Department of Energy
Albuquerque Operations
Los Alamos Area Office
Los Alamos, New Mexico 87544

P 403-671-203

RETURN RECEIPT REQUESTED

MAY 8 1991

CERTIFIED MAIL - RETURN RECEIPT REQUESTED

RECEIVED MAY 9 1991

A. Elizabeth Gordon, Ph.D., Permitting Supervisor
Hazardous and Radioactive Waste Bureau
New Mexico Environment Department
Harold Runnels Building
1190 St. Francis Drive
Santa Fe, New Mexico 87503

Dear Dr. Gordon:

Enclosed please find the supplemental documentation for a ground-water monitoring waiver at the TA-16 Surface Impoundment Closure. This documentation was requested by your office in a February 25, 1991 letter.

This documentation consists of four volumes containing five separate sections; they are: (1) Introduction; (2) Requirements for an Interim Status Ground-Water Monitoring Waiver and Certification; (3) Review of Background Information; (4) Summary; and (5) Reference Cited.

It is believed that this information demonstrates that ground-water monitoring is not necessary for this unit. Should you require further information, please feel free to call my staff at 665-5027.

Sincerely,

Monet Harrison, Acting Chief
Environment, Safety & Health Branch

Enclosure

cc w/o enclosure:
A. Tiedman, ADO, LANL, MS A120
J. Puckett, HSE-DO, LANL, MS K491
K. Hargis, HSE-8, LANL, MS K490

LESH:SS:0000

5922

Supporting Documentation for the

GROUND-WATER MONITORING WAIVER AT THE TA-16 SURFACE IMPOUNDMENT

prepared for

New Mexico Health and Environment Department

Environmental Improvement Division - Hazardous Waste Section

by the

Environmental Surveillance Group (HSE-8)

Los Alamos National Laboratory

Los Alamos, New Mexico

RCRA Number NM-0890010515

INTRODUCTION

Sometime between August 1985 and January 1986, barium concentration levels in the Technical Area (TA) 16 surface impoundment inadvertently exceeded 100 mg/l. At that time the impoundment was sampled for potential hazardous wastes and hazardous waste constituents. Contaminant indicator parameters for the impoundment included routine NPDES monitoring activities; and wastes exhibiting the characteristics of ignitability, corrosivity, reactivity, and Extraction Procedure (EP) toxicity. Subsequent sampling efforts included soil and water analyses for volatile (VOA) and semi-volatile (SVOA) organic compounds that are included on the U.S. Environmental Protection Agency's (EPA) Contract Laboratory Program (CLP) list, in addition to the parameters mentioned above. Analytical results from all of these sampling efforts have been summarized in the original closure plan document, and in a subsequent modification (IT, Inc., 1986; and HSE-8, 1988a). Barium above EP toxicity limits and certain volatile organic solvents above detection limits were identified in the impoundment fluids. Hence the TA-16 surface impoundment became a regulated unit under the Resource Conservation and Recovery Act (RCRA) of 1976, as amended. All other indicator parameters were below either detection or background limits, or were below regulated concentration levels.

The surface impoundment was declared a RCRA regulated unit in November 1986, by Los Alamos National Laboratory's (LANL) Environmental Surveillance Group (HSE-8) following completion of sample analyses. At that time an interim status closure plan (IT, Inc., 1986) was submitted to the New Mexico Environmental Improvement Division (NMEID) by the U.S. Department of Energy (DOE) for final clean closure under New Mexico Hazardous Waste Management Regulations (NMHWMR) 206.C.2.a through 206.C.2.k [40 CFR 265.110 through 120], and NMHWMR 206.C.6.f (40 CFR 265.228). As a RCRA regulated unit, this impoundment is required to have a ground-water monitoring plan under NMHWMR 206.C.1.a through e (40 CFR 265.90 through 94), unless it can be demonstrated under NMHWMR 206.C.1.a(3) [40 CFR 265.90(c)] that there is a low potential for migration of hazardous waste constituents from the facility via the uppermost aquifer to water supply wells or to surface water.

This document is a demonstration in support of a ground-water monitoring waiver at the TA-16 surface impoundment. This document will be maintained on file at the LANL HSE-8 office. It has been certified by Stephen G. McLin, a qualified ground-water hydrologist and geotechnical engineer, and by William D. Purtymun, a qualified geologist. Both of these individuals are staff members with HSE-8.

REQUIREMENTS FOR AN INTERIM STATUS GROUND-WATER MONITORING WAIVER

All or part of the ground-water monitoring requirements of NMHWMR 206.C.1 may be waived if the owner or operator can demonstrate that there is low potential for migration of hazardous waste or hazardous waste constituents from the facility via the uppermost aquifer to water supply wells or to surface water. This demonstration must be in writing, and must be kept at the facility. This demonstration must be certified by a qualified geologist or geotechnical engineer and must establish the following:

1. The potential for migration of hazardous waste or hazardous waste constituents from the facility to the uppermost aquifer by an evaluation of:

   a. A water balance of precipitation, evapotranspiration, runoff, and infiltration; and

   b. Unsaturated zone characteristics, including geologic materials, physical properties, and depth to ground-water; and

2. The potential for hazardous waste or hazardous waste constituents which enter the uppermost aquifer to migrate to a water supply well or surface water by an evaluation of:

   a. Saturated zone characteristics, including geologic materials, physical properties, and rate of ground-water flow; and

   b. The proximity of the facility to water supply wells or surface water.

This demonstration has been organized into several sections that follow. The "Review of Background Information" section is presented in a logical order to correspond with the numbered regulatory requirements for a monitoring waiver given above. Thus all information related to potential contaminant migration from the surface impoundments through the unsaturated zone and to the main aquifer is summarized first. Then all information related to the potential contaminant migration in the main aquifer to water supply wells or to surface water is summarized. A "Summary" section is then presented; these summary conclusions are ordered so as to correspond to the waiver requirements presented above. Finally a "References Cited" section lists all published and unpublished reports used by us in arriving at our stated conclusions.

REVIEW OF BACKGROUND INFORMATION

1.0 Migration Potential Through the Unsaturated Zone

1.0 (a) The Water Balance Equation

The water balance (precipitation, evapotranspiration, and surface runoff from precipitation) indicates there is little if any infiltration of precipitation through the soil zone into the underlying tuff and volcanic sediments. Hence there is no recharge to the uppermost aquifer beneath the mesa at TA-16 (Purtymun, 1962; Abrahams, et al., 1963; Cushman, 1965; Lane, 1981; NMEID, 1984; Purtymun, 1984; and Brown, et al., 1988). The uppermost aquifer beneath the western part of the plateau (i.e., the mesa at TA-16) lies at a depth of about 1,230 ft and is recharged from precipitation in the intermontane basins west of Los Alamos (Cushman, 1965; and Purtymun, 1984).

1.0 (b) Unsaturated Zone Characteristics

There are about 1,230 ft of unsaturated tuff and fanglomerate with interbedded volcanics underlying the mesa at TA-16 (Purtymun, 1968 and 1985; and Brown, et al., 1988). The thickness of the tuff is at its maximum along the western edge of the plateau, roughly delineated by New Mexico State Highway 4 west of Los Alamos National Laboratory (Weir and Purtymun, 1962; and Purtymun and Stoker, 1987). The thickness of the unsaturated tuff and sediments at TA-16 is indicated in the table shown below.

Geologic Section at TA-16	Thickness (ft)	Depth (ft)
BANDELIER TUFF		
Tshierege Member		
Unit 3	190	190
Unit 2	150	340
Unit 1	360	700
Otowi Member	210	910
Guaje Member	40	950
PUYE CONGLOMERATE		
Fanglomerate with interbedded volcanics	500	1,450
TESUQUE FORMATION		
Siltstones and sandstone, occasional conglomerates interbedded with volcanics, earlier volcanics and sediments	2,000	3,450
PRECAMBRIAN		
Basement Rocks	unknown	+3,450

The 950 ft of unsaturated tuff beneath the mesa at TA-16 consists of quartz and sanidine crystals and crystal fragments, and small rock fragments of latite, rhyolite, and pumice in a glassy gray ash matrix. The degree of welding of the tuff increases westward across the plateau toward the source area at Valles Caldera. The increase in welding of the tuff reduces the porosity and capillary size of the pores. This in turn reduces the intrinsic permeability and specific yield, while increasing the specific retention. Hence the hydraulic transmitting characteristics of the tuff are reduced as the degree of welding increases. Hydrologic investigations of the tuff that form the upper part of the plateau indicate that aqueous transport of contaminants through the unsaturated Bandelier Tuff is not a viable mechanism for contaminant migration (Purtymun, et al., 1978a; BEF, 1985a, 1985b, 1986a, and 1986b; and IT Inc., 1987). The physical and hydrologic characteristics of the Bandelier Tuff are discussed by Purtymun (1962 and 1973); Abrahams (1963); Purtymun and Koopman (1966); Purtymun and Kennedy (1966 and 1970); Purtymun and Abrahams (1967); Keller (1968); Purtymun, et al, (1978b and 1980b); Abeele, et al. (1981); Brown, et al. (1988); and Stephens (1988). The unsaturated tuff, sediments, and volcanics above the uppermost aquifer have also been evaluated in reference to air volume and energy exchange resulting from atmospheric pressure changes (Purtymun, et al., 1974).

2.0 Migration Potential in the Saturated Zone

2.0 (a) Saturated Zone Characteristics

The uppermost aquifer beneath the plateau at the TA-16 surface impoundment is the main aquifer of the Los Alamos area (Cushman 1965). It is the only aquifer in the area capable of water supply. Recharge to this aquifer is in the intermontane basins located west of Los Alamos. In general, water movement in the uppermost aquifer is from this recharge area toward the east and southeast beneath the plateau to the Rio Grande. A portion of this ground-water flow is discharged to the Rio Grande along White Rock Canyon through seeps and springs (Purtymun, et al., 1980a). The depth to the top of the main aquifer is about 1,300 ft along the western margin of the plateau (i.e., near TA-16) and decreases to about 600 feet along the eastern margin above the Rio Grande at White Rock Canyon. The age of water in the main aquifer has been estimated to be older than 1,500 years. It originated as precipitation recharge in the intermontane basin west of Los Alamos (Purtymun, 1984), and portions are discharged at the Pajarito well field (i.e., wells PM-1, PM-2, PM-3, PM-4, and PM-5) along the eastern edge of the plateau.

Tests in the main aquifer beneath the plateau indicate that the transmissivity ranges from 36,000 gpd/ft (490 ft of aquifer

penetration) to 94,000 gpd/ft (1,740 ft of aquifer penetration). The storage coefficient is estimated to range from 0.01 to 0.05. At a point located about three miles to the southeast of TA-16, the rate of ground-water movement in the upper 490 ft of the aquifer is toward the southeast at about 345 ft/yr (Purtymun, 1984). The quality of water in the main aquifer is monitored in supply wells, test wells, and springs; these data are reported in the Laboratory annual surveillance report (HSE-8, 1988b).

The geology and hydrology of the uppermost aquifer (main aquifer of the Los Alamos area) is documented in Theis and Conover (1962); Griggs and Hem (1964); Cushman (1965); Purtymun and Cooper (1969); Purtymun and Johansen (1974); Purtymun (1975 and 1984); Purtymun and Adams, (1980); and Purtymun and Stoker (1987 and 1988). The hydrologic characteristics of supply wells completed into the main aquifer have been documented in an annual report (Purtymun, et al., 1988).

2.0 (b) Proximity to Water Supply Wells or Surface Water

The nearest water supply wells to the TA-16 surface impoundment are wells PM-3 and PM-4. These wells lie about four miles to the east and east-southeast of the impoundment (Purtymun 1984); and are completed into the main aquifer. Movement of water in the main aquifer beneath the TA-16 area changes from east to southeast as it moves toward the Rio Grande. The Rio Grande flows to the southwest, forming White Rock Canyon by a down cutting action. This canyon forms the eastern edge of the plateau. The Rio Grande, the nearest perennial surface water body to the TA-16 area, lies about 8.5 miles southeast of the TA-16 surface impoundment.

SUMMARY

After reviewing the documents referenced herein, and from direct and extensive field observations at Los Alamos National Laboratory, we can summarize several important conclusions with regard to the surface impoundment at TA-16.

The potential for migration of hazardous wastes or hazardous waste constituents from the surface impoundment located at TA-16 to the uppermost aquifer is extremely low. This statement is supported by water balance studies which indicate that little to no precipitation recharges the main aquifer below Pajarito Plateau, by the presence of approximately 1,230 ft of unsaturated volcanic sediments below the TA-16 site, and the unsaturated hydraulic transmitting characteristics of the Bandelier Tuff. In addition, recent hydrologic investigations conducted on the tuff concluded that aqueous transport of contaminants through the unsaturated Bandelier Tuff is not a viable mechanism for contaminant transport.

In the highly unlikely event that hazardous wastes or hazardous waste constituents were to enter the uppermost aquifer from this surface impoundment, then there exists an extremely low potential for such constituents to migrate from this uppermost aquifer to water supply wells or to surface waters in concentration levels above minimum detection limits. This statement is supported by the large distances from the TA-16 impoundment to the nearest supply well and to the Rio Grande, by the hydraulic transmitting characteristics of the uppermost aquifer, by the moderately slow rate of ground-water movement, by the short time interval that the impoundment was in operation, by the relatively low barium concentration levels in the impoundment, and by periodic water quality sampling of the water supply wells and the Rio Grande.

These conclusions stated above are based on direct field observations made by us, and on physical evidence obtained from published and unpublished reports. All of the information used by us in arriving at these conclusions are cited below, and are intended to be part of this demonstration.

REFERENCES CITED

The following references are contained in Volume 1 of 4:

Abeele, W.V., M.L. Wheeler, and B.W. Burton, 1981, Geohydrology of the Bandelier Tuff; Los Alamos National Laboratory, Report No. LA-8962-MS, Los Alamos National Laboratory, Los Alamos, New Mexico.

Abrahams, J.H., J.E. Weir, and W.D. Purtymun, 1963, Distribution of moisture in soil and near-surface tuff on the Pajarito Plateau, Los Alamos County, New Mexico; U.S. Geological Survey, Short Articles in the Geologic and Hydrologic Sciences, Article No. 339, Washington, D.C.

Abrahams, J.H., 1963, Physical properties of and movement of water in the Bandelier Tuff, Los Alamos and Santa Fe Counties, New Mexico; U.S. Geological Survey, open file report, Albuquerque, New Mexico.

BEF, 1985a, Vadose zone characterization of Technical Area 54, Waste Disposal Areas G and L, Los Alamos National Laboratory, New Mexico: Report 1, Drilling and logging activities; Bendix Field Engineering Corporation report to Los Alamos National Laboratory, Los Alamos, New Mexico.

BEF, 1985b, Vadose zone characterization of Technical Area 54, Waste Disposal Areas G and L, Los Alamos National Laboratory, New Mexico: Report 2, Downhole instrumentation and pore-gas sampling and data collection procedures; Bendix Field Engineering Corporation report to Los Alamos National Laboratory, Los Alamos, New Mexico.

BEF, 1986a, Vadose zone characterization of Technical Area 54, Waste Disposal Areas G and L, Los Alamos National Laboratory, New Mexico: Report 3, Preliminary assessment of the hydrologic system; Bendix Field Engineering Corporation report to Los Alamos National Laboratory, Los Alamos, New Mexico.

BEF, 1986b, Vadose zone characterization of Technical Area 54, Waste Disposal Areas G and L, Los Alamos National Laboratory, New Mexico: Report 4, Preliminary assessment of the hydrologic system through fiscal year 1986; Bendix Field Engineering Corporation report to Los Alamos National Laboratory, Los Alamos, New Mexico.

The following references are contained in Volume 2 of 4:

Brown, F., W.D. Purtymun, A. Stocker, and A. Barr, 1988, Site geology of Technical Area 16 Area P; Los Alamos National Laboratory, Report No. LA-11209-MS, Los Alamos, New Mexico.

Cushman, R.L., 1965, An evaluation of aquifer and well characteristics of municipal well fields in Los Alamos and Guaje Canyons, near Los Alamos, New Mexico; U.S. Geological Survey, Water Supply Paper No. 1809-D, Washington, D.C.

Griggs, R.L., and J.D. Hem, 1964, Geology and ground-water resources of the Los Alamos area, New Mexico; U.S. Geological Survey, Water Supply Paper No. 1753, Washington, D.C.

HSE-8, 1988a, Supplemental report for the interim status closure plan at the TA-16 surface impoundment; unpublished report submitted to the New Mexico Environmental Improvement Division by Los Alamos National Laboratory, Santa Fe, New Mexico, dated November 18, 1988.

HSE-8, 1988b, Environmental surveillance at Los Alamos during 1987; Los Alamos National Laboratory, Environmental Surveillance Group (HSE-8), Report No. LA-11306-ENV, Los Alamos, New Mexico.

IT, Inc., 1986, Interim status closure and post-closure care plan, Technical Area 16 surface impoundment, Los Alamos National Laboratory; International Technology Corporation, Inc., report to Los Alamos National Laboratory, Los Alamos, New Mexico.

IT, Inc., 1987, Hydrogeologic assessment of Technical Area 54, areas G and L, Los Alamos National Laboratory; International Technology Corporation, Inc., final report to Los Alamos National Laboratory, Los Alamos, New Mexico.

Keller, M.D., 1968, Geologic studies and material properties investigations of Mesita de Los Alamos; Los Alamos Scientific Laboratory, Report No. LA-3728, Los Alamos National Laboratory, Los Alamos, New Mexico.

Lane, L., 1981, Estimated rainfall frequencies for Los Alamos; Los Alamos National Laboratory, unpublished inter-office memorandum from L. Lane (HSE-12) to Brent Bowen (HSE-8), dated August 11, 1981, Los Alamos, New Mexico.

NMEID, 1984, A reasonable worst-case water balance for LANL hazardous waste disposal areas with emphasis on TA-54; Attachment 1 of an unpublished report, New Mexico Environmental Improvement Division, Santa Fe, New Mexico, 15p.

Purtymun, W.D., and J.H. Abrahams, 1967, Hydrologic characteristics of an ash flow tuff at Frijoles Mesa, Los Alamos County, New Mexico; U.S. Geological Survey, open file report, Albuquerque, New Mexico.

Purtymun, W.D., and H. Adams, 1980, Geohydrology of Bandelier National Monument, New Mexico; Los Alamos Scientific Laboratory, Report No. LA-8461-MS, Los Alamos National Laboratory, Los Alamos, New Mexico.

The following references are contained in Volume 3 of 4:

Purtymun, W.D., and J.B. Cooper, 1969, Development of ground-water supplies on the Pajarito Plateau, Los Alamos County, New Mexico; U.S. Geological Survey, Professional Paper No. 650-B, pp. B149-B153, Washington, D.C.

Purtymun, W.D., R. Garde, and R. Peters, 1978a, Movement of fluids and plutonium from shafts at Los Alamos, New Mexico; Los Alamos Scientific Laboratory, Report No. LA-7379-MS, Los Alamos National Laboratory, Los Alamos, New Mexico.

Purtymun, W.D., and S. Johansen, 1974, General geology of the Pajarito Plateau; New Mexico Geological Society, Guidebook to the 25th field conference at Ghost Ranch, pp. 347-349, New Mexico Institute of Mining and Technology, Socorro, New Mexico.

Purtymun, W.D., and W.R. Kennedy, 1966, Distribution of moisture and radioactivity in the soil and tuff at the contamination waste pits near Technical Area 21, Los Alamos, New Mexico; U.S. Geological Survey, open file report, Albuquerque, New Mexico.

Purtymun, W.D., and W.R. Kennedy, 1970, Geology and hydrology of Mesita del Buey; Los Alamos Scientific Laboratory, Report No. LA-4660, Los Alamos National Laboratory, Los Alamos, New Mexico.

Purtymun, W.D., and F.C. Koopman, 1966, Physical characteristics of the Tshierege Member of the Bandelier Tuff with reference to use as a building and ornamental stone; U.S. Geological Survey, open file report, Albuquerque, New Mexico.

Purtymun, W.D., F.C. Koopman, S. Barr, and W.E. Clements, 1974, Air volume and energy transfer through test holes and atmospheric pressure effects on the main aquifer; Los Alamos Scientific Laboratory, Report No. LA-5725-MS, Los Alamos National Laboratory, Los Alamos, New Mexico.

Purtymun, W.D., R.J. Peters, and J.W. Owens, 1980a, Geohydrology of White Rock Canyon of the Rio Grande from Otowi to Frijoles Canyon; Los Alamos Scientific Laboratory, Report No. LA-8635-MS, Los Alamos National Laboratory, Los Alamos, New Mexico.

Purtymun, W.D., M.A. Rogers, and M.L. Wheeler, 1980b, Radiochemical analyses of samples from beneath a solid radioactive waste disposal pit at Los Alamos, New Mexico; Los

Alamos Scientific Laboratory, Report No. LA-8422-MS, Los Alamos National Laboratory, Los Alamos, New Mexico.

Purtymun, W.D., and A. Stoker, 1987, Environmental status of Technical Area 49, Los Alamos, New Mexico; Los Alamos National Laboratory, Report No. LA-11135-MS, Los Alamos, New Mexico.

Purtymun, W.D., and A. Stoker, 1988, Water supply at Los Alamos: Current status of wells and future water supply; Los Alamos National Laboratory, Report No. LA-11332-MS, Los Alamos, New Mexico.

Purtymun, W.D., A. Stoker, M. Maes, 1989, Water supply at Los Alamos in 1987; Los Alamos National Laboratory, Report No. LA-11478-PR, Los Alamos, New Mexico.

Purtymun, W.D., M.L. Wheeler, and M.A. Rogers, 1978b, Geologic description of cores from holes P-3 MH-1 through P-3 MH-5, Area G, Technical Area 54; Los Alamos Scientific Laboratory, Report No. LA-7308-MS, Los Alamos National Laboratory, Los Alamos, New Mexico.

Purtymun, W.D., 1962, The distribution of moisture in soil and underlying tuff at Technical Area 49, Frijoles Mesa, Los Alamos County, New Mexico; U.S. Geological Survey, open file report, Albuquerque, New Mexico.

Purtymun, W.D., 1968, Geology of the microseimograph station at S-site, Los Alamos County, New Mexico; U.S. Geological Survey, open file report, Albuquerque, New Mexico.

Purtymun, W.D., 1973, Underground movement of tritium from solid-waste storage shafts; Los Alamos Scientific Laboratory, Report No. LA-4660, Los Alamos National Laboratory, Los Alamos, New Mexico.

<u>The following references are contained in Volume 4 of 4</u>:

Purtymun, W.D., 1975, Geohydrology of the Pajarito Plateau with reference to quality of water, 1949-1972; Los Alamos Scientific Laboratory, unpublished informal report, Los Alamos National Laboratory, Los Alamos, New Mexico.

Purtymun, W.D., 1984, Hydrologic characteristics of the main aquifer in the Los Alamos area: Development of ground-water supplies; Los Alamos National Laboratory, Report No. LA-9957-MS, Los Alamos, New Mexico.

Purtymun, W.D., 1985, Geology and hydrology near S-site; Los Alamos National Laboratory, unpublished inter-office memorandum

from W.D. Purtymun to A. Drypolcher (HSE-8), dated 11-12-85, HSE-8 file no. HSE-8-85-1385, Los Alamos, New Mexico.

Stephens, D.B., 1988, Final data report on laboratory analyses of soil hydraulic properties of welded tuffs at Los Alamos National Laboratory; Daniel B. Stephens and Associates, Inc. report to Los Alamos National Laboratory, Los Alamos, New Mexico.

Theis, C.V., and C.S. Conover, 1962, Pumping tests in the Los Alamos Canyon well field near Los Alamos, New Mexico; U.S. Geological Survey, Water Supply Paper No. 1619-I, Washington, D.C.

Weir, J.E., and W.D. Purtymun, 1962, Geology and hydrology of Technical Area 49, Frijoles Mesa, Los Alamos County, New Mexico; U.S. Geological Survey, open file report, Albuquerque, New Mexico.

CERTIFICATION

GROUND-WATER MONITORING WAIVER AT THE TA-16 SURFACE IMPOUNDMENT

We the undersigned do hereby certify that this demonstration in support of a ground-water monitoring waiver for the above mentioned facility is correct and accurate, and that all supporting documentation in the reference section of the attached report has been reviewed by us, both individually and collectively. The opinions reached by us, and expressed herein, are based on direct field observations at Los Alamos National Laboratory, and the published and unpublished reports cited in this document. This demonstration consists of five separate sections; they are: (1) Introduction; (2) Requirements for an Interim Status Ground-Water Monitoring Waiver; (3) Review of Background Information; (4) Summary; and (5) References Cited. Copies of the references cited in this demonstration have been included in four separately bound volumes.

Stephen G. McLin

Stephen G. McLin, Ph.D., P.E.
Ground-Water Hydrologist and Geotechnical Engineer

William D. Purtymun

William D. Purtymun
Geohydrologist

LA-8962-MS

Los Alamos National Laboratory is operated by the University of California for the United States Department of Energy under contract W-7405-ENG-36.

Geohydrology of Bandelier Tuff

Los Alamos
Los Alamos National Laboratory
Los Alamos, New Mexico 87545

An Affirmative Action/Equal Opportunity Employer

This work was supported by the US Department of Energy, Office of Nuclear Waste Management.

DISCLAIMER

This report was prepared as an account of work sponsored by an agency of the United States Government. Neither the United States Government nor any agency thereof, nor any of their employees, makes any warranty, express or implied, or assumes any legal liability or responsibility for the accuracy, completeness, or usefulness of any information, apparatus, product, or process disclosed, or represents that its use would not infringe privately owned rights. References herein to any specific commercial product, process, or service by trade name, trademark, manufacturer, or otherwise, does not necessarily constitute or imply its endorsement, recommendation, or favoring by the United States Government or any agency thereof. The views and opinions of authors expressed herein do not necessarily state or reflect those of the United States Government or any agency thereof.

LA-8962-MS

UC-11
Issued: October 1981

Geohydrology of Bandelier Tuff

W. V. Abeele
M. L. Wheeler
B. W. Burton

Los Alamos
Los Alamos National Laboratory
Los Alamos, New Mexico 87545

CONTENTS

ABSTRACT 1

I. INTRODUCTION 1

II. PHYSICAL SETTING 3
A. Geology of the Los Alamos Area 3
B. Tuff Structure and Texture 6
C. General Climatology 6
D. Precipitation 7
1. Recent Climatic Records 7
2. Tree-Ring Evidence 8

III. SURFACE WATER 9

IV. SATURATED FLOW 11

V. GAUGING STATION, AREA G 12
A. Introduction 12
B. Location and Watershed Area 12
C. Weir and Stilling Basin 12
D. Runoff Events 14
E. Weir Calibration 14
1. Theoretical 14
2. Empirical 15
F. Rainfall-Runoff Calibration 15

VI. SATURATED AND UNSATURATED HYDRAULIC CONDUCTIVITIES 16
A. General 16
B. Crushed Tuff 17
1. Measurements 17
2. Predictive Methods 19
C. Solid Tuff 21
1. Measurements 21
2. Predictive Methods 21

VII. HYDROLOGIC MONITORING 22
A. Parameters Influencing Neutron Probe Readings 22
B. Prior Measurements 22
C. Current Monitoring 25
1. History 25
2. Data Discussion 25
a. Area C 25
b. Area G 27
c. Area F 29
d. TA-51 30
3. Geophysical Logging 30
4. Justification for Converting to "Inactive" 30

VIII. TRITIUM MIGRATION 31
A. Tritiated Water in Soils 31
B. Emanation of Tritiated Water 33

IX. STRATIGRAPHIC CONTROLS ON FLOW 37

X. RADIONUCLIDE TRANSPORT STUDIES 38
A. Downward Migration through Leaching 38
B. Upward Migration via Evapotranspiration 38

XI. SHEAR IN WET COHESIONLESS SOILS AND CRUSHED TUFF 39

ACKNOWLEDGMENTS 43
REFERENCES 43

APPENDIX

SUMMARY OF DEPTH RANGES AND MEASUREMENT DATES FOR MONITORING HOLES 46

FIGURES

1 Burial site map 2
2 Geologic stratigraphic relationships of Los Alamos County from Sierra de los Valles to the Rio Grande 3
3 Base map 10
4 Location of watershed and stilling basin, Area G, TA-54 13
5 Cross-section of stilling basin 13
6 Weir plate details 13
7 Precipitation and runoff, Area G weir 14
8 Calculated hydraulic conductivities compared with measured data 20
9 Saturation ratio as a function of matric potential (moisture characteristic curves) 22
10 Hydraulic conductivity as a function of matric potential 23
11 Hydraulic conductivity as a function of saturation ratio 23
12 Moisture distributions at TA-49 (Abrahams, Weir, & Purtymun, 1961) 24
13 Moisture distributions in Bandelier Tuff near TA-21 (Purtymun & Kennedy, 1966). 25
14 Moisture Hole CP2-1 26
15 Moisture Hole CP6-1 27
16 Moisture Hole GP1-1 28
17 Moisture Hole GS50-3 28
18 Moisture Hole GS50-5 29
19 Moisture Hole GP7-2 30
20 Resistance tests on tuff 40
21 Resistance tests on soil 41

TABLES

I PROPERTIES OF TUFF AS A FUNCTION OF DEGREE OF WELDING 5
II UPDATED PRECIPITATION WITH PROBABILITY LEVELS EQUAL TO OR LESS THAN (mm of ppt) 8
III DISCHARGE DATA FOR AREA G WEIR 15
IV PRECIPITATION AND RUNOFF ON JULY 10, 1980 16
V HYDRAULIC CHARACTERISTICS OF CRUSHED BANDELIER TUFF AS A FUNCTION OF MATRIC POTENTIAL 18
VI HYDRAULIC CONDUCTIVITY OF SOLID TUFF AS A FUNCTION OF MATRIC POTENTIAL 21
VII MOISTURE CONTENT OF BANDELIER TUFF 24
VIII HISTORY AND CURRENT STATUS AT MONITORING HOLES 26
IX DECREASE IN RADIOACTIVITY NEAR SHAFT 13 AS A FUNCTION OF DISTANCE FROM THE SHAFT ALONG A S-W AXIS 32
X DECREASE IN RADIOACTIVITY NEAR SHAFTS 50 AND 59 AS A FUNCTION OF DISTANCE FROM THE SHAFT 33
XI ACTIVITY AND FLUX OF TRITIATED WATER AT THE SOIL-ATMOSPHERE INTERFACE 4.7 m FROM THE CENTER OF GS-150 36
XII VANE SHEAR TEST ON SOIL 40
XIII VANE SHEAR TEST ON CRUSHED TUFF 40
XIV RESISTANCE TO PENETRATION IN TUFF 42
XV RESISTANCE TO PENETRATION IN SOIL 42
XVI RESISTANCE TO PENETRATION IN TUFF AFTER PUDDLING 43
XVII RESISTANCE TO PENETRATION IN SOIL AFTER PUDDLING 43

GEOHYDROLOGY OF BANDELIER TUFF

by

W. V. Abeele
M. L. Wheeler
B. W. Burton

ABSTRACT

The Los Alamos National Laboratory has been disposing of radioactive wastes since 1944. Environmental studies and monitoring for radioactive contamination started concurrently. In this report, only two mechanisms and rates by which the radionuclides can enter the environment are studied in detail: subsurface transport of radionuclides by migrating water, and diffusion of tritiated water (HTO) in the vapor phase. The report also includes a section concerning the influence of moisture on shear strength and possible resulting subsidences occurring in the pit overburdens. Because subsurface transport of radionuclides is influenced by the hydraulic conductivity and this in turn is regulated by the moisture content of any given material, a study was also undertaken involving precipitation, the most important climatic element influencing the geohydrology of any given area. Further work is in progress to correlate HTO emanation to atmospheric and pedological properties, especially including thermal characteristics of the tuff.

I. INTRODUCTION

Wastes containing plutonium and other radionuclides have been buried at Los Alamos National Laboratory since the beginning of Laboratory operations in the early 1940s. Open pits or trenches have provided the principal disposal facility, but vertical shafts and covered seepage pits have been used for special waste forms. All shafts, pits, and trenches have been excavated in the surface of the Bandelier tuff, the principal rock-type exposed in the Los Alamos area (Fig. 1). The tuff (a nonwelded to welded volcanic ash) comprises an upland area called the Pajarito Plateau. The Plateau is dissected by numerous canyons trending east-west, all of which drain into the Rio Grande. Most of the Laboratory facilities, including the waste disposal sites, are located on the tops of the resulting finger-like mesas.

A large variety of waste types have been buried at Los Alamos National Laboratory. The bulk of the material is room-generated trash, such as paper, packing material, protective clothing, broken glassware, obsolete contaminated equipment, etc., which is generally contained in cardboard boxes or wooden crates. A wide variety of disposal operations are performed, ranging from shaft disposal of cylinders containing millicurie quantities of tritium to demolition and burial of entire contaminated buildings. During the Laboratory's early years, liquid wastes were disposed directly to the ground by discharging them into seepage pits. Since 1952, the sludges resulting from liquid waste treatment have been placed in drums for burial or mixed with cement and poured into shafts.

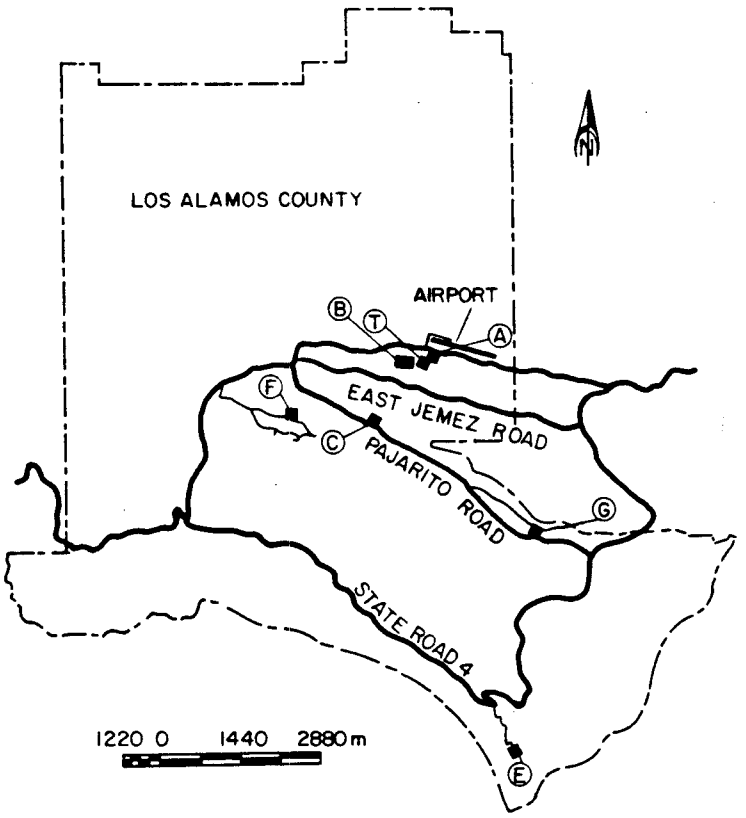

Fig. 1. Burial site map.

Presently, solid wastes are placed in open pits, characteristically about 10 m deep by 15 m wide by 130 m long. The wastes are placed in layers, with each layer covered with the crushed tuff excavated during construction of the pit. Location, physical description, and radionuclide content of the wastes are recorded in log books and on a computerized record keeping system. When a pit is filled to within approximately a meter of the ground surface, a cover of crushed tuff is overlaid and mounded about 1 m high to facilitate precipitation runoff. The surface is then reseeded with native vegetation for erosion control.

Present practices have evolved from a variety of burial procedures, but historically all practices are similar. Wastes are placed in trenches to within approximately a meter of the surface and the trench is then backfilled with uncontaminated crushed tuff. A records survey was made of the radionuclide content and composition of solid wastes disposed at Los Alamos National Laboratory since the beginning of the Laboratory (Rogers, 1977). Waste disposal records were highly variable in quality and quite incomplete until the mid-1950s. Detailed records of content and composition were not kept until 1959, and the quality of recording has improved steadily since that time. Guidelines for construction and use of solid waste disposal facilities at Area G, TA-54 have been in effect since 1956. The latest revision* is consistent with established Department of Energy (DOE) Burial Site Criteria.

Determining the potential impact of buried radioactive wastes on the environment requires definition of the mechanisms and rates by which the radionuclides can enter the environment. The various

*Memo H-7-80-660 To: Distribution (Operation Waste Management Committee), Through: Harry Jordan, H-DO; From: W. D. Purtymun, H-8, M. Wheeler, LS-6, and J. L. Warren, H-7 (December 10, 1980).

mechanisms can be divided into two major categories—natural phenomena more or less independent of human activity, and advertent acts by man, such as war, land excavation, sabotage, etc. All processes discussed here fall into the former category and can be further subdivided into two groups: chronic release processes, which occur at a more or less uniform rate when viewed on a time scale of tens to hundreds of years, and acute release processes consisting of single events separated by long periods of nonoccurrence. Chronic release mechanisms include exposure of the wastes by wind or water erosion, subsurface transport of radionuclides by migrating water, and plant or animal transfer of buried material to the surface.

This report is limited to the study of subsurface transport of radionuclides by migrating water or by diffusion of a radionuclide such as tritium in the vapor phase of tritiated water (HTO).

II. PHYSICAL SETTING

A. Geology of the Los Alamos Area

The volcanic and sedimentary rocks that occur in the Los Alamos area range in age from Miocene to Holocene. Rock types include sandstones and siltstones, crystalline rocks, and ash-flow tuffs (Fig. 2).

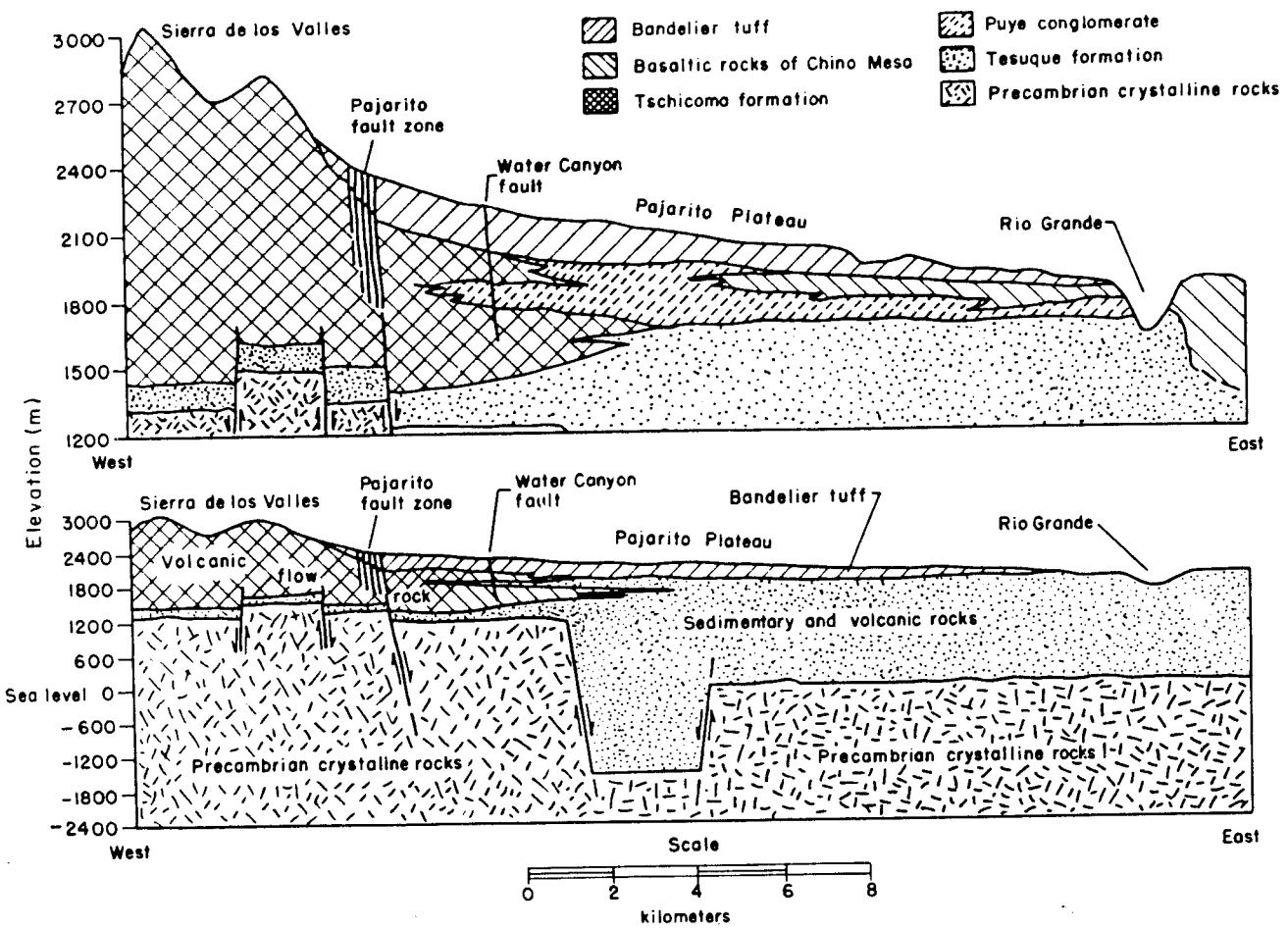

Fig. 2. Geologic stratigraphic relationships of Los Alamos County from Sierra de los Valles to the Rio Grande.

The oldest rock unit in the Los Alamos area is the Tesuque Formation, consisting of fossiliferous siltstones and sandstones with lenses of clay that were deposited as basin fill in the Rio Grande structural trough. Near Los Alamos these sediments are light pinkish-tan and include some interbedded basalts. The Tesuque underlies the Pajarito Plateau and is exposed at lower levels along the Puye Escarpment and in White Rock Canyon. The main water supply for Laboratory and domestic use is derived from the Tesuque. The age of the Tesuque is Miocene.

The Tschicoma Formation forms the major part of the interior mass of the central Jemez Mountains; thus, exposures are limited to the western and northern parts of the Los Alamos area. Rock types are porphyritic dacite, rhyodacite, and quartz latite containing phenocrysts of pyroxene, hornblende, biotite, plagioclase, and quartz (Bailey et al., 1969; Smith et al., 1970). Some units of latite and quartz latite in the Los Alamos area contain xenocrystic plagioclase that has been partially remelted, embayed, and resorbed, as well as subrounded and embayed quartz (Griggs, 1964). The maximum thickness of the 6.7 to 3.7 million-year-old (Myr) Tschicoma Formation exceeds 900 m (Bailey et al., 1969; Smith et al., 1970).

The Puye Formation, named for exposures in cliffs along the Puye Escarpment, is divided into two informal members, the lower Totavi Lentil, overlain by a fanglomerate. The basal Totavi Lentil (0 to 25 m thick) consists of well-rounded pebbles, cobbles, and small boulders of Precambrian quartzite and granite in a matrix of coarse arkosic sandstone. The upper unit is a poorly consolidated, silty, sandy conglomerate containing interlayered lapilli-tuff beds and volcanic mudflow deposits. The detritus is mostly dacite, rhyodacite, and quartz latite debris from erosion of the Tschicoma Formation (Bailey et al., 1979; Smith et al., 1970). The Puye is ~15 m thick in the eastern part of the Pajarito Plateau and thickens westward to ~220 m (Bailey et al., 1969). In the central and eastern parts of the plateau the Puye overlies the Tesuque Formation. It interfingers with basaltic andesite flows from the Cerros del Rio to the southeast and with younger flows of the Tschicoma to the west (DOE/EIS-0018, 1979).

The volcanic rocks of Cerros del Rio (Chino Mesa), which include some alkali olivine basalt, are mostly basaltic andesite flows and tuffs (0 to 460 m thick) containing xenocrysts of quartz (Smith et al., 1970). Some of these flows extend northwestward to form the steep walls of White Rock Canyon and cap high mesas to the east. Griggs (1964) mapped five units in the Los Alamos area. The volcanics of Cerros del Rio are less than 2.8 Myr old (Smith et al., 1970).

The basaltic andesite of Tank Nineteen (Smith et al., 1970) forms a broad shield volcano in the western part of the Cerros del Rio and ranges in thickness from 15 to 150 m. In the lower part of White Rock Canyon these flows overlie the Otowi Member of the Bandelier Tuff and tuffs of the Cerro Toledo Rhyolite.

Volcanism in the Jemez Mountains during the Pleistocene produced a series of rhyolite and quartz latite domes, ash flows, air-fall pumice, and obsidian. In the Los Alamos area these rocks are represented by the Cerro Toledo Rhyolite and the Bandelier Tuff.

The Cerro Toledo Rhyolite is a series of rhyolite domes, obsidian, tuffs, and tuff breccias that occur mostly within the Toledo Caldera (Smith et al., 1970). Exposures near Los Alamos occur in a small area in Rendija and Guaje Canyons. These reworked tuffs and sediments overlie the Puye Formation and are less than 30 m thick (DOE/EIS-0018, 1979).

The Bandelier Tuff is a sequence of nonwelded-to-welded rhyolite ash flows and pumice containing bi-pyramidal quartz and chatoyant sanidine (Smith et al., 1970). The tuff forms the upper parts of the Jemez Plateau on the western and the Pajarito Plateau on the eastern flanks of the Jemez Mountains. It is, therefore, the most important geologic unit at Los Alamos. All Laboratory facilities are constructed on the Bandelier Tuff. The formation is divided into two members, the lower Otowi and upper Tshirege, locally separated by tuffs of the Cerro Toledo Rhyolite. Each member is composed of a basal air-fall pumice overlain by a series of ash-flow units. The thickness of the tuff ranges from 10 to 320 m.

In the Los Alamos area the 1.4 Myr-old Otowi Member consists of a 0- to 10-m-thick basal bedded air-fall pumice (Guaje Pumice Bed) overlain by massive to poorly bedded nonwelded ash-flow deposits

containing abundant accidental lithic fragments. Ash flow units in the Otowi often easily erode to form characteristic pinnacle-shaped features. The thickness of this member in the Los Alamos area ranges from 0 to 80 m (DOE/EIS-0018, 1979).

The 1.1 Myr-old Tshirege Member consists of a 0.3-m-thick basal bedded air-fall pumice (Tsankawi Pumice Bed) overlain by nonwelded to welded ash flows containing genetically-related, hornblende-rich, quartz latite pumice and accidental lithic fragments (Bailey et al., 1969; Smith et al., 1970). The ash flows are often separated by pyroclastic surge deposits; pumice swarms occur intermittently. The Tshirege forms alternating vertical cliffs and steep slopes, caused by differential induration of the ash flows, resulting in units of varying hardness. The base of the Tshirege rests on the irregular erosional surface of the Otowi.

Physical properties of the tuff that may affect fluid flow result primarily from induration (which includes vapor-phase crystallization, devitrification, and welding) and jointing.

Vapor-phase crystallization results from the ash flows being partially fluidized by hot expanding gases during emplacement. After stabilization of the flows, these gases migrated upward and deposited dissolved materials as secondary minerals in void spaces between the glass shards. Vapor-phase minerals are predominantly cristobalite, alkalic feldspar, and tridymite. If a flow becomes welded before the vapor phase escapes, trapped gases may form cavities, which may or may not subsequently be filled with a solid phase.

Because volcanic glass (the major constituent of ash) is geologically unstable, it will spontaneously devitrify, yielding cristobalite, feldspar, and tridymite. Devitrification tends to be more prevalent in tuff that has undergone compaction and welding but may occur in more porous tuffs as well. Vapor-phase crystallization and devitrification can affect the hardness and porosity of the rock.

Depending on the temperature and water content of an ash flow, the constituent glass shards may deform and stick to one another, a process known as welding. Welding results in increased hardness and decreased porosity of the rock. The degree of welding in the Bandelier Tuff varies markedly. The majority of the Tshirege Member is moderately welded with some areas of more dense welding in the uppermost flow units (DOE/EIS-0018, 1979). Table I shows the variation in physical properties of the tuff as a result of welding.

Joints, formed by cooling of the ash flows, commonly divide the tuff into irregular blocks. The predominant joint sets are vertical or nearly vertical and joint frequency generally increases with increasing degree of welding. Joints range from closed to open as much as several centimeters; they may contain caliche near the surface, grading downward to clay (usually montmorillonite). In excavations, plant roots have been observed to extend to depths of at least 10 m in joints.

Moisture infiltrating into exposed tuff surfaces dissolves minute amounts of silica, which are redeposited as interstitial opaline material upon evaporation. This results in a "case hardened" surface layer a few centimeters thick that is highly resistant to wind and water erosion (DOE/EIS-0018, 1979). However, exposed pumice fragments weather readily, leaving a pitted surface on some units.

TABLE I

PROPERTIES OF TUFF AS A FUNCTION OF DEGREE OF WELDING[a]

	Nonwelded	Moderately Welded	Welded
Porosity (Vol %)	40-60	30-55	15-40
Cohesion of Shards	slight	moderate	good
Deformation of Shards	none	slight	strong, flattening of shards
Fracture	crumbly	somewhat brittle	brittle

[a]Data from DOE/EIS-0018,1979

B. Tuff Structure and Texture

The porosty of the tuff can be calculated from the real and apparent specific gravity where the per cent pore space =

$$1 - \frac{\text{bulk specific gravity}}{\text{real specific gravity}} \times 100 \cdot$$

The porosity of the tuff ranges from about 20% to about 60%. The size distribution of the pores, though, may be more important than total porosity in assessing aeration, permeability, and water-holding properties.

Equivalent pore size and matric potential applied to tuff relate in the following manner.

Pore Diameter (m)	Matric Potential (kPa)
$2 \cdot 10^{-4}$	1.5
$1 \cdot 10^{-4}$	3.0
$5 \cdot 10^{-5}$	6.0
$2 \cdot 10^{-5}$	15.0

The Tshirege Member reaches porosities of 60% that are comparable to those of the upper ranges encountered in fine clays (Abrahams, 1963). Such high porosities are, however, unusual for consolidated materials.

Abrahams shows that the bulk specific gravity of dry tuff can be divided into four separate, statistically significant groups, ranging from 1280 to 1840 kg m^{-3}.

There is, of course, a strong inverse correlation between the dry unit weight and porosity, while permeability has been shown to increase exponentially with the particle size and subsequent pore size. Particle sizes in the tuff average 46% of clay and silt and 53% sand and resembles a sandy silt (Abrahams, 1963).

Water in the smaller pores moves mostly by the slower processes of capillarity and vapor diffusion and, at saturation, contributes little to the bulk of the movement. Jointing, though, is common throughout the Tshirege Member and is sediment-free below a certain depth. Interconnected joints could provide paths for rapid water movement at saturation, if such a situation were to occur. Fears for this to happen are, however, unwarranted.

C. General Climatology

Maximum temperatures are generally below 32°C, with the extreme recorded at 35°C. A large diurnal variation keeps nocturnal temperatures in the 12°C to 15°C range. Winter temperatures are typically in the range of −10°C to 5°C, with the extreme recorded at −28°C. Many winter days are clear with light winds, and strong solar radiation makes conditions quite comfortable even when air temperatures are cold. The annual total of heating °C days is 3500, with January accounting for over 610 while July and August average zero degree days. Higher temperatures will increase evapotranspiration and occur at the origin of tuff desiccation. An annual observed value of about two-thirds the potential insolation is observed based on measured diurnal direct radiation. The reduction is caused by cloudiness, implying that approximately one-third of the daylight hours in one year were affected by cloudiness. The maximum cloud-free month (January) had 85% of potential insolation while the minimum (July) had 55%. A higher insolation with the same air temperature means a higher degree of desiccation of the tuff because of increased ground temperatures from radiation absorption.

Average relative humidity is 40%, ranging from 30% in May and June to above 50% in July, January, and February. The diurnal variation is very large and basically inverted to the diurnal temperature cycle. The summer months have nocturnal maxima of 80% and minima of 30%, while spring, the driest time, has a diurnal range from 15% to 50%. A lower relative humidity will enhance desiccation of the tuff because of an increased vapor pressure differential at the ground-atmosphere interface. A high relative humidity, however, may cause condensation to occur at the tuff surface provided the temperature depression in the tuff is sufficient.

At most sites near-calm wind conditions exist 10% to 15% of the time; 80% of the wind speeds are less than 3 m s^{-1}, and less than 1% of the time 10-minute-averaged winds are greater than 16 m s^{-1}. The nocturnal period, from 2000 to 0800 MST, is representative of stable thermal stratification. The nighttime winds show the greatest incidence of calm conditions.

During the period of insolation, 0800 to 1600 MST, the air is generally unstable, and 1600 to 2000 MST is a transition period during which the statistics are strongly affected by transient processes associated with sunset. Winds will remove layers of increased vapor pressure at the ground-atmosphere interface and consequently enhance desiccation of the tuff with increased wind speed.

Atmospheric diffusion depends on three primary considerations; source factors (size, duration, elevation above ground, temperature), terrain factors (roughness, slope, vegetative cover, solar heating), and meteorological factors (wind speed and direction, temperature stratification, turbulence energy). There is considerable interdependency among all of the factors listed and many of the available formulae for estimating atmospheric dispersion represent attempts at interrelating the impact of these factors. All these factors have to be taken into consideration in evaluating the tritiated water contamination of the atmosphere.

As expected, there is a distinct orientation of the concentration pattern parallel to the canyons. This feature suggests an important role of drainage winds in transporting effluents released in the western portion of the laboratory site. Stable thermal stratification is an integral feature of the drainage winds, as is a reduced level of turbulence. Therefore, these flows, quite frequent during nighttime hours, have the poorest capacity for dilution of released material. The stable temperature stratification inhibits vertical mixing, and horizontal mixing is constrained by the presence of the canyon walls. For purposes of estimation, the dilution within short travel distances may be neglected. Hence, for drainage within canyons that open into populated areas, the effective mixing length from release point to receptor is severely reduced. In particular, sites that have a drainage wind component into Pajarito Canyon can produce abnormally high concentrations of effluents in White Rock.

Another complicated transport process relevant to potential dispersion of materials from sites located in the bottom of canyons has been identified. Two mechanisms have been documented that can lead to an exchange of air between canyon and mesa tops. The first is convective mixing in an unstable atmosphere. This is basically a daytime phenomenon, probably most prevalent in the warm season. The second mechanism occurs under all stabilities when the cross-canyon wind exceeds 2 m s^{-1}, giving rise to a major roll eddy. This means that there are many circumstances under which material could be readily transported from the canyon bottom to the mesa top. (DOE/EIS-0018,1979, pp. 3-28 to 3-33).

D. Precipitation

1. Recent Climatic Records. The most important climatic element influencing the geohydrology of any given area is precipitation. Based on updated climatic records (1951 to 1980) for Los Alamos, New Mexico, precipitation equal to or less than an expected amount has been calculated for probability levels of 0.01 to 0.99. These values were determined based on the normal distribution obtained from precipitation data recorded in the last 30 years. Table II indicates those values on a yearly basis and shows that there is a 0.99 chance that the annual precipitation is less than 768 mm. It can also be interpreted that there is a 0.01 chance that the annual precipitation will exceed 768 mm. The updated (1980) mean annual precipitation for Los Alamos is 457 mm.

TABLE II

UPDATED PRECIPITATION WITH PROBABILITY LEVELS EQUAL TO OR LESS THAN (mm of ppt)

Level	0.01	0.05	0.10	0.20	0.30	0.40	0.50	0.60	0.70	0.80	0.90	0.95	0.99
Ppt	146	216	259	303	333	356	457	558	581	611	655	698	768

2. **Tree-Ring Evidence.** Dendroclimatology involves comparing modern meteorological records with contemporaneous tree ring widths and establishing, through regression analysis, the best statistical relationship existing between the tree ring index as the independent variable and, say, precipitation as the dependent variable. By then substituting tree ring indices in the equation, an estimate is obtained of previous precipitation patterns. Regions where temperature or rainfall is a severely limiting factor in growth yield the most clearly interpretable climatic indices. In Los Alamos, the one factor that can be notably limiting is precipitation. This should stimulate backward extension of precipitation gauge records by growth indices. The University of Arizona has supported a continuing search throughout the Western United States for the most sensitive trees, a fundamental phase of a research program with its main objective the derivation of centuries-long rainfall indices of quantitative value. No other region in the world is apparently so naturally favored as a source of dendroclimatic history (Schulman, 1951, 1952). Long-lived coniferous species, with abilities to survive very arid cycles, make selective studies possible. Tree ring indices have been obtained that showed a high dependency on annual rainfall.

In Los Alamos, the best correlations between tree ring indices and annual precipitation were found for the following, in order of goodness of fit:

a. Ponderosa pines, where precipitation (mm) = $543\ I_{Po}^{0.606}$. The corresponding correlation coefficient was found to be significant at the 0.99 level (I_{Po} = tree ring index for ponderosa pine).

b. Piñon, where precipitation (mm) = $467\ I_{Pi}^{0.619}$. The correlation coefficient in thise case was found to be still significant at the 0.99 level (I_{Pi} = tree ring index for piñon).

The similarity between these two equations is striking. The fact that in both cases the exponent of the index is <1 indicates that relatively small increases in precipitation could lead to sizable increases of tree ring indices in the Los Alamos area. A 100% increase of the index (doubling) corresponds to a 50% increase in precipitation, while a 50% decrease of the index (halving) represents a 33% decrease in precipitation.

The comparison between modern meteorological records and contemporaneous tree ring indices involves only the last 30 years. The mean tree ring index of 1, on the other hand, is based on records dating back to 1510 for ponderosa pine. If we substitute the mean tree ring index of 1 in the above formulae, a precipitation is obtained that is higher than the mean precipitation recorded during the last 30 years, because of a coefficient (e.g., 543) whose value exceeds the actual mean precipitation. This higher coefficient is because, during the 30 years to which the regression analysis was applied, the tree ring index was below average or <1. This also implies that during the period in question, precipitation was below average since 1510.

In conclusion, there seems to be agreement that an analysis of recent past recordings in the form of either climatic records or tree ring indices, is a good way to estimate the range of future pluvial variability.

The statistical relationship established between modern pluviometric records and contemporaneous tree ring indices allows one to estimate previous precipitation patterns. Good existing correlations for ponderosa pine permitted us to make the following estimates.

a. In the last 100 years, a maximum tree ring index of 1.85 occurred in 1919. Through regression analysis and use of derived formulae, this corresponds to an annual precipitation of 788 mm.

b. In the last 200 years a maximum tree ring index of 2.10 occurred in 1794. Through regression analysis and use of derived formulae, this corresponds to an annual precipitation of 851 mm.

c. The maximum tree ring index recorded in the Los Alamos area was 2.80 in 1597. This corresponds to an annual precipitation of 1013 mm.

d. The minimum tree ring indices recorded were in the years 1523, 1524, 1585, and 1685. According to the regression equation, this corresponds to annual precipitations of 144, 144, 113, and 58 mm, respectively. Statistics based on pluviometric records indicate that annual precipitation not exceeding 146 mm is likely to occur once in 100 years.

The above precipitation estimates correspond remarkably well with the estimated occurrences of maximum precipitation based on climatic records. Table I indicates that a maximum precipitation of 768 mm can be expected every century. This is only 2.5% different from the estimate reached by tree ring index analysis (Abeele, 1980).

III. SURFACE WATER

This section is a slightly modified version of DOE/EIS-0018, pp. 3-17 to 3-25, Final Environmental Impact Statement-Los Alamos Scientific Laboratory Site; U. S. Dept. of Energy, December 1979.

The Rio Grande, the master stream of the region, drains more than 37 000 km^2 in northern New Mexico and Colorado. The average discharge of the Rio Grande at the Otowi Bridge gauging station was about $1 \cdot 10^9$ m^3 per year or an average of 32 $m^3 s^{-1}$ for the 1955 to 1974 period. Suspended sediments discharged at the station for the period 1947 to 1974 ranged from 0.03 kg s^{-1} to 3900 kg s^{-1}.

Cochiti is a new reservoir, which began filling in 1976 (Fig. 3). It is designed to provide flood control, sediment retention, recreation, and fishery development. The dam is a 9-km-long, earthfilled dam located on the Rio Grande about 30 km southwest of Otowi Bridge and about 15 km from the southernmost point of the Laboratory boundary. The $5 \cdot 10^6$ m^2 surface area permanent pool will extend upstream approximately 12 km, reaching a point about 5 km from the southernmost point of the Laboratory boundary and will have a capacity of nearly $62 \cdot 10^6$ m^3. The flood-control pool extends upstream to the Otowi Bridge with a total volume of $750 \cdot 10^6$ m^3.

Essentially all downstream flow passes through the reservoir. Flood flows are temporarily stored and released at safe rates. The sediment-trapping function of the dam is expected to trap at least 90% of the sediments carried by the Rio Grande. Approximately $6.2 \cdot 10^6$ m^3 per year will be lost to evaporation from the permanent pool.

There are no municipal water supplies taken directly from the Rio Grande downstream from Los Alamos National Laboratory in New Mexico. Irrigation water is taken from the Rio Grande downstream from the Laboratory at numerous diversions starting below Cochiti Dam.

The quality of surface waters in the Upper Rio Grande Basin is generally good. The bacterial and chemical quality of all streams, with the exception of a reach of the Rio Grande between Española and Otowi Bridge, is considerably better than that required by the New Mexico State Water Quality Control Commission stream standards. The poor quality below Española to Otowi Bridge is attributed to the population concentration in the Española Valley. This reach is upstream of Los Alamos.

In the Los Alamos area, there is intermittent stream flow in canyons cut into the Pajarito Plateau. Perennial flow to the Rio Grande occurs in the Rito de los Frijoles to the south of the Laboratory and Santa Clara Canyon to the north. Springs between 2400- and 2700-m elevation on the slopes of the Sierra de los Valles supply base flow throughout the year to the upper reaches of Guaje, Los Alamos, Pajarito,

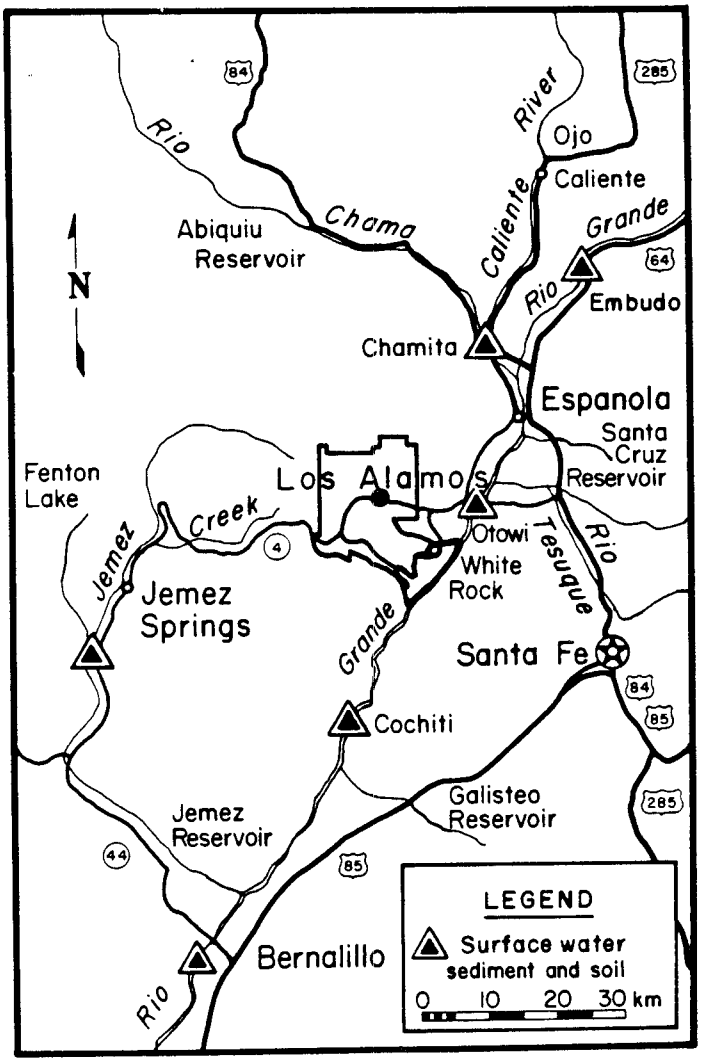

Fig. 3. Base map.

and Water Canyons, and Canyon del Valle. These springs discharge water perched in the Bandelier Tuff and Tschicoma Formation at rates from $1 \cdot 10^{-4}$ to $9 \cdot 10^{-3} m^3 s^{-1}$. The volume of flow from the springs is insufficient to maintain surface flow within more than the western third of the canyons before it is depleted by evaporation, transpiration, and infiltration into the underlying alluvium.

Sixteen drainage areas, with a total area of 212 km^2, pass through or originate within the Laboratory boundaries. Stream flow in these canyons is intermittent. Runoff from heavy thunderstorms or unusually heavy snowmelt will reach the Rio Grande. Four canyons — Pueblo, Los Alamos, Pajarito, and Water — have areas greater than 20 km^2. Ancho Canyon has 17 km^2, and all the rest have less than 10 km^2. Theoretical flood frequency and maximum discharge in 10 of the well-defined channels of the 16 drainage areas range from 1.1 $m^3 s^{-1}$ for a two-year frequency to 21 $m^3 s^{-1}$ for a 50-year frequency. Flooding does not pose a problem in the Los Alamos area. Highways may occasionally be closed for an hour when flash floods in canyons cross the pavement. Nearly all community and Laboratory structures are located on the mesa tops, which drain rapidly into the deep canyons.

Pajarito Site is located in Pajarito Canyon below a drainage area of 26 km^2. The 100-year storm (i.e., probability 0.01 in any year) will result in a discharge of 31 $m^3 s^{-1}$. The channel at the site that is restricted by a bridge will carry 42 $m^3 s^{-1}$.

Omega Site and W-Site are located in Los Alamos Canyon near the western edge of the Pajarito Plateau. The two sites are about 600 m apart with a drainage area of about 20.5 km^2 above the sites. The 100-year storm would produce a maximum flow of about 25 $m^3\ s^{-1}$ at the sites. An extrapolation indicates a 500-year flood (i.e., probability 0.002 in any year) would have a peak flow of about 37 $m^3\ s^{-1}$.

A box culvert at W-Site extends under the parking lot and has a carrying capacity of 156 $m^3\ s^{-1}$, while a restriction at the entrance of the channel at Omega Site will carry about 46 $m^3\ s^{-1}$. Thus, the channels at both sites should carry the maximum flow of 25 $m^3\ s^{-1}$ produced by a 100-year storm. If the channel should become clogged with debris, the resulting overflow would be carried by roadways or parking lots adjacent to the channel and would not cause damage to the structures in the area.

Another flood hazard considered was failure of the Los Alamos Canyon Reservoir. The dam is a concrete-core, rock and earthfilled dam with a capacity of $4.9 \cdot 10^4\ m^3$. The concrete spillway will carry a flow of 16 $m^3\ s^{-1}$, which is ample for the estimated flow of 12 $m^3\ s^{-1}$ produced by a 100-year storm.

Sanitary sewage effluents from both the townsite and the Laboratory are released into Pueblo and Sandia Canyons in sufficient volume to saturate the alluvium and maintain surface flows for a few hundred meters. Mortandad Canyon contains a small perennial stream maintained for about 1.5 km by effluents from a Laboratory cooling tower and an industrial-waste treatment plant.

IV. SATURATED FLOW

Ground water (subsurface water) occurs as perched water in alluvium and basalts and, in the zone of saturation, in sediments of the main aquifer of the Los Alamos area.

Two types of alluvium have developed in the stream channel. Drainage areas heading on the mountain flanks are made up of sand, gravels, cobbles, and boulders derived from the Tschicoma Formation and Bandelier Tuff. Drainage heading on the plateau contains only sands, gravels, and cobbles derived from the Bandelier Tuff. The alluvium is quite permeable, allowing rapid infiltration of rainfall and streamflow. The alluvium generally overlies the less permeable tuff. Water infiltrates downward in the alluvium until its movement is held back by the tuff. This results in the build-up of ground water perched within the alluvium. Saturated hydraulic conductivity of the alluvium ranges from $1.65 \cdot 10^{-3}\ m\ s^{-1}$ for a sand aquifer to $5.8 \cdot 10^{-4}\ m\ s^{-1}$ for a silty sand aquifer.

As water perched in the alluvium moves down the gradient, it is lost by evaporation and transpiration through plants and infiltration into underlying tuff. Vegetation is lush where surface or perched water in the alluvium is present. Water moving from the alluvium into the volcanic debris in the lower reach of Pueblo Canyon and the midreach of Los Alamos Canyon recharges a local body of perched water within the basaltic rock of Chino Mesa. Water from this perched aquifer discharges at the base of the basalt in Los Alamos Canyon west of the Rio Grande.

The hydraulic conductivity of this perched aquifer is $1.32 \cdot 10^{-3}\ m\ s^{-1}$.

Perched water is not found in the tuff, volcanic sediments, or basalts above the main aquifer in the central and western portions of the Plateau. Test holes in these areas penetrated numerous rock units that had the potential of perching water above the main aquifer. The absence of water in these test holes indicates that the infiltration of surface water through the alluvium and the tuff is limited. Age dating of water from the main aquifer further supports the inference of insignificant infiltration of surface water through the alluvium and tuff to the main aquifer.

The main aquifer in the Los Alamos area is located within the Tesuque Formation beneath the entire Plateau and Rio Grande Valley. The lower part of the Puye Conglomerate as well as the Tesuque Formation are within the main aquifer beneath the central and western portions of the Plateau. The depths to water below the mesa tops range from about 360 m along the western margin of the Plateau to about 180 m along the eastern part of the Plateau. The thickness of potable water in the aquifer is estimated to be at least 1200 m. The hydraulic gradient of the aquifer averages about 1.1% within the Puye Conglomerate but increases to about 20% along the eastern edge of the Plateau as the water in the aquifer enters the less permeable sediments of the Tesuque Formation. The average movement rate within the aquifer is about $3.5 \cdot 10^{-6}\ m\ s^{-1}$ toward the Rio Grande.

The hydraulic conductivity and transmissivity are different for various rock units within the main aquifer. Aquifer tests in wells penetrating the Puye Conglomerate indicated saturated hydraulic conductivities ranging from less than $1.15 \cdot 10^{-5}$ m s^{-1} to $1.50 \cdot 10^{-4}$ m s^{-1}. Supply wells in the Los Alamos Field penetrating sediments of the Tesuque Formation have an average transmissivity of $2.3 \cdot 10^{-3}$ m^2 s^{-1}, with an average hydraulic conductivity of less than 10^{-5} m s^{-1}. The wells in the Guaje Field, which penetrate basalts interbedded with sediments in the Tesuque Formation, have an average transmissivity of about 2.5 $m^2 s^{-1}$, with an average hydraulic conductivity of about 10^{-5} m s^{-1}. Supply wells in the Pajarito Well Field penetrated basalts interbedded with sediments in the Puye Conglomerate and the Tesuque Formation. The transmissivities ranged from $6 \cdot 10^{-3}$ to $4.6 \cdot 10^{-2}$ m^2 s^{-1}. The aquifer is under water table conditions in the western portion of the Plateau. Along the eastern margins the aquifer is artesian; that is, the water level in a well penetrating the aquifer will rise above the top of the saturated water-bearing material.

The major recharge area for the deep aquifer is in the intermountain basins formed by the Valles Caldera. The saturated sediments and volcanics in the basins are highly permeable and recharge the main aquifer in sediments of the Tesuque Formation and Puye Conglomerate. Minor amounts of recharge may occur in the deep canyons containing perennial streams on the flanks of the mountains.

The movement of water in the main aquifer is eastward toward the Rio Grande, where a part is discharged through springs and seeps into the river. It is estimated that the 18.4 km reach through White Rock Canyon below Otowi Bridge receives a discharge from the aquifer of 5.3 to $6.8 \cdot 10^6$ m^3 annually or an average of $1.92 \cdot 10^{-1} m^3 s^{-1}$.

V. GAUGING STATION, AREA G

A. Introduction

A potential exists for transport of radionuclides out of disposal sites by surface runoff. A gauging station was constructed at Area G, TA-54, to provide a sediment sampling point and to determine the volume of runoff from a representative portion of the area. Rainfall-runoff data from the gauging station will also be used to validate simulation models of the water balance at the disposal sites.

A catchment basin was constructed near the outlet of a major drainage from the site. A dam at the downstream end of the basin was fitted with a weir plate for discharge measurements.

B. Location and Watershed Area

The location of the weir is indicated in Fig. 4, as is the outline of the area draining through the weir. Asphalt runoff channels are indicated. There is a cutoff ditch along the slope north of the drainage basin, which directs flow to a discharge point below the weir. The total effective drainage area is 34 500 m^2, with slopes varying between 5 and 25%. The average slope for the watershed is about 10%.

C. Weir and Stilling Basin

A cross section of the weir dam is shown in Fig. 5. An aluminum weir plate, with a beveled 90° notch, was installed in the dam (Fig. 6). A cleaning port, sealed with a removable cover, is located in the bottom third of the plate.

The cross section (Fig. 5) also shows the original stilling basin profile. Sediment accumulation alters the volume of the basin below the weir notch with each runoff event. The volume of the basin from an elevation level with the bottom of the cleaning port to the bottom of the notch is approximately 17 m^3.

The water level in the stilling basin is recorded by a water level gauge installed in a stilling well (Fig. 5). The recorder is equipped with a spring-driven clock, adjustable for 1-day or 7-day service time. A special trigger mechanism starts the clock when the recorder float starts upward. Thus, the discharge record begins essentially at the start of each runoff event.

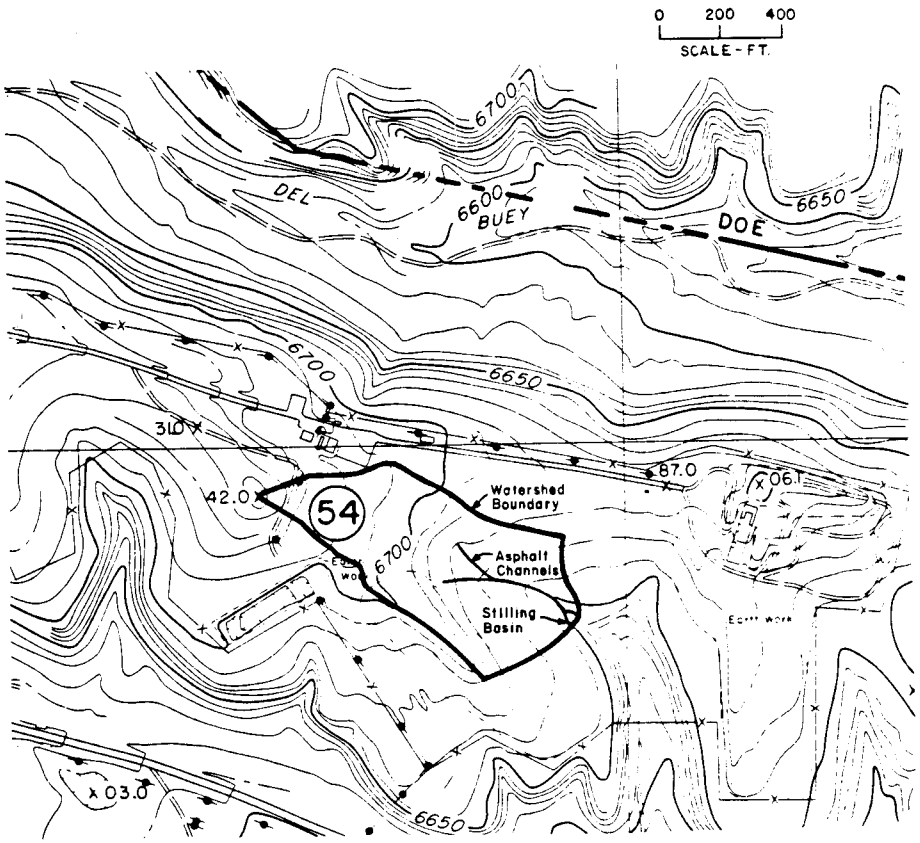

Fig. 4. Location of watershed and stilling basin, Area G, TA-54.

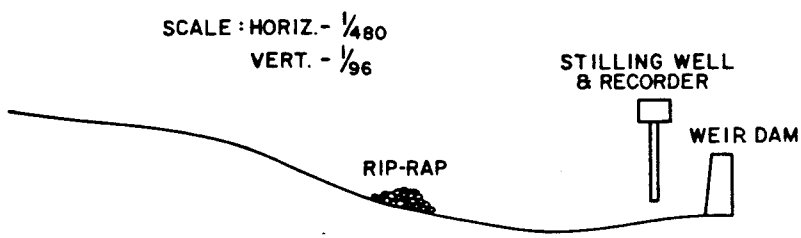

Fig. 5. Cross section of stilling basin.

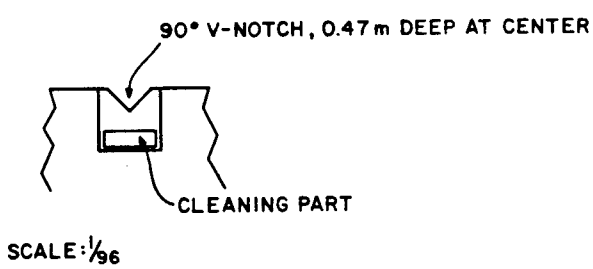

Fig. 6. Weir plate details.

D. Runoff Events

Installation of the recorder and weir was completed by mid-summer 1980. A major storm on 18 August produced runoff, but the recorder malfunctioned, and no runoff data were obtained; however, cumulative samplers downgradient from the weir were used to collect runoff samples (solution and suspended sediments) for plutonium analyses. The analyses were performed to determine if there was any measurable transport of plutonium from the surface of Area G. A similar sample was collected outside area G to provide background for the runoff event. The background analyses and analyses from the cumulative samplers were below the mean limits of detection for plutonium (<5 pCi/ℓ solution; 1 pCi/g suspended sediments).

A second storm complex delivered a total of 22.1 mm between 8 and 10 September 1980.

The hydrograph for 9 September 1980, together with observed precipitation, is given in Fig. 7. From 0100 hours on 10 September 1980, the water level showed a continuing decline caused by evaporation and gradual leakage from the stilling pond.

E. Weir Calibration

1. **Theoretical.** The discharge through a 90° V-notch weir is expressed by

$$Q = \frac{8}{15} \sqrt{2g}\, C_d h^{5/2} = 2.36\, C_d\, h^{5/2} \quad , \tag{1}$$

where

Q = Discharge - $m^3\ s^{-1}$,
g = Acceleration of gravity,
C_d = Coefficient of discharge, and
h = Water height above V-notch.

The value of C_d is approximately 1.0 but varies as an empirical function of the weir.

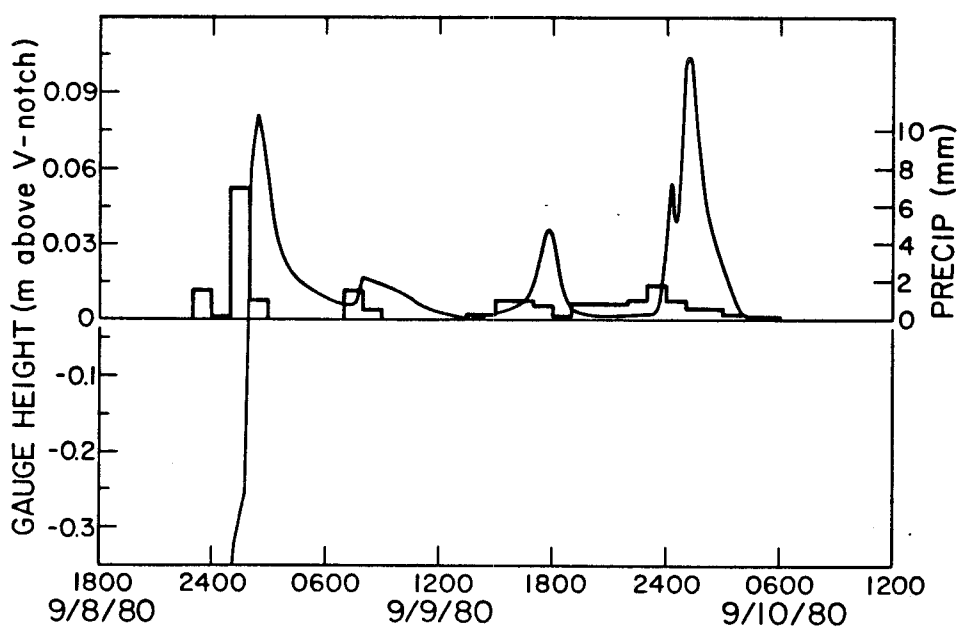

Fig. 7. Precipitation and runoff, Area G weir.

2. **Empirical.** A period was selected on 9 September 1980, when flow was occurring through the weir. A sequence of measurements was made, recording the time required for a fixed volume to flow through the weir. The water height, "h," was also recorded.

The measured discharge data are given in Table III.

The value of C_d for this weir can be determined, using Eq. (1), and the measured values of Q and h.

$$C_d = \frac{Q}{2.36\ h^{5/2}} = \frac{3.3 \cdot 10^5\ m^3\ s^{-1}}{2.36\ (1.21 \cdot 10^{-2})^{5/2}} = 0.87\ .$$

Thus, for flow in this range of discharge, the weir calibration is

$$Q = 2.1\ \ h^{5/2}\ .$$

Further calibration will be required to extend this relationship to significantly higher discharges.

F. Rainfall-Runoff Calibration

The storm event can also be used to evaluate the relationship between precipitation and runoff from the watershed. A rational formula is commonly used to estimate the peak discharge from precipitation on a small watershed. For conditions on this watershed the equation is

$$Q = 1.1 \cdot 10^{-7}\ (i)\ (A)\ ,$$

where

Q = Peak discharge, $m^3\ s^{-1}$
i = Precipitation rate, mm/h, and
A = Drainage area, m^2.

The observed precipitation and runoff are tabulated in Table IV, together with discharge calculated by the above formula.

The comparison shows that estimated discharges are significantly larger than measured values. However, the runoff formula is most applicable to high intensity storms (>25 mm/h) of 30 min to 1 h

TABLE III

DISCHARGE DATA FOR AREA G WEIR

Measurement Number	Flow (ℓ)	Elapsed Time (sec)	Discharge Rate ($m^3\ s^{-1}$)	Water Height (m)
1	3.5	105	$3.3 \cdot 10^{-5}$	$1.21 \cdot 10^{-2}$
2	3.5	113	$3.3 \cdot 10^{-5}$	$1.21 \cdot 10^{-2}$
3	3.5	113	$3.1 \cdot 10^{-5}$	$1.21 \cdot 10^{-2}$
		mean	$3.3 \cdot 10^{-5}$	$1.2 \cdot 10^{-2}$

TABLE IV

PRECIPITATION AND RUNOFF ON JULY 10, 1980

Time (hr)	Precipitation (mm/hr)	Discharge-m^3 s^{-1}	
		Observed	Calculated
1500	0.3	$6 \cdot 10^{-6}$	$1.2 \cdot 10^{-3}$
1600	1.0	$6 \cdot 10^{-6}$	$3.8 \cdot 10^{-3}$
1700	1.0	$9 \cdot 10^{-5}$	$3.8 \cdot 10^{-3}$
1800	0.8	$3.2 \cdot 10^{-4}$	$3.0 \cdot 10^{-3}$
1900	0.3	$1.3 \cdot 10^{-4}$	$1.2 \cdot 10^{-3}$

duration. Overestimation of discharge for small storms results from excessive infiltration and evaporation compared with larger storms. Further work, involving the inclusion of the dynamics of the rainfall-runoff process, may be required to improve agreement between estimated and actual runoffs. At present, the weir and stilling basin appear to be adequately sized for expected discharges.

VI. SATURATED AND UNSATURATED HYDRAULIC CONDUCTIVITIES

A. General

Precipitation, if occurring persistently and in large amounts, may reach the waste material in a disposal pit. Because potential evapotranspiration exceeds precipitation at the disposal sites, the majority of the percolating water is evaporated long before it reaches the waste material. The bottom of the soil horizon, consisting of a pronounced clay, is generally less than a meter deep. The clay horizon effectively restricts any further downward movement of water into the underlying Bandelier Tuff, where all the waste disposal sites at Los Alamos are located.

The fractures and joints are commonly filled with fine-grained weathering products within 10 m from the surface, while being open at greater depth with no sign of weathering. Roots penetrate filled fractures, attracted by the higher moisture availability in finer materials. Montmorillonite, present in considerable amount among the finer materials and expanding upon wetting, will seal fractures and strongly inhibit moisture movement. Moisture monitoring by means of a neutron moisture probe indicates that at depths exceeding 10 m the tuff rarely exceeds 10% of saturation. At such a low moisture ratio, only unsaturated and vapor flow can occur. As the degree of unsaturation augments, movement in the vapor phase becomes more preponderant. Here one needs to remember that fractures or joints, which are effective barriers to liquid unsaturated flow, are open pathways for unhindered diffusion of water in the vapor phase. Tritiated water vapor migration is consequently enhanced by the presence of such transportation channels. It must be remembered, however, that tritium is the only radionuclide at Los Alamos disposal sites to travel in the gaseous phase. All other radionuclides can be removed from their original location only through the movement of liquid water, barring a catastrophic event. Because fractures will act as barriers for unsaturated liquid flow, all radionuclides, except tritium, will be inhibited by the presence of these fractures in their movements through the tuff. Existence of low moisture content is further proven historically by the absence of weathering below 10 m (Wheeler et al., 1977). The hydraulic conductivity decreases strongly with the degree of saturation. The hydraulic conductivity was found to be a power function of the saturation ratio and will be expressed as such in the following chapters.

Saturation ratios of crushed fill overlying waste disposal pits remain constant below 3 m at a saturation ratio of 0.1 without even a sign of a significant seasonal variation.

Forces causing significant moisture movement result from gravity, moisture gradients, and temperature gradients. A difference in temperature or moisture content will also be the motive force to diffusion in the vapor phase. A moist or warm soil in contact with a dry or cool soil will create a vapor pressure gradient and a vapor diffusion into the drier or cooler area will occur.

Vertical liquid water flow at depths greater than 10 m, where there is no vapor pressure gradient, will be mainly a function of the hydraulic gradient ($\frac{h}{L}$), which is the energy loss per unit weight or head loss divided by the length of flow. Further, the vertical liquid water flow will be a function of the hydraulic conductivity of the tuff at a particular water content (K_θ). The moisture flow per unit area will consequently be described as

$$q = K_\theta \frac{h}{L} .$$

B. Crushed Tuff

1. Measurements. The essential parts of the laboratory apparatus used included a volumetric pressure plate extractor with a cell pressure control system accurate to 0.25%. The porous plate had a bubbling pressure of 200 kPa. The outflow measurement system consisted of a sealed Erlenmeyer flask into which the water was released. The flask was placed on a Mettler balance, which allowed for continuous weighing of the outflow. A burette was used to remove air from beneath the porous plate.

The simplest technique, described by Klute (1965), was first used to determine the unsaturated hydraulic conductivity. Although the experimental technique itself seemed to be flawless, no matching of Klute's theoretical diffusion equation plotted as the overlay or theoretical curve and the experimentally determined volume-outflow curve could be obtained without translation of the plots. An overlay was drawn for each applied matric potential. The conclusion was consequently reached that the assumption of a negligible head loss through the porous plate was not valid.

A series of corrective outflow overlays were drawn in accordance with the method suggested by Miller and Elrick (1958) for the determination of hydraulic conductivity extended to cases with non-negligible plate impedance. The corrective translation needed to obtain the matching of any of the overlays and the experimental curves turned out to be near an order of magnitude larger than Miller and Elrick assumed! Rijtema (1959) pointed out that unless good contact is established between the plate and the soil, an unknown flow impedance may prevail that could far outweigh the plate impedance itself. The plate impedance permitted a flow rate of $3.8 \cdot 10^{-8}$ m^3 s^{-1} m^{-2} kPa^{-1} or 1.37 cm^3 h^{-1} cm^{-2} bar^{-1} at saturation. The possible contact impedance could appear and grow as the matric potential or the saturation ratio was decreasing. Using Rijtema's method, the total impedance of the tuff sample is determined from the experimental outflow data for each applied matric potential (or pressure step). Data for $1 - Q_t/Q\infty$ are computed from the experimental values of the outflow Q_t at time t and the equilibrium yield $Q\infty$ obtained for a particular pressure step. Values of $1 - Q_t/Q\infty$ are plotted on a logarithmic scale against tL^{-2}, where t is the time elapsed for a particular outflow quantity Q_t and L is the thickness of the sample. Rijtema devised a method to calculate the diffusivity based on the ratio of the slope of the straight line drawn through the experimental points and a value derived directly from the intercept of that straight line and the $1 - Q_t/Q\infty$ axis. The hydraulic conductivity K at that particular pressure step can now be calculated by finding the product of the diffusivity D and the specific water capacity c. The equation for the time required for 0.99 of the outflow to occur is $t_{0.99} = 1.68\ L^2 D^{-1}$.

This equation was used to check what the magnitude of D must be if a 1-day equilibrium time was chosen. Computations show that D should be 2.5×10^{-8} m^2 s^{-1}. It was known from past experiments that the diffusivity of Bandelier tuff normally exceeded that value at matric potentials higher than −200 kPa. Consequently, the time for equilibrium was set at 1 day. Upon completion of the experiment, the sample was oven-dried, yielding an additional 41 g of water. The total amount of water present at

saturation was calculated to be 185 g. Knowing the dry weight of the tuff, it can be deduced that saturation is equivalent to 31% of water by weight. Table V shows how matric potential outflow, water ratio by mass, degree of saturation, specific water capacity, water diffusivity, and hydraulic conductivity correspond (Abeele, November 1979).

To determine if a thickness effect (of the soil layer under analysis) was taking place, 970 g of dry soil, 59 mm high, were put in the extractor and saturated. The total amount of water released, under a pressure of 30 kPa and 100 kPa, respectively, was measured. The ratio of released water (30 kPa vs 100 kPa) was 0.78, which is not very different from the ratio released during the former experiment (0.81). Desiccation of the soil submitted during 48 hours to a pressure of 100 kPa indicated a remaining moisture ratio of 0.789 in the top layer vs a remaining moisture ratio of 0.0893 in the bottom layer. The bulk of the soil yielded a remaining moisture ratio of 0.0847, which is very close to the one measured in the previous experiment (0.0848). This duplication seems to validate the previous experiment.

If matric potential vs saturation ratio, hydraulic conductivity vs saturation ratio, and hydraulic conductivity vs matric potential are plotted on a log-log graph, a straight line is obtained in every case corresponding to matric potentials lower than −11 kPa.

The range of matric potentials was limited to those below −11 kPa for the purpose of curve fitting because of the difficulty in measuring water outflow at the higher matric potential.

TABLE V

HYDRAULIC CHARACTERISTICS OF CRUSHED BANDELIER TUFF AS A FUNCTION OF MATRIC POTENTIAL

(Specific H_2O Capacity, H_2O Diffusivity and Hydraulic Conductivity were only measured at pressure steps <10%)

Matric Potential (−kPa)	Outflow (g)	Saturation Ratio	Specific Water Capacity (m^{-1})	Water Diffusivity ($m^2\ s^{-1}$)	Hydraulic Conductivity ($m\ s^{-1}$)
0	0.000	1.000			
10	20.082	0.890			
11	24.320	0.868	$8.98 \cdot 10^{-2}$	$1.02 \cdot 10^{-7}$	$9.18 \cdot 10^{-9}$
30	108.128	0.415			
33	110.261	0.405	$1.58 \cdot 10^{-2}$	$2.15 \cdot 10^{-7}$	$3.38 \cdot 10^{-9}$
42	117.407	0.368			
46	120.241	0.350	$1.50 \cdot 10^{-2}$	$1.38 \cdot 10^{-7}$	$2.07 \cdot 10^{-9}$
60	126.241	0.318			
66	127.841	0.310	$5.64 \cdot 10^{-3}$	$1.33 \cdot 10^{-7}$	$7.51 \cdot 10^{-10}$
80	131.589	0.290			
88	132.749	0.283	$3.07 \cdot 10^{-3}$	$1.40 \cdot 10^{-7}$	$4.30 \cdot 10^{-10}$
96	134.437	0.273	$2.98 \cdot 10^{-3}$	$1.21 \cdot 10^{-7}$	$3.60 \cdot 10^{-10}$
120	136.949	0.260			
132	137.949	0.255	$1.76 \cdot 10^{-3}$	$9.30 \cdot 10^{-8}$	$1.64 \cdot 10^{-10}$
146	139.315	0.248	$2.06 \cdot 10^{-3}$	$4.80 \cdot 10^{-8}$	$9.91 \cdot 10^{-11}$
161	140.543	0.240	$1.73 \cdot 10^{-3}$	$4.62 \cdot 10^{-8}$	$8.01 \cdot 10^{-11}$
177	142.643	0.230	$2.78 \cdot 10^{-3}$	$1.88 \cdot 10^{-8}$	$5.22 \cdot 10^{-11}$
195	144.057	0.223	$1.66 \cdot 10^{-3}$	$3.08 \cdot 10^{-8}$	$5.13 \cdot 10^{-11}$

If θ_v represents the water-filled porosity, θ or (θ/θ_s) the saturation ratio, ψ the matric potential in kPa, K_s the saturated hydraulic conductivity ($9.2 \cdot 10^{-7}$ m s^{-1}), K or $K(\theta)$ the unsaturated hydraulic conductivity, and r^2 the coefficient of determination, the following equations are obtained.

$$\theta = 1.21\ \psi^{-0.321}, \qquad r^2 = 0.993;$$
$$K = 2.43 \cdot 10^{-5}\ \psi^{-2.475}, \qquad r^2 = 0.990;$$
$$K = 5.04 \cdot 10^{-6}\ \theta^{7.623}, \qquad r^2 = 0.980.$$

As can be seen from the high values obtained for the coefficient of correlation, the above equations, if plotted on a log-log graph, will very closely match a straight line.

2. **Predictive Methods.** Because the hydraulic conductivity-water content relationship K (θ) is comparatively difficult to obtain, the possibility of predicting the hydraulic conductivity from the matric potential-water content relationship has been widely explored. Millington-Quirk (1961) and Campbell (1974), among others, developed equations for this purpose. Several authors treated a variety of predictive methods against experimental data and indicated the superiority of a "corrected" Millington-Quirk (MQ) method. A correction coefficient is introduced to match the observed vs the computed saturated conductivity. Jackson et al. (1965) and Kunze et al. (1968) modified the MQ formula by introducing a "matching factor" to improve the predictability of the equation. The MQ method uses the equation

$$K = 3.14 \cdot 10^{-2}\ \theta_v^{4/3}\ n^{-2}\ [h_1^{-2} + 3h_2^{-2} + \ldots + (2n-1)\ h_n^{-2}] \cdot K_s/K_{sc}\ (\mathrm{m\ s^{-1}})\ .$$

The water-filled porosity θ_v in cm^3 cm^{-3}, the pressure potential h in kPa and the total number of pore intervals n give the hydraulic conductivity units of ms^{-1}. In portions of the curve where data were scarce, curve fitting through regression analysis was applied to enhance the validity of the moisture characteristic curve. The constant is valid for laboratory experiments conducted at a temperature of 300K. K_s/K_{sc} is the matching factor (measured saturated conductivity/calculated saturated conductivity).

If the obtained conductivity data are fitted to the water-filled porosity, a power function is obtained where, for θ_v ranging from 0.02 to saturation (0.40),

$$K = 7.96 \cdot 10^{-4}\ \theta_v^{7.379} \text{ with } r = 0.9994 \text{ and}$$

$$K = 9.2 \cdot 10^{-7}\ \theta^{7.379} \text{ with } r = 0.9994\ .$$

As can be seen through comparison with the laboratory method (Rijtema's technique), the slopes are almost identical, the $K(\theta_v)$ function being somewhat steeper when measured (Rijtema, 1979). This is counterbalanced by the fact that the coefficient used in Rijtema's equation is less than 5.5 times higher than in the MQ equation. Consequently, *at any point*, the measured hydraulic conductivity will be *less* than 5.5 times higher than the predicted one using the MQ method (Abeele, November 1979).

Campbell's method for determining unsaturated conductivity from moisture retention data is simpler but agrees less with the laboratory method when applied to the Bandelier Tuff. An empirical expression relating water potential to water content for limited ranges of water content is, below matric potentials of −11 kPa,

$$\psi = \psi e\ (\theta/\theta_s)^{-b}\ ,$$

where ψe is the air-entry water potential and θ_s the saturated water content. The slope b can be determined from the above relationship and the unsaturated hydraulic conductivity is subsequently determined from the equation

$$K = K_s (\theta/\theta_s)^{2b+2}.$$

Through regression analysis, using the moisture retention data, $\psi/\psi_s = 0.0097(\theta/\theta_s)^{-3.0563}$, fixing the value of b at 3.0563. The unsaturated hydraulic conductivity is subsequently expressed as

$$K = 9.2 \cdot 10^{-7}\ \theta^{8.113}\ (\mathrm{m\ s^{-1}})\ .$$

Higher exponents in the three alternative regressions mean lower hydraulic conductivity, whereas higher coefficients mean higher values. Because the formula with the highest exponent is also the one with highest coefficient, the three methods result in hydraulic conductivities never exceeding one order of magnitude in difference. The superiority of the MQ method seems to be confirmed when matched with the measured values. Campbell's predictive method retains the advantage of being the easiest one to compute (Abeele, November 1979). For a graphic comparison of predicted conductivities vs measured conductivities, see Fig. 8.

A monitoring hole (GP1-1), drilled in fill material overlying a waste disposal pit, shows significant seasonal fluctuations in moisture content. The computed moisture flux was always found to be directed downward. This downward flux from the overburden averaged $3.76 \cdot 10^{-9}$ m s^{-1} or 0.12 m yr^{-1}. The downward flux from the overburden was computed to average $2.94 \cdot 10^{-10}$ m s^{-1} or 0.09 m yr^{-1} in 1978 and $4.75 \cdot 10^{-10}$ m s^{-1} or 0.15 m yr^{-1} in 1979. The higher average occurring in 1979 is probably caused by extremely high precipitations occurring at the end of 1978 and the beginning of 1979.

The flux $Q = K(\theta)\ \dfrac{\Delta(h-z)}{\Delta z}$,

where

z = depth,
h = matric potential corresponding to measured moisture content, and
$K(\theta)$ = hydraulic conductivity corresponding to measured moisture content.

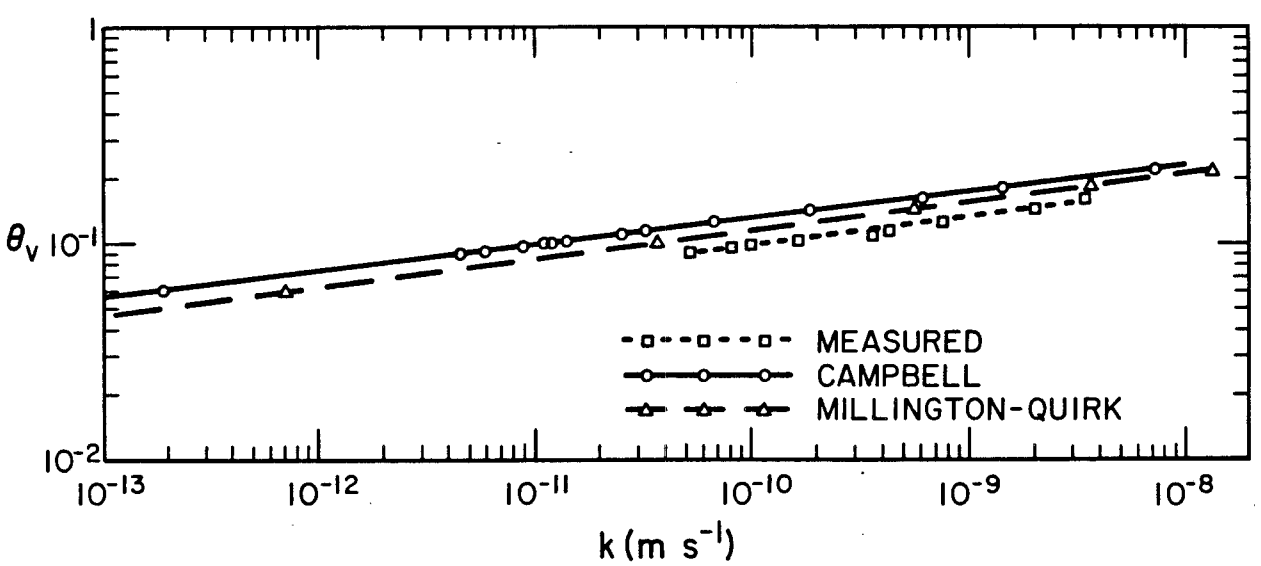

Fig. 8. Calculated hydraulic conductivities compared with measured data.

h and K(θ) are determined from the formerly expressed regression equation. These results are higher by a factor of 3 than the flux estimated in the 1979 Annual Report where the downward moisture flux was estimated at $9.5 \cdot 10^{-10}$ m s^{-1}.

The maximum downward moisture flux was computed to occur in December 1978 and found to be $2.2 \cdot 10^{-8}$ m s^{-1} or 0.694 m yr^{-1}. This followed an extremely wet November (1978) when close to 0.17 m of precipitation fell.

C. Solid Tuff

1. Measurements. The saturated hydraulic conductivity of solid tuff has been measured quite often. Widely differing measurements yield results from $2 \cdot 10^{-7}$ m s^{-1} to $4.7 \cdot 10^{-6}$ m s^{-1} when corrected for a temperature of 288K (Abrahams, 1963).

In the tuff used in these specific studies, a saturated hydraulic conductivity of $2.35 \cdot 10^{-6}$ m s^{-1} was measured. The unsaturated hydraulic conductivity was never measured.

2. Predictive Methods. The unsaturated hydraulic conductivity was predicted from the matric potential-water content relationship (moisture characteristic curve) according to the corrected MQ method. Table VI summarizes the characteristics that led to the computations of hydraulic conductivity as a function of matric potential. The acceptance of these results is based on the similarity found to exist between the predictive method according to Millington-Quirk and the measured values obtained for crushed tuff. A similar representation was assumed to exist for solid tuff.

The following equations were obtained through regression analysis for matric potentials lower than −15 kPa.

$$Q = 20.53\ \psi^{-1.050}, \qquad r^2 = 0.996;$$
$$K = 3.03 \cdot 10^{-4} \psi^{-2.989}, \qquad r^2 = 0.985;$$
$$K = 5.40 \cdot 10^{-8} \theta^{2.825}, \qquad r^2 = 0.973.$$

TABLE VI

HYDRAULIC CONDUCTIVITY OF SOLID TUFF AS A FUNCTION OF MATRIC POTENTIAL

Matric Potential (−kPa)	Saturation Ratio	Calculated Conductivity K_{sc} (m s^{-1})	Corrected Conductivity K (m s^{-1})
780	0.017	$9.8 \cdot 10^{-11}$	$1.4 \cdot 10^{-12}$
200	0.083	$1.6 \cdot 10^{-9}$	$2.3 \cdot 10^{-11}$
115	0.150	$9.1 \cdot 10^{-9}$	$1.3 \cdot 10^{-10}$
82	0.217	$3.0 \cdot 10^{-8}$	$4.3 \cdot 10^{-10}$
60	0.283	$7.7 \cdot 10^{-8}$	$1.1 \cdot 10^{-9}$
48	0.350	$1.6 \cdot 10^{-7}$	$2.3 \cdot 10^{-9}$
41	0.417	$3.2 \cdot 10^{-7}$	$4.5 \cdot 10^{-9}$
36	0.483	$5.4 \cdot 10^{-7}$	$7.7 \cdot 10^{-9}$
33	0.550	$8.5 \cdot 10^{-7}$	$1.2 \cdot 10^{-8}$
29	0.617	$1.3 \cdot 10^{-6}$	$1.8 \cdot 10^{-8}$
25	0.683	$2.0 \cdot 10^{-6}$	$2.8 \cdot 10^{-8}$
20	0.750	$2.8 \cdot 10^{-6}$	$4.0 \cdot 10^{-8}$
13	0.817	$4.2 \cdot 10^{-6}$	$6.0 \cdot 10^{-8}$
1	0.883	$6.5 \cdot 10^{-5}$	$9.2 \cdot 10^{-8}$

The tight power fit existing between saturation ratio and matric potential, hydraulic conductivity and matric potential, and, finally, hydraulic conductivity and saturation ratio are demonstrated by the very high coefficients of determination (r^2) existing below −15 kPa. Moisture characteristic curves for crushed and solid tuff are drawn in Fig. 9.

Graphic comparisons between the *calculated* hydraulic conductivities of solid tuff and the *measured* hydraulic conductivities of crushed tuff as a function of matric potential and saturation ratio are shown in Figs. 10 and 11.

VII. HYDROLOGIC MONITORING

A. Parameters Influencing Neutron Probe Readings

Often moisture must be measured with a neutron probe in access holes whose liner materials or diameters differ substantially from those the manufacturer considers ideal. The calibration chart accompanying the Troxler probe tested was valid for a thin-walled aluminum access pipe of 0.051 m outside diameter.

Computing soil moisture content with a neutron probe requires use of additional calibration curves that consider the hole diameter as well as the thermal neutron capture cross section of the hole liner, if those parameters are going to differ from those proposed by the manufacturer of the probe. The influence of steel, polyvinyl chloride, and aluminum casings that fit 0.051- to 0.102-m hole diameters was determined by comparison with neutron probe readings in uncased holes of corresponding diameters. Eccentricity of probe location was considered a potentially significant variable. The experiment was run in disturbed Bandelier tuff with an average dry density of 1350 kg m^{-3} and moisture content of 3.8 to 26.7% by volume. The casing material and hole diameter influenced the probe readings significantly, whereas eccentric location of the probe did not. Regression analyses showed an almost perfect inverse linear correlation between hole diameter and count rate (Abeele, October 1979).

B. Prior Measurements

Moisture relationships of the Bandelier tuff during the late 1950s and early 1960s (Abrahams, 1961) were extensively studied. Physical properties (density, porosity, etc.) and hydrologic properties

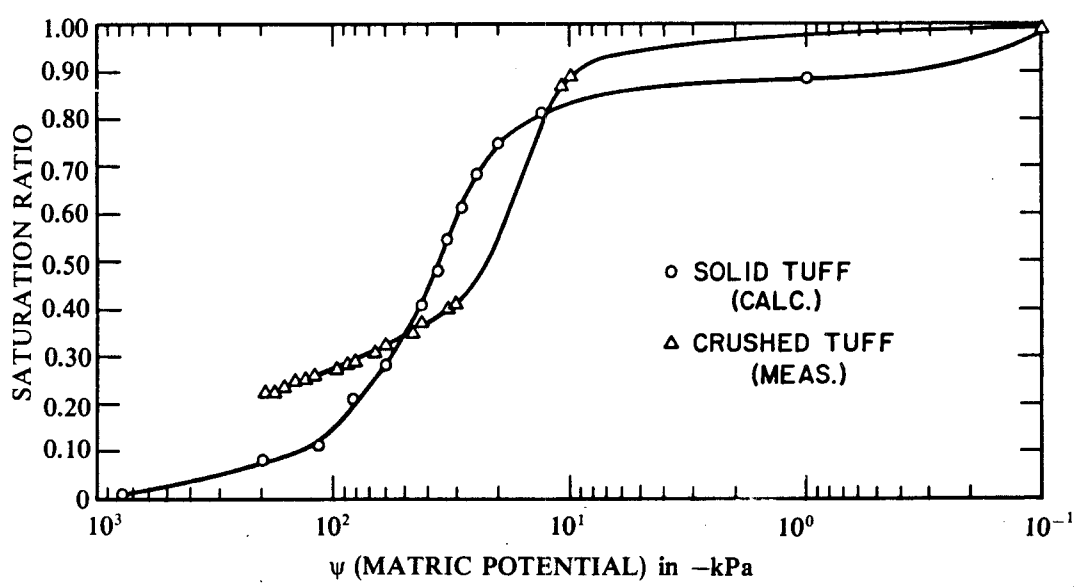

Fig. 9. Saturation ratio as a function of matric potential (moisture characteristic curves).

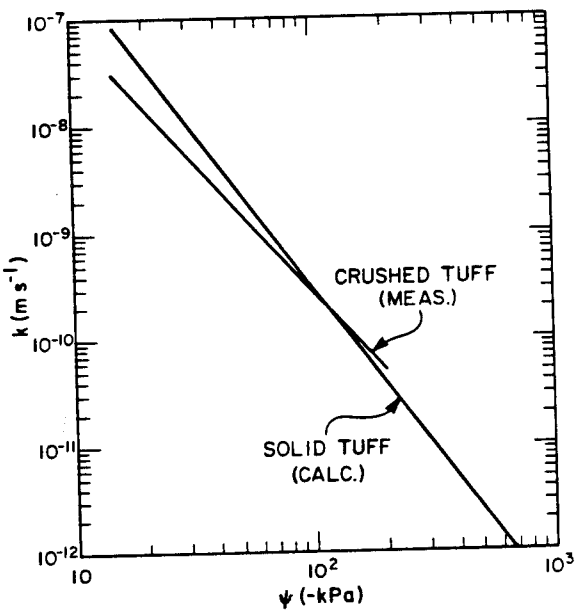

Fig. 10. Hydraulic conductivity as a function of matric potential.

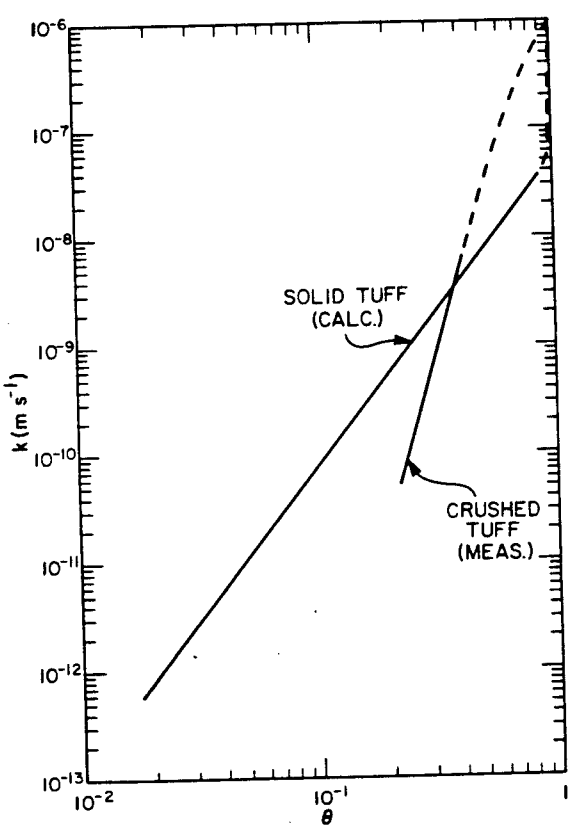

Fig. 11. Hydraulic conductivity as a function of saturation ratio.

(permeabilities, moisture tension curves, etc.) were measured on samples of tuff, and field experiments were conducted to investigate infiltration under high moisture conditions.

Data were also collected on the natural moisture conditions in the tuff, showing values of 5 to 10% by volume below a depth of a few meters. Variable amounts of precipitation infiltrate and percolate through the tuff or soil. Where the soil cover has not been disturbed, little if any water from precipitation infiltrates the underlying tuff (Purtymun and Kennedy, 1971). Where the soil cover was disturbed, as in the waste disposal areas, the moisture content of the tuff indicates a much higher degree of infiltration than the one that might have been implied by the moisture content fluctuations found in the undisturbed tuff.

Tests of precipitation infiltration in the disturbed tuff composing the pit overburden showed that moisture from a single storm may reach depths nearing 2 m, but in subsequent weeks is returned to the atmosphere by evaporation (Purtymun and Kennedy, 1971). Data on moisture contents of the tuff are presented in Table VII and Figs. 12 and 13.

TABLE VII

MOISTURE CONTENT OF BANDELIER TUFF[a]

Site	Depth (m)	Moisture Content (% by Vol.)
TA-49	0-30	2.1
	30-80	1.2
TA-33	0-2	16
	2-4	5.3
TA-3	0-3	16.5
	3-6	10.4

[a](From Abrahams, 1963)

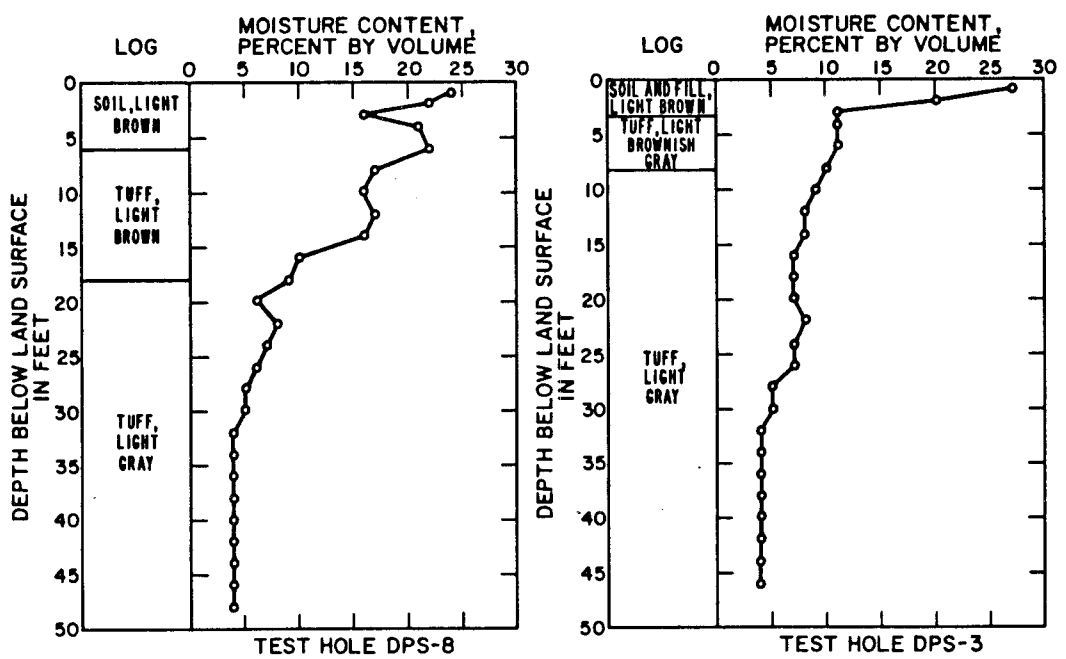

Fig. 12. Moisture distributions at TA-49 (Abrahams, Weir & Purtymun, 1961).

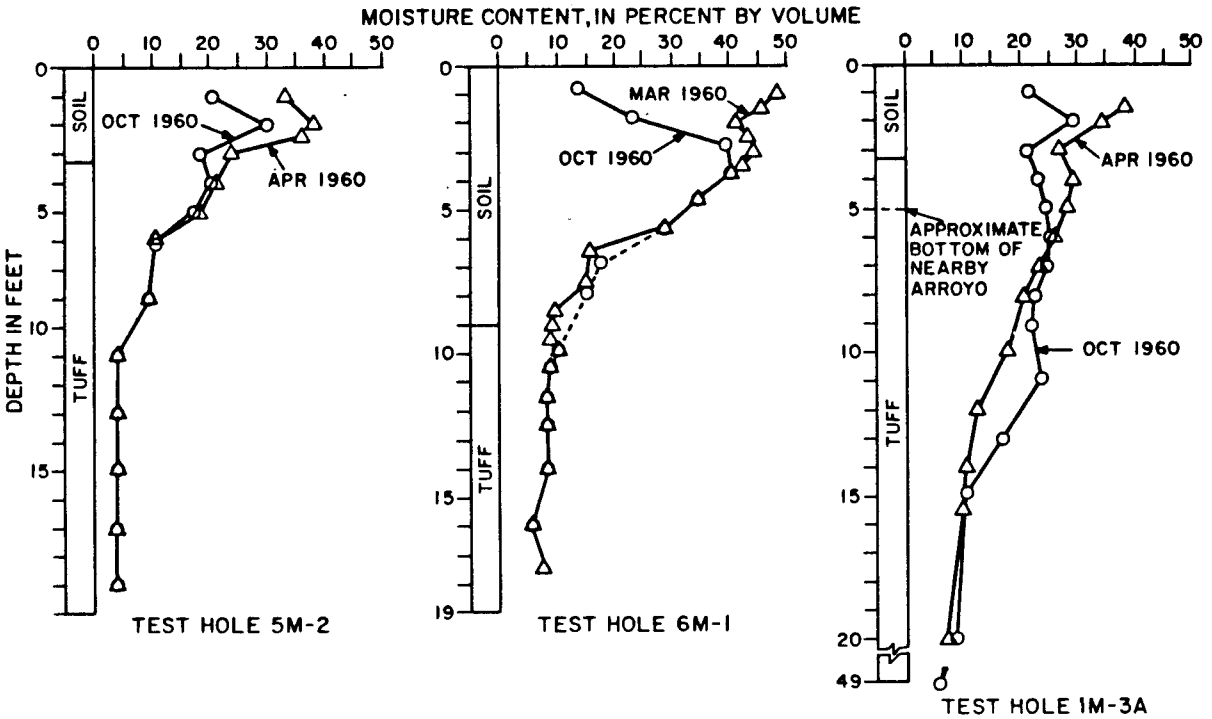

Fig. 13. Moisture distributions in Bandelier Tuff near TA-21 (Purtymun & Kennedy, 1966).

C. Current Monitoring

1. History. During the early 1970s there was renewed interest in establishing the dynamics of water and radionuclide movement within the Los Alamos radioactive waste disposal sites. A series of moisture access holes was drilled to allow monitoring of moisture depth distributions over a long time period. These investigations were also intended to establish the best means of installing access holes, optimum locations and measurement schedules, and the number of monitoring points required.

Measurements of the moisture content of solid and crushed tuff were made using a neutron moisture gauge (Abeele, October 1979). A description of the history and current status of the monitoring holes is presented in Appendix A. A summary of the measurement history is presented in Table VIII. The measurement data for these holes are on file with the Environmental Sciences Group, LS-6.

2. Data Discussion.

a. Area C. Four access holes were drilled in Area C in 1978. They are cased with aluminum tubing to about 1 m below the surface, below which the hole is open with an original diameter of about 8.5 cm. Geophysical logs of these holes revealed significant caving, to diameters of 25 cm in some cases, associated with low density zones such as pumice beds.

A summary of data from two of the holes (CP2-1, CP6-1), representative of all four, is presented in Figs. 14 and 15. Moisture contents below 30 m average between 6 and 7% by volume for CP2-1 and between 8 and 10% for CP6-1 and show no significant net gradient. Localized variations in moisture contents are probably caused by differences in the moisture tension relationships of various flow units. Moisture contents are expressed in per cent by volume or more often as Moisture Ratio by Volume (MRV).

A fifth hole, identified as TA52-1, was drilled just outside the perimeter fence at Area C, to obtain data on moisture conditions beneath undisturbed areas.

TABLE VIII

HISTORY AND CURRENT STATUS AT MONITORING HOLES

Hole	Original Depth (m)	Casing	Nominal Diam. (mm)	Current Status[a]
GP1-1	5.5	PVC	51	Active
GP1-2	3.5	PVC	51	Active
		PVC & Steel, to 1 m	51	Active
GS50-1	15	Open below to 2 m	102	Inactive
GP7-1	40	PVC	102	Inactive

[a]Status Types:
Active = Part of measurement net
Inactive = No measurement for > 2 yr (plugged/abandoned)

MONTHS 8,10,11 = 1978
MONTHS 13,14,15,17,18 = 1979
MONTHS 19,20,21,22,23 = 1979

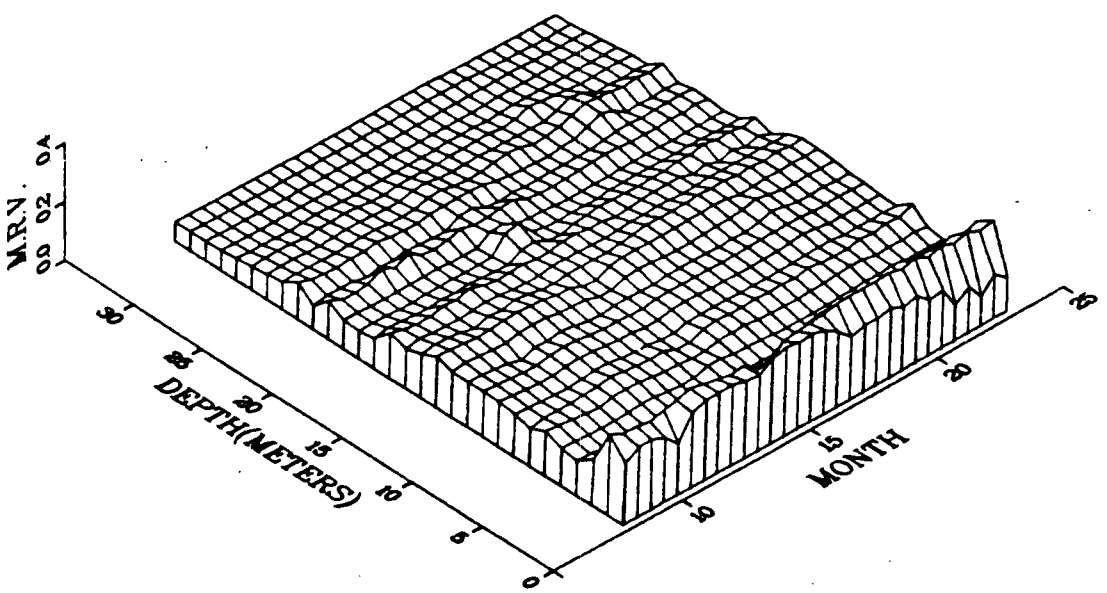

Fig. 14. Moisture Hole CP2-1.

MONTHS 8,10,11,12 = 1978
MONTHS 13,14,15,17,18 = 1979
MONTHS 19,20,21,22,23 = 1979

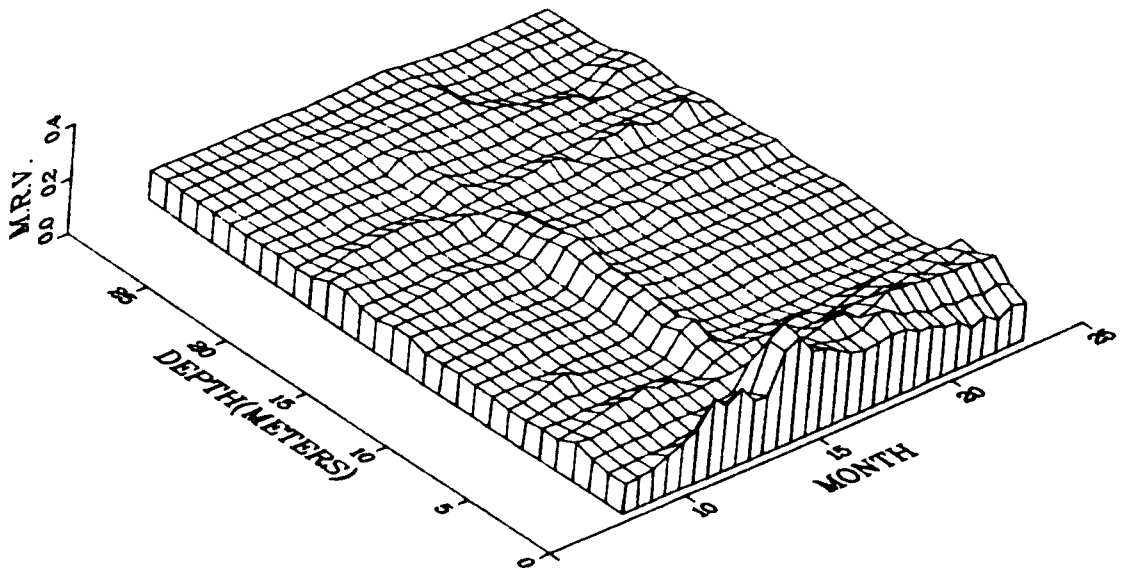

Fig. 15. Moisture Hole CP6-1.

b. Area G. Four holes were drilled in fill material overlying waste disposal pits (GP2-1, GP2-2, GP1-1, GP1-2) and cased with 5–cm PVC pipe. The former two were too shallow to obtain any significant data on depth distributions of soil moisture. Data from GP1-1, the deeper of the remaining two, is presented in Fig. 16. The data show significant seasonal fluctuations in moisture content to a depth of about 4 m, with a downward moisture flux below that depth. This flux, if it continues, will eventually raise the moisture content of the waste pit to a level above that of the surrounding undisturbed tuff, implying a gradual diffusion of moisture out of the waste pit. This condition results, in part, from the higher hydraulic conductivity of crushed tuff at high water content, compared with solid tuff. Changes in surface topography that reduced runoff are also partly responsible for disturbance of the natural moisture regime.

Six holes (GS50-1 to GS50-6) were drilled in solid tuff within the shaft disposal field. The holes are cased with steel pipe to a depth of about one meter, with an open hole of about 10.5 cm diameter below that depth. The holes were designed, in part, to detect possible moisture gradients away from Shaft 50, a source of tritium release from the shaft field (Wheeler and Warren, 1975). Data from two of these holes (GS50-3, GS50-5) are presented in Figs. 17 and 18. The data show seasonal fluctuations in moisture content in the upper 4 m, with no significant changes below that depth. The presence of stable "bulges" in the moisture content, underlain by regions of essentially constant moisture content, suggest that moisture is being held in the tuff, with no significant changes in moisture content during the measurement period. These bulges result, most probably, from variations in the moisture tension relationships of the tuff. For example, the bottom of the upper bulge coincides with the presence of a low-density pumice bed, a unit which would be expected to impede the downward flow of moisture. The moisture depth distributions show substantial stability over time, suggesting essentially steady-state conditions. No significant moisture gradients away from the shaft can be identified.

MONTHS 4,5,6,7,8,9,10,11,12 = 1978
MONTHS 13,14,15,16,17,18 = 1979
MONTHS 20,21,22,23,24 = 1979

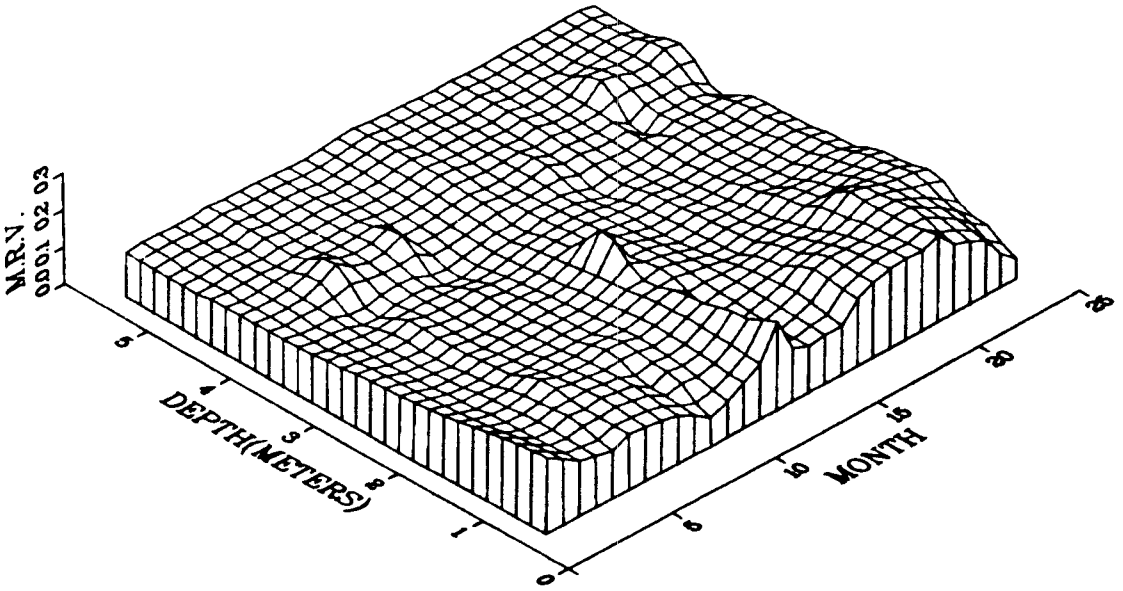

Fig. 16. Moisture Hole GP1-1.

MONTHS 4,5,6,7,8,9,10,11,12 = 1978
MONTHS 13,14,15,16,17,18 = 1979
MONTHS 19,20,21,22,23,24 = 1979

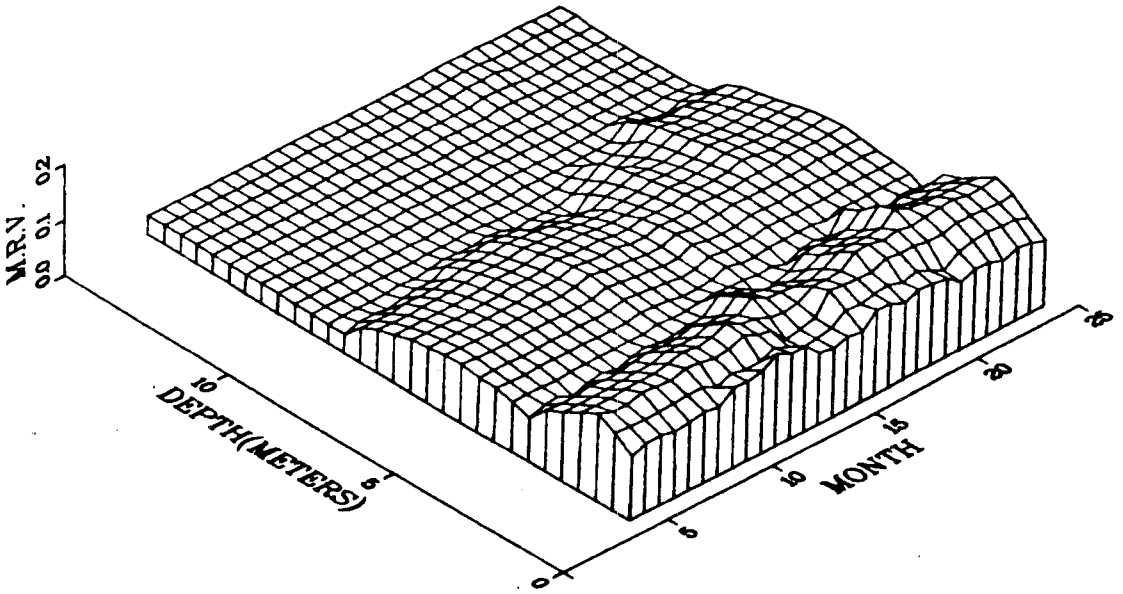

Fig. 17. Moisture Hole GS50-3.

MONTHS 4,5,6,7,8,9,10,11,12 = 1978
MONTHS 13,14,15,16,17,18 = 1979
MONTHS 19,20,21,22,23,24 = 1979

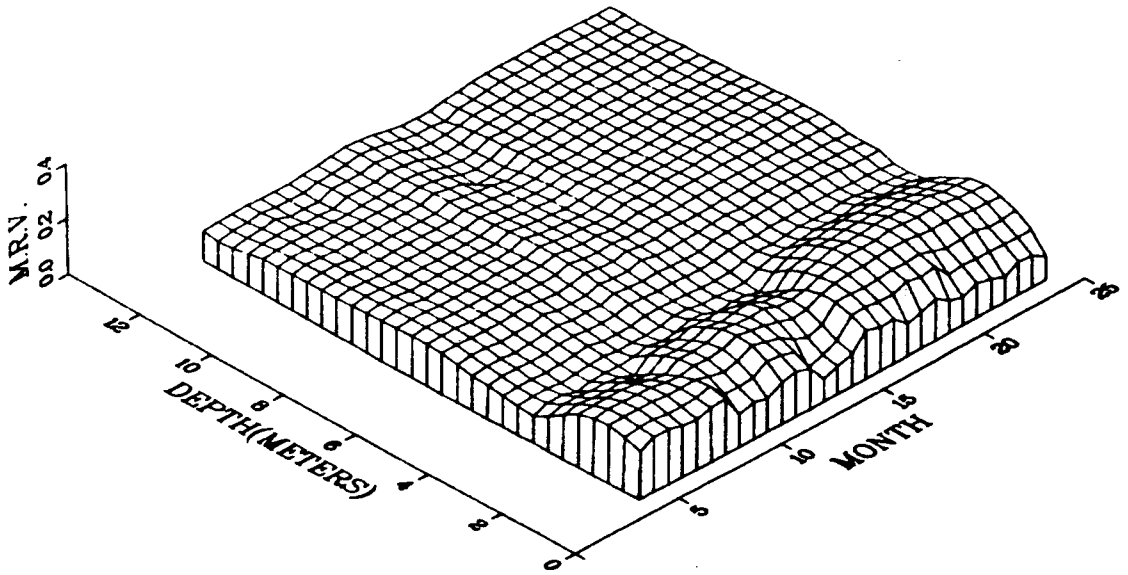

Fig. 18. Moisture Hole GS50-5.

Access holes were drilled in the bottom of Pits 7, 8, and 24 before backfilling was completed. Casings were extended to the surface before or during the filling process. All of the casings in Pit 8 were bent or broken beyond use during the filling process. Protective frameworks were constructed around the casings in Pits 7 and 24. However, several of these casings were also bent or broken beyond use during the filling process. Geophysical logs of two of these holes show extreme density variations (suggesting open voids) around the casings in GP7-2 and GP7-3, as well as breaks in both casings.

Moisture readings in the cased portions of the holes had been discontinued before these logs were collected because of the apparent meaningless nature of the data. Extreme variations in hole diameter and density are known to affect the readings (Abeele, October 1979). Data for Hole GP7-2 in the bottom of Pit 7 are presented in Fig. 19. The constantly low moisture distribution with depth, with the only exception occurring at the bottom of the pit (in the upper layers), suggests steady-state conditions with downward moisture flux due only to gravitational forces. Quantitative evaluation of this moisture flux suggests a downward rate of 10^{-11} m s^{-1} (0.3 mm per year).

One hole, GP26-1, was drilled in an undisturbed area. The hole is cased with 5-cm plastic pipe for the upper 0.5 m, below which the hole is open with an original diameter of about 10.5 cm. Geophysical logs indicate that some slumping of the sidewall has occurred, even though the hole was drilled only about 6 months before the logging. However, after the hole was constructed, pits were excavated near by, and the hole may provide data on the possible disturbance of the natural moisture regime by these pits. Only a limited amount of data have been collected from this hole and are not presented here.

c. Area F. A hole was drilled in the upper 0.5 m and cased with a 5-cm plastic pipe. The remainder of the hole was open, with a diameter of about 10.5 cm. The hole was intended to develop data on moisture contents of the tuff in a zone of relatively high precipitation, compared with Area C or Area G. However, insufficient data have been collected to date to make any such evaluations.

MONTHS 1,2,3,4,5,6 = 1978
MONTHS 7,8,9,10,11,12 = 1978
MONTHS 13,14,15,17,18 = 1979
MONTHS 19,20,21,22,23 = 1979

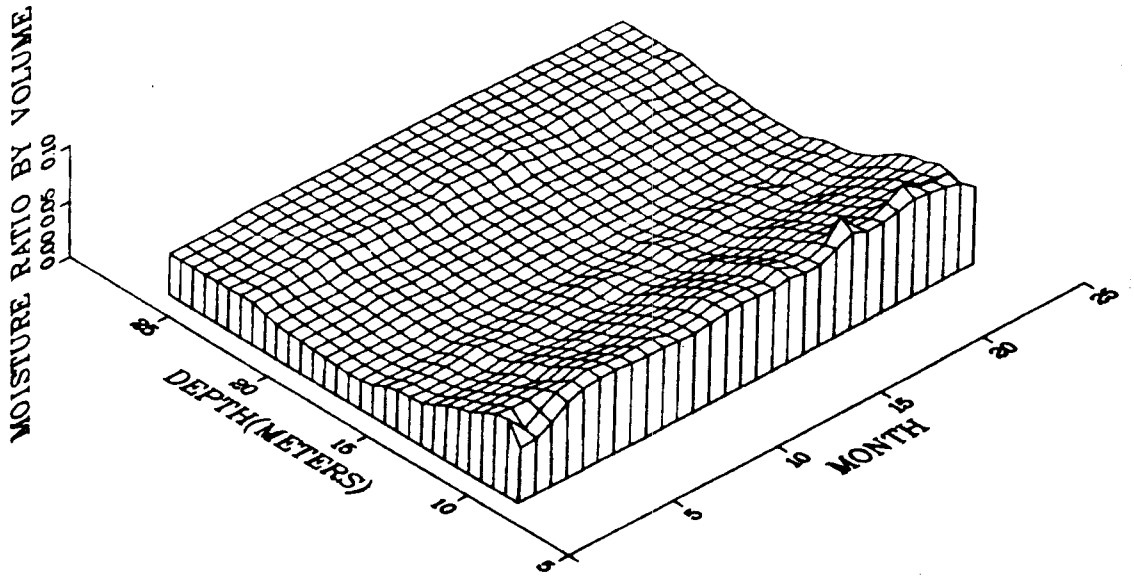

Fig. 19. Moisture Hole GP7-2.

d. TA-51. An access hole was drilled in an undisturbed area within TA-51 to obtain data on undisturbed moisture contents at a location midway between Areas C and G. Coincidentally, the area adjacent to the hole has been selected as the site of an experimental waste burial site. Although only limited data have been collected, background information on conditions in the area before construction at the adjacent site may be provided.

3. **Geophysical Logging.** Natural gamma, density (using gamma-gamma), neutron, and caliper logs were obtained for all of the holes described above. The caving of the holes in low-density zones has been discussed. The logs showed significant density variations with depth (see Section IX: Stratigraphic Controls on Flow). These density variations result from porosity changes in the tuff because of differing degrees of induration and material composition. Such variations have a significant effect on hydraulic properties, suggesting that detailed modeling of moisture flow will require extensive measurement of these properties for the various units. Conversely, the data collected during the past 6 years suggest that steady-state conditions prevail in all but near-surface portions of the tuff, and relatively simplistic analyses of the moisture flux may prove adequate to evaluate the potential for moisture and radionuclide flux within the disposal site.

The gamma logs proved useful in identifying unit contacts because of changes in natural radiation that occurred in the various units. These supported unit boundary identifications made with the density logs. The neutron logs, used primarily to determine porosity in saturated material, proved of little value for moisture content determinations. The particular probe used has a relatively long spacing between the source and detector (30 cm). Differences in chloride content of various units (determined by sample analysis) appear to result in differential neutron absorption. These differences are unrelated to moisture contents.

4. **Justification for Converting to "Inactive."** After extensive inspection of the data gathered in the existing monitoring holes, it was concluded that monitoring of several access holes should be eliminated.

This decision was based on similar moisture characteristics that seemed to prevail in adjacent monitoring holes (S50, P1, and P2). The decision concerning the P7 monitoring holes was more difficult because the part that goes through the pit is cased with PVC, whereas the part beneath the pit is uncased so that two different calibration curves had to be applied. An Analysis of Variance applied to the layer of soil that was backfilled in the pit around the monitoring hole showed a significant difference in moisture readings between monitoring holes. This could be caused by the presence of materials other than inorganic soils, or interference from the surrounding waste that could create preferential pathways for moisture into the soil around the monitoring holes because of successive layers of extremely permeable and impermeable waste material. These fluctuating moisture readings were therefore judged to be quite unreliable. The Analysis of Variance showed that there was no significant difference in undisturbed tuff moisture between P7-1 and P7-2 below 9 m.

As a consequence, and because shallow hole P2-1 was to be covered, monitoring of holes S50-1, S50-3, S50-5, P1-1, and P1-2 was retained. The monitoring of P7-1 and P7-3 was also continued below 9 m. P7-1 was chosen over P7-2 because of its greater depth.

VIII. TRITIUM MIGRATION

A. Tritiated Water in Soils

Radionuclides disposed of at the Los Alamos National Laboratory include significant amounts of transuranics (mostly plutonium and americum), uranium, fission products, activation products, and tritium. All investigations of the radioactive waste disposal areas revealed that, with the exception of tritium, no migration of these radionuclides has been detectable. Because of the high mobility of tritium in biological systems, there is a legitimate need to define and minimize the quantities of this radionuclide entering the environment from disposal areas (Wheeler et al., 1975). Migration of tritium from its disposal site was detected as early as 1970, although dissolution and subsequent migration of solid radionuclides in the disposal area is minimal. This has been verified continually by analysis of innumerable samples collected during the excavation of additional shafts in the disposal areas. Tritium, on the other hand, occurring principally as tritiated water, is nearly as free to move as water itself. Small quantities of tritium gas, disposed of by burial, convert very quickly to HTO on exposure to soil oxygen and moisture.

Before mid-1958, all tritium-containing wastes were disposed of by burial with other wastes in disposal pits. Since that time and until November 1973, unlined shafts, 8 to 20 m deep and possessing a diameter of 0.6 to 1.8 m, were used. Since November 1973, the walls and bottom of the disposal shafts for tritium waste have been coated with a 1- to 2-cm layer of asphalt. The primary motivation was an attempt to seal the many fractures in the tuff walls of the shaft, because it was believed that such fractures provided possible pathways for tritium migration (Wheeler et al., 1975). A study had previously shown that unlined tritium shafts were significant sources of soil contamination (Purtymun, 1973). In that study, it is shown that around an unlined shaft (number 13, Area G, Technical Area 54 on the Mesita del Buey), the tritium concentration in the surrounding tuff increased to a maximum between depths of 3 to 10 m and then decreased again with depth. Irregularities in the isotritium contours are seemingly influenced by the presence of open joints in the tuff, which provide for a much more rapid means of migration in the vapor phase. Close but irregular isotritium contours or high tritium gradients are to be found between the source (shaft) and an eventual transversal joint. The contours are elongated to the west of the shaft, indicating regions where either a radial joint was present or the outward (upward) movement of tritium was inhibited. High tritium gradients would consequently be an indication of swift, uninhibited aeration of tritium. A close and complete set of isotritium contour lines, which deserved close scrutiny, have been chosen along a southwest axis. The presence of tritium radioactivity decreases logarithmically with distance from the shaft. Table IX indicates the rate of decrease at various depths of radioactivity as a function of distance from the shaft. There were as many as seven contour lines intersecting the southwest

TABLE IX

DECREASE IN RADIOACTIVITY NEAR SHAFT 13 AS A FUNCTION OF DISTANCE FROM THE SHAFT ALONG A S-W AXIS

Depth (m)	Rate of Decrease (Bq m^{-3})	Coefficient of Correlation
3.75	$A = 3.1 \cdot 10^9 - 1.01 \cdot 10^9 \ln d$	$r = 0.96$
6.75	$A = 1.24 \cdot 10^{10} - 5.27 \cdot 10^9 \ln d$	$r = 0.97$
9.75	$A = 2.87 \cdot 10^9 - 1.04 \cdot 10^9 \ln d$	$r = 0.98$
12.75	$A = 1.23 \cdot 10^9 - 5.28 \cdot 10^8 \ln d$	$r = 0.96$

axis. The radioactivity is measured in Becquerels per cubic meter of water. Most interestingly, a vertical plane along the shaft axis showed that the maximum tritium concentration was located near the bottom of the shaft with the radioactivity decreasing upward according to $A = 1.11 \cdot 10^{10} - 6 \cdot 10^9 \ln d$ and $r = 0.97$. The similarity between the rate of decrease in radioactivity as a function of distance is striking along the vertical and horizontal planes! The closest match is between the horizontal rate of decrease as a function of distance from the shaft at 6.75-m depth and the vertical rate of decrease upward as a function of distance from the bottom of the shaft.

Shafts 50 and 59, also located in Area G, Technical Area 54 on the Mesita del Buey, have received tritium contaminated waste since 1973. Approximately the same time period elapsed between the placement of the waste and the collection of samples in shafts 50 and 59 as in shaft 13. Both shafts 50 and 59 were asphalt lined and asphalt containment was applied to the packaging of wastes placed in the shafts. Yet, on a percentage basis, significantly more tritium has migrated out of shafts where asphalt containment was used than from shafts where no asphalt was applied. Undoubtedly many factors contribute to this difference, including different waste forms and packaging before asphalting, variabilities in permeability of the tuff, and differences in the size and number of fractures intersected by the various shafts. However, the asphalting was intended to counteract and override these variabilities. It is concluded that the asphalting techniques, as applied in the past, did not significantly reduce the migration of tritium away from the disposal shafts. The shafts also appear to serve as a moisture source to the tuff, particularly at depth (Wheeler et al., 1975). This is probably because of the entrance of precipitation into the shafts during and between waste deliveries and before they are sealed off. The asphalted bottom serves as an inhibitor to the flow of moisture out of the shaft and this moisture in turn increases the total amount of water vapor to be diffused out of the shaft after its closure.

In this case also, tritium activity decreases logarithmically with distance from the shaft. Table X indicates, at two different depths, the rate of decrease of radioactivity as a function of distance from shafts 50 and 59. The fastest rate of decrease away from shaft 50 is along a SSW axis, while it seems fastest along the eastern axis originating at shaft 59. However, the tritium data are incomplete along the eastern axis, so that the next steepest gradient, along the northern axis, was chosen for analysis. For the tuff surrounding shafts 50 and 59, the radioactivity was measured using as basis a unit volume of tuff instead of water, as was used for the analyses surrounding shaft 13. Based on this fact, the constants in the regression equations should be quite a bit higher for shaft 13 for equal degrees of contamination. Since this is barely the case, it can be concluded that tritium contamination is substantially higher around shafts 50 and 59. The rates of decrease as a function of distance from the shaft are strikingly similar in both cases!

Because the preceding studies revealed that the asphalt was not significantly retarding tritium migration away from disposal shafts, a decision was made by the Waste Management Operations Group (H-7) to implement more rigorous packaging procedures involving the use of asphalt for tritium containing wastes. Asphalt coating of the shaft itself was eliminated.

TABLE X

DECREASE IN RADIOACTIVITY NEAR SHAFTS 50 AND 59 AS A FUNCTION OF DISTANCE FROM THE SHAFT

Shaft	Axis	Depth (m)	Rate of Decrease ($Bq\ m^{-3}$)	Coefficient of Correlation
50	SSW	3.75	$A = 1.01 \cdot 10^9 - 6.09 \cdot 10^8 \ln d$	$r = 0.98$
50	SSW	6.75	$A = 1.21 \cdot 10^9 - 5.61 \cdot 10^8 \ln d$	$r = 0.94$
59	N	3.75	$A = 1.03 \cdot 10^9 - 6.06 \cdot 10^8 \ln d$	$r = 0.96$
59	N	6.75	$A = 1.18 \cdot 10^9 - 5.73 \cdot 10^8 \ln d$	$r = 0.96$

To test the effectiveness of the new procedures, the new disposal shaft, No. 150, was located in an area where no prior tritium disposals had occurred. The extent of tritium migration into the tuff surrounding the shaft could then be related directly to the contents of the shaft. Disposal shaft 150 was drilled in the spring of 1976, with the first disposal occurring on 12 May 1976. In the winter of 1977, after more than $1 \cdot 10^{15}$ Bq (30 000 curies) of tritium had been disposed to the shaft, nine sampling holes were augered around the shaft. The samples were processed to remove the contained water, and the water was analyzed for tritium. The sampling holes were provided with surface casings and then sealed. Subsequently, in the fall of 1979, samples of the water vapor in the access holes were collected using silica gel as an absorbing medium. Water was distilled from the gel and analyzed for tritium. Also, the moisture content of the tuff surrounding the access holes was determined using a neutron moisture probe. The average water content in the tuff surrounding the shaft was about 4% by volume. This value agrees well with other measurements made in the area.

This latest study shows a release of 0.5 to 0.7% of the tritium in the shaft to the surrounding tuff vs an estimated 0.3 to 0.6% in the two previous cases. Thus, no substantial improvement in tritium containment was obtained by the new procedures. It is difficult to establish whether the packaging procedures themselves were inadequate, or the quality control on the procedures was inadequate.

Release of tritium to the surrounding tuff is not a significant health hazard; however, as the inventory of tritium in the disposal site continues to grow, improved methods will be necessary to provide additional containment. The results of this study have led to the design of further improvements in the techniques for tritium disposal. Sealed steel liners will be coated with asphalt and placed inside vertical shafts.

B. Emanation of Tritiated Water

1. The gradual mixture of tritiated water with natural soil moisture and subsequent evaporation of that water from the soil to the atmosphere results in a gaseous release from the burial ground. One study involved measuring the atmospheric release of tritiated water from Burial Pit 1, Area G. Soil borings in cover material overlying the waste showed tritium concentrations increasing from $7.4 \cdot 10^7$ Bq m^{-3} (2000 pCi/mℓ) of soil moisture at 15 cm to $4.6 \cdot 10^9$ Bq m^{-3} (125 000 pCi/mℓ) at 3.5 m. This gradient suggested an upward diffusion of tritiated water from the waste (at a depth below 3.5 m) to the surface soils. This tritiated water mixes with meteoritic soil moisture and is evaporated. The experimental measurements were designed to quantify the tritium flux and to establish the controlling factors.

Samples of evaporated soil moisture were collected on silica gel in covered sieves. Collection was at night, or on cloudy days, to reduce thermally induced lateral moisture fluxes. The average moisture flux and tritium flux were determined for the collection period. Atmospheric boundary layer data (vapor pressure) were collected. Soil moisture contents were measured from 0.5 to 1.5 m using a neutron moisture probe.

Correlations were made between tritiated water flux, (as dependent variable) and the various atmospheric and soil conditions. No significant correlation could be demonstrated between atmospheric conditions and tritiated water flux. The best correlation was obtained using soil moisture contents at 0.4 m and the soil moisture vapor pressure at 0.4 m. Measured tritiated water fluxes varied from $2 \cdot 10^{-3}$ Bq m^{-2} s^{-1} (0.005 μCi m^{-2} day^{-1}) to $2 \cdot 10^{-1}$ Bq m^{-2} s^{-1} (0.44 μCi m^{-2} day^{-1}). The actual surface area contributing to this flux was not established, but, as previously mentioned, measurements of the tritium distribution in the soil suggest that only a portion of this particular pit is contributing. Pit dimensions are approximately 30 m by 200 m ($6 \cdot 10^3$ m^2). If the entire pit were a source at the observed rate, atmospheric releases would range from 13 Bq s^{-1} to $1.1 \cdot 10^3$ Bq s^{-1} (30 μCi day^{-1} to 2640 μCi day^{-1}) during the measurement period. Because only some fraction of the total pit is actually contributing to tritium releases, the actual tritium released is less than this amount.

If the soil vapor pressure at 0.4 m is used as an independent variable together with the moisture ratio by volume at 0.4 m, measured with the neutron probe, a correlation coefficient of 0.7947 is obtained with tritiated water vapor aeration as the dependent variable. This coefficient of correlation is significant at the 1% level of confidence. Whether this highly significant coefficient of correlation is an indication of cause and effect relationship is somewhat arguable since temperature gradient, for example, could be the only reason for the existence of a vapor-pressure gradient. However, the relationship between temperature, moisture ratio by volume, and tritiated water aeration was not as good as the one between vapor pressure, moisture ratio by volume, and tritiated water aeration. The multiple correlation coefficient in that case was 0.7128. The difference is caused by the nonlinear relationship between temperature and saturated vapor pressure, but the lower values obtained using temperature as an independent variable do not exclude the fact that temperature *itself* is a cause for higher tritiated water vapor aeration. However, the higher correlation coefficients obtained using measurements taken at greater depths seem to indicate that liquid water flow is a more important factor in tritium aeration than vapor flow. This conclusion was reached because moisture content was increasing significantly with depth over the range considered and it is a known fact that liquid flow becomes more and more prevalent as the moisture content increases.

The addition of the atmospheric vapor pressure as an independent variable did not improve the multiple correlation coefficient. This is caused by the very nature of the experiment because the silica gel created a vapor pressure that was essentially zero in all cases at the soil-atmosphere interface. The moisture content was found to be maximum at 1 m; the loss of moisture in the upper meter, after correction for precipitation, was 9.95 mm between the 1st and 12th of June. This was measured using the neutron probe.

Based on the discontinuous nightly measurements using the silica–gel–filled sieve, and through interpolation, a total of 10.69 mm was predicted. The two above values seem to agree fairly well. The difference could be because of instrumental error, or higher evaporation induced by the presence of silica gel, or both.

2. Two sieves filled with silica gel and covered by a heavy aluminum plate were placed at spots equidistant from shafts 50 and 59, one at 6 m and the other at 10 m from the shafts, respectively. The activity measurements taken in February amounted to a tritiated water flux of 0.82 Bq s^{-1} m^{-2} ($2.22 \cdot 10^{-5}$μCi s^{-1} m^{-2}) and 0.22 Bq s^{-1} m^{-2} ($6 \cdot 10^{-6}$μCi s^{-1} m^{-2}), respectively.

3. Emanation of tritiated water was measured along 3 axes, A, B, C, 120° apart, around GS-150. The *measured* average concentration read $6.1 \cdot 10^8$ Bq m^{-3} of soil water ($1.65 \cdot 10^4$nCi/ℓ) for an area including 113.10 m^2. Because the evaporation rate was averaging $7.75 \cdot 10^{-9}$ m s^{-1}, the total release of tritiated water was: $6.1 \cdot 10^8$ Bq m^{-3} $\times$ $7.75 \cdot 10^{-9}$ m s^{-1} = 4.75 Bq m^{-2} s^{-1} ($1.11 \cdot 10^4$ nCi m^{-2} day^{-1}), or within the area under consideration (6 m radius): 535 Bq s^{-1} (1.25 mCi day^{-1}). Along each of the three axes, the rate of tritium emanation drops off with distance from the shaft according to a power function.

With d, the distance, expressed in meters and E, the tritiated water emanation, expressed in Bq m^{-2} s^{-1}, the regression analysis for the three different axes yields

$E = 95.5\ d^{-4.7546}$, with $r = 0.9902$;
$E = 104\ d^{-4.4050}$, with $r = 0.9972$; and
$E = 133\ d^{-5.0313}$, with $r = 0.9881$.

The average regression analysis for the three axes yields

$E = 110\ d^{-4.7000}$, with $r = 0.9932$.

This is an indication of an extremely fast decrease of tritium release with distance from the source (GS-150). This indicates further that water vapor emanation at the soil-atmosphere interface decreases faster with distance from the source than does the tritium dispersion in the soil, where the distribution behaves as a negative log function of distance. Further work is in progress to correlate tritium emanation to atmospheric and pedological properties of the GS-150 environment, especially including thermal characteristics of the tuff.

The thermal diffusivity (D) of the tuff at GS-150 was derived *in situ* from the measurements of daily temperature fluctuations (ΔT) at different depths (z) where

$$D = \left(- \frac{\Delta z}{\ell n(\Delta T_1/\Delta T_2)} \right)^2 \frac{\pi}{86400s}$$

averaged consistently $8 \cdot 10^{-7}$ m^2 s^{-1} during an extremely dry summer period, which kept the soil moisture content low, resulting in a low specific heat by volume leading to a higher thermal diffusivity. Representative tuff debris was hauled to the laboratory, where the density was accurately established as being $1.395 \cdot 10^3$ kg m^{-3}.

The specific heat (C_s) of the tuff was established in the laboratory using the standard method available for that purpose. A correction, obtained graphically, was used to correct for the thermal leakage of the thermally insulated container that was used as a calorimeter. The test was repeated four times and averaged C_s dry = 866J kg^{-1} K^{-1} or a heat capacity $C_v = 1.208 \cdot 10^6$ J m^{-3} K^{-1}. Since the Moisture Ratio by Volume *in situ* turned out to be 0.04, the actual heat capacity of the tuff under consideration is $C_{v0.04} = 1.375 \cdot 10^6$ J m^{-3} K^{-1}, with a standard deviation of $2.8 \cdot 10^4$ J m^{-3} K^{-1}. The thermal conductivity, λ, was estimated at $C_{v0.04}$ D = 1.1 W m^{-1} K^{-1}.

The above characteristics will help in determining the influence of the vapor gradient in the tuff on tritiated water emanation. Efforts are continuing to monitor temperature, heat flow, and water content at several depths, as well as atmospheric conditions capable of influencing tritium emanation. Relevant tritium elution data gathered so far are listed in Table XI. As one can readily observe, a seasonal pattern seems to emerge, with a peak of tritium release occurring in September. No detailed analysis has been made yet as the data base is far from complete, but the accumulated data would lead one to believe that the maximum releases of tritiated water occur when the vapor pressure within the shaft is driven to its maximum values, while the minimum releases of tritiated water occur when the vapor pressure within the shaft reaches a minimum. It seems evident that the maximum and minimum pressures within the shaft occur when temperatures below the surface reach a maximum or a minimum, respectively.

In conclusion, it should be pointed out that measurements of tritium emanation, taken in comparable locations and in the same seasonal period, yield results that form a good basis for comparison.

(1) Measurements taken on top of an assumed source of HTO over Pit 1 average 0.2 Bq m^{-2} s^{-1}.
(2) In February, at a point 6 m removed from both shafts 50 and 59, a release of 0.82 Bq m^{-2} s^{-1} was measured.
(3) By the end of December 1979, along the B axis originating from GS-150, the regression formula $E = 104\ d^{-4.405}$ then obtained yielded 0.11 Bq m^{-2} s^{-1} at 4.7 m from the shaft, a result that seems

TABLE XI

ACTIVITY AND FLUX OF TRITIATED WATER AT THE SOIL-ATMOSPHERE INTERFACE 4.7 m FROM THE CENTER OF GS-150

Date	HTO Concentration		Flux	
	10^6 Bq m^{-3}	μCi/ℓ	Bq m^{-2} s^{-1}	μCi m^{-2} day^{-1}
28 May 1980	79	2.13	0.58	1.35
4 June 1980	216	5.83	1.61	3.77
11 June 1980	293	7.92	2.00	4.67
18 June 1980	436	11.79	4.26	9.96
25 June 1980	496	13.40	4.47	10.45
2 July 1980	415	11.21	2.60	6.07
9 July 1980	284	7.68	1.63	3.81
16 July 1980	692	18.70	3.15	7.35
23 July 1980	688	18.60	2.62	6.11
30 July 1980	784	21.20	2.98	6.97
6 Aug. 1980	773	20.90	3.60	8.41
13 Aug. 1980	276	7.46	5.48	12.79
20 Aug. 1980	356	9.63	4.89	11.42
27 Aug. 1980	334	9.04	3.78	8.83
3 Sept. 1980	1088	29.40	9.62	22.47
10 Sept. 1980	350	9.45	4.13	9.65
17 Sept. 1980	518	14.00	5.54	12.94
24 Sept. 1980	607	16.40	5.67	13.25
1 Oct. 1980	492	13.30	4.15	9.70
8 Oct. 1980	470	12.70	2.41	5.64
15 Oct. 1980	205	5.54	1.21	2.83
22 Oct. 1980	168	4.55	1.21	2.83
29 Oct. 1980	112	3.03	0.43	1.01
5 Nov. 1980	138	3.73	0.95	2.21
12 Nov. 1980	128	3.46	0.72	1.65
19 Nov. 1980	135	3.64	0.60	1.41
3 Dec. 1980	89	2.40	0.43	1.00
17 Dec. 1980	28	0.75	0.29	0.67
23 Dec. 1980	26	0.69	0.22	0.51
30 Dec. 1980	19	0.50	0.14	0.32
7 Jan. 1981	21	0.57	0.12	0.28
14 Jan. 1981	20	0.5	0.11	0.25
21 Jan. 1981	40	1.08	0.16	0.38
28 Jan. 1981	46	1.25	0.13	0.31
4 Feb. 1981	55	1.49	0.15	0.36
11 Feb. 1981	63	1.70	0.24	0.55
18 Feb. 1981	75	2.03	0.41	0.96
25 Feb. 1981	126	3.40	0.46	1.07

to be quite compatible with actual measurements made by the end of December of the following year, when at 4.7 m from the shaft the emanation was 0.14 Bq m^{-2} s^{-1}.

Provided the *rate* of fall of tritium emanation with distance from the source remains the same throughout the seasons, the regression equation, during the period of maximum tritium release, is expected to adopt the form $E_{max} = 9095\ d^{-4.405}$. High release rates around the end of summer and beginning of fall are expected if the observations follow a seasonal pattern. Air concentrations in 1980 that are partly influenced by soil releases (absolute humidity, wind speed, and atmospheric convection will play an important role) also show a maximum during the warmer months and an overall minimum during the month of December.

At 4.7 m from the shaft center (GS-150), the flow of tritiated water averages 2.19 Bq m^{-2} s^{-1} (5.12 μCi m^{-2} day^{-1}) with the standard deviation = 2.20 Bq m^{-2} s^{-1} (5.17 μCi m^{-2} day^{-1}) at the soil surface. These measurements were taken during the 9 months preceding 25 March 1980.

IX. STRATIGRAPHIC CONTROLS ON FLOW

The study of the influence of sequential layers of tuff on moisture retention revolved mainly around the influence of related density differences on moisture retention. Densities and moisture contents were measured with nuclear probes that were lowered into monitoring holes. The density and moisture measurements obtained at each depth were then compared. A search for a cause and effect relationship between density and moisture content was subsequently performed through regression analysis.

After subtracting the measured moisture reading from the measured (wet) density, a regression analysis was run on 460 readings using the obtained dry density as the independent variable and the moisture ratio by volume as the dependent variable. The dry density was taken as the independent variable because it is obvious that some correlation would have to exist between the wet density and the moisture present because the moisture would necessarily increase the density measurement.

The dependence of the moisture ratio by volume (MRV) on the density (d) turned out to be

$$MRV = 0.0210 + 0.0809\ d \text{ with } r^2 = 0.0157\,,$$

indicating that 1.57% of the variation in MRV was associated with d!

More interesting is the fact that the equation shows a *slight* direct relationship between MRV and density, which is in direct contradiction with the observation made on page 52 in "Technical Reports Series No. 112, 1970" from the International Atomic Energy Agency, Vienna. Most authors fail to recognize an effect of soil density on soil moisture measurement in the normal soil density range and our findings can only support that view because of

(1) a low coefficient of determination between MRV and d.
(2) The small rate of change of MRV with d (an increase of 100 kg m^{-3} in density would mean an *increase* of 0.008 in the MRV).
(3) The proponents of a possible interaction between MRV and d indicate it would be an *inverse* correlation. The data presented do not give an indication of how strong (or weak) that correlation is supposed to be. The lack of interference of d in the moisture readings could only result in a narrowing of the confidence limits obtained when the moisture ratio is expressed as a function of the count ratio. Estimates of these confidence limits have been published and widely discussed (see Abeele, October 1979).

Subsequent logging by the US Geological Survey (USGS) showed that the actual monitoring hole diameter was, in some cases, not uniform, causing discrepancies in the moisture evaluation because of the application of the inappropriate calibration formula for that particular depth. An important parameter had consequently been overlooked. To remedy that, the regression analysis was repeated for the monitoring holes with irregular diameters. The analysis was applied over the depth range where the actual measured diameter matched the nominal diameter used in calibrating the neutron moisture probe readings. This obviously led to the elimination of the unwanted parameter. Somewhat different degrees of correlation were obtained for monitoring holes CS2-1, CS5-1, and CS6-1.

CS2-1	$MRV = -0.17 + 0.23d$	$r^2 = 0.17$
CS5-1	$MRV = 0.06 + 0.00074d$	$r^2 = 0.0019$
CS6-1	$MRV = 0.05 + 0.07d$	$r^2 = 0.07$

with r^2 being the coefficient of determination.

As can be seen, none of the correlations are significant. (In the case of CS5-1, one would have to try hard to obtain as bad a correlation between two columns of numbers chosen completely at random.) Moreover, in *every* case, the equations show again a slight *direct* relationship between MRV and density. The obvious conclusion of the study is that, in the range of tuff densities considered, there is no cause and effect relationship between density and moisture content.

X. RADIONUCLUDE TRANSPORT STUDIES

A. Downward Migration Through Leaching

Samples were collected along horizontal cores beneath Pit 3 in Area G for radiochemical analysis (Purtymun et al., 1978). For this purpose, a drill pad was constructed in a small canyon east of the pit from where five horizontal holes were cored under the pit. The study was performed in an attempt to detect possible migration of radionuclides from the waste pit into the tuff immediately underlying it. Core samples were analyzed for gross alpha, gross beta, ^{90}Sr, $^{238,239,240}Pu$, ^{241}Am, ^{137}Cs, and total uranium as contaminants in the waste. Filling of the pit was started 13 years before the core analysis study was begun. The tuff present on location was divided into several stratigraphic units, distinguishable from each other through their chemical and physical properties. Consequently, the natural concentrations of radionuclides vary from unit to unit.

The horizontal core holes were drilled in a fan-shaped array beneath the disposal pit. Samples of tuff beneath the pit and adjacent to it were analyzed for radionuclides known to be present in the pit, as well as for gross alpha and gross beta radiation. The analytical results from samples obtained beneath the pit were then compared statistically with the analytical results from samples obtained beside the pit. The analytical results were also grouped as a function of stratigraphic units.

The analytical results showed conclusively that the man-made radionuclides known to be present in the pit were not present at concentrations above the minimum detection limits in the samples collected beneath the pit. There were no statistically significant differences in gross alpha or gross beta radiation, or in concentrations of naturally occurring radionuclides in samples originating from under the pit compared with the samples obtained adjacent to the pit but pertaining to the same stratigraphic unit. In this context, it should be pointed out that the uranium concentrations varied between stratigraphic units but that the mean concentrations found in specific core samples were statistically undistinguishable from concentrations measured in related outcrops. Variabilities in gross alpha concentrations between units were found to be related to the already observed variability in uranium and other naturally occurring radionuclides.

Many of the waste containers in the pit were undoubtedly ruptured at the time of disposal through compaction by heavy earthmoving equipment. Also, much of the disposed waste, including contaminated soil, was not isolated from its environment. Thus, most of the radionuclides in the pit can be assumed to be available for dissolution and removal by moving soil moisture. The actual rates of dissolution and removal are not known but some must have happened locally in the 13 years that have elapsed since the initial use of the disposal pit. Results show, however, that any local radionuclide movement was restricted to the confines of the pit.

Expected water flow velocities, in the solid and crushed tuff, are known to be on the order of 10^{-12} m s^{-1} at the measured low soil moisture contents. This suggests that no migrating solutions would be detectable at depths exceeding a few millimeters beneath the pit. That expectation was not contradicted by the measurements taken in this study. No radionuclides, whose presence can be attributed to migration from the pit, were detected (Purtymun et al., 1980).

B. Upward Migration via Evapotranspiration

Surface contamination was known to exist in Area C, where the total activity in the top 5 cm of soil was calculated to be approximately $3 \cdot 10^{10}$ Bq. Several hypotheses have been advanced to account for the presence of the surface contamination (Trocki et al., in press).

(1) The nature of the disposal operations,
(2) the nature of known nuclear waste retrieval operations,
(3) burrowing animals,
(4) possible inadequate pit cover, and/or
(5) upward migration of radionuclides.

Core samples of several contaminated spots in Area C were analyzed for ^{238}Pu, ^{239}Pu, and ^{241}Am. Three corings, representative of how the activity was distributed as a function of depth, yielded the following regression equations (A is activity expressed in Bq kg^{-1} and d in meters depth).

I.D. No. CPS-16

^{238}Pu: $A = 1.04 \cdot 10^{-3} d^{-6}$

^{239}Pu: $A = 2.04 \cdot 10\ d^{-2.85}$

^{241}Am: $A = 0.91\ d^{-4.3}$

I.D. No. CPS-18

^{238}Pu: $A = 3.7 \cdot 10^{-3}\ d^{-4}$

^{239}Pu: $A = 1.37\ d^{-3.64}$

^{241}Am: $A = 2.59 \cdot 10^{-2}\ d^{-5}$

I.D. No. CPS-11

^{241}Am: $A = 0.74\ d^{-2.07}$

The above numbers are the identification of some of the contaminated spots under scrutiny in Area C.

These equations demonstrate a strong decrease of activity with depth. This strengthens the notion of surface spill as the source and no "upwelling" from the pit because of transport mechanisms involving evapotranspiration. The lack of uniformity, as far as the shape of the corresponding decreased activity curves is concerned, cannot be explained based on available information.

The decreasing activity with depth can only be a result of a slow leaching of radionuclides downward from their original surface spill location.

XI. SHEAR IN WET COHESIONLESS SOILS AND CRUSHED TUFF

Negative stress induced by capillary tension can be at the origin of increased soil shear strength. Capillary tension is the driving force that enables moist sand to maintain a molded or cut shape. Thin water films with small meniscus radii develop high-tensile stresses in the moisture wedges that hold soil particles in rigid contact. Fine sands and silts within the zone of capillary rise and fringe above a water table owe their strength to capillary tension and the resulting effective stresses in the granular structure. A point of maximum stress exists as a function of moisture content for a particular soil. Any drying or wetting away from that optimum moisture content will mean a decrease in maximum shear strength.The components of shear strength are friction and cohesion. The friction component is primarily affected by physical factors, while physiochemical factors affect the cohesion component. Cohesion is dependent on the attractive forces at work in clay-particle interactions. Water plays an important role in determining the magnitude of the cohesion component because it affects the distance between soil particles and, consequently, the attractive forces associated with air-water menisci (Baver et al., 1972). Excavation failures can sometimes be traced to a departure from a higher shear strength that existed when excavation was first begun.

A vane shear test was performed on soils and crushed tuff originating from the GS-150 area. As can be seen from Tables XII and XIII and Figs. 20 and 21, the decrease in strength caused by further wetting is much more drastic than that induced by eventual drying. For any granular material, the strength characteristics will depend heavily on the dry unit mass to which it is compacted. A higher dry unit mass

TABLE XII

VANE SHEAR TEST ON SOIL

Moisture Content by Mass (%)	Shear Strength (kPa)
2	7.25
8	7.2
12	7.6
16	8.0
20	6.0
24	3.0
26	0

TABLE XIII

VANE SHEAR TEST ON CRUSHED TUFF

Moisture Content by Mass (%)	Shear Strength (kPa)
1	1.0
10	5.8
12	8.2
14	12.8
16	14.0
18	14.2
20	14.6
22	16.2
24	16.2
26	10.2
28	0.0

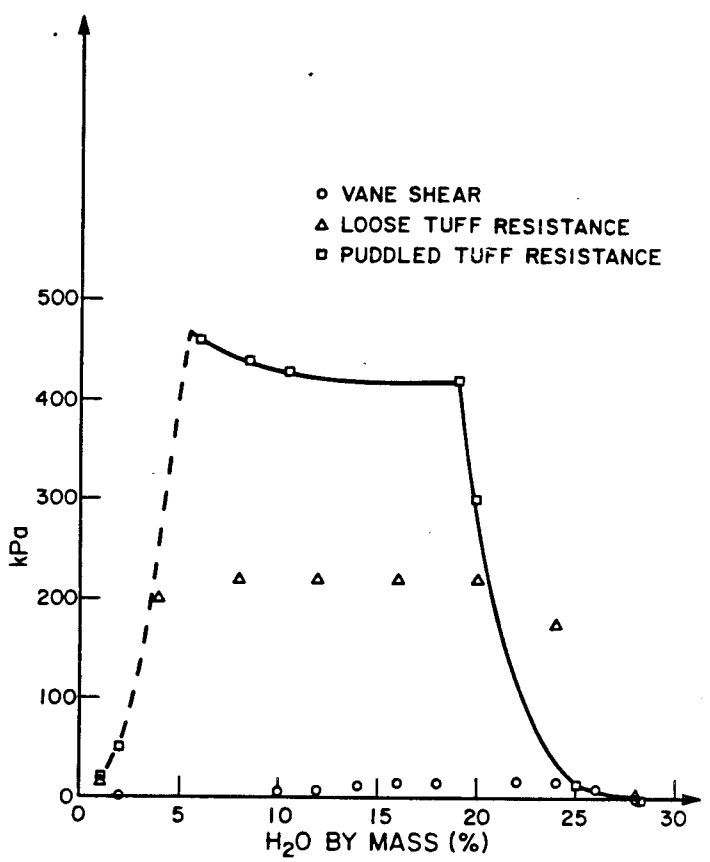

Fig. 20. Resistance tests on tuff.

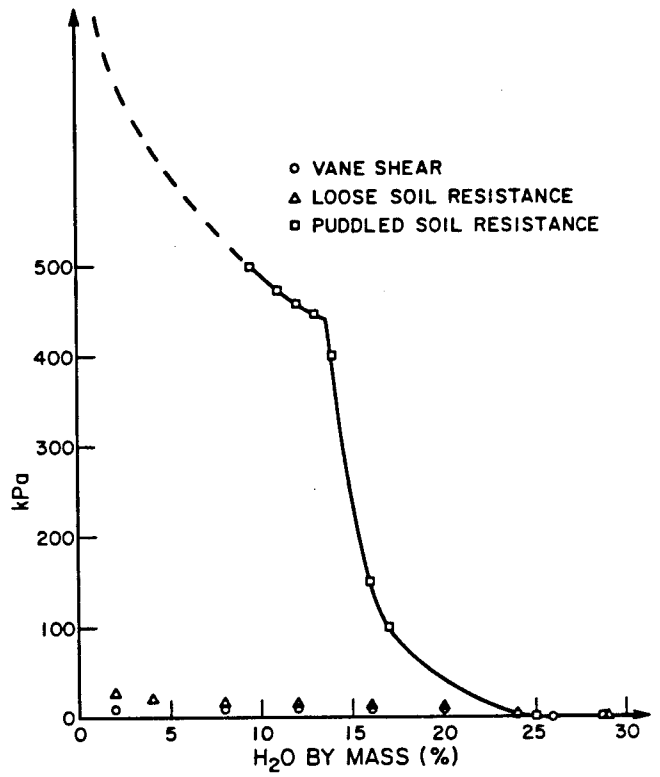

Fig. 21. Resistance tests on soil.

will correspond to a higher shear strength, all other parameters being equal. Changes in dry unit mass and shear strength are both influenced by the same independent variable, moisture content. A plot of dry density vs moisture content will indicate that compaction at any given energy level becomes more efficient as the moisture content increases toward an optimum moisture level beyond which the efficiency decreases.

The least expensive way to improve soil stabilization is precisely through compaction. Soil stabilization in turn means the improvement of several physical properties which, among other things, determine the shear strength of that soil. Besides an increase in shear strength, the other physical properties of a soil improved by compaction are the related increase in dry density and subsequent decreases in compressibility, permeability, and shrinkage (this last property mainly applicable to the montmorillonite clay that can be found on-site). As can be seen, adequate compaction of the pit overburden will improve several desirable properties important for good nuclear waste management.

The resistance to the penetration of a probing instrument is an integrated index of compaction, moisture content, texture, and type of material involved (crushed tuff, various clays, sand, etc.). As a penetrometer enters the soil, it will encounter resistance to compression, some friction between soil and metal and the shear resistance of the soil, which, as described above, involves both internal friction and cohesion (Baver et al., 1972).

The probe used in this study is a flat-bottom one. The tests show that soil moisture is a dominant factor influencing penetration resistance. There is a rapid decrease in resistance above 20% moisture by weight in crushed tuff and above 0% in the corresponding soil (Tables XIV and XV and Figs. 20 and 21). In tuff and soil the resistance to penetration at a moisture content of 16% by mass increases with depth of penetration.

TABLE XIV

RESISTANCE TO PENETRATION IN TUFF

Moisture Content by Mass (%)	Resistance (kPa)
1	15
4	200
8	220
12	220
16	220
20	220
24	175
28	0

TABLE XV

RESISTANCE TO PENETRATION IN SOIL

Moisture Content by Mass (%)	Resistance (kPa)
2	27
4	20
8	15
12	12
16	9
20	6
24	3
28	1

In tuff, the resistance to penetration, R, as a function of penetration depth, p, can be expressed as

$$R = 46p^{0.871} \qquad r^2 = 0.998$$

while in soil, the penetration resistance can be expressed as

$$R = 1.684p^{0.925} \qquad r^2 = 0.997$$

where R is expressed in kPa and p in mm.

The above results were obtained through regression analysis and in both cases the best results were obtained by adaptation of a power curve fit. As can be noticed, both expressions are nearly linear, which indicates that resistance to penetration increases *almost* proportionally with the penetration depth. If resistance to penetration is mainly a function of shear and compression resistance, it is fairly obvious from Figs. 20 and 21 that, for both tuff and soils, compression resistance is the most important component of the resistance to penetration and also the most sensitive to moisture content.

Application of similar compacting pressures on both crushed tuff and soil was at the origin of one notorious behavioral difference. The maintenance of that pressure caused practically no subsidence in the tuff as the moisture content was increased, while subsidence in the soil reached a high of 6%. This last phenomenon is well known to occur in soils, undoubtedly as a result of the enhanced ease of orientation of particles above the plastic limit. The soil in question, a very fine sandy loam, contains clay that has a platy or sheet-like structure. Because particle orientation is one of the major causes of subsidence (*or increased density)* during compression and because water is acting as a lubricant to facilitate such reorientation, it is to be expected that the soil under study will increase in density as the moisture content is increased. The near absence of that phenomenon in the crushed tuff indicates the absence of a platy structure and consequent minimum reorientation through lubrication (spherical particles do not possess a preferential orientation).

It should be noticed that in all of the above tests, the moisture was progressively *added* to loose, dry soil or tuff.

Tables XVI and XVII show how the resistance to penetration changes as a function of moisture after puddling and subsequent desiccation. It can be seen that the resistance to penetration reaches higher values using puddled materials. Drying of puddled soils produces maximum contact between particles, which causes high cohesion and strength due to interparticle attraction. Cohesion increases with a decrease in particle size distribution. Consequently, the point of maximum cohesion will increase with the

TABLE XVI

RESISTANCE TO PENETRATION IN TUFF AFTER PUDDLING

Percent H_2O	kPa
28	0
25	15
20	300
19	420
10.5	430
8.5	440
6.5	450
6	460
2	50
1	15

TABLE XVII

RESISTANCE TO PENETRATION IN SOIL AFTER PUDDLING

Percent H_2O	kPa
28	1
25	1
17	100
16	150
14	400
13	450
12	460
11	475
9.5	500
2	> 500
1	≫ 500

clay content of the materials under study. It is clear from Figs. 20 and 21 that the amount of cohesive soil is greater in soils than in crushed tuff. As a matter of fact, the resistance to penetration in soils increases rapidly beyond the measurement capabilities of the penetrometer in use. The dashed line in Fig. 21 indicates the suggested shape of the penetration resistance curve of puddled soil vs moisture content. Furthermore, it needs to be pointed out that the equation, expressing the resistance to penetration as a function of penetration depth, is not valid for dried puddled soils. Once the resistance of the "crust" is overcome, continued penetration occurs without any further increase in pressure. At very low moisture content (2%), the attraction between particles breaks down completely in tuff, while it continues to increase in soils, reaching its maximum at the lowest moisture content while tuff regains its complete loose state at 1% moisture content.

Just as the shear strength of crushed tuff, at a given moisture content, is very much a function of its dry density, so is the strength of undisturbed tuff equally dependent on its density (Purtymun et al., 1965). For several sites in the Los Alamos area, the influence of density (D) on resistance to crushing (RC) can be expressed as

$$RC = -383 + 51.72 \ln D$$

where the resistance to crushing is expressed in MPa and the bulk density in kg m^{-3}.

ACKNOWLEDGMENTS

Thanks are due to W. Herrera for computer plotting of the figures, to E. Trujillo and W. Herrera for sample collection, and to W. D. Purtymun for his pertinent advice.

REFERENCES

W. V. Abeele, "Future Credible Precipitation Occurrences in Los Alamos, New Mexico," Los Alamos Scientific Laboratory report LA-8523-MS (September 1980).

W. V. Abeele, "Determination of Hydraulic Conductivity in Crushed Bandelier Tuff," Los Alamos Scientific Laboratory report LA-8147-MS (November 1979).

W. V. Abeele, "The Influence of Access Hole Parameters on Neutron Moisture Probe Readings," Los Alamos Scientific Laboratory report LA-8094-MS (October 1979).

J. H. Abrahams, Jr., "Physical Properties of and Movement of Water in the Bandelier Tuff, Los Alamos and Santa Fe Counties, N.M.," US Dept. of the Interior Geological Survey, Albuquerque, New Mexico (January 1963).

J. H. Abrahams, Jr., J. E. Weir, Jr., and W. D. Purtymun, "Distribution of Moisture in Soil and Near-Surface Tuff on the Pajarito Plateau, Los Alamos County, N.M., U.S.G.S. Professional Paper 424D," Geological Research (1961).

R. A. Bailey, R. L. Smith, and C. S. Ross, "Stratigraphic Nomenclature of Volcanic Rocks in the Jemez Mountains, New Mexico," US Geol. Survey Bull. 1474 p. (1969).

L. D. Baver, W. H. Gardner, and W. R. Gardner, *Soil Physics* (John Wiley & Sons, New York, 1972), pp. 74-125.

G. S. Campbell, "A Simple Method for Determining Usaturated Conductivity from Moisture Retention Data," Soil Sci. 117:311-314 (1974).

DOE/EIS-0018, "Final Environmental Impact Statement - Los Alamos Scientific Laboratory Site, Los Alamos, New Mexico," US Department of Energy (December 1979).

R. L. Griggs, "Geology and Ground Water, Los Alamos Area, New Mexico," U. S. Geol. Survey Water Supply Paper, 1753 p. (1964).

International Atomic Energy Agency, "Neutron Moisture Gauges," Technical Report Series No. 112, Vienna (1970).

R. D. Jackson, R. J. Reginato, and C. H. M. Van Bavel, "Comparison of Measured and Calculated Hydraulic Conductivities of Unsaturated Soils," Water Resources Rev. 1, pp. 375-380 (1965).

A. Klute, "Water Diffusivity. Methods of Soil Analyses," Amer. Soc. of Agronomy, pp. 262-272 (1965).

R. J. Kunze, G. Vchara, and K. Graham, "Factors Important in the Calculation of Hydraulic Conductivity," Soil Sci. Soc. Amer. Proc. 32:760-765 (1968).

E. E. Miller and D. E. Elrick, "Dynamic Determination of Capillary Conductivity Extended for Nonnegligible Membrane Impedance," Soil Sci. Soc. Amer. Proc. 22:483-486 (1958).

R. J. Millington and J. P. Quirk, "Permeability of Porous Solids," Trans. Faraday Soc. 57:1200-1207 (1961).

W. D. Purtymun, "Underground Movement of Tritium from Solid Waste Storage Shafts," Los Alamos Scientific Laboratory report LA-5286-MS (May 1973).

W. D. Purtymun, M. L. Wheeler, and M. A. Rogers, "Geologic Description of Cores from Holes P-3 MH-1 through P-3 MH-5, Area G, Technical Area 54," Los Alamos Scientific Laboratory report LA-7308-MS (May 1978).

W. D. Purtymun and W. R. Kennedy, "Geology and Hydrology of Mesita del Buey," Los Alamos Scientific Laboratory report LA-4660 (May 1971).

W. D. Purtymun and W. E. Kennedy, "Distribution of Moisture and Radioactivity in Soil and Tuff at the Contaminated Waste-Pit Near Technical Area 21, Los Alamos, N.M.," US Geol. Survey Open File report (1966).

W. D. Purtymun and F. C. Koopman, "Physical Characteristics of the Tshirege Member of the Bandelier Tuff with Reference to Use as a Building and Ornamental Stone," US Geol. Survey Open File report, Albuquerque, N.M. (1965).

W. D. Purtymun, M. A. Rogers, and M. L. Wheeler, "Radiochemical Analyses of Samples from Beneath a Solid Radioactive Waste Disposal Pit at Los Alamos, N.M.," Los Alamos Scientific Laboratory report LA-8422-MS (June 1980).

P. E. Rijtema, "Calculation of Capillary Conductivity from Pressure Plate Outflow Data with Nonnegligible Membrane," Neth. J. Agr. Sci. 7:209-215 (1959).

M. A. Rogers, "History and Environmental Setting of LASL Near-Surface Land Disposal Facilities for Radioactive Wastes," Los Alamos Scientific Laboratory report LA-6848-MS (June 1977).

E. Schulman, 'Tree-Ring Indices of Rainfall, Temperature, and River Flow," Compendium of Meteorology (American Meteorological Society, Boston, 1951), pp. 1024-1029. See also Tree-Ring Bulletin 18, 10-18 (1952).

R. L. Smith, R. A. Bailey, and C. S. Ross, "Geologic Map of the Jemez Mountains, New Mexico," US Geol. Survey Misc. Geol. Investigation Map I - 571 (1970).

L. K. Trocki and W. V. Abeele, "Radioactivity Inventory of the Surface of Closed Waste Disposal Area C," Los Alamos National Laboratory report (in press).

M. L. Wheeler, W. J. Smith, and A. F. Gallegos, "A Preliminary Evaluation of the Potential for Plutonium Release from Burial Grounds at Los Alamos Scientific Laboratory," Los Alamos Scientific Laboratory report LA-6694-MS (February 1977).

M. L. Wheeler and J. L. Warren, "Tritium Containment After Burial of Contaminated Solid Waste," Proceedings of 23rd Conference on Remote Systems Technology (1975).

APPENDIX

SUMMARY OF DEPTH RANGES AND MEASUREMENT DATES FOR MONITORING HOLES - 1980

Number		Jan.	Feb.	Mar.	April	May	June
CP2180							
	Start	ND	00.50	00.50	00.50	00.50	00.50
	End		31.50	32.00	29.50	29.50	31.00
CP5180							
	Start	ND	00.50	00.50	00.50	00.50	ND
	End		29.50	27.50	27.50	27.50	
CP6180							
	Start	ND	00.50	00.50	00.50	00.50	00.50
	End		23.50	24.00	23.00	23.00	23.50
CS9980							
	Start	ND	00.50	00.50	00.50	00.50	00.50
	End		30.00	31.00	29.50	29.50	30.50
FP1180							
	Start	ND	00.50	00.50	00.50	00.50	ND
	End		21.00	21.00	21.00	21.00	21.00
GP1180							
	Start	ND	00.50	00.50	00.50	00.50	00.50
	End		5.50	5.50	5.00	5.00	5.00
GP1280							
	Start	ND	00.50	00.50	00.50	00.50	00.50
	End		3.50	3.50	3.50	3.50	3.00
GP2680							
	Start	ND	00.50	00.50	00.50	00.50	00.50
	End		33.00	31.50	31.00	31.00	31.50
GP7280							
	Start	ND	NE	9.00	9.00	9.00	9.00
	End			24.00	22.50	22.50	23.50
GP7380							
	Start	ND	9.00	9.00	9.00	9.00	9.00
	End		22.00	22.00	20.00	20.00	21.50
GS50380							
	Start	00.50	00.50	00.50	00.50	00.50	00.50
	End	11.50	12.00	12.00	11.50	11.50	12.00
GS50580							
	Start	00.50	00.50	00.50	00.50	00.50	00.50
	End	14.00	14.50	14.50	14.00	14.00	14.00
TA52180							
	Start	ND	00.50	00.50	00.50	00.50	00.50
	End		33.00	32.00	30.00	30.00	31.00
TA5180							
	Start	ND	00.50	00.50	00.50	00.50	ND
	End		33.00	31.50	30.00	30.00	(Lost Probe)

ND = No Data
NE = Data Not Entered

SUMMARY OF DEPTH RANGES AND MEASUREMENT DATES FOR MONITORING HOLES - 1979

Number		Jan.	Feb.	Mar.	April	May	June	July	Aug.	Sept.	Oct.	Nov.	Dec.
GS50319													
	Start	ND	ND	0.5	ND	0.5	0.5	0.5	0.5	0.5	0.5	0.5	0.5
	End			11.5		11.5	12.0	11.5	12.0	12.0	12.5	11.5	12.0
GS50579													
	Start	0.5	NM	0.5	ND	0.5	0.5	0.5	0.5	0.5	0.5	0.5	0.5
	End	14.0		14.0		14.0	14.0	14.0	15.0	14.0	15.0	15.0	14.5
GR1179													
	Start	0.5	0.5	0.5	ND	0.5	0.5	0.5	0.5	0.5	0.5	0.5	0.5
	End	5.0	5.0	5.0		5.0	5.5	5.0	5.0	5.0	5.5	5.0	5.5
GP1279													
	Start	0.5	0.5	0.5	ND	0.5	0.5	0.5	0.5	0.5	0.5	0.5	0.5
	End	3.5	3.5	3.5		3.5	4.0	3.5	4.0	3.5	4.0	3.5	4.0
GP7279													
	Start	9.0	9.0	9.0		9.0	9.0	9.0	9.0	9.0	9.0	9.0	ND
	End	22.5	24.5	22.5		23.0	23.5	23.0	23.5	23.5	26.0	23.5	
GP7379													
	Start	9.0	9.0	9.0	ND	9.0	9.0	9.0	9.0	9.0	9.0	9.0	ND
	End	20.0	21.0	20.0		20.5	22.5	20.5	21.5	20.5	22.5	20.5	
CP2179													
	Start	0.5	0.5	0.5	ND	0.5	0.5	0.5	0.5	0.5	0.5	0.10	ND
	End	29.5	25.5	29.5		29.5	29.5	29.5	26.0	29.5	32.5	29.5	
CP6179													
	Start	0.5	0.5	0.5	ND	0.5	0.5	0.5	0.5	0.5	0.5	0.10	ND
	End	24.0	30.0	24.50		24.0	22.0	22.5	23.5	28.0	24.5	23.0	
CS99179													
	Start	0.50	0.50	0.50	ND	0.50	0.50	0.5	0.5	0.5		0.5	ND
	End	30.50	20.00	30.50	ND	30.50	29.50	30.5	28.5	30.0	31.0	30.0	
CP5179													
	Start	0.5	0.5	ND	ND	0.5	0.5	0.5	0.5	0.5	0.5	0.10	ND
	End	27.5	30.5			27.5	29.0	27.5	28.5	28.0	29.5	27.5	
CP5179													
	Start	0.5	0.5	0.5		0.5	0.5	0.5	0.5	0.5	0.5	0.10	ND
	End	30.5	28.0	30.5		30.5	29.5	30.5	28.5	28.0	29.5	27.5	
FP1179													
	Start											0.5	ND
	End											21.0	
GP26179													
	Start											ND	0.5
	End												33.0
TA52179													
	Start											ND	0.5
	End												33.0
TA5179													
	Start											0.5	ND
	End											33.0	
CP5179													
	Start	0.5	0.5	ND	ND	0.5	0.5	0.5	0.5	0.5	0.5	0.5	0.5
	End	27.5	30.5	ND	ND	27.5	29.0	27.5	28.5	28.0	29.5	27.5	
CP5179													
	Start	0.5	0.5	0.5		0.5	0.5	0.5	0.5	0.5	0.5	0.10	ND
	End	30.5	28.0	30.5	30.5	29.5		30.5	28.5	28.0	29.5	27.5	
FP179													
	Start											0.5	ND
	End											21.0	

SUMMARY OF DEPTH RANGES AND MEASUREMENT DATES FOR MONITORING HOLES - 1976, Continued

Number	Jan.	Feb.	Mar.	April	May	June	July	Aug.	Sept.	Oct.	Nov.	Dec.
GP26179												
Start											ND	0.5
End												33.0
TA52179												
Start											ND	0.5
End												33.0
TA5179												
Start											0.5	ND
End											33.0	

SUMMARY OF DEPTH RANGES AND MEASUREMENT DATES FOR MONITORING HOLES - 1978

Number	Jan.	Feb.	Mar.	April	May	June	July	Aug.	Sept.	Oct.	Nov.	Dec.
CP2178												
Start							0.5	0.5		0.5	0.5	
End							29.5	29.5		29.5	31.0	
CPS178												
Start								0.5			0.5	0.5
End								31.0			31.5	30.5
GS50178												
Start	0.91	0.91	0.5	0.5	0.5	0.5	0.5	0.5	0.5	0.5	0.5	0.5
End	14.02	12.80	13.5	13.0	13.5	13.5	13.0	13.5	13.0	13.5	13.5	13.0
GS50378												
Start	0.5	0.5	0.5	0.5	0.5	0.5	0.5	0.5	0.5	0.5	0.5	0.5
End	11.0	11.0	12.0	12.0	12.5	11.5	11.5	12.0	11.5	11.5	12.0	11.5
GS50578												
Start	0.91	0.91	0.5	0.5	0.5	0.5	0.5	0.5	0.5	0.5	0.5	0.5
End	14.33	14.02	13.50	13.5	14.0	14.0	13.0	14.0	14.0	14.0	14.5	13.0
GA1178												
Start	0.61	0.61	0.5	0.5	0.5	0.5	0.5	0.5	0.5	0.5	0.5	0.5
End	5.49	5.49	5.00	5.0	5.0	5.0	5.0	5.0	5.0	5.0	5.0	5.0
GP1278												
Start	0.61	0.61	0.5	0.5	0.5	0.5	0.5	0.5	0.5	0.5	0.5	0.5
End	3.96	3.96	3.50	3.5	3.5	3.5	3.0	3.5	3.5	3.5	4.0	3.5
GP7178												
Start	8.53	8.53	9.0	9.0	9.0	9.0	9.0	9.0	9.0	9.0	9.0	9.0
End	24.68	24.07	23.0	23.0	23.0	24.0	25.0	23.5	23.0	23.0	23.5	23.0
GP7378												
Start	8.53	8.53	9.0	9.0	9.0	9.0	9.0	9.0	9.0	9.0	9.0	9.0
End	21.33	21.03	14.0	20.0	21.5	21.5	20.0	20.0	20.0	20.0	21.0	20.0
GP6178												
Start								0.5		0.5	0.5	0.5
End								24.0		24.0	25.5	24.0
GP5178												
Start								0.5	0.5	0.5	0.5	0.5
End								29.0	27.5	27.5	28.0	27.5

SUMMARY OF DEPTH RANGES AND MEASUREMENT DATES FOR MONITORING HOLES - 1977

Number		Jan.	Feb.	Mar.	April	May	June	July	Aug.	Sept.	Oct.	Nov.	Dec.
GS50177													
	Start	2.13	2.13	2.43	2.13	2.43	2.13	2.13	2.13	0.91	1.21	1.52	1.21
	End	11.58	9.45	11.58	8.53	14.62	9.45	9.14	14.33	14.02	14.02	14.02	13.72
GS50377													
	Start	1.82	1.82	2.13	2.43	2.43	2.13	2.13	1.82	1.82	1.21	1.21	0.91
	End	13.72	12.80	12.80	11.58	13.41	13.11	13.41	14.02	13.41	12.50	12.50	12.19
GS50577													
	Start	1.82	1.82	2.13	2.13	1.82	2.13	2.13	1.82	1.82	1.21	1.21	1.21
	End	9.45	9.45	9.75	9.14	13.72	9.45	14.33	14.64	14.63	13.41	14.02	14.02
GP177													
	Start	1.82	1.52	1.21	1.21	1.52	2.13	1.82		1.21	1.21	1.21	1.21
	End	5.49	5.49	4.57	5.18	5.49	5.49	5.79		5.49	5.49	5.79	5.49
GP1277													
	Start	1.82	1.52	1.52	1.21	1.52	1.52			1.52	1.21	1.21	1.21
	End	4.27	4.27	4.27	3.96	4.27	4.27			4.27	4.27	4.27	4.27
GP7177													
	Start	8.53	8.53	8.53		8.53	8.53	8.53		8.53	8.53	8.53	8.53
	End	24.38	14.33	14.02		24.07	14.02	14.94		24.07	22.86	22.86	22.86
GP7377													
	Start	8.53	8.53	8.53		8.53	8.53	8.53		8.53	8.53	8.53	8.53
	End	20.72	13.41	14.33		21.03	14.02	13.41		21.03	21.03	20.11	19.81

SUMMARY OF DEPTH RANGES AND MEASUREMENT DATES FOR MONITORING HOLES - 1976

Number		Jan.	Feb.	Mar.	April	May	June	July	Aug.	Sept.	Oct.	Nov.	Dec.
GS0176													
	Start	1.52		1.52				1.52	1.52				1.52
	End	13.41		9.75				7.62	8.53				7.92
GS50276													
	Start	1.52		1.52				1.52	1.52				1.52
	End	13.71		10.06				10.06	10.06				10.06
GS50376													
	Start	1.52		1.52				1.52	1.52				1.52
	End	13.41		10.06				9.75	9.45				10.06
GS50476													
	Start	1.52		1.52				1.52	1.52				1.52
	End	12.50		8.84				8.23	8.84				8.84
GS50576													
	Start	1.52		1.52				1.52	1.52				1.52
	End	13.41		10.06				7.92	7.92				8.23
GS50676													
	Start	1.52		1.52				1.52	1.52				1.52
	End	13.11		8.53				762	7.92				9.14
GP1176													
	Start	0.91						0.91	0.91				0.91
	End	4.88						4.88	4.88				4.88

SUMMARY OF DEPTH RANGES AND MEASUREMENT DATES FOR MONITORING HOLES - 1979, Continued

Number		Jan.	Feb.	Mar.	April	May	June	July	Aug.	Sept.	Oct.	Nov.	Dec.
GP1276													
	Start	0.91						0.91	0.91				0.91
	End	3.66						3.66	3.66				3.66
GP2176													
	Start	0.91						0.91	0.91				0.91
	End	2.74						3.05	2.74				2.44
GP2276													
	Start	0.91						0.91	0.91				0.91
	End							1.21	1.21				

SUMMARY OF DEPTH RANGES AND MEASUREMENT DATES FOR MONITORING HOLES - 1975

Number		Jan.	Feb.	Mar.	April	May	June	July	Aug.	Sept.	Oct.	Nov.	Dec.
GP1175													
	Start			0.30									
	End				4.55								
GP1275													
	Start			0.30									
	End			3.30									
GP1175													
	Start				0.30				0.30				
	End				4.55				4.55				
GP1275													
	Start				0.30				0.30				
	End				3.94				3.58				

SUMMARY OF DEPTH RANGES AND MEASUREMENT DATES FOR MONITORING HOLES - 1974

Number		Jan.	Feb.	Mar.	April	May	June	July	Aug.	Sept.	Oct.	Nov.	Dec.
GP1174													
	Start	0.30	0.30	0.30	0.30	0.30	0.30	0.30	0.30	0.30	0.30		
	End	5.12	4.85	4.85	4.85	5.10	4.24	2.42	5.10	5.10	4.24		
GP1274													
	Start	0.30	0.30	0.30	0.30	0.30	0.30	0.30	0.30	0.30	0.30		
	End	3.64	3.58	3.64	3.58	3.58	3.58	3.58	3.58	3.58	3.30		
GP2174													
	Start		0.30										
	End		2.73										
GP2274													
	Start		0.30										
	End		1.15										
GP2174													
	Start			0.30									
	End			2.73									
GP2274													
	Start			0.30									
	End			1.20									

☆U.S. GOVERNMENT PRINTING OFFICE: 1981—576-020/149

339. DISTRIBUTION OF MOISTURE IN SOIL AND NEAR-SURFACE TUFF ON THE PAJARITO PLATEAU, LOS ALAMOS COUNTY, NEW MEXICO

By JOHN H. ABRAHAMS, JR., JAMES E. WEIR, JR., and WILLIAM D. PURTYMUN, Albuquerque, N. Mex.

Work done in cooperation with the U.S. Atomic Energy Commission

The Pajarito Plateau adjoins the steep eastern flanks of the Sierra de los Valles in north-central New Mexico. It has been dissected by eastward-flowing streams into several fingerlike mesas. The plateau is underlain by pumice deposits, ash falls, and ash flows that were ejected from a large volcanic vent to the west. Ash flows that cap the plateau are welded rhyolite tuff. Soil on the middle part of the mesas is well developed on the flat uplands and is thought to be derived largely from tuff weathered in place. Three zones are recognizable: An A zone from which most of the clay has been leached, a B zone containing montmorillonite, and a C zone (transitional from soil to tuff) with a high clay content. The zone of saturation is more than 1,000 feet beneath the surface of the plateau in the areas studied (fig. 339.1).

Measurements of the rate and amount of water movement and of moisture content of the soil and tuff, both under natural conditions and in controlled infiltration experiments, were made as an essential part of studies

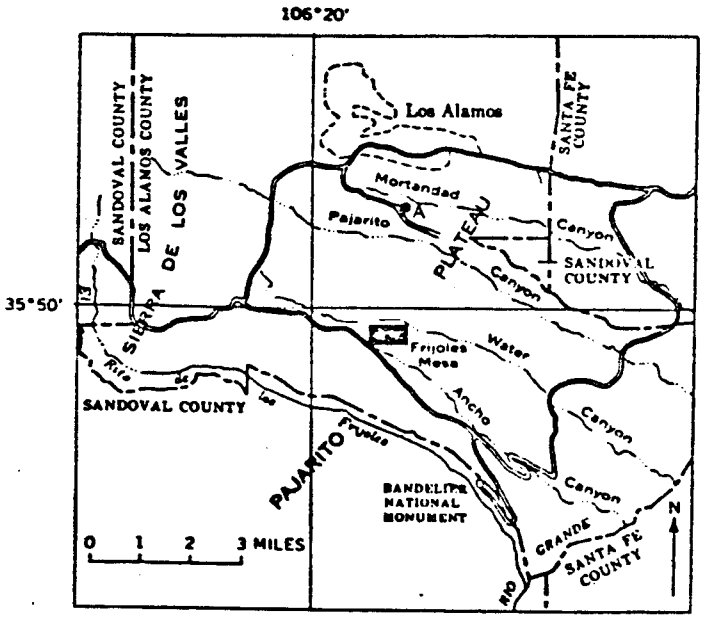

FIGURE 339.1.—Pajarito Plateau, N. Mex., showing area of moisture studies (shaded).

of aqueous movements of radioactive substances originating from liquid wastes or from leachable radioactive solids. These measurements were made as a part of the program with the Los Alamos Scientific Laboratory.

A neutron-scattering moisture probe was inserted into test holes cased with 2-inch plastic pipe to determine the moisture content of the rock and soil. The measurements were checked against laboratory determinations of moisture drill in cores. The moisture contents determined with the probe appeared to be about 1 to 2 percent higher than those made in the laboratory.

NATURAL DISTRIBUTION OF MOISTURE

Twenty-three test holes were drilled on Frijoles Mesa and moisture measurements were made in the spring, summer, and fall of 1960 to study natural infiltration in the soil and tuff. In general, the moisture content was found to increase from the surface to a depth of 2 to 3 feet, then decrease to a depth of 4 to 12 feet, and remain relatively constant at greater depths. There were some variations, however, that were apparently related to drainage and soil thickness. Data from the 23 test holes are summarized in the adjacent table.

	Thickness of soil (feet)		Depth at which moisture content was less than 10 percent (feet)		Depth at which moisture content was less than 5 percent (feet)	
	Range	Average	Range	Average	Range	Average
Fifteen test holes in well-drained areas	0.5–4.0	3.5	2.5–9.0	4.7	7.0–14.0	8.8
Eight test holes near arroyos, ditches, and in poorly drained areas	2.2–9.0	5.3	4.0–19.0+	9.5	(1)	

[1] Moisture content does not decrease to 5 percent; the holes range in depth from 19 to 49 feet.

The moisture content in the upper 5 or 6 feet was highest in March and April, as a result of late winter snow; it decreased to a minimum in October, owing to the high evapotranspiration rate during the summer and early fall.

Test-hole 5M–2 (fig. 339.2) is representative of the test holes in well-drained areas. Moisture measurements show that below a depth of 6 feet the moisture

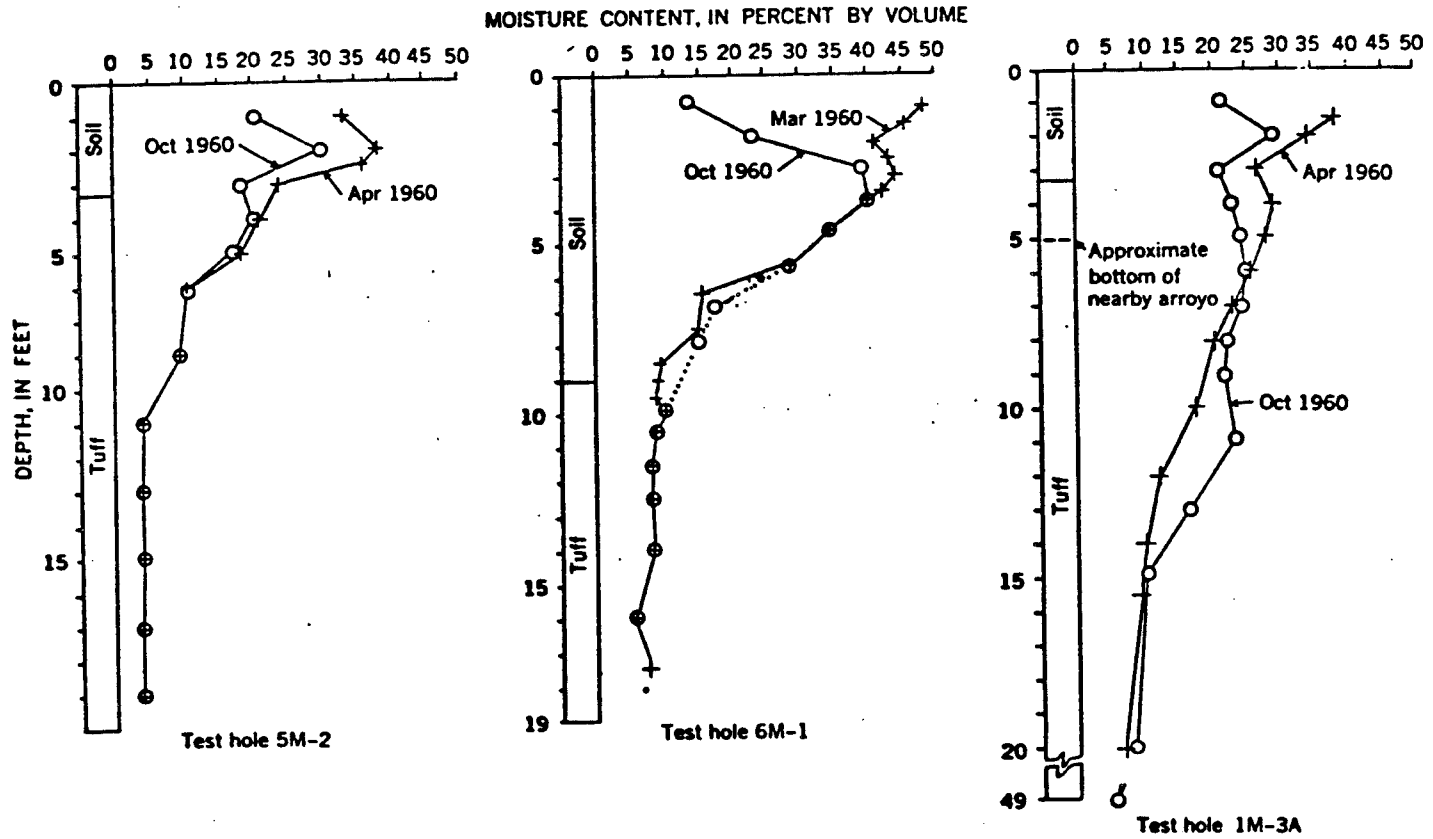

FIGURE 339.2.—Moisture measurements in selected test-holes on Frijoles Mesa, Los Alamos County, N. Mex.

content of the tuff remained unchanged and below 10 feet it was less than 4 percent.

Test holes near arroyos, ditches, and in poorly drained areas that received or retained water during periods of storm runoff are represented by test-holes 6M-1 and 1M-3A (fig. 339.2). Although moisture measurements in test-hole 6M-1 suggest a small increase in moisture content between about 6 and 10 feet in depth between March and October, they merely reflect the fact that measurements in this interval were made at slightly different depths. Thus, additional points on the October curve probably would have resulted in a curve that more nearly duplicated the March curve. In hole 6M-1 the moisture content below a depth of about 4 feet remained nearly the same, and the moisture content in the tuff ranged from 6 to 10 percent during both periods.

Construction near test-hole 1M-3A, on the bank of an arroyo, caused water to pond 2 to 4 inches deep several feet from the test-hole during wet periods. The ponded water percolated through the thin soil and sand in the bed of the arroyo and moved downward and laterally into the tuff as shown by the increase of moisture from 12 percent to 17 percent at a depth of

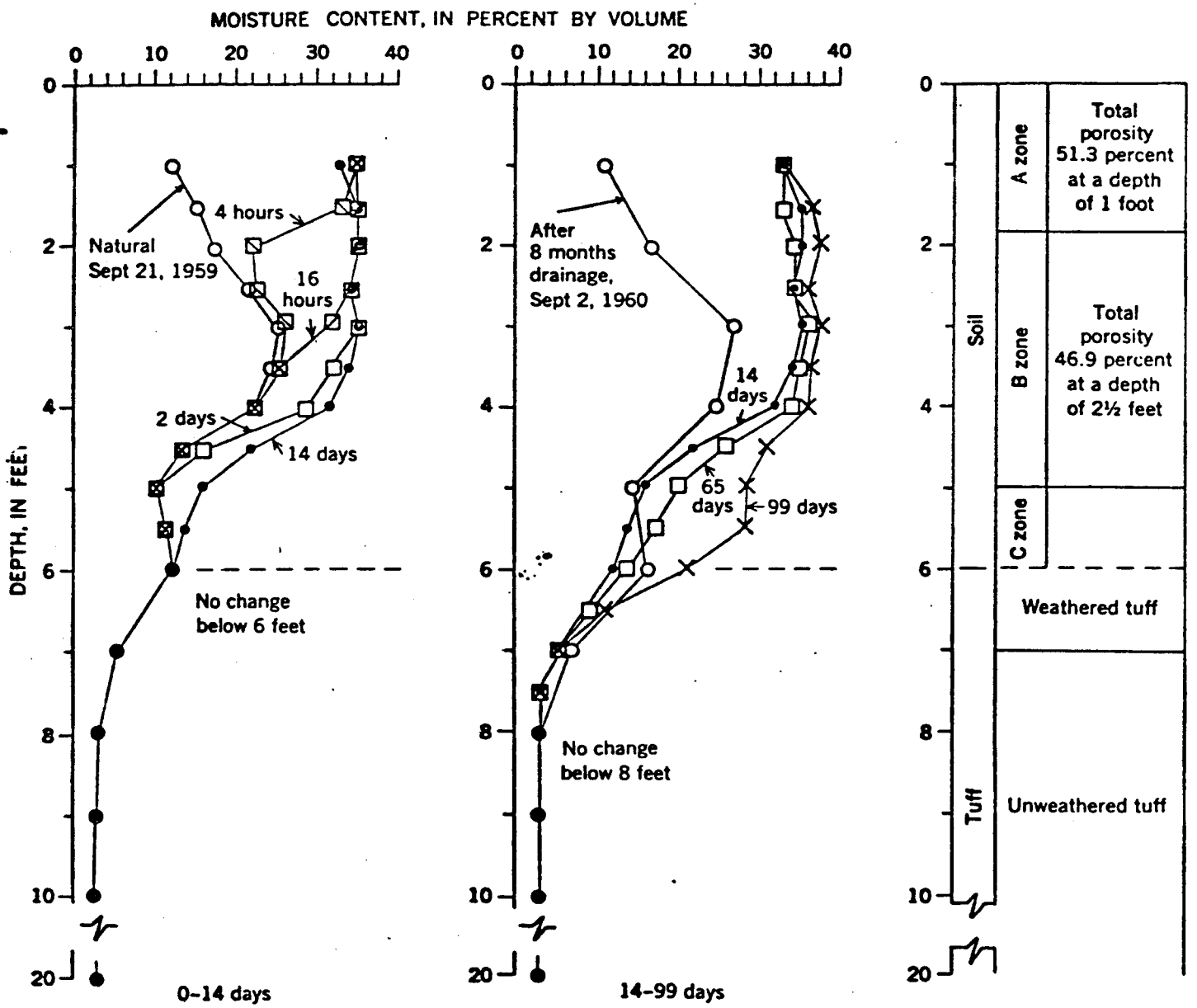

FIGURE 339.3.—Changes in moisture content beneath the infiltration pit at site A during 99 days of continuous infiltration, September 21 through December 29, 1959, and subsequent drainage for 8 months, Los Alamos County, N. Mex. Estimated rates of infiltration: 2nd day, 24 gallons per day per square foot; 10th day, 10 gpd per ft²; 20th day, 6 gpd per ft².

to 13 feet (fig. 339.2). Between 13 and 20 feet a all increase in moisture content is suggested, but ween 20 and 49 feet the moisture content remained out 6 to 8 percent.

INFILTRATION EXPERIMENT

At site A (fig. 339.1) an infiltration pit 2 feet in meter by 1 foot deep was constructed during Sep- nber 1956. The soil is similar to that on Frijoles esa; it is about 6 feet thick and is underlain by lded tuff. The area is moderately well drained. A t-hole 20 feet deep was drilled in the center of the iltration pit and a 2-inch plastic pipe was installed that it projected about 1 foot above the pit. Soil d tuff were packed around the casing to prevent page down alongside the casing. Moisture measure- nts were made prior to application of water. Water s introduced into the pit and a constant head main- ned at three-quarters of a foot for 99 days.

The wetted front (fig. 339.3) moved to a depth of out 4½ feet during the first 2 days of infiltration and a depth of about 6½ feet during the next 97 days, t water did not move through the transition zone o the tuff, except in the lower moisture range. The isture content decreased with depth from a maxi- m of about 38 percent in the B zone of the soil to s than 4 percent within a foot of the surface of the f.

Wat-- apparently was perched on the C zone of the l a. the moisture content within the B zone approached saturation. After the first several days of infiltration, most movement of water probably was lateral, as indicated by measurements in a series of holes around another infiltration pit nearby. Some water undoubtedly was lost by evaporation and transpiration.

Although the quantity of water used during the study was equivalent to almost 50 years of precipitation on the Pajarito Plateau, the moisture content in the A and B zones had returned to nearly normal after 8 months of drainage; the moisture content in the C zone and top 2 feet of tuff was slightly higher than before the experiment, and the moisture content of the tuff between 8 and 20 feet was unchanged. However, conditions during this study cannot be considered normal because the clogging or silting of pores probably was greatly accelerated when this volume of water moved into the soil within a period of 99 days without the normal seasonal distribution which involves alternate percolation and drainage.

CONCLUSIONS

Although water not removed by surface drainage infiltrates into the soil of the Pajarito Plateau, this study indicates that the downward movement of this water is impeded or stopped by the dense transition zone between the soil and the tuff. Thus, it seems that where the normal soil cover is undisturbed, there would be little or no recharge to the zone of saturation from precipitation on the surface of the plateau.

UNITED STATES
DEPARTMENT OF THE INTERIOR
GEOLOGICAL SURVEY
Albuquerque, New Mexico

Physical properties of and movement of water in the Bandelier Tuff, Los Alamos and Santa Fe Counties, New Mexico

By

John H. Abrahams, Jr.

Prepared in cooperation with the
Atomic Energy Commission and the
Los Alamos Scientific Laboratory

January 1963

Contents

	Page
Abstract	1
Introduction	4
Physical properties of the Bandelier Tuff	11
Porosity	12
Moisture content	15
Specific gravity	19
Dry unit weight	20
Moisture-tension relationship	22
Pore size	23
Hysteresis	29a
Particle-size distribution	30
Coefficient of permeability	33
Contacts between units in the Tshirege Member	34
Movement of water in the Bandelier Tuff	36
Site 1 - Tshirege tuff boulder in Pueblo Canyon	36
Site 3 - laundry pit	39
Site 4 - soil study	42
Site 5 - Mesita del Buey	48
Site 6 - DP-West	60
Conditions before infiltration	63
Infiltration studies, 1960 and 1961	67
The effects of joints and contacts on water movement	71
Summary and conclusions	75
Selected references	81

Illustrations--short list

(All illustrations in pocket)

	Reference page
Figure 1.--Index map of New Mexico showing Los Alamos County ------	4
2.--Map of the Los Alamos area showing the locations of study sites ----------	5
3.--Diagrammatic cross section of the Bandelier Tuff and older rocks ----------	7
4.--Deleted.	
5.--Energy relationship with moisture content of the tuff at Site 6 ----------	16
6-A.--Moisture-tension relationship and pore size in the tuff at Site 1 ----------	25
6-B.--Moisture-tension relationship and pore size in the tuff at Site 3 ----------	26
6-C.--Moisture-tension relationship and pore size in the tuff in the caisson area at Site 6 ----------	26
6-D.--Moisture-tension relationship and pore size in the tuff at Site 7 ----------	26
6-E.--Moisture-tension relationship and pore size in the tuff at Site 6 ----------	[illegible]
6-F.--Moisture-tension relationship and pore size in the tuff at Site 2 ----------	26
7.--Hysteresis curve showing the relation between moisture tension and moisture content of the tuff at Site 6 ---	32

Illustrations -- short list (Continued)

Reference Page

Figure 8.--~~Profile of hole at Site 8~~ Deleted. ~~[illegible]~~

9.--Sketch showing isohydral lines of moisture content in boulder at Site 1 ---------- 36

10.--Deleted.

11.--Moisture content of tuff at Site 3 ---------- 39

12-A.--Isohydral lines of moisture content at Site 4, 1958 ---------- 43

12-B.--Moisture content at Site 4, 1958 ---------- 43

13.--Moisture content in the soil and tuff beneath pit B at Site 4, ~~1959~~ ---------- 46

14.--~~Wetted areas on south wall of the disposal pit at Site 5 resulting from seepage from the infiltration pit back of the wall~~ Deleted. ~~[illegible]~~

15.--Relation of infiltration pit and access tubes to the disposal pit at Site 5 ---------- 48

16.--~~Deleted.~~ Wetted areas on south wall of the disposal pit at Site 5 resulting from seepage from the infiltration pit back of the wall - - - - - - 48

17.--Rate of infiltration from infiltration pit at Site 5, 1959-60 ---------- 49

18.--Moisture content and density of tuff in access tube 1 at Site 5, ~~1959-60~~ ---------- 50

19-A.--~~Profile I of an east-west section at Site 5 showing~~ isohydral lines of moisture content of the tuff, on Mar. 20, 1960, after about 3½ months of drainage ---------- 54

Illustrations--short list (Continued)

Reference Page

Figure 19-B.--~~Profile II of an east-west section at Site 5~~ ~~showing~~ isohydral lines of moisture content of the tuff, on June 2, 1960, after 40 days of infiltration ---------- 54

19-C.--~~Profile III of an east-west section at Site 5~~ ~~showing~~ isohydral lines of moisture content of the tuff, on July 28, 1960, after 99 days of infiltration ---------- 54

19-D.--~~Profile IV of an east-west section~~ at ~~Site 5~~ ~~showing~~ isohydral lines of moisture content of the tuff, on Dec. 6, 1960, after 230 days of infiltration ---------- 54

19-E.--~~Profile V of an east-west section at Site 5~~ ~~showing~~ isohydral lines of moisture content of the tuff, on Mar. 1, 1961, after about 3 months of drainage ---------- 54

20-A.--~~Profile I of a north-south section at Site 5~~ ~~showing~~ isohydral lines of moisture content of the tuff, on Apr. 20, 1960, after about 2½ months of drainage ---------- 55

20-B.--~~Profile II of a north-south section at Site 5~~ ~~showing~~ isohydral lines of moisture content of the tuff, on June 2, 1960, after 40 days of infiltration ---------- 55

Illustrations -- Short list (Continued)

Reference page

Figure 20-C.--~~Profile III of a north-south section at Site 5 showing~~ isohydral lines of moisture content of the tuff, on July 28, 1960, after 99 days of infiltration ---------- 55

20-D.--~~Profile IV of a north-south section at Site 5 showing~~ isohydral lines of moisture content of the tuff, on Sept. 1, 1960, after 134 days of infiltration ---------- 55

20-E.--~~Profile V of a north-south section at Site 5 showing~~ isohydral lines of moisture content of the tuff, on Dec. 6, 1960, after 230 days of infiltration ---------- 55

20-F.--~~Profile VI of a north-south section at Site 5 showing~~ isohydral lines of moisture content of the tuff, on Mar. 1, 1961, after about 3 months drainage ---------- 55

21.--Diagrammatic sketches of installations and caisson pit at Site 6 ---------- 61

22-A.--Section through Site 6 showing bending effect of the moisture content at one-third atmosphere tension. ---------- 64

22-B.--Section through Site 6 showing gross alpha activity ---------- 64

23.--Isohydral lines of moisture content of tuff below the bottom of disposal pit 1 at Site 6 ---------- 64

Illustrations -- Short list (Continued)

Reference page

Figure 24.--Deleted.

25.--Plan view showing locations of deep access tubes, sections through disposal pit, and moisture content of deep access tubes at Site 6 ---------- 69

26.--Sketch of Acid Canyon showing possible movement of water through joints in the Tshirege Member of the Bandelier Tuff at Site 5 ---------- 74

Illustrations--Long list

(All illustrations in pocket)

	Reference page
Figure 1.--Index map of New Mexico showing Los Alamos County ----	4
2.--Map of the Los Alamos area showing the locations of sites for studies of the physical properties and water movement in the Bandelier Tuff ----------	5
3.--Diagrammatic cross-section showing generalized stratigraphic relations of the Bandelier Tuff and older rocks in the Los Alamos area ----------	7
4.--Deleted	
5.--Energy relationship with moisture content of the Bandelier Tuff at Site 6 ----------	16
6-A.--Moisture-tension relationship and pore size in the tuff at Site 1 ----------	25
6-B.--Moisture-tension relationship and pore size in the tuff at Site 3 ----------	25
6-C.--Moisture-tension relationship and pore size in the tuff in the caisson area at Site 6 ----------	26
6-D.--Moisture-tension relationship and pore size in the tuff at Site 7 ----------	26

Illustrations--Long list - (Continued)

Reference page

Figure 6-E.--~~Curve showing relation of water content at several tensions to the size of pores~~ Moisture-tension relationship and pore size in the tuff beneath disposal pit at Site 6 ---------- 28

6-F.--~~Curve showing relation of water content at several tensions to the size of pores~~ Moisture-tension relationship and pore size in the tuff at Site 2 ---------- 28

7.--Hysteresis curve showing the relation between moisture tension and moisture content of a sample of the Bandelier Tuff at Site 6 ---------- 32

8.--~~Profile of hole at Site 8 showing a [illegible] relation between the physical properties of the Sahirge Mineral units of the Thirege~~ Deleted. ---------- [illegible]

9.--Sketch showing isohydral lines of moisture content, in percent by volume, and moisture content during capillary rise of water in boulder at Site 1 ------- 36

10.--Deleted.

11.--Moisture content of tuff beneath the disposal pit at Site 3 ---------- 39

12-A.--Isohydral lines of moisture content, in percent by volume, beneath pit A at Site 4 during intermittent infiltration and drainage, 1958 ---------- 43

12-B.--Moisture content beneath infiltration pit A at Site 4 during intermittent infiltration and drainage, 1958 ---------- 43

Illustrations--Long list - (Continued)

Reference page

Figure 13.--Moisture content in the soil and tuff beneath pit B at Site 4 during 99 days of continuous infiltration and subsequent drainage for 21 months, ~~1959~~ ---------- 46

14.--~~Wetted areas on south wall of the disposal pit at Site 5 resulting from seepage from the infiltration pit 16 feet back of the wall~~ Deleted ---------- ~~48~~

15.--Sketch showing relation of infiltration pit and access tubes to the disposal pit at Site 5 ---------- 48

16.--~~Deleted~~ Wetted areas on south wall of the disposal pit at Site 5 resulting from seepage from the infiltration pit 16 feet back of the wall --- 48a

17.--Rate of infiltration from infiltration pit at Site 5, 1959-60 ---------- 49

18.--Moisture content and density of tuff in access tube 1 at Site 5, ~~1959-60~~ ---------- 52

19-A.--Isohydral lines of moisture content of the tuff, in percent by volume, along an east-west section at Site 5 on Apr. 20, 1960, after about 3½ months of drainage ---------- 54

19-B.--Isohydral lines of moisture content of the tuff, in percent by volume, along an east-west section at Site 5 on June 2, 1960, after 42 days of infiltration ---------- 54

19-C.--Isohydral lines of moisture content of the tuff, in percent by volume, along an east-west section at Site 5 on July 28, 1960, after 99 days of infiltration ---------- 54

Illustrations--Long list - (Continued)

Reference page

Figure 19-D.--Isohydral lines of moisture content of the tuff, in percent by volume, along an east-west section at Site 5 on Dec. 6, 1960, after 230 days of infiltration ---------- 54

19-E.--Isohydral lines of moisture content of the tuff, in percent by volume, along an east-west section at Site 5 on Mar. 1, 1961, after about 3 months of drainage ---------- 54

20-A.--Isohydral lines of moisture content of the tuff, in percent by volume, along a north-south section at Site 5 on Apr. 20, 1960, after about 3½ months of drainage ---------- 55

20-B.--Isohydral lines of moisture content of the tuff, in percent by volume, along a north-south section at Site 5 on June 2, 1960, after 42 days of infiltration ---------- 55

20-C.--Isohydral lines of moisture content of the tuff, in percent by volume, along a north-south section at Site 5 on July 28, 1960, after 99 days of infiltration ---------- 55

20-D.--Isohydral lines of moisture content of the tuff, in percent by volume, along a north-south section at Site 5 on Sept. 1, 1960, after 134 days of infiltration ---------- 55

Illustrations--Long list - (Continued)

Reference page

Figure 20-E.--Isohydral lines of moisture content of the tuff, in percent by volume, along a north-south section at Site 5 on Dec. 6, 1960, after 250 days of infiltration ---------- 55

20-F.--Isohydral lines of moisture content of the tuff, in percent by volume, along a north-south section at Site 5 on Mar. 1, 1961, after about 3 months drainage ---------- 55

21.--Diagrammatic sketches of installations and caisson pit at Site 6 --------- ----- ---------- 61

22-A.--Section through Site 6 showing banding effect of the moisture content at one-third atmosphere tension ---------- 64

22-B.--Section through Site 6 showing gross alpha activity ---------- 65

23.--Isohydral lines of moisture content of tuff constructed from moisture readings in horizontal access tubes at 2, 8, 14, and 20 feet below the bottom of disposal pit 1 at Site 6 ---------- 65

24.--Deleted.

25.--Plan view showing locations of deep access tubes, sections through disposal pit, and moisture content of deep access tubes at Site 6 ---------- 69

Illustrations -- Long list (Continued)

Reference Page

Figure 26.--Sketch of Acid Canyon showing possible movement of water through joints in the Tshirege Member of the Bandelier Tuff and the location of a seep area in Acid Canyon at Site D ---------- 71

Tables

	Page
Table 1.--Sites investigated ----------	11a
Table 1-A.--Physical properties of Bandelier Tuff collected at 18 ~~different~~ sites and alluvium at one site on the Pajarito Plateau -----	11b
Table 2.--Standard deviation and deviation from means of the percent porosity at seven sites in the Los Alamos area ----------	14
Table 3.--Correlation coefficient of physical properties of samples from Sites 2, 6, 7, and 8 ----------	17a
Table 4-A.--Standard deviation, deviation from mean, and range of specific gravity at Site 7 ----------	19a
Table 4-B.--Comparison of specific gravity of the Tshirege Tuff from west to east across the Pajarito Plateau -----	19b
Table 5.--~~Average field capacity and porosity values for pore-size distribution curves and percentage of pores drained~~ Comparison of water drained from rock samples at one-third atmosphere tension with porosity----------	24a ~~24a~~
Table 6.--Particle-size distribution of samples of tuff from Sites 2, 3, and 6, in percent by weight ----------	30a ~~29a~~
Table 7.--Effects of transpiration by tumbleweed plants on the moisture content of tuff at Site 5, 1960 ------	50a
Table 8.--Description of material in caisson pit at Site 6 ----	63a
Table 9.--Averages of moisture content and gross alpha counts of tuff cores collected at Site 6 ----------	64a
Table 10.-Moisture content, in percent by volume, near the contact of the Guaje Member of the Bandelier Tuff and the Puye Conglomerate at Sites 17 and 18 -------	74a

Physical properties of and movement of water in the Bandelier Tuff, Los Alamos and Santa Fe Counties, New Mexico

By

John H. Abrahams, Jr.

Abstract

Radioactive wastes from the Los Alamos Scientific Laboratory near Los Alamos on the Pajarito Plateau in north-central New Mexico are released onto the surface and in the subsurface within the area. In the 1940's liquid wastes were processed for the removal of some radionuclides but the quantity of radioactivity discharged into open infiltration pits on the plateau or into natural drainage in deep canyons were not recorded. After waste treatment plants were built in 195-, supernatant liquids, separated from sludges containing most of the radioactivity, were treated to below off-site tolerances and discharged. The sludges are buried on the plateau after being mixed with concrete or vermiculite and placed in metal barrels.

The Pajarito Plateau is part of the Jemez Mountains volcanic complex. The altitude of the plateau ranges from about 7,800 feet at the base of the Sierra de Los Valles on the west to about 6,200 feet at an escarpment overlooking the Rio Grande on the east. The plateau has been dissected by east-west trending canyons as much as 1,000 feet deep.

The plateau is capped by the Bandelier Tuff of Pleistocene age that is at least 1,000 feet thick near the western margin of the plateau and thins eastward to less than 100 feet near White Rock Canyon. The Bandelier Tuff is divided, in ascending order, into the Guaje, Otowi, and Tshirege Members. In much of the plateau, the Tshirege comprises about three-fourths of the thickness of the Bandelier Tuff.

The Santa Fe Group of middle (?) Miocene and Pleistocene (?) age underlies the Bandelier Tuff and forms the main aquifer in the Los Alamos area.

Disposal of radioactivity wastes have been, for the most part, on the surface of or buried in the Tshirege Member. Most of the studies described in this report are with the Tshirege Member of the Bandelier Tuff, and reference to tuff in this report are to the Tshirege unless the Guaje and Otowi Members are mentioned specifically.

The Tshirege Member of the Bandelier Tuff contains sub-units that probably are individual beds of tuff. Water moving through the tuff is temporarily perched by variations in vertical permeability. The permeability varies from one bed to another, from one member to another, and from the Bandelier Tuff to underlying beds of the Santa Fe Group.

Joints are common throughout the Tshirege Member. The joints which are not filled with sediments or alteration products may interconnect across the contacts of sub-units and may provide paths for rapid movement of water which negate the effects of differences in the rock permeability. Nuclides in water moving through open joints would have a relatively limited opportunity to be absorbed into the tuff, as compared to nuclides in water that moved through the pores of the tuff.

Most of the gross alpha (plutonium) activity discharged into disposal pits was retained ~~within~~ in tuff at a depth less than 15 or 20 feet beneath the bottom of disposal pits, except for isolated areas where water carried the activity through joints to greater depth. There was an inverse relationship between gross alpha activity and the pH of water percolating through the tuff. (Christensen, Thomas, 1961)

The porosity of the tuff ranged from about 20 percent to about 60 percent. The porosity is inversely related to the moisture content at one-third atmospheric tension, which is roughly the average field capacity of the tuff. About 20 to 25 percent of the total pore space transmits most of the water which moves through the tuff. The average permeability is low--about ½ to 6 gallons per day per square foot.

The moisture content after 99 days of infiltration into a pit that penetrated a soil zone above one-half foot of a 5-foot thick, over underlying tuff ranged from about 39 percent by volume in the soil zone to less than 4 percent within a foot below the top of the underlying tuff. Soil cover reduces the amount of water that would infiltrate the tuff

The moisture content ranged from less than 1 percent by volume in undisturbed tuff to about 26 percent in tuff that was disturbed by man or nature. The average moisture content of the undisturbed tuff was less than 5 percent.

The moisture content during percolation of water through parts of the tuff that contained few joints or density gradients was in the 25 to 35 percent range. This range is slightly above the median of field capacity and porosity of the tuff. The rate of movement directly into dry tuff averaged about 2 feet per day during the first day, half a foot per day during the next 11 days, and about a tenth of a foot per day during the next 56 days. The moisture content of the tuff during upward capillary movement of water was less than the effective porosity. The temperature of the water, due to seasonal changes, apparently affected the rate of infiltration at the water-tuff interface to the extent that the rate of percolation exceeded the rate of infiltration when the water was near freezing.

Introduction

The Los Alamos area is on the Pajarito Plateau in north-central New Mexico, approximately 25 miles northwest of Santa Fe (fig. 1).

Figure 1.--Index map of New Mexico showing Los Alamos County.

It is mostly in Los Alamos County, but it extends a short distance into Santa Fe County. The area comprises about 30 square miles.

The Pajarito Plateau is part of the Jemez Mountains volcanic complex (fig. 2). The plateau slopes eastward from the Sierra de

Figure 2.--Map of the Los Alamos area showing the locations of sites for studies of the physical properties and water movement in the Bandelier Tuff.

los Valles, which forms the east rim of the Jemez Mountains caldera. The altitude of the plateau ranges from about 7,800 feet on the west side to about 6,200 feet on the east side at the escarpment overlooking the Rio Grande. The plateau has been dissected by deep canyons cut by streams flowing eastward from the Sierra de los Valles to the southward flowing Rio Grande. The canyons are 200 to 400 feet deep in the central and western parts of the plateau but are as much as 800 to 1,000 feet deep at the east side of the plateau where they join White Rock Canyon of the Rio Grande. The canyons are floored by ~~bedrock~~ volcanic rocks in the western part of the plateau. In the middle and eastern part of the plateau the canyons are floored by alluvium, in places as much as 80 feet thick. Nearly flat finger-like mesas extend east-southeastward between the canyons. The mesas are narrow, many a half mile wide or less, ~~and~~ They have a soil cover as much as 9 feet thick. The soil cover thins eastward as the canyons become wider and the mesas become narrower.

The plateau is heavily forested by Ponderosa pine, Pinon, and Juniper. A clump grass is common in the clearings.

The average annual precipitation is 20 to 25 inches on the western part of the plateau and 12 to 14 inches on the eastern part near the Rio Grande. Precipitation in the central part is 17 to 18 inches. Most of the precipitation occurs during summer thunder-showers, when several inches of rain may fall during as many hours. About a quarter of the precipitation occurs during the winter. Some precipitation percolates into the rock on the mesas or into the alluvium on the canyon floors. Some runoff from storms and from snowmelt reaches the Rio Grande.

The Pajarito Plateau is capped by the Bandelier Tuff of Pleistocene age (Griggs, 196_, Water-Supply Paper 1753, in press). The stratigraphic relations of the Bandelier and the rocks underlying the Bandelier are shown diagrammatically on figure 3. The Bandelier

Figure 3.--Diagrammatic cross-section showing generalized stratigraphic relations of the Bandelier Tuff and older rocks in the Los Alamos area.

is about 1,000 feet thick along the western margin of the plateau. The formation laps onto the Tschicoma Formation to the west and thins abruptly; it thins also to the east and is less than 100 feet thick on the east side of the plateau.

The Bandelier Tuff is divided into the Guaje, Otowi, and Tshirege Members, in ascending order. (Griggs, 196_, Water-supply Paper 1753, in press). The Guaje Member consists chiefly of rounded fragments of white, gray, and tan pumice in a glassy matrix; the Otowi Member consists of light-gray, pinkish-tan welded tuff and tuff breccia and beds of pumice fragments; the Tshirege Member is the caprock on the plateau and consists of welded tuff and tuff breccia. The Tshirege Member in much of the plateau comprises at least three-fourths of the thickness of the Bandelier Tuff.

The main ground-water body and aquifer in the Los Alamos area is in the Tschicoma Formation and the Santa Fe Group of middle (?) Miocene to Pleistocene (?) age (fig. 3). The depth to the top of this aquifer is about 1,200 feet beneath the surface in the western part of the Pajarito Plateau, about 1,000 feet beneath the surface ~~in the middle part of the plateau~~ near Los Alamos, and 300 to 900 feet below the canyon floors. The piezometric surface of the main aquifer slopes east-southeastward at about 60 to 80 feet per mile. The water in this aquifer moves east-southeastward to ~~its~~ natural discharge points along the Rio Grande valley.

The Bandelier Tuff is above the main aquifer (fig. 3), but ~~in~~ at places the Bandelier ~~it~~ contains perched water (Griggs, 196_, Water-supply Paper 1753, in press). Perched water occurs also in the alluvium in the canyons cut into the Bandelier.

Radioactive wastes from the laboratories near Los Alamos are released on the surface and in the subsurface within the area. The solid wastes, which consist mostly of materials such as metal objects, glassware, and garments, are buried in shallow pits on the mesas. Sludge wastes, obtained by concentrating liquid wastes, also are buried on the mesas after being mixed with concrete or vermiculite and placed in metal barrels. Liquid wastes are supernatant liquids that have been separated from the sludges. The liquid wastes are treated to below off-site tolerance limits and discharged into open infiltration pits on the mesas or into natural drainage channels in the canyons. From the early 1940's until the waste-treatment plants were built about 1951, liquid wastes were not treated, although some were processed for removal of certain nuclides, and the quantities of radioactivity discharged prior to 1951 were not recorded.

Water seeping into the rocks from precipitation and snowmelt could become contaminated with radionuclides from liquid waste in the infiltration pits, and in stream channels on canyon floors, and from buried solid wastes. If this contaminated water reached the main aquifer, the contamination would spread beyond the Los Alamos area. Ground water of the Los Alamos area does not remain stationary, but moves downgradient and becomes a part of the surface and ground water of the Rio Grande valley.

Water percolating into the ground and down toward the main aquifer in the Los Alamos area must pass through the Bandelier Tuff, and that formation probably offers the greatest resistance to water movement of any formation between land surface and the main aquifer. Because the Bandelier is particularly resistant to water movement, the present study was concerned with the hydraulic properties and radionuclide retention characteristics of that formation. Reference to tuff in this report will mean the Tshirege Member unless the Guaje and Otowi Members are mentioned specifically.

The investigation was made by the United States Geological Survey in cooperation with the United States Atomic Energy Commission and the University of California, Los Angeles Scientific Laboratory, to determine the direction and rate of movement of water and radioactive wastes from infiltration pits and the capacity of the surrounding rocks to retain radionuclides. Field studies were made by the Survey during 1958-61. The moisture movement and nuclide retention studies at Site 6 was a cooperative investigation with the Health Division (H-7) of the Los Alamos Scientific Laboratory. Moisture and density measuring equipment were provided and maintained by the Los Alamos Scientific Laboratory. Mr. William D. Purtymun, U. S. Geological Survey, participated in the construction and data collection at most of the sites that were studied.

Physical properties of the Bandelier Tuff

The site numbers, locations, and pertinent information about the study sites are summarized in table 1. The average values of the physical properties of the Bandelier Tuff including some for the Guaje and Otowi Members are summarized in table 1-A. The data contained in table 1 was obtained from physical analysis of samples collected from the various sites. The approximate number of samples collected were:

100	samples from Site 6	
80	samples from Site 5	(79 were moisture measurements only)
40	samples from Site 2	
32	samples from Site 7	(7 tests made on each sample)
12	samples from Site 8	
7	samples from Site 9	
6	samples from Site 3	
6	samples from Site 1	
1 or 2	samples from each of the other sites	

Data from Site 6 are used predominantly in the discussion on water retention in the tuff because of the comparatively large number of analyses made and the corresponding statistical control possible. Results of studies at the other sites commonly were parallel to those from Site 6, but generally they were not mathematically significant because of the small number of samples that were collected or because the samples were widely scattered.

Table 1.--Sites investigated

Site No.	1/ Location	Name of Site	Position in stratigraphic column	Description of site	Operation at site
1	NW¼NE¼ sec. 14, T. 19 N., R. 6 E.	Tshirege Tuff boulder in Pueblo Canyon	Tshirege Member of Bandelier Tuff. Stratigraphic position not known	Access holes in boulder embedded in alluvium, with water ponded against base of boulder.	Core samples of tuff collected; neutron meter moisture measurements made during capillary rise of water in boulder.
2	SE¼SE¼ sec. 18, T. 19 N., R. 7 E.	Road cut in lower part of Pueblo Canyon	Lower part of Tshirege Member	Core holes in northeast-facing wall of road cut.	Core samples of tuff collected.
3	NW¼SW¼ sec. 14, T. 19 N., R. 6 E.	Laundry pit	Middle part of Tshirege Member	Several access holes as much as 60 feet deep at different angles beneath a pit used occasionally for disposal of liquid radioactive wastes. Pit partly backfilled with gravel.	Samples of tuff collected and neutron meter moisture measurements made in access hole. Some water from precipitation and possible overflow from other pits.
4	NE¼SW¼ sec. 22, T. 19 N., R. 6 E.	Soil study	Middle part of Tshirege Member	Two infiltration pits about 2 feet in diameter and half a foot deep in soil about 5 feet thick overlying tuff. Five access tubes 3 to 5 feet deep in and around one pit. One access tube 28 feet deep in other.	Unconsolidated samples of tuff collected and neutron meter moisture measurement made in access tubes. Constant head of water in one pit during infiltration studies.
5	E½SW¼ sec. 31, T. 19 N., R. 7 E.	Southeast Mesita del Buey	Lower part of Tshirege Member	Eight access tubes to depths of about 40 feet around an infiltration pit adjacent to the south wall of a 29-foot deep disposal pit.	Unconsolidated samples of tuff collected and neutron meter moisture measurements made. Water into pit metered. Pool three-quarters of a foot deep maintained.
6	NE¼SE¼ sec. 14, T. 19 N., R. 6 E.	DP-West	Middle part of Tshirege Member	Horizontal and slanting access tubes beneath disposal pit backfilled with gravel. Slant holes 75 to 99 feet deep.	Core samples of tuff collected from horizontal holes. Unconsolidated samples of tuff collected from slant holes. Neutron meter moisture measurements made and sample of liquid wastes collected during and after infiltration of raw wastes and of tap water.
7	NW¼ sec. 3 and NE¼ sec. 4, T. 18 N., R. 6 E.	TA-49	Depth from 0 - 90 feet upper part of Tshirege Member. Depth from 90 - 275 feet middle part of Tshirege	Numerous holes in areaabout half mile in diameter. Most of the holes (commonly 6 feet in diameter) were less than 100 feet deep, but some small-diameter holes were as much as 275 feet deep.	Many core samples of tuff collected. Fractures in walls of hole were mapped.
8	NW¼NW¼ sec. 36, T. 19 N., R. 6 E.	Northwest Mesita del Buey	Lower part of Tshirege Member	One hole 6 feet in diameter and about 60 feet deep.	Some chunk samples of tuff collected and walls of hole inspected
9	Near cem. S½S½ sec. 23, T. 19 N., R. 6 E.	Beta hole	Middle part of Tshirege Member	One hole 6 feet in diameter and about 40 feet deep.	Some chunk samples of tuff collected.
10	NW¼SW¼ sec. 22, T. 19 N., R. 6 E.	TA-50	Middle part of Tshirege Member	Rectangular pits up to 20 feet deep for construction of building.	One chunk sample of tuff collected.
11	SW¼SE¼ sec. 9 and N½N½ sec. 16, T. 19 N., R. 6 E.	Acid Canyon	Middle part of Tshirege Member	Canyon floor and walls.	Three sets of core samples of tuff collected
12	SW¼SE¼ sec. 13, T. 18 N., R. 6 E.	TA-33	Lower part of Tshirege Member	Small pit into which small quantities of radioactive waste had been discharged.	Unconsolidated samples of tuff collected to depth of 12 feet beneath pit.
13	NE¼NE¼ sec. 20, T. 19 N., R 6 E.	Near Administration building	Upper part of Tshirege Member	Bore holes for foundation investigation.	Core samples of tuff collected by contractor.
14	SE¼NE¼ sec. 17, T. 19 N., R. 6 E.	Beneath bridge on Diamond Drive	Middle part of Tshirege Member	North wall of Los Alamos Canyon	Two core samples of tuff collected.
15	SE¼SE¼ sec. 9, T. 19 N., R. 6 E.	Lower part Acid Canyon	Alluvium on Otowi Member of Bandelier Tuff	Seep area downstream from contact of Tshirege and Otowi Members	Visited site numerous times to observe seep.
16	NW¼NW¼ sec. 20, T. 19 N., R. 7 E.	Otowi	Middle part of Otowi Member	South wall of Pueblo Canyon	One core sample of tuff collected.
17	SW¼NW¼ sec. 18, T. 19 N., R. 7 E.	Pueblo Canyon Site A	Contact of Guaje Member of Bandelier Tuff and Puye Conglomerate	In dry streambed	Two samples of tuff collected from Guaje Member near base and two samples of tuff collected from Puye Conglomerate near top.
18	NW¼SE¼ sec. 19, T. 19 N., R. 7 E.	Pueblo Canyon Site B	Contact of Guaje Member and Puye Conglomerate	In dry streambed	Two samples of tuff collected from Guaje Member near base and two samples of tuff collected from Puye Conglomerate near top.
19	SW¼NW¼ sec. 18, T. 19 N., R. 7 E.	Pueblo Canyon Site C	Contact of silt bed and underlying alluvium on canyon floor	Intermittent flow in streambed	Samples collected at base of silt and in underlying alluvium.

1/ Site numbers and locations shown on figure 2.

Table 1-A.--Physical properties of Bandelier Tuff collected at 18 sites and alluvium at one site on the Pajarito Plateau.

(Values given are average for each site.)

Site No.	Site name	Moisture content, in percent by volume	Dry Unit weight, in gm per cc	Specific gravity, rounded to nearest hundredth	Moisture content at one-third atmosphere tension in percent by volume	Specific retention in percent by volume	Total porosity ~~(avg)~~	Specific yield in percent by volume	Coefficient of permeability (gal per day per foot) vertical	Coefficient of permeability (gal per day per foot) horizontal
1	Tshirege Tuff boulder in Pueblo Canyon	5.4	1.63	-	23.9	-	a/ 35.8	-	-	-
2	Road cut in lower part of Pueblo Canyon	4.3	1.28	2.55	21.2	7.1	49.8	42.4	9.0	11.0
3	Laundry pit	24.9	1.44	2.56	21.0	12.6	43.7	32.9	1.7	.7
4	Soil Study	<1.0	-	-	b/ 14.5	-	-	-	-	-
5	Southeast Mesita del Buey	1.0	1.30	2.55	b/ 14.7	-	49.0	-	-	-
6	DP-West	23.1	1.47	2.56	20.6	16.7	42.1	25.8	2.6	6.5
7	TA-49 Depth, 0-90 feet	2.1	1.34	2.57	33.4	19.0	48.7	29.0	2.8	3.4
	Depth 90-275 feet c/	1.2	1.84	2.55	-	16.7	27.9	-	.4	-

Table 1-A.--Physical properties of Bandelier Tuff collected at 18 sites and alluvium at one site on the Pajarito Plateau. (Continued)

Site No.	Site name	Moisture content, in percent by volume	Dry Unit weight, in gm per cc	Specific gravity, rounded to nearest hundredth	Moisture content at one-third atmosphere tension in percent by volume	Specific retention in percent by volume	Total porosity	Specific yield in percent by volume	Coefficient of permeability (gal per day per foot) per foot)	
									vertical	horizontal
8	Northwest Mesita del Buey	-	1.50	2.55	14.4	12.5	d/ 41.3	28.8	3.8	-
9	Beta hole depth 0-20 feet	0.6	1.44	2.56	14.5	12.0	43.6	31.6	4.0	-
9	Beta hole depth 20-40 feet	.4	1.31	2.56	24.3	11.6	49.1	37.5	21.0	-
10	TA-50	-	1.57	2.56	-	-	38.7	27.1	2.0	-
11	Acid Canyon depth 0-1 feet below floor	7.4	-	-	-	-	-	-	-	-
11	Acid Canyon 5 feet below rim	7.6	-	-	-	-	-	-	-	-
11	Acid Canyon 0-5 feet below rim	12.7	-	-	-	-	-	-	-	-

Table 1-A.--Physical properties of Bandelier Tuff collected at 18 sites and alluvium at one site on the Pajarito Plateau. (Continued)

Site No.	Site name	Moisture content, in percent by volume	Dry Unit weight, in gm per cc	Specific gravity, rounded to nearest hundredth	Moisture content at one-third atmosphere tension in percent by volume	Specific retention in percent by volume	Total porosity	Specific yield in percent by volume	Coefficient of permeability (gal per day per foot/ per foot) vertical	Coefficient of permeability (gal per day per foot/ per foot) horizontal
12	TA-33 depth 0-7 feet	16.0	-	-	-	-	-	-	-	-
12	Depth 7-12 feet	5.3	-	-	-	-	-	-	-	-
13	Near Administration building;[e] depth 0-10 feet	16.5	-	-	-	-	-	-	-	-
13	Near Administration building;[e] depth 10-20 feet	10.4	-	-	-	-	-	-	-	-
14	Beneath bridge across upper Los Alamos Canyon	-	-	-	-	-	59.3	-	5.3	-

Table 1-A.--Physical properties of Bandelier Tuff collected at 18 sites and alluvium at one site on the Pajarito Plateau. (Continued)

Site No.	Site name	Moisture content, in percent by volume	Dry Unit weight, in gm per cc	Specific gravity, rounded to nearest hundredth	Moisture content at one-third atmosphere tension, in percent by volume	Specific retention in percent by volume	Total porosity	Specific yield in percent by volume	Coefficient of permeability (gal per day per foot/ per foot)	
									vertical	horizontal
15	Lower part Acid Canyon (observations only)	-	-	-	-	-	-	-	-	-
16	f/ Otowi	-	1.19	2.42	-	-	50.8	-	-	-
17	Pueblo Canyon site A-Base of Guaje	60.8	-	-	-	-	-	-	-	-
17	Pueblo Canyon site A-Top of Puye	34.2	-	-	-	-	-	-	-	-
18	Pueblo Canyon site B-Base of Guaje	30.6	-	-	-	-	-	-	-	-
18	Pueblo Canyon site B-Top of Puye	16.0	-	-	-	-	-	-	-	-

Table 1-A.--Physical properties of Bandelier Tuff collected at 18 sites and alluvium at one site on the Pajarito Plateau. (Continued)

Site No.	Site name	Moisture content, in percent by volume	Dry Unit weight, in gm per cc	Specific gravity, rounded to nearest hundredth	Moisture content at one-third atmosphere tension in percent by volume	Specific retention in percent by volume	Total porosity	Specific yield in percent by volume	Coefficient of permeability (gal per day per foot/ per foot)	
									vertical	horizontal
19	Pueblo Canyon site C-Base of silt bed	22	-	-	-	-	-	-	-	-
19	Pueblo Canyon site C-Alluvium below silt bed	12	-	-	-	-	-	-	-	-

a/ Effective porosity 32.7 percent
b/ Repacked-bulk
c/ Most samples from 200-275 foot intervals
d/ Effective porosity 39.4 percent
e/ Values of contractors
f/ Otowi Member of Bandelier Tuff

Porosity

Porosity is the ratio of the volume of the void spaces to the total volume of the rock or aggregate sample. The porosity of the Tshirege Member is as much as 60 percent in some zones, which is within the upper porosity range of fine clays. Such high porosity is unusual for consolidated sediment; however, samples of tuff collected ~~from the Tshirege~~ only a short distance vertically from zones of high porosity had porosities as low as 20 percent, which is within the range of many consolidated materials. The average porosities at study sites where three or more samples were collected ranged from 27.9 to 49.8 percent. An analysis of the variance of the porosity values indicates that the four different average groups of percentages, 27.9, 35.8, 42.1, and 43.7, and 48.7, and 49.8 (table 1-A) are significantly different at the 1 percent level. There is a difference of about 6 to 8 percent between groups, which may be of no significance.

The standard deviations (Snedecor, 1946, p. 36) show that the range of porosity values of the samples collected at most sites was relatively small. The ~~maximum~~ range of porosities was 36.2 to 48.0 percent for 38 porosity determinations at Site 6, but most porosity determinations were 42.1 percent, plus or minus 2.6 percent (table 2), probably because the area at Site 6 is relatively small. The high standard deviations of samples collected from the 0 to 90 and the 90 to 275 foot intervals at Site 7 are due to the relatively small number of samples representing a thick section of the Tshirege Member. The different average porosities of the 0-20 foot interval and the 20-40 foot interval at Site 9 and the small standard deviation of each indicate that the physical properties that control porosity of the tuff are different in the two intervals.

The porosity values shown in table 1-A are calculated total porosity and are slightly higher than the values of the measured effective porosity. Effective porosity is the ratio of the volume of the void spaces that will yield or transmit water to the total volume of the rock or aggregate sample. Total porosity includes all the pore space in the tuff, some of which water cannot move through because interconnection between pores is lacking, whereas effective porosity includes only the interconnected pore space and water can move between adjoining pores.

Table 2.--Standard deviation and deviation from means of the percent porosity at ~~six~~ seven sites in the Los Alamos area.

Site No.	Average porosity (from table 1)[A]	Standard deviation	Deviation from means
1	35.8	2.2	0.7
2	49.8	1.4	.5
3	43.7	1.9	.8
6	42.1	2.6	.4
7 (0-90 ft below surface)	49.4	4.0	1.0
(90-275 ft below surface)	27.9	6.2	2.3
8	41.3	2.5	.9
9 (0-20 ft below surface)	43.6	1.0	.8
(20-40 ft below surface)	49.1	1.1	.6

Moisture content

The moisture content of rock or soil is the ratio of the weight of water contained in the sample to the oven-dry sample, expressed as a percentage.

The moisture content of approximately 280 samples of tuff collected at or just below the surface of the plateau ranged from less than 1 percent by volume in samples from undisturbed areas (natural conditions) to about 26 percent by volume in samples from disturbed areas (any change from natural conditions). The moisture content of tuff from disturbed areas was generally less than 10 percent and commonly less than 5 percent by volume.

At most sites where the moisture content of near surface was relatively high, the moisture content decreased with depth to less than about 5 percent by volume. An example is Site 12, where the moisture content beneath the pit decreased to about 5 percent below 12 feet (table 1-A).

A curve denoting the relative position of the three known moisture values, oven-dry, air-dry, and one-third atmosphere moisture tension, of the tuff at several sites can be drawn to illustrate the energy relationships of moisture in the tuff. The curve (fig. 5)

Figure 5.--Energy relationship with moisture content of the Bandelier Tuff at Site 6.

shows that the air dry moisture content of the Tshirege Tuff is approximately 5 percent at Site 6. The moisture content at the 15 atmospheres moisture-tension point is about 8 percent (moisture tension is the attraction of rock or soil for water, Baver, 1956, p. 227-234), and is the moisture-tension point at which plants can no longer obtain water by capillary movement. The moisture content at the one-third atmosphere moisture-tension point (approximate field capacity, Colman, 1947, p. 380) is about 23 percent. At atmosphere pressures at altitudes over 5,000 feet above mean sea level the one-third atmosphere moisture-tension point is close to one-half atmosphere moisture tension. The approximate 15 percent moisture-content difference between the 15 atmosphere moisture-tension point and the approximate field capacity point is redistributed at depth and the moisture content of the tuff theoretically would eventually approach the 15 atmosphere moisture-tension point if aided by the influence of plant roots or movement of air through the rock. The moisture content of surrounding rocks, the amount of porosity, the size of the pores, and the temperature gradient all affect the length of time required for redistribution to take place. The saturated moisture content of the tuff is shown to be about 41 percent.

The placement of the curve for Bandelier Tuff (fig. 5) shows that the tuff at Site 6 is between those for a sandy loam and sand, which places the tuff in a range similar to sandy silt.

The negative correlation coefficient of the moisture content at the one-third atmosphere tension and porosity for sites 6 and 8, significant at the 1 percent level (chances out of 100), that figure is not an average of random figures is an indication that a larger volume of water will drain from the tuff as the porosity increases. The reason for the lack of correlation between the moisture content at the one-third tension values and the porosity at sites 2 and 7 is not clear, except possibly for the small number of samples involved at these sites (table 3). Data in table 3 show also that the one-third atmosphere tensions do not correlate with any other physical properties at site 2 although the four sets of non-significant correlations are given to show the trends and the degree of correlation.

Table 3.--Correlation coefficient of physical properties of samples from Sites 2, 6, 7, and 8

Site No.	Properties	Level of significance	Number of pairs of samples	Correlation coefficient	Approximate minimum coefficient necessary for significance at the 5 percent level
2	Moisture content at one-third atmosphere tension correlated with porosity	a/ NS	10	0.04	0.63
2	Moisture content at one-third atmosphere tension correlated with specific retention	a/ NS	9	.32	.67
2	Moisture content at one-third atmosphere tension correlated with dry unit weight	a/ NS	9	.53	.67
2	Specific retention of moisture correlated with porosity	a/ NS	9	.59	.67
6	Moisture content at one-third atmosphere tension correlated with porosity	c/ 0.01	39	-.63	-
6	Moisture content at one-third atmosphere tension correlated with undisturbed moisture content.	b/ .05	39	.34	-

17a

Table 3.--Continued

Site No.	Properties	Level of significance	Number of pairs of samples	Correlation coefficient	Approximate minimum coefficient necessary for significance at the 5 percent level
6	Moisture content at one-third atmosphere tension correlated with specific retention	c/ .01	9	.81	-
6	Moisture content correlated with dry unit weight	c/ .01	84	.39	-
6	Moisture content at one-third atmosphere tension correlated with dry unit weight	a/ NS	39	.26	0.32
7	Moisture content at one-third atmosphere tension correlated with porosity	a/ NS	-	-	-
7	Moisture content at one-third atmosphere tension correlated with specific retention	b/ .05	12	.65	-
8	Moisture content at one-third atmosphere tension correlated with porosity	c/ .01	12	-.95	-
8	Moisture content at one-third atmosphere tension correlated with dry unit weight	c/ .01	12	.95	-

a/ Not significant
b/ 5 percent level: chances are 19 out of 20 that figure is not an average at random values.
c/ 1 percent level: chances are 99 out of 100 that figure is [illegible] of random values.

Samples of the Bandelier Tuff that were tested for moisture content at one-third atmosphere tension fell into two general groups. The average moisture content of samples collected at sites 2, 3, 6, and from a depth of 20 to 40 feet at site 9 were 21.2, 21.0, 20.6, and 24.5 percent respectively, which is about 91 percent of the 24 percent average of moisture content of the tuff at sites 5 and 6 where water had been added to the tuff intermittently for years. The averages of samples collected at sites 4, 5, 8, and from a depth of 0 to 20 feet at site 9 were 14.5, 14.7, 14.4, and 14.5 respectively, which is about 55 percent of the 24 percent average of the wetted tuff at sites 5 and 6. The porosity of the samples seems unrelated to these differences of moisture contents, but the size of the pores in the tuff may be related to the differences.

Specific gravity

The specific gravity of the Bandelier Tuff on the Pajarito Plateau ranges from about 2.54 to 2.58, and most values range from about 2.56 to 2.57. These values are about the specific gravity of the major constituents of the tuff, which are quartz, 2.5 to 2.8, and orthoclase feldspar, 2.5 to 2.6 (Baver, 1956, p. 57). The specific gravity of particles in the 1- to 2-micron range, which are slightly smaller than the median size of tuff particles, is 2.56.

A decrease in specific gravity with depth similar to that which occurs at site 7 may indicate differences in vertical composition of the Tshirege Member (table 4-A). The specific gravity of the tuff may decrease from west to east across the plateau as indicated in table 4-B. This apparent decrease in specific gravity may indicate slight changes in the composition of the tuff or slight differences in the concentration of constituents of the tuff.

The decrease downward at site 7 and the apparent decrease eastward of the specific gravity of the tuff might indicate that the upper part of the Tshirege contains a larger percentage of feldspar than does the lower part, or it could indicate that the lower part contains less heavy minerals.

Table 4-A --Standard deviation, deviation from mean, and range of specific gravity at site 7

Interval	Ave/	Standard deviation	Deviation from mean	Range
0 - 90 ft.	2.568	0.015	0.005	2.555 - 2.581
90 -275 ft.	2.550	0.006	0.001	2.542 - 2.550

Table 4-B.--Comparison of specific gravity of the Tshirege Tuff from west to east across the Pajarito Plateau.

North line	-	2.560 (Site 3)	2.555 (Site 6)	-	-	2.550 (Site 2)	-
South line	2.560 (Site 10)	-	-	2.558 (Site 9)	2.552 (Site 8)	-	2.550 (Site 5)

nm 9

Dry unit weight

Dry unit weight is the weight in air of a given volume of oven-dry material. The dry unit weight of any material may be calculated from the formula $Y_d = \frac{W_d}{V}$ where Y_d = the dry unit weight of the sample, W_d = the oven-dry weight of the sample in grams, and V = the volume of the sample in cubic centimeters.

A statistical analysis of the dry unit weight of samples of tuff shows four significantly different groups of values: 1.84, 1.63, 1.44 and 1.47, 1.28, and 1.34, similar but opposite to those of porosity (table 1-A). Each group (for example, 1.44 and 1.47) is different significantly from each other at the 1 percent level. [~~(chances are 99 out of 100 that figures are not an average of random values)~~.]

The dry unit weight of different samples of a material vary inversely to the porosities of unit volumes of the samples. A difference in dry unit weight and porosity between two samples indicates a difference in composition. Evidence of vertical changes in the composition of the tuff is shown by the difference of the dry unit weight and the porosity in samples from Site 2. A statistical analysis of 28 cores collected from two holes drilled into the wall of the road cut indicates that the average dry unit weight is 1.28 (table 1-A). The average dry unit weight of samples from the upper hole is higher significantly than those in the hole about 3 feet stratigraphically lower in the tuff:

Location	Dry unit weight (gm per cc)	Porosity (percent)
Upper hole	a/ 1.30	b/ 49.2
Lower hole	a/ 1.26	b/ 50.4

a/ 1 percent level: chances are 99 out of 100 that figure is not an average of random values.

b/ 5 percent level: chances are 19 out of 20 that figure is not an average of random values.

The area involved is small, and the difference in average dry unit weights, though significant, is also small.

Moisture-tension relationship

Moisture-tension as used in this report is a contracted form of reference to the moisture content-moisture tension relationship. Moisture content has been described previously. Moisture tension is the equivalent negative gage pressure, or suction, in the soil moisture. Soil-moisture tension is equal to the equivalent negative or gauge pressure to which water must be subjected in order to be in hydraulic equilibrium, through a porous permeable wall or membrane, with the water in the soil. Moisture tension is a measure of the attractive force that rock or soil has for water. Tension is expressed in this report in centimeters of water or in units of atmospheric pressure. Tension of one-third atmosphere, or 344 centimeters of water, is comparable to field capacity (Colman, 1947, p. 280). This value of tension is used frequently in the report.

Many of the accepted concepts of flow of water below the water table cannot be applied directly to movement of water above the water table where pressure on the suspended or moving water is always less than one atmosphere. This pressure deficit is directly connected with the surface tension and the curvature existing on liquid and gas interfaces within the porous medium (Miller and Miller, 1956, p. 324). Much of the flow in the zone of aeration at moisture contents of less than field capacity is in thin films where resistance to flow is great (Kemper, 1961, p. 257). Capillary conductivity above field capacity is through thick films of water on the particles comprising the porous medium, whereas all the effective pore space in the zone of saturation or in laboratory studies of permeability is filled with water under pressure, and flow is predominantly through the middle of the flow channels.

Pore size

Equivalent pore size and moisture-tension relationship are related in the manner shown in the following table. (From capillary equation $h = \frac{2\gamma \cos\alpha}{r \rho_w g}$)

r = radius
ρ_w = den. of water
g = accel. of grav.
γ = surf. tens.
α = contact ∠

Pore diameter (mm)	Tension (cm of water)
0.20	15
.10	30
.05	60
.02	150

The non-capillary porosity (pore size sufficiently large that capillary rise of water is negligible) and the rate of percolation through soils vary directly with each other (Smith and others, 1944, p. 208), thus water will drain more rapidly from tuff containing a higher percentage of large pores spaces than from tuff containing few large pores even if the porosity is the same.

Little or no water can be withdrawn from a sand with nearly equal particles and pore sizes until a certain minimum tension value is reached (Youngs, 1960, p. 4027), and then only small additional tension is needed to empty many pores, whereas in the Bandelier Tuff pores of different size are randomly distributed throughout each sample and the large pores are interconnected by narrow necks so that each addition of tension increases the volume of water extracted. A tension of 1 cm (centimeter) of water applied to some samples, desaturated only a few large pores and increased tension drained progressively smaller pore spaces. Moisture measurements were made at tensions of 15 cm, 30 cm, 60 cm, 150 cm, and 344 cm tension on all samples. This system of tension measurements duplicated conditions of continuity of the sample similar to tuff in place.

The water content of various size pores at various tensions are shown in figures 6A-6F for samples of material from Sites 1, 2, 3, 6, and 7. An average curve for each group of samples is shown on the figures and represents a curve calculated from an estimated effective porosity and is used for comparison with curves from other sites. Most of the curves are similar but each curve has some characteristic that distinguishes it from the curves for samples from other sites. Table 5 summarizes some of the physical properties of the tuff and shows the estimated percentage of pores drained using estimated effective porosity values. The field capacities and porosities given in table 5 are slightly different from those given in table 1-A because all the data was not used in preparing table 5, and values for percentage of pores drained are rounded because the effective porosity is estimated.

l from rock samples at one-third atmosphere tension with porosity.

Water drained from saturated material			
Percent by volume at one-third atmosphere tension, or field capacity	Percent of total from pores larger than 0.1 mm[a]	Percent of total from pores larger than 0.2 mm[a]	Corresponding figure numbers
23.9	2	25	6-A
36.6	5	15	6-D
-	0	10	6-D
21.[illegible]	20	[illegible]	-B
22.[illegible]	20	50	6-C
22.6	20	50	6-D
20.8	5	[illegible]	-F
17.1	2	55	-F
20.1	1	55	6-C

The two moisture-tension curves on figure 6-A were constructed

Figure 6-A.--~~Curves showing moisture content at several tensions to the size of pores~~ Moisture-tension relationship and pore size in the tuff at Site 1.

from the same set of moisture-tension values and from laboratory determinations of total porosity and effective porosity. Curves prepared using data from samples taken from most other places on the Pajarito Plateau have the same general parallel relationship. The curve prepared using effective porosity data indicates 2 percent of the pores 0.20 mm (millimeter) in diameter and larger drain when the tension increases from zero (complete saturation) to 15 cm of water; about 25 percent of the pore spaces drain at one-third atmosphere tension (344 cm of water); and that about 75 percent of the pores are smaller than about 0.01 mm in diameter.

Samples for which moisture-tension curves type A were prepared in figures 6-B to 6-D have similar drainage properties. The position of those curves indicates that in these samples approximately 20 percent of the pores are larger than 0.20 mm in diameter and 40 to 50 percent are larger than 0.01 mm. Initial drainage from those groups of samples is relatively rapid because of the high percentage of large diameter pores and moderately high porosity, and approximately half the water in a saturated sample drains by gravity. The nearly horizontal trend of the moisture-~~[ons in]~~ tension curve on figure 6-C below 90 cm and the nearly vertical trend above 90 cm shows that about 40 percent of the pore space are relatively large and 60 percent are relatively small and that there are few intermediate size pores. This is similar to a typical field sand. The type A curves on figures 6-B and D indicate there is a relatively constant decrease in the size of the pores.

Figure 6-B.--~~Curve showing relation of water content at several tensions to the size of pores~~ Moisture-tension relationship and pore size in the tuff at Site 3.

Figure 6-C.--~~Curves showing relation of water content at several tensions to the size of pores~~ Moisture-tension relationship and pore size in the tuff in the caisson area at Site 6.

Figure 6-D.--~~Curves showing relation of water content at several tensions to the size of pores~~ Moisture-tension relationship and pore size in the tuff at Site 7.

The steep slopes of ~~two~~ type B and C curves on figure 6-D for samples of the Tshirege Member at site 7 indicate that the pores in these samples are ~~composed~~ almost entirely small [~~pore spaces~~]. The type B curve indicates that about 85 percent of the pores are smaller than 0.01 mm in diameter and do not drain by gravity, and the type C curve indicates that few pores are larger than 0.05 mm. These samples could represent a part of the Tshirege that would be relatively impermeable to vertical movement of water and wastes.

The type B curve on figure 6-C and the type A curves on figures 6-E and F indicate that only a small percentage of pores 0.20 mm in diameter drain initially and that more than half of the total pore space drains by gravity. The curves for samples collected at site 6 fall into two groups with the sandy material represented by the type A curve on figure 6-C. The curves of samples at depth adjacent to the disposal pit (type B curve on fig. 6-C) and at depth beneath the pit (type A curve on 6-E) are nearly parallel but the steeper slope beneath the flex point on figure 6-E may indicate that waste water moving through the tuff beneath the pit intermittently over a period of years has caused ~~some changes~~ a slight decrease in the size of the pores. The flat curve (fig. 6-F) indicating an even distribution of pores does not readily explain the comparatively low specific retention values of samples of the Tshirege Member from site 2.

Figure 6-E.--~~Curve showing relation of water content at several tensions to the size of pores in~~ Moisture-tension relationship and pore size in the [ ] Tuff at site 6, beneath disposal pit.

Figure 6-F.--~~Curve showing relation of water content at several tensions to the size of pores~~ Moisture-tension relationship and pore size in the [ ] Tuff at site 2.

The values listed below show the general relationship between pore size and percolation rate (Nelson and Baver, 1940, p. 73) and indicate that the rate of percolation through the 0.23-mm pore spaces is more than 60 times that through 0.02-mm pores. ~~These values are~~ used calculated the rate of percolation through tuff having about 20 percent pore

Pore size (mm)	Percolation rate (cc per 10 minutes)
0.230	723
0.151	335
0.122	285
0.067	133
0.020	12

space 0.20 mm or more in diameter and about 50 percent pore space 0.01 mm or more in diameter and high in porosity (table 5, site 6, upper half of caisson hole), is more than 100 times faster than the rate of movement through the boulder (table 5, site 1).

Hysteresis

Data obtained about the moisture-tension relationship during the draining or drying and wetting of a rock sample when plotted on graph paper produces two curves that join at two points to form a loop. There is marked hysteresis between the two curves, and the loop is commonly referred to as the "hysteresis loop".

The hysteresis loop (fig. 7) for a particular rigid porous

Figure 7.--Hysteresis curve showing the relation between moisture tension and moisture content of a sample of the Bandelier Tuff at Site 6.

medium is unique and its results are reproducible (Puri, 1949, p. 428). Hysteresis is due in part to the resistance of water adhesion within the small pore spaces during both the wetting and drying cycle. The moisture content on the drying cycle of the hysteresis loop at the one-third atmosphere tension in figure 7 is about 22 percent by volume and the moisture content at the same point on the wetting cycle is approximately 14 percent. These percentages are approximately the average for samples from Site 6. The maximum difference in moisture content on the two curves occurs between about 210 cm of water and 344 cm of water or one-third atmosphere tension.

Particle-size distribution

The particle size distribution of samples of tuff from four sites is listed in table 6. Many of the particles in the samples tested consisted in part of shards or glassy cementing material; thus the values in the table may be misleading, because some of the variations in the sizes of the particles may be due to the method of collecting the samples, which was by augering. The averages of 46 percent of clay and silt ~~fines~~ and 53 percent sand from table 6 is descriptive of a sandy silt.

The size of the particles in a porous medium have a direct effect on the movement of water because their arrangement and degree of packing determine the porosity and the pore sizes. Waldron and others (1961, p. 206) using glass beads 51 to 203 microns in diameter showed that open packing resulted in a porosity of 47.6 percent and that close packing resulted in a porosity of 26.0 percent. Lutz and Leamer (1940, p. 28) showed that permeability increases exponentially with the size of the particles and therefore with the size of pores, as follows: silt, 0.8 cc per min (cubic centimeters per minute); very fine sand, 3.7 cc per min; fine sand, 14.3 cc per min; and medium sand, 47.8 cc per min.

Table 6.--Particle-size distribution of samples of tuff from sites 2, 3, and 6, in percent by weight.

Sample Location	Number of Samples	Clay		Silt		Total, silt and clay		Sand		Gravel	
		Average	Range	Average	Range	Average	Range	Average	Range	Average	Range
e 2, side of oad cut.	2	-	4.2-6.9	-	34.2-38.5	-	38.4-45.4	-	54.6-61.6	-	-
e 3, beneath aundry isposal pit.	8	11.8	8.0-14.4	39.8	36.6-43.2	50.6	44.6-57.6	48.3	42.4-55.4	1.1	0.2-1.6
e 6, caisson ole.	2	-	6.2-7.0	-	29.2-30.4	-	36.2-36.6	-	62.3-62.6	-	1.1-1.2
e 6, beneath isposal pit.	4	-	-	-	-	38.4	21.3-49.3	60.1	50.0-78.3	1.5	0.4-4.2

A comparison of the one-third atmosphere tension values of drill cuttings and cores collected at site 6 showed that the values were reasonably close but that the dry unit weight, porosity, and permeability values were significantly different. The following are averages of analyses on samples collected at two depths:

Sample	Moisture content at one-third atmosphere tension in percent by volume	Dry unit weight	Porosity in percent	Coefficient of permeability (gpd per sq ft)
core	13.3	1.45	43.0	2.0
bulk	15.0	1.35	47.4	7.0

The results indicate that the laboratory analyses of samples of drill cuttings cannot be used for accurate interpretation of the physical properties, although values for the moisture content at one-third atmosphere tension were reasonably similar.

Coefficient of permeability

The average values of the permeability of the tuff (field coefficient of permeability is the number of gallons per day that flows through a cross section of 1 square foot under a unit hydraulic gradient, or through a section 1 foot high and 1 mile wide under a gradient of 1 foot per mile at prevailing conditions of water temperature. Laboratory determinations of the coefficient of permeability ~~are~~ (corrected to a temperature of 60°F) ranged from 0.4 gpd per sq ft (gallons per day per square foot) in the 90 to 275 foot zone at Site 7 to 10 gpd per sq ft at Site 2, but the range at each site was sufficiently narrow to assign a general value. The lowest average values of permeability coincided with the lowest porosity, and the highest values of permeability coincided with approximately the highest porosity (table 1-A). This indicates a gross relation which may not be true at individual sites. The relation between permeability and porosity, except for the extremes, appears to be random and cluster within 1.7 to 4.0 gpd per sq ft for the permeability and 38.7 and 49.8 percent for the porosity. The difference between vertical and horizontal permeability in the tuff is small. In general the horizontal permeability is larger than the vertical permeability and is probably related to density gradients within the flows, or to bedding.

Joints have increased the permeability of the Tshirege Member. Near the surface of the mesas joints are filled with clay, but at depth the joints are free of sediment. The width of joints ranges from 0 to as much as 3 inches. Most of the joints are vertical and extend to great depth in the Tshirege. At places, joints probably are open and interconnected through the Tshirege and form avenues through which water can move readily to depth. *

Joint spacing is irregular but widespread. The average density near site 9 is about one joint per square yard.

The Tshirege Member of the Bandelier Tuff contains sub-units that probably are individual beds of tuff. Water moving through the tuff is temporarily perched by variations in vertical permeability. The permeability varies from one bed to another, from one member to another, and from the Bandelier Tuff to underlying beds of the Santa Fe Group.

Movement of water in Bandelier Tuff

Site 1 - Tshirege tuff boulder in Pueblo Canyon

A boulder of Tshirege tuff embedded in alluvium in Pueblo Canyon was used for the study of capillary movement of water from a ponded surface. Six holes 3 inches in diameter and a maximum of 6 feet deep were drilled and cored into the boulder perpendicular to the steep west-facing slope of the boulder, and three pair of access tubes were installed during the fall of 1960 (fig. 9). Water was

Figure 9.--Sketch showing isohydral lines of ~~equal~~ moisture content, in percent by volume, and moisture content during capillary rise of water in boulder at Site 1.

ponded against the lower part of the boulder on the east and north sides to provide a constant supply of water in direct contact with the boulder at a controlled distance below the bottom of the access tubes.

The pond was filled and a constant head was established on September 18, 1960. Nine days later on September 27 the moisture content in the boulder was about 10 percent about 3 feet above and west of the pond (fig. 9), and was approximately 30 percent near the level of the land surface, which is approximately half a foot above pond level. On October 6, after 18 days, the 10 percent isohydral line had moved upward another 2 to 3 feet; the 15, 20, and 25 percent isohydral lines were unevenly spaced beneath the 10 percent line. The maximum moisture content measured in the boulder was about 30 percent on Dec. 8, the 81st day after the constant head in the pond had been established. The capillary movement through the boulder was not a sharp "front" as commonly takes place in the downward movement of moisture but was uneven.

The pattern formed by the isohydral lines on figure 9 indicates that the water moved laterally, ~~in~~ nearly saturating that part of the boulder beneath the land surface for several feet before it moved vertically. [~~This suggests that the boulder was saturated for several feet from the pond.~~] However, evaporation from the east face of the boulder may have about the same effect on the isohydral lines.

During the winter of 1960-61, the pond was frozen over or empty, and the decrease in moisture content in the boulder was not recorded. In 1961, the pond was refilled, and a second study of capillary movement in the boulder was made. A maximum moisture content of about 30 percent was measured on May 11, 1961, the 49th day following the start of the second study. The faster movement of water in the boulder, recorded in the second study, suggests that the boulder was still moist from the first study, and that the rate of capillary rise is faster in wetted material than in dry material.

The effective porosity of the tuff in the boulder, from core analysis, was 32.8 (table 1A). Thus, the approximate 3 percent difference between the maximum moisture content reached in the boulder and the effective porosity may indicate that the capillary fringe was not completely saturated under conditions of the study. A slight density gradient in the boulder may have had some effect on the movement of water. The density apparently is higher near the center and may indicate weathering of the outer layers of the boulder.

Site 3 - laundry pit

The study at Site 3 was to determine the possibility of using the site for a long-term infiltration experiment. Since about 1945, liquid radioactive wastes from contaminated laundry had been discharged into pit 1; overflow was piped to the lower pits 2 and 3 ~~through buried pipes~~ (fig. 11). The quantity reaching pit 3 was not determined

Figure 11.--Moisture content of the tuff beneath the disposal pit at Site 3.

but is believed to have been small, thus, most of the moisture in the tuff beneath the pit probably is from precipitation.

The moisture content of samples collected at depths of 3 and 4 feet beneath the south side of pit 3 (at letter "A" on figure 11) decreased with depth from 29 percent to 18 percent, and the permeability decreased from 0.3 gpd per sq ft to 0.006 gpd per sq ft. The decrease in permeability is not readily explained by the pore-size distribution curve (fig. 6B) because the percent of large pores for samples of tuff collected beneath the pit at letter "A" was moderately high (table 5), and the difference in total porosity was small. The low permeability may have been caused in part by clogged pores rather than by the physical properties of the tuff, as indicated by the clay, roots, and rootlets associated with the samples collected. A bulk sample collected at a depth of about ~~seven~~ 7 feet in hole 2 had a moisture content of 30 percent and became hard when it was dried in the oven. ~~which indicates weathered tuff.~~

Moisture contents as high as 30 percent in holes 1 and 2 beneath the zone of low permeability possibly represent water that moved laterally from the gravel fill near the center of the pit. This is indicated, too, by the moisture content in hole 2 near the gravel fill, which was generally higher than at hole 1. The high moisture content between depths of 15 and 25 feet in hole 2 and the sharp decrease at a depth of about 25 feet suggest the presence of semi-permeable layers that perch the water. The high moisture content of about 30 percent in hole 1 apparently represents another perching layer below 33 feet. The density of the tuff at 30 to 33 feet is almost 6 pounds per square foot less than above or below that interval. Decreasing moisture content above 25 feet at hole 1 on October 12, 1961, when the moisture content between 32 and 33 feet at hole 2 increased, indicates vertical as well as lateral movement beneath the pit.

Discharge to the pits was to be discontinued in late 1961, therefore additional experiments at this site were not ~~further~~ considered.

Site 4 - soil study

The studies at Site 4 were intended to ascertain the effect that a soil cover and the transition zone will have on the quantity of water that moves into the underlying tuff. The vertical and horizontal movement of water in the soil was also studied. The site was near the middle of a finger mesa, which sloped southeastward at about 1 to 2 percent. Cores for natural moisture-content determinations were collected at the site on Oct. 10, 1958.

Infiltration tests were made in 1958 and 1959, (Abrahams and others, 1961, p. D-144). Installations consisted of two shallow infiltration pits slightly less than 2 feet in diameter, one or more access tubes in each pit, and a supply of water. The tests during 1958 were made in the soil zone beneath pit A, and the tests during 1959 were made in the soil zone in the underlying tuff at pit B. The water supply at pit A was intermittent; at pit B the head was constant during the period of the test.

At pit A lateral movement is indicated by a higher moisture content in access tube 1, downgradient from the pit (fig. 12-A, profile I).

Figure 12-A.--Isohydral lines of moisture content, in percent by volume, beneath pit A at Site 4 during intermittent infiltration and drainage, 1958.

Moisture penetration was less than ~~three~~ 3 feet in holes 2 and 3, but probably more than ~~four~~ 4 feet in hole 1 after ~~four~~ 4 feet of water had infiltrated into pit A in 6 hours following 14 days of drainage. The rapidly increasing moisture content at the 1-foot depth in hole 1 indicates some lateral movement (fig. 12-B, profile I).

Figure 12-B.--Moisture content beneath infiltration pit A at Site 4 during intermittent infiltration and drainage, 1958.

The rate of percolation, after 19 days of drainage, averaged about one-half foot per day during the first 3 days of infiltration (fig. 12-A, profile II). The front became diffused during further infiltration and the rate of percolation could not be determined.

The maximum moisture content after 23 days of infiltration at pit A was about 37 percent at hole 1 (fig. 12-B, profiles II and III); the moisture content of the soil moved downward at approximately the same percent of saturation. The total porosity of the soil at a depth of about 1 foot was approximately 51 percent, and at 2 feet was approximately 49 percent, which indicated that the moisture content of 37 percent probably was well above field capacity but did not represent saturated conditions.

The rate of infiltration at pit B during the 99 day study decreased approximately logarithmically throughout most of the period as follows:

1 gpd/ft² = .07 in/hr.

1st and 2d days - 20 gpd per sq ft

4th to 18th days - 10 gpd per sq ft

18th to 31st days - 5 gpd per sq ft

31st to 51st days - 2 gpd per sq ft

51st to 69th days - less than 1 gpd per sq ft

Evapotranspiration was relatively constant. The infiltrating water followed two courses; (1) some went downward; and (2) some went to support evapotranspiration. As downward rates slowed, and a constant rate to evaporation was maintained, the ratio of between the two changed.

The wetted front moved to a depth of about 5 feet during the first 2 days of infiltration at pit B (fig. 13) and to a depth of

Figure 15.--Moisture content in the soil and tuff beneath pit B at Site 4 during 99 days of continuous infiltration and subsequent drainage for 21 months.

about 6½ feet within about 99 days. The decrease in the rate of movement of the front was logarithmically. The moisture content decreased with depth from a maximum of about 39 percent in the soil to less than 4 percent about 1 foot below the top of the tuff. After 8 months of drainage the moisture content was about the same as before infiltration started.

The high moisture content beneath the pit before infiltration started was due in part to heavy rains in August 1959 and the relatively poor drainage in the sandy surface soil. The May 19, 1961 measurements were high because of snowmelt, and the Oct. 2, 1961 measurements were low because of low precipitation.

The water use per square foot during this study was equivalent to about 40 or 50 years of precipitation on the Pajarito Plateau; however, natural conditions were not duplicated because the seasonal distribution of alternating percolation and drainage could not be duplicated. The fact that water did not penetrate the dense transition zone between the soil and tuff during the study or in the following year, indicates that the soil cover will impede vertical movement into the underlying tuff. Capillary rise, evaporation, and transpiration were perhaps the principal reasons that the water did not penetrate the underlying tuff, rather than the low permeability of the transition zone.

Site 5 - Mesita del Buey

Site 5 is adjacent to the south wall of a solid-waste disposal pit 29 feet deep (~~fig. 14~~), near the eastern end of Mesita del Buey,

~~Figure 14.--Wetted areas on south wall of the disposal pit at Site 5 resulting from seepage from the infiltration pit 10 feet back of the wall.~~ deleted

a finger mesa. The study at this site was to investigate movement of water and nuclides during continuous infiltration.

An infiltration pit, access tubes, and a water-storage tank were installed near the edge of the vertical wall of the disposal pit (fig. 15).

Figure 15.--Sketch showing relation of infiltration pit and access tubes to the disposal pit at Site 5.

The center of the infiltration pit was 10 feet south of the south edge of the waste disposal pit. The upper 2 feet of the infiltration pit was shored with wood planks within the soil and fill material, and the lower 1 foot was dug into the unweathered tuff. Water entered the pit through a 3/4-inch pipe connected to a value box adjacent to a 3,000-gallon storage tank. A float valve in the infiltration pit maintained a constant head of water of about three-fourths foot. Eight holes 40 feet deep lined with plastic tubing were installed in and near the infiltration pit (fig. 15).

Periodic measurements of water losses from the storage tank were made to determine the volume of water moving to the infilration pit.

The infiltration experiment started when water was put into the pit October 8, 1959. Between December 29, 1959 and January 6, 1960 the water line froze and the pit dried up. The infiltration phase of the experiment was suspended until April 20, 1960 and then restarted. About December 9, 1960 the water line froze again and the infiltration phase of the experiment was stopped, but moisture measurements were made in access tubes for several months to observe drainage patterns.

Photographic evidence that water moved into the tuff from the infiltration pit was a wet patch (fig. 16) that developed on the wall

Figure 16.--Wetted areas on south wall of the disposal pit at Site 5 resulting from seepage from the infiltration pit 10 feet back of the wall.

of the disposal pit 10 feet to the north. Evaporation from the wall discharged water that would have moved deeper in the tuff.

The rate of infiltration of water through the pit at Site 5 is shown graphically on figure 17. The slope of the log curve of

---

Figure 17.--Rate of infiltration from infiltration pit at Site 5, 1959-60.

---

the rate of infiltration for the 1959 study shows that the rate of infiltration decreased from about 0.75 gph per sq ft (gallons per hour per square foot) to about 0.2 gph per sq ft.

Significant seasonal changes in the log curve of the rate of infiltration for the 1960 study occur during the months of April and September. The steeper parts of the curve show a relatively rapid decrease in the rate of infiltration with time during the months in which the average temperature is less than about 50 degrees. The flatter part of the curve shows the rate of infiltration during months in which the average temperature is above 50 degrees. In these months the rate of infiltration decreased from about 0.4 gph per sq ft to about 0.2 gph per sq ft. The range of the temperature of the water in the pit, from near freezing during the winter to about 80 degrees in the summer, was enough to cause seasonal differences in the rate of infiltration into the tuff due to changes in viscosity (Horton, 1940, p. 417) In addition, seasonal temperature variances in the tuff beneath the infiltration pit may have been sufficient to cause some small differences in the rate of percolation.

The flatter part of the log curve of infiltration includes the time of the growing season at Los Alamos, and it is possible that evapotranspiration of tumbleweed on the soil and fill pad consumed small amount of water moving from the pit. However, when most of the plants were removed no measurable effect on the rate of infiltration took place. Several plants growing with their tap roots along the side of access tubes were kept in place. The moisture content of the upper 2 feet of material (table 7) was reduced at access tubes 2 and 3 where the tumbleweeds were growing; the moisture content increased after the plants were removed September 1. The moisture content at all the other tubes remained high throughout the growing season.

Table 7.--Effects of transpiration by (Tumbleweed) plants on the moisture content of tuff at Site 5, 1960.

Hole No.	Remarks	1960					
		May 18	June 2	July 1	July 29	Sept. 1	Dec. 6
		Moisture content, in percent by volume					
3	Tumbleweed at side of access tube.	22.5	16.5	12.5	8	6	20
2	Tumbleweed at side of access tube.	27.5	27.5	23.5	19	14	21
4	No Tumbleweed nearby.	26	26	27.5	25.5	24	26
6	No Tumbleweed nearby.	27.5	29	27.5	27	27.5	29
8	Tumbleweed removed from near access tube.	20	19.5	19	19.5	15	18

No evidence was found that water moved through the soil and fill pad and evaporated from the surface in quantities sufficient to affect the rate of infiltration in the pit. The moisture content of the upper foot of the soil ranged between 5 and 10 percent by volume, which generally is too low to transmit much water. The sandy material tends to form a barrier that reduces evaporation (Willis, 1960, p. 241).

The rate of infiltration during the warmer months (5 to 12 gpd per sq ft) was within or somewhat above the range of permeability determined from cores in the Laboratory. The field permeability (rate of percolation) in the zone of aeration cannot be directly compared to the saturated permeability (laboratory measurement) because water in the infiltration pit not only moved downward but also moved laterally as much as 8.5 feet from the edge of the infiltration pit (fig. 14). Thus, the rate of percolation, particularily from a small source of water located in a layered medium, is substantially less than the saturated permeability, because the water is subject to forces not involved in saturated flow.

The wetting front moving into the unsaturated tuff was sharpest in the early part of the 1959 study, but it became thicker and more diffuse as infiltration continued (fig. 18, profile I). Energy barriers

Figure 18.--Moisture content and density of tuff in access tube 1 at Site 5, 1~~959-60~~.

at the front retard the movement until the moisture content behind the front is raised to a maximum or optimum value (Bodman and Colman, 1944, p. 117-118). The thickness of the zone of transmission, the area between the unwetted tuff and the maximum moisture content attained during the vertical movement, ~~apparently~~ probably was a function of layering in the tuff. The average rate of movement of the part of the front containing a moisture content of 25 to 28 percent by volume was about 2 feet during the first day, about half a foot per day during the next 11 days, and about a tenth of a foot per day during the next 56 days, with additional movement in the lower moisture range to a total depth of about 18 feet. The rate of movement of the front in 1960 was higher (fig. 19, profile II) than in 1959 probably because the rock was wetted and fewer energy barriers existed to reduce the rate of movement and less water was needed to reach field capacity. (See ~~also~~ fig. 19 and 20.).

The moisture content of 25 to 28 percent apparently was the maximum attained away from the pit (fig. 18, profiles II and III) at Site 5. This moisture content is several percent above field capacity but is considerably less than saturation. The maximum moisture content 1 foot beneath the infiltration pit was about 40 percent, which is 6 to 7 percent less than the estimated effective porosity. The 6 to 7 percent ~~figure~~ probably represents the large pore spaces from which water drained into the underlying material, although it may also represent entrapped air. However, entrapped air should not be a problem in this study because of the large volume of porous medium involved and the probability that entrapped air beneath the infiltrating water would escape and not be surrounded or compressed (Free and Palmer, 1940, p. 395).

The moisture content of the tuff decreased steadily above an apparent Bulk density change at about 25 feet beneath the infiltration pit to a range of 5 to 16 percent after about 9½ months drainage (fig. 18, profile IV). The moisture content below the apparent density change slowly increased during drainage and after about 2 months reached a moisture content of about 8 percent. The 8 percent saturation extended below the bottom of the access tube.

The movement of water during the 1960 study at Site 5, and subsequent drainage, is shown on figures 19 and 20 by the changing

Figure 19-A.--Isohydral lines of moisture content of the tuff, in percent by volume, along an east-west section at Site 5 on Apr. 20, 1960, after about 3½ months of drainage.

19-B.--Isohydral lines of moisture content of the tuff, in percent by volume, along an east-west section at Site 5 on June 2, 1960, after 42 days of infiltration.

19-C.--Isohydral lines of moisture content of the tuff, in percent by volume, along an east-west section at Site 5 on July 28, 1960, after 99 days of infiltration.

19-D.--Isohydral lines of moisture content of the tuff, in percent by volume, along an east-west section at Site 5 on Dec. 6, 1960, after 230 days of infiltration.

19-E.--Isohydral lines of moisture content of the tuff, in percent by volume, along an east-west section at Site 5 on Mar. 1, 1961, after about 3 months of drainage.

patterns of isohydral line of moisture content.

Figure 20-A.--Isohydral lines of moisture content of the tuff, in percent by volume, along a north-south section at Site 5 on Apr. 20, 1960, after about 5½ months of drainage.

20-B.--Isohydral lines of moisture content of the tuff, in percent by volume, along a north-south section at Site 5 on June 2, 1960, after 42 days of infiltration.

20-C.--Isohydral lines of moisture content of the tuff, in percent by volume, along a north-south section at Site 5 on July 28, 1960, after 99 days of infiltration.

20-D.--Isohydral lines of moisture content of the tuff, in percent by volume, along a north-south section at Site 5 on Sept. 1, 1960, after 134 days of infiltration.

20-E.--Isohydral lines of moisture content of the tuff, in percent by volume, along a north-south section at Site 5 on Dec. 6, 1960, after 230 days of infiltration.

20-F.--Isohydral lines of moisture content of the tuff, in percent by volume, along a north-south section at Site 5 on Mar. 1, 1961, after about 3 months drainage.

Isohydral lines are shown on both figures for the day infiltration was restarted (April 20, 1960); after 42, 99, and 230 days of infiltration; and about 3 months after infiltration of water from the pit ceased. In addition, isohydral lines 134 days after infiltration started are shown on figure 20. The effect of density gradients in the tuff is reflected in the moisture pattern changes in figure 19. The effect of evaporation from the wall of the adjacent disposal pit is reflected prominently in the moisture patterns in figure 20. The expanding wet area on the wall of the disposal pit as outlined in figure 16 correlates to some degree with the moisture patterns in figure 20.

The positions of the isohydral lines on the day infiltration started, after 42, 99, and 230 days of infiltration, and after about 3 months drainage with no infiltration of water from the pit are shown in figures 19 and 20. The position after 134 days of infiltration is also included in figure 20. The effect of the density gradients in the tuff and evaporation from the disposal pit wall are reflected in the moisture patterns in figure 19. The effect of evaporation from the wall of the disposal pit on the movement of water in the tuff is shown by the moisture patterns. This sequence can be followed to some degree by the changes in the patch of wet area on the south wall of the disposal pit outlined in figure 16.

Water was retained in the tuff to near field capacity between the depths of 8 and 14 feet beneath the bottom of the pit approximately 3½ months after the infiltration phase of the experiment was suspended in January 1960 (figs. 19-A and 20-B). The slight bunching of the 10, 15, and 20 percent isohydral lines to the east in figures 19 A-E may indicate movement down dip in the tuff, or because of density changes at access tubes 4 and 5. The effects of density gradients were prominent on the east-west section at holes 4 and 5 and were beginning to show at a depth of about 20 to 25 feet at hole 2. Moisture content with respect to depth below the infiltration pit was greater to the south in figure 20. The ~~apparent trend of water~~ moisture content gradient in the tuff north of the infiltration pit indicates that water moved toward the wall of the disposal pit under the influence of forces ~~caused by~~ resulting from evaporation of water from the wall of the disposal pit. The apparent increasing rate of evaporation from the wall, with the approach of longer and warmer days, is evident on the north-south section. Little or no increase in moisture was apparent at depth at holes 6 and 7. Figures 19B and 20B show approximately the position and maximum extent of the tuff that contained a moisture content of 20 percent or more.

The closing of the 25 percent isohydral line and the constriction of the 20 percent isohydral line on 19-C and 20-C probably indicate that water evaporated from the wall of the disposal pit faster than it moved into the tuff from the infiltration pit. The 25 percent isohydral line closed late in June after 60 to 65 days of infiltration. The 10 and 15-percent isohydral lines did not advance significantly in any direction from the positions shown on figures 19-B and 20-C, except possibly at hole 1, although the rate of infiltration decreased only a small amount. The 2-percent isohydral line on figure 19-B showed a tendency to flatten, probably because of a density gradient at a depth of about 25 feet at hole 1. The lower moisture content at the upper part of holes 2 and 3 was due to evapotranspiration by the tumbleweeds growing there. Figure 20-D shows a continuing decrease of the area within the 25-percent isohydral line and almost total closure of the 20-percent lines beneath the infiltration pit.

Moisture measurements, made on December 6 after 230 days of infiltration, (figs. 19-D and 20-E) show a decrease in the moisture content of the tuff from that of previous measurements. Although the rate of evaporation from the disposal pit wall decreased steadily during the fall, because of the decreasing temperature, the rate of infiltration probably also decreased because of the greater viscosity of the water. The rate of infiltration at the near-freezing temperatures in the pit in December was probably only about half that during the middle of summer (Mavis and Wilsey, 1936, p. 17). Water in the pit probably froze during extremely cold nights late in November and early in December before the permanent freeze, thus completely stopping infiltration for periods of several hours. The rate of percolation exceeded the rate of infiltration from the pit when the water was near freezing.

On March 1, 1961, after about three months of drainage (figs. 19-E and 20-F), the isohydral lines assumed about the same positions and shapes as of ~~January~~ April 20, 1960, except in the lower moisture range directly beneath the infiltration pit where a low moisture content column 3 or 4 feet in diameter formed below a depth of about 30 feet.

A total of about 11,100 gallons of water moved through the infiltration pit during the 230 days of the study, most of which infiltrated during the summer months. A water budget cannot be calculated, however, because of the unknown quantities lost by evaporation.

Site 6, DP-West

Site DP-West is within one of the original disposal areas at Los Alamos technical area DP-West, and lies between the axis and the north rim of a finger-mesa.

The disposal area consists of four pits about 20 feet wide, 100 feet long, and 5 feet deep that were dug into the tuff and backfilled with layers of sand and gravel, and connected in pairs by buried pipes. Plutonium wastes dissolved in hydrofluoric acid were discharged into the pits between 1943 and 1952. The pits were ~~Some water~~ not roofed and ~~derived from~~ precipitation contributed water ~~[illegible]~~ to the pits ~~since 1952.~~ The objectives of the present study were to determine if and where ~~were to study the movement of~~ water moved beneath a disposal pit and to ascertain if waste products moved with the water. Samples of water, extracted with porous cups placed beneath the pit, were analyzed for chemical and radiochemical quality. The moisture content beneath the pit was measured in horizontal access tubes, and in tubes placed at an angle beneath the pit to a depth of about 100 feet.

A caisson 30 feet deep, 6 feet wide and 12 feet long was excavated about 6 feet north-northeast of the eastern quarter of pit 1 (fig. 21). The caisson was shored with planks and

Figure 21.--Diagrammatic sketches of installations and caisson pit at Site 6.

reinforced with timbers and contained three platforms 6 feet apart vertically. [~~A vacuum system capable of about one atmosphere was installed.~~]

Twelve pairs of holes 3 inches in diameter and 8 to 12 feet long and dipping downward at about ½-inch per foot were drilled at 2-foot intervals through the south wall of the caisson into the tuff beneath the pit (fig. 21). The uppermost hole was about 6 feet below the berm and less than half a foot beneath the bottom of the pit. A plastic tube approximately 2 inches in diameter was installed in one hole of each pair for moisture measurements. The annular space between the access tube and the wall of the drilled hole was not backfilled. The other hole of the pair contained a porous cup placed at the back of the hole and connected to ~~the~~ a vacuum system that was capable of about one atmosphere. The holes were backfilled around the vacuum tubes with crushed tuff emplaced with compressed air.

Six holes 4 to 6 inches in diameter and 75 to 99 feet in depth were drilled near the edge of the pit. Four of these holes were slanted to penetrate the tuff beneath the pit. The holes were lined with plastic access tubes approximately two inches in diameter and the annular space between the tubes and the walls of the holes was backfilled with crushed tuff.

Conditions before infiltration

Several facies in the tuff exposed during the construction of the caisson created special problems of data interpretation (sketch D on fig. 21). These facies types were an upper tuffaceous sand that was slightly consolidated and partly weathered and contained numerous roots and rootlets (bed A, fig. 21 and table 8); a pumiceous tuff that appeared to pinch out several feet south of the caisson (bed B, fig. 21); and an underlying welded tuff that was weathered, especially along joint faces along which wastes may have moved (bed C, fig. 21). A clay zone 6 to 12 inches thick overlies the welded tuff.

Table 8.--Description of material

in caisson pit at Site 6.

Position on figure 21	Description [a]
A	Sand, light orange-brown, weathered yellowish; consists of subround to subangular silt to coarse grains of quartz, sanidine, pumice, and minor amounts of mafic minerals, some grains pitted.
B	Tuff, light orange-gray, weathered throughout; much clay present.
C	Tuff, light gray, weathered yellowish around devitrified pumice fragments and adjacent to joints, locally weathered into clay, weathering more intense in bottom of pit; consists of ash and some mafic minerals.

a/ by William D. Purtymun

The banding effect of the one-third atmosphere tension moisture values (fig. 22-A) parallel to the clay development (sketch C, fig. 21)

Figure 22-A.--Section through Site 6 showing banding effect of the moisture content at one-third atmosphere tension.

suggests that waste-water movement may have changed some of the physical properties of the tuff, such as pore and particle sizes. Some of the wastes discharged in the east end of the disposal pit may have moved laterally through the sandy material (Bed A on sketch C and D, fig. 21) along the sloping top of the tuff and then vertically into the tuff. The lower moisture values (fig. 22-A) seem to coincide with areas of tuff in which the greatest amount of staining had occurred. The stained areas may indicate a different stage of weathering than that at the clay layer due to alternate wetting and drying cycles. A trend towards banding in the tuff is indicated also by the dry unit weight, specific retention, porosity values, and by the pattern (fig. 22-B) formed by plotting the gross alpha count on the section through the study area.

The moisture content and gross alpha activity of the cores collected in the study area decreased significantly from east to west and with depth (table 9), which indicates that much of the liquid discharged into the pit moved only a short distance laterally through the sandy material before infiltrating the tuff. The average moisture c ontent of the third horizontal group was significantly lower at the one percent level than that of the two upper groups, but not significantly less than that of the fourth group.

Table 9.--Averages of moisture content and gross alpha counts of tuff cores collected at site 6.

Group of holes by depth	Depth (feet)	Moisture content (in percent by volume)	Difference from lowest moisture content (18.4)	Least significant difference	Gross alpha counts per minute per dry gram[a]
First	0, 2, and 4	29.6	11.2	9.0	1,817
Second	6, 8, and 10	26.0	7.6	7.2	501
Third	12, 14, and 16	18.4	-	-	238
Fourth	18, 20, and 22	21.3	2.9	-	148
East	0, 6, 12, and 18	25.0	-	-	1,188
Middle	2, 8, 14, and 20	23.6	-	-	563
West	4, 10, 16, and 22	20.5	-	-	482

a/ Analysis by Los Alamos Scientific Laboratory.

The tuff is extensively jointed (fig. 21), and the tendency for liquid to move through the joints is indicated by higher gross alpha activity in local areas as shown by the gross alpha count of 1,000 per minute per dry gram at the 20 foot depth on figure 22-B.

Figure 22-B.--Section through Site 6 showing gross alpha activity.

In the east group of holes (fig. 21) the joints become more numerous with increasing depth. Several open joints on the south wall of the caisson were found below a depth of 25 feet. Waste water had penetrated the fineline joints to depths of at least 22 feet and subsequently altered the tuff adjacent to the joint as much as one-quarter to one-half inch. Clays developed locally and impeded drainage so that the joints retained water to the extent that the moisture content of the tuff was locally as much as 35 percent (fig. 23, profile I).

Figure 23.--Isohydral lines of moisture content of tuff constructed ~~drawn~~ from moisture readings in horizontal access tubes ~~holes~~ at 2, 8, 14, and 20 feet ~~depths~~ below the bottom of disposal pit 1 at Site 6.

The isohydral lines of the June 30 measurements (fig. 23, profile II) show a lateral movement of moisture from the disposal pit towards the caisson area before infiltration began. This increase in moisture content of the tuff probably was caused by infiltration of snowmelt and by the above normal precipitation in June (3.40 inches).

The moisture content of chunk samples collected at various depths during excavation of the caisson in October 1959 indicate that water from the disposal pit had moved northward only a short distance. Some water had moved through the sandy materials above the clay layer as indicated by moisture contents of 19 and 16 percent, respectively, at the 0 and 4 foot levels. Little or no water had reached the 12 and 14 foot levels although some had moved laterally at the 18 and 22 foot depth.

Infiltration studies, 1960 and 1961

The flow of water into the disposal pit was continuous for two months in both 1960 and 1961. Both studies were during the summer months when the temperature of the water, and other conditions, probably were comparable. The dates and approximate rates of flow of wastes and tap water into the pit are shown below (Christenson and Thomas, 1962, p. 261).

	Raw waste discharge		Tap water discharge	
1960	July 6-July 31	approximately 8,000 gallons per day	Aug. 1-Sept. 7	approximately 6,500 gallons per day
1961	June 30-Aug. 1	approximately 6,400 gallons per day	Aug. 2-Aug. 26	approximately 7,100 gallons per day

The moisture content of the tuff during continuous infiltration ranged from less than 30 to more than 35 percent (fig. 23, profile III). Isolated areas having a moisture content of 35 to 40 percent developed locally during August, suggesting movement through open joints. Drainage in the 10 to 15 foot zone below the pit was relatively slow after infiltration stopped (fig. 23, profile IV) probably because the caisson acted as a barrier to the lateral movement of water.

The moisture content before the 1961 study after almost 9½ months of drainage (fig. 23, profile V) was about the same or slightly lower than before the 1960 study, probably because of less rainfall. The moisture content through July 1961 also was about the same as during the 1960 study (fig. 23, profile VI), but during August the moisture content of the tuff increased (fig. 23, profile VII). The high moisture content of 45 percent at a depth of 8 feet indicates that water drained from a joint directly into the annular space around the access tube and that water may have been standing in the hole. Drainage from this area was relatively rapid (fig. 23, profile VIII), again suggesting movement through open joints.

Gross alpha activity in water samples from the 8 foot depth averaged several times higher than the activity in samples from other depths (Christenson and Thomas, 1962). Samples from other depths also contained relatively high alpha activity, which indicated movement through joints. There was an inverse relationship between gross alpha activity and the pH of the solution. Total hardness and total solids increased with depth, suggesting solution and resolution of previously deposited materials.

~~Deep~~ Access tubes (fig. 25) were installed in deep holes drilled

Figure 25.--Plan view showing locations of deep access tubes, sections through disposal pit, and moisture content of deep access tubes at site 6.

~~without water (except DPW-1A)~~ in February 1961. Pre-test moisture content or gross alpha counts were not determined. High gross alpha activity of drill cuttings at a depth of about 30 feet in hole DPW-2 as listed below probably was due to a zone of free water perched on the facies change noted in the walls of the caisson pit.

Hole number	1	1A	2	3	4	5
Gross alpha counts per minute per dry gram	2	24	698	3	$1\frac{1}{2}$	3

The moisture content during March and April ranged between 20 and 35 percent around the upper part of the tubes, due in part to snowmelt and impeded drainage and was about 10 percent or less around the bottom of all the access tubes except DPW-1A. The moisture at the bottom of access tube DPW-1A may have been due to drilling water; drilling water was not used in the construction of other h. At depth below about 20 or 30 feet the moisture content was highest around tubes near the northeast part of the disposal pit.

Most of the water discharged into the disposal pit infiltrated the tuff and percolated downward within a roughly 1,000 square foot area at the east end of the disposal pit near the caisson (fig. 25). Outside the oval shaped area of maximum infiltration (fig. 25), particularily to the north, is a fringe zone about 20 feet wide and about 60 feet deep where percolating water maintains the moisture content of the tuff slightly above field capacity.

The moisture content at most depths approached the pre-infiltration level about 2½ months after discharge of water into the pit was stopped. The moisture content of the tuff at DPW-3 and 4, adjacent to the western half of the disposal pit, increased only in the upper 20 to 30 feet after almost 2 months of infiltration, whereas the moisture content at the east side of the pit increased to depths of more than 92 feet. The irregularities in the curves of moisture content for access tubes DPW-1, 1A, and 2 probably are due to changes in permeability. The increases in moisture from depths of about 45 to 60 feet at DPW-1 and at 10 to 40 feet at DPW-2 probably is caused by water reaching these intervals through joints.

The effects of joints and contacts between subunits of the tuff on water movement

Water moves through the tuff in two ways--by capillary movement through the pores of the tuff, and by movement through open interconnected joints. Water entering open interconnected joints might move rapidly, downward, through the joints; however, if the joints are not continuous through contacts between subunits of the tuff the water might be perched above the contact and would tend to move laterally.

Liquid wastes are discharged periodically from a treatment plant onto the Tshirege Member in the floor of Acid Canyon. The point of discharge is about a quarter of a mile above a seep flowing several gallons per minute at the contact of the Tshirege and Otowi Members in Acid Canyon (fig. 26). The liquid wastes are discharged from the plant in

Figure 26.--Sketch of Acid Canyon showing possible movement of water through joints in the Tshirege Member of the Bandelier Tuff and the location of a seep area in Acid Canyon at Site 15.

slugs and cause intermittent surface flow on the canyon floor for periods of as much as one hour. Between intermittent flows the floor of the canyon normally is dry between the treatment plant and the seep; flow in the canyon is perennial below the seep.

The only known source of water emerging in the seep area is the liquid waste discharged from the treatment plant. Study of the area indicates that liquid waste percolates through joints in the Tshirege Member to the top of the massive Otowi Member where it is perched and then moves laterally along the contact to the seep area.

Liquid may also be moving along the subsurface contact of the two members to other points of discharge which have not as yet been found. The attitude of the contact is unknown; if it is relatively level water could be moving underground in all directions from the point of recharge.

Perched water occurs also at the contact between the Guaje Member and the underlying Puye Conglomerate. Moisture measurements of samples from Sites 17 and 18 from two holes drilled through the Guaje into the Puye indicated that the contact between the units forms a perching surface for percolating water. At both sites holes were drilled in the streambed in small canyons tributary to Pueblo Canyon and several yards upstream from the contact between the two units of the tuff.

The moisture contents above and below the Guaje-Puye contact were significantly different at both sites (table 13). The 60.8 percent average moisture content in the Guaje at Site 17 probably represents saturation or near saturation and the 34.2 percent in the clayey top of the Puye probably represents about field capacity or less. Apparently water infiltrates slowly across the contact and ~~percolates through~~ infiltrates the Puye after field capacity or above is attained in the Guaje. At Site 18, where less water is available because of a small drainage area, the average moisture content in the Guaje was 30.6 percent, or about half that at Site 17. The moisture content of the Puye at Site 18 was correspondingly low.

Samples were collected at the base of and below a compacted silt layer about 13 feet thick in the upper part of the Puye Conglomerate, and which perches the stream in part of Pueblo Canyon (Site 19). Moisture content of the samples show that little or no water infiltrates the silt layer. The moisture content at the bottom of the silt layer was about 22 percent by volume; the moisture content of the sandy sediments immediately beneath the layer was about 12 percent by volume.

Table 12.--Moisture content, in percent by volume, near the contact of the Guaje Member of the Bandelier Tuff and the Puye Conglomerate at Sites 17 and 18.

Site No.	Distance above or below contact (feet)	Moisture content (in percent by volume)	Stratigraphic Unit
17	1-2	61.0	Guaje Member
	0-1	60.7	Guaje Member
	0-1	34.2	Puye Conglomerate
18	2-4	29.9	Guaje Member
	0-2	31.4	Guaje Member
	0-2	15.9	Puye Conglomerate
	2-4	17.1	Puye Conglomerate

Summary and conclusions

The Bandelier Tuff is divided into three members--the Guaje Member at the base, the Otowi Member in the middle, and the Tshirege Member on top. Vertical density gradients in the Tshirege Member are caused by changes in the physical properties of the tuff. The bulk specific density gravity of the Bandelier Tuff decreases slightly with depth and also from west to east across the Pajarito Plateau.

The porosity of the tuff ranged from about 20 percent to about 60 percent and the deviation from the mean at any particular study area was generally only a few percent. The higher porosity values are within the upper parts of the units and within the upper few feet of the sub-units. The porosity is inversely related to the dry unit weight; the dry unit weight near the base of the units and sub-units is relatively high and the porosity relatively low. The porosity is also inversely related to the moisture content at one-third atmosphere tension, which was found to be roughly the average field capacity of the tuff. Pore-size distribution curves show that about 20 to 25 percent of the total pore space transmits most of the water which moves through the tuff, and that the water in the smaller pores moves mostly by the slower processes of capillarity and diffusion, and contributes little to the bulk of the movement. The average permeability is low--about $\frac{1}{2}$ to 6 gallons per day per square foot.

Jointing is common throughout the Tshirege Member. They are narrow and filled with sediments for a few feet below the land surface, but are sediment-free at depth. Joints interconnected to depth in the Tshirege could provide paths for rapid downward movement of water. In places, the movement of water through joints would negate the effect that a bed of low permeability would have caused had water movement been only through pores in the tuff. Nuclides in water moving through open joints would have a relatively limited opportunity to be absorbed onto the tuff, as compared to nuclides in water that moved through the pores of the tuff.

The moisture content during percolation of water through parts of the tuff that contain few joints or density gradients was in the 25 to 35 percent range. This range is slightly above midway between field capacity and porosity of the tuff. Slight changes in the physical properties of the tuff apparently caused local areas to become nearly saturated, but generally the moisture content during percolation through the bulk of the tuff was substantially less than saturation. Beneath restricting layers, water continued to move in the lower moisture range. The temperature of the water, due to seasonal changes, apparently affected the rate of infiltration at the water-tuff interface. The rate of percolation exceeded the rate of infiltration when the water was near freezing.

The rate of percolation in dry soil decreased from about half a foot per day during the first day to less than a quarter of a foot per day during the third day. In a wetted soil the wetted front moved to a depth of almost 5 feet during 2 days of infiltration. The maximum moisture content after 99 days of infiltration was about 39 percent in the soil zone and decreased to less than 4 percent within a foot of the top of the underlying tuff. The rate of movement directly into dry tuff averaged about 2 feet per day during the first day, half a foot per day during the next 11 days, and about a tenth of a foot per day during the next 56 days.

Water movement was monitored by moisture meter readings to a depth of about 90 feet below a disposal pit. Water in the low moisture range apparently moved to depths greater than 90 feet. Water in unknown quantities moves through open joints or joints enlarged by solvents in the wastes.

Alternate wetting and drying of the tuff due to intermittent or 'slug' discharge of wastes may cause different patterns of uptake of ions than continuous discharge. After the tuff has once been wetted and drained, the moisture content remains in the 10 to 20 percent range for a period of several months due to hysteresis, much of the movement being in the lower moisture range. Subsequent movement of water through the tuff is more rapid because the tuff is already wetted and an energy barrier is not created at the wetted front.

The effective and total porosity, pores sizes, pore size distribution, and the particle size each affect the movement of water in the Bandelier Tuff. Their individual and collective effects can be evaluated relative to various standard methods of studying water movement in a porous material, such as moisture content, tensions at different specific conductance and specific yield, and permeability. The water retention and water transmission properties of the tuff are functions of the porosity and the percent of large pore spaces, which in turn are related to the dry unit weight and particle size distribution.

Most of the gross alpha activity found beneath an infiltration pit was ~~[was obtained]~~ within tuff a short distance beneath the ~~[of the infiltration]~~ pit. Below a depth of about 15 to 20 feet the alpha activity was low, except for local areas of high alpha activity where water carried the activity along joints. Rapid movement of water through joints was substantiated during infiltration studies. The relationship between gross alpha activity and the pH of the solution was inverse. Total hardness and total solids increased with depth, suggesting solution and resolution of previously deposited materials.

Selected references

Abrahams, J. H., Jr., Weir, J. E., Jr., and Purtymun, W. D., 1961, Distribution of moisture in soil and near-surface tuff on the Pajarito Plateau, Los Alamos County, N. Mex.: U.S. Geol. Survey Prof. Paper 424-D, p. 142-145.

Abrahams, J. H., Jr., 1962, Movement of water and radionuclides in a tile field waste-disposal system at Jackass Flats, Nevada Test Site: construction and preliminar test, June 1958 through August 1959: in review.

Baltz, E. H., Abrahams, J. H., Jr., and Purtymun, W. D., 1962 Preliminary report on the geology and hydrology of Mortandad Canyon near Los Alamos, N. Mex., with reference to disposal of liquid, low level radioactive waste: in review.

Baver, L. D., 1956, Soil Physics: John Wiley and Sons, Inc., New York.

Bodman, G. B., and Coleman, E. A., 1944, Moisture and energy conditions during downward entry of water into soils: Soil Sci. Soc. America, v. 8, p. 116-122

Christenson, C. W., and Thomas, R. G., 1962, Paper presented at the Second Conference on Ground Disposal of Radioactive waste, Chalk River, Ontario, Sept. 26-29, 1961.

Coleman, E. A., 1947, A laboratory procedure for determining the field capacity of soils: Soil Sci., v. 63, p. 277-283.

Selected references - Continued

Free, G. R., and Palmer, V. J., 1941, Interrelationship of infiltration air movement, and pore-size distribution in graded silica sand: Soil Sci. Soc. America Proc., v. 5, p. 390-399.

Griggs, R. L., 196-, Geology and ground-water resources of the Los Alamos area, New Mexico: U.S. Geol. Survey, WSP 1753, in press.

Horton, R. E., 1940, An approach toward a physical interpretation of infiltration-capacity: Soil Sci. Soc. America Proc., v. 5, p. 399-417

Kemper, W. D., 1961 Movement of water as effected by free energy and pressure gradients: I. Application of classic equations and viscous and diffusive movements of the liquid phase in finely porous media: Soil Sci. Soc. America Proc., v. 25, no. 4, p. 255-260.

Krone, R. B., Ludwig, H. F., and Thomas, J. F., 1951, Porous tube devices for sampling soil solutions during water-spreading operations: Soil Sci., v. 73, No. 5, p. 211-219.

Lutz, J. F., and Leamer, R. W., 1940, Pore-size distribution as related to the permeability of soils: Soil Sci. Soc. America Proc., v. 4, p. 28-31.

Lyon, T. L., and Buckman, H. O., 1948, The nature and property of soils: The Macmillan Co., New York.

Selected references - Continued

Marshall, T. J., 1958, A relation between permeability and size distribution of pores: Jour. Soil Sci., v. 9, no. 1, p. 1-8.

Mavis, F. T., and Wilsey, E. F., 1936, A study of the permeability of sand: Bull. 7, University of Iowa, studies in Engineering, Iowa City, Iowa.

Miller, E. E., and Miller, R. D., 1956, Physical theory for capillary flow phenomena: Jour. Appl. Research, v. 27, no. 4, p. 324-332.

Nelson, W. R., and Baver, L. D., 1940, Movement of water through soils in relation to the nature of the pores: Soil Sci. Soc. America Proc., v. 5, p. 69-76.

Puri, A. H., 1949, Soils, their physics and chemistry: Reinhold distribution Corp., New York.

Smith, R. M., Browning, D. R., and Pohlman, G. G., 1944, Laboratory percolation through undisturbed soil samples in relation to pore-size distribution: Soil Sci., v. 57, no. 3, p. 197-213.

Snedecor, G. W., 1946, Statistical methods: The Iowa State College Press, Ames, Iowa.

Spiegel, Zane, and Baldwin, Brewster, 196-, Geology and water resources of the Santa Fe area, New Mexico: U.S. Geol. Survey Water-Supply Paper 1525, in press.

Van Bavel, C. H. M., Nielson, D. R., and Davidson, J. M., 1961, Calibration and characteristics of two neutron moisture probes: Soil Sci. Soc. America Proc., v. 25, no. 5, p. 329-334.

Selected references - Continued

Veimeyer, F. J., and Hendrickson, S., 1931, The moisture equivalent as a measure of the field capacity of soils: Soil Sci., v. 32, p. 181-193.

Waldon, L. J., McMurdie, J. L., and Vomocil, J. A., 1961, Water retention by capillary forces in an ideal soil; Soil Sci. Soc. America Proc., v. 25, no. 4, p. 265-267.

Weir, J. E., and Purtyman, W. D., 1962, Geology and hydrology of Technical Area 49, Frijoles Mesa, Los Alamos County, N. Mex.: U.S. Geol. Survey, in preparation.

Willis, W. O., 1960, Evaporation from layered soils in the presence of a water table: Soil Sci. Soc. America Proc., v. 24, no. 4, p. 239-243.

Youngs, E. G., 1960, The drainage of liquids from porous materials: Jour. Geophysical Research, v. 65, no. 12, p. 4025-4030.

GJ-37

VADOSE ZONE CHARACTERIZATION OF TECHNICAL AREA 54, WASTE DISPOSAL AREAS G AND L, LOS ALAMOS NATIONAL LABORATORY, NEW MEXICO

REPORT 1: DRILLING AND LOGGING ACTIVITIES

September 1985

Bendix Field Engineering Corporation
Grand Junction, Colorado

ALLIED Bendix Aerospace

This report was prepared as an account of work sponsored by an agency of the United States Government. Neither the United States Government nor any agency thereof, nor any of their employees, makes any warranty, express or implied, or assumes any legal liability or responsibility for the accuracy, completeness, or usefulness of any information, apparatus, product, or process disclosed in this report, or represents that its use would not infringe privately owned rights. Reference therein to any specific commercial product, process, or service by trade name, trademark, manufacturer, or otherwise, does not necessarily constitute or imply its endorsement, recommendation, or favoring by the United States Government or any agency thereof. The views and opinions of authors expressed herein do not necessarily state or reflect those of the United States Government or any agency thereof.

This report is a result of work performed by Bendix Field Engineering Corporation, Operating Contractor for the U.S. Department of Energy, Grand Junction Projects Office.

GJ-37

VADOSE ZONE CHARACTERIZATION OF TECHNICAL AREA 54, WASTE DISPOSAL AREAS G AND L, LOS ALAMOS NATIONAL LABORATORY, NEW MEXICO

REPORT 1: DRILLING AND LOGGING ACTIVITIES

Susan M. Rush and James J. Dexter

Bendix Field Engineering Corporation
Grand Junction Operations

September 1985

Prepared for
U.S. Department of Energy
Los Alamos National Laboratory
Los Alamos, New Mexico
in Conjunction with
U.S. Department of Energy
Grand Junction Projects Office
Grand Junction, Colorado
Under Contract No. DE-AC07-76GJ01664

CONTENTS LISTING

	Page
Foreword	v
Introduction	1
Background	1
Location	1
History of Waste Disposal Activity	1
Geologic Setting	3
Drilling and Sampling	3
Procedures	3
Results	5
Lithologic Logging	6
Procedures	6
Results	6
Geophysical Logging	34
Spectral Gamma and 3-Arm Caliper Logs	34
Natural Gamma, Epithermal Neutron, and Vertical Deviation Logs	35
Magnetic Susceptibility Logs	36
Moisture Logs	37
Gamma-Gamma Density, Natural Gamma, and 1-Arm Caliper Logs	37
Acknowledgements	38
References	38

LIST OF FIGURES

Figure 1.	Locations of Drill Holes in Areas G and L, Technical Area 54, Los Alamos National Laboratory, New Mexico	2
2.	Lithologic Log of Hole LLM-85-01	9
3.	Lithologic Log of Hole LLM-85-02	11
4.	Lithologic Log of Hole LLP-85-03	13
5.	Lithologic Log of Hole LLM-85-05	15
6.	Lithologic Log of Hole LGM-85-06	17
7.	Lithologic Log of Hole LGP-85-07	19
8.	Lithologic Log of Hole LGC-85-09	20
9.	Lithologic Log of Hole LGC-85-10	21
10.	Lithologic Log of Hole LGM-85-11	23
11.	Lithologic Log of Hole LLC-85-12	25
12.	Lithologic Log of Hole LLC-85-13	26
13.	Lithologic Log of Hole LLC-85-14	27
14.	Lithologic Log of Hole LLC-85-15	28
15.	Lithologic Log of Hole LLC-85-16	29
16.	Lithologic Log of Hole LLC-85-17	31
17.	Lithologic Log of Hole LLC-85-18	33

LIST OF TABLES

Page

Table 1. Total Depths of Core, Drill Hole, and Logging Activity for Los Alamos Drill Holes. 5

ATTACHMENTS

Geophysical logs for the Los Alamos drill holes are contained in 18 envelopes attached to this report, one envelope per hole labeled with the hole number.

FOREWORD

This report is the first of two interim reports, to be prepared prior to issuance of the final comprehensive characterization of the vadose zone in Areas G and L, Technical Area 54, Los Alamos National Laboratory, New Mexico. The second interim report is scheduled for completion in November of this year, with the final report due early in 1986.

In addition to the authors cited on the title page, a number of professionals of Bendix Field Engineering Corporation/Grand Junction Operations contributed significantly to the drilling and logging activities described in this report. These individuals and their respective contributions to this multidisciplinary effort are listed below.

- Sue Knutson and Dave Traub, Geophysical Loggers, who logged all of the drill holes and prepared most of the Bendix-generated geophysical logs.
- Sam Marutzky, Geophysical Engineer, who prepared the moisture logs from the epithermal neutron logging data.
- Jack McCaslin, Drilling Supervisor, who supervised drilling activities at Los Alamos.
- Steve Sturm, Geologist, who prepared many of the lithologic logs.
- Sandy Wagner, Chemist, who supervised monitoring of chemical hazards in the field.

INTRODUCTION

This report presents preliminary lithologic and geophysical data for Waste Disposal Areas G and L, located in Technical Area 54 at Los Alamos National Laboratory (LANL), New Mexico. These data, obtained via drilling and logging operations, will be used to aid in characterizing the vadose zone in Areas G and L. The study is being conducted by Bendix Field Engineering Corporation/ Grand Junction Operations (Bendix) in accord with a Statement of Work prepared by LANL, in response to a Resource Conservation and Recovery Act (RCRA) compliance order issued in May 1985 by the State of New Mexico.

The overall objective of this study of Areas G and L is twofold: to characterize the hydrology of the vadose zone at the site and to evaluate the potential for contaminant migration from these two waste-disposal areas, both of which are still actively used. Initial field activities for this study consisted of drilling and logging conducted over the period 30 July to 22 August 1985. The resulting lithologic and geophysical logs were completed on 13 September 1985. Due to the time constraints imposed on this first report, its scope is limited to a summary of these initial activities and presentation of the preliminary data with very little interpretation. A thorough interpretation of these data, including their integration with other results, will be presented in the comprehensive final report on this study, scheduled for completion early in 1986.

BACKGROUND

LOCATION

Drilling and logging activities took place in and around Waste Disposal Areas G and L in Technical Area 54 at the facilities of Los Alamos National Laboratory in Los Alamos County, New Mexico. Figure 1 shows the approximate locations of the drill holes. Areas G and L are located on Mesita del Buey, a narrow southeast-trending mesa which forms part of the large Pajarito Plateau in north-central New Mexico. Elevations of Mesita del Buey range from approximately 6600 to 6900 feet above sea level from the southeast to the northwest.

HISTORY OF WASTE DISPOSAL ACTIVITY

This summary of historical waste-disposal activity in Areas G and L was compiled from information presented in the Final Environmental Impact Statement on Los Alamos National Laboratory (U.S. Department of Energy, 1979).

Area G has been used since 1957 for the routine disposal in pits and shafts of laboratory-generated radioactive waste. Pits in Area G contain both contaminated trash-type waste and americium-241, the latter occurring in association with plutonium in drums of cement paste buried prior to 1967. In addition, through 1963, tritium wastes were routinely disposed of in pits. Even after the initiation of shaft disposal in 1963, a few instances of tritium-waste disposal in pits occurred up until 1967. Materials buried in shafts include tritium waste, scintillation vials, oils, high beta-gamma radioactive wastes, animal tissue, classified waste, and many other contaminated chemical wastes. Finally, solid waste contaminated with transuranic radionuclides at activity

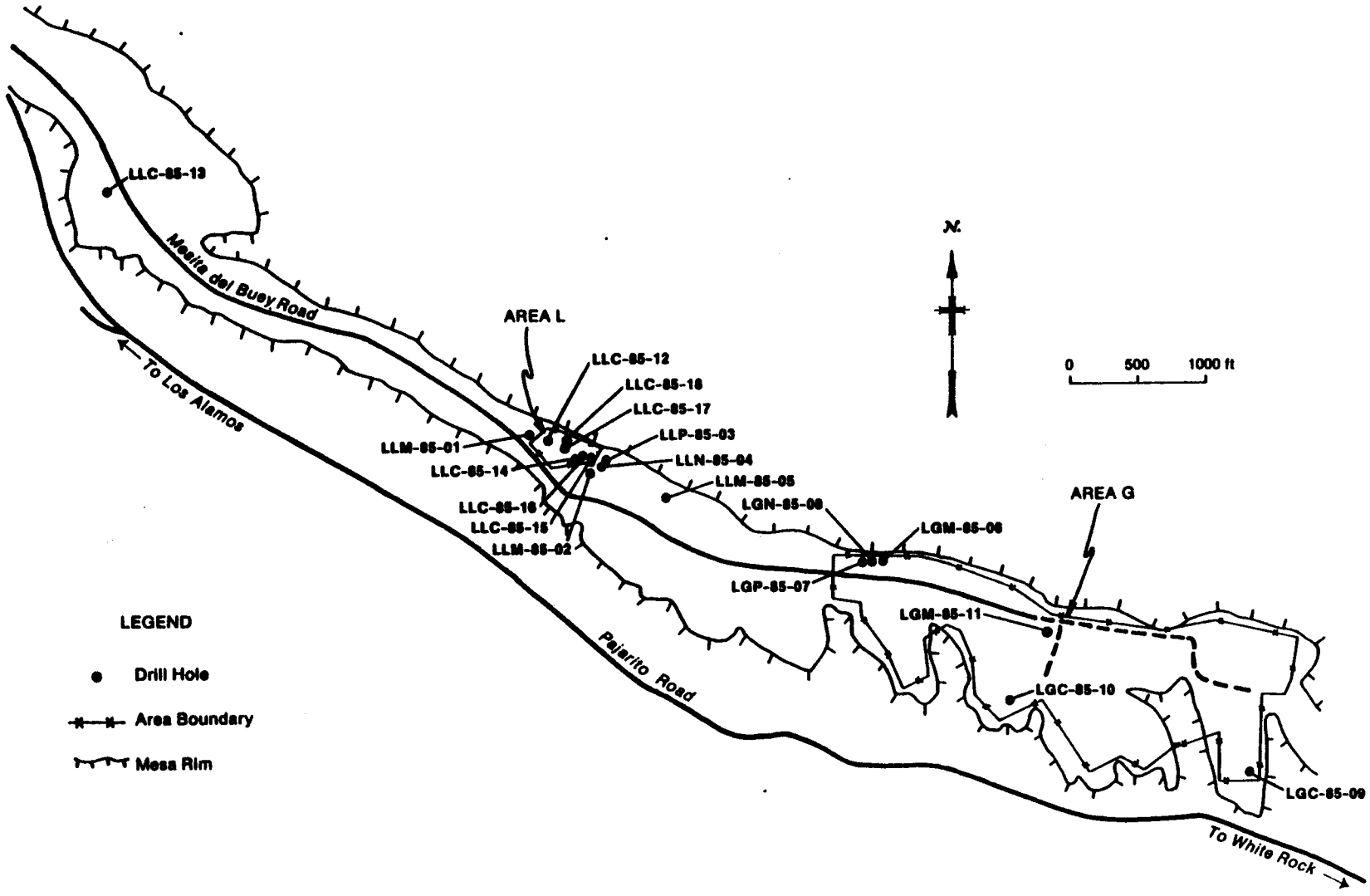

Figure 1. Locations of Drill Holes in Areas G and L, Technical Area 54, Los Alamos National Laboratory, New Mexico

levels greater than 10 nanocuries per gram of waste have been packaged and placed in 20-year retrievable storage in Area G since 1971, in accord with U.S. Department of Energy (DOE) regulations.

Area L is used for the disposal of hazardous wastes, including acids, bases, inorganic and organic solids and liquids, and reactive metals. The wastes have been disposed of by chemical type in deep shafts and shallow trenches. Separate shafts have also been used for burial of gas cylinders and drums containing bulk waste and solvents. Finally, bulk organic salts were previously disposed of in two separate shallow trenches. To date, no details are available regarding the actual composition of these wastes due to the lack of documentation of early waste-disposal practices.

GEOLOGIC SETTING

Mesita del Buey is underlain by rhyolitic ash-flow and airfall deposits of the Bandelier Tuff, which caps the regional topographic high known as the Pajarito Plateau (Purtymun and Kennedy, 1971). The Bandelier Tuff was derived from volcanism in the Jemez Mountains during the Pleistocene. This is the primary formation of interest because the LANL facilities are built on, and all waste-disposal pits, shafts, and trenches have been excavated in, the Bandelier Tuff.

The Bandelier Tuff is composed of two members: the lower Otowi Member, 1.4 million years old, and the upper Tshirege Member, 1.1 million years old (Bailey and others, 1969). The Otowi Member consists of a basal airfall pumice overlain by nonwelded ash-flow deposits containing abundant lithic fragments; it ranges in thickness in the Los Alamos area from 0 to 265 feet (Abeele and others, 1981). The upper Tshirege Member consists of a basal bedded airfall pumice overlain by nonwelded to welded ash flows containing abundant pumice and lithic fragments (Abeele and others, 1981). Only the Tshirege Member of the Bandelier Tuff has been penetrated by waste-disposal excavations in Technical Area 54.

The Tshirege Member can be subdivided into three units, two of which occur at Mesita del Buey (Purtymun and Kennedy, 1971). The characteristics used to distinguish these units and subunits are discussed in a subsequent section of this report (see Lithologic Logging).

DRILLING AND SAMPLING

PROCEDURES

All drilling for this study was accomplished using a Central Mining Equipment (CME) Model 55 drill rig equipped with hollow-stem augers and a continuous sampling system. In 16 of the 18 drill holes, continuous core was obtained using a 5-foot-long split-barrel sampler attached to the center drill stem of standard 6-5/8-inch-O.D. hollow-stem augers. Standard 4-inch-O.D. solid-stem augers were used to bore the two drill holes where no core recovery was desired (Holes LLN-85-04 and LGN-85-08). All drill holes were initially sampled or augered to a depth of approximately 4 feet. A 4-foot length of 8-inch-O.D. casing was then cemented in place and allowed to set overnight before drilling proceeded.

Core was obtained in 5-foot intervals, and those samples selected for gravimetric analysis were transferred to sealed containers immediately following retrieval. The rest of the cores were placed in labeled boxes. As soon as possible thereafter, samples were selected for analysis of Extraction Procedure (EP) toxicity and volatile organics. These samples were immediately placed in labeled containers, and the appropriate documentation completed, in accord with established procedures (Bendix Field Engineering Corporation, 1985a). Once the samples from a given interval had been selected, a lithologic log was prepared, also in accord with established procedures (Bendix Field Engineering Corporation, 1985a).

After each hole was cored to ~~the desired depth~~ 100 ft, the continuous sampling system was removed from the center drill stem and replaced with the standard center drill bit. The hole was then extended, in most cases approximately 20 feet below the desired final hole depth. The center drill stem and auger flights were then removed from the hole and the cuttings dropped downhole, filling the hole to the approximate desired total depth. The total depth of all holes is greater than 100ft. The average diameter was 7¼ inches, diameter of from the 3-arm [illegible]

Equipment was decontaminated between drill holes using the following procedures. For drill holes in and around Area L, the auger flights, center drill stem, and continuous sampler were steam-cleaned, then rinsed in methanol and allowed to dry in successive cattle tanks provided by LANL. For drill holes in Area G, all equipment was first monitored for radioactive contamination by LANL personnel (none was discovered); then the downhole equipment was decontaminated using the same procedure as above.

During all drilling activities, cuttings brought to the surface by the auger flights were immediately placed in 55-gallon drums to minimize the potential for adverse health effects occurring as a result of contaminated cuttings. In addition, as each 5-foot core interval was removed from a hole, measurements were taken at the hole and in the driller's breathing zone using an Organic Vapor Meter (OVM) and an Explosimeter, in accord with established procedures (Bendix Field Engineering Corporation, 1985b). Examination of the results indicated that no respiratory protection was needed.

The hole-numbering scheme is based primarily on the purpose for each hole and the drilling sequence (cf. Figure 1). The first letter, L, refers to Los Alamos. The second letter (G or L) identifies the waste-disposal area in or around which the hole is located. The third letter indicates the purpose for the hole, assigned according to the following designations:

- <u>M: Moisture Holes</u> - To be used to determine intrinsic permeability and hydraulic conductivity of the tuff.

- <u>C: Core and Pore-Gas Sampling Holes</u> - To be used to collect samples for EP-toxicity and volatile-organic analyses, and for the installation of pore-gas-sampling apparatus.

- <u>P: Psychrometer Holes</u> - To be used for the installation of thermocouple psychrometers and pressure transducers to determine local moisture conditions, temperature, and pressure.

- <u>N: Neutron Moisture Access Holes</u> - To be used by LANL for moisture measurements.

The middle designation, 85, indicates the year (1985) that these holes were drilled. The final two digits refer to drilling sequence.

RESULTS

Eighteen holes were drilled for a total footage of approximately 2190. Core totaling 1709 feet was collected from 16 drill holes. Of that total, 244 feet comprised samples for gravimetric, EP-toxicity, volatile-organic, moisture-characteristic, and petrologic analyses. The depth interval corresponding to each sample is indicated on the lithologic logs (see succeeding section). The core not preserved as samples from Hole LLC-85-18 was discarded; all other core was retained in core boxes.

Table 1 cites the total depth cored and total depth drilled in each hole, together with the maximum depths recorded during geophysical logging. The latter activity was accomplished by Bendix and by Century Geophysical Corporation using a total of four different probes (see subsequent discussion on Geophysical Logging). As the data indicate, total depths recorded during logging vary, largely because of the potential for the probes to sink into the loose cuttings at the base of the hole and the possibility of slight cave-in of the hole wall caused by the cable or the probes themselves.

Table 1. Total Depths of Core, Drill Hole, and Logging Activity for Los Alamos Drill Holes (depths in feet)

Drill-Hole Number	Total Depth Cored	Total Depth Drilled	Maximum Depth Measured During Logging	
			Bendix	Century Geophysical
LLM-85-01	124	140	121	116
LLM-85-02	124	145	126	125
LLP-85-03	99	120	97	97
LLN-85-04[a]	0	120	116	---
LLM-85-05	124	145	124	122
LGM-85-06 ok	124	145	127	121
LGP-85-07 LGP-08	49	60	53	53
LGN-85-08[a] LGN-07	0	60	54	---
LGC-85-09	99	120	106	107
LGC-85-10	99	120	109	108
LGM-85-11	124	145	130	126
LLC-85-12	99	120	106	108
LLC-85-13 (Bkgd)	99	120	113	116
LLC-85-14	99	120	112	112
LLC-85-15	99	120	115	119
LLC-85-16	99	120	117	119
LLC-85-17	149	150	140	140
LLC-85-18	99	120	105	107

[a]This hole was augered with a 4-inch-O.D. solid-stem auger.

Core recovery was 100 percent in 15 of the 16 cored drill holes, the exception being Hole LLC-85-18 which had 95 percent core recovery. Despite the poorly consolidated nature of the tuff, most of the core retrieved was in excellent condition. Core quality was governed by drilling speed and the physical condition of the shoe at the base of the continuous sampler. The sampler shoe was replaced several times in the course of drilling to maintain core quality.

LITHOLOGIC LOGGING

PROCEDURES

A lithologic log was prepared in accord with established field procedures (Bendix Field Engineering Corporation, 1985a) for each of the 16 holes cored with the continuous sampling system. These logs are presented in chronological order by hole number as Figures 2 through 17. The colors used to describe the core matrices are taken from the Rock Color Chart of Goddard and others (1975); the code in parentheses following a color description corresponds to the chart.

Also indicated on the logs are the numbers and depth intervals for samples collected for subsequent field or laboratory analysis. Samples identified by the three-letter prefix MCG- followed solely by a three-digit number were collected for gravimetric analysis. Those MCG-numbered samples denoted by a single asterisk (*) were collected for petrologic analysis, and those denoted by a double asterisk (**) were collected for laboratory analysis of moisture characteristics. Samples identified with the number 85 followed by a decimal point and five additional digits were collected for EP-toxicity and volatile-organic analyses by LANL; splits of these samples are identified by the addition of the letter A immediately following the sample number.

RESULTS

As previously mentioned, two of the three units of the Tshirege Member of the Bandelier Tuff underlie Mesita del Buey. These units dip 2 to 3 degrees to the southeast and become thinner in the direction of dip, away from their source in the Valles Caldera. Each of the units consists of two subunits which are described by Purtymun and Kennedy (1971). Their descriptions, together with characteristics observed in the actual core collected for this study, were used to distinguish between each of the subunits.

The lowermost subunit of the Tshirege Member encountered during this drilling program is Unit 1a, a nonwelded, light-orange to light-brown ash-flow tuff. The maximum thickness of Unit 1a encountered in the Los Alamos drill holes was 26 feet; no drill hole penetrated the entire unit. At Mesita del Buey, Unit 1a consists of very uniform, nonwelded, devitrified ash with numerous but scattered lumps of light-tan pumice lapilli and latitic to rhyolitic lithic lapilli.

The contact between Units 1a and 1b was discerned in the core on the basis of the increased degree of welding and the presence of brown and gray pumice lapilli in Unit 1b. The basal portion of Unit 1b contains distinctive, gold-colored, bipyramidal quartz crystals up to 4 mm in diameter and a bimodal

distribution of lithic lapilli. The lithic lapilli are abundant in the size range 1 to 4 mm in diameter, and occur less commonly in the size range 15 to 60 mm. They decrease in size and abundance toward the top of Unit 1b, where the occurrence of lithic lapilli is rare. The degree of welding in Unit 1b generally varies from non- to slightly welded at the base to moderately welded just above the base to slightly welded at the top. In four core holes where the entire section of Unit 1b was penetrated, the total thickness varies from approximately 29 to 52 feet.

The contact between Units 1b and 2a is transitional and therefore difficult to precisely identify in the core. In certain cases, the contact can be estimated on the basis of either a subtle color change in a non- to slightly welded portion of the core or the presence of brown, gray, and olive-colored pumice lapilli in the basal portion of Unit 2a. These pumice lapilli are generally larger than the predominantly brown pumice lapilli found in the upper portion of Unit 1b. In addition, the contact generally occurs in a zone where vapor-phase crystals of quartz and sanadine are small in size (less than 1 mm in diameter) and number. The contact between Units 1b and 2a may be more accurately defined when petrologic analyses of rock samples have been completed.

Unit 2a is an ash-flow tuff ranging in color from light pink to pale red to gray, and containing relatively large (5 to 30 mm) gray, brown, and olive pumice lapilli. Generally, Unit 2a varies from nonwelded at the base to moderately welded in the center to slightly to moderately welded at the top. At Mesita del Buey, however, this variation is not consistent from drill hole to drill hole. Unit 2a becomes thinner toward the southeast, as evidenced by a thickness exceeding 54 feet in the northwesternmost drill hole (LLC-85-13), to one averaging 40 feet in and around Area L, to one averaging 21 feet in Area G.

The contact between Units 2a and 2b is generally marked by a subtle color change within a non- to slightly welded zone of tuff. Purtymun and Kennedy (1971) identify this contact on the basis of the occurrence of thin, lenticular deposits of reworked tuff. However, this zone of reworked tuff was not observed in core collected during this drilling program. Moreover, the transition from Unit 2a to Unit 2b at Mesita del Buey appears to be marked by a decrease in the size and variety of pumice lapilli occurring in the basal portion of Unit 2b.

Unit 2b forms the cap rock at Mesita del Buey and consists of brownish-gray, light-gray, and pinkish-gray, slightly to moderately welded ash-flow tuff with light-gray and occasional brown pumice lapilli. Unit 2b comprises two flows that cooled as a single unit (Purtymun and Kennedy, 1971). The two flows can be distinguished on the basis of a color change, an increase in the abundance of pumice lapilli, or the occurrence of a thin deposit of reworked tuff between the two flows. The maximum and minimum thicknesses of Unit 2b encountered in the Los Alamos drill holes was 45 feet in the northwesternmost hole (LLC-85-13) and 28 feet in the southeasternmost hole (LGC-85-09), respectively.

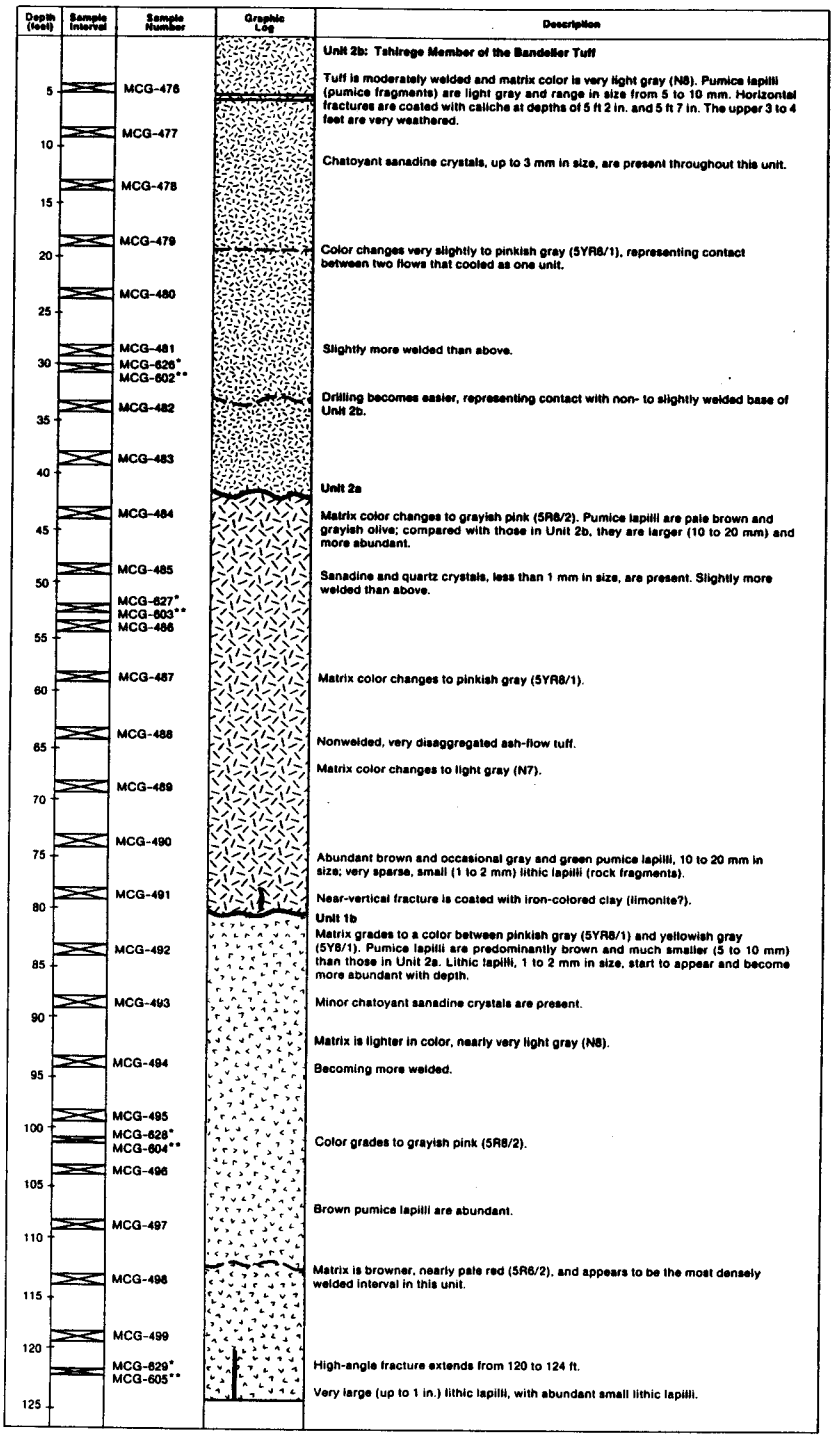

Figure 2. Lithologic Log of Hole LLM-85-01

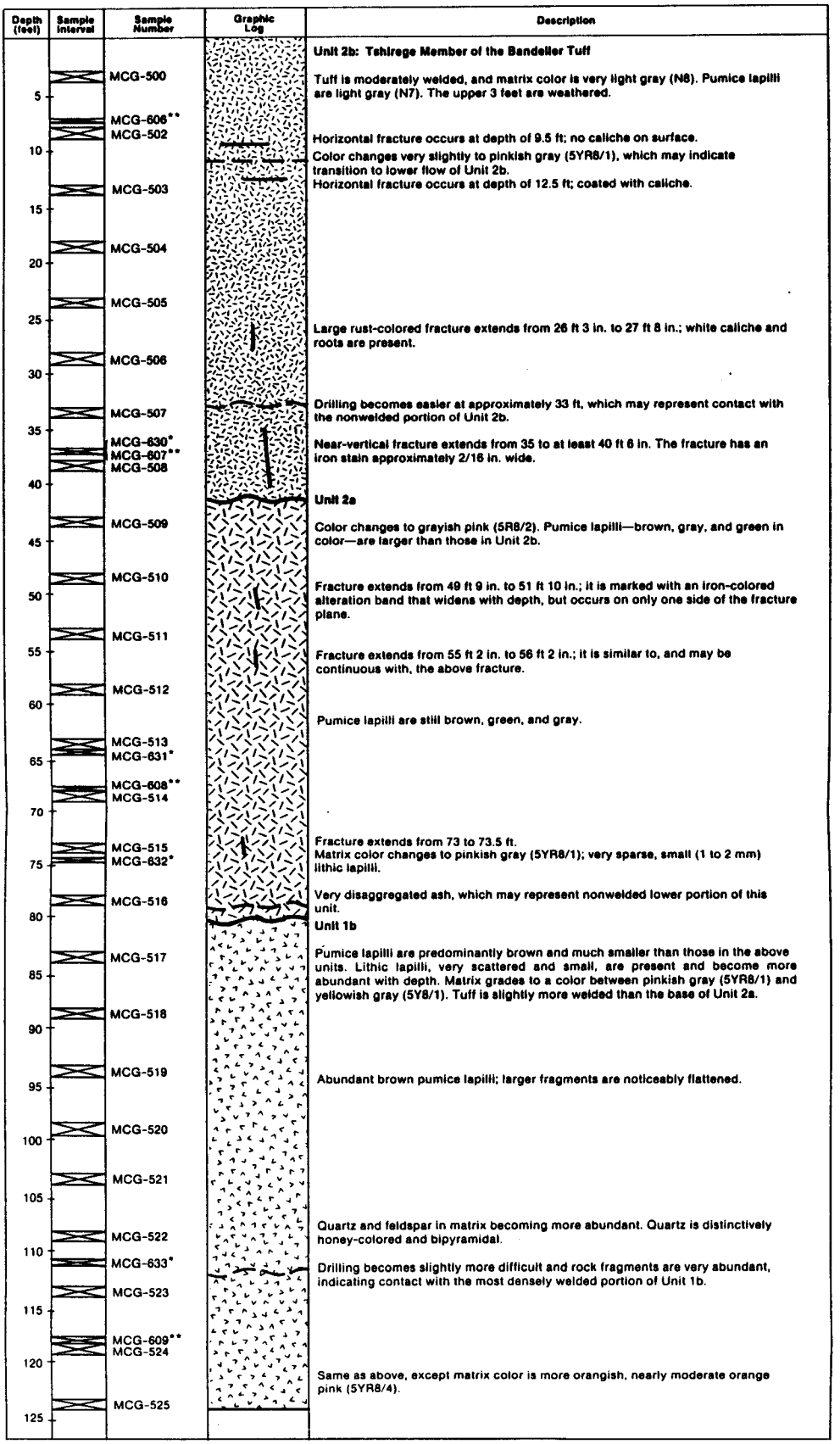

Figure 3. Lithologic Log of Hole LLM-85-02

Depth (feet)	Sample Interval	Sample Number	Graphic Log	Description
				Unit 2b: Tshirege Member of the Bandelier Tuff
				Tuff is more friable than that in Hole LLM-85-02. Matrix color is light gray (N7).
5				Horizontal fracture occurs at depth of 5 ft 10 in.; coated with caliche.
				Abundant quartz and sanadine crystals occur throughout this unit.
10				Matrix color changes slightly to pinkish gray (5YR8/1), which may represent the contact between two flows that cooled as a single unit.
15				
20				Drilling becomes easier at depth of approximately 20 ft.
				Gradational contact with lower, nonwelded portion of Unit 2b.
25				
				Matrix becomes slightly pinker, to grayish pink (5R8/2).
30				High-angle (nearly 90 degrees) fractures extend from 30 ft 8 in. to 31 ft 2 in., from 31 ft 8 in. to 32 ft 8 in., from 35 to 37 ft, and from 39.5 to 40 ft. All four are heavily stained with limonite. There appears to be a horizontal fracture lying between the upper two high-angle fractures.
35				
40				
				Unit 2a
45				Matrix becomes darker—to pale red (5R6/2)—at depth of 42 to 43 ft. Pumice lapilli are abundant, some longer than the core and appearing quite flattened. Occasional pumice lapilli are greenish (10Y4/2 to 10Y5/4).
50				
55				Small high-angle fracture occurs at depth of approximately 56 ft.
60				Pumice lapilli become more abundant and predominantly brown in color, but occasional gray and green fragments were observed.
65				
70				Some relatively large olive or greenish-colored pumice lapilli are still present. Very sparse, small (1 to 2 mm) lithic lapilli are also present.
75				**Unit 1b**
				Matrix changes to a color between light gray (N7) and yellowish gray (5Y8/1). Pumice lapilli are much smaller and predominantly brown.
80				
85				Minor amounts of quartz and sanadine crystals are present.
90				Drilling becomes very easy, indicative of nonwelded tuff.
				Quartz crystals become more abundant, but only traces of chatoyant sanadine occur in pumice lapilli.
95				Brown pumice lapilli are abundant and very flattened.
100				

Figure 4. Lithologic Log of Hole LLP-85-03

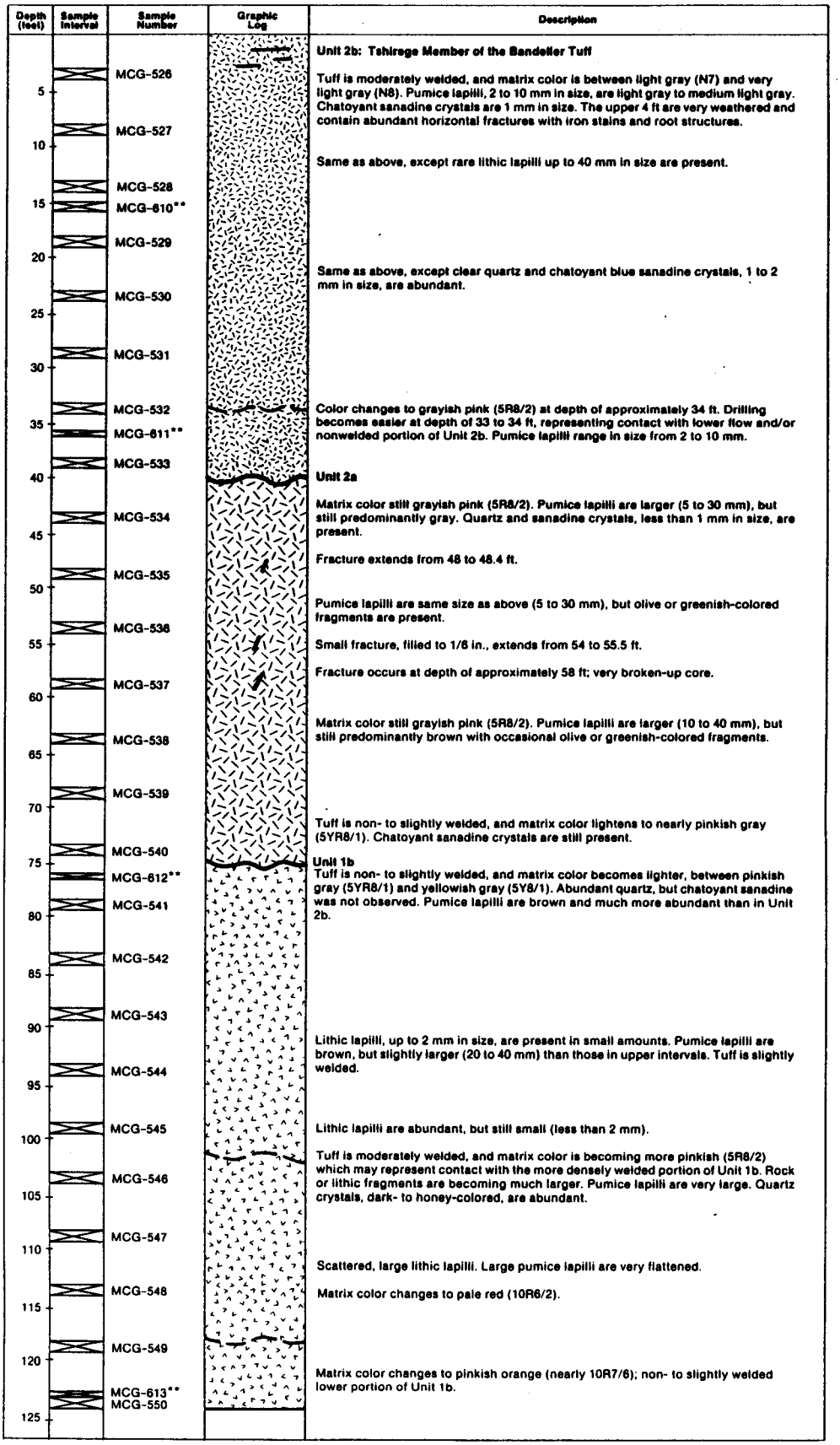

Figure 5. Lithologic Log of Hole LLM-85-05

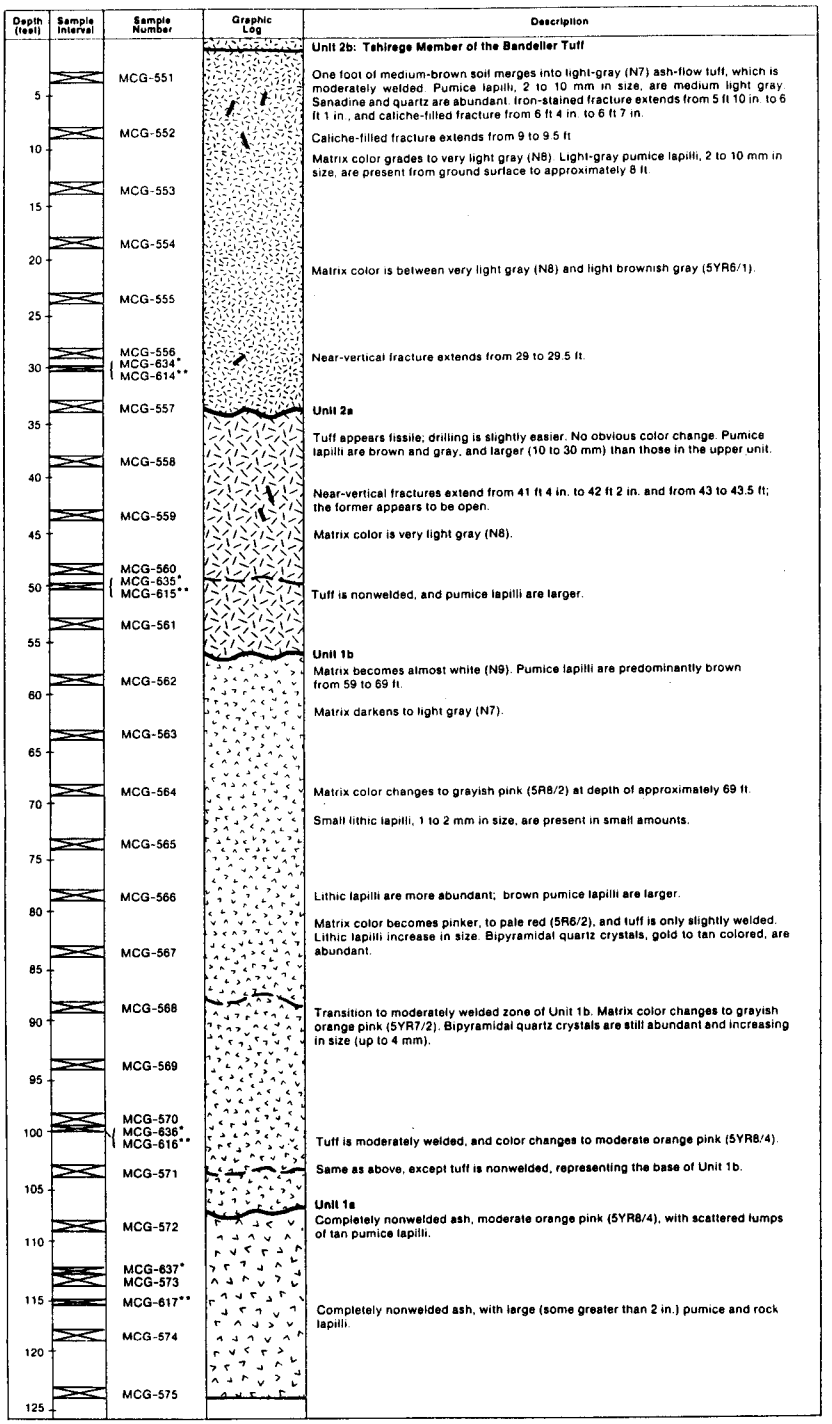

Figure 6. Lithologic Log of Hole LGM-85-06

Depth (feet)	Sample Interval	Sample Number	Graphic Log	Description
			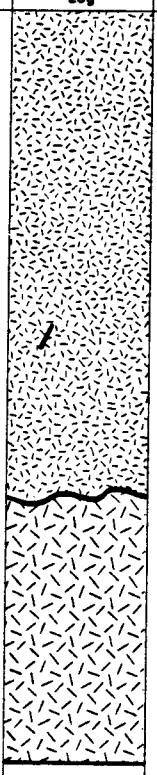	**Unit 2b: Tshirege Member of the Bandelier Tuff** Soil consisting of weathered tuff extends from ground surface to 5 ft, and contains scattered root material. Matrix color is between very light gray (N8) and light gray (N7). Pumice lapilli, 5 to 10 mm in size, are light gray. Tuff is moderately welded. Chatoyant sanadine and quartz crystals are abundant. Near-vertical, noncoated fracture (?), possibly open, extends from 21 ft 7 in. to 22 ft 1 in. **Unit 2a** Tuff appears fissile and less welded; drilling is easier. Matrix color is between light gray (N7) and very light brownish gray (5YR7/1). Pumice lapilli are larger (10 to 20 mm) and predominantly brown. Matrix color darkens to medium-light gray (N6).
5				
10				
15				
20				
25				
30				
35				
40				
45				
50				

Figure 7. Lithologic Log of Hole LGP-85-07

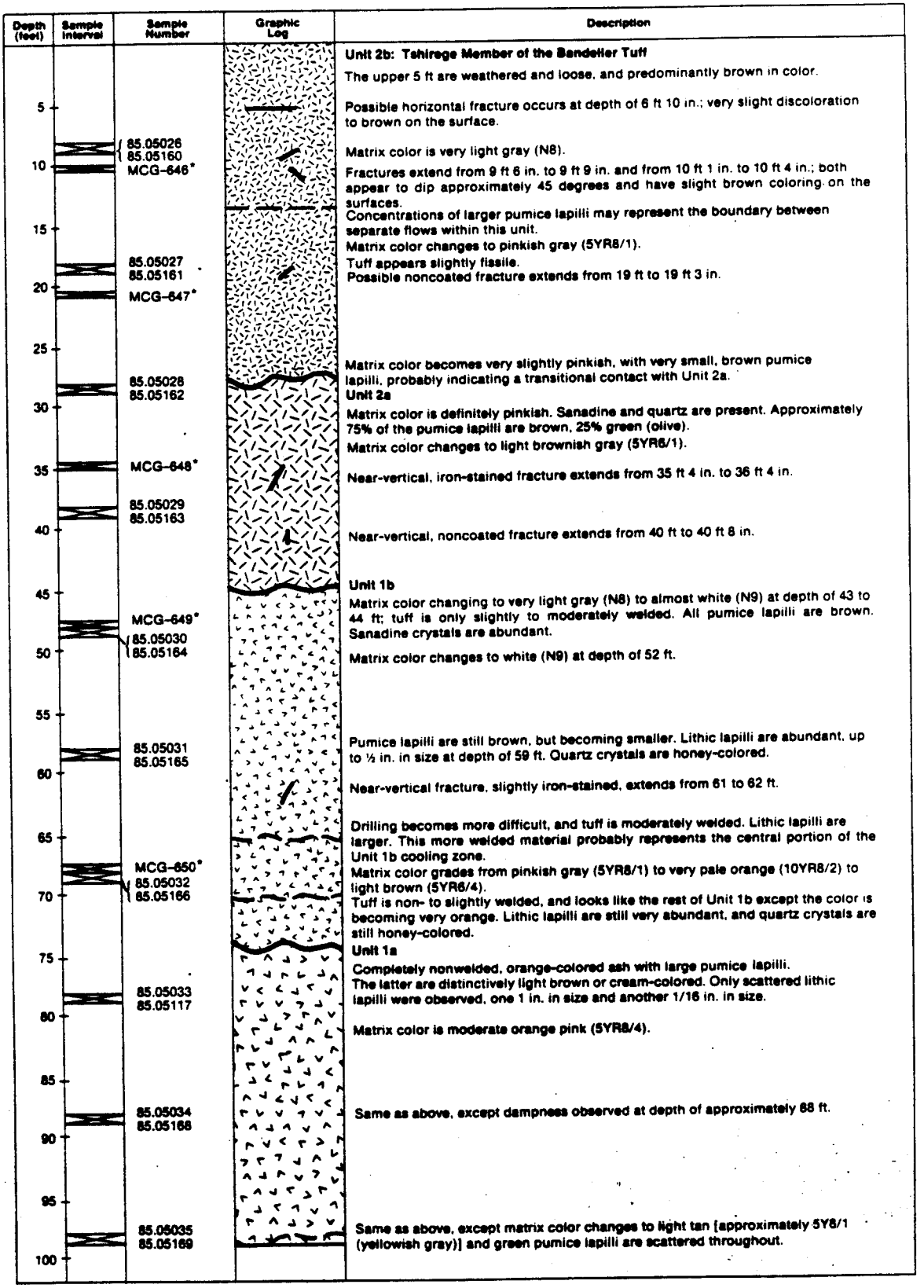

Figure 8. Lithologic Log of Hole LGC-85-09

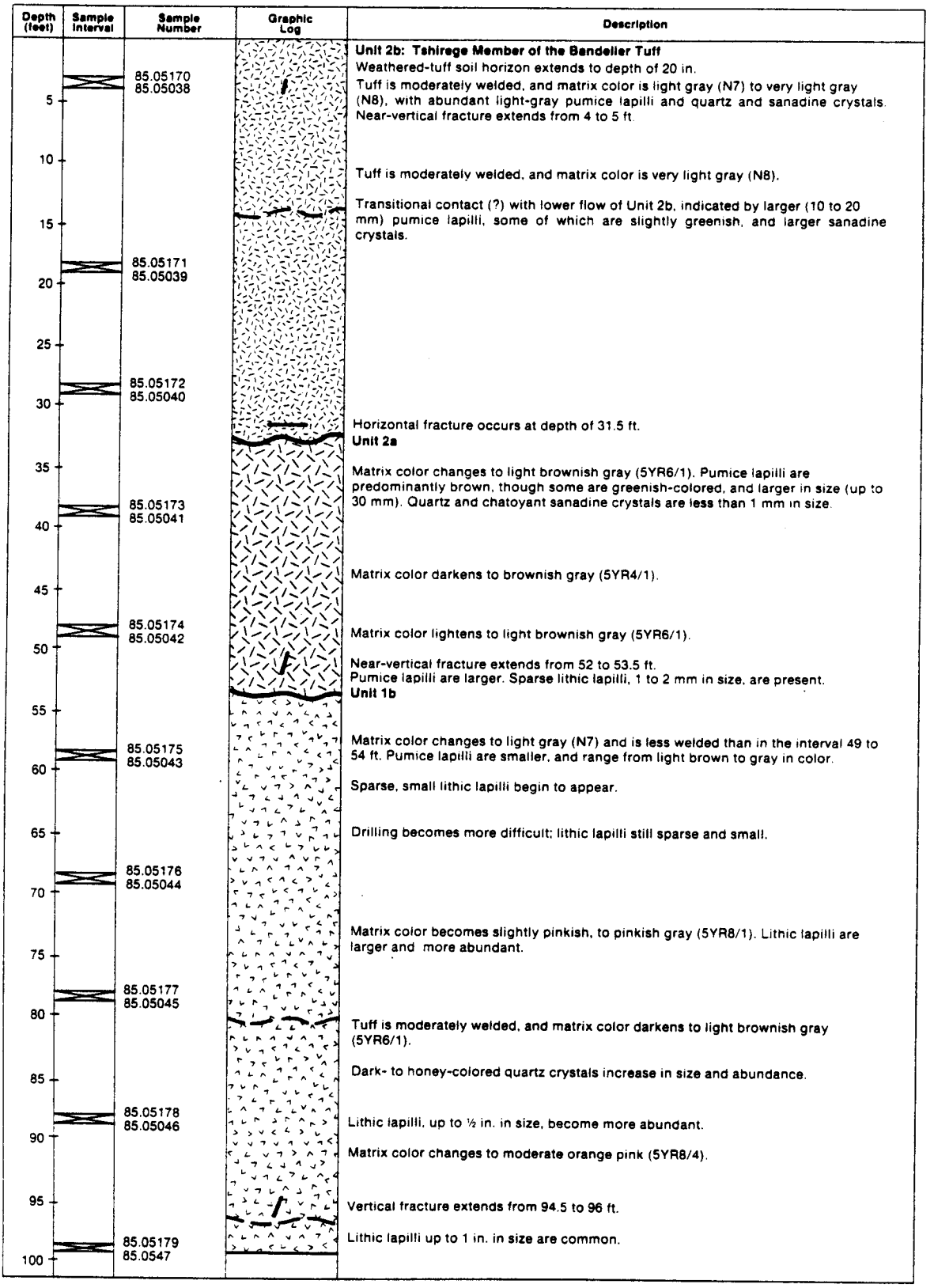

Figure 9. Lithologic Log of Hole LGC-85-10

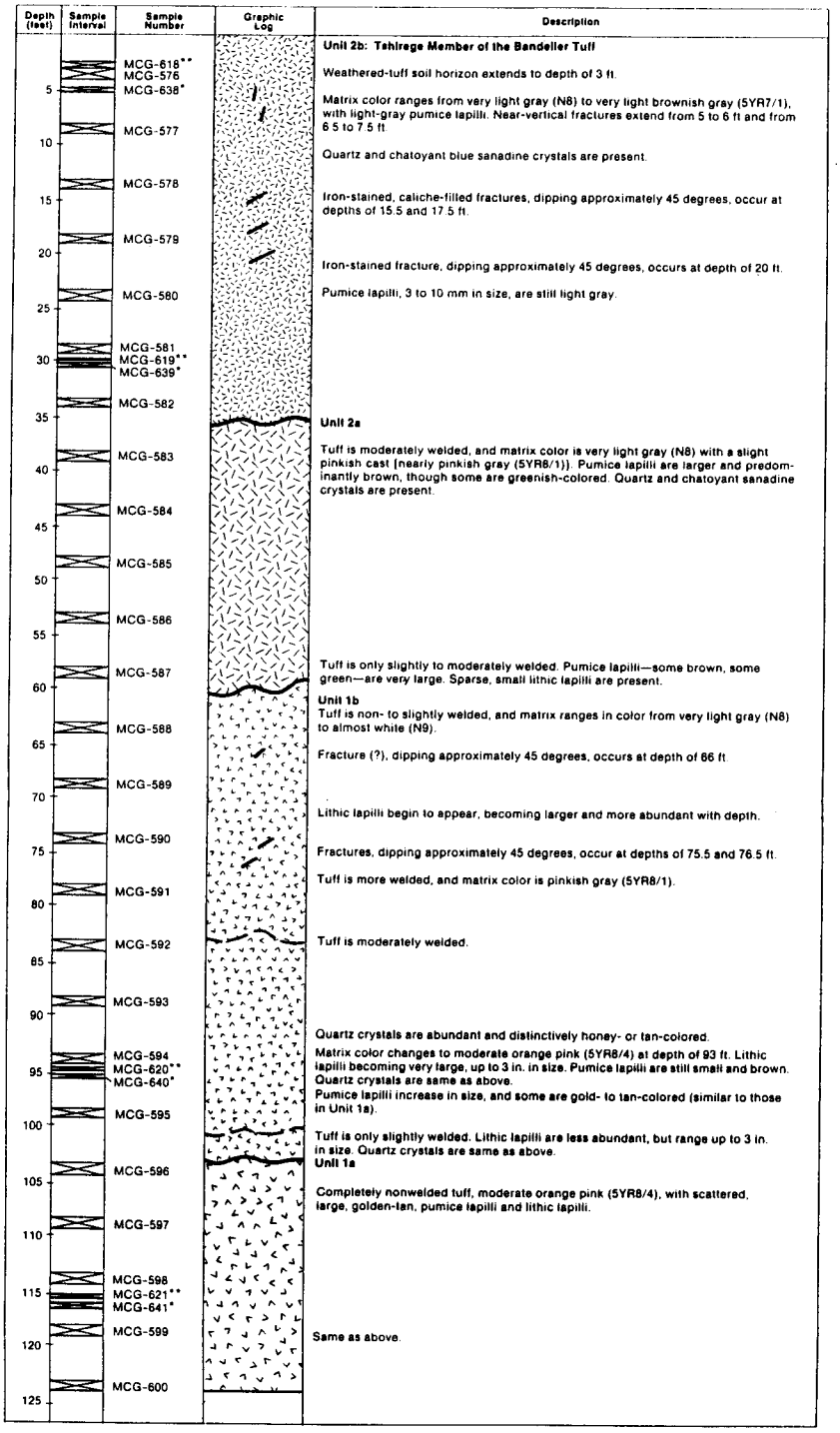

Figure 10. Lithologic Log of Hole LGM-85-11

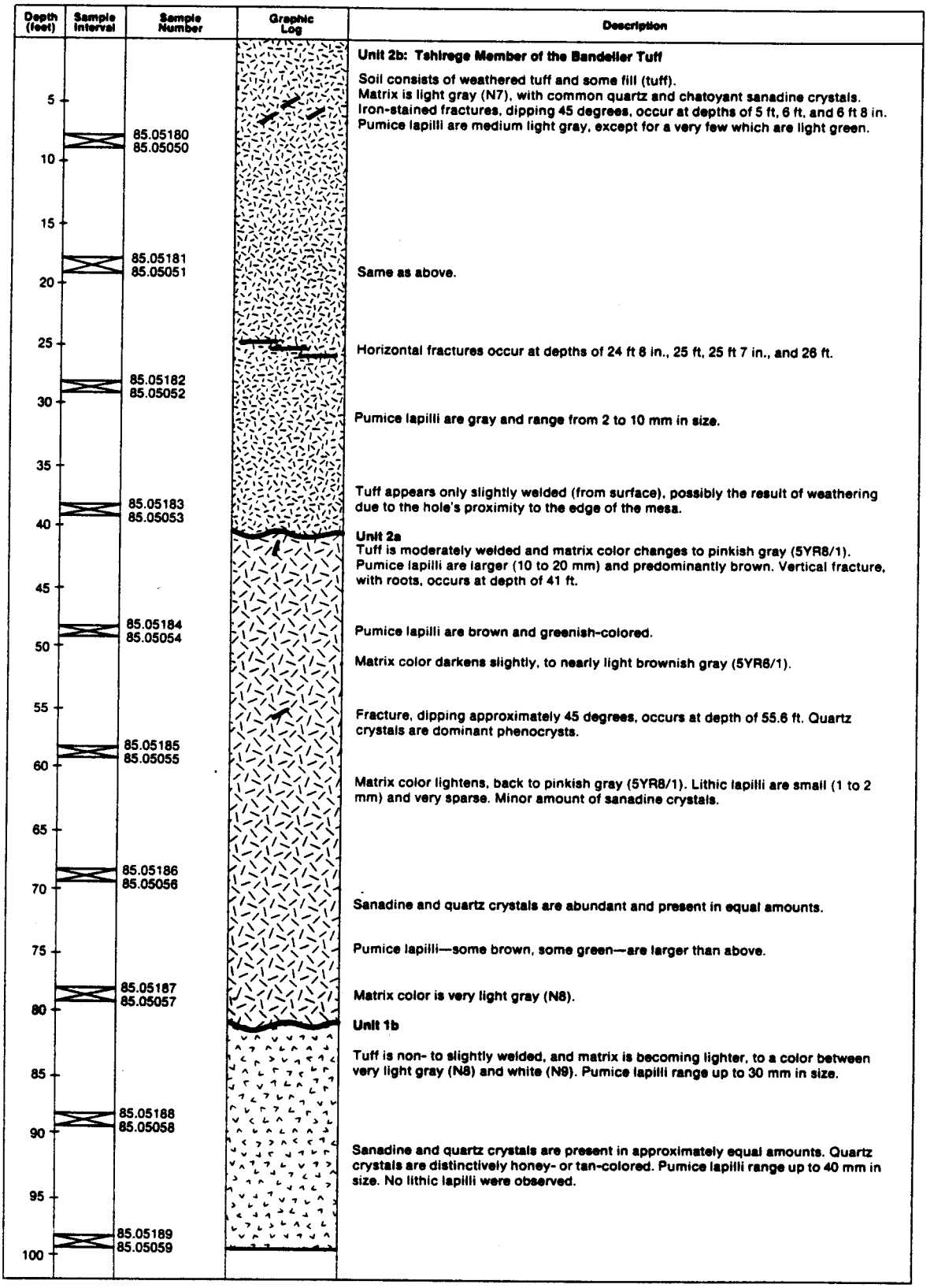

Figure 11. Lithologic Log of Hole LLC-85-12

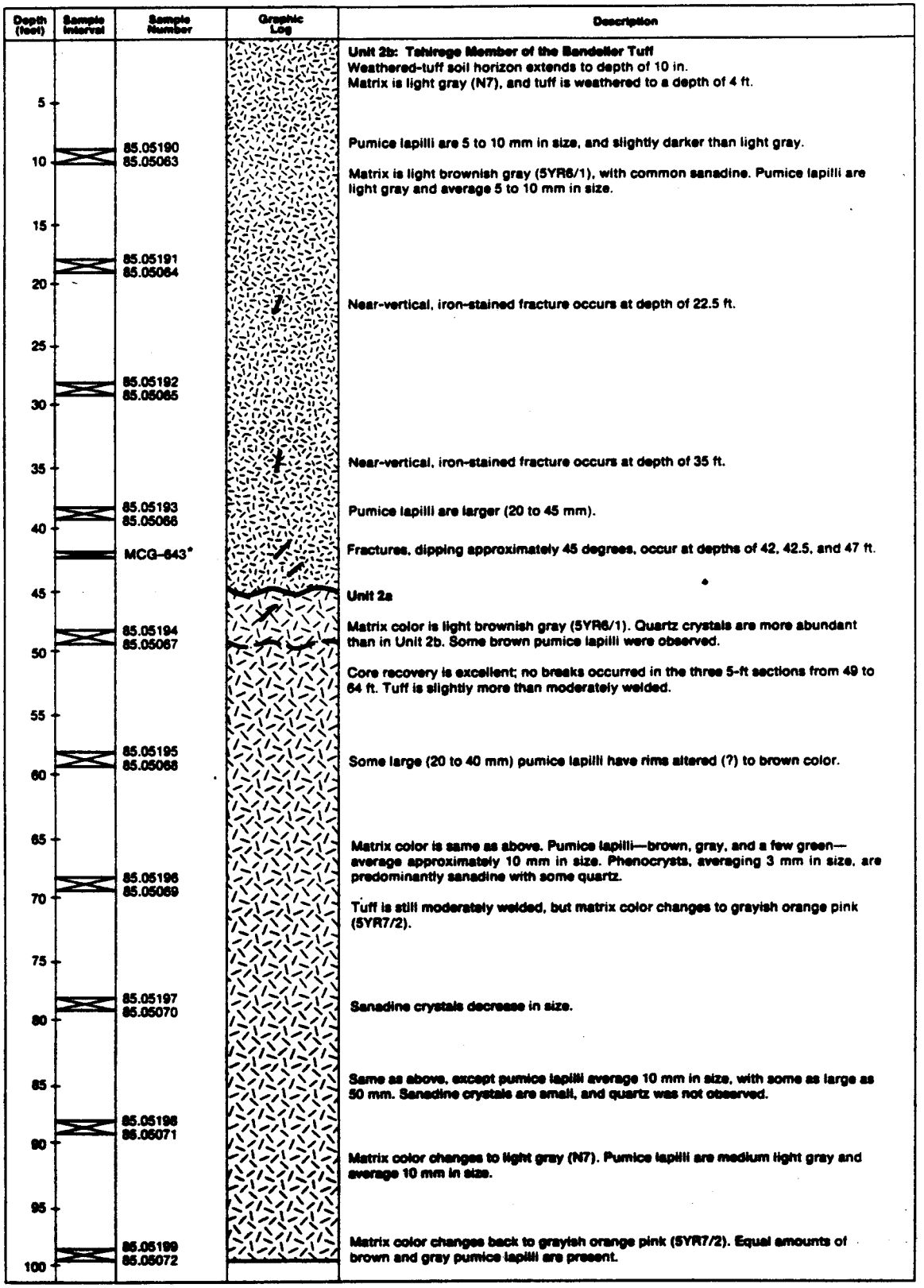

Figure 12. Lithologic Log of Hole LLC-85-13

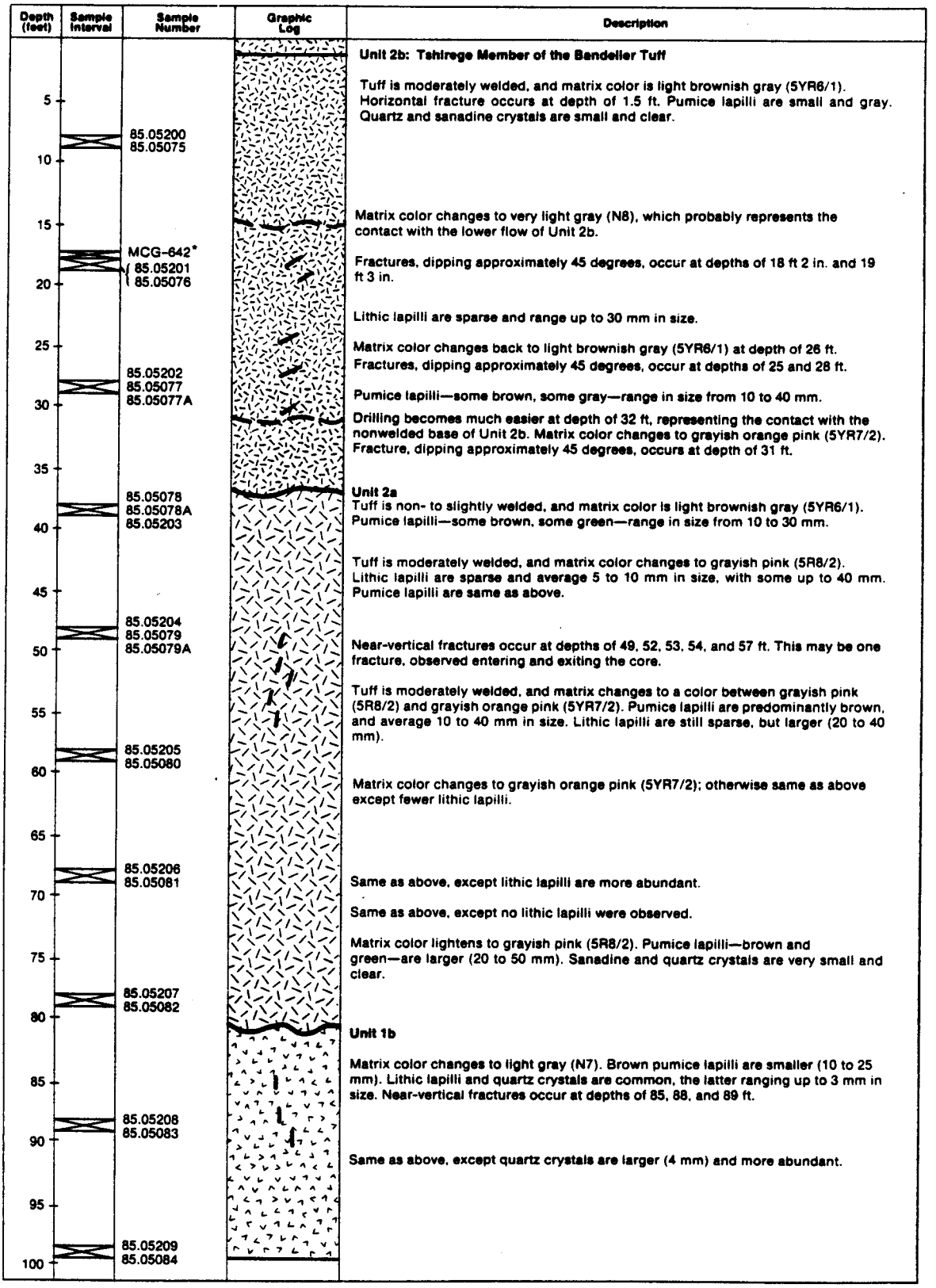

Figure 13. Lithologic Log of Hole LLC-85-14

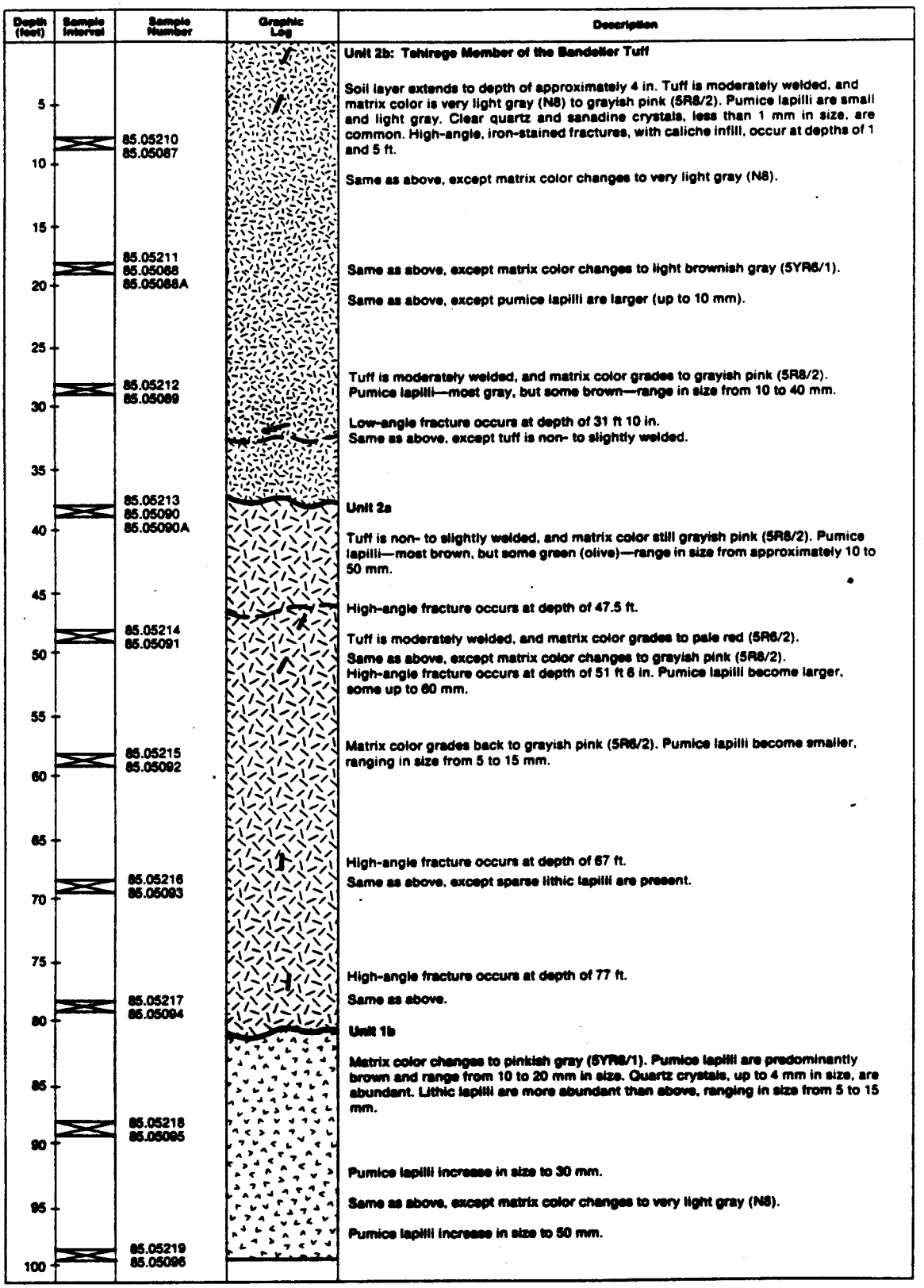

Figure 14. Lithologic Log of Hole LLC-85-15

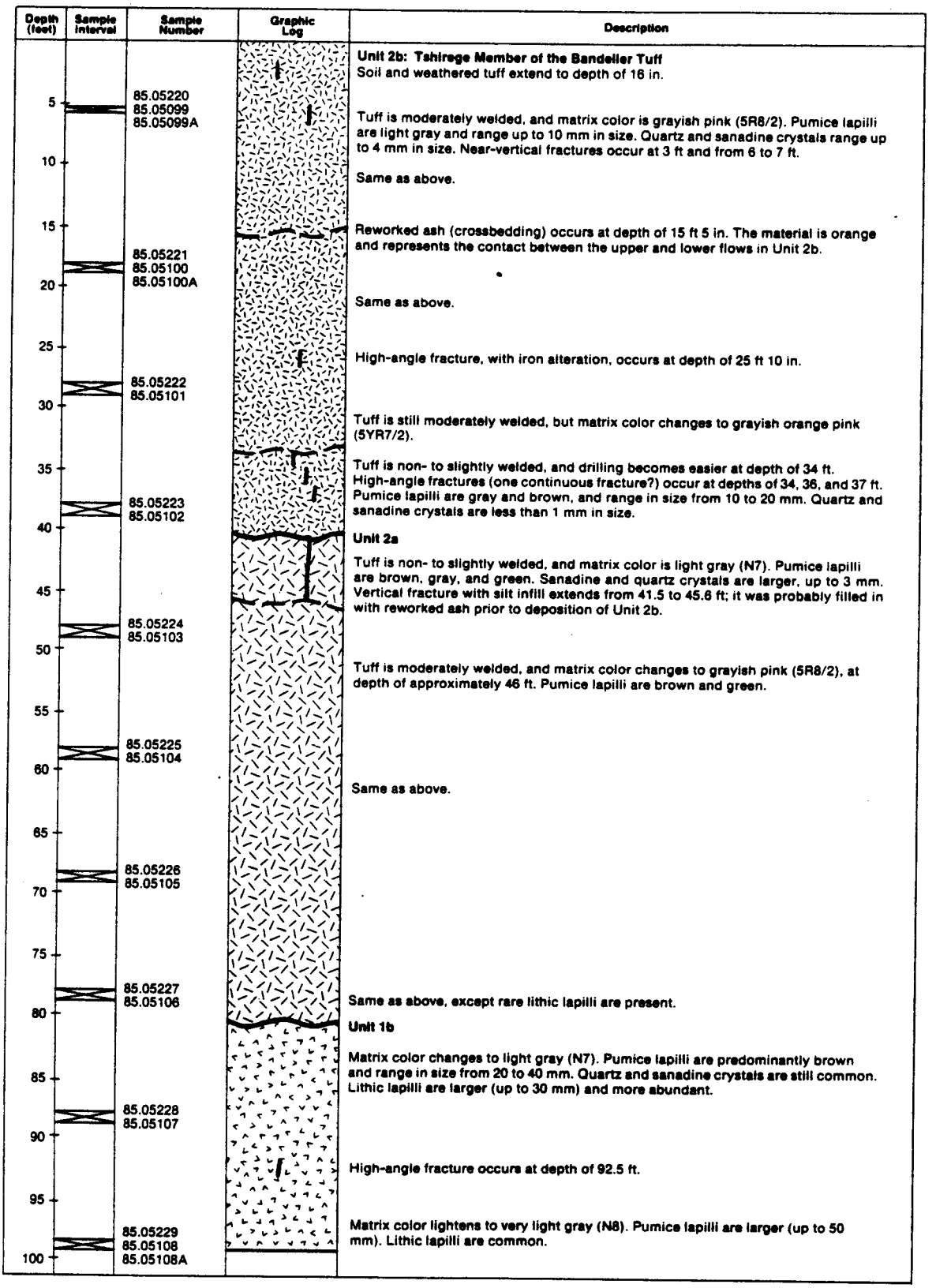

Figure 15. Lithologic Log of Hole LLC-85-16

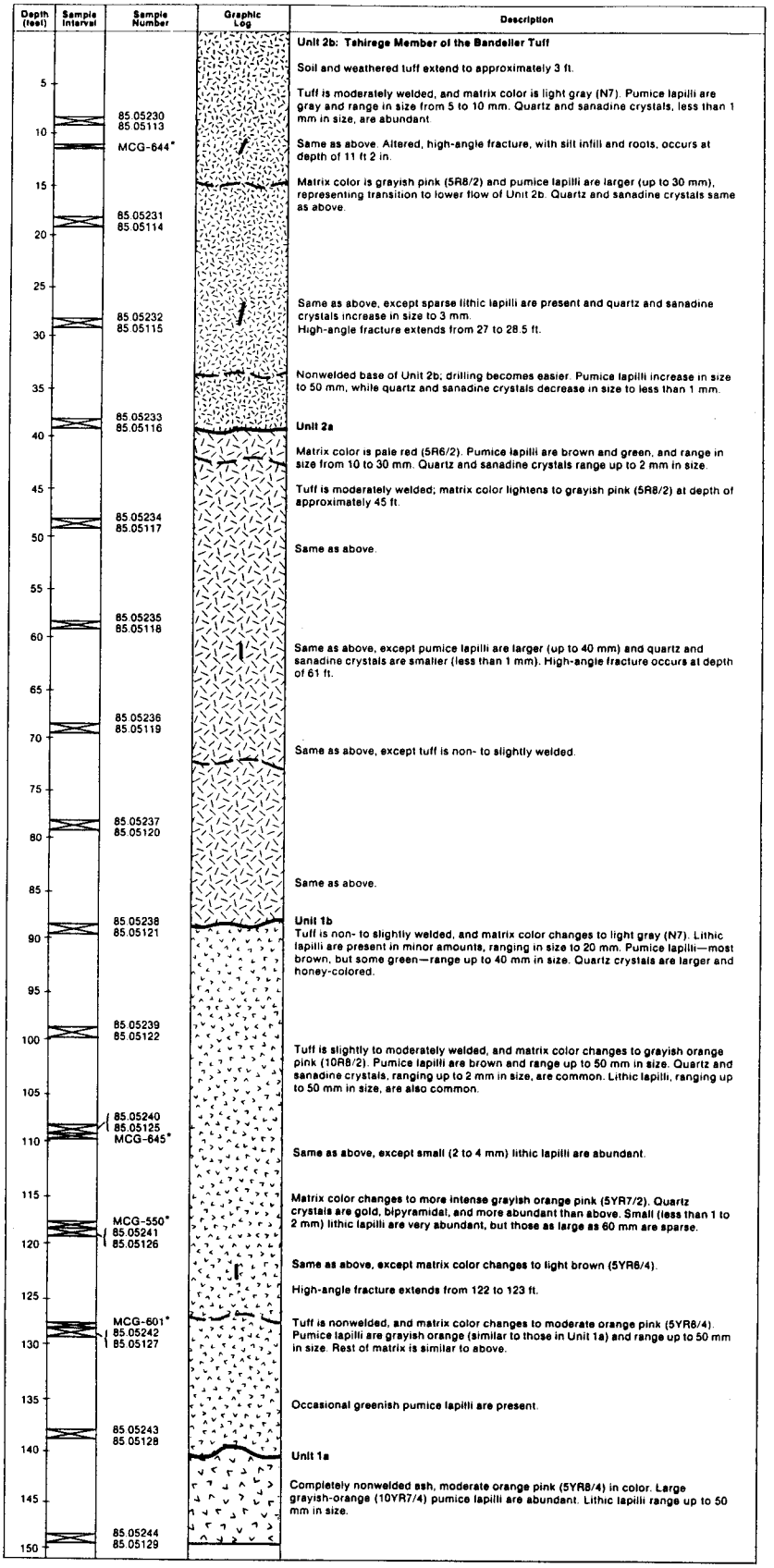

Figure 16. Lithologic Log of Hole LLC-85-17

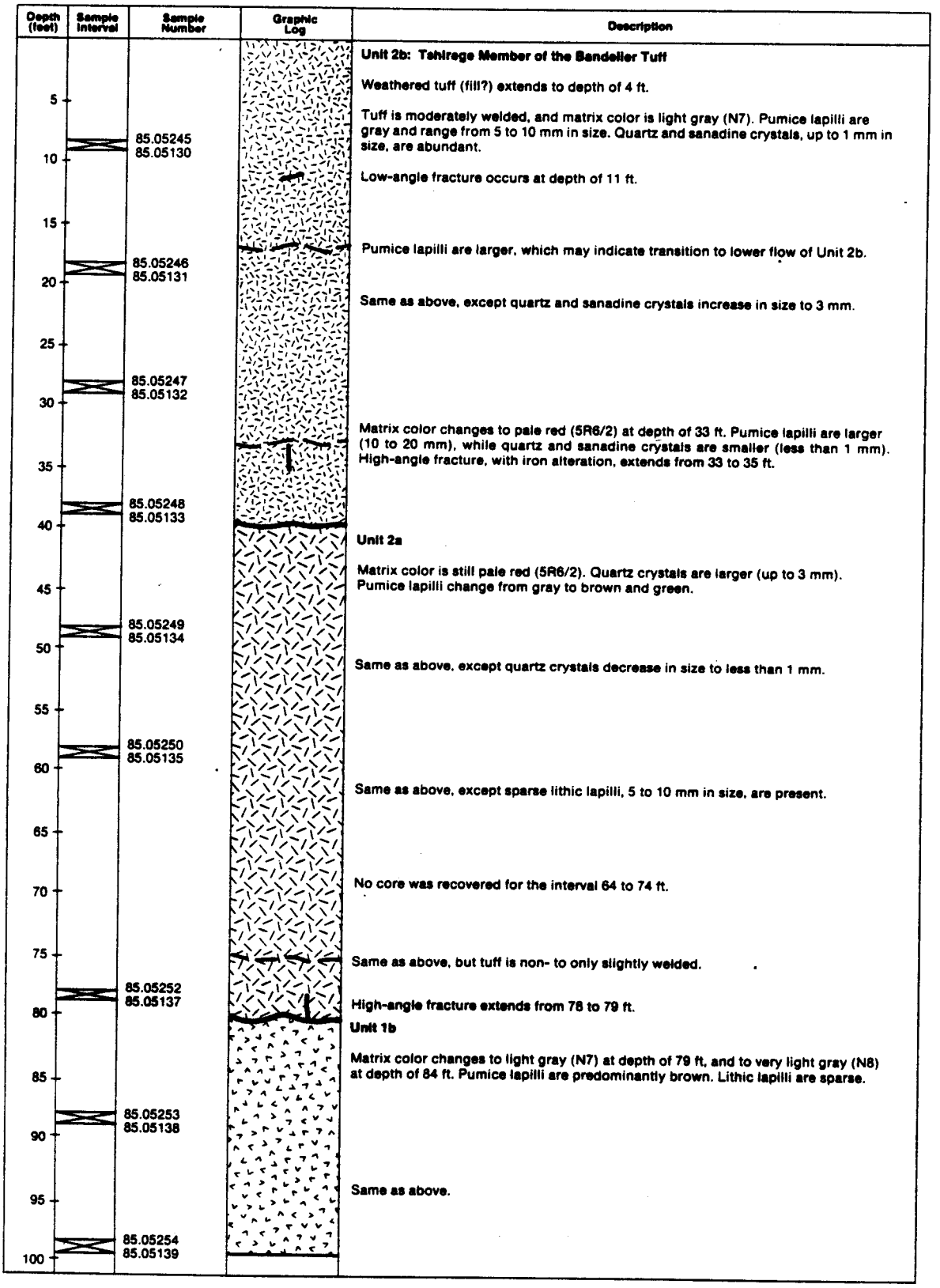

Figure 17. Lithologic Log of Hole LLC-85-18

GEOPHYSICAL LOGGING

Several different types of geophysical log were run in the open holes drilled for this study, using a total of four different probes. The data will be used to assist in characterizing the hydrologic and physical properties of the tuff underlying Areas G and L and in correlating those properties among all 18 drill holes at Mesita del Buey.

Bendix logged all 18 holes with three different probes to generate the following data:

- Spectral Gamma and 3-Arm Caliper Logs
- Natural Gamma, Epithermal Neutron, and Vertical Deviation Logs
- Magnetic Susceptibility Logs
- Moisture Logs Derived from the Epithermal Neutron Data

Century Geophysical Corporation logged 16 of the 18 holes with their 9030A probe to generate a gamma-gamma density, natural gamma, and 1-arm caliper log. The sets of geophysical logs for the Los Alamos drill holes are contained in separate envelopes attached to this report, one envelope per hole and labeled accordingly. Repeat logs were run by Bendix, but are not included in this report.

A discussion of each of the five types of logs is presented in the subsections that follow. These discussions include descriptions of the probe and any associated equipment, calibration information, and data-reduction methods. As noted earlier, however, the time constraints surrounding preparation of this initial report precluded all but very limited interpretation of the geophysical-logging data. As a consequence, only tentative results are suggested, based on preliminary examination of the logs. Thorough interpretations will be included in the final report, scheduled for completion early in 1986.

SPECTRAL GAMMA AND 3-ARM CALIPER LOGS

The spectral gamma probe (251A) contains two sodium-iodide (NaI) detectors with a manganese-54 source for gain-stabilization reference. Due to the low gamma activity in the Bandelier Tuff, however, only the larger 1-inch-by-12-inch NaI crystal was used as a detector in this study.

The associated hardware in the logging unit is set up to look at energy windows for measuring potassium, uranium, and thorium, using the following principal energy peaks:

- Potassium: K-40 - 1461 keV
- Uranium: Bi-214 - 1765 and 2204 keV
- Thorium: Tl-208 -2615 keV

The energy windows corresponding to these peaks are the following:

- Potassium: 1320 to 1575 keV
- Uranium: 1650 to 2389 keV
- Thorium: 2475 to 2765 keV

In addition, a total-count window is set up to measure gamma rays whose energies exceed 1 MeV. The count rates from each window are converted to concentrations of potassium in percent, uranium in ppm, and thorium in ppm.

Calibration data for the spectral gamma probe were collected at the U.S. Department of Energy (DOE) calibration facility in Grand Junction, Colorado, both before and after logging in Los Alamos. The calibration models at the DOE facility contain known concentrations of potassium, uranium, and thorium. Counts from the individual energy windows corresponding to potassium, uranium, and thorium were recorded and entered into the computer program CALBRT which derives a calibration matrix. This matrix was stored on tape and used to convert count rates to radioelement concentrations. The processed field data from the 1-inch-by-12-inch detector were then plotted versus depth, and the following curves are displayed:

- Potassium: % K from 0 to 16%; 1 inch = 4%
- Uranium: ppm U from 0 to 40 ppm; 1 inch = 10 ppm
  (backup scale: 0 to 100 ppm; 1 inch = 25 ppm)
- Thorium: ppm Th from 0 to 40 ppm; 1 inch = 10 ppm
  (backup scale: 0 to 100 ppm; 1 inch = 25 ppm)
- Total Counts: counts per second (cps) from 0 to 400 cps; 1 inch = 100 cps

A 3-arm caliper apparatus, capable of measuring hole diameters ranging from 2-1/8 inches to 22 inches, was used in conjunction with the spectral gamma probe. The results were plotted at a scale of 1 inch = 1 inch in the horizontal dimension.

Both the spectral gamma and 3-arm caliper logs for each hole were plotted at a vertical scale of 1 inch = 10 feet. Additional equipment data and logging data are summarized in the header for each log.

NATURAL GAMMA, EPITHERMAL NEUTRON, AND VERTICAL DEVIATION LOGS

The multifunction 9055A logging probe is capable of generating natural gamma-ray, self-potential, resistance, epithermal neutron, vertical deviation, and temperature logs. The self-potential and resistance logs were not applicable to this study because they must be run in a fluid-filled, uncased drill hole. The temperature log was also not run because of the shallow nature of the drill holes and the variable length of time elapsed between drilling and logging activities.

The natural gamma-ray system counts the entire spectrum of gamma rays above approximately 50 keV. The system was calibrated in the test models at the DOE calibration facility in Grand Junction, Colorado. However, since the more accurate spectral gamma system was also used to log the drill holes at Los Alamos, no attempt was made to convert these data from counts per second to

uranium concentration in ppm. Therefore, only the gross-gamma data were plotted on the logs, using a horizontal scale of 1 inch = 100 cps and a vertical scale of 1 inch = 10 feet.

The neutron system consists of an epithermal neutron detector used in conjunction with a 3-curie americium-beryllium neutron source. The system responds primarily to hydrogen present in the formation, in this case tuff. The neutron data were plotted on the logs using a horizontal scale of 1 inch = 250 cps and a vertical scale of 1 inch = 10 feet. These data were subsequently converted to moisture logs using corrections obtained from calibration models of known moisture content (see subsection below entitled Moisture Logs).

The vertical deviation system monitors the direction and angle that the drill hole deviates from vertical. This deviation is plotted in plan view such that the location of the hole with respect to the top is indicated for every 5-foot depth increment. The horizontal scale on the logs is 1 inch = 1 foot. The vertical deviation in the 18 drill holes at Los Alamos ranges from 1.1 to 4.1 feet, averaging 2.5 feet.

MAGNETIC SUSCEPTIBILITY LOGS

The magnetic susceptibility probe is calibrated in micro-cgs units in a granite block having a known value of susceptibility. The notation refers to the volume system for measuring magnetic susceptibility. Deflections are relative in magnitude to a baseline that must be established in an area of low or no magnetic susceptibility. Both the null calibration and the calibration in the granite block were performed at the DOE calibration facility in Grand Junction, Colorado. The null calibration was repeated in the field.

Unfortunately, in practical application, there is considerable baseline drift due to temperature changes in the sensing coil of the probe. For this reason, it is the shape of the curve plotted on the log that is significant, rather than the actual values displayed. At Los Alamos, repeat logs were run in every drill hole. Although the actual values on the main log differed from those on the repeat log, the credibility of the repeat log was established by overlaying it on the main log and verifying the similarity in the shape of the curve.

The magnetic susceptibility logs were plotted at a vertical scale of 1 inch = 10 feet. Additional equipment and logging data are noted in the header of each log. Preliminary examination of the logs suggests that there may be significant differences among the drill holes between certain units of the Tshirege Member of the Bandelier Tuff at Mesita del Buey. Should thorough examination confirm this initial indication, the magnetic susceptibility logs may prove to be a valuable aid in correlating the physical and hydrologic properties in the study area.

MOISTURE LOGS

The moisture logs are presented in a slightly different format from the other logs due to different data-reduction techniques. These logs were derived from the epithermal neutron data after applying several calibration factors and corrections to those data.

The epithermal neutron probe was calibrated in three test blocks having known moisture contents of 0.4, 7, and 28 percent. Because of the variability in the calibration data over such a large range in moisture content, two calibration equations were derived, one for moisture contents less than 7 percent and one for moisture contents greater than 7 percent. Uncertainties in the calculated moisture content at each 0.5-foot interval include those attributed to counting errors and an approximate 1 percent uncertainty due to the calibration parameters.

No hole-size correction was applied to the data due to the lack of an appropriate calibration model. However, the hole-size correction would most likely effect only a 1 percent difference in the calculated moisture content, well within the errors determined for most moisture-content calculations.

Furthermore, no corrections were applied to account for the casing and cement present in the uppermost 4 feet of each hole. As a consequence, the moisture contents reported for the first 4 feet of each hole should be regarded as qualitative.

GAMMA-GAMMA DENSITY, NATURAL GAMMA, AND 1-ARM CALIPER LOGS

Century Geophysical Corporation used its 9030A probe to run gamma-gamma density, natural gamma, and 1-arm caliper logs in 16 of the 18 drill holes at Los Alamos. The gamma-gamma density system was calibrated at the time it was installed on the logging truck. Subsequently, a calibration check was run on acrylic and aluminum blocks provided by Bendix, results of which indicated that the system was performing properly during logging operations at Los Alamos. The data collected in counts per second were immediately converted to apparent densities in grams per cubic centimeter (g/cm^3) using the calibration data obtained during installation of the logging system. The apparent densities were plotted at a horizontal scale of 1 inch = 0.2 g/cm^3. At first glance, it appears that these density logs may provide valuable insight into the physical and hydrologic characteristics of the tuff.

The natural gamma log run by Century Geophysial Corporation indicates the gross-gamma contribution above approximately 50 keV in uncalibrated API units. This log was requested primarily for purposes of cross-comparison with the Bendix-generated natural gamma log. The Century Geophysical natural gamma log was plotted at a horizontal scale of 1 inch = 200 API units.

The one-arm caliper log was run primarily to provide assurance that the probe was sidewalled in the drill holes during logging. These logs were plotted at a horizontal scale of 1 inch = 1 inch. Preliminary evaluation of the data suggests that the Bendix-generated 3-arm caliper logs provide a more accurate assessment of hole diameter than do the 1-arm caliper logs. However, none of the logs have yet been carefully examined or compared to determine the degree

of caving that may have occurred in any of the holes between the times that the 3-arm and 1-arm caliper measurements were made.

ACKNOWLEDGEMENTS

The authors acknowledge the many people who have contributed to this project to date. Particular thanks go to Micheline Devaurs, Bill Purtymun, Naomi Becker, and Dave McInroy, all of Los Alamos National Laboratory, HSE-8, for their direction and assistance.

REFERENCES

Abeele, W. V., M. L. Wheeler, and B. W. Burton, 1981. Geohydrology of Bandelier Tuff, LA-8962-MS, Los Alamos National Laboratory.

Bailey, R. A., R. L. Smith, and C. S. Ross, 1969. Stratigraphic Nomenclature of Volcanic Rocks in the Jemez Mountains, New Mexico, Bulletin 1274-P, U.S. Geological Survey.

Bendix Field Engineering Corporation, 1985a. Environmental Sciences Procedure Manual, Environmental Programs Division, internal document.

_____ 1985b. Health and Safety Manual for Chemical/Hazardous Materials, Remedial Action Projects, Environmental Programs Division, internal document.

Goddard, E. N., P. D. Trask, R. K. DeFord, O. N. Rove, J. T. Singewald, Jr., and R. M. Overbeck, 1975. Rock Color Chart, Geological Society of America, Boulder, Colorado.

Purtymun, W. D., and W. R. Kennedy, 1971. Geology and Hydrology of Mesita del Buey, LA-4660, Los Alamos Scientific Laboratory.

U.S. Department of Energy, 1979. Final Environmental Impact Statement - Los Alamos Scientific Laboratory Site, Los Alamos, New Mexico, DOE/EIS-0018.

GJ-43

VADOSE ZONE CHARACTERIZATION OF TECHNICAL AREA 54, WASTE DISPOSAL AREAS G AND L, LOS ALAMOS NATIONAL LABORATORY, NEW MEXICO

REPORT 2: DOWNHOLE INSTRUMENTATION AND PORE-GAS-SAMPLING/ DATA-COLLECTION PROCEDURES

November 1985

Bendix Field Engineering Corporation
Grand Junction, Colorado

ALLIED Bendix Aerospace

GJ-43

VADOSE ZONE CHARACTERIZATION OF TECHNICAL AREA 54, WASTE DISPOSAL AREAS G AND L, LOS ALAMOS NATIONAL LABORATORY, NEW MEXICO

REPORT 2: DOWNHOLE INSTRUMENTATION AND PORE-GAS-SAMPLING/DATA-COLLECTION PROCEDURES

Bendix Field Engineering Corporation
Grand Junction Operations

November 1985

Prepared for
U.S. Department of Energy
Los Alamos National Laboratory
Los Alamos, New Mexico
in Conjunction with
U.S. Department of Energy
Grand Junction Projects Office
Grand Junction, Colorado
Under Contract No. DE-AC07-76GJO1664

CONTENTS LISTING

		Page
1.0	Purpose and Scope	1
2.0	Instrument Installations	1
2.1	Pore-Gas Sampling Ports	1
2.2	Thermocouple Psychrometers and Pressure Transducers	13
3.0	Sampling and Data-Collection Procedures	18
3.1	Collection of Pore-Gas Samples	18
3.2	Collection of Water-Potential Data	21
3.3	Collection of Pressure Measurements	26
4.0	References	27

LIST OF FIGURES

Figure 2-1.	Diagram of a Pore-Gas Sampling Port	2
2-2.	Legends for the Instrument Installations	3
2-3.	Pore-Gas Sampling Port Installation for Hole LGC-85-09	4
2-4.	Pore-Gas Sampling Port Installation for Hole LGC-85-10	5
2-5.	Pore-Gas Sampling Port Installation for Hole LLC-85-12	6
2-6.	Pore-Gas Sampling Port Installation for Hole LLC-85-13	7
2-7.	Pore-Gas Sampling Port Installation for Hole LLC-85-14	8
2-8.	Pore-Gas Sampling Port Installation for Hole LLC-85-15	9
2-9.	Pore-Gas Sampling Port Installation for Hole LLC-85-16	11
2-10.	Installation of Thermocouple Psychrometers and Pressure Transducers in Hole LLP-85-03	16
2-11.	Installation of Thermocouple Psychrometers in Hole LGP-85-07	17
3-1.	Schematic of the DESAGA Gas Sampler	19
3-2.	Schematic of the RS-232C Cable Connections Between the HP-115 and the CI-30 Interface	24
3-3.	Schematic of the RS-232C Cable Connections Between the CI-30 Interface and the Computer/Printer	24

LIST OF TABLES

Table 2-1.	Installation Depths and Cooling Coefficients for Psychrometers in Hole LLP-85-03	14
2-2.	Installation Depths and Cooling Coefficients for Psychrometers in Hole LLP-85-07	15

1.0 PURPOSE AND SCOPE

This report describes the instrument installations and procedures for sample and data collection conducted in support of the vadose zone characterization of Waste Disposal Areas G and L, Technical Area 54, Los Alamos National Laboratory, New Mexico. The study was initiated in response to a Resource Conservation and Recovery Act (RCRA) Compliance Order/Schedule (Docket Number [illegible]:007) issued to the Laboratory by the Environmental Improvement Division of the State of New Mexico. The Compliance Order/Schedule, dated 7 May 1985, specifies acquisition of certain geotechnical information. The instrument installations described in this report were designed and emplaced by Bendix Field Engineering Corporation/Grand Junction Operations (Bendix) in accord with a Statement of Work issued by Los Alamos National Laboratory. Bendix is the Operating Contractor for the Department of Energy (DOE) Grand Junction, Colorado Projects Office.

This report is the second in a series of reports documenting the vadose zone characterization of the study area. The first report (Rush and Dexter, 1985) presented preliminary lithologic and geophysical data obtained via drilling and logging operations conducted over the period 30 July to 22 August 1985. This second report presents the instrument-completion diagrams for the nine boreholes in which instruments were installed and describes the procedures to be used in the collection of samples and other data.

2.0 INSTRUMENT INSTALLATIONS

2.[illegible] PORE-GAS SAMPLING PORTS

A total of 23 sampling ports were installed in seven boreholes in the study area in order to collect samples of pore gas at various locations in the boreholes. The sampling ports were constructed using low-pressure mobile-phase filters which were welded to standard 2-inch-I.D. galvanized pipe (see Figure 2-1). The filters consist of 2-micrometer, porous, stainless steel elements. Uphole access is provided via connection to 1/4-inch stainless steel tubing and stainless steel compression fittings.

Installation was accomplished by carefully lowering the string of galvanized pipe downhole. The annuli surrounding the pore-gas sampling ports were then filled with a fine-grained (sieve size of 80) silica sand, and isolated from upper and lower zones using powdered bentonite. (One zone in Hole LGC-85-09 was packed in tuff backfill due to cave-in of the hole.) Figure 2-2 presents the legend for the sampling-port installations; completion diagrams are shown in Figures 2-3 through 2-9 for the seven boreholes.

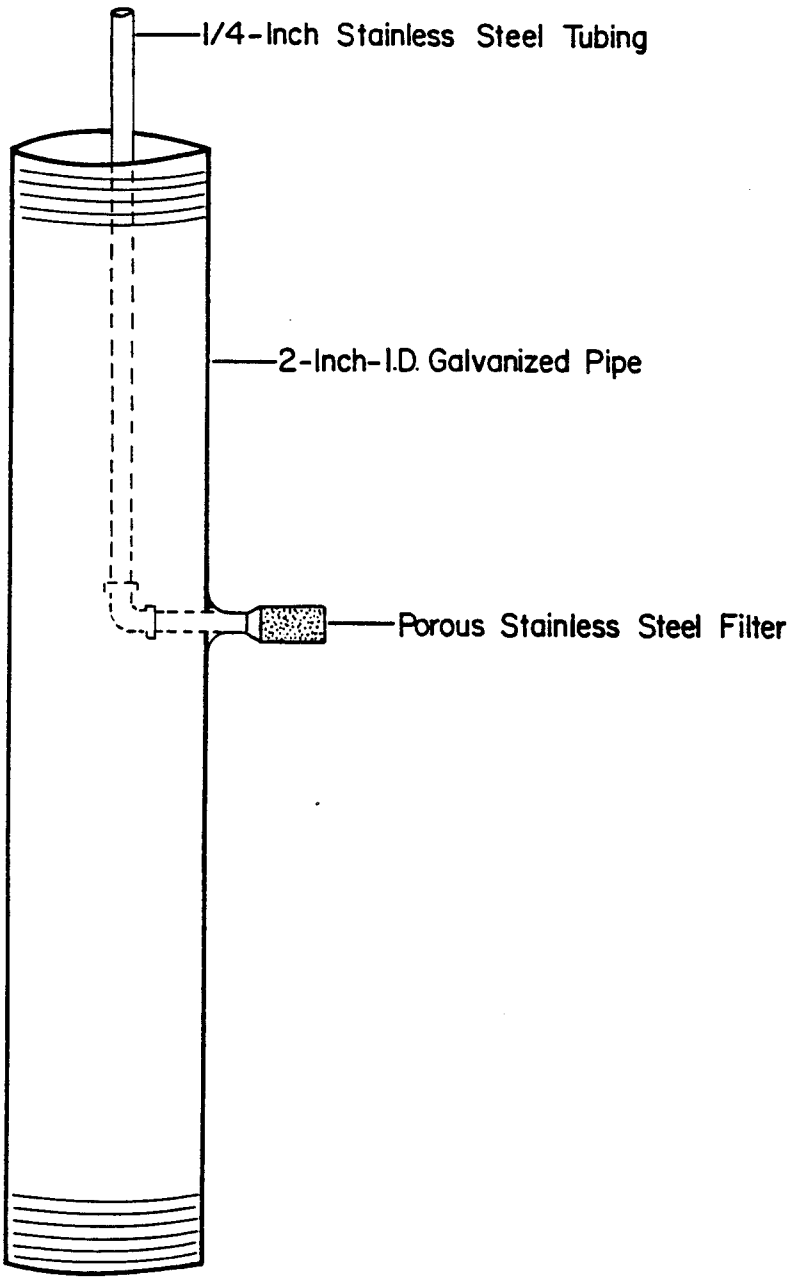

Figure 2-1. Diagram of a Pore-Gas Sampling Port

LEGEND FOR PORE-GAS SAMPLING-PORT INSTALLATIONS

Gravel (0.25-inch)

Gravel with Bentonite

Bentonite

Well Sand (approximate sieve size = 8)

Tuff Backfill from Unit 2b

Tuff Cave-In Material

Sampling Port

8-Inch Cemented Surface Casing

Stainless Steel Tubing Exiting
2-Inch-I.D. Galvanized Pipe, Showing Coupling

LEGEND FOR PSYCHROMETER AND TRANSDUCER INSTALLATIONS

Tuff Backfill

Bentonite

Psychrometer

Pressure Transducer

2-Inch PVC Pipe (used to support psychrometers and transducers)

Figure 2-2. Legends for the Instrument Installations

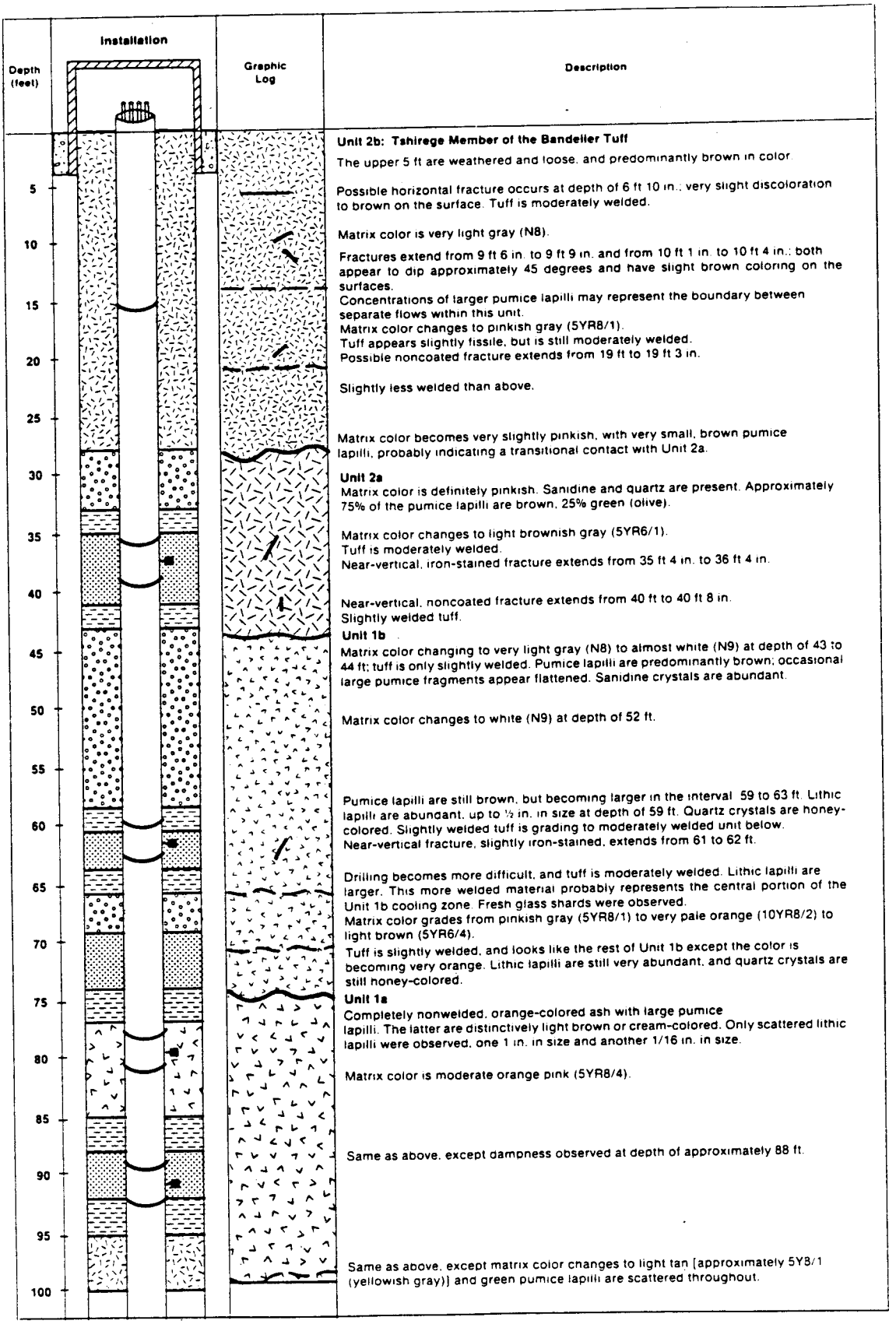

Figure 2-3. Pore-Gas Sampling Port Installation for Hole LGC-85-09

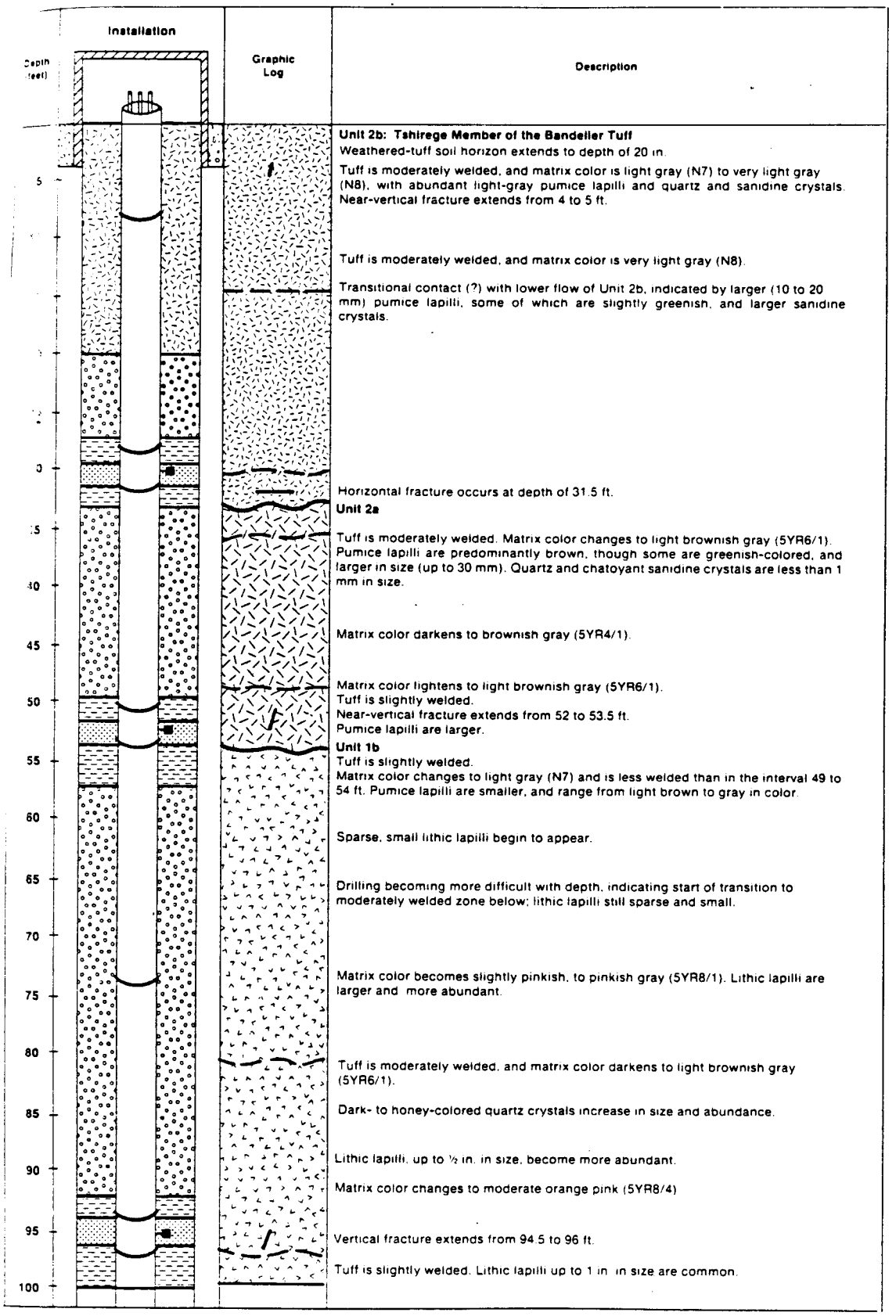

Figure 2-4. Pore-Gas Sampling Port Installation for Hole-LGC-85-10

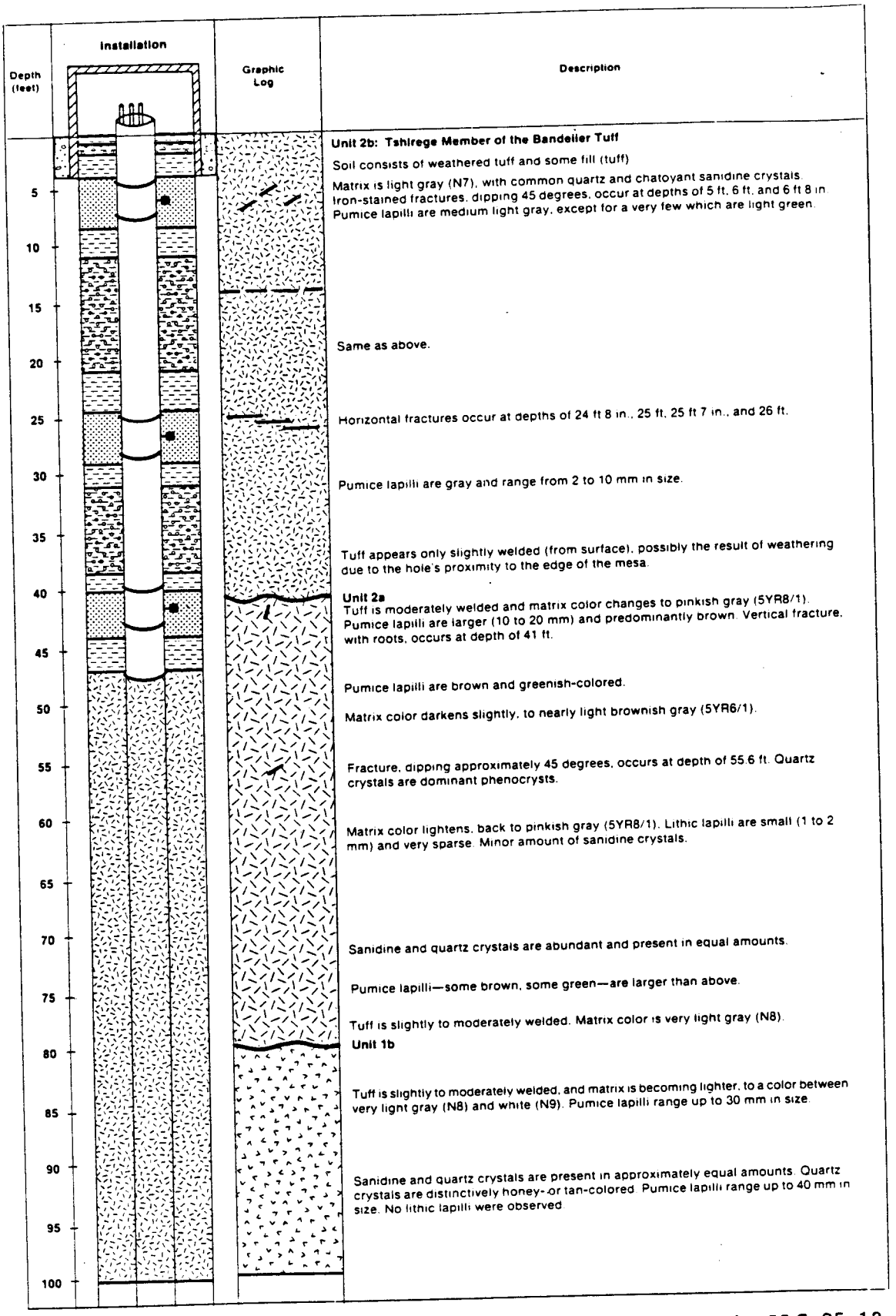

Figure 2-5. Pore-Gas Sampling Port Installation for Hole LLC-85-12

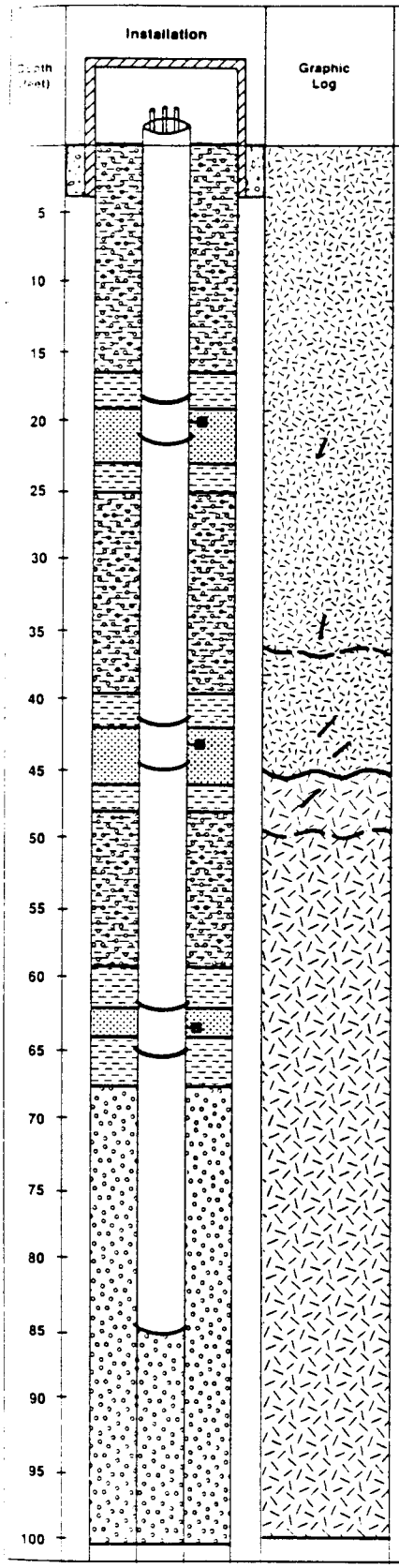

Figure 2-6. Pore-Gas Sampling Port Installation for Hole LLC-85-13

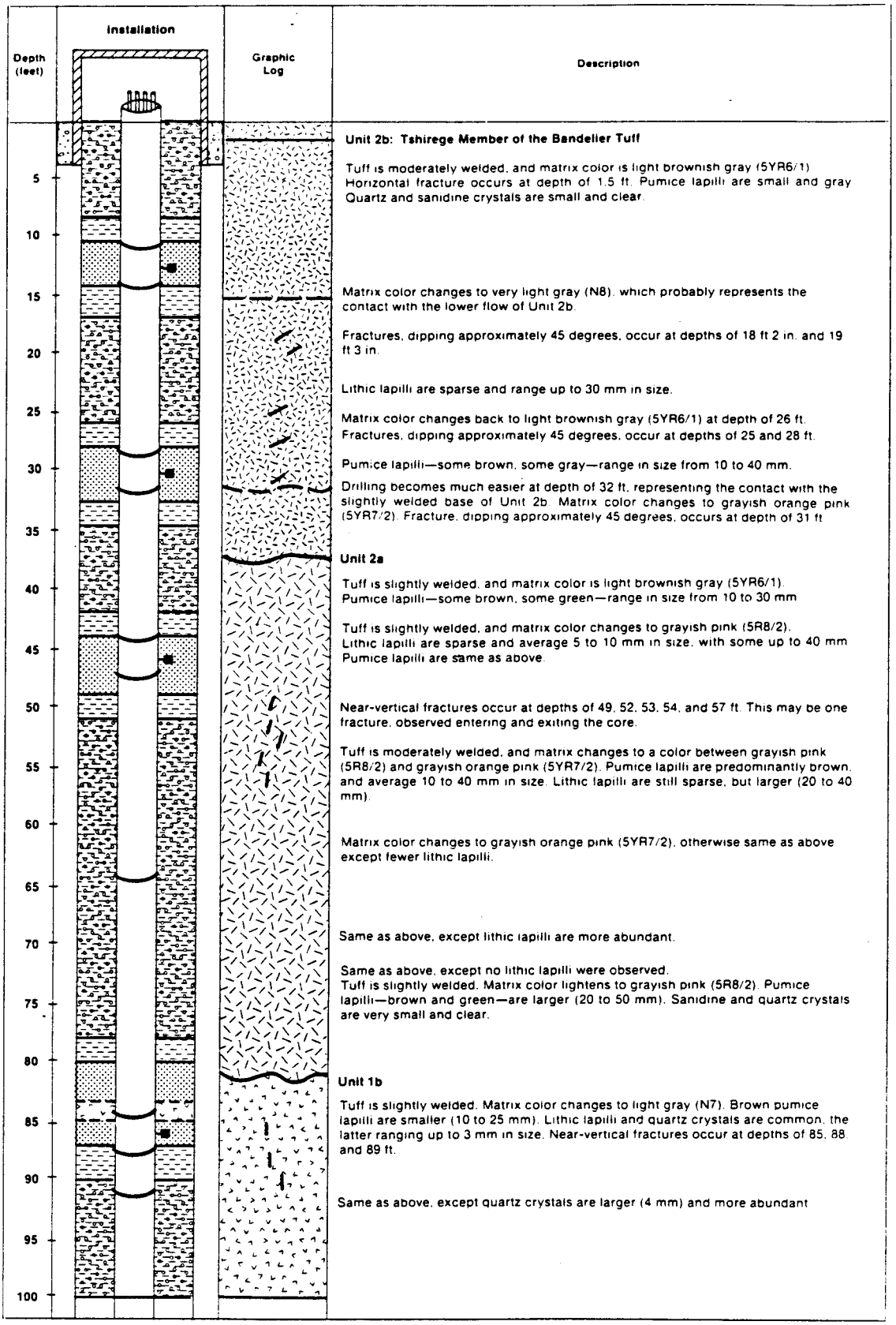

Figure 2-7. Pore-Gas Sampling Port Installation for Hole LLC-85-14

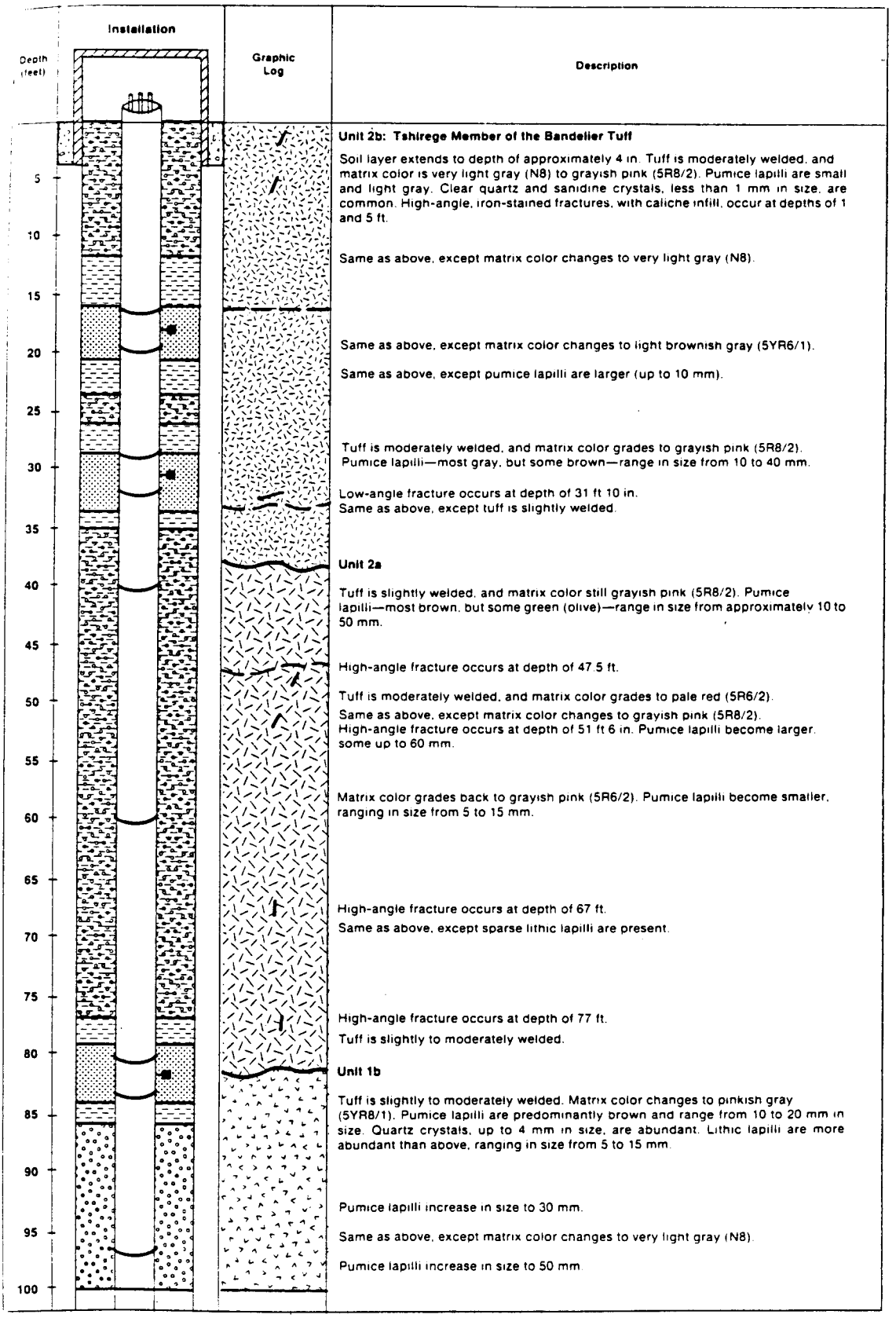

Figure 2-8. Pore-Gas Sampling Port Installation for Hole LLC-85-15

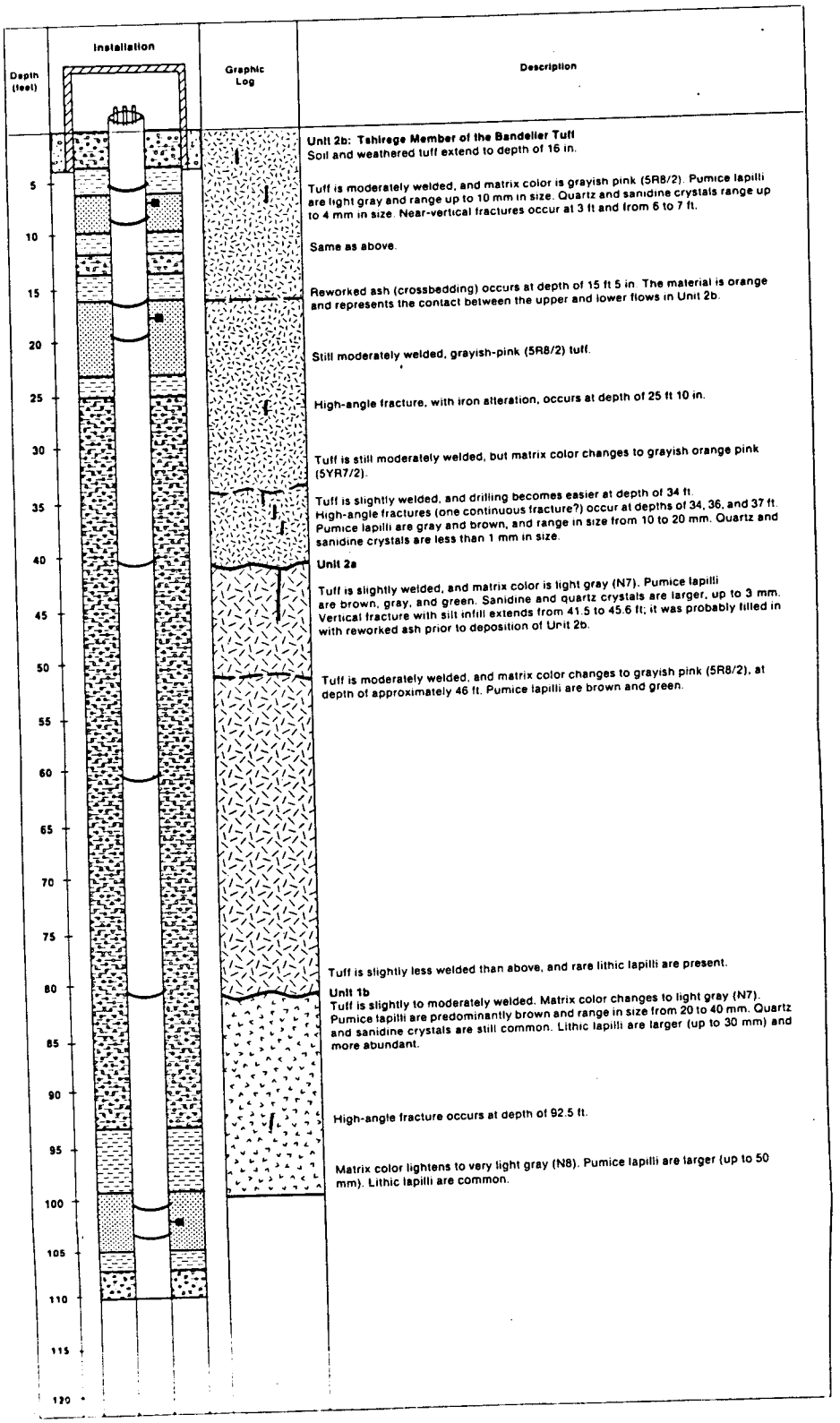

Figure 2-4. Pore-Gas Sampling Port Installation for Hole LLC-85-16

THERMOCOUPLE PSYCHROMETERS AND PRESSURE TRANSDUCERS

Thermocouple psychrometers and pressure transducers were installed at the study area in order to measure temperature, water potential, and pressure at various depths in selected boreholes. A total of 38 psychrometers were installed, 23 in Hole LLP-85-03 and 15 in Hole LGP-85-07. Because of the presence of surface casing in Hole LLP-85-03, a shallow boring was drilled adjacent to the main hole and five psychrometers were installed in this second hole close to the ground surface (depicted in the completion diagram as being in Hole LLP-85-03). A total of four pressure transducers were installed, three in Hole LLP-85-03 and one at ground surface near this hole.

Installations were accomplished by taping the instruments to a string of Schedule 40, 2-inch-I.D., polyvinylchloride (PVC) pipe and carefully lowering the string into the hole. The annulus surrounding the PVC pipe was then backfilled with auger cuttings from that drill hole. It was assumed that the density of this backfill material was similar to the in-situ density of the Bidelier Tuff, and that the relative humidity of the backfill material, as sensed by the instruments, would equilibrate with the relative humidity of the tuff. Fractured zones in Hole LLP-85-03 were isolated using powdered bentonite at selected intervals.

Installation depths, cooling coefficients, and scanner/channel identifications for the psychrometers in Holes LLP-85-03 and LGP-85-07 are presented in Tables 2-1 and 2-2, respectively. Completion diagrams of the psychrometer and transducer installations are shown in Figures 2-10 and 2-11; refer to Figure 2-2 for legend information for these installations. Calibration information will be presented in a subsequent report.

Table 2-1. Installation Depths and Cooling Coefficients for Psychrometers in Hole LLP-85-03

Psychrometer Serial Number	Scanner/Channel	Cooling Coefficient (microvolts)	Installation Depth (feet)
29414	I/1	54	Surface
29416[a]	I/2	56	2
29474[a]	I/3	57	4
29473[a]	I/4	54	6
29420[a]	I/5	59	8
29469[a]	I/6	56	10
29418	I/7	57	13
29483	I/8	62	13
29424	I/9	53	24
29479	I/10	57	24
29406	I/11	57	41
29462	I/12	61	41
29409	II/1	61	50
29475	II/2	60	50
29405	II/3	59	56
29477	II/4	64	56
29425	II/5	65	66
29455	II/6	65	66
29481	II/7	77	76
29422	II/8	59	76
29476	II/9	63	86
29458	II/10	62	96
29427	II/11	63	96

[a]Psychrometers in the upper 10 feet are located in a shallow boring adjacent to the main hole.

Table 2-2. Installation Depths and Cooling Coefficients for Psychrometers in Hole LGP-85-07

Psychrometer Serial Number	Scanner/Channel	Cooling Coefficient (microvolts)	Installation Depth (feet)
29415	III/1	59	4.5
29459	III/2	56	6.5
29410	III/3	60	8.5
29461	III/4	56	10
29411	III/5	57	12
29463	III/6	56	14
29417	III/7	57	17
29466	III/8	56	19
29403	III/9	61	22
29467	III/10	58	27
29407	III/11	57	32
29465	III/12	59	37
29464	III/13	57	42
29404	III/14	52	47
29468	III/15	57	52

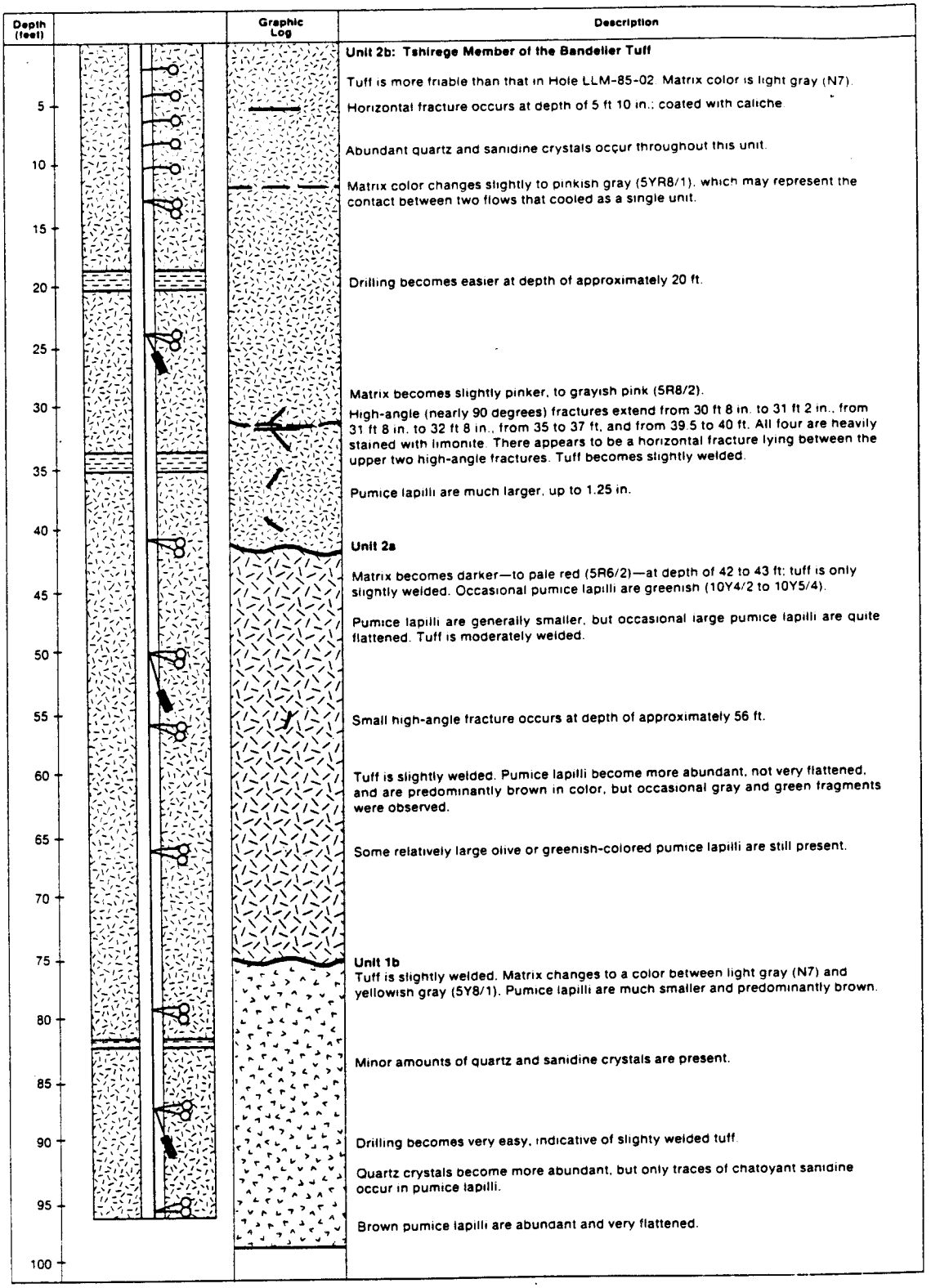

Figure 2-10. Installation of Thermocouple Psychrometers and Pressure Transducers in Hole LLP-85-03 (Note: The five psychrometers in the upper 10 feet are located in a shallow boring adjacent to the main hole.)

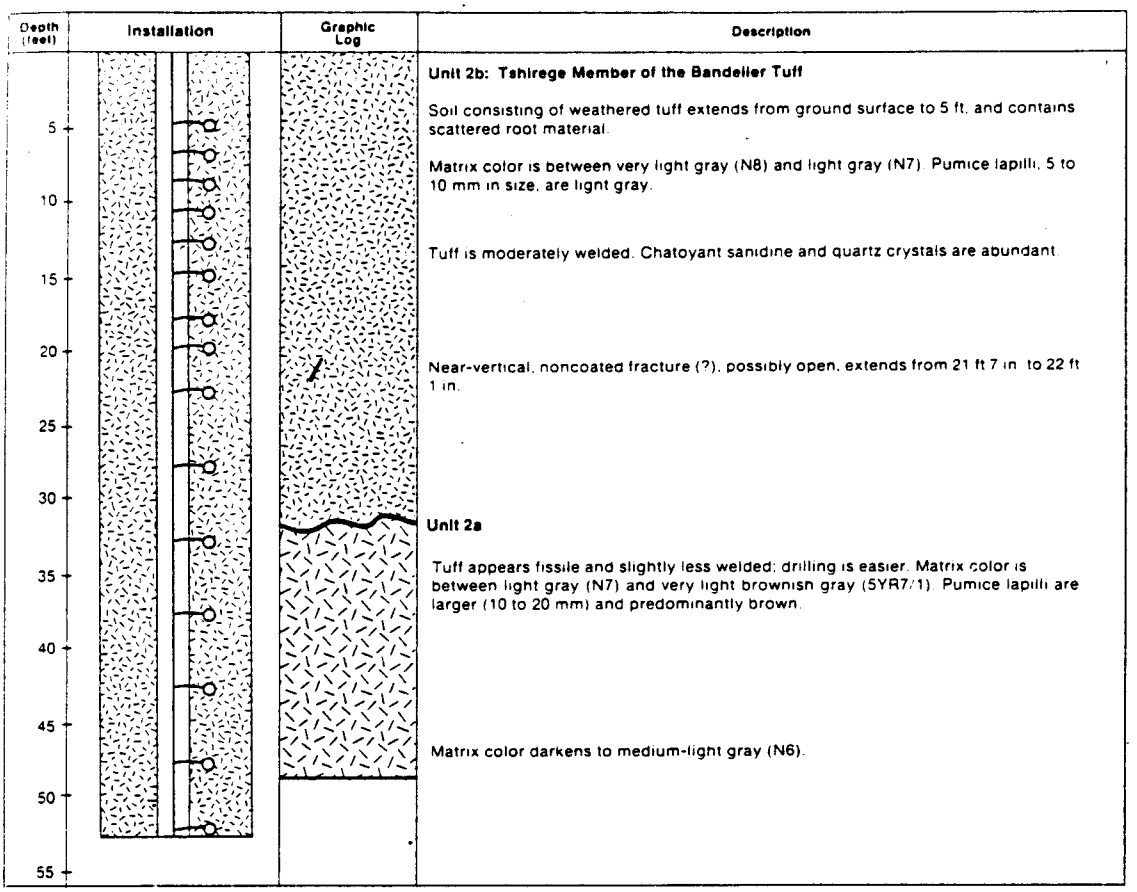

Figure 2-11. Installation of Thermocouple Psychrometers in Hole LGP-85-07

3.0 SAMPLING AND DATA-COLLECTION PROCEDURES

3.1 COLLECTION OF PORE-GAS SAMPLES

3.1.1 Introduction

These procedures were developed to collect samples of pore gas from boreholes located in Waste Disposal Areas G and L, Technical Area 54, Los Alamos National Laboratory, New Mexico. The samples are collected on either Tenax or charcoal-adsorption tubes. Notes on these procedures are presented at the end of the section (see Section 3.1.4).

3.1.2 Equipment

- DESAGA Gas Sampler [flow rate of 0.2 to 12 liters per minute (lpm)], Model GS-212 with Power Leads (TEKMAR Company, Cincinnati, Ohio)
- Orbo-32 Large Charcoal Tubes (Supelco No. 2-0228)
- Tenax Purge Trap Tubes (Supelco No. 2-0293)
- Silicone Tubing, 3/16-Inch I.D., 5/16-Inch O.D.
- Silicone Tubing, 3/32-Inch I.D., 5/32-Inch O.D.
- Swagelok Adapters, 1/8 to 1/4 Inch (two needed)

3.1.3 Procedures

3.1.3.1 Preparation

1. Connect the DESAGA gas sampler (see Figure 3-1) to a 12-Vdc automobile battery using the power leads.
2. Connect the inlet of the pump to the desired sampling port using 3/16-inch-I.D. silicone tubing.
3. Set the pump to continuous mode and maximum flow rate. Since the sampling intervals have a volume of approximately 50 liters, a total of 100 liters should be pumped from the sampling port to ensure subsequent collection of a representative sample. Once the purging process has been completed, disconnect the pump from the sampling port.
4. Proceed to Section 3.1.3.2 if a Tenax tube is to be used, or to Section 3.1.3.3 if a charcoal-adsorption tube is to be used.

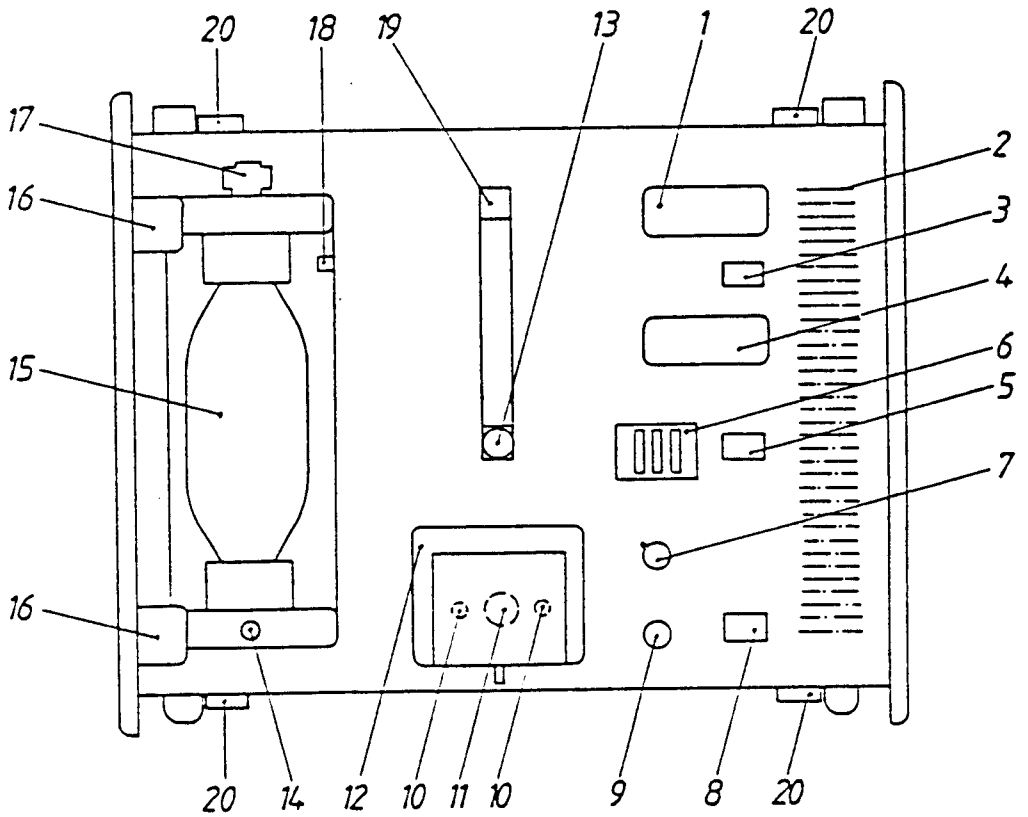

1 Temperature display (with GS 312 only)
2 Venting slits
3 Key for activating a temperature measurement (with GS 312 only)
4 Digital volume counter and state indicator
5 Key for starting and stopping a measurement cycle
6 Preset switches for the gas volume
7 Mode switch "Continuous" or "Preset"
8 Main switch
9 Socket for external control
10 DC power connection
11 DC fuse
12 Power adapter GN 220/12 (with GS 312 only)
13 Fine regulation valve for flow rate
14 Inlet
15 Absorber vessel
16 Mounts for stand rod
17 Lock for the absorber vessel
18 Outlet
19 Float-type flow meter
20 Lock for cover

Figure 3-1. Schematic of the DESAGA Gas Sampler

3.1.3.2 Tenax Tube Sampling Procedure

1. After completing the preparation steps, connect the inlet of the pump to the outlet of a Tenax purge trap sample tube using 3/16-inch-I.D. silicone tubing and a Swagelok adapter. The outlet of the tube is labeled "3% SP-2100."

2. Set the pump to PRESET mode and select the desired sample volume.

3. Set the pump to maximum flow rate (see Note 1). Turn on the pump and allow the flow rate to stabilize.

4. Turn the pump off momentarily to reset the volume meter.

5. Connect the inlet of the Tenax tube to the desired sampling port using silicone tubing and an adapter as before. Turn on the pump and continue pumping until the desired sample volume has been collected.

6. Disconnect the Tenax tube from the pump and the sampling port. Cap and label the tube for submittal to the laboratory (see Notes 2 and 3).

3.1.3.3 Charcoal Tube Sampling Procedure

1. After completing the preparation steps, uniformly break the sealed ends of a charcoal tube. If the tube should crack in the center, discard it.

2. Connect the inlet of the pump to the outlet of the charcoal tube using silicone tubing. The arrow on the tube indicates the correct airflow direction.

3. Set the pump to PRESET mode and select the desired sample volume.

4. Turn on the pump and set the flow rate to the desired value.

5. Turn the pump off momentarily to reset the volume meter.

6. Connect the inlet of the charcoal tube to the desired sampling port using silicone tubing. Turn on the pump and continue pumping until the desired sample volume has been collected.

7. Disconnect the charcoal tube from the pump and the sampling port. Cap and label the tube for submittal to the laboratory (see Notes 2 and 3).

3.1.4 Notes

1. Tenax tubes significantly restrict the flow rate, so the pump must be set at its maximum rate. The sample volume should be at least 1 liter to minimize errors in volume measurement due to the low flow rate.

2. The following information should be included on the label:

   - Well and Sampling-Port Identification
   - Date and Time of Sampling

- Sample Volume
- Flow Rate
- Temperature and Barometric Pressure at Time of Sampling (The volume displayed by the pump meter is at ambient conditions. Temperature and pressure measurements are therefore required in order to correct this volume to standard conditions.)
- Sampler's Signature

3. The sampling ports may eventually become clogged. As a preventive measure, the parts should be periodically "blown out" with compressed nitrogen.

3.2 COLLECTION OF WATER-POTENTIAL DATA

3.2 Introduction

procedures were developed to collect water-potential data from boreholes ed in Waste Disposal Areas G and L, Technical Area 54, Los Alamos nal Laboratory, New Mexico.

2 Equipment

psychrometers installed in Holes LLP-85-03 and LGP-85-07 may be read using utomated scanner. The scanner chosen for this study is the microprocessor-rolled HP-115 Water Potential Data System manufactured by Wescor. The 115 is a battery-powered scanning device, capable of determining water ential using either the dew-point (hygrometric) or the wet-bulb (psychro-ric) method. The equipment descriptions and operating procedures presented rein were taken from the Instruction Manual for the HP-115 (Wescor, undated).

maximum of 15 psychrometer leads can be plugged directly into the rear of the scanner, resulting in a 15-channel scanning capability. Measurements of temperature, zero offset, and psychrometer/hygrometer output are read from the psychrometer probes and automatically stored in memory for each scan. Time is also stored in memory at the beginning of each scanning cycle. A liquid crystal display (LCD) window located at the top of the instrument provides a means of monitoring the data-collecting operation. Data that have been stored in memory are then recovered via the RS-232C port located on the back panel of the instrument. Using this port, the memory contents may be transferred to a printer, a cassette, a telephone modem, or directly to a computer.

An internal rechargeable battery allows the HP-115 to run unattended for up to 60 days, or until the memory is filled. If desirable, an external battery can be connected to the rear panel of the instrument to permit longer periods of operation. The internal battery can be recharged from a wall socket by plugging the charging unit into the battery port located on the back of the instrument.

Since the scanner's memory limits the length of uninterrupted operating time, an equation is used to predict the time required to fill the memory. The maximum operating time of the scanner is given as

$$T = \frac{8112 \times 24}{S(6C + 2)}$$

where T is the time in hours, S is the number of scans per day, and C is the number of channels used. Example: Scanning 15 channels every 12 hours would fill the memory in 1058 hours (44 days).

3.2.3 Operating Procedure

A key is used to turn on the psychrometer scanner. When the scanner is switched on, it is best to remove the key from the switch because all the data and programming commands are lost once the instrument is switched off.

Based on conversations with the manufacturer, the scanning system works best in the psychrometric (wet-bulb) mode. Consequently, the operating procedure discussed herein focuses on the wet-bulb mode.

Several parameters must be programmed into the scanner memory when preparing the scanner for extended field use. These parameters are entered using the MODE selection dials, the SET selection dials, and the ENTER button. The various MODE options are discussed individually below.

1. MODE 00 - Time. Selection of Mode 00 by means of the MODE selection dial causes time to be displayed in hours and minutes from 0000 to 2400. To set time, dial in the correct time in hours and minutes on the SET dials, and press the ENTER button. Time may be synchronized to the second by turning on the system power synchronously with zero second of standard time prior to setting the hours and minutes as described above.

2. MODE 01 - Start Time. The next selection mode is the start time (MODE 01), used to preset the time when scanning is to begin. The start time can be any time from 0000 to 2400 hours. The desired time is selected on the SET dial and entered by pressing the ENTER button.

3. MODE 02 - Delay Time. Rotating the MODE dial to 02 causes the delay time (seconds) to be displayed. Delay time is the interval between the time that the cooling current is terminated and the time at which the reading is taken. In the psychrometric (wet-bulb) mode of operation, this delay time will allow the sensor to settle on the psychrometric plateau before a reading is taken. A delay time of 3 to 5 seconds will generally be sufficient for the sensor to reach a plateau. The desired time is selected on the SET dial and entered by pressing the ENTER button.

4. MODE 03 - Cooling Time. The cooling time is the length of time that a cooling current is passed through the psychrometer. The time interval selected must be long enough to permit water to condense on the thermocouple in the wet-bulb mode. Generally a cooling time of up to 30 seconds will be sufficient in the low-moisture ranges anticipated at Los Alamos. The cooling time is entered by means of the SET dials and the ENTER button.

5. MODES 04 and 05 - Cooling Coefficients. These modes refer to the cooling coefficients of the psychrometer probes. Since cooling coefficient settings are independent of the psychrometric (wet-bulb) mode of operation, they need not be set for the psychrometer probes at Los Alamos.

6. MODE 06 - Number of Sensors. Rotating the MODE dial to 06 causes the number of sensors being scanned to be displayed. This number may be changed by rotating the two rightmost digits of the SET dial to the appropriate number of sensors and pressing the ENTER button. Assuming that 15 psychrometer probes are to be scanned, the number of sensors should be set to 15.

7. MODE 07 - Scan Interval. Rotating the MODE dial to 07 causes the scan interval to be displayed. The scan interval is the elapsed time between successive scanning cycles. If the psychrometer probes are to be scanned twice daily, the scan interval (MODE 07) should be set to 1200 using the SET dial, and then the ENTER button should be pressed.

8. MODE 08 - Wet-Bulb Run. Rotating the MODE dial to 08 causes the SET time to be displayed until the first scanning cycle is complete. The initial scanning cycle is begun by pressing ENTER while in MODE 08. This initiates a primary scan of all the channels, after which the liquid crystal display (LCD) window will go blank. The LCD window will remain blank until the time in the scanner equals the start time designated in MODE 01. At this point, the LCD window will display time for approximately 14 seconds, and a new scanning cycle will begin.

During any scan, the temperature, offset, and wet-bulb readings will be displayed sequentially for each channel. All temperature readings are prefixed with a 4, followed by the value in tenths of a degree Celcius. Zero offset and wet-bulb readings, prefixed with a 5 and a 6, respectively, are displayed in tenths of microvolts. An example of the scanner readings is given below:

Temperature:	4205 = 20.5° Celcius
Zero Offset:	5010 = 1.0 microvolt
Wet Bulb:	6155 = 15.5 microvolts

9. MODE 13 - Data to RS-232C Port. Using Mode 13, data stored in the scanner's microprocessor may be transferred to a cassette tape while the scanner remains in the field. Wescor's CI-30 audio cassette interface is designed to interface the RS-232C port with the cassette recorder in this manner. The operating procedures for the CI-30 audio cassette interface are discussed below, and are based on the CI-30 Operating Manual (Wescor, 1982).

The CI-30 is equipped with an audio cable (Q4-275) and an RS-232C cable. The audio cable is simply a cord with a 1/8-inch phone jack on both ends. The RS-232C cable contains one end labeled INPUT and the other end labeled OUTPUT. Pinouts for the INPUT and OUTPUT ends of the RS-232C cable and their respective connections to the sending and receiving devices are shown in Figures 3-2 and 3-3. Data transfer via the RS-232C port is accomplished in the manner described below. Steps a through d

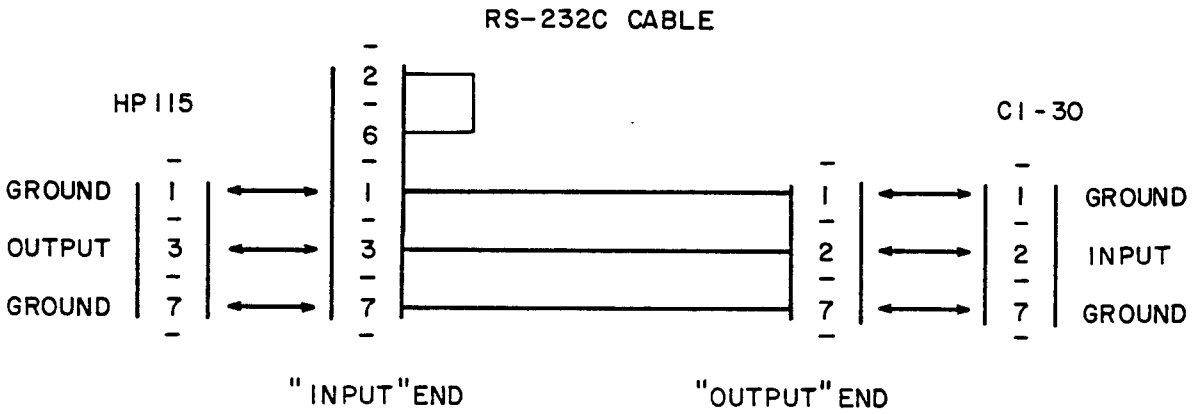

Figure 3-2. Schematic of the RS-232C Cable Connections Between the HP-115 and the CI-30 Interface

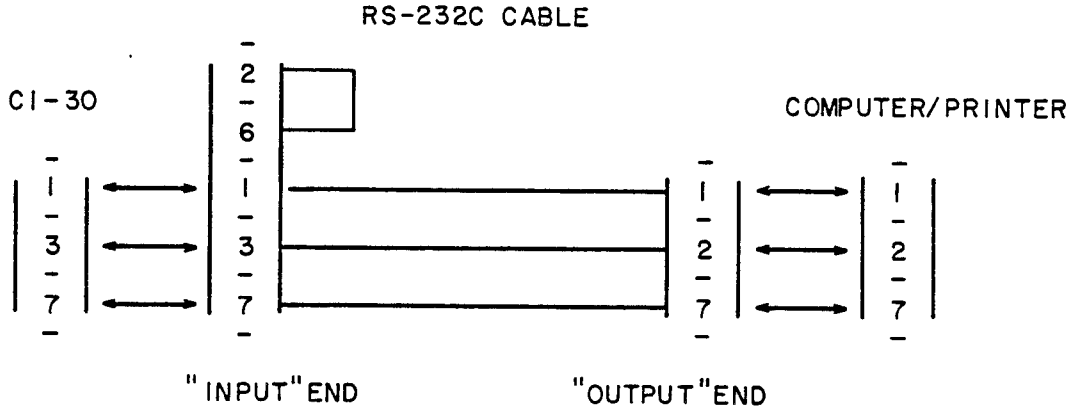

Figure 3-3. Schematic of the RS-232C Cable Connections Between the CI-30 Interface and the Computer/Printer

describe the transfer of data from the HP-115 scanner to the cassette recorder; Steps e through j describe data transfer from the cassette recorder to any computer.

a. Referring to Figure 3-2, connect the INPUT end of the RS-232C cable to the RS-232C port on the HP-115 scanner. Connect the OUTPUT end of the same cable to the RS-232C port on the CI-30 cassette interface.

b. Connect the audio cable (Q4-275) between the microphone jack on the CI-30 and the microphone jack on the cassette recorder. Advance the cassette tape until the clear leader is past the recording heads.

c. Switch the HP-115 to Mode 13. Turn on the CI-30 interface. Start the cassette recorder in RECORD mode and allow 10 seconds to pass. Initiate data transmission at the HP-115 by pressing the ENTER switch for 1 full second. This will cause the LCD window on the HP-115 to display four ones, i.e., 1111, indicating that data are being transmitted.

The data will continue to be transmitted to the cassette tape recorder until the HP-115 displays real time. Data transmissions can take anywhere from a few seconds to several minutes depending on the volume of data stored in the microprocessor. Upon completion of data transmission, turn the CI-30 interface off, stop the cassette recorder, rewind the tape, and disconnect both cables. Then set the MODE switch on the HP-115 to 08 and press the ENTER button to begin storing new data. The CI-30 and the cassette recorder can now be taken to the computer to enter the data.

d. The cable connections between the CI-30 and the computer are shown in Figure 3-3. Connect the INPUT end of the RS-232C cable to the RS-232C port on the CI-30. Connect the OUTPUT end to the RS-232C port on the computer.

f. Start the cassette recorder in the PLAY mode. When a high tone is heard, stop the recorder and connect the Q4-275 audio cable between the earphone jack on the cassette recorder and the earphone jack on the CI-30.

g. Prepare the computer to receive data. The parameters of the computer must match those of the sending device, i.e., the HP-115 scanner. Therefore, set the baud rate to 300, parity to none, and character length to 10 bits, which includes one start bit and one stop bit.

h. Adjust the volume control on the cassette recorder to between two-thirds and three-fourths of full volume, and start the cassette recorder in the PLAY mode. Allow the recorder to run in PLAY mode for 2 seconds prior to starting the computer and turning on the CI-30. It is important that the CI-30 be turned on last to prevent garbling of the data. The data are now being transmitted from the cassette recorder to the computer.

i. Upon completion of transmission, turn the CI-30 and the cassette recorder off and disconnect all cables. The wet-bulb and temperature data are now ready to be viewed at the computer terminal.

j. If errors appear in the data, repeat the above procedure. One possible source of error is the cassette tape. The tapes should be new, unrecorded tapes, preferably demagnetized. The recording and playing heads of the cassette recorder should also be thoroughly cleaned.

10. MODE 14 - Battery Percent Charge. Rotating the MODE dial to 14 causes the percent of battery charge to be displayed. In this and other operating modes, the decimals in the LCD window will flash whenever the battery charge drops below 10 percent of full charge.

3.3 COLLECTION OF PRESSURE MEASUREMENTS

3.3.1 Introduction

This procedure was developed to obtain pressure measurements from transducers installed in Hole LLP-85-03, located in Technical Area 54 at Los Alamos National Laboratory.

3.3.2 Equipment

The pressure-measurement system installed at Los Alamos consists of four electrical pressure transducers (cf. Figure 2-10) connected to an electro-piezo scanner recorder. The transducers use an absolute electrical pressure sensor with a strain-gauged, stainless steel diaphragm. A stainless steel disc filter permits direct burial of the transducers. The pressure range for the transducers is 0 to 25 pounds per square inch (psi) with a readability of 0.01 percent of scale.

The electro-piezo scanner recorder is a portable, battery-operated, ten-channel system for automatically recording transducer data. The date, time, and output from each of the transducers are recorded on an integral printer. The scanner records the output for a permanent record or can provide the output to an external device such as a computer, data terminal, paper punch, or magnetic tape recorder. The system can scan continuously or at variable scale intervals. The recorder can be completely sealed and left unattended to automatically record data at selected intervals.

3.3.3 Monitoring Procedure

The pressure-measurement system was installed in October 1985, and is presently collecting data. The major requirement for servicing the pressure-scanning system is periodic replacement of the printer paper. With the scan interval set at 1-hour periods, it is expected that the printer paper will need to be replaced once a month.

In addition, the scanner should be checked periodically to ensure that the power supply and the transducer connections are intact. A simple check of the battery-test system will demonstrate whether the power supply is connected. If the symbol O/C precedes a pressure reading on the printer paper, then the transducer connection is faulty. The transducer connector plug should be

removed from the scanner input port, checked, cleaned, and reattached. The system is then rechecked to ensure that a proper electrical connection has been achieved.

The channel numbers corresponding to the four transducers are as follows:

- CH00 - Surface Transducer
- CH01 - Transducer Buried at 26 Feet Below Ground Level
- CH02 - Transducer Buried at 54 Feet Below Ground Level
- CH03 - Transducer Buried at 90 Feet Below Ground Level

Channel 00 is the barometric pressure calibrated at sea level.

4.0 REFERENCES

Nyhan, S. M., and J. J. Dexter, 1985. Vadose Zone Characterization of Technical Area 54, Waste Disposal Areas G and L, Los Alamos National Laboratory, New Mexico - Report 1: Drilling and Logging Activities, GJ-37, Bendix Field Engineering Corporation, U.S. Department of Energy, Grand Junction Projects Office, Grand Junction, Colorado.

Wescor, 1982. CI-30 Audio Cassette Interface, Wescor, Inc., 459 South Main Street, Logan, Utah 84321.

Wescor, undated. Instruction Manual: Model HP-115 Microprocessor-Controlled Water Potential Data System, Wescor, Inc., 459 South Main Street, Logan, Utah 84321.

GJ-44

VADOSE ZONE CHARACTERIZATION OF TECHNICAL AREA 54, WASTE DISPOSAL AREAS G AND L, LOS ALAMOS NATIONAL LABORATORY, NEW MEXICO

REPORT 3: PRELIMINARY ASSESSMENT OF THE HYDROLOGIC SYSTEM

March 1986

Bendix Field Engineering Corporation
Grand Junction, Colorado

ALLIED Bendix Aerospace

This report was prepared as an account of work sponsored by an agency of the United States Government. Neither the United States Government nor any agency thereof, nor any of their employees, makes any warranty, express or implied, or assumes any legal liability or responsibility for the accuracy, completeness, or usefulness of any information, apparatus, product, or process disclosed in this report, or represents that its use would not infringe privately owned rights. Reference therein to any specific commercial product, process, or service by trade name, trademark, manufacturer, or otherwise, does not necessarily constitute or imply its endorsement, recommendation, or favoring by the United States Government or any agency thereof. The views and opinions of authors expressed herein do not necessarily state or reflect those of the United States Government or any agency thereof.

This report is a result of work performed by Bendix Field Engineering Corporation, Operating Contractor for the U.S. Department of Energy, Grand Junction Projects Office.

GJ-44

VADOSE ZONE CHARACTERIZATION OF TECHNICAL AREA 54, WASTE DISPOSAL AREAS G AND L, LOS ALAMOS NATIONAL LABORATORY, NEW MEXICO

REPORT 3: PRELIMINARY ASSESSMENT OF THE HYDROLOGIC SYSTEM

Peter M. Kearl, James J. Dexter, and Mark Kautsky

Bendix Field Engineering Corporation
Grand Junction Operations

March 1986

Prepared for
U.S. Department of Energy
Los Alamos National Laboratory
Los Alamos, New Mexico
in Conjunction with
U.S. Department of Energy
Grand Junction Projects Office
Grand Junction, Colorado
Under Contract No. DE-AC07-76GJ01664

CONTENTS LISTING

		Page
FOREWORD		vii
EXECUTIVE SUMMARY		ix
SECTION 1	INTRODUCTION	1
	1.1 Purpose and Scope	3
	1.2 Terminology and Units	4
	1.2.1 Terminology	4
	1.2.2 Units	5
	1.3 Previous Work by Bendix	5
SECTION 2	GEOLOGIC CHARACTERIZATION OF THE STUDY AREA	7
	2.1 Regional and Site Geology	9
	2.2 Welding and Correlation of Ash-Flow Units at Mesita del Buey	14
	2.3 Petrographic Analyses	14
	2.4 Interpretation of Geophysical Logs	17
	2.4.1 Natural Gamma and Epithermal Neutron Moisture Logs	19
	2.4.2 Spectral Gamma Logs	19
	2.4.3 Magnetic Susceptibility and Gamma-Gamma Logs	22
	2.5 Fractures	27
SECTION 3	HYDROLOGIC CHARACTERIZATION OF THE VADOSE ZONE	29
	3.1 General Characteristics	31
	3.1.1 Gravimetric Moisture Content	31
	3.1.2 Porosity	35
	3.1.3 Moisture Characteristic Curves	37
	3.2 Permeability Determinations	40
	3.2.1 Borehole-Injection Tests	40
	3.2.2 Vacuum Tests	49
	3.2.3 Laboratory Measurements	53
	3.2.4 Hydraulic Conductivity as a Function of Moisture Content	58
	3.2.5 Permeability Summary	59
	3.3 Gradient Determinations	64
	3.3.1 Temperature and Water-Potential Measurements	64
	3.3.2 Atmospheric/Rock-Pore Pressure Monitoring System	80
SECTION 4	NEUTRON MOISTURE MEASUREMENTS	83
	4.1 Purpose and Scope	85
	4.2 Casing Installations	85
	4.3 Calibration of the Neutron Probe	87
	4.4 Monitoring Program	87

CONTENTS LISTING (continued)

		Page
SECTION 5	PORE-GAS SAMPLING SYSTEM.	89
	5.1 Purpose and Scope.	91
	5.2 Design	91
	5.3 Installation	91
SECTION 6	CONCLUSIONS	95
SECTION 7	REFERENCES.	99

LIST OF APPENDICES

Appendix A.	Lithologic Logs and Instrument Completion Diagrams	A-1
Appendix B.	Petrographic Reports	B-1
Appendix C.	Moisture Characteristic Curves	C-1
Appendix D.	Effective Permeability as a Function of Saturation	D-1
Appendix E.	Listing of Fortran V Program for Converting Psychrometer Microvoltage Outputs to Water Potential	E-1

LIST OF FIGURES

Figure 2-1.	Location of the Study Area and Regional Geologic Relationships	10
2-2.	Geologic Cross Section from the Jemez Mountains on the West, Through the Pajarito Plateau, to the Rio Grande River on the East.	11
2-3.	Locations of Drill Holes in Areas G and L, Technical Area 54, Los Alamos National Laboratory, New Mexico . . .	12
2-4.	Cross Section Showing Parts of the Tshirege Member of the Bandelier Tuff, Drawn Through Mesita del Buey and Technical Area 54	15
2-5.	Epithermal Neutron, Natural Gamma, and Lithologic Logs for Hole LGC-85-10.	20
2-6.	Comparison of Moisture Curves for Hole LGM-85-06, Derived by Geophysical and Gravimetric Methods.	21
2-7.	Spectral Gamma and Lithologic Logs for Hole LGM-85-11 . .	23
2-8.	Magnetic Susceptibility, Apparent Density, and Lithologic Logs for Hole LGC-85-10.	24
2-9.	Magnetic Susceptibility, Apparent Density, and Lithologic Logs for Hole LLM-85-02.	25
2-10.	Magnetic Susceptibility, Apparent Density, and Lithologic Logs for Hole LGM-85-11.	26

LIST OF FIGURES (continued)

			Page
Figure	3-1.	Plots of Volumetric Moisture Content as a Function of Depth for Five Drill Holes.	34
	3-2.	Porosity of Battleship Rock Ash-Flow Tuff, Valles Mountains, New Mexico	38
	3-3.	Air-Injection Apparatus Used for In-Situ Permeability Measurements.	43
	3-4.	Water-Injection Apparatus Used for In-Situ Permeability Measurements.	44
	3-5.	Vacuum-Testing Apparatus Used for In-Situ Permeability Measurements.	50
	3-6.	Unsaturated Hydraulic Conductivities as Functions of Moisture Content and Water Potential for Samples MCG-603 and MCG-604	60
	3-7.	Unsaturated Hydraulic Conductivities as Functions of Moisture Content and Water Potential for Samples MCG-607 and MCG-613	61
	3-8.	Unsaturated Hydraulic Conductivities as Functions of Moisture Content and Water Potential for Samples MCG-616 and MCG-617	62
	3-9.	Unsaturated Hydraulic Conductivities as Functions of Moisture Content and Water Potential for Sample MCG-620	63
	3-10.	Sketch of the Single-Junction Stainless Steel Screen-Shielded Thermocouple Psychrometer.	66
	3-11.	Sketch of the Stainless Steel Calibration Chamber Showing Seals and Screen-Shielded Thermocouple Psychrometer . . .	68
	3-12.	Water Potential Versus Time for Selected Psychrometers in Hole LLP-85-03	71
	3-13.	Temperature Versus Time for Selected Psychrometers in Hole LLP-85-03	72
	3-14.	Water Potential Versus Time for Selected Psychrometers in Hole LGP-85-07	73
	3-15.	Temperature Versus Time for Selected Psychrometers in Hole LGP-85-07.	74
	3-16.	Air Temperature Versus Time at Hole LLP-85-03	75
	3-17.	Water Potential Versus Depth for Hole LLP-85-03	76
	3-18.	Temperature Versus Depth for Hole LLP-85-03	77
	3-19.	Water Potential Versus Depth for Hole LGP-85-07	78
	3-20.	Temperature Versus Depth for Hole LGP-85-07	79
	3-21.	Results from the Pressure Transducers Installed in Hole LLP-85-03.	82
	4-1.	Casing Installation and Depths of Neutron Probe Measurements in Hole LLN-85-04.	86
	4-2.	Casing Installation and Depths of Neutron Probe Measurements in Hole LGN-85-08.	88
	5-1.	Diagram of a Pore-Gas Sampling Port	92

LIST OF TABLES

			Page
Table	2-1.	Volume-Percent Quartz and Sanidine Determined from Point-Count Analysis of Thin Sections.	18
	2-2.	Number of Fractures Logged in the Los Alamos Drill Holes	28
	3-1.	Results of Porosity Determinations Using the Helium-Injection Method and Boyle's Law.	36
	3-2.	Hydraulic Conductivity Determined from Air-Injection Tests in Los Alamos Drill Holes	47
	3-3.	Hydraulic Conductivity Values Determined from Water-Injection Tests in Hole LLM-85-05	48
	3-4.	Comparison of Intrinsic Permeability Values Determined from Water-Injection and Air-Injection Tests in Hole LLM-85-05.	49
	3-5.	Permeability Values Determined from Vacuum Tests in Los Alamos Drill Holes.	54
	3-6.	Comparison of Intrinsic Permeability Values Determined from Air-Injection and Vacuum Tests in Los Alamos Drill Holes	55
	3-7.	Intrinsic Permeability Values Determined from Laboratory Analysis of Core Samples.	57
	3-8.	Comparison of Average Intrinsic Permeability Values for the Major Geologic Units of the Bandelier Tuff in the Study Area	64
	3-9.	Installation Depths and Calibration Coefficients for Psychrometers in Hole LLP-85-03	69
	3-10.	Installation Depths and Calibration Coefficients for Psychrometers in Hole LGP-85-07	70

FOREWORD

This study was initiated in response to a Compliance Order/Schedule (Docket Number 001007) issued by the State of New Mexico's Environmental Improvement Division under the authority of New Mexico's Hazardous Waste Management Act. The Order/Schedule, dated 7 May 1985, specifies a time line for obtaining certain geotechnical information regarding Waste Disposal Areas G and L in Technical Area 54, Los Alamos National Laboratory, New Mexico. This report addresses the informational requirements outlined in Paragraph 25, Tasks 1 through 5, of the Compliance Order/Schedule. The investigations described in this report were performed by personnel of Bendix Field Engineering Corporation, Grand Junction, Colorado, Operations Office.

The tasks requested by the State of New Mexico in Paragraph 25 of the Compliance Order/Schedule are addressed in the following sections of this report:

Compliance Order Task and Brief Title	Section in Report
1: Permeability Determinations	3.2.1, 3.2.2, 3.2.3
2: Moisture Characteristic Curves	3.1.3
3: Unsaturated Hydraulic Conductivity	3.2.4
4: Infiltration and Redistribution of Water	3.1.1, 3.3.1, 4.0
5: Pore-Gas-Sampling Installations	5.0

The emphasis of the Compliance Order/Schedule is on the quantification of capillary or liquid-flow transport processes. However, moisture data presented by Purtymun and Kennedy (1971) and Abeele and others (1981), as well as the moisture data presented in this report, indicate that movement by vapor phase is the major transport mechanism in the Bandelier Tuff in the study area. Thus, while much of the capillary-related information is useful, it can draw attention away from vapor transport. The reader is therefore asked to focus on relating the information presented in this report to vapor-transport processes.

In addition to the authors cited on the title page, a number of other professionals of Bendix Field Engineering Corporation/Grand Junction Operations contributed significantly to this study and to preparation of this report. These individuals and their respective contributions are listed below.

- Sue Rush who served as Project Manager and assisted in the drilling and the pore-gas-sampler installations.
- Nic Korte who served as Project Manager and assisted in the design and test of the pore-gas samplers.
- Steve Sturm who assisted in the drilling and the logging of core.
- Jeff Price who assisted in the hydrologic testing.

- Jack McCaslin who assisted in the drilling procurement as well as the drilling and the pore-gas-sampler installations.
- Steve Donivan who assisted in the design and test of the pore-gas samplers.
- Sandy Wagner who performed the field chemical monitoring and set up the analytical subcontract.
- Sue Knutson and Dave Traub who performed the geophysical logging.
- Rich Zinkl who provided the computer support.
- Bonnie Edwardson who performed the editing and document coordination.

The following personnel from Los Alamos National Laboratory also played a significant role in the completion of this study.

- Micheline Devaurs was the principal technical contact, assisted in the planning and conduct of field activities, and wrote Section 4 of this report.
- Dave McInroy assisted in several aspects of the field activities.
- Bill Purtymun recommended the drilling technique and provided much useful insight with respect to logging the Bandelier Tuff.

EXECUTIVE SUMMARY

The hydrologic characteristics of the vadose zone in Areas G and L, Technical Area 54, at Los Alamos National Laboratory are being investigated in response to a Compliance Order/Schedule (Docket Number 001007) issued to the Laboratory by the State of New Mexico's Environmental Improvement Division under the authority of New Mexico's Hazardous Waste Management Act. This report presents a preliminary assessment of the hydrologic system, specifically in response to Tasks 1 through 5, Paragraph 25, of the Compliance Order/Schedule. Bendix Field Engineering Corporation/Grand Junction Operations conducted the work described in this report.

The most significant conclusion resulting from this investigation is that vapor-phase transport is the predominant mechanism controlling the potential subsurface movement of contaminants in the study area. Evidence for this conclusion includes the low moisture content of the underlying rock and the high moisture-retention values observed in the moisture characteristic curves (Task 2 of the Compliance Order/Schedule). These results indicate that there is no interconnection or movement of liquid water in the interval of Bandelier Tuff examined in this study.

Permeability measurements were required by Task 1 (field tests) and Task 3 (laboratory tests) of the Compliance Order/Schedule. Field measurements were made using a vacuum-test method and by means of borehole injection with both air and water. Laboratory determinations were made using both the Klinkenberg Correction and the Dynamic methods. Agreement among the various methods was generally good, yielding an intrinsic permeability for the Bandelier Tuff in the range 10^{-8} to 10^{-9} cm^2.

Determination of the water distribution in the tuff was required by Task 4. Gravimetric results indicate a moisture content of 2 to 4 percent for the center portion of the profile, with generally higher contents in the lower portion of Unit 1b. Preliminary data from the thermocouple psychrometers indicate that water potentials range from -1 to -15 bar, suggesting low moisture conditions in the tuff. Neutron-measurement tools used for acquiring moisture data were also installed in two holes in the study area. Although data acquired with the probe were not available at the time of this writing, it is feared that the tuff may be too dry for such measurements to be effective.

The various field and laboratory activities conducted during this study permit an evaluation of the effects of porosity, pumice content, and degree of welding on the unsaturated transport processes. As expected, porosity and pumice content are highly correlated. The high porosity demonstrates that the tuff acts like a sponge: A quantity of water equal to approximately one-quarter of the rock volume is required to satisfy the capillary forces and permit the movement of water in the liquid phase. Permeability, on the other hand, is inversely proportional to porosity due to the significant amount of dead-end pore space which occurs in pumice. Finally, a high degree of welding apparently reduces the average radii of pores, the result being an increase in the capillary forces and the residual moisture content.

In partial fulfillment of the requirements of Task 5, installations for sampling pore gas in discrete subsurface zones were completed in certain holes. No data are yet available, but the rationale behind each sampling-port location is described in this report.

Another major objective of this study was to evaluate the role of fractures as avenues of transport in the Bandelier Tuff. Results obtained thus far, however, are inconclusive. The permeability of fractured zones, for example, is not significantly greater than that of the surrounding rock, even though certain fractured zones exhibit a higher moisture content. It is anticipated that results of the pore-gas sampling and analysis will be of particular benefit to the definition of the role of fractures in the vadose zone.

Section 1

INTRODUCTION

1.1 PURPOSE AND SCOPE

This report presents a preliminary assessment of the hydrologic processes that could contribute to transport of hazardous waste buried in the Bandelier Tuff at Los Alamos National Laboratory, New Mexico. More specifically, the study area encompasses Waste Disposal Areas G and L in Technical Area 54. The study was initiated in response to a Compliance Order/Schedule issued by the Environmental Improvement Division of the State of New Mexico. Included in the Order was a directive to obtain certain geotechnical information regarding the above-mentioned waste-disposal areas. The investigations described in this report were performed by Bendix Field Engineering Corporation/Grand Junction Operations (Bendix). Bendix is the operating contractor for the U.S. Department of Energy (DOE) Grand Junction, Colorado, Projects Office.

The report is organized into seven sections, followed by five appendices. The emphasis throughout is on the transport processes in the unsaturated zone that control potential contaminant migration in the Bandelier Tuff. Immediately following this Introduction, Section 2 defines the geologic framework through which these processes occur in the study area. Section 3 presents a characterization of the vadose zone in terms of the driving forces of transport, namely, gradients such as temperature and pressure. These evaluations require a considerable amount of data regarding the vadose zone, including permeability and such general parameters as moisture content and porosity. Thus, the early subsections of Section 3 describe the field and laboratory measurements conducted to acquire these data, together with the necessary calculations.

Sections 4 and 5 contain brief discussions of the neutron-moisture-measurement and pore-gas sampling-port installations, respectively; data and interpretations will be presented in a subsequent report. A comprehensive summary of this preliminary assessment is presented in Section 6, followed by a bibliography of the references (Section 7) cited throughout the text and appendices. Appendices A through E contain much of the data acquired throughout the course of this study, including lithologic logs, petrographic data, and moisture characteristic and permeability curves.

For this study, several experimental techniques were used to drill test holes and to measure important unsaturated flow parameters. In those cases, descriptions of the equipment, procedures, and assumptions associated with a specific test are included in the appropriate discussion.

Analysis of the rock core was hampered by several problems. From the core obtained during drilling, representative samples of the Tshirege Member of the Bandelier Tuff were selected and sent to TerraTek Research Laboratory of Salt Lake City, Utah, for analysis. Approximately 75 percent of this core was either completely unconsolidated or so friable that special handling techniques and procedures had to be developed. Moreover, mercury injection was not feasible on the unconsolidated samples, requiring that alternative laboratory techniques be substituted for the measurement of capillary forces. As a result, it was not possible to quantify the pore-size distributions and the imbibition or wetting curves for the porous media in the study area.

1.2 TERMINOLOGY AND UNITS

1.2.1 TERMINOLOGY

The terms 'vadose zone' and 'unsaturated zone' are often used synonymously in the literature, even though there is a distinction between the two. The unsaturated zone is defined as a subsurface area above the water table in which the porous material contains both air and water, the latter under pressures that are less than those of the atmosphere. The vadose zone also refers to the subsurface area above the water table composed of partially saturated porous material. The distinction lies in the fact that the vadose zone can contain perched zones of water, and the water in these perched zones is under pressures greater than those of the atmosphere. For purposes of this study, the term vadose zone will be used when referring to the subsurface area above the water table, but the processes controlling contaminant migration in that zone will be referred to as the 'unsaturated transport processes.'

Other potentially confusing terms used throughout the report include permeability, coefficient of permeability, hydraulic conductivity, and intrinsic permeability. Distinctions between these terms are summarized below.

- Permeability, when used alone, refers to the movement of a fluid through the porous or fractured media. No quantification is intended to be associated with the term.

- Hydraulic conductivity is the term used to quantify the permeability of the medium. It is dependent on the porous medium and the fluid, and must therefore be expressed in such a way that the fluid represented by the term is specified. The dimensions for hydraulic conductivity are length per unit time (L/t). The term coefficient of permeability is synonymous with hydraulic conductivity.

- Intrinsic permeability is a function of only the medium and has dimensions of length squared (L^2). Expressing permeability in this way permits comparison of permeability values obtained through different techniques using different fluids. (The relationship between hydraulic conductivity and intrinsic permeability is defined in Section 3.2.1.4.)

Laboratory results express the hydraulic conductivity as a function of the moisture content (Section 3.2.4) in terms of effective permeability (in units of millidarcys). Permeability expressed in this manner is considered an intrinsic permeability. For example, the effective permeability for water is a measurement of the intrinsic permeability of the void space occupied by water, so the value is expressed in terms which are independent of the fluid.

The terms capillary forces, capillary pressure, soil tension, and soil suction are used synonymously. For purposes of this report, capillary forces are quantified using the term water potential which is measured in pressure units of negative bars or negative pounds per square inch (psi).

One other term used throughout the report requires clarification. As used herein, lapilli is defined in a manner consistent with the definition presented by Ross and Smith (1961): Lapilli consist of either juvenile lava fragments, still plastic or liquid when ejected, or of broken rock of any sort

from the walls of the vent, or from the bedrock (country rock); in other words, they may be essential, accessory, or accidental ejecta. These authors state, however, that the term lapilli should be restricted to describing fragments in the size range 4 to 32 millimeters (mm); fragments of pyroclastic material larger than 32 mm are called blocks, whereas fragments smaller than 4 mm are called coarse ash (Ross and Smith, 1961). For purposes of simplification in this report, the size restriction for lapilli was ignored. For example, the presence of 'accessory' or 'accidental' lithic fragments (e.g., basalt fragments) less than 4 mm in diameter is one of the distinguishing characteristics of Unit 1b; these fragments are referred to as lithic lapilli in this report. In addition, fragments of pyroclastic ejecta of pumice or rock in the size range 32 to 60 mm (the latter value being the approximate diameter of the rock core obtained during this study) are also referred to as lapilli in this report.

1.2.2 UNITS

Inconsistencies in the unit systems used to express measurements occur throughout the report. Unfortunately, this inconsistency is unavoidable for the following reason. Several different types of instrument were used in the study, some of which display data in metric units (mks or cgs systems), while others are based on the British engineering system (fps system).* Conversion from one set of units to another is often cumbersome. For example, an instrument which measures pressure in the range 0 to 60 pounds per square inch (psi), with 0.2-psi increments, is described efficiently in British-system units. Conversion to the metric system results in an awkward description [i.e., 0 to 413.47 kilonewtons per square meter (kN/m^2) with 1.38-kN/m^2 increments]. Thus, for purposes of this report, both systems of units are given only when appropriate, in which cases the value in metric units is cited first, followed in parentheses by the equivalent value in British-engineering-system units.

1.3 PREVIOUS WORK BY BENDIX

This report is the third in a series of reports describing the preliminary hydrogeologic assessment of Waste Disposal Areas G and L in Technical Area 54, Los Alamos National Laboratory. The work has been performed by Bendix, in cooperation with the HSE-8 Environmental Surveillance Group at Los Alamos National Laboratory. The first report (Rush and Dexter, 1985) discusses the drilling and logging activities which were performed during the Summer of 1985. The second report (Bendix Field Engineering Corporation, 1985b) describes the procedures used for operating instruments installed at the site.

*For metric-system units, mks = meter-kilogram-second and cgs = centimeter-gram-second. For British-system units, fps = foot-pound-second.

Section 2

GEOLOGIC CHARACTERIZATION OF THE STUDY AREA

This description of the geologic characteristics of the Bandelier Tuff in the study area is divided into five subsections. The first describes regional and site geology, based on information contained in the literature and observations of core obtained from holes drilled at the site (Rush and Dexter, 1985). This is followed by a discussion of the degree of welding observed in the tuff and the correlation of ash-flow units across the study area. Results of petrographic analyses of core samples from the drill holes and interpretations of the geophysical logs from the holes are summarized in Sections 2.3 and 2.4, respectively. The final subsection describes fractures observed in the core, since the presence of fractures can affect the nature and direction of waste transport in the tuff.

2.1 REGIONAL AND SITE GEOLOGY

The study area is located just east of the southeastern boundary of the Colorado Plateau (see Figure 2-1), on the eastern flank of the Jemez Mountains, also known as the Pajarito Plateau. The Jemez Mountains lie at the intersection of the volcanically active Jemez Lineament and the tectonically active Rio Grande rift. The Jemez Lineament is an alignment of Late Cenozoic volcanic fields; volcanism along the lineament has been continuous since Pliocene time (Goff and Bolivar, 1983).

Waste Disposal Areas G and L, located within Technical Area 54 at Los Alamos National Laboratory, are situated on Mesita del Buey, which is part of the Pajarito Plateau (Figure 2-2). Mesita del Buey, a narrow, southeast-trending mesa approximately two miles long and one-quarter of a mile wide, is underlain by rhyolitic ash-flow and air-fall deposits of the Bandelier Tuff. The Bandelier Tuff is composed of two members: the lower Otowi Member, 1.4 million years old, and the upper Tshirege Member, 1.1 million years old (Bailey and others, 1969). The Otowi Member consists of basal, air-fall tuff overlain by nonwelded ash-flow deposits containing abundant lithic lapilli. The Tshirege Member, which overlies the Otowi, consists of basal, bedded, air-fall tuff overlain by nonwelded to welded ash-flow tuffs containing abundant pumice and lithic lapilli. The Otowi and Tshirege members are both over 100 feet (ft) thick under Mesita del Buey (Purtymun and Kennedy, 1971). All waste-disposal excavations in Technical Area 54 are located in the upper portion of the Tshirege Member of the Bandelier Tuff.

The Tshirege Member can be subdivided into three units, two of which occur at Mesita del Buey (Units 1 and 2); the third unit, a nonwelded to moderately welded pumiceous tuff, is absent in the study area (Purtymun and Kennedy, 1971). The first two units dip 2 to 3 degrees to the southeast and become thinner in the direction of dip, away from their source in the Valles Caldera. Each of the units consists of two subunits (a and b), which are described by Purtymun and Kennedy (1971). Their descriptions, together with characteristics observed in the actual core collected for this study, were used to distinguish between each of the subunits. Lithologic logs of Units 1a through 2b, derived from drill holes in the study area, are presented in Appendix A; drill-hole locations are shown in Figure 2-3.

The lowermost subunit of the Tshirege Member encountered during this study was Unit 1a, a nonwelded, light-orange to light-brown, rhyolitic, vitric-crystal,

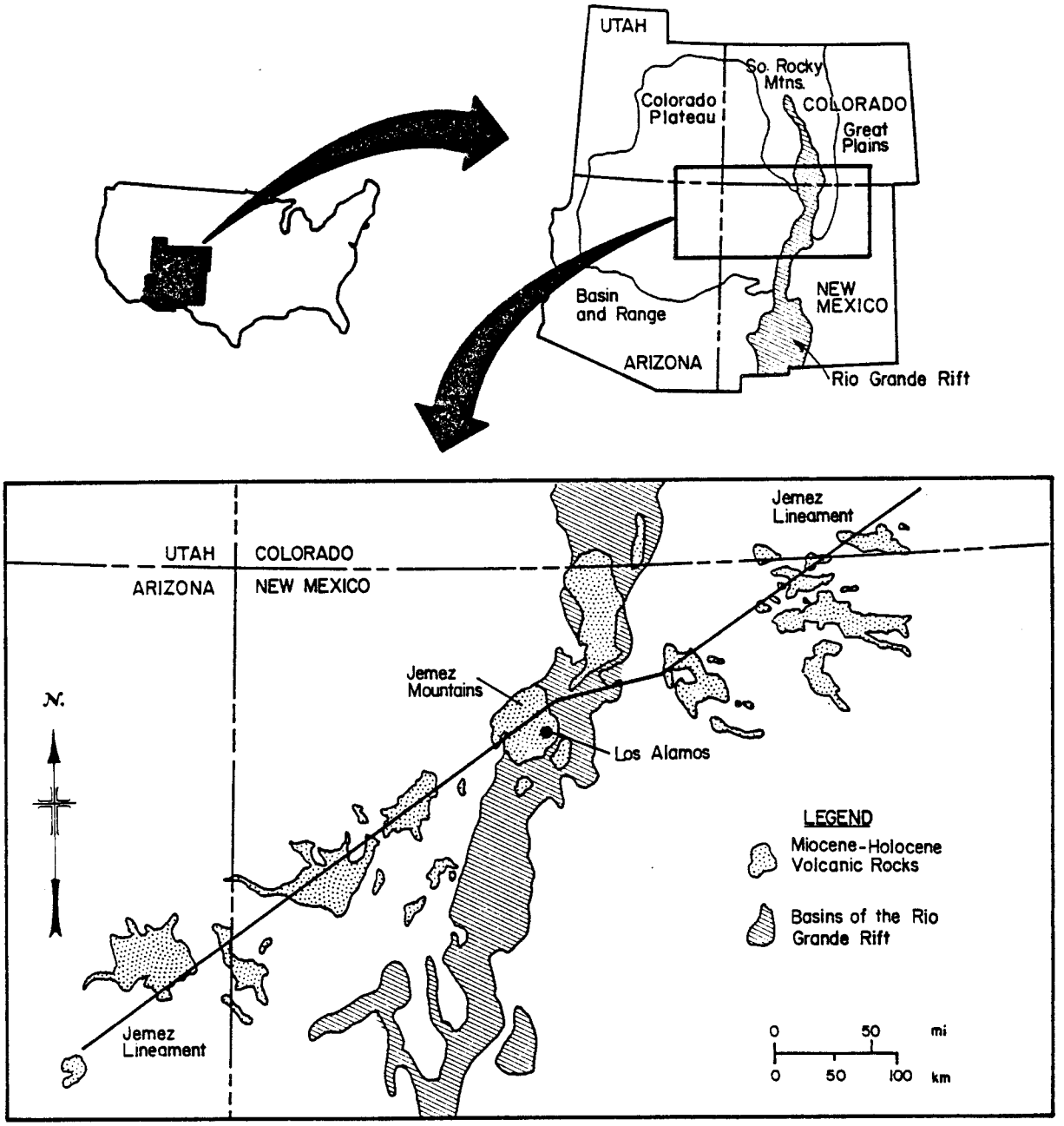

Figure 2-1. Location of the Study Area and Regional Geologic Relationships (modified from Goff and Bolivar, 1983)

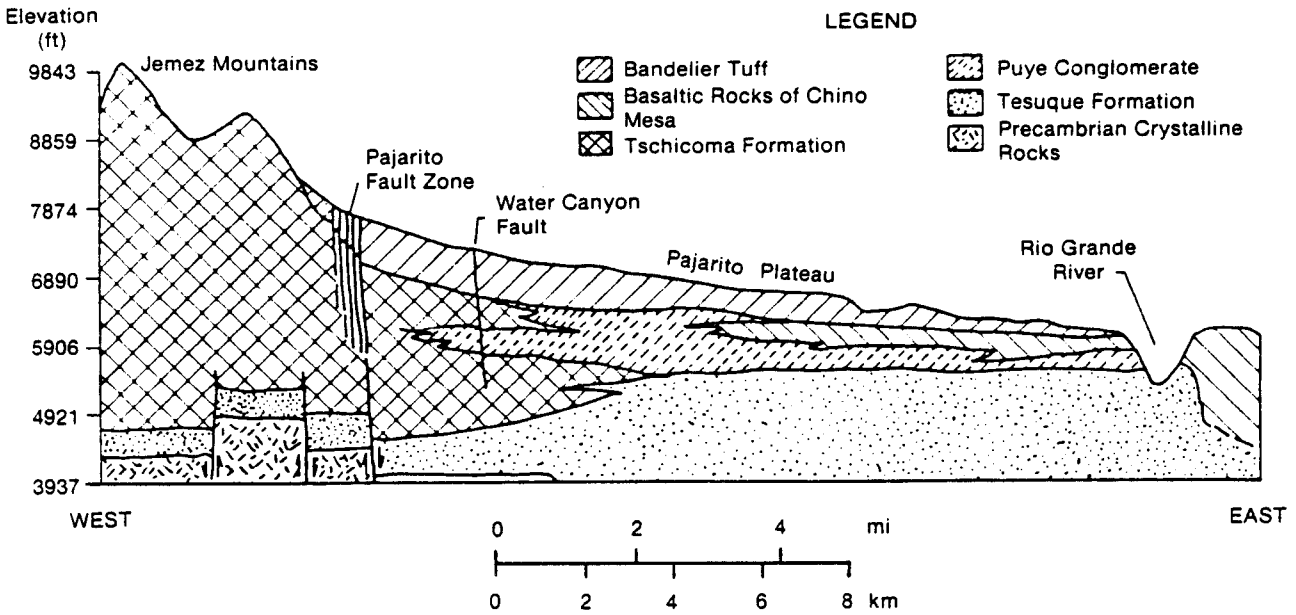

Figure 2-2. Geologic Cross Section from the Jemez Mountains on the West, Through the Pajarito Plateau, to the Rio Grande River on the East (modified from Abeele and others, 1981)

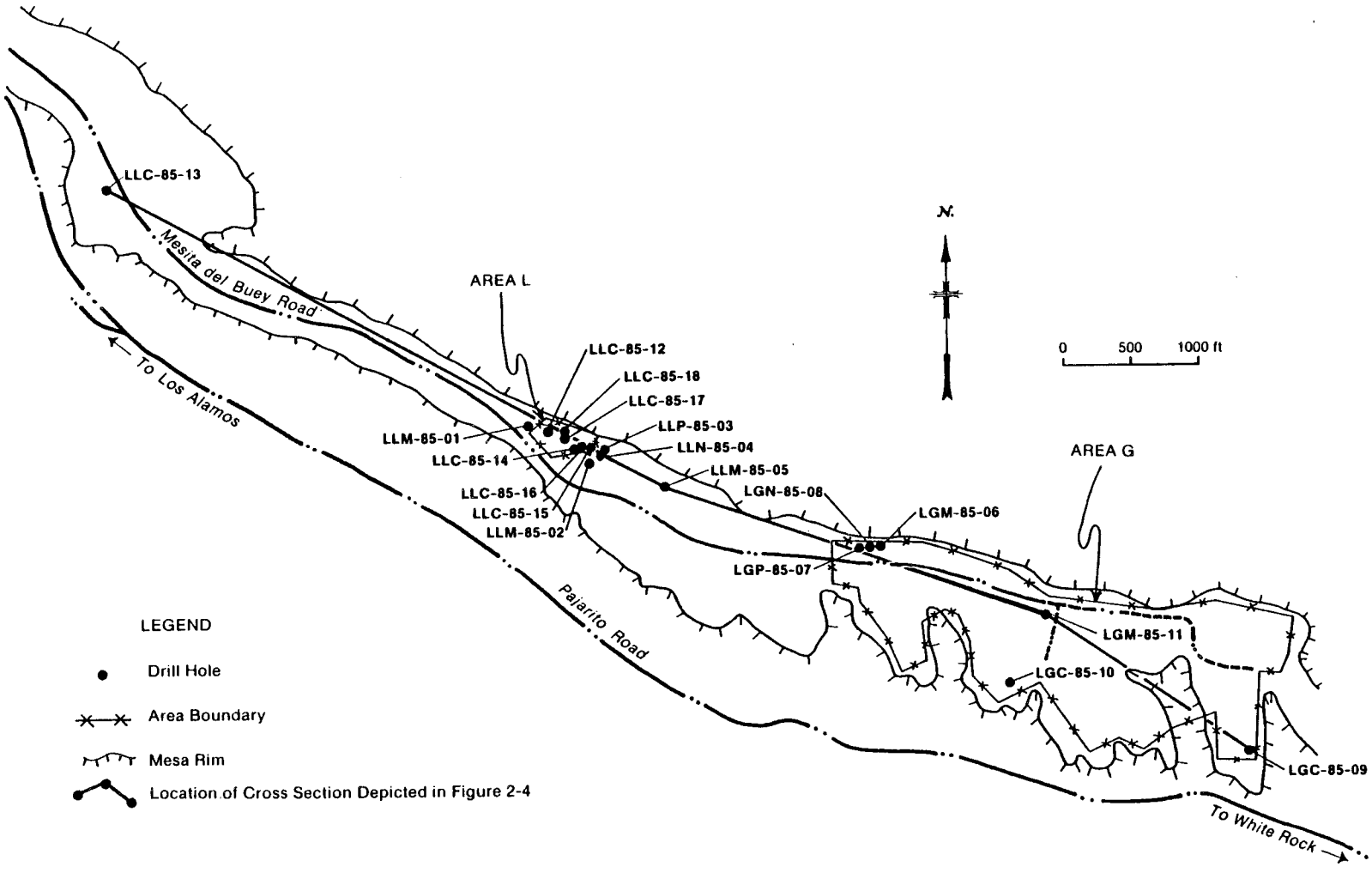

Figure 2-3. Locations of Drill Holes in Areas G and L, Technical Area 54, Los Alamos National Laboratory, New Mexico

ash-flow tuff. The maximum thickness of Unit 1a encountered in the Los Alamos drill holes was 26 ft; however, no drill hole penetrated the entire unit. At Mesita del Buey, Unit 1a consists of very uniform, nonwelded ash composed of brown glass shards and fine, flattened pumice lapilli, neither of which is devitrified. Also found in the ash are numerous but scattered lumps of light-tan pumice lapilli and latitic to rhyolitic lithic lapilli.

The contact between Units 1a and 1b is discerned in the core on the basis of the increased degree of welding and the presence of brown and gray pumice lapilli in Unit 1b. Unit 1b is a rhyolitic ash-flow tuff, ranging in color from light gray to pinkish gray near the top, and from pale red to moderate orange pink near the base. The lower portion of Unit 1b contains distinctive, gold-colored, bipyramidal quartz crystals up to 4 millimeters (mm) in diameter and a bimodal distribution of latitic to rhyolitic lithic lapilli. The lithic lapilli are abundant in the size range 1 to 4 mm in diameter, and occur less commonly in the size range 15 to 60 mm. They decrease in size and abundance toward the top of Unit 1b, where the occurrence of lithic lapilli is rare. The degree of welding in Unit 1b generally varies from slightly welded at the base to moderately welded just above the base to slightly welded at the top. In four core holes where the entire section of Unit 1b was penetrated, the total thickness varies from approximately 29 ft (on the southeast) to 52 ft (on the northwest).

The contact between Units 1b and 2a was difficult to identify precisely during coring operations. In certain cases, the contact can be estimated on the basis of either a subtle color change in a slightly welded portion of the core, or the presence of brown, gray, and olive-colored pumice lapilli in the basal portion of Unit 2a. These pumice lapilli are generally larger than the predominantly brown pumice lapilli found in the upper portion of Unit 1b. In addition, the contact seems to occur in a zone where vapor-phase crystals of quartz and sanidine are small (less than 1 mm in diameter) and sparse. Microscopic criteria for distinguishing between these units are described in Section 2.3 of this report.

Unit 2a consists of a lower ash flow and an upper ash fall (Purtymun and Kennedy, 1971), although no ash-fall unit was encountered during this study. The unit ranges in color from light pink to pale red to gray. It contains relatively large (5 to 30 mm) gray, brown, and olive-colored pumice lapilli, and varies from slightly to moderately welded. Unit 2a varies in thickness from greater than 54 ft in the northwesternmost drill hole (LLC-85-13) to 21 ft in the southeasternmost drill hole (LGC-85-09).

The contact between Units 2a and 2b is generally marked by a subtle color change within a slightly welded zone of tuff. Purtymun and Kennedy (1971) identify this contact on the basis of the occurrence of thin, lenticular deposits of reworked tuff. Although this zone of reworked tuff was not observed in core collected during this drilling program, the transition from Unit 2a to Unit 2b at Mesita del Buey appears to be marked by a decrease in the size and variety of pumice lapilli occurring in the basal portion of Unit 2b.

Unit 2b forms the cap rock at Mesita del Buey and consists of brownish-gray, light-gray, and pinkish-gray, slightly to moderately welded, rhyolitic ash-flow tuff with light-gray and occasional brown pumice lapilli. In some areas

on the Pajarito Plateau, this subunit may contain up to eight distinct flow units, separated by sandy partings and pumice concentrations (Goff and Bolivar, 1983). Field descriptions, apparent density logs, and magnetic susceptibility logs obtained during this study indicate that, at Mesita del Buey, Unit 2b consists of at least two separate flows that cooled as a single unit, and is generally separated from Unit 2a by a lower zone of slightly welded tuff. The maximum and minimum thicknesses of Unit 2b encountered in the Los Alamos drill holes were 45 ft in the northwesternmost hole (LLC-85-13) and 28 ft in the southeasternmost hole (LGC-85-09).

2.2 WELDING AND CORRELATION OF ASH-FLOW UNITS AT MESITA DEL BUEY

Welding of tuffaceous rocks at Mesita del Buey ranges from nonwelded to moderately welded. Although the degree of welding is gradational between these ranges, generalized definitions of each welding descriptor were formulated for use when describing rocks in the study area. These are summarized below:

- Nonwelded - Completely disaggregated; little to no flattening of pumice lapilli observed.
- Slightly Welded - Slightly coherent, but crumbles easily in the hand; occasional pumice lapilli are noticeably flattened.
- Moderately Welded - Tuff crumbles with difficulty in the hand and occasionally must be struck with a hammer to break; flattening of most pumice lapilli to varying degrees is noticeable.

Although the units are defined on the basis of individual or composite flows, general variations in welding within the units can be correlated across Mesita del Buey. A cross section showing these variations is presented in Figure 2-4; the location of the cross section in the study area is shown in Figure 2-3. Moderate welding is most consistently found in the lower portion of Unit 1b near its contact with Unit 1a, and in the middle and upper portions of Unit 2b. In general, the moderately welded portions of Unit 2a break or crumble in the hand more easily than the moderately welded portions of Units 1b and 2b. The welding characteristics of Unit 2a, however, are not consistent in a lateral sense. Also not laterally consistent are the slightly welded zones; in certain cases, the slightly welded zone more nearly approaches the definition of moderately welded, whereas in other cases, the slightly welded zone is almost nonwelded.

2.3 PETROGRAPHIC ANALYSES

Twenty-seven samples were submitted for petrographic analyses, results of which were used to establish recognition criteria for the different units within the ash-flow tuffs. Of this total, 23 were core samples of tuff and 4 were samples of lithic lapilli. The analyses were performed by the Bendix Petrology Laboratory in Grand Junction. Procedural details and the resulting petrographic reports are presented in Appendix B.

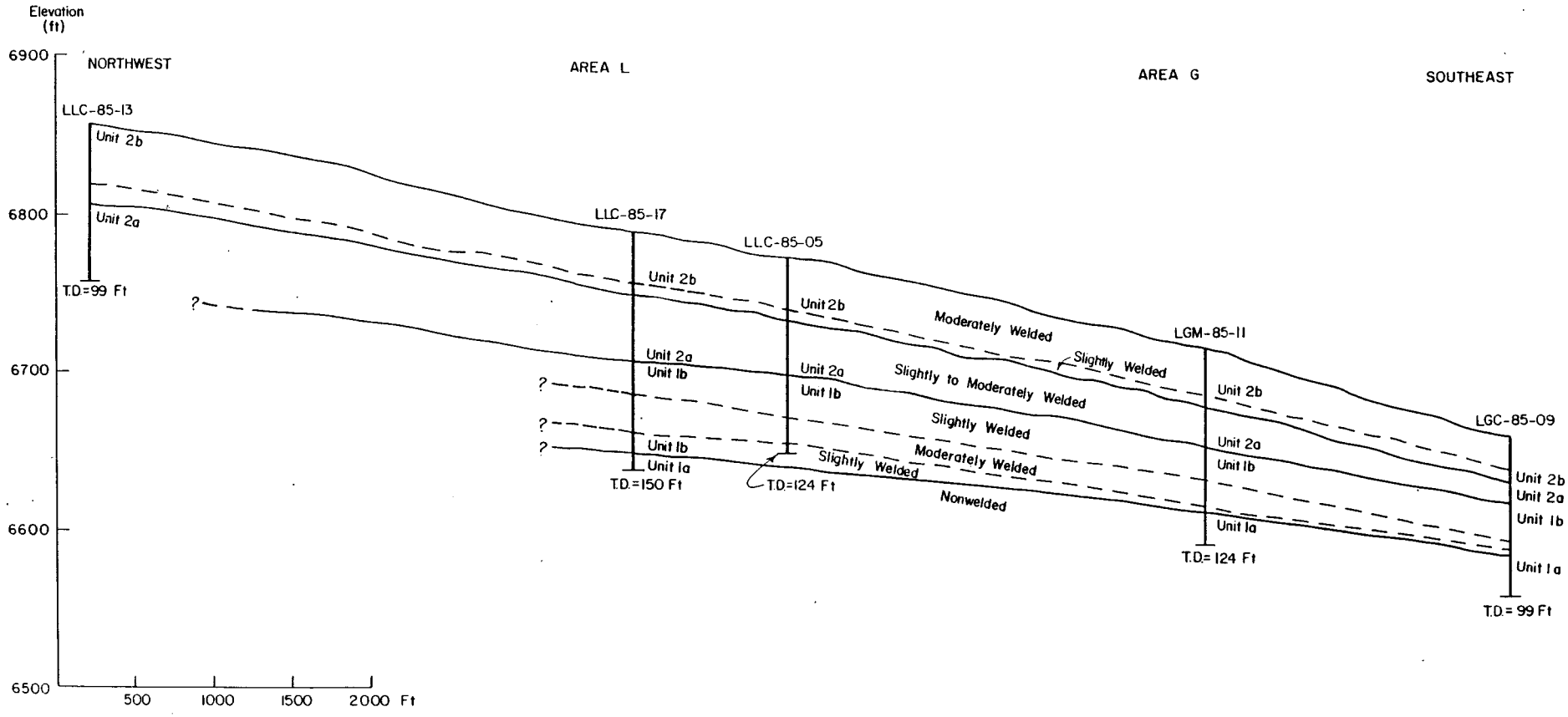

Figure 2-4. Cross Section Showing Parts of the Tshirege Member of the Bandelier Tuff, Drawn Through Mesita del Buey and Technical Area 54

Overall, the results indicate that the Tshirege Member of the Bandelier Tuff at Mesita del Buey is a rhyolitic tuff containing varied amounts of lithics (rock fragments), vitrics (pumice fragments and glass), and crystals (vapor-phase products and phenocrysts). Results of point-count analysis for quartz and sanidine (Table 2-1) indicate that Unit 1b generally contains less volume-percent sanidine (K-feldspar) than do Units 2a and 2b. Samples from Unit 1b have an average quartz/sanidine (Q/K) ratio of 0.9, while average ratios in Units 2a and 2b are 0.6. In addition, it was found that tridymite is generally absent in samples from Unit 1b. Units 1 and 2 are therefore compositionally distinct.

Other significant recognition criteria are the microscopic characteristics of pumice lapilli. Pumice lapilli in Unit 1b either are devitrified and display spherulitic textures with occasional vapor-phase mineralization by a radial-acicular zeolite, or consist of fresh glass; they also vary in shape from flattened to nonflattened in many samples. Pumice lapilli in Units 2a and 2b, on the other hand, are ubiquitously replaced by sanidine, tridymite, and occasionally a zeolite; in general, they are all at least partially flattened. Moreover, the average percentage of pumice lapilli (determined by point-count analysis of thin sections) is generally higher in Unit 1b (21 percent) than in Unit 2a (16 percent) or Unit 2b (13 percent). Evidently, the less flattened, more abundant nature of the pumice lapilli in Unit 1b is the primary reason for the fact that Unit 1b is less dense than Units 2a and 2b (see discussion of apparent density logs in Section 2.4.3).

2.4 INTERPRETATION OF GEOPHYSICAL LOGS

Several different types of geophysical log were obtained utilizing different downhole probes. Details regarding equipment and procedures were described in the first interim report (Rush and Dexter, 1985); a complete set of geophysical logs for all holes drilled during this study is included in that report.

The following geophysical-logging data were generated during this study:

- Natural Gamma, Epithermal Neutron (and derived moisture), and Vertical Deviation Logs
- Spectral Gamma and Caliper Logs
- Magnetic Susceptibility Logs
- Gamma-Gamma (Apparent Density) Logs

The caliper and vertical deviation logs were obtained prior to installation of instruments described in other parts of this report to determine sizes and types of downhole equipment that would be necessary to facilitate the installations. The vertical deviation in the 18 drill holes at Los Alamos averages 2.5 ft and ranges from 1 to 4 ft; in general, the diameters of the completed drill holes are between 7 and 8 inches.

Table 2-1. Volume-Percent Quartz and Sanidine Determined from Point-Count Analysis of Thin Sections

Sample Number	Hole Number	Depth (ft)	Volume-Percent Quartz	Volume-Percent Sanidine
UNIT 1b				
MCG-628	LLM-85-01	101	5.4	11.9
MCG-629	LLM-85-01	122	11.9	9.0
MCG-632	LLM-85-02	74	9.7	10.3
MCG-633	LLM-85-02	111	6.4	6.0
MCG-636	LGM-85-06	100	6.3	9.7
MCG-640	LGM-85-11	95	6.7	8.6
MCG-649	LGC-85-09	48	12.0	9.7
MCG-650	LGC-85-09	68	8.1	8.5
AVERAGE VALUES			8.3	9.2
UNIT 2a				
MCG-627	LLM-85-01	52	7.8	14.3
MCG-631	LLM-85-02	64	10.4	15.1
MCG-635	LGM-85-06	50	9.0	11.0
MCG-648	LGC-85-09	35	8.0	17.0
AVERAGE VALUES			8.8	14.3
UNIT 2b				
MCG-626	LLM-85-01	30	7.6	17.3
MCG-630	LLM-85-02	37	5.7	12.5
MCG-634	LGM-85-06	30	11.4	13.8
MCG-638	LGM-85-11	5	7.1	13.2
MCG-639	LGM-85-11	31	13.2	10.1
MCG-643	LLC-85-13	42	6.2	18.4
MCG-644	LLC-85-17	12	8.0	14.0
MCG-646	LGC-85-09	10	8.4	13.6
MCG-647	LGC-85-09	21	8.8	24.1
AVERAGE VALUES			8.5	15.2

Discussions of the remaining types of geophysical log are presented in the paragraphs that follow. These discussions focus primarily on interpreting the logs with a view to identifying the vertical variations of lithologies present in each drill hole. In general, most of the logs tend to confirm the presence of previously established boundaries and contacts within the ash-flow tuffs. In certain cases, however, information obtained from the geophysical logs required that modifications be made to the lithologic logs acquired during the

drilling of the study-area holes. Original versions of the lithologic logs were presented in the first interim report (Rush and Dexter, 1985); the subsequent modifications have been incorporated in the logs presented in this report (see Appendix A).

2.4.1 NATURAL GAMMA AND EPITHERMAL NEUTRON MOISTURE LOGS

The natural gamma probe counts the spectrum of gamma rays above approximately 50 kiloelectronvolts (keV). In the 18 holes drilled, gross-gamma radiation ranges from 300 to 700 counts per second (cps). The epithermal neutron system consists of a neutron detector used in conjunction with a neutron source. Values from the logs range from 600 to 1600 cps. Logs from both of these systems show the vertical distribution of these total-count ranges; few of the vertical changes in total count correlate with a known boundary within the ash-flow tuff. Only in two holes (LGC-85-09 and LGC-85-10) were confirmations of previously drawn contacts possible. Figure 2-5 presents the epithermal neutron, natural gamma, and lithologic logs for Hole LGC-85-10. As can be seen, changes in total count with depth suggest confirmation of contacts and boundaries drawn on the adjacent lithologic log. However, since some of the obvious vertical changes in total count do not correspond with known physical changes, it is not possible to identify contacts on the basis of the epithermal neutron and natural gamma logs alone.

Moisture logs were derived from the epithermal neutron data. These moisture logs have the same general shape as the moisture logs obtained by gravimetric methods (see Section 3.1.1). A comparison of the two methods is illustrated in Figure 2-6. In general, the values for moisture percent seen in the epithermal neutron log are higher than those seen in the gravimetric data. Although the epithermal neutron data are more detailed (data points were obtained every 0.5 ft whereas gravimetric samples were collected every 5 ft), it appears that the gravimetric data are more accurate. Uncertainties in the calculated (epithermal neutron) moisture content at each 0.5-ft interval are compounded by counting errors, errors associated with the calibration parameters, and errors associated with the fact that no hole-size corrections were applied to the data. The percent uncertainty represented by these errors often exceeds the calculated moisture value. In this study, for example, these errors are estimated to be ± 3.0 percent by volume (Marutzky, 1986).

2.4.2 SPECTRAL GAMMA LOGS

The spectral gamma probe counts energy produced by potassium (K), uranium (U), and thorium (Th); total counts obtained in the field were converted to concentrations of K in percent, and U and Th in parts per million (ppm).

The Bandelier Tuff drilled during this study averages approximately 4 percent potassium, 5 to 10 ppm uranium, and 20 to 30 ppm thorium. As with the logs described in the previous subsection, the spectral gamma logs can, at best, only help to confirm the existence of previously drawn contacts and boundaries. Since vertical changes in concentration are not consistent from one hole to another, the logs cannot be used to draw boundaries or modify previously drawn contacts.

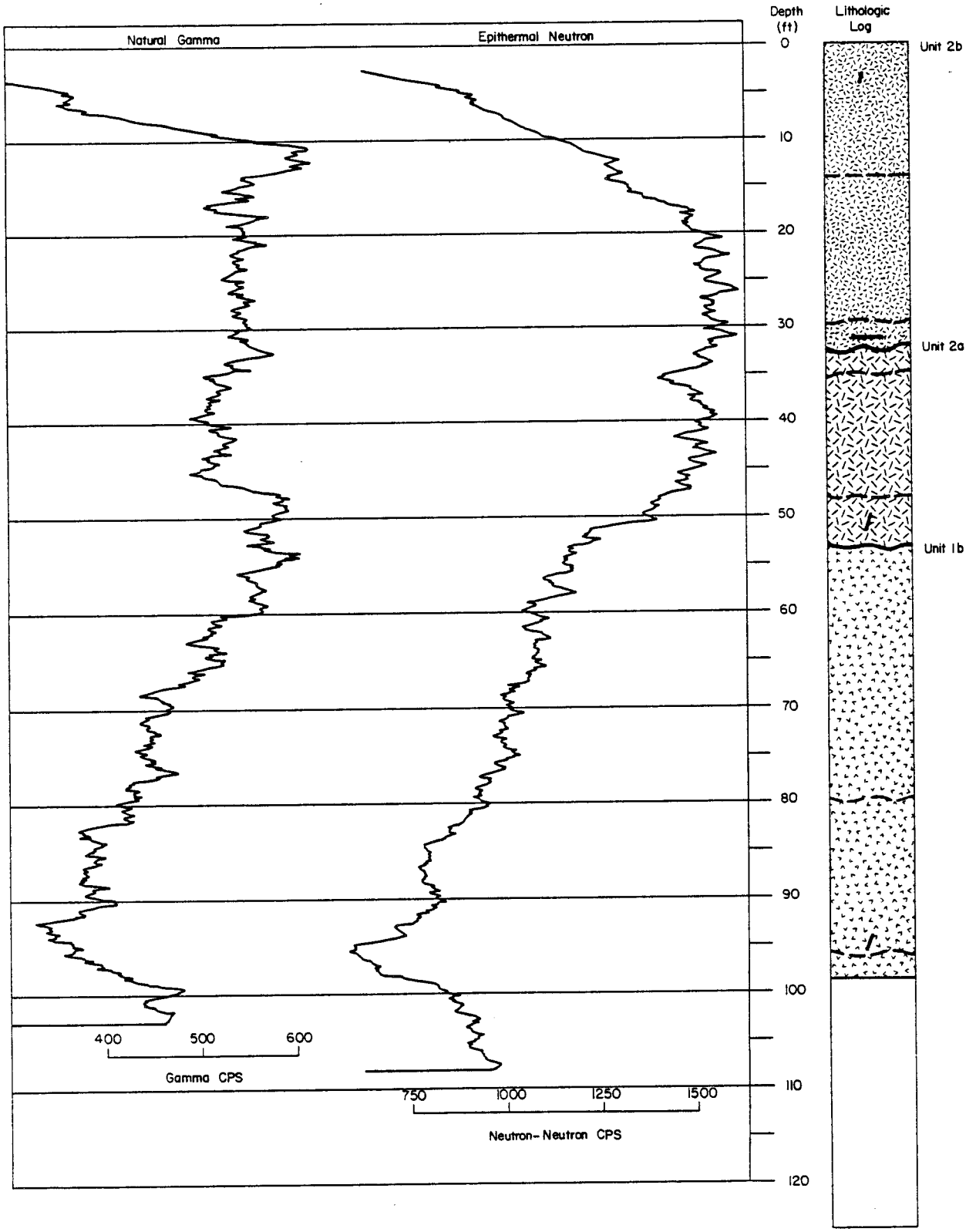

Figure 2-5. Epithermal Neutron, Natural Gamma, and Lithologic Logs for Hole LGC-85-10

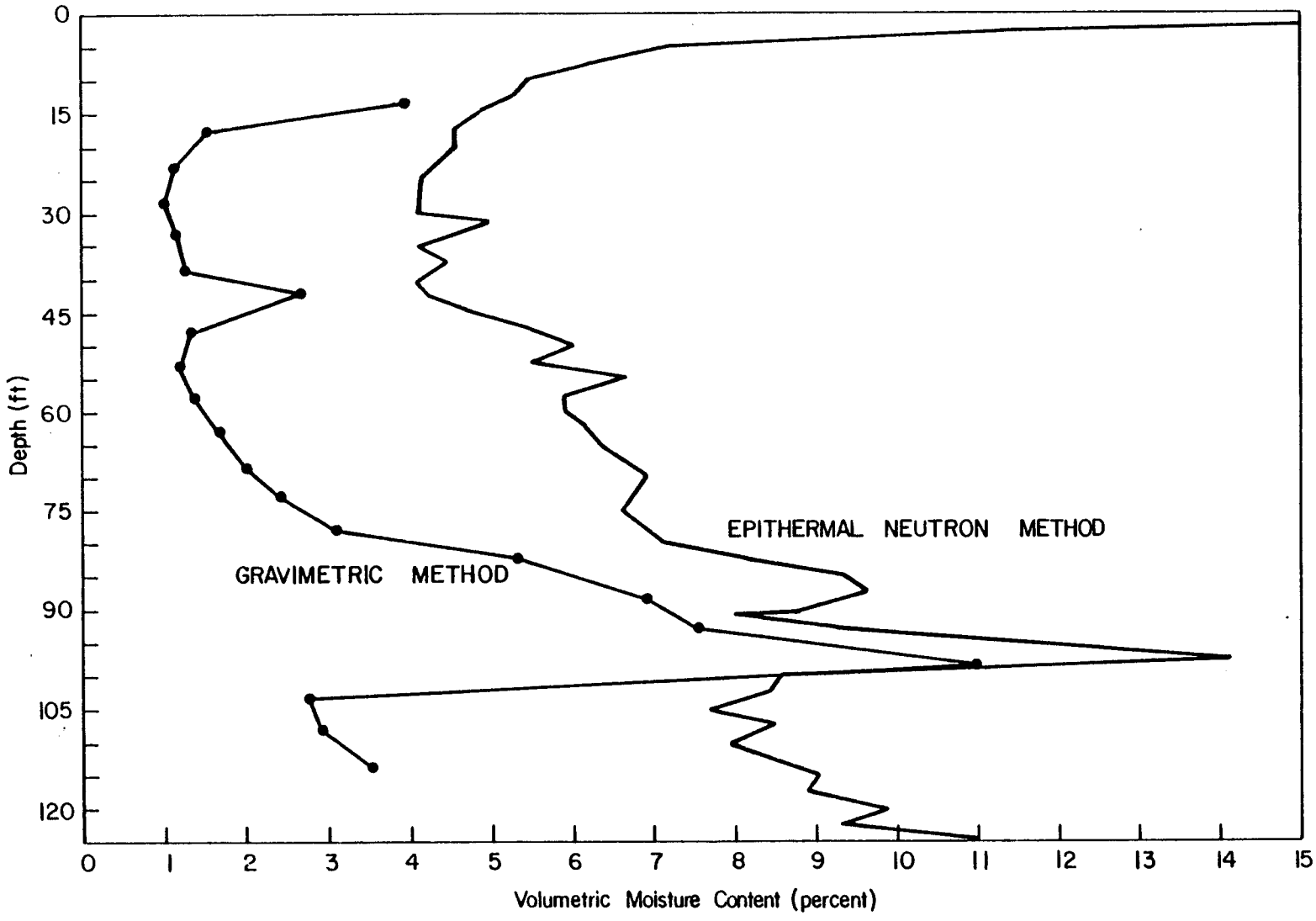

Figure 2-6. Comparison of Moisture Curves for Hole LGM-85-06, Derived by Geophysical and Gravimetric Methods

Figure 2-7 shows the spectral gamma and lithologic logs for Hole LGM-85-11. At first glance, there appears to be an inverse relationship between uranium and thorium. This is probably artificial and results from the use of a data-reduction program that strips away the energy contributions from uranium that overlap the energy window of thorium (and vice versa). At low concentrations of uranium and thorium, such as those displayed by the Bandelier Tuff in the study area, the stripping process results in apparent inverse relationships. As can be seen in Figure 2-7, however, this relationship is superseded by the simultaneous peaking of K, U, and Th at the boundary of Units 1b and 2a (61 ft), which is marked by an increase in uranium (to 10 ppm) and thorium (to 30 ppm). Similar increases in uranium and thorium at the contact of Units 1b and 2a were noted on spectral gamma logs from other holes as well, suggesting gross chemical differences between Unit 1 and Unit 2. This confirms the same conclusion drawn from the petrographic data on the basis of quartz and sanidine contents.

2.4.3 MAGNETIC SUSCEPTIBILITY AND GAMMA-GAMMA (APPARENT DENSITY) LOGS

The magnetic susceptibility (MS) and gamma-gamma (apparent density) logs proved to be the most valuable in terms of correlating physical and hydrologic properties in the study area. The MS probe is calibrated in micro-cgs* units and measures the degree to which the tuff is attracted to a magnet; essentially, this is an indirect measure of the iron content of the tuff. Because of considerable base-line drift due to temperature changes in the sensing coil of the probe, the shape of the curve, not the displayed values, is significant. The gamma-gamma probe collects data in counts per second that are immediately converted to apparent density in grams per cubic centimeter (g/cm^3) using the calibration data obtained during installation of the logging system. The density of the ash-flow tuffs is a function of welding, amounts of lithic and pumice lapilli, water content, and degree and amount of vapor-phase crystallization and devitrification.

Relationships between magnetic susceptibility, density, and lithology are shown schematically in Figures 2-8 through 2-10. For the most part, the MS logs show good correlations with contacts between individual ash flows, whereas the density logs show good correlations with boundaries based on welding characteristics. However, minute changes in magnetic susceptibility can delineate zones with different welding characteristics (see, for example, Figures 2-8 and A-9, Hole LGC-85-10, 83 to 97 ft), whereas minute changes in apparent density can delineate contacts between individual ash flows (Hole LGC-85-10 at a depth of 55 ft).

In some cases, the density log will indicate a contact between separate flows that is not visible on the MS log. For example, in Hole LGC-85-10 (Figure 2-8), the contact between separate flows within Unit 2b is marked only by an increase in the amount of pumice lapilli and is therefore visible only on the density log (at 14 ft). Concentrations of pumice lapilli are common at the tops, bottoms, and within ash-flow units. This feature is obvious on the density log in Figure 2-8; large negative peaks clearly demonstrate the increased concentration of pumice lapilli in the lower part of Unit 2a, from a depth of 50 to 54 ft. Another feature discernible on the density logs is the

*Centimeter-gram-second.

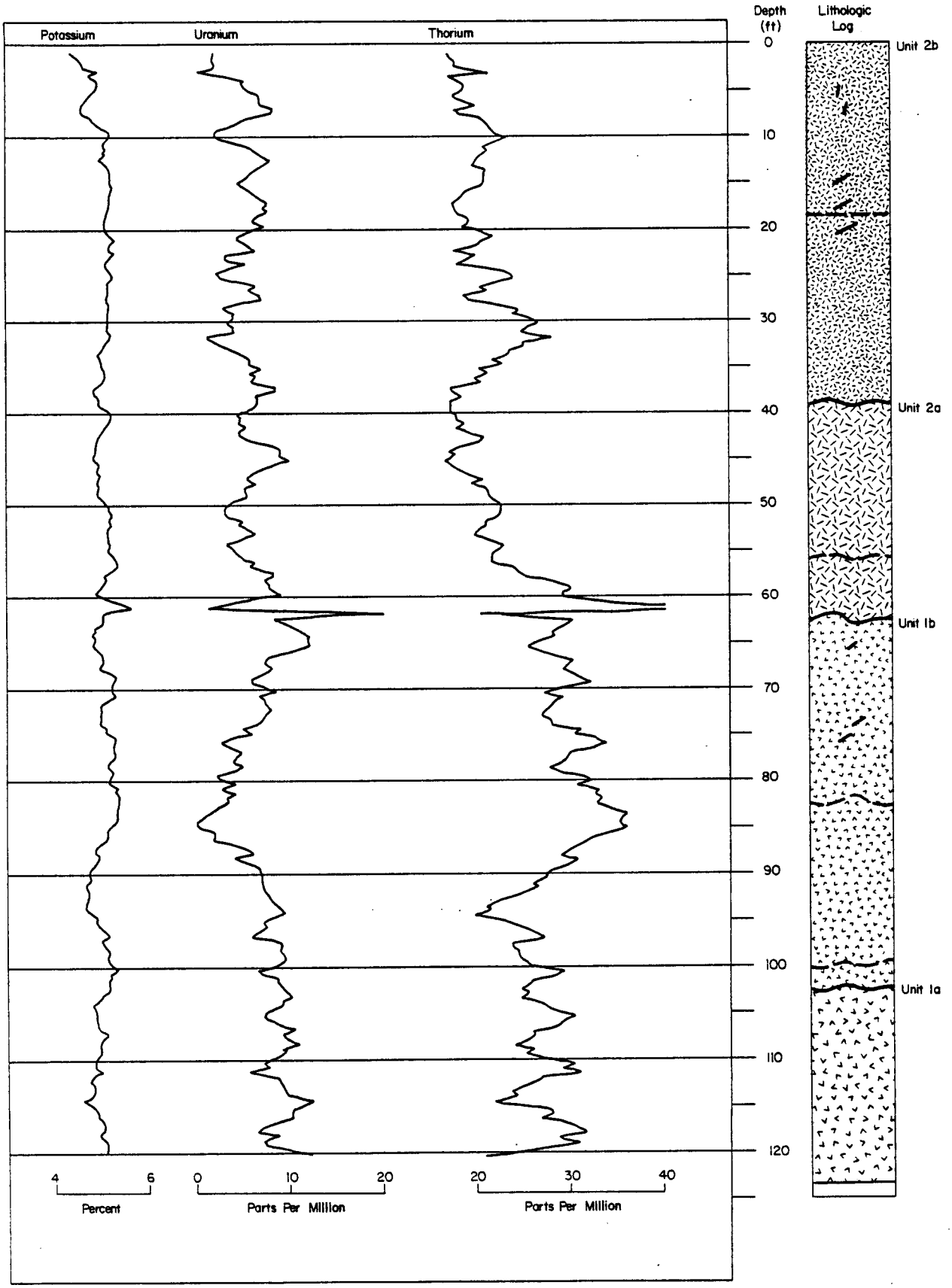

Figure 2-7. Spectral Gamma and Lithologic Logs for Hole LGM-85-11

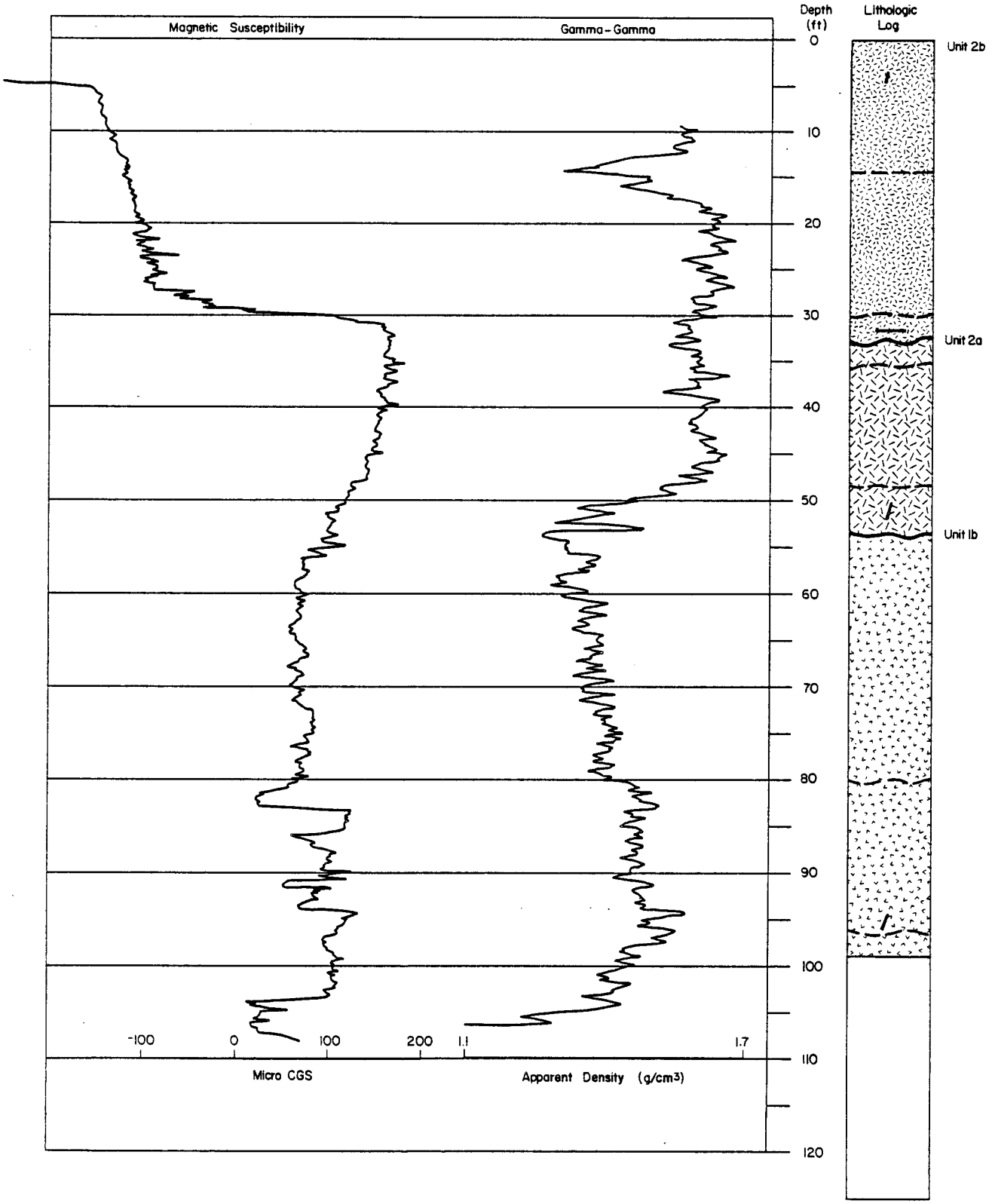

Figure 2-8. Magnetic Susceptibility, Apparent Density, and Lithologic Logs for Hole LGC-85-10

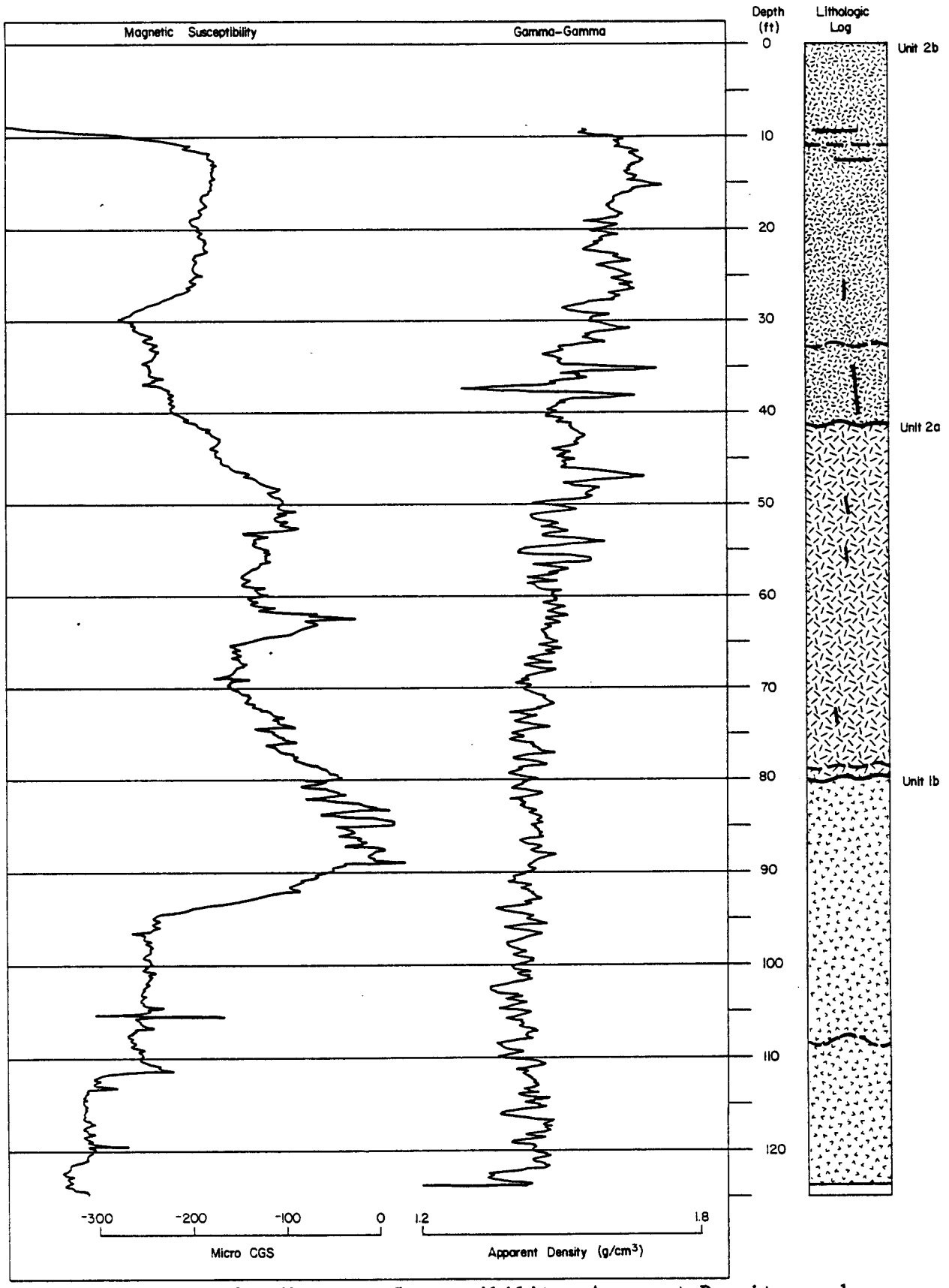

Figure 2-9. Magnetic Susceptibility, Apparent Density, and Lithologic Logs for Hole LLM-85-02

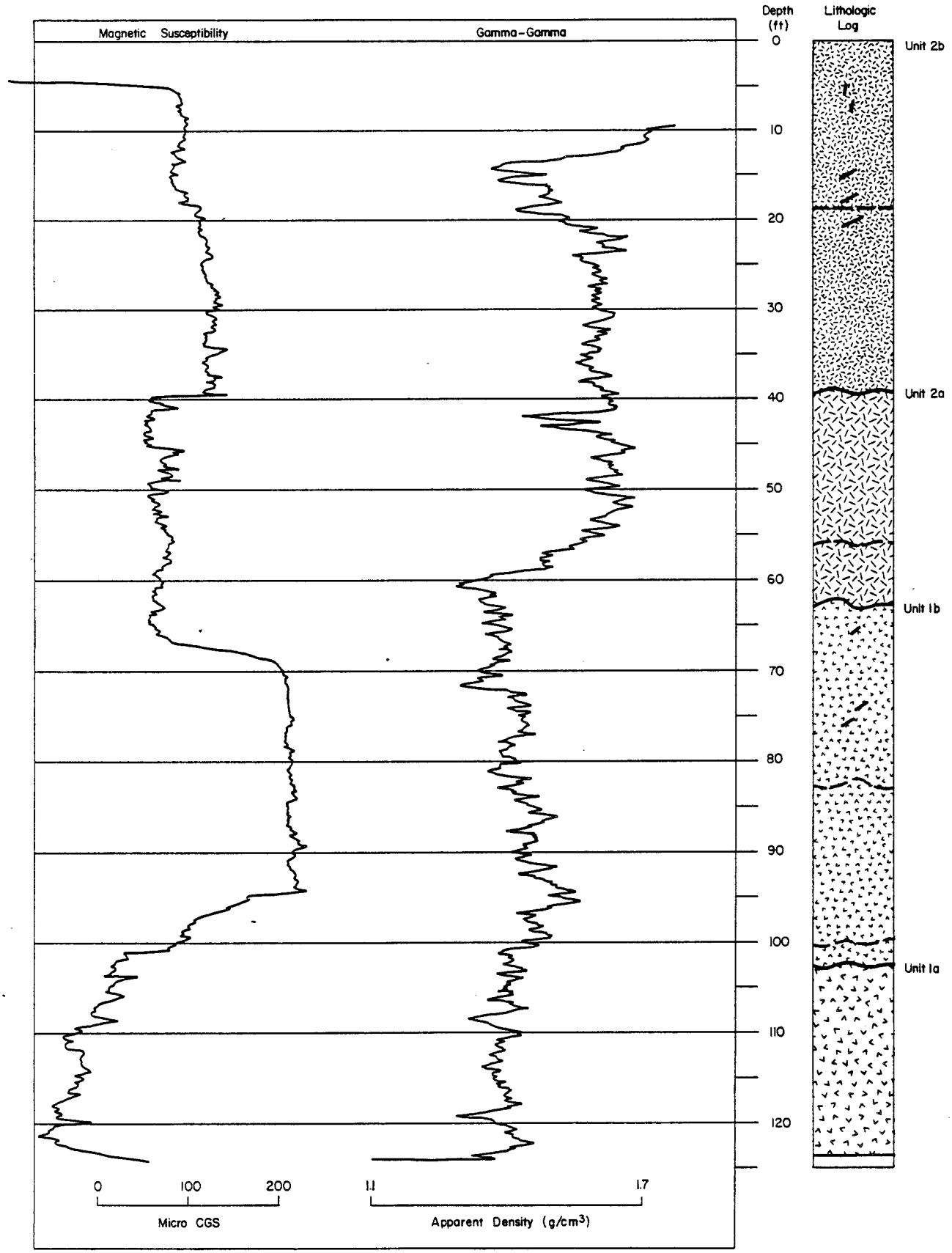

Figure 2-10. Magnetic Susceptibility, Apparent Density, and Lithologic Logs for Hole LGM-85-11

general decrease in the density of Unit 1b, which appears to be less dense on the whole than Units 2a or 2b. As noted earlier in the discussion of the petrologic data (Section 2.3), the decrease in the overall density of Unit 1b appears to be due to the fact that the pumice lapilli in the unit are more abundant and less flattened than those in Units 2b and 2a.

Occasionally the ability of the density logs to indicate contacts between distinct units, on the basis of minute density changes, is hampered by the presence of fractures. In Hole LLM-85-02 (Figure 2-9), the near-vertical fracture that extends from 35 to 40 ft obscures the minute changes in density that might be visible on the log were it not for the presence of the fracture. Induration of the tuff near the fracture, together with open spaces along the fracture, appears to result in both negative and positive apparent density peaks. A relationship between fractures and apparent density can also be seen in Figure 2-10 (Hole LGM-85-11) from a depth of 14 to 20 ft; large negative peaks on the apparent density log at 14, 16, and 19 ft correspond to observed fractures in core from this hole at 15.5, 17.5, and 20 ft. The differences in depth are probably due to the size of the core (2.5-inch diameter) versus the size of the hole that was probed (7- to 8-inch diameter). A potential application of the apparent density logs is in the determination of the extent to which fractures are open. Areas where fractures were logged via examination of the core are not always obvious on the density logs; fractures that are wholly to partially filled would probably not be characterized by a significant decrease in density.

The magnetic susceptibility log for Hole LGM-85-11 (Figure 2-10) indicates sharp boundaries which appear to define the gross differences between the four major subunits of the Tshirege Member; contacts between subunits at this location were refined based on this information. The MS log for Hole LLM-85-02 (Figure 2-9), on the other hand, does not appear to define the contacts between major subunits; consequently, the log can only be used to confirm, rather than modify, the boundaries and contacts identified during drilling operations.

In conclusion, it should be emphasized that care must be taken when interpreting MS logs. Because of the common 'base-line drift' mentioned previously, apparent boundary changes in the form of an MS shift are possible. Therefore, the MS logs should not be used alone to identify contacts between ash-flow cooling units.

2.5 FRACTURES

Fractures in the Tshirege Member at Mesita del Buey are predominantly tension joints formed as a result of contraction during initial cooling of the flows. Horizontal fractures, for the most part observed near the surface, are probably postdepositional fractures related to near-surface unloading along flow-foliation due to erosion of formerly overlying ash-flow tuff; most of these are filled with caliche and root material. During this study, horizontal fractures--a total of 11--were observed only in Unit 2b. No fractures were observed in Unit 1a, which is composed of completely nonwelded tuff. (Note: The entire thickness of Unit 1a was not penetrated in this study.)

A summary of the number of fractures logged during the drilling program of this study is presented in Table 2-2. Although most of these fractures are nearly vertical (between 70 and 90 degrees), approximately 20 fractures in both Units 2a and 2b have a dip of about 45 degrees (see the lithologic logs in Appendix A). The greatest number of fractures occurs in Unit 2b; this agrees with data collected by Purtymun and others (1978). These authors found that more than 70 percent of the fractures they logged in both Units 2b and 2a were filled with brown clay or caliche. Similarly, observations made during the drilling program for this study indicated that most of the fractures appeared to be partially to completely filled with either caliche, brown clay, or limonitic material. Samples of some of the filled fractures were submitted to the Bendix Petrology Laboratory for X-ray diffraction analysis. Both bulk fractions and clay-sized separates of the fracture coatings were analyzed. The results demonstrated that the bulk fractions had the same composition as the host samples. Clay-sized fractions consisted predominantly of smectite (montmorillonite), with moderate to minor amounts of illite/mica and kaolinite.

Most of the fractures logged during this study occur in moderately welded zones within the tuffs. This is to be expected since these zones retained heat longer than the slightly welded zones. A feature observed in one fracture (cf. Figure 2-9, Hole LLM-85-02, 35 to 44 ft) deserves to be mentioned. This fracture displays an effect similar to surficial 'case-hardening,' as described by Abeele and others (1981, page 5); the tuff near the fracture is quite hard, but the tuff is only slightly welded less than 2 inches from the joint surface. This feature may signify preferential movement of water or water vapor along open fractures during recent times, or may be a result of devolatization of the tuff during cooling. The fact that the gravimetric moisture data indicate an increase in moisture along at least one fracture (see Figure 2-6) lends support to the former theory.

Table 2-2. Number of Fractures Logged in the Los Alamos Drill Holes

Unit of Tshirege Member	Number of Fractures
Unit 2b	
Slightly Welded Zone	8
Moderately Welded Zone	39
Unit 2a	
Slightly Welded Zone	4
Moderately Welded Zone	24
Unit 1b	
Slightly Welded Zone	7
Moderately Welded Zone	3

Section 3

HYDROLOGIC CHARACTERIZATION OF THE VADOSE ZONE

This description of the hydrologic characteristics of the vadose zone in the study area is divided into three major subsections. Section 3.1 describes the general hydrologic characteristics of the tuff, including moisture content, which was determined gravimetrically; porosity, which was determined from helium-injection tests; and capillary force, determined from moisture characteristic curves. Permeability of the tuff is detailed in Section 3.2. Three field techniques were used to measure in-situ permeability, and two laboratory methods were used to measure permeability in core samples collected from the drill holes. Analyses of saturated and unsaturated hydraulic conductivity as a function of moisture content were also performed and are discussed in a separate subsection. A summary of all these permeability determinations concludes Section 3.2. Section 3.3 describes the gradient determinations, specifically measurements of temperature, water potential, and gas pressure, conducted to assess the driving forces of transport in the tuff.

This section of the report provides the geotechnical information specified in Tasks 1 through 4 of Paragraph 25 of the Compliance Order/Schedule. The specific subsections that address these tasks are highlighted with an asterisk and the corresponding task identified.

3.1 GENERAL CHARACTERISTICS

3.1.1 GRAVIMETRIC MOISTURE CONTENT

3.1.1.1 Purpose and Scope

Gravimetric moisture determinations were conducted to obtain a direct measurement of the in-situ water content of the tuff and to quantify the vertical moisture distribution. The moisture content as a function of depth is important when compared with results of permeability tests, water-potential measurements, and laboratory hydrologic testing as part of the quantification of moisture movement in the vadose zone.

This section describes the procedures for sample collection and moisture content calculations, and discusses the results of the gravimetric moisture-content determinations. Comparisons of the water-content results with other hydrologic measurements are presented in succeeding sections of this report (see Sections 3.1.3, 3.2.4, and 3.3.1).

3.1.1.2 Procedures

The specific procedure for the determination of gravimetric moisture consisted of the following steps. Core samples 1 ft in length were selected from the split-barrel sampler at 5-ft intervals and immediately placed in preweighed sample containers equipped with air-tight lids. The containers were weighed in the field and then delivered to the laboratory for drying. After drying for 24 hours at 105°C, the samples were reweighed to determine the moisture loss (Bendix Field Engineering Corporation, 1985a, 1985b).

Although gravimetric moisture determinations are relatively easy to perform, a number of precautions are necessary. For example, a major concern associated

with the drilling was that the heat produced by the auger would drive water out of the samples, resulting in inaccurate moisture-content measurements. Upon retrieval of the auger from the borehole, however, the temperature of the core barrel was observed to be cool. Apparently, the heat produced by the friction during drilling was minimal and confined to the outside of the auger, and therefore did not have a measurable effect on the moisture content in the core samples. Care was also taken to maintain the drying-oven temperature at 105°C to ensure that no structural water would be evolved and included in the apparent moisture content. Finally, the balance used to weigh the samples had a readability of 0.01 gram to ensure adequate accuracy for the low-moisture-content samples collected in this study.

3.1.1.3 Calculations

The amount of water in soil or rock can be expressed in the following ways:

- Water Content, Volume Fraction

$$\theta = V_l/V_t \tag{1}$$

- Water Content, Mass Basis

$$\theta_m = m_l/m_s \tag{2}$$

- Degree of Saturation

$$\theta_s = V_l/(V_l + V_g) \tag{3}$$

where

V_l = volume of liquid
V_t = total volume
m_l = mass of liquid
m_s = mass of solid
V_g = volume of the gas or air in the sample

Equations (1) and (2) are combined in order to convert from the mass basis to the volume fraction, a quantity that is generally more useful in field studies (Marshall and Holmes, 1979):

$$\theta = \theta_m \rho_b/\rho_l \tag{4}$$

where

ρ_b = dry bulk density
ρ_l = density of liquid

Values for mass were determined gravimetrically (Section 3.1.1.2). Values for dry bulk density were obtained from the gamma-gamma (apparent density) geophysical logs after subtracting the moisture content. Values for the density of water at different temperatures are readily available in the literature, but for most applications, it is sufficiently accurate to use the value 10^3 kg/m^3 (1.94 slugs/ft^3).

3.1.1.4 Results and Discussion

Gravimetric moisture determinations were performed in samples from five holes: LLM-85-01, LLM-85-02, LLM-85-05, LGM-85-06, and LGM-85-11 (see Figure 2-3 for drill-hole locations). The resulting volumetric moisture contents are plotted as a function of depth for all five holes in Figure 3-1.

Four distinct characteristics are apparent upon examination of these data:

- Low overall moisture content.
- Varying depths of water infiltration.
- Relatively high moisture content exhibited by the lower portion of Unit 1b.
- Higher moisture content observed in the vicinity of certain fractures.

The low overall moisture content is demonstrated by the 2 to 4 percent average moisture for the central portion of the profile. At such a low moisture content, interconnection of pore water would be minimal and capillarity as a major transport mechanism would be negligible. As a result, it can be concluded that vapor transport would be the major mechanism for moisture movement in the tuff (see the discussion in Section 3.1.3.4).

Infiltration depth depends on the specific area. Holes located in Area L, for example, show an increase in moisture content relative to depth of less than 10 ft. In Area G, the corresponding depth is closer to 15 ft. This difference in the depth of moisture penetration is unexplained at this time.

All of the moisture data indicate an increase in moisture content in the lower portion of Unit 1b. In Holes LGM-85-06 and -11, both of which fully penetrated Unit 1b, the increased moisture content correlates exactly with the moderately welded tuff encountered in Unit 1b (see lithologic logs in Appendix A). The degree of welding in the lower portion of Unit 1b was the highest observed in this study, with the exception of the upper portion of Unit 2b. As the degree of welding increases, the porosity of the formation decreases (Ross and Smith, 1961). It would be expected that as the porosity decreases so would the average pore-size radius, the result being an increase in capillary forces which would retain moisture in the more welded intervals of the tuff. The higher pumice content could also have a direct effect on the moisture-retention properties of Unit 1b. As welding increases, pumice clasts are flattened, both conditions resulting in a high concentration of gas tubes; these tubes form ideal capillary tubes which appear to exhibit strong capillary forces.

A higher moisture content is observed in samples located adjacent to certain fractures, indicating that some fractures do transport greater quantities of water vapor for absorption into the adjacent rock wall. Examples are the fractures located at 35 to 40 ft and 55 to 56 ft in Hole LLM-85-02, represented by the two moisture spikes at 38 and 55 ft, respectively (see Figure 3-1). Not all of the fractures exhibit this moisture anomaly, however, suggesting that not all of the fractures are open and available as avenues of transport for water vapor (see Section 2.5).

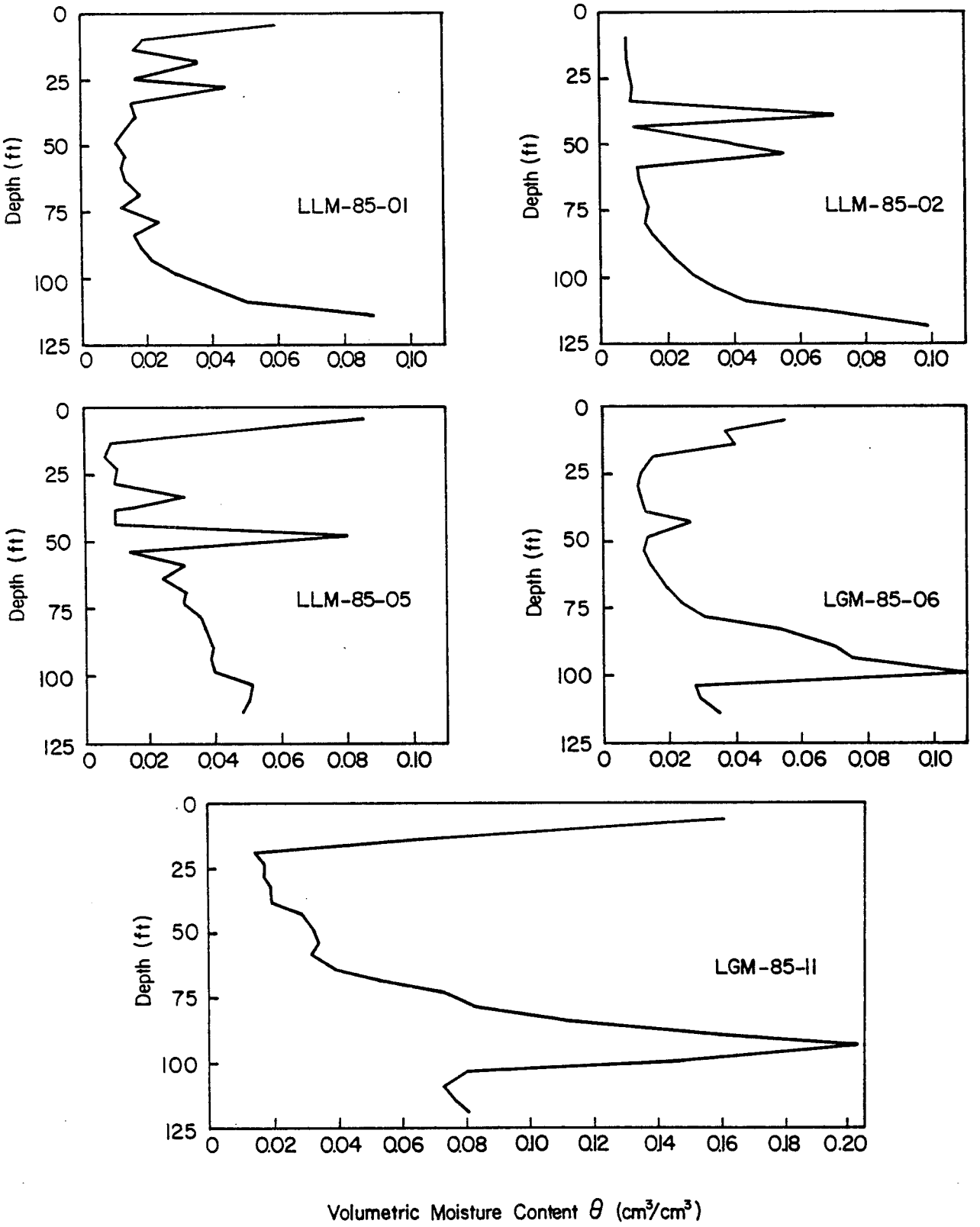

Figure 3-1. Plots of Volumetric Moisture Content as a Function of Depth for Five Drill Holes

3.1.2 POROSITY

3.1.2.1 Purpose and Scope

This section presents the results of helium-injection tests performed on 20 core samples for the purpose of measuring the porosity of the Bandelier Tuff. The laboratory work was performed by TerraTek Research Laboratory of Salt Lake City, Utah, at the direction of Bendix. The sample-preparation and laboratory-procedure sections that follow (3.1.2.2 and 3.1.2.3) are adapted from TerraTek's report (TerraTek Research Laboratory, 1985).

3.1.2.2 Sample Preparation

In order to obtain samples that were of the right size and shape for testing, it was necessary to plug the full diameter core material. This was done using air as the drill-bit coolant (to avoid any potentially adverse rock-fluid interaction). Plugging was done vertically due to the limited horizontal cross section of the core material. In all but one case (Sample MCG-616), attempts at sample plugging resulted in a partial disaggregation of the sample.

The samples thus obtained were placed in protective sheathing (one-inch-diameter heat-shrink teflon tubing*), with stainless steel end screens used for support and prevention of grain loss, and to allow for gas or fluid flow in testing. The samples were then subjected to a confining stress equal to that found at their burial depth in order to compact the grains to an orientation similar to that experienced in the formation. This was done to ensure that any void space between the sheathing and the sample did not affect the pore volume of the sample.

3.1.2.3 Procedure for Helium-Injection Tests

The samples were oven-dried prior to testing and placed under a slight overburden pressure (approximately 100 psi) in a hydrostatic core holder. Porosity measurements consisted of injecting helium into the samples (50-psi charging or injection pressure), monitoring pressure/volume relationships, and calculating porosity values using Boyle's Law.

3.1.2.4 Results and Discussion

Table 3-1 presents the results for the porosity determinations. Porosity values range from approximately 39 to 74 percent. Using a classification scheme presented by Abeele and others (1981), the degree of welding based on the porosity would range from nonwelded to moderately welded. This classification agrees with field and petrographic observations.

Since field determinations are very subjective, porosity appears to be a way of quantifying the degree of welding. The pumice content, however, must also be considered. The buoyancy of pumice in water is a consequence of its high

*Diameter cited is after shrinking.

Table 3-1. Results of Porosity Determinations Using the Helium-Injection Method and Boyle's Law

Hole Number	Geologic Unit	Sample Number	Depth (ft)	Degree of Welding[a]	Pumice Content (percent)[b]	Bulk Volume (cm^3)	Pore Volume (cm^3)	Porosity (percent)
LGM-85-11	2b	MCG-618	3	Moderately Welded	19	25.68	13.94	54.3
LLM-85-02	2b	MCG-606	7	Moderately Welded	--[c]	25.62	10.62	41.5
LLM-85-05	2b	MCG-610	15	Moderately Welded	--[c]	24.96	13.14	52.6
LLM-85-01	2b	MCG-602	30	Moderately Welded	15	27.44	10.87	39.6
LGM-85-11	2b	MCG-619	30	Slightly Welded	13	24.61	12.67	51.5
LLM-85-02	2b	MCG-607	36	Moderately Welded	11	24.00	11.15	46.5
LGM-85-06	2b	MCG-614	29	Moderately Welded	7	25.31	10.76	42.5
LLM-85-05	2b	MCG-611	36	Slightly Welded	--[c]	24.08	17.72	73.6
LLM-85-01	2a	MCG-603	52	Slightly Welded	33	24.20	15.58	64.4
LGM-85-06	2a	MCG-615	51	Slightly Welded	14	25.73	10.34	40.2
LLM-85-02	2a	MCG-608	67	Moderately Welded	6	24.69	10.69	43.3
LLM-85-05	2a/1b	MCG-612	76	Slightly Welded	--[c]	24.37	18.08	74.2
LLM-85-01	1b	MCG-604	101	Slightly Welded	27	26.76	16.62	62.1
LGM-85-06	1b	MCG-616	99	Moderately Welded	27	28.26	13.42	52.6
LGM-85-11	1b	MCG-620	94	Moderately Welded	17	26.08	16.76	64.3
LLM-85-02	1b	MCG-609	117	Moderately Welded	--[c]	25.69	12.46	48.5
LLM-85-05	1b	MCG-613	123	Slightly Welded	--[c]	26.23	17.20	65.6
LLM-85-01	1b	MCG-605	124	Moderately Welded	20	25.62	12.53	48.9
LGM-85-11	1a	MCG-621	115	Nonwelded	--[c]	24.16	14.51	60.1
LGM-85-06	1a	MCG-617	115	Nonwelded	--[c]	26.32	14.82	56.3

[a]Based on field observations.

[b]The percentage of pumice fragments in the sample was determined by thin-section analysis using the point-count method.

[c]Not measured.

porosity. As a result, a moderately welded sample could exhibit a relatively high porosity because of a high pumice content (e.g., compare Samples MCG-608 and MCG-620 in Table 3-1).

Ross and Smith (1961) demonstrate that porosity can be used to delineate degree of welding (Figure 3-2). However, it would be difficult to use porosity to classify the geologic units in the project area without greatly increasing the sampling frequency, because Units 2a and 2b are composed of more than one flow, each exhibiting significant variations in porosity and pumice content.

Based on the laboratory results, there appears to be no relationship between porosity and permeability (see Section 3.2). The reason could be that, for similar degrees of welding, an increase in the pumice content results in an increase in the porosity. Since the pumice lapilli contain a significant amount of dead-end pores, however, there is no significant increase in the effective permeability.

3.1.3 MOISTURE CHARACTERISTIC CURVES*

3.1.3.1 Purpose and Scope

A moisture characteristic curve is defined as the relationship between the capillary forces at varying degrees of saturation for a selected porous medium. This curve is particularly useful for the conversion of moisture data to capillary potential, and vice versa. This section of the report describes the procedure used to generate these curves, along with a discussion of the test results. The testing was performed by TerraTek Research Laboratory, and the description of the test procedures (Section 3.1.3.3) was adapted from their report (TerraTek Research Laboratory, 1985).

3.1.3.2 Sample Preparation

(See Section 3.1.2.2.)

3.1.3.3 Procedure for Centrifuge Tests

Prior to testing, the samples were vacuum-saturated with tap water. Complete saturation was verified by comparison with previous saturation data and the helium-injection data. Testing consisted of loading the samples into specially designed centrifuge cups and spinning them at six incremental speeds. Speeds ranged from a low of 130 revolutions per minute (rpm) to a high of 680 rpm. A stroboscope was used to monitor the speed of the centrifuge until it was stable. The speeds were converted mathematically to capillary pressure, and saturations were determined using displacement data. The average saturation derived from the displacement data was converted to a corrected wetting-fluid saturation value.

---

*Response to Task 2, Paragraph 25, Compliance Order/Schedule.

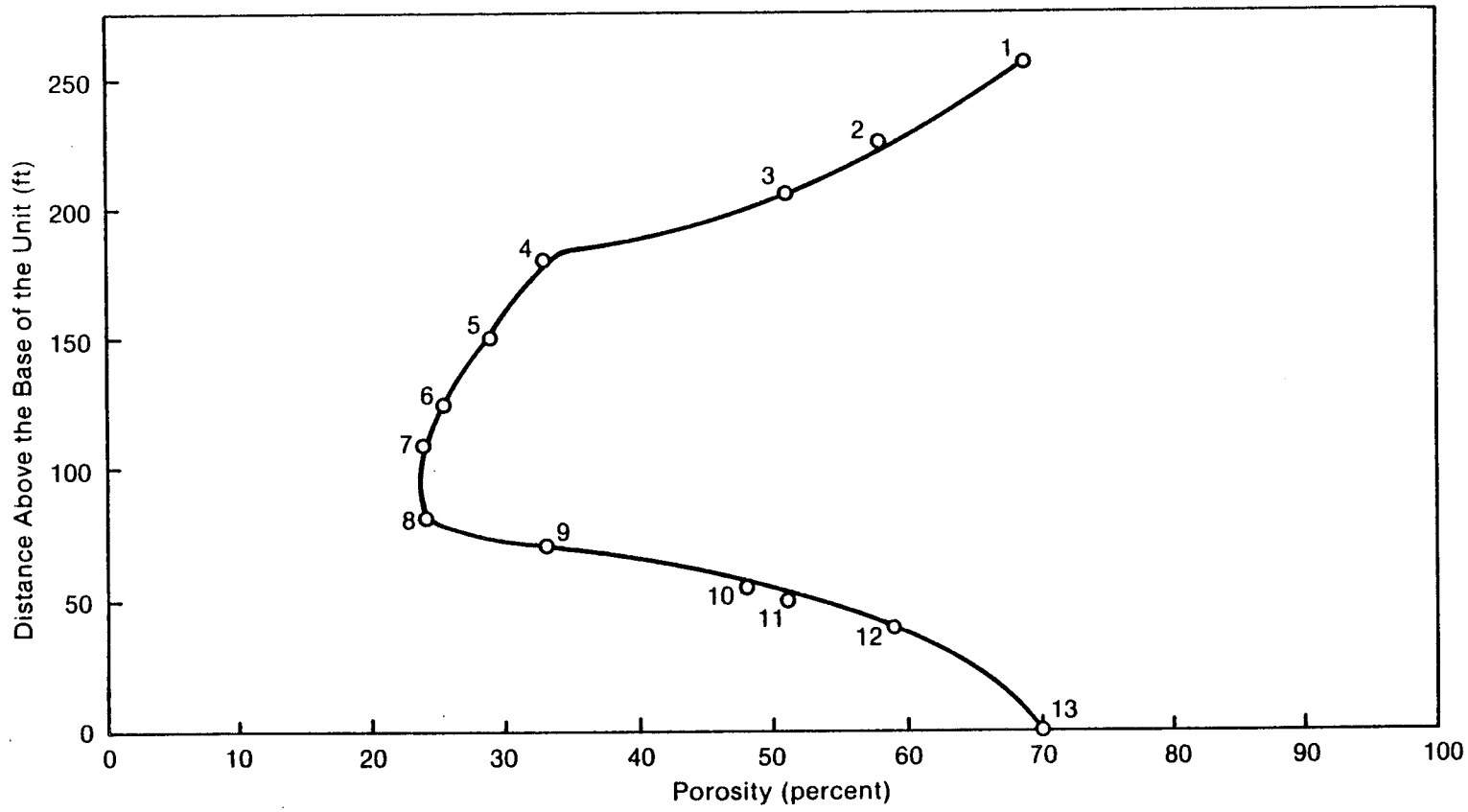

DATA PLOTTED IN THE GRAPH

Sample Number	Distance Below the Top of the Unit (ft)	Porosity (percent)	Sample Number	Distance Below the Top of the Unit (ft)	Porosity (percent)
1	0	69	8	175	24
2	30	58	9	185	33
3	50	51	10	200	48
4	75	33	11	205	51
5	105	29	12	215	59
6	130	25.5	13	255	70
7	145	24			

Figure 3-2. Porosity of Battleship Rock Ash-Flow Tuff, Valles Mountains, New Mexico (from Ross and Smith, 1961)

3.1.3.4 Results and Discussion

Moisture characteristic curves for 20 samples are presented in Appendix C. Only the drying curves were obtained because of the severe problems encountered when attempting to obtain imbibition (wetting) curves. Due to the highly porous nature of the samples, water was imbibed to such an extent that capillary-pressure determinations were impossible. Since the samples were too friable for mercury injection, it was decided to suspend attempts at obtaining these data.

After reviewing the moisture characteristic curves, the laboratory was requested to increase the centrifuge speed in order to evaluate lower water potentials (capillary pressures). Unfortunately, the samples disaggregated at these higher speeds. The laboratory was then requested to use the pressure-plate method to measure moisture characteristics, but those attempts were also unsuccessful due to sample disaggregation.

The most interesting data discernible from the moisture characteristic curves (Appendix C) are the extremely high moisture-retention (θ_r) values, which range up to 80 percent. The moisture-retention value is important because it represents the point at which capillarity as a transport mechanism breaks down. Since all of the moisture-content measurements for the Bandelier Tuff are significantly below this value, vapor transport is clearly the major mechanism of water transport.

The moisture characteristic data also demonstrate that only a minor amount of force is required to initiate the drainage of water from the saturated core sample, suggesting that the tuff has a low air-entry value. This information, coupled with the high residual moisture content, indicates that the tuff is characterized by a highly variable pore-size distribution.

It is interesting to compare the results of this study with those of a study performed by Abeele (1984), who presents moisture characteristic curves for crushed Bandelier Tuff. Residual saturation (θ_r) for the crushed tuff is approximately 0.2, as compared with an average of 0.5 for the solid rock cores. If it is assumed that both laboratory methods are reliable, then comparison of the unsaturated hydraulic properties of crushed versus natural tuff reveals a significant difference. One possible explanation is the destruction of the internal structure of the pumice lapilli in the crushed tuff. The gas tubes present in the pumice lapilli of uncrushed tuff are perfect little capillary tubes whose strong capillary forces retain significant amounts of water, resulting in higher θ_r values.

Knowledge of the average moisture-retention value enables one to calculate how much water must be supplied to the system in order for the capillary forces of the overlying tuff to be satisfied—a condition which must be met in order for recharge of liquid water to occur to the underlying groundwater system. Based on an average porosity of approximately 50 percent (Table 3-1) and an average moisture-retention value of approximately 50 percent (Appendix C), a recharge of 25 centimeters for each 1-meter thickness of tuff would be required to satisfy the capillary forces before recharge to the underlying groundwater system could occur. This scenario is quite unlikely in the study area due to

the large amount of water required and the fact that the potential evapotranspiration rates in the Jemez Mountains area exceed the annual precipitation amount (Abeele and others, 1981).

3.2 PERMEABILITY DETERMINATIONS

3.2.1 BOREHOLE-INJECTION TESTS*

3.2.1.1 Purpose and Scope

Borehole-injection tests, or packer tests, were used to measure the in-situ permeability of different intervals in the Bandelier Tuff. The tests were performed in accord with procedures described by the U.S. Department of the Interior (1974) and the University of Missouri at Rolla (1981). Usually the tests are performed with water, but injection of water near the waste-disposal areas at Los Alamos was not allowed (see succeeding subsection on Background for further discussion). One hole, LLM-85-05, located between Areas G and L, was tested with both air and water in order to permit a comparison between the two fluids.

Following the discussion on background, a detailed description of the field tests is presented, including equipment and procedures. The equations used to calculate hydraulic conductivity and intrinsic permeability are presented next, followed by a discussion of the results, including a comparison of the air and water values obtained for Hole LLM-85-05.

3.2.1.2 Background

Two methods are available to measure the in-situ saturated hydraulic conductivity, K_s, of the tuff above the water table. These are borehole-infiltration tests and borehole-injection tests. Borehole-infiltration tests require maintenance of a constant head of water in an open or cased borehole until the flow rate becomes steady. The method is described in papers by Stephens and Neuman (1982a, 1982b) and Stephens and others (1983). Borehole-injection tests involve installing packers in the borehole to isolate measurement intervals, followed by injection of air or water into the formation.

Prior to initiation of the investigations described in this report, Los Alamos National Laboratory requested that water not be injected into boreholes in the vicinity of Areas G and L. Since the majority of the holes for this study are in or adjacent to these areas, borehole infiltration as a method for determining in-situ permeabilities was eliminated. Instead, borehole injection was used to measure in-situ permeability in the study area, largely because packers can be used to isolate sections of the borehole for testing and because air can be used in place of water. However, the method, whether using air or water, is subject to a number of limitations and assumptions which warrant further discussion.

*Response to Task 1, Paragraph 25, Compliance Order/Schedule.

First, it should be emphasized that the air-injection method is experimental and may permit only a qualitative characterization of subsurface permeabilities. Miller and others (1974), for example, used an air-injection technique to study the fracturing around a tunnel in volcanic rock and were able to conclude only that the permeability of the rock was either high or low. Therefore, before any quantitative interpretation can be made; air-injection results must be compared with results of laboratory and other field tests.

Using air as an injection fluid for packer tests may require compensation or correction for these factors: gas compressibility, changes in the volume of the gas with respect to temperature, and variation in the atmospheric water-vapor content. To overcome potential problems related to these factors, certain assumptions were made and appropriate procedures were implemented.

Compressive effects are minimal under steady-state conditions. Hence, the flow of air was kept at a constant rate and under low pressure during the injection step. In addition, boundary effects were disregarded because capillary action should have no impact on air flow.

To permit compensation for temperature effects on the volume of gas, a probe was placed downhole just above the packer assembly. A description of the temperature probe and meter is presented in the Equipment subsection (Section 3.2.1.3.1).

Based on the results of a study by Loughborough (1966), who compared the permeability of concrete using air and water vapor versus dried air, the potential effects of varying amounts of water vapor were disregarded. Loughborough's results demonstrated an average difference in permeability of only 5 percent. It is expected that this difference would be even less in a more permeable medium such as the Bandelier Tuff, indicating that it is reasonable to assume no effect.

Finally, in order to accurately calculate permeability for an air-injection test, values for the fluid injection pressure and flow rate must be known. Depending on the injection rate and the permeability of the formation, the resulting pressure can be very low. Equipment used to measure the low injection flow rates and pressures are described in the Equipment subsection (Section 3.2.1.3.1).

The use of water as an injection fluid also has certain limitations, specifically for tests above the water table. The U.S. Department of Interior (1974) points out that water-injection tests are more accurate below the water table than above, since the describing equations assume that horizontal flow is inherent throughout the system. Another potential source of error associated with water-injection tests is that existing formulas for computing permeability disregard the effects of capillary flow in the vadose zone. Instead, the formulas are based on various approximations of the classical free surface theory, which assumes that flow takes place entirely within a saturated region, an approximation which could lead to significant errors as pointed out by Stephens and Neuman (1982a).

3.2.1.3 Description of Field Tests

3.2.1.3.1 Equipment. Figures 3-3 and 3-4 illustrate the equipment used for the air- and water-injection tests, respectively. Although the two configurations differ somewhat, each has the same essential parts: flow meter, pressure gauge or gauges, conduit pipe, downhole temperature probe, and pneumatic packers.

For the air-injection tests, a New Jersey Air Flow Meter was used to measure the volume of air injected into the formation. Since the quantity of air injected varied from hole to hole, two different meters with different flow ranges were used. One had a range of 0 to 40 cubic feet per minute (cfm) with 1-cfm increments, while the other had a range of 50 to 300 cfm with 5-cfm increments. For the water-injection tests, a Neptune Water Meter with 0.1-gallon increments replaced the New Jersey Air Flow Meter.

For both the air- and water-injection tests, a Heise pressure gauge was used to measure the downhole, or back injection, pressure. The Heise gauge has a range of 0 to 60 psi with 0.2-psi increments, and is calibrated for atmospheric pressure at sea level (14.7 psi). Such a sensitive gauge was necessary to accurately measure the low pressures which resulted from the small volumes of fluid injected.

Galvanized conduit pipe, 1-3/8 inches in diameter, was used to conduct fluid down the hole. Threaded sections and couplings were secured with Teflon tape to prevent leakage.

The probe used to measure downhole fluid temperatures was located in a small chamber at the base of the conduit pipe, just above the pneumatic packers. Both the chambers and the section of pipe to which it was welded contained holes that permitted small amounts of air to flow between the two. The temperature probe was connected to a YSI Model 42SC Tele-thermometer located at the surface. The Tele-thermometer had a range of -40 to 150°C with increments of 1°C.

Each 6-ft interval was isolated using a set of Tigre Tierra Model 610 Pneumatic Packers. The 4-ft-long packers expand up to 10 inches in diameter and can be inflated to 470 psi.

3.2.1.3.2 Procedure. The borehole-injection tests were conducted by isolating 6-ft intervals in the uncased boreholes using the pneumatic packers. The packers were inflated to 200 psi to ensure a good seal. (Several tests were performed before this inflation pressure was determined.) A known quantity of air or water was injected until a measurable pressure was obtained on the Heise gauge. The pressure, flow rate, and temperature were then periodically recorded until all readings were constant with respect to time. The flow rate was then increased and the procedure repeated. Once the higher flow rate became constant, the process was repeated using the lower flow rate to check reproducibility.

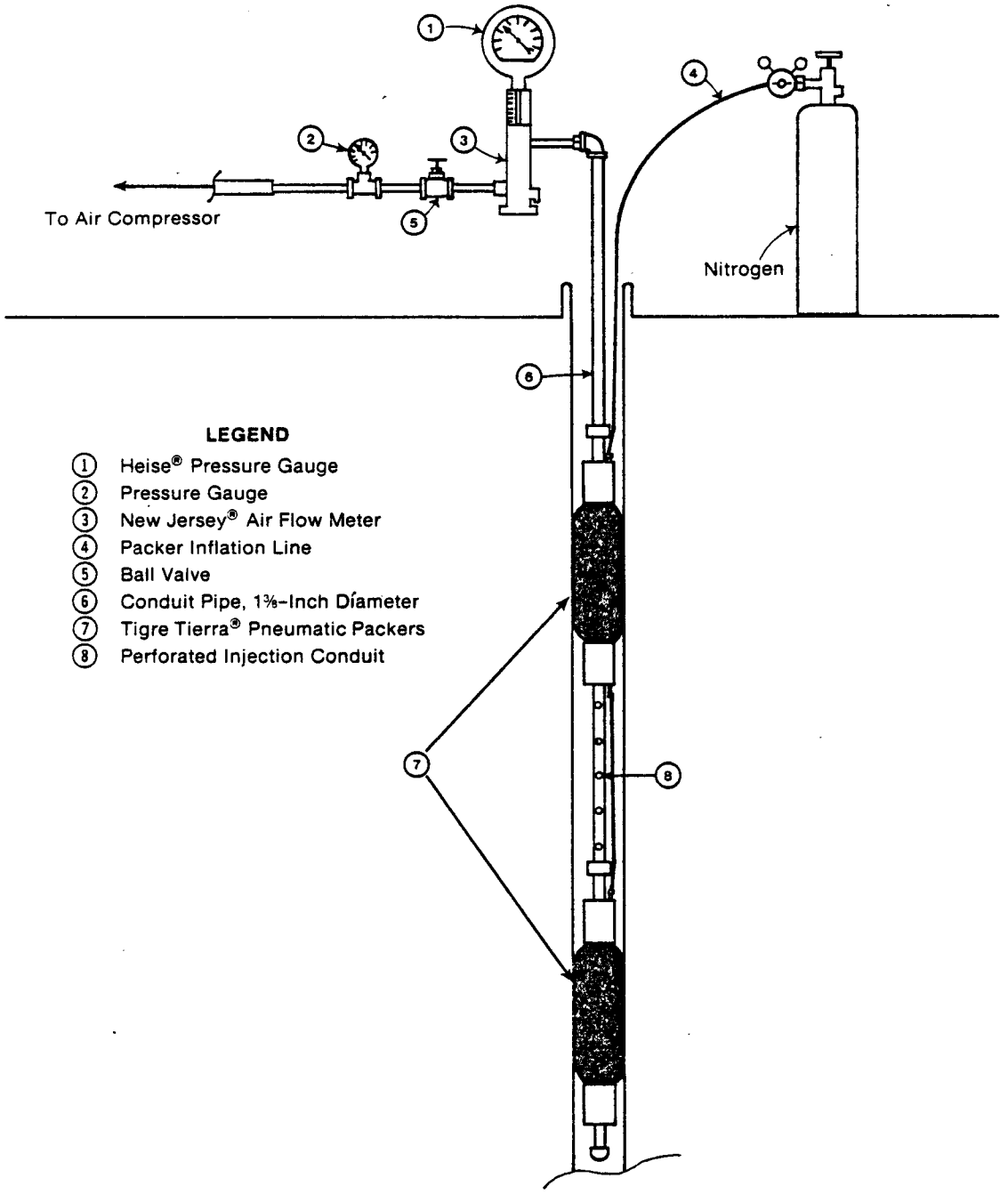

Figure 3-3. Air-Injection Apparatus Used for In-Situ Permeability Measurements

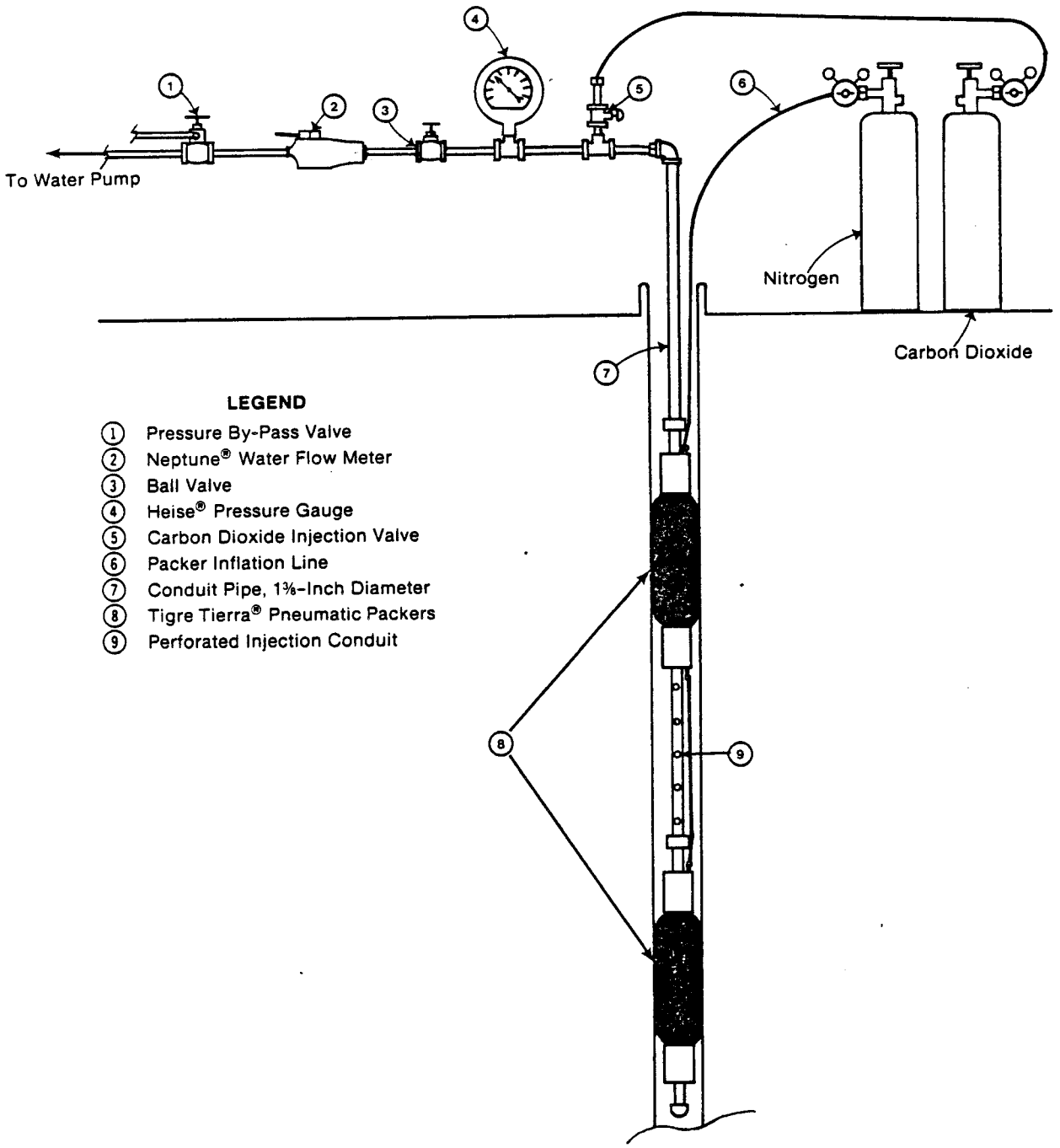

Figure 3-4. Water-Injection Apparatus Used for In-Situ Permeability Measurements

During the tests, the borehole was monitored for discharge of either air or water. If a discharge occurred, it was assumed that the packers were leaking and that the test was invalid.

3.2.1.4 Calculations

The rate at which a fluid can be injected into a geologic formation at a given pressure and through a known area is a function of the permeability of the formation. This relationship can be expressed in the following equation (U.S. Department of the Interior, 1974):

$$K = (Q/2\pi SH) \ln (S/r) \tag{5}$$

where

K = hydraulic conductivity (L/t)
Q = injection rate (L^3/t)
S = length of the test interval (L)
H = differential head of the fluid (L)
r = radius of the borehole (L)

Since the differential head is a combination of the height of the fluid column above the test interval and the pressure p at which the fluid is injected, p may be expressed as the height of the column of any fluid by the relationship

$$H = p/\gamma \tag{6}$$

where γ is the specific weight of the fluid.

Equation (5) is sufficient for the calculation of hydraulic conductivity when water is the injection fluid. However, modifications to Equation (5) are required when air is the injection fluid, because the specific weight of air is strongly dependent on the temperature and pressure. The specific weight of air can be determined from the equation of state for an ideal gas,

$$\gamma = gp_a/RT_a \tag{7}$$

where

γ = specific weight of the fluid (m/L^2t^2)
g = gravitational acceleration (L/t^2)
p_a = absolute pressure (force/L^2)
R = a gas constant
T_a = absolute temperature in degrees Rankine or Kelvin

For air, the value of R is 287 N-m/(kg)(°K) [1715 ft-lb/(slug)(°R)]. Substituting Equations (6) and (7) for the appropriate variables in Equation (5) yields

$$K = (Qgp_a/2\pi SpRT_a) \ln (S/r) \tag{8}$$

Since the flow rate of a gas through the New Jersey meter is also dependent on temperature and pressure, a combined correction factor, C_f, is required to

calculate the actual flow rate. Inserting the combined correction factor into Equation (8) yields the final equation for calculating the in-situ air-derived hydraulic conductivity,

$$K = (QC_f g p_a / 2\pi S p R T_a) \ln (S/r) \tag{9}$$

In order to compare the hydraulic conductivity derived from air injection versus that derived from water injection, it is convenient to use the term intrinsic permeability, k. Intrinsic permeability is a function of only the medium, whereas hydraulic conductivity is a function of both the medium and the fluid. The term k is widely used in the petroleum industry where the existence of gas, oil, and water in multiphase flow systems makes the use of a fluid-free conductance parameter attractive.

Intrinsic permeability and hydraulic conductivity can be related to one another by the equation (Nutting, 1930)

$$k = K\mu/\rho g \tag{10}$$

where

- k = intrinsic permeability (L^2)
- K = hydraulic conductivity (L/t)
- μ = absolute viscosity of the fluid ($F \cdot t/L^2$, where F = force)
- ρ = density of the fluid (m/L^3)
- g = gravitational acceleration (L/t^2)

Equation (10) will suffice for calculating k values from water-derived K values. However, modifications to Equation (10) are required for gas-derived conductivities because of the dependence of the density term on the pressure and temperature. Once again, the equation of state in the following form is used:

$$\rho = p_a/RT_a \tag{11}$$

Equation (11) is substituted for ρ in Equation (10) to yield the relationship between k and K for a gas,

$$k = K\mu RT_a/p_a g \tag{12}$$

Comparing the intrinsic permeability values calculated from the air- and water-injection tests can aid in the evaluation of any bias inherent in the individual methods.

3.2.1.5 Results and Discussion

Hydraulic conductivity values derived from the air-injection tests (Table 3-2) range from 10^{-3} to 10^{-5} centimeter per second (cm/s) [10^{-3} to 10^{-6} foot per second (ft/s)]. Conversions to intrinsic permeability indicate that the range of values is similar to those exhibited by a silty to clean sand (Freeze and Cherry, 1979). Based on field observations of the tuff, these permeability values appear to be reasonable.

Table 3-2. Hydraulic Conductivity Determined from Air-Injection Tests in Los Alamos Drill Holes

Hole Number	Geologic Unit	Test Interval[a] (ft)	Interval Description	Fractures Present?	Hydraulic Conductivity (K)	
					cm/s x 10^{-3}	ft/s x 10^{-5}
LLM-85-01	2b	9-15	Upper 2b, Moderately Welded	No	1.2	4.1
LLM-85-01	2b	30-36	Lower 2b, Moderately to Slightly Welded	No	0.70	2.3
LLM-85-02	2b	9-15	Upper 2b, Moderately Welded	Yes	0.094	0.31
LLM-85-02	2b	24-30	Middle 2b, Moderately Welded	No	0.11	0.37
LLM-85-05	2b	24-30	Mid-Lower 2b, Moderately Welded	No	0.91	3.0
LGM-85-11	2b	9-15	Upper 2b, Moderately Welded	No	1.5	5.0
LGM-85-11	2b	14-20	Middle 2b, Moderately Welded	Yes	1.4	4.7
LGM-85-11	2b/2a	35-41	Contact 2b/2a, Slightly Welded	No	0.12	0.40
LLM-85-01	2a	51-57	Middle 2a, Slightly Welded	No	0.33	1.1
LLM-85-01	2a	72-78	Lower 2a, Slightly Welded	Yes	0.14	0.45
LLM-85-02	2a	45.5-51.5	Upper 2a, Slightly Welded	Yes	0.14	0.45
LLM-85-02	2a	66.5-72.5	Mid-Lower 2a, Moderately Welded	No	0.14	0.45
LLM-85-05	2a	45-51	Upper 2a, Slightly Welded	Yes	2.8	9.3
LLM-85-05	2a	55-61	Middle 2a, Slightly Welded	Yes	1.9	6.2
LGM-85-06	2a	38-44	Upper 2a, Slightly Welded	Yes	0.067	0.22
LLM-85-05	2a/1b	75-81	Contact 2a/1b, Slightly Welded	No	0.052	0.17
LGM-85-11	2a/1b	56-62	Contact 2a/1b, Slightly Welded	No	0.52	1.7
LLM-85-01	1b	93-99	Mid-Upper 1b, Slightly Welded	No	0.082	0.27
LLM-85-02	1b	87-93	Upper 1b, Slightly Welded	No	0.085	0.28
LLM-85-05	1b	82-88	Upper 1b, Slightly Welded	No	0.061	0.20
LGM-85-06	1b	60-66	Upper 1b, Slightly Welded	No	0.64	2.1
LGM-85-06	1b	81-87	Middle 1b, Slightly to Moderately Welded	No	0.52	1.7
LGM-85-11	1a/1b	99-105	Contact 1a/1b, Slightly Welded	No	0.030	0.098
LGM-85-11	1b	77-83	Middle 1b, Slightly to Moderately Welded	No	0.23	0.77
LGM-85-11	1a	108-114	Upper 1a, Nonwelded	No	0.088	0.2

[a]Depth below ground level.

In general terms, the permeability of the tuff decreases with stratigraphic depth. Unit 2b shows an average air-derived hydraulic conductivity of 8.5 x 10^{-4} cm/s (2.8 x 10^{-5} ft/s); Unit 2a, 7.9 x 10^{-4} cm/s (2.6 x 10^{-5} ft/s); Unit 1b, 2.3 x 10^{-4} cm/s (7.7 x 10^{-6} ft/s); and Unit 1a, 8.8 x 10^{-5} cm/s (2.9 x 10^{-6} ft/s), this last being the only measurement obtained for Unit 1a.

The highest air-derived hydraulic conductivity was determined for a fractured zone in Unit 2a [2.8 x 10^{-3} cm/s (9.3 x 10^{-5} ft/s)]. However, the average K value determined for fractured zones [9.4 x 10^{-4} cm/s (3.1 x 10^{-5} ft/s)] was only slightly greater than values determined from the majority of air-injection tests in unfractured tuff. These results suggest that secondary fracture permeability does not appear to be significantly greater than the primary permeability of the tuff.

Water-derived hydraulic conductivities, presented in Table 3-3, are in the same range as those reported by Abeele (1984) for crushed tuff, i.e., 1.4 x 10^{-4} cm/s (4.6 x 10^{-6} ft/s). These values, like those derived from the air-injection tests, generally decrease with depth.

The reliability of the air-injection method is demonstrated by comparing the intrinsic permeability values calculated from both the air and water test for the same intervals (Table 3-4); results from the two lower zones in particular are in good agreement with one another. The largest discrepancy between the two methods is seen in the results for the interval 24 to 30 ft, where the value calculated from the water-injection test is an order of magnitude lower than the value calculated from the air-injection test. This water-injection test, however, was not performed in the same fashion as the others. Specifically, carbon dioxide was not injected prior to the tests as it was for the lower intervals. The purpose of injecting carbon dioxide is to minimize the effects of trapped air in the formation. Thus, permeability values might be less for tests performed without carbon dioxide injection. It would appear that these results support the use of carbon dioxide for water-injection tests in the vadose zone, as recommended by Stephens and others (1983).

Table 3-3. Hydraulic Conductivity Values Determined from Water-Injection Tests in Hole LLM-85-05

Test Interval (ft)[a]	Hydraulic Conductivity (K) cm/s	ft/s
10-16	9.4 x 10^{-4}	3.1 x 10^{-5}
24-30[b]	1.0 x 10^{-3}	3.3 x 10^{-5}
75-81	6.4 x 10^{-4}	2.1 x 10^{-5}
82-88	4.6 x 10^{-4}	1.5 x 10^{-5}

[a]Depth below ground level.
[b]Injection with carbon dioxide prior to water injection was not performed for this test interval.

Table 3-4. Comparison of Intrinsic Permeability Values Determined from Water-Injection and Air-Injection Tests in Hole LLM-85-05

Test Interval (ft)[a]	Intrinsic Permeability (k)			
	Air-Injection Test		Water-Injection Test	
	cm^2	ft^2	cm^2	ft^2
24-30[b]	1.8×10^{-7}	1.9×10^{-10}	1.3×10^{-8}	1.4×10^{-11}
75-81	7.5×10^{-9}	8.1×10^{-12}	8.4×10^{-9}	9.1×10^{-12}
82-88	9.0×10^{-9}	9.7×10^{-12}	6.0×10^{-9}	6.5×10^{-12}

[a]Depth below ground level.
[b]Injection with carbon dioxide prior to water injection was not performed for this test interval.

3.2.2 VACUUM TESTS*

3.2.2.1 Purpose and Scope

Vacuum tests were conducted in selected intervals of the Bandelier Tuff in order to obtain additional measurements of the in-situ permeability. These tests also involve sealing off the measurement interval using pneumatic packers and monitoring the changes in air pressure and flow rate after creating a pressure gradient. Unlike the air-injection tests, however, the pressure gradient is negative and is created by means of a vacuum pump. Detailed descriptions of the equipment and procedures, followed by discussions of the calculations and results, are presented in the succeeding paragraphs.

3.2.2.2 Description of Field Tests

3.2.2.2.1 Equipment. The vacuum-testing apparatus used for this study (see Figure 3-5) was designed to isolate a specified interval in the drill hole, to evacuate air by means of pumping, and to measure the resultant pressure response, flow rate, and air temperature. Isolation of the 1-meter-long (3.3 ft) test interval was accomplished by means of pneumatic packers similar to those used in the injection tests. A vacuum hose attached to the packer conduit pipe extended upward to the ground surface and was connected to a two-way valve that isolated the drill hole from the rest of the vacuum-testing equipment.

A capacitance manometer connected between the valve and the packers measured downhole pressure changes induced by pumping. The manometer was a tensioned-metal-diaphragm vacuum gauge having the capacity to measure pressure in the range of 1×10^{-4} torr to 1000 torr. (A torr is a unit of pressure equal to 1333.22 microbars, or the pressure required to support a column of mercury 1 millimeter high under standard conditions.) A pressure display module was connected to the manometer to provide direct readout of pressure in torr or millimeters.

*Response to Task 1, Paragraph 25, Compliance Order/Schedule.

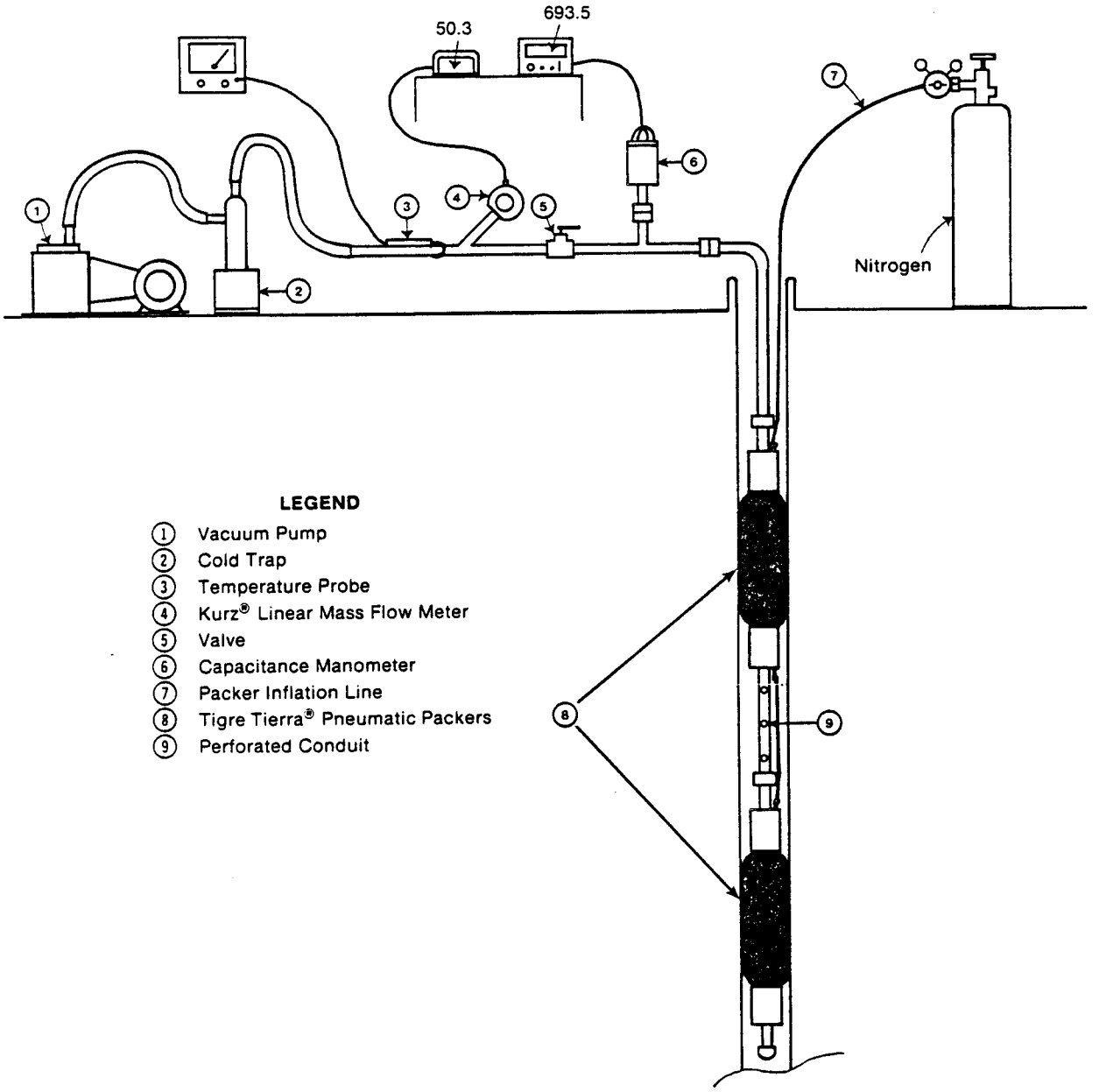

Figure 3-5. Vacuum-Testing Apparatus Used for In-Situ Permeability Measurements

The probe used to measure downhole air temperature was located in line with the system, in a small chamber welded to a section of pipe. Small holes connect the chamber and the pipe, allowing small amounts of air to flow between the two. The temperature probe was connected to a YSI Model 42SC Tele-thermometer, which has a range of -40 to 150°C with increments of 1°C.

A linear mass flow meter was located adjacent to the temperature probe in order to measure the gas flow rate induced by pumping. The meter consisted of two platinum windings: One winding was an ambient temperature detector; the other was heated to a constant temperature above that of the ambient or surrounding gas. A measure of the power required to maintain this temperature difference is a measure of the heat transfer from the winding, which in turn is a measure of the quantity of gas flowing past the sensor. The range of the meter was 0 to 1000 liters per minute (lpm), with an accuracy of 2 percent of the reading over a 10-to-1 range plus an additional one-half percent at full scale.

3.2.2.2.2 Procedure. Once a test interval had been selected, the pneumatic packers were lowered to the desired depth and inflated to isolate that particular section of the drill hole. The vacuum valve was closed, and the formation pressure prior to pumping was recorded in the field notebook.

With the vacuum pump running, the valve was opened to start the test. Pressure readings versus time were recorded at 5-second intervals. Pumping of the test section was continued as long as was necessary under the specified conditions dictated by the medium and the dead volume of the equipment. Generally, pumping was terminated after achieving steady-state flow. For tests in the Bandelier Tuff, it was observed that quasi steady-state conditions were obtained prior to 1 minute of pumping. Therefore, for all tests, the interval was pumped for a period of 1 minute. The temperature was recorded during the pumping phase of the tests, and the flow rate was recorded just prior to the end of the pumping phase.

After 1 minute of pumping, the vacuum valve was closed and the pressure buildup phase was begun. Pressure readings were once again recorded at 5-second intervals until the system returned to the prepumping pressure, signifying the end of the test.

3.2.2.3 Calculations

The vacuum-testing technique is based on methods used by the petroleum industry. In a paper presented by Horner (1951), the pressure buildup that results from closing gas wells is used to calculate the permeability of the subsurface formation. This method was modified by Jakubick (1983) for use in unsaturated materials by initiating the pressure buildup by means of vacuum pumping rather than by shutting-in the well. The equations used for the calculations in this study, however, were taken directly from Horner's paper, because Jakubick does not present the theory for his equations which are different from the original work by Horner. Moreover, Jakubick does not define the gas-constant term he used, nor does he maintain consistency in the units used in his equations.

Single-phase radial flow to a well completed in a reservoir, assumed to be homogeneous, horizontal, and of uniform thickness, may be expressed by the equation

$$(\partial^2 p/\partial r^2) + [(1/r)(\partial p/\partial r)] = (fc\mu/k)(\partial p/\partial t) \tag{13}$$

where

p = reservoir pressure
r = distance from the center line of the well
f = formation porosity
c = fluid compressibility
μ = fluid viscosity
k = intrinsic permeability of the formation
t = time

Horner presents the so-called 'point solution' to Equation (13) which yields

$$p = p_o + \{(q\mu/4\pi kh)E_i[-(r^2 f\mu c/4kt)]\} \tag{14}$$

where

p_o = initial reservoir pressure
q = a constant rate of production for the well
h = length of the test interval
E_i = the exponential integral

Considering a single well brought into production at t_o, which subsequently produced at a constant rate q, the well pressure p_w at the time $[(t_o + \varphi)/\varphi]$ may be obtained by superimposing two solutions of the form of Equation (14). For small values of its argument, the E_i function may be approximated by a logarithmic function. The result is the basic buildup equation for a single well in an infinite reservoir,

$$p_w = p_o - \{(q\mu/4\pi kh) \ln [(t_o + \varphi)/\varphi]\} \tag{15}$$

where φ is the time after close-in of the well.

For analysis of the data, it is convenient to change the natural logarithm, ln, to the base ten logarithm, $\log_{10}$, by the relationship

$$\ln x = (\log_{10} x)(\ln 10) \tag{16}$$

which yields

$$p_w = p_o - \{[(\ln 10)q\mu/4\pi kh] \log [(t_o + \varphi)/\varphi]\} \tag{17}$$

Analysis of the vacuum-test data using Equation (17) involves fitting a straight line through the data points. The slope of the line, m, from Equation (17) is defined as

$$m = -[(\ln 10)q\mu/4\pi kh] \tag{18}$$

The next step in the analysis involves plotting the well-pressure (p_w) data versus the log of $[(t_o + \varphi)/\varphi]$ and determining the slope of the resultant line. This graph is commonly referred to as a Horner plot. Once the slope of the line is determined, Equation (18) can be rearranged in terms of the intrinsic permeability as follows:

$$k = -[(\ln 10)q\mu/4\pi mh] = -[0.1832339(q\mu/mh)] \quad (19)$$

3.2.2.4 Results and Discussion

Intrinsic permeabilities determined from vacuum tests in the Bandelier Tuff (Table 3-5) range from 10^{-8} to 10^{-9} cm^2 (10^{-11} to 10^{-12} ft^2). The correlation coefficients for the linear regression used to fit a straight line through the data points on the Horner plots indicate a good linear relationship for the data; the lowest coefficient is 0.92 (see Table 3-5).

In general, the vacuum-test results, like those from the air-injection tests, indicate that permeability tends to decrease with depth. The lowest value, for example, was observed in the lower, moderately welded portion of Unit 1b. Results of the three tests performed in fractured zones indicate that there is no significant difference in permeability between fractured versus unfractured zones.

Table 3-6 compares intrinsic permeabilities derived from the air-injection tests versus the vacuum tests for similar intervals. The comparison demonstrates that the two methods yield results of the same order of magnitude. The vacuum-test results, however, are lower. A discussion of possible variations in vacuum-test and air-injection methods is presented in Section 3.2.5.

3.2.3 LABORATORY MEASUREMENTS*

3.2.3.1 Purpose and Scope

Laboratory measurements of permeability were also obtained on 20 core samples to provide a comparison with the field-test results. These determinations were conducted by TerraTek Research Laboratory using two procedures, one to measure permeability via gas injection and correction for gas slippage (Klinkenberg Correction Method) and the other to measure the gas-water relative permeability (Dynamic Method). The descriptions of these procedures are taken from TerraTek's report (TerraTek Research Laboratory, 1985). They are followed by a discussion of the laboratory results. A comparison of the laboratory and field data is presented in Section 3.2.5.

3.2.3.2 Sample Preparation

(See Section 3.1.2.2.)

*Response to Task 1, Paragraph 25, Compliance Order/Schedule.

Table 3-5. Permeability Values Determined from Vacuum Tests in Los Alamos Drill Holes

Hole Number	Geologic Unit	Test Interval[a] (ft)	Interval Description	Correlation Coefficient[b]	Fractures Present?	Intrinsic Permeability (k)	
						$cm^2 \times 10^{-9}$	$ft^2 \times 10^{-12}$
LLM-85-01	2b	30-33.3	Lower 2b, Moderately Welded	0.9409	No	39	42
LLM-85-02	2b	10-13.3	Upper 2b, Moderately Welded	0.9325	Yes	14	15
LLM-85-02	2b	25-28.3	Middle 2b, Moderately Welded	0.9267	Yes	22	24
LLM-85-05	2b	15-18.3	Middle 2b, Moderately Welded	0.9948	No	24	2.6
LGM-85-06	2b	10-13.3	Upper 2b, Moderately Welded	0.9675	No	38	41
LGM-85-11	2b/2a	35-38.3	Contact 2b/2a, Moderately Welded	0.9779	No	5.5	5.9
LLM-85-01	2a	70-73.3	Lower 2a, Nonwelded	0.9799	No	43	46
LLM-85-05	2a	40-43.3	Upper 2a, Slightly Welded	0.9196	No	8.4	9.1
LLM-85-05	2a	50-53.3	Middle 2a, Slightly Welded	0.9812	No	8.6	9.3
LLM-85-05	2a	60-63.3	Middle 2a, Moderately Welded	0.9882	No	8.6	9.3
LLM-85-06	2a	40-43.3	Middle 2a, Moderately Welded	0.9895	Yes	2.4	2.6
LLM-85-01	1b	80-83.3	Upper 1b, Slightly Welded	0.9946	No	5.6	6.0
LLM-85-01	1b	94-97.3	Upper 1b, Slightly Welded	0.9959	No	3.5	3.8
LLM-85-02	1b	87-90.3	Upper 1b, Slightly Welded	0.9966	No	9.3	10
LGM-85-06	1b	82-85.3	Middle 1b, Slightly Welded	0.9931	No	1.0	1.1
LGM-85-06	1b	100-103.3	Lower 1b, Moderately Welded	0.9932	No	0.84	0.90
LGM-85-11	1b	77-80.3	Middle 1b, Slightly Welded	0.9851	No	8.2	8.8
LGM-85-06	1b	60-63.3	Upper 1b, Slightly Welded	0.9903	No	8.7	9.4
LGM-85-11	1a	110-113.3	Upper 1a, Nonwelded	0.9963	No	2.7	2.9
LLM-85-02	1b	87-90.3	Upper 1b, Slightly Welded	0.9966	No	8.6	9.3
LLM-85-06	1b	87-90.3	Mid-Lower 2b, Moderately Welded	0.9609	No	2.4	2.6

[a]Depth below ground level.

[b]Correlation coefficient for the linear regression used to fit a straight line through the data points on the Horner plots (see Section 3.2.2.3).

Table 3-6. Comparison of Intrinsic Permeability Values Determined from Air-Injection and Vacuum Tests in Los Alamos Drill Holes

Hole Number	Test Interval (ft)[a]		Intrinsic Permeability (k)			
	Air-Injection Test	Vacuum Test	Air-Injection Test		Vacuum Test	
			$cm^2 \times 10^{-9}$	$ft^2 \times 10^{-12}$	$cm^2 \times 10^{-9}$	$ft^2 \times 10^{-12}$
LLM-85-01	30-36	30-33.3	130	140	39	42
LLM-85-02	9-15	10-13.3	10	11	15	16
LLM-85-02	24-30	25-28.3	16	17	22	24
LGM-85-11	35-41	35-38.3	17	18	5.5	5.9
LLM-85-01	72-78	70-73.3	19	21	43	46
LLM-85-01	93-99	94-97.3	7.6	8.2	3.5	3.8
LLM-85-02	87-93	87-90.3	3.3	9.5	9.3	10
LGM-85-06	60-66	60-63.3	120	130	8.7	9.4
LGM-85-06	81-87	82-85.3	84	90	1.0	1.1
LGM-85-11	99-105	100-103.3	3.3	3.6	0.84	0.90
LGM-85-11	77-83	77-80.3	32	35	8.2	8.8
LGM-85-11	108-114	110-113.3	7.2	7.8	2.7	2.9

[a]Depth below ground level.

3.2.3.3 Procedures

3.2.3.3.1 Klinkenberg Correction Method. Following porosity determinations, gas permeability measurements were performed on the 20 samples. These measurements were corrected for gas slippage, i.e., movement of gas along a boundary, using the Klinkenberg Correction Method. The measurement technique consisted of applying a confining pressure of approximately 100 psi and a slight pore pressure, and maintaining an approximate pressure drop of 2 psi across the sample during testing. Nitrogen gas was injected into the samples at four mean pressures (4, 9, 14, and 19 psi), and the permeability was calculated for each of these pressures. A plot was made of permeability versus the reciprocal mean pressures, and the intercept of a best-fit line through these four points, with the permeability axis at zero reciprocal mean pressure (infinite mean pressure), yielded the gas permeability corrected for gas slippage (Klinkenberg Correction).

3.2.3.3.2 Dynamic Method. Following completion of the gas permeability measurements, all 20 samples were subjected to gas-water relative permeability testing to determine intrinsic permeabilities (described in Section 3.2.3.4 below) and effective permeabilities (described in Section 3.2.4.1). Testing was begun by vacuum-saturating the samples with tap water (density = 0.995 g/cm^3 at room temperature). Complete saturation was verified by comparing these saturated-weight data with helium-injection data. Following saturation, each sample was placed in a hydrostatic core holder and subjected to a confining pressure of approximately 100 psi. Testing consisted of displacing the water from the samples with humidified nitrogen. (The gas was humidified to prevent drying or dehydration.) Incremental production of gas and water was monitored against time and flow rate at a constant injection pressure. These production data were used to calculate the gas-water relative permeabilities according to Johnson, Bossler, and Naumann's (1959) extension of Welge's (1952) derivation of relative permeability.

3.2.3.4 Results and Discussion

The laboratory permeability results (Table 3-7) are relatively uniform and consistent between the two methods, except for Sample MCG-607. The Klinkenberg result for this sample is probably unreliable as evidenced by its low correlation coefficient (0.714) and its poor comparison with the Dynamic Method result.

The results from both methods indicate only minor differences with depth or between geologic units. Klinkenberg permeabilities are approximately twice those determined by the Dynamic Method, but that is not considered significant for these types of measurement. More importantly, the average intrinsic permeability for both the Klinkenberg Correction Method and the Dynamic Method is 10^{-9} cm^2 (10^{-11} ft^2), a result that compares favorably with the field-test results.

Table 3-7. Intrinsic Permeability Values Determined from Laboratory Analysis of Core Samples

Hole Number	Geologic Unit	Sample Number	Depth of Sample (ft)[a]	Interval Description	Intrinsic Permeability/ Klinkenberg Method		Correlation Coefficient[b]	Intrinsic Permeability/ Dynamic Method	
					$cm^2 \times 10^{-9}$	$ft^2 \times 10^{-12}$		$cm^2 \times 10^{-9}$	$ft^2 \times 10^{-12}$
LGM-85-11	2b	MCG-618	3	Moderately Welded[c]	6.2	6.7	0.989	5.5	5.9
LLM-85-02	2b	MCG-606	7	Moderately Welded	6.6	7.1	0.745	4.5	4.9
LLM-85-05	2b	MCG-610	15	Moderately Welded	6.5	7.0	0.893	5.7	6.2
LLM-85-01	2b	MCG-602	30	Moderately Welded	2.7	2.9	0.958	1.1	1.2
LGM-85-11	2b	MCG-619	30	Moderately Welded	3.2	3.5	0.949	2.9	3.1
LLM-85-02	2b	MCG-607	36	Moderately Welded	11.0	12.0	0.714	1.2	1.3
LGM-85-06	2b	MCG-614	29	Moderately Welded	6.4	6.9	0.847	4.9	5.3
LLM-85-05	2b	MCG-611	36	Slightly Welded	3.5	3.8	0.984	2.4	2.6
LLM-85-01	2a	MCG-603	52	Slightly Welded	4.1	4.4	0.969	2.7	2.9
LGM-85-06	2a	MCG-615	51	Slightly Welded	2.5	2.7	0.954	0.86	0.93
LLM-85-02	2a	MCG-608	67	Moderately Welded	2.0	2.2	0.958	1.0	1.1
LLM-85-05	1b	MCG-612	76	Slightly Welded	2.1	2.3	0.944	1.3	1.4
LLM-85-01	1b	MCG-604	101	Slightly Welded	3.0	3.2	0.939	2.6	2.8
LGM-85-06	1b	MCG-616	99	Moderately Welded	18.0	19.0	0.917	13.0	14.0
LGM-85-11	1b	MCG-620	94	Moderately Welded	4.4	4.7	0.958	1.1	1.2
LLM-85-02	1b	MCG-609	117	Moderately Welded	3.3	3.6	0.973	1.7	1.8
LLM-85-05	1b	MCG-613	123	Slightly Welded	4.2	4.5	0.902	1.6	1.7
LLM-85-01	1b	MCG-605	124	Moderately Welded	6.0	6.5	0.850	2.3	2.5
LGM-85-11	1a	MCG-621	115	Nonwelded	3.4	3.7	0.933	1.8	1.9
LGM-85-06	1a	MCG-617	115	Nonwelded	1.4	1.5	0.970	0.93	1.0

[a]Below ground level.
[b]Determined for Klinkenberg permeabilities.
[c]Weathered.

3.2.4 HYDRAULIC CONDUCTIVITY AS A FUNCTION OF MOISTURE CONTENT*

3.2.4.1 Laboratory Tests

As noted above, the Dynamic Method was also used to determine permeability as a function of moisture content for the 20 samples of Bandelier Tuff (see Section 3.2.3.3.2). These values, called effective permeabilities, are plotted as a function of total air saturation in the graphs presented in Appendix D. Since the abscissa corresponds to total air saturation, the maximum effective permeabilities for water depicted on the curves occur at an air saturation of 0.000, which is equivalent to a water saturation (θ_s) of 1.000. Therefore, as the water saturation decreases, the effective permeability for water decreases, and the effective permeability for air increases.

The effective permeability values for the rock-core samples from the Bandelier Tuff range from 86.1 to 1301 millidarcys [(8.5×10^{-10} to 1.3×10^{-8} cm^2) or (9.1×10^{-13} to 1.4×10^{-11} ft^2)]. Residual water saturation following gas injection ranged from 0.64 to 0.95. Since moisture contents in the study area are much lower than this range (generally less than 10 percent), the effective permeabilities determined using the Dynamic Method are not indicative of the permeabilities one would expect to observe at depth in Areas G and L. These data are therefore only applicable to the estimation of near-surface conditions following a heavy rainfall, when moisture contents might exceed residual water saturation.

3.2.4.2 van Genuchten's Method

3.2.4.2.1 Purpose and Scope. A model described by van Genuchten (1978) was used to calculate the unsaturated hydraulic conductivity functions for the Bandelier Tuff. Inputs to the model are the saturated hydraulic conductivities and data from the moisture characteristic curves for the 20 core samples analyzed in the laboratory tests. The output function is a closed-form analytical expression that generates a plot of hydraulic conductivity versus moisture content and/or water potential. The output function is only valid over the moisture and water-potential ranges tested.

3.2.4.2.2 Procedure. A model described by Mualem (1976) was used to predict unsaturated hydraulic conductivities from the moisture characteristic curves (Appendix C) and the saturated hydraulic conductivities. Mualem's derivation yields an integral formula for determining the unsaturated hydraulic conductivity as a function of moisture content, which enables one to derive closed-form analytical expressions provided suitable equations for the moisture characteristic curves are available. The resulting conductivity expressions generally contain three independent, dimensionless parameters--α, n, and m--which are calculated using the nonlinear least-squares curve-fitting program described by van Genuchten (1978). The information required to calculate these parameters consists of saturated hydraulic conductivities and data obtained from the moisture characteristic curves, namely, the saturated and residual soil-moisture contents (θ_s, and θ_r, respectively) and the slope for the curve at midpoint [$(\theta_s + \theta_r)/2$].

*Response to Task 3, Paragraph 25, Compliance Order/Schedule.

All of this information was assembled into a data base and used as input into van Genuchten's model, which generates values for α, n, and m. The model then inputs these values into Mualem's integral formulas and plots the following two functions: $K(\theta)$ versus θ (moisture content) and $K(\psi)$ versus ψ (water potential). The intrinsic permeabilities determined using the Klinkenberg Correction Method (Table 3-7) were then used to calculate water-saturated hydraulic conductivities for input to the model. (See Section 3.2.1.4 for conversion of intrinsic permeability to hydraulic conductivity.) These values were used largely because they more closely reflect the in-situ permeabilities for air and water in the study area.

3.2.4.2.3 Results and Discussion. The modeling results are presented as graphs of unsaturated hydraulic conductivity versus volumetric moisture content [$K(\theta)$ versus θ] and of hydraulic conductivity versus water potential [$K(\psi)$ versus ψ]. Representative outputs from the model for 7 of the 20 samples are presented in Figures 3-6 through 3-9.

Unfortunately, these results are of limited value because they are based on partial moisture characteristic curves which do not extend over the range of water potentials and moisture contents measured in the field. For example, the water-potential values of the curves extend roughly to -0.3 bar (-300 cm of water), while those measured in the field range from -1 to -15 bar (see Section 3.3.1.3). Similarly, values for moisture content (θ) range from 0.4 to 0.6 on the curves, while those determined in the field are generally less than 0.1. As a consequence, the calculated unsaturated hydraulic conductivities are also outside the range of the field values.

Nevertheless, the calculated values can be used for near-surface infiltration studies when the moisture and water-potential ranges fall within those of the moisture characteristic curves. It should be noted, however, that these curves were obtained by drying the soil and therefore represent only the drying branch of the hysteresis loop. The drying branch has a higher moisture content for a given water potential than does the wetting branch; hence, a given soil is more retentive for drying than it is for wetting (Case and Welch, 1979).

3.2.5 PERMEABILITY SUMMARY

Table 3-8 compares the overall average intrinsic permeabilities of the geologic units as determined by the three methods used in this study, namely, in-situ borehole injection, in-situ vacuum testing, and laboratory testing of core samples. In contrast to the laboratory results, which show relative uniformity throughout the tuff, results of both field methods indicate a decrease in permeability with stratigraphic depth. This contrast is probably due in part to the fact that it was necessary to select the laboratory samples from those exhibiting the highest degree of consolidation; such samples would have lower permeabilities than the bulk formation from which they were taken. Furthermore, the laboratory tests measure a significantly smaller interval than that measured in the field. It was therefore concluded that the field-test results were the more reliable indicators of bulk permeabilities and that the permeabilities of the individual geologic units do indeed decrease with stratigraphic depth.

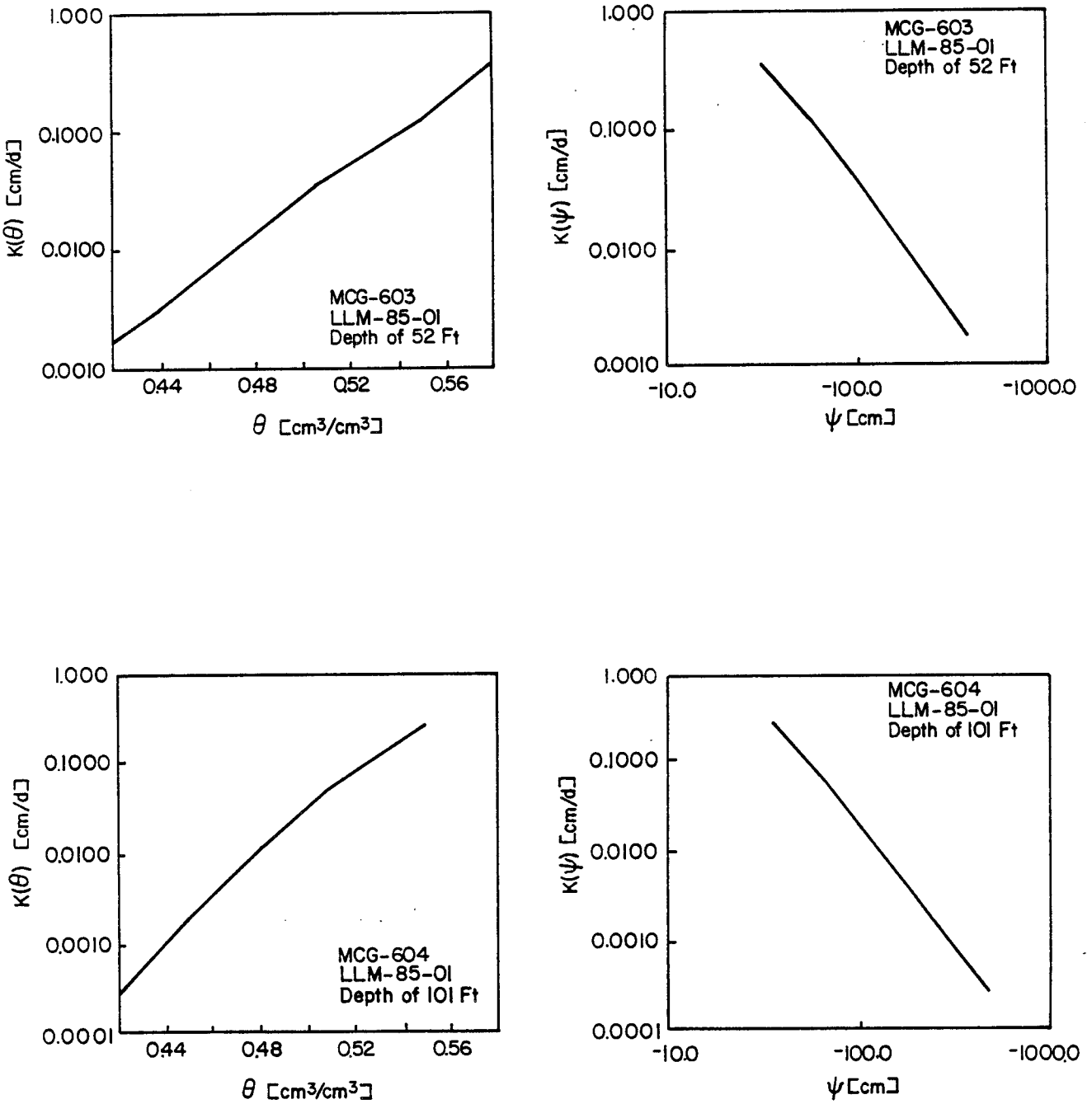

Figure 3-6. Unsaturated Hydraulic Conductivities as Functions of Moisture Content and Water Potential for Samples MCG-603 and MCG-604

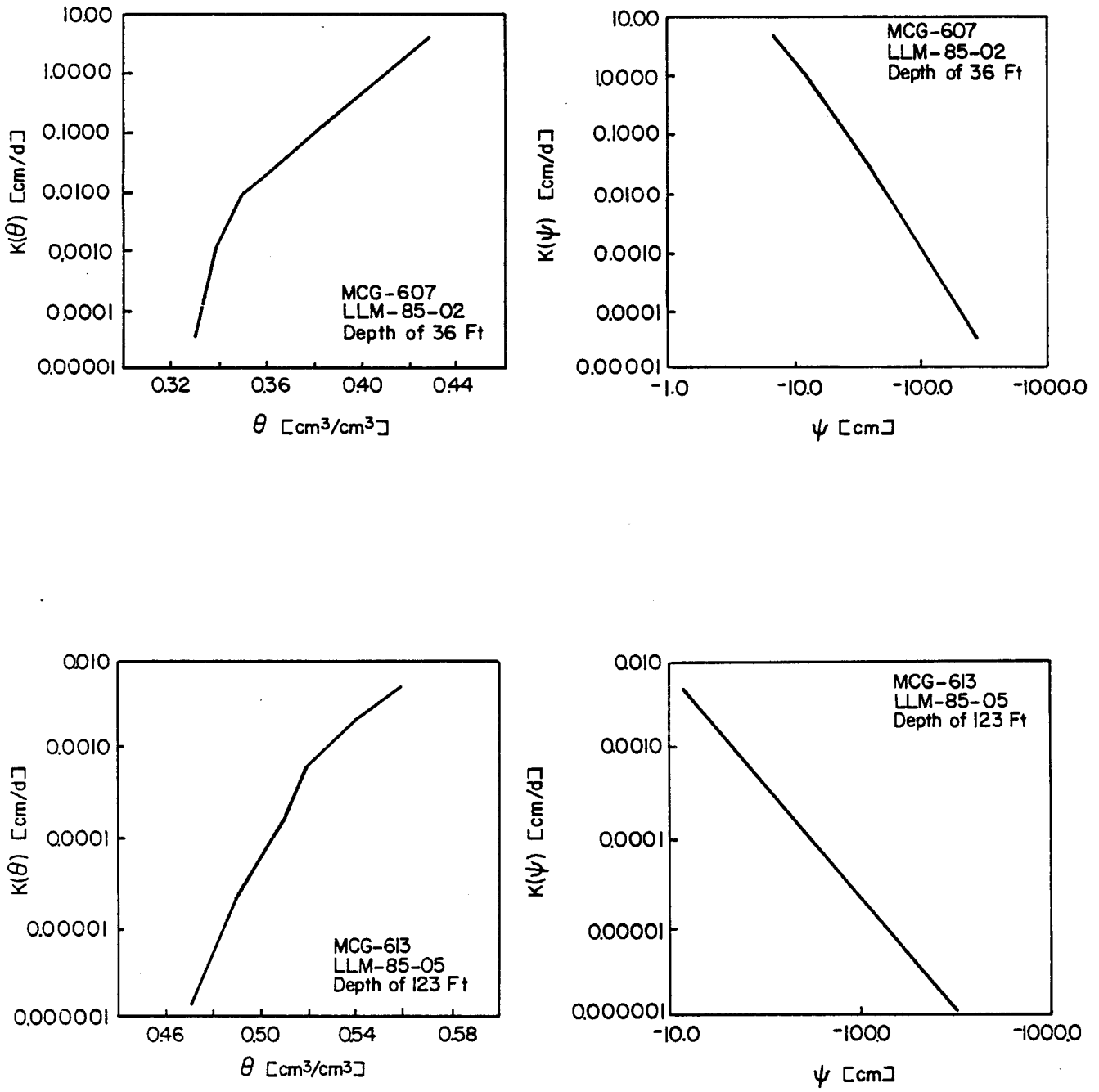

Figure 3-7. Unsaturated Hydraulic Conductivities as Functions of Moisture Content and Water Potential for Samples MCG-607 and MCG-613

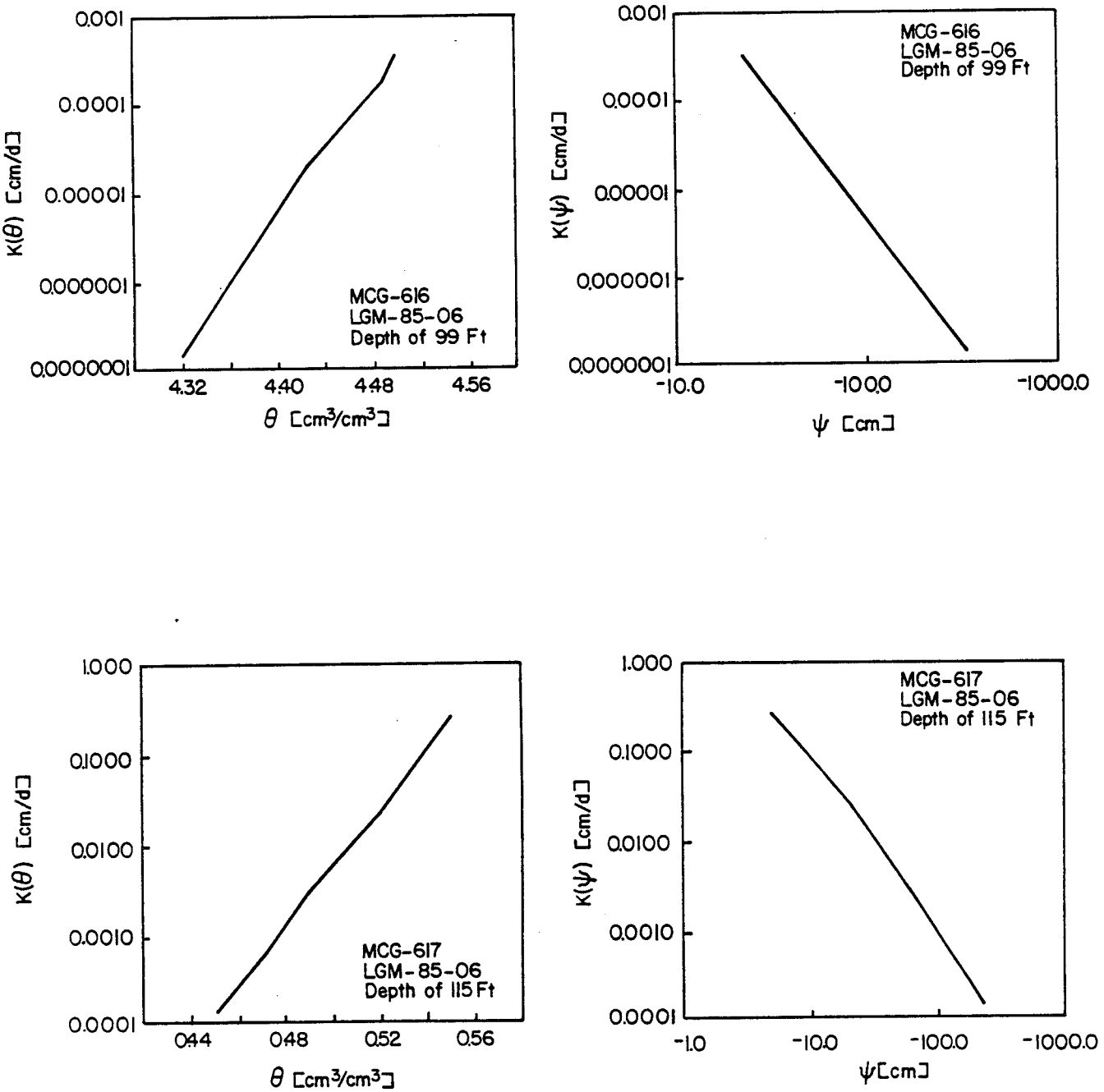

Figure 3-8. Unsaturated Hydraulic Conductivities as Functions of Moisture Content and Water Potential for Samples MCG-616 and MCG-617

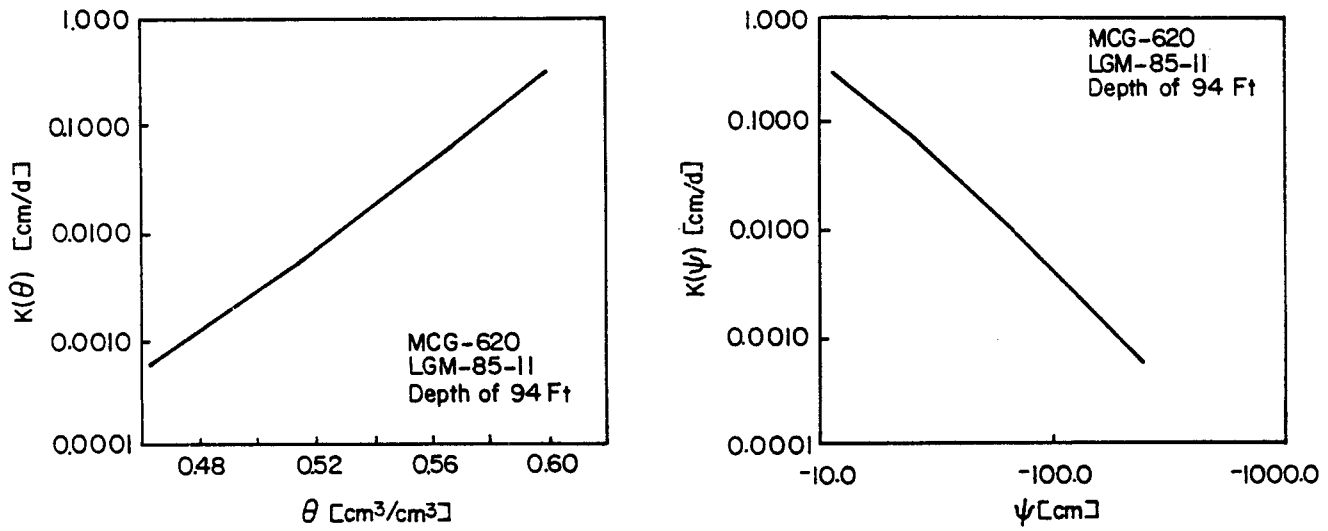

Figure 3-9. Unsaturated Hydraulic Conductivities as Functions of Moisture Content and Water Potential for Sample MCG-620

Table 3-8. Comparison of Average Intrinsic Permeability Values for the Major Geologic Units of the Bandelier Tuff in the Study Area

Unit	Intrinsic Permeability					
	Air-Injection Test		Vacuum Test		Laboratory Analysis	
	$cm^2 \times 10^{-9}$	$ft^2 \times 10^{-12}$	$cm^2 \times 10^{-9}$	$ft^2 \times 10^{-12}$	$cm^2 \times 10^{-9}$	$ft^2 \times 10^{-12}$
2b	93	100	23	25	5.7	6.2
2a	62	67	13	14	2.8	3.0
1b	26	28	5.7	6.2	5.7	6.2
1a	7.2[a]	7.8[a]	2.7[a]	2.9[a]	2.4	2.6

[a]Intrinsic permeability for this unit is based on only one measurement.

It should be noted that the lower average permeabilities determined by the vacuum test for Units 2b and 2a are probably due to the inability to perform the test in the more permeable portions of these units. A vacuum could not be established in the upper portions, so the test failed and no data were obtained. Thus, the average vacuum-test data do not include values for the most permeable zones in the units, resulting in average results which are biased low.

Results from all of the determinations do not permit a conclusive assessment of the effect of fractures on permeability. The moisture-content data indicate that the potential exists for fractures to cause preferential water movement; however, the enhancement may be less than the sensitivity of the measurement techniques. It follows that a better assessment would require additional testing, using methods having greater sensitivity. Similarly, additional tests, also having greater sensitivity, would be needed in order to fully assess the effects on permeability of such other sources of variation as pumice content.

3.3 GRADIENT DETERMINATIONS

3.3.1 TEMPERATURE AND WATER-POTENTIAL MEASUREMENTS*

3.3.1.1 Purpose and Scope

Temperature and water-potential measurements were made at the site to assess the magnitude and direction of the thermal and water-potential gradients in the study area. Knowledge of the gradients is used to determine whether temperature and water potential play a significant role in the transport of contaminants to the water table. A description of the instruments used to acquire these data, together with information on calibration, installation, and data reduction, is presented below, and is followed by a discussion of the results. The results are presented in the form of graphs plotting temperature and water potential versus time and depth.

*Response to Task 4, Paragraph 25, Compliance Order/Schedule.

3.3.1.2 Field Instrumentation

3.3.1.2.1 Description of the Thermocouple Psychrometers. Thermocouple psychrometers were used to obtain the water-potential measurements at Los Alamos because the low soil-water potential (less than -1 bar) precluded the use of tensiometers. The instruments actually measure voltage which is converted to soil-water potential by means of a calibration model (Brown and Bartos, 1982). Psychrometers are particularly convenient because they simultaneously measure temperature.

The thermocouple psychrometers used in this study were Models PCT-55 and PST-55 manufactured by Wescor, Inc., of Logan, Utah. The only difference between the two models is that the PST series is shielded with a stainless steel screen instead of a ceramic cup, and therefore has a faster response time. A diagram of a typical screen-shielded psychrometer is shown in Figure 3-10.

Operation of the psychrometers is based on the Peltier effect, in which a thermocouple is cooled below the dew point by passing an electric current across a junction composed of two dissimilar metal conductors. After water has condensed on the cooling junction, the electric current is discontinued and the junction immediately begins to warm up. The rate of warming is rapid at first, and then slows down until the latent heat of vaporization is overcome, at which time water condensed on the junction evaporates. The point at which the warming rate is at a minimum is known as the psychrometer plateau. The electromotive force (emf) generated across the junction during the psychrometer plateau is a measure of the relative humidity of the system (Spanner, 1951).

The relative humidity ($\bar{P}/P_o$) in soil is related to soil-water potential by the equation (Case and Welch, 1979)

$$\psi = (\rho k_B T/m) \ln (\bar{P}/P_o) = \psi_o \ln (\bar{P}/P_o) \qquad (20)$$

where

ρ = the density of water at temperature T
k_B = Boltzman's constant (1.38×10^{-16} erg/°K)
m = the mass of a water molecule (approximately 3×10^{-23} g)
$\bar{P}$ = the average vapor pressure in the soil
P_o = the pressure of the water vapor above a surface of infinite radius of curvature
$\psi_o \simeq 10^3$ bars at 300°K

3.3.1.2.2 Laboratory Calibration. Each psychrometer must be calibrated individually due to the variable thicknesses of the welded junction and wires used in fabrication. Saline solutions are convenient to use for calibration, since tables that relate salt concentrations and temperature to relative humidity are readily available (Lang, 1967). The ratio of microvoltage to theoretical water potential at a given temperature for a particular psychrometer provides the correction coefficient necessary for determining actual water potential in rock and soil systems.

In this study, reagent-grade sodium chloride was dissolved in deionized water to provide 0.5-, 1.0-, and 1.5-molal calibration solutions. Each psychrometer

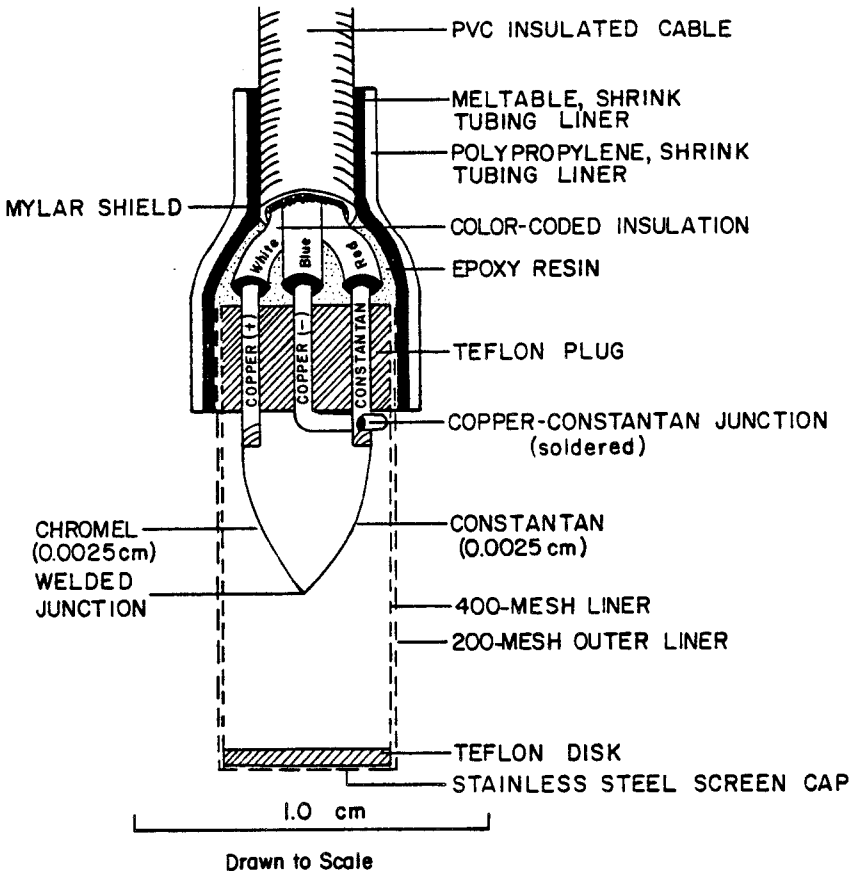

Figure 3-10. Sketch of the Single-Junction Stainless Steel Screen-Shielded Thermocouple Psychrometer (from Brown and Collins, 1980)

was calibrated using all three molal concentrations, independently, in the following manner. One milliliter of solution was decanted into a sample chamber. A psychrometer was then sealed into the chamber to create a closed system with a known water potential (see Figure 3-11). The sealed chamber was then placed in a wooden rack and equilibrated for at least 12 hours. Following equilibration, the voltage output of the thermocouples was read in psychrometric (wet-bulb) mode using a Wescor HR33T Dewpoint Microvoltmeter. Each molal concentration (water potential) was read three times for temperature and microvolts. These readings were then converted to water potential using the calibration model described below.

3.3.1.2.3 Psychrometer Calibration Model. The psychrometer calibration model developed by Brown and Bartos (1982) was used to accurately convert psychrometer outputs to water potential. This model is far more versatile than hand-drawn calibration curves because it can convert water potentials from 0 to -80 bar over a wide range of temperature and zero offset readings. Inputs to the model are temperature, cooling time, zero offset, psychrometer output in microvolts, and calibration coefficients, the last required for conversion of microvolts to water potential. The calibration coefficient B is defined as

$$\sum B = \sum WP / \sum \widehat{WP} \qquad (21)$$

where $\sum WP$ is the sum of the water potentials (sodium chloride solutions) used during calibration and $\sum \widehat{WP}$ is the sum of the water potentials estimated by the model. Calibration coefficients for each of the psychrometers installed in Holes LLP-85-03 and LGP-85-07 are presented in Tables 3-9 and 3-10, respectively. A listing of the Fortran V program for the model is reproduced as Appendix E. The output from the model is the water potential for the soil conditions as sensed by the psychrometer.

3.3.1.2.4 Field Installation. A total of 38 thermocouple psychrometers were installed at the study area, 23 in Hole LLP-85-03 and 15 in Hole LGP-85-07. Completion diagrams are provided in Appendix A. Because of the presence of surface casing in Hole LLP-85-03, a shallow boring was drilled adjacent to the main hole and five psychrometers were installed in this second hole close to the ground surface (depicted in Appendix A as being in the same hole). Installation was accomplished by taping the psychrometers to a string of Schedule 40, 2-inch-I.D., polyvinylchloride (PVC) pipe and carefully lowering the string into the hole. The annulus surrounding the PVC pipe was then backfilled with auger cuttings from that drill hole. It was assumed that the density of this backfill was similar to the in-situ density of the tuff, and that the relative humidity of the backfill, as sensed by the psychrometers, would equilibrate with the relative humidity of the adjacent tuff. Installation depths are included with the data presented in Tables 3-9 and 3-10 for Holes LLP-85-03 and LGP-85-07, respectively.

3.3.1.3 Results and Discussion

Psychrometer data were collected from Holes LLP-85-03 and LGP-85-07 over the period 22 October to 20 November 1985. The values for temperature and water potential were viewed in two ways, as plots of temperature or water potential versus time, and as plots of temperature or water potential versus depth. Selected plots of the former are presented in Figures 3-12 through 3-15. Air

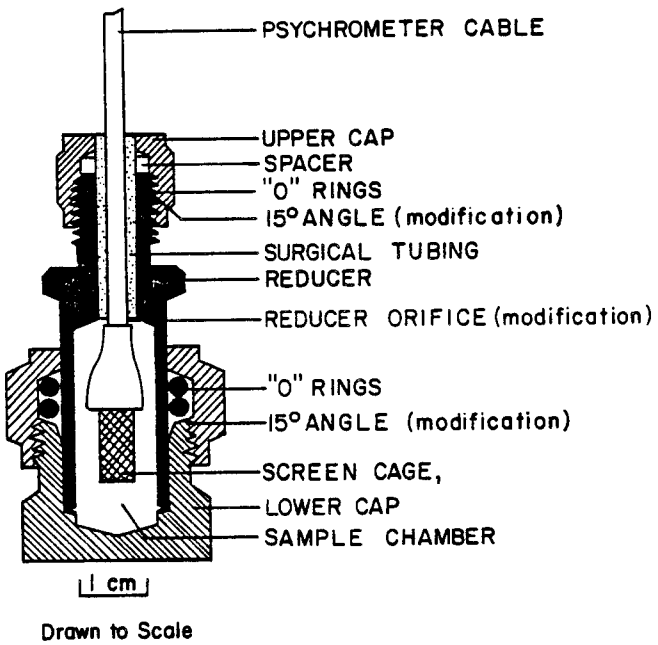

Figure 3-11. Sketch of the Stainless Steel Calibration Chamber Showing Seals and Screen-Shielded Thermocouple Psychrometer (from Brown and Collins, 1980)

temperature versus time at Hole LLP-85-03 is plotted in Figure 3-16. Box plots of water potential and temperature versus depth for the entire time period are presented in Figures 3-17 through 3-20. Since the box plots present the data in quartiles, the outlying values represent minimum and maximum values. The boxes enclose the 25- and 75-percent values, and the vertical lines connecting the boxes intersect the median-temperature or water-potential values for the time period.

The plot of air temperature versus time (Figure 3-16) demonstrates that a dramatic diurnal temperature variation exists at the site, and that the highs and lows generally decreased over this monitoring period. Plots of formation temperature versus time (Figures 3-13 and 3-15) for the psychrometers located within 15 ft of the ground surface demonstrate that the near-surface temperatures also decreased in response to the decrease in air temperature. Furthermore, as expected, a phase lag is evident when comparing the decreasing temperatures measured by successively deeper psychrometers.

Table 3-9. Installation Depths and Calibration Coefficients for Psychrometers in Hole LLP-85-03

Model Number[a]	Serial Number	Scanner/Channel	Calibration Coefficient for Water-Potential Model	Installation Depth (ft)
PCT-55	29414	I/1	--	Surface
PCT-55	29416[b]	I/2	0.85	2.0
PST-55	29474[b]	I/3	0.84	4.0
PST-55	29473[b]	I/4	0.84	6.0
PCT-55	29420[b]	I/5	0.89	8.0
PST-55	29469[b]	I/6	0.84	10
PCT-55	29418	I/7	0.81	13
PST-55	29483	I/8	0.88	13
PCT-55	29424	I/9	0.85	24
PST-55	29479	I/10	0.87	24
PCT-55	29406	I/11	0.90	41
PST-55	29462	I/12	1.00	41
PCT-55	29409	II/1	1.00	50
PST-55	29475	II/2	0.94	50
PCT-55	29405	II/3	0.85	56
PST-55	29477	II/4	1.03	56
PCT-55	29425	II/5	0.84	66
PST-55	29455	II/6	0.96	66
PST-55	29481	II/7	0.89	76
PCT-55	29422	II/8	0.94	76
PST-55	29476	II/9	0.90	86
PST-55	29458	II/10	1.00	96
PCT-55	29427	II/11	1.00	96

[a]The PCT series psychrometers are shielded with a ceramic cup, while the PST models are shielded with a stainless steel screen.

[b]Psychrometers in the upper 10 ft are located in a shallow boring adjacent to the main hole.

Table 3-10. Installation Depths and Calibration Coefficients for Psychrometers in Hole LGP-85-07

Model Number[a]	Serial Number	Scanner/Channel	Calibration Coefficient for Water-Potential Model	Installation Depth (ft)
PCT-55	29415	III/1	0.89	4.5
PST-55	29459	III/2	0.89	6.5
PCT-55	29410	III/3	0.85	8.5
PST-55	29461	III/4	0.91	10
PCT-55	29411	III/5	0.91	12
PST-55	29463	III/6	0.86	14
PCT-55	29417	III/7	0.84	17
PST-55	29466	III/8	0.87	19
PCT-55	29403	III/9	0.92	22
PST-55	29467	III/10	0.92	27
PCT-55	29407	III/11	1.00	32
PST-55	29465	III/12	1.04	37
PST-55	29464	III/13	0.95	42
PCT-55	29404	III/14	0.85	47
PST-55	29468	III/15	0.89	52

[a]The PCT series psychrometers are shielded with a ceramic cup, while the PST models are shielded with a stainless steel screen.

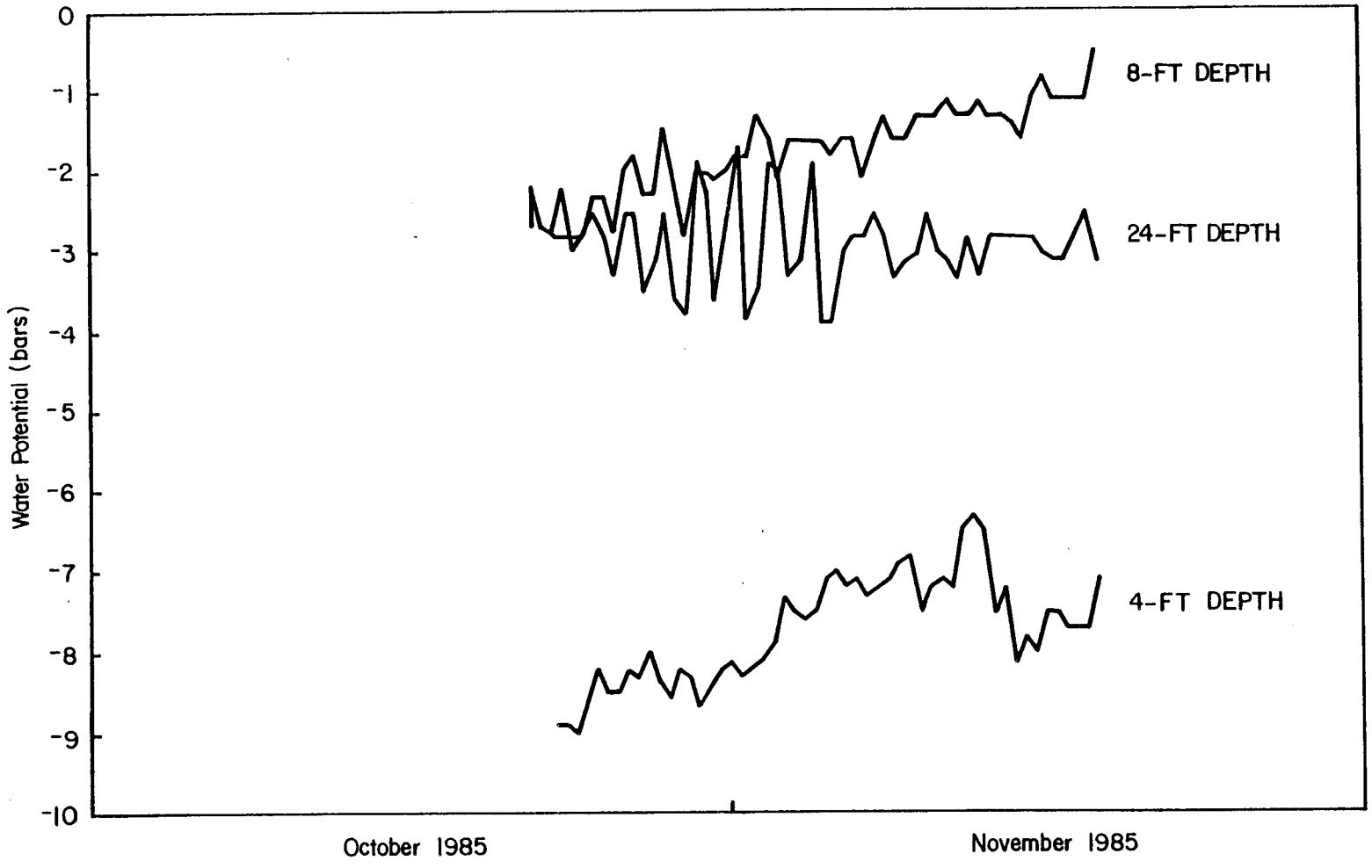

Figure 3-12. Water Potential Versus Time for Selected Psychrometers in Hole LLP-85-03

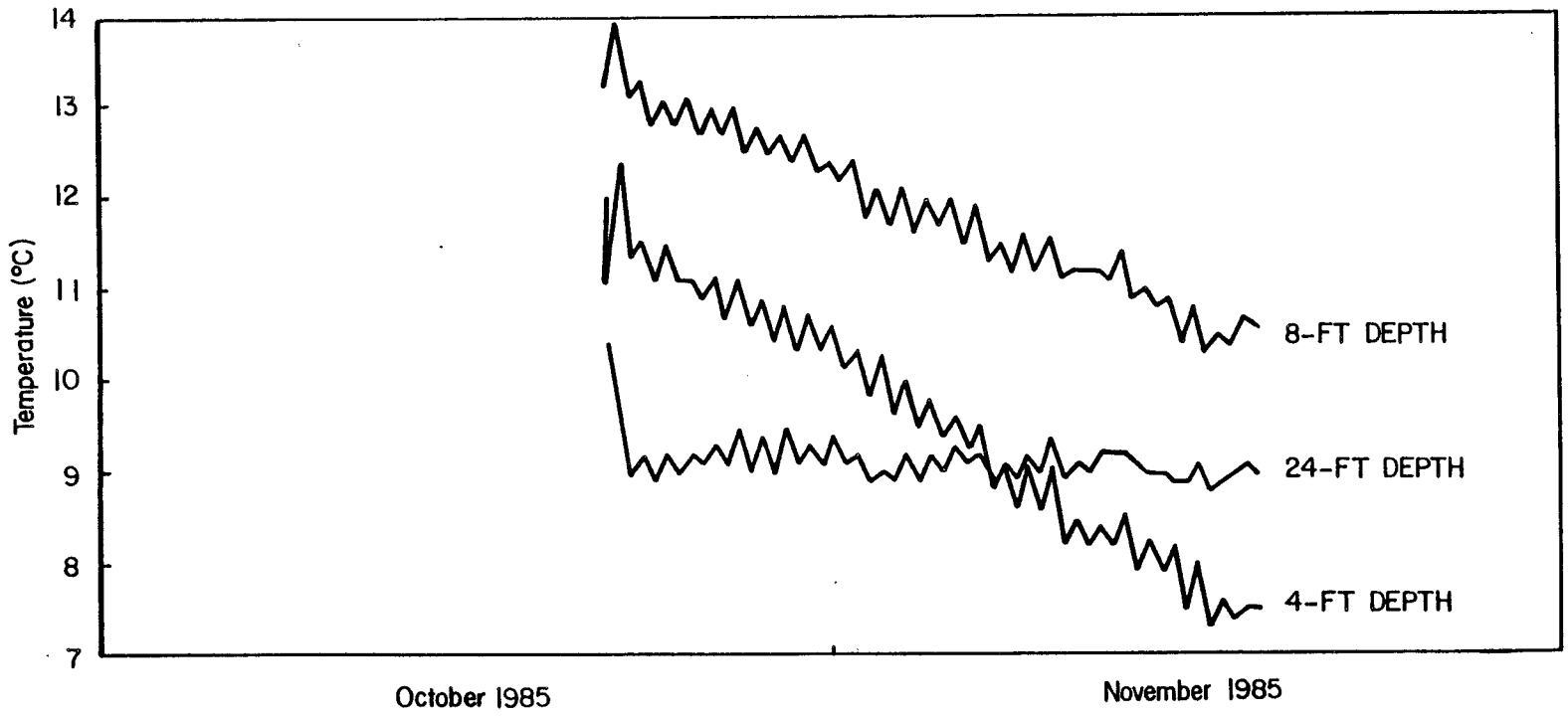

Figure 3-13. Temperature Versus Time for Selected Psychrometers in Hole LLP-85-03

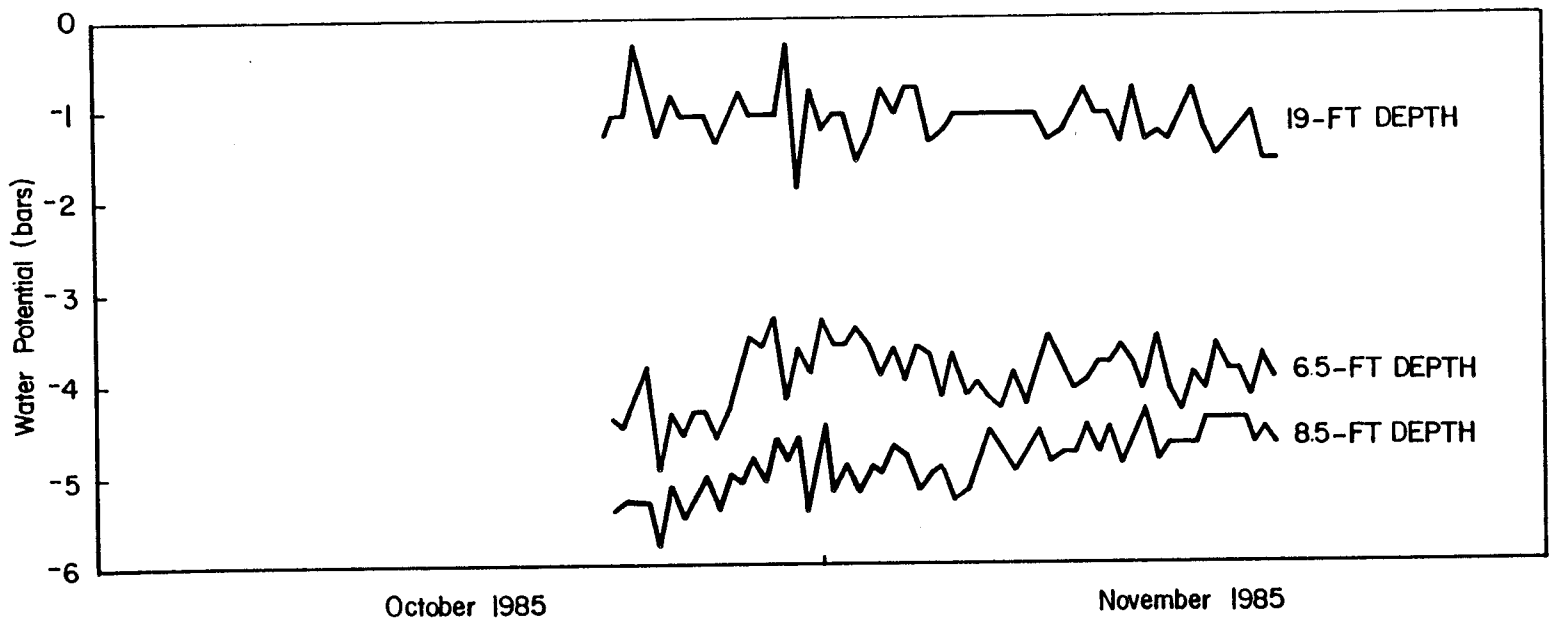

Figure 3-14. Water Potential Versus Time for Selected Psychrometers in Hole LGP-85-07

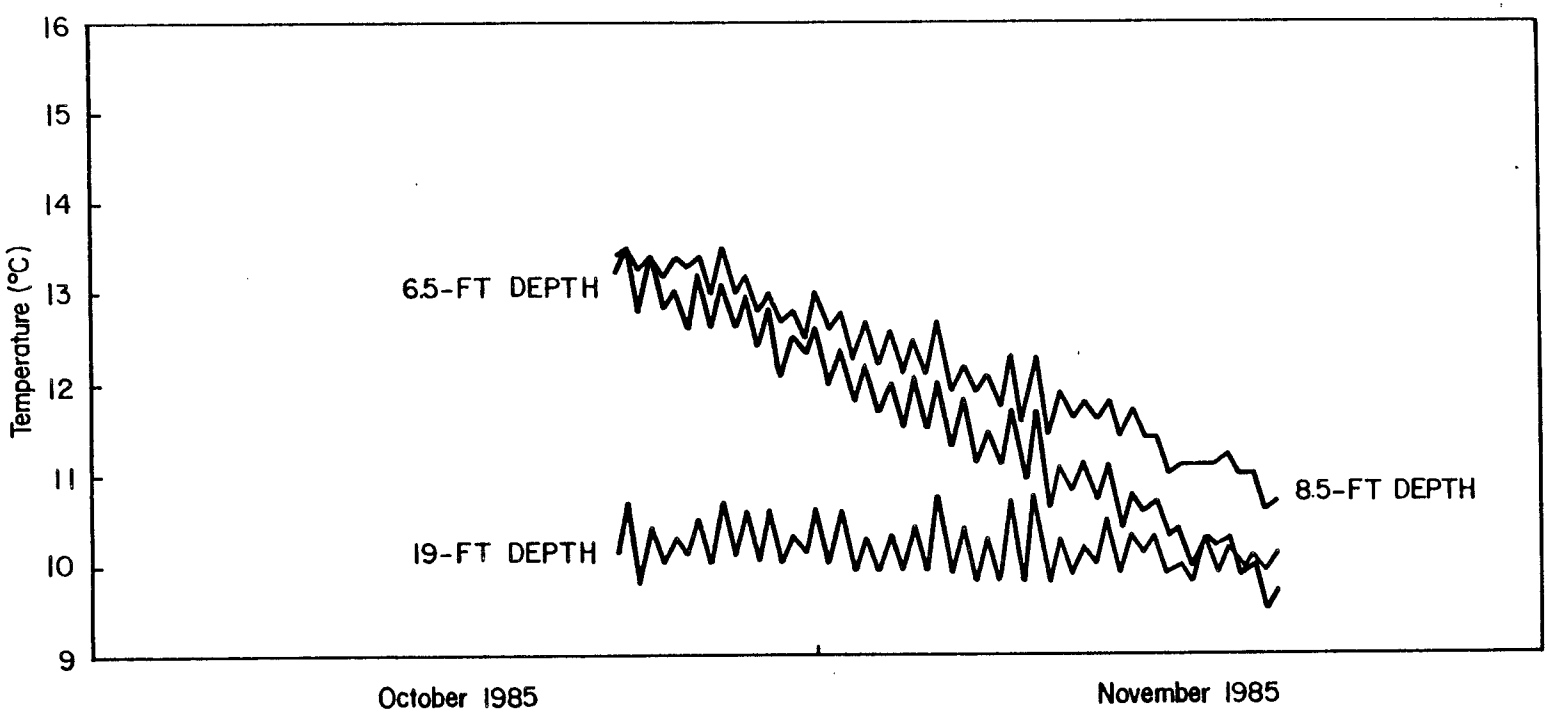

Figure 3-15. Temperature Versus Time for Selected Psychrometers in Hole LGP-85-07

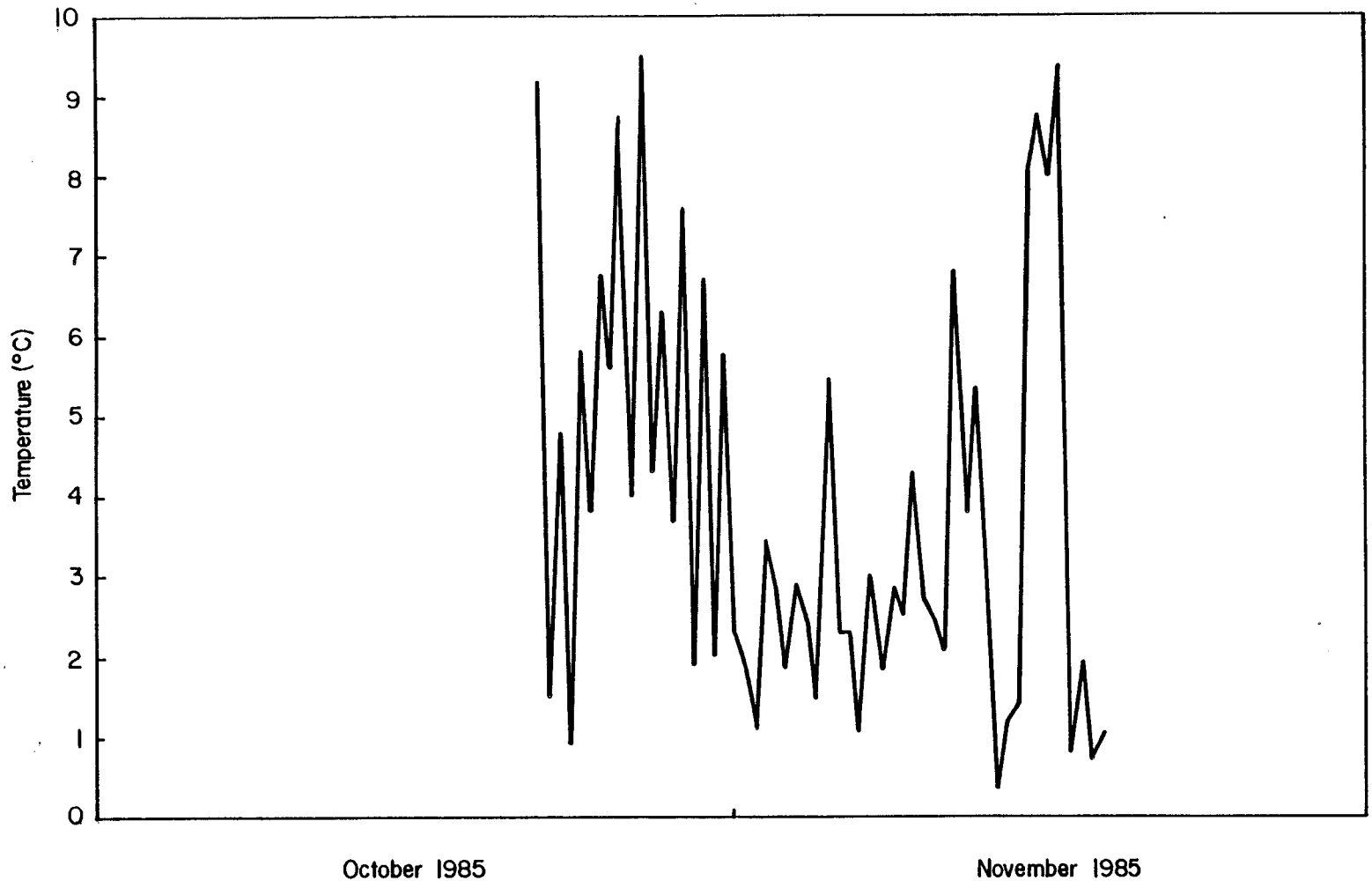

Figure 3-16. Air Temperature Versus Time at Hole LLP-85-03

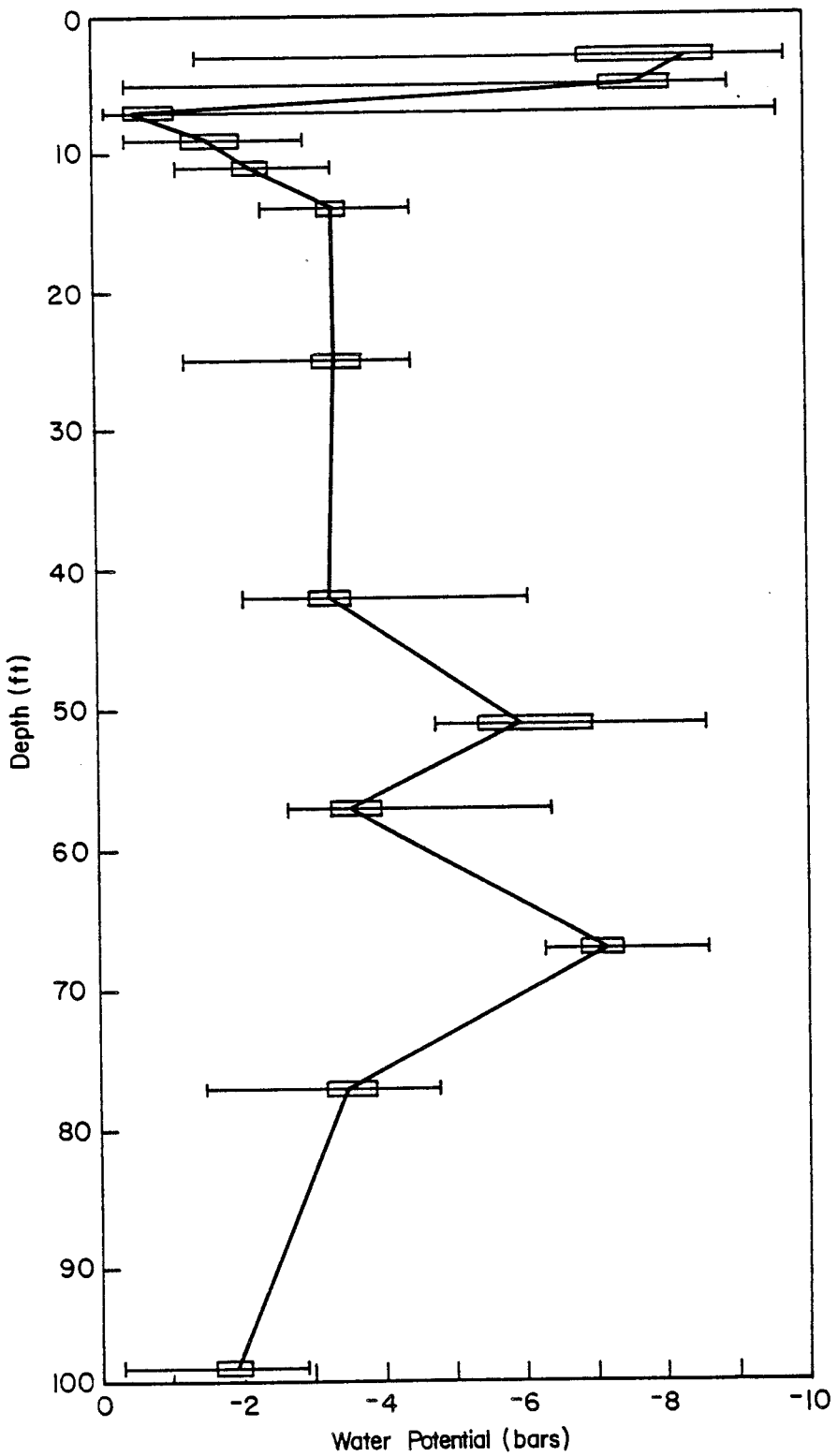

Figure 3-17. Water Potential Versus Depth for Hole LLP-85-03

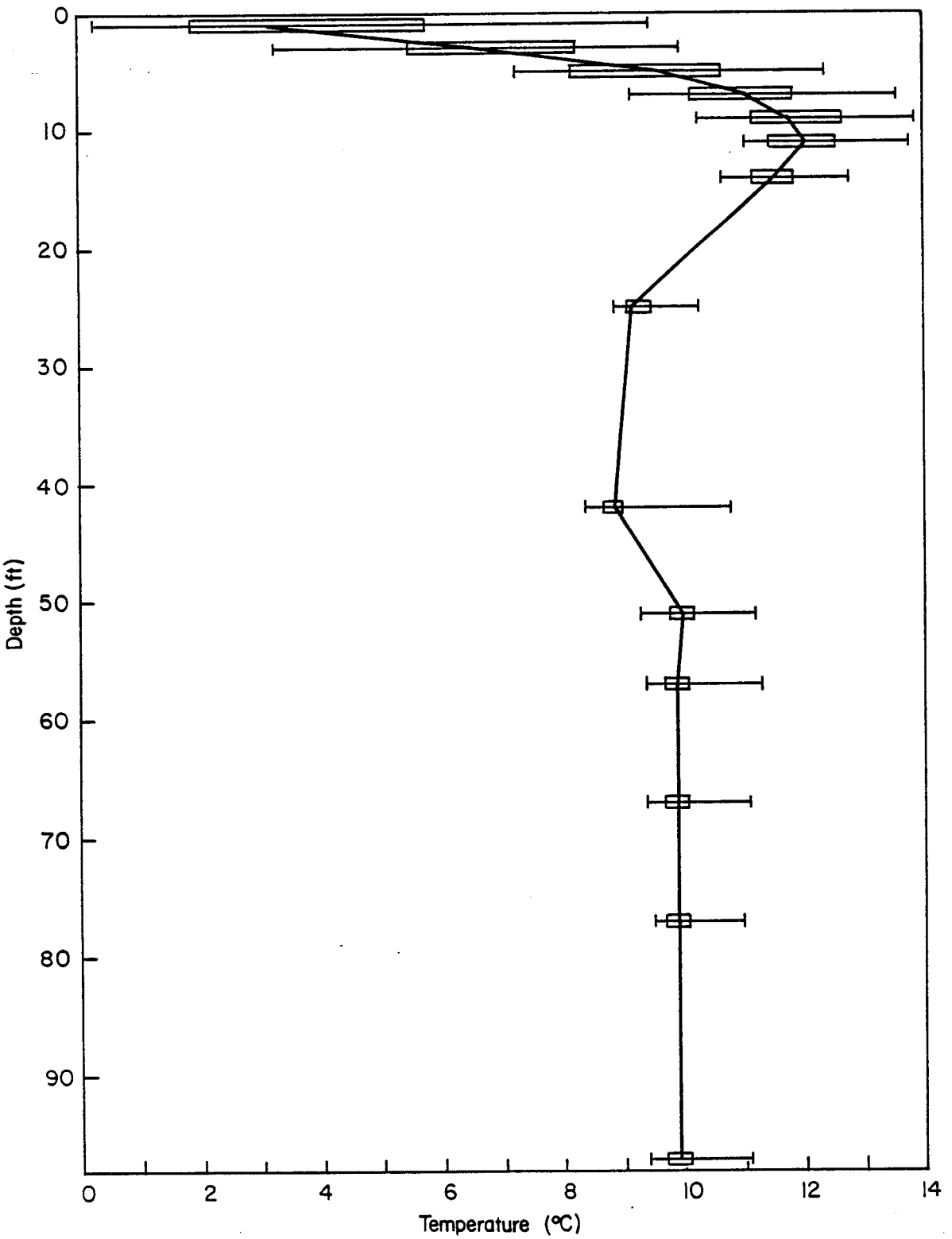

Figure 3-18. Temperature Versus Depth for Hole LLP-85-03

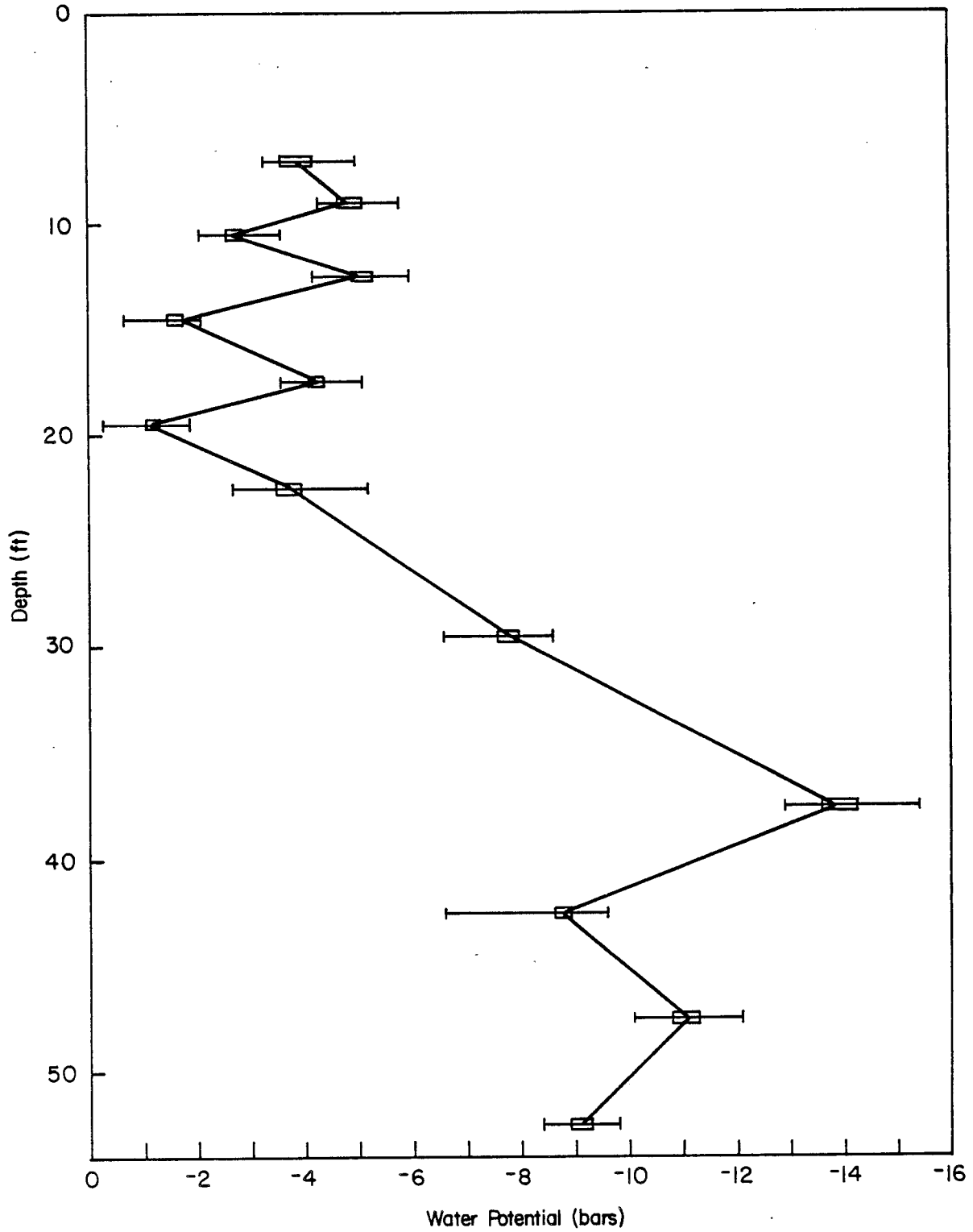

Figure 3-19. Water Potential Versus Depth for Hole LGP-85-07

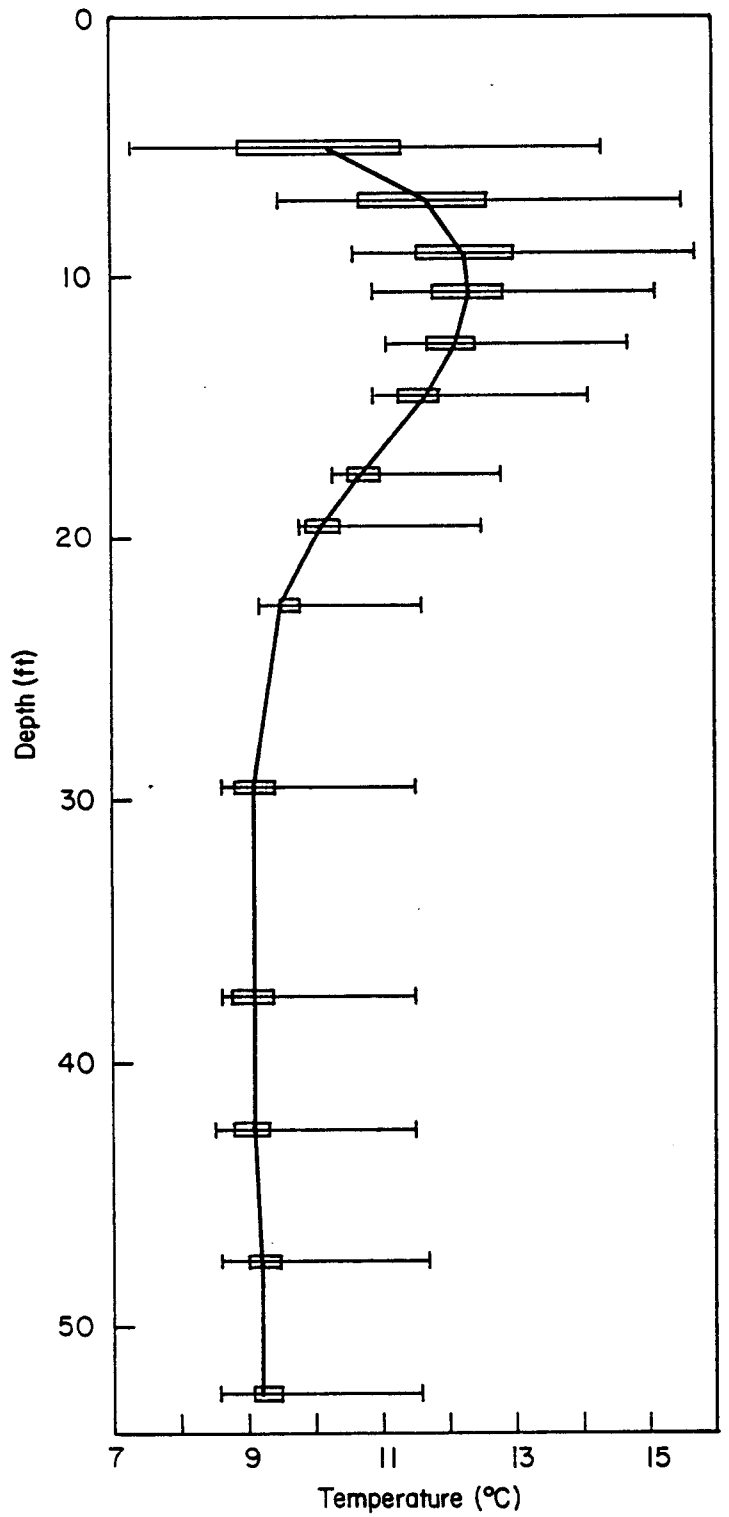

Figure 3-20. Temperature Versus Depth for Hole LGP-85-07

The plots of temperature versus depth (Figures 3-18 and 3-20) reveal a temperature bulge that probably represents the heat stored in the ground due to Summer heating. The position of the bulge indicates that the median gradient in temperature for this monitoring period is downward from about 10 to 20 ft and upward from about 10 ft.

The plots of water potential versus time for given depths (Figures 3-12 and 3-14) demonstrate that water potentials are subject to diurnal variations of about ±1 bar per day, and that there was little, if any, change in the average water potential during this monitoring period. Median water potentials range from approximately -0.5 bar to -8.7 bar in Hole LLP-85-03 (Figure 3-17) and from approximately -1.2 bar to -13.8 bar in Hole LGP-85-07 (Figure 3-19).

The large range of maximum and minimum values observed during this monitoring period limit gradient estimations to those that can be measured between successive psychrometers, i.e., within a single depth interval. Accurate assessments of an overall gradient in the study area will most likely require longer equilibration and monitoring times.

3.3.2 ATMOSPHERIC/ROCK-PORE PRESSURE MONITORING SYSTEM

3.3.2.1 Purpose and Scope

The purpose for installing the Atmospheric/Rock-Pore Pressure Monitoring System was to quantify the gas-pressure gradients in the Bandelier Tuff. Although these data were not required by the Compliance Order/Schedule, they can contribute significantly to the initial site assessment since differences in gas pressure can affect contaminant transport in the vapor phase.

Equipment and system installation are described in the paragraphs that follow. The subsection entitled Results and Discussion presents only a preliminary interpretation of the data; a broader, more reliable assessment of gas-pressure gradients would most likely require acquisition of pressure readings over a period of at least 1 year.

3.3.2.2 Equipment

The pressure-measurement system installed at Los Alamos consists of four electrical pressure transducers connected to an electro-piezo scanner/recorder. The transducers contain an absolute-electrical-pressure sensor equipped with a strain-gauged stainless steel diaphragm. A stainless steel disc filter permits direct burial of the transducers. Measurement capacity ranges from 0 to 25 pounds per square inch at sea level (psis), with a readability of 0.02 percent of scale. (Psis is calibrated in psi with zero being atmospheric pressure at sea level.)

The electro-piezo scanner/recorder is a portable, battery-operated system that automatically records ten transducer channels. The dates, times, and outputs from each of the transducers are recorded on the integral printer. This versatile scanner/recorder can permanently record the transducer outputs, or can provide the outputs to an external device such as a computer, data terminal, paper punch, or magnetic tape recorder. The pressure-measurement

system can be programmed to scan continuously or to scan at variable intervals. In the case of the latter, the recorder can be sealed and left unattended and will still record data at the preselected intervals.

3.3.2.3 Installation Design

The completion diagram for the pressure-transducer instrumentation installed in Hole LLP-85-03 is presented in Appendix A. The four transducers were installed at the following depths: ground surface, 26 ft, 54 ft (near a fracture), and 90 ft. The transducer located at ground surface measures the atmospheric pressure, while the buried transducers measure rock-pore gas pressures.

3.3.2.4 Results and Discussion

Pressure-measurement data were collected over the period 17 October through 15 November 1985 (Figure 3-21), except for the 7 days from 6 through 12 November when the system was inadvertently shut down. As noted previously, these limited data permit only a preliminary interpretation at this time. Characteristics which are discernible in Figure 3-21 include the following:

- Both the atmospheric and rock-pore pressures undergo daily fluctuations.
- The rock-pore pressure at 54 ft is consistently higher than the surrounding pressures, potentially a result of the nearby fracture.
- An increase in the atmospheric pressure for a period of several days is not reflected in the rock-pore pressures for the same period.

A broader assessment of the gas-pressure gradients in the study area requires acquisition of additional data, particularly with regard to identifying potential sources of variation in the data other than actual pressure variations.

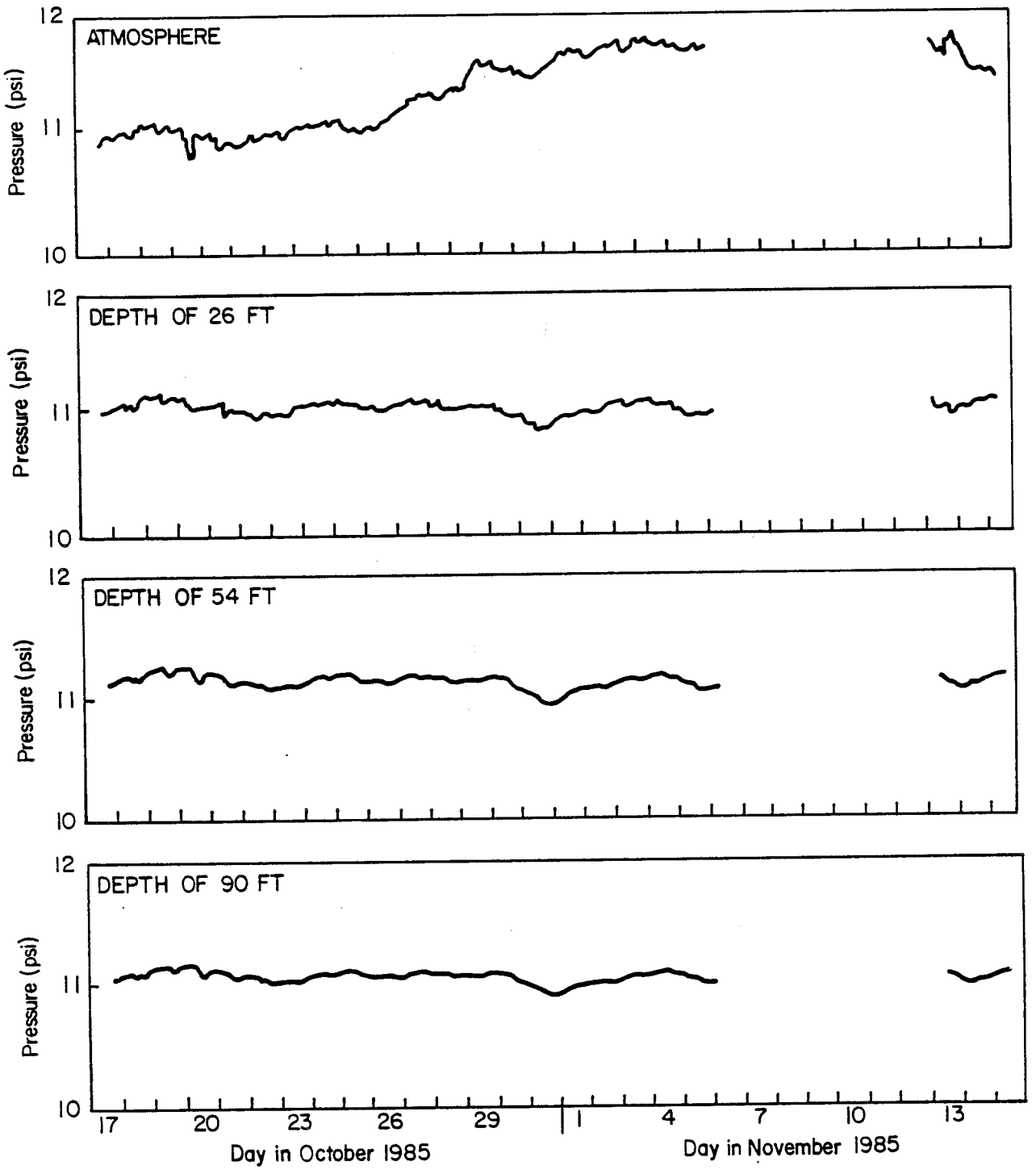

Figure 3-21. Results from the Pressure Transducers Installed in Hole LLP-85-03 (Note: The system was inadvertently shut down over the period 6-12 November 1985.)

Section 4

NEUTRON MOISTURE MEASUREMENTS

Note: This section responds to Task 4, Paragraph 25, of the Compliance Order/Schedule. The section was prepared by personnel of Los Alamos National Laboratory.

4.1 PURPOSE AND SCOPE

The moisture content of the Bandelier Tuff is being measured with a neutron probe in order to characterize the infiltration and redistribution of water in the tuff. Use of the neutron probe for moisture monitoring was specifically requested by the State of New Mexico in Task 4, Paragraph 25, of the Compliance Order/Schedule. Although data acquired with the probe were not yet available at the time of this writing, it is possible that the method will be of little value at Los Alamos due to the low moisture content of the tuff (see gravimetric moisture results in Section 3.1.1).

Two holes were identified for acquisition of biweekly neutron moisture readings, LLN-85-04 and LGN-85-08 (see Figure 2-3 for locations). Descriptions of the casing installations, probe calibration, and monitoring program are provided below. Data presentation and interpretation will be addressed in a subsequent report when data become available.

4.2 CASING INSTALLATIONS

The neutron access tubes, or casings, were constructed of cold drawn aluminum tubes, each 12 ft in length and having a wall thickness of 0.049 inch, an outside diameter of 2.5 inches, and an inside diameter of 2.402 inches. This inside diameter is approximately 0.25 inch larger than the outside diameter of the probe (1.865 inches), which prevents the probe from binding as it is maneuvered inside the casing. To further ensure free movement of the probe while it is being raised or lowered in the hole, the casing has no internal seams or obstructions.

Prior to transport to the field, the 12-ft lengths of tubing were welded together to make 24-ft sections and the sections pressure-tested to ensure a watertight seal. A cap was welded to one end of each of two sections, these to be installed at the bottom of the two holes. In the field, the 24-ft sections were joined together using 'no-hub' couplings rather than welding. This was done because the tubing wall is so thin that a watertight weld would be nearly impossible to accomplish with portable welding equipment. A no-hub coupling is a watertight rubber coupling, held in place by a corrugated stainless steel cover, on the ends of which are stainless steel hose clamps used for gripping the aluminum tubing.

The casings were installed in the drill holes in the following manner. The section with the bottom cap was lowered into the hole and held in place with a pipe vise. A second 24-ft section was joined to the first with a no-hub coupling. Silicon sealant was applied wherever rubber was exposed to slow decomposition of the material underground. Once the two sections were coupled, they were lowered into the ground and again held in place with the pipe vise while a second no-hub coupling was installed to join the now 48-ft section of tubing to another 12- or 24-ft section. This process was repeated until the bottom of the hole was reached. Any tubing remaining above ground level was cut off.

A diagram of the casing installation for Hole LLN-85-04 is presented in Figure 4-1. The depth of the uncased hole was 108 ft, so the casing required four 24-ft sections and one 12-ft section, joined together with four no-hub

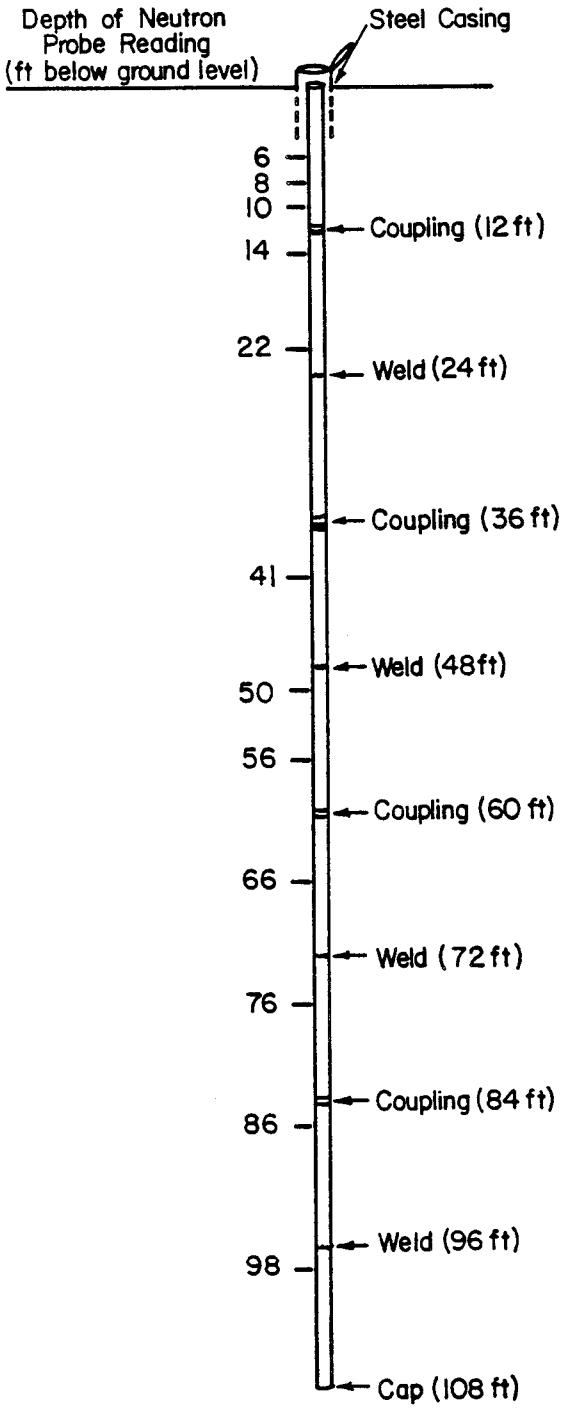

Figure 4-1. Casing Installation and Depths of Neutron Probe Measurements in Hole LLN-85-04

couplings. Hole LGN-85-08 (Figure 4-2) had an uncased depth of 50 ft, so the casing required two 24-ft sections and one 12-ft section, joined together with two no-hub couplings.

4.3 CALIBRATION OF THE NEUTRON PROBE

The neutron probe used at Los Alamos is a Campbell Pacific moisture gauge. Calibration of the instrument was accomplished by using it to measure moisture in five samples of Bandelier Tuff, each with a different but known moisture content. Instrument responses were recorded and used to generate a calibration curve.

The five samples of tuff consisted of three with varying moisture contents, one with no moisture, and one representing saturated conditions. The first three were prepared in the following manner. Crushed Bandelier Tuff was oven-dried at 250°C for 48 hours. A predetermined amount of dry tuff was then weighed and water added to it. The moistened tuff was packed in 15-cm lifts in a 55-gallon drum to achieve a bulk density of 1.5 g/cm^3, which is the average bulk density of the consolidated Bandelier Tuff at Los Alamos. The amounts of water added to the lifts varied from one drum to another, such that the volumetric water content of each drum was different. Samples were collected from each lift in each drum and analyzed gravimetrically to determine the moisture content and to ensure that the moisture content was constant throughout the entire drum.

The fourth drum was prepared in the same way as the first three except that no water was added. The fifth drum was also prepared as described above, except that water was added not to the lifts, but into the bottom of the drum through a 3/8-inch Tygon tube until the tuff was saturated to the drum surface. Samples from these drums were also analyzed so that the moisture contents would be known. Following preparation, all five drums were sealed by placing plastic sheeting between the drum surface and the cover. Silicon sealant was then applied on the edges to prevent evaporation.

Calibration measurements were taken by lowering the probe to the center of each drum and acquiring four 1-minute counts. These data and the known moisture contents were then subjected to a linear-regression analysis, which yields a calibration curve for the instrument. At the time of this writing, the calibration curve was not complete and is therefore not included in this report.

4.4 MONITORING PROGRAM

Biweekly neutron-moisture measurements were initiated in both drill holes on 17 December 1985. The depths of the probe readings are shown in Figures 4-1 and 4-2. The measurement depths in Hole LLN-85-04 correspond to the psychrometer-measurement depths in Hole LLP-85-03, while those in Hole LGN-85-08 correspond to psychrometers in Hole LGP-85-07 (see Appendix A for completion diagrams of Holes LLP-85-03 and LGP-85-07). In certain cases, identical correspondence was not possible due to the presence of the welds and couplings in the neutron-probe holes. As noted previously, no data are available at this time.

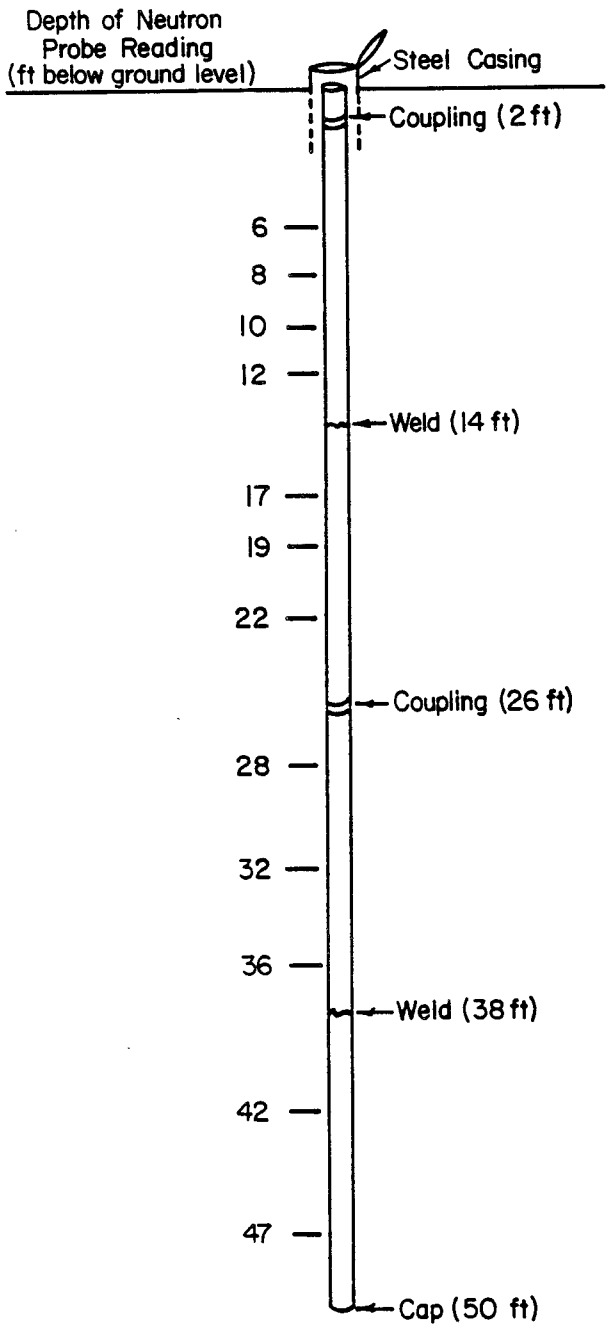

Figure 4-2. Casing Installation and Depths of Neutron Probe Measurements in Hole LGN-85-08

Section 5

PORE-GAS SAMPLING SYSTEM

Note: This section responds to Task 5, Paragraph 25, of the Compliance Order/Schedule.

5.1 PURPOSE AND SCOPE

Samples of pore gas from seven drill holes are being collected and analyzed in order to characterize the subsurface atmosphere in Areas G and L. The design and installation of the samplers are described in this section; included is a hole-by-hole description of the sampling-port locations and the rationale for choosing each location. At the time of this writing, laboratory analysis of the samples collected to date had not been completed. Data presentation and interpretation will therefore be addressed in a subsequent report.

5.2 DESIGN

The pore-gas sampling ports were constructed using low-pressure mobile-phase filters which were welded to standard 2-inch-I.D. galvanized pipe (Bendix Field Engineering Corporation, 1985b). The filters consist of 2-micrometer, porous, stainless steel elements; uphole access is provided via connection to 1/4-inch stainless steel tubing and stainless steel compression fittings. A diagram of a pore-gas sampling port is presented in Figure 5-1.

5.3 INSTALLATION

A total of 23 sampling ports were installed in seven drill holes in the study area; installation procedures were described in the second report (Bendix Field Engineering Corporation, 1985b). Installation diagrams are presented in Appendix A; drill-hole locations are shown in Figure 2-3. The following paragraphs describe the locations of the ports within each hole and the rationale for choosing these locations.

- Hole LGC-85-09. Since this was the only pore-gas sampling hole that penetrated Unit 1a, two ports were installed in that unit, one in the relatively moist section (below 88 ft) and the other in the relatively dry section, just above 80 ft. The third port was installed at about 63 ft to coincide with a fracture present in Unit 1b, and because the maximum waste-disposal depth in this area is approximately 60 ft. The fourth port was installed at 37 ft to coincide with fractures present in Unit 2a.

- Hole LGC-85-10. The deepest sampling port was installed at 95 ft to coincide with a near-vertical fracture present in the more densely welded portion of Unit 1b. The middle port was installed at about 53 ft to coincide with a fracture present in Unit 2a. The uppermost port was installed at 31 ft to coincide with a horizontal fracture and the Unit 2a/Unit 2b contact.

- Hole LLC-85-12. The deepest sampling port was installed at about 41 ft to coincide with a vertical fracture and the Unit 2a/Unit 2b contact. The middle port was installed at about 27 ft to sample the interval between 24 and 29 ft. This interval lies within Unit 2b and consists of a light-gray ash flow with numerous horizontal fractures. In addition, the Organic Vapor Meter (OVM) registered high readings [114 parts per million (ppm)

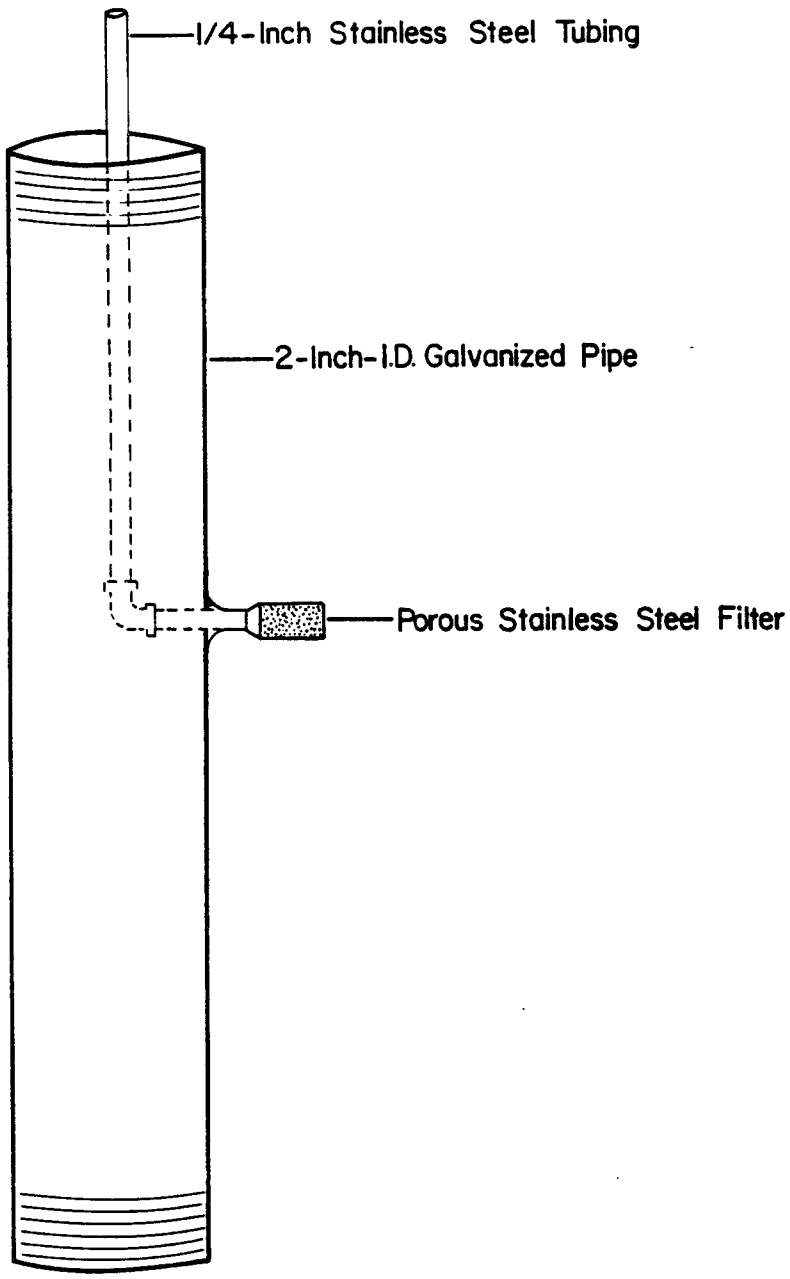

Figure 5-1. Diagram of a Pore-Gas Sampling Port

downhole] when the bottom of the auger string reached 24 ft, and again when the bottom of the string reached 29 ft (160 ppm). The uppermost gas-sampling port was installed at about 6 ft to coincide with several fractures present from 5 ft to 8 ft.

- Hole LLC-85-13. This is a 'background' hole located west of Area L. Only Units 2a and 2b were penetrated in this hole. The deepest sampling port was installed at about 65 ft in a moderately welded portion of Unit 2a. The middle port was installed at about 43 ft to coincide with several fractures and the Unit 2a/Unit 2b contact. The uppermost port was installed at about 21 ft to coincide with a near-vertical fracture present in Unit 2b.

- Hole LLC-85-14. The deepest sampling port was installed at about 86 ft to coincide with a fracture zone extending from 84 to 89 ft within Unit 1b. A relatively high OVM reading was recorded for this zone, which is separated from upper zones with high OVM readings by a zone of 'background' OVM readings. The second port was installed at about 46 ft to coincide with a nonfracture zone extending from 44 to 49 ft in Unit 2a where relatively high OVM readings were obtained. The third port was installed at about 31 ft to coincide with the interval 28 to 34 ft because the contact between two physically different zones of Unit 2b is present at 32 ft and field OVM readings were higher when crossing this interval. The contact is defined primarily by the transition into slightly welded or more easily drilled ash-flow tuff. Fractures are also present just above this contact. The uppermost sampling port was installed at about 13 ft to coincide with a moderately welded, nonfracture zone within Unit 2b. This zone, extending from 12 to 14 ft, exhibited relatively high OVM readings. In addition, sampling in this zone would permit comparison with results from known fracture zones.

- Hole LLC-85-15. The deepest port was installed at about 82 ft to sample pore gas in the interval 80 to 86 ft because a relatively high OVM reading was obtained near this interval. The other two sampling ports were installed at about 32 ft and 19 ft to coincide with the areas where the highest OVM readings were obtained in this hole.

- Hole LLC-85-16. The deepest sampling port was installed near the bottom of this hole to coincide with areas exhibiting high OVM readings. These areas are separated from the zones of additional high readings by 75 ft of relatively low OVM readings. The other two ports were installed near ground surface to coincide with zones that are both fractured and displayed relatively high OVM readings.

Section 6

CONCLUSIONS

The time constraints imposed on this study of Waste Disposal Areas G and L at Los Alamos permitted only a brief period for data acquisition and interpretation. As a consequence, the assessment presented herein of the vadose zone underlying Mesita del Buey is for the short term only. Nevertheless, some conclusions can be drawn from the data obtained thus far, the most important being that the dominant mode of transport in the interval of the Bandelier Tuff examined for this study is by vapor phase. In other words, the low moisture content of the tuff and the high moisture-retention values observed in the moisture characteristic curves indicate that interconnection of liquid water, and therefore movement of water in the liquid phase, is nonexistent. Additional conclusions are discussed in the paragraphs that follow.

- The geologic framework through which transport occurs can be characterized as a complex network of pumice and lithic clasts surrounded by a glass-shard/crystal matrix, with occasional fractures dissecting the porous media. Factors such as porosity, degree of welding, and pumice content have a direct effect on the unsaturated hydraulic characteristics.

- Taken together, the high values for porosity and moisture retention (both average approximately 50 percent) indicate that the tuff behaves much like a sponge. A quantity of water equal to approximately one quarter of the rock volume is required to satisfy capillary forces before recharge to the underlying groundwater system can occur. Based on the normal precipitation and the high evapotranspiration rates in the study area, this scenario is unlikely.

- Results from field and laboratory tests indicate that the overall range of intrinsic permeability for the Bandelier Tuff is 10^{-8} to 10^{-9} cm^2 (10^{-11} to 10^{-12} ft^2). These values are considered to represent moderate permeability.

- Permeability and porosity are not directly related, probably because of the tuff's pumice content; highly porous pumice lapilli contain a significant amount of dead-end pore space which greatly reduces permeability.

- The unsaturated hydraulic conductivities calculated using van Genuchten's model are of little value since the laboratory could only obtain moisture characteristic curves in the range 0 to -0.3 bar, with moisture contents (θ) of about 0.4 to 0.6. The calculated unsaturated hydraulic conductivities range from about 2 centimeters per day at saturation to about 1.0×10^{-6} centimeter per day at a water potential of -0.3 bar. In the field, however, water potentials range from -1 to -15 bar, and the moisture contents are below 0.1. Thus, the unsaturated hydraulic conductivities of the tuff in the field are actually much lower than the values calculated using van Genuchten's method.

- Unit 1b has a relatively higher degree of welding than the other units of Bandelier Tuff examined in this study. This higher degree of welding, coupled with the unit's high pumice content, results in strong capillary forces which are assumed to be responsible for the significant increase in moisture content in the lower portion of Unit 1b. Increases in the degree of welding are believed to reduce the pore-size radii, resulting in an increase in the capillary forces. Similarly, because there is a high

pumice content, there is a correspondingly high concentration of gas tubes; these tubes form ideal capillary tubes which appear to exhibit strong capillary forces.

- Test results indicate that permeability in and along fractures is very similar to the permeability of the surrounding porous media. Detection of the differences in the permeability, however, may be beyond the sensitivity of the testing methods, since several fracture zones show an increase in moisture content relative to the adjacent porous media.

- In certain cases, the magnetic susceptibility logs can be useful for estimating or confirming lithologic contacts. The gamma-gamma (apparent density) logs are useful for determining the degree of welding and possibly the relative pumice content of the various ash-flow units.

- Moisture characteristic curves for crushed tuff samples differ significantly from those obtained for core samples. As a consequence, interpretations of in-situ hydrogeologic transport cannot be reliably based on hydraulic data for crushed tuff.

Section 7

REFERENCES

Abeele, W. V., 1984. Hydraulic Testing of Crushed Bandelier Tuff, LA-10037-MS, UC-11, Los Alamos National Laboratory, New Mexico.

Abeele, W. V., M. L. Wheeler, and B. W. Burton, 1981. Geohydrology of Bandelier Tuff, LA-8962-MS, UC-11, Los Alamos National Laboratory, New Mexico.

Bailey, R. A., R. L. Smith, and C. S. Ross, 1969. Stratigraphic Nomenclature of Volcanic Rocks in the Jemez Mountains, New Mexico, Bulletin 1274-P, U.S. Geological Survey.

Bendix Field Engineering Corporation, 1985a. Environmental Sciences Procedure Manual, Environmental Programs Division, Grand Junction, Colorado, internal document.

Bendix Field Engineering Corporation, 1985b. Vadose Zone Characterization of Technical Area 54, Waste Disposal Areas G and L, Los Alamos National Laboratory - Report 2: Downhole Instrumentation and Pore-Gas-Sampling/Data-Collection Procedures, GJ-43, Bendix Field Engineering Corporation, Grand Junction Operations, U.S. Department of Energy, Grand Junction Projects Office, Grand Junction, Colorado.

Brown, R. W., and D. L. Bartos, 1982. A Calibration Model for Screen-Caged Peltier Thermocouple Psychrometers, Research Paper INT-293, U.S. Department of Agriculture, Intermountain Forest and Range Experiment Station.

Brown, R. W., and J. M. Collins, 1980. 'A Screen-Caged Thermocouple Psychrometer and Calibration Chamber for Measurements of Plant and Soil Water Potential,' Agronomy Journal, Vol. 72, pp. 851-854.

Case, C. M., and A. Welch, 1979. 'Pore Size Distribution, Suction and Hysteresis in Unsaturated Groundwater Flow,' Journal of Hydrology, Vol. 43, pp. 99-120.

Cook, E. F., 1965. Stratigraphy of Tertiary Volcanic Rocks of Eastern Nevada, Report No. 11, Nevada Bureau of Mines.

Environmental Improvement Division, 1985. Compliance Order/Schedule: Los Alamos National Laboratory, State of New Mexico, Santa Fe.

Freeze, R. A., and J. A. Cherry, 1979. Groundwater, Prentice-Hall, Inc., Englewood Cliffs, New Jersey.

Fukui, L. M., 1985. Petrography of the Tshirege Member of the Bandelier Tuff, Mesita del Buey, Los Alamos County, New Mexico, prepared for the Environmental Programs Division, Bendix Field Engineering Corporation, Grand Junction, Colorado.

Goddard, E. N., P. D. Trask, R. K. DeFord, O. N. Rove, J. T. Singewald, Jr., and R. M. Overbeck, 1975. Rock Color Chart, Geological Society of America, Boulder, Colorado.

Goff, F. E., and S. L. Bolivar, 1983. Field Trip Guide to the Valles Caldera and Its Geothermal Systems, LA-9963-OBES, Los Alamos National Laboratory, New Mexico.

Horner, R. D., 1951. 'Pressure Build-Up in Wells,' in Proceedings of the Third World Petroleum Congress, Section II, E. J. Bill, Leiden, Holland.

Jakubick, A. T., 1983. Permeability Measurements of the Near-Field of Excavations by Transient Pressure Testing, Atomic Energy of Canada, Technical Report, Whiteshell Nuclear Research Establishment, Pinawa, Manitoba.

Johnson, E. F., D. P. Bossler, and V. D. Naumann, 1959. 'Calculations of Relative Permeability from Displacement Experiments,' Transactions of the American Institute of Mining, Metallurgical, and Petroleum Engineers, Vol. 216, pp. 370-372.

Lai, Sung-Ho, J. M. Tiedje, and A. E. Erickson, 1976. 'In Situ Measurement of Gas Diffusion Coefficient in Soil,' Soil Science Society of America Journal, Vol. 40, pp. 3-6.

Lang, A. R. G., 1967. 'Osmotic Coefficients and Water Potentials of Sodium Chloride Solutions from 0 to 40°C,' Australian Journal of Chemistry, Vol. 20, No. 9, pp. 2017-2023.

Loughborough, M. T., 1966. 'Permeability of Concrete to Air,' Ontario Hydro Research Quarterly, First Quarter, Ontario, Canada.

Marshall, T. J., and J. W. Holmes, 1979. Soil Physics, Cambridge University Press, New York.

Marutzky, S. J., 1986. Personal Communication with S. J. Marutzky, Bendix Field Engineering Corporation, Grand Junction, Colorado, 18 February 1986.

Miller, C. H., D. R. Cunningham, and M. J. Cunningham, 1974. 'An Air Injection Technique to Study Intensity of Fracturing Around a Tunnel in Volcanic Rocks,' Bulletin of the Association of Engineering Geologists, Vol. II, No. 3.

Mualem, V., 1976. 'A New Model for Predicting the Hydraulic Conductivity of Unsaturated Porous Media,' Water Resources Research, Vol. 12, No. 3, pp. 513-522.

Nutting, P. G., 1930. 'Physical Analysis of Oil Sands,' Bulletin of the American Association of Petroleum Geologists, Vol. 14, pp. 1337-1349.

Purtymun, W. D., and W. R. Kennedy, 1971. Geology and Hydrology of Mesita del Buey, LA-4660, UC-41, Los Alamos National Laboratory, New Mexico.

Purtymun, W. D., M. L. Wheeler, and M. A. Rogers, 1978. Geologic Description of Cores from Holes P-3 MH-a through P-3 MH-5, Area G, Technical Area 54, LA-7308-MS, Informal Report, Los Alamos Scientific Laboratory, New Mexico.

Rogers, M. A., 1977. History and Environmental Setting of LASL Near-Surface Land Disposal Facilities for Radioactive Wastes, LA-6848-MS, Vol. 1, Los Alamos Scientific Laboratory.

Ross, C. S., and R. L. Smith, 1961. Ash-Flow Tuffs: Their Origin, Geologic Relationship, and Identification, USGS Professional Paper 366, Government Printing Office, Washington, D.C.

Rush, S. M., and J. J. Dexter, 1985. Vadose Zone Characterization of Technical Area 54, Waste Disposal Areas G and L - Report 1: Drilling and Logging Activities, GJ-37, Bendix Field Engineering Corporation, Grand Junction Operations, U.S. Department of Energy, Grand Junction Projects Office, Grand Junction, Colorado.

Spanner, D. C., 1951. 'The Peltier Effect and Its Use in the Measurement of Suction Pressure,' Journal of Experimental Botany, Vol. 2, No. 5, pp. 145-167.

Stephens, D. B., and S. P. Neuman, 1982a. 'Vadose Zone Permeability Tests: Summary,' Journal of the Hydraulics Division, American Society of Civil Engineers, Vol. 108, No. HY5, pp. 623-639.

Stephens, D. B., and S. P. Neuman, 1982b. 'Vadose Zone Permeability Tests: Steady State Results,' Journal of the Hydraulics Division, American Society of Civil Engineers, Vol. 108, No. HY5, pp. 640-659.

Stephens, D. B., S. Tyler, K. Lambert, and S. Yates, 1983. 'Field Experiments to Determine Saturated Hydraulic Conductivity in the Vadose Zone,' in Role of the Unsaturated Zone in Radioactive and Hazardous Waste Disposal, J. W. Mercer, P.S.C. Rao, and M. I. Wendell (eds.), Ann Arbor Scientific Publications, Ann Arbor, Michigan.

Streckeisen, A., 1967. 'Classification and Nomenclature of Igneous Rocks,' in Neues Jahrbuch fur Mineralogie, Abhandlungen, Vol. 107, pp. 144-240.

TerraTek Research Laboratory, 1985. Laboratory Analysis of Rock Core: Bandelier Formation, TR86-49, Salt Lake City, Utah.

U.S. Department of the Interior, 1974. Earth Manual: A Water Resource Technical Publication, Second Edition, Government Printing Office, Washington, D.C.

University of Missouri at Rolla, 1981. Seminar for Drillers and Exploration Managers, Orlando, Florida.

van Genuchten, Rien, 1978. Calculating the Unsaturated Hydraulic Conductivity with a New Closed-Form Analytical Model, Princeton University Water-Resources Program Report 78-WR-08.

Welge, H. J., 1952. 'A Simplified Method for Computing Oil Recovery by Gas or Water Drive,' Transactions of the American Institute of Mining, Metallurgical, and Petroleum Engineers, Vol. 195, pp. 91-98.

Wescor (undated). Instruction Manual for the Model HP-115 Microprocessor Controlled Water Potential Data System, Wescor, Inc., Logan, Utah.

Wescor, 1982. CI-30 Audio Cassette Interface, Wescor, Inc., Logan, Utah.

Appendix A

LITHOLOGIC LOGS AND INSTRUMENT COMPLETION DIAGRAMS

LITHOLOGIC LOGGING

A lithologic log was prepared in accord with established field procedures for each of the 16 holes cored with the continuous sampling system (Bendix Field Engineering Corporation, 1985a, 1985b). These logs are presented in chronological order by hole number as Figures A-2 through A-17. The colors used to describe the core matrices are taken from the Rock Color Chart of Goddard and others (1975); the code in parentheses following a color description corresponds to the chart.

For those holes in which no instruments were installed, the lithologic logs also show the numbers and depth intervals of samples collected for subsequent field or laboratory analysis. Samples identified by the three-letter prefix MCG- followed solely by a three-digit number were collected for gravimetric analysis. Those MCG-numbered samples denoted by a single asterisk (*) were collected for petrologic analysis, and those denoted by a double asterisk (**) were collected for laboratory analysis of moisture characteristics. Samples identified with the number 85 followed by a decimal point and five additional digits were collected for EP-toxicity and volatile-organic analyses by Los Alamos National Laboratory; splits of these samples are identified by the addition of the letter A immediately following the sample number.

For those holes in which instruments were installed (see discussion below), the columns on the lithologic logs originally used for sample identification have been replaced by instrument-completion diagrams. The reader is referred to the first report (Rush and Dexter, 1985) for information on sample numbers and intervals for those holes. It is important to note, however, that the lithologic data have been updated since publication of the first report. Consequently, the graphic log and description for a particular hole as they appeared in the first report may not match the information presented in this appendix.

INSTRUMENT COMPLETIONS

A total of 23 pore-gas sampling ports were installed in seven boreholes in the study area. Completion diagrams of the installations are presented in Figures A-8, A-9, and A-11 through A-15.

A total of 38 thermocouple psychrometers were installed at the study area, 23 in Hole LLP-85-03 and 15 in Hole LGP-85-07. Because of the presence of surface casing in Hole LLP-85-03, a shallow boring was drilled adjacent to the main hole and five psychrometers were installed in this second hole close to the ground surface (depicted in Figure A-4 as being in the same hole). Completion diagrams of the thermocouple-psychrometer installations are shown in Figures A-4 and A-7.

Finally, four pressure transducers were installed in Hole LLP-85-03, although the one at ground surface is actually in the shallow adjacent boring described above. The completion diagram is shown in Figure A-4.

Installation details were described in the second interim report (Bendix Field Engineering Corporation, 1985b). The legends for the instrument installations are presented in Figure A-1.

LEGEND FOR PORE-GAS SAMPLING-PORT INSTALLATIONS

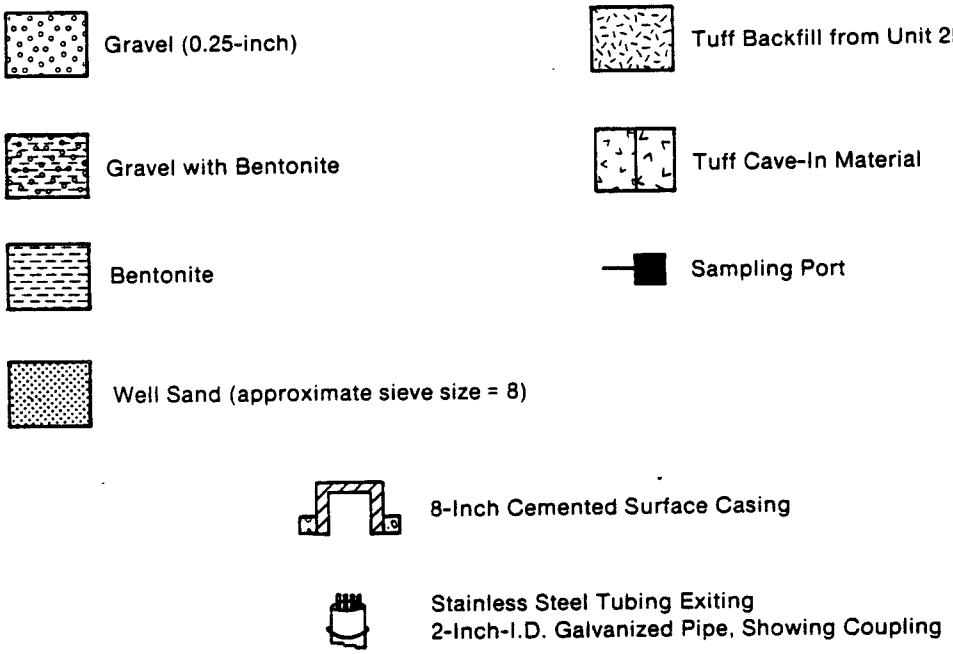

LEGEND FOR PSYCHROMETER AND TRANSDUCER INSTALLATIONS

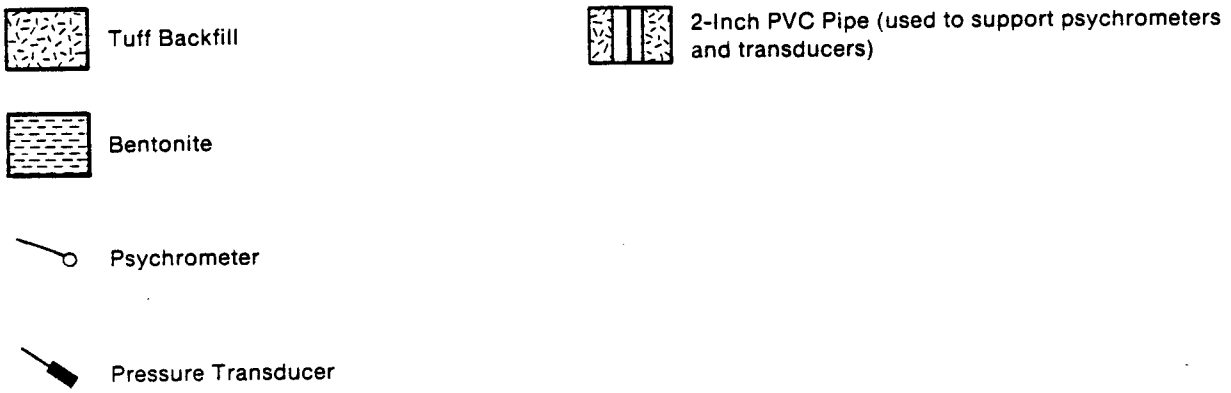

Figure A-1. Legends for the Instrument Installations

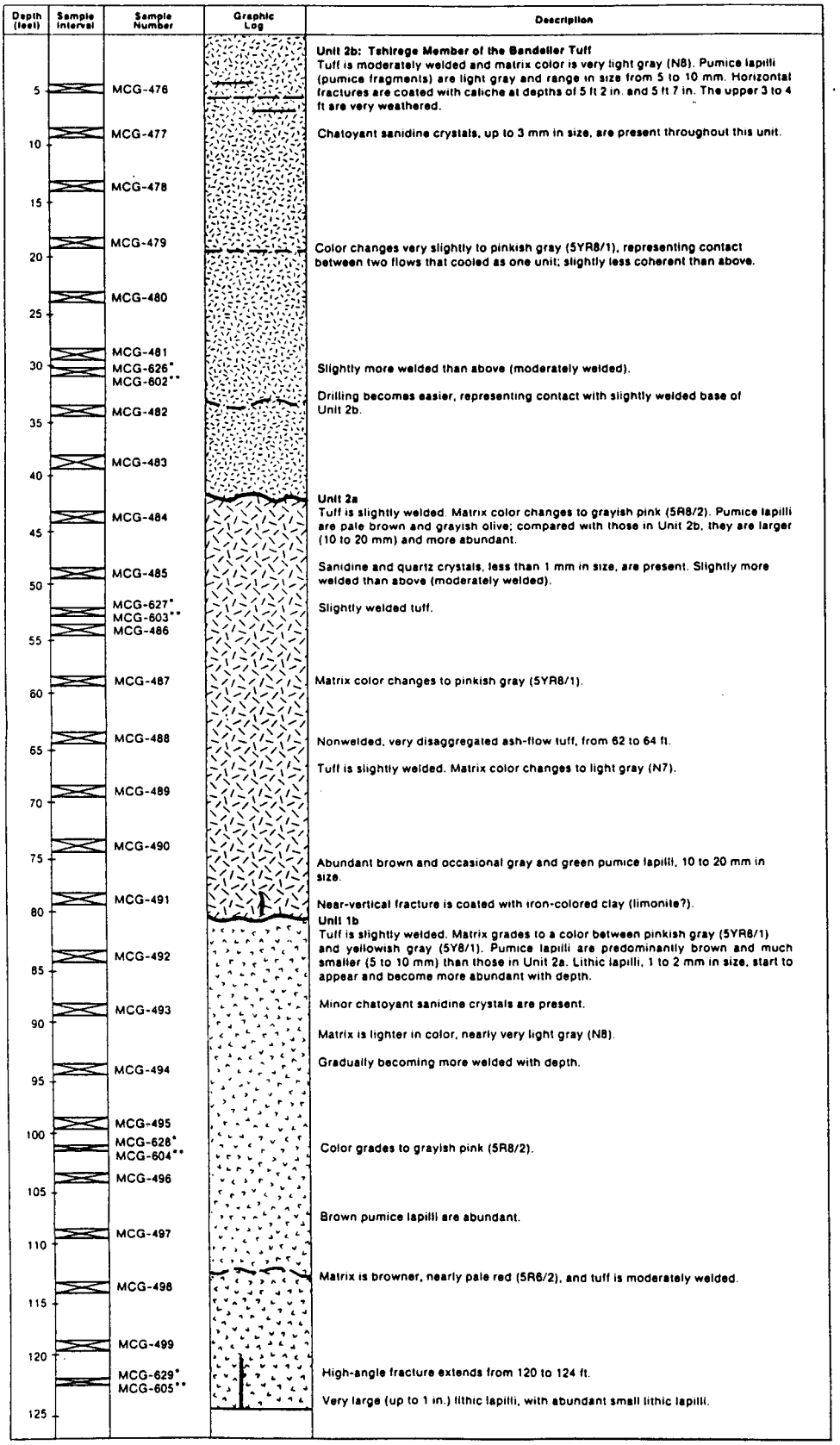

Figure A-2. Lithologic Log of Hole LLM-85-01

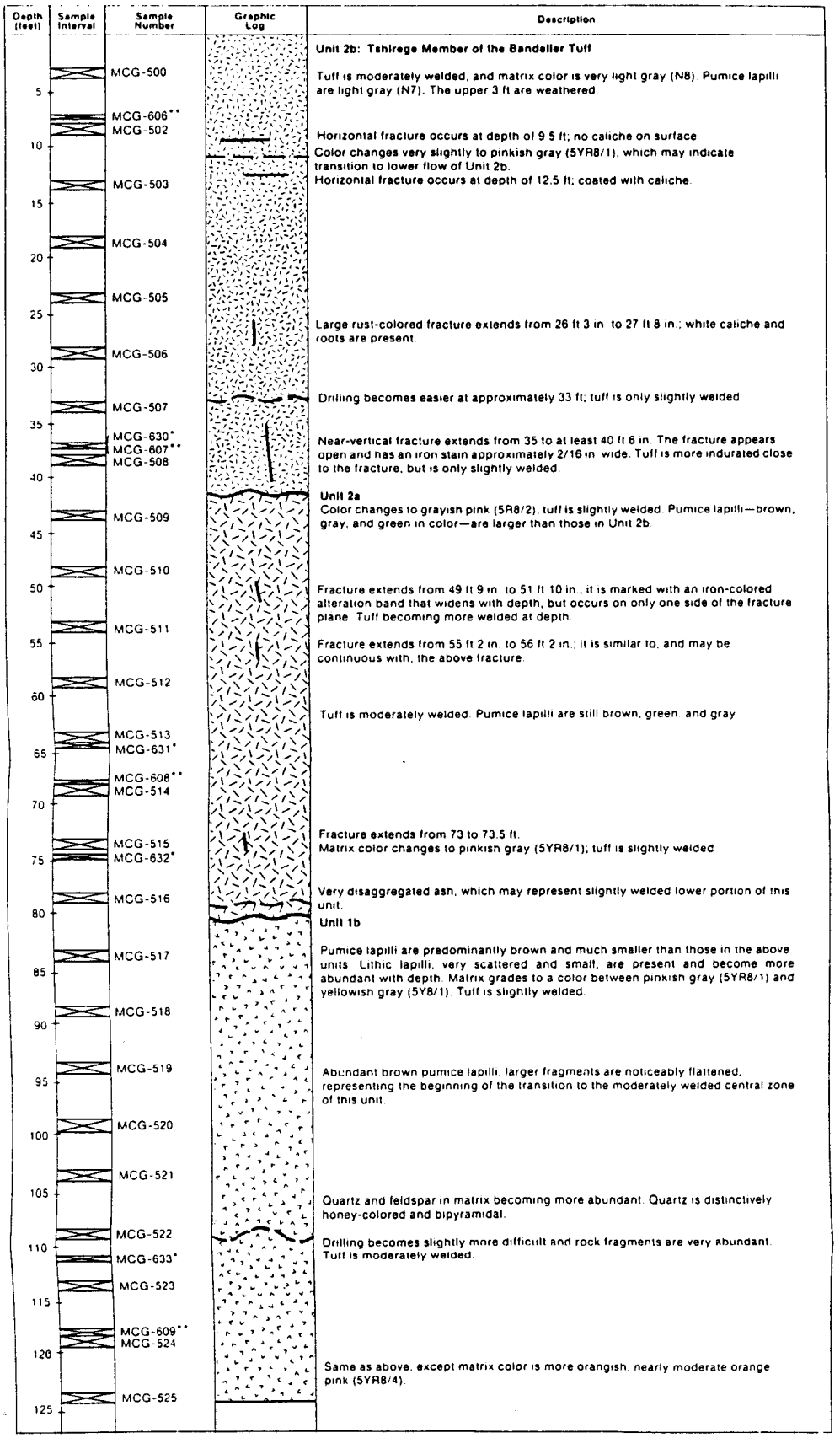

Figure A-3. Lithologic Log of Hole LLM-85-02

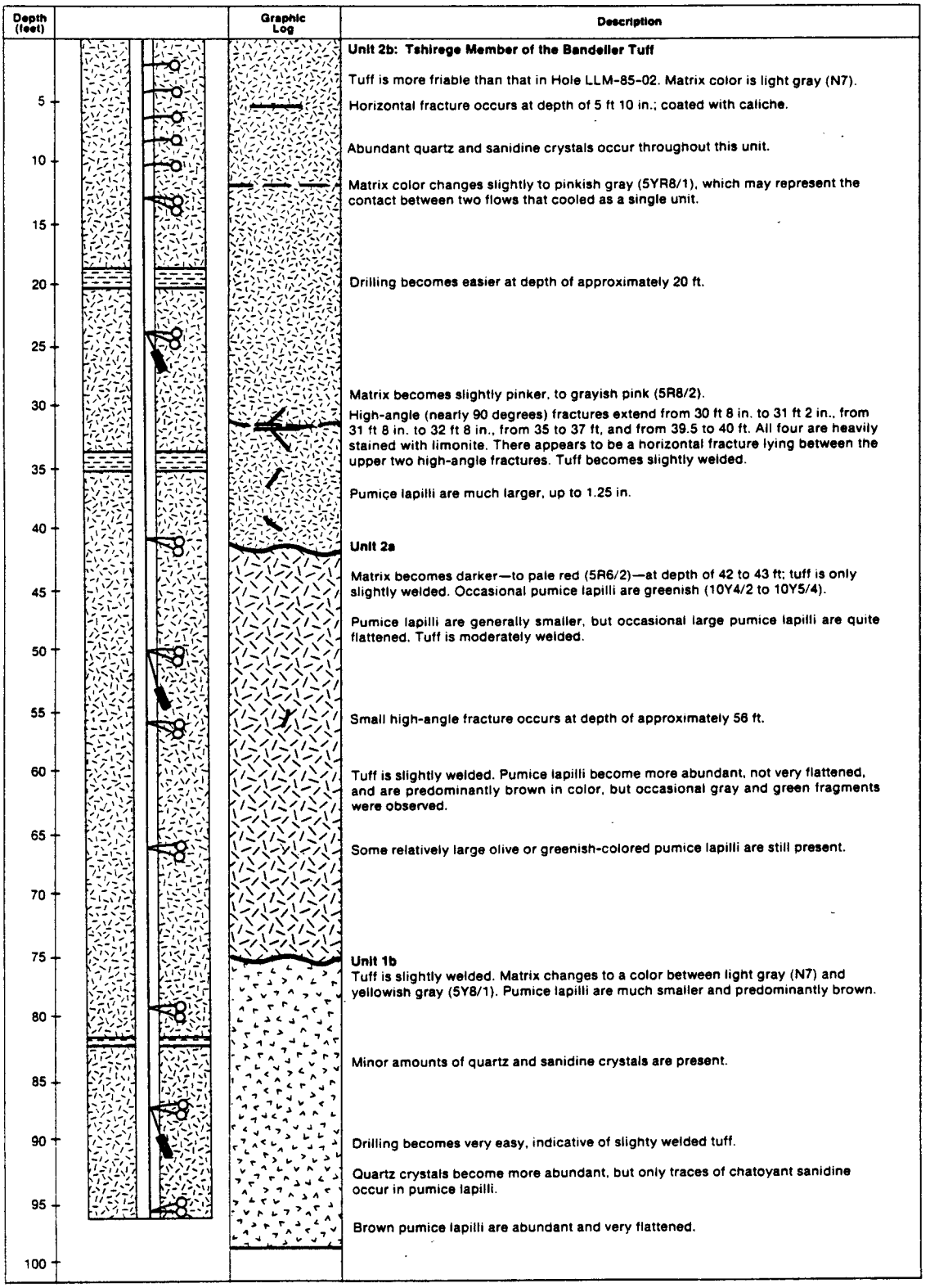

Figure A-4. Installation of Thermocouple Psychrometers and Pressure Transducers in Hole LLP-85-03 (Note: The psychrometers in the upper 10 ft are located in a shallow boring adjacent to the main hole.)

Depth (feet)	Sample Interval	Sample Number	Graphic Log	Description
				Unit 2b: Tshirege Member of the Bandelier Tuff
		MCG-526		Tuff is moderately welded, and matrix color is between light gray (N7) and very light gray (N8). Pumice lapilli, 2 to 10 mm in size, are light gray to medium light gray. Chatoyant sanidine crystals are 1 mm in size. The upper 4 ft are very weathered and contain abundant horizontal fractures with iron stains and root structures.
5				
		MCG-527		
10				Same as above, except rare lithic lapilli up to 40 mm in size are present.
		MCG-528		
15		MCG-610**		
		MCG-529		
20				Same as above, except clear quartz and chatoyant blue sanidine crystals, 1 to 2 mm in size, are abundant.
		MCG-530		
25				
		MCG-531		
30				
		MCG-532		Color changes to grayish pink (5R8/2) at depth of approximately 34 ft. Drilling becomes easier at depth of 33 ft, representing contact with lower flow and/or slightly welded portion of Unit 2b. Pumice lapilli range in size from 2 to 10 mm.
35		MCG-611**		
		MCG-533		
40				**Unit 2a**
		MCG-534		Matrix color still grayish pink (5R8/2); slightly welded tuff. Pumice lapilli are larger (5 to 30 mm), but still predominantly gray. Quartz and sanidine crystals, less than 1 mm in size, are present.
45				Fracture extends from 48 to 48.4 ft.
		MCG-535		
50				Tuff is slightly welded. Pumice lapilli are same size as above (5 to 30 mm), but olive or greenish-colored fragments are present.
		MCG-536		
55				Small fracture, filled to 1/6 in., extends from 54 to 55.5 ft.
				Fracture occurs at depth of approximately 58 ft; very broken-up core.
		MCG-537		
60				Tuff is gradually becoming moderately welded at depth.
				Matrix color still grayish pink (5R8/2). Pumice lapilli are larger (10 to 40 mm), but still predominantly brown with occasional olive or greenish-colored fragments.
		MCG-538		
65				
		MCG-539		
70				Tuff is slightly welded, and matrix color lightens to nearly pinkish gray (5YR8/1). Chatoyant sanidine crystals are still present.
		MCG-540		
75		MCG-612**		**Unit 1b**
		MCG-541		Tuff is slightly welded, and matrix color becomes lighter, between pinkish gray (5YR8/1) and yellowish gray (5Y8/1). Abundant quartz, but chatoyant sanidine was not observed. Pumice lapilli are brown and much more abundant than in Unit 2b.
80				
		MCG-542		
85				
		MCG-543		
90				Lithic lapilli, up to 2 mm in size, are present in small amounts. Pumice lapilli are brown, but slightly larger (20 to 40 mm) than those in upper intervals. Tuff is slightly welded.
		MCG-544		
95				
		MCG-545		Lithic lapilli are abundant, but still small (less than 2 mm).
100				Tuff is moderately welded, and matrix color is becoming more pinkish (5R8/2) which may represent contact with the more densely welded portion of Unit 1b. Rock or lithic fragments are becoming much larger. Pumice lapilli are very large. Quartz crystals, dark- to honey-colored, are abundant.
		MCG-546		
105				
		MCG-547		
110				Scattered, large lithic lapilli. Large pumice lapilli are very flattened.
		MCG-548		Matrix color changes to pale red (10R6/2).
115				
		MCG-549		
120				Matrix color changes to pinkish orange (nearly 10R7/6); slightly welded lower portion of Unit 1b.
		MCG-613**		
		MCG-550		
125				

Figure A-5. Lithologic Log of Hole LLM-85-05

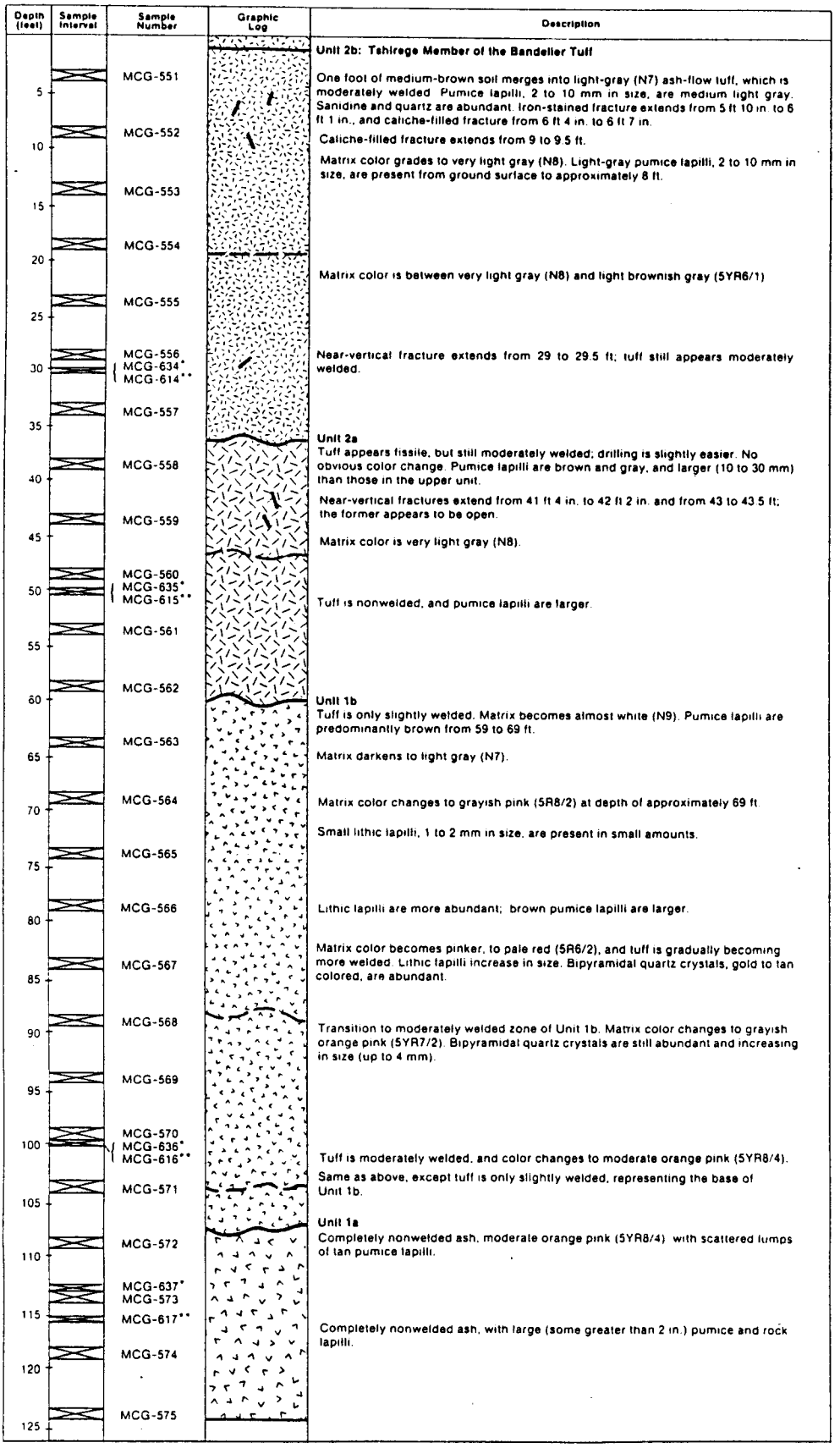

Figure A-6. Lithologic Log of Hole LGM-85-06

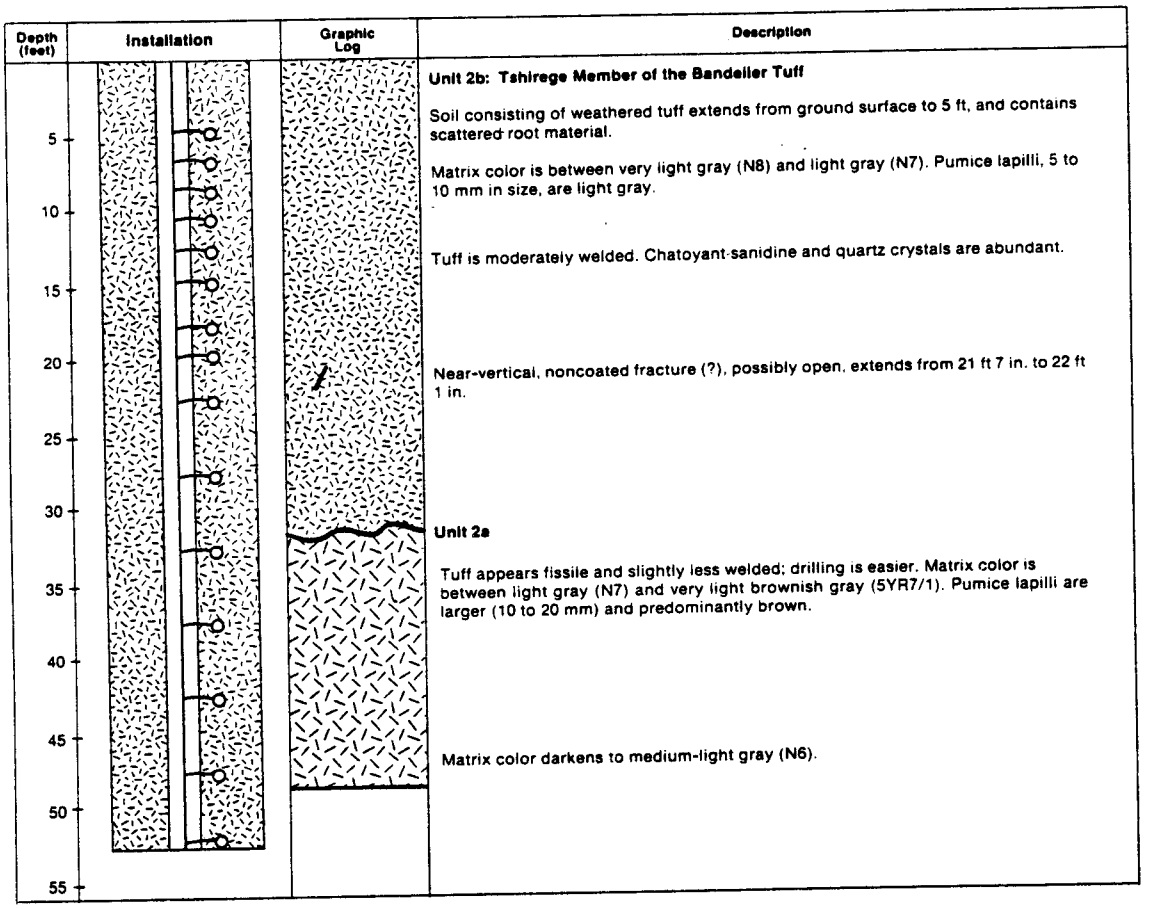

Figure A-7. Installation of Thermocouple Psychrometers in Hole LGP-85-07

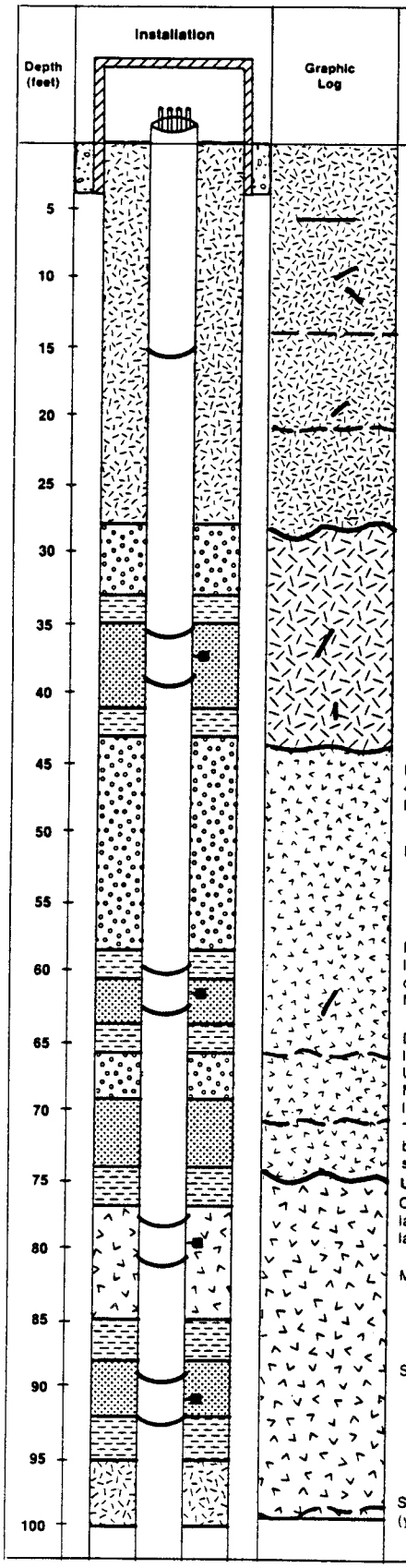

Description

Unit 2b: Tshirege Member of the Bandelier Tuff

The upper 5 ft are weathered and loose, and predominantly brown in color.

Possible horizontal fracture occurs at depth of 6 ft 10 in.; very slight discoloration to brown on the surface. Tuff is moderately welded.

Matrix color is very light gray (N8).

Fractures extend from 9 ft 6 in. to 9 ft 9 in. and from 10 ft 1 in. to 10 ft 4 in.; both appear to dip approximately 45 degrees and have slight brown coloring on the surfaces.
Concentrations of larger pumice lapilli may represent the boundary between separate flows within this unit.
Matrix color changes to pinkish gray (5YR8/1).
Tuff appears slightly fissile, but is still moderately welded.
Possible noncoated fracture extends from 19 ft to 19 ft 3 in.

Slightly less welded than above.

Matrix color becomes very slightly pinkish, with very small, brown pumice lapilli, probably indicating a transitional contact with Unit 2a.

Unit 2a

Matrix color is definitely pinkish. Sanidine and quartz are present. Approximately 75% of the pumice lapilli are brown, 25% green (olive).

Matrix color changes to light brownish gray (5YR6/1).
Tuff is moderately welded.
Near-vertical, iron-stained fracture extends from 35 ft 4 in. to 36 ft 4 in.

Near-vertical, noncoated fracture extends from 40 ft to 40 ft 8 in.
Slightly welded tuff.

Unit 1b

Matrix color changing to very light gray (N8) to almost white (N9) at depth of 43 to 44 ft; tuff is only slightly welded. Pumice lapilli are predominantly brown; occasional large pumice fragments appear flattened. Sanidine crystals are abundant.

Matrix color changes to white (N9) at depth of 52 ft.

Pumice lapilli are still brown, but becoming larger in the interval 59 to 63 ft. Lithic lapilli are abundant, up to ½ in. in size at depth of 59 ft. Quartz crystals are honey-colored. Slightly welded tuff is grading to moderately welded unit below.
Near-vertical fracture, slightly iron-stained, extends from 61 to 62 ft.

Drilling becomes more difficult, and tuff is moderately welded. Lithic lapilli are larger. This more welded material probably represents the central portion of the Unit 1b cooling zone. Fresh glass shards were observed.
Matrix color grades from pinkish gray (5YR8/1) to very pale orange (10YR8/2) to light brown (5YR6/4).
Tuff is slightly welded, and looks like the rest of Unit 1b except the color is becoming very orange. Lithic lapilli are still very abundant, and quartz crystals are still honey-colored.

Unit 1a

Completely nonwelded, orange-colored ash with large pumice lapilli. The latter are distinctively light brown or cream-colored. Only scattered lithic lapilli were observed, one 1 in. in size and another 1/16 in. in size.

Matrix color is moderate orange pink (5YR8/4).

Same as above, except dampness observed at depth of approximately 88 ft.

Same as above, except matrix color changes to light tan [approximately 5Y8/1 (yellowish gray)] and green pumice lapilli are scattered throughout.

Figure A-8. Installation of Pore-Gas Sampling Ports in Hole LGC-85-09

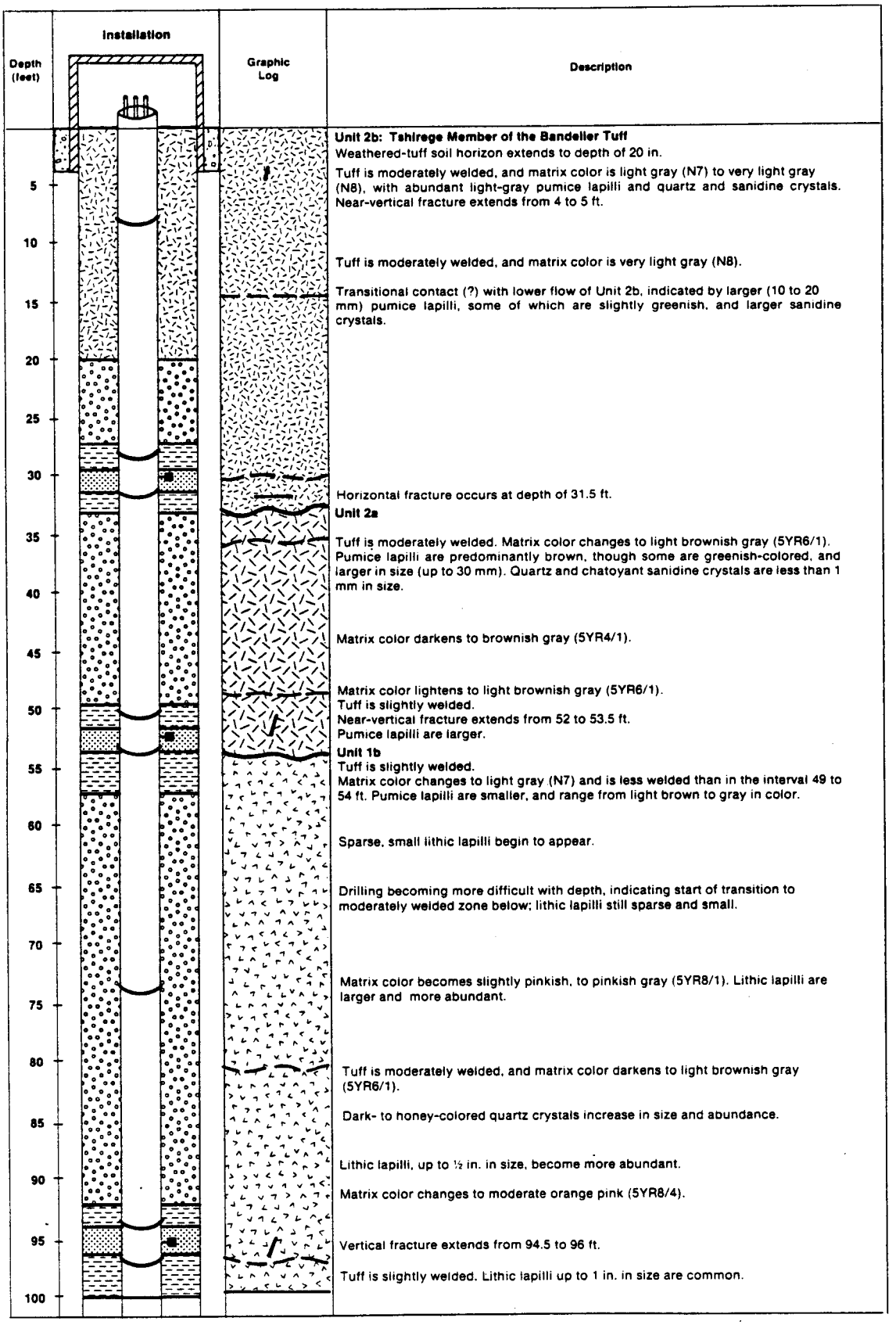

Figure A-9. Installation of Pore-Gas Sampling Ports in Hole LGC-85-10

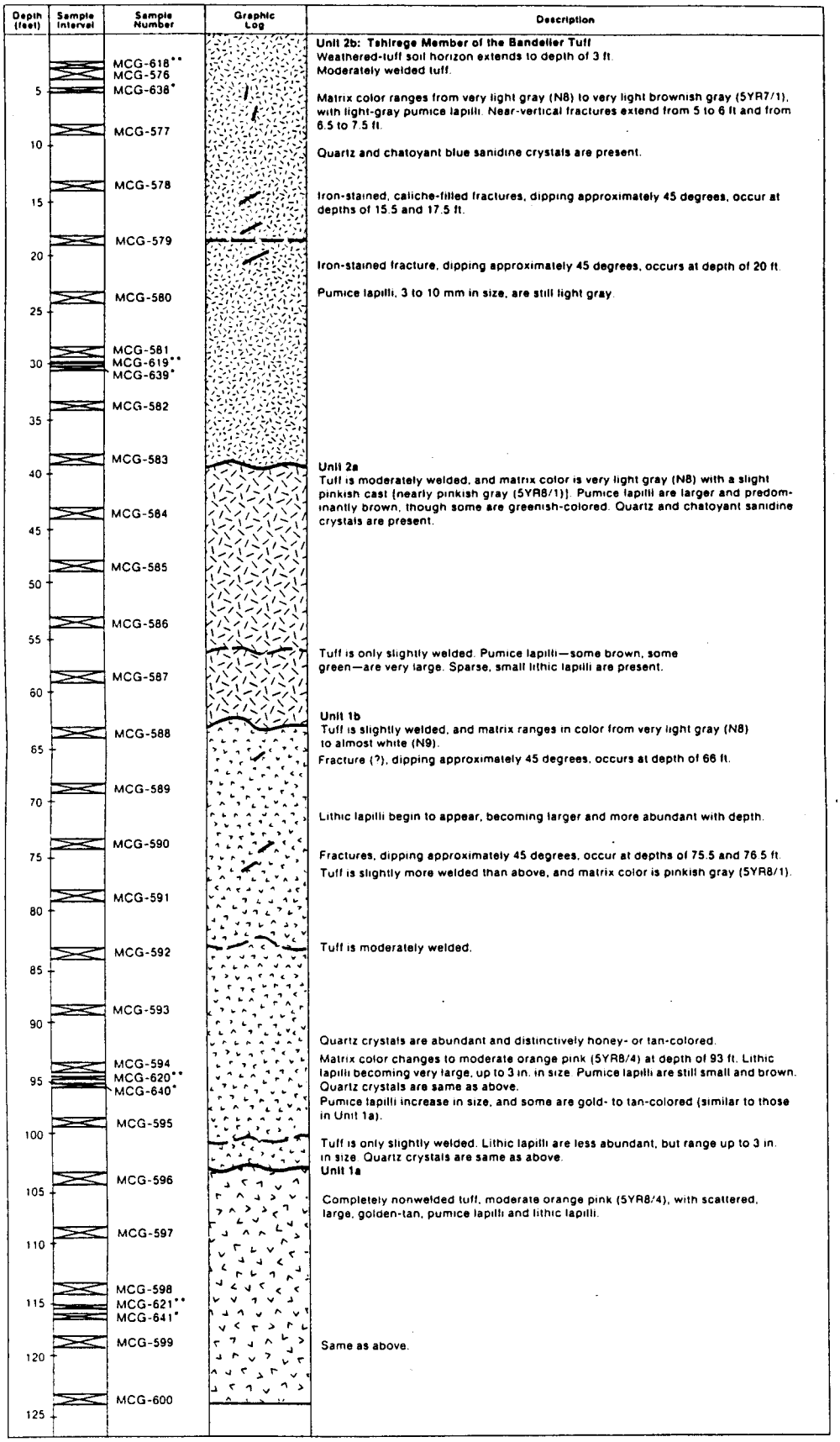

Figure A-10. Lithologic Log of Hole LGM-85-11

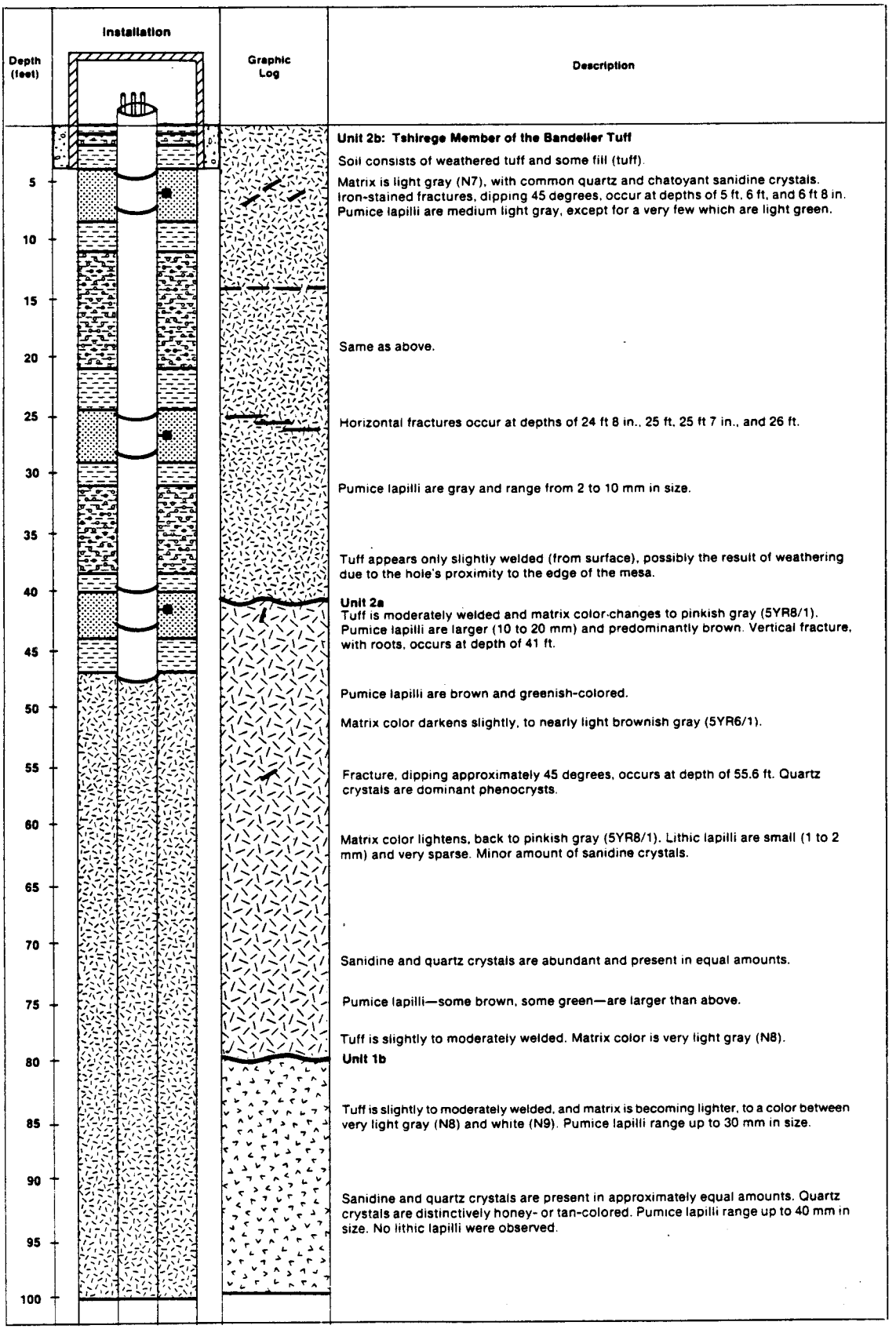

Figure A-11. Installation of Pore-Gas Sampling Ports in Hole LLC-85-12

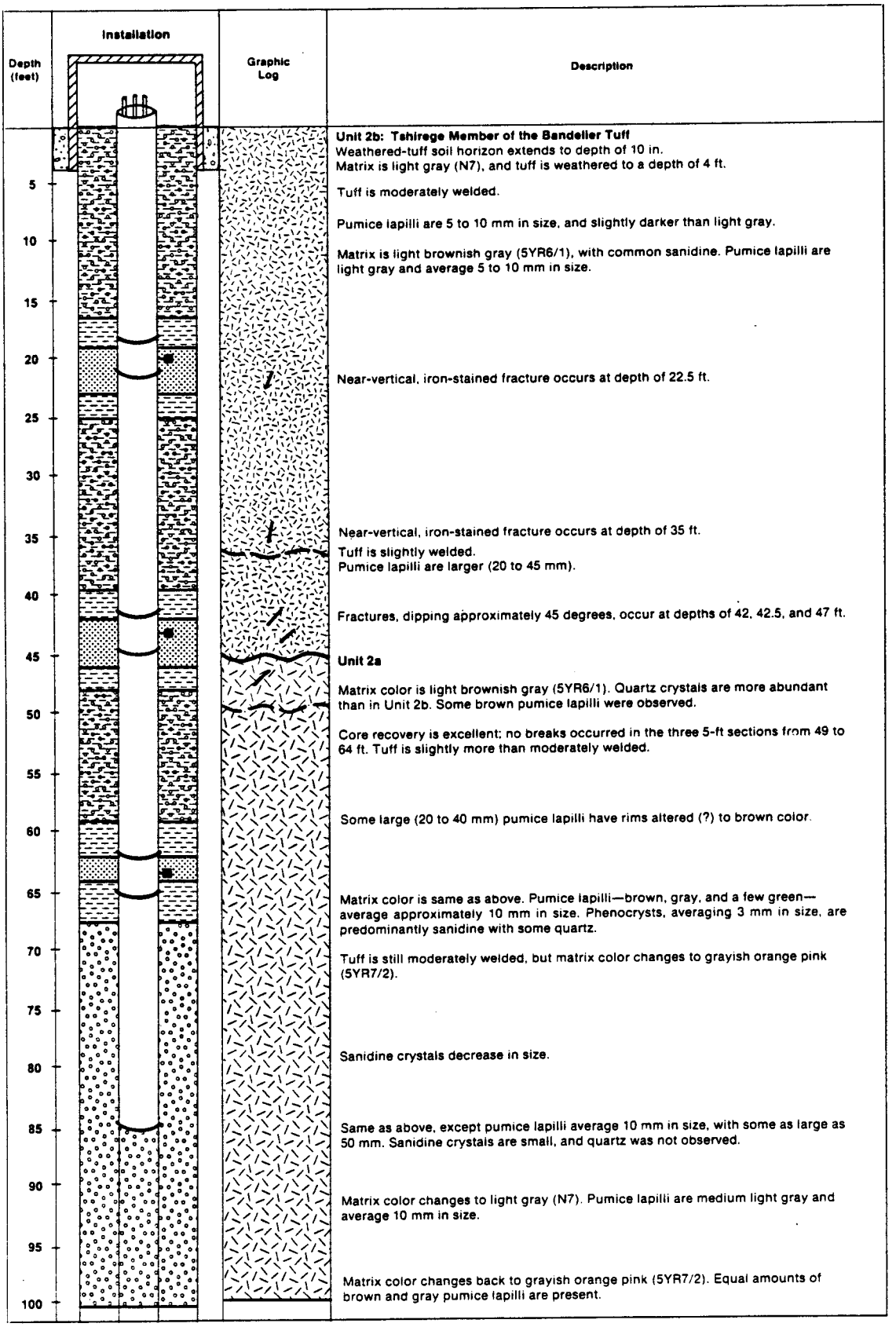

Figure A-12. Installation of Pore-Gas Sampling Ports in Hole LLC-85-13

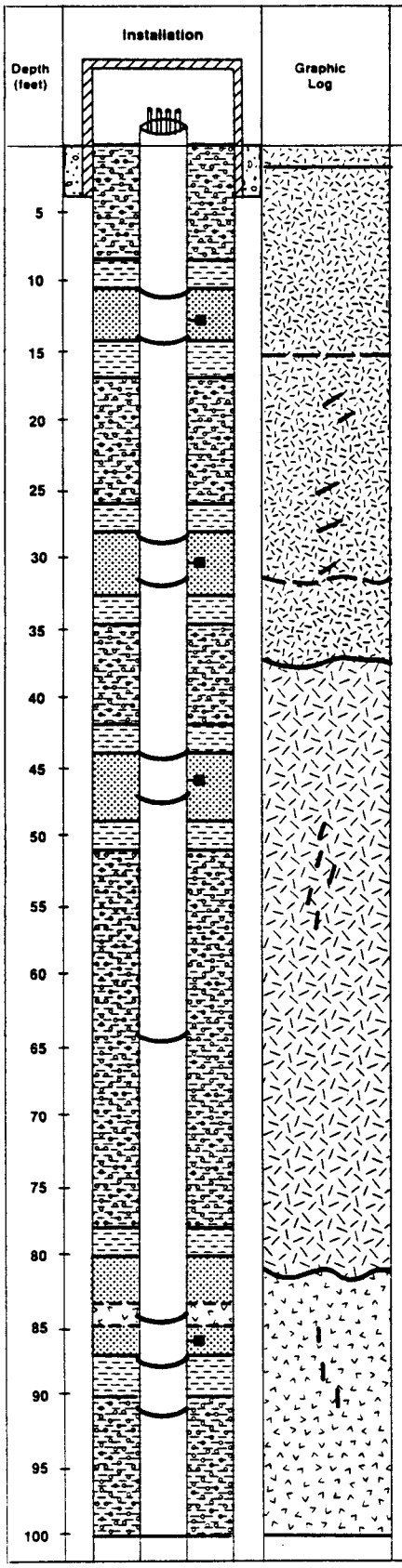

Description

Unit 2b: Tshirege Member of the Bandelier Tuff

Tuff is moderately welded, and matrix color is light brownish gray (5YR6/1). Horizontal fracture occurs at depth of 1.5 ft. Pumice lapilli are small and gray. Quartz and sanidine crystals are small and clear.

Matrix color changes to very light gray (N8), which probably represents the contact with the lower flow of Unit 2b.

Fractures, dipping approximately 45 degrees, occur at depths of 18 ft 2 in. and 19 ft 3 in.

Lithic lapilli are sparse and range up to 30 mm in size.

Matrix color changes back to light brownish gray (5YR6/1) at depth of 26 ft. Fractures, dipping approximately 45 degrees, occur at depths of 25 and 28 ft.

Pumice lapilli—some brown, some gray—range in size from 10 to 40 mm.

Drilling becomes much easier at depth of 32 ft, representing the contact with the slightly welded base of Unit 2b. Matrix color changes to grayish orange pink (5YR7/2). Fracture, dipping approximately 45 degrees, occurs at depth of 31 ft.

Unit 2a

Tuff is slightly welded, and matrix color is light brownish gray (5YR6/1). Pumice lapilli—some brown, some green—range in size from 10 to 30 mm.

Tuff is slightly welded, and matrix color changes to grayish pink (5R8/2). Lithic lapilli are sparse and average 5 to 10 mm in size, with some up to 40 mm. Pumice lapilli are same as above.

Near-vertical fractures occur at depths of 49, 52, 53, 54, and 57 ft. This may be one fracture, observed entering and exiting the core.

Tuff is moderately welded, and matrix changes to a color between grayish pink (5R8/2) and grayish orange pink (5YR7/2). Pumice lapilli are predominantly brown, and average 10 to 40 mm in size. Lithic lapilli are still sparse, but larger (20 to 40 mm).

Matrix color changes to grayish orange pink (5YR7/2); otherwise same as above except fewer lithic lapilli.

Same as above, except lithic lapilli are more abundant.

Same as above, except no lithic lapilli were observed.
Tuff is slightly welded. Matrix color lightens to grayish pink (5R8/2). Pumice lapilli—brown and green—are larger (20 to 50 mm). Sanidine and quartz crystals are very small and clear.

Unit 1b

Tuff is slightly welded. Matrix color changes to light gray (N7). Brown pumice lapilli are smaller (10 to 25 mm). Lithic lapilli and quartz crystals are common, the latter ranging up to 3 mm in size. Near-vertical fractures occur at depths of 85, 88, and 89 ft.

Same as above, except quartz crystals are larger (4 mm) and more abundant.

Figure A-13. Installation of Pore-Gas Sampling Ports in Hole LLC-85-14

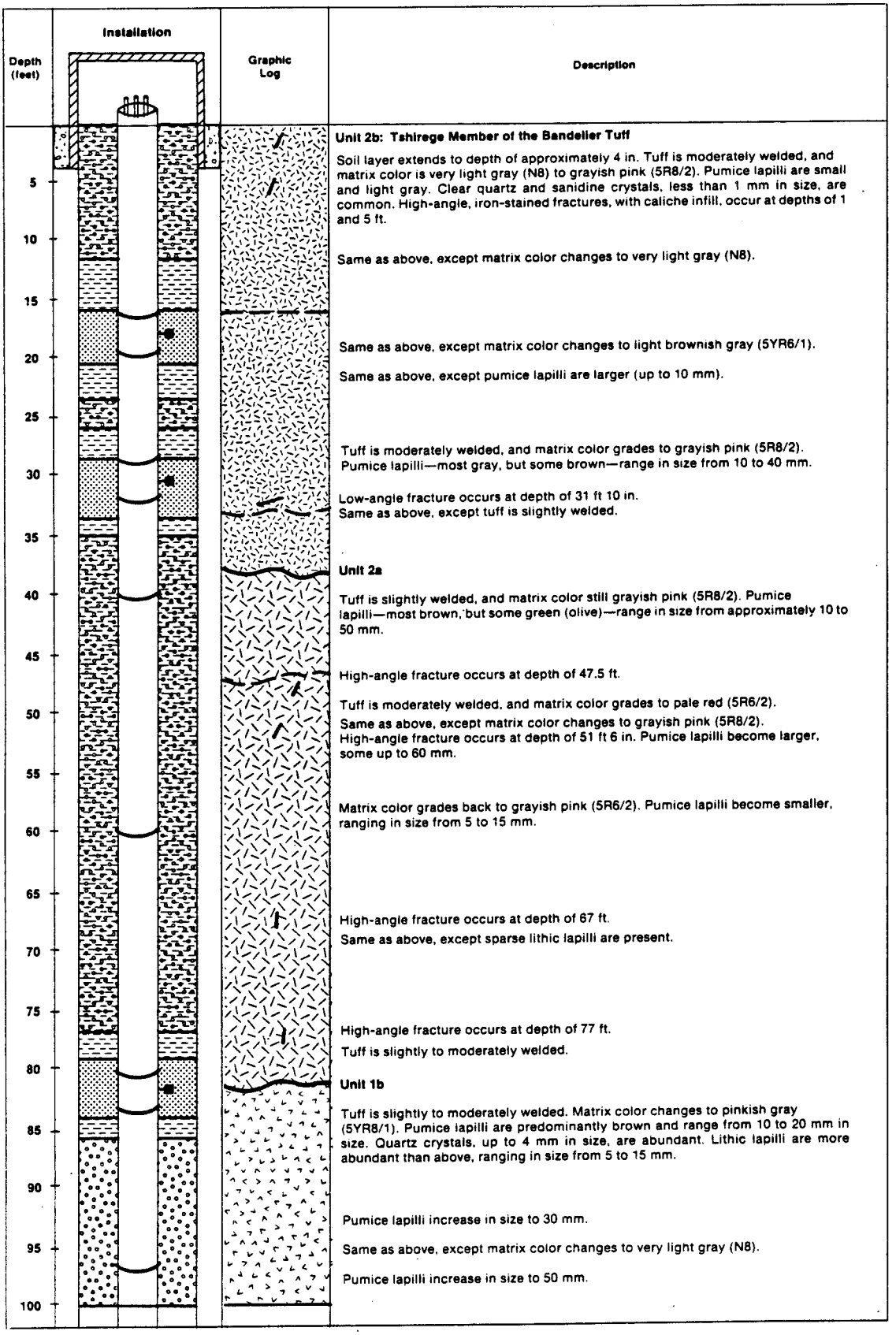

Figure A-14. Installation of Pore-Gas Sampling Ports in Hole LLC-85-15

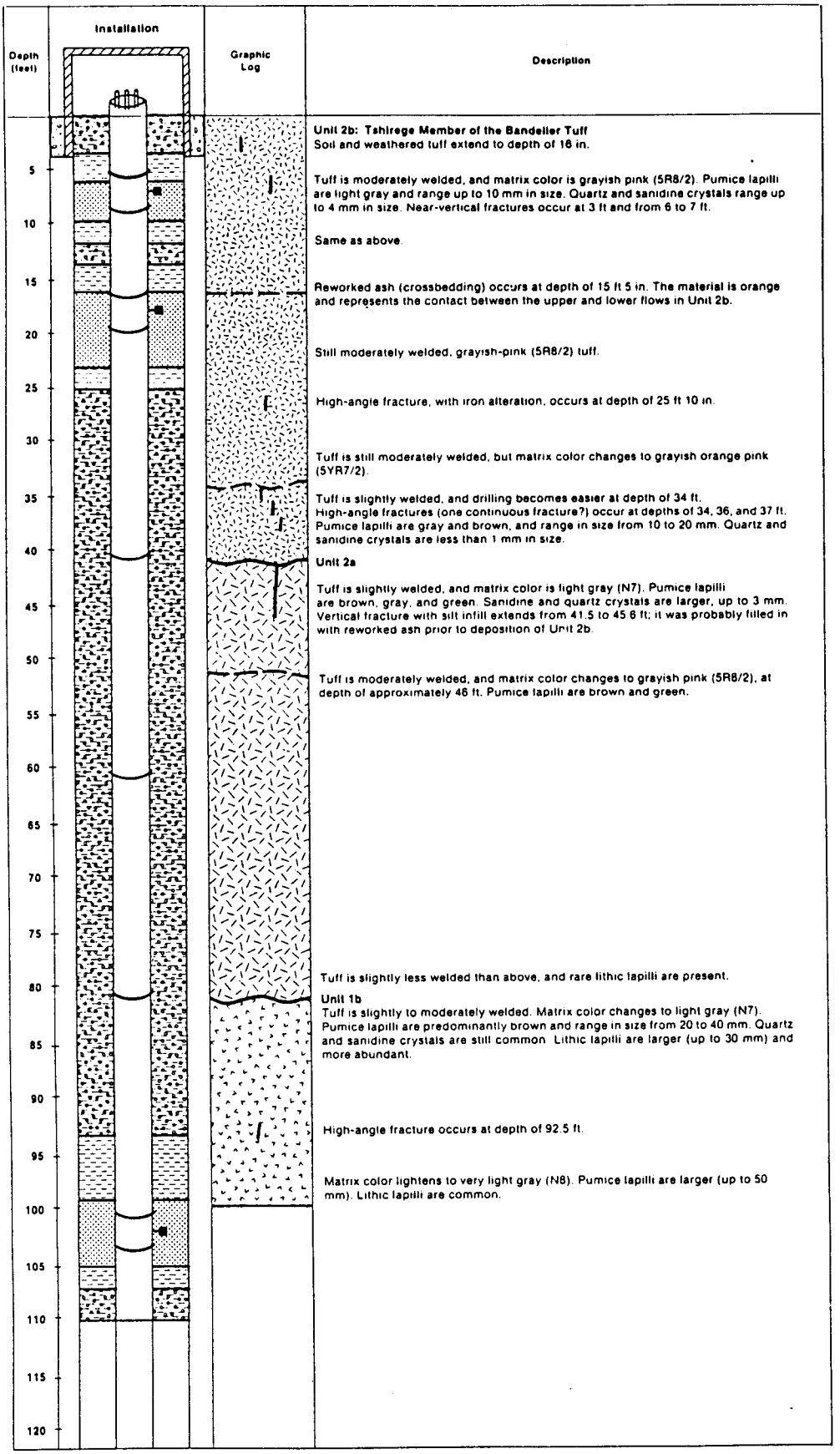

Figure A-15. Installation of Pore-Gas Sampling Ports in Hole LLC-85-16

A-25

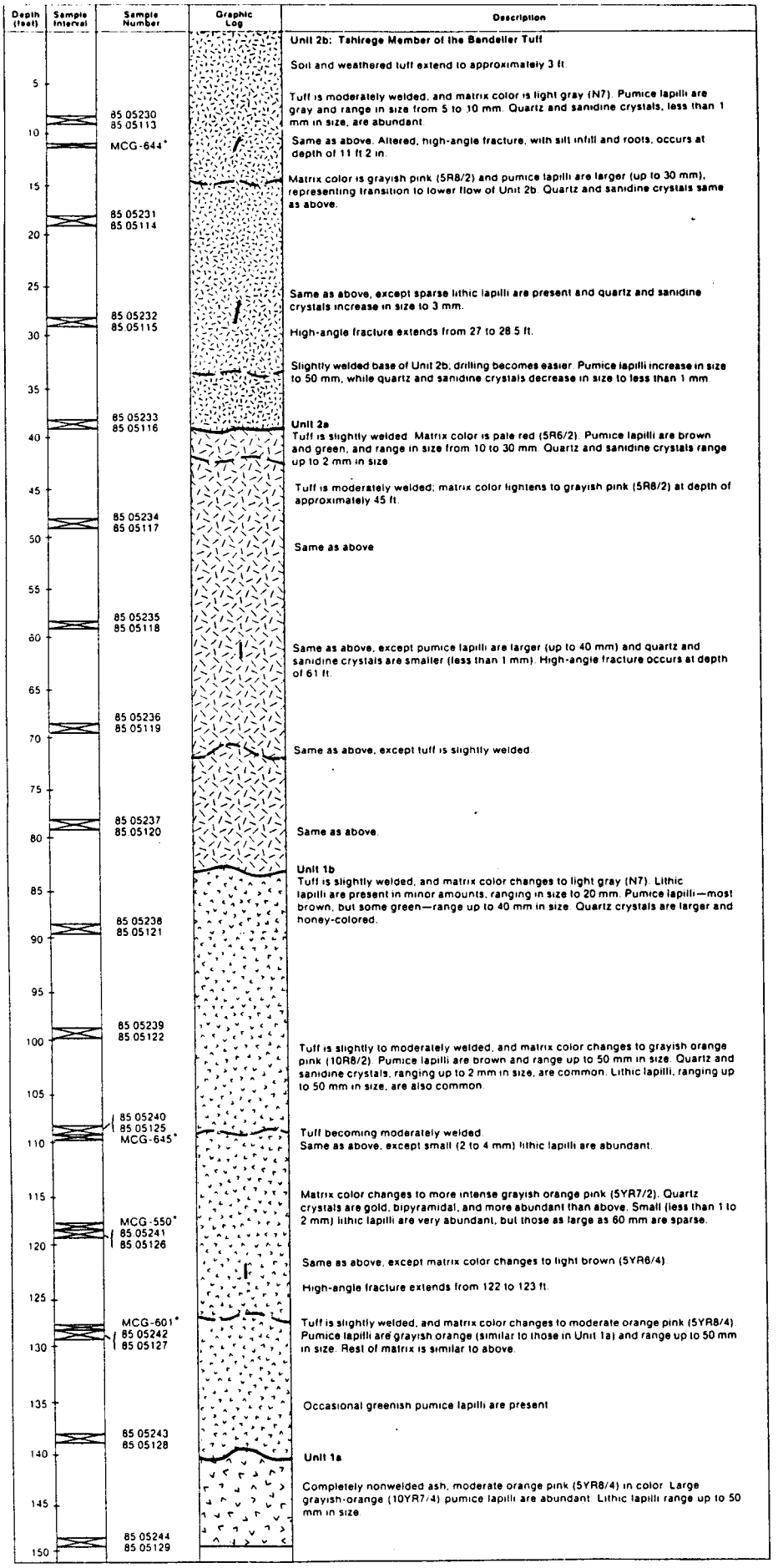

Figure A-16. Lithologic Log of Hole LLC-85-17

A-27

Depth (feet)	Sample Interval	Sample Number	Graphic Log	Description
				Unit 2b: Tshirege Member of the Bandelier Tuff
				Weathered tuff (fill?) extends to depth of 4 ft.
5				Tuff is moderately welded, and matrix color is light gray (N7). Pumice lapilli are gray and range from 5 to 10 mm in size. Quartz and sanidine crystals, up to 1 mm in size, are abundant.
		85.05245		
10		85.05130		Low-angle fracture occurs at depth of 11 ft.
15				Pumice lapilli are larger, which may indicate transition to lower flow of Unit 2b.
		85.05246		
20		85.05131		Same as above, except quartz and sanadine crystals increase in size to 3 mm.
25				
		85.05247		
30		85.05132		
35				Tuff is slightly to moderately welded. Matrix color changes to pale red (5R6/2) at depth of 33 ft. Pumice lapilli are larger (10 to 20 mm), while quartz and sanidine crystals are smaller (less than 1 mm). High-angle fracture, with iron alteration, extends from 33 to 35 ft.
		85.05248		
40		85.05133		**Unit 2a** Tuff is slightly to moderately welded. Matrix color is still pale red (5R6/2). Quartz crystals are larger (up to 3 mm). Pumice lapilli change from gray to brown and green.
45				
		85.05249		
50		85.05134		Same as above, except quartz crystals decrease in size to less than 1 mm.
55				
		85.05250		
60		85.05135		Same as above, except sparse lithic lapilli, 5 to 10 mm in size, are present.
65				
70				No core was recovered for the interval 64 to 74 ft.
75				Same as above, but tuff is only slightly welded.
		85.05252		
80		85.05137		High-angle fracture extends from 78 to 79 ft.
				Unit 1b Tuff is slightly welded. Matrix color changes to light gray (N7) at depth of 79 ft, and to very light gray (N8) at depth of 84 ft. Pumice lapilli are predominantly brown. Lithic lapilli are sparse.
85				
		85.05253		
90		85.05138		
95				Same as above.
		85.05254		
100		85.05139		

Figure A-17. Lithologic Log of Hole LLC-85-18

Appendix B

PETROGRAPHIC REPORTS

A total of 27 drill-core samples from the Tshirege Member of the Bandelier Tuff were submitted to the Bendix Petrology Laboratory for petrographic characterization. Nine samples were from Unit 2b, four from Unit 2a, eight from Unit 1b, two from Unit 1a, and four were lithic lapilli from various units. Analytical procedures and results are described below.

The samples as received consisted of sections of 5-cm-diameter drill core. From these samples, portions were removed using a core splitter for polished thin-section preparation. The samples were impregnated with blue-colored epoxy to emphasize the porosity in the thin sections.* Each thin section, with the exception of the nonwelded samples from Unit 1a, was subjected to point-count analysis (300 counts) to determine mineral and component abundance. Tuffaceous rocks were named according to the classification of Cook (1965). As shown in Figure B-1, the rocks from this study plot in the following fields: II (lithic-crystal tuff), III (lithic-vitric), IV (crystal-lithic), V (vitric-lithic), VII (crystal-vitric), and VIII (vitric-crystal).

The optical identifications of major and minor minerals, especially devitrification products, were confirmed using X-ray diffraction (XRD). The clay-sized fractions were separated from fracture coatings in Samples MCG-629, -630, -643, -644, and -648. These clay-sized separates were smeared or sedimented onto glass slides and analyzed in four different states: air-dried, glycolated, heated to 330°C, and heated to 550°C.

The compositional modifiers to tuffaceous rock names are based on the bulk XRD data. These modifiers were assigned according to the classification of Streckeisen (1967).

Petrographic descriptions of the samples are presented on the pages following Figure B-1. They are presented in consecutive order by sample number, although the drill-hole number, depth of the sample, and geologic unit are also identified near the top of the page. The volume percent of each mineral component is given, together with the petrographic description. Phenocrysts and groundmass are further subdivided into individual components, and these subcomponents are followed by a number in parentheses which indicates their volume percentage of the main component. The petrographic descriptions were taken from a report entitled Petrography of the Tshirege Member of the Bandelier Tuff, Mesita del Buey, Los Alamos County, New Mexico (Fukui, 1985).

*There is considerable discrepancy between porosity measured in thin section and that determined by means of helium injection (cf. Section 3.1.2). The significantly lower porosity determined in thin section is due to the fact that most of the thin sections were cut parallel to the core axis (parallel to the direction of flattening), resulting in erroneous extrapolation based on the cross section of the gas tubes rather than on their true shape.

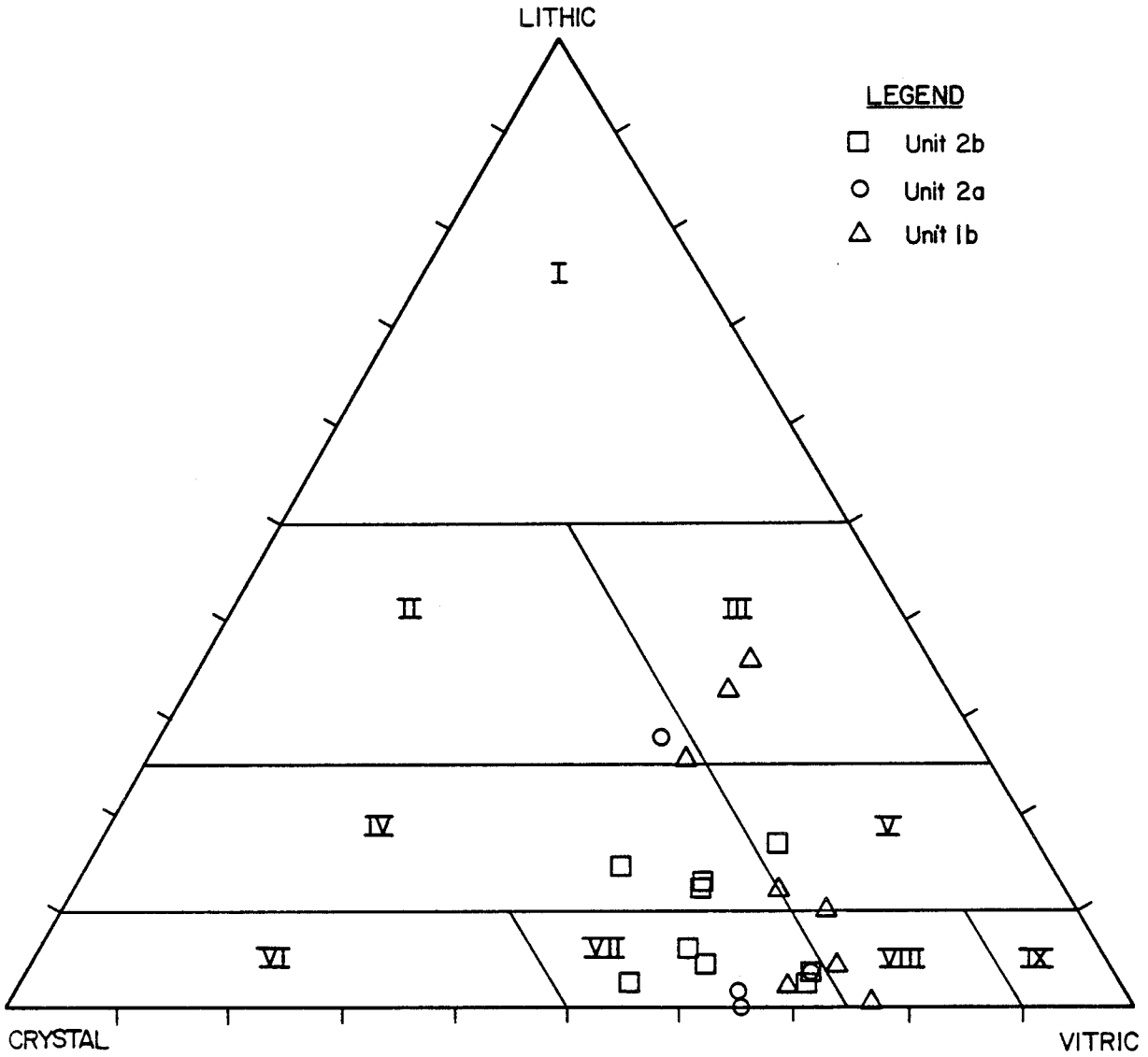

Figure B-1. Classification of Cook (1965) Used to Name Tuffaceous Rocks in This Study on the Basis of the Normalized Vitric (including pumice), Crystal, and Lithic Components Determined from the Modal Analysis

LANL VAPOR TRANSPORT STUDY
REQUEST NO.: 402553
PROJECT NO.: 6L0001000

SAMPLE NO.: MCG-550
DRILL HOLE LLM-85-17 UNIT 1B (LITHIC)
DRILL HOLE DEPTH (FT): 118

PHENOCRYST RATIO (Q/K/P): 1/6.67/0.33 DEGREE OF WELDING: Dense
POROSITY (VOL %): 10 OXIDATION STATE OF Fe-Ti OXIDES: C3-C4

ROCK NAME: Rhyolitic Vitric Tuff

GENERAL DESCRIPTION IN THIN SECTION: Densely welded glass with lithophysae filled by sanidine, tridymite, opaques, and late-stage alpha quartz. A few fine- to medium-grained phenocrysts are present.

MINERAL COMPONENT	VOL. %		COMMENTS
Groundmass		60	Densely welded glass with well-developed spherulitic devitrification. Glass is brown in part.
Vapor-Phase Minerals		28	
Sanidine	(73)		Porous, microcrystalline linings of lithophysae.
Tridymite	(18)		Fine grained, euhedral. Partially fills interiors of lithophysae. Wedge-shaped twins are common.
Alpha Quartz	(5)		Fine grained, anhedral. Late-stage filling of lithophysae.
Opaques	(4)		Fine grained, anhedral. Associated with sanidine stage of lithophysae filling. Magnetite/ilmenite altering to hematite.
Pore Space		10	Associated with vapor-phase crystallites.
Phenocrysts		2	
Sanidine	(83)		Fine to medium grained, euhedral to anhedral.
Alpha Quartz	(13)		Fine to medium grained, anhedral to euhedral. Embayed grains are present.
Plagioclase	(4)		Fine to medium grained, subhedral.
Opaques	(tr)		Fine grained, anhedral to subhedral. Magnetite intergrown with ilmenite.

LANL VAPOR TRANSPORT STUDY
REQUEST NO.: 402553
PROJECT NO.: 6L0001000

SAMPLE NO.: MCG-601
DRILL HOLE LLM-85-17 UNIT 1B (LITHIC)
DRILL HOLE DEPTH (FT): 128

POROSITY (VOL %): 1

OXIDATION STATE OF Fe-Ti OXIDES: C4

ROCK NAME: Hornblende Basalt Porphyry

GENERAL DESCRIPTION IN THIN SECTION: Fine- to medium-grained phenocrysts in a hyalopilitic groundmass. Glomeroporphyritic.

MINERAL COMPONENT	VOL. %		COMMENTS
Phenocrysts		32	
Plagioclase	(61)		Fine to medium grained, euhedral. Oscillatory zoning. Andesine. Embayed grains.
Hornblende(?)	(20)		Fine to medium grained, euhedral. Totally replaced by hematite and chlorite.
Biotite	(7)		Fine to medium grained, euhedral to subhedral. Partial replacement by hematite.
Pyroxene	(6)		Fine to medium grained, euhedral to subhedral. Hypersthene. Partial replacement by chlorite/serpentine.
Opaques	(5)		Fine grained, euhedral to subhedral. Magnetite with exsolved ilmenite; magnetite is oxidizing to hematite.
Olivine	(tr)		Medium grained, anhedral. Totally oxidized to hypersthene and magnetite.
Groundmass		68	Hyalopilitic.
Plagioclase	(94)		Felty laths.
Opaques	(2)		Magnetite oxidizing to hematite.
Glass	(1.5)		Brown-colored.
Pore Space	(1.5)		Microvugs in groundmass(?).
Biotite	(1)		Altered to chlorite and hematite.

LANL VAPOR TRANSPORT STUDY
REQUEST NO.: 402553
PROJECT NO.: 6L0001000

SAMPLE NO.: MCG-626
DRILL HOLE LLM-85-01 UNIT 2B
DRILL HOLE DEPTH (FT): 30

PHENOCRYST RATIO (Q/K/P): 1/2.26/0
POROSITY (VOL %): 23

DEGREE OF WELDING: Slight to Moderate
OXIDATION STATE OF Fe-Ti OXIDES: C4

ROCK NAME: Rhyolitic Crystal-Vitric Tuff

GENERAL DESCRIPTION IN THIN SECTION: Fine- to medium-grained phenocrysts (crystals) in a slightly to moderately welded glass groundmass. Intact glass bubble walls and Y-shaped shards are present.

MINERAL COMPONENT	VOL. %		COMMENTS
Groundmass		44	
Glass	(66)		Incipient axiolitic devitrification.
Pumice	(34)		Up to 2.59 mm. Replaced/mineralized by sanidine and tridymite. Phenocryst ratio (Q/K) = 1/3.
Phenocrysts		27	
Sanidine	(64)		Fine to medium grained, anhedral to subhedral.
Quartz	(28)		Fine to medium grained, anhedral to subhedral.
Opaques	(5)		Fine-grained, euhedral to subhedral. Ilmenite/magnetite altering to hematite.
Amphibole(?)	(3)		Fine grained, anhedral to subhedral. Lamprobolite, partially altered, with opaque rims.
Plagioclase	(tr)		Fine to medium grained, anhedral. Accidental crystal.
Biotite	(tr)		Fine grained, anhedral to subhedral.
Pore Space		23	
Lithic Fragments		5	Up to 10.4 mm. Consisting of an andesite, a rock similar to the host, and a plagioclase-sanidine fragment.
Zeolite		1	Very fine grained, euhedral. Isotropic; phase is probably analcime. Occurs in pore space.

LANL VAPOR TRANSPORT STUDY
REQUEST NO.: 402553
PROJECT NO.: 6L0001000

SAMPLE NO.: MCG-627
DRILL HOLE LLM-85-01 UNIT 2A
DRILL HOLE DEPTH (FT): 52

PHENOCRYST RATIO (Q/K/P): 1/1.79/0
POROSITY (VOL %): 13

DEGREE OF WELDING: Slight to Moderate
OXIDATION STATE OF Fe-Ti OXIDES: C2

ROCK NAME: Rhyolitic Crystal-Vitric Tuff

GENERAL DESCRIPTION IN THIN SECTION: Fine- to medium-grained phenocrysts in a groundmass that exhibits slight to moderate welding. Pumice fragments are generally coarser than those in Sample MCG-626 and the quartz phenocrysts are more embayed.

MINERAL COMPONENT	VOL. %		COMMENTS
Groundmass		62	
Pumice	(53)		Up to 13.9 mm. Replaced/mineralized by sanidine and tridymite. Phenocryst ratio (Q/K): 1/3. Some fragments altering to clay.
Glass	(47)		Incipient axiolitic devitrification.
Phenocrysts		23	
Sanidine	(62)		Fine to medium grained, subhedral to anhedral.
Quartz	(34)		Fine to medium grained, subhedral to euhedral. Some grains are embayed.
Opaques	(3)		Fine grained, euhedral to subhedral. Magnetite with exsolved ilmenite.
Pyroxene	(1)		Fine grained, anhedral to euhedral. Augite.
Pore Space		13	
Lithic Fragments		2	Up to 2.64 mm. Includes crystal-vitric tuffs with clay replacing the glass; strongly welded.
Unknown Component		tr	Rounded grain, 0.56 mm in longest axis, consisting of a thin rim of magnetite with randomly oriented clay (chlorite?) flakes and epidote or pyroxene grains.

LANL VAPOR TRANSPORT STUDY
REQUEST NO.: 402553
PROJECT NO.: 6L0001000

SAMPLE NO.: MCG-628
DRILL HOLE LLM-85-01 UNIT 1B
DRILL HOLE DEPTH (FT): 101

PHENOCRYST RATIO (Q/K/P): 1/2.25/0.06 DEGREE OF WELDING: Moderate
POROSITY (VOL %): 18 OXIDATION STATE OF Fe-Ti OXIDES: C2

ROCK NAME: Rhyolitic Vitric-Lithic Tuff

GENERAL DESCRIPTION IN THIN SECTION: Fine- to medium-grained phenocrysts in a moderately welded groundmass with incipient axiolitic devitrification. This sample contains more lithic fragments than Sample MCG-626 (Unit 2b) or Sample MCG-627 (Unit 2a).

MINERAL COMPONENT	VOL. %		COMMENTS
Groundmass		56	
Glass	(51)		Incipient axiolitic devitrification. Intact bubble walls and Y-shaped shards are present.
Pumice	(49)		Up to 8.89 mm. Spherulitic devitrification (rather than replaced by sanidine and tridymite as in Samples MCG-626 and -627). Phenocryst ratio (Q/K) = 1/3.67.
Phenocrysts		18	
Sanidine	(66)		Fine to medium grained, anhedral to euhedral.
Quartz	(30)		Fine to medium grained, anhedral to euhedral. Some grains are embayed.
Plagioclase	(2)		Medium grained, subhedral. Associated with pyroxene and magnetite-ilmenite. Zoned grain.
Opaques	(2)		Fine grained, anhedral to euhedral. Magnetite with exsolved ilmenite.
Pyroxene	(tr)		Fine grained, anhedral. One grain is coated by celadonite.
Pore Space		18	
Lithic Fragments		8	Up to 17.0 mm. Largest fragment is a thoroughly welded, crystal-vitric tuff. Other tuffs are altered to clay; basalts/andesites are present.

(continued on next page)

LANL VAPOR TRANSPORT STUDY
REQUEST NO.: 402553
PROJECT NO.: 6L0001000

SAMPLE NO.: MCG-628 (continued)
DRILL HOLE LLM-85-01 UNIT 1B
DRILL HOLE DEPTH (FT): 101

MINERAL COMPONENT	VOL. %	COMMENTS
Unknown Component	tr	Rounded grain, 0.62 mm in longest axis, consisting of clay (chlorite?) flakes in random orientation and magnetite with exsolved ilmenite. Magnetite is altering to hematite. Grain could be an altered mafic.

LANL VAPOR TRANSPORT STUDY
REQUEST NO.: 402553
PROJECT NO.: 6L0001000

SAMPLE NO.: MCG-629
DRILL HOLE LLM-85-01 UNIT 1B
DRILL HOLE DEPTH (FT): 122

PHENOCRYST RATIO (Q/K/P): 1/0.75/0
POROSITY (VOL %): 12

DEGREE OF WELDING: Moderate
OXIDATION STATE OF Fe-Ti OXIDES: C2-C3

ROCK NAME: Rhyolitic Vitric-Lithic Tuff

GENERAL DESCRIPTION IN THIN SECTION: Fine- to medium-grained phenocrysts in a moderately welded groundmass. Most shards show incipient alteration to clay. This sample is similar to MCG-628 except for the lack of significant devitrification of glass shards.

MINERAL COMPONENT	VOL. %		COMMENTS
Groundmass		55	
Glass	(63)		Shards are a mottled-brown color; this may be incipient alteration to clay. Intact bubble walls and Y-shaped shards are present.
Pumice	(37)		Up to 10.0 mm. Spherulitic devitrification. Phenocryst ratio (Q/K) = 1/4.25. One pumice fragment contains a pyroxene phenocryst.
Phenocryst		22	
Quartz	(54)		Fine to medium grained, anhedral to euhedral. Most grains are embayed.
Sanidine	(41)		Fine to medium grained, subhedral to euhedral.
Opaques	(5)		Fine grained, anhedral to euhedral. Magnetite with exsolved ilmenite.
Pyroxene	(tr)		Fine grained, anhedral to euhedral. Usually associated with opaques.
Pore Space		12	
Lithic Fragments		11	Up to 5.70 mm. Several thoroughly welded vitric-crystal tuffs with spherulitic devitrification are present. Also present are andesitic crystal-vitric tuffs that are moderately welded.

LANL VAPOR TRANSPORT STUDY
REQUEST NO.: 402553
PROJECT NO.: 6L0001000

SAMPLE NO.: MCG-630
DRILL HOLE LLM-85-02 UNIT 2B
DRILL HOLE DEPTH (FT): 37

PHENOCRYST RATIO (Q/K/P): 1/2.24/0.06 DEGREE OF WELDING: Moderate
POROSITY (VOL %): 16 OXIDATION STATE OF Fe-Ti OXIDES: C2

ROCK NAME: Rhyolitic Vitric-Lithic Tuff

GENERAL DESCRIPTION IN THIN SECTION: Fine- to medium-grained phenocrysts in a moderately welded groundmass. Shards show incipient axiolitic devitrification and clay coatings. Pumice fragments are mostly replaced by sanidine and tridymite as in Samples MCG-626 and -627.

MINERAL COMPONENT	VOL. %		COMMENTS
Groundmass		50	
Glass	(77)		Incipient axiolitic devitrification; glass is coated by clay. Y-shaped shards are present.
Pumice	(23)		Up to 8.74 mm. Replaced/mineralized by sanidine and tridymite. Phenocryst ratio (Q/K) = 1/4.
Phenocrysts		19	
Sanidine	(66)		Fine to medium grained, anhedral to euhedral. Some grains are embayed.
Quartz	(30)		Fine to medium grained, anhedral to euhedral. Some grains are embayed.
Plagioclase	(2)		Fine grained, subhedral.
Opaques	(2)		Fine grained, anhedral to euhedral. Magnetite with exsolved ilmenite.
Pyroxene	(tr)		Fine grained, anhedral to subhedral.
Amphibole	(tr)		Fine grained, anhedral.
Zircon	(tr)		Fine grained, euhedral.
Pore Space		16	
Lithic Fragments		14	Up to 15.8 mm. Several strongly welded, crystal-vitric tuffs with little or no devitrification of glass.

(continued on next page)

LANL VAPOR TRANSPORT STUDY
REQUEST NO.: 402553
PROJECT NO.: 6L0001000

SAMPLE NO.: MCG-630 (continued)
DRILL HOLE LLM-85-02 UNIT 2B
DRILL HOLE DEPTH (FT): 37

MINERAL COMPONENT	VOL. %	COMMENTS
Zeolite(?)	tr	Very fine grained, euhedral (radial acicular). Occupies pore space; too small for optical identification.
Unknown Component	tr	Euhedral grain shape (pyroxene?), 0.51 mm, at edge of thin section; consists of thin rim of magnetite and randomly oriented flakes of clay (chlorite?).

LANL VAPOR TRANSPORT STUDY
REQUEST NO.: 402553
PROJECT NO.: 6L0001000

SAMPLE NO.: MCG-631
DRILL HOLE LLM-85-02 UNIT 2A
DRILL HOLE DEPTH (FT): 64

PHENOCRYST RATIO (Q/K/P): 1/1.45/0
POROSITY (VOL %): 23

DEGREE OF WELDING: Moderate
OXIDATION STATE OF Fe-Ti OXIDES: C2-C3

ROCK NAME: Rhyolitic Crystal-Vitric Tuff

GENERAL DESCRIPTION IN THIN SECTION: Fine- to medium-grained phenocrysts in a moderately welded groundmass. Pumice fragments are mostly replaced by sanidine and tridymite.

MINERAL COMPONENT	VOL. %		COMMENTS
Groundmass		49	
Glass	(76)		Incipient axiolitic devitrification. Intact bubble walls and Y-shaped shards are present.
Pumice	(24)		Up to 7.26 mm. Replaced/mineralized by sanidine and tridymite. Phenocryst ratio (Q/K) = 1/4.
Phenocrysts		26	
Sanidine	(58)		Fine to medium grained, anhedral to euhedral.
Quartz	(40)		Fine to medium grained, anhedral to euhedral. Some grains are embayed.
Opaques	(1)		Fine grained, anhedral to euhedral. Magnetite-ilmenite intergrowths (exsolution).
Pyroxene	(1)		Fine grained, subhedral to euhedral. Usually associated with opaques.
Plagioclase	(tr)		Fine grained, euhedral.
Amphibole	(tr)		Fine grained, anhedral to euhedral.
Zircon	(tr)		Very fine grained, euhedral.
Pore Space		23	

(continued on next page)

LANL VAPOR TRANSPORT STUDY
REQUEST NO.: 402553
PROJECT NO.: 6L0001000

SAMPLE NO.: MCG-631 (continued)
DRILL HOLE LLM-85-02 UNIT 2A
DRILL HOLE DEPTH (FT): 64

MINERAL COMPONENT	VOL. %	COMMENTS
Lithic Fragments	1	Largest grain was on a corner of the thin section; grain is larger than 5.56 mm. Present are densely welded, partly devitrified vitric tuff; flow-banded rock; andesites; and other lithic types.
Zeolite(?)	1	Very fine grained, subhedral. Occurs in pore space.

LANL VAPOR TRANSPORT STUDY
REQUEST NO.: 402553
PROJECT NO.: 6L0001000

SAMPLE NO.: MCG-632
DRILL HOLE LLM-85-02 UNIT 2A (1B)
DRILL HOLE DEPTH (FT): 74

PHENOCRYST RATIO (Q/K/P): 1/1.07/0
POROSITY (VOL %): 21

DEGREE OF WELDING: Moderate
OXIDATION STATE OF Fe-Ti OXIDES: C3-C4

ROCK NAME: Rhyolitic Lithic-Crystal Tuff

GENERAL DESCRIPTION IN THIN SECTION: Fine- to medium-grained phenocrysts in a moderately welded groundmass. Pumice fragments resemble those in Samples MCG-628 and -629 (Unit 1b).

MINERAL COMPONENT	VOL. %	COMMENTS
Groundmass	38	
Glass	(64)	Incipient axiolitic devitrification. Intact bubble walls and Y-shaped shards are present.
Pumice	(36)	Up to 5.85 mm. Spherulitic devitrification. Phenocryst ratio (Q/K) = 1/3.83. Pyroxene phenocrysts are present. Some mineralization by tridymite or a zeolite.
Phenocrysts	21	
Sanidine	(49)	Fine to medium grained, anhedral to euhedral.
Quartz	(46)	Fine to medium grained, anhedral to euhedral. Some grains are embayed.
Opaques	(5)	Fine grained, anhedral to euhedral. Intergrown magnetite, ilmenite, and hematite.
Plagioclase	(tr)	Fine to medium grained, subhedral to euhedral.
Pyroxene	(tr)	Fine grained, anhedral to euhedral.
Amphibole	(tr)	Fine to medium grained, anhedral to euhedral.
Pore Space	21	

(continued on next page)

LANL VAPOR TRANSPORT STUDY
REQUEST NO.: 402553
PROJECT NO.: 6L0001000

SAMPLE NO.: MCG-632 (continued)
DRILL HOLE LLM-85-02 UNIT 2A (1B)
DRILL HOLE DEPTH (FT): 74

MINERAL COMPONENT	VOL. %	COMMENTS
Lithic Fragments	20	Up to 13.2 mm. Two large lithics fragments are strongly welded, crystal-vitric tuffs. Another large lithic is densely welded with totally devitrified glass. Andesites are also present.
Unknown Component	tr	Euhedral to subhedral grain shape, 0.54 mm, associated with sanidine and opaque grains in a glomerophenocryst. Grain has a thin, discontinuous rim of hematite with flakes of randomly oriented clay (chlorite?) and a grain of magnetite with exsolved ilmenite. Magnetite is altering to hematite. Grain also contains some remnant(?) pyroxene.

LANL VAPOR TRANSPORT STUDY
REQUEST NO.: 402553
PROJECT NO.: 6L0001000

SAMPLE NO.: MCG-633
DRILL HOLE LLM-85-02 UNIT 1B
DRILL HOLE DEPTH (FT): 111

PHENOCRYST RATIO (Q/K/P): 1/0.95/0
POROSITY (VOL %): 16

DEGREE OF WELDING: Moderate
OXIDATION STATE OF Fe-Ti OXIDES: C2-C3

ROCK NAME: Rhyolitic Lithic-Vitric Tuff

GENERAL DESCRIPTION IN THIN SECTION: Fine- to medium-grained phenocrysts in a moderately welded groundmass containing some brown glass. Large lithic fragments are present.

MINERAL COMPONENT	VOL. %	COMMENTS
Groundmass	41	
Glass	(61)	Incipient axiolitic devitrification. Mottled brown glass may indicate alteration to clay. Intact bubble walls and Y-shaped shards are present.
Pumice	(39)	Up to 9.11 mm. Spherulitic devitrification. Mineralization by a fibrous phase (zeolite?). Phenocryst ratio (Q/K) = 3/1.
Lithic Fragments	30	Up to 29.3 mm. Two major types: strongly welded, crystal-vitric tuff partially altered to clay, and a densely welded, vitric-crystal tuff that is totally devitrified.
Pore Space	16	
Phenocrysts	13	
Quartz	(49)	Fine to medium grained, anhedral to euhedral. Resorption features are common.
Sanidine	(46)	Fine to medium grained, anhedral to euhedral. Some embayments are present.
Opaques	(5)	Fine grained, anhedral to euhedral. Magnetite and ilmenite intergrowths.
Plagioclase	(tr)	Fine grained, subhedral to euhedral. Zoned grains are present.
Pyroxene	(tr)	Fine grained, anhedral. Associated with opaques.

LANL VAPOR TRANSPORT STUDY
REQUEST NO.: 402553
PROJECT NO.: 6L0001000

SAMPLE NO.: MCG-634
DRILL HOLE LLM-85-06 UNIT 2B
DRILL HOLE DEPTH (FT): 30

PHENOCRYST RATIO (Q/K/P): 1/1.20/0
POROSITY (VOL %): 25

DEGREE OF WELDING: Moderate
OXIDATION STATE OF Fe-Ti OXIDES: C3

ROCK NAME: Rhyolitic Crystal-Vitric Tuff

GENERAL DESCRIPTION IN THIN SECTION: Fine- to medium-grained phenocrysts in a moderately welded groundmass. Shards show axiolitic devitrification.

MINERAL COMPONENT	VOL. %		COMMENTS
Groundmass		45	
Glass	(84)		Axiolitic devitrification. Intact bubble walls and Y-shaped shards are present.
Pumice	(16)		Up to 8.15 mm. Two types are present: fragments replaced by sanidine and tridymite with quartz phenocrysts (dominant type), and andesitic fragments with plagioclase and amphibole phenocrysts and mineralization by tridymite.
Phenocrysts		26	
Sanidine	(53)		Fine to medium grained, anhedral to euhedral.
Quartz	(44)		Fine to medium grained, anhedral to euhedral. Embayments are present.
Opaques	(3)		Fine grained, anhedral to euhedral. Magnetite and ilmenite intergrowths.
Plagioclase	(tr)		Fine grained, euhedral to subhedral. Zoned grains are present.
Biotite	(tr)		Fine grained, anhedral.
Pyroxene	(tr)		Fine grained, anhedral to subhedral.
Amphibole	(tr)		Fine grained, anhedral.
Pore Space		25	

(continued on next page)

LANL VAPOR TRANSPORT STUDY
REQUEST NO.: 402553
PROJECT NO.: 6L0001000

SAMPLE NO.: MCG-634 (continued)
DRILL HOLE LLM-85-06 UNIT 2B
DRILL HOLE DEPTH (FT): 30

MINERAL COMPONENT	VOL. %	COMMENTS
Lithic Fragments	3	Up to 1.41 mm. Two types are present: densely welded, lithic tuff with spherulitic devitrification (see Samples MCG-550 and -645) and a strongly welded, vitric tuff which is devitrified.
Tridymite	tr	Occurs in pore spaces. Fine grained, euhedral.

LANL VAPOR TRANSPORT STUDY
REQUEST NO.: 402553
PROJECT NO.: 6L0001000

SAMPLE NO.: MCG-635
DRILL HOLE LLM-85-06 UNIT 2A
DRILL HOLE DEPTH (FT): 50

PHENOCRYST RATIO (Q/K/P): 1/1.22/0.07 DEGREE OF WELDING: Slight to Moderate
POROSITY (VOL %): 19 OXIDATION STATE OF Fe-Ti OXIDES: C3

ROCK NAME: Rhyolitic Lithic-Crystal Tuff

GENERAL DESCRIPTION IN THIN SECTION: Fine- to medium-grained phenocrysts in a slightly to moderately welded groundmass.

MINERAL COMPONENT	VOL. %		COMMENTS
Groundmass		36	
Glass	(61)		Incipient axiolitic devitrification. Intact bubble walls and Y-shaped shards are present.
Pumice	(39)		Up to 5.70 mm. Axiolitic devitrification and some replacement by sanidine and tridymite. Only quartz phenocrysts are present.
Phenocrysts		22	
Sanidine	(50)		Fine to medium grained, anhedral to euhedral.
Quartz	(41)		Fine to medium grained, anhedral to euhedral. Resorption features are common.
Opaques	(4.5)		Fine grained, anhedral to euhedral. Magnetite and ilmenite intergrowths.
Plagioclase	(3)		Fine grained, subhedral to euhedral. Zoned grains are present.
Pyroxene	(1.5)		Fine grained, euhedral to subhedral. Associated with opaques.
Lithic Fragments		22	Up to 19.3 mm. Predominant type of lithic is a strongly welded, crystal-vitric tuff containing pumice fragments from Unit 1b. Another type has a spongy lithology consisting of sanidine crystals.
Pore Space		19	

(continued on next page)

LANL VAPOR TRANSPORT STUDY
REQUEST NO.: 402553
PROJECT NO.: 6L0001000

SAMPLE NO.: MCG-635 (continued)
DRILL HOLE LLM-85-06 UNIT 2A
DRILL HOLE DEPTH (FT): 50

MINERAL COMPONENT	VOL. %	COMMENTS
Tridymite	1	Fine grained, euhedral. Occurs in pores.
Unknown Component	tr	Rounded grains, 0.54 and 0.91 mm, consisting of a discontinuous rim of hematite and magnetite with exsolved ilmenite. Some rutile is associated with grains of magnetite; magnetite is altering to hematite. The interiors of these rounded grains contain randomly oriented clay (chlorite?) flakes and epidote or pyroxene.

LANL VAPOR TRANSPORT STUDY
REQUEST NO.: 402553
PROJECT NO.: 6L0001000

SAMPLE NO.: MCG-636
DRILL HOLE LLM-85-06 UNIT 1B
DRILL HOLE DEPTH (FT): 99

PHENOCRYST RATIO (Q/K/P): 1/1.53/0
POROSITY (VOL %): 26

DEGREE OF WELDING: Moderate
OXIDATION STATE OF Fe-Ti OXIDES: C1-C2

ROCK NAME: Rhyolitic Vitric-Crystal Tuff

GENERAL DESCRIPTION IN THIN SECTION: Fine- to medium-grained phenocrysts in a fresh-glass groundmass. Glass in pumice fragments is fresh and not devitrified. Some pumice fragments are flattened.

MINERAL COMPONENT	VOL. %		COMMENTS
Groundmass		57	
Glass	(53)		Moderate welding, brown glass; not devitrified. Intact bubble walls and Y-shaped shards are present.
Pumice	(47)		Up to 5.93 mm. Some of the fragments are flattened. Glass is not devitrified. Phenocryst ratio (Q/K) for flattened pumice is 1/11; for non-flattened pumice, 1/1.25. Overall pumice phenocryst ratio is 1/3.20.
Pore Space		26	
Phenocrysts		17	
Sanidine	(57)		Fine to medium grained, anhedral to euhedral.
Quartz	(37)		Fine to medium grained, anhedral to euhedral.
Opaques	(4)		Fine grained, anhedral to euhedral. Magnetite, and magnetite with exsolved ilmenite.
Pyroxene	(2)		Fine grained, anhedral to euhedral.
Plagioclase	(tr)		Fine grained, anhedral.
Lithic Fragments		tr	Up to 1.42 mm. Hyalopilitic basalt/andesite.

LANL VAPOR TRANSPORT STUDY
REQUEST NO.: 402553
PROJECT NO.: 6L0001000

SAMPLE NO.: MCG-637
DRILL HOLE LLM-85-06 UNIT 1A
DRILL HOLE DEPTH (FT): 113

PHENOCRYST RATIO: Not Determined
DEGREE OF WELDING: Not Welded
POROSITY (VOL %): Not Determined
OXIDATION STATE OF Fe-Ti OXIDES: C3 (Pumice)

ROCK NAME: Rhyolitic Vitric-Crystal(?) Tuff

GENERAL DESCRIPTION IN THIN SECTION: The sample was not welded and the thin-section preparer provided a section of the pumice fragments only. Grain mounts of the fine fraction were prepared in immersion oil and Canada balsam. Each of these mounts contains brown-glass shards and a large proportion of fine, flattened pumice fragments. The glass in the shards and fine pumice fragments is not devitrified. Phenocrysts of sanidine, quartz, zoned plagioclase, opaques, pyroxene, and amphibole are present in the fine fraction. The medium fraction was examined using a binocular microscope. This fraction consisted of quartz and sanidine phenocrysts, pumice fragments, and lithic fragments. The coarse pumice fragments are similar to those in Sample MCG-636; some of these are flattened. Compositions of the coarse pumice fragments (based on phenocrysts) are rhyolitic to andesitic. The largest pumice fragment (26 mm) contains zoned plagioclase, euhedral lamprobolite, and anhedral pyroxene phenocrysts in a partially flattened pumice structure. Other pumice fragments range from not flattened to totally collapsed; glass is not devitrified.

LANL VAPOR TRANSPORT STUDY
REQUEST NO.: 402553
PROJECT NO.: 6L0001000

SAMPLE NO.: MCG-638
DRILL HOLE LLM-85-11 UNIT 2B
DRILL HOLE DEPTH (FT): 5

PHENOCRYST RATIO (Q/K/P): 1/1.82/0
POROSITY (VOL %): 22

DEGREE OF WELDING: Slight to Moderate
OXIDATION STATE OF Fe-Ti OXIDES: C3-C4

ROCK NAME: Rhyolitic Crystal-Vitric Tuff

GENERAL DESCRIPTION IN THIN SECTION: Fine- to medium-grained phenocrysts in a groundmass exhibiting slight to moderate welding and axiolitic devitrification of glass.

MINERAL COMPONENT	VOL. %		COMMENTS
Groundmass		55	
Glass	(65)		Axiolitic devitrification.
Pumice	(35)		Up to 2.52 mm. Replaced/mineralized by sanidine and tridymite. Phenocryst ratio (Q/K) = 1/2.25. Opaque and zircon phenocrysts are also present.
Pore Space		22	
Phenocrysts		21	
Sanidine	(63)		Fine to medium grained, anhedral to euhedral.
Quartz	(34)		Fine to medium grained, anhedral to euhedral. Some embayments are present.
Opaques	(3)		Fine grained, anhedral to euhedral. Magnetite, ilmenite, and hematite intergrowths.
Pyroxene	(tr)		Fine grained, anhedral to euhedral. Associated with opaques.
Plagioclase	(tr)		Fine grained, anhedral to subhedral. Zoned grains are present.
Amphibole	(tr)		Fine grained, anhedral.
Lithic Fragments		2	Up to 3.64 mm. Several types: strongly welded, vitric-crystal tuff, both devitrified and nondevitrified varieties; andesitic tuff, not devitrified; and hyalopilitic basalt.

LANL VAPOR TRANSPORT STUDY
REQUEST NO.: 402553
PROJECT NO.: 6L0001000

SAMPLE NO.: MCG-639
DRILL HOLE LLM-85-11 UNIT 2B
DRILL HOLE DEPTH (FT): 30.5

PHENOCRYST RATIO (Q/K/P): 1/0.77/0
POROSITY (VOL %): 24

DEGREE OF WELDING: Moderate
OXIDATION STATE OF Fe-Ti OXIDES: C4

ROCK NAME: Rhyolitic Crystal-Lithic Tuff

GENERAL DESCRIPTION IN THIN SECTION: Fine- to medium-grained phenocrysts in a moderately welded, devitrified groundmass.

MINERAL COMPONENT	VOL. %		COMMENTS
Groundmass		42	
Glass	(70)		Axiolitic devitrification. Intact bubble walls and Y-shaped shards are present.
Pumice	(30)		Up to 4.89 mm. Replaced/mineralized by sanidine and tridymite. Phenocryst ratio (Q/K) = 1/2.
Pore Space		24	
Phenocrysts		24	
Quartz	(55)		Fine to medium grained, anhedral to euhedral. Some embayments are present.
Sanidine	(42)		Fine to medium grained, anhedral to euhedral.
Opaques	(3)		Fine grained, anhedral to euhedral. Magnetite, ilmenite, and hematite intergrowths.
Pyroxene	(tr)		Fine grained, subhedral to euhedral.
Plagioclase	(tr)		Fine grained, euhedral. Zoned grains.
Amphibole	(tr)		Fine grained, subhedral.
Lithic Fragments		10	Up to 31.9 mm. Lenticular, strongly welded, crystal-vitric tuff with axiolitic devitrification and hyalopilitic basalts.

LANL VAPOR TRANSPORT STUDY
REQUEST NO.: 402553
PROJECT NO.: 6L0001000

SAMPLE NO.: MCG-640
DRILL HOLE LLM-85-11 UNIT 1B
DRILL HOLE DEPTH (FT): 95

PHENOCRYST RATIO (Q/K/P): 1/1.30/0
POROSITY (VOL %): 16

DEGREE OF WELDING: Moderate
OXIDATION STATE OF Fe-Ti OXIDES: C2

ROCK NAME: Rhyolitic Lithic-Vitric Tuff

GENERAL DESCRIPTION IN THIN SECTION: Fine- to medium-grained phenocrysts in a moderately welded groundmass.

MINERAL COMPONENT	VOL. %	COMMENTS
Groundmass	41	
Glass	(58)	Not devitrified; some brown glass is present.
Pumice	(42)	Up to 8.52 mm. Three types of pumice are present: nonflattened pumice with spherulitic devitrification [phenocryst ratio (Q/K) = 1/3]; flattened pumice that is not devitrified; and nonflattened pumice of andesitic composition.
Lithic Fragments	27	Up to 14.8 mm. Three types are present: strongly welded, crystal-vitric tuff; densely welded, vitric-crystal tuff that is totally devitrified; and altered basalt.
Pore Space	16	
Phenocrysts	16	
Sanidine	(54)	Fine to medium grained, anhedral to euhedral.
Quartz	(42)	Fine to medium grained, anhedral to euhedral. Some embayments are present.
Opaques	(2)	Fine grained, anhedral to euhedral. Magnetite with exsolved ilmenite.
Pyroxene	(2)	Fine grained, anhedral to euhedral.
Amphibole	(tr)	Fine grained, subhedral.

LANL VAPOR TRANSPORT STUDY
REQUEST NO.: 402553
PROJECT NO.: 6L0001000

SAMPLE NO.: MCG-641
DRILL HOLE LLM-85-11 UNIT 1A
DRILL HOLE DEPTH (FT): 116

PHENOCRYST RATIO: Not Determined
DEGREE OF WELDING: Not Welded
POROSITY (VOL %): Not Determined
OXIDATION STATE OF Fe-Ti OXIDES: C2 (Pumice)

ROCK NAME: Rhyolitic Vitric-Crystal(?) Tuff

GENERAL DESCRIPTION IN THIN SECTION: The sample was not welded and the thin-section preparer provided a section of the pumice fragments only. A grain mount of the fine fraction was prepared in Canada balsam. The fine fraction consists of glass shards, flattened pumice fragments, phenocrysts of quartz, sanidine, plagioclase, pyroxene, amphibole, and opaques. Goethite and goethite-stained material is present in the fine fraction. Glass is not devitrified in the shards and pumice fragments. The medium fraction was examined using a binocular microscope. This fraction consists of quartz, sanidine, opaque phenocrysts, and pumice (some flattened) and lithic fragments. The coarse pumice fragments have rhyolitic compositions based on the phenocrysts of sanidine, quartz, opaques, and (few) pyroxene. The pumice fragments vary from partially flattened to not flattened. Glass in the pumice fragments is not devitrified.

LANL VAPOR TRANSPORT STUDY
REQUEST NO.: 402553
PROJECT NO.: 6L0001000

SAMPLE NO.: MCG-642
DRILL HOLE LLM-85-14 UNIT 2B (LITHIC)
DRILL HOLE DEPTH (FT): 18

PHENOCRYST RATIO (Pl/Px): 4.57/1
POROSITY (VOL %): 5

DEGREE OF WELDING: Dense
OXIDATION STATE OF Fe-Ti OXIDES: C3-C4

ROCK NAME: Basalt Porphyry

GENERAL DESCRIPTION IN THIN SECTION: Fine- to medium-grained phenocrysts in a hyalopilitic groundmass.

MINERAL COMPONENT	VOL. %		COMMENTS
Groundmass		67	
Glass	(56)		Spherulitic devitrification.
Plagioclase Laths	(41)		Very fine grained, euhedral to subhedral.
Opaques	(3)		Very fine grained, anhedral to euhedral. Magnetite, ilmenite, and hematite.
Phenocrysts		28	
Plagioclase	(77)		Fine to medium grained, euhedral to anhedral. Spongy resorption textures.
Pyroxene	(17)		Fine to medium grained, euhedral to subhedral. Pigeonite.
Opaques	(6)		Fine grained, anhedral to euhedral. Magnetite, ilmenite, and hematite intergrowths.
Pore Space		5	Microporosity (in the groundmass) around and within some plagioclase phenocrysts.
Fracture Filling		tr	Goethite.

LANL VAPOR TRANSPORT STUDY
REQUEST NO.: 402553
PROJECT NO.: 6L0001000

SAMPLE NO.: MCG-643
DRILL HOLE LLM-85-13 UNIT 2B
DRILL HOLE DEPTH (FT): 42

PHENOCRYST RATIO (Q/K/P): 1/3.06/0.17 DEGREE OF WELDING: Moderate
POROSITY (VOL %): 28 OXIDATION STATE OF Fe-Ti OXIDES: C2

ROCK NAME: Rhyolitic Crystal-Lithic Tuff

GENERAL DESCRIPTION IN THIN SECTION: Fine- to medium-grained phenocrysts in a moderately welded groundmass with axiolitic devitrification. Glass has coatings of clay.

MINERAL COMPONENT	VOL. %		COMMENTS
Groundmass		34	
Glass	(81)		Axiolitic devitrification. Intact bubble walls and Y-shaped shards are present. Clay coatings are present.
Pumice	(19)		Up to 2.06 mm. Replaced/mineralized by sanidine and tridymite. No phenocrysts are present.
Pore Space		28	
Phenocrysts		27	
Sanidine	(68)		Fine to medium grained, anhedral to subhedral.
Quartz	(23)		Fine to medium grained, anhedral to euhedral. Embayed grains are present.
Plagioclase	(4)		Fine to medium grained, subhedral to euhedral.
Opaques	(4)		Fine grained, anhedral to euhedral. Magnetite with exsolved ilmenite; one grain contains an inclusion of pyrite.
Amphibole	(1)		Fine to medium grained, subhedral.
Pyroxene	(tr)		Fine grained, subhedral to euhedral.
Lithic Fragments		10	Up to 11.1 mm. Andesitic crystal-vitric tuff.
Tridymite		1	Very fine grained; occurs in pores.

LANL VAPOR TRANSPORT STUDY
REQUEST NO.: 402553
PROJECT NO.: 6L0001000

SAMPLE NO.: MCG-644
DRILL HOLE LLM-85-17 UNIT 2B
DRILL HOLE DEPTH (FT): 11

PHENOCRYST RATIO (Q/K/P): 1/1.75/0
POROSITY (VOL %): 25

DEGREE OF WELDING: Moderate
OXIDATION STATE OF Fe-Ti OXIDES: C3-C4

ROCK NAME: Rhyolitic Crystal-Lithic Tuff

GENERAL DESCRIPTION IN THIN SECTION: Fine- to medium-grained phenocrysts in a moderately welded groundmass. Although this sample has a fracture containing smectite, no clay was observed in thin section.

MINERAL COMPONENT	VOL. %		COMMENTS
Groundmass		41	
Glass	(71)		Axiolitic devitrification is present.
Pumice	(29)		Up to 3.39 mm. Replaced/mineralized by sanidine and tridymite. Phenocryst ratio (Q/K) = 1/1.
Pore Space		25	
Phenocrysts		23	
Sanidine	(61)		Fine to medium grained, anhedral to euhedral.
Quartz	(35)		Fine to medium grained, anhedral to subhedral. Some grains are embayed.
Opaques	(3)		Fine grained, anhedral to euhedral. Ilmenite with exsolved magnetite; grains of rutile are present.
Pyroxene	(1)		Fine grained, subhedral to anhedral.
Plagioclase	(tr)		Fine grained, euhedral. Zoned grains are present.
Lithic Fragments		10	Up to 12.7 mm. Several types: strongly welded, crystal-vitric tuff with fresh glass; densely welded, vitric-crystal tuff with coarse spherulitic devitrification; and a devitrified, andesitic/latitic vitric tuff.
Tridymite		1	Fine grained, euhedral. Occurs in pore spaces.

LANL VAPOR TRANSPORT STUDY
REQUEST NO.: 402553
PROJECT NO.: 6L0001000

SAMPLE NO.: MCG-645
DRILL HOLE LLM-85-17 UNIT 1B (LITHIC)
DRILL HOLE DEPTH (FT): 109

PHENOCRYST RATIO (Q/K/P): 1/4.33/0.67 DEGREE OF WELDING: Dense
POROSITY (VOL %): 9 OXIDATION STATE OF Fe-Ti OXIDES: C3-C4

ROCK NAME: Rhyolitic Vitric Tuff

GENERAL DESCRIPTION IN THIN SECTION: Densely welded glass with lithophysae filled by sanidine, tridymite, opaques, and late-stage alpha quartz. A few fine- to medium-grained phenocrysts are present.

MINERAL COMPONENT		VOL. %	COMMENTS
Groundmass		53	Densely welded glass with well-developed spherulitic devitrification. Glass is brown in part.
Vapor Phase Minerals		33	
Sanidine	(70)		Porous, microcrystalline linings of lithophysae.
Tridymite	(23)		Fine grained, euhedral. Partially fills interiors of lithophysae. Wedge-shaped twins are common.
Alpha Quartz	(4)		Fine grained, anhedral to euhedral. Late-stage lining and filling of lithophysae.
Opaques	(3)		Fine grained, anhedral. Associated with sanidine stage of lithophysae filling. Magnetite/ilmenite altering to hematite.
Pore Space		9	Associated with vapor-phase crystallites.
Phenocrysts		5	
Sanidine	(56)		Fine to medium grained, euhedral to subhedral.
Alpha Quartz	(44)		Fine grained, anhedral to euhedral. Embayed grains are present.
Opaques	(tr)		Fine grained, euhedral. Magnetite intergrown with ilmenite.
Plagioclase	(tr)		Fine grained, euhedral.

LANL VAPOR TRANSPORT STUDY
REQUEST NO.: 402553
PROJECT NO.: 6L0001000

SAMPLE NO.: MCG-646
DRILL HOLE LLM-85-09 UNIT 2B
DRILL HOLE DEPTH (FT): 10

PHENOCRYST RATIO (Q/K/P): 1/1.64/0
POROSITY (VOL %): 21

DEGREE OF WELDING: Moderate
OXIDATION STATE OF Fe-Ti OXIDES: C3-C4

ROCK NAME: Rhyolitic Crystal-Vitric Tuff

GENERAL DESCRIPTION IN THIN SECTION: Fine- to medium-grained phenocrysts in a moderately welded groundmass with axiolitic devitrification.

MINERAL COMPONENT	VOL. %		COMMENTS
Groundmass		55	
Glass	(68)		Axiolitic devitrification.
Pumice	(32)		Up to 9.93 mm. Replaced/mineralized by sanidine and tridymite.
Phenocrysts		22	
Sanidine	(62)		Fine to medium grained, anhedral to euhedral.
Quartz	(38)		Fine to medium grained, anhedral to euhedral. Embayed grains are present.
Pyroxene	(tr)		Fine grained, anhedral to subhedral.
Opaques	(tr)		Fine grained, anhedral to euhedral. Magnetite, ilmenite, hematite, and rutile.
Plagioclase	(tr)		Fine grained, euhedral. Zoned grain.
Allanite(?)	(tr)		Fine grained, euhedral.
Pore Space		21	
Lithic Fragments		2	Up to 1.70 mm. Mostly basalts.
Tridymite		tr	Fine grained, euhedral. Occurs in pore spaces.

LANL VAPOR TRANSPORT STUDY
REQUEST NO.: 402553
PROJECT NO.: 6L0001000

SAMPLE NO.: MCG-647
DRILL HOLE LLM-85-09 UNIT 2B
DRILL HOLE DEPTH (FT): 20

PHENOCRYST RATIO (Q/K/P): 1/2.77/0.04 DEGREE OF WELDING: Moderate
POROSITY (VOL %): 22 OXIDATION STATE OF Fe-Ti OXIDES: C2-C3

ROCK NAME: Rhyolitic Crystal-Vitric Tuff

GENERAL DESCRIPTION IN THIN SECTION: Fine- to medium-grained phenocrysts in a moderately welded groundmass with axiolitic devitrification.

MINERAL COMPONENT	VOL. %		COMMENTS
Groundmass		42	
Glass	(69)		Axiolitic devitrification.
Pumice	(31)		Up to 10.37 mm. Replaced/mineralized by sanidine and tridymite. Phenocryst ratio (Q/K) = 1/1.
Phenocrysts		34	
Sanidine	(71)		Fine to medium grained, anhedral to euhedral.
Quartz	(26)		Fine to medium grained, anhedral to euhedral.
Opaques	(2)		Fine grained, anhedral to euhedral. Magnetite and ilmenite intergrowths.
Plagioclase	(1)		Fine to medium grained, subhedral to euhedral. Some grains are zoned.
Pyroxene	(tr)		Fine grained, anhedral to subhedral.
Pore Space		22	
Lithic Fragments		2	Up to 1.30 mm. Mostly basalts.
Tridymite		tr	Fine grained, euhedral to anhedral. Occurs in pore space.
Unknown Component		tr	Rounded grain, 0.32 mm, consisting of a partial rim of hematite and randomly oriented flakes of clay (chlorite?). A grain of ilmenite with exsolved hematite is present as an inclusion.

LANL VAPOR TRANSPORT STUDY
REQUEST NO.: 402553
PROJECT NO.: 6L0001000

SAMPLE NO.: MCG-648
DRILL HOLE LLM-85-09 UNIT 2A
DRILL HOLE DEPTH (FT): 35

PHENOCRYST RATIO (Q/K/P): 1/2.17/0
POROSITY (VOL %): 26

DEGREE OF WELDING: Moderate
OXIDATION STATE OF Fe-Ti OXIDES: C3-C4

ROCK NAME: Rhyolitic Crystal-Vitric Tuff

GENERAL DESCRIPTION IN THIN SECTION: Fine- to medium-grained phenocrysts in a moderately welded groundmass with axiolitic devitrification. Although this sample has a fracture containing smectite, no clay was observed in thin section.

MINERAL COMPONENT	VOL. %		COMMENTS
Groundmass		48	
Glass	(70)		Axiolitic devitrification.
Pumice	(30)		Up to 4.70 mm. Replaced/mineralized by sanidine and tridymite. Phenocryst ratio (Q/K) = 1/1.
Pore Space		26	
Phenocrysts		25	
Sanidine	(68)		Fine to medium grained, anhedral to euhedral.
Quartz	(32)		Fine to medium grained, anhedral to euhedral. Embayed grains are present.
Pyroxene	(tr)		Fine grained, euhedral to anhedral.
Opaques	(tr)		Fine grained, subhedral to anhedral. Magnetite, ilmenite, and hematite.
Plagioclase	(tr)		Medium grained, euhedral. Zoned grain.
Amphibole	(tr)		Fine grained, anhedral.
Lithic Fragments		tr	Up to 1.67 mm. Mostly basalt/andesite.
Tridymite		tr	Fine grained, euhedral. Occurs in pore space.

(continued on next page)

LANL VAPOR TRANSPORT STUDY
REQUEST NO.: 402553
PROJECT NO.: 6L0001000

SAMPLE NO.: MCG-648 (continued)
DRILL HOLE LLM-85-09 UNIT 2A
DRILL HOLE DEPTH (FT): 35

MINERAL COMPONENT	VOL. %	COMMENTS
Unknown Component	tr	Two grains. One is rounded, 0.80 mm, with a thin rim of hematite and almost totally filled by sheaves of clay (chlorite?); inclusion of magnetite (altering to hematite) with exsolved ilmenite. The other is subhedral, 0.29 mm, with a thin rim of hematite and sparse, randomly oriented flakes of clay (chlorite?).

LANL VAPOR TRANSPORT STUDY
REQUEST NO.: 402553
PROJECT NO.: 6L0001000

SAMPLE NO.: MCG-649
DRILL HOLE LLM-85-09 UNIT 1B
DRILL HOLE DEPTH (FT): 47

PHENOCRYST RATIO (Q/K/P): 1/0.81/0.03 DEGREE OF WELDING: Moderate
POROSITY (VOL %): 21 OXIDATION STATE OF Fe-Ti OXIDES: C2-C3

ROCK NAME: Rhyolitic Crystal-Vitric Tuff

GENERAL DESCRIPTION IN THIN SECTION: Fine- to medium-grained phenocrysts in a groundmass containing glass that is not devitrified. Brown-colored glass is present in the groundmass and some pumice fragments.

MINERAL COMPONENT	VOL. %		COMMENTS
Groundmass		54	
Glass	(66)		Not devitrified. Some brown glass.
Pumice Fragments	(34)		Up to 7.78 mm. Some flattened fragments and andesitic compositions (based on phenocrysts). Phenocryst ratio in rhyolitic fragments (Q/K) = 1/1.83.
Phenocrysts		23	
Quartz	(52)		Fine to medium grained, anhedral to euhedral. Some grains are embayed.
Sanidine	(42)		Fine to medium grained, anhedral to euhedral.
Opaques	(4)		Fine grained, anhedral to euhedral. Magnetite and ilmenite intergrowths.
Plagioclase	(2)		Fine grained, subhedral. Zoned grain.
Pyroxene	(tr)		Fine grained, anhedral to euhedral.
Pore Space		21	
Lithic Fragments		2	Up to 0.97 mm. Several types: altered, flow-banded rock; altered, spherulitically devitrified rock; aphanitic rock; and hyalopilitic basalt.

LANL VAPOR TRANSPORT STUDY
REQUEST NO.: 402553
PROJECT NO.: 6L0001000

SAMPLE NO.: MCG-650
DRILL HOLE LLM-85-09 UNIT 1B
DRILL HOLE DEPTH (FT): 68

PHENOCRYST RATIO (Q/K/P): 1/1.04/0
POROSITY (VOL %): 24

DEGREE OF WELDING: Moderate
OXIDATION STATE OF Fe-Ti OXIDES: C3

ROCK NAME: Rhyolitic Vitric-Crystal Tuff

GENERAL DESCRIPTION IN THIN SECTION: Fine- to medium-grained phenocrysts in a moderately welded groundmass. Shards exhibit incipient axiolitic devitrification. Most pumice fragments have spherulitic devitrification.

MINERAL COMPONENT		VOL. %	COMMENTS
Groundmass		55	
Glass	(54)		Incipient axiolitic devitrification.
Pumice Fragments	(46)		Up to 6.74 mm. Most have spherulitic devitrification. Some are partially flattened. An andesitic composition (based on phenocrysts) is present. Phenocryst ratio (Q/K) in rhyolitic fragments is 1/1.33.
Pore Space		24	
Phenocrysts		18	
Sanidine	(47)		Fine to medium grained, anhedral to euhedral.
Quartz	(45)		Fine to medium grained, anhedral to euhedral. Resorption features are abundant.
Opaques	(6)		Fine grained, anhedral to euhedral. Ilmenite with exsolved magnetite.
Pyroxene	(2)		Fine grained, anhedral to euhedral. Most grains are associated with opaques; some grains are coated with celadonite.
Lithic Fragments		3	Up to 3.41 mm. Several types: altered basalt; hyalopilitic basalt; vitric tuff with spherulitic devitrification; granophyre; and an altered, flow-banded rock.

Appendix C

MOISTURE CHARACTERISTIC CURVES

Table C-1. Data Used to Plot the Moisture Characteristic Curves (drying curves only)

Hole Number	Sample Number	Depth (ft)	Capillary Pressure (psi)	Wetting Fluid Saturation (percent)
LLM-85-01	MCG-602	30	0.510	91.6
			0.906	86.4
			1.420	81.2
			2.055	76.1
			2.814	70.9
			3.701	65.8
LLM-85-01	MCG-603	52	0.455	90.0
			0.823	84.7
			1.385	79.7
			2.230	74.9
			3.495	70.2
			5.403	65.8
LLM-85-01	MCG-604	101	0.493	88.6
			0.955	82.1
			1.738	76.6
			3.220	71.9
			6.555	67.8
LLM-85-01	MCG-605	124	0.392	83.5
			0.620	76.9
			0.955	70.5
			1.450	64.4
			2.189	58.5
			3.319	52.9
LLM-85-02	MCG-606	7	0.392	88.6
			0.812	81.1
			1.450	73.9
			2.372	66.8
			3.663	60.0
			5.440	53.3
LLM-85-02	MCG-607	36	0.097	92.0
			0.181	87.3
			0.494	79.1
			0.799	75.8
			1.382	73.4
			2.975	71.8
LLM-85-02	MCG-608	67	0.424	90.7
			0.681	86.6
			1.050	82.6
			1.573	78.7
			2.315	75.0
			3.375	71.5

Table C-1 (continued). Data Used to Plot the Moisture Characteristic Curves (drying curves only)

Hole Number	Sample Number	Depth (ft)	Capillary Pressure (psi)	Wetting Fluid Saturation (percent)
LLM-85-02	MCG-609	117	0.252	94.2
			0.626	89.3
			1.135	84.2
			1.757	79.1
			2.474	73.9
			3.268	68.6
LLM-85-05	MCG-610	15	0.174	90.0
			0.328	84.5
			0.563	79.1
			0.913	73.9
			1.429	68.9
			2.188	64.2
LLM-85-05	MCG-611	36	0.259	96.1
			1.014	90.8
			1.879	85.0
			2.715	78.5
			3.482	71.4
			4.171	63.7
LLM-85-05	MCG-612	76	0.072	97.1
			0.344	94.0
			0.800	90.9
			1.424	87.8
			2.198	84.6
			3.109	81.4
LLM-85-05	MCG-613	123	0.166	85.1
			0.243	82.4
			0.382	79.7
			0.671	77.1
			1.426	74.6
			4.598	72.1
LGM-85-06	MCG-614	29	0.446	83.2
			0.679	77.2
			1.020	71.4
			1.526	65.8
			2.295	60.5
			3.500	55.4

Table C-1 (continued). Data Used to Plot the Moisture Characteristic Curves (drying curves only)

Hole Number	Sample Number	Depth (ft)	Capillary Pressure (psi)	Wetting Fluid Saturation (percent)
LGM-85-06	MCG-615	51	0.419	90.8
			0.650	86.9
			0.970	83.1
			1.411	79.5
			2.016	76.0
			2.850	72.6
LGM-85-06	MCG-616	99	0.322	85.6
			0.403	85.4
			0.542	84.5
			0.818	84.3
			1.527	83.4
			4.825	82.2
LGM-85-06	MCG-617	115	0.068	96.9
			0.309	92.3
			0.810	87.8
			1.716	83.6
			2.388	81.6
			3.259	79.6
LGM-85-11	MCG-618	3	0.296	88.7
			0.594	81.9
			1.063	75.3
			1.775	69.0
			2.841	62.9
			4.429	57.1
LGM-85-11	MCG-619	30	0.491	90.5
			1.188	81.6
			2.040	72.3
			2.976	62.6
			3.950	52.5
			4.934	42.0
LGM-85-11	MCG-620	94	0.161	93.3
			0.376	88.7
			0.734	84.2
			1.297	79.9
			2.163	75.8
			3.483	71.9

Table C-1 (continued). Data Used to Plot the Moisture Characteristic Curves (drying curves only)

Hole Number	Sample Number	Depth (ft)	Capillary Pressure (psi)	Wetting Fluid Saturation (percent)
LGM-85-11	MCG-621	115	0.270	92.3
			0.446	89.2
			0.727	86.3
			1.191	83.5
			1.991	80.9
			3.463	78.5

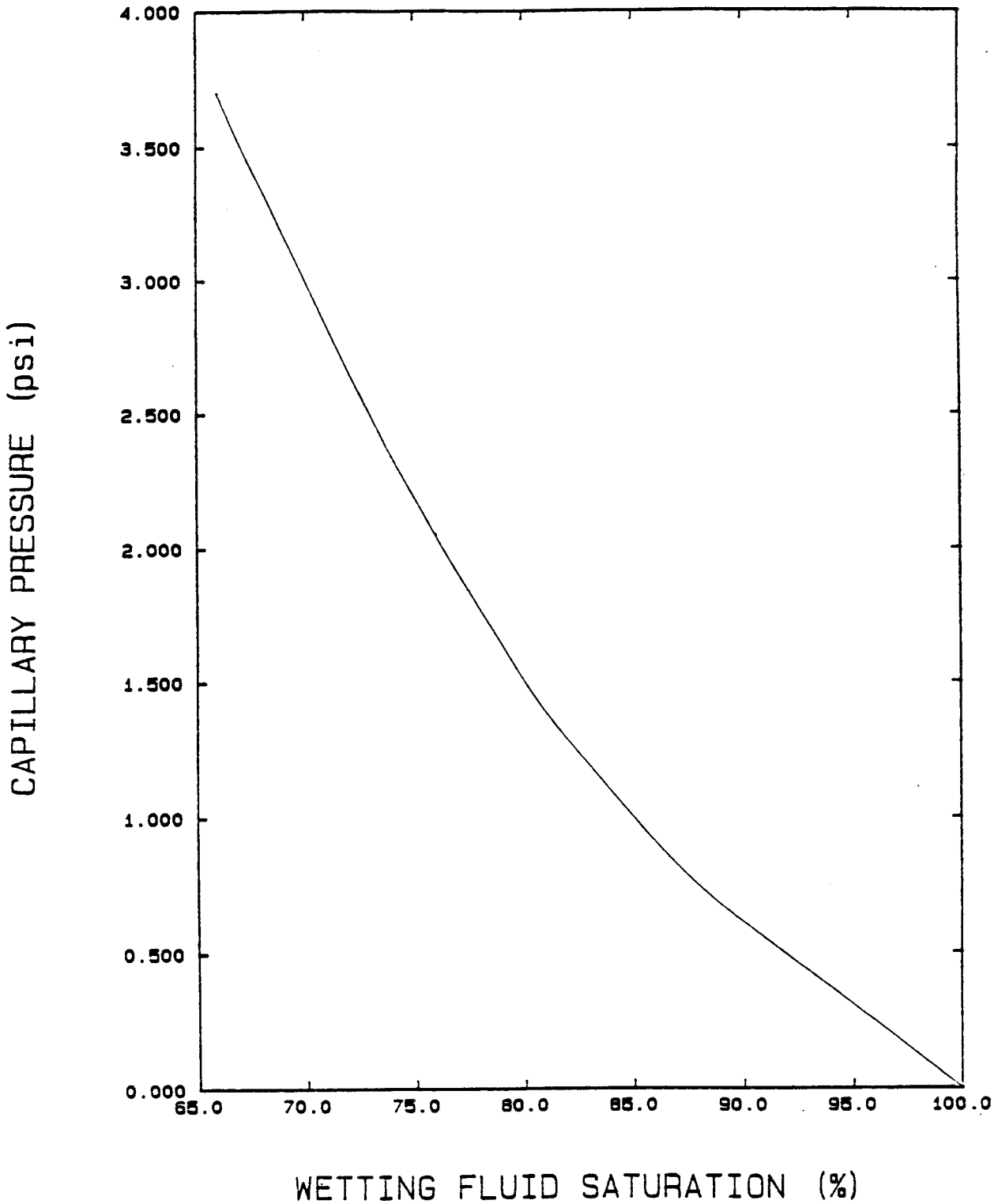

Figure C-1. Moisture Characteristic Curve for Sample MCG-602, Hole LLM-85-01, Depth of 30 Feet

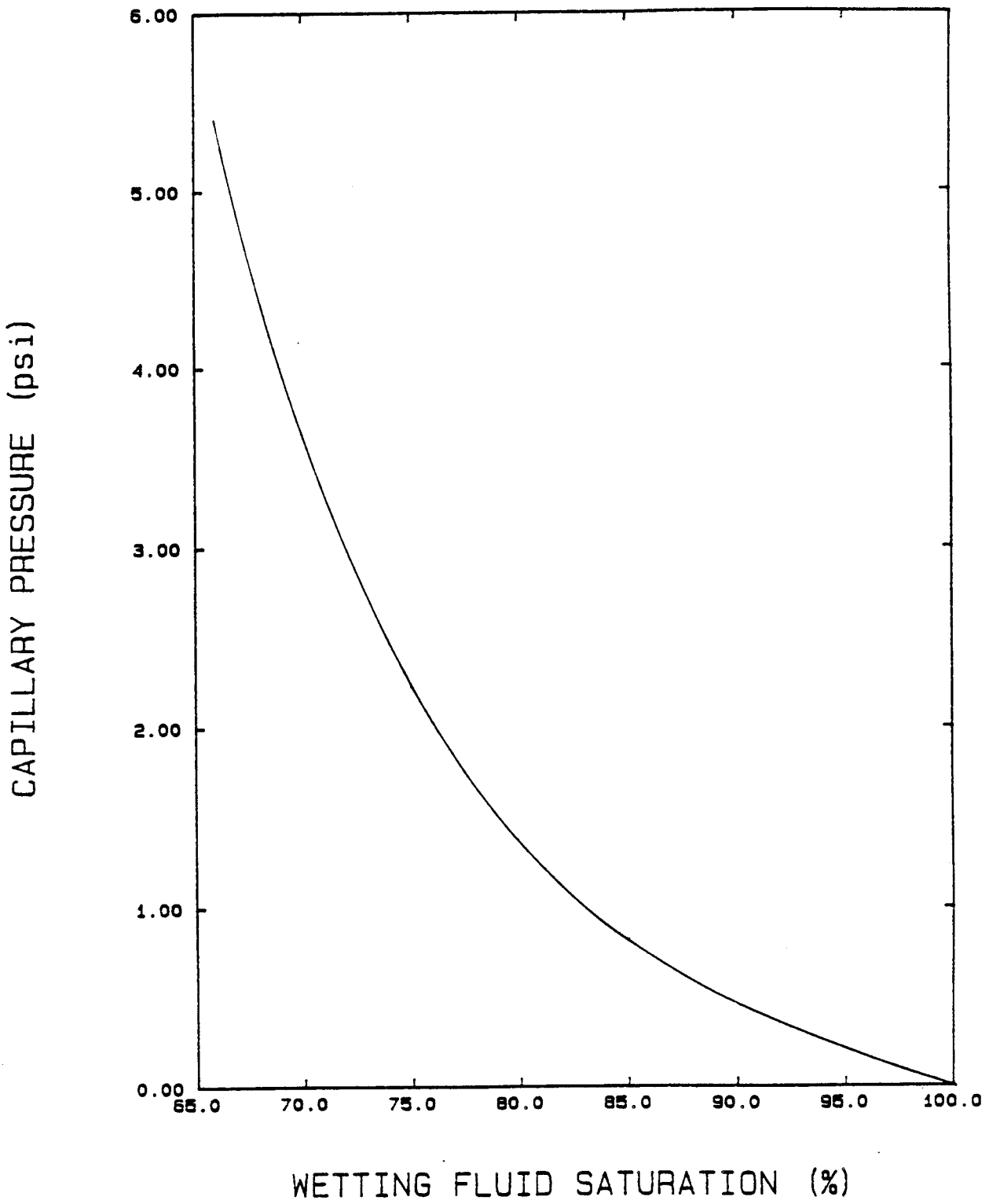

Figure C-2. Moisture Characteristic Curve for Sample MCG-603, Hole LLM-85-01, Depth of 52 Feet

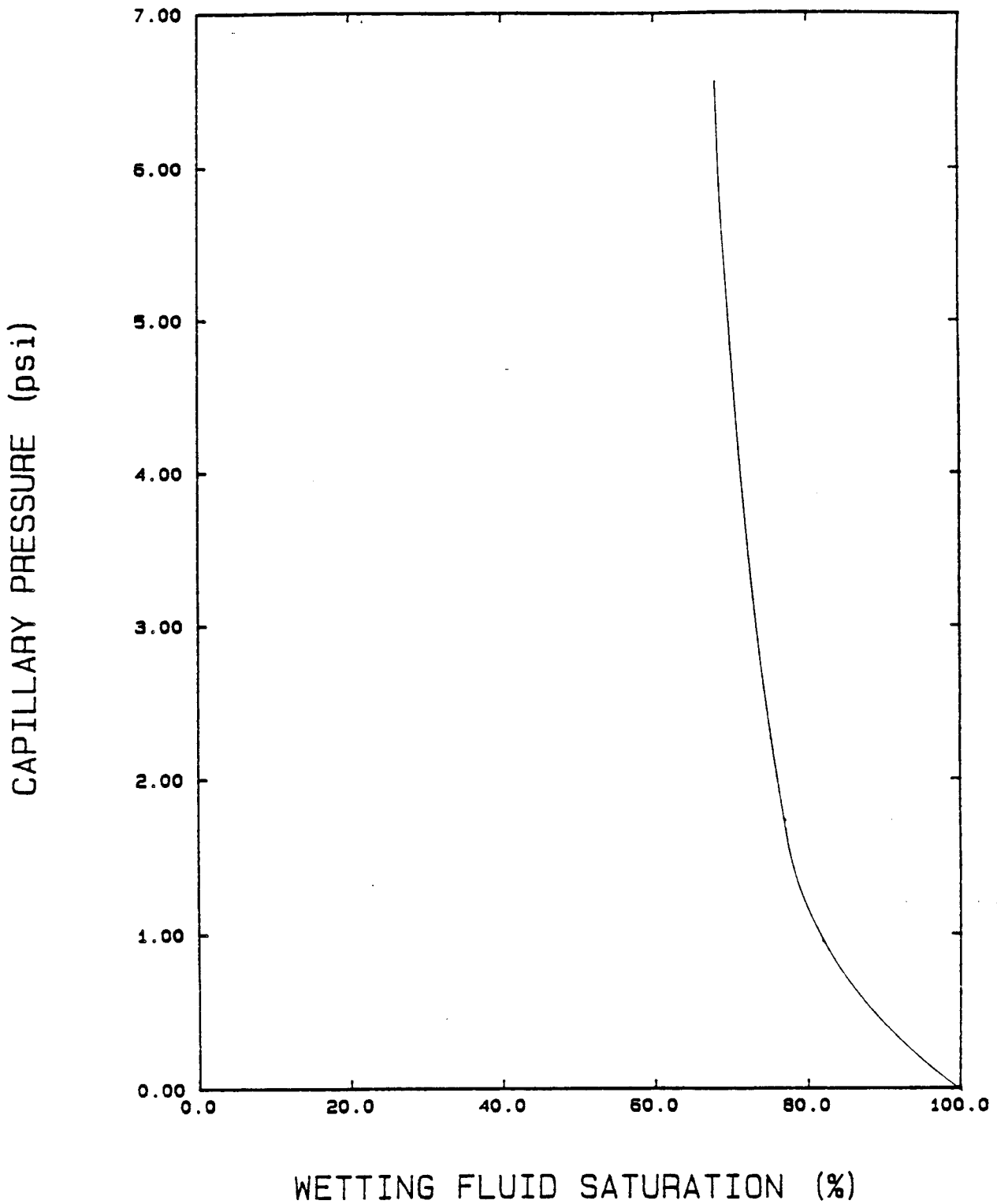

Figure C-3. Moisture Characteristic Curve for Sample MCG-604, Hole LLM-85-01, Depth of 101 Feet

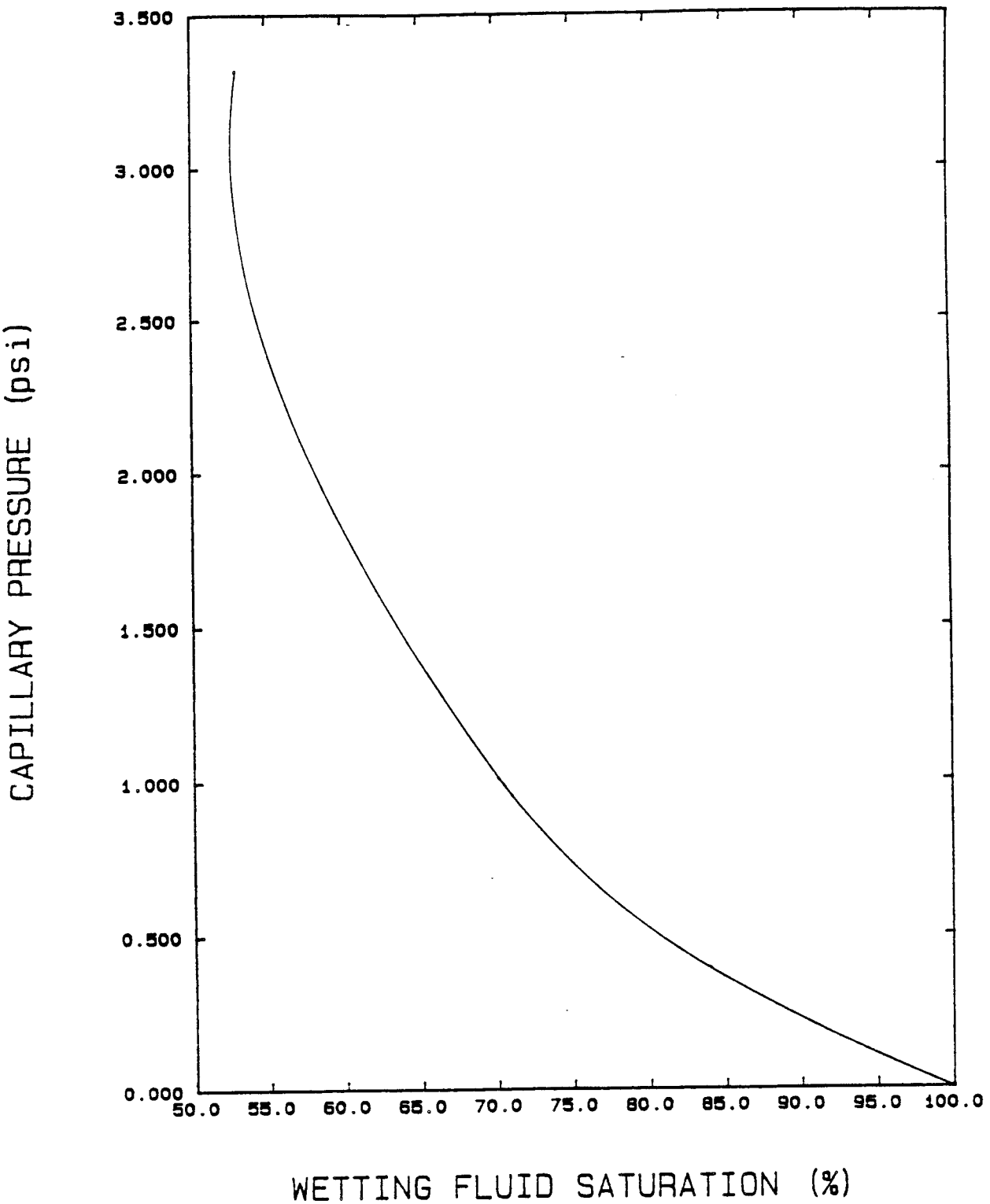

Figure C-4. Moisture Characteristic Curve for Sample MCG-605, Hole LLM-85-01, Depth of 124 Feet

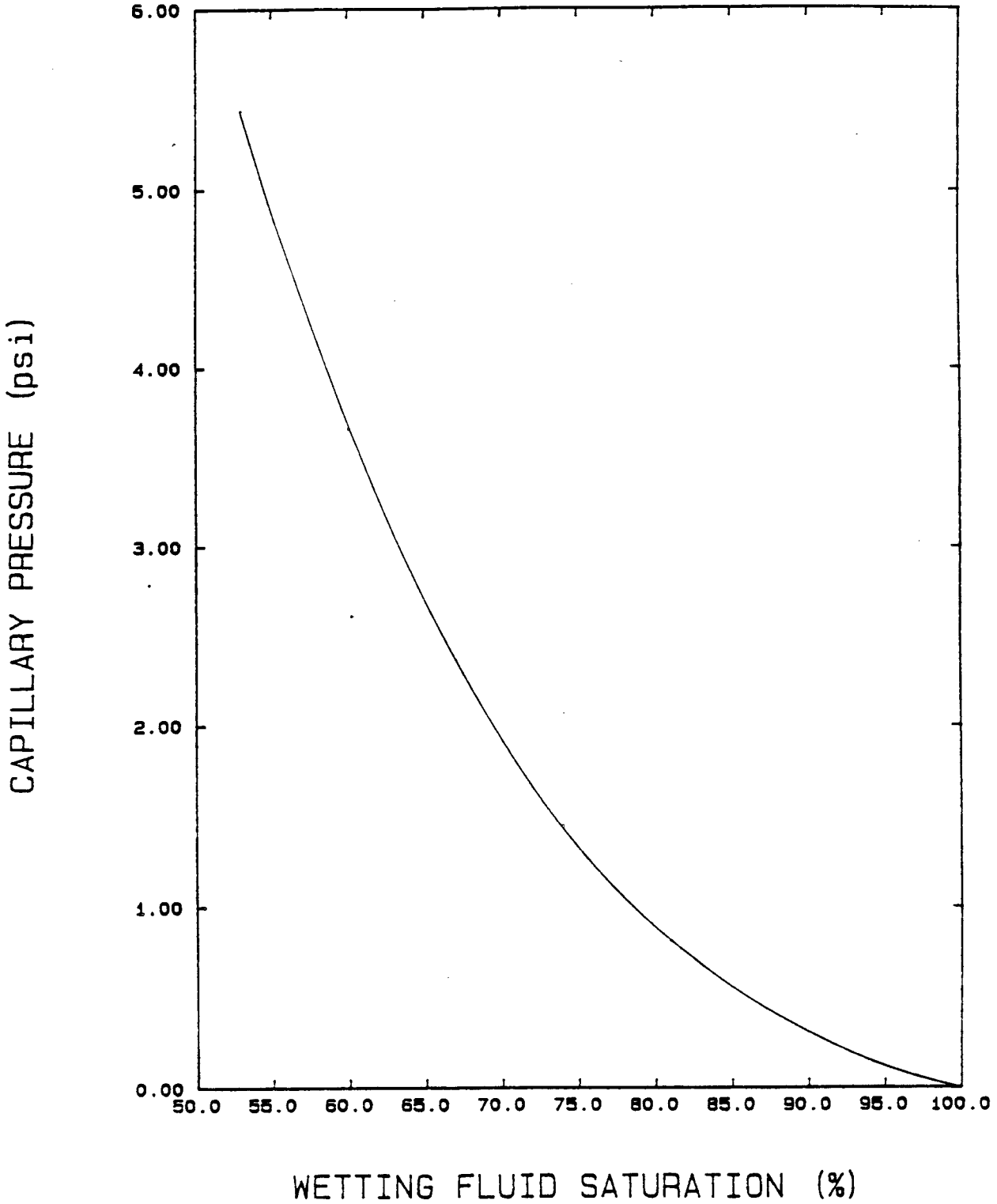

Figure C-5. Moisture Characteristic Curve for Sample MCG-606, Hole LLM-85-02, Depth of 7 Feet

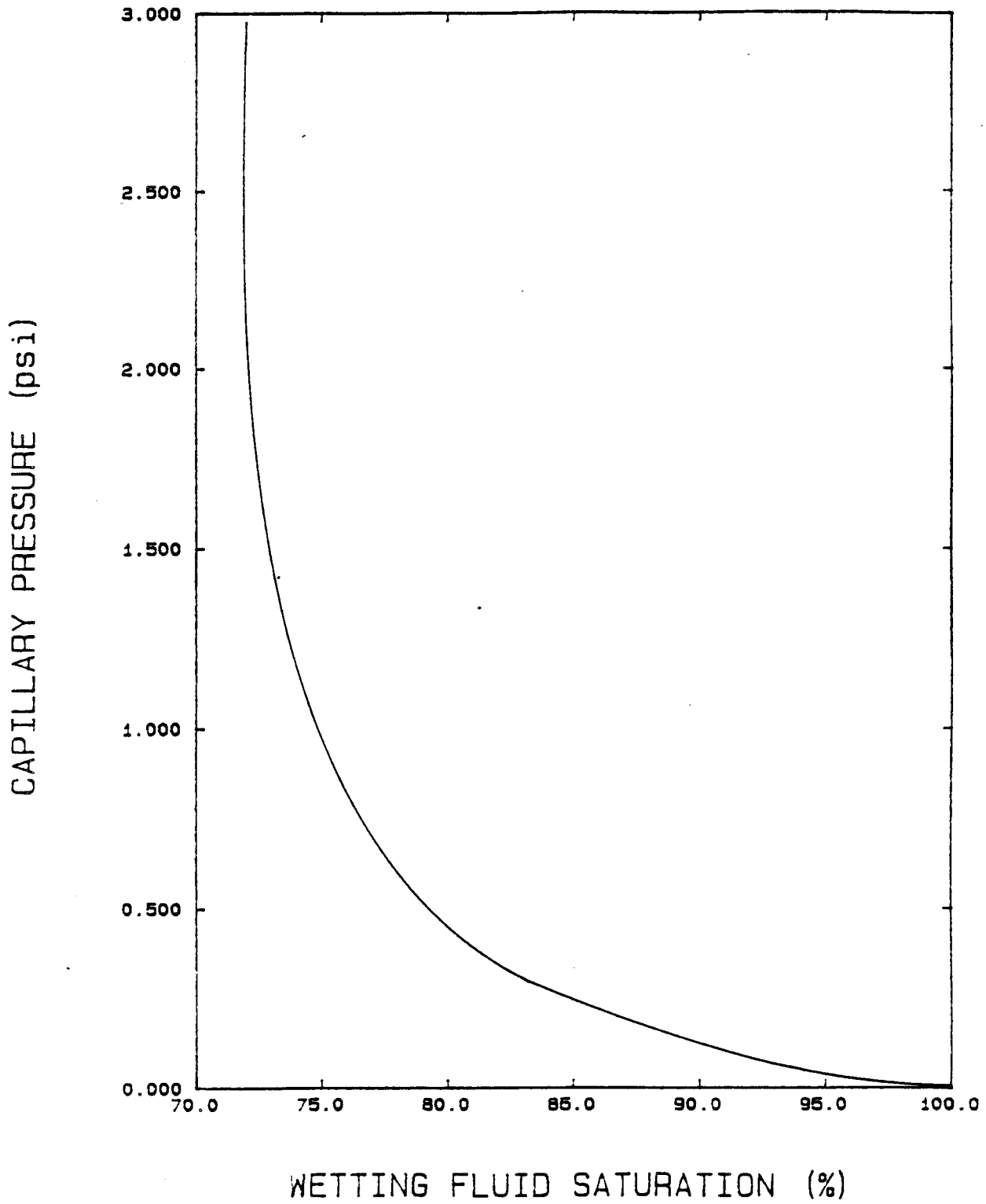

Figure C-6. Moisture Characteristic Curve for Sample MCG-607, Hole LLM-85-02, Depth of 36 Feet

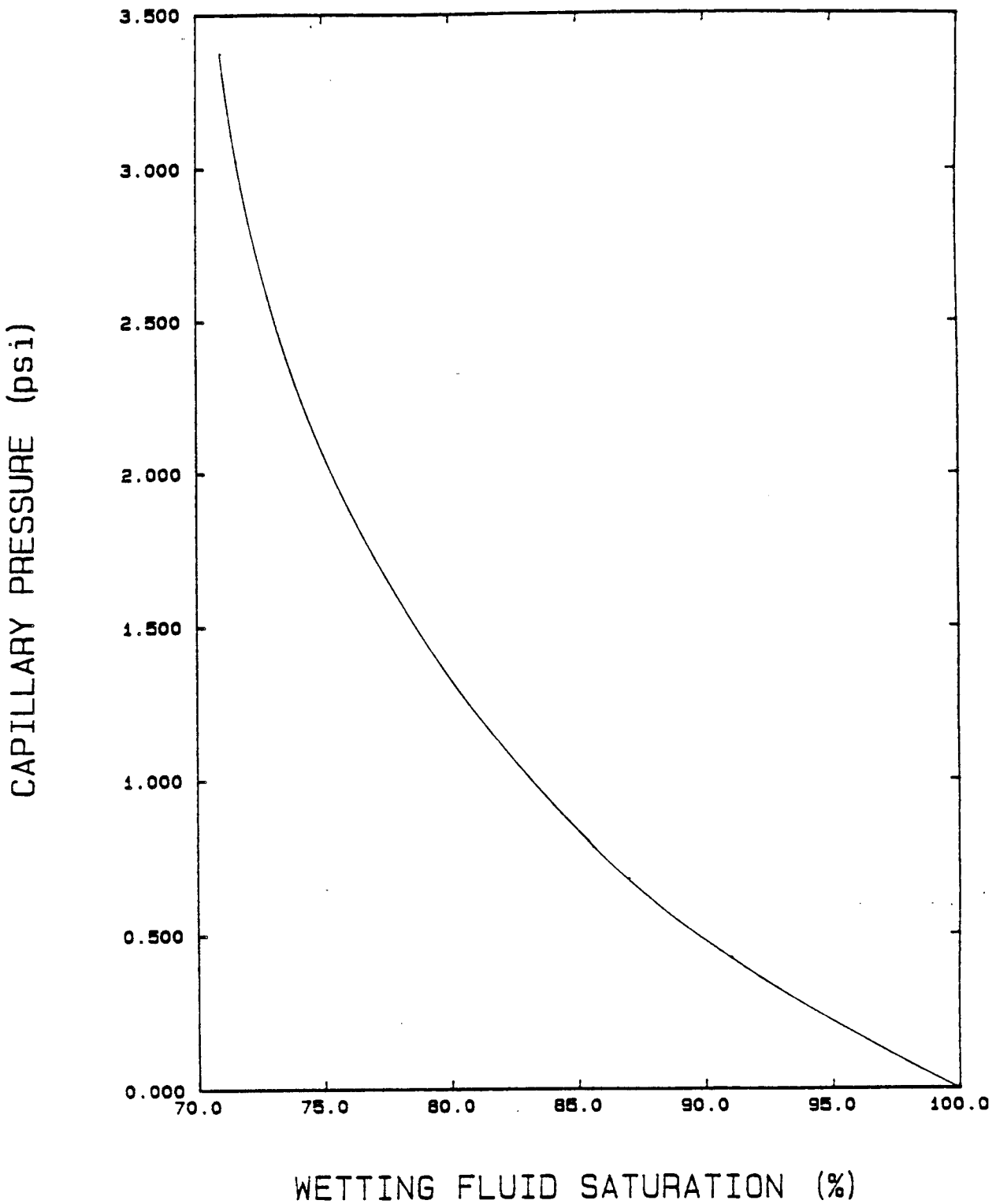

Figure C-7. Moisture Characteristic Curve for Sample MCG-608, Hole LLM-85-02, Depth of 67 Feet

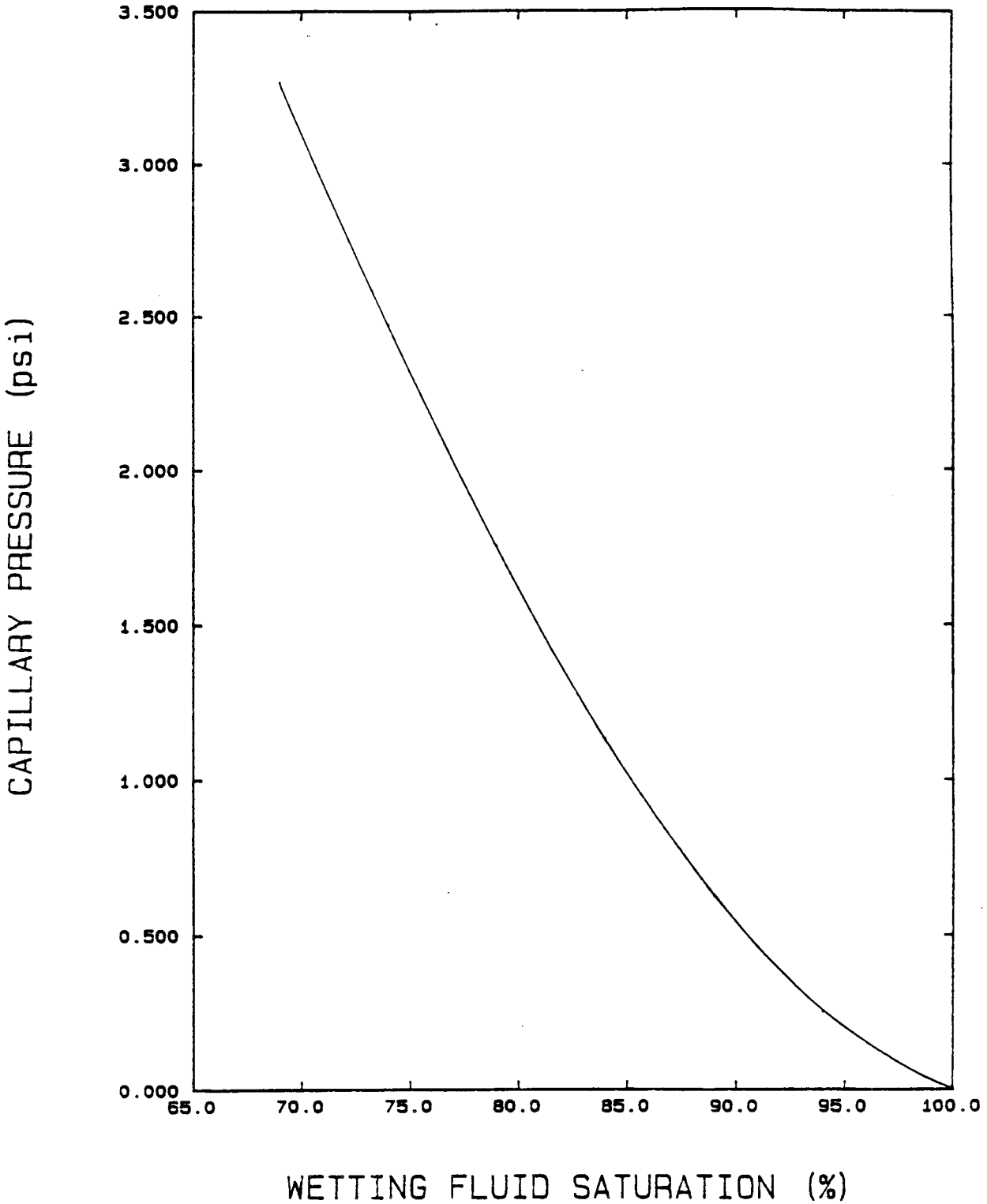

Figure C-8. Moisture Characteristic Curve for Sample MCG-609, Hole LLM-85-02, Depth of 117 Feet

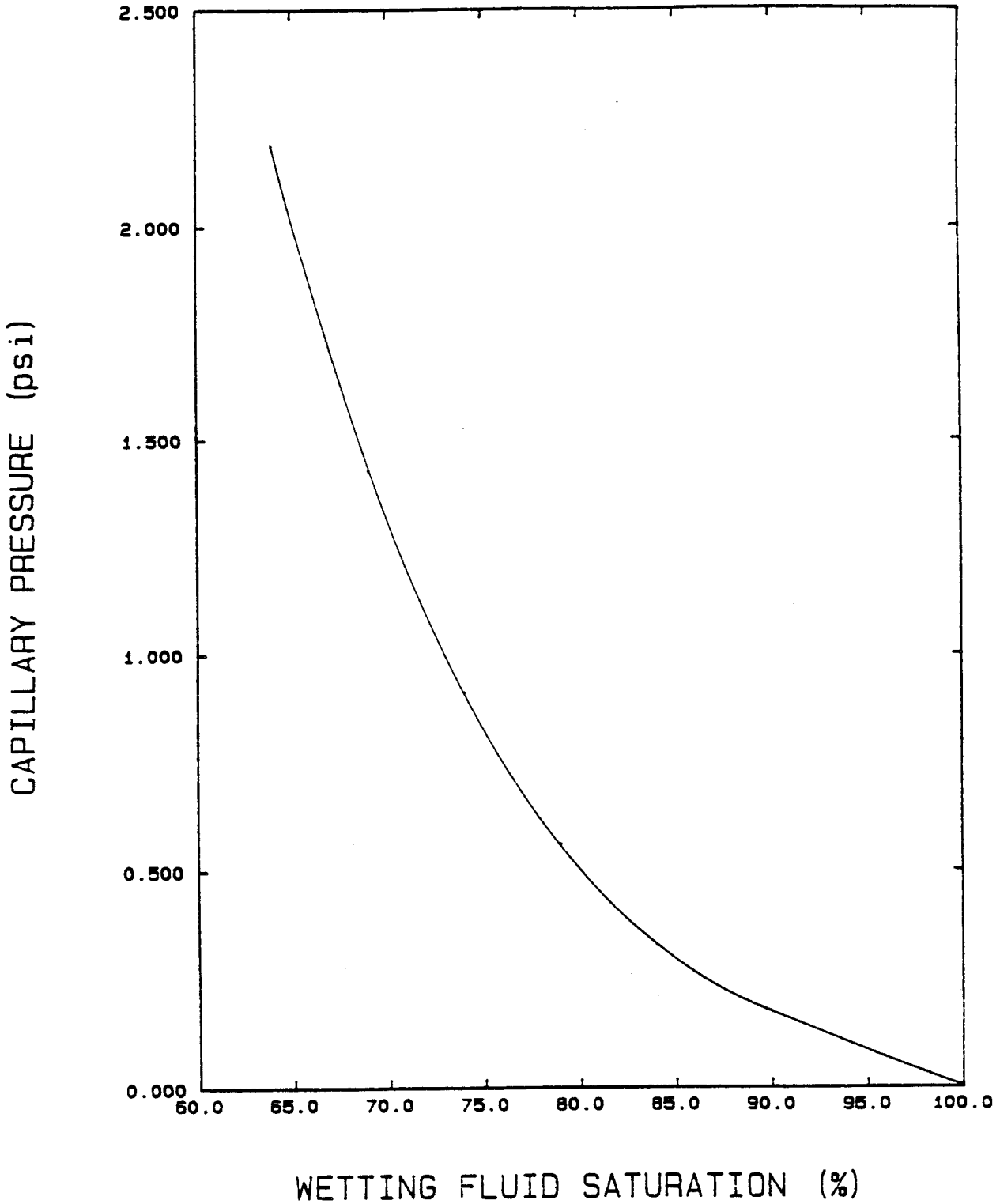

Figure C-9. Moisture Characteristic Curve for Sample MCG-610, Hole LLM-85-05, Depth of 15 Feet

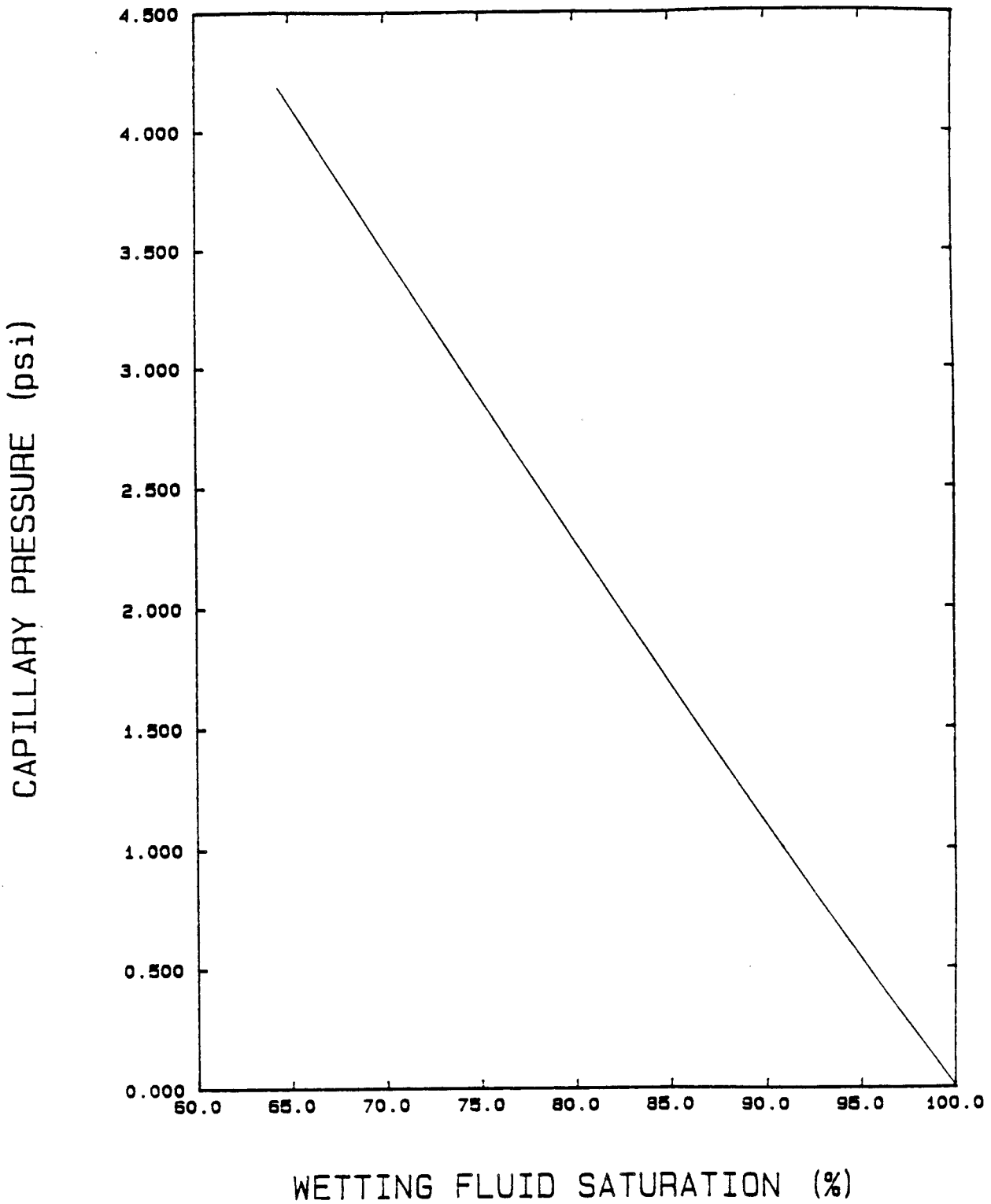

Figure C-10. Moisture Characteristic Curve for Sample MCG-611, Hole LLM-85-05, Depth of 36 Feet

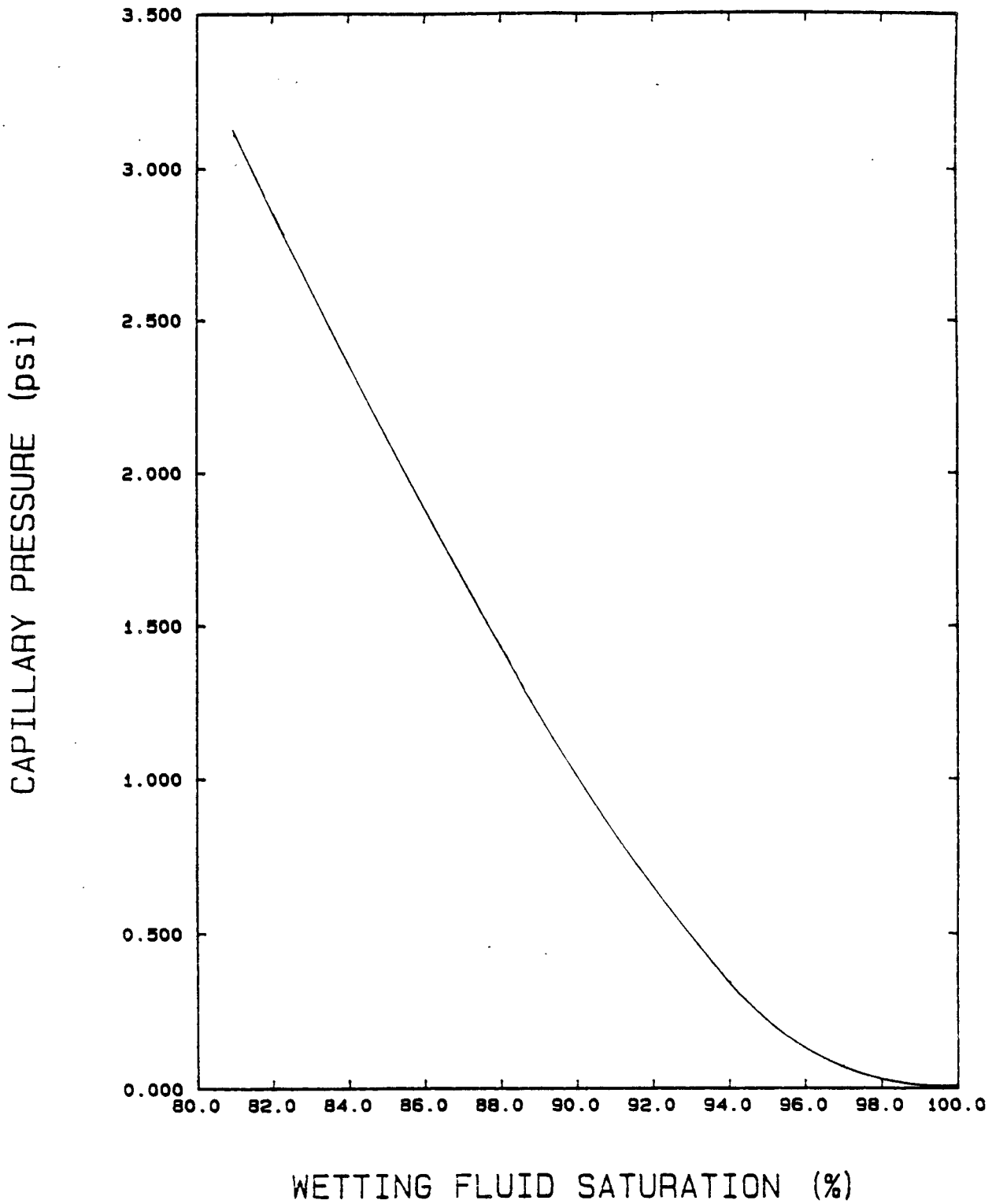

Figure C-11. Moisture Characteristic Curve for Sample MCG-612, Hole LLM-85-05, Depth of 76 Feet

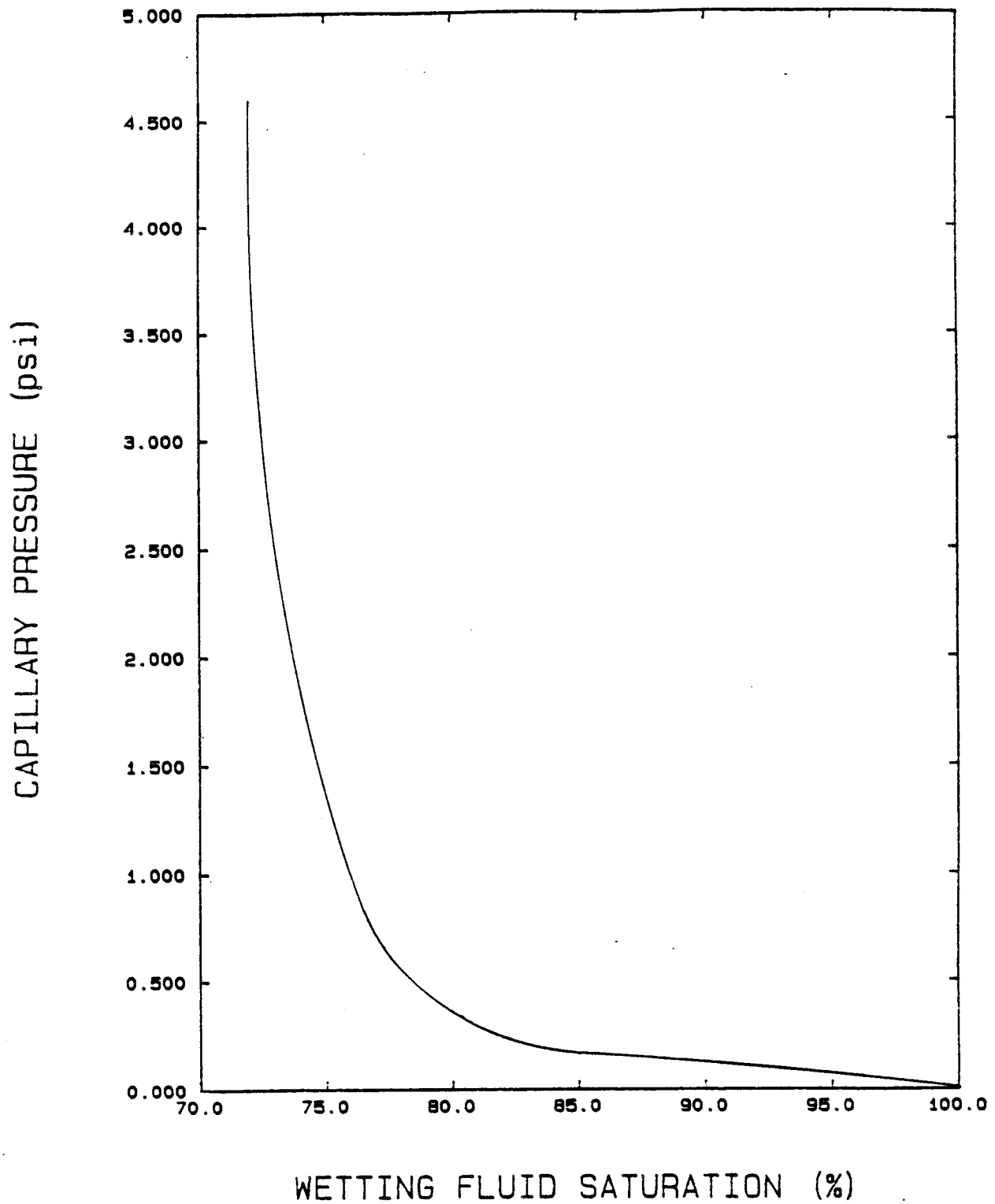

Figure C-12. Moisture Characteristic Curve for Sample MCG-613, Hole LLM-85-05, Depth of 123 Feet

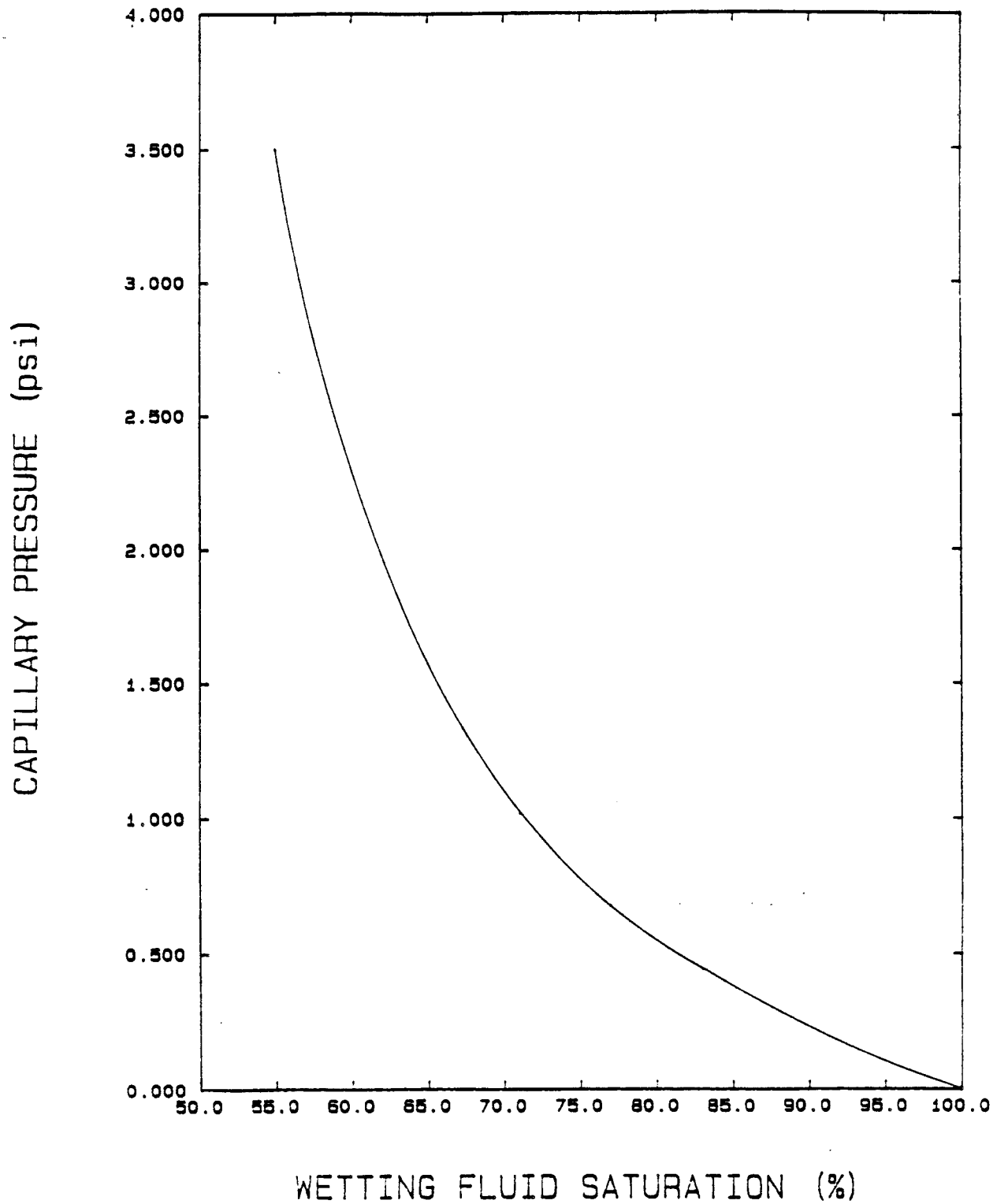

Figure C-13. Moisture Characteristic Curve for Sample MCG-614, Hole LGM-85-06, Depth of 29 Feet

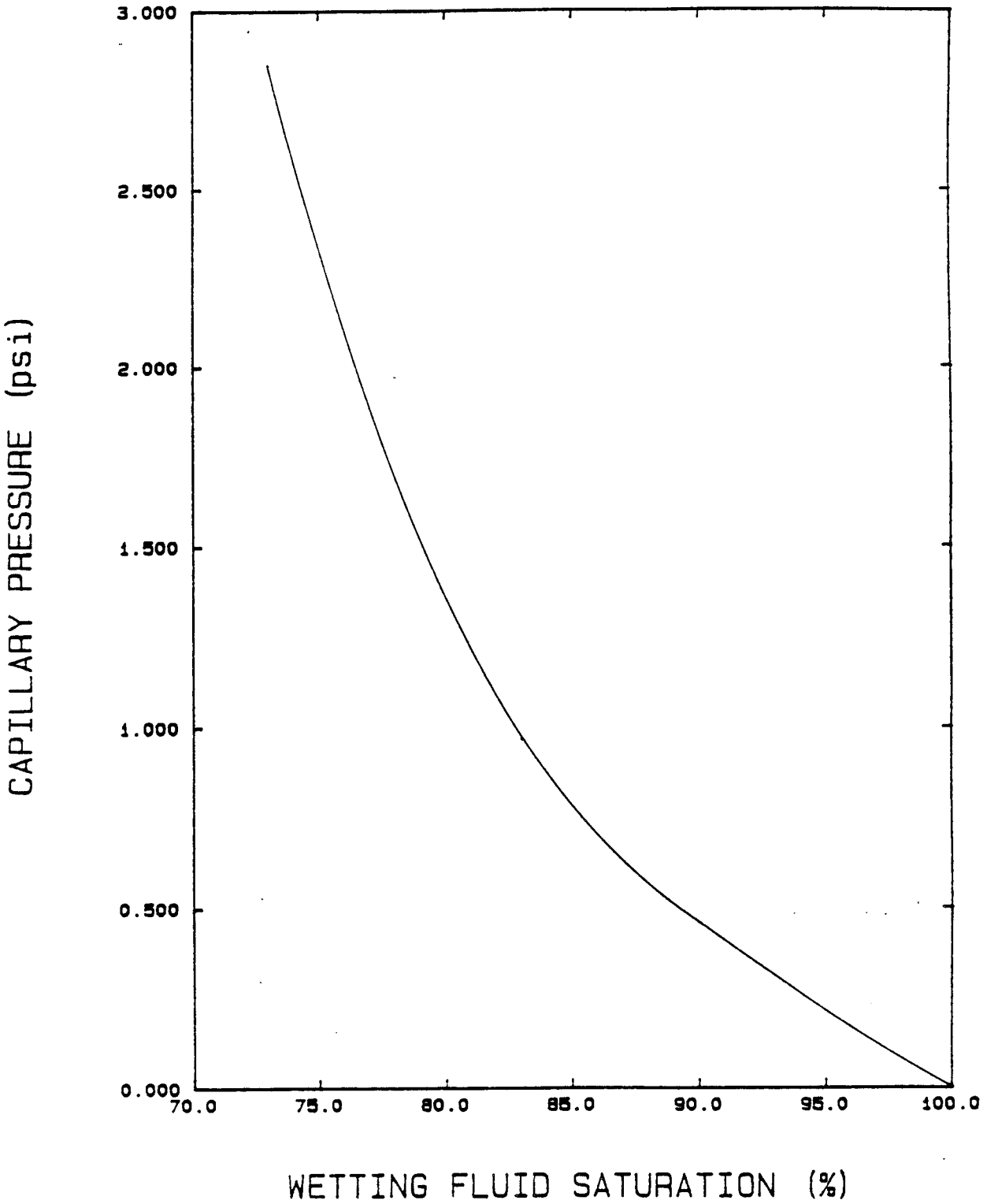

Figure C-14. Moisture Characteristic Curve for Sample MCG-615, Hole LGM-85-06, Depth of 51 Feet

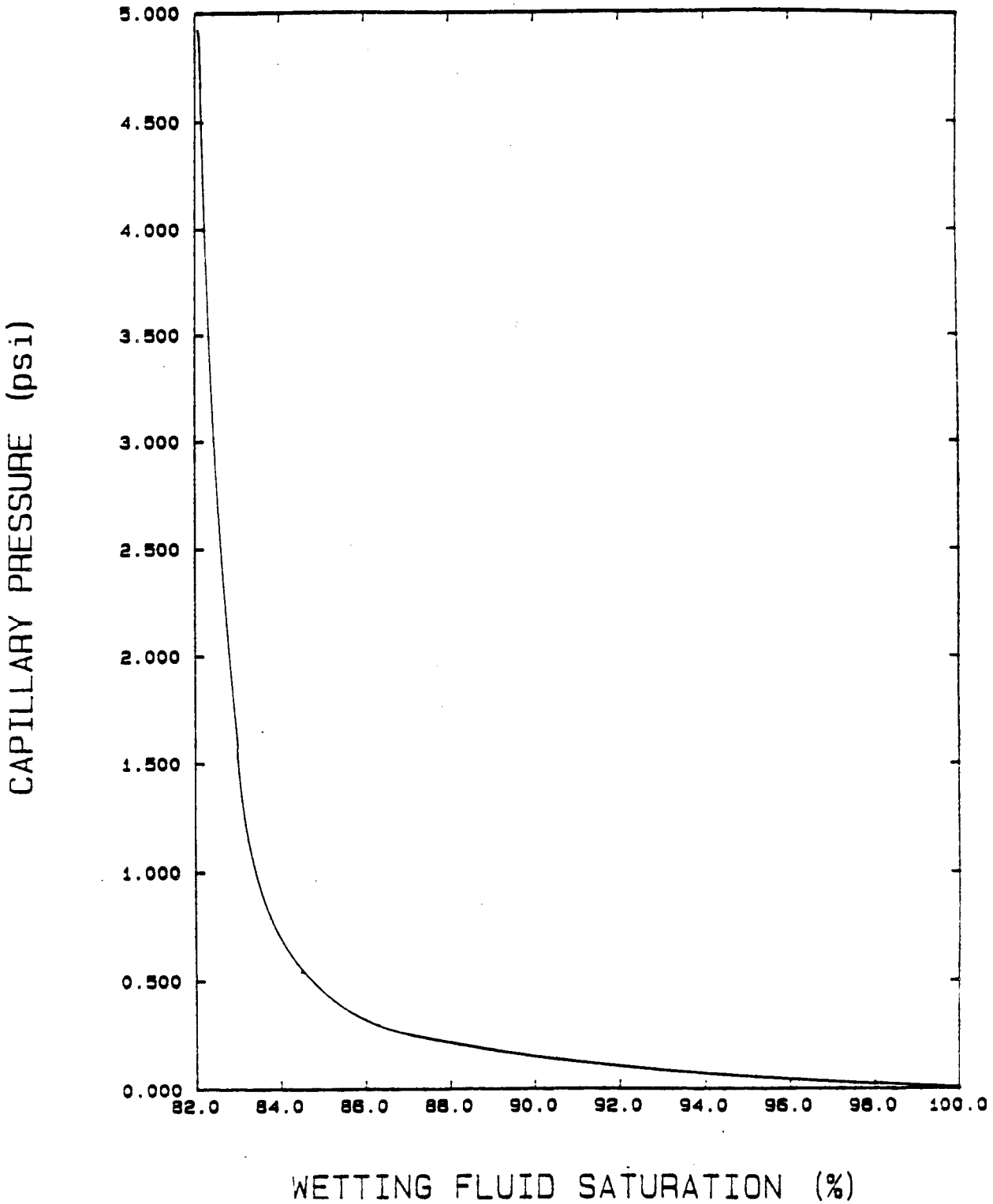

Figure C-15. Moisture Characteristic Curve for Sample MCG-616, Hole LGM-85-06, Depth of 99 Feet

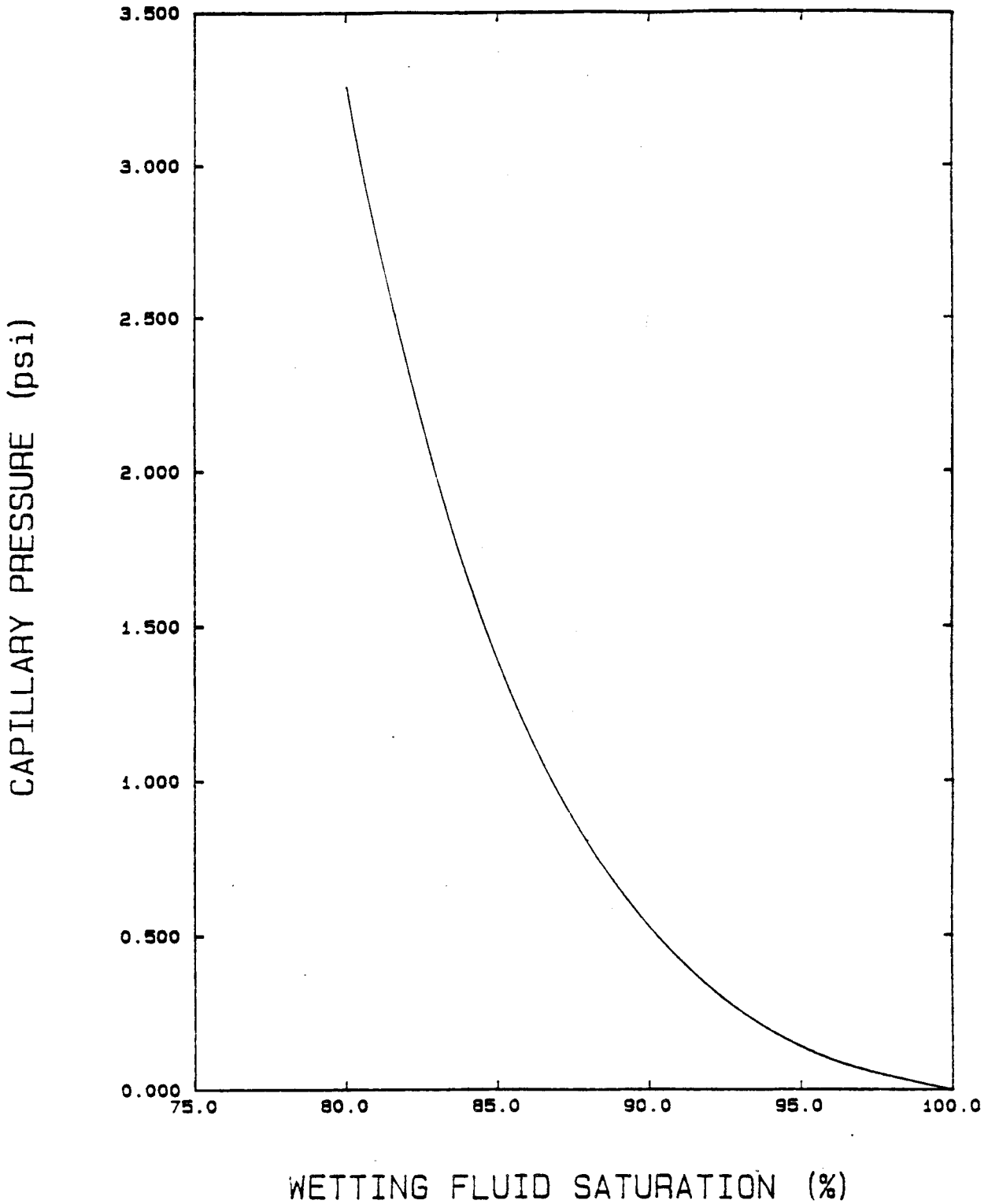

Figure C-16. Moisture Characteristic Curve for Sample MCG-617, Hole LGM-85-06, Depth of 115 Feet

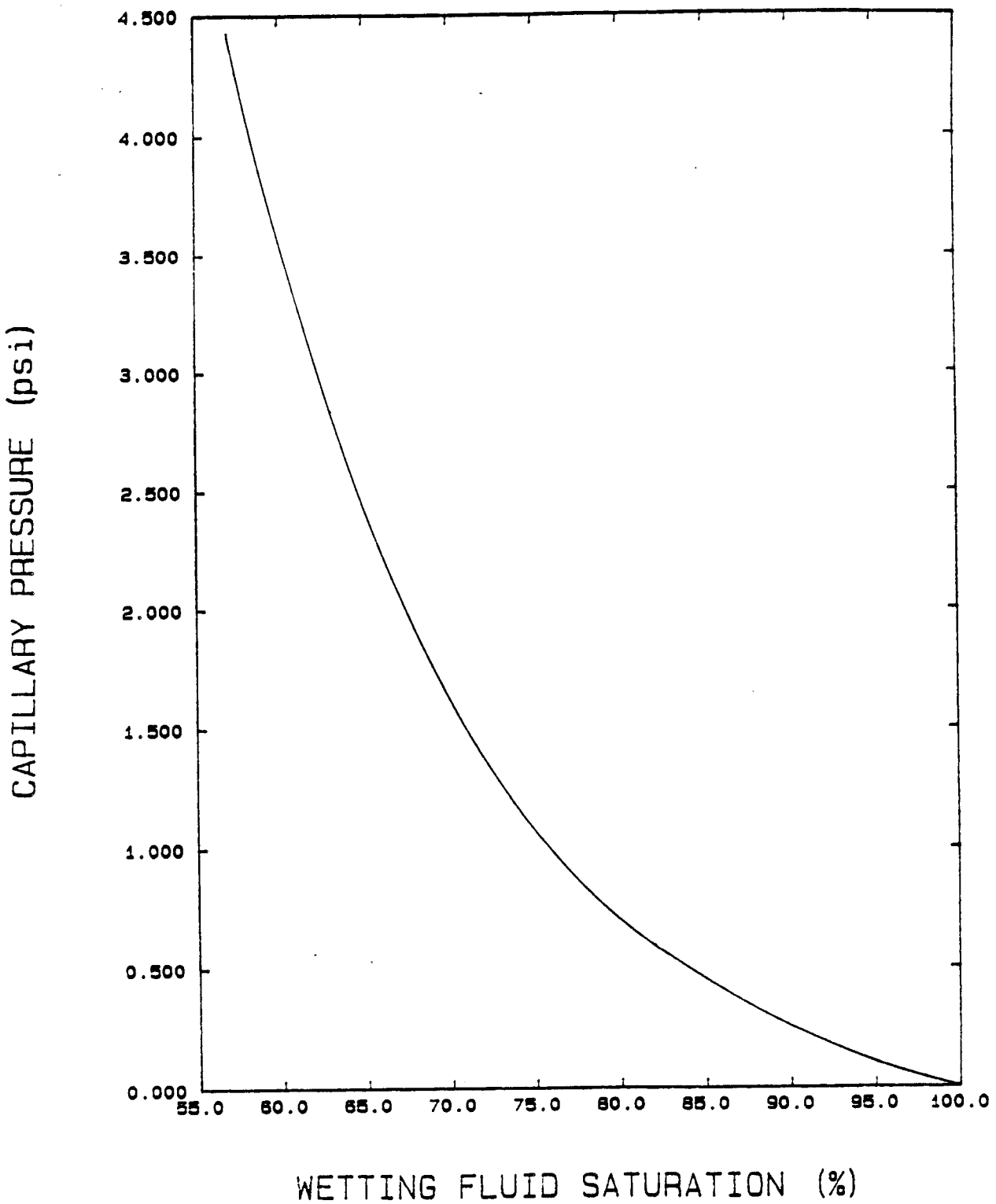

Figure C-17. Moisture Characteristic Curve for Sample MCG-618, Hole LGM-85-11, Depth of 3 Feet

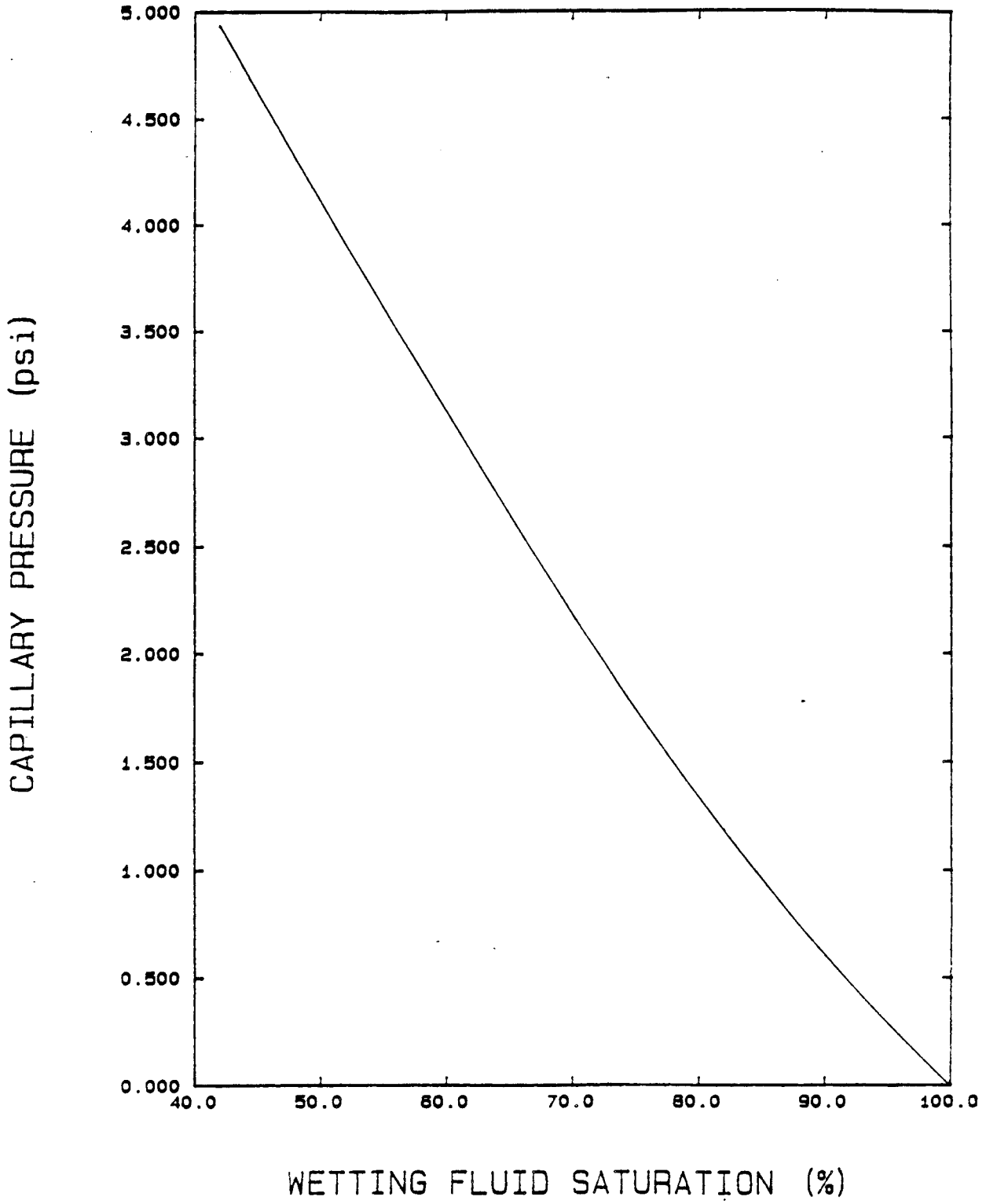

Figure C-18. Moisture Characteristic Curve for Sample MCG-619, Hole LGM-85-11, Depth of 30 Feet

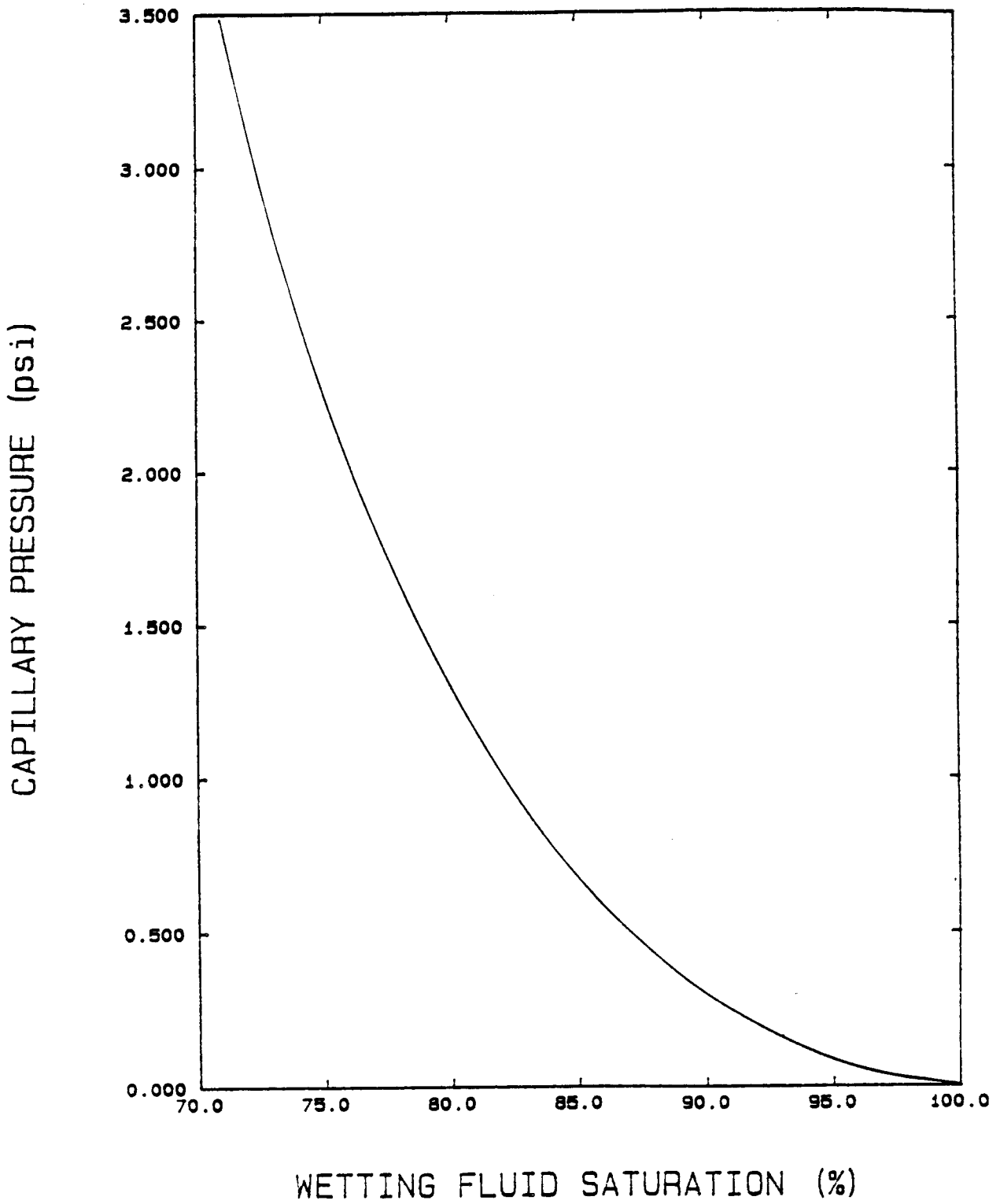

Figure C-19. Moisture Characteristic Curve for Sample MCG-620, Hole LGM-85-11, Depth of 94 Feet

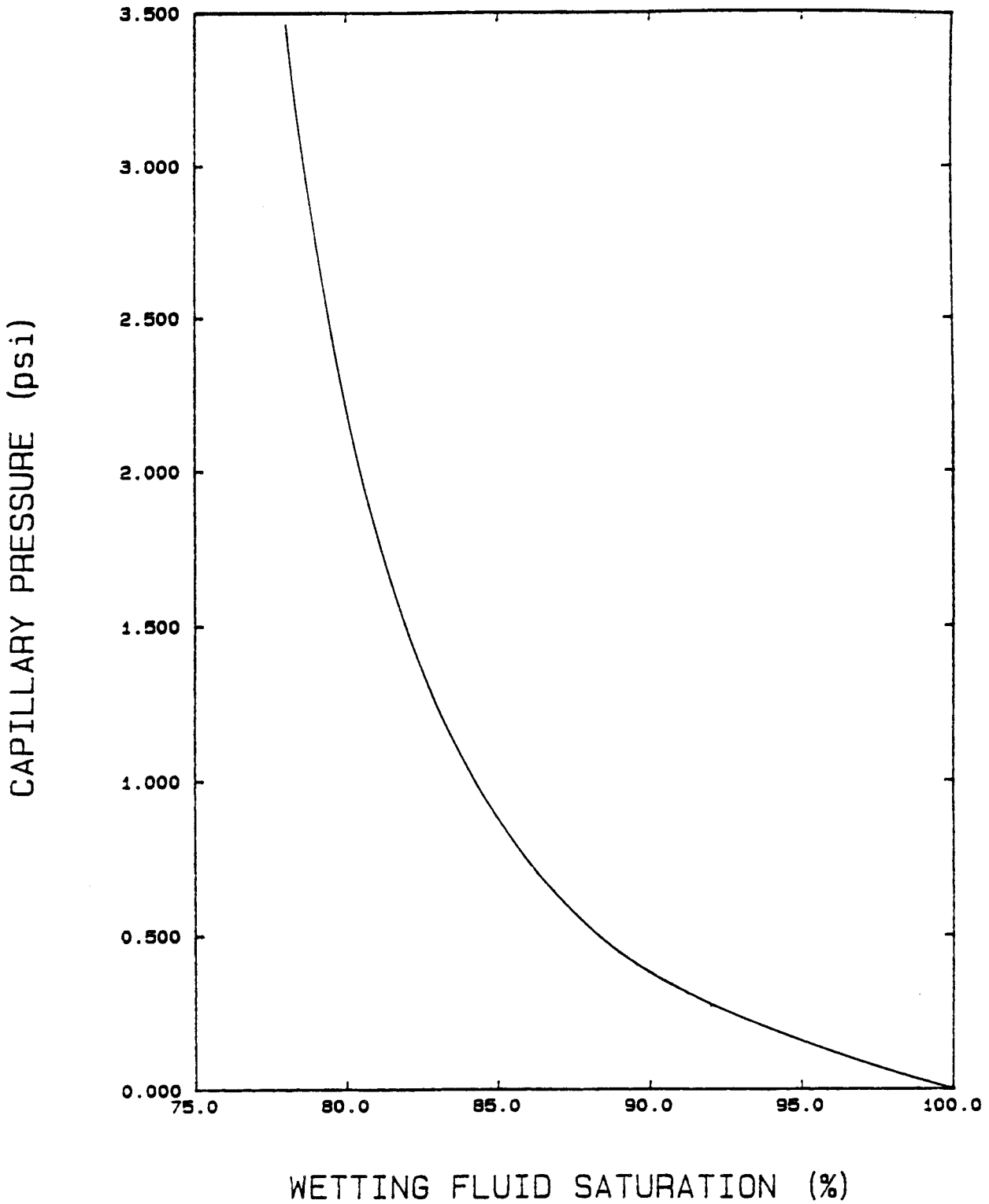

Figure C-20. Moisture Characteristic Curve for Sample MCG-621, Hole LGM-85-11, Depth of 115 Feet

Appendix D

EFFECTIVE PERMEABILITY AS A FUNCTION OF SATURATION

(saturation refers to total air saturation)

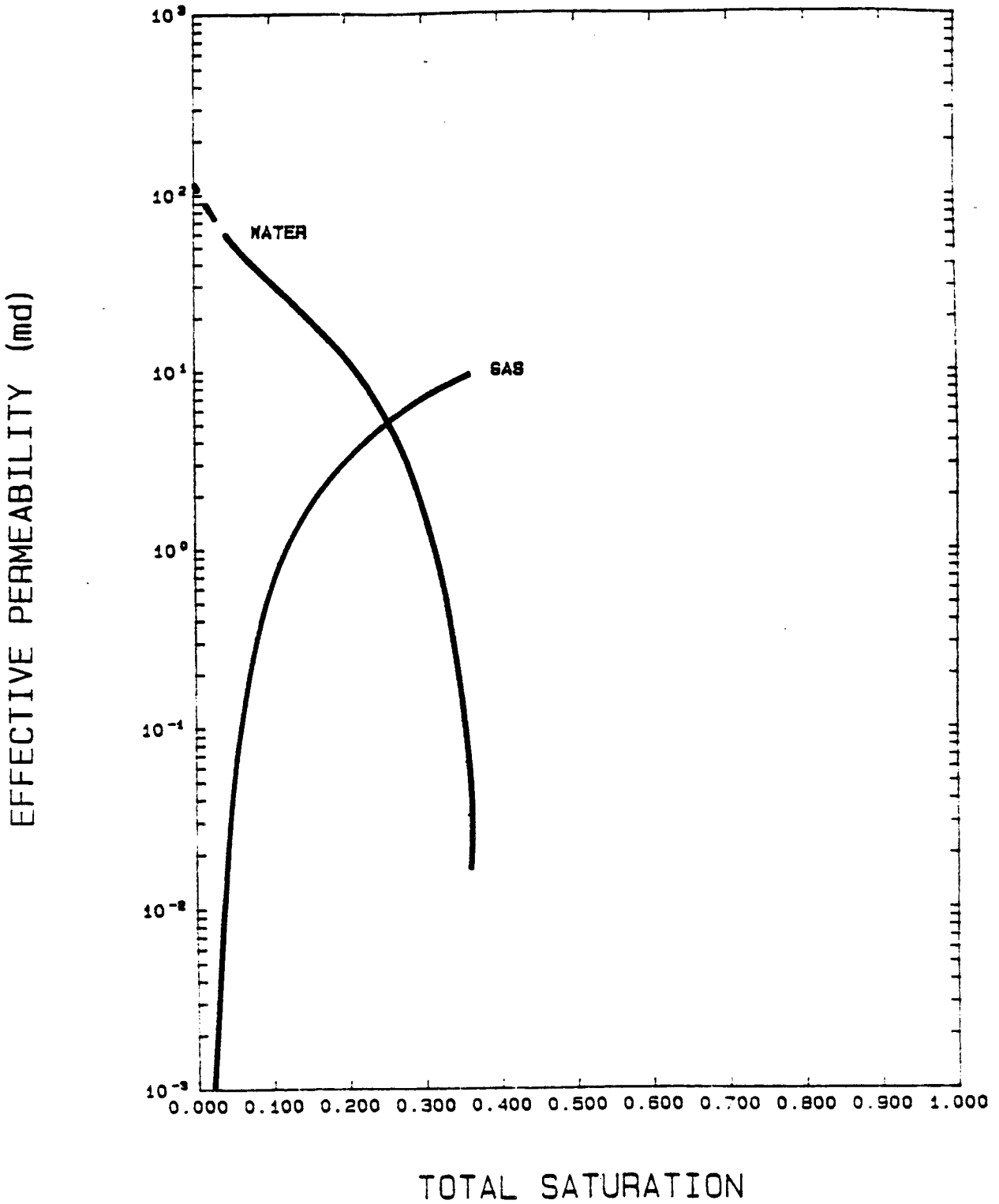

Figure D-1. Effective Permeability as a Function of Saturation for Sample MCG-602, Hole LLM-85-01, Depth of 30 Feet

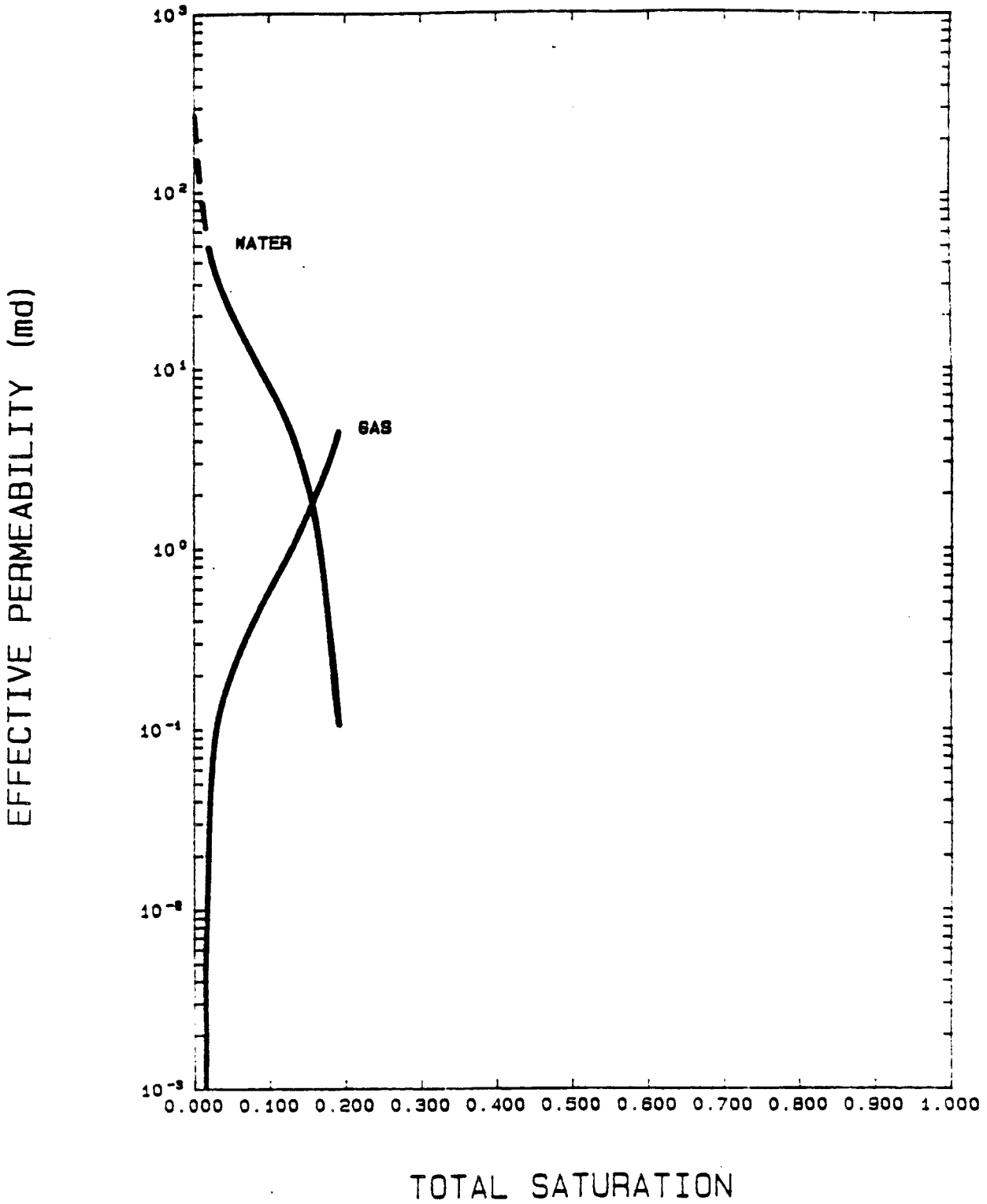

Figure D-2. Effective Permeability as a Function of Saturation for Sample MCG-603, Hole LLM-85-01, Depth of 52 Feet

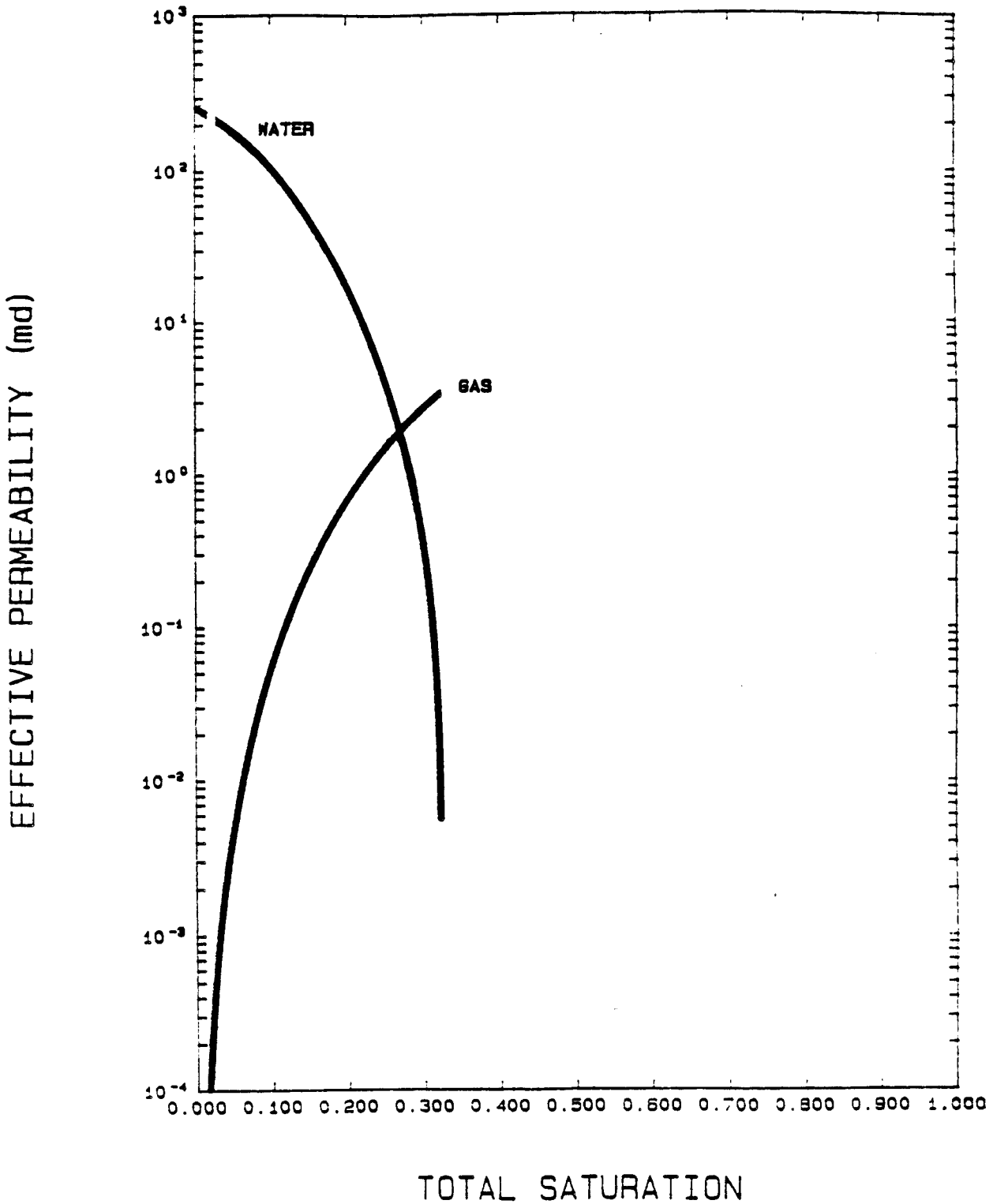

Figure D-3. Effective Permeability as a Function of Saturation for Sample MCG-604, Hole LLM-85-01, Depth of 101 Feet

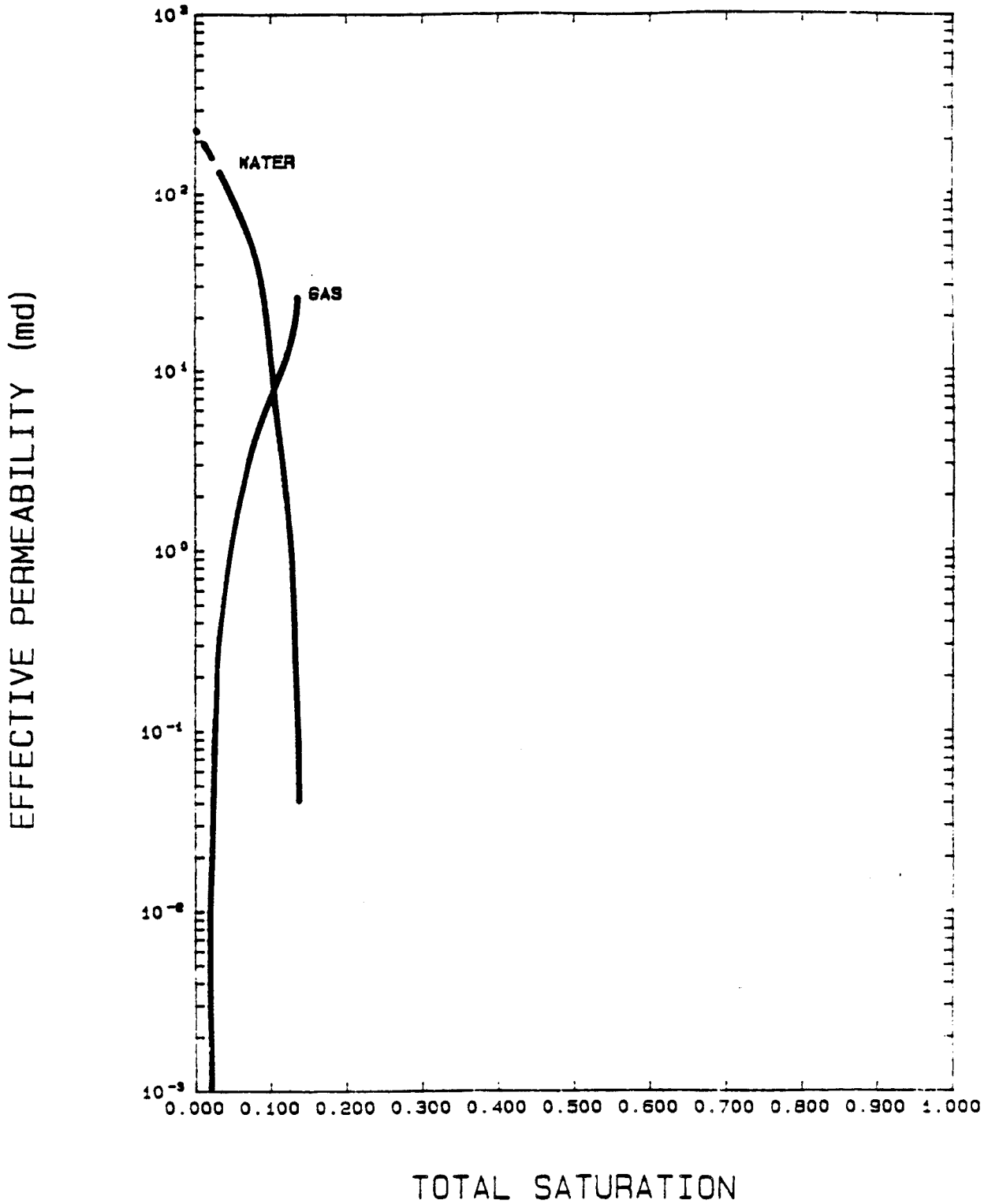

Figure D-4. Effective Permeability as a Function of Saturation for Sample MCG-605, Hole LLM-85-01, Depth of 124 Feet

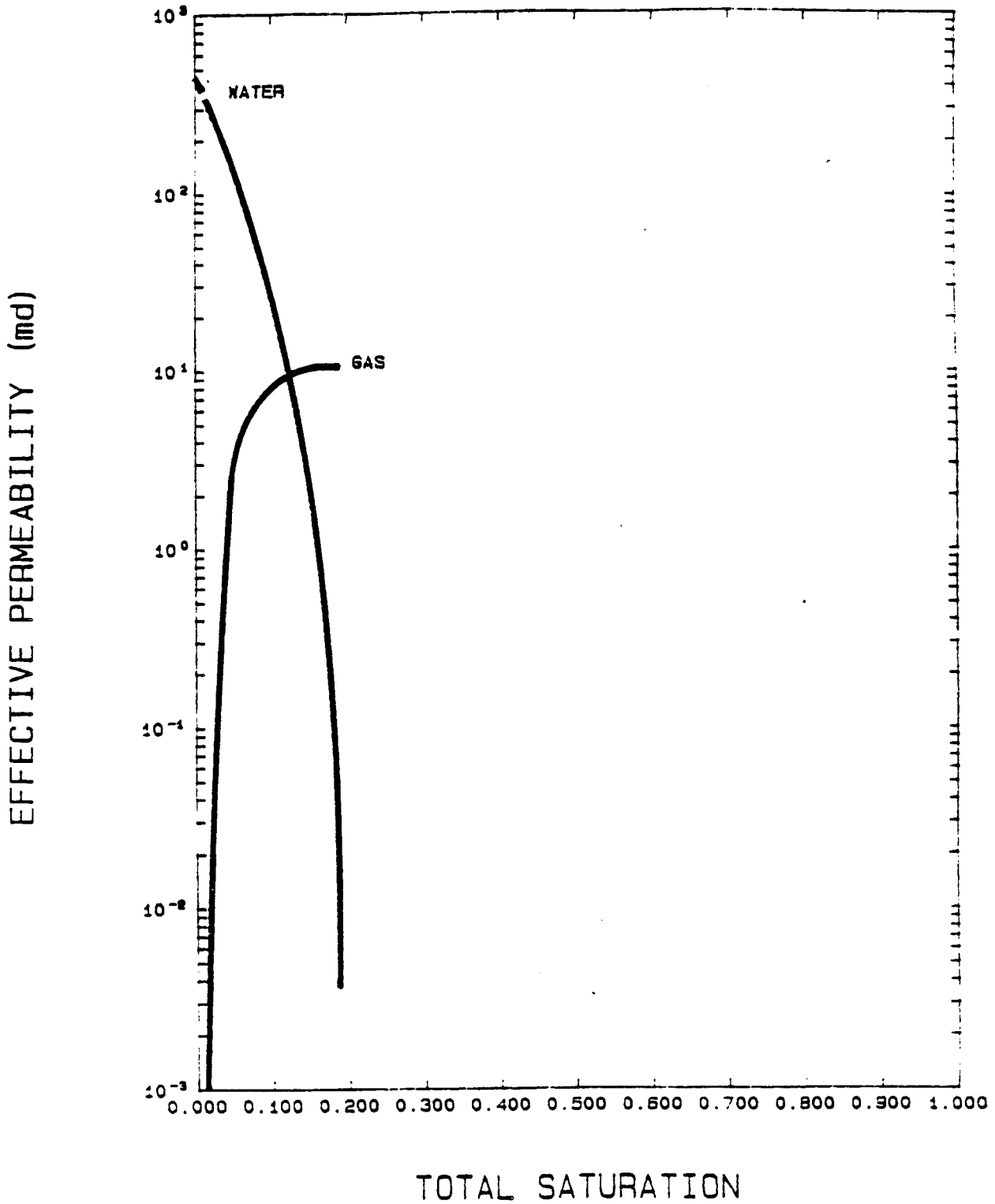

Figure D-5. Effective Permeability as a Function of Saturation for Sample MCG-606, Hole LLM-85-02, Depth of 7 Feet

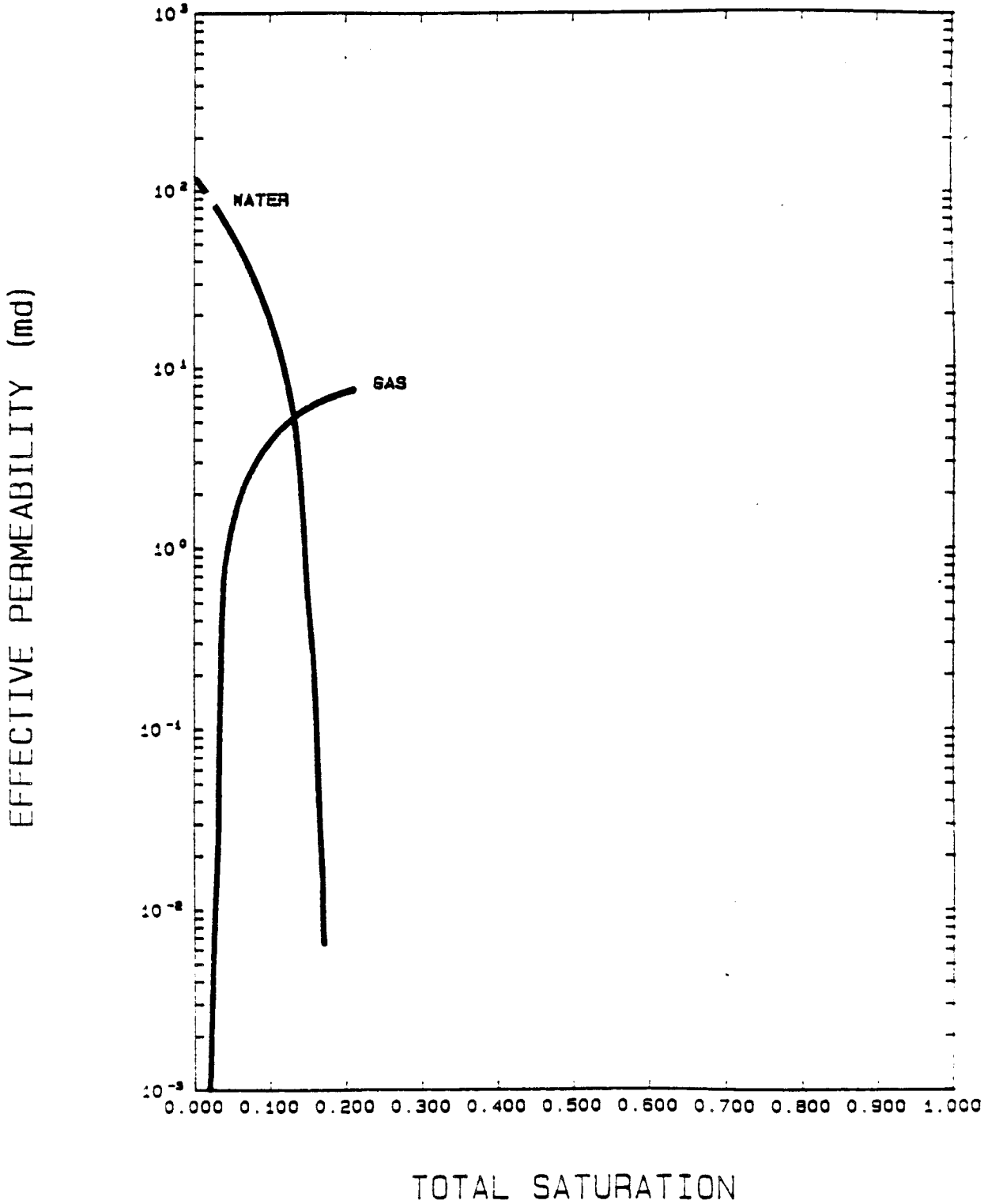

Figure D-6. Effective Permeability as a Function of Saturation for Sample MCG-607, Hole LLM-85-02, Depth of 36 Feet

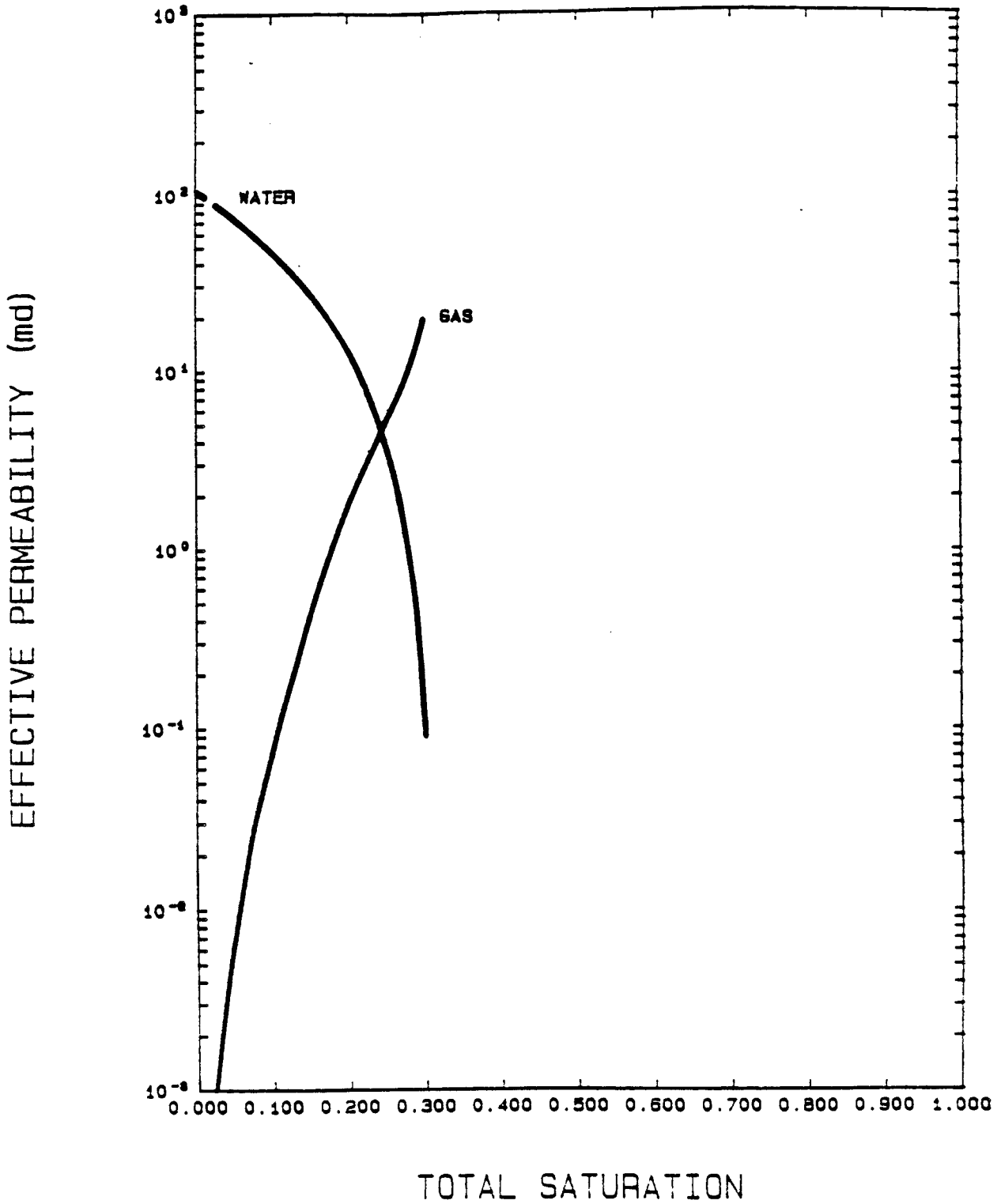

Figure D-7. Effective Permeability as a Function of Saturation for Sample MCG-608, Hole LLM-85-02, Depth of 67 Feet

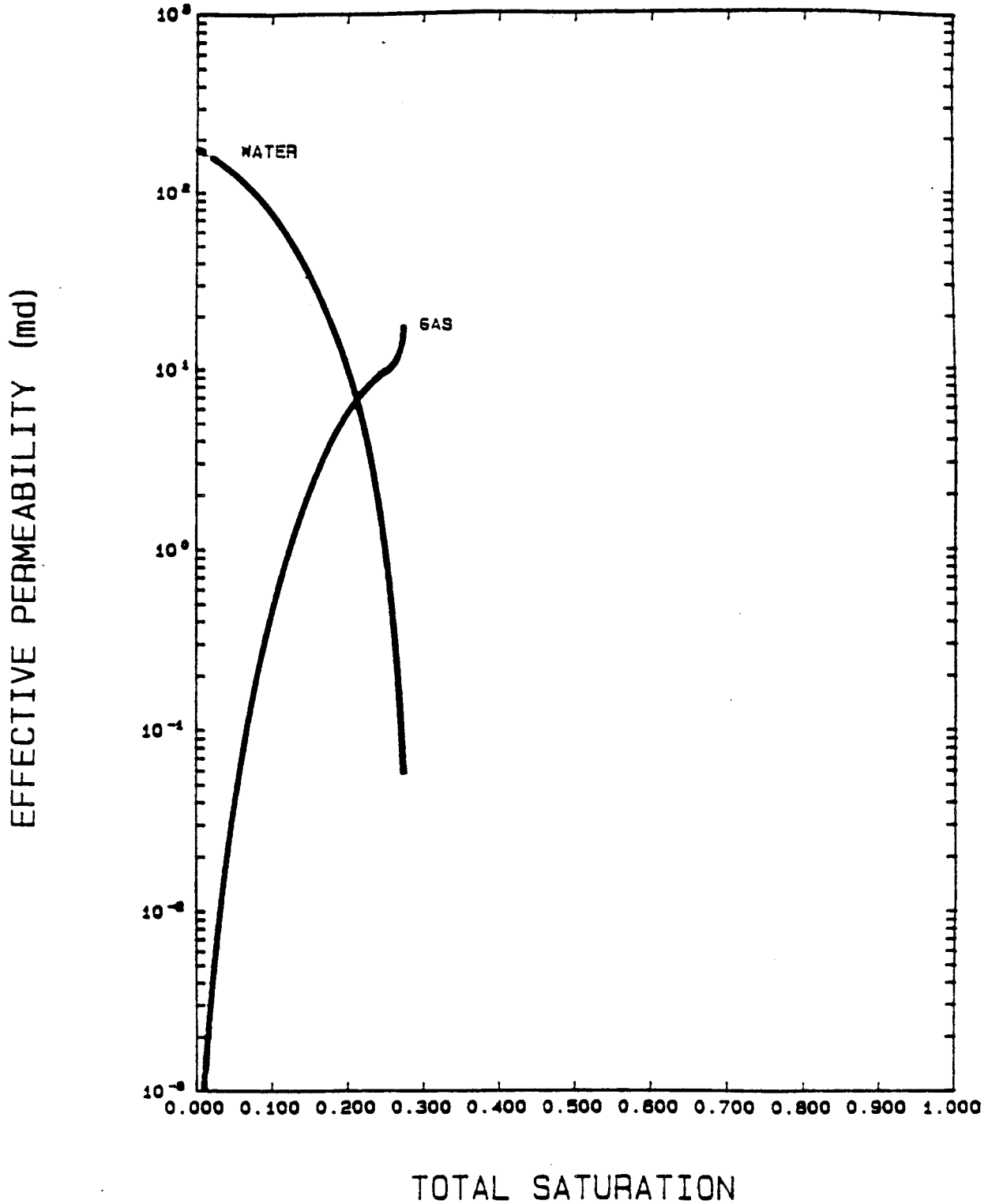

Figure D-8. Effective Permeability as a Function of Saturation for Sample MCG-609, Hole LLM-85-02, Depth of 117 Feet

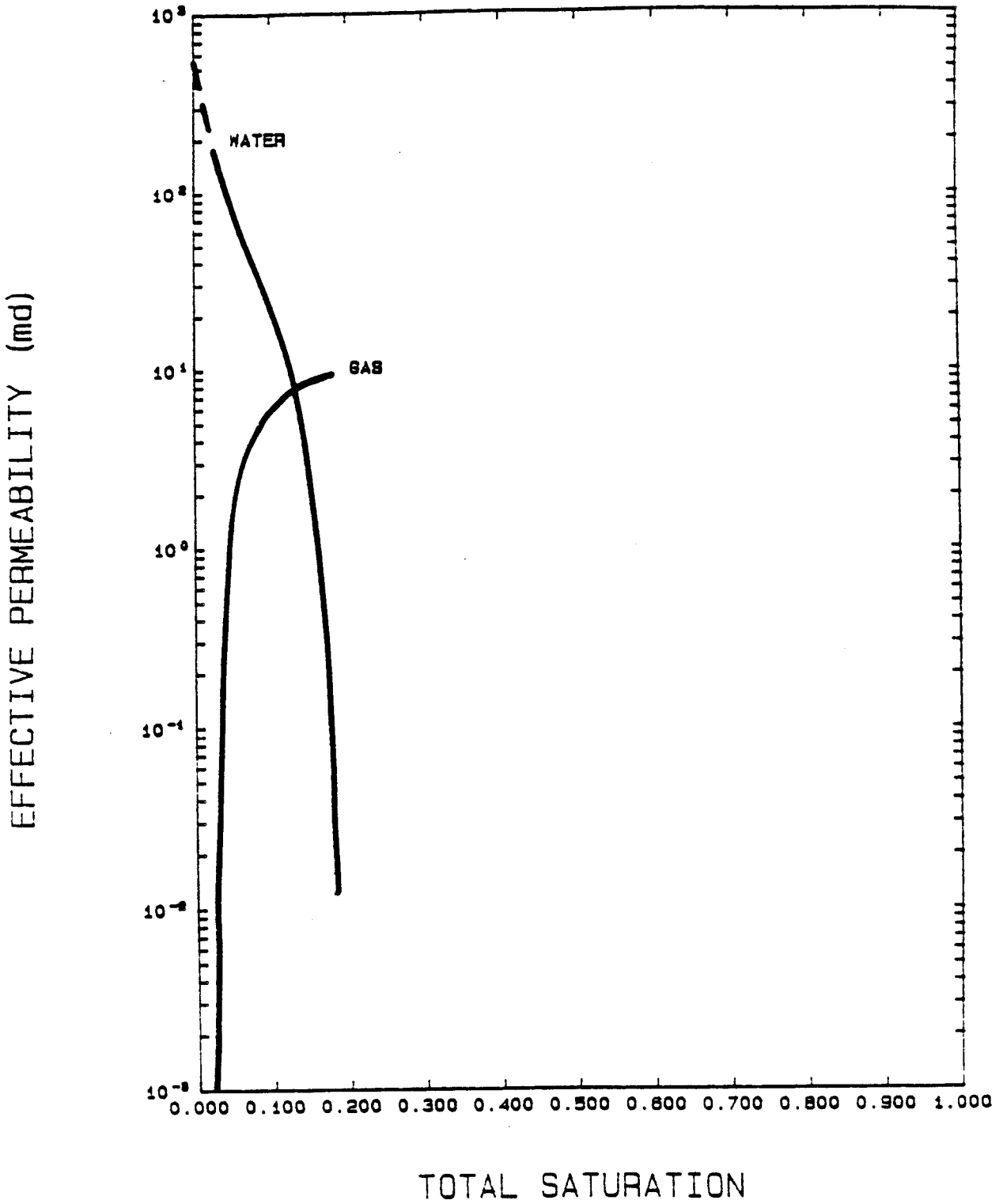

Figure D-9. Effective Permeability as a Function of Saturation for Sample MCG-610, Hole LLM-85-05, Depth of 15 Feet

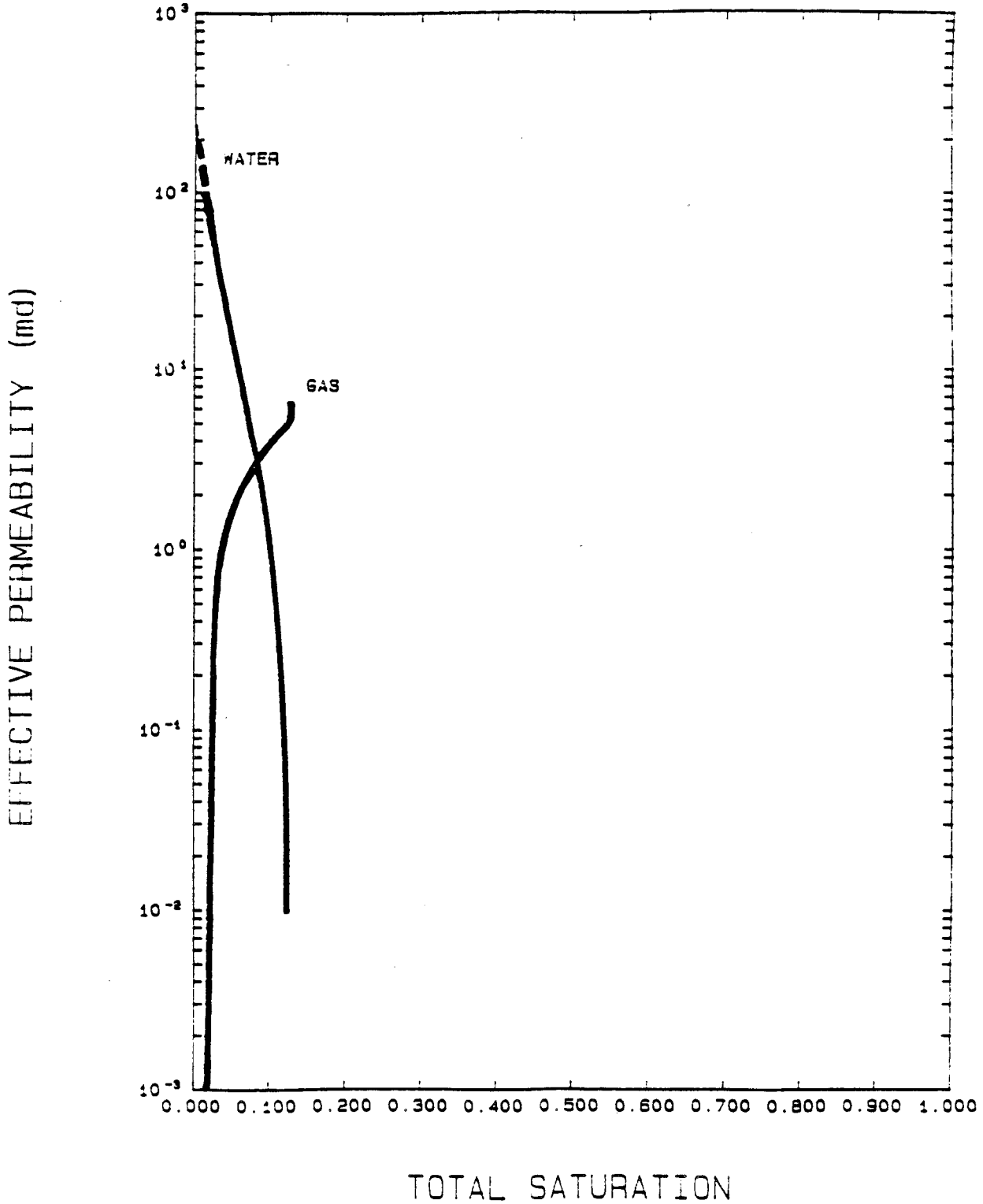

Figure D-10. Effective Permeability as a Function of Saturation for Sample MCG-611, Hole LLM-85-05, Depth of 36 Feet

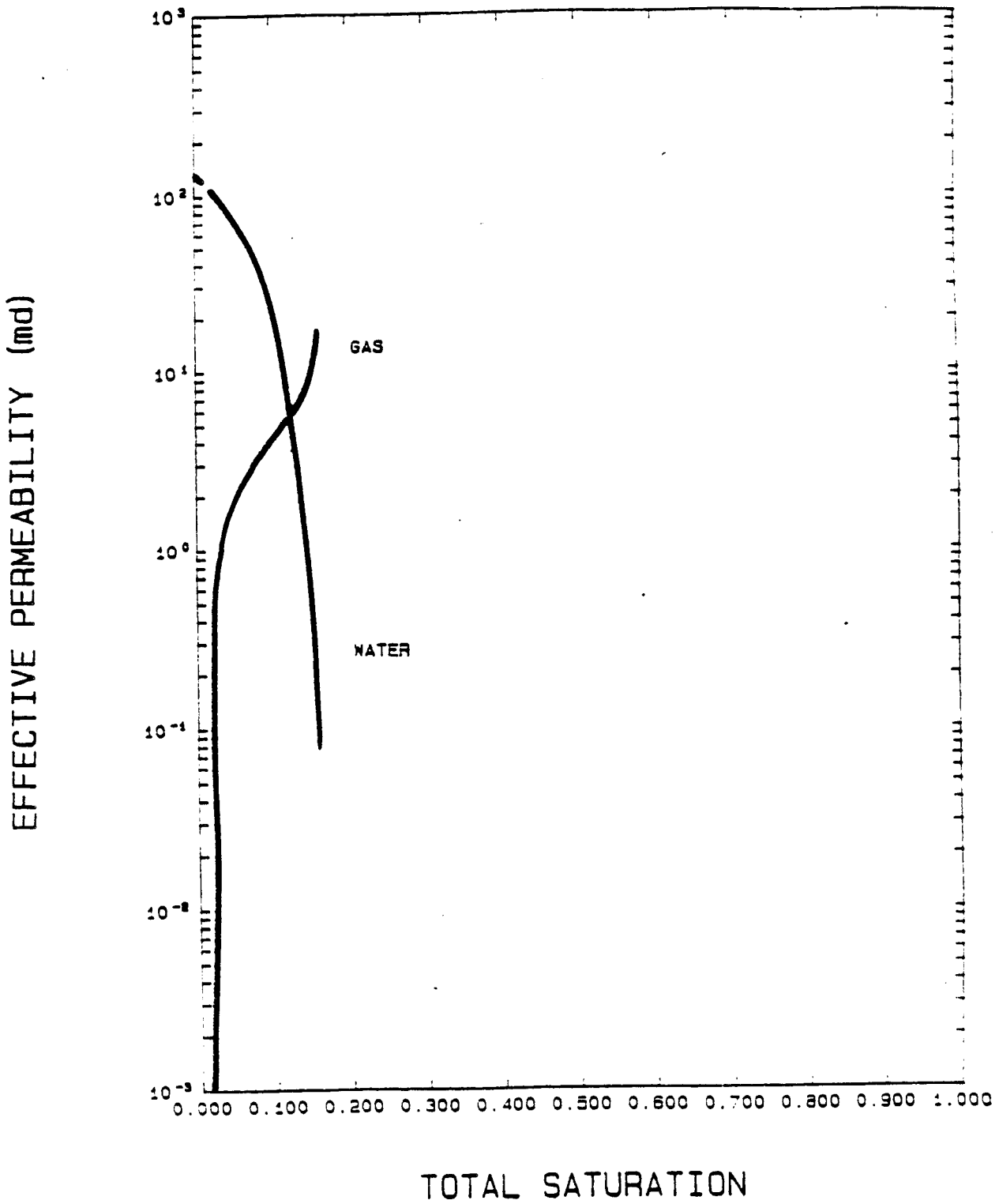

Figure D-11. Effective Permeability as a Function of Saturation for Sample MCG-612, Hole LLM-85-05, Depth of 76 Feet

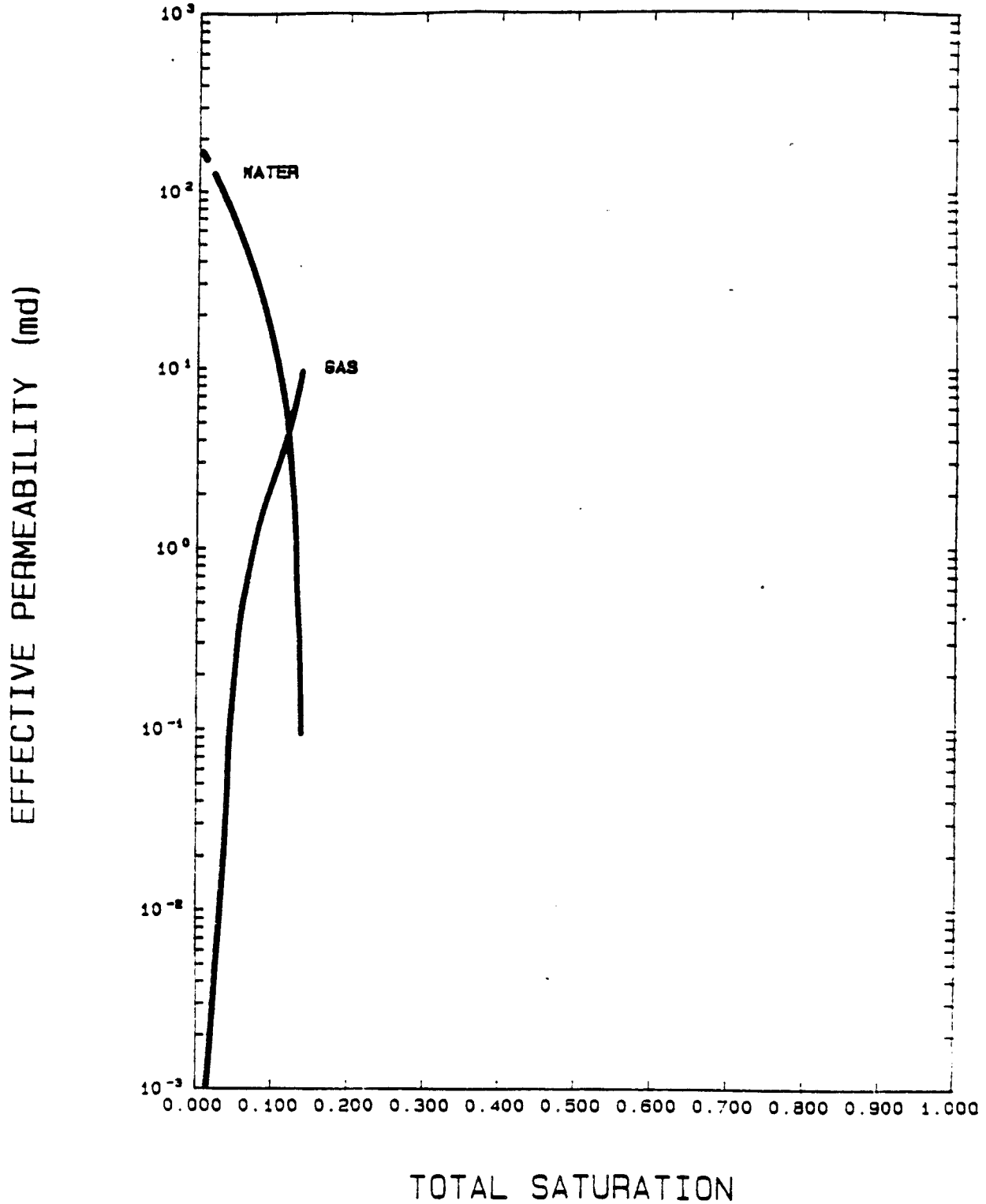

Figure D-12. Effective Permeability as a Function of Saturation for Sample MCG-613, Hole LLM-85-05, Depth of 123 Feet

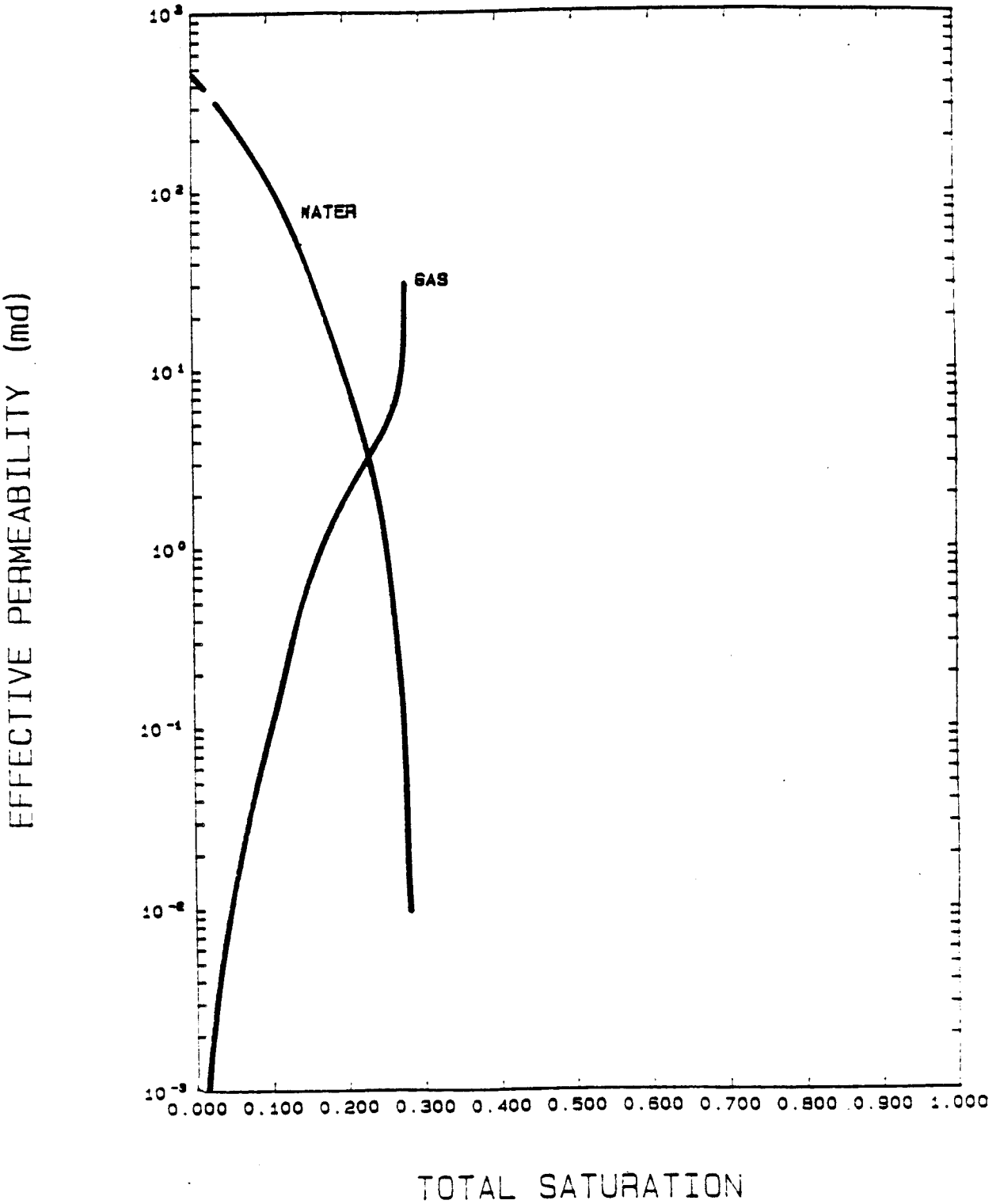

Figure D-13. Effective Permeability as a Function of Saturation for Sample MCG-614, Hole LGM-85-06, Depth of 29 Feet

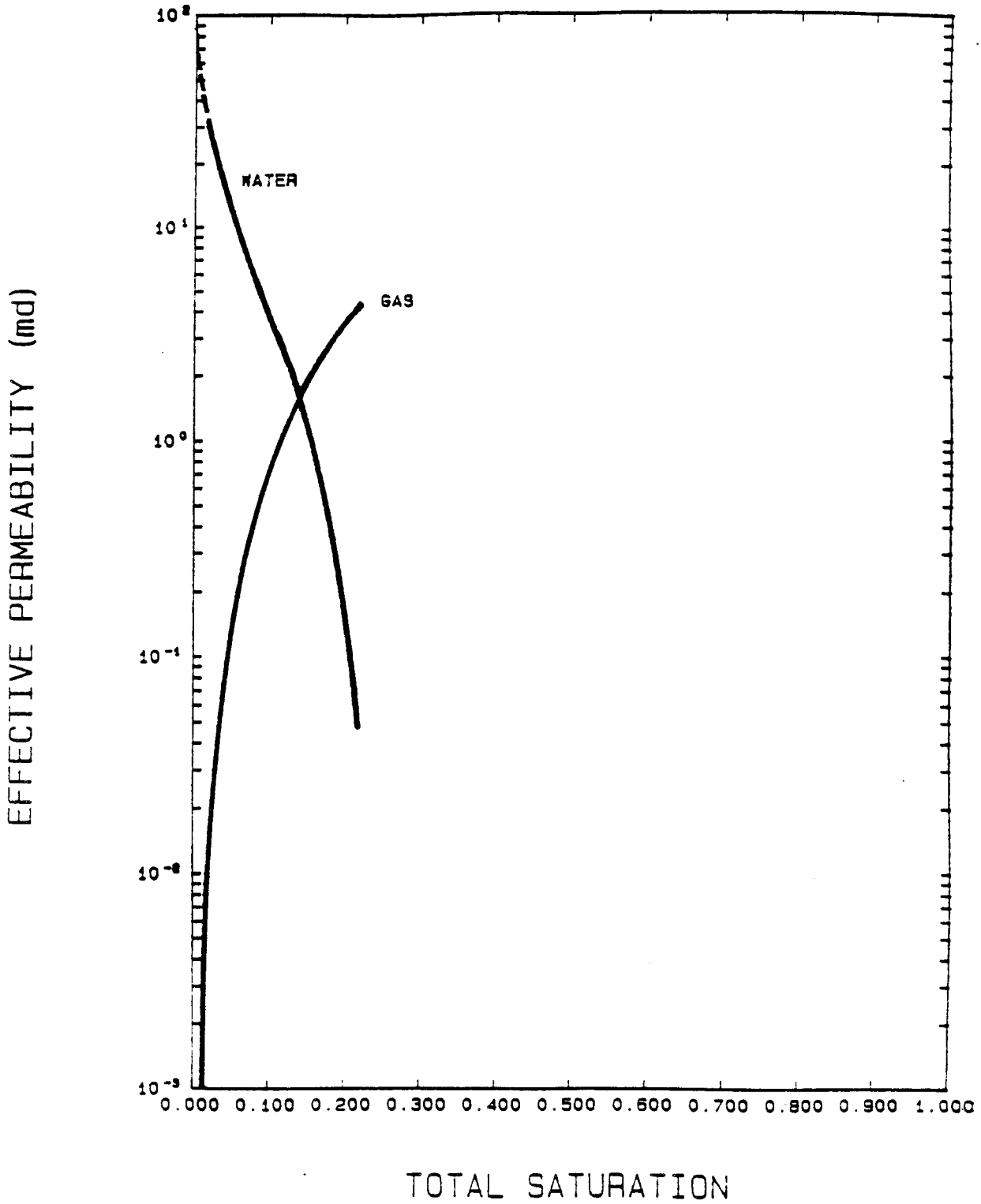

Figure D-14. Effective Permeability as a Function of Saturation for Sample MCG-615, Hole LGM-85-06, Depth of 51 Feet

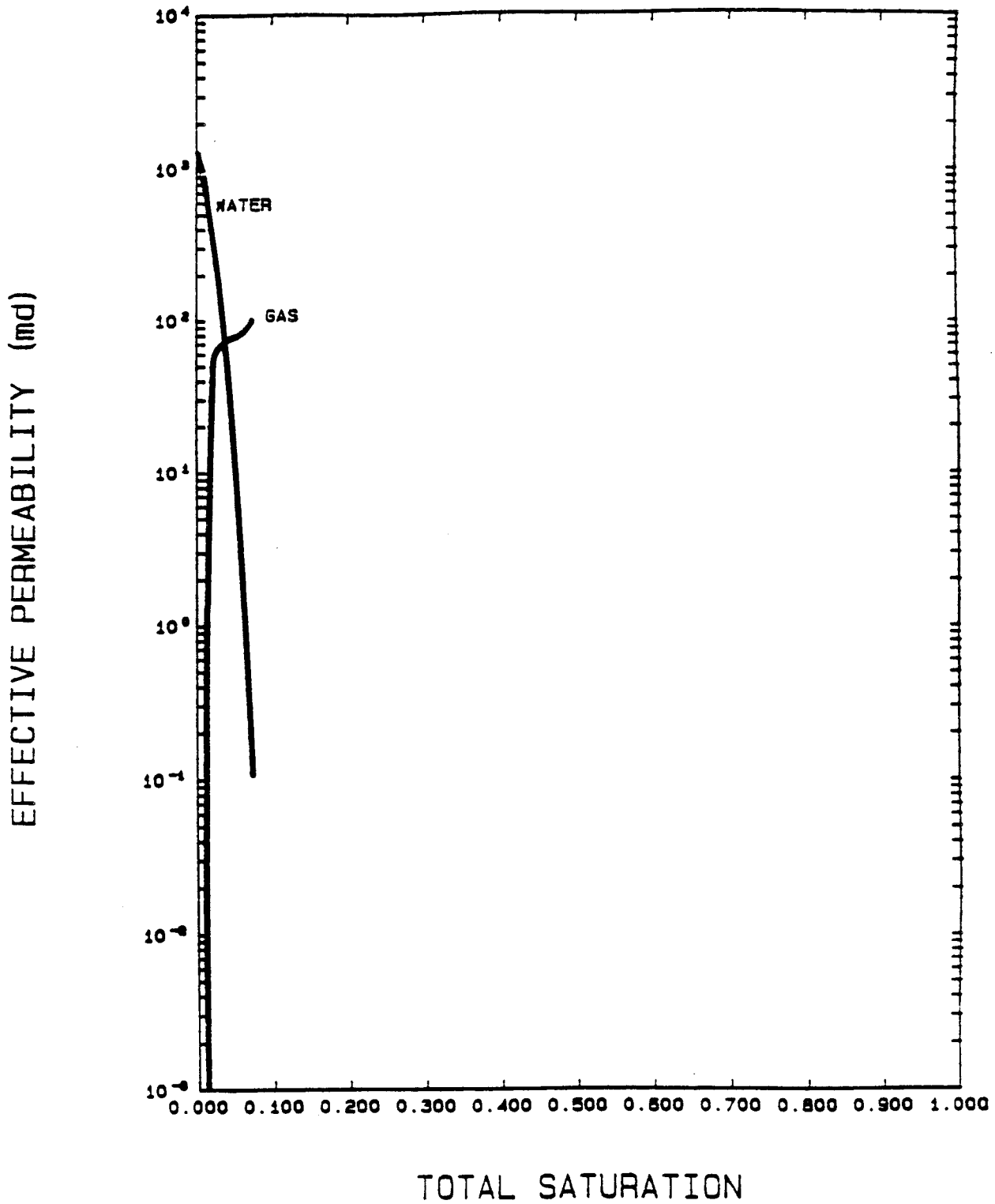

Figure D-15. Effective Permeability as a Function of Saturation for Sample MCG-616, Hole LGM-85-06, Depth of 99 Feet

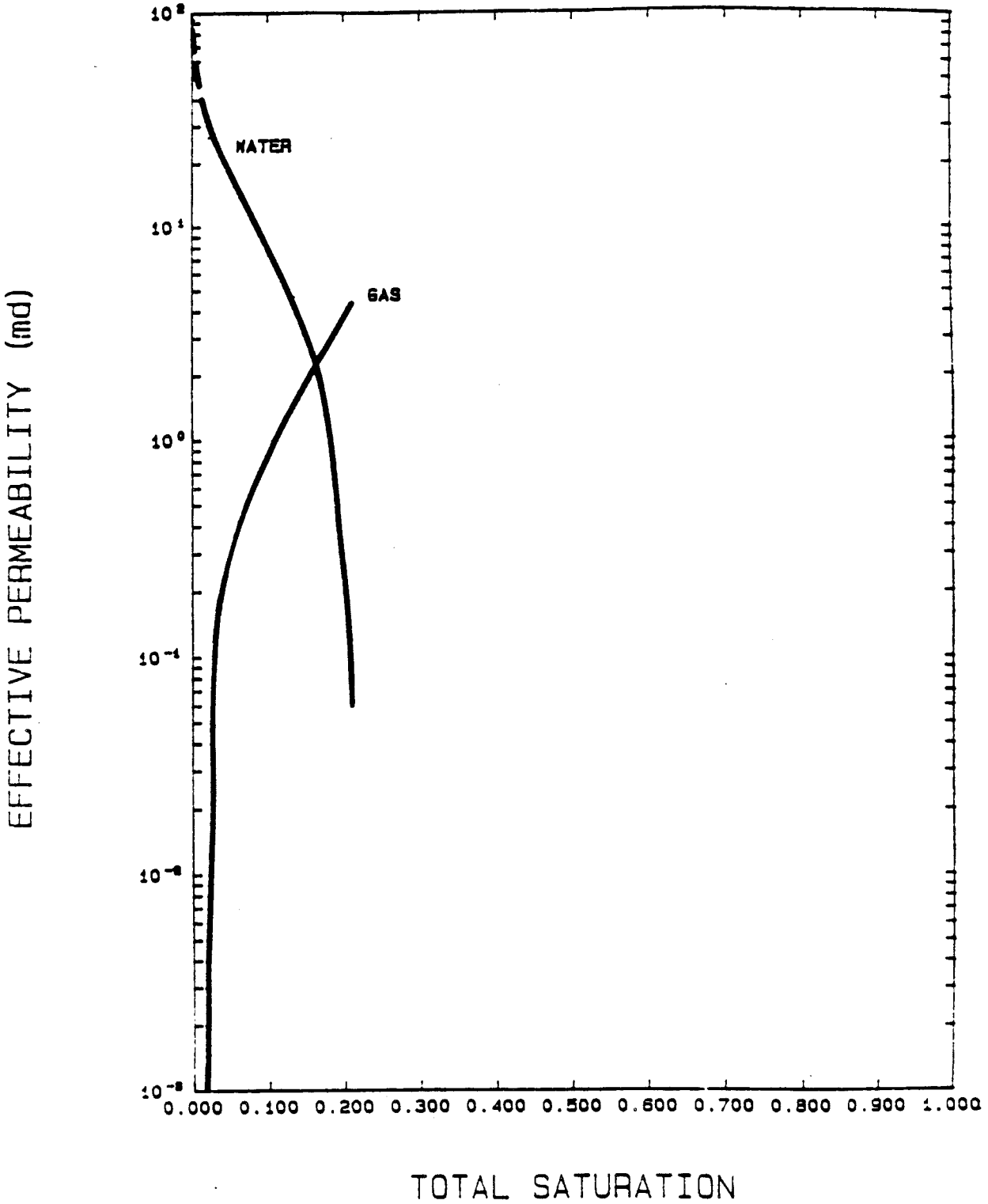

Figure D-16. Effective Permeability as a Function of Saturation for Sample MCG-617, Hole LGM-85-06, Depth of 115 Feet

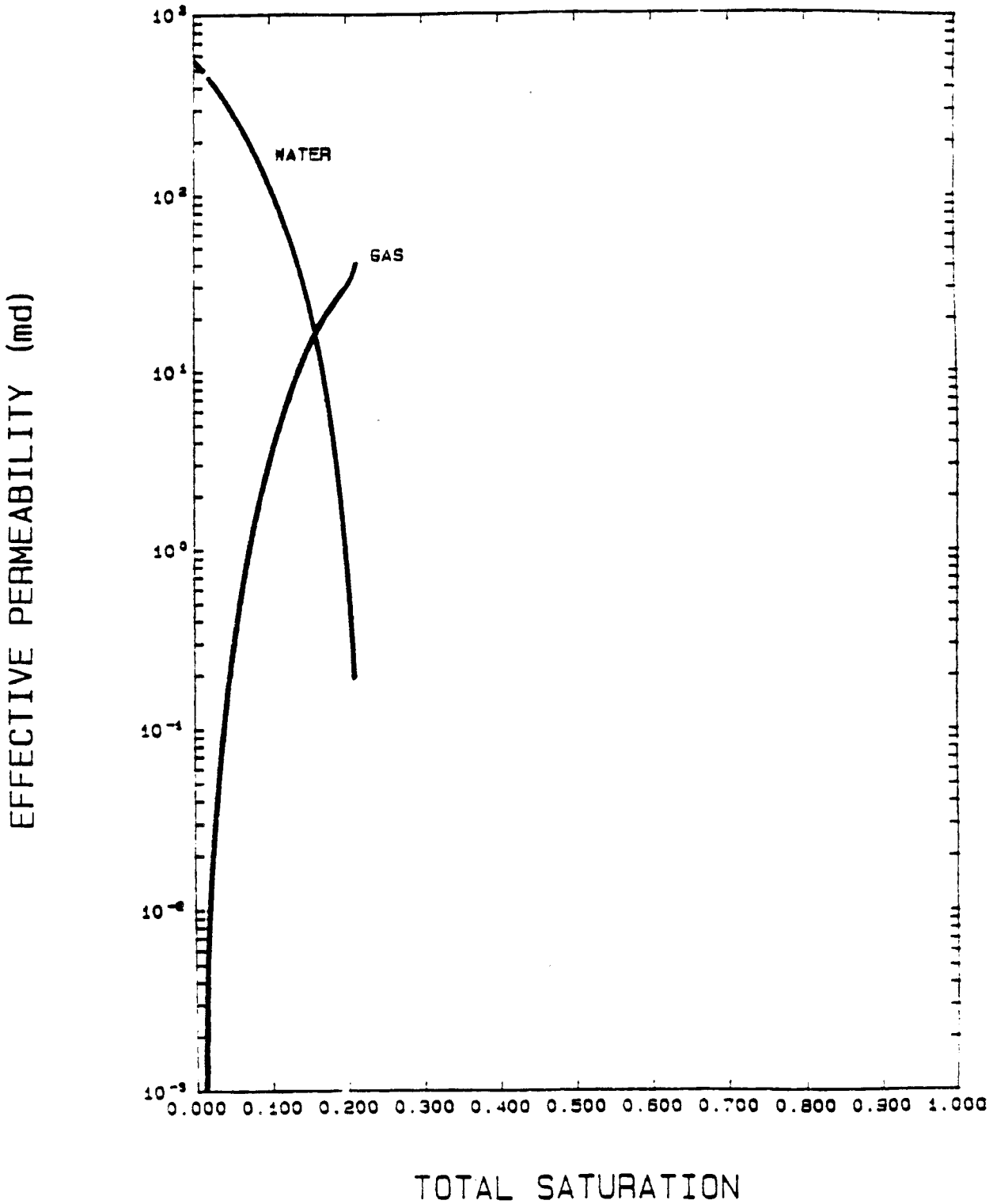

Figure D-17. Effective Permeability as a Function of Saturation for Sample MCG-618, Hole LGM-85-11, Depth of 3 Feet

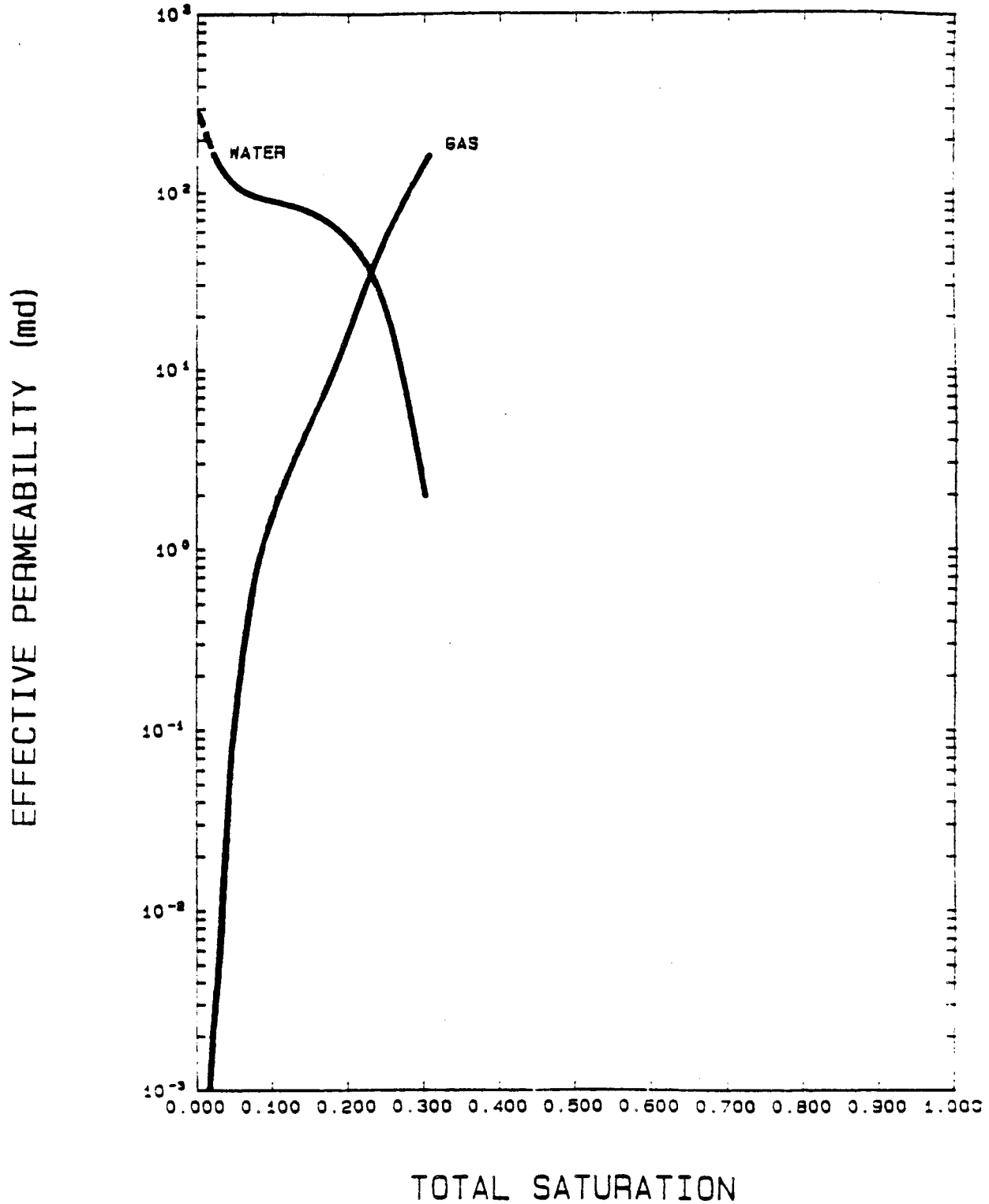

Figure D-18. Effective Permeability as a Function of Saturation for Sample MCG-619, Hole LGM-85-11, Depth of 30 Feet

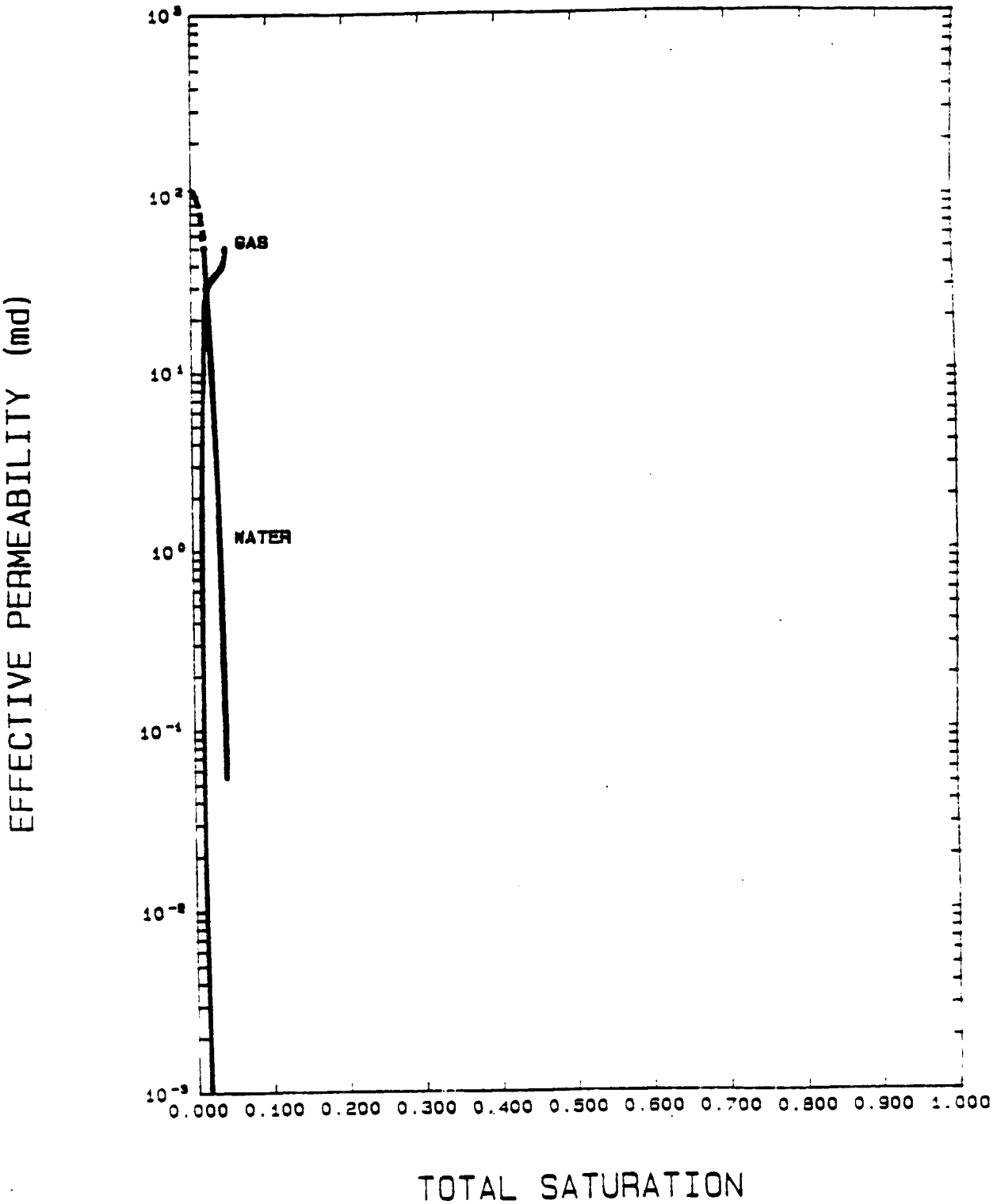

Figure D-19. Effective Permeability as a Function of Saturation for Sample MCG-620, Hole LGM-85-11, Depth of 94 Feet

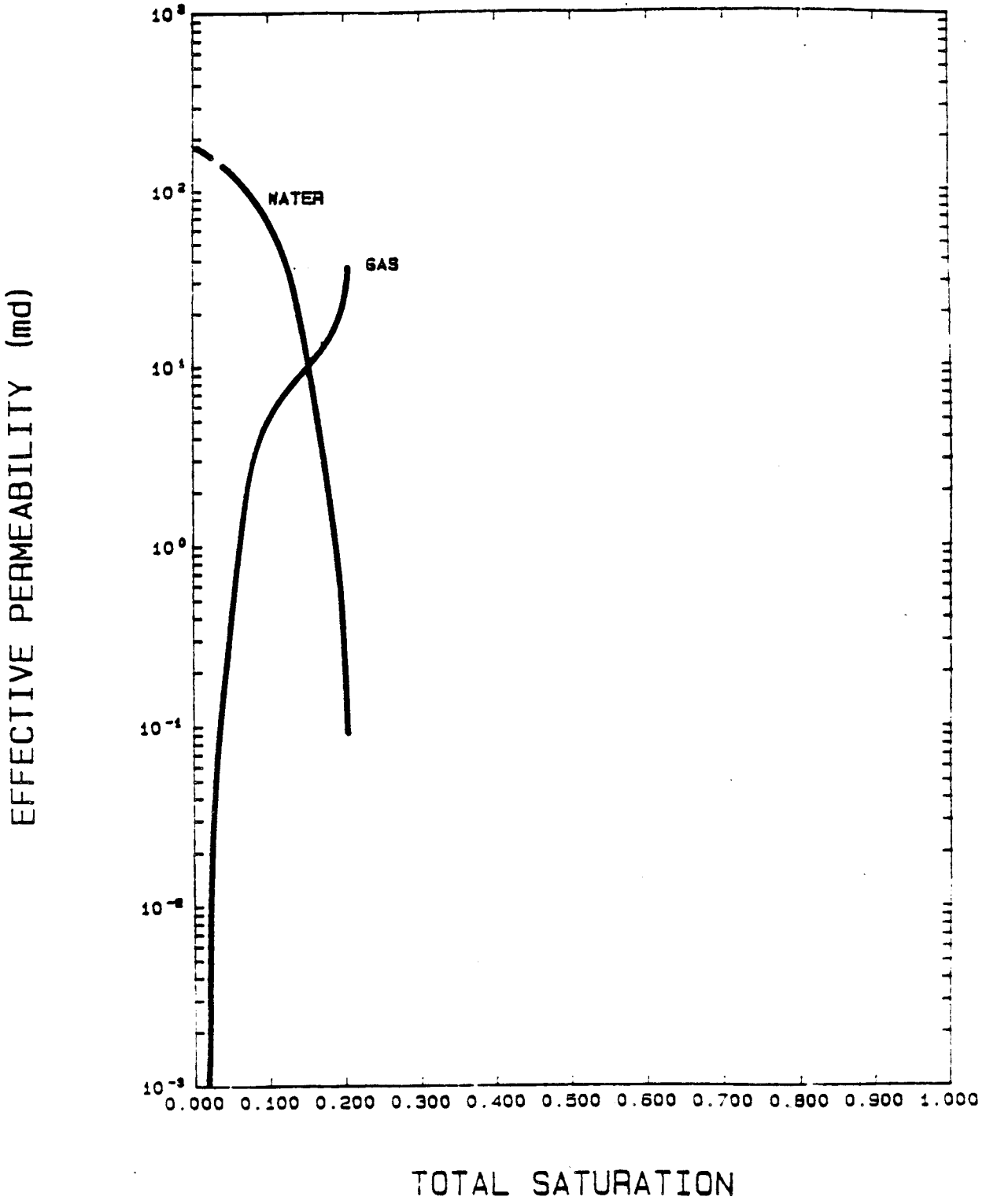

Figure D-20. Effective Permeability as a Function of Saturation for Sample MCG-621, Hole LGM-85-11, Depth of 115 Feet

Appendix E

LISTING OF FORTRAN V PROGRAM FOR CONVERTING PSYCHROMETER MICROVOLTAGE OUTPUTS TO WATER POTENTIAL

(modified from Brown and Bartos, 1982)

```
      PROGRAM H2OPOTU(INPUT,OUTPUT,TAPE5=INPUT,TAPE6=OUTPUT)
C**** LIMITS OF APPLICATION
C**** 14 < SEC < 61
C**** -1 < TEMP, DEGREES CEL < 41
C**** MV <= VIS*B*C
C**** -61 < OMV < 61
      REAL MV,MS,M15,IS,I15,LNS,LN15,NS,N15,MVS,MV15
      DATA SEC/15./
      IF(SEC.GE.14..AND.SEC.LE.61.) GO TO 10
      WRITE(6,5)
    5 FORMAT(' COOLING TIME IS NOT WITHIN MODEL RANGE')
      STOP
C
C**** READ INPUT DATA FOR FILE
   10 READ(22,20,END=100) I,DATE,TIME,B,TEMP,OMV,MV,DEPTH
   20 FORMAT(I4,A9,A7,F6.2,5F6.1)
      IF(TEMP.GE.-1..AND.TEMP.LE.41.) GO TO 30
      WRITE(6,25)
   25 FORMAT(' PSYCHROMETER TEMPERATURE IS NOT WITHIN MODEL RANGE')
      WP=-999.9
      GO TO 70
   30 IF(OMV.GE.-61..AND.OMV.LE.61.) GO TO 40
      WRITE(6,35)
   35 FORMAT(' ZERO OFFSET IS NOT WITHIN MODEL RANGE')
      WP=-999.9
      GO TO 70
   40 IF(MV.GT.0.) GO TO 50
      WRITE(6,45)
   45 FORMAT(' MICROVOLT READING .LE. 0.')
      WP=-999.9
      GO TO 70
C
   50 WPK=-22.5
      MS=2.5+EXP(-(ABS(((60.-SEC)/60.-1.)/.405)**3))
      M15=2.5+EXP(-(ABS(((60.-15.)/60.-1.)/.405)**3))
      IS=.45+.000333*SEC+1.9846E-19*SEC**10
      I15=.45+.000333*15.+1.9846E-19*15.**10
      RNS=EXP(-((1./(1.-IS))**MS))
      RN15=EXP(-((1./(1.-I15))**M15))
      DS=1.-RNS
      D15=1.-RN15
      X1AS=12.1-.003475*(60.-SEC)**1.63
      X1A15=12.1-.003475*(60.-15.)**1.63
      X1YS=39.2-.0004346*(60.-SEC)**2.45
      X1Y15=39.2-.0004346*(60.-15.)**2.45
      X2AS=88.-.0002579*(60.-SEC)**2.7
      X2A15=88.-.0002579*(60.-15.)**2.7
      X2YS=8.4+2.734E-07*(60.-SEC)**3.97
      X2Y15=8.4+2.734E-07*(60.-15.)**3.97
      LNS=EXP(-(ABS(((40.-TEMP)/40.-1.)/(1.-IS))**MS))
      LN15=EXP(-(ABS(((40.-TEMP)/40.-1.)/(1.-I15))**M15))
      NS=((LNS-RNS)/DS)*.185+1.18
      N15=((LN15-RN15)/D15)*.185+1.18
      UIS=X1AS+.017288*X1YS*TEMP**1.1
```

```
      UI15=X1A15+.017288*X1Y15*TEMP**1.1
      SPS=(X2AS-X2YS*.00017185*(40.-TEMP)**2.35)*(-1.)
      SP15=(X2A15-X2Y15*.00017185*(40.-TEMP)**2.35)*(-1.)
      MVS=(UIS-(UIS/(ABS(SPS)**NS))*(ABS(SPS-WPK)**NS))
      MV15=(UI15-(UI15/(ABS(SP15)**N15))*(ABS(SP15-WPK)**N15))
      ZOE=(.015*OMV+.001471*OMV*TEMP)
      C=(MVS+(MVS/MV15)*ZOE)/MVS
      R=UIS*C
      IF(MV.LE.R) GO TO 60
      WRITE(6,55)
   55 FORMAT(' MICROVOLT READING IS NOT WITHIN MODEL RANGE')
      WP=-999.9
      GO TO 70
   60 WP=((((ABS(SPS)**NS)*(UIS*C-MV))/(UIS*C))**(1./NS)+SPS)*B
      WP=-WP
   70 WRITE(23,20) I,DATE,TIME,B,TEMP,OMV,MV,DEPTH,WP
      GO TO 10
C
  100 CONTINUE
      STOP
      END
```

GJ-54

VADOSE ZONE CHARACTERIZATION OF TECHNICAL AREA 54, WASTE DISPOSAL AREAS G AND L, LOS ALAMOS NATIONAL LABORATORY, NEW MEXICO

REPORT 4: PRELIMINARY ASSESSMENT OF THE HYDROLOGIC SYSTEM THROUGH FISCAL YEAR 1986

By
Peter M. Kearl;
James J. Dexter;
Mark Kautsky

December 1986

UNC Service Through Technology

UNC Technical Services, Inc.
Grand Junction, Colorado

This report was prepared as an account of work sponsored by an agency of the United States Government. Neither the United States Government nor any agency thereof, nor any of their employees, makes any warranty, express or implied, or assumes any legal liability or responsibility for the accuracy, completeness, or usefulness of any information, apparatus, product, or process disclosed in this report, or represents that its use would not infringe privately owned rights. Reference herein to any specific commercial product, process, or service by trade name, trademark, manufacturer, or otherwise, does not necessarily constitute or imply its endorsement, recommendation, or favoring by the United States Government or any agency thereof. The views and opinions of authors expressed herein do not necessarily state or reflect those of the United States Government or any agency thereof.

GJ-54

VADOSE ZONE CHARACTERIZATION OF TECHNICAL AREA 54, WASTE DISPOSAL AREAS G AND L, LOS ALAMOS NATIONAL LABORATORY, NEW MEXICO

REPORT 4: PRELIMINARY ASSESSMENT OF THE HYDROLOGIC SYSTEM THROUGH FISCAL YEAR 1986

By
Peter M. Kearl;
James J. Dexter;
Mark Kautsky

December 1986

Work Performed Under Contract No. DE-AC07-86ID12584

Prepared for
U.S. Department of Energy
Assistant Secretary for Nuclear Energy
Los Alamos National Laboratory
Los Alamos, New Mexico
in Conjunction with
U.S. Department of Energy
Grand Junction Projects Office
Grand Junction, Colorado

Prepared by
UNC Technical Services, Inc.
Hazardous and Mixed Waste Program
Grand Junction, Colorado 81502

CONTENTS LISTING

		Page
FOREWORD		ix
EXECUTIVE SUMMARY		x
SECTION 1	INTRODUCTION	1
	1.1 Purpose and Scope	3
	1.2 Terminology and Units	4
	1.2.1 Terminology	4
	1.2.2 Units	5
	1.3 Previous Work	6
SECTION 2	GEOLOGIC CHARACTERIZATION OF THE STUDY AREA	7
	2.1 Regional and Site Geology	9
	2.2 Welding and Correlation of Ash-Flow Units at Mesita del Buey	14
	2.3 Petrographic Analyses	17
	2.4 Interpretation of Geophysical Logs	22
	2.4.1 Natural Gamma and Epithermal Neutron Moisture Logs	23
	2.4.2 Spectral Gamma Logs	23
	2.4.3 Magnetic Susceptibility and Gamma-Gamma Logs	26
	2.5 Fractures	32
	2.5.1 Subsurface Characteristics	32
	2.5.2 Surface Characteristics	33
SECTION 3	HYDROLOGIC CHARACTERIZATION OF THE VADOSE ZONE	35
	3.1 General Characteristics	37
	3.1.1 Gravimetric Moisture Content	37
	3.1.2 Porosity	45
	3.1.3 Moisture Characteristic Curves	47
	3.2 Permeability Determinations	50
	3.2.1 Borehole-Injection Tests	50
	3.2.2 Vacuum Tests	59
	3.2.3 Laboratory Measurements	63
	3.2.4 Hydraulic Conductivity as a Function of Moisture Content	68
	3.2.5 Permeability Summary	69
	3.3 Gradient Determinations	74
	3.3.1 Temperature and Water-Potential Measurements	74
	3.3.2 Atmospheric/Rock-Pore Pressure Monitoring System	90
SECTION 4	NEUTRON MOISTURE MEASUREMENTS	93
	4.1 Purpose and Scope	95
	4.2 Casing Installations	95
	4.3 Calibration of the Neutron Probe	97
	4.4 Monitoring Program	97

CONTENTS LISTING (continued)

		Page
SECTION 5	PORE-GAS SAMPLING SYSTEM	99
	5.1 Purpose and Scope	101
	5.2 Design	101
	5.3 Installation	101
SECTION 6	PETREX SURVEY	105
	6.1 Purpose and Scope	107
	6.2 Sampling and Analysis	107
	6.3 Results	107
SECTION 7	CONCLUSIONS	115
SECTION 8	REFERENCES	119

LIST OF APPENDICES

Appendix A.	Lithologic Logs and Instrument Completion Diagrams	A-1
Appendix B.	Petrographic Reports	B-1
Appendix C.	Moisture Characteristic Curves	C-1
Appendix D.	Effective Permeability as a Function of Saturation	D-1
Appendix E.	Listing of Fortran V Program for Converting Psychrometer Microvoltage Outputs to Water Potential	E-1
Appendix F.	Geophysical Logs	F-1

LIST OF FIGURES

Figure 2-1.	Location of the Study Area and Regional Geologic Relationships	10
2-2.	Geologic Cross Section from the Jemez Mountains on the West, Through the Pajarito Plateau, to the Rio Grande River on the East	11
2-3.	Locations of Drill Holes in Areas G and L, Technical Area 54, Los Alamos National Laboratory, New Mexico	12
2-4.	Cross Section Showing Parts of the Tshirege Member of the Bandelier Tuff, Drawn Through Mesita del Buey and Technical Area 54	15
2-5.	Fence Diagram Through Waste Disposal Area L Showing Subsurface Stratigraphy of the Bandelier Tuff	19
2-6.	Epithermal Neutron, Natural Gamma, and Lithologic Logs for Hole LGC-85-10	24
2-7.	Comparison of Moisture Curves for Hole LGM-85-06, Derived by Geophysical and Gravimetric Methods	25
2-8.	Spectral Gamma and Lithologic Logs for Hole LGM-85-11	27

LIST OF FIGURES (continued)

			Page
Figure	2-9.	Magnetic Susceptibility, Apparent Density, and Lithologic Logs for Hole LGC-85-10.	28
	2-10.	Magnetic Susceptibility, Apparent Density, and Lithologic Logs for Hole LLM-85-02.	30
	2-11.	Magnetic Susceptibility, Apparent Density, and Lithologic Logs for Hole LGM-85-11.	31
	2-12.	Rose Diagram of Joint Orientations of Exposed Fractures in Area L, Los Alamos National Laboratory	34
	3-1.	Plots of Volumetric Moisture Content as a Function of Depth for Drill Holes LLM-85-01, LLM-85-02, LLM-85-05, LGM-85-06, and LGM-85-11	40
	3-2.	Plots of Volumetric Moisture Content as a Function of Depth for Drill Holes LLC-86-19 and LLC-86-20	41
	3-3.	Plots of Volumetric Moisture Content as a Function of Depth for Drill Holes LLC-86-21 and LLC-86-22	42
	3-4.	Plots of Volumetric Moisture Content as a function of Depth for Drill Holes LLC-86-23 and LLC-86-24	43
	3-5.	Plots of Volumetric Moisture Content as a Function of Depth for Drill Hole LLC-86-25.	44
	3-6.	Porosity of Battleship Rock Ash-Flow Tuff, Valles Mountains, New Mexico	48
	3-7.	Air-Injection Apparatus Used for In-Situ Permeability Measurements.	53
	3-8.	Water-Injection Apparatus Used for In-Situ Permeability Measurements.	54
	3-9.	Vacuum-Testing Apparatus Used for In-Situ Permeability Measurements.	60
	3-10.	Unsaturated Hydraulic Conductivities as Functions of Moisture Content and Water Potential for Samples MCG-603 and MCG-604	70
	3-11.	Unsaturated Hydraulic Conductivities as Functions of Moisture Content and Water Potential for Samples MCG-607 and MCG-613	71
	3-12.	Unsaturated Hydraulic Conductivities as Functions of Moisture Content and Water Potential for Samples MCG-616 and MCG-617	72
	3-13.	Unsaturated Hydraulic Conductivities as Functions of Moisture Content and Water Potential for Sample MCG-620	73
	3-14.	Sketch of the Single-Junction Stainless Steel Screen-Shielded Thermocouple Psychrometer.	76
	3-15.	Sketch of the Stainless Steel Calibration Chamber Showing Seals and Screen-Shielded Thermocouple Psychrometer	78
	3-16.	Water Potential Versus Time for Selected Psychrometers in Hole LLP-85-03	81
	3-17.	Temperature Versus Time for Selected Psychrometers in Hole LLP-85-03	82
	3-18.	Water Potential Versus Time for Selected Psychrometers in Hole LGP-85-07	83

LIST OF FIGURES (continued)

			Page
Figure	3-19.	Temperature Versus Time for Selected Psychrometers in Hole LGP-85-07	84
	3-20.	Air Temperature Versus Time at Hole LLP-85-03	85
	3-21.	Water Potential Versus Depth for Hole LLP-85-03	86
	3-22.	Temperature Versus Depth for Hole LLP-85-03	87
	3-23.	Water Potential Versus Depth for Hole LGP-85-07	88
	3-24.	Temperature Versus Depth for Hole LGP-85-07	89
	3-25.	Results from the Pressure Transducers Installed in Hole LLP-85-03	92
	4-1.	Casing Installation and Depths of Neutron Probe Measurements in Hole LLN-85-04	96
	4-2.	Casing Installation and Depths of Neutron Probe Measurements in Hole LGN-85-08	98
	5-1.	Diagram of a Pore-Gas Sampling Port	102
	6-1.	Normalized Trichloroethylene Ion-Count Map, Waste Disposal Area L, Los Alamos National Laboratory, New Mexico	108
	6-2.	Normalized Tetrachloroethylene Ion-Count Map, Waste Disposal Area L, Los Alamos National Laboratory, New Mexico	109
	6-3.	Non-Normalized Benzene Ion-Count Map, Waste Disposal Area L, Los Alamos National Laboratory, New Mexico	110
	6-4.	Non-Normalized Toluene Ion-Count Map, Waste Disposal Area L, Los Alamos National Laboratory, New Mexico	111

LIST OF TABLES

			Page
Table	2-1.	Volume-Percent Quartz and Sanidine Determined from Point-Count Analysis of Thin Sections	21
	2-2.	Number of Fractures Logged in the Los Alamos Drill Holes	33
	3-1.	Results of Porosity Determinations Using the Helium-Injection Method and Boyle's Law	46
	3-2.	Hydraulic Conductivity Determined from Air-Injection Tests in Los Alamos Drill Holes	57
	3-3.	Hydraulic Conductivity Values Determined from Water-Injection Tests in Hole LLM-85-05	58
	3-4.	Comparison of Intrinsic Permeability Values Determined from Water-Injection and Air-Injection Tests in Hole LLM-85-05	59
	3-5.	Permeability Values Determined from Vacuum Tests in Los Alamos Drill Holes	64
	3-6.	Comparison of Intrinsic Permeability Values Determined from Air-Injection and Vacuum Tests in Los Alamos Drill Holes	65

LIST OF TABLES (continued)

			Page
Table	3-7.	Intrinsic Permeability Values Determined from Laboratory Analysis of Core Samples	67
	3-8.	Comparison of Average Intrinsic Permeability Values for the Major Geologic Units of the Bandelier Tuff in the Study Area	74
	3-9.	Installation Depths and Calibration Coefficients for Psychrometers in Hole LLP-85-03	79
	3-10.	Installation Depths and Calibration Coefficients for Psychrometers in Hole LGP-85-07	80

ATTACHMENTS

The 1986 geophysical logs for the Los Alamos National Laboratory drill holes are contained in the envelope attached to this report.

FOREWORD

This study was initiated in response to a Compliance Order/Schedule (Docket Number 001007) issued by the State of New Mexico's Environmental Improvement Division under the authority of New Mexico's Hazardous Waste Management Act. The Order/Schedule, dated 7 May 1985, specifies a time line for obtaining certain geotechnical information regarding Waste Disposal Areas G and L in Technical Area 54, Los Alamos National Laboratory, New Mexico. This report addresses the informational requirements outlined in Paragraph 25, Tasks 1 through 5, of the Compliance Order/Schedule. Certain field investigations performed in the Summer and Fall 1986 were above and beyond the requirements of the Compliance/Order Schedule. The investigations on which this report are based were performed by personnel of Bendix Field Engineering Corporation (Bendix), the contractor for the U.S. Department of Energy Grand Junction Projects Office (DOE/GJPO) through 30 September 1986. This report was prepared by the same professionals, now employed by UNC Technical Services, Inc., the current contractor.

The tasks requested by the State of New Mexico in Paragraph 25 of the Compliance Order/Schedule are addressed in the following sections of this report:

Compliance Order Task and Brief Title	Section in Report
1: Permeability Determinations	3.2.1, 3.2.2, 3.2.3
2: Moisture Characteristic Curves	3.1.3
3: Unsaturated Hydraulic Conductivity	3.2.4
4: Infiltration and Redistribution of Water	3.1.1, 3.3.1, 4.0
5: Pore-Gas-Sampling Installations	5.0

The emphasis of the Compliance Order/Schedule is on the quantification of capillary or liquid-flow transport processes. However, moisture data presented by Purtymun and Kennedy (1971) and Abeele and others (1981), as well as the moisture data presented in this report, indicate that movement by vapor phase is the major transport mechanism in the Bandelier Tuff in the study area. Thus, while much of the capillary-related information is useful, it can draw attention away from vapor transport. The reader is therefore asked to focus on relating the information presented in this report to vapor-transport processes.

In addition to the authors cited on the title page, a number of other contractor technical professionals at the Grand Junction Projects Office contributed significantly to this study and to preparation of this report. These individuals and their respective contributions are listed below.

- Sue Rush served as Project Manager and assisted in the drilling and the pore-gas-sampler installations.

- Nic Korte served as Project Manager and assisted in the design and test of the pore-gas samplers.

- Steve Sturm assisted in the drilling and the logging of core.

- Jeff Price assisted in the hydrologic testing.
- Jack McCaslin assisted in the drilling procurement as well as the drilling and the pore-gas-sampler installations.
- Steve Donivan assisted in the design and test of the pore-gas samplers.
- Sandy Wagner performed the field chemical monitoring and set up the analytical subcontract.
- Sue Knutson, Dave Traub, and Joseph Krabacher performed the geophysical logging.
- Rich Zinkl provided the computer support.
- Bonnie Edwardson and Marilynne Gossett performed the editing and document coordination.
- Kenneth Karp assisted with calibration and installation of psychrometers.

The following personnel from Los Alamos National Laboratory also played a significant role in the completion of this study.

- Micheline Devaurs was the principal technical contact, assisted in the planning and conduct of field activities, and wrote Section 4 of this report.
- Dave McInroy assisted in several aspects of the field activities.
- Bill Purtymun recommended the drilling technique and provided much useful insight with respect to logging the Bandelier Tuff.

EXECUTIVE SUMMARY

The hydrologic characteristics of the vadose zone in Areas G and L, Technical Area 54, at Los Alamos National Laboratory were investigated in response to a Compliance Order/Schedule (Docket Number 001007) issued to the Laboratory by the State of New Mexico's Environmental Improvement Division under the authority of New Mexico's Hazardous Waste Management Act. This report summarizes an assessment of the hydrologic system, specifically in response to Tasks 1 through 5, Paragraph 25, of the Compliance Order/Schedule. Vadose zone characterization work completed above and beyond the requirements of the Compliance Order/Schedule is also discussed herein.

The most significant conclusion resulting from this investigation is that vapor-phase transport is the predominant mechanism controlling the potential subsurface movement of contaminants in the study area. Evidence for this conclusion includes the low moisture content of the underlying rock and the high moisture-retention values observed in the moisture characteristic curves (Task 2 of the Compliance Order/Schedule). These results indicate that there is no interconnection or movement of liquid water in the interval of Bandelier Tuff examined in this study.

Permeability measurements were required by Task 1 (field tests) and Task 3 (laboratory tests) of the Compliance Order/Schedule. Field measurements were made using a vacuum-test method and by means of borehole injection with both air and water. Laboratory determinations were made using both the Klinkenberg Correction and the Dynamic methods. Agreement among the various methods was generally good, yielding an intrinsic permeability for the Bandelier Tuff in the range 10^{-8} to 10^{-9} cm^2.

Determination of the water distribution in the tuff was required by Task 4. Gravimetric results indicate a moisture content of 2 to 4 percent for the center portion of the profile, with generally higher contents in the lower portion of Unit 1b. Preliminary data from the thermocouple psychrometers indicate that water potentials range from -1 to -15 bar, suggesting low moisture conditions in the tuff. Neutron-measurement tools used for acquiring moisture data were also installed in two holes in the study area. Although data acquired with the probe were not available at the time of this writing, it is feared that the tuff may be too dry for such measurements to be effective.

The various field and laboratory activities conducted during this study permit an evaluation of the effects of porosity, pumice content, and degree of welding on the unsaturated transport processes. As expected, porosity and pumice content are highly correlated. The high porosity demonstrates that the tuff acts like a sponge: A quantity of water equal to approximately one-quarter of the rock volume is required to satisfy the capillary forces and permit the movement of water in the liquid phase. Permeability, on the other hand, is inversely proportional to porosity due to the significant amount of dead-end pore space which occurs in pumice. Finally, a high degree of welding apparently reduces the average radii of pores, the result being an increase in the capillary forces and the residual moisture content.

In partial fulfillment of the requirements of Task 5, installations for sampling pore gas in discrete subsurface zones were completed in certain holes. The rationale behind each sampling-port location is described in this report. Quarterly monitoring of the pore-gas samplers is being conducted by employees of the Laboratory; data from the monitoring were not available for this report.

Another major objective of this study was to evaluate the role of fractures as avenues of transport in the Bandelier Tuff. Results obtained thus far, however, are inconclusive. Although predominant northeasterly trends were measured, a bias in the data resulted from sampling limitations imposed by available exposures. The permeability of fractured zones, where fractures are filled, is not significantly greater than that of the surrounding rock. Certain fractured zones exhibit a higher moisture content and may be indicative of relatively open fractures. Petrex survey results indicate that ion counts of volatile organic compounds are not distributed uniformly in a radial pattern around the source. Instead, the distribution of volatile organic compounds is spatially variable, as if venting occurs in discrete zones whose fracture apertures and/or intensities may be locally elevated. Transport of contaminants from the source probably follows tortuous routes determined by a combination of fracture orientations and degree of dialation, and interconnections of fractures related to the position of infill materials. It is anticipated that results of the pore-gas sampling and analysis will be of particular benefit to the definition of the role of fractures in the vadose zone. In addition, more extensive Petrex surveys just under the rim of Mesita del Buey and in Area L may also better define the role of fractures relative to contaminant transport.

Section 1

INTRODUCTION

1.1 PURPOSE AND SCOPE

This report summarizes work conducted for Los Alamos National Laboratory (LANL) to assess the hydrologic processes that could contribute to transport of hazardous waste buried in the Bandelier Tuff at the LANL facility in New Mexico. More specifically, the study area encompasses Waste Disposal Areas G and L in Technical Area 54. The study was initiated in response to a Compliance Order/Schedule issued by the Environmental Improvement Division of the State of New Mexico. Included in the Order was a directive to obtain certain geotechnical information regarding the above-mentioned waste-disposal areas.

Work conducted during FY-1986 for this project included drilling, logging, and installation of monitoring equipment in additional boreholes. Seven new holes were drilled and two existing holes (drilled during FY-1985) were deepened. Pore-gas samplers were installed in selected holes. Geophysical logs were run in the new holes and lithologic logs were prepared to show monitoring equipment installation points. A Petrex survey was conducted to measure relative ion counts of organic vapors in the soil.

The FY-1986 work was conducted primarily to support preliminary conclusions based on results of earlier work. Consequently, this report has been prepared by amending and supplementing an earlier report by Kearl and others (1986). New material in this report includes a section on the Petrex survey, expansion of a section on pore-gas sampling, additional lithologic and geophysical logs, petrographic reports on FY-1986 samples, and a fence diagram showing the subsurface stratigraphy of Waste Area L.

The report is organized into eight sections, followed by six appendices. The emphasis throughout is on the transport processes in the unsaturated zone that control potential contaminant migration in the Bandelier Tuff. Immediately following this Introduction, Section 2 defines the geologic framework through which these processes occur in the study area. Section 3 presents a characterization of the vadose zone in terms of the driving forces of transport, namely, gradients such as temperature and pressure. These evaluations require a considerable amount of data regarding the vadose zone, including permeability and such general parameters as moisture content and porosity. Thus, the early subsections of Section 3 describe the field and laboratory measurements conducted to acquire these data, together with the necessary calculations.

Sections 4 and 5 contain discussions of the neutron-moisture-measurement and pore-gas sampling-port installations, respectively; Section 6 describes results of the Petrex survey. A comprehensive summary of results and conclusions is presented in Section 7, followed by a list of the references (Section 8) cited throughout the text and appendices. Appendices A through F contain much of the data acquired throughout the course of this study, including lithologic logs, petrographic data, moisture characteristic and permeability curves, and geophysical logs.

For this study, several experimental techniques were used to drill test holes and to measure important unsaturated flow parameters. In those cases, descriptions of the equipment, procedures, and assumptions associated with a specific test are included in the appropriate discussion.

Analysis of the rock core was hampered by several problems. From the core obtained during drilling, representative samples of the Tshirege Member of the Bandelier Tuff were selected and sent to TerraTek Research Laboratory of Salt Lake City, Utah, for analysis. Approximately 75 percent of this core was either completely unconsolidated or so friable that special handling techniques and procedures had to be developed. Moreover, mercury injection was not feasible on the unconsolidated samples, requiring that alternative laboratory techniques be substituted for the measurement of capillary forces. As a result, it was not possible to quantify the pore-size distributions and the imbibition or wetting curves for the porous media in the study area.

1.2 TERMINOLOGY AND UNITS

1.2.1 TERMINOLOGY

The terms 'vadose zone' and 'unsaturated zone' are often used synonymously in the literature, even though there is a distinction between the two. The unsaturated zone is defined as a subsurface area above the water table in which the porous material contains both air and water, the latter under pressures that are less than those of the atmosphere. The vadose zone also refers to the subsurface area above the water table composed of partially saturated porous material. The distinction lies in the fact that the vadose zone can contain perched zones of water, and the water in these perched zones is under pressures greater than those of the atmosphere. For purposes of this study, the term vadose zone will be used when referring to the subsurface area above the water table, but the processes controlling contaminant migration in that zone will be referred to as the 'unsaturated transport processes.'

Other potentially confusing terms used throughout the report include permeability, coefficient of permeability, hydraulic conductivity, and intrinsic permeability. Distinctions between these terms are summarized below.

- Permeability, when used alone, refers to the movement of a fluid through the porous or fractured media. No quantification is intended to be associated with the term.

- Hydraulic conductivity is the term used to quantify the permeability of the medium. It is dependent on the porous medium and the fluid, and must therefore be expressed in such a way that the fluid represented by the term is specified. The dimensions for hydraulic conductivity are length per unit time (L/t). The term coefficient of permeability is synonymous with hydraulic conductivity.

- Intrinsic permeability is a function of only the medium and has dimensions of length squared (L^2). Expressing permeability in this way permits comparison of permeability values obtained through different techniques using different fluids. (The relationship between hydraulic conductivity and intrinsic permeability is defined in Section 3.2.1.4.)

Laboratory results express the hydraulic conductivity as a function of the moisture content (Section 3.2.4) in terms of effective permeability (in units of millidarcys). Permeability expressed in this manner is considered an

intrinsic permeability. For example, the effective permeability for water is a measurement of the intrinsic permeability of the void space occupied by water, so the value is expressed in terms which are independent of the fluid.

The terms capillary forces, capillary pressure, soil tension, and soil suction are used synonymously. For purposes of this report, capillary forces are quantified using the term water potential which is measured in pressure units of negative bars or negative pounds per square inch (psi).

The terms residual moisture content, residual saturation, and moisture retention are also used synonymously. These terms refer to the undrainable quantity of water which remains in the sample even at increasingly higher capillary pressures. At these pressures, the water exists in discontinuous pockets or as thin films throughout the porous matrix. Vapor transport is the dominant transport mechanism below this range of saturation.

One other term used throughout the report requires clarification. As used herein, lapilli is defined in a manner consistent with the definition presented by Ross and Smith (1961): Lapilli consist of either juvenile lava fragments, still plastic or liquid when ejected, or of broken rock of any sort from the walls of the vent, or from the bedrock (country rock); in other words, they may be essential, accessory, or accidental ejecta. These authors state, however, that the term lapilli should be restricted to describing fragments in the size range 4 to 32 millimeters (mm); fragments of pyroclastic material larger than 32 mm are called blocks, whereas fragments smaller than 4 mm are called coarse ash (Ross and Smith, 1961). For purposes of simplification in this report, the size restriction for lapilli was ignored. For example, the presence of 'accessory' or 'accidental' lithic fragments (e.g., basalt fragments) less than 4 mm in diameter is one of the distinguishing characteristics of Unit 1b; these fragments are referred to as lithic lapilli in this report. In addition, fragments of pyroclastic ejecta of pumice or rock in the size range 32 to 60 mm (the latter value being the approximate diameter of the rock core obtained during this study) are also referred to as lapilli in this report.

1.2.2 UNITS

Inconsistencies in the unit systems used to express measurements occur throughout the report. Unfortunately, this inconsistency is unavoidable for the following reason. Several different types of instrument were used in the study, some of which display data in metric units (mks or cgs systems), while others are based on the British engineering system (fps system).* Conversion from one set of units to another is often cumbersome. For example, an instrument which measures pressure in the range 0 to 60 pounds per square inch (psi), with 0.2-psi increments, is described efficiently in British-system units. Conversion to the metric system results in an awkward description [i.e., 0 to 413.47 kilonewtons per square meter (kN/m^2) with 1.38-kN/m^2 increments]. Thus, for purposes of this report, both systems of units are given only when appropriate, in which cases the value in metric units is cited

*For metric-system units, mks = meter-kilogram-second and cgs = centimeter-gram-second. For British-system units, fps = foot-pound-second.

first, followed in parentheses by the equivalent value in British-engineering-system units.

1.3 PREVIOUS WORK

This report draws heavily on three earlier reports prepared for Los Alamos National Laboratory by the GJPO contractor personnel based on work conducted prior to FY-1986. The first report (Rush and Dexter, 1985) describes and discusses drilling and logging activities performed during the Summer of 1985. The second report (Bendix Field Engineering Corporation, 1985b) describes the procedures used for operating monitoring instruments installed for assessment of the hydrogeologic conditions of Waste Disposal Areas G and L in Technical Area 54. The third report (Kearl and others, 1986) presents a preliminary assessment of the hydrologic system based on FY-1985 work.

Section 2

GEOLOGIC CHARACTERIZATION OF THE STUDY AREA

This description of the geologic characteristics of the Bandelier Tuff in the study area is divided into five subsections. The first describes regional and site geology, based on information contained in the literature and observations of core obtained from holes drilled at the site (Rush and Dexter, 1985). This is followed by a discussion of the degree of welding observed in the tuff and the correlation of ash-flow units across the study area. Results of petrographic analyses of core samples from the drill holes and interpretations of the geophysical logs from the holes are summarized in Sections 2.3 and 2.4, respectively. The final subsection describes fractures observed in the core, since the presence of fractures can affect the nature and direction of waste transport in the tuff.

2.1 REGIONAL AND SITE GEOLOGY

The study area is located just east of the southeastern boundary of the Colorado Plateau (see Figure 2-1), on the eastern flank of the Jemez Mountains, also known as the Pajarito Plateau. The Jemez Mountains lie at the intersection of the volcanically active Jemez Lineament and the tectonically active Rio Grande rift. The Jemez Lineament is an alignment of Late Cenozoic volcanic fields; volcanism along the lineament has been continuous since Pliocene time (Goff and Bolivar, 1983).

Waste Disposal Areas G and L, located within Technical Area 54 at Los Alamos National Laboratory, are situated on Mesita del Buey, which is part of the Pajarito Plateau (Figure 2-2). Mesita del Buey, a narrow, southeast-trending mesa approximately two miles long and one-quarter of a mile wide, is underlain by rhyolitic ash-flow and air-fall deposits of the Bandelier Tuff. The Bandelier Tuff is composed of two members: the lower Otowi Member, 1.4 million years old, and the upper Tshirege Member, 1.1 million years old (Bailey and others, 1969). The Otowi Member consists of basal, air-fall tuff overlain by nonwelded ash-flow deposits containing abundant lithic lapilli. The Tshirege Member, which overlies the Otowi, consists of basal, bedded, air-fall tuff overlain by nonwelded to welded ash-flow tuffs containing abundant pumice and lithic lapilli. The Otowi and Tshirege members are both over 100 feet (ft) thick under Mesita del Buey (Purtymun and Kennedy, 1971). All waste-disposal excavations in Technical Area 54 are located in the upper portion of the Tshirege Member of the Bandelier Tuff.

The Tshirege Member can be subdivided into three units, two of which occur at Mesita del Buey (Units 1 and 2); the third unit, a nonwelded to moderately welded pumiceous tuff, is absent in the study area (Purtymun and Kennedy, 1971). The first two units dip 2 to 3 degrees to the southeast and become thinner in the direction of dip, away from their source in the Valles Caldera. Each of the units consists of two subunits (a and b), which are described by Purtymun and Kennedy (1971). Their descriptions, together with characteristics observed in the field and in the core collected for this study, were used to distinguish between each of the subunits. Lithologic logs of Units 1a through 2b, derived from drill holes in the study area, are presented in Appendix A; drill-hole locations are shown in Figure 2-3.

The lowermost subunit of the Tshirege Member encountered during this study was Unit 1a, a slightly welded to nonwelded, light-orange to light-brown,

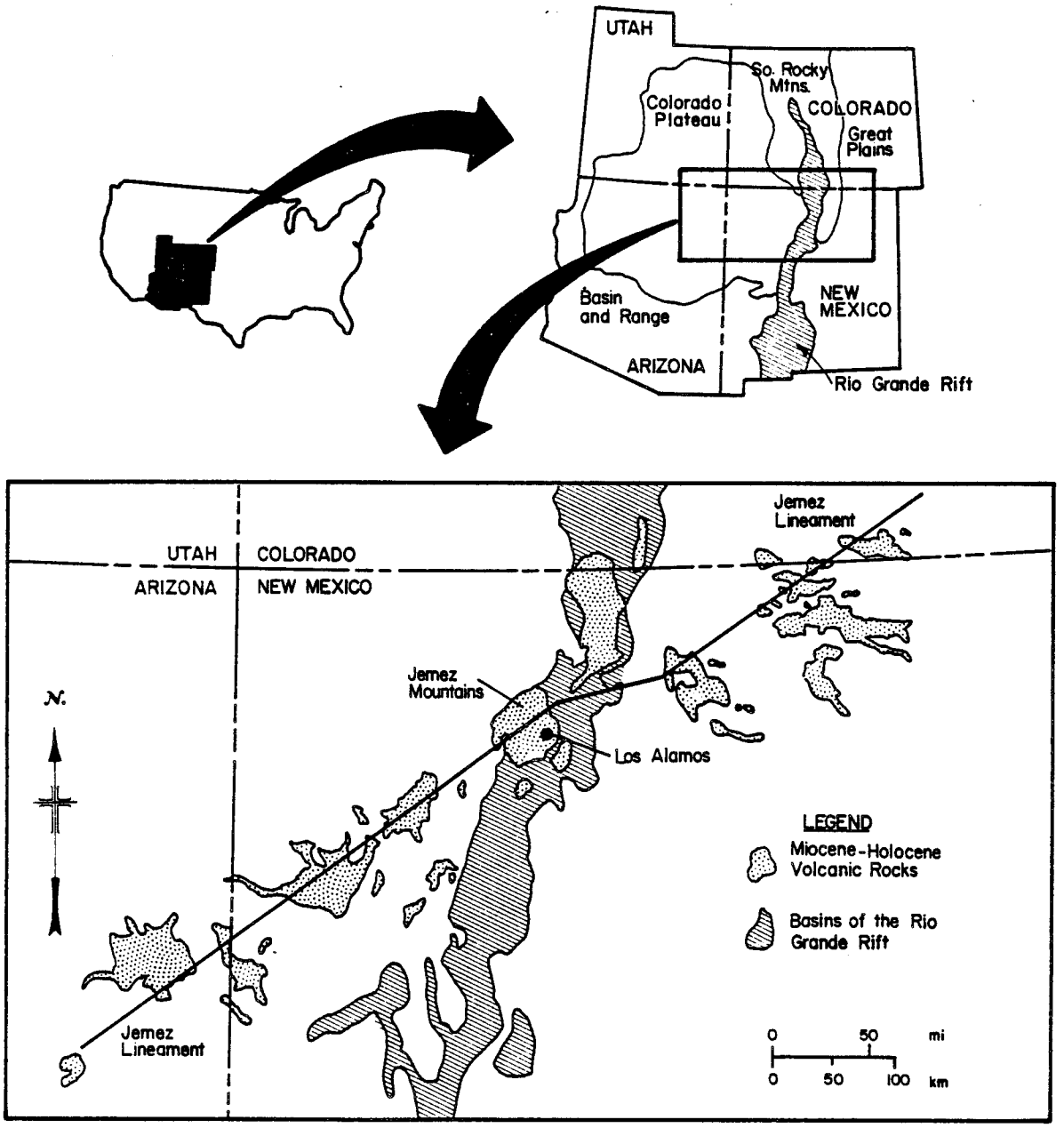

Figure 2-1. Location of the Study Area and Regional Geologic Relationships (modified from Goff and Bolivar, 1983)

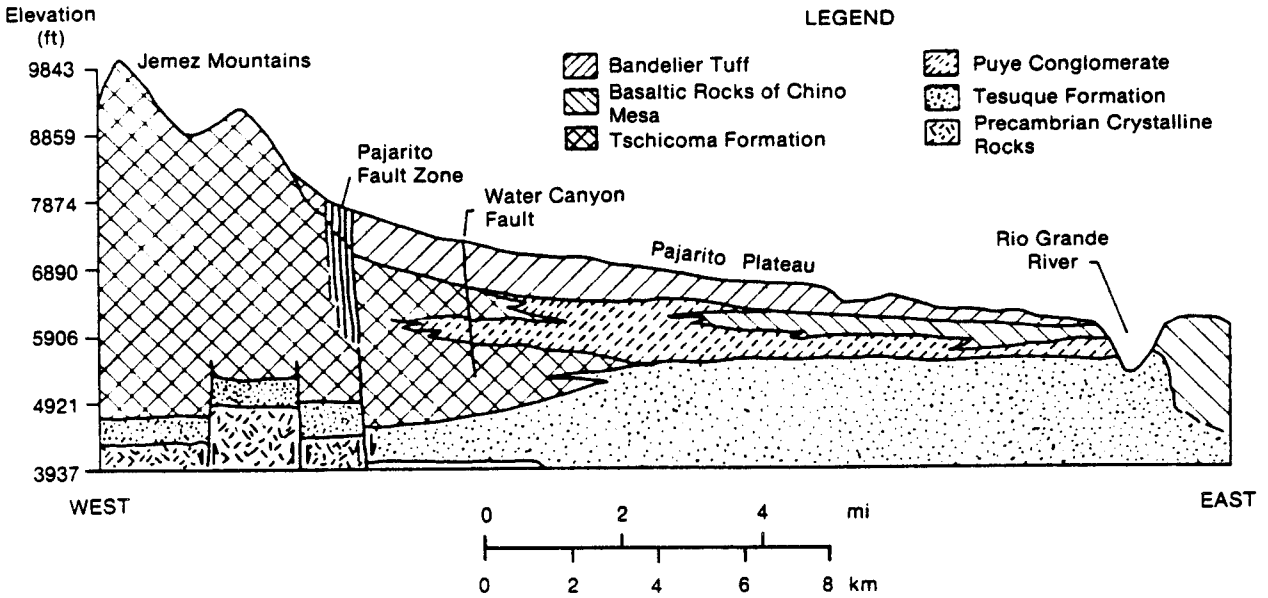

Figure 2-2. Geologic Cross Section from the Jemez Mountains on the West, Through the Pajarito Plateau, to the Rio Grande River on the East (modified from Abeele and others, 1981)

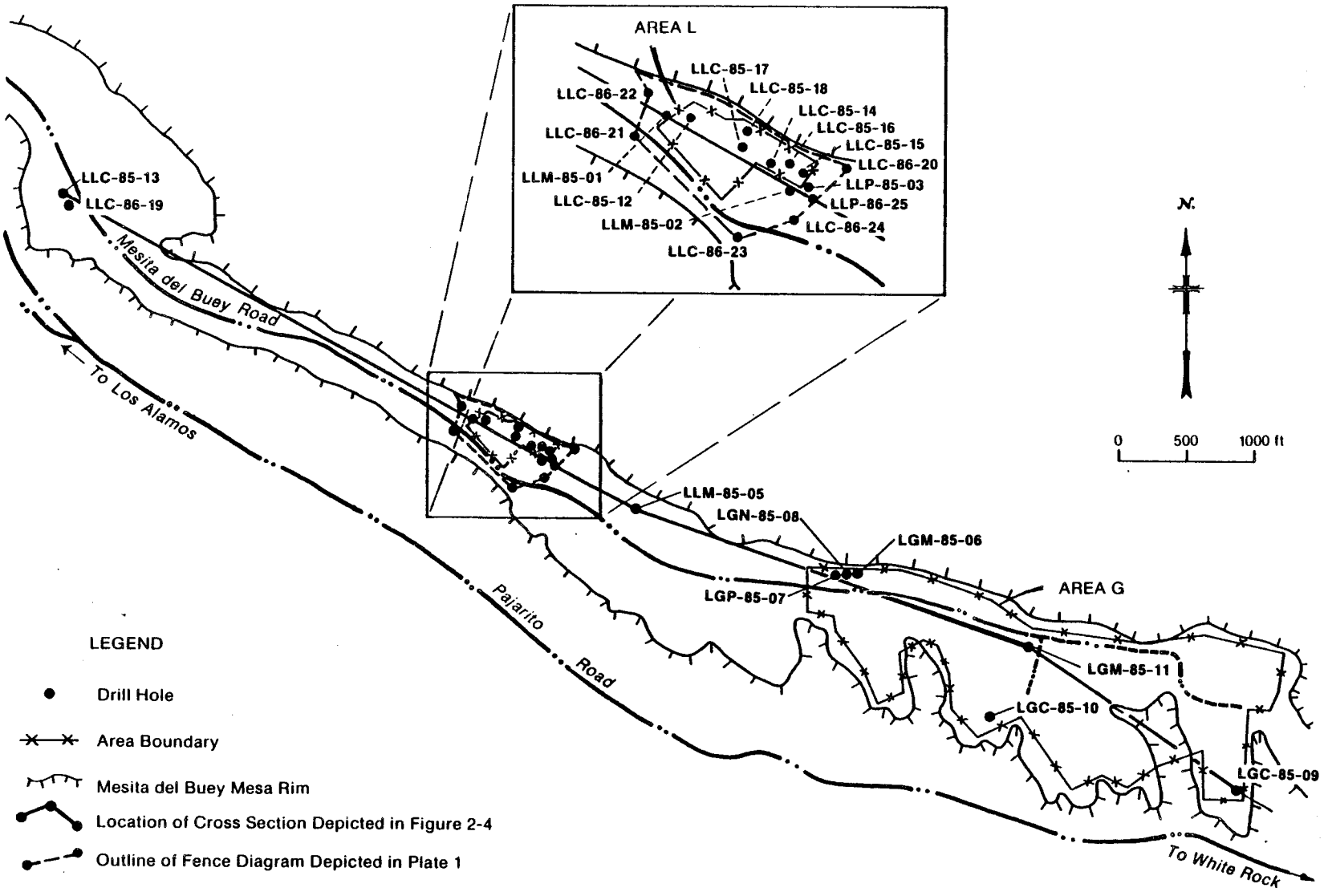

Figure 2-3. Locations of Drill Holes in Areas G and L, Technical Area 54, Los Alamos National Laboratory, New Mexico

rhyolitic, vitric-crystal ash-flow tuff. The maximum thickness of Unit 1a encountered in the Los Alamos drill holes was 64 ft; however, no drill hole penetrated the entire unit. At Mesita del Buey, Unit 1a consists of very uniform, nonwelded to slightly welded ash composed of brown glass shards and fine, flattened pumice lapilli, neither of which is devitrified. Also found in the ash are numerous but scattered lumps of light-tan pumice lapilli and latitic to rhyolitic lithic lapilli. In some of the deeper holes (1986 series), the lower, more tannish colored and slightly welded portions of the unit are noticeably damp immediately upon retrieval from the core barrel.

The contact between Units 1a and 1b is discerned in the core on the basis of the increased degree of welding and the presence of brown and gray pumice lapilli in Unit 1b. Unit 1b is a rhyolitic ash-flow tuff, ranging in color from light gray to pinkish gray near the top, and from pale red to moderate orange pink near the base. The lower portion of Unit 1b contains distinctive bipyramidal quartz crystals up to 4 millimeters (mm) in diameter and a bimodal distribution of latitic to rhyolitic lithic lapilli. The lithic lapilli are abundant in the size range 1 to 4 mm in diameter, and occur less commonly in the size range 15 to 60 mm. They decrease in size and abundance toward the top of Unit 1b, where the occurrence of lithic lapilli is rare. The degree of welding in Unit 1b generally varies from slightly welded at the base to moderately welded just above the base to slightly welded at the top. In 11 core holes where the entire section of Unit 1b was penetrated, the total thickness varies from approximately 29 ft (on the southeast) to 74 ft.

The contact between Units 1b and 2a was difficult to identify precisely during coring operations. In certain cases, the contact can be estimated on the basis of either a subtle color change in a slightly welded portion of the core, or the presence of brown, gray, and olive-colored pumice lapilli in the basal portion of Unit 2a. These pumice lapilli are generally larger than the predominantly brown pumice lapilli found in the upper portion of Unit 1b. In addition, the contact seems to occur in a zone where vapor-phase crystals of quartz and sanidine are small (less than 1 mm in diameter) and sparse. Microscopic criteria for distinguishing between these units are described in Section 2.3 of this report.

Unit 2a consists of a lower ash flow and an upper ash fall (Purtymun and Kennedy, 1971), although no ash-fall unit was encountered during this study. The unit ranges in color from light pink to pale red to gray. It contains relatively large (5 to 30 mm) gray-, brown-, and olive-colored pumice lapilli, and varies from slightly to moderately welded. Unit 2a varies in thickness from 67 ft in the northwest (Hole LLC-86-19) to 21 ft in the southeast (Hole LGC-85-09).

The contact between Units 2a and 2b is generally marked by a subtle color change within a slightly welded zone of tuff. Purtymun and Kennedy (1971) identify this contact on the basis of the occurrence of thin, lenticular deposits of reworked tuff. This zone of reworked tuff was observed in core from Holes LLC-86-21 and LLC-86-22. The transition from Unit 2a to Unit 2b at Mesita del Buey appears to be marked by a decrease in the variety of pumice lapilli occurring in the basal portion of Unit 2b; pumice lapilli in Unit 2b are dominantly gray in color, whereas the pumice lapilli in Unit 2a are gray-, brown-, and olive-colored. The contact between the two units is most easily seen in the outcrop; in many places the lenticular deposits of reworked tuff,

occasionally cross-bedded, are readily observable. In general, Unit 2a contains a greater amount of pumice lapilli and bombs than Unit 2b, resulting in sloping erosional surfaces. However, basal portions of Unit 2b often display an increase in the amounts of pumice lapilli and blocks, which can obviously confuse the issue when trying to discern this contact in the core. In outcrop, these basal, pumice-rich portions of Unit 2b are often continuous with the vertical cliff-forming nature of the rest of Unit 2b, down to its contact with Unit 2a, even though it is generally only slightly welded.

Unit 2b forms the cap rock at Mesita del Buey and consists of brownish-gray, light-gray, and pinkish-gray, slightly to moderately welded, rhyolitic ash-flow tuff with light-gray and occasional brown pumice lapilli. In some areas on the Pajarito Plateau, this subunit may contain up to eight distinct flow units, separated by sandy partings and pumice concentrations (Goff and Bolivar, 1983). Field descriptions, apparent density logs, and magnetic susceptibility logs obtained during this study indicate that, at Mesita del Buey, Unit 2b consists of several flows and is generally separated from Unit 2a by a lower zone of slightly welded tuff. The maximum and minimum thicknesses of Unit 2b encountered in the Los Alamos drill holes were 45 ft in the northwesternmost hole (LLC-85-13) and 28 ft in the southeasternmost hole (LGC-85-09).

2.2 WELDING AND CORRELATION OF ASH-FLOW UNITS AT MESITA DEL BUEY

Welding of tuffaceous rocks at Mesita del Buey ranges from nonwelded to moderately welded. Although the degree of welding is gradational between these ranges, generalized definitions of each welding descriptor were formulated for use when describing rocks in the study area. These are summarized below:

- Nonwelded - Completely disaggregated; little to no flattening of pumice lapilli observed.

- Slightly Welded - Slightly coherent, but crumbles easily in the hand; occasional pumice lapilli are noticeably flattened.

- Moderately Welded - Tuff crumbles with difficulty in the hand and occasionally must be struck with a hammer to break; flattening of most pumice lapilli to varying degrees is noticeable.

Although the units are defined on the basis of individual or composite flows, general variations in welding within the units can be correlated across Mesita del Buey. A cross section showing these variations is presented in Figure 2-4; the location of the cross section in the study area is shown in Figure 2-3. A general thinning of the ash-flow units can be seen on the cross section from northwest to southeast (away from the caldera). Moderate welding is most consistently found in the lower portion of Unit 1b near its contact with Unit 1a, and in the middle and upper portions of Unit 2b. In general, the moderately welded portions of Unit 2a break or crumble in the hand more easily than the moderately welded portions of Units 1b and 2b. The welding characteristics of Unit 2a, however, are not consistent in a lateral sense. Also not laterally consistent are the slightly welded zones; in certain cases,

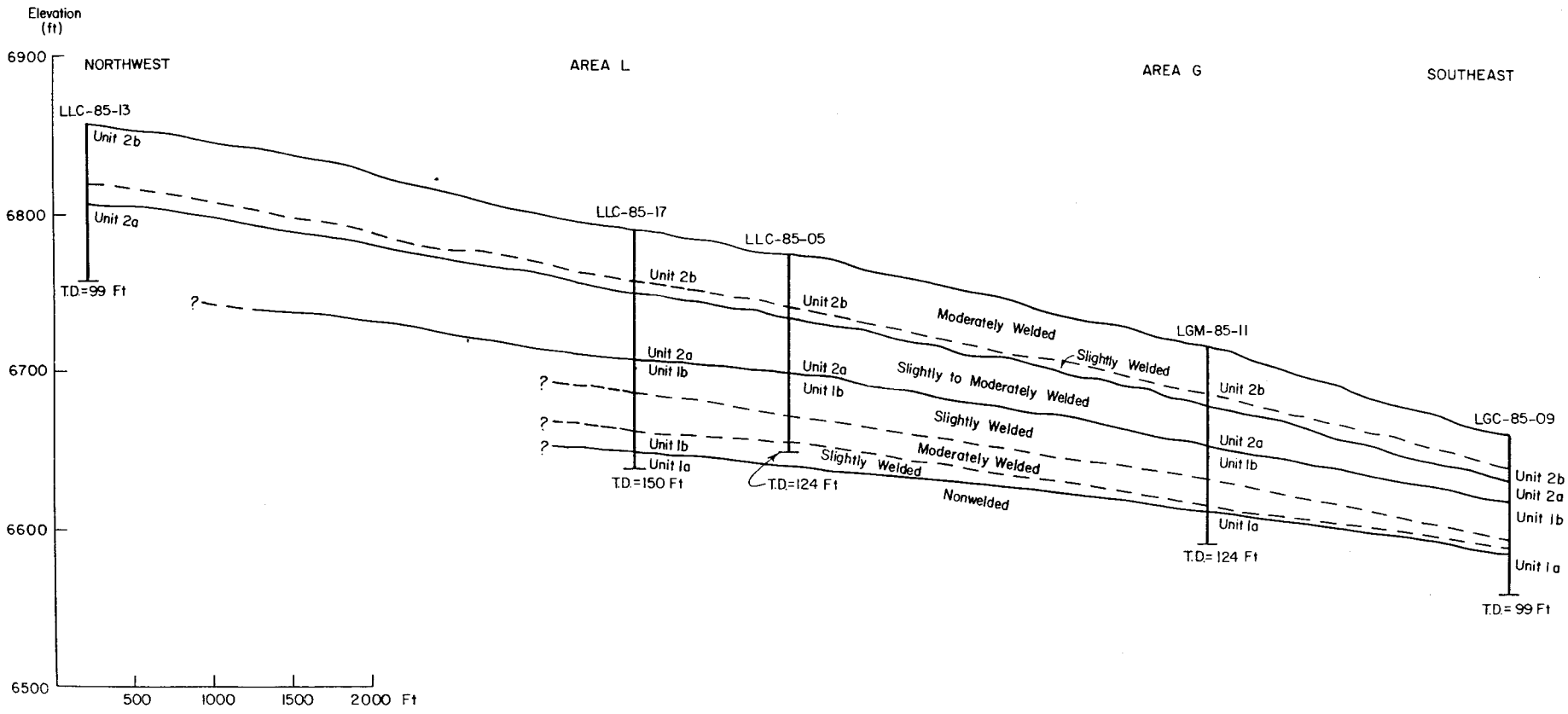

Figure 2-4. Cross Section Showing Parts of the Tshirege Member of the Bandelier Tuff, Drawn Through Mesita del Buey and Technical Area 54

the slightly welded zone more nearly approaches the definition of moderately welded, whereas in other cases, the slightly welded zone is almost nonwelded.

Holes were drilled during 1986 to 200-foot depths, and provided more detailed information about degree and continuity of welded zones. A fence or panel diagram, drawn on an isometric projection of a part of Mesita del Buey that includes Waste Disposal Area L, is presented in Figure 2-5. Because detailed records of recovery and rock quality designation (RQD) were kept during the 1986 drilling program, the welding characteristics of each unit were determined in greater detail than during the 1985 program.

The rock quality designation is an indirect measure of the number of fractures, the amount of softening, or the alteration present in the rock mass as observed in the core. The measure is obtained by summing up those pieces of core which are relatively hard and sound that are 4 inches in length or longer. In the case of the Bandelier Tuff, this can yield a qualitative measure of the degree of welding in zones with little to no fracturing. The welding in Unit 2a is not laterally consistent; observation of RQD parameters show that a central zone of more welded tuff is present throughout the unit. This central, moderately welded portion of Unit 2a is slightly less coherent than moderately welded zones in Units 2b and 1b.

The RQD parameters also help delineate different zones within Unit 2b; these zones can be seen on the individual logs in Appendix A, but were not included on the fence diagram (see Figure 2-5) because they are apparently only local in extent. These zones, together with the presence of sandy partings and pumice concentrations, also indicate that Unit 2b consists of several different ash flows. However, the widespread slightly welded zone at the base of Unit 2b, together with approximate compositional homogeneity and the cliff-forming nature of the unit, suggest that the ash flows of Unit 2b essentially cooled as a single unit. The basal, slightly welded zone of Unit 2b can be seen on the fence diagram (see Figure 2-5). Also visible on the fence diagram are minor variations of unit thickness on a local scale, and the slightly welded zone present at depth in Unit 1a.

2.3 PETROGRAPHIC ANALYSES

Thirty-eight samples were submitted for petrographic analyses, results of which were used to establish recognition criteria for the different units within the ash-flow tuffs. Of this total, 3 were outcrop samples of tuff, 27 were core samples of tuff, and 8 were samples of lithic and pumice lapilli. The outcrop samples were collected 600 feet northeast of Hole LLC-86-20. The analyses were performed by the GJPO Petrology Laboratory. Procedural details and the resulting petrographic reports are presented in Appendix B.

Overall, the results indicate that the Tshirege Member of the Bandelier Tuff at Mesita del Buey is a rhyolitic tuff containing varied amounts of lithics (rock fragments), vitrics (pumice fragments and glass), and crystals (vapor-phase products and phenocrysts). Results of point-count analysis for quartz and sanidine (Table 2-1) indicate that Unit 1b generally contains less volume-percent sanidine (K-feldspar) than do Units 2a and 2b. Samples from Unit 1b have an average quartz/sanidine (Q/K) ratio of 0.9, while average ratios in

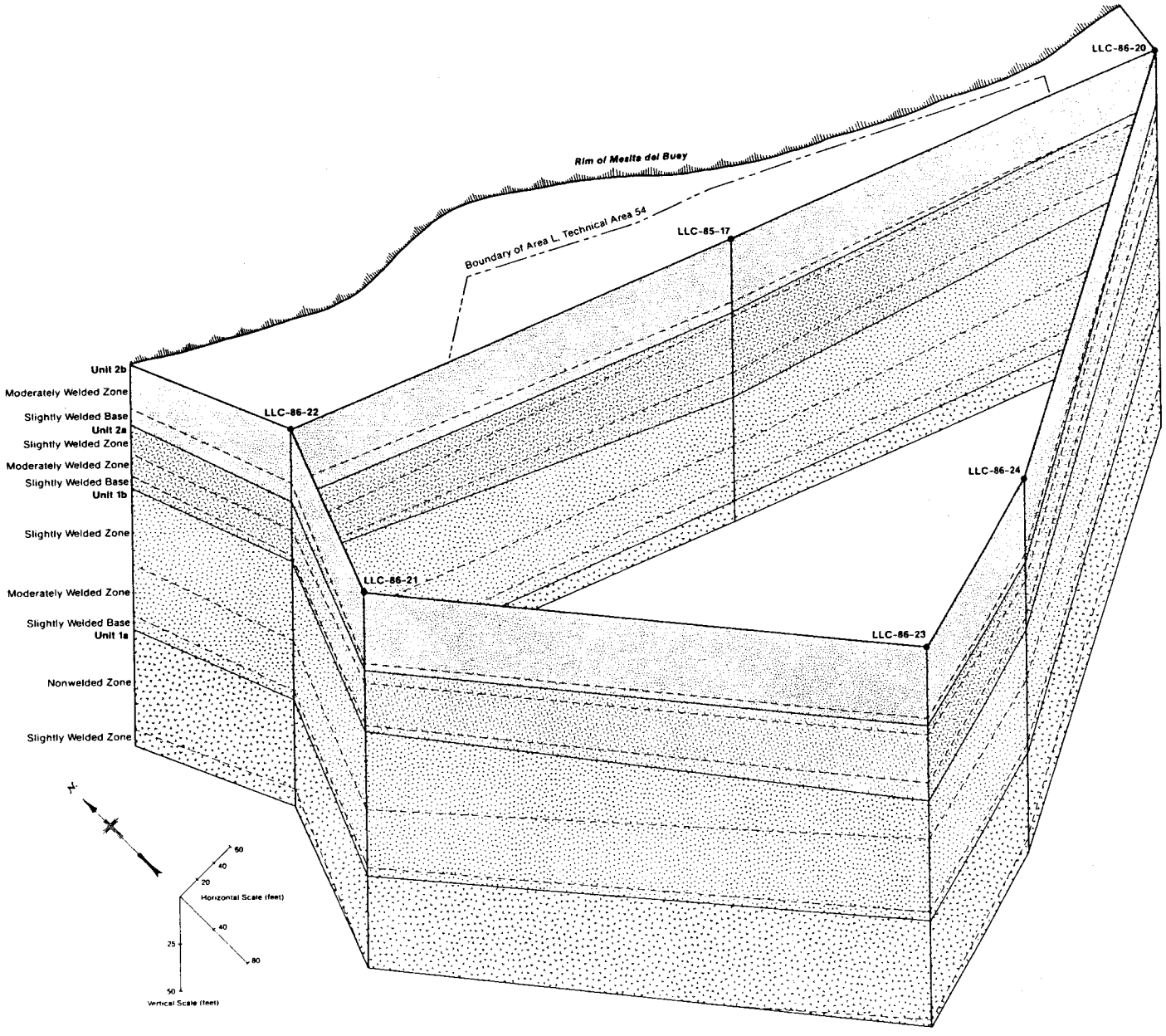

Figure 2-5. Fence Diagram Through Waste Disposal Area L Showing Subsurface Stratigraphy of the Bandelier Tuff

Units 2a and 2b are 0.6. In addition, it was found that tridymite is generally absent in samples from Unit 1b. Units 1 and 2 are therefore compositionally distinct.

Table 2-1. Volume-Percent Quartz and Sanidine Determined from Point-Count Analysis of Thin Sections

Sample Number	Hole Number	Depth (ft)	Volume-Percent Quartz	Volume-Percent Sanidine
UNIT 1b				
MCG-628	LLM-85-01	101	5.4	11.9
MCG-629	LLM-85-01	122	11.9	9.0
MCG-632	LLM-85-02	74	9.7	10.3
MCG-633	LLM-85-02	111	6.4	6.0
MCG-636	LGM-85-06	100	6.3	9.7
MCG-640	LGM-85-11	95	6.7	8.6
MCG-649	LGC-85-09	48	12.0	9.7
MCG-650	LGC-85-09	68	8.1	8.5
MCG-656	LLC-86-20	126	7.6	10.6
MCG-658	LLC-86-20	119	8.0	11.0
AVERAGE VALUES			8.2	9.5
UNIT 2a				
MCG-627	LLM-85-01	52	7.8	14.3
MCG-631	LLM-85-02	64	10.4	15.1
MCG-635	LGM-85-06	50	9.0	11.0
MCG-648	LGC-85-09	35	8.0	17.0
MCG-661	Outcrop	NA[a]	7.0	10.2
AVERAGE VALUES			8.4	13.5
UNIT 2b				
MCG-626	LLM-85-01	30	7.6	17.3
MCG-630	LLM-85-02	37	5.7	12.5
MCG-634	LGM-85-06	30	11.4	13.8
MCG-638	LGM-85-11	5	7.1	13.2
MCG-639	LGM-85-11	31	13.2	10.1
MCG-643	LLC-85-13	42	6.2	18.4
MCG-644	LLC-85-17	12	8.0	14.0
MCG-646	LGC-85-09	10	8.4	13.6
MCG-647	LGC-85-09	21	8.8	24.1
MCG-659	Outcrop	NA[a]	9.8	15.5
MCG-660	Outcrop	NA[a]	12.9	13.2
AVERAGE VALUES			9.0	15.1

[a]NA = Not Applicable.

Other significant recognition criteria are the microscopic characteristics of pumice lapilli. Pumice lapilli in Unit 1b either are devitrified and display spherulitic textures with occasional vapor-phase mineralization by a radial-acicular zeolite, or consist of fresh glass; they also vary in shape from flattened to nonflattened in many samples. Pumice lapilli in Units 2a and 2b, on the other hand, are ubiquitously replaced by sanidine, tridymite, and occasionally a zeolite; in general, they are all at least partially flattened. Moreover, the average percentage of pumice lapilli (determined by point-count analysis of thin sections) is generally higher in Unit 1b (21 percent) than in Unit 2a (16 percent) or Unit 2b (13 percent). Evidently, the less flattened, more abundant nature of the pumice lapilli in Unit 1b is the primary reason for the fact that Unit 1b is less dense than Units 2a and 2b (see discussion of apparent density logs in Section 2.4.3).

2.4 INTERPRETATION OF GEOPHYSICAL LOGS

Several different types of geophysical log were obtained utilizing different downhole probes. Details regarding equipment and procedures were described in the first interim report (Rush and Dexter, 1985); a complete set of geophysical logs for all holes drilled during the 1985 study is included in that report. Magnetic susceptibility and apparent density logs for holes drilled in 1986 are included in Appendix F.

The following geophysical-logging data were generated for many of the drillholes during this study:

- Natural Gamma, Epithermal Neutron (and derived moisture), and Vertical Deviation Logs
- Spectral Gamma and Caliper Logs
- Magnetic Susceptibility Logs
- Gamma-Gamma (Apparent Density) Logs

The caliper and vertical deviation logs were obtained prior to installation of instruments described in other parts of this report to determine sizes and types of downhole equipment that would be necessary to facilitate the installations. The vertical deviation in the 18 drill holes at Los Alamos averages 2.5 ft and ranges from 1 to 4 ft; in general, the diameters of the completed drill holes are between 7 and 8 inches.

Discussions of the remaining types of geophysical log are presented in the paragraphs that follow. These discussions focus primarily on interpreting the logs with a view to identifying the vertical variations of lithologies present in each drill hole. In general, most of the logs tend to confirm the presence of previously established boundaries and contacts within the ash-flow tuffs. In certain cases, however, information obtained from the geophysical logs required that modifications be made to the lithologic logs acquired during the drilling of the study-area holes. Original versions of the lithologic logs

were presented in the first interim report (Rush and Dexter, 1985); the subsequent modifications have been incorporated in the logs presented in this report (see Appendix A).

2.4.1 NATURAL GAMMA AND EPITHERMAL NEUTRON MOISTURE LOGS

The natural gamma probe counts the spectrum of gamma rays above approximately 50 kiloelectronvolts (keV). In the 18 holes drilled, gross-gamma radiation ranges from 300 to 700 counts per second (cps). The epithermal neutron system consists of a neutron detector used in conjunction with a neutron source. Values from the logs range from 600 to 1600 cps. Logs from both of these systems show the vertical distribution of these total-count ranges; few of the vertical changes in total count correlate with a known boundary within the ash-flow tuff. Only in two holes (LGC-85-09 and LGC-85-10) were confirmations of previously drawn contacts possible. Figure 2-6 presents the epithermal neutron, natural gamma, and lithologic logs for Hole LGC-85-10. As can be seen, changes in total count with depth suggest confirmation of contacts and boundaries drawn on the adjacent lithologic log. However, since some of the obvious vertical changes in total count do not correspond with known physical changes, it is not possible to identify contacts on the basis of the epithermal neutron and natural gamma logs alone.

Moisture logs were derived from the epithermal neutron data. These moisture logs have the same general shape as the moisture logs obtained by gravimetric methods (see Section 3.1.1). A comparison of the two methods is illustrated in Figure 2-7. In general, the values for moisture percent seen in the epithermal neutron log are higher than those seen in the gravimetric data. Although the epithermal neutron data are more detailed (data points were obtained every 0.5 ft whereas gravimetric samples were collected every 5 ft), it appears that the gravimetric data are more accurate. Uncertainties in the calculated (epithermal neutron) moisture content at each 0.5-ft interval are compounded by counting errors, errors associated with the calibration parameters, and errors associated with the fact that no hole-size corrections were applied to the data. The percent uncertainty represented by these errors often exceeds the calculated moisture value. In this study, for example, these errors are estimated to be ± 3.0 percent by volume (Marutzky, 1986).

2.4.2 SPECTRAL GAMMA LOGS

The spectral gamma probe counts energy produced by potassium (K), uranium (U), and thorium (Th); total counts obtained in the field were converted to concentrations of K in percent, and U and Th in parts per million (ppm).

The Bandelier Tuff drilled during this study averages approximately 4 percent potassium, 5 to 10 ppm uranium, and 20 to 30 ppm thorium. As with the logs described in the previous subsection, the spectral gamma logs can, at best, only help to confirm the existence of previously drawn contacts and boundaries. Since vertical changes in concentration are not consistent from one hole to another, the logs cannot be used to draw boundaries or modify previously drawn contacts.

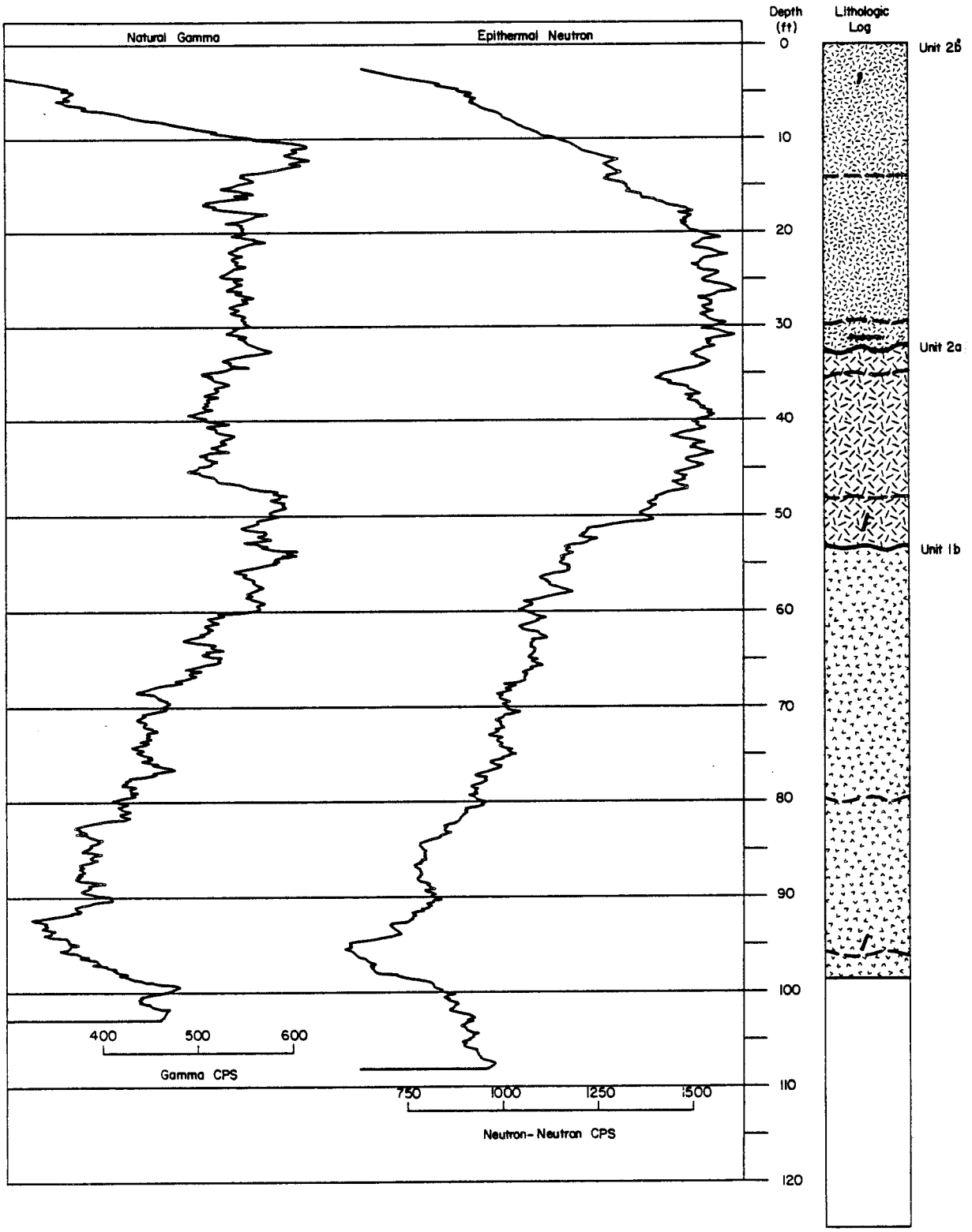

Figure 2-6. Epithermal Neutron, Natural Gamma, and Lithologic Logs for Hole LGC-85-10

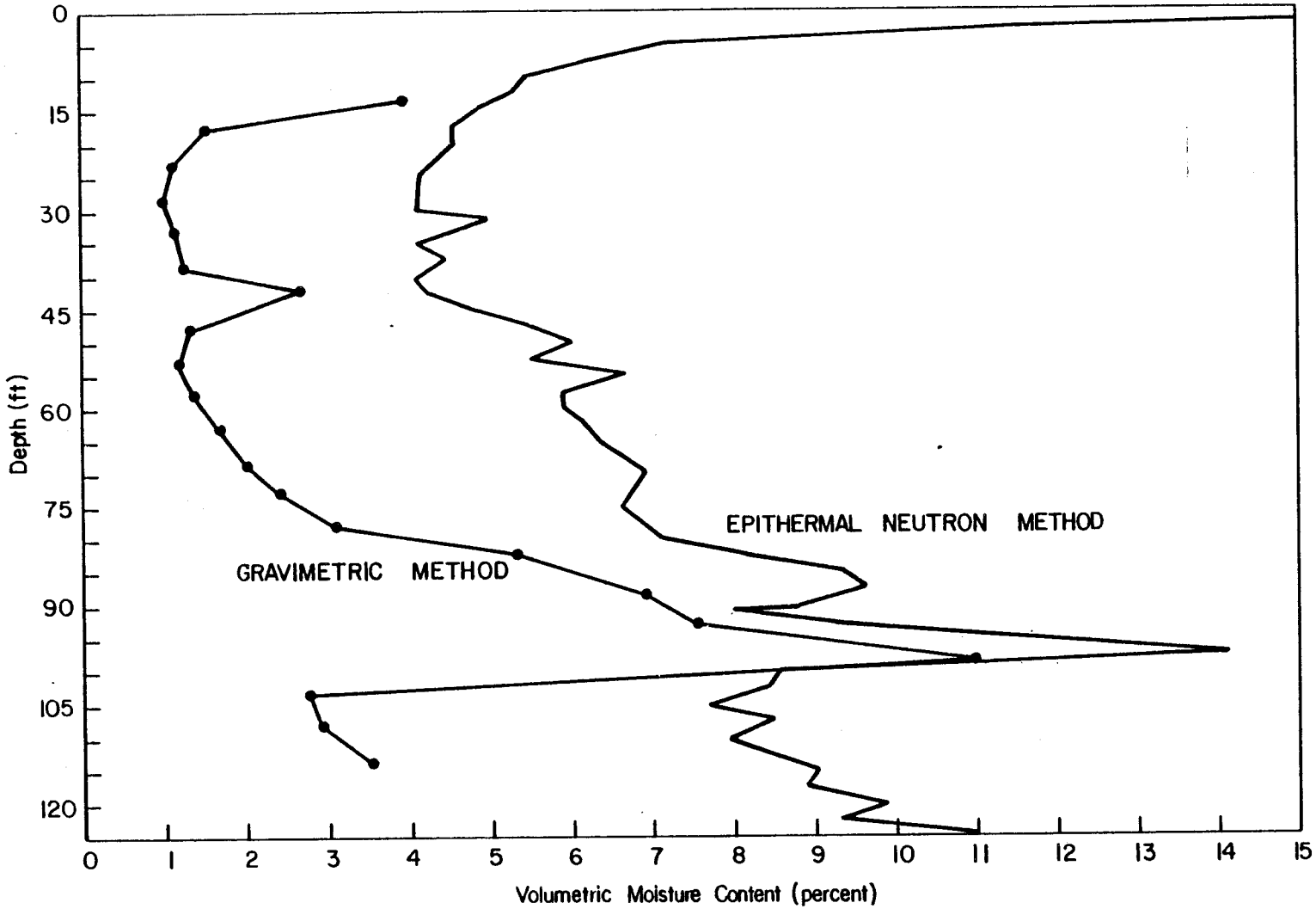

Figure 2-7. Comparison of Moisture Curves for Hole LGM-85-06, Derived by Geophysical and Gravimetric Methods

Figure 2-8 shows the spectral gamma and lithologic logs for Hole LGM-85-11. At first glance, there appears to be an inverse relationship between uranium and thorium. This is probably artificial and results from the use of a data-reduction program that strips away the energy contributions from uranium that overlap the energy window of thorium (and vice versa). At low concentrations of uranium and thorium, such as those displayed by the Bandelier Tuff in the study area, the stripping process results in apparent inverse relationships. As can be seen in Figure 2-8, however, this relationship is superseded by the simultaneous peaking of K, U, and Th at the boundary of Units 1b and 2a (61 ft), which is marked by an increase in uranium (to 10 ppm) and thorium (to 30 ppm). Similar increases in uranium and thorium at the contact of Units 1b and 2a were noted on spectral gamma logs from other holes as well, suggesting gross chemical differences between Unit 1 and Unit 2. This confirms the same conclusion drawn from the petrographic data on the basis of quartz and sanidine contents.

2.4.3 MAGNETIC SUSCEPTIBILITY AND GAMMA-GAMMA (APPARENT DENSITY) LOGS

The magnetic susceptibility (MS) and gamma-gamma (apparent density) logs proved to be the most valuable in terms of correlating physical and hydrologic properties in the study area. The MS probe is calibrated in micro-cgs* units and measures the degree to which the tuff is attracted to a magnet; essentially, this is an indirect measure of the iron content of the tuff. Because of considerable base-line drift due to temperature changes in the sensing coil of the probe, the shape of the curve, not the displayed values, is significant. The gamma-gamma probe collects data in counts per second that are immediately converted to apparent density in grams per cubic centimeter (g/cm^3) using the calibration data obtained during installation of the logging system. The density of the ash-flow tuffs is a function of welding, amounts of lithic and pumice lapilli, water content, and degree and amount of vapor-phase crystallization and devitrification.

Relationships between magnetic susceptibility, density, and lithology are shown schematically in Figures 2-9 through 2-11. For the most part, the MS logs show good correlations with contacts between individual ash flows, whereas the density logs show good correlations with boundaries based on welding characteristics. However, minute changes in magnetic susceptibility can delineate zones with different welding characteristics (see, for example, Figures 2-9 and A-9, Hole LGC-85-10, 83 to 97 ft), whereas minute changes in apparent density can delineate contacts between individual ash flows (Hole LGC-85-10 at a depth of 55 ft).

The MS and apparent density logs obtained from holes drilled Summer 1986 also correlate well with the lithologic logs. Since the 1986 holes penetrated the tuff at deeper levels, additional physical characteristics were substantiated. The moderately welded zone in Unit 1b was detected on the MS and apparent density logs. In Hole LLC-86-22, the core at a depth of 128 feet was noticeably damp upon retrieval (see Figure A-21, Appendix A). Although the apparent density log (see Appendix F) does not delineate the moderately welded zone very well (see comment on Figure A-21 stating that this zone is not as well defined as in other holes), a relatively dense zone is depicted from 125 to

*Centimeter-gram-second.

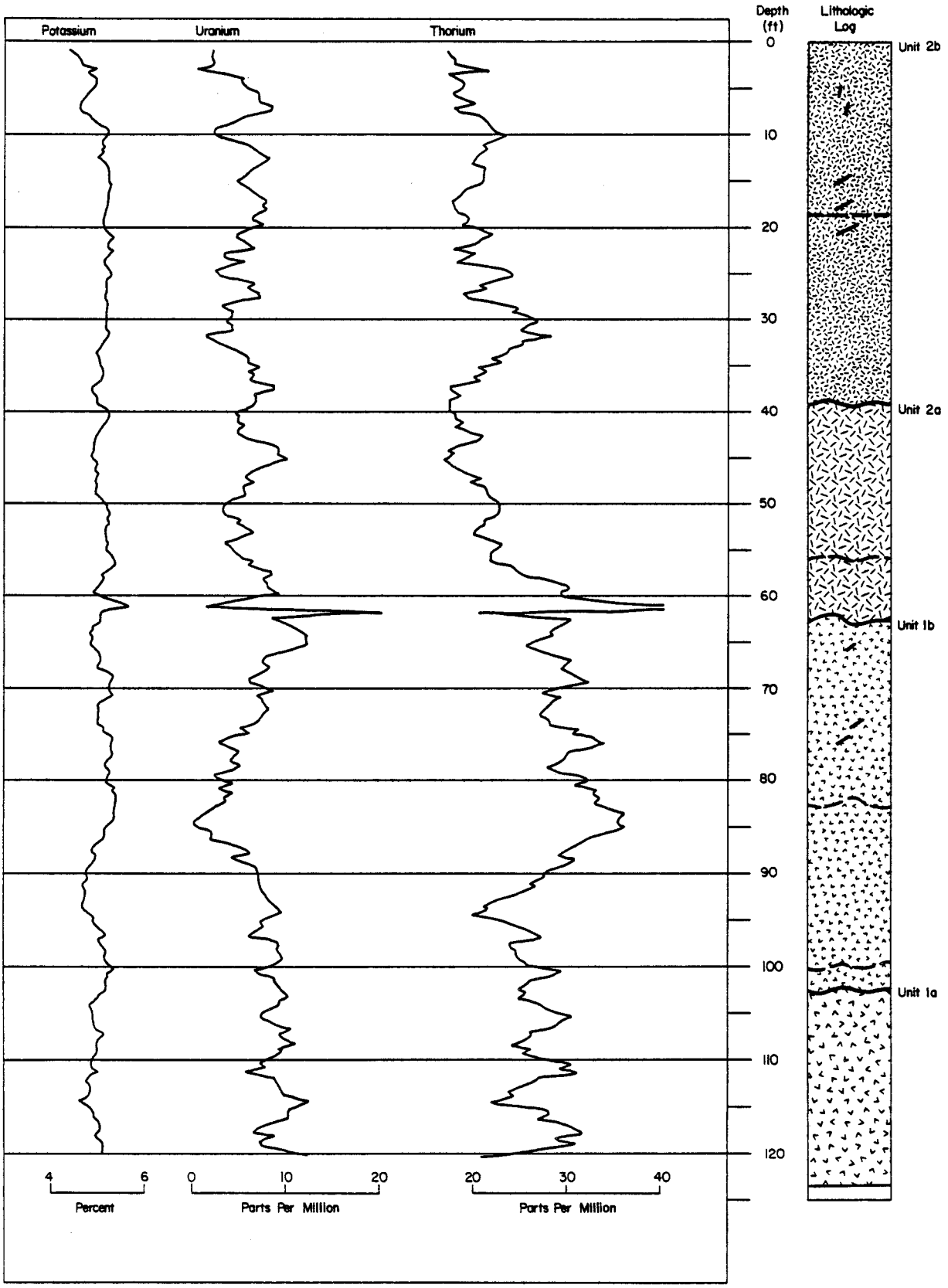

Figure 2-8. Spectral Gamma and Lithologic Logs for Hole LGM-85-11

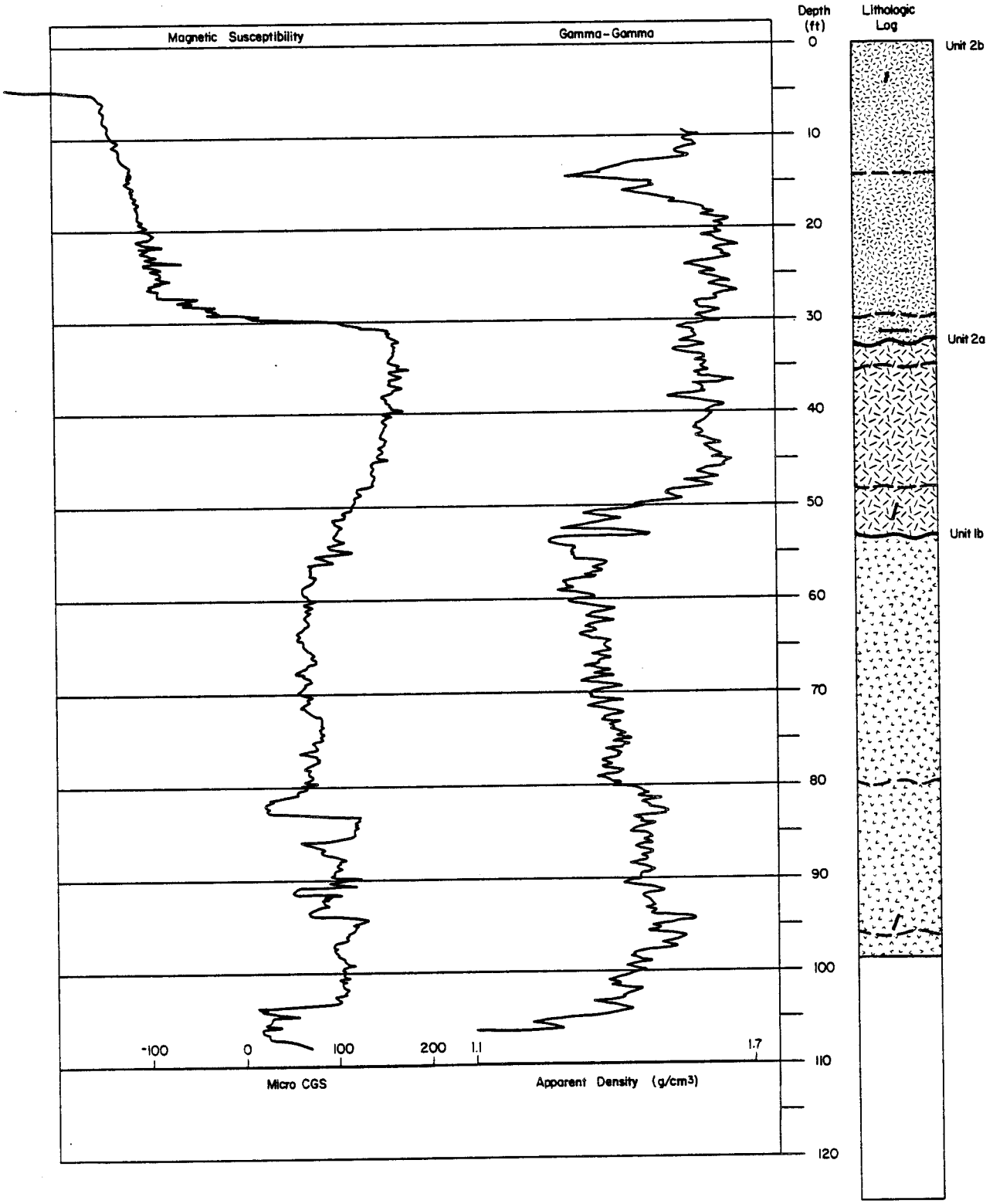

Figure 2-9. Magnetic Susceptibility, Apparent Density, and Lithologic Logs for Hole LGC-85-10

130 feet and defines the part of the zone with the highest moisture content. This 5-foot zone is in excellent agreement with the volumetric moisture data for this hole (see Figure 3-3, Hole LLC-86-22). The density log also indicates a gradual increase in density below a depth of 180 feet, where the Unit 1a tuff becomes noticeably damp and slightly welded. The MS log for this hole does not delineate this moderately welded zone, but does yield a striking match to the contact of Units 1a and 1b that was logged at approximately 142 feet during field operations; the MS log displays a large peak at a depth of 142 feet. In addition, the contact between Units 2a and 2b is substantiated by a large MS shift at 38 feet; the Units 2a and 1b contact is documented by a magnetic susceptibility spike at 72 feet. A large shift in magnetic susceptibility at a depth of 23 feet matches the subtle color change depicted on the lithologic log and probably represents the 'multiple-flow' nature of Unit 2b. The MS shift at a depth of 210 feet is probably significant, but core was not obtained below 198 feet so the shift cannot be interpreted; the MS shift could represent a simple color change in Unit 1a or the base of Unit 1a.

In some cases, the density log will indicate a contact between separate flows that is not visible on the MS log. For example, in Hole LGC-85-10 (Figure 2-9), the contact between separate flows within Unit 2b is marked only by an increase in the amount of pumice lapilli and is therefore visible only on the density log (at 14 ft). Concentrations of pumice lapilli are common at the tops, bottoms, and within ash-flow units. This feature is obvious on the density log in Figure 2-9; large negative peaks clearly demonstrate the increased concentration of pumice lapilli in the lower part of Unit 2a, from a depth of 50 to 54 ft. Another feature discernible on the density logs is the general decrease in the density of Unit 1b, which appears to be less dense on the whole than Units 2a or 2b. As noted earlier in the discussion of the petrologic data (Section 2.3), the decrease in the overall density of Unit 1b appears to be due to the fact that the pumice lapilli in the unit are more abundant and less flattened than those in Units 2b and 2a.

Occasionally the ability of the density logs to indicate contacts between distinct units, on the basis of minute density changes, is hampered by the presence of fractures. In Hole LLM-85-02 (Figure 2-10), the near-vertical fracture that extends from 35 to 40 ft obscures the minute changes in density that might be visible on the log were it not for the presence of the fracture. Induration of the tuff near the fracture, together with open spaces along the fracture, appears to result in both negative and positive apparent density peaks. A relationship between fractures and apparent density can also be seen in Figure 2-11 (Hole LGM-85-11) from a depth of 14 to 20 ft; large negative peaks on the apparent density log at 14, 16, and 19 ft correspond to observed fractures in core from this hole at 15.5, 17.5, and 20 ft. The differences in depth are probably due to the size of the core (2.5-inch diameter) versus the size of the hole that was probed (7- to 8-inch diameter). A potential application of the apparent density logs is in the determination of the extent to which fractures are open. Areas where fractures were logged via examination of the core are not always obvious on the density logs; fractures that are wholly to partially filled would probably not be characterized by a significant decrease in density.

The magnetic susceptibility log for Hole LGM-85-11 (Figure 2-11) indicates sharp boundaries which appear to define the gross differences between the four major subunits of the Tshirege Member; contacts between subunits at this

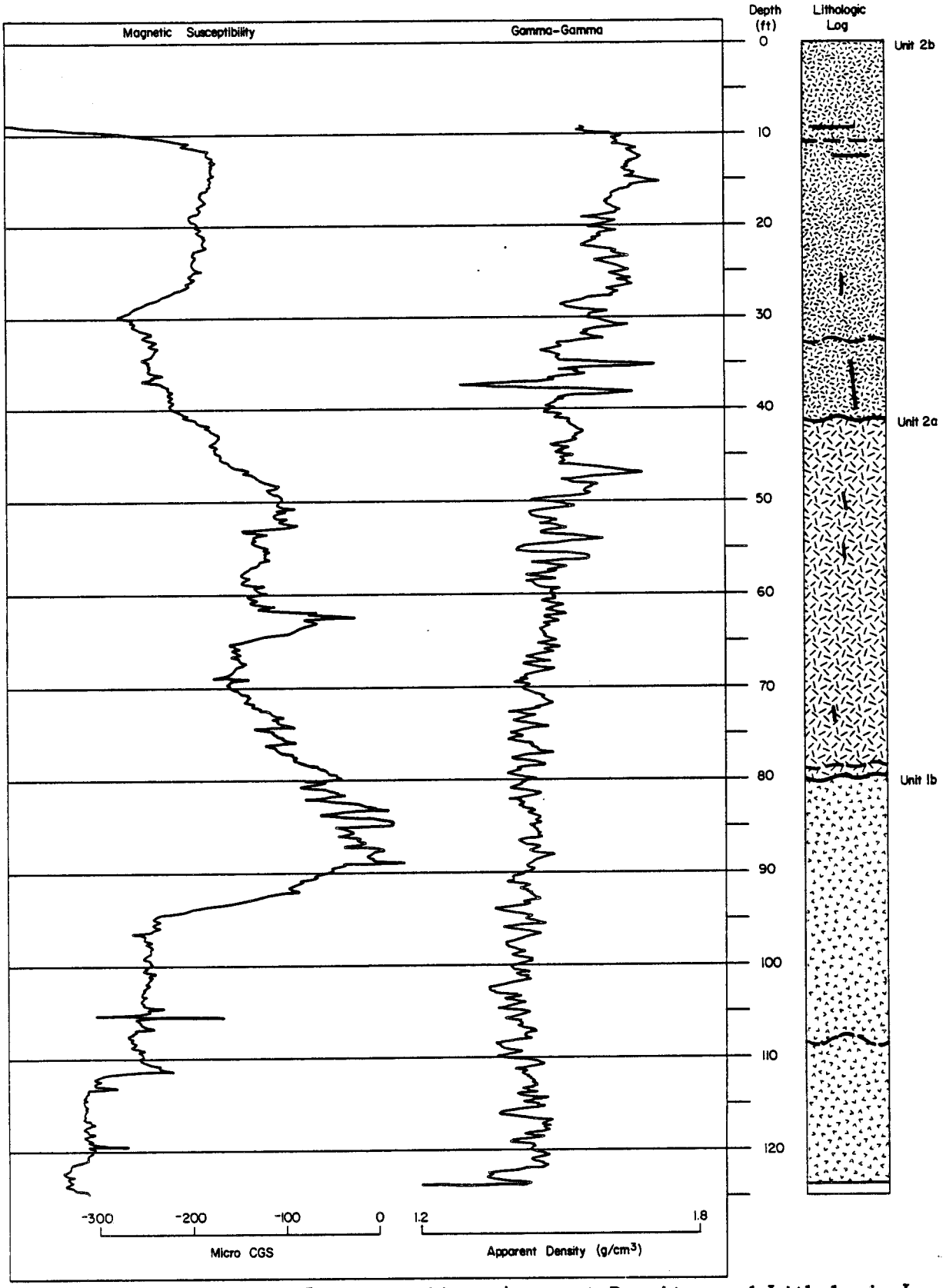

Figure 2-10. Magnetic Susceptibility, Apparent Density, and Lithologic Logs for Hole LLM-85-02

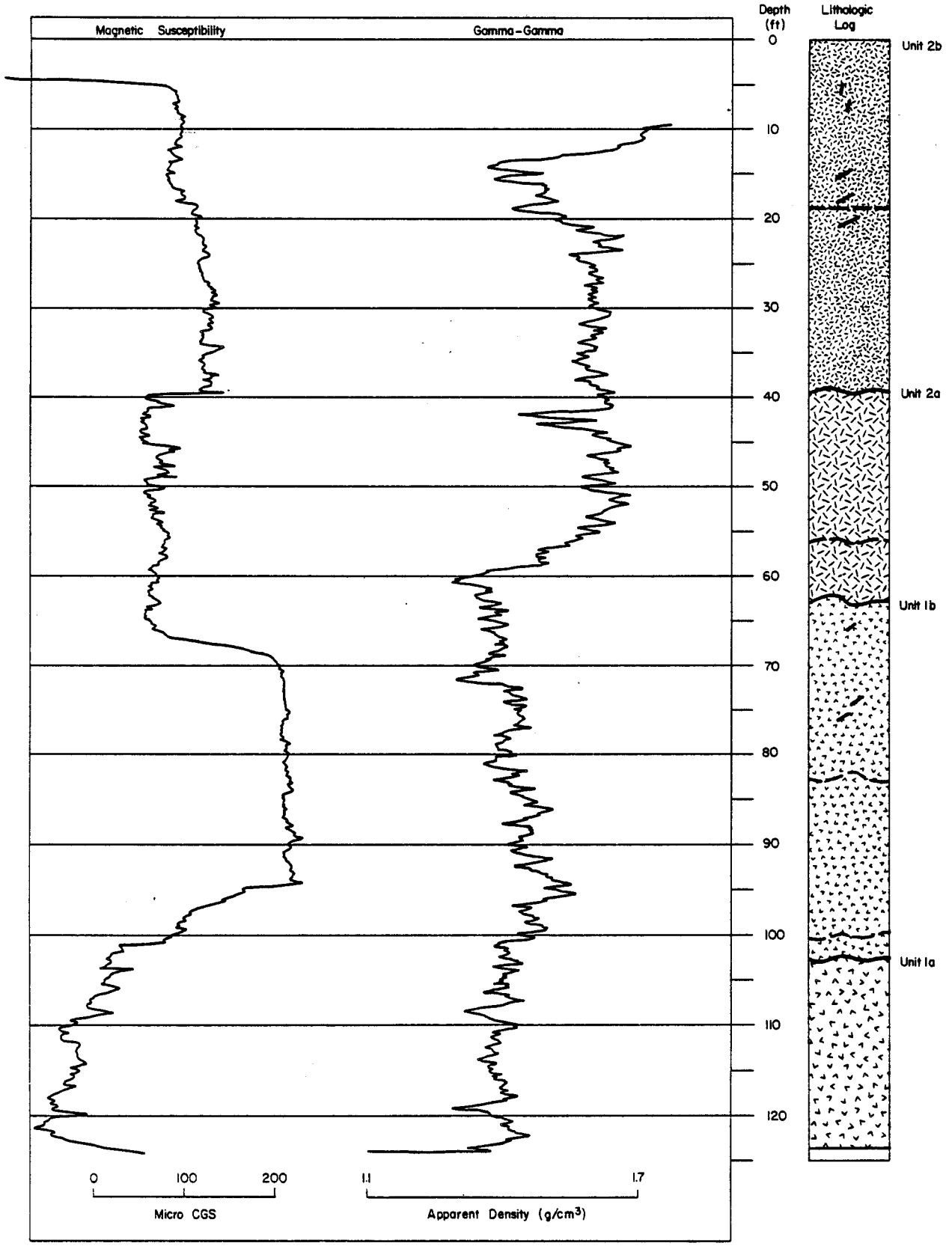

Figure 2-11. Magnetic Susceptibility, Apparent Density, and Lithologic Logs for Hole LGM-85-11

location were refined based on this information. The MS log for Hole LLM-85-02 (Figure 2-10), on the other hand, does not appear to define the contacts between major subunits; consequently, the log can only be used to confirm, rather than modify, the boundaries and contacts identified during drilling operations.

In conclusion, it should be emphasized that care must be taken when interpreting MS logs. Because of the common 'base-line drift' mentioned previously, apparent boundary changes in the form of an MS shift are possible. Therefore, the MS logs should not be used alone to identify contacts between ash-flow cooling units.

2.5 FRACTURES

2.5.1 SUBSURFACE CHARACTERISTICS

Fractures in the Tshirege Member at Mesita del Buey are predominantly tension joints formed as a result of contraction during initial cooling of the flows. Horizontal fractures, for the most part observed near the surface, are probably postdepositional fractures related to near-surface unloading along flow-foliation due to erosion of formerly overlying ash-flow tuff; most of these are filled with caliche and root material. During this study, horizontal fractures were observed only in Unit 2b. Only two fractures were observed in Unit 1a, which is composed of nonwelded to slightly welded tuff. (Note: The entire thickness of Unit 1a was not penetrated in this study.)

A summary of the number of fractures logged during the drilling program of this study is presented in Table 2-2. Although most of these fractures are nearly vertical (between 70 and 90 degrees), many fractures in both Units 2a and 2b have an apparent dip of about 45 degrees (see the lithologic logs in Appendix A). The greatest number of fractures occurs in Unit 2b; this agrees with data collected by Purtymun and others (1978). These authors found that more than 70 percent of the fractures they logged in both Units 2b and 2a were filled with brown clay or caliche. Similarly, observations made during the drilling program for this study indicated that most of the fractures appeared to be partially to completely filled with either caliche, brown clay, or limonitic material. Samples of some of the filled fractures were submitted to the GJPO Petrology Laboratory for X-ray diffraction analysis. Both bulk fractions and clay-sized separates of the fracture coatings were analyzed. The results demonstrated that the bulk fractions had the same composition as the host samples. Clay-sized fractions consisted predominantly of smectite (montmorillonite), with moderate to minor amounts of illite/mica and kaolinite.

Most of the fractures logged during this study occur in moderately welded zones within the tuffs. This is to be expected since these zones retained heat longer than the slightly welded zones. A feature observed in one fracture (cf. Figure 2-10, Hole LLM-85-02, 35 to 44 ft) deserves to be mentioned. This fracture displays an effect similar to surficial 'case-hardening,' as described by Abeele and others (1981, page 5); the tuff near the fracture is quite hard, but the tuff is only slightly welded less than 2 inches from the joint surface. This feature may signify preferential movement of water or

Table 2-2. Number of Fractures Logged in the Los Alamos Drill Holes

Unit of Tshirege Member	Number of Fractures[a]
Unit 2b	
Slightly Welded Zone	22
Moderately Welded Zone	81
Unit 2a	
Slightly Welded Zone	7
Moderately Welded Zone	45
Unit 1b	
Slightly Welded Zone	13
Moderately Welded Zone	26
Unit 1a	
Slightly Welded Zone	2

[a]Fracture zones are excluded where numerous fractures are present.

water vapor along open fractures during recent times, or may be a result of devolatization of the tuff during cooling. The fact that the gravimetric moisture data indicate an increase in moisture along several fractures (see Section 3.1.1) lends support to the former theory.

2.5.2 SURFACE CHARACTERISTICS

Because the distribution of fracture (joint) orientation may influence the anisotropy of the flow system associated with contaminants, a frequency-distribution study of joint orientations in Area L was conducted during the Summer of 1986. It was anticipated that results might further substantiate some of the apparent trends shown in part of the Petrex survey area (see Section 6). Joint orientations were measured using a Brunton compass and were plotted on a rose diagram (see Figure 2-12). Most of the 119 joints measured dip from 70 to 90 degrees.

A predominant northeast trend in the fracture orientations is depicted on the rose diagram (see Figure 2-12). However, because of the trend of Mesita del Buey and the configuration of its outcrop, a bias in the data resulted from the sampling limitation imposed by available exposures. Specifically, because the mesa trends northwest-southeast, the majority of the exposed fractures will be those oriented in a northeasterly direction; fractures having other orientations would be difficult to detect given the trend of the available exposures. Purtymun and Kennedy (1970) and Rogers (1977) reported diverse orientations on the mesa on the basis of measurements taken from trenches and pits away from the mesa rim. Purtymun and Kennedy concluded that 40 percent of the 1078 joints they measured in Unit 2b fall into three ranges of orientation: N. 30°-50° W., N. 60°-80° W., and N. 40°-60° E. Only the latter range was substantiated by measurements obtained during this study, but the diversity of trends found by Purtymun and Kennedy may help explain a similar

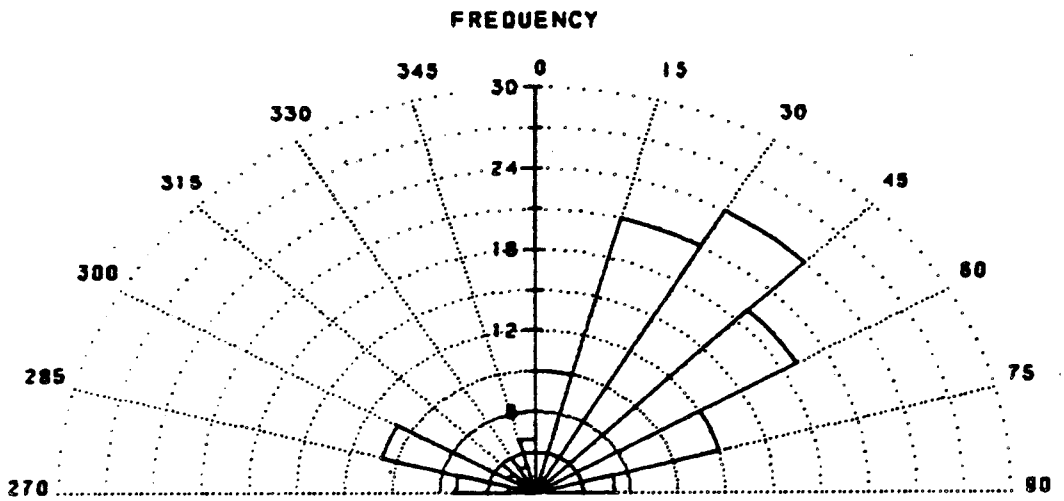

Figure 2-12. Rose Diagram of Joint Orientations of Exposed Fractures in Area L, Los Alamos National Laboratory (119 data points)

diversity in trends indicated by results of the Petrex survey (see Section 6). Therefore, although prominent northeast-trending fractures are recognized, it cannot be definitely concluded that the northeast orientation is the preferred avenue for contaminant transport.

The problem is further complicated by the fact that the physical nature of individual fractures may play an equally important, if not more important, role than the fracture orientation. As discussed previously, more than 70 percent of the fractures observed in the boreholes during this study, and by Purtymun and Kennedy (1970), are filled and therefore do not provide preferential pathways for contaminant migration. Fractures observed in freshly dug pits in Area G were noted by Rogers (1977) to range from tens of centimeters in width to tightly closed (or filled). According to Purtymun and Kennedy (1970), a single joint traced vertically through an ash flow may be closed in places and open in others, with openings ranging in width from 2 inches to less than 0.25 inch. Consequently, it is unlikely that any simple pattern of contaminant transport pathways can be inferred from fracture orientations. Rather, transport from the contaminant source to the surface probably follows tortuous routes determined by a combination of fracture orientations and degree of dilation, and interconnections of fractures related to the position of infill materials.

In summary, it appears that the mere occurrence of any 'preferred' fracture orientation is not sufficient to predict a simple, single direction of contaminant transport in Area L because transport is complicated by other fracture orientations and the closing of some fractures by secondary materials. The best method for determining the extent and dominant direction (if any) of contaminant transportation would be close monitoring and interpretation of chemical results from downhole pore-gas samples, in conjunction with more extensive Petrex surveys just under the rim of Mesita del Buey and in Area L.

Section 3

HYDROLOGIC CHARACTERIZATION OF THE VADOSE ZONE

This description of the hydrologic characteristics of the vadose zone in the study area is divided into three major subsections. Section 3.1 describes the general hydrologic characteristics of the tuff, including moisture content, which was determined gravimetrically; porosity, which was determined from helium-injection tests; and capillary force, determined from moisture characteristic curves. Permeability of the tuff is detailed in Section 3.2. Three field techniques were used to measure in-situ permeability, and two laboratory methods were used to measure permeability in core samples collected from the drill holes. Analyses of saturated and unsaturated hydraulic conductivity as a function of moisture content were also performed and are discussed in a separate subsection. A summary of all these permeability determinations concludes Section 3.2. Section 3.3 describes the gradient determinations, specifically measurements of temperature, water potential, and gas pressure, conducted to assess the driving forces of transport in the tuff.

This section of the report provides the geotechnical information specified in Tasks 1 through 4 of Paragraph 25 of the Compliance Order/Schedule. The specific subsections that address these tasks are highlighted with an asterisk and the corresponding task identified.

3.1 GENERAL CHARACTERISTICS

3.1.1 GRAVIMETRIC MOISTURE CONTENT

3.1.1.1 Purpose and Scope

Gravimetric moisture determinations were conducted to obtain a direct measurement of the in-situ water content of the tuff and to quantify the vertical moisture distribution. The moisture content as a function of depth is important when compared with results of permeability tests, water-potential measurements, and laboratory hydrologic testing as part of the quantification of moisture movement in the vadose zone.

This section describes the procedures for sample collection and moisture content calculations, and discusses the results of the gravimetric moisture-content determinations. Comparisons of the water-content results with other hydrologic measurements are presented in succeeding sections of this report (see Sections 3.1.3, 3.2.4, and 3.3.1).

3.1.1.2 Procedures

The specific procedure for the determination of gravimetric moisture consisted of the following steps. Core samples 1 ft in length were selected from the split-barrel sampler at 5-ft intervals and immediately placed in preweighed sample containers equipped with air-tight lids. The containers were weighed in the field and then delivered to the laboratory for drying. After drying for 24 hours at 105°C, the samples were reweighed to determine the moisture loss (Bendix Field Engineering Corporation, 1985a, 1985b).

Although gravimetric moisture determinations are relatively easy to perform, a number of precautions are necessary. For example, a major concern associated with the drilling was that the heat produced by the auger would drive water

out of the samples, resulting in inaccurate moisture-content measurements. Upon retrieval of the auger from the borehole, however, the temperature of the core barrel was observed to be cool. Apparently, the heat produced by the friction during drilling was minimal and confined to the outside of the auger, and therefore did not have a measurable effect on the moisture content in the core samples. Care was also taken to maintain the drying-oven temperature at 105°C to ensure that no structural water would be evolved and included in the apparent moisture content. Finally, the balance used to weigh the samples had a readability of 0.01 gram to ensure adequate accuracy for the low-moisture-content samples collected in this study.

3.1.1.3 Calculations

The amount of water in soil or rock can be expressed in the following ways:

- Water Content, Volume Fraction

$$\theta = V_l/V_t \tag{1}$$

- Water Content, Mass Basis

$$\theta_m = m_l/m_s \tag{2}$$

- Degree of Saturation

$$\theta_s = V_l/(V_l + V_g) \tag{3}$$

where

V_l = volume of liquid
V_t = total volume
m_l = mass of liquid
m_s = mass of solid
V_g = volume of the gas or air in the sample

Equations (1) and (2) are combined in order to convert from the mass basis to the volume fraction, a quantity that is generally more useful in field studies (Marshall and Holmes, 1979):

$$\theta = \theta_m \rho_b/\rho_l \tag{4}$$

where

ρ_b = dry bulk density
ρ_l = density of liquid

Values for mass were determined gravimetrically (Section 3.1.1.2). Values for dry bulk density were obtained from the gamma-gamma (apparent density) geophysical logs after subtracting the moisture content. Values for the density of water at different temperatures are readily available in the literature, but for most applications, it is sufficiently accurate to use the value 10^3 kg/m^3 (1.94 slugs/ft^3).

3.1.1.4 Results and Discussion

Gravimetric moisture determinations were performed in samples from 12 holes: LLM-85-01, LLM-85-02, LLM-85-05, LGM-85-06, LGM-85-11, LLC-86-19, LLC-86-20, LLC-86-21, LLC-86-22, LLC-86-23, LLC-86-24, and LLC-86-25 (see Figure 2-3 for drill-hole locations). The resulting volumetric moisture contents are plotted as a function of depth for all 12 holes in Figures 3-1, 3-2, 3-3, 3-4, and 3-5.

Four distinct characteristics are apparent upon examination of these data:

- Low overall moisture content.
- Varying depths of water infiltration.
- Relatively high moisture content exhibited by the lower portion of Unit 1b.
- Higher moisture content observed in the vicinity of certain fractures.

The low overall moisture content is demonstrated by the 2 to 4 percent average moisture for the central portion of the profile, while the lower portion of the profile, specifically Unit 1a, averaged a moisture content of 4 to 10 percent. At such low moisture contents, interconnection of pore water would be minimal and capillarity as a major transport mechanism would be negligible. As a result, it can be concluded that vapor transport would be the major mechanism for moisture movement in the tuff (see the discussion in Section 3.1.3.4).

Infiltration depth depends on the specific area. Holes located in Area L, for example, show an increase in moisture content relative to depth of less than 10 ft. In Area G, the corresponding depth is closer to 15 ft. This difference in the depth of moisture penetration is unexplained at this time.

All of the moisture data indicate an increase in moisture content in the lower portion of Unit 1b. In holes which fully penetrated Unit 1b, the increased moisture content correlates exactly with the moderately welded tuff encountered in Unit 1b (see lithologic logs in Appendix A). The degree of welding in the lower portion of Unit 1b was the highest observed in this study, with the exception of the upper portion of Unit 2b. As the degree of welding increases, the porosity of the formation decreases (Ross and Smith, 1961). It would be expected that as the porosity decreases so would the average pore-size radius, the result being an increase in capillary forces which would retain moisture in the more welded intervals of the tuff. The higher pumice content could also have a direct effect on the moisture-retention properties of Unit 1b. As welding increases, pumice clasts are flattened, both conditions resulting in a high concentration of gas tubes; these tubes form ideal capillary tubes which appear to exhibit strong capillary forces.

A higher moisture content is observed in samples located adjacent to certain fractures, indicating that some fractures do transport greater quantities of water vapor for absorption into the adjacent rock wall. Examples are the fractures located at 35 to 40 ft and 55 to 56 ft in Hole LLM-85-02, represented by the two moisture spikes at 38 and 55 ft, respectively (see

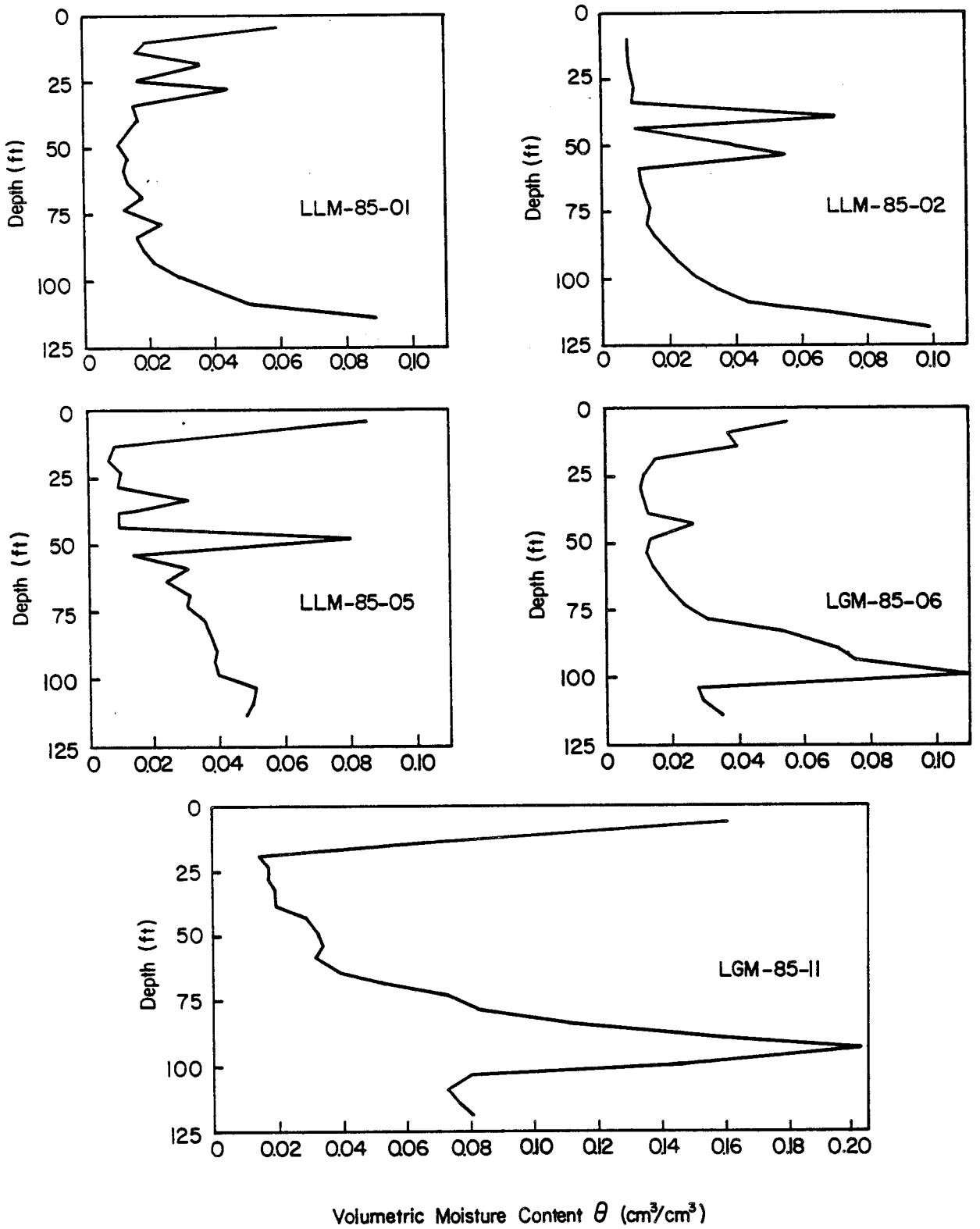

Figure 3-1. Plots of Volumetric Moisture Content as a Function of Depth for Drill Holes LLM-85-01, LLM-85-02, LLM-85-05, LGM-85-06, and LGM-85-11

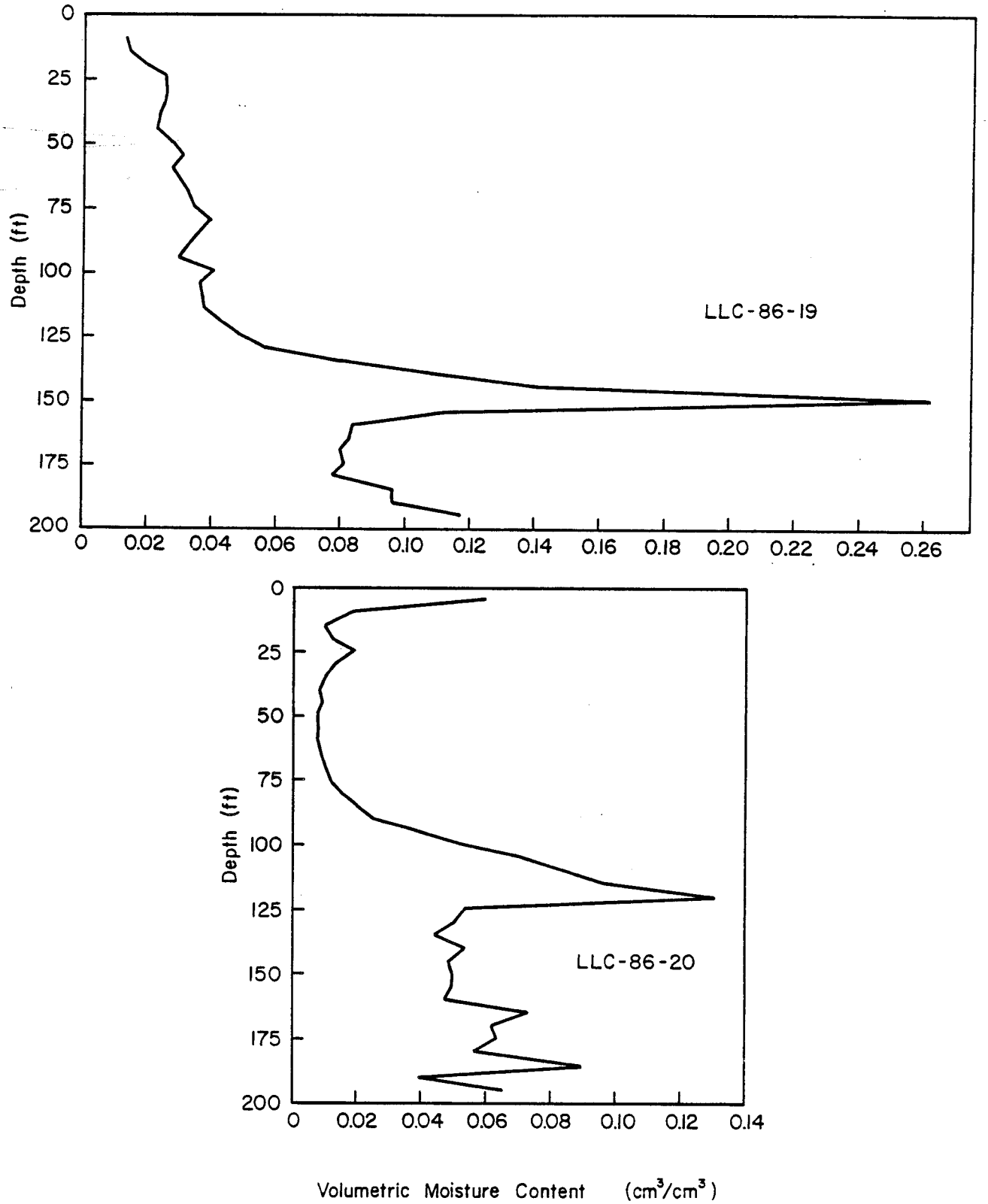

Figure 3-2. Plots of Volumetric Moisture Content as a Function of Depth for Drill Holes LLC-86-19 and LLC-86-20

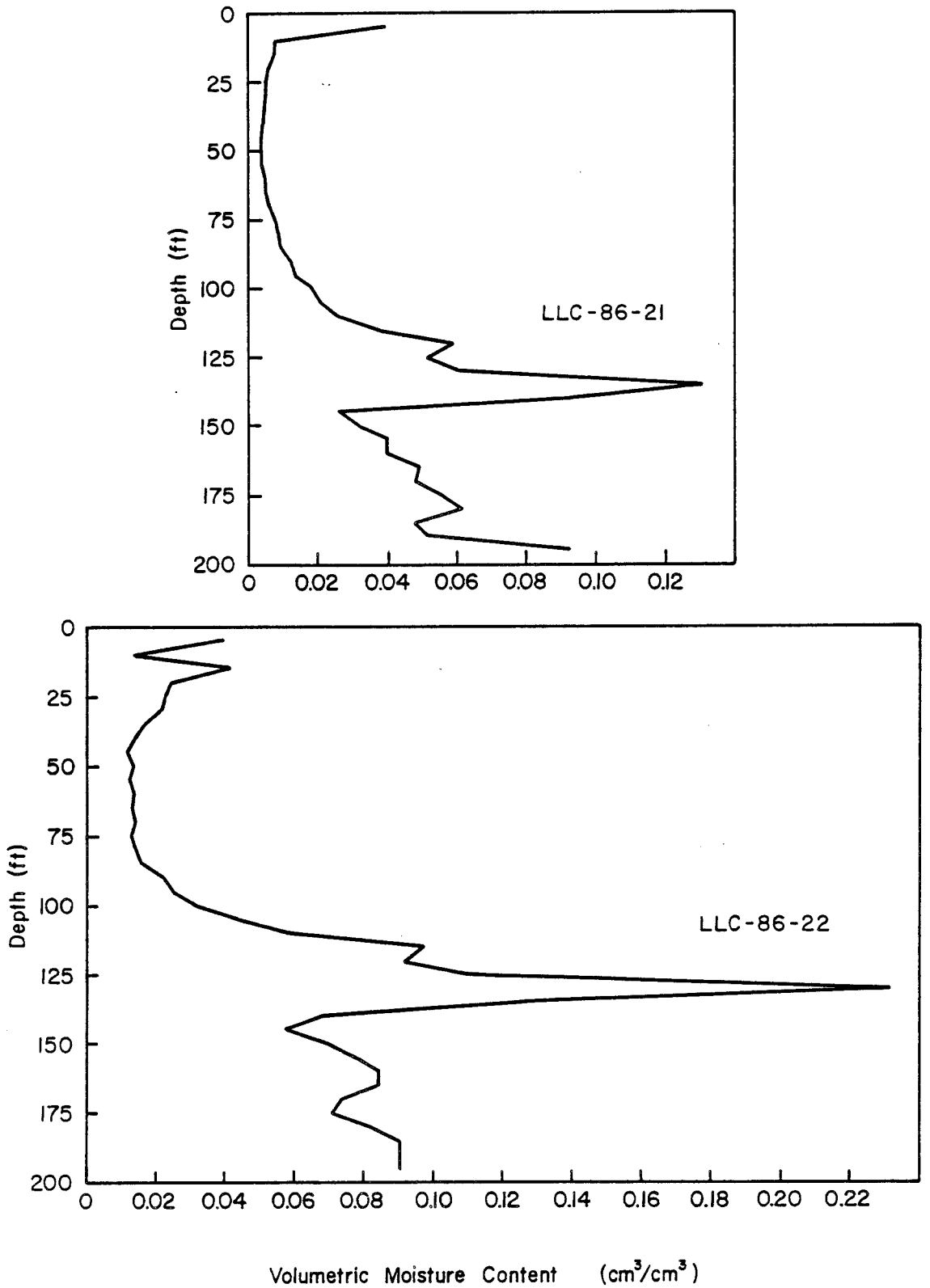

Figure 3-3. Plots of Volumetric Moisture Content as a Function of Depth for Drill Holes LLC-86-21 and LLC-86-22

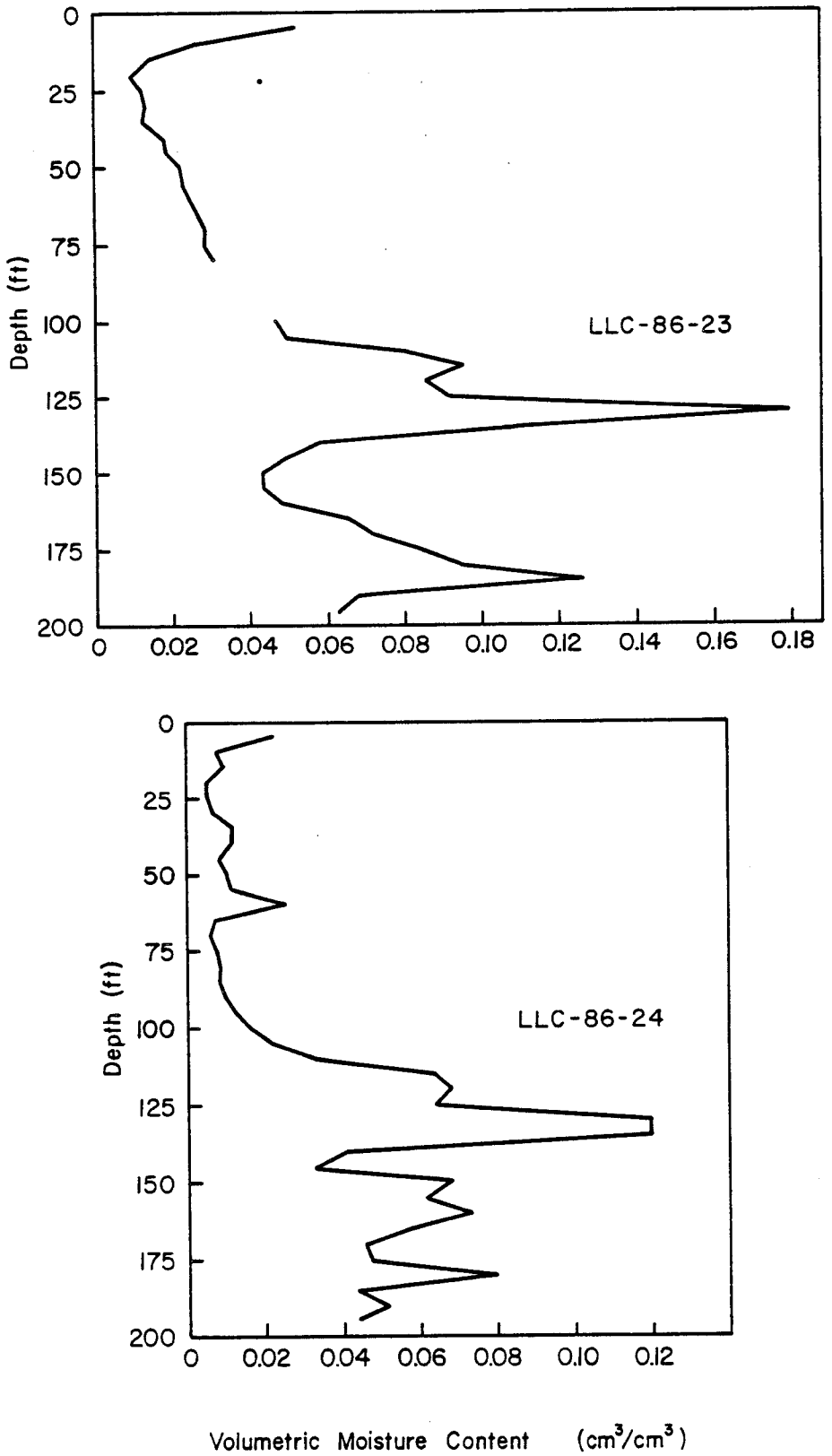

Figure 3-4. Plots of Volumetric Moisture Content as a Function of Depth for Drill Holes LLC-86-23 and LLC-86-24

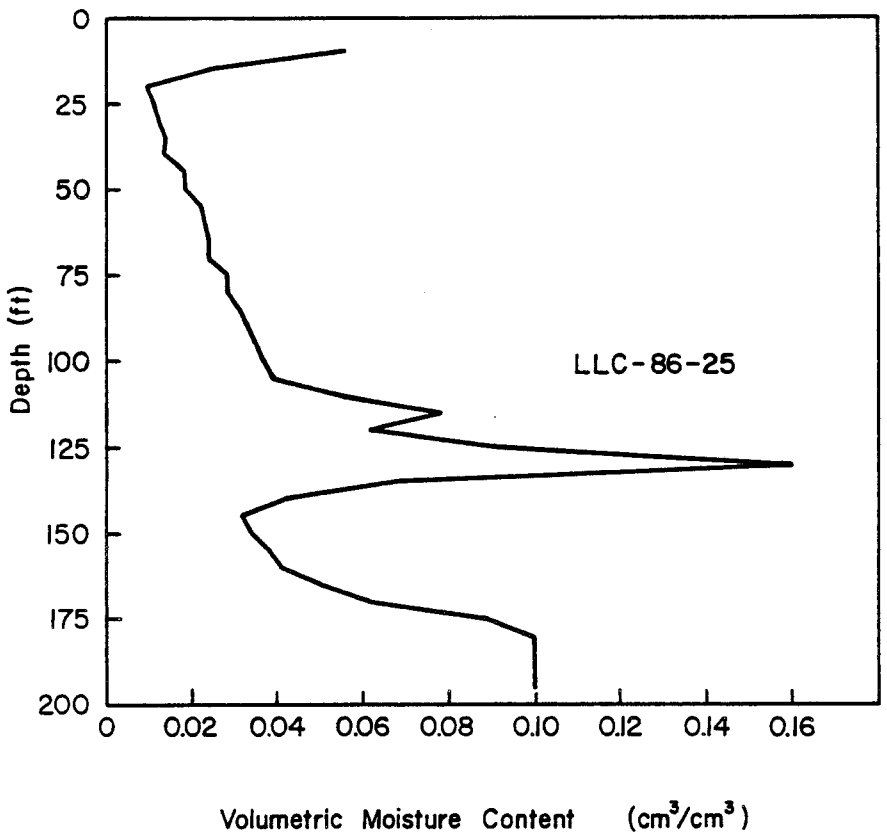

Figure 3-5. Plots of Volumetric Moisture Content as a Function of Depth for Drill Hole LLC-86-25

Figure 3-1). Not all of the fractures exhibit this moisture anomaly, however, suggesting that not all of the fractures are open and available as avenues of transport for water vapor (see Section 2.5).

3.1.2 POROSITY

3.1.2.1 Purpose and Scope

This section presents the results of helium-injection tests performed on 20 core samples for the purpose of measuring the porosity of the Bandelier Tuff. The laboratory work was performed by TerraTek Research Laboratory of Salt Lake City, Utah, at the direction of Bendix. The sample-preparation and laboratory-procedure sections that follow (3.1.2.2 and 3.1.2.3) are adapted from TerraTek's report (TerraTek Research Laboratory, 1985).

3.1.2.2 Sample Preparation

In order to obtain samples that were of the right size and shape for testing, it was necessary to plug the full diameter core material. This was done using air as the drill-bit coolant (to avoid any potentially adverse rock-fluid interaction). Plugging was done vertically due to the limited horizontal cross section of the core material. In all but one case (Sample MCG-616), attempts at sample plugging resulted in a partial disaggregation of the sample.

The samples thus obtained were placed in protective sheathing (one-inch-diameter heat-shrink Teflon tubing*), with stainless steel end screens used for support and prevention of grain loss, and to allow for gas or fluid flow in testing. The samples were then subjected to a confining stress equal to that found at their burial depth in order to compact the grains to an orientation similar to that experienced in the formation. This was done to ensure that any void space between the sheathing and the sample did not affect the pore volume of the sample.

3.1.2.3 Procedure for Helium-Injection Tests

The samples were oven-dried prior to testing and placed under a slight overburden pressure (approximately 100 psi) in a hydrostatic core holder. Porosity measurements consisted of injecting helium into the samples (50-psi charging or injection pressure), monitoring pressure/volume relationships, and calculating porosity values using Boyle's Law.

3.1.2.4 Results and Discussion

Table 3-1 presents the results for the porosity determinations. Porosity values range from approximately 39 to 74 percent. Using a classification scheme presented by Abeele and others (1981), the degree of welding based on the porosity would range from nonwelded to moderately welded. This classification agrees with field and petrographic observations.

---

*Diameter cited is after shrinking.

Table 3-1. Results of Porosity Determinations Using the Helium-Injection Method and Boyle's Law

Hole Number	Geologic Unit	Sample Number	Depth (ft)	Degree of Welding[a]	Pumice Content (percent)[b]	Bulk Volume (cm^3)	Pore Volume (cm^3)	Porosity (percent)
LGM-85-11	2b	MCG-618	3	Moderately Welded	19	25.68	13.94	54.3
LLM-85-02	2b	MCG-606	7	Moderately Welded	--[c]	25.62	10.62	41.5
LLM-85-05	2b	MCG-610	15	Moderately Welded	--[c]	24.96	13.14	52.6
LLM-85-01	2b	MCG-602	30	Moderately Welded	15	27.44	10.87	39.6
LGM-85-11	2b	MCG-619	30	Slightly Welded	13	24.61	12.67	51.5
LLM-85-02	2b	MCG-607	36	Moderately Welded	11	24.00	11.15	46.5
LGM-85-06	2b	MCG-614	29	Moderately Welded	7	25.31	10.76	42.5
LLM-85-05	2b	MCG-611	36	Slightly Welded	--[c]	24.08	17.72	73.6
LLM-85-01	2a	MCG-603	52	Slightly Welded	33	24.20	15.58	64.4
LGM-85-06	2a	MCG-615	51	Slightly Welded	14	25.73	10.34	40.2
LLM-85-02	2a	MCG-608	67	Moderately Welded	6	24.69	10.69	43.3
LLM-85-05	2a/1b	MCG-612	76	Slightly Welded	--[c]	24.37	18.08	74.2
LLM-85-01	1b	MCG-604	101	Slightly Welded	27	26.76	16.62	62.1
LGM-85-06	1b	MCG-616	99	Moderately Welded	27	28.26	13.42	52.6
LGM-85-11	1b	MCG-620	94	Moderately Welded	17	26.08	16.76	64.3
LLM-85-02	1b	MCG-609	117	Moderately Welded	--[c]	25.69	12.46	48.5
LLM-85-05	1b	MCG-613	123	Slightly Welded	--[c]	26.23	17.20	65.6
LLM-85-01	1b	MCG-605	124	Moderately Welded	20	25.62	12.53	48.9
LGM-85-11	1a	MCG-621	115	Nonwelded	--[c]	24.16	14.51	60.1
LGM-85-06	1a	MCG-617	115	Nonwelded	--[c]	26.32	14.82	56.3

[a]Based on field observations.

[b]The percentage of pumice fragments in the sample was determined by thin-section analysis using the point-count method.

[c]Not measured.

Since field determinations are very subjective, porosity appears to be a way of quantifying the degree of welding. The pumice content, however, must also be considered. The buoyancy of pumice in water is a consequence of its high porosity. As a result, a moderately welded sample could exhibit a relatively high porosity because of a high pumice content (e.g., compare Samples MCG-608 and MCG-620 in Table 3-1).

Ross and Smith (1961) demonstrate that porosity can be used to delineate degree of welding (Figure 3-6). However, it would be difficult to use porosity to classify the geologic units in the project area without greatly increasing the sampling frequency, because Units 2a and 2b are composed of more than one flow, each exhibiting significant variations in porosity and pumice content.

Based on the laboratory results, there appears to be no relationship between porosity and permeability (see Section 3.2). The reason could be that, for similar degrees of welding, an increase in the pumice content results in an increase in the porosity. Since the pumice lapilli contain a significant amount of dead-end pores, however, there is no significant increase in the effective permeability.

3.1.3 MOISTURE CHARACTERISTIC CURVES*

3.1.3.1 Purpose and Scope

A moisture characteristic curve is defined as the relationship between the capillary forces at varying degrees of saturation for a selected porous medium. This curve is particularly useful for the conversion of moisture data to capillary potential, and vice versa. This section of the report describes the procedure used to generate these curves, along with a discussion of the test results. The testing was performed by TerraTek Research Laboratory, and the description of the test procedures (Section 3.1.3.3) was adapted from their report (TerraTek Research Laboratory, 1985).

3.1.3.2 Sample Preparation

(See Section 3.1.2.2.)

3.1.3.3 Procedure for Centrifuge Tests

Prior to testing, the samples were vacuum-saturated with tap water. Complete saturation was verified by comparison with previous saturation data and the helium-injection data. Testing consisted of loading the samples into specially designed centrifuge cups and spinning them at six incremental speeds. Speeds ranged from a low of 130 revolutions per minute (rpm) to a high of 680 rpm. A stroboscope was used to monitor the speed of the centrifuge until it was stable. The speeds were converted mathematically to capillary pressure, and saturations were determined using displacement data. The average saturation derived from the displacement data was converted to a corrected wetting-fluid saturation value.

*Response to Task 2, Paragraph 25, Compliance Order/Schedule.

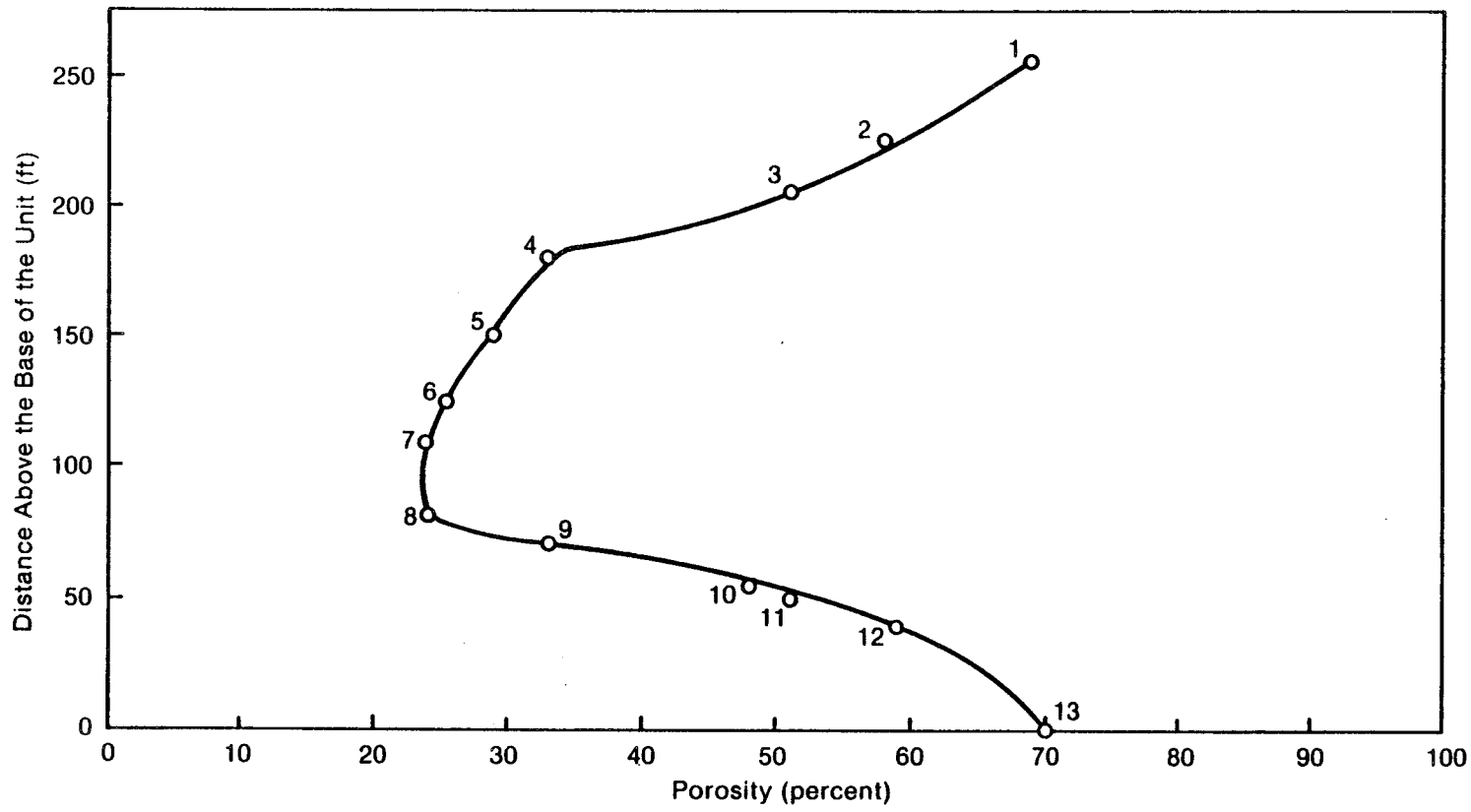

DATA PLOTTED IN THE GRAPH

Sample Number	Distance Below the Top of the Unit (ft)	Porosity (percent)	Sample Number	Distance Below the Top of the Unit (ft)	Porosity (percent)
1	0	69	8	175	24
2	30	58	9	185	33
3	50	51	10	200	48
4	75	33	11	205	51
5	105	29	12	215	59
6	130	25.5	13	255	70
7	145	24			

Figure 3-6. Porosity of Battleship Rock Ash-Flow Tuff, Valles Mountains, New Mexico (from Ross and Smith, 1961)

3.1.3.4 Results and Discussion

Moisture characteristic curves for 20 samples are presented in Appendix C. Only the drying curves were obtained because of the severe problems encountered when attempting to obtain imbibition (wetting) curves. Due to the highly porous nature of the samples, water was imbibed to such an extent that capillary-pressure determinations were impossible. Since the samples were too friable for mercury injection, it was decided to suspend attempts at obtaining these data.

After reviewing the moisture characteristic curves, the laboratory was requested to increase the centrifuge speed in order to evaluate lower water potentials (capillary pressures). Unfortunately, the samples disaggregated at these higher speeds. The laboratory was then requested to use the pressure-plate method to measure moisture characteristics, but those attempts were also unsuccessful due to sample disaggregation.

The most interesting data discernible from the moisture characteristic curves (Appendix C) are the extremely high moisture-retention (θ_r) values, which range up to 80 percent. The moisture-retention value is important because it represents the point at which capillarity as a transport mechanism breaks down. Since all of the moisture-content measurements for the Bandelier Tuff are significantly below this value, vapor transport is clearly the major mechanism of water transport.

The moisture characteristic data also demonstrate that only a minor amount of force is required to initiate the drainage of water from the saturated core sample, suggesting that the tuff has a low air-entry value. This information, coupled with the high residual moisture content, indicates that the tuff is characterized by a highly variable pore-size distribution.

It is interesting to compare the results of this study with those of a study performed by Abeele (1984), who presents moisture characteristic curves for crushed Bandelier Tuff. Residual saturation (θ_r) for the crushed tuff is approximately 0.2, as compared with an average of 0.5 for the solid rock cores. If it is assumed that both laboratory methods are reliable, then comparison of the unsaturated hydraulic properties of crushed versus natural tuff reveals a significant difference. One possible explanation is the destruction of the internal structure of the pumice lapilli in the crushed tuff. The gas tubes present in the pumice lapilli of uncrushed tuff are perfect little capillary tubes whose strong capillary forces retain significant amounts of water, resulting in higher θ_r values.

Knowledge of the average moisture-retention value enables one to calculate how much water must be supplied to the system in order for the capillary forces of the overlying tuff to be satisfied—a condition which must be met in order for recharge of liquid water to occur to the underlying groundwater system. Based on an average porosity of approximately 50 percent (Table 3-1) and an average moisture-retention value of approximately 50 percent (Appendix C), a recharge of 25 centimeters for each 1-meter thickness of tuff would be required to satisfy the capillary forces before recharge to the underlying groundwater system could occur. This scenario is quite unlikely in the study area due to the large amount of water required and the fact that the potential evapotrans-

piration rates in the Jemez Mountains area exceed the annual precipitation amount (Abeele and others, 1981).

3.2 PERMEABILITY DETERMINATIONS

3.2.1 BOREHOLE-INJECTION TESTS*

3.2.1.1 Purpose and Scope

Borehole-injection tests, or packer tests, were used to measure the in-situ permeability of different intervals in the Bandelier Tuff. The tests were performed in accord with procedures described by the U.S. Department of the Interior (1974) and the University of Missouri at Rolla (1981). Usually the tests are performed with water, but injection of water near the waste-disposal areas at Los Alamos was not allowed (see succeeding subsection on Background for further discussion). One hole, LLM-85-05, located between Areas G and L, was tested with both air and water in order to permit a comparison between the two fluids.

Following the discussion on background, a detailed description of the field tests is presented, including equipment and procedures. The equations used to calculate hydraulic conductivity and intrinsic permeability are presented next, followed by a discussion of the results, including a comparison of the air and water values obtained for Hole LLM-85-05.

3.2.1.2 Background

Two methods are available to measure the in-situ saturated hydraulic conductivity, K_s, of the tuff above the water table. These are borehole-infiltration tests and borehole-injection tests. Borehole-infiltration tests require maintenance of a constant head of water in an open or cased borehole until the flow rate becomes steady. The method is described in papers by Stephens and Neuman (1982a, 1982b) and Stephens and others (1983). Borehole-injection tests involve installing packers in the borehole to isolate measurement intervals, followed by injection of air or water into the formation.

Prior to initiation of the investigations described in this report, Los Alamos National Laboratory requested that water not be injected into boreholes in the vicinity of Areas G and L. Since the majority of the holes for this study are in or adjacent to these areas, borehole infiltration as a method for determining in-situ permeabilities was eliminated. Instead, borehole injection was used to measure in-situ permeability in the study area, largely because packers can be used to isolate sections of the borehole for testing and because air can be used in place of water. However, the method, whether using air or water, is subject to a number of limitations and assumptions which warrant further discussion.

---

*Response to Task 1, Paragraph 25, Compliance Order/Schedule.

First, it should be emphasized that the air-injection method is experimental and may permit only a qualitative characterization of subsurface permeabilities. Miller and others (1974), for example, used an air-injection technique to study the fracturing around a tunnel in volcanic rock and were able to conclude only that the permeability of the rock was either high or low. Therefore, before any quantitative interpretation can be made, air-injection results must be compared with results of laboratory and other field tests.

Using air as an injection fluid for packer tests may require compensation or correction for these factors: gas compressibility, changes in the volume of the gas with respect to temperature, and variation in the atmospheric water-vapor content. To overcome potential problems related to these factors, certain assumptions were made and appropriate procedures were implemented.

Compressive effects are minimal under steady-state conditions. Hence, the flow of air was kept at a constant rate and under low pressure during the injection step. In addition, boundary effects were disregarded because capillary action should have no impact on air flow.

To permit compensation for temperature effects on the volume of gas, a probe was placed downhole just above the packer assembly. A description of the temperature probe and meter is presented in the Equipment subsection (Section 3.2.1.3.1).

Based on the results of a study by Loughborough (1966), who compared the permeability of concrete using air and water vapor versus dried air, the potential effects of varying amounts of water vapor were disregarded. Loughborough's results demonstrated an average difference in permeability of only 5 percent. It is expected that this difference would be even less in a more permeable medium such as the Bandelier Tuff, indicating that it is reasonable to assume no effect.

Finally, in order to accurately calculate permeability for an air-injection test, values for the fluid injection pressure and flow rate must be known. Depending on the injection rate and the permeability of the formation, the resulting pressure can be very low. Equipment used to measure the low injection flow rates and pressures are described in the Equipment subsection (Section 3.2.1.3.1).

The use of water as an injection fluid also has certain limitations, specifically for tests above the water table. The U.S. Department of Interior (1974) points out that water-injection tests are more accurate below the water table than above, since the describing equations assume that horizontal flow is inherent throughout the system. Another potential source of error associated with water-injection tests is that existing formulas for computing permeability disregard the effects of capillary flow in the vadose zone. Instead, the formulas are based on various approximations of the classical free surface theory, which assumes that flow takes place entirely within a saturated region, an approximation which could lead to significant errors as pointed out by Stephens and Neuman (1982a).

3.2.1.3 Description of Field Tests

3.2.1.3.1 Equipment. Figures 3-7 and 3-8 illustrate the equipment used for the air- and water-injection tests, respectively. Although the two configurations differ somewhat, each has the same essential parts: flow meter, pressure gauge or gauges, conduit pipe, downhole temperature probe, and pneumatic packers.

For the air-injection tests, a New Jersey Air Flow Meter was used to measure the volume of air injected into the formation. Since the quantity of air injected varied from hole to hole, two different meters with different flow ranges were used. One had a range of 0 to 40 cubic feet per minute (cfm) with 1-cfm increments, while the other had a range of 50 to 300 cfm with 5-cfm increments. For the water-injection tests, a Neptune Water Meter with 0.1-gallon increments replaced the New Jersey Air Flow Meter.

For both the air- and water-injection tests, a Heise pressure gauge was used to measure the downhole, or back injection, pressure. The Heise gauge has a range of 0 to 60 psi with 0.2-psi increments, and is calibrated for atmospheric pressure at sea level (14.7 psi). Such a sensitive gauge was necessary to accurately measure the low pressures which resulted from the small volumes of fluid injected.

Galvanized conduit pipe, 1-3/8 inches in diameter, was used to conduct fluid down the hole. Threaded sections and couplings were secured with Teflon tape to prevent leakage.

The probe used to measure downhole fluid temperatures was located in a small chamber at the base of the conduit pipe, just above the pneumatic packers. Both the chambers and the section of pipe to which it was welded contained holes that permitted small amounts of air to flow between the two. The temperature probe was connected to a YSI Model 42SC Tele-thermometer located at the surface. The Tele-thermometer had a range of -40 to 150°C with increments of 1°C.

Each 6-ft interval was isolated using a set of Tigre Tierra Model 610 Pneumatic Packers. The 4-ft-long packers expand up to 10 inches in diameter and can be inflated to 470 psi.

3.2.1.3.2 Procedure. The borehole-injection tests were conducted by isolating 6-ft intervals in the uncased boreholes using the pneumatic packers. The packers were inflated to 200 psi to ensure a good seal. (Several tests were performed before this inflation pressure was determined.) A known quantity of air or water was injected until a measurable pressure was obtained on the Heise gauge. The pressure, flow rate, and temperature were then periodically recorded until all readings were constant with respect to time. The flow rate was then increased and the procedure repeated. Once the higher flow rate became constant, the process was repeated using the lower flow rate to check reproducibility.

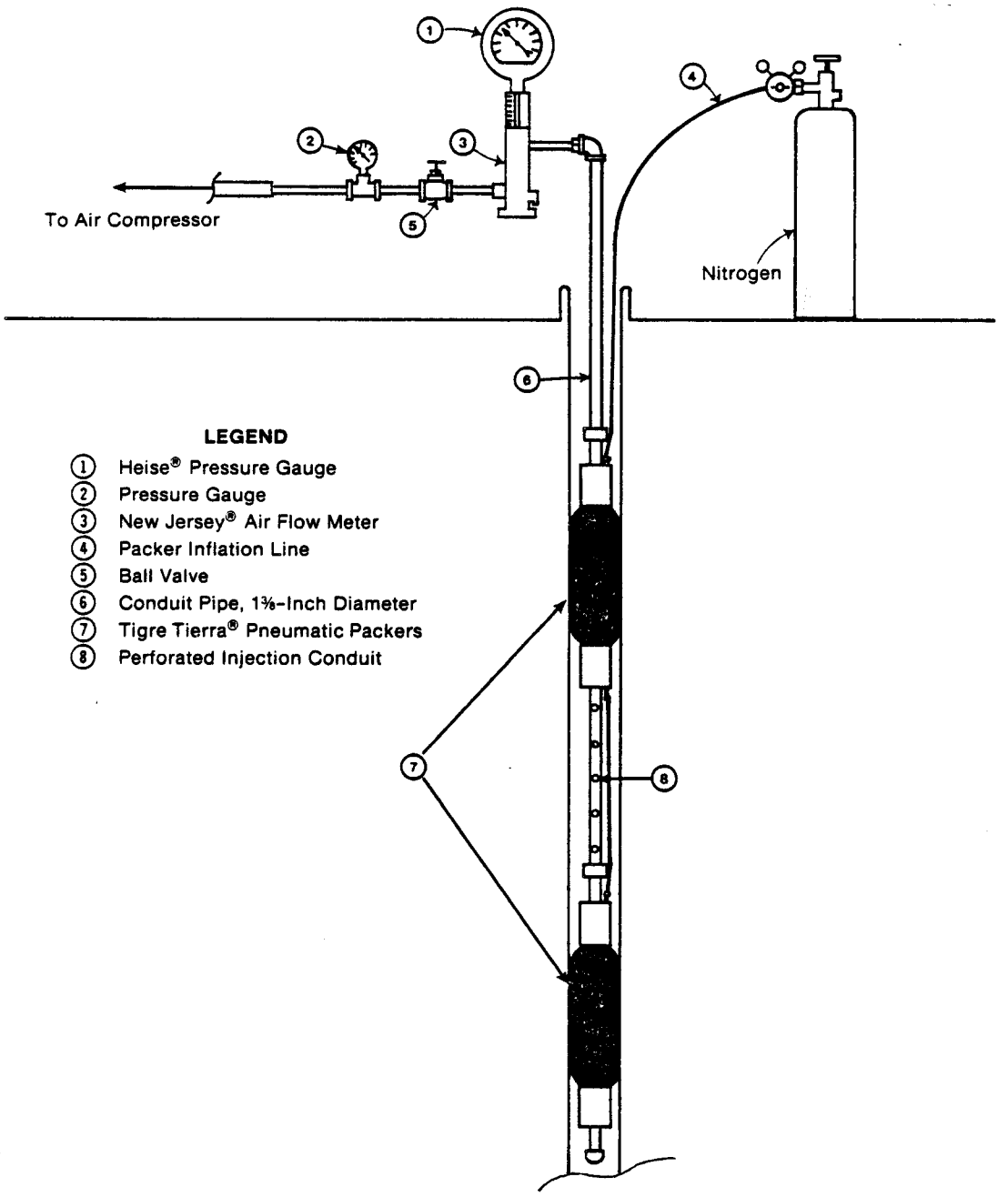

Figure 3-7. Air-Injection Apparatus Used for In-Situ Permeability Measurements

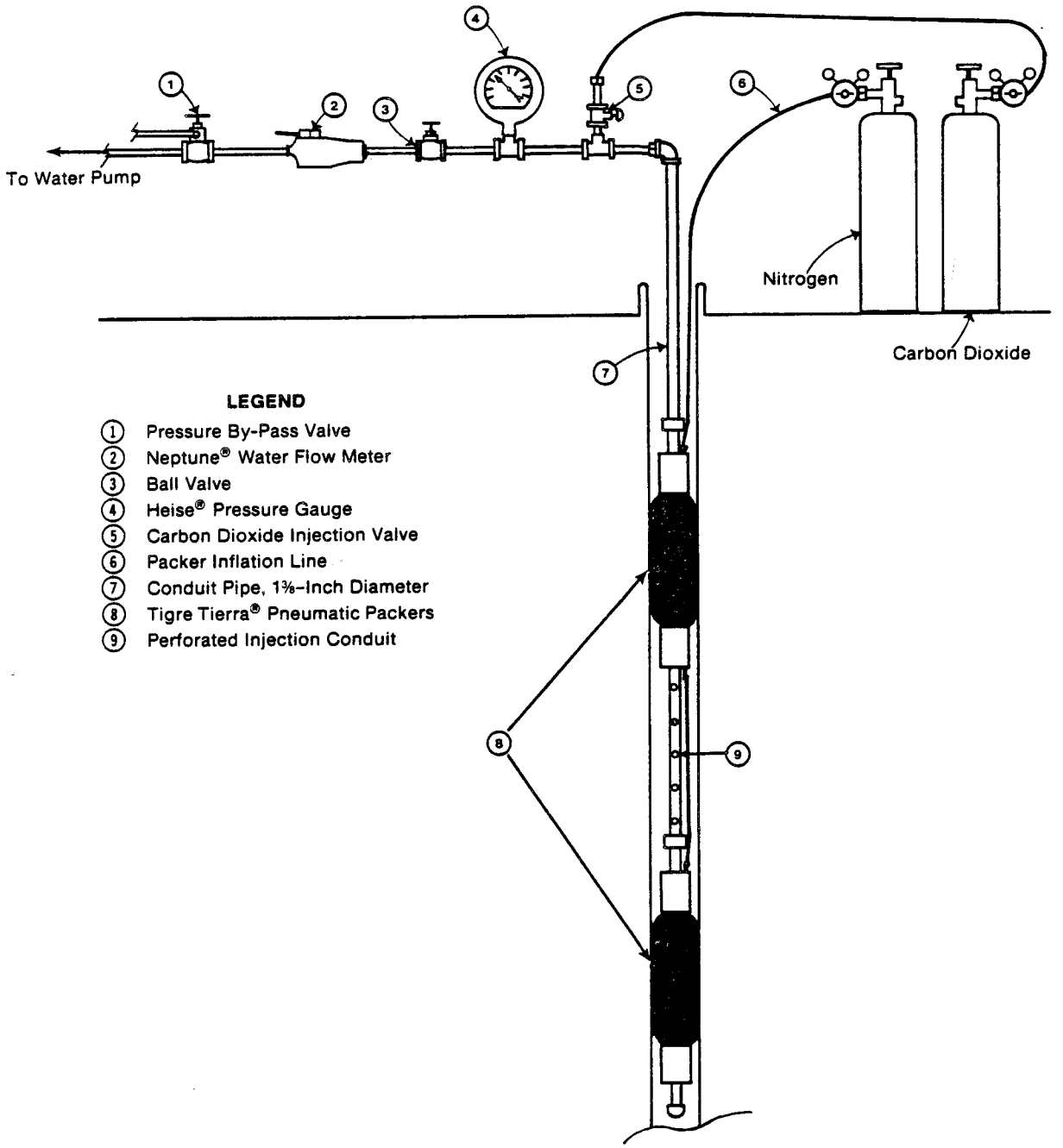

Figure 3-8. Water-Injection Apparatus Used for In-Situ Permeability Measurements

During the tests, the borehole was monitored for discharge of either air or water. If a discharge occurred, it was assumed that the packers were leaking and that the test was invalid.

3.2.1.4 Calculations

The rate at which a fluid can be injected into a geologic formation at a given pressure and through a known area is a function of the permeability of the formation. This relationship can be expressed in the following equation (U.S. Department of the Interior, 1974):

$$K = (Q/2\pi SH) \ln (S/r) \tag{5}$$

where

K = hydraulic conductivity (L/t)
Q = injection rate (L^3/t)
S = length of the test interval (L)
H = differential head of the fluid (L)
r = radius of the borehole (L)

Since the differential head is a combination of the height of the fluid column above the test interval and the pressure p at which the fluid is injected, p may be expressed as the height of the column of any fluid by the relationship

$$H = p/\gamma \tag{6}$$

where γ is the specific weight of the fluid.

Equation (5) is sufficient for the calculation of hydraulic conductivity when water is the injection fluid. However, modifications to Equation (5) are required when air is the injection fluid, because the specific weight of air is strongly dependent on the temperature and pressure. The specific weight of air can be determined from the equation of state for an ideal gas,

$$\gamma = gp_a/RT_a \tag{7}$$

where

γ = specific weight of the fluid (m/L^2t^2)
g = gravitational acceleration (L/t^2)
p_a = absolute pressure (force/L^2)
R = a gas constant
T_a = absolute temperature in degrees Rankine or Kelvin

For air, the value of R is 287 N-m/(kg)(°K) [1715 ft-lb/(slug)(°R)]. Substituting Equations (6) and (7) for the appropriate variables in Equation (5) yields

$$K = (Qgp_a/2\pi SpRT_a) \ln (S/r) \tag{8}$$

Since the flow rate of a gas through the New Jersey meter is also dependent on temperature and pressure, a combined correction factor, C_f, is required to calculate the actual flow rate. Inserting the combined correction factor into

Equation (8) yields the final equation for calculating the in-situ air-derived hydraulic conductivity,

$$K = (QC_f g p_a / 2\pi S p R T_a) \ln (S/r) \tag{9}$$

In order to compare the hydraulic conductivity derived from air injection versus that derived from water injection, it is convenient to use the term intrinsic permeability, k. Intrinsic permeability is a function of only the medium, whereas hydraulic conductivity is a function of both the medium and the fluid. The term k is widely used in the petroleum industry where the existence of gas, oil, and water in multiphase flow systems makes the use of a fluid-free conductance parameter attractive.

Intrinsic permeability and hydraulic conductivity can be related to one another by the equation (Nutting, 1930)

$$k = K\mu/\rho g \tag{10}$$

where

- k = intrinsic permeability (L^2)
- K = hydraulic conductivity (L/t)
- μ = absolute viscosity of the fluid ($F \cdot t/L^2$, where F = force)
- ρ = density of the fluid (m/L^3)
- g = gravitational acceleration (L/t^2)

Equation (10) will suffice for calculating k values from water-derived K values. However, modifications to Equation (10) are required for gas-derived conductivities because of the dependence of the density term on the pressure and temperature. Once again, the equation of state in the following form is used:

$$\rho = p_a/RT_a \tag{11}$$

Equation (11) is substituted for ρ in Equation (10) to yield the relationship between k and K for a gas,

$$k = K\mu RT_a/p_a g \tag{12}$$

Comparing the intrinsic permeability values calculated from the air- and water-injection tests can aid in the evaluation of any bias inherent in the individual methods.

3.2.1.5 Results and Discussion

Hydraulic conductivity values derived from the air-injection tests (Table 3-2) range from 10^{-3} to 10^{-5} centimeter per second (cm/s) [10^{-5} to 10^{-6} foot per second (ft/s)]. Conversions to intrinsic permeability indicate that the range of values is similar to those exhibited by a silty to clean sand (Freeze and Cherry, 1979). Based on field observations of the tuff, these permeability values appear to be reasonable.

Table 3-2. Hydraulic Conductivity Determined from Air-Injection Tests in Los Alamos Drill Holes

Hole Number	Geologic Unit	Test Interval[a] (ft)	Interval Description	Fractures Present?	Hydraulic Conductivity (K)	
					cm/s x 10^{-5}	ft/s x 10^{-5}
LLM-85-01	2b	9-15	Upper 2b, Moderately Welded	No	1.2	4.1
LLM-85-01	2b	30-36	Lower 2b, Moderately to Slightly Welded	No	0.70	2.3
LLM-85-02	2b	9-15	Upper 2b, Moderately Welded	Yes	0.094	0.31
LLM-85-02	2b	24-30	Middle 2b, Moderately Welded	No	0.11	0.37
LLM-85-05	2b	24-30	Mid-Lower 2b, Moderately Welded	No	0.91	3.0
LGM-85-11	2b	9-15	Upper 2b, Moderately Welded	No	1.5	5.0
LGM-85-11	2b	14-20	Middle 2b, Moderately Welded	Yes	1.4	4.7
LGM-85-11	2b/2a	35-41	Contact 2b/2a, Slightly Welded	No	0.12	0.40
LLM-85-01	2a	51-57	Middle 2a, Slightly Welded	No	0.33	1.1
LLM-85-01	2a	72-78	Lower 2a, Slightly Welded	Yes	0.14	0.45
LLM-85-02	2a	45.5-51.5	Upper 2a, Slightly Welded	Yes	0.14	0.45
LLM-85-02	2a	66.5-72.5	Mid-Lower 2a, Moderately Welded	No	0.14	0.45
LLM-85-05	2a	45-51	Upper 2a, Slightly Welded	Yes	2.8	9.3
LLM-85-05	2a	55-61	Middle 2a, Slightly Welded	Yes	1.9	6.2
LGM-85-06	2a	38-44	Upper 2a, Slightly Welded	Yes	0.067	0.22
LLM-85-05	2a/1b	75-81	Contact 2a/1b, Slightly Welded	No	0.052	0.17
LGM-85-11	2a/1b	56-62	Contact 2a/1b, Slightly Welded	No	0.52	1.7
LLM-85-01	1b	93-99	Mid-Upper 1b, Slightly Welded	No	0.082	0.27
LLM-85-02	1b	87-93	Upper 1b, Slightly Welded	No	0.085	0.28
LLM-85-05	1b	82-88	Upper 1b, Slightly Welded	No	0.061	0.20
LGM-85-06	1b	60-66	Upper 1b, Slightly Welded	No	0.64	2.1
LGM-85-06	1b	81-87	Middle 1b, Slightly to Moderately Welded	No	0.52	1.7
LGM-85-11	1a/1b	99-105	Contact 1a/1b, Slightly Welded	No	0.030	0.098
LGM-85-11	1b	77-83	Middle 1b, Slightly to Moderately Welded	No	0.23	0.77
LGM-85-11	1a	108-114	Upper 1a, Nonwelded	No	0.088	0.2

[a]Depth below ground level.

In general terms, the permeability of the tuff decreases with stratigraphic depth. Unit 2b shows an average air-derived hydraulic conductivity of 8.5 x 10^{-4} cm/s (2.8 x 10^{-5} ft/s); Unit 2a, 7.9 x 10^{-4} cm/s (2.6 x 10^{-5} ft/s); Unit 1b, 2.3 x 10^{-4} cm/s (7.7 x 10^{-6} ft/s); and Unit 1a, 8.8 x 10^{-5} cm/s (2.9 x 10^{-6} ft/s), this last being the only measurement obtained for Unit 1a.

The highest air-derived hydraulic conductivity was determined for a fractured zone in Unit 2a [2.8 x 10^{-3} cm/s (9.3 x 10^{-5} ft/s)]. However, the average K value determined for fractured zones [9.4 x 10^{-4} cm/s (3.1 x 10^{-5} ft/s)] was only slightly greater than values determined from the majority of air-injection tests in unfractured tuff. These results suggest that secondary fracture permeability does not appear to be significantly greater than the primary permeability of the tuff.

Water-derived hydraulic conductivities, presented in Table 3-3, are in the same range as those reported by Abeele (1984) for crushed tuff, i.e., 1.4 x 10^{-4} cm/s (4.6 x 10^{-6} ft/s). These values, like those derived from the air-injection tests, generally decrease with depth.

The reliability of the air-injection method is demonstrated by comparing the intrinsic permeability values calculated from both the air and water test for the same intervals (Table 3-4); results from the two lower zones in particular are in good agreement with one another. The largest discrepancy between the two methods is seen in the results for the interval 24 to 30 ft, where the value calculated from the water-injection test is an order of magnitude lower than the value calculated from the air-injection test. This water-injection test, however, was not performed in the same fashion as the others. Specifically, carbon dioxide was not injected prior to the tests as it was for the lower intervals. The purpose of injecting carbon dioxide is to minimize the effects of trapped air in the formation. Thus, permeability values might be less for tests performed without carbon dioxide injection. It would appear that these results support the use of carbon dioxide for water-injection tests in the vadose zone, as recommended by Stephens and others (1983).

Table 3-3. Hydraulic Conductivity Values Determined from Water-Injection Tests in Hole LLM-85-05

Test Interval (ft)[a]	Hydraulic Conductivity (K) cm/s	ft/s
10-16	9.4 x 10^{-4}	3.1 x 10^{-5}
24-30[b]	1.0 x 10^{-3}	3.3 x 10^{-5}
75-81	6.4 x 10^{-4}	2.1 x 10^{-5}
82-88	4.6 x 10^{-4}	1.5 x 10^{-5}

[a]Depth below ground level.

[b]Injection with carbon dioxide prior to water injection was not performed for this test interval.

Table 3-4. Comparison of Intrinsic Permeability Values Determined from Water-Injection and Air-Injection Tests in Hole LLM-85-05

Test Interval (ft)[a]	Intrinsic Permeability (k)			
	Air-Injection Test		Water-Injection Test	
	cm^2	ft^2	cm^2	ft^2
24-30[b]	1.8×10^{-7}	1.9×10^{-10}	1.3×10^{-8}	1.4×10^{-11}
75-81	7.5×10^{-9}	8.1×10^{-12}	8.4×10^{-9}	9.1×10^{-12}
82-88	9.0×10^{-9}	9.7×10^{-12}	6.0×10^{-9}	6.5×10^{-12}

[a]Depth below ground level.
[b]Injection with carbon dioxide prior to water injection was not performed for this test interval.

3.2.2 VACUUM TESTS*

3.2.2.1 Purpose and Scope

Vacuum tests were conducted in selected intervals of the Bandelier Tuff in order to obtain additional measurements of the in-situ permeability. These tests also involve sealing off the measurement interval using pneumatic packers and monitoring the changes in air pressure and flow rate after creating a pressure gradient. Unlike the air-injection tests, however, the pressure gradient is negative and is created by means of a vacuum pump. Detailed descriptions of the equipment and procedures, followed by discussions of the calculations and results, are presented in the succeeding paragraphs.

3.2.2.2 Description of Field Tests

3.2.2.2.1 Equipment. The vacuum-testing apparatus used for this study (see Figure 3-9) was designed to isolate a specified interval in the drill hole, to evacuate air by means of pumping, and to measure the resultant pressure response, flow rate, and air temperature. Isolation of the 1-meter-long (3.3 ft) test interval was accomplished by means of pneumatic packers similar to those used in the injection tests. A vacuum hose attached to the packer conduit pipe extended upward to the ground surface and was connected to a two-way valve that isolated the drill hole from the rest of the vacuum-testing equipment.

A capacitance manometer connected between the valve and the packers measured downhole pressure changes induced by pumping. The manometer was a tensioned-metal-diaphragm vacuum gauge having the capacity to measure pressure in the range of 1×10^{-4} torr to 1000 torr. (A torr is a unit of pressure equal to 1333.22 microbars, or the pressure required to support a column of mercury 1 millimeter high under standard conditions.) A pressure display module was connected to the manometer to provide direct readout of pressure in torr or millimeters.

*Response to Task 1, Paragraph 25, Compliance Order/Schedule.

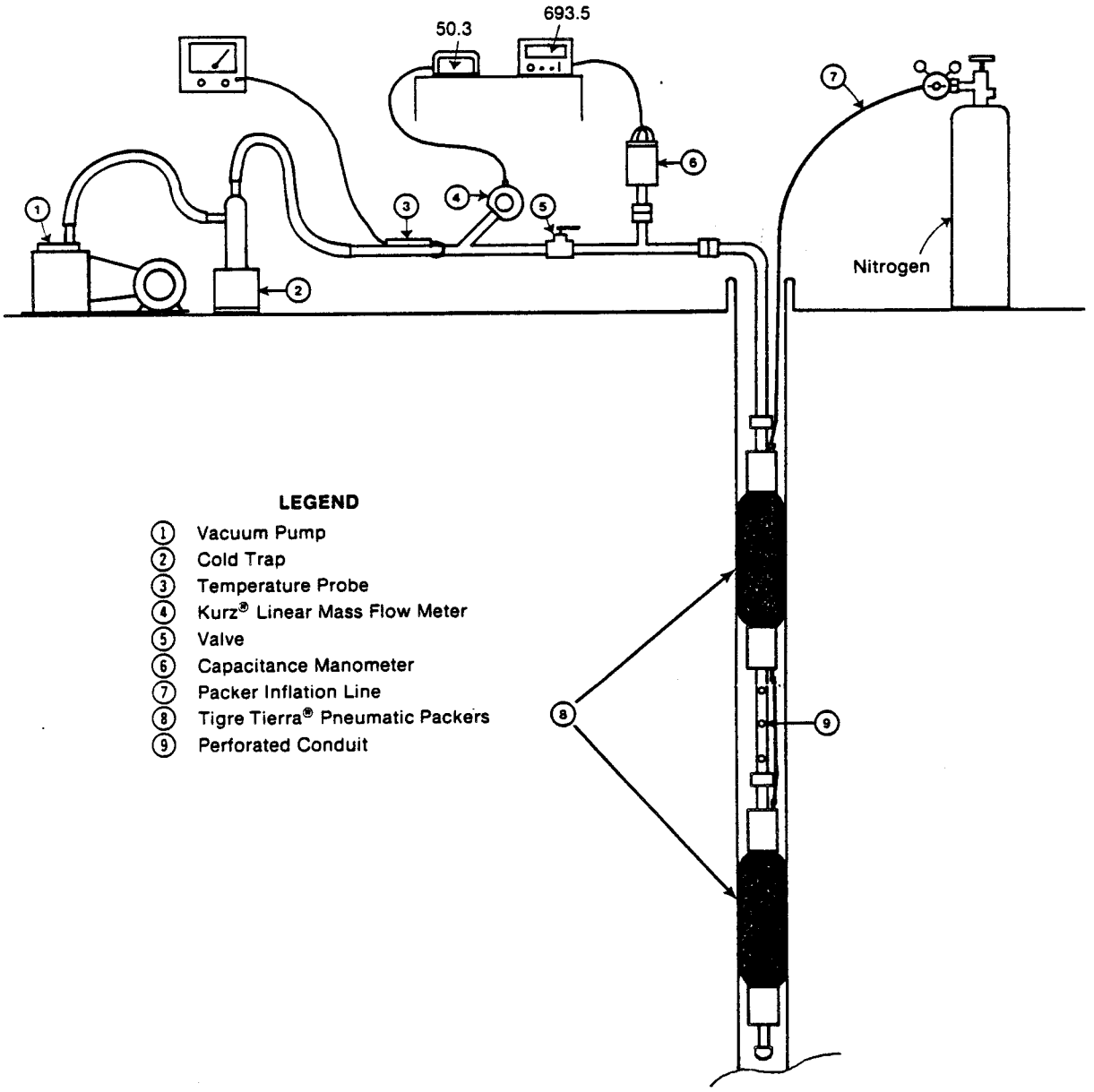

Figure 3-9. Vacuum-Testing Apparatus Used for In-Situ Permeability Measurements

The probe used to measure downhole air temperature was located in line with the system, in a small chamber welded to a section of pipe. Small holes connect the chamber and the pipe, allowing small amounts of air to flow between the two. The temperature probe was connected to a YSI Model 42SC Tele-thermometer, which has a range of -40 to 150°C with increments of 1°C.

A linear mass flow meter was located adjacent to the temperature probe in order to measure the gas flow rate induced by pumping. The meter consisted of two platinum windings: One winding was an ambient temperature detector; the other was heated to a constant temperature above that of the ambient or surrounding gas. A measure of the power required to maintain this temperature difference is a measure of the heat transfer from the winding, which in turn is a measure of the quantity of gas flowing past the sensor. The range of the meter was 0 to 1000 liters per minute (lpm), with an accuracy of 2 percent of the reading over a 10-to-1 range plus an additional one-half percent at full scale.

3.2.2.2.2 Procedure. Once a test interval had been selected, the pneumatic packers were lowered to the desired depth and inflated to isolate that particular section of the drill hole. The vacuum valve was closed, and the formation pressure prior to pumping was recorded in the field notebook.

With the vacuum pump running, the valve was opened to start the test. Pressure readings versus time were recorded at 5-second intervals. Pumping of the test section was continued as long as was necessary under the specified conditions dictated by the medium and the dead volume of the equipment. Generally, pumping was terminated after achieving steady-state flow. For tests in the Bandelier Tuff, it was observed that quasi steady-state conditions were obtained prior to 1 minute of pumping. Therefore, for all tests, the interval was pumped for a period of 1 minute. The temperature was recorded during the pumping phase of the tests, and the flow rate was recorded just prior to the end of the pumping phase.

After 1 minute of pumping, the vacuum valve was closed and the pressure buildup phase was begun. Pressure readings were once again recorded at 5-second intervals until the system returned to the prepumping pressure, signifying the end of the test.

3.2.2.3 Calculations

The vacuum-testing technique is based on methods used by the petroleum industry. In a paper presented by Horner (1951), the pressure buildup that results from closing gas wells is used to calculate the permeability of the subsurface formation. This method was modified by Jakubick (1983) for use in unsaturated materials by initiating the pressure buildup by means of vacuum pumping rather than by shutting-in the well. The equations used for the calculations in this study, however, were taken directly from Horner's paper, because Jakubick does not present the theory for his equations which are different from the original work by Horner. Moreover, Jakubick does not define the gas-constant term he used, nor does he maintain consistency in the units used in his equations.

Single-phase radial flow to a well completed in a reservoir, assumed to be homogeneous, horizontal, and of uniform thickness, may be expressed by the equation

$$(\partial^2 p/\partial r^2) + [(1/r)(\partial p/\partial r)] = (fc\mu/k)(\partial p/\partial t) \tag{13}$$

where

p = reservoir pressure
r = distance from the center line of the well
f = formation porosity
c = fluid compressibility
μ = fluid viscosity
k = intrinsic permeability of the formation
t = time

Horner presents the so-called 'point solution' to Equation (13) which yields

$$p = p_o + \{(q\mu/4\pi kh)E_i[-(r^2 f\mu c/4kt)]\} \tag{14}$$

where

p_o = initial reservoir pressure
q = a constant rate of production for the well
h = length of the test interval
E_i = the exponential integral

Considering a single well brought into production at t_o, which subsequently produced at a constant rate q, the well pressure p_w at the time $[(t_o + \varphi)/\varphi]$ may be obtained by superimposing two solutions of the form of Equation (14). For small values of its argument, the E_i function may be approximated by a logarithmic function. The result is the basic buildup equation for a single well in an infinite reservoir,

$$p_w = p_o - \{(q\mu/4\pi kh) \ln [(t_o + \varphi)/\varphi]\} \tag{15}$$

where is the time after close-in of the well.

For analysis of the data, it is convenient to change the natural logarithm, ln, to the base ten logarithm, $\log_{10}$, by the relationship

$$\ln x = (\log_{10} x)(\ln 10) \tag{16}$$

which yields

$$p_w = p_o - \{[(\ln 10)q\mu/4\pi kh] \log [(t_o + \varphi)/\varphi]\} \tag{17}$$

Analysis of the vacuum-test data using Equation (17) involves fitting a straight line through the data points. The slope of the line, m, from Equation (17) is defined as

$$m = -[(\ln 10)q\mu/4\pi kh] \tag{18}$$

The next step in the analysis involves plotting the well-pressure (p_w) data versus the log of $[(t_o + \varphi)/\varphi]$ and determining the slope of the resultant line. This graph is commonly referred to as a Horner plot. Once the slope of the line is determined, Equation (18) can be rearranged in terms of the intrinsic permeability as follows:

$$k = -[(\ln 10) q\mu/4\pi mh] = -[0.1832339(q\mu/mh)] \quad (19)$$

3.2.2.4 Results and Discussion

Intrinsic permeabilities determined from vacuum tests in the Bandelier Tuff (Table 3-5) range from 10^{-8} to 10^{-9} cm^2 (10^{-11} to 10^{-12} ft^2). The correlation coefficients for the linear regression used to fit a straight line through the data points on the Horner plots indicate a good linear relationship for the data; the lowest coefficient is 0.92 (see Table 3-5).

In general, the vacuum-test results, like those from the air-injection tests, indicate that permeability tends to decrease with depth. The lowest value, for example, was observed in the lower, moderately welded portion of Unit 1b. Results of the three tests performed in fractured zones indicate that there is no significant difference in permeability between fractured versus unfractured zones.

Table 3-6 compares intrinsic permeabilities derived from the air-injection tests versus the vacuum tests for similar intervals. The comparison demonstrates that the two methods yield results of the same order of magnitude. The vacuum-test results, however, are lower. A discussion of possible variations in vacuum-test and air-injection methods is presented in Section 3.2.5.

3.2.3 LABORATORY MEASUREMENTS*

3.2.3.1 Purpose and Scope

Laboratory measurements of permeability were also obtained on 20 core samples to provide a comparison with the field-test results. These determinations were conducted by TerraTek Research Laboratory using two procedures, one to measure permeability via gas injection and correction for gas slippage (Klinkenberg Correction Method) and the other to measure the gas-water relative permeability (Dynamic Method). The descriptions of these procedures are taken from TerraTek's report (TerraTek Research Laboratory, 1985). They are followed by a discussion of the laboratory results. A comparison of the laboratory and field data is presented in Section 3.2.5.

3.2.3.2 Sample Preparation

(See Section 3.1.2.2.)

*Response to Task 1, Paragraph 25, Compliance Order/Schedule.

Table 3-5. Permeability Values Determined from Vacuum Tests in Los Alamos Drill Holes

Hole Number	Geologic Unit	Test Interval[a] (ft)	Interval Description	Correlation Coefficient[b]	Fractures Present?	Intrinsic Permeability (k)	
						$cm^2 \times 10^{-9}$	$ft^2 \times 10^{-12}$
LLM-85-01	2b	30-33.3	Lower 2b, Moderately Welded	0.9409	No	39	42
LLM-85-02	2b	10-13.3	Upper 2b, Moderately Welded	0.9325	Yes	14	15
LLM-85-02	2b	25-28.3	Middle 2b, Moderately Welded	0.9267	Yes	22	24
LLM-85-05	2b	15-18.3	Middle 2b, Moderately Welded	0.9948	No	24	2.6
LGM-85-06	2b	10-13.3	Upper 2b, Moderately Welded	0.9675	No	38	41
LGM-85-11	2b/2a	35-38.3	Contact 2b/2a, Moderately Welded	0.9779	No	5.5	5.9
LLM-85-01	2a	70-73.3	Lower 2a, Nonwelded	0.9799	No	43	46
LLM-85-05	2a	40-43.3	Upper 2a, Slightly Welded	0.9196	No	8.4	9.1
LLM-85-05	2a	50-53.3	Middle 2a, Slightly Welded	0.9812	No	8.6	9.3
LLM-85-05	2a	60-63.3	Middle 2a, Moderately Welded	0.9882	No	8.6	9.3
LLM-85-06	2a	40-43.3	Middle 2a, Moderately Welded	0.9895	Yes	2.4	2.6
LLM-85-01	1b	80-83.3	Upper 1b, Slightly Welded	0.9946	No	5.6	6.0
LLM-85-01	1b	94-97.3	Upper 1b, Slightly Welded	0.9959	No	3.5	3.8
LLM-85-02	1b	87-90.3	Upper 1b, Slightly Welded	0.9966	No	9.3	10
LGM-85-06	1b	82-85.3	Middle 1b, Slightly Welded	0.9931	No	1.0	1.1
LGM-85-06	1b	100-103.3	Lower 1b, Moderately Welded	0.9932	No	0.84	0.90
LGM-85-11	1b	77-80.3	Middle 1b, Slightly Welded	0.9851	No	8.2	8.8
LGM-85-06	1b	60-63.3	Upper 1b, Slightly Welded	0.9903	No	8.7	9.4
LGM-85-11	1a	110-113.3	Upper 1a, Nonwelded	0.9963	No	2.7	2.9
LLM-85-02	1b	87-90.3	Upper 1b, Slightly Welded	0.9966	No	8.6	9.3
LLM-85-06	1b	87-90.3	Mid-Lower 2b, Moderately Welded	0.9609	No	2.4	2.6

[a]Depth below ground level.

[b]Correlation coefficient for the linear regression used to fit a straight line through the data points on the Horner plots (see Section 3.2.2.3).

Table 3-6. Comparison of Intrinsic Permeability Values Determined from Air-Injection and Vacuum Tests in Los Alamos Drill Holes

Hole Number	Test Interval (ft)[a]		Intrinsic Permeability (k)			
	Air-Injection Test	Vacuum Test	Air-Injection Test		Vacuum Test	
			$cm^2 \times 10^{-9}$	$ft^2 \times 10^{-12}$	$cm^2 \times 10^{-9}$	$ft^2 \times 10^{-12}$
LLM-85-01	30-36	30-33.3	130	140	39	42
LLM-85-02	9-15	10-13.3	10	11	15	16
LLM-85-02	24-30	25-28.3	16	17	22	24
LGM-85-11	35-41	35-38.3	17	18	5.5	5.9
LLM-85-01	72-78	70-73.3	19	21	43	46
LLM-85-01	93-99	94-97.3	7.6	8.2	3.5	3.8
LLM-85-02	87-93	87-90.3	3.3	9.5	9.3	10
LGM-85-06	60-66	60-63.3	120	130	8.7	9.4
LGM-85-06	81-87	82-85.3	84	90	1.0	1.1
LGM-85-11	99-105	100-103.3	3.3	3.6	0.84	0.90
LGM-85-11	77-83	77-80.3	32	35	8.2	8.8
LGM-85-11	108-114	110-113.3	7.2	7.8	2.7	2.9

[a]Depth below ground level.

3.2.3.3 Procedures

3.2.3.3.1 Klinkenberg Correction Method. Following porosity determinations, gas permeability measurements were performed on the 20 samples. These measurements were corrected for gas slippage, i.e., movement of gas along a boundary, using the Klinkenberg Correction Method. The measurement technique consisted of applying a confining pressure of approximately 100 psi and a slight pore pressure, and maintaining an approximate pressure drop of 2 psi across the sample during testing. Nitrogen gas was injected into the samples at four mean pressures (4, 9, 14, and 19 psi), and the permeability was calculated for each of these pressures. A plot was made of permeability versus the reciprocal mean pressures, and the intercept of a best-fit line through these four points, with the permeability axis at zero reciprocal mean pressure (infinite mean pressure), yielded the gas permeability corrected for gas slippage (Klinkenberg Correction).

3.2.3.3.2 Dynamic Method. Following completion of the gas permeability measurements, all 20 samples were subjected to gas-water relative permeability testing to determine intrinsic permeabilities (described in Section 3.2.3.4 below) and effective permeabilities (described in Section 3.2.4.1). Testing was begun by vacuum-saturating the samples with tap water (density = 0.995 g/cm^3 at room temperature). Complete saturation was verified by comparing these saturated-weight data with helium-injection data. Following saturation, each sample was placed in a hydrostatic core holder and subjected to a confining pressure of approximately 100 psi. Testing consisted of displacing the water from the samples with humidified nitrogen. (The gas was humidified to prevent drying or dehydration.) Incremental production of gas and water was monitored against time and flow rate at a constant injection pressure. These production data were used to calculate the gas-water relative permeabilities according to Johnson, Bossler, and Naumann's (1959) extension of Welge's (1952) derivation of relative permeability.

3.2.3.4 Results and Discussion

The laboratory permeability results (Table 3-7) are relatively uniform and consistent between the two methods, except for Sample MCG-607. The Klinkenberg result for this sample is probably unreliable as evidenced by its low correlation coefficient (0.714) and its poor comparison with the Dynamic Method result.

The results from both methods indicate only minor differences with depth or between geologic units. Klinkenberg permeabilities are approximately twice those determined by the Dynamic Method, but that is not considered significant for these types of measurement. More importantly, the average intrinsic permeability for both the Klinkenberg Correction Method and the Dynamic Method is 10^{-9} cm^2 (10^{-11} ft^2), a result that compares favorably with the field-test results.

Table 3-7. Intrinsic Permeability Values Determined from Laboratory Analysis of Core Samples

Hole Number	Geologic Unit	Sample Number	Depth of Sample (ft)[a]	Interval Description	Intrinsic Permeability/ Klinkenberg Method		Correlation Coefficient[b]	Intrinsic Permeability/ Dynamic Method	
					$cm^2 \times 10^{-9}$	$ft^2 \times 10^{-12}$		$cm^2 \times 10^{-9}$	$ft^2 \times 10^{-12}$
LGM-85-11	2b	MCG-618	3	Moderately Welded[c]	6.2	6.7	0.989	5.5	5.9
LLM-85-02	2b	MCG-606	7	Moderately Welded	6.6	7.1	0.745	4.5	4.9
LLM-85-05	2b	MCG-610	15	Moderately Welded	6.5	7.0	0.893	5.7	6.2
LLM-85-01	2b	MCG-602	30	Moderately Welded	2.7	2.9	0.958	1.1	1.2
LGM-85-11	2b	MCG-619	30	Moderately Welded	3.2	3.5	0.949	2.9	3.1
LLM-85-02	2b	MCG-607	36	Moderately Welded	11.0	12.0	0.714	1.2	1.3
LGM-85-06	2b	MCG-614	29	Moderately Welded	6.4	6.9	0.847	4.9	5.3
LLM-85-05	2b	MCG-611	36	Slightly Welded	3.5	3.8	0.984	2.4	2.6
LLM-85-01	2a	MCG-603	52	Slightly Welded	4.1	4.4	0.969	2.7	2.9
LGM-85-06	2a	MCG-615	51	Slightly Welded	2.5	2.7	0.954	0.86	0.93
LLM-85-02	2a	MCG-608	67	Moderately Welded	2.0	2.2	0.958	1.0	1.1
LLM-85-05	1b	MCG-612	76	Slightly Welded	2.1	2.3	0.944	1.3	1.4
LLM-85-01	1b	MCG-604	101	Slightly Welded	3.0	3.2	0.939	2.6	2.8
LGM-85-06	1b	MCG-616	99	Moderately Welded	18.0	19.0	0.917	13.0	14.0
LGM-85-11	1b	MCG-620	94	Moderately Welded	4.4	4.7	0.958	1.1	1.2
LLM-85-02	1b	MCG-609	117	Moderately Welded	3.3	3.6	0.973	1.7	1.8
LLM-85-05	1b	MCG-613	123	Slightly Welded	4.2	4.5	0.902	1.6	1.7
LLM-85-01	1b	MCG-605	124	Moderately Welded	6.0	6.5	0.850	2.3	2.5
LGM-85-11	1a	MCG-621	115	Nonwelded	3.4	3.7	0.933	1.8	1.9
LGM-85-06	1a	MCG-617	115	Nonwelded	1.4	1.5	0.970	0.93	1.0

[a]Below ground level.
[b]Determined for Klinkenberg permeabilities.
[c]Weathered.

3.2.4 HYDRAULIC CONDUCTIVITY AS A FUNCTION OF MOISTURE CONTENT*

3.2.4.1 Laboratory Tests

As noted above, the Dynamic Method was also used to determine permeability as a function of moisture content for the 20 samples of Bandelier Tuff (see Section 3.2.3.3.2). These values, called effective permeabilities, are plotted as a function of total air saturation in the graphs presented in Appendix D. Since the abscissa corresponds to total air saturation, the maximum effective permeabilities for water depicted on the curves occur at an air saturation of 0.000, which is equivalent to a water saturation (θ_s) of 1.000. Therefore, as the water saturation decreases, the effective permeability for water decreases, and the effective permeability for air increases.

The effective permeability values for the rock-core samples from the Bandelier Tuff range from 86.1 to 1301 millidarcys [(8.5×10^{-10} to 1.3×10^{-8} cm^2) or (9.1×10^{-13} to 1.4×10^{-11} ft^2)]. Residual water saturation following gas injection ranged from 0.64 to 0.95. Since moisture contents in the study area are much lower than this range (generally less than 10 percent), the effective permeabilities determined using the Dynamic Method are not indicative of the permeabilities one would expect to observe at depth in Areas G and L. These data are therefore only applicable to the estimation of near-surface conditions following a heavy rainfall, when moisture contents might exceed residual water saturation.

3.2.4.2 van Genuchten's Method

3.2.4.2.1 Purpose and Scope. A model described by van Genuchten (1978) was used to calculate the unsaturated hydraulic conductivity functions for the Bandelier Tuff. Inputs to the model are the saturated hydraulic conductivities and data from the moisture characteristic curves for the 20 core samples analyzed in the laboratory tests. The output function is a closed-form analytical expression that generates a plot of hydraulic conductivity versus moisture content and/or water potential. The output function is only valid over the moisture and water-potential ranges tested.

3.2.4.2.2 Procedure. A model described by Mualem (1976) was used to predict unsaturated hydraulic conductivities from the moisture characteristic curves (Appendix C) and the saturated hydraulic conductivities. Mualem's derivation yields an integral formula for determining the unsaturated hydraulic conductivity as a function of moisture content, which enables one to derive closed-form analytical expressions provided suitable equations for the moisture characteristic curves are available. The resulting conductivity expressions generally contain three independent, dimensionless parameters--α, n, and m--which are calculated using the nonlinear least-squares curve-fitting program described by van Genuchten (1978). The information required to calculate these parameters consists of saturated hydraulic conductivities and data obtained from the moisture characteristic curves, namely, the saturated and residual soil-moisture contents (θ_s, and θ_r, respectively) and the slope for the curve at midpoint [$(\theta_s + \theta_r)/2$].

---

*Response to Task 3, Paragraph 25, Compliance Order/Schedule.

All of this information was assembled into a data base and used as input into van Genuchten's model, which generates values for α, n, and m. The model then inputs these values into Mualem's integral formulas and plots the following two functions: $K(\theta)$ versus θ (moisture content) and $K(\psi)$ versus ψ (water potential). The intrinsic permeabilities determined using the Klinkenberg Correction Method (Table 3-7) were then used to calculate water-saturated hydraulic conductivities for input to the model. (See Section 3.2.1.4 for conversion of intrinsic permeability to hydraulic conductivity.) These values were used largely because they more closely reflect the in-situ permeabilities for air and water in the study area.

3.2.4.2.3 Results and Discussion. The modeling results are presented as graphs of unsaturated hydraulic conductivity versus volumetric moisture content [$K(\theta)$ versus θ] and of hydraulic conductivity versus water potential [$K(\psi)$ versus ψ]. Representative outputs from the model for 7 of the 20 samples are presented in Figures 3-10 through 3-13.

Unfortunately, these results are of limited value because they are based on partial moisture characteristic curves which do not extend over the range of water potentials and moisture contents measured in the field. For example, the water-potential values of the curves extend roughly to -0.3 bar (-300 cm of water), while those measured in the field range from -1 to -15 bar (see Section 3.3.1.3). Similarly, values for moisture content (θ) range from 0.4 to 0.6 on the curves, while those determined in the field are generally less than 0.1. As a consequence, the calculated unsaturated hydraulic conductivities are also outside the range of the field values.

Nevertheless, the calculated values can be used for near-surface infiltration studies when the moisture and water-potential ranges fall within those of the moisture characteristic curves. It should be noted, however, that these curves were obtained by drying the soil and therefore represent only the drying branch of the hysteresis loop. The drying branch has a higher moisture content for a given water potential than does the wetting branch; hence, a given soil is more retentive for drying than it is for wetting (Case and Welch, 1979).

3.2.5 PERMEABILITY SUMMARY

Table 3-8 compares the overall average intrinsic permeabilities of the geologic units as determined by the three methods used in this study, namely, in-situ borehole injection, in-situ vacuum testing, and laboratory testing of core samples. In contrast to the laboratory results, which show relative uniformity throughout the tuff, results of both field methods indicate a decrease in permeability with stratigraphic depth. This contrast is probably due in part to the fact that it was necessary to select the laboratory samples from those exhibiting the highest degree of consolidation; such samples would have lower permeabilities than the bulk formation from which they were taken. Furthermore, the laboratory tests measure a significantly smaller interval than that measured in the field. It was therefore concluded that the field-test results were the more reliable indicators of bulk permeabilities and that the permeabilities of the individual geologic units do indeed decrease with stratigraphic depth.

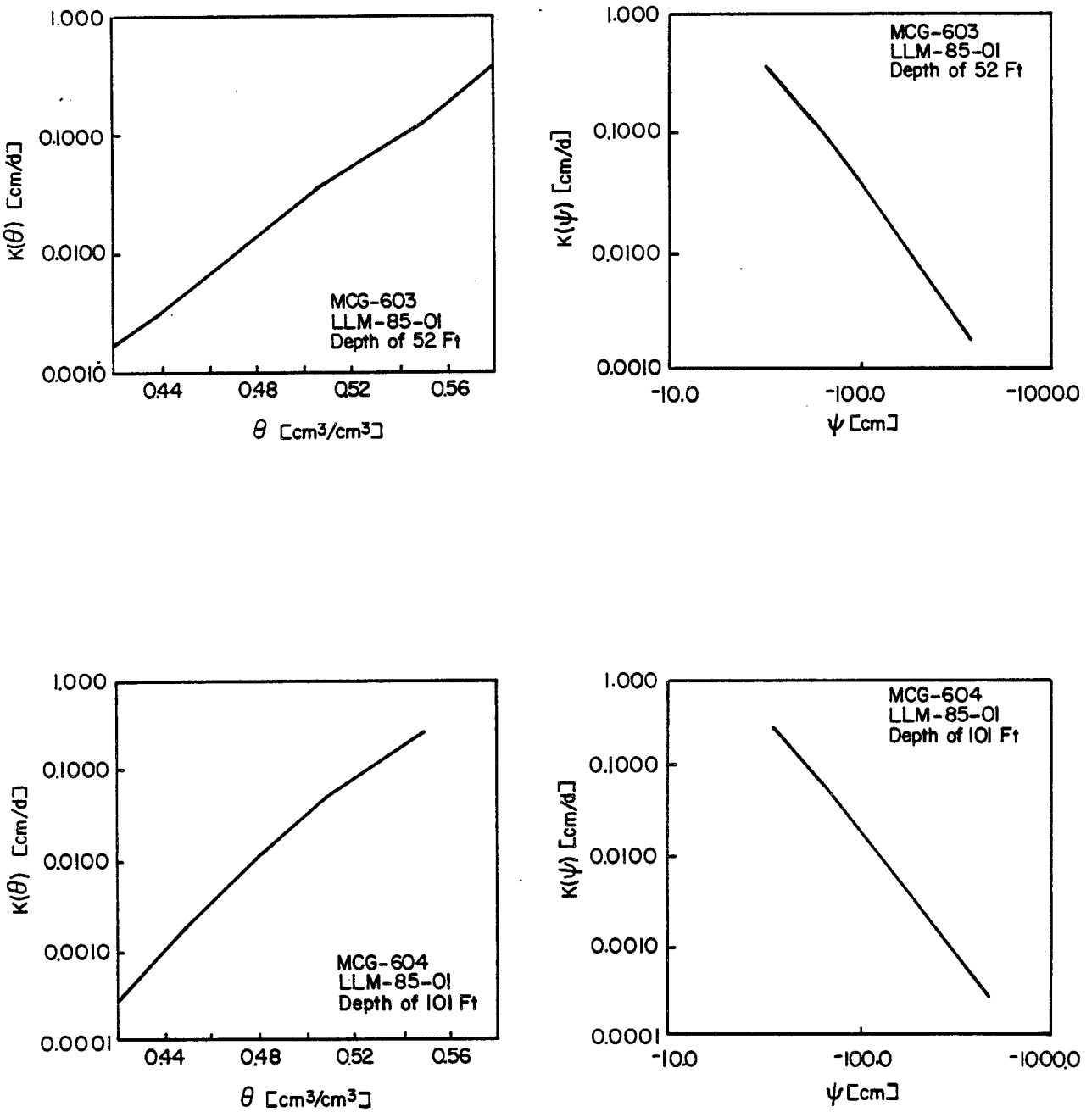

Figure 3-10. Unsaturated Hydraulic Conductivities as Functions of Moisture Content and Water Potential for Samples MCG-603 and MCG-604

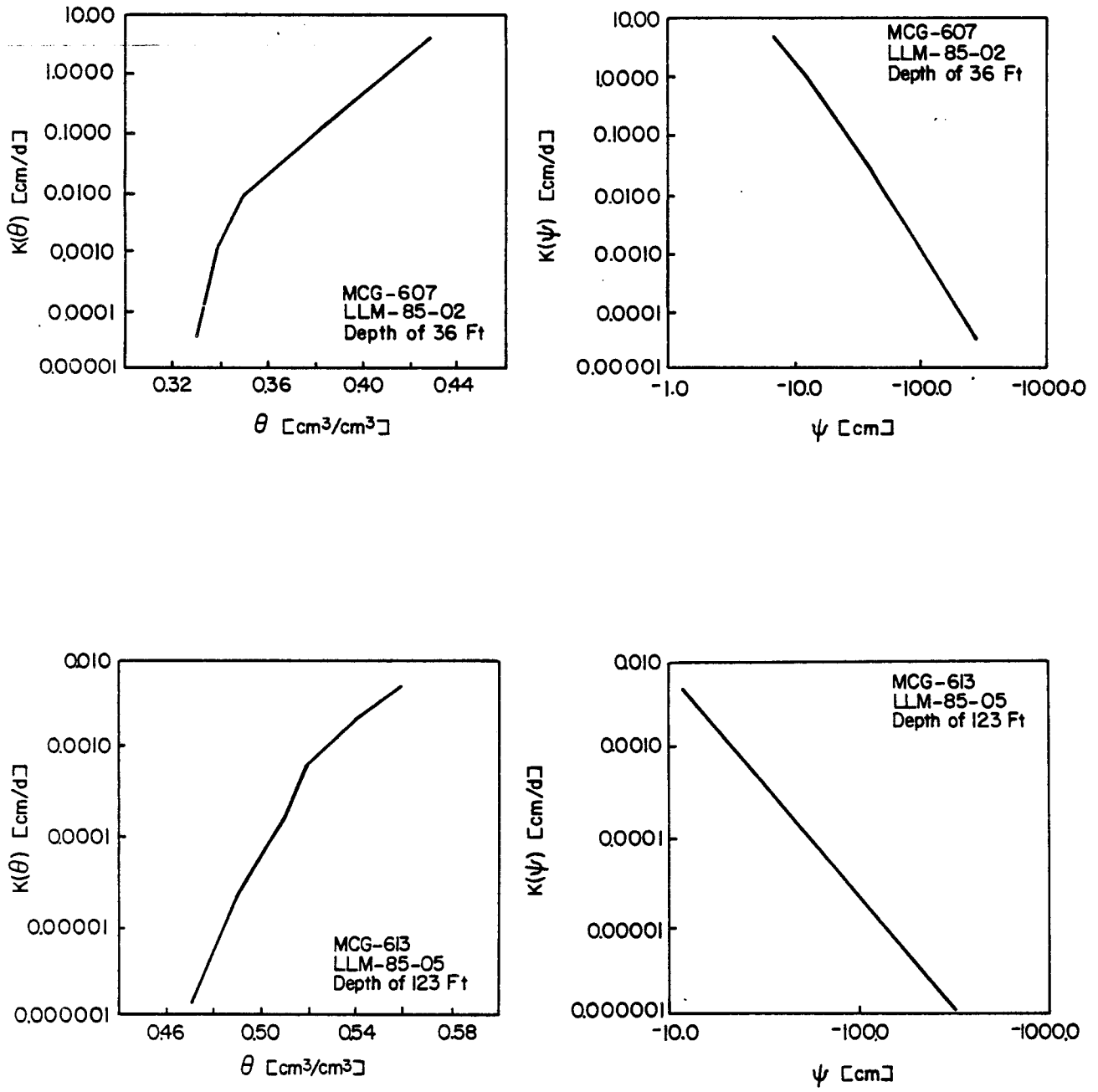

Figure 3-11. Unsaturated Hydraulic Conductivities as Functions of Moisture Content and Water Potential for Samples MCG-607 and MCG-613

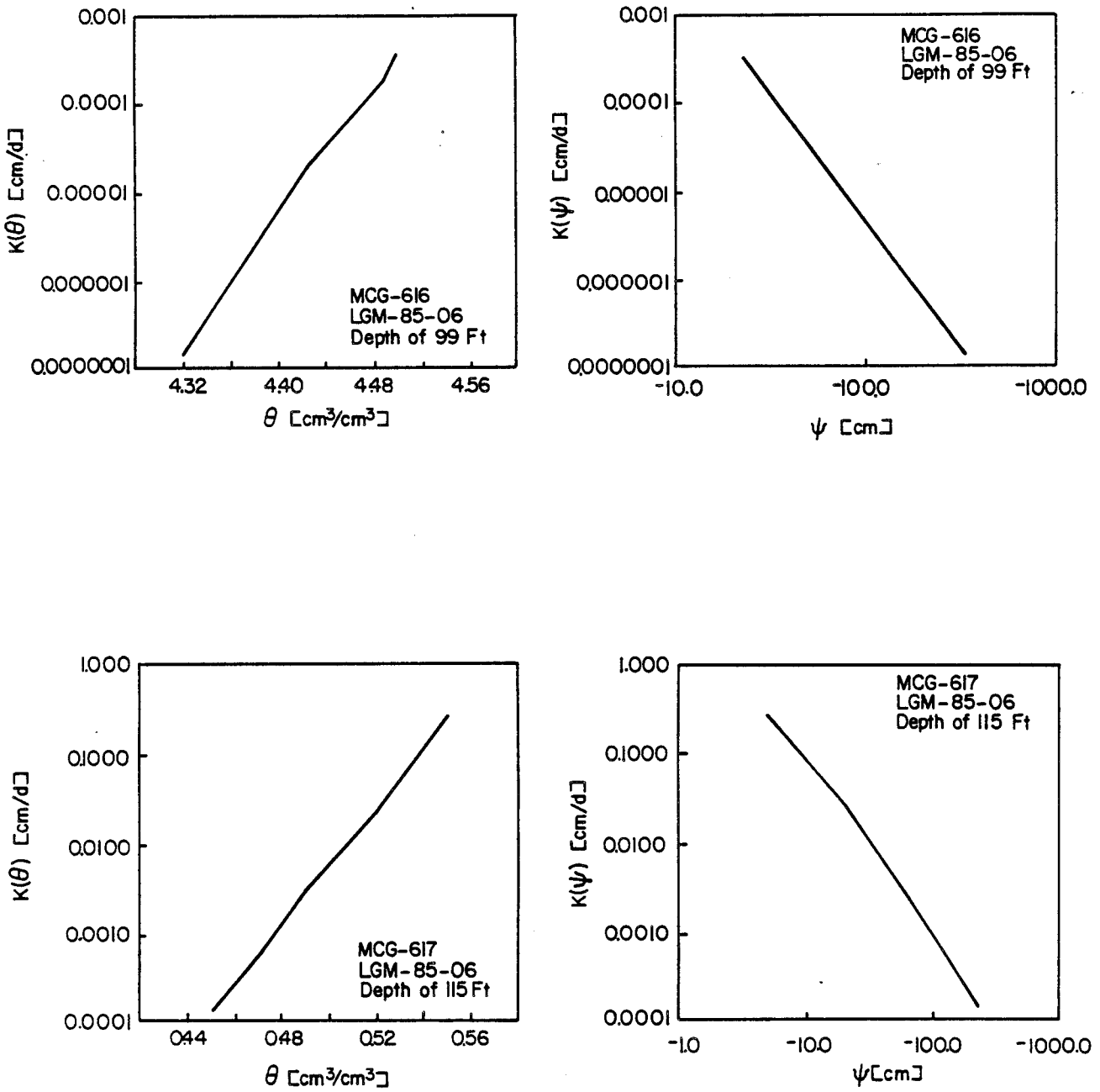

Figure 3-12. Unsaturated Hydraulic Conductivities as Functions of Moisture Content and Water Potential for Samples MCG-616 and MCG-617

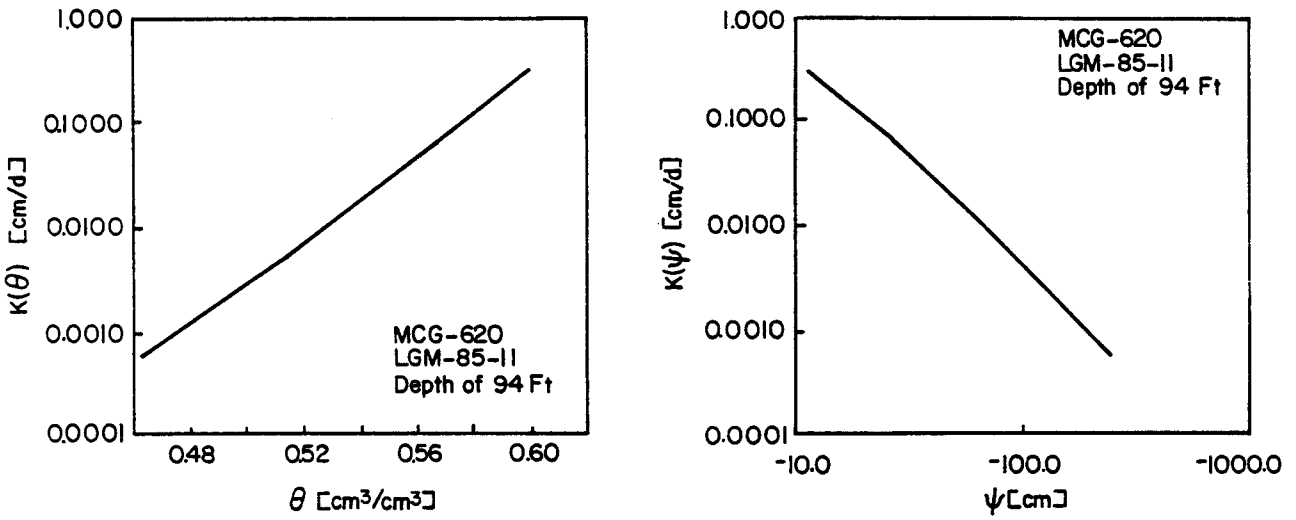

Figure 3-13. Unsaturated Hydraulic Conductivities as Functions of Moisture Content and Water Potential for Sample MCG-620

Table 3-8. Comparison of Average Intrinsic Permeability Values for the Major Geologic Units of the Bandelier Tuff in the Study Area

Unit	Intrinsic Permeability					
	Air-Injection Test		Vacuum Test		Laboratory Analysis	
	$cm^2 \times 10^{-9}$	$ft^2 \times 10^{-12}$	$cm^2 \times 10^{-9}$	$ft^2 \times 10^{-12}$	$cm^2 \times 10^{-9}$	$ft^2 \times 10^{-12}$
2b	93	100	23	25	5.7	6.2
2a	62	67	13	14	2.8	3.0
1b	26	28	5.7	6.2	5.7	6.2
1a	7.2[a]	7.8[a]	2.7[a]	2.9[a]	2.4	2.6

[a]Intrinsic permeability for this unit is based on only one measurement.

It should be noted that the lower average permeabilities determined by the vacuum test for Units 2b and 2a are probably due to the inability to perform the test in the more permeable portions of these units. A vacuum could not be established in the upper portions, so the test failed and no data were obtained. Thus, the average vacuum-test data do not include values for the most permeable zones in the units, resulting in average results which are biased low.

Results from all of the determinations do not permit a conclusive assessment of the effect of fractures on permeability. The moisture-content data indicate that the potential exists for fractures to cause preferential water movement; however, the enhancement may be less than the sensitivity of the measurement techniques. It follows that a better assessment would require additional testing, using methods having greater sensitivity. Similarly, additional tests, also having greater sensitivity, would be needed in order to fully assess the effects on permeability of such other sources of variation as pumice content.

3.3 GRADIENT DETERMINATIONS

3.3.1 TEMPERATURE AND WATER-POTENTIAL MEASUREMENTS*

3.3.1.1 Purpose and Scope

Temperature and water-potential measurements were made at the site to assess the magnitude and direction of the thermal and water-potential gradients in the study area. Knowledge of the gradients is used to determine whether temperature and water potential play a significant role in the transport of contaminants to the water table. A description of the instruments used to acquire these data, together with information on calibration, installation, and data reduction, is presented below, and is followed by a discussion of the results. The results are presented in the form of graphs plotting temperature and water potential versus time and depth.

*Response to Task 4, Paragraph 25, Compliance Order/Schedule.

3.3.1.2 Field Instrumentation

3.3.1.2.1 Description of the Thermocouple Psychrometers. Thermocouple psychrometers were used to obtain the water-potential measurements at Los Alamos because the low soil-water potential (less than -1 bar) precluded the use of tensiometers. The instruments actually measure voltage which is converted to soil-water potential by means of a calibration model (Brown and Bartos, 1982). Psychrometers are particularly convenient because they simultaneously measure temperature.

The thermocouple psychrometers used in this study were Models PCT-55 and PST-55 manufactured by Wescor, Inc., of Logan, Utah. The only difference between the two models is that the PST series is shielded with a stainless steel screen instead of a ceramic cup, and therefore has a faster response time. A diagram of a typical screen-shielded psychrometer is shown in Figure 3-14.

Operation of the psychrometers is based on the Peltier effect, in which a thermocouple is cooled below the dew point by passing an electric current across a junction composed of two dissimilar metal conductors. After water has condensed on the cooling junction, the electric current is discontinued and the junction immediately begins to warm up. The rate of warming is rapid at first, and then slows down until the latent heat of vaporization is overcome, at which time water condensed on the junction evaporates. The point at which the warming rate is at a minimum is known as the psychrometric plateau. The electromotive force (emf) generated across the junction during the psychrometric plateau is a measure of the relative humidity of the system (Spanner, 1951).

The relative humidity ($\bar{P}/P_o$) in soil is related to soil-water potential by the equation (Case and Welch, 1979)

$$\psi = (\rho k_B T/m) \ln (\bar{P}/P_o) = \psi_o \ln (\bar{P}/P_o) \qquad (20)$$

where

ρ = the density of water at temperature T
k_B = Boltzman's constant (1.38×10^{-16} erg/°K)
m = the mass of a water molecule (approximately 3×10^{-23} g)
$\bar{P}$ = the average vapor pressure in the soil
P_o = the pressure of the water vapor above a surface of infinite radius of curvature
$\psi_o \simeq 10^3$ bars at 300°K

3.3.1.2.2 Laboratory Calibration. Each psychrometer must be calibrated individually due to the variable thicknesses of the welded junction and wires used in fabrication. Saline solutions are convenient to use for calibration, since tables that relate salt concentrations and temperature to relative humidity are readily available (Lang, 1967). The ratio of microvoltage to theoretical water potential at a given temperature for a particular psychrometer provides the correction coefficient necessary for determining actual water potential in rock and soil systems.

In this study, reagent-grade sodium chloride was dissolved in deionized water to provide calibration solutions ranging in strength from 0.1 to 1.0 molal.

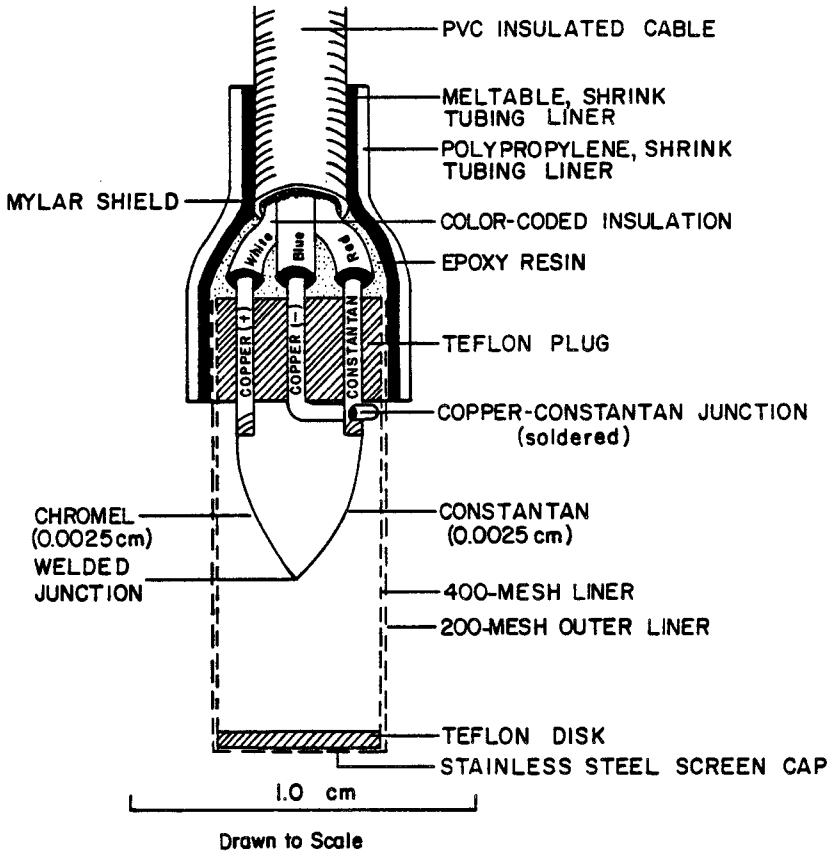

Figure 3-14. Sketch of the Single-Junction Stainless Steel Screen-Shielded Thermocouple Psychrometer (from Brown and Collins, 1980)

Each psychrometer was calibrated using at least three molal concentrations, independently, in the following manner. One milliliter of solution was decanted into a sample chamber. A psychrometer was then sealed into the chamber to create a closed system with a known water potential (see Figure 3-15). The sealed chamber was then placed in a wooden rack and equilibrated for at least 24 hours. Following equilibration, the voltage output of the thermocouples was read in psychrometric (wet-bulb) mode using either a Wescor HR33T Dewpoint Microvoltmeter or a Wescor HP-115 Microprocessor-Controlled Data Collection System. Each molal concentration (water potential) was read a minimum of three times for temperature and microvolts. These readings were then converted to water potential using the calibration model described below.

3.3.1.2.3 Psychrometer Calibration Model. The psychrometer calibration model developed by Brown and Bartos (1982) was used to accurately convert psychrometer outputs to water potential. This model is far more versatile than hand-drawn calibration curves because it can convert water potentials from -1 to -80 bar over a wide range of temperature and zero offset readings. Inputs to the model are temperature, cooling time, zero offset, psychrometer output in microvolts, and calibration coefficients, the last required for conversion of microvolts to water potential. The calibration coefficient B is defined as

$$\sum B = \sum WP / \sum W\hat{P} \qquad (21)$$

where $\sum WP$ is the sum of the actual water potentials (sodium chloride solutions) used during calibration, and $\sum W\hat{P}$ is the sum of the water potentials estimated by the model. Calibration coefficients for each of the psychrometers installed in Holes LLP-85-03 and LGP-85-07 are presented in Tables 3-9 and 3-10, respectively. A listing of the Fortran V program for the model is reproduced as Appendix E. The output from the model is the water potential for the soil conditions as sensed by the psychrometer.

3.3.1.2.4 Field Installation. On 22 October 1985, a total of 38 thermocouple psychrometers were installed at the study area, 23 in Hole LLP-85-03 and 15 in Hole LGP-85-07. Completion diagrams are provided in Appendix A. Because of the presence of surface casing in Hole LLP-85-03, a shallow boring was drilled adjacent to the main hole and five psychrometers were installed in this second hole close to the ground surface (depicted in Appendix A as being in the same hole). Installation was accomplished by taping the psychrometers to a string of Schedule 40, 2-inch-I.D., polyvinylchloride (PVC) pipe and carefully lowering the string into the hole. The annulus surrounding the PVC pipe was then backfilled with auger cuttings from that drill hole. It was assumed that the density of this backfill was similar to the in-situ density of the tuff, and that the relative humidity of the backfill, as sensed by the psychrometers, would equilibrate with the relative humidity of the adjacent tuff. Installation depths are included with the data presented in Tables 3-9 and 3-10, for Holes LLP-85-03 and LGP-85-07, respectively.

3.3.1.3 Results and Discussion

Psychrometer data were collected for Holes LLP-85-03 and LGP-85-07 over the period 22 October to 20 November 1985. The values for temperature and water potential were viewed in two ways, as plots of temperature or water potential versus time, and as plots of temperature or water potential versus depth.

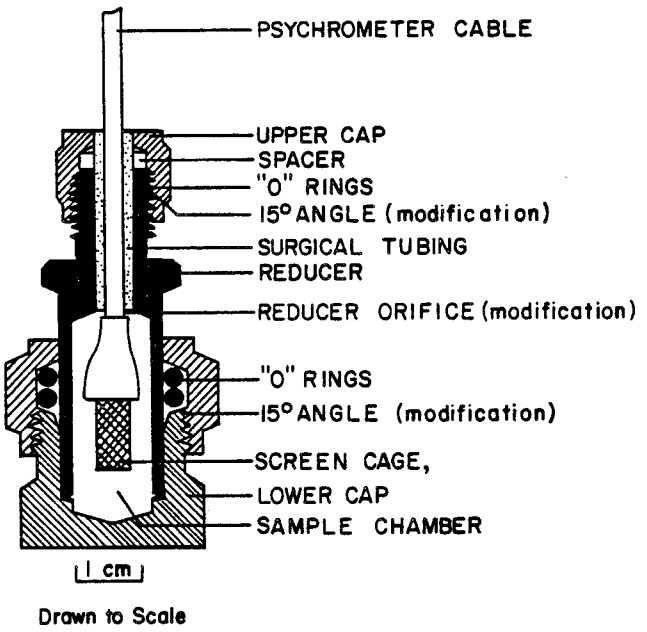

Figure 3-15. Sketch of the Stainless Steel Calibration Chamber Showing Seals and Screen-Shielded Thermocouple Psychrometer (from Brown and Collins, 1980)

Table 3-9. Installation Depths and Calibration Coefficients for Psychrometers in Hole LLP-85-03

Model Number[a]	Serial Number	Scanner/Channel	Calibration Coefficient for Water-Potential Model	Installation Depth (ft)
PCT-55	29414	I/1	--	Surface
PCT-55	29416[b]	I/2	0.85	2.0
PST-55	29474[b]	I/3	0.84	4.0
PST-55	29473[b]	I/4	0.84	6.0
PCT-55	29420[b]	I/5	0.89	8.0
PST-55	29469[b]	I/6	0.84	10
PCT-55	29418	I/7	0.81	13
PST-55	29483	I/8	0.88	13
PCT-55	29424	I/9	0.85	24
PST-55	29479	I/10	0.87	24
PCT-55	29406	I/11	0.90	41
PST-55	29462	I/12	1.00	41
PCT-55	29409	II/1	1.00	50
PST-55	29475	II/2	0.94	50
PCT-55	29405	II/3	0.85	56
PST-55	29477	II/4	1.03	56
PCT-55	29425	II/5	0.84	66
PST-55	29455	II/6	0.96	66
PST-55	29481	II/7	0.89	76
PCT-55	29422	II/8	0.94	76
PST-55	29476	II/9	0.90	86
PST-55	29458	II/10	1.00	96
PCT-55	29427	II/11	1.00	96

[a]The PCT series psychrometers are shielded with a ceramic cup, while the PST models are shielded with a stainless steel screen.

[b]Psychrometers in the upper 10 ft are located in a shallow boring adjacent to the main hole.

Table 3-10. Installation Depths and Calibration Coefficients for Psychrometers in Hole LGP-85-07

Model Number[a]	Serial Number	Scanner/Channel	Calibration Coefficient for Water-Potential Model	Installation Depth (ft)
PCT-55	29415	III/1	0.89	4.5
PST-55	29459	III/2	0.89	6.5
PCT-55	29410	III/3	0.85	8.5
PST-55	29461	III/4	0.91	10
PCT-55	29411	III/5	0.91	12
PST-55	29463	III/6	0.86	14
PCT-55	29417	III/7	0.84	17
PST-55	29466	III/8	0.87	19
PCT-55	29403	III/9	0.92	22
PST-55	29467	III/10	0.92	27
PCT-55	29407	III/11	1.00	32
PST-55	29465	III/12	1.04	37
PST-55	29464	III/13	0.95	42
PCT-55	29404	III/14	0.85	47
PST-55	29468	III/15	0.89	52

[a]The PCT series psychrometers are shielded with a ceramic cup, while the PST models are shielded with a stainless steel screen.

Selected plots of the former are presented in Figures 3-16 through 3-19. Air temperature versus time at Hole LLP-85-03 is plotted in Figure 3-20. Box plots of water potential and temperature versus depth for the entire time period are presented in Figures 3-21 through 3-24. Since the box plots present the data in quartiles, the outlying values represent minimum and maximum values. The boxes enclose the 25- and 75-percent values, and the vertical lines connecting the boxes intersect the median-temperature or water-potential values for the time period.

The plot of air temperature versus time (Figure 3-20) demonstrates that a dramatic diurnal temperature variation exists at the site, and that the highs and lows generally decreased over this monitoring period. Plots of formation temperature versus time (Figures 3-17 and 3-19) for the psychrometers located within 15 ft of the ground surface demonstrate that the near-surface temperatures also decreased in response to the decrease in air temperature. Furthermore, as expected, a phase lag is evident when comparing the decreasing temperatures measured by successively deeper psychrometers.

The plots of temperature versus depth (Figures 3-22 and 3-24) reveal a temperature bulge that probably represents the heat stored in the ground due to Summer heating. The position of the bulge indicates that the median gradient in temperature for this monitoring period is downward from about 10 to 20 ft and upward from about 10 ft.

The plots of water potential versus time for given depths (Figures 3-16 and 3-18) demonstrate that water potentials are subject to diurnal variations of about ±1 bar per day, and that there was little, if any, change in the average

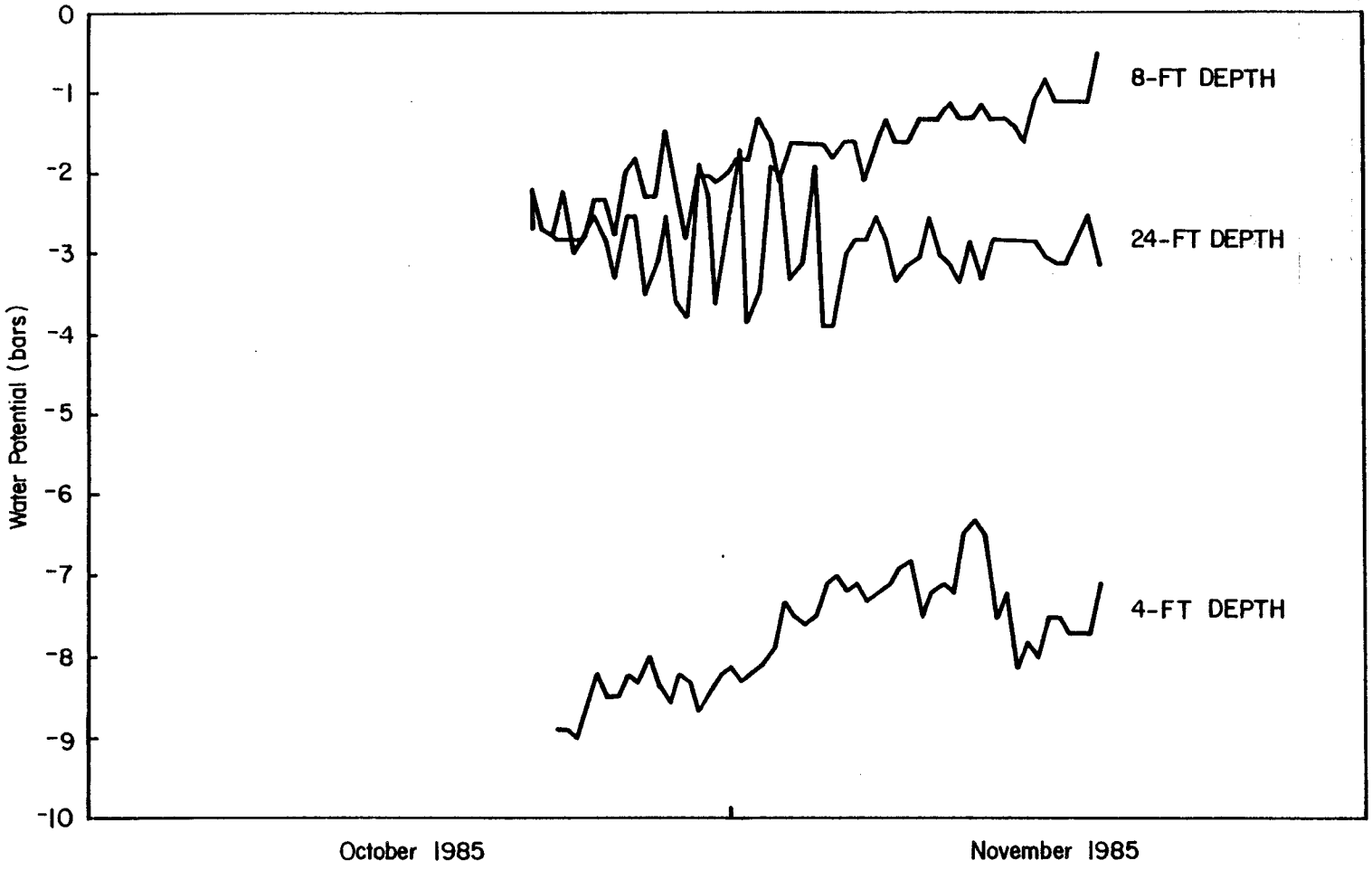

Figure 3-16. Water Potential Versus Time for Selected Psychrometers in Hole LLP-85-03

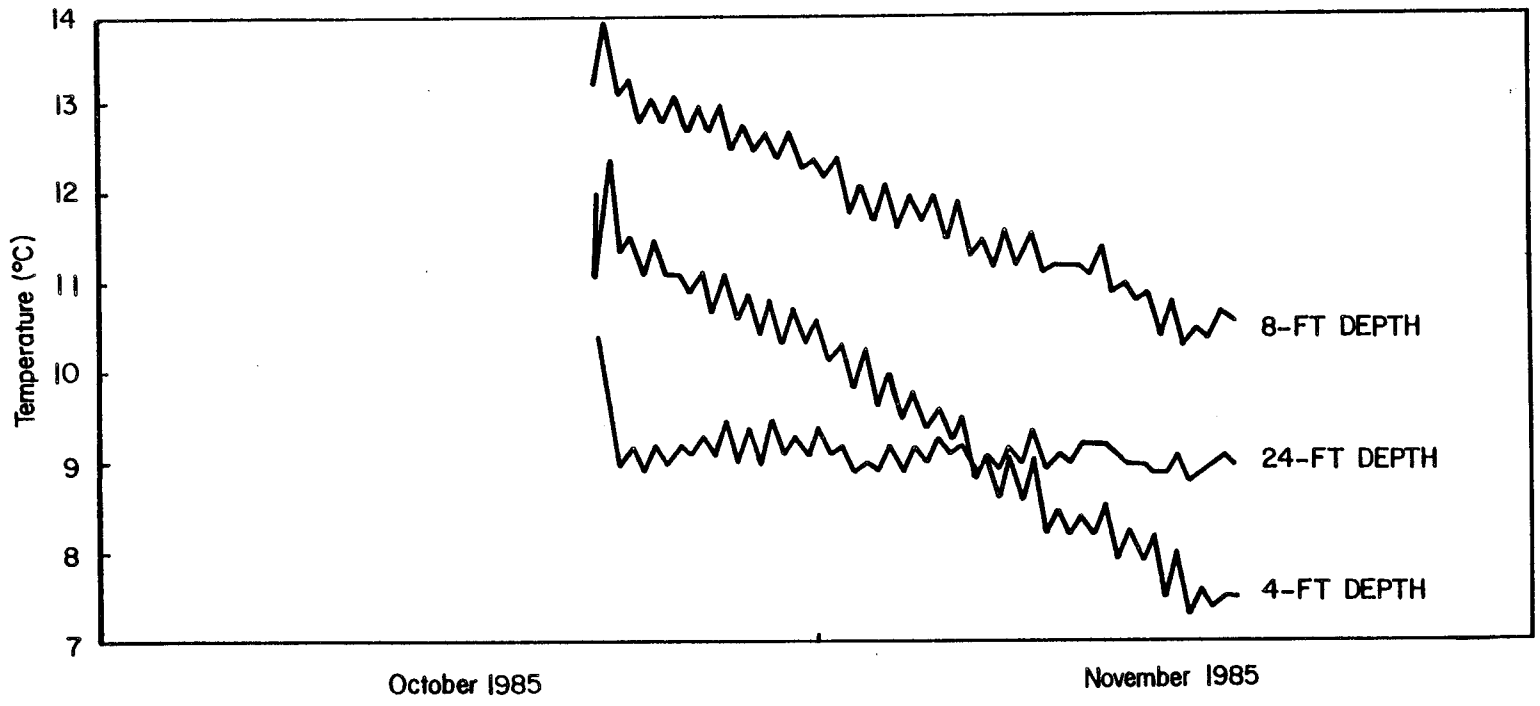

Figure 3-17. Temperature Versus Time for Selected Psychrometers in Hole LLP-85-03

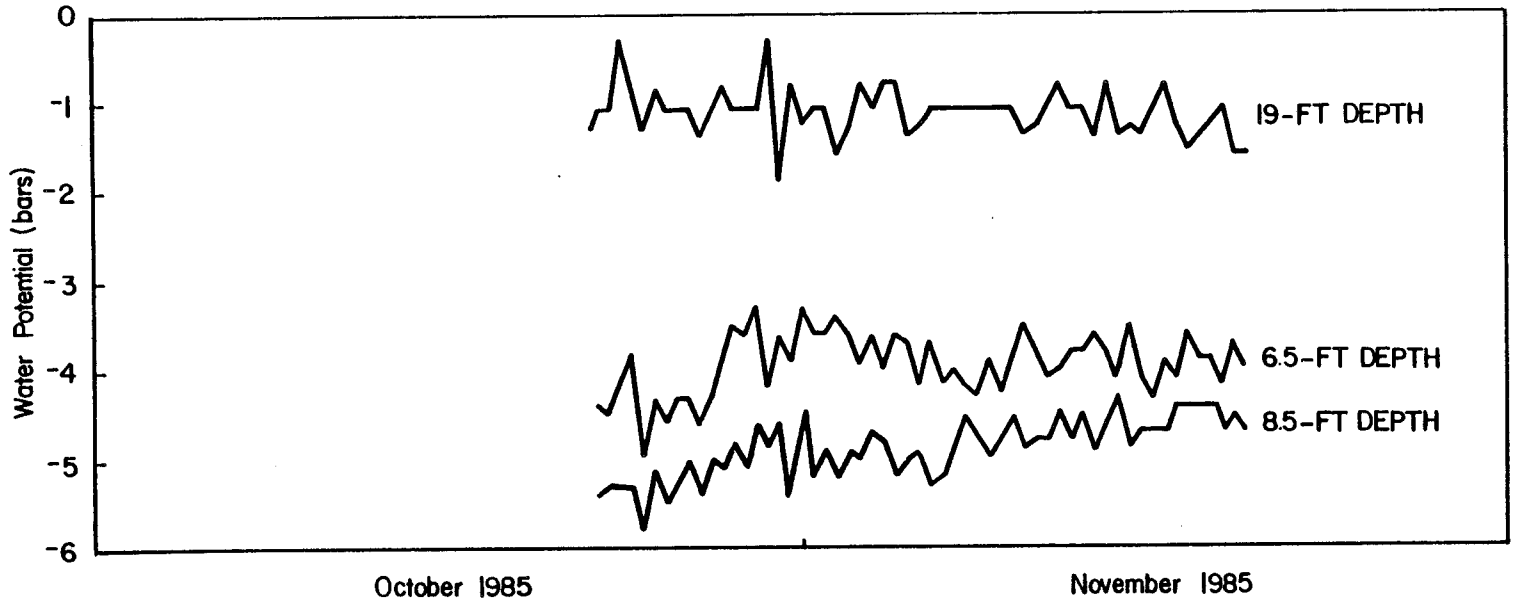

Figure 3-18. Water Potential Versus Time for Selected Psychrometers in Hole LGP-85-07

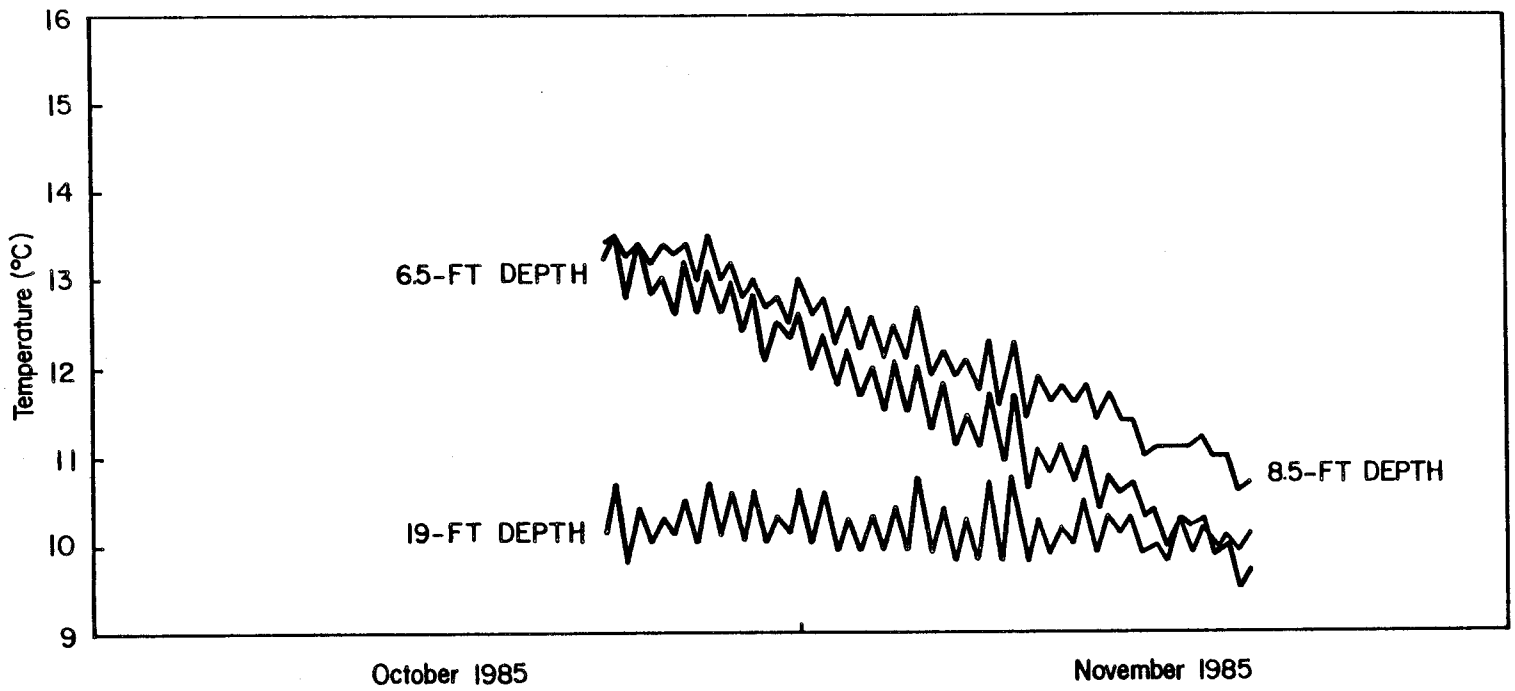

Figure 3-19. Temperature Versus Time for Selected Psychrometers in Hole LGP-85-07

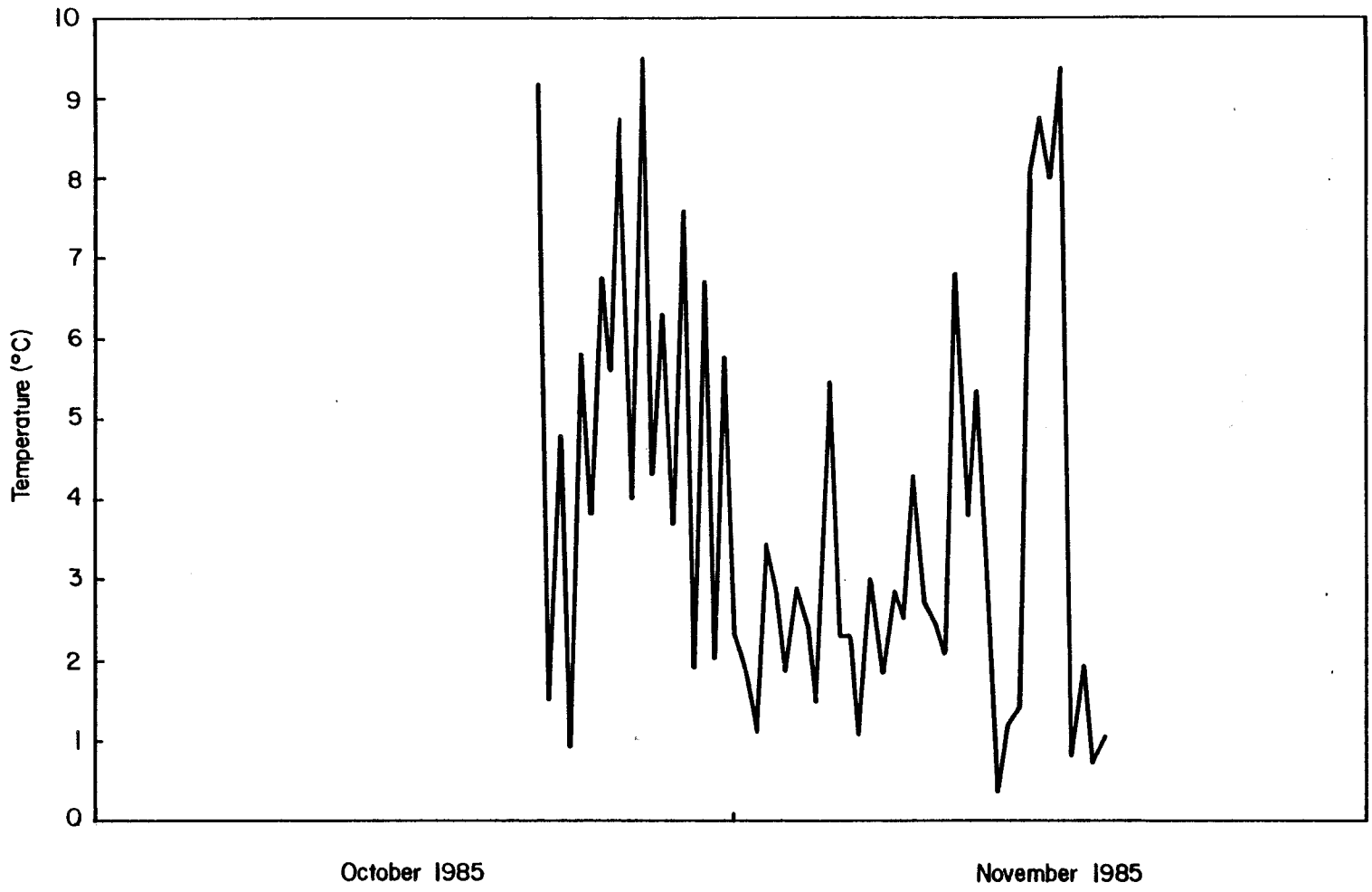

Figure 3-20. Air Temperature Versus Time at Hole LLP-85-03

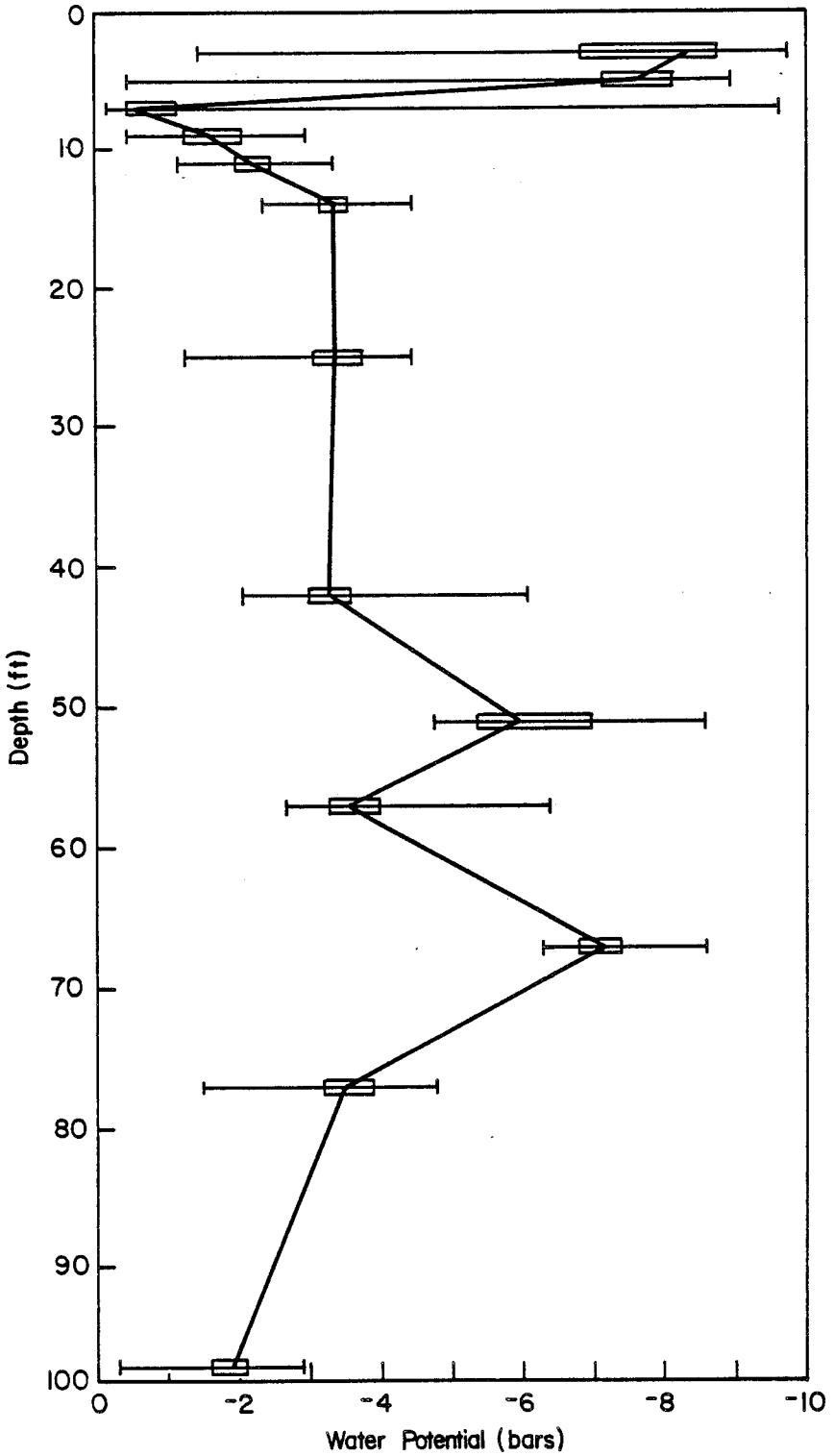

Figure 3-21. Water Potential Versus Depth for Hole LLP-85-03

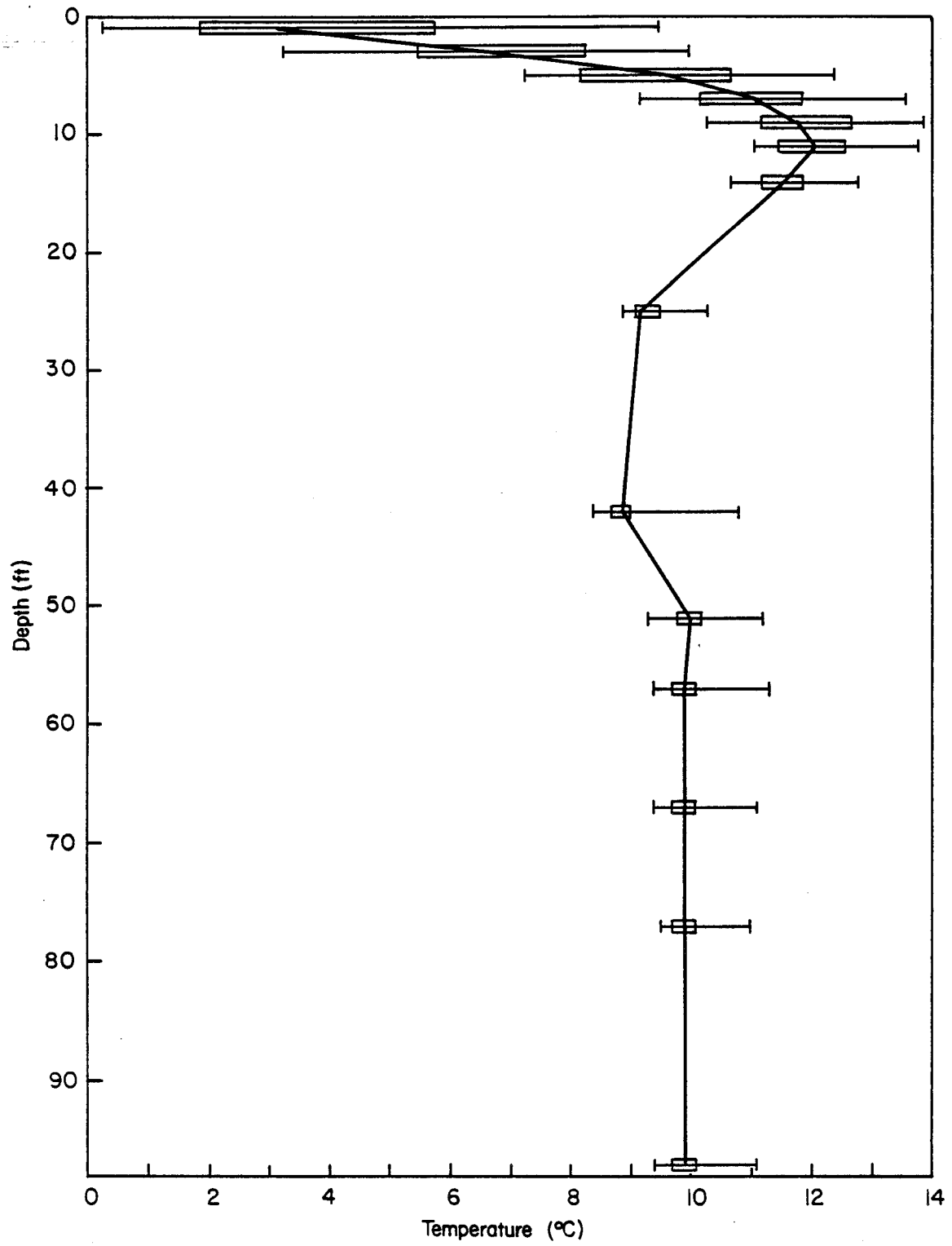

Figure 3-22. Temperature Versus Depth for Hole LLP-85-03

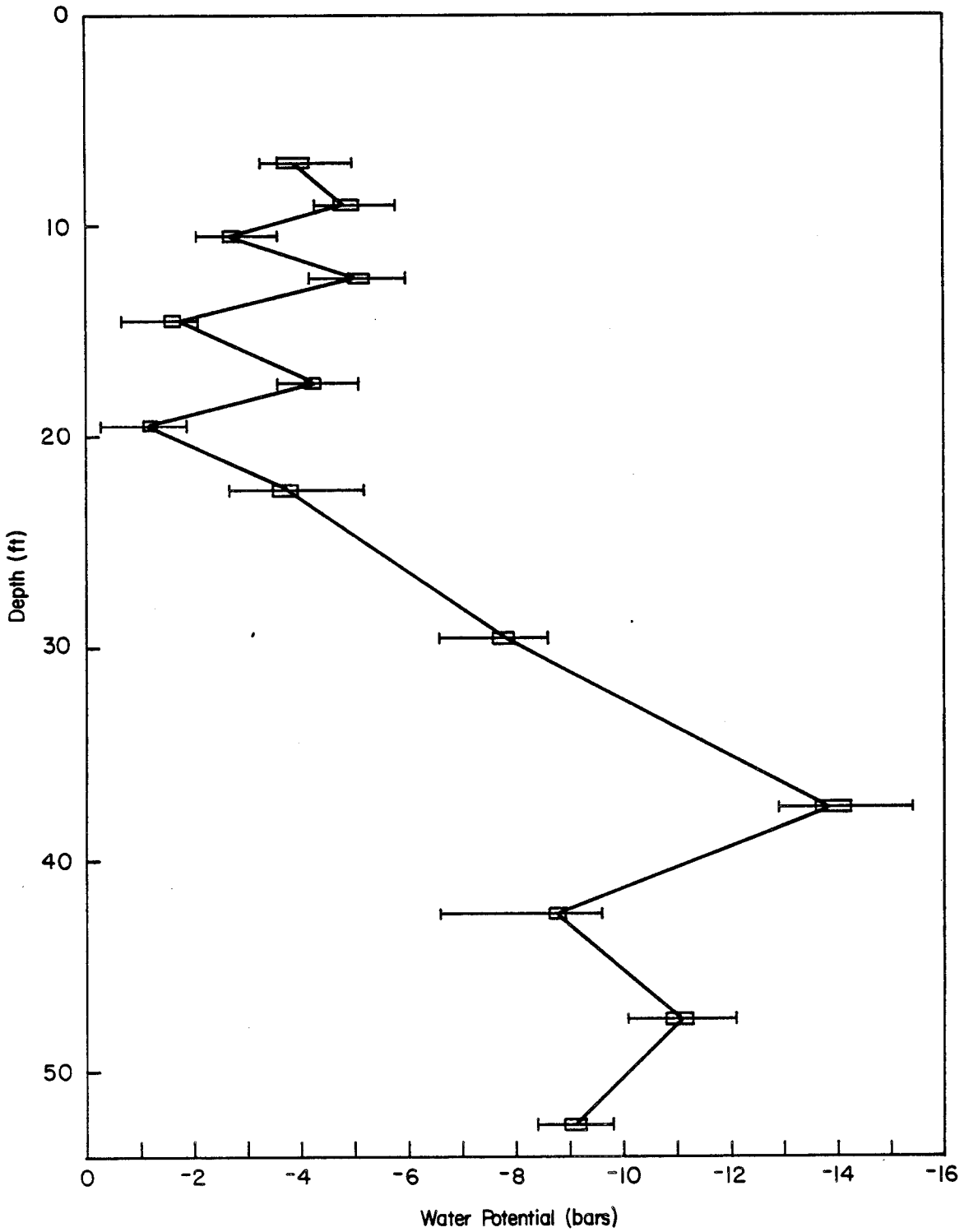

Figure 3-23. Water Potential Versus Depth for Hole LGP-85-07

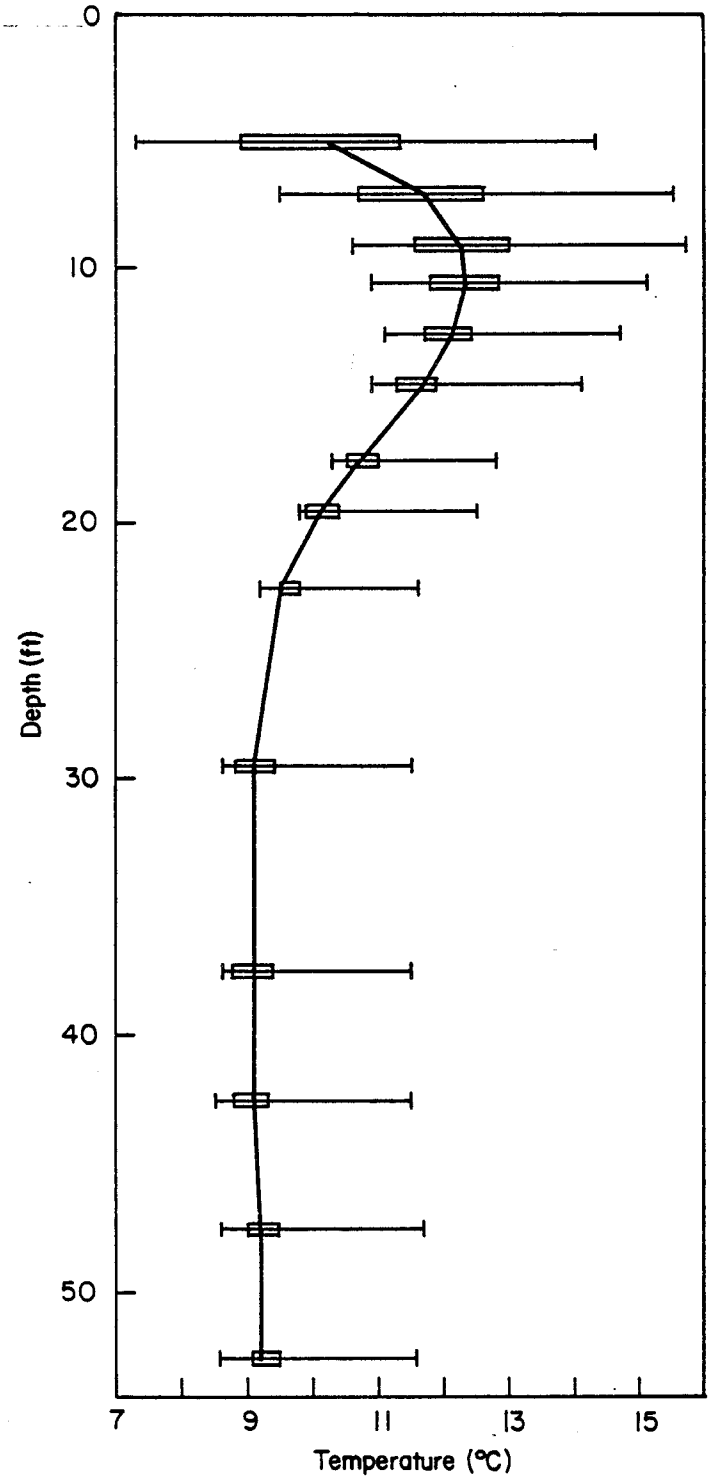

Figure 3-24. Temperature Versus Depth for Hole LGP-85-07

water potential during this monitoring period. Median water potentials range from approximately -0.5 bar to -8.7 bar in Hole LLP-85-03 (Figure 3-21) and from approximately -1.2 bar to -13.8 bar in Hole LGP-85-07 (Figure 3-23).

The large range of maximum and minimum values observed during this monitoring period limit gradient estimations to those that can be measured between successive psychrometers, i.e., within a single depth interval. Accurate assessments of an overall gradient in the study area will most likely require longer equilibration and monitoring times.

3.3.2 ATMOSPHERIC/ROCK-PORE PRESSURE MONITORING SYSTEM

3.3.2.1 Purpose and Scope

The purpose for installing the Atmospheric/Rock-Pore Pressure Monitoring System was to quantify the gas-pressure gradients in the Bandelier Tuff. Although these data were not required by the Compliance Order/Schedule, they can contribute significantly to the initial site assessment since differences in gas pressure can affect contaminant transport in the vapor phase.

Equipment and system installation are described in the paragraphs that follow. The subsection entitled Results and Discussion presents only a preliminary interpretation of the data; a broader, more reliable assessment of gas-pressure gradients would most likely require acquisition of pressure readings over a period of at least 1 year.

3.3.2.2 Equipment

The pressure-measurement system installed at Los Alamos consists of four electrical pressure transducers connected to an electro-piezo scanner/recorder. The transducers contain an absolute-electrical-pressure sensor equipped with a strain-gauged stainless steel diaphragm. A stainless steel disc filter permits direct burial of the transducers. Measurement capacity ranges from 0 to 25 pounds per square inch at sea level (psis), with a readability of 0.02 percent of scale. (Psis is calibrated in psi with zero being atmospheric pressure at sea level.)

The electro-piezo scanner/recorder is a portable, battery-operated system that automatically records ten transducer channels. The dates, times, and outputs from each of the transducers are recorded on the integral printer. This versatile scanner/recorder can permanently record the transducer outputs, or can provide the outputs to an external device such as a computer, data terminal, paper punch, or magnetic tape recorder. The pressure-measurement system can be programmed to scan continuously or to scan at variable intervals. In the case of the latter, the recorder can be sealed and left unattended and will still record data at the preselected intervals.

3.3.2.3 Installation Design

The completion diagram for the pressure-transducer instrumentation installed in Hole LLP-85-03 is presented in Appendix A. The four transducers were installed at the following depths: ground surface, 26 ft, 54 ft (near a fracture), and 90 ft. The transducer located at ground surface measures the

atmospheric pressure, while the buried transducers measure rock-pore gas pressures.

3.3.2.4 Results and Discussion

Pressure-measurement data were collected over the period 17 October through 15 November 1985 (Figure 3-25), except for the 7 days from 6 through 12 November when the system was inadvertently shut down. As noted previously, these limited data permit only a preliminary interpretation at this time. Characteristics which are discernible in Figure 3-25 include the following:

- Both the atmospheric and rock-pore pressures undergo daily fluctuations.
- The rock-pore pressure at 54 ft is consistently higher than the surrounding pressures, potentially a result of the nearby fracture.
- An increase in the atmospheric pressure for a period of several days is not reflected in the rock-pore pressures for the same period.

A broader assessment of the gas-pressure gradients in the study area requires acquisition of additional data, particularly with regard to identifying potential sources of variation in the data other than actual pressure variations.

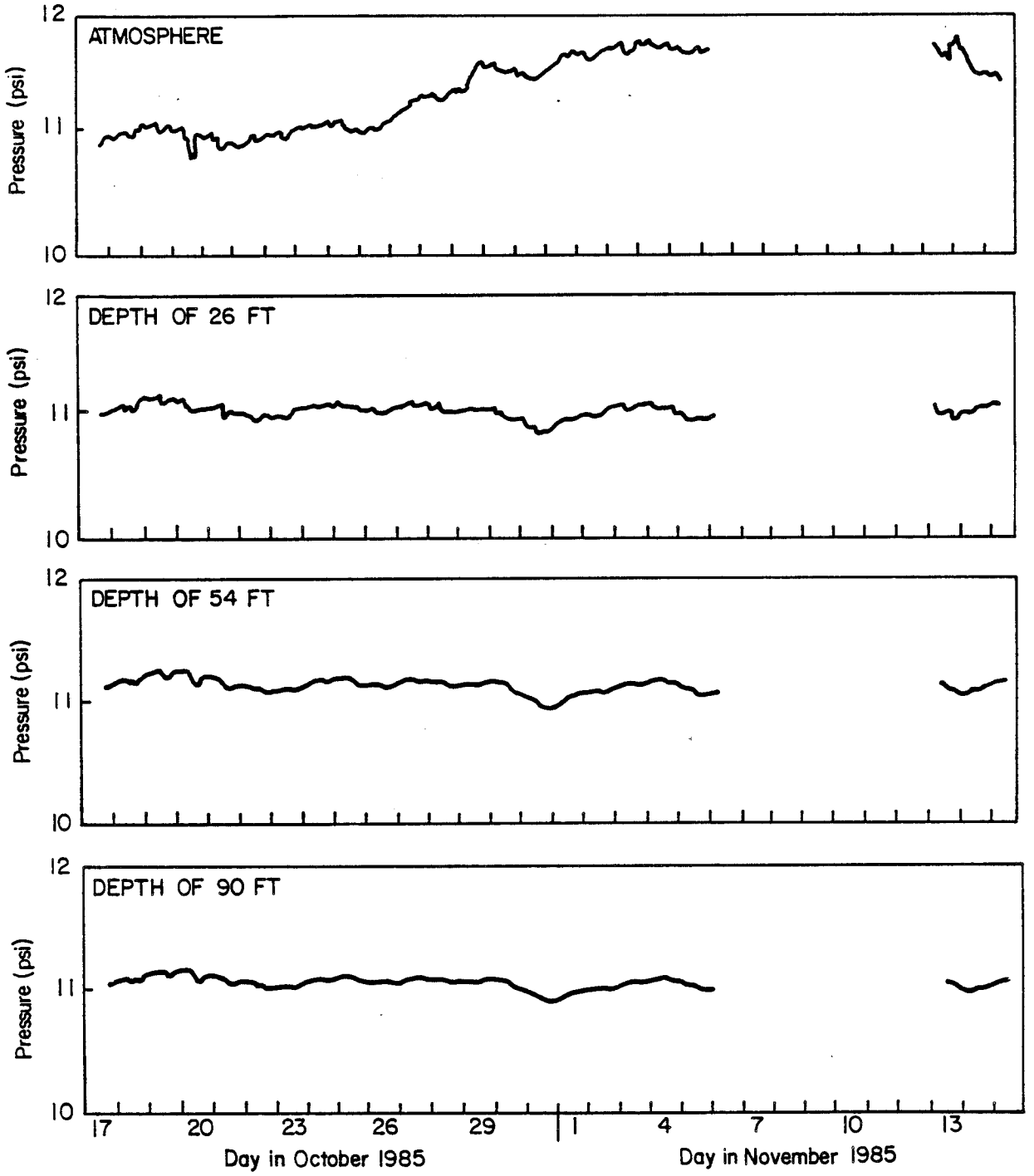

Figure 3-25. Results from the Pressure Transducers Installed in Hole LLP-85-03 (Note: The system was inadvertently shut down over the period 6-12 November 1985.)

Section 4

NEUTRON MOISTURE MEASUREMENTS

Note: This section responds to Task 4, Paragraph 25, of the Compliance Order/Schedule. The section was prepared by personnel of Los Alamos National Laboratory.

4.1 PURPOSE AND SCOPE

The moisture content of the Bandelier Tuff is being measured with a neutron probe in order to characterize the infiltration and redistribution of water in the tuff. Use of the neutron probe for moisture monitoring was specifically requested by the State of New Mexico in Task 4, Paragraph 25, of the Compliance Order/Schedule. Although data acquired with the probe were not yet available at the time of this writing, it is possible that the method will be of little value at Los Alamos due to the low moisture content of the tuff (see gravimetric moisture results in Section 3.1.1).

Two holes were identified for acquisition of biweekly neutron moisture readings, LLN-85-04 and LGN-85-08 (see Figure 2-3 for locations). Descriptions of the casing installations, probe calibration, and monitoring program are provided below. Data presentation and interpretation will be addressed in a subsequent report when data become available.

4.2 CASING INSTALLATIONS

The neutron access tubes, or casings, were constructed of cold drawn aluminum tubes, each 12 ft in length and having a wall thickness of 0.049 inch, an outside diameter of 2.5 inches, and an inside diameter of 2.402 inches. This inside diameter is approximately 0.25 inch larger than the outside diameter of the probe (1.865 inches), which prevents the probe from binding as it is maneuvered inside the casing. To further ensure free movement of the probe while it is being raised or lowered in the hole, the casing has no internal seams or obstructions.

Prior to transport to the field, the 12-ft lengths of tubing were welded together to make 24-ft sections and the sections pressure-tested to ensure a watertight seal. A cap was welded to one end of each of two sections, these to be installed at the bottom of the two holes. In the field, the 24-ft sections were joined together using 'no-hub' couplings rather than welding. This was done because the tubing wall is so thin that a watertight weld would be nearly impossible to accomplish with portable welding equipment. A no-hub coupling is a watertight rubber coupling, held in place by a corrugated stainless steel cover, on the ends of which are stainless steel hose clamps used for gripping the aluminum tubing.

The casings were installed in the drill holes in the following manner. The section with the bottom cap was lowered into the hole and held in place with a pipe vise. A second 24-ft section was joined to the first with a no-hub coupling. Silicon sealant was applied wherever rubber was exposed to slow decomposition of the material underground. Once the two sections were coupled, they were lowered into the ground and again held in place with the pipe vise while a second no-hub coupling was installed to join the now 48-ft section of tubing to another 12- or 24-ft section. This process was repeated until the bottom of the hole was reached. Any tubing remaining above ground level was cut off.

A diagram of the casing installation for Hole LLN-85-04 is presented in Figure 4-1. The depth of the uncased hole was 108 ft, so the casing required four 24-ft sections and one 12-ft section, joined together with four no-hub

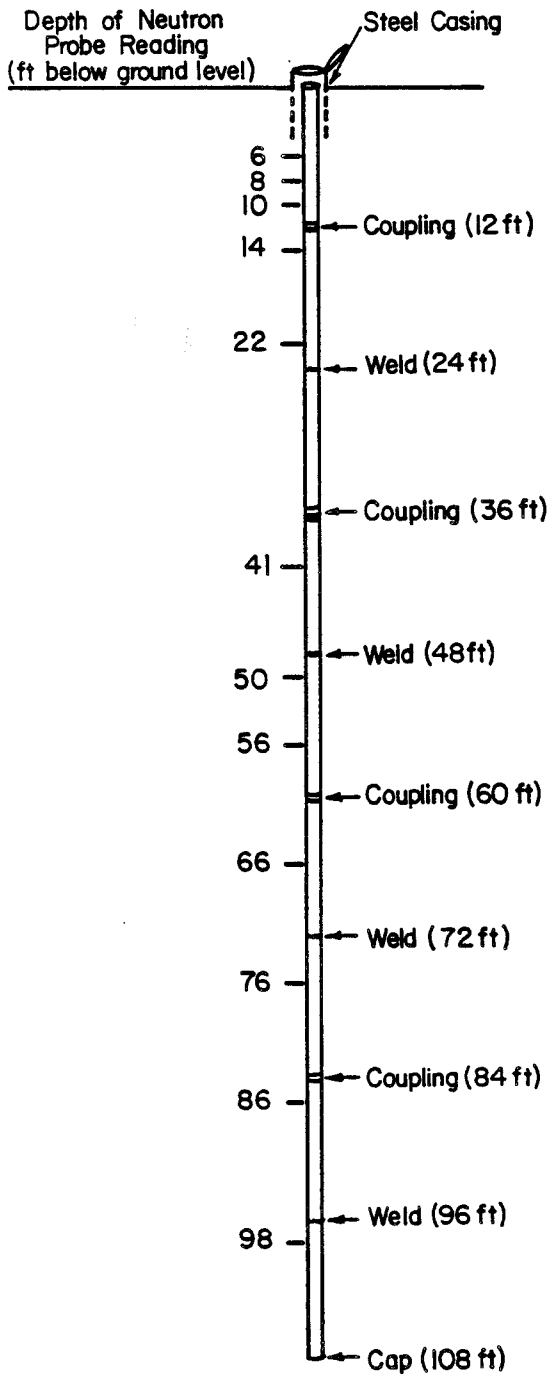

Figure 4-1. Casing Installation and Depths of Neutron Probe Measurements in Hole LLN-85-04

couplings. Hole LGN-85-08 (Figure 4-2) had an uncased depth of 50 ft, so the casing required two 24-ft sections and one 12-ft section, joined together with two no-hub couplings.

4.3 CALIBRATION OF THE NEUTRON PROBE

The neutron probe used at Los Alamos is a Campbell Pacific moisture gauge. Calibration of the instrument was accomplished by using it to measure moisture in five samples of Bandelier Tuff, each with a different but known moisture content. Instrument responses were recorded and used to generate a calibration curve.

The five samples of tuff consisted of three with varying moisture contents, one with no moisture, and one representing saturated conditions. The first three were prepared in the following manner. Crushed Bandelier Tuff was oven-dried at 250°C for 48 hours. A predetermined amount of dry tuff was then weighed and water added to it. The moistened tuff was packed in 15-cm lifts in a 55-gallon drum to achieve a bulk density of 1.5 g/cm^3, which is the average bulk density of the consolidated Bandelier Tuff at Los Alamos. The amounts of water added to the lifts varied from one drum to another, such that the volumetric water content of each drum was different. Samples were collected from each lift in each drum and analyzed gravimetrically to determine the moisture content and to ensure that the moisture content was constant throughout the entire drum.

The fourth drum was prepared in the same way as the first three except that no water was added. The fifth drum was also prepared as described above, except that water was added not to the lifts, but into the bottom of the drum through a 3/8-inch Tygon tube until the tuff was saturated to the drum surface. Samples from these drums were also analyzed so that the moisture contents would be known. Following preparation, all five drums were sealed by placing plastic sheeting between the drum surface and the cover. Silicon sealant was then applied on the edges to prevent evaporation.

Calibration measurements were taken by lowering the probe to the center of each drum and acquiring four 1-minute counts. These data and the known moisture contents were then subjected to a linear-regression analysis, which yields a calibration curve for the instrument. At the time of this writing, the calibration curve was not complete and is therefore not included in this report.

4.4 MONITORING PROGRAM

Biweekly neutron-moisture measurements were initiated in both drill holes on 17 December 1985. The depths of the probe readings are shown in Figures 4-1 and 4-2. The measurement depths in Hole LLN-85-04 correspond to the psychrometer-measurement depths in Hole LLP-85-03, while those in Hole LGN-85-08 correspond to psychrometers in Hole LGP-85-07 (see Appendix A for completion diagrams of Holes LLP-85-03 and LGP-85-07). In certain cases, identical correspondence was not possible due to the presence of the welds and couplings in the neutron-probe holes. As noted previously, no data are available at this time.

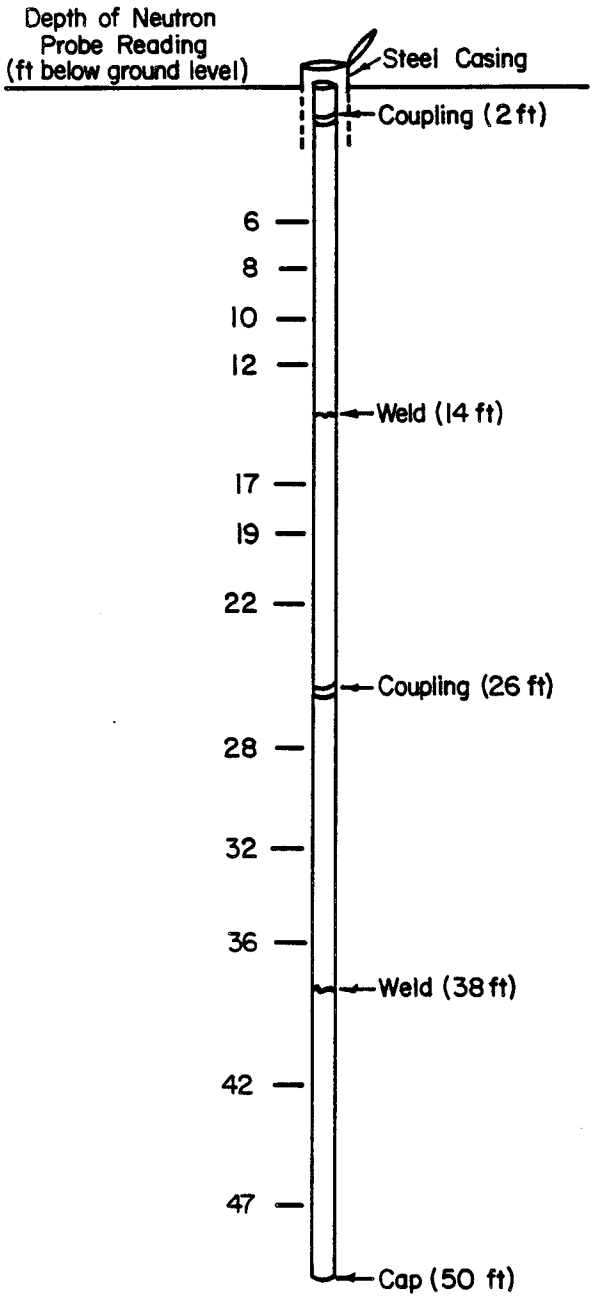

Figure 4-2. Casing Installation and Depths of Neutron Probe Measurements in Hole LGN-85-08

Section 5

PORE-GAS SAMPLING SYSTEM

Note: This section responds to Task 5, Paragraph 25, of the Compliance Order/Schedule.

5.1 PURPOSE AND SCOPE

Samples of pore gas from 14 drill holes are being collected and analyzed in order to characterize the subsurface atmosphere in Areas G and L. The design and installation of the samplers are described in this section; included is a hole-by-hole description of the sampling-port locations and the rationale for choosing each location. At the time of this writing, laboratory analysis of the samples collected to date were not available. Data presentation and interpretation will therefore not be addressed in this report.

5.2 DESIGN

Two pore-gas sampling port designs were implemented for this study. The first design was utilized during the installations completed during Summer 1985, while the second design was used during the installation completed during Fall 1986. During Summer 1985, the pore-gas sampling ports were constructed using low-pressure mobile-phase filters which were welded to standard 2-inch-I.D. galvanized pipe (Bendix Field Engineering Corporation, 1985b). The filters consist of 2-micrometer, porous, stainless steel elements; uphole access is provided via connection to 1/4-inch stainless steel tubing and stainless steel compression fittings. A diagram of a pore-gas sampling port is presented in Figure 5-1. During Summer 1986, the pore-gas samplers were simply assembled by connecting the mobile-phase filters to 1/4-inch stainless steel tubing with stainless steel compression fittings. No elbows were used. Consequently, the sampling port and line assembly were built for installation without the galvanized pipe used in Summer 1985.

5.3 INSTALLATION

In Summer 1986, 70 pore-gas sampling ports were installed in seven 200-ft-deep boreholes. The borehole locations were cited based upon the Petrex Survey (Section 6) results. As requested by Los Alamos National Laboratory, the sampling ports were installed at 20-ft intervals to a depth of 200 ft. A total of 10 sampling ports were placed into each hole. Installation diagrams are presented in Appendix A; drill hole locations are shown in Figure 2-3. In Summer 1985, a total of 23 sampling ports were installed in seven drill holes in the study area; installation procedures were described in the second report (Bendix Field Engineering Corporation, 1985b). Installation diagrams are presented in Appendix A; drill-hole locations are shown in Figure 2-3. The following paragraphs describe the locations of the ports within each hole and the rationale for choosing these locations.

- Hole LGC-85-09. Since this was the only pore-gas sampling hole that penetrated Unit 1a, two ports were installed in that unit, one in the relatively moist section (below 88 ft) and the other in the relatively dry section, just above 80 ft. The third port was installed at about 63 ft to coincide with a fracture present in Unit 1b, and because the maximum waste-disposal depth in this area is approximately 60 ft. The fourth port was installed at 37 ft to coincide with fractures present in Unit 2a.

- Hole LGC-85-10. The deepest sampling port was installed at 95 ft to coincide with a near-vertical fracture present in the more densely welded

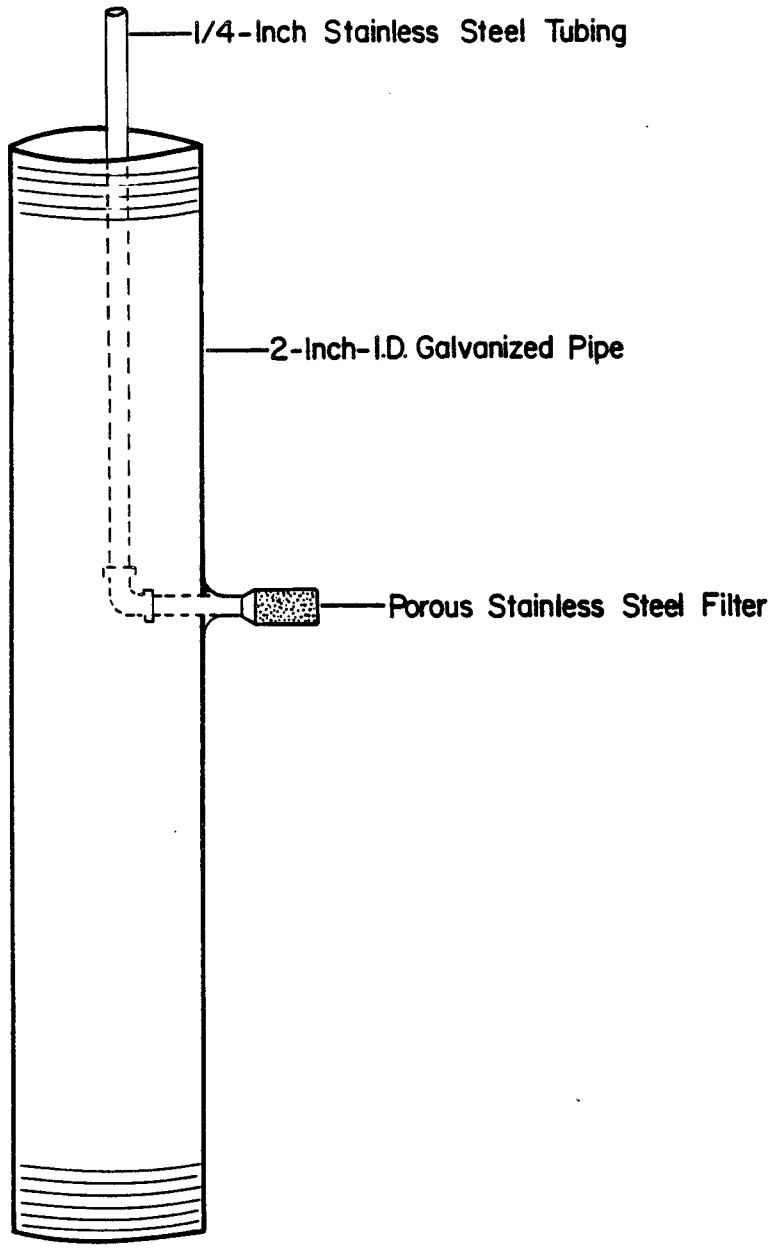

Figure 5-1. Diagram of a Pore-Gas Sampling Port

portion of Unit 1b. The middle port was installed at about 53 ft to coincide with a fracture present in Unit 2a. The uppermost port was installed at 31 ft to coincide with a horizontal fracture and the Unit 2a/Unit 2b contact.

- Hole LLC-85-12. The deepest sampling port was installed at about 41 ft to coincide with a vertical fracture and the Unit 2a/Unit 2b contact. The middle port was installed at about 27 ft to sample the interval between 24 and 29 ft. This interval lies within Unit 2b and consists of a light-gray ash flow with numerous horizontal fractures. In addition, the Organic Vapor Meter (OVM) registered high readings [114 parts per million (ppm) downhole] when the bottom of the auger string reached 24 ft, and again when the bottom of the string reached 29 ft (160 ppm). The uppermost gas-sampling port was installed at about 6 ft to coincide with several fractures present from 5 ft to 8 ft.

- Hole LLC-85-13. This is a 'background' hole located west of Area L. Only Units 2a and 2b were penetrated in this hole. The deepest sampling port was installed at about 65 ft in a moderately welded portion of Unit 2a. The middle port was installed at about 43 ft to coincide with several fractures and the Unit 2a/Unit 2b contact. The uppermost port was installed at about 21 ft to coincide with a near-vertical fracture present in Unit 2b.

- Hole LLC-85-14. The deepest sampling port was installed at about 86 ft to coincide with a fracture zone extending from 84 to 89 ft within Unit 1b. A relatively high OVM reading was recorded for this zone, which is separated from upper zones with high OVM readings by a zone of 'background' OVM readings. The second port was installed at about 46 ft to coincide with a nonfracture zone extending from 44 to 49 ft in Unit 2a where relatively high OVM readings were obtained. The third port was installed at about 31 ft to coincide with the interval 28 to 34 ft because the contact between two physically different zones of Unit 2b is present at 32 ft and field OVM readings were higher when crossing this interval. The contact is defined primarily by the transition into slightly welded or more easily drilled ash-flow tuff. Fractures are also present just above this contact. The uppermost sampling port was installed at about 13 ft to coincide with a moderately welded, nonfracture zone within Unit 2b. This zone, extending from 12 to 14 ft, exhibited relatively high OVM readings. In addition, sampling in this zone would permit comparison with results from known fracture zones.

- Hole LLC-85-15. The deepest port was installed at about 82 ft to sample pore gas in the interval 80 to 86 ft because a relatively high OVM reading was obtained near this interval. The other two sampling ports were installed at about 32 ft and 19 ft to coincide with the areas where the highest OVM readings were obtained in this hole.

- Hole LLC-85-16. The deepest sampling port was installed near the bottom of this hole to coincide with areas exhibiting high OVM readings. These areas are separated from the zones of additional high readings by 75 ft of relatively low OVM readings. The other two ports were installed near ground surface to coincide with zones that are both fractured and displayed relatively high OVM readings.

Section 6

PETREX SURVEY

6.1 PURPOSE AND SCOPE

A Petrex survey, utilizing the K-V Fingerprint Technique, was conducted at Waste Disposal Area L as a screening tool to guide the placement of additional pore-gas sampling wells. The survey was also used to qualitatively define the extent of migration of volatile organic compounds away from waste-disposal shafts and trenches. The K-V Fingerprint Technique, marketed by Petrex, Golden, Colorado, permits passive or static gas sampling and analysis of the soil to identify organic compounds and determine the relative number of ions sorbed onto the sampling element per unit time. The ion counts per unit time represent a relative flux of ions venting to the ground surface. The volatile organic compounds studied were trichloroethylene (TCE), tetrachloroethylene (PCE), benzene, and toluene.

6.2 SAMPLING AND ANALYSIS

The sampling device used in the Petrex survey consists of a 0.02-inch-diameter by 4-inch-long wire filament, which is coated with a monolayer of charcoal and inserted in a glass tube. The tube is then placed in a 12- to 14-inch deep hole and covered with soil. The sampling tube remains in the ground for a sufficient period to expose the filament, and is then removed. For this investigation, a period of 10 days was used. The volatile organic compounds sorbed onto the charcoal filament from the soil atmosphere are purged in a pyrolyzer, using the filament as a heat source. The volatilized compounds are then passed to a mass spectrometer for analysis.

A total of 101 samplers were installed at a 30-foot grid in and around Waste Disposal Area L. The sampler spacing was selected to be broad enough to provide information on the lateral extent of the plume and narrow enough to contour the ion-count data. The designated spacing interval of the samplers was also chosen to be close enough to determine the orientation of any plumes.

Natural background measurements were also performed to provide a perspective from which to analyze the sampling results. The natural background was determined by placing an array of five samplers at 30-foot intervals along a northerly projection away from background Hole LLC-85-13 (see Figure 2-3). The background samplers were removed from the soil 10 days after emplacement.

6.3 RESULTS

Four maps were constructed to show the relative vapor ion counts emanating from Waste Disposal Area L. Figures 6-1 through 6-4 show results of the Petrex survey for the organic compounds trichloroethylene, tetrachloroethylene, benzene, and toluene, respectively.

The toluene ion counts were the highest of the compounds surveyed. Toluene ion counts exceed 60,000 at a number of locations, and more than 90,000 at one location at the east-central margin of the survey grid. The counts for benzene were the next highest, although they were much lower than the counts

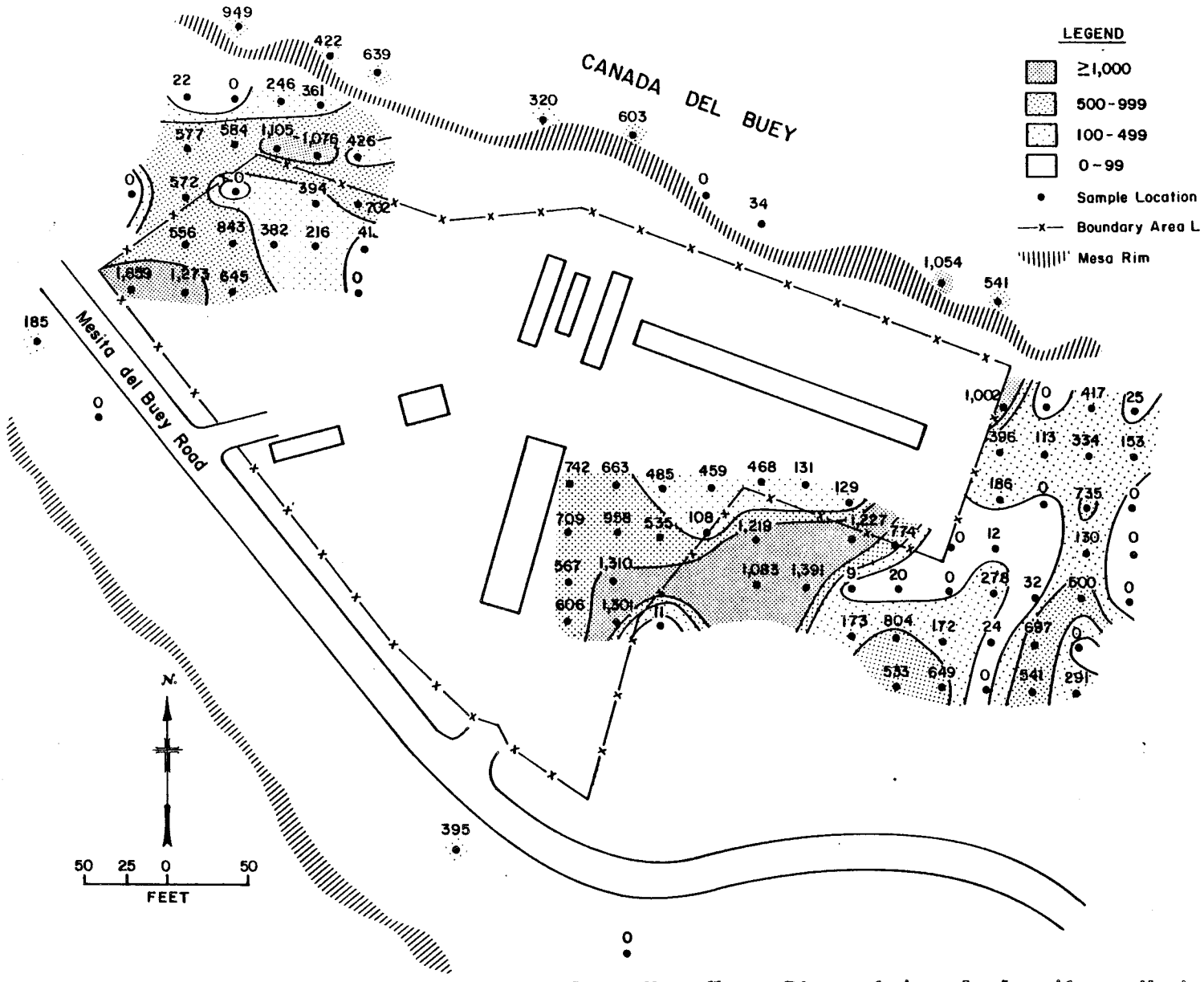

Figure 6-1. Normalized Trichloroethylene Ion-Count Map, Waste Disposal Area L, Los Alamos National Laboratory, New Mexico

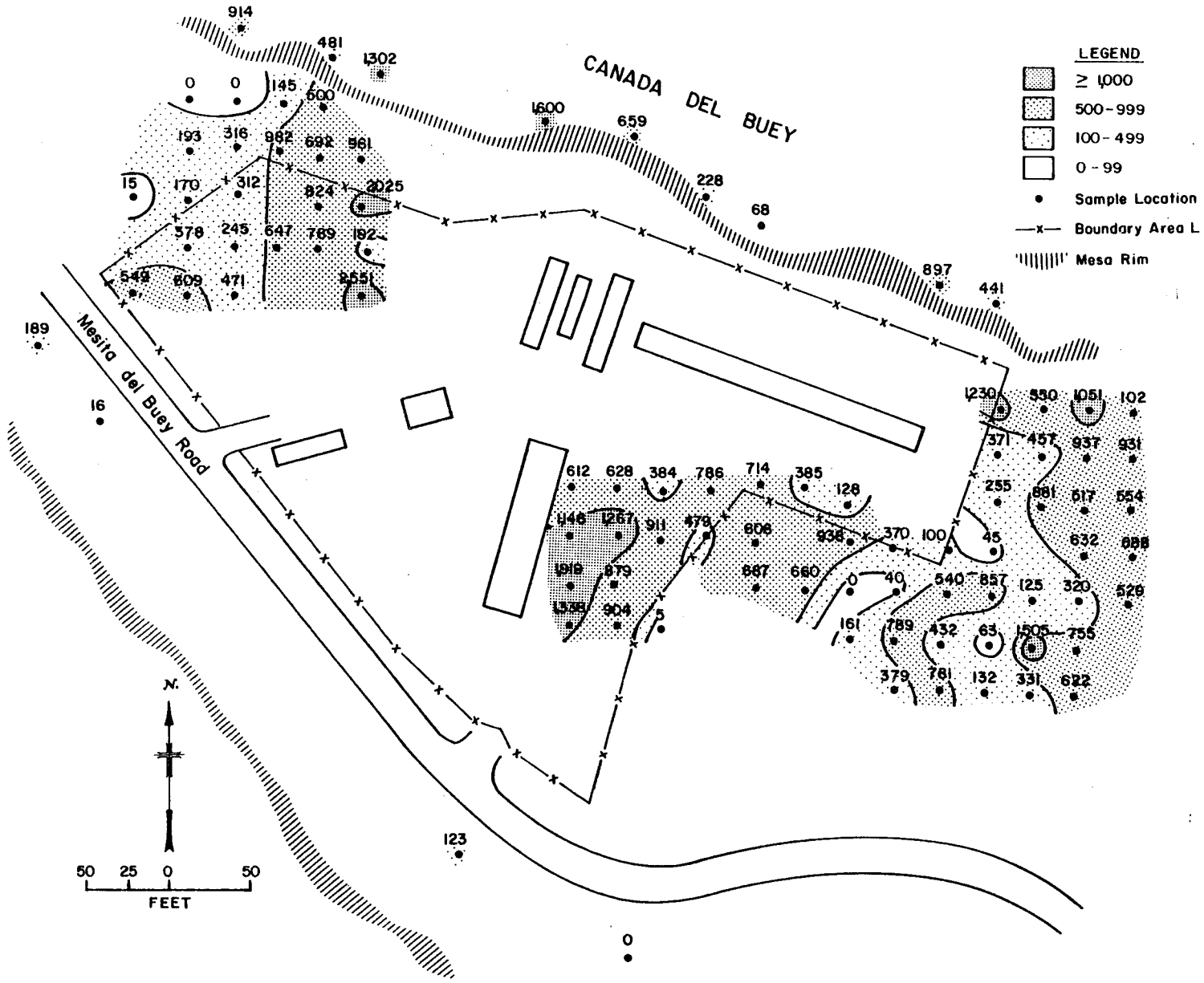

Figure 6-2. Normalized Tetrachloroethylene Ion-Count Map, Waste Disposal Area L, Los Alamos National Laboratory, New Mexico

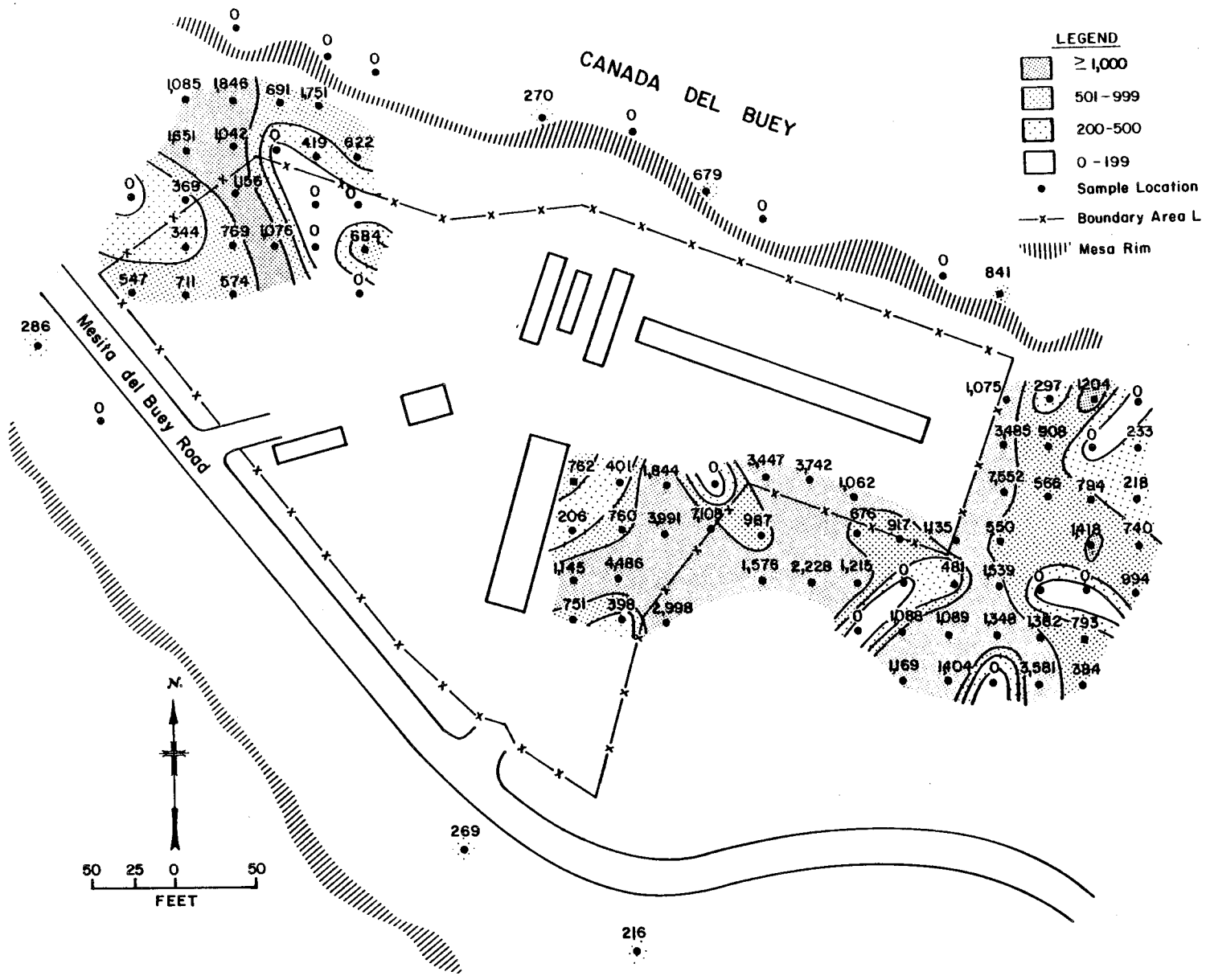

Figure 6-3. Non-Normalized Benzene Ion-Count Map, Waste Disposal Area L, Los Alamos National Laboratory, New Mexico

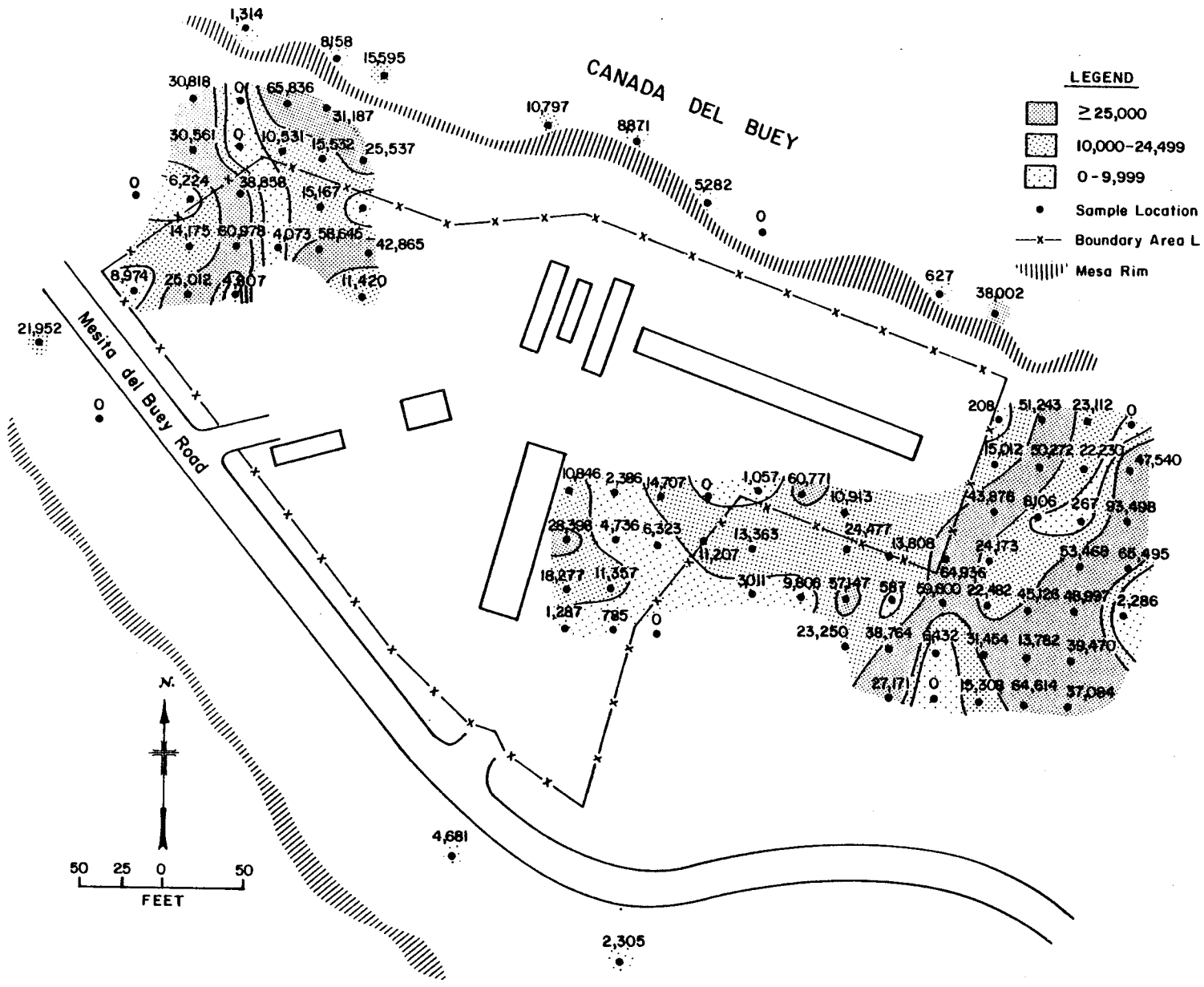

Figure 6-4. Non-Normalized Toluene Ion-Count Map, Waste Disposal Area L, Los Alamos National Laboratory, New Mexico

for toluene. Trichloroethylene and tetrachloroethylene had the lowest total ion counts.

The trichloroethylene and tetrachloroethylene data presented in Figures 6-1 and 6-2, respectively, were normalized by dividing the specific ion counts by the total ion counts less atmospheric compounds. The benezene and toluene ion counts are non-normalized and represent total uncorrected specific ion counts. The ion counts for a specific compound are not absolute and, therefore, should not be used to compare individual compounds as a means of determining relative abundances of the compounds present. The ion counts of a particular compound, however, may be used to show the relative flux distribution of specific ions.

Background ion counts for benzene and toluene ranged from 0 to 1,078 and 0 to 27,998, respectively. The background values are quite high when compared to the ion counts taken at Waste Disposal Area L. The gases given off by plant roots in the soil zone are suspected of having a chemical structure similar to benzene and toluene; the plant-root gases overprint and likely predominate over the counts observed at Area L. Since the range in background counts is so high for benzene and toluene, it is likely that even a wider range of background counts could be expected if more than five samplers were used to survey the background. The existing five-sample array of background counts is, therefore, insufficient to characterize the background accurately because the maximum observed counts could be well below the probable maximum background value. Furthermore, analytical results of core samples collected during the drilling phase of the project have not indicated that benzene or toluene were even present in the pore-gas fraction of the rock (Rocky Mountain Analytical Laboratory, 1986). The benzene and toluene maps (see Figures 6-3 and 6-4), consequently, are not recommended for use in delineating the vapor-phase contamination at Area L.

Background ion counts for trichloroethylene and tetrachloroethylene were found to be very low to nonexistent. As a result, the ion counts shown in Figures 6-1 and 6-2 more accurately reflect the relative flux of these vapors emanating from Area L. Trichloroethylene and tetrachloroethylene would, therefore, be good compounds to define the extent of migration away from the waste-disposal shafts and trenches.

From the distribution of the ion-count data observed in Figures 6-1 through 6-2, there is no readily apparent single trend in the data at any location surveyed. There are locally high ion-count locations, which may simply indicate proximity to waste trenches and pits. The distribution of ion counts, however, is not concentric around the source. Locally contoured areas with high ion counts, some of which are linear trends, may indicate areas where the fracture intensity or the fracture aperture is relatively large. Where the trends do exist, it may indicate preferential movement through open joints, which would be more effective in transmitting organic vapors than the intervening blocks of tuff.

It should be noted that the lateral extent of the ion-count plume could not be defined conclusively because substantial ion counts were detected at the margins of the sample area. It can be assumed that these elevated ion counts extend beyond the limits of the present survey. Consequently, additional pore-gas sampling holes were located beyond the limits of the existing Petrex grid to aid in defining the extent of the organic vapor contamination plume. No analytical data on the newly installed, pore-gas monitoring ports were available at the time of this report.

Section 7

CONCLUSIONS

The time constraints imposed on this study of Waste Disposal Areas G and L at Los Alamos permitted only a brief period for data acquisition and interpretation. As a consequence, the assessment presented herein of the vadose zone underlying Mesita del Buey is for the short term only. Nevertheless, some conclusions can be drawn from the data obtained thus far, the most important being that the dominant mode of transport in the interval of the Bandelier Tuff examined for this study is by vapor phase. In other words, the low moisture content of the tuff and the high moisture-retention values observed in the moisture characteristic curves indicate that interconnection of liquid water, and therefore movement of water in the liquid phase, is nonexistent. Additional conclusions are discussed in the paragraphs that follow.

- The geologic framework through which transport occurs can be characterized as a complex network of pumice and lithic clasts surrounded by a glass-shard/crystal matrix, with occasional fractures dissecting the porous media. Factors such as porosity, degree of welding, and pumice content have a direct effect on the unsaturated hydraulic characteristics.

- Taken together, the high values for porosity and moisture retention (both average approximately 50 percent) indicate that the tuff behaves much like a sponge. A quantity of water equal to approximately one quarter of the rock volume is required to satisfy capillary forces before recharge to the underlying groundwater system can occur. Based on the normal precipitation and the high evapotranspiration rates in the study area, this scenario is unlikely.

- Results from field and laboratory tests indicate that the overall range of intrinsic permeability for the Bandelier Tuff is 10^{-8} to 10^{-9} cm^2 (10^{-11} to 10^{-12} ft^2). These values are considered to represent moderate permeability.

- Permeability and porosity are not directly related, probably because of the tuff's pumice content; highly porous pumice lapilli contain a significant amount of dead-end pore space which greatly reduces permeability.

- The unsaturated hydraulic conductivities calculated using van Genuchten's model are of little value since the laboratory could only obtain moisture characteristic curves in the range 0 to -0.3 bar, with moisture contents (θ) of about 0.4 to 0.6. The calculated unsaturated hydraulic conductivities range from about 2 centimeters per day at saturation to about 1.0×10^{-6} centimeter per day at a water potential of -0.3 bar. In the field, however, water potentials range from -1 to -15 bar, and the moisture contents are below 0.1. Thus, the unsaturated hydraulic conductivities of the tuff in the field are actually much lower than the values calculated using van Genuchten's method.

- Unit 1b has a relatively higher degree of welding than the other units of Bandelier Tuff examined in this study. This higher degree of welding, coupled with the unit's high pumice content, results in strong capillary forces which are assumed to be responsible for the significant increase in moisture content in the lower portion of Unit 1b. Increases in the degree of welding are believed to reduce the pore-size radii, resulting in an increase in the capillary forces. Similarly, because there is a high

pumice content, there is a correspondingly high concentration of gas tubes; these tubes form ideal capillary tubes which appear to exhibit strong capillary forces.

- Test results indicate that permeability in and along fractures is very similar to the permeability of the surrounding porous media. Detection of the differences in the permeability, however, may be beyond the sensitivity of the testing methods, since several fracture zones show an increase in moisture content relative to the adjacent porous media.

- In certain cases, the magnetic susceptibility logs can be useful for estimating or confirming lithologic contacts. The gamma-gamma (apparent density) logs are useful for determining the degree of welding and possibly the relative pumice content of the various ash-flow units.

- Moisture characteristic curves for crushed tuff samples differ significantly from those obtained for core samples. As a consequence, interpretations of in-situ hydrogeologic transport cannot be reliably based on hydraulic data for crushed tuff.

- Petrex survey results indicate that organic-vapor ion-count contours are not distributed concentrically surrounding the contaminant source at Area L. Venting of organic vapors may occur in discrete zones where fracture apertures and/or intensities are locally elevated.

- A dominant northeast trend of fractures was determined by measuring joints on Mesita del Buey; however, a bias in the data resulted from sampling limitations imposed by available exposures. Occurrence of 'preferred' fracture orientation is not a sufficient single criteria for predicting direction of contaminant migration; transport from a contaminant source to the surface probably follows tortuous routes determined by a combination of fracture orientations and degree of dilation, and interconnections of fractures related to the position of infill materials.

- The best method for determining the extent and direction of contaminant transportation would be close monitoring and interpretation of analytical results from pore-gas samples, together with more extensive Petrex surveys just under the rim of Mesita del Buey and in Waste Disposal Area L.

Section 8

REFERENCES

Abeele, W. V., 1984. Hydraulic Testing of Crushed Bandelier Tuff, LA-10037-MS, UC-11, Los Alamos National Laboratory, New Mexico.

Abeele, W. V., M. L. Wheeler, and B. W. Burton, 1981. Geohydrology of Bandelier Tuff, LA-8962-MS, UC-11, Los Alamos National Laboratory, New Mexico.

Bailey, R. A., R. L. Smith, and C. S. Ross, 1969. Stratigraphic Nomenclature of Volcanic Rocks in the Jemez Mountains, New Mexico, Bulletin 1274-P, U.S. Geological Survey.

Bendix Field Engineering Corporation, 1985a. Environmental Sciences Procedure Manual, Environmental Programs Division, Grand Junction, Colorado, internal document.

Bendix Field Engineering Corporation, 1985b. Vadose Zone Characterization of Technical Area 54, Waste Disposal Areas G and L, Los Alamos National Laboratory - Report 2: Downhole Instrumentation and Pore-Gas-Sampling/Data-Collection Procedures, GJ-43, Bendix Field Engineering Corporation, Grand Junction Operations, U.S. Department of Energy, Grand Junction Projects Office, Grand Junction, Colorado.

Brown, R. W., and D. L. Bartos, 1982. A Calibration Model for Screen-Caged Peltier Thermocouple Psychrometers, Research Paper INT-293, U.S. Department of Agriculture, Intermountain Forest and Range Experiment Station.

Brown, R. W., and J. M. Collins, 1980. 'A Screen-Caged Thermocouple Psychrometer and Calibration Chamber for Measurements of Plant and Soil Water Potential,' Agronomy Journal, Vol. 72, pp. 851-854.

Case, C. M., and A. Welch, 1979. 'Pore Size Distribution, Suction and Hysteresis in Unsaturated Groundwater Flow,' Journal of Hydrology, Vol. 43, pp. 99-120.

Chemical Rubber Company, 1986-1987. Handbook of Chemistry and Physics: 47th Edition, Robert C. Weast (editor-in-chief), Cleveland, Ohio.

Cook, E. F., 1965. Stratigraphy of Tertiary Volcanic Rocks of Eastern Nevada, Report No. 11, Nevada Bureau of Mines.

Environmental Improvement Division, 1985. Compliance Order/Schedule: Los Alamos National Laboratory, State of New Mexico, Santa Fe.

Freeze, R. A., and J. A. Cherry, 1979. Groundwater, Prentice-Hall, Inc., Englewood Cliffs, New Jersey.

Fukui, L. M., 1985. Petrography of the Tshirege Member of the Bandelier Tuff, Mesita del Buey, Los Alamos County, New Mexico, prepared for the Environmental Programs Division, Bendix Field Engineering Corporation, Grand Junction, Colorado.

_____ 1986. Petrography of the Tshirege Member of the Bandelier Tuff, Mesita del Buey, Los Alamos County, New Mexico: Second Report, prepared for the Environmental Programs Division, Bendix Field Engineering Corporation, Grand Junction, Colorado.

Goddard, E. N., P. D. Trask, R. K. DeFord, O. N. Rove, J. T. Singewald, Jr., and R. M. Overbeck, 1975. Rock Color Chart, Geological Society of America, Boulder, Colorado.

Goff, F. E., and S. L. Bolivar, 1983. Field Trip Guide to the Valles Caldera and Its Geothermal Systems, LA-9963-OBES, Los Alamos National Laboratory, New Mexico.

Horner, R. D., 1951. 'Pressure Build-Up in Wells,' in Proceedings of the Third World Petroleum Congress, Section II, E. J. Bill, Leiden, Holland.

Jakubick, A. T., 1983. Permeability Measurements of the Near-Field of Excavations by Transient Pressure Testing, Atomic Energy of Canada, Technical Report, Whiteshell Nuclear Research Establishment, Pinawa, Manitoba.

Johnson, E. F., D. P. Bossler, and V. D. Naumann, 1959. 'Calculations of Relative Permeability from Displacement Experiments,' Transactions of the American Institute of Mining, Metallurgical, and Petroleum Engineers, Vol. 216, pp. 370-372.

Kearl, P. M., J. J. Dexter, and M. Kautsky, 1986. Vadose Zone Characterization of Technical Area 54, Waste Disposal Areas G and L, Los Alamos National Laboratory, New Mexico - Report 3: Preliminary Assessment of the Hydrologic System, GJ-44, Bendix Field Engineering Corporation, Grand Junction Operations, U.S. Department of Energy, Grand Junction Projects Office, Grand Junction, Colorado.

Lai, Sung-Ho, J. M. Tiedje, and A. E. Erickson, 1976. 'In Situ Measurement of Gas Diffusion Coefficient in Soil,' Soil Science Society of America Journal, Vol. 40, pp. 3-6.

Lang, A. R. G., 1967. 'Osmotic Coefficients and Water Potentials of Sodium Chloride Solutions from 0 to 40°C,' Australian Journal of Chemistry, Vol. 20, No. 9, pp. 2017-2023.

Loughborough, M. T., 1966. 'Permeability of Concrete to Air,' Ontario Hydro Research Quarterly, First Quarter, Ontario, Canada.

Marshall, T. J., and J. W. Holmes, 1979. Soil Physics, Cambridge University Press, New York.

Marutzky, S. J., 1986. Personal Communication with S. J. Marutzky, Bendix Field Engineering Corporation, Grand Junction, Colorado, 18 February 1986.

McBeth Division, Kollmorgen Corporation, 1975. Munsell™ Soil Color Chart, McBeth Division, Kollmorgen Corporation, Baltimore, Maryland.

Miller, C. H., D. R. Cunningham, and M. J. Cunningham, 1974. 'An Air Injection Technique to Study Intensity of Fracturing Around a Tunnel in Volcanic Rocks,' Bulletin of the Association of Engineering Geologists, Vol. II, No. 3.

Mualem, V., 1976. 'A New Model for Predicting the Hydraulic Conductivity of Unsaturated Porous Media,' Water Resources Research, Vol. 12, No. 3, pp. 513-522.

Nutting, P. G., 1930. 'Physical Analysis of Oil Sands,' Bulletin of the American Association of Petroleum Geologists, Vol. 14, pp. 1337-1349.

Purtymun, W. D., and W. R. Kennedy, 1971. Geology and Hydrology of Mesita del Buey, LA-4660, UC-41, Los Alamos National Laboratory, New Mexico.

Purtymun, W. D., M. L. Wheeler, and M. A. Rogers, 1978. Geologic Description of Cores from Holes P-3 MH-a through P-3 MH-5, Area G, Technical Area 54, LA-7308-MS, Informal Report, Los Alamos Scientific Laboratory, New Mexico.

Rocky Mountain Analytical Laboratory Division, ENSECO, Inc., 1986. Analytical Results for Bendix Field Engineering Corporation, Rocky Mountain Analytical Laboratory Division, ENSECO, Inc., Arvada, Colorado.

Rogers, M. A., 1977. History and Environmental Setting of LASL Near-Surface Land Disposal Facilities for Radioactive Wastes, LA-6848-MS, Vol. 1, Los Alamos Scientific Laboratory.

Ross, C. S., and R. L. Smith, 1961. Ash-Flow Tuffs: Their Origin, Geologic Relationship, and Identification, USGS Professional Paper 366, Government Printing Office, Washington, D.C.

Rush, S. M., and J. J. Dexter, 1985. Vadose Zone Characterization of Technical Area 54, Waste Disposal Areas G and L - Report 1: Drilling and Logging Activities, GJ-37, Bendix Field Engineering Corporation, Grand Junction Operations, U.S. Department of Energy, Grand Junction Projects Office, Grand Junction, Colorado.

Spanner, D. C., 1951. 'The Peltier Effect and Its Use in the Measurement of Suction Pressure,' Journal of Experimental Botany, Vol. 2, No. 5, pp. 145-167.

Stephens, D. B., and S. P. Neuman, 1982a. 'Vadose Zone Permeability Tests: Summary,' Journal of the Hydraulics Division, American Society of Civil Engineers, Vol. 108, No. HY5, pp. 623-639.

Stephens, D. B., and S. P. Neuman, 1982b. 'Vadose Zone Permeability Tests: Steady State Results,' Journal of the Hydraulics Division, American Society of Civil Engineers, Vol. 108, No. HY5, pp. 640-659.

Stephens, D. B., S. Tyler, K. Lambert, and S. Yates, 1983. 'Field Experiments to Determine Saturated Hydraulic Conductivity in the Vadose Zone,' in Role of the Unsaturated Zone in Radioactive and Hazardous Waste Disposal, J. W. Mercer, P.S.C. Rao, and M. I. Wendell (eds.), Ann Arbor Scientific Publications, Ann Arbor, Michigan.

Streckeisen, A., 1967. 'Classification and Nomenclature of Igneous Rocks,' in Neues Jahrbuch fur Mineralogie, Abhandlungen, Vol. 107, pp. 144-240.

TerraTek Research Laboratory, 1985. Laboratory Analysis of Rock Core: Bandelier Formation, TR86-49, Salt Lake City, Utah.

U.S. Department of the Interior, 1974. Earth Manual: A Water Resource Technical Publication, Second Edition, Government Printing Office, Washington, D.C.

University of Missouri at Rolla, 1981. Seminar for Drillers and Exploration Managers, Orlando, Florida.

van Genuchten, Rien, 1978. Calculating the Unsaturated Hydraulic Conductivity with a New Closed-Form Analytical Model, Princeton University Water-Resources Program Report 78-WR-08.

Welge, H. J., 1952. 'A Simplified Method for Computing Oil Recovery by Gas or Water Drive,' Transactions of the American Institute of Mining, Metallurgical, and Petroleum Engineers, Vol. 195, pp. 91-98.

Wescor (undated). Instruction Manual for the Model HP-115 Microprocessor Controlled Water Potential Data System, Wescor, Inc., Logan, Utah.

Wescor, 1982. CI-30 Audio Cassette Interface, Wescor, Inc., Logan, Utah.

Appendix A

LITHOLOGIC LOGS AND INSTRUMENT COMPLETION DIAGRAMS

LITHOLOGIC LOGGING

A lithologic log was prepared in accord with established field procedures for each of the 23 holes cored with the continuous sampling system (Bendix Field Engineering Corporation, 1985a, 1985b). These logs are presented in chronological order by hole number as Figures A-2 through A-24. The colors used to describe the core matrices are taken from the Rock Color Chart of Goddard and others (1975) and the Munsell™ Soil Color Chart, Macbeth Division of Kollmorgen Corporation, Baltimore, Maryland (1975); the code in parentheses following a color description corresponds to the charts.

For most of the holes, the lithologic logs also show the numbers and depth intervals of samples collected for subsequent field or laboratory analysis. Samples identified by the three-letter prefix MCG- followed solely by a three-digit number were collected for gravimetric analysis. Those MCG-numbered samples denoted by a single asterisk (*) were collected for petrologic analysis, and those denoted by a double asterisk (**) were collected for laboratory analysis of moisture characteristics. Samples identified with the number 85 followed by a decimal point and five additional digits were collected for EP-toxicity and volatile-organic analyses by Los Alamos National Laboratory for drilling conducted during Summer 1985. Splits of these samples are identified by the addition of the letter A immediately following the sample number. Samples identified with the prefix R5 were collected for volatile-organic analyses by Rocky Mountain Analytical Laboratory, Arvada, Colorado. Results of these analyses were presented to Los Alamos National Laboratory 7 October 1986.

Lithologic logs for holes drilled during 1986 (designated with an '86' in the log number) and Holes LLM-85-01 and LLM-85-02 have a specific installation column for instrument-completion diagrams (except LLC-86-25). The lithologic logs for the remainder of the holes in which instruments were installed show instrument-completion diagrams in the column originally used for sample identification. The reader is referred to the first report (Rush and Dexter, 1985) for information on sample numbers and intervals for those holes. It is important to note, however, that the lithologic data have been updated since publication of the first report. Consequently, the graphic log and description for a particular hole as they appeared in the first report may not match the information presented in this appendix.

INSTRUMENT COMPLETIONS

A total of 93 pore-gas sampling ports were installed in 14 boreholes in the study area. Completion diagrams of the installations are presented in Figures A-2, A-3, A-8, A-9, A-11 through A-15, and A-19 through A-23.

A total of 38 thermocouple psychrometers were installed at the study area, 23 in Hole LLP-85-03 and 15 in Hole LGP-85-07. Because of the presence of surface casing in Hole LLP-85-03, a shallow boring was drilled adjacent to the main hole and five psychrometers were installed in this second hole close to the ground surface (depicted in Figure A-4 as being in the same hole). Completion diagrams of the thermocouple-psychrometer installations are shown in Figures A-4 and A-7. Four pressure transducers were installed in Hole LLP-85-03, although the one at ground surface is actually in the shallow

adjacent boring described above. The completion diagram is shown in Figure A-4.

Installation details were described in the second interim report (Bendix Field Engineering Corporation, 1985b). The legends for the instrument installations are presented in Figure A-1.

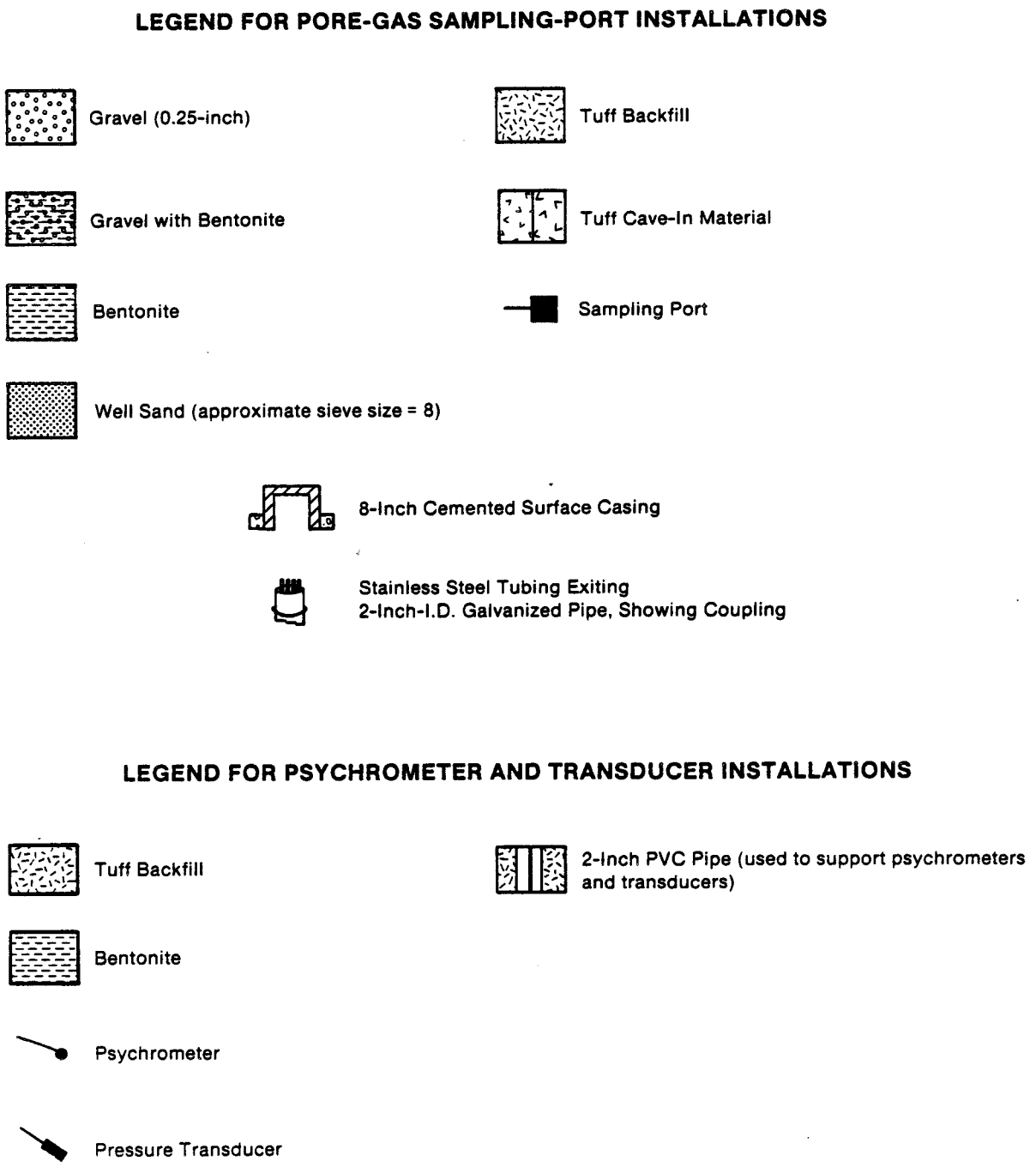

Figure A-1. Legends for the Instrument Installations

Depth (feet)	Sample Interval	Sample Number	Rock Quality Designation/ Recovery (%)	Installation	Graphic Log	Description
						Unit 2b: Tshirege Member of the Bandelier Tuff Tuff is moderately welded and matrix color is very light gray (N8). Pumice lapilli (pumice fragments) are light gray and range in size from 5 to 10 mm. Horizontal fractures are coated with caliche at depths of 5 ft 2 in. and 5 ft 7 in. The upper 3 to 4 ft are very weathered.
5		MCG-476				
		MCG-477				
10						Chatoyant sanidine crystals, up to 3 mm in size, are present throughout this unit.
		MCG-478				
15						
		MCG-479				
20						Color changes very slightly to pinkish gray (5YR8/1), representing contact between two flows that cooled as one unit; slightly less coherent than above.
		MCG-480				
25						
		MCG-481				
30		MCG-626* MCG-602**				Slightly more welded than above (moderately welded).
		MCG-482				Drilling becomes easier, representing contact with slightly welded base of Unit 2b.
35						
		MCG-483				
40						**Unit 2a**
		MCG-484				Tuff is slightly welded. Matrix color changes to grayish pink (5R8/2). Pumice lapilli are pale brown and grayish olive; compared with those in Unit 2b, they are larger (10 to 20 mm) and more abundant.
45						
		MCG-485				Sanidine and quartz crystals, less than 1 mm in size, are present. Slightly more welded than above (moderately welded).
50		MCG-627* MCG-603**				Slightly welded tuff.
		MCG-486				
55						
		MCG-487				Matrix color changes to pinkish gray (5YR8/1).
60						
		MCG-488				
65						Nonwelded, very disaggregated ash-flow tuff, from 62 to 64 ft.
		MCG-489				Tuff is slightly welded. Matrix color changes to light gray (N7).
70						
		MCG-490				
75						Abundant brown and occasional gray and green pumice lapilli, 10 to 20 mm in size.
		MCG-491				Near-vertical fracture is coated with iron-colored clay (limonite?).
80						**Unit 1b**
		MCG-492				Tuff is slightly welded. Matrix grades to a color between pinkish gray (5YR8/1) and yellowish gray (5Y8/1). Pumice lapilli are predominantly brown and much smaller (5 to 10 mm) than those in Unit 2a. Lithic lapilli, 1 to 2 mm in size, start to appear and become more abundant with depth.
85						
		MCG-493				Minor chatoyant sanidine crystals are present.
90						Matrix is lighter in color, nearly very light gray (N8).
		MCG-494				Gradually becoming more welded with depth.
95						
		MCG-495				
100		MCG-628* MCG-604**				Color grades to grayish pink (5R8/2).
		MCG-496				
105						
		MCG-497				Brown pumice lapilli are abundant.
110						
		MCG-498				Matrix is browner, nearly pale red (5R6/2), and tuff is moderately welded.
115						
		MCG-499				
120		MCG-629* MCG-605**				High-angle fracture extends from 120 to 124 ft.
125						Very large (up to 1 in.) lithic lapilli, with abundant small lithic lapilli.
130						
135						
140						
145						
150						
155						
160						Undifferentiated tuff below 125 ft.
165						
170						
175						
180						
185						
190						
195						
200						

Figure A-2. Lithologic Log of Hole LLM-85-01

Depth (feet)	Sample Interval	Sample Number	Rock Quality Designation/ Recovery (%)	Installation	Graphic Log	Description
		MCG-500				**Unit 2b: Tshirege Member of the Bandelier Tuff**
5						Tuff is moderately welded, and matrix color is very light gray (N8). Pumice lapilli are light gray (N7). The upper 3 ft are weathered.
		MCG-606**				Horizontal fracture occurs at depth of 9.5 ft; no caliche on surface.
		MCG-502				Color changes very slightly to pinkish gray (5YR8/1), which may indicate transition to lower flow of Unit 2b.
10						Horizontal fracture occurs at depth of 12.5 ft; coated with caliche.
		MCG-503				
15						
		MCG-504				
20						
		MCG-505				
25						Large rust-colored fracture extends from 26 ft 3 in. to 27 ft 8 in.; white caliche and roots are present.
		MCG-506				
30						
		MCG-507				Drilling becomes easier at approximately 33 ft; tuff is only slightly welded.
35		MCG-630*				
		MCG-607**				Near-vertical fracture extends from 35 to at least 40 ft 6 in. The fracture appears open and has an iron stain approximately 2/16 in. wide. Tuff is more indurated close to the fracture, but is only slightly welded.
		MCG-508				
40						**Unit 2a**
		MCG-509				Color changes to grayish pink (5R8/2); tuff is slightly welded. Pumice lapilli—brown, gray, and green in color—are larger than those in Unit 2b.
45						
		MCG-510				
50						Fracture extends from 49 ft 9 in. to 51 ft 10 in.; it is marked with an iron-colored alteration band that widens with depth, but occurs on only one side of the fracture plane. Tuff becoming more welded at depth.
		MCG-511				
55						Fracture extends from 55 ft 2 in. to 56 ft 2 in.; it is similar to, and may be continuous with, the above fracture.
		MCG-512				
60						Tuff is moderately welded. Pumice lapilli are still brown, green, and gray.
		MCG-513				
65		MCG-631*				
		MCG-608**				
70		MCG-514				
		MCG-515				Fracture extends from 73 to 73.5 ft.
75		MCG-632*				Matrix color changes to pinkish gray (5YR8/1); tuff is slightly welded.
		MCG-516				Very disaggregated ash, which may represent slightly welded lower portion of this unit.
80						**Unit 1b**
		MCG-517				Pumice lapilli are predominantly brown and much smaller than those in the above units. Lithic lapilli, very scattered and small, are present and become more abundant with depth. Matrix grades to a color between pinkish gray (5YR8/1) and yellowish gray (5Y8/1). Tuff is slightly welded.
85						
		MCG-518				
90						
		MCG-519				Abundant brown pumice lapilli; larger fragments are noticeably flattened, representing the beginning of the transition to the moderately welded central zone of this unit.
95						
		MCG-520				
100						
		MCG-521				Quartz and feldspar in matrix becoming more abundant. Quartz is distinctively honey-colored and bipyramidal.
105						
		MCG-522				Drilling becomes slightly more difficult and rock fragments are very abundant. Tuff is moderately welded.
110		MCG-633*				
		MCG-523				
115						
		MCG-609**				
120		MCG-524				Same as above, except matrix color is more orangish, nearly moderate orange pink (5YR8/4).
		MCG-525				
125						
130						
135						
140						
145						
150						
155						
160						Undifferentiated tuff below 125 ft.
165						
170						
175						
180						
185						
190						
195						
200						

Figure A-3. Lithologic Log of Hole LLM-85-02

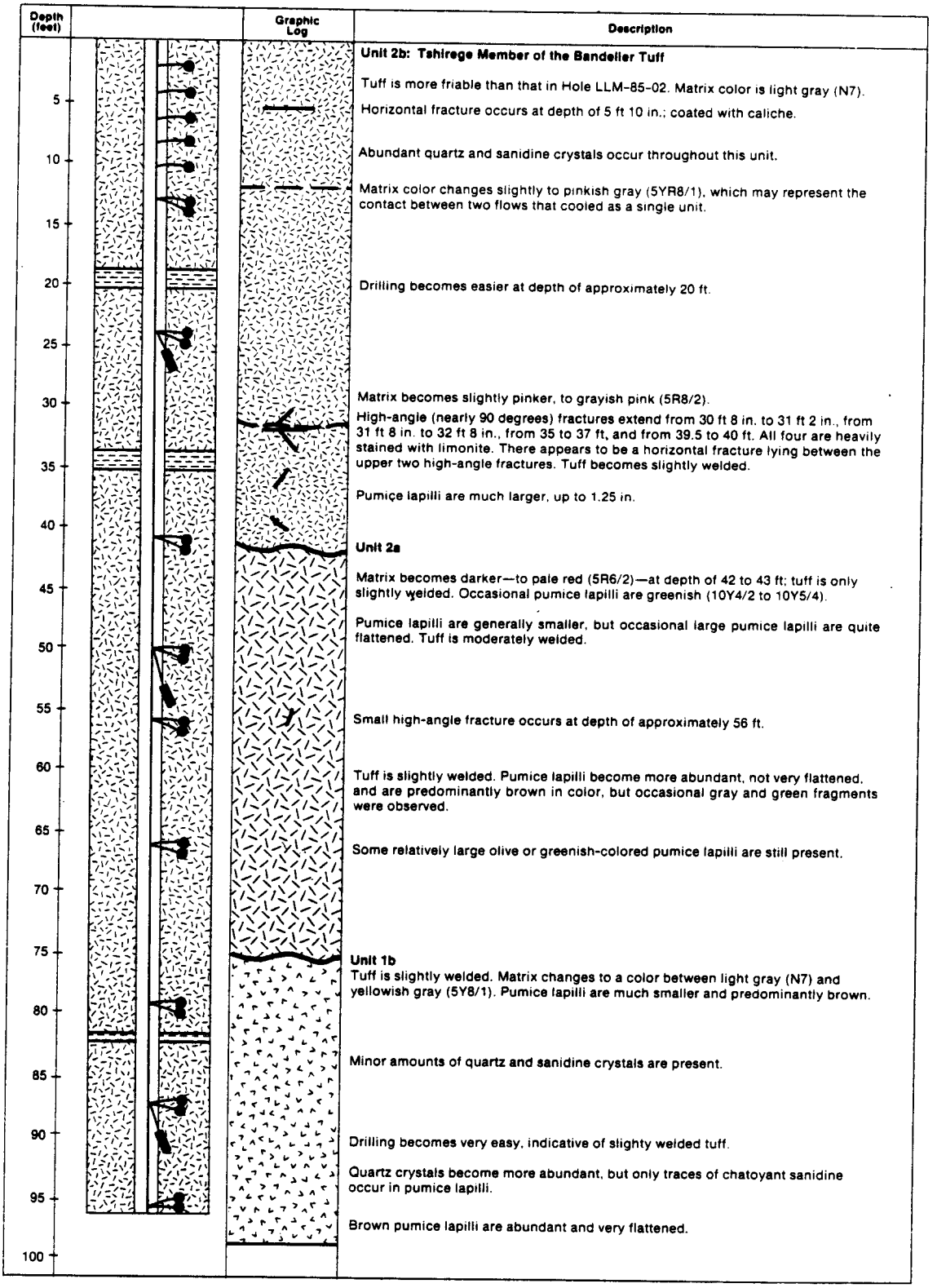

Figure A-4. Installation of Thermocouple Psychrometers and Pressure Transducers in Hole LLP-85-03 (Note: The psychrometers in the upper 10 ft are located in a shallow boring adjacent to the main hole.)

Depth (feet)	Sample Interval	Sample Number	Graphic Log	Description
				Unit 2b: Tshirege Member of the Bandelier Tuff
		MCG-526		Tuff is moderately welded, and matrix color is between light gray (N7) and very light gray (N8). Pumice lapilli, 2 to 10 mm in size, are light gray to medium light gray. Chatoyant sanidine crystals are 1 mm in size. The upper 4 ft are very weathered and contain abundant horizontal fractures with iron stains and root structures.
5				
		MCG-527		
10				Same as above, except rare lithic lapilli up to 40 mm in size are present
		MCG-528		
15		MCG-610**		
		MCG-529		
20				Same as above, except clear quartz and chatoyant blue sanidine crystals, 1 to 2 mm in size, are abundant.
		MCG-530		
25				
		MCG-531		
30				
		MCG-532		Color changes to grayish pink (5R8/2) at depth of approximately 34 ft. Drilling becomes easier at depth of 33 ft, representing contact with lower flow and/or slightly welded portion of Unit 2b. Pumice lapilli range in size from 2 to 10 mm.
35		MCG-611**		
		MCG-533		
40				**Unit 2a**
		MCG-534		Matrix color still grayish pink (5R8/2); slightly welded tuff. Pumice lapilli are larger (5 to 30 mm), but still predominantly gray. Quartz and sanidine crystals, less than 1 mm in size, are present.
45				Fracture extends from 48 to 48.4 ft.
		MCG-535		
50				Tuff is slightly welded. Pumice lapilli are same size as above (5 to 30 mm), but olive or greenish-colored fragments are present.
		MCG-536		
55				Small fracture, filled to 1/6 in., extends from 54 to 55.5 ft.
		MCG-537		Fracture occurs at depth of approximately 58 ft; very broken-up core.
60				Tuff is gradually becoming moderately welded at depth.
		MCG-538		Matrix color still grayish pink (5R8/2). Pumice lapilli are larger (10 to 40 mm), but still predominantly brown with occasional olive or greenish-colored fragments.
65				
		MCG-539		
70				Tuff is slightly welded, and matrix color lightens to nearly pinkish gray (5YR8/1). Chatoyant sanidine crystals are still present.
		MCG-540		
75		MCG-612**		**Unit 1b**
		MCG-541		Tuff is slightly welded, and matrix color becomes lighter, between pinkish gray (5YR8/1) and yellowish gray (5Y8/1). Abundant quartz, but chatoyant sanidine was not observed. Pumice lapilli are brown and much more abundant than in Unit 2b.
80				
		MCG-542		
85				
		MCG-543		
90				Lithic lapilli, up to 2 mm in size, are present in small amounts. Pumice lapilli are brown, but slightly larger (20 to 40 mm) than those in upper intervals. Tuff is slightly welded.
		MCG-544		
95				
		MCG-545		Lithic lapilli are abundant, but still small (less than 2 mm).
100				Tuff is moderately welded, and matrix color is becoming more pinkish (5R8/2) which may represent contact with the more densely welded portion of Unit 1b. Rock or lithic fragments are becoming much larger. Pumice lapilli are very large. Quartz crystals, dark- to honey-colored, are abundant.
		MCG-546		
105				
		MCG-547		
110				Scattered, large lithic lapilli. Large pumice lapilli are very flattened.
		MCG-548		Matrix color changes to pale red (10R6/2).
115				
		MCG-549		
120				Matrix color changes to pinkish orange (nearly 10R7/6); slightly welded lower portion of Unit 1b.
		MCG-613**		
		MCG-550		
125				

Figure A-5. Lithologic Log of Hole LLM-85-05

Depth (feet)	Sample Interval	Sample Number	Graphic Log	Description
				Unit 2b: Tshirege Member of the Bandelier Tuff
		MCG-551		One foot of medium-brown soil merges into light-gray (N7) ash-flow tuff, which is moderately welded. Pumice lapilli, 2 to 10 mm in size, are medium light gray. Sanidine and quartz are abundant. Iron-stained fracture extends from 5 ft 10 in. to 6 ft 1 in., and caliche-filled fracture from 6 ft 4 in. to 6 ft 7 in.
5				
		MCG-552		Caliche-filled fracture extends from 9 to 9.5 ft.
10				Matrix color grades to very light gray (N8). Light-gray pumice lapilli, 2 to 10 mm in size, are present from ground surface to approximately 8 ft.
		MCG-553		
15				
		MCG-554		
20				Matrix color is between very light gray (N8) and light brownish gray (5YR6/1).
		MCG-555		
25				
		MCG-556		Near-vertical fracture extends from 29 to 29.5 ft; tuff still appears moderately welded.
30		MCG-634*, MCG-614**		
		MCG-557		
35				**Unit 2a**
		MCG-558		Tuff appears fissile, but still moderately welded; drilling is slightly easier. No obvious color change. Pumice lapilli are brown and gray, and larger (10 to 30 mm) than those in the upper unit.
40				Near-vertical fractures extend from 41 ft 4 in. to 42 ft 2 in. and from 43 to 43.5 ft; the former appears to be open.
		MCG-559		
45				Matrix color is very light gray (N8).
		MCG-560		
50		MCG-635*, MCG-615**		Tuff is nonwelded, and pumice lapilli are larger.
		MCG-561		
55				
		MCG-562		
60				**Unit 1b** Tuff is only slightly welded. Matrix becomes almost white (N9). Pumice lapilli are predominantly brown from 59 to 69 ft.
		MCG-563		
65				Matrix darkens to light gray (N7).
		MCG-564		Matrix color changes to grayish pink (5R8/2) at depth of approximately 69 ft.
70				Small lithic lapilli, 1 to 2 mm in size, are present in small amounts.
		MCG-565		
75				
		MCG-566		Lithic lapilli are more abundant; brown pumice lapilli are larger.
80				
		MCG-567		Matrix color becomes pinker, to pale red (5R6/2), and tuff is gradually becoming more welded. Lithic lapilli increase in size. Bipyramidal quartz crystals, gold to tan colored, are abundant.
85				
		MCG-568		Transition to moderately welded zone of Unit 1b. Matrix color changes to grayish orange pink (5YR7/2). Bipyramidal quartz crystals are still abundant and increasing in size (up to 4 mm).
90				
		MCG-569		
95				
		MCG-570		
100		MCG-636*, MCG-616**		Tuff is moderately welded, and color changes to moderate orange pink (5YR8/4).
		MCG-571		Same as above, except tuff is only slightly welded, representing the base of Unit 1b.
105				**Unit 1a**
		MCG-572		Completely nonwelded ash, moderate orange pink (5YR8/4), with scattered lumps of tan pumice lapilli.
110				
		MCG-637*, MCG-573		
115		MCG-617**		Completely nonwelded ash, with large (some greater than 2 in.) pumice and rock lapilli.
		MCG-574		
120				
		MCG-575		
125				

Figure A-6. Lithologic Log of Hole LGM-85-06

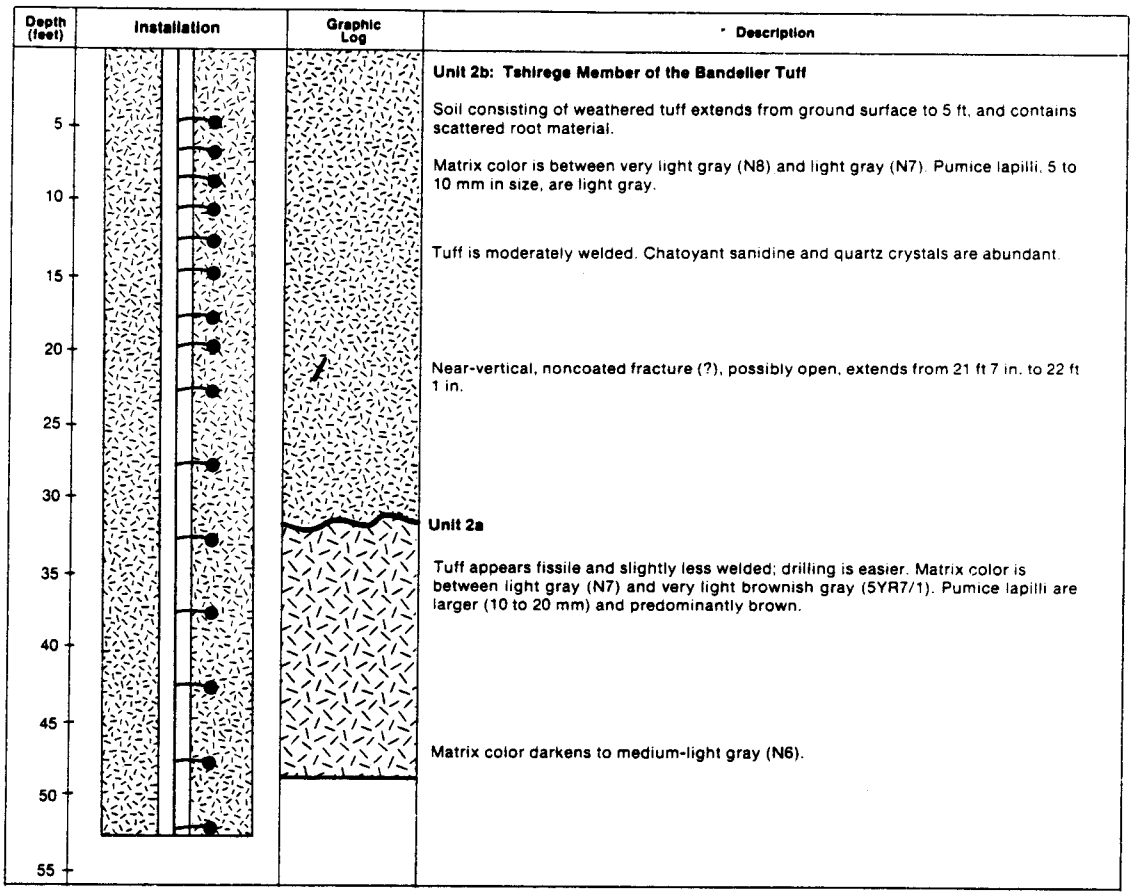

Figure A-7. Installation of Thermocouple Psychrometers in Hole LGP-85-07

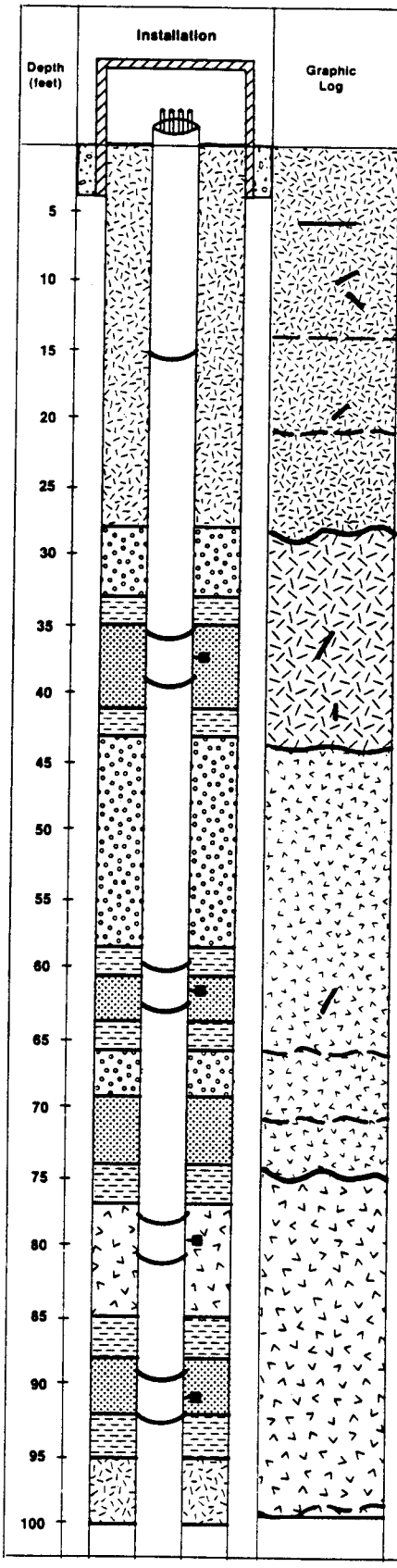

Description

Unit 2b: Tshirege Member of the Bandelier Tuff

The upper 5 ft are weathered and loose, and predominantly brown in color.

Possible horizontal fracture occurs at depth of 6 ft 10 in.; very slight discoloration to brown on the surface. Tuff is moderately welded.

Matrix color is very light gray (N8).

Fractures extend from 9 ft 6 in. to 9 ft 9 in. and from 10 ft 1 in. to 10 ft 4 in.; both appear to dip approximately 45 degrees and have slight brown coloring on the surfaces.
Concentrations of larger pumice lapilli may represent the boundary between separate flows within this unit.
Matrix color changes to pinkish gray (5YR8/1).
Tuff appears slightly fissile, but is still moderately welded.
Possible noncoated fracture extends from 19 ft to 19 ft 3 in.

Slightly less welded than above.

Matrix color becomes very slightly pinkish, with very small, brown pumice lapilli, probably indicating a transitional contact with Unit 2a.

Unit 2a
Matrix color is definitely pinkish. Sanidine and quartz are present. Approximately 75% of the pumice lapilli are brown, 25% green (olive).

Matrix color changes to light brownish gray (5YR6/1).
Tuff is moderately welded.
Near-vertical, iron-stained fracture extends from 35 ft 4 in. to 36 ft 4 in.

Near-vertical, noncoated fracture extends from 40 ft to 40 ft 8 in.
Slightly welded tuff.

Unit 1b
Matrix color changing to very light gray (N8) to almost white (N9) at depth of 43 to 44 ft; tuff is only slightly welded. Pumice lapilli are predominantly brown; occasional large pumice fragments appear flattened. Sanidine crystals are abundant.

Matrix color changes to white (N9) at depth of 52 ft.

Pumice lapilli are still brown, but becoming larger in the interval 59 to 63 ft. Lithic lapilli are abundant, up to ½ in. in size at depth of 59 ft. Quartz crystals are honey-colored. Slightly welded tuff is grading to moderately welded unit below.
Near-vertical fracture, slightly iron-stained, extends from 61 to 62 ft.

Drilling becomes more difficult, and tuff is moderately welded. Lithic lapilli are larger. This more welded material probably represents the central portion of the Unit 1b cooling zone. Fresh glass shards were observed.
Matrix color grades from pinkish gray (5YR8/1) to very pale orange (10YR8/2) to light brown (5YR6/4).
Tuff is slightly welded, and looks like the rest of Unit 1b except the color is becoming very orange. Lithic lapilli are still very abundant, and quartz crystals are still honey-colored.

Unit 1a
Completely nonwelded, orange-colored ash with large pumice lapilli. The latter are distinctively light brown or cream-colored. Only scattered lithic lapilli were observed, one 1 in. in size and another 1/16 in. in size.

Matrix color is moderate orange pink (5YR8/4).

Same as above, except dampness observed at depth of approximately 88 ft.

Same as above, except matrix color changes to light tan [approximately 5Y8/1 (yellowish gray)] and green pumice lapilli are scattered throughout.

Figure A-8. Installation of Pore-Gas Sampling Ports in Hole LGC-85-09

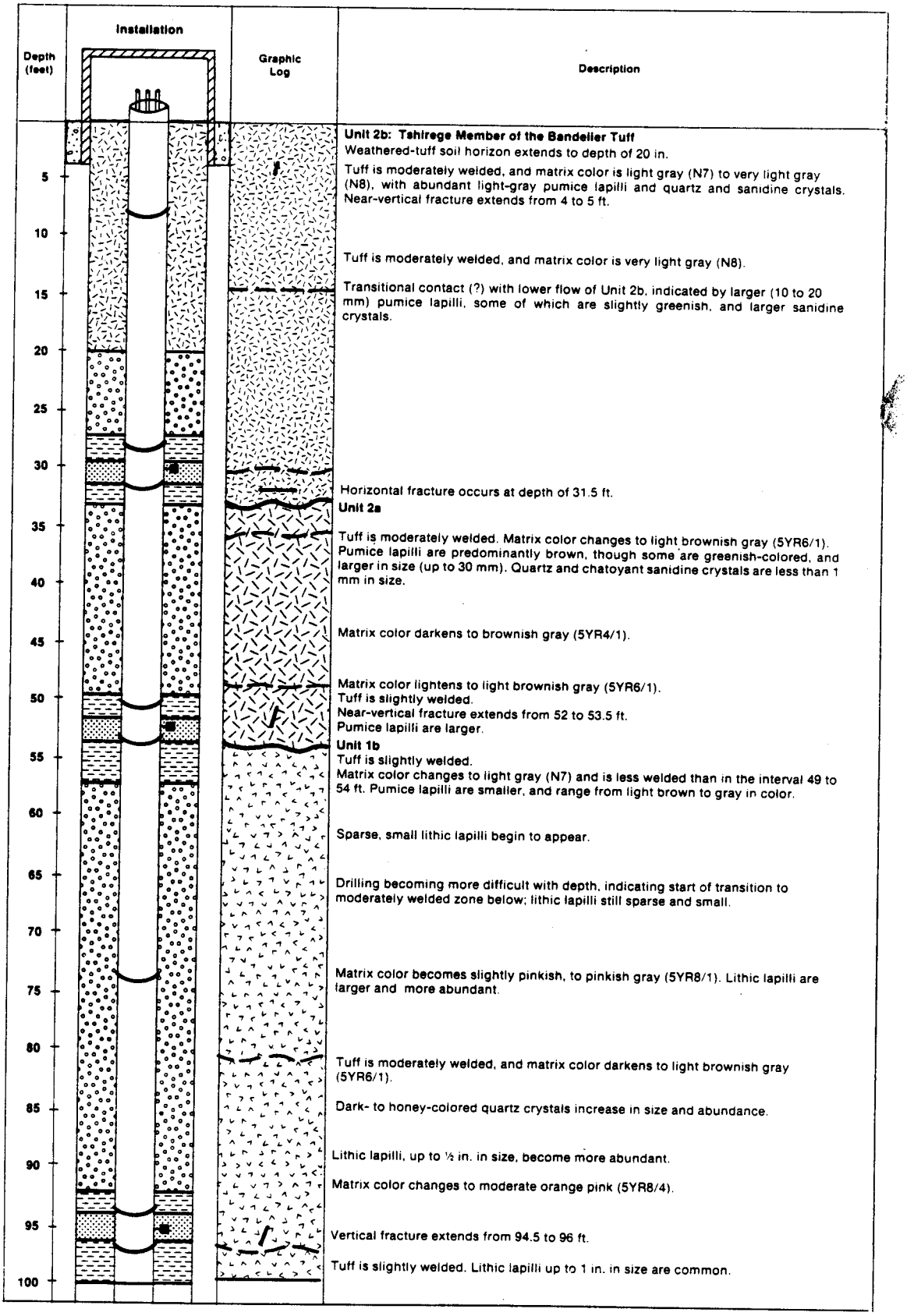

Figure A-9. Installation of Pore-Gas Sampling Ports in Hole LGC-85-10

Depth (feet)	Sample Interval	Sample Number	Graphic Log	Description
		MCG-618**		**Unit 2b: Tshirege Member of the Bandelier Tuff** Weathered-tuff soil horizon extends to depth of 3 ft. Moderately welded tuff.
		MCG-576		
5		MCG-638*		Matrix color ranges from very light gray (N8) to very light brownish gray (5YR7/1), with light-gray pumice lapilli. Near-vertical fractures extend from 5 to 6 ft and from 6.5 to 7.5 ft.
		MCG-577		
10				Quartz and chatoyant blue sanidine crystals are present.
		MCG-578		
15				Iron-stained, caliche-filled fractures, dipping approximately 45 degrees, occur at depths of 15.5 and 17.5 ft.
		MCG-579		
20				Iron-stained fracture, dipping approximately 45 degrees, occurs at depth of 20 ft.
		MCG-580		Pumice lapilli, 3 to 10 mm in size, are still light gray.
25				
		MCG-581		
30		MCG-619**		
		MCG-639*		
		MCG-582		
35				
		MCG-583		**Unit 2a**
40				Tuff is moderately welded, and matrix color is very light gray (N8) with a slight pinkish cast [nearly pinkish gray (5YR8/1)]. Pumice lapilli are larger and predominantly brown, though some are greenish-colored. Quartz and chatoyant sanidine crystals are present.
		MCG-584		
45				
		MCG-585		
50				
		MCG-586		
55				Tuff is only slightly welded. Pumice lapilli—some brown, some green—are very large. Sparse, small lithic lapilli are present.
		MCG-587		
60				**Unit 1b**
		MCG-588		Tuff is slightly welded, and matrix ranges in color from very light gray (N8) to almost white (N9).
65				Fracture (?), dipping approximately 45 degrees, occurs at depth of 66 ft.
		MCG-589		
70				Lithic lapilli begin to appear, becoming larger and more abundant with depth.
		MCG-590		
75				Fractures, dipping approximately 45 degrees, occur at depths of 75.5 and 76.5 ft. Tuff is slightly more welded than above, and matrix color is pinkish gray (5YR8/1).
		MCG-591		
80				
		MCG-592		Tuff is moderately welded.
85				
		MCG-593		
90				Quartz crystals are abundant and distinctively honey- or tan-colored.
		MCG-594		Matrix color changes to moderate orange pink (5YR8/4) at depth of 93 ft. Lithic lapilli becoming very large, up to 3 in. in size. Pumice lapilli are still small and brown. Quartz crystals are same as above.
95		MCG-620**		
		MCG-640*		Pumice lapilli increase in size, and some are gold- to tan-colored (similar to those in Unit 1a).
		MCG-595		
100				Tuff is only slightly welded. Lithic lapilli are less abundant, but range up to 3 in. in size. Quartz crystals are same as above.
		MCG-596		**Unit 1a**
105				Completely nonwelded tuff, moderate orange pink (5YR8/4), with scattered, large, golden-tan, pumice lapilli and lithic lapilli.
		MCG-597		
110				
		MCG-598		
115		MCG-621**		
		MCG-641*		
		MCG-599		Same as above.
120				
		MCG-600		
125				

Figure A-10. Lithologic Log of Hole LGM-85-11

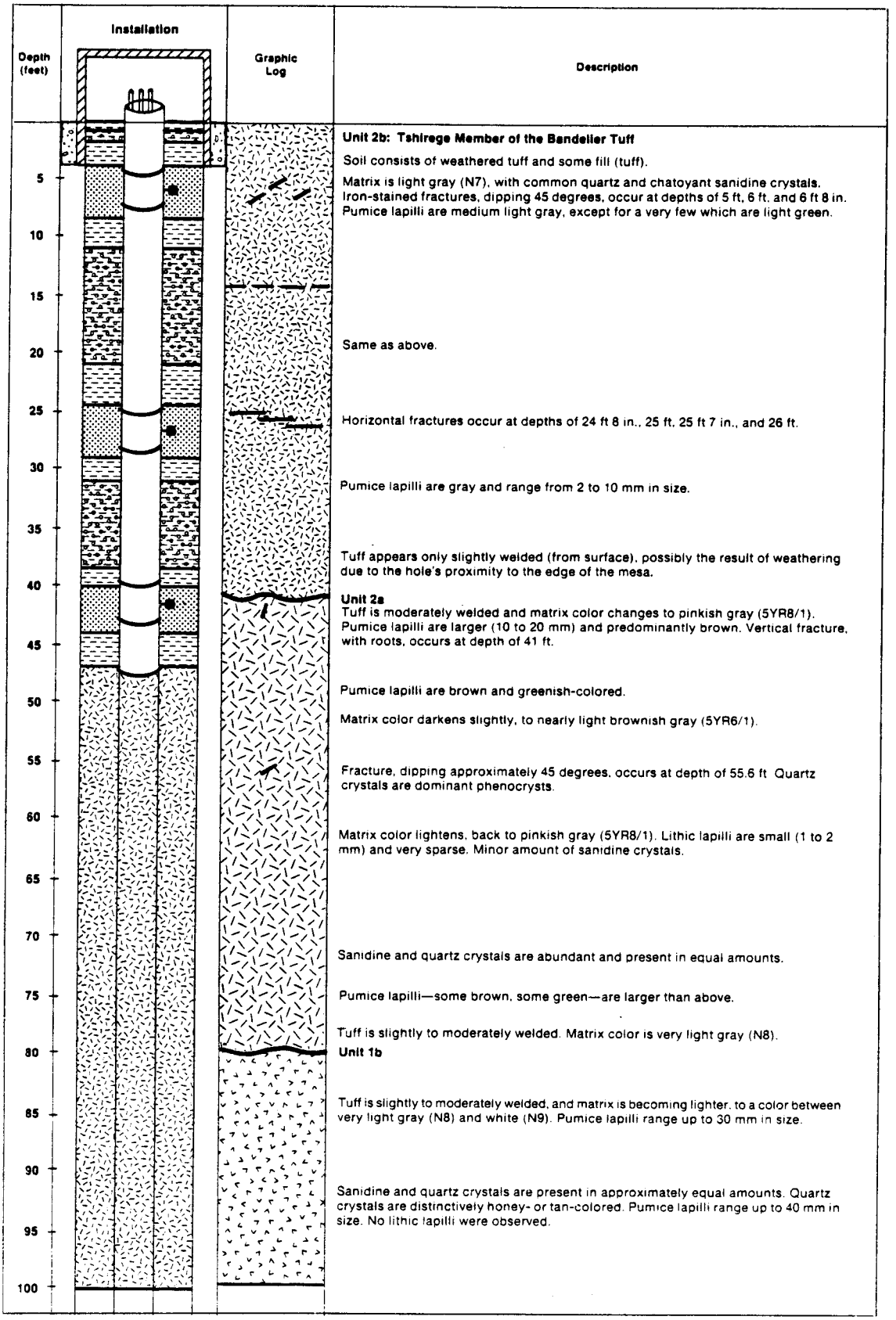

Figure A-11. Installation of Pore-Gas Sampling Ports in Hole LLC-85-12

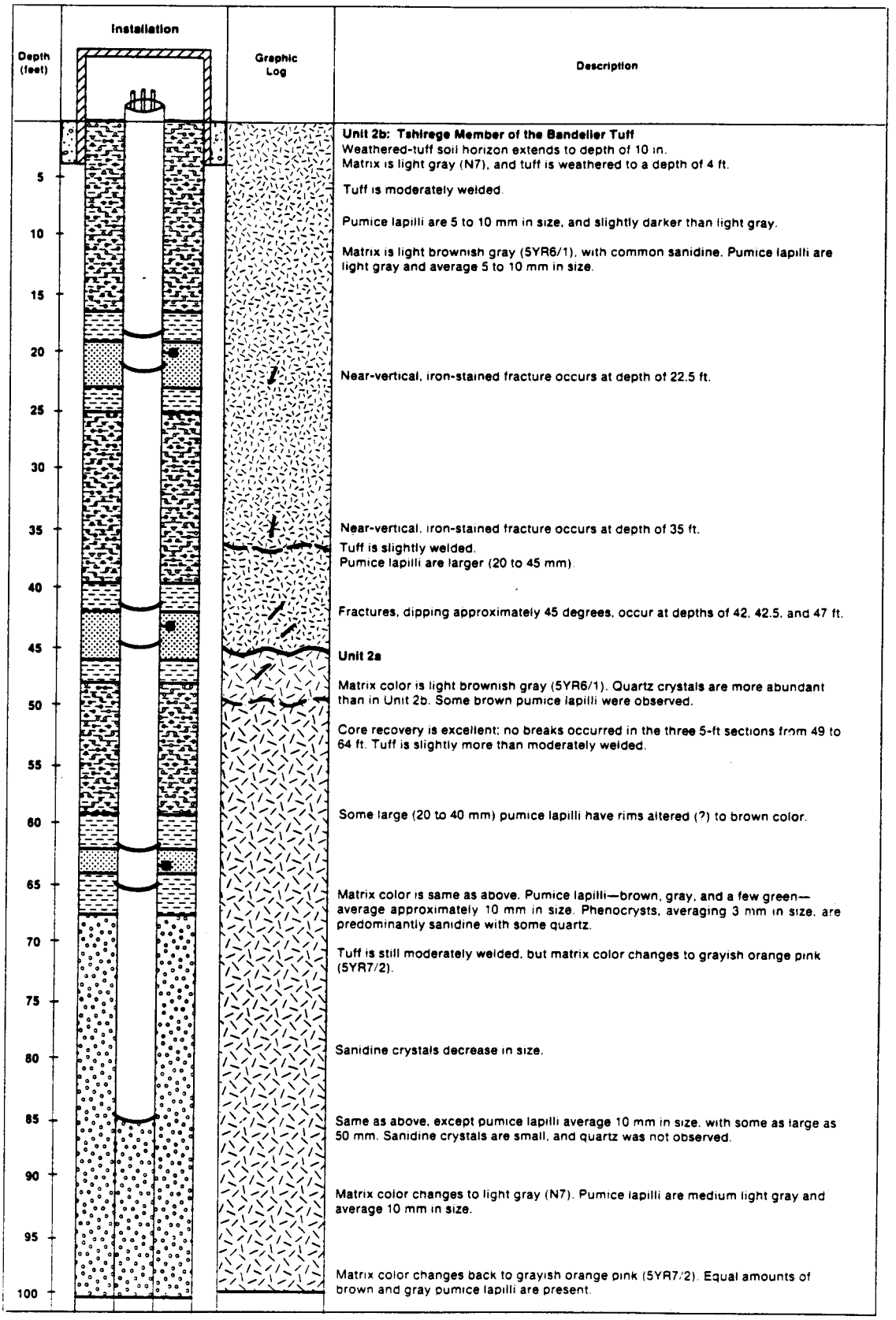

Figure A-12. Installation of Pore-Gas Sampling Ports in Hole LLC-85-13

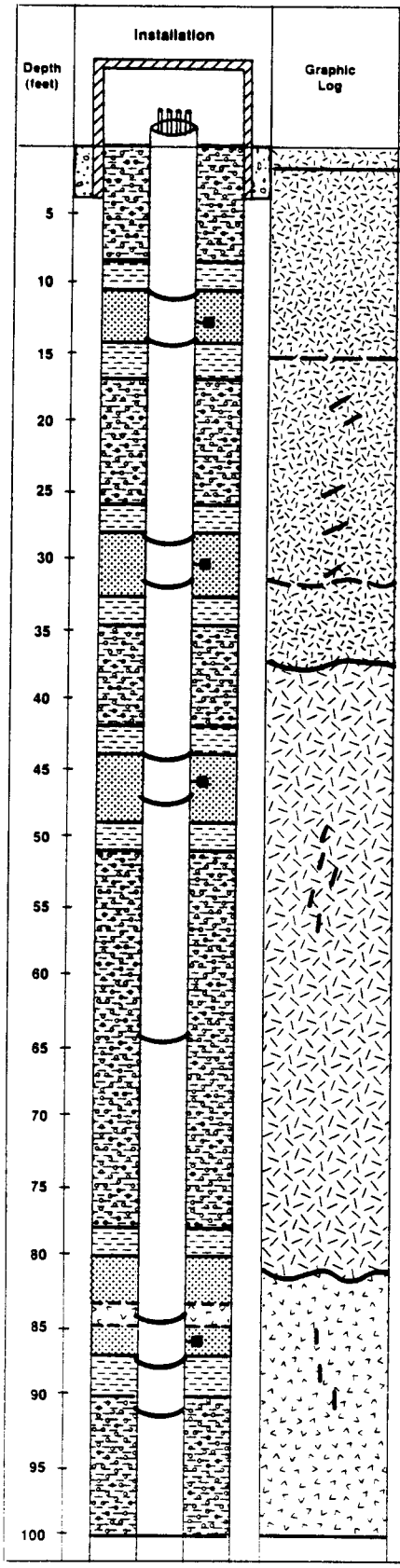

Description

Unit 2b: Tshirege Member of the Bandelier Tuff

Tuff is moderately welded, and matrix color is light brownish gray (5YR6/1). Horizontal fracture occurs at depth of 1.5 ft. Pumice lapilli are small and gray. Quartz and sanidine crystals are small and clear.

Matrix color changes to very light gray (N8), which probably represents the contact with the lower flow of Unit 2b.

Fractures, dipping approximately 45 degrees, occur at depths of 18 ft 2 in. and 19 ft 3 in.

Lithic lapilli are sparse and range up to 30 mm in size.

Matrix color changes back to light brownish gray (5YR6/1) at depth of 26 ft. Fractures, dipping approximately 45 degrees, occur at depths of 25 and 28 ft.

Pumice lapilli—some brown, some gray—range in size from 10 to 40 mm.

Drilling becomes much easier at depth of 32 ft, representing the contact with the slightly welded base of Unit 2b. Matrix color changes to grayish orange pink (5YR7/2). Fracture, dipping approximately 45 degrees, occurs at depth of 31 ft.

Unit 2a

Tuff is slightly welded, and matrix color is light brownish gray (5YR6/1). Pumice lapilli—some brown, some green—range in size from 10 to 30 mm.

Tuff is slightly welded, and matrix color changes to grayish pink (5R8/2). Lithic lapilli are sparse and average 5 to 10 mm in size, with some up to 40 mm. Pumice lapilli are same as above.

Near-vertical fractures occur at depths of 49, 52, 53, 54, and 57 ft. This may be one fracture, observed entering and exiting the core.

Tuff is moderately welded, and matrix changes to a color between grayish pink (5R8/2) and grayish orange pink (5YR7/2). Pumice lapilli are predominantly brown, and average 10 to 40 mm in size. Lithic lapilli are still sparse, but larger (20 to 40 mm).

Matrix color changes to grayish orange pink (5YR7/2); otherwise same as above except fewer lithic lapilli.

Same as above, except lithic lapilli are more abundant.

Same as above, except no lithic lapilli were observed.
Tuff is slightly welded. Matrix color lightens to grayish pink (5R8/2). Pumice lapilli—brown and green—are larger (20 to 50 mm). Sanidine and quartz crystals are very small and clear.

Unit 1b

Tuff is slightly welded. Matrix color changes to light gray (N7). Brown pumice lapilli are smaller (10 to 25 mm). Lithic lapilli and quartz crystals are common, the latter ranging up to 3 mm in size. Near-vertical fractures occur at depths of 85, 88, and 89 ft.

Same as above, except quartz crystals are larger (4 mm) and more abundant.

Figure A-13. Installation of Pore-Gas Sampling Ports in Hole LLC-85-14

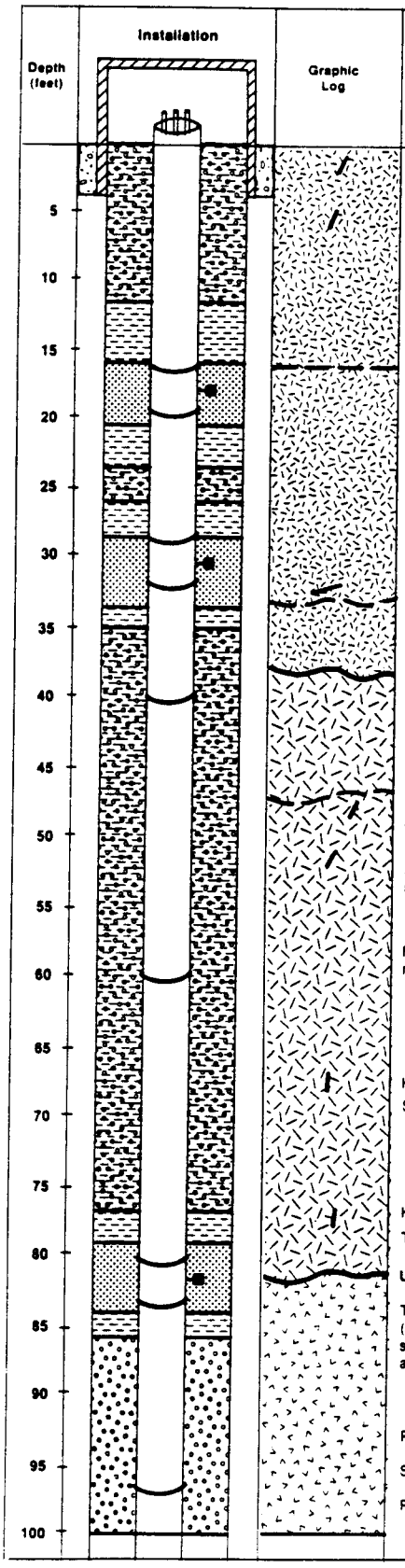

Unit 2b: Tshirege Member of the Bandelier Tuff

Soil layer extends to depth of approximately 4 in. Tuff is moderately welded, and matrix color is very light gray (N8) to grayish pink (5R8/2). Pumice lapilli are small and light gray. Clear quartz and sanidine crystals, less than 1 mm in size, are common. High-angle, iron-stained fractures, with caliche infill, occur at depths of 1 and 5 ft.

Same as above, except matrix color changes to very light gray (N8).

Same as above, except matrix color changes to light brownish gray (5YR6/1).

Same as above, except pumice lapilli are larger (up to 10 mm).

Tuff is moderately welded, and matrix color grades to grayish pink (5R8/2). Pumice lapilli—most gray, but some brown—range in size from 10 to 40 mm.

Low-angle fracture occurs at depth of 31 ft 10 in.
Same as above, except tuff is slightly welded.

Unit 2a

Tuff is slightly welded, and matrix color still grayish pink (5R8/2). Pumice lapilli—most brown, but some green (olive)—range in size from approximately 10 to 50 mm.

High-angle fracture occurs at depth of 47.5 ft.

Tuff is moderately welded, and matrix color grades to pale red (5R6/2).
Same as above, except matrix color changes to grayish pink (5R8/2).
High-angle fracture occurs at depth of 51 ft 6 in. Pumice lapilli become larger, some up to 60 mm.

Matrix color grades back to grayish pink (5R6/2). Pumice lapilli become smaller, ranging in size from 5 to 15 mm.

High-angle fracture occurs at depth of 67 ft.
Same as above, except sparse lithic lapilli are present.

High-angle fracture occurs at depth of 77 ft.
Tuff is slightly to moderately welded.

Unit 1b

Tuff is slightly to moderately welded. Matrix color changes to pinkish gray (5YR8/1). Pumice lapilli are predominantly brown and range from 10 to 20 mm in size. Quartz crystals, up to 4 mm in size, are abundant. Lithic lapilli are more abundant than above, ranging in size from 5 to 15 mm.

Pumice lapilli increase in size to 30 mm.

Same as above, except matrix color changes to very light gray (N8).

Pumice lapilli increase in size to 50 mm.

Figure A-14. Installation of Pore-Gas Sampling Ports in Hole LLC-85-15

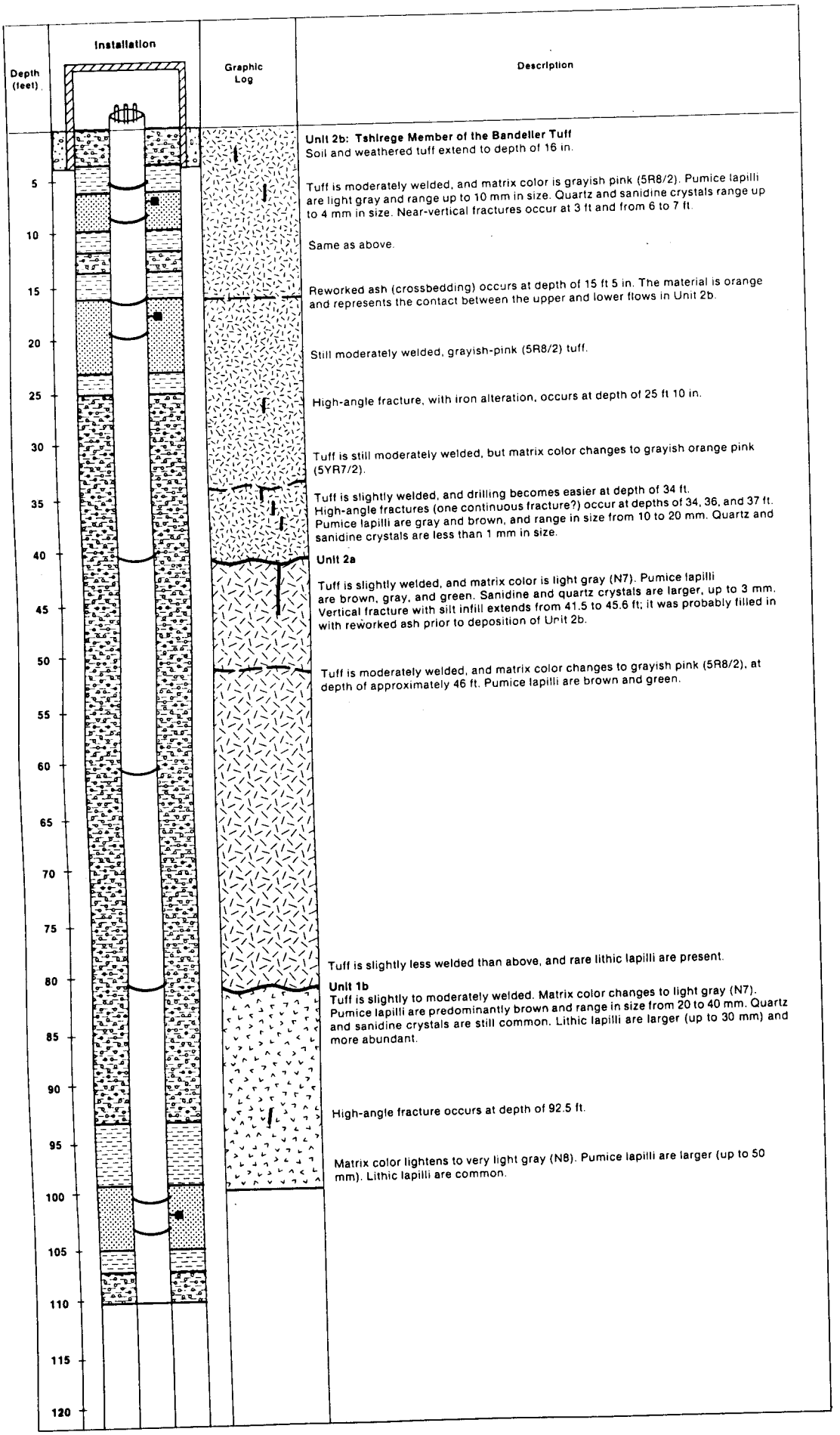

Figure A-15. Installation of Pore-Gas Sampling Ports in Hole LLC-85-16

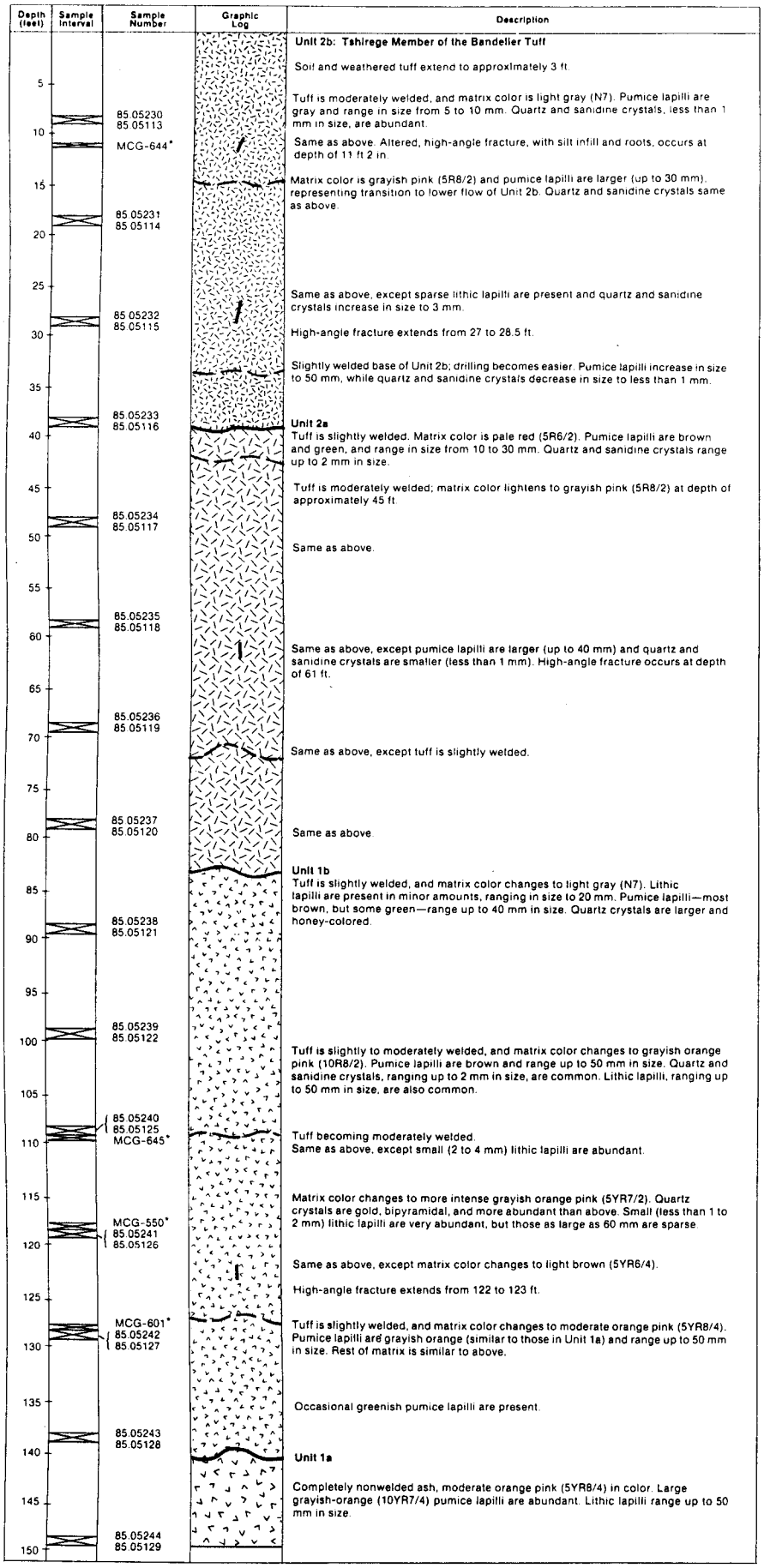

Figure A-16. Lithologic Log of Hole LLC-85-17

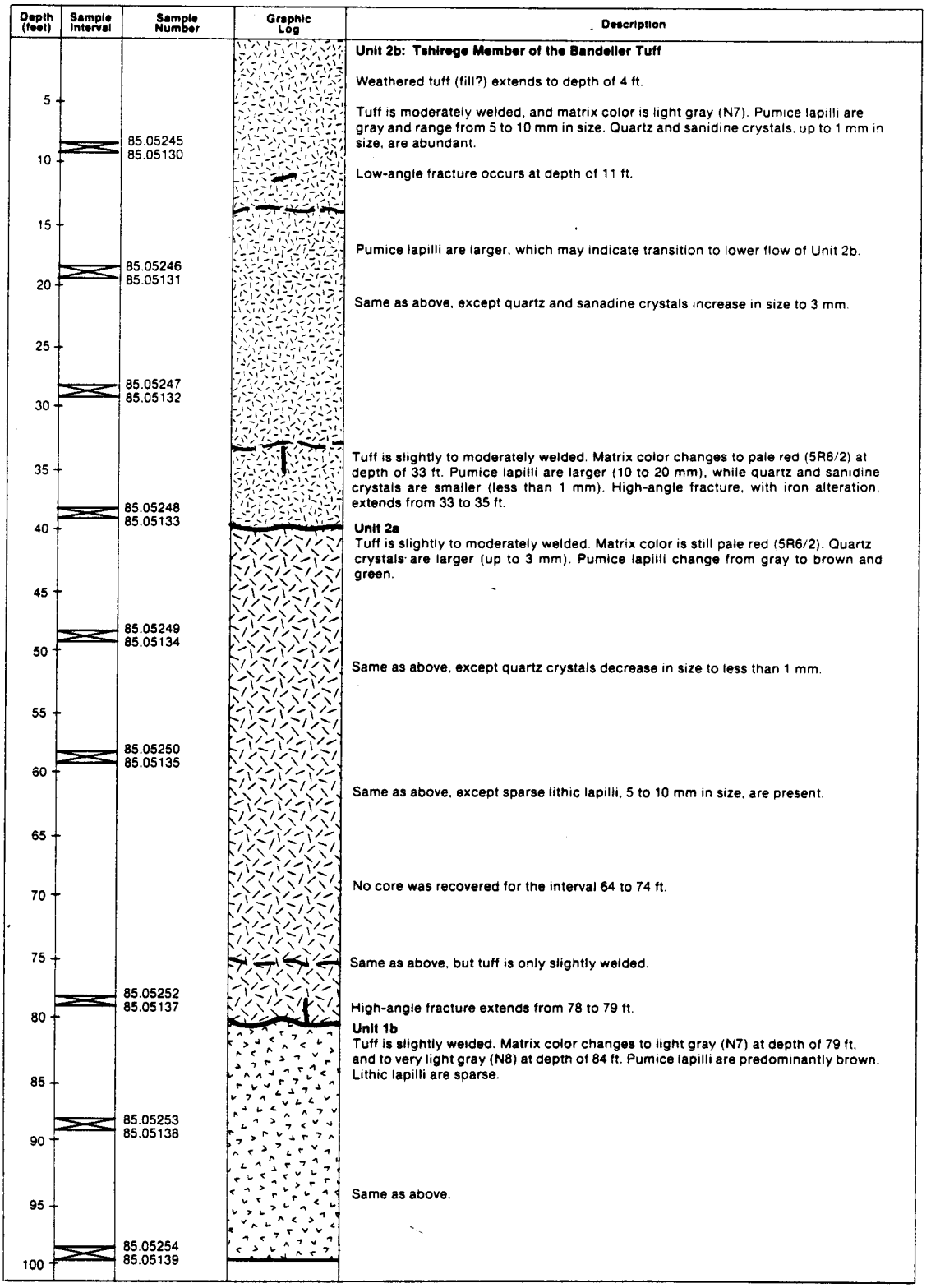

Figure A-17. Lithologic Log of Hole LLC-85-18

Depth (feet)	Sample Interval	Sample Number	Rock Quality Designation/ Recovery (%)	Installation	Graphic Log	Description
						Unit 2b: Tshirege Member of the Bandelier Tuff Soil horizon extends to about 10 in. in depth. Matrix is light gray (N7). Pumice lapilli are light gray to gray and have iron-stained alteration rims. Tuff is moderately welded
5			?/0			
10		R5-1	90/100			Near horizontal iron-stained fracture at depth of 10 ft. Abundant phenocrysts of quartz (3-5 mm) and sanidine (1-3 mm).
15		R5-2	80/90			Matrix color changes to grayish orange pink (5YR 7/2). Scattered lithic lapilli up to 10 mm are present.
20		R5-3	0/100			Color as above; tuff is slightly welded.
25			100/100			Pumice lapilli slightly darker than above (5YR 6/1) and are occasionally flattened. Scattered lithic lapilli up to 30 mm are present. Tuff becomes moderately welded. Near-vertical fractures with iron-staining are present at depths of 23 and 25 ft.
30		R5-4	30/100			Tuff becoming slightly welded. Small, 1- to 2-mm spots of rust colloration are present.
35			0/100			**Unit 2a**
40		R5-5	0/100			Tuff appears fissile and is nearly non-welded. Matrix color is still grayish orange pink (5YR 7/2). Tuff still contains abundant spots of local iron-staining.
45			0/100			Tuff is slightly welded. Pumice lapilli appear slightly larger than above, and some are greenish-gray in color.
50		R5-6	0/100			Vertical fracture with only minor iron-staining from a depth of 50 to 53 ft.
55			14/100			Tuff is more coherent than above, but still only slightly welded. Scattered pumice lapilli are up to 30 mm in size but most average around 3-4 mm.
60		R5-7	0/100			As above; tuff is slightly welded.
65			0/100			
70		R5-8	5/90			Lithic lapilli around 2 mm in size begin to appear. Pumice lapilli are mostly gray and display alteration rinds of rust-color.
75			5/100			
80		R5-9	60/100			Tuff becomes moderately welded. Occasional lithic fragments up to 30 mm. Matrix color becoming grayer (5YR 7/1). Iron rust-spots (1 to 2 mm) are still common. Pumice lapilli appear slightly flattened.
85			100/20			
90		R5-10	15/100			Tuff becomes slightly welded. Pumice lapilli average 6 to 8 mm, are not flattened, and are about 70% gray and 30% greenish-colored. Trace of 1- to 2-mm sanidine is present.
95			0/100			Rare lithic lapilli are up to 30 mm in size. Matrix color between pinkish gray and pinkish white (5YR 7/2 to 5YR 8/2).
100		R5-11	20/100			**Unit 1b**
105			13/100			Matrix color is pinkish white (5YR 8/2). Tuff is slightly welded. Brown-colored pumice lapilli predominate. Minor amounts of quartz and sanidine are present.
110		R5-12	0/100			Matrix color is white (5YR 8/1).
115			26/100			Pumice lapilli are dominantly brown in color. Lithic lapilli from less than 1 to 5 mm becoming abundant.
120		R5-13	18/100			Scattered white colored pumice lapilli are present. Quartz phenocrysts (many obviously bipyramidal) are becoming more abundant. Minor sanidine phenocrysts are present; these are not chatoyant, but can be identified on the basis of striated crystal faces.
125			26/100			Golden color of quartz phenocrysts is due to iron staining of the tuff immediately surrounding the quartz.
130		R5-14	20/100			Matrix color darkening slightly to pinkish white (5YR 8/2). Lithic lapilli becoming larger, up to 35 mm, but most fall into size range of 1-5 mm.
135			20/100			
140		R5-15	40/100			Transition to moderately welded portion of Unit 1b.
145			30/100			Matrix color changes to orange (5YR 7/4). Tuff feels damp to the touch immediately upon retrieval.
150		R5-18	84/100			Care must be struck with a hammer to break and is moderately welded. Probable vertical fracture present from 152 to 153 ft.
155			30/100			Tuff becomes slightly welded.
160		R5-19 MCG-653	0/80			**Unit 1a** Tuff is non-welded. Lithic lapilli predominantly from 2-5 mm in size with some up to 30 to 60 mm. Quartz phenocrysts, similar to above units, increase in number. Matrix color as above. Pumice lapilli are a distinctive tan color. Scattered reddish-yellow (5YR 6/6) pumice lapilli.
165			0/80			
170		R5-20	0/100			Matrix color changes to a tannish color (7.5YR 7/4) at 169.5 ft.
175		MCG-652	0/100			Occasional tan pumice lapilli up to 45 mm.
180		R5-21	0/100			
185			0/100			
190		R5-22 MCG-651	0/100			Color changes to pink (5YR 7/3).
195			0/100			Tuff becomes slightly welded at 194 ft.
200		R5-23				

Figure A-18. Lithologic Log of Hole LLC-86-19

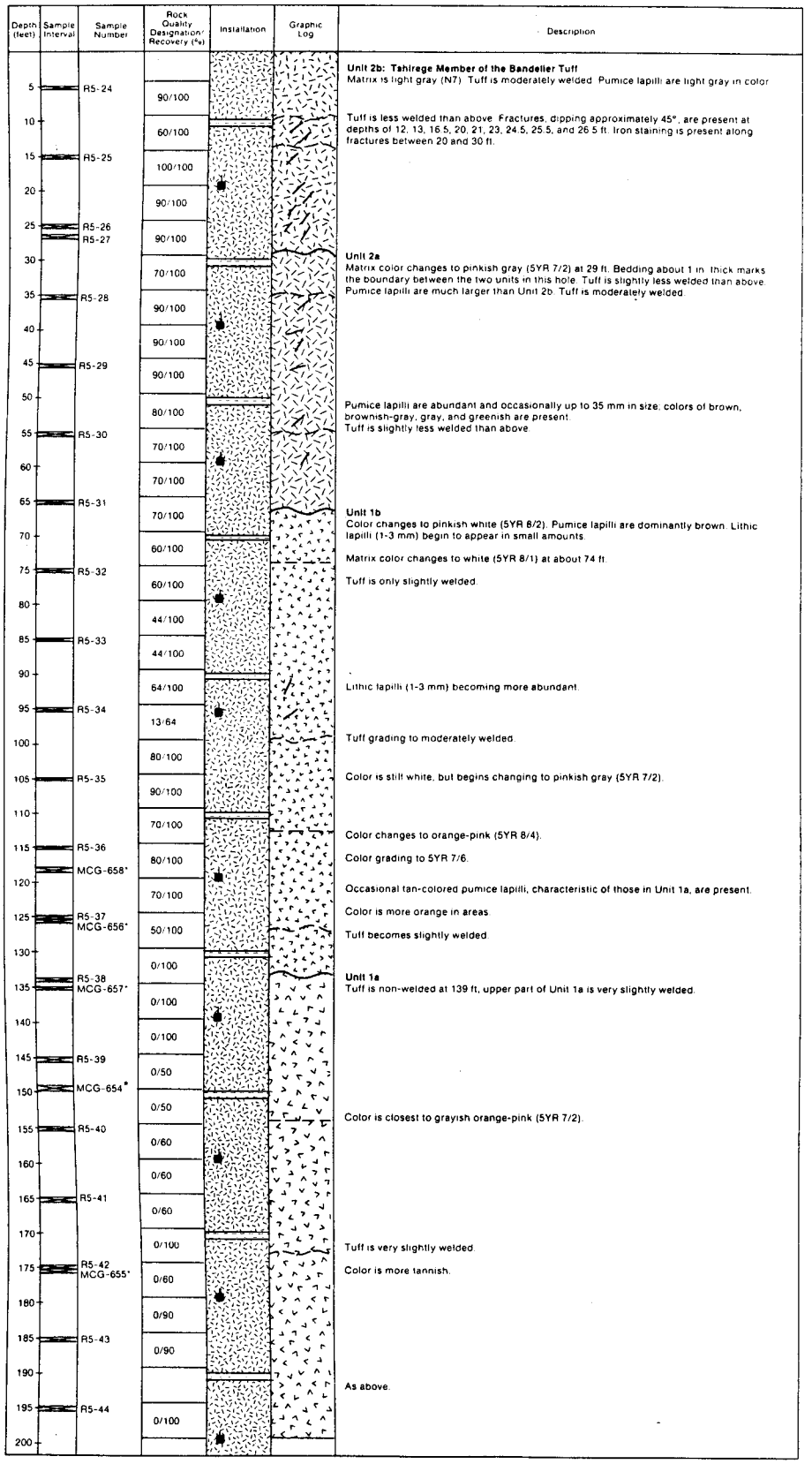

Figure A-19. Lithologic Log of Hole LLC-86-20

Depth (feet)	Sample Interval	Sample Number	Rock Quality Designation/ Recovery (%)	Installation	Graphic Log	Description
						Unit 2b: Tshirege Member of the Bandelier Tuff Matrix color is pinkish white (5YR 8/2). Tuff is moderately welded. High-angle fracture(s) are present at 6 and 8 ft depths, both with caliche infill.
5			90/100			
10			100/100			Color grades to white (5YR 8/1)
15		R5-48	90/100			Pumice lapilli are gray, visibly flattened, and average from 2-6 mm in size
20			72/100			Tuff is slightly less welded than above, but still moderately welded
25		R5-49	70/100			Matrix color as above.
30			90/100			Tuff is moderately welded. Lithic fragments, few up to 10 mm, most 2-4 mm, are present. High-angle fracture(s) are present at 33 and 34 ft depths. Pumice lapilli becoming larger (some greater than 2 in. diameter) and more abundant at a depth of 30 ft.
35		R5-50	90/100			
40			20/100			Tuff grades into slightly welded base. Pumice lapilli are smaller and mostly flattened. **Unit 2a**
45		R5-51	30/100			Reworked tuff zone from 41 to 41.13 ft marks boundary between two units. Matrix color still white, but closer to 7.5YR N 8/1. Pumice lapilli become larger, many up to 20 mm, and are slightly flattened. Slightly welded upper portion of unit grades to moderately welded at approximately 49 ft depth.
50			78/100			
55		R5-52	60/100			
60			60/100			Pumice lapilli dominantly gray in color.
65		R5-53	64/100			
70			48/100			Tuff becomes slightly welded. **Unit 1b**
75		R5-54	50/100			Contact marked by vivid color change to pinkish gray (5YR 7/2) at 73.2 ft. Pumice lapilli are dominantly brown in color. Very small (1 to 2 mm) lithic lapilli are present but sparse. Fracture (45°) with no infill at around 79 ft. Quartz phenocrysts are rare and mostly < 1 mm. Lithic lapilli still sparse but up to 4 mm.
80			42/100			
85		R5-55	20/100			Fracture(s) present at 85, 87, and 88 ft, none with infill, all around 45°.
90			20/100			Matrix color changes gradually to pinkish white (5YR 8/2).
95		R5-56	18/100			Lithic lapilli range in size up to 7 mm. Quartz phenocrysts become more abundant. Matrix color is closer to white (5YR 8/1).
100			18/100			
105		R5-57	18/100			Pumice lapilli are larger. Lithic lapilli are more abundant and range up to 15 mm in size.
110			22/100			Pumice lapilli are smaller and range from 5 to 20 mm. Lithic lapilli are dominantly from 1-3 mm in size; few range up to 10 mm. Matrix color changes to pinkish white (5YR 8/2).
115		R5-58	90/100			Tuff becomes moderately welded at a depth of 114 ft.
120			20/100			Tuff is highly fractured from 120 to 133 ft, but is still moderately welded. Fractures have no infill.
125		R5-59	30/100			
130			50/100			
135		R5-60	40/100			Color changes to pinkish orange (5YR 7/4) at 133 ft. Fractures, dipping at 45°, are present at 134.5 and 138 ft.
140			90/100			Tannish pumice lapilli typical of Unit 1a begin appearing. Fracture(s) present at 140 and 141 ft, dipping around 45°.
145		R5-61	0/100			Tuff becomes slightly welded at around 145 ft.
150			0/100			**Unit 1a** Tuff grades from slightly welded to nonwelded at 154 ft. Lithic lapilli are smaller and less abundant. Abundant tannish pumice lapilli are present.
155		R5-62	0/80			
160			0/90			Matrix color gradually changing to pinkish gray (5YR 7/2) at around 163 ft.
165		R5-63	0/80			Pumice lapilli are abundant and range in size from 5-25 mm. Lithic lapilli are scattered and range in size up to 5 mm.
170			0/80			
175		R5-64	0/60			
180			0/60			As above.
185		R5-65	0/60			
190			0/60			
195		R5-66	0/40			
200						

Figure A-20. Lithologic Log of Hole LLC-86-21

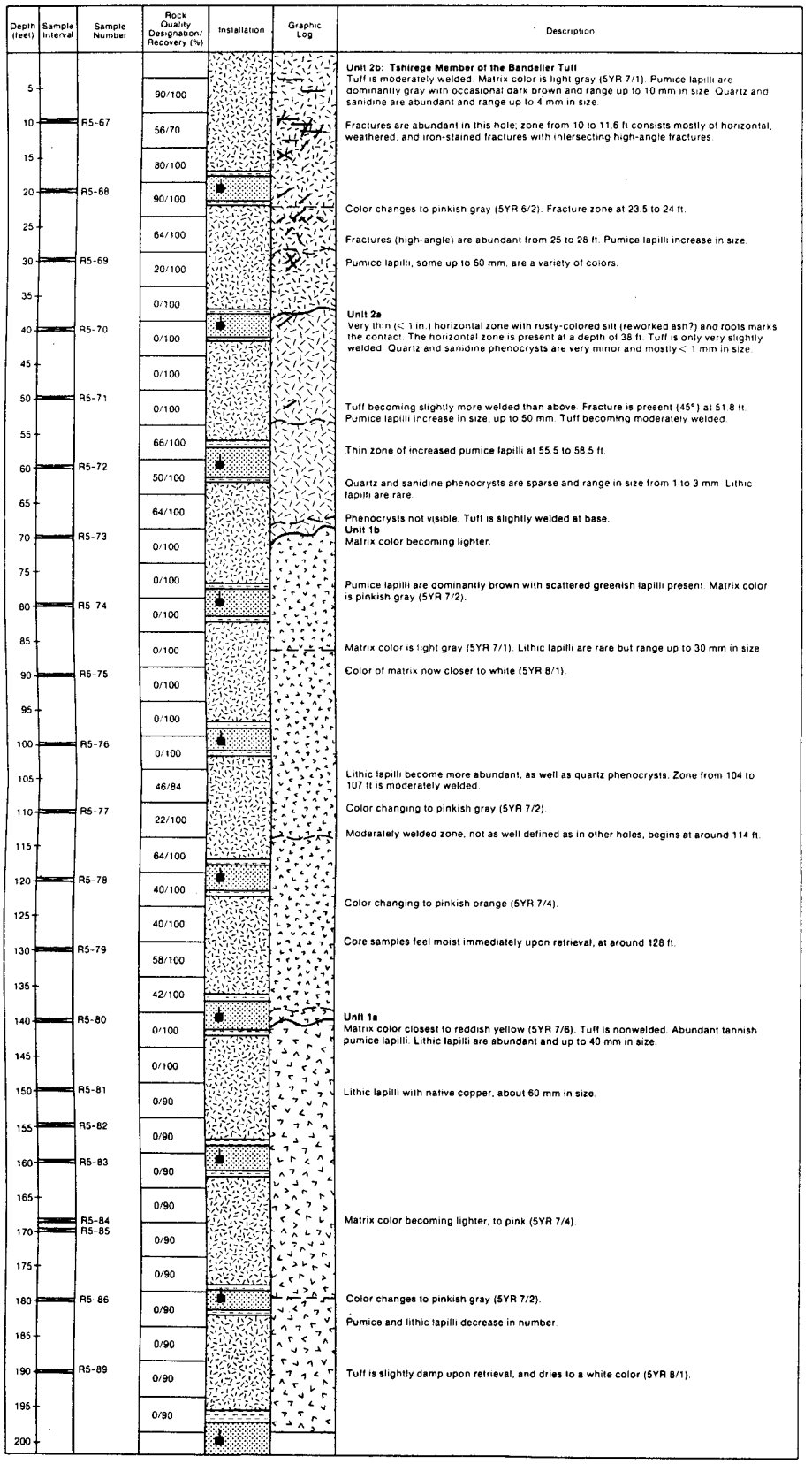

Figure A-21. Lithologic Log of Hole LLC-86-22

Depth (feet)	Sample Interval	Sample Number	Rock Quality Designation/ Recovery (%)	Installation	Graphic Log	Description
						Unit 2b: Tshirege Member of the Bandelier Tuff Tuff is moderately welded, matrix color is light gray (N7). Pumice lapilli is light gray, non-altered. Quartz and sanidine phenocrysts are 2-3 mm in size. 45° fractures at 4, 5, 6½, and 9 ft with iron infill and roots.
5		R5-90	70/100			
10			74/100			Fractures at depths of 13, 16½, and 18½ ft with iron infill and roots. Fractured zone from 18½-25 ft.
15		R5-91	30/100			
20			30/100			
25		R5-92	40/100			60° fractures at depths of 28, 33, and 31½ ft.
30			60/100			Tuff is moderately welded, matrix is light gray (N7). Pumice lapilli is gray and slightly flattened. Quartz phenocrysts to 3 mm in size.
35		R5-93	70/100			
40			46/100			Tuff becoming slightly less welded. **Unit 2a** Tuff is moderately welded, matrix color changes to 5YR 7/3 at 45 ft. Pumice lapilli is red/brown and not altered. Bimodal sizes, 2-3 mm and 10-30 mm. Quartz phenocrysts to 2 mm.
45		R5-94	76/100			
50			80/100			
55		R5-95	65/100			
60			85/100			
65		R5-96	70/100			Tuff is moderately welded, matrix color is pink (5YR 7/3). Pumice lapilli predominantly reddish brown, 2-3 mm in size, rare gray lapilli 5-8 mm.
70			50/100			Tuff is slightly welded. Matrix color changes to 10YR 7/1 (light gray). Pumice lapilli predominantly brown, 5-20 mm in size, a few gray pumice lapilli to 5 mm. Lithic lapilli rare, 2-10 mm.
75		R5-97	70/100			
80			70/100			**Unit 1b**
85			-/0			
90			-/0			
95			-/0			Split barrel accidentally dropped down hole, resulting in a 15 ft interval of lost core, from 83.5-98.5 ft.
100		R5-98	45/100			Tuff moderately welded, matrix color (white) 5YR 8/1. Pumice lapilli increase in size to 5-50 mm, (brown). Quartz phenocrysts are common and 2-4 mm in size. Lithic lapilli more common.
105			75/100			
110		R5-99	50/100			
115		R5-100	35/100			Matrix color more pink (5YR 8/2). Vertical fracture from 111 to 118½ ft with altered clay infill.
120			60/100			Olive pumice lapilli appear. Quartz phenocrysts common, bipyramidal, and golden. Tuff moderately welded, matrix color change to 5YR 8/4 at 127 ft. Lithic lapilli of 2-10 mm in size are common, a few up to 60 mm.
125		R5-101	0/100			
130			52/100			
135		R5-102	60/100			Tannish pumice lapilli, characteristic of Unit 1a, begin to appear. Matrix more orange (5YR 7/4).
140			20/100			Tuff slightly welded. Pumice predominantly tannish in color.
145		R5-103	0/100			**Unit 1a** Tuff nonwelded at 145 ft. Pumice lapilli, tannish 10-40 mm in size. Lithic lapilli rare. Matrix color now typical of Unit 1a (5YR 7/6).
150			0/85			
155		R5-104	0/90			Lithic lapilli increase in number; size up to 50 mm.
160			0/80			
165		R5-105	0/80			
170			0/80			Matrix color less orange to 5YR 7/4. Pumice lapilli increase in size, 40-60 mm. Tuff is non-welded.
175		R5-106	0/90			
180			0/90			Tuff matrix gradually becoming more gray to 5YR 7/3. Lithic lapilli rare, 5-10 mm in size.
185		R5-107	0/90			
190			0/100			Pumice lapilli are dominantly gray with large quartz transparent phenocrysts up to 4 mm. Matrix color 5YR 8/2.
195		R5-108	0/95			Tuff is slightly welded. Moisture apparent. Lithic lapilli 5-10 mm in size.
200						

Figure A-22. Lithologic Log of Hole LLC-86-23

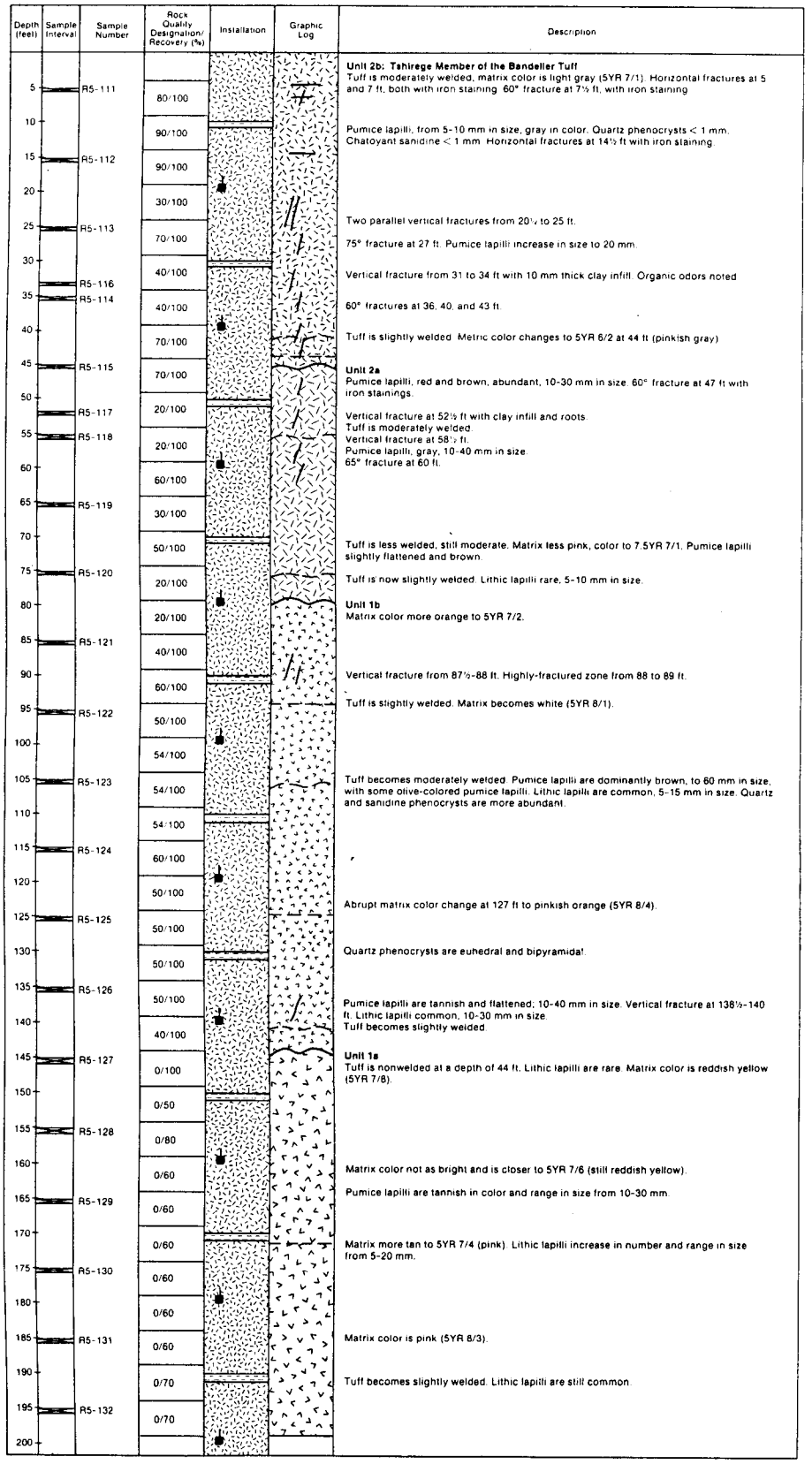

Figure A-23. Lithologic Log of Hole LLC-86-24

Depth (feet)	Sample Interval	Sample Number	Rock Quality Designation Recovery (%)	Graphic Log	Description
					Unit 2b: Tshirege Member of the Bandelier Tuff
5		R5-135	60/100		Moderately welded tuff. Matrix color is light gray (5YR 7/1). Pumice lapilli are gray and range in size from 5-10 mm. Quartz and sanidine phenocrysts are visible but are less than 1 mm in size
10			100/100		Fracture, dipping around 45°, at depth of 10.7 ft. Matrix changes color to pinkish white (5YR 8/2) at 13 ft
15		R5-136	80/100		
20			80/100		Quartz phenocrysts are up to 4 mm in size. High angle fractures are present at depths of 20, 21, 22.5 ft, iron staining is present on surface
25		R5-137	50/100		Fracture zone from 23 to 26 ft, organic vapor odors were detected. Matrix color is gray (5YR 6/1). Quartz and sanidine crystals are abundant
30			60/100		
35		R5-138	80/100		Tuff is still moderately welded. Fractures dipping about 45° are present at depths of 30.5, 33, 34, and 35 ft, organic vapor odors are stronger than above
40			60/100		**Unit 2a** Matrix is pinkish gray (5YR 7/2). Tuff is slightly less welded than above
45		R5-139	60/100		
50			60/100		Fractures were noted at 50 and 55 ft depths, both dipping about 45°
55		R5-140	50/100		Quartz and sanidine are abundant and are up to 2mm in size
60			40/100		Pumice lapilli becoming larger, up to 30 mm.
65		R5-141	64/100		Matrix color is light gray (5YR 7/1). Phenocrysts are not visible. Fractures are present at 65.7 and 66.6 ft. Tuff is slightly welded
70			40/100		**Unit 1b**
75		R5-142	34/100		Matrix color changes to pinkish white (5YR 8/2). Tuff is slightly welded. Lithic lapilli up to 2 mm were noted. Quartz phenocrysts are less than 1 mm in size. Pumice lapilli are mostly brown in color
80			20/100		Matrix color closer to white (5YR 8/1).
85		R5-143	30/100		Lithic lapilli increase in size (up to 30 mm).
90			20/100		Pumice lapilli range in size from 10 to 30 mm
95		R5-144	20/100		
100		R5-145	16/100		Rig shutdown because of strong organic vapors in breathing zone
105		R5-146	20/100		Matrix color as above. Quartz phenocrysts becoming more abundant and range in size up to 3 mm. Pumice lapilli range in size from 10-20 mm. Lithic lapilli more prominent, some up to 20 mm in size. High angle fractures are present at depths of 105, 106, 107, and 112.5 ft
110		R5-147	40/100		
115		R5-148	60/100		Tuff becomes moderately welded
120		R5-149	70/100		
125		R5-150	60/100		Matrix color is pinkish orange (5YR 8/4). Fractures are present at depths of 122, 127, and 127.5 ft, with a dip of approximately 45°
130		R5-151	60/100		Matrix color darkens to reddish yellow (5YR 7/6). Tannish pumice lapilli such as those common in Unit 1a begin to appear at around 130 ft
135		R5-152	30/100		Tuff becomes slightly welded
140		R5-153	0/90		**Unit 1a** Matrix color as above only mottled up to 5YR 7/8 in spots. Tuff is nonwelded
145		R5-154	0/95		
150		R5-155	0/40		
155		R5-156	0/30		Large tannish pumice lapilli are common, few up to <60 mm in size
160		R5-157	0/40		Matrix color changes to pinkish gray (5YR 7/2) at 161 ft
165		R5-158	0/40		
170		R5-159	0/70		
175		R5-160	0/60		Matrix color closer to 5YR 7/3. Tannish pumice lapilli appear slightly flattened
180		R5-161	0/80		Matrix color is pink (5YR 7/2)
185		R5-162	0/100		Tuff becomes slightly welded. Pumice lapilli (the typical tannish color) are extremely flattened
190		R5-163	0/100		High-angle fractures are present at depths of 191 and 192 ft
195		R5-164	0/70		Matrix color changes to pinkish gray
200					

Figure A-24. Lithologic Log of Hole LLC-86-25

Appendix B

PETROGRAPHIC REPORTS

NOTE

Appendix B comprises two sections to reflect work completed during two fiscal years; each section addresses the analysis of petrographic samples from a particular set of drill-hole and outcrop samples. Section B.1 contains results of samples obtained from Holes LLM-85-01, -02, -06, -09, -11, -13, -14, and -17, which were cored as part of the Fiscal Year (FY) 1985 fieldwork. Sample numbers corresponding to this suite of samples are MCG-550, -601, and -626 through -650 (a total of 27 samples). Section B.2 consists of results of samples from Holes LLC-86-19 and LLC-86-20, cored during the FY 1986 field season, and from outcrops on the study site (also obtained during FY 1986). Sample numbers corresponding to these samples are MCG-651 through -661 (a total of 11 samples).

B.1 FISCAL YEAR 1985 FIELDWORK

A total of 27 drill-core samples from the Tshirege Member of the Bandelier Tuff were submitted to the GJPO Petrology Laboratory for petrographic characterization. Nine samples were from Unit 2b, four from Unit 2a, eight from Unit 1b, two from Unit 1a, and four were lithic lapilli from various units. Analytical procedures and results are described below.

The samples as received consisted of sections of 5-cm-diameter drill core. From these samples, portions were removed using a core splitter for polished thin-section preparation. The samples were impregnated with blue-colored epoxy to emphasize the porosity in the thin sections.* Each thin section, with the exception of the nonwelded samples from Unit 1a, was subjected to point-count analysis (300 counts) to determine mineral and component abundance. Tuffaceous rocks were named according to the classification of Cook (1965). As shown in Figure B-1, the rocks from this study plot in the following fields: II (lithic-crystal tuff), III (lithic-vitric), IV (crystal-lithic), V (vitric-lithic), VII (crystal-vitric), and VIII (vitric-crystal).

The optical identifications of major and minor minerals, especially devitrification products, were confirmed using X-ray diffraction (XRD). The clay-sized fractions were separated from fracture coatings in Samples MCG-629, -630, -643, -644, and -648. These clay-sized separates were smeared or sedimented onto glass slides and analyzed in four different states: air-dried, glycolated, heated to 330°C, and heated to 550°C.

The compositional modifiers to tuffaceous rock names are based on the bulk XRD data. These modifiers were assigned according to the classification of Streckeisen (1967).

Petrographic descriptions of the samples are presented on the pages following Figure B-1. They are presented in consecutive order by sample number, although the drill-hole number, depth of the sample, and geologic unit are also identified near the top of the page. The volume percent of each mineral component is given, together with the petrographic description. Phenocrysts and groundmass are further subdivided into individual components, and these subcomponents are followed by a number in parentheses which indicates their volume percentage of the main component. The petrographic descriptions were taken from a report entitled Petrography of the Tshirege Member of the Bandelier Tuff, Mesita del Buey, Los Alamos County, New Mexico (Fukui, 1985).

*There is considerable discrepancy between porosity measured in thin section and that determined by means of helium injection (cf. Section 3.1.2). The significantly lower porosity determined in thin section is due to the fact that most of the thin sections were cut parallel to the core axis (parallel to the direction of flattening), resulting in erroneous extrapolation based on the cross section of the gas tubes rather than on their true shape.

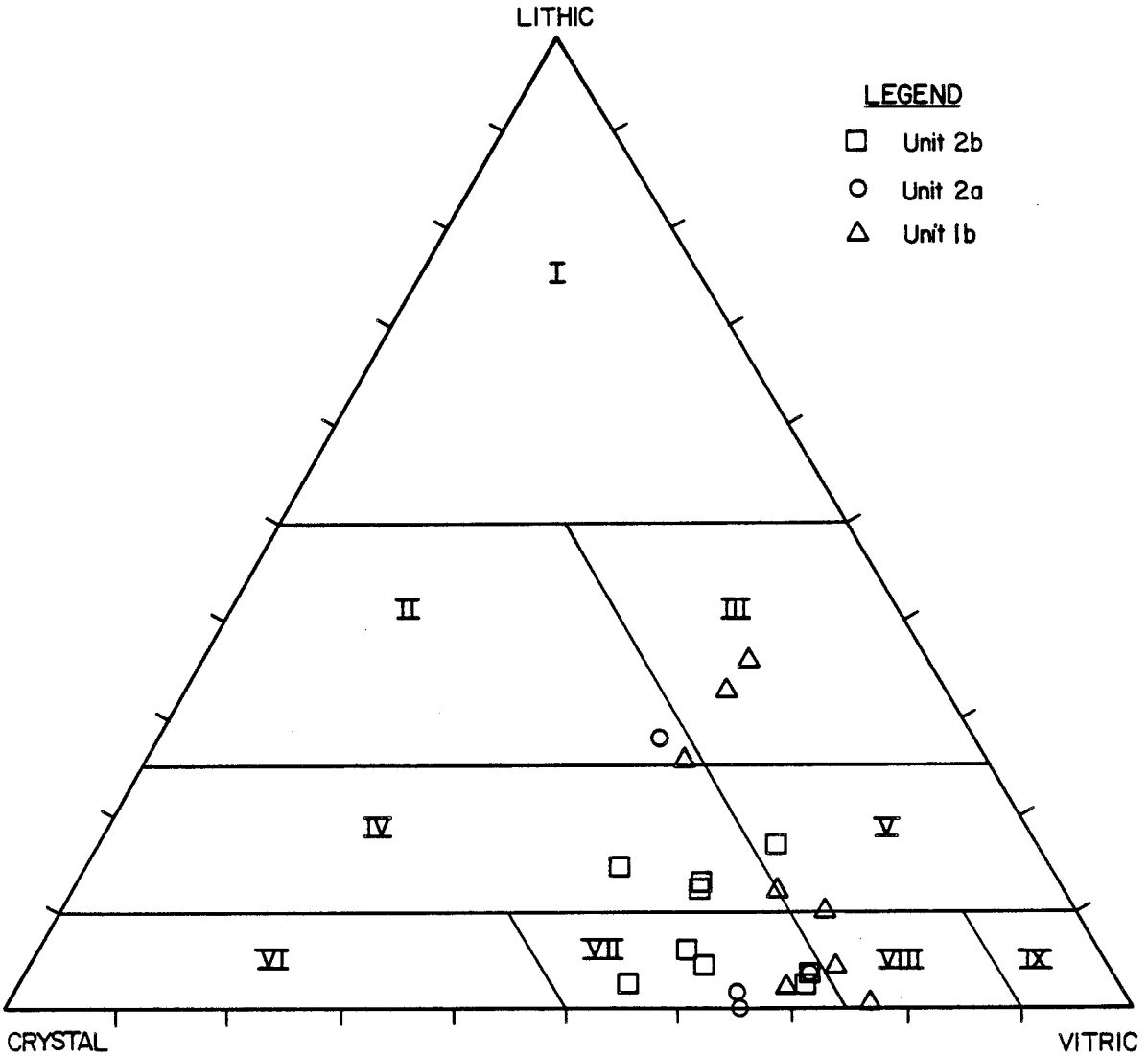

Figure B-1. Classification of Cook (1965) Used to Name Tuffaceous Rocks in This Study on the Basis of the Normalized Vitric (including pumice), Crystal, and Lithic Components Determined from the Modal Analysis

LANL VAPOR TRANSPORT STUDY
REQUEST NO.: 402553
PROJECT NO.: 6L0001000

SAMPLE NO.: MCG-550
DRILL HOLE LLM-85-17 UNIT 1B (LITHIC)
DRILL HOLE DEPTH (FT): 118

PHENOCRYST RATIO (Q/K/P): 1/6.67/0.33 DEGREE OF WELDING: Dense
POROSITY (VOL %): 10 OXIDATION STATE OF Fe-Ti OXIDES: C3-C4

ROCK NAME: Rhyolitic Vitric Tuff

GENERAL DESCRIPTION IN THIN SECTION: Densely welded glass with lithophysae filled by sanidine, tridymite, opaques, and late-stage alpha quartz. A few fine- to medium-grained phenocrysts are present.

MINERAL COMPONENT	VOL. %		COMMENTS
Groundmass		60	Densely welded glass with well-developed spherulitic devitrification. Glass is brown in part.
Vapor-Phase Minerals		28	
Sanidine	(73)		Porous, microcrystalline linings of lithophysae.
Tridymite	(18)		Fine grained, euhedral. Partially fills interiors of lithophysae. Wedge-shaped twins are common.
Alpha Quartz	(5)		Fine grained, anhedral. Late-stage filling of lithophysae.
Opaques	(4)		Fine grained, anhedral. Associated with sanidine stage of lithophysae filling. Magnetite/ilmenite altering to hematite.
Pore Space		10	Associated with vapor-phase crystallites.
Phenocrysts		2	
Sanidine	(83)		Fine to medium grained, euhedral to anhedral.
Alpha Quartz	(13)		Fine to medium grained, anhedral to euhedral. Embayed grains are present.
Plagioclase	(4)		Fine to medium grained, subhedral.
Opaques	(tr)		Fine grained, anhedral to subhedral. Magnetite intergrown with ilmenite.

LANL VAPOR TRANSPORT STUDY
REQUEST NO.: 402553
PROJECT NO.: 6L0001000

SAMPLE NO.: MCG-601
DRILL HOLE LLM-85-17 UNIT 1B (LITHIC)
DRILL HOLE DEPTH (FT): 128

POROSITY (VOL %): 1

OXIDATION STATE OF Fe-Ti OXIDES: C4

ROCK NAME: Hornblende Basalt Porphyry

GENERAL DESCRIPTION IN THIN SECTION: Fine- to medium-grained phenocrysts in a hyalopilitic groundmass. Glomeroporphyritic.

MINERAL COMPONENT	VOL. %	COMMENTS
Phenocrysts	32	
Plagioclase	(61)	Fine to medium grained, euhedral. Oscillatory zoning. Andesine. Embayed grains.
Hornblende(?)	(20)	Fine to medium grained, euhedral. Totally replaced by hematite and chlorite.
Biotite	(7)	Fine to medium grained, euhedral to subhedral. Partial replacement by hematite.
Pyroxene	(6)	Fine to medium grained, euhedral to subhedral. Hypersthene. Partial replacement by chlorite/serpentine.
Opaques	(5)	Fine grained, euhedral to subhedral. Magnetite with exsolved ilmenite; magnetite is oxidizing to hematite.
Olivine	(tr)	Medium grained, anhedral. Totally oxidized to hypersthene and magnetite.
Groundmass	68	Hyalopilitic.
Plagioclase	(94)	Felty laths.
Opaques	(2)	Magnetite oxidizing to hematite.
Glass	(1.5)	Brown-colored.
Pore Space	(1.5)	Microvugs in groundmass(?).
Biotite	(1)	Altered to chlorite and hematite.

LANL VAPOR TRANSPORT STUDY
REQUEST NO.: 402553
PROJECT NO.: 6L0001000

SAMPLE NO.: MCG-626
DRILL HOLE LLM-85-01 UNIT 2B
DRILL HOLE DEPTH (FT): 30

PHENOCRYST RATIO (Q/K/P): 1/2.26/0
POROSITY (VOL %): 23

DEGREE OF WELDING: Slight to Moderate
OXIDATION STATE OF Fe-Ti OXIDES: C4

ROCK NAME: Rhyolitic Crystal-Vitric Tuff

GENERAL DESCRIPTION IN THIN SECTION: Fine- to medium-grained phenocrysts (crystals) in a slightly to moderately welded glass groundmass. Intact glass bubble walls and Y-shaped shards are present.

MINERAL COMPONENT	VOL. %		COMMENTS
Groundmass		44	
Glass	(66)		Incipient axiolitic devitrification.
Pumice	(34)		Up to 2.59 mm. Replaced/mineralized by sanidine and tridymite. Phenocryst ratio (Q/K) = 1/3.
Phenocrysts		27	
Sanidine	(64)		Fine to medium grained, anhedral to subhedral.
Quartz	(28)		Fine to medium grained, anhedral to subhedral.
Opaques	(5)		Fine-grained, euhedral to subhedral. Ilmenite/magnetite altering to hematite.
Amphibole(?)	(3)		Fine grained, anhedral to subhedral. Lamprobolite, partially altered, with opaque rims.
Plagioclase	(tr)		Fine to medium grained, anhedral. Accidental crystal.
Biotite	(tr)		Fine grained, anhedral to subhedral.
Pore Space		23	
Lithic Fragments		5	Up to 10.4 mm. Consisting of an andesite, a rock similar to the host, and a plagioclase-sanidine fragment.
Zeolite		1	Very fine grained, euhedral. Isotropic; phase is probably analcime. Occurs in pore space.

LANL VAPOR TRANSPORT STUDY
REQUEST NO.: 402553
PROJECT NO.: 6L0001000

SAMPLE NO.: MCG-627
DRILL HOLE LLM-85-01 UNIT 2A
DRILL HOLE DEPTH (FT): 52

PHENOCRYST RATIO (Q/K/P): 1/1.79/0
POROSITY (VOL %): 13

DEGREE OF WELDING: Slight to Moderate
OXIDATION STATE OF Fe-Ti OXIDES: C2

ROCK NAME: Rhyolitic Crystal-Vitric Tuff

GENERAL DESCRIPTION IN THIN SECTION: Fine- to medium-grained phenocrysts in a groundmass that exhibits slight to moderate welding. Pumice fragments are generally coarser than those in Sample MCG-626 and the quartz phenocrysts are more embayed.

MINERAL COMPONENT	VOL. %		COMMENTS
Groundmass		62	
Pumice	(53)		Up to 13.9 mm. Replaced/mineralized by sanidine and tridymite. Phenocryst ratio (Q/K): 1/3. Some fragments altering to clay.
Glass	(47)		Incipient axiolitic devitrification.
Phenocrysts		23	
Sanidine	(62)		Fine to medium grained, subhedral to anhedral.
Quartz	(34)		Fine to medium grained, subhedral to euhedral. Some grains are embayed.
Opaques	(3)		Fine grained, euhedral to subhedral. Magnetite with exsolved ilmenite.
Pyroxene	(1)		Fine grained, anhedral to euhedral. Augite.
Pore Space		13	
Lithic Fragments		2	Up to 2.64 mm. Includes crystal-vitric tuffs with clay replacing the glass; strongly welded.
Unknown Component		tr	Rounded grain, 0.56 mm in longest axis, consisting of a thin rim of magnetite with randomly oriented clay (chlorite?) flakes and epidote or pyroxene grains.

LANL VAPOR TRANSPORT STUDY
REQUEST NO.: 402553
PROJECT NO.: 6L0001000

SAMPLE NO.: MCG-628
DRILL HOLE LLM-85-01 UNIT 1B
DRILL HOLE DEPTH (FT): 101

PHENOCRYST RATIO (Q/K/P): 1/2.25/0.06 DEGREE OF WELDING: Moderate
POROSITY (VOL %): 18 OXIDATION STATE OF Fe-Ti OXIDES: C2

ROCK NAME: Rhyolitic Vitric-Lithic Tuff

GENERAL DESCRIPTION IN THIN SECTION: Fine- to medium-grained phenocrysts in a moderately welded groundmass with incipient axiolitic devitrification. This sample contains more lithic fragments than Sample MCG-626 (Unit 2b) or Sample MCG-627 (Unit 2a).

MINERAL COMPONENT	VOL. %		COMMENTS
Groundmass		56	
Glass	(51)		Incipient axiolitic devitrification. Intact bubble walls and Y-shaped shards are present.
Pumice	(49)		Up to 8.89 mm. Spherulitic devitrification (rather than replaced by sanidine and tridymite as in Samples MCG-626 and -627). Phenocryst ratio (Q/K) = 1/3.67.
Phenocrysts		18	
Sanidine	(66)		Fine to medium grained, anhedral to euhedral.
Quartz	(30)		Fine to medium grained, anhedral to euhedral. Some grains are embayed.
Plagioclase	(2)		Medium grained, subhedral. Associated with pyroxene and magnetite-ilmenite. Zoned grain.
Opaques	(2)		Fine grained, anhedral to euhedral. Magnetite with exsolved ilmenite.
Pyroxene	(tr)		Fine grained, anhedral. One grain is coated by celadonite.
Pore Space		18	
Lithic Fragments		8	Up to 17.0 mm. Largest fragment is a thoroughly welded, crystal-vitric tuff. Other tuffs are altered to clay; basalts/andesites are present.

(continued on next page)

LANL VAPOR TRANSPORT STUDY
REQUEST NO.: 402553
PROJECT NO.: 6L0001000

SAMPLE NO.: MCG-628 (continued)
DRILL HOLE LLM-85-01 UNIT 1B
DRILL HOLE DEPTH (FT): 101

MINERAL COMPONENT	VOL. %	COMMENTS
Unknown Component	tr	Rounded grain, 0.62 mm in longest axis, consisting of clay (chlorite?) flakes in random orientation and magnetite with exsolved ilmenite. Magnetite is altering to hematite. Grain could be an altered mafic.

LANL VAPOR TRANSPORT STUDY
REQUEST NO.: 402553
PROJECT NO.: 6L0001000

SAMPLE NO.: MCG-629
DRILL HOLE LLM-85-01 UNIT 1B
DRILL HOLE DEPTH (FT): 122

PHENOCRYST RATIO (Q/K/P): 1/0.75/0
POROSITY (VOL %): 12

DEGREE OF WELDING: Moderate
OXIDATION STATE OF Fe-Ti OXIDES: C2-C3

ROCK NAME: Rhyolitic Vitric-Lithic Tuff

GENERAL DESCRIPTION IN THIN SECTION: Fine- to medium-grained phenocrysts in a moderately welded groundmass. Most shards show incipient alteration to clay. This sample is similar to MCG-628 except for the lack of significant devitrification of glass shards.

MINERAL COMPONENT	VOL. %		COMMENTS
Groundmass		55	
Glass	(63)		Shards are a mottled-brown color; this may be incipient alteration to clay. Intact bubble walls and Y-shaped shards are present.
Pumice	(37)		Up to 10.0 mm. Spherulitic devitrification. Phenocryst ratio (Q/K) = 1/4.25. One pumice fragment contains a pyroxene phenocryst.
Phenocryst		22	
Quartz	(54)		Fine to medium grained, anhedral to euhedral. Most grains are embayed.
Sanidine	(41)		Fine to medium grained, subhedral to euhedral.
Opaques	(5)		Fine grained, anhedral to euhedral. Magnetite with exsolved ilmenite.
Pyroxene	(tr)		Fine grained, anhedral to euhedral. Usually associated with opaques.
Pore Space		12	
Lithic Fragments		11	Up to 5.70 mm. Several thoroughly welded vitric-crystal tuffs with spherulitic devitrification are present. Also present are andesitic crystal-vitric tuffs that are moderately welded.

LANL VAPOR TRANSPORT STUDY
REQUEST NO.: 402553
PROJECT NO.: 6L0001000

SAMPLE NO.: MCG-630
DRILL HOLE LLM-85-02 UNIT 2B
DRILL HOLE DEPTH (FT): 37

PHENOCRYST RATIO (Q/K/P): 1/2.24/0.06 DEGREE OF WELDING: Moderate
POROSITY (VOL %): 16 OXIDATION STATE OF Fe-Ti OXIDES: C2

ROCK NAME: Rhyolitic Vitric-Lithic Tuff

GENERAL DESCRIPTION IN THIN SECTION: Fine- to medium-grained phenocrysts in a moderately welded groundmass. Shards show incipient axiolitic devitrification and clay coatings. Pumice fragments are mostly replaced by sanidine and tridymite as in Samples MCG-626 and -627.

MINERAL COMPONENT	VOL. %		COMMENTS
Groundmass		50	
Glass	(77)		Incipient axiolitic devitrification; glass is coated by clay. Y-shaped shards are present.
Pumice	(23)		Up to 8.74 mm. Replaced/mineralized by sanidine and tridymite. Phenocryst ratio (Q/K) = 1/4.
Phenocrysts		19	
Sanidine	(66)		Fine to medium grained, anhedral to euhedral. Some grains are embayed.
Quartz	(30)		Fine to medium grained, anhedral to euhedral. Some grains are embayed.
Plagioclase	(2)		Fine grained, subhedral.
Opaques	(2)		Fine grained, anhedral to euhedral. Magnetite with exsolved ilmenite.
Pyroxene	(tr)		Fine grained, anhedral to subhedral.
Amphibole	(tr)		Fine grained, anhedral.
Zircon	(tr)		Fine grained, euhedral.
Pore Space		16	
Lithic Fragments		14	Up to 15.8 mm. Several strongly welded, crystal-vitric tuffs with little or no devitrification of glass.

(continued on next page)

LANL VAPOR TRANSPORT STUDY
REQUEST NO.: 402553
PROJECT NO.: 6L0001000

SAMPLE NO.: MCG-630 (continued)
DRILL HOLE LLM-85-02 UNIT 2B
DRILL HOLE DEPTH (FT): 37

MINERAL COMPONENT	VOL. %	COMMENTS
Zeolite(?)	tr	Very fine grained, euhedral (radial acicular). Occupies pore space; too small for optical identification.
Unknown Component	tr	Euhedral grain shape (pyroxene?), 0.51 mm, at edge of thin section; consists of thin rim of magnetite and randomly oriented flakes of clay (chlorite?).

LANL VAPOR TRANSPORT STUDY
REQUEST NO.: 402553
PROJECT NO.: 6L0001000

SAMPLE NO.: MCG-631
DRILL HOLE LLM-85-02 UNIT 2A
DRILL HOLE DEPTH (FT): 64

PHENOCRYST RATIO (Q/K/P): 1/1.45/0
POROSITY (VOL %): 23

DEGREE OF WELDING: Moderate
OXIDATION STATE OF Fe-Ti OXIDES: C2-C3

ROCK NAME: Rhyolitic Crystal-Vitric Tuff

GENERAL DESCRIPTION IN THIN SECTION: Fine- to medium-grained phenocrysts in a moderately welded groundmass. Pumice fragments are mostly replaced by sanidine and tridymite.

MINERAL COMPONENT	VOL. %		COMMENTS
Groundmass		49	
Glass	(76)		Incipient axiolitic devitrification. Intact bubble walls and Y-shaped shards are present.
Pumice	(24)		Up to 7.26 mm. Replaced/mineralized by sanidine and tridymite. Phenocryst ratio (Q/K) = 1/4.
Phenocrysts		26	
Sanidine	(58)		Fine to medium grained, anhedral to euhedral.
Quartz	(40)		Fine to medium grained, anhedral to euhedral. Some grains are embayed.
Opaques	(1)		Fine grained, anhedral to euhedral. Magnetite-ilmenite intergrowths (exsolution).
Pyroxene	(1)		Fine grained, subhedral to euhedral. Usually associated with opaques.
Plagioclase	(tr)		Fine grained, euhedral.
Amphibole	(tr)		Fine grained, anhedral to euhedral.
Zircon	(tr)		Very fine grained, euhedral.
Pore Space		23	

(continued on next page)

LANL VAPOR TRANSPORT STUDY
REQUEST NO.: 402553
PROJECT NO.: 6L0001000

SAMPLE NO.: MCG-631 (continued)
DRILL HOLE LLM-85-02 UNIT 2A
DRILL HOLE DEPTH (FT): 64

MINERAL COMPONENT	VOL. %	COMMENTS
Lithic Fragments	1	Largest grain was on a corner of the thin section; grain is larger than 5.56 mm. Present are densely welded, partly devitrified vitric tuff; flow-banded rock; andesites; and other lithic types.
Zeolite(?)	1	Very fine grained, subhedral. Occurs in pore space.

LANL VAPOR TRANSPORT STUDY
REQUEST NO.: 402553
PROJECT NO.: 6L0001000

SAMPLE NO.: MCG-632
DRILL HOLE LLM-85-02 UNIT 2A (1B)
DRILL HOLE DEPTH (FT): 74

PHENOCRYST RATIO (Q/K/P): 1/1.07/0
POROSITY (VOL %): 21

DEGREE OF WELDING: Moderate
OXIDATION STATE OF Fe-Ti OXIDES: C3-C4

ROCK NAME: Rhyolitic Lithic-Crystal Tuff

GENERAL DESCRIPTION IN THIN SECTION: Fine- to medium-grained phenocrysts in a moderately welded groundmass. Pumice fragments resemble those in Samples MCG-628 and -629 (Unit 1b).

MINERAL COMPONENT	VOL. %	COMMENTS
Groundmass	38	
Glass	(64)	Incipient axiolitic devitrification. Intact bubble walls and Y-shaped shards are present.
Pumice	(36)	Up to 5.85 mm. Spherulitic devitrification. Phenocryst ratio (Q/K) = 1/3.83. Pyroxene phenocrysts are present. Some mineralization by tridymite or a zeolite.
Phenocrysts	21	
Sanidine	(49)	Fine to medium grained, anhedral to euhedral.
Quartz	(46)	Fine to medium grained, anhedral to euhedral. Some grains are embayed.
Opaques	(5)	Fine grained, anhedral to euhedral. Intergrown magnetite, ilmenite, and hematite.
Plagioclase	(tr)	Fine to medium grained, subhedral to euhedral.
Pyroxene	(tr)	Fine grained, anhedral to euhedral.
Amphibole	(tr)	Fine to medium grained, anhedral to euhedral.
Pore Space	21	

(continued on next page)

LANL VAPOR TRANSPORT STUDY
REQUEST NO.: 402553
PROJECT NO.: 6L0001000

SAMPLE NO.: MCG-632 (continued)
DRILL HOLE LLM-85-02 UNIT 2A (1B)
DRILL HOLE DEPTH (FT): 74

MINERAL COMPONENT	VOL. %	COMMENTS
Lithic Fragments	20	Up to 13.2 mm. Two large lithics fragments are strongly welded, crystal-vitric tuffs. Another large lithic is densely welded with totally devitrified glass. Andesites are also present.
Unknown Component	tr	Euhedral to subhedral grain shape, 0.54 mm, associated with sanidine and opaque grains in a glomerophenocryst. Grain has a thin, discontinuous rim of hematite with flakes of randomly oriented clay (chlorite?) and a grain of magnetite with exsolved ilmenite. Magnetite is altering to hematite. Grain also contains some remnant(?) pyroxene.

LANL VAPOR TRANSPORT STUDY
REQUEST NO.: 402553
PROJECT NO.: 6L0001000

SAMPLE NO.: MCG-633
DRILL HOLE LLM-85-02 UNIT 1B
DRILL HOLE DEPTH (FT): 111

PHENOCRYST RATIO (Q/K/P): 1/0.95/0
POROSITY (VOL %): 16

DEGREE OF WELDING: Moderate
OXIDATION STATE OF Fe-Ti OXIDES: C2-C3

ROCK NAME: Rhyolitic Lithic-Vitric Tuff

GENERAL DESCRIPTION IN THIN SECTION: Fine- to medium-grained phenocrysts in a moderately welded groundmass containing some brown glass. Large lithic fragments are present.

MINERAL COMPONENT	VOL. %		COMMENTS
Groundmass		41	
Glass	(61)		Incipient axiolitic devitrification. Mottled brown glass may indicate alteration to clay. Intact bubble walls and Y-shaped shards are present.
Pumice	(39)		Up to 9.11 mm. Spherulitic devitrification. Mineralization by a fibrous phase (zeolite?). Phenocryst ratio (Q/K) = 3/1.
Lithic Fragments		30	Up to 29.3 mm. Two major types: strongly welded, crystal-vitric tuff partially altered to clay, and a densely welded, vitric-crystal tuff that is totally devitrified.
Pore Space		16	
Phenocrysts		13	
Quartz	(49)		Fine to medium grained, anhedral to euhedral. Resorption features are common.
Sanidine	(46)		Fine to medium grained, anhedral to euhedral. Some embayments are present.
Opaques	(5)		Fine grained, anhedral to euhedral. Magnetite and ilmenite intergrowths.
Plagioclase	(tr)		Fine grained, subhedral to euhedral. Zoned grains are present.
Pyroxene	(tr)		Fine grained, anhedral. Associated with opaques.

LANL VAPOR TRANSPORT STUDY
REQUEST NO.: 402553
PROJECT NO.: 6L0001000

SAMPLE NO.: MCG-634
DRILL HOLE LLM-85-06 UNIT 2B
DRILL HOLE DEPTH (FT): 30

PHENOCRYST RATIO (Q/K/P): 1/1.20/0
POROSITY (VOL %): 25

DEGREE OF WELDING: Moderate
OXIDATION STATE OF Fe-Ti OXIDES: C3

ROCK NAME: Rhyolitic Crystal-Vitric Tuff

GENERAL DESCRIPTION IN THIN SECTION: Fine- to medium-grained phenocrysts in a moderately welded groundmass. Shards show axiolitic devitrification.

MINERAL COMPONENT	VOL. %		COMMENTS
Groundmass		45	
Glass	(84)		Axiolitic devitrification. Intact bubble walls and Y-shaped shards are present.
Pumice	(16)		Up to 8.15 mm. Two types are present: fragments replaced by sanidine and tridymite with quartz phenocrysts (dominant type), and andesitic fragments with plagioclase and amphibole phenocrysts and mineralization by tridymite.
Phenocrysts		26	
Sanidine	(53)		Fine to medium grained, anhedral to euhedral.
Quartz	(44)		Fine to medium grained, anhedral to euhedral. Embayments are present.
Opaques	(3)		Fine grained, anhedral to euhedral. Magnetite and ilmenite intergrowths.
Plagioclase	(tr)		Fine grained, euhedral to subhedral. Zoned grains are present.
Biotite	(tr)		Fine grained, anhedral.
Pyroxene	(tr)		Fine grained, anhedral to subhedral.
Amphibole	(tr)		Fine grained, anhedral.
Pore Space		25	

(continued on next page)

LANL VAPOR TRANSPORT STUDY
REQUEST NO.: 402553
PROJECT NO.: 6L0001000

SAMPLE NO.: MCG-634 (continued)
DRILL HOLE LLM-85-06 UNIT 2B
DRILL HOLE DEPTH (FT): 30

MINERAL COMPONENT	VOL. %	COMMENTS
Lithic Fragments	3	Up to 1.41 mm. Two types are present: densely welded, lithic tuff with spherulitic devitrification (see Samples MCG-550 and -645) and a strongly welded, vitric tuff which is devitrified.
Tridymite	tr	Occurs in pore spaces. Fine grained, euhedral.

LANL VAPOR TRANSPORT STUDY
REQUEST NO.: 402553
PROJECT NO.: 6L0001000

SAMPLE NO.: MCG-635
DRILL HOLE LLM-85-06 UNIT 2A
DRILL HOLE DEPTH (FT): 50

PHENOCRYST RATIO (Q/K/P): 1/1.22/0.07 DEGREE OF WELDING: Slight to Moderate
POROSITY (VOL %): 19 OXIDATION STATE OF Fe-Ti OXIDES: C3

ROCK NAME: Rhyolitic Lithic-Crystal Tuff

GENERAL DESCRIPTION IN THIN SECTION: Fine- to medium-grained phenocrysts in a slightly to moderately welded groundmass.

MINERAL COMPONENT	VOL. %		COMMENTS
Groundmass		36	
Glass	(61)		Incipient axiolitic devitrification. Intact bubble walls and Y-shaped shards are present.
Pumice	(39)		Up to 5.70 mm. Axiolitic devitrification and some replacement by sanidine and tridymite. Only quartz phenocrysts are present.
Phenocrysts		22	
Sanidine	(50)		Fine to medium grained, anhedral to euhedral.
Quartz	(41)		Fine to medium grained, anhedral to euhedral. Resorption features are common.
Opaques	(4.5)		Fine grained, anhedral to euhedral. Magnetite and ilmenite intergrowths.
Plagioclase	(3)		Fine grained, subhedral to euhedral. Zoned grains are present.
Pyroxene	(1.5)		Fine grained, euhedral to subhedral. Associated with opaques.
Lithic Fragments		22	Up to 19.3 mm. Predominant type of lithic is a strongly welded, crystal-vitric tuff containing pumice fragments from Unit 1b. Another type has a spongy lithology consisting of sanidine crystals.
Pore Space		19	

(continued on next page)

LANL VAPOR TRANSPORT STUDY
REQUEST NO.: 402553
PROJECT NO.: 6L0001000

SAMPLE NO.: MCG-635 (continued)
DRILL HOLE LLM-85-06 UNIT 2A
DRILL HOLE DEPTH (FT): 50

MINERAL COMPONENT	VOL. %	COMMENTS
Tridymite	1	Fine grained, euhedral. Occurs in pores.
Unknown Component	tr	Rounded grains, 0.54 and 0.91 mm, consisting of a discontinuous rim of hematite and magnetite with exsolved ilmenite. Some rutile is associated with grains of magnetite; magnetite is altering to hematite. The interiors of these rounded grains contain randomly oriented clay (chlorite?) flakes and epidote or pyroxene.

LANL VAPOR TRANSPORT STUDY
REQUEST NO.: 402553
PROJECT NO.: 6L0001000

SAMPLE NO.: MCG-636
DRILL HOLE LLM-85-06 UNIT 1B
DRILL HOLE DEPTH (FT): 99

PHENOCRYST RATIO (Q/K/P): 1/1.53/0
POROSITY (VOL %): 26

DEGREE OF WELDING: Moderate
OXIDATION STATE OF Fe-Ti OXIDES: C1-C2

ROCK NAME: Rhyolitic Vitric-Crystal Tuff

GENERAL DESCRIPTION IN THIN SECTION: Fine- to medium-grained phenocrysts in a fresh-glass groundmass. Glass in pumice fragments is fresh and not devitrified. Some pumice fragments are flattened.

MINERAL COMPONENT	VOL. %		COMMENTS
Groundmass		57	
Glass	(53)		Moderate welding, brown glass; not devitrified. Intact bubble walls and Y-shaped shards are present.
Pumice	(47)		Up to 5.93 mm. Some of the fragments are flattened. Glass is not devitrified. Phenocryst ratio (Q/K) for flattened pumice is 1/11; for non-flattened pumice, 1/1.25. Overall pumice phenocryst ratio is 1/3.20.
Pore Space		26	
Phenocrysts		17	
Sanidine	(57)		Fine to medium grained, anhedral to euhedral.
Quartz	(37)		Fine to medium grained, anhedral to euhedral.
Opaques	(4)		Fine grained, anhedral to euhedral. Magnetite, and magnetite with exsolved ilmenite.
Pyroxene	(2)		Fine grained, anhedral to euhedral.
Plagioclase	(tr)		Fine grained, anhedral.
Lithic Fragments		tr	Up to 1.42 mm. Hyalopilitic basalt/andesite.

LANL VAPOR TRANSPORT STUDY
REQUEST NO.: 402553
PROJECT NO.: 6L0001000

SAMPLE NO.: MCG-637
DRILL HOLE LLM-85-06 UNIT 1A
DRILL HOLE DEPTH (FT): 113

PHENOCRYST RATIO: Not Determined
DEGREE OF WELDING: Not Welded
POROSITY (VOL %): Not Determined
OXIDATION STATE OF Fe-Ti OXIDES: C3 (Pumice)

ROCK NAME: Rhyolitic Vitric-Crystal(?) Tuff

GENERAL DESCRIPTION IN THIN SECTION: The sample was not welded and the thin-section preparer provided a section of the pumice fragments only. Grain mounts of the fine fraction were prepared in immersion oil and Canada balsam. Each of these mounts contains brown-glass shards and a large proportion of fine, flattened pumice fragments. The glass in the shards and fine pumice fragments is not devitrified. Phenocrysts of sanidine, quartz, zoned plagioclase, opaques, pyroxene, and amphibole are present in the fine fraction. The medium fraction was examined using a binocular microscope. This fraction consisted of quartz and sanidine phenocrysts, pumice fragments, and lithic fragments. The coarse pumice fragments are similar to those in Sample MCG-636; some of these are flattened. Compositions of the coarse pumice fragments (based on phenocrysts) are rhyolitic to andesitic. The largest pumice fragment (26 mm) contains zoned plagioclase, euhedral lamprobolite, and anhedral pyroxene phenocrysts in a partially flattened pumice structure. Other pumice fragments range from not flattened to totally collapsed; glass is not devitrified.

LANL VAPOR TRANSPORT STUDY
REQUEST NO.: 402553
PROJECT NO.: 6L0001000

SAMPLE NO.: MCG-638
DRILL HOLE LLM-85-11 UNIT 2B
DRILL HOLE DEPTH (FT): 5

PHENOCRYST RATIO (Q/K/P): 1/1.82/0
POROSITY (VOL %): 22

DEGREE OF WELDING: Slight to Moderate
OXIDATION STATE OF Fe-Ti OXIDES: C3-C4

ROCK NAME: Rhyolitic Crystal-Vitric Tuff

GENERAL DESCRIPTION IN THIN SECTION: Fine- to medium-grained phenocrysts in a groundmass exhibiting slight to moderate welding and axiolitic devitrification of glass.

MINERAL COMPONENT	VOL. %		COMMENTS
Groundmass		55	
Glass	(65)		Axiolitic devitrification.
Pumice	(35)		Up to 2.52 mm. Replaced/mineralized by sanidine and tridymite. Phenocryst ratio (Q/K) = 1/2.25. Opaque and zircon phenocrysts are also present.
Pore Space		22	
Phenocrysts		21	
Sanidine	(63)		Fine to medium grained, anhedral to euhedral.
Quartz	(34)		Fine to medium grained, anhedral to euhedral. Some embayments are present.
Opaques	(3)		Fine grained, anhedral to euhedral. Magnetite, ilmenite, and hematite intergrowths.
Pyroxene	(tr)		Fine grained, anhedral to euhedral. Associated with opaques.
Plagioclase	(tr)		Fine grained, anhedral to subhedral. Zoned grains are present.
Amphibole	(tr)		Fine grained, anhedral.
Lithic Fragments		2	Up to 3.64 mm. Several types: strongly welded, vitric-crystal tuff, both devitrified and nondevitrified varieties; andesitic tuff, not devitrified; and hyalopilitic basalt.

LANL VAPOR TRANSPORT STUDY
REQUEST NO.: 402553
PROJECT NO.: 6L0001000

SAMPLE NO.: MCG-639
DRILL HOLE LLM-85-11 UNIT 2B
DRILL HOLE DEPTH (FT): 30.5

PHENOCRYST RATIO (Q/K/P): 1/0.77/0
POROSITY (VOL %): 24

DEGREE OF WELDING: Moderate
OXIDATION STATE OF Fe-Ti OXIDES: C4

ROCK NAME: Rhyolitic Crystal-Lithic Tuff

GENERAL DESCRIPTION IN THIN SECTION: Fine- to medium-grained phenocrysts in a moderately welded, devitrified groundmass.

MINERAL COMPONENT	VOL. %		COMMENTS
Groundmass		42	
Glass	(70)		Axiolitic devitrification. Intact bubble walls and Y-shaped shards are present.
Pumice	(30)		Up to 4.89 mm. Replaced/mineralized by sanidine and tridymite. Phenocryst ratio (Q/K) = 1/2.
Pore Space		24	
Phenocrysts		24	
Quartz	(55)		Fine to medium grained, anhedral to euhedral. Some embayments are present.
Sanidine	(42)		Fine to medium grained, anhedral to euhedral.
Opaques	(3)		Fine grained, anhedral to euhedral. Magnetite, ilmenite, and hematite intergrowths.
Pyroxene	(tr)		Fine grained, subhedral to euhedral.
Plagioclase	(tr)		Fine grained, euhedral. Zoned grains.
Amphibole	(tr)		Fine grained, subhedral.
Lithic Fragments		10	Up to 31.9 mm. Lenticular, strongly welded, crystal-vitric tuff with axiolitic devitrification and hyalopilitic basalts.

LANL VAPOR TRANSPORT STUDY
REQUEST NO.: 402553
PROJECT NO.: 6L0001000

SAMPLE NO.: MCG-640
DRILL HOLE LLM-85-11 UNIT 1B
DRILL HOLE DEPTH (FT): 95

PHENOCRYST RATIO (Q/K/P): 1/1.30/0
POROSITY (VOL %): 16

DEGREE OF WELDING: Moderate
OXIDATION STATE OF Fe-Ti OXIDES: C2

ROCK NAME: Rhyolitic Lithic-Vitric Tuff

GENERAL DESCRIPTION IN THIN SECTION: Fine- to medium-grained phenocrysts in a moderately welded groundmass.

MINERAL COMPONENT	VOL. %		COMMENTS
Groundmass		41	
Glass	(58)		Not devitrified; some brown glass is present.
Pumice	(42)		Up to 8.52 mm. Three types of pumice are present: nonflattened pumice with spherulitic devitrification [phenocryst ratio (Q/K) = 1/3]; flattened pumice that is not devitrified; and nonflattened pumice of andesitic composition.
Lithic Fragments		27	Up to 14.8 mm. Three types are present: strongly welded, crystal-vitric tuff; densely welded, vitric-crystal tuff that is totally devitrified; and altered basalt.
Pore Space		16	
Phenocrysts		16	
Sanidine	(54)		Fine to medium grained, anhedral to euhedral.
Quartz	(42)		Fine to medium grained, anhedral to euhedral. Some embayments are present.
Opaques	(2)		Fine grained, anhedral to euhedral. Magnetite with exsolved ilmenite.
Pyroxene	(2)		Fine grained, anhedral to euhedral.
Amphibole	(tr)		Fine grained, subhedral.

LANL VAPOR TRANSPORT STUDY
REQUEST NO.: 402553
PROJECT NO.: 6L0001000

SAMPLE NO.: MCG-641
DRILL HOLE LLM-85-11 UNIT 1A
DRILL HOLE DEPTH (FT): 116

PHENOCRYST RATIO: Not Determined
DEGREE OF WELDING: Not Welded
POROSITY (VOL %): Not Determined
OXIDATION STATE OF Fe-Ti OXIDES: C2 (Pumice)

ROCK NAME: Rhyolitic Vitric-Crystal(?) Tuff

GENERAL DESCRIPTION IN THIN SECTION: The sample was not welded and the thin-section preparer provided a section of the pumice fragments only. A grain mount of the fine fraction was prepared in Canada balsam. The fine fraction consists of glass shards, flattened pumice fragments, phenocrysts of quartz, sanidine, plagioclase, pyroxene, amphibole, and opaques. Goethite and goethite-stained material is present in the fine fraction. Glass is not devitrified in the shards and pumice fragments. The medium fraction was examined using a binocular microscope. This fraction consists of quartz, sanidine, opaque phenocrysts, and pumice (some flattened) and lithic fragments. The coarse pumice fragments have rhyolitic compositions based on the phenocrysts of sanidine, quartz, opaques, and (few) pyroxene. The pumice fragments vary from partially flattened to not flattened. Glass in the pumice fragments is not devitrified.

LANL VAPOR TRANSPORT STUDY
REQUEST NO.: 402553
PROJECT NO.: 6L0001000

SAMPLE NO.: MCG-642
DRILL HOLE LLM-85-14 UNIT 2B (LITHIC)
DRILL HOLE DEPTH (FT): 18

PHENOCRYST RATIO (P_l/P_x): 4.57/1
POROSITY (VOL %): 5

DEGREE OF WELDING: Dense
OXIDATION STATE OF Fe-Ti OXIDES: C3-C4

ROCK NAME: Basalt Porphyry

GENERAL DESCRIPTION IN THIN SECTION: Fine- to medium-grained phenocrysts in a hyalopilitic groundmass.

MINERAL COMPONENT	VOL. %		COMMENTS
Groundmass		67	
Glass	(56)		Spherulitic devitrification.
Plagioclase Laths	(41)		Very fine grained, euhedral to subhedral.
Opaques	(3)		Very fine grained, anhedral to euhedral. Magnetite, ilmenite, and hematite.
Phenocrysts		28	
Plagioclase	(77)		Fine to medium grained, euhedral to anhedral. Spongy resorption textures.
Pyroxene	(17)		Fine to medium grained, euhedral to subhedral. Pigeonite.
Opaques	(6)		Fine grained, anhedral to euhedral. Magnetite, ilmenite, and hematite intergrowths.
Pore Space		5	Microporosity (in the groundmass) around and within some plagioclase phenocrysts.
Fracture Filling		tr	Goethite.

LANL VAPOR TRANSPORT STUDY
REQUEST NO.: 402553
PROJECT NO.: 6L0001000

SAMPLE NO.: MCG-643
DRILL HOLE LLM-85-13 UNIT 2B
DRILL HOLE DEPTH (FT): 42

PHENOCRYST RATIO (Q/K/P): 1/3.06/0.17 DEGREE OF WELDING: Moderate
POROSITY (VOL %): 28 OXIDATION STATE OF Fe-Ti OXIDES: C2

ROCK NAME: Rhyolitic Crystal-Lithic Tuff

GENERAL DESCRIPTION IN THIN SECTION: Fine- to medium-grained phenocrysts in a moderately welded groundmass with axiolitic devitrification. Glass has coatings of clay.

MINERAL COMPONENT	VOL. %		COMMENTS
Groundmass		34	
Glass	(81)		Axiolitic devitrification. Intact bubble walls and Y-shaped shards are present. Clay coatings are present.
Pumice	(19)		Up to 2.06 mm. Replaced/mineralized by sanidine and tridymite. No phenocrysts are present.
Pore Space		28	
Phenocrysts		27	
Sanidine	(68)		Fine to medium grained, anhedral to subhedral.
Quartz	(23)		Fine to medium grained, anhedral to euhedral. Embayed grains are present.
Plagioclase	(4)		Fine to medium grained, subhedral to euhedral.
Opaques	(4)		Fine grained, anhedral to euhedral. Magnetite with exsolved ilmenite; one grain contains an inclusion of pyrite.
Amphibole	(1)		Fine to medium grained, subhedral.
Pyroxene	(tr)		Fine grained, subhedral to euhedral.
Lithic Fragments		10	Up to 11.1 mm. Andesitic crystal-vitric tuff.
Tridymite		1	Very fine grained; occurs in pores.

LANL VAPOR TRANSPORT STUDY
REQUEST NO.: 402553
PROJECT NO.: 6L0001000

SAMPLE NO.: MCG-644
DRILL HOLE LLM-85-17 UNIT 2B
DRILL HOLE DEPTH (FT): 11

PHENOCRYST RATIO (Q/K/P): 1/1.75/0
POROSITY (VOL %): 25

DEGREE OF WELDING: Moderate
OXIDATION STATE OF Fe-Ti OXIDES: C3-C4

ROCK NAME: Rhyolitic Crystal-Lithic Tuff

GENERAL DESCRIPTION IN THIN SECTION: Fine- to medium-grained phenocrysts in a moderately welded groundmass. Although this sample has a fracture containing smectite, no clay was observed in thin section.

MINERAL COMPONENT	VOL. %		COMMENTS
Groundmass		41	
Glass	(71)		Axiolitic devitrification is present.
Pumice	(29)		Up to 3.39 mm. Replaced/mineralized by sanidine and tridymite. Phenocryst ratio (Q/K) = 1/1.
Pore Space		25	
Phenocrysts		23	
Sanidine	(61)		Fine to medium grained, anhedral to euhedral.
Quartz	(35)		Fine to medium grained, anhedral to subhedral. Some grains are embayed.
Opaques	(3)		Fine grained, anhedral to euhedral. Ilmenite with exsolved magnetite; grains of rutile are present.
Pyroxene	(1)		Fine grained, subhedral to anhedral.
Plagioclase	(tr)		Fine grained, euhedral. Zoned grains are present.
Lithic Fragments		10	Up to 12.7 mm. Several types: strongly welded, crystal-vitric tuff with fresh glass; densely welded, vitric-crystal tuff with coarse spherulitic devitrification; and a devitrified, andesitic/latitic vitric tuff.
Tridymite		1	Fine grained, euhedral. Occurs in pore spaces.

LANL VAPOR TRANSPORT STUDY
REQUEST NO.: 402553
PROJECT NO.: 6L0001000

SAMPLE NO.: MCG-645
DRILL HOLE LLM-85-17 UNIT 1B (LITHIC)
DRILL HOLE DEPTH (FT): 109

PHENOCRYST RATIO (Q/K/P): 1/4.33/0.67 DEGREE OF WELDING: Dense
POROSITY (VOL %): 9 OXIDATION STATE OF Fe-Ti OXIDES: C3-C4

ROCK NAME: Rhyolitic Vitric Tuff

GENERAL DESCRIPTION IN THIN SECTION: Densely welded glass with lithophysae filled by sanidine, tridymite, opaques, and late-stage alpha quartz. A few fine- to medium-grained phenocrysts are present.

MINERAL COMPONENT	VOL. %		COMMENTS
Groundmass		53	Densely welded glass with well-developed spherulitic devitrification. Glass is brown in part.
Vapor Phase Minerals		33	
Sanidine	(70)		Porous, microcrystalline linings of lithophysae.
Tridymite	(23)		Fine grained, euhedral. Partially fills interiors of lithophysae. Wedge-shaped twins are common.
Alpha Quartz	(4)		Fine grained, anhedral to euhedral. Late-stage lining and filling of lithophysae.
Opaques	(3)		Fine grained, anhedral. Associated with sanidine stage of lithophysae filling. Magnetite/ilmenite altering to hematite.
Pore Space		9	Associated with vapor-phase crystallites.
Phenocrysts		5	
Sanidine	(56)		Fine to medium grained, euhedral to subhedral.
Alpha Quartz	(44)		Fine grained, anhedral to euhedral. Embayed grains are present.
Opaques	(tr)		Fine grained, euhedral. Magnetite intergrown with ilmenite.
Plagioclase	(tr)		Fine grained, euhedral.

LANL VAPOR TRANSPORT STUDY
REQUEST NO.: 402553
PROJECT NO.: 6L0001000

SAMPLE NO.: MCG-646
DRILL HOLE LLM-85-09 UNIT 2B
DRILL HOLE DEPTH (FT): 10

PHENOCRYST RATIO (Q/K/P): 1/1.64/0
POROSITY (VOL %): 21

DEGREE OF WELDING: Moderate
OXIDATION STATE OF Fe-Ti OXIDES: C3-C4

ROCK NAME: Rhyolitic Crystal-Vitric Tuff

GENERAL DESCRIPTION IN THIN SECTION: Fine- to medium-grained phenocrysts in a moderately welded groundmass with axiolitic devitrification.

MINERAL COMPONENT	VOL. %		COMMENTS
Groundmass		55	
Glass	(68)		Axiolitic devitrification.
Pumice	(32)		Up to 9.93 mm. Replaced/mineralized by sanidine and tridymite.
Phenocrysts		22	
Sanidine	(62)		Fine to medium grained, anhedral to euhedral.
Quartz	(38)		Fine to medium grained, anhedral to euhedral. Embayed grains are present.
Pyroxene	(tr)		Fine grained, anhedral to subhedral.
Opaques	(tr)		Fine grained, anhedral to euhedral. Magnetite, ilmenite, hematite, and rutile.
Plagioclase	(tr)		Fine grained, euhedral. Zoned grain.
Allanite(?)	(tr)		Fine grained, euhedral.
Pore Space		21	
Lithic Fragments		2	Up to 1.70 mm. Mostly basalts.
Tridymite		tr	Fine grained, euhedral. Occurs in pore spaces.

LANL VAPOR TRANSPORT STUDY
REQUEST NO.: 402553
PROJECT NO.: 6L0001000

SAMPLE NO.: MCG-647
DRILL HOLE LLM-85-09 UNIT 2B
DRILL HOLE DEPTH (FT): 20

PHENOCRYST RATIO (Q/K/P): 1/2.77/0.04 DEGREE OF WELDING: Moderate
POROSITY (VOL %): 22 OXIDATION STATE OF Fe-Ti OXIDES: C2-C3

ROCK NAME: Rhyolitic Crystal-Vitric Tuff

GENERAL DESCRIPTION IN THIN SECTION: Fine- to medium-grained phenocrysts in a moderately welded groundmass with axiolitic devitrification.

MINERAL COMPONENT	VOL. %		COMMENTS
Groundmass		42	
Glass	(69)		Axiolitic devitrification.
Pumice	(31)		Up to 10.37 mm. Replaced/mineralized by sanidine and tridymite. Phenocryst ratio (Q/K) = 1/1.
Phenocrysts		34	
Sanidine	(71)		Fine to medium grained, anhedral to euhedral.
Quartz	(26)		Fine to medium grained, anhedral to euhedral.
Opaques	(2)		Fine grained, anhedral to euhedral. Magnetite and ilmenite intergrowths.
Plagioclase	(1)		Fine to medium grained, subhedral to euhedral. Some grains are zoned.
Pyroxene	(tr)		Fine grained, anhedral to subhedral.
Pore Space		22	
Lithic Fragments		2	Up to 1.30 mm. Mostly basalts.
Tridymite		tr	Fine grained, euhedral to anhedral. Occurs in pore space.
Unknown Component		tr	Rounded grain, 0.32 mm, consisting of a partial rim of hematite and randomly oriented flakes of clay (chlorite?). A grain of ilmenite with exsolved hematite is present as an inclusion.

LANL VAPOR TRANSPORT STUDY
REQUEST NO.: 402553
PROJECT NO.: 6L0001000

SAMPLE NO.: MCG-648
DRILL HOLE LLM-85-09 UNIT 2A
DRILL HOLE DEPTH (FT): 35

PHENOCRYST RATIO (Q/K/P): 1/2.17/0
POROSITY (VOL %): 26

DEGREE OF WELDING: Moderate
OXIDATION STATE OF Fe-Ti OXIDES: C3-C4

ROCK NAME: Rhyolitic Crystal-Vitric Tuff

GENERAL DESCRIPTION IN THIN SECTION: Fine- to medium-grained phenocrysts in a moderately welded groundmass with axiolitic devitrification. Although this sample has a fracture containing smectite, no clay was observed in thin section.

MINERAL COMPONENT	VOL. %		COMMENTS
Groundmass		48	
Glass	(70)		Axiolitic devitrification.
Pumice	(30)		Up to 4.70 mm. Replaced/mineralized by sanidine and tridymite. Phenocryst ratio (Q/K) = 1/1.
Pore Space		26	
Phenocrysts		25	
Sanidine	(68)		Fine to medium grained, anhedral to euhedral.
Quartz	(32)		Fine to medium grained, anhedral to euhedral. Embayed grains are present.
Pyroxene	(tr)		Fine grained, euhedral to anhedral.
Opaques	(tr)		Fine grained, subhedral to anhedral. Magnetite, ilmenite, and hematite.
Plagioclase	(tr)		Medium grained, euhedral. Zoned grain.
Amphibole	(tr)		Fine grained, anhedral.
Lithic Fragments		tr	Up to 1.67 mm. Mostly basalt/andesite.
Tridymite		tr	Fine grained, euhedral. Occurs in pore space.

(continued on next page)

LANL VAPOR TRANSPORT STUDY
REQUEST NO.: 402553
PROJECT NO.: 6L0001000

SAMPLE NO.: MCG-648 (continued)
DRILL HOLE LLM-85-09 UNIT 2A
DRILL HOLE DEPTH (FT): 35

MINERAL COMPONENT	VOL. %	COMMENTS
Unknown Component	tr	Two grains. One is rounded, 0.80 mm, with a thin rim of hematite and almost totally filled by sheaves of clay (chlorite?); inclusion of magnetite (altering to hematite) with exsolved ilmenite. The other is subhedral, 0.29 mm, with a thin rim of hematite and sparse, randomly oriented flakes of clay (chlorite?).

LANL VAPOR TRANSPORT STUDY
REQUEST NO.: 402553
PROJECT NO.: 6L0001000

SAMPLE NO.: MCG-649
DRILL HOLE LLM-85-09 UNIT 1B
DRILL HOLE DEPTH (FT): 47

PHENOCRYST RATIO (Q/K/P): 1/0.81/0.03 DEGREE OF WELDING: Moderate
POROSITY (VOL %): 21 OXIDATION STATE OF Fe-Ti OXIDES: C2-C3

ROCK NAME: Rhyolitic Crystal-Vitric Tuff

GENERAL DESCRIPTION IN THIN SECTION: Fine- to medium-grained phenocrysts in a groundmass containing glass that is not devitrified. Brown-colored glass is present in the groundmass and some pumice fragments.

MINERAL COMPONENT	VOL. %		COMMENTS
Groundmass		54	
Glass	(66)		Not devitrified. Some brown glass.
Pumice Fragments	(34)		Up to 7.78 mm. Some flattened fragments and andesitic compositions (based on phenocrysts). Phenocryst ratio in rhyolitic fragments (Q/K) = 1/1.83.
Phenocrysts		23	
Quartz	(52)		Fine to medium grained, anhedral to euhedral. Some grains are embayed.
Sanidine	(42)		Fine to medium grained, anhedral to euhedral.
Opaques	(4)		Fine grained, anhedral to euhedral. Magnetite and ilmenite intergrowths.
Plagioclase	(2)		Fine grained, subhedral. Zoned grain.
Pyroxene	(tr)		Fine grained, anhedral to euhedral.
Pore Space		21	
Lithic Fragments		2	Up to 0.97 mm. Several types: altered, flow-banded rock; altered, spherulitically devitrified rock; aphanitic rock; and hyalopilitic basalt.

LANL VAPOR TRANSPORT STUDY
REQUEST NO.: 402553
PROJECT NO.: 6L0001000

SAMPLE NO.: MCG-650
DRILL HOLE LLM-85-09 UNIT 1B
DRILL HOLE DEPTH (FT): 68

PHENOCRYST RATIO (Q/K/P): 1/1.04/0
POROSITY (VOL %): 24

DEGREE OF WELDING: Moderate
OXIDATION STATE OF Fe-Ti OXIDES: C3

ROCK NAME: Rhyolitic Vitric-Crystal Tuff

GENERAL DESCRIPTION IN THIN SECTION: Fine- to medium-grained phenocrysts in a moderately welded groundmass. Shards exhibit incipient axiolitic devitrification. Most pumice fragments have spherulitic devitrification.

MINERAL COMPONENT	VOL. %		COMMENTS
Groundmass		55	
Glass	(54)		Incipient axiolitic devitrification.
Pumice Fragments	(46)		Up to 6.74 mm. Most have spherulitic devitrification. Some are partially flattened. An andesitic composition (based on phenocrysts) is present. Phenocryst ratio (Q/K) in rhyolitic fragments is 1/1.33.
Pore Space		24	
Phenocrysts		18	
Sanidine	(47)		Fine to medium grained, anhedral to euhedral.
Quartz	(45)		Fine to medium grained, anhedral to euhedral. Resorption features are abundant.
Opaques	(6)		Fine grained, anhedral to euhedral. Ilmenite with exsolved magnetite.
Pyroxene	(2)		Fine grained, anhedral to euhedral. Most grains are associated with opaques; some grains are coated with celadonite.
Lithic Fragments		3	Up to 3.41 mm. Several types: altered basalt; hyalopilitic basalt; vitric tuff with spherulitic devitrification; granophyre; and an altered, flow-banded rock.

B.2 FISCAL YEAR 1986 FIELDWORK

A total of 11 drill-core and outcrop samples from the Tshirege Member of the Bandelier Tuff were submitted to the GJPO Petrology Laboratory for petrographic characterization. There were two samples each from Unit 1a, Unit 1b, and Unit 2b; one sample from Unit 2a; and four lithic lapilli and pumice fragments from Unit 1a.

The samples as received consisted of sections of 5-cm-diameter drill core and irregular samples from outcrops. From these samples, portions were removed using a core splitter for polished-thin-section preparation. The samples were impregnated with blue-colored epoxy to emphasize the porosity in the thin sections.* Each thin section was subjected to point-count analysis (300 counts) to determine mineral and component abundance. Tuffaceous rocks were named according to the classification of Cook (1965). As shown in Figure B-2, the rocks from this study plot in the following fields: VII (crystal-vitric tuff) and VIII (vitric-crystal).

The optical identifications of major and minor minerals, especially devitrification products, were confirmed using X-ray diffraction (XRD). The compositional modifiers to tuffaceous rock names are based on bulk XRD data. These modifiers were assigned according to the classification of Streckeisen (1967).

Petrographic descriptions of these samples are presented on the pages following Figure B-2. They are presented in consecutive order by sample number, although the drill-hole number, depth of the sample, and geologic unit are also identified near the top of the page. The volume percent of each mineral component is given, together with the petrographic description. Phenocrysts and groundmass are further subdivided into individual components, and these subcomponents are followed by a number in parentheses which indicates their volume percentage of the main component. The petrographic descriptions were taken from a report entitled Petrography of the Tshirege Member of the Bandelier Tuff, Mesita del Buey, Los Alamos County, New Mexico: Second Report (Fukui, 1986).

*There is considerable discrepancy between porosity measured in thin section and that determined by means of helium injection (see Section 3.1.2). The significantly lower porosity determined in thin section is due to the fact that most of the thin sections were cut parallel to the core axis (parallel to the direction of flattening), resulting in erroneous extrapolation based on the cross section of the gas tubes rather than on their true shape.

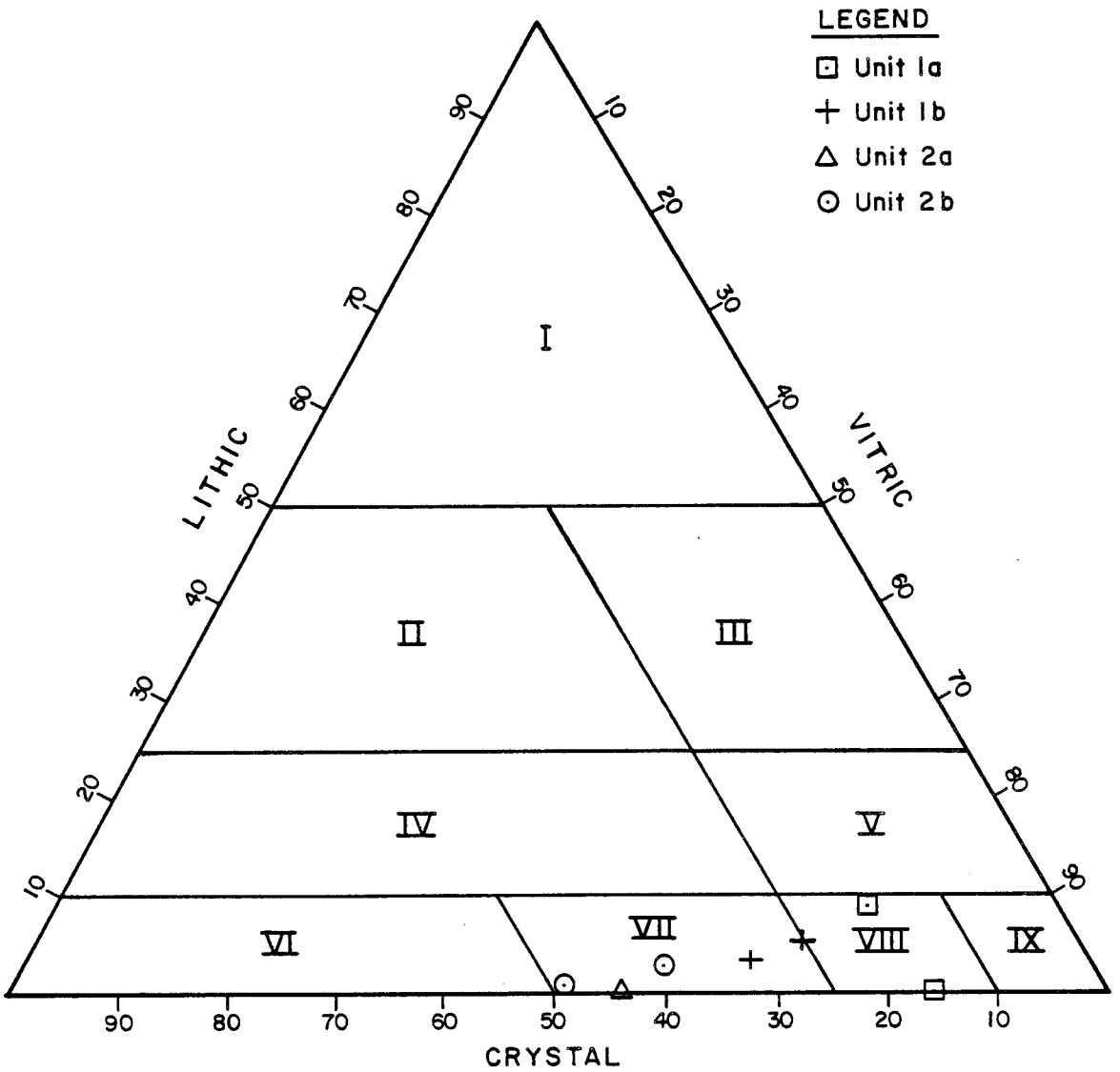

Figure B-2. Classification of Cook (1965) Used to Name Tuffaceous Rocks in This Study on the Basis of the Normalized Vitric (including pumice), Crystal, and Lithic Components Determined From the Modal Analysis.

LANL VAPOR TRANSPORT STUDY
REQUEST NO.: 403353
PROJECT NO.: 6L0001000

SAMPLE NO.: MCG-651
DRILL HOLE LLC-86-19 UNIT 1a (Lithic)
DRILL HOLE DEPTH (FT): 190

BANDELIER TUFF PHENOCRYST-RATIO (Q/K/P): 1/7.3/5.5
DEGREE OF WELDING: Strong
POROSITY (VOL. %): 1
OXIDATION STATE OF Fe-Ti OXIDES: C7

ROCK NAME: Altered Crystal-Vitric Tuff

GENERAL DESCRIPTION IN THIN SECTION: Lithic fragment with feldspar phenocrysts replaced by analcime(?).

MINERAL COMPONENT	VOL. %		COMMENTS
Groundmass		62	
Glass	(93)		Glass appears partially altered to clay that is iron stained. The glass is not devitrified. Shard structure is preserved.
Opaques	(7)		Hematite.
Phenocrysts		35	
Plagioclase	(44)		Pseudomorphic replacement by analcime. Compositional-zoning structure is preserved.
K-feldspar	(33)		Pseudomorphic replacement by analcime.
Biotite	(13)		Totally altered to chlorite and hematite.
Pyroxene(?)	(9)		Altered to serpentine(?) and hematite.
Opaques	(tr)		Altered to pseudobrookite and hematite.
Lithics(?)		3	Altered.
Vug		2	Vugs are lined by opal and filled by chalcedony.
Pore Space		1	

LANL VAPOR TRANSPORT STUDY
REQUEST NO.: 403353
PROJECT NO.: 6L0001000

SAMPLE NO.: MCG-652
DRILL HOLE LLC-86-19 UNIT 1a (Lithic)
DRILL HOLE DEPTH (FT): 175

BANDELIER TUFF PHENOCRYST-RATIO (Q/K/P): Unknown
DEGREE OF WELDING: Strong
POROSITY (VOL. %): 22
OXIDATION STATE OF Fe-Ti OXIDES: C7

ROCK NAME: Altered, Crystal-Vitric Tuff

GENERAL DESCRIPTION IN THIN SECTION: Groundmass is silicified. Phenocrysts are replaced by clay minerals. Vague features in the rock may be pumice and lithic fragments.

MINERAL COMPONENT	VOL. %		COMMENTS
Groundmass		67	
Glass	(91)		Replaced by quartz and clay minerals.
Pumice Fragments	(9)		Up to 5.45 mm. Replaced by silica. Texturally, these resemble the pumice in Units 2a and 2b.
Pore Space		22	
Phenocrysts		6	
Feldspars(?)	(68)		Totally replaced by clay.
Opaques	(32)		Totally replaced by pseudobrookite and hematite.
Lithic Fragments(?)		5	Vague textural features.

LANL VAPOR TRANSPORT STUDY
REQUEST NO.: 403353
PROJECT NO.: 6L0001000

SAMPLE NO.: MCG-653
DRILL HOLE LLC-86-19 UNIT 1a (Lithic)
DRILL HOLE DEPTH (FT): 162

BANDELIER TUFF PHENOCRYST-RATIO (Q/K/P): 1/3.4/0
DEGREE OF WELDING: Strong
POROSITY (VOL. %): 13
OXIDATION STATE OF Fe-Ti OXIDES: C4

ROCK NAME: Rhyolitic Vitric Tuff

GENERAL DESCRIPTION IN THIN SECTION: Fine- to medium-grained phenocrysts in a strongly welded groundmass with axiolitic and spherulitic devitrification and vapor-phase mineralization.

MINERAL COMPONENT		VOL. %	COMMENTS
Groundmass		73	Strongly welded glass with axiolitic and spherulitic devitrification.
Pore Space		13	
Vapor-Phase Minerals		9	Fills vugs.
Sanidine	(53)		
Tridymite	(29)		
Alpha Quartz	(18)		
Phenocrysts		5	
Sanidine	(63)		
Opaques	(31)		Ilmenite, magnetite, and hematite.
Alpha Quartz	(6)		
Pyroxene	(tr)		Augite. Rimmed by goethite.

LANL VAPOR TRANSPORT STUDY
REQUEST NO.: 403353
PROJECT NO.: 6L0001000

SAMPLE NO.: MCG-654
DRILL HOLE LLC-86-20 UNIT 1a
DRILL HOLE DEPTH (FT): 148

BANDELIER TUFF PHENOCRYST-RATIO (Q/K/P): NA
DEGREE OF WELDING: Slight
POROSITY (VOL. %): 46
OXIDATION STATE OF Fe-Ti OXIDES: C2-C3

ROCK NAME: Andesitic Pumice Fragment

GENERAL DESCRIPTION IN THIN SECTION: Sample is a pumice fragment; fine- to medium-grained phenocrysts in fresh glass. The pumice is not flattened.

MINERAL COMPONENT	VOL. %		COMMENTS
Pore Space		46	
Phenocrysts		36	
Plagioclase	(76)		Medium-grained phenocrysts exhibit normal zoning; finer grains do not appear to be zoned. Fresh.
Amphibole	(23)		Basaltic hornblende (lamprobolite).
Opaques	(1)		Magnetite and ilmenite.
Groundmass (Pumice)		18	Fresh, colorless glass.

LANL VAPOR TRANSPORT STUDY
REQUEST NO.: 403353
PROJECT NO.: 6L0001000

SAMPLE NO.: MCG-655
DRILL HOLE LLC-86-20 UNIT 1a
DRILL HOLE DEPTH (FT): 176

BANDELIER TUFF PHENOCRYST-RATIO (Q/K/P): .1/1.4/0.06
DEGREE OF WELDING: Slight
POROSITY (VOL. %): 33
OXIDATION STATE OF Fe-Ti OXIDES: C2-C3

ROCK NAME: Rhyolitic Vitric-Crystal Tuff

GENERAL DESCRIPTION IN THIN SECTION: Fine-to medium-grained phenocrysts in a slightly welded, fresh-glass groundmass. Glass in pumice fragments is also fresh. Some pumice fragments are flattened.

MINERAL COMPONENT	VOL. %		COMMENTS
Groundmass		49	
Pumice Fragments	(59)		Up to 6.73 mm. Fresh glass. Some fragments are totally flattened. The only phenocrysts in the fragments are sanidine, amphibole, and opaques.
Glass	(41)		Fresh. Y-shaped shards are present.
Pore Space		33	
Phenocrysts		12	
Sanidine	(49)		
Quartz	(49)		Embayed grains are common.
Opaques	(2)		Magnetite and ilmenite.
Pyroxene	(tr)		Augite.
Amphibole	(tr)		Lamprobolite.
Lithic Fragments		6	Up 2.56 mm. Mostly basaltic tuffs.

LANL VAPOR TRANSPORT STUDY
REQUEST NO.: 403353
PROJECT NO.: 6L0001000

SAMPLE NO.: MCG-656
DRILL HOLE LLC-86-20 UNIT 1b
DRILL HOLE DEPTH (FT): 126

BANDELIER TUFF PHENOCRYST-RATIO (Q/K/P): 1/2/0.01
DEGREE OF WELDING: Slight
POROSITY (VOL. %): 38
OXIDATION STATE OF Fe-Ti OXIDES: C3-C4

ROCK NAME: Rhyolitic Crystal-Vitric Tuff

GENERAL DESCRIPTION IN THIN SECTION: Fine- to medium-grained phenocrysts in a slightly welded, fresh-glass groundmass. Glass in pumice fragments is also fresh. Some pumice fragments are flattened.

MINERAL COMPONENT	VOL. %		COMMENTS
Groundmass		41	
Glass	(66)		Fresh; brown-colored.
Pumice	(46)		Up to 5.45 mm. Some pumice fragments are totally flattened. Phenocryst ratio in pumice is two sanidine for every quartz.
Pore Space		38	
Phenocrysts		19	
Sanidine	(56)		
Quartz	(40)		Many grains are embayed.
Opaques	(4)		Ilmenite, magnetite, and hematite.
Pyroxene	(tr)		Augite.
Plagioclase	(tr)		
Amphibole	(tr)		Lamprobolite.
Lithic Fragments		2	Up to 3.45 mm. Altered and fresh hyalopilitic basalts; altered lithic-vitric tuff with abundant basaltic material; altered, thoroughly welded, spherulitically devitrified, vitric tuff; and silicified vitric tuff.

LANL VAPOR TRANSPORT STUDY
REQUEST NO.: 403353
PROJECT NO.: 6L0001000

SAMPLE NO.: MCG-657
DRILL HOLE LLC-86-20 UNIT 1a
DRILL HOLE DEPTH (FT): 134

BANDELIER TUFF PHENOCRYST-RATIO (Q/K/P): 1/1.3/0.1 (In Pumice Fragments)
DEGREE OF WELDING: Slight
POROSITY (VOL. %): 53
OXIDATION STATE OF Fe-Ti OXIDES: C3-C4

ROCK NAME: Rhyolitic Vitric-Crystal Tuff

GENERAL DESCRIPTION IN THIN SECTION: Fine- to medium-grained phenocrysts in a groundmass consisting mainly of fresh-glass, pumice fragments. Many pumice fragments are partially flattened.

MINERAL COMPONENT		VOL. %	COMMENTS
Pore Space		53	
Groundmass		40	
Pumice Fragments	(85)		Up to 34 mm. Many pumice fragments are partially flattened. Glass is fresh. Some brown-colored glass.
Glass	(15)		Fresh; brown colored. Y-shaped shards and intact bubble walls indicate slight welding.
Phenocrysts		7	Mainly in pumice fragments.
Sanidine	(50)		
Quartz	(36)		
Opaques	(14)		Ilmenite, magnetite, and hematite.
Pyroxene	(tr)		Augite.

LANL VAPOR TRANSPORT STUDY
REQUEST NO.: 403353
PROJECT NO.: 6L0001000

SAMPLE NO.: MCG-658
DRILL HOLE LLC-86-20 UNIT 1b
DRILL HOLE DEPTH (FT): 119

BANDELIER TUFF PHENOCRYST-RATIO (Q/K/P): 1/1.5/0.01
DEGREE OF WELDING: Slight to Moderate POROSITY (VOL. %): 21
OXIDATION STATE OF Fe-Ti OXIDES: C4

ROCK NAME: Rhyolitic Vitric-Crystal Tuff

GENERAL DESCRIPTION IN THIN SECTION: Fine- to medium-grained phenocrysts in a slightly to moderately welded, fresh-glass groundmass. Some pumice fragments are flattened.

MINERAL COMPONENT	VOL. %		COMMENTS
Groundmass		55	
Glass	(75)		Mostly fresh, incipient alteration to clay. Minor amounts of brown-colored glass are present.
Pumice	(25)		Up to 7.73 mm. Some fragments are flattened. Phenocryst ratio is 1:1 quartz to sanidine.
Pore Space		21	
Phenocrysts		20	
Sanidine	(55)		
Quartz	(40)		
Opaques	(3)		Magnetite, ilmenite, rutile, and hematite.
Plagioclase	(2)		
Pyroxene	(tr)		Augite
Lithic Fragments		4	Up to 2.88 mm. Altered hyalopilitic basalts and vitric tuffs; a vitric tuff with spherulitic devitrification; and a fresh, porous, basaltic crystal-vitric tuff.

LANL VAPOR TRANSPORT STUDY
REQUEST NO.: 403353
PROJECT NO.: 6L0001000

SAMPLE NO.: MCG-659
OUTCROP SAMPLE
UNIT 2b

BANDELIER TUFF PHENOCRYST-RATIO (Q/K/P): 1/2.5/0.01
DEGREE OF WELDING: Slight
POROSITY (VOL. %): 34
OXIDATION STATE OF Fe-Ti OXIDES: C4

ROCK NAME: Rhyolitic Crystal-Vitric Tuff

GENERAL DESCRIPTION IN THIN SECTION: Fine- to medium-grained phenocrysts in a slightly welded groundmass. Shards show axiolitic devitrification. Pumice fragments are replaced by sanidine and tridymite.

MINERAL COMPONENT		VOL. %	COMMENTS
Groundmass		38	
Glass	(67)		Axiolitic devitrification. Y-shaped shards are present.
Pumice Fragments	(33)		Up to 2.58 mm. Replaced/mineralized by sanidine and tridymite. Phenocryst ratio (Q/K) = 1/2.5.
Pore Space		34	
Phenocrysts		26	
Sanidine	(60)		
Quartz	(38)		Some grains are embayed.
Opaques	(2)		Ilmenite, magnetite, rutile, and hematite.
Pyroxene	(tr)		
Plagioclase	(tr)		One zoned grain.
Lithic Fragments		2	Up to 2.61 mm. Basalts.

LANL VAPOR TRANSPORT STUDY
REQUEST NO.: 403353
PROJECT NO.: 6L0001000

SAMPLE NO.: MCG-660
OUTCROP SAMPLE
UNIT 2b

BANDELIER TUFF PHENOCRYST-RATIO (Q/K/P): 1/2.5/0.04
DEGREE OF WELDING: Slight
POROSITY (VOL. %): 43
OXIDATION STATE OF Fe-Ti OXIDES: C4

ROCK NAME: Rhyolitic Crystal-Vitric Tuff

GENERAL DESCRIPTION IN THIN SECTION: Fine- to medium-grained phenocrysts in a slightly welded groundmass. Shards show axiolitic devitrification. Pumice fragments are replaced by sanidine and tridymite.

MINERAL COMPONENT	VOL. %		COMMENTS
Pore Space		43	
Groundmass		29	
Glass	(69)		Axiolitic devitrification.
Pumice	(31)		Up to 6.15 mm. Replaced/mineralized by sanidine and tridymite. Some pumice fragments contain a fibrous zeolite, others have amphibole, pyroxene, and zoned-plagioclase phenocrysts. One pumice fragment had a phenocryst ratio (Q/K) = 1/1.5.
Phenocrysts		28	
Sanidine	(47)		May have oriented overgrowths of sanidine; this may be vapor-phase mineralization.
Quartz	(46)		
Opaques	(5)		Ilmenite, magnetite, rutile, and hematite.
Plagioclase	(1)		
Amphibole	(1)		Lamprobolite.
Pyroxene	(tr)		Augite.
Lithic Fragments		tr	Up to 1.45 mm. Altered tuff and grains consisting of pyroxene and opaques, possibly from a basalt.

LANL VAPOR TRANSPORT STUDY
REQUEST NO.: 403353
PROJECT NO.: 6L0001000

SAMPLE NO.: MCG-661
OUTCROP SAMPLE
UNIT 2a

BANDELIER TUFF PHENOCRYST-RATIO (Q/K/P): 1/3.2/0.05
DEGREE OF WELDING: Slight
POROSITY (VOL. %): 44
OXIDATION STATE OF Fe-Ti OXIDES: C4

ROCK NAME: Rhyolitic Crystal Vitric Tuff

GENERAL DESCRIPTION IN THIN SECTION: Fine- to medium-grained phenocrysts in a slightly welded groundmass. Shards show axiolitic devitrification. Pumice fragments are replaced by sanidine and tridymite.

MINERAL COMPONENT	VOL. %		COMMENTS
Pore Space		44	
Groundmass		31	
Glass	(59)		Axiolitic devitrification. Y-shaped shards and intact bubble-walls.
Pumice Fragments	(41)		Up to 4.03 mm. Replaced/mineralized by sanidine and tridymite. Some pumice fragments are andesitic (plagioclase and amphibole phenocrysts); the other pumice only contain quartz phenocrysts.
Phenocrysts		25	
Sanidine	(41)		Some sanidine phenocrysts have been partially dissolved (intragranular porosity).
Quartz	(28)		
Opaques	(14)		Ilmenite, magnetite, rutile, and hematite.
Plagioclase	(3)		Zoned grains.
Amphibole	(tr)		Lamprobolite.
Biotite	(tr)		
Pyroxene	(tr)		Augite.
Lithic Fragment		tr	The lithic is a silicified tuff and measures 1.82 mm.

Appendix C

MOISTURE CHARACTERISTIC CURVES

Table C-1. Data Used to Plot the Moisture Characteristic Curves (drying curves only)

Hole Number	Sample Number	Depth (ft)	Capillary Pressure (psi)	Wetting Fluid Saturation (percent)
LLM-85-01	MCG-602	30	0.510	91.6
			0.906	86.4
			1.420	81.2
			2.055	76.1
			2.814	70.9
			3.701	65.8
LLM-85-01	MCG-603	52	0.455	90.0
			0.823	84.7
			1.385	79.7
			2.230	74.9
			3.495	70.2
			5.403	65.8
LLM-85-01	MCG-604	101	0.493	88.6
			0.955	82.1
			1.738	76.6
			3.220	71.9
			6.555	67.8
LLM-85-01	MCG-605	124	0.392	83.5
			0.620	76.9
			0.955	70.5
			1.450	64.4
			2.189	58.5
			3.319	52.9
LLM-85-02	MCG-606	7	0.392	88.6
			0.812	81.1
			1.450	73.9
			2.372	66.8
			3.663	60.0
			5.440	53.3
LLM-85-02	MCG-607	36	0.097	92.0
			0.181	87.3
			0.494	79.1
			0.799	75.8
			1.382	73.4
			2.975	71.8
LLM-85-02	MCG-608	67	0.424	90.7
			0.681	86.6
			1.050	82.6
			1.573	78.7
			2.315	75.0
			3.375	71.5

Table C-1 (continued). Data Used to Plot the Moisture Characteristic Curves (drying curves only)

Hole Number	Sample Number	Depth (ft)	Capillary Pressure (psi)	Wetting Fluid Saturation (percent)
LLM-85-02	MCG-609	117	0.252	94.2
			0.626	89.3
			1.135	84.2
			1.757	79.1
			2.474	73.9
			3.268	68.6
LLM-85-05	MCG-610	15	0.174	90.0
			0.328	84.5
			0.563	79.1
			0.913	73.9
			1.429	68.9
			2.188	64.2
LLM-85-05	MCG-611	36	0.259	96.1
			1.014	90.8
			1.879	85.0
			2.715	78.5
			3.482	71.4
			4.171	63.7
LLM-85-05	MCG-612	76	0.072	97.1
			0.344	94.0
			0.800	90.9
			1.424	87.8
			2.198	84.6
			3.109	81.4
LLM-85-05	MCG-613	123	0.166	85.1
			0.243	82.4
			0.382	79.7
			0.671	77.1
			1.426	74.6
			4.598	72.1
LGM-85-06	MCG-614	29	0.446	83.2
			0.679	77.2
			1.020	71.4
			1.526	65.8
			2.295	60.5
			3.500	55.4

Table C-1 (continued). Data Used to Plot the Moisture Characteristic Curves (drying curves only)

Hole Number	Sample Number	Depth (ft)	Capillary Pressure (psi)	Wetting Fluid Saturation (percent)
LGM-85-06	MCG-615	51	0.419	90.8
			0.650	86.9
			0.970	83.1
			1.411	79.5
			2.016	76.0
			2.850	72.6
LGM-85-06	MCG-616	99	0.322	85.6
			0.403	85.4
			0.542	84.5
			0.818	84.3
			1.527	83.4
			4.825	82.2
LGM-85-06	MCG-617	115	0.068	96.9
			0.309	92.3
			0.810	87.8
			1.716	83.6
			2.388	81.6
			3.259	79.6
LGM-85-11	MCG-618	3	0.296	88.7
			0.594	81.9
			1.063	75.3
			1.775	69.0
			2.841	62.9
			4.429	57.1
LGM-85-11	MCG-619	30	0.491	90.5
			1.188	81.6
			2.040	72.3
			2.976	62.6
			3.950	52.5
			4.934	42.0
LGM-85-11	MCG-620	94	0.161	93.3
			0.376	88.7
			0.734	84.2
			1.297	79.9
			2.163	75.8
			3.483	71.9

Table C-1 (continued). Data Used to Plot the Moisture Characteristic Curves (drying curves only)

Hole Number	Sample Number	Depth (ft)	Capillary Pressure (psi)	Wetting Fluid Saturation (percent)
LGM-85-11	MCG-621	115	0.270	92.3
			0.446	89.2
			0.727	86.3
			1.191	83.5
			1.991	80.9
			3.463	78.5

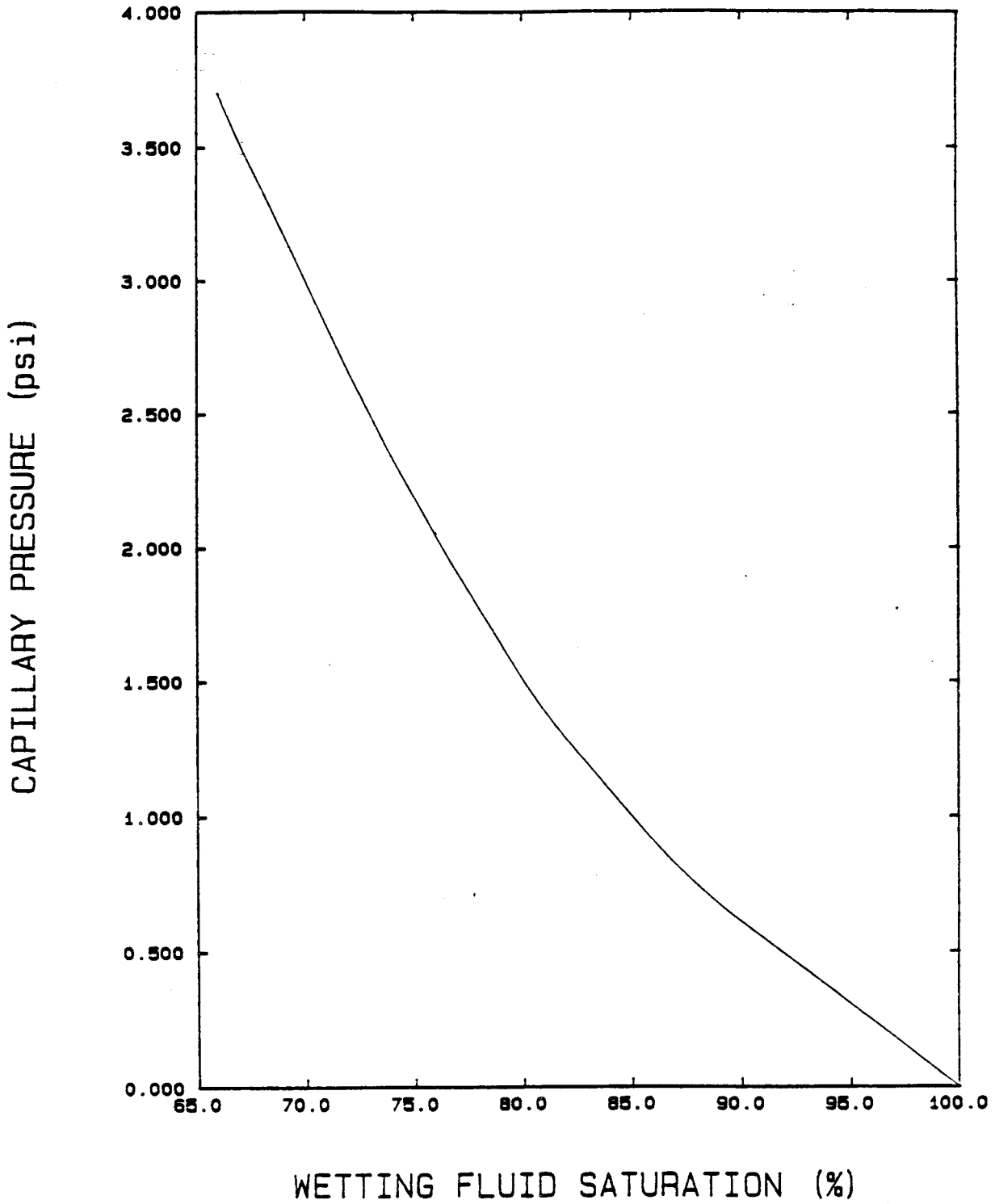

Figure C-1. Moisture Characteristic Curve for Sample MCG-602, Hole LLM-85-01, Depth of 30 Feet

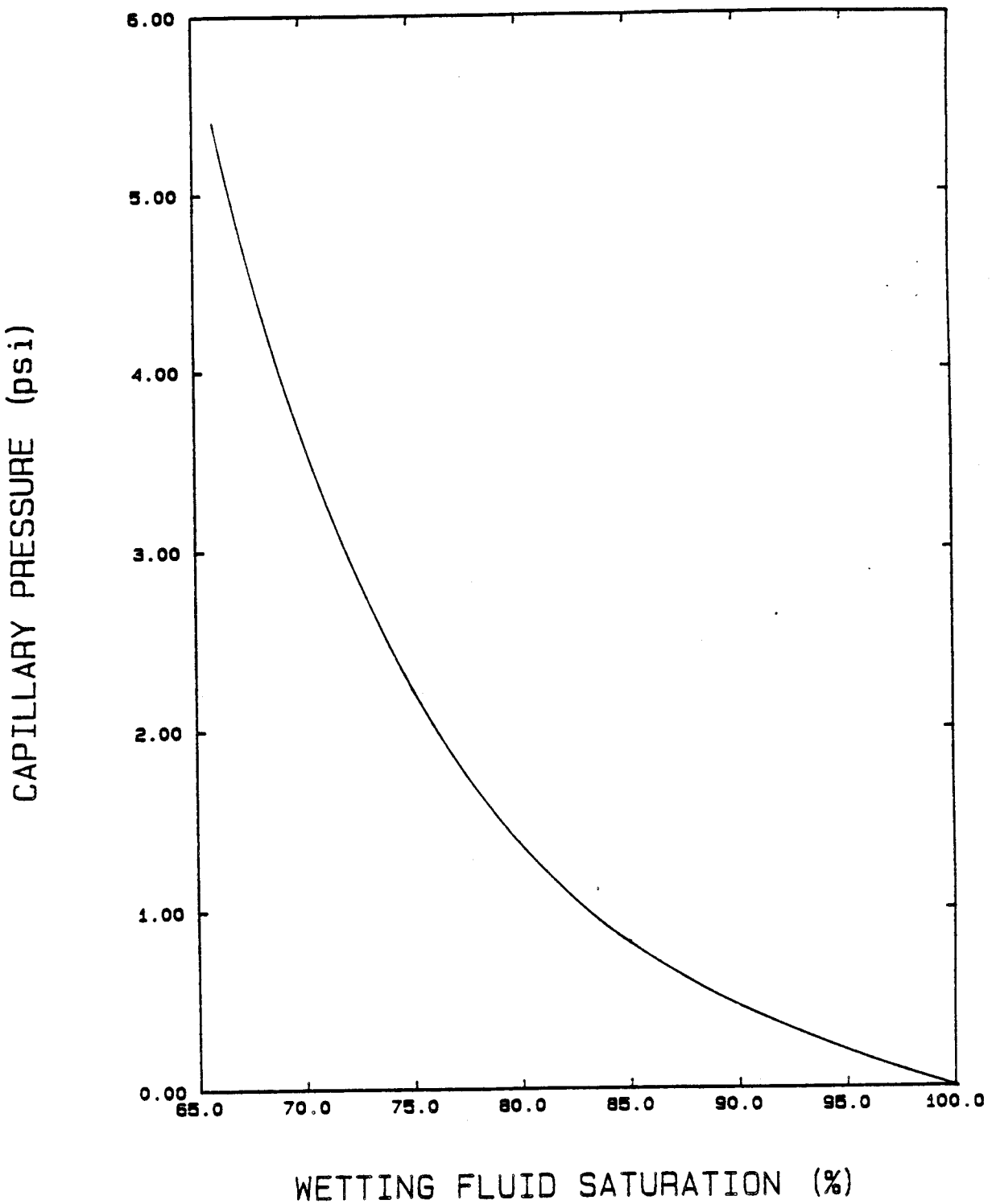

Figure C-2. Moisture Characteristic Curve for Sample MCG-603, Hole LLM-85-01, Depth of 52 Feet

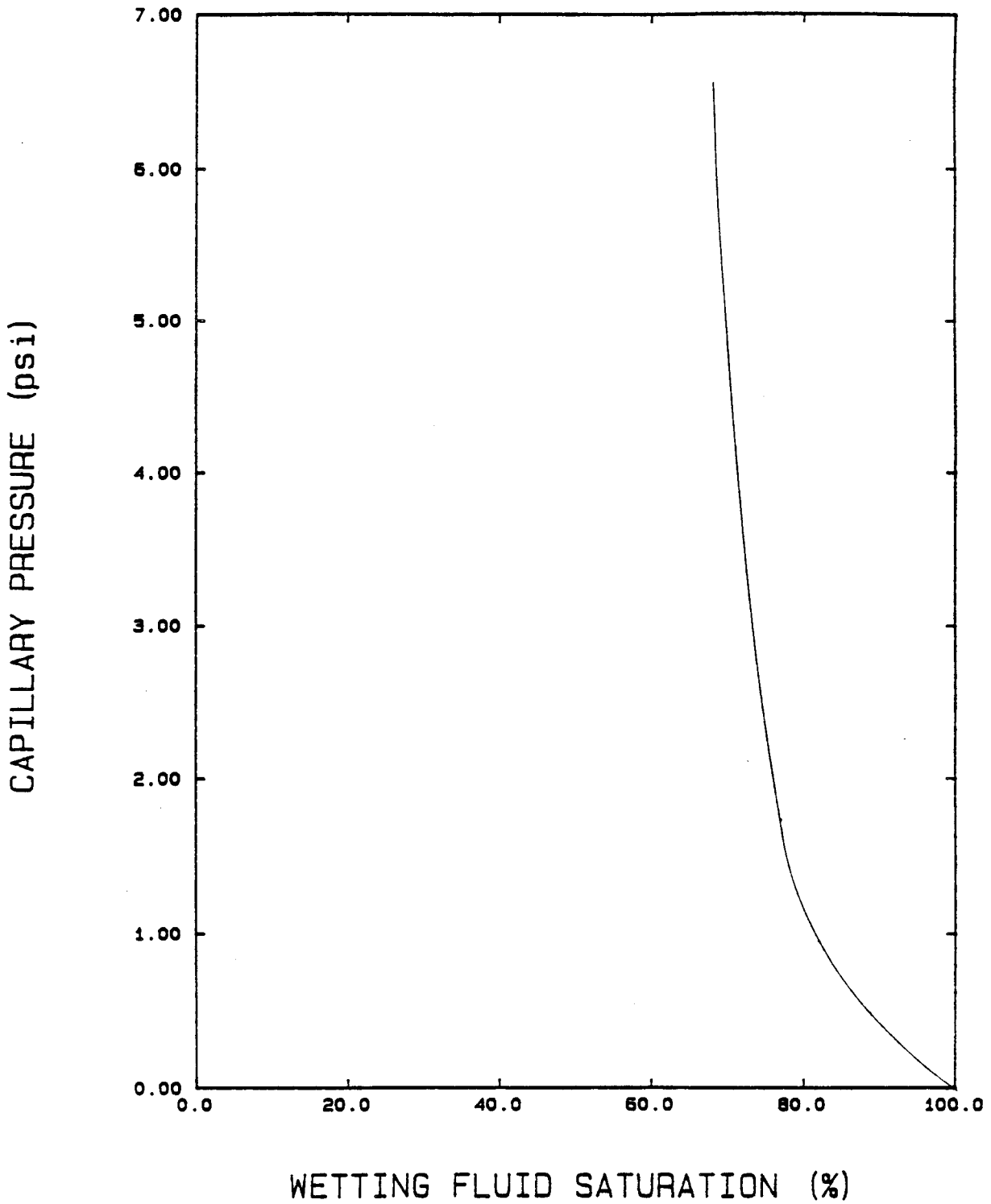

Figure C-3. Moisture Characteristic Curve for Sample MCG-604, Hole LLM-85-01, Depth of 101 Feet

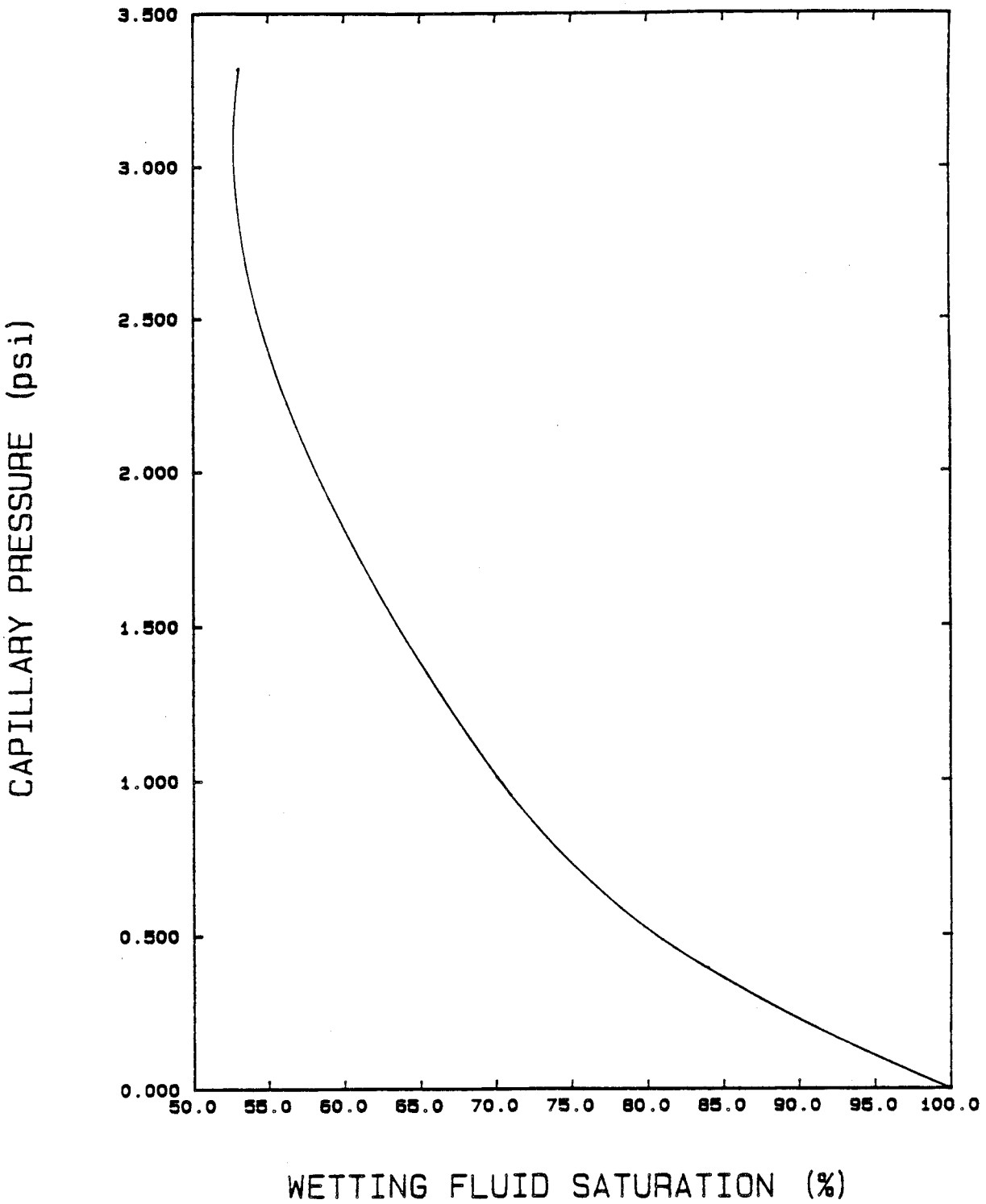

Figure C-4. Moisture Characteristic Curve for Sample MCG-605, Hole LLM-85-01, Depth of 124 Feet

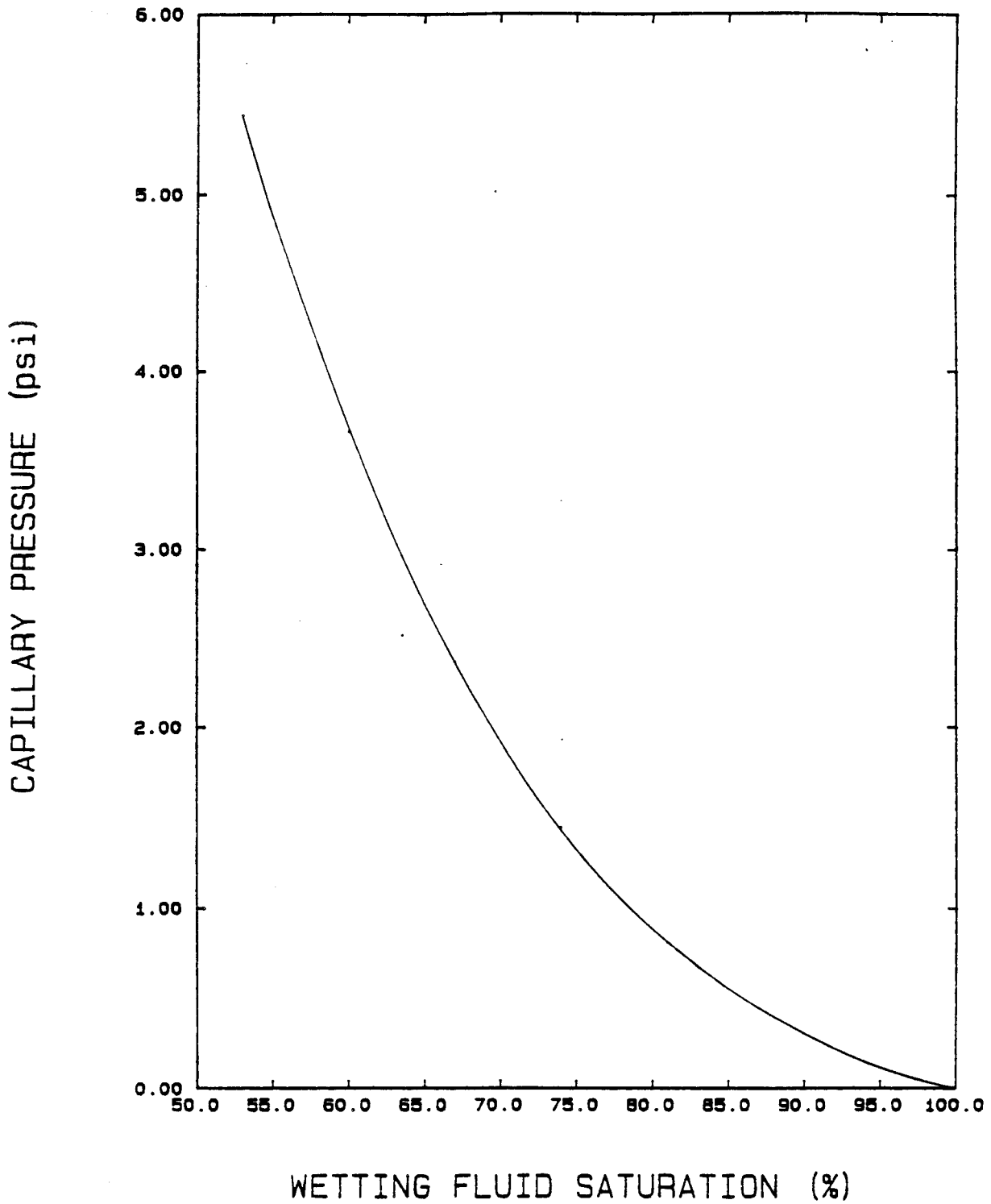

Figure C-5. Moisture Characteristic Curve for Sample MCG-606, Hole LLM-85-02, Depth of 7 Feet

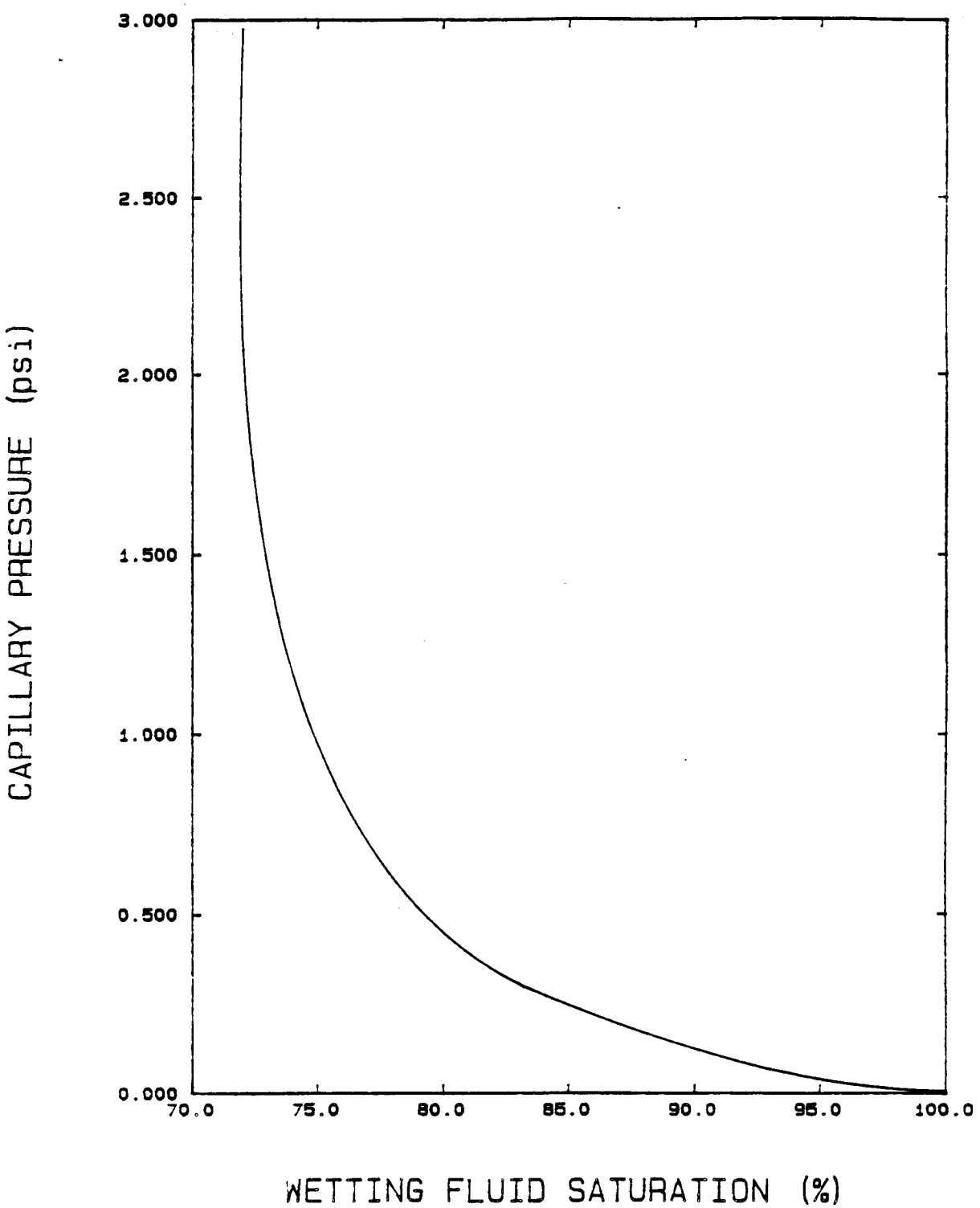

Figure C-6. Moisture Characteristic Curve for Sample MCG-607, Hole LLM-85-02, Depth of 36 Feet

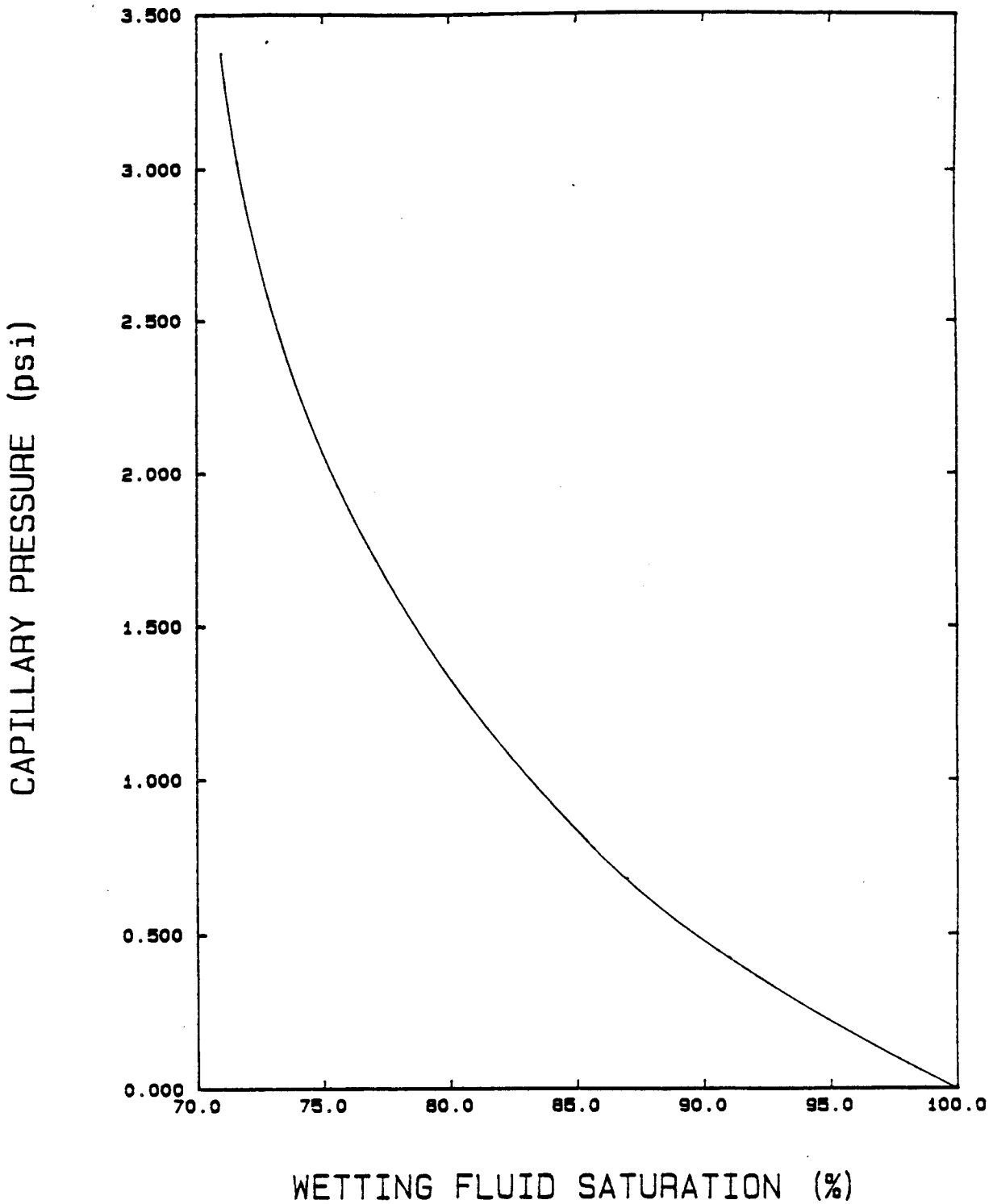

Figure C-7. Moisture Characteristic Curve for Sample MCG-608, Hole LLM-85-02, Depth of 67 Feet

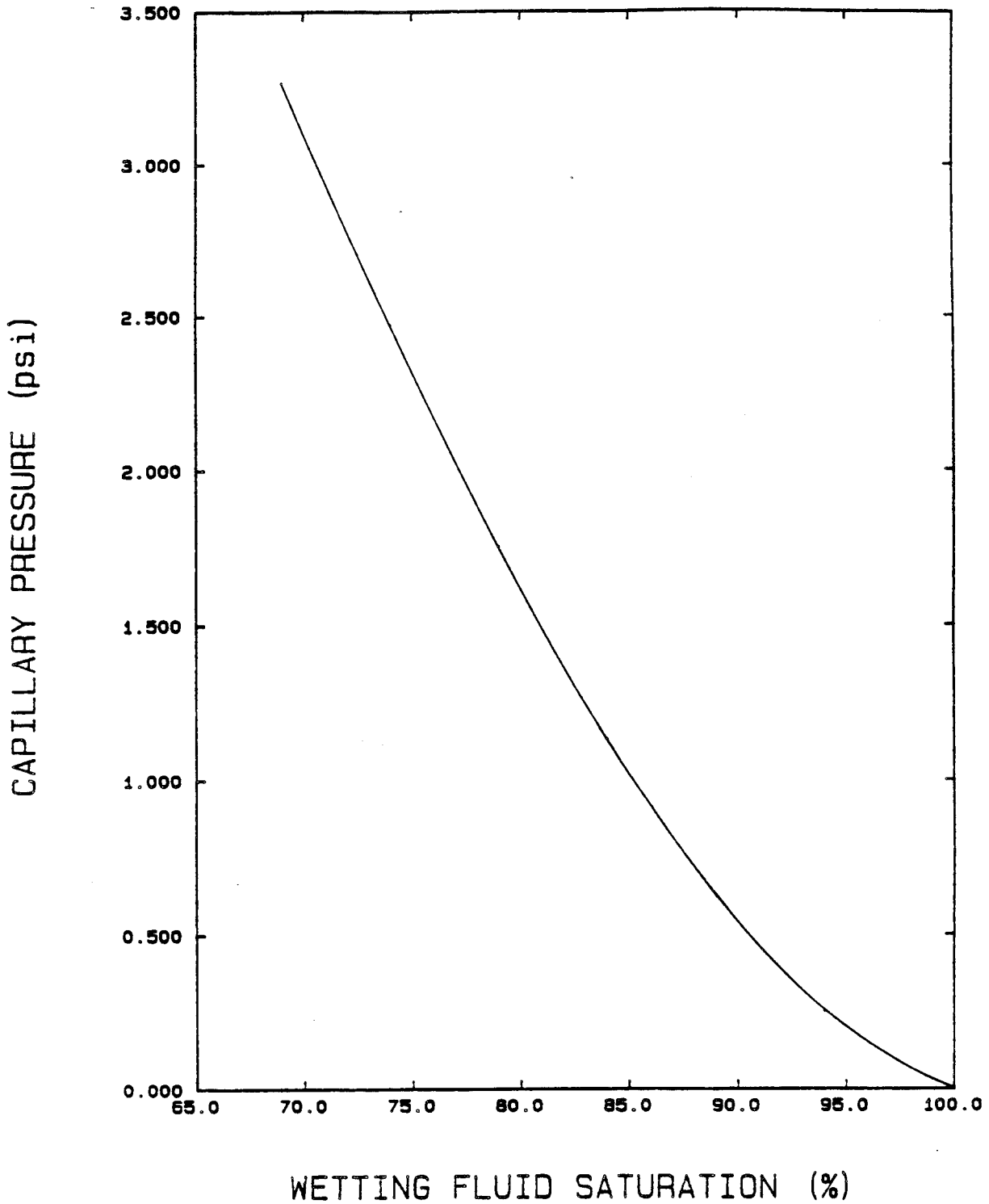

Figure C-8. Moisture Characteristic Curve for Sample MCG-609, Hole LLM-85-02, Depth of 117 Feet

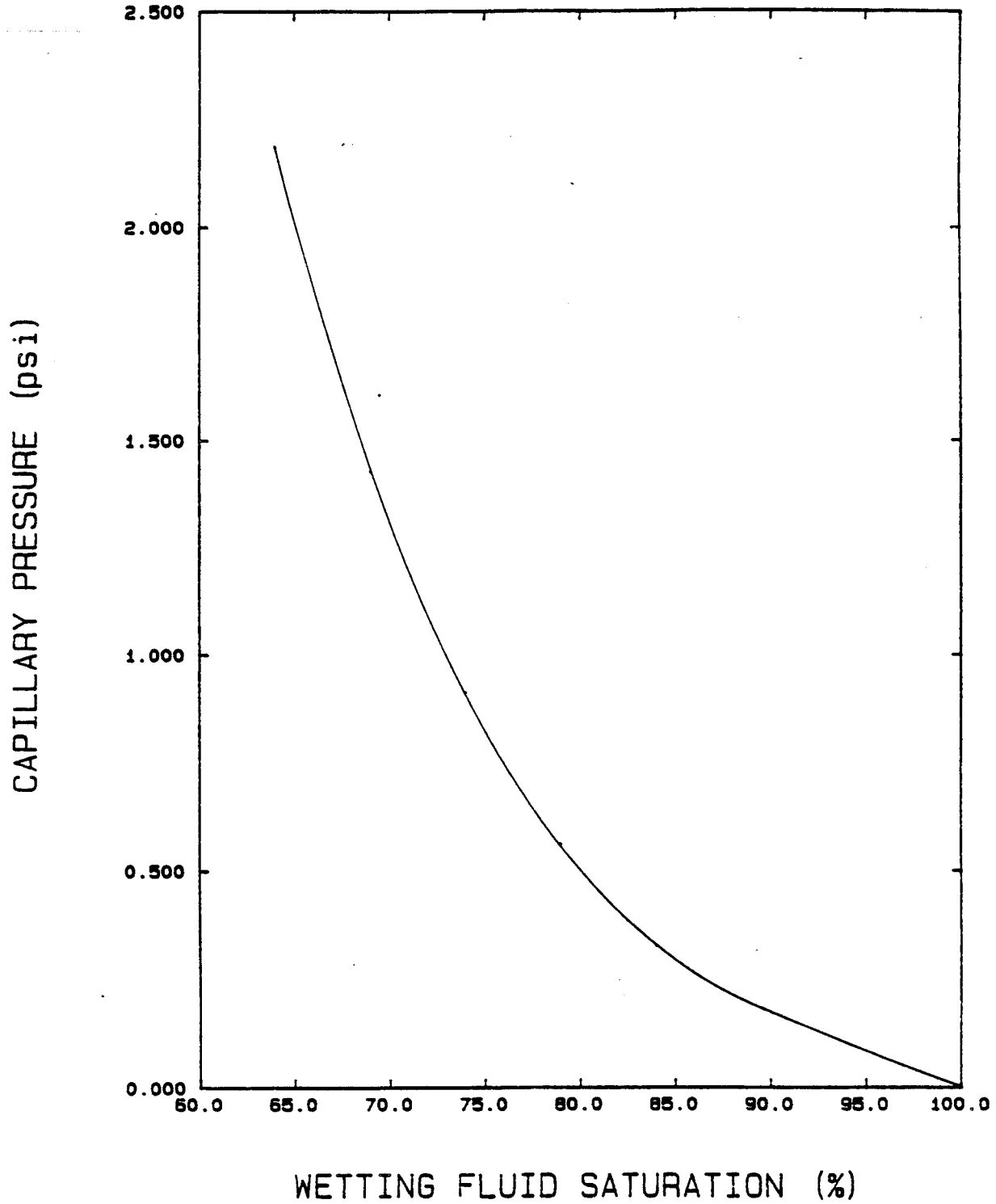

Figure C-9. Moisture Characteristic Curve for Sample MCG-610, Hole LLM-85-05, Depth of 15 Feet

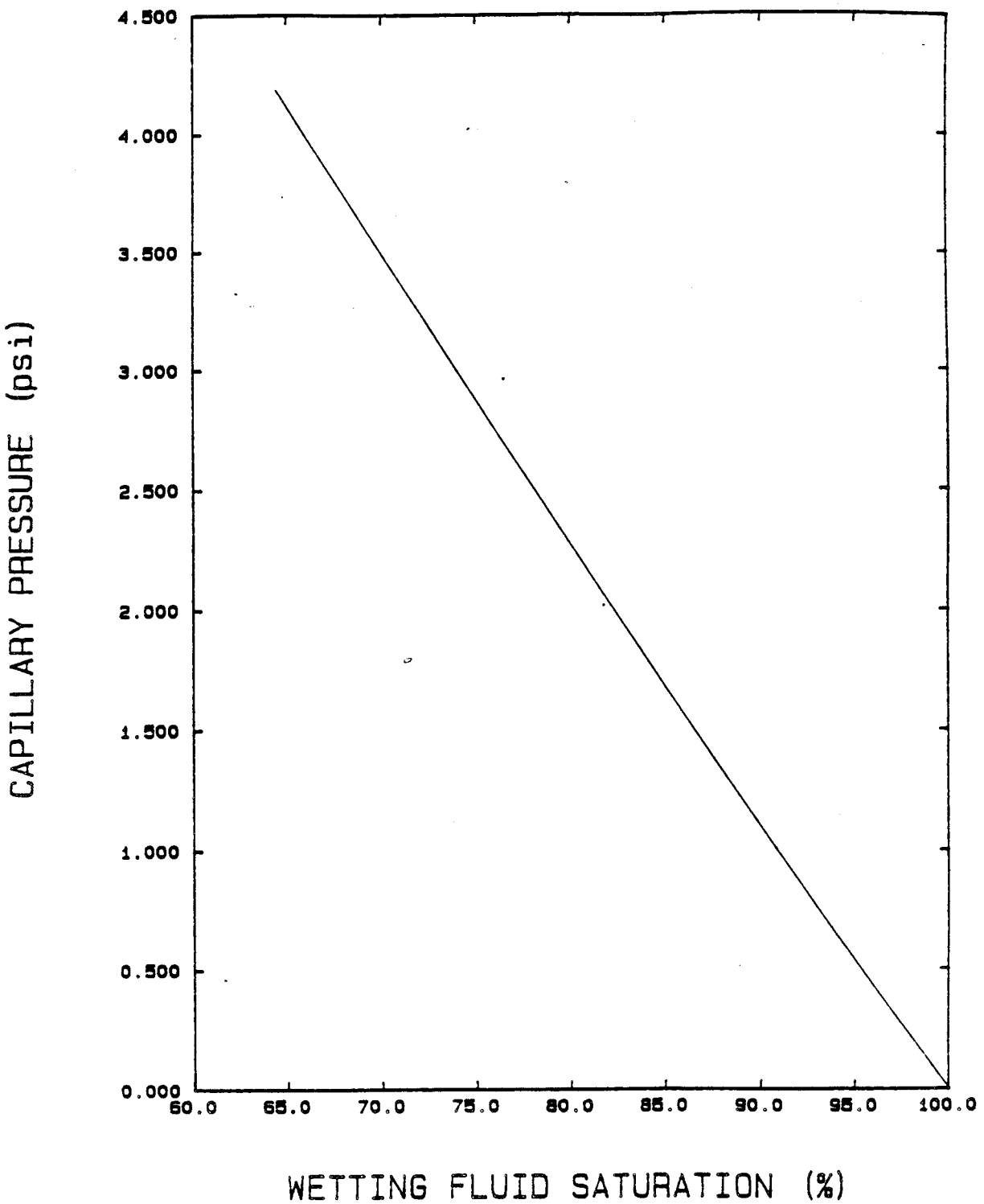

Figure C-10. Moisture Characteristic Curve for Sample MCG-611, Hole LLM-85-05, Depth of 36 Feet

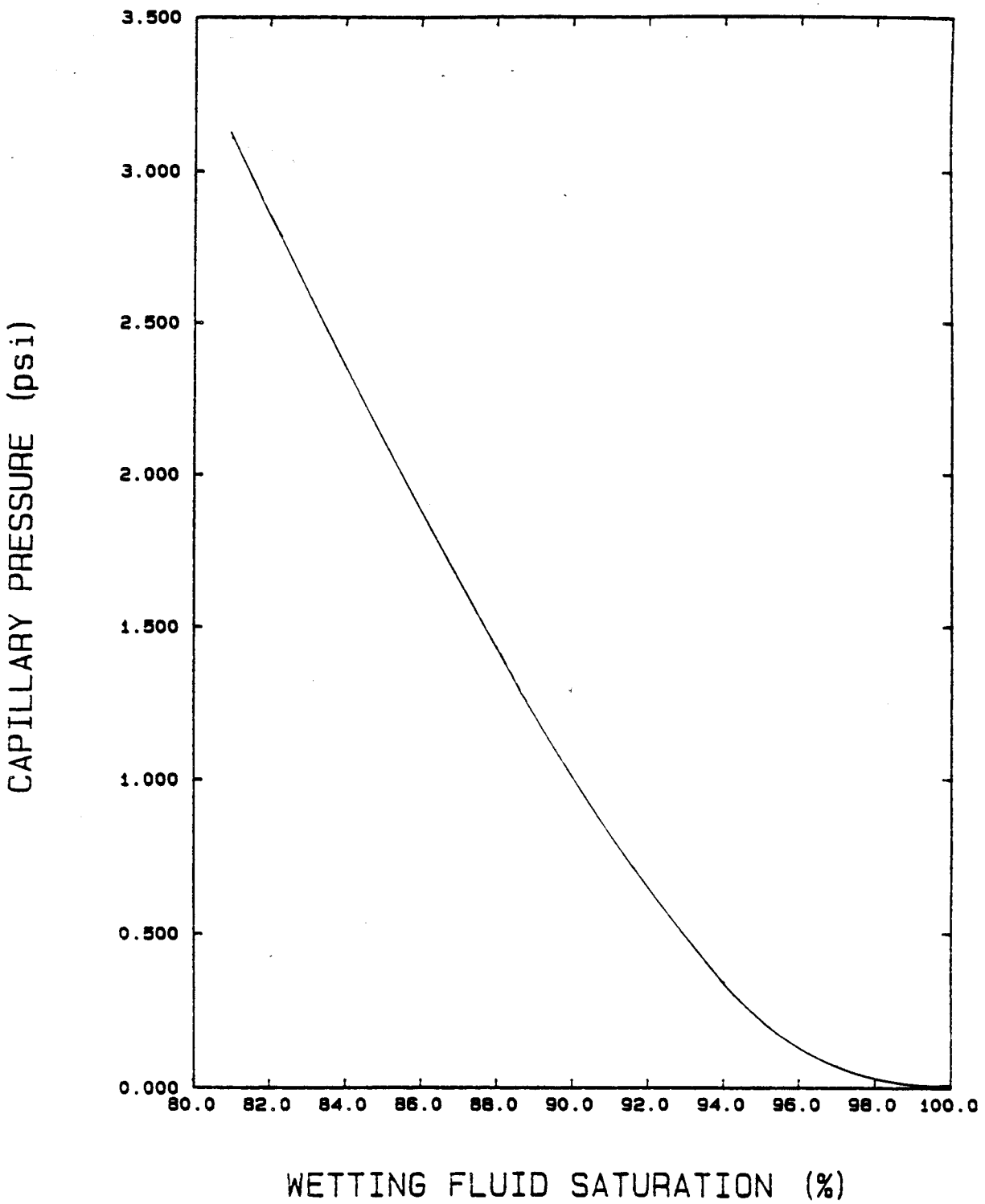

Figure C-11. Moisture Characteristic Curve for Sample MCG-612, Hole LLM-85-05, Depth of 76 Feet

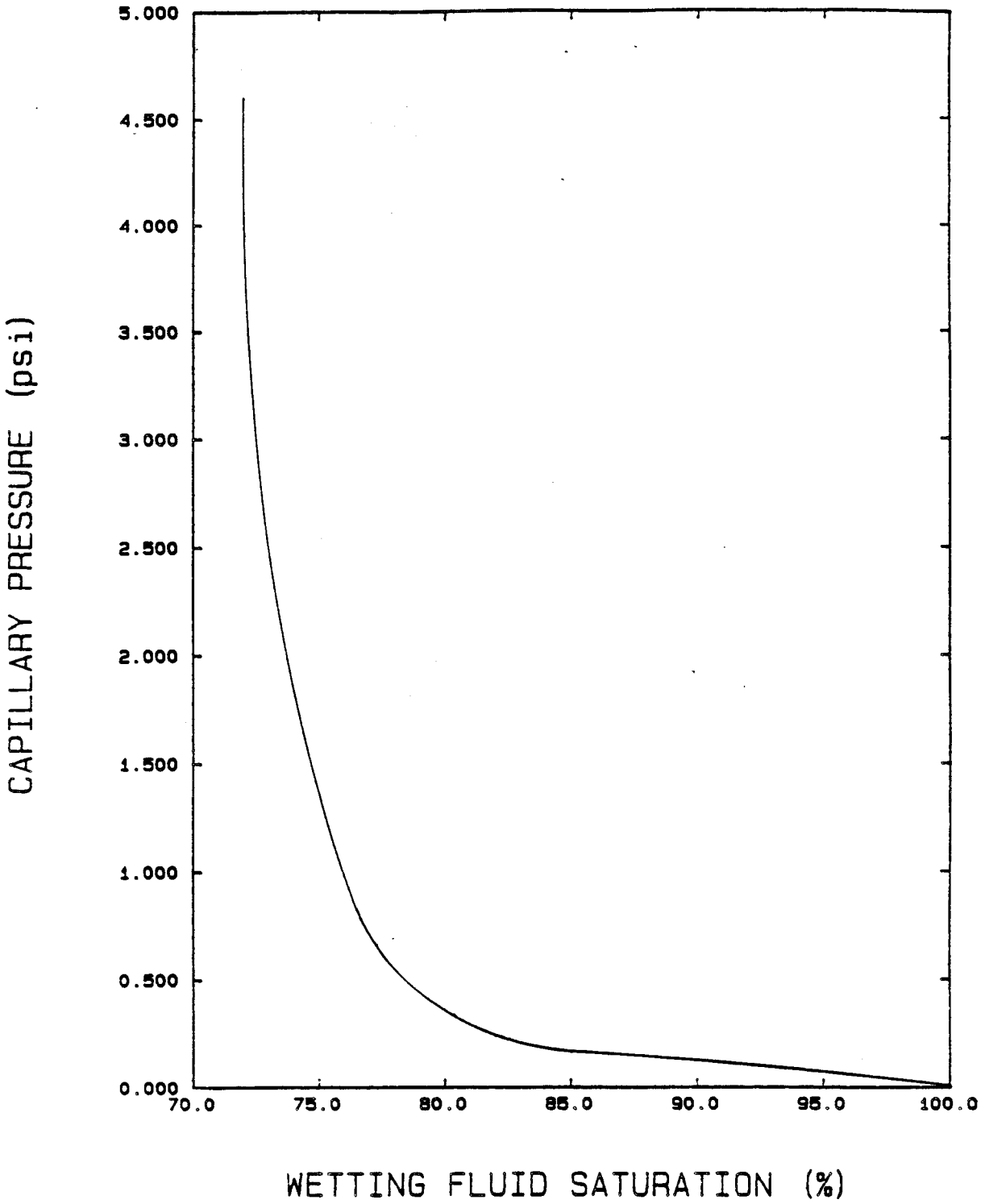

Figure C-12. Moisture Characteristic Curve for Sample MCG-613, Hole LLM-85-05, Depth of 123 Feet

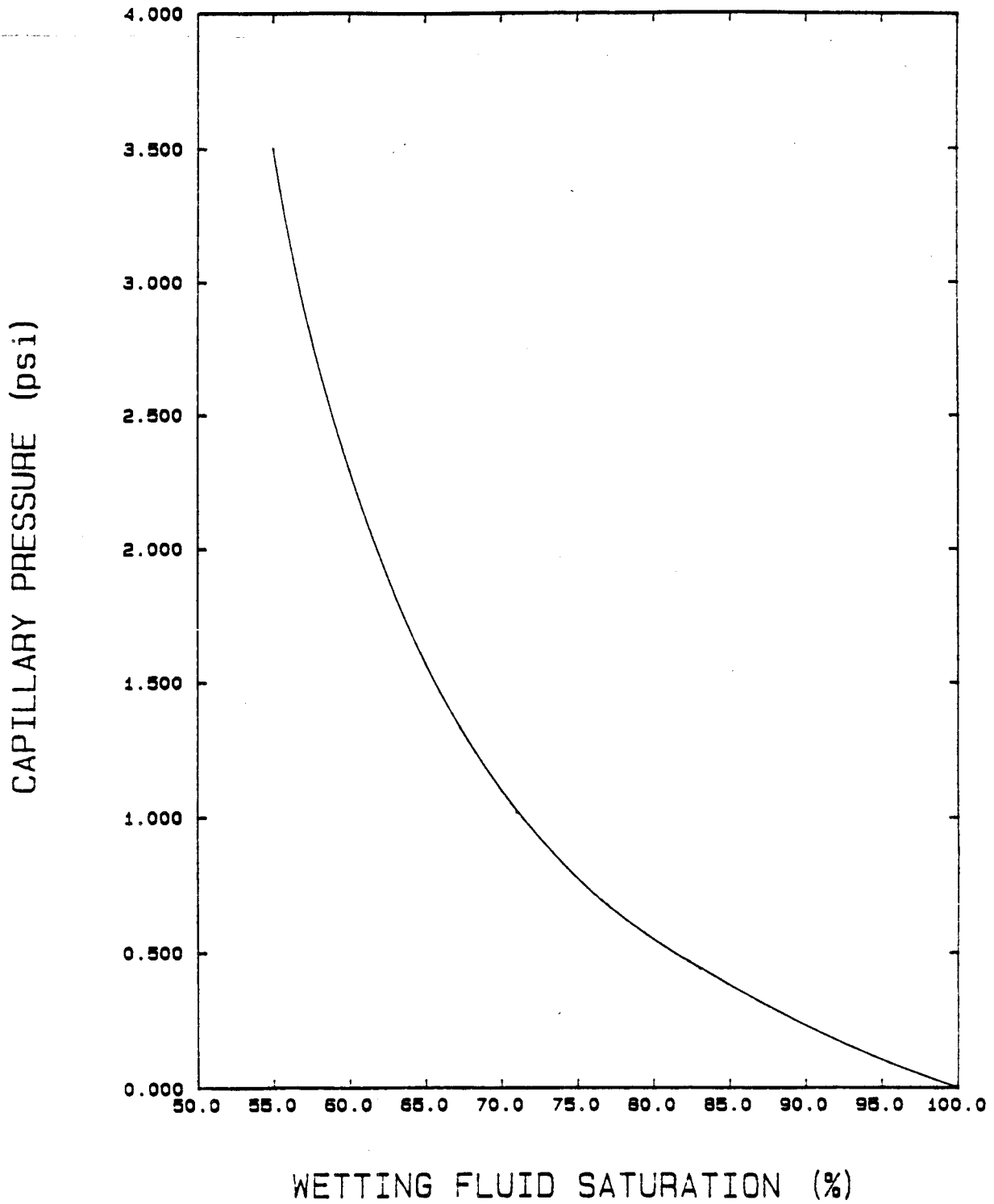

Figure C-13. Moisture Characteristic Curve for Sample MCG-614, Hole LGM-85-06, Depth of 29 Feet

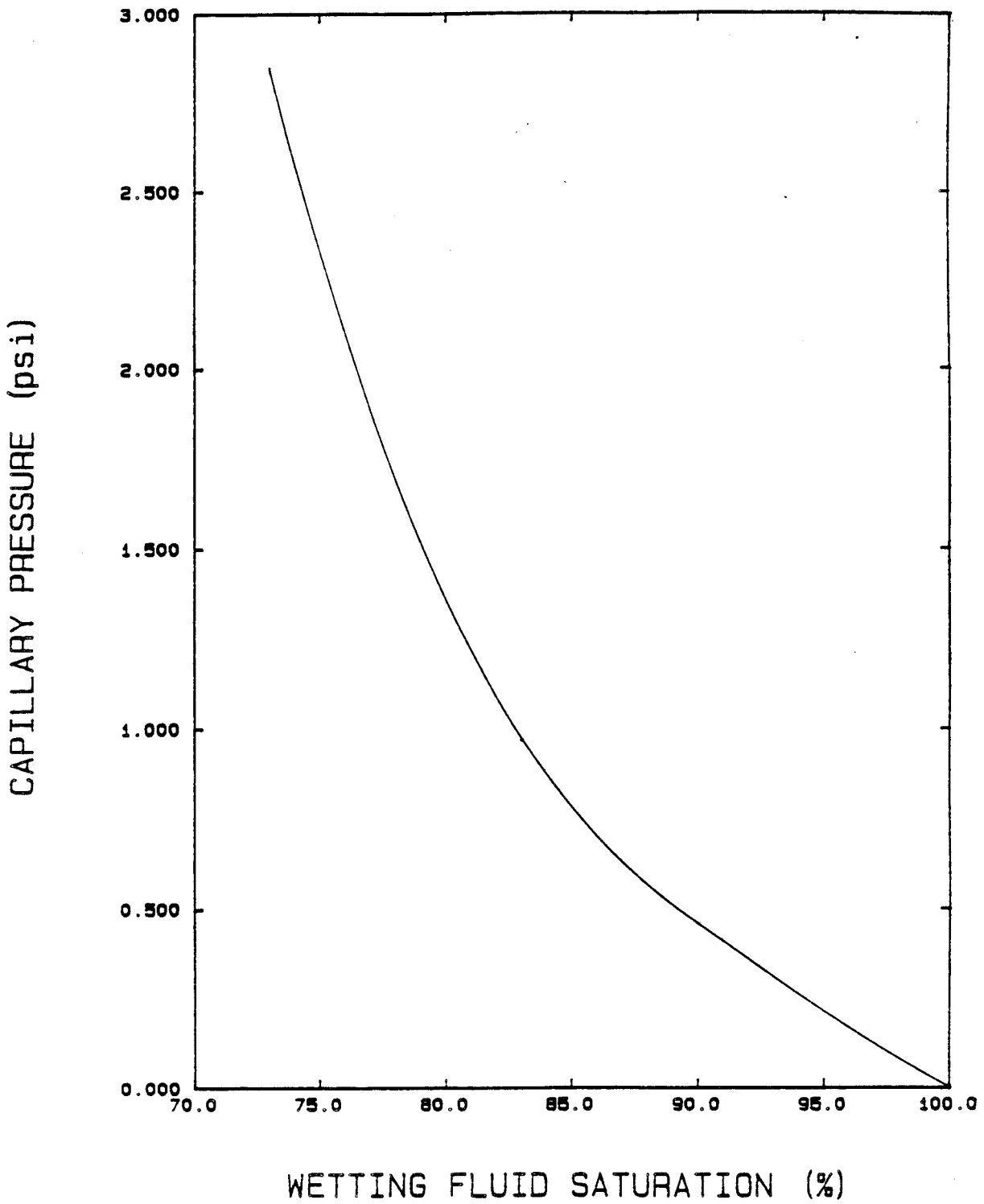

Figure C-14. Moisture Characteristic Curve for Sample MCG-615, Hole LGM-85-06, Depth of 51 Feet

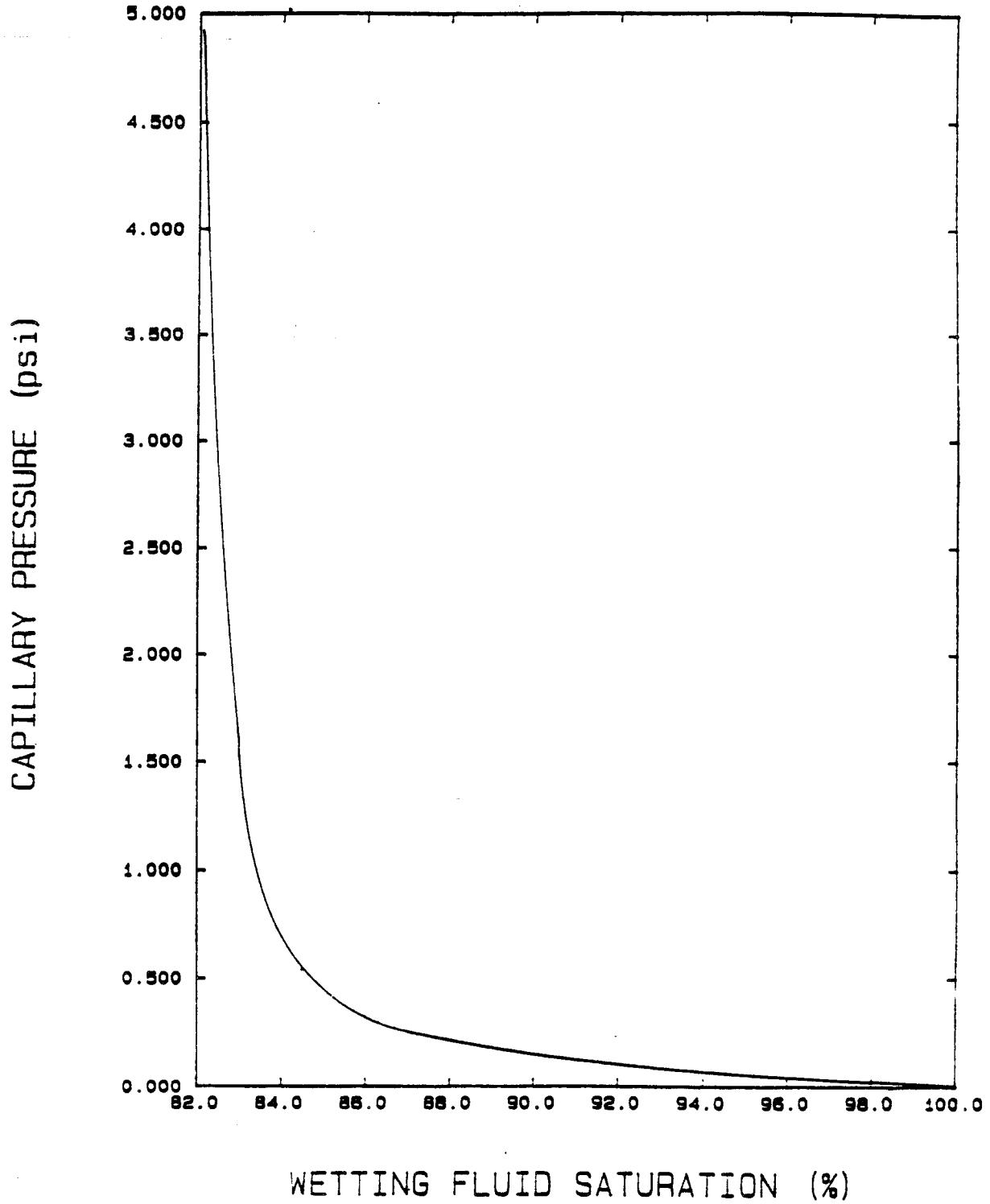

Figure C-15. Moisture Characteristic Curve for Sample MCG-616, Hole LGM-85-06, Depth of 99 Feet

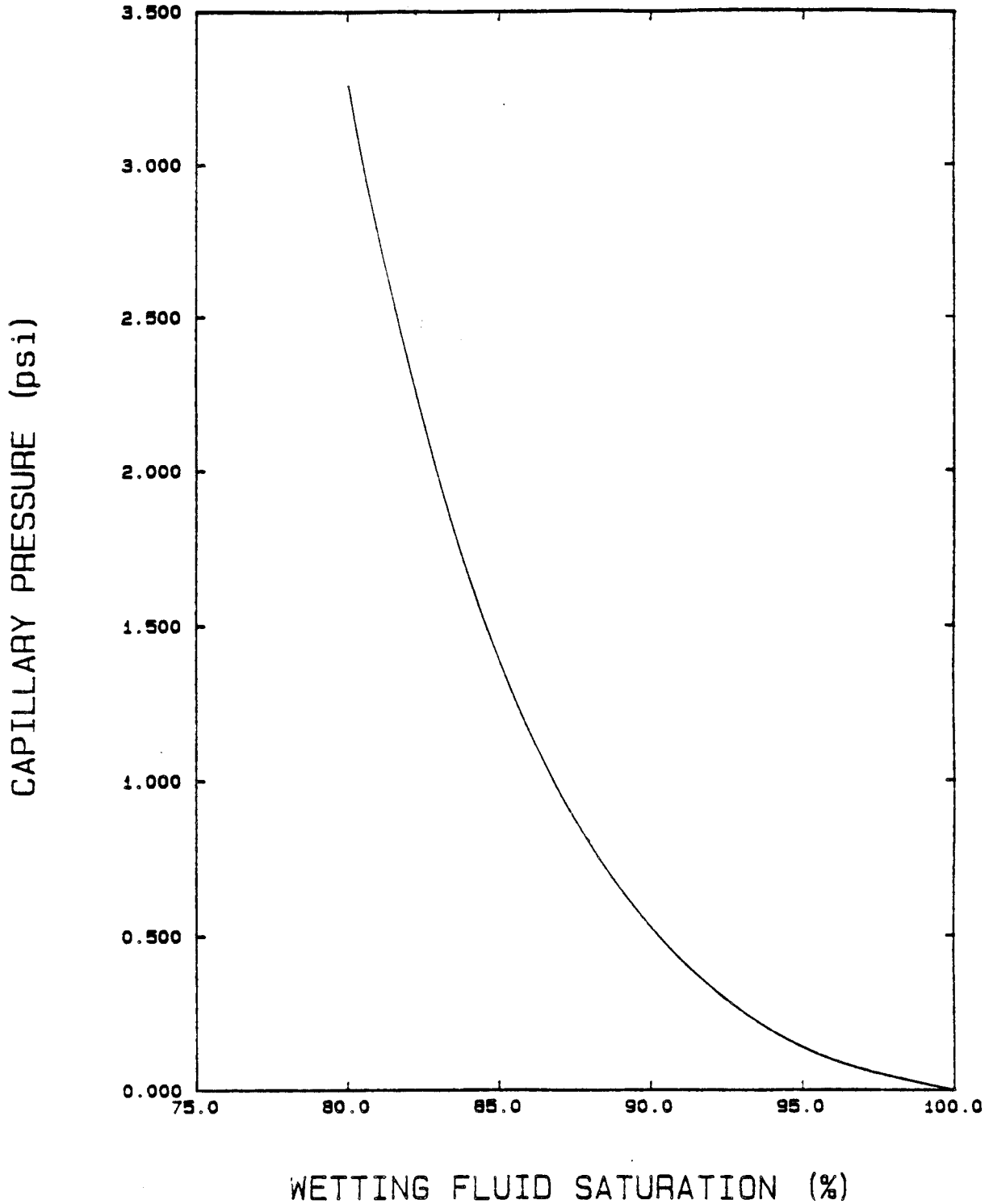

Figure C-16. Moisture Characteristic Curve for Sample MCG-617, Hole LGM-85-06, Depth of 115 Feet

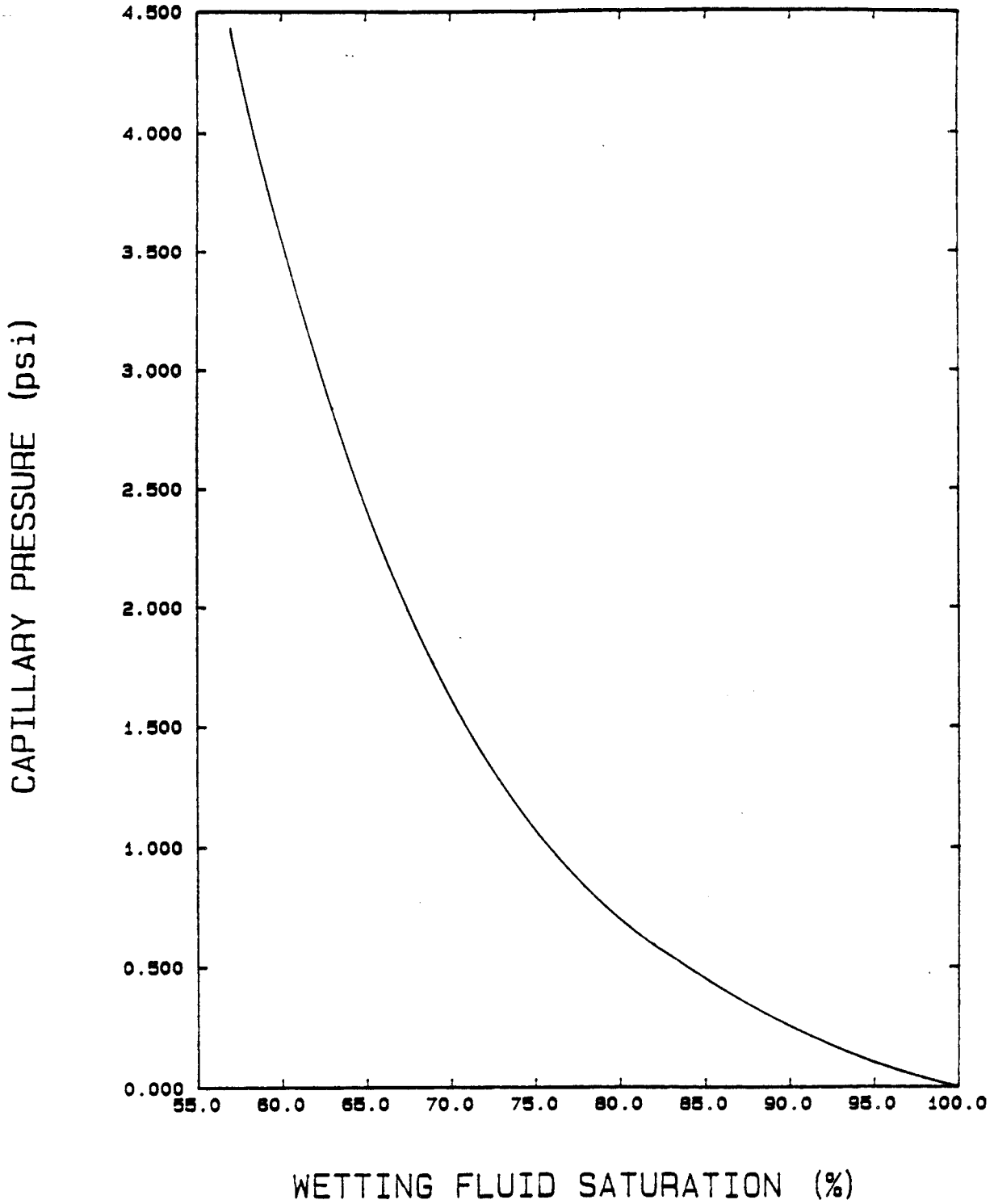

Figure C-17. Moisture Characteristic Curve for Sample MCG-618, Hole LGM-85-11, Depth of 3 Feet

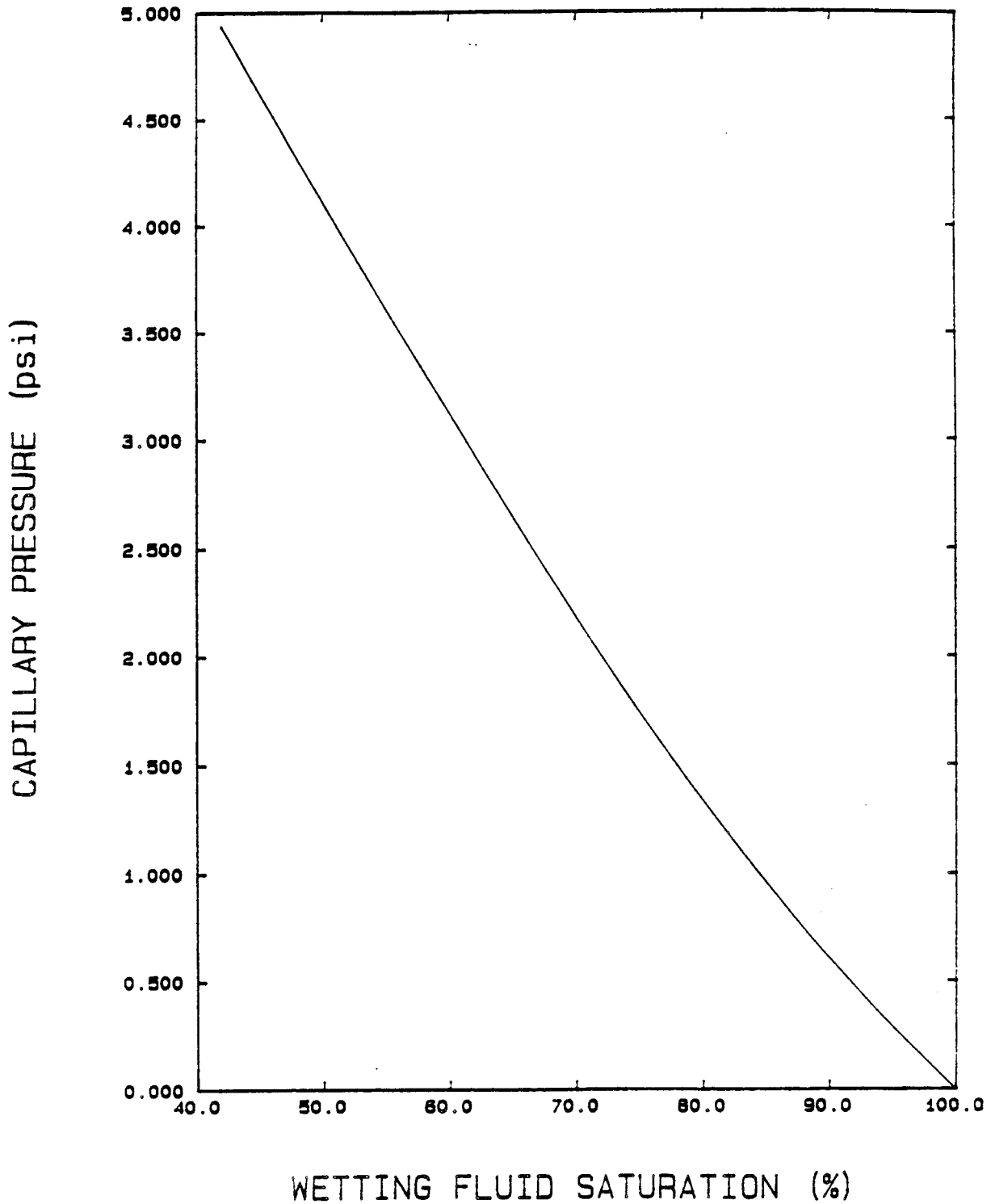

Figure C-18. Moisture Characteristic Curve for Sample MCG-619, Hole LGM-85-11, Depth of 30 Feet

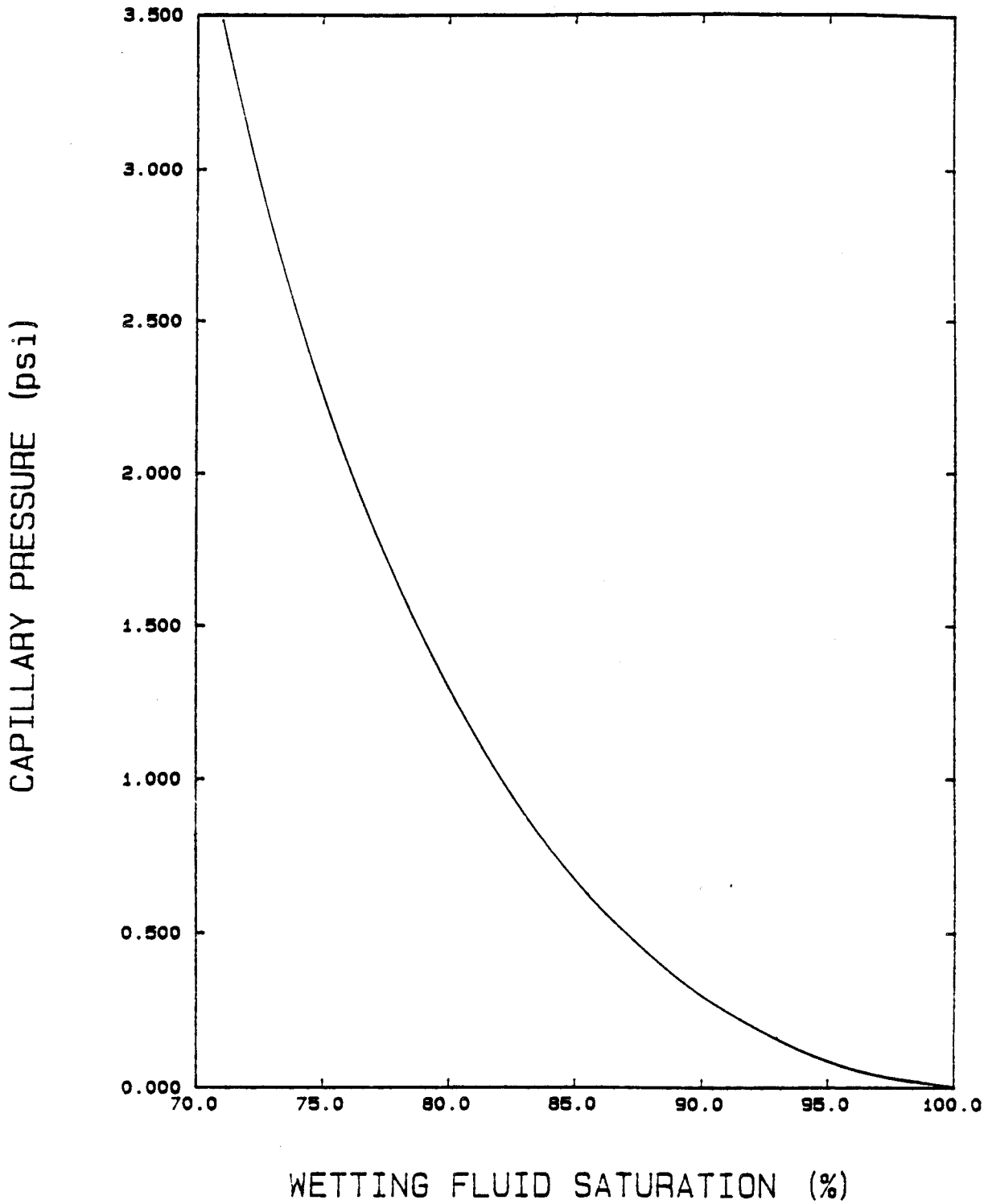

Figure C-19. Moisture Characteristic Curve for Sample MCG-620, Hole LGM-85-11, Depth of 94 Feet

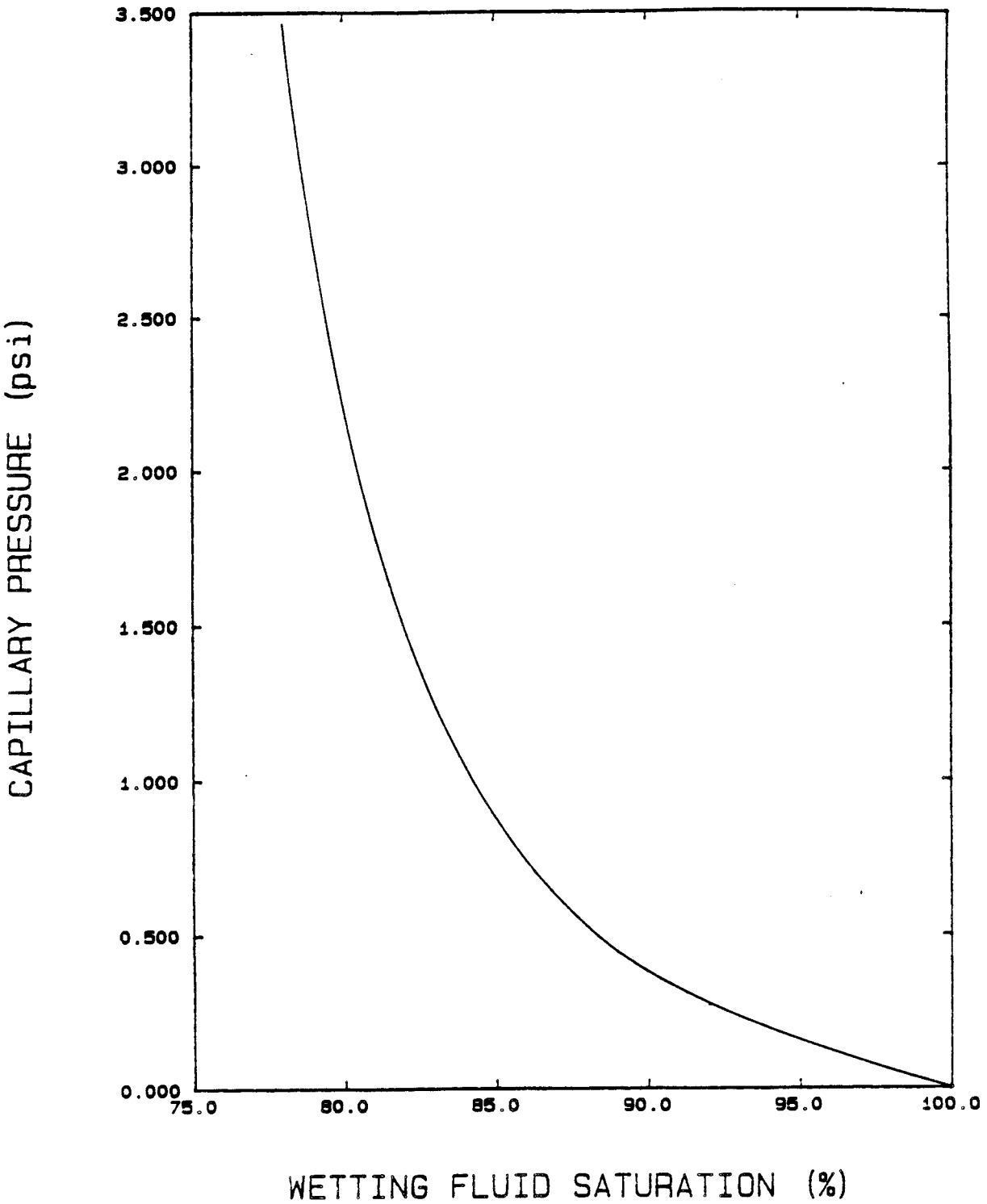

Figure C-20. Moisture Characteristic Curve for Sample MCG-621, Hole LGM-85-11, Depth of 115 Feet

Appendix D

EFFECTIVE PERMEABILITY AS A FUNCTION OF SATURATION

(saturation refers to total air saturation)

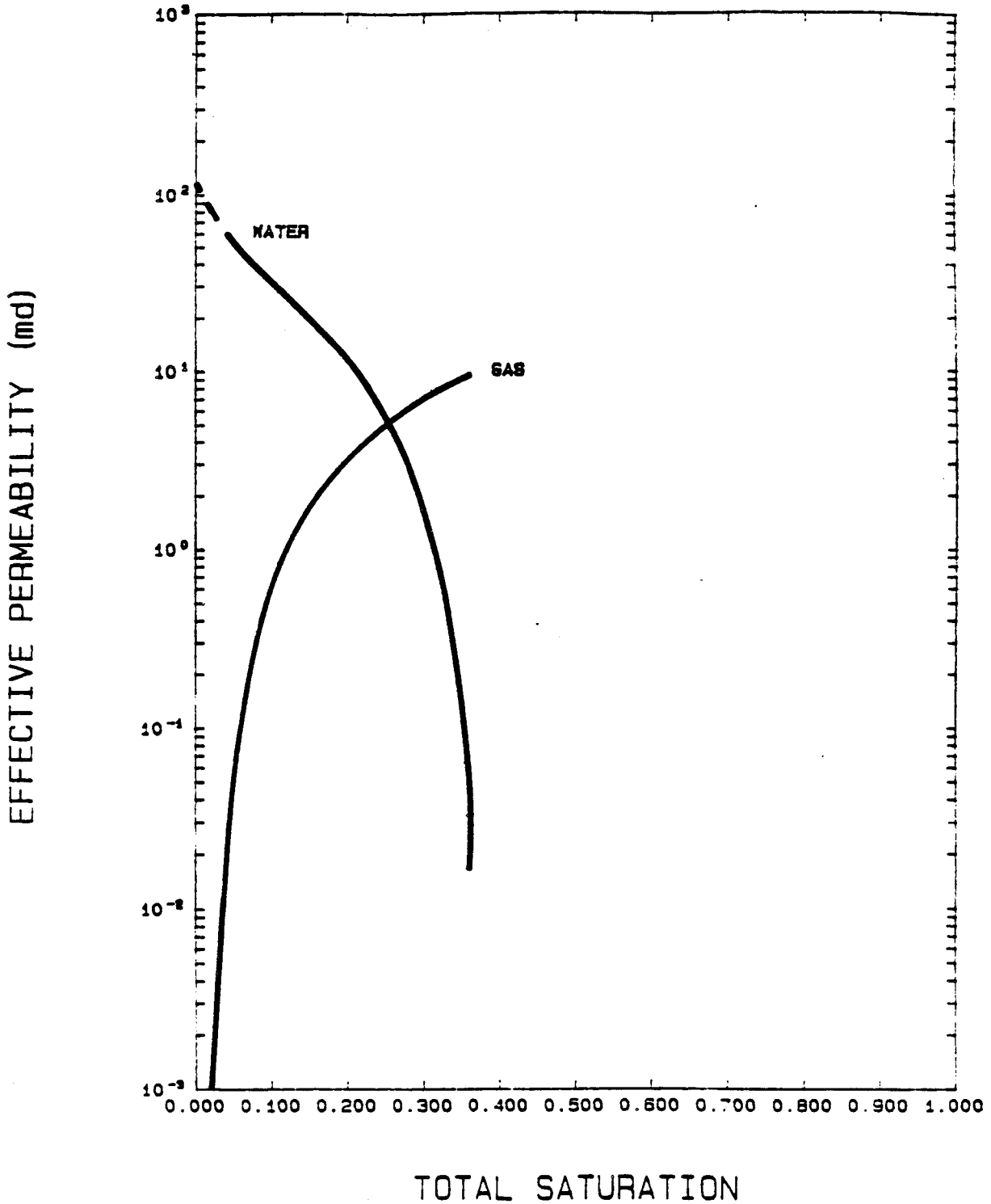

Figure D-1. Effective Permeability as a Function of Saturation for Sample MCG-602, Hole LLM-85-01, Depth of 30 Feet

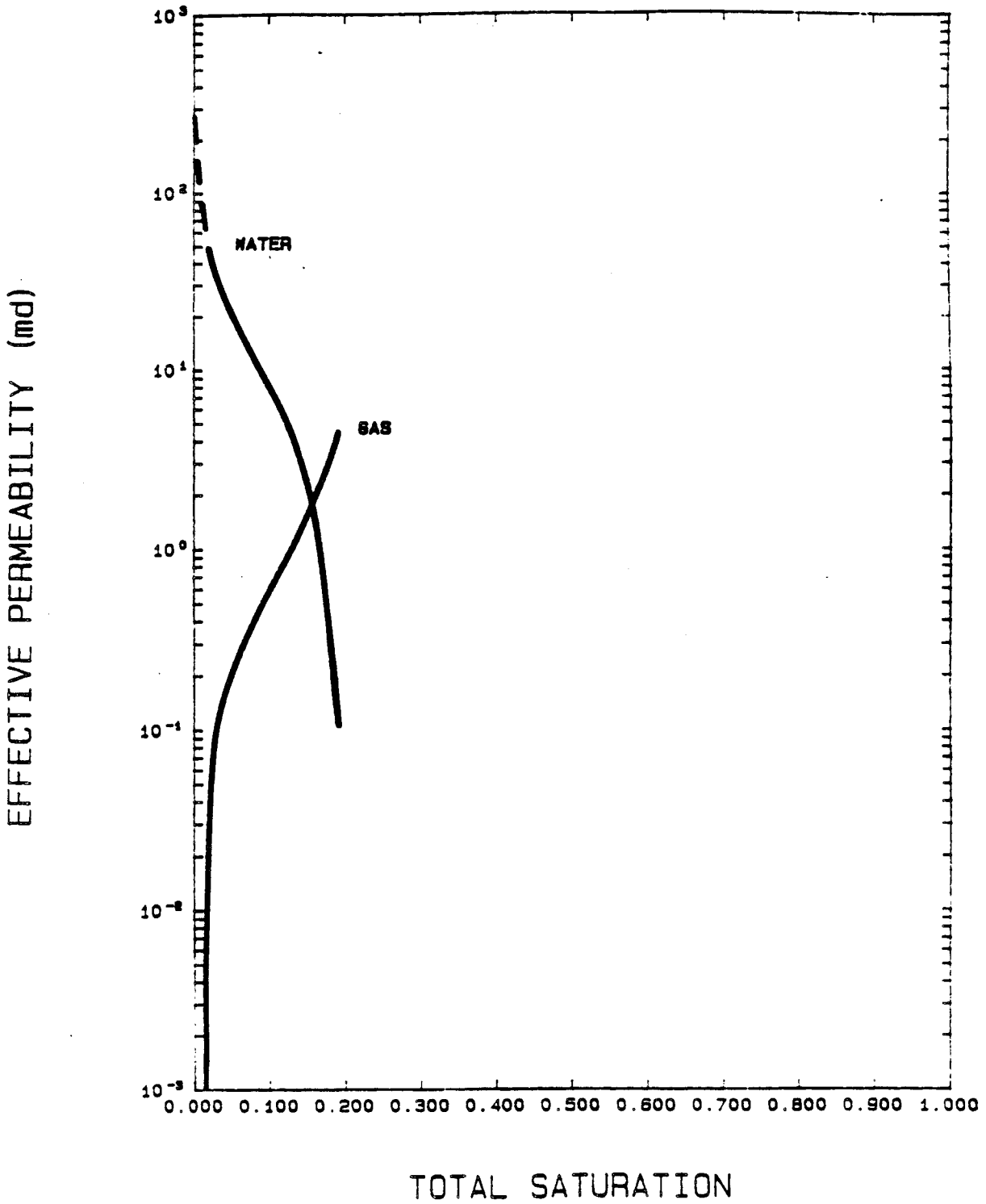

Figure D-2. Effective Permeability as a Function of Saturation for Sample MCG-603, Hole LLM-85-01, Depth of 52 Feet

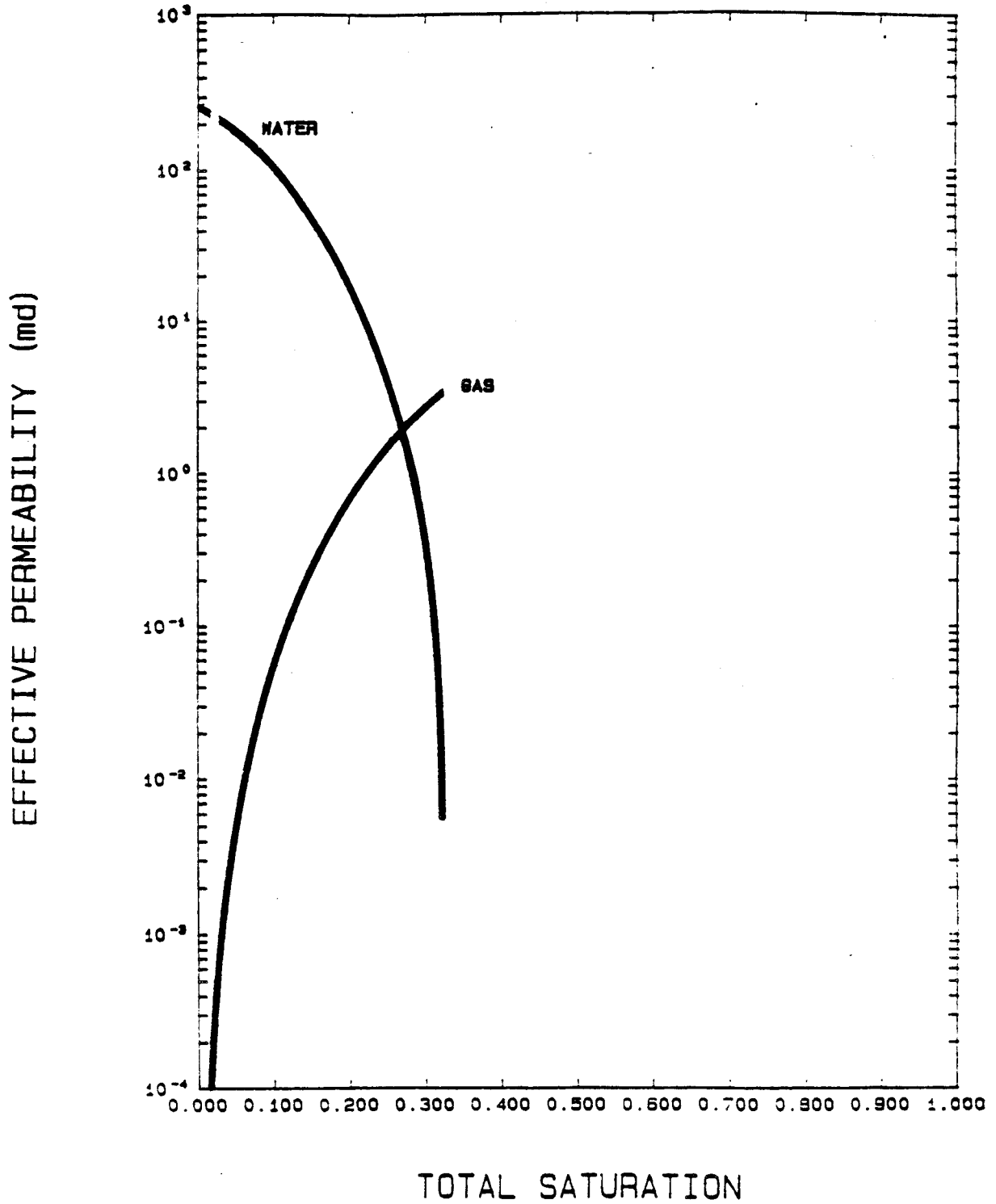

Figure D-3. Effective Permeability as a Function of Saturation for Sample MCG-604, Hole LLM-85-01, Depth of 101 Feet

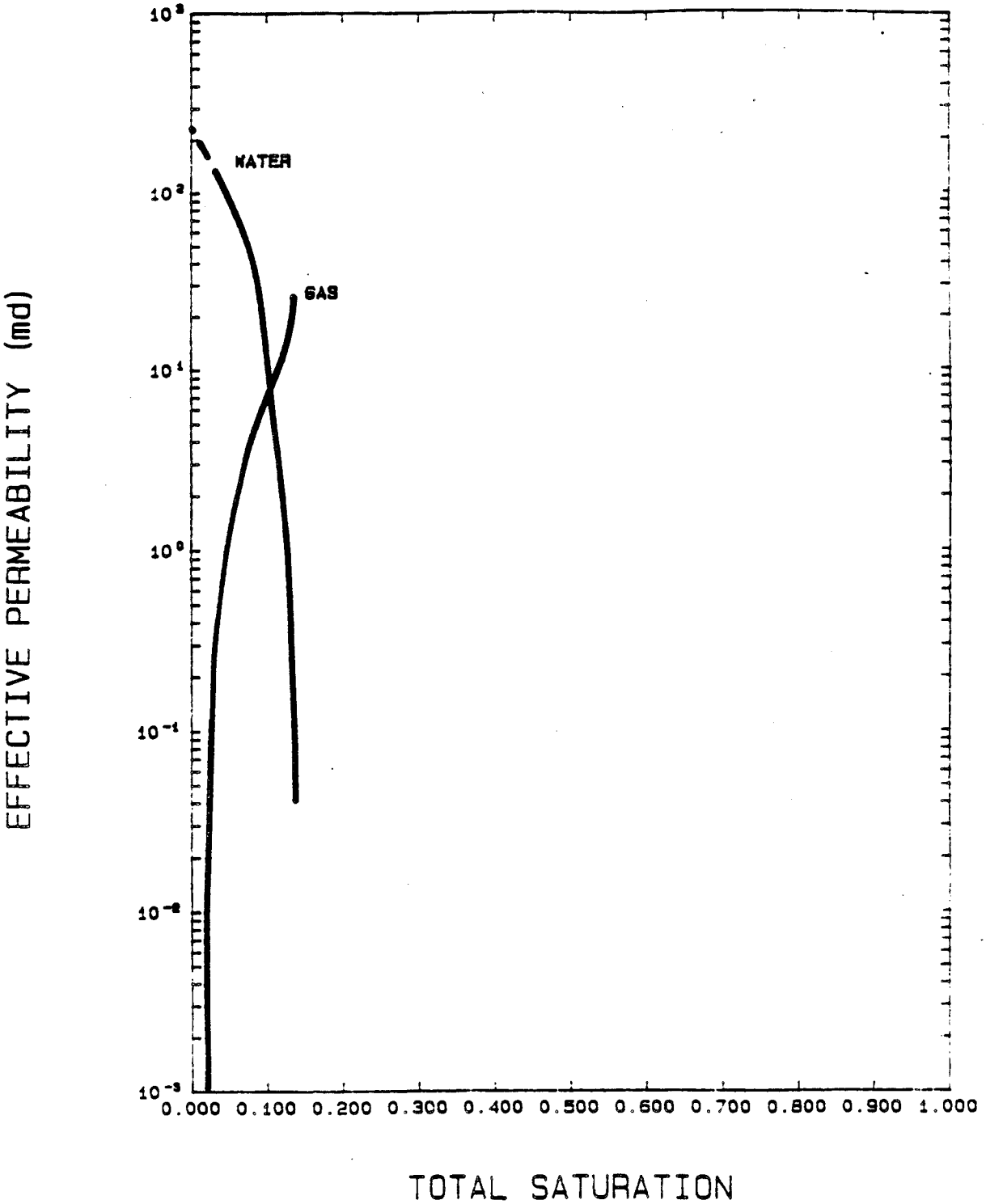

Figure D-4. Effective Permeability as a Function of Saturation for Sample MCG-605, Hole LLM-85-01, Depth of 124 Feet

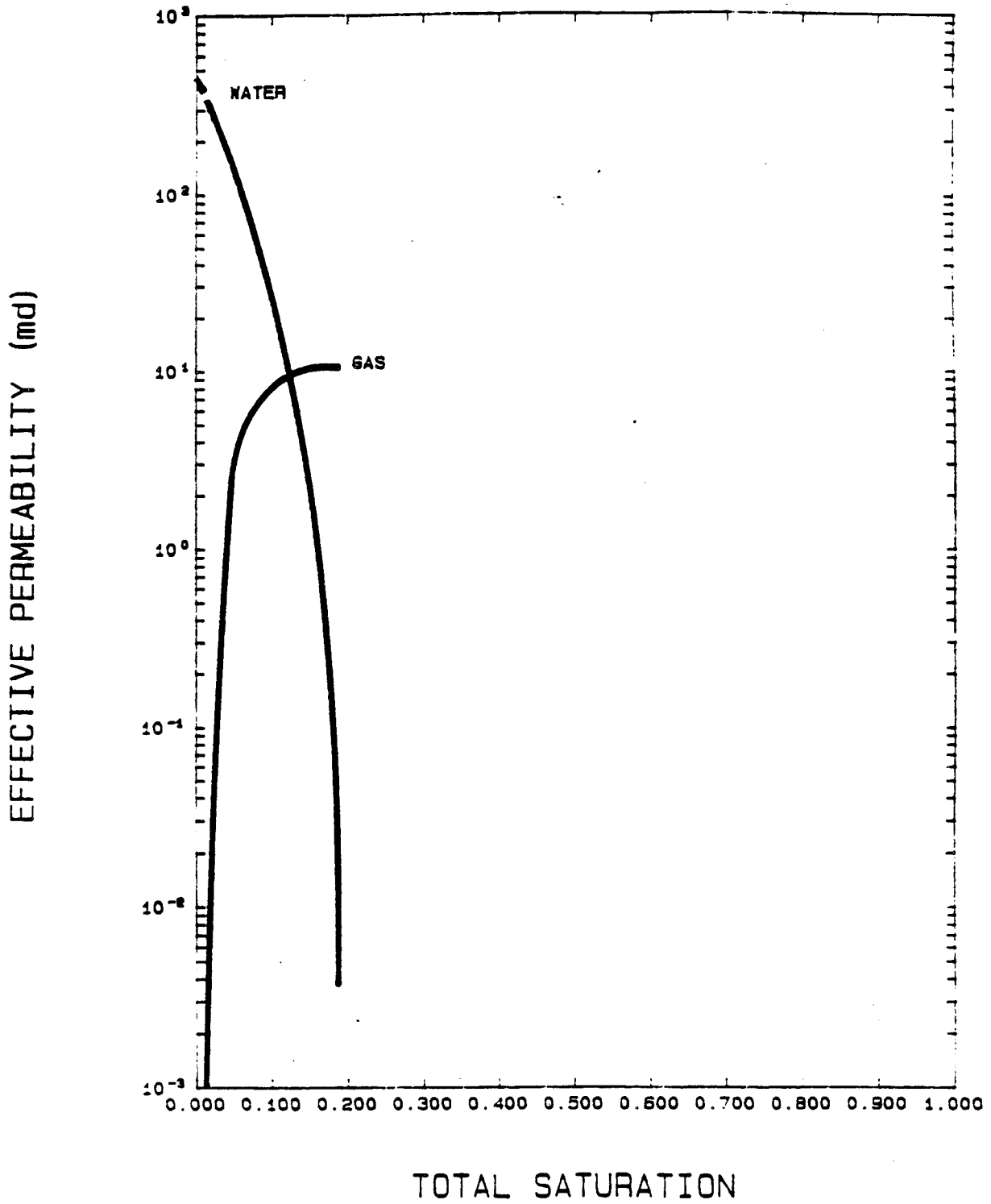

Figure D-5. Effective Permeability as a Function of Saturation for Sample MCG-606, Hole LLM-85-02, Depth of 7 Feet

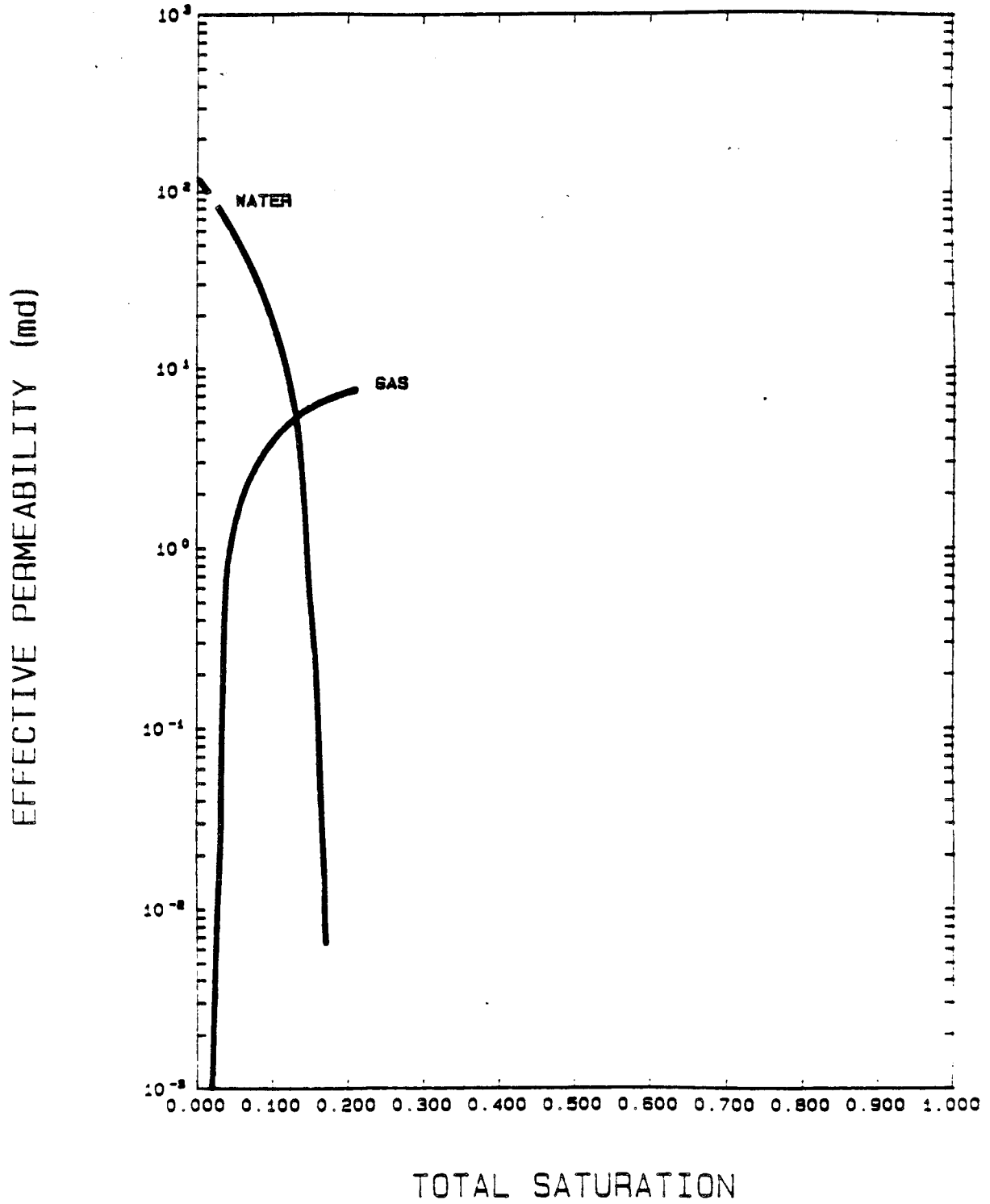

Figure D-6. Effective Permeability as a Function of Saturation for Sample MCG-607, Hole LLM-85-02, Depth of 36 Feet

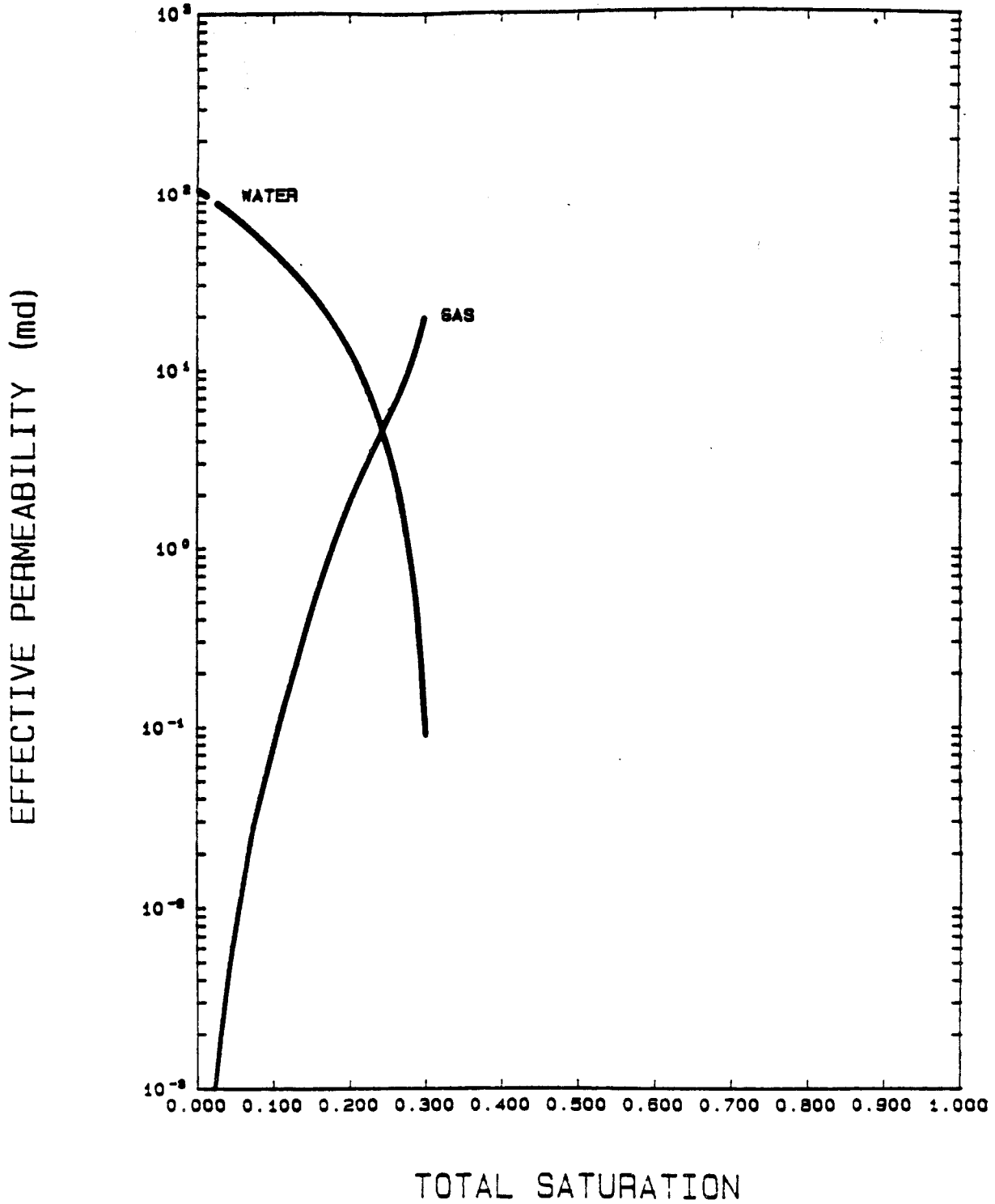

Figure D-7. Effective Permeability as a Function of Saturation for Sample MCG-608, Hole LLM-85-02, Depth of 67 Feet

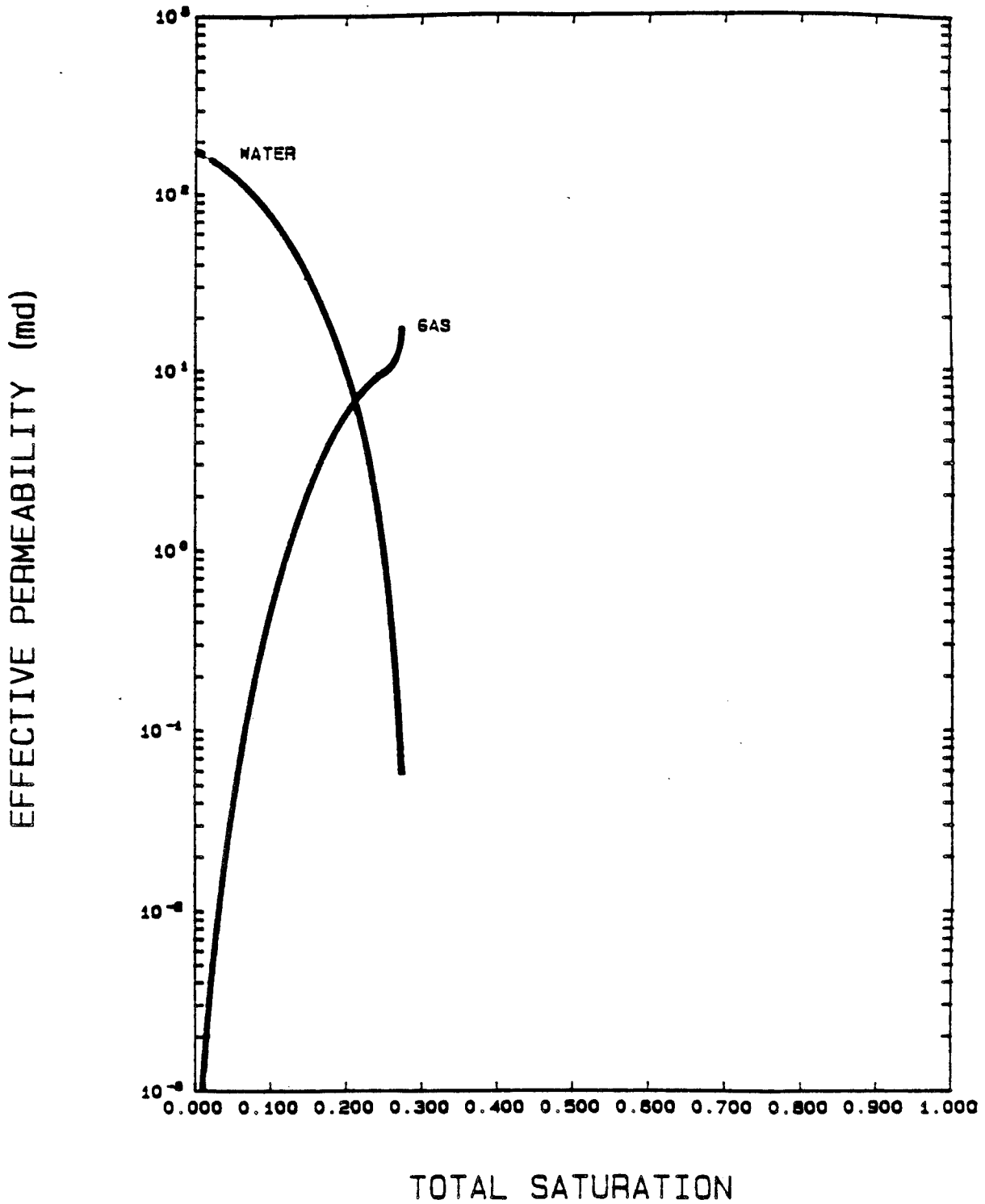

Figure D-8. Effective Permeability as a Function of Saturation for Sample MCG-609, Hole LLM-85-02, Depth of 117 Feet

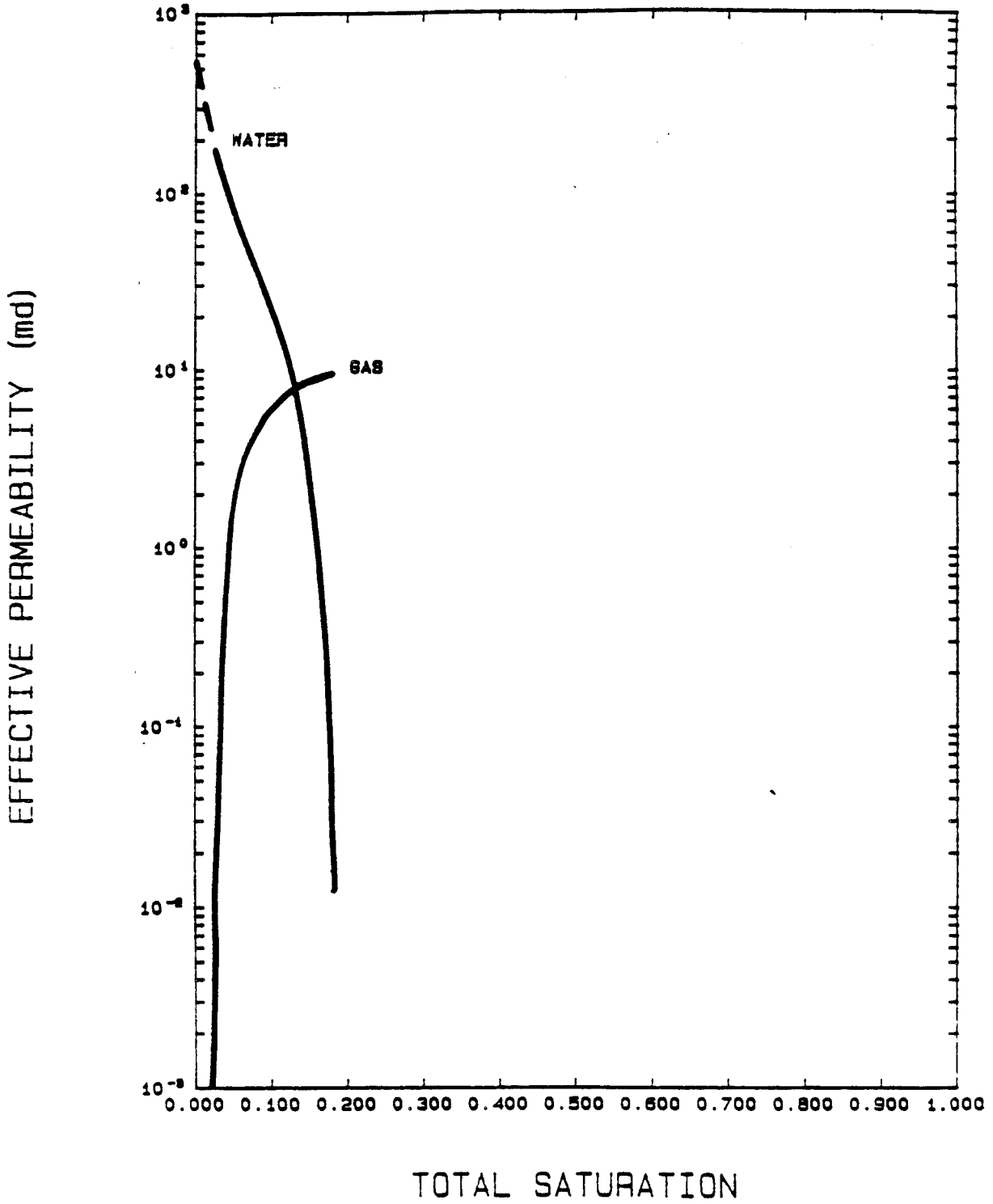

Figure D-9. Effective Permeability as a Function of Saturation for Sample MCG-610, Hole LLM-85-05, Depth of 15 Feet

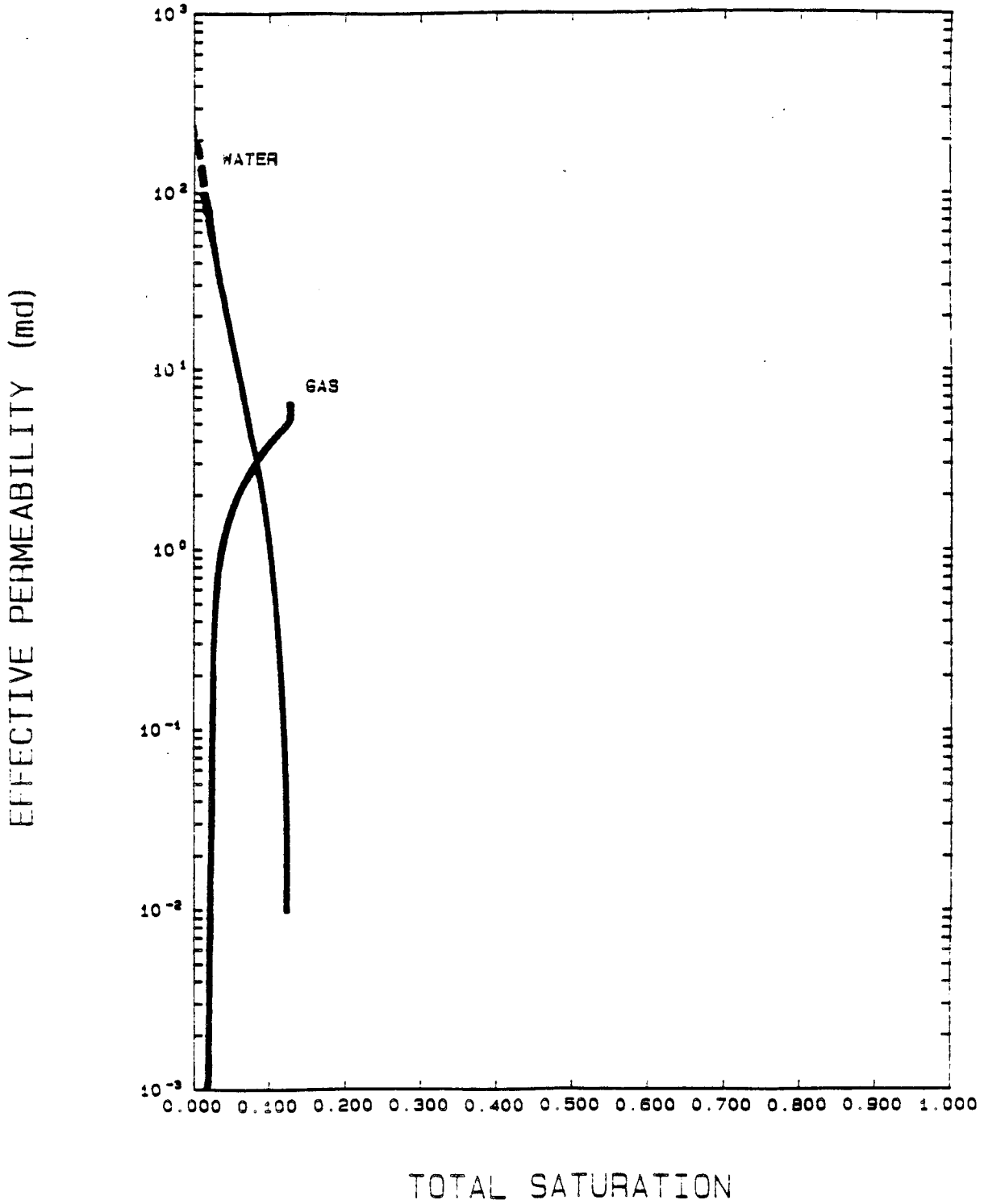

Figure D-10. Effective Permeability as a Function of Saturation for Sample MCG-611, Hole LLM-85-05, Depth of 36 Feet

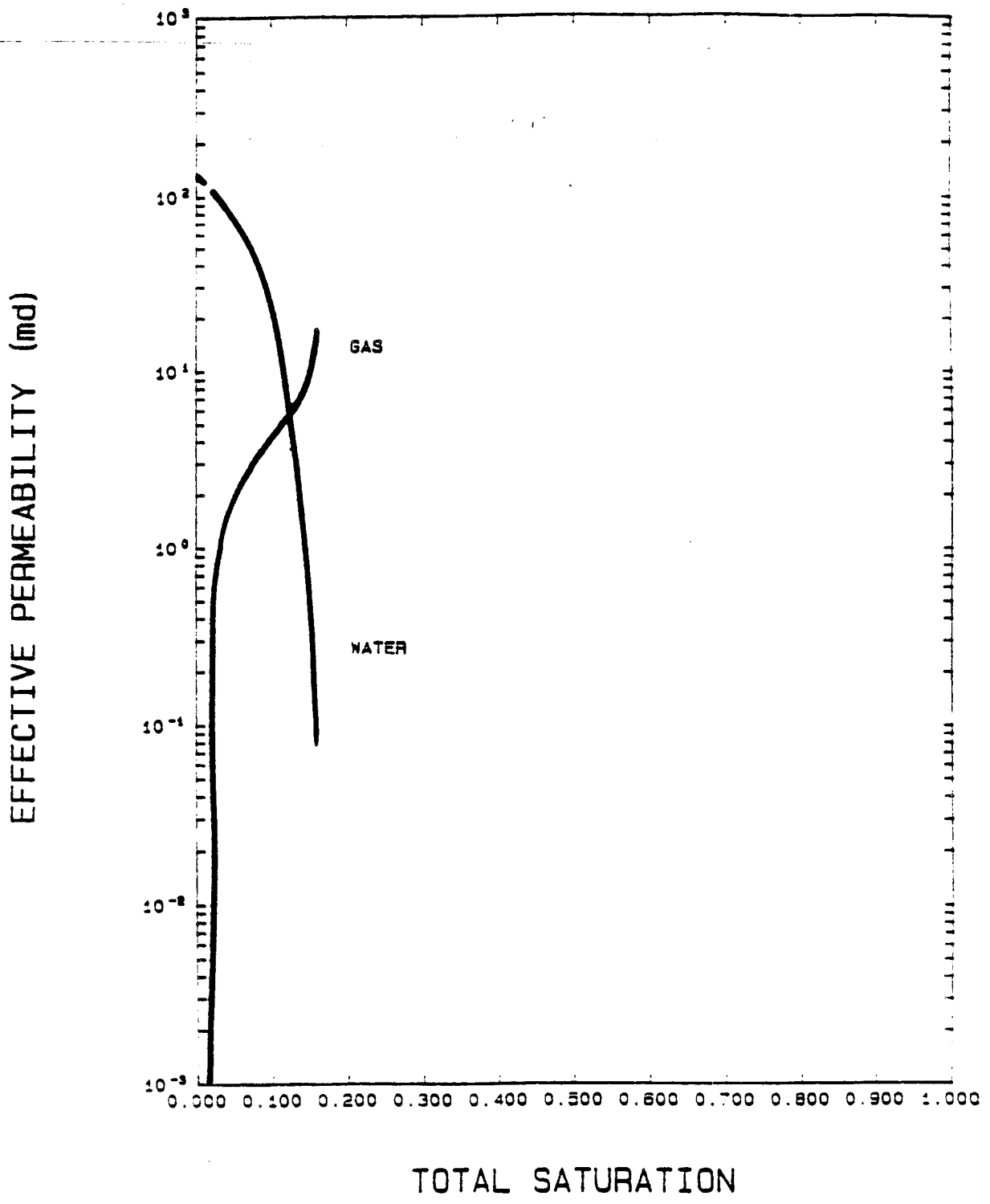

Figure D-11. Effective Permeability as a Function of Saturation for Sample MCG-612, Hole LLM-85-05, Depth of 76 Feet

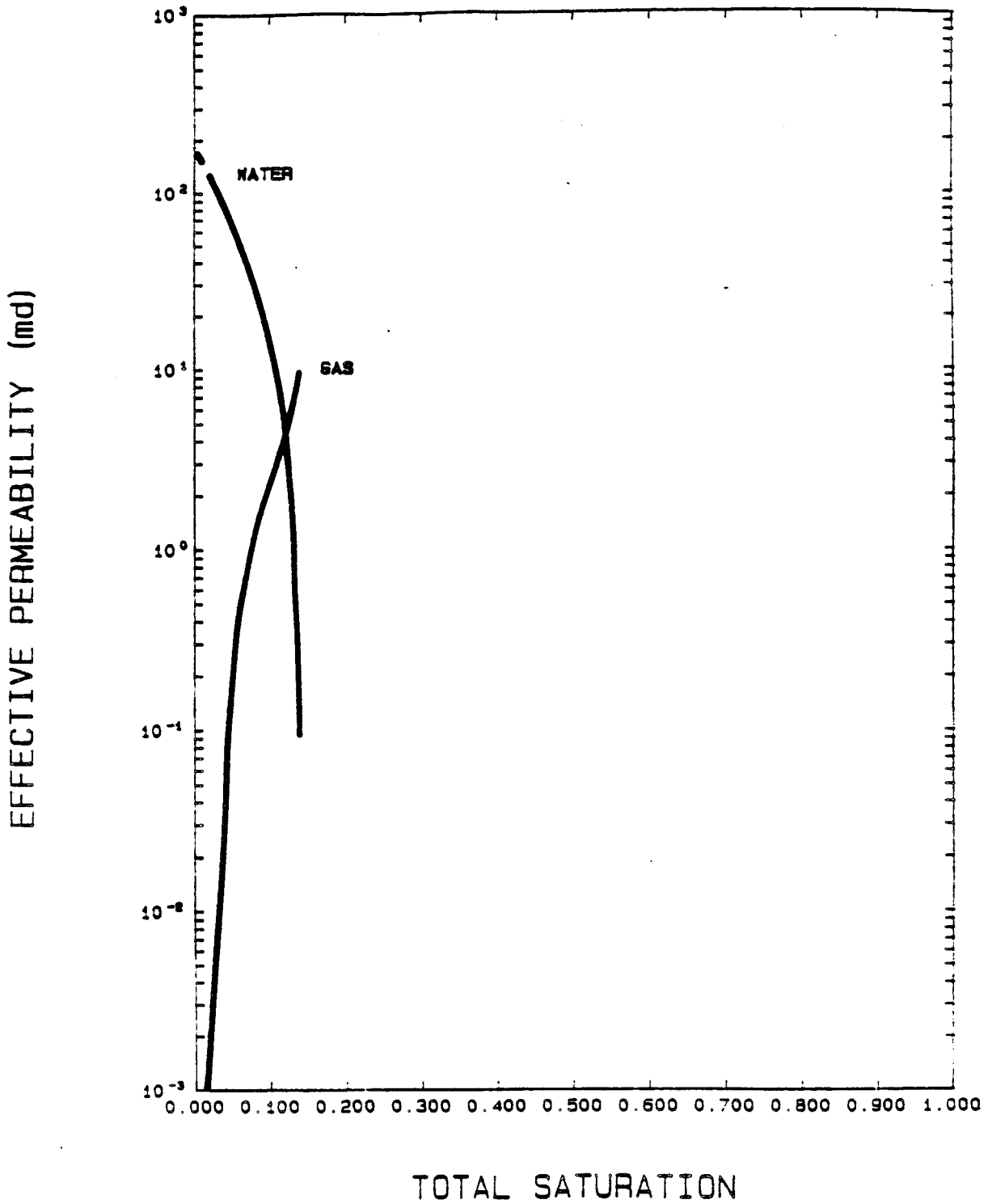

Figure D-12. Effective Permeability as a Function of Saturation for Sample MCG-613, Hole LLM-85-05, Depth of 123 Feet

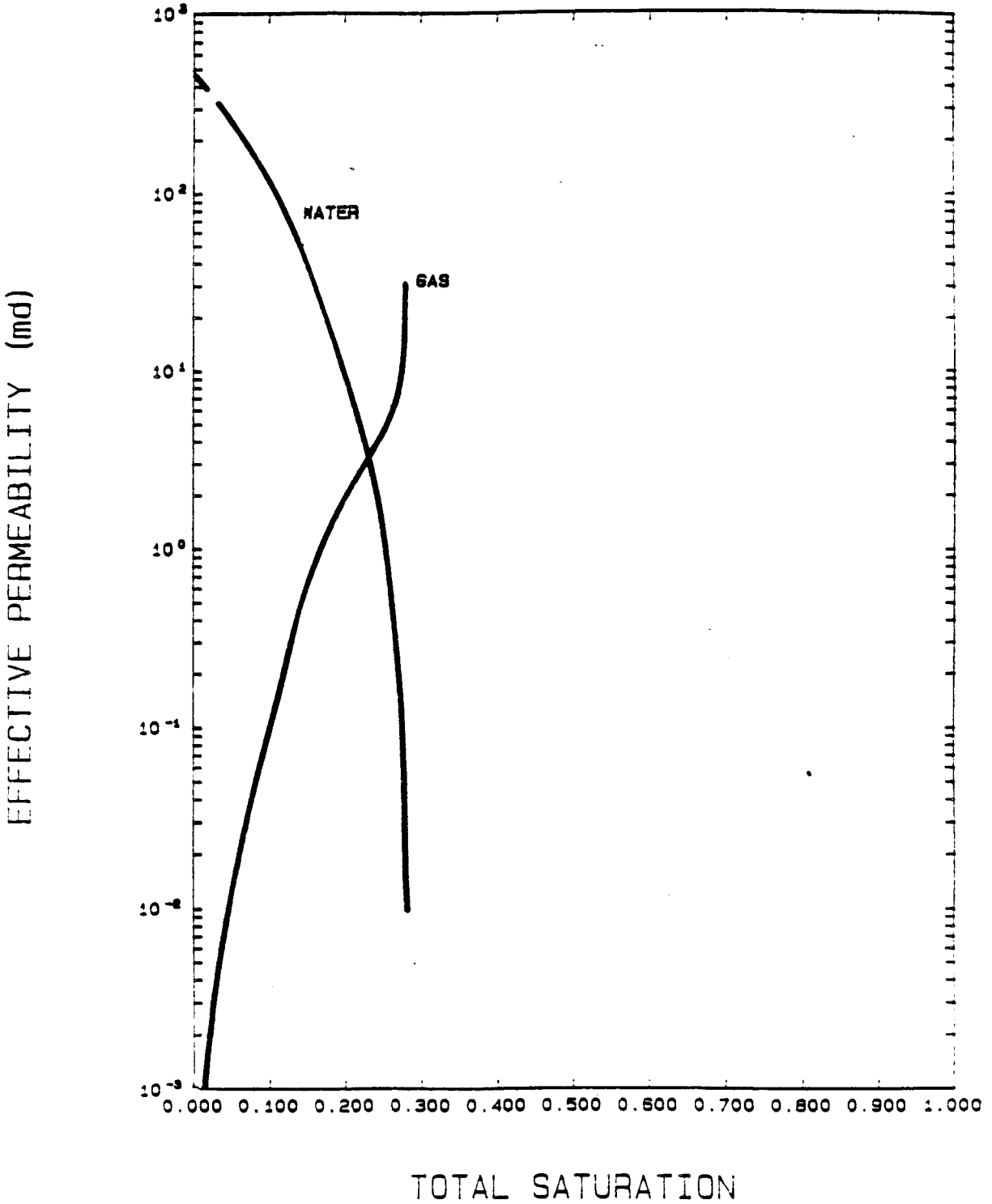

Figure D-13. Effective Permeability as a Function of Saturation for Sample MCG-614, Hole LGM-85-06, Depth of 29 Feet

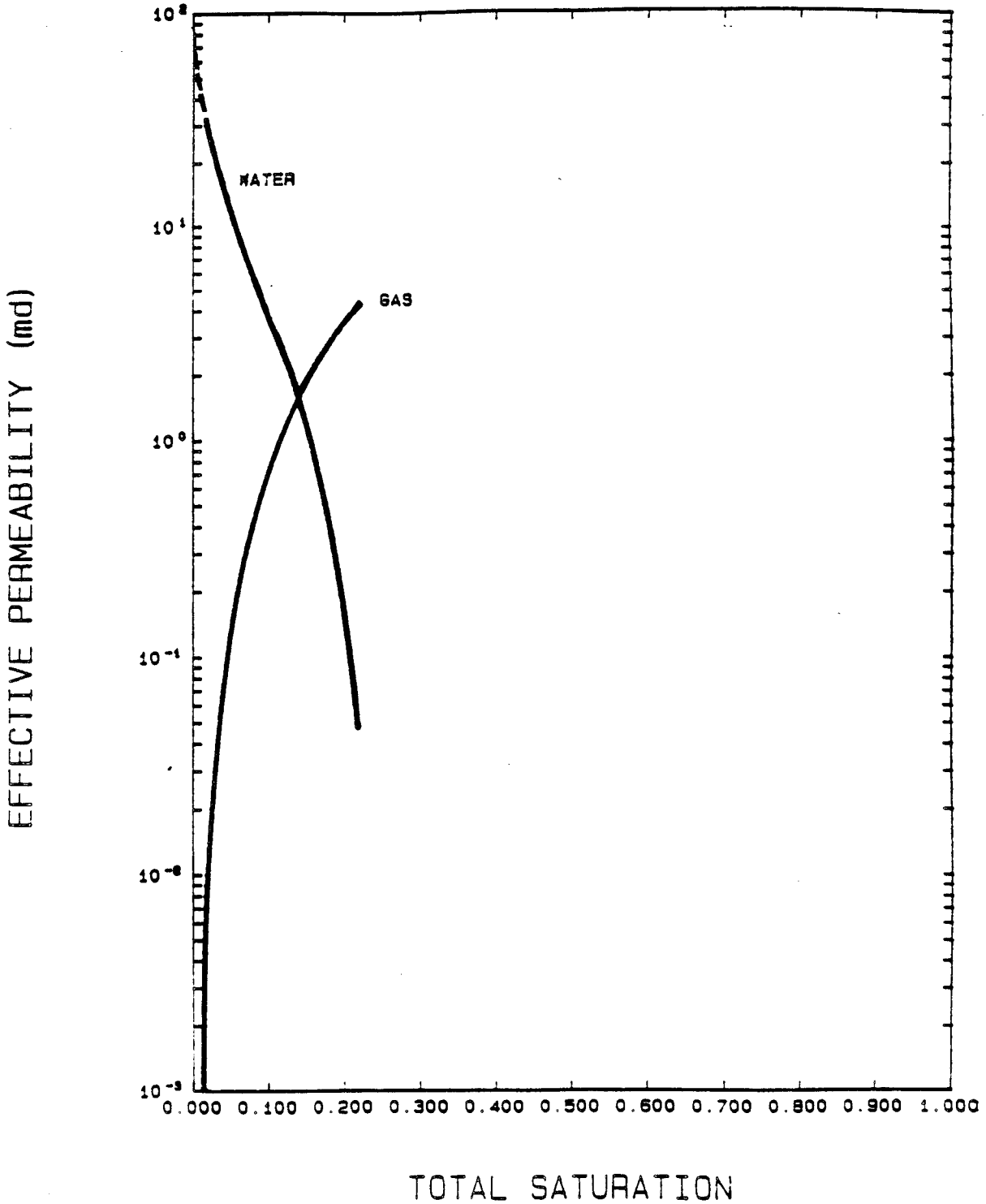

Figure D-14. Effective Permeability as a Function of Saturation for Sample MCG-615, Hole LGM-85-06, Depth of 51 Feet

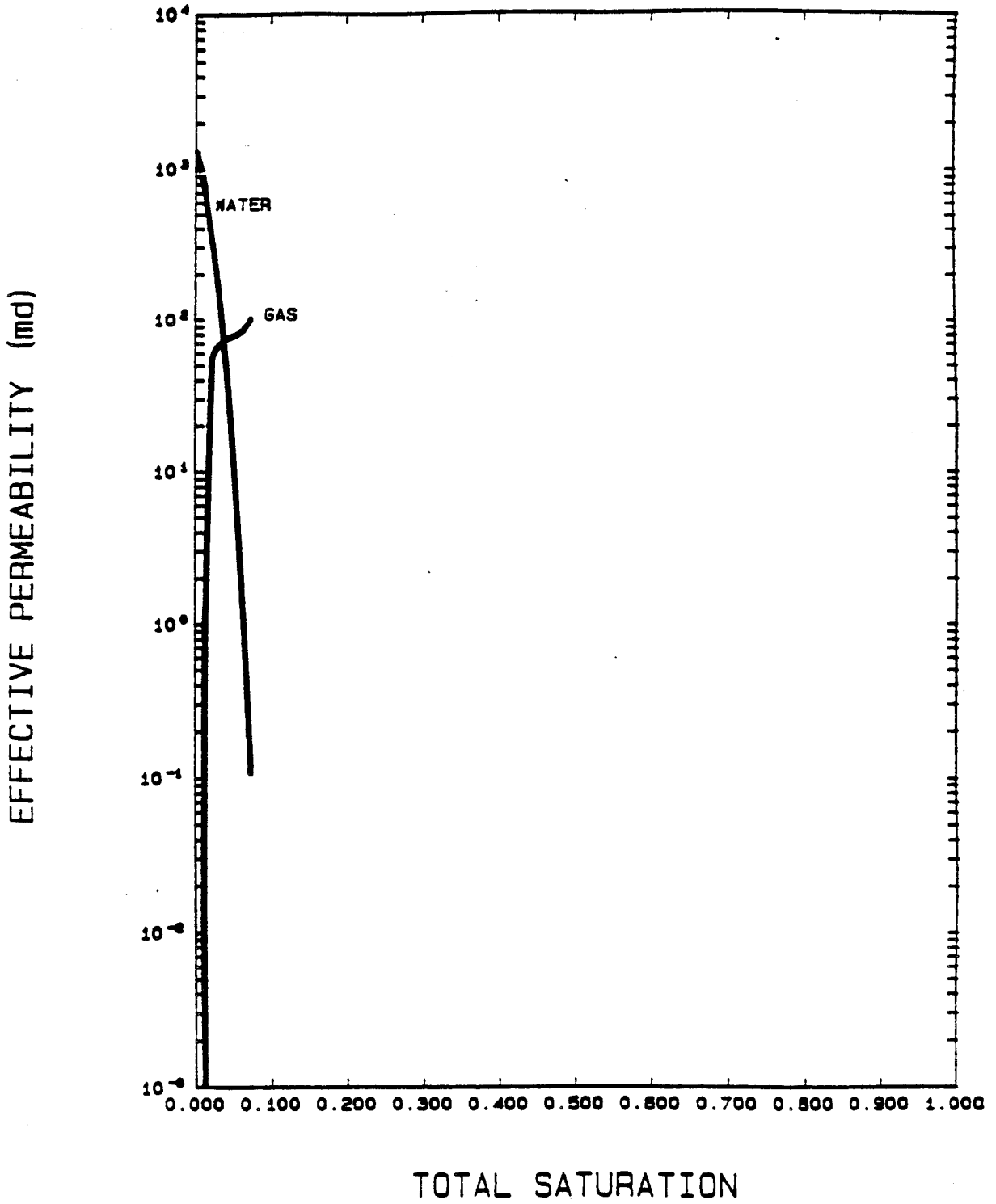

Figure D-15. Effective Permeability as a Function of Saturation for Sample MCG-616, Hole LGM-85-06, Depth of 99 Feet

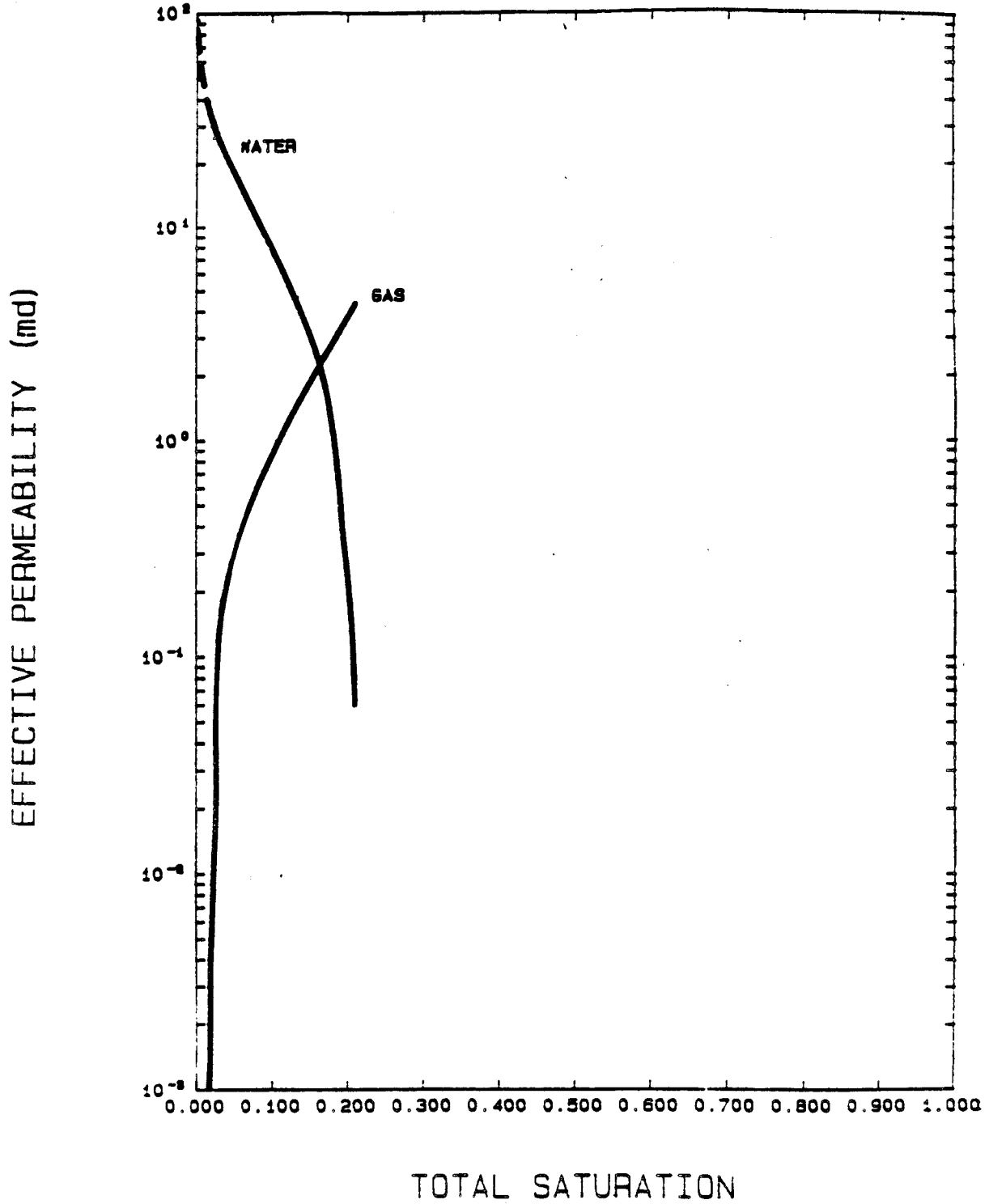

Figure D-16. Effective Permeability as a Function of Saturation for Sample MCG-617, Hole LGM-85-06, Depth of 115 Feet

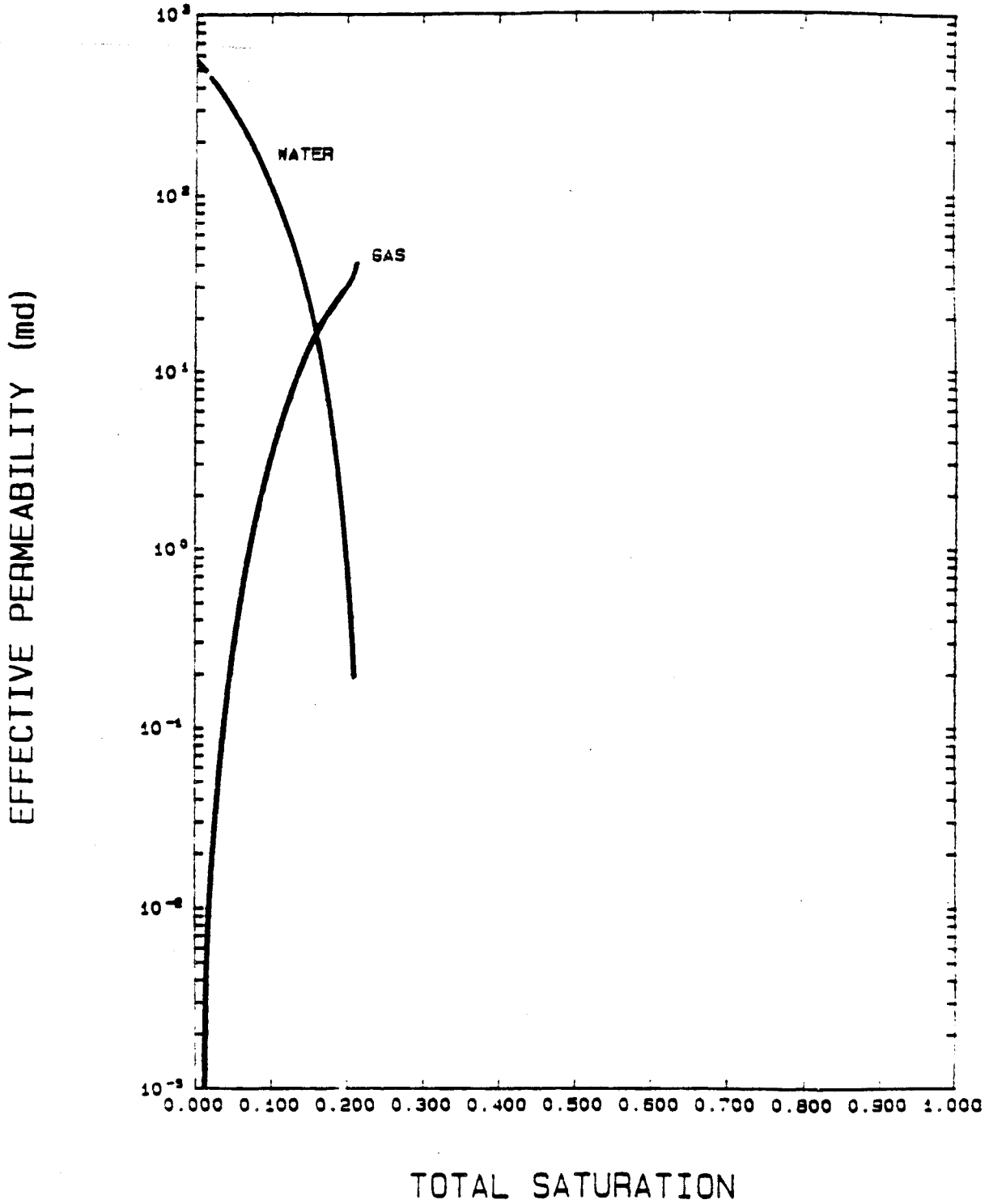

Figure D-17. Effective Permeability as a Function of Saturation for Sample MCG-618, Hole LGM-85-11, Depth of 3 Feet

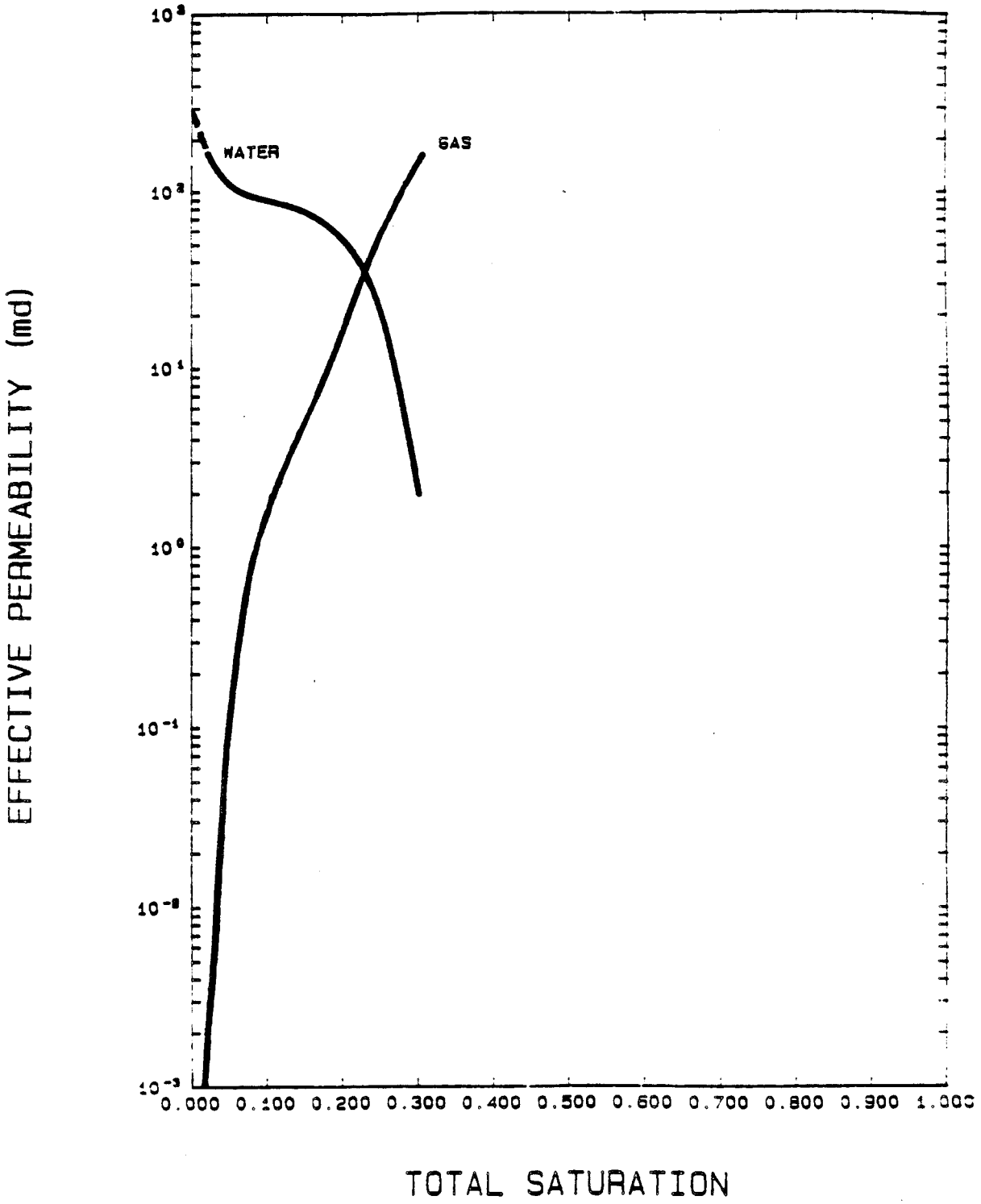

Figure D-18. Effective Permeability as a Function of Saturation for Sample MCG-619, Hole LGM-85-11, Depth of 30 Feet

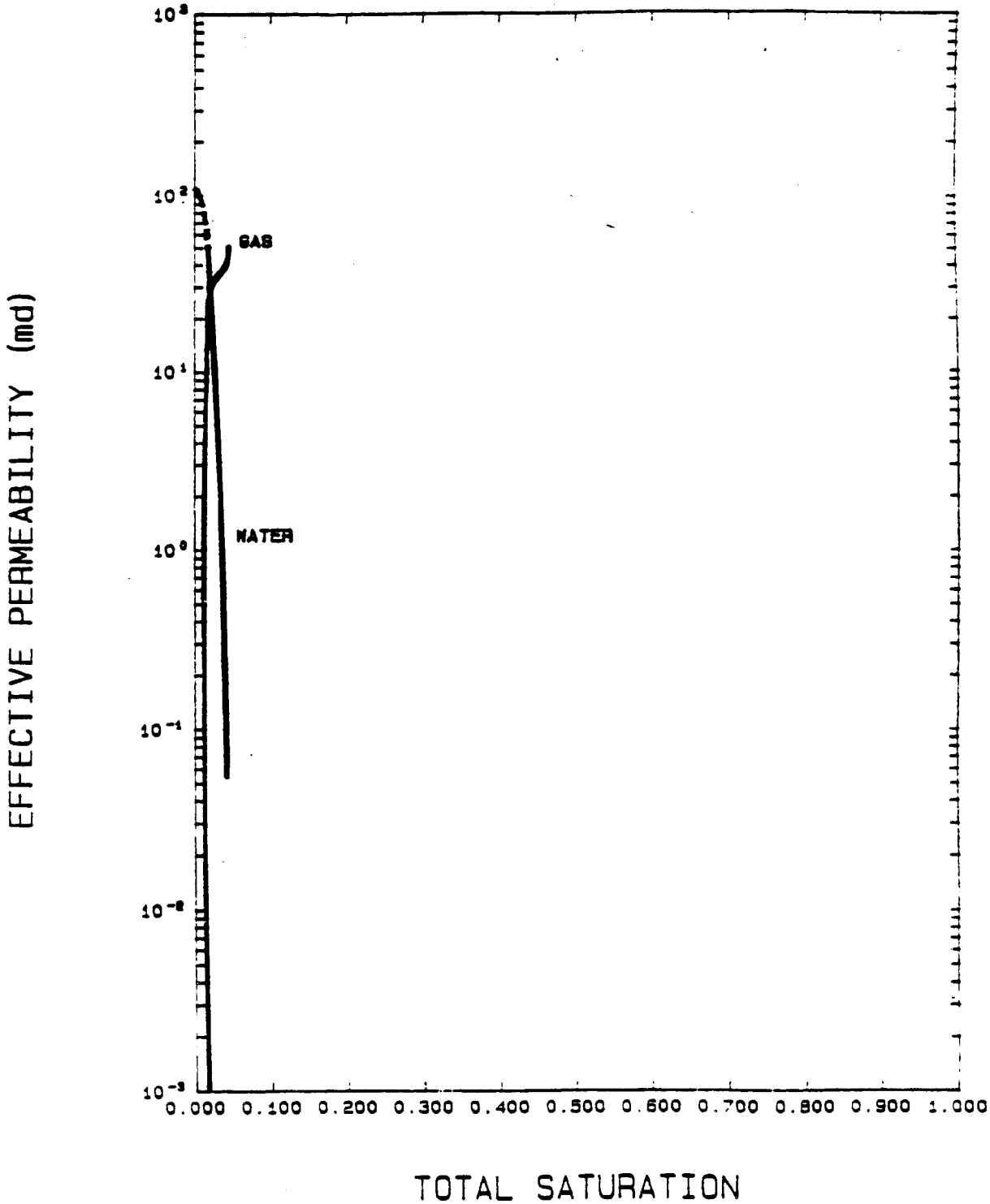

Figure D-19. Effective Permeability as a Function of Saturation for Sample MCG-620, Hole LGM-85-11, Depth of 94 Feet

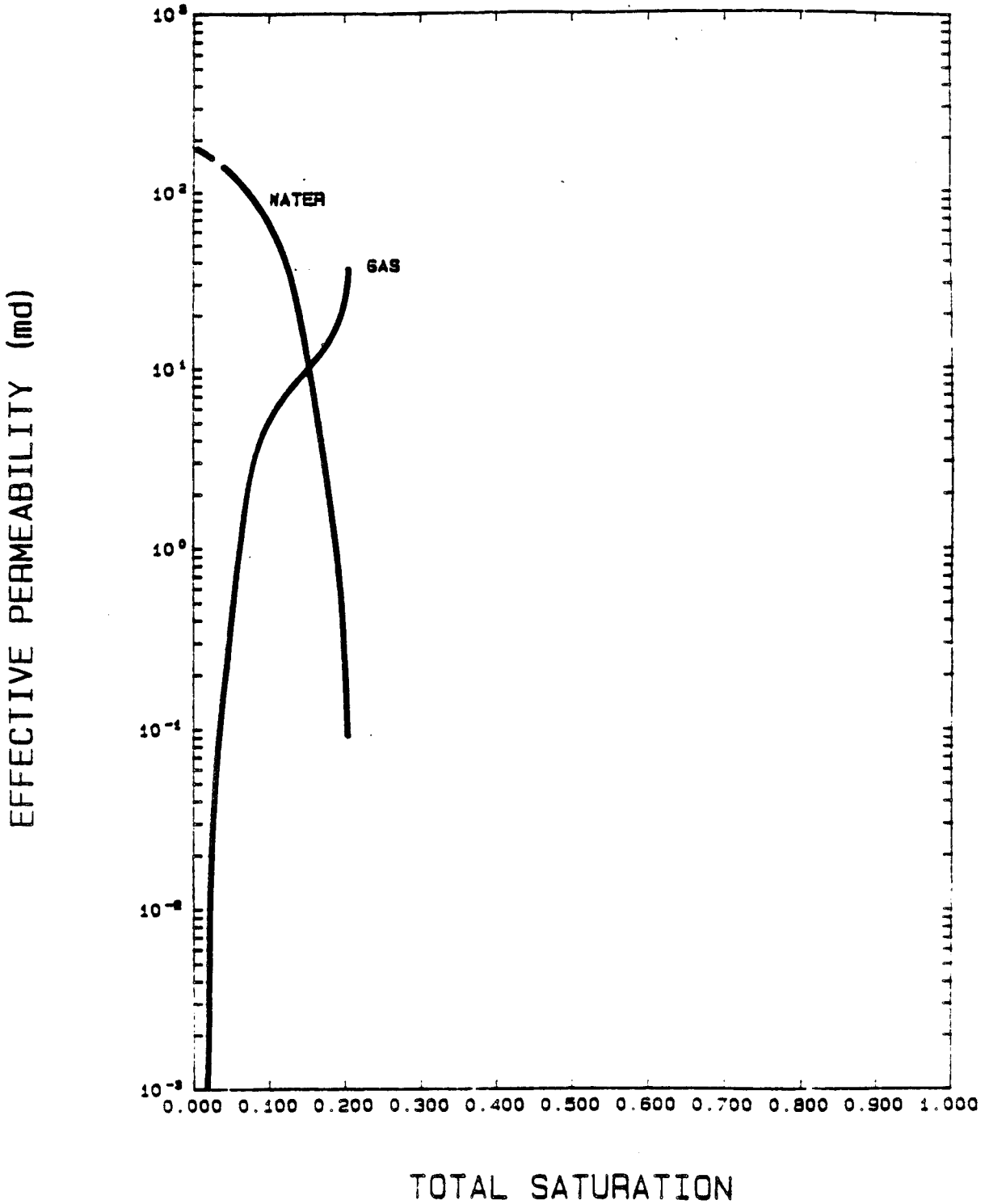

Figure D-20. Effective Permeability as a Function of Saturation for Sample MCG-621, Hole LGM-85-11, Depth of 115 Feet

Appendix E

LISTING OF FORTRAN V PROGRAM FOR CONVERTING PSYCHROMETER MICROVOLTAGE OUTPUTS TO WATER POTENTIAL

(modified from Brown and Bartos, 1982)

```
      PROGRAM H2OPOTU(INPUT,OUTPUT,TAPE5=INPUT,TAPE6=OUTPUT)
C**** LIMITS OF APPLICATION
C**** 14 < SEC < 61
C**** -1 < TEMP, DEGREES CEL < 41
C**** MV <= VIS*B*C
C**** -61 < OMV < 61
      REAL MV,MS,M15,IS,I15,LNS,LN15,NS,N15,MVS,MV15
      DATA SEC/15./
      IF(SEC.GE.14..AND.SEC.LE.61.) GO TO 10
      WRITE(6,5)
    5 FORMAT(' COOLING TIME IS NOT WITHIN MODEL RANGE')
      STOP
C
C**** READ INPUT DATA FOR FILE
   10 READ(22,20,END=100) I,DATE,TIME,B,TEMP,OMV,MV,DEPTH
   20 FORMAT(I4,A9,A7,F6.2,5F6.1)
      IF(TEMP.GE.-1..AND.TEMP.LE.41.) GO TO 30
      WRITE(6,25)
   25 FORMAT(' PSYCHROMETER TEMPERATURE IS NOT WITHIN MODEL RANGE')
      WP=-999.9
      GO TO 70
   30 IF(OMV.GE.-61..AND.OMV.LE.61.) GO TO 40
      WRITE(6,35)
   35 FORMAT(' ZERO OFFSET IS NOT WITHIN MODEL RANGE')
      WP=-999.9
      GO TO 70
   40 IF(MV.GT.0.) GO TO 50
      WRITE(6,45)
   45 FORMAT(' MICROVOLT READING .LE. 0.')
      WP=-999.9
      GO TO 70
C
   50 WPK=-22.5
      MS=2.5+EXP(-(ABS(((60.-SEC)/60.-1.)/.405)**3))
      M15=2.5+EXP(-(ABS(((60.-15.)/60.-1.)/.405)**3))
      IS=.45+.000333*SEC+1.9846E-19*SEC**10
      I15=.45+.000333*15.+1.9846E-19*15.**10
      RNS=EXP(-((1./(1.-IS))**MS))
      RN15=EXP(-((1./(1.-I15))**M15))
      DS=1.-RNS
      D15=1.-RN15
      X1AS=12.1-.003475*(60.-SEC)**1.63
      X1A15=12.1-.003475*(60.-15.)**1.63
      X1YS=39.2-.0004346*(60.-SEC)**2.45
      X1Y15=39.2-.0004346*(60.-15.)**2.45
      X2AS=88.-.0002579*(60.-SEC)**2.7
      X2A15=88.-.0002579*(60.-15.)**2.7
      X2YS=8.4+2.734E-07*(60.-SEC)**3.97
      X2Y15=8.4+2.734E-07*(60.-15.)**3.97
      LNS=EXP(-(ABS(((40.-TEMP)/40.-1.)/(1.-IS))**MS))
      LN15=EXP(-(ABS(((40.-TEMP)/40.-1.)/(1.-I15))**M15))
      NS=((LNS-RNS)/DS)*.185+1.18
      N15=((LN15-RN15)/D15)*.185+1.18
      UIS=X1AS+.017288*X1YS*TEMP**1.1
```

```
      UI15=X1A15+.017288*X1Y15*TEMP**1.1
      SPS=(X2AS-X2YS*.00017185*(40.-TEMP)**2.35)*(-1.)
      SP15=(X2A15-X2Y15*.00017185*(40.-TEMP)**2.35)*(-1.)
      MVS=(UIS-(UIS/(ABS(SPS)**NS))*(ABS(SPS-WPK)**NS))
      MV15=(UI15-(UI15/(ABS(SP15)**N15))*(ABS(SP15-WPK)**N15))
      ZOE=(.015*OMV+.001471*OMV*TEMP)
      C=(MVS+(MVS/MV15)*ZOE)/MVS
      R=UIS*C
      IF(MV.LE.R) GO TO 60
      WRITE(6,55)
   55 FORMAT(' MICROVOLT READING IS NOT WITHIN MODEL RANGE')
      WP=-999.9
      GO TO 70
   60 WP=((((ABS(SPS)**NS)*(UIS*C-MV))/(UIS*C))**(1./NS)+SPS)*B
      WP=-WP
   70 WRITE(23,20) I,DATE,TIME,B,TEMP,OMV,MV,DEPTH,WP
      GO TO 10
C
  100 CONTINUE
      STOP
      END
```

Appendix F

GEOPHYSICAL LOGS
(in attached envelope)

LA-11209-MS

Site Geology and Hydrology of Technical Area 16, Area P

Los Alamos

Los Alamos National Laboratory is operated by the University of California for the United States Department of Energy under contract W-7405-ENG-36.

Composition by Gloria Brito, Group HSE-8

An Affirmative Action/Equal Opportunity Employer

This report was prepared as an account of work sponsored by an agency of the United States Government. Neither the United States Government nor any agency thereof, nor any of their employees, makes any warranty, express or implied, or assumes any legal liability or responsibility for the accuracy, completeness, or usefulness of any information, apparatus, product, or process disclosed, or represents that its use would not infringe privately owned rights. Reference herein to any specific commercial product, process, or service by trade name, trademark, manufacturer, or otherwise, does not necessarily constitute or imply its endorsement, recommendation, or favoring by the United States Government or any agency thereof. The views and opinions of authors expressed herein do not necessarily state or reflect those of the United States Government or any agency thereof.

LA-11209-MS

UC-11
Issued: February 1988

Site Geology and Hydrology of Technical Area 16, Area P

Fred Brown
William Purtymun
Alan Stoker
Alice Barr

Los Alamos National Laboratory
Los Alamos, New Mexico 87545

SITE GEOLOGY AND HYDROLOGY OF TECHNICAL AREA 16, AREA P

by

Fred Brown, William Purtymun, Alan Stoker, and Alice Barr

ABSTRACT

Two distinct units of the Quaternary Upper Bandelier Tuff were encountered during a geological investigation of Technical Area 16, Area P, at Los Alamos National Laboratory, Los Alamos, New Mexico. Unit 3, the uppermost unit encountered, consists of four distinct ashflows, and is characterized by a high degree of welding and low-moisture content. Unit 2, the lowermost unit encountered, is densely welded, and noticeably impeded drilling operations. The Water Canyon Fault Zone, which lies approximately 500 ft to the east of Area P, exhibits 10 to 15 ft of displacement in the subsurface with little surface expression apparent. No evidence for the existence of groundwater was detected.

I. INTRODUCTION

Technical Area 16, Area P (TA-16, Area P), at Los Alamos National Laboratory (LANL) has been used since the 1950s as an industrial landfill, and is regulated under the New Mexico Environmental Improvement Division's Hazardous Waste Management Regulations due to barium residues in excess of the Extraction Procedure (EP) toxicity limits. LANL desires to permanently close the landfill, and in an effort to address closure and postclosure requirements required by RCRA (Resource Conservation and Recovery Act), a geological site investigation was conducted by the LANL Environmental Surveillance Group (HSE-8) during the summer of 1987.

II. REGIONAL GEOLOGY

The regional geology of Los Alamos has been previously reported in detail (i.e., Smith and Bailey, 1966; Purtymun, 1974; Gardner and Goff, 1986). In summary, Los Alamos National Laboratory is located on the eastern flank of the Jemez Mountains, an area dominated by volcanic deposits associated with the formation and collapse of the Valle and Toledo Calderas. Eruptive activity culminated with the deposition of a large volume (about 400 km^3) of Quaternary Bandelier Tuff, a rhyolitic tuff ranging in thickness from 30 to 1000 ft. The Bandelier Tuff is composed of a series of ashfall and ashflow tuffs unconformably resting on Chino Mesa Basalt and Puye Conglomerate of the Santa Fe Group. Depth

to the main aquifer in the vicinity of Area P is about 1230 ft (Purtymun, 1984) (Fig. 1).

Deposits of Bandelier Tuff form broad plateaus that encircle the Jemez Mountains and dip gently away from the Valle Caldera. The plateau on the eastern side of the Jemez Mountains, the Pajarito Plateau, consists of a series of east to southeast trending mesas separated by deeply incised canyons. The Bandelier Tuff itself consists of upper (Tshirege) and lower (Otowi) members, each containing a prominent ashfall bed at the base. Generally, the upper (Tshirege) member is the more densely welded of the two, and welding tends to increase with proximity to caldera sources (Bailey et al., 1969; Gardner et al., 1986).

Four fault zones have been recognized in the Pajarito Plateau: Pajarito, Water Canyon, Guaje Mt., and Rendija Canyon Fault Zones (Dransfield and Gardner, 1985). The Water Canyon Fault Zone, which extends through TA-16, trends roughly north to northeast with about 30 to 100 ft of down-to-the-east displacement. Approximately 10 to 15 ft of displacement can be seen in the subsurface adjacent to Area P, with little or no surface expression apparent.

III. GEOLOGY OF AREA P

Area P lies near the eastern margin of the Jemez Mountains, in the saddle of a short east-west trending mesa. The Water Canyon Fault Zone cuts through the tuff approximately 500 ft to the east. To the north, the Canon de Valle has cut through the fault scarp, draining an area on the west of the Sierra de los Valles flanks. To the south is a small unnamed canyon containing intermittent discharge from local outfalls. The main technical centers of TA-16 are located west of Area P (Fig. 2).

The mesa is capped by approximately 800 ft of Bandelier Tuff (Purtymun, 1968). Five distinct units, composed of groups of ashflows, have been recognized in the Tshirege Member of the Bandelier Tuff (Griggs, 1964; Smith and Bailey, 1966), of which two units were encountered during drilling operations at Area P (Brown, 1987). In addition, scattered outcrops of El Cajete Pumice occur in the area.

In order to establish the shallow subsurface geology of Area P, a series of 17 boreholes (numbered P-0 through P-16) was drilled in the summer of 1987. Drilling was done with a CME-55 rotary drilling rig and 4-inch conventional auger. Continuous auger cuttings were retrieved for lithologic logging and moisture analysis, and one set of continuous core was recovered using 6-inch hollow stem auger and split-spoon core barrels.

Borehole logging of lithology was done on the basis of four characteristics: (1) color (Goddard et al., 1984), (2) degree of welding, (3) shape and abundance of pumice lapilli, and (4) distribution of lithic fragments. Four distinct types of welding were recognized during drilling operations:

1. Nonwelded: high porosity, low cohesion of glassy fragments and crumbly texture. In core samples, this can be recognized by disaggregation and little or no flattening of pumice lapilli.

2. Moderately welded: less porosity, moderate cohesion, brittle texture, and slight deformation of glassy fragments. In core samples, this texture crumbles easily in the hand and contains some noticeably flattened pumice lapilli.

3. Welded: low porosity, good cohesion, brittle texture, and noticeable deformation of glassy fragments. This texture normally requires a hammer to break, and the majority of pumice fragments are noticeably flattened.

4. Densely welded: texture noticeably impedes or halts drilling, with little or no penetration; poor core recovery.

Two major lithologic units have been recognized at Area P (person. comm., W. Purtymun, 1987). Unit 3, the uppermost unit encountered during drilling operations, consists of four individual ashflows that appear to have cooled contemporaneously, forming a single compound unit. These ashflows are herein designated as Subunits 3a, 3b,

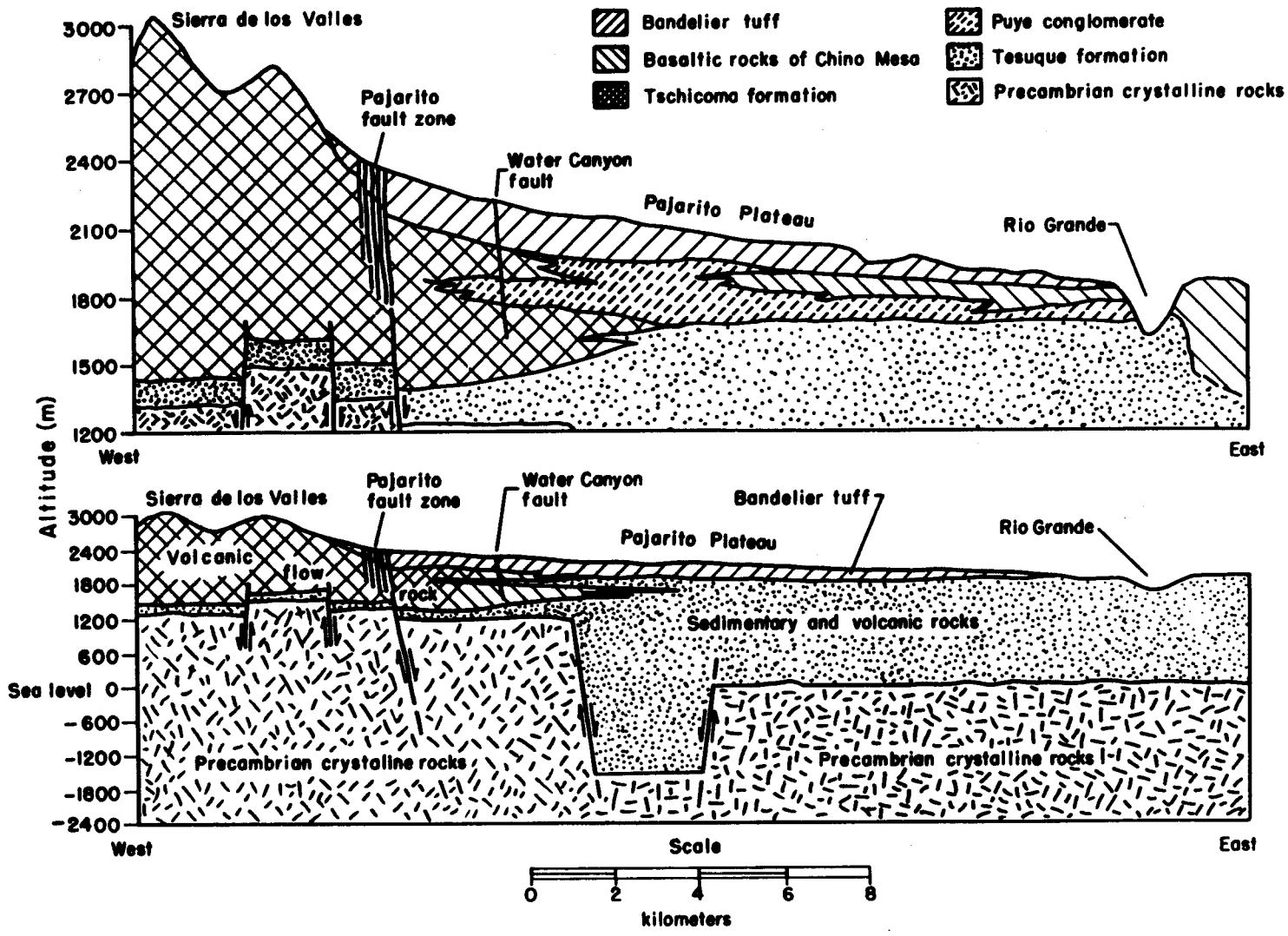

Figure 1. Geologic cross section through the Pajarito Plateau.

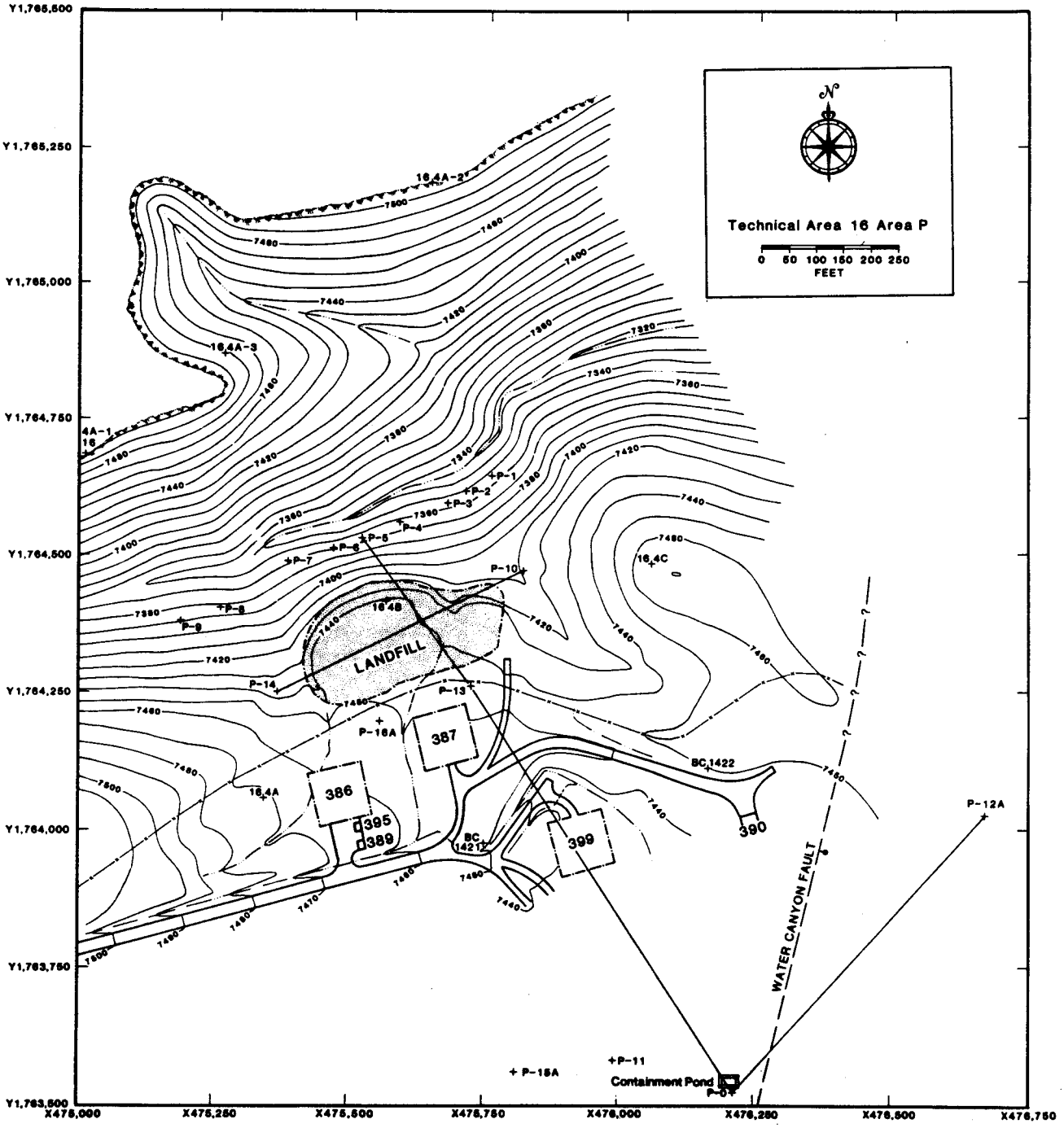

Figure 2. Site map of Technical Area 16, Area P. Boreholes are marked with crosses, numbered P-O through P-16A. Additional crosses are surveyer's marks.

3c, and 3d (bottom to top). Unit 3 rests conformably above Unit 2, the lowermost unit encountered. In general, the Bandelier Tuff dips 2 to 5° towards the east; in the vicinity of Area P dip is negligible, and the units are essentially horizontal and of uniform thickness.

Subunit 3a consists of a welded dark yellowish brown tuff, with rare pumice lapilli (slightly flattened), and abundant pebble-sized red porphyritic quartz latite and grey rhyolite lithic fragments. The ratio of quartz latite to rhyolite increases towards the base of the subunit. The contact between Subunit 3a and Unit 2 tends to be densely welded. East of the Water Canyon Fault this unit appears to be nonwelded.

Subunit 3b consists of a welded pale yellowish brown tuff, with common grey and red pumice lapilli, (noticeably flattened), and rare pebble-sized rhyolite lithic fragments. This unit weathers to a dark brown, and contains abundant clayey pumice lapilli to the northwest.

Subunit 3c consists of a moderately welded brownish grey to yellowish brown tuff, with common grey pumice lapilli (noticeably flattened), and rare pebble-sized rhyolite lithic fragments. Clay-filled vertical fractures are common throughout this subunit. The contact between 3c and 3d tends to be densely welded.

Subunit 3d outcrops along the higher rim of the saddle, and consists of a moderately welded yellowish brown tuff, with rare pebble-sized rhyolite lithic fragments and common grey pumice lapilli. Subunit 3d is overlain by scattered deposits of El Cajete Pumice.

Locally, Unit 2 consists of a welded to densely welded tuff, light grey to pinkish grey in color, with common pumice lapilli and pebble-sized rhyolite fragments. Due to dense welding, the drill bit was only able to penetrate the upper 5 to 10 ft of Unit 2 (Fig. 3).

IV. *IN SITU* MOISTURE CONTENT

Hydrologic characteristics of tuff depend primarily on the degree of welding, with porosity and hydraulic conductivity decreasing as the degree of welding increases. At Los Alamos, saturated hydraulic conductivity for a moderately welded tuff ranges from 0.1 to 1.7 ft/day, and for a welded tuff ranges from 0.009 to 0.26 ft/day (Abeele et al., 1981). Samples of tuff recovered during drilling operations at Area P were not saturated.

Gravimetric moisture determinations were conducted to obtain a direct measurement of *in situ* water content of the tuff. Samples were taken from drill cuttings every 5 or 10 ft, and moisture determinations were made by weighing samples immediately after collection and after oven-drying 24 hrs at 105°C.

Although gravimetric moisture determinations are relatively easy to perform, care must be taken to ensure that the heat produced by drilling does not bias the samples collected. In the few cases where drill cuttings were noticeably warm to the touch, or water vapor was noticed coming from the borehole, samples were not collected for analysis. Care was also taken to maintain the drying oven at 105°C to ensure that no structural water was driven off.

Table I provides a summary of gravimetric data collected for Unit 3, and indicates a low overall moisture content for Area P. Although a range of 1.9 to 24.7% is considered low, this value slightly exceeds the gravimetric moisture content determined for technical areas further to the east [5-11% for TA-33 (Abrahams, 1963), 2-20% for TA-54 (Kearl et al., 1986)]. This higher range may be due to increased

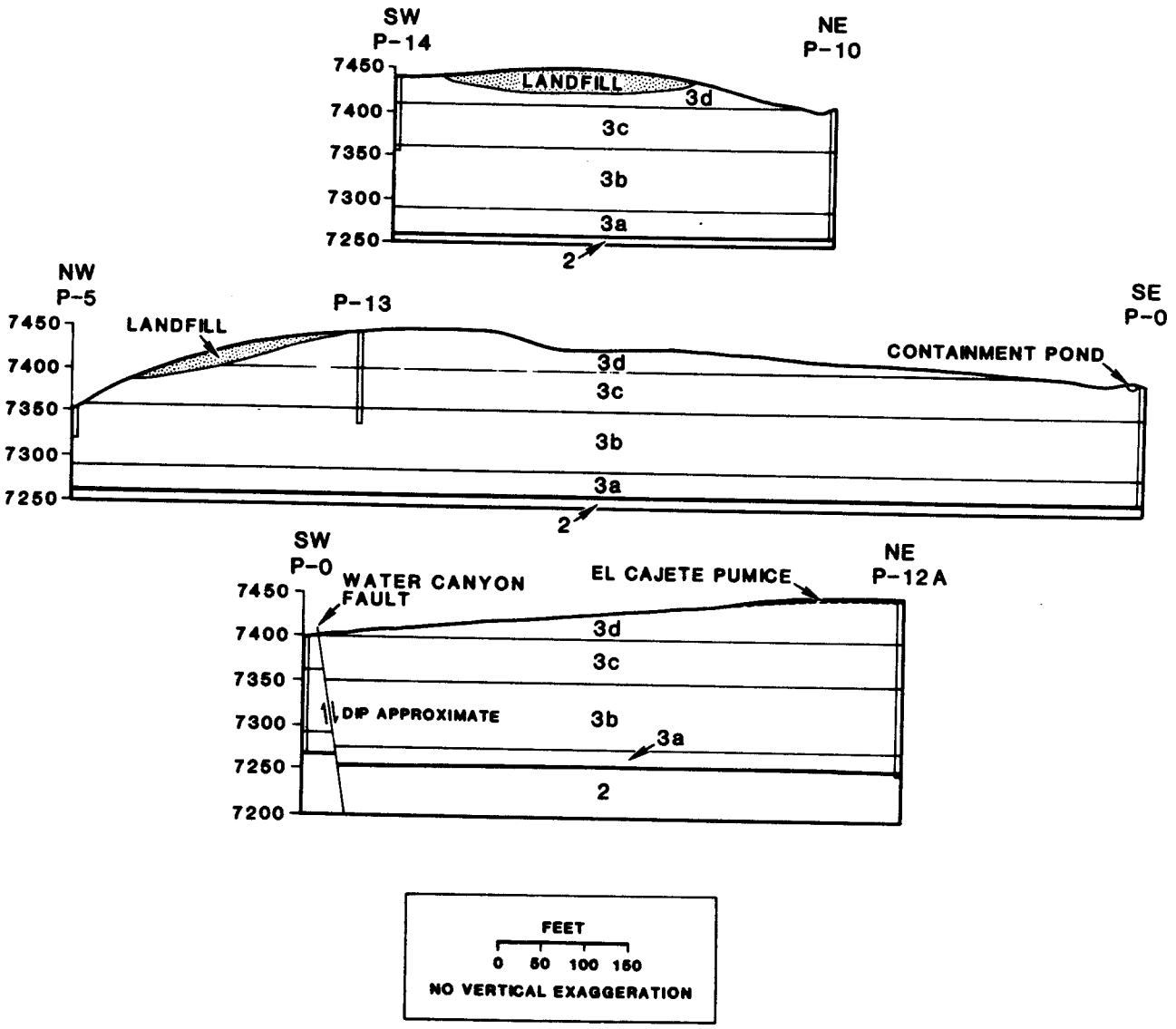

Figure 3. Geologic cross sections through Area P. Section lines are shown in Figure 2.

rainfall at TA-16, the result of orographic effects caused by the adjacent Jemez Mountains.

The energy relationship with moisture content for the Tshirege Member of the Bandelier Tuff was derived for volumetric moisture content by Abrahams (1963). Volumetric values can be converted to gravimetric values by dividing volumetric values by the average bulk density of the tuff. Repeated neutron and gamma probe calibration runs have established an average bulk density for the Tshirege Member of 1.4 g/cm^3. In addition, the density of 10 random samples was obtained after drying by weighing crushed tuff of a known volume. Average density for the 10 samples was 1.47 g/cm^3, with a standard deviation of 0.12.

Table I. Average Gravimetric Moisture Content. STD = Standard Deviation

Subunit	Mean (%)	STD	Range (%)
3d	5.2	3.6	2.2-17.7
3c	6.1	3.5	1.9-24.7
3b	5.7	2.1	2.3-11.4
3a	3.8	1.4	2.3-5.8
Total Unit	5.8	3.0	1.9-24.7

TA-16, Area P, lies in the vadose zone of the Bandelier Tuff, a zone defined by Everett et al. (1984) as existing beneath the topsoil and above the water table, in which moisture in pore spaces coexists with air or in which geological materials are unsaturated. Based on the results of Abrahams (1963), saturation of the Tshirege Member of the Bandelier Tuff, and thus groundwater, occurs when gravimetric moisture content is about 29%. When moisture content is below 7%, there is no movement of water; between 7 to 21% moisture is redistributed by diffusion; between 21 to 29% moisture distribution is by gravity and capillarity, and above 29% movement is by gravity drainage (Fig. 4). Table I suggests that the primary mechanism for moisture distribution at Area P is diffusion.

In summary, the shallow geology of TA-16, Area P, consists of two distinct units. The upper Unit 3 consists of four ashflows that appear to form a single compound unit. The lower Unit 2, a separate compound unit, is densely welded in the vicinity of Area P, and noticeably impeded drilling operations. There is no evidence of groundwater at Area P. The results of this investigation will be incorporated in the LANL landfill closure plan for Area P.

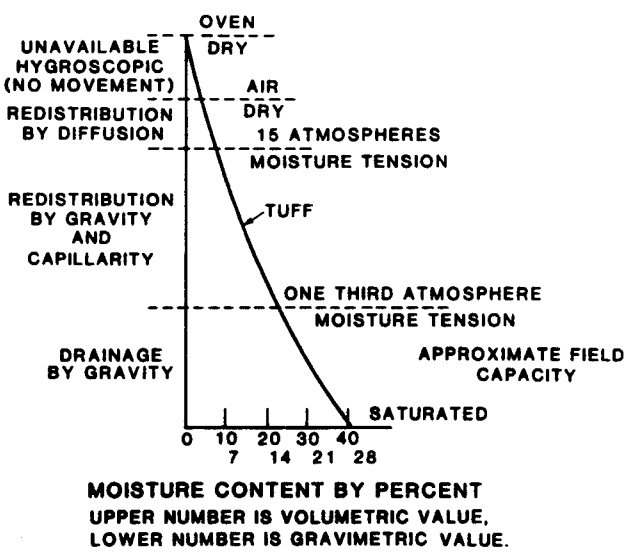

Figure 4. Energy relationship with moisture content of Bandelier Tuff (modified from Abrahams, 1963).

V. REFERENCES

Abeele, W. V., M. L. Wheeler, and B. W. Burton, "Geohydrology of Bandelier Tuff," Los Alamos National Laboratory report LA-8962-MS (1981).

Abrahams J. H., "Physical Properties of and Movement of Water in the Bandelier Tuff, Los Alamos and Santa Fe Counties, New Mexico," U.S.G.S. Open File Report, (1963).

Bailey, R. A., R. L. Smith, and C. S. Ross, "Stratigraphic Nomenclature of the Volcanic Rocks of the Jemez Mountains, New Mexico," U.S.G.S. Bulletin 1274-P (1969).

Brown, F., "Test Hole P-87-0, TA-16, Area P," Los Alamos National Laboratory memorandum HSE8-87-842 to Alice R. Barr (July 29, 1987).

Dransfield, B. J., and J. N. Gardner, "Subsurface Geology of the Pajarito Plateau, Espanola Basin, New Mexico," Los Alamos National Laboratory report LA-10455-MS (1985).

Everett, L. G., L. G. Wilson, and E. W.Holyman, "Vadose Zone Monitoring for Hazardous Waste Sites," Noyes Data Corporation, Park Ridge, New Jersey (1984).

Gardner, J. N, and F. Goff, "Stratigraphic Relations and Lithologic Variations in the Jemez Volcanic Field, New Mexico," *Journal of Geophysical Research*, **91**, 1763-1778 (1986).

Goddard, E. N., P. D. Trask, and R. K. De Ford, et al., *Rock Color Chart*, Geological Society of America (1984).

Griggs, R. L., "Geology and Groundwater Resources in the Los Alamos Area," U.S.G.S. Water Supply Paper 1753 (1964).

Kearl, M. P., J. J. Dexter, and M. Kautsky, "Vadose Zone Characterization of Technical Area 54, Waste Disposal Areas G and L," Report 3: Preliminary Assessment of the Hydrologic System, Bendix Field Engineering (1986).

Purtymun W., "Geology of the Microseismic Station at S-Site, Los Alamos County, Los Alamos," U.S.G.S. Administrative report (1968).

Purtymun, W., "General Geohydrology of the Pajarito Plateau, in *New Mexico Geologic Society Guidebook*, 25th Field Conference (1974).

Purtymun, W., "Hydrological Characteristics of the Main Aquifer in the Los Alamos Area," Los Alamos National Laboratory report LA-9957-MS (1984).

Smith, R. L. and R. A. Bailey, "The Bandelier Tuff - A Study of Ash-Flow Eruption Cycles from Zoned Magma Chambers," Bulletin Volcanologique **29**, 83-104 (1966).

Printed in the United States of America
Available from
National Technical Information Service
US Department of Commerce
5285 Port Royal Road
Springfield, VA 22161

Microfiche (A01)

Page Range	NTIS Price Code	Page Range	NTIS Price Code	Page Range	NTIS Price Code	Page Range	NTIS Price Code
001-025	A02	151-175	A08	301-325	A14	451-475	A20
026-050	A03	176-200	A09	326-350	A15	476-500	A21
051-075	A04	201-225	A10	351-375	A16	501-525	A22
076-100	A05	226-250	A11	376-400	A17	526-550	A23
101-125	A06	251-275	A12	401-425	A18	551-575	A24
126-150	A07	276-300	A13	426-450	A19	576-600	A25
						601-up*	A99

*Contact NTIS for a price quote.

Los Alamos National Laboratory
Los Alamos, New Mexico 87545

An Evaluation of Aquifer and Well Characteristics of Municipal Well Fields in Los Alamos and Guaje Canyons, Near Los Alamos, New Mexico

By R. L. CUSHMAN

CONTRIBUTIONS TO THE HYDROLOGY OF THE UNITED STATES

GEOLOGICAL SURVEY WATER-SUPPLY PAPER 1809-D

Prepared in cooperation with the U.S. Atomic Energy Commission and published with the permission of the Commission

UNITED STATES GOVERNMENT PRINTING OFFICE, WASHINGTON : 1965

Geology and Ground-Water Resources of The Los Alamos Area New Mexico

By ROY L. GRIGGS

With a section on QUALITY OF WATER

By JOHN D. HEM

GEOLOGICAL SURVEY WATER-SUPPLY PAPER 1753

Prepared in cooperation with the Atomic Energy Commission

UNITED STATES GOVERNMENT PRINTING OFFICE, WASHINGTON : 1964

SUPPLEMENTAL REPORT FOR THE INTERIM STATUS CLOSURE PLAN AT THE TA-16 SURFACE IMPOUNDMENT

prepared for

New Mexico Health and Environment Department
Environmental Improvement Division - Hazardous Waste Section

by the

Environmental Surveillance Group (HSE-8)
Solid Waste and Remedial Action Section

Los Alamos National Laboratory
Los Alamos, New Mexico 87545
RCRA Number NM-0890010515

February 6, 1989

VOLUME II OF II

SUPPLEMENTAL REPORT FOR THE
INTERIM STATUS CLOSURE PLAN AT THE TA-16 SURFACE IMPOUNDMENT

Facility ID No.....NM890010515
Facility Name.....Los Alamos National Laboratory
Legal Owner.....United States Department of Energy
Legal Operator.....University of California
Address.....Los Alamos Area Office
City, State.....Los Alamos, New Mexico 87545
Contact Person.....Mr. Harold Valencia, Area Manager
Phone.....(505) 667-5105
Originally Dated.....November 18, 1988
Date Modified.....February 6, 1989

LA-11306-ENV

UC-41
Issued: May 1988

Environmental Surveillance at Los Alamos During 1987

Environmental Surveillance Group

Los Alamos
Los Alamos National Laboratory
Los Alamos, New Mexico 87545

FOREWORD

Suggestions on How to Read this Report

This report addresses both the lay person and the scientist. Each reader may have limited or comprehensive interest in this report. We have tried to make it accessible to all without compromising its scientific integrity. Following are directions advising each audience on how best to use this document.

1. **Lay Person with Limited Interest.** Read Part I, the Executive Summary, which describes the Laboratory's environmental monitoring operations and summarizes environmental data for this year. Emphasis is on the significance of findings and environmental regulatory compliance. A glossary is in the back.

2. **Lay Person with Comprehensive Interest.** Follow directions for the "Lay Person with Limited Interest" given above. Also, summaries of each section of the report are in boldface type and precede the technical text. Read summaries of those sections that interest you. Further details are in the text following each summary. Appendix A (Standards for Environmental Contaminants) and Appendix F (Description of Technical Areas and Their Associated Programs) may also be helpful.

3. **Scientists with Limited Interest.** Read Part I, the Executive Summary, to determine the parts of the Laboratory's environmental program that interest you. You may then read summaries and technical details of these parts in the body of the report. Detailed data tables are in Appendix G.

4. **Scientists with Comprehensive Interest.** Read Part I, the Executive Summary, which describes the Laboratory's environmental programs and summarizes environmental data for this year. Read the boldface summaries that head each major subdivision of this report. Further details are in the text and appendixes.

For further information about this report, contact the Los Alamos National Laboratory's Environmental Surveillance Group (HSE-8):

Environmental Surveillance Group (HSE-8)
Los Alamos National Laboratory
P. O. Box 1663
Los Alamos, New Mexico--87545
Attn: Dr. Lars F. Soholt
Mail Stop K490
Commercial Telephone: (505) 667-5021
Federal Telephone System: 843-5021

ACKNOWLEDGMENTS

This report was compiled by the Environmental Surveillance Group (HSE-8) of the Laboratory's Health, Safety, and Environment Division. Personnel in HSE-8 include:

Marjorie Martz Emerson, Group Leader
Alice Barr
Naomi Becker
Roy Bohn
Brent Bowen
Thomas Buhl
Ili Chen
Marie Conn
Kathy Derouin
Jean Dewart
Anthony Drypolcher
Craig Eberhart
Malcolm Ennis
Teralene Foxx
Anthony Gallegos
Anthony Grieggs
Barbara Hargis
Belinda Harrigan
Keith Jacobsen
Carla Jacquez
Beverly Larson
Eddie Lujan
Max Maes
David McInroy
David Nochumson
Charles Nylander
Colleen Olinger
William Olsen
Betty Perkins
William Purtymun
Steven Rae
Richard Romero
John Salazar
Tina Marie Sandoval
Wayne Scoggins
Lars Soholt
Alan Stoker
Daniel Talley
Gail Tierney
Michael Trujillo
Donald VanEtten
Ralph Ward
James White

Kathy Derouin and Gloria Brito did the word processing and assembly of this report in a very professional manner. Environmental data were provided by the following groups in the Laboratory's Health, Safety, and Environmental Division: Radiation Protection (HSE-1), Industrial Hygiene (HSE-5), Waste Management (HSE-7), Health and Environmental Chemistry (HSE-9), Accelerator Health Protection (HSE-11), and Environmental Sciences (HSE-12).

CONTENTS

ABSTRACT 1

I. EXECUTIVE SUMMARY 2
- A. Monitoring Operations 2
- B. Estimated Doses and Risks from Radiation Exposure 2
  - 1. Radiation Doses 2
  - 2. Risk Estimates 3
- C. External Penetrating Radiation 4
- D. Air Monitoring 5
- E. Water, Soil, and Sediment Monitoring 7
- F. Foodstuffs Monitoring 7
- G. Unplanned Release 7
  - 1. March 18 Tritium Release at the Van de Graaff Facility at TA-3 7
  - 2. December 11-12 Tritium Release at TA-33 7
- H. Environmental Compliance Activities 8
  - 1. Resource Conservation and Recovery Act 8
  - 2. Clean Water Act 8
  - 3. National Environment Policy Act 8
  - 4. Clean Air Act 8
  - 5. Safe Drinking Water Act 8
  - 6. Federal Insecticide, Fungicide, and Rodenticide Act 8
  - 7. Archaeological and Historical Protection 8
  - 8. Threatened/Endangered Species and Floodplains/Wetlands Protection 9
  - 9. Comprehensive Environmental Response, Compensation, and Liability Act 9
  - 10. Toxic Substances Control Act 9
  - 11. Emergency Planning and Community Right-to-Know Act 9

II. INTRODUCTION TO THE LOS ALAMOS AREA 11
- A. Geographic Setting 11
- B. Land Use 11
- C. Geology-Hydrology 12
- D. Climatology 14
- E. Population Distribution 15
- F. Programs at Los Alamos National Laboratory 15

III. RADIATION DOSES 17
- A. Background 17
- B. Estimate of Radiation Doses 18
  - 1. Doses from Natural Background Radiation and Medical and Dental Radiation 18
  - 2. Dose to Individuals from External Penetrating Radiation from Airborne Emissions 20
  - 3. Doses to Individuals from Inhalation of Airborne Emissions 20
  - 4. Modeled Doses from Airborne Emissions 21
  - 5. Doses from Direct Penetrating Radiation 21
  - 6. Doses to Individuals from Treated Liquid Effluents 21
  - 7. Doses to Individuals from Ingestion of Foodstuffs 21
  - 8. Cumulative Effective Dose Equivalents 22

C. Risk to an Individual from Laboratory Releases 23
1. Estimating Risk 23
2. Risk from Natural Background Radiation and Medical and Dental Radiation 24
3. Risk from Laboratory Operations 24

IV. MEASUREMENT OF EXTERNAL PENETRATING RADIATION 25
A. Background 25
B. Environmental TLD Network 25
C. Los Alamos Meson Physics Facility (LAMPF) TLD Network 26
D. TLD Network for Low-Level Radioactive Waste Management Areas 26

V. AIR MONITORING 29
A. Radionuclides in Ambient Air 29
1. Background 29
2. Airborne Emissions 29
3. Gross Beta Radioactivity 30
4. Tritium 30
5. Plutonium and Americium 33
6. Uranium 33
B. Nonradioactive Chemicals in Ambient Air 33
1. Air Quality 33
a. Bandelier National Atmospheric Deposition Program Station 33
b. Particulate Air Quality Measurements 33
2. Beryllium Operations 33
3. Steam Plants and Power Plant 33
4. Motor Vehicle Emissions 34
5. Asphalt Plant 35
6. Burning and Detonation of Explosives 35
7. Lead Pouring Facility 36

VI. WATER, SOILS, AND SEDIMENTS MONITORING 37
A. Effluent Quality 37
B. Radiochemical and Chemical Quality of Surface and Ground Waters 38
1. Background 38
2. Regional Stations 38
a. Radiochemical Analyses 39
b. Chemical Analyses 42
3. Perimeter Stations 42
a. Radiochemical Analyses 42
b. Chemical Analyses 44
4. On-site Stations 44
a. Noneffluent Release Areas 44
b. On-site Effluent Release Areas 44
5. Transport of Radionuclides in Surface Run-Off 47
C. Radioactivity in Soils and Sediments 47
1. Background Levels of Radioactivity in Soils and Sediments 47
2. Regional Soils and Sediments 47
3. Perimeter Soil and Sediments 48
4. On-site Soils and Sediments 51
5. Sediments in Regional Reservoirs 52

6. Transport in Sediments and Run-Off from an Active Waste Management Area (Area TA-54) 53

VII. FOODSTUFFS MONITORING 57
A. Background 57
B. Produce 57
C. Fish 57

VIII. ENVIRONMENTAL COMPLIANCE 59
A. Resource Conservation and Recovery Act (RCRA) 59
1. Background 59
2. Permit Application 59
3. Area P Landfill and Lagoons 59
4. Other RCRA Activities 62
B. Clean Water Act 62
1. Laboratory Liquid Waste Discharge Permits 62
2. Federal Facility Compliance Agreement 63
3. Clean Water Act Audits 63
4. Administrative Order 63
5. Fenton Hill Geothermal Project NPDES Permit 63
6. Spill Prevention Control and Countermeasure (SPCC) Plan 65
7. Sanitary Wastewater Systems Consolidation 65
8. Interim Improvements at TA-3 Sanitary Wastewater Treatment Plant 66
9. Interim Improvements at Other Sanitary Wastewater Treatment Plants 66
10. Septic Tank System Survey and Registration 66
11. Treatment of Chemical Oxygen Demands at TA-16 66
C. National Environmental Policy Act (NEPA) 66
D. Clean Air Act 67
1. Federal Regulations 67
a. National Emissions Standards for Hazardous Air Pollutants (NESHAPS) 67
b. National Ambient Air Quality Standards 67
c. Prevention of Significant Deterioration (PSD) 67
d. New Source Performance Standards (NSPS) 67
2. State Regulations 69
a. New Mexico Air Quality Control Regulation (NMAQCR) 301 69
b. NMAQCR 501 69
c. NMAQCR 604 69
d. NMAQCR 702 70
e. Other Regulations 70
E. Safe Drinking Water Act (Municipal and Industrial Water Supply) 70
1. Background 70
2. Radioactivity in Municipal and Industrial Water Supply 72
3. Chemical Quality of Municipal and Industrial Water Supply 72
F. Federal Insecticide, Fungicide, and Rodenticide Act 72
G. Archaeological and Historical Protection 72
H. Threatened/Endangered Species and Floodplains/Wetlands Protection 76

I. Comprehensive, Environmental Response, Compensation, and Liability Act (CERCLA) 76
J. Toxic Substances Control Act (TSCA) 76
K. Emergency Planning and Community Right-to-Know Act 76
L. DOE Headquarters' Environmental Survey 78
M. Health, Safety, and Environmental Appraisal of Laboratory Operations and Facilities 78
N. Engineering Quality Assurance 79

IX. ENVIRONMENTAL SUPPORT ACTIVITIES 81
A. Meteorological Monitoring 81
1. Weather Summary 81
2. Wind Roses 82
3. Precipitation Summary 86
B. Environmental Restoration 86
C. Vadose Zone Characterization at Area L and Area G 88
D. Remedial Investigations at the Proposed White Rock Y Interchange 88
E. Environmental Monitoring at the Fenton Hill Site 89
F. Distribution of Radionuclides in Channel Alluvium of Mortandad Canyon 90
G. Underground Storage Tanks 93
H. PCB Inventory at the Laboratory 95
I. Biomonitoring of the Laboratory's Liquid Effluents 95
J. National Atmospheric Deposition Program (NADP) Network Station 96
K. Vadose Zone Characterization at TA-16, Area P 96
L. Environmental Studies of TA-49 97
M. Quality of Surface and Ground Water Adjacent to the Los Alamos National Laboratory: Organic Compounds 98
N. Radiation Levels from LAMPF Emissions 99

X. PUBLICATIONS 101

XI. REFERENCES 103

APPENDIX A--STANDARDS FOR ENVIRONMENTAL CONTAMINANTS 107

APPENDIX B--PROCEDURES FOR SAMPLING, DATA HANDLING, AND QUALITY ASSURANCE 113

APPENDIX C--ANALYTICAL CHEMISTRY METHODOLOGY 118

APPENDIX D--METHODS FOR DOSE CALCULATIONS 140

APPENDIX E--UNITS OF MEASUREMENT 147

APPENDIX F--DESCRIPTIONS OF TECHNICAL AREAS AND THEIR ASSOCIATED PROGRAMS 148

APPENDIX G--ENVIRONMENTAL DATA TABLES 151

GLOSSARY 265

DISTRIBUTION LIST 271

FIGURES

1. Regional location of Los Alamos 3
2. Summary of estimated maximum individual and Laboratory boundary doses (excluding contributions from cosmic, terrestrial, and medical diagnostic sources) from Laboratory operations 4
3. Topography of the Los Alamos area 11
4. Technical areas (TAs) of Los Alamos National Laboratory in relation to surrounding landholdings 12
5. Conceptual illustration of geologic-hydrologic relationships in Los Alamos area 13
6. Thermoluminescent dosimeter (TLD) locations on or near the Laboratory site 22
7. Thermoluminescent dosimeter (TLD) measurements (includes contributions from cosmic, terrestrial, and Laboratory radiation) 26
8. Air sampler locations on or near the Laboratory site 30
9. Summary of tritium releases (airborne emissions and liquid effluents) 31
10. Summary of plutonium releases (airborne emissions and liquid effluents) 31
11. Airborne activation product emissions (principally ^{11}C, ^{10}C, ^{13}N, ^{16}N, ^{14}O, ^{15}O, ^{41}Ar) from the Los Alamos Meson Physics Facility (TA-53) 32
12. Atmospheric gross beta activity at a regional (background) station and an on-site station during 1987 32
13. Summary of strontium and cesium liquid effluent releases 37
14. Regional surface water, sediment, and soil sampling locations 38
15. Surface and ground water sampling locations on and near the Laboratory site 39
16. Locations of surface run-off sampling stations at the Laboratory 48
17. Soil sampling on an near the Laboratory site 51
18. Sediment sampling locations on an near the Laboratory site 52
19. Special regional sediment sampling locations 53
20. Surface water gaging station in Area G (TA-54) and sediment sampling stations adjacent to Area G 55
21. Fish and produce sampling locations 57
22. Locations of beehives 58
23. 1987 Summary of Clean Water Act Compliance, NPDES Permit NM0028353 63
24. Locations of reservoirs, well fields, supply wells, and gallery water supply 71
25. Summary of 1987 weather in Los Alamos (data from Occupational Health Laboratory, OHL, TA-59 82
26. Daytime wind roses at Laboratory stations during 1987 83
27. Nighttime wind roses at Laboratory stations during 1987 84
28. Cumulative wind roses at Laboratory stations in 1987 85
29. Summer (June-August) and annual rainfall during 1987 (inches) 87
30. Sampling stations for surface and ground water near the Fenton Hill Site (TA-57) 90

31. Sediment sampling stations in Mortandad Canyon 92
32. Location of experimental areas and test wells at TA-49 98
33. Surface and ground water locations sampled for organic analyses 99

TABLES

1. Number of Sampling Locations 4
2. Added Individual Lifetime Cancer Mortality Risks Attributable to 1987 Radiation Exposure 5
3. Comparison of 1986 and 1987 Radioactive Releases from the Laboratory 6
4. 1987 Population Within 80 km of Los Alamos 16
5. Summary of Annual, Effective Dose Equivalents Due to 1987 Laboratory Operations 19
6. Estimated Population Effective Dose Equivalents (person-rem) During 1987 23
7. Doses (mrem) Measured by TLDs at On-site Waste Areas During 1987 27
8. Particulate Air Quality 34
9. Particulate Air Quality, Seasonal Averages 34
10. Estimate of Air Pollutant Emissions Associated with the Operation of the Vehicle Fleet 35
11. Asphalt Plant Particulate Emissions 35
12. Estimated Air Pollutant Emissions from the Open Burning of Waste Explosives 36
13. Maximum Concentrations of Radioactivity in Surface and Ground Waters from Off-site and On-site Stations 40
14. Maximum Chemical Concentrations in Surface and Ground Waters 43
15. Average Plutonium Concentrations in Summer Run-off in Canyons Draining the Laboratory 45
16. Maximum Concentrations of Radioactivity in Soils and Sediments from Regional, Perimeter, and On-site Stations 49
17. Radiochemical Analyses of Sediments from Reservoirs on the Rio Chama and Rio Grande 54
18. Major Regulatory Requirements of the Hazardous and Solid Waste Amendments of 1984 Impacting Waste Management at Los Alamos National Laboratory 60
19. Environmental Permits Under Which the Laboratory Operated in 1987 61
20. Environmental Appraisals Conducted at the Laboratory in 1987 64
21. National and New Mexico Ambient Air Quality Standards 68
22. Maximum Concentrations of Radioactivity in Municipal Water Supply, Well and Distribution System 73
23. Maximum Chemical Concentrations in Water Supply and Distribution Systems 75
24. Quantities (kg) of PCB Contaminated Articles Discarded at TA-54 in 1987 77
25. Tentative Findings by Topical Area and Category from the DOE Headquarters' Environmental Survey of Los Alamos National Laboratory 1987 79
26. Quality of Surface and Ground Waters at Fenton Hill Geothermal Site 91
27. Transuranics in Mortandad Canyon Channel Alluvium June 16, 1987 93
28. Radionuclides in Mortandad Canyon Channel Alluvium, June 16, 1987
29. Summary of Underground Petroleum Storage Tanks Removed in 1987 96

APPENDIX TABLES

A-1. DOE Radiation Protection Standards for External and Internal Exposures 108
A-2. DOE's Derived Concentration Guides (DCG) for Uncontrolled Areas and Concentration Guides (CG) for Controlled Areas 110
A-3. Maximum Contaminant Level (MCL) in Water Supply for Inorganic Chemicals and Radiochemicals 111
A-4. Minimum Concentrations of Inorganic Contaminants for Meeting EPA's Extraction Procedure (EP) Toxicity Characteristic for Hazardous Waste 112

C-1. Analytical Methods for Various Stable Constituents 119
C-2. Method Summary (Organics) 121
C-3. Volatiles Determined by Purge and Trap 122
C-4. Volatiles Determined by SW-846 Method 8010 123
C-5. Volatiles Determined by SW-846 Method 8020 124
C-6. Volatiles Determined in Air 125
C-7. EP Toxicity Organic Contaminants 126
C-8. Summary of HSE-9 Quality Assurance Tests for Data from January 1, 1987 to December 31, 1987 (Stable Element Analyses Performed by HSE-9) 127
C-9. Summary of HSE-9 Quality Assurance Tests for Data from January 1, 1987 to December 31, 1987 (Stable Element Analyses Performed by Contractors) 129
C-10. Summary of HSE-9 Quality Assurance Tests for Data from January 1, 1987 to December 31, 1987 (Organic Analyses Performed by HSE-9) 130
C-11. Summary of HSE-9 Quality Assurance Tests for Data from January 1, 1987 to December 31, 1987 (Organic Analyses Performed by Contractors) 132
C-12. Summary of HSE-9 Quality Assurance Tests for Data from January 1, 1987 to December 31, 1987 (Radiochemical Analyses Performed by HSE-9) 133
C-13. Detection Limits for Analyses of Typical Environmental Samples 134

D-1. Dose Conversion Factors (rem/μCi Intake) for Calculating Internal Doses 141
D-2. Dose Conversion Factors [(mrem/yr/(μCi/mL)] for Calculating External Doses 143

E-1. Prefixes Used with SI (Metric) Units 147
E-2. Approximate Conversion Factors for Selected SI (Metric) Units 147

G-1. Estimated Maximum Individual 50-Year Dose Commitments from 1987 Airborne Radioactivity 152
G-2. Airborne Radioactive Emissions Totals 153
G-3. Thermoluminescent Dosimeter Measurements 154
G-4. Location of Air Sampling Stations 155
G-5. Average Background Concentrations of Radioactivity in the Atmosphere 156
G-6. Estimated Aerial Concentrations of Toxic Elements Aerosolized by Dynamic Experiments 157

G-7. Atmospheric Tritiated Water Concentrations for 1987 158
G-8. Atmospheric $^{239,240}Pu$ Concentration for 1987 160
G-9. Atmospheric ^{241}Am Concentration for 1987 162
G-10. Atmospheric Uranium Concentration for 1987 163
G-11. Emissions (tons/yr) and Fuel Consumption (10^9 Btu/yr) from the TA-3 Power Plant and Steam Plants 165
G-12. Quality of Effluent from the TA-50 Liquid Radioactive Waste Treatment Plan for 1987 166
G-13. Quality of Effluent from the Los Alamos Meson Physics Facilities (TA-53) Lagoons for 1987 167
G-14. Location of Surface and Ground Water Sampling Stations 168
G-15. Radiochemical Quality of Surface Water from Regional Stations 172
G-16. Chemical Quality of Surface Water from Regional Stations 173
G-17. Radiochemical Quality of Surface and Ground Waters from Perimeter Stations 174
G-18. Radiochemical Quality of Surface Waters from White Rock Canyon, October 1987 175
G-19. Chemical Quality of Surface and Ground Waters from Perimeter Stations 177
G-20. Primary Chemical Quality of Surface and Ground Waters from White Rock Canyon, October 1987 178
G-21. Secondary Chemical Quality of Surface and Ground Waters from White Rock Canyon, October 1987 180
G-22. Chemical Quality of Surface and Ground Waters from White Rock Canyon, October 1987 182
G-23. Radiochemical Quality of Surface and Ground Waters from On-site Stations 184
G-24. Radiochemical Quality of Shallow Ground Water in Pajarito Canyon 186
G-25. Chemical Quality of Surface and Ground Waters from On-site Stations 187
G-26. Chemical Quality of Shallow Ground Water in Pajarito Canyon 188
G-27. Radiochemical Quality of Surface and Ground Waters from Acid-Pueblo Canyon 189
G-28. Radiochemical Quality of Surface and Ground Waters from DP-Los Alamos Canyon 190
G-29. Radiochemical Quality of Surface and Shallow Ground Water from Mortandad Canyon 191
G-30. Radiochemical Quality of Surface Waters from Sandia Canyon 192
G-31. Chemical Quality of Surface and Ground Waters from Acid-Pueblo Canyons 193
G-32. Chemical Quality of Surface and Shallow Ground Waters in DP-Los Alamos Canyon 194
G-33. Chemical Quality of Surface and Shallow Ground Waters in Mortandad Canyon 195
G-34. Chemical Quality of Surface Water from Sandia Canyon 196
G-35. Background Radiochemical Quality of Run-off (Solution and Suspended Sediments) in the Los Alamos Area 197
G-36. Plutonium in Spring Run-off in Solution and Suspended Sediments 198
G-37. Radiochemistry of Storm Run-off in Sediment Traps, Mortandad
G-38. Locations of Soil and Sediment Sampling Stations 202
G-39. Radiochemical Analyses of Regional Soils and Sediments 203
G-40. Radiochemical Analyses of Perimeter Soils and Sediments 206
G-41. Suburanic and Gross Gamma Radiochemical Analyses of On-site Soils and Sediments 208

G-42. Uranium and Transuranic Radiochemical Analyses of On-site Soils and Sediments 211
G-43. Inorganic Chemical Parameters in Solution Extracted from Sediments Downgradient from Areas G and L, TA-54 214
G-44. Radionuclides in Local and Regional Produce 215
G-45. Radionuclides in Fish 217
G-46. Locations of Beehives 219
G-47. Selected Radionuclides in Local and Regional Honey 220
G-48. Selected Radionuclides in Local and Regional Bees 221
G-49. Hazardous Waste Management Facilities at Los Alamos National Laboratory 222
G-50. 1987 RCRA Interactions Among the Laboratory, Environmental Protection Agency (EPA), and New Mexico's Environmental Improvement Division (EID) 223
G-51. Types of Discharges and Parameters Monitored at the Laboratory Under its NPDES Permit NM0028355 224
G-52. NPDES Permit Effluent Quality Monitoring of Sanitary Sewage Treatment Outfalls 225
G-53. Limits Established by NPDES Permit NM0028355 for Industrial Outfall Discharges 227
G-54. NPDES Permit Effluent Quality Monitoring of Industrial Outfalls 229
G-55. Schedule and Status of Upgrading the Laboratory's Waste Water Outfalls 231
G-56. Federal Facility Compliance Agreement Interim Compliance Limits and Compliance Schedule 233
G-57. Environmental Documentation Approved by the Laboratory Environmental Review Committee in 1987 235
G-58. Radiochemical Analyses of Water from Municipal Supply and Distribution System 237
G-59. Gross Radioactivity in Water from Municipal Supply and Distribution Systems 240
G-60. Primary Chemical Quality for Water Supply and Distribution System 243
G-61. Secondary Chemical Quality for Water Supply 247
G-62. Miscellaneous Chemical Analyses 249
G-63. Los Alamos Climatological Survey (1911-1987) Temperature and Precipitation Means and Extremes 251
G-64. Los Alamos Precipitation (inches) for 1987 253
G-65. Los Alamos Climatological Summary for 1987 254
G-66. Weather Highlights of 1987 256
G-67. Wet Deposition Measurements 259
G-68. Radiochemical Analyses of Sediments at TA-49 260
G-69. Chemical Concentrations in Solution Extracted from Sediments Downgradient form Experimental Areas at TA-49 262
G-70. Storm Run-off from TA-49 263
G-71. Chemical Quality of Storm Run-off from TA-49 264

ENVIRONMENTAL SURVEILLANCE AT

LOS ALAMOS DURING 1987

by

ENVIRONMENTAL SURVEILLANCE GROUP

ABSTRACT

This report describes the environmental surveillance program conducted by Los Alamos National Laboratory during 1987. Routine monitoring for radiation and radioactive or chemical materials is conducted on the Laboratory site as well as in the surrounding region. Monitoring results are used to determine compliance with appropriate standards and to permit early identification of potentially undesirable trends. Results and interpretation of data for 1987 cover: external penetrating radiation; quantities of airborne emissions and liquid effluents; concentrations of chemicals and radionuclides in ambient air, surface and ground waters, municipal water supply, soils and sediments, and foodstuffs; and environmental compliance. Comparisons with appropriate standards, regulations, and background levels provide the basis for concluding that environmental effects from Laboratory operations are insignificant and do not pose a threat to the public, Laboratory employees, or the environment.

I. EXECUTIVE SUMMARY

A. Monitoring Operations

The Laboratory maintains an ongoing environmental surveillance program as required by US Department of Energy (DOE) Orders 5480.1A ("Environmental Protection, Safety, and Health Protection Programs," August 1981) and 5484.1 ("Environmental Protection, Safety, and Health Protection Information Reporting Requirements," February 1981). The surveillance program maintains routine monitoring for radiation, radioactive materials, and chemical substances on the Laboratory site and in the surrounding region. These activities document compliance with appropriate standards, identify trends, provide information for the public, and contribute to general environmental knowledge. More detailed, supplemental environmental studies are carried out to determine the extent of the potential problems, to provide the basis for any remedial actions, and to provide further information on surrounding environments. The monitoring program also supports the Laboratory's policy to protect the public, employees, and environment from harm that could be caused by Laboratory activities and to reduce environmental impacts to the greatest degree practicable. Environmental monitoring information complements data on specific releases, such as those from radioactive liquid-waste treatment plants and stacks at nuclear research facilities.

Monitoring and sampling locations for various types of measurements are organized into three groups: (1) Regional stations are located within the five counties surrounding Los Alamos County (Fig. 1) at distances up to 80 km (50 mi) from the Laboratory. They provide a basis for determining conditions beyond the range of potential influence from normal Laboratory operations. (2) Perimeter stations are located within about 4 km (2.5 mi) of the Laboratory boundary, and many are in residential and community areas. They document conditions in areas regularly occupied by the public and potentially affected by Laboratory operations. (3) On-site stations are within the Laboratory boundary, and most are in areas accessible only to employees during normal working hours. They document environmental conditions at the Laboratory where the public has limited access.

Samples of air particulates and gases, waters, soils, sediments, and foodstuffs are routinely collected at these stations for subsequent analyses (Table 1). External penetrating radiation from cosmic, terrestrial, and Laboratory sources is also measured.

Additional samples are collected and analyzed to gain information about particular events, such as major surface run-off events, nonroutine releases, or special studies. More than 25 000 analyses for chemical and radiochemical constituents were carried out for environmental surveillance during 1987. Resulting data were used for dose calculations, for comparisons with standards and background levels, and for interpretation of the relative risks associated with Laboratory operations.

B. Estimated Doses and Risks from Radiation Exposure

1. Radiation Doses. Estimated individual radiation doses to the public attributable to Laboratory operations are compared with applicable standards in this report. Doses are expressed as a percentage of DOE's Radiation Protection Standard (RPS). The RPS is for doses from exposures excluding contributions from natural background, fallout, and radioactive consumer products. Estimated doses are those believed to be potential doses to individuals under realistic conditions of exposure.

Historically, estimated doses from Laboratory operations have been less than 7% of the 500 mrem/yr standard that was in effect prior to 1985 (Fig. 2). These doses have principally resulted from external radiation from the Laboratory's airborne releases. In 1985, DOE issued interim guidelines that lowered its RPS to 100 mrem/yr (effective dose equivalent) from all exposure pathways. In addition, exposure via the air pathway is further limited to 25 mrem/yr (whole body) in accordance with requirements of the US Environmental Protection Agency (EPA) (Appendix A). In 1987 the estimated maximum individual dose was 6.1 mrem, 24% of the EPA's 25-mrem standard. This dose resulted mostly from external radiation from short-lived airborne emissions from a linear particle accelerator, the Los Alamos Meson Physics Facility (LAMPF).

Another perspective is gained by comparing these estimated doses with the estimated whole-body dose attributable to background radiation. The highest estimated dose caused from Laboratory operations was about 2% of the 327 mrem received from background radioactivity in Los Alamos during 1987.

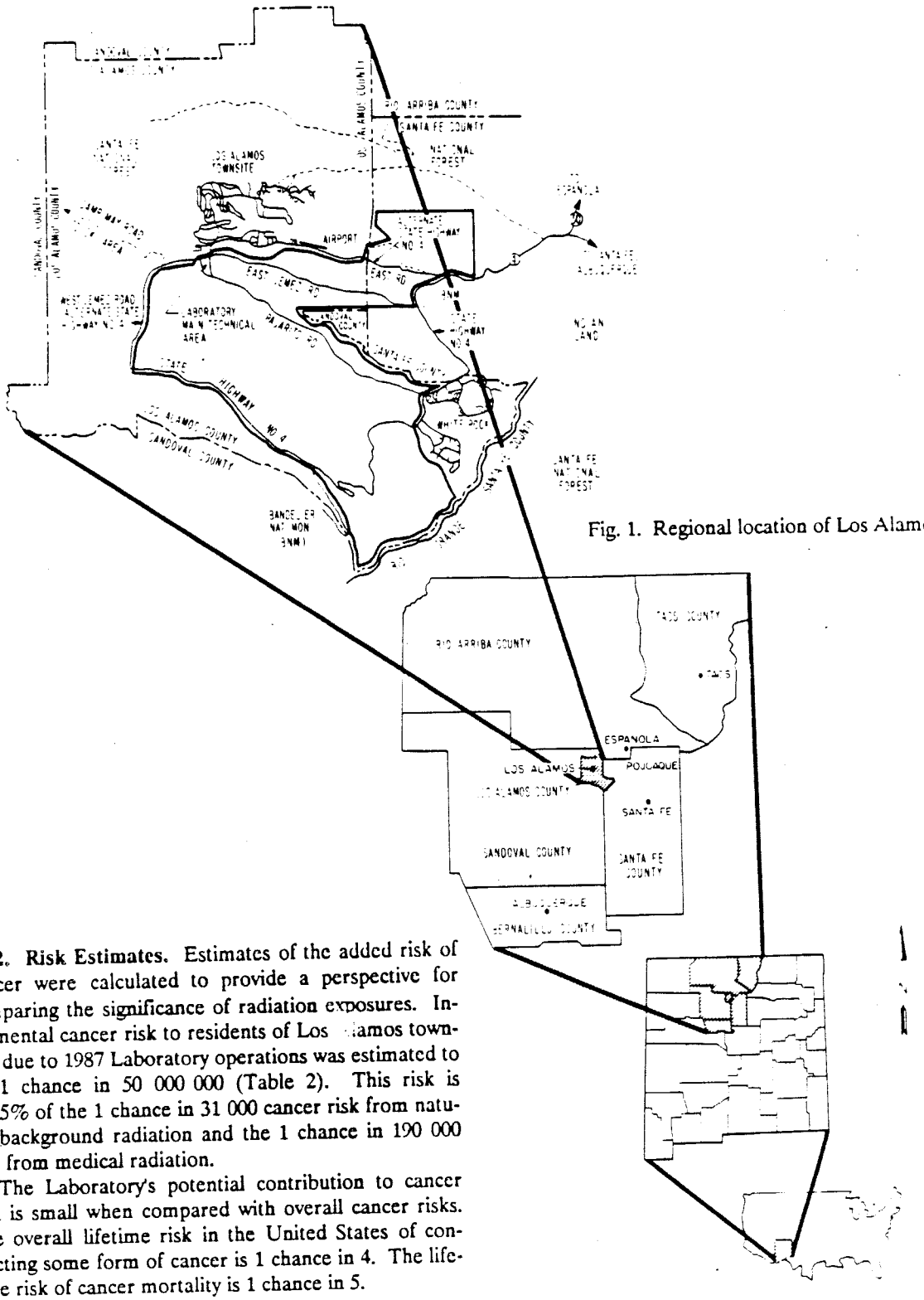

Fig. 1. Regional location of Los Alamos.

2. Risk Estimates. Estimates of the added risk of cancer were calculated to provide a perspective for comparing the significance of radiation exposures. Incremental cancer risk to residents of Los Alamos townsite due to 1987 Laboratory operations was estimated to be 1 chance in 50 000 000 (Table 2). This risk is <0.5% of the 1 chance in 31 000 cancer risk from natural background radiation and the 1 chance in 190 000 risk from medical radiation.

The Laboratory's potential contribution to cancer risk is small when compared with overall cancer risks. The overall lifetime risk in the United States of contracting some form of cancer is 1 chance in 4. The lifetime risk of cancer mortality is 1 chance in 5.

Table 1. Number of Sampling Locations

Typing of Monitoring	Regional	Perimeter	Onsite
External radiation	4	12	139
Air	3	11	12
Surface and ground waters[a]	6	32	37
Soils and sediments	16	16	34
Foodstuffs	10	8	11

[a]An additional 22 stations for the water supply and 33 special surface and ground water stations related to the Fenton Hill Geothermal Program were also sampled and analyzed as part of the monitoring program.

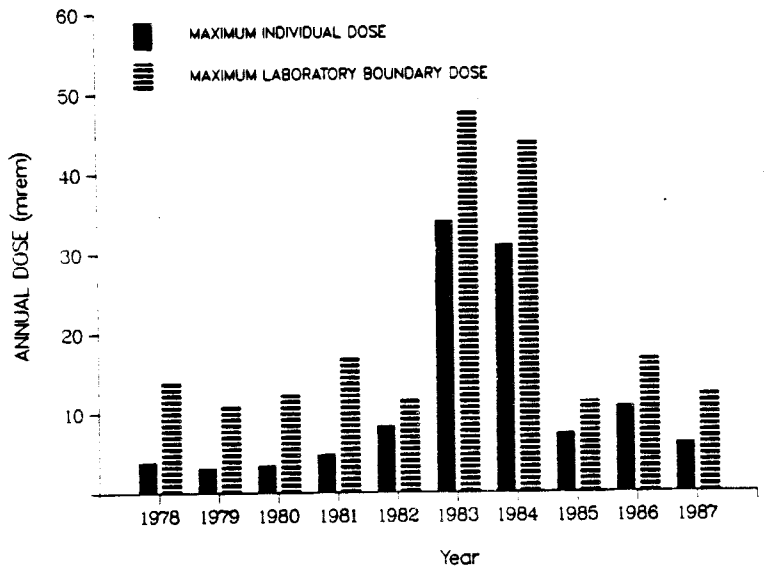

Fig. 2. Summary of estimated maximum individual and Laboratory boundary doses (excluding contributions from cosmic, terrestrial, and medical diagnostic sources) from Laboratory operations.

C. External Penetrating Radiation

Levels of external penetrating radiation (including X and gamma rays and charged particle contributions from cosmic, terrestrial, and manmade sources) in the Los Alamos area are monitored with thermoluminescent dosimeters (TLDs) at 147 locations.

The TLD network monitoring radiation from airborne activation products released by the LAMPF measured about 12 ± 5 mrem/yr (excludes background radiation from cosmic and terrestrial sources). This measured external radiation level was used to calculate radiation dose by taking into account shielding by buildings and self-shielding by the body. The value

Table 2. Added Individual Lifetime Cancer Mortality Risks Attributable to 1987 Radiation Exposure

Exposure Source	Incremental Effective Dose Equivalent (mrem) Used in Risk Estimate	Added Risk (Chance) to an Individual of Cancer Mortality
Average exposure from Laboratory Operations		
Los Alamos Townsite	0.21	1 in 50 000 000
White Rock Area	0.17	1 in 60 000 000
Natural Radiation		
Cosmic, Terrestrial, Self-Irradiation and Radon Exposure[a]		
Los Alamos and White Rock	327[a]	1 in 31 000[b]
Medical X-Rays (Diagnostic Procedures)		
Average Whole Body Exposure	53	1 in 190 000

[a]An effective dose equivalent of 200 mrem was used to estimate the risk from inhaling ^{222}Rn and its transformation products.
[b]The risks from natural radiation from non-radon sources were estimated to be 1 chance in 79,000 in Los Alamos and in White Rock. The risk of lung cancer from radon exposure was estimated to be 1 chance in 50,000 for both locations. Risk estimates are derived from ICRP Publication 26 and NCRP Report 93.

measured in 1987 is lower than the measured 18 ± 2 mrem/yr obtained in 1986 (Fig. 2). The difference is probably caused by variation in weather patterns between the two years rather than differences in LAMPF operations, because the estimate of airborne activity emitted from LAMPF increased in 1987 (Table 3).

Radiation levels (including natural background radiation from cosmic and terrestrial sources) are also measured at regional, perimeter, and on-site locations in the Environmental TLD Network. Some measurements at on-site stations were above background levels, as expected, reflecting ongoing research activities at or historical releases from Laboratory facilities.

D. Air Monitoring

Airborne radioactive emissions were monitored at 87 release points at the Laboratory. Total airborne 26 sampling stations. Measurements of radioactivity in the air are compared with concentration guides based upon DOE's RPS. These guides are concentrations of radioactivity in air breathed continuously throughout the year that result in effective doses equal to DOE's RPS of 100 mrem/yr for off-site areas (Derived Concentration Guides for Uncontrolled Areas) and to the occupational RPS (see Appendix A) for on-site areas (Concentration Guides for Controlled Areas). Hereafter they are called guides for on-site and off-site areas.

Only the on-site tritium air concentrations showed any measurable impact due to Laboratory operations. Annual average concentrations of tritium remained <0.1% of DOE's guides at all stations and posed no environmental or health problems in 1987. Annual average concentrations of longer-lived radionuclides in air were also <0.1% of the guides during 1987.

Table 3. Comparison of 1986 and 1987 Radioactive Releases from the Laboratory

Airborne Emissions

Radionuclide	Units	Activity Released 1986	Activity Released 1987	Ratio 1987:1986
^{3}H	Ci	10 700	3 180	0.3
^{32}P	µCi	70	48	0.7
^{41}Ar	Ci	276	232	0.8
^{131}I	µCi	38	0	0
Uranium	µCi	847	1 080	1.3
Plutonium	µCi	207	73	0.4
Gaseous Mixed Activation Products	Ci	112 000	150 000	1.3
Mixed Fission Products	µCi	2 570	1 290	0.5
Particulate/Vapor Activation Products	Ci	0.1	0.2	2.0
Total	Ci	122 976	153 412	1.2

Liquid Effluents

Radionuclide	Activity Released (mCi) 1986	Activity Released (mCi) 1987	Ratio 1987:1986
^{3}H	89 710	110 000	1.2
$^{89,90}Sr$	9.9	65	6.6
^{137}Cs	18	8.1	0.4
^{234}U	2.4	1.6	0.7
$^{238,239,240}Pu$	5.1	4.6	0.9
^{241}Am	3.2	3.6	1.1
Other	1 166.7	610.5	0.5
Total	90 915.3	110 693.4	1.2

E. Water, Soil, and Sediment Monitoring

Liquid effluents containing low levels of radioactivity were routinely released from one waste treatment plant and one sanitary sewage lagoon system. Concentrations at all discharge points were well below the DOE's concentration guides for on-site areas. The dominant change was an increase in tritium discharge from TA-50's radioactive liquid-waste treatment facility due to increased concentrations in the released waters (Table 3).

Surface and ground waters are monitored to detect potential dispersion of radionuclides from Laboratory operations. Only the surface and shallow ground waters in on-site liquid effluent release areas contained radioactivity in concentrations that are above natural terrestrial and worldwide fallout levels. These concentrations are minute fractions (<0.1%) of DOE's guides for on-site areas. These on-site waters are not a source of industrial, agricultural, or municipal water supplies. The radiochemical quality of water from regional, perimeter, and on-site areas that have received no direct discharge showed no significant effects from Laboratory releases.

The potable water supply met all applicable EPA radiochemical and chemical standards. Lack of a hydrologic connection to the deep aquifer was confirmed by lack of radioactive or chemical contamination in municipal water supply sources.

Measurements of radioactivity in samples of soils and sediments provide data on less direct pathways of exposure. These measurements are useful for understanding hydrological transport of radioactivity in intermittent stream channels near low-level radioactive waste management areas. On-site areas within Pueblo, Los Alamos, and Mortandad canyons all had concentrations of radioactivity on sediments at levels slightly higher than attributable to natural terrestrial sources or worldwide fallout. The low levels of cesium, plutonium, and strontium in Mortandad Canyon are due to liquid effluents from a waste treatment plant. No above-background radioactivity on sediments or in water has been measured in locations beyond the Laboratory boundary in Mortandad Canyon. However, small amounts of radioactivity on sediments in Pueblo Canyon (from pre-1964 effluents) and Los Alamos Canyon (from 1952 to current treated effluents) have been transported to the Rio Grande. Theoretical estimates, confirmed by measurements, show the incremental effect on Rio Grande sediments is insignificant when compared with background concentrations in soils and sediments.

Environmental monitoring is done at 1 active and 11 inactive waste management areas at the Laboratory. The general public is excluded from these controlled-access sites. Surface run-off has transported some low-level contamination from the active disposal area and several of the inactive areas into controlled-access canyons. Leachate extracts (following EPA guidelines) from the surface contamination indicate the presence of no constituents in excess of EPA criteria for hazardous waste determination.

F. Foodstuffs Monitoring

Most fruit, vegetable, fish, bee, and honey samples from regional and perimeter locations showed no radioactivity distinguishable from that attributable to natural sources or worldwide fallout. Some produce samples from on-site locations had slightly elevated tritium concentrations at levels $\leq$2% of DOE's guides for tritium in water (there are no concentration guides for produce).

G. Unplanned Releases

During 1987, there were two unplanned releases of radioactive or hazardous materials. Both involved release of tritium. The quantities of tritium released were small and resulted in radiation doses that were fractions of the Radiation Protection Standard.

1. March 18 Tritium Release at the Van de Graaff Facility at TA-3. On March 18, 1987, 375 Ci of tritium (as elemental tritium gas) were released from the Van de Graaff facility at TA-3. Air samples collected from four downwind air samplers were within normal ranges for tritium at these locations. All measured concentrations were <0.1% of the DOE's Derived Concentration Guide for tritium in off-site areas. Calculations from meteorological modeling estimated a dose to the maximum exposed individual of 0.003 mrem to the lung, <0.1% of the EPA's air emission standard of 75 mrem/yr (any organ) to a member of the public.

2. December 11-12 Tritium Release at TA-33. Approximately 165 Ci of elemental tritium gas were inadvertently released from TA-33 on December 11-12, 1987. Air samples were collected at five downwind locations. All measured air concentrations were found to

be within their normal range and <0.1% of the DOE's Derived Concentration Guide for tritium. The highest estimated dose to a member of the public was 0.001 mrem to the lung, <0.1% of the 75 mrem/yr EPA air emission standard.

H. Environmental Compliance Activities

1. Resource Conservation and Recovery Act. The Resource Conservation and Recovery Act (RCRA) regulates hazardous wastes from generation to ultimate disposal. The EPA has transferred full authority (with the exception of the Hazardous and Solid Waste Amendment of 1984) for administering RCRA to New Mexico's Environmental Improvement Division (EID). In 1987, the Laboratory had numerous interactions with EID and prepared documentation to comply with RCRA requirements. The Laboratory has revised RCRA Parts A and B permit applications, originally submitted in 1985. The latest revisions were submitted November 1987.

2. Clean Water Act. Regulations under the Clean Water Act set water quality standards and effluent limitations. The two primary programs at the Laboratory to comply with the Clean Water Act are the National Pollutant Discharge Elimination System (NPDES) and the Spill Prevention Control and Countermeasure (SPCC) programs.

The NPDES requires permits for nonradioactive constituents at all point source discharges. A single NPDES permit for the Laboratory authorizes liquid effluent discharges from 98 industrial outfalls and 10 sanitary sewage treatment outfalls; the permit expires in March 1991. The Laboratory was in compliance with the NPDES permit in about 96% and 99% of the analyses done on samples collected for compliance monitoring at sanitary and industrial waste discharges, respectively. Chronically noncompliant discharges are being upgraded under an EPA/DOE Federal Facility Compliance Agreement.

Another NPDES permit authorizes liquid effluent discharge from the Fenton Hill Geothermal Project. The permit for a single outfall was issued to regulate the discharge of mineral-laden water from the recycle loop of the geothermal wells.

The SPCC program provides for cleanup of spills and requires preparation of a SPCC Plan. The Laboratory has many elements that are required in a SPCC plan and has assembled a Laboratory-wide formal SPCC Plan that was adopted and implemented in 1987.

3. National Environmental Policy Act. The Laboratory Environmental Review Committee reviews environmental documentation required by National Environmental Policy Act legislation as well as identifies other environmental items of concern to the Laboratory. An Environmental Evaluations Coordinator helps prepare required DOE documentation and identify other items requiring committee attention. Documentation usually consists of Action Description Memorandums (brief environmental evaluations) or Environmental Assessments (more detailed evaluations). During 1987, the committee approved 20 Action Description Memorandums and 1 Environmental Assessment and forwarded this documentation to DOE.

4. Clean Air Act. During 1987, the Laboratory's operations remained in compliance with all federal and state air quality regulations. State regulations are required to be as stringent as federal regulations, and many state standards are more stringent. Over 180 asbestos removal jobs involved the disposal of 270 m^3 (9500 ft^3) of asbestos. All beryllium shops met emissions performance requirements. The Laboratory applied to EPA for approval to construct the Independent Management Activity facility. This program will emit depleted uranium similar to other dynamic testing projects at the Laboratory. Approval was obtained from EPA in January, 1988.

5. Safe Drinking Water Act. Municipal and industrial water supply for the Laboratory and community is from 16 deep wells and 1 gallery (collection system fed by springs). The wells range in depth from 265 to 942 m (869 to 3090 ft). The chemical quality of the water easily met EPA's National Interim Primary Drinking Water Standards (40 CFR 141) in 1987.

6. Federal Insecticide, Fungicide, and Rodenticide Act. The Federal Insecticide, Fungicide, and Rodenticide Act (FIFRA) requires registration of all pesticides, restricts use of certain pesticides, recommends standards for pesticide applicators, and regulates disposal and transportation of pesticides. The Laboratory stores, uses, and discards pesticides in compliance with this act.

7. Archaeological and Historical Protection. The Laboratory's Environmental Evaluation Coordination and Quality Assurance programs provide protection as mandated by law for the hundreds of archaeological

and historical resources located on Laboratory land. Pursuant to federal regulations implementing Section 106 of the National Historic Preservation Act of 1966, as amended, clearance for construction where no resource will be affected and mitigation of unavoidable adverse effects from Laboratory activity is determined in consultation with New Mexico's State Historical Preservation Office. During 1987, archaeologists performed 28 cultural resource surveys, monitored 7 projects, fenced 1 site, and undertook adverse impact mitigation at 2 sites.

8. Threatened/Endangered Species and Floodplains/Wetlands Protection. The DOE and Laboratory must comply with the Endangered Species Act of 1973, as amended, and with Executive orders 11988, Floodplain Management, and 11990, Protection of Wetlands Environmental Review Requirements. Three Floodplains/Wetlands notifications were prepared for publication in the Federal Register. Laboratory biologists surveyed 17 proposed construction sites for potential impact. They identified no endangered or rare species at these sites.

9. Comprehensive Environmental Response, Compensation, and Liability Act. The Comprehensive Environmental Response, Compensation, and Liability Act (CERCLA) of 1980 mandated cleanup of toxic and hazardous contaminants at closed and abandoned hazardous waste sites. The Superfund Amendments and Reauthorization Act (SARA) of 1986 extensively amended CERCLA. Laboratory compliance activities at hazardous waste sites are part of DOE's Albuquerque Operations Office's Comprehensive Environmental Restoration Program (CERP). The program is evaluating all areas at the Laboratory for possible contamination.

10. Toxic Substances Control Act. The Toxic Substances Control Act (TSCA) regulates the manufacture, processing, distribution, use, storage, and labeling of chemical substances, including polychlorinated biphenyls (PCBs). The Laboratory has EPA authorization to dispose of PCB wastes at its chemical waste landfill (Area L) and burn PCB contaminated wastes at its Controlled Air Incinerator (99.9999% combustion efficiency). The Laboratory is in compliance with EPA's permit conditions for authorizing on-site disposal of PCB contaminated wastes.

11. Emergency Planning and Community Right-to-Know Act. Title III of SARA, also known as the Emergency Planning and Community Right-to-Know Act (EPCRA), is the centerpiece of federal policy on chemical disaster prevention and response. In response to this legislation, the state of New Mexico has established an Emergency Response Commission (ERC) within the State Police Department's Hazardous Materials Emergency Response Division; the commission has designated Los Alamos County as the local Emergency Planning District, and the Laboratory's Emergency Management Office will continue to develop and coordinate a comprehensive laboratory-wide, all-hazards emergency response plan that is compatible with the county's overall plan.

The Industrial Hygiene (HSE-5) and Environmental Surveillance (HSE-8) groups provided a preliminary list of 137 chemical substances used on-site to the Emergency Management Office. In addition, individual Materials Safety Data Sheets for each of these 137 chemicals have also been provided to the Emergency Management Office to facilitate county planning.

II. INTRODUCTION TO THE LOS ALAMOS AREA

A. Geographic Setting

Los Alamos National Laboratory and the associated residential areas of Los Alamos and White Rock are located in Los Alamos County, northcentral New Mexico, approximately 100 km (60 mi) NNE of Albuquerque and 40 km (25 mi) NW of Santa Fe (Fig. 1). The 111 km^2 (43 mi^2) Laboratory site and adjacent communities are situated on Pajarito Plateau. The plateau consists of a series of finger-like mesas separated by deep eastwest oriented canyons cut by intermittent streams (Fig. 3). Mesa tops range in elevation from approximately 2400 m (7800 ft) on the flank of the Jemez Mountains to about 1800 m (6200 ft) at their eastern termination above the Rio Grande valley.

All Los Alamos County and vicinity locations referenced in this report are identified by the Laboratory Cartesian coordinate system, which is based upon US Customary units of measurement. This system is standard throughout the Laboratory, but is independent of the US Geological Survey and New Mexico State Survey coordinate systems. The major coordinate markers shown on the maps are at 3 km (10 000 ft) intervals, and for the purpose of this report, locations are reported to the nearest 0.03 km (100 ft).

The DOE controls the area within the Laboratory boundary and has the option to completely restrict access. This control can be instituted if necessary.

B. Land Use

Most Laboratory and community developments are confined to mesa tops (see the inside front cover). The surrounding land is largely undeveloped with large tracts of land north, west, and south of the Laboratory site held by the Santa Fe National Forest, Bureau of Land Management, Bandelier National Monument, General Services Administration, and Los Alamos County (see the inside back cover). The San Ildefonso Pueblo borders the Laboratory to the east.

Laboratory land is used for building sites, test areas, waste disposal locations, roads, and utility rights-of-way (Fig. 4 and Appendix F). However, these account for only a small fraction of the total land area. Most land provides isolation for security and safety and is a reserve for future structure locations. The Long Range Site Development Plan (Engineering 1982) assures adequate planning for the best possible future uses of available Laboratory lands.

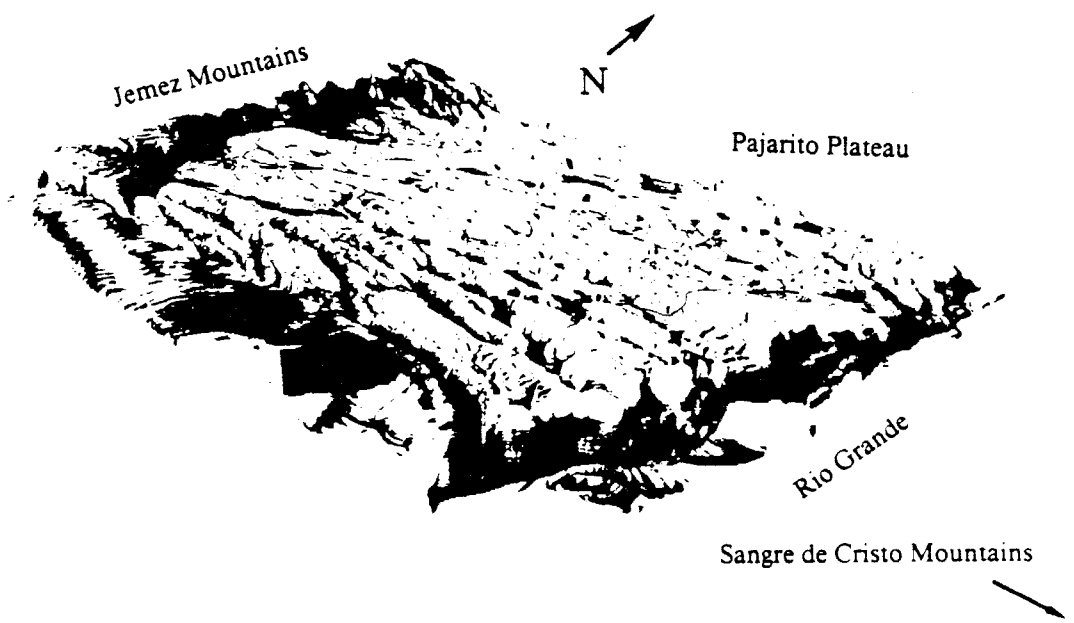

Fig. 3. Topography of the Los Alamos area.

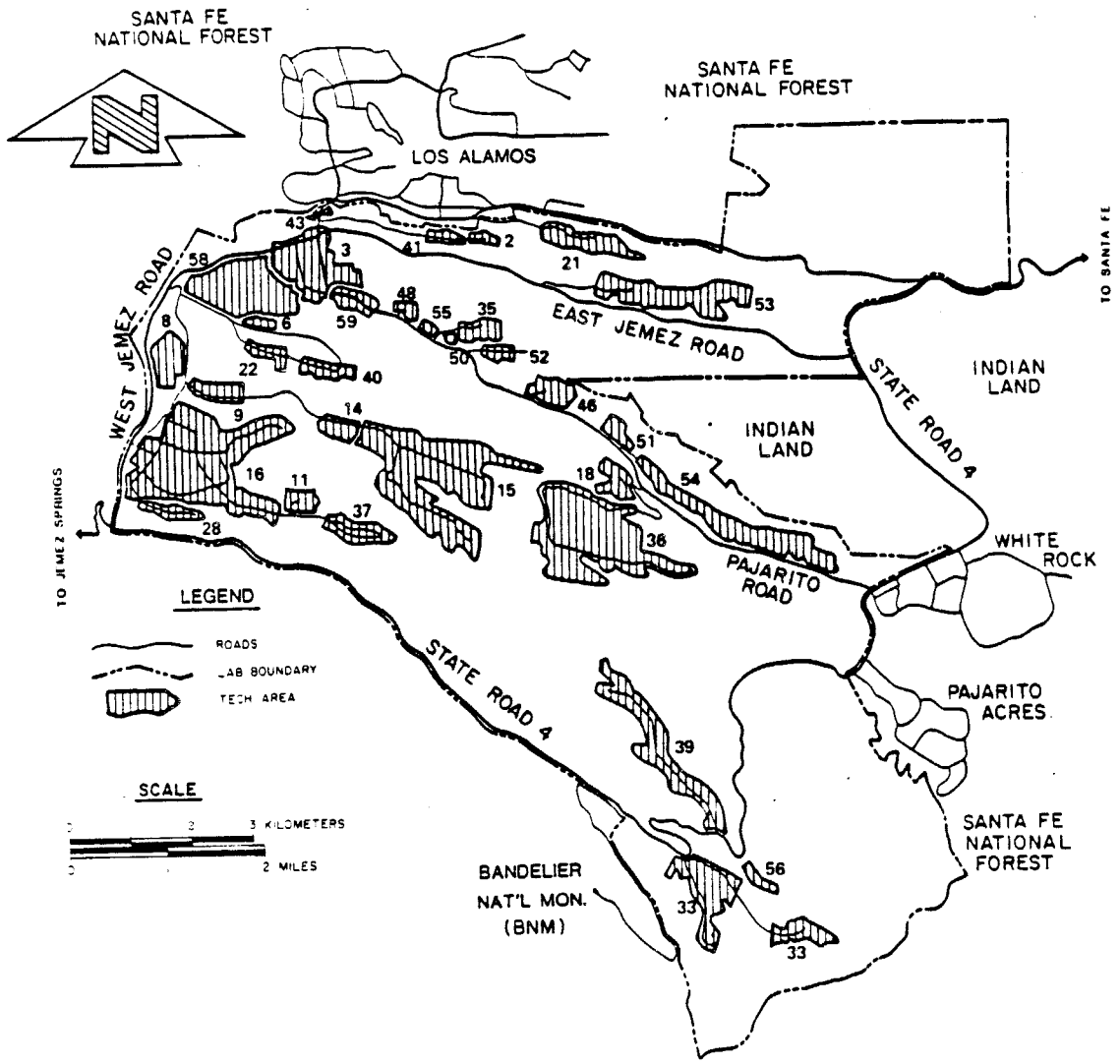

Fig. 4. Technical areas (TAs) of Los Alamos National Laboratory in relation to surrounding landholdings.

Limited access by the public is allowed in certain areas of the Laboratory reservation. An area north of Ancho Canyon between the Rio Grande and State Road 4 is open to hikers, rafters, and hunters, but woodcutting and vehicles are prohibited. Portions of Mortandad and Pueblo canyons are also open to the public. An archaeological site (Otowi Tract) northwest of State Road 4, near the White Rock Y, is open to the public subject to restrictions of cultural resource protection regulations.

C. Geology-Hydrology

Most of the finger-like mesas in the Laboratory area are found in Bandelier Tuff (Fig. 5). Ashfall, ashfall pumice, and rhyolite tuff form the surface of

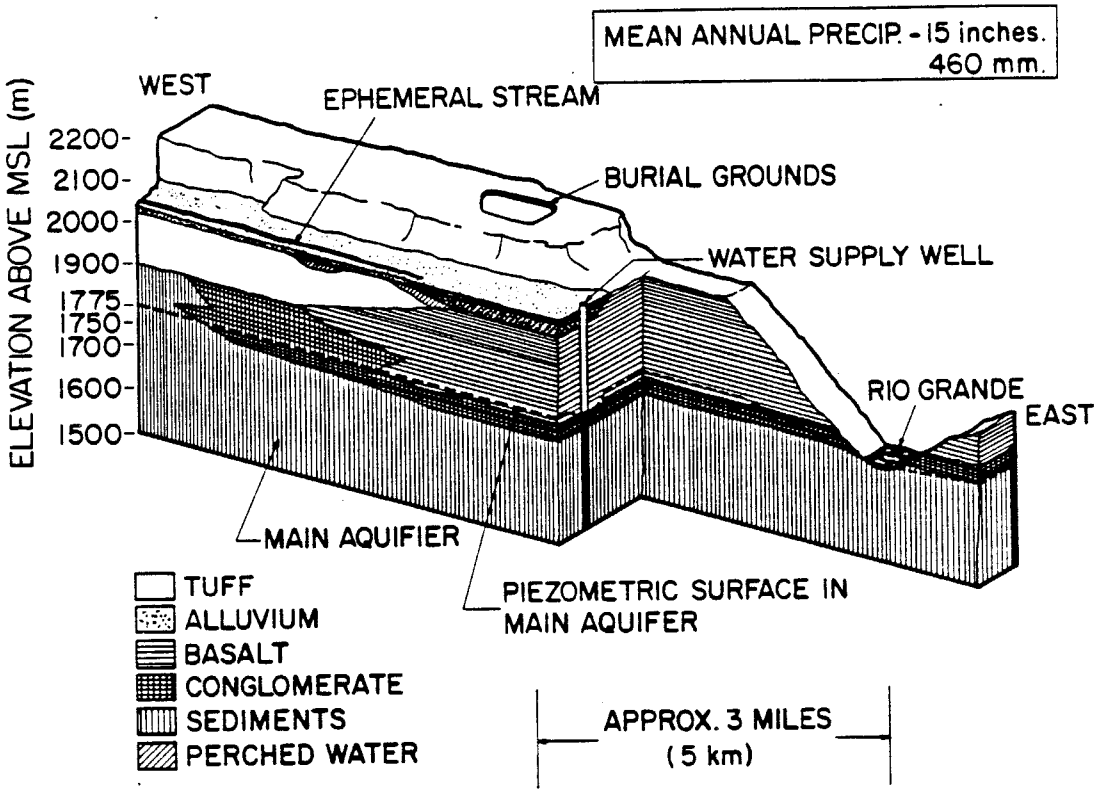

Fig. 5. Conceptual illustration of geologic-hydrologic relationships in Los Alamos area.

Pajarito Plateau. The tuff ranges from nonwelded to welded and is in excess of 300 m (1000 ft) thick in the western part of the plateau and thins to about 80 m (260 ft) eastward above the Rio Grande. It is deposited as the result of a major eruption of a volcano in the Jemez Mountains about 1.1 to 1.4 million years ago.

The tuffs overlap onto older volcanics of the Tschicoma Formation, which form the Jemez Mountains. They are underlain by the conglomerate of the Puye Formation (Fig. 5) in the central and eastern edge along the Rio Grande. Chino Mesa basalts (Fig. 5) interfinger with the conglomerate along the river. These formations overlay the sediments of the Tesuque Formation (Fig. 5), which extends across the Rio Grande valley and is in excess of 1000 m (3300 ft) thick.

Los Alamos area surface water is primarily in intermittent streams. Springs on flanks of the Jemez Mountains supply base flow into upper reaches of some canyons, but the amount is insufficient to maintain surface flows across the Laboratory site before it is depleted by evaporation, transpiration, and infiltration. Run-off from heavy thunderstorms or heavy snowmelt reaches the Rio Grande several times a year in some drainages. Effluents from sanitary sewage, industrial waste treatment plants, and cooling tower blowdown are released to some canyons at rates sufficient to maintain surface flows for about 1.5 km (1 mi).

Ground water occurs in three modes in the Los Alamos area: (1) water in shallow alluvium in canyons, (2) perched water (a ground water body above an impermeable layer that is separated from the underlying main body of ground water by an unsaturated zone), and (3) the main aquifer of the Los Alamos area (Fig. 5).

Intermittent stream flows in canyons of the plateau have deposited alluvium that ranges from less than 1 m (3 ft) to as much as 30 m (100 ft) in thickness.

The alluvium is quite permeable, in contrast to the underlying volcanic tuff and sediments. Intermittent run-off in canyons infiltrates the alluvium until its downward movement is impeded by the less permeable tuff and volcanic sediment. This results in a shallow alluvial ground water body that moves downgradient in the alluvium. As water in the alluvium moves downgradient, it is depleted by evapotranspiration and movement into underlying volcanics (Purtymun 1977).

Perched water occurs in comglomerate and basalts beneath the alluvium in a limited area about 40 m (120 ft) in the mid-reach of Pueblo Canyon and in a second area about 50 to 70 m (150 to 200 ft) beneath the surface in lower Pueblo and Los Alamos canyons near their confluence. The second area is mainly in basalts (Fig. 5) and has one discharge point at Basalt Springs in Los Alamos Canyon.

The main aquifer of the Los Alamos area is the only aquifer in the area capable of serving as a municipal water supply. The surface of the aquifer rises westward from the Rio Grande within the Tesuque Formation into the lower part of the Puye Formation beneath the central and western part of the plateau. Depth of the aquifer decreases from 360 m (1200 ft) along the western margin of the plateau to about 180 m (600 ft) at the eastern margin. The main aquifer is isolated from alluvial and perched waters by about 110 to 190 m (350 to 620 ft) of dry tuff and volcanic sediments. Thus, there is little hydrologic connection or potential for recharge to the main aquifer from alluvial or perched water.

Water in the main aquifer is under water table conditions in the western and central part of the plateau and under artesian conditions in the eastern part and along the Rio Grande (Purtymun 1974B). The major recharge to the main aquifer is from the intermountain basin of the Valles Caldera in the Jemez Mountains west of Los Alamos. The water table in the caldera is near land surface. The underlying lake sediment and volcanics are highly permeable and recharge the aquifer through Tschicoma Formation interflow breccias (rock consisting of sharp fragments embedded in a fine-grained matrix) and the Tesuque Formation. The Rio Grande receives ground water discharge from springs fed by the main aquifer. The 18.4 km (11.5 mi) reach of the river in White Rock Canyon between Otowi Bridge and the mouth of Rito de Frijoles receives an estimated 5.3 to 6.8 x 10^3 m^3 (4300 to 5500 acre-feet) annually from the aquifer.

D. Climatology

Los Alamos has a semiarid, temperate mountain climate. Average, annual precipitation is nearly 45 cm (18 in). Precipitation was heavy during 1987, totalling 60 cm (23.6 in.). It was the third consecutive year with precipitation at least 130% of normal. Forty per cent of the annual precipitation normally occurs during July and August due to thundershowers. Officially, at TA-59, rainfall was normal during the summer of 1987. However, other areas in Los Alamos were below normal for the summer. Winter precipitation falls primarily as snow, with accumulations of about 130 cm (51 in.) annually. Record snowfalls in January and February and heavy snow in December of 1987 helped produce a record annual snowfall of 453 cm (178 in.).

Summers are generally sunny with moderate warm days and cool nights. Maximum temperatures are usually below 32°C (90°F). Brief afternoon and evening thundershowers are common, especially in July and August. High altitude, light winds, clear skies, and dry atmosphere allow night temperatures to drop below 15°C (59°F) after even the warmest day. Winter temperatures typically range from about -9 to -4°C (15 to 25°F) during the night and from -11 to 10°C (30 to 50°F) during the day. Occasionally, temperatures drop to near -18°C (0°F) or below. Many winter days are clear with light winds, so strong sunshine can make conditions quite comfortable even when air temperatures are cold.

Snowstorms with accumulations exceeding 10 cm (4 in.) are common in Los Alamos. Some storms can be associated with strong winds, frigid air, and dangerous wind chills. Several severe storms occurred during the year. One storm dumped 122 cm (48 in.) officially with up to 152 cm (60 in.) along the mountains during January 15-17, 1987. It was the heaviest snowfall on record in Los Alamos for one storm. Another severe storm dropped nearly 66 cm (26 in.) of snow during February 18-19.

Surface winds in Los Alamos often vary dramatically with time-of-day and with location because of complex terrain. With light, large-scale winds and clear skies, a distinct daily wind cycle often exists: a light southeasterly to southerly upslope wind during the day and a light westerly to northwesterly drainage wind during the night. However, several miles to the east toward the edge of Pajarito Plateau, near the Rio Grande Valley, a different daily wind cycle is common: a moderate southwesterly up-valley wind during the

day and either a light northwesterly to northerly drainage wind or moderate southwesterly wind at night. On the whole, the predominant winds are southerly to northwesterly over western Los Alamos County and southwesterly and northeasterly toward the Rio Grande Valley. The year 1987 followed normal patterns in wind.

Historically, no tornadoes have been reported to have touched down in Los Alamos County. Numerous funnel clouds were reported near Santa Fe on August 24-25, 1987. Strong dust devils can produce winds up to 35 m/sec (75 mph) at isolated spots in the county, especially at lower elevations. Strong winds with gusts exceeding 27 m/sec (60 mph) are common and widespread during the spring. Lightning is very common over Pajarito Plateau. There are 58 thunderstorm days during an average year, with most occurring during the summer. Lightning protection is an important design factor for most facilities at the Laboratory. Hail damage can also occur. Hailstones with diameters up to 0.64 cm (0.25 in.) are common, whereas 1.3-cm (0.5-in.) diameter hailstones are rare.

Atmospheric mixing or dispersion characteristics affect the transport of contaminants released into the air. Good mixing conditions result in greater dilution of released contaminants. Under poorer mixing conditions, the potential increases for exposure to higher concentrations of released contaminants.

Frequent clear skies and light winds promote good daytime atmospheric dispersion at Los Alamos. Complex terrain and forested vegetation also enhance vertical and horizontal mixing of the atmosphere and contaminants released into the air. During the night, light winds and clear skies favor the formation of temperature inversions, restricting vertical atmospheric dispersion. Air flow channeling by terrain features also reduces nighttime dispersion. Poor atmospheric dispersion conditions frequently exist in canyon bottoms. The frequency of atmospheric stability, an estimate of the dispersion capability of the atmosphere, is approximately 40% unstable (good mixing), 35% neutral (fair mixing), and 25% stable (poor mixing) on the mesa tops of the Los Alamos area.

E. Population Distribution

Los Alamos County has an estimated 1987 population of approximately 18 370 (based on the 1980 census adjusted for 1987). Two residential and related commercial areas exist in the county (Fig. 4). The Los Alamos townsite, the original area of development (and now including residential areas known as the Eastern Area, the Western Area, North Community, Barranca Mesa, and North Mesa), has an estimated population of 11 480. The White Rock area (including the residential areas of White Rock, La Senda, and Pajarito Acres) has about 6820 residents. About one-third of those employed in Los Alamos commute from other counties. Population estimates for 1987 place about 193 000 people within an 80 km (50 mi) radius of Los Alamos (Table 4).

F. Programs at Los Alamos National Laboratory

The Laboratory is administered by the University of California for the Department of Energy. The Laboratory's environmental program, conducted by the Environmental Surveillance Group, is part of a continuing investigation and documentation program.

Since its inception in 1943, the Laboratory's primary mission has been nuclear weapons research and development. Programs include weapons development, magnetic and inertial fusion, nuclear fission, nuclear safeguards and security, and laser isotope separation. There is also basic research in the areas of physics, chemistry, and engineering that supports such programs. Research on peaceful uses of nuclear energy has included space applications, power reactor programs, radiobiology, and medicine. Major research programs in elementary particle physics are carried out at the Laboratory's linear proton accelerator. Other programs include applied photochemistry, astrophysics, earth sciences, energy resources, nuclear fuel safeguards, lasers, computer sciences, solar energy, geothermal energy, biomedical and environmental research, and nuclear waste management research. Appendix F summarizes activities at the Laboratory's 32 active Technical Areas (TAs).

In August 1977, the Laboratory site, encompassing 111 km^2 (43 mi^2), was dedicated as a National Environmental Research Park. The ultimate goal of programs associated with this regional facility is to encourage environmental research that will contribute understanding of how people can best live in balance with nature while enjoying the benefits of technology. Park resources are available to individuals and organizations outside of the Laboratory to facilitate self-supported research on these subjects deemed compatible with the Laboratory programmatic mission (DOE 1979).

Table 4. 1987 Population Within 80 km of Los Alamos[a,b]

Direction	1-2	2-4	4-8	8-15	15-20	20-30	30-40	40-60	60-80
N	1	---	---	---	---	---	1 114	---	360
NNE	---	---	---	554	---	531	1 697	1 761	216
NE	1	---	---	---	311	14 798	990	1 104	3 730
ENE	---	---	---	1 745	1 533	2 443	2 592	1 164	2 216
E	---	---	75	23	500	1 030	626	---	1 455
ESE	---	---	---	---	---	263	20 829	1 062	1 470
SE	---	---	6 820	---	---	---	48 152	2 198	7
SSE	---	---	---	---	---	---	383	3 911	85
S	---	---	---	50	---	267	516	5 720	---
SSW	---	---	---	20	---	686	169	6 917	28 115
SW	---	---	---	---	---	---	264	3 490	---
WSW	---	---	---	---	---	264	263	2 137	174
W	---	---	---	---	---	---	---	138	111
WNW	---	1 448	6 595	---	---	---	---	---	2 587
NW	---	528	1 737	---	---	---	---	1 410	---
NNW	---	583	584	---	---	---	---	62	61

[a]This distribution represents the resident, nonworkforce population with respect to the Los Alamos Meson Physics Facility's stack at TA-53. A slightly different distribution for Los Alamos County townsites was used to model releases from the TA-2 stack, which is located closer to Los Alamos.
[b]Total population within 80 km of Los Alamos is 192 649.

A Final Environmental Impact Statement (DOE 1979) that assesses potential cumulative environmental impacts associated with current, known future, and continuing activities at the Laboratory was completed in 1979. The report provides environmental input for decisions regarding continuing activities at the Laboratory. It also provides more detailed information on the environment of the Los Alamos area.

III. RADIATION DOSES

Some incremental radiation doses--above those received from natural background, resuspended fallout, and medical and dental diagnostic procedures--are received by Los Alamos County residents as a result of Laboratory operations. The largest estimated dose at an occupied location was about 6 mrem to the whole body or 24% of EPA's air emission standard of 25 mrem/yr. This dose estimate is principally due to airborne radiation from the linear particle accelerator at the Los Alamos Meson Physics Facility. The effective dose equivalent to the maximum exposed individual from all pathways was also approximately 6 mrem. This is 6% of the DOE Radiation Protection Standard of 100 mrem/yr.

No significant exposure pathways are believed to exist for radioactivity released in treated liquid waste discharges. Most released radionuclides are retained in alluvial sediments within Laboratory boundaries. A small fraction is transported off-site in stream channel sediments during heavy run-off. Radionuclide concentrations in these sediments, however, are only slightly above background levels. Other minor pathways include direct radiation and foodstuffs.

The cumulative effective dose equivalent attributable to Laboratory operations received by the population living within 80 km (50 mi) of the Laboratory was conservatively estimated to be 3.5 person-rem during 1987. This is <0.01% of the 61 000 person-rem cumulative effective dose equivalent received by the same population from natural radiation sources and 0.03% of the 10 000 person-rem cumulative effective dose equivalent received from diagnostic medical procedures. About 90% of this dose, 3.0 person-rem, was received by persons living in Los Alamos County. This dose is 0.05% of the 6000 person-rem received by the population of Los Alamos County from background radiation and 0.3% of the 970 person-rem from diagnostic medical and dental procedures.

In 1987, the average, added risk of cancer mortality to Los Alamos townsite residents was 1 chance in 50 000 000 due to radiation from this year's Laboratory operations; this is much less than 1 chance in 31 000 from background radiation. The EPA has estimated average lifetime risk for overall cancer incidence as 1 chance in 4 and for cancer mortality as 1 chance in 5.

A. Background

The impact of environmental releases of radioactivity is evaluated by estimating doses received by the public from exposure to these releases. These doses are then compared with applicable standards and with doses from background radiation and medical and dental radiation.

The DOE's Radiation Protection Standard (RPS) limits the effective dose equivalent to 100 mrem/yr for all pathways of exposure (DOE 1985). The effective dose equivalent is the hypothetical whole-body dose that carries the same risk of cancer or genetic disorders as a given dose to a particular organ (see Glossary). Using this dose, which was introduced by the International Commission on Radiological Protection (ICRP 1977), allows direct comparison of exposures to different organs.

In accordance with federal EPA regulations (40 CFR 61), whole-body doses received via the air pathway only are limited to 25 mrem/yr and individual organ doses are limited to 75 mrem/yr via this pathway. The principal pathway of exposure at Los Alamos has been via release of radionuclides into the air resulting in external radiation doses to the whole body. Other pathways contribute finite but negligible doses. Detailed discussion of standards is presented in Appendix A.

The exposure pathways considered for the Los Alamos area are atmospheric transport of airborne radioactive emissions, hydrologic transport of treated liquid effluents, food chains, and direct exposure to external penetrating radiation. Exposure to radioactive materials or radiation in the environment was determined by direct measurements of airborne and

waterborne contaminants, of contaminants in foodstuffs, and of external penetrating radiation. Theoretical dose calculations based on atmospheric dispersion modeling were made for other airborne emissions present at levels too low for measurement.

Doses were calculated from measured or derived exposures using models based on the recommendations of the International Commission of Radiological Protection (Appendix D). These doses are summarized in Table 5 for the most important exposure categories, as defined in DOE Order 5484.1 (DOE 1981) as:

1. *Maximum Boundary Dose, or "Fence-Post" Dose Rate:* Maximum dose at the Laboratory boundary where the highest dose rate occurs. This dose does not take into account shielding or occupancy and does not require that an individual actually receive this dose.
2. *Maximum Individual Dose:* Maximum dose to an individual in the off-site location where the highest dose rate occurs and where there is a person present. It includes corrections for shielding (for example, for being inside a building) and occupancy (what fraction of the year the person is in the area).
3. *Average Dose:* Average doses to residents of Los Alamos and White Rock.
4. *Whole-Body Cumulative Dose:* The whole-body cumulative dose for the population within an 80-km (50-mi) radius of the Laboratory. The cumulative effective dose equivalent for the 80 km area is also given in accordance with the DOE Radiation Protection Standard (DOE 1985).

The maximum boundary and the individual doses over the past 9 years are summarized in Fig. 2. Over 95% of each of these doses resulted from airborne emissions of activation products from the Los Alamos Meson Physics Facility (LAMPF).

The effective dose equivalent is taken to be the same as the whole-body dose equivalent for whole-body external radiation. The effective dose equivalent for internal radiation is the weighed sum of the doses to individual organs (see Glossary).

All internal radiation doses (via inhalation or ingestion) are 50-year dose commitments (Appendix D). This is the total dose received from intake of a radionuclide for 50 years following intake.

In addition to compliance with dose standards, which define an upper limit for doses to the public, there is a concurrent commitment to maintain radiation exposure to individuals and population groups to levels as low as reasonably achievable (ALARA). This policy is followed at the Laboratory by applying strict controls on airborne emissions, liquid effluents, and operations to minimize doses to the public and to limit releases of radioactive materials to the environment. Ambient monitoring described in this report documents the effectiveness of these controls.

B. Estimate of Radiation Doses

1. Doses from Natural Background Radiation and Medical and Dental Radiation. Effective dose equivalents from natural background and from medical and dental uses of radiation are estimated to provide a comparison with doses resulting from Laboratory operations. Doses from global fallout are only a small fraction of these doses (<1%) and are not considered further here. Exposure to natural background radiation results principally in whole-body doses and in localized doses to the lung and other organs. For convenience, these doses are divided into those resulting from exposure to radon and its decay products that mainly affect the lung, and those from nonradon sources that mainly affect the whole body.

Estimates of background radiation are based on a recent comprehensive report by the National Council on Radiation Protection and Measurements (NCRP 1987). This document contains some minor differences from a 1975 NCRP report that had been used in previous environmental surveillance reports. These differences include using 20% (instead of 10%) shielding by structures for cosmic radiation and 30% (instead of 20%) self-shielding by the body for terrestrial radiation. The 1987 NCRP document also gives an effective dose equivalent for radon exposure. These changes were incorporated into this report to obtain the most current estimates of background radiation. This resulted in some small differences from the procedure used in previous reports for determining background doses.

Whole-body external dose is incurred from exposure to cosmic rays, external terrestrial radiation from naturally occurring radioactivity in the earth's surface and from global fallout. Effective dose equivalents from internal radiation are due to radionuclides deposited in the body through inhalation or ingestion.

Nonradon effective dose equivalents from background radiation vary each year depending on factors such as snow cover and the solar cycle (Sec. IV). Estimates of background from nonradon sources are

Table 5. Summary of Annual, Effective Dose Equivalents Due to 1987 Laboratory Operations

	Maximum Dose at Laboratory Boundary[a]	Maximum Dose to an Individual[b]	Average Dose to Nearby Residents		Cumulative Dose to Population Within 80 km of the Laboratory
			Los Alamos	White Rock	
Dose	12 ± 5 mrem	6.1 mrem	0.21 mrem	0.17 mrem	3.5 person-rem
Location	Boundary N. of TA-53	Residence N. of TA-53	Los Alamos	White Rock	Area within 80 km of Laboratory
DOE Radiation Protection Standard	--	100 mrem	100 mrem	100 mrem	--
% of Radiation Protection Standard	--	6%	0.2%	0.2%	--
Background	327 mrem	327 mrem	327 mrem	327 mrem	61 000 person-rem
% of Background	4%	2%	0.06%	0.05%	0.006%

[a]Maximum boundary dose is the dose to a hypothetical individual at the Laboratory boundary where the highest dose rate occurs with no correction for shielding. It assumes that the hypothetical individual is at the Laboratory boundary continuously (24 hours a day, 365 days a year).

[b]Maximum individual dose is the dose to an individual at or outside the Laboratory where the highest dose rate occurs and where there is a person. It takes into account occupancy (the fraction of time a person is actually at that location), self-shielding, and shielding by buildings.

based on measured external radiation background levels of 102 mrem (Los Alamos) and 106 mrem (White Rock) due to irradiation from charged particles, X rays, and gamma rays. These uncorrected, measured doses were adjusted for shielding by reducing the cosmic ray component (60 mrem at Los Alamos, 52 mrem at White Rock) by 20% to allow for shielding by structures, and the terrestrial component (42 mrem at Los Alamos and 54 mrem at White Rock) by 30% to allow for self-shielding by the body (NCRP 1987). To these estimates, based on measurements, were added 10 mrem at Los Alamos and 8 mrem at White Rock from neutron cosmic radiation (20% shielding assumed) and 40 mrem from internal radiation (NCRP 1987). The estimated whole-body dose from background, nonradon radiation is 127 mrem at Los Alamos and White Rock.

In addition to these nonradon doses, a second component of background radiation is dose to the lung from inhalation of ^{222}Rn and its decay products. The ^{222}Rn is produced by decay of ^{226}Ra, a member of the uranium series, which is naturally present in the construction materials in a building and in its underlying soil. The effective dose equivalent from exposure to background ^{222}Rn and its decay products is taken to be 200 mrem/year (NCRP 1987). This background estimate may be revised if a nationwide study of background levels of ^{222}Rn and its decay products in homes is undertaken as recommended by the NCRP (1984A, 1987).

The total effective dose equivalent to residents at Los Alamos and White Rock is 327 mrem/yr (Table 5), or 127 mrem/yr from nonradon sources and 200 mrem/yr from radon.

The use of medical and dental radiation in the United States accounts for an annual average, per capita, effective dose equivalent of 53 mrem (NCRP 1987). This estimate includes doses from both X rays and radiopharmaceuticals.

2. Dose to Individuals from External Penetrating Radiation from Airborne Emissions. The thermoluminescent dosimeter network at the Laboratory boundary north of LAMPF indicated a 12.4 mrem increment above cosmic and terrestrial background radiation during 1987 (Sec. IV). This increment is attributed to emission of air activation products from LAMPF. Based on 30% shielding from being inside buildings (NRC 1977), 30% self-shielding (NCRP 1987), and 100% occupancy, this 12.4 mrem increment translates to an estimated 6.1 mrem whole-body dose to an individual living along State Road 4 north of LAMPF (Table G-1). The 6.1 mrem is 24% of EPA's air emission standard of 25 mrem/yr for a member of the public (Appendix A). This location north of LAMPF has been the area where the highest boundary and individual doses have been measured since the dosimeter monitoring began.

Because these doses are from external penetrating radiation, all whole-body doses reported in this section are numerically equal to effective dose equivalents. Consequently, the doses are not only less than EPA's air emission standard of 25 mrem/yr (whole body), but also less than DOE's Radiation Protection Standard of 100 mrem/yr (effective dose equivalent).

A maximum on-site dose to a member of the public from external penetrating radiation from all Laboratory airborne emissions was estimated using a Gaussian dispersion meteorological model (Slade 1968). The estimated maximum on-site dose was 0.001 mrem (whole body) for 1987. This is <0.005% of the EPA's 25 mrem air emission standard for protection of a member of the public (Appendix A). This dose was calculated (using credible worst-case conditions) for a person spending 4 hours at the Laboratory's science museum, an area readily accessible to the public.

Average dose to residents in Los Alamos townsite attributable to Laboratory operations was 0.21 mrem to the whole body. The corresponding dose to White Rock residents was 0.17 mrem to the whole body. The doses are 0.8% and 0.7%, respectively, of EPA's 25 mrem air emission standard. They were estimated using an air dispersion model, measured stack releases (Table G-2), and 1987 meteorological data. These doses were dominated by external radiation from airborne releases at LAMPF.

3. Doses to Individuals from Inhalation of Airborne Emissions. The maximum individual doses attributable to inhalation of airborne emissions are summarized in Table G-1 and are below the EPA air emission standards for whole-body doses, 25 mrem/yr, and the limit for organ doses, 75 mrem/yr (Appendix A).

Exposure to airborne ^{3}H (as tritiated water vapor), uranium, ^{238}Pu, ^{239,240}Pu, and ^{241}Am were determined by measurement (Sec. V). Correction for background was made assuming that natural radioactivity and worldwide fallout were represented by data from the three regional sampling stations at Espanola, Pojoaque, and Santa Fe. Doses were calculated using the procedures described in Appendix D.

The inhalation dose that was the highest percentage of the EPA's air emission standard was 0.11 mrem to the bone surface; this is 0.1% of the 75 mrem/yr standard for dose to any organ from the air pathway.

Emissions of air activation products from LAMPF resulted in negligible inhalation exposures.

All other atmospheric releases of radioactivity (Table G-2) were evaluated by theoretical calculations. All potential doses from these other releases were less than the smallest ones presented in this section and were thus considered insignificant.

4. Modeled Doses from Airborne Emissions. For compliance with 40 CFR Part 61, Subpart H, the federal EPA requires that radiation doses be determined with the computer code AIRDOS-EPA (EPA 1985A). The AIRDOS-EPA code was run with 1987 meteorology data and radioactive emissions data given in Table G-2. As expected, over 98% of the maximum individual dose resulted from external exposure to the air activation products from LAMPF. The maximum individual whole-body dose as determined by AIRDOS-EPA was 10.9 mrem corrected to include shielding due to buildings (30% reduction). This dose, which would occur in the area just north of LAMPF, is 44% of the EPA's air emission standard of 25 mrem/yr (whole body).

The maximum organ dose was calculated by AIRDOS-EPA to be 12.8 mrem to the lung, or 17% of EPA's air emission standard of 75 mrem/yr to any organ. This dose would also occur in the area just north of LAMPF. Of the 12.8 mrem, approximately 95% is due to external penetrating radiation from LAMPF air emissions and 5% from other Laboratory emissions.

5. Doses from Direct Penetrating Radiation. No direct penetrating radiation from Laboratory operations was detected by TLD monitoring in off-site areas. The only off-site TLD measurements showing any effect from Laboratory operations were those taken north of LAMPF. These were due to airborne emissions and are discussed above. On-site TLD measurements of external penetrating radiation reflected Laboratory operations and do not represent potential exposure to the public except in the vicinity of TA-18 on Pajarito Road. Members of the public using the DOE-controlled road passing by TA-18 would likely receive no more than 2 mrem/yr of direct gamma and neutron radiation, which is 2% of the DOE's 100 mrem/yr standard for protection from exposure by all pathways (Appendix A). This value was based on 1987 field measurements of gamma plus neutron dose rates using thermoluminescent dosimeters.

The on-site thermoluminescent dosimeter station (Station 24, Fig. 6) near the northeastern Laboratory boundary recorded an above-background dose of about 70 mrem. This reflects direct radiation from a localized accumulation of ^{137}Cs on sediments transported from treated effluent released from TA-21 prior to 1964. No one resides near this location.

6. Doses to Individuals from Treated Liquid Effluents. Treated, liquid effluents do not flow beyond the Laboratory boundary but are retained in alluvium of the receiving canyons (Sec. VI). These treated effluents are monitored at their point of discharge and their behavior in the alluvium of the canyons below outfalls has been studied (Hakonson 1976A, 1976B, and Purtymun 1971, 1974A).

Small quantities of radioactive contaminants transported during periods of heavy run-off have been measured in canyon sediments beyond the Laboratory boundary in Los Alamos Canyon. Calculations made with radiological data from Acid, Pueblo, and Los Alamos canyons (ESG 1981) indicate a minor exposure pathway (eating liver from a steer that drinks water from and grazes in lower Los Alamos Canyon) to man from these canyon sediments. This pathway could potentially result in a maximum 50-year dose commitment of 0.0013 mrem to bone.

7. Doses to Individuals from Ingestion of Foodstuffs. Data from sampling of produce, fish, and honey during 1987 (Section VII) were used to estimate doses received from eating these foodstuffs. All calculated effective dose equivalents are 0.1% or less of the DOE's 100 mrem/yr standard (Appendix A).

Fruit and vegetable samples were analyzed for six radionuclides (^{3}H, ^{137}Cs, total uranium, ^{238}Pu, and $^{239,240}Pu$). Maximum committed effective dose equivalent that would result from ingesting one quarter of an annual consumption of fruits and vegetables (160 kg) from the off-site locations was 0.07 mrem. This dose is 0.07% of the DOE's Radiation Protection Standards for protecting members of the public (Appendix A).

Ingestion of produce collected on-site is not a significant exposure pathway because of the small amount of edible material, low radionuclide concentrations, and limited access to these foodstuffs.

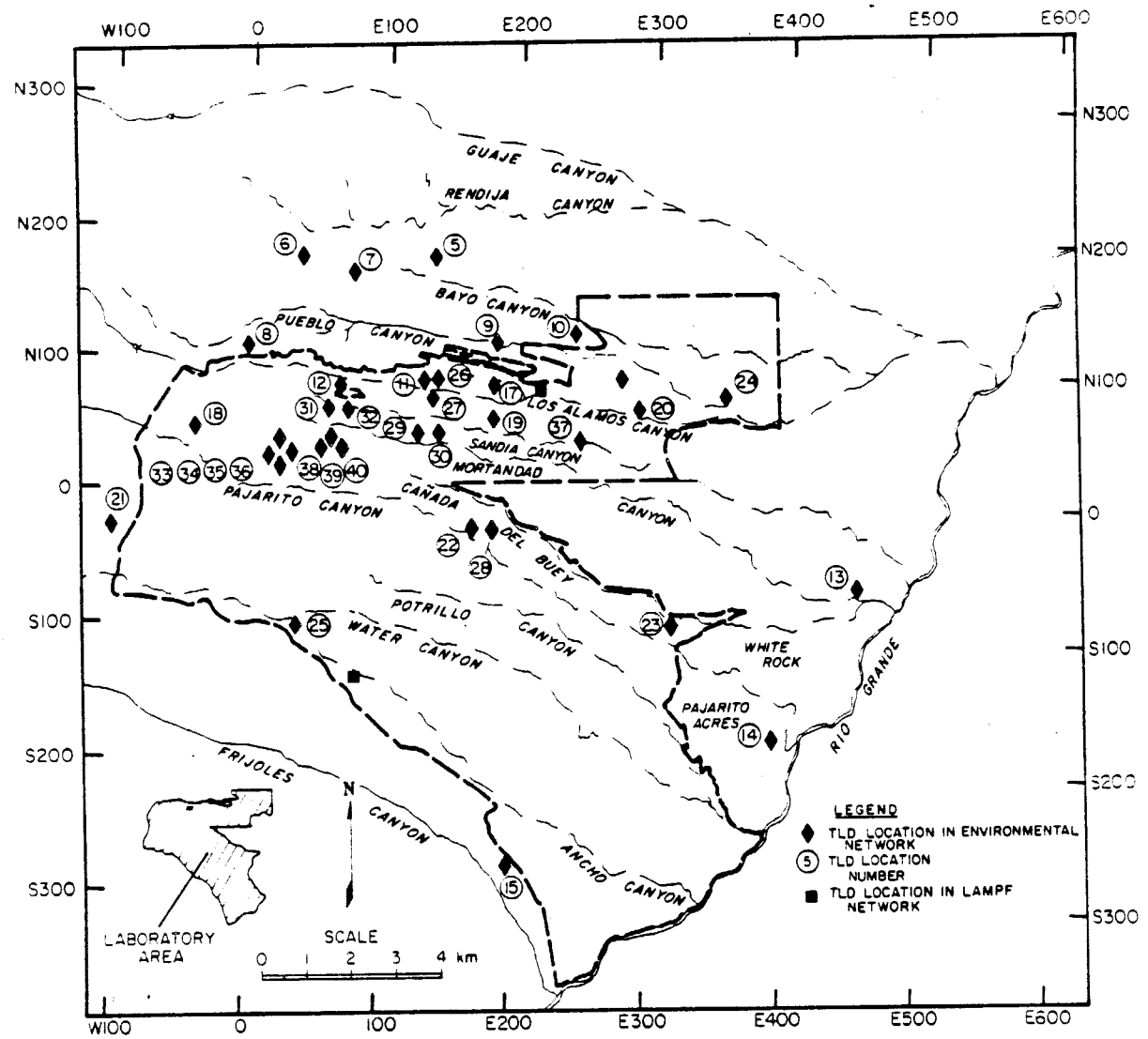

Fig. 6. Thermoluminescent dosimeter (TLD) locations on or near the Laboratory site.

Fish samples were analyzed for ^{90}Sr, ^{137}Cs, natural uranium, ^{238}Pu, and $^{239,240}Pu$. Radionuclide concentrations in fish from Cochiti Reservoir, the sampling location downstream from the Laboratory, are compared with concentrations in fish taken from upstream. The maximum effective dose equivalent to an individual eating 21 kg of fish from Cochiti Reservoir is 0.03 mrem, which is 0.03% of DOE's 100 mrem standard (DOE 1985). Maximum organ dose is 0.3 mrem to bone surface.

Trace amounts of radionuclides were found in honey. The maximum effective dose equivalent one would get from eating 5 kg of this honey, if it were made available for consumption, would be 0.02 mrem, which is 0.02% of DOE's 100 mrem standard.

8. Cumulative Effective Dose Equivalents. The 1987 population cumulative effective dose equivalents attributable to Laboratory operations to persons living within 80 km (50 mi) of the Laboratory was calculated

to be 3.5 person-rem. This dose is <0.01% of the 61 000 person-rem exposure from natural background radiation and 0.03% of the 10 000 person-rem exposure from medical radiation (Table 6). The 1987 population whole-body dose equivalent is also 3.5 person-rem. This is because the dose is dominated by external whole-body radiation from LAMPF emissions. Whole-body doses received from external radiation equal total effective doses.

The population dose from Laboratory operations was calculated from measured radionuclide emission rates (Table G-2), atmospheric modeling using measured meteorological data for 1987, and population data based on the 1980 Bureau of Census count adjusted to 1987 (Table 4 and Appendix D).

The population dose from natural background radiation was calculated using the background radiation levels given above. The dose to the 80-km population from medical and dental radiation was calculated using a mean annual dose of 53 mrem per capita. The population distribution in Table 4 was used in both these calculations to obtain the total population dose.

Also shown in Table 6 is the population effective dose equivalent in Los Alamos County from Laboratory operations, natural background radiation, and medical and dental radiation. Approximately 90% of the total population dose from Laboratory operations is to Los Alamos County residents. This dose is 0.05% of the population effective dose equivalent from background and 0.3% of the population dose from medical and dental radiation, respectively.

Population centers outside of Los Alamos County are farther away, so dispersion, dilution, and decay in transit (particularly for ^{11}C, ^{13}N, ^{14}O, ^{15}O, and ^{41}Ar) reduce their dose to less than 10% of the total. The population dose to residents outside of Los Alamos County and within 80 km (50 mi) of the Laboratory is 0.001% of the dose from natural background radiation and 0.004% of the dose from medical and dental radiation.

C. Risk to an Individual from Laboratory Releases

1. Estimating Risk. Risk estimates of possible health effects from radiation doses to the public

Table 6. Estimated Population Effective Dose Equivalents (person-rem) During 1987

Exposure Mechanism	Los Alamos County (18 400 persons)	80-km Region (193 000 persons)[a]
Total Due to Laboratory Releases	3.1[b]	3.5
Natural Background		
Non-Radon	2300	22 000
Radon	3700	39 000
Total Due to Natural Sources of Radiation	6000	61 000
Diagnostic Medical Exposure [~53 mrem/yr per person (NCRP 1987)]	970	10 000

[a]Includes doses reported for Los Alamos County.
[b]Calculations are based on thermoluminescent dosimeter measurements. They include a 30% reduction in cosmic radiation from shielding by structures and a 30% reduction in terrestial radiation from self-shielding by the body.

resulting from Laboratory operations have been made to provide perspective in interpreting these radiation doses. These calculations, however, may overestimate actual risk for low-LET (linear energy transfer) radiation. The National Council on Radiation Protection and Measurements (NCRP 1975A) has warned "risk estimates for radiogenic cancers at low doses and low dose rates derived on the basis of linear (proportional) extrapolation from the rising portions of the dose incidence curve at high doses and high dose rates...cannot be expected to provide realistic estimates of the actual risks from low level, low-LET radiation, and have such a high probability of overestimating the actual risk as to be of only marginal value, if any, for purposes of realistic risk-benefit evaluation."

Low-LET radiation, which includes gamma rays, is the principal type of environmental radiation resulting from Laboratory operations. Estimated doses from high-LET radiation, such as neutron or alpha particle radiation, are less than 3% of estimated low-LET radiation doses. Consequently, risk estimates in this report may overestimate the true risks.

The International Commission on Radiological Protection (ICRP 1977) estimated that the total risk of cancer mortality from uniform, whole-body radiation for individuals is 0.0001 per rem, that is, there is 1 chance in 10 000 that an individual exposed to 1000 mrem (1 rem) of whole-body radiation would develop a fatal cancer during his lifetime due to that exposure. This same risk factor applies to the risk of cancer mortality per rem of effective dose equivalent. In developing risk estimates, the International Commission on Radiological Protection has warned "radiation risk estimates should be used only with great caution and with explicit recognition of the possibility that the actual risk at low doses may be lower than that implied by a deliberately cautious assumption of proportionality" (ICRP 1977).

2. Risk from Natural Background Radiation and Medical and Dental Radiation. During 1987, persons living in Los Alamos and White Rock received an average effective dose equivalent of 127 mrem of non-radon (principally to the whole body) radiation from natural sources (including cosmic, terrestrial, and self-irradiation sources with allowances for shielding and cosmic neutron exposure). Thus the added cancer mortality risk attributable to natural, whole-body radiation in 1987 was 1 chance in 79 000 in Los Alamos and White Rock (Table 2).

Natural background radiation also includes exposure to the lung from ^{222}Rn and its decay products (see above), in addition to exposure to whole body radiation. This exposure to the lung also carries a chance of cancer mortality due to natural radiation sources that was not included in the estimate for whole body radiation. For the background effective dose equivalent of 200 mrem/yr, the added risk due to exposure to natural ^{222}Rn and its decay products is 1 chance in 50 000.

The total cancer mortality risk from natural background radiation is 1 chance in 31 000 for Los Alamos and White Rock. The additional risk of cancer mortality from exposure to medical and dental radiations is 1 chance in 190 000.

3. Risk from Laboratory Operations. The risks calculated above from natural background radiation and medical and dental radiation can be compared with the incremental risk due to radiation from Laboratory operations. The average doses to individuals in Los Alamos and White Rock because of 1987 Laboratory activities were 0.21 mrem and 0.17 mrem, respectively. These doses are estimated to add lifetime risks of about 1 chance in 50 000 000 in Los Alamos and White Rock to an individual's risk of cancer mortality (Table 2). These risks are <0.1% of the risk attributed to exposure to natural background radiation or to medical and dental radiation.

For Americans the average lifetime risk is a 1 in 4 chance of contracting a cancer and a 1 in 5 chance of dying of cancer (EPA 1979A). The Los Alamos incremental dose attributable to Laboratory operations is equivalent to the additional exposure from cosmic rays a person would get from flying in a commercial jet aircraft for 57 min.

The exposure from Laboratory operations to Los Alamos County residents is well within variations in exposure to these people from natural cosmic and terrestrial sources and global fallout. For example, amount of snow cover and position in the solar sunspot cycle can account for a 10 mrem variation from year to year. Energy conservation measures, such as sealing and insulating houses and installing passive solar systems, are likely to contribute more to the total risk to Los Alamos County residents than Laboratory operations because of increased ^{222}Rn levels inside homes.

IV. MEASUREMENT OF EXTERNAL PENETRATING RADIATION

Levels of external penetrating radiation--including X and gamma rays and charged particle contributions from cosmic, terrestrial, and manmade sources--are monitored in the Los Alamos area with thermoluminescent dosimeters. Measurements for regional locations showed a statistically discernible decrease in radiation levels for 1987. The only boundary or perimeter measurements showing an effect attributable to laboratory operations were those from dosimeters located north of the Los Alamos Meson Physics Facility (a linear particle accelerator). They showed an above-background radiation measurement of about 12 ± 5 mrem in 1987. This is a decrease from the 1986 measurement of 18 ± 3 mrem, although not statistically significant. Some on-site measurements were above background levels, as expected, reflecting research activities and waste management operations at the Laboratory.

A. Background

Natural external penetrating radiation comes from terrestrial and cosmic sources. The natural terrestrial component results from decay of ^{40}K and of radioactive nuclides in the decay chains of ^{232}Th, ^{235}U, and ^{238}U. Natural terrestrial radiation in the Los Alamos area is highly variable with time and location. During any year, external radiation levels can vary 15 to 25% at any location because of changes in soil moisture and snow cover (NCRP 1975B). There is also spatial variation because of different soil and rock types in the area (ESG 1978).

The cosmic source of natural ionizing radiation increases with elevation because of reduced shielding by the atmosphere. At sea level, it produces measurements between 25 and 30 mrem/yr. Los Alamos, with a mean elevation of about 2.2 km (1.4 mi), receives about 60 mrem/yr from the cosmic component. However, the regional locations range in elevation from about 1.7 km (1.1 mi) at Espanola to 2.7 km (1.7 mi) at Fenton Hill, resulting in a corresponding range between 45 and 90 mrem/yr for the cosmic component. The cosmic component can vary about ±5% because of solar modulations (NCRP 1975B).

Fluctuations in natural background ionizing radiation make it difficult to detect an increase in radiation levels from manmade sources. This is especially true when the size of the increase is small relative to the magnitude of natural fluctuations. Therefore, in order to measure contributions to external radiation from operation of the Los Alamos Meson Physics Facility (LAMPF), arrays of 48 thermoluminescent dosimeters (TLDs) each have been deployed near LAMPF and in background areas.

Levels of external penetrating radiation--including X and gamma rays and charged particle contributions from cosmic, terrestrial, and manmade sources--in the Los Alamos area are measured with TLDs deployed in three independent networks. These networks are used to measure radiation levels at: (1) the Laboratory and regional areas, (2) the Laboratory boundary north of LAMPF, and (3) low-level radioactive waste management areas.

B. Environmental TLD Network

The environmental network consists of 40 stations divided into three groups. The regional group consists of four locations, 28 to 44 km (17 to 27 mi) from the Laboratory boundary in the neighboring communities of Espanola, Pojoaque, and Santa Fe as well as the Fenton Hill Site 30 km (19 mi) west of Los Alamos. The off-site perimeter group consists of 12 stations within 4 km (2.5 mi) of the boundary. Within the Laboratory boundary, 24 locations comprise the on-site group (Fig. 6). Details of methodology for this network are found in Appendix B.

Annual averages for the groups were significantly lower in 1987 than 1986 ($p < 0.05$, 2-way analysis of variance) (Fig. 7). Regional and perimeter stations showed no statistically discernible increase in radiation levels attributable to Laboratory operations (Table G-3). Annual measurements at off-site stations ranged from 70 to 124 mrem.

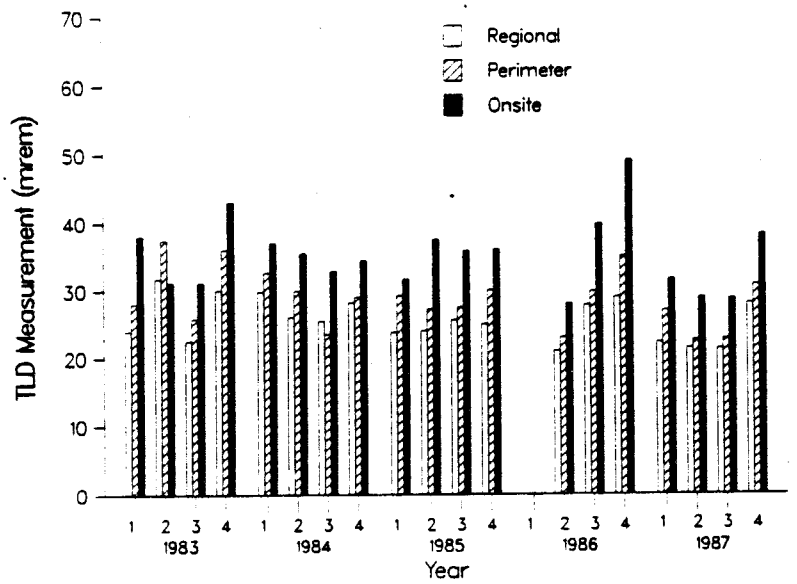

Fig. 7. Thermoluminescent dosimeter (TLD) measurements (includes contributions from cosmic, terrestrial, and Laboratory radiation sources).

Some comparisons provide a useful perspective for evaluating these measurements. For instance, the average person in the United States receives about 53 mrem/yr for medical diagnostic procedures (NCRP 1987). The DOE's RPS is 100 mrem/yr, effective dose received from all pathways, and the dose received via air is restricted by EPA's standard of 25 mrem/yr (whole body) (Appendix A). These values are in addition to normal background, consumer products, and medical sources. The standards apply to locations of maximum probable exposure to an individual in an off-site, uncontrolled area.

C. Los Alamos Meson Physics Facility (LAMPF) TLD Network

This network monitors external radiation from airborne activation products (gases, particles, and vapors) released by LAMPF, TA-53. The prevailing winds are from the south and southwest (Sec. II). Twelve TLD sites are located downwind at the Laboratory boundary north of LAMPF along 800 m (0.5 mi) of canyon rim. Twelve background TLD sites are about 9 km (5.5 mi) from the facility along a canyon rim near the southern boundary of the Laboratory (Fig. 6). This background location is not influenced by any Laboratory external radiation sources.

The TLDs at the 24 sites are changed each calendar quarter or sooner, if LAMPF's operating schedule dictates (start-up or shut-down of the accelerator for extended periods midway in a calendar quarter). The radiation measurement (above background) for this network was about 12 $\pm$ 5 mrem for 1987. This value is obtained by subtracting the annual measurement at the background sites from the annual measurement at the Laboratory's boundary north of LAMPF (Appendix B). This year's measurement is about two-thirds of the value measured in 1986 (Fig. 2) even though estimated emissions from LAMPF increased in 1987 (Table 3).

D. TLD Network for Low-Level Radioactive Waste Management Areas

This network of 92 locations monitors radiation levels at 1 active and 11 inactive low-level radioactive waste management areas. These waste management areas are controlled-access areas and are not accessible to the general public. Active and inactive waste areas are monitored for external penetrating radiation with arrays of TLDs (Table 7). Averages at all sites but Area X were higher than average perimeter values. However, the ranges at most sites largely overlapped the range of values found at perimeter and

regional stations (Tables 7 and G-3). The extremes at Area G, the active radioactive waste area, and Area T, an inactive waste area, have been noted in previous years. These are the results of past and present radioactive waste management activities.

Table 7. Doses (mrem) Measured by TLDs at On-site Waste Areas During 1987

Area	Number of TLDs	Mean	Minimum	Maximum
A	5	118	112	121
B	14	118	107	126
C	10	116	104	149
E	4	119	113	125
F	4	108	102	111
G	27	132	111	174
T	7	133	109	198
U	4	115	112	119
V	4	117	111	122
W	2	110	107	113
X	1	91	---	---
AB	10	106	96	114

V. AIR MONITORING

Airborne radioactive emissions were released from 87 points at the Laboratory during 1987. The largest airborne release was 150 000 Ci of short-lived (2 to 20 minute half-lives) air activation products from the Los Alamos Meson Physics Facility (LAMPF). Ambient air is routinely sampled at several locations on-site, along the Laboratory perimeter, and in distant areas which serve as regional background stations. Concentrations of airborne tritium, uranium, plutonium, americium, and gross beta activity are measured. The highest measured and annual average activity concentrations of these radioactive materials were much less than 0.1% of levels that exceed DOE's Radiation Protection Standards. Nonradiological airborne emissions from the Laboratory remained below federal and state limits.

A. Radionuclides in Ambient Air

1. Background. The ambient air sampling network for radioactivity consists of 26 continuously operating stations (see Appendix B for a complete description of sampling procedures). The regional monitoring stations, 28 to 44 km (18 to 28 mi) from the Laboratory, are located at Espanola, Pojoaque, and Santa Fe (Fig. 8). The results from these stations are used as reference points for determining regional background levels of airborne radioactivity. The 11 perimeter stations are within 4 km (2.5 mi) of the Laboratory boundary; 12 stations are located within the Laboratory boundary (Fig. 8, Table G-4).

Natural fallout radioactivity levels in air fluctuate and affect measurements made by the Laboratory's air sampling program. Worldwide background airborne radioactivity is largely composed of fallout from past above-ground nuclear weapon tests, natural radionuclides from the transformation products of thorium and uranium attached to dust particles, and materials resulting from interactions with cosmic radiation (e.g., tritiated water vapor produced by interactions of cosmic radiation and stable water). Background, airborne radioactivity concentrations are summarized in Table G-5.

Particulate matter in the atmosphere is primarily caused by resuspension of soil which is dependent upon meteorological conditions. Windy, dry days can increase soil resuspension, whereas precipitation (rain or snow) can wash out particulate matter from the atmosphere. Consequently, there are often large daily and seasonal fluctuations in airborne radioactivity concentrations caused by changing meteorological conditions.

2. Airborne Emissions. Radioactive airborne emissions are discharged at the Laboratory from 87 stacks. These emissions consist primarily of filtered exhausts from gloveboxes, experimental facilities, operational facilities (such as liquid waste treatment plants), a nuclear research reactor, and a linear particle accelerator at LAMPF. The emissions receive appropriate treatment prior to discharge, such as filtration for particulates as well as catalytic conversion and adsorption for activation gases. Quantities of airborne radioactivity released depend on the nature of ongoing research activities and vary significantly from year to year (Figs. 9-11).

During 1987, as in previous years, the most significant releases were from LAMPF (Fig. 11 and Table G-2). The amount released for the year was 150 000 Ci of air activation products (gases, particulates, and vapors). These emissions were about 30% above 1986 amounts. The principal airborne activation products (half-lives in parentheses) were ^{11}C (20 min), ^{13}N (10 min), ^{14}O (71 sec), ^{15}O (123 sec), and ^{41}Ar (1.83 h). Over 95% of the radioactivity was from ^{11}C, ^{13}N, ^{14}O, and ^{15}O. However, the radioactivity from these radionuclides declines rapidly because of the short half-lives.

Airborne tritium emissions decreased by 70% from 10 700 Ci in 1986 to 3180 Ci in 1987 (Table 3). This was principally due to decreases in tritium releases from facilities at TA-3, TA-33, and TA-41.

In addition to releases from facilities, some depleted uranium (uranium consisting primarily of ^{238}U) is dispersed by experiments that use conventional high explosives. About 98 kg (220 lb) of depleted uranium was used in such experiments in 1987 (Table G-6). This mass contains about 46 mCi of radioactivity.

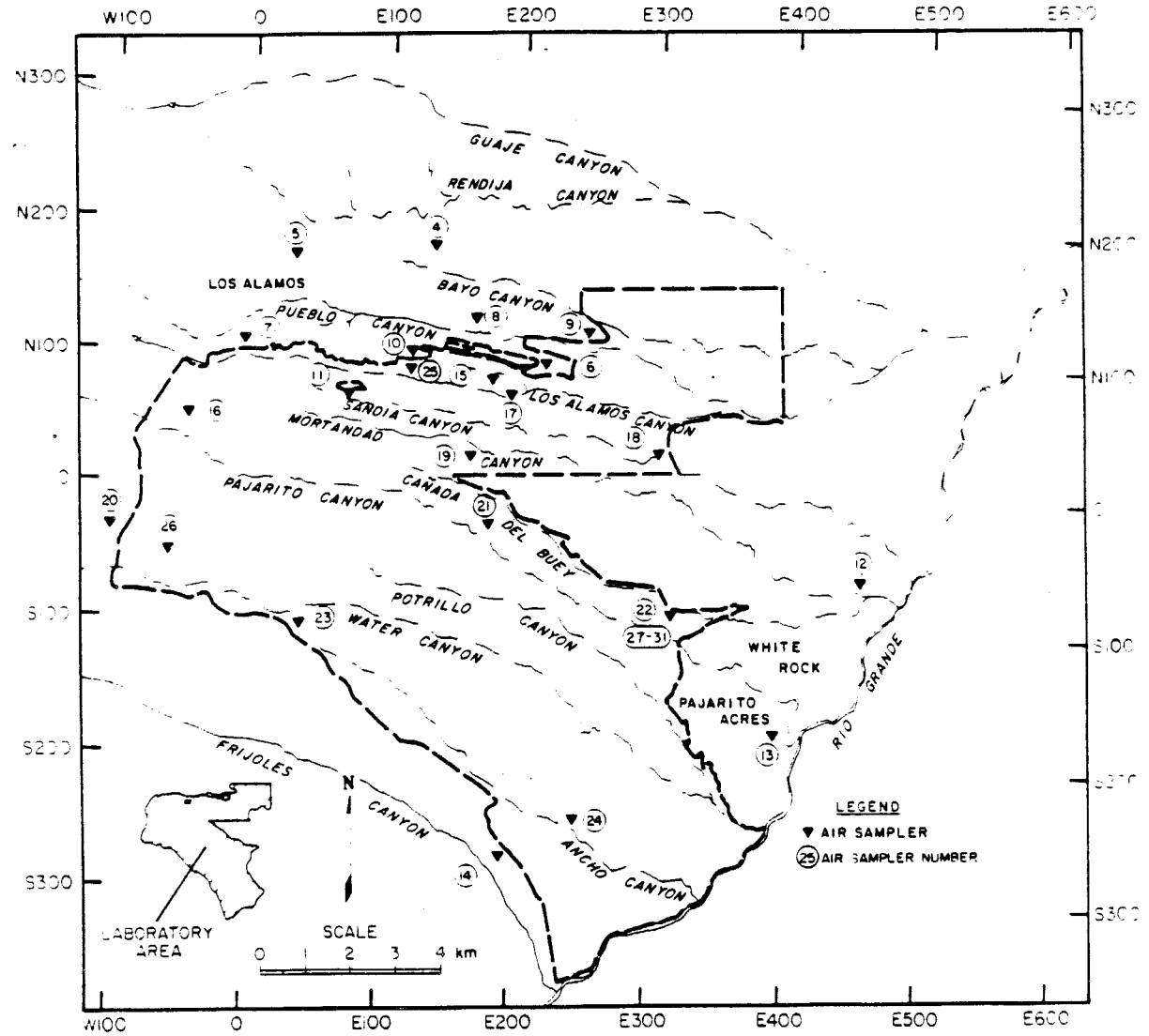

Fig. 8. Air sampler locations on or near the Laboratory site.

Most of the debris from these experiments is deposited on the ground in the vicinity of the firing sites. Limited experimental data indicate that about 10% of the depleted uranium becomes airborne. Dispersion calculations indicate that resulting airborne concentrations are in the same range as attributable to the natural abundance of uranium resuspended in dust particles originating from the earth's crust. This is confirmed by monitoring of airborne uranium concentrations (see below).

3. Gross Beta Radioactivity. Gross beta analyses help in evaluating general radiological air quality. Figure 12 shows gross beta concentrations at a regional sampling location (Espanola), about 30 km (20 mi) from the Laboratory, and at an on-site sampling location (TA-59).

4. Tritium. In 1987, the regional mean (4.1 x 10^{-12} μCi/mL) and the perimeter annual mean (11.0 x 10^{-12} μCi/mL) were slightly but statistically

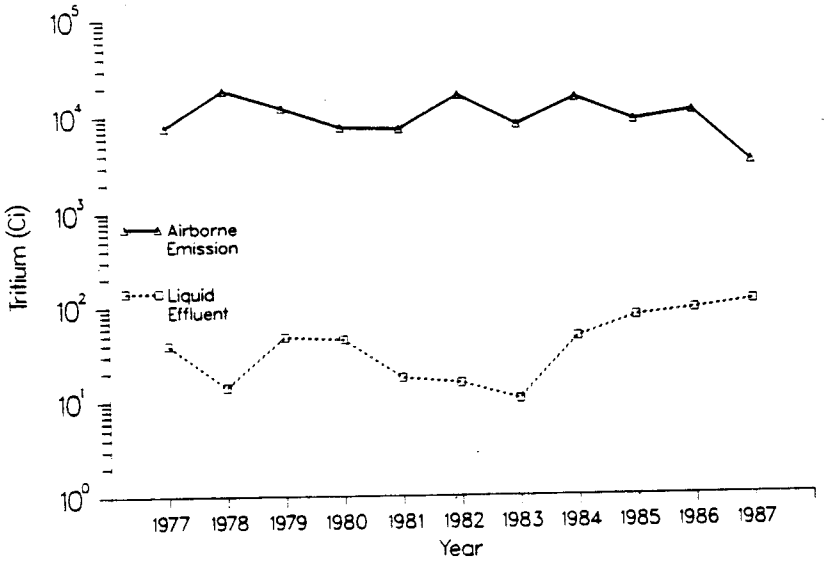

Fig. 9. Summary of tritium releases (airborne emissions and liquid effluents).

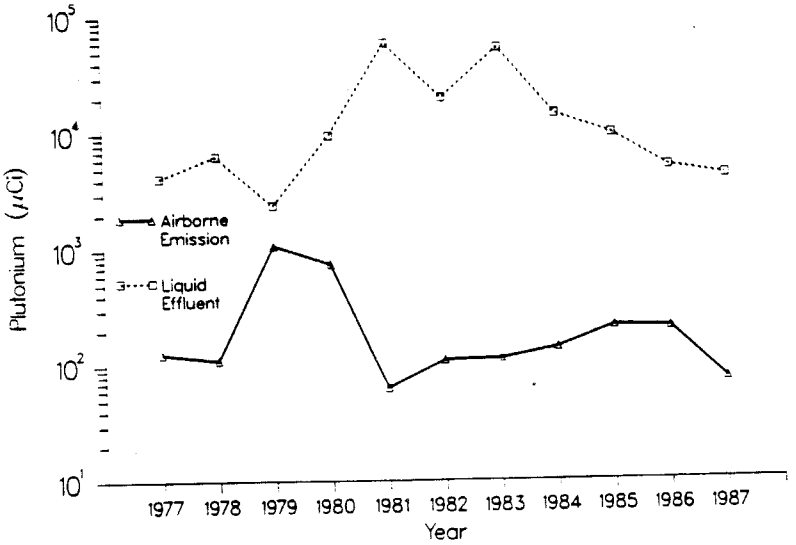

Fig. 10. Summary of plutonium releases (airborne emissions and liquid effluents).

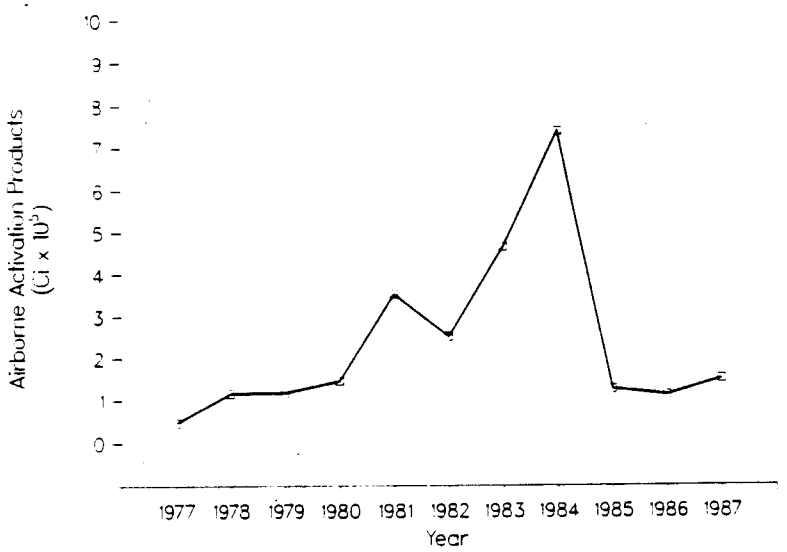

Fig. 11. Airborne activation product emissions (principally ^{11}C, ^{10}C, ^{13}N, ^{16}N, ^{14}O, ^{15}O, ^{41}Ar) from the Los Alamos Meson Physics Facility (TA-53).

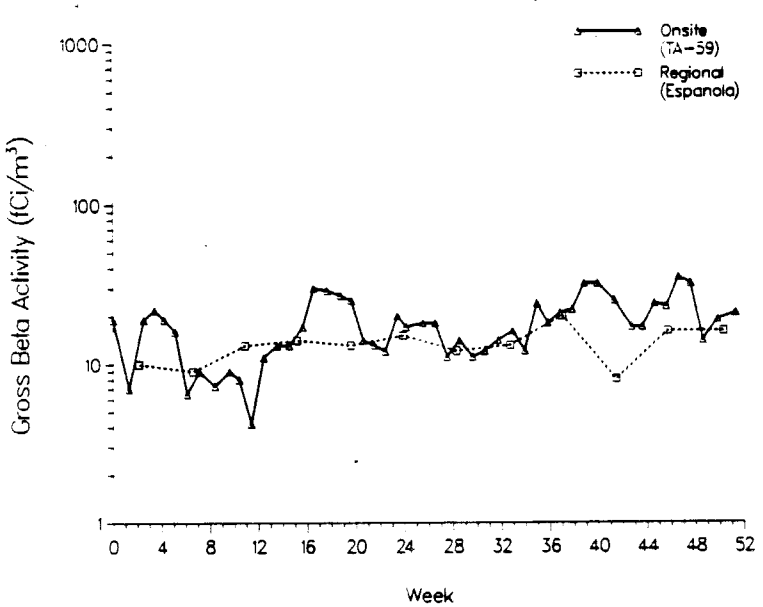

Fig. 12. Atmospheric gross beta activity at a regional (background) station and an on-site station during 1987.

significantly lower than the on-site annual mean (21.7 x 10^{-12} μCi/mL) (Table G-7). This reflects the slight impact of Laboratory operations. The TA-21 (Station 15) and TA-54 (Station 22) annual means of 51.8 x 10^{-12} and 32.3 x 10^{-12} μCi/mL, respectively, were the two highest means measured in 1987. Both of these stations are located within the Laboratory boundary near areas where tritium is disposed of or used in operations. These tritium concentrations are <0.1% of the concentration guide for tritium in air based on DOE's RPS for Controlled Areas (Appendix A).

5. Plutonium and Americium. Of the 101 air sample analyses performed in 1987 for ^{238}Pu, only three were above the minimum detectable limit of 2 x 10^{-18} μCi/mL. The highest concentration occurred at TA-54 (6.3 ± 1.4 x 10^{-18} μCi/mL) and represents <0.1% of the DOE's Derived Concentration Guide for ^{238}Pu in off-site areas, 2 x 10^{-12} μCi/mL (Appendix A). The results of the ^{238}Pu analyses are not tabulated in this report because of the large number of results below the minimum detectable activity.

The 1987 annual means for ^{239,240}Pu concentrations in air for the regional (0.7 x 10^{-18} μCi/mL), perimeter (0.9 x 10^{-18} μCi/mL), and on-site (1.8 x 10^{-18} μCi/mL) stations were all <0.1% of concentration guides.

Measured concentrations of ^{241}Am were also <0.1% of the concentration guides for Controlled and Uncontrolled Areas (Appendix A).

The detailed results are in Tables G-8 and G-9.

6. Uranium. Because uranium is a naturally occurring radionuclide in soil, it is found in airborne soil particles that have been resuspended by wind or mechanical forces (for example, vehicles or construction activity). As a result, uranium concentrations in air are heavily dependent on the immediate environment of the air sampling station. Those stations with relatively higher annual averages or maximums are in dusty areas, where a higher filter dust loading accounts for collection of more natural uranium from resuspended soil particles.

The 1987 means were: regional, 74 pg/m^3; perimeter, 33 pg/m^3; and on-site, 31 pg/m^3 (Table G-10). All measured annual means were less than 0.1% of the concentration guides for uranium in off-site and on-site areas (Appendix A). No effects attributable to Laboratory operations were observed.

B. Nonradioactive Chemicals in Ambient Air

1. Air Quality

a. Bandelier National Atmospheric Deposition Program Station. The Laboratory operates a wet deposition station located at the Bandelier National Monument. The station is part of the National Atmospheric Deposition Program Network. The sampling results are presented in Section IX.

b. Particulate Air Quality Measurements. Measurements of total suspended particulates (TSP) in Los Alamos and White Rock and applicable state and federal standards are reported in Table 8. The measurements are made once every 6 days at a site on West Road in Los Alamos and at the sewage treatment plant in White Rock by the NMEID. The 24-hour average standards are not to be exceeded more than once per year. There is both a primary and a secondary standard for TSP. The primary standard is to protect human health and the secondary standard is to protect general welfare, such as the prevention of soiling and material damage. The state 24-hour standard is as stringent as the federal secondary standard.

The state and federal ambient air quality standards were met in both Los Alamos and White Rock. The seasonally averaged TSP concentrations are shown in Table 9.

2. Beryllium Operations. Beryllium machining operations are located in shop 4 at TA-3-39, in shop 13 at TA-3-102, and the beryllium shop at TA-35-213. Beryllium machining takes place intermittently, a few days per year. A new beryllium processing facility located at TA-3-141 began operation in 1987. Exhaust air from each of these operations passes through air pollution control equipment before exiting from a stack. A baghouse type filter is used to control emissions from shop 4. The other operations use HEPA filters to control emissions. The air pollution control systems have >99.9% particulate removal efficiencies.

3. Steam Plants and Power Plant. Fuel consumption and emissions estimates for the three steam plants and the TA-3 power plant are reported in Table G-12. The NO_x emissions from the TA-3 power plant

Table 8. Particulate Air Quality ($\mu g/m^3$)

Federal and State Ambient Air Quality Standards		Measurements	
Type	Concentration	Los Alamos	White Rock
24-hour average[a]		70.2[b] (150.8)[c]	46.2[b] (53.3)[c]
State[c]	150		
Federal			
Primary	260		
Secondary	150		
7-day average[d]	110		
30-day average[d]	90		
Annual Geometric Mean		23.8	29.7
Primary	75		
Secondary	60		

---

[a]Not to be exceeded more than once per year.
[b]Second highest
[c]Highest.
[d]New Mexico state standard only.

Table 9. Particulate Air Quality, Seasonal Averages ($\mu g/m^3$)

	Winter	Spring	Summer	Fall
Los Alamos	22.5	26.4	24.0	17.8
White Rock	19.6	34.7	29.0	45.9

were estimated based upon boiler exhaust gas measurements. Exhaust gas measurements indicated that SO_x levels exhaust gases were below minimum detectable levels. Emission factors from EPA were used in making the other emission estimates (EPA 1984). The change in emissions from 1986 to 1987 reflects the change in fuel consumption. The Western Area steam plant, used as a standby plant, was operated only one month during 1987.

4. Motor Vehicle Emissions. Estimates of air pollutant emissions associated with the operation of the motor vehicle fleet are reported in Table 10. Emissions increased due to increases in mileage and fuel use. Direct emissions from the vehicles as well as emissions caused by evaporative losses from fuel storage tanks were estimated. Hydrocarbons, carbon monoxide, nitrogen oxides, sulfur oxides, and particulate emissions were estimated based upon motor

Table 10. Estimate of Air Pollutant Emissions Associated With the Operation of the Vehicle Fleet (metric tons)

	1986	1987	Incremental % Change
Fuel Storage Evaporative Losses	4.8	6.7	39.8
Hydrocarbons	10.4	12.4	18.9
Carbon Monoxide	120.2	133.6	11.2
Nitrogen Oxides	11.9	13.3	11.4
Sulfur Oxides	1.4	1.8	30.6
Particulates			
Exhaust	0.6	0.8	32.7
Tire Wear	1.3	1.7	30.1

Table 11. Asphalt Plant Particulate Emissions

Year	Production (tons/yer)	Emissions (lb/year)	Incremental % Change from 1986
1986	6 980	232	---
1987	8 083	269	15.8

vehicle class, age, and the vehicle miles traveled (EPA 1981, EPA 1984). Fuel storage evaporative losses were estimated based upon the fuel usage.

5. Asphalt Plant. Annual production figures and estimates of particulate emissions from the asphalt concrete plant are found in Table 11. The particulate emissions from the plant are low, but have increased from 1986 to 1987 because of an increase in production. There has been a substantial decrease in production since 1985 because of the purchase of the asphalt from outside vendors. A multicyclone and a wet scrubber are used to clean the exhaust gas stream before it is released into the atmosphere. The particulate emission estimate was based upon stack testing data (Kramer 1977) and production data.

6. Burning and Detonation of Explosives. During 1987, a total of 18 400 kg (20 tons) of high-explosive wastes were disposed of by open burning at the TA-16 burn ground. Estimates of emissions resulting from this burning are reported in Table 12. The emissions were 7.7% lower than those for 1986. These estimates were made by using data from experimental work carried out by Mason and Hanger - Silas Co., Inc. (MHSM 1976).

Dynamic experiments employing conventional explosives are routinely conducted in certain test areas at the Laboratory. In some experiments these explosives contain toxic metals including uranium, beryllium, and lead. Through November 1987, uranium emissions had decreased 51.3%, lead emissions

Table 12. Estimated Air Pollutant Emissions from the Open Burning of Waste Explosives (kg)

Pollutant	1986	1987
Oxides of Nitrogen	602.1	555.7
Particulates	358.9	331.2
Carbon Monoxide	155.5	143.5
Hydrocarbons	2.0	1.8

decreased 26.9%, and beryllium emissions decreased 4.8% from 1986 levels.

Estimates of average concentrations of these toxic metals downwind from the detonations are reported in Table G-6. Applicable standards are also presented in this table. Estimated concentrations were <0.01% of applicable standards. These estimates are based upon information concerning the proportion of material aerosolized provided from limited field experiments involving aircraft sampling and the amounts of toxic metals used in the experiments through November 1987.

7. Lead Pouring Facility. Pan Am World Services operates a lead pouring facility for producing lead castings that is located at TA-3-38. Approximately 11 700 kg (25 800 lb) of lead were estimated to have been poured during 1987. The estimated 1987 annual lead emissions from this facility were 5.1 kg (11.2 lb); maximum quarterly emissions were 1.8 kg (3.9 lb). The emission estimates were based upon the amounts of lead poured and an EPA emission factor for lead casting operations (EPA 1984).

Both federal and state ambient air quality standards for lead are 1.5 g/m^3 averaged over a calendar quarter. Air dispersion procedures recommended by the EPA (EPA 1977, 1986) were used to estimate the maximum quarterly average lead concentrations caused by emissions from the lead pouring facility. These procedures provide conservative concentration estimates. The maximum quarterly concentration for 1987 was estimated to be 0.11 $\mu g/m^3$, 7% of the standard.

VI. WATER, SOILS, AND SEDIMENTS MONITORING

Surface and ground waters, soils, and sediments were sampled and analyzed to monitor dispersion of radionuclides and chemicals from Laboratory operations. Radionuclide and chemical concentrations of water from areas where there has been no direct release of treated effluents evidenced no observable effects due to Laboratory operations. The chemical quality of surface waters from areas with no effluent release varied with seasonal fluctuations. Water in on-site areas where treated effluent has been released contained radionuclides below DOE's concentration guides. The quality of water in these release areas reflected some impact of Laboratory operations, but these waters are confined within the Laboratory and are not a source of municipal, industrial, or agricultural water supply.

Most regional and perimeter soil and sediment stations contained radioactivity at or near background levels. Concentrations that did exceed background were low and not considered significant. Sediments from areas where treated discharges have been released contained radionuclides in excess of background. Concentrations of plutonium in sediments from regional reservoirs on the Rio Chama and Rio Grande reflected worldwide fallout.

A. Effluent Quality

In the past, treated liquid effluents containing low levels of radioactivity have been released from the Central Liquid Waste Treatment Plant (TA-50), a smaller plant serving laboratories at TA-21, and a sanitary sewage lagoon system serving LAMPF (TA-53) (Tables 3, G-12, G-13, and Figs. 9, 10, and 13). In 1987, there were no releases from TA-21.

Radionuclide concentrations in treated effluents from the larger radioactive liquid waste-treatment plant (TA-50) were well below DOE's concentration guides for on-site areas (Table G-12). The total activity released in 1987 (ca. 110 Ci) was 120% of that

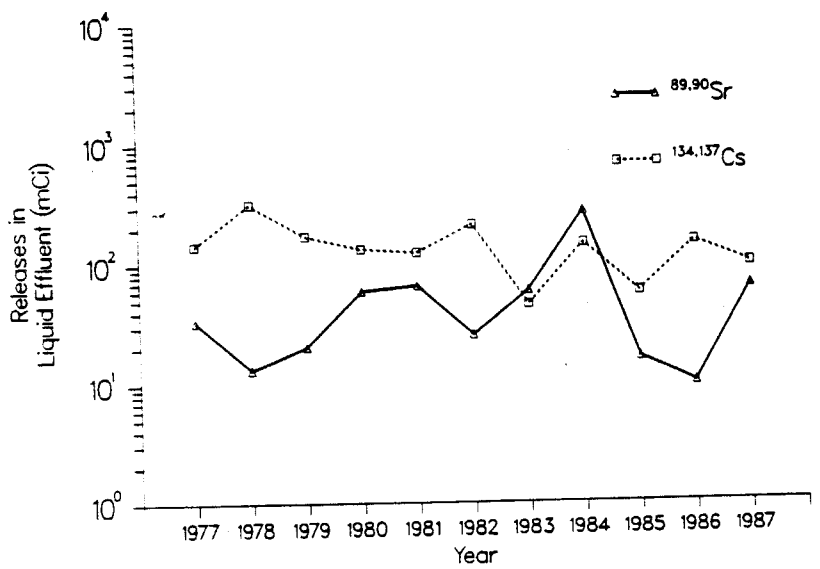

Fig. 13. Summary of strontium and cesium liquid effluent releases.

released in 1986 (ca. 91 Ci) (Table 3). Release of ^{89}Sr increased six-fold because of additional processing of LAMPF isotopes at the TA-48 hot cells. Effluents from TA-50 are discharged into the normally dry stream channel in Mortandad Canyon, where surface flow has not passed beyond the Laboratory's boundary since before the plant began operation in 1963.

Concentrations found in the TA-53 lagoon effluent in 1987 were higher than in 1986 for some radionuclides and lower for others (Table G-13). The source of the radioactivity was activated nuclides in water from the beam-stop cooling systems. The volume discharged from the lagoons decreased slightly in 1987. There was no discharge after April 8, 1987. All radionuclide concentrations were well below DOE's concentration guides for on-site areas (Table G-13). The discharge from the lagoons sinks into the alluvium of Los Alamos Canyon within the Laboratory's boundary.

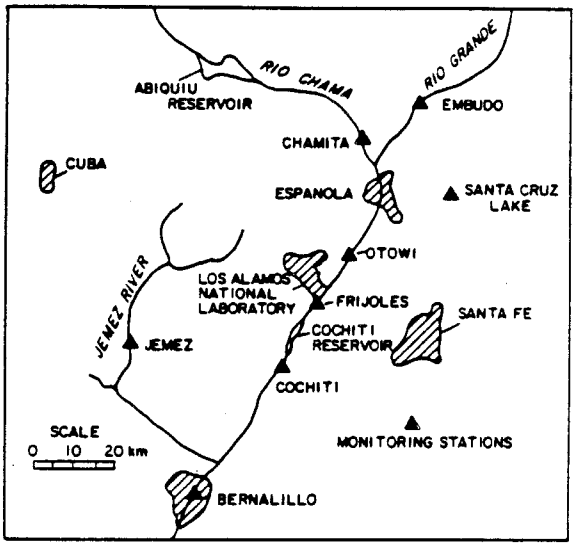

Fig. 14. Regional surface water, sediment, and soil sampling locations.

B. Radiochemical and Chemical Quality of Surface and Ground Waters

1. Background. Surface and ground waters from regional, perimeter, and on-site stations are monitored to provide routine surveillance of Laboratory operations (Figs. 14 and 15, Table G-14). If a sample from a particular station was not taken this year, it was because the station was dry or a water pump was broken. Concentrations of radionuclides in water samples are compared with guides derived from DOE's Radiation Protection Standard (RPS) (Appendix A). Concentration guides do not account for concentrating mechanisms that may exist in environmental media. Consequently, other media such as sediments, soils, and foodstuffs are also monitored (see subsequent sections).

Routine chemical analyses of water samples have been carried out for many constituents over a number of years. Although surface and shallow ground waters are not a source of municipal or industrial water supply, results of these analyses are compared with EPA drinking water standards as these are the most restrictive related to water use.

2. Regional Stations. Regional surface water samples were collected within 75 km (47 mi) of the Laboratory from 6 stations on the Rio Grande, Rio Chama, and Jemez River (Fig. 14). The six sampling stations were located at U.S. Geological Survey Gaging Stations. These waters provided baseline data for radiochemical and chemical analyses in areas beyond the Laboratory boundary. Stations on the Rio Grande were: Embudo, Otowi, Cochiti, and Bernalillo. The Rio Grande at Otowi, just east of Los Alamos, has a drainage area of 37 000 km^2 (14 300 mi^2) in southern Colorado and northern New Mexico. Discharge for the period of record (1895-1905, 1909-1986) has ranged from a minimum of 1.7 m^3/sec (60 ft^3/sec) in 1902 to 691 m^3/sec (24 400 ft^3/sec) in 1920. The discharge for water year 1986 (October 1985 to September 1986) ranged from 12 m^3/sec (408 ft^3/sec) in September to 220 m^3/sec (7900 ft^3/sec) in June (USGS 1987).

The Rio Chama is tributary to the Rio Grande upstream from Los Alamos (Fig. 14). At Chamita on the Rio Chama, the drainage area above the station is 8143 km^2 (3143 mi^2) in northern New Mexico with a small area in southern Colorado. Since 1971, some flow has resulted from transmountain diversion water from the San Juan Drainage. Flow at the gage is governed by release from several reservoirs. Discharge at Chamita during water year 1986 ranged from 1.8 m^3/sec (65 ft^3/sec) in December to 98 m^3/sec (3460 ft^3/sec) in May.

The station at Jemez on the Jemez River drains an area of the Jemez Mountains west of Los Alamos. The Fenton Hill Hot Dry Rock Geothermal Facility

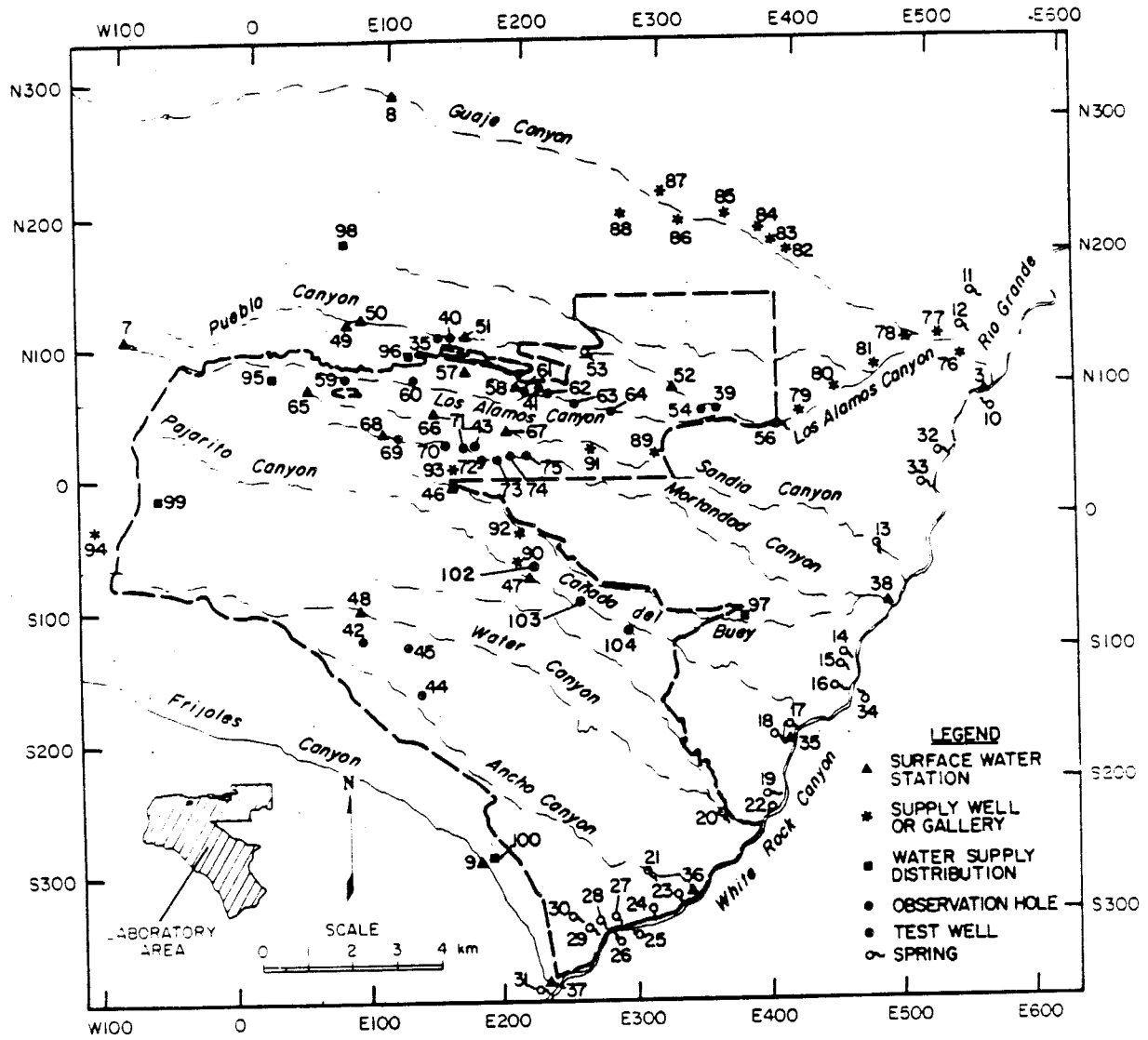

Fig. 15. Surface and ground water sampling locations on and near the Laboratory site.

(TA-57) is located within this drainage. The drainage area is small, about 1220 km^2 (471 mi^2). During water year 1986, discharge ranged from 0.34 m^3/sec (12 ft^3/sec) in February to 54 m^3/sec (1900 ft^3/sec) in July. The river is tributary to the Rio Grande downstream from Los Alamos.

Surface waters from the Rio Grande, Rio Chama, and Jemez River are used for irrigation of crops in the valleys both upstream and downstream from Los Alamos. Water from these rivers is part of recreational areas on state and federal lands.

a. Radiochemical Analyses. Surface water samples from regional stations were collected in February and September 1987. Cesium, plutonium, tritium, and total uranium activity levels in these waters were low (Tables 13 and G-15). Samples collected downgradient from the Laboratory showed no

Table 13. Maximum Concentrations of Radioactivity in Surface and Ground Waters from Off-site and On-site Stations

	Number of Stations[a]	^{137}Cs (10^{-9} µCi/mL)	^{238}Pu (10^{-9} µCi/mL)	$^{239,240}Pu$ (10^{-9} µCi/mL)	^{3}H (10^{-6} µCi/mL)	Total U (µg/L)
Analytical Limits of Detection		40	0.009	0.03	0.7	1.0
Off-site Stations (Uncontrolled Areas)						
Derived Concentration Guide (DCG) for Uncontrolled Areas[b]		3000	400	300	2000	800
Regional	6	1200 (414)	0.011 (0.012)	0.025 (0.014)	0.2 (0.3)	3.0 (1.0)
Perimeter						
Adjacent	6	98 (62)	0.036 (0.016)	0.037 (0.041)	0.4 (0.3)	12.5 (1.3)
White Rock	20	149 (71)	0.027 (0.015)	0.009 (0.006)	13 (1.0)	22 (2.4)
Off-site Station Group Summary:						
Maximum Concentration		1200	0.036	0.037	13	22
Maximum Concentration as % DCG for Uncontrolled Areas		40	<1	<1	<1	3
On-site Stations (Controlled Areas)						
Concentration Guide (CG) for Controlled Areas[b]		400 000	100 000	100 000	100 000	60 000
Noneffluent Areas						
Groundwater (Main Aquifer)	7	136 (63)	0.035 (0.037)	0.022 (0.016)	0.5 (0.3)	0.0 (0.1)
Surface Water	3	44 (55)	0.010 (0.023)	0.006 (0.018)	0.6 (0.3)	7.0 (1.0)
Pajarito Canyon	3	111 (68)	0.035 (0.016)	0.015(0.015)	0.7 (0.3)	1.0 (1.0)

Table 13 (cont)

	Number of Stations[a]	^{137}Cs (10^{-9} µCi/mL)	^{238}Pu (10^{-9} µCi/mL)	$^{239,240}Pu$ (10^{-9} µCi/mL)	^{3}H (10^{-6} µCi/mL)	Total U (µg/L)
Effluent Areas						
Acid-Pueblo Canyon	8	167 (71)	0.010 (0.015)	2.38 (0.126)	1.4 (0.4)	
DP-Los Alamos Canyon	8	188 (86)	0.028 (0.015)	0.124 (0.024)	19 (2.0)	1.0 (1.0)
Sandia Canyon	3	135 (58)	0.002 (0.004)	0.012 (0.032)	0.8 (0.3)	1.8 (0.1)
Mortandad Canyon	7	213 (84)	30.0 (3.00)	90.0 (5.00)	12000 (1000)	5.7 (0.6)
On-site Group Summary:						
Maximum Concentration		213	30.0	90.0	12000	5.7
Maximum Concentration as % CG for Controlled Areas		<1	<1	<1	1	<1

effect from the Laboratory's operation. Results from 1987 exhibited no significant differences from 1986. Maximum concentrations of radioactivity in regional surface water samples were well below DOE's concentration guides for off-site areas.

b. Chemical Analyses. Surface water samples from regional stations were collected in February 1987. Maximum concentrations in regional water samples were well below drinking water standards (Tables 14 and G-16). There were some variations from previous years' results. These fluctuations result from chemical changes that occur with variations in discharges at the sampling stations. This is normal and no inference can be made that the water quality at these stations is deteriorating.

3. **Perimeter Stations.** Perimeter stations within 4 km (2.5 mi) of Los Alamos included surface water stations at Los Alamos Reservoir, Guaje Canyon, Frijoles Canyon, and three springs (La Mesita, Indian, and Sacred springs). Other perimeter stations were in White Rock Canyon along the Rio Grande just east of the Laboratory. Included in this group were stations at 23 springs, 3 streams, and a sanitary effluent release (Fig. 15 and Table G-14).

Los Alamos Reservoir in upper Los Alamos Canyon on the flanks of the mountains, west of Los Alamos, has a capacity of 51 000 m^3 (41 acre-ft) and a drainage area of 16.6 km^2 (6.4 mi^2) above the intake. The reservoir is used for storage and recreation. Water flows by gravity through about 10.2 km (6.4 mi) of water lines for irrigation of lawns and shrubs at the Laboratory's Health Research Laboratory (TA-43), the Los Alamos High School, and University of New Mexico's Los Alamos Branch.

The station in Guaje Canyon is below Guaje Reservoir. Guaje Reservoir in upper Guaje Canyon has a capacity of 0.9 x 10^3 m^3 (0.7 acre-ft) and a drainage area above the intake of about 14.5 km^2 (5.6 mi^2). The reservoir is used for diversion rather than storage as flow in the canyon is maintained by perennial springs. Water flows by gravity through 9.0 km (5.6 mi) of water lines for irrigation of lawns and shrubs at Los Alamos Middle School and Guaje Pines Cemetery. The stream and reservoir are also used for recreation.

The water lines from Guaje and Los Alamos reservoirs are not a part of the municipal or industrial water supply at Los Alamos. They are owned by DOE and operated by Pan Am World Services. Diversion for irrigation is usually from May through October.

Surface flow in Frijoles Canyon was sampled at Bandelier National Monument Headquarters. Flow in the canyon is from spring discharge in the upper reach of the canyon. Flow decreases as the stream crosses Pajarito Plateau because of seepage and evapotranspiration losses. The drainage area above the monument headquarters is about 45 km^2 (17 mi^2) (Purtymun 1980A).

La Mesita Spring is east of the Rio Grande, whereas Indian and Sacred springs are west of the river in lower Los Alamos Canyon. These springs discharge from faults in the siltstones and sandstones of the Tesuque Formation and from small seep areas. Total discharge at each spring is probably less than 1 L/sec (0.3 gal/sec).

Perimeter stations in White Rock Canyon are composed of four groups of springs. The springs discharge from the main aquifer. Three groups (Group I, II, and III) have similar, aquifer-related, chemical quality. Water from these springs is from the main aquifer beneath the Pajarito Plateau (Purtymun 1980B). Chemical quality of Spring 3B (Group IV) reflects local conditions in the aquifer discharging through a fault in volcanics.

Part of the heavy run-off in the Rio Grande in 1987 was stored in Cochiti Reservoir. In October, when the springs were sampled, seven springs were below the reservoir level and could not be sampled.

Three streams that flow to the Rio Grande were also sampled. Streams in Pajarito and Ancho canyons are fed from Group I springs. The stream in Frijoles Canyon at the Rio Grande is fed by a spring on the flanks of the mountains west of Pajarito Plateau and flows through Bandelier National Monument to the Rio Grande.

Treated sanitary effluent from the community of White Rock was also sampled in Mortandad Canyon at its confluence with the Rio Grande.

Detailed results of radiochemical and chemical analyses of samples collected from the perimeter stations are shown in Tables G-17 through G-22.

a. Radiochemical Analyses. Cesium, plutonium, tritium, and total uranium activity for samples collected at perimeter stations were low and well below DOE's concentration guides for off-site areas (Table 13).

Table 14. Maximum Chemical Concentrations in Surface and Ground Waters

	Number of Stations	mg/L				
		Cl	F	NO_3 (as N)	TDS	pH
EPA Drinking Water Standard[a]	--	250	2.0	10	500	6.5-8.5
Off-site Stations						
Regional Stations	6	47	0.8	<1	174	8.3
Perimeter Stations						
Adjacent	6	32	0.5	2	208	8.1
White Rock Canyon	20	43	1.5	12	467	8.6
Summary: Off-site Stations						
Maximum Concentration		47	1.5	12	208	8.6
Maximum Concentration as Per Cent of Standard		19	75	120	42	101
On-site Stations						
Noneffluent Areas						
Ground Water	7	32	0.5	7	253	8.4
Surface Water	3	36	9.3	<1	188	7.8
Pajarito Canyon	3	73	0.6	0.4	462	7.5
Effluent Release Areas						
Acid-Pueblo Canyon	8	86	0.9	6.0	343	8.0
DP-Los Alamos Canyon	8	101	2.5	1.4	306	8.1
Sandia Canyon	3	159	1.0	1.8	1129	7.9
Mortandad Canyon	7	39	3.9	118	1011	9.9
Summary: On-site Stations						
Maximum Concentration		159	9.3	118	1129	9.9
Maximum Concentration as Per Cent of Standard		80	465	1180	225	116

[a]EPA (1976, 1979B).

b. Chemical Analyses. Maximum chemical concentrations in samples from the perimeter stations were within drinking water standards except for nitrate (as N) in waters (sanitary effluent) from Mortandad Canyon at the Rio Grande (Tables 15 and G-20). The effluent also exceeded secondary standards for copper, iron, and pH at the Rio Grande (Table G-21). Table G-22 presents miscellaneous data for chemical quality of water in White Rock Canyon. Concentrations in water samples from the 16 springs and 3 streams in White Rock Canyon were also within drinking water standards.

4. On-site Stations. On-site sampling stations are grouped as those that are not located in effluent release areas and those that are located in areas receiving or that have received treated industrial effluents (Fig. 15, Table G-14).

a. Noneffluent Release Areas. On-site, noneffluent sampling stations consist of seven deep test wells, three surface water sources, and three new, shallow observation wells. The deep test wells are completed into the main aquifer.

Test Wells 1 and 2 are in the lower and middle reaches of Pueblo Canyon. Depths to the top of the main aquifer are 181 to 231 m (594 and 758 ft), respectively. Test Well 3 is in the midreach of Los Alamos Canyon with a depth of 228 m (748 ft) to the top of the main aquifer. These wells are in canyons that have received (Pueblo Canyon) or are now receiving (Los Alamos Canyon) industrial effluents. Test Wells DT-5A, DT-9, and DT-10 are at the southern edge of the laboratory. Depths to the top of the main aquifer are 359, 306, and 332 m (1180, 1006, and 1090 ft), respectively. Test Well 8 is in the midreach of Mortandad Canyon, an area that receives industrial effluents. The top of the aquifer here lies at about 295 m (968 ft) below the surface. These test wells are constructed to seal out all water above the main aquifer. The wells monitor any possible effects that the Laboratory's operation may have on water quality in the main aquifer.

Surface water samples are collected in Canada del Buey and Pajarito and Water canyons downstream from technical areas to monitor the quality of run-off from these sites.

Three shallow observation wells were drilled in 1985 and cased through the alluvium (thickness about 4 m [12 ft]) in Pajarito Canyon (Fig. 15 and Table G-14). Water in the alluvium is perched on the underlying tuff and is recharged through storm run-off. The observation wells were constructed to determine if technical areas in the canyon or adjacent mesas were affecting the quality of shallow ground water (Tables 13, 14, and G-23).

Radiochemical concentrations from surface and ground water sources showed no effects of laboratory operations (Tables 13, G-23, and G-24). Concentrations of tritium, cesium, and plutonium were at or below limits of detection. Concentrations of all radionuclides were well below DOE's concentration guides for on-site areas.

Chemical quality of ground water from the test wells into the main aquifer reflected local conditions of the aquifer around the well. Quality of surface water and of observation wells in Pajarito Canyon varied slightly. The effect, if any, was small, probably as the result of seasonal fluctuations. Maximum concentrations of five chemical constituents in the on-site surface and ground water samples were within drinking water standards, except for fluoride (9.3 mg/L) in water from Canada del Buey (Tables 14, G-25, and G-26).

b. On-site Effluent Release Areas. On-site effluent release areas are canyons that receive or have received treated industrial or sanitary effluents. These include DP-Los Alamos, Sandia, and Mortandad canyons. Also included is Acid-Pueblo Canyon, which is a former release area for industrial effluents. Acid-Pueblo Canyon received untreated and treated industrial effluents, which contained residual radionuclides from 1944 to 1964 (ESG 1981). The canyon also receives treated sanitary effluents from the Los Alamos County treatment plants in the upper and middle reaches of Pueblo Canyon. Sanitary effluents form some perennial flow in the canyon, but do not reach State Road 4.

Water occurs seasonally in the alluvium dependent on the volume of surface flow from sanitary effluents and storm run-off. Hamilton Bend Springs discharges from alluvium in the lower reach of Pueblo Canyon and is dry part of the year. The primary sampling stations are surface water stations at Acid Weir, Pueblo 1, Pueblo 2, and Pueblo 3 (Table G-14). Other sampling stations are Test Well T-2A [drilled to a depth of 40.5 m (133 ft)], which penetrates the alluvium and Bandelier Tuff and is completed into the Puye conglomerate. Aquifer tests indicated the perched aquifer is of limited extent. Water level measurements over a period of time indicate that the perched

Table 15. Average Plutonium Concentrations in Snowmelt Run-off in Canyons Draining the Laboratory

Location	Number of Analyses	Solution		Suspended Sediments	
		^{238}Pu (10^{-9} µCi/mL)	$^{239,240}Pu$ (10^{-9} µCi/mL)	^{238}Pu (pCi/g)	$^{239,240}Pu$ (pCi/g)
Water Canyon at SR-4	8	0.004 (0.011)	0.005 (0.017)	0.056 (0.118)	0.115 (0.268)
Pajarito Canyon at SR-4	14	−0.002 (0.016)	0.013 (0.037)	0.068 (0.138)	0.128 (0.242)
Los Alamos Canyon at SR-4	14	0.006 (0.026)	0.015 (0.015)	0.093 (0.093)	1.96 (1.01)
Pueblo Canyon at SR-4	7	−0.002 (0.016)	0.007 (0.010)	0.016 (0.016)	2.86 (2.38)
Los Alamos Canyon at Otowi	11	0.004 (0.022)	0.007 (0.009)	0.216 (0.561)	0.827 (0.829)
Rio Grande at Otowi	1	−0.016 (0.011)	−0.024 (0.014)	0.001 (0.004)	0.001 (0.002)
Background[a]		0.030	0.026	0.135	0.830

[a] $\bar{x}$ + 2s from Table G-35.

aquifer is hydrologically connected to the stream in Pueblo Canyon.

Perched water in the basaltic rocks is sampled from Test Well 1A, in lower Pueblo Canyon, and Basalt Springs, further eastward in lower Los Alamos Canyon. Recharge to the perched aquifer in the basalt occurs near Hamilton Bend Springs. Travel time from the recharge area near Hamilton Bend Spring to Test Well 1A is estimated to be 1 to 2 months with another 2 to 3 months to reach Basalt Springs.

DP-Los Alamos Canyon has received treated industrial effluents, which contain some radionuclides and some sanitary effluents from treatment plants at TA-21. Treated industrial effluents have been released into the canyon since 1952. During 1987, there were no liquid discharges from TA-21. In the upper reaches of Los Alamos Canyon (above Station LAO-1), there are occasional releases of cooling water from the research reactor at TA-2. Los Alamos Canyon also receives discharge from the lagoons at LAMPF (TA-53). On the flanks of the mountains, Los Alamos Reservoir impounds run-off from snowmelt and rainfall. Stream flow from this impoundment into the canyon is intermittent, dependent on precipitation to cause run-off to reach the laboratory boundary at State Road 4.

Infiltration of treated effluents and natural run-off maintains a shallow body of water in the alluvium of Los Alamos Canyon. Water levels are highest in late spring from snowmelt run-off and late summer from thundershowers. Water levels decline during the winter and early summer as storm run-off is at a minimum. Sampling stations consist of two surface water stations in DP Canyon and six observation wells completed into alluvium (about 66 m [20 ft] thick) in Los Alamos Canyon (Table G-14).

Sandia Canyon has a small drainage area that heads on Pajarito Plateau in TA-3. The canyon receives cooling tower blowdown from the TA-3 power plant and treated sanitary effluents from TA-3. Treated effluents from a sanitary treatment plant form a perennial stream in a short reach of the upper canyon. Only during heavy summer thundershowers in the drainage area does stream flow reach the Laboratory boundary at State Road 4. Two monitoring wells in the lower canyon just west of State Road 4 indicated no perched water in the alluvium in this area. There are three surface water sampling stations in the reach of the canyon that contains perennial flow (Table G-14).

Mortandad Canyon has a small drainage area that heads in TA-3. Industrial liquid wastes containing radionuclides are collected and processed at the Industrial Waste Treatment Plant at TA-50. After treatment that removes most of the radioactivity, the effluents are released into Mortandad Canyon. Velocity of water movement in the perched aquifer ranges from 18 m/day (59 ft/day) in the upper reach to about 2 m/day (7 ft/day) in the lower reach (Purtymun 1974C, 1983). The top of the main aquifer is about 290 m (950 ft) below the perched aquifer. Hydrologic studies in the canyon began in 1960. Since that time, there has been no surface flow beyond the Laboratory's boundary because the small drainage area in the upper part of the canyon results in limited run-off and a thick section of unsaturated alluvium in the lower canyon allows rapid infiltration and storage of run-off when it does occur. Monitoring stations in the canyon are one surface water station (Gaging Station 1, GS-1) and six observation wells completed into the shallow alluvial aquifer. At times, wells in the lower reach of the canyon are dry.

Acid-Pueblo (Table G-27), DP-Los Alamos (Table G-28), Mortandad (Table G-29), and Sandia (Table G-30) canyons all contained surface and shallow ground waters with measurable amounts of radioactivity. Radioactivity is well below DOE's concentration guides for on-site areas (Table 13). Radionuclide concentrations from treated effluents decreased downgradient in the canyon due to dilution and adsorption of radionuclides on alluvial sediments. Surface and shallow ground waters in these canyons are not a source of municipal, industrial, or agricultural supply. Only during periods of heavy precipitation or snowmelt would waters from Acid-Pueblo, DP-Los Alamos, or Sandia canyons extend beyond Laboratory boundaries and reach the Rio Grande. In Mortandad Canyon there has been no surface run-off to the Laboratory's boundary since hydrologic studies were initiated in 1960. This was 3 years before the treatment plant at TA-50 began releasing treated effluents into the canyon (Purtymun 1983).

Relatively high concentrations of chlorides, nitrates, fluorides, and total dissolved solids have resulted from effluents released into some of the canyons (Tables G-31 through G-34). Relatively high fluoride and nitrate concentrations were found in waters from Mortandad Canyon, which receives the largest volume of industrial effluents (Purtymun 1977). Though the concentrations of some chemical constituents in the waters of these canyons were high

when compared with drinking water standards (Table 14), these on-site waters are not a source of municipal, industrial, or agricultural supply.

Maximum chemical concentrations occurred in water samples taken near treated effluent outfalls (Table G-31 through G-34). Chemical quality of the water improved downgradient from the outfalls. Surface flows in Acid-Pueblo and DP-Los Alamos canyons reach the Rio Grande only during spring snowmelt or heavy summer thunderstorms. There has been no surface run-off to Laboratory boundaries recorded in Mortandad Canyon since 1960, when observations began.

5. Transport of Radionuclides in Surface Run-Off. The major transport of radionuclides from canyons that have received treated, low-level radioactive effluents is by surface run-off. Radionuclides in the effluents may become adsorbed or attached to sediment particles in the stream channels. Concentrations of radioactivity in the alluvium is highest near the treated effluent outfall and decreases in concentration downgradient in the canyon as the sediments and radionuclides are transported and dispersed by other treated industrial effluents, sanitary effluents, and surface run-off.

Surface run-off occurs in two modes. Spring snowmelt run-off occurs over a long period of time (days) at a low discharge rate and sediment load. Summer run-off from thunderstorms occurs over a short period of time (hours) at a high discharge rate and sediment load. During 1987, no summer run-off samples were collected.

Spring snowmelt samples of run-off from 13 stations (Fig. 16) were analyzed for radionuclides in solution and suspended sediments. Radioactivity in solution is defined as the filtrate passing through a 0.45 μm pore-size filter, whereas radioactivity in suspended sediments is defined as a residue on the filter. For background samples, the solution was analyzed for ^{3}H, ^{137}Cs, total U, ^{238}Pu, $^{239,240}Pu$, and gross gamma, whereas suspended sediments were analyzed for ^{238}Pu and $^{239,240}Pu$. Only plutonium was analyzed in samples from the other stations.

Background values are presented in Table G-35. Plutonium levels at the six sampling stations were below background (Tables 15 and G-36). Suspended sediments collected in Los Alamos Canyon at SR-4 contained ^{238}Pu above background levels; $^{239,240}Pu$ in sediments from Los Alamos and Pueblo Canyon at SR-4 were above background. Los Alamos Canyon and Pueblo Canyon west of SR-4 have received treated effluents containing plutonium. The plutonium in the suspended sediments in these canyons are dispersed and diluted by storm run-off before reaching the Rio Grande. The plutonium in suspended sediments from Los Alamos Canyon was below background in the Rio Grande (Table 15).

In lower Mortandad Canyon just below Well MCO-7 (Fig. 15 and Table G-14), three sediment traps were constructed. The upper part of the canyon receives treated, low-level radioactive effluents from the treatment plant at TA-50. A run-off event into the upper sediment trap in June was sampled for radionuclides. Transuranics in solution and in suspended sediments was above background indicating run-off transport from the upper canyon (Table G-37).

C. Radioactivity in Soils and Sediments

1. Background Levels of Radioactivity in Soils and Sediments. Samples were routinely collected and analyzed for radionuclides from regional stations from 1974 through 1985 (Purtymun 1987A). They were used to establish background levels of ^{137}Cs, ^{238}Pu, $^{239,240}Pu$, ^{90}Sr, total U, ^{3}H, and gross gamma radioactivity in soils and sediments (Table 16). Average concentrations plus twice the standard deviation were used to establish the upper limits of the background concentrations. The number of analyses used to establish background levels ranged from 29 (^{90}Sr) to 76 (^{238}Pu, $^{239,240}Pu$) for soils and 36 (^{90}Sr) to 113 (^{238}Pu, $^{239,240}Pu$) for sediments. Samples were collected from 5 regional soil stations and 10 regional sediments stations. Background concentrations may be exceeded slightly by 1987 surveillance results due to changes in instrument background or a modification of analytical procedures. See Appendix B for description of methods for collection of soil and sediment samples.

2. Regional Soils and Sediments. Regional soil and sediment samples were collected in the same general locations as the regional water samples (Fig. 14). Additional regional sediment samples were collected along the Rio Grande from Otowi Bridge to Cochiti Reservoir. The locations are listed in Table G-38 and the detailed results of radiochemical analyses of the regional soils and sediments are in Table G-39.

In 1987, soil and sediment samples were collected from seven stations and analyzed for six types of radioactivity (Table 16). Radioactivity ranged within background as reported by Purtymun (1987A).

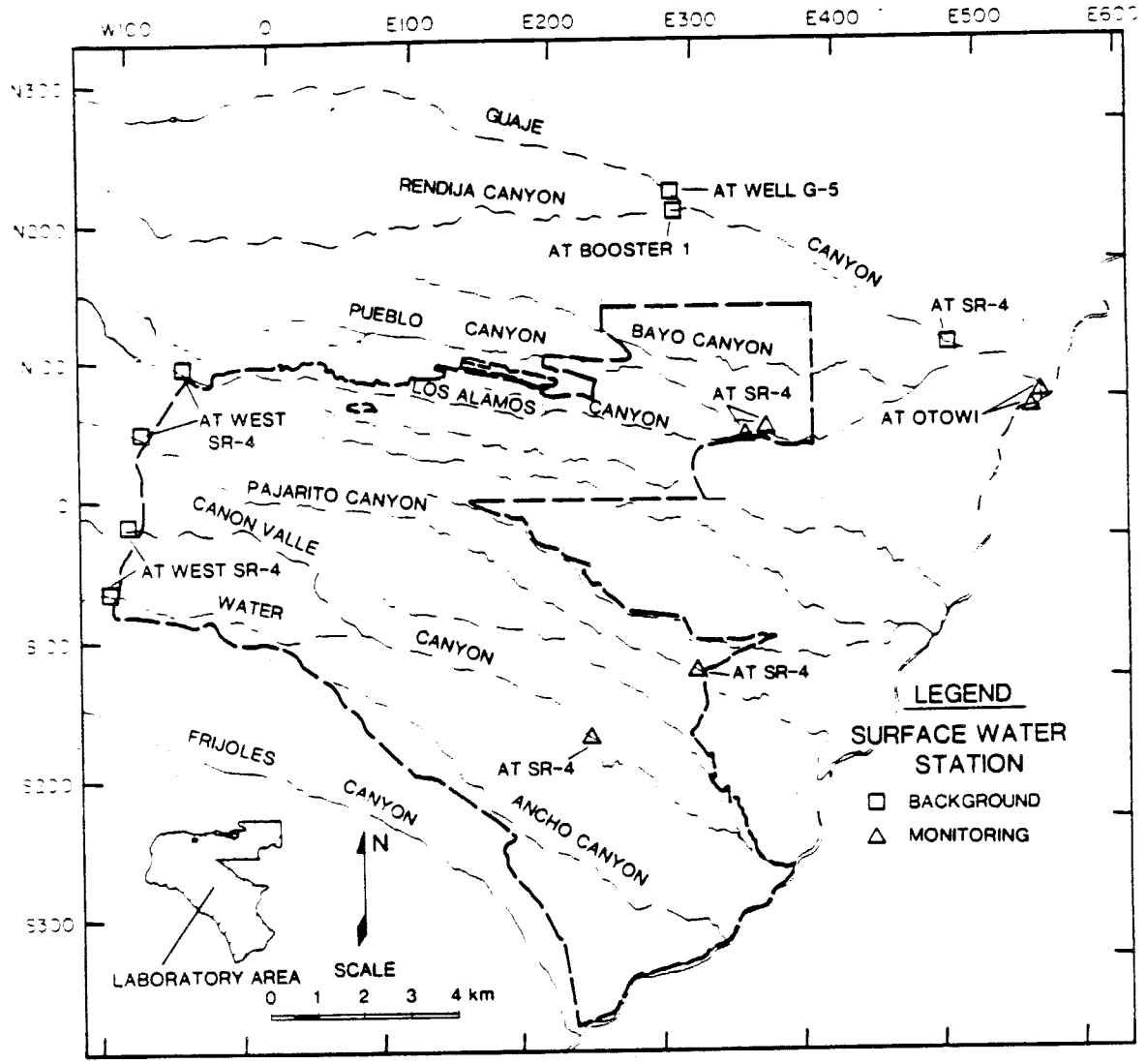

Fig. 16. Locations of surface run-off sampling stations at the Laboratory.

3. Perimeter Soil and Sediments. Six perimeter soil stations were sampled within 4 km (2.5 mi) of the Laboratory. Seventeen sediment stations near the Laboratory boundary and in intermittent streams that cross the Pajarito Plateau were also sampled (Figs. 17 and 18). The perimeter soil and sediment sampling stations are listed in Table G-38 and detailed analytical results are found in Table G-40.

Analyses of the perimeter soil samples indicated that background concentrations were slightly exceeded in 1987 for ^{238}Pu (one sample), ^{239,240}Pu (one sample), and ^{137}Cs (one sample). Uranium and gross gamma levels result from naturally occurring radiation in soil and sediments (Table 16).

Analyses of sediments from the 17 perimeter stations indicated that concentrations of most radionuclides were below background levels with the exception of total uranium, which exceeded background in one sample (Table 16).

Table 16. Maximum Concentrations of Radioactivity in Soils and Sediments from Regional, Perimeter, and On-site Stations

	Number of Stations	^{3}H (10^{-6} µCi/mL)	^{137}Cs (pCi/g)	Total U (µg/g)
Analytical Limits of Detection	--	0.7	0.1	0.03
Soil				
Background (1974-1986)[a]	--	7.2	1.09	3.4
Regional Stations	7	13	0.60	5.4
Perimeter Stations	6	2.8 (0)[c]	1.3 (1)	5.3 (5)
On-site Stations	10	10 (1)	0.79 (0)	4.6 (7)
Sediments				
Background (1974-1986)[a]	--	13	0.44	4.4
Regional Stations[b]	7	0.7	0.38	8.5
Perimeter Stations	17	0.5 (0)	0.39 (0)	3.2 (0)
On-site Station, Effluent Release Areas				
Acid-Pueblo Canyon	6	---	0.27 (0)	3.4 (0)
DP-Los Alamos Canyon	11	---	10.7 (6)	5.0 (1)
Mortandad Canyon	7	---	38 (3)	4.8 (1)

---

[a] $\bar{x}$ + 2s of a number of background analyses for soils and bed sediments (Purtymun 1987).
[b] Regional background 1987.
[c] Number in parentheses indicates number of stations exceeding background concentrations.

Table 16 (cont)

	Number of Stations	^{238}Pu (pCi/g)	$^{239,240}Pu$ (pCi/g)	Gross Gamma (Counts/min/g)
Analytical Limits of Detection	--	0.003	0.002	0.1
Soil				
Background (1974-1986)[a]	--	0.005	0.025	6.6
Regional Stations[b]	7	0.002	0.016	6.4
Perimeter Stations	6	0.029 (1)	0.026 (1)	9.0 (4)
On-site Stations	10	0.005 (0)	0.038 (1)	7.5 (3)
Sediments				
Background (1974-1986)[a]	--	0.006	0.023	7.9
Regional Stations[b]	7	0.001	0.007	3.8
Perimeter Stations	17	0.002 (0)	0.006 (0)	2.5 (0)
On-site Station, Effluent Release Areas				
Acid-Pueblo Canyon	6	0.026 (1)	0.612 (3)	0.8 (0)
DP-Los Alamos Canyon	11	0.196 (8)	0.615 (10)	5.8 (0)
Mortandad Canyon	7	7.59 (2)	30.7 (2)	54 (2)

---

[a] $\bar{x}$ + 2s of a number of background analyses for soils and bed sediments (Purtymun 1987).
[b] Regional background 1987.
[c] Number in parentheses indicates number of stations exceeding background concentrations.

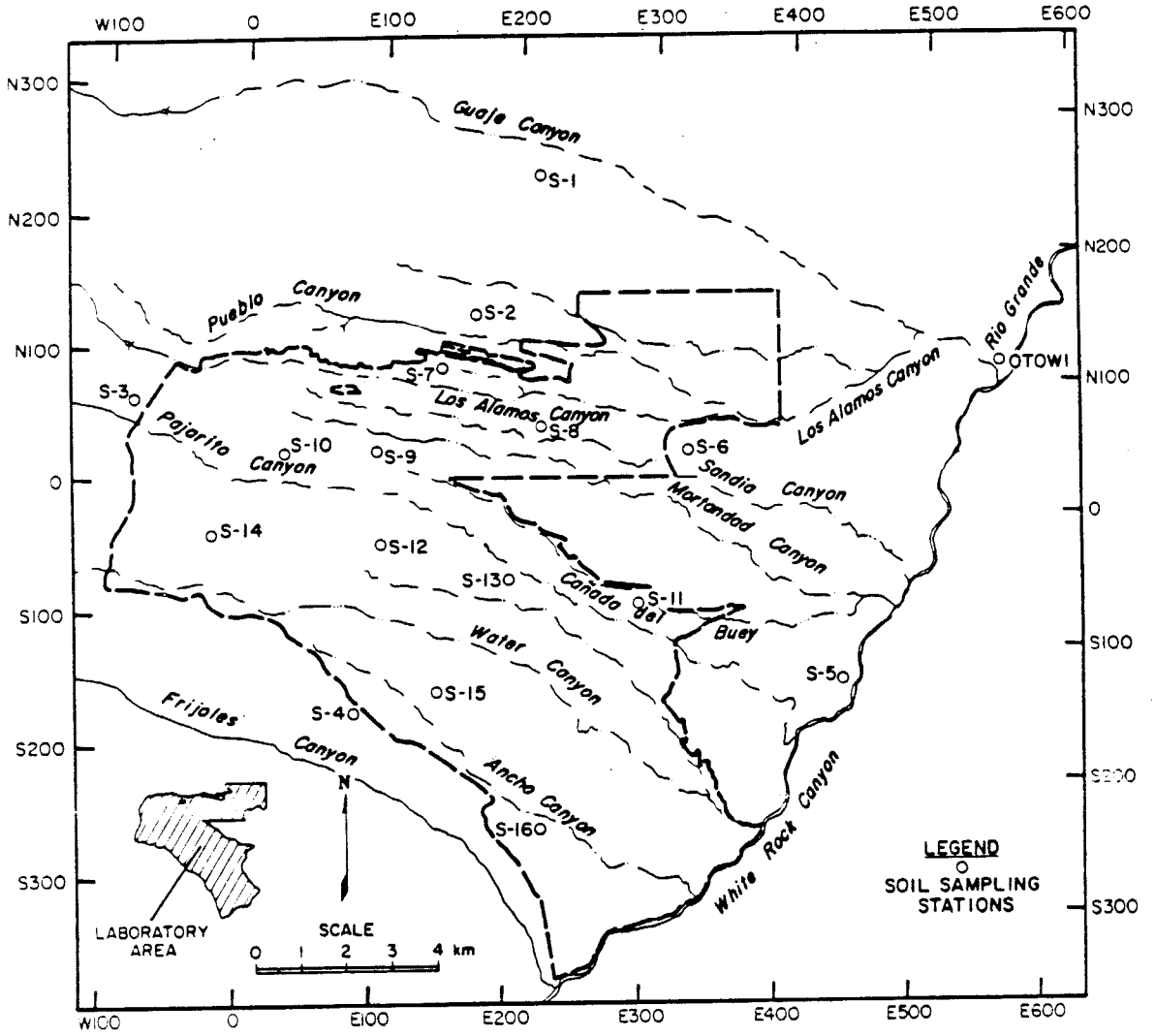

Fig. 17. Soil sampling on an near the Laboratory site.

4. On-site Soils and Sediments. On-site soil samples were collected from 10 stations within the Laboratory boundaries. On-site sediments were collected from 24 stations within areas that have received treated liquid effluent (Table G-38, Figs. 17 and 18).

The maximum ^{137}Cs and ^{238}Pu concentrations in the 10 soil samples were below regional background levels (Tables 16, G-41, and G-42). The concentrations of $^{239,240}Pu$ at two stations (near TA-55, Plutonium Facility) were above background (Tables 16 and G-42). The ^{3}H concentrations from soil at two stations (one near TA-33, Tritium Facility) were above background. The uranium background concentration was exceeded at seven stations, and gross gamma background activity was exceeded at three stations. Uranium and gross gamma are low and do not reflect contamination from Laboratory operations but rather variation in natural radioactivity in the soil minerals.

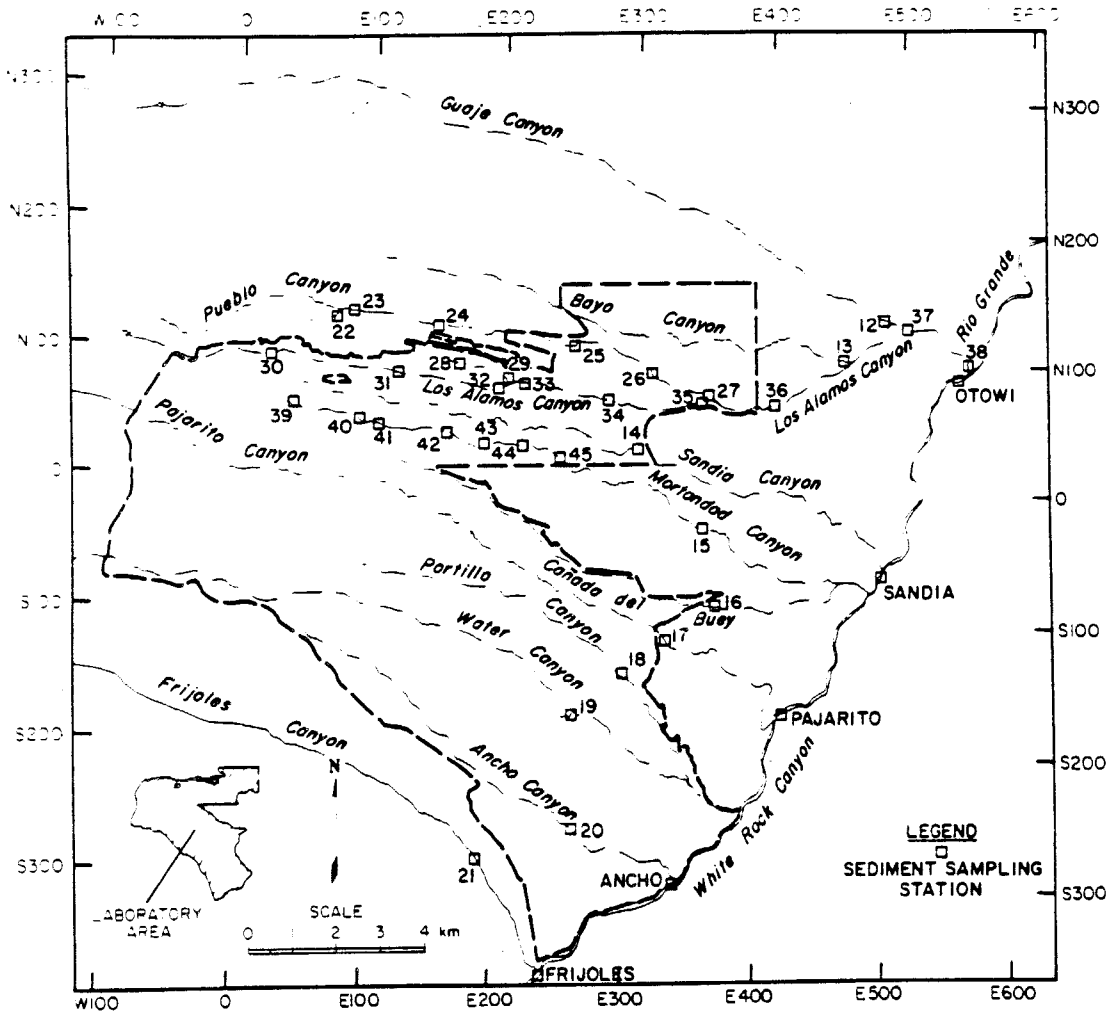

Fig. 18. Sediment sampling locations on and near the Laboratory site.

Three canyons received or are receiving treated, low-level radioactive effluents: Acid-Pueblo, DP-Los Alamos, and Mortandad canyons. The concentrations of radionuclides in these canyons exceeded regional background levels (Table 16). The concentrations in sediments of Pueblo and DP-Los Alamos canyons decrease downgradient as the radionuclides are dispersed and mixed with uncontaminated sediments (Tables G-41 and G-42). The concentrations in Mortandad also decrease downgradient in the canyon; however, the concentrations at the Laboratory boundary do not indicate any transport to this point or beyond. The radionuclides in these canyons are derived from low-level radioactive effluents released from the treatment plants. The concentrations are low and pose no health or environmental problems.

5. Sediments in Regional Reservoirs. Reservoir sediments were collected from three stations in Abiquiu Reservoir on the Rio Chama and three stations in Cochiti Reservoir on the Rio Grande south of Los Alamos (Fig. 19). The samples were analyzed for ^{238}Pu and ^{239,240}Pu using 1 kg (2 lb, dry weight) samples (100 times the usual mass used for analyses)

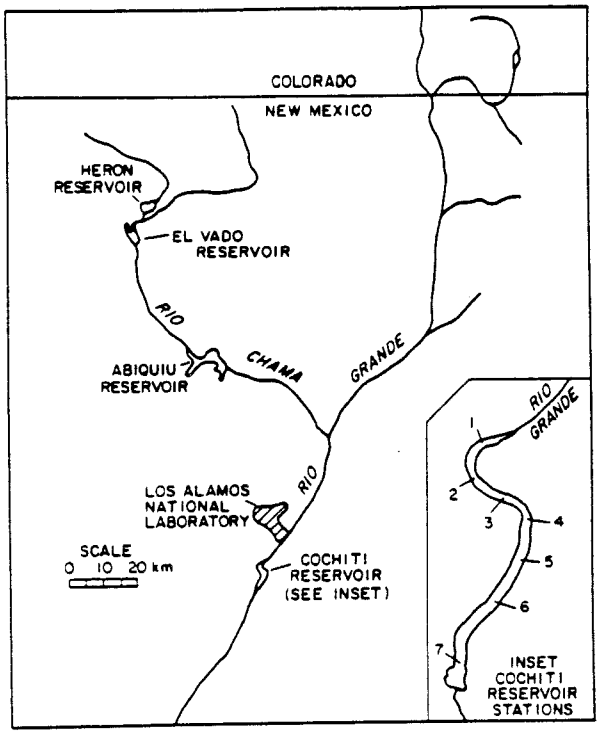

Fig. 19. Special regional sediment sampling locations.

of regular sediments. These large samples increase the sensitivity of the plutonium analyses, which is necessary to effectively evaluate background plutonium concentrations in fallout from atmospheric tests.

Average ^{238}Pu concentrations ranged from 0.00003 pCi/g to 0.00135 pCi/g; ^{239,240}Pu concentrations were slightly higher, ranging from 0.00020 pCi/g to 0.02910 pCi/g (Table 17). The distribution of plutonium was similar to samples collected in previous years (1979, 1982, 1984, 1985, and 1986). Analyses of the current and previous years' data revealed significantly higher levels ($p<0.05$) of plutonium in Cochiti than in Abiquiu reservoir. Sediments in Cochiti reservoirs contained a higher fraction of finer particles and organic materials than sediments from Abiquiu. These features enhance the capacity of the sediment to adsorb plutonium and other metal ions. The difference does not appear to be attributable to Laboratory operations. The ratios of ^{239,240}Pu to ^{238}Pu in the Cochiti sediments do not differ significantly from the ratio characteristic of worldwide fallout, about the same as found in sediment at Abiquiu Reservoir. The plutonium concentrations in sediments from the two reservoirs are low, within the range of worldwide fallout and are not a health or environmental concern.

6. Transport in Sediments and Run-Off from an Active Waste Management Area (Area TA-54). Radionuclides transported by surface run-off have an affinity for attachment to sediment particles by ion exchange or adsorption. Thus, radionuclides in surface run-off tend to concentrate in sediments. Nine sampling stations were established in 1982 outside the perimeter fence at Area G (TA-54) to monitor possible transport of radionuclides by storm run-off from the waste storage and disposal area (Fig. 20). The samples collected in September 1987 for radiochemical analyses were lost, and another set collected in February 1988 will be reported with 1988 monitoring data.

All surface run-off from Area L is into Canada del Buey. Sediment samples were analyzed for a number of inorganics (Table G-43). Eight constituents have EPA criteria set for toxic concentrations. The inorganics analyzed for EPA's Extraction Procedure (EP) toxicity criteria were well below criteria concentrations and below limits of detection. The other five were at or below limits of detection. The pH was slightly alkaline, ranging from 7.0 to 8.0.

Table 17. Radiochemical Analyses of Sediments from Reservoirs on the Rio Chama and Rio Grande[a]

Reservoir	^{137}Cs (pCi/g)	Total U (μg/g)	^{90}Sr (pCi/g)	^{238}Pu (pCi/g)	$^{239,240}Pu$ (pCi/g)	Ratio of $^{239,240}Pu$ to ^{238}Pu
Rio Chama						
Abiquiu Reservoir						
Upper	0.10 (0.08)	3.3 (0.3)	0.00 (0.10)	0.00009 (0.00002)	0.00020 (0.00011)	--
Middle	0.21 (0.09)	3.8 (0.4)	-0.03 (0.10)	0.00020 (0.00004)	0.00502 (0.00026)	--
Lower	0.35 (0.11)	3.6 (0.4)	-0.10 (0.20)	0.00024 (0.00003)	0.00602 (0.00026)	--
$\bar{x}$ (s)	0.22 (0.13)	3.6 (0.25)	-0.04 (0.5)	0.00018 (0.00008)	0.00375 (0.00311)	21
Rio Grande						
Cochiti Reservoir						
Upper	0.26 (0.11)	3.8 (0.4)	0.07 (0.05)	0.00003 (0.00001)	0.00256 (0.00011)	--
Middle	0.15 (0.09)	3.8 (0.4)	0.03 (0.06)	0.00110 (0.00006)	0.02970 (0.00107)	--
Lower	0.51 (0.12)	3.8 (0.4)	0.08 (0.09)	0.00135 (0.00010)	0.02020 (0.00089)	--
$\bar{x}$ (s)	0.31 (0.18)	3.8 (0.0)	0.06 (0.03)	0.00083 (0.00070)	0.01749 (0.01377)	21

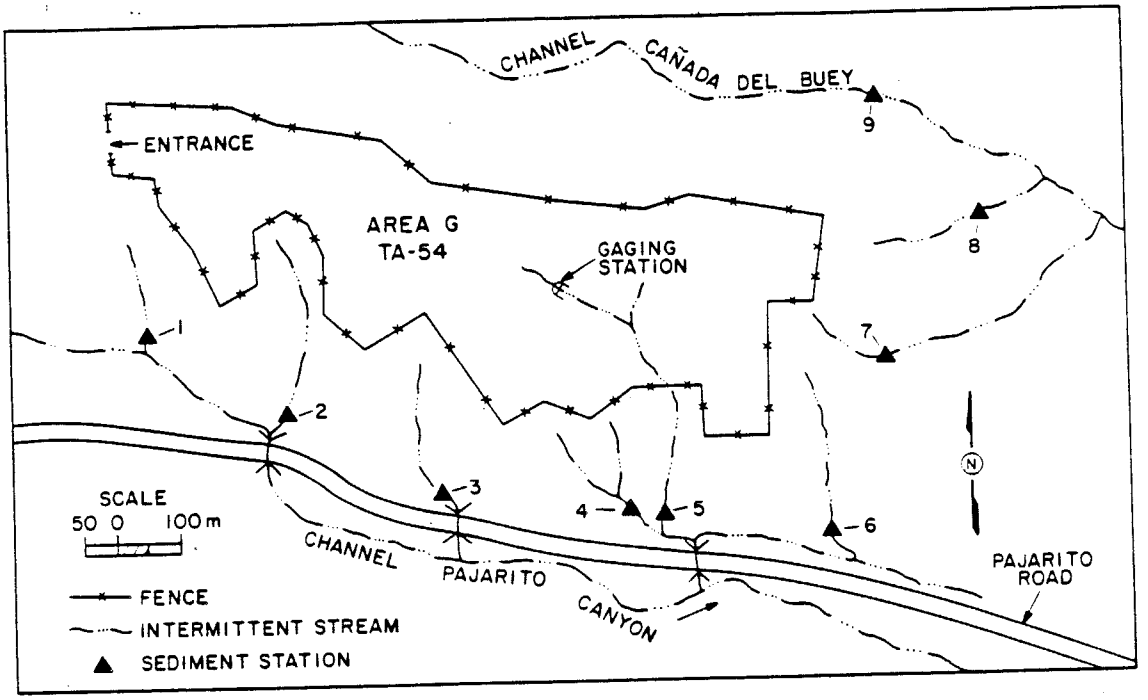

Fig. 20. Surface water gaging station in Area G (TA-54) and sediment sampling stations adjacent to Area G.

VII. FOODSTUFFS MONITORING

Most produce, fish, and honey samples collected near the Laboratory showed no influence from Laboratory operations. Some on-site samples contained slightly elevated levels of tritium and uranium. Concentrations of radionuclides in foodstuffs contributed only a minute fraction of the Laboratory's contribution to individual and population doses received by the public.

A. Background

Produce, garden soil, fish, and honey have been routinely sampled to monitor for potential radioactivity from Laboratory operations. Produce and honey collected in the Espanola Valley and fish collected at Abiquiu Reservoir are not affected by Laboratory operations (Fig. 21). These regional sampling locations are upstream from the confluence of the Rio Grande and intermittent streams that cross the Laboratory. They are also sufficiently distant from the Laboratory as to be unaffected by airborne emissions (Sec. V). Consequently, these regional areas are used as background sampling locations for the foodstuffs sampling program.

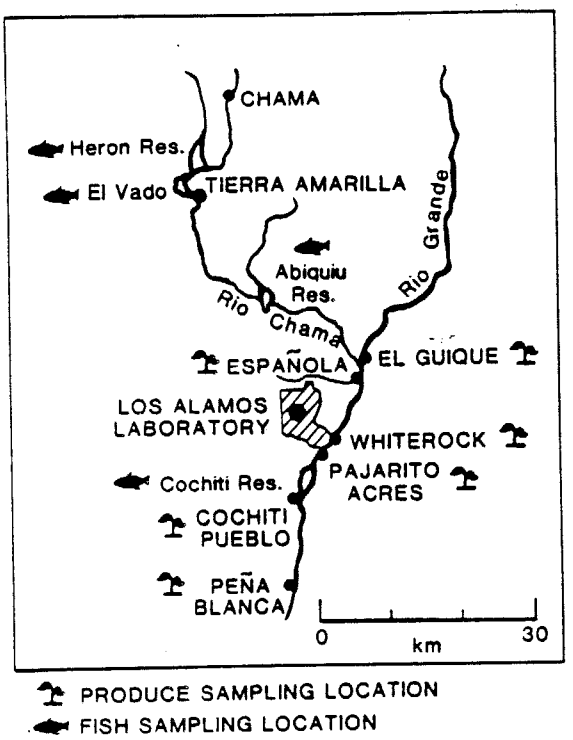

Fig. 21. Fish and produce sampling locations.

B. Produce

Data in Table G-44 summarize produce sample results for ^{3}H (in tissue water), ^{90}Sr, ^{137}Cs, ^{238}Pu, $^{239,240}Pu$, and total uranium. Sampling and preparation methods are described in Appendix B.

Concentrations of ^{137}Cs, ^{238}Pu, and $^{239,240}Pu$ in produce from regional, perimeter, and on-site sampling locations were statistically indistinguishable (one-way analysis of variance at the 95% confidence level). Significantly higher levels of ^{3}H ^{90}Sr, and uranium were found in on-site produce than in produce from some other sites.

Elevated radionuclide levels in on-site samples are probably the result of Laboratory operations. However, on-site produce is not a regular component of the diet of either Laboratory employees or the general public. The Laboratory contributions to doses received in produce consumption pose no threat to the health and safety of the general public (Sec. III).

C. Fish

Fish were sampled in two reservoirs (Fig. 21). Abiquiu Reservoir is upstream from the Laboratory on the Rio Chama and serves as a background sampling location. Cochiti Reservoir could potentially be affected by Laboratory effluents because it is downstream from the Laboratory on the Rio Grande. Sampling procedures are described in Appendix B. Edible tissue was radiochemically analyzed within fish species for ^{90}Sr, ^{137}Cs, ^{238}Pu, $^{239,240}Pu$, and total uranium.

Results for fish are presented in Table G-45. For ^{137}Cs, ^{238}Pu, and $^{239,240}Pu$, no differences were apparent (two-factor analysis of variance, 95% confidence level) between the upstream and downstream samples.

Thus, significantly higher concentrations of plutonium in Cochiti sediments (Table 17) were not reflected in the food chain. In some previous years, higher levels of ^{137}Cs had been observed in fish upstream. As in previous years, uranium levels within species exhibited distinct patterns. Body burdens in bottom-feeding catfish tended to be higher than those found in crappie. Uranium levels were significantly higher in Cochiti fish, although the difference remained low (6 $\mu g/g$). Levels of ^{90}Sr in crappie were significantly higher in upstream samples, reflecting increased global fallout at higher elevations.

The data indicate that Laboratory operations do not result in significant doses received by the general public consuming fish from Cochiti Reservoir (Sec. III).

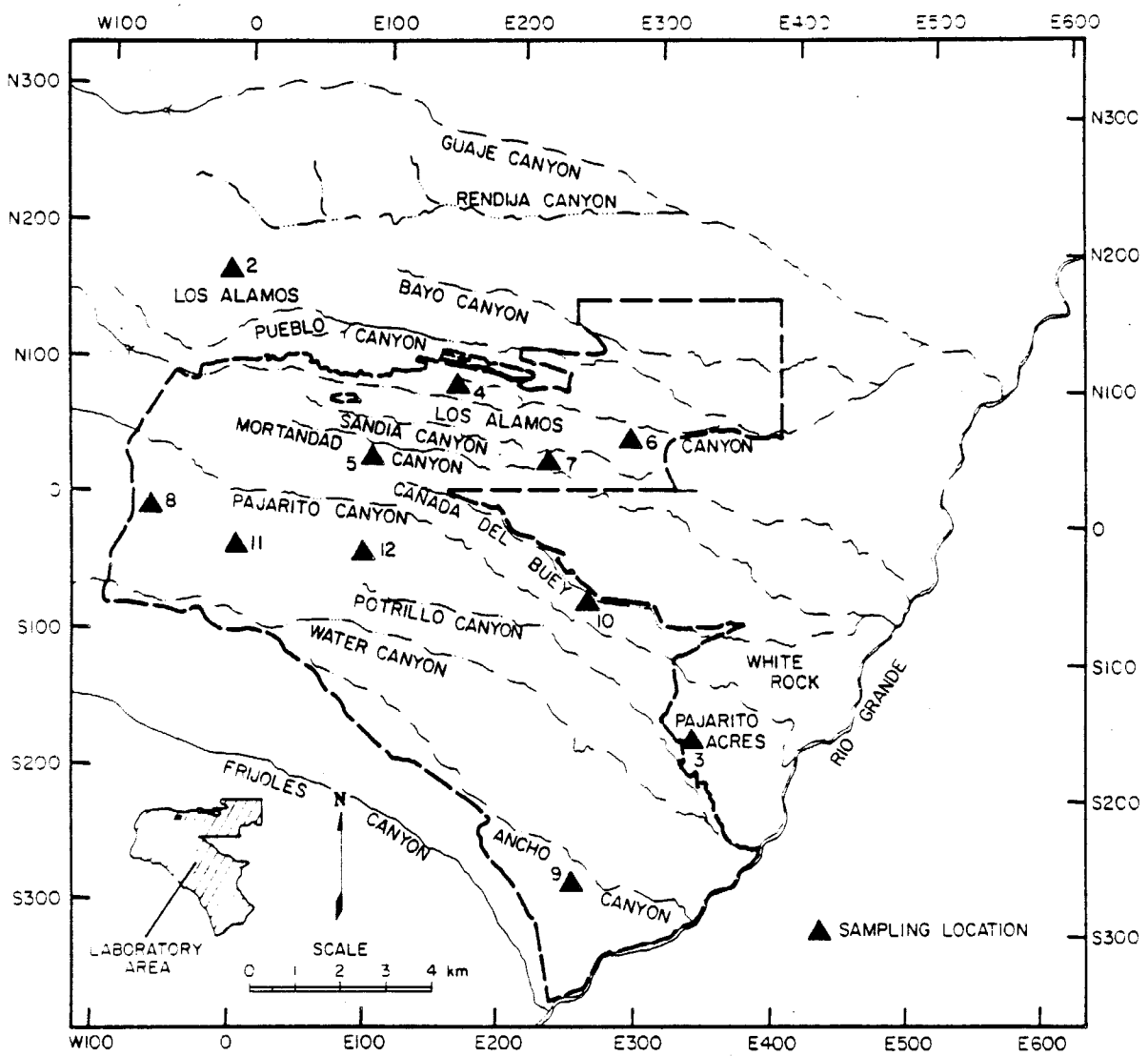

Fig. 22. Locations of beehives.

VIII. ENVIRONMENTAL COMPLIANCE

In accordance with the policy of the Department of Energy, the Laboratory complies with federal and state environmental requirements. These requirements address handling, transport, release, and disposal of hazardous materials as well as protection of ecological, archaeological, historical, atmospheric, and aquatic resources. The Laboratory is currently applying for federal and state permits for operating hazardous waste storage areas as well as renewing a permit for discharge of liquid effluents. The Laboratory was in compliance with treated liquid discharge permit limits in 96% and 99% of monitoring analyses from sanitary and industrial effluent outfalls, respectively. Sanitary waste treatment facilities are currently being upgraded to improve compliance. All airborne releases were well within regulatory limits during 1987. A total of 180 asbestos removal jobs were carried out during the year, and appropriate notification was provided to state regulators. Concentrations of constituents in the drinking water distribution system remained within federal water supply standards, although a few constituents exceeded limits at the wellhead. The Laboratory carried out two mitigation actions at cultural sites. During 1987, 21 documents were prepared to ensure environmental compliance by new Laboratory activities.

A. Resource Conservation and Recovery Act (RCRA)

1. Background. The Resource Conservation and Recovery Act (RCRA) (as amended by the Hazardous and Solid Waste Amendments of 1984 [HSWA]) mandates a comprehensive program to regulate hazardous wastes from generation to ultimate disposal. Major emphasis of the amendments is to reduce hazardous waste volume and toxicity and to minimize land disposal of hazardous waste. Major requirements under HSWA that impact waste handling at the Laboratory are presented in Table 18.

The EPA has granted New Mexico interim RCRA authorization transferring regulatory control of hazardous wastes to the state's Environmental Improvement Division (NMEID). State authority for hazardous waste regulation is the New Mexico State Hazardous Waste Act and Hazardous Waste Management Regulation (HWMR). However, NMEID has not yet obtained authorization for implementing all of the 1984 RCRA amendments.

The Laboratory produces a wide variety of hazardous wastes. Small volumes of all chemicals listed under 40 CFR 261.33 could occur at the Laboratory as a result of ongoing research. Process wastes are generated from ongoing manufacturing operations that support research, such as liquid wastes from circuit board preparation and lithium hydride scrap from metal machining. Although they occur in larger volumes than discarded laboratory chemicals, process wastes are few in number, well defined, and not acutely toxic. High-explosive wastes include small pieces of explosives and contaminated sludges that are thermally treated on-site.

2. Permit Application. The Los Alamos Area Office of DOE has submitted both Part A and Part B applications under RCRA and the New Mexico Hazardous Waste Act for the Laboratory (Table 19). In response to changes in waste handling, comments from NMEID, and changes in regulations, DOE submitted revised applications in November 1987.

Landfilling of hazardous wastes was discontinued in 1985, and existing landfills will be closed under interim authority after the NMEID approves closure plans. Storage facilities holding wastes for less than 90 days need not obtain a Part B permit. All facilities listed in Table G-49 as having interim status, but not included in the Part B application, must be closed before the application is approved.

3. Area P Landfill and Lagoons. The Area P landfill and surface impoundment are located in a remote area of the northeastern section of TA-16, adjacent to burning pads. The landfill was used from the

Table 18. Major Regulatory Requirements of the Hazardous and Solid Waste Amendments of 1984 Impacting Waste Management at Los Alamos National Laboratory

The Hazardous and Solid Waste Amendments of 1984:

- o prohibit placement of bulk liquids, containerized liquid hazardous waste, or free bulk or free liquids, even with adsorbents, in landfills.
- o prohibit landfill disposal of certain waste and require that the EPA review all listed wastes to determine their suitability for land disposal.
- o establish minimum technology requirements for landfills to include double liners and leak detection.
- o require EPA to establish minimum technology requirements for underground tanks.
- o require that generators of manifested wastes certify that they have minimized the volume and toxicity of wastes to the degree economically feasible.
- o require that the operators of landfills or surface impoundments certify that a ground water monitoring program is in place or a waiver demonstrated by November 8, 1985, with failure to do so resulting in loss of interim status on November 23, 1985.
- o require that federal installations submit an inventory of hazardous waste facilities by January 31, 1986.
- o require the preparation by August 8, 1985, of a health assessment for landfills and surface impoundments seeking a Part B permit.

early 1950s until about 1982 to dispose of high-explosive (HE) contaminated materials. The surface impoundment received filtered liquid extract from HE contaminated wastewater associated with activities at Buildings 401 and 406. Both sites received soluble barium nitrate in excess of EPA's criteria for defining toxic materials and are considered to contain hazardous wastes under RCRA. Neither site was included in the Laboratory's original or updated RCRA permit applications. The Laboratory chose to separately close each of these sites under 40 CFR 265 interim status standards. Appropriate closure and post-closure plans were submitted to New Mexico's EID in 1985, and both plans are awaiting final approval.

A modified landfill closure and post-closure plan was prepared for submittal to the NMEID in late 1987. Modifications were necessary because the landfill will eventually be subject to permitted standards under 40 CFR 264 once the NMEID issues the Laboratory its RCRA permit. Furthermore, HSE-8 desired to establish a 30-year post-closure ground water monitoring plan that would be consistent with regard to monitoring parameters and would fulfill requirements under both interim and permitted standards. To this end, HSE-8 personnel constructed nine ground water monitoring wells and five neutron moisture access monitoring wells. To date no recoverable amounts of ground water have been observed; average unsaturated gravimetric borehole moisture contents range from 2% to 24%. Based on these and other hydrogeologic data, a ground water monitoring waiver was requested from the NMEID in December 1987. If this waiver is eventually approved, then the 30-year,

Table 19. Enviromental Permits Under Which the Laboratory Operated in 1987

Type	Permitted Activity	Issue Date	Expiration Date	Administering Agency
RCRA Hazardous Waste Facility	Hazardous Waste Handling	Revised Application Submitted November 1987	--	NMEID[a]
PCB	Disposal of PCBs	June 5, 1980	--	EPA[b]
PCB Oil	Incineration of PCB Oils	May 21, 1984	--	EPA
NPDES-Los Alamos	Discharge of Industrial and Sanitary Liquid Effluents	Modified Permit May 29, 1987	March 1, 1991	EPA
NPDES-Fenton Hill	Discharge of Industrial and Sanitary Liquid Effluents	October 15, 1983[c]	--	EPA
Ground Water Discharge Plan-Fenton Hill	Discharge to Ground Water	June 5, 1985	June 1990	NMOCD[d]
NESHAPS	Construction and Operation of Four Beryllium Facilities	December 26, 1985 and March 19, 1986	--	NMEID
Open Burning	Burning at TA-16-412	May 26, 1987	May 26, 1988	NMEID

[a] New Mexico Enviromental Improvement Division.
[b] US Enviromental Protection Agency.
[c] Renewal pending.
[d] New Mexico Oil Conservation Division.

post-closure ground water monitoring requirements at the landfill will be terminated.

Closure and post-closure plans for the lagoon did not require modification because all of the impoundment's wastewater was completely removed in 1987 and shipped off-site for final treatment and disposal. In addition, the lagoon's synthetic membrane underliner was completely removed along with all contaminated subbase soils. This "clean" closure approach dictates interim status standards be followed rather than permitted standards since it occurred prior to the issuance of a RCRA permit. Furthermore, this lagoon closure plan does not require the typical 30-year, post-closure care requirements for in situ closure. The same process could not be used for the landfill because explosion hazards preclude landfill excavations.

4. Other RCRA Activities. Areas L and G are located at TA-54 on Mesita del Buey and have been used for disposal of hazardous wastes and are subject to RCRA regulation. A ground water monitoring waiver application for both Area L and Area G has been submitted to the NMEID. Vadose zone (partially saturated zone above the water table) monitoring beneath the landfills and perched water monitoring in the adjacent canyons is being conducted to support this application (Sec. IX). Quarterly reports of the pore gas sampling and perched water analysis have been submitted to the NMEID.

Table G-49 lists several storage areas and one thermal treatment area currently under interim status but for which a Part B permit is not being sought. Area TA-3-102, used to store drummed lithium hydride scrap, will be closed under interim authority in 1988 and reopened as a <90-day storage area. Areas TA-22-24 and TA-40-2 are magazines used for storage of high-explosive wastes. These will be closed to waste storage in 1988 and replaced by other satellite storage units. The TA-40 scrap detonation pit used for destroying scrap high explosives has been closed to waste detonation. All scrap generated will be handled at other detonation sites included in the Part B application. Closure plans for these facilities have been submitted to NMEID.

A controlled air incinerator with interim status for treating hazardous waste is located at TA-50-37. A trial burn was conducted in October 1986. The raw data were submitted to the NMEID in December 1986 and a final report for the test burn was submitted on March 5, 1987. These data and report will support the laboratory's application for a hazardous waste permit for this facility.

An inventory of underground storage tanks (UST) was submitted to the NMEID on May 5, 1986, in accordance with the Hazardous and Solid Waste Amendments. A revised inventory has been completed. Some tanks have been removed and others added including one at the Life Sciences Division's facility at Kirtland Air Force Base. A total of 104 tanks are now identified for the underground storage of regulated substances under Subtitle I of RCRA. Nine unused USTs were removed during 1987 and disposed of along with any contaminated soil.

In July 1987, EPA/NMEID conducted a joint hazardous waste compliance inspection (Table G-50). Violations were noted and a notice of violations will be issued in January 1988. Corrective actions will have to take place addressing these violations. The EPA was the lead agency for this inspection.

B. Clean Water Act

1. Laboratory Liquid Waste Discharge Permits. The primary goal of the Clean Water Act (33 U.S.C. 446 et seq.) is to restore and maintain the chemical, physical, and biological integrity of the nation's waters. The act established the National Pollutant Discharge Elimination System (NPDES) that requires permitting all point-source effluent discharges to the nation's waters. The permit establishes specific chemical, physical, and biological criteria that an effluent must meet prior to discharge. The DOE has two NPDES permits, one for Laboratory facilities in Los Alamos and one for the Fenton Hill Geothermal Project facility, located 50 km (30 mi) west of Los Alamos in the Jemez Mountains (Table 19). Both permits are issued and enforced by EPA's Region VI, Dallas, Texas. However, through a federal/state agreement and grant, NMEID performs compliance monitoring and reporting as agents for EPA.

The NPDES permit in effect for the Laboratory in 1987 (NM0028355) was reissued May 29, 1987, and will expire on March 1, 1991. As of December 31, 1987, the permit regulates 98 industrial outfalls and 10 sanitary outfalls (Table G-51). Each outfall represents a sampling station for permit compliance monitoring.

The Laboratory forwarded three NPDES permit modification requests to DOE for transmittal to EPA during 1987. The first requested addition of two new outfalls: outfall No. 128, which discharges effluent from a printed circuit board discharge at TA-22-91;

and outfall No. 129, which discharges effluent from boiler blowdown at TA-21-357. The second modification request addressed elimination of 22 outfalls that are no longer discharging; reactivation of outfall No. 007 at the TA-16 steam plant; combination of outfalls at three locations within the Laboratory; correction of outfall descriptions at four locations; and addition of three new outfalls (outfall No. 130 discharges effluent from a cooling tower located at TA-11-30, outfall No. 131 discharges effluent from once-through cooling water at TA-48-1, and outfall No. 132 discharges photographic waste effluent from TA 35-87. The third request contained information regarding 16 new wastewater outfalls consisting of eleven noncontact cooling water discharges, four treated cooling water discharges, and one sanitary wastewater discharge. The modification request also contained information about modifying six existing outfalls and eliminating two existing outfalls because wastewater has been diverted to other permitted outfalls.

Weekly sampling results are tabulated in a Discharge Monitoring Report (DMR) and submitted through DOE to EPA and NMEID on a monthly basis. Deviations from NPDES permit limits are explained separately to EPA and NMEID with the monthly submittal (Tables G-52 through G-54). During 1987, 96.3% and 98.7% of monitoring analyses complied with NPDES limits at sanitary and industrial outfalls, respectively (Fig. 23).

2. **Federal Facility Compliance Agreement.** On July 18, 1986, the Federal Facility Compliance Agreement (FFCA) between DOE's Los Alamos Area Office (LAAO) and EPA became effective. The FFCA contains interim effluent limitations and a schedule of compliance for several outfalls and outfall categories that had experienced frequent noncompliance with the NPDES permit limitations (Tables G-55 and G-56). Throughout 1987, required FFCA quarterly progress reports indicated that the Laboratory was well ahead of schedule in meeting final compliance milestones, with the exception of corrective actions on outfall 06S (TA-41). The completion of these corrections was delayed until November due to contract negotiations. At the end of December 1987, completion of only one project was needed to meet the FFCA schedule of compliance.

3. **Clean Water Act Audits.** The EPA conducted one audit under the Clean Water Act in 1987 (Table 20). An EPA Compliance Evaluation Inspection (CEI) was conducted on April 23, 1987. The CEI report received from EPA indicated that the permit deficiencies previously noted during the CEI had been corrected, and that the permittee was in compliance with permit requirements. The report stated that, "overall, this is a well run, well managed facility."

4. **Administrative Order.** On August 6, 1987, EPA's Region VI issued an Administrative Order (AO) to DOE regarding NPDES Permit NM0028355. The AO was based on self-monitoring reports submitted by the Laboratory that identified a number of individual parameter violations occurring at outfalls during 1986 and 1987, as well as alleged reporting violations. DOE responded to the AO in a submittal to EPA dated September 3, 1987.

5. **Fenton Hill Geothermal Project NPDES Permit.** The NPDES permit for the Fenton Hill

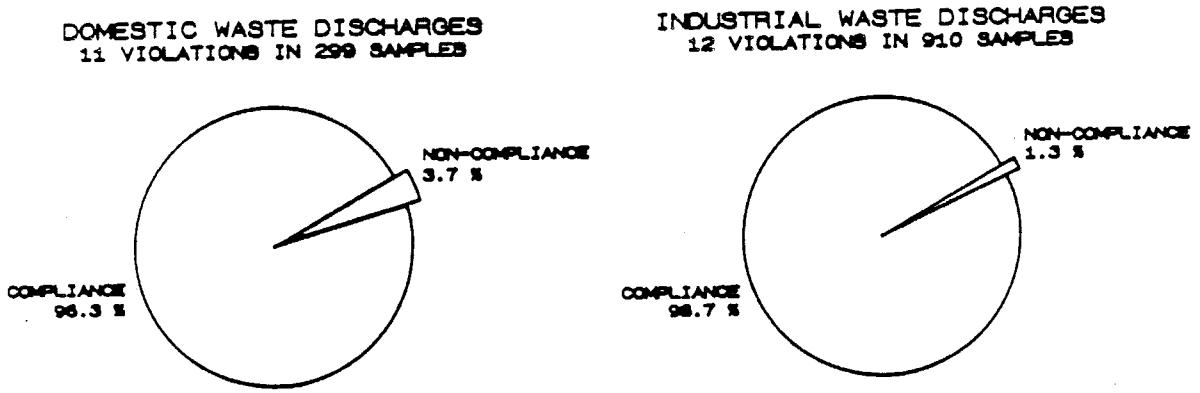

Fig. 23. 1987 Summary of Clean Water Act Compliance, NPDES Permit NM0028353

DOMESTIC WASTE DISCHARGES
11 VIOLATIONS IN 299 SAMPLES

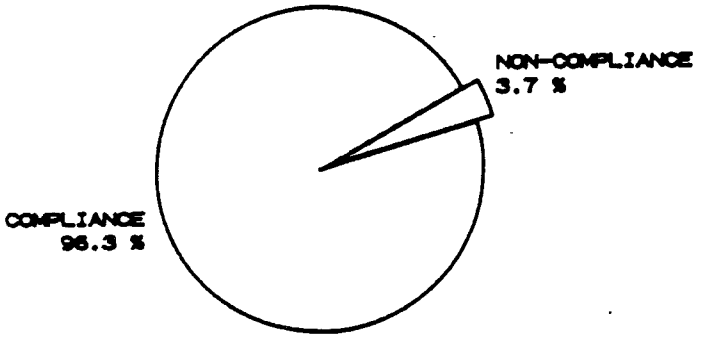

INDUSTRIAL WASTE DISCHARGES
12 VIOLATIONS IN 910 SAMPLES

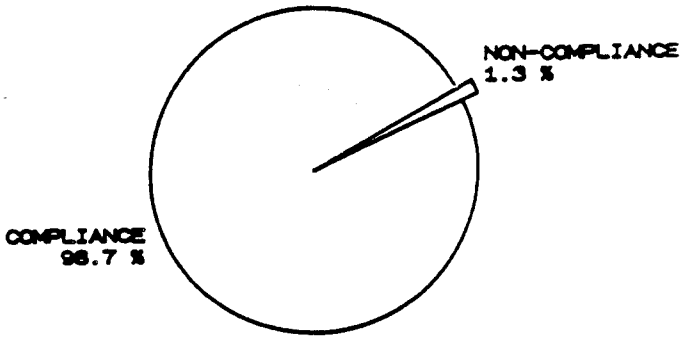

LA-1130C-ENV
Fig. 23 p. 63
6-½ in. wide on final

Table 20. Environmental Appraisals Conducted at the Laboratory in 1987

Day	Purpose	Performing Agency
January 28-29	Hazardous Waste Management Inspection	New Mexico's Environmental Improvement Division (EID) and U.S. Environmental Protection Agency (EPA)
January 27-31	Review of Environmental Monitoring Program	Albuquerque Operations Office U.S. Department of Energy (ALO/DOE)
January 27-29	Reconnaissance Survey of Zia Motor Pool	Laboratory's Environmental Surveillance Group, HSE-8
March 30-April 17	Environmental Survey	DOE Headquarters
April 23	NPDES Compliance Evaluation Inspection - Main Technical Area	EPA
May 1	Inspection of Air Pollution Compliance	EPA and EID
June 19	Compliance Inspection Federal Facility Compliance Agreement	EPA
June 24	Groundwater Discharge Plan Inspection - Fenton Hill	OCD
August 11	NPDES Compliance Evaluation Inspection - Fenton Hill	EID
October 27	Evaluation of RCRA Permit	EID
November 9	NPDES Site Inspection - Fenton Hill	EID and OCD

Geothermal Project was issued to regulate the discharge of mineral-laden water from the recycle loop of the geothermal wells (Table 19). NPDES permit NM0028576 was issued October 15, 1979, with an expiration date of June 30, 1983. Although the Laboratory applied for permit renewal more than 180 days prior to the expiration date, until April 1987 EPA Region VI had not acted upon the application. The existing permit has been administratively continued until supplanted by a new permit.

On April 15, 1987, EPA requested an updated application for the permit in order to reflect present conditions at the site, and DOE submitted an application package on May 20. Subsequently, EPA issued a proposed permit for comment and state certification (pursuant to Section 401, 33 U.S.C. 466 et seq.). The proposed permit included effluent monitoring and reporting requirements for flow, pH, and phenols.

Because proposed NPDES permits are subject to state review and certification, a meeting was held with

the NMEID and New Mexico Oil Conservation Division (NMOCD) to discuss the proposed permit and the environmental concerns of the state agencies. Subsequent to the meeting, a site inspection was held at Fenton Hill on November 9, 1987, to review the discharge location(s), inspect treatment systems, sample the wastewater, and survey the drainage system affected by the discharge. In December an information package containing a description of all water and wastewater piping and storage at the site was mailed by DOE/LAAO to the state agencies. State certification was granted by NMEID on January 8, 1988, with no additional state-imposed permit conditions. Issuance of the final NPDES permit is anticipated during the first quarter of 1988.

The original Fenton Hill NPDES permit regulates a single outfall. The daily monitoring requirements for the outfall during discharge include: arsenic, boron, cadmium, fluoride, lithium, pH, and flow. Concentrations for each of these parameters are to be reported. However, only the parameter pH has a limit, i.e., it must be within the range of 6.0 to 9.0 standard units.

The proposed Fenton Hill NPDES permit also will regulate the same single outfall. The daily monitoring requirements for the outfall during discharge will include: flow, pH, and phenols.

On August 11, 1987 the NMEID conducted a CEI at the Fenton Hill Geothermal Site. The results of the inspection were transmitted to DOE/LAAO on September 11, 1987. The inspection report indicated some deficiencies in flow measurement, pH monitoring, and analytical reporting, and record-keeping. All deficiencies were corrected.

A discharge plan for the Fenton Hill Geothermal Project was submitted to the NMOCD in June 1984 and approved in June 1985 (Table 19). The discharge plan approval is for a period of 5 years. The discharge plan approval letter states that there will be no routine monitoring or reporting requirements other than those mentioned above.

On April 27, 1987, DOE/LAAO submitted to NMOCD a request to modify the ground water discharge plan (GW-31) by using chemical tracers in various experiments conducted to evaluate the geothermal reservoir. In order to fully evaluate the discharge plan modification, NMOCD conducted a site inspection at Fenton Hill on June 24, 1987. After considering all of the information available to them, NMOCD approved the discharge plan modification on September 8, 1987.

6. Spill Prevention Control and Countermeasure (SPCC) Plan. During 1987 technical and administrative reviews of the Laboratory's Spill Prevention Control and Countermeasure (SPCC) Plan were completed. The SPCC Plan was distributed to the Senior Management Group and to divisional environmental coordinators during October 1987. The plan was accompanied by a VHS video cassette that included a 15-minute overview of the plan, as well as two short videos on safe drum handling and polychlorinated biphenyls (PCBs) at the Laboratory, topics related to the SPCC plan.

The SPCC plan addresses facilities improvements (e.g., dikes, berms, or other secondary spill containment measures), operational procedures, and mechanisms for reporting of hazardous substances and oil spills to the appropriate managerial and regulatory authorities. The plan complements existing Administrative Requirements in the Laboratory's Health and Safety Manual for accidental oil and chemical spills and environmental protection. Its goal is to minimize off-site oil and hazardous chemical discharges and to provide a spill response system.

7. Sanitary Wastewater Systems Consolidation. Many of the existing sanitary wastewater treatment facilities at the Laboratory are over 30 years old and do not consistently meet NPDES permit requirements. The cost of operation of these facilities has increased over the years due to maintenance and replacement of old equipment and other factors. In 1985, the Laboratory initiated the Sanitary Wastewater Systems Consolidation (SWSC) project to replace most of these facilities and to provide an area-wide wastewater treatment system.

The proposed SWSC project will be designed to meet current and anticipated future discharge requirements and reduce operation and maintenance costs. The new wastewater treatment plant will be located near TA-46 and will utilize the extended aeration process. The proposed plant will include preliminary treatment works, flow equalization basins, an oxidation ditch, a secondary clarifier and facilities for disinfection of effluent. Effluent from the plant will be reused for cooling water at the TA-3 power plant and for other nonpotable uses. Excess effluent will be discharged to Canada del Buey under a new NPDES permit. Upon completion, the proposed SWSC project will replace 8 wastewater treatment plants and 32 septic tank systems currently maintained by the Laboratory.

During 1987, the final design criteria for the SWSC project were approved, and construction is scheduled to be completed in 1992. When complete, the SWSC project will eliminate noncomplying discharges. The project will reduce operation and maintenance costs associated with the existing treatment plants and septic tank systems. Also, the number of discharge points requiring sampling, analyses and reporting will be reduced.

8. Interim Improvements at TA-3 Sanitary Wastewater Treatment Plant. The TA-3 Wastewater Treatment Plant is presently the largest sanitary wastewater facility at the Laboratory and provides treatment for about 1.15×10^6 liter (0.3×10^6 gal.) of wastewater per day. The TA-3 plant is a trickling filter plant with two parallel trains of treatment units. Effluent from the plant exceeds biochemical oxygen demand (BOD) standards at times during the winter months. During cold periods, biological activity in the trickling filters is reduced and removal of dissolved organic matter from the wastewater declines. Installation of a steam injection system was selected from several alternatives considered to improve BOD removal at the plant. No discharge violations for BOD have occurred since completion of the system. Additional testing is being conducted in order to fine-tune the temperature setting and to determine the optimum amount of steam for meeting permit requirements.

In addition to the steam injection system, a new chlorination system was installed at the plant to prevent occasional violations of the fecal coliform limit. Since installation of this system, no violations of fecal coliform requirements have occurred.

9. Interim Improvements At Other Sanitary Wastewater Treatment Plants. The wastewater treatment facilities serving TA-18 include two lined lagoons that are operated in parallel. Effluent from these lagoons has contained total suspended solids in excess of NPDES limits. A conceptual design was completed for the construction of two sand filters to be located below the lagoons for removal of suspended solids. The old wastewater treatment facilities that served TA-41 were replaced by a high-pressure system, which now carries wastewater to the TA-3 plant. This new pumping system has eliminated all effluent discharges at TA-41.

10. Septic Tank System Survey And Registration. During 1987, a survey of all septic tank systems at the Laboratory found a total of 61 systems receiving <2,000 gal./day that required registration under New Mexico's Liquid Waste Disposal Regulations. Each septic tank system was registered with the Health, Safety, and Environment Section of Los Alamos County. In addition, a manual for selecting on-site wastewater disposal systems was completed. The manual provides Laboratory design engineers and project reviewers with information on the alternatives available for treatment and disposal of sanitary wastewater and on meeting state regulations when connection to the central collection system is not possible.

11. Treatment of Chemical Oxygen Demands at TA-16. The industrial wastewater at TA-16 originates from explosives processing and includes several organic wastes. Effluent from industrial outfall No. 055 at TA-16 has exceeded the chemical oxygen demand (COD) NPDES limit of 150 mg/L. In order to consistently meet COD permit limitations, a new treatment unit was combined with the existing facilities in 1987.

The new treatment unit includes two activated carbon tanks designed to reduce organics contributing to COD. Preliminary results indicate that adsorption by activated carbon is selective and that some organics remain in the effluent. Additional testing is needed to determine the most effective types of activated carbon or other filter media available for the organics present.

C. National Environmental Policy Act (NEPA)

The National Environmental Policy Act of 1969 (NEPA) requires that proposed federal actions be evaluated for their potential environmental impacts. The DOE's compliance with NEPA generally takes the form of an Action Description Memorandum (ADM). The ADM provides a brief description of the proposed action and serves as a basis for determining the required level of any further NEPA documentation. Further documentation is carried out at the request of DOE and may consist of either an Environmental Assessment (EA) or an Environmental Impact Statement (EIS). The Laboratory Environmental

Review Committee (LERC) reviews NEPA documentation. A Laboratory Environmental Evaluation Coordinator assists project personnel to prepare the appropriate documentation and present it to the committee.

The LERC approved 18 ADMs, 2 revised ADMs, and 1 EA in 1987 (Table G-57). The Laboratory instituted a new procedure for identifying project environmental, health, and safety requirements which has reduced the volume of paperwork required for NEPA documentation.

D. Clean Air Act

1. Federal Regulations

a. National Emissions Standards for Hazardous Air Pollutants (NESHAPS). This regulation sets reporting, emissions control, disposal, stack testing, and other requirements for specified operations involving hazardous air pollutants. New Mexico's EID has responsibility for administering these regulations. Laboratory operations that are regulated by NESHAPS include radionclide handling, asbestos disposal and removal, and beryllium machining.

The EPA has promulgated regulations for control of airborne radionuclide releases from DOE facilities (40 CFR 61, Subpart H). Since 1985, DOE and its contractors have been subject to EPA's radionuclide air emissions limits for exposure of the general public via the air pathway (DOE 1985). Laboratory operations are in compliance with these standards (Sec. III). Further discussion is presented in Appendix A. During 1987, the DOE and the Laboratory submitted an application to construct facilities for the Independent Management Activity program, as required under 40 CFR 61, Subpart A. This application was approved by EPA in January 1988.

Notification, emissions control, and disposal requirements for operations involving the removal of friable asbestos are specified under the NESHAPS regulations. The NMEID requires asbestos disposal certification forms be filled out and sent to them for each large asbestos removal job and an annual one for all small renovation jobs. Four certification forms, including the annual notification for the small disposal jobs, were sent to NMEID. Nearly 270 m^3 (9500 ft^3) of asbestos contaminated wastes were disposed at TA-54 in 1987.

During 1987, 180 asbestos jobs involved the removal of 2080 m (6825 ft) of asbestos materials on pipe and 96 m^2 (1032 ft^2) on other facility components. Six notifications of asbestos removal were sent to NMEID in 1987, including the notification for small removal jobs. Ninety-seven percent of the asbestos removed, including 53.5% of the length of asbestos removed from pipe, involved small renovation jobs that required no job-specific notification to the state.

The NESHAPS includes notification, emission limit, and stack performance testing requirements for beryllium machine shops. A modification to an existing permit was issued by NMEID during 1987 for one processing operation (Table 19).

b. National Ambient Air Quality Standards. Federal and state Ambient Air Quality Standards are shown in Table 21. Based upon available monitoring data and modeling, Laboratory emissions have not exceeded federal or state standards (Sec. V). Pollutants emitted by Laboratory sources include: sulfur dioxide, particulates, carbon monoxide, nitrogen dioxide, lead, beryllium, heavy metals, and nonmethane hydrocarbons. Laboratory sources that emit these pollutants include beryllium machining and processing, the TA-3 power plant, the steam plants, the motor vehicle fleet, the asphalt plant, the lead pouring facility, the burning and detonation of high explosives, and the burning of potentially high-explosive contaminated wastes (Sec. V).

A new federal particulate standard (the PM_{10} standard) for particles less than 10 microns in diameter went into effect this year.

c. Prevention of Significant Deterioration (PSD). The PSD regulations have stringent requirements (preconstruction review, permitting, best available control technology for emissions, air quality increments not to be exceeded, visibility protection requirements and air quality monitoring) for the construction of any new major stationary source or major modification located near a Class I Area, such as Bandelier National Monument's Wilderness Area. To date, the DOE and Laboratory have not been subject to PSD.

d. New Source Performance Standards (NSPS). The NSPS applies to 72 source categories. Its provisions include emission standards, notification, and emission testing procedures and reporting and emission monitoring requirements. The DOE and Laboratory have not been subject to NSPS. A proposed

Table 21. National and New Mexico Ambient Air Quality Standards

Pollutant	Averaging Time	Units	New Mexico	Federal Primary	Federal Secondary
Sulfur Dioxide	Annual Arithmetic Mean	ppm	0.02	0.03	---
	24 hour[a]	ppm	0.10	0.14	---
	3 hour[a]	ppm	---	---	0.5
Total Suspended Particulates	Annual Geometric Mean	g/m^3	60	75	60
	30 days	$\mu g/m^3$	90	---	---
	7 days	$\mu g/m^3$	110	---	---
	24 hour[a]	$\mu g/m^3$	150	260	150
PM_{10}[c]	Annual Arithmetic Mean	$\mu g/m^3$	50	50	50
	24 hour	$\mu g/m^3$	150	150	150
Carbon Monoxide	8 hour[a]	ppm	8.7	9	---
	1 hour[a]	ppm	13.1	35	---
Ozone	1 hour[b]	ppm	0.06	0.12	0.12
Nitrogen Dioxide	Annual Arithmetic Mean	ppm	0.05	0.053	0.053
	24 hour[a]	ppm	0.10	---	---
Lead	Calendar Quarter	$\mu g/m^3$	1.5	1.5	1.5
Beryllium	30 days	$\mu g/m^3$	0.01	---	---

Table 21 (cont)

Pollutant	Averaging Time	Units	New Mexico	Federal Primary	Federal Secondary
Asbestos	30 days	$\mu g/m^3$	0.01	---	---
Heavy Metals (Total Combined)	30 days	$\mu g/m^3$	10	---	---
Non-Methane Hydrocarbons	3 hour	ppm	0.19	---	---

[a]Maximum concentration not to be exceeded more than once per year.
[b]The standard is attained when the expected number of days per calendar year with maximum hourly average concentrations above the limit is equal to or less than one.
[c]PM_{10} covers particles less than 10 microns in diameter.

solid-waste-fired-boiler would easily meet NSPS limits for incinerators.

2. State Regulations

a. New Mexico Air Quality Control Regulation (NMAQCR) 301. Under this regulation, open burning of explosive materials is permitted where transport to other facilities may be dangerous. The DOE and Laboratory are permitted to burn waste explosives and explosive-contaminated wastes. Burning of waste explosives is done at the TA-16 burn ground, whereas burning of potentially high-explosive contaminated wastes is done at the TA-16 open incinerator.

The open incinerator is in the process of being replaced by an enclosed incinerator, with two-stage combustion. Complete combustion would occur within the two-stage incinerator, and an open burning permit is not required. An air pollution review of the planned incinerator estimated ambient air pollutant concentrations that were not of concern. The estimated emissions were too low to require either a permit or registration.

b. NMAQCR 501. The NMAQCR 501 sets emission standards according to process rate and requires the control of fugitive emissions from asphalt processing equipment. The asphalt concrete plant operated by Pan Am World Services is subject to this regulation. This plant is old, subject to leaking, and is inspected annually. During the annual inspection, leaks causing fugitive emissions were discovered and repaired.

The asphalt plant meets the stack emission standard for particulates as specified in this regulation. The plant, which has a 75 000 kg/h (75 ton/h) capacity, is required to meet an emission limit of 16 kg (35 lb) particulates per hour. A stack test of the asphalt plant in 1977 indicated an average emission rate of 0.8 kg/h (1.8 lb/h) and a maximum rate of 1.0 kg/h (2.2 lb/h) over 3 tests (Kramer 1977). Although the plant is old and not required to meet NSPS stack-emission limits for asphalt plants, it meets these standards (Kramer 1977).

c. NMAQCR 604. The NMAQCR 604 requires gas burning equipment built prior to January 10, 1973, to meet an emission standard for NO_x of 0.3 lb/10^6 Btu when natural gas consumption exceeds 10^{12} Btu/yr/unit. The TA-3 power plant's boilers have the potential to operate at heat inputs that exceed the 10^{12} Btu/yr/unit but have not operated beyond this limit.

Thus, these boilers have not been subject to this regulation. The TA-3 power plant meets the emission standard, although it is not required to do so. The emission standard is equivalent to a flue gas concentration of 248 ppm. The TA-3 boilers meet the standard with measured flue gas concentrations of 15 to 22 ppm.

d. NMAQCR 702. The NMAQCR 702 requires the permitting of any new or modified source if it exceeds a given emissions rate and is not addressed by other regulations. When new Laboratory emission sources or modifications to existing sources are planned, an air pollution regulatory compliance review is carried out. This review evaluates the steps to be followed to comply with state and federal air pollution regulations. As part of the permitting process, NMEID reviews new or modified sources for compliance with all state and federal air pollution regulations. Under this regulation, the NMEID issued the modification to the permit for the beryllium processing operation at TA-3-141.

Group HSE-8 is assisting Facilities Engineering (ENG) Division in obtaining an air quality construction permit for a steam production facility consisting of two solid-waste-fired boilers (SWFB) and two gas-fired auxiliary boilers. This facility is proposed to replace the TA-16 steam plant. The facility will burn county and Laboratory refuse as well as natural gas and generate steam for TA-16. The permit application has been submitted and has been ruled complete by the NMEID. Meteorological air-dispersion modeling of emitted substances has demonstrated that impact on the local air quality, including impacts at the Bandelier Wilderness Area, will be negligible.

The NMEID has proposed amendments to this regulation that would require the permitting of an additional 600-700 substances. The NMEID has called this new class of substances "toxic air pollutants." If adopted, the proposed amendments would have a major impact on Laboratory operations and would be expensive to comply with. The Laboratory has hundreds of laboratories and shops that use these substances. Reconstruction of existing facilities and the construction of new facilities would be impacted by the proposed amendments.

e. Other Regulations. The NMEID proposed new regulations requiring one-time registration of all sources that have emissions of toxic air pollutants that exceed specified levels. The New Mexico Environmental Improvement Board (NMEIB) adopted these regulations on June 12, 1987, and they went into effect on September 17, 1987. The Laboratory is required to comply with these regulations by September 17, 1988. The Laboratory, with the assistance of a subcontractor, has completed a survey to obtain the necessary information and is in the process of using this information to develop an emission inventory for all of the Laboratory sources. A computerized data base system is being developed to process the large amount of information that has been collected. The data base will also be used to meet future permitting and internal requirements.

E. Safe Drinking Water Act (Municipal and Industrial Water Supplies)

1. Background. The federal Safe Drinking Water Act (42 U.S.C. 300f et seq.), as amended, requires the adoption of national drinking water regulations as part of the effort to protect the quality of drinking water in the United States. The U.S. Environmental Protection Agency (EPA) is responsible for the administration of the act and has promulgated National Interim Primary Drinking Water regulations. Although EPA is designated by law as the administrator of the Act, assignment of responsibilities to a state is permitted, and primacy for administration and enforcement of federal drinking water regulations has been approved for New Mexico.

The state of New Mexico administers and enforces the drinking water requirements through regulations adopted by New Mexico's EIB and implemented by NMEID. During 1987, reports on trihalomethane, radiological, microbiological, and inorganic chemical concentrations in the Laboratory's water supply were prepared for the NMEID pursuant to NMEIB regulations. Municipal and industrial water supplies for the Laboratory and community easily met the regulations.

The main aquifer is the only aquifer in the area capable of municipal and industrial water supply (Sec. II). Water for the Laboratory and community is supplied from 17 deep wells in 3 well fields and 1 gallery. The well fields are on Pajarito Plateau and in canyons east of the Laboratory (Fig. 24). The gallery is west of the Laboratory on the flanks of the mountains. Production from the wells and gallery for 1987 was 6.1 x 10^9 L (1.6 x 10^9 gal).

The Los Alamos well field is composed of five producing wells and one standby well. Well LA-6 is on

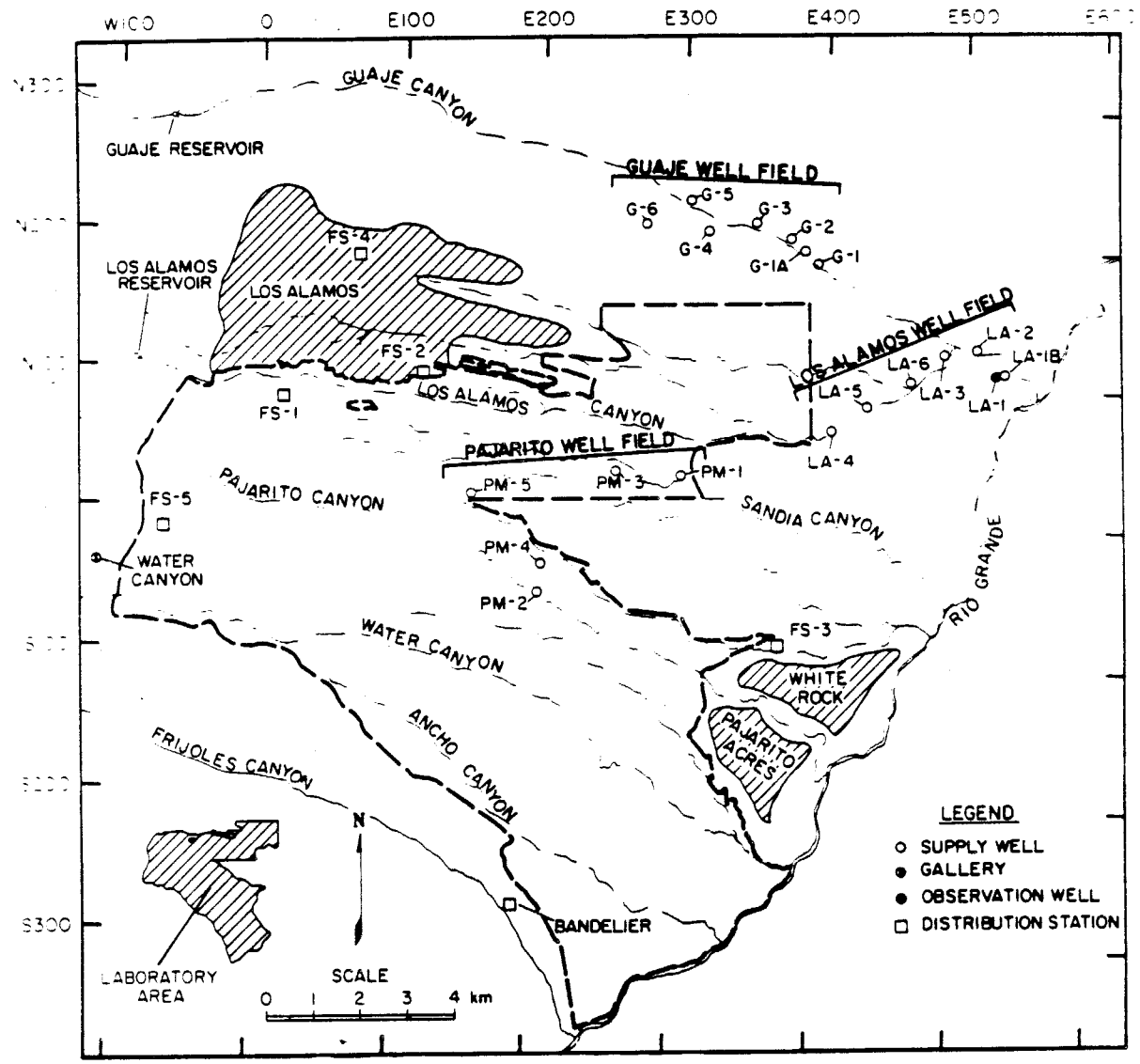

Fig. 24. Locations of reservoirs, well fields, supply wells, and gallery water supply

standby status, to be used only in case of emergency. Water from Well LA-6 contains excessive amounts of natural arsenic (up to 0.200 mg/L) that cannot be reduced to acceptable limits by mixing in the distribution system (Purtymun 1977). Well LA-4 was down for repairs and was not sampled. Wells in the field range in depth from 265 to 600 m (870 to 2000 ft). Movement of water in the upper 411 m (1350 ft) of the main aquifer in this area is eastward at about 6 m/yr (20 ft/yr) (Purtymun 1984).

The Guaje well field is composed of seven producing wells. During 1987, Well G-3 was down for repairs and was not sampled. Wells in the field range in depth from 463 to 610 m (1520 to 2000 ft). Movement in water in the upper 430 m (1410 ft) of the aquifer is southeastward at about 11 m/yr (36 ft/yr) (Purtymun 1984).

The Pajarito well field is composed of five wells that range in depth from 701 to 942 m (2300 to 3090

ft). Movement of water in the upper 535 m (1750 ft) of the aquifer is eastward at 29 m/yr (85 ft/yr).

The Water Canyon gallery collects spring discharge from a perched water zone in the volcanics on the flanks of the mountains west of Los Alamos and Pajarito Plateau (Fig. 24). The canyon supplies a small but important part of the production with use of little energy.

Water for drinking and industrial use is also obtained from a well at the Laboratory's experimental geothermal site (Fenton Hill, TA-57) about 45 km (28 mi) west of Los Alamos. The well is about 133 m (436 ft) deep completed in volcanics. During 1987, the well produced about 20 x 10^6 L (5.4 x 10^6 gal). The TA-57 water is not a part of the Los Alamos supply.

All water comprising the municipal and industrial supply is pumped from wells, piped through transmission lines, and lifted by booster pumps into reservoirs for distribution to the community and Laboratory. Water from the gallery flows by gravity through a microfilter station and is pumped into one of the reservoirs for distribution. All supply water is chlorinated prior to entering the distribution system.

Water in the distribution systems was sampled at five community and Laboratory locations (fire stations), Bandelier National Monument, and Fenton Hill (Fig. 24, Table G-14). Although federal and state standards (Appendix A) require analyses every 3 years, the Laboratory performs the analyses annually.

2. Radioactivity in Municipal and Industrial Water Supply. The maximum radioactivity concentrations found in the supply (wells and gallery) and distribution (including Fenton Hill) systems are in compliance with the EPA's National Interim Primary Drinking Water Standards (Tables 22, G-58, and G-59).

3. Chemical Quality of Municipal and Industrial Water Supply. Water from most wells and the distribution systems complied with EPA's primary and secondary standards (Tables 23 and G-60 through G-62). The concentration of fluoride from Well LA-1B was above primary standards (Table G-60). This is consistent with previous years. Mixing in the distribution system reduced concentrations to acceptable levels (Table 23). The concentration of lead from Well PM-5 also exceeded the primary standard (Table G-60). Well PM-5 was resampled and lead (<0.001 mg/L) was well below the primary standard.

The quality of water from the wells varied with local conditions within the same aquifer (Tables G-60 through G-62). Water quality depends on well depth, lithology of aquifer adjacent to well, and yield from beds within the aquifer.

F. Federal Insecticide, Fungicide, and Rodenticide Act

The Federal Insecticide, Fungicide, and Rodenticide Act (FIFRA) requires registration of all pesticides, restricts use of certain pesticides, recommends standards for pesticide applicators, and regulates disposal and transportation of pesticides. A pesticide is defined as any substance intended to prevent, destroy, repel, or mitigate pests. The Laboratory stores, uses, and discards pesticides in compliance with the provisions of FIFRA. A Laboratory pest control policy was established in June 1984 to establish procedures and identify suitable pesticides for control of plant and animal pests. Anything outside the scope of the policy must be approved by the Pest Control Oversight Committee. No unusual events associated with compliance occurred during 1987.

G. Archaeological and Historical Protection

Laboratory lands contain about 900 known archaeological and historical sites. Protection of cultural resources is mandated by numerous laws and regulations, including the National Historic Preservation Act of 1966, as implemented by 36 CFR Part 800 Protection of Historic and Cultural Properties, and the New Mexico Cultural Properties Act of 1969, as amended. The Laboratory's Environmental Evaluation Coordinator oversees management and protection of cultural resources.

Laboratory archaeologists survey project sites in advance of construction to determine the presence or absence of cultural resources. During 1987, the Laboratory conducted 28 cultural resource surveys, monitored construction at 7 sites, had permanent protective fencing erected at 1 site, and undertook adverse impact mitigation at 2 sites. During surveys of one project in Mortandad Canyon, archaeologists discovered a pit house site that indicates earlier prehistoric occupation of the area than heretofore thought.

The DOE granted an Archaeological Resource Protection Act permit to the Museum of New Mexico, Laboratory of Anthropology, for archaeological testing at the White Rock Y Intersection, site of a proposed new highway interchange.

Table 22. Maximum Concentrations of Radioactivity in Municipal Water Supply, Well and Distribution System

	Number of Stations	^{3}H (10^{-6} µCi/mL)	^{137}Cs (10^{-9} µCi/mL)	Total U (µg/L)	^{238}Pu (10^{-9} µCi/mL)
Analytical Limits of Detection	--	0.7	40	1.0	0.009
Maximum Contamination Level (MCL)[a]	--	20	200	1800[b]	15
Wells	16	0.3 (0.7)	42 (48)	6.0 (1.0)	0.011 (0.009)
	--	(2%)[c]	(21%)	(<1%)	(<1%)
Distribution System (Los Alamos)	6	2.1 (0.7)	71 (42)	2.0 (1.0)	0.012 (0.012)
	--	(11%)	(36%)	(<1%)	(<1%)
Distribution System (Fenton Hill)	1	0.1 (0.3)	113 (50)	1.0 (1.0)	0.000 (0.010)
	--	(<1%)	(57%)	(<1%)	(<1%)

Table 22 (cont)

	Number of Stations	$^{239,240}Pu$ (10^{-9} µCi/mL)	Gross Alpha (10^{-9} µCi/mL)	Gross Beta (10^{-9} µCi/mL)	Gross Gamma (Counts/min/L)
Analytical Limits of Detection	--	0.03	3	3	50
Maximum Contamination Level (MCL)[a]	--	15	15[d]	--	--
Wells	16	0.044 (0.007)	-5.0 (2.0)	3.2 (0.5)	-40 (100)
	--	(<1%)	(<1%)	--	--
Distribution System (Los Alamos)	6	0.037 (0.017)	2.4 (0.9)	42 (4.0)	500 (90)
	--	(<1%)	(16%)	--	--
Distribution System (Fenton Hill)	1	0.004 (0.004)	-0.2 (0.8)	6.1 (0.8)	350 (90)
	--	(<1%)	(<1%)	--	--

[a]EPA (1976).
[b]Level recommended by International Commission on Radiological Protection.
[c]Percentage of EPA's MCL is shown in parentheses.
[d]Environmental Protection Agency's Maximum Contaminant Level (MCL) for gross alpha is 15 x 10^{-9} µCi/mL. However, if gross alpha results exceed EPA's limit of 5 x 10^{-9} Ci/mL, isotopic analysis to determine radium content is required.

Table 23. Maximum Chemical Concentrations in Water Supply and Distribution Systems (results in mg/L)

Inorganic Chemical Contaminant	Standards	Supply: Well and Gallery	Supply: Per Cent of Standard	Distribution: Los Alamos Bandelier TA-57	Distribution: Per Cent of Standard
Primary[a]					
Ag	0.05	<0.001	<2	<0.001	<2
As	0.05	0.044	88	0.017	34
Ba	1.0	0.084	8	0.107	11
Cd	0.01	<0.0005	<5	<0.0005	<5
Cr	0.05	0.022	44	0.011	22
F	2.0	3.2	160	1.0	50
Hg	0.002	0.0003	15	<0.0002	10
$NO_3(N)$	10	<1	<10	<1	<10
Pb	0.05	0.092	184	0.031	62
Se	0.01	<0.002	<20	<0.002	<20
Secondary[b]					
Cl	250	17	7	45	18
Cu	1.0	0.266	27	0.024	2
Fe	0.3	0.095	32	0.110	37
Mn	0.05	0.009	18	<0.001	<2
SO_4	250	39	16	10	4
Zn	5.0	0.250	5	0.096	<2
TDS	500	430	86	276	55
pH	6.5 - 8.5	8.6	101	8.4	99

[a]EPA (1976).
[b]EPA (1979B).

Pursuant to federal regulations implementing Section 106 of the National Historic Preservation Act of 1966, as amended, clearance for construction and mitigation of unavoidable adverse impact to cultural resources is determined in consultation with the New Mexico State Historic Preservation Office (SHPO) and, if necessary, with the Advisory Council on Historic Preservation. The SHPO was consulted concerning potential impact to surveyed project areas.

The SHPO and Advisory Council approved stabilization and restoration work on the historic Pond Cabin at TA-18. The Laboratory completed work on this project during 1987. The cabin will be nominated for inclusion on the State Register of Cultural Properties. Surveys of prehistoric Indian cavates along the south slope of Mesita del Buey using volunteer Laboratory staff supervised by Laboratory archaeologists were completed, and a report was submitted to the Laboratory. Analysis of archaeological and botanical data recovered from the Romero Cabin homesteading site was completed and draft reports prepared.

The DOE and the Museum of New Mexico established a curatorial Programmatic Memorandum of Agreement (PMOA). Archaeological and historical artifacts from Laboratory projects will be curated professionally at the Museum's Laboratory of Anthropology. A draft procedural PMOA among DOE, SHPO, and the Advisory Council for Historic Preservation was prepared and is under DOE review. The PMOA will streamline Section 106 consultation requirements of the National Historic Preservation Act of 1966.

H. Threatened/Endangered Species and Floodplains/Wetlands Protection

The DOE and Laboratory must comply with the Endangered Species Act of 1973, as amended, and with Executive orders 11988, Floodplain Management, and 11990, Protection of Wetlands Environmental Review Requirements. Three Floodplain/Wetland notifications were prepared for publication in the Federal Register: Live Firing Range Extension, Sandia Canyon; Pulsed Power Assembly Building, TA-39, Ancho Canyon; and White Rock Y Interchange, Pueblo and Los Alamos canyons. Laboratory biologists surveyed 17 proposed construction sites for potential impact. They identified no endangered or rare animal or plant species at these sites.

A draft management plan for the endangered peregrine falcon was prepared and is under review. Computer mapping and analysis of raptor aeries and prey habitat in Los Alamos and Water canyons were initiated.

I. Comprehensive Environmental Response, Compensation, and Liability Act (CERCLA)

The Comprehensive Environmental Response, Compensation, and Liability Act (CERCLA) of 1980 and Superfund Amendments and Reauthorization Act (SARA) of 1986 mandate cleanup of toxic and hazardous contaminants at closed and abandoned hazardous waste sites. The CERCLA/SARA-related action at hazardous waste sites at the Laboratory are being addressed under the DOE Albuquerque Operations Office's Environmental Restoration (ER) Program.

J. Toxic Substances Control Act (TSCA)

The TSCA (15 U.S.C. et seq.) establishes a list of toxic chemicals for which the manufacture, use, storage, handling, and disposal are regulated. This is accomplished by requiring premanufacturing notification for new chemicals, testing of new or existing chemicals suspected of presenting unreasonable risk to human health or the environment, and control of chemicals found to pose an unreasonable risk.

Part 761 of TSCA contains the regulations applicable to polychlorinated biphenyls (PCBs). This part applies to all persons who manufacture, process, distribute in commerce, use, or dispose of PCBs or PCB items. Substances that are regulated by this rule include, but are not limited to, dielectric fluids, contaminated solvents, oils, waste oils, heat transfer fluids, hydraulic fluids, paints, sludges, slurries, dredge spoils, soils, and materials contaminated as a result of spills. Most of the provisions of the regulations apply to PCBs only if they are present in concentrations above a specified level. For example, the regulations regarding storage and disposal of PCBs generally apply to materials at PCB concentrations of 50 parts per million (ppm) and above. At the Laboratory, materials with >500 ppm PCBs are transported off-site for disposal.

During 1987, the Laboratory continued to inventory and mark PCB articles such as transformers and capacitors. The Laboratory's inventory of in-service PCB transformers >500 ppm, PCB transformers >50 but <500 ppm, and PCB capacitors includes 136, 137, and 2,777 units, respectively, as of July 1, 1987. Visual inspection of PCB transformers was conducted at least quarterly during 1987, and inspection records maintained pursuant to regulations. An annual report summarizing PCB disposal, transportation, storage, and in-service use for the time period July 1, 1986, through June 30, 1987, is available pursuant to federal regulation. During September 1987, HSE-8 prepared a 15-minute video film summarizing PCB use and regulation at the Laboratory. The video film will be used as a training aid to acquaint Laboratory personnel with PCBs and familiarize them with the federal regulations governing their use and disposal.

The Laboratory has EPA approval (Region VI) to dispose of PCB-contaminated articles, oils, and materials in the chemical waste landfill located at TA-54, Area G (Table 19). The approval requires semiannual reporting to EPA regarding the type and weight of PCB articles disposed of, and monitoring information regarding chemical quality of storm water run-off and natural springs in the area. The cumulative weights of specific types of PCB articles which were disposed at TA-54 during 1987 are listed in Table 24.

K. Emergency Planning and Community Right-to-Know Act

Title III of SARA, also known as the Emergency Planning and Community Right-to-Know Act (EPCRA), became effective on May 17, 1987. The EPCRA is the centerpiece of federal policy on chemical disaster prevention and response. The act is intended to encourage and support emergency planning

Table 24. Quantities (kg) of PCB Contaminated Articles Discarded at TA-54 in 1987[a]

PCB Article(s)	Shaft C11	Shaft C12	Pit 29	Pit 32
Transformer Carcases		907		522
Absorbed PCB Oil (<500 ppm)				
Rags/Dirt (drummed)				
Empty Drums				
Asphalt/dirt (noncontainerized)		9 616		1 361
Capacitors				
Generators				
Power Supply				
PCB Clean-Up Drum	722		41	
PCB Contaminated Equipment			175	2 359
Misc				
Total	722	10 523	216	4 242
Grand Total	15 703			

[a]PCB article and oils that contain ≥500 ppm PCB are shipped out-of-state for disposal.

efforts at state and local levels. Its implementation provides the public and local governments with information concerning potential toxic and chemical hazards present in their communities. The act is organized into three subtitles; the Laboratory will only be directly affected by Subtitle B, which provides the mechanism for community awareness of hazardous chemicals present in a given facility. However, it has voluntarily taken an active role in coordinating local community emergency response planning activities under Subtitle A.

The Laboratory is required to report its hazardous chemical substance inventory and safety handling procedures to the newly-created Los Alamos District Emergency Planning Commission, the state Emergency Response Commission, and the Los Alamos County Fire Department. The Laboratory's Emergency Management Office (EMO) coordinates all reporting, planning, and response efforts with the preexisting Los Alamos County Office of Emergency Preparedness, which acts as the district emergency planning group. Groups HSE-5 and HSE-8 provided a preliminary list of 137 on-site chemical substances that are on either the EPA's Chemical Emergency Preparedness Program (CEPP) list of 369 chemicals that are considered to be extremely hazardous (40 CFR 355, Appendices A and B) or on the list of 717 hazardous substances that are subject to CERCLA reportable quantity provisions (40 CFR 302, Table 302.4). In addition, individual Materials Safety Data Sheets (MSDS) for each of these substances have been provided to the EMO. These sheets, which were organized according to health and physical hazards, were originally developed in response to the Occupational Health and Safety Administration's (OSHA) Hazard Communication Standard (29 CFR 1910.1200). They are designed to inform individuals of specific chemical dangers and methods to avoid potential hazards.

In order for a listed chemical substance to qualify for EPCRA reporting requirements, the Laboratory must have a combined total amount of that chemical substance in excess of either its threshold planning quantity or its reportable quantity. For those chemical substances with no established reportable quantities, the Laboratory must have at least 0.45 kg (1 lb) of that substance before it qualifies for reporting requirements. Once a given listed chemical substance has been determined to be reportable, future annual reporting requirements dictate that the Laboratory must disclose individual building storage locations and the average annual quantity on-hand at each location where that substance is located. Once reported, this information becomes public property. These requirements may conflict with national security guidelines enforced by DOE and may require future DOE reporting directives if conflicting requirements are to be fully satisfied.

L. DOE Headquarters' Environmental Survey

The DOE Headquarters conducted an environmental survey of the Laboratory during March 30 through April 17, 1987. The purpose of the survey was to provide a no-fault identification, inventory, prioritization, and review of environmental issues and practices at the Laboratory. Similar surveys have been conducted at other DOE facilities, and evaluation of findings from all the surveys will lead to a DOE-wide prioritization of environmental problems (due in October 1989).

Findings of the survey were separated into four categories based upon potential for environmental impact:

> Category I: Finding addresses situations that pose an immediate threat to employees, public, or environment. Immediate action required.
>
> Category II: Finding addresses situations that cannot wait for action to be taken until the final report of the survey is published in approximately 3 years. The Laboratory should start new programs or continue existing programs, as appropriate, to address this finding before the 3-year period expires.
>
> Category III: Finding addresses situations that hold a "potential" for contamination from existing operations. The Laboratory is encouraged to continue existing programs or start new programs to address this finding as appropriate.
>
> Category IV: Finding is an observation only.

The findings were further subdivided into eight topical areas (Table 25). The majority (87%) of the findings were in categories III and IV. Most (63%) addressed hazardous materials handling and storage.

A preliminary report that will list the findings at Los Alamos from the survey will be published by DOE in March 1988. The DOE Survey Team will conduct environmental sampling at the Laboratory in the summer of 1988 and results of this sampling may affect the findings.

The Laboratory has drafted an implementation plan based on the tentative findings and has started to implement appropriate remedial actions.

M. Health, Safety, and Environmental Appraisal of Laboratory Operations and Facilities

Laboratory policy requires line management to establish an effective health, safety, and environmental (HSE) protection program. These programs must be appraised periodically to evaluate their effectiveness. The HSE Division began an appraisal program in November 1987, and over the next three years will perform operational and facility appraisals of the HSE programs of all Divisions. Appraisal teams are comprised of one representative each from the Safety (HSE-3), Industrial Hygiene (HSE-5), Waste Management (HSE-7), and Environmental Surveillance (HSE-8) groups. The responsibility of HSE-8 is to determine the effectiveness of divisional and facilities programs for ensuring compliance with applicable Laboratory policy, DOE orders and guidelines, federal and state regulations, and prudent management practices for protection of the environment and the general public.

Group HSE-8's appraisal includes evaluations of air emissions, liquid effluents, toxic substances use, waste management practices, and archaeological/cultural resources protection as applicable. The

Table 25. Tentative Findings by Topical Area and Category from the DOE Headquarters' Environmental Survey of Los Alamos National Laboratory 1987

Topical Area	Category I	Category II	Category III	Category IV
Air	0	0	0	2
Surface Water	0	2	3	3
Ground Water	0	0	1	2
Active Waste Disposal Areas	0	1	5	1
Chemical Handling	0	1	5	2
Hazardous Materials	0	1	2	1
Inactive Waste Disposal Areas	0	0	5	0
Quality Assurance	0	0	1	0

Group also evaluates whether the operation or facility is in accord with applicable environmental documentation such as an EIS, EA, ADM, or completed HSE Preliminary Project Questionnaire. The Group takes the opportunity during the appraisal to inform operations and facilities of potential environmental problems and of the availability of support from the Group for addressing these problems.

The HSE programs of Life Sciences and Facilities Engineering divisions were appraised in the last quarter of 1987.

N. Engineering Quality Assurance

The Laboratory has a Quality Assurance program (Facilities 1983) for engineering, construction, modification, installation, and maintenance of DOE facilities. The purpose of the program is to minimize the chance of deficiencies in construction; to improve the cost effectiveness of facility design, construction, and operation; and to protect the environment. A major goal of engineering quality assurance is to ensure operational compliance with all applicable environmental regulations. The quality assurance program is implemented from inception of design through completion of construction by a project team approach. The project team consists of individuals from the DOE's program division, the DOE's Albuquerque Operations, and Los Alamos Area Offices, the Laboratory's operating group(s), the Laboratory's Facility Engineering Division, design contractor, inspection organization, and construction contractor. Each proposed project is reviewed by personnel from the Environmental Surveillance Group (HSE-8) to ensure environmental integrity is maintained.

IX. ENVIRONMENTAL SUPPORT ACTIVITIES

In addition to environmental surveillance and compliance activities, the Laboratory carried out a number of related environmental activities. Selected studies are briefly described below. Many of these are ongoing and provide information for surveillance and compliance activities at the Laboratory.

A. Meteorological Monitoring (Brent Bowen, Jean Dewart, William Olsen, I-li Chen, and Margaret Salazar)

1. Weather Summary. Los Alamos received heavy precipitation for the third consecutive year, with 60 cm (23.6 in.) of water equivalent falling during 1987. Much of the precipitation was from record snowfall in January and February and from heavy rainfall in May and June. Snowfall totaled a record 453 cm (178.4 in.) for the year, over 3.5 times normal. Record snow fell in both January and February, including a record 122 cm (48 in.) from one storm during January. Heavy rains fell during May and locally (TA-59) during June. Temperatures were quite warm during October. Arctic air and several storms gave Los Alamos a cold December with near-record snowfall. The year as a whole had slightly cooler than normal temperatures. The annual summary is shown in Fig. 25 and other data are shown in Table G-63 through G-66.

A stormy pattern became established over the southwestern United States during January. One storm dropped nearly 25 cm (10 in.) on Los Alamos during the 7-8th and the record snowfall from one storm fell during the 15-17th. Even larger accumulations of 152-178 cm (60-70 in.) were reported in northern Los Alamos. The storm closed the Laboratory and the townsite. The locally large snowfall resulted from a stationary storm in Arizona forcing relatively warm air northward over the Pajarito Plateau and an arctic air mass. Only several inches fell in the Rio Grande Valley and Santa Fe. The snowfall helped give Los Alamos its snowiest month on record of nearly 165 cm (65 in.), exceeding the old record by nearly 61 cm (2 ft). Also, the 102 cm (40 in.) of snow on the ground on the 16th and 17th set a record. After 5 cm (2 in.) of snowfall two days later, temperatures rose dramatically, reaching 12.2°C (54°F) on the 27th. Except for another 10 cm (4 in.) of snow on January 31st, temperatures remained warm through the middle of February, with the snow cover shrinking to 2.5 cm (1 in.) by the 14th. The stormy pattern returned, however, with a 11.4 cm (4.5 in.) snowfall on the 16th. Then, an intense storm dropped nearly 68 cm (27 in.) of snow during the 18-20th, including 51 cm (20 in.) on the 19th. This snowfall became the largest for February on record. A week later, another storm dropped 43 cm (17 in.) of snow during the 24-26th. Some of the snow was accompanied by thunder and lightning. The total snow of 123 cm (48.5 in.) was the largest on record for February and second only to the previous month for all months. In addition, this month became the wettest February on record with 7.1 cm (2.78 in.) of water equivalent precipitation.

Winter weather moderated during March, with near-normal weather. Except for a storm that dropped 30 cm (12 in.) of wet snow on April 4-5th, warm weather prevailed during April. Frequent thundershowers produced 7.2 cm (2.83 in.) of rain during May, nearly 2-1/2 times the normal. One thunderstorm produced up to 7.6 cm (3 in.) of hail on the 23rd.

The summer began with a downpour at TA-59 on June 7th. A local thunderstorm dropped 5.5 cm (2.16 in.) of rain, with 5.4 cm (2.11 in.) falling in two hours. The two hour rainfall represented a near 50 year rainfall. Very little or no rain fell at other sites. Rainfall was scant in July with 3.5 cm (1.37 in.), less than half of normal. Rainfall was normal during August with 10.9 cm (4.29 in.). Thunderstorms produced a funnel cloud on the 24th and numerous funnel clouds on the 25th near Santa Fe.

Near-normal weather conditions prevailed during September. A strong high-pressure system centered over the Western United States gave Los Alamos a warm and dry October. High temperatures for the month averaged (19.1°C) (66.4°F), nearly 2°C (4°F) above normal. Rainfall was light at 1.2 cm (0.49 in.), less than one-third of normal. Near-record snows fell during December, with a total of over 91 cm (36 in.). The biggest snowfall of 48 cm (19 in.) on the 24-25th gave Los Alamos its whitest Christmas on record, with 41 cm (16 in.) of snow on the ground. The year ended with 453 cm (178.4 in.) of snow, exceeding the previous record of 287 cm (112.8 in.) set in 1984.

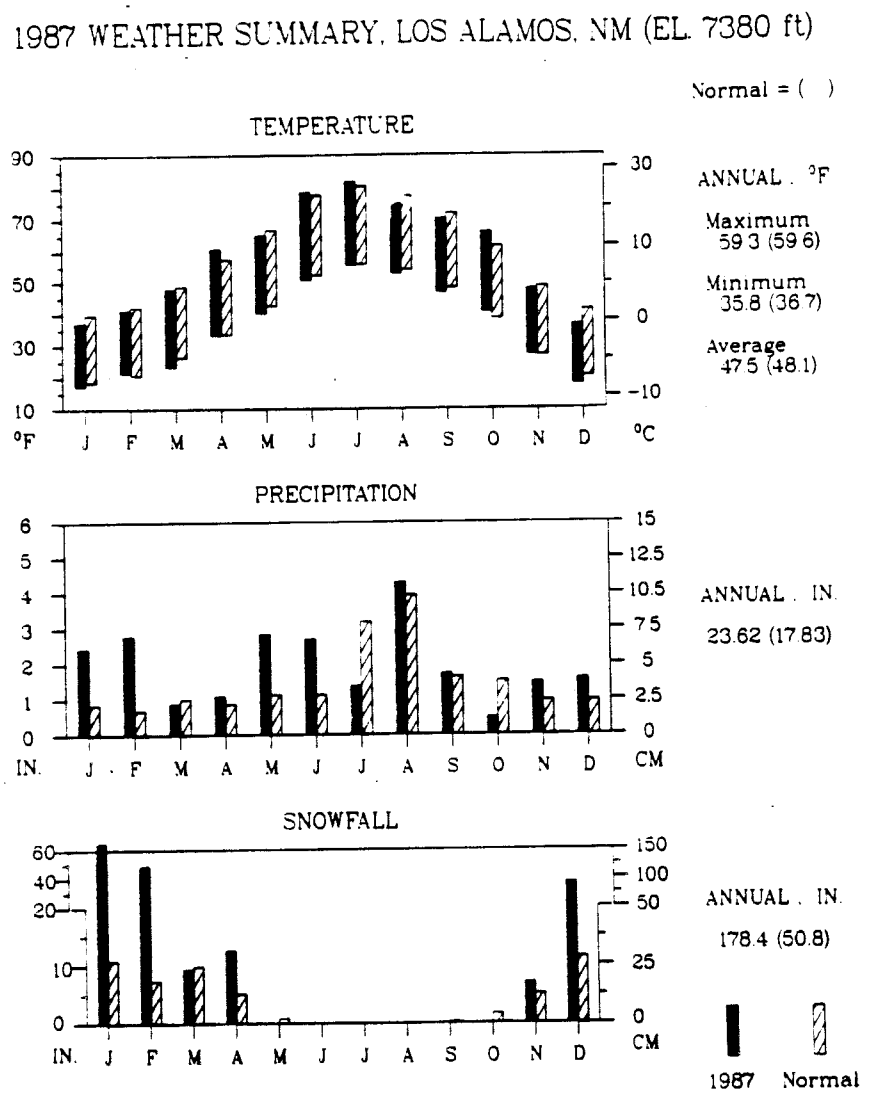

Fig. 25. Summary of 1987 weather in Los Alamos (data from Occupational Health Laboratory, OHL, TA-59.

2. **Wind Roses.** The 1987 surface wind speed and direction measured from three sites at Los Alamos are plotted in wind roses for day, night, and total hours (Figs. 26 through 28). A wind rose is a circle with lines extending from the center representing the direction *from* which the wind blows. The length of each line is proportional to the frequency of the wind speed interval from that particular direction. Each direction is one of 16 primary compass points (N, NNE, etc.) and is centered on a 22.5 sector of the circle. The frequency of the calm winds, defined as those having speeds less than 0.5 m/s (1.1 mph), is given in the circle's center. Day and night are defined by the times of sunrise and sunset.

The wind roses represent winds at TA-50 (2216 m above sea level or MSL [7019 ft]), East Gate (2140 m MSL [7019 ft]), and Area-G (2039 m MSL [6688 ft]). Surface winds were measured at a height of about

1987 WEATHER SUMMARY, LOS ALAMOS, NM (EL. 7380 ft)

Normal = ( )

TEMPERATURE

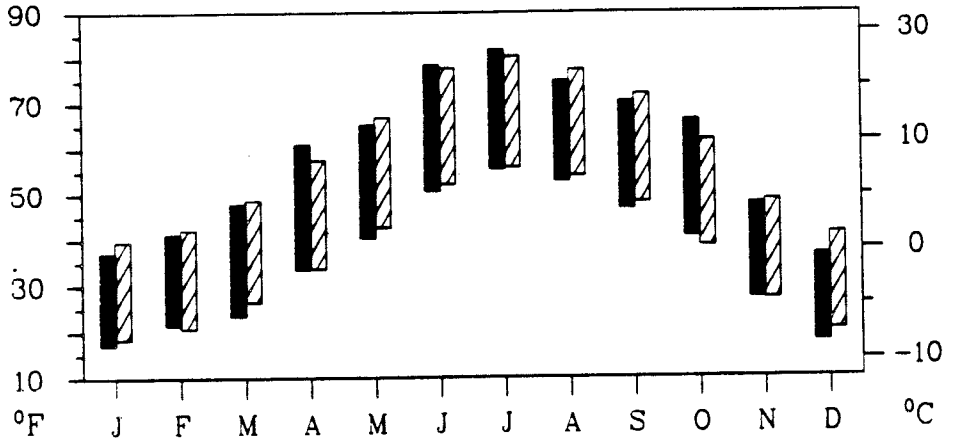

ANNUAL , °F

Maximum
59.3 (59.6)

Minimum
35.8 (36.7)

Average
47.5 (48.1)

PRECIPITATION

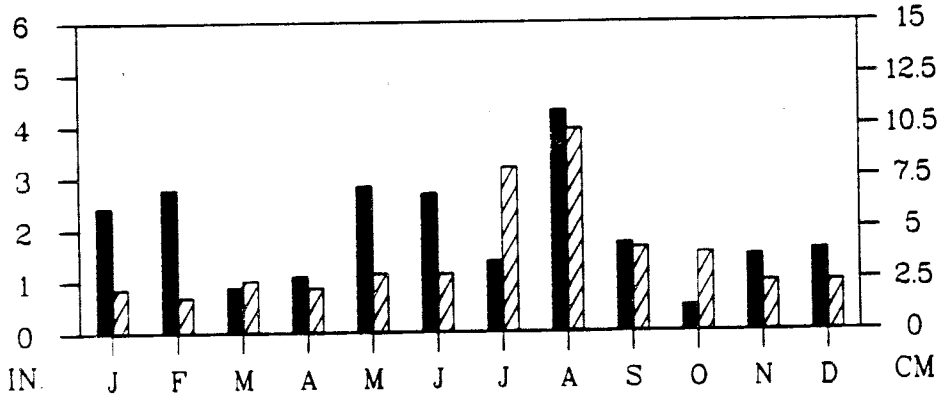

ANNUAL , IN.

23.62 (17.83)

SNOWFALL

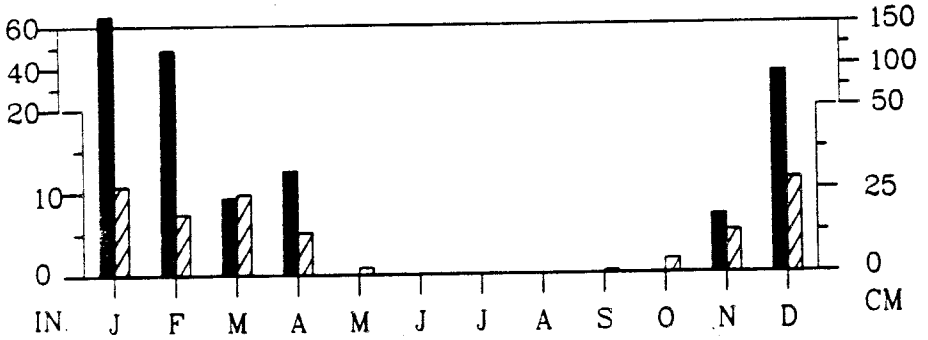

ANNUAL , IN.

178.4 (50.8)

1987 Normal

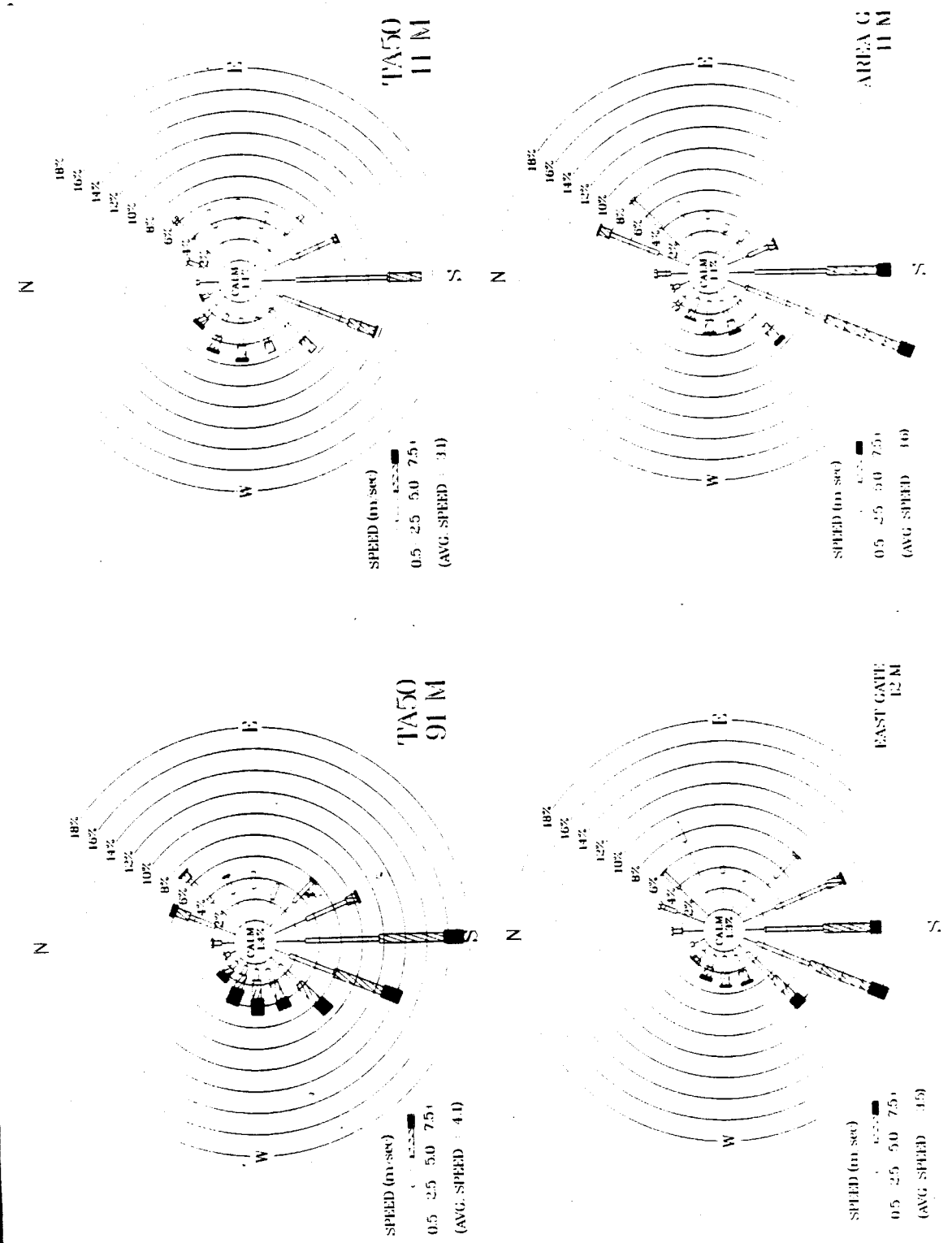

Fig. 26. Daytime wind roses at Laboratory stations during 1987.

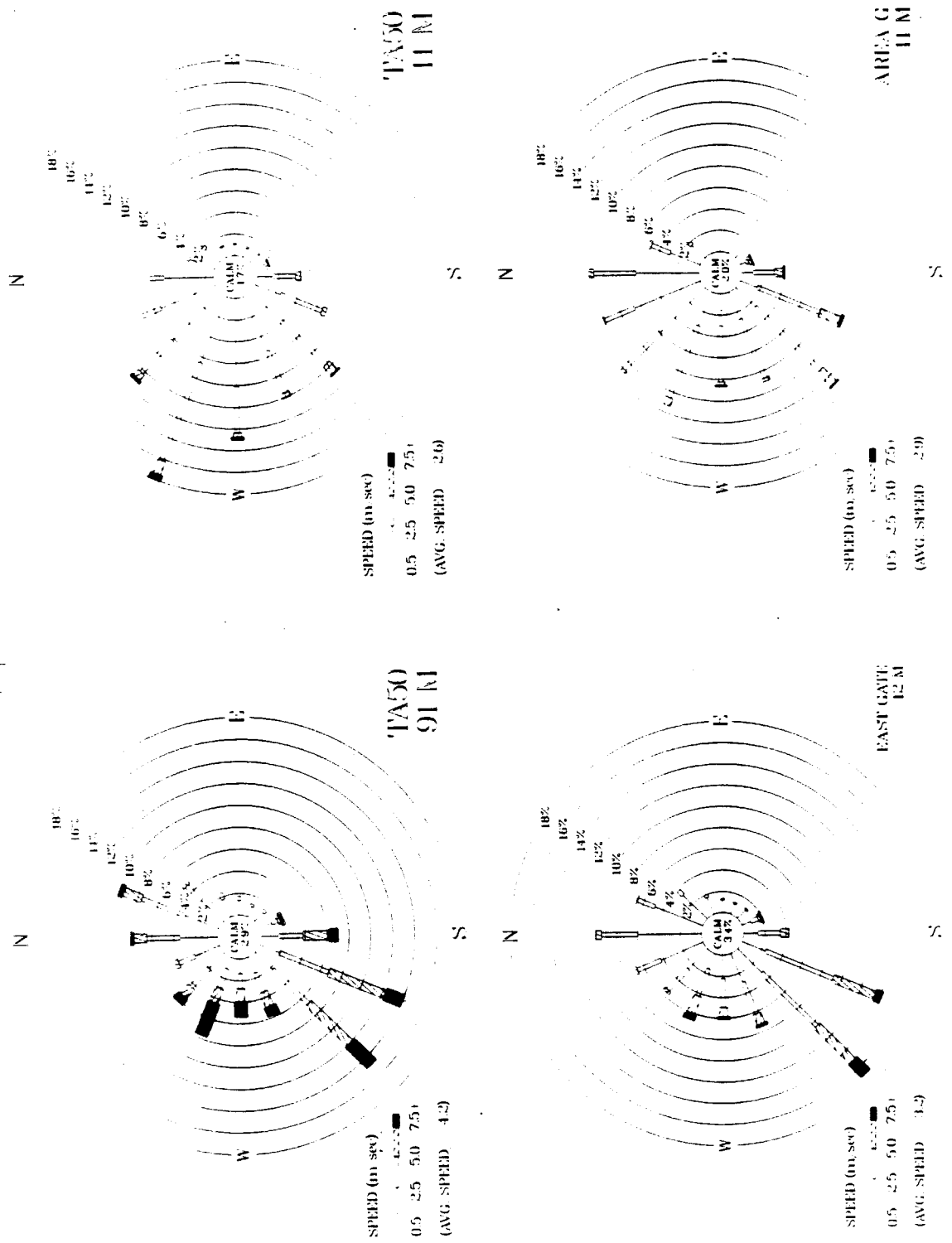

Fig. 27. Nighttime wind roses at Laboratory stations during 1987.

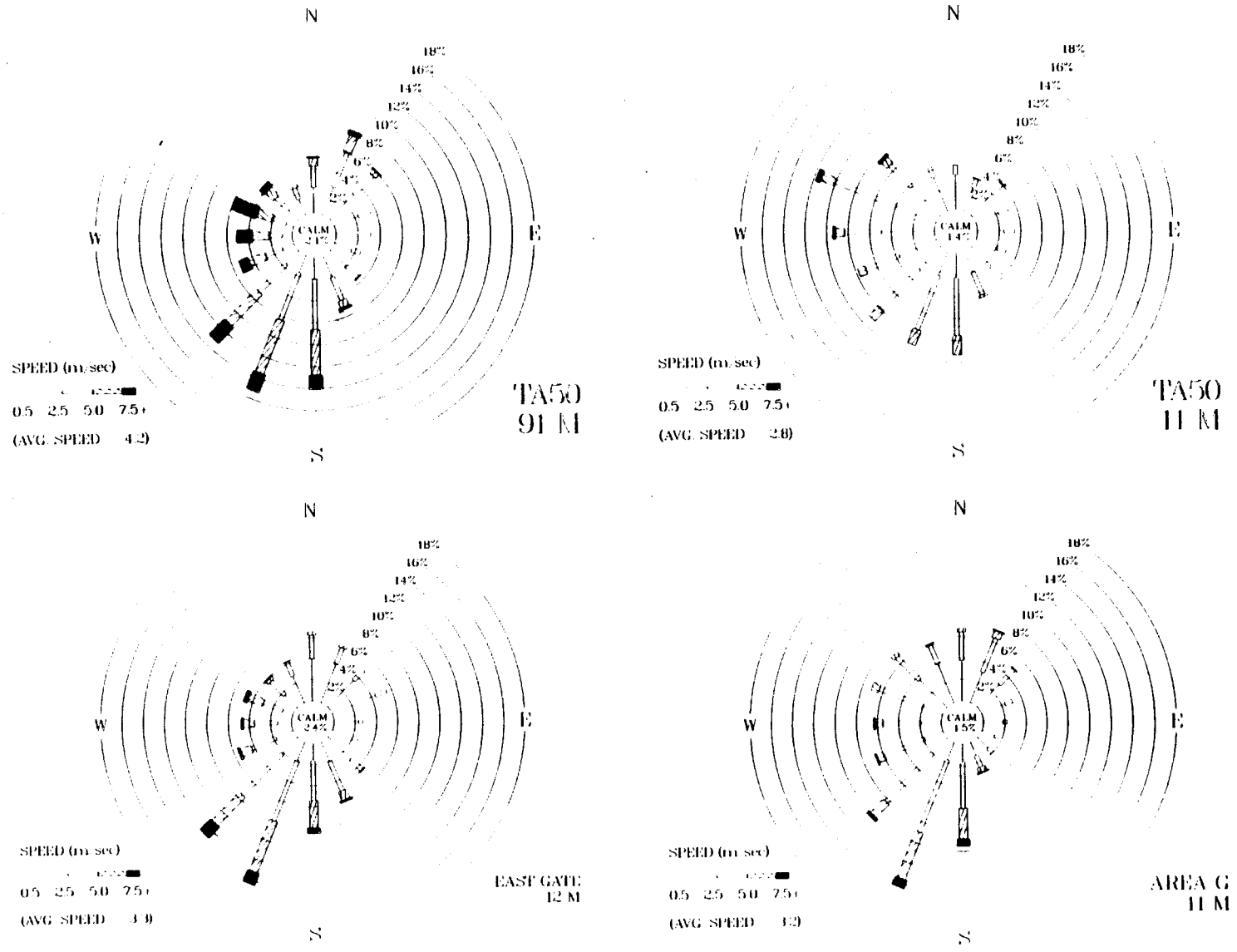

Fig. 28. Cumulative wind roses at Laboratory stations in 1987.

11 m (36 ft) at the three sites and an upper level wind rose is shown for the 91 m (300 ft) level at TA-50. Data recovery exceeded 96% at all sites.

Surface winds at Los Alamos are generally light with the average speed of nearly 3 m/s (7 mph). Wind speeds greater than 5 m/s (11 mph) occurred with frequencies ranging from 10% at TA-50 to 21% at East Gate. Many of the strong winds occurred during the spring. Over 40% of surface winds at all sites were less than 2.5 m/s (5.5 mph). The average wind speed increases to over 4 m/s (9 mph) at 91 m (300 ft). Wind speeds greater than 5 m/s (11 mph) occurred 34% of the time while speeds less than 2.5 m/s (5.5 mph) occurred 29% of the time at the higher level.

Distribution of winds varies with site, height above ground, and time of day primarily because of the terrain features found at Los Alamos. On days with sunshine and light large-scale winds, a deep, thermally driven upslope wind develops over the Pajarito Plateau. Note the high frequency of SE through S winds during the day at TA-50 (both levels) and East Gate (Fig. 26). Upslope winds are generally light, less than 2.5 m/s (5.5 mph). Winds become more SSW and S at Area G (i.e., at lower elevations). The winds here are more affected by the Rio Grande Valley than the plateau. Channeling of regional-scale winds by the valley contributes to the high frequency of SSW and NNE or NE winds. In addition, a thermally driven up-valley wind probably causes some of the SSW winds under 2.5 m/s (5.5 mph) at Area G.

Winds display a reversal during the night. A shallow drainage wind often forms and flows down the plateau on clear nights with light, large-scale winds. These winds are generally less than 2.5 m/s (5.5 mph). Surface wind peaks from the NW through W are evident at TA-50, whereas the drainage wind at Area G is evenly distributed from the WNW through the N. Downslope winds are much less frequent at East Gate. The TA-50 wind rose at 91 m (300 ft) shows dramatically different winds from those at the surface, with valley-channeled winds dominating. A high frequency of winds are up-valley (SW and SSW) and down-valley (N through NE). Note that less frequent channeled winds also occur at the lower sites, East Gate and Area G, during the night.

3. **Precipitation Summary.** Precipitation in Los Alamos County was heavy during 1987, with as much as 61 cm (24 in.) falling in the North Community and at TA-59. Figure 29 shows analyses of rainfall for the summer season (June-August) and the entire year. Monthly precipitation totals are presented in Table G-64. Record January and February and near-record December snowfalls helped to push 1987 precipitation to about 30% above normal at the western sites near the Jemez Mountains. Summer rainfall was generally below normal. The maximum area of summer rainfall included TA-59. A thunderstorm dumped 5 cm (2 in.) of rain locally at TA-59 during a single day in June. Precipitation was generally the highest in the northwestern part of the area, near the mountains and where the highest terrain is. Precipitation decreased with decreasing elevation and distance from mountains.

B. Environmental Restoration (ER) Program (Kenneth Rea, Robert Vocke, Roger Ferenbaugh, Robert Gonzales, Marjorie Martz-Emerson, Betty Perkins, and Alan Stoker)

The DOE facilities operate under a policy of full compliance with applicable environmental regulations. The DOE's Albuquerque Operations Office (AL) Environmental Restoration (ER) Program is being implemented to help fulfill that commitment at installations within the AL complex, including facilities in California, Colorado, Florida, Missouri, New Mexico, Ohio, and Texas. The program assists DOE in setting environmental priorities and in justifying funding enhancements of existing programs or remedial actions. Implementation of the ER Program is being accomplished through the combined efforts of the AL complex. The Laboratory is providing programmatic guidance/management and technical support to AL for ER implementation.

The program is designed to identify, assess, and correct existing or potential environmental concerns. The scope includes the review of major environmental regulations, with emphasis on CERCLA/SARA and RCRA. The program includes evaluation of management practices for hazardous substances. Additionally, assessment of pollution control of and monitoring programs for hazardous substances emphasizes both adequate understanding of environmental pathways and regulatory compliance. Implementation of the ER Program is intended to help fulfill DOE's obligations for federal facilities under the EPA's CERCLA/SARA. The program was initially implemented in five phases (i.e., Installation Assessment, Remedial Investigation, Feasibility Study, Remedial Action, and Compliance and Verification).

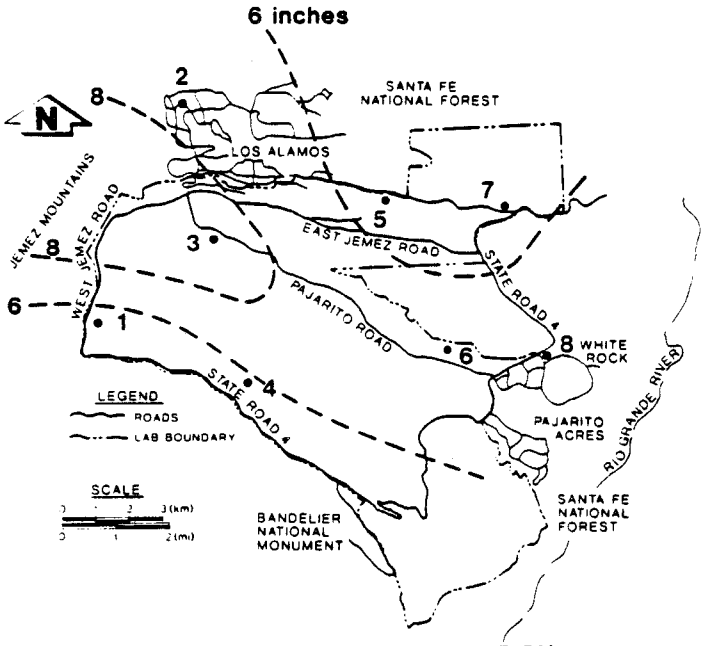

1987 SUMMER PRECIPITATION

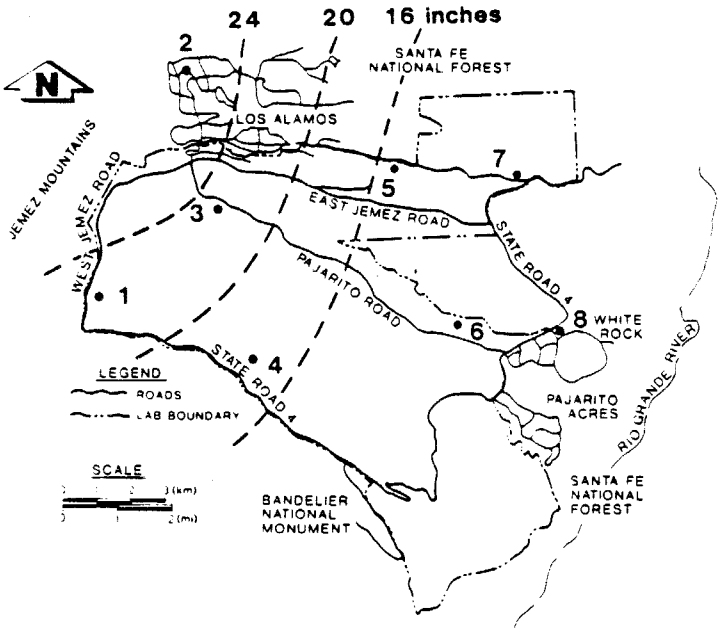

1987 TOTAL PRECIPITATION

Fig. 29. Summer (June-August) and annual rainfall during 1987 (inches).

During 1987, the Phase I reports for Pinellas, Sandia National Laboratories-Livermore and Los Alamos National Laboratory were released to the EPA and appropriate states. The Phase I reports for the other major AL installations were released in 1986.

Remedial investigation plan (RIP) development and remedial investigations proceeded at all eight AL installations during 1987. The installation generic monitoring plans (IGMPs) that have been prepared for each DOE/AL installation are being tiered to the DOE/AL CERP generic monitoring plan (CGMP), which was prepared during 1986. Remedial investigation plans that will be prepared for each AL installation will be tiered to the appropriate IGMP.

The draft Phase I report for Los Alamos was released to the state of New Mexico and the EPA during October 1987. The Laboratory's IGMP will be ready for internal review during early 1988. Several site-specific RIPs will be prepared for the Laboratory during 1988.

Remedial investigations at Los Alamos during 1987 consisted of the White Rock Y and the Potrillo Canyon studies. Reconnaissance geophysics studies were also conducted at TA-21. Additionally, substantial information was acquired for preparing site-specific RIPs at TA-21, TA-33, and TA-49.

C. Vadose Zone Characterization at Areas L and G (Alice Barr, Anthony Grieggs, and David McInroy)

The Resource Conservation and Recovery Act (RCRA) requires that hazardous waste disposal facilities such as the Laboratory either (1) perform ground water monitoring, or (2) obtain a waiver of ground water monitoring requirements, provided there is a low potential for migration of hazardous waste or constituents from the disposal areas to water supply wells via the uppermost aquifer. A vadose zone (unsaturated zone above the main aquifer) characterization program was initiated to substantiate the Laboratory's request for a ground water monitoring waiver.

At Areas L and G (TA-54), the uppermost aquifer is approximately 300 m (1000 ft) below the surface. The zone above the aquifer (the vadose zone) was studied to characterize its hydrogeology and evaluate the potential for contaminant migration. Data were collected to determine intrinsic permeability, moisture characteristic curves, unsaturated hydraulic conductivity, pore gas distribution, and actual contaminant presence in the vadose zone. Several conclusions were reached from this study, including the following: (1) the dominant mechanism of subsurface transport is through vapor phase migration--aqueous transport of contaminants is highly unlikely; (2) perched water is confined to the alluvium in the adjacent canyon and does not extend beneath the mesa or connect hydraulically to the main aquifer; (3) some metal contamination exists at shallow depths in Area L; (4) organic vapor contamination exists in Areas L and G; (5) no contamination was evident in the perched canyon water; and (6) vertical cooling fractures are present in the disposal areas but their ability to transport contaminants and water has not been determined. A final report presenting these findings and the data collected was submitted to the NMEID's Hazardous Waste Program on March 31, 1987.

The analytical results of this study indicated the presence of organic vapor contamination at depths up to 30 m (100 ft). As a result, the Laboratory has initiated a program to determine the vertical and horizontal extent of this contamination and appropriate remediation, if deemed necessary. The program consists of four phases: (1) an initial experimental effort to determine the most effective method for monitoring hole completion and sampling; (2) an expanded sampling and analytical program to delineate the extent of contamination; (3) interpretation of results and proposal of any necessary remedial action; and (4) the remediation itself.

The first phase is now in progress. Four different (1 existing, 3 new) borehole completions have been sampled. Initial analytical results indicate the new sampling technique is more effective in determining a concentration gradient. Also, the three new completion methods surpass the existing borehole in sensitivity, ease of installation and cost. Additional sampling will be performed to substantiate these findings before proceeding to the second phase.

D. Remedial Investigations at the Proposed White Rock Y Interchange (Lars Soholt, Richard Romero Eddie Lujan, John Salazar and Thomas Buhl)

The state of New Mexico is proposing to construct an interchange to improve the intersection of State Road 4 (SR 4) and the Main Hill Road (Alternate SR 4) into the Los Alamos townsite. The DOE intends to grant an easement to the state for construction and maintenance of the interchange on DOE-managed lands. The easement area would include

parts of Los Alamos and Lower Pueblo canyons that are known to have residual radioactivity at levels above background. This residual radioactivity is the result of liquid discharges from TA-2, TA-21, and TA-45. As part of DOE's ER Program, the Environmental Surveillance Group (HSE-8) carried out an investigation to determine if the lands were suitable for release to the state without remedial action to lower levels of residual radioactivity. The results of this remedial investigation indicate that the lands in Los Alamos and Lower Pueblo canyons are suitable for construction of the White Rock Y interchange without need for remedial action.

Above-background, residual radioactivity in Los Alamos Canyon is dominated by cesium-137 (up to 50 pCi/g) and strontium-90 (up to 13 pCi/g). Uranium and transuranics are also present at above-background levels, but activity concentrations are lower. These radionuclides have deposited in the alluvial accumulation of sediment where the canyon's stream intersects State Road 4. Within Lower Pueblo Canyon, plutonium-239 is the dominant residual radionuclide (up to 15 pCi/g), and uranium is also present at above-background levels. These radionuclides have deposited where the canyon's stream widens, upstream from its confluence with Los Alamos Canyon.

Transport pathways analyses were carried out using conservative scenarios to determine if the levels of residual radioactivity indicated that remedial action was necessary prior to granting an easement to the state. The two scenarios that were considered were:

- Construction activity in Los Alamos and Lower Pueblo canyons; and
- Removal of soil material for use in a home garden.

Potential pathways of exposure within the construction scenario include worker inhalation of dust suspended during earth-moving activities and direct exposure to gamma radiation from residual cesium-137. Within the home garden scenario, it was assumed that material was removed from the construction site for use as garden soil. Potential pathways for exposure of a home gardener include direct gamma radiation from cesium-137, inhalation of dust suspended during gardening activities, ingestion of produce grown in the garden, and ingestion of water from a nearby well which has received radionuclides leached from garden soils.

For residual radioactivity in Los Alamos Canyon, the pathways analyses resulted in a calculated commitment of 9 mrem/yr effective dose equivalent within the construction scenario and 29 mrem/yr effective dose equivalent within the home-garden scenario. For residual radioactivity in Lower Pueblo Canyon, the pathways analyses resulted in a calculated commitment of 4 mrem/yr effective dose equivalent within the construction scenario and 9 mrem/yr effective dose equivalent within the home-garden scenario. All of these doses are less than the 100 mrem/yr effective dose equivalent commitment that serves as DOE's radiation protection standard for protection of the general public. Maximum concentrations of airborne radionuclides during construction would be less than 15% of DOE's limits for exposure of the general public.

E. Environmental Monitoring at the Fenton Hill Site [William Purtymun, Roger Ferenbaugh, (HSE-9), Max Maes and Mary Williams (HSE-9)]

The Laboratory is currently evaluating the feasibility of extracting thermal energy from the hot dry rock geothermal reservoir at the Fenton Hill Geothermal Site (TA-57). The site is located about 45 km (28 mi) west of Los Alamos on the southern edge of the Valles Caldera. The hot dry rock energy concept involves drilling two deep holes, connecting these holes by hydraulic fracturing, and bringing thermal energy to the surface by circulating water through the system. Environmental monitoring is performed adjacent to the site to assess any impacts from the geothermal operations.

The chemical quality of surface and ground waters in the vicinity of TA-57 (Fig. 30) has been determined for use in geohydrologic and environmental studies. These water quality studies began before construction and testing of the hot dry rock system (Purtymun 1974D). The most recent samples were collected in November 1987.

Surface water stations (13 on the Jemez River, the Rio Guadalupe, and their tributaries) are divided into four general groups based on the predominate ions and TDS (Table 26). The predominate ions are (1) sodium and chloride, (2) calcium and bicarbonate, (3) calcium and sulfate, and (4) sodium and bicarbonate. Ground water stations (five mineral and hot springs, one well, and five springs) are also grouped according to predominate ions. These ions are (1) sodium and chloride, (2) calcium and bicarbonate, and (3) sodium and bicarbonate (Table 26).

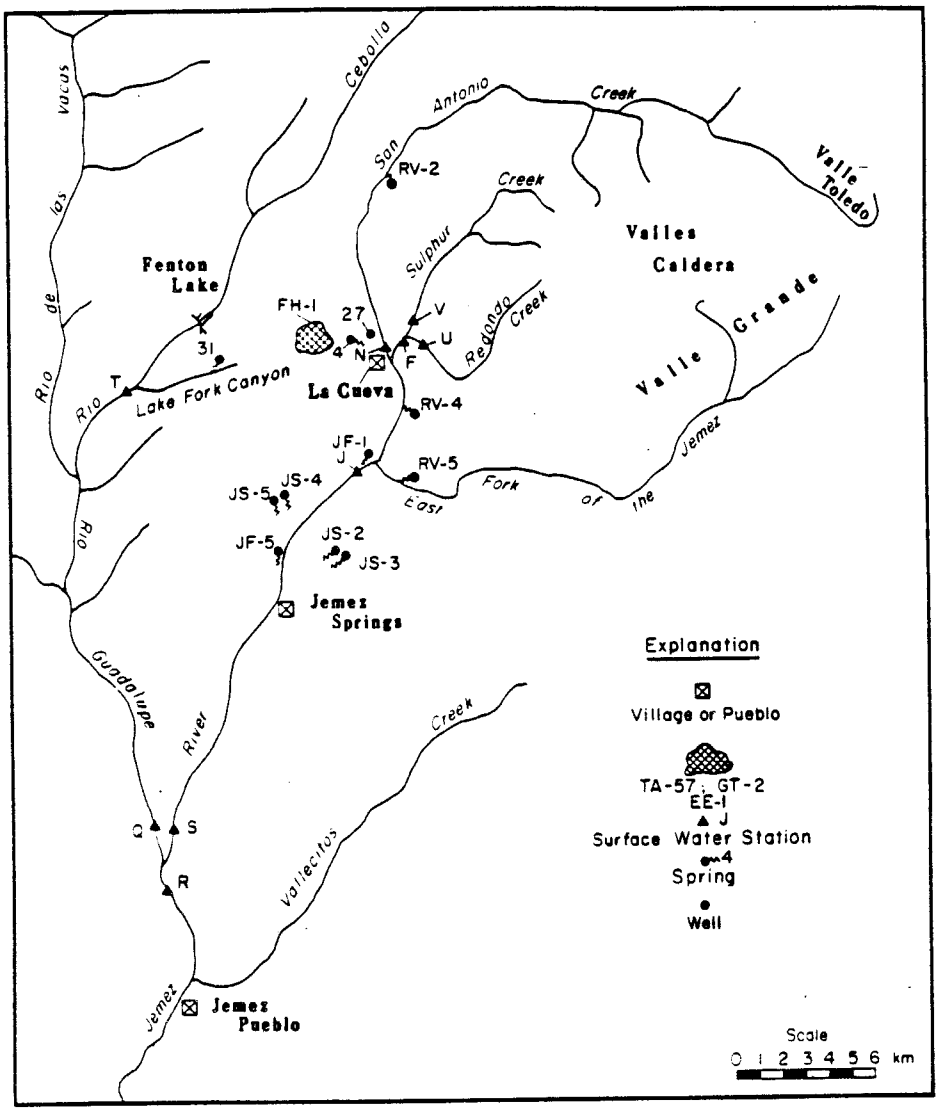

Fig. 30. Sampling stations for surface and ground water near the Fenton Hill Site (TA-57).

There were no significant changes in the chemical quality of surface and ground water at the individual stations from previous years (Purtymun 1988A).

F. Distribution of Radionuclides in Channel Alluvium of Mortandad Canyon [Donald VanEtten, William Purtymun, Max Maes, and Richard Peters (HSE-9)]

Trace amounts of radionuclides remaining in effluent are released from the treatment plant at TA-50 into the adjacent Mortandad Canyon (Table G-12). The effluent recharges a shallow body of ground water in the alluvium. The radionuclides in the effluent are adsorbed or bound to the sediments in the channel, reducing the amount found in the water of the shallow aquifer. This shallow aquifer is of limited extent and lies within the Laboratory boundary.

The sediments and radionuclides in the stream channel alluvium are subject to transport by additional releases of effluent or by storm run-off. The small drainage area of the canyon and the ability of the thick

Table 26. Quality of Surface and Groundwaters at Fenton Hill Geothermal Site
(concentrations in mg/L)
November

Surface Water

	Na	Cl	TDS
Sodium Chloride			
Redondo Creek (U)	10	15	126
Jemez River (R)	75	97	436
Jemez River (S)	85	132	388

	Na	HCO_3	TDS
Calcium Bicarbonate			
San Antonio Creek (N)	16	62	141
Rio Cebolla (T)	10	88	118
Rio Guadalupe (Q)	15	170	228
Lake Fork 1 (LF-1)	10	54	132
Lake Fork 2 (LF-2)	17	71	168
Lake Fork 3 (LF-3)	13	50	220
Lake Fork 4 (LF-4)	15	72	284

	Ca	SO_4	TDS
Calcium Sulfate			
Sulphur Creek (V)	52	305	456
Sulphur Creek (F)	28	66	150

	Na	HCO_3	TDS
Sodium Bicarbonate			
Jemez River (J)	16	59	104

Groundwater

	Na	Cl	TDS
Sodium Chloride			
Loc. JF-1 (Hot Spr)	460	1000	1940
Loc. JF-5 (Hot Spr)	960	2300	3830

	Ca	HCO_3	TDS
Calcium Bicarbonate			
FH-1 (Supply Well)	48	117	280
Loc. 39 (Spr)	13	41	52

	Na	HCO_3	TDS
Sodium Bicarbonate			
JS-2, 3 (Spr)	17	80	160
JS-4, 5 (Spr)	17	72	154
Loc. 4 (Spr)	16	55	92
Loc. 31 (Spr)	11	62	110
RV-2 (Hot Spr)	22	45	114
RV-4 (Hot Spr)	52	123	168
RV-5 (Hot Spr)	20	83	78

---

[a]See Fig. 30 for sampling locations. One sample taken at each location.

section of unsaturated alluvium to store the run-off has prevented transport to the Laboratory boundary. To confine the surface run-off and contaminants within the Laboratory, there has been a series of sediment traps installed in the canyon since early 1970. The traps range from gravel-filled galleries to stilling basins that contain suspended solids as well as bed sediment (alluvium).

A storm on June 7, 1987, produced a record 50-year, 2-hr rainfall of 5.5 cm (2.16 in.). The rainfall resulted in the largest run-off event in Mortandad Canyon since hydrologic studies began in 1960. The peak discharge in the upper canyon at gaging station GS-1 was estimated to be 4.5 m^3/s (160 ft^3/s [cfs]). Two other large run-off events occurred in August 1968 (3.2 m^3/s [115 cfs]) and November 1987 (2.9 m^3/s [102 cfs]). The peak discharge at the sediment traps of the June 1987 event was about 3 m^3/s (100 cfs). The run-off filled the two sediment traps and overflowed into the third. The estimated volume of run-off was 3500 m^3 (930 000 gal.).

A set of sediment samples were collected in the canyon on June 16 and analyzed for transuranics and gamma emitting radionuclides (Fig. 31). The concentrations of plutonium and americium above the effluent outfall from TA-50 (stations 1, 2, and A) were background (Table 27). The ^{238}Pu concentrations between gaging station GS-1 to station 7 just above the sediment trap ranged from 3.3 to 11.7 pCi/g, and the $^{239,240}Pu$ in the same reach of canyon ranged from 12.2 to 39.3 pCi/g. The ^{241}Am for this same sampling area ranged from 11.72 to 33.81 pCi/g. The largest concentrations of transuranics in sediments were in sediment trap 1 with 18 pCi/g of ^{238}Pu, 58.9 pCi/g of $^{239,240}Pu$, and 79.50 pCi/g of ^{241}Am. The concentrations decreased in trap 2 and decreased further in trap 3. All of the bed sediments and most of the suspended sediments were retained in trap 1, resulting in higher concentrations here than in traps 2 and 3.

Gamma-emitting radionuclides followed the same trends as transuranics (Table 28). The concentrations above the effluent outfall were background. The highest concentrations were for ^{137}Cs with a range from 15.3 to 62.9 pCi/g in the channel above the traps and 96.7 pCi/g in trap 1. Trace amounts of ^{134}Cs, $^{59,60}Co$, and ^{75}Se were found in the channel sediment samples with the highest concentrations in the sediment traps.

The sediments from traps 1 and 2 were analyzed using EPA's toxic characteristic leach procedure (TCLP) to identify hazardous wastes. Analyses were carried out for pesticides (8 compounds), extractable organics (15 compounds), volatile organics (18 compounds), and metal (8 elements). None of these were detected.

Previous run-off events have not been contained in the area of the sediment traps. The analyses of sediments below the traps indicated that run-off events had carried radionuclides to station 10. Below station 10 and still within the Laboratory, the concentrations of radionuclides were at or below background. The

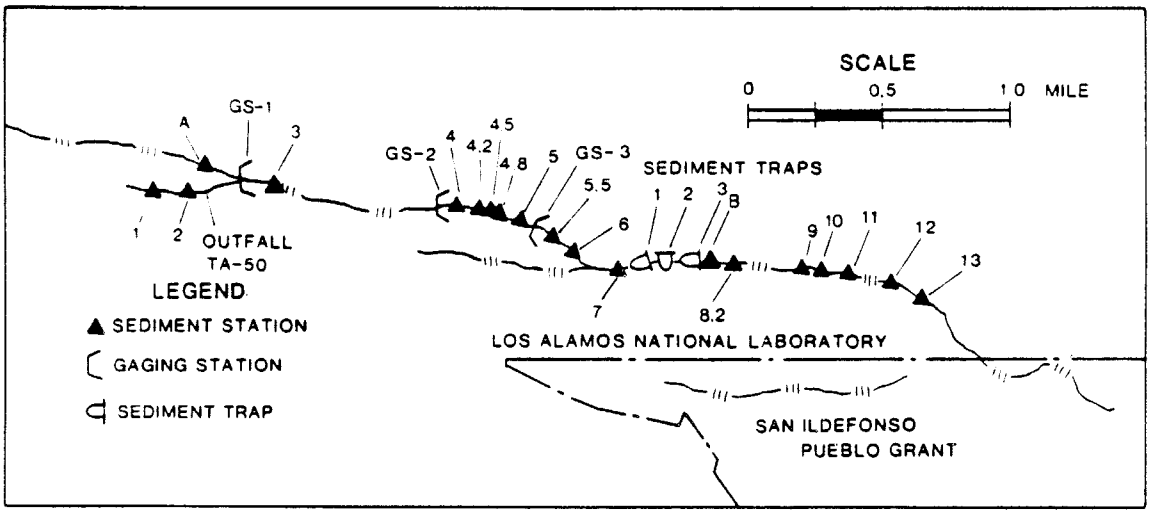

Fig. 31. Sediment sampling stations in Mortandad Canyon.

Table 27. Transuranics in Mortandad Canyon Channel Alluvium, June 16, 1987[a]

Station	^{238}Pu (pCi/g)		$^{239,240}Pu$ (pCi/g)		^{241}Am (pCi/g)	
Effluent Canyon						
1	0.012	(0.007)	0.024	(0.011)	-0.008	(0.002)
2	0.011	(0.006)	0.033	(0.011)	0.130	(0.050)
TA-50 Outfall	0.712	(0.058)	1.81	(0.107)	0.970	(0.050)
Mortandad Canyon						
A	0.005	(0.009)	0.033	(0.010)	0.02	(0.002)
GS-1	3.91	(0.330)	16.2	(1.20)	11.72	(0.14)
3	7.69	(0.580)	17.6	(1.30)	16.79	(0.17)
GS-2	7.00	(0.560)	24.6	(1.80)	31.96	(0.24)
4	7.27	(0.550)	26.2	(1.80)	33.81	(0.24)
4.2	11.7	(0.070)	39.3	(2.30)	22.08	(0.20)
4.5	4.69	(0.37)	18.9	(1.30)	19.85	(0.20)
4.8	4.26	(0.390)	18.1	(1.40)	28.76	(0.22)
5	7.11	(0.690)	29.7	(2.20)	20.51	(0.19)
GS-3	4.67	(0.450)	20.1	(1.60)	22.60	(0.19)
5.5	5.67	(0.430)	24.5	(1.60)	27.71	(0.22)
6	6.29	(0.610)	16.2	(1.40)	14.60	(0.16)
7	3.30	(0.171)	12.2	(0.519)	16.53	(0.17)
Sediment Trap 1	18.2	(1.30)	58.9	(3.90)	79.50	(0.40)
Sediment Trap 2	9.71	(0.750)	35.8	(2.60)	51.42	(0.31)
Sediment Trap 3	2.06	(0.126)	7.06	(0.329)	10.11	(0.13)
3	2.13	(0.24)	7.17	(0.64)	12.53	(0.15)
8.2	0.105	(0.018)	0.399	(0.037)	0.56	(0.03)
10	0.09	(0.02)	0.33	(0.04)	0.31	(0.03)
11	0.095	(0.024)	0.330	(0.042)	0.01	(0.002)
12	-0.025	(0.017)	0.010	(0.012)	0.1	(0.01)
13	-0.010	(0.011)	0.089	(0.020)	0.8	(0.002)

[a]Location of sediment stations shown on Fig. 31; counting uncertainty in parentheses.

maintenance of the sediment traps is essential to contain residual radioactivity within the Laboratory boundaries.

G. Underground Storage Tanks (James White, Alice Barr, David McInroy, and Steven McLin)

Subtitle I of the Hazardous and Solid Waste Amendments to the Resource Conservation and Recovery Act has broadened the scope of underground tank regulations. Previously, only Subtitle C of RCRA regulated those underground tanks that contained hazardous waste. Subtitle I now brings underground tanks that contain regulated substances under RCRA regulation. Along with the requirement for EPA to promulgate specific regulations, several major provisions have been included in this new program. Among them are: the requirement to notify of existing tanks; the provision granting EPA authority to inspect the test tanks and to enforce regulatory requirements through the use of administrative orders, injunctions or civil penalties; the provision subjecting tanks controlled by the federal government to Subtitle I; and the requirement to satisfy statutory standards for new tanks.

Table 28. Radionuclides in Mortandad Canyon Channel Alluvium, June 16, 1987[a]

Station	^{137}Cs (pCi/g)	^{134}Cs (pCi/g)	^{60}Co (pCi/g)	^{57}Co (pCi/g)	^{75}Se (pCi/g)
Effluent Canyon					
1	0.24 (0.10)	0.11 (0.09)	0.07 (0.14)	0.39 (0.21)	-0.11 (0.14)
2	0.005 (0.07)	-0.12 (0.09)	-0.07 (0.12)	0.02 (0.14)	-0.03 (0.09)
TA-50 Outfall	0.69 (0.14)	0.28 (0.12)	0.16 (0.13)	1.56 (0.33)	0.71 (0.17)
Mortandad Canyon					
A	0.13 (0.09)	0.03 (0.08)	-0.10 (0.11)	0.09 (0.014)	0.003 (0.008)
GS-1	15.30 (2.31)	0.83 (0.17)	1.73 (0.30)	15.60 (2.36)	2.82 (0.44)
3	30.20 (4.55)	0.25 (0.18)	0.73 (0.20)	8.23 (1.26)	2.13 (0.36)
GS-2	48.90 (7.36)	0.10 (0.09)	0.40 (0.16)	4.30 (0.69)	2.00 (0.34)
4	62.90 (9.46)	0.97 (0.18)	0.35 (0.14)	3.52 (0.55)	1.92 (0.31)
4.2	31.60 (4.76)	0.34 (0.11)	0.23 (0.17)	3.00 (0.53)	1.27 (0.24)
4.5	37.30 (5.63)	0.56 (0.16)	0.18 (0.17)	1.80 (0.35)	0.73 (0.17)
4.8	43.20 (6.50)	0.78 (0.15)	0.12 (0.12)	1.99 (0.33)	1.33 (0.23)
5	23.50 (3.55)	0.29 (0.12)	0.02 (0.15)	1.75 (0.36)	0.79 (0.18)
GS-3	39.50 (5.95)	0.84 (0.16)	0.20 (0.12)	1.45 (0.25)	0.76 (0.15)
5.5	55.40 (8.33)	0.98 (0.19)	0.24 (0.12)	2.08 (0.35)	1.24 (0.23)
6	53.30 (8.01)	0.16 (0.11)	0.11 (0.16)	1.02 (0.29)	0.21 (0.12)
7	29.70 (4.48)	0.34 (0.10)	-0.18 (0.12)	0.85 (0.21)	0.34 (0.12)
Sediment Trap 1	96.70 (19.5)	0.24 (0.12)	1.36 (0.26)	11.70 (1.79)	7.64 (1.17)
Sediment Trap 2	96.50 (14.5)	1.68 (0.28)	0.71 (0.18)	5.52 (0.85)	3.41 (0.52)
Sediment Trap 3	15.10 (2.29)	0.16 (0.10)	-0.19 (0.14)	1.37 (0.36)	0.61 (0.17)
B	27.40 (4.13)	0.37 (0.16)	0.21 (0.19)	0.70 (0.32)	0.38 (0.19)
8.2	3.12 (0.48)	0.29 (0.10)	-0.14 (0.13)	0.48 (0.21)	0.07 (0.14)
10	1.60 (0.26)	0.23 (0.11)	-0.09 (0.14)	0.66 (0.22)	0.16 (0.14)
11	0.46 (0.13)	0.02 (0.08)	-0.27 (0.14)	-0.06 (0.12)	0.09 (0.09)
12	0.63 (0.15)	0.19 (0.11)	-0.20 (0.14)	0.66 (0.24)	0.01 (0.12)
13	0.23 (0.08)	-0.08 (0.09)	-0.05 (0.12)	-0.16 (0.14)	0.09 (0.09)

[a]Location of sediment stations shown in Fig. 31; counting uncertainty in parentheses.

In response to these requirements, underground storage tanks at the Laboratory were inventoried and the results submitted to New Mexico's EID. Leak testing was conducted on 27 of the 105 tanks subject to Subtitle I, and several leaking tanks were found. The major leaks were corrected. Further mitigation will be implemented as the need is identified in development of a tank management plan. An underground storage tank management program is currently being developed that will provide background information, descriptions of the tank population and associated regulatory requirements, a leak detection program, and a software package to facilitate data manipulation.

For new USTs installed after 1988, there is little difference between the newly proposed and existing regulations regardless of the substance stored. These requirements basically mandate design and construction standards, secondary containment provisions, corrosion protection, leak detection monitoring, and spill and overfill control. However, for existing USTs that hold regulated substances under Subtitle I of RCRA, there are some important differences: (1) a ten-year transition period during which existing USTs must be upgraded to new UST standards or removed from service; (2) a three to five year period during which existing USTs must be retrofitted with corrosion protection and spill prevention safeguards; and (3) a regulatory exemption for all USTs that are contained within an underground vault, or otherwise having complete secondary containment. This last provision in the proposed rules was the main driving force behind the development of a vault design concept for all new USTs at the Laboratory below.

During 1987, 32 inactive USTs that were used to store petroleum products were identified at the laboratory. The majority of these tanks were installed in the mid-1940s. These tanks were prioritized for removal according to age, tank size, and overall environmental concerns. Residual fuels in these tanks were removed by pumping and sold to a recycling firm in Albuquerque after being tested to verify their chemical composition. Complete removal of the first nine of these tanks began in August 1987 and included the removal of the tank, all associated piping, and any contaminated soils which might have been affected by leaking hydrocarbons. These excavated materials were then decontaminated before final off-site landfill disposal. Two leaded gasoline and seven diesel fuel tanks were completely removed by late October. A summary of these tanks is shown in Table 29.

During the remainder of 1987, the other twenty-three abandoned USTs were emptied of their contents. Pan Am World Services has estimated the costs of removing these twenty-three USTs at approximately $10,000 per tank; during FY 1988 Pan Am will continue removal operations as funding permits.

H. PCB Inventory at the Laboratory (Roy Bohn)

In order to comply with federal, state, and Laboratory environmental regulations, the Laboratory's Environmental Surveillance Group (HSE-8) coordinated a Laboratory-wide program to inventory and label polychlorinated biphenyls (PCBs).

A PCB hotline was installed and operated by HSE-8 personnel to record any messages or questions regarding PCB contaminated items owned or operated by any user group throughout the Laboratory. Each division appointed a PCB representative whose responsibilities included notifying HSE-8, through the PCB hotline, of any equipment owned or operated by the division that contained or was suspected to contain PCBs.

Once notified of equipment containing or suspected of containing PCBs, HSE-8 sampled the equipment and submitted the samples to the Laboratory's Health and Environmental Chemistry Group (HSE-9) for PCB analysis. The analytical results along with other information on sample origin (i.e., location and type of equipment) are entered into the HSE-8 computer data base. The equipment is then labeled either as containing PCBs (in concentrations found present) or as containing no PCBs.

The HSE-8 computer data base contains data on 931 samples analyzed for PCBs in 1987.

I. Biomonitoring of the Laboratory's Liquid Effluents (Roy Bohn and Charles Nylander)

HSE-8 has initiated a biomonitoring program at the Laboratory in support of its NPDES program. Biomonitoring is used as a strategy to evaluate the overall toxic impact of effluents without specifically identifying individual contaminants.

With over 100 NPDES permitted outfalls at the Laboratory, consistent monitoring of each effluent is not feasible. Outfalls were segregated into nine basic categories according to wastewater source. Biomonitoring samples are collected from one representative outfall of each category. Biomonitoring assays using

Table 29. Summary of Underground Petroleum Storage Tanks Removed in 1987

Tank Structure Number	Size (gallons)	Substance Stored
TA-3-318	5,000	Diesel
TA-6-47	2,000	Diesel
TA-8-60	2,000	Diesel
TA-8-61	2,000	Diesel
TA-15-52	6,000	Diesel
TA-15-274	218	Leaded Gasoline
TA-16-16	1,000	Diesel
TA-16-196	4,000	Leaded Gasoline
TA-52-12	400	Diesel

Daphnia pulex as a test organism are conducted for each representative effluent and LC50 values are calculated. To date each outfall has been sampled three times and preliminary results indicate that overall water quality of effluents is good. Biomonitoring sampling will continue in 1988.

J. National Atmospheric Deposition Program (NADP) Network Station (David Nochumson and Michael Trujillo)

Group HSE-8 operates a wet deposition station that is part of the NADP Network. The station is located at the Bandelier National Monument. Composition precipitation samples are collected on a weekly basis. The samples are initially weighed and analyzed for pH and conductivity before being sent out for the analysis of the composition of ionic species. The samples are sent out for analysis to a laboratory located at Colorado State University. Summary statistics of the data for the four latest completed quarters are presented in Table G-67.

The magnitude of the ionic species deposition was generally highest in the third quarter of 1987 and lowest during the second quarter of 1987. The amount of precipitation was also lowest during the second quarter of 1987. The amount of deposition is quite variable. This variation reflects the variability in the cleanliness of the atmosphere that the storm clouds have contacted. The ions in the rainwater are from nearby and distant as well as manmade and natural sources. High nitrate and sulfate deposition are most likely from manmade sources (motor vehicles, copper smelters, and power plants).

The natural pH of the rainfall, without manmade contribution, is unknown. The natural pH is most likely higher than 5.6, for rainwater in equilibrium with atmospheric carbon dioxide because of the contribution from alkaline soils. For the latest 4 quarters, all but two of the weekly samples had pHs below 5.6, which indicates contributions from acidic species other than carbon dioxide.

K. Vadose Zone Characterization at TA-16, Area P (Steven McLin, David McInroy, and Anthony Grieggs)

The hydrologic transmitting characteristics of the vadose zone in Area P are presently under detailed investigation. These efforts will support the ground water monitoring waiver that was requested in December 1987 as required under 40 CFR 265, Subpart F. This waiver must demonstrate that there is low potential for migration of hazardous wastes or their components from the landfill via the uppermost aquifer to water supply wells or to surface water in Canon de Valle. Based on currently available information, major potential migratory pathways from the landfill include (in decreasing order of importance): (1) surface erosion into Canon de Valle waters and subsequent sediment transport; (2) shallow percolation into the underlying unsaturated tuff with hydraulic interconnection to the surface stream; and (3) deep percolation to the major freshwater aquifer. Soluble barium nitrate is the major contaminant of concern, although other substances may also be present in the landfill. During a December 1987 survey of locations adjacent to the landfill, barium concentrations did not exceed 3 mg/L; in the

past, barium concentrations have occasionally exceeded 100 mg/L.

Five neutron moisture access wells and nine ground water monitoring wells were installed around the landfill in 1987. Additional boreholes were also located approximately 240 m (800 ft) south to verify suspected stratigraphic unit correlations within the unsaturated Bandelier Tuff and to obtain continuous core samples from a third borehole for laboratory testing. A thin veneer of alluvium (i.e., locally less than 1.5 m (5 ft) has been deposited on the floor of Canyon de Valle; however, the entire landfill site is underlaid by the Bandelier Tuff. Two major lithologic subunits were identified at Area P, based on degree of welding. The uppermost subunit varies in thickness from about 40 to 60 m (140 to over 200 ft) and consists of unsaturated, friable to moderately welded, yellowish-brown tuff. The lower subunit is also unsaturated, and consists of a densely welded, grey tuff. The top of the major freshwater aquifer is estimated to be between 240 and 370 m (800 and 1200 ft) below the surface of Area P.

Continuous core samples were recovered from well P-16A, located immediately south of the western portion of the Area P landfill. Total borehole depth was about 25 m (80 ft); this test hole was converted to a neutron moisture access well when 2.5-in. aluminum casing was set. Laboratory testing on selected core segments included a determination of saturated hydraulic conductivity utilizing both a constant and falling head procedure, moisture retention characteristics using the hanging column and pressure plate apparatuses, initial gravimetric and volumetric moisture contents, bulk density, porosity, and unsaturated hydraulic conductivity as a function of both negative pore pressure head and volumetric moisture content. This information will be utilized in a numerical simulation of potential barium migration from the landfill through these upper Bandelier Tuff units in order to evaluate the likelihood deep ground water contamination. A detailed water balance computation and sediment erosion characterization study for Canon de Valle will complete the efforts required under the waiver request.

L. Environmental Studies of TA-49 (William Purtymun, Alan Stoker, and Max Maes)

From 1959 to 1961, hydronuclear experiments were conducted in underground shafts at the Laboratory's TA-49. Area TA-49 is located on Frijoles Mesa in the southwest corner of the Laboratory between TA-28 and TA-33 (Fig. 4). These experiments involved a combination of conventional (chemical) high explosives, usually in a nuclear weapon configuration, and fissile material whose quantity was reduced far below the amount required for a nuclear explosion. A total of 35 hydronuclear experiments and 9 related equation-of-state and criticality experiments, all involving some fissile material, were conducted. Other experiments involving high explosives, but no fissile materials, were conducted through the same period.

A total of about 41 kg (90 lb) of plutonium, 93 kg (200 lb) of enriched uranium, 82 kg (180 lb) of depleted uranium, and 15 kg (33 lb) of beryllium was utilized. These materials were dispersed in the bottoms of the shafts by detonation of the conventional (chemical) high explosives.

Some plutonium contamination was measured at the surface in one experimental area in December 1960 and was traced to cuttings from a shaft drilled during October and November. Plutonium had apparently been dispersed through fractures in the tuff by the detonation of an experiment in an adjacent, experimental shaft. All surface soil contamination ascertainable by standard procedures and instruments of the time was cleaned up and placed back in the shaft from which it originated (Purtymun 1987B).

Three deep test wells (DT-5A, DT-9, and DT-10) are drilled from the surface of the mesa at TA-49 into the main aquifer of the Los Alamos area (Fig. 23). The depth to the main aquifer is about 360 m (1200 ft). There is no water perched in beds between the surface of the mesa and top of main aquifer. The chemical and radiochemical quality of water from these wells indicated no contamination from activities at TA-49 (Sec. VI).

Eleven sediment surface stations were established in 1972 in natural drainage from the experimental areas. A twelfth station was added in 1981 as the drainage was changed (Fig. 32). Samples collected in 1986 and 1987 indicated sediments at Station A-3 contained plutonium concentrations in excess of background (Table G-68). The concentrations are below cleanup levels (100 pCi/g) and are from the chemistry building (removed) at Area 11. The ^{3}H, ^{137}Cs, total U and gross gamma analytical results were at or near background levels.

Sediments from the twelve stations were analyzed for chemical constituents extracted from sediments downgradient from the experimental area (Fig. 31). The results of the analyses indicated constituents were

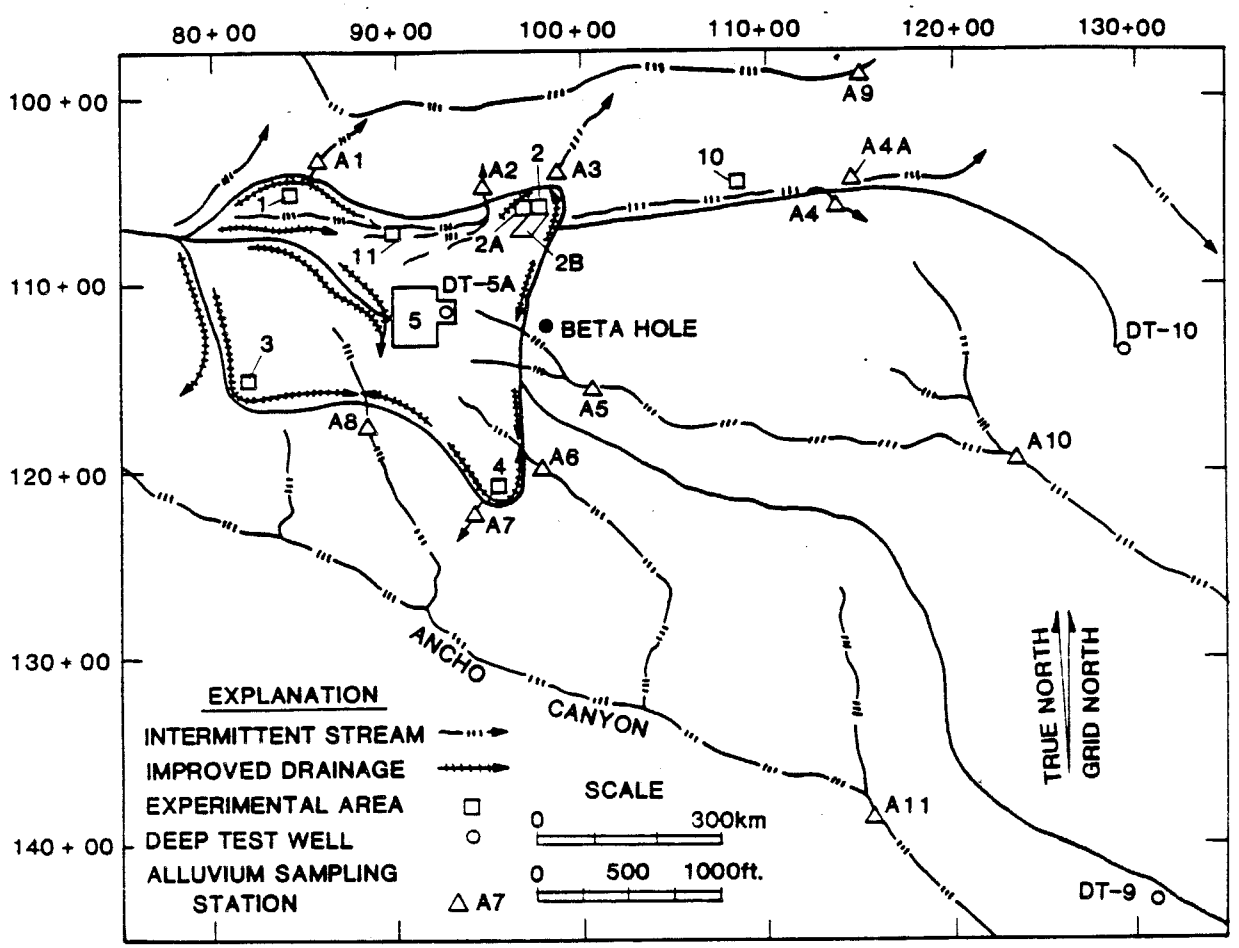

Fig. 32. Location of experimental areas and test wells at TA-49.

below limits of detection or EP toxic criteria concentrations where applicable (Table G-69).

Storm run-off samples were taken from four stations in late August and early September. The ^{137}Cs and plutonium in solution and plutonium in suspended sediments were at or below background indicating no detectable transport in storm run-off (Table G-70).

The chemical quality of the run-off contained only naturally occurring constituents (Table G-71).

M. Quality of Surface and Ground Water Adjacent to the Los Alamos National Laboratory: Organic Compounds (William Purtymun, Roger Ferenbaugh, and Max Maes)

Surface and ground water samples were collected from 43 stations representing the major occurrences of natural and municipal water and industrial and sanitary effluents in the Los Alamos area (Fig. 33). The

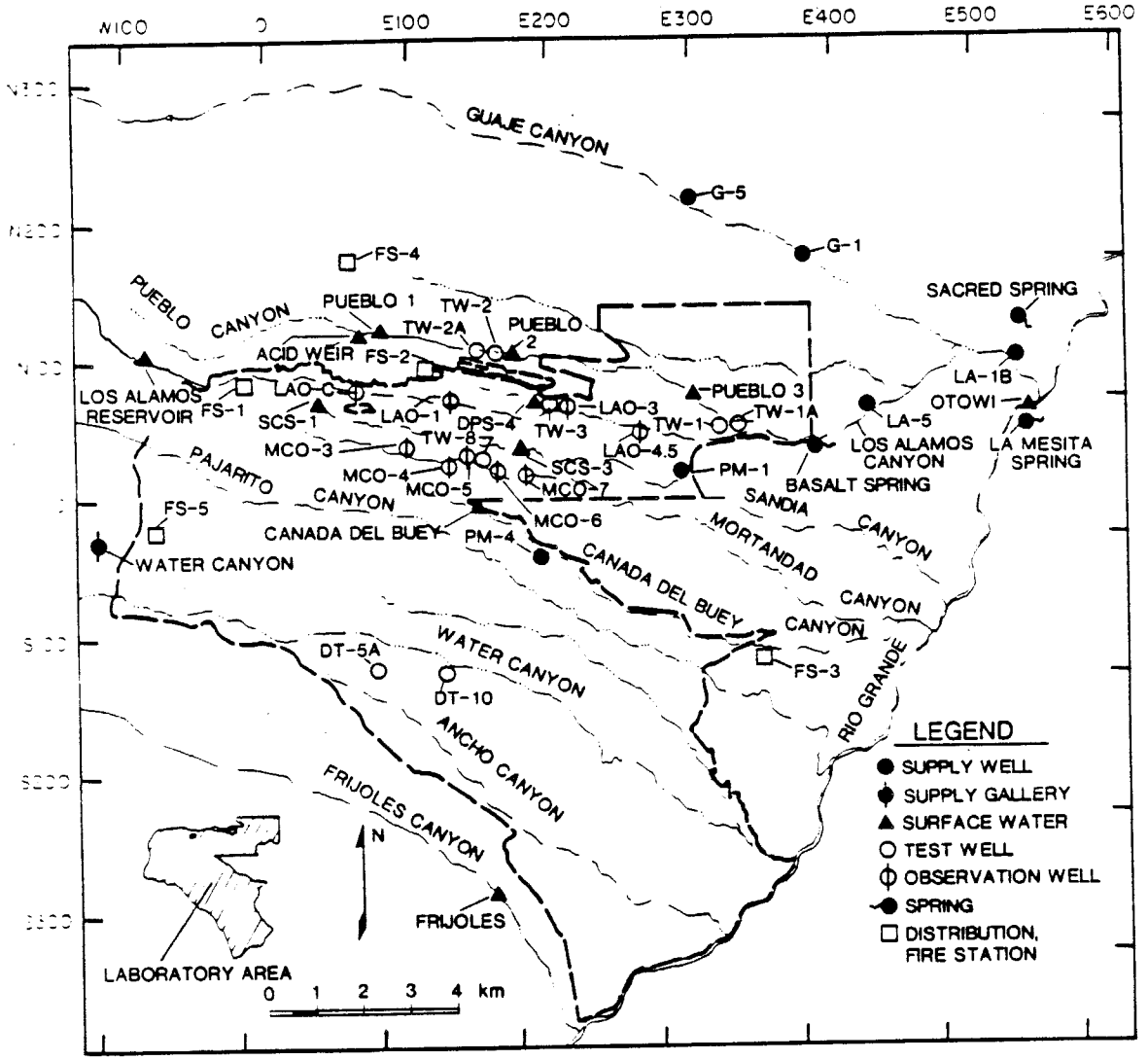

Fig. 33. Surface and ground water locations sampled for organic analyses.

samples were analyzed for volatile organics (35 compounds), semi-volatile organics (65 compounds), BNA fraction, pesticides (20 compounds), herbicides (3 compounds), polychlorinated biphenyls (7 compounds), and cyanides. The investigation was made to investigate possible areas of organic contamination for further study; however, the impact of organic contamination in surface and ground water is minimal. A limited program of organic monitoring will be incorporated into the annual surveillance of surface and ground water in and adjacent to the Laboratory at Los Alamos (Purtymun 1988).

N. Radiation Levels from LAMPF Emissions (Brent Bowen, William Olsen, I-li Chen, and Donald VanEtten)

The monitoring network of high-pressure ionization chambers (HPICs) used to measure external radiation from LAMPF emissions was expanded to seven

units during 1987. Three HPICs continued to monitor external radiation levels north, north-northeast, and northeast of LAMPF, across the Los Alamos Canyon during most of the LAMPF operating cycle, June through November. The other four units were placed at various locations for shorter periods of time. Locations included Kwage Mesa (2.0 km [1.2 mi] north of LAMPF), Bayo sewage treatment plant (2.3 km [1.4 mi] northeast of LAMPF in Bayo Canyon), locations north-northwest and east-northeast of LAMPF across Los Alamos Canyon, 0.8 km (0.5 mi) east of LAMPF, 0.5 km (0.3 mi) northwest of LAMPF in Los Alamos Canyon, sites 1.2-2.6 km (0.7-1.6 mi) south to southwest of LAMPF on mesas, and a site west-southwest of LAMPF in Mortandad Canyon. Most of the siting took advantage of the high frequency of south to southwesterly and north to northeasterly winds caused by Rio Grande Valley channeling.

Results to date confirm that the highest external radiation levels are transported toward the northeast and north-northeast. However, the highest short-term (an hour or so) levels of over 100 μR/hour were found east of LAMPF, with over the mesa transport. Higher short-term levels were also found north of LAMPF. External radiation dropped off by 50% or so with increases in downwind distance of 0.8-2.0 km (0.5-1.2 mi). Above-background external radiation was detected at all canyon sites, especially in Los Alamos Canyon, at 0.5 km (0.3 mi) downwind. Radiation levels occasionally exceeded 50-60 μR/h at this site. Much of these levels may be a result of shine of the LAMPF plume traveling overhead. Predicted external radiation levels using on-site meteorological data and release data agree well with measured concentrations at all sites.

X. PUBLICATIONS

B. M. Bowen, W. A. Olsen, I. Chen, and D. M. VanEtten, "Measurement and Modeling of External Radiation During 1985 from LAMPF Emissions," Los Alamos National Laboratory report LA-11150-MS (November 1987).

T. Buhl, D. Van Etten, and W. Hansen, "Investigation of Thorium Contamination at Two Target Areas at White Sands Missile Range," Los Alamos National Laboratory report LA-10893-MS (February 1987).

Environmental Surveillance Group, HSE-8, "Quality Assurance Project Plans," Los Alamos National Laboratory report (February 1987).

Environmental Surveillance Group, "Environmental Surveillance at Los Alamos in 1986," Los Alamos National Laboratory report LA-10992-ENV (April 1987).

W. Purtymun, R. Ferenbaugh, N. Becker, M. Williams, and M. Maes, "Water Quality in the Vicinity of Fenton Hill, 1983 and 1984", Los Alamos National Laboratory report LA-10892-PR (January 1987).

W. D. Purtymun, R. J. Peters, T. E. Buhl, M. N. Maes, and F.H. Brown, "Background Concentrations of Radionuclides in Soils and River Sediments in Northern New Mexico, 1974-1986," Los Alamos National Laboratory report LA-11134-MS (November 1987).

W. D. Purtymun and A.K. Stoker, "Environmental Status of Technical Area 49, Los Alamos, New Mexico," Los Alamos National Laboratory report LA-11135-MS (November 1987).

W. D. Purtymun, A. K. Stoker, and M. N. Maes, "Water Supply at Los Alamos During 1986," Los Alamos National Laboratory report LA-11046-PR (August 1987).

G. Tierney, "New Mexico Weed History," in Proceedings of the Southwestern Native Plant Symposium, L. Johnson and J. Phillips, Eds. (Albuquerque, New Mexico, October 1987), pp. 31-34.

D. VanEtten and W. Olsen, "Improvement of a Portable Pressurized Ionization Chamber with the Addition of a Microprocessor Datalogger," Los Alamos National Laboratory report LA-11014-MS (July 1987).

W. J. Wenzel, A. J. Gallegos, T. S. Foxx, G. Tierney, and J. C. Rodgers, "Cesium-137, Plutonium 239/240, Total Uranium and Scandium in Trees and Shrubs Growing in Transuranic Waste at Area B," Los Alamos National Laboratory report LA-11126-MS (November 1987).

XI. REFERENCES

DOE 1979: US Department of Energy, "Final Environmental Impact Statement: Los Alamos Scientific Laboratory Site, Los Alamos, New Mexico," US Department of Energy report DOE/EIS0018 (December 1979).

DOE 1981: US Department of Energy Order 5484.1, Chapter III, "Effluent and Environmental Monitoring Program Requirements" (February 1981).

DOE 1985: US Department of Energy, "DOE-Derived Concentration Guides for Drinking Water and Breathing Air Contaminated with Radionuclides by Members of the Public (sic)," attachments to memorandum from R. J. Stern, Director, Office of Environmental Guidance, US Department of Energy (February 28, 1986).

Engineering 1982: Engineering Division, "Los Alamos National Laboratory Long-Range Site Development Plan," for Los Alamos National Laboratory (September 1982).

EPA 1976: US Environmental Protection Agency, "National Interim Primary Drinking Water Regulations," US Environmental Protection Agency report EPA-570/9-76-0033 (1976).

EPA 1979: US Environmental Protection Agency, "National Secondary Drinking Water Regulations," Federal Register 44 (140), July 19, 1979.

EPA 1981: US Environmental Protection Agency, "Compilation of Air Pollutant Emission Factors: Highway Mobile Sources," US Environmental Protection Agency report EPA 460/3-81-005 (1981).

EPA 1984: US Environmental Protection Agency, "Compilation of Air Pollutant Emission Factors," US Environmental Protection Agency report AP-42, Supplement 15, Third Edition (January 1984).

EPA 1986: US Environmental Protection Agency, "Guideline On Air Quality Models (Revised)," US Environmental Protection Agency report EPA-450/2-78-027R (July 1986).

ESG 1978: Environmental Surveillance Group, "Environmental Surveillance at Los Alamos During 1977," Los Alamos Scientific Laboratory report LA-7263-MS (April 1978).

ESG 1981: Environmental Surveillance Group, "Radiological Survey of the Site of a Former Radioactive Liquid Waste Treatment Plant (TA-45) and the Effluent Receiving Areas of Acid, Pueblo, and Los Alamos Canyons, Los Alamos, New Mexico, Final Report," Los Alamos National Laboratory report LA-8890-ENV/US Department of Energy report DOE/EV-0005/30 (May 1981).

Facilities 1983: Facilities Engineering Division, "Laboratory Quality Assurance Manual for Engineering and Construction," Los Alamos National Laboratory Manual (September 1983, Revision 5).

Hakonson 1976A: T.E. Hakonson and K.V. Bostick, "Cesium-137 and Plutonium in Liquid Waste Discharge Areas at Los Alamos," F. R. Miera, Jr., and R. J. Peters, "The Distribution of Plutonium and Cesium of Alluvial Soils in the Los Alamos Environs," both in *Radioecology and Energy Resources* (Dowden, Hutchinson, and Ross, Inc., Stroudsburg, Pennsylvania, 1976).

Hakonson 1976B: T. E. Hakonson, J. W. Nyhan, and W. D. Purtymun, "Accumulation and Transport of Soil Plutonium in Liquid Waste Discharge Areas at Los Alamos," Proc. Transuranium Nuclides in the Environment, International Atomic Energy Agency report IAEA-SM-199/99 (1976).

ICRP 1977: International Commission on Radiological Protection, "Recommendations of the International Commission on Radiological Protection," adopted January 17, 1977, Annals of the ICRP 1 (3) (1977), ICRP Publication No. 26.

Kramer 1977: Kramer, Callahn, and Associates, "Particulate Analyses of Drier Exhaust Emissions at the Zia Company Asphalt Plant, Los Alamos, New Mexico" (September 1977).

MHSM 1976: Mason and Hanger-Silas Mason Co., Inc., "Disposal of Water or Excess High Explosives," MHSM quarterly progress reports (January 1971 through March 1976).

NCRP 1975: National Council on Radiation Protection and Measurements, "Review of the Current State of Radiation Protection Philosophy," National Council on Radiation Protection and Measurements report No. 43 (1975).

NCRP 1975B: National Council on Radiation Protection and Measurements, "Natural Background Radiation in the United States," National Council on Radiation Protection and Measurements report No. 45 (November 1975).

NCRP 1987: National Council on Radiation Protection and Measurements, "Ionizing Radiation Exposure of the Population of the Unites States," National Council on Radiation Protection and Measurements report No. 93 (September 1987).

NRC 1977: Nuclear Regulatory Commission, "Calculation of Annual Doses to Man from Routine Releases of Reactor Effluents for the Purpose of Evaluating Compliance with 10 CFR Part 50, Appendix I," Nuclear Regulatory Commission report Regulatory Guide 1.109 (October 1977).

Purtymun, 1971: W. D. Purtymun, "Plutonium in Stream Channel Alluvium in the Los Alamos Area, New Mexico," Los Alamos Scientific Laboratory report LA-4561 (1971).

Purtymun 1974A: W. D. Purtymun, "Storm Runoff and Transport of Radionuclides in DP Canyon, Los Alamos County, New Mexico," Los Alamos Scientific Laboratory report LA-5744 (1974).

Purtymun, 1974B: W. D. Purtymun and S. Johansen, "General Geohydrology of the Pajarito Plateau," New Mexico Geological Society Guidebook, 25th Field Conference, Ghost Ranch, New Mexico (1974).

Purtymun 1974C: W. D. Purtymun, "Dispersion and Movement of Tritium in a Shallow Aquifer in Mortandad Canyon," Los Alamos Scientific Laboratory report LA-5716-MS (September 1974).

Purtymun 1974D: W. D. Purtymun, F. G. West, and W. H. Adams, "Preliminary Study of Quality of Water in the Drainage Area of the Jemez River and Rio Guadalupe," Los Alamos Scientific Laboratory report LA-5595-MS (April 1974).

Purtymun 1977: W. D. Purtymun, J. R. Bucholz, and T. E. Hakonson, "Chemical Quality of Effluents and the influence on Water Quality in a Shallow Aquifer," J. of Environmental Quality 6 (1) (January-March 1977).

Purtymun 1980B: W. D. Purtymun, R. J. Peters, and J. W. Owens, "Geohydrology of White Rock Canyon of the Rio Grande from Otowi to Frijoles Canyon," Los Alamos Scientific Laboratory report LA-8635-MS (December 1980).

Purtymun 1983: W. D. Purtymun, W. R. Hansen, and R. J. Peters, "Radiochemical Quality of Water in the Shallow Aquifer in Mortandad Canyon 1967-1978," Los Alamos National Laboratory report LA-9675-MS (March 1983).

Purtymun 1984: W. D. Purtymun, "Hydrologic Characteristics of the Main Aquifer in the Los Alamos Area: Development of Groundwater Supplies," Los Alamos National Laboratory report LA-9957-MS (January 1984).

Purtymun 1987A: W. D. Purtymun, R. J. Peters, T. E. Buhl, M. N. Maes, and F. H. Brown, "Background Concentrations of radionuclides in Soils and River Sediments in Northern New Mexico, 1974-1986," Los Alamos National Laboratory report LA-11134-MS (November 1987).

Purtymun 1987B: William D. Purtymun and Alan K. Stoker, "Environmental Status of Technical Area 49, Los Alamos, New Mexico," Los Alamos National Laboratory report LA-11135-MS (November 1987).

Purtymun 1988A: W. D. Purtymun, R. W. Ferenbaugh, M. C. Williams, and M. N. Maes, "Water Quality in the Vicinity of Fenton Hill, 1985 and 1986," Los Alamos National Laboratory report LA-11210-PR (March 1988).

Purtymun 1988B: William Purtymun, Roger Ferenbaugh, and Max Maes, "Quality of Surface and Ground Water at and Adjacent to the Los Alamos National Laboratory: Organic Compounds," Los Alamos National Laboratory report (in preparation).

Slade 1968: D. H. Slade, Ed., "Meteorology and Atomic Energy 1967," US Atomic Energy Commission documented TID-24190 (1968).

USGS 1987: U. S. Geological Survey, "Water Resource Data for New Mexico Water Year 1986," U.S. Geological Survey water data NM-86-1 (1987).

APPENDIX A

STANDARDS FOR ENVIRONMENTAL CONTAMINANTS

Throughout this report, concentrations of radioactive and chemical constituents in air and water samples are compared with pertinent standards and guidelines in regulations of federal and state agencies. No comparable standards for soils, sediments, and foodstuffs are available. Laboratory operations are conducted in accordance with directives and procedures regarding compliance with environmental standards. These directives are contained in DOE Orders 5480.1B (Environmental Protection, Safety, and Health Protection Program for DOE Operations), 5480.1 (Environmental Protection, Safety, and Health Protection Standards) and 5480.11 (Requirements for Radiation Protection); and DOE Order 5484.1 (Environmental Radiation Protection, Safety, and Health Protection Information Reporting Requirements), Chapter III (Effluent and Environmental Monitoring Program Requirements). All of these DOE orders are being revised.

The DOE regulates radiation exposure to the public and the worker by limiting the radiation dose that can be received. Because some radionuclides remain in the body and result in exposure long after intake, DOE requires consideration of the dose commitment caused by inhalation, ingestion, or absorption of such radionuclides. This involves integrating the dose received from radionuclides over a standard period of time. For this report, 50-yr dose commitments were calculated using dose factors from Reference A1. The dose factors adopted by DOE are based on the recommendations of Publication 30 of the International Commission on Radiological Protection (ICRP).[A2] Those factors used in this report are presented in Appendix D.

In 1985, DOE adopted interim limits that lowered its Radiation Protection Standard (RPS) for members of the general public.[A3] Table A-1 lists currently applicable RPS for operations at the Laboratory. Concentrations of radionuclides that are measured at on-site stations are compared with DOE's Concentration Guides (CGs) for Controlled Areas as listed in DOE Order 5480.1, Chapt. 11 (Table A-2). Off-site measurements are compared with DOE's Derived Concentration Guides (DCGs) for Uncontrolled Areas, based upon a revised RPS for the general public of 100 mrem/yr effective dose equivalent.[A4] These DCGs represent the smallest estimated concentrations in water or air, taken in continuously for a period of 50 yr, that will result in annual effective dose equivalents equal to the RPS of 100 mrem. The new RPSs and the information in Reference A1 are based on recommendations of the ICRP and of the National Commission on Radiation Protection and Measurements (NCRP).[A2,A3,A4]

The effective dose equivalent is the hypothetical whole-body dose that would result in the same risk of radiation-induced cancer or genetic disorder as a given exposure to an individual organ. The effective dose is the sum of the individual organ doses, weighted to account for the sensitivity of each organ to radiation-induced damage. The weighting factors are taken from the recommendations of the ICRP. The effective dose equivalent includes dose from both internal and external exposure.

Radionuclide concentrations in air and water in uncontrolled areas measured by the Laboratory's surveillance program are compared to DCGs in this report. In addition to the 100 mrem/yr effective dose RPS, exposures from the air pathway are also limited by the EPA's standard of 25 mrem/yr (whole body) and 75 mrem/yr (any organ) (Table A-1). To demonstrate compliance with these standards, doses from the air pathway are compared directly with the EPA dose limits.

For chemical constituents in drinking water, standards have been promulgated by the EPA and adopted by the New Mexico Environmental Improvement Division (Table A-3). The EPA's primary Maximum Contaminant Level (MCL) is the maximum permissible level of a contaminant in water that is delivered to the outlet of the ultimate user of a public water system.[A7] The EPA's secondary water standards control contaminants in drinking water that primarily affect esthetic qualities associated with public acceptance of drinking water.[A8] At considerably higher concentrations of these contaminants, health implications may arise.

Radioactivity in drinking water is regulated by EPA regulations contained in 40 CFR 141.[A8] These regulations provide that combined ^{226}Ra and ^{228}Ra may not exceed 5×10^{-9} μCi/mL. Gross alpha activity (including ^{226}Ra, but excluding radon and uranium) may not exceed 15×10^{-9} μCi/mL.

Table A-1. DOE Radiation Protection Standards for External and Internal Exposures

Exposure of Any Member of the Public[a]

1. All Pathways

	Annual Effective Dose Equivalent[b] at Point of Maximum Probable Exposure
Occasional annual[c] exposure	500 mrem
Prolonged annual[c] exposure	100 mrem

No individual organ shall receive an annual dose equivalent in excess of 5000 mrem.

2. Air pathway only[d]

	Annual Dose Equivalent at Point of Maximum Probable Exposure
Whole body dose	25 mrem
Any organ	75 mrem

Occupational Exposures[a]

Type of Exposure	Exposure Period	Dose Equivalent
Whole body, head and trunk, gonads, lens of the eye[e], red bone marrow, active blood forming organs	Year Calendar Quarter	5 000 mrem 3 000 mrem
Unlimited area of the skin (except hands and forearms); other organs, tissues, and organ systems (except bone)	Year Calendar Quarter	15 000 mrem 5 000 mrem
Bone	Year Calendar Quarter	30 000 mrem 10 000 mrem
Forearms[f]	Year Calendar Quarter	30 000 mrem 10 000 mrem
Hands and feet[f]	Year Calendar Quarter	75 000 mrem 25 000 mrem

Table A-1 (cont)

---

[a]In keeping with DOE policy, exposures shall be limited to as small a fraction of the respective annual dose limits as practicable. These Radiation Protection Standards apply to exposures from routine Laboratory operation, excluding contributions from cosmic, terrestrial, global fallout, self-irradiation, and medical diagnostic sources of radiation. Routine operation means normal, planned operation and does not include actual or potential accidental or unplanned releases. Exposure limits for any member of the general public are taken from Reference A3. Limits for occupational exposure are taken from DOE Order 5480.11.

[b]As used by DOE, effective dose equivalent includes both the effective dose equivalent from external radiation and the committed effective dose equivalent to individual tissues from ingestion and inhalation during the calendar year.

[c]For the purposes of DOE's Radiation Protection Standard, a prolonged exposure will be one that lasts, or is predicted to last, longer than 5 years.

[d]These levels are from EPA's regulations promulgated under the Clean Air Act(40 CFR 61, Subpart H).

[e]Beta exposure below 700 keV will not penetrate the lens of the eye; therefore, the applicable limit for beta radiation of these energies would be that for skin, 15 000 mrem/year.

[f]All reasonable effort should be made to keep exposure of forearms and hands within the general limit for skin.

Table A-2. DOE's Derived Concentration Guides (DCG) for Uncontrolled Areas and Concentration Guides (CG) for Controlled Areas (μCi/mL)[a]

Nuclide	DCGs for Uncontrolled Areas		CGs for Controll Areas	
	Air	Water	Air	Water
^{3}H	1×10^{-7}	2×10^{-3}	5×10^{-6}	1×10^{-1}
^{7}Be	5×10^{-8}	1×10^{-3}	1×10^{-6}	5×10^{-2}
^{89}Sr	3×10^{-10}	2×10^{-5}	3×10^{-8}	3×10^{-4}
^{90}Sr[b]	9×10^{-12}	1×10^{-6}	1×10^{-9}	1×10^{-5}
^{137}Cs	4×10^{-10}	3×10^{-6}	1×10^{-8}	4×10^{-4}
^{234}U	9×10^{-14}	5×10^{-7}	1×10^{-10}	1×10^{-4}
^{235}U	1×10^{-13}	6×10^{-7}	1×10^{-10}	1×10^{-4}
^{238}U	1×10^{-13}	6×10^{-7}	7×10^{-11}	2×10^{-5}
^{238}Pu	3×10^{-14}	4×10^{-7}	2×10^{-12}	1×10^{-4}
^{239}Pu[b]	2×10^{-14}	3×10^{-7}	2×10^{-12}	1×10^{-4}
^{240}Pu	2×10^{-14}	3×10^{-7}	2×10^{-12}	1×10^{-4}
^{241}Am	2×10^{-14}	6×10^{-7}	6×10^{-12}	1×10^{-4}
	(pg/m^3)	(mg/L)	(pg/m^3)	(mg/L)
U, natural[c]	$1 \times 10^{+5}$	8×10^{-1}	$2 \times 10^{+8}$	$6 \times 10^{+1}$

---

[a]Guides for uncontrolled areas are based upon DOE's Radiation Protection Standard (RPS) for the general public;[A5] those for controlled areas are based upon occupational RPSs for DOE Order 5480.11. Guides apply to concentrations in excess of those occurring naturally or due to fallout.

[b]Guides for ^{239}Pu and ^{90}Sr are the most appropriate to use for gross alpha and gross beta, respectively.

[c]One curie of natural uranium is equivalent to 3000 kg of natural uranium. Therefore, uranium masses may be converted to DOE's "uranium special curie" by multiplying by 3.3×10^{-13} μCi/pg.

Table A-3. Maximum Contaminant Level (MCL) in Water Supply for Inorganic Chemicals and Radiochemicals[a]

Inorganic Chemical Contaminant	MCL (mg/L)	Radiochemical Contaminant	MCL (µCi/mL)
Primary Standard			
Ag	0.05		
As	0.05	Gross alpha[b]	15×10^{-9}
Ba	1	^{3}H	20×10^{-6}
Cd	0.010	^{238}Pu	15×10^{-9}
Cr	0.05	^{239}Pu	15×10^{-9}
F[c]	2.0		
Hg	0.002		
NO_3 (as N)	10		
Pb	0.05		
Se	0.01		
Secondary Standards			
Cl	250		
Cu	1		
Fe	0.3		
Mn	0.05		
SO_4	250		
Zn	5.0		
TDS	500		
pH	6.5 - 8.5		

---

[a]Source: References A7 and A8.
[b]See text for duscussion of application of gross alpha MCL and gross beta screening level of 5×10^{-9} µCi/mL.
[c]Based on annual average of the maximum daily air temperature of 14.7 to 17.6°C.

A screening level of 5 x 10^{-9} Ci/mL is established to determine when analysis specifically for radium isotopes is necessary. In this report, plutonium concentrations are compared with the gross alpha standard for drinking water (Table A-3). For manmade beta and photon emitting radionuclides, drinking water concentrations are limited to concentrations that would result in doses not exceeding 4 mrem/yr, calculated according to a specified procedure.

The EPA established minimum concentrations of certain contaminants in a water extract from wastes for designation of these wastes as hazardous by reason of toxicity.[A9] The Extraction Procedure (EP) must follow steps outlined by EPA in 40 CFR 261, Appendix II. In this report, the EP toxicity minimum concentrations (Table A-4) are used to compare to concentrations of selected constituents in extracts from the Laboratory's active waste areas.

Table A-4. Minimum Concentrations of Inorganic Contaminants for Meeting EPA's Extraction Procedure (EP) Toxicity Characteristic for Hazardous Waste[a]

Contaminant	Criteria Concentration (mg/L)
Arsenic	5.0
Barium	100.0
Cadmium	1.0
Chromium	1.0
Lead	5.0
Mercury	0.2
Selenium	1.0
Silver	5.0

[a]Source: Reference A9.

REFERENCES

A1. U.S. Department of Energy, "Committed Dose Equivalent Tables for U.S. Department of Energy Population Dose Calculations," prepared by J. P. Corley, Ed. for the U.S. Department of Energy (draft, 1985).

A2. International Commission on Radiological Protection, "Limits for Intakes of Radionuclides by Workers," ICRP Publication 30, Parts 1, 2, and 3, and their Supplements, Annals of the ICRP, Vol. 2, No. 3/4 through Vol. 8, No. 4 (1979-1982).

A3. U.S. Department of Energy, "Radiation Standards for the Protection of the Public in the Vicinity of DOE Facilities," memorandum from William A. Vaughan, Assistant Secretary for Environment, Safety, and Health, U.S. Department of Energy (August 5, 1985).

A4. U.S. Department of Energy, "DOE-Derived Concentration Guides for Drinking Water and Breathing Air Contaminated with Radionuclides by Members of the Public [sic]," attachment to memorandum from R. J. Stern, Director, Office of Environmental Guidance, U.S. Department of Energy (February 28, 1986).

A5. U.S. Environmental Protection Agency, "National Emission Standard for Radionuclide Emissions from Department of Energy Facilities," Code of Federal Regulations, Title 40, Part 61, Subpart H (1985).

A6. International Commission on Radiological Protection, "Report of the Task Group on Reference Man," ICRP Publication 23 (1975).

A7. U.S. Environmental Protection Agency, "National Interim Primary Drinking Water Regulations," U.S. Environmental Protection Agency report EPA-570/9-70-003 (1976) and 40 CFR 141.

A8. U.S. Environmental Protection Agency, "National Secondary Drinking Water Regulations," Federal Register 44 (140) (July 19, 1979).

A9. U.S. Environmental Protection Agency, "Part 261 - Identification and listing of hazardous waste. Table I - Maximum concentration of contaminants for characteristics of EP toxicity," Federal Register 45: 33122 (May 19, 1980).

APPENDIX B

PROCEDURES FOR SAMPLING, DATA HANDLING, AND QUALITY ASSURANCE

A. Thermoluminescent Dosimeters

The thermoluminescent dosimeters (TLDs) used at the Laboratory are lithium fluoride (LiF) chips, 6.4 mm square by 0.9 mm thick. The TLDs, after being exposed to radiation, emit light upon being heated. The amount of light is proportional to the amount of radiation to which the TLD was exposed. The TLDs used in the Laboratory's environmental monitoring program are insensitive to neutrons, so the contribution of cosmic neutrons to natural background radiation is not measured.

The chips are annealed to 400°C (752°F) for 1 h and then cooled rapidly to room temperature. This followed by annealing at 100°C (212°F) for 1 h and again cooling rapidly to room temperature. In order for the annealing conditions to be repeatable, chips are put into rectangular borosilicate glass vials that hold 48 LiF chips each. These vials are slipped into a borosilicate glass rack so they can be placed at once into the ovens maintained at 400°C and 100°C.

Four LiF chips constitute a dosimeter. The LiF chips are contained in a two part threaded assembly made of an opaque yellow acetate plastic. A calibration set is prepared each time chips are annealed. The calibration set is read at the start of the dosimetry cycle. The number of dosimeters and exposure levels are determined for each calibration in order to efficiently use available TLD chips and personnel. Each set contains from 20 to 50 dosimeters. These are irradiated at levels between 0 mR and 80 mR using an 8.5 mCi ^{137}Cs source calibrated by the National Bureau of Standards.

A factor of 1 rem (tissue) = 1.050 mR is used in evaluating the dosimeter data. This factor is the reciprocal of the product of the roentgen-to-rad conversion factors of 0.958 for muscle ^{137}Cs and of 0.994, which corrects for attenuation of the primary radiation beam at electronic equilibrium thickness. A rad-to-rem conversion factor of 1.0 for gamma rays is used as recommended by the International Commission on Radiation Protection.[B1,B2] A method of weighted least squares linear regression is used to determine the relationship between TLD reader response and dose (weighting factor is the variance).[B3]

The TLD chips used are all from the same production batch and were selected by the manufacturer so that the measured standard deviation in thermoluminescent sensitivity is 2.0 to 4.0% of the mean at a 10 R exposure. At the end of each field cycle, whether calendar quarter or the Los Alamos Meson Physics Facility operation cycle, the dose at each network location is estimated from the regression along with the regression's upper and lower 95% confidence limits at the estimated value.[B4] At the end of the calendar year, individual field cycle doses are summed for each location. Uncertainty is calculated as summation in quadrature of the individual uncertainties.[B3]

Further details are provided in the TLD quality assurance project plan.[B5]

B. Air Sampling

Samples are collected monthly at 26 continuously operating stations.[B6] Air pumps with flow rates of about 3 L/sec are used. Airborne aerosols are collected on 79 mm diameter polystyrene filters. Each filter is mounted on a cartridge that contains charcoal. This charcoal is not routinely analyzed for radioactivity. However, if an unplanned release occurs, the charcoal can be analyzed for any ^{131}I it may have collected. Part of the total air flow is passed through a cartridge containing silica get to absorb atmospheric water vapor for tritium analyses. Air flow rates through both sampling cartridges are measured with rotameters and sampling times recorded. The entire air sampling train at each station is cleaned, repaired, and calibrated as-needed.

Two clean, control filters are used to detect any possible contamination of the 26 sampling filters while they are in transit. The control filters accompany the 26 sampling filters when they are placed in the air samplers and when they are retrieved. The control filters are analyzed for radioactivity along with the 26 sampling filters. Analytical results for the control filters are subtracted from the appropriate gross results to obtain net data.

At one on-site location (N050 E040), airborne radioactivity samples are collected weekly. Airborne

particulate matter on each filter is counted for gross alpha and gross beta activities, which help trace temporal variations in radionuclide concentrations in ambient air. The same measurements are made monthly on a filter from the Espanola (Station 1) regional air sampler.

On a quarterly basis, the monthly filters for each station are cut in half. The filter halves are combined to produce two quarterly composite samples for each station. The first group is analyzed for ^{238}Pu, $^{239,240}Pu$, and ^{241}Am (on selected filters). The second group of filter halves is saved for uranium analysis.

Filters from the first composite group are ignited in platinum dishes, treated with $HF\text{-}HNO_3$ to dissolve silica, wet ashed with $HNO_3\text{-}H_2O_2$ to decompose organic residue, and treated with HNO_3-HC1 to ensure isotopic equilibrium. Plutonium is separated from the resulting solution by anion exchange. For 11 selected stations, americium is separated by cation exchange from the eluant solutions resulting from the plutonium separation process. The purified plutonium and americium samples are separated, electrodeposited, and measured for alpha-particle emission with a solid state alpha detection system. Alpha particle energy groups associated with decay of ^{238}Pu, $^{239,240}Pu$, and ^{241}Am are integrated and the concentration of each radionuclide in its respective filter sample calculated. This technique does not differentiate between ^{239}Pu and ^{240}Pu. Uranium analyses by neutron activation analysis (see Appendix C) are done on the second group of filter halves.

Silica gel cartridges from the 26 air sampling stations are analyzed monthly for tritiated water. The cartridges contain blue "indicating" gel to indicate the degree of desiccant saturation. During cold months of low absolute humidity, sampling flow rates are increased to ensure collection of enough water vapor for analysis. Water is distilled from each silica get cartridge and an aliquot of the distillate is analyzed for tritium by liquid scintillation counting. The amount of water absorbed by the silica get is determined by the difference between weights of the gel before and after sampling.

Analytical quality control for analyses done in the air sampling program are described in Appendix C. In brief, both blanks and standards are analyzed in conjunction with normal analytical procedures. About 10% of the analyses are devoted to quality control.

Further details may be found in the air sampling quality assurance project plan. [B7]

C. Water Sampling

Surface and ground water sampling stations are grouped by location (regional, perimeter, onsite) and hydrologic similarity. Water samples are taken once or twice a year. Samples from wells are collected after sufficient pumpage or bailing to ensure that the sample is representative of the aquifer. Spring samples (ground water) are collected at the discharge point.

The water samples are collected in 4 L (for radiochemical) and 1 L (for chemical) polyethylene bottles. The 4-L bottles are acidified in the field with 5 mL of concentrated nitric acid and returned to the laboratory within a few hours of sample collection for filtration through a 0.45-μm pore membrane filter. The samples are analyzed radiochemically for ^{3}H, ^{137}Cs, total U, ^{238}Pu and $^{239,240}Pu$, and as well as for gross alpha, beta, and gamma activities. Water samples for chemical analyses are handled similarly.

Storm run-off samples are analyzed for radionuclides in solution and suspended sediments. The samples are filtered through a 0.45- m filter. Solution is defined as filtrate passing through the filter, while suspended sediment is defined as the residue on the filter.

Further details may be found in the water sampling quality assurance project plan.[B8]

D. Soil and Sediment Sampling

Two soil sampling procedures are used. The first procedure is used to take surface composite samples. Soiled samples are collected by taking 5 plugs, 75 mm (3.0 in.) in diameter and 50 mm (2.0 in.) deep, at the center and corners of a square area 10 m (33 ft) on a side. The five plugs are combined to form a composite sample for radiochemical analysis

The second procedure is used to take surface and subsurface samples at one sampling location. Samples are collected from three layers in the top 30 cm (12 in.) of soil. A steel ring is placed on the surface of the soil at the sampling point. The soil enclosed by the ring is then collected by undercutting the ring with a metal spatula. A second spatula is then placed on top of the ring and the sample is transferred into a plastic bag and labelled.

All three layers are preserved by freezing. All equipment used for collection of these samples is washed with a soap and water solution and dried with paper towels. This is done before each sample is taken to reduce the potential for cross contamination.

Sediment samples are collected from dune buildup behind boulders in the main channels of perennially flowing streams. Samples from the beds of intermittently flowing streams are collected in the main channel.

Depending on the reason for taking a particular soil or sediment sample, it may be analyzed to detect any of the following: gross alpha and beta activities, ^{90}Sr, total uranium, ^{137}Cs, ^{238}Pu, and $^{239,240}Pu$. Moisture distilled from soiled samples may be analyzed for ^{3}H.

Further details may be found in the soil and sediment sampling quality assurance plan.[B8]

E. Foodstuffs Sampling

Local and regional produce are sampled annually. Fish are sampled annually from reservoirs upstream and downstream from the Laboratory.

Produce and soil samples are collected from local gardens in the fall of each year.[B9] Each produce or soil sample is sealed in a labeled, plastic bag. Samples are refrigerated until preparation for chemical analysis. Produce samples are washed as if prepared for consumption and quantitative wet, dry, and ash weights are determined. Soils are split and dried at 100°C (212°F) before analysis. A complete sample bank is kept until all radiochemical analyses are completed. Water is distilled from samples and submitted for tritium analysis. Produce ash and dry soil are submitted for analyses of ^{90}Sr, ^{137}Cs, total uranium, ^{238}Pu, and $^{239,240}Pu$.

At each reservoir, hook and line, trot line, or gill nets are used to capture fish.[B9] Fish, sediment, and water samples are transported under ice to the Laboratory for preparation. Sediment and water samples are submitted directly for radiochemical analysis. Fish are individually washed as if for consumption, dissected, and wet, dry, and ash weights determined. Ash is submitted for analysis of ^{90}Sr, ^{137}Cs, total uranium, ^{238}Pu, and $^{239,240}Pu$.

Further information may be found in the foodstuffs sampling quality assurance project plan.[B10]

F. Meteorological Monitoring

Meteorological data are continuously monitored on instrumented towers at five Laboratory locations. Measurements include wind speed and direction, standard deviations of wind speed and direction, vertical wind speed and its standard deviation, air temperature, dewpoint temperature, relative humidity, solar radiation, and precipitation.

These parameters are measured at discrete levels on the towers at heights ranging from ground level to 91 m (300 ft). Each parameter is measured every 3 to 5 sec and averaged or summed over 15 minute intervals. Data are recorded on digital cassette tape or transmitted by phone line to a microcomputer at the Occupational Health Laboratory at TA-59.

Data validation is accomplished with automated and manual screening techniques. One computer code compares measured data with expected ranges and make comparisons based on known meteorological relationships. Another code produces daily plots of data from each tower. These graphics are reviewed to provide another check of the data. This screening also helps to detect problems with the instrumentation that might develop between the annual or semi-annual (depending upon the instrument) calibrations.

Further details may be found in the meteorological monitoring quality assurance project plan.[B11]

G. Data Handling

Measurements of the radiochemical samples require that analytical or instrumental backgrounds be subtracted to obtain net values. Thus, net values that are lower than the minimum detection limit of an analytical technique (see Appendix C) are sometimes obtained. Consequently, individual measurements can result in values of zero and negative numbers. Although a negative value does not represent a physical reality, a valid long-term average of many measurements can be obtained only if the very small and negative values are included in the population.[B12]

For individual measurements, uncertainties are reported as the standard deviation. These values are associated with the estimated variance of counting, and indicate the precision of the counts.

Standard deviations (s) for the station and group (regional, perimeter, onsite) means are calculated using the following equation:

$$s = \sqrt{\frac{\sum_{i=1}^{N} (\bar{c}-c_i)^2}{(N-1)}}$$

where,

c_i = concentration for sample i,
$\bar{c}$ = means of samples from a given station or group, and
N = number of samples comprising a station or a group.

This value is reported as the uncertainty for the station and group means.

H. Quality Assurance

Collection of samples for chemical and radiochemical analyses follow a set procedure to ensure proper sample collection, documentation, submittal for chemical analysis, and posting of analytical results.

Before sample collection, the schedule and procedures to be followed are discussed with the chemist or chemists involved with doing the analyses. The discussion includes:

1. Number and type of samples.
2. Type of analyses and required limits of detection.
3. Proper sample containers.
4. Preparation of sample containers with preservative, if needed.
5. Sample schedule to ensure minimum holding time of analyses to comply with EPA criteria.

The Health and Environmental Chemistry Group (HSE-9) issues to the collector a block of sample numbers (e.g., 86.0071) with individual numbers assigned by the collector to individual station. These sample numbers follow the sample from collection through analyses and posting of individual results.

Each number, a single sample, is assigned to a particular station and is entered into the collector's log book. After the sample is collected, the date, time, temperature (if water), other pertinent information, and remarks are entered opposite sample number and station previously listed in the log book.

The sample container is labeled with station name, sample number, date, and preservative, if added.

After the sample is collected, it is delivered to the Group HSE-9 section leader. The section leader makes out a numbered request form entitled "HSE-9 Analytical Chemical Request." The request form number is entered in the collector's log book opposite sample numbers submitted along with the date delivered to chemist. The analytical request form serves as "chain-of-custody" for the samples.

The analytical request form contains the following information related to ownership and sample program submitted as (1) requestor (i.e., sample collector), (2) program code, (3) sample owner (i.e., program manager), (4) date, and (5) total number of samples. The second part of the request form contains (1) sample number or numbers, (2) matrix (e.g., water), (3) types of analyses (i.e., specific radionuclide and/or chemical constituent), (4) technique (i.e., analytical method to be used for individual constituents), (5) analyst (i.e., chemist to perform analyses), (6) priority of sample or samples, and (7) remarks. One copy of the form goes to the collector for his file and the other copies follow the sample.

Quality control, analytical methods and procedures, and limits of detection related to Group HSE-9's analytical work are presented in Appendix C.

The analytical results are returned to the sample collector who posts data according to sample and station taken from the log book. These data sheets are included in the report and are used to interpret data for the report.

Further details may be found in the quality assurance project plan for each program.[B5,B7,B8,B10,B11]

REFERENCES

B1. H. E. John and J. R. Cunningham, The Physics of Radiobiology 3rd Edition (C.C. Thomas, Springfield, Illinois, 1974).

B2. International Commission on Radiological Protection, "Protection Against Ionizing Radiation from External Sources," International Commission on Radiological Protection Report No. 15 (Pergamon Press, New York, 1970).

B3. P. R. Bevington, "Data Reduction and Error Analysis for the Physical Sciences" (McGraw-Hill, New York, 1969).

B4. M. G. Natrella, "Experimental Statistics" (National Bureau of Standards Handbook 91, Washington, D.C. 1963).

B5. D. Talley, "Environmental Thermoluminescent Dosimetry Quality Assurance Program of the Los Alamos National Laboratory's Environmental Surveillance Group, HSE-8," in *Environmental Surveillance Group*, "Quality

Assurance Project Plans," Los Alamos National Laboratory report LA-UR-87-1076 (February 1987).

B6. T. C. Gunderson, "Environmental and Emergency Response Capabilities of Los Alamos Scientific Laboratory's Radiological Air Sampling Program," Los Alamos Scientific Laboratory report LA-8379-MS (May 1980).

B7. T. Buhl, "Quality Assurance Plan for the Radiological Air Sampling Network, Los Alamos National Laboratory," in *Environmental Surveillance Group*, "Quality Assurance Project Plans," Los Alamos National Laboratory report LA-UR-87-1076 (February 1987).

B8. W. Purtymun, "Quality Assurance Plan for Water, Soil, Sediments, and Water Supply Sampling at Los Alamos National Laboratory," in *Environmental Surveillance Group*, "Quality Assurance Project Plans," Los Alamos National Laboratory report LA-UR-87-1076 (February 1987).

B9. J. G. Salazar, "Produce and Fish Sampling Program of Los Alamos National Laboratory's Environmental Surveillance Group," Los Alamos National Laboratory report LA-10186-MS (September 1984).

B10. L. Soholt, "Quality Assurance project Plan--Foodstuffs Monitoring at Los Alamos National Laboratory," in *Environmental Surveillance Group*, "Quality Assurance Project Plans," Los Alamos National Laboratory report LA-UR-87-1075 (February 1987).

B11. W. Olsen and J. Dewart, "Meteorological Quality Assurance Program of the Los Alamos National Laboratory's Environmental Surveillance Group, HSE-8," in *Environmental Surveillance Group*, "Quality Assurance Project Plans," Los Alamos National Laboratory report LA-UR-87-1076 (February 1987).

B12. R. O. Gilbert, "Recommendations Concerning the Computation and Reporting of Counting Statistics for the Nevada Applied Ecology Group", Battelle Pacific Northwest Laboratories report BNWL-B-368 (September 1975).

APPENDIX C

ANALYTICAL CHEMISTRY METHODOLOGY

Most analytical chemistry is provided by the Environmental and Health Chemistry Group (HSE-9). Overflow work is contracted to several commercial laboratories.

A. Radioactive Constituents

Environmental samples are routinely analyzed for the following radioactive constituents: gross alpha, beta, and gamma, isotopic plutonium, americium, uranium, cesium, tritium, and strontium. The detailed procedures have been published in this appendix in previous years.[C1,C2] Occasionally other radionuclides from specific sources are determined: ^{7}Be, ^{22}Na, ^{40}K, ^{51}Cr, ^{60}Co, ^{65}Zn, ^{83}Rb, ^{106}Ru, ^{134}Cs, ^{140}Ba, ^{152}Eu, ^{154}Eu, and ^{226}Ra. All but ^{226}Ra are determined by gamma-ray spectrometry on large Ge(Li) detectors. Depending upon the concentration and matrix, ^{226}Ra is measured by emanation[C3] or by gamma-ray spectrometry of its ^{214}Bi decay product.[C4] Uranium isotopic ratios ($^{235}U/^{238}U$) are measured by neutron activation analysis where precisions of $\pm 5\%$ are adequate.[C5] More precise work require mass spectrometry. Group HSE-9 acquired a VG-Instruments PLASMAQUAD Inductively Coupled Plasma Mass Spectrometer (ICPMS) in early 1986. Uranium isotopic ratios can be readily determined in environmental materials with precisions of 1-2% RSD at considerably reduced cost relative to neutron activation.

B. Stable Constituents

A number of analytical methods are used for various stable isotopes. The choice of method is based on many criteria, including the operational state of the instruments, time limitations, expected concentrations in samples, quantity of sample available, sample matrix, and Environmental Protection Agency (EPA) regulations.

Instrumental techniques available include neutron activation, atomic absorption, ion chromatography, color spectrophotometry (manual and automated), potentiometry, combustion analysis, and ICPMS. Standard chemical methods are also used for many of the common water quality tests. Atomic absorption capacities include flame, furnace, mercury cold vapor, and hydride generation, as well as flame emission spectrophotometry. The methods used and references for determination of various chemical constituents are summarized in Table C-1. In 1986 the EPA Region-6 administration granted HSE-9 limited approval for alternative test procedures for uranium in drinking water (delayed neutron assay) and for flow injection (without distillation) for chloride in drinking water and waste water. EPA approved for other modified methods is being actively sought.

C. Organic Constituents

Environmental water samples are analyzed by EPA or modified EPA methodology. Methods in use are supported by the use of documented spike/recovery studies, method and field blanks, matrix spikes, surrogate spikes, and blind quality control samples. EPA procedures are modified in order to take advantages of recent advances in analytical separation and analysis techniques. Volatile organics are analyzed by a modification of EPA 624 [purge and trap/gas chromatography/mass spectrometry (PT/GC/MS)]. Semivolatile organics are analyzed by a variety of methods including 604 (phenols), 606 (phthalate esters), 608 (organochlorine pesticides and PBCs), 609 (nitroaromatics), 610 (polynuclear aromatic hydrocarbons), 612 (chlorinated hydrocarbons), and 625 (semivolatiles by GC/MS). For samples in a solid matrix, comparable methods found within EPA's document SW-846 are used with suitable modifications as needed. Manual and automated methods have been developed using neutron activation to screen oil samples for potential PCB contamination via total chlorine determination.

Instrumentation available for organic analysis includes gas chromatographs with a variety of detector systems including mass spectrometry, flame ionization, and electron capture. Also available is a high pressure liquid chromatograph equipped with a UV and refractive index detection system, an infrared spectrophotometer, and a UV/visible spectrophotometer for colorimetric analyses. Methods used for sample preparation include solvent extraction, soxhlet extraction, liquid/liquid extraction, kuderna danish concentration,

Table C-1. Analytical Methods for Various Stable Constituents

Technique	Stable Constituents Measured	References
Standard Chemical Methods	Total Alkalinity, Hardness, SO_3^{-2}, SO_4^{-2}, TDS, Conductivity, COD	C6, C65
Color Spectrophotometry	NO_3^-, PO_4^{-3}, Si, Pb, Ti, B	C6, C65
Neutron Activation Instrumental Thermal	Al, Sb, As, Ba, Br, Ca, Ce, Cs, Cl, Cr, Co, Dy, Eu, Au, Hf, In, I, Fe, La, Lu, Mg, Mn, K, Rb, Sm, Sc, Se, Na, Sr, S, Ta, Tb, Th, Ti, W, V, Yb, Zn	C7, C12, C13, C14, C15 C65
Instrumental Epithermal	Al, Sb, As, Ba, Br, Cs, Cr, F, Ga, Au, In, I, La, Mg, Mn, Mo, Ni, K, Sm, Se, Si, Na, Sr, Th, Ti, W, U, Zn, Zr	C7, C9, C16, C17, C18, C19, C20, C21, C65
Thermal Neutron Capture Gamma Ray	Al, B, Ca, Cd, C, Gd, H, Fe, Mg, N, P, K, Si, Na, S, Ti	C7, C22, C23, C24, C25, C26, C27, C29, C65
Radiochemical	Sb, As, Cu, Au, Ir, Hg, Mo, Os, Pd, Pt, Ru, Se, Ag, Te, Th, W, U, La, Ce, Pr, Nd, Sm, Eu, Gd, Tb, Dy, Ho, Er, Yb, Lu, $^{235}U/^{238}U$, ^{238}Pu, ^{239}Pu	C5, C6, C7, C30, C31, C32, C33, C34, C35, C36, C37, C38, C51, C65
Delayed Neutron Assay	U	C7, C8, C10, C11, C39, C40, C65
Atomic Absorption	Sb, As, Ba, Be, Bi, Cd, Ca, Cr, Co, Cu, Ga, In, Fe, Pb, Li, Mg, Mn, Hg, Mo, Ni, K, Se, Ag, Na, Sr, Te, Tl, Sn, Ti, V, Zn, Al	C6, C41, C43, C44, C45, C46, C47, C48, C52, C53, C54, C65

Table C-1 (cont)

Technique	Stable Constituents Measured	References
Inductively Coupled Plasma Mass Spectrometry	Sb, As, Ba, Be, B, Bi, Cd, Cr, Co, Cu, Ga, In, Pb, Li, Mn, Hg, Mo, Ni, Se, Br, Ag, Sr, Te, Ti, Sn, Ti, V, Zn	C65
Ion Chromatograpy	F^-, Cl^-, Br^-, NO_2^-, NO_3^- SO_4^{-2}, PO_4^{-3}	C49, C65
Potentiometric	F^-, NH_4^+, pH, Br^-, Cl_2 (total) Cl_2 (free)	C50, C55, C65
Combustion	C, N, H, S, Total Organic Carbon	C29, C62, C63, C65
Corrosivity	--	C56, C57
Ignitability (Flash point)	--	C56, C58
Automated Colorimetry	CN^-, NH_4^-, PO_4^{-3}, NO_3^- NO_2^-, Cl^-, COD, TKN Si, B, SO_4^{-2}, Cr^{+6}	C6, C59, C60, C62, C65

column separation, headspace, and purge and trap. The methods used for analyses in 1987 along with references are shown in Table C-2. Tables C-3 through C-7 show compounds determined by these methods and representative detection limits.

D. Analytical Chemistry Quality Evaluation Program

1. Introduction. Control samples are analyzed in conjunction with normal analytical chemistry workload. Such samples consist of several general types: calibration standards, reagent blanks, process blanks, matrix blanks, duplicates, and standard reference materials. Analysis of control samples fills two needs in the analytical work. First, it provides quality control over analytical procedures so that problems that might occur can be identified and corrected. Secondly, data obtained from analysis of control samples permit evaluation of the capabilities of a particular analytical technique for determination of a given element or constituent under a certain set of circumstances. The former function is analytical quality control; the latter is quality assurance.

No attempt is made to conceal the identity of control samples from the analyst. They are submitted to the laboratory at regular intervals and analyzed in association with other samples; that is, they are not handled as a unique set of samples. We feel it would be difficult for analysts to give the samples special attention, even if they are so inclined. We endeavor to run at least 10% of stable constituent analyses and

Table C-2. Method Summary (Organics)

Analyte	Matrix	Method	Technique[a]	Reference
Volatiles	air	---	GC/MS	C65
Volatiles	soil	8010	PT/GC/MS	C64 C65
		8020		C66
Volatiles	water	625	PT/GC/MS	C64
EP Toxicity	soil	1310, 8080 8150	GC/ECD	C66
PCBs	water	606	GC/ECD	C64
	soil	8080	GC/ECD	C66
	oil	IH 320	GC/ECD	C65

[a]GC - gas chromatography, PT - purge and trap, ECD - electron capture detection, and MS - mass spectrometry.

selected radioactive constituent analyses as quality assurance samples using the materials described above. A detailed description of our Quality Assurance program and a complete listing of our annual results have been published annually.[C67-C76]

2. Radioactive Constituents. Quality control and quality assurance samples for radioactive constituents are obtained from outside agencies as well as prepared internally. The Quality Assurance Division of the Environmental Monitoring Systems Laboratory (EPA-Las Vegas) provides water, foodstuff, and air filter samples for analysis of gross alpha, gross beta, ^{3}H, ^{40}K, ^{60}Co, ^{65}Zn, ^{90}Sr, ^{106}Ru, ^{134}Cs, ^{137}Cs, ^{226}Ra, and $^{239,240}Pu$ as part of an ongoing laboratory intercomparison program. The National Bureau of Standards (NBS) provides several soil and sediment Standard Reference Materials (SRM) for environmental radioactivity. These SRMs are certified for ^{60}Co, ^{90}Sr, ^{137}Cs, ^{226}Ra, ^{238}Pu, $^{239,240}Pu$, ^{241}Am, and several other nuclides. The DOE's Environmental Measurements Laboratory also provides quality assurance samples.

Soil, rock, and ore samples obtained from the Canadian Geological Survey (CGS) are used for quality assurance of uranium and thorium determinations in silicate matrices. Our own "inhouse" standards are prepared by adding known quantities of liquid NBS radioactivity SRMs to blank matrix materials.

3. Stable Constituents. Quality assurance for the stable constituent analysis program is maintained by analysis of certified or well-characterized environmental materials. The NBS has a large set of silicate, water, and biological SRMs. The EPA distributes mineral analysis and trace analysis water standards. Rock and soil reference materials have been obtained from the CGS and the United States Geological Survey (USGS and NBS), Details of this program have also been published elsewhere.[C76]

The analytical quality control program for a specific batch of samples is the combination of many factors. These include the "fit of the calibration," instrument drift, calibration of the instrument and/or reagents, recovery for SRMs, and precision of results. In addition, there is a program for evaluation of the quality of results for an individual water sample.[C77] These individual water sample quality ratios are the sum of the milliequivalent (meq) cations to the sum of meq anions, the meq hardness of the sum of meq

Table C-3. Volatiles Determined by Purge and Trap

Compound	Representative Detection Limits (μg/L)
Methylene chloride	1.0
1,1-Dichloroethane	1.0
1,1-Dichloroethene	1.0
cis-1,2-Dichloroethene	1.0
1,2-Dichloroethane	1.0
Chloroform	1.0
Bromoform	1.0
Carbon tetrachloride	1.0
Bromodichloromethane	1.0
Dibromochloromethane	1.0
Dibromomethane	1.0
4-Methyl-2-pentanone	1.0
1,1,1-Trichloroethane	1.0
1,1,2-Trichloroethane	1.0
1,2-Dichloropropane	1.0
cis-1,3-Dichloropropene	5.0
trans-1,3-Dichloropropene	5.0
1,2-Dibromo-3-chloropropane	1.0
Trichloroethene	1.0
2-chloroethylvinyl ether	5.0
1,1,2,2-Tetrachloroethane	1.0
Tetrachloroethene	1.0
Chlorobenzene	1.0
1,2-Dichlorobenzene	1.0
1,3-Dichlorobenzene	1.0
1,4-Dichlorobenzene	1.0
Benzene	1.0
Acetone	5.0
Carbon disulfide	5.0
Toluene	1.0
Ethyl benzene	1.0
Styrene	5.0
o-xylene	1.0
m-xylene/p-xylene	1.0

Column: Supelco SPB-5 60 m x 0.25 mm x 1.0 μm. Limits of detection estimated by minimum signal required to yield identifiable mass spectral scan.

Ca^{+2} and Mg^{+2}, the observed total dissolved solids (TDS) to the sum of solids, the observed conductivity to the sum of contributing conductivities, as well as the two ratios obtained by multiplying (0.01) x (conductivity) and dividing by the meq cations and the meq anions.

4. Indicators of Accuracy and Precision. Accuracy is the degree of difference between average test results and true results, when the latter are known or assumed. Precision is the degree of mutual agreement among replicate measurements (frequently assessed by calculating the standard deviation of a set of data

Table C-4. Volatiles Determined by SW-846 Method 8010

Compound	Detection Limits (μg/kg)[a]
Bis (2-chloroethoxy) methane	--
Bis (2-chlorisopropy) ether	--
Bromobenzene	2300
Bromodichloromethane	1000
Bromoform	1000
Carbon tetrachloride	2100
Chloracetaldehyde	--
Chlorobenzene	1200
Chloroethane	--
Chloroform	1000
1-Chlorohexane	--
2-Chloroethyl vinyl ether	--
Chloromethane	--
Chlorotoluene	--
Dibromochloromethane	1000
Dibromomethane	--
1,2-Dichlorobenzene	500
1,3-Dichlorobenzene	500
1,4-Dichlorobenzene	500
Dichlorodifluoromethane	--
1,1-Dichloroethane	1000
1,2-Dichloroethane	800
1,1-Dichloroethylene	--
trans-1,2-Dichloroethylene	500
Dichloromethane	500
1,2-Dichloropropane	500
trans- 1,3-Dichloropropylene	--
1,1,2,2-Tetrachloroethane	2100
1,1,1,2-Tetrachloroethane	--
Tetrachloroethylene	2100
1,1,1-Trichloroethane	1600
1,1,2-Trichloroethane	1500
Trichloroethylene	500
Trichlorofluoromethane	--
Trichloropropane	--
Vinyl chloride	--

---

[a]Column: 60 m x 0.32 mm SPB-5 fused silica capillary, using methanolic partition with purge-and-trap. Detection limits is calculated from intercept of external calibration curve using a Flame Ionization Detector.

Table C-5. Volatiles Determined by SW-846 Method 8020

Compound	Detection Limits (μg/kg)[a]
Benzene	500
Chlorobenzene	1200
1,4-Dichlorobenzene	500
1,3-Dichlorobenzene	500
1,2-Dichlorobenzene	500
Toluene	500
Ethyl Benzene	800
Xylenes	--

[a]Column: 60 m x 0.32 mm SPB-5 fused silica capillary, using methanolic partition with purge-and-trap. Detection limits is calculated from intercept of external calibration curve using a Flame Ionization Detector.

points). Accuracy and precision are evaluated from results of analysis of reference materials. These results are normalized to the known quality in the reference material to permit comparison among reference materials of similar matrix containing different concentrations of the analyte:

$$r = \frac{\text{Reported Quantity}}{\text{Known Quantity}}$$

A mean value (R) for all normalized analyses of a given type is calculated as follows for a given matrix type (N is total number of analytical determinations):

$$R = \frac{\Sigma_i r_i}{N}.$$

The standard deviation(s) of R is calculated assuming a normal distribution of the population of analytical determinations (N):

$$s = \sqrt{\frac{\Sigma_i (R - r_i)^2}{(N - 1)}}$$

These calculated values are presented in Table C-8 through C-12. The mean value of R is a measure of the accuracy of a procedure. Values of R greater than unity indicate a positive bias and values less than unity a negative bias in the analysis.

The standard deviation is a measure of precision. Precision is a function of the concentration of analyte; that is, as the absolute concentration approaches the limit of detection, precision deteriorates. For instances, the precision for some determinations is quite large because many standards approached the limits of detection of a measurement. We are attempting to address this issue by calculating a new quality assurance parameter:

$$|\bar{X}_E - \bar{X}_c| < 1.96 \quad (S_E)^2 + (S_c)^2$$

where X_E and X_c are the experimentally determined and certified or consensus mean elemental concentrations, respectively. The S_E and S_c parameters are the standard deviations associated with $\bar{X}_E$ and $\bar{X}_c$, respectively. An analysis will be considered under control when this condition is satisfied for a certain element in a given matrix. Details on this approach are presented elsewhere.[C76]

Data on analytical detection limits are in Table C-13.

Table C-6. Volatiles Determined in Air

Compound	Representative Detection Limits (μg/tube)
1,1-Dichloroethane	3.0
1,1-Dichloroethene	3.0
cis-1,2-Dichloroethene	3.0
Chloroform	3.0
Bromoform	3.0
Bromodichloromethane	3.0
Dibromochloromethane	3.0
Dibromomethane	3.0
1,1,1-Trichloroethane	3.0
1,1,2-Trichloroethane	3.0
1,2-Dichloropropane	3.0
cis-1,3-Dichloropropene	5.0
trans-1,3-Dichloroprepene	5.0
1,2-Dibromo-3-chloropropane	3.0
Trichlorethene	3.0
2-chloroethylvinyl ether	5.0
1,1,2,2-Tetrachloroethane	3.0
Tetrachloroethene	3.0
Chlorobenzene	3.0
1,2-Dichlorobenzene	3.0
1,3-Dichlorobenzene	3.0
1,4-Dichlorobenzene	3.0
Trichlorofluoromethane	5.0
Toluene	3.0
Ethyl benzene	3.0
o-xylene	3.0
m-xylene/p-xylene	3.0

Column: Supelco SPB-5 60 m x 0.25 mm x 1.0 μm.
Method: Carbon disulfide desorbtion of charcoal tubes followed by GC/MS analysis.

Table C-7. EP Toxicity Organic Contaminants

Contaminant	Maximum Concentration (mg/L)	Representative Detection Limits (mg/L)[a]
Endrin (1,2,3,4,10,10-Hexachloro-1 7-epoxy-1,4,4a,5,6,7,8,8a-octahydro-1 4-endo, endo-5, 8-dimethanoaphthalene)	0.02	0.006
Lindane (1,2,3,4,5,6-Hexachlorocyclohexane, gamma isomer)	0.4	0.0002
Methoxychlor (1,1,1-Trichloro-2,2-bis (p-methoxphenyl)ethane)	10.0	0.004
Toxaphene ($C_{10}H_{10}Cl_8$ Technical chlorinated camphene, 67-69% chlorine)	0.5	0.020
2,4-D (2,4-Dichlorophenoxyacetic acid)	10.0	0.016
2,4,5-TP (Silvex) (2,4,5-Trichlorophenoxypropionic acid)	1.0	0.005

---

[a]Column: 30 m x 0.32 mm SPB-5 fused silica capillary. Detection limit is calculated from GC response being equal to four times the GC background noise using an electron capture detector.

Table C-8. Summary of HSE-9 Quality Assurance Tests for Data from January 1, 1987 to December 31, 1987 (Stable Element Analyses Performed by HSE-9)

ELE	BIOLOGICAL Mean ± SD (n)	SLUDGE Mean ± SD (n)	EP-TOX Mean ± SD (n)	FILTER Mean ± SD (n)	BULK Mean ± SD (n)	SILICATE Mean ± SD (n)	WATER Mean ± SD (n)
Ag	---	---	1.07 ± 0.06 (31)	---	1.17 ± 0.01 (3)	---	1.02 ± 0.07 (130)
Al	---	---	---	1.04 ± 0.02 (3)	---	---	1.01 ± 0.11 (19)
As	0.96 ± 0.22 (12)	0.92 ± 0.09 (9)	1.05 ± 0.05 (51)	1.01 ± 0.07 (27)	---	1.33 ± 0.39 (6)	1.05 ± 0.10 (92)
B	0.99 ± 0.10 (7)	---	---	1.08 (1)	---	---	1.02 ± 0.06 (42)
Ba	---	---	1.03 ± 0.08 (35)	---	0.91 ± 0.02 (3)	1.15 (2)	1.02 ± 0.11 (93)
Be	---	---	1.02 ± 0.07 (9)	0.95 ± 0.09 (93)	---	1.42 ± 0.37 (9)	1.04 ± 0.06 (35)
Bi	---	---	---	1.05 ± 0.11 (10)	---	---	---
Br	0.93 ± 0.18 (14)	---	---	---	---	0.98 (1)	0.91 ± 0.07 (26)
C	0.99 ± 0.02 (25)	---	---	---	---	---	---
Ca	0.78 (1)	---	---	---	---	---	0.99 ± 0.04 (39)
Cd	---	0.94 ± 0.08 (15)	1.05 ± 0.08 (78)	0.96 ± 0.11 (32)	1.08 ± 0.04 (3)	1.00 (1)	0.98 ± 0.08 (127)
Ce	---	---	---	---	---	1.13 (2)	---
Cl	0.93 (1)	---	---	---	---	---	1.00 ± 0.05 (89)
Cl2	---	---	---	---	---	---	0.96 ± 0.16 (13)
CN	---	---	---	---	---	---	0.87 ± 0.09 (175)
Co	---	---	0.94 (2)	---	---	2.88 ± 2.77 (10)	1.00 ± 0.08 (4)
COD	---	---	---	---	---	---	1.02 ± 0.06 (54)
COND	---	---	---	---	---	---	1.01 ± 0.04 (52)
Cr	---	---	1.02 ± 0.06 (60)	---	0.96 ± 0.08 (4)	0.89 (2)	1.01 ± 0.16 (115)
Cr(+6)	---	---	---	---	---	---	0.92 ± 0.06 (109)
Cs	1.65 ± 0.08 (7)	---	---	---	---	0.97 (2)	---
Cu	1.06 (1)	---	0.97 ± 0.05 (13)	1.03 ± 0.03 (6)	---	1.09 (1)	1.01 ± 0.08 (108)
Eu	---	---	---	---	---	1.02 ± 0.08 (8)	---
F	---	---	---	---	---	---	1.02 ± 0.11 (104)
Fe	---	---	---	---	---	0.98 ± 0.04 (9)	1.03 ± 0.07 (102)
FLASH PT.	---	---	---	---	1.01 ± 0.02 (27)	---	---
Ga	---	---	---	1.04 ± 0.06 (13)	---	1.08 ± 0.38 (7)	---
Gd	---	---	---	0.97 ± 0.06 (4)	---	---	---
H	0.99 ± 0.04 (31)	---	---	---	---	---	---
HARD	---	---	---	---	---	---	1.00 ± 0.05 (17)
HEATCAP	---	---	---	---	1.06 ± 0.14 (8)	---	---
Hf	---	---	---	---	---	0.99 (2)	---
Hg	---	---	0.85 ± 0.26 (21)	---	---	1.09 ± 0.21 (135)	1.00 ± 0.10 (70)
I	---	---	---	---	---	---	0.94 ± 0.02 (6)
K	0.95 (1)	---	---	---	---	1.13 ± 0.16 (4)	1.02 ± 0.09 (26)

Table C-8 (cont)

ELE	BIOLOGICAL Mean ± SD	(n)	SLUDGE Mean ± SD	(n)	EP-TOX Mean ± SD	(n)	FILTER Mean ± SD	(n)	BULK Mean ± SD	(n)	SILICATE Mean ± SD	(n)	WATER Mean ± SD	(n)
La	---		---		---		---		---		0.95 ± 0.08	(12)	---	
Li	---		---		0.99	(2)	1.20 ± 0.01	(3)	---		---		1.01 ± 0.05	(40)
Lu	---		---		---		---		---		1.16	(1)	---	
Mg	---		---		---		---		---		---		0.96 ± 0.12	(40)
Mn	1.04	(1)	---		0.89 ± 0.03	(3)	1.01 ± 0.01	(3)	---		---		1.07 ± 0.12	(41)
Mo	1.00 ± 0.02	(4)	---		---		---		---		---		1.13 ± 0.08	(7)
N	0.95 ± 0.06	(65)	---		---		---		---		---		---	
Na	1.00	(1)	---		---		---		---		0.97 ± 0.02	(4)	1.03 ± 0.04	(29)
NH3-N	---		---		---		---		---		---		0.98 ± 0.06	(138)
Ni	---		---		1.02 ± 0.07	(22)	---		---		0.90	(1)	1.00 ± 0.08	(61)
NO3-N	---		---		---		---		---		---		1.00 ± 0.05	(77)
P	---		---		---		---		---		---		0.95 ± 0.11	(86)
Pb	---		1.03 ± 0.04	(17)	1.06 ± 0.08	(73)	1.01 ± 0.12	(49)	1.02	(2)	---		1.01 ± 0.11	(144)
pH	---		---		---		---		---		---		1.00 ± 0.01	(474)
Rb	---		---		---		---		---		0.95 ± 0.05	(8)	---	
S	0.97 ± 0.06	(138)	---		---		---		---		0.69 ± 0.09	(99)	---	
Sb	---		---		---		---		---		1.18	(2)	---	
Sc	0.97 ± 0.02	(4)	---		---		1.00 ± 0.11	(19)	---		1.00 ± 0.06	(8)	---	
Se	---		---		0.97 ± 0.14	(42)	---		---		1.12	(2)	1.05 ± 0.14	(73)
Si	---		---		---		---		---		---		0.99 ± 0.06	(85)
Sm	---		---		---		---		---		0.96 ± 0.05	(4)	---	
SO4	---		---		---		---		---		---		0.97 ± 0.06	(80)
Ta	---		---		---		---		---		0.86	(2)	---	
TALK	---		---		---		---		---		---		0.98 ± 0.03	(47)
Tb	---		---		---		---		---		1.11	(1)	---	
TDS	---		---		---		---		1.04	(1)	---		0.98 ± 0.12	(34)
Th	---		---		---		---		---		1.03 ± 0.20	(20)	1.00 ± 0.10	(6)
Ti	---		1.32 ± 0.25	(10)	---		1.01 ± 0.01	(3)	---		---		---	
Tl	---		---		---		---		---		---		1.04 ± 0.12	(8)
TOX	---		---		---		---		1.08 ± 0.10	(9)	---		---	
TSS	---		---		---		---		---		---		0.66	(1)
U	1.08 ± 0.08	(25)	---		---		0.99 ± 0.07	(29)	---		0.98 ± 0.03	(81)	1.02 ± 0.06	(62)
V	1.29	(1)	1.92 ± 0.15	(32)	0.99	(2)	1.02 ± 0.01	(3)	---		1.09 ± 0.13	(3)	1.03 ± 0.08	(4)
W	0.79 ± 0.06	(4)	---		---		---		---		---		---	
Yb	---		---		---		---		---		0.95 ± 0.11	(10)	---	
Zn	---		1.05 ± 0.07	(58)	1.01 ± 0.06	(5)	0.98 ± 0.10	(32)	---		---		1.00 ± 0.09	(93)

Table C-9. Summary of HSE-9 Quality Assurance Tests for Data from January 1, 1987 to December 31, 1987 (Stable Element Analyses Performed by Contractors)

ELEMENT	BULK Mean ± SD (n)	SILICATE Mean ± SD (n)	WATER Mean ± SD (n)
Ag	---	---	1.43 (1)
Al	---	0.93 ± 0.06 (20)	1.11 (1)
As	---	---	0.92 (1)
Ba	---	---	0.98 (1)
Br	0.98 ± 0.12 (11)	---	---
Ca	---	0.96 ± 0.06 (20)	---
Cd	---	---	1.00 (1)
Cl	0.91 ± 0.22 (13)	0.96 ± 0.20 (20)	1.06 ± 0.04 (7)
Cr	---	---	1.06 (1)
Dy	---	0.97 ± 0.16 (20)	---
F	1.85 ± 1.16 (11)	---	---
Fe	---	---	1.23 (2)
I	1.02 ± 0.09 (11)	---	---
Mg	---	0.83 ± 0.12 (20)	---
Mn	---	1.01 ± 0.03 (20)	---
Na	---	0.97 ± 0.03 (20)	---
Pb	---	---	1.81 (1)
Ti	---	0.95 ± 0.06 (20)	---
V	---	1.03 ± 0.04 (20)	---

Table C-10. Summary of HSE-9 Quality Assurance Tests for Data from January 1, 1987 to December 31, 1987 (Organic Analyses Performed by HSE-9)

COMPOUND	FILTER Mean ± SD	(n)	BULK Mean ± SD	(n)	SILICATE Mean ± SD	(n)	TUBE Mean ± SD	(n)	WATER Mean ± SD	(n)
Acetone	---		---		---		---		0.07	(1)
Aldrin	---		---		---		---		1.16	(2)
Aroclor 1221	---		---		---		---		1.03	(2)
Aroclor 1242	1.04 ± 0.06	(5)	0.97 ± 0.11	(64)	0.66 ± 0.24	(8)	---		0.99 ± 0.19	(3)
Aroclor 1254	1.15	(1)	0.90 ± 0.10	(6)	0.67	(2)	---		---	
Aroclor 1260	1.00	(2)	0.92 ± 0.11	(56)	0.93	(2)	---		0.88	(2)
Benzene	---		0.89	(1)	0.48	(1)	0.92 ± 0.27	(16)	1.00 ± 0.28	(4)
Benzo-k-fluoranthene	---		---		---		---		0.83	(1)
Bis(2-chloroethoxy)methane	---		---		---		---		0.82	(1)
Bromodichloromethane	---		---		0.55	(1)	0.87	(2)	0.83 ± 0.05	(8)
Bromoform	---		---		0.68	(1)	---		0.97 ± 0.16	(6)
2-Butanone	---		0.75	(1)						
Camphene, chlorinated	---		---		---		---		3.10	(2)
Carbon tetrachloride	---		---		---		1.07 ± 0.15	(18)	0.68 ± 0.23	(11)
Cellosolve acetate	---		---		---		1.02 ± 0.04	(3)	---	
Chlorobenzene	---		---		0.60	(2)	0.85	(2)	0.85	(2)
Chlorodibromomethane	---		---		---		0.76	(2)	0.93 ± 0.15	(5)
Chloroform	---		---		0.47	(1)	1.01 ± 0.22	(18)	0.85 ± 0.21	(8)
2-Chloronaphthalene	---		---		---		---		1.03	(1)
2,4-D	---		---		1.74	(1)	---		1.18 ± 0.44	(7)
Dibromochloromethane	---		---		---		0.76	(2)	0.93 ± 0.15	(5)
Dibromomethane	---		---		---		---		0.99	(1)
o-Dichlorobenzene (1,2)	---		---		---		1.01	(1)	0.99	(1)
m-Dichlorobenzene (1,3)	---		---		---		---		0.98	(2)
p-Dichlorobenzene (1,4)	---		---		---		---		1.06	(2)
Dichlorobromomethane	---		---		0.55	(1)	0.87	(2)	0.83 ± 0.05	(8)
1,1-Dichloroethane	---		---		0.47	(2)	1.03 ± 0.08	(16)	0.92 ± 0.20	(3)
1,1-Dichloroethane	0.96	(2)								
1,1-Dichloroethene	---		---		---		---		1.64 ± 0.69	(4)
2,4-Dichlorophenol	---		---		---		---		1.14	(1)
1,4-Dioxane	---		---		---		1.26	(1)	---	

Table C-10 (cont)

COMPOUND	FILTER Mean ± SD (n)	BULK Mean ± SD (n)	SILICATE Mean ± SD (n)	TUBE Mean ± SD (n)	WATER Mean ± SD (n)
Endrin	---	---	---	---	0.95 (2)
Ethyl acetate	---	---	---	1.09 (1)	---
Ethylbenzene	---	0.88 (1)	---	1.47 ± 0.05 (4)	0.72 ± 0.09 (4)
Ethylene chloride	---	---	---	1.03 ± 0.08 (16)	0.92 ± 0.20 (3)
Hexachloro-1,3-butadiene	---	---	---	---	0.96 (1)
Hexane	---	---	---	0.82 (1)	---
Lindane	---	---	2.75 (1)	---	1.23 ± 0.36 (6)
Methoxychlor	---	---	---	---	1.79 ± 0.39 (3)
Methylchloroform	---	---	---	---	0.68 ± 0.16 (7)
Methylene chloride	---	---	---	---	1.68 ± 0.76 (4)
Methylethyl ketone	---	0.75 (1)	---	---	---
Naphthalene	---	---	---	0.45 (2)	---
Phenol	---	---	---	---	0.92 (1)
Silvex	---	---	---	---	0.96 ± 0.24 (7)
Styrene	---	---	---	1.00 (1)	---
1,1,2,2-Tetrachloroethane	---	---	---	---	1.05 (2)
Tetrachloroethylene	---	---	---	0.40 (1)	0.81 (1)
Tetrahydrofuran	---	---	---	0.31 (4)	---
Toluene	---	---	0.21 ± 0.08 (5)	0.97 ± 0.06 (18)	0.82 (2)
Toxaphene	---	---	---	---	3.10 (2)
Tribromomethane	---	---	0.68 (1)	---	0.97 ± 0.16 (6)
1,1,2-Trichloroethane	---	---	---	---	1.35 ± 0.60 (3)
1,1,1-Trichloroethane	---	---	---	---	0.68 ± 0.16 (7)
Trichloroethylene	---	---	---	0.97 ± 0.15 (13)	1.14 ± 0.42 (3)
Vinyl acetate	---	---	---	---	1.29 (1)
Vinylidene chloride	---	---	---	---	1.64 ± 0.69 (4)
o-Xylene	---	---	---	1.09 ± 0.30 (15)	---
p-Xylene	---	---	---	1.30 (2)	0.77 (1)

Table C-11. Summary of HSE-9 Quality Assurance Tests for Data from January 1, 1987 to December 31, 1987 (Organic Analyses Performed by Contractors)

COMPOUND	WATER Mean ± SD	(n)	BULK Mean ± SD	(n)	SILICATE Mean ± SD	(n)	TUBE Mean ± SD	(n)
Acenaphthene	0.87	(1)	---		---		---	
Anthracene	0.35	(1)	---		---		---	
Aroclor 1242	---		0.74 ± 0.14	(10)	---		---	
Aroclor 1254	---		0.71 ± 0.22	(5)	---		---	
Aroclor 1260	---		0.78 ± 0.46	(9)	---		---	
1,2-Benzanthracene	0.62	(2)	---		---		---	
1,2-Benzanthracene (d12)	0.62	(2)	---		---		---	
Benzo-a-pyrene	0.63	(1)	---		---		---	
Benzo-b-fluoranthene	1.11	(1)	---		---		---	
Benzo-k-fluoranthene	0.53	(2)	---		---		---	
Bis(2-chloroethoxy)methane	0.66	(2)	---		---		---	
Bis(2-chloroethyl)ether	0.56	(2)	---		---		---	
Bis(2-chloroisopropyl)ether	0.66	(1)	---		---		---	
Bis(2-ethylhexyl)phthalate	0.48 ± 0.47	(3)	---		---		---	
Bromodichloromethane	0.62	(2)	---		---		---	
Bromoform	0.70	(2)	---		---		---	
4-Bromophenylphenyl ether	0.76	(1)	---		---		---	
Butylbenzyl phthalate	0.67	(1)	---		---		---	
Carbon tetrachloride	0.99 ± 0.58	(6)	0.87	(1)	---		0.77 ± 0.43	(5)
Chlorobenzene	---		---		0.07 ± 0.04	(4)	---	
Chlorodibromomethane	0.69	(2)	---		---		---	
Chloroform	0.64	(2)	---		---		---	
2-Chloronaphthalene	0.23	(2)	---		---		---	
4-Chlorophenylphenyl ether	0.62	(1)	---		---		---	
Chrysene	0.70	(1)	---		---		---	
Di-n-butyl phthalate	1.59	(2)	---		---		---	
Dibromochloromethane	0.69	(2)	---		---		---	
Dibutyl phthalate	1.59	(2)	---		---		---	
o-Dichlorobenzene (1,2)	0.42	(2)	---		---		---	
m-Dichlorobenzene (1,3)	0.54	(2)	---		---		---	
p-Dichlorobenzene (1,4)	0.59	(1)	---		---		---	
Dichlorobromomethane	0.62	(2)	---		---		---	
1,2-Dichloroethane	0.89	(2)	---		---		---	
Diethyl phthalate	0.92	(2)	---		---		---	
Dimethyl phthalate	0.46	(1)	---		---		---	
2,4-Dinitrotoluene	0.76	(2)	---		---		---	
2,6-Dinitrotoluene	0.76	(2)	---		---		---	
Ethylbenzene	---		---		0.13 ± 0.07	(5)	---	
Ethylene chloride	0.89	(2)	---		---		---	
Fluoranthene	0.78	(1)	---		---		---	
Fluorene	1.67	(1)	---		---		---	
HCB	0.41	(2)	---		---		---	
Hexachloro-1,3-butadiene	0.30	(2)	---		---		---	
Hexachlorobenzene	0.41	(2)	---		---		---	
Hexachlorobutadiene	0.30	(2)	---		---		---	
Hexachloroethane	0.46	(1)	---		---		---	
Isophorone	0.57	(2)	---		---		---	
Methylchloroform	0.73	(2)	---		---		---	
Methylene chloride	---		---		0.36	(2)	---	
Nitrobenzene	0.57	(1)	---		---		---	
N-Nitrosodi-n-propylamine	0.24	(2)	---		---		---	
Phenanthrene	0.72	(2)	---		---		---	
Phenanthrene (d10)	0.72	(2)	---		---		---	
Tetrachloroethylene	0.41	(2)	---		---		---	
Tribromomethane	0.70	(2)	---		---		---	
1,1,1-Trichloroethane	0.73	(2)	---		---		---	
Trichloroethylene	0.59 ± 0.17	(4)	---		200.	(2)	0.05	(2)
o-Xylene	---		---		0.16 ± 0.04	(5)	---	

Table C-12. Summary of HSE-9 Quality Assurance Tests for Data from January 1, 1987 to December 31, 1987 (Radiochemical Analyses Performed by HSE-9)

NUCLIDE	BIOLOGICAL Mean ± SD (n)	FILTER Mean ± SD (n)	SILICATE Mean ± SD (n)	WATER Mean ± SD (n)
Alpha	---	0.93 ± 0.06 (72)	---	1.07 ± 0.13 (546)
Am-241	1.23 ± 0.09 (3)	1.12 ± 0.10 (7)	1.00 ± 0.16 (6)	1.04 ± 0.08 (66)
Be-7	---	1.80 ± 0.31 (6)	---	---
Beta	---	0.94 ± 0.04 (72)	---	1.03 ± 0.47 (549)
Co-57	---	---	---	1.15 ± 0.09 (53)
Co-60	1.19 ± 0.10 (4)	0.92 ± 0.01 (3)	---	0.91 ± 0.41 (72)
Cs-134	---	---	---	1.03 ± 0.24 (66)
Cs-137	1.13 ± 0.66 (35)	1.34 ± 0.32 (6)	0.92 ± 0.11 (43)	1.00 ± 0.11 (108)
Gamma	---	---	0.93 ± 0.04 (5)	0.92 ± 0.11 (21)
H-3	---	---	---	1.07 ± 0.23 (307)
I-131	1.11 ± 0.13 (9)	---	---	---
K-40	---	---	---	---
Mn-54	---	---	3.29 ± 0.02 (3)	---
Na-22	---	1.05 ± 0.03 (3)	---	1.07 ± 0.07 (56)
Pu-238	0.95 ± 0.21 (22)	---	---	1.01 ± 0.03 (49)
Pu-239	1.15 ± 0.37 (34)	---	1.09 ± 0.44 (18)	1.05 ± 0.10 (58)
Ra-226	---	1.33 ± 0.60 (9)	1.20 ± 0.62 (25)	1.00 ± 0.17 (81)
Ru-106	---	---	---	0.94 ± 0.06 (15)
Sr-90	0.98 ± 0.13 (23)	1.49 ± 0.07 (3)	---	1.07 ± 0.36 (10)
U-234	---	1.01 ± 0.07 (4)	1.16 ± 0.46 (7)	0.94 ± 0.05 (18)
U-235	---	---	---	0.93 ± 0.10 (26)
U-235/238	---	---	---	0.89 ± 0.13 (23)
		---	---	0.95 (2)

Table C-13. Detection Limits for Analyses of Typical Environmental Samples

Parameter	Approximate Sample Volume or Weight	Count Time	Detection Limit Concentration
Air Sample			
Tritium	3 m^3	50 min	1×10^{-10} µCi/m^3
^{238}Pu	2.0×10^4 m^3	8×10^4 sec	2×10^{-18} µCi/m^3
$^{239,240}Pu$	2.0×10^4 m^3	8×10^4 sec	3×10^{-18} µCi/m^3
^{241}Am	2.0×10^4 m^3	8×10^4 sec	2×10^{-18} µCi/m^3
Gross alpha	6.5×10^3 m^3	100 min	4×10^{-16} µCi/m^3
Gross beta	6.5×10^3 m^3	100 min	4×10^{-16} µCi/m^3
Uranium (delayed neutron)	2.0×10^4 m^3	60 sec	1 pg/m^3
Water Sample			
Tritium	0.005 L	50 min	7×10^{-7} µCi/mL
^{137}Cs	0.5 L	5×10^4 sec	4×10^{-8} µCi/mL
^{238}Pu	0.5 L	8×10^4 sec	9×10^{-12} µCi/mL
$^{239,240}Pu$	0.5 L	8×10^4 sec	3×10^{-11} µCi/mL
^{241}Am	0.5 L	8×10^4 sec	2×10^{-10} µCi/mL
Gross alpha	0.9 L	100 min	3×10^{-9} µCi/mL
Gross beta	0.9 L	100 min	3×10^{-9} µCi/mL
Uranium (delayed neutron)	0.025 L	50 sec	1 µg/L
Soil Sample			
Tritium	1 kg	50 min	0.003 pCi/g
^{137}Cs	100 g	5×10^4 sec	10^{-1} pCi/g
^{238}Pu	10 g	8×10^4 sec	0.003 pCi/g
$^{239,240}Pu$	10 g	8×10^4 sec	0.002 pCi/g
^{241}Am	10 g	8×10^4 sec	0.01 pCi/g
Gross alpha	2 g	100 min	1.4 pCi/g
Gross beta	2 g	100 min	1.3 pCi/g
Uranium (delayed neutron)	2 g	20 sec	0.03 µg/g

REFERENCES

C1. Environmental Surveillance Group, "Environmental Surveillance at Los Alamos During 1979," Los Alamos Scientific Laboratory report LA-8200-ENV (April 1980).

C2. Environmental Surveillance Group, "Environmental Surveillance at Los Alamos during 1980," Los Alamos National Laboratory report LA-8810-ENV (April 1981).

C3. J. H. Harley, Ed. (1972 with annual supplements), Environmental Measurements Laboratory Procedures Manual HASL-300.

C4. E. S. Gladney, W. Eberhardt, and R. J. Peters, "The Determination of ^{226}Ra in CCRMP Reference Samples by Independent Nuclear Methods," Geostandards Newsletter 6,5-6 (1982).

C5. E. S. Gladney, D. R. Perrin, and R. J. Peters, "The Determination of U-235/U-238 Ratio in Natural Waters by Chelex-100 Ion Exchange and Neutron Activation Analysis," Anal. Chem. 55:976-977 (1983).

C6. American Public Health Association, American Water Works Association, and the Water Pollution Control Federation, *Standard Methods for the Examination of Water and Wastewater*, 15th edition (1980).

C7. E. S. Gladney, D. B. Curtis, D. R. Perrin, J. W. Owens, and W. E. Goode, "Nuclear Techniques for the Chemical Analysis of Environmental Materials," Los Alamos National Laboratory report LA-8192-MS (1980).

C8. E. S. Gladney, J. W. Owens, and J. W. Starner, "Simultaneous Determination of Uranium and Thorium in Ores by Instrumental Epithermal Neutron Activation Analysis," Anal. Chim Acta 104, 120 (1979).

C9. E. S. Gladney, D. R. Perrin, J. P. Balagna, and C. L. Warner, "Evaluation of a Boron Filtered Epithermal Neutron Irradiation Facility," Anal. Chem. 52, 2128 (1980).

C10. S. A. Amiel, "Analytical Applications of Delayed Neutron Emission in Fissionable Elements," Anal. Chem. 34, 1683 (1962).

C11. E. S. Gladney, W. K. Hensley, and M. M. Minor, "Comparison of Three Techniques for the Measurement of Depleted Uranium in Soils," Anal. Chem. 50, 652 (1978).

C12. G. E. Gordon, K. Randle, G. G. Goles, J. B. Corliss, M. H. Beeson, and S. S. Oxley, "Instrumental Activation Analysis of Standard Rocks with High Resolution -Ray Detectors," Geochim. et. Cosmochim. Acta 32, 369 (1968).

C13. R. Dams, J. A. Robbins, K. A. Rahn, and J. W. Winchester, "Nondestructive Neutron Activation Analysis of Air Pollution Particulates," Anal. Chem. 42, 861 (1970).

C14. B. Salbu, E. Steinnes, and A. C. Pappas, "Multielement Neutron Activation of Fresh Water Using Ge(Li) Gamma Spectrometry," Anal. Chem. 47, 1011 (1975).

C15. G. R. Van der Linden, F. DeCorte, and J. Hoste, "Activation Analysis of Biological Materials with Ruthenium as a Multi-Isotopic Comparator," Anal. Chim. Acta 71, 263 (1974).

C16. E. Steinnes, "Epithermal Neutron Activation Analysis of Geological Materials," in *Activation Analysis in Geochemistry and Cosmochemistry*, A. O. Brumfelt and E. Steinnes, Eds., UNIVERSITETSFORLAGET, Oslo, Norway, pp. 113-128 (1971).

C17. E. S. Gladney, L. E. Wangen, and R. D. Aguilar, "Comparison of Three Techniques for Rapid Determination of Sr in Soils and Vegetation," Anal. Lett. 10, 1083 (1977).

C18. L. E. Wangen and E. S. Gladney, "Determination of As and Ga in Standard Materials by Instrumental Epithermal Neutron Activation Analysis," Anal. Chim. Acta 96, 271 (1978).

C19. E. S. Gladney, J. W Owens, M. L. Marple, and D. L. Dreesen, "A Comparison of Thermal and Epithermal Neutron Activation for the Measurement of Se in Vegetation," Anal. Lett. **A11**, 1001 (1978).

C20. E. S. Gladney and D. R. Perrin, "Quantitative Analysis of Silicates by Instrumental Epithermal Neutron Activation Using (n,p) Reactions," Anal. Chem. **51**, 2297 (1979).

C21. E. S. Gladney and D. R. Perrin, "Determination of Bromine in Biological, Soil, and Geological Standard Reference Materials by Instrumental Epithermal Neutron Activation Analysis," Anal. Chem. **51**, 2015 (1979).

C22. E. S. Gladney, E. T. Jurney, and D. B. Curtis, "Nondestructive Determination of Boron and Cadmium in Environmental Materials by Thermal Neutron Prompt Gamma-Ray Spectrometry," Anal. Chem. **48**, 2139 (1976).

C23. E. T. Jurney, D. B. Curtis, and E. S. Gladney, "Nondestructive Determination of Sulfur in Environmental Materials by Thermal Neutron Prompt Gamma-Ray Spectroscopy," Anal. Chem. **49**, 1741 (1977).

C24. E. S. Gladney, D. B. Curtis, and E. T. Jurney, "Multielement Analysis of Major and Minor Elements by Thermal Neutron Capture Gamma-Ray Spectrometry," J. Radional. Chem. **46**, 299 (1978).

C25. D. B. Curtis, E. S. Gladney, and E. T. Jurney, "Potential Interference in the Determination of Sulfur by Thermal Neutron Induced Prompt Gamma-Ray Spectrometry," Anal. Chem. **51**, 158 (1979).

C26. E. S. Gladney, D. B. Curtis, and E. T. Jurney, "Simultaneous Determination of Nitrogen, Carbon, and Hydrogen Using Thermal Neutron Prompt GammaRay Spectrometry," Anal. Chim. Acta **110**, 339 (1979).

C27. E. S. Gladney, "A Literature Survey of Chemical Analysis by Thermal Neutron Induced Capture Gamma-Ray Spectrometry," Los Alamos Scientific Laboratory report LA-8028-MS (Sept. 1979).

C28. M. P. Failey, D. L. Anderson, W. H. Zoller, G. E. Gordon, and R. M. Lindstrom, "Neutron Capture Prompt Gamma-Ray Activation Analysis for Multielement Determination in Complex Samples," Anal. Chem. **51**, 2209 (1979).

C29. T. G. Schofield, E. S. Gladney, F. R. Miera, and P. E. Trujillo, "Comparative Determination of Carbon, Nitrogen, and Hydrogen in Environmental Standard Reference Materials by Instrumental Combustion Analysis and Thermal Neutron Capture Gamma Ray Spectrometry," Anal. Lett. **A13**, 75 (1980).

C30. E. S. Gladney and H. L. Rook, "Determination of Tellurium and Uranium in Environmental Materials," Anal. Chem. **47**, 1554 (1975).

C31. E. S. Gladney, J. W. Owens, and J. W. Starner, "The Determination of Uranium in Natural Waters by Neutron Activation Analysis," Anal. Chem. **48**, 973 (1976).

C32. E. S. Gladney, "Copper Determination in Standard Materials Using Neutron Activation and Srafion NMRR Anion Exchange Resin," Anal. Chim. Acta **91**, 353 (1977).

C33. E. S. Gladney, "Determination of As, Sb, Mo, Th, and W in Silicates by Thermal Neutron Activation and Inorganic Ion Exchange," Anal. Lett. **A11**, 429 (1978).

C34. E. S. Gladney and J. W. Owens, "Determination of As, W, and Sb in Natural Waters by Neutron Activation and Inorganic Ion Exchange," Anal. Chem. **48**, 2220 (1976).

C35. R. A. Nadkarni and G. H. Morrison, "Determination of the Nobel Metals in Geologic Materials by Neutron Activation Analysis," Anal. Chem. **46**, 232 (1974).

C36. R. A. Nadkarni and G. H. Morrison, "Determination of Molybdenum by Neutron Activation and Srafion NMRR Ion Exchange Resin Separation," Anal. Chem. **50**, 294 (1978).

C37. R. A. Nadkarni and G. H. Morrison, Determination of Silver in rocks by Neutron Activation Analysis," Anal. Chem. **47**, 2285 (1975).

C38. D. Knab and E. S. Gladney, "Determination of Selenium in Environmental Materials by Neutron Activation and Inorganic Ion Exchange," Anal. Chem. **52**, 825 (1980).

C39. E. S. Gladney, D. R. Perrin, W. K. Hensley, and M. E. Bunker, "Uranium Content of 25 Silicate Standard Materials," Geostandards Newsletter **4**, 243 (1980).

C40. E. S. Gladney, D. R. Perrin, and W. K. Hensley, "Determination of Uranium in NBS Biological Standard Reference Materials by Delayed Neutron Assay," J. Radioanal. Chem. **59**, 249 (1980).

C41. Perkin-Elmer Corporation, "Analytical Methods Using the HGA Graphite Furnace," Perkin-Elmer, Norwalk, Connecticut (1977).

C42. R. D. Ediger, "Atomic Absorption Analysis with the Graphite Furnace Using Matrix Modification," Atomic Absorption Newslett. **14**, 127 (1975).

C43. J. W. Owens and E. S. Gladney, "Determination of Beryllium in Environmental Materials by Flameless Atomic Absorption Spectrometry," Atomic Absorption Newslett. **15**, 95 (1976).

C44. J. W. Owens and E. S. Gladney, "Lithium Metaborate Fusion and the Determination of Trace Metals in Fly Ash by Flameless Atomic Absorption," Atomic Absorption Newslett. **15**, 95 (1976).

C45. J. W. Owens and E. S. Gladney, "The Determination of Arsenic in Natural Waters by Flameless Atomic Absorption," Atomic Absorption Newslett. **15**, 47 (1976).

C46. E. S. Gladney, "Matrix Modification for the Determination of Bi by Flameless Atomic Absorption," Atomic Absorption Newslett. **16**, 114 (1977).

C47. E. S. Gladney and J. W. Owens, "Determination of Hg Using a Carrier-Free Combustion Separation and Flameless Atomic Absorption," Anal. Chim. Acta **90**, 271 (1977).

C48. E. S. Gladney, J. W. Owens, and D. R. Perrin, "The Determination of Mercury in Environmental Materials," Los Alamos Scientific Laboratory report LA-7865-MS (June 1979).

C49. F. C. Smith and R. A. Wetzel, "Operation and Maintenance Manual for Dionex Model 10 and Model 14 Ion Chromatographs," Dionex Corp., Sunnyvale, California (1978).

C50. American Society for Testing and Materials, *1977 Annual Book of ASTM Standards: Part 31: Water*, ASTM, Philadelphia, Pennsylvania (1977).

C51. E. S. Gladney and D. Knab, "Determination of 13 Rare Earth Elements in Geological Materials via Thermal and Epithermal Neutron Activation with Pre-irradiation Chemical Separation," (in preparation).

C52. F. J. Fernandez, M. M. Beaty, and W. B. Barnett, "Use of L'Vov Platform for Furnace Atomic Absorption Applications," Atomic Spectroscopy **2**, 16 (1981).

C53. T. C. Rains, M. S. Epstein, and S. R. Koirtyohann, "Atomic Absorption Spectroscopy," American Chemical Society-A Short Course.

C54. C. R. Parker, "Water Analysis by Atomic Spectroscopy," Varian Techtron Ltd, Springvale, Australia (1972).

C55. D. Knab, "An Investigation of the Analysis of Environmental Samples for Fluoride" (in preparation).

C56. Code of Federal Regulations, Protection Environment 40 Parts 190-399, Office of the Federal Register, National Archives and Record Service, General Services Administration (1983).

C57. NACE Standard TM-01-67, "Laboratory Corrosion Testing of Metals for the Process Industries," National Association of Corrosion Engineers, Houston, Texas (1972).

C58. ASTM Method 093-77 or D93-80, American Society for Testing Materials, Philadelphia, Pa.

C59. Methods for Chemical Analysis of Water and Waste, Environmental Monitoring and Support Laboratory, Office of Research and Development, U.S. Environmental Protection Agency, Cincinnati, Ohio (1983).

C60. Industrial Methods for Technician Auto Analyzer II, Technicon Industrial Systems, Tarrytown, NY (1977-1982).

C61. M. C. Williams, "Automated Method for the Determination of Cyanide" (in preparation).

C62. B. B. Bernard and D. L. Vann, "Model 700: Total Organic Carbon Analyzer Operating Procedures and Service Manual," OIC Corp. (1984).

C63. N. W. Bower, E. S. Gladney, and R. W. Ferenbaugh, "Critical Comparison of X-Ray Fluorescence and Combustion-Infrared Methods for the Determination of Sulfur in Biological Matrices," Analyst, 111:105-106 (1986).

C64. Federal Register, Part III (December 3, 1979).

C65. M. A. Gautier and E. S. Gladney (editors), "Health and Environmental Chemistry at Los Alamos: Analytical Techniques, Data Management and Quality Assurance," Los Alamos National Laboratory report LA-10300, Vol. 1 (1986).

C66. USEPA, "Test Methods for Evaluating Solid Waste: Physical/Chemical Methods, SW-846 Second Edition (July 1982).

C67. E. S. Gladney, J. W. Owens, T. C. Gunderson, and W. E. Goode, "Quality Assurance for Environmental Analytical Chemistry: 1976-1979," Los Alamos Scientific Laboratory report LA-8730-MS (1981).

C68. E. S. Gladney, W. E. Goode, D. R. Perrin, and C. E. Burns, "Quality Assurance for Environmental Analytical Chemistry: 1980," Los Alamos National Laboratory report LA-8966-MS (1981).

C69. E. S. Gladney, C. E. Burns, D. R. Perrin, and R. D. Robinson, "Quality Assurance for Environmental Analytical Chemistry: 1981," Los Alamos National Laboratory report LA-9579-MS (1982).

C70. E. S. Gladney, C. E. Burns, D. R. Perrin, R. D. Robinson, and D. Knab, "Quality Assurance for Environmental Analytical Chemistry: 1982," Los Alamos National Laboratory report LA-9950-MS (1984).

C71. E. S. Gladney, D. R. Perrin, and W. E. Goode, "Quality Assurance for Environmental Analytical Chemistry at Los Alamos," Proceedings of the 4th DOE Environmental Protection Information Meeting, Denver, Co., Dec. 7-9, 1982, CONF-821215, pp. 107-118 (1983).

C72. E. S. Gladney, C. E. Burns, D. R. Perrin, R. D. Robinson, and N. A. Raybold, "Quality Assurance for Environmental Analytical Chemistry: 1983," Los Alamos National Laboratory report LA-10115-MS (1984).

C73. M. A. Gautier, E. S. Gladney, and D. R. Perrin, "Quality Assurance for Health and Environmental Chemistry: 1984,:" Los Alamos National Laboratory report LA-10508-MS (1985).

C74. M. A. Gautier, E. S. Gladney, and B. T. O'Malley, "Quality Assurance for Health and Environmental Chemistry: 1985, Los Alamos National Laboratory report LA-10813-MS (1986).

C75. M. A. Gautier, E. S. Gladney, W. D. Moss, M. B. Phillips, and B. T. O'Malley, "Quality Assurance for Health and Environmental Chemistry: 1986," Los Alamos National Laboratory report (LA-11114-MS (1987).

C76. M. A. Gautier, E. S. Gladney, M. B. Phillips, and B. T. O'Malley, "Quality Assurance for Health and Environmental Chemistry: 1987," Los Alamos National Laboratory report (in press).

C77. R. D. Robinson, D. Knab, and D. R. Perrin, "An Individual Water Sample Quality Assurance Program," Los Alamos National Laboratory report LA-10163-MS (1985).

APPENDIX D

METHODS FOR DOSE CALCULATIONS

A. Introduction

Annual radiation doses are evaluated for three principal exposure pathways: inhalation, ingestion, and external exposure (which includes exposure from immersion in air containing photon-emitting radionuclides and direct and scattered penetrating radiation). Estimates are made of:

(1) Maximum boundary organ doses and effective dose equivalents to a hypothetical individual at the laboratory boundary where the highest dose rate occurs. It assumes the individual is outdoors at the Laboratory boundary continuously (24 hours a day, 365 days a year).

(2) Maximum individual organ doses and effective dose equivalents to an individual at or outside the Laboratory boundary where the highest dose rate occurs and a person actually is present. It takes into account occupancy (the fraction of time that a person actually occupies that location), shielding by buildings, and self-shielding.

(3) Average organ by body tissues and effective dose equivalents to nearby residents.

(4) Collective effective dose equivalent for the population living within an 80-km (50-mi) radius of the Laboratory.

Results of environmental measurements are used as much as possible in assessing doses to individual members of the public. Calculations based on these measurements follow procedures recommended by federal agencies to determine radiation doses.[D1,D2]

If the impact of Laboratory operations is not detectable by environmental measurements, individual and population doses attributable to Laboratory activities are estimated through modeling of releases.

Dose conversion factors used for inhalation and ingestion calculations are given in Table D-1. These adose conversion factors are taken from the DOE[D3] and are based on factors in Publication 30 of the International Commission on Radiological Protection (ICRP).[D4]

The dose conversion factors for inhalation assume a 1 um activity median aerodynamic diameter, as well as the lung solubility category that will maximize the effective dose equivalent (for comparison with DOE's 100 mrem/yr Radiation Protection Standard [RPS]) if more than one category is given. Similarly, the ingestion dose conversion factors are chosen to maximize the effective dose or organ dose if more than one gastrointestinal tract uptake is given (for comparison with DOE's 100 mrem/yr RPS for all pathways).

These dose conversion factors calculate the 50-yr dose commitment for internal exposure. The 50-yr dose commitment is the total dose received by an organ during the 50-yr period following the intake of a radionuclide that is attributable to that intake.

External doses are calculated using the dose-rate conversion factors published by Kocher.[D5] These factors, which are given in Table D-2, give the photon dose rate in mrem/yr per unit radionuclide air concentration in uCi/mL. The factors are used in the calculation of the population effective dose equivalent from external radiation for the 80-km (50-mi) area.

B. Inhalation Dose

Annual average air concentrations of ^{3}H, total U, ^{238}Pu, $^{239,240}Pu$, and ^{241}Am, determined by the Laboratory's air monitoring network, are corrected for background by subtracting the average concentrations measured at regional stations. These net concentrations are then multiplied by a standard breathing rate of 8400 m^3/yr[D6] to determine total annual intake via inhalation, in uCi/yr, for each radionuclide. Each intake is multiplied by appropriate dose conversion factors to convert radionuclide intake into 50-yr dose commitments. Following ICRP methods, doses are calculated for all organs that contribute over 10% of the total effective dose equivalent for each radionuclide (see Appendix A for definition of effective dose equivalent).

The dose calculated for inhalation of ^{3}H is increased by 50% to account for absorption through the skin.

This procedure for dose calculation conservatively assumes that a hypothetical individual is exposed to the measured air concentration continuously throughout the entire year (8760 h). This assumption is made for the boundary dose, dose to the maximum exposed individual, and dose to the population living within 80 km (50 mi) of the site.

Table D-1. Dose Conversion Factors (rem/uCi Intake) for Calculating Internal Doses

INHALATION

Radionuclide	Target Organ: Soft Tissue	Lung	Bone Surface	Red Marrow	Liver	Gonads	Effective Dose
^{3}H	6.3×10^{-5}						6.3×10^{-5}
^{234}U		$1.1 \times 10^{+3}$					$1.3 \times 10^{+2}$
^{235}U		$1.0 \times 10^{+3}$					$1.2 \times 10^{+2}$
^{238}U		$1.0 \times 10^{+3}$					$1.2 \times 10^{+2}$
^{238}Pu			$8.1 \times 10^{+3}$	$6.7 \times 10^{+2}$	$1.8 \times 10^{+3}$	$1.0 \times 10^{+2}$	$4.6 \times 10^{+2}$
$^{239,240}Pu$			$9.3 \times 10^{+3}$	$7.4 \times 10^{+2}$	$2.0 \times 10^{+3}$	$1.2 \times 10^{+2}$	$5.1 \times 10^{+2}$
^{241}Am			$9.3 \times 10^{+3}$	$7.4 \times 10^{+2}$	$2.0 \times 10^{+3}$	$1.2 \times 10^{+2}$	$5.2 \times 10^{+2}$

INGESTION

Radionuclide	Bone Surface	Red Marrow	Liver	Gonads	Kidney	Lungs	Breast	Thyroid
^{3}H								
^{7}Be		4.4×10^{-3}		2.1×10^{-4}				
^{90}Sr	1.6	7.0×10^{-1}						
^{137}Cs	4.8×10^{-2}	4.8×10^{-2}		5.2×10^{-2}		4.8×10^{-3}	4.4×10^{-3}	4.8 x 10
^{234}U	4.1	2.7×10^{-1}			1.7			
^{235}U	3.7	2.5×10^{-1}			1.6			
^{238}U	3.7	2.5×10^{-1}			1.5			
^{238}Pu	6.7	5.5×10^{-1}	1.5	8.5×10^{-2}				
$^{239,240}Pu$	7.8	5.9×10^{-1}	1.6	9.6×10^{-2}				
^{241}Am	$4.1 \times 10^{+1}$	3.1	8.5	5.2×10^{-1}				

Table D-1 (cont)

Radionuclide	Target Organ: Soft Tissue	LLI[a] Wall	SI[a] Wall	ULI[a] Wall	Remainder	Effective Dose
^{3}H	6.3×10^{-5}					6.3×10^{-5}
^{7}Be		4.4×10^{-4}	2.0×10^{-4}	2.7×10^{-4}		1.1×10^{-4}
^{90}Sr						1.3×10^{-1}
^{137}Cs		5.2×10^{-2}	5.2×10^{-2}		5.5×1^{-2}	5.0×10^{-2}
^{234}U						2.6×10^{-1}
^{235}U		2.0×10^{-1}				2.5×10^{-1}
^{238}U						2.3×10^{-1}
^{238}Pu						3.8×10^{-1}
$^{239,240}Pu$						4.3×10^{-1}
^{241}Am						2.2

---

[a]LLI = lower lower-intestine; SI = small intestine; ULI = upper-intestine.

Table D-2. Dose Conversion Factors [(mrem/yr)/(μCi/mL)] for Calculating External Doses[a]

^{10}C	$9.8 \times 10^{+9}$
^{11}C	$5.6 \times 10^{+9}$
^{13}N	$5.6 \times 10^{+9}$
^{16}N	$2.5 \times 10^{+10}$
^{14}O	$1.8 \times 10^{+10}$
^{15}O	$5.6 \times 10^{+9}$
^{41}Ar	$7.5 \times 10^{+9}$

[a]Dose conversion factors for ^{11}C, ^{13}N, ^{15}O, and ^{41}Ar were taken from Kocher.[D5] Dose conversion factors for the remaining radionuclides, which were not presented by Krocher, were calculated from:

$$DCF\ [(mrem/yr)/(\mu Ci/mL)] = 0.25 \times E \times 3.2 \times 10^{+10}$$

where E is the average gamma ray energy in MeV. The calculated factors were reduced by 30% to account for self-shielding by the body, so that they would be directly comparable with the factors from Kocher.

Organ doses and effective dose equivalent are determined at all sampling sites for each radionuclide. A final calculation estimates the total inhalation organ doses and effective dose equivalent by summing over all radionuclides.

C. Ingestion Dose

Results from foodstuff sampling (Sec. VII) are used to calculate organ doses and effective dose equivalents from ingestion for individual members of the public. The procedure is similar to that used in the previous section. Corrections for background are made by subtracting the average concentrations from sampling stations not affected by Laboratory operations. The radionuclide concentration in a particular foodstuff is multiplied by the annual consumption rate[D2] to obtain total annual intake of that radionuclide. Multiplication of the annual intake by the radionuclide's ingestion dose conversion factor for a particular organ gives the estimated dose to the organ. Similarly, effective dose equivalent is calculated using the effective dose equivalent conversion factor (Table D-1).

Doses are evaluated for ingestion of ^{3}H, ^{137}Cs, total U, ^{238}Pu, and $^{239,240}Pu$ in fruits and vegetables; ^{3}H, ^{7}Be, ^{22}Na, ^{54}Mn, ^{57}Co, ^{83}Rb, ^{134}Cs, ^{137}Cs, and total U in honey; and ^{90}Sr, ^{137}Cs, total U, ^{238}Pu, and $^{239,240}Pu$ in fish.

D. External Radiation

Environmental thermoluminescent dosimeter (TLD) measurements are used to estimate external radiation doses.

Nuclear reactions with air in the target areas at the Los Alamos Meson Physics Facility (LAMPF, TA-53) cause the formation of air activation products, principally ^{11}C, ^{13}N, ^{14}O, and ^{15}O. These isotopes are all positron emitters and have 20.4 min, 10 min, 71 sec, and 122 sec half-lives, respectively. Neutron reactions with air at the Omega West Reactor (TA-2) and the LAMPF also form ^{41}Ar, which has a 1.8 h half-life.

The radioisotopes ^{11}C, ^{13}N, ^{14}O, and ^{15}O are sources of photon radiation because of formation of two 0.511 MeV photons through positron-electron annihilation. The ^{14}O emits a 2.3 MeV gamma with 99% yield. The ^{41}Ar emits a 1.29 MeV gamma with 99% yield.

The TLD measurements are corrected for background to determine the contribution to the external radiation field from Laboratory operations. Background estimates at each site, based on historical data, consideration of possible nonbackground contributions, and, if possible, values measured at locations of similar geology and topography, are then subtracted from each measured value. This net dose is assumed to represent the dose from Laboratory activities that an individual would receive if he or she were to spend 100% of his or her time during an entire year at the monitoring location.

The individual dose is estimated from these measurements by taking into account occupancy and shielding. At offsite locations where residences are present, an occupancy factor of 1.0 was used.

Two types of shielding are considered: shielding by buildings and self-shielding. Each shielding type is estimated to reduce the external radiation dose by 30%.[D9,D10]

Boundary and maximum individual doses from ^{41}Ar releases from the Omega West Reactor are estimated using a standard Gaussian dispersion model and measured stack releases (from Table G-2). Procedures used in making the calculations are described in the following section.

Neutron doses from the critical assemblies at TA-18 were based on 1987 measurements. Neutron fields were monitored principally with TLDs placed in cadmium-hooded 23-cm (9-in.) polyethylene spheres.

At onsite locations at which above-background doses were measured, but at which public access is limited, doses based on a more realistic estimate of exposure time are also presented. Assumptions used in these estimates are in the text.

E. Population Dose

Calculation of collective effective dose equivalent estimates (in person-rem) are based on measured data to the extent possible. For background radiation, average measured background doses for Los Alamos, White Rock, and regional stations are multiplied by the appropriate population number. Tritium average doses are calculated from average measured concentrations in Los Alamos and White Rock above background (as measured by the regional stations).

These doses are multiplied by population data incorporating results of the 1980 census (Sec. II.E). The population data have been slightly modified (increased from 155 077 in 1980 to 192 649 persons in 1987 within 80 km [50 mi] of the boundary) to account for population changes between 1980 and 1987. These changes are extrapolated from an estimate of the 1986 New Mexico population, by county, that was made by the U.S. Bureau of the Census.[D7]

Radionuclides emitted by the LAMPF and, to a lesser extent, by the Omega West Reactor, contribute over 95% of the population dose.

For ^{41}Ar, ^{11}C, ^{13}N, ^{14}O, and ^{15}O, atmospheric dispersion models are used to calculate an average dose to individuals living in the area in question. The air concentration of the isotope ($\chi[r,\theta]$) at a location (r,θ) due to its emission from a particular source is found using the annual average meteorological dispersion coefficient ($\chi[r,\theta]/Q$) (based on Gaussian plume dispersion models[D8]) and the source term Q. Source terms, obtained by stack measurements, are in Table G-2.

The dispersion factors were calculated from 1987 meteorological data collected near LAMPF during the actual time periods when radionuclides were being released from the stacks. Dispersion coefficients used to calculate the χ/Q's were determined from measurements of the standard deviations of wind direction. The χ/Q includes the reduction of the source term due to radioactive decay.

The gamma dose rate in a semi-infinite cloud at time t, $\gamma_\infty(r,\theta,t)$, can be represented by the equation

$$\gamma_\infty(r,\theta,t) = (DCF)\,(r,\theta,t)$$

where

$\gamma_\infty(r,\theta,t)$ = gamma dose rate in mrem/yr at time t, at a distance r, and angle θ,

DCF = dose rate conversion factor from Kocher,[D5] or calculated from Slade[D8]

$\chi(r,\theta,t)$ = plume concentration in μCi/mL.

The annual dose is multiplied by the appropriate population figure to give the estimated population dose.

REFERENCES

D1. U.S. Department of Energy, "A Guide for Environmental Radiological Surveillance at U.S. Department of Energy Installations," U.S. Department of Energy report DOE/ EP-0023 (July 1981).f

D2. U.S. Nuclear Regulatory Commission, "Calculation of Annual Doses to Man from Routine Releases of Reactor Effluents for the Purpose of Evaluating Compliance with 10 CFR Part 50, Appendix I," U.S. Nuclear Regulatory Commission Regulatory Guide 1.109 (1977).

D3. U.S. Department of Energy, "Committed Dose Equivalent Tables for U.S. Department of Energy Population Dose Calculations," prepared by J. P. Corley, Ed., for the U.S. Department of Energy, U.S. Department of Energy report DOE/EH- (draft, 1985).

D4. International Commission on Radiological Protection, "Limits for Intakes of Radionuclides by Workers," ICRP Publication 30, Parts 1, 2, and 3, and their Supplements, Annals of the ICRP, Vol. 2, No. 3/4 through Vol. 8, No. 4 (1979-1982).

D5. D. C. Kocher, "Dose-Rate Conversion Factors for External Exposure to Photon and Electron Radiation from Radionuclides Occurring in Routine Releases from Nuclear Fuel Cycle Facilities," Health Physics, Vol. 38, pp. 543-621 (1980).

D6. International Commission on Radiological Protection, "Report on the Task Group on Reference Man," ICRP Publication 23 (1975).

D7. U.S. Bureau of the Census, Provisional Data for 1986 for New Mexico counties.

D8. D. H. Slade, Ed., "Meteorology and Atomic Energy 1968," U.S. Atomic Energy Commission document TID-24190 (1968).

D9. National Council on Radiation Protection and Measurements, "Natural Background Radiation in the United States," NCRP Report Number 45 (1975).

D10. National Council on Radiation Protection and Measurements, "Ionizing Radiation Exposure of the Population of the United States," NCRP Report Number 93 (1987).

APPENDIX E

UNITS OF MEASUREMENT

Throughout this report the International (SI) or Metric system of measurements has been used, with some exceptions. For units of radiation activity, exposure, and dose, customary units [i.e., Curie (Ci), Roentgen (R), rad, and rem] are retained because current standards are written in terms of these units. The equivalent SI units are the Becquerel (Bq), coulomb per kilogram (C/kg), Gray (Gy), and Sievert (Sv), respectively. Table E-1 presents prefixes used in this report to define fractions or multiples of the base units of measurements. Table E-2 presents conversion factors for converting from SI units to U.S. Customary Units.

Table E-1. Prefixes Used with SI (Metric) Units

Prefix	Factor	Symbol
mega-	1,000,000 or 10^{+6}	M
kilo-	1,000 or 10^{+3}	k
centi-	0.01 or 10^{-2}	c
milli-	0.001 or 10^{-3}	m
micro-	0.000001 or 10^{-6}	µ
nano-	0.000000001 or 10^{-9}	n
pico-	0.000000000001 or 10^{-12}	p
femto-	0.000000000000001 or 10^{-15}	f
atto-	0.000000000000000001 or 10^{-18}	a

Table E-2. Approximate Conversion Factors for Selected SI (Metric) Units

Multiply SI (Metric) Unit	By	To Obtain US Customary Unit
Celsius (°C)	9/5, +32	Fahrenheit (°F)
Centimeters (cm)	0.39	Inches (in.)
Cubic Meters (m^3)	35	Cubic Feet (ft^3)
Hectares (ha)	2.5	Acres
Grams (g)	0.035	Ounces (oz)
Kilograms (kg)	2.2	Pounds (lb)
Kilometers (km)	0.62	Miles (mi)
Liters (L)	0.26	Gallons (gal)
Meters (m)	3.3	Feet (ft)
Micrograms per Gram (g/g)	1	Parts per Million (ppm)
Milligrams per Liter (mg/L)	1	Parts per Million (ppm)
Square Kilometers (km^2)	0.39	Square Miles (mi^2)

APPENDIX F

DESCRIPTIONS OF TECHNICAL AREAS AND THEIR ASSOCIATED PROGRAMS

Locations of the 32 active technical areas (TA) operated by the Laboratory are shown in Fig. 4. The main programs conducted at each are listed in this appendix.

TA-2, Omega Site: Omega West Reactor, an 8 megawatt nuclear research reactor, is located here. It serves as a research tool in providing a source of neutrons for fundamental studies in nuclear physics and associated fields.

TA-3, South Mesa Site: In this main technical area of the Laboratory is the Administration Building that contains the Director's office and administrative offices and laboratories for several divisions. Other buildings house the Central Computing Facility, Administration offices, Materials Department, the science museum, Chemistry and Materials Science Laboratories, Physics Laboratories, technical shops, cryogenics laboratories, a Van de Graaff accelerator, and cafeteria.

TA-6, Two Mile Mesa Site: This is one of three sites (TA-22 and TA-40 are the other two sites) used in development of special detonators for initiation of high explosive systems. Fundamental and applied research in support of this activity includes investigation of phenomena associated with initiation of high explosives, and research in rapid shock-induced reactions with shock tubes.

TA-8, GT Site (or Anchor Site West): This is a nondestructive testing site operated as a service facility for the entire Laboratory. It maintains capability in all modern nondestructive testing techniques for ensuring quality of material, ranging from test weapon components to checking of high pressure dies and molds. Principal tools include radiographic techniques (X ray machines to 1 million volts, a 24-MeV betatron), radioactive isotopes, ultrasonic testing, penetrant testing, and electromagnetic methods.

TA-9, Anchor Site East: At this site, fabrication feasibility and physical properties of explosives are explored. New organic compounds are investigated for possible use as explosives. Storage and stability problems are also studied.

TA-11, K-Site: Facilities are located here for testing explosive components and systems under a variety of extreme physical environments. The facilities are arranged so testing may be controlled and observed remotely, and so that devices containing explosives or radioactive materials, as well as those containing nonhazardous materials, may be tested.

TA-14, Q-Site: This firing site is used for running various tests on relatively small explosive charges and for fragment impact tests.

TA-15, R-Site: This is the home of PHERMEX--a multiple cavity electron accelerator capable of producing a very large flux of X rays for certain weapons development problems and tests. This site is also used for the investigation of weapon functioning and weapon system behavior in nonnuclear tests, principally by electronic recording means.

TA-16, S-Site: Investigations at this site include development, engineering design, pilot manufacture, environmental testing, and stockpile production liaison for nuclear weapon warhead systems. Development and testing of high explosives, plastics and adhesives, and process development for manufacture of items using these and other materials are accomplished in extensive facilities.

TA-18, Pajarito Laboratory Site: The fundamental behavior of nuclear chain reactions with simple, low-power reactors called "critical assemblies" is studied here. Experiments are operated by remote control and observed by closed circuit television. The machines are housed in buildings known as "kivas" and are used primarily to provide a controlled means of assembling a critical amount of fissionable materials. This is done to study the effects of various shapes, sizes and configurations. These machines are also used as source of fission neutrons in large quantities for experimental purposes.

TA-21, DP-Site: This site has two primary research areas, DP West and DP East. DP West is concerned with chemistry research. DP East is the high temperature chemistry and tritium site.

TA-22, TD Site: See TA-6.

TA-28, Magazine Area "A": Explosives storage area.

TA-33, HP-Site: A major high-pressure tritium handling facility is located here. Laboratory and office space for Geosciences Division related to the Hot Dry Rock Geothermal Project are also here.

TA-35, Ten Site: Nuclear safeguards research and development, which is conducted here, is concerned with techniques for nondestructive detection, identification, and analysis of fissionable isotopes. Research in reactor safety and laser fusion is also done here.

TA-36, Kappa Site: Various explosive phenomena, such as detonation velocity, are investigated here.

TA-37, Magazine Area "C": Explosives storage area.

TA-39, Ancho Canyon Site: Nonnuclear weapon behavior is studied here, primarily by photographic techniques. Investigations are also made into various phenomenological aspects of explosives, interactions of explosives, and explosions with other materials.

TA-40, DF-Site: See TA-6.

TA-41, W-Site: Personnel in this site are engaged primarily in engineering design and development of nuclear components, including fabrications and evaluation of test materials for weapons.

TA-43, Health Research Laboratory: The Biomedical Research Group does research here in cellular radiobiology, biophysics, mammalian radiobiology, and mammalian metabolism. A large medical library, special counters used to measure radioactivity in humans and animals, and animal quarters for dogs, mice and monkeys are also located in this building.

TA-46, WA-Site: Here, applied photochemistry, which includes development of technology for laser isotope separation and laser-enhancement of chemical processes, is investigated. Solar energy research, particularly in the area of passive solar heating for residences, is done.

TA-48, Radiochemistry Site: Laboratory scientists and technicians at this site study nuclear properties of radioactive materials by using analytical and physical chemistry. Measurements of radioactive substances are made and "hot cells' are used for remote handling of radioactive materials.

TA-50, Waste Management Site: Personnel at this site have responsibility for treating and disposing of most industrial liquid waste received from Laboratory technical areas, for development of improved methods of solid waste treatment, and for containment of radioactivity removed by treatment. Radioactive liquid waste is piped to this site for treatment from most technical areas.

TA-51, Animal Exposure Facility: Here, animals are exposed to nonradioactive toxic materials to determine biological effects of high and low exposures.

TA-52, Reactor Development Site: A wide variety of activities related to nuclear reactor performance and safety are done here.

TA-53, Meson Physics Facility: The Los Alamos Meson Physics Facility (LAMPF), a linear particle accelerator, is used to conduct research in the areas of basic physics, cancer treatment, material studies, and isotope production.

TA-54, Waste Disposal Site: This is a disposal area for solid radioactive and toxic wastes.

TA-55, Plutonium Processing Facilities: Processing of plutonium and research in plutonium metallurgy are done here.

TA-57, Fenton Hill Site: This is the location of the Laboratory's Hot Dry Rock geothermal project. Here scientists are studying the possibility of producing energy by circulating water through hot, dry rock located hundreds of meters below the earth's surface. The water is heated and then brought to the surface to drive electric generators.

TA-58, Two Mile Mesa: Undeveloped technical area.

TA-59, Occupational Health Site: Occupational health and environmental science activities are conducted here.

APPENDIX G

ENVIRONMENTAL DATA TABLES

Table G-1. Estimated Maximum Individual 50-Year Dose Commitments from 1987 Airborne Radioactivity[a]

Isotope	Critical Organ	Location	Estimated Dose (mrem/yr)	Percentage of Radiation Protection Standard
^{3}H	Whole Body	Royal Crest (Station 11)[b]	0.02	<0.1%
$^{11}C, ^{13}N, ^{14}O, ^{15}O, ^{41}Ar$	Whole Body	East Gate (Station 6)[b]	6.1	24%
$U, ^{238}Pu, ^{239,240}Pu, ^{241}Am$	Bone Surface	Exxon Station (Station 10)[b]	0.11	0.1%

[a]Estimated maximum individual dose is the dose from Laboratory operations (excluding dose contributions from cosmic, terrestial, medical diagnostics, and other non-Laboratory sources) to an individual at or outside the Laboratory boundary where the highest dose rate occurs and where there is a person. It takes into account occupancy factors.
[b]See Fig. 8 for station locations.

Table G-2. Airborne Radioactive Emissions Totals[a]

Location	$^{238,239,240}Pu$[b] (μCi)	$^{235,238}U$[c] (μCi)	Mixed Fission Products (μCi)	^{41}Ar[d] (Ci)	^{32}P (μCi)	^{3}H (Ci)	Activation Products: Gaseous[e] (Ci)	Activation Products: Particulate/Vapor[f] (Ci)
TA-2				232				
TA-3	64.9	868	21.6			851		
TA-21	1.4	207	0.2			596		
TA-33						1000		
TA-35	0.6					155		
TA-41						470		
TA-43	0.5				48.4			
TA-46								
TA-48	0.6	1.6	1250					
TA-50	4.5		21.6					
TA-53						15.2	150 000	0.2
TA-54	<0.1							
TA-55	0.2					85.4		
Totals	72.8	1080	1290	232	48.4	3180	150 000	0.2

---

[a]As reported on DOE Forms F-5821.1

[b]Plutonium values contain indeterminant traces of ^{241}Am, a transformation product of ^{241}Pu.

[c]Does not include aerosolized uranium from explosives testing (Table G-6).

[d]Does not include 600 Ci of ^{41}Ar present in gaseous, mixed activation products.

[e]Includes the following constituents: ^{16}N - 3.7%; ^{10}C - 1.4%; ^{14}O - 0.6%; ^{15}O - 43.7%; ^{13}N - 15.1%; ^{11}C - 35.1%; ^{41}Ar - 0.4%.

[f]Includes 37 nuclides, dominated by ^{183}Os and ^{7}Be.

Table G-3. Thermoluminescent Dosimeter Measurements

Station Location	Coordinates	Annual[a] Measurement (mrem)
Regional Stations (28-44 km)--Uncontrolled Areas		
1. Espanola	--	70 (8)[a]
2. Pojoaque	--	88 (8)
3. Santa Fe	--	90 (8)
4. Fenton Hill	--	124 (8)
Perimeter Stations (0-4 km)--Uncontrolled Areas		
5. Barranca School	N180 E130	98 (8)
6. Arkansas Avenue	N170 E030	85 (8)
7. Cumbres School	N150 E090	103 (8)
8. 48th Street	N110 W010	107 (8)
9. LA Airport	N110 E170	98 (8)
10. Bayo Canyon	N120 E250	106 (10)
11. Exxon Station	N090 E120	115 (8)
12. Royal Crest Trailer Court	N080 E080	108 (8)
13. White Rock	S080 E420	122 (8)
14. Pajarito Acres	S210 E380	90 (8)
15. Bandelier Lookout Station	S280 E200	95 (8)
16. Pajarito Ski Area	N150 W200	112 (8)
Onsite Stations--Controlled Areas		
17. TA-21 (DP West)	N095 E140	83 (8)
18. TA-6 (Two-Mile Mesa)	N025 E030	97 (8)
19. TA-53 (LAMPF)	N070 E090	115 (8)
20. Well PM-1	N030 E305	115 (8)
21. TA-16 (S-Site)	S035 W025	113 (7)
22. Booster P-2	S030 E220	112 (8)
23. TA-54 (Area G)	S080 E290	93 (8)
24. State Hwy 4	N070 E350	176 (8)
25. Frijoles Mesa	S165 E085	102 (8)
26. TA-2 (Omega Stack)	N075 E120	117 (8)
27. TA-2 (Omega Canyon)	N085 E1210	149 (7)
28. TA-18 (Pajarito Site)	S040 E205	153 (8)
29. TA-35 (Ten Site A)	N040 E105	116 (8)
30. TA-35 (Ten Site B)	N040 E110	122 (8)
31. TA-59 (Occupational Health Lab)	N050 E040	111 (8)
32. TA-3 (Van de Graaff)	N050 E020	121 (8)
33. TA-3 (Guard Station)	N050 E020	219 (8)
34. TA-3 (Alarm Building)	N050 E020	211 (8)
35. TA-3 (Guard Building)	N050 E020	165 (8)
36. TA-3 (Shop)	N050 E020	112 (8)
37. Pistol Range	N040 E240	110 (8)
38. TA-55 (Plutonium Facility South)	N040 E240	106 (8)
39. TA-55 (Plutonium Facility West)	N040 E080	117 (8)
40. TA-55 (Plutonium Facility North)	N040 E080	118 (8)

[a]Measurement (95% confidence increments).

Table G-4. Location of Air Sampling Stations

Station	Latitude or N-S Coord	Longitude or E-W Coord
Regional (28-44 km)		
1. Espanola	36°00'	106°06'
2. Pojoaque	35°52'	106°02'
3. Santa Fe	35°40'	106°56'
Perimeter (0-4 km)		
4. Barranca School	N180	E130
5. Arkansas Avenue	N170	E030
6. East Gate	N090	E210
7. 48th Street	N110	W010
8. LA Airport	N110	E170
9. Bayo Canyon	N120	E250
10. Exxon Station	N090	E120
11. Royal Crest	N080	E080
12. White Rock	S080	E420
13. Pajarito Acres	S210	E380
14. Bandelier	S280	E200
Onsite		
15. TA-21	N095	E140
16. TA-6	N025	E030
17. TA-53 (LAMPF)	N070	E090
18. Well PM-1	N030	E305
19. TA-52	N020	E155
20. TA-16	S035	W025
21. Booster P-2	S030	E180
22. TA-54	S080	E290
23. TA-49	S165	E085
24. TA-33	S245	E225
25. TA-2	N082	E110
26. TA-16-450	S055	W070

Table G-5. Average Background Concentrations of Radioactivity in the Atmosphere

Radioactive Constituent	Units	EPA[a] 1983-1986	Laboratory[b] 1987	Uncontrolled Area Guide[c]
Gross beta	10^{-15} μCi/mL	10 ± 20	13 ± 3	9000
^{3}H	10^{-12} μCi/mL	Not reported	4.1 ± 17.0	200 000
U(natural)	pg/m^{3}	68 ± 25	74 ± 35	100 000
^{238}Pu	10^{-18} μCi/mL	0.3 ± 0.4	0.4 ± 0.3[d]	30 000
$^{239,240}Pu$	10^{-18} μCi/mL	0.8 ± 0.9	0.7 ± 0.4[e]	20 000
^{241}Am	10^{-18} μCi/mL	Not reported	1.4 ± 0.4[d]	20 000

[a]Environmental Protection Agency, "Environmental Radiation Data," Reports 33 through 45. Data are from Santa Fe, New Mexico sampling location and were taken from January 1983 through June 1986, excluding the periods from May 1983 through February 1984 and January 1985 through February 1985 for which data were not available.
[b]Data are annual averages from the regional stations (Espanola, Pojoaque, Santa Fe) and were taken during calendar year 1987.
[c]See Appendix A. These values are presented for comparison.
[d]Minimum detectable limit is 2 x 10^{-18} μCi/mL.
[e]Minimum detectable limit is 3 x 10^{-18} μCi/mL.

Table G-6. Estimated Aerial Concentrations of Toxic Elements Aerosolized by Dynamic Experiments[a]

Element	1987 Total Usage (kg)	Fraction Aerosolized (%)	Annual Average Concentration (ng/m^3) (4 km)	Annual Average Concentration (ng/m^3) (8 km)	Applicable Standard (ng/m^3)
Uranium	97.6	10	9.5×10^{-3}	3.8×10^{-3}	9000[b]
Beryllium	2.0	2	5.5×10^{-5}	1.6×10^{-5}	10[c]
Lead	70.8	100[d]	7.6×20^{-2}	3.0×10^{-2}	1500[e]

[a]Through November.
[b]DOE 1981.
[c]Thirty day average. New Mexico Air Quality Control Regulation 201.
[d]Assumed percentage aerosolized.
[e]Three-month average, 40 CFR 50.12.

Table G-7. Airborne Tritiated Water Concentrations for 1987

Station Location[a]	Total Air Volume (m^3)	Number of Monthly Samples	Number of Samples <MDL[b]	Concentrations--pCi/m^3 (10^{-12} µCi/mL) Max[c]	Min[c]	Mean[c]	Mean as % Guide[d]
Regional Stations (24-44 km)--Uncontrolled Areas							
1. Espanola	111.31	11	7	31.0 (6.0)	-8.0 (2.0)	3.1 (10.0)	<0.1
2. Pojoaque	104.96	11	7	90.0 (20.0)	-7.0 (2.0)	9.1 (27.6)	<0.1
3. Santa Fe	111.66	11	8	5.0 (2.0)	-7.0 (2.0)	0.0 (3.7)	<0.1
Regional Group Summary	326.93	33	22	90.0 (20.0)	-8.0 (2.0)	4.1 (17.0)	<0.1
Perimeter Stations (0-4 km)--Uncontrolled Areas							
4. Barranca School	122.26	12	2	60.0 (10.0)	-3.0 (1.0)	11.7 (16.8)	<0.1
5. Arkansas Avenue	116.71	12	5	30.0 (6.0)	-2.5 (0.6)	9.4 (10.9)	<0.1
6. East Gate	121.19	12	1	28.0 (5.0)	0.7 (0.6)	9.0 (6.9)	<0.1
7. 48th Street	119.99	12	4	120.0 (20.0)	-3.6 (1.0)	27.0 (41.6)	<0.1
8. LA Airport	118.14	12	0	37.0 (7.0)	3.5 (0.8)	11.5 (9.0)	<0.1
9. Bayo STP	113.21	11	5	7.0 (1.0)	-1.3 (0.4)	2.9 (2.8)	<0.1
10. Exxon Station	123.49	12	2	25.0 (5.0)	-1.8 (0.6)	8.9 (8.2)	<0.1
11. Royal Crest	108.75	12	0	140.0 (30.0)	3.0 (1.0)	27.3 (39.0)	<0.1
12. White Rock	106.36	12	7	49.0 (9.0)	-6.0 (2.0)	7.7 (15.2)	<0.1
13. Pajarito Acres	120.93	12	9	7.0 (1.0)	-4.0 (1.0)	0.6 (3.0)	<0.1
14. Bandelier	105.59	12	4	13.0 (3.0)	-0.8 (0.6)	4.4 (3.8)	<0.1
Perimeter Group Summary	1276.62	131	39	140.0 (30.0)	-6.0 (2.0)	11.0 (20.4)	<0.1

Table G-7 (cont)

Station Location[a]	Total Air Volume (m^3)	Number of Monthly Samples	Number of Samples <MDL[b]	Concentrations--pCi/m^3 (10^{-12} µCi/mL) Max[c]	Min[c]	Mean[c]	Mean as % Guide[d]
On-site Stations--Controlled Areas							
15. TA-21	94.84	11	0	460.0 (90.0)	2.5 (0.8)	51.8 (135.6)	<0.1
16. TA-6	116.66	12	5	90.0 (20.0)	-2.9 (0.9)	10.9 (25.6)	<0.1
17. TA-53 (LAMPF)	106.20	12	2	70.0 (10.0)	-4.0 (1.0)	15.1 (21.3)	<0.1
18. Well PM-1	107.70	12	2	51.0 (10.0)	-5.0 (1.0)	12.3 (15.8)	<0.1
19. TA-52	105.85	12	2	130.0 (30.0)	-3.6 (1.0)	19.2 (37.4)	<0.1
20. TA-16	121.59	12	6	39.0 (8.0)	-6.0 (1.0)	3.9 (11.5)	<0.1
21. Booster P-2	95.73	12	3	140.0 (30.0)	-5.0 (1.0)	19.6 (41.2)	<0.1
22. TA-54	114.93	12	1	100.0 (20.0)	-2.0 (2.0)	32.3 (35.7)	<0.1
23. TA-49	99.71	12	8	160.0 (30.0)	-7.0 (2.0)	17.9 (46.8)	<0.1
24. TA-33	120.35	12	0	32.0 (6.0)	7.0 (1.0)	19.5 (7.5)	<0.1
25. Ta-2	90.70	12	0	120.0 (20.0)	3.0 (1.0)	27.4 (33.9)	<0.1
26. TA-16-450	79.03	12	7	180.0 (30.0)	-12.0 (3.0)	15.8 (52.1)	<0.1
On-site Group Summary	1253.29	143	36	460.0 (90.0)	-12.0 (3.0)	21.7 (51.5)	<0.1

---

[a]See Fig. 8 for map of station locations.
[b]Minimum detectable limit = 2×10^{-12} µCi/mL.
[c]Uncertainties are in parentheses (see Appendix B).
[d]Controlled Area DOE Concentration Guide = 5×10^{-6} µCi/mL;
uncontrolled Area Derived Concentration Guide = 1×10^{-7} µCi/mL.

Table G-8. Airborne $^{239,240}Pu$ Concentrations for 1987

Station Location[a]	Total Air Volume (m^3)	Number of Quarterly Samples	Number of Samples <MDL[b]	Concentrations--aCi/m^3 (10^{-18} µCi/mL) Max[c]	Min[c]	Mean[c]	Mean as % Guide[d]
Regional Stations (28-44 km)--Uncontrolled Areas							
1. Espanola	91 077	4	4	1.0 (1.5)	0.5 (0.5)	0.8 (0.2)	<0.1
2. Pojoaque	84 739	4	4	1.3 (0.6)	0.0 (0.5)	0.5 (0.6)	<0.1
3. Santa Fe	96 114	4	4	1.2 (0.6)	0.3 (0.7)	0.7 (0.4)	<0.1
Regional Group Summary	271 930	12	12	1.3 (0.6)	0.0 (0.5)	0.7 (0.4)	<0.1
Perimeter Stations (0-49 km)--Uncontrolled Areas							
4. Barranca School	72 961	3	3	1.4 (2.3)	0.2 (0.3)	0.6 (0.6)	<0.1
5. Arkansas Avenue	74 296	3	3	0.8 (0.7)	0.5 (0.4)	0.7 (0.2)	<0.1
6. East Gate	73 328	4	4	3.8 (3.0)	0.2 (0.5)	1.5 (1.6)	<0.1
7. 48th Street	59 630	3	3	0.5 (0.5)	0.0 (0.5)	0.3 (0.3)	<0.1
8. LA Airport	93 632	4	3	2.1 (0.6)	0.6 (0.4)	1.2 (0.7)	<0.1
9. Bayo STP	88 374	4	3	2.1 (0.9)	0.7 (1.3)	1.2 (0.6)	<0.1
10. Exxon Station	87 022	4	2	3.1 (0.8)	0.6 (0.6)	2.1 (1.0)	<0.1
11. Royal Crest	86 622	4	4	1.4 (4.2)	0.0 (0.5)	0.6 (0.6)	<0.1
12. White Rock	92 885	4	4	1.1 (0.5)	0.0 (0.6)	0.7 (0.5)	<0.1
13. Pajarito Acres	105 964	4	4	1.1 (0.5)	0.2 (0.2)	0.5 (0.4)	<0.1
14. Bandelier	88 466	4	4	0.6 (0.4)	0.1 (0.4)	0.3 (0.2)	<0.1
Perimeter Group Summary	923 180	41	37	3.8 (3.0)	0.0 (0.5)	0.9 (0.9)	<0.1

Table G-8 (cont)

Station Location[a]	Total Air Volume (m^3)	Number of Quarterly Samples	Number of Samples <MDL[b]	Concentrations--aCi/m^3 (10^{-18} µCi/mL) Max[c]	Min[c]	Mean[c]	Mean as % Guide[d]
On-site Stations--Controlled Areas							
15. TA-21	94 118	4	4	1.8 (0.5)	0.4 (0.4)	1.1 (0.6)	<0.1
16. TA-6	87 428	4	4	1.0 (0.5)	0.4 (0.4)	0.6 (0.3)	<0.1
17. TA-53 (LAMPF)	104 546	4	4	0.8 (0.6)	0.0 (0.4)	0.4 (0.4)	<0.1
18. Well PM-1	110 612	4	4	0.3 (0.2)	0.1 (0.1)	0.2 (0.1)	<0.1
19. TA-52	94 263	4	4	0.3 (0.4)	0.0 (0.5)	0.2 (0.1)	<0.1
20. TA-16	103 821	4	4	0.9 (0.4)	0.5 (0.4)	0.7 (0.2)	<0.1
21. Booster P-2	91 987	4	3	3.8 (1.0)	0.0 (0.4)	1.6 (1.6)	<0.1
22. TA-54	91 599	4	0	36.8 (3.6)	2.8 (0.7)	13.5 (15.7)	<0.1
23. TA-49	77 741	4	4	0.7 (0.8)	0.4 (0.2)	0.6 (0.1)	<0.1
24. TA-33	105 211	4	4	1.7 (0.6)	0.1 (0.4)	0.8 (0.7)	<0.1
25. TA-2	89 097	4	3	3.2 (1.0)	0.2 (0.4)	1.0 (1.5)	<0.1
26. TA-16-450	67 011	4	4	1.6 (0.9)	0.3 (0.6)	0.8 (0.6)	<0.1
On-site Group Summary	1 117 434	48	42	36.8 (3.6)	0.0 (0.4)	1.8 (5.4)	<0.1

---

[a]See Fig. 8 for map of station locations.
[b]Minimum detectable limit = 3×10^{-18} µCi/mL.
[c]Uncertainties are in parentheses (see Appendix B).
[d]Controlled Area DOE Concentration Guide = 2×10^{-12} µCi/mL.
Uncontrolled Area Derived Concentration Guide = 2×10^{-14} µCi/mL.

Table G-9. Airborne ^{241}Am Concentrations for 1987

Station Location[a]	Total Air Volume (m^3)	Number of Quarterly Samples	Number of Samples <MDL[b]	Concentrations--aCi/m^3 (10^{-18} µCi/mL) Max[c]	Min[c]	Mean[c]	Mean as % Guide[d]
Regional Stations (28-44 km)--Uncontrolled Areas							
3. Santa Fe	71 629	3	3	1.8 (0.8)	1.0 (0.8)	1.4 ± 0.4	<0.1
Perimeter Stations (0-40 km)--Uncontrolled Areas							
6. East Gate	55 655	3	3	1.7 (0.7)	0.3 (0.7)	1.1 (0.7)	<0.1
8. LA Airport	24 931	1	1	1.7 (0.8)	1.7 (0.8)	1.7 (0.8)	<0.1
9. Bayo STP	66 204	3	3	1.7 (0.7)	0.3 (0.4)	1.0 (0.7)	<0.1
12. White Rock	92 885	4	4	1.3 (0.8)	0.5 (0.7)	0.8 (0.3)	<0.1
Perimeter Group Summary	239 675	11	11	1.7 (0.8)	0.3 (0.7)	1.0 (0.5)	<0.1
On-site Stations--Controlled Areas							
16. TA-6	87 428	4	4	1.9 (0.9)	0.8 (0.5)	1.5 (0.5)	<0.1
17. TA-53 (LAMPF)	104 546	4	4	1.0 (0.5)	0.5 (0.4)	0.8 (0.2)	<0.1
20. TA-16	103 821	4	4	1.6 (0.8)	0.6 (0.5)	1.0 (0.4)	<0.1
21. Booster P-2	91 987	4	4	1.9 (0.9)	0.8 (0.6)	1.3 (0.5)	<0.1
22. TA-54	91 599	4	0	26.3 (2.4)	3.3 (1.0)	9.5 (11.2)	<0.1
23. TA-49	77 741	4	4	2.5 (1.5)	0.4 (0.7)	1.2 (0.9)	<0.1
On-site Group Summary	557 122	24	20	26.3 (2.4)	0.4 (0.7)	2.5 (5.2)	<0.1

[a]See Fig. 8 for map of station locations.
[b]Minimum detectable limit = 2×10^{-18} µCi/mL.
[c]Uncertainties are in parentheses (see Appendix B).
[d]Controlled Area DOE Concentration Guide = 6×10^{-12} µCi/mL.
Uncontrolled Area Derived Concentration Guide = 2×10^{-14} µCi/mL.

Table G-10. Airborne Uranium Concentrations for 1987

Station Location[a]	Total Air Volume (m^3)	Number of Quarterly Samples	Number of Samples <MDL[b]	Concentrations--pg/m^3 Max[c]	Min[c]	Mean[c]	Mean as % Guide[d]
Regional Stations (28-44 km)--Uncontrolled Areas							
1. Espanola	91 077	4	0	118.9 (11.9)	28.1 (2.8)	78.9 (40.5)	<0.1
2. Pojoaque	84 739	4	0	124.8 (12.5)	88.0 (8.8)	103.0 (15.6)	<0.1
3. Santa Fe	96 114	4	0	48.5 (4.9)	31.6 (3.2)	40.4 (7.0)	<0.1
Regional Group Summary	271 930	12	0	124.8 (12.5)	28.1 (2.8)	74.1 (35.4)	<0.1
Perimeter Stations (0-4 km)--Uncontrolled Areas							
4. Barranca School	96 881	4	0	49.0 (4.9)	29.7 (3.0)	36.2 (8.9)	<0.1
5. Arkansas Avenue	97 921	4	0	27.1 (2.7)	14.9 (1.5)	21.4 (5.0)	<0.1
6. East Gate	73 328	4	0	47.9 (4.8)	28.0 (2.8)	36.9 (8.4)	<0.1
7. 48th Street	77 435	4	0	34.0 (3.4)	24.4 (2.4)	28.5 (4.5)	<0.1
8. LA Airport	93 632	4	0	69.8 (7.0)	35.4 (3.5)	50.1 (16.6)	<0.1
9. Bayo STP	88 374	4	0	39.2 (3.9)	18.0 (1.8)	28.0 (10.9)	<0.1
10. Exxon Station	87 022	4	0	66.8 (6.7)	38.3 (3.8)	52.4 (13.2)	<0.1
11. Royal Crest	86 622	4	0	68.1 (6.8)	24.2 (2.4)	41.6 (18.8)	<0.1
12. White Rock	92 885	4	0	31.5 (3.1)	24.1 (2.4)	27.6 (3.7)	<0.1
13. Pajarito Acres	105 964	4	0	25.5 (2.5)	11.3 (1.1)	19.8 (6.0)	<0.1
14. Bandelier	88 466	4	0	33.6 (3.4)	11.6 (1.2)	21.8 (11.3)	<0.1
Perimeter Group Summary	988 530	44	0	69.8 (7.0)	11.3 (1.1)	33.1 (14.5)	<0.1

Table G-10 (cont)

Station Location[a]	Total Air Volume (m^3)	Number of Quarterly Samples	Number of Samples <MDL[b]	Concentrations--pg/m^3 Max[c]	Min[c]	Mean[c]	Mean as % Guide[d]
On-site Stations--Controlled Areas							
15. TA-21	94 118	4	0	42.5 (4.3)	24.9 (2.5)	34.6 (7.9)	<0.1
16. TA-6	87 428	4	0	74.4 (7.4)	18.2 (1.8)	39.8 (24.4)	<0.1
17. TA-53 (LAMPF)	104 546	4	0	34.5 (3.4)	26.8 (2.7)	30.3 (3.2)	<0.1
18. Well PM-1	110 612	4	0	20.9 (2.1)	15.4 (1.5)	19.0 (2.6)	<0.1
19. TA-52	94 263	4	0	50.9 (5.1)	21.0 (2.1)	39.1 (13.4)	<0.1
20. TA-16	103 821	4	0	27.5 (2.7)	15.6 (1.6)	20.7 (5.4)	<0.1
21. Booster P-2	91 987	4	0	37.0 (3.7)	28.1 (2.8)	30.5 (4.4)	<0.1
22. TA-54	91 599	4	0	88.6 (8.9)	35.0 (3.5)	53.8 (24.0)	<0.1
23. TA-49	77 741	4	0	28.3 (2.8)	13.2 (1.3)	20.2 (6.8)	<0.1
24. TA-33	105 211	4	0	70.2 (7.0)	15.3 (1.5)	32.8 (25.2)	<0.1
25. TA-2	89 097	4	0	56.4 (5.6)	23.1 (2.3)	34.1 (15.3)	<0.1
26. TA-16-450	67 011	4	0	18.6 (1.9)	12.8 (1.3)	16.5 (2.6)	<0.1
On-site Group Summary	1 117 434	48	0	88.6 (8.9)	12.8 (1.3)	30.9 (16.2)	<0.1

[a]See Fig. 8 for map of station locations.
[b]Minimum detectable limit = 1 pg/m^3.
[c]Uncertainties are in parentheses (see Appendix B).
[d]Controlled Area DOE Concentration Guide = 2×10^8 pg/m^3.
Uncontrolled Area Derived Concentration Guide = 1×10^5 pg/m^3.

Note: One curie of natural uranium is equivalent to 3000 kg of natural uranium. Hence, uranium masses can be converted to the DOE "uranium special curie" by using the factor 3.3×10^{-13} $\mu Ci/pg$.

Table G-11. Emissions (tons/yr) and Fuel Consumption (10^9 Btu/yr) from the TA-3 Power Plant and Steam Plants

		Location				
Parameter	Year	TA-3	TA-16	TA-21	Western Area	Total
Particulates	1986	1.8	0.4	0.1	0.00	2.3
	1987	1.5	0.5	0.1	0.00	2.1
	% Change	-14.9	11.6	-1.7	--	-9.3
Oxides of Nitrogen	1986	15.1	19.6	5.5	0.00	40.2
	1987	12.8	21.8	5.4	0.07	40.1
	% Change	-15.3	11.4	-1.2	--	-0.2
Carbon Monoxide	1986	23.6	4.9	1.4	0.00	29.9
	1987	20.1	5.5	1.4	0.02	26.9
	% Change	-15.0	11.6	-1.2	--	-10.0
Hydrocarbons	1986	1.0	0.8	0.2	0.00	2.0
	1987	0.9	0.9	0.2	0.00	2.0
	% Change	-14.6	11.6	-1.2	--	-2.5
Fuel Consumption	1986	1313	310	87	0	1710.0
	1987	1098	341	85	1	1525.0
	% Change	-16.3	10.0	-2.8	--	-10.8

Table G-12. Quality of Effluent from the TA-50 Liquid Radioactive Waste Treatment Plan for 1987[a]

Radionuclide	Activity Released (mCi)	Mean Concentration (μCi/mL)	Mean as % DOE's CG[b]
^{3}H	100 000	3.8×10^{-3}	3.8
^{89}Sr	64	2.4×10^{-6}	0.8
^{90}Sr	1.0	3.9×10^{-8}	0.4
^{137}Cs	8.1	3.0×10^{-7}	0.1
^{234}U	1.6	6.0×10^{-8}	<0.1
^{238}Pu	1.4	5.3×10^{-8}	<0.1
$^{239,230}Pu$	3.2	1.2×10^{-7}	0.1
^{241}Am	3.6	1.3×10^{-7}	0.1

Nonradioactive Constituents	Mean Concentration (mg/L)
Cd[c]	1.1×10^{-3}
Ca	170
Cl	150
Total Cr[c]	2.4×10^{-2}
Cu[c]	0.33
F	12
Hg[c]	4.9×10^{-4}
Mg	1.1
Na	920
Pb[c]	5.1×10^{-2}
Zn[c]	0.32
CN	0.3
COD	100
NO_3-N	476
PO_4	1.5
TDS	4150
pH[c]	6.98 - 7.77

Total Effluent Volume = 2.66×10^{7} L

---

[a]As reported on DOE forms F-5821.1.
[b]Department of Energy's Concentration Guide for Controlled Areas (Appendix A).
[c]Constituents regulated by National Pollutant Discharge Elimination System permit.

Table G-13. Quality of Effluent from the Los Alamos Meson Physics Facilities (TA-53) Lagoons for 1987[a]

Radionuclide	Activity Released (mCi)	Mean Concentration (μCi/mL)	Mean as % DOE's CG[b]
^{3}H	10 900	2.7×10^{-3}	2.7
^{7}Be	330	8.0×10^{-5}	0.2
^{22}Na	89	2.2×10^{-5}	2.2
^{54}Mn	23	5.6×10^{-6}	0.1
^{57}Co	81	2.0×10^{-5}	<0.1
^{60}Co	8.5	2.1×10^{-6}	0.2
^{134}Cs	79	1.9×10^{-5}	6.4

Total Effluent Volume = 4.109×10^{6} L

---

[a]As reported on DOE forms F-5821.1.
[b]Department of Energy's Concentration Guide for Controlled Areas (Appendix A).

Table G-14. Location of Surface and Ground Water Sampling Stations

Station	Latitude or N-S Coordinate	Longitude or E-W Coordinate	Map Designation[a]	Type[b]
Regional Surface Water				
Rio Chama at Chamita	30°05'	106°07'	---	SW
Rio Grande at Embudo	36°12'	105°58'	---	SW
Rio Grande at Otowi	35°52'	106°08'	---	SW
Rio Grande at Cochiti	35°37'	106°19'	---	SW
Rio Grande at Bernalillo	35°17'	106°36'	---	SW
Jemez River	35°40'	106°44'	---	SW
Perimeter Stations				
Los Alamos Reservoir	N105	W090	7	SW
Guaje Canyon	N300	E100	8	SW
Frijoles	S280	E180	9	SW
La Mesita Spring	N080	E550	10	GWD
Sacred Spring	N170	E540	11	GWD
Indian Spring	N140	E530	12	GWD
White Rock Canyon				
Group I				
Sandia Spring	S030	E470	13	SWR
Spring 3	S110	E450	14	SWR
Spring 3A	S120	E445	15	SWR
Spring 3AA	S140	E440	16	SWR
Spring 4	S170	E110	17	SWR
Spring 4A	S150	E395	18	SWR
Spring 5	S220	E390	19	SWR
Sprng 5A	S240	E360	20	SWR
Ancho Spring	S280	E305	21	SWR
Group II				
Spring 5A	S230	E390	22	SWR
Spring 6	S300	E330	23	SWR
Spring 6A	S310	E310	24	SWR
Spring 7	S330	E295	25	SWR
Spring 8	S335	E285	26	SWR
Spring 8A	S315	E280	27	SWR
Spring 9	S270	E270	28	SWR
Spring 9A	S325	E265	29	SWR
Doe Spring	S320	E250	30	SWR
Spring 10	S370	E230	31	SWR
Group III				
Spring 1	N040	E520	32	SWR
Spring 2	N015	E505	33	SWR

Table G-14 (cont)

Station	Latitude or N-S Coordinate	Longitude or E-W Coordinate	Map Designation[a]	Type[b]
White Rock Canyon				
Group IV				
Spring 3B	S150	E465	34	SWR
Streams				
Pajarito	S180	E410	35	SWR
Ancho	S295	E340	36	SWR
Frijoles	S365	E235	37	SWR
Sanitary Effluent				
Mortandad	S070	E480	38	SWR
Onsite Stations				
Test Well 1	N070	E345	39	GWD
Test Well 2	N120	E150	40	GWD
Test Well 3	N080	E215	41	GWD
Test Well DT-5A	S110	E090	42	GWD
Test Well 8	N035	E170	43	GWD
Test Well DT-9	S155	E140	44	GWD
Test Well DT-10	S120	E125	45	GWD
Canada del Buey	N010	E150	46	SW
Pajarito	S060	E215	47	SW
Water Canyon at Beta	S090	E090	48	SW
Pajarito Canyon (Onsite)				
PCO-1	S054	E212	102	GWS
PCO-2	S081	E255	103	GWS
PCO-3	S098	E293	104	GWS
Effluent Release Areas				
Acid-Pueblo Canyon				
Acid Weir	N125	E070	49	SW
Pueblo 1	N130	E080	50	SW
Pueblo 2	N120	E155	51	SW
Pueblo 3	N085	E315	52	SW
Hamilton Bend Springs	N110	E250	53	S
Test Well 1A	N070	E335	54	GWS
Test Well 2A	N120	E140	55	GWS
Basalt Spring	N065	E395	56	S

Table G-14 (cont)

Station	Latitude or N-S Coordinate	Longitude or E-W Coordinate	Map Designation[a]	Type[b]
DP-Los Alamos Canyon				
DPS-1	N090	E160	57	SW
DPS-4	N080	E200	58	SW
LAO-C	N085	E070	59	GWS
LAO-1	N080	E120	60	GWS
LAO-2	N080	E210	61	GWS
LAO-3	N080	E220	62	GWS
LAO-4	N070	E245	63	GWS
LAO-4.5	N065	E270	64	GWS
Sandia Canyon				
SCS-1	N080	E040	65	SW
SCS-2	N060	E140	66	SW
SCS-3	N050	E185	67	SW
Mortandad Canyon				
GS-1	N040	E100	68	SW
MCO-3	N040	E110	69	GWS
MCO-4	N035	E150	70	GWS
MCO-5	N030	E160	71	GWS
MCO-6	N030	E175	72	GWS
MCO-7	N025	E180	73	GWS
MCO-7.5	N030	E190	74	GWS
MCO-8				
Water Supply and Distribution				
Los Alamos Well Field				
Well LA-1B	N115	E530	76	GWD
Well LA-2	N125	E505	77	GWD
Well LA-3	N130	E490	78	GWD
Well LA-4	N070	E405	79	GWD
Well LA-5	N076	E435	80	GWD
Well LA-6	N105	E465	81	GWD
Guaje Well Field				
Well G-1	N190	E385	82	GWD
Well G-1A	N197	E380	83	GWD
Well G-2	N205	E365	84	GWD
Well G-3	N215	E350	85	GWD
Well G-4	N213	E315	86	GWD
Well G-5	N228	E295	87	GWD
Well G-6	N215	E270	88	GWD

Table G-14 (cont)

Station	Latitude or N-S Coordinate	Longitude or E-W Coordinate	Map Designation[a]	Type[b]
Pajarito Well Field				
Well PM-1	N030	E305	89	GWD
Well PM-2	S055	E202	90	GWD
Well PM-3	N040	E255	91	GWD
Well PM-4	S030	E205	92	GWD
Well PM-5	N015	E155	93	GWD
Water Canyon Gallery	S040	W125	94	GWD
Fire Station 1	N080	E015	95	D
Fire Station 2	N100	E120	96	D
Fire Station 3	S085	E375	97	D
Fire Station 4	N185	E070	98	D
Fire Station 5	S010	W065	99	D
Bandelier National Monument Headquarters	S270	E190	100	D
Fenton Hill (TA-57)	35°53'	106°40'	101	D

[a]Regional surface water sampling locations in Fig. 15; Perimeter, White Rock Canyon, On-site, and Effluent Release Area sampling locations in Fig. 16.
[b]SW = surface water, GWD = deep or main aquifer, GWS = shallow or alluvial aquifer, SWR = spring at White Rock Canyon, and D = water supply distribution system.

Table G-15. Radiochemical Quality of Surface Water from Regional Stations[a]

Station	^{3}H (10^{-6} µCi/mL)	^{137}Cs (10^{-9} µCi/mL)	Total U (µg/L)	^{238}Pu (10^{-9} µCi/mL)	$^{239,240}Pu$ (10^{-9} µCi/mL)	Gross Gamma (Counts/min/L)
Rio Chama at Chamita	-0.7 (0.7)	32 (44)	1.3 (1.0)	0.008 (0.012)	0.017 (0.012)	-70 (100)
Rio Chama at Chamita	0.2 (0.3)	95 (62)	2.0 (1.0)	0.011 (0.012)	-0.004 (0.004)	260 (80)
Rio Grande at Embudo	-1.6 (0.7)	80 (57)	2.2 (1.0)	0.000 (0.010)	0.006 (0.010)	30 (100)
Rio Grande at Embudo	-0.2 (0.3)	21 (53)	2.0 (1.0)	-0.008 (0.008)	-0.008 (0.006)	460 (90)
Rio Grande at Otowi	-0.9 (0.7)	8 (44)	2.1 (1.0)	0.000 (0.010)	-0.004 (0.010)	-150 (100)
Rio Grande at Otowi	0.2 (0.3)	1200 (414)	2.0 (1.0)	0.018 (0.018)	-0.004 (0.012)	260 (80)
Rio Grande at Cochiti	-0.7 (0.7)	38 (55)	2.3 (1.0)	0.000 (0.010)	0.000 (0.010)	20 (100)
Rio Grande at Cochiti	0.1 (0.3)	--	2.0 (1.0)	-0.005 (0.005)	0.000 (0.010)	360 (90)
Rio Grande at Bernalillo	-0.4 (0.7)	41 (45)	2.4 (1.0)	-0.012 (0.018)	-0.025 (0.013)	-300 (100)
Rio Grande at Bernalillo	0.2 (0.3)	139 (65)	3.0 (1.0)	0.000 (0.010)	-0.008 (0.008)	380 (90)
Jemez River at Jemez	-1.4 (0.7)	108 (58)	1.6 (1.0)	-0.004 (0.009)	0.025 (0.014)	-180 (100)
Jemez River at Jemez	-0.1 (0.3)	58 (58)	2.0 (1.0)	0.004 (0.008)	-0.004 (0.004)	400 (90)
No. of Analyses	12	11	12	12	12	12
Average	-0.4	165	2.1	0.001	-0.001	122
S	0.6	345	0.4	0.008	0.013	261
Minimum	-1.6 (0.7)	8 (44)	1.3 (1.0)	-0.012 (0.018)	-0.025 (0.013)	-300 (100)
Maximum	0.2 (0.3)	1200 (414)	3.0 (1.0)	0.011 (0.012)	0.025 (0.014)	460 (90)
Limits of Detection	0.7	40	1	0.009	0.03	50

[a]Samples collected in February and September; counting uncertainty in parentheses.

Table G-16. Chemical Quality of Surface Water from Regional Stations (mg/L)[a]

Station	SiO_2	Ca	Mg	K	Na	CO_3	HCO_3	P	SO_4	Cl	F	N	TDS	Total Hardness	pH	Conductivity (mS/m)
Rio Chama at Chamita	11	32	8.2	1.8	17	0	89	<0.2	80	3	0.2	<1	174	217	8.2	34
Rio Grande at Embudo	24	30	6.0	2.3	15	0	92	<0.2	34	5	0.5	<1	103	177	8.0	26
Rio Grande at Otowi	26	30	6.1	2.2	15	0	93	<0.2	34	5	0.5	<1	101	175	8.2	26
Rio Grande at Cochiti	17	38	7.1	1.9	16	0	96	<0.2	56	4	0.3	<1	127	195	8.1	30
Rio Grande at Bernalillo	18	39	7.3	2.0	18	0	95	<0.2	62	5	0.3	<1	126	203	8.0	32
Jemez River at Jemez	38	37	5.5	5.9	44	2	141	<0.2	17	47	0.8	<1	123	279	8.3	45
Summary																
No. of Analyses	6	6	6	6	6	6	6	6	6	6	6	6	6	6	6	6
Average	22	34	6.7	2.6	20	<1	101	--	47	11	0.4	--	126	208	8.1	32
S	9	4	1.0	1.6	11	1	20	--	23	17	0.2	--	26	38	0.1	7
Minimum	11	30	5.5	1.8	15	0	89	--	17	3	0.2	--	101	175	8.0	26
Maximum	38	39	8.2	5.9	44	2	141	<0.2	80	47	0.8	<1	174	279	8.3	45*

[a]Samples collected in February.

Table G-17. Radiochemical Quality of Surface and Ground Waters from Perimeter Stations

Station	^{3}H (10^{-6} µCi/mL)	^{137}Cs (10^{-9} µCi/mL)	Total U (µg /L)[a]	^{238}Pu (10^{-9} µCi/mL)	$^{239,240}Pu$ (10^{-9} µCi/mL)	Gross Gamma (Counts/min/L)
Los Alamos Reservoir	-0.7 (0.3)	8 (54)	1.0 (1.0)	0.021 (0.015)	-0.004 (0.011)	---
Los Alamos Reservoir	0.0 (0.3)	42 (62)	1.0 (1.0)	-0.002 (0.006)	-0.004 (0.006)	-70 (80)
Guaje Reservoir	-2.7 (0.7)	-24 (55)	0.2 (0.1)	0.036 (0.016)	0.011 (0.010)	-400 (100)
Frijoles Canyon	-2.0 (0.7)	88 (51)	0.2 (0.1)	0.016 (0.018)	0.016 (0.014)	160 (100)
Frijoles Canyon	0.4 (0.3)	98 (62)	1.0 (1.0)	0.008 (0.006)	0.008 (0.005)	-20 (80)
La Mesita Spring	-1.5 (0.7)	59 (44)	12.5 (1.3)	-0.014 (0.014)	-0.014 (0.012)	-180 (100)
La Mesita Spring	0.0 (0.3)	24 (53)	--	0.002 (0.006)	-0.002 (0.005)	-80 (80)
Indian Spring	-1.1 (0.7)	80 (56)	9.6 (1.0)	-0.007 (0.019)	0.029 (0.023)	-30 (100)
Indian Spring	0.0 (0.3)	59 (68)	6.0 (1.0)	-0.005 (0.008)	0.000 (0.005)	80 (80)
Sacred Spring	-1.7 (0.7)	13 (38)	2.1 (1.0)	0.001 (0.010)	0.037 (0.041)	-50 (100)
Sacred Spring	-0.1 (0.3)	-2 (60)	4.0 (1.0)	0.010 (0.009)	0.002 (0.005)	160 (80)
Summary						
No. of Analyses	11	11	10	11	11	10
Average	-0.8	40	3.8	0.006	0.007	-43
S	1.0	40	4.3	0.014	0.015	166
Minimum	-2.7 (0.7)	-24 (55)	0.2 (0.1)	-0.014 (0.012)	-0.014 (0.012)	-400 (100)
Maximum	0.4 (0.3)	98 (62)	12.5 (1.3)	0.036 (0.016)	0.037 (0.041)	160 (100)
Limits of Detection	0.7	40	1	0.009	0.03	50

[a]Samples collected in March and September; counting uncertainty in parentheses.

Table G-18. Radiochemical Quality of Surface Waters from White Rock Canyon, October 1987

Station	^{3}H (10^{-6} µCi/mL)	^{137}Cs (10^{-9} µCi/mL)	Total U (µg/L)	^{238}Pu (10^{-9} µCi/mL)	$^{239,240}Pu$ (10^{-9} µCi/mL)	Gross Gamma (Counts/min/L)
Group I						
Sandia Spring	-0.8 (0.3)	122 (64)	1.0 (1.0)	0.020 (0.014)	-0.004 (0.004)	100 (80)
Spring 3	-0.8 (0.3)	-6 (65)	1.0 (1.0)	0.000 (0.010)	0.004 (0.008)	0 (80)
Spring 3A	-1.2 (0.3)	94 (62)	1.0 (1.0)	-0.019 (0.010)	0.000 (0.010)	0 (80)
Spring 3AA	-0.9 (0.3)	40 (62)	1.0 (1.0)	0.004 (0.004)	0.000 (0.010)	60 (80)
Spring 4	0.7 (0.3)	103 (64)	1.0 (1.0)	0.012 (0.013)	-0.008 (0.008)	-110 (80)
Spring 4A	-0.1 (0.3)	87 (60)	1.0 (1.0)	0.022 (0.011)	-0.004 (0.004)	0 (80)
Spring 5	-0.1 (0.3)	99 (63)	1.0 (1.0)	0.009 (0.009)	0.005 (0.008)	10 (80)
Spring 5AA	-0.2 (0.3)	74 (61)	1.0 (1.0)	0.004 (0.008)	-0.004 (0.004)	10 (80)
Ancho Spring	-0.7 (0.3)	38 (69)	1.0 (1.0)	-0.008 (0.010)	0.000 (0.010)	190 (80)
Group II						
Spring 8A	-0.9 (0.3)	100 (62)	1.0 (1.0)	0.013 (0.013)	0.000 (0.010)	160 (80)
Spring 9	-0.6 (0.3)	-49 (62)	1.0 (1.0)	-0.004 (0.007)	0.000 (0.010)	90 (80)
Spring 9A	-1.0 (0.3)	13 (61)	1.0 (1.0)	0.004 (0.011)	0.008 (0.012)	170 (80)
Doe Spring	-0.8 (0.3)	149 (71)	1.0 (1.0)	0.008 (0.005)	0.000 (0.010)	130 (80)
Group III						
Spring 1	-1.1 (0.3)	103 (61)	1.0 (1.0)	0.004 (0.010)	-0.013 (0.008)	30 (80)
Spring 2	-0.8 (0.3)	24 (67)	3.9 (1.0)	0.004 (0.008)	0.009 (0.006)	220 (80)
Group IV						
Spring 3B	-0.2 (0.3)	29 (60)	2.2 (2.4)	0.000 (0.010)	0.004 (0.004)	60 (80)
Streams						
Pajarito	13 (1.0)	64 (68)	1.3 (1.0)	0.027 (0.015)	-0.004 (0.004)	10 (80)
Ancho	-0.7 (0.3)	-2 (60)	1.0 (1.0)	-0.008 (0.008)	0.000 (0.010)	160 (80)
Frijoles	-0.8 (0.3)	-45 (61)	1.0 (1.10)	0.020 (0.018)	-0.004 (0.009)	190 (80)

Table G-18 (cont)

Station	^{3}H (10^{-6} µCi/mL)	^{137}Cs (10^{-9} µCi/mL)	Total U (µg/L)	^{238}Pu (10^{-9} µCi/mL)	$^{239,240}Pu$ (10^{-9} µCi/mL)	Gross Gamma (Counts/min/L)
Sanitary Effluent						
Mortandad	-0.2 (0.3)	-39 (68)	1.0 (1.0)	0.000 (0.010)	0.000 (0.010)	70 (80)
No. of Analyses	20	20	20	20	20	20
Maximum	13 (1.0)	149 (71)	22 (2.4)	0.027 (0.015)	0.009 (0.006)	
Limits of Detection	0.7	40	1	0.009	0.03	50

---

[a]Counting uncertainty in parentheses; Springs 5A, 5B, 6, 6A, 7, 8, and 10 covered by Cochiti Reservoir.

Table G-19. Chemical Quality of Surface and Ground Waters from Perimeter Stations (mg/L)[a]

Station	SiO_2	Ca	Mg	K	Na	CO_3	HCO_3	P	SO_4	Cl	F	N	TDS	Total Hardness	pH	Conductivity mS/m
Los Alamos Reservoir	28	7	0.9	2.5	3	0	27	<0.2	7	2	<0.2	<1	78	24	7.8	7
Guaje Canyon	49	10	3.1	1.7	6	0	37	<0.2	8	2	0.2	<1	106	37	7.7	10
Frijoles at Nat. Mon.	54	9	3.1	2.1	8	0	42	<0.2	6	3	<0.2	<1	111	33	7.8	11
La Mesita Spring	27	33	0.8	2.4	30	0	118	<0.2	14	8	0.3	2	174	90	8.1	30
Indian Spring	42	27	2.7	2.7	27	0	110	<0.2	7	32	0.5	<1	208	95	7.5	32
Sacred Spring	32	22	0.4	2.9	23	0	99	<0.2	7	3	0.5	<1	135	56	7.7	20
Summary																
No. of Analyses	6	6	6	6	6	6	6	6	6	6	6	6	6	6	6	6
Average	37	18	1.8	2.4	16	--	72	--	8	8	<0.3	<1	135	56	7.8	18
S	11	11	1.3	0.4	12	--	41	--	3	12	0 .1	0.4	48	30	0.2	11
Minimum	27	7	0.8	1.7	3	--	27	--	6	2	<0.2	<1	78	24	7.7	7
Maximum	54	33	3.1	2.9	30	0	118	<0.2	14	32	0.5	2	208	90	8.1	32

[a]Samples collected in February and March.

Table G-20. Primary Chemical Quality of Surface and Ground Waters from White Rock Canyon, October 1987 (mg/L)

Stations	Ag	As	Ba	Cd	Cr	F	Hg	N	Pd	Se
Group I										
Sandia Spring	<0.001	0.002	0.132	<0.001	0.003	0.6	0.002	0.2	0.003	<0.002
Spring 3	<0.001	0.002	0.035	<0.001	0.005	0.5	0.001	0.8	<0.001	<0.002
Spring 3A	<0.001	0.003	0.031	<0.001	0.005	0.5	<0.001	0.5	<0.001	<0.002
Spring 3AA	<0.001	0.003	0.021	<0.001	0.011	0.5	<0.001	0.5	0.001	<0.002
Spring 4	<0.001	0.002	0.039	<0.001	0.005	0.6	<0.001	1.0	<0.001	<0.002
Spring 4A	<0.001	<0.001	0.043	<0.001	0.005	0.6	<0.001	1.1	<0.001	<0.002
Spring 5	<0.001	0.002	0.031	<0.001	0.005	0.5	<0.001	0.4	<0.001	<0.002
Spring 5AA	<0.001	0.002	0.194	<0.001	0.002	0.5	<0.001	<0.2	0.001	<0.002
Ancho Spring	<0.001	0.001	0.028	<0.001	0.004	0.4	<0.001	<0.2	<0.001	<0.002
Group II										
Spring 8A	<0.001	0.001	0.024	<0.001	0.001	0.5	<0.001	<0.2	<0.001	<0.002
Spring 9	<0.001	0.001	0.016	<0.001	0.003	0.5	0.002	<0.2	<0.001	<0.002
Spring 9A	<0.001	0.001	0.013	<0.001	0.007	0.5	0.001	<0.2	<0.001	<0.002
Doe Spring	<0.001	0.001	0.022	<0.001	0.002	0.6	<0.001	<0.2	<0.001	<0.002
Group III										
Spring 1	<0.001	0.004	0.061	<0.001	0.003	0.7	<0.001	<0.2	0.001	<0.002
Spring 2	<0.001	0.024	0.081	<0.001	0.001	1.5	<0.001	<0.2	0.001	<0.002
Group IV										
Spring 3B	<0.001	0.011	0.044	<0.001	0.008	0.9	<0.001	2.1	<0.001	<0.002
Streams										
Pajarito	<0.001	0.002	0.038	<0.001	0.004	0.5	<0.001	0.7	<0.001	<0.002
Ancho	<0.001	<0.001	0.026	<0.001	0.004	0.4	<0.001	<0.2	<0.001	<0.002
Frijoles	<0.001	<0.001	0.017	<0.001	0.001	0.2	<0.001	<0.2	<0.001	<0.002

Table G-20 (cont)

Stations	Ag	As	Ba	Cd	Cr	F	Hg	N	Pd	Se
Sanitary Effluent										
Mortandad	<0.001	0.005	0.053	0.005	0.003	0.9	<0.001	12	<0.001	<0.002
Summary										
No. of Analyses										
Maximum Concentration	<0.001	0.024	0.194	0.005	0.011	1.5	0.002	12	0.003	<0.002
USEPA and NMEID Primary Maximum Concentrations[a]	0.05	0.05	1.0	0.01	0.05	2.0	0.002	10	0.05	0.01
Maximum Concentrations as % of primary maximum	<2	48	19	50	22	75	100	120	6	<20

[a]Reference (USEPA 1976); comparison of primary and secondary maximum concentration to spring and stream maximum concentrations for comparison only, spring and stream not a source of water supply.

Table G-21. Secondary Chemical Quality of Surface and Ground Waters from White Rock Canyon, October 1987 (mg/L)

Stations	Cl	Cu	Fe	Mn	SO_4	Zn	TDS	pH
Group I								
Sandia Spring	4	<0.001	0.137	0.042	5	<0.001	195	8.1
Spring 3	4	<0.001	0.145	<0.001	5	<0.001	145	8.1
Spring 3A	3	0.002	0.114	<0.001	5	0.001	140	7.9
Spring 3AA	3	0.002	1.71	<0.001	4	0.006	131	7.8
Spring 4	7	<0.001	0.070	<0.001	10	0.001	168	7.6
Spring 4A	6	<0.001	0.010	<0.001	7	<0.001	170	7.8
Spring 5	5	0.001	0.540	<0.001	6	<0.001	160	7.9
Spring 5AA	8	0.001	1.99	0.179	10	0.003	214	7.6
Ancho Spring	2	<0.001	0.020	0.002	3	0.001	140	7.4
Group II								
Spring 8A	2	<0.001	0.127	0.002	2	<0.001	146	7.8
Spring 9	2	<0.001	0.101	0.003	2	<0.001	142	7.7
Spring 9A	2	<0.001	0.817	0.003	2	<0.001	134	7.7
Doe Spring	2	<0.001	0.174	<0.001	2	<0.001	143	7.8
Group III								
Spring 1	4	<0.001	2.90	0.056	8	0.005	153	7.9
Spring 2	4	0.001	1.57	0.120	7	0.003	224	8.1
Group IV								
Spring 3B	4	<0.001	0.054	0.010	17	<0.001	403	8.0
Streams								
Pajarito	6	<0.001	0.049	0.002	6	<0.001	175	8.1
Ancho	3	<0.001	0.174	0.004	3	<0.001	143	8.6
Frijoles	4	<0.001	0.240	0.005	5	<0.001	133	7.9
Sanitary Effluent								
Mortandad	43	33	0.627	0.021	32	0.027	467	7.3

Table 21 (cont)

Stations	Cl	Cu	Fe	Mn	SO_4	Zn	TDS	pH
Summary								
No. of Analyses	20	20	20	20	20	20	20	20
Maximum Concentration	43	33	2.90	0.042	32	0.027	467	8.6
USEPA and NMEID								
Secondary Maximum Concentration[a]	250	1.0	0.3	0.5	250	5.0	500	6.5-8.5
Maximum Concentration as % of Secondary Maximum Concentration	17	3300	967	8	6	<1	93	101

[a]Reference (USEPA 1976); comparison of primary and secondary maximum concentration to spring and stream maximum concentrations for comparison only, spring and stream not a source of water supply.

Table G-22. Chemical Quality of Surface and Ground Waters from White Rock Canyon, October 1987 (mg/L)

Station	SiO_2	Ca	Mg	K	Na	CO_3	HCO_3	Mo	Ni	Total Hard-ness	Cond (mS/M)
Group I											
Sandia Spring	42	38	2.7	2.9	17	0	131	<0.001	0.002	108	26
Sandia 3	49	21	1.6	2.9	17	0	81	<0.001	<0.001	59	17
Spring 3A	49	21	1.7	2.9	16	0	81	<0.001	<0.001	58	17
Spring 3AA	41	18	<0.5	2.9	18	0	77	<0.001	<0.001	45	16
Spring 4	52	23	3.7	2.7	15	0	85	<0.001	<0.001	77	21
Spring 4A	67	22	4.6	2.2	13	0	81	<0.001	0.002	73	19
Spring 5	66	18	4.8	2.0	12	0	79	<0.001	<0.001	65	18
Spring 5AA	59	32	6.0	3.5	14	0	122	<0.001	0.001	112	28
Ancho Spring	72	12	3.1	2.0	11	0	60	<0.001	0.001	42	13
Group II											
Spring 8A	76	12	3.2	2.1	12	0	62	<0.001	0.001	39	14
Spring 9	72	11	3.1	1.5	11	0	61	<0.001	0.001	39	12
Spring 9A	70	11	3.1	1.4	10	0	58	<0.001	0.001	39	12
Doe Spring	72	12	3.3	1.5	2	0	64	<0.001	0.001	43	13
Group III											
Spring 1	32	19	1.2	2.2	34	0	109	0.002	0.002	57	24
Spring 2	32	21	1.0	1.4	61	0	172	0.002	<0.001	58	34
Group IV											
Spring 3B	44	22	1.9	4.8	127	0	316	0.004	<0.001	66	64
Streams											
Pajario	68	20	4.4	2.5	14	0	86	<0.001	<0.001	70	19
Ancho	76	12	3.2	1.9	11	4	64	<0.001	<0.001	47	13
Frijoles	59	9	2.4	2.2	10	0	53	<0.001	<0.001	39	12

Table G-22 (cont)

Station	SiO_2	Ca	Mg	K	Na	CO_3	HCO_3	Mo	Ni	Total Hard-ness	Cond (mS/M)
Sanitary Effluent											
Mortandad	93	26	7.7	16	85	0	132	<0.001	0.029	110	64
Summary											
No. of Analyses	20	20	20	20	20	20	20	20	20	20	20
Maximum Concentration	93	38	7.7	16	127	20	316	0.004	0.027	108	64

NOTE: Springs 5A, 5B, 6, 6A, 7, 8, and 10 covered by Cochito Reservoir: The 20 locations also analyzed for following constituents: CN <0.01 mg/L; P <0.2 mg/L, except Mortandad 12 mg/L; Sb <0.001 mg/L; Th <0.001 mg/L; Tl <0.001 mg/L;

Table G-23. Radiochemical Quality of Surface and Ground Waters from On-site Stations[a]

Station	^{3}H (10^{-6} µCi/mL)	^{137}Cs (10^{-9} µCi/mL)	Total U (µg/L)	^{238}Pu (10^{-9} µCi/mL)	$^{239,240}Pu$ (10^{-9} µCi/mL)	Gross Gamma (Counts/min/L)
Test Well 1	-2.4 (0.7)	77 (58)	2.9 (1.0)	-0.005 (0.008)	0.005 (0.013)	-400 (100)
Test Well 1						
Test Well 2	-2.1 (0.7)	90 (52)	0.3 (0.1)	0.000 (0.010)	0.000 (0.010)	-200 (100)
Test Well 2						
Test Well 3	-1.4 (0.7)	8 (61)	0.6 (0.1)	0.022 (0.027)	0.022 (0.016)	-200 (100)
Test Well 3	0.3 (0.3)	65 (60)	1.0 (1.0)	0.021 (0.019)	0.011 (0.011)	10 (80)
Test Well DT-5A	-2.0 (0.7)	-37 (55)	0.3 (0.1)	-0.009 (0.009)	0.005 (0.011)	-300 (100)
Test Well DT-5A	0.1 (0.3)	58 (52)	1.0 (1.0)	0.002 (0.005)	0.002 (0.006)	130 (80)
Test Well 8	-2.1 (0.7)	86 (50)	0.0 (0.1)	0.035 (0.037)	0.000 (0.010)	-300 (100)
Test Well 8	0.5 (0.3)	38 (67)	1.0 (1.0)	-0.010 (0.010)	0.010 (0.010)	190 (80)
Test Well DT-9	0.0 (0.3)	-13 (58)	1.0 (1.0)	-0.002 (0.006)	0.008 (0.007)	-60 (80)
Test Well DT-10	-1.6 (0.7)	-93 (50)	0.3 (0.1)	0.005 (0.012)	0.000 (0.010)	-40 (100)
Test Well DT-10	0.2 (0.3)	136 (63)	0.3 (0.1)	0.002 (0.008)	0.002 (0.004)	-10 (80)
Canada del Buey	-0.6 (0.7)	44 (55)	0.4 (0.1)	0.010 (0.023)	0.005 (0.014)	-500 (100)
Canada del Buey	0.3 (0.3)	-25 (60)	1.0 (1.0)	-0.002 (0.003)	0.002 (0.003)	-70 (80)
Pajarito Canyon	-1.2 (0.7)	29 (54)	0.3 (0.1)	0.000 (0.010)	0.006 (0.018)	110 (100)
Pajarito Canyon	0.6 (0.3)	33 (58)	1.0 (1.0)	0.004 (0.007)	0.002 (0.004)	-280 (80)
Water Canyon at Beta Hole	-2.0 (0.7)	21 (55)	0.0 (0.1)	-0.004 (0.004)	0.000 (0.010)	-400 (100)
Water Canyon at Beta Hole	0.1 (0.3)	67 (60)	1.0 (1.0)	-0.004 (0.008)	0.000 (0.010)	80 (80)

Table G-23 (cont)

Station	^{3}H (10^{-6} µCi/mL)	^{137}Cs (10^{-9} µCi/mL)	Total U (µg/L)	^{238}Pu (10^{-9} µCi/mL)	$^{239,240}Pu$ (10^{-9} µCi/mL)	Gross Gamma (Counts/min/L)
Summary						
No. of Analyses	17	17	17	17	17	17
Average	-0.8	34	0.7	0.004	0.005	-132
S	1.1	55	0.7	0.012	0.007	208
Minimum	-2.4 (0.7)	-93 (50)	0.0 (0.1)	-0.010 (0.010)	0.000 (0.010)	-500 (100)
Maximum	0.6 (0.3)	-136 (63)	22.9 (1.0)	0.035 (0.037)	0.022 (0.016)	190 (80)
Limits of Detection	0.7	40	1	0.009	0.03	50

[a]Samples collected in March and September; counting uncertainty in parentheses.

Table G-24. Radiochemical Quality of Shallow Ground Water in Pajarito Canyon

Station	^{3}H (10^{-6} µCi/mL)	^{137}Cs (10^{-9} µCi/mL)	Total U (µg/L)	^{238}Pu (10^{-9} µCi/mL)	$^{239,240}Pu$ (10^{-9} µCi/mL)	Gross Gamma (Counts/min/L)
Well PCO-1	0.4 (0.3)	111 (68)	1.0 (1.0)	0.005 (0.018)	0.015 (0.015)	130 (80)
Well PCO-2	0.7 (0.3)	89 (69)	1.0 (1.0)	0.035 (0.016)	-0.004 (0.004)	210 (80)
Well PCO-3	0.3 (0.3)	-3 (67)	1.0 (1.0)	-0.004 (0.010)	0.004 (0.010)	110 (80)
Summary						
No. of Analyses	3	3	3	3	3	3
Average	0.5	66	1.0	0.012	0.005	150
S	0.2	60	0.020	0.010	0.010	53
Minimum	0.3 (0.3)	-3 (67)	--	-0.004 (0.010)	-0.004 (0.004)	110 (80)
Maximum	0.7 (0.3)	111 (68)	1.0 (1.0)	0.035 (0.016)	0.015 (0.015)	210 (80)

Table G-25. Chemical Quality of Surface and Ground Waters from On-site Stations (mg/L)[a]

Station	SiO_2	Ca	Mg	K	Na	CO_3	HCO_3	P	SO_4	Cl	F	N	TDS	Total Hardness	pH	Conductivity (mS/m)
Test Well 1	50	49	9.1	4.1	14	0	102	<0.2	24	32	0.5	7	253	164	8.0	40
Test Well 2	65	16	4.0	1.1	9	0	66	<0.2	2	2	0.5	<1	136	52	7.9	14
Test Well 3	72	19	5.7	2.2	12	0	80	<0.2	3	4	0.4	<1	165	67	7.8	18
Test Well DT-5A	67	9	2.6	1.6	11	0	52	<0.2	2	2	0.3	<1	123	30	7.9	11
Test Well 8	5	4	1.1	1.3	11	3	38	<0.2	<1	2	0.3	<1	27	12	8.7	8
Test Well DT-10	56	14	3.8	1.2	11	0	63	<0.2	6	2	0.3	<1	107	48	8.4	13
Canada del Buey	21	6	1.5	1.4	12	0	27	<0.2	4	8	9.3	<1	77	18	7.1	9
Pajarito Canyon	22	28	7.1	2.9	26	0	87	<0.2	7	36	0.3	<1	188	98	7.7	31
Water at Beta Hole	37	13	4.6	3.4	18	0	42	<0.2	11	19	0.3	<1	148	55	7.8	17
Summary																
No. of Analyses	9	9	9	9	9	9	9	9	9	9	9	9	9	9	9	9
Average	44	18	4.4	2.1	14	<1	62	--	<7	12	1.4	<2	136	60	7.9	18
S	24	14	2.6	1.1	5	<1	25	--	7	14	3.0	2	65	47	0.4	11
Minimum	5	4	1.1	1.1	9	0	27	--	<1	2	0.3	<1	27	18	7.1	9
Maximum	72	49	9.1	4.1	26	3	102	<0.2	24	36	9.3	7	253	164	8.0	40

[a]Samples collected in February and March.

Table G-26. Chemical Quality of Shallow Ground Water in Pajarito Canyon (mg/L)

Station	SiO_2	Ca	Mg	K	Na	CO_3	HCO_3	P	SO_4	Cl	F	N	TDS	Total Hardness	pH	Conductivity (mS/m)
Well PCO-1	49	76	13	4.9	52	0	250	<0.2	8	70	0.6	0.2	462	269	7.3	70
Well PCO-2	49	74	13	4.0	52	0	247	<0.2	8	71	0.6	0.4	434	263	7.5	71
Well PCO-3	48	77	12	4.0	105	0	249	<0.2	8	73	0.6	0.3	447	262	7.5	72
Summary																
No. of Analyses	3	3	3	3	3	3	3	3	3	3	3	3	3	3	3	3
Average	49	76	12.7	4.3	70	0	249	<0.2	8	71	0.6	0.3	448	265	7.5	71
S	1	2	0.6	0.5	30	0	2	0	0	2	0	0.1	14	4	0.2	1
Minimum	48	74	12	4.0	52	--	247	--	--	70	--	0.2	434	262	7.3	70
Maximum	49	77	13	4.9	105	0	250	<0.2	8	73	0.6	0.4	462	269	7.5	72

Table G-27. Radiochemical Quality of Surface and Ground Waters from Acid-Pueblo Canyon[a]

Station	^{3}H (10^{-6} µCi/mL)	^{137}Cs (10^{-9} µCi/mL)	Total U (µg/L)	^{238}Pu (10^{-9} µCi/mL)	$^{239,240}Pu$ (10^{-9} µCi/mL)	Gross Gamma (Counts/min/L)
Acid Weir	-2.2 (0.7)	2 (43)	0.6 (0.1)	0.010 (0.015)	0.068 (0.018)	300 (100)
Acid Weir	0.0 (0.3)	-58 (50)	2.0 (1.0)	0.017 (0.015)	2.38 (0.126)	130 (80)
Pueblo 1	-1.7 (0.7)	-16 (42)	0.6 (0.1)	0.007 (0.015)	0.083 (0.028)	200 (100)
Pueblo 1	-0.2 (0.4)	44 (60)	1.0 (1.0)	-0.009 (0.009)	0.006 (0.010)	-10 (80)
Pueblo 2	-1.5 (0.7)	-8 (43)	0.6 (0.1)	-0.062 (0.055)	0.062 (0.069)	-2500 (300)
Pueblo 2	0.1 (0.3)	82 (70)	1.0 (1.0)	-0.010 (0.012)	0.031 (0.014)	700 (100)
Pueblo 3	-1.8 (0.7)	41 (43)	0.9 (0.1)	0.012 (0.034)	0.092 (0.043)	-90 (100)
Pueblo 3	-0.3 (0.3)	118 (63)	1.0 (1.0)	0.000 (0.010)	0.031 (0.015)	580 (100)
Hamilton Bend Springs	-2.3 (0.7)	46 (21)	0.6 (0.1)	-0.009 (0.011)	-0.004 (0.008)	100 (100)
Hamilton Bend Springs (Dry)	--	--	--	--	--	--
Test Well 1A	-1.7 (0.7)	24 (48)	0.0 (1.0)	0.010 (0.017)	-0.010 (0.012)	-300 (100)
Test Well 1A	0.3 (0.3)	13 (59)	1.0 (1.0)	0.005 (0.004)	-0.002 (0.005)	-270 (80)
Test Well 2A	0.5 (0.7)	--	0.0 (1.0)	0.000 (0.010)	0.032 (0.018)	-500 (100)
Test Well 2A	1.4 (0.4)	167 (71)	1.0 (1.0)	-0.005 (0.005)	0.005 (0.005)	580 (100)
Basalt Spring	-0.9 (0.7)	131 (65)	1.3 (1.0)	-0.011 (0.012)	0.000 (0.010)	-300 (100)
Basalt Spring	-0.4 (0.3)	40 (62)	1.0 (1.0)	0.002 (0.003)	0.002 (0.002)	420 (90)
Summary						
No. of Analyses	15	14	15	15	15	15
Average	-0.7	45	0.8	-0.003	0.180	-64
S	1.1	62	0.5	0.019	0.610	765
Minimum	-2.3 (0.7)	-58 (50)	0.0 (1.0)	-0.062 (0.055)	-0.004 (0.008)	-2500 (300)
Maximum	1.4 (0.4)	167 (71)	2.0 (1.0)	0.010 (0.015)	2.38 (0.012)	700 (100)
Limits of Detection	0.7	50	1	0.009	0.03	50

[a]Samples collected in March and September; counting uncertainty in parentheses.

Table G-28. Radiochemical Quality of Surface and Ground Waters from DP-Los Alamos Canyon[a]

Station	^{3}H (10^{-6} µCi/mL)	^{137}Cs (10^{-9} µCi/mL)	Total U (µg/L)	^{238}Pu (10^{-9} µCi/mL)	$^{239,240}Pu$ (10^{-9} µCi/mL)	Gross Gamma (Counts/min/L)
DPS-1	-1.5 (0.7)	27 (44)	1.0 (0.1)	0.021 (0.016)	0.114 (0.024)	300 (100)
DPS-1	0.5 (0.3)	16 (75)	1.0 (1.0)	-0.005 (0.012)	0.014 (0.013)	700 (100)
DPS-4	-0.6 (0.7)	33 (44)	0.8 (0.1)	0.008 (0.018)	0.041 (0.027)	200 (100)
DPS-4	1.2 (0.4)	188 (80)	1.0 (1.0)	0.019 (0.012)	0.034 (0.013)	530 (100)
LAO-C	-0.3 (0.8)	56 (48)	0.1 (0.1)	0.000 (0.010)	0.005 (0.015)	-400 (100)
LAO-C	0.6 (0.3)	89 (69)	1.0 (1.0)	0.015 (0.015)	0.015 (0.016)	580 (100)
LAO-1	-0.4 (0.7)	-20 (48)	0.2 (0.1)	-0.006 (0.010)	-0.017 (0.010)	40 (100)
LAO-1	19 (2.0)	68 (67)	1.0 (1.0)	-0.017 (0.013)	0.008 (0.008)	700 (100)
LAO-2	-1.6 (0.7)	7 (42)	0.2 (0.1)	0.000 (0.010)	0.029 (0.023)	-60 (100)
LAO-2	1.3 (0.4)	116 (71)	1.0 (1.0)	0.009 (0.019)	0.009 (0.015)	350 (90)
LAO-3	-0.8 (0.7)	-56 (38)	0.3 (0.1)	0.015 (0.018)	0.015 (0.021)	-100 (100)
LAO-3	1.5 (0.4)	13 (58)	1.0 (1.0)	0.015 (0.011)	-0.004 (0.010)	240 (80)
LAO-4	-0.5 (0.7)	78 (50)	0.3 (0.1)	0.028 (0.015)	0.124 (0.024)	0 (100)
LAO-4	1.3 (0.4)	155 (79)	1.0 (1.0)	0.004 (0.013)	0.004 (0.015)	90 (80)
LAO-4.5	0.0 (0.7)	-39 (43)	0.3 (0.1)	0.000 (0.010)	0.021 (0.018)	-200 (100)
LAO-4.5	1.7 (0.4)	128 (77)	1.0 (1.0)	0.017 (0.017)	0.000 (0.010)	120 (80)
Summary						
No. of Analyses	16	16	16	16	16	16
Average	1.3	54	0.7	0.008	0.026	193
S	4.8	79	0.4	0.012	0.039	321
Minimum	-1.6 (0.7)	-56 (38)	0.1 (0.1)	-0.017 (0.013)	-0.017 (0.010)	-400 (100)
Maximum	19 (2.0)	188 (86)	1.0 (1.0)	0.028 (0.015)	0.124 (0.008)	700 (100)
Limits of Detection	0.7	40	1	0.009	0.03	50

[a]Samples collected in March and November; counting uncertainty in parentheses.

Table G-29. Radiochemical Quality of Surface and Shallow Ground Waters from Mortandad Canyon[a]

Station	^{3}H (10^{-6} µCi/mL)	^{90}Sr (10^{-9} µCi/mL)	^{137}Cs (10^{-9} µCi/mL)	Total U (µg/L)	^{238}Pu (10^{-9} µCi/mL)	$^{239,240}Pu$ (10^{-9} µCi/mL)	Gross Gamma (Counts/min/L)
GS-1	8400 (800)	6.2 (0.3)	-29 (55)	3.3 (0.3)	30.0 (3.00)	90.0 (5.00)	8500 (900)
GS-1	120 (10)	--	213 (84)	1.0 (1.0)	0.677 (0.033)	4.51 (0.185)	9700 (1000)
MCO-3	12 000 (1000)	9.5 (0.7)	66 (51)	3.8 (0.4)	24.2 (1.50)	68.0 (4.00)	10 000 (1000)
MCO-3	140 (10)	--	-2 (68)	1.0 (1.0)	0.921 (0.066)	5.23 (0.219)	11 000 (1000)
MCO-4	210 (20)	0.4 (0.4)	18 (56)	2.4 (0.2)	0.165 (0.034)	0.278 (0.044)	-300 (100)
MCO-4	480 (50)	--	-62 (75)	4.0 (1.0)	0.093 (0.023)	0.097 (0.021)	210 (80)
MCO-5	210 (20)	-0.6 (0.5)	73 (56)	1.7 (0.2)	0.053 (0.025)	0.337 (0.052)	-500 (100)
MCO-5	490 (50)	--	-20 (59)	4.0 (1.0)	0.150 (0.025)	0.382 (0.041)	270 (80)
MCO-6	400 (40)	56 (1.0)	95 (56)	2.7 (0.3)	0.941 (0.142)	3.35 (0.281)	1200 (200)
MCO-6	500 (50)	--	22 (68)	4.0 (1.0)	0.138 (0.026)	0.333 (0.039)	270 (80)
MCO-7	480 (50)	--	68 (60)	5.6 (0.6)	0.037 (0.044)	0.037 (0.040)	60 (100)
MCO-7	470 (50)	--	7 (62)	3.0 (1.0)	0.038 (0.018)	0.021 (0.015)	190 (80)
MCO-7.5	406 (40)	--	68 (49)	5.7 (0.6)	0.075 (0.026)	0.091 (0.026)	-300 (100)
MCO-7.5	490 (50)	--	53 (69)	3.0 (1.0)	0.030 (0.018)	0.066 (0.020)	180 (80)
Summary							
No. of Analyses	14	5	14	14	14	14	14
Average	1770	14	41	3.2	4.11	12.3	2891
S	3643	24	67	1.4	9.81	28.6	4578
Minimum	120 (10)	-0.6 (0.5)	-62 (75)	1.0 (1.0)	0.036 (0.018)	0.021 (0.015)	-500 (100)
Maximum	12 000 (1000)	56 (1.0)	213 (84)	5.7 (0.6)	30.0 (3.00)	90.0 (5.00)	11 000 (1000)
Limits of Detection	0.7	0.01	40	1	0.009	0.03	50

[a]Samples collected in March and November; counting uncertainty in parentheses.

Table G-30. Radiochemical Quality of Surface Waters from Sandia Canyon[a]

Station	^{3}H (10^{-6} µCi/mL)	^{137}Cs (10^{-9} µCi/mL)	Total U (µg/L)	^{238}Pu (10^{-9} µCi/mL)	$^{239,240}Pu$ (10^{-9} µCi/mL)	Gross Gamma (Counts/min/L)
SCS-1	-0.9 (0.7)	-47 (44)	1.8 (0.1)	0.000 (0.010)	0.012 (0.032)	40 (100)
SCS-1	0.7 (0.3)	29 (61)	1.0 (1.0)	0.002 (0.004)	0.000 (0.005)	30 (80)
SCS-2	-0.1 (0.7)	83 (57)	0.5 (0.1)	-0.076 (0.039)	-0.019 (0.033)	-130 (100)
SCS-2	0.8 (0.3)	36 (61)	1.0 (1.0)	0.000 (0.005)	0.002 (0.002)	160 (80)
SCS-3	-0.3 (0.7)	32 (48)	0.5 (0.1)	-0.054 (0.033)	-0.027 (0.019)	-40 (100)
SCS-3	0.0 (0.3)	135 (58)	1.0 (1.0)	-0.002 (0.007)	0.000 (0.005)	0 (80)
Summary						
No. of Analyses	6	6	6	6	6	6
Average	0.3	45	0.9	-0.022	-0.005	56
S	0.6	60	0.5	0.034	0.015	155
Minimum	-0.9 (0.7)	-47 (44)	0.5 (0.1)	-0.076 (0.039)	-0.027 (0.019)	-130 (100)
Maximum	0.8 (0.3)	135 (58)	1.8 (0.1)	0.002 (0.004)	0.012 (0.032)	306 (80)
Limits of Detection	0.7	40	1	0.009	0.03	50

[a]Samples collected in March and September; counting uncertainty in parentheses.

Table G-31. Chemical Quality of Surface and Shallow Ground Waters in Acid-Pueblo Canyon (mg/L)[a]

Station	SiO_2	Ca	Mg	K	Na	CO_3	HCO_3	P	SO_4	Cl	F	N	TDS	Total Hardness	pH	Conductivity (mS/m)
Acid Weir	25	18	3.6	5.0	70	0	56	1.7	19	85	0.5	2	265	59	7.4	45
Pueblo 1	26	18	3.7	5.3	69	0	56	1.7	20	86	0.5	2	277	60	7.3	44
Pueblo 2	26	18	3.5	4.9	68	0	56	1.7	20	85	0.5	2	274	58	7.5	45
Pueblo 3	32	19	3.5	6.8	76	0	75	3.7	23	74	0.8	6	302	60	7.7	48
Hamilton Bend Spring	55	15	4.3	9.2	74	0	110	6.5	23	47	0.9	2	287	51	8.0	44
Test Well 1A	50	30	8.2	8.2	69	0	119	4.3	30	60	0.7	9	343	114	7.9	55
Test Well 2A	35	34	6.8	3.5	22	0	79	<0.2	23	54	0.4	<1	211	109	7.0	36
Basalt Spring	40	24	6.7	3.8	17	0	80	<0.2	17	16	0.6	2	173	89	7.7	26
Summary																
No. of Analyses	8	8	8	8	8	8	8	8	8	8	8	8	8	8	8	8
Average	36	22	5.0	5.8	58	0	79	<2.5	22	64	0.6	<3	266	75	7.6	43
S	11	7	1.9	2.0	24	--	24	2.2	4	24	0.2	3	53	25	0.3	9
Minimum	25	15	3.5	3.5	17	--	56	<0.2	17	16	0.4	<1	173	51	7.0	26
Maximum	55	34	8.2	9.2	76	--	119	6.5	30	86	0.9	6	343	114	8.0	55

[a]Samples collected in March.

Table G-32. Chemical Quality of Surface and Shallow Ground Waters in DP-Los Alamos Canyon (mg/L)[a]

Station	SiO_2	Ca	Mg	K	Na	CO_3	HCO_3	P	SO_4	Cl	F	N	TDS	Total Hardness	pH	Conductivity (mS/m)
DPS-1	17	26	2.2	4.9	78	0	84	<0.2	18	101	0.6	1.2	306	75	7.8	51
	19	16	1.0	3.5	32	0	77	<0.2	9	13	0.7	<0.2	152	44	7.5	23
DPS-4	21	15	1.7	10.5	90	0	90	0.4	26	94	2.5	1.2	306	44	8.1	52
	44	18	3.4	4.5	46	0	89	<0.2	13	34	0.6	1.0	216	57	7.0	32
LAO-C	27	8	2.6	2.2	7	0	21	<0.2	9	10	<0.2	<0.2	96	28	7.5	9
	32	10	2.1	2.7	34	0	57	<0.2	7	31	0.3	<0.2	157	32	7.0	23
LAO-1	29	12	3.5	2.5	22	0	26	<0.2	9	39	<0.2	<1	142	42	7.6	20
	23	13	1.1	10.5	65	0	129	0.4	16	21	2.4	0.7	228	39	7.8	37
LAO-2	30	13	3.7	2.8	29	0	32	<0.2	9	49	0.3	<1	165	52	7.4	25
	40	18	3.9	8.6	35	0	95	<0.2	14	21	1.1	0.5	186	58	7.0	30
LAO-3	33	14	4.0	3.1	30	0	32	<0.2	10	56	0.3	<1	184	54	7.6	25
	41	18	3.9	8.5	35	0	93	<0.2	14	21	1.1	0.4	184	57	7.0	27
LAO-4	31	13	3.7	3.3	30	0	34	<0.2	10	52	0.3	<1	169	49	7.4	26
	41	16	2.8	12.4	59	0	126	0.3	17	23	2.0	0.8	231	47	7.1	38
LAO-4.5	33	15	4.0	3.5	31	0	33	<0.2	10	57	0.3	1.4	183	58	7.6	26
	42	16	2.8	12.1	59	0	125	0.3	17	24	2.0	0.7	229	44	7.1	37
Summary																
No. of Analyses	16	16	16	16	16	16	16	16	16	16	16	16	16	16	16	16
Average	31	15	2.9	5.9	42	0	71	0.2	13	40	0.9	<0.8	196	49	7.4	30
S	8	4	1.0	3.7	22	0	38	0.0	5	27	0.8	<0.4	55	11	0.3	11
Minimum	17	8	1.0	2.2	7	0	21	<0.2	7	13	<0.2	<0.2	96	28	7.0	9
Maximum	44	26	4.0	12.4	90	0	129	0.4	26	101	2.5	1.4	306	75	8.1	52

[a]Samples collected in March and April.

Table G-33. Chemical Quality of Surface and Shallow Ground Waters in Mortandad Canyon (mg/L)[a]

Station	SiO_2	Ca	Mg	K	Na	CO_3	HCO_3	P	SO_4	Cl	F	N	TDS	Total Hardness	pH	Conductivity (mS/m)
GS-1	44	109	2.7	54.9	54	0	257	<0.2	81	35	6.0	45	780	256	7.9	130
	57	38	3.1	20.0	85	0	124	<0.2	24	4	1.1	37	492	110	7.8	71
MCO-3	44	130	2.9	66.8	132	0	306	<0.2	102	40	7.7	56	963	315	7.9	160
	62	39	3.3	21.4	92	0	124	<0.2	25	28	1.2	42	426	112	7.8	73
MCO-4	33	37	2.8	35.1	74	2	142	<0.2	24	30	2.4	31	492	97	8.4	76
	65	9	<0.5	18.9	165	66	133	<0.2	60	38	3.9	44	601	24	9.9	91
MCO-5	30	20	4.7	7.3	220	0	176	<0.2	21	28	1.9	37	551	76	7.7	85
	27	39	5.7	34.2	228	0	164	<0.2	48	37	3.0	118	1010	107	7.5	145
MCO-6	29	18	4.1	8.2	155	0	176	<0.2	29	29	2.3	37	548	63	7.6	85
	42	21	2.8	26.2	190	19	150	<0.2	53	39	3.3	75	751	61	9.0	115
MCO-7	30	17	4.2	4.9	223	0	214	<0.2	37	30	2.4	62	775	61	8.3	118
	31	12	2.4	4.0	178	0	182	<0.2	40	35	3.3	46	622	37	7.6	92
MCO-7.5	30	17	4.2	4.9	229	0	215	<0.2	38	30	2.5	62	777	62	8.3	120
	31	13	2.5	4.1	178	0	183	<0.2	40	35	3.2	47	592	43	7.7	92
Summary																
No. of Analyses	14	14	14	14	14	14	14	14	14	14	14	14	14	14	14	14
Average	40	37	3.2	22.2	157	6	182	<0.2	45	31	3.2	53	677	102	8.1	104
S	13	37	1.2	19.7	61	18	52	0.0	23	9	1.8	22	168	83	0.5	28
Minimum	29	9	<0.5	4.0	74	0	124	<0.2	24	4	1.1	37	492	24	7.5	72
Maximum	65	130	5.7	66.8	229	66	306	<0.2	102	39	3.9	118	1010	315	9.9	160

[a]Samples collected in March.

Table G-34. Chemical Quality of Surface Water from Sandia Canyon (mg/L)[a]

Station	SiO_2	Ca	Mg	K	Na	CO_3	HCO_3	P	SO_4	Cl	F	N	TDS	Total Hardness	pH	Conductivity (mS/m)
SCS-1	96	34	4.7	8.1	215	--	--	1.4	768	83	1.0	1.3	1129	100	--	300
SCS-2	46	22	3.8	8.5	126	0	68	1.5	40	157	0.8	1.8	465	71	7.8	80
SCS-3	46	19	3.7	8.6	130	0	62	1.5	40	159	0.8	1.8	468	66	7.9	81
Summary																
No. of Analyses	3	3	3	3	3	2	2	3	3	3	3	3	3	3	2	3
Average	63	25	4.1	8.4	157	0	65	1.5	283	133	0.9	1.6	687	79	7.8	153
S	29	8	0.6	0.3	50	--	4	0.1	420	43	0.1	0.3	382	18	0.1	127
Minimum	46	19	3.8	8.1	126	--	62	1.4	40	83	0.8	1.3	465	66	7.8	80
Maximum	96	34	4.7	8.6	215	0	68	1.5	768	159	1.0	1.8	1129	100	7.9	300

[a]Samples collected in March.

Table G-35. Background Radiochemical Quality of Run-off (Solution and Suspended Sediments) in the Los Alamos Area[a]

Station	1987 Date	In Solution: ^{3}H (10^{-6} µCi/mL)	In Solution: ^{137}Cs (10^{-9} µCi/mL)	In Solution: Total U (µg/L)	In Solution: Gross Gamma (counts/min/L)
West SR-4 at Water Canyon	4/29	0.4 (0.3)	69 (60)	1.0 (1.0)	20 (80)
West SR-4 at Canon Valle	4/29	0.5 (0.3)	117 (62)	1.0 (1.0)	120 (80)
West SR-4 at Pajarito Canyon	4/29	0.7 (0.3)	138 (71)	1.0 (1.0)	130 (80)
West SR-4 at Los Alamos Canyon	4/29	0.4 (0.3)	−91 (50)	1.0 (1.0)	150 (80)
Guaje Canyon at Well G-5	4/29	0.5 (0.3)	13 (75)	1.0 (1.0)	170 (80)
$\bar{x}$ (s)		0.5 (0.1)	64 (67)	1.0 (1.0)	118 (58)

Station	1987 Date	In Solution: ^{238}Pu (10^{-9} µCi/mL)	In Solution: $^{239,240}Pu$ (10^{-9} µCi/mL)	Suspended Sediments: ^{238}Pu (pCi/g)	Suspended Sediments: $^{239,240}Pu$ (pCi/g)
West SR-4 at Water Canyon	4/29	0.000 (0.010)	0.009 (0.027)	0.077 (0.045)	0.033 (0.037)
West SR-4 at Canon Valle	4/29	0.031 (0.015)	0.010 (0.010)	0.000 (0.019)	0.034 (0.034)
West SR-4 at Pajarito Canyon	4/29	0.000 (0.010)	0.004 (0.010)	0.034 (0.075)	0.006 (0.045)
West SR-4 at Los Alamos Canyon	4/29	0.013 (0.017)	0.004 (0.008)	0.064 (0.013)	1.32 (0.071)
Rendija Canyon at Booster 1	3/12	0.013 (0.012)	−0.004 (0.010)	−0.010 (0.001)	0.020 (0.012)
Guaje Canyon at Well G-5	4/29	−0.004 (0.012)	0.014 (0.013)	−0.004 (0.004)	0.011 (0.005)
	5/4-7	0.007 (0.012)	0.014 (0.010)	−0.016 (0.016)	0.056 (0.027)
	5/11-14	0.015 (0.009)	0.011 (0.008)	0.066 (0.050)	0.089 (0.054)
	5/26-28	−0.009 (0.014)	0.000 (0.010)	0.020 (0.061)	−0.020 (0.035)
	6/4	−0.019 (0.014)	0.000 (0.010)	0.176 (0.117)	0.106 (0.093)
	6/8-11	0.010 (0.010)	0.010 (0.010)	0.022 (0.071)	0.000 (0.039)
Guaje Canyon at SR-4	4/20	0.004 (0.011)	−0.004 (0.007)	0.001 (0.001)	0.012 (0.002)
	4/30	0.010 (0.010)	0.029 (0.014)	0.011 (0.003)	0.233 (0.014)
	5/18-21	0.009 (0.016)	−0.009 (0.013)	−0.032 (0.045)	0.032 (0.051)
$\bar{x}$ (s)		0.006 (0.012)	0.006 (0.010)	0.029 (0.053)	0.138 (0.346)

[a]Location of stations shown in Fig. 16; counting uncertainty in parentheses.

Table G-36. Plutonium in Spring Run-off in Solution and Suspended Sediments

Station	1987 Date	Solution ^{238}Pu (10^{-9} µCi/mL)	Solution $^{239,240}Pu$ (10^{-9} µCi/mL)	Suspended Sediments ^{238}Pu (pCi/g)	Suspended Sediments $^{239,240}Pu$ (pCi/g)
Water Canyon at SR-4	4/14	-0.017 (0.020)	0.033 (0.026)	0.000 (0.140)	0.000 (0.140)
	4/20	0.000 (0.010)	0.024 (0.016)	0.018 (0.060)	-0.062 (0.038)
	4/30	0.010 (0.019)	-0.010 (0.013)	-0.012 (0.032)	0.024 (0.042)
	5/4-7	0.018 (0.014)	0.004 (0.004)	0.004 (0.006)	0.004 (0.004)
	5/11-14	0.000 (0.010)	-0.004 (0.011)	0.342 (0.343)	0.770 (0.356)
	5/18-21	0.004 (0.008)	-0.004 (0.004)	0.000 (0.132)	0.058 (0.101)
	5/26-28	0.000 (0.001)	0.009 (0.009)	0.066 (0.066)	0.066 (0.081)
	6/4	0.015 (0.015)	-0.015 (0.008)	0.028 (0.048)	0.056 (0.040)
$\bar{x}$ (s)		0.004 (0.011)	0.005 (0.017)	0.056 (0.118)	0.115 (0.268)
Pajarito Canyon at SR-4	3/5	0.035 (0.019)	0.004 (0.010)	-0.134 (0.164)	0.067 (0.178)
	3/2-5	-0.010 (0.007)	0.014 (0.008)	0.945 (0.069)	0.942 (0.131)
	3/6-19	-0.004 (0.015)	-0.004 (0.004)	0.021 (0.044)	0.000 (0.022)
	3/23-26	-0.018 (0.022)	-0.018 (0.018)	-0.026 (0.070)	0.079 (0.087)
	3/30-4/2	0.004 (0.012)	0.000 (0.010)	0.150 (0.011)	0.060 (0.110)
	4/6-9	-0.005 (0.012)	0.017 (0.017)	0.020 (0.040)	0.066 (0.052)
	4/20	0.000 (0.010)	0.000 (0.000)	0.030 (0.030)	0.000 (0.030)
	4/30	0.000 (0.010)	0.134 (0.010)	0.116 (0.084)	0.093 (0.080)
	5/4-7	-0.120 (0.009)	-0.004 (0.009)	-0.034 (0.034)	0.034 (0.059)
	5/11-14	-0.011 (0.012)	0.007 (0.007)	0.161 (0.105)	0.095 (0.056)
	5/18-21	-0.024 (0.016)	0.034 (0.016)	0.172 (0.150)	0.000 (0.079)
	5/26-28	0.016 (0.014)	0.004 (0.011)	0.040 (0.069)	0.120 (0.090)
	6/4	-0.022 (0.011)	0.000 (0.010)	0.000 (0.227)	0.218 (0.218)
	6/8-11	-0.012 (0.013)	0.000 (0.010)	-0.014 (0.024)	0.014 (0.014)
$\bar{x}$ (s)		-0.002 (0.016)	0.013 (0.037)	0.068 (0.138)	0.128 (0.242)

Table G-36 (cont)

Station	1987 Date	Solution ^{238}Pu (10^{-9} µCi/mL)	Solution $^{239,240}Pu$ (10^{-9} µCi/mL)	Suspended Sediments ^{238}Pu (pCi/g)	Suspended Sediments $^{239,240}Pu$ (pCi/g)
Los Alamos Canyon at SR-4	3/2-5	-0.011 (0.019)	0.011 (0.024)	0.190 (0.061)	2.84 (0.219)
	3/16-19	0.030 (0.016)	0.035 (0.015)	0.105 (0.014)	0.770 (0.048)
	3/23-26	0.012 (0.013)	0.020 (0.012)	0.026 (0.004)	0.426 (0.024)
	3/30-31,4/1-2	0.000 (0.010)	-0.004 (0.004)	0.033 (0.023)	3.50 (0.400)
	4/6-9	-0.059 (0.066)	0.040 (0.040)	-0.040 (0.040)	0.230 (0.110)
	4/14-17	0.054 (0.020)	0.010 (0.012)	0.018 (0.018)	2.20 (0.160)
	4/20	0.021 (0.016)	0.036 (0.006)	0.118 (0.024)	1.65 (0.110)
	4/30	0.008 (0.011)	0.008 (0.011)	0.074 (0.019)	2.08 (0.121)
	5/4-7	0.029 (0.018)	0.000 (0.010)	0.055 (0.021)	1.63 (0.128)
	5/11-14	-0.004 (0.009)	0.014 (0.012)	0.023 (0.069)	1.59 (0.209)
	5/18-21	0.009 (0.013)	0.014 (0.014)	0.117 (0.060)	2.52 (0.228)
	5/26-27	0.000 (0.010)	0.000 (0.010)	0.212 (0.071)	3.32 (0.304)
	6/4	0.004 (0.004)	0.031 (0.013)	0.314 (0.105)	2.79 (0.328)
	6/8-11	-0.009 (0.011)	-0.004 (0.010)	0.051 (0.102)	1.94 (0.241)
$\bar{x}$ (s)		0.006 (0.026)	0.015 (0.015)	0.093 (0.093)	1.96 (1.01)
Pueblo Canyon at SR-4	3/5	-0.014 (0.025)	0.014 (0.032)	0.021 (0.010)	4.63 (0.232)
	3/2-5	-0.026 (0.015)	0.000 (0.010)	0.036 (0.008)	0.742 (0.047)
	3/16-19	-0.008 (0.010)	0.023 (0.014)	0.011 (0.005)	1.60 (0.095)
	3/23-26	0.000 (0.010)	-0.007 (0.007)	0.015 (0.004)	1.17 (0.050)
	3/30-31,4/1-2	0.021 (0.014)	0.000 (0.010)	0.005 (0.002)	1.35 (0.058)
	4/6-9	0.012 (0.015)	0.012 (0.013)	0.034 (0.014)	7.27 (0.310)
	4/14-17	0.000 (0.010)	0.010 (0.010)	-0.009 (0.009)	3.27 (0.210)
$\bar{x}$ (s)		-0.002 (0.016)	0.007 (0.010)	0.016 (0.016)	2.86 (2.38)

Table G-36 (cont)

Station	1987 Date	Solution ^{238}Pu (10^{-9} µCi/mL)	Solution $^{239,240}Pu$ (10^{-9} µCi/mL)	Suspended Sediments ^{238}Pu (pCi/g)	Suspended Sediments $^{239,240}Pu$ (pCi/g)
Los Alamos Canyon at Otowi	3/2-5	-0.033 (0.025)	0.011 (0.019)	0.181 (0.012)	0.401 (0.022)
	3/16-19	0.008 (0.012)	0.011 (0.011)	0.059 (0.008)	1.40 (0.069)
	4/20	0.000 (0.010)	0.000 (0.010)	0.036 (0.006)	0.930 (0.047)
	4/30	0.000 (0.010)	0.008 (0.013)	0.004 (0.002)	0.121 (0.010)
	5/4-7	0.004 (0.004)	-0.004 (0.004)	0.019 (0.005)	0.264 (0.021)
	5/11-14	0.000 (0.010)	0.018 (0.018)	0.009 (0.005)	0.167 (0.97)
	5/18-21	0.000 (0.010)	0.021 (0.018)	0.029 (0.011)	0.228 (0.029)
	5/26-28	0.054 (0.021)	0.009 (0.009)	0.018 (0.009)	0.268 (0.036)
	6/4	0.027 (0.017)	0.013 (0.012)	0.058 (0.041)	0.878 (0.164)
	6/8-11	-0.005 (0.013)	0.005 (0.015)	0.064 (0.034)	2.74 (0.202)
	6/14-17	-0.011 (0.017)	-0.011 (0.011)	1.90 (0.060)	1.70 (0.160)
$\bar{x}$ (s)		0.004 (0.022)	0.007 (0.009)	0.216 (0.561)	0.827 (0.829)
Rio Grande at Otowi	3/12	-0.016 (0.011)	-0.024 (0.014)	0.001 (0.004)	0.001 (0.002)

Table G-37. Radiochemistry of Storm Run-off in Sediment Traps, Mortandad Canyon

	Uranium and Plutonium Analyses				
	Solution			Suspended Sediments	
Station	Total U (μg/L)	^{238}Pu (10^{-9} μCi/mL)	$^{239,240}Pu$ (10^{-9} μCi/mL)	^{238}Pu (pCi/g)	$^{239,240}Pu$ (pCi/g)
Sediment Trap 1	2.0 (1.0)	0.225 (0.225)	1.24 (0.331)	39.2 (1.72)	137 (5.17)
Sediment Trap 2	1.0 (1.0)	0.767 (0.334)	1.34 (0.363)	31.1 (1.43)	107 (4.13)
Sediment Trap 3	1.0 (1.0)	-0.212 (0.150)	0.265 (0.206)	21.5 (1.04)	75.3 (2.97)

	Tritium, Cesium, and Gross Radioactivity Analyses				
	Solution				
Station	^{3}H (10^{-6} μCi/mL)	^{137}Cs (10^{-9} μCi/mL)	Gross Alpha (10^{-9} μCi/mL)	Gross Beta (10^{-9} μCi/mL)	Gross Gamma (counts/min/L)
Sediment Trap 1	9.0 (1.0)	-18 (59)	5.0 (1.0)	35 (4.0)	---
Sediment Trap 2	4.7 (0.6)	26 (40)	1.5 (0.7)	26 (3.0)	---
Sediment Trap 3	5.9 (0.7)	3 (59)	2.4 (0.9)	17 (2.0)	---

Table G-38. Locations of Soil and Sediment Sampling Stations

Station	Latitude or N-S Coord	Longitude or E-W Coord	Map Designation[a]
Regional Sediments			
Chamita	36°05'	106°07'	--
Embudo	36°12'	105°58'	--
Otowi	35°52'	106°08'	--
Sandia	S060	E490	--
Pajarito	S185	E410	--
Ancho	S305	E335	--
Frijoles	S375	E235	--
Cochiti	35°37'	106°19'	--
Bernalillo	35°17'	106°36'	--
Jemez River	35°40'	106°44'	--
Perimeter Sediments			
Guaje at SR-4	N135	E480	12
Bayo at SR-4	N100	E455	13
Sandia at SR-4	N025	E315	14
Mortandad at SR-4	S030	E350	15
Canada del Buey at SR-4	S090	E360	16
Pajarito at SR-4	S105	E320	17
Potrillo at SR-4	S145	E295	18
Water at SR-4	S170	E260	19
Ancho at SR-4	S255	E250	20
Frijoles at National Monument Headquarters	S280	E185	21
Effluent Release Area Sediments			
Acid Pueblo Canyon			
Acid Weir	N125	E070	22
Pueblo 1	N130	E085	23
Pueblo 2	N120	E145	24
Hamilton Bend Spring	N105	E255	25
Pueblo 3	N090	E315	26
Pueblo at SR-4	N070	E350	27
DP-Los Alamos Canyon			
DPS-1	N090	E160	28
DPS-4	N075	E205	29
Los Alamos at Bridge	N095	E020	30
Los Alamos at LAO-1	N080	E120	31
Los Alamos at GS-1	N075	E200	32
Los Alamos at LAO-3	N075	E215	33
Los Alamos at LAO-4.5	N065	E270	34
Los Alamos at SR-4	N065	E355	35
Los Alamos at Totavi	N065	E405	36
Los Alamos at LA-2	N125	E510	37
Los Alamos at Otowi	N100	E560	38

Table G-38 (cont)

Station	Latitude or N-S Coord	Longitude or E-W Coord	Map Designation[a]
Mortandad Canyon			
Mortandad near CMR	N060	E036	39
Mortandad west of GS-1	N045	E095	40
Mortandad at GS-1	N040	E105	41
Mortandad at MCO-5	N035	E155	42
Mortandad at MCO-7	N025	E190	43
Mortandad at MCO-9	N030	E215	44
Mortandad at MCO-13	N015	E250	45
Regional Soils			
Rio Chama	36°05'	106°07'	--
Embudo	36°12'	105°58'	--
Otowi	35°52'	106°08'	--
Near Santa Cruz	35°59'	105°54'	--
Cochiti	35°37'	106°19'	--
Bernalillo	35°17'	106°36'	--
Jemez	35°40'	106°44'	--
Perimeter Soils			
Sportsman's Club	N240	E215	S1
North Mesa	N134	E168	S2
TA-8	N060	W075	S3
TA-49	S165	E085	S4
White Rock (east)	S055	E385	S5
Tsankawi	N020	E310	S6
Onsite Soils			
TA-21	N095	E140	S7
East of TA-53	N051	E218	S8
TA-50	N035	E095	S9
Two Mile Mesa	N025	E030	S10
East of TA-54	S080	E295	S11
R-Site Road East	S042	E103	S12
Potrillo Drive	S065	E195	S13
S-Site	S035	W025	S14
Near Test Well DT-9	S150	E140	S115
Near TA-33	S245	E225	S16

[a]Soil sampling locations in Figs. 14 and 17; sediment sampling locations in Figs. 14 and 18.

Table G-39. Radiochemical Analyses of Regional Soils and Sediments[a]

Location	^{3}H (10^{-6} µCi/mL)	^{137}Cs (pCi/g)	Total U (µg/g)	^{238}Pu (pCi/g)	$^{239,240}Pu$ (pCi/g)	^{241}Am (pCi/g)	Gross Gamma (counts/min/g)
Soils							
Chamita	0.2 (0.5)	0.24 (0.07)	5.4 (0.5)	0.002 (0.001)	0.008 (0.002)	--	6.4 (0.8)
Embudo	0.1 (0.5)	0.25 (0.10)	4.8 (0.5)	0.000 (0.001)	0.007 (0.002)	--	6.0 (0.8)
Otowi	-0.8 (0.5)	0.02 (0.06)	5.0 (0.5)	0.000 (0.001)	0.008 (0.002)	--	6.1 (0.8)
Near Santa Cruz Lake	--	0.41 (0.10)	3.1 (0.3)	0.000 (0.001)	0.007 (0.002)	--	4.6 (0.7)
Cochiti	4.7 (0.7)	0.43 (0.09)	3.0 (0.3)	0.000 (0.001)	0.016 (0.003)	--	4.1 (0.7)
Bernalillo	13 (1.0)	0.60 (0.13)	1.9 (0.2)	0.002 (0.001)	0.013 (0.003)	--	3.7 (0.7)
Jemez	4.3 (0.7)	0.23 (0.08)	2.1 (0.2)	0.001 (0.001)	0.010 (0.003)	--	1.7 (0.6)
Summary							
No. of Analyses	6	7	7	7	7	--	7
Average	3.6	0.31	3.6	0.001	0.010	--	4.7
S	5.2	0.19	1.4	0.001	0.003	--	1.7
Minimum	-0.8 (0.5)	0.02 (0.06)	1.9 (0.2)	0.000 (0.001)	0.007 (0.002)	--	1.7 (0.6)
Maximum	13 (1.0)	0.60 (0.13)	5.4 (0.5)	0.002 (0.001)	0.016 (0.003)	--	6.4 (0.8)
Sediments							
Rio Chama at Chamita	--	0.00 (0.06)	1.9 (0.2)	-0.001 (0.001)	-0.002 (0.001)	-0.160 (0.081)	-3.5 (0.7)
Rio Grande at Embudo	--	0.14 (0.10)	2.3 (0.2)	0.000 (0.001)	0.000 (0.001)	-0.146 (0.177)	-4.1 (0.7)
Rio Grande at Otowi	--	0.06 (0.06)	2.0 (0.2)	0.001 (0.002)	0.000 (0.001)	-0.078 (0.081)	-5.5 (0.8)
Rio Grande at Sandia	0.7 (0.4)	0.38 (0.11)	8.5 (0.9)	0.001 (0.002)	0.002 (0.001)	--	3.8 (0.7)
Rio Grande at Pajarito	0.2 (0.4)	0.12 (0.10)	3.4 (0.4)	0.000 (0.001)	0.007 (0.002)	--	1.8 (0.6)
Rio Grande at Ancho[b]	--	--		--	--	--	--
Rio Grande at Frijoles[b]	--	--	--	--	--	--	--
Rio Grande at Bernalillo	--	0.13 (0.09)	2.8 (0.3)	0.000 (0.001)	0.004 (0.002)	-3.26 (0.520)	-1.6 (0.6)
Jemez River at Jemez	--	0.09 (0.08)	1.1 (0.2)	0.000 (0.002)	0.001 (0.001)	--	--

Table G-39 (cont)

Location	^{3}H (10^{-6} µCi/mL)	^{137}Cs (pCi/g)	Total U (µg/g)	^{238}Pu (pCi/g)	$^{239,240}Pu$ (pCi/g)	^{241}Am (pCi/g)	Gross Gamma (counts/min/g)
Summary							
No. of Analyses	2	7	7	7	7	4	6
Average	0.4	0.13	3.1	0.000	0.002	-0.911	-1.5
S	0.3	0.12	2.5	0.001	0.003	1.57	3.6
Minimum	0.2 (0.4)	0.00 (0.06)	1.1 (0.2)	-0.001 (0.001)	-0.002 (0.001)	-3.26 (0.520)	-3.5 (0.7)
Maximum	0.7 (0.4)	0.38 (0.11)	8.5 (0.9)	0.001 (0.002)	0.007 (0.002)	-0.078 (0.081)	3.8 (0.7)
Limits of Detection	0.7	0.1	0.3	0.003	0.002	0.01	0.1

---

[a]Samples collected in April; counting uncertainty in parentheses.

[b]Sampling station covered by reservoir.

Table G-40. Radiochemical Analyses of Perimeter Soils and Sediments

Location	^{3}H (10^{-6} µCi/mL)	^{137}Cs (pCi/g)	Total U (µg/g)	^{238}Pu (pCi/g)	$^{239,240}Pu$ (pCi/g)	^{241}Am (pCi/g)	Gross Gamma (counts/min/g)
Perimeter Soils							
Sportmans Club	1.1 (0.5)	0.29 (0.09)	4.2 (0.4)	0.001 (0.001)	0.018 (0.003)	--	4.4 (0.7)
North Mesa	0.4 (0.5)	0.25 (0.08)	3.8 (0.4)	0.001 (0.001)	0.008 (0.002)	--	6.3 (0.8)
TA-8	0.6 (0.5)	1.3 (0.22)	3.1 (0.3)	0.002 (0.001)	0.026 (0.004)	--	7.3 (0.9)
TA-49	-0.1 (0.5)	0.34 (0.09)	4.8 (0.5)	0.000 (0.001)	0.004 (0.002)	--	7.1 (0.9)
White Rock	2.8 (0.6)	0.24 (0.08)	4.0 (0.4)	0.001 (0.001)	0.010 (0.002)	--	7.5 (0.9)
Tsankawi	1.5 (0.5)	0.27 (0.07)	5.3 (0.5)	0.029 (0.004)	0.009 (0.002)	--	9.0 (1.0)
Summary							
No. of Analyses	6	6	6	6	6		6
Average	1.0	0.44	4.2	0.006	0.013	--	6.9
S	1.0	0.42	0.8	0.011	0.008	--	1.5
Minimum	-0.1 (0.5)	0.24 (0.08)	3.1 (0.3)	0.000 (0.001)	0.004 (0.002)	--	4.4 (0.7)
Maximum	2.8 (0.6)	1.3 (0.22)	5.3 (0.5)	0.029 (0.004)	0.026 (0.004)	--	9.0 (1.0)
Perimeter Sediments							
Guaje at SR-4	--	0.06 (0.06)	2.8 (0.3)	0.000 (0.001)	0.002 (0.001)	-0.016 (0.068)	-2.4 (0.6)
Bayo at SR-4	--	0.34 (0.11)	3.2 (0.3)	-0.001 (0.002)	0.002 (0.002)	0.028 (0.202)	-0.8 (0.6)
Sandia at SR-4	--	0.06 (0.06)	1.8 (0.2)	0.001 (0.001)	0.001 (0.001)	0.010 (0.081)	-2.1 (0.6)
Mortandad at SR-4	--	0.00 (0.07)	1.7 (0.2)	-0.000 (0.001)	0.002 (0.001)	--	-1.2 (0.6)
Canada del Buey at SR-4	--	0.13 (0.09)	2.1 (0.2)	0.002 (0.002)	0.001 (0.002)	0.054 (0.179)	-23 (2.0)
Pajarito at SR-4	--	0.10 (0.06)	2.6 (0.3)	-0.001 (0.002)	0.005 (0.003)	0.043 (0.096)	0.2 (0.6)
Potrillo at SR-4	--	0.04 (0.09)	2.5 (0.3)	0.001 (0.001)	0.002 (0.001)	0.311 (0.188)	-1.6 (0.6)
Water at SR-4	--	0.15 (0.08)	1.7 (0.2)	0.000 (0.001)	0.002 (0.001)	--	-2.6 (0.6)
Ancho at SR-4	--	0.12 (0.07)	2.3 (0.3)	0.000 (0.001)	0.006 (0.002)	0.110 (0.097)	-1.2 (0.6)
Frijoles at Bandelier	--	0.24 (0.10)	3.2 (0.3)	-0.001 (0.001)	0.001 (0.001)	0.230 (0.185)	-0.9 (0.6)
Sandia at Rio Grande	--	0.39 (0.12)	2.0 (0.2)	0.000 (0.001)	0.001 (0.002)	--	-1.5 (0.6)
Canada del Ancha at Rio Grande	--	0.14 (0.09)	1.3 (0.2)	-0.001 (0.001)	0.001 (0.001)	--	-0.8 (0.6)

Table G-40 (cont)

Location	^{3}H (10^{-6} µCi/mL)	^{137}Cs (pCi/g)	Total U (µg/g)	^{238}Pu (pCi/g)	$^{239,240}Pu$ (pCi/g)	^{241}Am (pCi/g)	Gross Gamma (counts/min/g)
Mortandad At Rio Grande	0.3 (0.4)	0.03 (0.10)	1.7 (0.2)	0.000 (0.000)	0.002 (0.001)	--	-0.7 (0.6)
Pajarito at Rio Grande	0.5 (0.4)	0.36 (0.11)	2.9 (0.3)	0.000 (0.001)	0.003 (0.002)	--	-0.0 (0.6)
Water at Rio Grande	--	0.09 (0.09)	1.8 (0.2)	0.001 (0.001)	0.001 (0.001)	--	-2.9 (0.6)
Ancho at Rio Grande	0.2 (0.4)	0.08 (0.08)	1.2 (0.2)	0.000 (0.001)	0.000 (0.001)	--	-4.8 (0.7)
Frijoles at Rio Grande	0.4 (0.4)	0.13 (0.10)	2.8 (0.3)	-0.001 (0.001)	0.002 (0.001)	--	2.5 (0.6)
Summary							
No. of Analyses	4	17	17	17	17	8	17
Average	0.3	0.14	2.2	0.000	0.002	0.096	-2.6
Std. Dev.	0.1	0.12	0.6	0.001	0.002	0.116	5.5
Minimum	0.2 (0.4)	0.00 (0.07)	1.2 (0.2)	-0.001 (0.002)	0.000 (0.001)	-0.016 (0.068)	-2.3 (2.0)
Maximum	0.5 (0.4)	0.39 (0.12)	3.2 (0.3)	0.002 (0.002)	0.006 (0.002)	0.311 (0.188)	2.5 (0.6)
Limits of Detection	0.7	0.1	0.3	0.003	0.002	0.002	0.1

[a]Samples collected in April; counting uncertainty in parentheses.

Table G-41. Suburanic and Gross Gamma Analyses of On-site Soils and Sediments[a]

Location	^{3}H (10^{-6} µCi/mL)	^{137}Cs (pCi/g)	Gross Gamma (counts/min/g)
On-site Soils			
TA-21	1.9 (0.5)	-0.01 (0.08)	6.6 (0.9)
East of TA-53	1.0 (0.5)	0.17 (0.08)	7.5 (0.9)
TA-50	2.3 (0.5)	0.11 (0.08)	6.8 (0.9)
Two-Mile Mesa	0.7 (0.5)	0.51 (0.11)	4.7 (0.7)
East of TA-54	-0.5 (0.5)	0.14 (0.07)	6.0 (0.8)
R-Site Road East	0.4 (0.5)	0.05 (0.05)	6.4 (0.8)
Potrillo Drive	2.4 (0.6)	0.25 (0.09)	5.2 (0.8)
S-Site	0.7 (0.5)	0.12 (0.06)	5.8 (0.8)
Near DT-9	-0.2 (0.5)	0.79 (0.15)	5.1 (0.7)
Near TA-33	10 (1.0)	0.25 (0.07)	7.2 (0.9)
Summary			
No. of Analyses	10	10	10
Average	1.9	0.24	6.1
S	3.0	0.24	0.9
Minimum	-0.5 (0.5)	-0.01 (0.08)	4.7 (0.7)
Maximum	10 (1.0)	0.79 (0.15)	7.5 (0.9)
Sediments: Effluents			
Release Areas			
Pueblo Canyon			
Acid Weir	---	0.18 (0.10)	0.8 (0.6)
Pueblo 1	---	0.20 (0.10)	-2.2 (0.6)
Pueblo 2	---	-0.02 (0.06)	-0.8 (0.6)
Hamilton Bend Spring	---	0.27 (0.09)	-0.3 (0.6)
Pueblo 3	---	0.02 (0.07)	-1.3 (0.6)
Pueblo at SR-4	---	-0.01 (0.09)	-3.4 (0.7)

Table G-41 (cont)

Location	^{3}H (10^{-6} µCi/mL)	^{137}Cs (pCi/g)	Gross Gamma (counts/min/g)
Summary			
No. of Analyses	---	6	6
Average	---	0.11	-1.2
S	---	0.12	1.5
Minimum	---	-0.02 (0.06)	-3.4 (0.7)
Maximum	---	0.27 (0.09)	0.8 (0.6)
Los Alamos Canyon			
DP Canyon at DPS-1	---	7.2 (1.1)	5.4 (0.8)
DP Canyon at DPS-4	---	10.7 (1.6)	---
Los Alamos at Bridge	---	0.30 (0.10)	-3.9 (0.7)
Los Alamos at LAO-1	---	1.1 (0.19)	1.1 (0.6)
Los Alamos at GS-1	---	0.20 (0.09)	3.6 (0.7)
Los Alamos at LAO-3	---	0.20 (0.07)	-0.9 (0.6)
Los Alamos at LAO-4.5	---	0.62 (0.14)	0.9 (0.6)
Los Alamos at SR-4	---	1.8 (0.28)	3.5 (0.7)
Los Alamos at Totavi	---	0.85 (0.16)	3.4 (0.7)
Los Alamos at LA-2	---	0.31 (0.09)	3.6 (0.7)
Los Alamos at Otowi	---	0.30 (0.10)	0.8 (0.6)
Summary			
No. of Analyses	---	11	10
Average	---	2.1	1.8
S	---	3.5	2.7
Minimum	---	0.20 (0.09)	-3.9 (0.7)
Maximum	---	10.7 (1.6)	5.4 (0.8)

Table G-41 (cont)

Location	^{3}H (10^{-6} µCi/mL)	^{137}Cs (pCi/g)	Gross Gamma (counts/min/g)
Mortandad Canyon			
Mortandad at CMR	---	0.08 (0.06)	-1.4 (0.6)
Mortandad West of GS-1	---	0.11 (0.09)	-2.1 (0.6)
Mortandad at GS-1	---	-0.06 (0.06)	0.2 (0.6)
Mortandad at MCO-5	---	38 (5.7)	54 (5.0)
Mortandad at MCO-7	---	16 (2.4)	17 (2.0)
Mortandad at MCO-9	---	0.28 (0.10)	4.9 (0.8)
Mortandad at MCO-13	---	0.56 (0.13)	--
Summary			
No. of Analyses	---	7	16
Average	---	7.85	12
S	---	14.5	22
Minimum	---	-0.06 (0.06)	-2.1 (0.6)
Maximum	---	38 (5.7)	54 (5.0)
Limits of Detection	0.7	0.1	0.1

[a]Samples collected in April and May; counting uncertainty in parentheses.

Table G-42. Uranium and Transuranic Radiochemical Analyses of On-site Soils and Sediments[a]

Location	Total U (µg/g)	^{238}Pu (pCi/g)	$^{239,240}Pu$ (pCi/g)	^{241}Am (pCi/g)
On-site Soils				
TA-21	3.8 (0.4)	0.005 (0.004)	0.002 (0.002)	---
East of TA-53	4.6 (0.5)	0.000 (0.002)	0.012 (0.001)	--
TA-50	4.2 (0.5)	0.002 (0.001)	0.038 (0.003)	--
Two-Mile Mesa	2.9 (0.3)	0.002 (0.002)	0.020 (0.005)	--
East of TA-54	3.4 (0.3)	0.002 (0.002)	0.008 (0.004)	--
R-Site Road East	3.9 (0.4)	0.003 (0.001)	0.002 (0.002)	--
Potrillo Drive	3.9 (0.4)	0.000 (0.001)	0.000 (0.001)	--
S-Site	4.1 (0.4)	0.001 (0.002)	0.000 (0.001)	--
Near DT-9	3.1 (0.4)	0.000 (0.001)	0.016 (0.003)	--
Near TA-33	3.6 (0.4)	0.001 (0.001)	0.009 (0.002)	--
Summary				
No. of Analyses	10	10	10	--
Average	3.7	0.002	0.011	--
S	0.5	0.002	0.012	--
Minimum	2.9 (0.3)	0.000 (0.002)	0.000 (0.001)	--
Maximum	4.6 (0.5)	0.005 (0.004)	0.038 (0.003)	--
Sediments: Effluent Release Area				
Pueblo Canyon				
Acid Weir	3.2 (0.3)	0.001 (0.002)	0.004 (0.002)	1.28 (0.251)
Pueblo 1	2.4 (0.2)	-0.036 (0.018)	0.009 (0.027)	-1.83 (0.330)
Pueblo 2	2.9 (0.3)	0.026 (0.014)	0.612 (0.062)	2.51 (0.401)
Hamilton Bend Spring	3.4 (0.3)	0.001 (0.008)	0.167 (0.010)	2.29 (0.373)
Pueblo 3	3.2 (0.3)	0.000 (0.001)	0.004 (0.002)	1.31 (0.254)
Pueblo at SR-4	2.7 (0.3)	0.002 (0.001)	0.399 (0.021)	2.37 (0.382)

Table G-42 (cont)

Location	Total U (µg/g)	^{238}Pu (pCi/g)	$^{239,240}Pu$ (pCi/g)	^{241}Am (pCi/g)
Summary				
No. of Analyses	6	6	6	6
Average	2.9	-0.001	0.199	1.93
S	0.4	0.020	0.254	0.54
Minimum	2.4 (0.2)	-0.036 (0.018)	0.004 (0.002)	1.28 (0.251)
Maximum	3.4 (0.3)	0.026 (0.014)	0.612 (0.062)	2.51 (0.401)
Sediments: Effluent Release Area				
Los Alamos Canyon				
DP Canyon at DPS-1	2.5 (0.3)	0.067 (0.019)	0.139 (0.026)	2.88 (0.457)
DP Canyon at DPS-4	5.0 (0.5)	0.196 (0.012)	0.609 (0.029)	--
Los Alamos at Bridge	2.8 (0.3)	-0.001 (0.001)	0.002 (0.011)	-1.27 (0.223)
Los Alamos at LAO-1	3.4 (0.3)	0.021 (0.004)	0.239 (0.014)	1.65 (0.301)
Los Alamos at GS-1	4.4 (0.4)	0.002 (0.001)	0.516 (0.026)	1.38 (0.291)
Los Alamos at LAO-3	3.0 (0.3)	0.005 (0.002)	0.183 (0.011)	1.37 (0.260)
Los Alamos at LAO-4.5	3.2 (0.3)	0.008 (0.002)	0.267 (0.015)	-1.48 (0.278)
Los Alamos at SR-4	4.2 (0.4)	0.029 (0.004)	0.414 (0.023)	1.24 (0.246)
Los Alamos at Totavi	4.4 (0.4)	0.062 (0.006)	0.493 (0.025)	-2.71 (0.442)
Los Alamos at LA-2	4.3 (0.4)	0.006 (0.002)	0.615 (0.030)	2.43 (0.390)
Los Alamos at Otowi	3.6 (0.4)	0.006 (0.002)	0.131 (0.010)	-2.43 (0.391)
Summary				
No. of Analyses	11	11	11	10
Average	3.7	0.036	0.328	0.306
S	0.8	0.058	0.211	2.06
Minimum	2.5 (0.3)	-0.001 (0.001)	0.002 (0.011)	-2.43 (0.391)
Maximum	5.0 (0.5)	0.196 (0.012)	0.615 (0.030)	2.88 (0.457)

Table G-42 (cont)

Location	Total U (μg/g)	^{238}Pu (pCi/g)	$^{239,240}Pu$ (pCi/g)	^{241}Am (pCi/g)
Sediments: Effluent Release Area, Mortandad Canyon				
Mortandad at CMR	1.8 (0.2)	0.021 (0.003)	0.006 (0.002)	1.16 (0.225)
Mortandad West of GS-1	1.5 (0.2)	0.008 (0.017)	0.000 (0.001)	1.39 (0.290)
Mortandad at GS-1	2.3 (0.2)	-0.028 (0.013)	-0.005 (0.012)	3.99 (0.613)
Mortandad at MCO-5	2.9 (0.3)	7.59 (0.520)	30.7 (1.90)	24.6 (3.71)
Mortandad at MCO-7	1.7 (0.2)	1.52 (0.082)	6.02 (0.246)	4.22 (0.649)
Mortandad at MCO-9	4.8 (0.5)	-0.035 (0.013)	0.005 (0.011)	1.50 (0.304)
Mortandad at MCO-13	2.4 (0.2)	0.002 (0.001)	0.023 (0.003)	--
Summary				
No. of Analyses	7	7	7	6
Average	2.5	1.30	5.25	6.14
S	1.1	2.83	11.4	9.14
Minimum	1.5 (0.2)	-0.035 (0.013)	-0.005 (0.012)	1.16 (0.225)
Maximum	4.8 (0.5)	7.59 (0.520)	30.7 (1.90)	24.6 (3.71)
Limits of Detection	1	0.003	0.002	0.001

---

[a]Samples collected in April and May; counting uncertainty in parentheses.

Table G-43. Inorganic Chemical Parameters in Solution Extracted from Sediments Downgradient from Areas G and L, TA-54

Parameters[b]	Maximum EP Toxic Concentration[c]	Limits of Detection	Station Numbers[a]								
			1	2	3	4	5	6	7	8	9
Arsenic	5.0	0.05	BLD	BLD	BLD	BLD	BLD	BLD	BLD	BLD	BLD
Barium	100	0.5	BLD	BLD	BLD	BLD	BLD	BLD	BLD	BLD	BLD
Cadmium	1.0	0.01	BLD	BLD	BLD	BLD	BLD	BLD	BLD	BLD	BLD
Chromium	5.0	0.05	BLD	BLD	BLD	BLD	BLD	BLD	BLD	BLD	BLD
Lead	5.0	0.05	BLD	BLD	BLD	BLD	BLD	BLD	BLD	BLD	BLD
Mercury	2.0	0.001	BLD	BLD	BLD	BLD	BLD	BLD	BLD	BLD	BLD
Selenium	1.0	0.01	BLD	BLD	BLD	BLD	BLD	BLD	BLD	BLD	BLD
Silver	5.0	0.05	BLD	BLD	BLD	BLD	BLD	BLD	BLD	BLD	BLD
Nickel	--	0.01	BLD	BLD	BLD	BLD	BLD	BLD	BLD	BLD	BLD
Beryllium[d]	--	0.005	BLD	BLD	BLD	BLD	BLD	BLD	BLD	BLD	BLD
Sulfate	--	0.2	BLD	BLD	BLD	BLD	BLD	BLD	BLD	BLD	BLD
Nitrate	--	0.2	0.3	BLD	0.7	0.2	BLD	0.3	BLD	BLD	BLD
Cyanide	--	0.01	BLD	BLD	BLD	BLD	BLD	BLD	BLD	BLD	BLD
pH[e]	--	--	8.0	7.4	7.5	7.3	7.2	7.0	7.9	7.2	7.0

---

[a]Samples collected in September; station number location in Figure 20.
[b]Concentrations in mg/L except as noted; BLD = Below Detection Limit.
[c]New Mexico Hazardous Waste Management Regulations (HWMR) 201 B.5.; Extraction procedure.
[d]Units are μg/g.
[e]Standard units.

Table G-44. Radionuclides in Local and Regional Produce

	^{3}H (pCi/mL)	^{90}Sr (10^{-3} pCi/dry g)	^{137}Cs (10^{-3} pCi/dry g)	U (ng/dry g)	^{238}Pu (10^{-5} pCi/dry g)	$^{239,240}Pu$ (10^{-5} pCi/dry g)
Cochiti/Santo Domingo						
N	7	7	7	7	7	7
Mean	0.8	4.6	96	4.1	0.7	1.8
Std. Dev.	0.4	5.4	52	3.5	1.9	3.6
Minimum	0.0 (0.4)	0.6 (0.6)	-99 (130)	0.8 (0.8)	-2.8 (5.0)	-1.7 (1.7)
Maximum	1.2 (0.4)	12.6 (2.4)	180 (130)	8.0 (0.8)	3.2 (5.5)	8.7 (5.5)
Espanola						
N	7	7	7	7	7	7
Mean	1.1	6.9	45	6.3	3.5	7.7
Std. Dev.	0.8	6.0	98	7.3	4.1	4.8
Minimum	-0.3 (0.4)	0.5 (1.5)	36 (65)	0.5 (0.05)	0.0 (6.7)	0.0 (1.9)
Maximum	1.5 (0.4)	14.2 (1.8)	180 (120)	21 (2.1)	10.7 (8.0)	15 (8.5)
San Ildefonso						
N	2	2	2	2	2	2
Mean	1.0	0.6	24	0.5	0.2	0.7
Std. Dev.	0.5	0.4	52	0.1	1.4	2.2
Minimum	0.7 (0.4)	0.9 (0.6)	-13 (22)	0.5 (0.05)	-0.8 (0.8)	-0.8 (0.8)
Maximum	1.4 (0.4)	0.3 (0.5)	61 (32)	0.6 (0.06)	1.2 (1.2)	2.3 (1.2)
Los Alamos/White Rock						
N	8	8	8	8	8	8
Mean	2.3	13	45	4.4	0.5	13
Std. Dev.	0.7	12	41	4.6	1.3	29
Minimum	1.4 (0.4)	1.8 (1.2)	-18 (46)	1.0 (0.1)	-1.4 (1.4)	-15 (15)
Maximum	3.4 (0.5)	33.2 (1.6)	100 (71)	13 (1.3)	2.5 (3.3)	78 (13)

Table G-44 (cont)

	^{3}H (pCi/mL)	^{90}Sr (10^{-3} pCi/dry g)	^{137}Cs (10^{-3} pCi/dry g)	U (ng/dry g)	^{238}Pu (10^{-5} pCi/dry g)	$^{239,240}Pu$ (10^{-5} pCi/dry g)
On-site						
N	17	17	17	17	17	17
Mean	24	20	54	19	20	15
Std. Dev.	50	16	60	26	42	32
Minimum	1.0 (0.4)	2.5 (1.4)	-30 (81)	1.0 (0.1)	-13 (36)	-18 (33)
Maximum	200 (20)	51.8 (1.2)	240 (100)	97 (9.7)	170 (21)	120 (16)
Minimum Detectable Limit	0.7	0.5 (1.5)	100	2	20	10

[a]Counting uncertainties within parentheses.

Table G-45. Radionuclides in Fish

	^{90}Sr (10^{-3} pCi/dry g)	^{137}Cs (10^{-3} pCi/dry g)	U (ng/dry g)	^{238}Pu (10^{-5} pCi/dry g)	^{239}Pu (10^{-5} pCi/dry g)
CATFISH					
Abiquiu					
N	10	10	10	5	5
Mean	42	130	5.2	3	3
Std. Dev.	36	90	2.0	4	3
Minimum	14 (2)[a]	-35 (78)	1.4 (0.1)	0 (4)	0 (6)
Maximum	140 (8)	290 (99)	9.3 (0.9)	10 (10)	7 (4)
Cochiti					
N	10	10	10	5	5
Mean	52	100	11.5	5	1
Std. Dev.	72	120	5.0	8	6
Minimum	12 (2)	-140 (100)	6.2 (0.6)	-5 (5)	-5 (4)
Maximum	240 (26)	270 (100)	19 (1.9)	14 (1)	8 (6)
CRAPPIE					
Abiquiu					
N	10	10	10	5	5
Mean	190	60	1.4	-3	6
Std. Dev.	150	130	0.42	8	1
Minimum	26 (2)	-210 (120)	0.45 (0.1)	-14 (11)	5 (8)
Maximum	500 (25)	240 (170)	1.9 (0.2)	5 (6)	8 (8)

Table G-45 (cont)

	^{90}Sr (10^{-3} pCi/dry g)	^{137}Cs (10^{-3} pCi/dry g)	U (ng/dry g)	^{238}Pu (10^{-5} pCi/dry g)	^{239}Pu (10^{-5} pCi/dry g)
Cochiti					
N	10	10	10	5	5
Mean	53	120	2.4	5	5
Std. Dev.	42	93	0.58	10	6
Minimum	15 (1)	-70 (120)	1.2 (0.1)	-8 (7)	-3 (3)
Maximum	120 (13)	245 (130)	2.6 (0.3)	17 (10)	12 (5)
Minimum Detectable Limit	--	10	3	30	20

[a]Counting uncertainties in parentheses.

Table G-46. Locations of Beehives

Stations	N-S Coordinate	E-W Coordinate
Regional Stations (28-44 km)--Uncontrolled Area		
1. Chimayo	--	--
13. San Pedro	--	--
Perimeter Stations (0-4 km)--Uncontrolled Areas		
2. Northern Los Alamos County	N180	W020
3. Pajarito Acres	S210	E380
On-site Stations--Controlled Areas		
4. TA-21 (DP Canyon)	N095	E180
5. TA-50 (Upper Mortandad Canyon)	N040	E095
6. TA-53 (LAMPF)	N050	E220
7. Lower Mortandad Canyon	N020	E185
8. TA-8 (Anchor Site W)	S020	W065
9. TA-33 (HP-Site)	S260	E265
10. TA-54 (Area G)	N050	E220
11. TA-9 (Anchor Site E)	S005	W040
12. TA-15 (R-Site)	S020	E065
14. Frijoles Mesa	S160	E105
15. TA-16 (S-Site)	S055	W080

Table G-47. Selected Radionuclides in Local and Regional Honey[a]

	Chimayo	San Pedro	Pajarito Acres	Lower Mortandad	TA-8	TA-9	TA-15	TA-21	TA-33	TA-35	TA-53
^{3}H (pCi/L)	300 (400)[b]	1400 (400)	2300 (400)	8400 (1000)	400 (400)	4500 (400)	4300 (600)	7500 (900)	33 000 (3000)	8400 (1000)	120 (10)
^{7}Be (pCi/L)	1430 (1190)	-550 (1330)	-140 (568)	41 (1000)	1830 (1270)	130 (461)	1920 (996)	1130 (564)	1710 (1250)	-422 (1210)	1040 (1110)
^{57}Co (pCi/L)	69 (64)	65 (60)	217 (70)	101 (48)	13 (69)	69 (47)	107 (50)	160 (58)	60 (71)	16 (79)	92 (49)
^{137}Cs (pCi/L)	488 (94)	509 (102)	4 (40)	88 (51)	24 (52)	61 (45)	5 (36)	24 (43)	-52 (52)	73 (56)	62 (48)
^{54}Mn (pCi/L)	76 (56)	72 (53)	99 (42)	93 (47)	54 (52)	73 (41)	77 (41)	53 (40)	118 (56)	52 (51)	3 (38)
^{22}Na (pCi/L)	62 (55)	-32 (58)	43 (46)	40 (43)	20 (57)	609 (111)	105 (47)	82 (49)	481 (106)	70 (64)	30 (49)
^{83}Rb (pCi/L)	330 (215)	216 (197)	48 (139)	145 (146)	55 (187)	36 (132)	52 (180)	-50 (115)	145 (194)	62 (192)	138 (207)

[a]Density of honey was about 1860 g/L; data from 1986.
[b]Counting uncertainty in parentheses.

Table G-48. Selected Radionuclides in Local and Regional Bees[a]

	Chimayo	San Pedro	Pajarito Acres	Lower Mortandad	TA-8	TA-9	TA-15	TA-33	TA-35	TA-53
^{3}H (pCi/L)	2400 (500)[b]	5000 (700)	4600 (600)	14 000 (2000)	7700 (900)	12 000 (1000)	5300 (700)	8700 (1000)	21 000 (2000)	6100 (800)
^{7}Be (pCi/g)	1.7 (1.1)	4.1 (2.3)	0.0 (2.1)	0.9 (2.2)	6.6 (2.4)	5.4 (2.4)	2.6 (1.3)	1.2 (1.3)	1.2 (1.3)	1.6 (1.1)
^{57}Co (pCi/g)	0.44 (0.13)	0.14 (0.094)	0.30 (0.12)	0.26 (0.14)	0.18 (0.15)	0.26 (0.11)	0.27 (0.13)	0.24 (0.11)	0.31 (0.12)	0.16 (0.11)
^{137}Cs (pCi/g)	0.020 (0.069)	0.009 (0.072)	-0.041 (0.060)	0.022 (0.11)	-0.066 (0.10)	0.14 (0.063)	0.002 (0.079)	0.11 (0.074)	0.079 (0.071)	-0.041 (0.070)
^{54}Mn (pCi/g)	0.20 (0.096)	0.024 (0.088)	0.18 (0.11)	0.25 (0.11)	0.006 (0.098)	0.17 (0.099)	0.14 (0.082)	0.086 (0.081)	0.084 (0.092)	0.21 (0.11)
^{22}Na (pCi/g)	-0.11 (0.086)	-0.042 (0.083)	0.082 (0.099)	1.2 (0.22)	0.008 (0.087)	0.077 (0.086)	0.079 (0.087)	--	0.11 (0.088)	0.22 (0.10)
^{83}Rb (pCi/g)	0.31 (0.27)	0.13 (0.28)	0.28 (0.32)	-0.25 (0.28)	0.31 (0.33)	0.24 (0.29)	-0.19 (0.23)	0.012 (0.23)	0.083 (0.17)	-0.086 (0.20)
Uranium (ng/g)[b]	63 (6.3)	200 (19)	57 (5.7)	62 (6.2)	57 (5.7)	73 (7.3)	88 (8.8)	160 (16)	75 (7.50)	89 (9.0)

[a]Data from 1986.
[b]Counting uncertainty in parentheses.

Table G-49. Hazardous Waste Management Facilities at Los Alamos National Laboratory

Technical Area	Facility Type	Interim Status or <90-Day Storage	Part B Permit Application
TA-54 Area L	Tank Treatment	Yes	Yes
	Container Storage	Yes	Yes
	Landfill[a]	No	No
TA-54 Area G	Landfill[a]	No	No
TA-50-1	Batch Treatment	Yes	Yes
	Container Storage	Yes	Yes
TA-50-37	Controlled Air Incinerator	Yes	Yes
	Container Storage	<90-day	Yes
TA-3-102	Container Storage	<90-day	No
TA-3-40	Container Storage	<90-day	No
TA-14	Thermal Treatment	Yes	Yes
TA-15	Thermal Treatment	Yes	Yes
TA-36	Thermal Treatment	Yes	Yes
TA-39	Thermal Treatment	Yes	Yes
TA-22-24	Container Storage	Yes	No[b]
TA-53-2	Container Storage	<90-day	No
TA-40-2	Container Storage	Yes	No[b]
TA-40 SDS	Thermal Treatment	Yes	No
TA-16	Thermal Treatment	Yes	Yes
TA-16 Area P	Landfill[a]	No	No
TA-46	Tank Storage	<90-day	No

---

[a]Interim status was terminated in November 1985. These landfills are in the process of being closed in accordance with New Mexico Hazardous Waste Regulations.
[b]To be closed under interim status.

Table G-50. 1987 RCRA Interactions Among the Laboratory, Environmental Protection Agency (EPA), and New Mexico's Environmental Improvement Division (EID)

January 30, 1987	EID affirms LANL's RCRA permit application is complete and that they are proceeding with the technical review.
March 5, 1987	Trial burn report for the TA-50 controlled air incinerator submitted to the EID.
July 14, 1987	EPA/EID hazardous waste inspection.
August 17, 1987	Submit revised Part A including mixed wastes. DOE dirrective.
September 9, 1987	EID denies LANL request to modify the Part A. Inadequate justification and no authority to regulate mixed waste.
October 16, 1987	Request from the EID for the post-closure care permit application for hazardous waste landfills. Due by 9/30/88.
October, 1987	Respond to EID Part A denial.
October 23, 1987	EPA National Survey of Hazardous Waste Treatment, Storage, Disposal and Recycling Facilities submitted.
November 12, 1987	Received Notice of Violation letter (November 10) as result of July 14, 1987 EPA/EID inspection.
November 20, 1987	EID informs LANL that no comments were received on the closure plans for TA-40-2, TA-3-102, and TA-22-24.
November 24, 1987	Letter for EID rescinding the November 10 NOV.
November 25, 1987	Submitted revised permit application (Parts A and B) to the EID.
December 8, 1987	Submitted post-closure care permit application to the EID. See 10/16/87 above.
December 22, 1987	Request to the EID for a ground water monitoring waiver for Area P.

Table G-51. Types of Discharges and Parameters Monitored at the Laboratory Under its NPDES Permit NM0028355

EPA ID #	Type of Discharge	Number Outfalls	Monitoring Required and Sample Frequency
01A	Power Plant	1	Total Suspended Solids, Free Available Chlorine, pH, Flow (monthly)
02A	Boiler Blowdown	1	pH, Total Suspended Solids, Flow Copper, Iron, Phosphorous, Sulfite, Total Chromium (weekly)
03A	Treated Cooling Water	35	Total Suspended Solids, Free Available Chlorine, Phosphorous, pH, Flow (weekly)
04A	Noncontact Cooling Water	28	pH, Flow (weekly)
050 051	Radioactive Waste Treatment Plants	2	Ammonia, Chemical Oxygen Demand, Total Suspended Solids, Cadmium, Chromium, Copper, Iron Lead, Mercury, Zinc, pH, Flow (weekly)
05A	High Explosive Discharge	18	Chemical Oxygen Demand, pH, Flow, Total Suspended Solids (weekly)
06A	Photo Wastes	12	Cyanide, Silver, pH, Flow (weekly)
128	Printed Circuit Board	1	pH, Chemical Oxygen Demand, Total Suspended Solids, Iron, Copper, Silver, Flow (weekly)
SS	Sanitary Wastes	10	Biochemical Oxygen Demand, Flow, pH, Total Suspended Solids, Fecal Coliform Bacteria, (variable frequency, from 3 per month to quarterly)

Table G-52. NPDES Permit Effluent Quality Monitoring of Sanitary Sewage Treatment Outfalls

Discharge Location	Permit Parameters	Number of Deviations	Range of Deviation
TA-3	BOD[a]	0	--
	TSS[b]	1	51.3
	Fecal Coliforms[c]	3	3500.0 to 227,200
	pH[d]	0	--
TA-8	BOD	0	--
	TSS (90)	0	--
	pH	0	--
TA-9	BOD	0	--
	TSS	0	--
	pH	0	--
TA-16	BOD	0	--
	TSS	1	165.5
	pH	0	--
TA-18	BOD	0	--
	TSS (90)	0	--
	pH	2	9.4 to 10.1
TA-21	BOD	0	--
	TSS	0	--
	pH	1	10.6
TA-35	BOD	0	--
	TSS (90)	0	--
	pH	0	--
TA-41	BOD	0	--
	TSS	0	--
	Fecal Coliforms	1	4800.0
	pH	0	--
TA-46	BOD	0	--
	TSS	0	--
	pH	1	5.7
TA-48	BOD	0	--
	TSS	0	--
	pH	0	--

Table G-52 (cont)

Discharge Location	Permit Parameters	Number of Deviations	Range of Deviation
TA-53	BOD	0	--
	TSS (90)	0	--
	pH	1	10.2

---

[a]Biochemical oxygen demand (BOD) permit limits are 30 mg/L (20-day average) and 45 mg/L (7-day average).
[b]Total suspended solids (TSS) permit limits are 30 mg/L (20-day average) and 45 mg/L or 90 mg/L (7-day average).
[c]Fecal coliform limits are 1000 organisms/100 mL (20-day average) and 2000 organisms/100 mL (7-day average).
[d]Range of permit pH limits is >6.0 and <9.0 standard units.

Table G-53. Limits Established by NPDES Permit NM0028355 for Industrial Outfall Discharges

Discharge Category	Parameter Limited	Daily Average	Daily Maximum	Units of Measurement
Power Plant	TSS	30.0	100.0	mg/L
	Free Cl	0.2	0.5	mg/L
	pH	6-9	6-9	standard units
Boiler Blowdown	TSS	30	100	mg/L
	Fe	10	40	mg/L
	Cu	1	1	mg/L
	P	20	40	mg/L
	SO_3	35	70	mg/L
	Cr	Report	Report	mg/L
	pH	6-9	6-9	standard units
Treated Cooling Water	TSS	30.0	100.0	mg/L
	Free Cl	0.2	0.5	mg/L
	P	5.0	5.0	mg/L
Noncontact Cooling Water	pH	6-9	6-9	standard units
Radioactive Waste Treatment Plants	COD[a]	18.8	37.5	lb/day
	COD[b]	94.0	156.0	lb/day
	TSS[a]	3.8	12.5	lb/day
	TSS[b]	18.8	62.6	lb/day
	Cd[a]	0.01	0.06	lb/day
	Cd[b]	0.06	0.3	lb/day
	Cr[a]	0.02	0.08	lb/day
	Cr[b]	0.19	0.38	lb/day
	Cu[a]	0.13	0.13	lb/day
	Cu[b]	0.63	0.63	lb/day
	Fe[a]	0.13	0.13	lb/day
	Fe[b]	1.0	2.0	lb/day
	Pb[a]	0.01	0.03	lb/day
	Pb[b]	0.06	0.15	lb/day
	Hg[a]	0.007	0.02	lb/day
	Hg[b]	0.003	0.09	lb/day
	Zn[a]	0.13	0.37	lb/day
	Zn[b]	0.62	1.83	lb/day
	pH[a]	6-9	6-9	standard units
	pH[b]	6-9	6-9	standard units
High Explosives	COD	150.0	250.0	mg/L
	TSS	30.0	45.0	mg/L
	pH	6-9	6-9	standard units

Table G-53 (cont)

Discharge Category	Parameter Limited	Daily Average	Daily Maximum	Units of Measurement
Photo Wastes	CN	0.2	0.2	mg/L
	Ag	0.5	1.0	mg/L
	pH	6-9	6-9	standard units
Printed Circuit Board	COD	1.9,	3.8	lb/dy
	TSS	1.25	2.5	lb/dy
	Fe	0.05	0.1	lb/dy
	Cu	0.05	0.1	lb/dy
	Ag	Report	Report	lb/dy
	pH	6-9	6-9	standard units

---

[a]Limitations for outfall 050 located at TA-21-257.
[b]Limitations for outfall 051 located at TA-50-1.

Table G-54. NPDES Permit Effluent Quality Monitoring of Industrial Outfalls[a]

Discharge Category	Number of Outfalls	Permit Parameter	Number of Deviations	Range of Deviations	Number of Outfalls With Deviations
Power Plant	1	TSS[b]	0	---	0
		Free Cl	1	2.0	1
		pH	0	---	0
Boiler Blowdown	1	pH	0	---	0
		TSS	0	---	0
		Cu	0	---	0
		Fe	0	---	0
		P	0	---	0
		SO_3	0	---	0
		Cr	0	---	0
Treated Cooling Water	35	TSS	0	---	0
		Free Cl	3	0.60 to 1.5	3
		P	0	---	0
		pH	3	9.2 to 9.3	2
Noncontact Cooling Water	28	pH	0	---	0
Radioactive Waste Treatment Plant	2	COD[c]	0	180.2 to 787.33	0
		TSS	0	---	0
		Cd	0	---	0
		Cr	0	---	0
		Cu	0	---	0
		Fe	0	---	0
		Pb	0	---	0
		Hg	0	---	0
		Zn	0	---	0
		pH	1	4.9	1
High Explosives	18	COD	2	360.0 to 410.0	2
		TSS	0	---	0
		pH	0	---	0

Table G-54 (cont)

Discharge Category	Number of Outfalls	Permit Parameter	Number of Deviations	Range of Deviations	Number of Outfalls With Deviations
Photo Wastes	12	CN	0	---	0
		Ag	0	---	0
		TSS	0	---	0
		pH	1	9.9	1
Printed Circuit Board	1	pH	1	9.4	1
		COD	0	---	0
		Ag			
		Fe	0	---	0
		Cu	0	---	0
		TSS	0	---	0

---

[a]Limits set by the NPDES permit are presented in Table G-40.
[b]Total suspended solids.
[c]Chemical oxygen demand.

Table G-55. Schedule and Status of Upgrading the Laboratory's Waste Water Outfalls

Outfalls	Date	Status
01A		
Final design complete	August 1986	Completed
Advertisement of construction contract	September 1986	Completed
Award of construction contract	October 1986	Completed
Construction completion	December 1986	Completed
In compliance with final limits	January 1987	Completed
03A		
Final design complete	August 1986	Completed
Advertisement of construction contract	September 1986	Completed
Award of construction contract	October 1986	Completed
Construction completion	December 1986	Completed
In compliance with final limits	January 1987	Completed
05A		
Final design complete	September 1986	Completed
Advertisement of construction contract	October	Completed
Award of construction contract	November 1986	Completed
Construction completion	May 1987	Completed
In compliance with final limits	June 1987	Completed
01S		
Final design complete	Completed	Completed
Advertisement of construction contract	Completed	Completed
Award of construction contract	July 1986	Completed
Construction completion	May 1987	Completed
In compliance with final limits	August 1987	Completed
04S		
Final design complete	January 1987	Completed
Advertisement of construction contract	February 1987	Completed
Award of construction contract	March 1987	Completed
Construction complete	December 1987	Completed
In compliance with final limits	January 1988	Completed
05S		
Final design complete	Completed	Completed
Advertisement of construction contract	Completed	Completed
Award of construction contract	July 1986	Completed
Construction completion	January 1988	Completed
In compliance with final limits	May 1988	--

Table G-55 (cont)

Outfalls	Date	Status
06S		
Final design complete	Completed	Completed
Advertisement of construction contract	July 1986	Completed
Award of construction contract	August 1986	Completed
Construction completion	August 1987	Completed
In compliance with final limits	September 1987	Completed
10S		
Final design complete	Completed	Completed
Advertisement of construction contract	Completed	Completed
Award of construction contract	Completed	Completed
Construction completion	Completed	Completed
In compliance with final limits	September 1986	Completed
11S		
Final design complete	Completed	Completed
Advertisement of construction contract	Completed	Completed
Award of construction contract	July 1986	Completed
Construction complete	November 1986	Completed
In compliance with final limits	January 1987	Completed

Table G-56. Federal Facility Compliance Agreement Interim Compliance Limits and Compliance Schedule

Effluent Characteristic	Discharge Limitation Daily Avg. (lb/day)	Daily Avg. (mg/L)	7-Day Avg. (mg/L)
Industrial Outfalls			
Outfall 01A (Power Plant)			
Flow[a]	N/A	N/A	N/A
Total suspended solids	N/A	30	100
Free available chlorine	N/A	1.0	5.0
Outfall 03A (Treated Cooling Water)			
Flow	N/A	N/A	N/A
Total suspended solids	N/A	30	100
Free available chlorine	N/A	1.0	5.0
Total phosphorous	N/A	5	5
Outfall 05A (High Explosive)			
Flow	N/A	N/A	N/A
Chemical oxygen demand	N/A	1000	2000
Total suspended solids	N/A	60	90
Sanitary Waste Water Outfalls			
Outfall 01S (Located at TA-3)			
Flow	N/A	N/A	N/A
Biochemical oxygen demand	225.2	70	105
Total suspended solids	225.2	55	105
Fecal coliform	N/A	10,000	200,000
Outfall 04S (Located at TA-18)			
Flow	N/A	N/A	N/A
Biochemical oxygen demand	10	60	95
Total suspended solids	10	70	125
Outfall 05S (Located at TA-21)			
Flow	N/A	N/A	N/A
Biochemical oxygen demand	6.8	60	95
Total suspended solids	7.3	60	100

Table G-56 (cont)

Effluent Characteristic	Discharge Limitation		
	Daily Avg. (lb/day)	Daily Avg. (mg/L)	7-Day Avg. (mg/L)
Outfall 06S (Located at TA-41)			
Flow	N/A	N/A	N/A
Biochemical oxygen demand	11.4	55	60
Total suspended solids	6.2	30	45
Fecal coliform bacteria	N/A	20,000	100,000
Outfall 10S (Located at TA-35)			
Flow	N/A	N/A	N/A
Biochemical oxygen demand	23.2	115	185
Total suspended solids	26.1	130	170
Outfall 11S (Located at TA-8)			
Flow	N/A	N/A	N/A
Biochemical oxygen demand	N/A	60	95
Total suspended solids	N/A	70	125

---

[a]Flow must be monitored and reported in millions of gallons per day.
NOTE: The pH shall not be less than 6.0 nor greater than 9.0.

Table G-57. Environmental Documentation Approved by the Laboratory Environmental Review Committee in 1987

Action Description Memorandums

Laboratory-Wide

- Core Hole, Valles Caldera (VC-2B), Sulphur Springs, Document No. 87-15
- Dwarf Mistletoe Control with Ethrel, A Growth Regulator, Document No. 87-10
- Live Firing Range Extension, Sandia Canyon, Document 87-9
- Seismic Trench, Cabra Canyon, Document No. 87-4

TA-3

- Beryllium Facility, TA-3-141, Document No. 87-8
- Lethality Test System, TA-3-253, -322, 218, Document No. 87-2
- Remote Handled Transuranic Waste Close-out, Document No. 87-16

TA-15

- Dual Axis Radiography Hydrotest Facility, Document No. 87-14

TA-16

- New Tritium Processing Facility, Document No. 87-6

TA-35

- Confinement Physics Research Facility, TA-35/52, Document No. 87-5
- Confinement Physics Research Facility, Revised TA-35/52, Document No. 87-5 rev
- Plutonium Gas Gun Facility, Document No. 87-7

TA-50

- Combustible Chemical and Radioactive Waste Storage/Staging Facility, TA 50-37, Document No. 87-11

Table G-57 (cont)

TA-52

- High density Z-Pinch (ZEBRA), Document No. 87-19

TA-53

- Neutron Time of Flight Program, Document No. 87-3
- Neutron Time of Flight Program, Revised, Document No. 87-3 rev

TA-54

- Polychlorinated Biphenyl (PCB) Storage Facility, LJ 8002 Document No. 87-1

TA-55

- Accelerated Residue Recovery Project, Document No. 87-20
- Special Nuclear Materials (SNM) Research and Development Laboratory, Document No. 87-13

TA-59

- Organic Chemistry Standards Preparation Facility, TA-59-1, Rm B4, Document No. 87-17

Environmental Assessments

Transuranic (TRU) Waste Inventory Work-Off Plan

Other

An additional document, a CEARP/CERCLA Remedial Investigation Plan, was processed as the functional equivalent to the ADM for compliance with the requirements of NEPA:

- Comprehensive Environmental Assessment and Response Program, White Rock Y Interchange Remedial Investigation Plan, Synopsis

Table G-58. Radiochemical Analyses of Water from Municipal Supply and Distribution System[a]

Stations	^{3}H (10^{-6} µCi/mL)	^{137}Cs (10^{-9} µCi/mL)	Total U (µg/L)	^{238}Pu (10^{-9} µCi/mL)	$^{249,240}Pu$ (10^{-9} µCi/mL)
Los Alamos Field					
Well LA-1B	-1.4 (0.7)	-31 (49)	6.0 (1.0)	0.011 (0.009)	-0.003 (0.009)
Well LA-2	-1.4 (0.7)	42 (48)	6.0 (1.0)	-0.007 (0.005)	0.000 (0.010)
Well LA-3	-0.6 (0.7)	42 (43)	2.0 (1.0)	0.000 (0.010)	0.024 (0.016)
Well LA-4	--	--	--	--	--
Well LA-5	-1.1 (0.7)	33 (42)	5.0 (1.0)	0.000 (0.010)	0.000 (0.010)
Guaje Field					
Well G-1	-1.0 (0.7)	40 (44)	1.0 (1.0)	-0.013 (0.010)	0.044 (0.010)
Well G-1A	-0.9 (0.7)	-33 (44)	1.0 (1.0)	0.004 (0.010)	-0.004 (0.007)
Well G-2	-0.7 (0.7)	-16 (36)	1.0 (1.0)	-0.039 (0.012)	-0.008 (0.010)
Well G-3	--	--	--	--	--
Well G-4	-0.6 (0.7)	9 (44)	1.0 (1.0)	-0.024 (0.011)	0.000 (0.010)
Well G-5	-0.9 (0.7)	-7 (36)	1.0 (1.0)	0.000 (0.010)	0.004 (0.010)
Well G-6	-1.4 (0.7)	19 (43)	1.0 (1.0)	-0.018 (0.013)	-0.004 (0.008)
Pajarito Field					
Well PM-1	0.0 (0.7)	-6 (37)	2.0 (1.0)	-0.004 (0.007)	-0.021 (0.011)
Well PM-2	0.0 (0.7)	3 (44)	0.0 (1.0)	-0.011 (0.013)	-0.011 (0.008)
Well PM-3	-0.8 (0.7)	42 (42)	1.0 (1.0)	-0.013 (0.010)	-0.004 (0.008)
Well PM-4	0.3 (0.7)	-77 (44)	0.0 (1.0)	0.000 (0.010)	0.012 (0.012)
Well PM-5	0.2 (0.7)	-22 (38)	0.0 (1.0)	-0.012 (0.009)	0.000 (0.010)

Table G-58 (cont)

Stations	^{3}H (10^{-6} µCi/mL)	^{137}Cs (10^{-9} µCi/mL)	Total U (µg/L)	^{238}Pu (10^{-9} µCi/mL)	$^{249,240}Pu$ (10^{-9} µCi/mL)
Gallery (Water Canyon)	-1.2 (0.7)	10 (50)	1.0 (1.0)	-0.005 (0.008)	-0.014 (0.011)
Supply Summary					
No. of Analyses	16	16	16	16	16
Average	-0.7	5.7	2	-0.002	0.001
S	0.6	33.5	2	0.015	0.015
Minimum	-1.4 (0.7)	-77 (44)	0.0 (1.0)	-0.039 (0.012)	-0.021 (0.011)
Maximum	0.3 (0.7)	42 (48)	6.0 (1.0)	0.011 (0.009)	0.044 (0.007)
Distribution					
Fire Station 1	0.5 (0.7)	-5 (42)	1.0 (1.0)	0.006 (0.016)	0.037 (0.017)
Fire Station 1	-0.3 (0.3)	71 (56)	1.0 (1.0)	-0.012 (0.009)	-0.006 (0.006)
Fire Station 2	-0.1 (0.7)	-32 (43)	2.0 (1.0)	0.000 (0.010)	0.005 (0.009)
Fire Station 2	-0.4 (0.3)	2 (58)	1.0 (1.0)	0.000 (0.010)	0.000 (0.010)
Fire Station 3	0.9 (0.7)	18 (44)	1.0 (1.0)	0.000 (0.010)	-0.008 (0.008)
Fire Station 3	0.5 (0.3)	17 (61)	1.0 (1.0)	0.004 (0.012)	0.019 (0.013)
Fire Station 4	2.1 (0.7)	47 (44)	1.0 (1.0)	0.000 (0.010)	0.019 (0.010)
Fire Station 4	-0.2 (0.3)	62 (59)	1.0 (1.0)	0.009 (0.011)	0.000 (0.010)
Fire Station 5	-1.9 (0.7)	65 (45)	1.0 (1.0)	0.008 (0.018)	0.000 (0.010)
Fire Station 5	0.2 (0.3)	-48 (64)	1.0 (1.0)	0.012 (0.012)	0.000 (0.010)
Bandelier Nat. Mon.	-2.4 (0.7)	-24 (45)	1.0 (1.0)	0.000 (0.010)	0.025 (0.018)
Bandelier Nat. Mon.	0.2 (0.3)	-12 (61)	1.0 (1.0)	-0.004 (0.011)	0.004 (0.010)

Table G-58 (cont)

Stations	^{3}H (10^{-6} µCi/mL)	^{137}Cs (10^{-9} µCi/mL)	Total U (µg/L)	^{238}Pu (10^{-9} µCi/mL)	$^{249,240}Pu$ (10^{-9} µCi/mL)
Distribution Summary					
No. of Analyses	12	12	12	12	12
Average	−0.1	13	1	0.002	0.008
S	1.2	40	0	0.006	0.014
Minimum	−2.4 (0.7)	−48 (64)	1.0 (1.0)	−0.012 (0.009)	−0.008 (0.008)
Maximum	2.1 (0.7)	71 (56)	2.0 (1.0)	0.012 (0.012)	0.037 (0.017)
Fenton Hill (TA-57)	−0.9 (0.7)	113 (50)	1.0 (1.0)	0.000 (0.010)	0.004 (0.008)
Fenton Hill (TA-57)	0.1 (0.3)	−42 (60)	1.0 (1.0)	0.000 (0.010)	0.004 (0.004)
Standby Well (not part of Water Supply) Well LA-6	−1.6 (0.7)	50 (43)	4.0 (1.0)	0.000 (0.010)	0.012 (0.012)
USEPA Maximum Concentration[b]	20	200	1800[c]	15	15
Limits of Detection	0.7	40	1	0.009	0.03

---

[a]Well samples collected in February; distribution samples collected in February and September; counting uncertainty in parentheses.
[b]Reference (EPA 1976).
[c]Levels recommended by International Commission on Radiological Protection.

Table G-59. Gross Radioactivity in Water from Municipal Supply and Distribution Systems[a]

Stations	Gross Alpha (10^{-9} µCi/mL)	Gross Beta (10^{-9} µCi/mL)	Gross Gamma (Counts/min/L)
Los Alamos Field			
Well LA-1B	-6.0 (4.0)	7.2 (0.8)	-40 (100)
Well LA-2	-7.0 (2.0)	1.7 (0.4)	-160 (100)
Well LA-3	6.0 (2.0)	2.5 (0.5)	-300 (100)
Well LA-4	--	--	--
Well LA-5	-5.0 (2.0)	1.7 (0.4)	-400 (100)
Guaje Field			
Well G-1	-6.0 (2.0)	2.8 (0.5)	-300 (100)
Well G-1A	-5.0 (1.0)	1.8 (0.4)	-140 (100)
Well G-2	-8.0 (2.0)	3.1 (0.5)	-300 (100)
Well G-3	--	--	--
Well G-4	-7.0 (2.0)	1.2 (0.4)	-220 (100)
Well G-5	-6.0 (2.0)	3.0 (0.5)	-300 (100)
Well G-6	-6.0 (2.0)	2.9 (0.5)	-120 (100)
Pajarito Field			
Well PM-1	-8.0 (2.0)	4.3 (0.6)	-170 (100)
Well PM-2	-6.0 (2.0)	1.8 (0.4)	-140 (100)
Well PM-3	-9.0 (2.0)	3.2 (0.5)	-110 (100)
Well PM-4	-7.0 (2.0)	1.9 (0.4)	-140 (100)
Well PM-5	-6.0 (2.0)	2.3 (0.4)	-190 (100)

Table G-59 (cont)

Stations	Gross Alpha (10^{-9} µCi/mL)	Gross Beta (10^{-9} µCi/mL)	Gross Gamma (Counts/min/L)
Gallery (Water Canyon)	-6.0 (2.0)	2.2 (0.4)	70 (100)
Supply Summary			
No. of Analyses	16	16	16
Average	-6.5	2.7	-185
S	1.1	1.4	116
Minimum	-9.0 (2.0)	1.2 (0.4)	-400 (100)
Maximum	-5.0 (2.0)	3.2 (0.5)	-40 (100)
Distribution			
Fire Station 1	-7.0 (2.0)	1.7 (0.4)	-120 (100)
Fire Station 1	2.4 (0.9)	3.0 (0.5)	310 (80)
Fire Station 2	-7.0 (2.0)	42 (4.0)	-40 (100)
Fire Station 2	2.1 (1.0)	3.5 (0.5)	500 (90)
Fire Station 3	-7.0 (2.0)	8.3 (1.0)	90 (100)
Fire Station 3	2.0 (0.9)	4.7 (0.6)	330 (90)
Fire Station 4	-7.0 (2.0)	2.3 (0.4)	90 (100)
Fire Station 4	1.5 (0.9)	4.1 (0.6)	420 (90)
Fire Station 5	-6.0 (2.0)	2.5 (0.4)	-80 (100)
Fire Station 5	1.9 (0.9)	2.7 (0.5)	340 (90)
Bandelier Nat. Mon.	-7.0 (2.0)	1.7 (0.4)	60 (100)
Bandelier Nat. Mon.	2.0 (1.0)	5.3 (0.7)	270 (90)

Table G-59 (cont)

Stations	Gross Alpha (10^{-9} µCi/mL)	Gross Beta (10^{-9} µCi/mL)	Gross Gamma (Counts/min/L)
Distribution Summary			
No. of Analyses	12	12	12
Average	-2.4	6.8	180
S	4.6	11	207
Minimum	-0.7 (2.0)	1.7 (0.4)	-120 (100)
Maximum	2.4 (0.9)	42 (4.0)	500 (90)
Fenton Hill (TA-57)	-11 (3.0)	4.9 (0.6)	20 (100)
Fenton Hill (TA-57)	-0.2 (0.8)	6.1 (0.8)	350 (90)
Standby Well (not part of Water Supply) Well LA-6	-6.0 (2.0)	1.0 (0.4)	-150 (100)
USEPA Maximum Concentration Limits[b]	15	--	--
Limits of Detection	3	3	50

[a]Well samples collected in February; distribution samples collected in February and September; counting uncertainty in parentheses.

[b]The Environmental Protection Agency MCL for gross alpha is 15 x 10^{-9} µCi/mL; however, if gross alpha in the system exceeds 5 x 10^{-9} µCi/mL, isotopic analyses of radium content is required.

Table G-60. Primary Chemical Quality for Water Supply and Distribution Systems (mg/L)[a]

Stations	Ag	As	Ba	Cd	Cr
Supply					
Los Alamos Field					
Well 1B	<0.001	0.034	0.032	<0.0005	0.022
Well 2	<0.001	0.013	0.084	<0.0005	0.021
Well 3	<0.001	0.006	0.053	<0.0005	0.008
Well 4	--	--	--	--	--
Well 5	<0.001	0.017	0.075	<0.0005	0.007
Guaje Field					
Well G-1	<0.001	0.003	0.062	<0.0005	0.007
Well G-1A	<0.001	0.012	0.037	<0.0005	0.008
Well G-2	<0.001	0.044	0.064	<0.0005	0.013
Well G-3	--	--	--	--	--
Well G-4	<0.001	0.002	0.017	<0.0005	0.005
Well G-5	<0.001	0.002	0.013	<0.0005	0.004
Well G-6	<0.001	0.003	0.007	<0.0005	0.007
Pajarito Field					
Well PM-1	<0.001	0.001	0.075	<0.0005	0.006
Well PM-2	<0.001	0.001	0.028	<0.0005	0.008
Well PM-3	<0.001	0.002	0.047	<0.0005	0.008
Well PM-4	<0.001	<0.001	0.026	<0.0005	0.007
Well PM-5	<0.001	<0.001	0.027	<0.0005	0.007
Gallery (Water Canyon)	<0.001	<0.001	0.018	<0.0005	<0.004
Supply Summary					
No. of Analyses	16	16	16	16	16
Maximum	<0.001	0.044	0.084	<0.0005	0.022

Table G-60 (cont)

Stations	Ag	As	Ba	Cd	Cr
Distribution					
Fire Station 1	<0.001	0.002	0.025	<0.0005	0.008
Fire Station 2	<0.001	0.017	0.043	<0.0005	0.010
Fire Station 3	<0.001	0.001	0.051	<0.0005	0.008
Fire Station 4	<0.001	0.016	0.030	<0.0005	0.011
Fire Station 5	<0.001	0.013	0.030	<0.0005	0.007
Bandelier National Monument	<0.001	0.012	0.027	<0.0005	0.001
Distribution Summary					
No. of Analyses	6	6	6	6	6
Maximum	<0.001	0.017	0.051	<0.0005	0.011
Fenton Hill (TA-57)	<0.001	<0.001	0.107	<0.0005	<0.001
Standby Well (not part of Water Supply) Well LA-6	<0.001	0.142	0.072	<0.0005	0.024
EPA and NMEID Primary Maximum Concentration Levels [b]	0.05	0.05	1.0	0.01	0.05

Table G-60 (cont)

Stations	F	Hg	N	Pb	Se
Supply					
Los Alamos Field					
Well 1B	3.2	<0.0002	<1	0.008	<0.002
Well 2	2.2	<0.0002	<1	0.006	<0.002
Well 3	0.7	0.0003	<1	0.002	<0.002
Well 4	--	--	--	--	--
Well 5	0.9	<0.0002	<1	0.041	<0.002
Guaje Field					
Well G-1	0.4	<0.0002	<1	0.002	<0.002
Well G-1A	0.6	<0.0002	<1	0.008	<0.002
Well G-2	0.9	<0.0002	<1	0.011	<0.002
Well G-3	--	--	--	--	--
Well G-4	0.3	<0.0002	<1	0.005	<0.002
Well G-5	0.4	0.0003	<1	0.003	<0.002
Well G-6	0.3	<0.0002	<1	0.001	<0.002
Pajarito Field					
Well PM-1	0.3	0.0003	<1	0.004	<0.002
Well PM-2	0.3	0.0002	<1	0.034	<0.002
Well PM-3	0.4	0.0003	<1	0.012	<0.002
Well PM-4	0.3	0.0003	<1	0.020	<0.002
Well PM-5	0.3	0.0003	<1	0.092	<0.002
Gallery (Water Canyon)	0.2	0.0002	<1	<0.001	<0.002
Supply Summary					
No. of Analyses	16	16	16	16	16
Maximum	3.2	0.0003	<1	0.092	<0.002

Table G-60 (cont)

Stations	F	Hg	N	Pb	Se
Distribution					
Fire Station 1	0.3	<0.0002	<1	<0.001	<0.002
Fire Station 2	0.1	<0.0002	<1	0.031	<0.002
Fire Station 3	0.6	<0.0002	<1	<0.001	<0.002
Fire Station 4	0.6	<0.0002	<1	<0.001	<0.002
Fire Station 5	0.8	<0.0002	<1	0.004	<0.002
Bandelier National Monument	0.8	<0.0002	<1	0.003	<0.002
Distribution Summary					
No. of Analyses	6	6	6	6	6
Maximum	1.0	<0.0002	<1	0.031	<0.002
Fenton Hill (TA-57)	<0.2	<0.0002	<1	0.001	<0.002
Standby Well (not part of Water Supply) Well LA-6	--	0.0002	<1	0.007	<0.002
EPA and NMEID Primary Maximum Concentration Levels[b]	2.0	0.002	10	0.05	0.01

---

[a]Samples collected in February.
[b]Reference (EPA 1976).

Table G-61. Secondary Chemical Quality for Water Supply (mg/L)[a]

Stations	Cl	Cu	Fe	Mn	SO_4	Zn	TDS	pH
Supply								
Los Alamos Field								
Well 1B	17	0.090	0.014	0.009	39	0.030	430	8.6
Well 2	17	0.024	0.015	<0.001	17	0.015	244	8.4
Well 3	4	0.005	0.071	0.001	7	0.006	155	8.2
Well 4	--	--	--	--	--	--	--	--
Well 5	2	0.266	0.065	0.004	5	0.250	155	8.5
Guaje Field								
Well G-1	3	0.008	0.061	0.001	5	0.006	193	8.3
Well G-1A	3	0.014	0.022	<0.001	4	0.009	173	8.4
Well G-2	3	0.004	0.021	0.001	4	0.005	203	8.4
Well G-3	--	--	--	--	--	--	--	--
Well G-4	3	0.035	0.017	0.007	4	0.013	167	8.2
Well G-5	3	0.008	0.008	<0.001	4	0.011	169	8.0
Well G-6	3	0.008	0.008	<0.001	3	0.008	152	8.2
Pajarito Field								
Well PM-1	8	0.037	0.019	0.001	6	0.019	201	8.1
Well PM-2	2	0.018	0.017	0.005	2	0.011	150	8.1
Well PM-3	8	0.036	0.010	0.002	6	0.011	203	8.4
Well PM-4	2	0.013	0.024	<0.001	2	0.010	174	8.0
Well PM-5	2	0.032	0.030	0.008	2	0.043	155	8.0
Gallery (Water Canyon)	1	0.001	0.095	0.004	4	0.002	111	7.7
Supply Summary								
No. of Analyses	16	16	16	16	16	16	16	16
Maximum	17	0.266	0.095	0.009	39	0.250	430	8.6

Table G-61 (cont)

Stations	Cl	Cu	Fe	Mn	SO_4	Zn	TDS	pH
Distribution								
Fire Station 1	3	0.001	0.010	<0.001	3	0.030	150	8.0
Fire Station 2	6	0.006	0.020	<0.001	10	0.002	184	8.4
Fire Station 3	8	0.024	0.007	<0.001	6	0.002	217	8.1
Fire Station 4	4	0.006	0.022	<0.001	5	0.002	163	8.3
Fire Station 5	5	0.003	0.110	<0.001	8	0.046	193	8.3
Bandelier Nat. Mon.	5	0.014	0.084	<0.001	8	0.096	187	8.3
Distribution Summary								
No. of Analyses	6	6	6	6	6	6	6	6
Maximum	8	0.024	0.110	<0.001	10	0.096	217	8.4
Fenton Hill (TA-57)	45	0.002	0.048	<0.001	10	0.015	276	8.0
Standby Well (not part of Water Supply) Well LA-6	4	0.024	0.100	0.167	6	0.664	230	8.8
EPA Secondary Maximum Concentration Levels[b]	250	1.0	0.3	0.05	250	5.0	500	6.5-8.5

---

[a]Standard units.
[b]Reference: EPA 1979.

Table G-62. Miscellaneous Chemical Analyses (mg/L)[a]

Stations	SiO_2	Ca	Mg	K	Na	CO_3	HCO_3	P	Total Hard-ness	Conduc-tivity (mS/m)
Los Alamos Field										
Well LA-1B	38	8	0.4	2.4	166	7	316	<0.2	18	68
Well LA-2	31	7	0.1	1.1	77	3	141	<0.2	15	36
Well LA-3	34	13	0.3	1.6	35	0	86	<0.2	31	20
Well LA-4	--	--	--	--	--	--	--	--	--	--
Well LA-5	37	9	0.1	1.4	45	3	101	<0.2	23	22
Guaje Field										
Well G-1	88	13	0.5	3.1	22	0	75	<0.2	32	16
Well G-1A	70	10	0.4	2.7	32	0	84	<0.2	24	18
Well G-2	69	11	0.5	2.7	38	2	100	<0.2	27	22
Well G-3	--	--	--	--	--	--	--	--	--	--
Well G-4	52	18	3.6	2.0	13	0	72	<0.2	58	16
Well G-5	56	18	3.8	2.0	12	0	76	<0.2	58	16
Well G-6	51	13	2.1	2.2	19	0	73	<0.2	43	16
Pajarito Field										
Well PM-1	72	27	6.4	3.6	20	0	117	<0.2	91	26
Well PM-2	87	9	3.3	2.0	13	0	57	<0.2	36	12
Well PM-3	82	25	7.7	3.6	19	3	112	<0.2	97	26
Well PM-4	83	11	3.9	2.3	13	0	61	<0.2	43	14
Well PM-5	73	9	3.3	2.0	13	0	60	<0.2	36	12
Gallery (Water Canyon)	34	7	3.3	2.0	7	0	39	<0.2	43	9
Supply Summary										
No. of Analyses	16	16	16	16	16	16	16	16	16	16
Maximum	88	27	7.7	3.6	166	7	316	<0.2	97	68

Table G-62 (cont)

Stations	SiO_2	Ca	Mg	K	Na	CO_3	HCO_3	P	Total Hard-ness	Conduc-tivity (mS/m)
Distribution										
Fire Station 1	82	11	3.3	2.1	14	0	65	<0.2	41	14
Fire Station 2	54	11	1.0	2.1	50	0	112	<0.2	31	26
Fire Station 3	82	25	7.0	3.6	20	0	118	<0.2	94	26
Fire Station 4	60	13	1.6	2.8	27	0	87	<0.2	38	18
Fire Station 5	52	11	1.7	2.2	38	0	91	<0.2	31	22
Bandelier Nat. Mon.	48	12	1.8	2.1	38	1.2	101	<0.2	35	24
Distribution Summary										
No. of Analyses	6	6	6	6	6	6	6	6	6	6
Maximum	82	25	7.0	3.6	50	1.2	118	<0.2	94	26
Fenton Hill (TA-57)	67	53	5.0	5.2	17	0	127	<0.2	160	40
Standby Well (not part of Water Supply) Well LA-6	30	3	<0.1	0.9	70	8	144	<0.2	8	30

[a]Supply samples collected in February; distribution samples collected in February and September.

Table G-63. Los Alamos, New Mexico,[a] Climatological Survey (1911-1987)
Temperature and Precipitation Means[b] and Extremes

Temperature(°F)[c]

	Normals			Extremes							
Month	Mean Max	Mean Min	Avg	High Avg	Year	Low Avg	Year	High Daily Max	Date	Low Daily Min	Date
Jan	39.7	18.5	29.1	37.6	1986	20.9	1930	64	1/12/81	-18	1/13/63
Feb	43.0	21.5	32.2	37.4	1934	23.0	1939	69	2/25/86	-14	2/1/51
Mar	48.7	26.5	37.6	45.8	1972	32.1	1948	71	3/27/86[d]	-3	3/11/48
Apr	57.6	33.7	45.6	54.3	1954	39.7	1973	79	4/23/38	5	4/9/28
May	67.0	42.8	54.9	60.5	1956	50.1	1957	89	5/29/35	24	5/1/76[d]
Jun	77.8	52.4	65.1	69.4	1980	60.4	1965	95	6/22/81	28	6/3/19
Jul	80.4	56.1	68.2	71.4	1980	63.3	1926	95	7/11/35	37	7/7/24
Aug	77.4	54.3	65.8	70.3	1936	60.9	1929	92	8/10/37	40	8/16/47
Sept	72.1	48.4	60.2	65.8	1956	56.2	1965	94	9/11/34	23	9/29/36
Oct	62.0	38.7	50.3	54.7	1963	42.8	1984	84	10/1/80	15	10/19/76
Nov	48.7	27.1	37.9	44.4	1949	30.5	1972	72	11/1/50	-14	1/28/76
Dec	41.4	20.3	30.8	38.4	1980	24.6	1931	64	12/27/80	-13	12/9/78
Annual	59.6	36.7	48.1	52.0	1954	46.2	1932	95	6/22/81[d]	-18	1/13/63

Table G-63 (cont)

Month	Precipitation (in.)[c] Precipitation[e] Mean	Max	Year	Daily Max	Date	Snow Mean	Max	Year	Daily Max	Date	Mean Number of Days Per Year Precip >0.10 in.	Max Temp >90°F	Min Temp <32°F
Jan	0.85	6.75	1916	2.45	1/12/76	10.7	64.8	1987	22.0	1/15/87	2	0	30
Feb	0.68	2.78	1987	1.05	2/20/15	7.3	48.5	1987	20.0	2/19/87	2	0	26
Mar	1.01	4.11	1973	2.25	3/30/16	9.7	36.0	1973	18.0	3/30/16	3	0	24
Apr	0.86	4.64	1915	2.00	4/12/75	5.1	33.6	1958	20.0	4/12/75	2	0	13
May	1.13	4.47	1929	1.80	5/21/29	0.8	17.0	1917	12.0	5/2/78	3	0	2
Jun	1.12	5.67	1986	2.51	6/10/13	0	---	---	---	---	3	0	0
Jul	3.18	7.98	1919	2.47	7/31/68	0	---	---	---	---	8	1	0
Aug	3.93	11.18	1952	2.26	8/1/51	0	---	---	---	---	9	0	0
Sept	1.63	5.79	1941	2.21	9/22/29	0.1	6.0	1913	6.0	9/25/13	4	0	0
Oct	1.52	6.77	1957	3.48	10/5/11	1.7	20.0	1984	9.0	10/31/72	3	0	7
Nov	0.96	6.60	1978	1.77	11/25/78	5.0	34.5	1957	14.0	11/22/31	2	0	22
Dec	0.96	3.21	1984	1.60	12/6/78	11.4	41.3	1967	22.0	12/6/78	3	0	30
Annual	17.83	30.34	1941	3.48	10/5/11	50.8	178.4	1987	22.0	1/15/87	43	2	154
Season							153.2	1986-1987		12/6/78			

---

[a] Latitude 35° 32′ north, longitude 106° 19′ west; elevation 2249 m.
[b] Means based on standard 30-year period: 1951-1980.
[c] Metric conversions: 1 in. = 2.5 cm; °F = 9/5 °C + 32.
[d] Most recent occurrence.
[e] Includes liquid water equivalent of frozen precipitation.

Table G-64. Los Alamos Precipitation (inches) for 1987[a]

	S-Site (1)	North Community (2)	TA-59 (3)	Bandelier (4)	East Gate (5)	Area G (6)	White Rock Y (7)	White Rock (8)
January	2.60	3.43	2.43	1.67	1.72	0.94	1.39	0.94
February	3.39	3.44	2.78	2.11	1.71	1.37	1.43	1.26
March	0.75	0.90	0.88	0.43	0.34	0.30	0.30	0.38
April	1.12	1.24	1.09	0.66	0.57	0.43	0.43	0.49
May	2.25	1.75	2.83	2.29	2.15	1.54	3.13	2.35
June	1.88	1.22	2.69	0.68	0.64	0.64	0.95	0.52
July	1.02	0.76	1.37	1.29	1.03	1.38	0.85	1.28
August	4.48	4.97	4.29	3.67	2.92	4.76	3.79	4.83
September	1.00	2.24	1.72	0.76	1.19	0.62	1.00	0.96
October	0.74	0.58	0.49	0.41	0.45	0.43	0.47	0.49
November	1.66	1.79	1.47	0.99	1.17	0.94	0.59	0.75
December	1.79	2.20	1.58	1.71	1.34	1.04	1.34	1.19
Annual	22.68	24.52	23.62	16.67	15.23	14.39	15.67	15.44

[a]See Figure 29 for site locations.

Table G-65. Los Alamos Climatological Summary for 1987

	Temperature (°F)[a]						
	Means			Extremes			
Month	Mean Max	Mean Min	Avg	High	Date	Low	Date
Jan	37.1	17.2	27.2	54	12,27	-3	18
Feb	41.3	21.6	31.4	54	11	7	21,28
Mar	47.9	23.5	35.7	61	6	7	30
Apr	61.0	33.5	47.3	76	17	21	7
May	65.4	40.5	52.9	76	31	31	3
Jun	78.6	50.9	64.7	88	24	42	5
Jul	81.9	55.8	68.8	87	5 dates	51	14,17
Aug	75.3	53.3	64.0	87	1	43	27
Sept	70.5	46.9	58.7	77	1	40	15
Oct	66.4	40.8	53.6	77	4	28	20
Nov	48.0	27.2	37.6	63	4	15	28
Dec	36.7	17.8	27.3	60	4	1	27
Annual	59.3	35.8	47.5	88	6/24	-3	1/18

Table G-65 (cont)

Month	Precipitation (in.)[a] Water Equivalent Total	Water Equivalent Daily Max	Water Equivalent Date	Snow Total	Snow Daily Max	Snow Date	Number of Days Precip >0.10 in.	Max Temp >90°F	Min Temp <32°F
Jan	2.43	0.68	15	64.8	22.0	15	6	0	31
Feb	2.78	0.97	19	48.5	20.0	19	6	0	28
Mar	0.88	0.34	10	9.3	5.3	28	2	0	31
Apr	1.09	0.58	4	12.5	7.5	4	3	0	15
May	2.83	0.59	23	0	0	--	9	0	1
Jun	2.69	2.16	7	0	0	--	3	0	0
Jul	1.37	0.63	16	0	0	--	3	0	0
Aug	4.29	1.00	26	0	0	--	10	0	0
Sept	1.72	0.73	6	0	0	--	5	0	0
Oct	0.49	0.22	14	0	0	--	2	0	1
Nov	1.47	0.57	1	7.0	4.5	26	4	0	24
Dec	1.58	0.47	18,24	36.3	12.0	24	6	0	29
Annual	23.62	2.16	6/7	178.4	22.0	1/15	59	0	160

[a]Metric conversions: 1 in. = 2.5 cm; °F = 9/5°C + 32

Table G-66. Weather Highlights of 1987

January	Record snowfall: 64.8 in. Snowiest January on record (previous: 39.3 in. in 1949). Snowiest month on record (previous: 41.3 in. in December 1967). Precip = 2.43 in. (normal = 0.85 in.). Storm dropped 48.0 in. during 15-17th with 60-70 in. reported in North Community - LANL closed and townsite paralyzed. Record snowfall from one storm, 48.0 in. (previous: 34.5 in. during 12/12 to 12/15/84). Set daily record snowfall for January with 22.0 in. on 15th (previous: 15.0 in. on 1/5/13). Tied daily record snowfall for any month with 22.0 in. on 15th (also 12/6/78). Set record for most snow on ground in January with 40 in. on 16th and 17th (previous: 27 in., 1/30-1/31/79). Set record for most snow on ground in any month (previous: 28 in., 3/4 to 3/5/15). Strong winds with gusts = 59 mph on 5th. SMDP on the 7th: 0.41 in. SMDS on the 15th: 22.0 in. SMDS on the 16th: 21.0 in. SMDS on the 17th: 5.0 in.
February	Record snowfall and precip. Record February snowfall: 48.5 in. (previous: 36.4 in., 1982). 2nd snowiest month (most: 64.8 in., January 1987). Record February precip.: 2.78 in. (previous: 2.44 in., 1948). Storm drops 26.7 in. of snow 18th-20th. Record snowfall from one storm in February (previous: 21.5 in., 2/3 to 2/5/82). Strong winds with gusts = 56 mph on 14th. SMDP on the 16th: 0.27 in. SMDS on the 16th: 4.5 in. SMDP on the 18th: 0.30 in. SMDP on the 19th: 0.97 in. (Also record for most daily precip. in February - previous: 0.96 in., 2/15/75). SMDS on the 19th: 20.0 in. (Also record for most daily snow in February - previous: 19.0 in., 2/4/82). SMDP on the 26th: 0.63 in. SMDS on the 26th: 9.0 in.
March	Cooler than normal. Strong winds with gusts = 50 mph on 20th.

Table G-66 (cont)

April	Mild and above normal snow. Average maximum temperature = 61.0°F (Normal = 57.6°F) Snowfall = 12.5 in. (Normal = 5.1 in.).
May	Wet and cool. Precipitation = 2.83 in. (Normal = 1.13 in.). SMDP on the 16th: 0.41 in. SMDP on the 23rd: 0.59 in. Hail accumulation of 3 in. on 23rd.
June	Wet. Precipitation = 2.69 in. (Normal = 1.12 in.). SMDP on the 7th: 2.16 in. Thunderstorm on 7th gives near 50-year rainfall for 2 hours: 2.11 in. Strong winds with gusts = 58 mph on 18th, some windows blown out in townsite.
July	Dry. Precipitation = 1.37 in. (Normal = 3.18 in.). Some one-inch diameter hail, but little accumulation on 13th.
August	Funnel clouds reported near Santa Fe on 24-25th. SMDP on the 26th: 1.00 in. SMDL on the 29th: 44°F.
September	Hazy 4th-10th from Western U.S. forest fires. SMDP on the 6th: 0.73 in.
October	Warm and dry. Mean temperature = 53.6°F (Normal = 50.3). Mean max temperature = 66.4°F (Normal = 62.0°F). Precipitation = 0.49 in. (Normal = 1.52 in.). TMDH on the 4th: 77°F.
November	SMDP on the 1st: 0.57 in.

Table G-66 (cont)

December	Snowy and cold. Snowfall = 36.3 in. (Normal = 11.4 in.). 3rd snowiest December on record. Storm drops 19.0 in. snow with up to 26 in. in North Community during 24-25th. Mean temperature = 27.3°F (Normal = 30.8°F). Mean max temperature = 36.7°F (Normal = 41.4°F). TMDH on the 4th: 60°F. SMDS on the 12th: 4.5 in. SMDL on the 15th: 3°F. SMDP on the 18th: 0.47 in. SMDS on the 18th: 6.0 in. SMDP on the 24th: 0.47 in. SMDS on the 24th: 12.0 in. SMDS on the 25th: 7.0 in. Record snow on ground for Christmas: 16.0 in. High temperatures only 19, 14, and 17°F, respectively, on 25, 26, and 27th.
Annual	1987 mean temperature = 47.5°F (Normal = 48.1°F). 1987 precipitation = 23.62 in. (Normal = 17.83 in.). 3rd consecutive year with precipitation >30% above normal. 1987 snowfall = 178.4 in. or 14.9 ft. (Normal = 50.8 in.). Snowiest year on record (previous: 112.8 in., 1984). 1986-1987 winter season snowfall = 153.2 in. Snowiest winter season on record (previous: 123.6 in., 1957-1958).

Key for Abbreviations:

SMDH: Set Maximum Daily High Temperature Record
TMDH: Tied Maximum Daily High Temperature Record
SMDL: Set Minimum Daily Low Temperature Record
TMDL: Tied Minimum Daily Low Temperature Record
SMDP: Set Maximum Daily Precipitation Record
SMDS: Set Maximum Daily Snowfall Record

Table G-67. Wet Deposition Measurements ($\mu eq/m^2$ unless specified)[a]

Parameter	Fourth Quarter 1986	First Quarter 1987	Second Quarter 1987	Third Quarter 1987
Precipitation (in.)	0.45 (0.0-2.0)	0.27 (0.0-.83)	0.17 (0.0-.77)	0.40 (0.0-1.49)
Field pH	4.8 (4.6-5.1)	4.8 (4.0-5.8)	4.7 (4.6-4.9)	4.7 (4.1-5.5)
Calcium	68 (0.5-470)	92 (1.5-290)	66 (0.5-200)	180 (1.0-580)
Magnesium	9.4 (0.0-48)	14 (1.6-29	12 (0.0-31)	29 (0.0-86)
Potassium	4.2 (0.0-25)	3.4 (0.0-6.6)	7.8 (0.0-37)	9.8 (0.0-32)
Sodium	31 (0.0-90)	34 (1.7-90)	15 (0.0-43.9)	39 (1.3-84)
Ammonium	110 (1.1-47)	63 (1.1-270)	79 (0.55-270)	110 (4.4-300)
Nitrate	130 (0.8-450)	133 (16-310)	120 (0.58-300)	300 (32-60)
Chloride	19 (3.4-51)	26 (2.0-64)	15 (0.84-63)	41 (1.1-100)
Sulfate	280 (2.1-1000)	150 (21-430)	140 (1.5-390)	280 (31-590)
Phosphate	-- --	-- --	6.9 --	2.2 --

[a]Mean; range in parentheses.

Table G-68. Radiochemical Analyses of Sediments at TA-49

Station No.	Date	^{3}H (10^{-6} pCi/g)	^{137}Cs (10^{-9} pCi/g)	Total U (µg/g)	^{238}Pu (10^{-9} pCi/g)	$^{239,240}Pu$ (10^{-9} pCi/g)	Gross Gamma (Counts/min/g)
A-1	8-6-86	2.4 (0.5)	0.11 (0.05)	3.0 (0.3)	0.000 (0.001)	0.004 (0.002)	4.0 (0.7)
A-1	4-13-87	--	0.08 (0.07)	2.3 (0.2)	0.004 (0.002)	0.003 (0.002)	7.3 (0.9)
A-2	8-6-86	5.4 (0.7)	0.35 (0.10)	4.2 (0.4)	0.005 (0.002)	0.022 (0.004)	5.2 (0.7)
A-2	4-13-87	--	0.22 (0.08)	3.7 (0.4)	0.001 (0.001)	0.004 (0.005)	9.0 (1.0)
A-3	8-6-86	3.4 (0.5)	1.2 (0.21)	5.3 (0.5)	0.216 (0.013)	10.7 (0.425)	6.5 (0.7)
A-3	4-13-87	--	0.29 (0.08)	4.7 (0.5)	0.001 (0.000)	0.083 (0.010)	10 (1.0)
A-4	8-6-87	5.7 (0.7)	-0.20 (0.05)	4.2 (0.4)	0.000 (0.001)	0.004 (0.002)	5.5 (0.8)
A-4	4-13-87	--	0.16 (0.09)	3.4 (0.3)	0.001 (0.002)	0.006 (0.002)	9.0 (1.0)
A-4A	8-6-86	3.1 (0.5)	0.70 (0.15)	4.0 (0.4)	0.001 (0.001)	0.000 (0.001)	6.5 (0.8)
A-4A	4-13-87	--	0.23 (0.09)	3.4 (0.3)	0.001 (0.001)	0.008 (0.002)	9.0 (1.0)
A-5	8-6-86	3.0 (0.5)	-0.08 (0.02)	3.8 (0.4)	0.001 (0.002)	0.042 (0.006)	5.8 (0.8)
A-5	4-13-87	--	0.39 (0.11)	3.4 (0.3)	0.000 (0.001)	0.016 (0.004)	9.0 (1.0)
A-6	8-6-86	4.7 (0.6)	0.49 (0.10)	4.2 (0.4)	0.002 (0.001)	0.012 (0.002)	6.3 (0.8)
A-6	4-13-87	--	0.14 (0.08)	3.5 (0.4)	0.000 (0.001)	0.001 (0.001)	9.0 (1.0)
A-7	8-6-86	4.1 (0.6)	0.48 (0.10)	4.1 (0.4)	0.003 (0.002)	0.016 (0.003)	6.3 (0.8)
A-7	4-13-87	--	0.37 (0.11)	3.9 (0.4)	0.002 (0.001)	0.016 (0.003)	8.0 (1.0)
A-8	8-6-86	3.8 (0.6)	0.20 (0.06)	2.6 (0.3)	0.001 (0.001)	0.001 (0.002)	4.4 (0.7)
A-8	4-13-87	--	0.17 (0.09)	3.4 (0.3)	-0.001 (0.002)	0.004 (0.002)	7.8 (0.9)
A-9	8-6-86	6.4 (0.8)	0.10 (0.06)	3.9 (0.4)	0.000 (0.001)	0.003 (0.002)	6.1 (0.8)
A-9	4-13-87	--	0.09 (0.09)	2.9 (0.3)	0.000 (0.001)	0.002 (0.002)	6.3 (0.8)
A-10	8-6-86	8.0 (0.9)	0.10 (0.07)	2.6 (0.3)	0.000 (0.001)	0.004 (0.002)	4.8 (0.7)
A-10	4-13-87	--	0.45 (0.11)	3.7 (0.4)	0.005 (0.001)	0.014 (0.003)	9.0 (1.0)

Table G-68 (cont)

Station No.	Date	^{3}H (10^{-6} pCi/g)	^{137}Cs (10^{-9} pCi/g)	Total U (μg/g)	^{238}Pu (10^{-9} pCi/g)	$^{239,240}Pu$ (10^{-9} pCi/g)	Gross Gamma (Counts/min/g)
A-11	8-6-86	2.9 (0.5)	0.03 (0.06)	3.2 (0.3)	0.000 (0.001)	0.003 (0.002)	5.9 (0.8)
A-11	4-13-87	--	0.57 (0.13)	2.6 (0.3)	0.002 (0.002)	0.010 (0.002)	7.0 (0.9)
A Background	4-13-87	--	0.20 (0.09)	3.4 (0.3)	0.000 (0.001)	0.005 (0.002)	5.7 (0.8)
B Background	4-13-87	--	0.05 (0.08)	2.9 (0.3)	0.004 (0.003)	0.001 (0.003)	3.1 (0.6)
Limits of Detection		0.3	0.1	0.1	0.002	0.002	0.1
Maximum Concentration		8.0	1.2 (0.21)	5.3 (0.5)	0.216 (0.013)	10.7 (0.425)	10 (1.0)
Regional Background		7.2	0.44	4.4	0.006	0.023	7.9
Maximum as % of Regional Background		111	272	120	3600	4652	126

Note: Station number shown in Fig. 33; counting uncertainty in parentheses.

Table G-69. Chemical Concentrations in Solution Extracted from Sediments Downgradient from Experimental Areas at TA-49

Chemical[b]	Maximum EP Toxic Concentration[c]	Limit of Detection	Stations Numbers[a]												Background[a]	
			A-1	A-2	A-3	A-4	A-4A	A-5	A-6	A-7	A-8	A-9	A-10	A-11	A	B
Arsenic	5.0	0.05	BLD	BLD	BLD	BLD	BLD	BLD	BLD	BLD	BLD	BLD	BLD	BLD	BLD	BLD
Barium	100	0.5	0.6	BLD	0.6	BLD	0.8	0.5	0.7	BLD	0.6	BLD	BLD	BLD	0.5	1.3
Cadmium	1.0	0.01	BLD	BLD	BLD	BLD	BLD	BLD	BLD	BLD	BLD	BLD	BLD	BLD	BLD	BLD
Chromium	5.0	0.05	BLD	BLD	BLD	BLD	BLD	BLD	BLD	BLD	BLD	BLD	BLD	BLD	BLD	BLD
Lead	5.0	0.05	BLD	0.06	BLD	BLD	BLD	BLD	BLD	BLD	BLD	BLD	BLD	BLD	BLD	BLD
Mercury	2.0	0.005	BLD	BLD	BLD	BLD	BLD	BLD	BLD	BLD	BLD	BLD	BLD	BLD	BLD	BLD
Selenium	1.0	0.01	BLD	BLD	BLD	BLD	BLD	BLD	BLD	BLD	BLD	BLD	BLD	BLD	BLD	BLD
Silver	---	0.05	BLD	BLD	BLD	BLD	BLD	BLD	BLD	BLD	BLD	BLD	BLD	BLD	BLD	BLD
Nickel	---	0.01	BLD	BLD	BLD	BLD	BLD	BLD	BLD	BLD	BLD	BLD	BLD	BLD	BLD	BLD
Beryllium[d]	---	0.001	BLD	BLD	BLD	BLD	BLD	BLD	BLD	BLD	BLD	BLD	BLD	BLD	BLD	BLD
Sulfate	---	0.2	BLD	BLD	BLD	0.4	BLD	BLD	0.3	BLD	1.1	BLD	BLD	BLD	BLD	0.5
Nitrate	---	0.2	BLD	BLD	BLD	BLD	BLD	BLD	BLD	BLD	BLD	BLD	BLD	BLD	BLD	BLD
Uranium[d]	---	1.0	BLD	BLD	BLD	BLD	BLD	BLD	BLD	BLD	BLD	BLD	BLD	BLD	BLD	7.9

[a]Station number shown in Figure 31; background stations are Bandelier National Monument, entrance (A) and small canyon north of supply well PM-1 (B).

[b]Concentrations in mg/L except as noted; BLD = Below Limit of Detection.

[c]New Mexico Hazardous Waste Management Regulations (HWMR) 201 B.5.; Extraction procedure.

[d]Units are μg/g.

Table G-70. Storm Run-off from TA-49

Station	Date 1987	Solution ^{137}Cs (10^{-9} µCi/ml)	Solution ^{238}Pu (10^{-9} µCi/ml)	Solution $^{239,240}Pu$ (10^{-9} µCi/ml)	Suspended Sediments ^{238}Pu (pCi/g)	Suspended Sediments $^{239,240}Pu$ (pCi/g)
A-1	8-24	152 (65)	0.007 (0.011)	0.010 (0.008)	0.000 (0.001)	0.027 (0.006)
A-1	8-24	15 (60)	-0.008 (0.011)	0.000 (0.010)	-0.004 (0.008)	0.048 (0.013)
A-2	8-24	38 (60)	-0.057 (0.033)	0.000 (0.010)	0.001 (0.001)	0.002 (0.001)
A-5	8-24	-13 (60)	-0.009 (0.015)	0.033 (0.018)	0.000 (0.001)	0.007 (0.033)
A-5	8-28	67 (61)	0.008 (0.008)	0.025 (0.010)	0.000 (0.001)	0.006 (0.002)
A-5	9-10	82 (61)	0.011 (0.014)	-0.004 (0.004)	0.004 (0.002	0.024 (0.004)
A-8	8-24	45 (53)	0.000 (0.010)	0.000 (0.010)	0.001 (0.001)	0.001 (0.001)
A-8	8-28	-27 (60)	0.021 (0.017)	0.005 (0.014)	0.000 (0.001)	0.028 (0.004)

Table G-71. Chemical Quality of Storm Run-off from TA-49

Station	Date 1987	mg/L As	Cr	N	SO_4	pH
A-1	8-24	0.002	0.02	1.2	2	6.0
A-1	8-24	0.002	0.03	0.3	3	7.8
A-2	8-24	0.003	0.02	0.2	2	7.7
A-5	8-24	0.003	0.03	0.2	2	7.6
A-5	8-28	0.002	0.04	1.0	2	7.1
A-5	9-10	0.003	0.03	0.2	2	7.0
A-8	8-24	0.003	0.04	0.7	4	8.1
A-8	8-28	0.008	0.04	0.7	2	7.0
Standard[a]		0.05	0.05	10	250	

Constituent[b]	Concentration (mg/L)	Standards[a] (mg/L)
Ag	<0.05	0.05
Ba	<0.1	1.0
Be	<0.01	--
CN	<0.01	--
Cd	<0.01	0.01
Hg	<0.002	0.002
Ni	<0.01	--
Pb	<0.01	0.05
Se	<0.02	0.01

---

[a]Primary or secondary drinking water standards (EPA 1976, 1979).

[b]Analyzed from stations for each run-off event.

GLOSSARY

alpha particle	A charged particle (identical to the helium nucleus) composed of two protons and two neutrons that is emitted during decay of certain radioactive atoms. Alpha particles are stopped by several centimeters of air or a sheet of paper.
activation products	In nuclear reactors and some high energy research facilities, neutrons and other subatomic particles that are being generated can produce radioactive species through interaction with materials such as air, construction materials, or impurities in cooling water. These "activation products" are usually distinguished, for reporting purposes, from "fission products."
background radiation	Ionizing radiation from sources other than the laboratory. It may include cosmic radiation; external radiation from naturally occurring radioactivity in the earth (terrestrial radiation), air, and water; internal radiation from naturally occurring radioactive elements in the human body; and radiation from medical diagostic procedures.
beta particle	A charged particle (identical to the electron) that is emitted during decay of certain radioactivity atoms. Most beta particles are stopped by 0.6 cm of aluminum or less.
Concentration Guide (CG)	The concentration of a radionuclide in air or water that results in a whole body or organ dose in the 50th year of exposure equal to the Department of Energy's Radiation Protection Standard for external and internal exposures. This dose is calculated assuming the air is continuously inhaled or the water is the sole source of liquid nourishment for 50 years.
Controlled Area	Any Laboratory area to which access is controlled to protect individuals from exposure to radiation and radioactive materials.

cosmic radiation	High-energy particulate and electromagnetic radiations that originate outside the earth's atmosphere. Cosmic radiation is part of natural background radiation.
curie (Ci)	A special unit of radioactivity. One curie equals 3.70×10^{10} nuclear transformations per second.
dose	A term denoting the quantity of radiation energy absorbed.
dose, absorbed	The energy imparted to matter by ionizing radiation per unit mass of irradiated material. (The unit of absorbed dose is the rad.)
dose, effective	The hypothetical whole body dose that would give the same risk of cancer mortality and/or serious genetic disorder as a given exposure, that may be limited to just a few organs. The effective dose equivalent is equal to the sum of individual organ doses each weighted by degree of risk that the organ dose carries. For example, a 100 mrem dose to the lung, which has a weighting factor of 0.112, gives an effective dose equivalent to (100 x 0.12 =) 12 mrem.
dose, equivalent	A term used in radiation protection that expresses all types of radiation (alpha, beta, and so on) on a common scale for calculating the effective absorbed dose. It is the product of the absorbed dose in rads and certain modifying factors. (The unit of dose equivalent is the rem.)
dose, maximum boundary	The greatest dose commitment, considering all potential routes of exposure from a facility's operation, to a hypothetical individual who is in an Uncontrolled Area where the highest dose rate occurs. It assumes that the hypothetical individual is present for 100% of the time (full occupancy) and does not take into account shielding (for example, by buildings).
dose, maximum individual	The greatest dose commitment, considering all potential routes of exposure from a facility's operation, to an individual at or outside the Laboratory boundary where the highest dose rate occurs. It takes into account shielding and occupancy factors that would apply to a real individual.
dose, population	The sum of the radiation doses to individuals of a population. It is expressed in units of person-rem (for example, if 1000 people each received a radiation dose of 1 rem, their population dose would be 1000 person-rem.

dose, whole body	A radiation dose commitment that involves exposure of the entire body (as opposed to an organ dose that involves exposure to a single organ or set of organs).
exposure	A measure of the ionization produced in air by x or gamma radiation. (The unit of exposure is the reontgen).
external radiation	Radiation originating from a source outside the body.
fission products	Those atoms created through the splitting of larger atoms into smaller ones, accompanied by release of energy.
gallery	An underground collection basin for spring discharges.
gamma radiation	Short-wavelength electromagnetic radiation of nuclear origin that has no mass or charge. Because of its short wavelength (high energy), gamma radiation can cause ionization. Other electromagnetic radiation (microwaves, visible light, radiowaves, etc.) have longer wavelengths (lower energy) and cannot cause ionization.
gross alpha	The total amount of measured alpha activity without identification of specific radionuclides.
gross beta	The total amount of measured beta activity without identification of specific radionuclides.
groundwater	A subsurface body of water in the zone of saturation.
half-life, radioactive	The time required for the activity of a radioactive substance to decrease to half its value by inherent radioactive decay. After two half-lives, one-fourth of the original activity remains (1/2 x 1/2), after three half-lives, one-eighth (1/2 x 1/2 x 1/2), and so on.
internal radiation	Radiation from a source within the body as a result of deposition of radionuclides in body tissues by processes, such as ingestion, inhalation, or implantation. Potassium-40, a naturally occurring radionuclide, is a major source of internal radiation in living organisms.
Laboratory	Los Alamos National Laboratory.

Maximum Contaminant Level (MCL)	Maximum permissible level of a contaminant in water that is delivered to the free-flowing outlet of the ultimate user of a public water system (see Appendix A and Table A-III). The MCLs are specified by the Environmental Protection Agency.
mrem	Millirem (10^{-3} rem). See rem definition.
perched water	A groundwater body above an impermeable layer that is separated from an underlying main body of groundwater by an unsaturated zone.
person-rem	The unit of population dose, it expresses the sum of radiation exposures received by a population. For example, two persons each with a 0.5 rem exposure have received 1 person-rem. Also, 500 people each with an exposure of 0.002 rem have received 1 person-rem.
rad	A special unit of absorbed dose from ionizing radiation. A dose of 1 rad equals the absorption of 100 years of radiation energy per gram of absorbing material.
radiation	The emission of particles or energy as a result of an atomic or nuclear process.
Radiation Protection Standard	A standard for external and internal exposure to radioactivity as defined in Department of Energy Order 5480.1A, Chapter XI (see Appendix A and Table A-II in this report).
rem	The unit of radiation dose equivalent that takes into account different kinds of ionizing radiation and permits them to be expressed on a common basis. The dose equivalent in rems is numerically equal to the absorbed dose in rads multiplied by the necessary modifying factors.
roentgen (R)	A unit of radiation exposure that expresses exposure in terms of the amount of ionization produced by x rays in a volume of air. One roentgen (R) is 2.58×10^{-4} coulombs per kilogram of air.
terrestrial radiation	Radiation emitted by naturally occurring radionuclides, such as ^{40}K, the natural decay chains ^{235}U, ^{238}U, or ^{232}Th, or from cosmic-ray induced radionuclides in the soil.

thermoluminescent dosimeter (TLD)	A material (the Laboratory users lithium fluoride) that, after being exposed to radiation, luminesces upon being heated. The amount of light the material emits is proportional to the amount of radiation (dose) to which it was exposed.
tritium	A radionuclide of hydrogen with a half-life of 12.3 years. The very low energy of its radioactivity decay makes it one of the least hazardous radionuclides.
tuff	Rock of compacted volcanic ash and dust.
Uncontrolled Area	An area beyond the boundaries of a Controlled Area (see definition of "Controlled Area" in this Glossary).
uranium, depleted	Uranium consisting primarily of ^{238}U and having less than 0.72 wt% ^{235}U. Except in rare cases occurring in nature, depleted uranium is manmade.
uranium, total	The amount of uranium in a sample assuming the uranium has the isotopic content of uranium in nature (99.27 wt% ^{238}U 0.72 wt% ^{235}U, 0.0057 wt% ^{234}U).
Working Level Month (WLM)	A unit of exposure to ^{222}Rn and its decay products. Working Level (WL) is any combination of the short-lived ^{222}Rn decay products in 1 liter of air that will result in the emission of 1.3×10^5 MeV potential alpha energy. At equilibrium, 100 pCi/L of ^{222}Rn corresponds to one WL. Cumulative exposure is measured in Working Level Months, which is 170 WL-hours.

DISTRIBUTION LIST

STANDARD UC-41 (HEALTH AND SAFETY DISTRIBUTION)

DEPARTMENT OF ENERGY
Office of Military Application (2)
General G. Whithers
Technical Information Center
D. Bost
Albuquerque Operations Office (20)
J. Themelis
R. Miller
C. Soden
Los Alamos Area Office (3)
H. Valencia
D. Gallegos
Environmental Measurements Laboratory
H. Volchok
E. Hardy, Jr.
Idaho Operations Office
M. Williamson
Nevada Operations Office
B. Church
Oak Ridge Operations Office
R. Sleeman
Savannah River Operations Office
S. Wright
Department of Energy Contractors
Argonne National Laboratory
N. Golchert
Battelle, Pacific Northwest Laboratories
R. Jaquish
Brookhaven National Laboratory
L. Day
Rockwell International - Rocky Flats Plant
G. Setlock
Lawrence Livermore National Laboratory
D. Brekke
Mound Laboratory
D. Carfagno
Oak Ridge National Laboratory
T. Kitchings
Pantex Plant
W. Laseter
Sandia National Laboratories, Albuquerque
G. Millard
Savannah River Plant
R. Kump

Other External
University of California
Environmental, Health, and Safety Office
Environmental Protection Agency
S. Meyers, ORP, Washington, DC
C. Costa, EMSL, Las Vegas, NV
R. Layton, Region 6, Dallas, TX
A. Davis, Region 6, Dallas, TX
J. Highland, Region 6, Dallas, TX
New Mexico Governor
G. Garruthers
New Mexico Health and Environment Dept., Environmental Improvement Division
M. Burkhart, Director
S. Hill
C. Clayton
M. Brown
K. Jones
R. Mitzelfelt
J. Thompson
New Mexico Oil Conservation Division
W. J. LeMay
New Mexico Energy and Minerals Department
A. Lockhart
New Mexico Natural Resources Department
M. Barr
New Mexico State Engineer
S. Reynolds
US Forest Service
Bandelier National Monument
Pan Am World Services
T. Holm-Hansen
J. Lopez
Individuals
J. White, Army Corps of Engineers
J. Daniel, US Geological Survey, Albuquerque, NM
R. Faus, TP Pump and Pipe Co.
Media
The Monitor, Los Alamos, NM
The New Mexican, Santa Fe, NM
The Reporter, Santa Fe, NM
The Rio Grande Sun, Espanola, NM
Albuquerque Journal, Albuquerque, NM
Albuquerque Tribune, Albuquerque, NM

New Mexico Independent, Albuquerque, NM
KRSN Radio, Los Alamos, NM
New Mexico Congressional Delegation
Senator P. Domenici
Senator J. Bingaman
Representative M. Lujan, Jr.
Representative J. Skeen
Representative W. Richardson
Elected Officials
City of Espanola
R. Lucero, Mayor
City of Santa Fe
S. Pick, Mayor
County of Los Alamos
N. Bartlitt, Chairman of Los Alamos Council
S. Stoddard, State Senator
D. Sundberg, State Representative
New Mexico Office of Indian Affairs
Bureau of Indian Affairs
Administrative Manager
Eight Northern Pueblos
Governor, Nambe Pueblo
Governor, Picuris Pueblo
Governor, Pojoaque Pueblo
Governor, San Ildefonso Pueblo
Governor, San Juan Pueblo
Governor F. Gutierrez, Santa Clara Pueblo
Governor J. Cordova, Taos Pueblo
Governor J. Hena, Tesuque Pueblo
Mesa Public Library, Los Alamos, NM

Internal Distribution

Director's Office
S. Hecker, Director
A. Tiedman, Associate Director for Support
J. Mitchell, Laboratory Counsel
J. Breen, Public Affairs Officer (2)
Health, Safety, and Environment Division Office (10)
J. Puckett
T. Gunderson
R. Stafford
D. Garvey
Environmental Restoration Program Technical Support Office
K. Rea
R. Vocke
Group HSE-1, Radiation Protection
A. Valentine
J. Graf
F. Guevara
R. Miller
Group HSE-3, Safety
W. Courtright
Group HSE-5, Industrial Hygiene
J. Jackson
Group HSE-7, Waste Management
R. Koenig
R. Garde
K. Balo
J. Buchholz
J. Warren
Group HSE-8, Environmental Surveillance
M. Martz-Emerson
T. Buhl
A. Drypolcher
L. Soholt
Group HSE-9, Health and Environmental Chemistry
R. Gooley
E. Gladney
Group HSE-10, Chemistry Health Protection
Group HSE-11, Accelerator Health Protection
J. Miller
R. Dvorak
Group HSE-12, Environmental Sciences
T. Hakonson
C. Reynolds
Group IS-1, Publications
C. Rodriguez
Group IS-4, Library Services (15)
Group IS-10, Technical Information (2)
Group ENG-11, Long Range Facilities Planning
S. Coonley
Laboratory Environmental Review Committee
D. Garvey
T. Gunderson
L. Bays
S. Coonley
M. McCorkle
C. Olinger, ex officio

McLIN

INTERNATIONAL TECHNOLOGY CORPORATION

Project No. 301215
February 6, 1989

Interim Status Closure Plan

Tech Area 16 Surface Impoundment

Los Alamos National Laboratory
Los Alamos, New Mexico

RESPONSIVE TO THE NEEDS OF ENVIRONMENTAL MANAGEMENT

S.G. McLin

Interim Status Closure Plan

VOLUME I OF II

INTERIM STATUS CLOSURE PLAN, TA-16 SURFACE IMPOUNDMENT

Facility ID No..... NM890010515
Facility Name..... Los Alamos National Laboratory
Legal Owner..... United States Department of Energy
Legal Operator..... University of California
Address..... Los Alamos Area Office
City, State..... Los Alamos, New Mexico 87545
Contact Person..... Mr. Harold Valencia, Area Manager
Phone..... (505) 667-5105
Dated..... February 6, 1989

NT NATIONAL
EC..NOLOGY
ORPORATION

Project No. 301017.02
March, 1987

Final Report

ogeologic Assessment of Technical 54, Areas G and L
\lamos National Laboratory

t Number: NMHWA 001007

amos National Laboratory
'amos, New Mexico

RESPONSIVE TO THE NEEDS OF ENVIRONMENTAL MANAGEMENT

Hydrogeologic Assessment of Technical Area 54, Areas G and L Los Alamos National Laboratory

Docket Number: NMHWA 001007

EXECUTIVE SUMMARY

1.0 INTRODUCTION

Los Alamos National Laboratory has operated two chemical waste disposal facilities in Technical Area 54 on Mesita del Buey located in the southern half of Section 31, T19N, R7E (N.M.P.M.). These areas, designated Areas G and L, occupy 63 acres and approximately 2.5 acres, respectively. Area G, used primarily for disposal of low-level radioactive materials, has been in operation since 1957 and is expected to remain active through the foreseeable future. In addition to low-level waste, small quantities of asbestos, beryllium residues, empty pesticide containers, polychlorinated biphenyl (PCB) contaminated solids and solid trash-type wastes contaminated with known or suspected carcinogens were disposed of at Area G. Area L served as the Laboratory's principal chemical waste disposal area between 1964 and 1985 and a wide variety of organic and inorganic wastes were disposed of at this area. Wastes were disposed of in Areas G and L by emplacement in shafts, trenches and pits excavated in the Bandelier Tuff to depths of up to 65 feet.

This report presents a summary of the hydrogeology of Areas G and L and other data and discussions relevant to the potential for migration of hazardous waste from the disposal areas. This report was prepared in response to a Compliance Order/Schedule, dated May 7, 1985, issued to the Laboratory by the New Mexico Environmental Improvement Division, pursuant to the New Mexico Hazardous Waste Act. Paragraph 25 of the Order mandated that certain tests and investigations be performed at Areas G and L to obtain information on the hydrologic characteristics of the waste disposal areas relevant to the potential for migration of waste constituents into the area ground water.

Work was initiated in late 1985 to fulfill the testing requirements of the Order. Eighteen 100- to about 135-foot deep boreholes were drilled into the Bandelier Tuff from the top of Mesita del Buey, and approximately 1,700 feet of core were obtained. In addition, a 60-foot deep borehole was sunk near a surface impoundment at Area L. Selected core samples were analyzed for numerous parameters, and hydrologic testing and geophysical logging were performed in the boreholes. Selected boreholes were completed for pore gas sampling, neutron moisture monitoring, and psychrometer installation. In addition to the boreholes drilled from the top of the mesa, holes were drilled

in the adjacent canyons to investigate possible alluvial aquifers. Table ES-1 provides a list of Compliance Order Paragraph 25 tasks and a description of the activities undertaken to fulfill the task requirements. The purpose of this report is to summarize the results of the recent work (published and unpublished) and to combine these data with published information on site characteristics into a cogent report on the potential for chemical waste migration in the lithosphere at Areas G and L.

2.0 GEOLOGY

Los Alamos National Laboratory is located on the Pajarito Plateau on the east-central edge of the Jemez mountains. These mountains are formed by a complex pile of volcanic rocks along the northwest margin of the Rio Grande rift in north-central New Mexico. The plateau, which forms an apron of volcanic and sedimentary rocks along the eastern flank of the mountains, is aligned approximately north-south and is about 20 to 25 miles in length and five to ten miles wide. The plateau slopes gently eastward from an elevation of about 7,500 feet near the mountains toward the Rio Grande where it terminates at an elevation of about 6,200 feet in steep slopes and cliffs formed by down cutting of the river. The plateau has been dissected into a number of narrow mesas by southeastward-trending intermittent streams. One of these mesas, Mesita del Buey, near the eastern edge of the Pajarito Plateau, is the site of Technical Area 54, Areas G and L. Mesita del Buey is bounded on the north by Cañada del Buey and on the south by Pajarito Canyon.

The stratigraphy of Mesita del Buey is a series of sediments and volcanic extrusive rocks and is typical of a terrane produced by concurrent sedimentation and volcanism. In ascending order, the following rock units are present at Mesita del Buey: Tesuque Formation, Puye Conglomerate, basaltic rocks of Chino Mesa, and the Bandelier Tuff. The Tesuque, consisting of siltstone and sandstone with conglomerate lenses and basalt layers, is overlain by the conglomerates and sandstones of the Puye Conglomerate. Overlying and interfingering with the Puye are the dense basalt flows and scoria of the basaltic Chino Mesa rocks. The Bandelier Tuff, which consists of numerous ashfall and ashflow units and overlies the Puye and Chino Mesa flows, caps the mesa. The three to four-foot layer of soil present along the axis of the mesa thins appreciably towards the canyons, exposing the tuff in places.

Surface mapping and subsurface correlation of ash flow units, as well as the seismic line of the mesa, indicate no displacement (faults) of the tuff. The most prevalent structural features in the mesa rocks are the fractures or joints in the volcanic rocks caused by shrinkage upon cooling after deposition. Both horizontal and vertical joints have been observed in the Bandelier Tuff; however, vertical joints are much more prevalent. A joint traced vertically through an ashflow may be closed in places and open in others. Joints near the base of the soil are often clay-filled for three to four feet below the surface and either filled, or open with clay plating, below this depth. Vertical joint frequencies observed in horizontal borings are about one joint per three to six feet of core recovered.

3.0 HYDROLOGICAL CHARACTERIZATION OF THE VADOSE ZONE

Vadose zone characterization studies were undertaken in Technical Area 54, Areas G and L to provide a quantitative analysis of moisture movement in the Bandelier Tuff. These analyses aid in determining the likelihood of contaminants from Areas G and L migrating through the vadose zone and into ground water beneath the sites. A two-tiered approach to quantify moisture movement in tuff was utilized: (1) rock characteristics and hydraulic head were measured to calculate seepage velocity and rates of moisture flux, and (2) moisture content of the tuff following precipitation events was measured to determine changes in moisture content with depth.

To permit calculation of seepage velocity and rates of moisture flux in the tuff, hydrologic testing was performed in boreholes at Areas G and L and in the laboratory on core samples from the boreholes. The intrinsic permeability of the tuff was measured in boreholes through air injection and vacuum tests; laboratory tests included gas injection with correction for slippage and the Dynamic Method to measure gas-water relative permeability. Air injection tests were performed in five open boreholes on 25, six-foot test intervals, including seven intervals adjacent to fracture zones. Intrinsic permeability was found to range from about 10^{-8} to 10^{-9} square centimeters (cm^2) for fractured and unfractured intervals. Similar data were obtained from water injection tests performed in one borehole to verify the results of the air

injection tests. No significant difference between fractured and unfractured tuff was noted. Vacuum tests performed on 18 intervals in the same boreholes yielded slightly lower permeability values, but with an average also in the 10^{-8} to 10^{-9} cm^2 range. Laboratory tests of intrinsic permeability of core samples of the Bandelier Tuff yielded values in the low 10^{-9} cm^2 range. Lower values are expected for laboratory tests because discontinuities that occur in the rock intersected by the borehole are not typically present in the laboratory-tested core.

Gravimetric moisture content, soil-moisture characteristic curves, and unsaturated hydraulic conductivity of tuff samples for boreholes at Areas G and L were measured in the laboratory. The gravimetric moisture content of core segments from 12 drill holes was found to range generally from two to four percent with isolated intervals ranging up to 10 to 28 percent. Soil moisture characteristic curves were determined for 20 samples of the Bandelier Tuff. Moisture content was determined for capillary pressures in the range of -0.03 to -0.34 bar [0.5 to 5 pounds per square inch (psi)]. Attempts to measure moisture contents at lower capillary pressures were unsuccessful because samples disaggregated. Thus, moisture characteristic curves could only be determined for volumetric moisture contents above 22 percent, which is considerably higher than the values observed from testing core samples of field measurements. However, some conclusions can be reached from the characteristic curve data. Moisture retention values of the tuff are extremely high, ranging up to 80 percent (60 percent volumetric moisture). Since all of the moisture content measurements for the tuff are significantly below 80 percent, capillary transport of liquids does not contribute to moisture movement and vapor transport is clearly the major mechanism of water transport.

Actual measurement of moisture content at depth in the tuff tends to verify the conclusion regarding moisture movement. Neutron logging of one borehole in each of Areas G and L was performed every two weeks for an approximately eight month period. Borehole logging was also performed daily for a period after three major precipitation events in the area. Moisture profiles measured in this manner show the upper 10 to 20 feet of the tuff to be affected by precipitation events and subject to seasonal fluctuations. Below 20 feet, however, moisture content is extremely low and in the range of the gravimetric moisture determination.

To measure capillary potential, thermocouple psychrometers were installed at numerous depths in one borehole in each of Areas G and L. Though data obtained from the psychrometers are highly variable, they indicate soil moisture tensions ranging from 1 to 15 bars. Utilizing measured hydraulic conductivity values for the tuff and hydraulic head data from the psychrometers, moisture flux calculations were performed to determine maximum rates of moisture movement in the tuff. For Area L, a maximum downward flux of 0.25 feet per year (ft/yr) and a maximum upward flux of 0.20 ft/yr were calculated. For Area G, maximum downward and maximum upward fluxes of 0.49 ft/yr and 0.041 ft/yr, respectively, were calculated. These calculated flux rates very likely overestimate the moisture flux values at Areas G and L because only hydraulic conductivity values at higher percentages of saturation than those observed in the field are available. Because hydraulic conductivity in the vadose zone typically increases with increases in percent saturation, the measured hydraulic conductivity values are certainly greater than actual field conditions. Lower values of flux rates (by about an order of magnitude) are predicted if calculated (rather than measured) hydraulic conductivity values are used. Though highly conservative, these moisture flux values show that very long periods of time would be required for water and contaminants to move by **unsaturated** flow from the disposal facilities to the ground water. In addition, there is no evidence to suggest that saturation of the tuff and subsequent transport of contaminants by saturated flow is possible.

4.0 CHEMICAL CHARACTERIZATION OF THE VADOSE ZONE

Chemical characterization data on the Bandelier Tuff at Areas G and L were obtained by analysis of core samples and by sampling and analysis of gases in the rock pores. Core samples were collected at about ten-foot intervals from seven boreholes at Areas G and L for a total of 70 samples. With the exception of two samples in Area L, all cores exhibited Extraction Procedure (EP) Toxic metals below detection limit concentrations (which are well below EP Toxic regulated concentrations). One sample collected from the zero to ten-foot depth interval had a detectable (though below regulatory limit) EP concentration of barium. A second sample collected from the ten- to twenty-foot depth slightly exceeded the EP Toxic limit for chromium. All core

samples were also analyzed for volatile organic compounds. No volatile organics were detected in core samples from Area G; however, the lower limit of detection for most of the compounds was in the parts per million range, not permitting detection of trace concentrations possibly present. Volatile organics were detected in core samples from various depths in all four boreholes from which samples were obtained at Area L. The detected compounds, ranging from part per billion to part per million concentrations at depths up to 100 feet, consist of a suite of common solvents and ketones (i.e., methylene chloride, acetone, tetrahydrofuran, methyl ethyl ketone, etc.).

A total of 23 sampling ports were installed in the seven test holes to permit collection of pore gas at various depths. Pore gases were collected by pumping air from the sampling port through charcoal adsorption tubes. After collection, volatile organics were extracted from the charcoal and analyzed. The results of the analyses indicate that volatile organic compound vapors are present in the pore gas of the tuff in part per million concentrations at depths up to about 100 feet.

Core analyses and pore gas data suggest that volatile organic constituents of the waste disposed of at Area G and/or Area L have migrated into the tuff. Based on the vadose zone characterization studies, vapor diffusion is the most probable migration mechanism.

5.0 GROUND WATER HYDROLOGY IN AREAS G AND L

The main aquifer in the Los Alamos area is the only aquifer capable of producing a municipal and industrial water supply. The hydraulic and chemical properties of the main aquifer are reasonably well known from information obtained from supply wells, stock wells, test wells, and springs. The upper surface of the main aquifer slopes eastward from the major recharge area in the Valles Caldera (west of the Pajarito Plateau) to the Rio Grande (east of the plateau) where it discharges as springs and seeps into the river.

Beneath Areas G and L, the upper surface of the main aquifer is contained in the poorly consolidated conglomerates, sandstones and siltstones of the Tesuque Formation. The main aquifer was encountered at a depth of about 875

feet below the land surface just west of Areas G and L. Based on data from supply wells in the Los Alamos area, the Tesuque has an average saturated thickness of 1,470 feet and a hydraulic gradient of 0.015. Using this hydraulic gradient value for calculation, the depth to the main aquifer beneath Areas G and L is 850 feet and 950 feet, respectively. Based on test data obtained from supply wells and an assumed porosity value of 30 percent, the velocity of water in the main aquifer is about 0.18 feet per day.

Test holes were drilled and monitoring wells were installed in Cañada del Buey (bounding Mesita del Buey on the north) and Pajarito Canyon (which bounds the mesa to the south) to investigate the alluvial perched water systems potentially present in these canyons. The alluvium in Cañada del Buey was found to be confined to the canyon, and all test holes in the alluvium were dry. In Pajarito Canyon, the alluvium also does not extend beneath the mesa. In this canyon, however, a perched water system was intersected by the boreholes. The top of the perched water is about one to five feet below the surface of the alluvium, and the water level fluctuates significantly over short periods of time. The approximate saturated thickness encountered by the wells is eight to ten feet, and also exhibits substantial fluctuations.

Water samples were collected from the Pajarito Canyon wells and analyzed for volatile organic compounds, selected metals and radiological parameters. No volatile organics were detected in the samples and metal concentrations and radiological parameters were found to be below drinking water standards. Thus, there appears to be no discernable effect on water quality in Pajarito Canyon from disposal operations at Areas G and L.

6.0 CONCLUSIONS

Several specific conclusions, based on the hydrogeologic investigations performed at Mesita del Buey in 1985 and 1986 and on previous work, can be reached relative to the characteristics of Areas G and L and the potential for migration of contaminants from waste disposal units in these areas:

1. The Bandelier Tuff stratigraphy at Areas G and L is similar to that of the tuff throughout the western Pajarito Plateau.

2. Vertical and near-vertical fractures (formed during cooling of the volcanically deposited material) are common in the Bandelier Tuff on Mesita del Buey (and elsewhere), though the degree of openness or pervasiveness of individual fractures is not well characterized.

3. No major fault zones that could serve as conduits from the shallow subsurface to the regional water table are known to exist at or near Areas G and L.

4. The combination of very low moisture content in the tuff, empirical determination that moisture from precipitation does not infiltrate below a depth of ten to 22 feet, and very low calculated flux rates all suggest that aqueous transport of contaminants through Bandelier Tuff is not a viable mechanism for contaminant migration at Areas G and L.

5. Volatile organic waste constituents have migrated (probably in the vapor phase) from land disposal units at Areas G and L based on the results of core and pore gas analyses conducted in 1985 and 1986.

6. Metals contamination from the land disposal units at Areas G and L was detected in only two samples from shallow depths (20 feet or less) at Area L.

7. Chemical data from the core and pore gas analyses (and information obtained from vadose zone characterization) support vapor phase migration from Areas G and L as the dominant transport mechanism, based on the presence of volatile organic vapors at depths of up to 100 feet.

8. No perched bodies of water, which could be hydraulically connected to the main aquifer, have been detected beneath Areas G and L.

9. Perched water in Pajarito Canyon is confined to alluvium within the canyon and does not extend vertically or horizontally into the Bandelier Tuff which forms Mesita del Buey. No perched water was detected in Cañada del Buey.

10. There is no evidence of migration of hazardous waste constituents from Areas G and L into the perched water contained in the alluvium of Pajarito Canyon.

TABLE ES-1

SUMMARY OF REQUIREMENTS AND COMPLIANCE WITH COMPLIANCE ORDER PARAGRAPH 25

PARAGRAPH 25 REQUIREMENTS				TESTS CONDUCTED TO SATISFY REQUIREMENT		
TASK	ACCEPTABLE METHODS	SAMPLE FREQUENCY	SAMPLE LOCATIONS	TEST CONDUCTED	BOREHOLE	INTERVAL TESTED (FEET BELOW SURFACE)
1. Intrinsic Permeability of Tuff, k	• Constant head test • Flow test • Pressure transient test	• 5 holes 125 ft deep • 1 test per horizon • 6 tests per hole	• TA-54 Area G • TA-54 Area L	• Laboratory (Dynamic, Klinkenberg)	LLM-85-01 LLM-85-02 LLM-85-05 LGM-85-06 LGM-85-11	30, 52, 101, 124 7, 36, 67, 117 15, 36, 76, 123 29, 51, 99, 115 3, 30, 94, 115
				• Field Vacuum Tests (Pressure Transient)	LLM-85-01 LLM-85-02 LLM-85-05 LGM-85-06 LGM-85-11	30-33, 70-73, 80-83, 94-97 10-13, 25-28, 87-90, 87-90 15-18, 40-43, 50-53, 60-63 10-13, 40-43, 60-63, 82-85, 87-90, 100-103 35-38, 77-80, 110-113
				Air Injection Tests (Pressure Transient)	LLM-85-01 LLM-85-02 LLM-85-05 LGM-85-06 LGM-85-11	9-15, 30-36, 51-57, 72-78, 93-99 9-15, 24-30, 45-51, 66-72, 87-93 24-30, 45-51, 55-61, 75-81, 82-88 38-44, 60-66, 81-87 9-15, 14-20, 35-41, 56-62, 77-83, 99-105, 108-114
2. Moisture Characteristic Curves, $\psi(\theta)$	• Any standard lab method • Drying curve only • More than one method needed	• 5 samples from each of 4 horizons	• TA-54 Area G • TA-54 Area L	• Centrifugal Method	LLM-85-01 LLM-85-02 LLM-85-05 LGM-85-06 LGM-85-11	30, 52, 101, 124 7, 36, 67, 117 15, 36, 76, 123 29, 51, 99, 115 3, 30, 94, 115
				• Pressure Plate Method	Samples Disaggregated	

TABLE ES-1
SUMMARY OF REQUIREMENTS AND COMPLIANCE WITH COMPLIANCE ORDER PARAGRAPH 25
(Continued)

PARAGRAPH 25 REQUIREMENTS				TESTS CONDUCTED TO SATISFY REQUIREMENT		
TASK	ACCEPTABLE METHODS	SAMPLE FREQUENCY	SAMPLE LOCATIONS	TEST CONDUCTED	BOREHOLE	INTERVAL TESTED (FEET BELOW SURFACE)
3. Unsaturated Hydraulic Conductivity of Tuff K(θ)	• Theoretical and laboratory methods required • Sufficient number of different methods must be employed to give trustworty predictions	• 5 samples from each of 4 horizons	• TA-54 Area G • TA-54 Area L	• Laboratory (Dynamic Method)	LLM-85-01 LLM-85-02 LLM-85-05 LGM-85-06 LGM-85-11	30, 52, 101, 124 7, 36, 67, 117 15, 36, 76, 123 29, 51, 99, 115 3, 30, 94, 115
				• Theoretical (Van Genuchten Method)	LLM-85-01 LLM-85-02 LLM-85-05 LGM-85-06 LGM-85-11	52, 101 36 123 99, 115 94
4. Infiltration and Redistribution of Meteoric Water Into Tuff	• Neutron logging and • Moisture blocks or psychrometry	• 4 holes, 2-50 ft deep and 2 100-ft deep • Neutron log each 2 weeks with daily logs after 2 autumn storms • 10 potential sensors per hole	• 2 at TA-54 Area G • 2 at TA-54 Area L	• Neutron Logging	LLN-85-04 LGN-85-08	108 ft 50 ft
				• Psychrometers	LLP-85-03 LGP-85-07	95 ft, 23 sensors 52 ft, 15 sensors

TABLE ES-1
SUMMARY OF REQUIREMENTS AND COMPLIANCE WITH COMPLIANCE ORDER PARAGRAPH 25
(Continued)

PARAGRAPH 25 REQUIREMENTS				TESTS CONDUCTED TO SATISFY REQUIREMENT		
TASK	ACCEPTABLE METHODS	SAMPLE FREQUENCY	SAMPLE LOCATIONS	TEST CONDUCTED	BOREHOLE	INTERVAL TESTED (FEET BELOW SURFACE)
5. Core and Pore Gas Analyses	• Standard methods for inorganics • GC or GC/MS for volatile organics	• At least 6 holes of varying depths • Cores analyzed for inorganics and volatile organics at 10 ft intervals • Pore gas samplers in bottom of holes • Analyze quarterly	• 2 at TA-54 Area G • 4 at TA-54 Area L	• Core Analyses	LGC-85-09	10 ft intervals
					LGC-85-10	10 ft intervals
					LLC-85-12	10 ft intervals
					LLC-85-14	10 ft intervals
					LLC-85-15	10 ft intervals
					LLC-85-16	10 ft intervals
				• Pore Gas Samplers	LGC-85-09	37, 63, 80, 91
					LGC-85-10	31, 53, 95
					LLC-85-12	6, 27, 41
					LLC-85-13	21, 43, 65
					LLC-85-14	13, 31, 46, 86
					LLC-85-15	19, 32, 82
					LLC-85-16	7, 17, 102
6. Analysis of Perched Water	• Observation wells in side canyons • Report summarizing applicability of research in Mortandad Canyon	• 6 wells bottoming in tuff • Samples and water levels collected quarterly	• 3 wells in Cañada del Buey • 3 wells in Pajarito Canyon	• Well Installation	CDBO-1	15 ft
					CDBO-2	18 ft
					CDBO-3	12 ft
					CDBO-4	12 ft
					PCO-1	22 ft
					PCO-2	22 ft
					PCO-3	20 ft
					PCM-1	60 ft
					PCM-2	120 ft
					PCM-3	60 ft
					PCM-4	60 ft

TABLE OF CONTENTS

	PAGE
LIST OF TABLES	iv
LIST OF FIGURES	viii
1.0 INTRODUCTION	1-1
1.1 PURPOSE AND SCOPE	1-1
1.2 DESCRIPTION OF WASTE MANAGEMENT OPERATIONS	1-2
1.2.1 Area G	1-2
1.2.1.1 Waste Disposal Pits	1-2
1.2.1.2 Area G Trenches	1-3
1.2.1.3 Disposal Shafts	1-3
1.2.2 Area L	1-3
1.3 DESCRIPTION OF 1985-1986 INVESTIGATIONS	1-4
1.3.1 Drilling Activities	1-4
1.3.2 Hydrologic Testing	1-6
1.3.3 Chemical Analyses	1-6
2.0 GEOLOGY	2-1
2.1 REGIONAL GEOLOGY	2-1
2.2 SITE GEOLOGY	2-2
2.2.1 Stratigraphy	2-3
2.2.1.1 General Stratigraphy of the Pajarito Plateau	2-3
2.1.1.2 Stratigraphy of Mesita del Buey	2-4
2.2.2 Structure	2-8
2.2.2.1 General Structure of the Pajarito Plateau	2-8
2.2.2.2 Structure of Mesita del Buey	2-9
3.0 HYDROLOGIC CHARACTERIZATION OF THE VADOSE ZONE	3-1
3.1 LOCAL CLIMATE	3-3
3.2 INTRINSIC PERMEABILITY OF THE VADOSE ZONE	3-3
3.2.1 Field Permeability Tests	3-4
3.2.1.1 Injection Tests	3-4
3.2.1.2 Vacuum Tests	3-5
3.2.2 Laboratory Permeability Tests	3-7
3.2.3 Summary of Intrinsic Permeability Testing	3-8
3.3 VADOSE ZONE MOISTURE CHARACTERISTICS	3-8
3.3.1 Gravimetric Moisture Content	3-8

TABLE OF CONTENTS

(Continued)

	PAGE
3.3.2 Soil Moisture Characteristic Curves	3-9
3.4 UNSATURATED HYDRAULIC CONDUCTIVITY AS A FUNCTION OF MOISTURE CONTENT	3-11
3.4.1 Measurements of Unsaturated Hydraulic Conductivity (Dynamic Method)	3-11
3.4.2 Theoretical Determination of Unsaturated Hydraulic Conductivity	3-13
3.5 VADOSE ZONE MOISTURE MONITORING	3-14
3.5.1 Neutron Moisture Logging	3-14
3.5.2 Measurement of Capillary Potential	3-17
3.6 GRADIENT DETERMINATIONS AND MOISTURE MOVEMENT	3-19
3.7 SUMMARY OF VADOSE ZONE HYDROLOGY	3-22
4.0 CHEMICAL CHARACTERIZATION OF THE VADOSE ZONE	4-1
4.1 TEST HOLE CORING AND PORE GAS ANALYSES	4-1
4.2 TEST HOLE CORE	4-1
4.2.1 Core Sampling	4-1
4.2.2 Analytical Methods	4-2
4.2.3 Results of EP Toxicity Analyses	4-2
4.2.4 Results of Core Analyses for Volatile Organic Compounds	4-3
4.3 TEST HOLE PORE GAS ANALYSES	4-4
4.3.1 Pore Gas Sampling	4-5
4.3.2 Analytical Method	4-5
4.3.3 Results of Pore Gas Analyses	4-6
4.4 SUMMARY OF CHEMICAL CHARACTERIZATION	4-7
5.0 GROUND WATER HYDROLOGY IN AREAS G AND L	5-1
5.1 MAIN AQUIFER	5-1
5.1.1 Hydraulic Characteristics of the Main Aquifer	5-1
5.1.2 Chemical Quality of the Main Aquifer Near Mesita del Buey	5-2
5.2 HYDROGEOLOGY OF PERCHED WATERS ADJACENT TO MESITA DEL BUEY	5-3
5.2.1 Relevant Hydrologic Studies in Mortandad Canyon	5-3
5.2.2 Cañada del Buey	5-5
5.2.3 Pajarito Canyon	5-5

TABLE OF CONTENTS

(Continued)

		PAGE
5.2.3.1	Nature and Extent of Perched Water in Pajarito Canyon	5-6
5.2.3.2	Hydraulic Properties of the Perched Water in Pajarito Canyon	5-7
5.2.3.3	Quarterly Water Sampling Procedures in Pajarito Canyon	5-8
5.2.3.4	Chemical Quality of Perched Water in the Alluvium of Pajarito Canyon	5-9
5.2.3.5	Summary of Perched Water Investigation in Pajarito Canyon	5-11
5.3	SUMMARY OF GROUND WATER HYDROLOGY IN AREAS G AND L	5-11
6.0	CONCLUSIONS	6-1
7.0	REFERENCES	7-1

APPENDIX A NEW MEXICO ENVIRONMENTAL IMPROVEMENT DIVISION COMPLIANCE ORDER/ SCHEDULE DATED MAY 7, 1985

APPENDIX B AREA L WASTE LOGS

APPENDIX C LITHOLOGIC LOGS AND CONSTRUCTION DETAILS FOR 1985 BOREHOLES

APPENDIX D GLOSSARY OF VADOSE ZONE TERMINOLOGY

APPENDIX E 1985-1986 PRECIPITATION MEASUREMENTS, LOS ALAMOS NATIONAL LABORATORY

APPENDIX F SOIL-MOISTURE CHARACTERISTIC CURVES AND UNSATURATED HYDRAULIC CONDUCTIVITY

APPENDIX G AREAS G AND L NEUTRON MOISTURE MEASUREMENTS AND NEUTRON PROBE CALIBRATION DATA

APPENDIX H AREAS G AND L THERMOCOUPLE PSYCHROMETER DATA

APPENDIX I HYDRAULIC HEAD AND MOISTURE FLUX CALCULATION WORKSHEETS

APPENDIX J CORE AND WATER ANALYSIS FOR VOLATILE ORGANIC COMPOUNDS, PURGE AND TRAP METHOD

APPENDIX K ANALYTICAL PROCEDURE FOR ANALYSIS OF VOLATILE ORGANICS PRESENT ON CHARCOAL TUBES

LIST OF TABLES

TABLE NO.	TITLE
1-1	Compliance Order Paragraph 25 Tasks and Corresponding Report Sections
1-2	Total Depths of Core and Drill Hole For Los Alamos 1985 Test Holes
3-1	Mean Monthly Precipitation, Los Alamos, New Mexico
3-2	Precipitation Measured at TA-54 Area G, 1986
3-3	Hydraulic Conductivity Determined From Air-Injection Tests in Los Alamos Drill Holes
3-4	Permeability Values Determined From Vacuum Tests in Los Alamos Drill Holes
3-5	Comparison of Intrinsic Permeability Values Determined From Air-Injection and Vacuum Tests in Los Alamos Drill Holes
3-6	Intrinsic Permeability Values Determined From Laboratory Analysis for Core Samples
3-7	Comparison of Average Intrinsic Permeability Values From Major Geologic Units of Bandelier Tuff in the Study Area
3-8	Results of Moisture/Tension Relationship Testing for Intact Cores of Bandelier Tuff
3-9	Water Effective Permeability and Unsaturated Hydraulic Conductivity of Samples of Bandelier Tuff
3-10	Model Predicted Hydraulic Conductivity of Bandelier Tuff at Minimum Measured Moisture Content
3-11	Summary of Data From Selected Psychrometers at TA-54 Areas G and L
3-12	Summary of Moisture Flux Calculations
4-1	EP Toxicity Analytical Results For Core From Drill Hole Number LLC-85-12
4-2	EP Toxicity Analytical Results For Core From Drill Hole Number LLC-85-13
4-3	EP Toxicity Analytical Results For Core From Drill Hole Number LLC-85-14
4-4	EP Toxicity Analytical Results For Core From Drill Hole Number LLC-85-15

LIST OF TABLES
(Continued)

TABLE NO.	TITLE
4-5	EP Toxicity Analytical Results For Core From Drill Hole Number LLC-85-16
4-6	EP Toxicity Analytical Results For Core From Drill Hole Number LLC-85-17
4-7	EP Toxicity Analytical Results For Core From Drill Hole Number LLC-85-18
4-8	EP Toxicity Analytical Results For Core From Drill Hole LLC-85-A
4-9	EP Toxicity Analytical Results For Surface Impoundment Core Samples
4-10	EP Toxicity Analytical Results For Core From Drill Hole Number LGC-85-09
4-11	EP Toxicity Analytical Results For Core From Drill Hole Number LGC-85-10
4-12	Miscellaneous Chemical Analytical Results For Six Background Soil Samples Taken Near Area L
4-13	Location and Description of Area L Background Soil Samples
4-14	Miscellaneous Chemical Analytical Results For Core From Drill Hole Number LLC-85-17
4-15	Miscellaneous Chemical Analytical Results For Core From Drill Hole Number LLC-85-18
4-16	Miscellaneous Chemical Analytical Results For Core From Drill Hole Number LLC-85-A
4-17	Miscellaneous Chemical Analytical Results For Surface Impoundment Core Samples
4-18	Volatile Organic Compounds Analyzed by Los Alamos National Laboratory in Cores From Drill Holes
4-19	Volatile Organic Compounds Analyzed by Rocky Mountain Analytical Laboratory in Cores From Drill Holes
4-20	Volatile Organic Analytical Results For Drill Hole Cores - August 1985

LIST OF TABLES
(Continued)

TABLE NO.	TITLE
4-21	Volatile Organic Compounds Analyzed in Pore Gas by Los Alamos National Laboratory
4-22	Volatile Organic Compound Detection Limits For Representative Analytes
4-23	1986 Pore Gas Sampling, Drill Hole LLC-85-12
4-24	1986 Pore Gas Sampling, Drill Hole LLC-85-13
4-25	1986 Pore Gas Sampling, Drill Hole LLC-85-14
4-26	1986 Pore Gas Sampling, Drill Hole LLC-85-15
4-27	1986 Pore Gas Sampling, Drill Hole LLC-85-16
4-28	1986 Pore Gas Sampling, Drill Hole LGC-85-09
4-29	1986 Pore Gas Sampling, Drill Hole LGC-85-10
5-1	Lithologic Log of Water-Supply Well Pajarito Mesa #2 (PM-2)
5-2	Construction and Hydrologic Data for Wells in the Pajarito Field, Los Alamos
5-3	Hydrologic Data for Springs in the White Rock Canyon Area
5-4	Lithologic Logs of Monitoring Wells in Cañada del Buey
5-5	Summary of Monitoring Well Construction in Pajarito Canyon and Mesita del Buey
5-6	Summary of Water-Level Measurements and Elevations for Monitoring Wells in Cañada del Buey
5-7	Moisture Content of Cuttings from the PCM-Series Test Holes
5-8	Lithologic Logs of Monitoring Wells in Pajarito Canyon
5-9	Lithologic Logs of the PCM-Series Test Holes in Pajarito Canyon
5-10	Lithologic Logs of Test Holes T-5 and T-6 in Pajarito Canyon
5-11	Summary of Water-Level Measurements and Elevations for Monitoring Wells in Pajarito Canyon

LIST OF TABLES
(Continued)

TABLE NO.	TITLE
5-12	Summary of Inorganic Parameters Routinely Analyzed in Monitoring Well Samples
5-13	Summary of Volatile Organic Compounds Routinely Analyzed in Monitoring Well Samples
5-14	Inorganic Water-Quality Results from Monitoring Well PCO-1 in Pajarito Canyon
5-15	Inorganic Water-Quality Results from Monitoring Well PCO-2 in Pajarito Canyon
5-16	Inorganic Water-Quality Results from Monitoring Well PCO-3 in Pajarito Canyon
5-17	Volatile Organic Water-Quality Results from Monitoring Well PCO-1 in Pajarito Canyon
5-18	Volatile Organic Water-Quality Results from Monitoring Well PCO-2 in Pajarito Canyon
5-19	Volatile Organic Water-Quality Results from Monitoring Well PCO-3 in Pajarito Canyon

LIST OF FIGURES

FIGURE NO.	TITLE
1-1	Location Map for Mesita del Buey and Technical Area 54
1-2	Area G Land Disposal Facilities (TA-54 Area G)
1-3	TA-54 Area L Waste Management Facilities
1-4	Location Map for Instrumented Boreholes, Test Holes, and Monitoring Wells in Technical Area 54, Areas G and L
2-1	Physiographic Features of the Jemez Mountains
2-2	Generalized Geologic Cross-Section of Pajarito Plateau
2-3	Generalized Stratigraphic Column for Mesita del Buey
2-4	Generalized Geologic Cross-Section (East-West) Showing Relationship of the Chino Mesa Basalt to the Bandelier Tuff
2-5	Geologic Cross-Section of the Tshirege Member of the Bandelier Tuff at Mesita Del Buey
2-6	Location of Technical Area 54 Facility Relative to the Nearby Fault Traces
3-1	Volumetric Moisture Profiles of Bandelier Tuff From Selected Borings in TA-54 Areas G and L
3-2	Soil Moisture Characteristic Curve for a Typical Sample of Bandelier Tuff
3-3	Moisture Content Versus Depth, Area G, December 1986 Through May 1986
3-4	Moisture Content Versus Depth, Area G, June 1986 Through December 1986
3-5	Moisture Content Versus Depth, Area L, December 1985 Through May 1986
3-6	Moisture Content Versus Depth, Area L, June 1986 Through December 1986
3-7	Moisture Content at Selected Depths, Area G, October 1986
3-8	Moisture Content at Selected Depths, Area G, November 1986
3-9	Moisture Content at Selected Depths, Area L, October 1986

LIST OF FIGURES
(Continued)

FIGURE NO.	TITLE
3-10	Moisture Content at Selected Depths, Area L, November 1986
3-11	Average Soil-Water Tension, TA-54 Area G
3-12	Average Soil-Water Tension, TA-54 Area L
4-1	Diagram of a Pore Gas Sampling Port
4-2	1,1,1-Trichloroethane Concentrations in Pore Gas Samples From Drill Hole LLC-85-12, 1986
4-3	1,1,1-Trichloroethane Concentrations in Pore Gas Samples From Drill Hole LLC-85-14, 1986
4-4	1,1,1-Trichloroethane Concentrations in Pore Gas Samples From Drill Hole LLC-85-15, 1986
4-5	1,1,1-Trichloroethane Concentrations in Pore Gas Samples From Drill Hole LLC-85-16, 1986
4-6	1,1,1-Trichloroethane Concentrations in Pore Gas Samples From Drill Hole LGC-85-09, 1986
4-7	1,1,1-Trichloroethane Concentrations in Pore Gas Samples From Drill Hole LGC-85-10, 1986
5-1	Location of Supply Wells, Test Wells, Stock Wells, and Springs in the Los Alamos Area
5-2	Potentiometric Surface Map of the Main Aquifer in the Los Alamos Area
5-3	Rate of Movement of Water in the Main Aquifer in the Los Alamos Area
5-4	Stiff Diagrams for the Main Aquifer Near Mesita del Buey
5-5	Graphic Comparison of Chemical Constituents in the Main Aquifer from Supply Wells, Test Wells, Stock Wells, and Springs
5-6	Construction Schematic of Monitoring Wells in Pajarito Canyon and Cañada del Buey
5-7	Topographic Profiles A-A' and B-B' and Geologic Cross-Sections of Pajarito Canyon and Cañada del Buey

LIST OF FIGURES
(Continued)

FIGURE NO.	TITLE
5-8	Topographic Profiles C-C' and D-D' and Geologic Cross-Sections of Pajarito Canyon and Cañada del Buey
5-9	Contour Map of Technical Area 54 Showing the Locations of Monitoring Wells and Cross-Sections
5-10	Northwest-Southeast Topographic Profiles and Geologic Cross Sections of Mesita del Buey and Pajarito Canyon
5-11	Plot of Water-Level Elevations Versus Time for Pajarito Canyon Monitoring Wells
5-12	Summary of the 1985-1986 Precipitation Data in Area G
5-13	Stiff Diagrams for Monitoring Well PCO-1 in Pajarito Canyon
5-14	Stiff Diagrams for Monitoring Well PCO-2 in Pajarito Canyon
5-15	Stiff Diagrams for Monitoring Well PCO-3 in Pajarito Canyon

1.0 INTRODUCTION

1.1 PURPOSE AND SCOPE

This report presents a summary of the geohydrology of Waste Disposal Areas G and L in Technical Area (TA) 54 at Los Alamos National Laboratory (see Figure 1-1 for site location). Also presented are other pertinent data and discussions relevant to the potential for migration of hazardous waste from the disposal areas. This report was prepared in response to a Compliance Order/ Schedule dated May 7, 1985 (Docket Number 001007) issued to the U.S. Department of Energy, Los Alamos Area Office and the University of California, Los Alamos National Laboratory by the Environmental Improvement Division (EID) of the State of New Mexico Health and Environment Department. The Order, issued pursuant to the New Mexico Hazardous Waste Act, mandated that certain tests and investigations be performed at Areas G and L to obtain information on the geohydrological characteristics of the waste disposal area relevant to the potential for migration of contaminants into the area ground water. A copy of the Order is included as Appendix A.

Work was initiated in late 1985 to fulfill the testing requirements in the Order, and numerous reports on the results of individual tests or groups of tests have been prepared by Bendix Field Engineering Corporation/Grand Junction (BFEC, now UNC Technical Services, Inc.) and Los Alamos National Laboratory. Also, data have been obtained since publication of the most recent reports that are relevant to geohydrologic characterization of Areas G and L. The purpose of this report is to summarize the results of the recent work (published and unpublished) and to combine these data with published information on site characteristics into a cogent "publishable" report on the chemical waste migration potential in the lithosphere at Areas G and L.

The report is divided into six sections. The remainder of this section provides a brief summary of waste disposal operations at TA-54, Areas G and L, and a general description of the activities performed to satisfy individual test requirements in the Order. Section 2.0 provides a summary description of the regional and site geology. Sections 3.0 and 4.0 describe the hydrologic characteristics and chemical characteristics, respectively, of Areas G and L. A discussion of the ground water hydrology at Areas G and L is given in

Section 5.0 and a brief summary and conclusions are provided in Section 6.0. Table 1-1 provides a list of the tasks required by the Order and the numbers of the sections of this report that discuss the test and test results.

1.2 DESCRIPTION OF WASTE MANAGEMENT OPERATIONS

Los Alamos National Laboratory has operated two waste disposal facilities in Technical Area 54 on Mesita del Buey located in the southern half of Section 31, T19N, R7E (Figure 1-1). These areas, designated Areas G and L, occupy 63 acres and about 2.5 acres, respectively. Area G, used primarily for disposal of low-level radioactive materials, has been in operation since 1957 and is expected to remain active through the foreseeable future. Area L served as the Laboratory's principal chemical waste disposal area between 1964 and 1985. Currently, no disposal of hazardous chemical waste occurs at these areas.

1.2.1 Area G

Low-level radioactive waste has been disposed of in Area G since 1957. In addition to the low-level waste, small amounts of asbestos, beryllium residues, empty pesticide containers, PCB contaminated solids, and solid trash-type wastes contaminated with known or suspected carcinogens were disposed of at Area G. The Laboratory was granted approval in 1980 by the U.S. Environmental Protection Agency to dispose of PCB solid wastes in facilities at Area G. Hazardous wastes regulated under RCRA represent less than one percent of the total waste at Area G. Waste disposal practices at Area G include use of shafts, trenches and pits. Figure 1-2 shows the location of the waste disposal units.

1.2.1.1 Waste Disposal Pits

Currently there are 31 active and filled pits in Area G, 28 have been filled and 3 are open; some pits are yet to be excavated (see Figure 1-2). Burial pits vary in dimensions, the deepest being 65 feet deep; 15 feet is maintained between pits, and all pits are located a minimum of 50 feet from the edge of the mesa (Zygmunt, 1984).

After excavation of each pit into the Bandelier Tuff, geologic and photographic records are made of the floor and walls. Pit floors are then layered

with a one-half-foot blanket of compacted crushed tuff. Solid or solidified wastes are placed in the pits in layers with one-half-foot layers of crushed tuff between layers of waste. When the pits are filled to within about three feet of the lowest point of the pit rim, they are covered with crushed tuff and topsoil to minimize run-on and erosion (Zygmunt, 1984).

1.2.1.2 Area G Trenches

Eight trenches for storage of waste are present in Area G, four of which are not yet excavated. Trenches A and B are cored in the tuff with three-foot diameters by two-foot holes on about three-foot centers. Casks which contain waste are placed within the trenches. Each waste cask stores two 30-gallon drums of waste. After an array of casks has been placed into a trench, the trenches are backfilled with crushed tuff to the level of the casks. Corrugated decking is placed on top of the cask lids and the trenches are filled to the surface with crushed tuff (Rogers, 1977).

1.2.1.3 Disposal Shafts

About 100 disposal shafts in the Bandelier tuff are located in Area G disposal shaft field and are used for disposal of low-level radioactive waste (Rogers, 1977). The first shafts were completed at the end of 1965 and were put into use in early 1967. Two types of shafts were utilized in Area G: lined and unlined. Lined shafts, 14 through 23, used primarily for storage of tritium-contaminated waste, consist of three foot diameter borings, 25 feet deep; one foot diameter steel pipe is centered in the boring, and the annulus is filled with concrete. The remaining shafts range from two feet to six feet in diameter and 25 feet to 60 feet in depth. The Area G shafts are separated by a minimum distance of 7.5 feet. Wastes are layered in the shafts with one-half-foot layers of crushed tuff between layers of waste, shafts are filled to within about three feet of the lowest point of the shaft rim, covered with one-half foot of crushed tuff and finally covered with about three feet of uncontaminated concrete (Zygmunt, 1984).

1.2.2 Area L

Area L has been the principal chemical waste handling and disposal area at the Laboratory since 1964. From 1964 through May 1975, all chemical wastes were disposed of in one pit at the site, Pit A (Figure 1-3). Beginning in June

1975, the disposal pit was covered and shafts in the tuff were used for disposal of chemical waste until 1985. A surface impoundment that may have been used for hazardous waste disposal was also open during part of this time. All disposal of chemical waste at Area L was discontinued in 1985.

Thirty-four shafts are present in Area L; all have been sealed. Figure 1-3 shows the location of each shaft and contains information about the period of use and type of waste deposited in each. The Area L shafts are similar to those in Area G. They range from three feet to eight feet in diameter and are approximately 60 feet deep. The shafts are typically spaced about 15 feet apart (center to center). Upon completion of shafts, geologic records and photographs were made and a three-foot thick layer of crushed tuff was placed in the bottom. Containerized wastes were lowered into the shafts with one-half-foot layers of crushed tuff separating drums. As with the Area G shafts, when the shafts were filled to within about three feet of the surface, the wastes were covered with compacted crushed tuff and sealed with a minimum of three feet of concrete (Zygmunt, 1984).

Each shaft was dedicated to accept only compatible waste materials. A list of the hazardous waste materials which are known to have been placed into shafts 19 through 34 is provided in Appendix B. Waste disposal records for earlier shafts are incomplete. Prior to 1982, shaft disposal of liquid chemicals was conducted without the addition of absorbents. Calculations in DOE (1984) show that the volume of non-absorbed liquids is insufficient to support significant downward migration of liquid contaminants.

1.3 DESCRIPTION OF 1985-1986 INVESTIGATIONS

1.3.1 Drilling Activities

During 1985, test holes were drilled both from the top of Mesita del Buey and in the adjacent canyons to investigate the upper part of the vadose zone (Figure 1-4 and Table 1-2). Eighteen test holes were drilled into the Bandelier Tuff from the top of Mesita del Buey (the location of Technical Area 54, Areas G and L). The locations of these holes are shown on Figures 1-2 and 1-3. The 18 holes were drilled using a Central Mining Equipment (CME) Model 55 drilling rig equipped with standard six and five-eighth-inch outside diameter hollow-stem augers and a continuous sampling system. Core was

obtained using a two-inch diameter, five-foot long, split-barrel sampler attached to the center drill stem of the augers. Of the about 2,190 total footage drilled, 1,709 feet of core were obtained from 16 of the holes (Table 1-2). Standard four-inch outside diameter solid stem augers were used to bore the two drill holes from which no core was desired. Core was obtained in five-foot intervals and samples for the various tests planned were collected from the core and appropriately preserved. After samples were selected, a lithologic log was prepared (lithologic logs are provided in Appendix C) and the core was placed in labeled boxes for transfer to a storage facility. All down-hole equipment was decontaminated by steam cleaning followed by a methanol rinse and air-drying after completion of each test hole to obviate the potential for cross-contamination. In addition to these 18 holes, a 60-foot deep borehole was sunk near the surface impoundment at Area L (Figure 1-3) to obtain core samples for chemical analysis.

After drilling was complete, each hole was geophysically logged using four different probes to generate the following data: 1) spectral gamma and three-arm caliper logs, 2) natural gamma, epithermal neutron and vertical deviation logs, 3) magnetic susceptibility logs, and 4) moisture logs derived from epithermal neutron data. In addition, 16 of the 18 holes were logged with another probe to generate a gamma-gamma density, natural gamma and one-arm caliper log. Copies of all logs run are provided in BFEC (1985a).

The manner in which each test hole was completed depended on its primary purpose. The hole numbering scheme provides a code that indicates the general completion configuration for each hole and the sequence in which the holes were drilled. The first letter in each hole number, L, refers to Los Alamos. The second letter, G or L, identifies the waste disposal area in or near which the hole is located. The third letter indicates the primary purpose for which the hole was drilled; the codes were assigned as follows:

- M: Moisture Holes - To be used to determine intrinsic permeability and hydraulic conductivity of the tuff

- C: Core and Pore-Gas Sampling Holes - To be used to collect samples for EP-toxicity and volatile-organic analyses, and for the installation of pore-gas sampling apparatus

- P: Psychrometer Holes - To be used for the installation of thermocouple psychrometers and pressure transducers to determine local moisture conditions, temperature, and pressure

- N: Neutron Moisture Access Holes - To be used by LANL for moisture measurements.

The middle designation, 85, indicates the year that the test holes were drilled, and the final two digits refer to the drilling sequence. The construction details for each of the test holes are shown on the figures in Appendix C.

In addition to the holes drilled on Mesita del Buey, test holes were also sunk in the canyons that bound the mesa (Figure 1-4 and Table 1-2). Four test holes were drilled into the alluvium of Cañada del Buey and seven holes were sunk in Pajarito Canyon alluvium. These holes were drilled using a truck-mounted, continuous flight hollow-stem auger drilling rig. Test holes penetrated the alluvium and were drilled several feet into the underlying Bandelier Tuff. Lithologic logs were prepared during drilling and are included in Appendix C. All four holes in Cañada del Buey and three of the seven holes in Pajarito Canyon were completed as monitoring (or observation) wells. Construction details for these monitoring wells are also provided in Appendix C.

1.3.2 Hydrologic Testing

Samples of core from the holes drilled on Mesita del Buey were tested for a number of parameters that have import on the hydrologic behavior of the Bandelier Tuff. These tests, described in Sections 3.3 and 3.4 included those necessary to determine gravimetric moisture content, porosity, soil moisture characteristic curves, permeability and hydraulic conductivity. Samples of alluvium from some holes drilled in Cañada del Buey and Pajarito Canyon were also tested to determine gravimetric moisture content (see Section 5.2 for details).

In addition to laboratory tests to determine pertinent hydrologic parameters, field tests were also conducted in the test holes drilled on Mesita del Buey. These tests included two types of borehole injection tests and vacuum tests

(Section 3.2). Other investigations performed in these test holes over a period of months included atmospheric/rock-pore pressure monitoring, measurements of temperature and water potential, and neutron moisture measurements (Section 3.5). Hydrologic investigation activities in the holes in the canyons consisted only of measuring water levels over a period of months in those holes that encountered perched water (Section 5.2).

1.3.3 Chemical Analyses

Analyses of rock core and pore gases from the Mesita del Buey test holes and water samples collected from the canyon monitoring wells were performed for a selected group of parameters. Parameters included those needed to detect constituents of wastes disposed of at Areas G and L. A discussion of the sampling and analytical regimens and the analytical results for core samples and pore gas samples are presented in Sections 4.2 and 4.3, respectively. For water samples, analytical results are presented in Section 5.2.

TABLE 1-1

COMPLIANCE ORDER PARAGRAPH 25 TASKS AND CORRESPONDING REPORT SECTIONS

COMPLIANCE ORDER PARAGRAPH 25 TASK	REPORT SECTION
Task 1. Intrinsic Permeability of Tuff, k	3.2
Task 2. Soil Moisture Characteristic Curves, $\Psi(\theta)$	3.3.2
Task 3. Unsaturated Hydraulic Conductivity of Tuff, $K(\theta)$	3.4
Task 4. Infiltration and Redistribution of Meteoric Water into Tuff	3.5
Task 5. Core and Pore Gas Analyses	4.1, 4.2, 4.3
Task 6. Analysis of Perched Water	5.2

TABLE 1-2

TOTAL DEPTHS OF CORE AND DRILL HOLE FOR LOS ALAMOS 1985 TEST HOLES
(depths in feet)

DRILL-HOLE NUMBER	TOTAL DEPTH CORED	TOTAL DEPTH DRILLED
LLM-85-01	124	140
LLM-85-02	125	145
LLP-85-03	99	120
LLN-85-04[1]	0	120
LLM-85-05	124	145
LGM-85-06	124	145
LGP-85-07	49	60
LGN-85-08[1]	0	60
LGC-85-09	99	120
LGC-85-10	99	120
LGM-85-11	124	145
LLC-85-12	99	120
LLC-85-13	99	120
LLC-85-14	99	120
LLC-85-15	99	120
LLC-85-16	99	120
LLC-85-17	149	150
LLC-85-18	99	120
PCO-1	0	22
PCO-2	0	22
PCO-3	0	20
PCM-1	0	60
PCM-2	0	120
PCM-3	0	60
PCM-4	0	60
CDBO-1	0	15
CDBO-2	0	18
CDBO-3	0	12
CDBO-4	0	12

[1] Hole augered with a 4-inch-O.D. solid-stem auger.

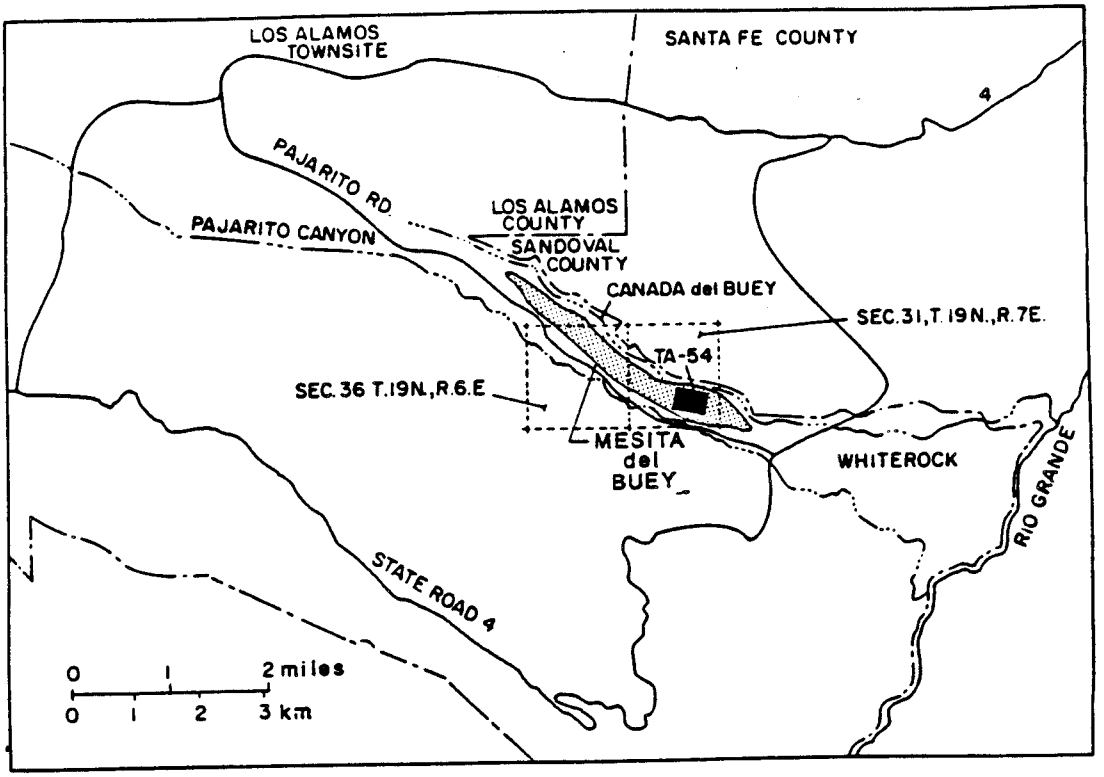

From Rogers (1977)

FIGURE 1-1

LOCATION MAP
FOR MESITA DEL BUEY
AND TECHNICAL AREA 54

PREPARED FOR

LOS ALAMOS NATIONAL LABORATORY
LOS ALAMOS, NEW MEXICO

... Creating a Safer Tomorrow

© 1984 IT CORPORATION
ALL COPYRIGHTS RESERVED
Do Not Scale This Drawing

DRAWN BY LLF 2/27/87
CHECKED BY 3/25
APPROVED BY
3/25/87
DRAWING NUMBER 301017 02.A20
65360

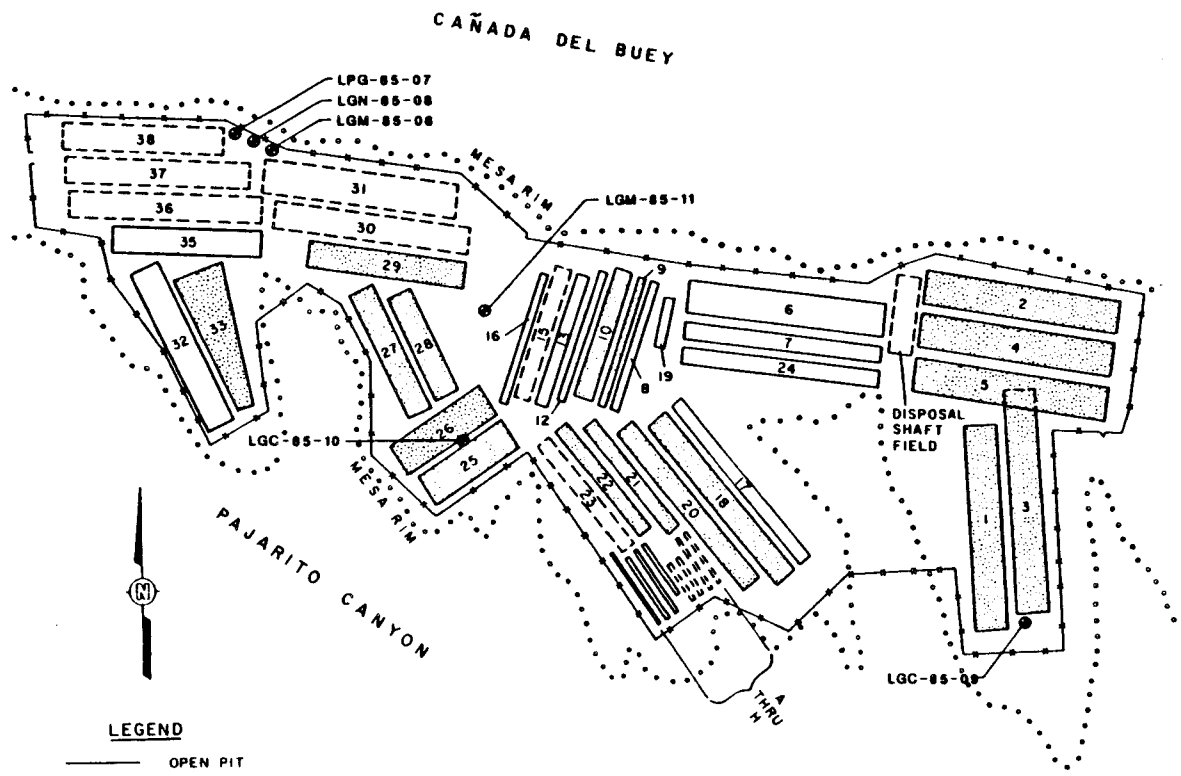

LEGEND

OPEN PIT

PLANNED PIT

FILLED PIT

DRILL HOLE FOR VADOSE ZONE CHARACTERIZATION

FIGURE 1-2

AREA G LAND DISPOSAL FACILITIES

(TA-54 AREA G)

PREPARED FOR

LOS ALAMOS NATIONAL LABORATORY

LOS ALAMOS, NEW MEXICO

Creating a Safer Tomorrow

DRAWN BY	L.I.F.	CHECKED BY		DRAWING NUMBER 301017 B17
	10/16/84	APPROVED BY		

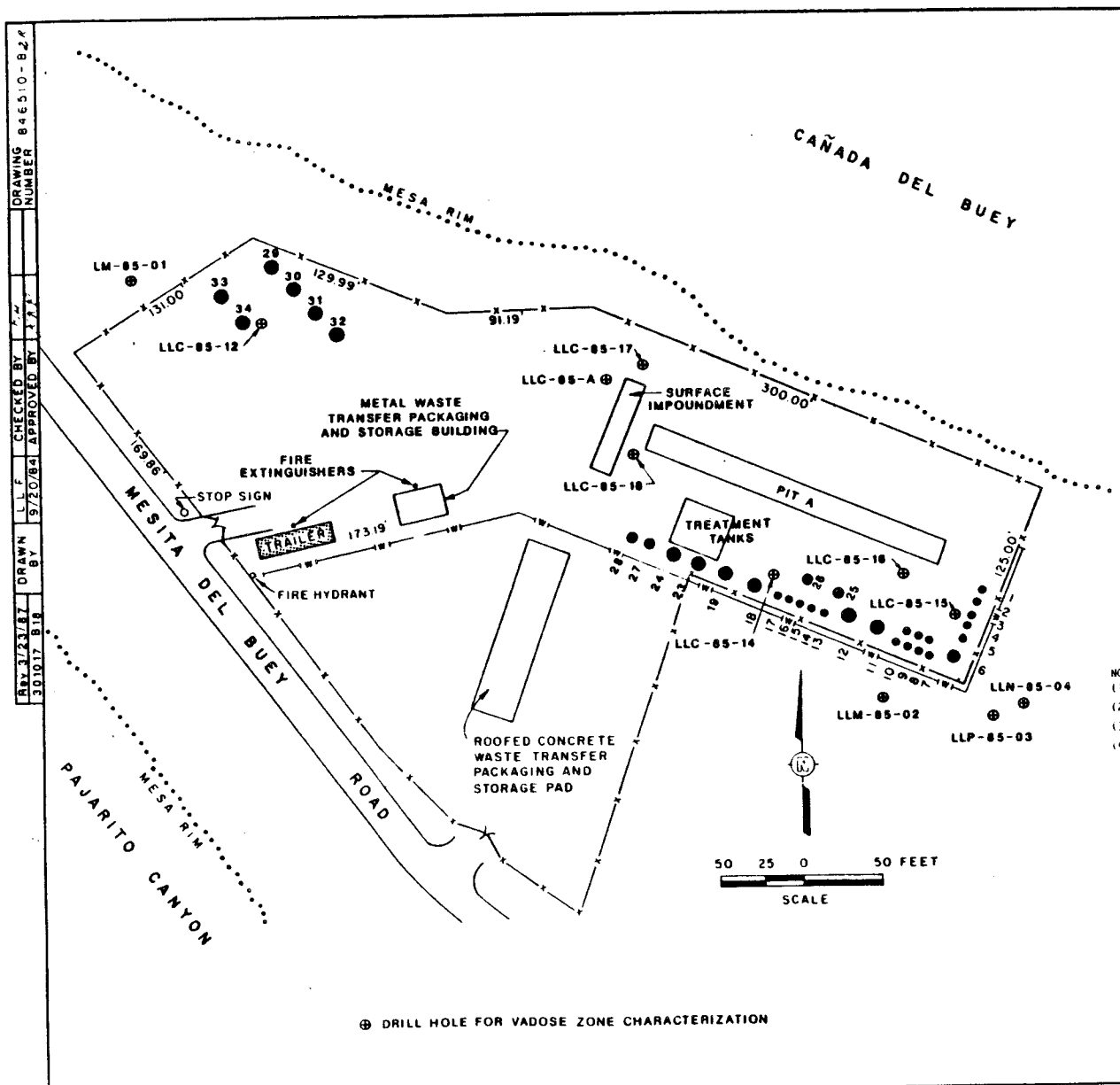

AREA L SHAFTS[1]
(INFORMATION CURRENT MARCH 1985)

SHAFT NO.	SHAFT DIAMETER (FEET)	DATE DRILLED	DATE CAPPED	CONTENTS
1	3	4/80	9/83	ORGANICS[2]
2	3	2/75	7/79	ACIDS & BASES
3	3	2/75	11/78	INORGANIC
4	3	2/75	5/80	ORGANIC
5	3	2/75	6/77	WASTE OIL
6	4	6/75	6/79	REACTIVE
7	3	6/75	6/79	REACTIVE
8	3	6/75	6/79	REACTIVE
9	3	6/75	6/79	GAS CYLINDERS
10	3	6/77	6/79	WASTE OIL
11	8	1/78	7/79	WASTE OIL/SOLVENT
12	4	1/78	7/79	WASTE OIL/SOLVENT
13	3	6/79	5/82	INORGANIC
14	3	6/79	5/82	REACTIVE
15	3	6/79	5/82	REACTIVE
16	3	6/79	5/82	GAS CYLINDERS
17	3	6/79	5/82	ORGANIC
18	8	6/79	6/80	WASTE OIL
19	8	4/80	5/82	WASTE OIL
20	3	4/80	9/83	INORGANIC
21	3	4/80	1/86	GAS CYLINDERS
22	3	4/80	9/83	ORGANIC
23[3]	8	4/82	3/84	WASTE OIL
24[4]	8	4/82	4/84	ORGANIC & WASTE OIL
25	6	3/82	5/85	INORGANIC
26	6	3/82	3/84	ORGANIC
27	4	1/83	2/85	SPECIAL[5]
28	4	1/82	5/85	SPECIAL
29	6	12/83	3/84	ORGANIC
30	6	12/83	3/84	ORGANIC
31	6	12/83	3/84	ORGANIC
32	4	3/84	3/84	ORGANIC
33	5	3/84	2/85	ORGANIC
34	6	2/85	5/85	ORGANIC

NOTES:
(1) ALL SHAFTS ARE APPROXIMATELY 60 FEET DEEP.
(2) PRIOR TO SHAFT 23, LIQUIDS WERE DISPOSED OF IN DRUMS WITHOUT ADDING ABSORBENTS.
(3) MIDDLE SECTION OF THIS SHAFT NOT USED.
(4) USED FOR MISCELLANEOUS WASTE REQUIRING GREATER ISOLATION.

FIGURE 1-3

TA-54 AREA L
WASTE MANAGEMENT FACILITIES

PREPARED FOR

LOS ALAMOS NATIONAL LABORATORY
LOS ALAMOS, NEW MEXICO

IT CORPORATION

DRAWING NUMBER 846510-B2
CHECKED BY
APPROVED BY
DRAWN BY L.L.F. 9/20/84
Rev 3/23/87 301017 B18

9-1-53 HERCULENE A&B SMITH CO. PGH. PA.

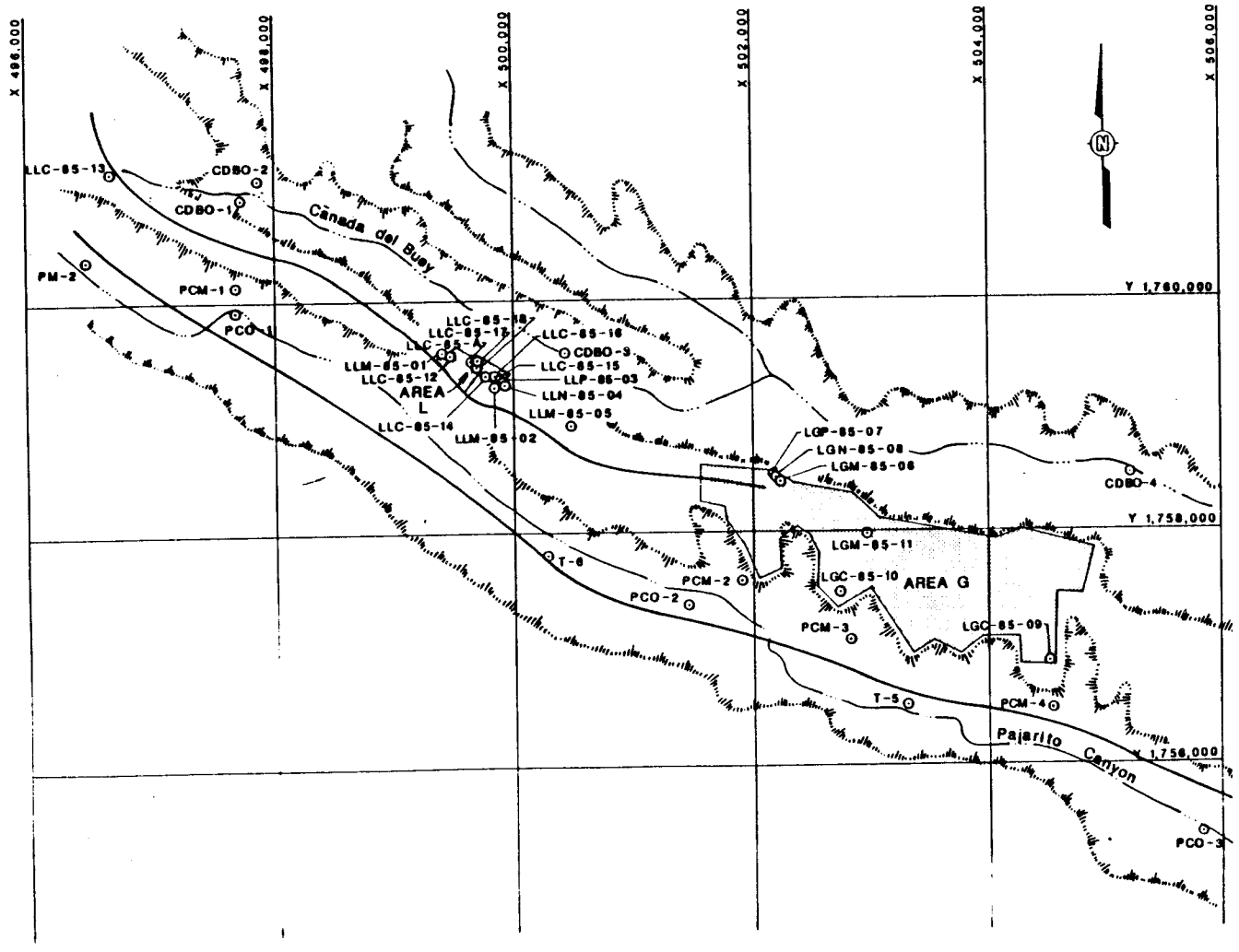

WELL NO.	Y-COORDINATE	X-COORDINATE	ELEVATION (LAND SURFACE DATUM)
CDBO-1	1,760,881.92	497,724.37	6757.5
CDBO-2	1,761,041.07	497,874.80	6748.2
CDBO-3	1,759,548.98	500,432.90	6673.2
CDBO-4	1,758,484.91	505,230.80	65[illegible].5
LLM-85-01	1,759,552.34	499,402.86	6797.4
LLM-85-02	1,759,260.86	499,853.04	679[illegible].7
LLP-85-03	1,759,269.11	499,923.76	6788.7
LLN-85-04	1,759,265.96	499,924.24	6788.3
LLM-85-05	1,758,919.02	500,471.44	6772.5
LGM-85-06	1,758,437.40	502,239.90	6730.3
LGP-85-07	1,758,462.39	502,195.69	673[illegible]
LGN-85-08	1,758,457.04	502,205.42	673[illegible].5
LGC-85-09	1,756,884.15	504,521.44	6659.3
LGC-85-10	1,757,487.94	502,748.67	6707.[illegible]
LGM-85-11	1,757,977.36	502,978.01	6715.5
LLC-85-12	1,759,536.30	499,477.89	6794.[illegible]
LLC-85-13	1,761,119.07	496,644.14	6856
LLC-85-14	1,759,355.53	499,782.26	679[illegible].4
LLC-85-15	1,759,315.73	499,895.35	6787.5
LLC-85-16	1,759,350.09	499,850.10	6788.3
LLC-85-17	1,759,485.35	499,703.83	6788.4
LLC-85-18	1,759,440.61	499,698.48	6790.4
PCO-1	1,759,928.36	497,674.98	6687.3
PCO-2	1,757,379.51	501,455.63	6618.3
PCO-3	1,755,423.76	505,841.81	65[illegible].3
PM-2	1,760,367.72	496,447.87	6713.2
T-5	1,756,514.61	503,312.12	659[illegible]
T-6	1,757,817.74	500,272.15	664[illegible]
PCM-1			664[illegible]
PCM-2			66[illegible]
PCM-3			66[illegible]
PCM-4			65[illegible]

FIGURE 1-4

LOCATION MAP FOR INSTRUMENTED BOREHOLES, TEST HOLES, AND MONITORING WELLS IN TECHNICAL AREA 54, AREAS G AND L

PREPARED FOR

LOS ALAMOS NATIONAL LABORATORY
LOS ALAMOS, NEW MEXICO

⊙ INSTRUMENTED BOREHOLES, TEST HOLES, AND MONITORING WELLS

IT Creating a Safer Tomorrow

DRAWN BY	MJG	7/25/87	CHECKED BY		APPROVED BY		DRAWING NUMBER	301017 816

1984 IT CORPORATION
ALL COPYRIGHTS RESERVED
Do Not Scale This Drawing

2.0 GEOLOGY

Numerous subsurface geological investigations of the Pajarito Plateau and the Mesita del Buey portion of the plateau (the part of the plateau on which Areas G and L are located) have been performed during at least the past 40 years. Many studies of the plateau have been conducted in conjunction with hydrologic investigations performed to ascertain the adequacy of ground water resources for the Laboratory. Many other studies, concentrated solely on the geology of the plateau, have been undertaken to gain further basic knowledge of volcanic tuffs or the Jemez volcanic assemblage. In addition to studies of the entire Pajarito Plateau, detailed investigations of the geology of Mesita del Buey have been conducted during the past 20 years to ensure that the mesita terrane provides adequate containment for land disposal of hazardous and radioactive wastes. The more recent of these studies, performed by BFEC and the Laboratory primarily in 1985 and early 1986 and described in the previous section, have added detail to the knowledge of the upper 100 feet or so of the geology of Mesita del Buey. The results of these efforts have been combined with previously published information and are presented in the sections that follow to provide the geologic framework necessary to an understanding of the Mesita del Buey hydrology.

2.1 REGIONAL GEOLOGY

Los Alamos National Laboratory is located on the east-central edge of the Jemez Mountains. The Jemez Mountains are formed by a complex pile of volcanic rocks along the northwest margin of the Rio Grande rift in north-central New Mexico (Figure 2-1). The immense volume of Pliocene and Quaternary extrusive rocks that represents the Jemez volcanic field covers an area of over 30 miles east-to-west and 50 miles north-to-south and is over 4000 feet in thickness near the center (Woodward, 1974).

The Jemez volcanic field unconformably overlies the eastern part of the Nacimiento uplift and the southern Chama basin. The Chama basin, the San Juan Basin and the Gallina-Archuleta arch are part of the Colorado Plateau, whereas the Brazos and Nacimiento uplifts (Figure 2-1) are generally included with the Southern Rocky Mountains (Woodward, 1974). These features attained their present structural outlines during the Laramide orogeny of Late Cretaceous and

early Tertiary time. Superimposed on these Laramide structures is the Rio Grande rift that began to form during the Miocene. Volcanism in the Jemez area began in Pliocene time after initial development of the rift with extrusive rocks accumulating along the western margin of the rift contemporaneously with late stages of rifting (Woodward, 1974). Initial eruptions were dominantly mafic to intermediate flows, which probably formed low, coalescing shields. Eruptive activity culminated in the early Pleistocene with explosive, caldera-forming eruptions of ashflow tuffs, which covered most of the shields and formed two calderas, the largest and youngest of which is the Valles Caldera located seven to ten miles west of Los Alamos, New Mexico (Kudo, 1974). Extensive studies of the Jemez volcanism have been performed by Ross et al. (1961), Bailey et al. (1969), Smith and Bailey (1966, 1968) and Smith et al. (1970).

Major tectonic features here are dominated by vertical movements. Minor horizontal shift and compressional features, however, occur in parts of the Colorado Plateau and Southern Rocky Mountain structures. The stratigraphy, structure and tectonics of the Jemez Mountains and surrounding area have been the topics of a large number of reconnaissance and detailed studies (c.f., Dane, 1948; Kelley, 1954, 1955; Griggs, 1964; Woodward, et al., 1972, 1973, 1974).

2.2 SITE GEOLOGY

The Los Alamos facilities are located on the western part of the Pajarito Plateau (Figure 2-1), which forms an apron of volcanic and sedimentary rocks around the eastern flanks of the Jemez Mountains. The plateau is aligned approximately north-south and is about 20 to 25 miles in length and five to ten miles wide. It is bounded on the east by White Rock Canyon (which contains the Rio Grande), on the north and northeast by the Puye Escarpment and on the west by Sierra de los Valles. The plateau slopes gently eastward from an elevation of about 7,500 feet near the mountains toward the Rio Grande where it terminates at an elevation of about 5,400 feet in steep slopes and cliffs formed by down cutting of the river. The plateau has been dissected into a number of narrow mesas by southeastward-trending intermittent streams. One of these mesas, Mesita del Buey, is the site of Technical Area 54, Areas G and L, which have been utilized for disposal of Laboratory radioactive and hazardous waste.

Mesita del Buey is a narrow southeastward-trending mesa about two miles in length and one quarter mile wide. The mesa surface slopes gently from an altitude of about 6,900 feet at its western margin to about 6,600 feet near its eastern end (Purtymun and Kennedy, 1971). It is bounded on the north by Cañada del Buey and on the south by Pajarito Canyon. The canyons have cut 50 to 100 feet below the surface of the mesa producing near-vertical cliffs from the mesa top to the canyon floors. The stratigraphy [illegible] re of Mesita del Buey and the Pajarito Plateau are described below.

2.2.1 Stratigraphy

2.2.1.1 General Stratigraphy of the Pajarito Plateau

The Pajarito Plateau is formed by a series of sediments and volcanic extrusive rocks and is typical of a terrane produced by concurrent sedimentation and volcanism. A generalized cross-section of the Pajarito Plateau is shown in Figure 2-2. The base of the plateau is represented by the Miocene Tesuque Formation, which in this area consists of friable to moderately well cemented siltstone and sandstones that contain lenses of conglomerate and clay (Purtymun and Johansen, 1974). Some basalt flows are interbedded with the sediments in the formation. The lower part of the Tesuque is comprised of fine arkosic sand and the upper part is composed of very coarse arkosic sand, latitic gravels and volcanic detritus. The late Pliocene to early Pleistocene basaltic rocks of Chino Mesa form the steep walls of White Rock Canyon and cap the high mesas to the east (Griggs, 1964). The basalts represent a series of flows that overlie the Tesuque Formation east of Pajarito Plateau and interfinger with and overlie the Puye Formation on the plateau.

Overlying the Tesuque Formation are the volcanic extrusives of the Pliocene to early Pleistocene Tschicoma Formation, which consist of latite, quartz-latite flows and pyroclastic rocks. The Tschicoma has been extruded through the Tesuque west of Los Alamos, forming the lower part of the Jemez Volcanic Pile. Penecontemporaneous with the Tschicoma Formation is the Puye Formation (Bailey, et al., 1969). It is described as a broad alluvial and pyroclastic fan flanking the east side of the northern Jemez Mountains. It interbeds with the Tschicoma Formation and the basalts of Chino Mesa and unconformably overlies the Tesuque Formation.

Blanketing much of the Pajarito Plateau are the ashflow and ashfall rhyolitic tuffs of the Pleistocene Bandelier Tuff. The Bandelier Tuff has been subdivided into three members (Griggs, 1964), which are from lowermost upward: the Guaje Member, a bedded pumice-fall deposit; the Otowi Member, a massive pumiceous tuff breccia of ashflow origin; and the Tshirege Member, a succession of cliff-forming welded ashflows. Other workers (e.g., Bailey et al., 1969) divide the Bandelier into two members, the Otowi and the Tshirege. Because most of the geologic investigations of Mesita del Buey and the Laboratory area consider the Bandelier Tuff to consist of three members, a three-member nomenclature will be used in this discussion.

A thin layer of soil cover overlies the Bandelier Tuff over much of the Pajarito Plateau although the soil thins considerably near canyon edges. Recent alluvium is present in the canyons cutting the plateau (Rogers, 1977). This alluvium consists primarily of detritus derived from the canyon walls formed by the Tschicoma Formation along the western edge of the plateau and by the Bandelier Tuff farther east.

2.1.1.2 Stratigraphy of Mesita del Buey

The general stratigraphy of Mesita del Buey is reasonably typical of the remainder of the Pajarito Plateau (Figure 2-2). However, the large number of drillholes that have been sunk on and adjacent to the mesa (Figure 1-4) permit detailed descriptions of the upper portion of the mesa stratigraphy. All of the boreholes shown on Figure 1-4 extend only into the Bandelier Tuff with the exception of boreholes PM-2, T-5 and T-6, which are of sufficient depth to penetrate portions of the Tesuque Formation, basalts of Chino Mesa and the Puye Conglomerate, respectively. Graphic lithologic logs for all boreholes (except PM-2 and LLC-85-A) are provided in Appendix C.

Borehole PM-2 penetrated the top 1,190 feet of the Tesuque Formation (Rogers, 1977), which in this location consists of a series of coarse sediments and basalt layers (Figure 2-3). The sediment layers range in thickness from about 75 to 250 feet and are comprised of silty sandstones, sandstones with lenses of clay and pebbly conglomerates (Purtymun and Kennedy, 1971). The two basalt layers encountered in PM-2 have thicknesses of about 50 to 100 feet.

Overlying the Tesuque Formation at Mesita del Buey are the Totavi Lentil and Fanglomerate Member of the Puye Conglomerate. West of Mesita del Buey, the Tschicoma Formation is often found above the Tesuque on the Pajarito Plateau; however, it is thought that the Tschicoma does not extend as far east as Mesita del Buey (Figure 2-2). The Totavi Lentil, the lower member of the Puye Conglomerate, consists of about 70 feet of subrounded quartzite, chalcedony and cobble-chip gravels in a sand matrix. The Fanglomerate Member of the Puye is comprised of a series of basalt, latite and quartzite gravel, pebble and cobble layers intercalated with sandy gravel layers. The Fanglomerate Member is about 640 feet in thickness at borehole PM-2.

Overlying and interfingering with the Puye Conglomerate at Mesita del Buey are the basaltic rocks of Chino Mesa (Figure 2-4). The Chino Mesa flows are described from boreholes PM-2 and T-5 to consist of layers of dense, olivene-containing, vuggy basalts intercalated with vuggy, scoria-containing basalt. Borehole logs from PM-2 indicate that the basalts of Chino Mesa are approximately 270 feet in thickness.

The ashfall and ashflow tuffs of the Bandelier Tuff overlie the Chino Mesa basalts. The Bandelier has been divided into three members, which are in ascending order, the Guaje, the Otowi and the Tshirege Members (Figure 2-3). The Guaje Member is an ashfall pumice with a thin layer of pumiceous tuff at its base. The Guaje consists of gray lump-pumice fragments as large as two inches in diameter, and glass shards and quartz and sanidine crystals are present in the cellular structure (Purtymun and Kennedy, 1971). The upper two to three feet of the member are reworked pumice and tuff. The Guaje ranges in thickness from about 30 feet on the western edge of Mesita del Buey to approximately ten feet at borehole T-5.

The Otowi Member is a light grey, nonwelded pumiceous, rhyolitic tuff, which contains quartz crystals, glass shards and minor amounts of mafic minerals. Also present are varying amounts of rock fragments of rhyolite, latite and pumice in a fine-grained ash (Purtymun and Kennedy, 1971). The Otowi is primarily ashflows but contains several beds of reworked tuff and pumice in the upper part of the member. The thickness of the Otowi Member ranges from about

120 to 180 feet at Mesita del Buey as recorded in borehole logs from T-5 and T-6 (Rogers, 1977). The thickness of the Otowi in borehole PM-2 is noted as 375 feet, however, the overlying Tshirege Member was not identified from borehole cuttings and may have been included with the Otowi.

The Tshirege Member of the Bandelier Tuff has been divided into three units, two of which (Units 1 and 2) occur at Mesita del Buey (Figure 2-5). The third unit, a non-welded to moderately welded pumiceous tuff is absent (Purtymun and Kennedy, 1971). The first two units dip two to three degrees to the southeast and thin in the direction of the dip and with increasing distance from their source in Valles Caldera. Each of Units 1 and 2 has been subdivided into two subunits (a and b) and are described as they appear at Mesita del Buey by Purtymun and Kennedy (1971) and BFEC (1986).

The lowermost subunit of the Tshirege Member (Unit 1a) is a non-welded, light orange to light brown, rhyolitic, vitric crystal, ashflow tuff (BFEC, 1986). At Mesita del Buey, Unit 1a consists of very uniform, non-welded ash composed of brown glass shards and fine, flattened pumice lapilli, neither of which has undergone discernable detrification. The ash also contains varying amounts of lumps of pumice lapilli and latitic to rhyolitic lithic lapilli. In the western part of Mesita del Buey, Unit 1a is about 30 feet thick (Purtymun and Kennedy, 1971), and though not entirely penetrated by any of the recent boreholes, at least 25 feet in thickness at Areas G and L (BFEC, 1986).

Unit 1b, which overlies Unit 1a, is differentiated from Unit 1a by a slight color change (light orange-brown of Unit 1a to grayish brown) and by the presence of larger quartz crystals and fewer and smaller rock fragments. In addition, magnetic susceptibility geophysical logs help locate the Unit 1a - Unit 1b contact in some boreholes (BFEC, 1986). Unit 1b is a rhyolitic ashflow tuff, ranging in color from pale red to orange-pink near its base to light gray to pink-gray near its top. The lower portion of Unit 1b contains gold-colored, bipyramidal quartz crystals up to about 3/16-inch in diameter (BFEC, 1986). At Mesita del Buey, the thickness of Unit 1b was found to range from about 30 feet in the southeast to 50 feet in the northwest.

Unit 2a is a light gray pumiceous tuff that contains rock fragments of pumice, latite and rhyolite, with some quartz crystals in a light gray ash (Purtymun and Kennedy, 1971). The contact between Units 1b and 2a is difficult to identify because Unit 1b is transitional into Unit 2a. In some cases, the contact can be estimated based on subtle color changes or by an increase in the size of the pumice lapilli from Unit 1b to Unit 2a. In addition, the magnetic susceptibility and apparent density geophysical logs run in some of the boreholes on Mesita del Buey helped to identify the Unit 1b - Unit 2a contact (BFEC, 1986). Unit 2a is thought to consist of two ashflows or ashfalls. In the western part of Mesita del Buey, Unit 2a appears as a moderately welded tuff that forms a vertical wall along the canyons. The unit becomes progressively less well welded eastward and is described as nonwelded along the eastern edge of Mesita del Buey (Purtymun and Kennedy, 1971). The nonwelded portion of Unit 2a is thought to be an ashfall, rather than ashflow tuff. Unit 2a is about 85 feet thick along the western edge of Mesita del Buey (Purtymun and Kennedy, 1971) and thins to approximately 20 feet along the eastern edge of the mesa (BFEC, 1986).

Unit 2b forms the cap rock at Mesita del Buey and consists of brownish gray, light gray and pinkish gray, slightly to moderately weldea, rhyolitic ashflow tuff with light gray and occasional brown pumice lapilli (BFEC, 1986). Unit 2b is separated from the underlying Unit 2a by an erosional contact, marked by a thin layer of silt, sand and pumice (Purtymun and Kennedy, 1971). On Mesita del Buey, Unit 2b is composed of at least two ashflows that cooled as a single unit, based on field descriptions and apparent density and magnetic susceptibility geophysical logs (BFEC, 1986). The average thickness of Unit 2b on Mesita del Buey is about 60 feet (Purtymun and Kennedy, 1971); however, at the eastern edge of the mesa (the location of Areas G and L), the thickness of the unit (encountered in boreholes) ranges from about 45 to 28 feet (BFEC, 1986).

A three to four-foot layer of soil covers Unit 2b along the axis of the mesa. The soil cover thins appreciably towards the canyon rims, however, and the tuff is exposed in places along the mesa edges (Purtymun and Kennedy, 1971). The alluvium in the stream channels north of Mesita del Buey is up to 10 to 12 feet thick. It consists of sand-size quartz and sanidine crystals and crystal fragments and pebble to cobble-size fragments of latite, rhyolite

and pumice derived from weathering and erosion of the tuff (Purtymun and Kennedy, 1971). The alluvium in Pajarito Canyon, south of the mesa, is up to 30 feet thick and is generally composed of the same tuff weathering products as the streams north of the mesa.

2.2.2 Structure

2.2.2.1 General Structure of the Pajarito Plateau

The geologic structure of surface rocks on Pajarito Plateau is simple, although the structure of underlying strata may be complex. The regional dip of surface rocks of the Pajarito Plateau is one to two degrees east. Beds of the Tesuque Formation, however, dip gently to the west in the easternmost part of the plateau (Griggs, 1964).

The rocks of the Pajarito Plateau are broken by several northward-trending normal faults. The Pajarito fault zone is located near the the western edge of the plateau in the southern part of the area (Figures 2-2 and 2-6). In this area, the Bandelier Tuff is downthrown about 300 feet on the east side of the Pajarito fault (Griggs, 1964). Farther north, the fault splits into two smaller subparallel faults, both downthrown to the east. Displacement decreases northward until both faults die out. The fault planes dip steeply to the east (note the vertical exaggeration on Figure 2-2). Just east of and parallel to the Pajarito fault zone is a normal fault with a displacement of about 30 feet. This fault, which extends through the Bandelier Tuff, also dips steeply to the east.

Two other normal faults, en echelon to Pajarito zone, are located to the northeast (Figure 2-6). These faults are downthrown to the west, and the fault planes also dip to the west. The westernmost of the faults extends southward for a short distance subparallel to the northern extension of the Pajarito zone. The area between the faults is a shallow syncline. The Bandelier Tuff is displaced about 50 feet along the en echelon faults; however, the Tschicoma Formation may be displaced as much as 500 feet along the easternmost fault. The difference in displacement seems to indicate recurring movement along a pre-Bandelier fault (Griggs, 1964).

The ashflows of the Bandelier Tuff are broken into a number of blocks by joints formed by shrinkage as the ashflow cooled. The near vertical attitude of most of the joints and the curved form of some are indicative of formation by cooling. The joints are more numerous in welded than in nonwelded tuffs because the welded tuffs were deposited at higher temperatures (Purtymun and Kennedy, 1971). The jointing in the Bandelier and other volcanic units in the Mesita del Buey area is discussed in the following section.

2.2.2.2 Structure of Mesita del Buey

No faults are known to break the rocks of Mesita del Buey (Figures 2-4 and 2-6). The ashflows of the Bandelier Tuff thin eastward because of the topographically high basalts of Chino Mesa on which they were deposited (Purtymun and Kennedy, 1971).

The most prevalent structural features in the rocks of Mesita del Buey are the fractures or joints in the volcanic rocks caused by shrinkage upon cooling after deposition. A good description of the jointing observed in the Bandelier Tuff is provided in Purtymun and Kennedy (1971); portions of their text have been reproduced below.

> The joints are classified as master and minor joints. Master joints are numerous and long, and may pass through one or more ashflows. A single unit may contain several ashflows emplaced at different times, but the joint pattern of the older layer may tend to govern formation of joints in the younger layer as it cools. Also, two or more ashflows may be laid down in rapid succession and cool as a single unit with joints forming in the flows at the same time.
>
> The master joints are vertical or nearly vertical and generally dip 70 degrees from the horizontal. The vertical trend may be straight or slightly curved. The dip is deflected slightly when the joint enters a unit with different density or degree of welding.
>
> Minor joints dip at angles less than 70 degrees. They are more numerous near the tops of ashflows and do not persist as they intersect the master joints.
>
> A joint traced vertically through an ashflow may be closed in places and open in others. Locally the opening may be as much as 2 in. wide, but most openings are less than 1/4 in. wide. Joints terminating in the base of the soil zone or in exposed tuff on the mesa surface are filled with

> light-brown clay which may extend 3 to 4 feet below the surface. Below the brown clay, the joint openings are filled, or the joint faces are plated, with a light-gray clay. The light-gray clay is derived from weathering of the tuff and from minerals leached from the tuff by water and precipitated along joint openings before development of the near-surface brown clay that seals the joint at the surface.
>
> The master joints are tension joints formed by the contraction of the tuff as it cooled. In a cooling homogeneous molten liquid, rupture occurs as three vertical fractures intersecting at angles of 120 degrees and radiating out from numerous centers. If the centers are evenly distributed, the fractures bound vertical hexagonal columns. A rose diagram illustrating the orientation of joints formed from a homogeneous molten liquid would show three joint sets (a number of joints with the same characteristic pattern) intersecting at angles of 60 degrees.
>
> The heterogeneous characteristics of the tuff did not allow joint sets to form vertical hexagonal columns. A rose diagram prepared using the orientation of 1,078 master joints [at Mesita del Buey] showed the average of the three joint sets intersecting at angles of 30 and 90 degrees. The three joint sets, N30°W to N50°W, N60°W to N80°W and N40°E to N60°E, comprise 40% of the joints measured for the study.
>
> The blocks formed by the joints range from a few square feet to as much as 500 square feet at the surface. In the walls of the pits there is about one master joint for every seven feet of horizontal wall.

Investigations of the subsurface at Areas G and L have also described jointing in the Bandelier Tuff. Purtymun and others (1978) drilled a number of subhorizontal core holes beneath a waste disposal pit (Pit 3) at Area G. The five borings, which extended 240 to 304 feet into Units 2a and 2b of the Bandelier, encountered near-vertical joints at frequencies ranging from about three to six feet of core recovered. Most of the joints were filled or plated with brown clay. The remainder were open with joint faces slightly weathered or plated with caliche. Many of the drillholes sunk by BFEC in 1985 encountered fractures in the upper three units of the Bandelier Tuff (BFEC, 1986). No fractures were intersected in Unit 1a; however, the entire thickness of this unit was not penetrated by any of the 1985 drillholes. Most of the fractures encountered are nearly vertical. Some of the fractures intersected in Units 2a and 2b have a dip of about 45 degrees and others, only in Unit 2b, are

nearly horizontal. Similar to the fractures described by Purtymun and Kennedy (1971) and Purtymun and others (1978), the fractures were found to be partially or completely filled with caliche, brown clay or limonitic material (BFEC, 1986). The locations of these fractures are noted on the lithologic logs in Appendix C.

In addition to the fractures or joints in the Bandelier Tuff, it is likely that similar features exist to some extent in the basaltic rocks of Chino Mesa at Mesita del Buey. Zones of lost circulation in the Chino Mesa rocks are noted at various depths in the borehole PM-2 drilling logs and in the drilling logs from other water supply wells drilled on Pajarito Plateau (Cooper et al., 1965). Whether the lost circulation zones represent subvertical fractures or cooling joints in the basalts or coarse sediment layers between flows is unknown.

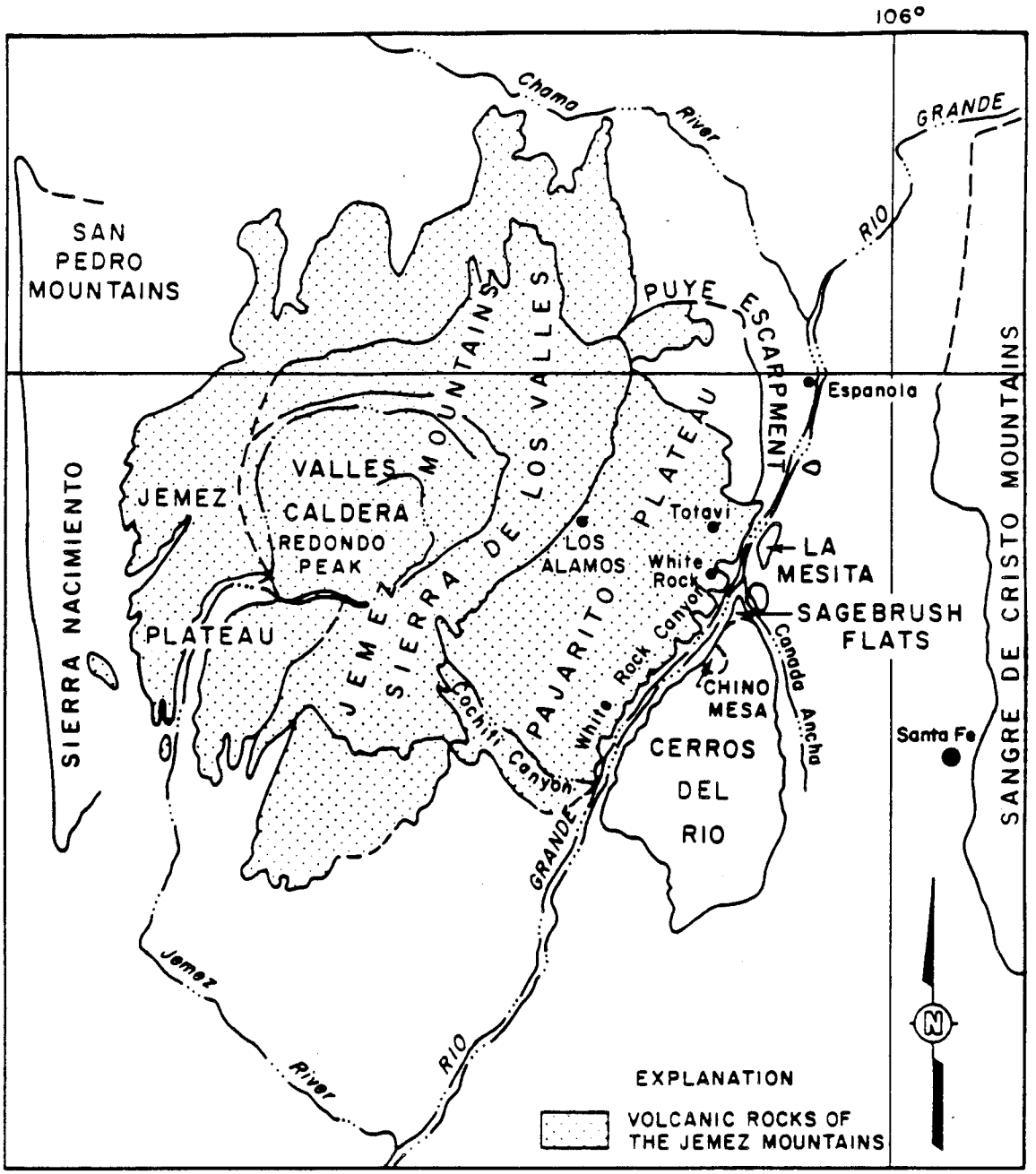

Reference; R.L. Griggs, 1954

5 0 5 10 MILES

SCALE

FIGURE 2-1

PHYSIOGRAPHIC FEATURES OF THE JEMEZ MOUNTAINS

PREPARED FOR

LOS ALAMOS NATIONAL LABORATORY

LOS ALAMOS, NEW MEXICO

IT CORPORATION

301017 A50	DP	MJG 9/24/84	CHECKED BY		DRAWING NUMBER 84
Rev 2/24/87			APPROVED BY		

A8

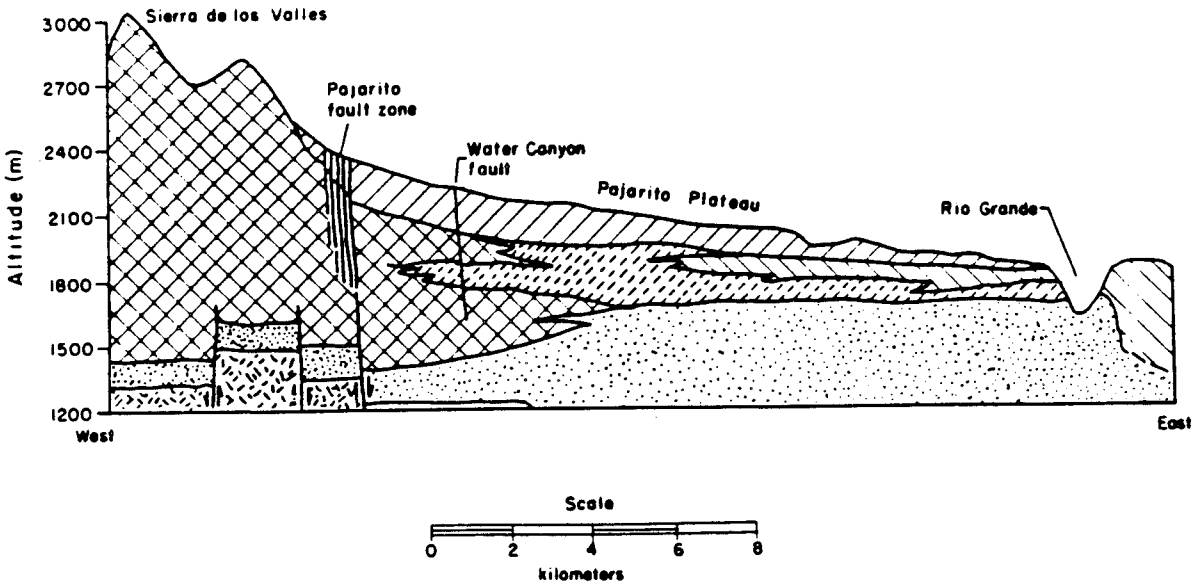

LEGEND

- Bandelier tuff
- Basaltic rocks of Chino Mesa
- Tschicoma formation
- Puye conglomerate
- Tesuque formation
- Precambrian crystalline rocks

Purtymun (Unpublished) as Cited in Rogers (1977)

FIGURE 2-2

GENERALIZED GEOLOGIC CROSS-SECTION OF PAJARITO PLATEAU

PREPARED FOR

LOS ALAMOS NATIONAL LABORATORY
LOS ALAMOS, NEW MEXICO

© 1984 IT CORPORATION
ALL COPYRIGHTS RESERVED
Not to Scale This Drawing

IT ... Creating a Safer Tomorrow

DRAWN BY	LLF	2/24/87
CHECKED BY	SaJS	3/25/87
APPROVED BY		3/25/87
DRAWING NUMBER	301017 A 23	

65360

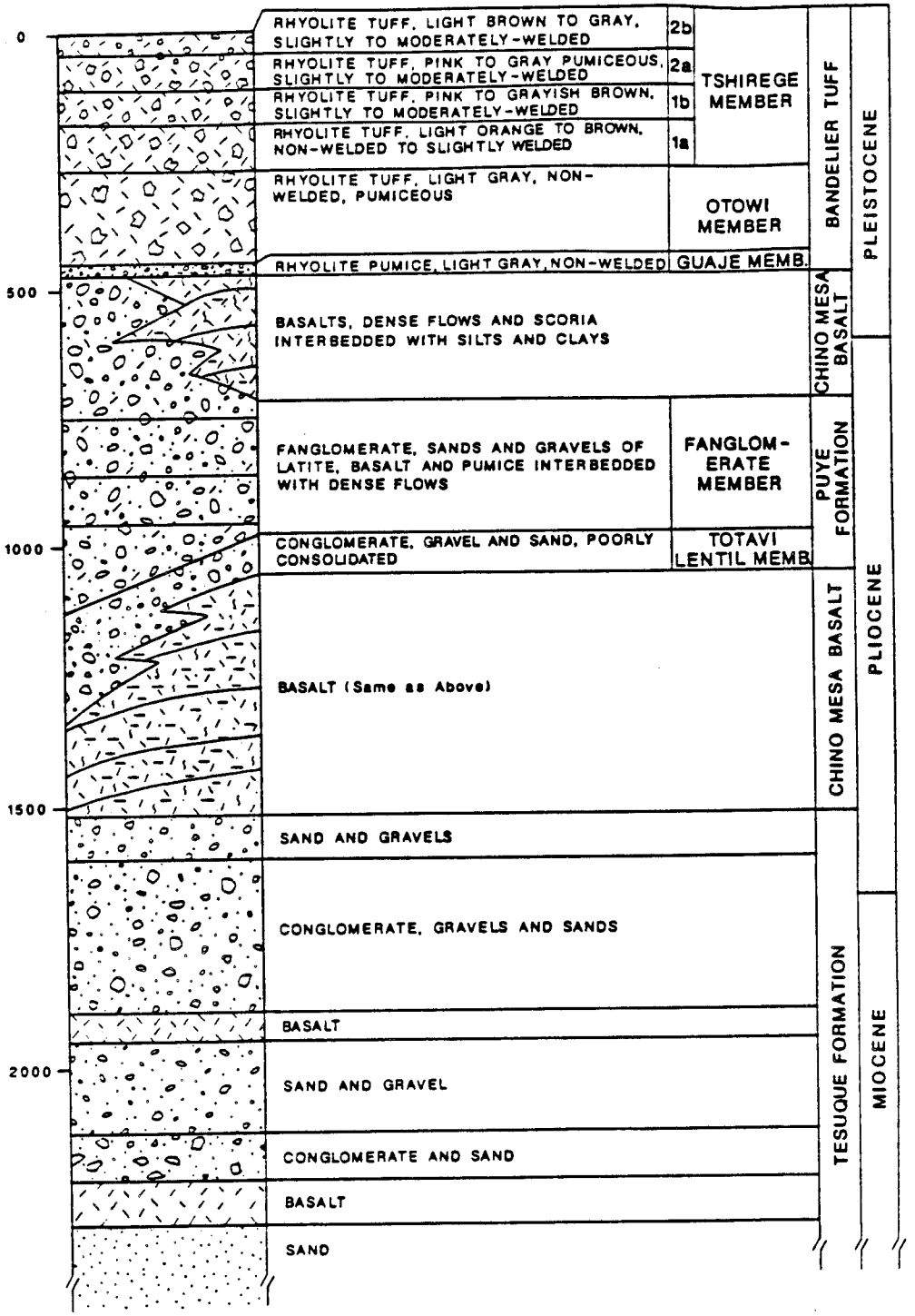

FIGURE 2-3

Compiled from: BFEC (1985a), Devaurs (1985), Griggs (1964), Rogers (1977)

GENERALIZED STRATIGRAPHIC COLUMN FOR MESITA DEL BUEY

PREPARED FOR

LOS ALAMOS NATIONAL LABORATORY
LOS ALAMOS, NEW MEXICO

© 1984 IT CORPORATION
ALL COPYRIGHTS RESERVED

IT ... Creating a Safer Tomorrow

DRAWING NUMBER 301...7 A 24

CHECKED BY / APPROVED BY: MJG / 3/25/87 — SWJS / 3/25/87

65360

Do Not Scale This Drawing

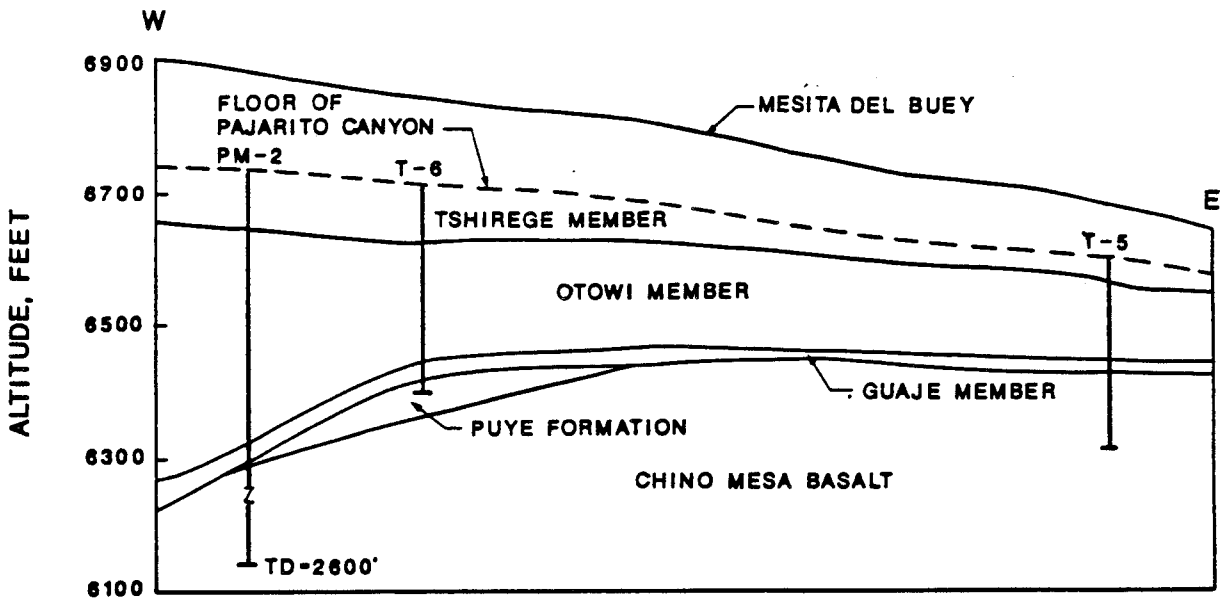

From Purtymun and Kennedy (1971)

FIGURE 2-4

GENERALIZED GEOLOGIC CROSS-SECTION (EAST-WEST) SHOWING RELATIONSHIP OF THE CHINO MESA BASALT TO THE BANDELIER TUFF

PREPARED FOR

LOS ALAMOS NATIONAL LABORATORY
LOS ALAMOS, NEW MEXICO

© 1984 IT CORPORATION
ALL COPYRIGHTS RESERVED

... Creating a Safer Tomorrow

Do Not Scale This Drawing

DRAWING NUMBER 30.017 ~25
3/25/87
SWS
CHECKED BY
APPROVED BY
LLF
2/24/87
65360

D...	LLF	CHECKED BY	SWS	8/25/87	DRAWING
	2/24/87	APPROVED BY	[illegible]	3/25/87	NUMBER 301[illegible]./ A26

65360

© 1984 IT CORPORATION
ALL COPYRIGHTS RESERVED

Do Not Scale This Drawing

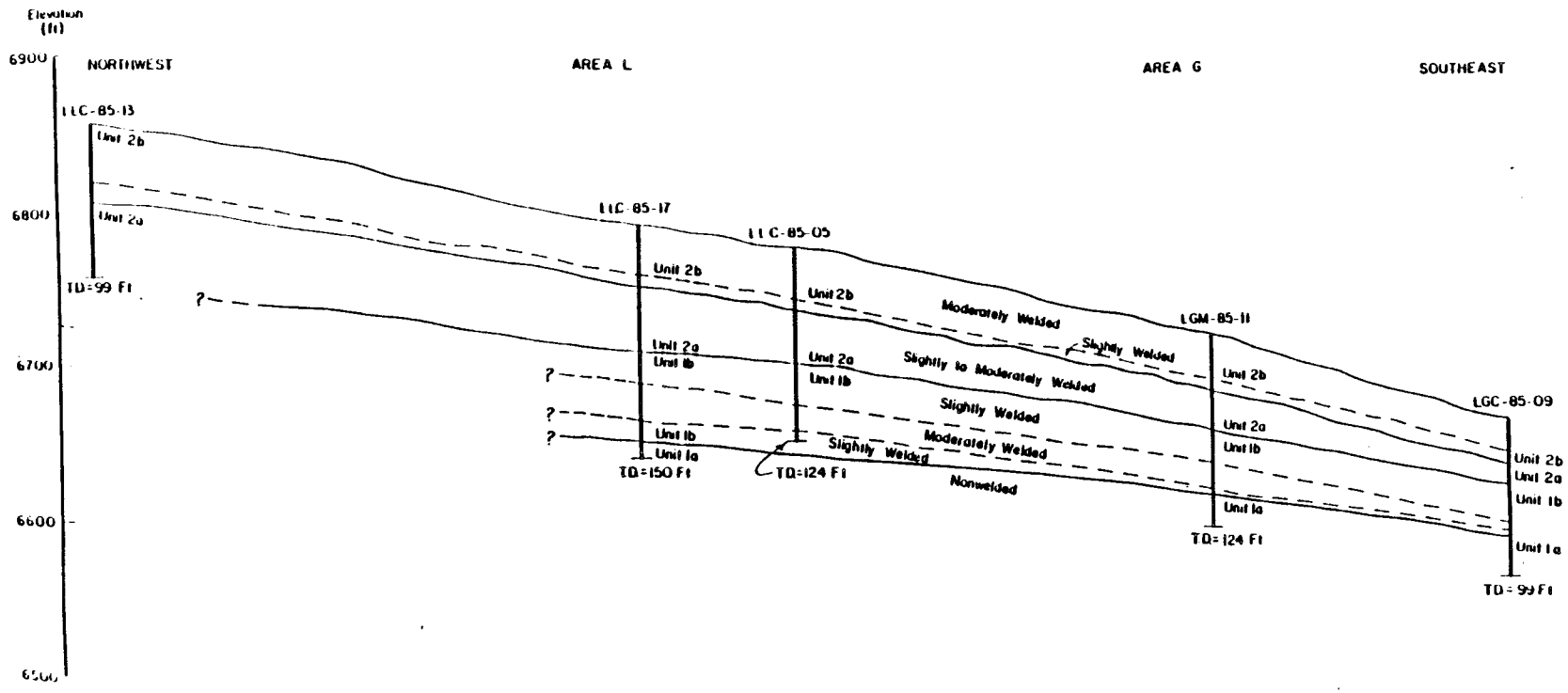

1000 500 0 2000 FEET

HORIZONTAL SCALE

From BFEC (1986)

FIGURE 2-5

GEOLOGIC CROSS-SECTION
OF THE TSHIREGE MEMBER
OF THE BANDELIER TUFF
AT MESITA DEL BUEY

PREPARED FOR

LOS ALAMOS NATIONAL LABORATORY
LOS ALAMOS, NEW MEXICO

IT ... Creating a Safer Tomorrow

301017 02 A27

DRAWN BY	MJS	CHECKED BY	SWS	3/25/83	DRAWING NUMBER	86510-B4
	10/17/84	APPROVED BY		3/25/83		

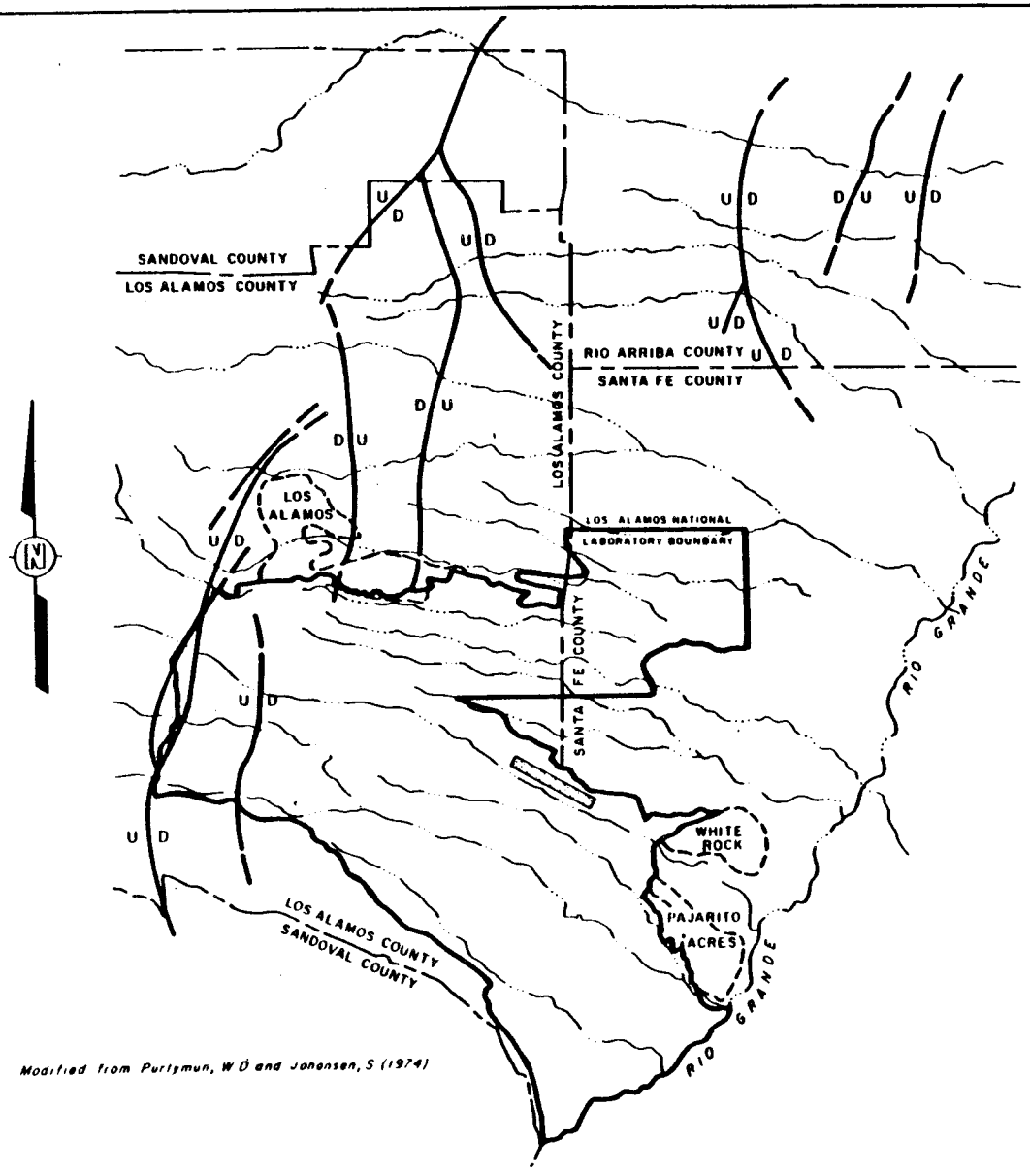

Modified from Purtymun, W D and Johansen, S (1974)

EXPLANATION

U/D MAJOR FAULTS, D INDICATES DOWNTHROWN SIDE, U INDICATES UPTHROWN SIDE

TECHNICAL AREA 54

1 0 1 2 MILES

SCALE

FIGURE 2 8

LOCATION OF TECHNICAL AREA 54 FACILITY RELATIVE TO THE NEARBY FAULT TRACES

PREPARED FOR

LOS ALAMOS NATIONAL LABORATORY
LOS ALAMOS, NEW MEXICO

IT CORPORATION

10 1293 HERCULENE ADD SMITH CO PGH PA

3.0 HYDROLOGIC CHARACTERIZATION OF THE VADOSE ZONE

Vadose zone hydrologic characterization studies were undertaken in Technical Area 54, Areas G and L to provide a quantitative analysis of moisture movement through the unsaturated Bandelier Tuff. These analyses aid in determining the likelihood of contaminants from Areas G and L migrating through the vadose zone and into the main aquifer approximately 850 to 950 feet beneath the sites. No perched water has been detected above the main aquifer; therefore, studies of moisture movement have been concentrated on unsaturated flow processes. The studies presented in this section fulfill requirements of paragraph 25, tasks 1-4 of the compliance order issued to the Laboratory on May 7, 1985 (see Section 1.0).

The Laboratory utilized a two-tiered approach to quantify moisture movement in the tuff: 1) hydrologic characteristics of the tuff and hydraulic head were measured in order to calculate seepage velocity and rates of moisture flux, and 2) moisture content of the tuff following precipitation events was measured to empirically determine changes in moisture content with depth. Tasks one through four of the compliance order are focused on collection of data necessary to calculate seepage velocity and rates of unsaturated flow; however, the order does not specify these analyses be conducted. The Laboratory has included these calculations for completeness.

The approach to calculation of seepage velocity and moisture flux rates for fluid movement through the vadose zone is similar to the approach used in determining rates of ground water movement within aquifers. Rates of ground water movement are primarily controlled by the hydraulic conductivity of an aquifer and changes in hydraulic head. The hydraulic conductivity of a saturated medium is a function both of the physical properties of the medium and the fluid. Hydraulic head (H) is equal to the sum of the elevation of the measuring point (z) and the pressure head (ψ) of the fluid at the measuring point. These two properties, hydraulic conductivity and hydraulic head, also govern rates of moisture movement in the vadose zone. However, in the vadose zone unsaturated hydraulic conductivity and pressure head are functions of moisture content (θ); that is, conductivity and pressure head decrease with decreasing moisture. In addition, pressure head (also termed capillary or matric potential) in the vadose zone is less than zero.

As described above, calculation of moisture flux in the vadose zone entails determination of unsaturated hydraulic conductivity and hydraulic head. Unsaturated hydraulic conductivity can be measured directly or it can be determined through measurement of rock permeability and relationships between moisture content and pressure head, also known as soil moisture characteristic curves [$\psi(\theta)$]. Therefore, in order to calculate rates of moisture flux the permeability, moisture content, relationships between moisture content and pressure head, unsaturated hydraulic conductivity, and pressure head of materials in the vadose zone must be determined. The very dry conditions present within the tuff pose difficulties in measuring the above listed properties. These difficulties will be explained along with discussion of data collection techniques.

Empirical determinations of moisture movement can be made directly with instruments such as neutron moisture probes. Also, pressure head can be monitored and converted to moisture determinations via the soil moisture characteristic curves.

The discussion provided below presents, summarizes and interprets data collected in order to quantify moisture movement in the vadose zone underlying Areas G and L during approximately the past eighteen months. Much of the data was collected by Bendix Field Engineering Company, Inc. (BFEC) and Laboratory personnel. Results of previous research are also incorporated as appropriate. The discussion relies heavily on BFEC (1986) as this report presents much of the collected data and the details of data collection methods.

Section 3.1 provides a brief discussion of the local climate and the importance of precipitation on evaluation of the vadose zone hydrology. Section 3.2 discusses permeability testing of the Bandelier Tuff (task 1). Section 3.3 discusses field moisture conditions, and measurement of soil moisture characteristic curves (task 2). Section 3.4 discusses unsaturated hydraulic conductivity determinations (task 3) and Section 3.5 presents the vadose zone moisture monitoring program at Areas G and L (task 4). In addition, empirical measurements of infiltration are provided in this section. Calculations of moisture flux rates are presented in Section 3.6 and the vadose zone hydrology

is summarized in Section 3.7. Definitions of terms and units used throughout this section are presented in Appendix D.

Units of measurement utilized in this report vary from British (foot, pound, second) to the International System (SI) and are sometimes inconsistent within each system. This is due to the different measurement units used in the original studies. Attempts were not made to convert these units to one system due to the loss of precision encountered in some conversions and the resulting "awkward" values associated with unit changes.

3.1 LOCAL CLIMATE

The climate of the study area can be characterized as a semi-arid, temperate mountain climate. Laboratory wide precipitation averages approximately 18 inches per year, with approximately 40 percent of this amount occurring in July and August. Temperatures are moderate, rarely exceeding 90°F (32°C) during the summer months or falling below 0°F (-18°C) during the winter. Mean monthly precipitation data for the Los Alamos area are presented in Table 3-1. Because studies of vadose zone hydrology presented herein are focused on quantitative analysis of moisture movement and redistribution of moisture within the tuff, it becomes important to determine if moisture conditions at the site are typical of those normally encountered at the site. Unusually wet or dry conditions during the study period may cause measurements of moisture content or pressure head to be abnormal. The Laboratory maintains a precipitation gage at TA-54, Area G. This is the closest weather data station to Areas G and L. Area G precipitation data for the year 1986 are presented in Appendix E and summarized in Table 3-2. Compared to mean precipitation data for Area G in Table 3-1, precipitation in 1986 was approximately 30 percent above average (18.85 inches as compared to 13.45 inches), thus, analyses of vadose zone hydrology conducted in 1986 should represent wetter than normal moisture conditions in Areas G and L.

3.2 INTRINSIC PERMEABILITY OF THE VADOSE ZONE

A variety of methods, including both field and laboratory procedures, were utilized to determine the intrinsic permeability (k) of the vadose zone at Areas G and L. Intrinsic permeability is a basic characteristic of the vadose zone that requires evaluation to determine the magnitude of fluid movement

through the tuff. Tests conducted to determine intrinsic permeability also fulfill requirements of paragraph 25 - task 1 of the compliance order issued to the Laboratory on May 7, 1985, by the State of New Mexico. The compliance order specifies that at least five boreholes 125 ft deep be tested; and at least one test per horizon per hole with a minimum of six tests per hole be included.

Field methods for determining intrinsic permeability included air injection and vacuum tests and a water injection test which is used for result comparison with air tests. Laboratory methods used were gas injection with correction for slippage (Klinkenberg Correction Method) and the Dynamic Method to measure gas-water relative permeability. Procedures utilized for conducting the tests and reduction of test data are presented in BFEC (1986).

3.2.1 Field Permeability Tests

3.2.1.1 Injection Tests

Conventional field methods for determination of unsaturated zone intrinsic permeability and hydraulic conductivity usually involve maintenance of a constant head of water in a borehole until flow becomes steady, e.g., Stephens and Neuman (1982a, 1982b) and Stephens and others (1983). Due to the potential for mobilization of contaminants in the vadose zone in Areas G and L by percolating water during and after infiltration tests, permeability tests involving injection of water at depth were discouraged; rather, injection and vacuum tests using air as the testing fluid were selected due to their lower potential for mobilizing contaminants. In addition, the use of water as an injection fluid above the water table has limitations as equations used to reduce data assume that horizontal flow occurs throughout the system (see BFEC, 1986).

It should be emphasized that air injection methods for determining vadose zone permeability are currently experimental and may permit only a qualitative analysis of the tested material. The use of air as an injection fluid requires compensation for gas compressibility and volume changes caused by changes in temperature and water vapor content. Attempts were made to compensate for these factors during testing through use of additional instrumentation which closely monitored temperature. Corrections to pressure data

necessary due to temperature changes could then be applied. Analysis of test data assumes tests are conducted at sufficiently low pressures such that gas compressibility is not significant.

Permeability tests using air injection were conducted in five boreholes such that each stratigraphic unit in each borehole was tested. Six-foot test intervals were isolated in open boreholes with a straddle packer assembly so that 25 intervals, including seven adjacent to fractured zones, were tested. BFEC (1986) describes test procedures and data reduction techniques. Table 3-3 presents the results of these tests. Eight, nine, seven, and one interval(s) in units 2b, 2a, 1b, and 1a were tested, respectively. Hydraulic conductivity results are expressed as air relative values in 10^{-3} centimeters per second (cm/s). The values range from a maximum of 2.8×10^{-3} cm/s along a fractured zone in unit 2a at a depth of 45 - 51 feet to a minimum of 3.0×10^{-5} cm/s in an unfractured interval of units 1a and 1b at 99 to 105 feet below the surface. The average hydraulic conductivity for fractured zones is 9.3×10^{-4} cm/s, based on 7 measurements, and the average for unfractured zones is 4.1×10^{-4} cm/s (18 measurements). The average conductivity for stratigraphic units 2b, 2a, 1b, and 1a are 7.5×10^{-4}, 6.8×10^{-4}, 2.4×10^{-4}, and 8.8×10^{-5} cm/s respectively, indicating a slight decrease in hydraulic conductivity with depth. Again, care should be used in application of these data as the test method used is currently experimental.

Permeability and hydraulic conductivity measurements of each stratigraphic unit were performed in borehole LLM-85-05 using a water injection test. Water was used in this borehole because it is located outside of Areas G and L and potential mobilization of contaminants was not of great concern. Testing procedures are described in BFEC (1986). The water injection tests yielded hydraulic conductivity measurements ranging from 1.0×10^{-3} cm/s to 4.6×10^{-4} cm/s with an average of 7.6×10^{-4} cm/s. These measurements compare favorably to those determined by air injection and thus lend credibility to the air injection method.

3.2.1.2 Vacuum Tests

In addition to the air injection tests described above, the Laboratory conducted a series of air vacuum tests to verify injection test results and

further characterize the in situ permeability of the Bandelier Tuff. Vacuum tests were conducted in the same boreholes as injection tests: LLM-85-01, LLM-85-02, LLM-85-05, LGM-85-06, and LGM-85-11. Twenty-one tests were conducted over one meter intervals. As with the injection tests, tested intervals were isolated by using a straddle packer assembly in an uncased borehole. Tests could not be performed in certain intervals due to the inability of the vacuum pump to sufficiently evacuate the test interval. Six, five, nine and one interval(s) in stratigraphic units 2b, 2a, 1b, and 1a were tested, respectively.

The air-vacuum test is based on methods used by the petroleum industry in evaluating permeability of gas producing intervals and is a pressure transient test. Horner (1951) presents a description and analysis of pressure buildup which results from closing in a gas well after a period of production. A similar analysis is used in the air-vacuum testing procedures. BFEC (1986) provides a detailed discussion of test procedures and data reduction techniques.

Table 3-4 presents results of the vacuum permeability tests conducted in Areas G and L. The average intrinsic permeability for test intervals adjacent to fractured zones is 1.28×10^{-8} cm^2 (square centimeters) (3 measurements), while permeability in unfractured zones averages 1.25×10^{-8} cm^2 (18 measurements); thus, vacuum tests, as described in BFEC (1986), do not yield differing results between fractured and unfractured zones of boreholes. As determined by vacuum tests, the average permeability of stratigraphic units 2b, 2a, 1b, and 1a are 2.37×10^{-8} cm^2, 1.42×10^{-8} cm^2, 5.3×10^{-9} and 2.7×10^{-9} cm^2. These averages indicate an order of magnitude decrease in intrinsic permeability with stratigraphic depth in the tuff.

Table 3-5 compares field derived intrinsic permeability values from air-injection with vacuum tests performed in the same boreholes at the same stratigraphic interval. Vacuum-test permeabilities are generally lower than permeabilities derived from air-injection tests although both methods indicate a decrease in permeability with depth. BFEC (1986) attributes the difference to the inability to perform vacuum tests in more permeable portions of the tuff, thus biasing samples to lower permeability zones.

3.2.2 Laboratory Permeability Tests

Intrinsic permeability of 20 core samples was determined in the laboratory by TerraTek Research Laboratory. TerraTek utilized two procedures for permeability determination, gas injection with correction for slippage (Klinkenberg Correction Method), and the Dynamic Method to measure gas-water relative and effective permeability. The following discussion of laboratory procedures are taken from BFEC (1986) and TerraTek Research Laboratory (1985).

> The measurement technique for the Klinkenberg Method consists of applying a confining pressure of approximately 100 psi and a slight pore pressure, and maintaining an approximate pressure drop of two psi across the sample during testing. Nitrogen gas is injected into the samples at mean pressure of 4, 9, 14, and 19 psi, and the permeability is calculated for each of the pressures. A graph of permeability versus the reciprocal mean pressure is constructed and the intercept of a best fit line through the data points with the permeability axis at zero reciprocal mean pressure yields the gas permeability corrected for gas slippage (Klinkenberg correction).
>
> The Dynamic Method measures the gas-water relative permeability of samples. Testing begins by vacuum-saturating the samples with tap water. Following saturation, each sample is placed in a hydrostatic core holder and subjected to a confining pressure of approximately 100 psi. Testing consists of displacing water from the samples with humidified nitrogen. Incremental production of gas and water is monitored against time and flow rate at constant injection pressure. The production data are used to calculate gas-water relative permeabilities according to the method of Johnson, Bossler, and Naumann (1959), and Welge (1952).

Laboratory derived intrinsic permeability values for samples of Bandelier Tuff are presented in Table 3-6. Results for the two methods are very similar with intrinsic permeability on the order of 10^{-9} cm^2. In general the Dynamic Method yielded slightly lower results. Klinkenberg Method permeabilities range from 1.4×10^{-9} cm^2 at a depth of 115 feet in borehole LGM-85-06 to 18.0×10^{-9} cm^2 at a depth of 99 feet for the same borehole. The average Klinkenberg permeability for units 2b, 2a, 1b, and 1a are 5.75×10^{-9} cm^2, 2.86×10^{-9} cm^2, 5.85×10^{-9} cm^2, and 2.4×10^{-9} cm^2 respectively. Laboratory derived intrinsic permeabilities do not appear to change systematically with depth.

3.2.3 Summary of Intrinsic Permeability Testing

Comparisons of average intrinsic permeability measurements determined by field and laboratory methods for the four stratigraphic units of Bandelier Tuff are presented in Table 3-7. Field derived permeability measurements tend to decrease with stratigraphic depth. In addition, laboratory derived permeabilities are generally lower than field derived values, which may be attributed to the fact that samples selected for laboratory analysis were those exhibiting the highest degree of consolidation (BFEC, 1986) and, thus, lower permeability. Also, field derived permeabilities are measured over a larger interval and may be more representative of actual formation permeability. However, it should be noted that methods utilized to determine field permeability values are experimental in nature and interpretation of these data should be made cautiously. Field methods do not indicate an increase in permeability in the vicinity of fractured intervals; although, field observations such as "case hardening" of fractures and measurements of moisture content indicate that some fractures may provide areas of increased permeability (see Section 2.2.2.2).

3.3 VADOSE ZONE MOISTURE CHARACTERISTICS

As discussed previously in this section, moisture characteristics of the vadose zone play a key role in determining unsaturated hydraulic conductivity and rates of fluid movement in the unsaturated zone. This section provides discussions of measurements of moisture content of the tuff under field conditions, and measurement of soil moisture characteristic curves.

3.3.1 Gravimetric Moisture Content

Gravimetric moisture content determinations were conducted on core segments of Bandelier Tuff recovered from 12 drill holes in Areas G and L to determine vertical moisture profiles in the tuff and to aid in interpretation of other vadose zone analyses. Although not specifically required by the compliance order, determination of moisture profiles within the tuff is critical to analysis of unsaturated flow and moisture movement in the vadose zone because hydraulic properties of the vadose zone change with changing moisture content.

Cores were collected and analyzed for moisture content by BFEC. Core was obtained using a split-barrel sampler in accordance with procedures discussed

in Section 1.0. Moisture determinations were made by weighing samples soon after removal from the borehole and after oven-drying at 105°C. Details of sampling procedure, analysis, and data reduction are presented in Section 3.1.1 of BFEC (1986).

Figure 3-1 presents typical moisture profiles of the tuff. In general, the tuff is characterized by very low volumetric moisture content. Moisture content for the tuff is typically 2 to 4 percent (volumetric), with isolated intervals ranging up to 10 to 28 percent. Many of the moisture profiles indicate an increase in moisture content in an interval between 100 to 150 feet below the surface. BFEC (1986) correlates the zone of increased moisture to the lower portion of Unit 1b which contains a moderately welded tuff zone. Additionally, BFEC observes that higher moisture contents occur in the vicinity of certain fractured intervals.

3.3.2 Soil Moisture Characteristic Curves

Soil moisture characteristic curves, relationships between moisture content and pressure head, have been determined for 20 samples of Bandelier Tuff so that hydrologic properties of the tuff could be analyzed and unsaturated hydraulic conductivity could be predicted. These analyses fulfill the requirements set forth in paragraph 25, task 2 of the May 7, 1985 compliance order issued to the Laboratory. The compliance order specifies that at least five samples from each of at least four horizons be tested by any of the standard lab methods and that more than one method is needed to include all moisture conditions.

Soil moisture characteristic curves are useful in vadose zone studies as they provide a means of converting moisture content measurements into capillary potential information. Both types of data are necessary in evaluating unsaturated flow of water and contaminants through the vadose zone.

Soil moisture characteristic curves were determined for 20 samples of intact Bandelier Tuff. The samples were collected by BFEC during the 1985 drilling program (see Section 1.0). Testing of the samples was performed by TerraTek Research Laboratory and consisted of vacuum-saturating the samples with tap water and spinning in a centrifuge at various speeds to simulate a range of

capillary pressures and determining the moisture content remaining in the sample. Drying curves only were determined for the samples and effects of hysteresis were not considered. BFEC (1986) provides additional discussion of procedures.

Results of the analyses and identification of the borehole, depth, and stratigraphic unit from which samples were obtained, are listed in Table 3-8. Moisture content was determined, in general, for capillary pressures in the range of -0.03 to -.34 bar [0.5 to 5 pounds per square inch (psi)] and 22 to 72 percent moisture. Graphical depictions of these data are contained in Appendix C of BFEC (1986). Attempts to increase centrifuge speed so that lower capillary pressures could be evaluated resulted in disaggreation of the samples. Attempts were made to use the pressure-plate method to measure soil water moisture characteristics at lower moisture-tension conditions. Even though cores displaying the greatest degree of consolidation were selected for testing, this attempt was also unsuccessful due to sample disaggreation (see BFEC, 1986, Section 3.1.3.4).

Measurements of moisture content from cores of Bandelier Tuff show that field moisture conditions range from 2 to 10 percent, occasionally ranging to 28 percent. Table 3-8 shows that capillary potential was determined for minimum volumetric moisture content of approximately 22 to 60 percent. Figure 3-2 presents a representative example of the characteristic curves.

BFEC (1986) draws the following conclusions from analysis of the soil moisture-characteristic curves:

> The most interesting data discernible from the moisture characteristic curves (BFEC, 1986 Appendix C) are the extremely high moisture-retention (θ_r) values, which range up to 80 percent. The moisture-retention value is important because it represents the point at which capillarity as a transport mechanism breaks down. Since all of the moisture-content measurements for the Bandelier Tuff are significantly below this value, vapor transport is clearly the major mechanism of water transport.

As used above, the term capillarity refers to the process of unsaturated flow, and the moisture retention value of 80 percent indicates that no liquid transport can occur at moisture content below this value.

Note that the moisture retention value of 80 percent discussed above, as are all the BFEC characteristic curve data, are presented in terms of percent saturation. The 80 percent value above represents approximately 60 percent volumetric moisture.

3.4 UNSATURATED HYDRAULIC CONDUCTIVITY AS A FUNCTION OF MOISTURE CONTENT

Two methods were utilized to determine the unsaturated hydraulic conductivity of the vadose zone as a function of moisture content $K(\theta)$: the Dynamic Method, described in Section 3.2, and a theoretical method described by Mualem (1976). These analyses fulfill the requirements of paragraph 25, task 3 of the May 7, 1985 compliance order which specifies that five samples from each of at least four horizons be sampled. Analyses were conducted on four samples taken from each of five boreholes.

3.4.1 Measurement of Unsaturated Hydraulic Conductivity (Dynamic Method)

Freeze and Cherry (1979) explain that unsaturated flow is actually a special case of multiphase flow with two phases, air and water coexisting in the pore channels; therefore, each rock possesses two characteristic curves of fluid content versus pressure head, one for water and air. They further explain that when determining conductivity relationships, it is preferable to work with permeability (k) rather than hydraulic conductivity since k is independent of fluid properties. Flow parameters k_w and k_a are defined as the effective permeabilities of the medium to water and air. Each rock has characteristic curves of effective permeability versus pressure head for air $k_a(\psi)$ and water $k_w(\psi)$. Effective permeability depends not only on the rock, but also upon the relative amounts of different fluids in the pores (Schlumberger, 1972).

The following discussion of laboratory testing of unsaturated hydraulic conductivity by the Dynamic Method is taken from BFEC (1986).

> The Dynamic Method was also used to determine permeability as a function of moisture content for the 20 samples of Bandelier Tuff. These values, called effective permeabilities, are plotted as a function of total air saturation in the graphs presented in Appendix D of BFEC, 1986. Since the abscissa corresponds to total air saturation, the maximum effective permeabilities for water depicted on

the curves occur at an air saturation of 0.000, which is equivalent to a water saturation (θ_s) of 1.000. Therefore, as the water saturation decreases, the effective permeability for water decreases and the effective permeability for air increases.

The effective permeability values for the rock-core samples from the Bandelier Tuff range from 86.1 to 1301 millidarcys [(8.5×10^{-10} to 1.3×10^{-3} cm^2) or (9.1×10^{-13} to 1.4×10^{-11} ft^2)]. Residual water saturation following gas injection ranged from 0.64 to 0.95. Since moisture contents in the study area are much lower than this range (generally less than 10 percent), the effective permeabilities determined using the Dynamic Method are not indicative of the permeabilities one would expect to observe at depth in areas G and L. These data are therefore only applicable to the estimation of near-surface conditions following a heavy rainfall, when moisture contents might exceed residual water saturation.

It follows from the previous discussion that unsaturated hydraulic conductivity may be calculated from effective permeability data by the following equation:

$$K = \frac{k\rho g}{\mu} \qquad (3\text{-}1)$$

where

K = hydraulic conductivity at moisture content θ
k = effective water permeability at moisture content θ
ρ = density of water
g = gravitational acceleration
μ = dynamic viscosity of water

Since unsaturated hydraulic conductivity is proportional to moisture content, (i.e., conductivity decreases with decreasing moisture) and the permeability data collected are measured for greater moisture contents than observed in the field, calculations of unsaturated hydraulic conductivity are presented for the minimum moisture conditions measured in the laboratory. These data represent hydraulic conductivities greater than the maximum likely to be encountered under field conditions.

Effective permeability at minimum moisture content was measured from graphs of air and water permeability versus percent saturation presented in Appendix D

of BFEC (1986). These data and the results of hydraulic conductivity calculations are presented in Table 3-9. Constants used in the calculation of unsaturated conductivities are typical of ground water (Freeze and Cherry, 1979) and are as follows: $\rho = 1.0\ g/cm^3$, $g = 980\ cm/s^2$, and $\mu = 1.124$ cP (centipoise). Unsaturated hydraulic conductivity calculated from measured effective permeability for 64 to 95 percent water saturation (25.2 to 61.3 percent volumetric water content) ranges from 1.63×10^{-7} to 3.01×10^{-9} cm/s (Table 3-9). Sample LGM-85-11, 30 feet, yielded a very high conductivity, two orders of magnitude above the average. The result of tests on this sample are thought to be erroneous due to its large deviation from the norm.

3.4.2 Theoretical Determination of Unsaturated Hydraulic Conductivity

Unsaturated hydraulic conductivity as a function of moisture content, $K(\theta)$, and as a function of capillary pressure, $K(\psi)$, was determined for samples of Bandelier Tuff using models described by van Genuchten (1978) and Mualem (1976). The models output graphs of $K(\psi)$ and $K(\theta)$ from saturated hydraulic conductivities and soil moisture characteristic curves. Saturated hydraulic conductivity values were calculated from intrinsic permeability measurements yielded by the Klinkenberg method. Additional discussion of the models used, input data, and methodology for determination of $K(\psi)$ and $K(\theta)$ are presented in BFEC (1986).

Graphs of unsaturated hydraulic conductivity as a function of moisture content and capillary pressure for representative samples of Bandelier Tuff are presented in Appendix F. The curves are of limited use because one of the model input parameters, the $\psi(\theta)$ relationship, could not be determined in the range of conditions present within the tuff [i.e., moisture content less than 10 percent and capillary pressure between -1 and -10 bar. However, since hydraulic conductivity decreases with decreasing capillary pressure and moisture content and $K(\psi)$ and $K(\theta)$ were determined for ranges higher than field conditions, it can be concluded that lowest measured $K(\psi)$ above the range of field conditions represents hydraulic conductivity greater than the maximum likely to be encountered in the field. Table 3-10 contains hydraulic conductivity derived for minimum moisture content as determined from the model outputs.

The average theoretically derived hydraulic conductivity for the minimum moisture conditions for which $K(\theta)$ was measured is approximately 7.8×10^{-3} cm/day or 9.1×10^{-8} cm/s at 36 percent moisture (volumetric). This is on the same order of magnitude as values determined from measurement of effective permeability (Table 3-9), thus the two methods of determining $K(\theta)$ support each other for the moisture conditions measured.

3.5 VADOSE ZONE MOISTURE MONITORING

Since late 1985 the Laboratory has been conducting a vadose zone moisture monitoring program at Areas G and L to analyze the infiltration and redistribution of meteoric water into the Bandelier Tuff and to monitor capillary potential in the tuff. This monitoring program fulfills the requirements of paragraph 25 - task 4 of the May 7, 1985 compliance order issued to the Laboratory. The monitoring system utilizes neutron logging to monitor moisture conditions at Areas G and L and thermocouple psychrometers at various depths for monitoring capillary potential.

Under ideal circumstances, soil moisture data collected by neutron moisture measurements can be converted to estimates of capillary pressure and capillary pressure measurements can be converted to soil moisture data through use of the $\psi(\theta)$ relationship or the soil characteristic curve. However, due to difficulties in measuring $\psi(\theta)$ relationships for very low moisture conditions present in the tuff, accurate conversions between moisture and tension data cannot be made.

3.5.1 Neutron Moisture Logging

The moisture content of the Bandelier Tuff is being measured with a neutron moisture probe in order to analyze infiltration and redistribution of moisture in the tuff.

Two boreholes, one each in Areas G and L, have been completed with cold drawn aluminum casing for neutron probe access. Boring numbers LLN-85-04 and LGN-85-08 have been completed to depths of 108 and 50 feet, respectively. The annular space around the casings were backfilled with cuttings from the borehole and compacted with a cement vibrator. Details of installation procedures for the access wells are provided in BFEC (1986) Section 4.2.

The Laboratory utilizes a Campbell Pacific moisture gauge to conduct measurements. Calibration of the instrument is conducted by recording the number of thermalized neutron counts in 16 second intervals from samples of known moisture content. Calibration curves for the instrument are then constructed. Further discussion of calibration procedures are presented in BFEC (1986).

Neutron moisture measurements were initiated on December 17, 1985 at the two areas. Measurements were collected approximately every two weeks through June 1986, after which data were not collected until early October due to equipment malfunction. The original moisture probe, a Campbell Pacific model 501DR was replaced during this time period with a model 503DR. The new probe was calibrated using the same procedures as for the model 501DR, using only the high and low moisture calibration samples, an internal auto calibration feature interpolates intermediate moisture conditions. Calibration data and curves for each of the instruments are provided in Appendix G. After calibration of the model 503DR, daily moisture profiles were collected from each area after precipitation events and the biweekly schedule was then continued.

Measurements of volumetric moisture content of Bandelier Tuff in Areas G and L are presented in tabular form in Appendix G. Figures 3-3 through 3-6 display monthly moisture-depth profiles for Areas G and L. As can be seen from comparing the graphs, moisture content remains essentially the same below 15 feet indicating that very little precipitation infiltrates below this depth. The moisture content of the tuff in both areas varies very little and remains between two and five percent; this range is comparable to the measured gravimetric moisture content of the tuff. The graphs also show a bimodal distribution of data, with data collected prior to October 1986 being grouped approximately one to one and one-half percent below data collected after October 1986. The uniformity of the apparent difference in moisture content with depth suggests that the change is due to instrument measurement rather than an actual change in moisture content. Data collected prior to October 1986 were collected with the Model 501DR while data collected after October were collected with the model 503DR. Slight differences in instrument calibration, source strength, and/or counting time may account for the small shift in moisture determinations.

In accordance with requirements of task four, measurements of soil moisture conditions were collected daily after autumn storms. Three storms were recorded in October and early November 1986. Precipitation data from Area G (Appendix E) indicate that 0.34 inches of rain fell between October 5 and 7, 1.63 inches between October 10 and 12, and 1.49 inches between November 1 and 4. Daily measurements of volumetric moisture content in the tuff, as measured by the neutron probe after each precipitation event, are presented in Appendix G and graphically summarized in Figures 3-7 through 3-10.

Graphs of moisture content versus time are presented for depths below the surface of 2, 6, 10, 22, 41, and 50 feet for Area L and 2, 6, 10, 22, 42, and 47 feet for Area G. Graphs for October storms (Figures 3-7 and 3-9) indicate slight increases in moisture after precipitation to a depth of ten feet; these changes are more visible in Area L data than Area G. Changes of one-half to one percent volumetric moisture appear to be indicated approximately six days after precipitation at ten foot depth (Figure 3-9). Moisture content of the tuff below ten feet depth does not appear to be influenced by autumn precipitation events. The difference in depth of infiltration between Areas G and L may be due to geographic differences at the sites such as wind sheltering, local differences in precipitation and evaporation or variable amounts of ground disturbance.

Precision of the instrument places limitations on measurement of low moisture conditions. Manufacturers of the neutron moisture probe calculate precision of the instrument as follows:

$$\% \text{ error} = \frac{100}{(x \bullet t/16)^{\frac{1}{2}}} \qquad (3\text{-}2)$$

where

x = number of slow neutron counts
t = counting time in seconds

The two point calibration for the model 503DR instrument yields an average of 157 counts per 16 second counting period at 0.075 percent moisture. These data yield a 7.98 percent error in precision for low moisture conditions.

Moisture profiles measured in 1986 in Areas G and L are consistent with moisture measurements conducted in previous studies of the Bandelier Tuff. Abeele and others (1981) present neutron-moisture data of the tuff for various locations at the Laboratory measured between 1960 and 1980; typically, the upper 10 to 15 feet of tuff exhibit moisture conditions ranging from 10 to 40 percent by volume. Moisture rarely exceeded 5 to 10 percent below 15 feet of depth. The data presented by Abeele and others for Area G show that significant seasonal fluctuations in moisture content exist in the uppermost four meters of disturbed areas in Area G. These older data are consistent with the 1986 data (Figures 3-3 and 3-4).

Gravimetric moisture data, and neutron-moisture data collected during the 1985-86 and 1960-70 studies are consistent in showing the following trends:

- The moisture content of the tuff throughout the area is low, typically between 2 to 5 percent with intervals ranging up to 10 to 28 percent
- Seasonal variation of moisture content occurs in the upper 10 to 20 feet of the tuff. Seasonal variations are not measurable below approximately 20 feet
- Precipitation from monitored autumn storms does not infiltrate below approximately ten feet.

Empirical studies of neutron-moisture measurement, described above, lead to the conclusion that the tuff is not saturated, in fact it is very dry, and moisture from precipitation does not appear to infiltrate to significant depth. Therefore, infiltration of meteoric water would not seem to be a viable process for transport of waste constituents from Areas G and L through the unsaturated zone.

3.5.2 Measurement of Capillary Potential

Task four of the compliance order specifies that in addition to neutron-moisture measurements, the Laboratory must monitor capillary potential with either moisture blocks or by psychrometry. Psychrometers were used rather than tensiometers or moisture blocks because the high soil water tensions present precluded the use of tensiometers and many problems are associated with use of moisture blocks. Psychrometers however also have inherent deficiencies in measuring high soil water tensions. Care must be taken in

interpreting the psychrometer data due to the placement and backfill surrounding the sensors. Everett and others (1984) explain that nonrepresentative measurements of tension may occur if a good contact is not maintained between the psychrometer cup and the surrounding formation. Proper contacts are especially difficult to achieve in coarse material, at greater depths, or when sensors are surrounded by well indurated material. Any or all of these factors may be present in the Area G and L boreholes and may account for fluctuation in data.

Boreholes LLP-85-03 and LGP-85-07 were instrumented with 23 and 15 psychrometers, respectively (Appendix C, Figures C-4 and C-7). Thermocouple psychrometers are designed to measure negative soil water pressure from relative humidity versus output voltage relationships. Details of the installation, calibration, and operation of the psychrometers at Areas G and L are provided in BFEC (1986), Section 3.3.1, and BFEC (1985b). Everett and others (1984) provide additional discussion of the use of psychrometers.

Each psychrometer is connected to an automatic data recorder which records soil water potential once per day. Psychrometers in borehole LGP-85-07 are connected to one data recorder, psychrometers below a depth of 41 feet in borehole LLP-85-03 are connected to a second recorder and psychrometers above 41 feet at Area L are connected to a third recorder. The psychrometers have been operational since October 1985. Data collected through November 1986 are presented in Appendix H. Data recording errors are indicated as zero soil-water potential in this appendix. The zero values are assigned to the reading and do not represent saturated conditions. Additionally, several blocks of data are not available due to malfunction of the data recorders. Table 3-11 contains a summary of data collected from selected psychrometers in Areas G and L. Monthly averages, maximum and minimum soil tension measurements are presented for Area G psychrometers at 22, 42,and 52 feet below the surface. Similar data are presented for Area L psychrometers at depths of 24, 50, 76, and 96 feet. These intervals were selected to provide a reasonable number of data to summarize and do not have any known hydrologic significance. Unfortunately, data below 41 feet in Area L are absent for several months due to data recording errors in the third recorder. Data from the 41 foot psychrometer are included in the table for periods in which psychrometer data are

unavailable for 50 to 96 foot depths. These data are also presented graphically in Figures 3-11 and 3-12.

The most apparent characteristic of the psychrometer data from Areas G and L is the high variability of the readings. The data range from less than one bar tension to over 18 bars. Monthly averages of soil water tension in Area L range from 2.96 to 6.95 bars and from 2.42 to 10.22 bars in Area G. Both the Area G and L psychrometers display a high rate of change during the October-November 1985 period. This is interpreted as a period of moisture conditions in the boreholes equilibrating with surrounding formation. After the initial one to two month equilibration period, the average readings tend to be more stable and fluctuate in the two to seven bar tension range.

Due to the data recording malfunctions described earlier, and the period required for the tensiometers to stabilize, tension measurements are not available through a complete year; thus, seasonal variations in matric forces cannot be evaluated.

Due to the inherent difficulty in measuring soil water tension at very low moisture conditions, the variability displayed in the psychrometer data collected, and the difficulty encountered in quantifying soil moisture characteristic curves, the psychrometer data are best utilized as a qualitative tool in judging relative moisture content. The data do, however, prove to be useful in calculation of average hydraulic head (Section 3.6).

3.6 GRADIENT DETERMINATIONS AND MOISTURE MOVEMENT

Moisture flux is defined as the volume of water crossing a unit area of porous material per unit time and is given by the equation:

$$J = -K(\theta)\nabla H \qquad \text{(Everett and others, 1984)} \qquad (3\text{-}3)$$

where

- J = specific discharge or flux (volume per unit area per unit time)
- $K(\theta)$ = hydraulic conductivity, expressed as a function of water content, θ
- H = total hydraulic head, the sum of soil-water pressure head, ψ, and potential head, z
- ∇H = the hydraulic gradient, expressed in vector form

Flux has units of velocity. The negative sign in the above equation is used by convention to indicate flow occurs in the direction of decreasing hydraulic head.

Hillel (1980, p. 108) describes the process of unsaturated flow as the movement of water along hydration films over particle surfaces in a tendency to equilibrate hydraulic potential. Additionally, Hillel explains that large interaggregate (or interparticle) spaces, which confer high hydraulic conductivity at saturation, become barriers to liquid flow when emptied. The process of unsaturated flow, and moisture flux calculations, therefore, assumes that a continuum of moisture exists throughout the region of flow. Given the very low moisture content of the tuff and the degree of discontinuity (e.g., fractures) it is doubtful that flow processes are continuous throughout the vadose zone. However, the following calculations of moisture flux are presented, assuming that moisture is uniformly and continuously distributed, to provide a logical completion of analysis of data collected under tasks one through four of compliance order paragraph 25.

The hydraulic conductivity of the Bandelier Tuff was determined via two methods: 1) measurement of gas-water effective permeability at various moisture content and calculation of hydraulic conductivity at given moisture conditions, and 2) a theoretical method based on the characteristic curves (Section 3.3.2.2). Due to experimental difficulties, $K(\theta)$ could not be determined for the range of conditions encountered in the field; however, the derived values serve well as estimates of maximum possible $K(\theta)$ likely to be encountered in the field. Values of $K(\theta)$ are presented in Tables 3-9 and 3-10; the two methods yield similar results with model predicted values being slightly greater than measured values, the average model predicted value at minimum measurable moisture conditions is 9.3×10^{-8} cm/s (2.64×10^{-4} ft/day) and 4.66×10^{-8} cm/s (1.32×10^{-4} ft/day) for measured conductivities.

Hydraulic head gradients are determined from monthly soil tension averages as measured by psychrometers located in Areas G and L. The total hydraulic head (H) can be calculated by the formula:

$$H = \psi + z \qquad \text{(Freeze and Cherry, 1979)} \qquad (3\text{-}4)$$

where

ψ = capillary pressure
z = elevation
In the unsaturated zone $\psi < 0$

Elevations in feet above mean sea level were determined for psychrometers located at depths of 24, 41, 50, 76, and 96 feet in area L and at depths of 22, 42, and 52 feet in area G; and mean monthly capillary pressure (Table 3-11) was added to the elevation to determine hydraulic head. These datum were arbitrarily selected as calculation intervals and do not represent any known hydrologic significance. Further, it is assumed that unsaturated flow occurs within the surface to 22 foot interval, as demonstrated by neutron moisture measurements. However, the emphasis of this study is to determine the likelihood of contaminant transport downward through the tuff, below the waste disposal facilities; therefore, analysis of the surface to 22 foot interval is unwarranted.

Hydraulic gradients were calculated between psychrometers by dividing the change in hydraulic head between two psychrometers by the distance separating the measuring points. Calculation spreadsheets showing the calculation procedures and data are presented in Appendix I. By convention, a change in hydraulic head less than zero indicates a decrease in hydraulic head in the downward direction. Moisture flux is next calculated using Equation 3-3. Calculations are shown using the average measured and average theoretical hydraulic conductivities. Table 3-12 summarizes the results of these calculations; more detailed results are presented in Appendix I. Moisture flux calculations were conducted for intervals between 24-50 feet, 50-76 feet, and 76-96 feet below the surface in Area L and 22-42 feet and 42-52 feet below the surface for Area G. The 24- to 41-foot interval was used in calculations for Area L during the month when data below 41 feet were not available. The flux calculations were conducted for 12-month periods using the average soil tension for that month.

Results of the calculations using model predicted hydraulic conductivity (2.64×10^{-4} ft/day) range from a maximum downward flux of 0.508 ft/yr (15.5 cm/yr)

to a maximum upward flux of 0.397 ft/yr (12.1 cm/yr) in Area L. Results of flux calculations in Area G using the model derived hydraulic conductivity range from a downward rate of 0.982 ft/yr (29.9 cm/yr) to a maximum upward rate of 0.081 ft/yr (2.5 cm/yr). Flux rates calculated using average measured hydraulic conductivity an Area L ranged from a maximum downward rate of 0.254 ft/yr (7.74 cm/yr) to a maximum upward rate of 0.198 ft/yr (6.03 cm/yr); Area G rates range from downward flux of 0.491 ft/yr (1.49 cm/yr) to upward flux of 0.041 ft/yr (1.25 cm/yr).

The calculations of flux should be viewed as highly conservative, representing the maximum movement of fluid likely to be encountered under field conditions as hydraulic conductivities used in the flux calculations are determined for moisture content above field conditions and therefore are of greater magnitude. Even though estimates of flux are conservative, they show that very long periods of time are required for water and contaminants to move by porous flow through the tuff and that aqueous movement of contaminants through the porous flow in the vadose zone is not a viable mechanism for contamination of ground water.

As described in Section 2.2.2 the tuff underlying Areas G and L contains numerous fractures and joints. These fractures may effectively serve as barriers to unsaturated flow of water and contaminants due to interruption of capillary pathways. Fractures however, may provide pathways for migration of vapor phase contaminants.

3.7 SUMMARY OF VADOSE ZONE HYDROLOGY

Based on the data collected in this report and from other studies the following conclusions can be made concerning the hydrologic characterization of the vadose zone and possible aqueous phase migration of chemical contaminants.

- The Bandelier Tuff is characterized by very low moisture content, typically in the range of two to five percent. This value is well below the porosity and thus moisture movement via unsaturated flow processes predominate over saturated flow.

- The tuff is very porous, averaging 50 percent porosity and has high moisture retention properties.

- Field and laboratory intrinsic permeability tests indicate average permeability of the tuff to be 10^{-8} to 10^{-9} cm^2. This represents moderate permeability similar to that of silty sand.

- Field permeability tests do not indicate increased permeability in zones adjacent to fractures in boreholes; however, the aperture, trace, and degree of fracture filling is variable and the permeability along fractures may vary significantly.

- The unsaturated hydraulic conductivity of the tuff was determined to be approximately 10^{-8} cm/s at approximately 20 to 40 percent moisture content as determined by measured effective permeability and using van Genuchten's model. Actual moisture conditions and $K(\theta)$ are likely lower than these values.

- Soil-characteristic curves for intact cores of Bandelier Tuff could not be determined for the range of moisture/tension conditions present in the field due to the low moisture content in the tuff and the low degree of consolidation within the tuff.

- Soil water tension as measured by thermocouple psychrometers range from one to fifteen bars. Monthly averages typically range from two to seven bars.

- Neutron measurements of vadose zone moisture show that seasonal variation of moisture occurs in the upper 10 to 15 feet of the vadose zone. Moisture content below 15 feet does not appear to change with time. Neutron measurements of moisture after precipitation events indicate the maximum depth of wetting to be approximately ten feet. No influence of precipitation on moisture content was observed at a depth of 22 feet and moisture is assumed to be returned to the surface by evapotranspiration.

- Maximum calculated moisture flux rates for porous flow are 0.508 ft/yr and 0.982 ft/yr for Areas L and G respectively. Mean flux rates for the areas are 0.070 and 0.421 ft/yr. These calculations are based on unsaturated hydraulic conductivities for greater moisture content than observed in the field and thus are greater than actual flux rates. The assumptions that underlie these calculations make it unlikely that unsaturated flow occurs over any significant distance.

Each of the above statements support the conclusion that aqueous transport of contaminants through Bandelier Tuff by saturated or unsaturated flow processes is not a viable mechanism for contaminant migration at Areas G and L.

TABLE 3-1
MEAN MONTHLY PRECIPITATION (INCHES)
LOS ALAMOS, NEW MEXICO[1]

	JAN	FEB	MAR	APR	MAY	JUNE	JULY	AUG	SEPT	OCT	NOV	DEC	ANNUAL
White Rock	0.25	0.24	0.24	0.32	1.20	1.50	2.29	3.68	1.73	1.02	0.39	0.67	13.50
TA-59/TA-3	0.82	0.67	1.14	0.82	1.16	1.10	3.20	3.86	1.73	1.47	0.99	0.97	17.93
Los Alamos	0.84	0.70	1.01	1.01	1.25	1.33	3.29	3.69	2.01	1.61	0.70	0.93	18.37
TA-54													13.45[2]

(1) From NMEID (1985).
(2) Five years of record; annual total based on 75 percent of TA-59/TA-3.

LAN:1702-T3-1

TABLE 3-2
PRECIPITATION MEASURED AT TA-54 AREA G, 1986

MONTH	JAN	FEB	MAR	APR	MAY	JUNE	JULY	AUG	SEPT	OCT	NOV	DEC	Annual
Precipitation (inches)	0	0.91	0.81	1.46	1.38	3.45	2.19	1.12	2.34	2.10	2.45	0.64	18.85

TABLE 3-3
HYDRAULIC CONDUCTIVITY DETERMINED FROM AIR-INJECTION TESTS IN LOS ALAMOS DRILL HOLES

HOLE NUMBER	GEOLOGIC UNIT	TEST INTERVAL[1] (ft)	INTERVAL DESCRIPTION	FRACTURES PRESENT?	HYDRAULIC CONDUCTIVITY (K) cm/s x 10^{-3}	ft/s x 10^{-5}
LLM-85-01	2b	9-15	Upper 2b, Moderately Welded	No	1.2	4.1
LLM-85-01	2b	30-36	Lower 2b, Moderately to Slightly Welded	No	0.70	2.3
LLM-85-02	2b	9-15	Upper 2b, Moderately Welded	Yes	0.094	0.31
LLM-85-02	2b	24-30	Middle 2b, Moderately Welded	No	0.11	0.37
LLM-85-05	2b	24-30	Mid-Lower 2b, Moderately Welded	No	0.91	3.0
LGM-85-11	2b	9-15	Upper 2b, Moderately Welded	No	1.5	5.0
LGM-85-11	2b	14-20	Middle 2b, Moderately Welded	Yes	1.4	4.7
LGM-85-11	2b/2a	35-41	Contact 2b/2a, Slightly Welded	No	0.12	0.40
LLM-85-01	2a	51-57	Middle 2a, Slightly Welded	No	0.33	1.1
LLM-85-01	2a	72-78	Lower 2a, Slightly Welded	Yes	0.14	0.45
LLM-85-02	2a	45.5-51.5	Upper 2a, Slightly Welded	Yes	0.14	0.45
LLM-85-02	2a	66.5-72.5	Mid-Lower 2a, Moderately Welded	No	0.14	0.45
LLM-85-05	2a	45-51	Upper 2a, Slightly Welded	Yes	2.8	9.3
LLM-85-05	2a	55-61	Middle 2a, Slightly Welded	Yes	1.9	6.2
LGM-85-06	2a	38-44	Upper 2a, Slightly Welded	Yes	0.067	0.22
LLM-85-05	2a/1b	75-81	Contact 2a/1b, Slightly Welded	No	0.052	0.17
LGM-85-11	2a/1b	56-62	Contact 2a/1b, Slightly Welded	No	0.52	1.7
LLM-85-01	1b	93-99	Mid-Upper 1b, Slightly Welded	No	0.082	0.27
LLM-85-02	1b	87-93	Upper 1b, Slightly Welded	No	0.085	0.28
LLM-85-05	1b	82-88	Upper 1b, Slightly Welded	No	0.061	0.20

[1] Depth below ground level

TABLE 3-3

HYDRAULIC CONDUCTIVITY DETERMINED FROM AIR-INJECTION TESTS IN LOS ALAMOS DRILL HOLES

(Continued)

HOLE NUMBER	GEOLOGIC UNIT	TEST INTERVAL[1] (ft)	INTERVAL DESCRIPTION	FRACTURES PRESENT?	HYDRAULIC CONDUCTIVITY (K) cm/s x 10^{-3}	ft/s x 10^{-5}
LGM-85-06	1b	60-66	Upper 1b, Slightly Welded	No	0.64	2.1
LGM-85-06	1b	81-87	Middle 1b, Slightly to Moderately Welded	No	0.52	1.7
LGM-85-11	1a/1b	99-105	Contact 1a/1b, Slightly Welded	No	0.030	0.098
LGM-85-11	1b	77-83	Middle 1b, Slightly to Moderately Welded	No	0.23	0.77
LGM-85-11	1a	108-114	Upper 1a, Nonwelded	No	0.088	0.2

From BFEC (1986)

TABLE 3-4

PERMEABILITY VALUES DETERMINED FROM VACUUM TESTS IN LOS ALAMOS DRILL HOLES

HOLE NUMBER	GEOLOGIC UNIT	TEST INTERVAL[1] (ft)	INTERVAL DESCRIPTION	FRACTURES PRESENT?	INTRINSIC PERMEABILITY (k) $cm^2 \times 10^{-9}$	$ft^2 \times 10^{-12}$
LLM-85-01	2b	30-33.3	Lower 2b, Moderately Welded	No	39	42
LLM-85-02	2b	10-13.3	Upper 2b, Moderately Welded	Yes	14	15
LLM-85-02	2b	25-28.3	Middle 2b, Moderately Welded	Yes	22	24
LLM-85-05	2b	15-18.3	Middle 2b, Moderately Welded	No	24	2.6
LGM-85-06	2b	10-13.3	Upper 2b, Moderately Welded	No	38	41
LGM-85-11	2b/2a	35-38.3	Contact 2b/2a, Moderately Welded	No	5.5	5.9
LLM-85-01	2a	70-73.3	Lower 2a, Nonwelded	No	43	46
LLM-85-05	2a	40-43.3	Upper 2a, Slightly Welded	No	8.4	9.1
LLM-85-05	2a	50-53.3	Middle 2a, Slightly Welded	No	8.6	9.3
LLM-85-05	2a	60-63.3	Middle 2a, Moderately Welded	No	8.6	9.3
LLM-85-06	2a	40-43.3	Middle 2a, Moderately Welded	Yes	2.4	2.6
LLM-85-01	1b	80-83.3	Upper 1b, Slightly Welded	No	5.6	6.0
LLM-85-01	1b	94-97.3	Upper 1b, Slightly Welded	No	3.5	3.8
LLM-85-02	1b	87-90.3	Upper 1b, Slightly Welded	No	9.3	10
LGM-85-06	1b	82-85.3	Middle 1b, Slightly Welded	No	1.0	1.1
LGM-85-06	1b	100-103.3	Lower 1b, Moderately Welded	No	0.84	0.90
LGM-85-11	1b	77-80.3	Middle 1b, Slightly Welded	No	8.2	8.8
LGM-85-06	1b	60-63.3	Upper 1b, Slightly Welded	No	8.7	9.4
LGM-85-11	1a	110-113.3	Upper 1a, Nonwelded	No	2.7	2.9
LLM-85-02	1b	87-90.3	Upper 1b, Slightly Welded	No	8.6	9.3
LLM-85-06	1b	87-90.3	Mid-Lower 2b, Moderately Welded	No	2.4	2.6

Modified From BFEC (1986)

[1] Depth below ground level.

TABLE 3-5
COMPARISON OF INTRINSIC PERMEABILITY VALUES DETERMINED FROM AIR-INJECTION AND VACUUM TESTS IN LOS ALAMOS DRILL HOLES

HOLE NUMBER	TEST INTERVAL (ft)[1]		INTRINSIC PERMEABILITY (k)			
	AIR-INJECTION TEST	VACUUM TEST	AIR-INJECTION TEST		VACUUM TEST	
			$cm/^2 \times 10^{-9}$	$ft^2 \times 10^{-12}$	$cm/^2 \times 10^{-9}$	$ft^2 \times 10^{-12}$
LLM-85-01	30-36	30-33.3	130	140	39	42
LLM-85-02	9-15	10-13.3	10	11	15	16
LLM-85-02	24-30	25-28.3	16	17	22	24
LGM-85-11	35-41	35-38.3	17	18	5.5	5.9
LLM-85-01	72-78	70-73.3	19	21	43	46
LLM-85-01	93-99	94-97.3	7.6	8.2	3.5	3.8
LLM-85-02	87-93	87-90.3	3.3	9.5	9.3	10
LGM-85-06	60-66	60-63.3	120	130	8.7	9.4
LGM-85-06	81-87	82-85.3	84	90	1.0	1.1
LGM-85-11	99-105	100-103.3	3.3	3.6	0.84	0.90
LGM-85-11	77-83	77-80.3	32	35	8.2	8.8
LGM-85-11	108-114	110-113.3	7.2	7.8	2.7	2.9

From BFEC (1986)

---

[1] Depth below ground level

LAN:1702-T3-5

TABLE 3-6
INTRINSIC PERMEABILITY VALUES DETERMINED FROM LABORATORY ANALYSIS OF CORE SAMPLES

HOLE NUMBER	GEOLOGIC UNIT	SAMPLE NUMBER	DEPTH OF SAMPLE (ft)[2]	INTERVAL DESCRIPTION	INTRINSIC PERMEABILITY/ KLINKENBERG METHOD $cm^2 \times 10^{-9}$	INTRINSIC PERMEABILITY/ KLINKENBERG METHOD $ft^2 \times 10^{-12}$	CORRELATION COEFFICIENT[1]	INTRINSIC PERMEABILITY/ DYNAMIC METHOD $cm^2 \times 10^{-9}$	INTRINSIC PERMEABILITY/ DYNAMIC METHOD $ft^2 \times 10^{-12}$
LGM-85-11	2b	MCG-618	3	Moderately Welded[3]	6.2	6.7	0.989	5.5	5.9
LLM-85-02	2b	MCG-606	7	Moderately Welded	6.6	7.1	0.745	4.5	4.9
LLM-85-05	2b	MCG-610	15	Moderately Welded	6.5	7.0	0.893	5.7	6.2
LLM-85-01	2b	MCG-602	30	Moderately Welded	2.7	2.9	0.958	1.1	1.2
LGM-85-11	2b	MCG-619	30	Moderately Welded	3.2	3.5	0.949	2.9	3.1
LLM-85-02	2b	MCG-607	36	Moderately Welded	11.0	12.0	0.714	1.2	1.3
LGM-85-06	2b	MCG-614	29	Moderately Welded	6.4	6.9	0.847	4.9	5.3
LLM-85-05	2b	MCG-611	36	Slightly Welded	3.5	3.8	0.984	2.4	2.6
LLM-85-01	2a	MCG-603	52	Slightly Welded	4.1	4.4	0.969	2.7	2.9
LGM-85-06	2a	MCG-615	51	Slightly Welded	2.5	2.7	0.954	0.86	0.93
LLM-85-02	2a	MCG-608	67	Moderately Welded	2.0	2.2	0.958	1.0	1.1
LLM-85-05	1b	MCG-612	76	Slightly Welded	2.1	2.3	0.944	1.3	1.4
LLM-85-01	1b	MCG-604	101	Slightly Welded	3.0	3.2	0.939	2.6	2.8
LGM-85-06	1b	MCG-616	99	Moderately Welded	18.0	19.0	0.917	13.0	14.0
LGM-85-11	1b	MCG-620	94	Moderately Welded	4.4	4.7	0.958	1.1	1.2
LLM-85-02	1b	MCG-609	117	Moderately Welded	3.3	3.6	0.973	1.7	1.8
LLM-85-05	1b	MCG-613	123	Slightly Welded	4.2	4.5	0.902	1.6	1.7
LLM-85-01	1b	MCG-605	124	Moderately Welded	6.0	6.5	0.850	2.3	2.5
LGM-85-11	1a	MCG-621	115	Nonwelded	3.4	3.7	0.933	1.8	1.9
LGM-85-06	1a	MCG-617	115	Nonwelded	1.4	1.5	0.970	0.93	1.0

FROM BFEC (1986)

(1) Determined for Klinkenberg permeabilities
(2) Below ground level
(3) Weathered

LAN:1702-T3-6

TABLE 3-7
COMPARISON OF AVERAGE INTRINSIC PERMEABILITY VALUES FOR THE MAJOR GEOLOGIC UNITS OF THE BANDELIER TUFF IN THE STUDY AREA

UNIT	INTRINSIC PERMEABILITY					
	AIR-INJECTION TEST		VACUUM TEST		LABORATORY ANALYSIS	
	$cm/^2 \times 10^{-9}$	$ft^2 \times 10^{-12}$	$cm/^2 \times 10^{-9}$	$ft^2 \times 10^{-12}$	$cm/^2 \times 10^{-9}$	$ft^2 \times 10^{-12}$
2b	93	100	23	25	5.7	6.2
2a	62	67	13	14	2.8	3.0
1b	26	28	5.7	6.2	5.7	6.2
1a	7.8(1)	7.8(1)	2.7(1)	2.9	2.4	2.6

From BFEC (1986)

(1) Intrinsic permeability for this unit is based on only one measurement.

TABLE 3-8

RESULTS OF MOISTURE/TENSION RELATIONSHIP TESTING FOR INTACT CORES OF BANDELIER TUFF[1]

BORING NUMBER	SAMPLE NUMBER	DEPTH (ft)	STRATIGRAPHIC UNIT	CAPILLARY PRESSURE (psi)	WETTING FLUID SATURATION (percent)	VOLUMETRIC MOISTURE (percent)
LLM-85-01	MCG-602	30	2b	0.510	91.6	36.3
				0.906	84.6	33.5
				1.420	81.2	32.1
				2.055	76.1	30.1
				2.814	70.9	28.1
				3.701	65.8	26.0
LLM-85-01	MCG-603	52	2a	0.455	90.0	58.
				0.823	84.7	54.5
				1.385	79.7	51.3
				2.230	74.9	48.2
				3.495	70.2	45.2
				5.403	65.8	42.4
LLM-85-01	MCG-604	101	1b	0.493	88.6	55.0
				0.955	82.1	51.
				1.738	76.6	47.6
				3.220	71.9	44.6
				6.555	67.8	42.1
LLM-85-01	MCG-605	124	1b	0.392	83.5	40.8
				0.620	76.9	37.6
				0.955	70.5	34.5
				1.450	64.4	31.5
				2.189	58.5	28.6
				3.319	52.9	25.9
LLM-85-02	MCG-606	7	2b	0.392	88.6	36.8
				0.812	81.1	33.7
				1.450	73.9	30.7
				2.372	66.8	27.7
				3.663	60.0	24.9
				5.440	53.3	22.1
LLM-85-02	MCG-607	36	2b	0.097	92.0	42.8
				0.181	87.3	40.6
				0.494	79.1	36.8
				0.799	75.8	35.2
				1.382	73.4	34.1
				2.975	71.8	33.4

[1] Modified from BFEC (1986)

TABLE 3-8

RESULTS OF MOISTURE/TENSION RELATIONSHIP TESTING FOR INTACT CORES OF BANDELIER TUFF
(Continued)

BORING NUMBER	SAMPLE NUMBER	DEPTH (ft)	STRATIGRAPHIC UNIT	CAPILLARY PRESSURE (psi)	WETTING FLUID SATURATION (percent)	VOLUMETRIC MOISTURE (percent)
LLM-85-02	MCG-608	67	2a	0.424	90.7	39.3
				0.681	86.6	37.5
				1.050	82.6	35.8
				1.573	78.7	34.1
				2.315	75.0	32.5
				3.375	71.5	30.9
LLM-85-02	MCG-609	117	1b	0.252	94.2	45.7
				0.626	89.3	43.3
				1.135	84.2	40.8
				1.757	79.1	38.4
				2.474	73.9	35.8
				3.268	68.6	33.3
LLM-85-05	MCG-610	15	2b	0.174	90.0	47.3
				0.328	84.5	44.4
				0.563	79.1	41.6
				0.913	73.9	38.9
				1.429	68.9	52.0
				2.188	64.2	33.8
LLM-85-05	MCG-611	36	2b	0.259	96.1	70.7
				1.014	90.8	66.8
				1.879	85.0	62.6
				2.715	78.5	57.8
				3.482	71.4	52.6
				4.171	63.7	46.9
LLM-85-05	MCG-612	76	1b	0.072	97.1	72.0
				0.344	94.0	69.7
				0.800	90.9	67.4
				1.424	87.8	65.1
				2.198	84.6	62.8
				3.109	81.4	60.4
LLM-85-05	MCG-613	123	1b	0.166	85.1	55.8
				0.243	82.4	54.1
				0.382	79.7	52.3
				0.671	77.1	50.6
				1.426	74.6	48.9
				4.598	72.1	47.3

TABLE 3-8
RESULTS OF MOISTURE/TENSION RELATIONSHIP TESTING FOR INTACT CORES OF BANDELIER TUFF

(Continued)

BORING NUMBER	SAMPLE NUMBER	DEPTH (ft)	STRATIGRAPHIC UNIT	CAPILLARY PRESSURE (psi)	WETTING FLUID SATURATION (percent)	VOLUMETRIC MOISTURE (percent)
LGM-85-06	MCG-614	29	2b	0.446	83.2	35.4
				0.679	77.2	32.8
				1.020	71.4	30.3
				1.526	65.8	28.0
				2.295	60.5	25.7
				3.500	55.4	23.5
LGM-85-06	MCG-615	51	2a	0.419	90.8	36.5
				0.650	86.9	34.9
				0.970	83.1	33.4
				1.411	79.5	32.0
				2.016	76.0	30.6
				2.850	72.6	29.2
LGM-85-06	MCG-616	99	1b	0.322	85.6	45.0
				0.403	85.4	44.9
				0.542	84.5	44.4
				0.818	84.3	44.3
				1.527	83.4	43.9
				4.825	82.2	43.2
LGM-85-06	MCG-617	115	1a	0.068	96.9	54.6
				0.309	92.3	52.0
				0.810	87.8	49.4
				1.716	83.6	47.1
				2.388	81.6	45.9
				3.259	79.6	44.8
LGM-85-11	MCG-618	3	2b	0.296	88.7	48.2
				0.594	81.9	44.5
				1.063	75.3	40.9
				1.775	69.0	37.5
				2.841	62.9	34.2
				4.429	57.1	31.0
LGM-85-11	MCG-619	30	2b	0.491	90.5	46.6
				1.188	81.6	42.0
				2.040	72.3	37.2
				2.976	62.6	32.2
				3.950	52.5	27.0
				4.934	42.0	21.6

TABLE 3-8
RESULTS OF MOISTURE/TENSION RELATIONSHIP TESTING FOR
INTACT CORES OF BANDELIER TUFF

(Continued)

BORING NUMBER	SAMPLE NUMBER	DEPTH (ft)	STRATIGRAPHIC UNIT	CAPILLARY PRESSURE (psi)	WETTING FLUID SATURATION (percent)	VOLUMETRIC MOISTURE (percent)
LGM-85-11	MCG-620	94	1b	0.161	93.3	60.0
				0.376	88.7	57.0
				0.734	84.2	54.1
				1.297	79.9	51.4
				2.163	75.8	48.7
				3.483	71.9	46.2
LGM-85-11	MCG-621	115	1a	0.270	92.3	55.5
				0.446	89.2	53.6
				0.727	86.3	51.9
				1.191	83.5	50.2
				1.991	80.9	48.6
				3.463	7[illegible].5	47.2

TABLE 3-9

WATER EFFECTIVE PERMEABILITY AND UNSATURATED HYDRAULIC CONDUCTIVITY OF BANDELIER TUFF

WELL	DEPTH (ft)	PERCENT WATER SATURATION	VOLUMETRIC MOISTURE (percent)	EFFECTIVE PERMEABILITY (MD)	K (cm/s)	K (ft/day)
LLM-85-01	30	64	25	1.5×10^{-2}	1.29×10^{-8}	3.66×10^{-5}
LLM-85-01	52	80	51	9×10^{-2}	7.74×10^{-8}	2.19×10^{-4}
LLM-85-01	101	68	42	5×10^{-3}	4.3×10^{-9}	1.22×10^{-5}
LLM-85-01	124	86	42	4×10^{-2}	3.44×10^{-8}	9.75×10^{-5}
LLM-85-02	7	81	34	3.5×10^{-3}	3.01×10^{-9}	8.53×10^{-6}
LLM-85-02	36	83	39	6×10^{-3}	5.16×10^{-9}	1.46×10^{-5}
LLM-85-02	67	71	31	9×10^{-2}	7.74×10^{-8}	2.19×10^{-4}
LLM-85-02	117	72	35	5.5×10^{-2}	4.73×10^{-8}	1.34×10^{-4}
LLM-85-05	15	82	43	1.2×10^{-2}	1.03×10^{-8}	2.92×10^{-5}
LLM-85-05	36	87	64	9×10^{-3}	7.74×10^{-9}	2.19×10^{-5}
LLM-85-05	76	83	62	7×10^{-2}	6.02×10^{-8}	1.71×10^{-4}
LLM-85-05	123	85	56	9×10^{-2}	7.74×10^{-8}	2.19×10^{-4}
LGM-85-06	29	73	31	9.5×10^{-3}	8.17×10^{-9}	2.32×10^{-5}
LGM-85-06	51	77	31	4.5×10^{-2}	3.87×10^{-8}	1.09×10^{-4}
LGM-85-06	99	93	49	1×10^{-1}	8.6×10^{-8}	2.44×10^{-4}
LGM-85-06	115	78	44	6×10^{-2}	5.16×10^{-8}	1.46×10^{-4}
LGM-85-11	3	78	42	1.9×10^{-1}	1.63×10^{-7}	4.62×10^{-4}
LGM-85-11	30	69	36	2×10^{0}	1.72×10^{-6}	4.88×10^{-3}
LGM-85-11	94	95	61	5×10^{-2}	4.3×10^{-8}	1.22×10^{-4}
LGM-85-11	115	79	47	9×10^{-2}	7.74×10^{-8}	2.19×10^{-4}

TABLE 3-10

MODEL PREDICTED HYDRAULIC CONDUCTIVITY AT MINIMUM MEASURED MOISTURE

BORING	SAMPLE DEPTH	VOLUMETRIC MOISTURE (%)	K (cm/d)[1]	K (cm/s)
LLM-85-01	30	26	$2x10^{-2}$	$2.3x10^{-7}$
LLM-85-01	52	42	$2x10^{-3}$	$2.3x10^{-8}$
LLM-85-01	101	42	$3x10^{-4}$	$3.5x10^{-9}$
LLM-85-01	124	26	$5x10^{-4}$	$5.8x10^{-9}$
LLM-85-02	7	22	$5x10^{-3}$	$5.8x10^{-8}$
LLM-85-02	36	33	$3x10^{-5}$	$3.5x10^{-10}$
LLM-85-02	67	31	$1x10^{-3}$	$1.2x10^{-8}$
LLM-85-02	117	33	$1x10^{-2}$	$1.2x10^{-7}$
LLM-85-05	15	34	$2x10^{-3}$	$2.3X10^{-8}$
LLM-85-05	36	46	$1x10^{-1}$	$1.2x10^{-6}$
LLM-85-05	76	60	$1x10^{-3}$	$1.2x10^{-8}$
LLM-85-05	123	47	$1x10^{-6}$	$1.2x10^{-11}$
LGM-85-06	29	24	$1x10^{-3}$	$1.2x10^{-8}$
LGM-85-06	51	29	$4x10^{-3}$	$4.6x10^{-8}$
LGM-85-06	99	43	$1x10^{-7}$	$1.2x10^{-12}$
LGM-85-06	115	45	$1x10^{-4}$	$1.2x10^{-9}$
LGM-85-11	3	30	$9x10^{-4}$	$1.0x10^{-8}$
LGM-85-11	30	22	$8x10^{-3}$	$9.3x10^{-8}$
LGM-85-11	94	47	$7x10^{-4}$	$8.1x10^{-9}$
LGM-85-11	115	47	$2x10^{-4}$	$2.3x10^{-9}$

[1] Graphically determined from BFEC (1986)

TABLE 3-11

SUMMARY OF DATA FROM SELECTED PSYCHROMETERS AT TA-54 AREAS G AND L

AREA	MONTH	DEPTH	NUMBER OF READINGS	CAPILLARY POTENTIAL (-BARS) MEAN	MAX	MIN
L	Oct 85	24	20	3.02	4.24	0.78
L	Oct 85	50	16	4.24	8.55	0.29
L	Oct 85	76	16	3.92	5.98	2.97
L	Oct 85	96	16	3.14	5.35	1.26
L	Nov 85	24	60	3.41	8.32	0.57
L	Nov 85	50	53	5.85	11.33	0.3
L	Nov 85	76	60	3.50	5.77	1.85
L	Nov 85	96	62	3.10	6.66	0.97
L	Dec 85	24	16	3.63	4.59	2.84
L	Dec 85	50	38	6.95	10.96	2.89
L	Dec 85	76	38	2.97	4.47	1.42
L	Dec 85	96	38	2.96	5.17	0.98
L	Feb 86	24	55	5.61	9.45	1.68
L	Feb 86	41	54	5.54	10.69	1.24
L	Mar 86	24	32	4.48	8.17	1.03
L	Mar 86	41	30	5.60	11.14	0.25
L	Apr 86	24	34	5.92	8.75	1.69
L	Apr 86	50	34	6.60	10.97	0.31
L	Apr 86	76	34	4.90	7.55	1.89
L	Apr 86	96	33	4.11	10.07	1.33
L	May 86	24	59	4.92	9.16	0.75
L	May 86	50	37	5.28	11.53	0.59
L	May 86	76	39	3.90	8.49	0.56
L	May 86	96	39	3.62	7.82	0.31
L	Jun 86	24	30	4.81	8.09	0.79
L	Jun 86	50	16	5.86	9.29	0.30
L	Jun 86	76	16	3.31	6.00	1.19
L	Jun 86	96	15	3.68	11.01	0.34
L	Aug 86	24	30	5.67	8.82	1.31
L	Aug 86	41	29	5.52	10.36	1.33
L	Sep 86	24	59	6.00	10.12	1.98
L	Sep 86	41	56	5.63	10.59	0.30

TABLE 3-11
SUMMARY OF DATA FROM SELECTED PSYCHROMETERS AT TA-54 AREAS G AND L
(Continued)

AREA	MONTH	DEPTH	NUMBER OF READINGS	CAPILLARY POTENTIAL (-BARS) MEAN	MAX	MIN
L	Oct 86	24	56	5.57	10.49	0.88
L	Oct 86	41	55	5.45	11.44	0.30
L	Nov 86	24	33	4.94	11.19	0.95
L	Nov 86	41	32	4.91	11.49	0.92
G	Oct 85	22	10	3.29	3.85	1.36
G	Oct 85	42	10	8.79	12.95	6.57
G	Oct 85	52	10	10.22	18.	8.63
G	Nov 85	22	7	3.81	4.15	3.55
G	Nov 85	42	7	8.66	9.09	8.31
G	Nov 85	52	6	9.03	9.61	8.78
G	Mar 86	22	5	2.67	5.18	0.86
G	Mar 86	42	5	6.27	7.92	2.68
G	Mar 86	52	5	6.42	8.78	4.79
G	Apr 86	22	24	2.73	5.52	0.88
G	Apr 86	42	24	5.96	9.06	2.62
G	Apr 86	52	22	5.41	6.98	2.14
G	May 86	22	30	2.77	4.33	1.07
G	May 86	42	30	3.43	5.57	1.96
G	May 86	52	30	5.27	7.44	2.41
G	Jun 86	22	30	3.20	4.27	0.82
G	Jun 86	42	29	2.50	4.50	0.29
G	Jun 86	52	29	4.81	6.37	3.24
G	Jul 86	22	17	2.90	4.36	1.28
G	Jul 86	42	17	2.42	4.04	0.30
G	Jul 86	52	17	4.98	6.84	3.37
G	Oct 86	22	28	4.16	7.06	0.89
G	Oct 86	42	28	4.12	7.83	1.82
G	Oct 86	52	28	5.09	7.48	2.90
G	Nov 86	22	18	3.65	8.75	1.14
G	Nov 86	42	18	5.60	9.18	1.38
G	Nov 86	52	18	5.39	8.80	4.07

TABLE 3-12

SUMMARY OF MOISTURE FLUX CALCULATIONS

AREA	HYDRAULIC CONDUCTIVITY (FT/DAY)	MAXIMUM DOWNWARD FLUX (FT/YR)	MINIMUM DOWNWARD FLUX (FT/YR)	MEAN FLUX (FT/YR)
L	2.64×10^{-4} (1)	0.508	-0.397 (2)	0.070
L	1.32×10^{-4} (3)	0.254	-0.198	0.036
G	2.64×10^{-4}	0.982	-0.081	0.421
G	1.32×10^{-4}	0.491	-0.041	0.211

(1) Average unsaturated hydraulic conductivity determined from theoretical methods.
(2) Flux rates <0 indicate upward movement.
(3) Average unsaturated hydraulic conductivity determined from measurement methods.

301017
2/24/87

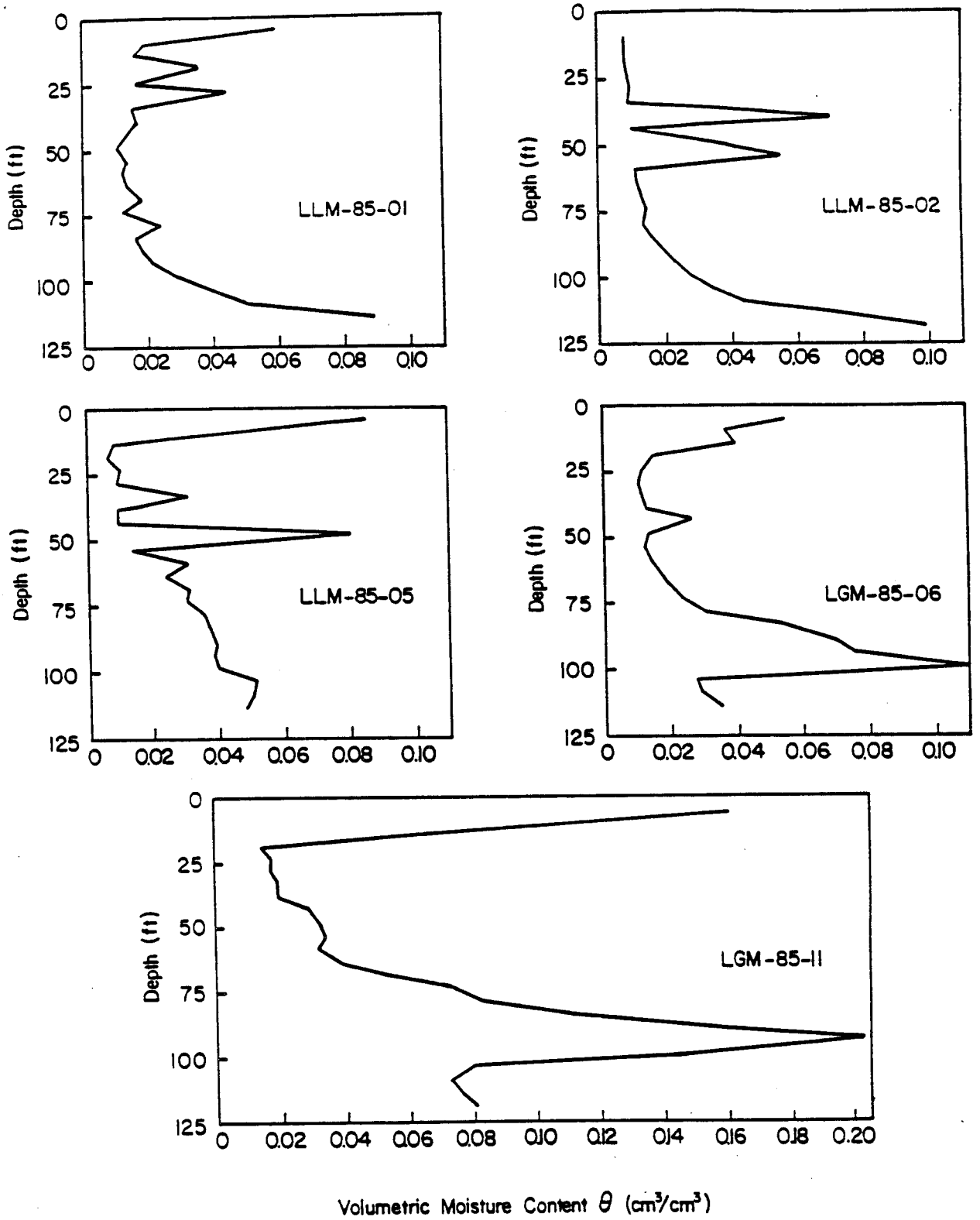

FIGURE 3-1 VOLUMETRIC MOISTURE PROFILES OF BANDELIER TUFF FROM SELECTED BORINGS IN TA-54 AREAS G AND L (BFEC, 1986)

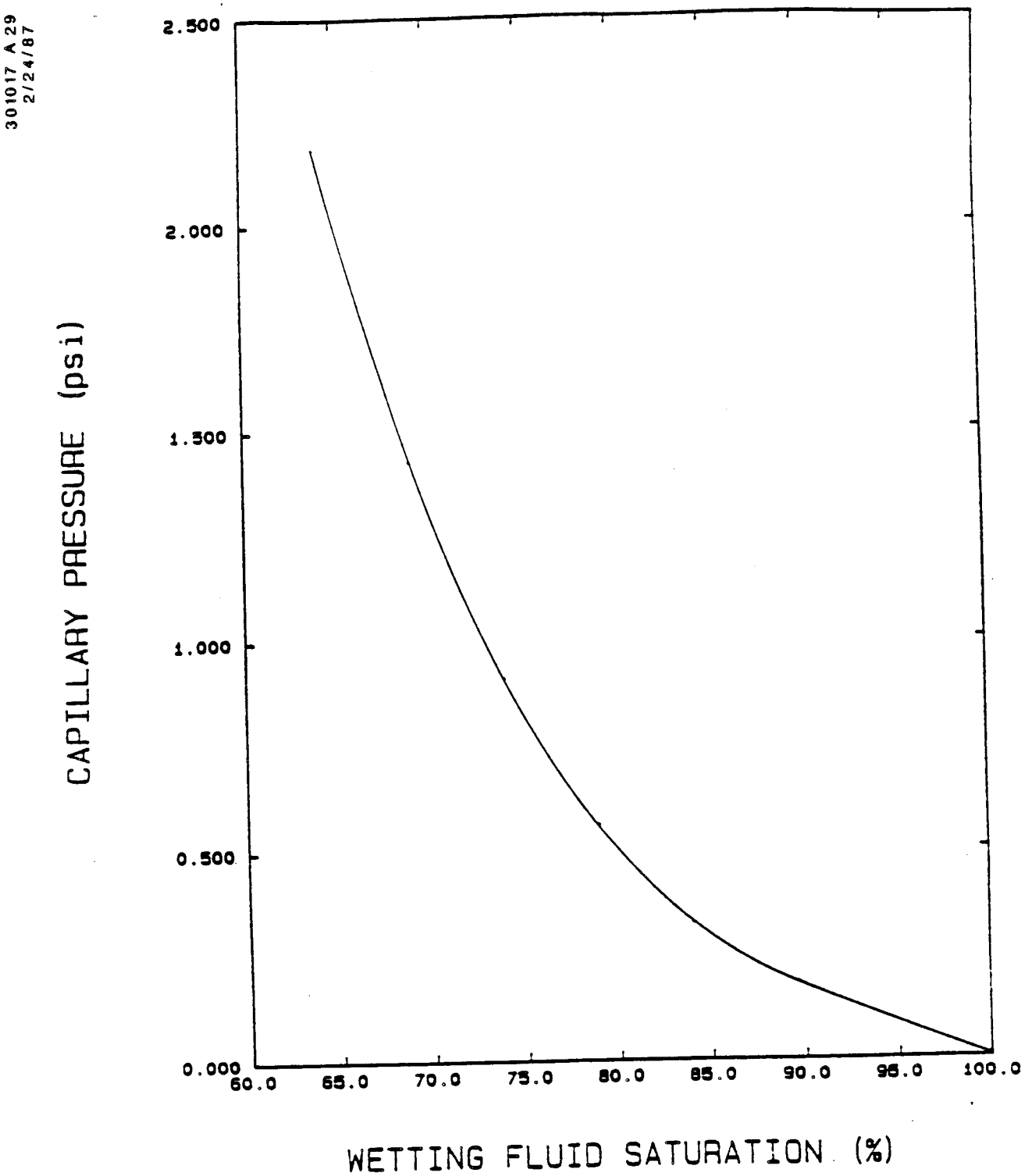

FIGURE 3-2. SOIL MOISTURE CHARACTERISTIC CURVE FOR A TYPICAL SAMPLE OF BANDELIER TUFF (BFEC, 1986)

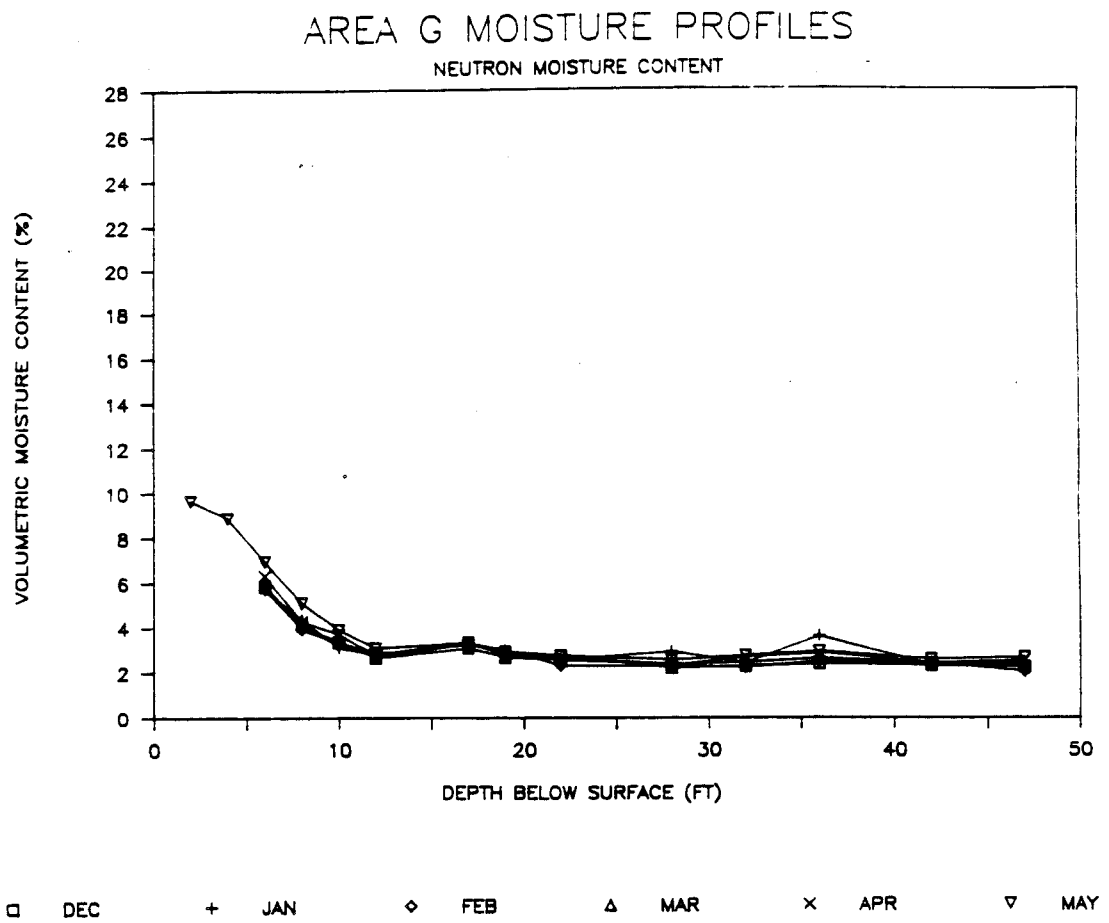

FIGURE 3-3

VOLUMETRIC MOISTURE CONTENT VERSUS DEPTH, IN AREA G, DECEMBER 1986 THROUGH MAY 1986

PREPARED FOR

LOS ALAMOS NATIONAL LABORATORY
LOS ALAMOS, NEW MEXICO

© 1984 IT CORPORATION
ALL COPYRIGHTS RESERVED

IT ... Creating a Safer Tomorrow

Do Not Scale This Drawing

LLF 12/24/87 | CHECKED BY SWS | APPROVED BY | 3/25/87 | DRAWING NUMBER 30.

65380

DRAWN BY	LLF	CHECKED BY		3/25/87	DRAWING NUMBER 301017 A39
	2/24/87	APPROVED BY		3/25/87	

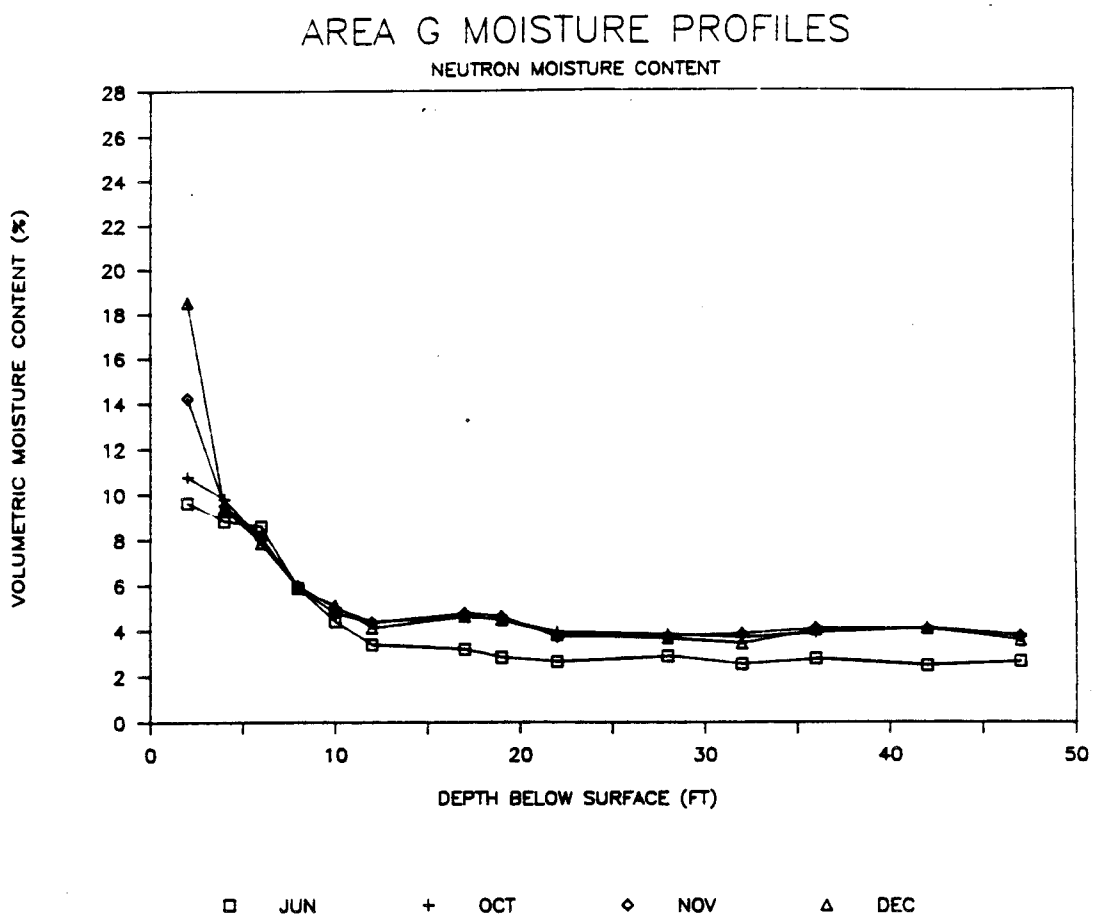

FIGURE 3-4

VOLUMETRIC MOISTURE CONTENT
VERSUS DEPTH, IN AREA G,
JUNE 1986 THROUGH DECEMBER 1986

PREPARED FOR

LOS ALAMOS NATIONAL LABORATORY
LOS ALAMOS, NEW MEXICO

© 1984 IT CORPORATION
ALL COPYRIGHTS RESERVED

IT ... Creating a Safer Tomorrow

65360

Do Not Scale This Drawing

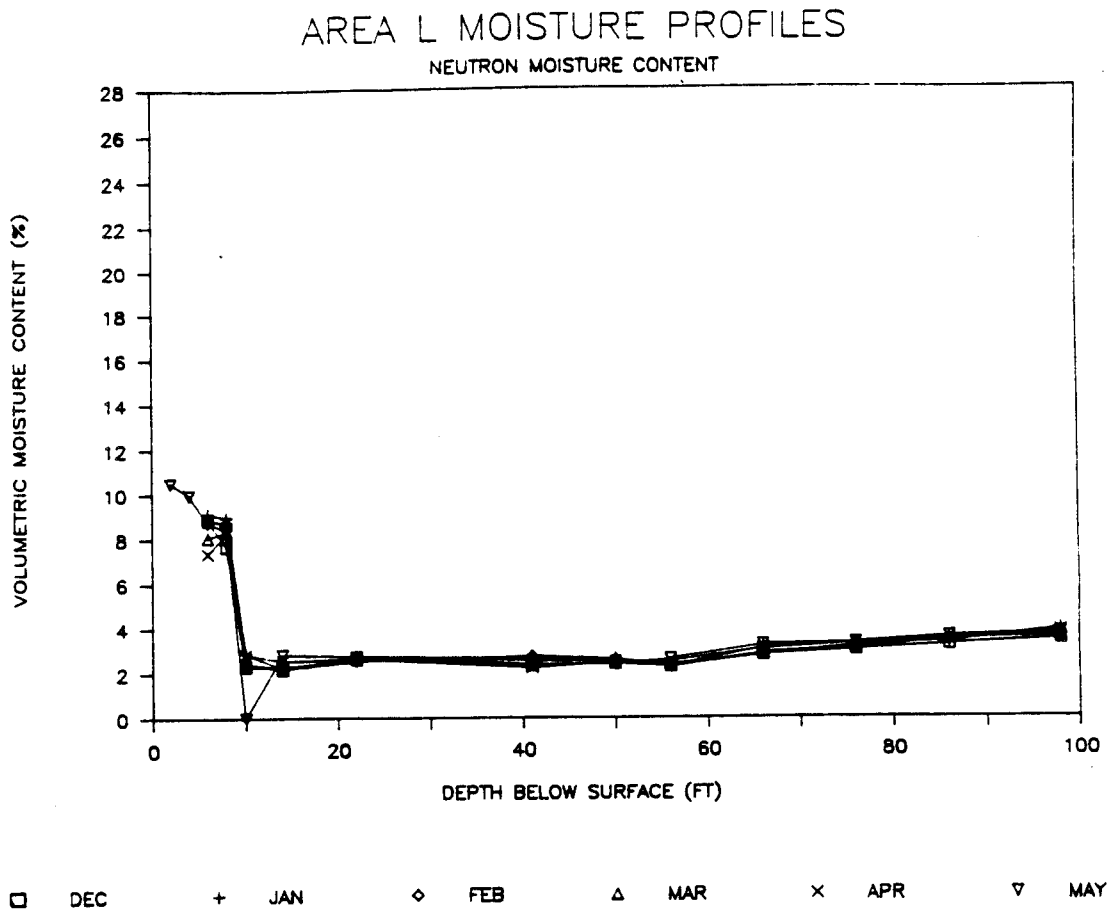

FIGURE 3-5

VOLUMETRIC MOISTURE CONTENT
VERSUS DEPTH, IN AREA L,
DECEMBER 1985 THROUGH MAY 1986

PREPARED FOR

LOS ALAMOS NATIONAL LABORATORY
LOS ALAMOS, NEW MEXICO

© 1984 IT CORPORATION
ALL COPYRIGHTS RESERVED

IT ... Creating a Safer Tomorrow

Do Not Scale This Drawing

LLF 2/24/87 | CHECKED BY SWS 3/25/87 | APPROVED BY 3/25/87 | DRAWING NUMBER 36

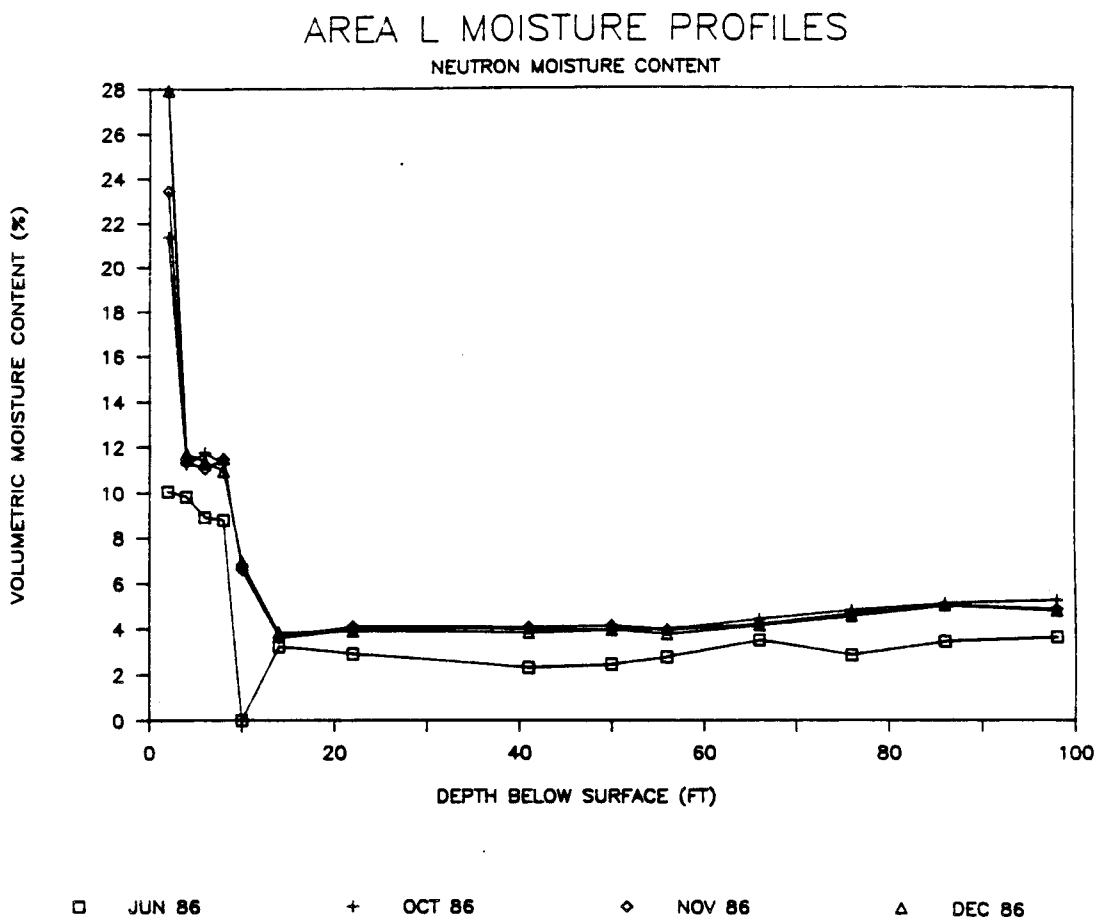

FIGURE 3-6

VOLUMETRIC MOISTURE CONTENT
VERSUS DEPTH, IN AREA L,
JUNE 1986 THROUGH DECEMBER 1986

PREPARED FOR

LOS ALAMOS NATIONAL LABORATORY
LOS ALAMOS, NEW MEXICO

© 1984 IT CORPORATION
ALL COPYRIGHTS RESERVED

... Creating a Safer Tomorrow

Do Not Scale This Drawing

LLF	CHECKED BY	SWS	3/25/87	DRAWING NUMBER 301017 A41
2/24/87	APPROVED BY		3/25/87	

65360

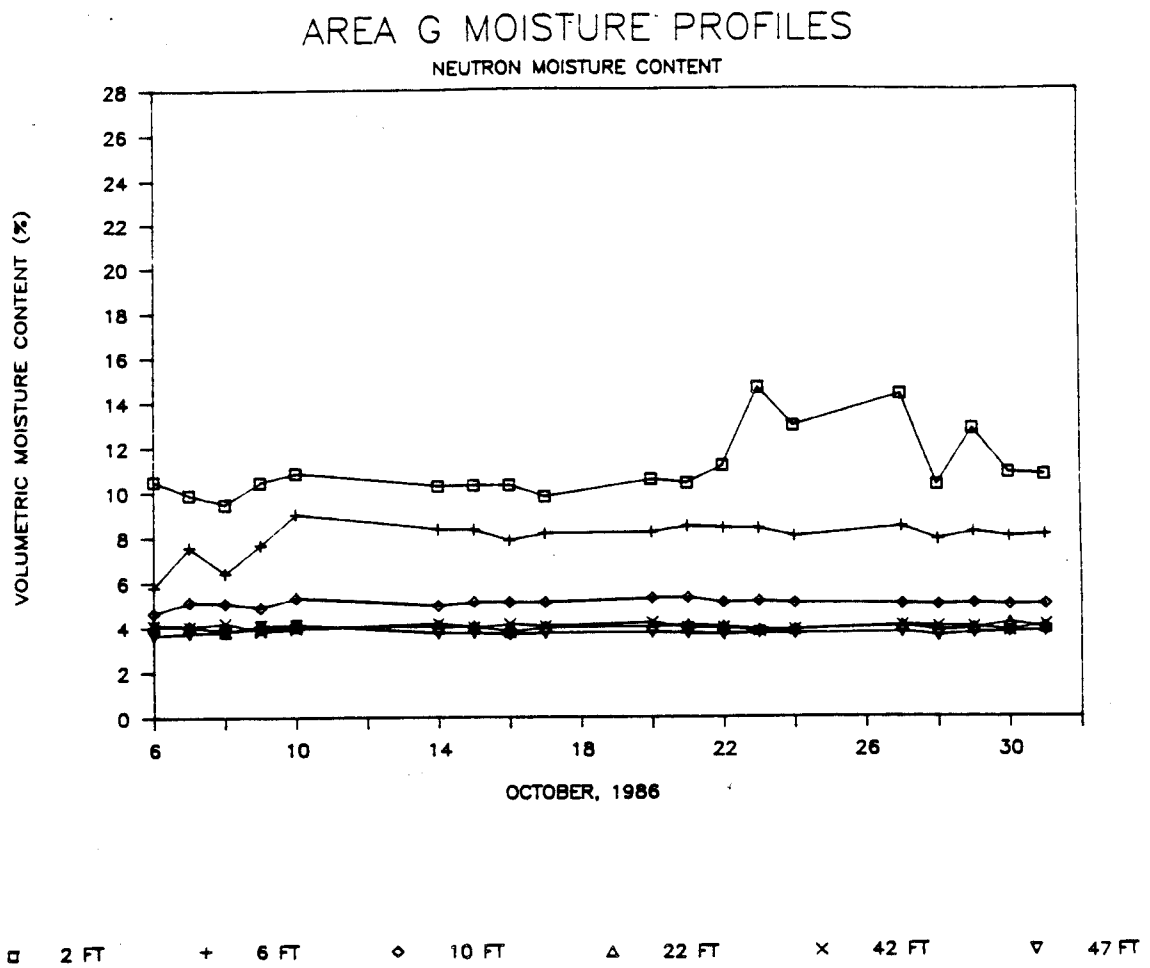

FIGURE 3-7

VOLUMETRIC MOISTURE CONTENT
AT SELECTED DEPTHS,
IN AREA G, OCTOBER 1986

PREPARED FOR

LOS ALAMOS NATIONAL LABORATORY
LOS ALAMOS, NEW MEXICO

© 1984 IT CORPORATION
ALL COPYRIGHTS RESERVED

IT ... Creating a Safer Tomorrow

Do Not Scale This Drawing

LLF	CHECKED BY	SWS	3/25/87	DRAWING NUMBER	301017 A
12/24/87	APPROVED BY		3/25/87		

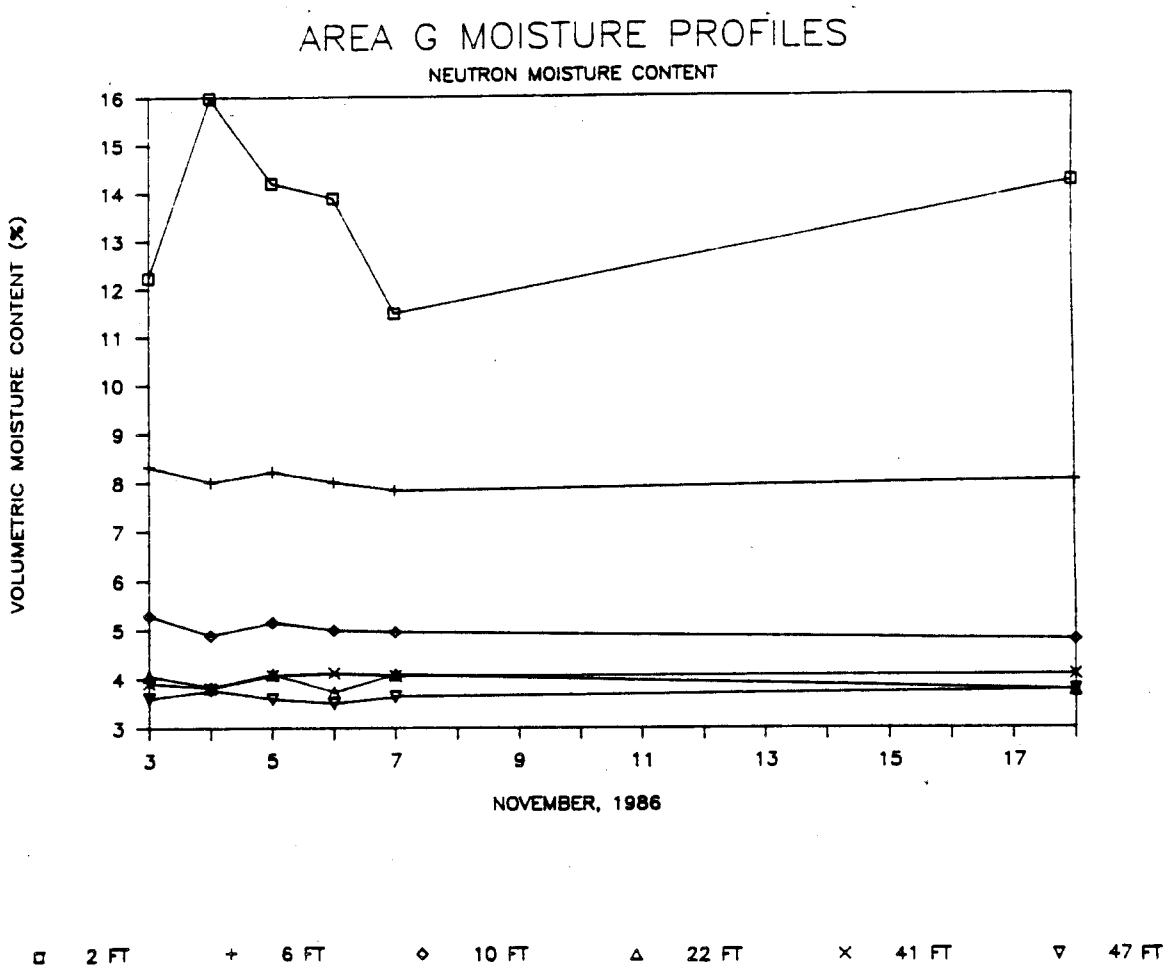

FIGURE 3-8

VOLUMETRIC MOISTURE CONTENT
AT SELECTED DEPTHS,
IN AREA G, NOVEMBER 1986

PREPARED FOR

LOS ALAMOS NATIONAL LABORATORY
LOS ALAMOS, NEW MEXICO

LLF	CHECKED BY	SWS	9/25/87	DRAWING NUMBER	301017 A43
2/24/87	APPROVED BY		9/25/87		

© 1984 IT CORPORATION
ALL COPYRIGHTS RESERVED

IT ... Creating a Safer Tomorrow

Do Not Scale This Drawing

65360

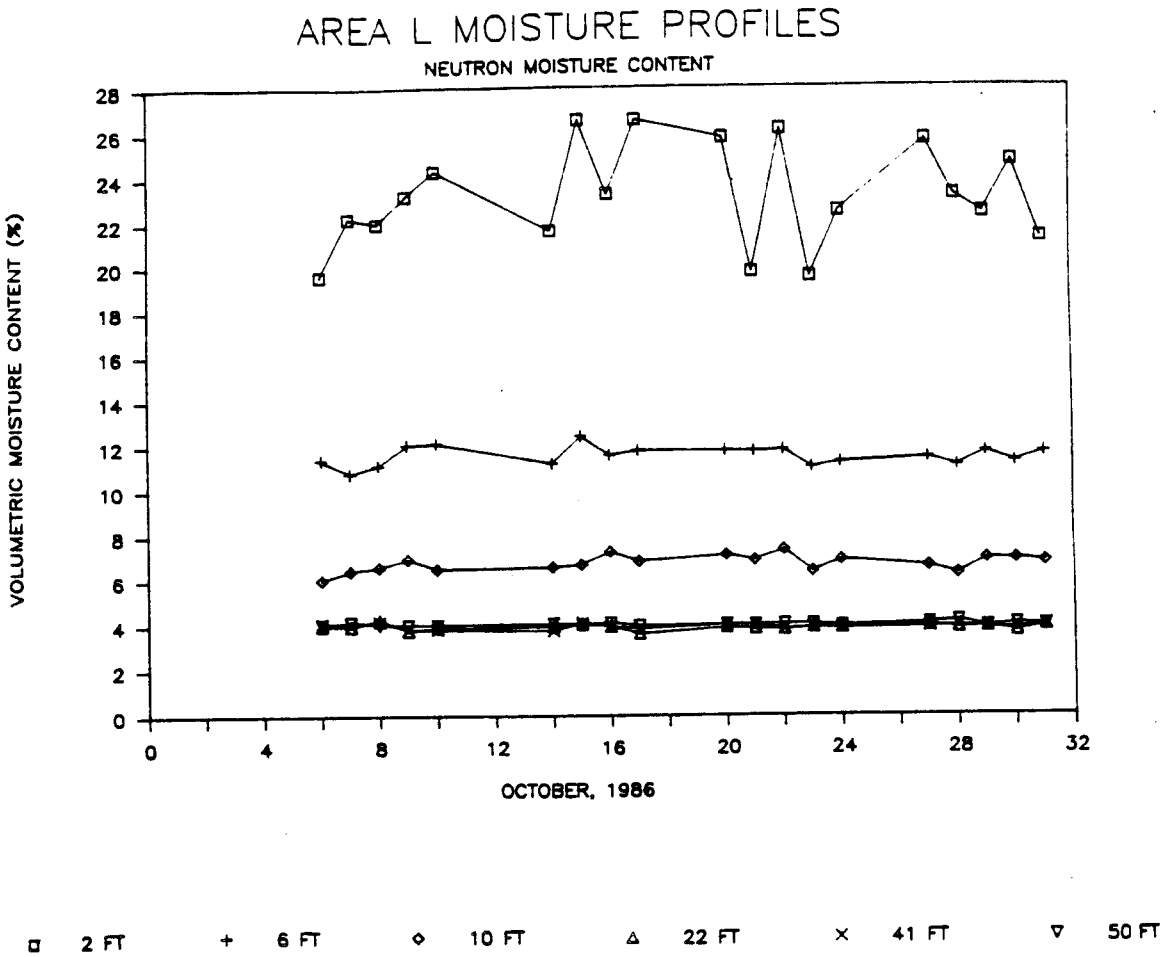

FIGURE 3-9

VOLUMETRIC MOISTURE CONTENT
AT SELECTED DEPTHS,
IN AREA L, OCTOBER 1986

PREPARED FOR

LOS ALAMOS NATIONAL LABORATORY
LOS ALAMOS, NEW MEXICO

LLF	CHECKED BY	SWS	3/25/87
2/24/87	APPROVED BY		3/25/87

DRAWING NUMBER 30

C

© 1984 IT CORPORATION
ALL COPYRIGHTS RESERVED

IT ... Creating a Safer Tomorrow

65360

Do Not Scale This Drawing

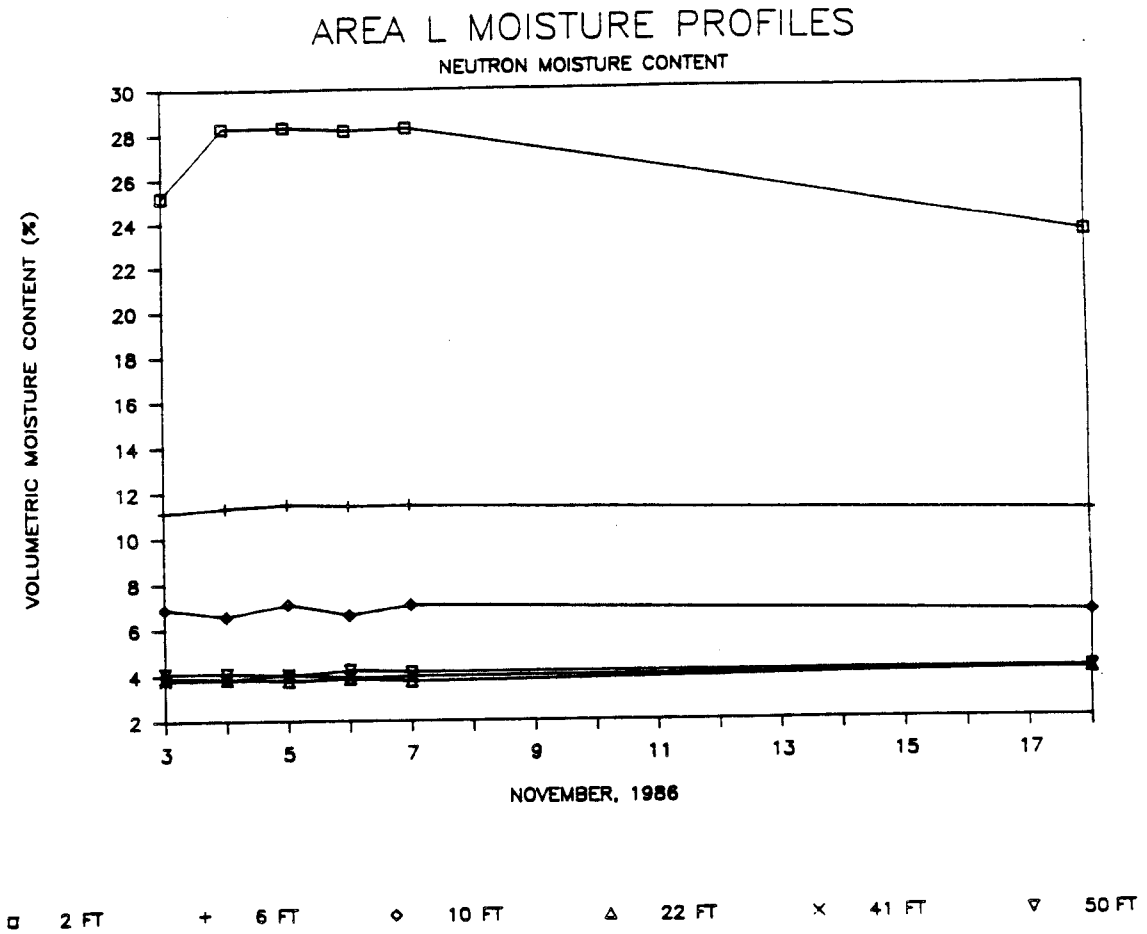

FIGURE 3-10

VOLUMETRIC MOISTURE CONTENT
AT SELECTED DEPTHS,
IN AREA L, NOVEMBER 1986

PREPARED FOR

LOS ALAMOS NATIONAL LABORATORY
LOS ALAMOS, NEW MEXICO

LLF	CHECKED BY	Scus	3/25/87	DRAWING NUMBER 30. A45
2/24/87	APPROVED BY	JKR	3/25/87	

© 1984 IT CORPORATION
ALL COPYRIGHTS RESERVED

IT ... Creating a Safer Tomorrow

65360

Do Not Scale This Drawing

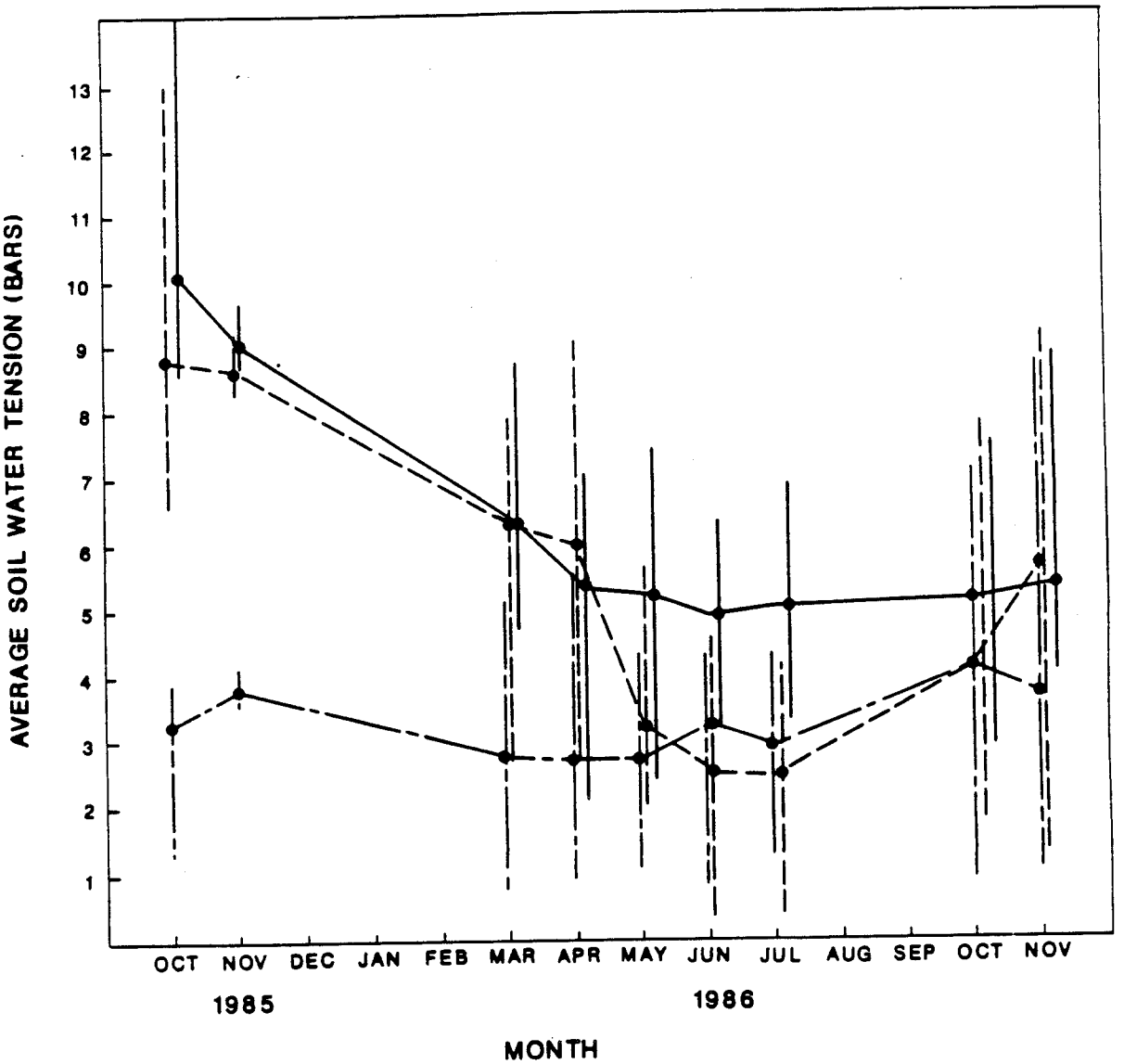

LEGEND

22 Feet

42 Feet

52 Feet

FIGURE 3-11

TA-54 AREA G

AVERAGE SOIL WATER TENSION

PREPARED FOR

LOS ALAMOS NATIONAL LABORATORY
LOS ALAMOS, NEW MEXICO

IT ... Creating a Safer Tomorrow

© 1984 IT CORPORATION
ALL COPYRIGHTS RESERVED

Do Not Scale This Drawing

65360

JPK	CHECKED BY	SWS	3/25/87	DRAWING NUMBER 3C
2/17/87	APPROVED BY		3/25/87	

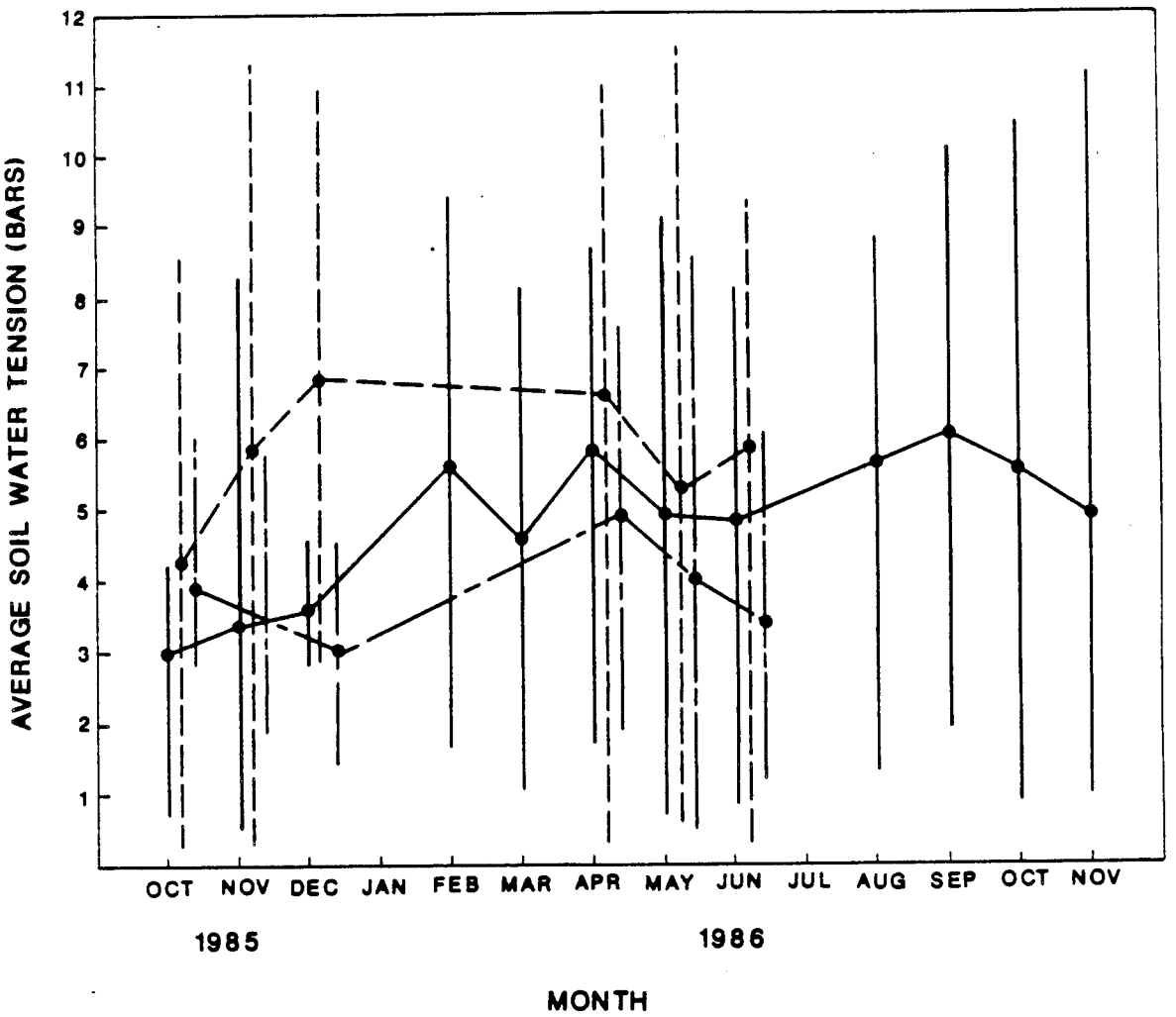

LEGEND

24 Feet

50 Feet

76 Feet

FIGURE 3-12

TA-54 AREA L

AVERAGE SOIL WATER TENSION

PREPARED FOR

LOS ALAMOS NATIONAL LABORATORY
LOS ALAMOS, NEW MEXICO

© 1984 IT CORPORATION
ALL COPYRIGHTS RESERVED

IT ... Creating a Safer Tomorrow

Do Not Scale This Drawing

65360

DI	JPK	CHECKED BY	SWS	3/25/87	DRAWING NUMBER 301011-A47
br	2/17/87	APPROVED BY		3/25/87	

4.0 CHEMICAL CHARACTERIZATION OF THE VADOSE ZONE

4.1 TEST HOLE CORING AND PORE GAS ANALYSES

Seven test hole locations were selected for coring and installation of pore gas samplers on Mesita del Buey to fulfill the requirements of Paragraph 25, Task 5 of the Order. One background test hole (LLC-85-13) was selected on the western end of the mesa. Of the remaining six test holes, two were located at Area G (LGC-85-09 and LGC-85-10) and four were located at Area L (LLC-85-12, LLC-85-14, LLC-85-15, and LLC-85-16) (Devaurs, 1985). In addition, three test hole locations were selected for coring adjacent to the Area L surface impoundment (LLC-85-17, LLC-85-18, and LLC-85-A) together with one shallow test hole location selected within the surface impoundment in conjunction with related investigatory activities required by Paragraph 24 of the Order (Department of Energy, 1986f). Six surface soil samples were also collected to establish background soil chemistry in Area L. The locations of the test holes in Areas G and L are shown on Figures 1-2 and 1-3, respectively.

4.2 TEST HOLE CORE

Core sampling was conducted in accordance with EPA procedures (U.S. EPA, 1985a). Two representative samples were taken from each ten feet of core, one for inorganic analyses and one for volatile organic analyses. Samples were collected in 500 ml wide-mouth glass bottles (Devaurs, 1985). The laboratories performing analyses on these samples were the Health and Environmental Chemistry Group (HSE-9) at Los Alamos National Laboratory and Rocky Mountain Analytical Laboratory in Colorado.

4.2.1 Core Sampling

Each 500 ml container for inorganic analyses was filled with rock core, labeled, and sealed in Parafilm® (intended to ensure sample integrity). A chain-of-custody tag was attached to each sample container. The seal had to be broken to open the container. Information pertinent to sampling was recorded in a field log book and samples were placed in boxes for transport to the laboratory. At the laboratory, sample custody was transferred to an inorganic chemist and samples were stored in a locked refrigerator in a secure laboratory. A sample analysis request sheet accompanied each sample to track laboratory analyses (Devaurs, 1985).

Prior to sample collection, sample jars were washed with soap and rinsed with distilled water. The jars were stored at 105°C until taken to the field for sample collection.

Sampling containers for organic analyses were completely filled with rock core and the jar cap sealed by teflon liner. Each was labeled and sealed in Parafilm® (intended to ensure sample integrity). A chain-of-custody tag was attached to each sample container. The seal had to be broken to open the container. Information pertinent to sampling was recorded in a field log book. In the field, samples were stored on ice in ice chests immediately after sample collection. For each drill hole, a water field blank was submitted with the samples. The blank consisted of a jar with organic-free water which was open to the atmosphere at the site while the hole was being drilled. Samples were transported to the laboratory on ice in ice chests and sample custody transferred to an organic chemist. Until analyses were conducted, samples were stored in a locked refrigerator in a secure laboratory. A sample analysis request sheet accompanied each sample to track laboratory analyses (Devaurs, 1985).

4.2.2 Analytical Methods

Core samples were analyzed for inorganic metals (EP Toxic) and volatile organics. All EP toxic metals were extracted and analyzed [by the Los Alamos Environmental Chemistry Group (HSE-9)] by an atomic absorption spectrophotometer using EPA methods. The volatile organic compounds were analyzed by HSE-9 using a purge and trap, gas chromatograph flame ionization detector (FID) procedure and gas chromatography/mass spectrometry (GC/MS) for confirmation (Devaurs, 1985). The methods of extraction and analysis for volatile organic compounds are provided in Appendix J and include modifications and compilations of recommended procedures (U.S. EPA, 1984; U.S. EPA, 1985a). Selected samples were also analyzed by the Rocky Mountain Analytical Laboratory (RMA) for volatile organic compounds using GC/MS.

4.2.3 Results of EP Toxicity Analyses

Results of the EP Toxicity analyses for the core samples are provided in Tables 4-1 through 4-11. All EP Toxic metals for test holes outside of the

Area L surface impoundment were below the EP Toxic regulated concentration (New Mexico Environmental Improvement Board, 1985a) with the exception of one chromium measurement in the 10 to 20 foot depth interval of core from drill hole LLC-85-18 (Table 4-7). Chromium and cadmium concentrations were also above the EP Toxic levels in the 8 to 29 inch (0.67-2.42 feet) depth interval in samples cored directly into the surface impoundment (Table 4-9). In addition, barium was detected at levels below the EP Toxic concentration in drill hole LGC-85-10 in the 0-10 foot depth interval (see Table 4-11). Miscellaneous chemical analytical results are presented in Tables 4-12 through 4-17.

4.2.4 Results of Core Analyses for Volatile Organic Compounds

Core samples from all ten test holes were analyzed for volatile organics by HSE-9 (Devaurs, 1985; Department of Energy, 1986f). Table 4-18 summarizes the volatile organic compounds analyzed for in each of the core samples. A limited number of core samples from selected test holes, were split for duplicate analyses by RMA. A summary of the volatile organic compounds analyzed for by RMA is given in Table 4-19. In general, the two laboratories conducted comparable volatile organic compound screens. However, the detection limit reported by RMA for each of the samples was more sensitive (parts per billion) than the detection limits reported by HSE-9 (parts per million). This difference in reported detection limits may account for the fewer number of compounds detected and reported by HSE-9 (Table 4-20).

No volatile organic compounds were detected by HSE-9 in the cores from Area G (LGC-85-09 and LGC-85-10) and no duplicate Area G core analyses were performed by RMA. In the background test hole, LLC-85-13, HSE reported 2-pentanone at a depth of 48 feet (Table 4-20). Because this test hole is located a great distance from Area L (3,200 feet), it is probable that the presence of 2-pentanone in the sample in a concentration at the reported detection limit, is due to laboratory contamination or sample/equipment handling during coring.

In Area L, volatile organic compounds were detected in core samples from various depth intervals in five of the seven test holes (LLC-85-12, LLC-85-14, LLC-85-15, LLC-85-16, and LLC-85-18; see Table 4-20). The compounds present are a suite of solvents and ketones [i.e., methylene chloride, acetone, tetrahydrofuran, 4-methyl-2-pentanone (MEK), etc.]. The compounds were detected in

parts per billion concentrations by RMA with the exception of acetone at a concentration of 4.3 mg/kg (parts per million) in test hole LLC-85-15 (18-19 foot interval) and acetonitrile at a concentration of 1.1 mg/kg in test hole LLC-85-14 (48-49 foot interval). In contrast, for compounds detected by both laboratories (i.e., tetrahydrofuran, acetone, etc.) the compound concentrations reported by HSE-9 are all in the part per million range whereas, RMA reported concentrations in the part per billion range. While identification of volatile organic compounds by HSE-9 appear accurate, the reported concentrations should be considered qualitative only, since the volatile organic concentrations reported in the HSE-9 data are very near the reported detection limits.

4.3 TEST HOLE PORE GAS ANALYSES

Following coring, a total of 23 sampling ports were installed in the seven test holes cored to fulfill Paragraph 25 of the Order to collect samples of pore gas at various depths (Devaurs and Bell, 1986). The sampling ports were constructed using low-pressure mobile-phase filters welded to a two-inch (I.D.) galvanized pipe (Figure 4-1). The filters consist of two-micrometer, porous, stainless steel elements. The ports are accessed on the surface via ¼-inch stainless steel tubing (Devaurs and Bell, 1986).

The sampling ports were installed by lowering the pre-assembled string of galvanized pipe downhole. The sampling ports were packed with sieve size 80 silica sand, isolated above and below with powdered bentonite. Due to concerns regarding the introduction of water into the vadose zone and the subsequent potential for mobilization of waste constituents, no water was mixed with the bentonite. As a result, there is some uncertainty as to the degree of isolation between sample ports. Additionally, one zone in test hole LGC-85-09 was packed with crushed tuff backfill due to caving of the hole (Devaurs and Bell, 1986).

Diagrams of the sampling port installations are provided in Appendix C. The selection of sampling port zones within each test hole was based on the stratigraphic unit encountered, the presence of fractures, and the presence of high organic vapor meter readings during drilling. Detailed information regarding the selection of each sampling port is provided in BFEC (1986).

4.3.1 Pore Gas Sampling

Pore gas samples were collected from each sampling port using a DESAGA gas sampler (BFEC, 1985b). The samples were initially collected monthly (January through April 1986) as procedures and protocols were refined and subsequently were collected quarterly as required by the Order. As a result of an auto-sampler malfunction, however, data from the third quarter (July through October 1986) are not available.

The DESAGA gas sampler pumps a known volume of gas through charcoal adsorption tubes which collect the organic compounds from the gas. Prior to sampling, a minimum of 50 liters of gas was purged through each sampling port (Devaurs and Bell, 1986). Between January and December 1986, pore gas samples of five, two and one liters were collected from the sampling ports. Initially, a gas sample volume of five liters was collected, but breakthrough (saturation of the quantitative region of the charcoal tube) occurred. Pore gas samples were subsequently reduced to two, and then one, liter volumes to eliminate the occurrence of breakthrough (Devaurs and Bell, 1986). Following collection, all charcoal tube samples were kept sealed and refrigerated until the samples were extracted by HSE-9 personnel.

4.3.2 Analytical Method

The charcoal tubes are desorbed with a carbon disulfide solution containing an internal standard. The extracted solution is then directly injected into a gas chromatograph/mass selective detector (GC/MSD) for analysis (Devaurs and Bell, 1986). Table 4-21 summarizes the volatile organic compounds analyzed for in the extract and representative detection limits are provided in Table 4-22. A detailed discussion of the analytical procedure is provided in Appendix K.

Analytical uncertainty exists in quantification of benzene and carbon tetrachloride in the January and February 1986 results. These two compounds co-elute and interferences were observed from benzene impurities in the carbon disulfide. In February 1986, 1,1-dichloroethene was detected. However, because 1,1-dichloroethene co-elutes with carbon disulfide, only qualitative information is provided for 1,1-dichloroethene (Devaurs and Bell, 1986).

4.3.3 Results of Pore Gas Analyses

Analytical results for pore gas samples collected January through April 1986 are summarized in Tables 4-23 through 4-29. During this period, no volatile organic compounds have been detected in the background hole LLC-85-13 (Table 4-24) which supports the conclusion that the one measurement of 2-pentanone (acetone) in core from the test hole is probably related to cross-contamination in the field or in the laboratory. In Areas G and L, a similar suite of volatile organic compounds were found in all test holes. In the two Area G test holes, 1,1,1-trichloroethane is the most prevalent compound and has been detected at concentrations ranging from 55 to 980 µg/ℓ air (parts per billion). Trichloroethene and tetrachloroethane were also found in both holes at low part per billion concentrations (less than 10 µg/ℓ air, see Tables 4-28 and 4-29).

In the four Area L test holes, the volatile organic compounds detected (in decreasing concentrations) are as follows:

- 1,1,1-trichloroethane
- trichlorofluoromethane
- trichloroethene
- toluene
- chloroform
- tetrachloroethene
- total xylenes
- ethylbenzene
- chlorobenzene
- carbon tetrachloride
- dichlorodifluoroethane
- 1,1-dichloroethene

While the compounds listed above occur at varying concentrations at different depths in different test holes, a comparison of 1,1,1-trichloroethane concentrations provides a common datum for a discussion of results. Figures 4-2 through 4-5 provide a graphical representation of 1,1,1-trichloroethane concentrations with depth in the Area L test holes. The highest concentrations of the compound occur in test holes LLC-85-14 and LLC-85-15 (approximately 10,000 µg/ℓ in the pore gas) which are located adjacent to organic waste shafts number 17 and number 4, respectively (see Figure 1-3). By comparison, the concentrations of 1,1,1-trichloroethane in Area G (approximately 300 µg/ℓ

in the pore gas), where a smaller volume of organic compounds have been disposed, are an order of magnitude less than the Area L concentrations (see Figures 4-6 and 4-7).

On the basis of existing pore gas data, there appears to be no relationship between the concentration of any volatile organic compounds and the stratigraphic unit or structural feature sampled for pore gas. For example, there were no significant increases in volatile organic concentrations from samples collected in test hole LLC-85-14 at the Tshirege Member Unit 2b-2a interface, 2a-1b interface, or at fractured zones.

4.4 SUMMARY OF CHEMICAL CHARACTERIZATION

No EP Toxic metals were detected in any test hole cores below a depth of 20 feet in Areas G and L. The core analyses and pore gas analyses do, however, indicate that volatile organic compounds are present at depths of up to 100 feet below the ground surface in Areas G and L. The suite of organic ketone compounds detected in the core analyses is different than the aromatic and halogenated hydrocarbons detected in the pore gas samples. This difference may be related to sampling device efficiencies, analytical detection limits, and the intrinsic physical properties of the volatile organic compounds (i.e., boiling point, specific gravity, etc.).

Based on the available chemical data, the results of the rock core and pore gas analyses indicate the following:

- No EP Toxic metals have been detected below a depth of 20 feet in Areas G or L in the cores analyzed
- Volatile organic compounds are present in rock core samples at 100 feet at part per billion concentrations in Area L (no volatile organic compounds were detected in rock core samples in Area G)
- Volatile organic compounds are present in pore gas samples at 100 feet at part per million concentrations in Area L and part per billion concentrations in Area G
- There is no apparent correlation between high pore gas concentrations and subsurface stratigraphy (ashflow interfaces) or structure (fractures)

- The highest pore gas concentrations of volatile organic compounds have been detected in test holes (LLC-85-14 and LLC-85-15) nearest organic disposal shafts (shaft numbers 17 and 4).

TABLE 4-1
EP TOXICITY ANALYTICAL RESULTS FOR
CORE FROM DRILL HOLE NUMBER LLC-85-12[1]

PARAMETER	EP TOXIC REGULATED CONCEN-TRATION[2] (mg/ℓ)	DETECTION LIMIT[3] (mg/ℓ)	DEPTH INTERVALS IN FEET									
			0-10	10-20	20-30	30-40	40-50	50-60	60-70	70-80	80-90	90-100
Arsenic	5.0	0.1 ± 0.05	ND	ND	ND	ND	ND	ND	ND	ND	ND	ND
Barium	100.0	1.0 ± 1.0	ND	ND	ND	ND	ND	ND	ND	ND	ND	ND
Cadmium	1.0	0.1 ± 0.1	ND	ND	ND	ND	ND	ND	ND	ND	ND	ND
Chromium	5.0	0.2 ± 0.2	ND	ND	ND	ND	ND	ND	ND	ND	ND	ND
Lead	5.0	0.5 ± 0.5	ND	ND	ND	ND	ND	ND	ND	ND	ND	ND
Mercury	0.2	0.01 ± 0.01	ND	ND	ND	ND	ND	ND	ND	ND	ND	ND
Selenium	1.0	0.05 ± 0.020	ND	ND	ND	ND	ND	ND	ND	ND	ND	ND
Silver	5.0	0.5 ± 0.5	ND	ND	ND	ND	ND	ND	ND	ND	ND	ND

(1) From Devaurs, 1985.
(2) New Mexico Environmental Improvement Board, 1985a.
(3) ND = Not detected.
The ± value represents the uncertainty term for the analysis.

TABLE 4-2
EP TOXICITY ANALYTICAL RESULTS FOR
CORE FROM DRILL HOLE NUMBER LLC-85-13[1]

PARAMETER	EP TOXIC REGULATED CONCEN-TRATION[2] (mg/ℓ)	DETECTION LIMIT[3] (mg/ℓ)	DEPTH INTERVALS IN FEET									
			0-10	10-20	20-30	30-40	40-50	50-60	60-70	70-80	80-90	90-100
Arsenic	5.0	0.05 ± 0.025	ND	ND	ND	ND	ND	ND	ND	ND	ND	ND
Barium	100.0	1.0 ± 1.0	ND	ND	ND	ND	ND	ND	ND	ND	ND	ND
Cadmium	1.0	0.1 ± 0.1	ND	ND	ND	ND	ND	ND	ND	ND	ND	ND
Chromium	5.0	0.2 ± 0.2	ND	ND	ND	ND	ND	ND	ND	ND	ND	ND
Lead	5.0	0.5 ± 0.5	ND	ND	ND	ND	ND	ND	ND	ND	ND	ND
Mercury	0.2	0.01 ± 0.01	ND	ND	ND	ND	ND	ND	ND	ND	ND	ND
Selenium	1.0	0.05 ± 0.025	ND	ND	ND	ND	ND	ND	ND	ND	ND	ND
Silver	5.0	0.5 ± 0.5	ND	ND	ND	ND	ND	ND	ND	ND	ND	ND

(1) From Devaurs, 1985.
(2) New Mexico Environmental Improvement Board, 1985a.
(3) ND = Not detected.
The ± value represents the uncertainty term for the analysis.

TABLE 4-3
EP TOXICITY ANALYTICAL RESULTS FOR
CORE FROM DRILL HOLE NUMBER LLC-85-14[1]

PARAMETER	EP TOXIC REGULATED CONCEN-TRATION[2] (mg/ℓ)	DETECTION LIMIT[3] (mg/ℓ)	DEPTH INTERVALS IN FEET									
			0-10	10-20	20-30	30-40	40-50	50-60	60-70	70-80	80-90	90-100
Arsenic	5.0	0.05 ± 0.025	ND	ND	ND	ND	ND	ND	ND	ND	ND	ND
Barium	100.0	1.0 ± 1.0	ND	ND	ND	ND	ND	ND	ND	ND	ND	ND
Cadmium	1.0	0.1 ± 0.1	ND	ND	ND	ND	ND	ND	ND	ND	ND	ND
Chromium	5.0	0.2 ± 0.2	ND	ND	ND	ND	ND	ND	ND	ND	ND	ND
Lead	5.0	0.5 ± 0.5	ND	ND	ND	ND	ND	ND	ND	ND	ND	ND
Mercury	0.2	0.01 ± 0.01	ND	ND	ND	ND	ND	ND	ND	ND	ND	ND
Selenium	1.0	0.05 ± 0.025	ND	ND	ND	ND	ND	ND	ND	ND	ND	ND
Silver	5.0	0.5 ± 0.5	ND	ND	ND	ND	ND	ND	ND	ND	ND	ND

(1) From Devaurs, 1985.
(2) New Mexico Environmental Improvement Board, 1985a.
(3) ND = Not detected.
The ± value represents the uncertainty term for the analysis.

TABLE 4-4
EP TOXICITY ANALYTICAL RESULTS FOR
CORE FROM DRILL HOLE NUMBER LLC-85-15[1]

PARAMETER	EP TOXIC REGULATED CONCEN-TRATION[2] (mg/ℓ)	DETECTION LIMIT[3] (mg/ℓ)	DEPTH INTERVALS IN FEET									
			0-10	10-20	20-30	30-40	40-50	50-60	60-70	70-80	80-90	90-100
Arsenic	5.0	0.05 ± 0.025	ND	ND	ND	ND	ND	ND	ND	ND	ND	ND
Barium	100.0	1.0 ± 1.0	ND	ND	ND	ND	ND	ND	ND	ND	ND	ND
Cadmium	1.0	0.1 ± 0.1	ND	ND	ND	ND	ND	ND	ND	ND	ND	ND
Chromium	5.0	0.2 ± 0.2	ND	ND	ND	ND	ND	ND	ND	ND	ND	ND
Lead	5.0	0.5 ± 0.5	ND	ND	ND	ND	ND	ND	ND	ND	ND	ND
Mercury	0.2	0.01 ± 0.01	ND	ND	ND	ND	ND	ND	ND	ND	ND	ND
Selenium	1.0	0.05 ± 0.025	ND	ND	ND	ND	ND	ND	ND	ND	ND	ND
Silver	5.0	0.5 ± 0.5	ND	ND	ND	ND	ND	ND	ND	ND	ND	ND

(1) From Devaurs, 1985.
(2) New Mexico Environmental Improvement Board, 1985a.
(3) ND = Not detected.
The ± value represents the uncertainty term for the analysis.

TABLE 4-5
EP TOXICITY ANALYTICAL RESULTS FOR
CORE FROM DRILL HOLE NUMBER LLC-85-16[1]

PARAMETER	EP TOXIC REGULATED CONCEN-TRATION[2] (mg/ℓ)	DETECTION LIMIT[3] (mg/ℓ)	DEPTH INTERVALS IN FEET									
			0-10	10-20	20-30	30-40	40-50	50-60	60-70	70-80	80-90	90-100
Arsenic	5.0	0.05 ± 0.025	ND	ND	ND	ND	ND	ND	ND	ND	ND	ND
Barium	100.0	1.0 ± 1.0	ND	ND	ND	ND	ND	ND	ND	ND	ND	ND
Cadmium	1.0	0.1 ± 0.1	ND	ND	ND	ND	ND	ND	ND	ND	ND	ND
Chromium	5.0	0.2 ± 0.2	ND	ND	ND	ND	ND	ND	ND	ND	ND	ND
Lead	5.0	0.5 ± 0.5	ND	ND	ND	ND	ND	ND	ND	ND	ND	ND
Mercury	0.2	0.01 ± 0.01	ND	ND	ND	ND	ND	ND	ND	ND	ND	ND
Selenium	1.0	0.05 ± 0.025	ND	ND	ND	ND	ND	ND	ND	ND	ND	ND
Silver	5.0	0.5 ± 0.5	ND	ND	ND	ND	ND	ND	ND	ND	ND	ND

(1) From Devaurs, 1985.
(2) New Mexico Environmental Improvement Board, 1985a.
(3) ND = Not detected.
The ± value represents the uncertainty term for the analysis.

TABLE 4-6
EP TOXICITY ANALYTICAL RESULTS FOR
CORE FROM DRILL HOLE NUMBER LLC-85-17[1]

PARAMETER	EP TOXIC REGULATED CONCEN-TRATION[2] (mg/ℓ)	DETECTION LIMIT[3] (mg/ℓ)	DEPTH INTERVALS IN FEET														
			0-10	10-20	20-30	30-40	40-50	50-60	60-70	70-80	80-90	90-100	100-110	110-120	120-130	130-140	140-150
Arsenic	5.0	0.05 ± 0.025	ND	ND	ND	ND	ND	ND	ND	ND	ND	ND	ND	ND	ND	ND	ND
Barium	100.0	1.0 ± 1.0	ND	ND	ND	ND	ND	ND	ND	ND	ND	ND	ND	ND	ND	ND	ND
Cadmium	1.0	0.1 ± 0.1	ND	ND	ND	ND	ND	ND	ND	ND	ND	ND	ND	ND	ND	ND	ND
Chromium	5.0	0.5 ± 0.5	ND	ND	ND	ND	ND	ND	ND	ND	ND	ND	ND	ND	ND	ND	ND
Lead	5.0	0.5 ± 0.5	ND	ND	ND	ND	ND	ND	ND	ND	ND	ND	ND	ND	ND	ND	ND
Mercury	0.2	0.01 ± 0.01	ND	ND	ND	ND	ND	ND	ND	ND	ND	ND	ND	ND	ND	ND	ND
Selenium	1.0	0.05 ± 0.025	ND	ND	ND	ND	ND	ND	ND	ND	ND	ND	ND	ND	ND	ND	ND
Silver	5.0	0.5 ± 0.5	ND	ND	ND	ND	ND	ND	ND	ND	ND	ND	ND	ND	ND	ND	ND

(1) From Devaurs, 1985.
(2) New Mexico Environmental Improvement Board, 1985a.
(3) ND = Not detected.
The ± value represents the uncertainty term for the analysis.

TABLE 4-7
EP TOXICITY ANALYTICAL RESULTS FOR
CORE FROM DRILL HOLE NUMBER LLC-85-18[1]

PARAMETER	EP TOXIC REGULATED CONCEN-TRATION[2] (mg/ℓ)	DETECTION LIMIT[3] (mg/ℓ)	DEPTH INTERVALS IN FEET									
			0-10	10-20	20-30	30-40	40-50	50-60	60-70[4]	70-80	80-90	90-100
Arsenic	5.0	0.05 ± 0.025	ND	ND	ND	ND	ND	ND	---	ND	ND	ND
Barium	100.0	1.0 ± 1.0	ND	ND	ND	ND	ND	ND	---	ND	ND	ND
Cadmium	1.0	0.1 ± 0.1	ND	ND	ND	ND	ND	ND	---	ND	ND	ND
Chromium	5.0	0.5 ± 0.5	ND	6.6	ND	ND	ND	ND	---	ND	ND	ND
Lead	5.0	0.5 ± 0.5	ND	ND	ND	ND	ND	ND	---	ND	ND	ND
Mercury	0.2	0.01 ± 0.01	ND	ND	ND	ND	ND	ND	---	ND	ND	ND
Selenium	1.0	0.05 ± 0.025	ND	ND	ND	ND	ND	ND	---	ND	ND	ND
Silver	5.0	0.5 ± 0.5	ND	ND	ND	ND	ND	ND	---	ND	ND	ND

(1) From Devaurs, 1985.
(2) New Mexico Environmental Improvement Board, 1985a.
(3) ND = Not detected.
(4) No sample available; no core recovery.

TABLE 4-8
EP TOXICITY ANALYTICAL RESULTS FOR
CORE FROM DRILL HOLE LLC-85-A[1]

PARAMETER	EP TOXIC REGULATED CONCEN-TRATION[2] (mg/ℓ)	DETECTION LIMIT[3] (mg/ℓ)	DEPTH INTERVALS IN FEET													
			0-5	5-6	9-10	14-15	19-20	24-25	29-30	34-35	39-40	44-45	49-50	49-50	54-55	59-60
Arsenic	5.0	0.5 ± 0.5	ND	ND	ND	ND	ND	ND	ND	ND	ND	ND	ND	ND	ND	ND
Barium	100.0	0.22 ± 0.20	ND	ND	ND	ND	ND	0.26	ND	ND	ND	ND	ND	ND	ND	ND
Cadmium	1.0	0.01 ± 0.01	ND	ND	ND	ND	ND	0.02	ND	ND	ND	ND	ND	ND	ND	ND
Chromium	5.0	0.23 ± 0.20	ND	ND	ND	ND	ND	0.77	0.57	ND	ND	ND	ND	ND	ND	ND
Lead	5.0	0.07 ± 0.07	ND	ND	ND	ND	ND	ND	ND	ND	ND	ND	ND	ND	ND	ND
Mercury	0.2	0.0002 ± 0.0002	0.0003	0.0002	0.0003	0.0003	0.0011	0.0003	ND	0.0003	ND	ND	ND	ND	ND	ND
Selenium	1.0	0.01 ± 0.01	ND	ND	ND	ND	ND	ND	ND	ND	ND	ND	ND	ND	ND	ND
Silver	5.0	0.20 ± 0.20	ND	ND	ND	ND	ND	ND	ND	ND	ND	ND	ND	ND	ND	ND

(1) From Department of Energy, 1986f.
(2) New Mexico Environmental Improvement Board, 1985a.
(3) ND = Not detected.
NOTE: The ± value represents the uncertainty term for the analysis.

TABLE 4-9
EP TOXICITY ANALYTICAL RESULTS FOR
SURFACE IMPOUNDMENT CORE SAMPLES[1]

PARAMETER	EP TOXIC REGULATED CONCEN-TRATION[2] (mg/ℓ)	DETECTION LIMIT (mg/ℓ)	DEPTH INTERVALS IN INCHES					
			0-4	4-8	8-12	12-16	16-20	20-29
Arsenic	5.0	0.002	0.015	0.006	0.005	0.002	0.002	0.002
Barium	100.0	0.10	0.184	<0.13	<0.13	0.87	0.83	<0.13
Cadmium	1.0	0.01	0.013	0.014	2.15	11.10	3.59	1.04
Chromium	5.0	0.05	0.23	1.06	8.51	20.8	15.8	13.2
Lead	5.0	0.50	<0.50	0.50	<0.50	<0.50	<0.50	<0.50
Mercury	0.2	0.02	<0.02	<0.02	<0.02	<0.02	<0.02	<0.02
Silver	5.0	0.024	<0.024	<0.024	<0.024	<0.024	<0.024	<0.024

(1) From Department of Energy, 1986f.
(2) New Mexico Environmental Improvement Board, 1985a.

TABLE 4-10
EP TOXICITY ANALYTICAL RESULTS FOR
CORE FROM DRILL HOLE NUMBER LGC-85-09[1]

PARAMETER	EP TOXIC REGULATED CONCEN-TRATION[2] (mg/ℓ)	DETECTION LIMIT[3] (mg/ℓ)	DEPTH INTERVALS IN FEET									
			0-10	10-20	20-30	30-40	40-50	50-60	60-70	70-80	80-90	90-100
Arsenic	5.0	0.1 ± 0.05	ND	ND	ND	ND	ND	ND	ND	ND	ND	ND
Barium	100.0	1.0 ± 1.0	ND	ND	ND	ND	ND	ND	ND	ND	ND	ND
Cadmium	1.0	0.1 ± 0.1	ND	ND	ND	ND	ND	ND	ND	ND	ND	ND
Chromium	5.0	0.2 ± 0.2	ND	ND	ND	ND	ND	ND	ND	ND	ND	ND
Lead	5.0	0.5 ± 0.5	ND	ND	ND	ND	ND	ND	ND	ND	ND	ND
Mercury	0.2	0.01 ± 0.01	ND	ND	ND	ND	ND	ND	ND	ND	ND	ND
Selenium	1.0	0.05 ± 0.02	ND	ND	ND	ND	ND	ND	ND	ND	ND	ND
Silver	5.0	0.5 ± 0.5	ND	ND	ND	ND	ND	ND	ND	ND	ND	ND

(1) From Devaurs, 1985.
(2) New Mexico Environmental Improvement Board, 1985a.
(3) ND = Not detected.
The ± value represents the uncertainty term for the analysis.

TABLE 4-11
EP TOXICITY ANALYTICAL RESULTS FOR
CORE FROM DRILL HOLE NUMBER LGC-85-10[1]

PARAMETER	EP TOXIC REGULATED CONCEN-TRATION[2] (mg/ℓ)	DETECTION LIMIT[3] (mg/ℓ)	DEPTH INTERVALS IN FEET									
			0-10	10-20	20-30	30-40	40-50	50-60	60-70	70-80	80-90	90-100
Arsenic	5.0	0.1 ± 0.05	ND	ND	ND	ND	ND	ND	ND	ND	ND	ND
Barium	100.0	1.0 ± 1.0	1.50 ±0.40	ND	ND	ND	ND	ND	ND	ND	ND	ND
Cadmium	1.0	0.1 ± 0.1	ND	ND	ND	ND	ND	ND	ND	ND	ND	ND
Chromium	5.0	0.2 ± 0.2	ND	ND	ND	ND	ND	ND	ND	ND	ND	ND
Lead	5.0	0.5 ± 0.5	ND	ND	ND	ND	ND	ND	ND	ND	ND	ND
Mercury	0.2	0.01 ± 0.01	ND	ND	ND	ND	ND	ND	ND	ND	ND	ND
Selenium	1.0	0.05 ± 0.02	ND	ND	ND	ND	ND	ND	ND	ND	ND	ND
Silver	5.0	0.5 ± 0.5	ND	ND	ND	ND	ND	ND	ND	ND	ND	ND

(1) From Devaurs, 1985.
(2) New Mexico Environmental Improvement Board, 1985a.
(3) ND = Not detected.
The ± value represents the uncertainty term for the analysis.

TABLE 4-12
MISCELLANEOUS CHEMICAL ANALYTICAL RESULTS FOR SIX BACKGROUND SOIL SAMPLES TAKEN NEAR AREA L[1]

PARAMETER	SAMPLE NUMBER NO. 1	NO. 2	NO. 3	NO. 4	NO. 5	NO. 6	MEAN ± STD. DEV.
Lithium (mg/ℓ)	<0.05	<0.05	<0.05	<0.05	<0.05	<0.05	<0.05 ± 0
Copper (mg/ℓ)	<0.20	<0.20	<0.20	<0.20	<0.20	<0.20	<0.20 ± 0
NH_3-N (mg/ℓ)	0.0	0.02	0.14	0.0	0.0	0.0	0.03 ± 0.05
Fluoride (mg/ℓ)	0.32	<0.20	0.32	0.25	0.46	0.49	0.34 ± 0.11
TDS (mg/ℓ)	58	29	61	24	74	40	48 ± 20
pH	9.3	7.2	8.2	7.2	7.2	6.7	7.6 ± 1.0
Soil Moisture (%)	9.1	12.0	9.5	7.9	10.5	10.2	9.9 ± 1.4

[1] From Department of Energy, 1986f.

TABLE 4-13
LOCATION AND DESCRIPTION OF AREA L BACKGROUND SOIL SAMPLES[1]

SAMPLE IDENTIFICATION	SAMPLE LOCATION
No. 1	Two feet outside the Area L storage pad in tuff used as fill originating from Area G.
No. 2	24 feet west of the northwest corner of the Area L storage pad in undisturbed tuff.
No. 3	70 feet east of the northeast corner of the Area L storage pad in native, but disturbed, tuff.
No. 4	One foot outside the northeast corner of the Area L fence.
No. 5	20 feet outside the center of the east Area L fence.
No. 6	Ten feet outside the northwest corner of the Area L fence.

[1] From Department of Energy, 1986f.

TABLE 4-14
MISCELLANEOUS CHEMICAL ANALYTICAL RESULTS FOR CORE FROM DRILL HOLE NUMBER LLC-85-17[1]

PARAMETER	BACKGROUND LEVEL[2]	DEPTH INTERVALS IN FEET														
		0-10	10-20	20-30	30-40	40-50	50-60	60-70	70-80	80-90	90-100	100-110	110-120	120-130	130-140	140-150
Lithium (mg/ℓ)	<0.05 ± 0	<0.05	<0.05	<0.05	<0.05	<0.05	<0.05	<0.05	<0.05	<0.05	<0.05	<0.05	<0.05	<0.05	<0.05	<0.05
Copper (mg/ℓ)	<0.20 ± 0	<0.1	<0.1	<0.1	<0.1	<0.1	0.12	<0.1	<0.1	<0.1	<0.1	<0.1	<0.1	<0.1	<0.1	<0.1
NH_3-N (mg/ℓ)	0.03 ± 0.05	0.41	0.22	0.97	3.10	0.83	0.90	0.24	1.30	0.25	0.25	0.32	0.82	0.087	0.32	0.33
Fluoride (mg/ℓ)	0.34 ± 0.11	0.31	3.59	3.76	1.44	3.96	5.59	5.10	6.64	4.90	5.68	6.66	6.68	6.87	6.80	6.27
TDS (mg/ℓ)	48 ± 20	17	54	79	185	34	40	43	47	27	30	51	39	74	66	46
pH	7.6 ± 1.0	6.6	6.0	7.9	8.8	5.9	5.8	5.5	6.0	5.9	6.0	5.8	5.8	6.1	6.1	6.6
Soil Moisture (%)	9.9 ± 1.4	9.1	4.0	7.4	5.5	4.1	0.7	0.9	0.6	1.2	2.5	5.3	5.7	8.4	3.0	4.3

(1) From Department of Energy, 1986f.
(2) Determined from six soil samples taken in Area L (see Table 4-12).

TABLE 4-15
MISCELLANEOUS CHEMICAL ANALYTICAL RESULTS FOR
CORE FROM DRILL HOLE NUMBER LLC-85-18[1]

PARAMETER	BACKGROUND LEVEL[2]	DEPTH INTERVALS IN FEET									
		0-10	10-20	20-30	30-40	40-50	50-60	60-70[3]	70-80	80-90	90-100
Lithium (mg/ℓ)	<0.05 ± 0	<0.05	0.12	<0.05	<0.05	<0.05	<0.05	---	<0.05	<0.05	<0.05
Copper (mg/ℓ)	<0.20 ± 0	<0.1	10.0	<0.1	<0.1	<0.1	<0.1	---	<0.1	<0.1	<0.1
NH_3-N (mg/ℓ)	0.03 ± 0.05	0.30	0.38	0.38	0.20	0.34	0.053	---	0.18	0.10	0.15
Fluoride (mg/ℓ)	0.34 ± 0.11	0.37	17.0	2.63	3.51	3.30	3.45	---	2.31	6.86	7.53
TDS (mg/ℓ)	48 ± 20	22	188	88	37	52	113	---	91	75	79
pH	7.6 ± 1.0	5.5	3.8	8.6	5.9	7.4	8.7	---	7.9	6.2	6.8
Soil Moisture (%)	9.9 ± 1.4	11.6	6.3	9.0	8.4	8.3	5.7	---	2.5	0.1	1.6

(1) From Department of Energy, 1986f.
(2) Determined from six soil samples taken in Area L (see Table 4-12).
(3) No sample available; all core lost in drilling accident.

TABLE 4-16
MISCELLANEOUS CHEMICAL ANALYTICAL RESULTS FOR CORE FROM DRILL HOLE NUMBER LLC-85-A[1]

PARAMETER	BACKGROUND LEVEL[2]	DEPTH INTERVALS IN FEET													
		0-5	5-6	9-10	14-15	19-20	24-25	29-30	34-35	39-40	44-45	49-50	49-50	54-55	59-60
Lithium (mg/ℓ)	<0.05 ± 0	<0.02	<0.02	3.0	0.13	0.64	1.10	0.06	<0.02	<0.02	<0.02	<0.02	<0.02	<0.02	<0.02
Copper (mg/ℓ)	<0.20 ± 0	<0.03	<0.03	0.22	1.60	1.50	4.90	1.10	0.03	0.14	0.04	0.03	0.03	0.09	<0.03
NH_3-N (mg/ℓ)	0.03 ± 0.05	3.2	4.0	11.0	11.0	7.0	25.0	16.0	7.4	1.1	4.7	1.0	1.7	0.64	0.15
Fluoride (mg/ℓ)	0.34 ± 0.11	0.0139	0.0049	0.0053	0.0027	0.0028	0.0021	0.0015	0.0007	0.0013	0.0022	0.0030	0.0032	0.0030	0.0044
TDS (mg/ℓ)	48 ± 20	56.0	30.0	651.0	237.0	128.0	528.0	505.0	341.0	225.0	245.0	273.0	261.0	54.0	72.0
Soil Moisture (%)	9.9 ± 1.4	9.3	11.5	12.4	6.9	9.5	20.3	19.9	7.9	7.3	6.4	5.7	5.6	2.6	4.7

(1) From Department of Energy, 1986f.
(2) Determined from six soil samples taken in Area L (see Table 4-12).

TABLE 4-17
MISCELLANEOUS CHEMICAL ANALYTICAL RESULTS FOR SURFACE IMPOUNDMENT CORE SAMPLES[1]

PARAMETER	BACKGROUND LEVEL[2]	DEPTH INTERVALS IN INCHES					
		0-4	4-8	8-12	12-16	16-20	20-29
Lithium (mg/ℓ)	<0.05 ± 0	0.45	0.24	0.27	0.60	0.39	0.33
Copper (mg/ℓ)	<0.20 ± 0	13.6	7.6	73.4	178	93.5	61.0
Nitrate (mg/ℓ)	0.03 ± 0.05	<30.	<30.	<30.	<30.	<30.	<30.
Fluoride (mg/ℓ)	0.34 ± 0.11	28	28	13	10	10	10
TDS (mg/ℓ)	48 ± 20	2,928	973	941	2,159	1,894	1,404
pH	7.6 ± 1.0	8.9	8.9	8.6	8.4	8.0	8.0
Soil Moisture (%)	9.9 ± 1.4	----	----	----	----	----	----
Conductivity (mg/ℓ)	---	4,500	2,300	2,800	3,590	3,150	2,500
Chloride (mg/ℓ)	---	980	440	340	210	200	200
Sulfate (mg/ℓ)	---	36	20	19	490	540	440

(1) From Department of Energy, 1986f.
(2) Determined from six soil samples taken in Area L (see Table 4-12).

TABLE 4-18

VOLATILE ORGANIC COMPOUNDS ANALYZED BY LOS ALAMOS NATIONAL LABORATORY IN CORES FROM DRILL HOLES[1]

TARGET COMPOUNDS	DETECTION LIMIT (µg/kg)
1,1-Dichloroethylene	---
Methylene Chloride	521
T-1,2-Dichloroethylene	521
1,1-Dichloroethane	1,042
Chloroform	1,042
1,1,1-Trichloroethane	1,563
1,2-Dichloroethane	833
Benzene	521
Carbon Tetrachloride	2,083
Trichloroethylene	521
1,2-Dichloropropane	521
Bromodichloromethane	1,042
Toluene	521
1,1,2-Trichloroethane	1,527
Chlorodibromomethane	1,042
Tetrachloroethylene	2,083
Chlorobenzene	1,250
Ethylbenzene	833
Bromoform	1,042
1,1,2,2-Tetrachloroethane	2,083
Bromobenzene	2,292
1,3-Dichlorobenzene	521
1,4-Dichlorobenzene	---
1,2-Dichlorobenzene	521

NON-TARGET COMPOUNDS

2-Hexanone
2-Pentanone
Acetone
Tetrahydrofuran
1-Butanol
1,4-Dioxane

[1] From Devaurs, 1985

TABLE 4-19

VOLATILE ORGANIC COMPOUNDS ANALYZED BY
ROCKY MOUNTAIN ANALYTICAL LABORATORY IN CORES FROM DRILL HOLES[1]

PRIORITY POLLUTANT PARAMETERS	DETECTION LIMIT (µg/kg)
Acrolein	100
Acrylonitrile	100
Benzene	5
Bromoform	5
Carbon tetrachloride	5
Chlorobenzene	5
Chlorodibromomethane	5
Chloroethane	10
2-Chloroethylvinyl ether	5
Chloroform	5
Dichlorobromomethane	5
1,1-Dichloroethane	5
1,2-Dichloroethane	5
1,1-Dichloroethylene	5
1,2-Dichloropropane	5
1,3-Dichloropropylene	5
Ethylbenzene	5
Methylbromide	10
Methylchloride	10
Methylene chloride	10
1,1,2,2-Tetrachloroethane	5
Tetrachlroethylene	5
Toluene	5
1,2-trans-Dichloroethylene	5
1,1,1-Trichloroethane	5
1,1,2-Trichloroethane	5
Trichloroethylene	5
Vinyl chloride	10

NON-PRIORITY POLLUTANT PARAMETERS

Acetone	Dimethoxymethane	Propanol
1,4-Dioxane	Ethanol	1-Butanol
Acetonitrile	2-Propanol	Tetramethyl pentanone
Tetrahydrofuran	2-Methyl-2-Propanol	Chlorodifluoromethane
2-Butanone	4-Methyl-2-Pentanone	Bisoxymethane

[1] From Rocky Mountain Analytical Laboratory, 1985.

TABLE 4-20

VOLATILE ORGANIC ANALYTICAL RESULTS FOR DRILL HOLE CORES
AUGUST 1985[1]

DRILL HOLE NUMBER	DEPTH INTERVAL (ft)	VOLATILE ORGANIC COMPOUND	CONCENTRATION (µg/kg)	DETECTION LIMIT (µg/kg)
LLC-85-12	38-39	2-Hexanone	3,710-4,130[a][c]	3,300
LLC-85-13	48-49	2-Pentanone (Acetone)	3,300[c]	3,300
LLC-85-14	28-29	Acetone	60[b]	---
		1,4-Dioxane	40[b]	---
		Tetrahydrofuran	16[c]	---
	38-39	2-Pentanone (Acetone)	3,640[c]	3,300
	38-39 (split)[f]	Acetone	190[b]	---
		Acetonitrile	27[b]	---
		Tetrahydrofuran	67[c]	---
	48-49	1-Butanol	83,330[c]	62,500

[a] Range given because two samples were prepared since portions of one sample were spilled.
[b] Concentration determined from analysis of analytical standard.
[c] Concentration estimated using total ionization peak area relative to the internal standard.
[d] Best computer match is [2,2'-Methylene bis (oxy)] bis propane.
[e] Several other volatile compounds were present in this drillhole, but they could not be definitely identified. The Mass spectrometer scans of these compounds were consistent with small chain alcohols. They were most concentrated at depth intervals of 18-19, 28-29, and 38-39 feet.
[f] Samples analyzed by Rocky Mountain Analytical Laboratory.
[1] Compiled from Devaurs, 1985, and Rocky Mountain Analytical Laboratory, 1985.

LAN:1702-T47:1

TABLE 4-20
VOLATILE ORGANIC ANALYTICAL RESULTS FOR DRILL HOLE CORES
AUGUST 1985
(Continued)

DRILL HOLE NUMBER	DEPTH INTERVAL (ft)	VOLATILE ORGANIC COMPOUND	CONCENTRATION (µg/kg)	DETECTION LIMIT (µg/kg)
LLC-85-14 (continued)	48-49 (split)[f]	Acetone	670[b]	---
		2-Butanone	100[b]	---
		4-Methyl-2-Pentanone	110[b]	---
		Acetonitrile	1,100[b]	---
		Tetrahydrofuran	520[c]	---
		Dimethoxymethane	25[c]	---
		Unknown (oxygenated HC)	10[c][d]	---
		Unknown (oxygenated HC)	7[c]	---
LLC-85-15	18-19[e]	Tetrahydrofuran	4,500[c]	3,000
	18-19 (split)[f]	Methylene Chloride	17	10
		Toluene	12	5
		Acetone	4,300[b]	---
		2-Butanone	470[b]	---
		4-Methyl-2-Pentanone	140[b]	---
		Ethanol	5[c]	---
		2-Propanol	6[c]	---
		Tetrahydrofuran	210[c]	---
		2-Methyl-2-Propanol	11[c]	---
	28-29	1,4-Dioxane	1,500[c]	1,500
	38-39	1,4-Dioxane	1,500[c]	1,500
		1-Butanol	100,000[c]	62,500

TABLE 4-20
VOLATILE ORGANIC ANALYTICAL RESULTS FOR DRILL HOLE CORES
AUGUST 1985
(Continued)

DRILL HOLE NUMBER	DEPTH INTERVAL (ft)	VOLATILE ORGANIC COMPOUND	CONCENTRATION (μg/kg)	DETECTION LIMIT (μg/kg)
LLC-85-15 (continued)	38-39 (split)[f]	Acetone	300[b]	---
		2-Butanone	170[b]	---
		4-Methyl-2-Pentanone	420[b]	---
		Ethanol	170[c]	---
		Bisoxymethane	270[c]	---
		Propanol	270[c]	---
		Propanol (Isomer)	150[c]	
		2-Methyl-2-Propanol	77[c]	---
		1,4-Dioxane	200[c]	---
		1-Butanol	280[c]	---
	88-89	2-Pentanone (Acetone)	3,300[b]	3,300
LLC-85-16	5.5-7.0[f]	1,2-Dichloroethane	19	5
		Methylene chloride	30	10
		Acetone	110[b]	---
		4-Methyl-2-Pentanone	27[b]	---
		2-Propanol	6[c]	---
		1-Butanol	17[c]	---
		Fluorinated Aliphatic	6[c]	---
		Tetramethylpentanone	7[c]	---
	17-19[f]	Methylene Chloride	18	10
		Acetone	82[c]	---
	97-99[f]	Methylene Chloride	15	10
		Acetone	110[b]	---
		4-Methyl-2-Pentanone	5[b]	---
		Chlorodifluoromethane	10[c]	---

LAN:1702-T47:3

TABLE 4-20
VOLATILE ORGANIC ANALYTICAL RESULTS FOR DRILL HOLE CORES
AUGUST 1985
(Continued)

DRILL HOLE NUMBER	DEPTH INTERVAL (ft)	VOLATILE ORGANIC COMPOUND	CONCENTRATION (μg/kg)	DETECTION LIMIT (μg/kg)
LLC-85-18	18-19[f]	Methylene Chloride	17	10
		Acetone	130[b]	---
		Chlorodifluoromethane	12[c]	---
		Unknown Hydrocarbon	20[c]	---
		Ethanol	190[c]	---
		C_6-Hydrocarbon	9[c]	---
	78-79[f]	Acetone	70[b]	---
		2-Butanone	55[b]	---
		Unknown Hydrocarbon	9[c]	---

TABLE 4-21

VOLATILE ORGANIC COMPOUNDS ANALYZED IN PORE GAS BY LOS ALAMOS NATIONAL LABORATORY

Chloromethane
Bromomethane
Vinyl Chloride
Chloroethane
Methylene Chloride
Acetone
1,1-Dichloroethane
1,1-Dichloroethene
trans-1,2-Dichloroethene
Chloroform
1,2-Dichloroethane
2-Butanone
1,1,1-Trichloroethane
Carbon Tetrachloride
Vinly Acetate
Bromodichloromethane
1,1,2,2-Tetrachloroethane
1,2-Dichloropropane
trans-1,3-Dichloropropene
Trichloroethene
Dibromochloromethane
1,1,2-Trichloroethane
Benzene
cis-1,3-Dichloropropene

Bromoform
2-Hexanone
4-Methyl-2-Pentanone
Tetrachloroethene
Toluene
Chlorobenzene
Ethylbenzene
Styrene
Total Xylenes
Trichlorofluoromethane
Tetrahydrofuran

TABLE 4-22

VOLATILE ORGANIC COMPOUND
DETECTION LIMITS FOR REPRESENTATIVE ANALYTES[1]

1986
DETECTION LIMITS
µg/TUBE

COMPOUND	JAN	FEB	MAR	APR	DEC
Trichlorofluoromethane	3	4.5	1	1	3.0
Dichlorodifluoromethane	3	---	---	---	---
Chloroform	1	1.2	1	1	3.0
1,1,1-Trichloroethane	3	1.3	1	1	3.0
Carbon Tetrachloride	1	---	1	1	3.0
Trichloroethene	1	1.2	1	1	3.0
Toluene	0.8	0.8	1	1	3.0
Tetrachloroethene	1.0	1.0	1	1	3.0
Total Xylenes	1.1	1.0	1	1	3.0
Chlorobenzene	---	1.2	---	1	3.0
1,1-Dichloroethene	---	---	1	---	3.0
Ethylbenzene	---	1.2	---	1	3.0

[1] Compiled from Devaurs and Bell, 1986; Department of Energy, 1986e; and unpublished laboratory data report (December).

TABLE 4-23

1986 PORE GAS SAMPLING[1]
DRILL HOLE LLC-85-12
μg/L AIR

COMPOUND	6 FT JAN	6 FT FEB	6 FT MAR	6 FT APR	6 FT DEC[2]	27 FT JAN	27 FT FEB	27 FT MAR	27 FT APR	27 FT DEC[2]	41 FT JAN	41 FT FEB	41 FT MAR	41 FT APR	41 FT DEC[2]
Dichlorodifluoromethane	ND<3	---	---	---	---	ND<3	---	---	---	---	ND<3	---	---	---	---
Trichlorofluoromethane	90	36	ND<1	ND<1	ND<3.0	273	32	ND<1	---	42.9	146	33	ND<1	ND<1	ND<3.0
Chloroform	ND<1	24	11	25	7.6	ND<1	37	29	---	25.5	3.8	88	47	30	38.3
1,1,1-trichloroethane	252	882	697	429	888.3	2,803	1,006	786	---	1,108.6	3,540	868	673	517	983.1
Carbon tetrachloride	19	TR<1.0	>0.5*	ND<1	>3.0	64	TR<1.0	>0.5*	---	>3.0	46	TR<1.0	>0.5*	ND<1	>3.0
Trichloroethene	988	384	416	223	410.6	1,355	580	440	---	726.7	760	394	273	260	609.0
Toluene	126	52	36	0.6	21.9	935	270	169	---	129.3	213	46	34	26	26.6
Tetrachloroethene	17	11	ND<1	ND<1	3.7	14	10	7.5	---	5.9	175	12	ND<1	ND<1	6.1
Total Xylenes	ND<1.1	ND<1.0	ND<1	ND<1	ND<3.0	14	3.6	ND<1	---	ND<3.0	1.1	ND<1.0	ND<1	ND<1	ND<3.0
Chlorobenzene	---	ND<1.2	---	ND<1	ND<3.0	---	ND<1.2	---	---	ND<3.0	---	ND<1.2	---	ND<1	ND<3.0
1,1-dichloroethene	---	---	ND<1	---	---	---	---	ND<1	---	---	---	---	ND<1	---	---
Ethylbenzene	---	ND<1.2	---	ND<1	ND<3.0	---	ND<1.2	---	---	ND<3.0	---	ND<1.2	---	ND<1	ND<3.0

*Calculated from tentative results.
ND = This compound was not detected; the limit of detection for this analysis is less than the amount stated in the table above.
TR = Trace; this compound was present, but was below the level at which concentration could be determined.
NA = Not available
(1) Compiled from Devaurs and Bell, 1986, and Department of Energy, 1986e.
(2) From unpublished Laboratory data report; analytical uncertainty ±15 percent μg/tube.

LAN:017-TABLE/3

TABLE 4-24

1986 PORE GAS SAMPLING[1]
DRILL HOLE LLC-85-13
μg/L AIR

COMPOUND	21 FT JAN	21 FT FEB	21 FT MAR	21 FT APR	21 FT DEC[2]	43 FT JAN	43 FT FEB	43 FT MAR	43 FT APR	43 FT DEC[2]	65 FT JAN	65 FT FEB	65 FT MAR	65 FT APR	65 FT DEC[2]
Dichlorodifluoromethane	ND<3	---	---	---	---	ND<3	---	---	---	---	ND<3	---	---	---	---
Trichlorofluoromethane	ND<3	ND<4.5	ND<1	ND<1	ND<3.0	ND<3	ND<4.5	ND<1	ND<1	ND<3.0	ND<3	ND<4.5	ND<1	ND<1	ND<3.0
Chloroform	ND<1	ND<1.2	ND<1	ND<1	ND<3.0	ND<1	ND<1.2	ND<1	ND<1	ND<3.0	ND<1	ND<1.2	ND<1	ND<1	ND<3.0
1,1,1-trichloroethane	ND<3	ND<1.3	ND<1	ND<1	ND<3.0	ND<3	ND<1.3	ND<1	ND<1	ND<3.0	ND<3	ND<1.3	ND<1	ND<1	ND<3.0
Carbon tetrachloride	ND<1	---	ND<1	ND<1	ND<3.0	ND<1	---	ND<1	ND<1	ND<3.0	ND<1	---	ND<1	ND<1	ND<3.0
Trichloroethene	ND<1	ND<1.2	ND<1	ND<1	ND<3.0	ND<1	ND<1.2	ND<1	ND<1	ND<3.0	ND<1	ND<1.2	ND<1	ND<1	ND<3.0
Toluene	ND<0.8	ND<0.8	ND<1	ND<1	ND<3.0	ND<0.8	ND<0.8	ND<1	ND<1	ND<3.0	ND<0.8	ND<0.8	ND<1	ND<1	ND<3.0
Tetrachloroethene	ND<1.0	ND<1.0	ND<1	ND<1	ND<3.0	ND<1.0	ND<1.0	ND<1	ND<1	ND<3.0	ND<1.0	ND<1.0	ND<1	ND<1	ND<3.0
Total Xylenes	ND<1.1	ND<1.0	ND<1	ND<1	ND<3.0	ND<1.1	ND<1.0	ND<1	ND<1	ND<3.0	ND<1.1	ND<1.0	ND<1	ND<1	ND<3.0
Chlorobenzene	---	ND<1.0	---	ND<1	ND<3.0	---	ND<1.2	---	ND<1	ND<3.0	---	ND<1.2	---	ND<1	ND<3.0
1,1-dichloroethene	---	---	ND<1	---	---	---	---	ND<1	---	---	---	---	ND<1	---	---
Ethylbenzene	---	ND<1.2	---	ND<1	ND<3.0	---	ND<1.2	---	ND<1	ND<3.0	---	ND<1.2	---	ND<1	ND<3.0

ND = This compound was not detected; the limit of detection for this analysis is less than the amount stated in the table above.
NA = Not available
(1) Compiled from Devaurs and Bell, 1986, and Department of Energy, 1986e.
(2) From unpublished Laboratory data report; analytical uncertainty ±15 percent μg/tube.

TABLE 4-25

1986 PORE GAS SAMPLING[1]
DRILL HOLE LLC-85-14
μg/L AIR

COMPOUND	JAN	FEB	13 FT MAR	APR	DEC[2]	JAN	FEB	31 FT MAR	APR	DEC[2]	JAN	FEB	46 FT MAR	APR	DEC[2]	JAN	FEB	86 FT MAR	APR	DEC[2]
Dichlorodifluoromethane	BRK	---	---	---	---	BRK	---	---	---	---	BRK	---	---	---	---	BRK	---	---	---	---
Trichlorofluoromethane	BRK	ND<4.5	ND<1	ND<1	ND<3.0	BRK	45	ND<1	ND<1	ND<3.0	BRK	ND<4.5	ND<1	ND<1	ND<3.0	BRK	ND<4.5	<5*	ND<1	14.4
Chloroform	BRK	67	ND<1	86	ND<3.0	BRK	182	ND<1	109	68.5	BRK	184	ND<1	120	83.1	BRK	175	124	86	71.8
1,1,1-trichloroethane	BRK	7,335	BRK	7,554	9,463.4	BRK	BRK	BRK	9,148	12,117.4	BRK	171,080	BRK	10,140	12,367.3	BRK	BRK	BRK	8,717	11,546.2
Carbon tetrachloride	BRK	TR<1.0	ND<1	TR<1	>3.0	BRK	TR<1.0	ND<1	TR<1	>3.0	BRK	TR<1.0	ND<1	TR<1	>3.0	BRK	TR<1.0	>0.5*	TR<1	>3.0
Trichloroethene	BRK	ND<1.2	713	912	800.5	BRK	1,350	879	946	1,039.6	BRK	2,715	1,036	812	931.1	BRK	1,060	730	720	918.3
Toluene	BRK	3	ND<1	ND<1	ND<3.0	BRK	51	ND<1	28	12.2	BRK	61	ND<1	37	311.3	BRK	101	64	58	31.0
Tetrachloroethene	BRK	2	ND<1	16	10.7	BRK	37	ND<1	25	20.0	BRK	52	ND<1	20	21.5	BRK	ND<1.0	<7.5*	17	23.9
Total Xylenes	BRK	14	ND<1	ND<1	ND<3.0	BRK	74	ND<1	57	ND<3.0	BRK	46	ND<1	18	ND<3.0	BRK	ND<1.0	ND<1	ND<1	ND<3.0
Chlorobenzene	---	ND<1.2	---	ND<1	ND<3.0	---	11	---	4.6	5.2	---	13	---	5.4	5.9	---	ND<1.2	---	ND<1	3.5
1,1-dichloroethene	---	---	ND<1	---	---	---	---	ND<1	---	---	---	---	ND<1	----	---	---	---	ND<1	---	---
Ethylbenzene	---	5	---	ND<1	3.0	---	30	---	23	8.0	---	16	---	6.3	12.8	---	ND<1.2	---	ND<1	5.1

*Calculated from tentative results.
ND = This compound was not detected; the limit of detection for this analysis is less than the amount stated in the table above.
TR = Trace; this compound was present, but was below the level at which concentration could be determined.
BRK = Breakthrough in charcoal tubes.
NA = Not available
(1) Compiled from Devaurs and Bell, 1986, and Department of Energy, 1986e.
(2) From unpublished Laboratory data report; analytical uncertainty ±15 percent μg/tube.

LAN:017-TABLE/5

TABLE 4-26

1986 PORE GAS SAMPLING[1]
DRILL HOLE LLC-85-15
μg/L AIR

COMPOUND	19 FT JAN	19 FT FEB	19 FT MAR	19 FT APR	19 FT DEC[2]	32 FT JAN	32 FT FEB	32 FT MAR	32 FT APR	32 FT DEC[2]	82 FT JAN	82 FT FEB	82 FT MAR	82 FT APR	82 FT DEC[2]
Dichlorodifluoromethane	BRK	---	ND<1	---	---	BRK	---	ND<1	---	---	BRK	---	ND<1	---	---
Trichlorofluoromethane	BRK	ND<4.5	ND<1	ND<1	ND<3.0	BRK	BRK	ND<1	28	46.3	BRK	4,120	ND<1	167	19.2
Chloroform	BRK	47	308	142	115.9	BRK	BRK	510	399	283.7	BRK	240	ND<1	121	228.0
1,1,1-trichloroethane	BRK	1,045	BRK	4,833	3,586.4	BRK	BRK	BRK	8,294	15,218.9	BRK	12,927	BRK	8,618	8,713.3
Carbon tetrachloride	BRK	ND<1.0	ND<1	TR<1	>3.0	BRK	BRK	ND<1	TR<1	>3.0	BRK	ND<1.0	ND<1	TR<1	>3.0
Trichloroethene	BRK	188	1,354	852	1,029.4	BRK	BRK	1,850	1,823	2,923.9	BRK	BRK	1,310	1,464	324.1
Toluene	BRK	40	512	139	90.5	BRK	BRK	817	573	624.8	BRK	593	482	349	1,008.8
Tetrachloroethene	BRK	111	457	406	395.4	BRK	BRK	635	48	406.9	BRK	111	ND<1	80	71.0
Total Xylenes	BRK	6	160	27	ND<3.0	BRK	BRK	332	219	ND<3.0	BRK	149	ND<1	107	ND<3.0
Chlorobenzene	---	---	---	7.7	97.1	---	BRK	---	21	25.6	---	ND<1.2	---	ND<1	ND<3.0
1,1-dichloroethene	---	---	---	---	---	---	---	---	---	---	---	---	---	---	--
Ethylbenzene	---	4.2	---	12	17.9	---	BRK	---	52	71.3	---	ND<1.2	---	22	11.6

ND = This compound was not detected; the limit of detection for this analysis is less than the amount stated in the table above.
TR = Trace; this compound was present, but was below the level at which concentration could be determined.
BRK = Breakthrough in charcoal tubes.
NA = Not available
(1) Compiled from Devaurs and Bell, 1986, and Department of Energy, 1986e.
(2) From unpublished Laboratory data report; analytical uncertainty ±15 percent μg/tube.

TABLE 4-27

1986 PORE GAS SAMPLING[1]
DRILL HOLE LLC-85-16
μg/L AIR

COMPOUND	7 FT JAN	7 FT FEB	7 FT MAR	7 FT APR	7 FT DEC[2]	17 FT JAN	17 FT FEB	17 FT MAR	17 FT APR	17 FT DEC[2]	102 FT JAN	102 FT FEB	102 FT MAR	102 FT APR	102 FT DEC[2]
Dichlorodifluoromethane	ND<3	---	---	---	---	ND<3	---	---	---	---	BRK	---	---	---	---
Trichlorofluoromethane	39	11	ND<1	NA	ND<3.0	ND<3	12	ND<1	ND<1	ND<3.0	BRK	BRK	ND<1	27	25.6
Chloroform	47	12	43	NA	72.7	92	16	20	82	ND<3.0	BRK	BRK	20	76	ND<3.0
1,1,1-trichloroethane	1,856	2,548	1,817	NA	4,143.2	2,030	3,326	3,081	3,625	4,786.7	BRK	BRK	3,745	5,901	7,403.1
Carbon tetrachloride	4.8	TR<1.0	>0.5*	NA	>3.0	ND<1	TR<1.0	>0.5*	ND<1	>3.0	BRK	ND<1.0	---	ND<1	>3.0
Trichloroethene	547	748	452	NA	1,050.8	749	1,126	870	950	1,220.6	BRK	1,080	757	999	1,181.6
Toluene	ND<0.8	ND<0.8	ND<1	NA	ND<3.0	ND<0.8	ND<0.8	ND<1	34	ND<3.0	BRK	300	ND<1	105	88.5
Tetrachloroethene	21	10	30	NA	21.1	45	13	50	ND<1	17.5	BRK	12	27	28	11.2
Total Xylenes	ND<1.1	ND<1.0	ND<1	NA	ND<3.0	ND<1.1	ND<1.0	ND<1	ND<1	ND<3.0	BRK	4	7.5	ND<1	ND<3.0
Chlorobenzene	---	---	---	NA	ND<3.0	---	---	---	ND<1	ND<3.0	---	---	---	ND<1	ND<3.0
1,1-dichloroethene	---	ND<18	ND<1	---	---	---	ND<18	ND<1	---	---	---	TR<18	ND<1	---	---
Ethylbenzene	---	ND<1.2	---	NA	ND<3.0	---	ND<1.2	---	ND<1	ND<3.0	---	1.8	---	ND<1	8.0

*Calculated from tentative results.
ND = This compound was not detected; the limit of detection for this analysis is less than the amount stated in the table above.
TR = Trace; this compound was present, but was below the level at which concentration could be determined.
BRK = Breakthrough in charcoal tubes.
NA = Not available
(1) Compiled from Devaurs and Bell, 1986, and Department of Energy, 1986e.
(2) From unpublished Laboratory data report; analytical uncertainty ±15 percent μg/tube.

LAN:017-TABLE/7

TABLE 4-28

1986 PORE GAS SAMPLING[1]
DRILL HOLE LGC-85-09
μg/L AIR

COMPOUND	JAN	FEB	37 FT MAR	APR	DEC[2]	JAN	FEB	63 FT MAR	APR	DEC[2]	JAN	FEB	80 FT MAR	APR	DEC[2]	JAN	FEB	91 FT MAR	APR	DEC[2]
Dichlorodifluoromethane	ND<3	---	---	---	---	ND<3	---	---	---	---	---	---	---	---	---	ND<3	---	---	---	---
Trichlorofluoromethane	ND<3	ND<4.5	ND<1	ND<1	ND<3.0	ND<3	ND<4.5	ND<1	ND<1	ND<3.0	---	ND<4.5	ND<1	ND<1	ND<3.0	ND<3	ND<4.5	ND<1	ND<1	ND<3.0
Chloroform	ND<1	ND<1.2	ND<1	ND<1	ND<3.0	ND<1	ND<1.2	ND<1	ND<1	ND<3.0	---	ND<1.2	ND<1	ND<1	ND<3.0	ND<1	ND<1.2	ND<1	ND<1	ND<3.0
1,1,1-trichloroethane	384	380	<250*	349	561.5	980	472	<250*	466	644.0	---	210	<250*	374	421.0	312	406	>250*	90	ND<3.0
Carbon tetrachloride	ND<1	ND<1.0	ND<1	ND<1	ND<3.0	ND<1	ND<1.0	ND<1	ND<1	ND<3.0	---	ND<1.0	ND<1	ND<1	ND<3.0	ND<1	ND<1.0	ND<1	ND<1	ND<3.0
Trichloroethene	1.3	1.6	1	ND<1	ND<3.0	1.8	2.2	1.64	2.2	ND<3.0	---	1.2	1.6	2.7	ND<3.0	1.6	2.2	0.98	1.4	ND<3.0
Toluene	ND<0.8	ND<0.8	ND<1	ND<1	ND<3.0	ND<0.8	ND<0.8	ND<1	ND<1	ND<3.0	---	ND<0.8	ND<1	ND<1	ND<3.0	ND<0.8	0.4	ND<1	ND<1	ND<3.0
Tetrachloroethene	3.2	3.8	4	ND<1	ND<3.0	4.1	4.6	5	ND<1	ND<3.0	---	3	>0.5*	ND<1	ND<3.0	2.9	4	2.57	ND<1	ND<3.0
Total Xylenes	ND<1.1	ND<1.0	ND<1	ND<1	ND<3.0	ND<1.1	ND<1.0	ND<1	ND<1	ND<3.0	---	ND<1.0	ND<1	ND<1	ND<3.0	ND<1.1	0.8	ND<1	ND<1	ND<3.0
Chlorobenzene	---	---	---	ND<1	ND<3.0	---	---	---	ND<1	ND<3.0	---	---	---	ND<1	ND<3.0	---	---	---	ND<1	ND<3.0
1,1-dichloroethene	---	ND<18.0	>0.5*	---	---	---	TR<18.0	>0.5*	---	---	---	ND<18.0	>0.5*	---	---	---	TR<18.0	>0.5*	---	---
Ethylbenzene	---	ND<1.2	---	ND<1	ND<3.0	---	ND<1.2	---	ND<1	ND<3.0	---	ND<1.2	---	ND<1	ND<3.0	---	ND<1.2	---	ND<1	ND<3.0

*Calculated from tentative results.
ND = This compound was not detected; the limit of detection for this analysis is less than the amount stated in the table above.
TR = Trace; this compound was present, but was below the level at which concentration could be determined.
NA = Not available
(1) Compiled from Devaurs and Bell, 1986, and Department of Energy, 1986e.
(2) From unpublished Laboratory data report; analytical uncertainty ±15 percent μg/tube.

LAN:017-TABLE/1

TABLE 4-29

1986 PORE GAS SAMPLING[1]
DRILL HOLE LGC-85-10
μg/L AIR

COMPOUND	31 FT JAN	31 FT FEB	31 FT MAR	31 FT APR	31 FT DEC[2]	53 FT JAN	53 FT FEB	53 FT MAR	53 FT APR	53 FT DEC[2]	95 FT JAN	95 FT FEB	95 FT MAR	95 FT APR	95 FT DEC[2]
Dichlorodifluoromethane	ND<3	---	---	---	---	4	---	---	---	---	4.4	---	---	---	---
Trichlorofluoromethane	18	14	9.5	ND<1	ND<3.0	18	14	10.6	ND<1	ND<3.0	7.4	7.6	7.2	ND<1	ND<3.0
Chloroform	ND<1	ND<1.2	ND<1	ND<1	ND<3.0	ND<1	ND<1.2	ND<1	ND<1	ND<3.0	ND<1	ND<1.2	ND<1	ND<1	ND<3.0
1,1,1-trichloroethane	184	314	>250*	99	138.0	152	168	>250*	147	208.0	79	101	>250*	55	90.0
Carbon tetrachloride	ND<1	ND<1.0	ND<1	ND<1	ND<3.0	ND<1	ND<1.0	ND<1	ND<1	ND<3.0	ND<1	ND<1.0	ND<1	ND<1	ND<3.0
Trichloroethene	2.6	2.6	2.2	ND<1	ND<3.0	4.4	4.4	4.15	ND<1	ND<3.0	ND<1	6.4	6.5	3.4	ND<3.0
Toluene	ND<0.8	ND<0.8	ND<1	ND<1	ND<3.0	ND<0.8	ND<0.8	ND<1	ND<1	ND<3.0	ND<0.8	ND<0.8	ND<1	ND<1	ND<3.0
Tetrachloroethene	2.8	3.0	3.19	ND<1	ND<3.0	3.4	3.6	4.08	ND<1	ND<3.0	2.8	3.2	3.55	ND<1	ND<3.0
Total Xylenes	ND<1.1	ND<1.0	ND<1	ND<1	ND<3.0	ND<1.1	ND<1.0	ND<1	ND<1	ND<3.0	ND<1.1	ND<1.0	ND<1	ND<1	ND<3.0
Chlorobenzene	---	---	---	ND<1	ND<3.0	---	---	---	ND<1	ND<3.0	---	---	---	ND<1	ND<3.0
1,1-dichloroethene	---	ND<18.0	ND<1	---	---	---	ND<18.0	ND<1	---	---	---	ND<18.0	ND<1	---	---
Ethylbenzene	---	ND<1.2	---	ND<1	ND<3.0	---	ND<1.2	---	ND<1	ND<3.0	---	ND<1.2	---	ND<1	ND<3.0

*Calculated from tentative results.
ND = This compound was not detected; the limit of detection for this analysis is less than the amount stated in the table above.
NA = Not available
(1) Compiled from Devaurs and Bell, 1986, and Department of Energy, 1986e.
(2) From unpublished Laboratory data report; analytical uncertainty ±15 percent μg/tube.

301017 02 A48

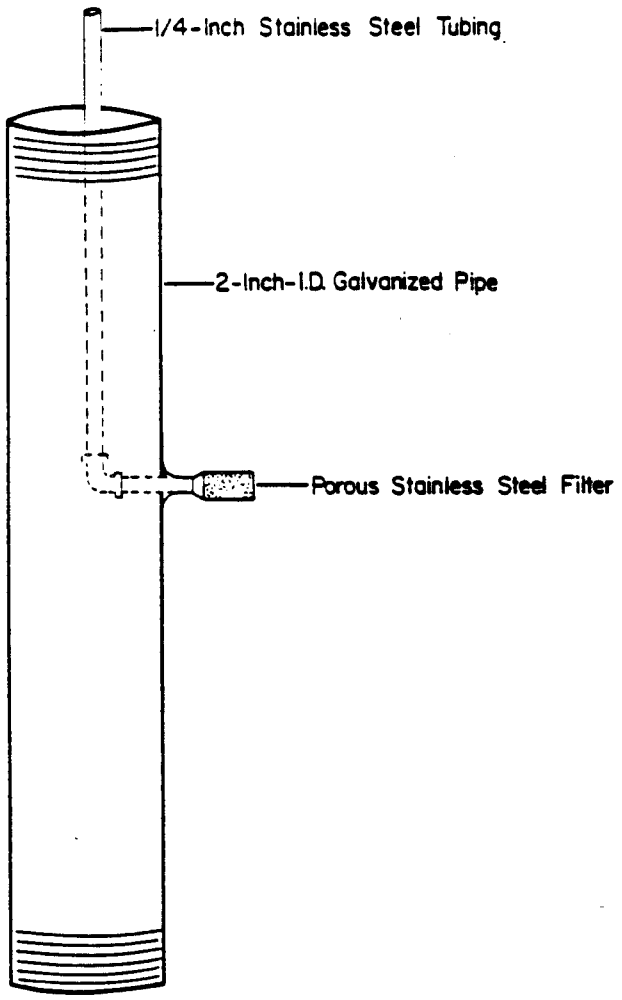

FIGURE 4-1. DIAGRAM OF A PORE-GAS SAMPLING PORT (DEVAURS AND BELL, 1986)

DRILLHOLE LLC-85-12

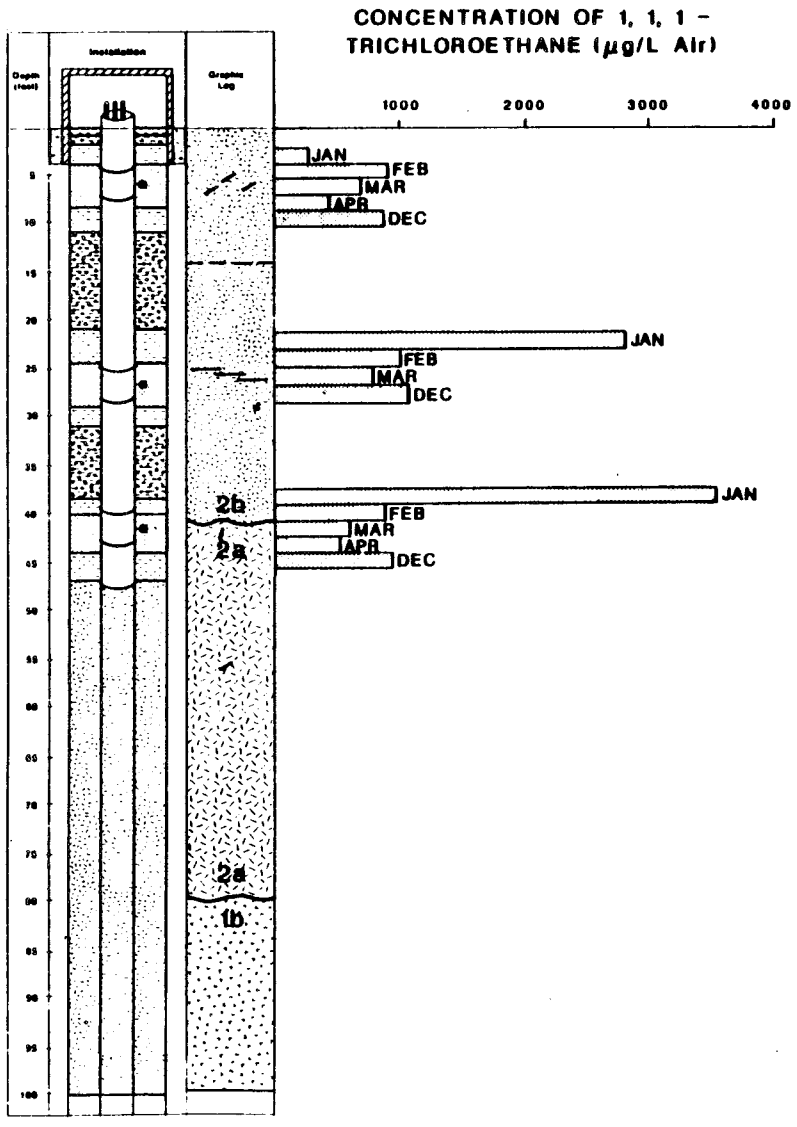

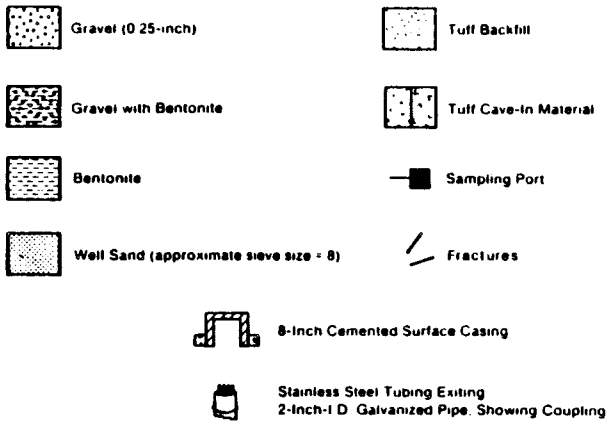

(Figure modified from BFEC, 1986; chemical data from Devaurs and Bell, 1986 and Department of Energy, 1986e)

FIGURE 4-2

1,1,1-TRICHLOROETHANE CONCENTRATIONS IN PORE GAS SAMPLES DRILLHOLE LLC-85-12, 1986

PREPARED FOR

LOS ALAMOS NATIONAL LABORATORY
LOS ALAMOS, NEW MEXICO

IT Creating a Safer Tomorrow

DRAWING NUMBER 901017 02 B7

DRAWN BY | CHECKED BY | APPROVED BY

© 1984 IT CORPORATION
ALL COPYRIGHTS RESERVED
Do Not Scale This Drawing

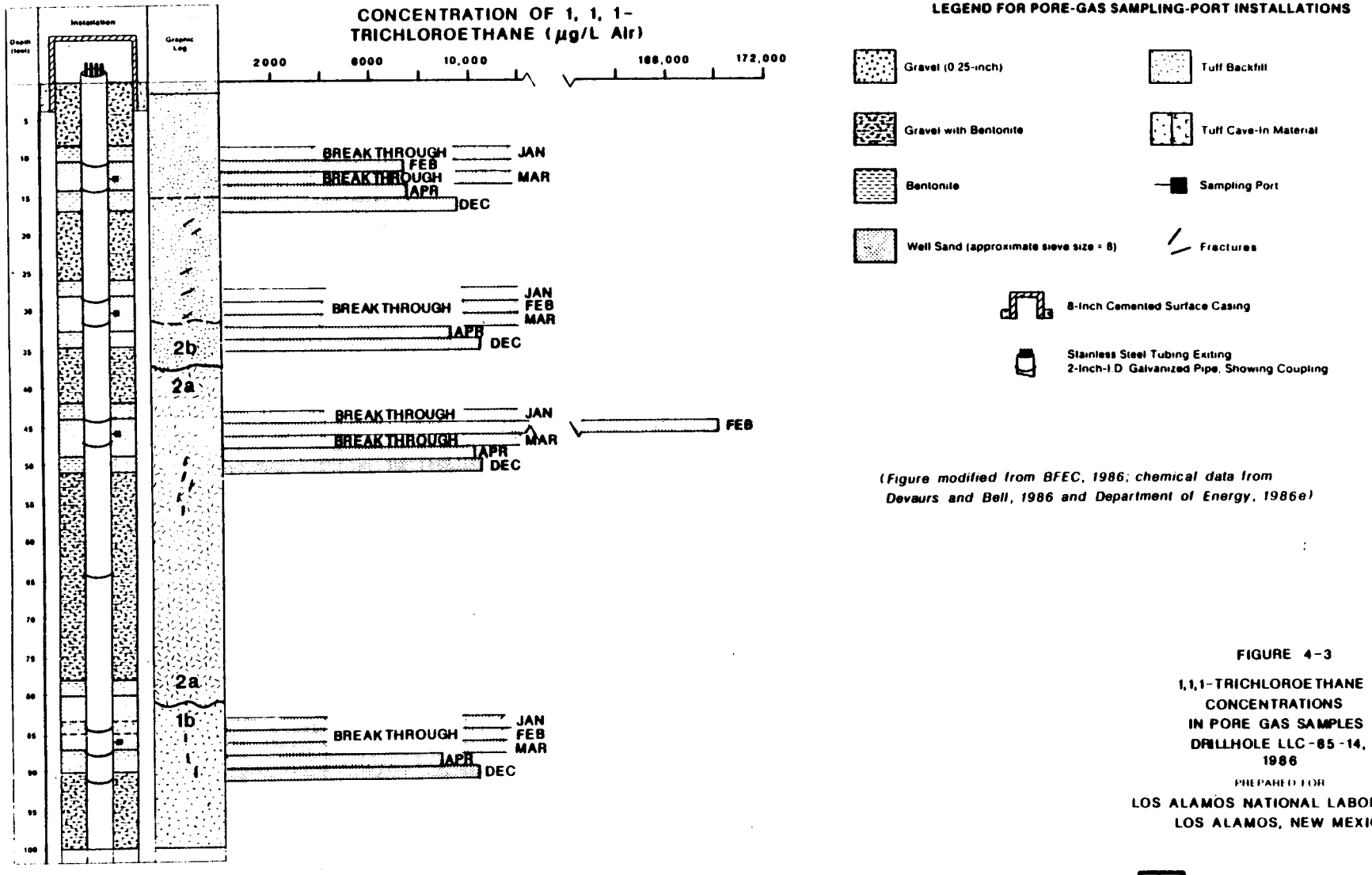

(Figure modified from BFEC, 1986; chemical data from Devaurs and Bell, 1986 and Department of Energy, 1986e)

FIGURE 4-3

1,1,1-TRICHLOROETHANE CONCENTRATIONS IN PORE GAS SAMPLES DRILLHOLE LLC-85-14, 1986

PREPARED FOR

LOS ALAMOS NATIONAL LABORATORY
LOS ALAMOS, NEW MEXICO

IT Creating a Safer Tomorrow

DRAWN BY LLF 2/28/87 CHECKED BY APPROVED BY DRAWING NUMBER 301017 02 86

© 1984 IT CORPORATION
ALL COPYRIGHTS RESERVED
Do Not Scale This Drawing

DRILLHOLE LLC-85-15

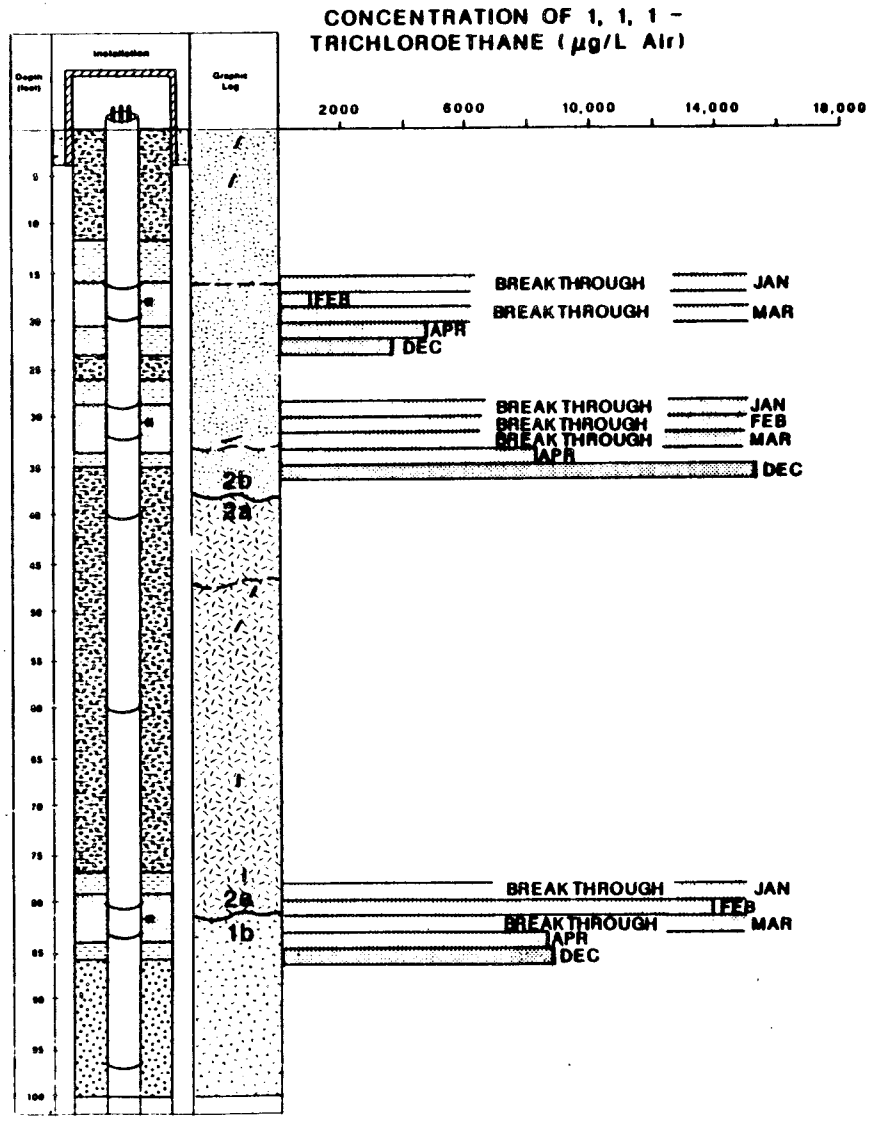

LEGEND FOR PORE-GAS SAMPLING-PORT INSTALLATIONS

- Gravel (0.25-inch)
- Tuff Backfill
- Gravel with Bentonite
- Tuff Cave-In Material
- Bentonite
- Sampling Port
- Well Sand (approximate sieve size = 8)
- Fractures
- 8-Inch Cemented Surface Casing
- Stainless Steel Tubing Exiting 2-Inch-I.D. Galvanized Pipe, Showing Coupling

(Figure modified from BFEC, 1986; chemical data from Devaurs and Bell, 1986 and Department of Energy, 1986e)

FIGURE 4-4

1,1,1-TRICHLOROETHANE CONCENTRATIONS IN PORE GAS SAMPLES DRILLHOLE LLC-85-15, 1986

PREPARED FOR

LOS ALAMOS NATIONAL LABORATORY
LOS ALAMOS, NEW MEXICO

IT Creating a Safer Tomorrow

DRAWN BY	CHECKED BY	APPROVED BY	DRAWING NUMBER
LLF 2/28/87	DEC		301017 02 B9

© 1984 IT CORPORATION
ALL COPYRIGHTS RESERVED
Do Not Scale Drawing

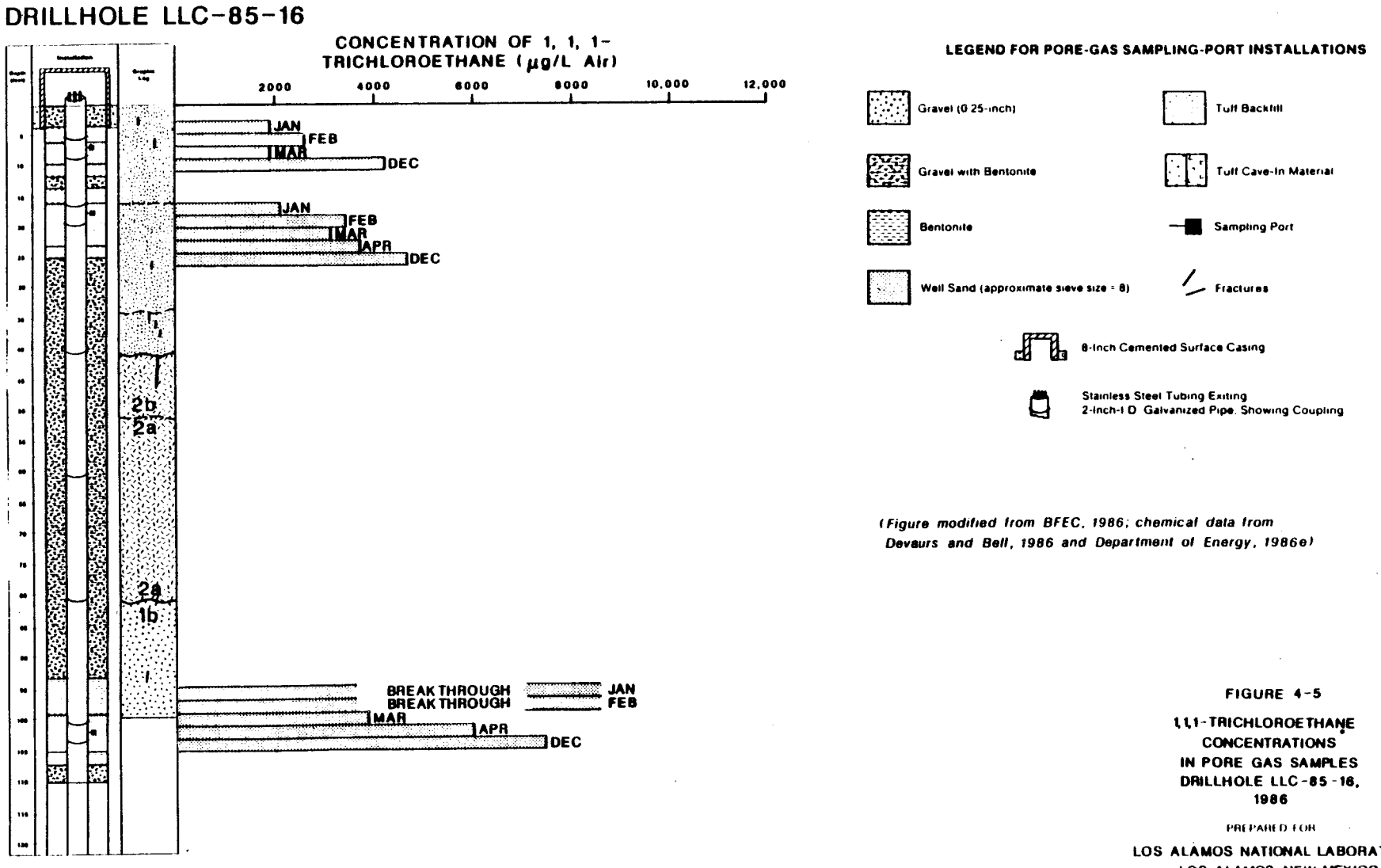

(Figure modified from BFEC, 1986; chemical data from Devaurs and Bell, 1986 and Department of Energy, 1986e)

FIGURE 4-5

1,1,1-TRICHLOROETHANE CONCENTRATIONS IN PORE GAS SAMPLES DRILLHOLE LLC-85-16, 1986

PREPARED FOR

LOS ALAMOS NATIONAL LABORATORY
LOS ALAMOS, NEW MEXICO

IT Creating a Safer Tomorrow

DRAWN BY | DATE 2/28/87 | CHECKED BY | APPROVED BY | DATE 3/16/87 | DRAWING NUMBER 301017 02 810

© 1984 IT CORPORATION
ALL COPYRIGHTS RESERVED
Do Not Scale This Drawing

DRILLHOLE LGC-85-09

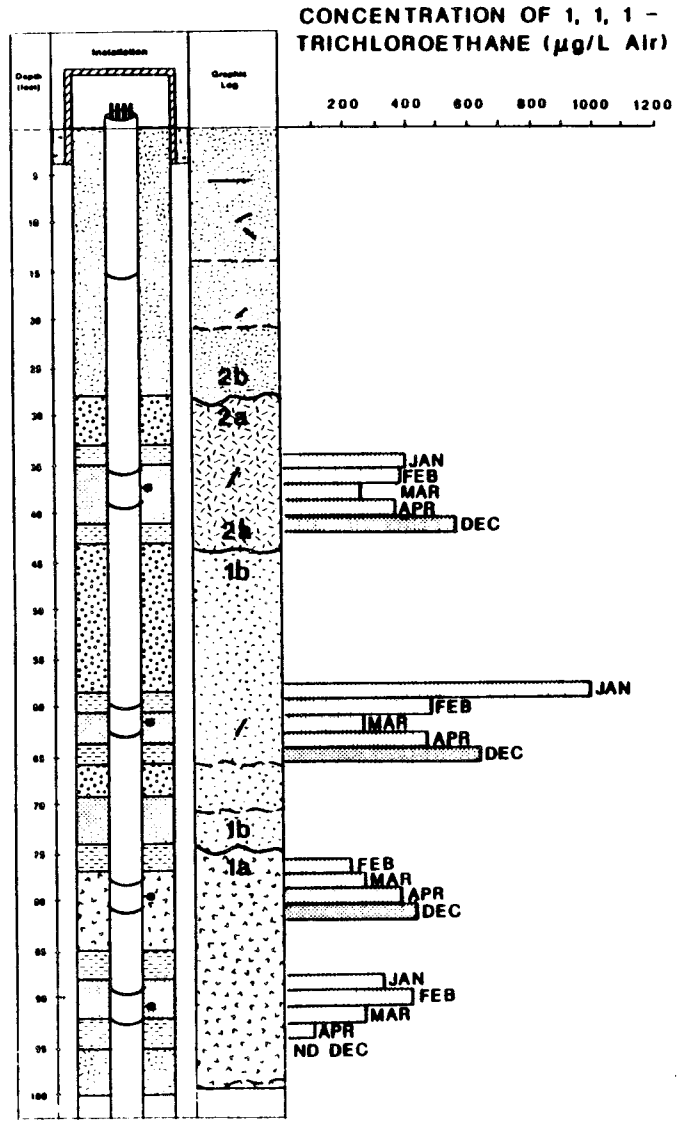

LEGEND FOR PORE-GAS SAMPLING-PORT INSTALLATIONS

- Gravel (0.25-inch)
- Gravel with Bentonite
- Bentonite
- Well Sand (approximate sieve size ÷ 8)
- Tuff Backfill
- Tuff Cave-In Material
- Sampling Port
- Fractures
- 8-Inch Cemented Surface Casing
- Stainless Steel Tubing Exiting 2-Inch-I.D. Galvanized Pipe, Showing Coupling

(Figure modified from BFEC, 1986; chemical data from Devaurs and Bell, 1986 and Department of Energy, 1986e)

FIGURE 4-6

1,1,1-TRICHLOROETHANE CONCENTRATIONS IN PORE GAS SAMPLES DRILLHOLE LGC-85-09, 1986

PREPARED FOR

LOS ALAMOS NATIONAL LABORATORY LOS ALAMOS, NEW MEXICO

IT Creating a Safer Tomorrow

DRAWN BY | CHECKED BY | APPROVED BY | DRAWING NUMBER 301017 02 B41

© 1984 IT CORPORATION ALL COPYRIGHTS RESERVED
Do Not Scale Drawing

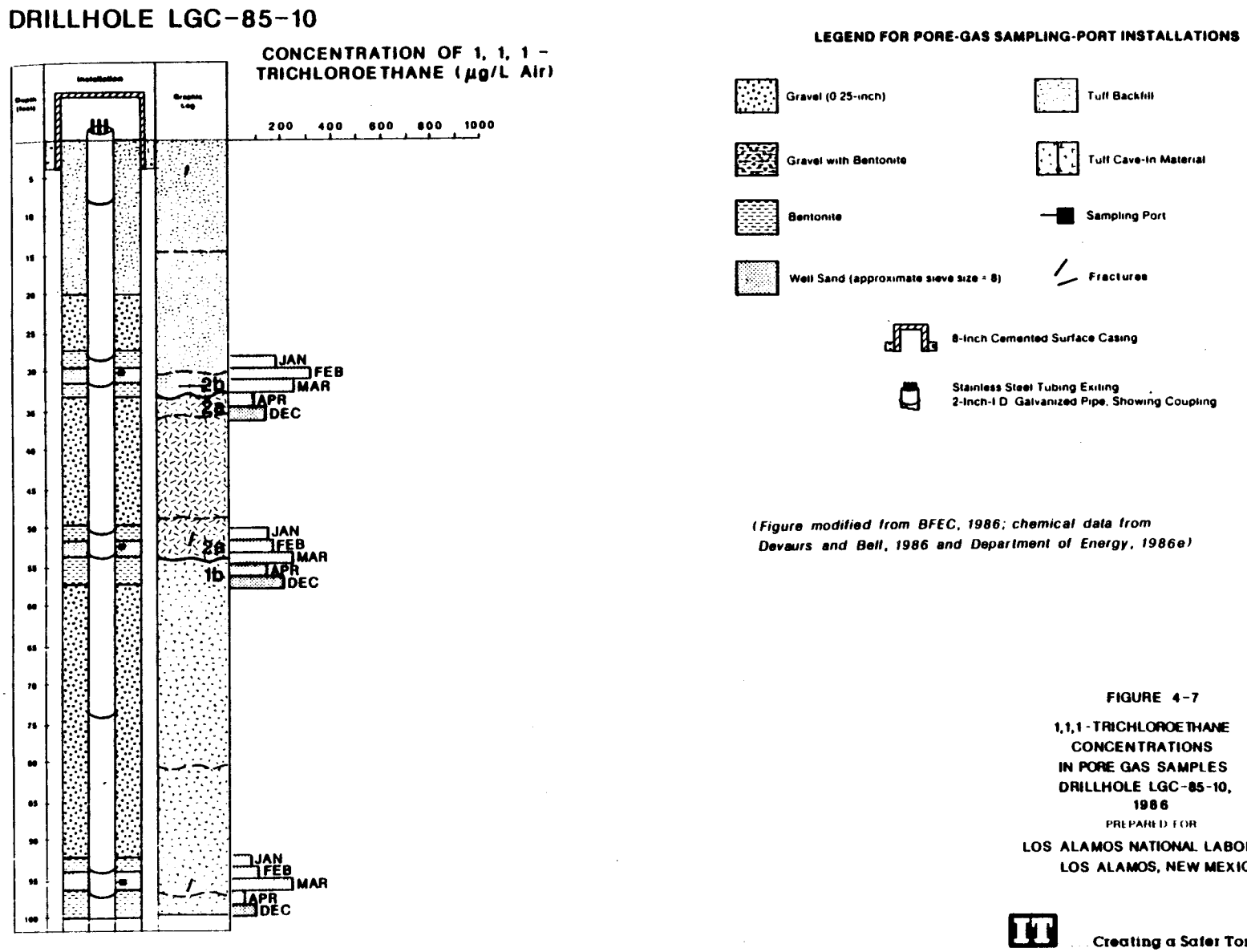

(Figure modified from BFEC, 1986; chemical data from Devaurs and Bell, 1986 and Department of Energy, 1986e)

FIGURE 4-7

1,1,1-TRICHLOROETHANE CONCENTRATIONS IN PORE GAS SAMPLES DRILLHOLE LGC-85-10, 1986

PREPARED FOR

LOS ALAMOS NATIONAL LABORATORY
LOS ALAMOS, NEW MEXICO

IT Creating a Safer Tomorrow

© 1984 IT CORPORATION
ALL COPYRIGHTS RESERVED
Do Not Scale This Drawing

DRAWN BY LLF 2/28/87 CHECKED BY APPROVED BY DRAWING NUMBER 301017 02 B12

5.0 GROUND WATER HYDROLOGY IN AREAS G AND L

5.1 MAIN AQUIFER

5.1.1 Hydraulic Characteristics of the Main Aquifer

The main aquifer in the Los Alamos area is the only aquifer capable of producing a municipal and industrial water supply (Purtymun, 1984). Characterization of the hydraulic and chemical properties of the main aquifer, therefore, can be based on information obtained from supply wells, stock wells, test wells, and springs (Figure 5-1). The upper surface of the main aquifer slopes eastward from the major recharge area in the Valles Caldera to the Rio Grande where it discharges as springs and seeps into the river (Purtymun, 1984).

The major recharge area for the aquifer is an intermountain basin formed by the Valles Caldera (Figure 2-1). The basin is filled with lacustrine deposits underlain by volcanic debris resulting from the collapse of the Caldera (Conover, et al., 1963). The saturated basin fill is highly permeable and provides a source of recharge to sediments of the Tesuque Formation (Purtymun, 1984). Beneath Mesita del Buey, the main aquifer is contained in the poorly-consolidated conglomerates of the Puye Formation and the conglomerates, sandstones, and siltstones of the Tesuque Formation (see Section 2.2). The main aquifer was encountered at 874 feet below land surface when PM-2 was drilled in 1965 (Figure 5-1) (Cooper, et al., 1965). While the drillers reported a show of water at 335 feet in the lithologic log, subsequent geophysical logging did not confirm the presence of any water in this zone. It is probable, as is common with water-filled holes drilled with a cable tool rig, that circulation fluid lost from an upper fractured zone was re-encountered at this deeper zone. A summary of the lithologic log for PM-2 is provided in Table 5-1. In the Pajarito Well Field, the aquifer has an average saturated thickness of 1,470 feet and hydraulic gradient of 0.015 foot per foot (Figure 5-2). Based on the main aquifer elevation in well PM-2 and the hydraulic gradient, the depth to the main aquifer beneath Areas G and L is 850 feet and 950 feet, respectively. The transit time from recharge of the aquifer to discharge along the Rio Grande is estimated between 50 and 1,400 years based on tritium and carbon-14 analyses, respectively (Purtymun, 1984). The rate of movement of the main aquifer beneath Mesita del Buey can be estimated using the Darcian flow equation:

$$v = \frac{KI}{n} \qquad (5\text{-}1)$$

where

v = velocity (meters per second)
K = hydraulic conductivity (meters per second)
I = hydraulic gradient (meters per meter)
n = porosity

The hydraulic conductivity of the main aquifer as calculated for this study from pump testing of PM-2 is 4.2 feet per day. Transmissivity was calculated by Purtymun (1984) to be 40,000 gallons per day per foot. Using these values, together with an assumed sand to silt porosity of 30 percent (Freeze and Cherry, 1979), the velocity of ground water within the main aquifer beneath Mesita del Buey is 0.18 feet per day (5.7×10^{-2} meters per day). This rate correlates with the 95 feet per year (0.26 feet per day) movement calculated by Purtymun (1984) and shown in Figure 5-3.

5.1.2 Chemical Quality of the Main Aquifer Near Mesita del Buey

The chemical quality of the main aquifer has been characterized by sampling wells and in White Rock Canyon springs near the Rio Grande. In general, the water quality depends on the well depth, lithology of the aquifers, and yields from individual beds within the aquifer (Purtymun, 1984). In 1981, water samples from the Pajarito Well Field (Figure 5-1) were collected from well heads after periods of pumping. A summary of the Pajarito Well Field construction and water-quality results is provided in Table 5-2. Water from wells PM-2 and PM-4, the two wells nearest Mesita del Buey, are sodium bicarbonate water (Figure 5-4), while PM-1 and PM-3 are dominantly calcium bicarbonate (Figure 5-5). Although there are numerous deep canyons cut into the Bandelier Tuff of the Pajarito Plateau, there are no documented springs or seeps along the canyon wells (Griggs, 1964). Springs are located along White Rock Canyon near the Rio Grande and were sampled in 1981. Springs 4 and 5A in White Rock Canyon are both calcium bicarbonate (Figure 5-4). A summary of the hydrologic data for springs in White Rock Canyon is provided in Table 5-3.

5.2 HYDROGEOLOGY OF PERCHED WATERS ADJACENT TO MESITA DEL BUEY

Mesita del Buey is bounded on the north by Cañada del Buey and on the south by Pajarito Canyon (Figure 1-4). In response to Task 6 (paragraph 25) of the Compliance Order, the Laboratory investigated the alluvium in Cañada del Buey and Pajarito Canyon to determine:

1. If perched water is present in the alluvium and underlying tuff
2. The horizontal and vertical extent of the perched water
3. The chemical quality of the perched water
4. The hydrologic similarities among Cañada del Buey, Pajarito Canyon and Mortandad Canyon, and the applicability of previous research in Mortandad Canyon to items 1, 2, and 3 above.

In order to investigate the alluvial systems, test holes were drilled and monitoring wells were installed in both canyons. Test holes were drilled April 16-18, 1985 (PCO and CDBO series) and October 22, 1985 (PCM series) using a truck-mounted, continuous flight hollow-stem auger. The test holes penetrated the alluvium and were drilled to various depths into the underlying Bandelier Tuff. Monitoring wells were installed in selected test holes by casing the holes with four-inch diameter, schedule 40, PVC casing. The PVC casing was perforated with 0.25-inch holes and wrapped with approximately 0.050 slotted stainless steel mesh (Devaurs, 1985). The annular space between the test hole wall and the casing was gravel-packed to within two feet of the ground surface and completed with a concrete collar. Each monitoring well casing is protected with a nine-inch diameter steel casing with a locking cap. The wells were developed by jetting and pumping with a centrifugal pump (Devaurs, 1985). A construction schematic of the monitoring wells is given in Figure 5-6. Monitoring wells and test holes elevations were surveyed with horizontal and vertical control.

5.2.1 Relevant Hydrologic Studies in Mortandad Canyon

The following discussion of extensive hydrologic studies of Mortandad Canyon are largely derived from Purtymun (1975) and Devaurs and Purtymun (1985). The discussion focuses on hydrologic and geologic similarities among Cañada del Buey, Pajarito Canyon, and Mortandad Canyon.

Mortandad Canyon is a southeast-trending canyon approximately ten miles in length cut into the Pajarito Plateau, north of Cañada del Buey (Figure 5-1). The canyon drains an area of 2.86 square miles to the eastern Laboratory boundary and is a tributary to the Rio Grande in White Rock Canyon. Alluvium on the canyon floor ranges from less that 3 feet in the headwaters to over 120 feet to the east, and consists mainly of silt, sand, and gravel derived from erosion and weathering of tuff in the canyon. Thus, the geologic setting of Mortandad Canyon is comparable to those of Pajarito Canyon and Cañada del Buey. Portions of Mortandad Canyon are perennial due to the National Pollutant Discharge Elimination System (NPDES) permitted discharge of effluent from the TA-50 industrial waste water treatment plant. The plant began discharging treated liquid water in 1963. Prior to initiation of these discharges, no perennial flow existed in the canyon; however, alluvium in the canyon contained a small perched water body (Baltz, et al., 1963). Recharge of the alluvial system in the canyon currently occurs from infiltration of storm and snow melt runoff and from infiltration of the TA-50 discharge.

Several hydrologic studies of Mortandad Canyon have been conducted over the last 25 years to define the horizontal and vertical extent of saturation within the alluvium and surrounding consolidated deposits; c.f., Abrahams et al. (1962), Baltz et al. (1963), Purtymun (1974), Purtymun (1975), Purtymun et al. (1983), and Environmental Surveillance Group (1984). These studies have entailed installation of shallow observation wells, neutron-moisture access wells, and deep test wells. The above studies conclude that perched water in Mortandad Canyon is confined to alluvium within the channel and saturation does not extend horizontally or vertically into the tuff.

The similarities in the geologic setting among the three canyons suggests that the canyons may also be hydrologically similar. Mortandad Canyon, which receives perennial flow from the TA-50 industrial waste water treatment plant, does not contribute to recharge of the main aquifer within the study area; thus, it is likely that no recharge of the main aquifer occurs from the ephemeral flows in Cañada del Buey or Pajarito Canyon.

5.2.2 Cañada del Buey

Cañada del Buey bounds Mesita del Buey to the north and has a drainage area of 3.4 square miles within the Laboratory's boundary (Purtymun, 1975). Stream flow in the canyon is ephemeral and flows only in response to storm runoff or snow-melt. Four test holes (CDBO-1 through CDBO-4) were drilled into the Cañada del Buey alluvium near Mesita del Buey, two in the upper reach, one in the middle reach, and one in the lower reach (Figure 1-4). Based on the test hole borings, the alluvium in Cañada del Buey is derived from weathered Bandelier tuff (Devaurs and Purtymun, 1985) and is comprised of sands, silts, and clay with a few gravels. The alluvium is thin in the canyon, ranging from 9 to 12 feet in thickness (Table 5-4; see Appendix C for lithologic logs). The alluvium is confined to the canyon and does not extend beneath the Mesita del Buey. The stream channel in Cañada del Buey is not well-defined, braiding out in places along the canyon floor (Devaurs and Purtymun, 1985). During drilling operations, the alluvium was noted to appear relatively dry, containing an estimated ten percent moisture.

All four test holes were completed as monitoring wells in Cañada del Buey. Screens were set opposite the alluvium in the wells and a summary of the CDBO-Series well construction is given in Table 5-5. The wells are monitored quarterly and during the period June 1985 through September 1986, no water was detected in any of the four wells (Table 5-6). Consequently, no water samples have been collected for chemical analyses.

The current investigation of Cañada del Buey indicates that the alluvium contains no perched water. The absence of perched water is likely related to the small drainage area which produces little surface water to form and recharge a body of water in the alluvium (Devaurs and Purtymun, 1985) combined with a high evapotranspiration rate for the area (New Mexico Environmental Improvement Division, 1985).

5.2.3 Pajarito Canyon

Pajarito Canyon, which bounds Mesita del Buey to the south, heads on the flanks of Sierra de los Valles and drains an area of 10.6 square miles (Purtymun, 1975). While the canyon contains a perennial stream on the mountain flanks and western half of the Pajarito Plateau, stream flow on the

eastern half of the plateau near Mesita del Buey is ephemeral and flows only in response to storm runoff and snow-melt (Devaurs and Purtymun, 1985).

5.2.3.1 Nature and Extent of Perched Water in Pajarito Canyon

Seven test holes were drilled in Pajarito Canyon in 1985 to determine the presence and extent of perched water in the alluvium (Figure 1-4). Three of the seven test holes encountered perched water and were completed as monitoring wells designated PCO-1, PCO-2, and PCO-3. Well construction for the three monitoring wells is summarized in Table 5-5. The remaining four test holes (PCM-1 through PCM-4) were dry when drilled through the alluvium and were completed into the tuff. The PCM test holes were blank-cased with four-inch schedule 40 PVC (Devaurs and Purtymun, 1985). Drilling cuttings from the PCM-Series test holes were analyzed for moisture using a direct oven-drying method. The procedure involved weighing the cuttings before and after drying at 105°C and then calculating the original water content per unit mass of oven-dry soil. The average moisture content in the cuttings was 11 percent, ranging from 6 to 16 percent. A summary of the moisture contents is presented in Table 5-7. Based on the lithologic logs of three PCO-series monitoring wells, the alluvium in Pajarito Canyon is derived from Bandelier Tuff and Tschicoma Formation (Devaurs and Purtymun, 1985) and is comprised of boulders, cobbles, and gravels in a silty sand matrix (see Appendix C for lithologic logs). The alluvium ranges from 9 to 12 feet in thickness in the existing canyon channel (PCO-Series, Table 5-8) and thins towards the canyon flanks (PCM-Series, Table 5-9). Lithologic logs and installation diagrams for all seven test holes are provided in Appendix C.

In addition to the seven test holes drilled in 1985, the laboratory drilled two test holes in the canyon during March of 1950 as part of a water-supply study (Griggs, 1964; Purtymun, 1975). These holes, identified as T-5 and T-6 (Figure 1-4), were drilled to depths of 263 feet and 300 feet, respectively, and completely penetrated the Bandelier Tuff beneath the floor of Pajarito Canyon (Table 5-10; see Appendix C for lithologic logs). Although the test holes were blank-cased through the alluvium, no water was encountered in the underlying tuff and volcanic sediments (Griggs, 1964; Purtymun, 1975). The holes were also dry when measured in the spring of 1985 (Devaurs and Purtymun, 1985).

Nineteen test holes were drilled into the Bandelier Tuff on top of Mesita del Buey in Areas G (6 test holes), L (12 test holes), and one background hole northwest of Area L. One test hole in Area L (LLC-85-A) was abandoned following coring. In Area G, the test holes ranged in depth from 50 to 125 feet. Test holes LGC-85-09 and LGM-85-11 were drilled 40 feet and 9 feet, respectively, beneath the base of the alluvium in Pajarito Canyon. Neither of the test holes encountered perched water in the Bandelier Tuff. In Area L the test holes ranged in depth from 60 feet to 200 feet. Test holes LLC-85-17, LLM-85-01 and LLM-85-02 were drilled to depths extending approximately 2, 43, and 48 feet (respectively) beneath the base of alluvium in Pajarito Canyon. None of these three test holes encountered perched water in the Bandelier Tuff. A summary of the lithologic logs and installation diagrams for each test hole, with the exception of the abandoned test hole LLC-85-A, is provided in Appendix C.

Topographic profiles and geologic cross-sections through Mesita del Buey and the adjacent alluvium-filled canyons (Figures 5-7 and 5-8) illustrate that the perched water, found only in Pajarito Canyon, does not extend horizontally beneath the mesa into the adjacent tuff. Locations of sections A-A' through D-D' are shown on Figure 5-9. Figure 5-10 is a longitudinal channel cross-section through Pajarito Canyon which shows the hydrogeologic relationship between the deeper test holes (e.g., T-5) and perched water in the alluvium. These test holes illustrate that the perched water in the alluvium does not extend vertically into the basalts and sedimentary deposits which lie beneath the tuff.

5.2.3.2 Hydraulic Properties of the Perched Water in Pajarito Canyon

Water-levels in the PCO-Series monitoring wells have been measured quarterly since June 1985. Water-levels are measured to the nearest 0.01 foot using a weighted graduated steel tape. The depth to water is measured from the top of the well casing. A summary of the water-level measurements from June 1985 through September 1986 is given in Table 5-11 and water-level elevations for that same period are shown in Figure 5-11. Maximum fluctuations in water-levels, or maximum fluctuations in the saturated thickness of the perched water are 1.1 feet in PCO-1, 3.34 feet in PCO-2, and 0.59 feet in PCO-3. The

saturated thickness in wells PCO-1 and PCO-3 average 10.01 and 8.93, respectively. In contrast, the saturated thickness in PCO-2 is approximately one-half the thickness of the other two wells, averaging 3.91 feet. The greater range of water-level elevations in PCO-2 may reflect the thinner saturated thickness and bedrock channel configuration.

Seasonal fluctuations in water-levels were documented during the period June 1985 through September 1986, with the highest water-levels generally measured during the summer months (June through August) and the lowest water-levels measured during the winter months (December through March). While there are no direct discharge measurements in Pajarito Canyon during this time period, precipitation data from the Area G station are available for 1985-1986 (Figure 5-12). There appears to be a correlation in wells PCO-1 and PCO-2 between large precipitation events (October 10, 1985 and June 26, 1986) and increases in water-level elevations in all three wells. These correlations are preliminary, however, in the absence of actual precipitation-runoff relationship data for Pajarito Canyon. Summer thunderstorms in New Mexico are typically convective in nature (Environmental Surveillance Group, 1986), and therefore, precipitation duration, precipitation intensity, and antecedent moisture can vary significantly throughout the Pajarito Canyon drainage area.

The rate of movement of perched water in the Pajarito Canyon alluvium can be estimated using the Darcian flow equation (see Section 5.1). The average gradient measured in the monitoring wells is 0.015. Hydraulic conductivities in the alluvium ranges from 1.65×10^{-3} meters per second for a sand aquifer to 5.8×10^{-4} meters per second for a silty sand aquifer (Purtymun, 1981). Using these values, together with an assumed sand to silt porosity of 30 percent (Freeze and Cherry, 1979), the velocity of the perched water ranges from 8 to 23 feet per day (2 to 7 meters per day).

5.2.3.3 Quarterly Water Sampling Procedures in Pajarito Canyon

Prior to sampling, each monitoring well is purged to remove stagnant water from the well borehole. The borehole water is removed by bailing with a two-inch diameter brass bailer until a minimum of three borehole volumes are removed (or the well is bailed dry). Water samples are collected for inorganic and volatile organic analyses conducted by the Health and Environmental Chemistry Group (HSE-9).

Inorganic analyses performed each quarter include general chemistry, selected metals, and radiological parameters. Table 5-12 presents a summary of the inorganic parameters routinely quantified. One-gallon polyethylene bottles are used to collect water samples for inorganic analysis. The first one gallon unfiltered water sample is acidified with nitric acid in the field (for radiological parameters) and returned with the second unfiltered, non-acidified water sample within four hours to the laboratory's analytical facilities. Two aliquots are withdrawn from the unfiltered, non-acidified gallon sample. One aliquot is filtered and acidified with nitric acid for metals analyses and the second unfiltered, non-acidified aliquot is analyzed for general chemistry. All inorganic analyses are performed using approved EPA methods (U.S. EPA, 1976; U.S. EPA, 1979) and 40 CFR 141 regulations for radiological analyses. Water samples are also collected from each monitoring well in 40 milliliter vials with teflon-coated septa. These samples are analyzed for volatile organic compounds using purge and trap gas chromatography (GC) with gas chromatography/mass spectrometry (GC/MS) confirmation. Table 5-13 summarizes the volatile organic compounds routinely quantified. Volatile organic analyses are performed according to approved EPA methods (U.S. EPA, 1985a).

All samples are labeled in the field and sealed with a parafilm seal to ensure sample integrity. A chain of custody tag is attached to each sample container. The samples are placed in an ice chest and transferred to the laboratory's analytical facilities. Information pertinent to sampling is recorded in a field logbook and chain of custody is maintained on all samples. After sample custody is transferred to appropriate laboratory analytical personnel, the samples are placed in locked refrigerators in a secured building. A sample analysis request sheet accompanies each sample to track sample analyses.

5.2.3.4 Chemical Quality of Perched Water in the Alluvium of Pajarito Canyon

The concentration of dissolved solids in the perched water in the alluvium of Pajarito Canyon increases downgradient as shown by the analytical results of water samples collected from monitoring wells PCO-1, PCO-2, and PCO-3 (see Figure 1-4 for well locations). The water is characteristically sodium

bicarbonate upgradient in well PCO-1 (Figure 5-13). In well PCO-2, located approximately mid-reach, the water is a sodium-calcium bicarbonate (Figure 5-14). Downgradient, in well PCO-3 the water is characteristically calcium bicarbonate (Figure 5-15). Dissolved metals and radiological parameters (i.e., calcium, copper, zinc, manganese, total uranium and tritium, etc.) generally increase in concentration downgradient. Although the perched water in the alluvium of Pajarito Canyon is not a drinking water source, U.S. EPA and New Mexico Environmental Improvement Board (NMEIB) numeric drinking water standards have been included in Tables 5-14 through 5-16 for relative comparison of perched water quality. All chemical and radiological constituents were detected at concentrations below the primary and secondary maximum contaminant levels specified for drinking water (U.S. EPA, 1976; U.S. EPA, 1979; New Mexico Environmental Improvement Board, 1985b) with the exception of manganese (several quarterly measurements in PCO-1, PCO-2, and PCO-3), total uranium (one quarterly measurement each in PCO-2 and PCO-3) and total dissolved solids (one quarterly measurement in PCO-3). Tables 5-14 through 5-16 summarize the results of inorganic analyses conducted on well samples collected during the period June 1985 through September 1986.

In addition to changes in perched water quality downgradient, seasonal fluctuations in water quality related to saturated thickness were also observed in data collected from well PCO-3. Between December 1985 and March 1986, the concentrations of dissolved constituents (metals, anions, and radiological parameters) increased to two to three times the previous quarter's concentrations (see Table 5-16). This same time period corresponds to the minimum saturated thickness ("low-flow") of perched water measured in the alluvium. Concentrations of these same dissolved constituents are diluted during the "high-flow" spring and summer months which is in response to snow melt and precipitation runoff.

Results of volatile organic analyses of the perched water collected from each of the monitoring wells is summarized in Tables 5-17 through 5-19. None of the volatile organic compounds routinely analyzed (see Table 5-13) have ever been detected in any of the wells, including samples collected during periods of "low-flow" in the alluvium (December and March samples).

5.2.3.5 Summary of Perched Water Investigation in Pajarito Canyon

The investigation of the perched water system contained in Pajarito Canyon alluvium indicates that:

1. The canyon contains a body of perched water in the alluvium which was perennial during the period June 1985 through September 1986.

2. The perched water in the alluvium does not extend horizontally or vertically into the adjacent tuff that forms Mesita del Buey.

3. The concentration of dissolved solids in the perched water in the alluvium increases downgradient.

4. Chemical quality of the perched water in the alluvium is dependent on water volume which, in turn, is dependent on seasonal precipitation-runoff characteristics in the canyon.

5. The concentration of dissolved solids in the perched water in the alluvium decreased during periods of high-flow as a result of dilution.

5.3 SUMMARY OF GROUND WATER HYDROLOGY IN AREAS G AND L

Studies of the main aquifer (Purtymun, 1984) and perched water (Purtymun, 1975; Devaurs and Purtymun, 1985) at the Areas G and L supports the following findings:

- The depth to the main aquifer beneath Areas G and L is approximately 850 feet and 950 feet, respectively

- There are no perched bodies of water beneath Areas G and L which are hydraulically connected to the main aquifer

- There are no springs or seeps on the canyon walls in Pajarito Canyon or Cañada del Buey

- The perched body of water contained in the alluvium of Pajarito Canyon adjacent to Areas G and L does not extend horizontally or vertically into the adjacent tuff (similar to hydrologic findings in Mortandad Canyon) and is not hydraulically connected to the main aquifer

- Based on the available data, chemical quality of perched water in the alluvium has not been affected by the hazardous waste disposal areas on Mesita del Buey.

TABLE 5-1

LITHOLOGIC LOG OF WATER-SUPPLY WELL PAJARITO MESA #2 (PM-2)[1][2]

GEOLOGIC UNIT	LITHOLOGIC DESCRIPTION	DEPTH (FT) TO	FROM
Alluvium	Boulders and clay; boulders of latite as large as 12 inches and grayish-brown clay, some sand and gravel	0	7
	Sand and gravel; sand is light-gray, fine-to-coarse and composed of crystals and fragments of sanidine and quartz; gravel is fine-to-coarse and composed of latite and tuff	7	30
Bandelier Tuff (Otowi Member)	Tuff; buff, silty, consists mostly of sanidine and quartz crystals, many fragments of rhyolite and latite, trace of pumice near 105 feet	30	125
	Tuff; mostly crystals of sanidine and quartz with rhyolite and latite fragments; much white and tan pumice	125	165
	Tuff; light-gray, consists of crystals and fragments of sanidine, quartz, and glass, and many brown and gray rhyolite fragments to 1/8 inch	165	225
	Pumice; buff	225	235
	Tuff; crystals and fragments of sanidine, quartz, glass in sand-sized grains, and gravel of rhyolite, latite, and basalt, much white pumice	235	300
	Pumice; light-gray to tan	300	315
	Tuff; crystals and fragments of sanidine, quartz, glass and dark volcanic rocks with much white pumice (show of water at 335 feet)[3]	315	345

[1] From Cooper et al., 1965.
[2] PM-2 drilled in 1965.
[3] Show of water not confirmed by subsequent geophysical logging.

TABLE 5-1
LITHOLOGIC LOG OF WATER-SUPPLY WELL PAJARITO MESA #2 (PM-2)
(Continued)

GEOLOGIC UNIT	LITHOLOGIC DESCRIPTION	DEPTH (FT) TO	FROM
Bandelier Tuff (Otowi Member) (continued)	Tuff; gray, composed of sand-sized grains sanidine, quartz, and glass crystals and many gravels of rhyolite and latite, trace pumice	345	390
	Tuff; crystals and fragments of sand-sized sanidine, quartz, and glass	390	405
Bandelier Tuff (Guaje Member)	Pumice; light-tan to light-gray, lumps as large as 1/4 inch	405	432
Chino Mesa Basalt (Unit 3)	Basalt; black, dense, with some iron-staining, trace tan clayey silt, minor olivene, pyrite, and white crystalline material	432	505
	Basalt; dark reddish-brown and dark-gray, dense	505	515
	Basalt; dark-gray, dense with buff, clay and silt (caliper log indicates a zone of lost circulation 522-534 feet)	515	530
	Basalt; dark-gray to black, vuggy, trace olivene	530	550
	Basalt; scoria, dark-gray to reddish-brown, vuggy, trace buff clay (caliper log indicates a zone of lost circulation 546-564 feet)	550	570
	Basalt; gray to greenish-gray, granular to fine-grained glassy structure, much olivene and feldspar crystals	570	590
	Basalt; black, brown, and red, vuggy, contains scoria	590	605
	Basalt; dark grayish-red, dense, trace olivene and feldspar crystals	605	617
	Basalt (No samples. Electric logs and driller's logs indicate this interval to be basalt. Hole was drilled without circulation.)	617	700

TABLE 5-1
LITHOLOGIC LOG OF WATER-SUPPLY WELL PAJARITO MESA #2 (PM-2)
(Continued)

GEOLOGIC UNIT	LITHOLOGIC DESCRIPTION	DEPTH (FT) TO	FROM
Puye Conglomerate (Fanglomerate Member)	Conglomerate (No samples. Electric logs and driller's logs indicate this interval to be conglomerate. Hole was drilled without circulation.)	700	730
	Conglomerate; sand is fine-to-coarse, quartz, frosted and rounded; gravel is mostly latite, much basalt	730	734
	Basalt; dark-gray, dense	734	738
	Conglomerate; as 730 to 734 feet	738	758
	Basalt; as 734 to 738 feet	758	770
	Conglomerate; greenish-gray, sand is fine-to-coarse, subrounded-to-rounded frosted quartz and subrounded-to-subangular basalt and latite; gravel sizes are subangular-to-subrounded basalt and latite; contains crystals and fragments of sanidine, quartz, and glass	770	1,000
	Conglomerate; as 770 to 1,000 feet, but contains much larger percentage of gravel size particles and some chert and tan silty clay	1,000	1,168
	Conglomerate; as 1,000 to 1,168 feet, but contains white and tan fibrous pumice	1,168	1,186
	Conglomerate; gray-to-tan, mostly sand composed of subrounded basalt and latite and frosted quartz, occasional gravel size; contains tan pumice, and white to light-gray silt	1,186	1,250
	Conglomerate; mostly gravel size, subangular-to-subrounded basalt and latite, much pumice from 1,250 to 1,280	1,250	1,340
Puye Conglomerate (Totavi Lentil)	Gravel and sand; composed of subrounded gravels of quartzite, chalcedony, and quartz, and large chips from cobbles	1,340	1,410

TABLE 5-1
LITHOLOGIC LOG OF WATER-SUPPLY WELL PAJARITO MESA #2 (PM-2)
(Continued)

GEOLOGIC UNIT	LITHOLOGIC DESCRIPTION	DEPTH (FT) TO	FROM
Tesuque Formation	Sand; light pinkish-gray to dark-gray, fine-to-coarse, subrounded-to-rounded, quartz, some fine-to-coarse gravels of quartz and quartzite	1,410	1,548
	Conglomerate; sand is grayish-pink, subangular-to-subrounded quartz; gravel is subrounded quartz and quartzite and a few gravels of vuggy basalt	1,548	1,840
	Basalt; black to dark-gray, coarse crystalline with gray to green waxey clay filling some vugs and some vug lining of white crystals	1,840	1,892
	Sand and gravel; mostly sand-sized grains of fine-medium subrounded quartz, some subrounded gravels of basalt and latite, many chips of basalt. Interval may contain thin basalt flows	1,892	2,108
	Conglomerate; sand, well-sorted, fine-to-coarse, and subrounded gravels of latite and quartzite	2,108	2,218
	Basalt; brown, red, and black, weathered appearance, contains clay and white crystals in vugs	2,218	2,312
	Sand; grayish-pink, very fine-to-medium, subangular-to-subrounded, quartz, contains tan and cream clay and a few rounded basalt gravels	2,312	2,370
	Sand; as 2,312 to 2,370 feet, but coarser grained with white clay	2,370	2,410
	Sand; grayish-pink, coarse-to-very coarse, rounded-to-subrounded, quartz, some white and tan clay	2,410	2,460
	Clayey sand; fine-to-coarse sand with much white and tan clay	2,460	2,490

TABLE 5-1
LITHOLOGIC LOG OF WATER-SUPPLY WELL PAJARITO MESA #2 (PM-2)
(Continued)

GEOLOGIC UNIT	LITHOLOGIC DESCRIPTION	DEPTH (FT) TO	FROM
Tesuque Formation (continued)	Clay; tan to white, sandy	2,490	2,510
	Clayey sand; as 2,460 to 2,490, contains much basalt (possible basalt layer at 2,506 to 2,508 according to electric logs)	2,510	2,530
	Sand; pinkish-gray to tan, fine-to-coarse, Subangular-to-subrounded quartz and white to tan clay	2,530	2,600

Note 1: Sample obtained from bottom of drill bit after removal from hole at 2,600.feet is tan sandy clay and subangular fragments up to 1 inch of dark-gray, hard, structureless, very fine silty, non-calcareous shale. Exterior of shale fragments have lining of calcareous material on weathered surface.

Note 2: Samples of the drill cuttings were collected by the contractor at 5-foot intervals from 0 to 617 feet and at 10-foot intervals from 617 to 2,600 feet. These samples were then washed by the Geological Survey and studied under the binocular microscope. The samples were described dry. Thickness and depth intervals of drill cutting samples have been correlated with data interpreted from electric logs and driller's logs.

TABLE 5-2
CONSTRUCTION AND HYDROLOGIC DATA FOR WELLS IN THE PAJARITO WELL FIELD, LOS ALAMOS[1]

	Pajarito Field				
	PM-1	PM-2	PM-3	PM-4	PM-5
Date of Completion	1965	1965	1966	1981	1982
Elevation of LSD (ft)	6520	6715	6640	6920	7095
Construction					
Depth drilled (ft)	2501	2600	2552	2920	3120
Depth completed (ft)	2499	2300	2552	2875	3093
Diameter (in.)[b]	12	14	14	16	16
Water Levels					
Date	1982	1982	1982	1982	1982
Depth below LSD (ft)	748	874	762	1047	1208
Elevation (ft)	5772	5841	5878	5873	5887
Water-Level Fluctuations					
Period (yr)	1965-1982	1966-1982	1968-1982	1981-1982	---
Change (ft)	-2	-48	-19	5	---
Annual rate (ft/yr)	-0.1	-2.8	-1.3	---	---
Aquifer					
Formation	QTp-Tsf	QTp-Tsf	QTp-Tsf	QTp-Tsf	QTp-Tsf
Saturated thickness (ft)	1751	1426	1790	1828	1885
Yield					
Date	1982	1982	1982	1982	1982
Rate (gpm)	589	1386	1402	1473	1225
Drawdown (ft)	22	60	23	40	144
Specific capacity (gpm/ft)	26.8	23.1	60.9	36.8	8.5
Transmissivity (gpd/ft)	55 000	40 000	320 000	44 000	10 000
Field coefficient of permeability (gpd/ft^2)	31	28	179	24	5.3
Production					
Period (yr)	1965-1982	1966-1982	1968-1982	1982	---
Pumpage (10^6 gal.)	1593	5863	3478	76	---
Quality of Water					
Date	3-18-81	3-18-81	3-18-81	8-3-81	8-4-81
Chemical (mg/ℓ)					
SiO_2	77	81	88	87	86
Ca	28	8	24	9	14
Mg	6.9	3.1	8.4	3	4
Na	18	10	18	11	24
CO_3	0	0	0	0	0
HCO_3	144	65	148	70	106
SO_4	5	3	7	4	10
Cl	4	9	10	2	4
F	0.3	0.3	0.4	0.3	0.3
NO_3	2.0	<0.1	1.8	2	8
TDS	212	140	216	165	211
Hard	90	36	90	36	52
Specific conductance (μmho)	260	130	250	120	190
pH	8.0	7.8	8.3	8.2	8.2
Radiochemical					
Total uranium (μg/ℓ)	2.4 ± 0.8	0.0 ± 0.8	1.0 ± 0.8	0.8 ± 0.8	2.2 ± 0.4
Temperature (°F)	71	69	71	69	73

[a]Well was abandoned in 1956; data were not used in the average hydrologic characteristics. It is located 150 ft SW of well LA-1B.

[b]Wells have two different diameter sizes of casing; i.e., 12 (650 ft) 10 reads: 12-in. diameter to 650 ft. then 10-in. diameter to completed depth of well.

Note: QTp = Puye Conglomerate; Tsf = Tesuque Formation.

[1]From Purtymun, 1984.

TABLE 5-3
HYDROLOGIC DATA FOR SPRINGS IN THE WHITE ROCK CANYON AREA[1]

	Spring 3	Spring 3B	Spring 4	Spring 5A	Spring 5B	Spring 6	Spring 8A	Spring 10
Elevation of LSD (ft)	5560	5500	5500	5430	5400	5380	5370	5360
Aquifer	QTp	Tsf	QTp	Tsf	Tsf	Tsf	Tsf	Tsf
Discharge at Rio Grande (gpm)	20	30	80	30	10	60	30	20
Quality of Water								
Date	10 13 81	10 13 81	10-13 81	10-13-81	10-14-81	10-14-81	10-14-81	10-15 81
Chemical (mg/ℓ)								
SiO_2	52	46	60	60	64	74	75	69
Ca	20	24	28	24	17	12	11	12
Mg	1.6	2.0	5.7	2.7	4.4	3.6	2.8	3.2
Na	16	139	15	22	12	11	13	13
CO_3	0	0	0	0	0	0	0	0
HCO_3	99	392	132	124	87	74	56	80
SO_4	4	4	6	7	2	2	3	3
Cl	5	6	8	6	4	4	5	4
F	0.4	0.6	0.5	0.3	0.5	0.3	0.4	0.4
NO_3	2.6	8.4	<0.4	1.7	2.0	<0.4	<0.4	1.7
TDS	125	374	168	186	152	134	152	146
Hardness	56	64	92	69	56	44	39	42
Specific conductance (μmho)	210	610	220	240	150	140	130	120
pH	8.1	7.5	7.0	7.4	7.4	7.0	9.0	7.8
Radiochemical								
Total uranium (μg/ℓ)	2.3 ± 0.8	19 ± 4.0	1.5 ± 0.8	2.2 ± 0.8	1.9 ± 0.8	1.0 ± 0.8	1.7 ± 0.8	1.7 ± 0.8
Temperature (°F)	72	68	66	70	61	73	72	66

Note: Tsf = Tesuque Formation and QTp = Puye Conglomerate.

[1] From Purtymun, 1984.

TABLE 5-4

LITHOLOGIC LOGS OF MONITORING WELLS IN CAÑADA DEL BUEY[1]

WELL	LITHOLOGIC DESCRIPTION	DEPTH (FT) TO	FROM
CDBO-1	Alluvium; light brown, silty sand with some clay	0	9
	Tuff; brown, weathered with quartz and sanidine crystals and crystal fragments, some rock fragments (weathered tuff contains an estimated 20-30 percent silt and clay)	9	15
CDBO-2	Alluvium; light brown, silty sand with some clay	0	12
	Tuff; brown, weathered with quartz and sanidine crystals and crystal fragments, some rock fragments (weathered tuff contains an estimated 20-30 percent silt and clay)	12	18
CDBO-3	Alluvium; light brown, silty sand with some clay	0	8
	Tuff; light gray, quartz and sanidine crystals and crystal fragments, some small rock fragments, slight amount of clay as a result of weathering	8	12
CDBO-4	Alluvium; light brown, silty sand with some clay	0	9
	Tuff; light gray, quartz and sanidine crystals and crystal fragments, some small rock fragments, slight amount of clay as a result of weathering	9	12

[1] From Devaurs, 1985

TABLE 5-5

SUMMARY OF MONITORING WELL CONSTRUCTION AND TEST HOLE COMPLETION IN PAJARITO CANYON AND CAÑADA DEL BUEY[1]

WELL	LAND SURFACE ELEVATION (FT)	HEIGHT OF STEEL CASING[2] (FT)	TOTAL DEPTH[2] (FT)	CASED INTERVAL[2] (FT)	PERFORATED INTERVAL[2] (FT)	DATE INSTALLED
PAJARITO CANYON						
PCO-1	6687.0	1.2	12.3	0-4.3[3]	4.3-12.3[3]	4/16/85
PCO-2	6618.3	1.0	9.5	0-1.5[3]	1.5- 9.5[3]	4/17/85
PCO-3	6546.3	1.2	17.7	0-5.7[3]	5.7-17.7[3]	4/17/85
PCM-1	6697.6	1.35	60	0-8.3[3]	---	10/22/85
PCM-2	6640.1	1.35	120	0-7.2[3]	---	10/22/85
PCM-3	6615.0	1.35	60	0-8.3[3]	---	10/22/85
PCM-4	6584.7	0.7	60	0-9.7[3]	---	10/22/85
T-5	6591.6	2.0	263	0-22[4]	---	3/1950
T-6	6642.1	2.75	300	0-30[4]	---	3/1950
CAÑADA DEL BUEY						
CDBO-1	6757.6	1.37	13.1	0-5.1[3]	5.1-13.1[3]	4/17/85
CDBO-2	6748.2	1.30	17.9	0-5.9[3]	5.9-17.9[3]	4/18/85
CDBO-3	6670.2	1.20	12.4	0-4.4[3]	4.4-12.4[3]	4/18/85
CDBO-4	6564.5	1.30	12.1	0-4.1[3]	4.1-12.1[3]	4/18/85

(1) Modified from Devaurs, 1985.
(2) All lengths cited in this table are measured from the land surface datum.
(3) Cased with four-inch O.D PVC pipe.
(4) Cased with six-inch carbon steel pipe.

TABLE 5-6

SUMMARY OF WATER-LEVEL MEASUREMENTS AND ELEVATIONS FOR MONITORING WELLS IN CAÑADA DEL BUEY[1]

WELL	CDBO-1	CDBO-2	CDBO-3	CDBO-4
LAND SURFACE ELEVATION (FT)	(6757.6)	(6748.2)	(6670.2)	(6564.5)
DATE MEASURED				
05/28/85	Dry	Dry	Dry	Dry
09/04/85	Dry	Dry	Dry	Dry
12/02/85	Dry	Dry	Dry	Dry
03/06/86	Dry	Dry	Dry	Dry
06/10/86	Dry	Dry	Dry	Dry
07/03/86	Dry	Dry	Dry	Dry
08/08/86	Dry	Dry	Dry	Dry
09/03/86	Dry	Dry	Dry	Dry

[1] From Department of Energy, 1987

TABLE 5-7

MOISTURE CONTENT OF CUTTINGS FROM THE PCM-SERIES TEST HOLES[1]

DEPTH (FT)	PERCENT MOISTURE BY WEIGHT			
	PCM-1	PCM-2	PCM-3	PCM-4
3	8.7	12.3	12.9	12.0
8	5.7	6.5	15.7	5.6
13	9.0	3.8	5.4	6.0
18	11.0	2.9	11.5	2.1
23	11.1	5.6	8.9	2.5
28	11.1	7.3	6.8	4.1
33	11.7	4.4	6.8	6.6
38	11.7	4.2	6.8	8.4
43	12.1	4.8	7.6	9.5
48	12.2	5.3	7.7	11.5
53	14.4	5.4		12.6
58		6.5		
63		6.4		
68		8.2		
73		8.9		
78		7.9		
83		9.2		
88		9.6		
93		9.5		
98		9.7		
103		9.6		
108		9.8		
113		9.2		
118		9.2		

[1] From McInroy, 1985

TABLE 5-8

LITHOLOGIC LOGS OF MONITORING WELLS IN PAJARITO CANYON[1]

WELL	LITHOLOGIC DESCRIPTION	DEPTH (FT) TO	FROM
PCO-1	Alluvium; light brown, gravels, cobbles, and boulders intermixed with clays, silts and sands	0	11
	Tuff; light reddish-brown, non- to moderately-welded, quartz and sanidine crystals and crystal fragments, few small rock fragments	11	22
PCO-2	Alluvium; light brown, gravels, cobbles, and boulders intermixed with clays, silts, and sands	0	9
	Tuff; light reddish-brown, non- to moderately-welded, quartz and sanidine crystals and crystal fragments, few small rock fragments	9	22
PCO-3	Alluvium; light brown, gravels with a few cobbles in a matrix of silty sand	0	12
	Tuff; light gray to light brown, weathered, some quartz and sanidine crystals and crystal fragments, a few small rock fragments in a matrix of weathered tuff, mostly silts and clay	12	20

[1] From Devaurs, 1985

TABLE 5-9

LITHOLOGIC LOGS OF THE PCM-SERIES TEST HOLES IN PAJARITO CANYON[1]

TEST BORING	LITHOLOGIC DESCRIPTION	DEPTH (FT) TO	FROM
PCM-1	Alluvium	0	8
	Tuff; reddish-brown, pumice layer at 44 feet	8	60
PCM-2	Alluvium (weathered tuff)	0	6
	Tuff; light gray to pinkish-brown tuff, pumice fragments, and rock fragments	6	120
PCM-3	Alluvium	0	8
	Tuff; rock fragments at 13 feet, pink tuff and numerous pumice fragments at 14 feet	8	60
PCM-4	Alluvium	0	1
	Tuff; light grayish-pink, brownish-gray at 13 feet, pumice fragments at 14 feet, reddish brown tuff at 25 feet	1	60

[1] From McInroy, 1985

TABLE 5-10
LITHOLOGIC LOGS OF TEST HOLES T-5 AND T-6 IN PAJARITO CANYON[1][2]

	GEOLOGIC UNIT	DEPTH (FT) TO	FROM
T-5			
	Alluvium	0	23
	Bandelier Tuff		
	Tshirege Member	23	40
	Otowi Member	40	160
	Guaje Member	160	171
	Chino Mesa Basalt	171	263
T-6			
	Alluvium	0	25
	Bandelier Tuff		
	Tshirege Member	25	85
	Otowi Member	85	265
	Guaje Member	265	285
	Puye Formation		
	(Fanglomerate Member)	285	300

(1) From Purtymun, 1975.
(2) Test holes drilled in March 1950.

TABLE 5-11

SUMMARY OF WATER-LEVEL MEASUREMENTS AND ELEVATIONS FOR MONITORING WELLS IN PAJARITO CANYON[1]

WELL	PCO-1			PCO-2			PCO-3		
LAND SURFACE ELEVATION (FT)		(6687.0)			(6618.3)			(6546.3)	
DATE MEASURED	DEPTH BELOW LAND DATUM (FT)	ELEVATION (FT)	SATURATED THICKNESS (FT)	DEPTH BELOW LAND DATUM (FT)	ELEVATION (FT)	SATURATED THICKNESS (FT)	DEPTH BELOW LAND DATUM (FT)	ELEVATION (FT)	SATURATED THICKNESS (FT)
06/11/85	1.25	6685.75	9.75	3.63	6614.67	5.37	2.98	6543.32	9.02
09/12/85	1.29	6685.71	9.71	5.05	6613.25	3.95	3.30	6543.00	8.70
12/13/85	1.28	6685.72	9.72	6.26	6612.04	2.75	3.01	6543.29	8.99
03/06/86	1.59	6685.41	9.41	6.93	6611.37	2.07	3.08	6543.22	8.92
03/12/86	1.62	6685.38	9.38	6.97	6611.33	2.03	3.11	6543.19	8.89
06/10/86	0.78	6686.22	10.22	3.88	6614.42	5.12	3.29	6543.01	8.71
06/18/86	0.72	6686.28	10.28	3.83	6614.47	5.17	3.18	6543.12	8.82
07/03/86	0.54	6686.46	10.46	3.86	6614.44	5.14	2.71	6543.59	9.29
07/16/86	0.52	6686.48	10.48	3.99	6614.31	5.01	2.94	6543.36	9.06
08/08/86	0.69	6686.31	10.31	4.94	6613.36	4.06	3.03	6543.27	8.97
08/27/86	0.84	6686.16	10.16	5.48	6612.82	3.52	3.19	6543.11	8.81
09/03/86	0.86	6686.14	10.14	5.78	6612.52	3.22	3.13	6543.17	8.87
09/18/86	0.85	6686.15	10.15	5.61	6612.69	3.39	3.00	6543.30	9.00

[1] From Department of Energy, 1987

LAN:1702-T48b

TABLE 5-12
SUMMARY OF INORGANIC PARAMETERS ROUTINELY ANALYZED
IN MONITORING WELL SAMPLES

GENERAL CHEMISTRY	METALS	RADIOLOGICAL PARAMETERS
Calcium	Silver	Cesium-137
Magnesium	Arsenic	Plutonium-238
Potassium	Barium	Plutonium-239, 240
Sodium	Cadmium	Tritium
Chloride	Chromium	Total Uranium
Sulfate	Mercury	Gross Alpha
Nitrate (NO_3 as N)	Lead	Gross Beta
Fluoride	Selenium	Gross Gamma
Carbonate	Copper	
Bicarbonate	Iron	
Phosphorus	Manganese	
Total Hardness	Zinc	
Conductivity		
pH		
Total Dissolved Solids		
Silica		

TABLE 5-13

SUMMARY OF VOLATILE ORGANIC COMPOUNDS ROUTINELY ANALYZED IN MONITORING WELL SAMPLES

1,4-Dichlorobenzene
1,2-Dichlorobenzene
Chloromethane
Bromomethane
Vinyl Chloride
Chloroethane
Acetone
2-Butanone
Vinyl Acetate
trans-1,3-Dichloropropene
cis-1,3-Dichloropropene
2-Hexanone
4-Methyl-2-Pentanone
Styrene
Total Xylenes
Trichlorofluoromethane
Tetrahydrofuran
Dibromochloromethane
Dibromomethane
1,2-Dibromo-3-Chloropropane
2-Chloroethylvinyl Ether
Carbon Disulfide
Purgeable Gases[1]

1,1-Dichloroethylene
Methylene Chloride
1,2-Dichloroethylene
1,1-Dichloroethane
Chloroform
1,1,1-Trichloroethane
1,2-Dichloroethane
Benzene
Carbon Tetrachloride
Trichloroethylene
1,2-Dichloropropane
Bromodichloromethane
Toluene
1,1,2-Trichloroethane
Chlorodibromomethane
Tetrachloroethylene
Chlorobenzene
Ethylbenzene
Bromoform
1,1,2,2-Tetrachloroethane
Bromobenzene
1,3-Dichlorobenzene

[1] Includes chloromethane, chloroethane, bromomethane, and vinyl chloride.

TABLE 5-14
INORGANIC WATER QUALITY RESULTS FROM MONITORING WELL
PCO-1 IN PAJARITO CANYON[1]

DATE SAMPLED		06/11/85	09/03/85	12/04/85	03/06/86	06/10/86	09/18/86	NMEIB/ NMWQCC[2]	U.S. EPA[3]
GENERAL CHEMISTRY									
Ca	mg/ℓ	33	22	17	18	19	16		
Mg	mg/ℓ	9.9	6.6	5.1	4.9	6	5		
K	mg/ℓ	5.7	5.3	3.7	3.7	4.3	4.2		
Na	mg/ℓ	47	36	27	28	26	22		
Cl	mg/ℓ	68	35	16.7	22	27	10.7	250.0	250.0
SO_4	mg/ℓ	18.5	13.4	9.5	7.7	9	5.5	600.00	250.0
NO_3 (N)	mg/ℓ	1.7	0.2	<0.1	0.30	1.3	<0.2	10.0	10.0
F	mg/ℓ	0.5	0.4	<0.1	0.3	0.2	0.4	1.6	4.0
CO_3	mg/ℓ	0	0	<0.5	0.0	0.0	0.0		
HCO_3	mg/ℓ	97	101	92	93	82	88		
P	mg/ℓ	<0.2	<0.2	<0.1	0.0	<0.2	<0.2		
Total Hardness	mg/ℓ	122	89	68	88	74	55		
Conductivity	µmohs/cm	48	350	250	260	275	225		
pH		6.7	7.04	6.77	7.4	7.5	6.9	6-9	6.5-8.5
TDS	mg/ℓ	298	217	153	170	188	160	1,000.0	500.0
SiO_2	mg/ℓ	31	39	28	25.7	27	24		

(1) Compiled from Devaurs, 1985; Department of Energy (DOE), 1986a; DOE 1986b, DOE 1986c; DOE 1986d; DOE 1987.
(2) From New Mexico Environmental Improvement Board, 1985b; New Mexico Water Quality Control Commission, 1986.
(3) From U.S. EPA, 1976; U.S. EPA 1979.

LAN:1702-T/1

TABLE 5-14
INORGANIC WATER QUALITY RESULTS FROM MONITORING WELL PCO-1 IN PAJARITO CANYON[1]
(Continued)

DATE SAMPLED		06/11/85	09/03/85	12/04/85	03/06/86	06/10/86	09/18/86	NMEIB/ NMWQCC[2]	U.S. EPA[3]
METALS									
Ag	mg/ℓ	<0.001	<0.001	<0.001	<0.001	<0.005	<0.001	0.05	0.05
As	mg/ℓ	0.004	<0.001	0.001	<0.002	0.002	<0.001	0.05	0.05
Ba	mg/ℓ	0.196	0.148	0.138	0.12	0.076	0.07	1.0	1.0
Cd	mg/ℓ	<0.001	0.005	0.00	<0.002	<0.001	0.0005	0.01	0.01
Cr	mg/ℓ	0.006	0.003	0.037	<0.003	0.0224	<0.001	0.05	0.05
Hg	mg/ℓ	<0.002	<0.001	<0.002	<0.005	<0.002	<0.002	0.002	0.002
Pb	mg/ℓ	<0.003	<0.001	<0.001	<0.005	0.003	0.003	0.05	0.05
Se	mg/ℓ	<0.003	<0.003	<0.001	<0.001	<0.002	<0.001	0.01	0.01
Cu	mg/ℓ	0.014	0.010	<0.010	0.010	0.005	0.004	1.0	1.0
Fe	mg/ℓ	0.095	0.012	0.098	0.005	0.017	<0.003	1.0	0.3
Mn	mg/ℓ	0.018	0.051	0.065	0.32	<0.003	0.115	0.2	0.05
Zn	mg/ℓ	0.029	0.025	0.013	0.005	<0.02	<0.001	10.0	5.0

(1) Compiled from Devaurs, 1985; Department of Energy (DOE), 1986a; DOE 1986b, DOE 1986c; DOE 1986d; DOE 1987.
(2) From New Mexico Environmental Improvement Board, 1985b; New Mexico Water Quality Control Commission, 1986.
(3) From U.S. EPA, 1976; U.S. EPA, 1979.

TABLE 5-14
INORGANIC WATER QUALITY RESULTS FROM MONITORING WELL
PCO-1 IN PAJARITO CANYON[1]
(Continued)

DATE SAMPLED		06/11/85	09/03/85	12/04/85	03/06/86	06/10/86	09/18/86	NMEIB/ NMWQCC[2]	U.S. EPA[3]
RADIOLOGICALS									
Cs-137	pCi/ℓ	74 ± 98	-17.3 ± 120	-36.1 ± 76.4	-17.4 ± 61	-28 ± 72	74 ± 41		200
Pu-238	pCi/ℓ	0.000 ± 0.020	0.013 ± 0.024	0.005 ± 0.02	0.016 ± 0.02	-0.010 ± 0.025	0.001 ± 0.01		15
Pu-239,240	pCi/ℓ	0.005 ± 0.016	0.000 ± 0.02	0.037 ± 0.032	0.021 ± 0.02	0.005 ± 0.033	0.01 ± 0.01		15
H-3	pCi/ℓ	-400 ± 800	3,200 ± 1,000	400 ± 800	-1,400 ± 800	800 ± 800	4,100 ± 600	20,000	20,000
Total U	mg/ℓ	1.4 ± 1.0	0.8 ± 0.4	0.5 ± 0.6	0.0 ± 0.2	1.0 ± 0.6	---	5.0	5.0
Gross Alpha	pCi/ℓ	2.0 ± 4.0	0.300 ± 1.6	1.7 ± 1.4	1.1 ± 1.4	0.8 ± 2	11.0 ± 3.0	15.0	15.0
Gross Beta	pCi/ℓ	8.0 ± 1.8	6.3 ± 1.6	1.7 ± 1.0	2.6 ± 1.0	5.9 ± 1.6	10.0 ± 1.0		
Gross Gamma	cpm/ℓ	-50 ± 120	160 ± 120	70.0 ± 120	-40 ± 120	-120 ± 120	146 ± 100		

(1) Compiled from Devaurs, 1985; Department of Energy (DOE), 1986a; DOE 1986b, DOE 1986c; DOE 1986d; DOE 1987.
(2) From New Mexico Environmental Improvement Board, 1985b; New Mexico Water Quality Control Commission, 1986.
(3) From U.S. EPA, 1976; U.S. EPA, 1979.

TABLE 5-15
INORGANIC WATER QUALITY RESULTS FROM MONITORING WELL
PCO-2 IN PAJARITO CANYON[1]

DATE SAMPLED		06/11/85	09/03/85	12/04/85[2]	03/06/86[2]	06/10/86	09/18/86	NMEIB/ NMWQCC[3]	U.S. EPA[4]
GENERAL CHEMISTRY									
Ca	mg/ℓ	18	19	---	---	21	19		
Mg	mg/ℓ	5.1	5.7	---	---	6	5		
K	mg/ℓ	3.9	3.8	---	---	3.5	3.4		
Na	mg/ℓ	18	19	---	---	21	19		
Cl	mg/ℓ	14	17	---	---	25	14.2	250.0	250.0
SO_4	mg/ℓ	10.0	7.8	---	---	8	5.1	600.00	250.0
NO_3 (N)	mg/ℓ	0.3	0.3	---	---	0.8	<0.2	10.0	10.0
F	mg/ℓ	0.3	0.4	---	---	0.24	0.4	1.6	4.0
CO_3	mg/ℓ	0	0	---	---	0.0	0.0		
HCO_3	mg/ℓ	66	88	---	---	82	88		
P	mg/ℓ	<0.2	<0.2	---	---	<0.2	<0.2		
Total Hardness	mg/ℓ	62	80	---	---	75	61		
Conductivity	µmohs/cm	19	250	---	---	255	225		
pH		6.89	6.83	---	---	7.4	7.0	6-9	6.5-8.5
TDS	mg/ℓ	143	156	---	---	175	152	1,000.0	500.0
SiO_2	mg/ℓ	26	31	---	---	27	23		

(1) Compiled from Devaurs, 1985; Department of Energy (DOE), 1986a; DOE 1986b, DOE 1986c; DOE 1986d; DOE 1987.
(2) Volume of water in monitoring well insufficient to collect sample.
(3) From New Mexico Environmental Improvement Board, 1985b, New Mexico Water Quality Control Commission, 1986.
(4) From U.S. EPA, 1976; U.S. EPA, 1979.

TABLE 5-15
INORGANIC WATER QUALITY RESULTS FROM MONITORING WELL
PCO-2 IN PAJARITO CANYON[1]
(Continued)

DATE SAMPLED		06/11/85	09/03/85	12/04/85[2]	03/06/86[2]	06/10/86	09/18/86	NMEIB/ NMWQCC[3]	U.S. EPA[4]
METALS									
Ag	mg/ℓ	<0.001	<0.001	---	---	<0.005	<0.001	0.05	0.05
As	mg/ℓ	0.001	<0.001	---	---	<0.002	<0.001	0.05	0.05
Ba	mg/ℓ	0.069	0.090	---	---	0.018	0.18	1.0	1.0
Cd	mg/ℓ	<0.001	0.002	---	---	0.0014	<0.0002	0.01	0.01
Cr	mg/ℓ	0.006	0.007	---	---	0.0206	<0.001	0.05	0.05
Hg	mg/ℓ	<0.002	<0.001	---	---	<0.002	<0.002	0.002	0.002
Pb	mg/ℓ	0.006	<0.001	---	---	0.003	<0.001	0.05	0.05
Se	mg/ℓ	<0.003	<0.003	---	---	<0.002	<0.001	0.01	0.01
Cu	mg/ℓ	<0.005	<0.005	---	---	<0.022	0.001	1.0	1.0
Fe	mg/ℓ	0.072	0.051	---	---	<0.002	<0.003	1.0	0.3
Mn	mg/ℓ	0.371	0.321	---	---	<0.003	0.291	0.2	0.05
Zn	mg/ℓ	<0.01	<0.010	---	---	0.01	<0.001	10.0	5.0

(1) Compiled from Devaurs, 1985; Department of Energy (DOE), 1986a; DOE 1986b, DOE 1986c; DOE 1986d; DOE 1987.
(2) Volume of water in monitoring well insufficient to collect sample.
(3) From New Mexico Environmental Improvement Board, 1985b; New Mexico Water Quality Control Commission, 1986.
(4) From U.S. EPA, 1976; U.S. EPA, 1979.

TABLE 5-15
INORGANIC WATER QUALITY RESULTS FROM MONITORING WELL
PCO-2 IN PAJARITO CANYON[1]
(Continued)

DATE SAMPLED		06/11/85	09/03/85	12/04/85[2]	03/06/86[2]	06/10/86	09/18/86	NMEIB/ NMWQCC[3]	U.S. EPA[4]
RADIOLOGICALS									
Cs-137	pCi/ℓ	70 ± 82	97.8 ± 86	---	---	-38. ± 56	40 ± 38		200
Pu-238	pCi/ℓ	0.000 ± 0.0001	0.000 ± 0.02	---	---	0.006 ± 0.029	-0.02 ± 0.02		15.0
Pu-239,240	pCi/ℓ	0.000 ± 0.024	0.000 ± 0.02	---	---	-0.011 ± 0.027	0.01 ± 0.02		15.0
H-3	pCi/ℓ	600 ± 800	3,700 ± 1000	---	---	800 ± 800	3,600 ± 600	20,000	20,000
Total U	mg/ℓ	3.8 ± 1.6	5.1 ± 0.5	---	---	2.5 ± 0.6	---	5.0	5.0
Gross Alpha	pCi/ℓ	9.0 ± 26.0	6.0 ± 4.0	---	---	0.4 ± 2	14.0 ± 3.0	15.0	15.0
Gross Beta	pCi/ℓ	16.0 ± 4.0	17.0 ± 4.0	---	---	11 ± 2.0	15.0 ± 2.0		
Gross Gamma	cpm/ℓ	60 ± 120	190 ± 120	---	---	-190 ± 120	146 ± 100		

(1) Compiled from Devaurs, 1985; Department of Energy (DOE), 1986a; DOE 1986b, DOE 1986c; DOE 1986d; DOE 1987.
(2) Volume of water in monitoring well insufficient to collect sample.
(3) From New Mexico Environmental Improvement Board, 1985b; New Mexico Water Quality Control Commission, 1986.
(4) From U.S. EPA, 1976; U.S. EPA, 1979.

TABLE 5-16
INORGANIC WATER QUALITY RESULTS FROM MONITORING WELL
PCO-3 IN PAJARITO CANYON[1]

DATE SAMPLED		06/11/85	09/03/85	12/04/85	03/06/86	06/10/86	09/18/86	NMEIB/ NMWQCC[2]	U.S. EPA[3]
GENERAL CHEMISTRY									
Ca	mg/ℓ	40	39	125	87	55	80		
Mg	mg/ℓ	9.8	9.5	29.7	18	12	16		
K	mg/ℓ	3.6	3.8	4.4	3.2	3.9	2.9		
Na	mg/ℓ	24	23	57	41	32	18		
Cl	mg/ℓ	22	22	74	40	24	42.7	250.0	250.0
SO_4	mg/ℓ	7.6	7.3	5.2	9.4	19	0.8	600.00	250.0
NO_3 (N)	mg/ℓ	0.5	<0.1	<0.1	0.0	0.9	<0.2	10.0	10.0
F	mg/ℓ	0.7	0.7	0.4	0.6	0.54	0.3	1.6	4.0
CO_3	mg/ℓ	0	0	<0.5	0.0	0.0	0.0		
HCO_3	mg/ℓ	150	158	477	287	212	281		
P	mg/ℓ	<0.2	<0.2	<0.1	0.0	<0.2	<0.2		
Total Hardness	mg/ℓ	141	149	478	302	183	229		
Conductivity	µmohs/cm	38	390	1080	660	520	650		
pH		7.5	7.46	7.32	8.0	7.8	7.0	6-9	6.5-8.5
TDS	mg/ℓ	251	246	659	438	350	408	1,000.0	500.0
SiO_2	mg/ℓ	35	38	35	34.9	30	32		

(1) Compiled from Devaurs, 1985; Department of Energy (DOE), 1986a; DOE 1986b, DOE 1986c; DOE 1986d; DOE 1987.
(2) From New Mexico Environmental Improvement Board, 1985b; New Mexico Water Quality Control Commission, 1986.
(3) From U.S. EPA, 1976; U.S. EPA, 1979.

TABLE 5-16
INORGANIC WATER QUALITY RESULTS FROM MONITORING WELL
PCO-3 IN PAJARITO CANYON[1]
(Continued)

DATE SAMPLED		06/11/85	09/03/85	12/04/85	03/06/86	06/10/86	09/18/86	NMEIB/ NMWQCC[2]	U.S. EPA[3]
METALS									
Ag	mg/ℓ	<0.001	<0.001	<0.001	<0.001	<0.005	<0.001	0.05	0.05
As	mg/ℓ	0.001	0.002	0.001	<0.002	<0.002	0.002	0.05	0.05
Ba	mg/ℓ	0.104	0.100	0.303	0.17	0.099	0.04	1.0	1.0
Cd	mg/ℓ	<0.001	0.003	0.009	0.002	<0.001	0.0013	0.01	0.01
Cr	mg/ℓ	0.005	0.003	0.014	<0.003	0.0226	0.002	0.05	0.05
Hg	mg/ℓ	<0.002	<0.001	<0.002	<0.005	<0.002	<0.002	0.002	0.002
Pb	mg/ℓ	<0.003	<0.001	<0.001	<0.005	0.003	<0.001	0.05	0.05
Se	mg/ℓ	<0.003	<0.003	<0.001	<0.001	<0.002	<0.001	0.01	0.01
Cu	mg/ℓ	0.038	0.028	0.054	0.05	0.021	0.025	1.0	1.0
Fe	mg/ℓ	0.005	0.007	0.040	<0.003	0.019	0.003	1.0	0.3
Mn	mg/ℓ	0.388	0.026	2.86	1.72	<0.003	0.395	0.2	0.05
Zn	mg/ℓ	0.052	0.029	0.061	0.035	<0.01	<0.001	10.0	5.0

(1) Compiled from Devaurs, 1985; Department of Energy (DOE), 1986a; DOE 1986b, DOE 1986c; DOE 1986d; DOE 1987.
(2) From New Mexico Environmental Improvement Board, 1985b; New Mexico Water Quality Control Commission, 1986.
(3) From U.S. EPA, 1976; U.S. EPA, 1979.

TABLE 5-16
INORGANIC WATER QUALITY RESULTS FROM MONITORING WELL
PCO-3 IN PAJARITO CANYON[1]

(Continued)

DATE SAMPLED		06/11/85	09/03/85	12/04/85	03/06/86	06/10/86	09/18/86	NMEIB/ NMWQCC[2]	U.S. EPA[3]
RADIOLOGICALS									
Cs-137	pCi/ℓ	-10 ± 84	48.1 ± 100	-29.3 ± 66.4	-44.5 ± 70	-10 ± 64	31 ± 43		200
Pu-238	pCi/ℓ	0.024 ± 0.030	0.004 ± 0.02	0.000 ± 0.02	0.012 ± 0.02	-0.027 ± 0.034	0.00 ± 0.001		15
Pu-239,240	pCi/ℓ	0.016 ± 0.022	0.014 ± 0.02	0.032 ± 0.02	0.015 ± 0.02	-0.005 ± 0.016	0.00 ± 0.01		15
H-3	pCi/ℓ	1,300 ± 800	4,800 ± 1,200	9,000 ± 800	1,200 ± 800	900 ± 800	1,900 ± 500	20,000	20,000
Total U	mg/ℓ	1.5 ± 1.0	1.4 ± 0.4	6.2 ± 1.2	0.5 ± 0.4	3.7 ± 0.8	---	5.0	5.0
Gross Alpha	pCi/ℓ	3.0 ± 4.0	0.3 ± 1.6	-40 ± 3.2	2.0 ± 4.0	0.1 ± 2	9.0 ± 3.0	15.0	15.0
Gross Beta	pCi/ℓ	4.8 ± 1.2	3.6 ± 1.0	2.3 ± 1.0	3.1 ± 1.0	10 ± 2.0	12.0 ± 1.0		
Gross Gamma	cpm/ℓ	40 ± 120	120 ± 120	0.0 ± 120	-50 ± 120	-160 ± 120	219 ± 100d		

(1) Compiled from Devaurs, 1985; Department of Energy (DOE), 1986a; DOE 1986b, DOE 1986c; DOE 1986d; DOE 1987.
(2) From New Mexico Environmental Improvement Board, 1985b; New Mexico Water Quality Control Commission, 1986.
(3) From U.S. EPA, 1976; U.S. EPA, 1979.

TABLE 5-17
VOLATILE ORGANIC WATER QUALITY RESULTS FROM MONITORING WELL
PCO-1 IN PAJARITO CANYON[1]

DATE SAMPLED	06/11/85	09/03/85	12/04/85	03/06/86	06/10/86	09/18/86	NMWQCC[2]	U.S. EPA[3]
VOLATILE ORGANICS (mg/ℓ)								Proposed MCL's
1,1-Dichloroethylene	---	---	---	ND<0.001	ND<0.001	ND<0.001	0.005	0.007
Methylene Chloride	---	ND<0.005	ND<0.005	ND<0.001	ND<0.001	ND<0.001	0.10	
1,2-Dichloroethylene	---	ND<0.005	ND<0.005	ND<0.001	ND<0.001	ND<0.001		
1,1-Dichloroethane	---	ND<0.010	ND<0.010	ND<0.001	ND<0.001	ND<0.001	0.025	
Chloroform	---	ND<0.010	ND<0.010	ND<0.001	ND<0.001	ND<0.001	0.10	
1,1,1-Trichloroethane	---	ND<0.015	ND<0.015	ND<0.001	ND<0.001	ND<0.001	0.06	0.20
1,2-Dichloroethane	---	ND<0.008	ND<0.008	ND<0.001	ND<0.001	ND<0.001	0.01	0.005
Benzene	---	ND<0.005	ND<0.005	ND<0.001	ND<0.001	ND<0.001	0.01	0.005
Carbon Tetrachloride	---	ND<0.020	ND<0.020	ND<0.001	ND<0.001	ND<0.001	0.01	0.005
Trichloroethylene	---	ND<0.005	ND<0.005	ND<0.001	ND<0.001	ND<0.001	0.10	0.005
1,2-Dichloropropane	---	ND<0.005	ND<0.005	ND<0.001	ND<0.001	ND<0.001		
Bromodichloromethane	---	ND<0.010	ND<0.010	ND<0.001	ND<0.001	ND<0.001		
Toluene	---	ND<0.005	ND<0.005	ND<0.001	ND<0.001	ND<0.001	0.75	
1,1,2-Trichloroethane	---	ND<0.015	ND<0.015	ND<0.001	ND<0.001	ND<0.001	0.01	
Chlorodibromomethane	---	ND<0.010	ND<0.010	ND<0.005	ND<0.005	---		
Tetrachloroethylene	---	ND<0.020	ND<0.020	ND<0.001	ND<0.001	ND<0.001	0.02	
Chlorobenzene	---	ND<0.012	ND<0.012	ND<0.001	ND<0.001	ND<0.001		
Ethylbenzene	---	ND<0.008	ND<0.008	ND<0.001	ND<0.001	ND<0.001	0.750	
Bromoform	---	ND<0.010	ND<0.010	ND<0.001	ND<0.001	ND<0.001		
1,1,2,2-Tetrachloroethane	---	ND<0.020	ND<0.020	ND<0.001	ND<0.001	ND<0.001	0.01	
Bromobenzene	---	ND<0.022	ND<0.022	---	---	---		
1,3-Dichlorobenzene	---	ND<0.005	ND<0.005	---	---	ND<0.001		

(1) Compiled from Devaurs, 1985; Department of Energy (DOE), 1986a; DOE 1986b, DOE 1986c; DOE 1986d; DOE 1987.
(2) From New Mexico Water Quality Control Commission, 1986.
(3) From U.S. EPA, 1985b.

TABLE 5-17
VOLATILE ORGANIC WATER QUALITY RESULTS FROM MONITORING WELL PCO-1 IN PAJARITO CANYON[1]
(Continued)

DATE SAMPLED	06/11/85	09/03/85	12/04/85	03/06/86	06/10/86	09/18/86	NMWQCC[2]	U.S. EPA[3]
								Proposed MCL's
VOLATILE ORGANICS (mg/ℓ) (Continued)								
1,4-Dichlorobenzene	---	---	---	---	---	ND<0.001		0.75
1,2-Dichlorobenzene	---	ND<0.005	ND<0.005	---	---	ND<0.001		
Chloromethane	---	---	---	ND<0.005	ND<0.005	---		
Bromomethane	---	---	---	ND<0.005	ND<0.005	---		
Vinyl Chloride	---	---	---	ND<0.005	ND<0.005	---	0.001	0.001
Chloroethane	---	---	---	ND<0.005	ND<0.005	---		
Acetone	---	---	---	ND<0.005	ND<0.005	ND<0.005		
2-Butanone	---	---	---	ND<0.005	ND<0.005	---		
Vinyl Acetate	---	---	---	ND<0.005	ND<0.005	---		
trans-1,3-Dichloropropene	---	---	---	ND<0.005	ND<0.005	ND<0.005		
cis-1,3-Dichloropropene	---	---	---	ND<0.005	ND<0.005	ND<0.005		
2-Hexanone	---	---	---	ND<0.005	ND<0.005	---		
4-Methyl-2-Pentanone	---	---	---	ND<0.001	ND<0.001	ND<0.001		
Styrene	---	---	---	ND<0.005	ND<0.005	ND<0.005		
Total Xylenes	---	---	---	ND<0.001	ND<0.001	ND<0.001	0.620	
Trichlorofluoromethane	---	---	---	ND<0.005	ND<0.005	---		
Tetrahydrofuran	---	---	---	ND<0.005	ND<0.005	---		
Dibromochloromethane	---	---	---	---	---	ND<0.001		
Dibromomethane	---	---	---	---	---	ND<0.001		

(1) Compiled from Devaurs, 1985; Department of Energy (DOE), 1986a; DOE 1986b, DOE 1986c; DOE 1986d; DOE 1987.
(2) From New Mexico Water Quality Control Commission, 1986.
(3) From U.S. EPA, 1985b.

LAN:1702-T/5

TABLE 5-17
VOLATILE ORGANIC WATER QUALITY RESULTS FROM MONITORING WELL PCO-1 IN PAJARITO CANYON[1]
(Continued)

DATE SAMPLED	06/11/85	09/03/85	12/04/85	03/06/86	06/10/86	09/18/86	NMWQCC[2]	U.S. EPA[3]
VOLATILE ORGANICS (mg/ℓ) (Continued)								Proposed MCL's
1,2-Dibromo-3-Chloropropane	---	---	---	---	---	ND<0.001		
2-Chloroethylvinyl Ether	---	---	---	---	---	ND<0.005		
Carbon Disulfide	---	---	---	---	---	ND<0.005		
Purgeable Gases[4]	---	---	---	---	---	ND<0.010		

(1) Compiled from Devaurs, 1985; Department of Energy (DOE), 1986a; DOE 1986b, DOE 1986c; DOE 1986d; DOE 1987.
(2) From New Mexico Water Quality Control Commission, 1986.
(3) From U.S. EPA, 1985b.
(4) Includes chloromethane, chloroethane, bromomethane, and vinyl chloride.

TABLE 5-18
VOLATILE ORGANIC WATER QUALITY RESULTS FROM MONITORING WELL PCO-2 IN PAJARITO CANYON[1]

DATE SAMPLED	06/11/85	09/03/85	12/04/85[2]	03/06/86[2]	06/10/86	09/18/86	NMWQCC[3]	U.S. EPA[4]
								Proposed MCL's
VOLATILE ORGANICS (mg/ℓ)								
1,1-Dichloroethylene	---	---	---	---	ND<0.001	ND<0.001	0.005	0.007
Methylene Chloride	---	ND<0.005	---	---	ND<0.001	ND<0.001	0.10	
1,2-Dichloroethylene	---	ND<0.005	---	---	ND<0.001	ND<0.001		
1,1-Dichloroethane	---	ND<0.010	---	---	ND<0.001	ND<0.001	0.025	
Chloroform	---	ND<0.010	---	---	ND<0.001	ND<0.001	0.10	
1,1,1-Trichloroethane	---	ND<0.015	---	---	ND<0.001	ND<0.001	0.06	0.20
1,2-Dichloroethane	---	ND<0.008	---	---	ND<0.001	ND<0.001	0.01	0.005
Benzene	---	ND<0.005	---	---	ND<0.001	ND<0.001	0.01	0.005
Carbon Tetrachloride	---	ND<0.020	---	---	ND<0.001	ND<0.001	0.01	0.005
Trichloroethylene	---	ND<0.005	---	---	ND<0.001	ND<0.001	0.10	0.005
1,2-Dichlorepropane	---	ND<0.005	---	---	ND<0.001	ND<0.001		
Bromodichloromethane	---	ND<0.010	---	---	ND<0.001	ND<0.001		
Toluene	---	ND<0.005	---	---	ND<0.001	ND<0.001	0.75	
1,1,2-Trichloroethane	---	ND<0.015	---	---	ND<0.001	ND<0.001	0.01	
Chlorodibromomethane	---	ND<0.010	---	---	ND<0.005	---		
Tetrachloroethylene	---	ND<0.020	---	---	ND<0.001	ND<0.001	0.02	
Chlorobenzene	---	ND<0.012	---	---	ND<0.001	ND<0.001		
Ethylbenzene	---	ND<0.008	---	---	ND<0.001	ND<0.001	0.750	
Bromoform	---	ND<0.010	---	---	ND<0.001	ND<0.001		
1,1,2,2-Tetrachloroethane	---	ND<0.020	---	---	ND<0.001	ND<0.001	0.01	

(1) Compiled from Devaurs, 1985; Department of Energy (DOE), 1986a; DOE 1986b, DOE 1986c; DOE 1986d; DOE 1987.
(2) Volume of water in monitoring well insufficient to collect sample.
(3) From New Mexico Water Quality Control Commission, 1986.
(4) From U.S. EPA, 1985b.

TABLE 5-18
VOLATILE ORGANIC WATER QUALITY RESULTS FROM MONITORING WELL PCO-2 IN PAJARITO CANYON[1]

(Continued)

DATE SAMPLED	06/11/85	09/03/85	12/04/85[2]	03/06/86[2]	06/10/86	09/18/86	NMWQCC[3]	U.S. EPA[4]
VOLATILE ORGANICS (mg/ℓ) (Continued)								Proposed MCL's
Bromobenzene	---	ND<0.022	---	---	---	---		
1,3-Dichlorobenzene	---	ND<0.005	---	---	---	ND<0.001		
1,4-Dichlorobenzene	---	---	---	---	---	ND<0.001		0.75
1,2-Dichlorobenzene	---	ND<0.005	---	---	---	ND<0.001		
Chloromethane	---	---	---	---	ND<0.005	---		
Bromomethane	---	---	---	---	ND<0.005	---		
Vinyl Chloride	---	---	---	---	ND<0.005	---	0.001	0.001
Chloroethane	---	---	---	---	ND<0.005	---		
Acetone	---	---	---	---	ND<0.005	ND<0.005		
2-Butanone	---	---	---	---	ND<0.005	---		
Vinyl acetate	---	---	---	---	ND<0.005	---		
trans-1,3-Dichloropropene	---	---	---	---	ND<0.005	ND<0.005		
cis-1,3-Dichloropropene	---	---	---	---	ND<0.005	ND<0.005		
2-Hexanone	---	---	---	---	ND<0.005	---		
4-Methyl-2-Pentanone	---	---	---	---	ND<0.005	ND<0.001		
Styrene	---	---	---	---	ND<0.005	ND<0.005		
Total Xylenes	---	---	---	---	ND<0.005	ND<0.001	0.620	
Trichlorofluoromethane	---	---	---	---	ND<0.005	---		
Tetrahydrofuran	---	---	---	---	ND<0.005	---		

(1) Compiled from Devaurs, 1985; Department of Energy (DOE), 1986a; DOE 1986b, DOE 1986c; DOE 1986d; DOE 1987.
(2) Volume of water in monitoring well insufficient to collect sample.
(3) From New Mexico Water Quality Control Commission, 1986.
(4) From U.S. EPA, 1985b.

LAN:1702-T/11

TABLE 5-18
VOLATILE ORGANIC WATER QUALITY RESULTS FROM MONITORING WELL PCO-2 IN PAJARITO CANYON[1]
(Continued)

DATE SAMPLED	06/11/85	09/03/85	12/04/85[2]	03/06/86[2]	06/10/86	09/18/86	NMWQCC[3]	U.S. EPA[4]
VOLATILE ORGANICS (mg/ℓ) (Continued)								Proposed MCL's
Dibromochloromethane	---	---	---	---	---	ND<0.001		
Dibromomethane	---	---	---	---	---	ND<0.001		
1,2-Dibromo-3-Chloropropane	---	---	---	---	---	ND<0.001		
2-Chloroethylvinyl Ether	---	---	---	---	---	ND<0.005		
Carbon Disulfide	---	---	---	---	---	ND<0.005		
Purgeable Gases[5]	---	---	---	---	---	ND<0.010		

(1) Compiled from Devaurs, 1985; Department of Energy (DOE), 1986a; DOE 1986b, DOE 1986c; DOE 1986d; DOE 1987.
(2) Volume of water in monitoring well insufficient to sample.
(3) From New Mexico Water Quality Control Commission, 1986.
(4) From U.S. EPA, 1985b.
(5) Includes chloromethane, chloroethane, bromomethane, and vinyl chloride.

TABLE 5-19
VOLATILE ORGANIC WATER QUALITY RESULTS FROM MONITORING WELL PCO-3 IN PAJARITO CANYON[1]

DATE SAMPLED	06/11/85	09/03/85	12/04/85	03/06/86	06/10/86	09/18/86	NMWQCC[2]	U.S. EPA[3]
VOLATILE ORGANICS (mg/ℓ)								Proposed MCL's
1,1-Dichloroethylene	---	---	---	ND<0.001	ND<0.001	ND<0.001	0.005	0.007
Methylene Chloride	---	ND<0.005	ND<0.005	ND<0.001	ND<0.001	ND<0.001	0.10	
1,2-Dichloroethylene	---	ND<0.005	ND<0.005	ND<0.001	ND<0.001	ND<0.001		
1,1-Dichloroethane	---	ND<0.010	ND<0.010	ND<0.001	ND<0.001	ND<0.001	0.025	
Chloroform	---	ND<0.010	ND<0.010	ND<0.001	ND<0.001	ND<0.001	0.10	
1,1,1-Trichloroethane	---	ND<0.015	ND<0.015	ND<0.001	ND<0.001	ND<0.001	0.06	0.20
1,2-Dichloroethane	---	ND<0.008	ND<0.008	ND<0.001	ND<0.001	ND<0.001	0.01	0.005
Benzene	---	ND<0.005	ND<0.005	ND<0.001	ND<0.001	ND<0.001	0.01	0.005
Carbon tetrachloride	---	ND<0.020	ND<0.020	ND<0.001	ND<0.001	ND<0.001	0.01	0.005
Trichloroethylene	---	ND<0.005	ND<0.005	ND<0.001	ND<0.001	ND<0.001	0.10	0.005
1,2-Dichloropropane	---	ND<0.005	ND<0.005	ND<0.001	ND<0.001	ND<0.001		
Bromodichloromethane	---	ND<0.010	ND<0.010	ND<0.001	ND<0.001	ND<0.001		
Toluene	---	ND<0.005	ND<0.005	ND<0.001	ND<0.001	ND<0.001	0.75	
1,1,2-Trichloroethane	---	ND<0.015	ND<0.015	ND<0.001	ND<0.001	ND<0.001	0.01	
Chlorodibromomethane	---	ND<0.010	ND<0.010	ND<0.005	ND<0.005	---		
Tetrachlorethylene	---	ND<0.020	ND<0.020	ND<0.001	ND<0.001	ND<0.001	0.02	
Chlorobenzene	---	ND<0.012	ND<0.012	ND<0.001	ND<0.001	ND<0.001		
Ethylbenzene	---	ND<0.008	ND<0.008	ND<0.001	ND<0.001	ND<0.001	0.750	
Bromoform	---	ND<0.010	ND<0.010	ND<0.001	ND<0.001	ND<0.001		
1,1,2,2-Tetrachloroethane	---	ND<0.020	ND<0.020	ND<0.001	ND<0.001	ND<0.001	0.01	

(1) Compiled from Devaurs, 1985; Department of Energy (DOE), 1986a; DOE 1986b, DOE 1986c; DOE 1986d; DOE 1987.
(2) From New Mexico Water Quality Control Commission, 1986.
(3) From U.S. EPA, 1985b.

LAN:1702-T/16

TABLE 5-19
VOLATILE ORGANIC WATER QUALITY RESULTS FROM MONITORING WELL PCO-3 IN PAJARITO CANYON[1]
(Continued)

DATE SAMPLED	06/11/85	09/03/85	12/04/85	03/06/86	06/10/86	09/18/86	NMWQCC[2]	U.S. EPA[3]
VOLATILE ORGANICS (mg/ℓ) (Continued)								Proposed MCL's
Bromobenzene	---	ND<0.022	ND<0.022	---	---	---		
1,3-Dichlorobenzene	---	ND<0.005	ND<0.005	---	---	ND<0.001		
1,4-Dichlorobenzene	---	---	---	---	---	ND<0.001		0.75
1,2-Dichlorobenzene	---	ND<0.005	ND<0.005	---	---	ND<0.001		
Chloromethane	---	---	---	ND<0.005	ND<0.005	---		
Bromomethane	---	---	---	ND<0.005	ND<0.005	---		
Vinyl Chloride	---	---	---	ND<0.005	ND<0.005	---	0.001	0.001
Chloroethane	---	---	---	ND<0.005	ND<0.005	---		
Acetone	---	---	---	ND<0.005	ND<0.005	ND<0.005		
2-Butanone	---	---	---	ND<0.005	ND<0.005	---		
Vinyl Acetate	---	---	---	ND<0.005	ND<0.005	---		
trans-1,3-Dichloropropene	---	---	---	ND<0.005	ND<0.005	ND<0.005		
cis-1,3-Dichloropropene	---	---	---	ND<0.005	ND<0.005	ND<0.005		
2-Hexanone	---	---	---	ND<0.005	ND<0.005	---		
4-Methyl-2-Pentanone	---	---	---	ND<0.001	ND<0.001	ND<0.001		
Styrene	---	---	---	ND<0.005	ND<0.005	ND<0.005		
Total Xylenes	---	---	---	ND<0.001	ND<0.001	ND<0.001	0.620	
Trichlorofluoromethane	---	---	---	ND<0.005	ND<0.005	---		
Tetrahydrofuran	---	---	---	ND<0.005	ND<0.005	---		

(1) Compiled from Devaurs, 1985; Department of Energy (DOE), 1986a; DOE 1986b, DOE 1986c; DOE 1986d; DOE 1987.
(2) From New Mexico Water Quality Control Commission, 1986.
(3) From U.S. EPA, 1985b.

LAN:1702-T/17

TABLE 5-19
VOLATILE ORGANIC WATER QUALITY RESULTS FROM MONITORING WELL PCO-3 IN PAJARITO CANYON[1]
(Continued)

DATE SAMPLED	06/11/85	09/03/85	12/04/85	03/06/86	06/10/86	09/18/86	NMWQCC[2]	U.S. EPA[3]
VOLATILE ORGANICS (mg/ℓ) (Continued)								Proposed MCL's
Dibromochloromethane	---	---	---	---	---	ND<0.001		
Dibromomethane	---	---	---	---	---	ND<0.001		
1,2-Dibromo-3-Chloropropane	---	---	---	---	---	ND<0.001		
2-Chloroethylvinyl Ether	---	---	---	---	---	ND<0.005		
Carbon Disulfide	---	---	---	---	---	ND<0.005		
Purgeable Gases[4]	---	---	---	---	---	ND<0.010		

(1) Compiled from Devaurs, 1985; Department of Energy (DOE), 1986a; DOE 1986b, DOE 1986c; DOE 1986d; DOE 1987.
(2) From New Mexico Water Quality Control Commission, 1986.
(3) From U.S. EPA, 1985b.
(4) Includes chloromethane, chloroethane, bromomethane, and vinyl chloride.

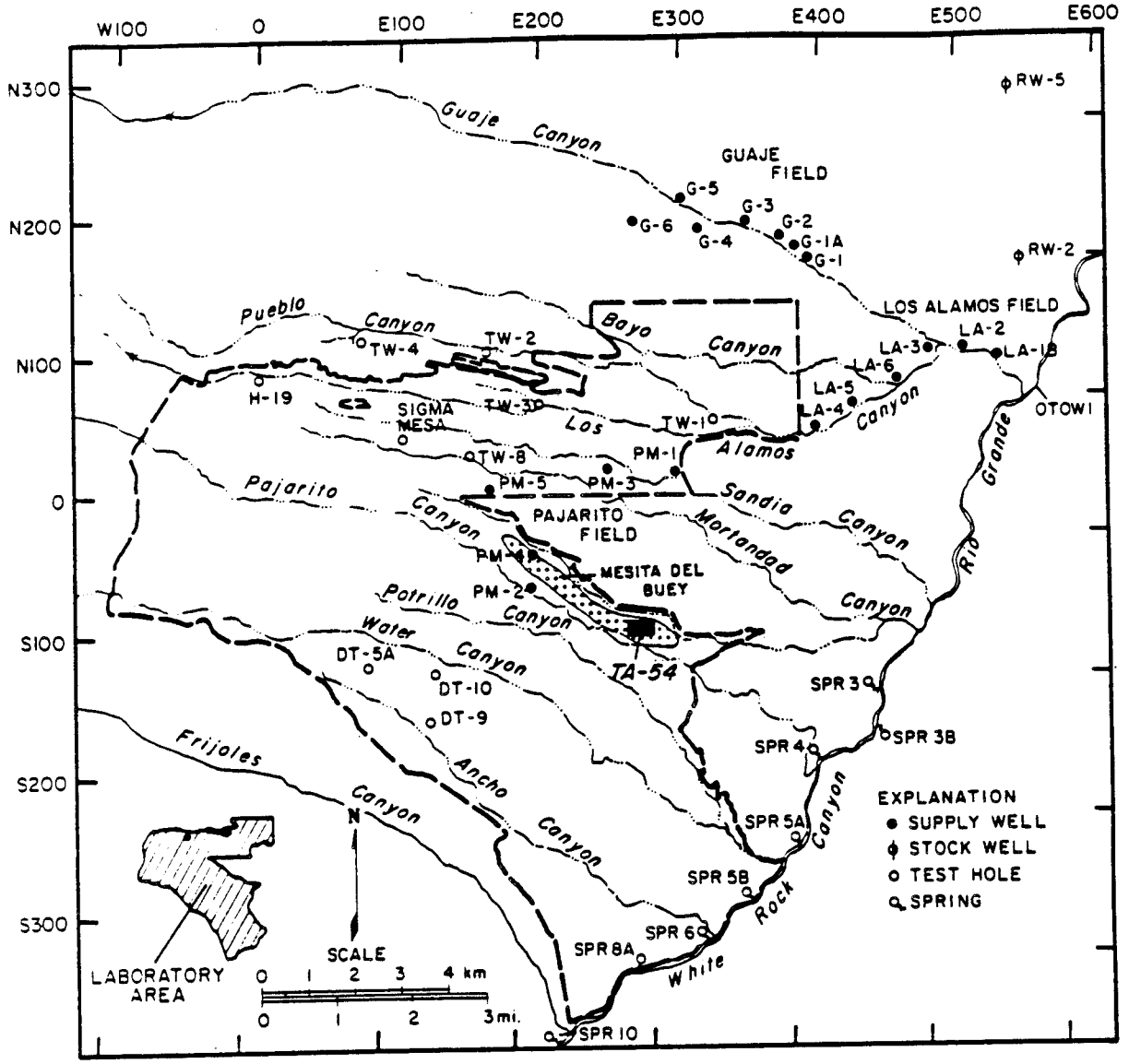

FIGURE 5-1 LOCATION OF SUPPLY WELLS, TEST WELLS, STOCK WELLS, AND SPRINGS IN THE MAN AQUIFER IN THE LOS ALAMOS AREA (PURTYMUN, 1984)

301017 02 A50

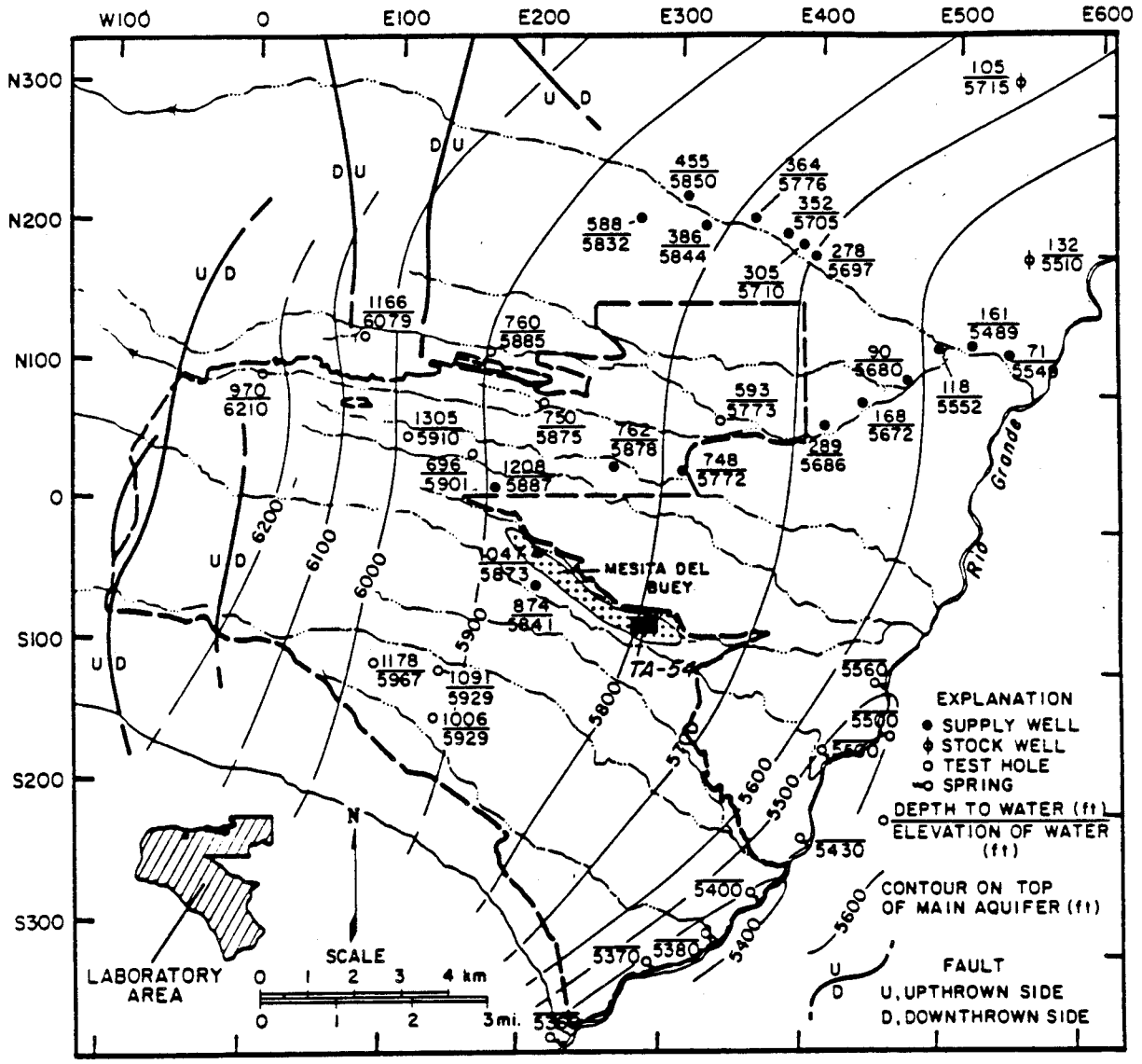

FIGURE 5-2 POTENTIOMETRIC SURFACE MAP OF THE MAIN AQUIFER IN THE LOS ALAMOS AREA (PURTYMUN, 1984)

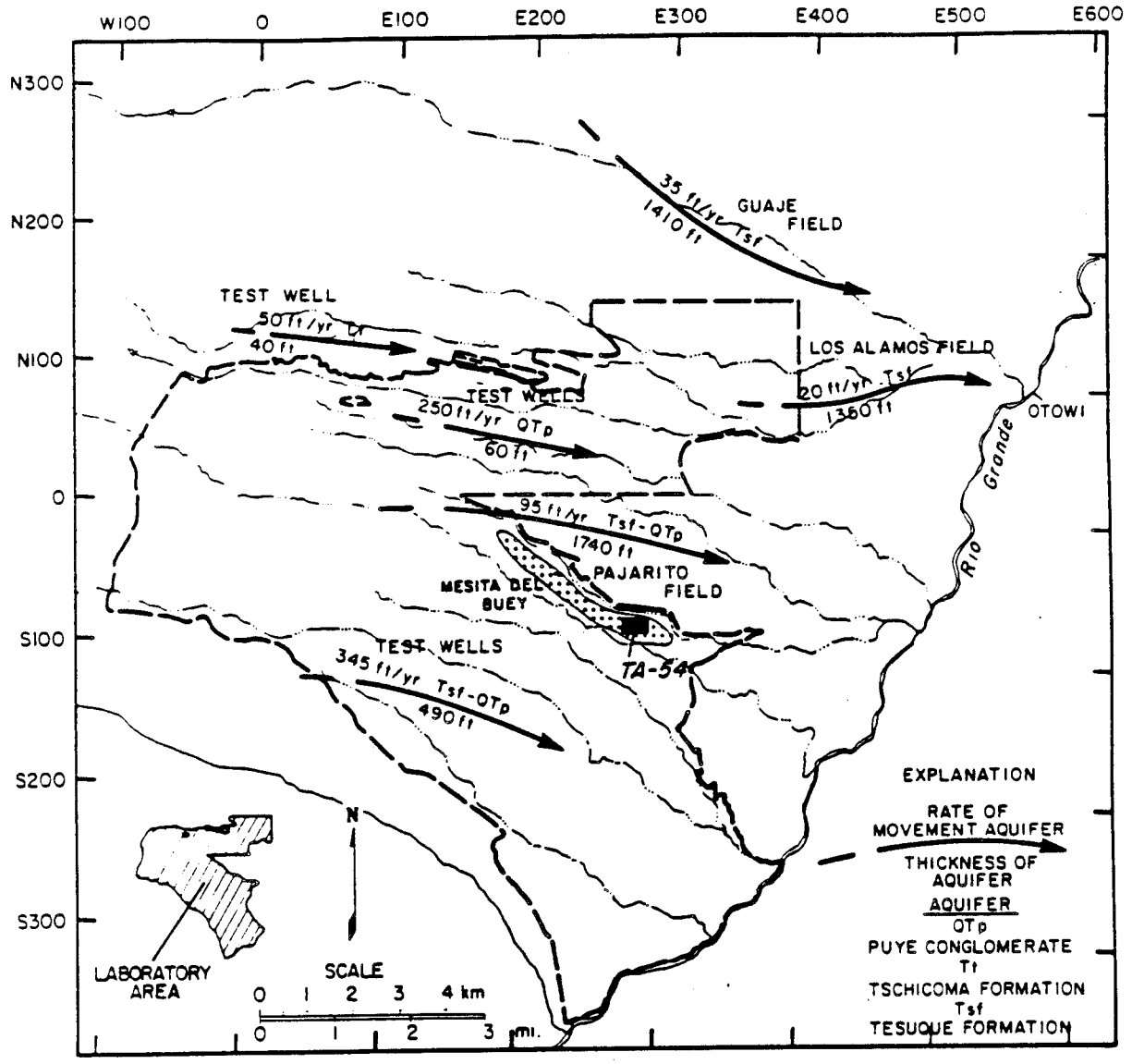

FIGURE 5-3 RATE OF MOVEMENT OF WATER IN THE MAIN AQUIFER IN THE LOS ALAMOS AREA (PURTYMUN, 1984)

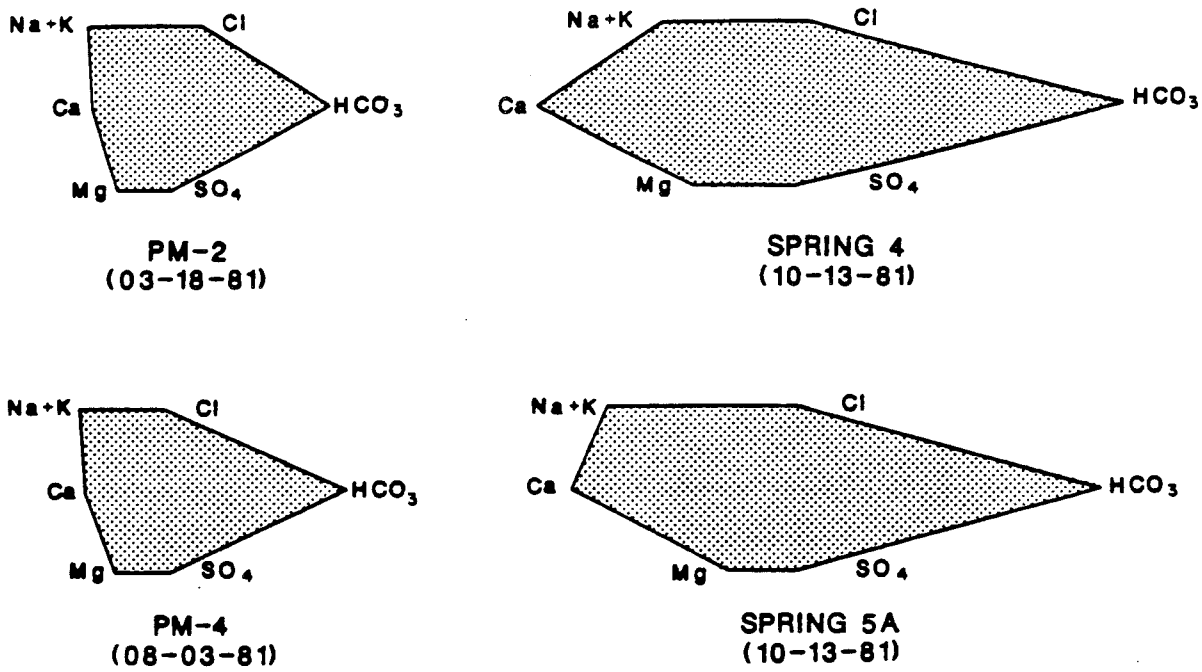

FIGURE 5-4

STIFF DIAGRAMS
FOR THE MAIN AQUIFER
NEAR MESITA DEL BUEY

PREPARED FOR

LOS ALAMOS NATIONAL LABORATORY
LOS ALAMOS, NEW MEXICO

DRAWING NUMBER	301017 A52
	3/25/82
	3/25/82
CHECKED BY	SWS
APPROVED BY	
LLF	2/17/86
AW BY	

© 1984 IT CORPORATION
ALL COPYRIGHTS RESERVED

IT ... Creating a Safer Tomorrow

65360

Do Not ... ile This Drawing

301017 02.A53

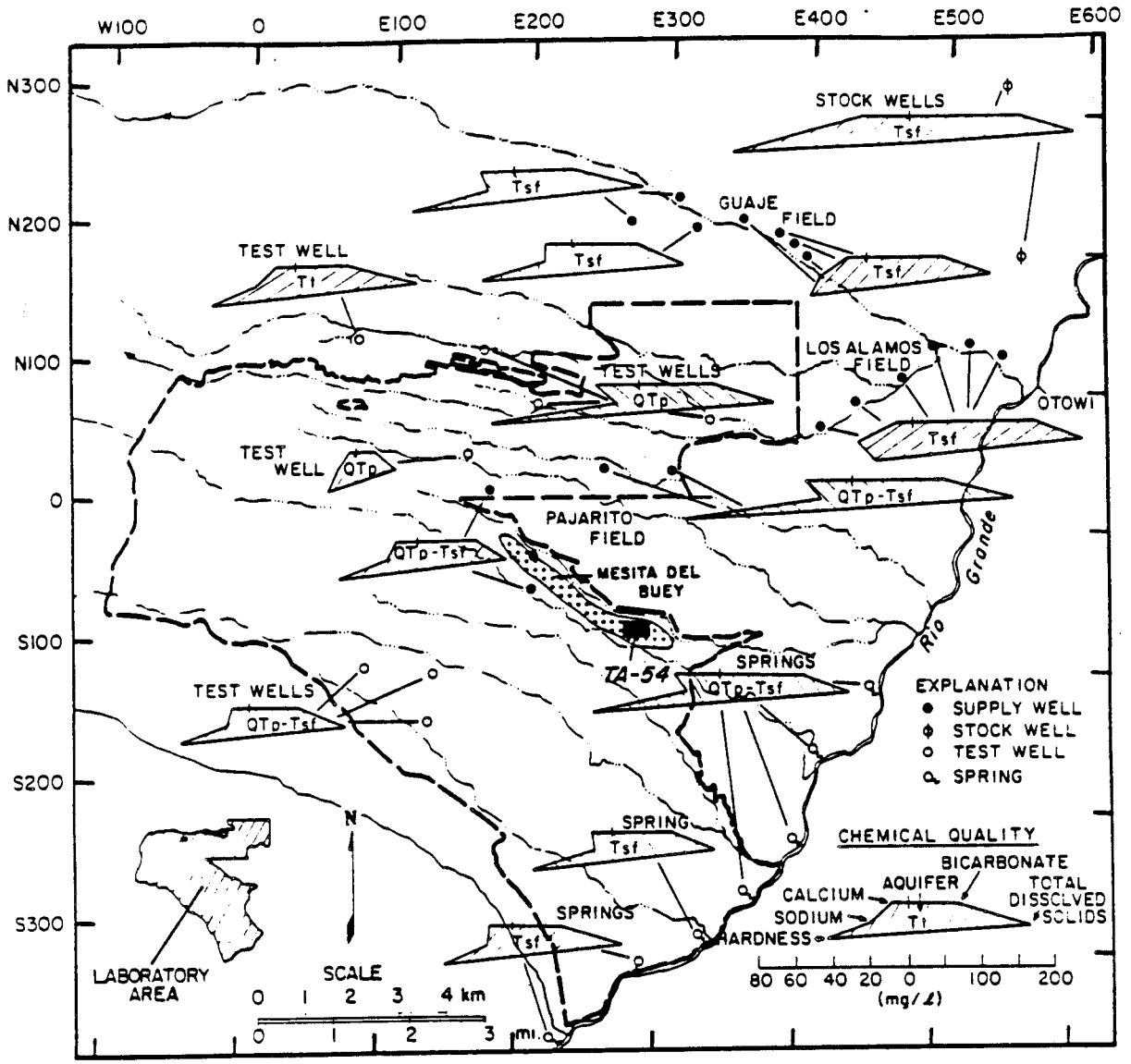

FIGURE 5-5 GRAPHIC COMPARISON OF CHEMICAL CONSTITUENTS IN THE MAIN AQUIFER FROM SUPPLY WELLS, TEST WELLS, STOCK WELLS, AND SPRINGS (PURTYMUN, 1984)

301017

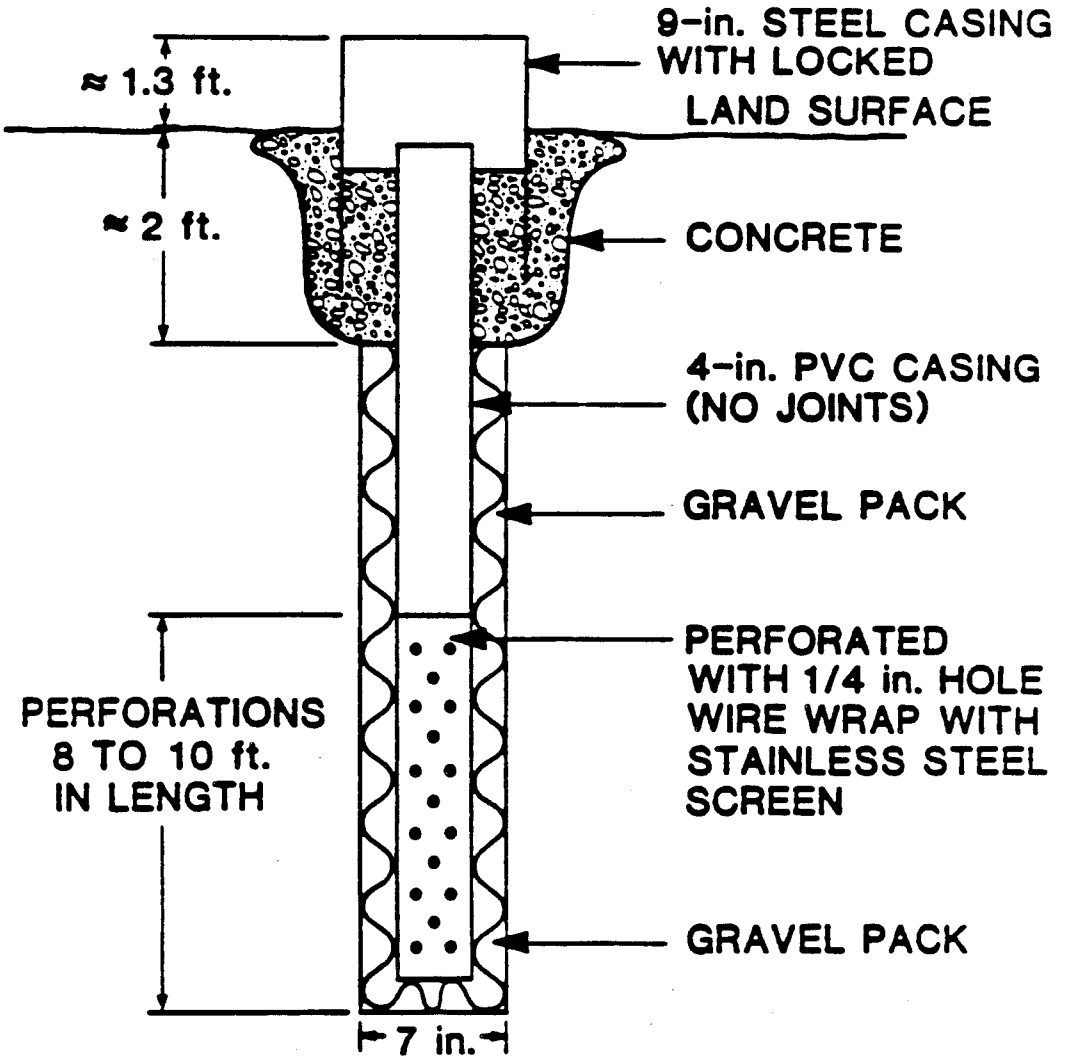

FIGURE 5-6 CONSTRUCTION SCHEMATIC OF MONITORING WELLS IN PAJARITO CANYON AND CAÑADA DEL BUEY (DEVAURS, 1985)

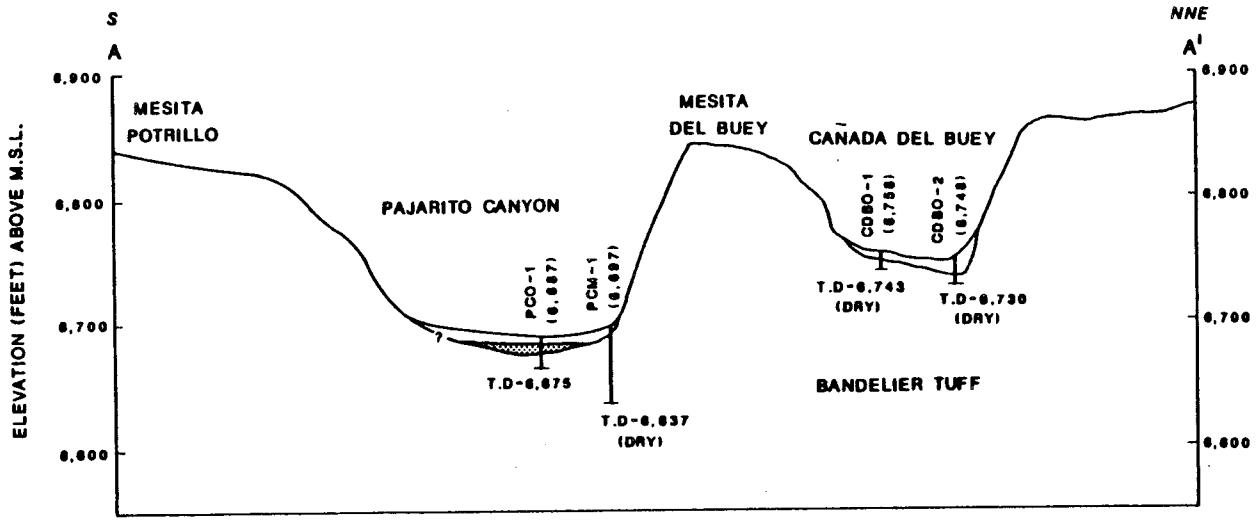

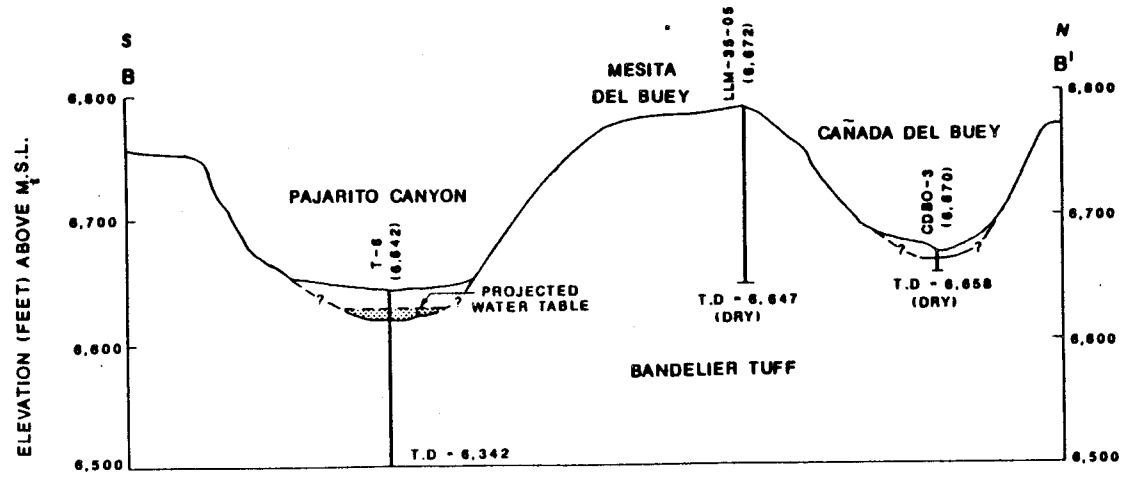

PERCHED WATER IN ALLUVIUM

400 200 0 400 FEET

HORIZONTAL SCALE

FIGURE 5-7

TOPOGRAPHIC PROFILES A-A' AND B-B' AND GEOLOGIC CROSS-SECTIONS THROUGH MESITA DEL BUEY

PREPARED FOR

LOS ALAMOS NATIONAL LABORATORY
LOS ALAMOS, NEW MEXICO

IT Creating a Safer Tomorrow

DRAWN BY	CHECKED BY	APPROVED BY	DRAWING NUMBER
JPK 2/19/87	2/25/87	2/25/87	301017 B13

© 1984 IT CORPORATION
ALL COPYRIGHTS RESERVED
Do Not Scale This Drawing

65380

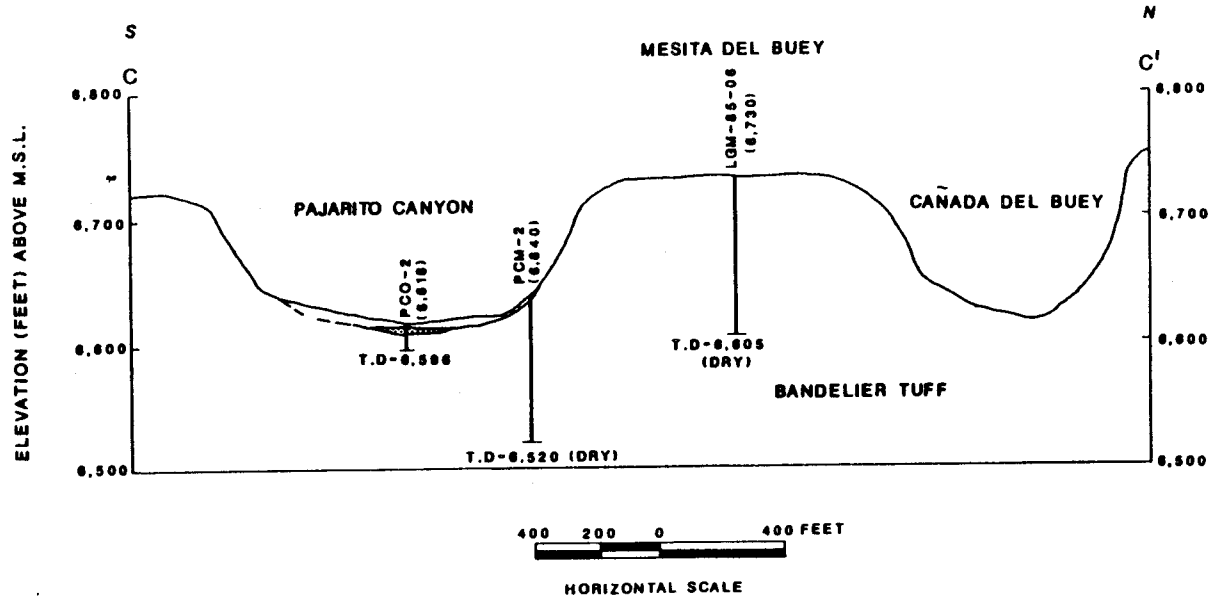

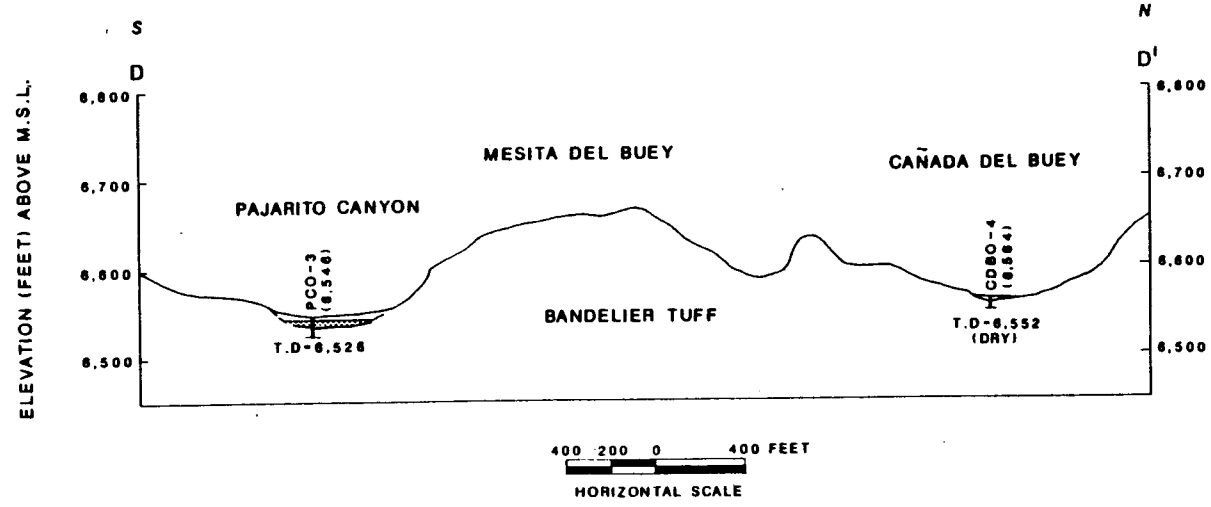

PERCHED WATER IN ALLUVIUM

FIGURE 5-8
TOPOGRAPHIC PROFILES
C-C' AND D-D' AND
GEOLOGIC CROSS-SECTIONS
OF MESITA DEL BUEY
PREPARED FOR
LOS ALAMOS NATIONAL LABORATORY
LOS ALAMOS, NEW MEXICO

IT Creating a Safer Tomorrow

DRAWN BY	LLF	CHECKED BY			DRAWING NUMBER 301017 B14
	2/23/87	APPROVED BY			

55380 © 1984 IT CORPORATION
ALL COPYRIGHTS RESERVED
Do Not Scale This Drawing

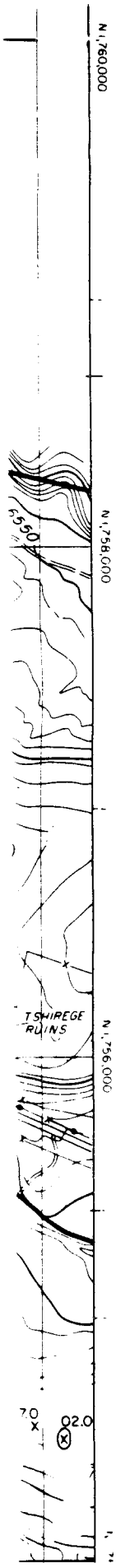

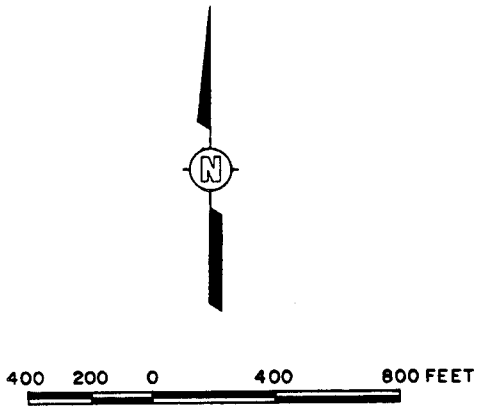

FIGURE 5-9

CONTOUR MAP OF TECHNICAL AREA 54
SHOWING THE LOCATIONS OF
MONITORING WELLS AND CROSS-SECTIONS

PREPARED FOR

LOS ALAMOS NATIONAL LABORATORY
LOS ALAMOS, NEW MEXICO

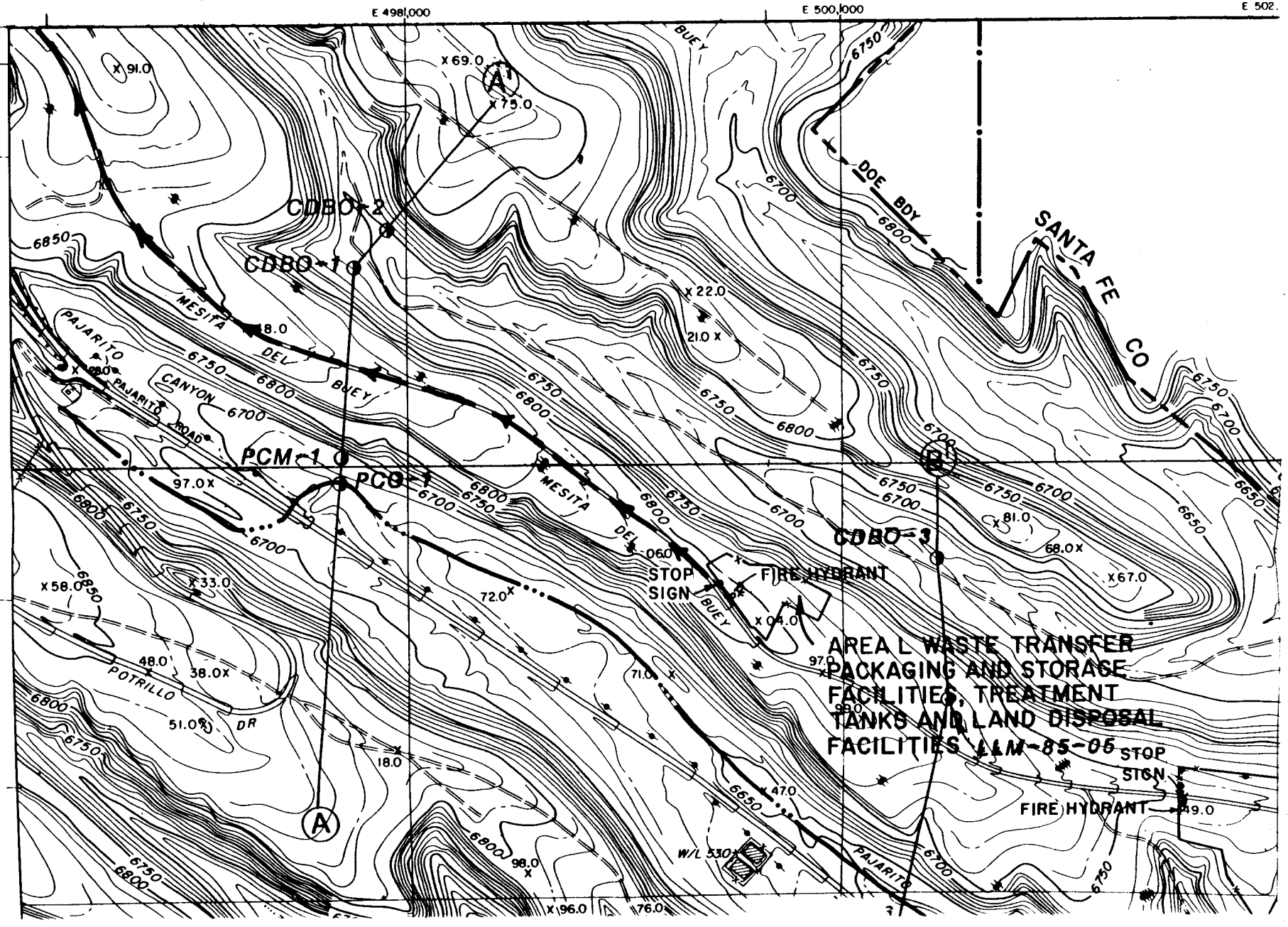
E 498,000
E 500,000
E 502.
3,967,000 N
S 40+00
S 60+00
3,966,000 N
A'
A
B'
B
CDBO-2
CDBO-1
CDBO-3
PCM-1
PCO-1
DOE BDY
SANTA FE CO
MESITA DEL BUEY
PAJARITO CANYON
PAJARITO ROAD
POTRILLO DR
STOP SIGN
FIRE HYDRANT
W/L 530
AREA L WASTE TRANSFER PACKAGING AND STORAGE FACILITIES, TREATMENT TANKS AND LAND DISPOSAL FACILITIES LLM-85-05

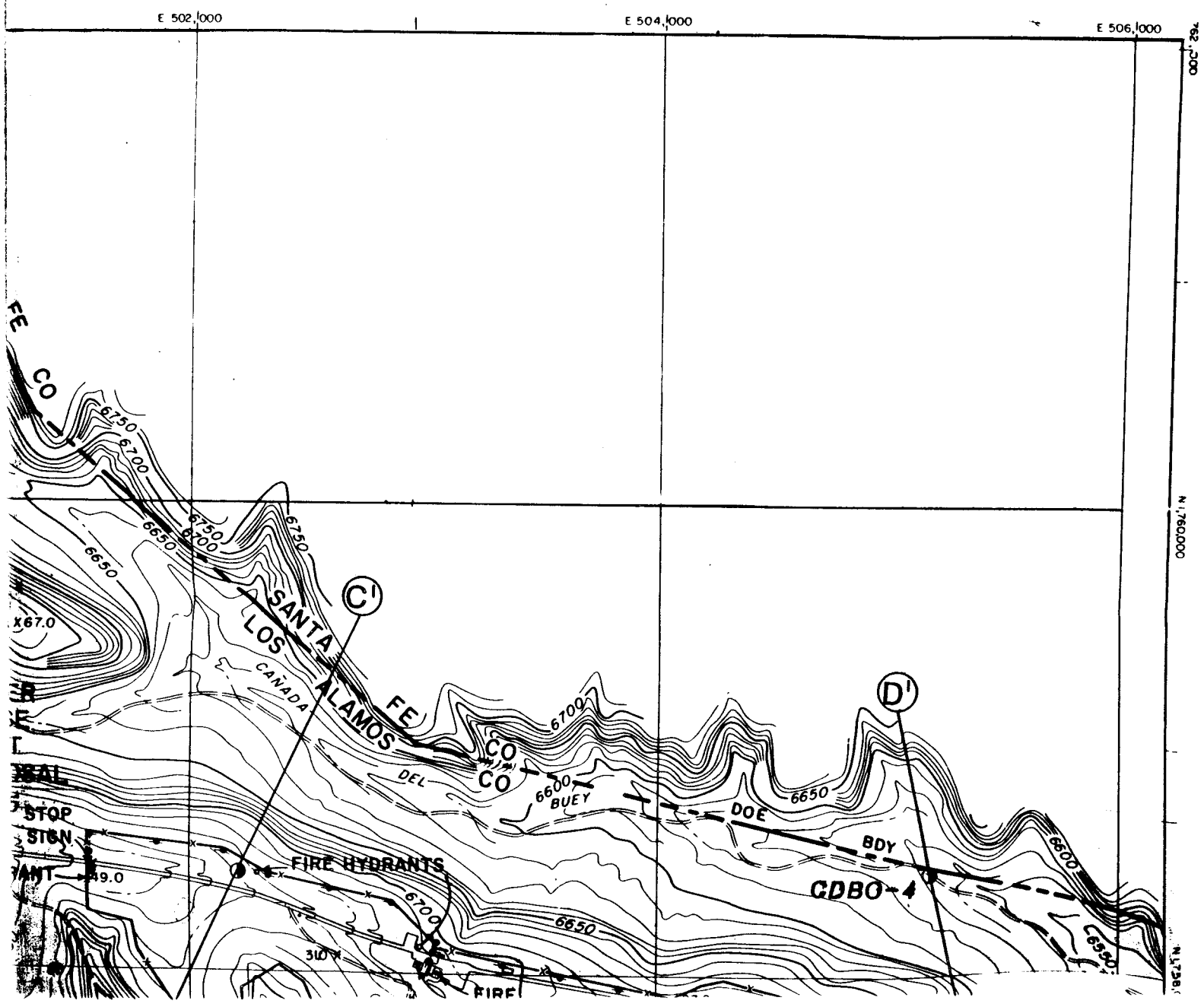
E 502,000
E 504,000
E 506,000
N 1,760,000
N 1,758,000
6750
6700
6650
6600
6550
SANTA FE CO
LOS ALAMOS CO
CANADA DEL BUEY
DOE BDY
CDBO-4
C'
D'
FIRE HYDRANTS
STOP SIGN
FIRE
X67.0
49.0
310

L

MONITORIN

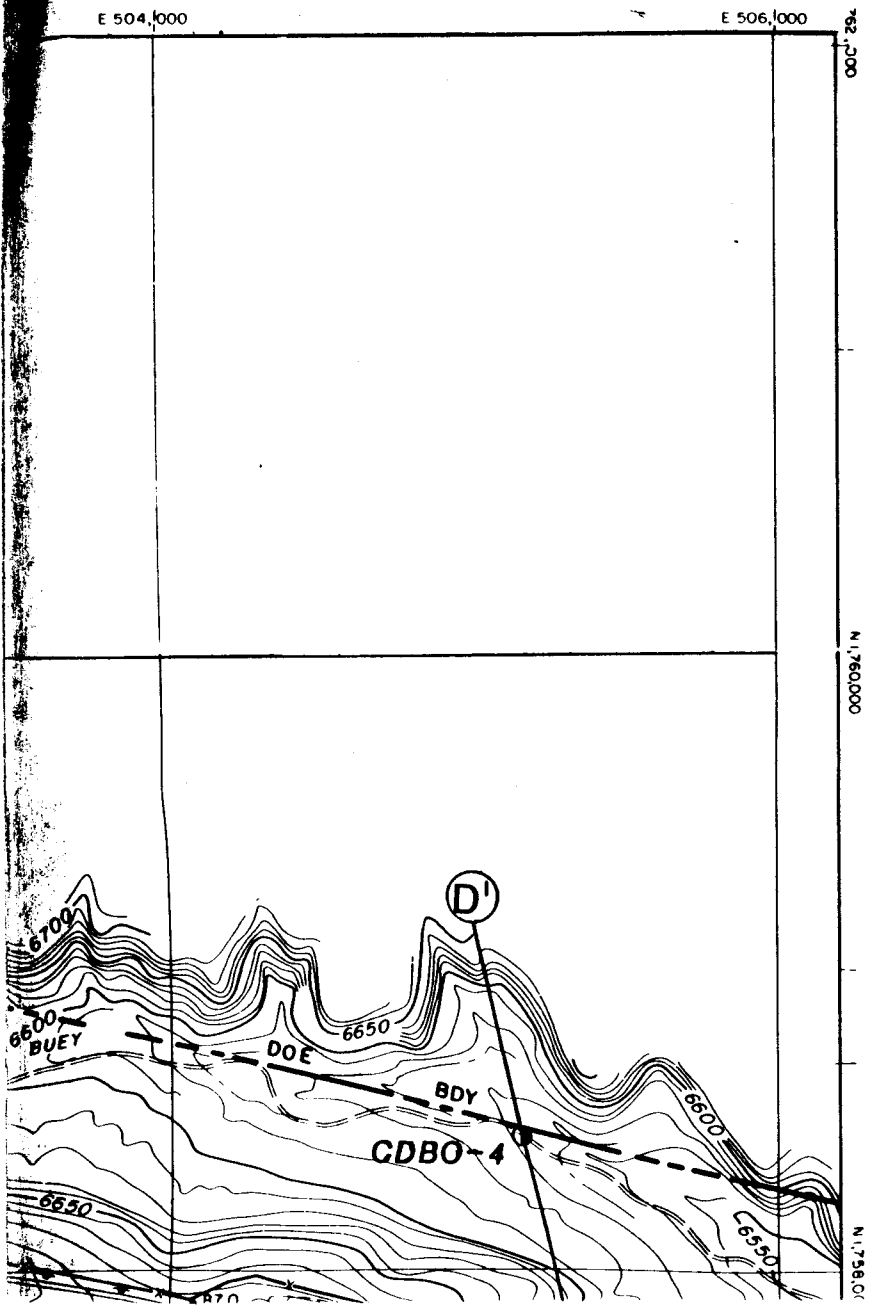

LEGEND

◑ MONITORING WELLS AND TEST HOLES

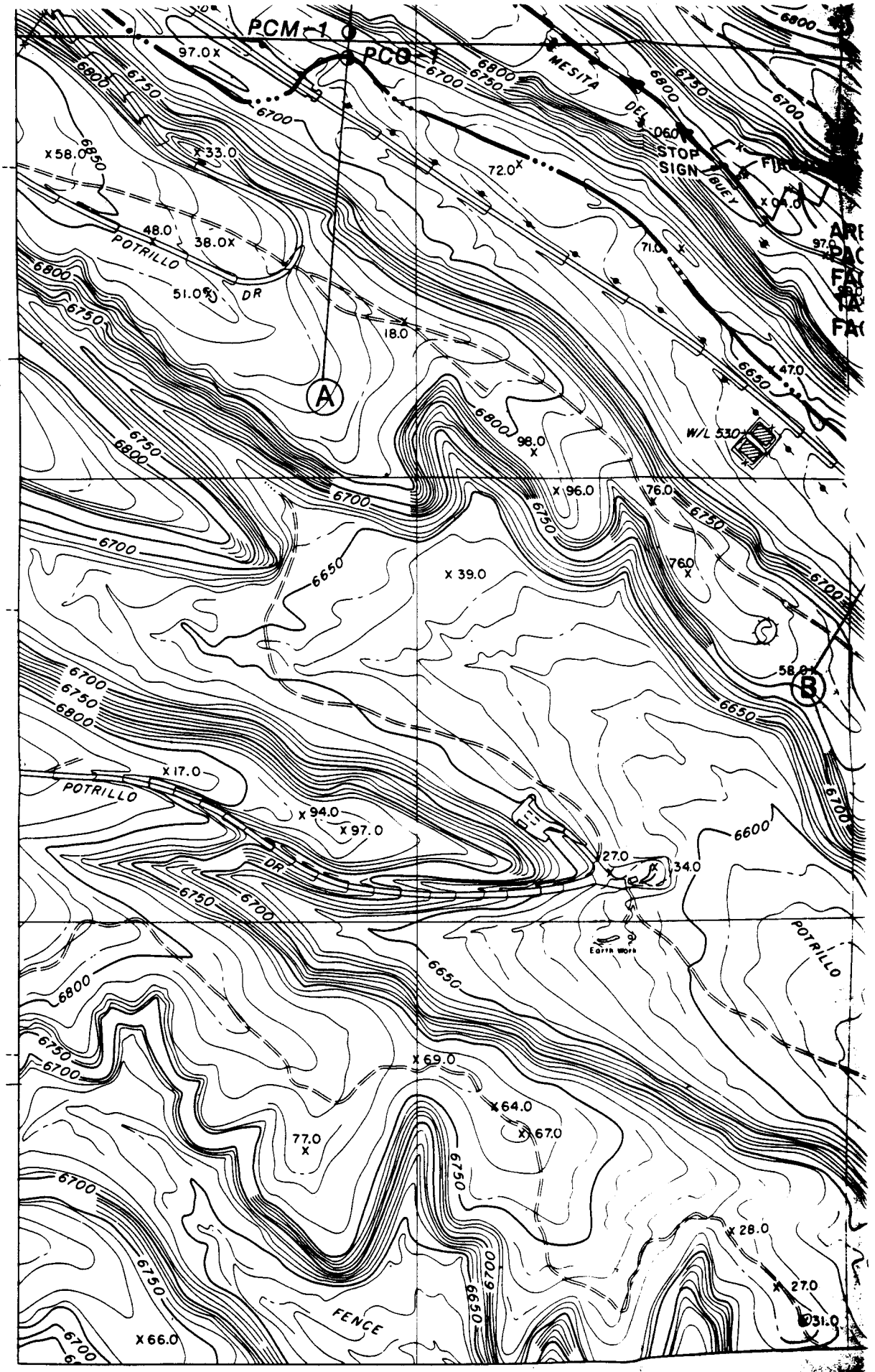
PCM-1
PCO-1
MESITA DEL GUEY
STOP SIGN
POTRILLO DR
POTRILLO
W/L 530
Earth Work
FENCE
A
B
S60+00
3,966,000 N
S 80+00
3,965,000 N S100+00

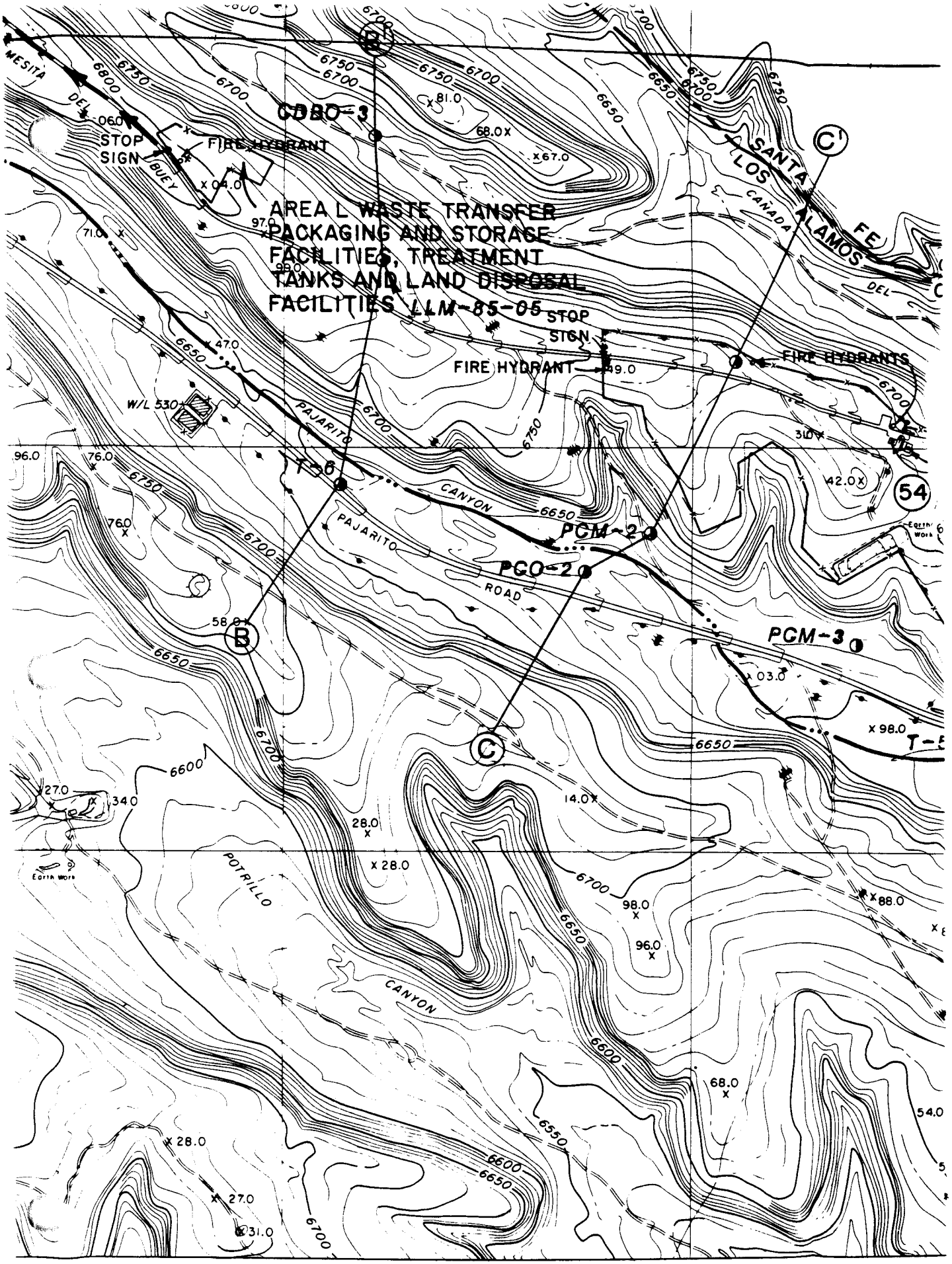
AREA L WASTE TRANSFER
PACKAGING AND STORAGE
FACILITIES, TREATMENT
TANKS AND LAND DISPOSAL
FACILITIES LLM-85-05
CDBO-3
STOP SIGN
FIRE HYDRANT
STOP SIGN
FIRE HYDRANT
FIRE HYDRANTS
W/L 530
T-6
PCM-2
PCO-2
PCM-3
B
B'
C
C'
54
SANTA FE
LOS ALAMOS
CANADA
DEL
MESITA
BUEY
PAJARITO
CANYON
PAJARITO
ROAD
POTRILLO
CANYON
Earth Work
Earth Work
6800
6750
6700
6650
6600
6550

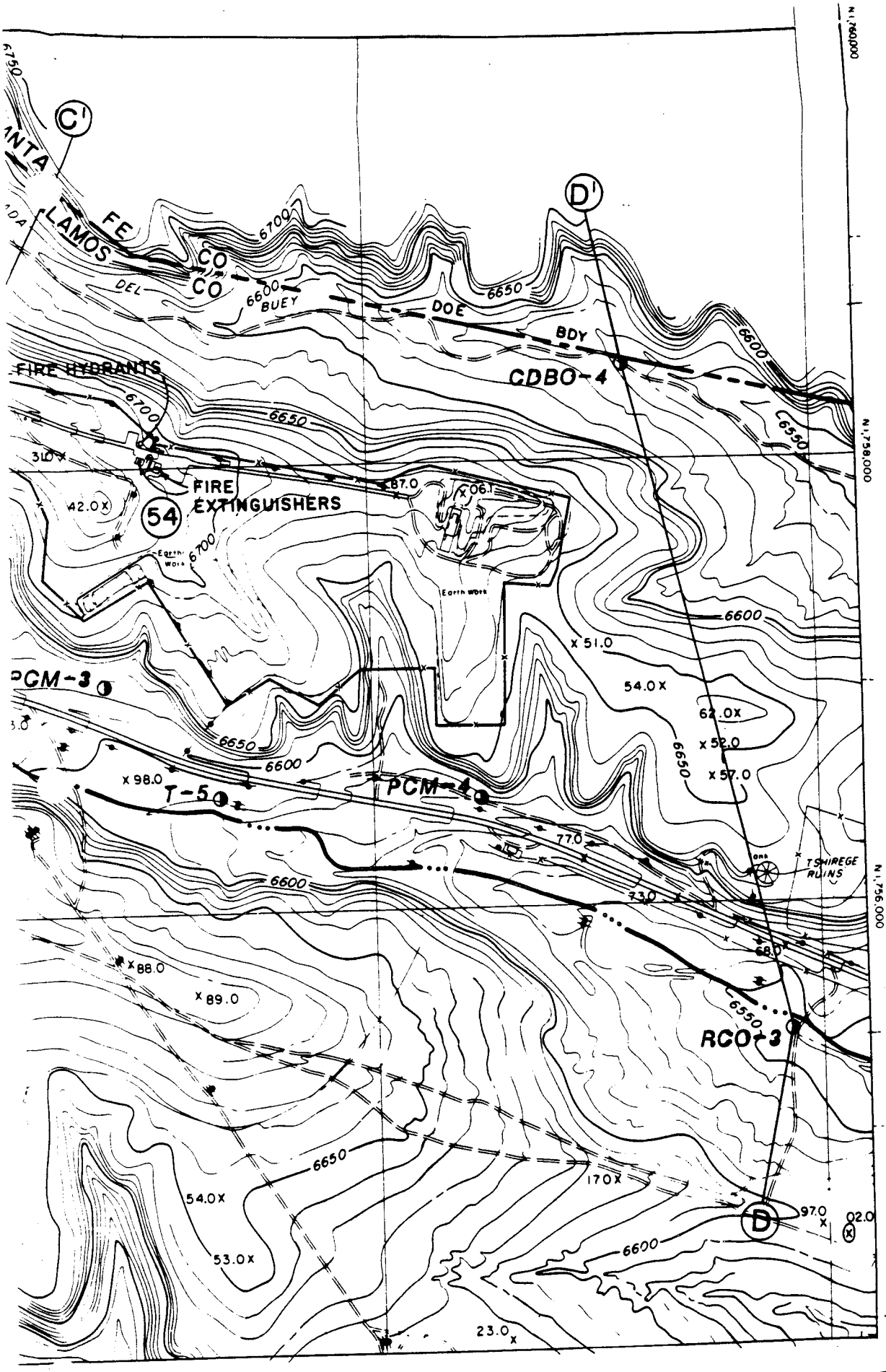

CONTO

MONITOR

LOS

THIS PAGE INTENTIONALLY LEFT BLANK

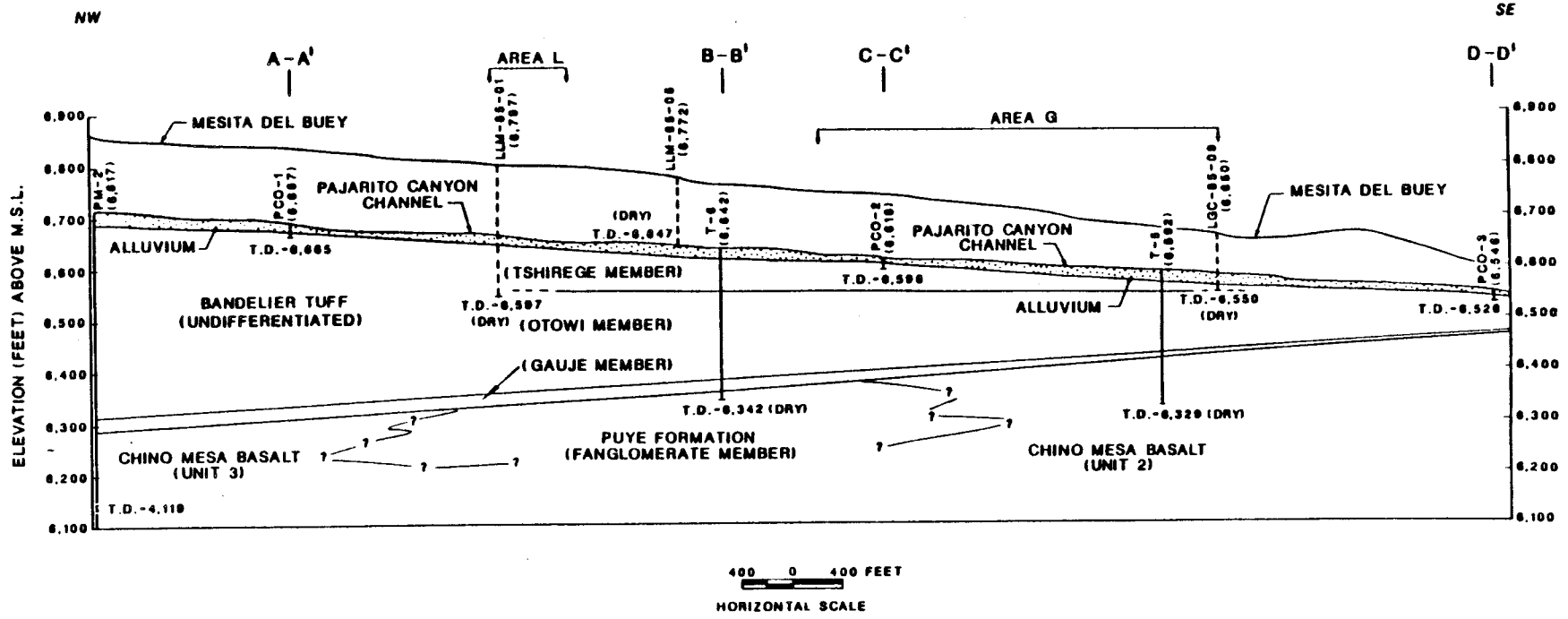

FIGURE 5-10

NORTHWEST - SOUTHEAST TOPOGRAPHIC PROFILES AND GEOLOGIC CROSS-SECTIONS OF MESITA DEL BUEY AND PAJARITO CANYON

PREPARED FOR

LOS ALAMOS NATIONAL LABORATORY
LOS ALAMOS, NEW MEXICO

Creating a Safer Tomorrow

1984 IT CORPORATION
ALL COPYRIGHTS RESERVED

DRAWN BY LLP 2/23/87 | CHECKED BY | APPROVED BY | DRAWING NUMBER 301017 815

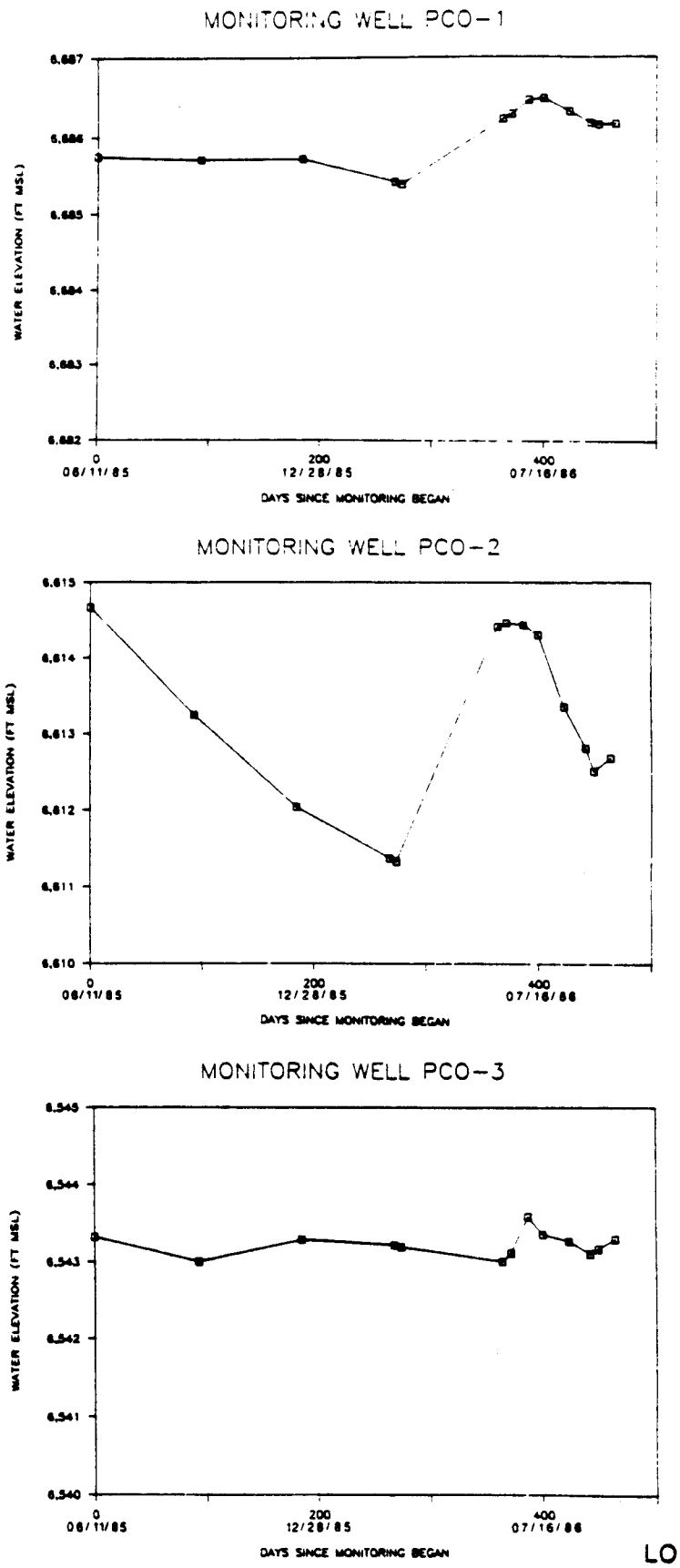

FIGURE 5-11

PLOT OF WATER-LEVEL ELEVATION VERSUS TIME FOR PAJARITO CANYON MONITORING WELLS

PREPARED FOR

LOS ALAMOS NATIONAL LABORATORY
LOS ALAMOS, NEW MEXICO

LLF | CHECKED BY | SWS | 3/25/87 | DRAWING
2/27/87 | APPROVED BY | 3/25/87 | NUMBER 301017 02 A55

© 1984 IT CORPORATION
ALL COPYRIGHTS RESERVED

IT ... Creating a Safer Tomorrow

Do Not Scale This Drawing

05360

DRAWN BY	LLF	CHECKED BY	SWS	3/25/87	DRAWING NUMBER 301017 02 A56
	2/27/87	APPROVED BY		3/25/87	

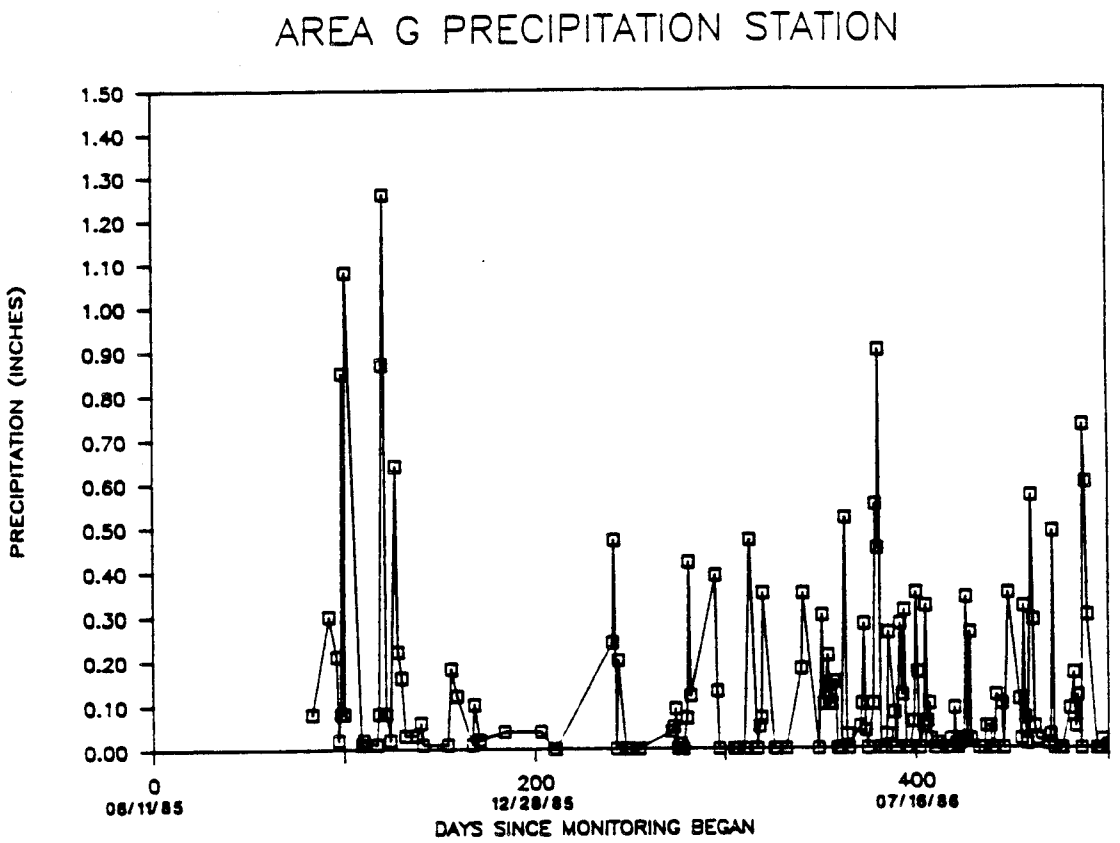

NOTE: 1985-1986 precipitation data is tabulated in Appendix F

FIGURE 5-12

SUMMARY OF THE 1985-1986 PRECIPITATION DATA IN AREA G

PREPARED FOR

LOS ALAMOS NATIONAL LABORATORY
LOS ALAMOS, NEW MEXICO

© 1984 IT CORPORATION
ALL COPYRIGHTS RESERVED

IT ... Creating a Safer Tomorrow

65360

Do Not Scale This Drawing

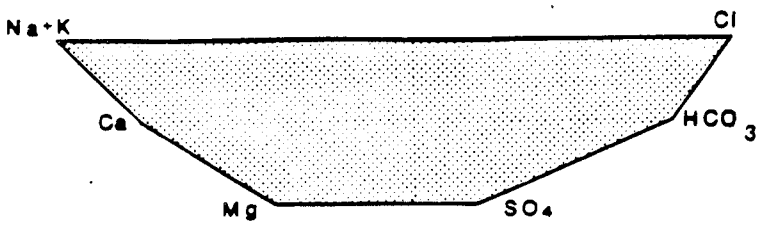

06-11-85

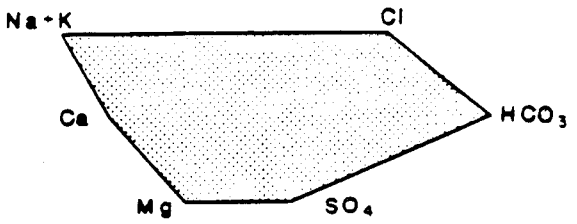

06-10-86

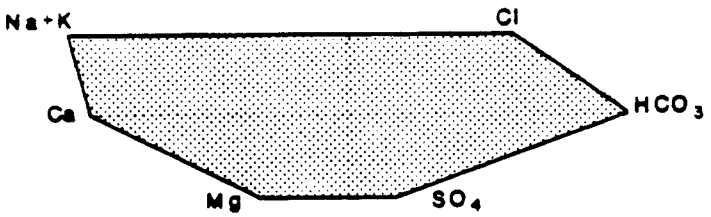

09-03-85

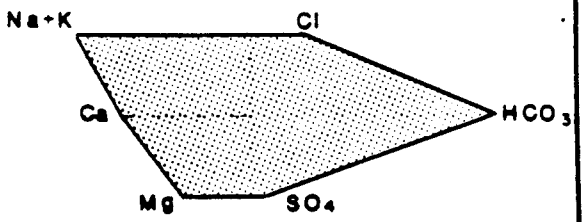

09-18-86

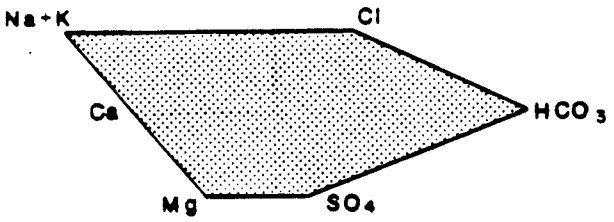

12-04-85

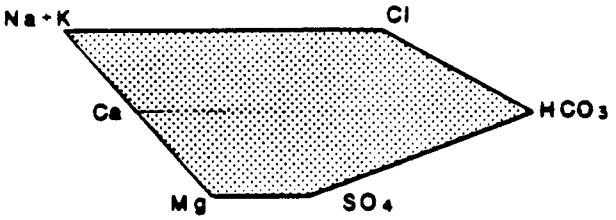

03-06-86

FIGURE 5-13

STIFF DIAGRAMS FOR PERCHED WATER IN MONITORING WELL PCO-1 PAJARITO CANYON

PREPARED FOR

LOS ALAMOS NATIONAL LABORATORY
LOS ALAMOS, NEW MEXICO

DR	LLF 17/86	CHECKED BY SWS	DRAWING NUMBER 3010
	APPROVED BY	3/25/87	3/25/87

© 1984 IT CORPORATION
ALL COPYRIGHTS RESERVED

IT ... Creating a Safer Tomorrow

05360

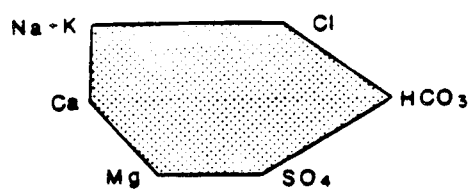

06-11-85

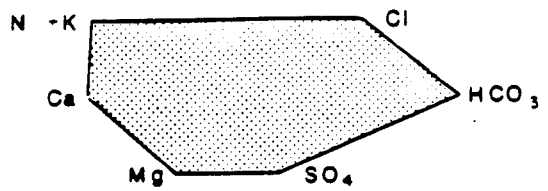

06-10-86

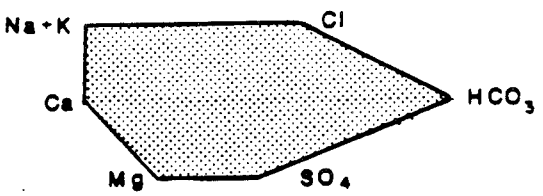

09-03-85

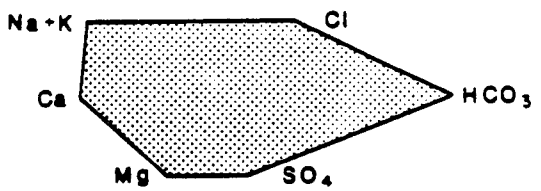

09-18-86

12-04-85
(NOT AVAILABLE)

03-06-86
(NOT AVAILABLE)

FIGURE 5-14

STIFF DIAGRAMS FOR PERCHED WATER IN MONITORING WELL PCO-2 PAJARITO CANYON

PREPARED FOR

LOS ALAMOS NATIONAL LABORATORY
LOS ALAMOS, NEW MEXICO

© 1984 IT CORPORATION
ALL COPYRIGHTS RESERVED

IT ... Creating a Safer Tomorrow

Do Not Scale This Drawing

DRAWN BY	LLF 2/17/86	CHECKED BY	SGJS	DRAWING NUMBER 301017 A58
		APPROVED BY		

85360

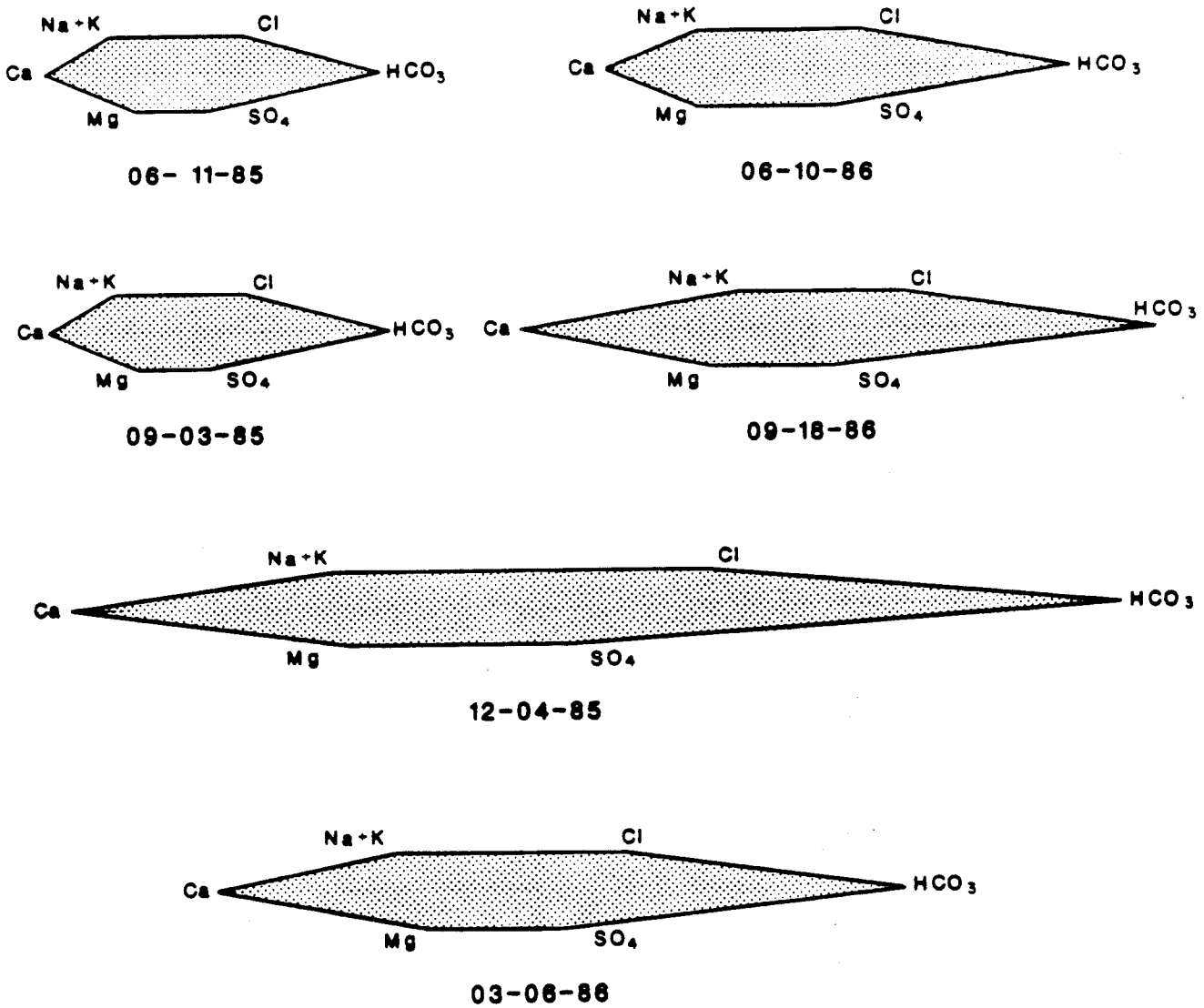

FIGURE 5-15
STIFF DIAGRAMS FOR PERCHED WATER
IN MONITORING WELL PCO-3
PAJARITO CANYON

PREPARED FOR

LOS ALAMOS NATIONAL LABORATORY
LOS ALAMOS, NEW MEXICO

© 1984 IT CORPORATION
ALL COPYRIGHTS RESERVED

IT ... Creating a Safer Tomorrow

DRAWING NUMBER 301017 A

CHECKED BY

APPROVED BY

LLF

7.0 REFERENCES

Abeele, W. V., M. L. Wheeler, and B. W. Burton, 1981, Geohydrology of Bandelier Tuff, LA-8962-MS, UC-11, Los Alamos National Laboratory, NM.

Abrahams, J. H., E. H. Baltz, and W. D. Purtymum, 1962, Movement of Perched Ground Water in Alluvium Near Los Alamos, New Mexico, U.S. Geological Survey Professional Paper 450-B.

BFEC, 1985a, Vadose Zone Characterization of Technical Area 54, Waste Disposal Areas G and L, Los Alamos National Laboratory, New Mexico. Report 1: Drilling and Logging Activities, Bendix Field Engineering Corporation, 38 pp.

BFEC, 1985b, Vadose Zone Characterization of Technical Area 54, Waste Disposal Areas G and L, Los Alamos National Laboratory, New Mexico. Report 2: Down-hole Instrumentation and Pore-Gas-Sampling/Data-Collection Procedures, Bendix Field Engineering Corporation, 27 pp.

BFEC, 1986, Vadose Zone Characterization of Technical Area 54, Waste Disposal Areas G and L, Los Alamos National Laboratory, New Mexico. Report 3: Preliminary Assessment of the Hydrologic System, Bendix Field Engineering Corporation, 103 pp. and Appendices.

Bailey, R. A., R. L. Smith and C. S. Ross, 1969, Volcanic Rocks in the Jemez Mountains, New Mexico, U.S. Geological Survey Bulletin 1274-P, 29 pp.

Baltz, E. H., J. H. Abrahams, and W. D. Purtymun, 1963, Preliminary Report on the Geology and Hydrology of Mortandad Canyon Near Los Alamos, New Mexico, U.S. Geological Survey Open File Report.

Cooper, J. B., W. D. Purtymun, and E. G. John, 1965, Records of Water Supply Wells Guaje Canyon 6, Pajarito Mesa 1 and Pajarito Mesa 2, Los Alamos, New Mexico -- Basic Data Report, U.S. Geological Survey, 89 pp.

Conover, C. S., C. V. Theis, and R. L. Griggs, 1963, Geology and Hydrology of the Valle Grande and Valle Toledo, Sandoval County, New Mexico, U.S. Geological Survey Water Supply Paper 1619-Y.

Dane, C. H., 1948, Geologic Map of Part of Eastern San Juan Basin, Rio Arriba County, New Mexico, U.S. Geological Survey Oil and Gas Investigations Preliminary Map 78.

Department of Energy, 1987, Quarterly Report: September 1986 Observation Well Data from Canyons Adjacent to Mesita del Buey Waste Disposal Areas, Los Alamos National Laboratory, unpublished Report.

Department of Energy, 1986a, Quarterly Report: September 1985 Observation Well Data from Canyons Adjacent to Mesita del Buey Waste Disposal Areas, Los Alamos National Laboratory, unpublished Report.

Department of Energy, 1986b, Quarterly Report: December 1985 Observation Well Data from Canyons Adjacent to Mesita del Buey Waste Disposal Areas, Los Alamos National Laboratory, unpublished Report.

Department of Energy, 1986c, Quarterly Report: March 1986 Observation Well Data from Canyons Adjacent to Mesita del Buey Waste Disposal Areas, Los Alamos National Laboratory, unpublished Report.

Department of Energy, 1986d, Quarterly Report: June 1986 Observation Well Data from Canyons Adjacent to Mesita del Buey Waste Disposal Areas, Los Alamos National Laboratory, unpublished Report.

Department of Energy, 1986e, Quarterly Report: Results of March and April 1986 Pore Gas Sampling Conducted at Technical Area 54 Waste Disposal Areas L and G, Los Alamos National Laboratory, unpublished Report.

Department of Energy, 1986f, Results of Area L Surface Impoundment Characterization, Los Alamos National Laboratory Report HSE-8-86-1296, 11-18.

Department of Energy, 1984, Correspondence, H. E. Valencia to D. Fort, October 31, 1984.

Devaurs, M., 1985, Core Analyses and Observation Well Data from Mesita del Buey Waste Disposal Areas and in Adjacent Canyons, Los Alamos National Laboratory, unpublished Report, 52 pp.

Devaurs, M., and S. Bell, 1986, Results of Initial Pore Gas Sampling Conducted at Technical Area 54 Waste Disposal Areas L and G, Los Alamos National Laboratory Report LA-UR-862370, 35 pp.

Devaurs, M., and W. D. Purtyman, 1985, Hydrologic Characteristics of the Alluvial Aquifers in Mortandad, Cañada del Buey, and Pajarito Canyons, Los Alamos National Laboratory, unpublished Report, 27 pp.

Environmental Surveillance Group, 1984, Environmental Surveillance at Los Alamos During 1983, Los Alamos National Laboratory Report LA-10100-ENV.

Environmental Surveillance Group (HSE-8), 1986, Environmental Surveillance at Los Alamos During 1985, Los Alamos National Laboratory Report, LA-10721-ENV.

Everett, L. G., L. G. Wilson, and E. W. Hoylman, 1984, Vadose Zone Monitoring for Hazardous Waste Sites, Noyes Data Corporation, New Jersey, 358 pp.

Freeze, R. A., and J. A. Cherry, 1979, Groundwater, Prentice-Hall, Inc., New Jersey, 604 pp.

Griggs, R. L., 1964, Geology and Ground-Water Resources of the Los Alamos Area, New Mexico, U.S. Geological Survey Water Supply Paper 1753, 107 pp.

Hillel, D., 1980, Introduction to Soil Physics, Academic Press, Inc., New York, NY, 364 pp.

Horner, R. D., 1951, "Pressure Build-Up in Wells," in Proceedings of the Third World Petroleum Conference, Section II, E. J. Bill, Leiden, Holland.

Johnson, E. F., D. P. Bossler, and V. D. Naumann, 1959, "Calculations of Relative Permeability from Displacement Experiments," Transactions of the American Institute of Mining, Metallurgical, and Petroleum Engineers, Vol. 216, pp. 370-372.

Kelley, V. C., 1954, Tectonic Map of a Part of the Upper Rio Grande Area, U.S. Geologic Survey Oil and Gas Investigations Map OM-157.

Kelley, V. C., 1955, Regional Tectonics of the Colorado Plateau and Relationship to the Origin and Distribution of Uranium, University of New Mexico Publications on Geology, No. 5, 120 pp.

Kudo, A. M., 1974, "Outline of the Igneous Geology of the Jemez Mountains Volcanic Field," New Mexico Geological Society Guidebook, 25th Field Conference, Central-Northern New Mexico, pp. 287-289.

McInroy, D., 1985-1986, RCRA Monitoring Field Notebook A-001180, Environmental Surveillance Group (HSE-8), Los Alamos National Laboratory, unpublished notes.

Mualem, V., 1976, "A new Model for Predicting the Hydraulic Conductivity of Unsaturated Porous Media," Water Resources Research, Vol. 12, No. 3, pp. 513-522.

New Mexico Environmental Improvement Board, 1985a, New Mexico Hazardous Waste Management Regulations (NMHWMR-3).

New Mexico Environmental Improvement Board, 1985b, Regulations Governing Water Supplies, (EIB/WSR1).

New Mexico Environmental Improvement Division, 1985, A reasonable Worst-Case Water Balance for LANL Hazardous Waste Disposal Areas, with Emphasis on TA-54, Unpublished Report, (May 7, 1985).

New Mexico Water Quality Control Commission, 1986, Water Quality Control Commission Regulations (WQCC 82-1).

Purtymun, W. D., 1974, Dispersion and Movement of Tritium in a Shallow Aquifer in Mortandad Canyon at Los Alamos Scientific Laboratory, Los Alamos Scientific Laboratory Report LA-5716-MS.

Purtymun, W. D., 1975, Geohydrology of the Pajarito Plateau with Reference to Quality of Water, 1949-1975, Los Alamos National Laboratory informal Report, 343 pp.

Purtymun, W. D., 1981, Geohydrology of the Bandelier Tuff, Los Alamos National Laboratory Report LA-8962-MS, 50 pp.

Purtymun, W. D., 1984, Hydrologic Characteristics of the Main Aquifer in the Los Alamos Area: Development of Ground Water Supplies, Los Alamos National Laboratory Report LA-9957-MS, 44 pp.

Purtymun, W. D., and S. Johansen, 1974, "General Geohydrology of the Pajarito Plateau," New Mexico Geological Society Guidebook, 25th Field Conference, Central Northern New Mexico, pp. 347-349.

Purtymun, W. D. and W. R. Kennedy, 1971, Geology and Hydrology of Mesita del Buey, Los Alamos Scientific Laboratory Report LA-4660, 11 pp.

Purtymun, W. D., M. L. Wheeler and M. A. Rogers, 1978, Geologic Description of Cores From Holes P-3 MH-1 Through P-3 MH-5, Area G, Technical Area 54, Los Alamos Scientific Laboratory Report LA-7308-MS, 13 pp.

Purtymun, W. D., W. R. Hansen, and R. J. Peters, 1983, Radiochemical Quality of Water in the Shallow Aquifer in Mortandad Canyon, 1967-1978, Los Alamos National Laboratory Report LA-9675-MS.

Rocky Mountain Analytical Laboratory, 1985, Results of Volatile Organic Analyses, letter report dated September 24, 1985.

Rogers, M. A., 1977, History and Environmental Setting of LASL Near-Surface Land Disposal Facilities for Radioactive Wastes (Areas A, B, C, D, E, F, G, and T), Los Alamos Scientific Laboratory, informal Report LA-6848-MS, Vol. I and II.

Ross, C. S, R. L. Smith and R. A. Bailey, 1961, "Outline of the Geology of the Jemez Mountains, New Mexico," New Mexico Geological Society Guidebook, 12th Field Conference, Albuquerque Country, pp. 139-143.

Schlumberger, 1972, Log Interpretation, Vol. I - Principles, Schlumberger Limited, New York, 113 pp.

Smith, R. L., and R. A. Bailey, 1966, "The Bandelier Tuff - A study of Ash-Flow Eruption Cycles From Zoned Magma Chambers," Bulletin of Volcanology, Series 2, Vol. 29, pp. 83-104.

Smith. R. L., and R. A. Bailey, 1968, Resurgent Cauldrons, Geological Society of America Memoir 116, pp. 613-662.

Smith, R. L., R. A. Bailey and C. S. Ross, 1970, Geologic Map of the Jemez Mountains, New Mexico, U.S. Geological Survey Miscellaneous Investigations Map I-571.

Stephens, D. B., and S. P. Neuman, 1982a, "Vadose Zone Permeability Test: Summary," Journal of the Hydraulics Division, American Society of Civil Engineers, Vol. 108, No. HY5, pp. 623-639.

Stephens, D. B., and S. P. Neuman, 1982b, "Vadose Zone Permeability Test: Steady State Results," Journal of the Hydraulics Division, American Society of Civil Engineers, Vol. 108, No. HY5, pp. 640-659.

Stephens, D. B., S. Tyler, K. Lambert, and S. Yates, 1983, "Field Experiments to Determine Saturated Hydraulic Conductivity in the Vadose Zone," in Role of Unsaturated Zone in Radioactive and Hazardous Waste Disposal, J. W. Mercer, P. S. C. Rao, and M. I. Wendell (eds.), Ann Arbor Scientific Publications, Ann Arbor, Michigan.

TerraTek Research Laboratory, 1985, Laboratory Analysis of Rock Core: Bandelier Formation, TR86-49, Salt Lake City, Utah.

U.S. EPA, 1976, National Interim Primary Drinking Water Regulations, U.S. Environmental Protection Agency, 40 CFR 141.

U.S. EPA, 1979, National Secondary Drinking Water Regulations, U.S. Environmental Protection Agency, 40 CFR 143.

U.S. EPA, 1984, A Characterization of Hazardous Waste Sites - A Methods Manual, Vol. III, Available Laboratory Analytical Methods, U.S. Environmental Protection Agency Report, EPA-600/4-84-038.

U.S. EPA, 1985a, Test Methods for Evaluating Solid Waste, Physical/Chemical Methods, EPA-SW-846, U.S. Government Printing Office.

U.S. EPA, 1985b, National Primary Drinking Water Regulations; Volatile Synthetic Organic Chemicals, U.S. Environmental Protection Agency, 40 CFR 141 and 142.

van Genuchten, Rien, 1978, Calculating the Unsaturated Hydraulic Conductivity with a New Closed-Form Analytical Model, Princeton University Water-Resources Program Report 78-WR-08.

Welge, H. J., 1952, "A Simplified Method for Computing Oil Recovery by Gas or Water Drive," Transactions of the American Institute of Mining, Metallurgical, and Petroleum Engineers, Vol. 195, pp. 91-98.

Woodward, L. A., 1974, "Tectonics of Central-Northern New Mexico," New Mexico Geological Society Guidebook, 25th Field Conference, Central-Northern New Mexico, pp. 123-129.

Woodward, L. A., and R. Martinez, 1974, Geologic Map and Sections of the Holy Ghost Spring Quadrangle, New Mexico, New Mexico Bureau of Mines and Mineral Resources Geologic Map 29.

Woodward, L. A., W. H. Kaufman and J. B. Anderson, 1972, "Nacimiento Fault and Related Structures, Northern New Mexico," Geological Society of America Bulletin, Vol. 83, pp. 2383-2396.

Woodward, L. A., W. H. Kaufman, J. B. Anderson and R. K. Reed, 1973, Geologic Map and Sections of the San Pablo Quadrangle, New Mexico, New Mexico Bureau of Mines and Mineral Resources Geologic Map 26.

Zygmunt, S., 1984, Facility Description for Part B Hazardous Waste Permit, Los Alamos National Laboratory, unpublished report.

6.0 SUMMARY AND CONCLUSIONS

Hydrogeologic investigations of waste disposal Areas G and L at Los Alamos National Laboratory were conducted in response to a Compliance Order issued to the Laboratory by the State of New Mexico on May 7, 1985. Based on the investigations conducted during 1985 and 1986 in fulfillment of the Order and on previous investigations, several conclusions which reflect the current state of knowledge relative to the potential migration of hazardous waste constituents from the areas can be reached. These conclusions and brief summaries of data supporting each are provided below. Comprehensive discussions of data and conclusions concerning each area are provided in the accompanying text.

6.1 GEOLOGY OF TECHNICAL AREA 54, AREAS G AND L

Areas G and L are located on Mesita del Buey, a narrow southeast-trending mesa located on the western edge of the Pajarito Plateau. The plateau is comprised of an apron of volcanic and sedimentary rocks exceeding 2,000 feet in thickness on the eastern flanks of the Jemez mountains. Mesita del Buey is formed by approximately 475 feet of ashflows and ashfalls of the Bandelier Tuff which dip gently two to three degrees to the southeast. The tuff is underlain by 1,050 feet of interbedded Chino Mesa basalt and conglomerates of the Puye Formation. The Tesuque Formation, which underlies the Chino Mesa Basalt and Puye Formation, is comprised of coarse sediments interbedded with basalt flows and exceeds 1,000 feet in thickness beneath Mesita del Buey.

The geologic structure of the surface rocks which form Mesita del Buey are relatively simple; no faults are known to break the rocks of Mesita del Buey. The most prevalent structural features of Mesita del Buey are fractures in the volcanic rocks caused by shrinkage upon cooling after deposition. These fractures are nearly vertical with an average opening of ¼-inch. Most of the fractures encountered in the tuff are filled or plated with brown clay. The remainder are open with joint faces slightly weathered or plated with caliche. On the basis of this study and previous work the following conclusions concerning the geology of Mesita del Buey can be drawn:

- **The stratigraphy at Areas G and L is similar to that of the tuff throughout the western Pajarito Plateau**

- **Vertical and near-vertical fractures (formed during cooling of the volcanically deposited material) are common in the Bandelier Tuff on Mesita del Buey (and elsewhere), though the degree of openness or pervasiveness of individual fractures is not well characterized**

- **No major fault zones that could serve as conduits from the shallow subsurface to the regional water table are known to exist at or near Areas G and L.**

6.2 HYDROLOGIC CHARACTERIZATION OF THE VADOSE ZONE

Tasks one through four, paragraph 25 of the Order issued to the Laboratory specify testing and monitoring programs to be carried out to characterize the vadose zone hydrology at Areas G and L. The four tasks taken together provide the information necessary to calculate rates of moisture flux by unsaturated fluid flow through porous media. Task four also requires empirical measurement of infiltration and moisture redistribution within the tuff.

Task one requires measurement of the intrinsic permeability of the tuff. This task was satisfied utilizing both field and laboratory methods. Field methods included air injection and vacuum testing of five boreholes. (Due to the potential for mobilization of contaminants in the vadose zone by water introduced by testing, air permeability tests, which are experimental in nature, were utilized for field investigations). Water injection permeability tests were conducted in one borehole for comparison with results of air tests; tests conducted with water yield permeability of the same order of magnitude as air tests. Including both field methods, a minimum of nine intervals were tested in each borehole. Intrinsic permeability of four samples from each borehole was determined in the laboratory via the Klinkenberg Method and the Dynamic Method. Field methods yield intrinsic permeability in the range of 10^{-8} to 10^{-9} cm^2 and laboratory methods yield values of 10^{-9} cm^2. These values represent moderate permeability similar to that of silty sand. Each method indicates a slight decrease in intrinsic permeability with depth. In addition, intervals tested adjacent to fractures do not exhibit increased permeability.

Task two requires determination of soil moisture characteristic curves for five samples from each of at least four horizons. This requirement was satisfied by testing four samples (one per horizon) from five boreholes. The soil

moisture characteristic curves were determined by the centrifugal method. This method yielded characteristic curves in the 0.03 bar (0.5 psi) to 0.34 bar (5 psi) soil water tension range. Field conditions of soil water tension range from 1 to 15 bars. Attempts to evaluate higher tension ranges (lower moisture content) were made utilizing the centrifugal and pressure plate methods. These methods were unsuccessful due to sample disaggregation at higher tensions.

Task three of paragraph 25 requires determination of unsaturated hydraulic conductivity of the Bandelier Tuff; five samples from each of four horizons are required. Theoretical and laboratory methods were utilized to determine the unsaturated conductivity of four samples from five boreholes. Due to difficulties with the material strength of the tuff (sample disaggregation) discussed above, the hydraulic conductivity of samples in the range of moisture conditions naturally encountered in the tuff could not be determined. However, since hydraulic conductivity decreases with decreasing moisture content and the conductivity of samples was determined for moisture ranges above field moisture conditions, the determined values serve as maximum estimates of unsaturated hydraulic conductivity likely to be encountered under field conditions. Theoretical methods of determining hydraulic conductivity yield an average of 2.64×10^{-4} ft/day and measured values average 1.32×10^{-4} ft/day. Thus, the two methods yield similar results.

Task four requires an analysis of infiltration and redistribution of meteoric water into the tuff by neutron logging and either moisture blocks and/or psychrometry. The Laboratory satisfied this requirement by conducting neutron-moisture monitoring and measuring matric potential with thermocouple psychrometers. Neutron moisture monitoring and gravimetric moisture measurements indicate that the volumetric moisture content of the tuff below ten feet is approximately two to four percent. In addition, analysis of daily moisture logs after autumn precipitation indicate the depth of infiltration of meteoric water is approximately ten feet. Moisture is not observed to move deeper than this depth and is assumed to be returned to the surface through evapotranspiration. Psychrometers indicate that soil tensions range from just less than one bar to approximately 15 bars. Vertical hydraulic gradients, as determined by psychrometers, range from downward values of 10.20 ft/ft to upward gradients of 4.12 ft/ft.

The primary emphasis of tasks one through four of paragraph 25 of the Order is to gather data required to assess rates of liquid movement through the Bandelier Tuff both by calculation and empirically. Empirical measurements of moisture content in the tuff following precipitation events indicate that slight (0.5 percent) increases in moisture are observed at depths up to ten feet below the surface; no effects of precipitation or moisture were observed at 22 feet. Thus, empirical measurement of redistribution of meteoric water suggests that effects of precipitation are confined to the uppermost 22 feet of the vadose zone and therefore do not provide a viable means of contaminant transport below this depth.

Calculation of liquid flux rates through porous media using field derived hydraulic gradients and laboratory derived unsaturated hydraulic conductivities yield mean flux rates of 0.036 and 0.211 feet per year for Areas L and G, respectively. The calculations should be viewed as extremely conservative for the following reasons. Hillel (1980, p. 108) explains that unsaturated flow occurs in response to hydraulic gradients by fluid movement along hydration films over particle surfaces in a tendency to equilibrate the potential. At very low moisture content (two to four percent), it is doubtful whether or not continuous hydration films exist to provide for fluid movement. Further, fractures which may range from microstructures to master joint sets, may provide effective barriers to capillary flow.

Assuming that moisture is evenly distributed throughout the tuff, the flux rates determined by calculations may still be viewed as conservative because of values used for hydraulic conductivity. As stated previously, hydraulic conductivity decreases with decreasing moisture content. Unsaturated hydraulic conductivity for use in flux calculations was determined for wetting fluid saturations of 40 to 70 percent (22 to 60 percent volumetric moisture content) while in situ moisture measurements of tuff indicate two to four percent volumetric moisture. Thus, hydraulic conductivities utilized in flux calculations are greater than values under field conditions and therefore yield greater flux rates than can be reasonably expected to occur in the field. Though highly conservative, these moisture flux values show that very long periods of time would be required for water and contaminants to move by unsaturated flow from the disposal facilities to the ground water.

The discussion of vadose zone hydrologic characterization presented above leads to the following conclusion:

- **The combination of very low moisture content in the tuff, empirical determination that moisture from precipitation does not infiltrate below a depth of ten to 22 feet, and very low calculated flux rates all suggest that aqueous transport of contaminants through Bandelier Tuff is not a viable mechanism for contaminant migration at Areas G and L.**

6.3 CHEMICAL CHARACTERIZATION OF THE VADOSE ZONE

Seven test hole locations were selected for core and pore gas analyses of the Bandelier Tuff at Mesita del Buey to fulfill the requirements of Task 5 of the Order. In 1985, four test holes were drilled at Area L, two test holes at Area G, and one background hole on the western end of the mesa. Core samples were collected from each ten foot interval in all seven test holes and analyzed for EP Toxicity and volatile organic compounds.

No EP toxic metals were detected in test hole cores below a depth of 20 feet in Areas G and L. Part per million concentrations of volatile organic compounds were present in core samples from test holes in Area L at depths up to 100 feet (the maximum depth sampled). In Area G, no volatile organic compounds were detected at part per million concentrations (detection limit for Area G samples).

A total of 23 sampling ports were installed in the seven test holes (three or four per test hole) to collect samples of pore gas from the tuff at various depths. Samples were collected by pumping the pore gas through charcoal adsorption tubes and volatile organic analyses were subsequently performed on the charcoal desorption solution. Volatile organic compounds were detected in Area L in part per million concentrations at all depths sampled. There remains, however, some uncertainty as to the degree of isolation between sample ports within tests holes. In Area G, volatile organic compounds were detected in part per billion concentrations at all depths sampled. From this data, the following conclusions can be inferred:

- **Hazardous waste constituents have migrated from land disposal units at Areas G and L based on the results of core and pore gas analyses conducted in 1985 and 1986**

- **Chemical data from the core and pore gas analyses (and information obtained from vadose zone characterization) support vapor phase migration from Areas G and L as the dominant transport mechanism, based on the presence of volatile organic vapors at depths of up to 100 feet.**

6.4 GROUND WATER HYDROLOGY IN AREAS G AND L

Two distinct ground water systems are present within the Pajarito Plateau near Areas G and L on Mesita del Buey; the main aquifer which occurs at great depth in the Tesuque Formation and a shallow perched water system contained in the alluvium of Pajarito Canyon. No perched water is contained in the alluvium of Cañada del Buey. The main aquifer is the only ground water system in the Los Alamos area capable of producing a municipal and industrial water supply. Characterization of the hydraulic and chemical properties of the main aquifer is, therefore, based on information obtained from supply wells, stock wells, test wells, and springs. The main aquifer is located at a depth of approximately 950 and 850 feet below Areas L and G, respectively, and has an average saturated thickness of 1,470 feet. Beneath Mesita del Buey, the aquifer moves east-southeast towards the Rio Grande at a velocity of about 65 feet per year. Water from wells PM-2 and PM-4, the two supply wells nearest Mesita del Buey, are sodium bicarbonate and have less than 200 mg/ℓ total dissolved solids concentration.

Between June 1985 and September 1986, the alluvium in Pajarito Canyon contained a perennial body of perched water. Based on the 27 test holes drilled on Mesita del Buey and in Pajarito Canyon, the perched water contained in the alluvium does not extend horizontally or vertically into the tuff which forms Mesita del Buey. The saturated thickness of the perched water ranges from four to ten feet in the wells monitored and is dependent on both the channel bedrock configuration and the thickness of the alluvial deposits. The perched water moves east through the canyon to the Rio Grande with a velocity ranging from 8 to 23 feet per day. Upgradient from Areas G and L, the perched water is characteristically sodium bicarbonate with an average annual total dissolved solids concentration of 180 mg/ℓ. The perched water gradually becomes calcium bicarbonate downgradient and the average total dissolved solids concentration increases to 420 mg/ℓ. All chemical and radiological constituents in the perched water are at concentrations below the primary

standards for drinking water. No volatile organic compounds have been detected in the perched water. Fluctuations in the inorganic chemical quality in the perched water system are dependent on the saturated thickness of the water in the alluvium and, during periods of high flow, the concentrations of dissolved constituents are typically diluted.

Studies of the main aquifer and perched water systems near Mesita del Buey indicate that:

- **No perched bodies of water, which could be hydraulically connected to the main aquifer, are known to exist beneath Areas G and L**
- **Perched water in Pajarito Canyon is confined to alluvium within the canyon and does not extend vertically or horizontally into the Bandelier Tuff which forms Mesita del Buey**
- **There is no evidence of migration of hazardous waste constituents from Areas G and L into the perched water contained in the alluvium of Pajarito Canyon.**

LA-3728
UC-28, PARTICLE ACCELERATORS
AND HIGH-VOLTAGE MACHINES
TID-4500

LOS ALAMOS SCIENTIFIC LABORATORY
of the
University of California
LOS ALAMOS • NEW MEXICO

Report written: June 1968

Report distributed: November 14, 1968

Geologic Studies and Material Properties Investigations of Mesita de Los Alamos

Compiled by

M. Dean Keller

TABLE OF CONTENTS

ABSTRACT 1

1. INTRODUCTION AND SUMMARY 1

2. GEOLOGY OF LOS ALAMOS 2

History 2

Seismic Probability 3

Other Physical Characteristics 8

3. NEAR-SURFACE ROCKS 9

Geology 9

Bandelier Formation 12

Tshirege Member 12

Structure 12

Physical Characteristics 14

4. GROUND VIBRATION CHARACTERISTICS 18

Units and Definitions 18

Equipment and Instrumentation 18

Impact Tests 20

Procedure 20

Computation of Results 20

Conclusions 21

High-Explosive Detonation Tests 21

Procedure 21

Computation of Results 22

Limitations 22

Conclusions 22

Seismic Records 22

Attenuation Characteristics 26

Fourier Spectra 27

Project Gasbuggy 27

Procedure 27

Discussion of Results 27

Conclusions 27

Microseisms 29

Frequency 29

Velocity: Zero to peak displacement and acceleration 29

Conclusions 29

Traffic Effects 30

Procedure 30

Computation of Results 30

Conclusions 30

5. DEFORMATION CHARACTERISTICS 32
Precision Leveling 34
Factors Affecting Accuracy of Theoretical Analysis 34
Modulus of Elasticity 34
Strata Depth 35
Foundation Stiffness 35
Qualitative Tests 36
Iron House 36
Pajarito Reservoir No. 3 36
Comparison of Calculated to Empirical Deformation 37
Pajarito Reservoir No. 2 37
Mesita de Los Alamos 38
Assumptions 39
Calculated versus Empirical Deformation 39
Computer Analysis for Deformation 42
Deformation under Sustained Loading 42
Pajarito Reservoir No. 2 42
Mesita de Los Alamos, Location No. 1 42
Mesita de Los Alamos, Location No. 2 46
Conclusions 46
Deformation under Load 46
Deformation under Sustained Loading 46
ACKNOWLEDGMENTS 49

GEOLOGIC STUDIES AND MATERIAL PROPERTIES INVESTIGATIONS OF MESITA DE LOS ALAMOS

Compiled by
M. Dean Keller

ABSTRACT

Investigations were conducted to verify the competence of the foundation material for the Los Alamos Meson Physics Facility and to provide relevant quantitative data for use by the architect-engineers in their facility design work. These investigations included geologic history, seismic probability, physical characteristics of the near-surface rocks, ground vibration characteristics, and deformation characteristics.

1. INTRODUCTION AND SUMMARY

The Los Alamos Meson Physics Facility, encompassing as its primary entity an 800-MeV linear proton accelerator of unprecedented current-carrying capability, is planned for location on Mesita de Los Alamos, a site on the Pajarito Plateau in Los Alamos County. The accelerator and its associated facilities will constitute a significant adjunct to the research capabilities of the Los Alamos Scientific Laboratory and to the scientific community at large, under the auspices of the Atomic Energy Commission. When the facility is completed, the scientific staff will embark upon extensive research programs concerned with seeking new insights into, and understanding of, the complexities of the atomic nucleus and related problems.

The characteristics of and the geographical location for this accelerator and its supporting laboratories have been carefully considered during the past few years. Preliminary studies have all indicated that Mesita de Los Alamos is a desirable location for an accelerator of this type. The geologic history of the area, the stability of the mesa, and the load-bearing qualities of the tuffaceous rock ensure a firm and quiescent base for this half-mile long machine. However, detailed quantitative descriptions of all relevant geologic features

must be obtained to permit the architect-engineers to proceed with designs for the various buildings and accelerator structures with the assurance that not only will the required stability be realized, but also that the design will be accomplished in an economical manner.

The seismic probability of the Los Alamos area as determined by history, geology, and field research is presented in this report, and the probability of other geological hazards is discussed. The geological units of Mesita de Los Alamos are described along with data pertinent thereto such as density, moisture content, temperature gradient, and discontinuities.

Tests were conducted to determine vibratory characteristics of the volcanic tuff on Mesita de Los Alamos. Driving forces duplicated for this study included heavy truck traffic, impact loading, and the detonation of high explosives. Microseisms were recorded.

The deformation and creep characteristics of the volcanic tuff were determined by load tests, and correlation to analytical methods was achieved.

2. GEOLOGY OF LOS ALAMOS

History

Griggs has described the geology of the Los Alamos area,[1] and Smith et al. have summarized the area's volcanic history.[2]

Los Alamos is situated on mesas of the Pajarito Plateau on the east flank of the Jemez Mountains (Fig. 2-1). The area has had intermittent volcanic activity for several million years. The culmination of this activity was the cataclysmic eruptions that produced the welded tuff deposits of the Bandelier Formation. The lower member of this formation was erupted from vents that were later obscured by a major collapse of the Toledo caldera. This caldera, in turn, was modified and obscured by eruptions of the upper member of the Bandelier Formation and the consequent collapse to produce the Valles caldera.

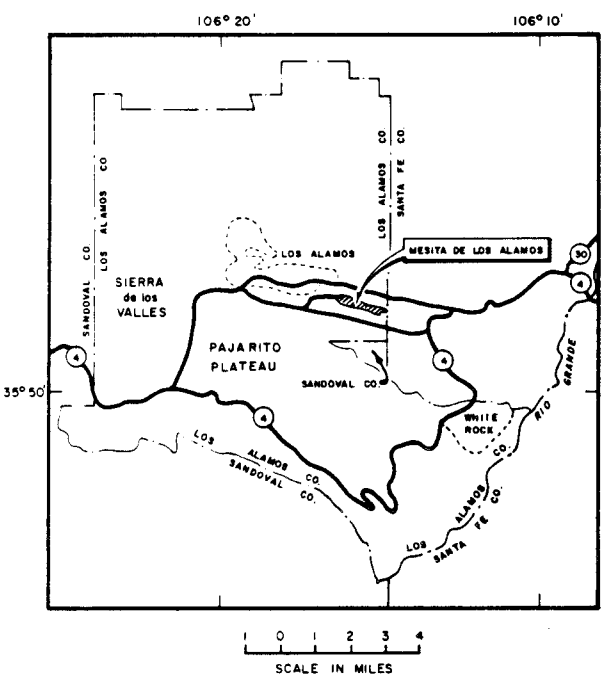

Fig. 2-1. Los Alamos area.

The upper member of the Bandelier Formation caps the mesas in the vicinity of Los Alamos. These mesas have been incised to depths as great as 800 ft by east-flowing streams. This depth of downcutting and the radiometric age of 1.1 million years for the upper member of the Bandelier Formation[3] permit calculating a rate of downcutting by the major streams of 5 to 8 x 10^{-4} ft per year.

Subsequent to the development of the Valles caldera, rhyolite domes were extruded within the caldera and the youngest of these--South Mountain, which has a radiometric age of about 400,000 years[4] -- is partially blanketed by a pumice sheet that issued from El Cajete. An exposure of the El Cajete pumice in a road cut on State Highway 4 about 1 mile west of the Triple H Ranch is shown in Fig. 2-2. A presumed correlative unit of this sheet locally known as "popcorn tuff" is exposed in a

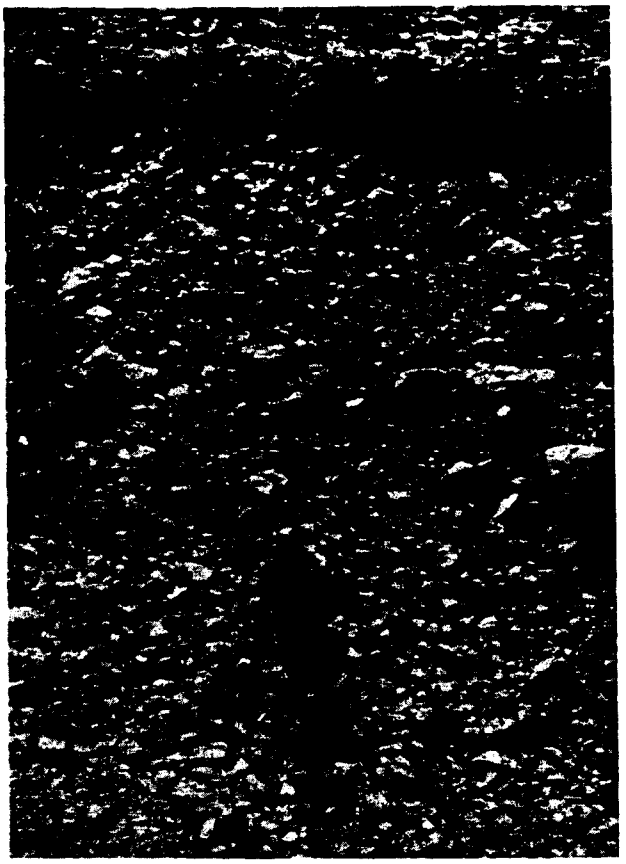

Fig. 2-2. El Cajete pumice.

Fig. 2-3. Popcorn tuff.

road cut on State Highway 4 about 400 ft northwest of its intersection with West Jemez Road (Fig. 2-3).

It is estimated that the El Cajete pumice may be as young as 50,000 to 100,000 years.[3] Samples of the two pumice deposits were unsuitable for radiometric dating. Subsequent to the volcanic activity of El Cajete, the area has been dormant except for some thermal springs and fumaroles.

Seismic Probability

The Los Alamos area has had a long history of faulting and, presumably, earthquakes principally related to the development of the Rio Grande graben which lies immediately east of the Jemez Mountains. Most of the modern earthquake history of New Mexico has been along the Rio Grande graben in the area south of Albuquerque. The Valles caldera and the older Toledo caldera developed by collapse on ring fractures, and the area probably suffered some earth shaking during their development.

The Pajarito fault extends along the east front of the Jemez Mountains immediately west of Los Alamos. This fault is part of a zone of faults that forms the western boundary of the Rio Grande graben and, as such, has probably had a long history of movement. The inferred development of the Pajarito fault is shown in Fig. 2-4, which also shows a gravity profile across the west side of the Rio Grande graben. The basement rocks have been displaced more than the precaldera volcanic rocks, which in turn have been displaced more than the Bandelier Formation. The Pajarito fault also displaces the pumice sheet (popcorn tuff) that is believed to be correlative with the El Cajete pumice. The pumice sheet (popcorn tuff) is preserved on the downthrown block and has

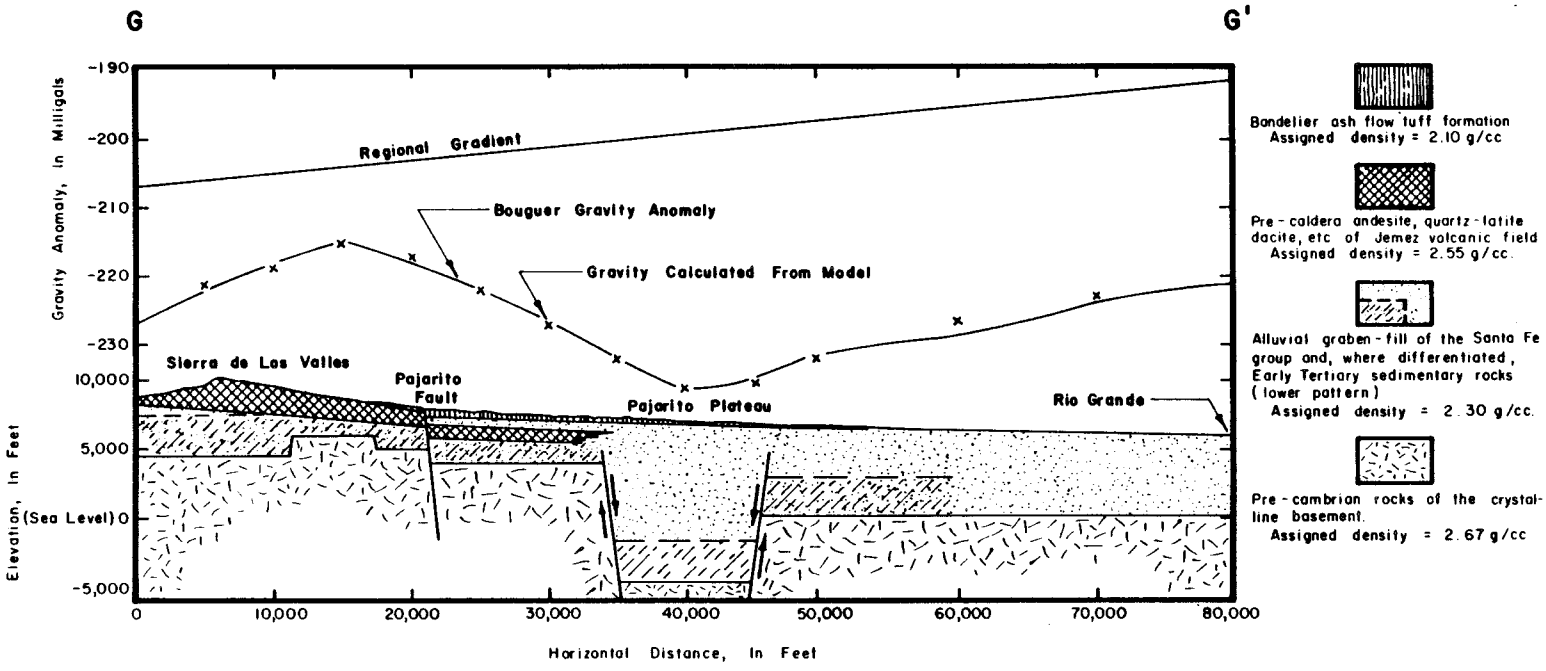

Fig. 2-4. Geologic cross section and gravity profile from the Jemez Mountains to the Rio Grande. (Section cut on Figure 2-7.)

been completely eroded from the uplifted block.

The present-day scarp on the Pajarito fault has a maximum height of about 400 ft where the fault splits into two strands in the vicinity of Canon de Valle, and the height of the two scarps total about 500 ft. This 400 to 500 ft of displacement may all be younger, or only a small fraction of it may be younger, than the pumice sheet, but the displaced pumice sheet permits the determination of a maximum frequency of fault displacement. If it is assumed that the pumice sheet is 50,000 years old and it has been offset the maximum of 500 ft and if it is further assumed that the displacement has been by small increments that may average 10 ft, then one such increment has occurred every 1,000 years. Should the pumice be older and the postpumice displacement appreciably smaller than assumed, the frequency could be drastically reduced.

Considerable evidence suggests that the rate of faulting is very much lower, if it has not ceased altogether. Pinnacles eroded in the soft formation are common features in the vicinity of the Jemez Mountains. Ross and Smith[5] described those in the Bandelier tuff (welded volcanic ash of the Bandelier Formation) as

> ...conical shaped pinnacles... that are locally known as tent rocks because of their resemblance to conical tents or tepees. There is a tendency for the formation of these in nearly all the nonwelded parts of the ash-flow tuff deposits but they are particularly outstanding in two members of the Bandelier Formation. The Bandelier Formation occupies an area of about 400 square miles and at least one of the tent rock members is present over most of this area. Some of the tent rocks are cones only a few feet high while others are 100 or more feet high... There are all gradations in size and of varying degrees of perfection in symmetry. Some cones are capped by large boulders that were rafted from the ground surface traversed by the ash flow during its emplacement. Some of these boulders weighing as much as several hundred pounds tend to retard erosion and produce boulder-capped pinnacles. Not rarely this results in whole colonies of pinnacles capped by boulders of varying size.

Boulder-capped pinnacles eroded in the Puye conglomerate are prominent in Rendija Canyon (Fig. 2-5). These pinnacles are 10 to 60 ft high and the capping boulders are from 2 to 5 times the diameter of the neck supporting them.

These pinnacles, particularly the boulder-capped ones, are unstable landforms and probably could not survive a strong earthquake in their vicinity. The height of

Fig. 2-5. Boulder-capped pinnacles eroded in Puye conglomerate in Rendija Canyon.

the pinnacles indicates a long period of ground stability. A 60-ft pinnacle would require 75,000 to 120,000 years to develop with the indicated rate of downcutting for the major canyons in the area.

The continuously inhabited Indian dwellings in the area and the absence of mention of earthquakes in the Spanish and Mexican records show that earthquakes have either not occurred in the area or have been so minor as to not deserve mention. Houses of unreinforced adobe construction (Fig. 2-6) in Indian pueblos have little lateral strength and would probably be severely damaged or destroyed during a strong earthquake. The prehistoric Indian ruins in the area also attest to a long, continued period of ground stability.

A recent instrumental study of New Mexico earthquakes by Sanford[6] shows very low seismicity compared to such regions as southern California. During the 2-1/2 year period covered by his study, no shocks as strong as magnitude 3.5 were recorded. Predictions of activity based on the observed shocks are much lower than the known historical activity.

An instrumental record of ground stability in the area was desirable despite the uncertainty of predicting seismicity from short periods of observation and despite the geologic and cultural evidence indicating an absence of geologically recent faulting. Therefore, four portable continuous-recording seismograph stations were installed at four locations (Fig. 2-7) in the vicinity of Los Alamos and operated for a 9-day period (March 25 to April 2, 1967).

Three of the stations were instrumented with one vertical and two horizontal Electrotech EV-17 seismometers, and the fourth with only a vertical seismometer. The seismometers were placed about 10 ft apart in holes about 1 ft deep. The signals from the seismometer were amplified and recorded on tape recorders, which were powered by thermoelectric generators.

All of the sites were noisy during the working day and seismic events could be identified with certainty only between the hours of 1900 and 0600. The quality of the seismograms is shown in Fig. 2-8.

Approximately 13 seismic events were recorded during the 9 days of operation. Of these events, one-half are teleseisms originating at great distances from Los Alamos. Most of the remaining events originated at least 100 km away; some of these could not be clearly identified as earthquakes. No local (less than 20 km away) seismic events were recorded. The nearest event was an

Fig. 2-6. Partially ruined adobe building at San Ildefonso Pueblo.

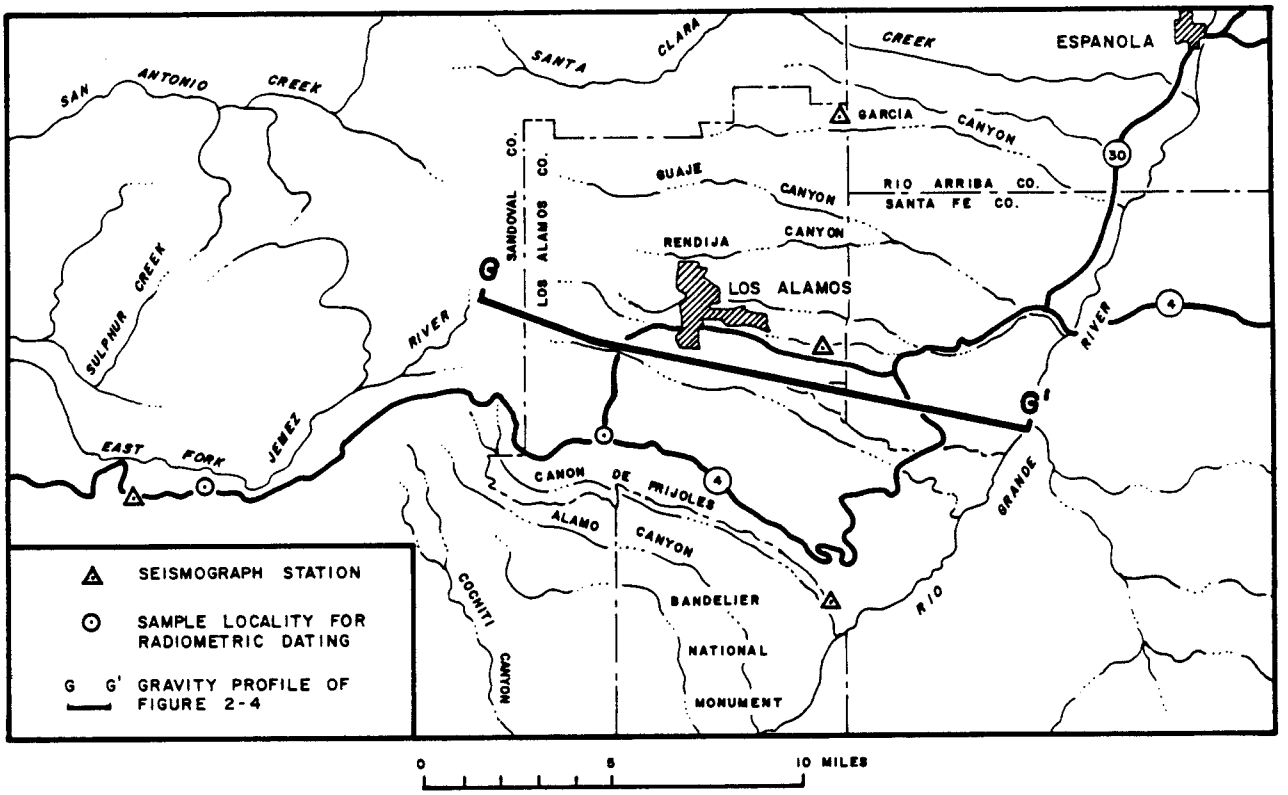

Fig. 2-7. Seismograph stations and sample localities.

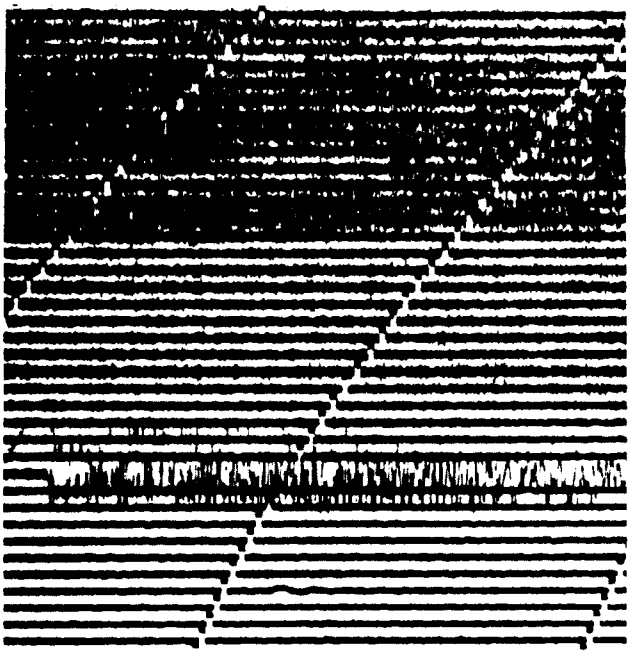

Fig. 2-8. Portion of seismogram recorded at the most northerly station. Note the high noise level in the upper part, recorded during working hours. The event shown in the lower part originated at about 200 km from the station. The time ticks are 1 min. apart.

earthquake of small magnitude that occurred about 20 km west of the seismograph location.

Local events of magnitude at least as low as 1.0 would have been recorded with the instrument settings used in this study. Because no such events were recorded, we conclude that the instrumental study of ground stability, although of far too short a term to be definitive, corroborates the geologic and cultural evidence of very stable ground in the Los Alamos area.

The likelihood of severe seismic damage to installations in the vicinity of Los Alamos seems remote. There was no active, creeping fault at Los Alamos during the observation period. Sanford reported [6] that his data resulted in a prediction for west-central New Mexico of a strongest shock of magnitude 3.5 for a 25-year period. He acknowledges that "this contradicts the known seismicity of the region because at least four shocks of this magnitude occurred within 50 km of Socorro from 1960 to 1961." In view of the seeming absence of earthquakes at Los Alamos, Sanford's figure of a maximum shock

of magnitude 3.5 per 25-year period might be taken as an upper limit for the seismicity at Los Alamos.

Other Physical Characteristics

Geologic hazards of possible significance in planning building construction in the vicinity of Los Alamos, other than seismic hazards, include ground compaction due to withdrawal of water, landslides, and renewed volcanism. Of these the possibility of renewed volcanism in the area probably deserves the most serious study.

Ground compaction due to withdrawal of water is not considered to be a significant geologic hazard because pumping to the present time has lowered the water table significantly only in the vicinity of the well fields. The aquifers are silty sandstones, sandstones, and conglomerates and, as such, are not particularly susceptible to compaction when the water is withdrawn.

Landslides, except for isolated rock falls from the mesa rims, are an unlikely hazard at Los Alamos because of the dry climate, the deep water table, and the rock formation characteristics. The Bandelier Formation is a nearly flat-lying cohesive unit with a low specific gravity, producing a relatively small load on the underlying formations. These rocks are essentially dry to a depth of several feet below the canyon bottoms. Thus, ground and climatic conditions conducive to landslide development are generally not present at Los Alamos. Landslides, except rock falls at the base of the mesa-rim cliffs, are virtually nonexistent topographic features in the area, which indicates that favorable conditions for their development have not existed in the geologically recent past.

The area of the Jemez Mountains has a long history of volcanism[2] and it is possible that volcanism has not ended. This volcanism has been characterized[2] by alternating periods of dormancy and activity, some of which produced catastrophic eruptions.

Whether the present quiescent period is a dormant interval or marks the end of volcanism in the area is unknown. Smith[4] has stated that when he began work in the area about 20 years ago there were active fumaroles within the Valles caldera and boiling water issued from some of the thermal springs. The fumaroles have now ceased to play and the temperature of the springs is much lower. The failing of the fumaroles might be due to lowering of ground temperatures, which would also account for the cessation of the fumaroles.

References

1. R. L. Griggs, "Geology and Ground-Water Resources of the Los Alamos Area, New Mexico", with a section on Quality of Water by J. D. Hem, U.S. Geological Survey, Water Supply Paper 1753, 1964.
2. R. L. Smith, R. A. Bailey, and C. S. Ross, "Structural Evolution of the Valles Caldera, New Mexico, and Its Bearing on the Emplacement of Ring Dikes," U. S. Geological Survey, Professional Paper 424-D, 1961, pp. D-145 to D-149.
3. R. L. Smith, private communication, May 1966.
4. R. L. Smith, private communication, March 1966.
5. C. S. Ross and R. L. Smith, "Ash-flow Tuffs: Their Origin, Geologic Relations, and Identification," U. S. Geological Survey, Professional Paper 366, 1961.
6. O. R. Sanford, "An Instrumental Study of New Mexico Earthquakes," New Mexico Bureau of Mines and Mineral Resources, Circular 78, 1965.

3. NEAR-SURFACE ROCKS

The Pajarito Plateau, formed by a series of ashflows and ashfalls of rhyolite tuff, is dissected into a number of finger-like mesas by eastward-flowing intermittent streams that are tributary to the Rio Grande. Mesita de Los Alamos is one of these mesas bounded on the north by Los Alamos Canyon and on the south by Sandia Canyon. The canyon floors are 200 to 400 ft below the surface of the mesa. There is a small east-west ridge along the northern edge of the mesa, and the surface of the mesa slopes southward from the ridge at an altitude of about 7,035 to about 6,920 ft along the southeastern edge of the mesa.

The geologic investigation was made in conjunction with the drilling of 25 test holes by Albuquerque Testing Laboratory to determine the load-bearing capacities of the tuff. The major structure of the facility is the injector building to be built near test holes TH-1 and TH-2 (Fig. 3-1). A concrete tunnel (beam channel) covered with crushed tuff will extend from near test hole TH-2 to TH-12 to the experimental building, located between TH-12 and TH-14. The foundations of these structures are approximately 6,966 ft above mean sea level. Most of the test holes in a line with the beam channel were drilled and tested to an altitude of 6,960 ft. In the eastern part of the proposed tunnel and experimental building area, core recovery was poor or penetration tests indicated low bearing capacities; hence, the holes were bored to greater depths.

A geologic map and cross sections of the upper surface of the mesa were compiled. Temperature measurements were made in three of the test holes, and continuous temperature recordings were made to a depth of 3 ft in two types of soil and one type of tuff. Moisture and density measurements were made along the walls of the test holes. Gamma ray and caliper logs were run in the test holes to aid in the stratigraphic correlation of the tuff.

Geology

Mesita de Los Alamos is composed of the Bandelier Formation of Pleistocene age. Underlying the Bandelier Formation are rocks of the Santa Fe Group of middle (?) Miocene to Pleistocene (?) age. In the Los Alamos area the rocks of the Santa Fe Group are, in ascending order, the Tesuque Formation, the Puye conglomerate, and the basaltic rocks of Chino Mesa (Fig. 3-2).

The Tesuque Formation is composed of siltstone and sandstones with some conglomerate and clay lenses. The formation exceeds a total thickness of 2,400 ft in the area. The Puye conglomerate is composed of the Totavi Lentil.

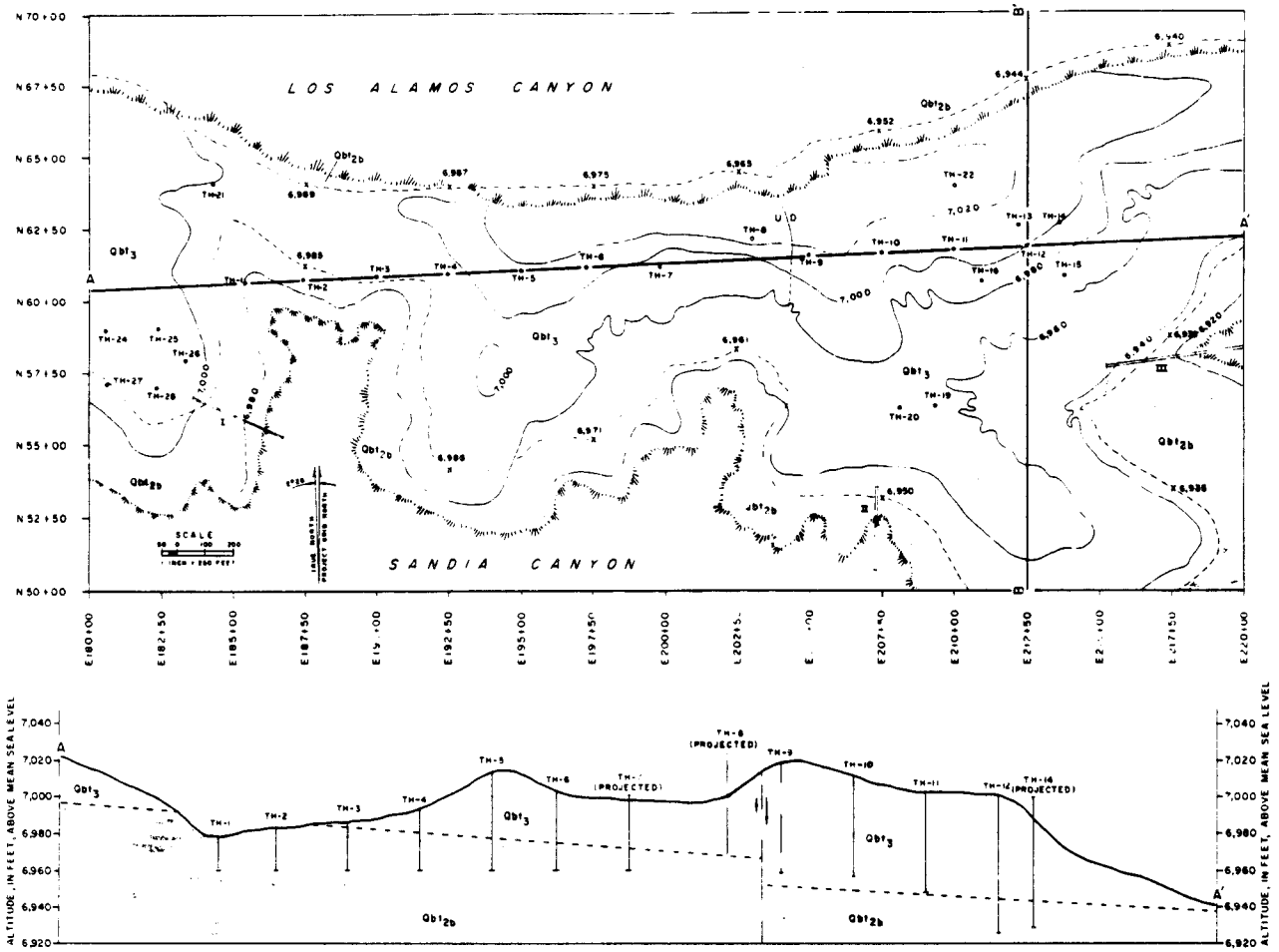

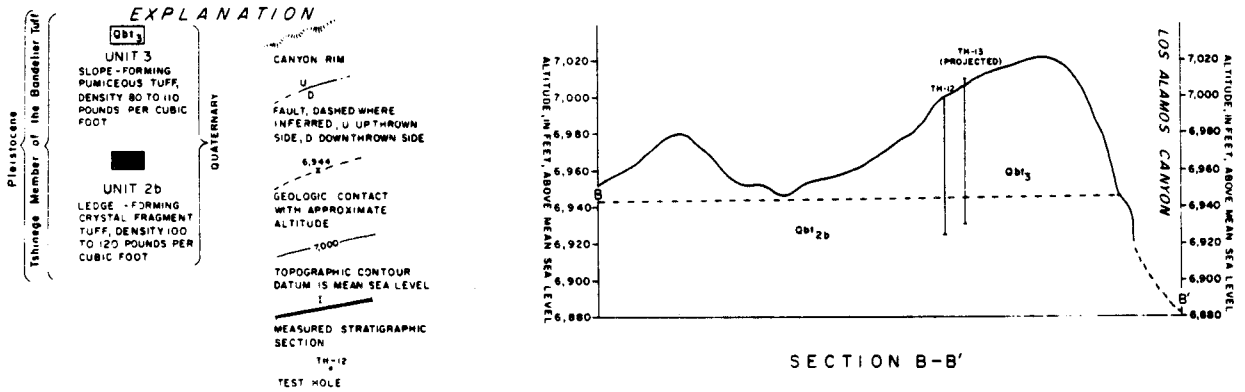

Fig. 3-1. Geologic map and sections showing location of test holes at Mesita de Los Alamos.

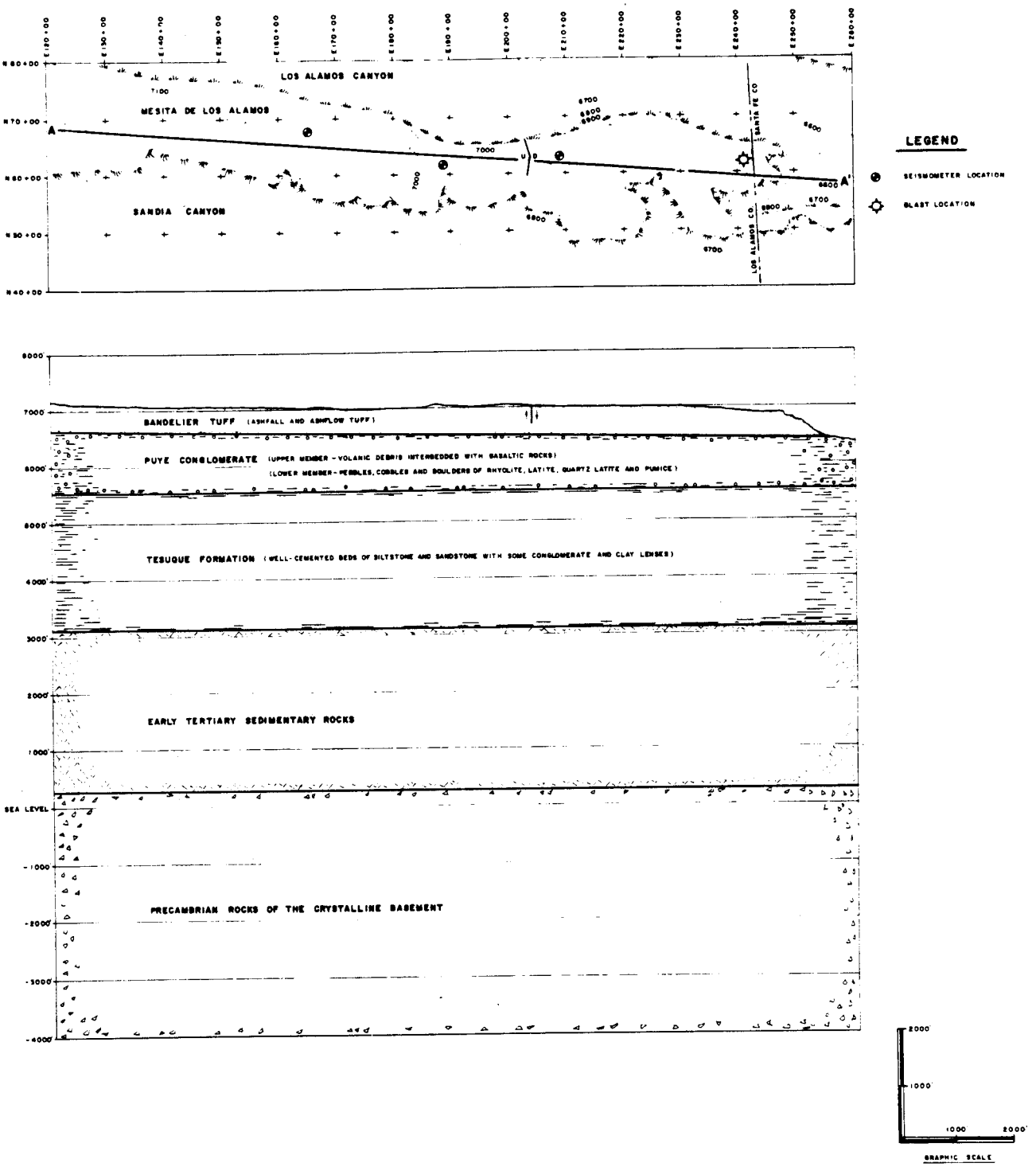

Fig. 3-2. West-east cross section (A-A').

a poorly consolidated channel fill deposit, and an overlying fanglomerate member composed of volcanic debris interbedded with the basaltic rocks of Chino Mesa. The total thickness of the Puye conglomerate and the basaltic rocks of Chino Mesa at well T-3 in Los Alamos Canyon immediately north of Mesita de Los Alamos exceeds 640 ft.

Bandelier Formation

The Bandelier Formation consists of ashfalls and ashflow rocks that are draped over older rocks, filling the lows and initially forming a smoother surface than that of the older rocks. The Bandelier Formation is composed of three members. In ascending order they are: the Guaje Member, an ashfall pumice about 35 ft thick, found in the subsurface at Mesita de Los Alamos; the Otowi Member, a friable ashflow about 235 ft thick, partly exposed in the lower wall of Los Alamos Canyon adjacent to Mesita de Los Alamos; and the Tshirege Member, a series of ashflow tuffs which cap Mesita de Los Alamos. Only units of the Tshirege Member were studied.

Tshirege Member

The Tshirege Member is composed of a series of rhyolite tuff ashflows that contain quartz and sanidine crystals and crystal fragments; some mafic minerals; and rock fragments of pumice, rhyolite, and latite in a fine ash matrix. The ashflows vary from a nonwelded to a welded tuff.[1] The Tshirege Member is about 300 ft thick under the ridge at Mesita de Los Alamos. Five units of the Tshirege Member (units 1a, 1b, 2a, 2b, and 3) described by Baltz et al.[2] are present.

Structure

The units of the Tshirege Member dip gently eastward at Mesita de Los Alamos. Units 2b and 3 form the upper part of the mesa dipping 3 to 6° toward the east-southeast.

Unit 2b outcrops at TH-1 and TH-2. The dip of the unit causes the contact between units 2b and 3 to cross the foundation elevation between TH-7 and TH-8. Thus, due to the dip of the two units, the foundation of the buildings and tunnel west of TH-7 will be in unit 2b and the foundation east of TH-7 will be in unit 3 (Fig. 3-1).

The units 2b and 3 are broken by a normal strike slip fault between TH-8 and TH-9 (Fig. 3-1). The units on the east have moved down about 14 ft relative to the units west of the fault. Slickensides in the fault zone indicate the units on the east have moved about 14 ft south relative to the units west of the fault. Surface expression of the fault is a gouge zone 6 to 18 in. wide that stands 2 to 3 ft above the land surface for a distance of about 20 ft along the southern flank of the east-west trending ridge. This gouge zone consists of reddish tuff that has been welded by the movement, thus forming a more competent rock than unit 3, which forms the ridge. Along the crest of the ridge the gouge zone narrows and is eroded level with the land surface. The fault plane is nearly vertical as indicated by the remnants of the gouge zone in Los Alamos Canyon.

The cause of the fault is unknown. It may be due to compaction of the underlying members of the Bandelier tuff as the upper units of the Tshirege Member were laid down or it may be related to the tectonic forces that formed the Rio Grande depression.

The numerous joints in units 2b and 3 probably are tension joints formed during the cooling of the ashflows. The most prominent and numerous joints are nearly vertical and some are slightly open. Near-surface joints are filled with clay and weathering products of the tuff.

Units 1a and 1b. The lower part of the Tshirege Member consists of two ledge-forming layers of pumiceous tuff breccia similar in lithology, but slightly different in color and weathering characteristics. The lower layer is unit 1a (Fig. 3-3), a massive orange-weathering pumiceous tuff breccia forming a near vertical cliff above the alluvium in Sandia Canyon. This lower unit contains pumice fragments of obsidian and rhyolite in a fine glassy ash matrix. The weathered outer 1 to 3 in. of tuff is casehardened, protecting the unweathered rock from erosion. The thickness of unit 1a varies because of the irregular erosion surface at the top of the Otowi Member

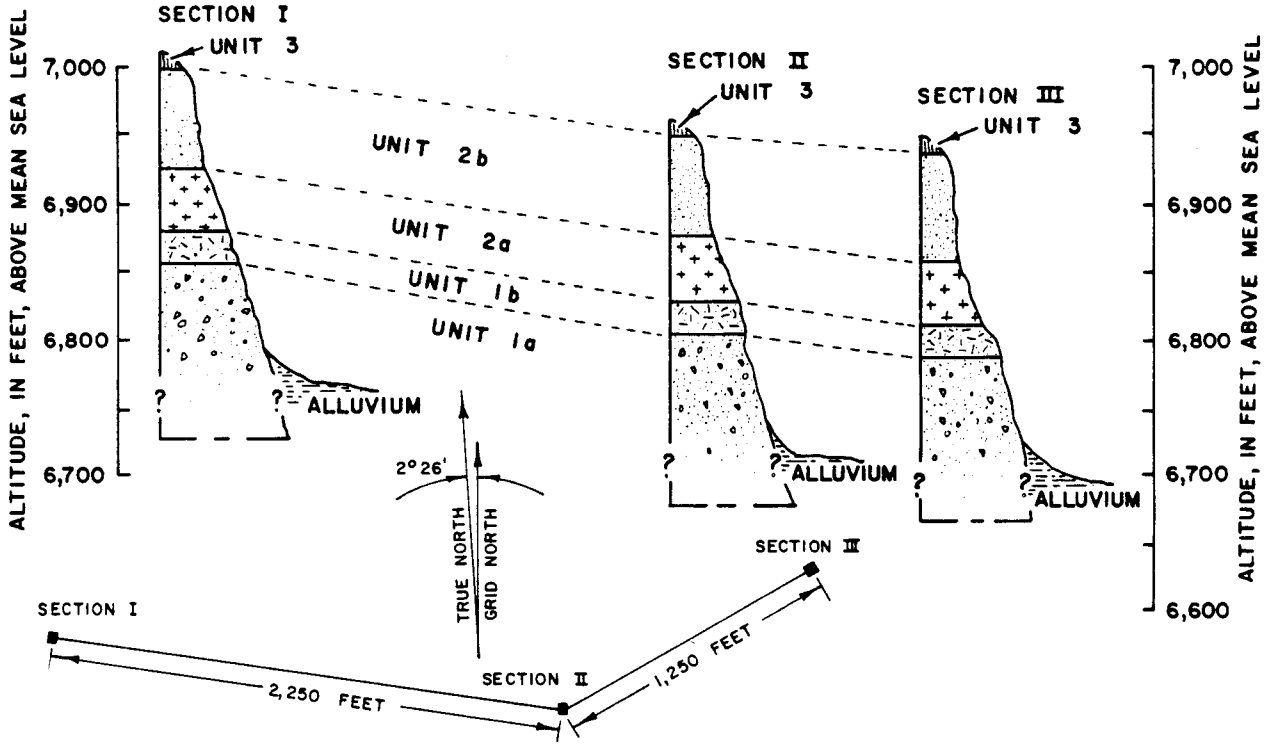

Fig. 3-3. Stratigraphic sections of the Tshirege Member of the Bandelier tuff at Mesita de Los Alamos and Mesita del Buey.

upon which it rests; it may be as much as 80 ft thick near the center of the mesa.

Unit 1b (Fig. 3-3) rests conformably on unit 1a and weathers to a dull grayish-brown. It is a tuff breccia with a fine-grained pink ash matrix similar to the underlying unit 1a; however, the pumice fragments are smaller and 15 to 20% of the material consists of granule-sized quartz-crystal fragments and fragments of dense volcanic rocks. Unit 1b is slightly less resistant to erosion than the unit 1a and forms a ledge set back from the lower unit. At some places both layers form near-vertical cliffs where the units can be distinguished by a soft bed of pumice at the base of the upper unit, which weathers to a persistent notch in the cliffs. The thickness is fairly uniform, ranging from 21 to 23 ft along the southern edge of Mesita de Los Alamos.

Units 2a and 2b. The lower unit 2a (Fig. 3-3) is a light-gray pumiceous tuff consisting of moderately welded pumiceous ash containing fragments of pumice, dense rhyolite, and latite fragments as much as 3 in. long. The unit weathers to a dull gray with a casehardened rind several inches thick. It forms a steep smooth slope set back from unit 1 and is separated from the overlying unit 2b by an erosional unconformity. The thickness ranges from 47 to 51 ft along the southern edge of the mesa.

The overlying unit 2b (Fig. 3-3) is a light pink to brown-weathering, moderately welded tuff (porosity from 30 to 50% by volume) composed of quartz and sanidine crystals and fragments in a matrix of light-pink fine-grained ash. Some rock fragments of pumice and latite are 1/2 in. long. The unit is resistant to erosion and forms ledges and benches above the steep rounded slopes of basal unit 2a. The unit ranges from 76 to 83 ft thick along the southern edge of the mesa, where it forms the uppermost rim of Sandia Canyon. Along Los Alamos Canyon, unit 2b forms a bench along the wall. Unit 2b underlies the proposed foundation of the injector building and tunnel in the western part of the mesa.

Unit 3. This unit (Fig. 3-3) rests conformably on

unit 2b and grades downward into it. Unit 3 consists primarily of light-gray, light-tan, and white nonwelded to moderately welded pumiceous tuff breccia (porosity from 30 to 60% by volume). The rock is composed of fine pumice fragments and glassy shards and contains numerous layers of pebble and cobble-sized pumice fragments and some gray dense rhyolite. Most of the unit is relatively soft and has eroded to form smooth, round slopes with a rind of casehardened material several inches thick.

The unit has eroded along the southern and extreme eastern edges of the mesa. The thickest section of unit 3 (about 75 ft thick) occurs near the center of the east-west trending ridge along the northern edge of the mesa. This unit forms the foundation of the east end of the tunnel and the experimental building.

Physical Characteristics

Density. The density measurements of units 2b and 3 were made by a density gauge manufactured by Nuclear-Chicago Corporation. A probe emitting gamma rays was lowered into the test holes and pulses from the probe, counted by a scaler at 5-ft depth intervals, were converted to densities.

The bulk density of the tuff of unit 2b as determined by density logging ranged from 100 to 120 lb/ft^3; the density of unit 3 ranged from 80 to 110 lb/ft^3. Differential cooling of an ashflow unit results in density changes of the unit in a vertical section (Table 3-I); rapid cooling of an ashflow after emplacement results in a more porous and pumiceous tuff at the upper and lower contacts.

Penetration tests, and bearing capacities determined from cores, indicate that bearing capacity of the tuff increases with density.

Moisture content. The moisture content of the bore walls of some test holes was determined with a neutron-scattering moisture probe manufactured by Nuclear-Chicago Corporation. Pulses from the probe were counted with a portable scaler and converted to moisture content.

The moisture content of the tuff beneath the soil zone or near surface tuff in TH-1, TH-2, TH-3, TH-4, and TH-5 was below 5% by volume. The moisture content of the other holes was not determined because water was added during drilling. Measurements in six test holes drilled in January 1964 indicate that the moisture content of the tuff below foundation altitude was less than 5% by volume.[3] Other studies[4] of moisture distribution in the soil and tuff in the Los Alamos area indicate that the natural moisture content of the tuff beneath the mesas is generally less than 5% by volume in areas where the natural soil cover and drainage have not been disturbed.

Temperature. Test holes in tuff inhale and exhale air in response to atmospheric pressure changes. Inflatable plastic packings were placed in the test holes to eliminate the effect of transient air movement during the measurement of bore-wall temperatures. Standard calibrated laboratory thermometers were placed between the packers and bore walls at selected depths. Thermometer carriers had an oil reservoir around the bulbs with sufficient heat capacity to maintain constant temperature during removal from the test holes. The temperatures of three test holes given in Table 3-II were measured by this technique.

The lower temperatures measured in TH-1 are due in part to the physical characteristics of the tuff. TH-1 is completely in unit 2b, which is less permeable to air than unit 3 in TH-7 and TH-11. The tuff at TH-7 and TH-11 also receives more solar heat because these test holes are on the south-facing slope of the east-west ridge, where the combination of higher permeability and higher solar radiation probably accounts for the slightly higher temperatures. The cause of the 1 to 2° temperature increase of the tuff at depth in TH-7 and TH-11 is unknown.

Temperatures were recorded at 2-hr intervals at depths of 0.5, 1, 2, and 3 ft on the surface of the mesa in a sandy soil overlying the light gray pumice tuff of unit 3 (Table 3-III), a clay soil (Table 3-IV), and in the light gray pumice tuff of unit 3 (Table 3-V). Concurrent air temperatures are also shown in each table. Daily temperature changes appear to affect the soil or tuff only to a 1-ft depth. Daily temperature extremes in the fall and early spring probably extend slightly deeper.

Table 3-I

Density of the Tuff in Test Holes TH-1, TH-7, and TH-11 as Determined by Density Logging

TH-1			TH-7			TH-11		
Depth (ft)	Unit of Tshirege Member	Density (lb/ft^3)	Depth (ft)	Unit of Tshirege Member	Density (lb/ft^3)	Depth (ft)	Unit of Tshirege Member	Density (lb/ft^3)
3	2b	114	5	3	94	5	3	80
6	2b	112	10	3	105	10	3	97
9	2b	115	15	3	107	15	3	105
12	2b	113	20	3	105	20	3	105
15	2b	110	25	3	110	25	3	105
-	-	-	30	3	102	30	3	108
-	-	-	34	2b	110	35	3	105
-	-	-	39	2b	109	40	3	105
-	-	-	-	-	-	45	3	90
-	-	-	-	-	-	49	3	103

Table 3-II

Temperature Gradients in the Tuff in Test Holes TH-1, TH-7, and TH-11 (June 1966)

TH-1		TH-7		TH-11	
Depth (ft)	Temperature (^oF)	Depth (ft)	Temperature (^oF)	Depth (ft)	Temperature (^oF)
3	60	3	62	3	63
8	53	8	61	8	56
13	50	18	52	13	53
16	50	28	52	23	53
-	-	38	54	33	54
-	-	-	-	43	54

Table 3-III

Air Temperature and Temperature at Depth in a Sandy Soil

Tuff (Unit 3) (June 7-13, 1966)

Time	Air Temp. (°F)	Soil Temp. at 0.5 ft (°F)	Air Temp. (°F)	Soil Temp. at 1.0 ft (°F)	Air Temp. (°F)	Tuff Temp. at 2.0 ft (°F)	Air Temp. (°F)	Tuff Temp. at 3.0 ft (°F)
00:00	58	72	50	63	60	63	60	61
02:00	57	71	50	62	50	63	58	61
04:00	51	68	50	62	54	63	54	61
06:00	50	68	50	62	54	63	54	61
08:00	74	65	54	62	70	63	70	61
10:00	75	64	65	62	73	63	77	61
12:00	76	68	70	62	78	63	76	61
14:00	77	72	64	62	78	63	76	61
16:00	72	74	57	62	-	-	74	61
18:00	74	75	57	62	75	63	72	61
20:00	66	74	50	62	64	63	62	61
22:00	61	74	50	62	62	63	57	61

Table 3-IV

Air Temperature and Temperature at Depth in a Clay Soil

(June 13-20, 1966)

Time	Air Temp. (°F)	Soil Temp. at 0.5 ft (°F)	Air Temp. (°F)	Soil Temp. at 1.0 ft (°F)	Air Temp. (°F)	Soil Temp. at 2.0 ft (°F)	Air Temp. (°F)	Soil Temp. at 3.0 ft (°F)
00:00	59	72	60	70	60	66	53	64
02:00	58	71	54	70	53	66	50	64
04:00	54	70	52	70	53	66	50	64
06:00	60	68	52	69	56	66	50	64
08:00	76	68	74	68	80	66	65	64
10:00	80	68	81	68	80	66	74	64
12:00	81	69	82	68	80	66	74	64
14:00	85	71	80	68	80	66	72	64
16:00	90	74	80	68	78	66	68	64
18:00	82	75	84	70	76	66	68	64
20:00	62	75	68	70	70	66	62	64
22:00	60	74	60	70	64	66	52	64

Table 3-V

Air Temperature and Temperature at Depth in a Pumiceous Tuff (Unit 3) (June 7-13, 1966)

Time	Air Temp. (°F)	Tuff Temp. at 0.5 ft (°F)	Air Temp. (°F)	Tuff Temp. at 1.0 ft (°F)	Air Temp. (°F)	Tuff Temp. at 2.0 ft (°F)	Air Temp. (°F)	Tuff Temp. at 3.0 ft (°F)
00:00	60	67	56	66	44	61	58	60
02:00	54	65	54	66	44	61	59	60
04:00	51	62	53	65	44	61	58	60
06:00	48	60	50	64	45	61	52	60
08:00	53	60	54	64	48	61	58	60
10:00	64	60	62	62	54	61	68	60
12:00	72	61	66	62	58	61	76	60
14:00	80	62	72	62	66	61	78	60
16:00	85	68	-	-	73	62	88	60
18:00	84	70	79	64	66	62	84	60
20:00	72	71	72	65	61	62	74	60
22:00	64	70	58	66	52	62	64	60

References

1. W. D. Purtymun and F. C. Koopman, "Physical Characteristics of the Tshirege Member of the Bandelier Tuff with Reference to Use as Building and Ornamental Stone," U. S. Geological Survey, Open-File Report, 1965.
2. E. H. Baltz, J. H. Abrahams, Jr., and W. D. Purtymun, "Preliminary Report on the Geology and Hydrology of Mortandad Canyon near Los Alamos, New Mexico, with Reference to Disposal of Liquid Low-Level Radioactive Wastes," U. S. Geological Survey, Open-File Report, 1963.
3. W. D. Purtymun, U. S. Geological Survey, February 5, 1964, written communication to C. R. Wherritt, ENG-1, LASL.
4. J. H. Abrahams, Jr., J. E. Weir, Jr., and W. D. Purtymun, "Distribution of Moisture in Soil and Near-Surface Tuff on the Pajarito Plateau, Los Alamos County, New Mexico," U. S. Geological Survey, Professional Paper 424-D, 1961, pp. D-142 to D-145.

4. GROUND VIBRATION CHARACTERISTICS

Units and Definitions

Velocity	=	v	μ/sec (maximum).
Frequency	=	f	cps.
Period	=	T	sec.
Displacement	=	d	μ (zero to peak).
Acceleration	=	a	μ/sec/sec (maximum).

$f = 1/T.$

$v = 2\pi f\, d = 2\pi(\frac{1}{T})d = \mu/\text{sec}.$

$d = \frac{vT}{2\pi} = \frac{(\text{microns/sec})\,(\text{sec})}{2\pi} = \mu$

$a = 4\pi^2 f^2\, d = 4\pi^2(\frac{1}{T})^2\, d = \mu/\text{sec/sec}.$

$g = 9.8 \times 10^6\ \mu/\text{sec/sec}.$

Equipment and Instrumentation

The U. S. Coast and Geodetic Survey supplied and operated the following equipment:

Type No. 21 seismometer, National Geophysical Corporation.

Model L5 amplifiers, National Geophysical Corporation.

Model VR3300 magnetic tape recorder, Central Electronics Company, Inc.

Model 4D camera, National Geophysical Corporation.

Model 905 WWV radio receiver, Beckman Instruments, Inc.

Model TS 100 timer, W. F. Sprengnether Instrument Company.

The response curve for this equipment is essentially flat between 1.5 and 80 cps with a negligible correction factor between 1.0 and 1.5 cps (Fig. 4-1). For 16 and 100-cps cutoff filters, the NGC-21 seismometer is flat to 10 and 100 cps, respectively (Fig. 4-2). The computer programs used in analyzing the data were limited to a range of 1.0 through 16.0 cps since the frequencies beyond this limit attenuated rapidly and were, therefore, well within the flat portion of the instrument response curve. A 16-cps cutoff filter was based on the seismometers. The data were recorded with the Model 4D camera, which recorded simultaneously 13 channels of information.

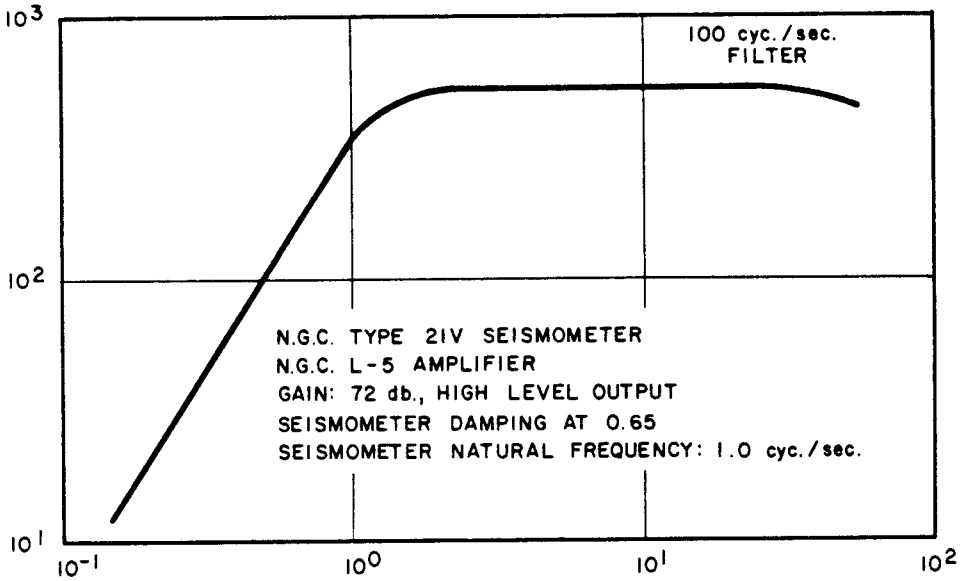

Fig. 4-1. Seismograph velocity sensitivity versus frequency, from calibrations.

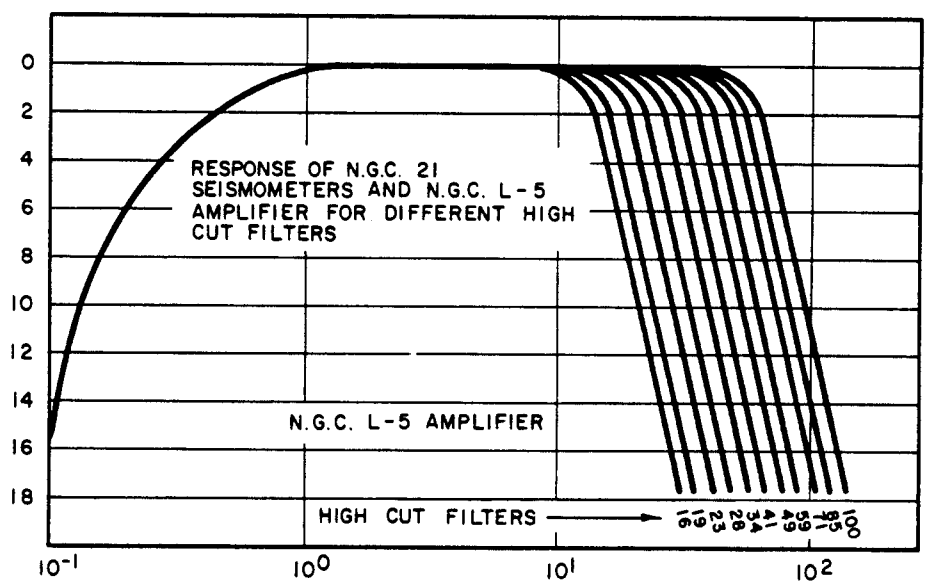

Fig. 4-2. Amplifier relative voltage sensitivity versus frequency.

Impact Tests

Procedure

These tests were conducted with a cast carbon-steel block measuring 0.3 x 1.0 x 5.8 m and weighing 12,000 kg. Two seismograph recorders were located 107 and 137 m from where the weight was dropped. The initial test was conducted by lifting the weight 0.3 m with a crane with the 5.8- x 1.0- m side parallel to the ground. The weight was then dropped by releasing the crane brake, and the resulting ground motion was recorded. This test was repeated, and then the weight was dropped 0.9 m and then 1.5, each test being conducted twice.

Computation of Results

The records for the 0.3-m test, trial 2, were digitized. This test was selected because its record had fewer truncated points due to instrument saturation than other tests. Selected wave forms for the 0.3-, 0.9-, and 1.5-m tests were measured to determine the period and amplitude of each cycle. From these data the frequency, velocity, acceleration, and ground displacement were calculated using the CDC 6600 digital computer. The number of occurrences for each frequency was plotted (Fig. 4-3). Over 90% of the frequencies recorded were between 6 and 16 cps; the predominant frequency was approximately 10 cps.

The average acceleration for selected cycles was calculated and plotted for each test (Fig. 4-4). The ground acceleration for the 1.5-m drop was not appreciably greater than that for the 0.9-m drop, and it was slightly less for the vertical orientation nearest the drop site. This may be due to the weight being dropped on the same spot for each test, which pulverized the tuff. The impact for the 1.5-m drop was thereby cushioned. The seismograph nearest the drop point recorded the largest ground acceleration. The difference can be observed in Fig. 4-4.

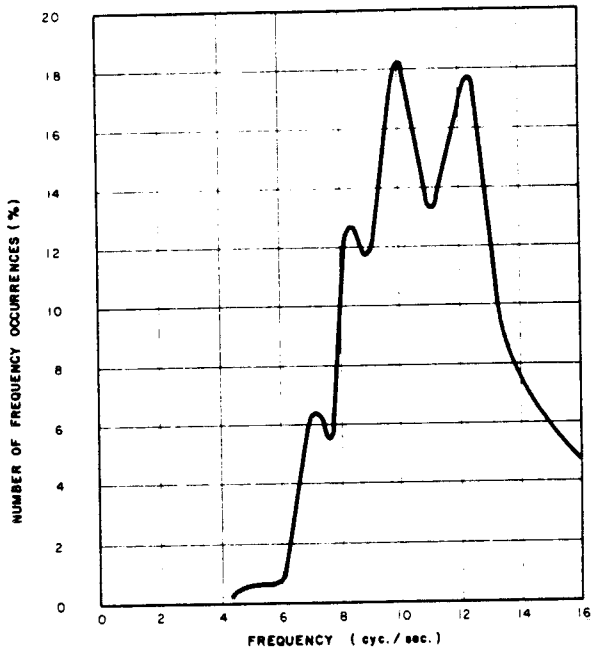

Fig. 4-3. Frequency versus number of frequency occurrences.

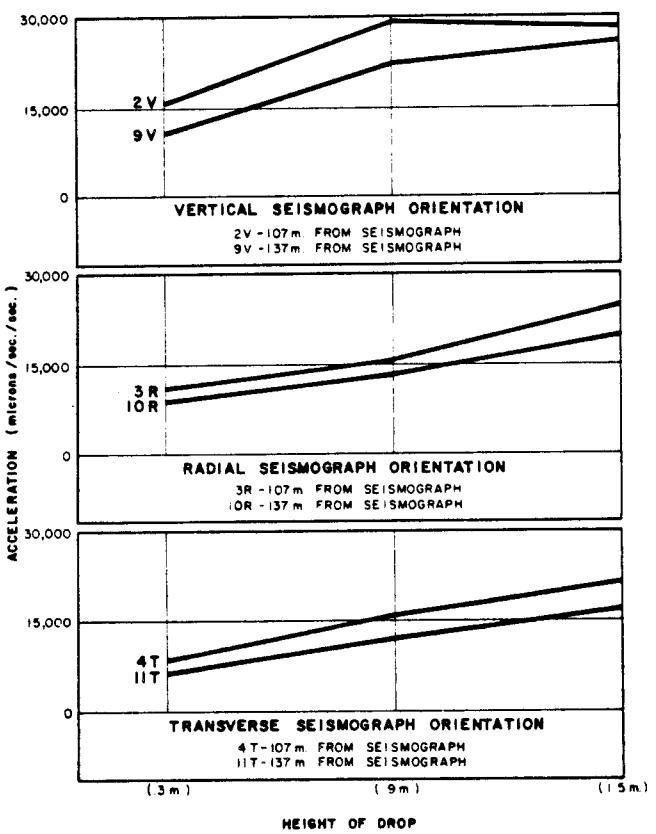

Fig. 4-4. Ground acceleration versus height of drop.

The digitized record of the 0.3-m drop was processed using a computer program for a Fourier series analysis. The Fourier spectra, plotted by a Stromberg - Carlson 4020 plotter (Figs. 4-5 and 4-6), indicate that for frequencies of approximately 9 to 12 cps the greatest Fourier coefficient amplitudes result. Frequencies of 4 to 5 cps also had relatively high amplitudes, but the 9- to 12-cps range was more prevalent in the impact tests.

Conclusions

There was a difference in prevalent frequencies between the impact- and high-explosive test data. The impact-test spectra were relatively flat, whereas the high-explosives test spectra attenuated rapidly from the peak frequency. The most plausible explanation for this difference is the proximity of the seismograph recorders to the drop site.

High-Explosive Detonation Tests

These tests were conducted to determine the vibratory characteristics of Mesita de Los Alamos with respect to shock forces. Using proper correlation between detonations and seismic disturbances, these tests were interpreted to determine resonant characteristics of the mesa for the inception of seismic response spectra. In addition, the velocity of the shock waves in the tuff was calculated and a means of predicting the effects of detonations at a distance was established for the Los Alamos area.

Procedure

The high explosive was Composition C, with an energy rating 1.4 times that of TNT. As shown in Fig. 3-2, the charges were detonated on Mesita de Los Alamos approximately 15 m from the county line. The sizes of these charges in the order fired were 2.3, 4.5, 6.8, 9.1, 9.1, 13.6, 13.6, and 3.6 kg. Seismographs orientated in the vertical, transverse, and radial directions were at three stations, positioned as follows:

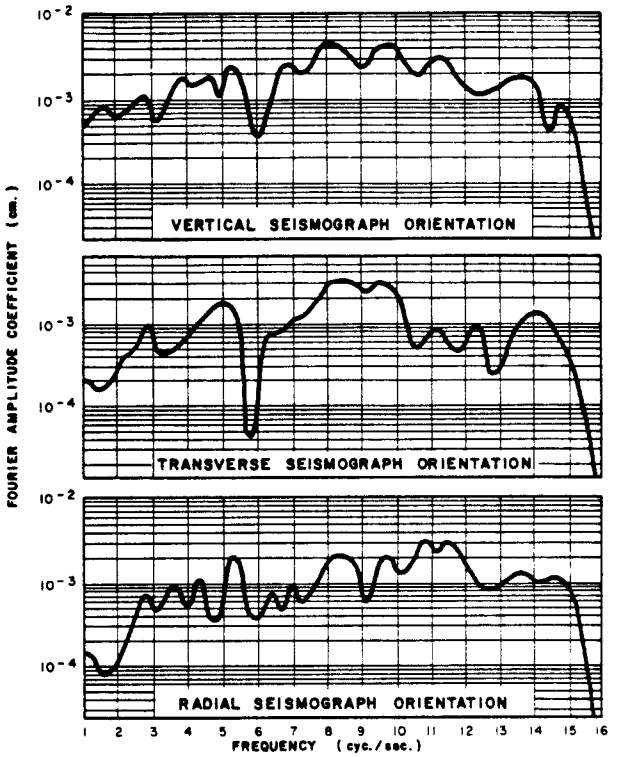

Fig. 4-5. Peak amplitude values, Fourier spectra. Seismograph located 107 m from impact.

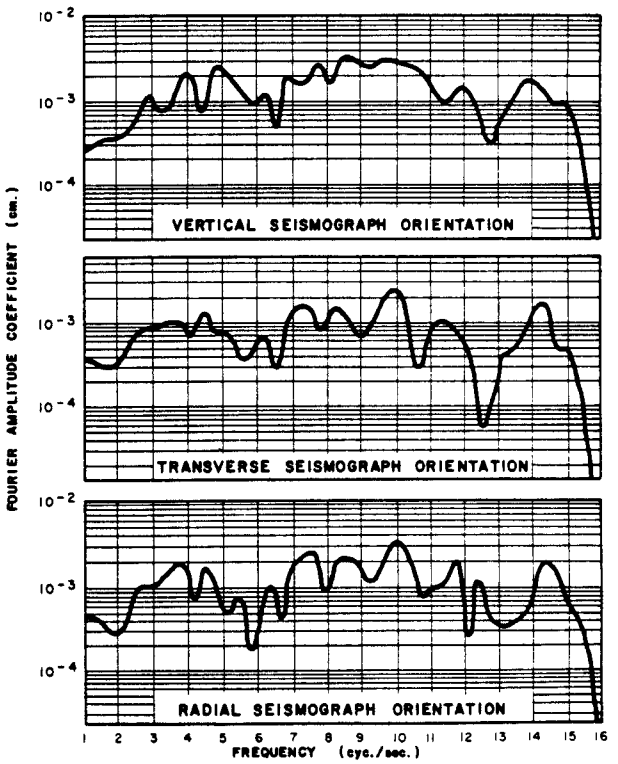

Fig. 4-6. Peak amplitude values, Fourier spectra. Seismograph located 137 m from impact.

Station	Distance from Shot (m)
2	996
1	1559
3	2303

The charges were placed in holes approximately 1 m in diameter and approximately 1 m deep drilled to firm tuff. Backfill, consisting of the excavated material, was placed over each charge to couple it to the earth; coupling was adequate to obtain signals for analysis, but a considerable amount of energy was dissipated into the atmosphere. A transducer close to the charges transmitted a detonation signal through wires to the seismograph. This signal appears as a blip on channel 11 of the seismograph record, and indicates zero time for the detonation.

Computation of Results

The data obtained from the seismometers were recorded by the Model 4D camera (Figs. 4-7 and 4-8). Two methods were used to derive results from these data. In one method the seismic wave forms were measured and the results were processed through the CDC 6600 computer to calculate velocity, displacement, and acceleration. The wave forms were matched; i.e., the corresponding wave forms for the different sizes of explosive charges were compared to obtain the data presented in this section. The wave forms for the stations at various distances from the shots were not matched, but the same time increment was compared, thus yielding a comparison of average values at distances from the shots (Table 4-I). The ground acceleration versus the size of charge (Fig. 4-9) and the ground acceleration versus the distance from the detonation (Fig. 4-10) were plotted from the data given in Table 4-I. For the second method the seismic records for the 4.5-kg Composition C detonation were digitized and a computer program was used to calculate Fourier spectra (Figs. 4-11, 4-12, and 4-13).

Limitations

The seismograph records used for the Fourier spectra analysis and for the other graphs presented here were not segregated according to the type of signal. These records represent compression, shear, and surface waves. Reflection of waves from various discontinuities has, no doubt, changed their forms. It is believed, however, that the spectra developed do represent the distribution of frequencies that would be experienced from a shock excitation. A different origin for the shock force would possibly yield slightly different spectra, but with similar characteristics. The curves developed from Table 4-I would not be affected greatly by reflection of waves because the same waves for the various size charges were studied.

A limitation that must be considered when comparing formulas developed using the test data is that the coupling of the charges to the ground was not as positive as the coupling attained during underground tests. The slope of curves, however, should be characteristic of the medium (tuff) being tested.

Conclusions

Seismic Records. The time at which the compression, shear, and surface waves arrived is shown in Figs. 4-7 and 4-8. Station 2 was 996 m from the point of detonation, and the initial compression wave arrived 0.82 sec after detonation. The velocity of this shock wave through the tuff (all unit 3) was 1215 m/sec. Based on this velocity, the reflected "P" wave traveled 1460 m. This would indicate that the reflection occurred at the 5500-ft elevation, at the transition from the Puye conglomerate to the Tesuque Formation (Fig. 3-2). The "P" wave is not strong due to the imperfect coupling of the detonation to the tuff, and the surface waves obliterate the reflected "P" waves when they arrive.

Station 1, 1559 m from the point of detonation, was in unit 2b of the Bandelier tuff, as was the point of detonation. This unit is a more competent material than unit 3, having a modulus of elasticity of approximately 14,000 kg/cm^2 compared to approximately 1,400 kg/cm^2 for unit 3. The velocity of the compression wave in unit 2b is 1470 m/sec.

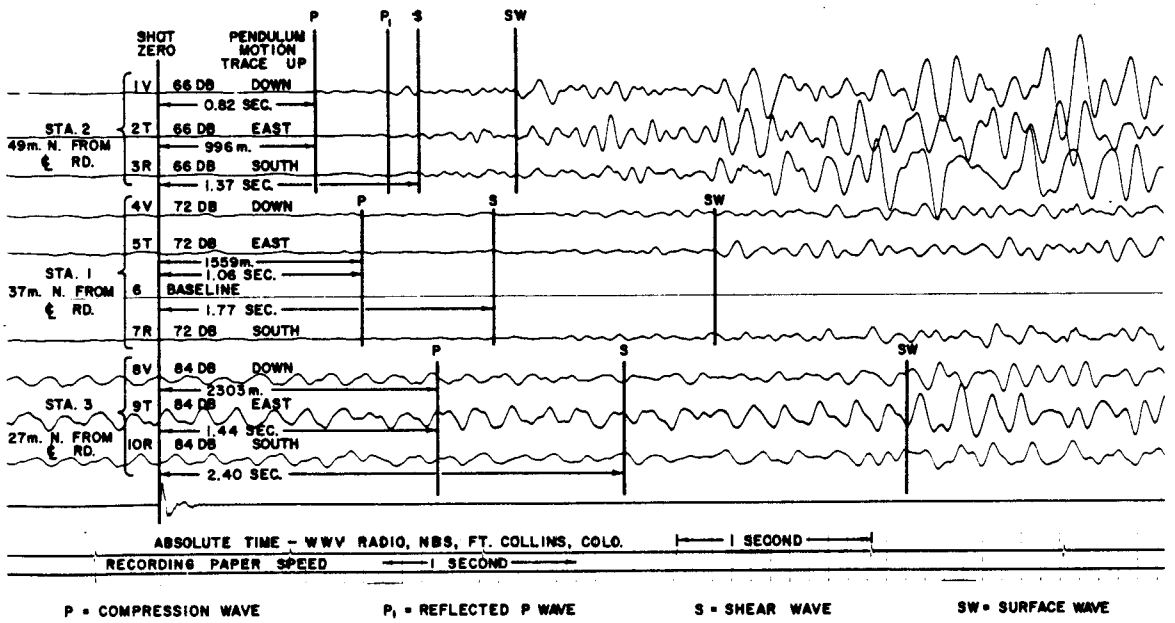

Fig. 4-7. Seismic records: test 3, phase 2; 4.5 kg Composition C.

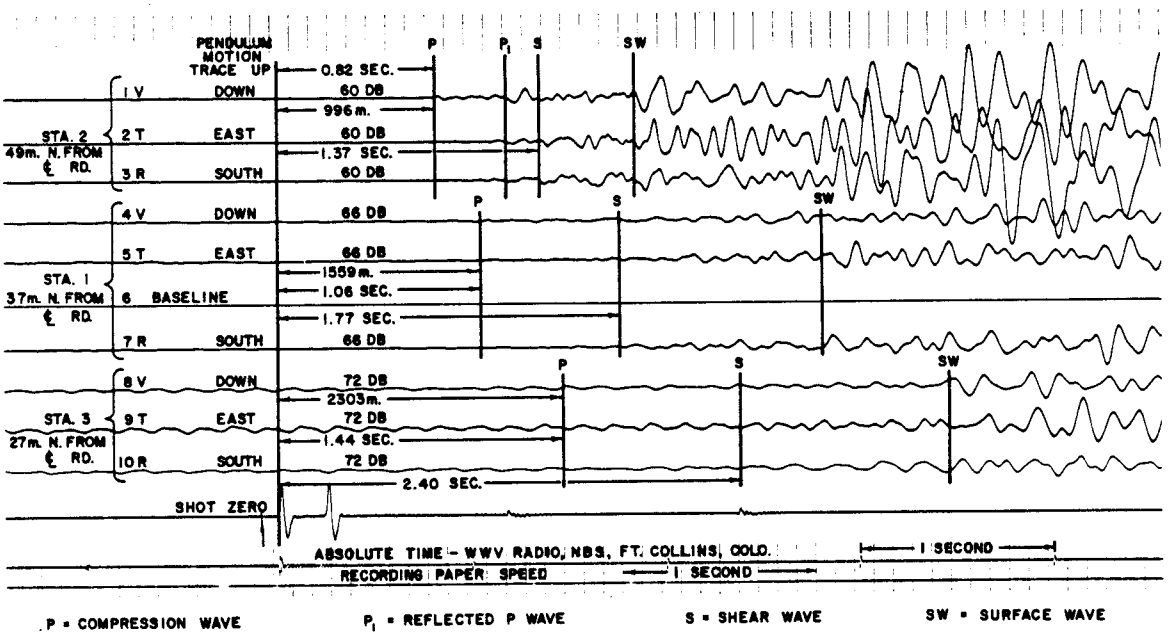

Fig. 4-8. Seismic records: test 3, phase 6; 13.6 kg Composition C.

Table 4-I

High-Explosive Detonations

		Seismometer Orientation								
		Vertical			Transverse			Radial		
		STA. 2	STA. 1	STA. 3	STA. 2	STA. 1	STA. 3	STA. 2	STA. 1	STA. 3
		(IV)	(4V)	(8V)	(2T)	(5T)	(9T)	(3R)	(7R)	(10R)
	Vel.	26.34	8.03	2.52	18.64	9.63	3.76	18.64	10.97	3.01
2.3 kg	Disp.	0.679	0.266	0.076	0.432	0.289	0.122	0.473	0.335	0.104
	Acc.	1064.	254.	84.	830.	342.	126.	780.	371.	91.
	Vel.	43.92	12.86	5.89	33.81	14.23	4.61	39.98	17.75	4.35
4.5 kg	Disp.	1.201	0.434	0.180	0.850	0.427	0.170	1.049	0.588	0.151
	Acc.	1598.	396.	194.	1392.	499.	134.	1565.	596.	127.
	Vel.	63.95	18.01	9.01	49.69	20.82	7.57	55.41	27.77	6.93
6.8 kg	Disp.	1.745	0.637	0.286	1.228	0.631	0.269	1.580	0.898	0.250
	Acc.	2392.	526.	287.	2077.	735.	229.	2044.	878.	199.
	Vel.	84.77	25.35	11.81	59.43	30.64	10.98	82.06	35.80	10.06
9.1 kg	Disp.	2.470	0.910	0.385	1.546	1.027	0.394	2.511	1.178	0.377
	Acc.	2961.	730.	369.	2361.	961.	334.	2794.	1108.	261.
	Vel.	150.24	39.08	14.76	84.17	51.02	18.78	120.98	51.97	14.33
13.6 kg	Disp.	4.537	1.396	0.526	2.192	1.715	0.703	3.840	1.738	0.572
	Acc.	5041.	1134.	424.	3359.	1600.	522.	4099.	1577.	370.

Vel. μ/sec

Disp. μ

Acc. μ/sec/sec

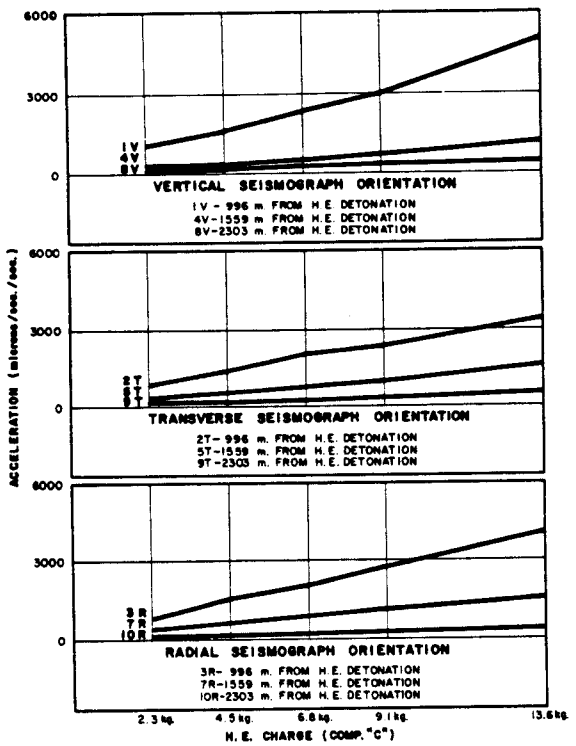

Fig. 4-9. H. E. detonation tests: ground acceleration versus size of charge.

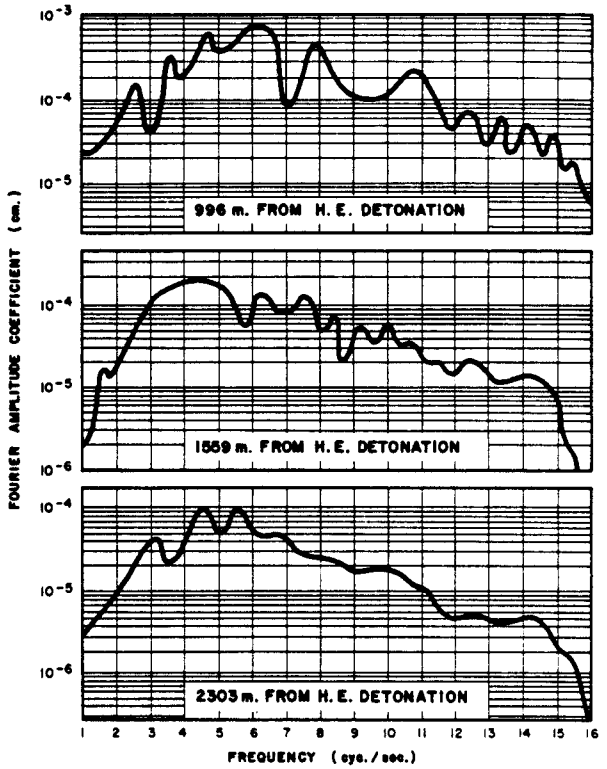

Fig. 4-11. Peak amplitude values: Fourier spectra, vertical seismograph orientation.

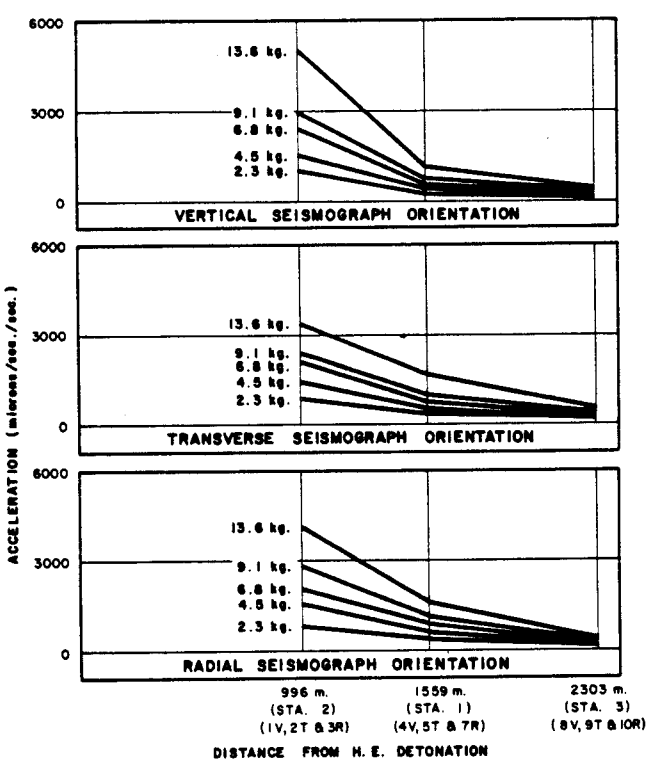

Fig. 4-10. H. E. detonation tests: ground acceleration versus distance from detonation.

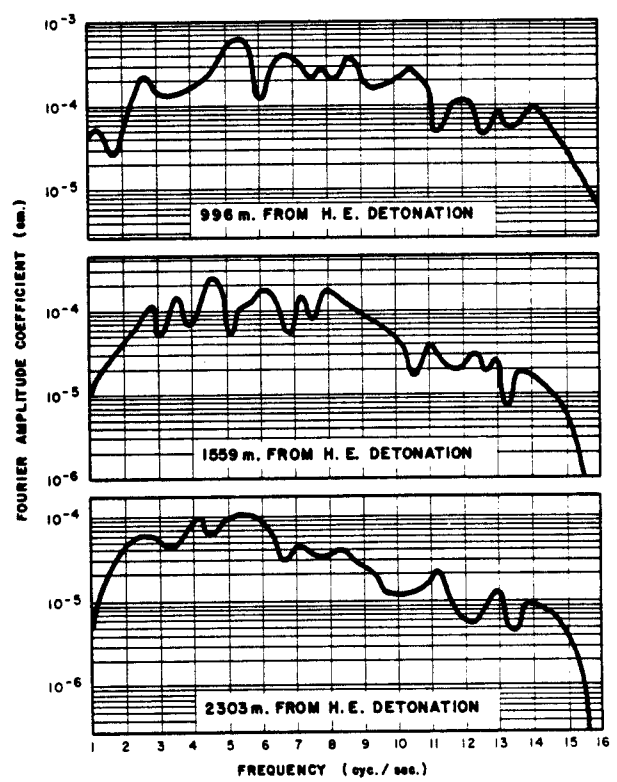

Fig. 4-12. Peak amplitude values: Fourier spectra, transverse seismograph orientation.

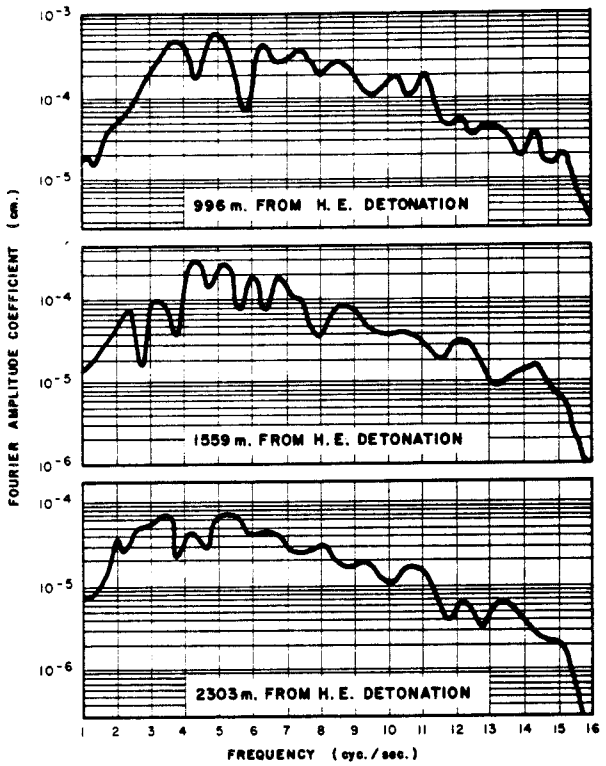

Fig. 4-13. Peak amplitude values: Fourier spectra, radial seismograph orientation.

At Station 3, 2303 m from the point of detonation, the compression waves were more difficult to detect. The arrival of the surface waves was, however, obvious. The proposed initial points for the compression, shear, and surface waves, are shown in Figs. 4-7 and 4-8. The average velocity of the compression waves in the unit 2b and unit 3 tuff was calculated as 1600 m/sec.

Attenuation Characteristics. Empirical formulas for predicting earth motion resulting from the detonation of underground nuclear devices were developed by the United States Coast and Geodetic Survey.[1] The energy ratings of the detonations for the study conducted on Mesita de Los Alamos were below those of detonations for which the formulas were developed. Also, the ground coupling of the detonations on Mesita de Los Alamos was not comparable to that from which the formulas were developed. A comparison was made, however, to see to what extent our accelerations deviated from those predicted by the empirical formulas. The accelerations, chosen from our records, were the average of the three peak accelerations, usually surface waves. One formula[2] developed by the U. S. Coast and Geodetic Survey follows:

$$A = K_a W^{0.54} R^{-1.4}$$

where

K_a = constant = 0.0103 for tuff,

W = size of detonation in tons equivalent TNT (1 ton = 907.18 kg),

R = distance to detonation, in kilometers,

A = acceleration in g's where 1 g = 9.8×10^6 μ/sec/sec.

The comparison of predicted accelerations to those recorded by our seismometers is given in Table 4-II. The comparison becomes more favorable as the size of the charge increases and as the distance from the detonation decreases. This formula could be used to conservatively predict the effects of detonations within Los Alamos County on the Meson Physics Facility. At a distance of 7 km, an equivalent of 0.05 tons of TNT well-coupled to the earth will cause an acceleration of less than 130×10^{-6} g. This is less than the disturbance caused by a loaded truck passing the site and is approximately one-eighth the perception threshold for acceleration.

Table 4-II
Acceleration ($g \times 10^{-6}$)

Equivalent TNT (Tons)	Comparison	Distance to Detonation (km) 0.996	1.559	2.303
0.007	C. & G. S. Formula	705	379	219
	Measured	276	66	24
0.014	C. & G. S. Formula	1030	553	319
	Measured	557	129	53
0.021	C. & G. S. Formula	1280	666	395
	Measured	1080	151	70

The formula developed by Mickey and the empirical results obtained from the test conducted on Mesita de Los Alamos coincide at approximately 1 km and 0.025 tons of TNT. A conservative formula developed from the empirical results has the form

$$A = 0.0150\, W^{0.68} R^{-3.26},$$

using the same nomenclature as the U.S. Coast and Geodetic Survey formula. Note that the greatest change is in R, the distance factor.

The effects predicted by this formula of a loosely coupled detonation of 0.05 tons of TNT at a distance of 7 km would be an acceleration of less than 4×10^{-6}g, which is less than weekend background noise. This is borne out by the fact that detonations at distant sites were not detected on Mesita de Los Alamos.

Fourier Spectra. Fourier spectra were developed for the seismic records generated by a shock force. Almost all of the data developing this spectra were caused by waves. Generally, the Fourier amplitude coefficient is of a greater magnitude between 3 and 9 cps than below or above this range. The least attenuation occurred between 4 and 6 cps. It is proposed that the predominant frequency of the mesa is approximately 4.5 cps for localized detonations.

Transverse movement is higher than would be expected of a shock wave emitted from a point source. This may be explained by reflection of P, S, and SW waves from the walls of the mesa.

Project Gasbuggy

Procedure

On December 10, 1967, a nuclear device equivalent to 26,000 tons of TNT was detonated at a depth of 4,250 ft, approximately 123.5 km northwest of Mesita de Los Alamos. A U.S. Coast and Geodetic survey team measured ground motions at Mesita de Los Alamos generated by this detonation. Detailed information on equipment and procedure may be obtained from Ref. 4.

Discussion of Results

The maximum amplitude at Mesita de Los Alamos was slightly lower than predicted, and the seismic first arrival times indicated a propagation velocity of about 6 km/sec. At these distances the first arrivals did not penetrate to the Mohorovicic discontinuity. The maximum motions were probably propagated as a surface wave, progressing at velocities of 3.5 to 4.8 km/sec. The vibrations had decayed to one-tenth of maximum at about 95 sec. The motion had not returned to normal preshot background at 4 min after zero.

The Gasbuggy seismogram was analyzed for maximum motions at dominant visual frequencies. This could be grossly equivalent to a Fourier spectra analysis. Dynamic response spectra for single-degree-of-freedom elastic systems have been used by structural engineers to design earthquake resistant buildings. These spectra are usually computed with seismic data from earthquakes as an input. A method for estimating response spectra has been devised that uses the maximum earth motions. A spectra envelope can be made using 2 times maximum acceleration, 1.5 times maximum particle velocity, and 1 times maximum displacement. This approaches the response for a system with 5 to 10% critical damping.

Fig. 4-14 was constructed using this method. This graph infers that a one-degree-of-freedom oscillator (or building) with a natural frequency of 1 Hz would experience ground motions in terms of acceleration, velocity, and displacement of 1.0×10^{-4}g, 1.5×10^{-2}cm/sec. and 2.2×10^{-3}cm from Gasbuggy. Similarly, a 4-Hz building would respond 1.5×10^{-3}cm, 5.3×10^{-2}cm/sec, and 2.1×10^{-3}cm.

The visual dominant spectra for all traces were derived. The average frequency for the maximum motions was 2.6 Hz with lower and upper limits of 2.2 and 3.1 Hz. The vibrations decrease rapidly with increased frequency.

Conclusions

The frequencies of maximum motion from Gasbuggy were between 2 and 3 Hz. The amplitudes of vibrations on Mesita de Los Alamos generated by the Gasbuggy detonation were generally as predicted by formulas derived from previous nuclear detonations.

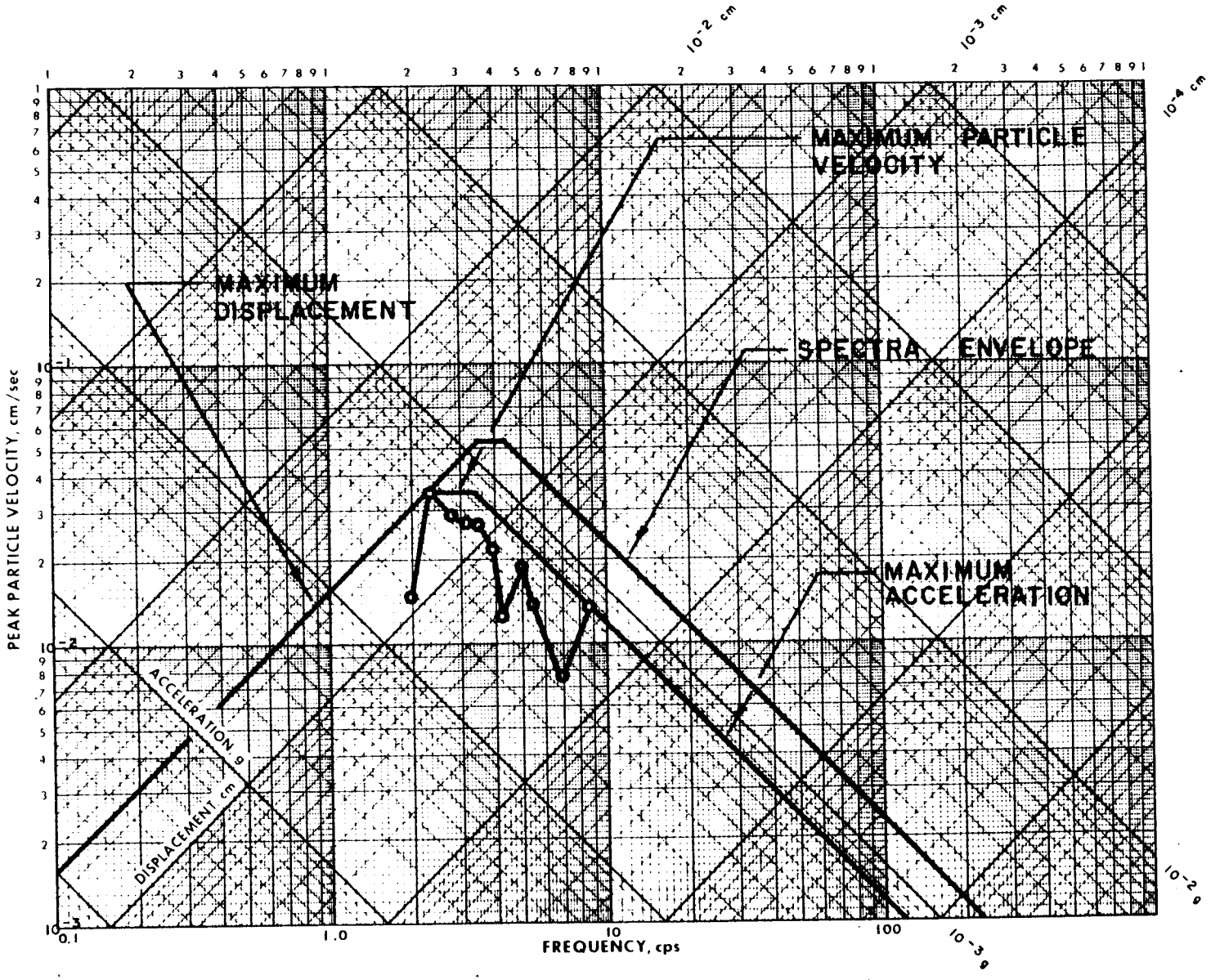

Fig. 4-14. Response spectra - Los Alamos area, Gasbuggy experiment.

Microseisms

Microseisms of natural or artificial origin will affect the operation of the Meson Physics Facility only if their amplitude is excessive. In his final report, Hof stated[3] that he was unable to find anyone having machine-tool problems caused by natural microseisms. It does not appear that there is a possibility of any disturbance to equipment in the Meson Physics Facility from microseisms of natural origin, so this phase of the report is limited to a determination of frequency characteristics and the calculation of ground-motion characterictics for the more intense microseisms generated by artificial means. The difference in intensity of these microseisms for working hours and for nights and weekends is noted as well as the intensity in two different tuffs.

Frequency

A random sampling of frequencies through a 10-sec period indicated a predominance of frequencies in the 5- to 7-cps range. This sampling was taken for the vertical component only; the horizontal components appeared to be similar (Table 4-III).

Velocity: Zero to Peak Displacement and Acceleration.

Table 4-III presents values for velocity, displacement, acceleration, and period for week end and working-hours microseisms. Unit 3 and unit 2b are the geologic members of the Bandelier tuff previously described.

Conclusions

The microseisms recorded on Mesita de Los Alamos are comparable to those presented in the Hof report.[3] In most cases, the microseisms recorded on Mondays are twice the magnitude of those recorded on Sundays. There appears to be no discernible difference in the magnitude of the microseisms in the more competent (unit 2b) as compared to the more friable (unit 3) tuff.

Table 4-III
Microseisms

Geologic Member	Orientation	Velocity	Displacement	Acceleration	Period
Microseisms, Sunday, October 23, 1966, 11:15 A.M.					
Unit 3	Vertical	1.14	0.027	72	0.15
Unit 2b	Vertical	1.14	0.025	72	0.10
Unit 3	Transverse	1.37	0.043	53	0.20
Unit 2b	Transverse	1.37	0.030	60	0.14
Unit 3	Radial	2.51	0.070	115	0.20
Unit 2b	Radial	1.36	0.032	57	0.15
Microseisms, Monday, October 24, 1966, 10:10 A.M.					
Unit 3	Vertical	2.51	0.076	99	0.16
Unit 2b	Vertical	1.83	0.047	72	0.16
Unit 3	Transverse	2.97	0.071	103	0.15
Unit 2b	Transverse	3.20	0.107	96	0.21
Unit 3	Radial	2,05	0.068	61	0.21
Unit 2b	Radial	3.65	0.116	116	0.20

Velocity μ/sec.
Displacement μ.
Acceleration μ/sec/sec.
Period sec.

Traffic Effects

The transportation of large quantities of shielding to the experimental building will be necessary. The vibrations generated by heavy truck traffic could be of a magnitude requiring engineering design of equipment supports to attenuate these vibrations. The effects of heavy truck traffic were studied.

Procedure

A trailer truck was loaded with two 12,200-kg weights. The total weight of truck and weights was 26,592 kg. This truck traveled along an unimproved road past two seismograph stations. The seismographs were oriented perpendicular to the road at 37 and 89 m from the center line of the road, respectively. After records were taken of vibrations caused by truck traffic, the truck was stopped at a point closest to the seismograph stations. It was assumed that the braking action of the truck would generate a greater magnitude of vibration than the passing of the trucks.

Computation of Results

The data obtained from the seismometers and amplifiers were recorded simultaneously on 13 channels by the Model 4D camera. Magnetic tape records were also obtained on a CEC Model UR 3300 recorder but were not digitized because they were not considered necessary for this report. Two methods were used to derive results from these data. In one method the seismic wave forms were measured and the results were processed by the CDC 6600 computer to calculate values of velocity, displacement, and acceleration. The maximum values of vibration for the braking action are given in Table 4-IV. In the other method the records for the truck passing the stations were digitized, and a computer program was used to generate Fourier spectra for this event. These spectra are illustrated in Figs. 4-15 and 4-16.

Conclusions

The vibrations generated by truck braking action are 30 to 40 times greater than from natural microseisms of the area. It appears that attenuation of vibrations was greater in the more competent tuff (unit 2b) than in the more friable tuff (unit 3).

The vibrations generated by the truck braking are of the same order of magnitude as those of the truck passing. The road was rough, however, and much of the vibration was generated when the truck tires hit holes in the road. For a smooth road[4] vibrations from the truck passing were an order of magnitude lower than vibrations from the braking action. Braking action on a smooth road resulted in vibrations approximately one-half of the magnitude of the same action on a rough road.[4] A study of the frequency of vibrations indicated a predominance between 8 and 14 cps.

The Fourier spectra for all stations indicate a response across the spectra. However, a general peaking around 2.3, 4.5, 8.5, and 13 cps was noted, and the attenuation at these frequencies was not as pronounced as the attenuation at other frequencies. No amplification of signals was noted at any frequency, although the forcing function may be considered repetitive.

References

1. R. Willden and E. E. Criley, "Study of the Possibility of Seismic Hazards in the Vicinity of Los Alamos, New Mexico," U.S. Geological Survey, Open-File Report, 1966.
2. W. V. Mickey, "Seismic Wave Propagation," U.S. Department of Commerce, Coast and Geodetic Survey, 1964.
3. G. J. Hof, "Seismic Noise Study at Los Alamos Scientific Laboratory," Sandia Corporation Report SCTM170-62(25), 1962.
4. W.V. Mickey, J.F. Devine, and A.V.C. Meyer. "Project Gasbuggy, Response of the Mesita de Los Alamos to the Gasbuggy Experiment and Induced Vibrations," U.S. Department of Commerce, Coast and Geodetic Survey, E.S.S.A., April 1968.

Table 4-IV
Truck Passing and Braking

Geologic Member	Seismometer Orientation	Velocity (μ/sec) 37 m	Velocity (μ/sec) 89 m	Displacement (μ) 37 m	Displacement (μ) 89 m	Acceleration (μ/sec/sec) 37 m	Acceleration (μ/sec/sec) 89 m
Truck Braking							
Unit 3	Vertical	47.1	47.1	1.27	0.93	2020	1870
Unit 2b	Vertical	30.9	17.3	0.74	0.38	1520	773
Unit 3	Transverse	21.7	18.1	0.62	0.75	980	568
Unit 2b	Transverse	3.9	3.0	0.07	0.09	254	118
Unit 3	Radial	27.2	18.1	0.61	0.63	1220	645
Unit 2b	Radial	42.7	19.1	0.88	0.47	2070	862
Truck Passing							
Unit 3	Vertical	42.7	12.7	1.29	0.39	1410	412
	Transverse	30.0	11.8	0.76	0.30	1170	460
	Radial	30.9	12.7	0.59	0.32	1620	500

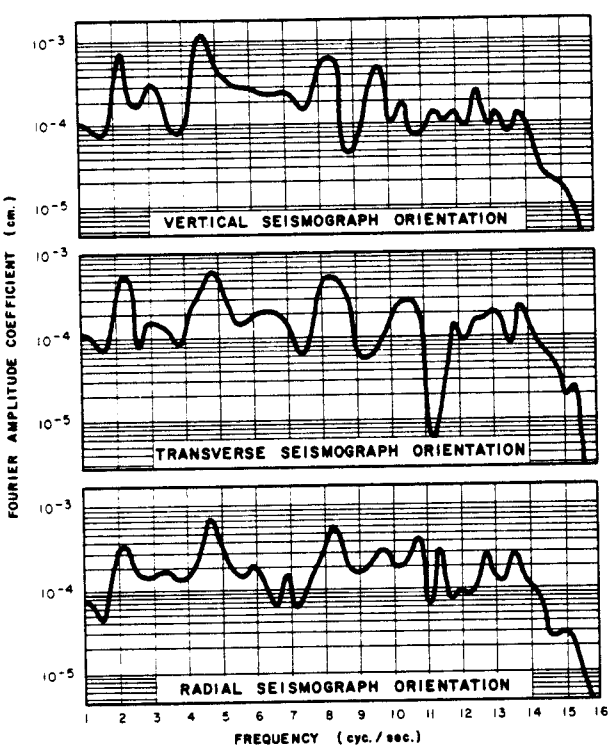

Fig. 4-15. Peak amplitude values; Fourier spectra. Seismograph located 37 m from the center line of the road.

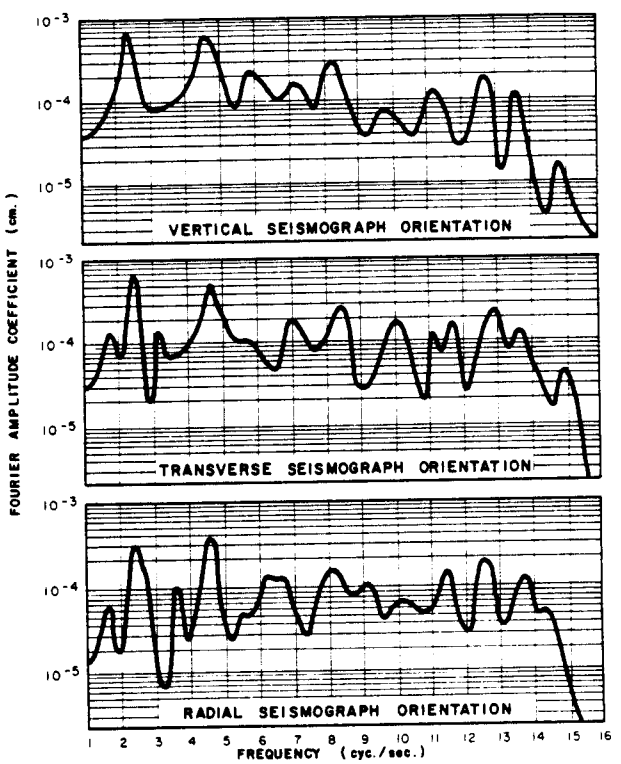

Fig. 4-16. Peak amplitude values; Fourier spectra. Seismograph located 89 m from the center line of the road.

5. DEFORMATION CHARACTERISTICS

To correlate the geological composition of Mesita del Buey to that of Mesita de Los Alamos and to describe the geological composition of Mesita de Los Alamos, a stratigraphic section of the Tshirege Member was measured at Mesita del Buey near Pajarito Reservoir No. 2 and the geologic units of the section were correlated with a section previously measured at Mesita de Los Alamos near the proposed location of the experimental building (Figs. 5-1 and 5-2). Correlations of the geologic units were made by the lithology of the units and their weathering characteristics. The units were also traced southward from Mesita de Los Alamos to Mesita del Buey. A datum was established on the prominent marker bed of tuff between units 1a and 1b, which is light orange and weathers to a slight notch. It is a persistent and readily identified geologic feature that is present where the two units are exposed on the plateau.

Units 1b and 2a thicken slightly from Mesita de Los Alamos southward to Mesita del Buey (Table 5-I); unit 2b thins about 47 ft. The difference in unit 2b' s thickness on the two mesas may be due to the direction of the ejection of the ash flow that formed this unit and the origin of the flow (an area west of the Pajarito Plateau) and in part to topography that existed in pre-Bandelier time. The thickness of the Tshirege Member decreases rapidly east of the section at Mesita del Buey to the vicinity of White Rock, where the tuff lies directly on the basalt.

The basalt formed a topographic high in pre-Bandelier time. The upper part of unit 3 is eroded on both mesas. The thickness of the remaining part of unit 3 is 45 ft at Mesita del Buey and 98 ft at Mesita de Los Alamos.

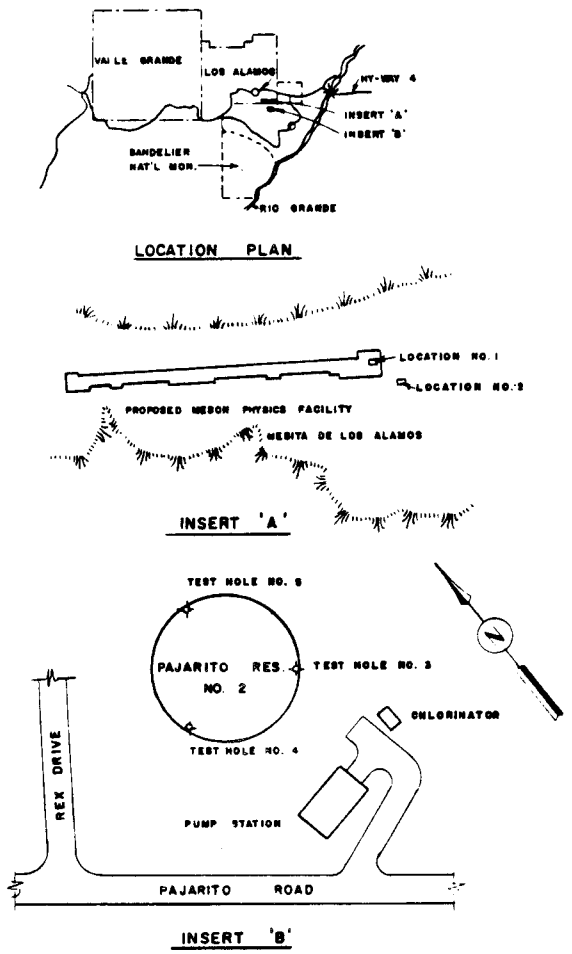

Fig. 5-1. Test site locations.

The altitudes of the two test areas at Mesita de Los Alamos are 6,970 and 6,990 ft; the altitude of the test area at Mesita del Buey is 6,935 ft. The test areas on both mesas are in unit 3 but at different stratigraphic positions in the unit (Table 5-II).

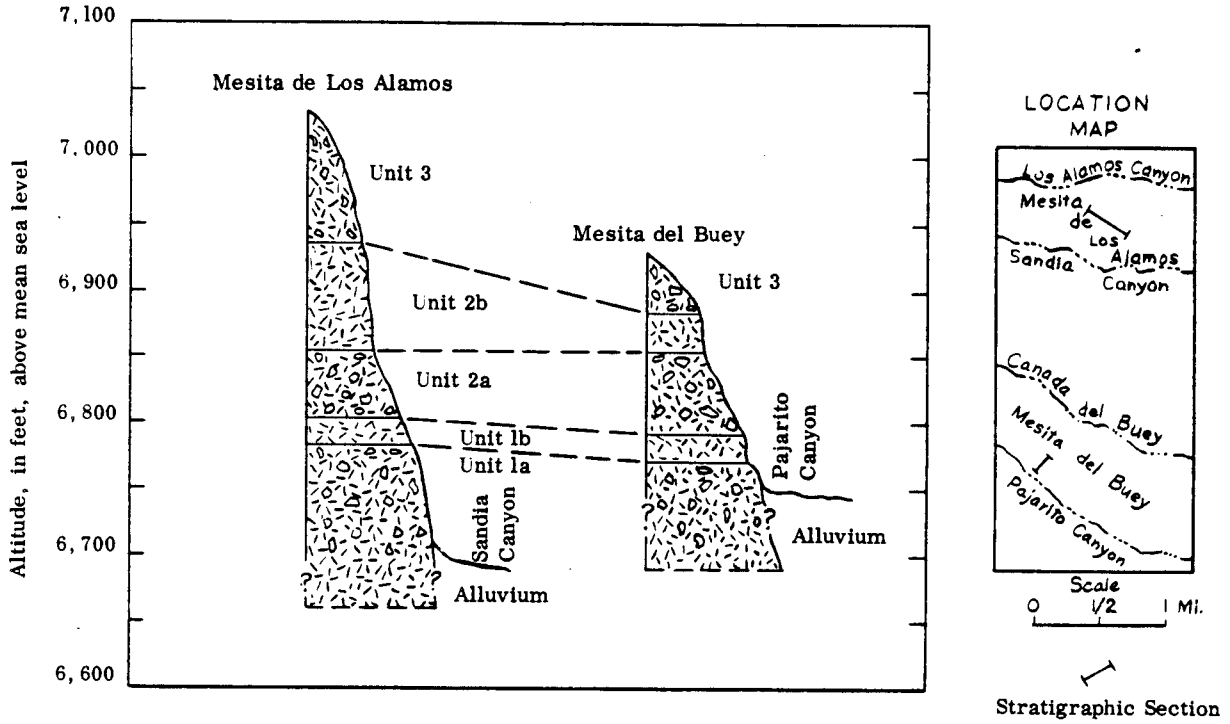

Fig. 5-2. Stratigraphic sections of the Tshirege Member of the Bandelier tuff at Mesita de Los Alamos and at Mesita del Buey.

Table 5-I

Thickness of Geologic Units at Stratigraphic Sections

Geologic Units	Mesita de Los Alamos a/ (ft)	Mesita del Buey b/ (ft)	Remarks
3	98	45	Upper part eroded
2b	76	29	
2a	51	60	
1b	21	23	
1a	74	16	Lower part covered

a/ Altitude at top of section--7,034 ft

b/ Altitude at top of section --6,935 ft

The physical characteristics of units 2a and 3, which will support the Meson Physics Facility structures, apply to both Mesita de Los Alamos and Mesita del Buey.

The foundation material in the Los Alamos area is composed primarily of a welded volcanic ash, usually deposited as an ash flow. As such it is an anisotropic material which exhibits different characteristics depending on the orientation of the sample being tested. It is remarkable that the foundation material can be cut with a saw or bulldozer, but can maintain its integrity while having a vertical face 100 ft high. Bearing capacity of the more competent tuff may conservatively be estimated at 10 tons/ft^2. Modulus of elasticity values of from 20,000 to over 150,000 psi are common, depending on the density of the material and the degree of welding.

The degree of welding is classified at Los Alamos as nonwelded, moderately welded, and welded tuff. The transition between nonwelded (porosity as much as 60%) to welded tuff (porosity as small as 15%) is due to compaction and fusing by heat of the crystals, crystal fragments, and rock fragments in the ash matrix. The degree of welding and the amounts and size of pumice, latite, and rhyolite rock fragments determine the physical characteristics of the tuff; i.e., porosity, density, and bearing capacity.

Table 5-II

Thickness of Geologic Units at Test Areas

Geologic Units	Mesita de Los Alamos a/ (ft)	Mesita de Los Alamos b/ (ft)	Mesita del Buey c/ (ft)	Remarks
3	54	34	45	
2b	76	76	29	
2a	51	51	60	
1b	21	21	23	
1a	74	74	16	Lower part covered

a/ Altitude at test area--6,990 ft

b/ Altitude at test area--6,970 ft

c/ Altitude at test area--6,935 ft

Precision Leveling

The equipment used for the precise readings consisted of: a Wild-Herrbrugg Instruments, Inc., N-3 precision level with optical micrometer; a Keuffel and Esser Co., precise level rod; a rod level; and a thermometer.

In general, the procedures and instrumentation of the precise leveling program conformed to U. S. G. S. second-order practice. Field notes included all pertinent data and comments.

The reliability of the reading obtained under field conditions is probably good to the nearest 0.001 ft. Although the optical micrometer scale can be interpolated to 0.0001 ft by estimation between the 0.0005-ft scale graduations, other variables such as bubble creep, air refraction, superimposing of the cross hairs on the eye graduation, eye strain, relief of internal stresses in the tripod, and movement occasioned by the shifting weight of the level man while taking the readings tend to offset the seemingly higher accuracy capabilities of the equipment.

Factors Affecting Accuracy of Theoretical Analysis

Modulus of Elasticity

A deformation analysis of Mesita de Los Alamos should be an elastic analysis based on Hooke's law. Two variables in this analysis are (1) the pressure at various depths and distances from the load and (2) the modulus of elasticity. The pressures at various depths can be predicted if the characteristics of the foundation are known.

In the unit 3 tuff, it is difficult to obtain a core sample to test for modulus of elasticity because the sample disintegrates when it is disturbed. It is necessary to determine modulus of elasticity values by testing samples taken at or near the surface and by estimating values at depths based upon geological and physical characteristics of the tuff. Samples may be taken close to the surface by excavation with hand tools. This method was used to determine modulus of elasticity values for Pajarito Reservoir No. 2 and for the locations on Mesita de Los Alamos. Because the tuff is an anisotropic material, correct orientation was maintained during the tests. The results of these tests are considered conservative in that lateral pressure was not used to simulate the in situ condition of the tuff. The ash matrix contains intrusions of pumice, latite, and rhyolite. These intrusions are usually small, i.e., approximately 6 to 10 in.^{3}, and do not adversely affect deformation characteristics. An intrusion in a tuff sample, however, will greatly affect that sample's strength and modulus of elasticity. Samples which exhibit values much smaller than the average value of a group should be disregarded and a new average value established.

The value of the modulus of elasticity obtained from tests conducted on tuff samples is representative of the

in situ modulus for the sample area, or is conservative.

Strata Depth

The depth of each stratum may be estimated by borings. Indications of changes in strata are a change in the unit weight of the tuff or an increase in resistance to penetration. There is no precise correlation between unit weight and modulus of elasticity.

It is necessary to estimate the modulus of elasticity at various depths by using the modulus of elasticity at the surface, the unit weight of the material, and the results of borings taken in the more competent tuff. This has been done for the analytical analysis of the load test on Mesita de Los Alamos.

Foundation Stiffness

To compare theoretical analysis to empirical data, the stiffness of the foundation must be established. For tests involving water tanks, the load is imposed on the foundation material through a thin steel plate. It may be assumed that the foundation is flexible and that the analytical approach such as the Boussinesq equation for vertical stress or Newmark's chart will apply.[1,2] Test loads imposed on Mesita de Los Alamos were composed of steel counterweights, which were relatively stiff; therefore, it was necessary to determine what effect this stiffness will have on the theoretical analysis. An analysis by Timoshenko and Goodier[3] indicated that for a circular surface footing the theoretical settlement of a rigid footing is approximately 7-1/2% smaller than the corresponding average settlement due to the same total load uniformly distributed under the footing.

The distribution of pressure under the rigid circular footing is not uniform: a concentration of pressure exists around the perimeter of the footing, and the smallest value of pressure is at the center. Since the footing is rigid, this uneven distribution of pressure results in the smaller theoretical settlement. Timoshenko's analysis was based upon the pressure exerted on metal by a rigid die.

Casagrande[4] states that, for a perfectly elastic soil, the reactions of a rigid footing would be larger on the perimeter than in the center of the footing, but for sand the opposite would be true. The volcanic tuff in Los Alamos is more like an elastic than an inelastic material, and a larger stress concentration would be expected around the perimeter of the footing.

The preceding assumptions are based on rigid foundations. It was necessary to consider empirical results to determine the rigidity of the test weights. The pressure coefficients at various depths, assuming a foundation 19 ft x 9 ft 9 in. and using the Newmark chart, are given in Table 5-III. The total pressure at the center of the short edge is approximately 0.8 times the total pressure at the center of the long edge. The total pressure at the corner is approximately 0.6 times the total pressure at the center of the long edge. Assuming that the deformation ratio will be the same, the theoretical distribution of the total deformation around the perimeter of the test load can be determined. In Table 5-IV the measured deformation is compared to an assumed average deformation (with the assumption that the foundation is rigid) and to a theoretical deformation assuming that, for this foundation, the Newmark chart and the Boussinesq equation for vertical stress are valid; i.e., the foundation is flexible. The average percentage difference is twice as much for a rigid as for a flexible foundation. This indicates that redistribution of stress occurs in the tuff, allowing the use of the Newmark chart and the Boussinesq equation for this analysis.

Table 5-III
Newmark Pressure Coefficients

Depth (ft)	Center of Long Edge	Center of Short Edge	Corner
5	94	80	46
8	78	63	43
10	68	52	39
15	48	38	31
20	32	25	24
30	17	15	15
40	11	11	11
60	5	5	5
Total	353	289	214

Table 5-IV

Mesita de Los Alamos

Location No. 1

Corner	Measured Deformation 11/23/66 (ft)	Average Deformation 11/23/66	Difference From Average	Percentage Difference	Theoretical Distribution Newmark Chart	Difference Deformation and Newmark Theoretical Deformation	Percentage Difference
NW	0.0115	0.0143	-0.0028	-19.5	0.0114	0.0001	0.9
W	0.0162	0.0143	0.0019	13.3	0.0152	0.0010	7.2
SW	0.0097	0.0143	-0.0046	-32.0	0.0114	-0.0017	-15.0
S	0.0172	0.0143	0.0029	20.3	0.0190	-0.0018	-9.5
SE	0.0127	0.0143	-0.0016	-11.2	0.0114	0.0013	11.4
E	0.0112	0.0143	-0.0031	-21.7	0.0152	-0.0040	-26.3
NE	0.0110	0.0143	-0.0033	-23.1	0.0114	-0.0004	-3.5
N	0.0248	0.0143	0.0105	73.3	0.0190	0.0058	30.5
Average	0.0143	0.0143		26.8			13.1

Qualitative Tests

Two loadings, one a structure constructed of iron counterweights (Iron House) and the other a water reservoir, were observed during construction and filling, respectively, to establish procedures for tests to be conducted later. Subsoil information was not available for these projects, nor was it possible to maintain the integrity of the bench marks. It was decided that only qualitative results could be obtained.

Iron House

The characteristics of the tuff under the Iron House are unknown. It may be assumed that it is a competent material. However, fill had been placed over the tuff approximately 6 to 10 ft deep on the south side of the Iron House, with lesser amounts on the east side. Most of the benchmarks did not penetrate the fill; two on the east side of the building did penetrate the fill.

The area covered by the Iron House was approximately 44 x 19 ft, with the load being imposed around the perimeter of the building. Counterweights 19 ft long, 3 ft 3 in. wide, and 2 ft thick were used as a floor. This floor, no doubt, helped to distribute the load across the width of the building. The total load was in excess of 1,000 tons, or approximately 1.2 ton/ft^2.

Reference points were 3/4-in. -diam reinforcing bars, 5 ft long, driven into the ground allowing 6 in. to project.

A small amount of creep occurred, but whether in the tuff or in the fill is unknown. Some heaving occurred on the east reference points.

Pajarito Reservoir No. 3

The volcanic tuff at Pajarito Reservoir No. 3 is classified as hard. The tuff near the edge of the mesa is broken and fractured. The tuff under the tank may be assumed to be competent with a modulus of elasticity of approximately 150,000 psi (unit 2b).

The capacity of Pajarito Reservoir No. 3 is one million gallons, or approximately 4,160 tons. The head of water is 35 ft, resulting in a uniform pressure on the bottom of the tank of 2,180 lb/ft^2.

Reference point N-O, which is located approximately 1 ft from the edge of the tank, was deformed 0.0050 ft

under load. This compares to a deformation of 0.0104 ft for N-1 and 0.0077 ft for E-1, which are located an equal distance from the edge of the tank at Pajarito Reservoir No. 2. Reference point N-2, which is located approximately 9 ft from the edge of the tank, deflected 0.0042 ft. This compares to an average of 0.0054 ft for Pajarito Reservoir No. 2.

Comparison of Calculated to Empirical Deformation

Pajarito Reservoir No. 2

This reservoir is at the intersection of Pajarito Road and Rex Drive (Fig. 5-3). It has a capacity of 1.5 million gallons and imposes a total load of 6,250 tons over an area of 5,740 ft^2, or about 2,180 lb/ft^2. The maximum head of water is 35 ft. The radius of the tank is 42 ft, 7 in. The bottom of the tank is at elevation 6,935 ft.

Reinforcing bars were driven into undisturbed tuff at locations E-0, E-1, etc., as shown in Fig. 5-3. Prior to the filling of the tank on September 10, 1966, readings were taken on these bench marks to establish a base for measuring future deformation. Readings were then taken approximately every two weeks to establish a record of creep for the loaded area. On January 11, 1967, the tank water level was lowered to 4.5 ft to measure rebound. The tank was refilled and readings with 29.75 ft of water were taken on January 18, 1967, and with 33.0 ft of water on March 6, 1967.

Assumptions. The water reservoirs impose loads on the soil in agreement with Boussinesq's theory, and the Newmark chart applies. The solution for the theoretical deformation under load was derived using the Newmark chart. The pressure at predetermined depths in the foundation material was computed, and the deformation at these depths was calculated using Hooke's law. This analysis assumed that the foundation material is an isotropic uniform material.

Volcanic tuff of both the units 3 and 2b strata was excavated and tested by the Zia Company's Material Testing Laboratory. The samples were oriented in three directions for testing: vertical, north-south (horizontal), and east-west (horizontal). Average values for the modulus of elasticity for the unit 3 tuff were as follows:

Vertical	21,390 psi
East-West	15,340 psi
North-South	14,080 psi

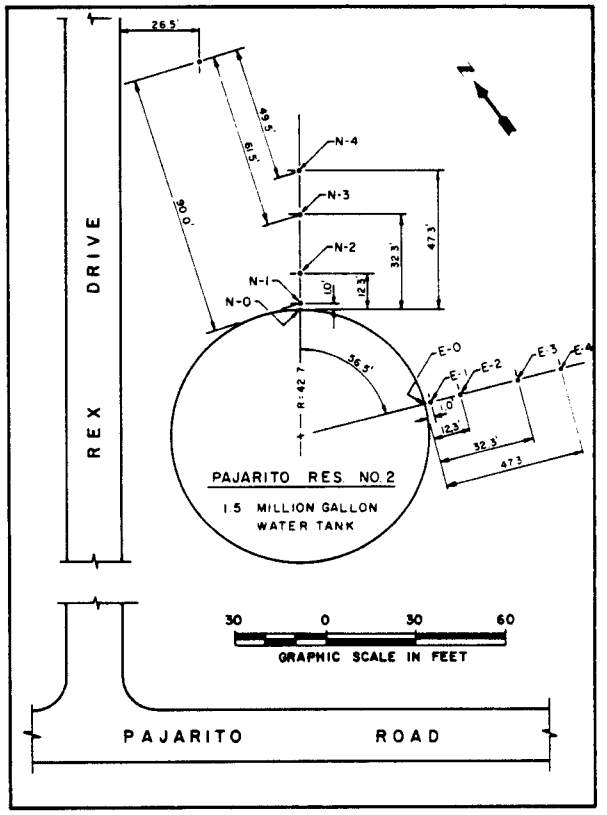

Fig. 5-3. Plan, Pajarito Reservoir No. 2.

A value of 20,000 psi for the modulus of elasticity was used in the calculations for deformation for unit 3 tuff. The depth of this stratum was assumed to be 50 ft. Over 75% of the total deformation occurs in the first 50 ft below ground level.

The value for the modulus of elasticity in the vertical direction at the surface of the unit 2b tuff was approximately 100,000 psi. This value was used in the calculations for the tuff from 50 to 75 ft below the surface. Below this stratum a value of 150,000 psi was used, based on borings taken on Mesita de Los Alamos.

Calculated versus Empirical Deformation. To minimize error, five readings representing one month under full load were averaged to obtain the empirical deformation curves given in Fig. 5-4. These curves represent the measured deformation as a function of distance from the center line of the tank in the north and east directions. The calculated deformation curve was derived using the Newmark chart, and the modulus of elasticity determined by tests conducted by The Zia Company.

The agreement between calculated and empirical deformation is approximately the same as the agreement between the deformation recorded in the east and west directions. The agreement is poorest near the tank and becomes more favorable as the distance from the tank increases. Near the tank the localized effect of the tank ring wall may cause some deviation from theoretical prediction.

In general, the theoretical deformation is within 0.002 ft of the empirical deformation at the greater distances from the tank, and is conservative closer to the tank.

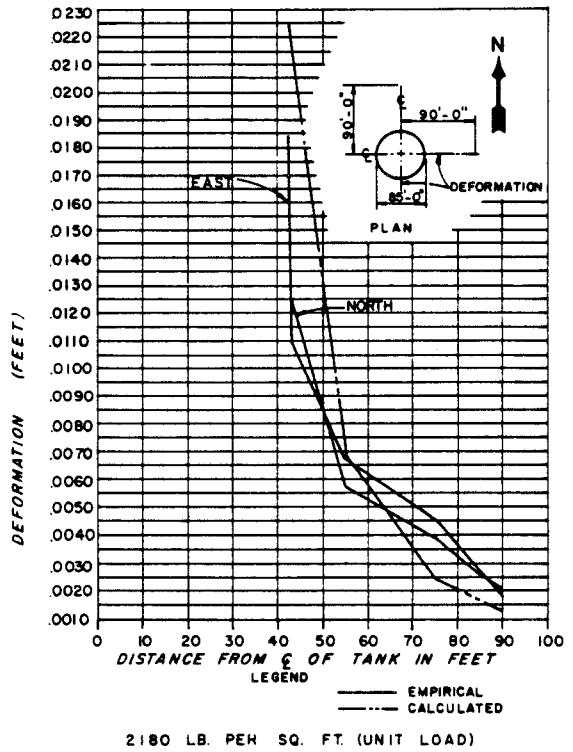

Fig. 5-4. Pajarito Reservoir No. 2, deformation versus distance.

Mesita de Los Alamos

Surplus Atlas silo counterweights were used to impose loads on Mesita de Los Alamos. The dimensions and weights of the counterweights are as follows:

No.	Size	Weight Each (lbs)	Total Weight (tons)
39	19.0 x 3.25 x 1.0 ft	26,887	524.3
21	19.0 x 3.25 x 0.5 ft	14,638	153.
11	9.0 x 3.25 x 1.0 ft	12,712	69.9

The area on which the weights were imposed was first leveled to undisturbed tuff. A 4-in. layer of pulverized tuff was placed and compacted over this area to assure an equal distribution of load to the undisturbed tuff below. Empirical data obtained from the load test were used to determine the type of analysis; i.e., flexible or rigid foundation.

On October 24 and 25, 1966, counterweights weighing 750 tons were placed at location No. 1 on Mesita de Los Alamos. Three counterweights, 19 ft x 3.25 ft, 3 in. x 1 ft, were placed on the bottom followed by five counterweights, 9 x 3.25 x 1 ft, to distribute the load. The remaining counterweights were then placed with the 19-ft dimension in the east-west direction. The total area on which the load was imposed was approximately 185 ft^2; the total load imposed was 4.05 ton/ft^2. Deformation was recorded for five weeks, at which time all creep appeared to have stopped. On December 9 and 10, 1966, the weights were transferred from location No. 1 to location No. 2, where 4.05 ton/ft^2 were imposed on the tuff. The final reading at this position was taken on December 27, 1966, which allowed two weeks for deformation. It was noted that most of the deformation occurred during the first two-week period at location No. 1, and that little

would be gained by applying the load at location No. 2 for a longer time.

On December 27 and December 28, 1966, the test weights were transferred from location No. 2 to location No. 1. Three counterweights measuring 9 x 3.25 x 1 ft were placed on the bottom followed by three counterweights, 9 x 3.25 x 1 ft to distribute the load. The remaining counterweights were then placed with the long direction running east-west. Additional bench marks were driven into the ground at the four corners of the new configuration prior to the placing of the counterweights. The total area on which the weight was imposed was 87.5 ft^2; the load imposed on this area was 8.55 ton/ft^2.

On March 8, 1967, the test weights were relocated to location No. 2, where 8.55 ton/ft^2 were imposed on the tuff. Additional bench marks were driven at the four corners of the new configuration as was done at location No. 1. Deformation was recorded and the effect of creep was noted. This test was discontinued when contractor's equipment was moved into the immediate area.

Assumptions. The Newmark influence chart for computation of vertical stress and a computer program using the Boussinesq equation for vertical stress were used to determine the stress at various depths below the surface. The deformations at these depths were determined using Hooke's law.

Values for the modulus of elasticity were obtained from the study conducted by the Albuquerque Testing Laboratory (1966). In the unit 3 tuff, in the vicinity of the test areas, values of 25,600, 30,600, and 23,300 psi were determined from tests. A value of 25,000 psi was used in the calculation for deformation for the unit 3 tuff. At location No. 1 the depth of stratum for unit 3 tuff was assumed to be 50 ft based upon information from test boring No. 12, (Albuquerque Testing Laboratory, 1966). At location No. 2, based upon information from test boring No. 15, the depth of stratum for unit 3 tuff was assumed to be 25 ft. The unit 2b tuff was assumed to have a modulus of elasticity of 160,000 psi based upon the test conducted at elevation 6,932 on a sample from test boring No. 12. Deformation was calculated for a depth of 85 ft after which the additional increments of deformation were considered negligible.

Calculated versus Empirical Deformation.

Location No. 1, 4.05 ton/ft^2

To minimize error, a total of five readings representing a period of over one month was averaged to obtain the empirical deformation curves given in Figs. 5-5 and 5-6. These curves represent the measured deformation as a function of distance from the center line of the test load in the north (Fig. 5-5) and in the east (Fig. 5-6) directions. A review of readings taken on a secondary bench mark indicates that the primary bench mark was not disturbed. Very little creep is indicated by the readings taken during this month, and the difference between the high and low readings for a particular bench mark may be attributed to survey inaccuracy.

The results of this phase of the load test indicate a close correlation between empirical and calculated deformations. The largest deviation noted was 0.001 ft with the exception of the closest east bench mark, which was probably disturbed during erection of the load test weights; a much smaller difference was noted between empirical and calculated values at location No. 2 for a bench mark at a similar location.

Location No. 1, 8.55 ton/ft^2

A total of seven readings representing a five-week period were averaged to obtain the empirical deformation curves given in Fig. 5-7. These curves represent the measured deformation as a function of distance from the center line of the test load in the north and in the east directions. A review of readings taken on a secondary bench mark indicates that the primary bench mark was not disturbed. Very little or no creep is indicated by the deformation recorded during this five-week period, and the difference between the high and the low readings for a particular bench mark may be attributed to survey accuracy limitations.

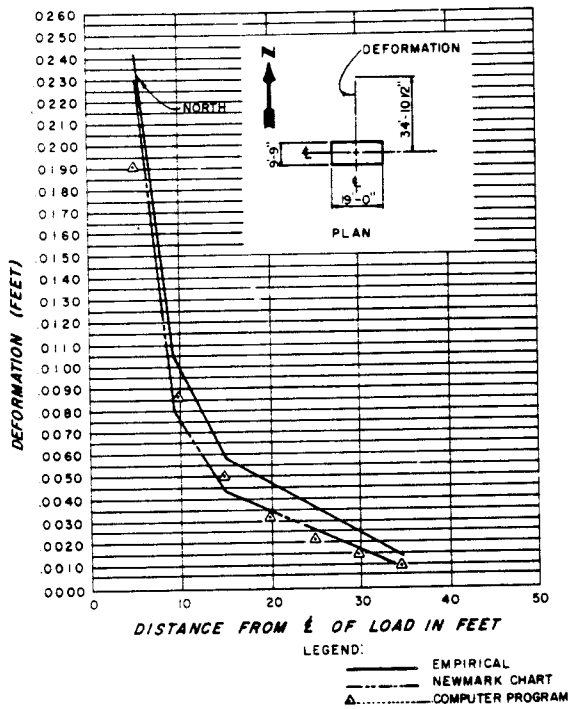

Fig. 5-5. Deformation versus distance: location No. 1 (4.05 ton/ft^2), Mesita de Los Alamos.

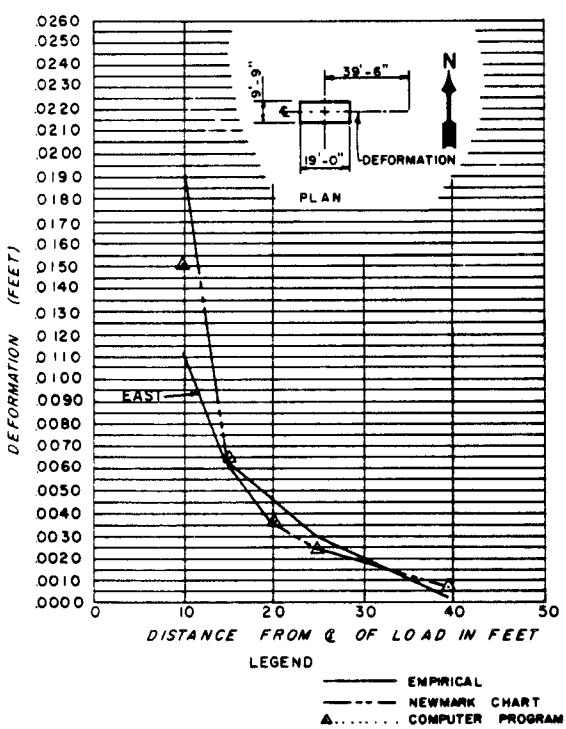

Fig. 5-6. Deformation versus distance: location No. 1 (4.05 ton/ft^2), Mesita de Los Alamos.

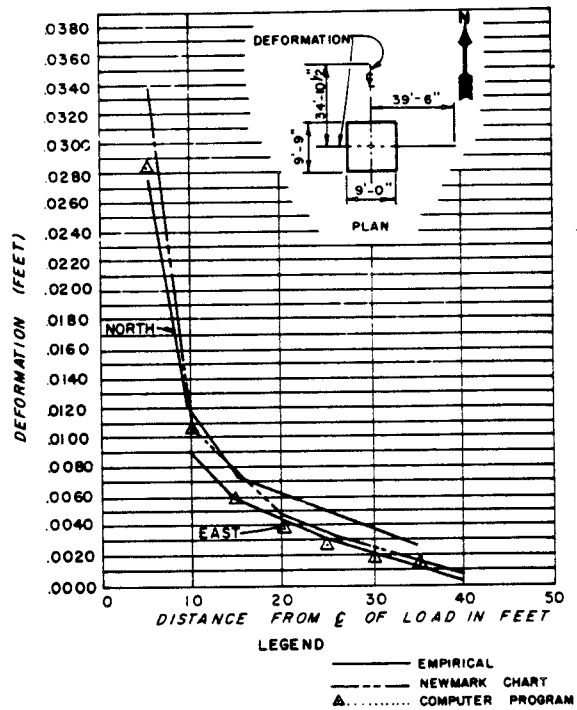

Fig. 5-7. Deformation versus distance: location No. 1 (8.55 ton/ft^2), Mesita de Los Alamos.

Agreement within 0.001 ft is noted from 10 ft to 40 ft from the center line of the test load. A larger difference is noted 5 ft from the center line of the test load but the deformation-distance curve is steep at this point and the locations of the bench marks with respect to the center line of the test load are not precisely known. The agreement between empirical and analytical results is good.

Location No. 2, 4.05 ton/ft^2

This loading was imposed at location No. 2 for approximately two weeks. The bench marks for location No. 2 were modified to allow more precise readings, and the accuracy of the readings at this location is considered good. The average of two independent readings was used to derive the empirical results shown in Figs. 5-8 and 5-9. Very little creep is indicated for the two-week period. As seen in Figs. 5-8 and 5-9, the agreement between empirical and analytical results is exceptionally good.

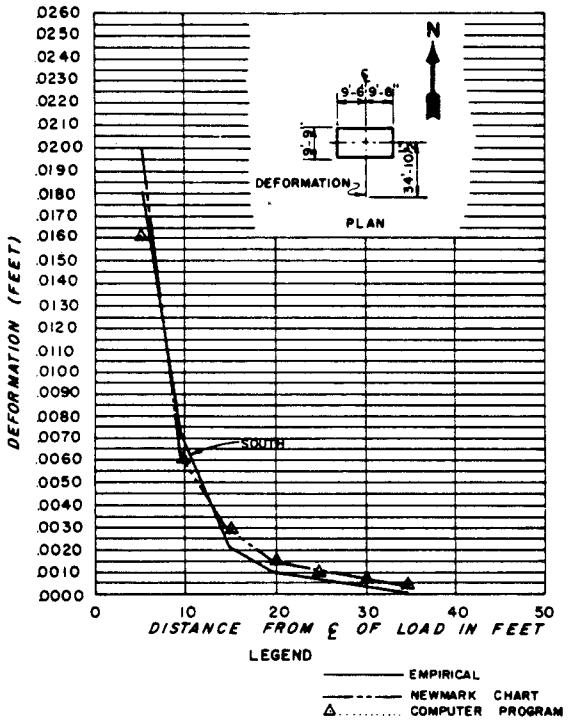

Fig. 5-8. Deformation versus distance: location No. 2 (4.05 ton/ft^2), Mesita de Los Alamos.

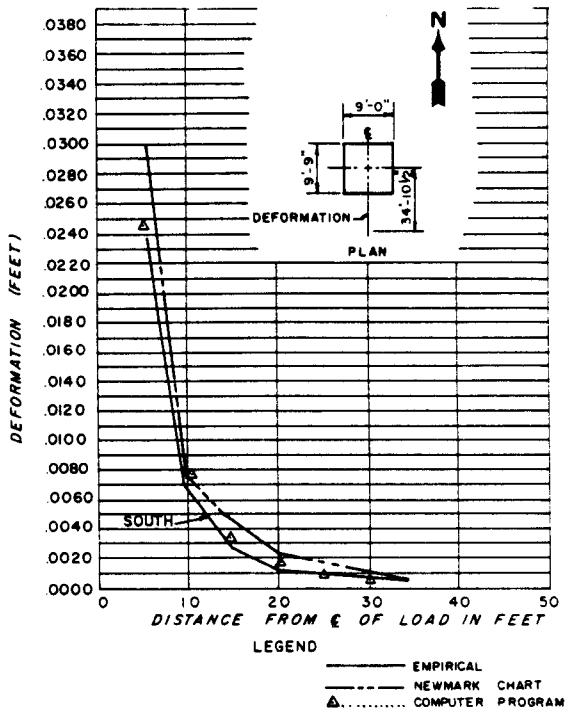

Fig. 5-10. Deformation versus distance: location No. 2 (8.55 ton/ft^2), Mesita de Los Alamos.

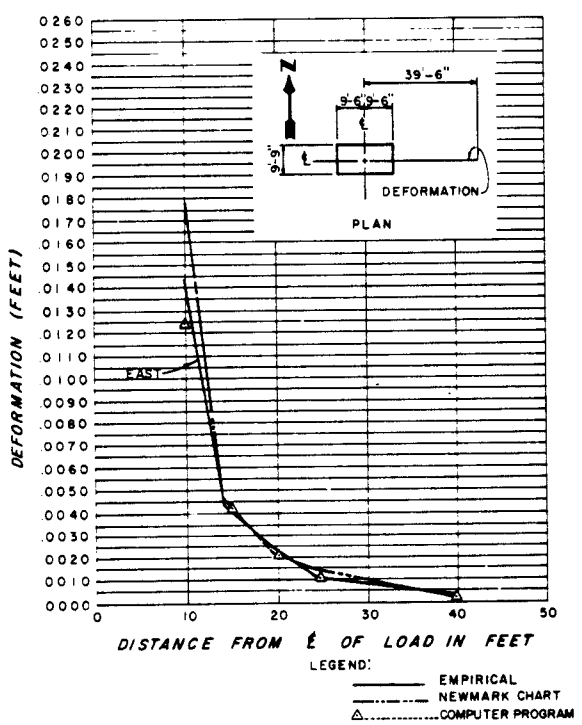

Fig. 5-9. Deformation versus distance: location No. 2 (4.05 ton/ft^2), Mesita de Los Alamos.

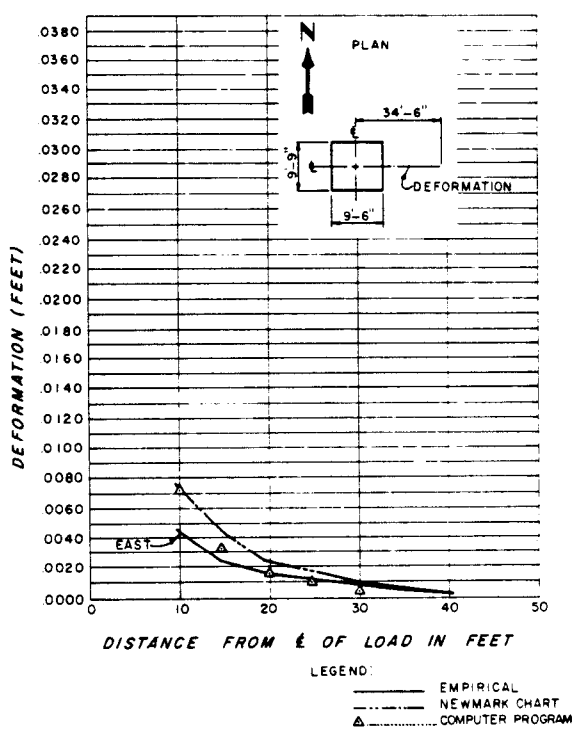

Fig. 5-11. Deformation versus distance: location No. 2 (8.55 ton/ft^2), Mesita de Los Alamos.

Location No. 2, 8.55 ton/ft^2

This loading was imposed on the tuff at location No. 2 on March 8, 1967. Upon inspection of the test load, it was determined that localized failure had occurred and that the weights were leaning to the north and west. The northerly lean was 3-1/4 in. in 12 ft which, after two weeks, had become 2-3/4 in. in 12 ft. The westerly lean was 2-3/4 in. in 12 ft, and after two weeks the test load was plumb in the east-west direction.

Figures 5-10 and 5-11 record the deformation due to the 8.55 ton/ft^2 loading. The agreement between theoretical and empirical deformation is not as good as for the 4.05 ton/ft^2 loading, but it is within 0.002 ft at all points 10 ft or more from the center line of the test load. Usually the theoretical deformation is greater than the empirical results and is therefore conservative. Figures 5-10 and 5-11 are based on the readings taken March 10, 1967; readings taken after this date were discounted because of increased construction activity in the area.

Computer Analysis for Deformation. A computer program was written to calculate deformation at various distances from the center of the test load using Boussinesq's equation for vertical stress and Hooke's law. Results of this computer analysis are shown as triangles on Figs. 5-5 through 5-11. The correlation between computer and empirical results is good.

Deformation Under Sustained Loading

The deformation of the tuff at selected bench marks was studied to determine if a creep factor could be associated with the Bandelier tuff. The bench marks selected were those closest to the test load which, therefore, experienced the greatest deformation. By choosing these bench marks, the inaccuracies attributed to surveying are reduced compared to the total deformation.

Pajarito Reservoir No. 2

The test load at this location cannot be considered steady because the water level within the tank is constantly changing. The tank gauge readings are shown on Figs. 5-12 and 5-13. There appears to be no discernible creep recorded at bench mark N-1 or E-1 over the five months of observation. The variations in the readings may be attributed to survey inaccuracies or water-level fluctuations.

Mesita de Los Alamos, Location No. 1

Figures 5-14 through 5-17 are records for bench marks S-O, E-O, N-O, and W-O, respectively, for the test at location No. 1 for the period between October 21, 1966, and March 17, 1967. The reliability of readings taken after March 17, 1967, should be discounted because of construction activity in the area. Particular attention should be given to the deformation under load during (1) the time period October 26 to November 30, 1966, when a test load of 4.05 ton/ft^2 was imposed on the tuff and (2) the time period between December 28, 1966, and March 3, 1967, when a test load of 8.55 ton/ft^2 was imposed. Another interesting comparison is one of deformation prior to initial loading, after the 4.05 ton/ft^2 load was removed.

October 26 to November 30, 1966. During this period E-O and W-O, Figs. 5-15 and 5-17, respectively, show no creep; N-O, Fig. 5-16, shows minor creep under sustained load; and S-O, Fig. 5-14, shows a small negative creep (recovery) under sustained load. The change in readings at N-O and S-O could be attributed to survey inaccuracies or to a redistribution of stress in the tuff. During this five-week period there was no indication of a large amount of deformation due to creep. The load imposed during this period was 4.05 ton/ft^2.

December 28, 1966, to March 3, 1967. During this nine-week period a load (8.55 ton/ft^2) which approached the ultimate bearing capacity of the tuff was imposed. S-O (Fig. 5-14) and N-O (Fig. 5-16) located 5 ft, 4-1/2 in. from the center line of the test load recorded larger deformations than E-O and W-O, which were located 10 ft from the center line of the test load.

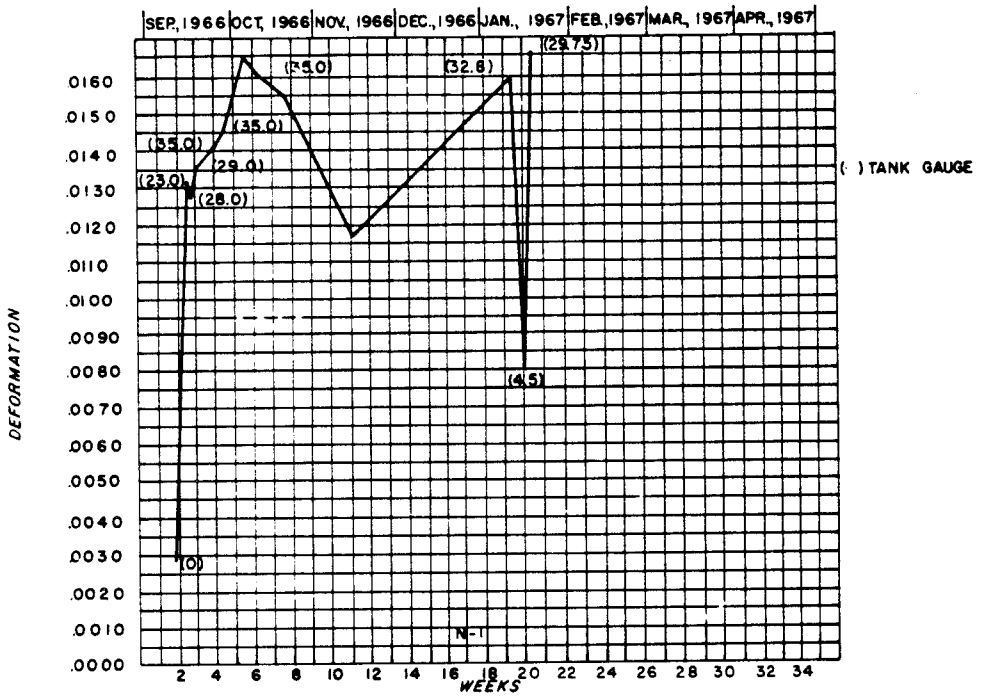

Fig. 5-12. Deformation versus time: Pajarito Reservoir No. 2, bench mark N-1.

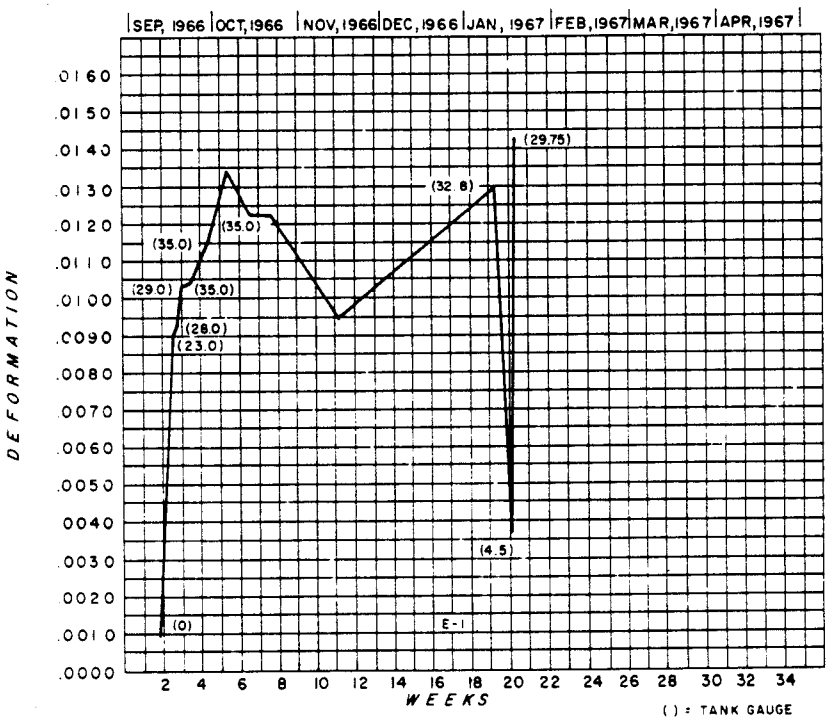

Fig. 5-13. Deformation versus time: Pajarito Reservoir No. 2, bench mark E-1.

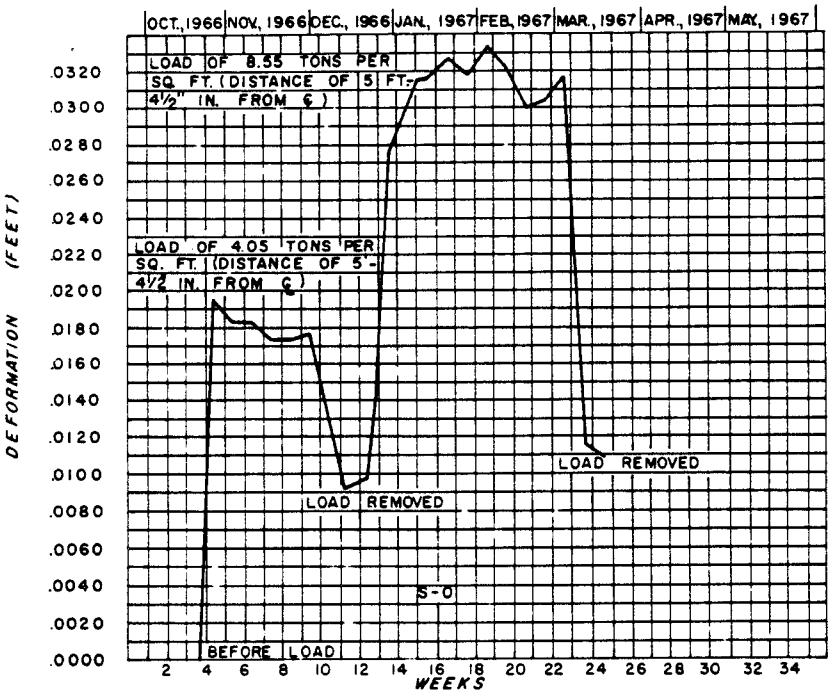

Fig. 5-14. Deformation versus time: location No. 1, Mesita de Los Alamos, bench mark S-O.

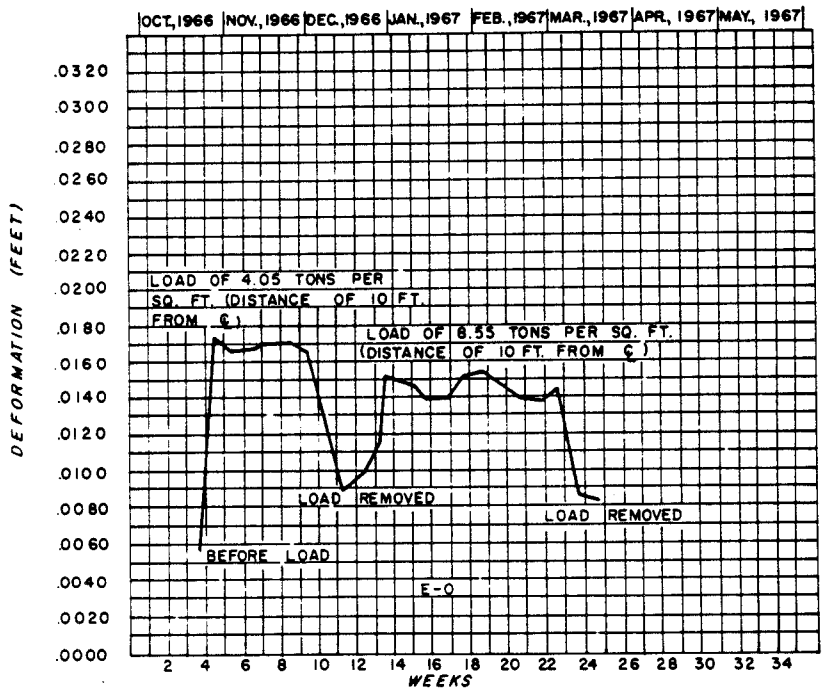

Fig. 5-15. Deformation versus time: location No. 1, Mesita de Los Alamos, bench mark E-O.

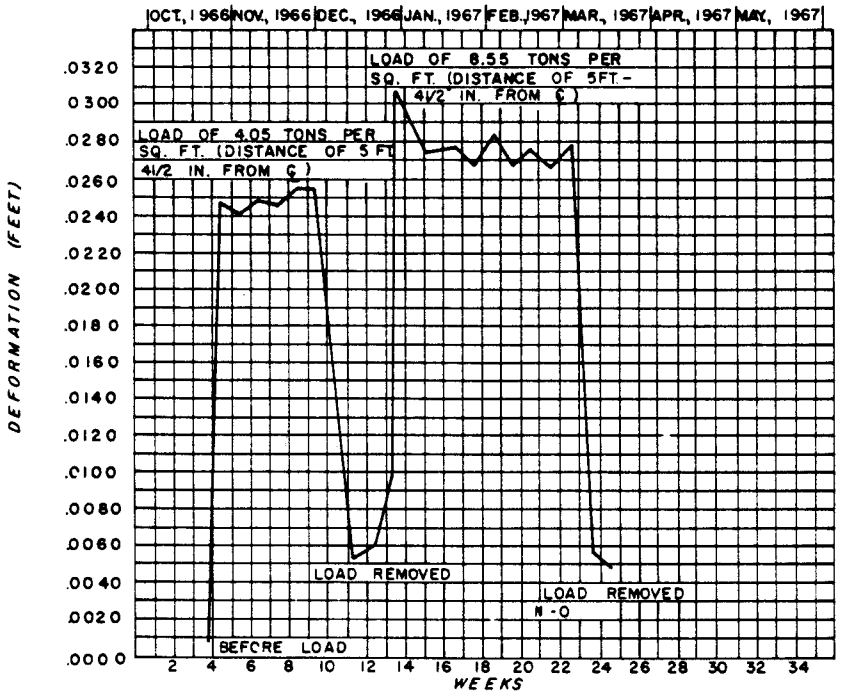

Fig. 5-16. Deformation versus time: location No. 1, Mesita de Los Alamos, bench mark N-O.

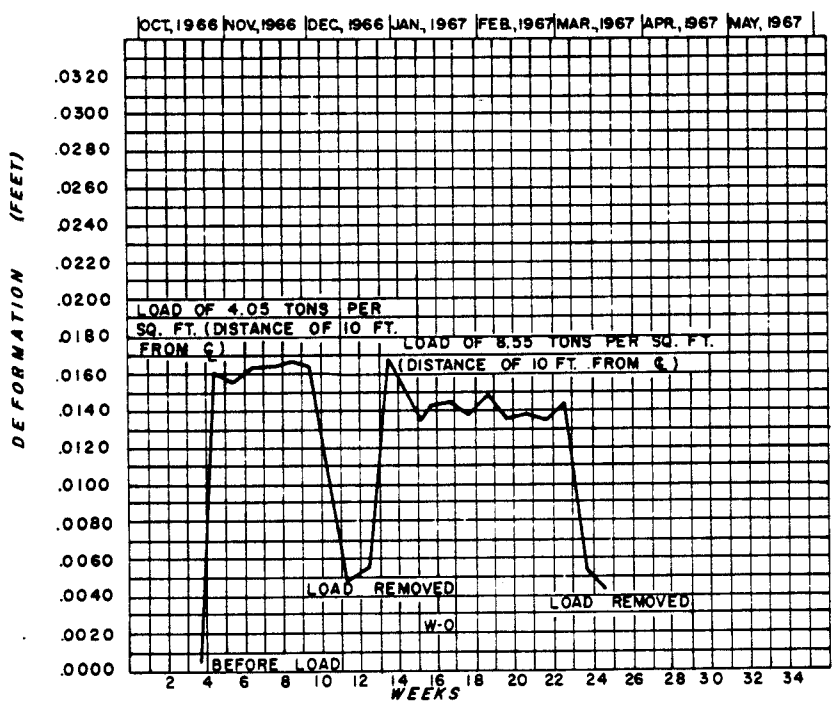

Fig. 5-17. Deformation versus time: location No. 1, Mesita de Los Alamos, bench mark W-O.

For all four bench marks, there is little indication of an increase in deformation due to creep.

Irrecoverable Deformation. At S-O a large (0.01 ft) permanent deformation was recorded between the no-load condition on the undisturbed tuff and the no-load condition after the 4.05-ton/ft^2 load was removed. This large permanent deformation did not occur from the time the 4.05-ton/ft^2 load was removed to the time the 8.55-ton/ft^2 load was removed. For bench marks E-O, N-O, and W-O. the permanent deformation from a no-load condition on undisturbed soil to a no-load condition after the 4.05-ton/ft^2 load was removed is much smaller (about 0.004 ft). There appears to be no further permanent deformation caused by the application of the 8.55-ton/ft^2 load.

Mesita de Los Alamos, Location No. 2

Figures 5-18 through 5-20 record the deformation experienced at E-O, N-O, and S-O at location No. 2. E-O was located 10 ft from the center line of the test load; S-O and N-O were located 5 ft, 4-1/2 in. from the center line of the test load. Unfortunately, the test load at location No. 2 was not imposed for a long enough period to obtain a good record of creep deformation. However, all three records indicate that from December 12 to December 27, 1966, a large amount of creep deformation did not take place. From December 28, 1966, to March 3, 1967, a period of approximately 9 weeks during which there was no load imposed at location No. 2, negative creep (recovery) did not take place either. For location No. 2, after the load was removed, bench marks E-O, N-O, and S-O were either at or below the same elevation as prior to the original loading of 4.05 ton/ft^2. The test load of 8.55 ton/ft^2 imposed at location No. 2 on March 8, 1967, caused the volcanic tuff to yield. Localized failure caused the test load to lean towards the north 3-1/4 in. in 12 ft and towards the west 2-3/4 in. in 12 ft. After approximately two weeks under load, the north-south lean had been reduced to 2-3/4 in. in 12 ft, and in the east-west direction the test load was plumb. This can be attributed to a localized failure of the volcanic tuff on the west side of the test load followed by a localized failure on the east side. At N-O and S-O, which were the closest bench marks to the test load, the 8.55 ton/ft^2 load caused a deformation comparable to that experienced at location No. 1, even though localized failure occurred under the test load. It is proposed that the localized failure resulted in a shear and bearing failure of the tuff around the perimeter of the test load, and that the effect of this failure beyond the perimeter is negligible.

Conclusions

The test conducted on Mesita del Buey and on Mesita de Los Alamos did not answer all of the questions that a designer could ask. The effects of vibratory loading and of numerous repetitive loadings on deformation must still be determined. The tests do give adequate information for the design of foundations to limit deformation with respect to static loading, and thus encompass the majority of loadings to be imposed by the Meson Physics Facility.

Deformation under Load

Newmark's chart or the Boussinesq equation for calculating vertical stress may be used to determine the stress in the tuff. The application of Hooke's law will yield values for deformation due to this stress. Empirical results indicate a correlation between this theoretical approach and actual deformation. Incorrect values for the modulus of elasticity of the foundation material are the more likely reasons for errors. Care must be taken to assure that the modulus of elasticity used in design is representative of the in situ modulus of elasticity of the volcanic tuff in the vicinity of the loaded area.

Deformation under Sustained Loading

Based upon the tests conducted for this study, the following is proposed. The initial deformation under load is comprised of an elastic deformation and a permanent deformation. This permanent deformation is about 20% for the unit 3 tuff; it would be less for the unit 2b

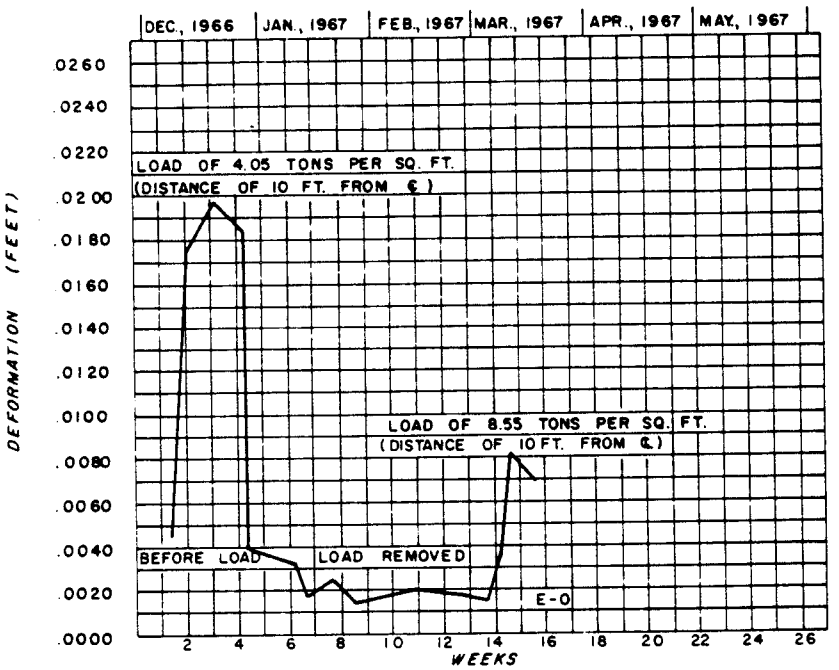

Fig. 5-18. Deformation versus time: location No. 2, Mesita de Los Alamos, bench mark E-O.

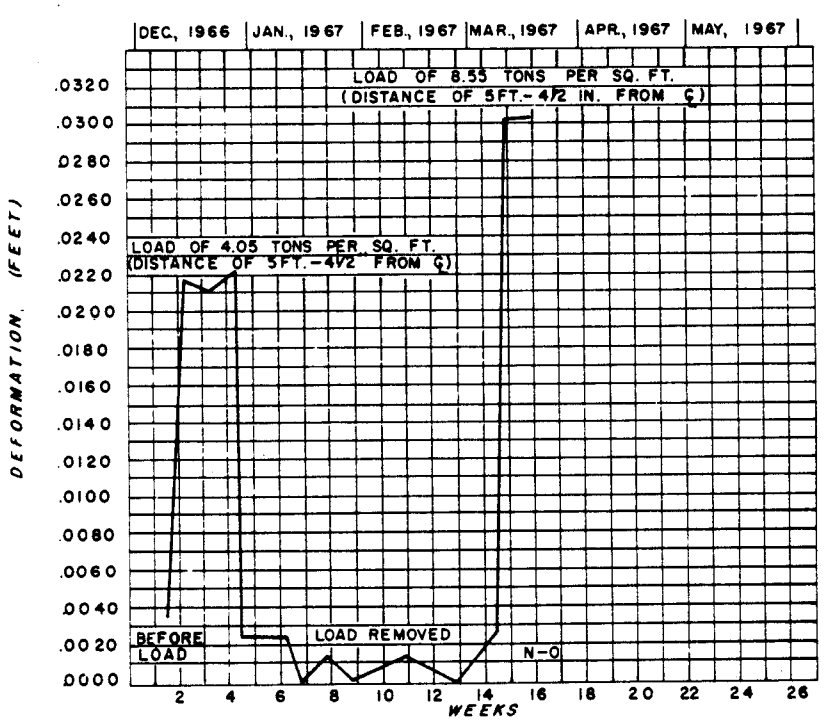

Fig. 5-19. Deformation versus time: location No. 2, Mesita de Los Alamos, bench mark N-O.

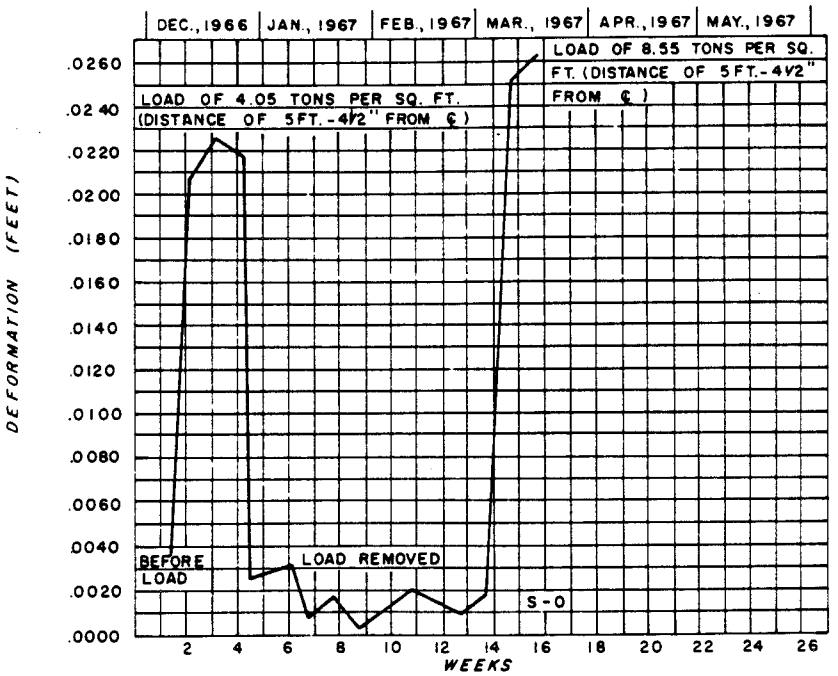

Fig. 5-20. Deformation versus time: location No. 2, Mesita de Los Alamos, bench mark S-O.

tuff. This permanent deformation occurs with the initial loading and is not recoverable. It is caused by a breakdown of the tuff, probably under the first 2 ton/ft^2 load.

After the permanent deformation has taken place, usually in the first few hours of loading, the tuff reacts as an elastic material. The effects of vibratory loading on creep is not yet known.

References

1. G. P. Tschebotarioff, Soil Mechanics, Foundations, and Earth Structures, 1st Edition, McGraw-Hill Book Company, New York (1951), Chap. 9.
2. J. Comrie, ed., Civil Engineering Reference Book, 2nd Edition, Butterworths, London (1961), Vol. 2, pp. 54-60.
3. S. Timoshenko and J. N. Goodier, Theory of Elasticity, 2nd Edition, McGraw-Hill Book Company, New York (1951).
4. A. Casagrande, "Application of Soil Mechanics in Designing Building Foundations," Proceedings, American Society of Civil Engineers, Vol. 68, November 1942, p. 1487.

ACKNOWLEDGMENTS

The following acknowledgments of contribution to this document are made:

Section 2, Geology of Los Alamos, was derived from work done by the U. S. Geological Survey, Branch of Crustal Studies, under contract to the Los Alamos Scientific Laboratory. Authors of this section were Ronald Willden and Edward E. Criley, both of the U. S. Geological Survey.

Section 3. Near-Surface Rocks, was derived from work done by the U. S. Geological Survey, Water Resources Branch, under contract to the Los Alamos Scientific Laboratory. The author of this section was William D. Purtymun of the U. S. Geological Survey.

Section 4, Ground Vibration Characteristics, was written by Eric S. Foster, P. E., and M. Dean Keller, P. E., of the Los Alamos Scientific Laboratory, and Frank H. Werner of the U. S. Coast and Geodetic Survey.

Section 5, Deformation Characteristics, was written by M. Dean Keller.

Technical assistance was rendered by Roland A. Pettitt, P. E., head of The Zia Company's Materials Testing Laboratory; B. P. Williams, P. E., of the Los Alamos Scientific Laboratory Engineering Department; and W. V. Mickey, Chief of the Vibrations and Engineering Projects Branch, Seismology Division, E. S. S. A., Coast and Geodetic Survey. Ralland Christiansen of the Los Alamos Scientific Laboratory assisted in the calculation of data and in the preparation of charts. Mrs. Grace Roybal and Mrs. Freda Grote endured through numerous rough drafts and the final typing of this document.

Los Alamos
Los Alamos National Laboratory
Los Alamos, New Mexico 87545

memorandum

TO: Brent Bowen, H-8, MS-490

DATE: August 11, 1981

THRU:

MAIL STOP/TELEPHONE: 495, 7-3021

FROM: Leonard Lane, LS-6

SYMBOL: LS6-81-285

SUBJECT: ESTIMATED RAINFALL FREQUENCIES FOR LOS ALAMOS

Based on the isopluvials in NOAA atlas-2 for 6-hr and 24-hr precipitation depths, I have computed the rainfall frequency estimates shown in Table 1 and Fig. 1. As you know, precipitation depths are interpolated from the isopluvials after locating the point of interest on the maps. As this requires locating the same point on a series of 12 maps, there may be some slight registration differences in the printing, and precise interpolation between isolines is difficult, there is the possibility of an error while reading the maps. I would suggest an independent computation of the values shown in Table 1.

I also went back to your original records and tabulated the maximum 24-hr precipitation depths for Los Alamos. These data are plotted in Fig. 2. Also shown in Fig. 2 are the corresponding estimates from NOAA Atlas-2. Notice that the NOAA Atlas-2 estimates are some 20% higher than the observations suggest. These differences are illustrated in Fig. 3. However, the relationship shown in Fig. 3 is linear and very close to a straight line. This suggests to me that although there are differences in the absolute amounts of maximum 24-hr precipitation for the return periods, the relationships between amounts for the various return periods are very well represented by the NOAA Atlas-2 estimates.

In view of the differences between observed data and NOAA Atlas-2 estimates shown in Figs. 2 and 3, the NOAA Atlas-2 estimates may be high for the 24-hr period. However, since no data were available on shorter time periods (1 hr, 6 hr, etc.) the quality of these estimates (Table 1) are unknown. In the absence of actual data for periods shorter than 6-hr, I would recommend use of the data shown in Table 1.

If you should have an opportunity to check my calculations in Table 1 or if you have any information on shorter time periods I would like to know. Thank you for the use of NOAA Atlas-2 and the opportunity to use your records.

LL:em Leonard J. Lane

xc: W. Purtymun, H-8
J. Rogers, LS-6
J. Nyhan, LS-6
T. Hakonson, LS-6

ABLE 1. Precipitation Frequency Estimates for Los Alamos, NM (106°19'W, 35°52'N, Elev. = 7410 Ft) From Precipitation Frequency Atlas, "NOAA Atlas-2" (Miller, et. al., 1973).[1]

RETURN PERIOD	ESTIMATED RAINFALL DEPTHS IN INCHES FOR THE GIVEN TIME PERIOD AND THE GIVEN RETURN PERIOD							
Tr	15-MIN	30-MIN	60-MIN	2-HR	3-HR	6-HR	24-HR	ANNUAL[2]
(YEARS)	P_{15}	P_{30}	P_{60}	P_2	P_3	P_6	P_{24}	P_A
2	0.56	0.77	0.98	1.11	1.20	1.36	1.76	17.99
5	0.72	1.00	1.26	1.42	1.53	1.74	2.32	24.06
10	0.82	1.13	1.43	1.62	1.75	2.00	2.67	25.79
25	0.95	1.31	1.66	1.89	2.04	2.32	3.14	27.9[3]
50	1.07	1.49	1.88	2.13	2.30	2.61	3.57	29.0[3]
100	1.19	1.64	2.08	2.36	2.55	2.90	4.00	30.24

1. Source: Miller, J.F., Frederick, R.H., and Tracey, R.J. 1973. NOAA Atlas-2, "Precipitation-Frequency Atlas of the Western United States, Volume IV-New Mexico," U.S. Dept. of Commerce, NOAA, National Weather Service, Silver Spring, MD.

2. Source: Abeele, W.V., Wheeler, M.L., and Burton, B.W. 1981. "Geohydrology of Bandelier Tuff" Los Alamos National Laboratory report, Manuscript in press.

3. Interpolated values.

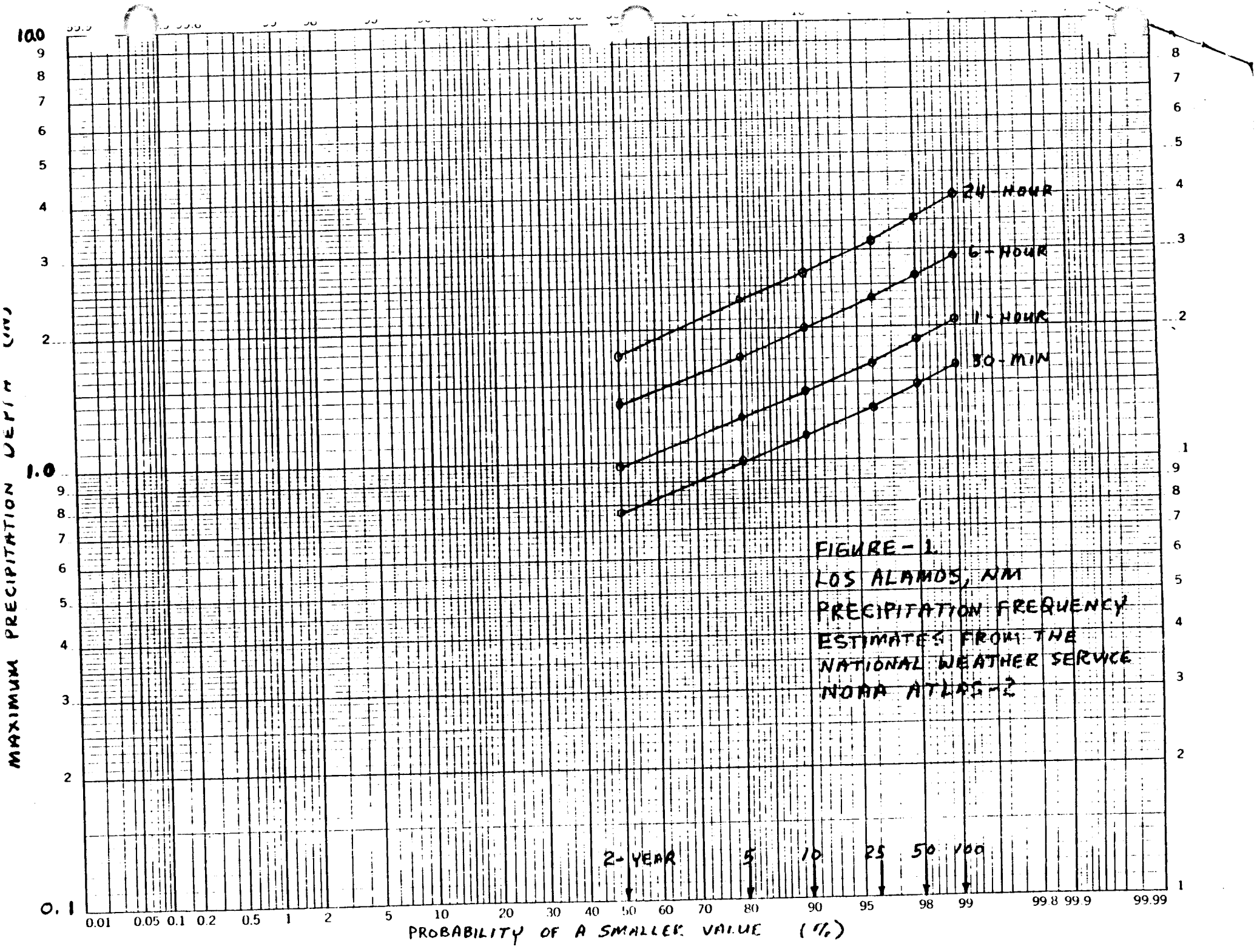

FIGURE - 1.
LOS ALAMOS, NM
PRECIPITATION FREQUENCY
ESTIMATES FROM THE
NATIONAL WEATHER SERVICE
NOAA ATLAS-2

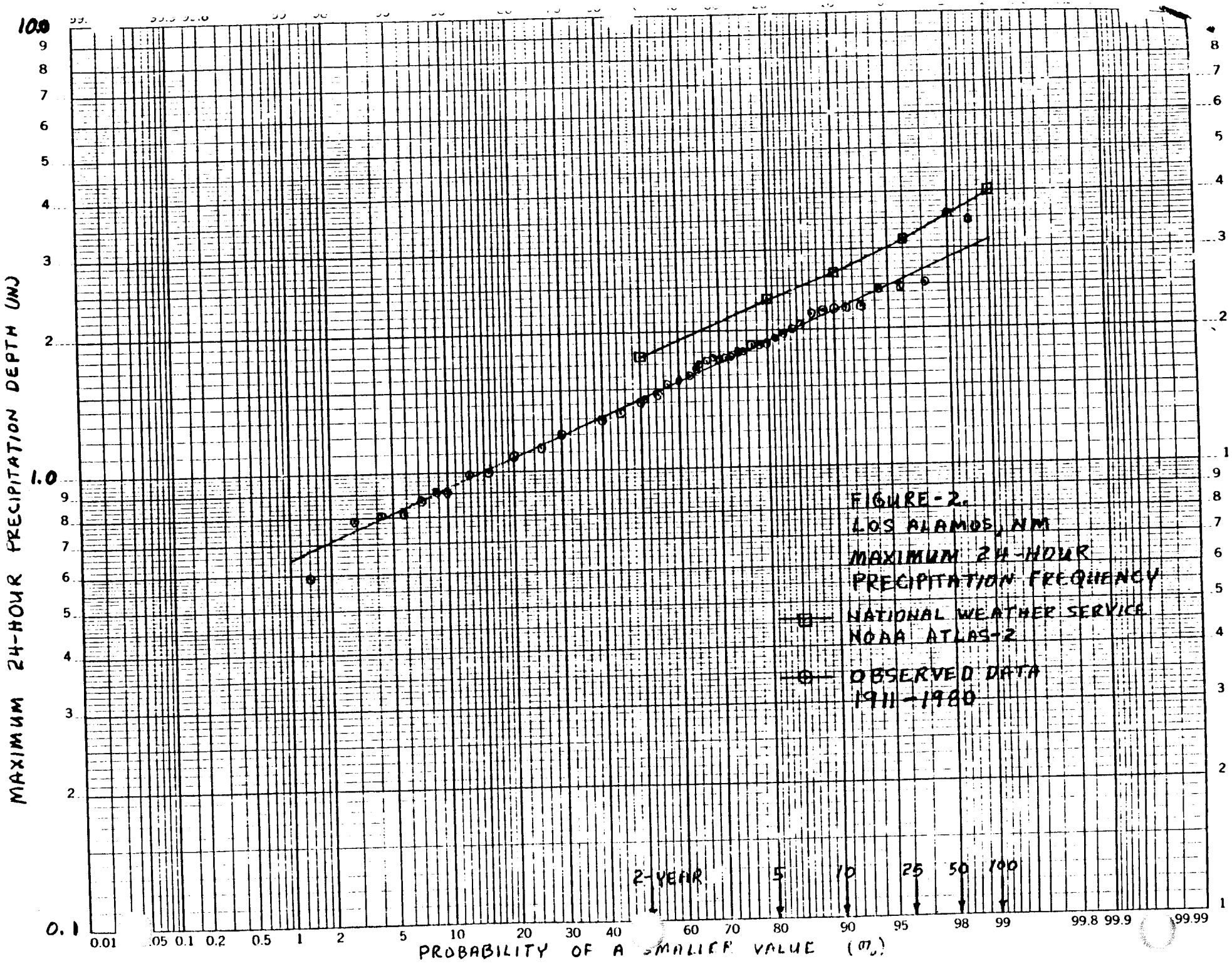

FIGURE-2.
LOS ALAMOS, NM
MAXIMUM 24-HOUR
PRECIPITATION FREQUENCY

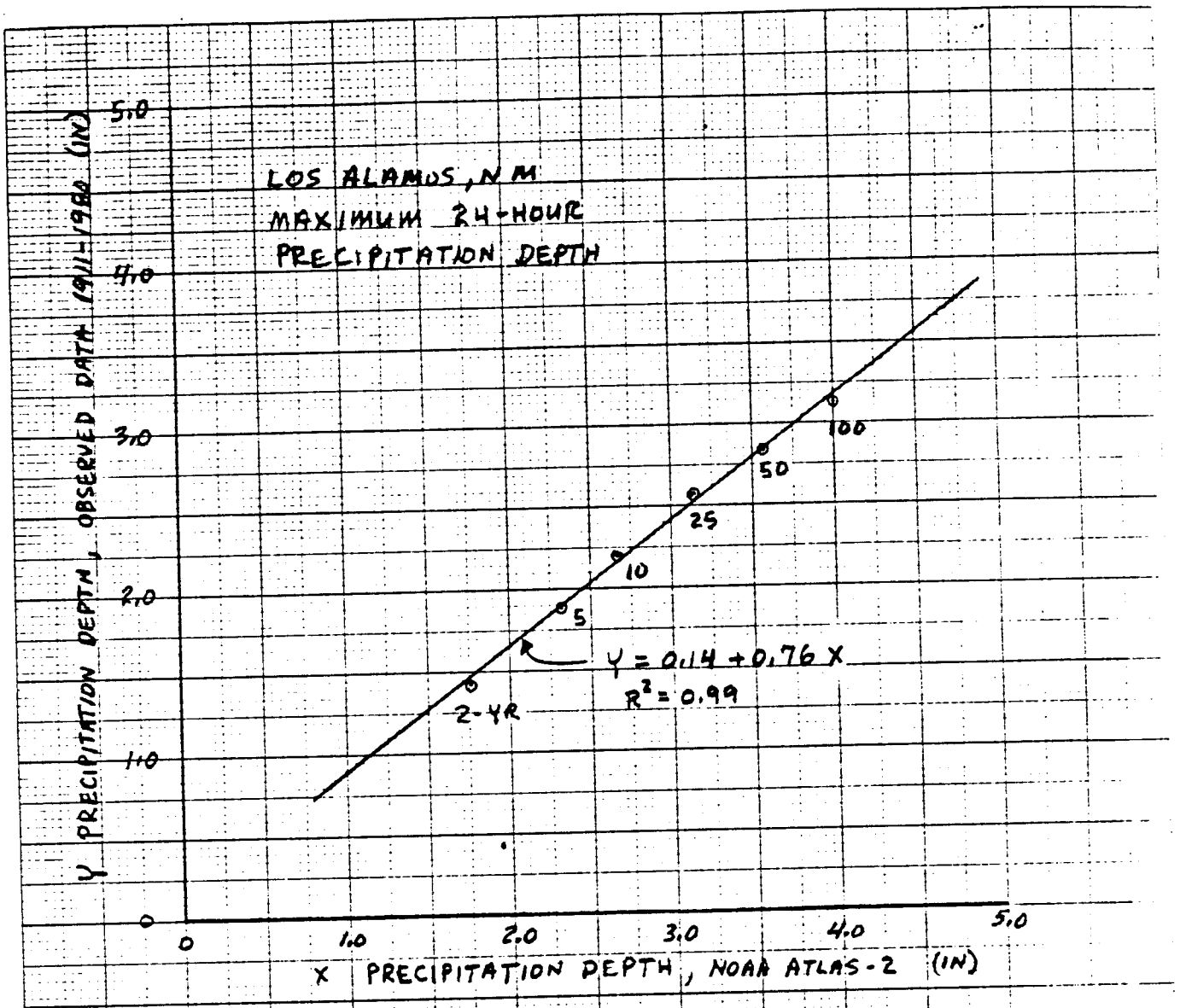

FIGURE-3. RELATION BETWEEN OBSERVED AND ESTIMATED MAXIMUM 24-HOUR PRECIPITATION AMOUNTS AT LOS ALAMOS FOR RETURN PERIODS OF 2 TO 100 YEARS.

NMEID 1984

ATTACHMENT 1

A Reasonable Worst-Case Water Balance for LANL Hazardous Waste Disposal Areas, With Emphasis on TA-54

The water balance for LANL's hazardous waste disposal areas submitted to EID by LANL on November 1, 1984, did not adequately estimate the potential for infiltration at those areas. Since this submittal was LANL's second attempt at a water balance, the EID drew up the following water balance.

1. Precipitation

The EID is aware of four precipitation stations relevant to LANL hazardous waste disposal areas. The data we currently have available from these stations is shown on page two.

These records show that winters at White Rock - and, presumably, at TA-54, which is only two miles away - are significantly drier than at Los Alamos or TA-59/TA-3. Since the non-summer months are the ones most likely to experience precipitation in excess of evapotranspiration (ET) requirements, applying precipitation data from TA-59/3 or from Los Alamos to TA-54 will tend to overestimate both annual precipitation at TA-54 and the proportion of that precipitation that may be available for infiltration.

For the Los Alamos station, a LANL employee has estimated the frequencies of occurence of annual precipitation totals that equal or exceed given values (Lane, 1981). These are:

RETURN PERIOD	ANNUAL PRECIPITATION IN INCHES
2 years	17.99 (i.e., 17.99 is the median annual precipitation)
5	24.06
10	25.79
25	27.93
50	29.03
100	30.24

To round out this picture, it is desirable to gain some idea of past rainfall from the interpretation of local tree-ring data. In one careful recent study, the authors found no reason to discard their initial premise that the quantity of annual precipitation for the Santa Fe area has remained roughly the same for the last 1000 years (Rose, Dean, and Robinson, 1981). Their work showed that excursions in 10-year averages of annual precipitation at Arroyo Hondo have not exceeded about three inches in the 1000-year record they examined.

Precipitation Data Relevant to a Water Balance at LANL Disposal Areas

Location	Average Precipitation by Month in Inches												Annual Total
	J	F	M	A	M	J	J	A	S	O	N	D	
White Rock	0.25	0.24	0.24	0.32	1.20	1.50	2.29	3.68	1.73	1.02	0.39	0.67	13.50
(9 years of record here; elevation circa 6700')													
TA-59/TA-3	0.82	0.67	1.14	0.82	1.16	1.10	3.20	3.86	1.73	1.47	0.99	0.97	17.93
(33 years combined record; elevation circa 7400')													
Los Alamos	0.84	0.70	1.01	1.01	1.25	1.33	3.29	3.69	2.01	1.61	0.70	0.93	18.37
(60 years of record; elevation 7410')													
TA-54													(13.45)
(5 years of record; annual total based on 75% of TA-59/3, as per Appendix II, p. 41; elevation circa 6700')													

(Data from Appendix II, Gabin and Lesperance, and

LANL's water balance cites an article which apparently throws a dark cloud on all of dendroclimatalogy, but we have not yet been able to access this article. Only note that, if rising CO_2 levels in the air are a competent cause of decreased tree ring response to moisture, even on semi-arid sites low in other plant nutrients, the effect will be to bias dendro-climatologists toward over-estimating past rainfall. LANL's water balance analyzes possible infiltration from a synthetic rainfall year composed of each of the highest monthly precipitation totals recorded at TA-59/3. This gives an annual total of 57.47 inches, almost twice the estimated 100-year annual precipitation. This figure is roughly equal to the average annual precipitation in Vancouver, B.C.; it is not clear that such a precipitation year could ever occur at Los Alamos without the climatic conditions that may have prevailed here in the Pleistocene. Hence, EID believes LANL's precipitation scenarios to be overly conservative.

A recent LANL study (Abeele, Wheeler, and Burton, 1981) used methods which were not explicit to study Los Alamos tree rings. In the period examined (which apparently extended at least back to 1523), the maximum annual precipitation indicated by the tree ring data was roughly 40 inches, in 1597.

A more reasonable approach than that of the LANL water balance might be to analyze the water balance under a suite of reasonable worst-case assumptions. If significant infiltration could occur under any of these regimes, one must determine both the robustness of this result and where this infiltrated water would be likely to go. The synthetic precipitation regimes that will be examined for TA-54 are shown on page 4.

For LANL disposal areas at roughly the elevation of TA-59/3, the first scenario on page 4 represents typical, rather than worst-case, conditions. The remaining sections of this report will focus on TA-54; generalizations to wetter areas are left to the reader. Note that the second and third synthetic records shown on page 4 slightly exceed the 100-year annual rainfall at Los Alamos.

2. Runoff

The LANL water balance estimates runoff at a flat 20% of incident precipitation, ostensibly based on an SCS Curve Number of 82. There are at least four reasons why this approach will overestimate runoff:

a. Precipitation is assumed to occur as rainfall only. The months of greatest interest experience significant snowfall; snow is less likely to produce runoff than rain.

b. To apply the SCS method, the frequency spectrum of individual storm magnitudes must be known in detail. Appendix II assumes storms deposit an average of roughly 1.25" of rain per storm; this is far too great.

c. What is locally runoff may become infiltration elsewhere, e.g. by running down a ramp into an active pit.

"Worst-Case" Precipitation Scenarios for TA-54

Scenario	Precipitation by Month												Annual Total
	J	F	M	A	M	J	J	A	S	O	N	D	
1. Wet decade	0.84	0.70	1.01	1.01	1.25	1.33	3.29	3.69	2.01	1.61	0.70	0.93	18.37
at TA-54; data shown is the average recorded for Los Alamos.													
2. Wet single	0.82	0.67	1.14	0.82	1.16	1.10	3.20	3.86	4.55	6.77	6.60	2.85	33.54
year at TA-54; data shown are monthly autumn maxima from TA-59/3: balance of year is average TA-59/3 data.													
3. Wet single	2.81	1.87	4.11	3.23	3.50	3.40	3.20	3.86	1.73	1.47	0.99	0.97	31.14
year at TA-54; data shown are monthly spring maxima from TA-59/3: balance of year is average TA-59/3 data.													

d. Moist (neither wet nor dry) antecedent moisture conditions are assumed in the LANL water balance. Most storms will occur with dry antecedent conditions.

A reasonable worst case analysis would assume that the precipitation of greatest interest (that is, precipitation with the greatest potential for infiltration) falls either as slow-melting snow or as individual storms of less than 0.5" in magnitude. These conditions will produce little or no runoff from TA-54, and no abstraction for runoff will be made in the water balances to follow.

3. Interception and Depression Storage

To the extent that evapotranspiration (ET) figures are computed from data for crops or natural vegetation that receive water from rain, snow, or artifical sprinkling, these ET figures already include interception losses. While in forested areas or other situations involving a high leaf area index, or in situations involving roofs, interception is important, it is not likely to be very important at TA-54 due to the sparse plant cover. The potential interception from a 2" grass lawn has been estimated to be only 0.01" (Lull and Sopper, 1969); other estimates and references can be found in Dunne and Leopold (1978). In the following analyses, an interception of zero will be assumed.

In order for depression storage to be significant in preventing infiltration, impervious depressions must be present. These conditions are not, to our knowledge, present at TA-54 to any significant extent.

4. Evapotranspiration

Discussions of evapotranspiration (ET) are often lent an unnecessarily abstract quality by the use of the "potential" ET (PET) concept. PET cannot be measured either directly or indirectly; nevertheless several traditional formulae exist to predict what it would be if it could be measured. What can be measured is the actual ET of a site, and this has unfortunately not been measured at any of the LANL disposal areas.

Observation of low moisture levels in the tuff at TA-54, and the apparent invariance of this low level with depth beyond a certain depth, lend credence to the idea that infiltration is small at TA-54 (e.g., Abrahams, Weir, and Purtymun, date unknown). Since runoff is not large either, except perhaps in summer thunderstorm events, a close upper bound for the average annual actual ET is simply the precipitation that falls on the site.

In a wet year, transpiration by plants, as well as evaporation from bare soil and snow, will increase above this average value. Winter transpiration alone will not increase very much, however, and will hardly increase at all if only winter-dormant species are involved. Summer transpiration will also increase in a wet year, but not indefinitely and not to the extent that would be possible in denser vegetation communities. The upshot is that while ET will be greater in wet years, there is no guarantee that it will increase sufficiently to prevent infiltration. The

incontrovertible evidence that infiltration does occasionally occur is discussed in a later section.

The Blaney-Criddle method for computing the consumptive use of an irrigated perennial crop will be used to predict the maximum ET that could be experienced in a given month (i.e., the PET). This empirical formula uses day length and mean air temperature to calculate PET. The version of this formula used here (Soil Conservation Service, 1970, cited in Dunne and Leopold, 1978) is more recent, and significantly different, than that used in Appendix II (Cruff and Thompson, 1967). The table below gives the PET for mature alfalfa (a highly water-intensive crop) grown in Los Alamos. That is, these values purport to predict consumptive water use by freely-irrigated alfalfa in Los Alamos.

Month	k	PET
J	0.63	0.39 in.
F	0.73	0.49 in.
M	0.86	0.91 in.
A	0.99	1.89 in.
M	1.08	3.68 in.
J	1.13	5.84 in.
J	1.11	6.53 in.
A	1.06	5.42 in.
S	0.99	3.63 in.
O	0.91	1.99 in.
N	0.78	0.70 in.
D	0.64	0.42 in.
Annual Total:		31.86 in.

Here PET = $0.3937(0.142T_a + 1.095)(T_a + 17.8)kd$ when T_a 3^oC, and PET = $0.3937(T_a + 17.8)kd$ when T_a 3^oC. Here PET is in inches, k is the crop coefficient for alfalfa shown above, and d is a day length variable (Dunn and Leopold, 1978).

The potential ET for bare crushed tuff backfill, or with a cover of sparse grass and widely spaced trees, will be less than the PET for alfalfa shown above. Note that the annual PET computed for TA-54 in LANL's water balance was 41.89", using an earlier version of the Blaney-Criddle formula. This is unreasonably high.

Regional actual ET values have been measured for vegetation types that may approximate in some cases, and bracket, in other cases, the LANL situation. The following actual ETs show, in a broad way, that ETs for forested land tend to be greater than those for brush or grass and are in every case less than that for the alfalfa discussed above (cases cited in Rich and Thompson, 1974):

Cover Type	Location	Season	ET for Season
grassland	CO	June-Sept.	9.5 inches
grassland	UT	May-Nov.	10.0
brush	UT	May-Nov.	13.9
pine	AZ	May-Oct.	23.6
aspen	CO	June-Sept.	18.8

The following annual values for ET have been obtained in three instrumented watersheds south of Flagstaff on the Mogollon Rim. These watersheds lie in elevations between 5000' and 8000' and have soils derived from basalt and volcanic cinders which range from clay to clay

loams and which restrict infiltration. Actual ET figures were obtained by subtracting streamflow from precipitation, and so contain interception, snow sublimation, and any ground water recharge (this last is believed to be very small) (Baker, 1982).

	Dominant Vegetation Type		
	Utah Juniper (lower elevation)	Alligator Juniper (medium elevation)	Ponderosa Pine (highest elevation)
Annual Precip.	18.03 in.	20.71 in.	25.50 in.
Annual ET	16.97	15.94	19.94
Basal area per acre	60 ft^2	20 ft^2	125 ft^2

These watersheds are located at approximately the latitude and elevation of Los Alamos and receive annual precipitation, on the average, that is at least that received at LANL's disposal areas. Although the basal areas shown do not define dense forests, these ET values include whatever brush and herbaceous species that may be present in the understory, and the transpiratory ability of these associations is probably at least that present at TA-54.

At LANL, deep-rooting plants (including all trees) are prevented from growing on backfilled areas at Area G, and at any other areas where hazardous materials (such as tritium) may be drawn to the surface by transpiration. Trees will certainly send roots preferentially into disposal pits, both because it is mechanically easier to grow there and because increased infiltration in those areas may create a more favorable moisture environment for plant growth. Studies cited in a LANL report (Rogers, 1977) document tritium uptake by plants at Area G.

It follows that the Arizona watersheds provide a reasonable high estimate of actual ET for LANL disposal areas. ET at TA-54 could not reasonably be expected to be greater than 20" except in the wettest years, and on the average would be somewhat less than the 16-17" experienced in the juniper-dominated watersheds. It is reassuring that these numbers are at least in the same range as the incident precipitation at LANL.

Unfortunately, the only way to a priori distribute, without actual measurement, these annual estimates of ET among the 12 months of the year is to refer to the estimates of PET we have made above. Assuming these estimates are good ones, and assuming we are happy with a 12-interval discretization of the year's hydrology, we must then translate PET into actual ET.

If the soil is thoroughly penetrated by roots, and if the plants involved are actively transpiring, ET will proceed at the PET rate until the soil moisture tension reaches some threshold level, after which it will fall off according to some (unknown) relationship. The ratio of ET/PET when

moisture is limiting has been investigated by many researchers, with conflicting results that apparently depend on factors unique to the particular experiments. Reviews of this work along with the results of experiments in New Mexico can be found in the bibliography (Sammis, et.al., 1979; Gregory and Hanson, 1976; Al-Khafaf, et.al., 1979; Spurr and Barnes, 1973; Dunne and Leopold, 1978).

In the dormant season, when ET is of most interest to us (and of least interest to the agricultural researchers), ET/PET apparently falls off more quickly than when roots are active. According to one review, soil evaporation falls off to an "insignificant value" after 0.2 to 0.4 inches of water has evaporated, due to the formation of a dry soil mulch at the surface (Dunne and Leopold, 1973).

It follows from the above discussion that it is crucial to know the species, active seasons, rooting depths, and cover densities of vegetation both now and in the future at LANL's disposal areas, if we are to understand the present and future water balance at those areas. Even though the native vegetation appears to have been capable of establishing an ET regime that has led to a constant and low moisture content in the tuff at depth, the treeless shallow-rooted vegetation that has been described as present at TA-54 now may not either be able to extract water as efficiently, or for as many months of the year, as the original vegetation.

In the present rough-and-ready analysis, vegetative dormancy (and the "dry-soil-mulch" effect) are not considered beyond the extent they may already be incorporated into the Blaney-Criddle formula. The present analysis may, therefore, overestimate winter ET and underestimate winter infiltation, to some extent.

Actual ET for the ith month is computed as follows:

$$ET = (PET/AWC)(SM_{i-1} + SM_i)/2$$

where: PET is potential evapotranspiration in inches
AWC is the available water capacity of the soil in inches
SM_{i-1} is the soil moisture at the end of the previous month in inches, and
SM_i is the soil moisture at the end of the current month in inches.

SM_i is, in turn,

$$SM_i = SM_i' \text{ if } 0 \leq SM_i' \leq AWC, \text{ and}$$
$$= AWC \text{ if } SM_i' > AWC$$

where $SM_i' = SM_{i-1} + P - ET$.

Eliminating ET gives $SM_i' = [SM_{i-1} (1 - PET/2AWC) + P] / (1 + PET/2AWC)$.

This is the linear assumption of Thornthwaite applied to discrete monthly intervals, i.e., ET/PET when soil moisture is limiting is proportional to the difference between soil moisture level and field capacity. Other

assumptions could be used, but the main conclusions that will be reached are, we believe, robust with respect to the functional form of the ET/soil moisture relationship.

5. Soil Moisture Storage

In the interest of time, the approach used in Appendix II to model moisture storage in the soil is provisionally applied here. Note that the discharge and storage of soil moisture is assumed to take place evenly throughout the soil profile in this approach, and soil and tuff beneath the average rooting depth is assumed to not contribute to ET. It almost certainly does contribute to ET, as will be discussed later.

In the water balances below, the value for available water capacity (AWC) given in Appendix II of 4.96 inches (for crushed tuff) is used. By comparison Appendix II uses an AWC value of 5.43 for undisturbed soil.

6. Water Balances

The water balance which obtains from Scenario 1 precipitation is shown as Case 1 in the following table and graphically on page 12. The soil moisture cycle represented by case 1 is quickly reached from a variety of initial conditions, as shown in Cases 3 and 4, and perturbations, such as a very wet month as shown in Case 2, quickly die out. Under Scenario 1, April arrives with the soil just reaching field capacity, and no infiltration ever occurs; actual ET is equivalent to precipitation.* Recall that this represents a fairly wet year at TA-54, and represents a typical year at the Los Alamos weather station (or at TA-59/3, which has a similar elevation and precipitation record).

If a single wet month occurs in the fall, or if the soil should enter the fall nearly saturated due to unusually heavy rains in September, infiltration will occur in every subsequent month until April. As can be seen in Case 2, the total amounts of infiltration can be significant under these assumptions.

Scenarios 2 and 3 result in very large amounts of infiltration in several months, giving up to 7 months of infiltration in the case of Scenario 2. These scenarios, which have long return periods (>>100 years at TA-54) will not be discussed further.

At TA-54, winters (and April) are significantly drier than at Los Alamos, on the average. Nevertheless, it is hard to see why infiltration would not occasionally occur there, as it does at Los Alamos, during periods of wet weather. Unlike at the Los Alamos station, however, PET exceeds rainfall in every month except December, and the propect of several months of infiltration occurring after a wet fall month does not seem to be very likely, unless those following months are also unusually wet.

*Actually, in a soil at field capacity, slow drainage does in fact occur. Note that we have essentially assumed, in the above, that a dense crop of mature alfalfa is ready, all the time, to transpire moisture at TA-54. In

LANL Water Balance: Case 1: Steady-State

	Jan	Feb	Mar	Apr	May	Jun	Jul	Aug	Sep	Oct	Nov	Dec
Precip.	0.84	0.70	1.01	1.01	1.25	1.33	3.29	3.69	2.01	1.61	0.70	0.93
PET	0.39	0.49	0.91	1.89	3.68	5.84	6.53	5.42	3.63	1.99	0.70	0.41
Soil Moisture	4.61	4.84	4.95	4.22	2.85	1.52	2.30	3.06	2.89	3.27	3.49	4.11
ET	0.34	0.47	0.90	1.75	2.62	2.57	2.51	2.93	2.17	1.23	0.48	0.31
Potential Infiltration	0	0	0	0	0	0	0	0	0	0	0	0

Case 2: Very Wet November

Precip.	0.84	0.70	1.01	1.01	1.25	1.33	3.29	3.69	2.01	1.61	6.60	0.93
PET	0.39	0.49	0.91	1.89	3.68	5.84	6.53	5.42	3.63	1.99	0.70	0.41
Soil Moisture	4.96	4.96	4.96	4.22	2.85	1.52	2.30	3.06	2.89	3.27	4.96	4.96
ET	0.39	0.49	0.91	1.75	2.62	2.57	2.51	2.93	2.17	1.23	0.58	0.41
Potential Infiltration	0.45	0.21	0.10	0	0	0	0	0	0	0	4.33	0.52

LANL Water Balance: Case 3: Beginning from the wilting point in May

	Jan	Feb	Mar	Apr	May	Jun	Jul	Aug	Sep	Oct	Nov	Dec
Precip.	0.84	0.70	1.01	1.01	1.25	1.33	3.29	3.69	2.01	1.61	0.70	0.93
PET	0.39	0.49	0.91	1.89	3.68	5.84	6.53	5.42	3.63	1.99	0.70	0.41
Soil Moisture	4.60	4.83	4.94	4.21	0*	0.84	2.16	3.02	2.87	3.25	3.48	4.10
ET	0.34	0.23	0.90	1.74		0.49	1.97	2.83	2.16	1.23	0.47	0.31
Potential Infiltration	0	0	0	0	0	0	0	0	0	0	0	0

Case 4: Beginning with soil at field capacity in January

Precip	0.84	0.70	1.01	1.01	1.25	1.33	3.29	3.69	2.01	1.61	0.70	0.93
PET	0.39	0.49	0.91	1.89	3.68	5.84	6.53	5.42	3.63	1.99	0.70	0.41
Soil Moisture	4.96	4.96	4.96	4.22	2.85	0.84	2.16	3.02	2.87	3.25	3.48	4.10
ET	0.39	0.49	0.91	1.75	2.62	0.49	1.97	2.83	2.16	1.23	0.47	0.31
Potential Infiltration	0.45	0.21	0.10	0	0	0	0	0	0	0	0	0

*initial month

Potential Evapotranspiration, Computed Average Actual Transpiration, and Precipitation at Los Alamos, NM

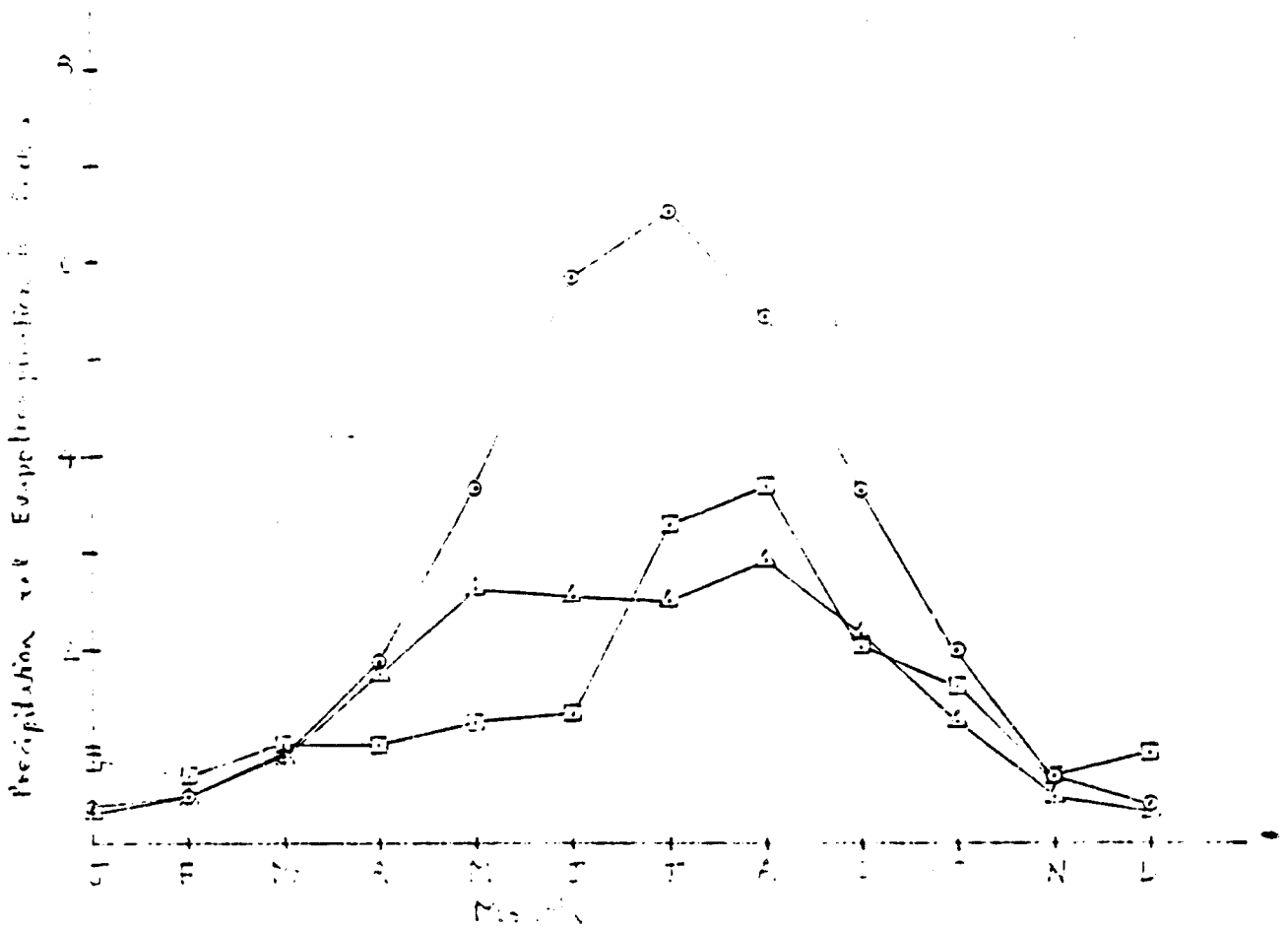

⊙ potential ET (Blaney-Criddle alfalfa). See text for assumptions.
△ average actual ET under Los Alamos precipitation (Scenario 1). See text for assumptions.
⊡ average Los Alamos precipitation.

the case of bare or nearly-bare soil, actual ET values will be lower, and infilitration higher, than the figures given.

7. Evidence of Infiltration

The average relative humidity at Los Alamos is circa 40% (DOE, 1979). The soil moisture tension which will equilibrate with this humidity is more than 1000 bars (for pure water) (Hillel, 1980). The circa 4% wetness found in the tuff in some investigations (Abrahams, Weir, and Purtymun, date unknown) is, presumably, much greater than the wetness which would produce 1000 bars of tension. (Unfortunately, moisture tensions do not appear to have been measured in the field at LANL to date). This high wetness must either be a "fossil" wetness remaining from past climates (presumably > 1000 years ago; see section 1) or a quasi-equilbrium established in the present infiltration, percolation, and ET regime. Even the 1% wetness reported for tuff at depth (30-80 meters) at TA-49 (Abeele, Wheeler, and Burton, 1981) appears to result in a suction that is less than the wilting point (see the calculated moisture characteristic curve in this same publication).

One of the papers cited above (Abrahams, Weir, and Purtymun, date unknown) measured little infiltration below ten feet with most infiltration not sinking below a depth of six feet. Unfortunately, these results cannot be applied directly to TA-54 because: 1) the degree of welding in the tuff may not be the same; 2) the clayey layer which was so effective in preventing infiltration may not be continuous at the experimental site, let alone at TA-54, where soil cover is not continuous; and 3) disposal pits have no developed clay layer to impede infiltration. Note that if moisture tension is constant with depth, a net downward water flux is occurring, assuming the osmotic tension is constant with depth. Therefore the constant soil-moisture-with-depth curves shown in the above publications are consistent with the existence of net infiltration. Soil moisture tensions would have to increase roughly 3 bars every 100 ft to counteract the effect of gravity.

Measurements at a neutron probe hole in backfilled material in Area G (location unknown to us) showed a total of 9.44 inches of infiltration in 1978 and 1979, due at least in part to an extemely wet November in 1978. Prompt infiltration to 25 meters was also observed at Area C (Abeele, Wheeler, and Burton, 1981). It is unfortunate that LANL has not installed (to our knowledge) a set of comparable long-term soil moisture holes that would allow construction of a wetness spectrum from the "high"-infiltration areas at LANL's western boundary to the low-infiltration areas on its eastern boundary.

One detailed LANL report (Rogers, 1977) shows photographic evidence of wet patches alternating with dry patches in tuff following a large storm event. In addition, water was observed to issue into an open disposal pit from the soil/tuff interface during this storm event, and to run out from open joints into the pit. These processes will presumably occur with or without crushed tuff backfill and suggest that flow patterns in the tuff will focus in excavated (higher permeability) areas, as would be predicted theoretically.

GM:egr

References

Abeele, W.V., Wheeler, M.L., and Burton, B.W., 1981. Geohydrology of Bandelier Tuff. LA-8962-MS.

Abrahams, J.H., Weir, J.E., and Purtymun, W.D., date unknown. Distribution of moisture in soil and near-surface tuff on the Pajarito Plateau, Los Alamos County, New Mexico. MS. published in an unknown publication, in files of New Mexico Environmental Improvment Division, Santa Fe, NM.

Al-Khafaf, S., Wierenga, D.J., and Williams, B.C., 1979. Improved method of estimating crop consumptive use and distribution of soil water in irrigated soil profiles. New Mexico Water Resources Research Institute Report No. 103, Las Cruces, NM.

Baker, M.B., 1981. Hydrologic regimes of forested areas in the Beaver Creek watershed. USDA Forest Service General Technical Report RM-90, Rocky Mountain Forest and Range Experiment Station, Ft. Collins, CO.

Cruff, R.W., and Thompson, T.H., 1967. A comparison of methods of estimating potential evapotranspiration from climatological data in arid and subhumid environments. US Geological Survey Water-Supply Paper 1339-M.Dunne, T., and Leopold, L.B., 1978. Water in Environmental Planning. W.H. Freeman and Co., San Francisco.

Gabin, V.L., and Lesperance, L.E., 1977. New Mexico Climatological Data: Precipitation, Temperature, Evaporation, and Wind: Monthly and Annual Means. W.K. Summers and Assoc., Socorro, NM.

Gregory, E.J., and Hanson, E.G., 1976. Predicting comsumptive use with climatological data. New Mexico Water Resources Research Institute Report No. 066, Las Cruces, NM.

Hillel, D., 1980. Fundamentals of Soil Physics. Academic Press, NY.

Lane, Leonard, 1981. August 11 memorandum to Brent Bowen, LANL, titled "Estimated Rainfall Frequencies for Los Alamos". LANL LSG-81-285.

Lull, H.W., and Sopper, W.E., 1969. Hydrolic effects from urbanization of forested watersheds in the northeast. USDA Forest Service Research Paper NE-146, Northeastern Forest Experiment Station, Upper Darby, PA.

Rich, L.R., and Thompson, J.R., 1974. Watershed management in Arizona's mixed conifer forests: the status of our knowledge. USDA Forest Service Research Paper RM-130.

Rogers, M.A., 1977. History and environmental setting of LASL near-surface land disposal facilities for radioactive wastes (Areas A, B, C, D, E, F, G, and T). LA-6848-MS.

Rose, M.R., Dean, J.S., and Robinson, W.J., 1981. The Past Climate of Arroyo Hondo, New Mexico, Reconstructed from Tree Rings. School of American Research Press, Santa Fe, NM.

Sammis, T.W., et.al., 1979. Consumptive use and yields of crops in New Mexico. New Mexico Water Resources Research Institute Report No. 115, Las Cruces, NM.

Spurr, S.H., and Barnes, B.V., 1973. Forest Ecology, 2nd edition. Ronald Press, NY.

US Department of Energy, 1979. Final Environmental Impact Statement: Los Alamos Scientific Laboratory Site. US DOE, Washington, DC.

USGS-
Unpublished Rept
Santa Fe, NM
1967

Hydrologic characteristics of an ash flow tuff at Frijoles Mesa, Los Alamos County, New Mexico

By

William D. Purtymun and John H. Abrahams, Jr.

Albuquerque, N. Mex.

Abstract

The specific yield of an ash flow tuff is related to porosity while the coefficient of permeability is independent of the porosity and is related to the pore size distribution. Fluid movement in the lower third of the flow as it cools could result in larger horizontal permeability in direction of movement than vertical permeabilities.

Hydrologic characteristics of an ash flow tuff at Frijoles Mesa, Los Alamos County, New Mexico

By

William D. Purtymun and John H. Abrahams, Jr.

Work done in cooperation with the
U.S. Atomic Energy Commission

Frijoles Mesa in Los Alamos County is about 5 miles south of the city of Los Alamos, in north-central New Mexico. The mesa is underlain by a series of ash falls and ash flows more than 900 feet thick. The hydrologic characteristics, porosity, specific yield, pore-size distribution, and coefficient of permeability of the uppermost flow were determined in a study made in cooperation with the Los Alamos Scientific Laboratory at Los Alamos, New Mexico.

The ash flow is composed of rhyolite tuff and is as much as 80 feet thick near the center of the mesa. It is a light gray to light pinkish gray, containing phenocrysts of quartz, sanidine, devitrified pumice, rhyolite and latite rock fragments in a ground mass of devitrified glass shards. The ash flow exhibits zonal variations of welding of a simple cooling unit (Smith, 1961) by changes in porosity in a vertical section. The greater porosities occur in the upper and basal parts of the flow. Smaller porosities (zone of denser welding) occur in the lower third of the flow. The pore size distribution indicates that the larger pore size decreases with increased depth.

The specific yield of the tuff is related to the porosity and with a general decrease in porosity there is a decrease in specific yield (fig. 1). The coefficient of permeability is related to pore

Figure 1 (caption on next page) belongs near here.

size distribution rather than porosity. The permeability decreases at increased depth with a decrease in pore size greater than 0.1 mm (table 1).

Figure 1 The relationship of specific yield to porosity of an ash flow tuff.

Table 1.--Hydrologic characteristics of an ash flow tuff, Frijoles Mesa, Los Alamos County, New Mexico. (analyses by the U.S. Geol. Survey)

Height above base of flow (feet)	Porosity (percent)	Coefficient of permeability (gallons per day per square foot)		Pore size distribution (percent of porosity)	
		Vertical	Horizontal	>.01 mm	< .01 mm
59	54	2	-	-	-
47	50	3	3	39	61
47	54	6	5	26	74
40	51	4	4	20	80
29	49	1	-		
22	41	.1	2	20	80
20	47	2	2	15	85
19	42	1	.8	-	
12	38	.9	1	-	
1	51	1	-	17	83
1	49	.9	2	10	80

The variations in vertical and horizontal permeabilities in the lower third of the flow may be due to fluid movement and compaction of the ash flow as it cools. Fluid movement of the flow as it cools could result in elongation of the pores in a horizontal plane and permeability along the direction of movement may be greater than that taken vertically or at right angles to this movement. Three of the five horizontal permeabilities in the lower third of the flow reflect a larger horizontal permeability (table 1); however, the permeabilities were taken in random directions and no attempt was made to orient them in the probable direction of movement of the flow as it cooled.

Reference

Smith, R. L., 1960, "Zones and zonal variations in welded ash flows," U.S. Geol. Survey Prof. Paper 354-F, 10 p.

Illustrations

Figure 1.--Relationship of specific yield to porosity of an ash flow tuff.

Tables

Table 1.--Hydrologic characteristics of an ash flow tuff, Frijoles Mesa, Los Alamos County, New Mexico.

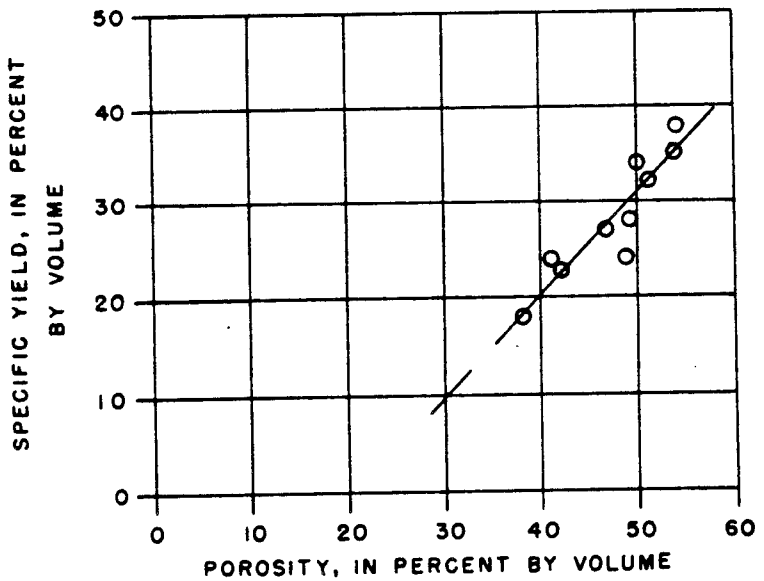

Figure 1.--Relationship of specific yield to porosity of an ash flow tuff.

LA-8461-MS

Informal Report

Geohydrology of Bandelier National Monument, New Mexico

University of California

LOS ALAMOS SCIENTIFIC LABORATORY
Post Office Box 1663 Los Alamos, New Mexico 87545

An Affirmative Action/Equal Opportunity Employer

This report was not edited by the Technical Information staff.

This report was prepared as an account of work sponsored by the United States Government. Neither the United States nor the United States Department of Energy, nor any of their employees, makes any warranty, express or implied, or assumes any legal liability or responsibility for the accuracy, completeness, or usefulness of any information, apparatus, product, or process disclosed, or represents that its use would not infringe privately owned rights. Reference herein to any specific commercial product, process, or service by trade name, mark, manufacturer, or otherwise, does not necessarily constitute or imply its endorsement, recommendation, or favoring by the United States Government or any agency thereof. The views and opinions of authors expressed herein do not necessarily state or reflect those of the United States Government or any agency thereof.

UNITED STATES
DEPARTMENT OF ENERGY
CONTRACT W-7405-ENG. 36

LA-8461-MS
Informal Report
UC-11
Issued: July 1980

Geohydrology of Bandelier National Monument, New Mexico

William D. Purtymun
Howard Adams

GEOHYDROLOGY OF BANDELIER NATIONAL MONUMENT, NEW MEXICO

by

William D. Purtymun and Howard Adams

ABSTRACT

Bandelier National Monument is located on the eastern slopes of the Sierra de los Valles and the Pajarito Plateau. The Pajarito Plateau was formed by a series of ashflow and ashfall of rhyolite tuff. Perennial and intermittent streams have cut the surface of the plateau into a number of narrow southeast-trending mesas separated by deep canyons. Perennial surface flow occurs in Cañon de los Frijoles and in the upper and middle reaches of Alamo, Capulin, Medio, and Sanchez Canyons. Of the five springs in and adjacent to the Monument, three discharge from perched aquifers and two from the main aquifer. Water in the deep main aquifer moves south to southeast in the Monument. Along the western edge of the Monument, the intrusion of volcanic rock of the San Miguel Mountains forms a barrier to the movement of water from the recharge area in the Valles Caldera. About 46.4 km^2 of the drainage area in the upper and middle reaches of Cañon de los Frijoles, Alamo, Lummis and Capulin Canyons were burned over by a wildfire (the La Mesa Fire) in June 1977. The geohydrology of the area was determined to assess the availability of surface and ground water in the Monument and to determine the impact of the wildfire on these water resources.

I. INTRODUCTION

Bandelier National Monument is located on the eastern slopes of the Sierra de los Valles and Pajarito Plateau, west of the Rio Grande, in north-central New Mexico (Fig. 1). The elevation ranges from 1620 m along the Rio Grande in the southeast corner of the Monument to 3109 m in the northwest corner on the crest of the Sierra de los Valles. The major part of the Monument is on the Pajarito Plateau. The plateau forms a broad apron around the flanks of the mountains, with its surface sloping gently from mountains toward the Rio Grande. The eastern edge of the plateau is terminated along the deep canyon of the Rio Grande. Southeast trending streams have cut the surface of the plateau into a series of long narrow mesas separated by deep canyons.

Near the western boundary of the Monument, extruded volcanic rocks form the San Miguel Mountains, which bifurcate the plateau into an east and west segment. The crest of the mountains (St. Peter's Dome) rises to an elevation of about 2580 m. North of the San Miguel Mountains near the Monument boundary, the western part of the plateau is uplifted about 100 m along a north-south trending fault scarp. South and east of the San Miguel Mountains the plateau slopes gently toward the canyon of the Rio Grande.

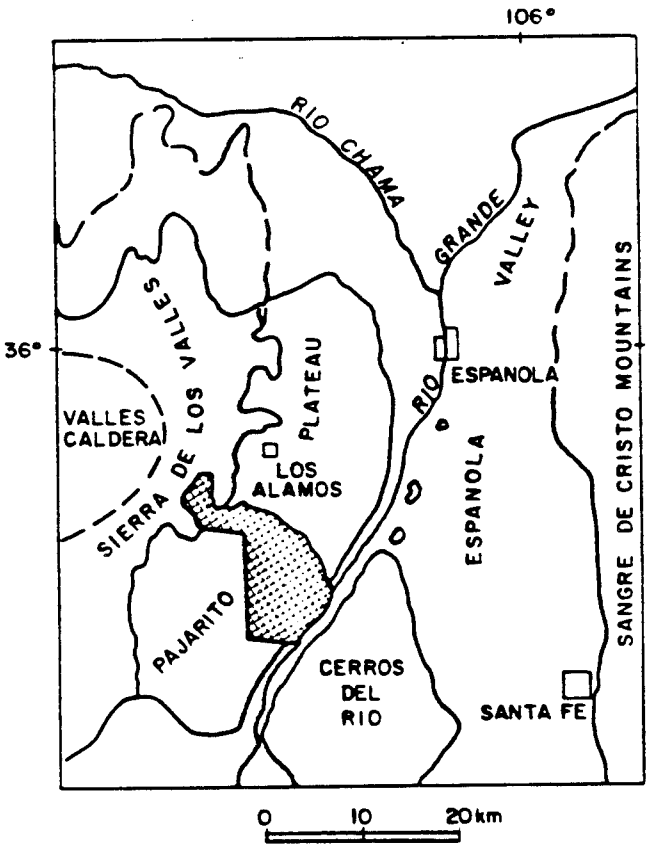

Fig. 1.
Physiographic features in the vicinity of Bandelier National Monument.

The wide range of elevations results in climate and vegetation changes from the Rio Grande to the crest of the Sierra de los Valles. Average precipitation increases from about 23 cm along the river to as much as 76 cm along the crest of the mountains. The average precipitation on the plateau is about 46 cm, with about 70% of the precipitation occurring in late June, July, and August during summer thunder showers.

The average July temperature at the lower elevations is about 23°C and on the plateau about 19°C, while average January temperatures along the river are −6°C and on the plateau −7°C. Juniper-grass lands with Russian Olive, some willow, cottonwood, and salt cedar are found along the river. The eastern two-thirds of the plateau is covered with pinon and juniper, while the western third and lower slopes of the mountains are covered with pine. Spruce, fir, and aspen intermingle with pine on the upper slopes of the mountains. Alpine meadows are found on the south-facing slopes of the mountains. In June 1977, the La Mesa Fire consumed about 61.9 km² of pinon, juniper, spruce, aspen and pine in and adjacent to the Monument.

The purpose of this report is to present the general geohydrology in and adjacent to the Monument in order to evaluate the effects of the wildfire on the water resources. The study was made in cooperation with the National Park Service at Bandelier National Monument. It is based on hydrologic data collected by the Monument and by the Los Alamos Scientific Laboratory (LASL). The report includes data through 1978.

The data are expressed in metric units. The following table, conversion from metric to English units, is included for the convenience of the reader.

To Convert From	To	Multiply By
cm	in	3.94×10^{-1}
m	ft	3.28
km	mi	6.22×10^{-1}
m^3	acre-ft	8.11×10^{-4}
km^2	mi^2	3.85×10^{-1}
ℓ/s	gal/min	15.85
m^3/s	ft^3/s	35.3
ℓ/s/m	gal/min/ft	4.82
m^2/day	ft^2/day	10.76
$m^3/s/km^2$	$ft^3/s/mi^2$	91.5
kg	ton	1.10×10^{-3}
kg/km^2	lb/mi^2	5.71

The generalized geology is presented as a basis for understanding the hydrology of the area. Detailed geology can be found in Ross et al. (1961), Smith et al. (1962), Griggs (1964), Bailey et al. (1969), and Smith et al. (1970).[1-5]

The Monument is located on the southeastern flank of the Valles Caldera, thus most of the rocks that outcrop are from volcanic cycles of eruption from the Caldera (Fig. 1). The generalized geologic map groups the outcrops in the area from oldest to youngest as the Galisteo Formation, Santa Fe Formation, basaltic rocks of the Rio Grande, volcanic rocks of the Valles Caldera, volcanic rocks of the Pajarito Plateau, and alluvium (Fig. 2 and Table I). The volcanic rocks of the Pajarito Plateau (Bandelier tuff) are a part of the eruption sequence of the Valles Caldera, but are shown separately on

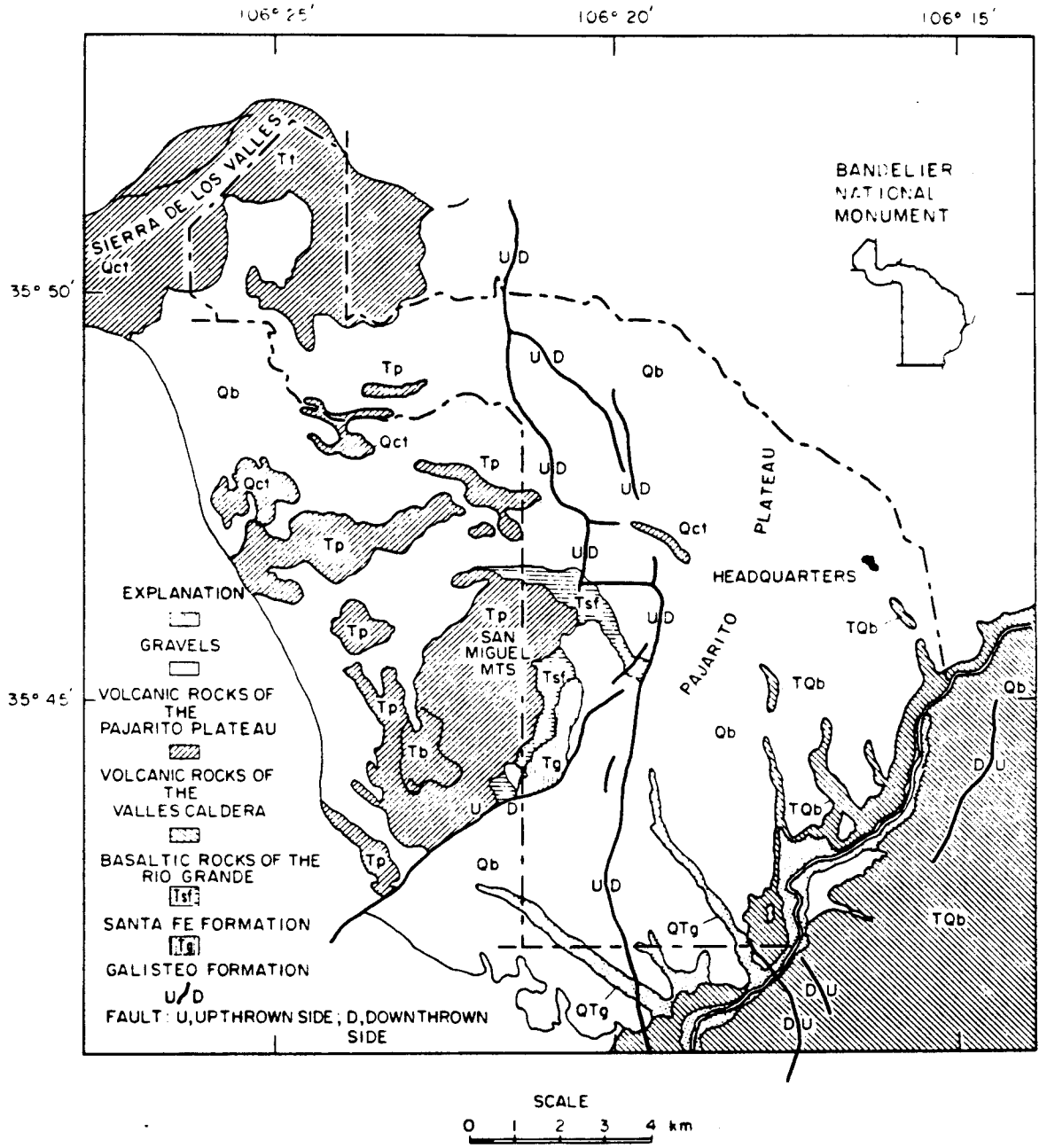

Fig. 2.
Generalized geologic map of Bandelier National Monument (see Table II for description of units).

the map as they form the upper surface of the Pajarito Plateau (Fig. 2). The volcanic rocks of the Valles Caldera form the Sierra de los Valles and San Miguel Mountains, while the basaltic rock of the Rio Grande outcrops along the Rio Grande. A large area of basalts occur east of the river. Alluvium is found along the Rio Grande and in the canyons cut into the plateau in the southern part of the area (Fig. 2).

The Monument is located on the western side of the Rio Grande depression, a structural basin that extends from southern Colorado through central New Mexico into northern Mexico.[6] Major faults

TABLE I

GENERALIZED STRATIGRAPHY OF MAP UNITS

Map Unit	Description
Alluvium	River gravels of recent age in Capulin and Sanchez Canyons; Old alluvium and pediment gravels of late Pliocene or early Pleistocene age in lower Capulin and Medio Canyon and midreach of Sanchez Canyon. All are shown as QTg in Figure 2.
Volcanic Rocks of the Pajarito Plateau	Bandelier Tuff (Qb) composed of ashflow and ashfalls of rhyolite tuff in units ranging from nonwelded to welded.
Volcanic Rocks of the Valles Caldera	Cerro Toledo Rhyolite (Qct) of rhyolite tuff and tuff breccias; Tschicoma Formation (Tt) of dacite and quartz latite forming thick massive flows and domes of the Sierra de Valles; Bearshead Rhyolite (Tb) of rhyolitic volcanic flows, domes, and intrusions; and the Paliza Canyon Formation (Tp) olivine-augite basalt, andesite-olivine basaltic andesite, and dacite and quartz latite in massive flows and domes.
Basaltic Rocks of the Rio Grande	Basaltic andesites of the Tank Nineteen basalts and basaltic lavas and tuff of Cerro del Rio (TQb) and including interbedded sediments containing basaltic debris.
Santa Fe Formation	Arkosic siltstone and sandstone with lenses of clay and pebbly conglomerate (Tsf).
Galisteo Formation	Shales, siltstone and conglomerate (Tg).

along the western boundary of the Monument are part of the faulting associated with the Rio Grande depression (Fig. 2).

II. SURFACE WATER

Major canyons that originate in or cross the Monument are Cañon de los Frijoles, Lummis, Alamo, Capulin, Medio and Sanchez. All are tributaries to the Rio Grande.

A. Rio Grande and Cochiti Reservoir

The Rio Grande is the master stream in north central New Mexico. The drainage area above Otowi (U.S. Geol. Survey Gaging Station), about 18 km upstream from the mouth of Cañon de los Frijoles, is about 37×10^3 km^2 in southern Colorado and northern New Mexico.

The discharge at Otowi for 78 years of record to 1978 has ranged from 1.7 m^3/s in 1902 to 691 m^3/s in 1920. During 1977 the discharge ranged from 4.8 m^3/s to 74 m^3/s, with 5.3×10^8 m^3 of water passing through the station. The daily sediment concentrations in 1977 ranged from 53 to 17 500 mg/ℓ, with about 8.1×10^8 kg of sediments carried by the station.[7]

During 1978 the discharge at Otowi ranged from 6.8 m^3/s to 114 m^3/s with 8.6×10^8 m^3 of water passing through the station. The daily sediment concentrations ranged from 76 to 6000 mg/ℓ with about

TABLE II

CAPACITY OF COCHITI RESERVOIR BASED ON ELEVATION

Elevation		Storage	
(m)	(ft)	(m^3)	(Ac-ft)
1621.5	5,320	56.7×10^6	46,010
1624.6	5,330	72.4×10^6	58,730
1627.7	5,340	90.5×10^6	73,410

1.1×10^9 kg of sediments carried through the station.[8]

Since 1973 a part of the flow of the Rio Grande has been impounded at Cochiti reservoir, about 9.6 km south of the Monument. Water impounded by the reservoir extends up the canyon into the Monument. In 1977, the maximum impoundment was at an elevation of 1622.4 m or near the mouth of Alamo Canyon (Fig. 3).[7] In 1978, the maximum impoundment reached an elevation of 1625 m. The capacity of the reservoir, based on elevations, is shown in Table II.

Based on surface water records at Otowi and Cochiti before construction of the reservoir, it was estimated that the Rio Grande gained about 0.71 m^3/s of ground water inflow in a 41.6 km reach of the river from Otowi to Cochiti.[9] Seepage investigations of the river in 1963 and 1964 indicated that 0.42 m^3/s were discharged to the river in the reach between Otowi and the mouth of Cañon de Frijoles. In the reach from Cañon de los Frijoles to Cochiti the river was losing water to the sediments and volcanics underlying the river channel.[10]

B. Chaquihui Canyon

Chaquihui Canyon heads on the eastern edge of the Pajarito Plateau and has a drainage area of 4.7 km^2 above the Rio Grande (Table III). Only a small part of the drainage area is within the Monument (Fig. 3). The channel is cut into tuff, basalts, and volcanic sediments, and has a steep gradient of about 9%. The middle reach of the canyon has perennial flow for a short distance from springs and seeps (Doe Spring) in the volcanic sediments.

C. Cañon de los Frijoles

Cañon de los Frijoles heads on the eastern slopes of the Sierra de los Valles and has a drainage area of 51.5 km^2 above the junction with the Rio Grande (Fig. 3). Almost all of the drainage area lies within the Monument. The canyon in the upper reach west of the Upper Crossing (Site No. D) is underlain by some andesite and latite, but is mainly cut into the tuff. East of the upper crossing and across the Pajarito Plateau the channel is cut into the tuff to near the Rio Grande where basalts and volcanic sediments underlie the channel. The basalts have limited downcutting of the canyon to the west. The gradient of the channel in the upper reach is about 7%, while to the east across the plateau the slope decreases to about 3%. Near the Rio Grande where the channel is cut into basalts the gradient increases to about 7%.

The surface flow in the canyon is perennial and generally extends to the Rio Grande except for short periods during the summer. The base flow is from springs that emerge from a densely welded tuff at an elevation of about 2570 km in the north and the west forks of the canyon as it cuts into the slopes of the Sierra de los Valles (Fig. 3).

The U.S. Geological Survey made a series of low-flow measurements in the canyon from 1958 through 1960 in order to determine increases or decreases in discharge in the various reaches of the canyon (Fig. 3).[11,12] Stream discharge increased slightly from the springs in the upper canyon downstream to the Site No. D, Upper Crossing (Table IV). The Upper Crossing is near the major fault that crosses the canyon (Fig. 2). The flow increase in this reach of the canyon is probably due to thinning of the alluvium west of the fault (return flow from alluvium), to seepage from coalluvium on the canyon walls, and in part to the fault zone as water from higher elevations moves downward through the brecciated zone. The canyon walls west of Upper Crossing range from 120 to 250 m in height. Surface flow decreases across the plateau by evapotranspiration with some loss of water into the alluvium and underlying tuff. The alluvium in the canyon appears to be thin, probably less than 6 m. East of the Monument Headquarters the alluvium thins further and the channel is cut onto basalts and volcanic sediments.

A surface water gaging station was operated near the Upper Crossing during 1960-62 (Table V). The

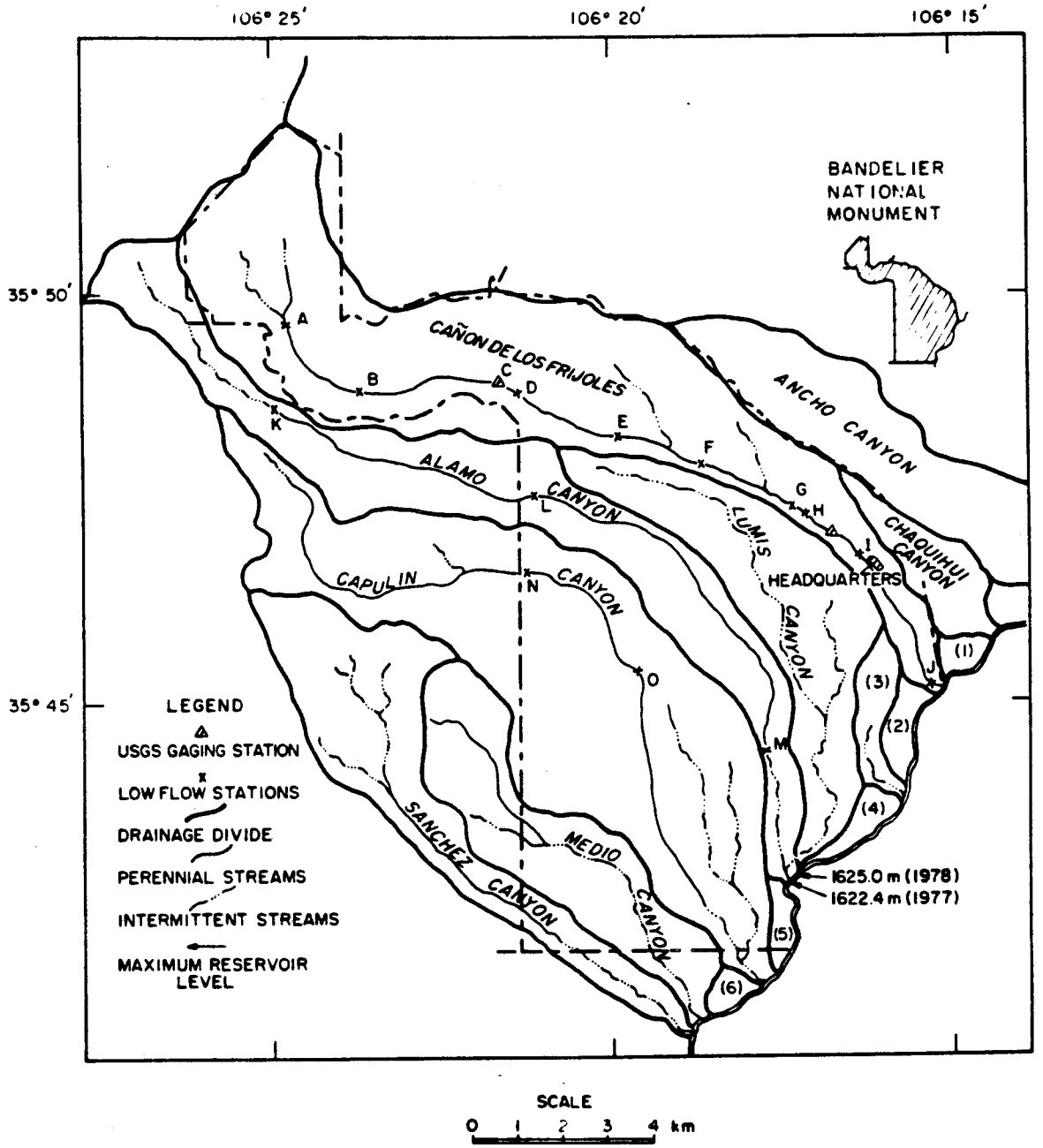

Fig. 3.
Drainage area and location of hydrologic stations.

drainage area above the station was 23.1 km². The annual runoff (i.e., drainage area to volume of runoff) ranged from 6.4 to 7.1 cm. This station was moved in 1963 into a reach of the canyon above the Monument Headquarters (Fig. 3). The drainage area above the relocated station was about 45.3 km². Runoff at the lower station ranged from 1.5 to 3.3 cm as the result of surface waters loss across the plateau (Table V).

The gaging station above the headquarters was activated in July 1977 after the wildfire. The fire burned about 26.2 km² or about 58% of the drainage area above the station. Runoff in 1978, after the

TABLE III

DRAINAGE AND BURN AREAS OF CANYONS

Canyon	Drainage Area[a] km²	Drainage Area[a] mi²	Burn Area km²	Burn Area mi²
Chaquihui	4.7	1.8	---	---
Slope 1 to Rio Grande	0.8	0.3	---	---
Canon de Frijoles	51.5	19.9	26.2	10.1
Slope 2 to Rio Grande	1.3	0.5	---	---
Canyon 3 to Rio Grande	2.3	0.9	---	---
Slope 4 to Rio Grande	1.3	0.5	---	---
Lummis[b]	19.7	7.6	6.0	2.3
Alamo	49.7	19.2	11.1	4.3
Slope 5 to Rio Grande	1.0	0.4	---	---
Capulin	51.0	19.7	3.1	1.2
Slope 6 to Rio Grande	0.8	0.3	---	---
Medio	17.1	6.6	---	---
Sanchez	19.9	7.7	---	---
Total			46.4	17.9

[a]At Rio Grande.

[b]Tributary to Capulin.

burn, was 128.2×10^4 m³ or about the same as occurred at the station (1964-69) before the fire (Table V). Though it appears that the volume of runoff has not changed, the time of collection and retention of precipitation in the drainage area has decreased. This resulted in larger discharge from runoff events.

The largest runoff event (1964-69) was 0.53 m³/s in June 1965. During the post-fire period, July 1977 through September 1978, 20 runoff events exceeded the discharge of 0.53 m³/s in 1965 (Table VI). The largest events, 51 m³/s and 88.5 m³/s were in July 1978.[7,8]

The burn removed most of the vegetation in the drainage area, thus reducing the holding capacity of precipitation. This has resulted in larger discharge yields from summer storms. The maximum yield prior to the burn was 0.012 m³/s/km². In a smaller canyon to the north the yield for a season of summer runoff events in 1967 averaged 0.024 m³/s/km².[13] The discharge yield since the fire for the 20 events in Cañon de los Frijoles has ranged from 0.015 to 1.95 m³/s/km². The discharge yield is highly variable as the precipitation from summer storms is highly localized and rainfall intensity varies in a long narrow drainage area such as Cañon de los Frijoles.

TABLE IV

LOW-FLOW MEASUREMENTS OF RITO DE LOS FRIJOLES (m³/s)

	1958	1959					1960		
Site No.[a]	10-20	4-16	4-29	6-3	9-3	10-12	5-16	6-20	Av
A	---	---	0.025	0.014	0.008	0.003	0.025	0.014	0.015
B	---	---	0.040	0.025	0.017	0.017	0.040	0.025	0.027
C	---	---	0.059	0.042	0.034	0.034	0.045	0.034	0.041
D	0.054	0.076	---	0.045	---	0.040	0.059	0.034	0.051
E	0.034	0.074	---	0.042	0.034	0.028	0.042	0.023	0.040
F	0.042	0.068	---	0.031	0.034	0.031	---	0.025	0.038
G	0.034	0.062	---	0.037	0.034	0.028	0.048	0.028	0.038
H	0.037	0.074	---	0.031	0.031	0.028	0.042	0.023	0.038
I	0.034	0.045	---	0.031	0.034	0.023	0.040	0.023	0.032
J	---	---	---	---	0.020	0.014	0.034	0.008	0.019

[a]For location, see Fig. 3.

TABLE V

ANNUAL RUNOFF AT GAGING STATIONS

Water Year	Volume		Runoff	
	10^4 m^3	Acre-feet	cm	in.
1960	164.3	1332	7.11	2.8
1961	145.5	1180	6.35	2.5
1962	152.9	1240	6.60	2.6
1963	---	---	---	---
1964	71.5	580	1.52	0.6
1965	102.3	830	2.03	0.8
1966	90.6	735	2.03	0.8
1967	83.0	673	1.78	0.7
1968	155.4	1260	3.30	1.3
1969	128.2	1040	2.78	1.1
1978[a]	128.2	1040	2.78	1.1

[a]After burn.

Note: 1960-62 drainage area 23.1 km^2 (8.9 mi^2); 1964-69 and 1978 drainage area 45.3 km^2 (17.5 mi^2).

D. Lummis Canyon

Lummis Canyon heads on the Pajarito Plateau and has a drainage area of 19.7 km^2 above the Rio Grande (Fig. 3). About 6.0 km^2 or 30% of the drainage area was burned over in the 1977 fire. The canyon is cut into the tuff in the upper and middle reaches and into the basalts and sediments along the Rio Grande. The gradient of the channel is about 4%.

Stream flow in the canyon is a result of snowmelt runoff or summer type storms. On July 5, 1977, after the burn, precipitation in the drainage area produced a runoff event, with a discharge estimated at 6.5 m^3/s. The drainage area discharge yield for the event was 0.33 $m^3/s/km^2$, or slightly less than the 0.41 $m^3/s/km^2$ that occurred in Cañon de los Frijoles on the same day (Table VI).

E. Alamo Canyon

Alamo Canyon heads on the flanks of the Sierra de los Valles and has a drainage area of 49.7 km^2 above the Rio Grande (Table II). About 11.1 km^2 or 22% of the drainage area was burned over in 1977. The upper and middle reach of the canyon cuts mainly into the tuff and small segments of other volcanic rocks, while the lower reach above the Rio Grande is cut into basalts and sediments (Fig. 2). The gradient of the channel in the upper reach west of the Monument boundary is about 7%, while in the middle and lower reach of the canyon the gradient is about 4%.

Stream flow in the upper, middle, and part of the lower reach is perennial. The base flow is from springs and seeps in the upper reach of the channel. Flow decreases eastward in the canyon as water is lost to evapotranspiration and infiltration into the underlying alluvium and volcanic rocks. Base flow in July 1977 was 0.002 m^3/s at Station K, 0.001 m^3/s at Station L, and 0.0006 m^3/s at station O (Fig. 3).

On July 5, 1977, precipitation produced a runoff event similar to that in Cañon de los Frijoles and Lummis Canyon. The discharge was estimated at 7.6 m^3/s. The drainage area yielded about 0.15 $m^3/s/km^2$ or less than occurred from the same storm in Cañon de los Frijoles and Lummis Canyon. The percent of burn in the drainage area decreased from 42% in Cañon de los Frijoles to 30% in Lummis and 22% in Alamo, with runoff yield of 0.41 $m^3/s/km^2$, 0.33 $m^3/s/km^2$, and 0.15 $m^3/s/km^2$, respectively for the same storm.

F. Capulin Canyon

Capulin Canyon heads on the Pajarito Plateau but also receives part of the drainage from the San Miguel Mountains. The drainage area is about 51.0 km^2 above the Rio Grande. About 3.1 km^2 or 6% of the drainage area was burned over in 1977. The channel is cut into tuff and volcanics in the upper reach west of the Monument boundary. East of the boundary on the Pajarito Plateau the middle reach is cut into the tuff and older sediments of the Santa Fe Formation. The lower reach is underlain by gravels, some recent and some older sediments. The gradient of the channel in the upper reach is about 6% and in the middle and lower reaches is about 4%.

Stream flow in the upper, middle, and part of the lower reaches of the canyon is perennial. The base flow is from springs and seep in the upper reach of the canyon. Base flow in July 1977 was 0.02 m^3/s at

TABLE VI

MAXIMUM DISCHARGES ABOVE 0.54 m³/s (19 cfs) AND RUNOFF JULY—SEPTEMBER 1977-78

Date	Time	Discharge		Runoff	
		m³/s	ft³/s	m³/s/km²	ft³/s/mi²
July 5, 1977	(Unknown)	18.5	653	0.408	37.3
July 8, 1977	(18:00)	2.18	77	0.048	4.4
July 9, 1977	(19:30)	2.55	90	0.056	5.1
July 27, 1977	(15:30)	10.8	382	0.238	21.8
Aug. 12, 1977	(08:45)	10.9	386	0.241	22.1
Aug. 12, 1977	(15:15)	0.68	24	0.015	1.4
Aug. 16, 1977	(01:30)	1.42	50	0.031	2.8
Aug. 17, 1977	(20:15)	1.05	37	0.023	2.1
Aug. 19, 1977	(20:30)	6.63	234	0.146	13.4
Aug. 20, 1977	(15:15)	14.7	519	0.325	29.7
Aug. 20, 1977	(21:30)	7.48	264	0.165	15.1
Aug. 22, 1977	(16:30)	10.1	358	0.223	20.5
Sept. 2, 1977	(15:45)	1.59	56	0.035	3.2
Sept. 3, 1977	(14:30)	2.10	74	0.046	4.3
Oct. 4, 1977	(17:00)	1.25	44	0.028	2.5
June 30, 1978	(13:00)	8.38	296	0.185	16.9
July 12, 1978	(15:00)	51.0	1800	1.13	103
July 21, 1978	(13:45)	88.5	3030	1.95	173
Aug. 9, 1978	(20:30)	1.39	49	0.031	2.8
Sept. 24, 1978	(06:00)	0.99	35	0.22	2.0

Stations N and O (Fig. 3). Stream flow east of Station O (Base Camp) decreases with evapotranspiration and infiltration into gravels that make up the stream channel.

G. Medio Canyon

Medio Canyon heads on the southern flanks of the San Miguel Mountains and has a drainage area of about 17.1 km² above the Rio Grande. Only the middle reach of the canyon is within the Monument. The upper reach of the channel west of the Monument boundary is cut into the volcanic rocks associated with the Valles Caldera. The middle reach is cut into the tuff while the lower reach above the Rio Grande is underlain by older gravels, basalts and associated sediments. The gradient of the upper reach is about 13%, while in the middle and lower reaches the gradient is about 4%. The stream flow in the upper reach of the canyon is perennial, fed by springs and seeps in the volcanic rocks.

H. Sanchez Canyon

Sanchez Canyon heads on the western flanks of the San Miguel Mountains and has a drainage area of about 19.9 km². Only a small part of the canyon is within the Monument (Fig. 3). The channel is cut into the tuff and other volcanic rocks west of the Monument boundary and into gravels and sediments both recent and older as it extends eastward across the Monument to the Rio Grande. The gradient of the channel west of the boundary is 8% and east of the boundary to the Rio Grande is about 4%. The middle reach of the canyon contains perennial flow from small springs and seeps (Fig. 3).

I. Other Drainage Areas

Six smaller drainage areas are located near the Monument boundary adjacent to the Rio Grande (Fig. 3). All, except one described below, are steep slopes at the end of the mesas between major canyons. The slopes contain no well defined stream channels. Runoff from the slopes is intermittent and occurs in many small channels during excessive precipitation. Slope 1 contains a small seep area high on the canyon wall. The seep is in sediments associated with basalts and is covered by an area of vegetation.

The one exception is Canyon 3 below Cañon de los Frijoles with a drainage area of 2.3 km^2 (Fig. 3). The upper reach of the canyon is cut into the tuff and near the Rio Grande it is cut into basalts and sediments. The gradient of the channel is about 8%.

III. GROUND WATER

Ground water occurs as springs in or adjacent to the Monument. Some of these springs form base flow in several of the canyons. Five springs, two adjacent to and three within the Monument are described. There are no wells or test holes within the Monument. Hydrology of the Main Aquifer of the Los Alamos area (deep ground water body) is described from data collected adjacent to the Monument.[3,14-18]

A. Springs

Springs adjacent to the Monument are Doe and Turkey Springs (Fig. 4). Doe Spring discharges from sediments below a basalt flow in Chaquihui Canyon. The spring is a large seep area on the north wall of the canyon. The seep area forms several deep pools in a short reach of the canyon. Turkey Spring discharges from volcanic rocks associated with the Valles Caldera. The spring discharge is about 1.4 ℓ/s. This spring maintains surface flow in the upper reach of the canyon tributary to Capulin Canyon (Fig. 4).

Springs in the Monument are located in the North Fork of Cañon de los Frijoles (Station 3), Apache Spring (Station 7), and near the mouth of Cañon de los Frijoles (Station 10).

The spring at Station 3, North Fork of Cañon de los Frijoles, discharges from volcanics associated with the Valles Caldera. The source, perched aquifer in fractured, densely welded latites, is rather large as the discharge from this aquifer in both the north and west fork of the canyon forms the base flow in Cañon de los Frijoles (Fig. 4). Base flow in the canyon below the junction is about 0.015 m^3/s. Recharge to the aquifer is probably from a shallow water bearing zone in the Valles Caldera.

The spring at Station 7 (Apache Spring) discharges from a welded unit of tuff on the north side of Cañon de los Frijoles (Fig. 3). The water body, perched in the tuff, is small as flow from the collection tank (built by Civil Conservation Corps in the 1930s) is <0.06 ℓ/s.

The spring near the mouth of Cañon de los Frijoles (Station 10) discharges from volcanic sediments associated with basalts. The discharge is about 0.1 ℓ/s and is from the main aquifer.

About 20 springs and seeps discharge from the main aquifer along the Rio Grande north of Cañon de los Frijoles. There are no springs and seeps south of Cañon de los Frijoles along the Rio Grande.[10]

B. Main Aquifer of the Los Alamos Area

The surface of the main aquifer rises westward from the Rio Grande from basalts and associated sediments into a fanglomerate which lies below the tuff. North of the Monument along the western edge of the Pajarito Plateau the surface of the aquifer lies at a depth of 300 to 375 m; the surface slopes gently eastward at about 10 m/km. The water in the aquifer moves from the major recharge area in the Valles Caldera eastward to the Rio Grande, where a part is discharged through seeps and springs north of the mouth of Cañon de los Frijoles.

Tests of the main aquifer (in two test holes) on the plateau north of the Monument indicated a transmissivity of 450 m^3/day with 72 m of penetration of the aquifer and 750 m^3/day with 152 m of penetration. The test, at a pumping rate of 5 ℓ/s, indicated specific capacity of 3.3 ℓ/s/m and 4.6 ℓ/s/m of drawdown for a 24-hr test. Based on the gradient of the potentiometric surface of the aquifer and hydrologic characteristics of the aquifer, the rate of movement in the aquifer was calculated to be about 120 m/yr.

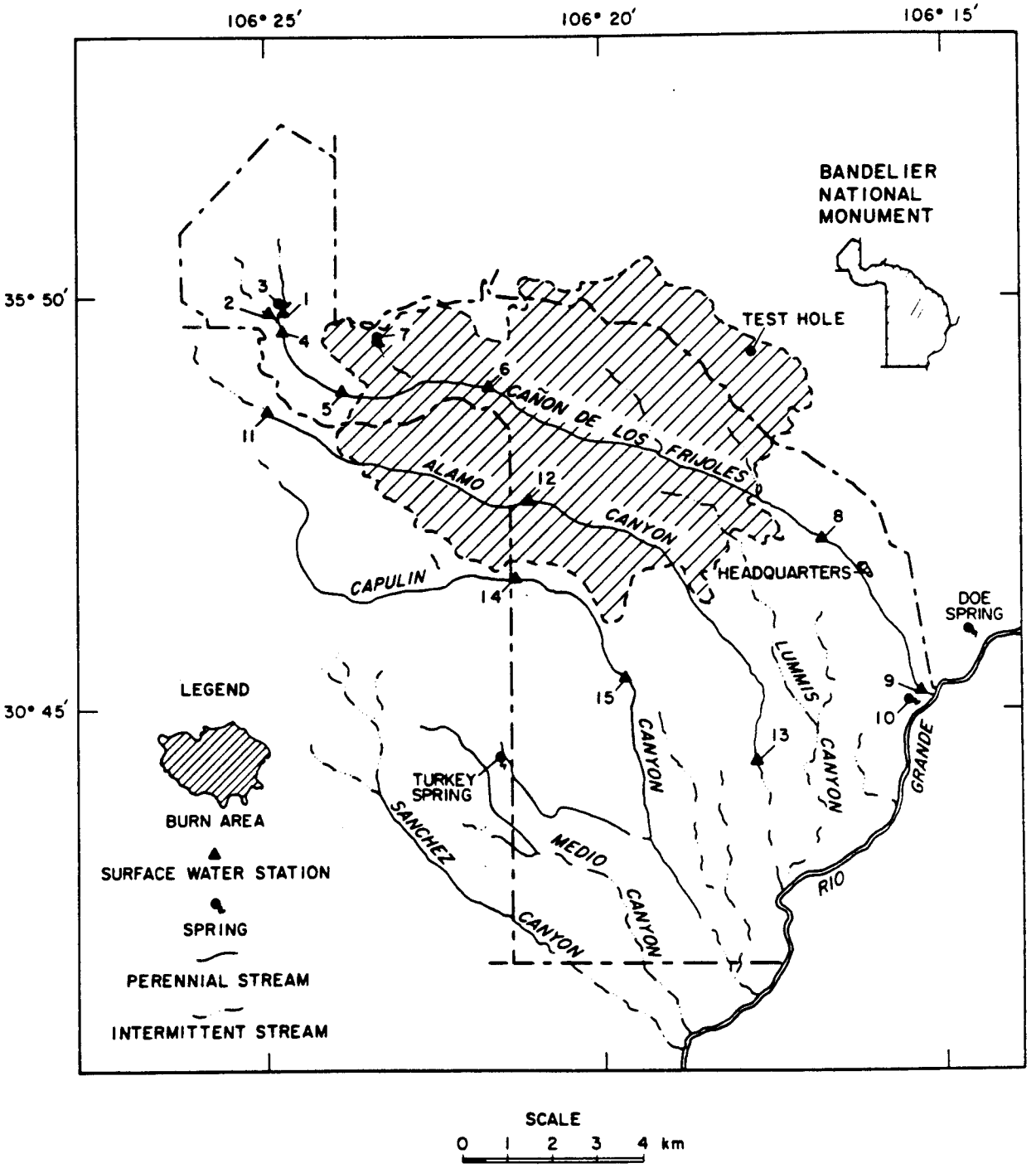

Fig. 4.
Burn area and location of water sampling stations.

Generalized contours of the potentiometric surface of the main aquifer were extrapolated from the Los Alamos area to the north into the eastern part of the Monument using the additional control of a well in Cochiti Canyon southwest of the Monument and wells and test holes east of the Rio Grande.[19] The Rio Grande above the mouth of Cañon de los Frijoles is a gaining stream (ground water discharge to the river) while below the mouth of the canyon the river is a losing stream (river recharging the aquifer). Thus the surface of the aquifer north of Cañon de los Frijoles along the Rio Grande is at or slightly above the river level while the surface of the aquifer to the south is at an elevation below the river level (Fig. 5).

The movement of water in the southern part of the Monument trends more to the south than southeast in the Los Alamos area. A small ground water depression forms west of the river south of the Monument.[20] This depression, offset west of the river, extends into the Bernalillo-Albuquerque area to the south.[21] The major faults along the western edge of the Monument and the intrusion of volcanic rocks of the Valles Caldera that form the San Miquel Mountains apparently restrict the movement of water in the western part of the Monument and west of the Monument boundary from the main recharge area in the Valles Caldera. Depth to the top of the main aquifer at Monument Headquarters is estimated to be 108 m, and at Base Camp in Capulin Canyon at 185 m (Fig. 5).

IV. QUALITY OF WATER

Water quality data were obtained from samples of surface water in the Rio Grande and Cañon de los Frijoles and several springs prior to the wildfire in 1977 (Table VII). After the fire, two sets of samples, 1977 and 1978, were collected in and adjacent to the Monument of surface water in major canyons and at springs (Table VIII). Routine analyses of these samples included calcium, magnesium, sodium, carbonate, bicarbonate, chloride, fluoride, nitrate, total dissolved solids (TDS), total hardness, specific conductance and pH.

Samples of base flow and runoff events were collected in Cañon de los Frijoles and Alamo and Capulin Canyons by Monument personnel. These samples were analyzed by Environmental Consultants Inc. (Clarksville, Indiana). The analyses included a number of different constituents. Those showing the largest change were barium, calcium, bicarbonate, manganese, magnesium, lead, phenol, and zinc, as shown in Table IX.

A. Surface Water

Water samples are routinely collected from the Rio Grande at Otowi north of the Monument and from the Rio Grande below Cochiti Dam south of the Monument. Water in the river contains principal ions of calcium and bicarbonate (Tables VII, VIII). The chemical quality of the water in the Rio Grande will vary at a given station during the year because of dilution of base flow with storm runoff from various parts of the drainage area (Fig. 6).

Water samples have been collected from Cañon de los Frijoles at the Monument Headquarters since 1957. The principal ions in the stream water are calcium and bicarbonate. The water is typical of mountain streams in the area with TDS ranging from 84 to 168 mg/ℓ for samples collected prior to the fire in 1977. Variations in constituent concentrations occurs as the result of increase discharge due to storm runoff resulting in dilution of base flow (Table VII). Debris washed into the stream after the fire caused a slight increase in some chemical constituents (Table VIII).

During the 1958-60 low-flow investigations, water samples were collected at various stations and analyzed for calcium-carbonate, sodium, and chloride (Table X). The average calcium-carbonate and sodium concentration increased only slightly downgradient; chloride varied considerably but also generally increased downgradient.[22] The slight increase in constituent concentrations is caused by minerals taken into solution from the alluvium.

In July 1977 after the fire, water samples were collected from six stations above and below the burn (Fig. 4). These stations and one additional station were sampled a year later in June and July 1978. A graphic comparison by station of calcium, sodium, chloride, TDS, and bicarbonate of samples taken in 1977 shows a general increase in these constituents downgradient in the canyon. The largest increase occurs between stations 5 and 6 where the stream enters the burn area (Fig. 7). Chemicals leached from the fire debris in the burn area enter the stream increasing certain chemical concentrations. In 1978,

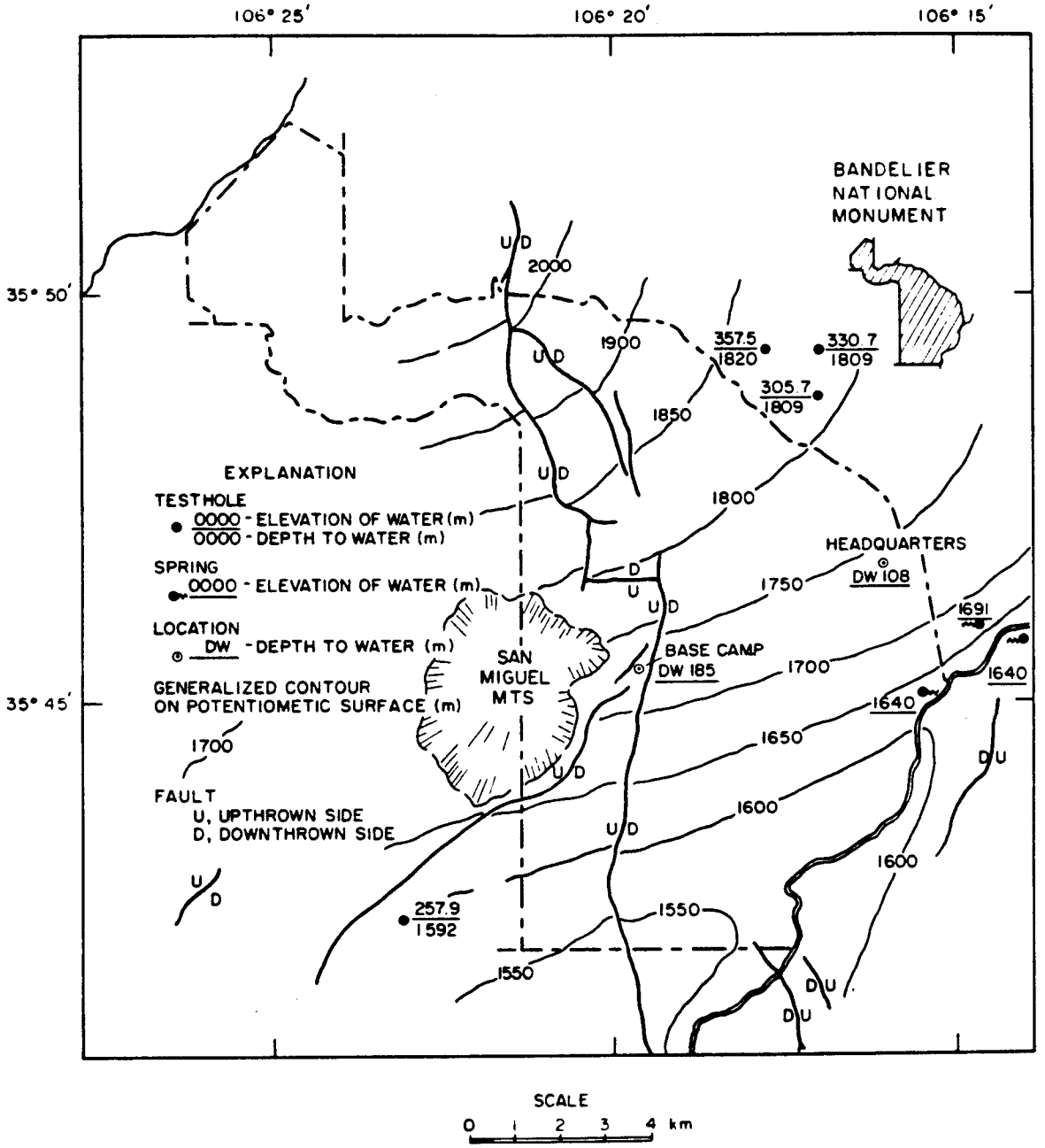

Fig. 5.
Generalized contours on the potentiometric surface of the main aquifer.

the constituents increased at station 6 (near Monument Headquarters), then decreased slightly at the Rio Grande. A comparison of the constituents in 1977 to those in 1978 show considerable variation but below station 6 a general decrease in most concentrations is indicated.

The burn brought about a slight increase in calcium, bicarbonate, chloride, fluoride, and TDS in base flow at the Monument Headquarters (Fig. 8). TDS concentrations increased after the fire from 110 mg/ℓ in March 1977 to 214 mg/ℓ in July 1977. After July, the TDS concentrations declined slightly (Fig.

TABLE VII

CHEMICAL QUALITY OF SURFACE AND GROUND WATER, AUGUST 1957-MARCH 1977

Station	Location	Date	Ca	Mg	Na	CO_3	HCO_3	Cl	F	NO_3	TDS	Total Hard	Specific Conductance (µmho)	pH
			mg/l											
Adjacent to Monument														
...	Rio Grande at Otowi	3-8-77	44	7	23	0	124	8	0.4	0.8	316	138	390	8.0
...	Rio Grande at Cochiti	3-8-77	44	8	22	0	136	2	0.4	0.4	308	142	390	8.2
...	Doe Spring	10-27-74	13	2	13	0	66	4	0.5	0.8	138	42	130	7.1
...	Test Well-Plateau	3-11-77	9	1	11	0	56	3	0.2	0.3	106	28	130	7.7
5	Frijoles, Upper Crossing	5-13-66	6	3	13	0	34	1	0.2	0.4	111	28	80	7.4
Inside Monument														
7	Apache Spring	6-7-61	---	---	5	0	67	1	0.1	0.1	---	44	120	7.1
8	Frijoles, Mon. Hdq													
		1957-1976												
	No. of Analyses		13	13	23	23	23	23	22	22	13	23	23	23
	Minimum		6	2	5	0	34	<1	<0.1	0.1	84	28	70	7.1
	Maximum		11	11	15	0	82	8	0.9	1.6	168	68	145	8.4
	Average		9	5	10	0	56	3	0.3	0.4	137	39	106	7.6
	Standard Deviation		1	2	3	0	11	2	0.2	0.3	25	9	17	0.3
		3-8-77	8	2	10	0	48	2	0.2	<0.4	110	30	120	7.9
9	Frijoles at Rio Grande	9-12-73	13	3	11	0	56	4	<0.1	0.4	174	44	120	7.8
10	Spring	9-1-73	11	4	9	0	68	6	0.2	0.8	206	44	120	7.4
		10-3-74	13	2	13	0	66	4	0.5	0.8	138	42	130	7.1

TABLE VIII

CHEMICAL QUALITY OF SURFACE AND GROUND WATER, JUNE 1977-SEPTEMBER 1978

Station	Location	Date	mg/ℓ SiO_2	Ca	Mg	K	Na	CO_3	HCO_3	SO_4	Cℓ	F	NO_3	TDS	Total Hard	Specific Conductance (μmho)	pH	Total Uranium (μg/ℓ)	Temp (°C)
Adjacent to Monument																			
---	Rio Grande at Otowi	3-6-78	---	38	9	---	24	0	139	---	6	0.5	<0.4	394	131	350	8.5	---	---
---	Rio Grande at Cochiti	3-7-78	---	36	8	---	25	0	156	---	2	0.5	<0.4	410	123	350	8.3	---	---
---	Doe Spring	9-20-78	---	8	3	---	11	0	78	---	2	0.5	0.4	160	33	140	---	---	---
---	Test Well—Plateau	10-27-77	---	8	4	---	17	0	58	---	2	0.2	0.2	149	36	130	7.6	---	---
---	Turkey Spring	7-10-77	---	24	5	2.5	11	0	104	---	3	0.2	<0.1	166	80	250	7.8	2.0 ± 0.3	19
---		7-10-78	69	23	7	---	11	0	100	<1	4	0.3	<0.1	188	87	215	8.4	---	---
Inside Monument																			
01	Frijoles, North Fork	7-8-77	---	13	3	3.2	5	0	48	---	12	0.1	0.1	154	44	130	7.3	1.9 ± 0.6	10
01		6-27-78	63	7	4	---	9	0	46	5	4	0.2	0.1	158	32	120	7.8	---	---
02	Frijoles, West Fork	7-8-77	---	10	2	0.7	9	0	48	---	5	0.2	0.1	164	34	130	7.8	2.5 ± 0.6	16
02		6-27-78	70	4	2	---	11	0	40	9	2	0.3	<0.1	168	19	90	7.7	---	---
03	Spring, North Fork	7-8-77	---	12	3	2.3	8	0	66	---	2	0.1	0.1	150	44	130	7.8	2.5 ± 0.6	10
03		6-27-78	79	6	2	---	15	0	54	6	1	0.3	0.1	174	23	120	7.9	---	---
04	Frijoles, Confluence	6-27-78	60	6	6	9	9	0	48	4	4	0.2	0.1	158	38	120	7.9	---	---
05	Frijoles above Burn	7-8-77	---	10	<1	0.2	9	0	62	---	5	0.1	0.1	140	26	100	7.7	2.8 ± 0.6	15
05		6-27-78	66	6	4	---	15	0	46	6	<1	0.2	<0.1	162	31	110	7.9	---	---
06	Frijoles, Upper Crossing	7-8-77	---	17	3	1.1	9	0	84	---	6	0.1	0.2	166	56	170	7.6	3.4 ± 0.8	17
06		6-27-78	69	9	4	---	10	0	56	4	4	0.2	0.1	164	39	130	8.0	---	---
07	Apache Spring	7-8-77	---	13	5	3.5	14	0	60	---	22	0.1	0.1	222	54	200	7.5	2.0 ± 0.6	7
07		7-10-78	55	10	6	---	10	0	56	5	5	0.3	0.1	110	50	160	7.7	---	---
08	Frijoles, Mon. Hdq	7-10-77	---	32	4	1.9	10	0	120	---	7	0.2	0.3	214	96	220	7.6	5.5 ± 0.8	13
08		11-1-77	---	13	<1	---	22	0	78	---	7	0.3	1.6	190	32	180	7.9	---	---
08		3-8-78	48	5	3	---	10	0	185	18	9	0.6	7.0	162	27	120	8.2	0.2 ± 0.1	---
08		6-26-78	63	11	4	---	11	0	66	<1	2	0.3	0.1	120	44	150	8.0	---	---
08		3-12-79	26	6	3	2.5	10	0	56	11	3	0.2	<0.1	162	25	130	8.3	0.2 ± 0.4	---
09	Frijoles at Rio Grande	7-10-77	---	34	4	4.5	13	0	124	---	2	<0.1	0.5	246	102	260	7.5	6.8 ± 1.0	17
09		9-14-77	---	22	4	---	17	0	102	---	6	0.2	0.4	182	72	210	8.5	---	17
09		6-26-78	65	13	5	---	11	0	74	<1	2	0.3	<0.1	126	52	180	7.8	---	---
10	Spring 10	9-14-77	---	13	2	---	11	0	62	---	4	0.5	0.3	138	41	140	7.8	---	18
10		6-26-78	67	10	5	---	11	0	66	<1	1	0.4	0.2	118	47	150	8.0	---	---
10		9-20-78	62	8	3	---	11	0	78	2	2	0.5	0.4	160	70	140	---		

TABLE VIII (cont)

CHEMICAL QUALITY OF SURFACE AND GROUND WATER, JUNE 1977-SEPTEMBER 1978

Station	Location	Date	mg/ℓ												Total Hard	Specific Conductance (μmho)	pH	Total Uranium (μg/ℓ)	Temp (°C)
			SiO_2	Ca	Mg	K	Na	CO_3	HCO_3	SO_4	Cℓ	F	NO_3	TDS					
11	Alamo Canyon	7-10-77	---	13	3	4.1	3	0	50	---	2	0.2	0.2	148	44	140	7.2	2.5 ± 0.6	11
11		7-10-78	20	6	3	---	4	0	34	<1	1	0.2	<0.1	68	29	100	7.0	---	---
12	Alamo Canyon	7-10-77	---	29	4	6.3	8	0	98	---	1	0.1	0.1	176	90	260	7.6	2.4 ± 0.6	15
12		7-10-78	51	19	6	---	9	0	80	11	2	0.3	<0.1	114	71	200	8.1	---	---
13	Alamo Canyon	7-10-77	---	33	5	4.0	11	0	122	---	3	0.1	0.3	232	104	240	7.7	3.7 ± 0.8	22
13		7-10-78	43	24	6	---	9	0	82	6	3	0.6	<0.1	178	83	210	8.2	---	---
14	Capulin Canyon	7-10-77	---	15	3	2.3	10	0	72	---	3	0.1	0.1	148	51	170	7.7	1.9 ± 0.6	17
14		7-10-78	69	12	5	---	10	0	66	<1	3	0.5	<0.1	162	51	145	8.5	---	---
15	Capulin Canyon	7-9-77		21	4	4.5	8	0	92	---	2	0.2	0.1	178	70	220	7.8	2.4 ± 0.6	18
15		7-10-78	61	14	4	---	10	0	72	<1	3	0.4	<0.1	162	54	160	8.3	---	---

TABLE IX

CHEMICAL QUALITY OF BASE FLOW AND STORM RUNOFF

(Analyses in mg/ℓ)

Station	Location	Type of Flow	Date	Ba	Ca	Fe	HCO_3	Mg	Mn	Pb	Phenol	Zn
8	Frijoles, Mon. Hdq.	Storm	8-12-77	1.5	164	42	262	9	9.3	0.58	0.068	0.6
		Base	8-27-77	<0.5	100	2.4	92	14	0.4	<0.03	<0.005	<0.5
		Base	9-15-77	<0.5	101	0.8	88	13	<0.1	<0.03	<0.001	<0.5
		Base	10-1-77	<0.5	19	0.9	89	6	<0.1	<0.03	<0.001	0.6
		Base	2-8-78	<0.5	3	<0.5	67	1	<0.1	<0.03	0.003	<0.5
		Storm	6-19-78	1.3	58	240	112	28	14	1.0	0.023	1.2
13	Alamo Canyon	Base	9-1-77	<0.5	87	0.6	80	11	<0.1	<0.3	<0.001	<0.5
		Base	10-6-77	<0.5	20	<0.5	85	5	0.1	<0.3	0.002	<0.5
		Base	6-2-77	<0.5	6	<0.5	95	1	<0.1	<0.3	<0.001	<0.5
15	Capulin Canyon	Storm	8-17-77	0.8	112	3.7	52	20	1.2	<0.3	<0.001	<0.5
		Base	9-9-77	<0.5	65	<0.5	72	13	<0.1	<0.3	<0.001	<0.5
		Base	4-30-78	<0.5	5	<0.5	81	1	<0.1	<0.3	<0.001	<0.5
		Base	11-30-78	<0.5	6	<0.5	56	7	<0.1	<0.3	<0.001	<0.5

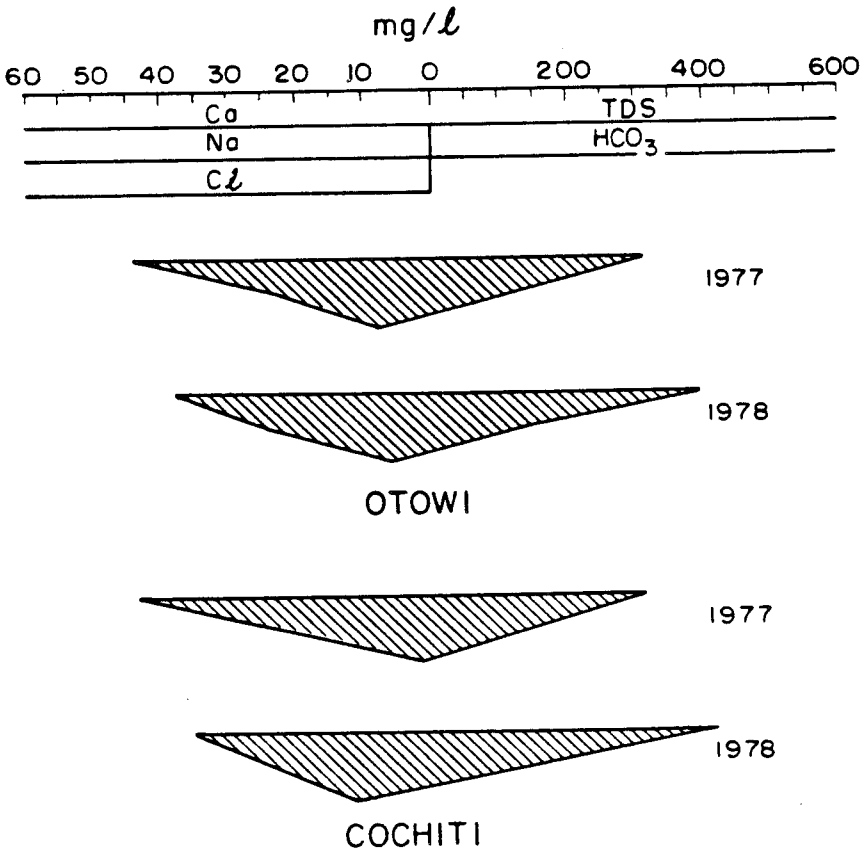

Fig. 6.
Calcium, sodium, chloride, total dissolved solids, and bicarbonates at Otowi and Cochiti on the Rio Grande.

8). Sodium and fluoride varied slightly but showed no significant trend (Table VIII). These constituents in base flow have shown a general decline in concentration as the fire debris and ash are removed from the channel by continued runoff.

Samples of base flow and storm runoff were collected in Cañon de los Frijoles, indicating barium, calcium, iron, bicarbonate, manganese, lead, phenol, and zinc concentrations were elevated in storm runoff when compared to base flow (Table IX). Phenol is attributed to decay of vegetation. Other constituents, with the exception of lead, can be attributed to the runoff from the burn area. Lead could be from automobile emissions, as it was not reported in a similar runoff event in Capulin Canyon, which is remote from vehicle traffic (Fig. 9).

Three surface water samples were collected in Alamo Canyon in July 1977 and 1978 above, within, and downgradient from the burn (Fig. 4). The water

TABLE X

AVERAGE CALCIUM BICARBONATE, SODIUM, AND CHLORIDE AT LOW-FLOW STATIONS, 1958-60

Low-Flow Stations	mg/ℓ		
	$CaCO_3$	Na	Cℓ
C	30	8.2	2.0
D	30	8.8	1.6
E	31	8.8	1.8
F	32	9.0	1.9
G	32	8.6	1.8
H	32	9.2	1.8
I	33	9.3	1.7
J	34	10.5	2.5

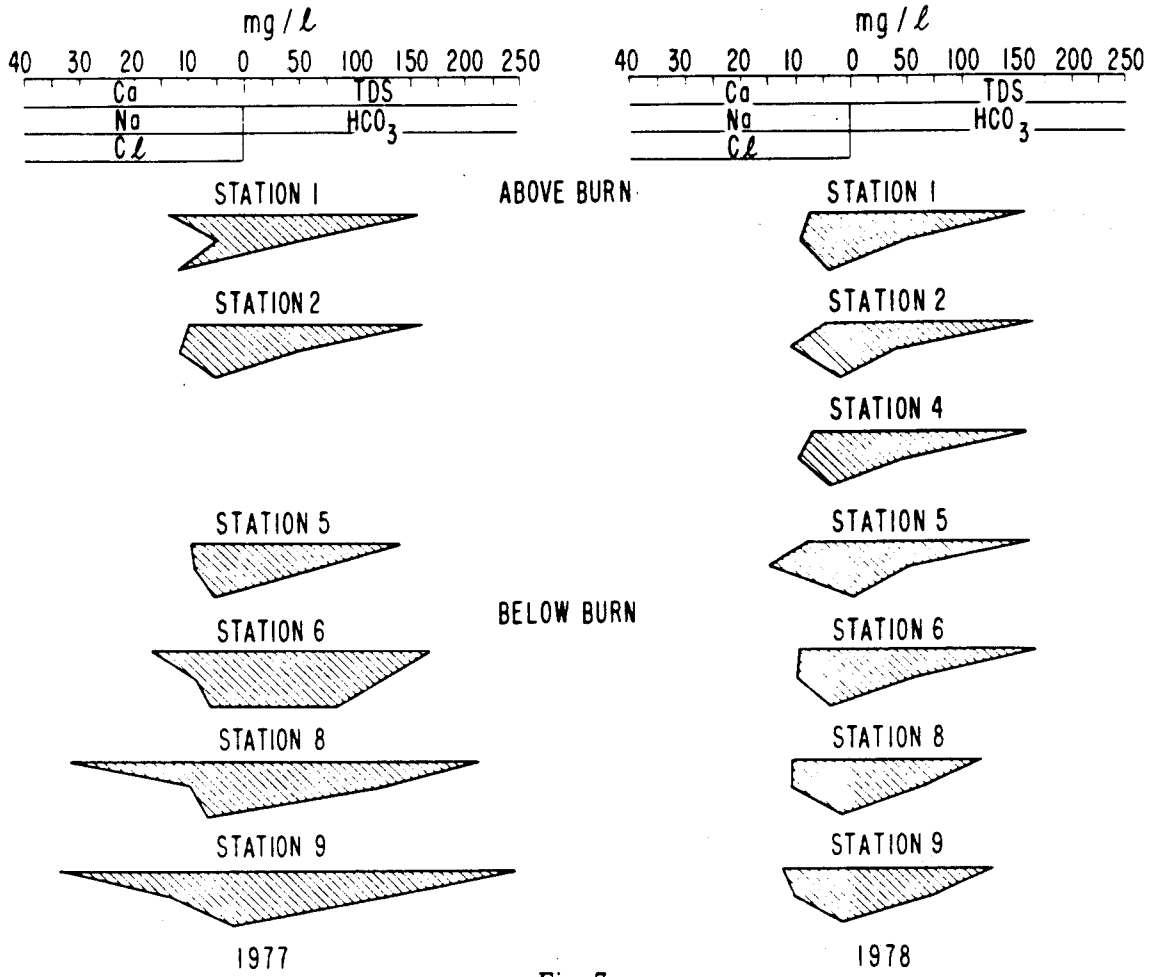

Fig. 7.
Calcium, sodium, chloride, total dissolved solids, and bicarbonate in surface water from Cañon de los Frijoles.

contains principal ions of calcium and bicarbonate (Table VIII). A comparison of the water quality at the three stations in 1977 shows the effect of the burn, with a slight increase of calcium, sodium, bicarbonate, and TDS (Fig. 10). Analyses of samples collected in 1978 indicated a decrease in most of these constituents,. Three analyses of base flow for barium, calcium, iron, bicarbonate, magnesium, manganese, lead, phenol, and zinc are shown in Table IX. Only calcium and magnesium decreased during the year. The remaining constituents varied but showed no significant trends.

Surface water below the burn in Capulin Canyon was sampled in 1977 and 1978 (Fig. 4). The base flow contains principal ions of calcium and bicarbonate (Table VIII). The concentrations of calcium, bicarbonate, and TDS generally increase downgradient in the canyon. The concentrations of these constituents decreased from 1977 to 1978 when compared at individual stations.

Samples of base flow and storm runoff at Station 15 (Base Camp) were analyzed for barium, calcium, iron, bicarbonate, magnesium, manganese, lead, phenol, and zinc (Table IX). Barium, calcium, iron, and manganese concentrations were elevated during runoff events. Bicarbonate varied but showed no significant trend. Phenols and lead were below analytical limits.

B. Ground Water

Ground water from springs in and adjacent to the Monument has been analyzed for routine chemical constituents. Included in ground water data are one

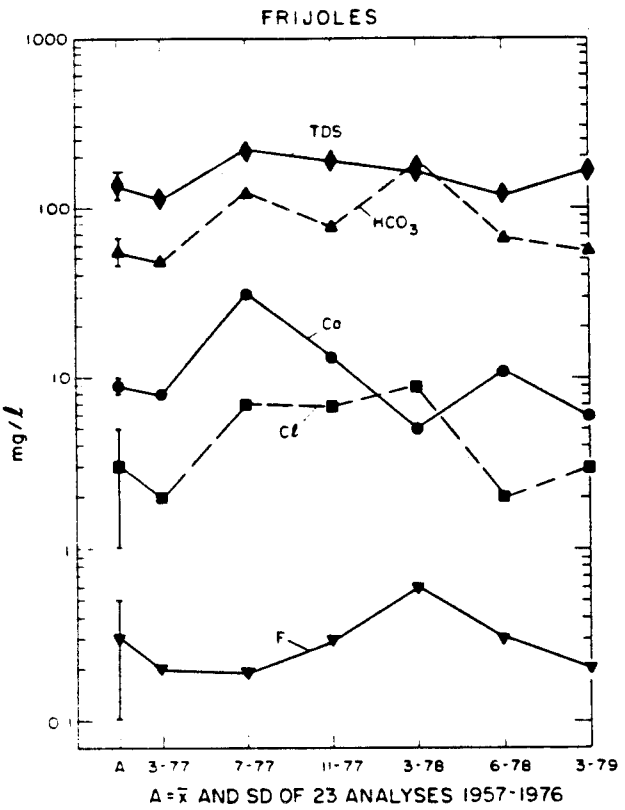

Fig. 8.
Base flow chemical constituent variation in Cañon de los Frijoles before and after the La Mesa Fire.

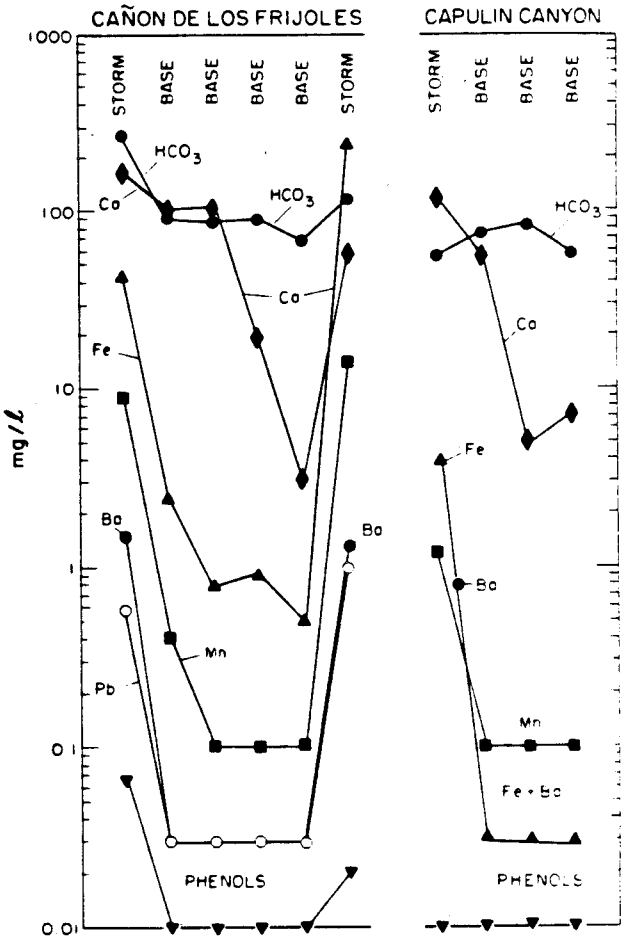

Fig. 9.
Base flow and storm runoff chemical constituent variations in Cañon de los Frijoles and Capulin Canyon after the La Mesa Fire.

chemical analysis from a test hole completed in the main aquifer on the plateau north of the Monument.

Doe and Turkey Springs are located adjacent to the Monument (Fig. 4). The principal ions in water from Doe Spring are sodium and bicarbonate (Fig. 11). The TDS is low, below 200 mg/ℓ with a water temperature of 18°C (Tables VII, VIII). The principal ions in water from Turkey Spring are calcium and bicarbonate (Fig. 11). TDS is under 250 mg/ℓ with water temperature of 19°C.

Three springs in the Monument are at Station 3 (North Fork of Cañon de los Frijoles), Station 7 (Apache Spring), and Station 10 (near mouth of Canon de los Frijoles). The discharge of the spring at Station 3 forms a part of the base flow in Cañon de los Frijoles. The water contains principal ions of calcium and bicarbonate (Tables VII, VIII). TDS are less than 175 mg/ℓ with a water temperature of about 10°C. Station 7 is a small seep with principal ions of calcium-sodium and bicarbonate (Fig. 11). TDS are low, less than 150 mg/ℓ, with a water temperature of 9°C. Water from the spring at Station 10 contains principal ions of sodium and bicarbonate with a water temperature of about 19°C. TDS are less than 200 mg/ℓ (Tables VII, VIII).

The chemical quality of water from the seep at Station 7 (Apache Spring) has shown some effect of recharge from the burn area. In July 1977, after the fire, the TDS were 222 mg/ℓ, while in 1978 they had decreased to 110 mg/ℓ. It is apparent that recharge to the small perched aquifer is rapid, usually within a month. Between the fire in early June and samples collected in early July there were only three periods of precipitation. The chemical quality of water from the other springs (outside the burn area; Doe,

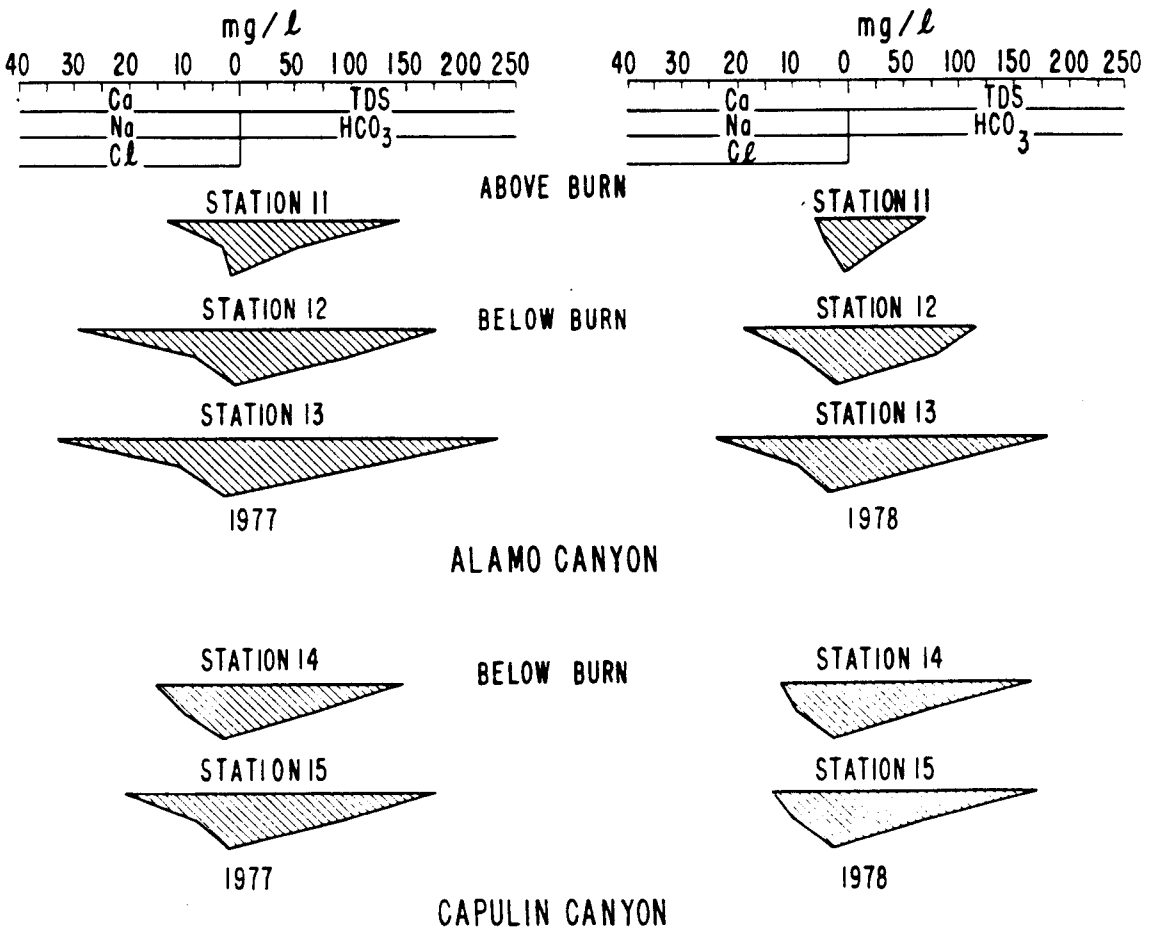

Fig. 10.
Calcium, sodium, chloride, total dissolved solids, and bicarbonate in surface water in Alamo and Capulin Canyons.

Turkey, Stations 3 and 10) have shown no significant changes between sampling periods.

Water from the main aquifer at a test well north of the Monument on the plateau contains principal ions of sodium and bicarbonate (Fig. 11). The TDS are less than 150 mg/ℓ at a water temperature of 21°C.

The quality of water from Doe Spring and Station 10 is quite similar in chemical constituents, both have the same chemical concentrations and principal ions of sodium and bicarbonate (Fig. 11). The spring discharges from the main aquifer near the Rio Grande. The water quality of these springs is comparable to the water from the test well on the plateau.

C. Suspended Sediments

Soils in the drainage area of Cañon de los Frijoles above the gaging station near the Monument Headquarters are derived from the weathering of tuff and volcanic rocks of the Valles Caldera. Overland runoff moves loose, erodible particles from the land surface into the stream channel. Once in the channel the sediment particles are transported by the stream either as suspended or bed sediments. The suspended sediments are classified as having a mean diameter <6 mm (6 mm is the intake size of the DH-48 samples used in the study). Only the suspended sediment loads were determined for base flow and two small runoff events.

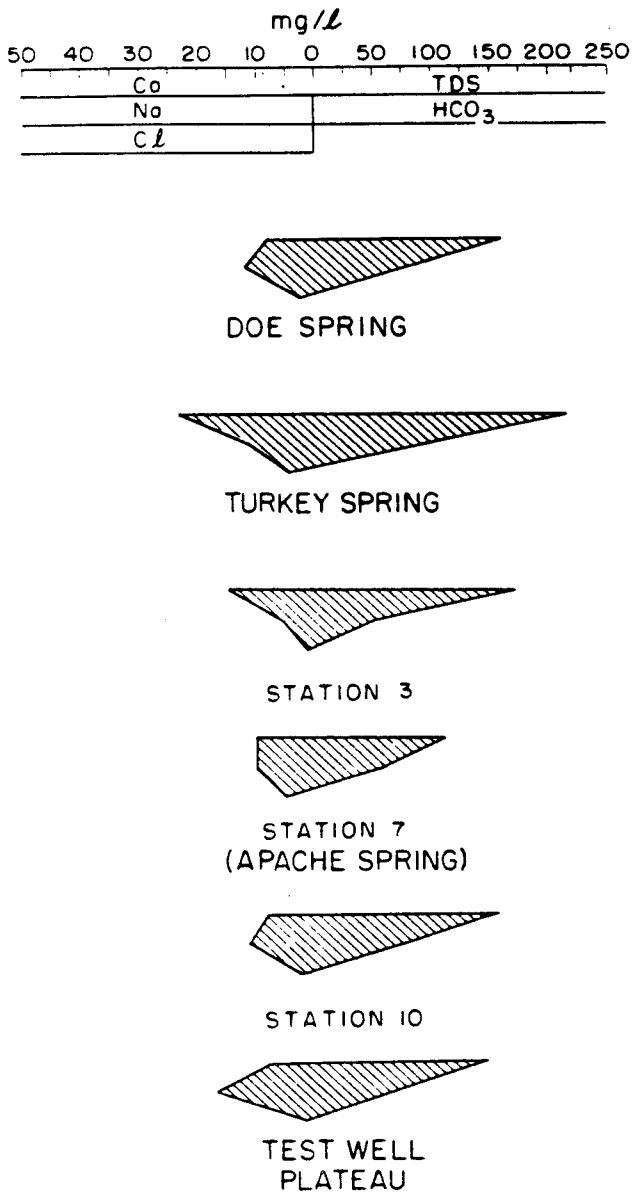

Fig. 11.
Calcium, sodium, chloride, total dissolved solids, and bicarbonate in ground water from springs and a test hole.

The base flow in Cañon de los Frijoles, about 0.03 m^3/ℓ, carries a small amount of suspended sediment. The average suspended sediment concentration in base flow for a 15-day period in July 1977 was about 140 mg/ℓ at the Monument Headquarters. During a 24-h period the stream carried about 381 kg of suspended sediments in 2.7×10^3 m^3 of water through the station. The suspended sediments yield of the base flow is about 8.4 kg/km^2.

TABLE XI

DISCHARGE AND SEDIMENT CONCENTRATION OF TWO STORM RUNOFF EVENTS, 1977

Date and Time		Discharge (m^3/s)	Discharge (ft^3/s)	Suspended Sediments (mg/ℓ)
Aug. 12	7:45	4.13	146	39,600
	11:15	0.48	17	11,200
	16:10	0.18	6.5	4,930
	17:20	0.10	3.7	1,310
	18:05	0.08	2.9	1,250
	20:15	0.07	2.5	560
Aug. 20	14:20	0.11	3.8	785
	15:20	12.3	433	98,800
	15:50	8.86	313	94,600
	16:25	5.49	194	54,100
	17:30	1.95	69	29,600
	19:00	0.85	30	12,600
	19:30	0.71	25	8,820
	20:00	0.62	22	7,120

The suspended sediment load in storm runoff increased as the vegetation cover holding the soil in place was destroyed in the fire. Also, the burned area is in the upper reaches of the canyon where channel gradients are steep. The resulting high flow velocities increase the transport of suspended sediments. Two runoff events were used to illustrate the amount of sediment transported through the gaging station near Monument Headquarters after the fire.

The maximum discharge on August 12, 1977 was 4.1 m^3/s with a maximum suspended sediment concentration of 39.6×10^3 mg/ℓ (Table XI). The mean discharge for the 15.2 h event was 0.14 m^3/s with a mean suspended sediment concentration of 2.1×10^3 mg/ℓ. About 16.6×10^3 kg of suspended sediments were carried through the gaging station in 7.9×10^3 m^3 of runoff. The suspended sediment yield for the event was 3.7×10^2 kg/km^2.

The maximum discharge of the second event, August 20, 1977, was 12.3 m^3/s with a maximum suspended sediment concentration of 98.8×10^3 mg/ℓ (Table XI). The mean discharge for the 5.7 h

event was 0.57 m^3/s with a mean suspended sediment concentration of 5.8×10^3 mg/ℓ. About 6.7×10^4 kg of suspended sediments were carried through the gaging station in 11.6×10^3 m^3 of runoff. The suspended sediment yield for the event was 1.5×10^3 kg/km^2.

V. SUMMARY AND CONCLUSIONS

Cañon de los Frijoles contains a perennial stream from the mountains across the plateau to the Rio Grande. Four other canyons (Alamo, Capulin, Medio and Sanchez) contain perennial streams in short reaches from the flanks of the mountains on to part of the plateau. The base flow in these canyons is from springs and seeps along the base of the mountains. Low-flow investigations in Cañon de los Frijoles indicate decreased flow across the plateau where water is lost to evapotranspiration and infiltration into the underlying volcanic rocks and sediments.

Gradients in the stream channels are greater on the flanks of the mountains, decreasing across the plateau. The gradient increases in lower Cañon de los Frijoles because the basalt in the channel has limited the downcutting of the canyon to the west. The 1977 wildfire occurred mainly in the upper reaches of the canyons in areas of the greater channel gradients. This results in increased flow velocities during summer storms and increased transport of suspended sediments from erosion.

Available data on runoff from summer storms indicates the discharge yield increased from 0.012 $m^3/s/km^2$ to a maximum of 1.95 $m^3/s/km^2$ in Cañon de los Frijoles in a 15 month period after the burn. The discharge yield of a single runoff event in Lummis and Alamo Canyons was 0.33 $m^3/s/km^2$ and 0.15 $m^3/s/km^2$, respectively. The loss of the vegetative cover by burn has resulted in decreased collection and retention time for runoff resulting in larger discharge from runoff events. As the vegetation cover increases in the drainage area through seeding and natural growth, the discharge yield and suspended sediment yield will decrease.

The chemical quality of surface water in Cañon de los Frijoles changed slightly after the burn. The most noticeable change was an increase in calcium, chloride, bicarbonate, and TDS. Analyses taken over a 21-month period after the burn indicated a general decline in most of these constituents. Similar analyses of surface water in Alamo and Capulin Canyon indicate similar results over a 12-month period.

Analyses of samples collected of summer storm runoff compared with base flow in Cañon de los Frijoles indicated that higher concentrations of barium, calcium, iron, bicarbonate, manganese, lead, phenols, and zinc occurred in storm runoff than in the base flow.

Precipitation and runoff from the burn area will remove the fire debris allowing the quality of water of the streams to return to normal. The past two years data indicates the water quality of the base flow should return to normal three to five years after the fire.

Ground water occurs as springs and seeps in and adjacent to the Monument. There are no wells or test holes in the Monument. Two springs in Upper Cañon de los Frijoles discharge from a perched aquifer. The spring in the north fork of Cañon de los Frijoles (Station 3) discharges from a perched aquifer which is probably recharged from the upper water bearing zone in the Valles Caldera to the west. The spring contributes a part of the base flow for the stream in the canyon. Station 7 (Apache Spring) is a small spring on the north wall of Cañon de los Frijoles which discharges from a perched aquifer of limited extent. The TDS in the water from Apache Spring increased shortly after the burn, indicating rapid recharge. Turkey Spring, west of the Monument boundary, contributes a part of the base flow in a tributary to Capulin Canyon. This spring lies outside the burn area and was unaffected by the fire.

Two springs, Doe Spring in Chaquihui Canyon north of the Monument and the spring at Station 10 in lower Cañon de los Frijoles, discharge from the main aquifer. The main aquifer lies at a depth of 300 to 375 m along the western edge of the plateau north of the Monument. The surface slopes gently toward the Rio Grande where a part of the water is discharged into the river. North of the Monument the Rio Grande is a gaining stream with ground water discharged to the river, while to the south along the eastern boundary of the Monument, water from the river is lost into the underlying rocks. Contours on the potentiometric surface of the aquifer north of the Monument indicate water in the aquifer moves to the southeast. In the Monument the movement changes to a more southernly direction. Major

recharge to the main aquifer is from the Valles Caldera. In the eastern part of the Monument, the intrusion of volcanic rocks which form the San Miguel Mountains have restricted the movement of water in the aquifer causing a ground water depression to form west of the Rio Grande and south of the Monument.

REFERENCES

1. C. S. Ross, R. L. Smith, and R. A. Bailey, "Outline of Geology of the Jemez Mountains, New Mexico," New Mexico Geological Society Guidebook of the Albuquerque Country, 12th Field Conf. (1961).

2. R. L. Smith, R. A. Bailey, and C. S. Ross, "Structural Evolution of the Valles Caldera, New Mexico and Its Bearing on Emplacement of Ring Dikes," U.S.Geol. Survey Prof. Paper 424-D (1961).

3. R. L. Griggs, "Geology and Ground-Water Resources of the Los Alamos Area, New Mexico," U.S. Geol. Survey Water-Supply Paper 1753 (1964).

4. R. A. Bailey, R. L. Smith, and C. S. Ross, "Stratigraphic Nomenclature of the Volcanic Rock of the Jemez Mountains, New Mexico," U.S. Geol. Survey Bulletin 1274-P (1969).

5. R. L. Smith, R. A. Bailey, and C. S. Ross, "Geologic Map of the Jemez Mountains, New Mexico," U.S. Geol. Survey Misc. Geol. Inv. Map I-571 (1970).

6. V. C. Kelley, "The Rio Grande Depression from Taos to Santa Fe," New Mexico Geological Society Guidebook of the Southeastern Sangre de Cristo Mountains, New Mexico, 7th Field Conf. (1956).

7. U.S. Geol. Survey, "Water Resources Data for New Mexico, Water Year 1977," U.S. Geol. Survey Water-Data report NM-77-1 (1978).

8. U.S. Geol. Survey, "Water Resources Data for New Mexico, Water year 1978," U.S. Geol. Survey Water-Data report NM-78-1 (1979).

9. Z. E. Spiegel, "Geology and Water Resources of the Santa Fe Area, New Mexico," U.S. Geol. Survey Water-Supply Paper 1525 (1963).

10. W. D. Purtymun, "Geology and Hydrology of White Rock Canyon from Otowi to the Confluence of Frijoles Canyon, Los Alamos and Santa Fe Counties, New Mexico," U.S. Geol. Survey open-file report (1966).

11. U.S. Geol. Survey, "Surface Water Supply of the United States, Part 8, Western Gulf of Mexico Basins," U.S. Geol. Survey Water-Supply Paper 1632 (1959).

12. U.S. Geol. Survey, "Surface Water Supply of the United States, Part 8, Western Gulf of Mexico Basins," U.S. Geol. Survey Water-Supply Paper 1712 (1960).

13. W. D. Purtymun, "Storm Runoff and Transport of Radionuclides in DP Canyon, Los Alamos County, New Mexico," Los Alamos Scientific Laboratory report LA-5744 (1977).

14. C. V. Theis and C. S. Conover, "Pumping Test in the Los Alamos Canyon Well Field near Los Alamos, New Mexico," U.S. Geol. Survey Water-Supply Paper 1619-I (1962).

15. C. S. Conover, C. V. Theis, and R. L. Griggs, "Geology and Hydrology of the Valle Grande and Valle Toledo, Sandoval County, New Mexico," U.S. Geol. Survey Water-Supply Paper 1619-Y (1963).

16. R. L. Cushman, "An Evaluation of Aquifer and Well Characteristics of Municipal Well Fields in Los Alamos and Guaje Canyons Near Los Alamos, New Mexico," U.S. Geol. Water-Supply Paper 1809-D (1965).

17. W. D. Purtymun and J. B. Cooper, "Development of Ground-Water Supplies on the Pajarito Plateau, Los Alamos County, New Mexico, "U.S. Geol. Survey Prof. Paper 650-B (1969).

18. W. D. Purtymun and S. Johansen, "General Geohydrology of the Pajarito Plateau," New Mexico Geological Society Guidebook, Ghost Ranch (Central-Northern, New Mexico), 25th Field Conf. (1974).

19. R. L. Borton, "A Listing of Geohydrological Data for 106 Exploratory Holes Drilled by Nuclear Dynamics, in Rio Arriba, Sandoval, and Santa Fe Counties, 1970-72," New Mexico State Engineer open-file report (1974).

20. F. B. Titus, Jr., "Ground-Water Geology of the Rio Grande Trough in North-Central New Mexico, with Sections on the Jemez Caldera and Lucero Uplift," New Mexico Geological Society Guidebook, Albuquerque Country, 12th Field Conf. (1961).

21. L. J. Bjorklund and B. W. Maxwell, "Availability of Ground Water in the Albuquerque Area, Bernalillo and Sandoval Counties, New Mexico," New Mexico State Engineer Tech. Rept 21 (1961).

22. U.S. Geol. Survey, "Quality of Surface Water of the United States, Parts 7 and 8, Lower Mississippi River Basin and Western Gulf of Mexico Basins," U. S. Geol. Survey (1960).

DEVELOPMENT OF GROUND-WATER SUPPLIES ON THE PAJARITO PLATEAU, LOS ALAMOS COUNTY, NEW MEXICO

By WILLIAM D. PURTYMUN and JAMES B. COOPER,
Santa Fe, N. Mex., Albuquerque, N. Mex.

Work done in cooperation with the U.S. Atomic Energy Commission and the Los Alamos Scientific Laboratory

Abstract.—The Pajarito Mesa well field, completed in 1966 on the Pajarito Plateau, contributed 37 percent of the total water supply to Los Alamos in 1967. Two wells in the field are capable of yields of 1,400 gallons per minute each. This yield is about three times that of any of the other 13 supply wells in the water-supply system. The high yield of the two wells is attributed to the occurrence of coarse volcanic debris and arkosic sediment in the Puye and Tesuque Formations of the Santa Fe Group that make up the main aquifer beneath the Pajarito Plateau.

The town of Los Alamos and laboratories of the U. S. Atomic Energy Commission and the Los Alamos Scientific Laboratory are located on the Pajarito Plateau in north-central New Mexico (fig. 1). Since the community was established in 1943 the demand for water, created by population growth and the expansion of the laboratories, has equaled and at times exceeded the amount of water that had been developed.

The initial water supply was obtained from small streams and springs in the mountains west of the town. These sources soon became inadequate, and in 1949 a ground-water supply was established. Since conversion of the water-supply system to ground-water sources, the U.S. Geological Survey has assisted the U.S. Atomic Energy Commission in the development and management of the ground-water supply.

HYDROGEOLOGIC CONDITIONS OF THE PAJARITO PLATEAU

The Pajarito Plateau forms a topographically high area that slopes gently eastward from the flanks of the Sierra de los Valles toward the Rio Grande (Kelley, 1952, p. 93). The plateau is formed by rocks of the Santa Fe Group of middle (?) Miocene to Pleistocene(?) age, and volcanic rocks of Pliocene and Pleistocene age (Griggs, 1964, fig. 8). Figure 2 is a diagrammatic section showing the geologic units in the Los Alamos area.

The Santa Fe Group comprises the Tesuque and the Puye Formations, and the basaltic rocks of Chino Mesa. These formations crop out along the eastern margin of the Pajarito Plateau. The permeable sediments of the Tesuque Formation are the main aquifer penetrated by the wells in Los Alamos and Guaje Canyons.

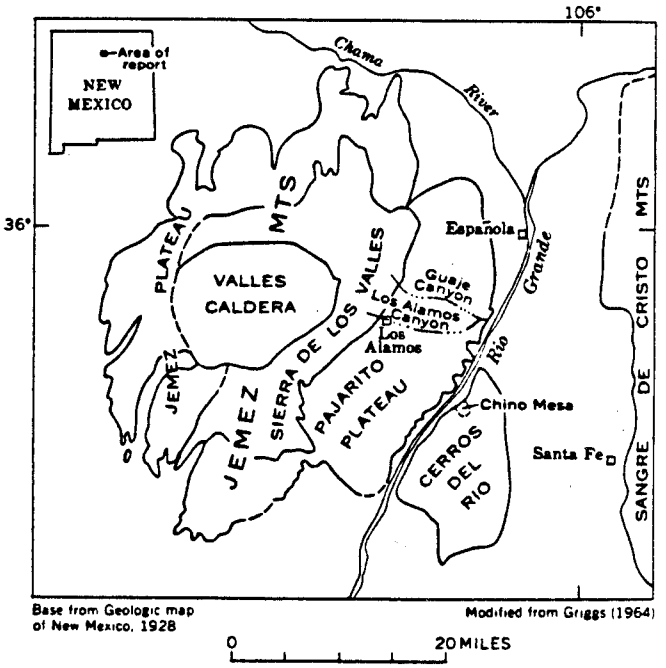

FIGURE 1.—Map of the Los Alamos area, showing topographic features mentioned in the text.

U.S. GEOL. SURVEY PROF. PAPER 650-B, PAGES B149-B153

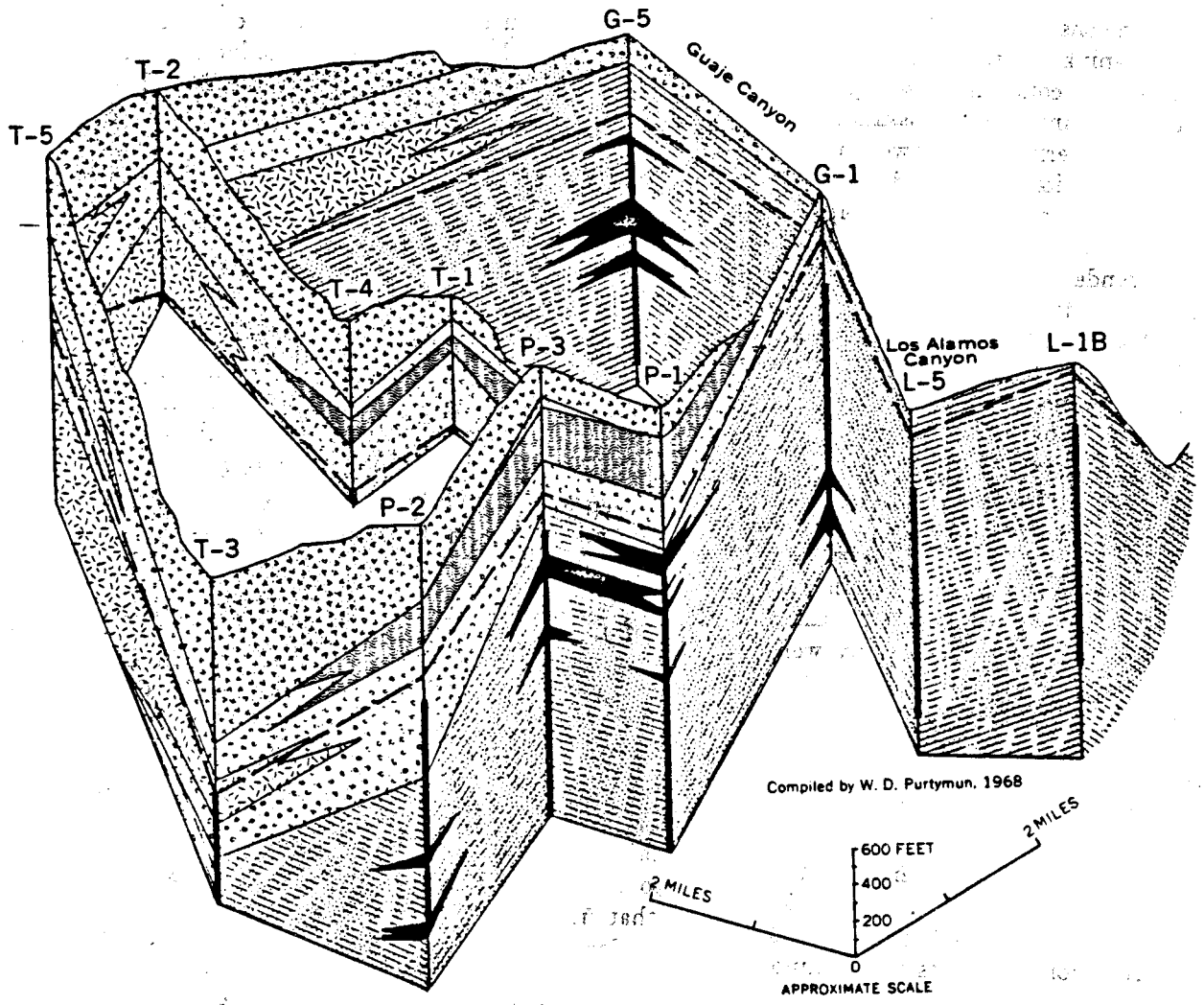

EXPLANATION

Bandelier Tuff

Puye Formation

Basaltic rocks of Chino Mesa

Tschicoma Formation

Tesuque Formation

Basalt in the Tesuque Formation

Well

Heavy line shows section that is all or partly open to the aquifer

Top of main aquifer

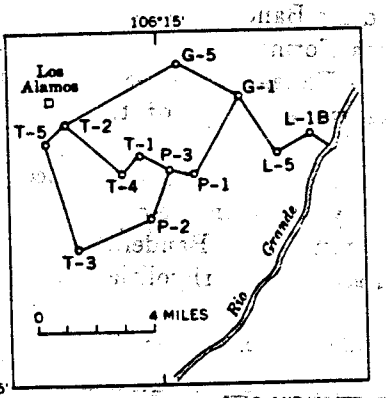

LOCATION OF WELLS AND LINES OF SECTION

FIGURE 2.—Diagrammatic section of geologic units in the Los Alamos area.

The Tesuque Formation consists of friable to moderat[illegible] well cemented light-pinkish-gray to light-brown silt[illegible]ne and sandstone that contains lenses of conglo[illegible]ate and clay and some interbedded basalt flows. The sedimentary rocks were derived from two sources. The lower part of the formation penetrated by wells in Los Alamos and Guaje Canyons consists principally of fine arkosic quartz sand derived from source areas to the east of the Rio Grande. The upper part consists of very coarse arkosic quartz sand, latitic gravels, and volcanic detritus, derived from sources both east and west of the Rio Grande (Griggs, 1964, p. 22).

The Puye Formation is a poorly consolidated conglomerate channel-fill deposit overlain by a fanglomerate composed of volcanic debris. The channel-fill deposits are gray and consist of fragments of quartzite, schist, gneiss, and granite, ranging in size from sand to boulders. The fanglomerate is generally gray and consists of pebbles and cobbles of rhyolite, latite, quartz-latite, and pumice, in a matrix of silt and sand. Sorting is poor, but tongues and lenses of fairly well sorted pumiceous siltstone and water-laid pumice are present within the fanglomerate. The rocks were derived from flows associated with the volcanic rocks of the Jemez Mountains.

The basaltic rocks of Chino Mesa consist of basalt a[illegible]asalt breccia that overlie the Puye along the Rio Gra[illegible]de and interfinger with the conglomerate to the we[illegible]eneath the Pajarito Plateau (fig. 2). The basalt, which thickens southward along the river and thins westward, originated from volcanic vents near Chino Mesa (fig. 1).

The volcanic rocks consist of the Tschicoma Formation of Pliocene age and the Bandelier Tuff of Pleistocene age. The Tschicoma Formation forms the mountains of the Sierra de los Valles, and is present in the subsurface beneath the western edge of the plateau (fig. 2). The deposits are composed of latite, quartz-latite flows, and pyroclastic rocks. The Tschicoma Formation is overlain by the Bandelier Tuff along the flanks of the mountains. The Bandelier Tuff, a series of ash flows and ash falls of rhyolitic tuff, caps the Pajarito Plateau and unconformably overlies the Puye Formation and basaltic rocks of Chino Mesa in the central and eastern parts of the plateau. The Tschicoma Formation, the Bandelier Tuff, and the basaltic rocks of Chino Mesa contain only small amounts of water, which usually is perched above a confining layer.

DEVELOPMENT OF GROUND-WATER SUPPLIES

The first water-supply wells drilled in the Las Alamos area were located along the eastern edge of the Pajarito Plateau in Los Alamos Canyon and Guaje Canyon, which are tributary to the Rio Grande (fig. 1). The wells were located in the canyons rather than in the higher elevations of the Pajarito Plateau in order to keep drilling depths to a minimum and to be as close as possible to the then-known aquifers in the Santa Fe Group. The wells yielded satisfactory quantities of water, 500 gallons per minute or more, and several of them have been in continuous service for 20 years or more. In 1967, six wells located in Los Alamos Canyon and seven wells located in Guaje Canyon supplied 63 percent of the total amount of water (1.3 billion gallons) used by Los Alamos (table 1).

In 1963, because of increasing water demands and lack of additional space for new wells in Los Alamos and Guaje Canyons, new locations were sought on the Pajarito Plateau. Test drilling on the plateau indicated that the main aquifer, entirely within the Tesuque Formation in the lower part of Los Alamos and Guaje Canyons, rises stratigraphically westward, and that beneath the central part of the plateau the lower part of the overlying Puye Formation is saturated and becomes a part of the aquifer.

These data, as well as extensive knowledge of the surface geology, suggested that the saturated portion of the Puye Formation and the sediments in the upper part of the Tesuque Formation would yield considerable quantities of water to a well that penetrated deeply into the zone of saturation. Even though wells on the plateau might need to be as much as a thousand

TABLE 1.—*Pumping rate, total pumpage, and specific capacities of wells in Los Alamos Canyon, Guaje Canyon, and Pajarito Mesa well fields, 1967*

Location	Number of wells	Pumping rate (gpm)			Total pumpage		Specific capacity (gpm per ft of drawdown)		
		Range		Average	Millions of gallons	Percent of total	Range		Average
		From	To				From	To	
Los Alamos Canyon	6	360	565	495	373	28	2	14	6
Guaje Canyon	7	395	560	425	465	35	2	13	6
P[illegible]ito Mesa	[1] 2	635	1,425	1,030	481	37	15	26	20

[1] Does not include well P-3, which was added to the system in January 1968.

feet deeper than wells drilled at lower elevations in the canyons, the economic savings resulting from shorter pipelines and greater choice for well locations, le such drilling feasible.

The first deep well, P–1, of the Pajarito Mesa well field (well-field designation of the U.S. Atomic Energy Commission) was drilled in 1964 to a depth of 2,500 feet on the Pajarito Plateau. It penetrated about 1,800 feet of saturated sediments and volcanic rocks in the Puye and Tesuque Formations. The coefficient of transmissibility at the well and specific capacity of the well are greater than that of wells in the Los Alamos and Guaje Canyons (table 2).

Data from well P–1 enabled further interpretation of the geology and hydrology beneath the plateau, and sites for additional wells were established to the west, at even higher elevations on the plateau. In 1965 a second well (P–2) was completed at a depth of 2,300 feet, and in 1966 a third well (P–3) was completed at a depth of 2,550 feet. These wells were constructed to accommodate pumps capable of producing 1,400 gpm each. The specific capacity of these wells on the plateau is four to six times greater than that of the Los Alamos and Guaje Canyons wells (table 2).

QUALITY OF WATER

The chemical quality of water may vary within a l field owing to local conditions that exist in the aquifer in the vicinity of the well. In general the water from the supply wells is of good quality for domestic use (table 3), as it contains less than 500 parts per million of dissolved solids (U.S. Public Health Service, 1962, p. 33). In the Pajarito Mesa well field the quality and temperature of water from wells P–1 and P–3 are similar, but water from well P–2 is some what different. The major yield to wells P–1 and P–3 is from the coarse sediments of the Tesuque Formation, whereas a large part of the yield to P–2 is from a thick saturated section of Puye Formation. The section of each well that is open to the aquifer, either throughout the indicated section or at intervals within it, is shown on figure 2.

The silica concentration of water from the three wells ranges from 74 to 82 ppm. The silica and calcium-magnesium concentrations, particularly of P–1 and P–3, may require special treatment for some industrial uses inasmuch as these constituents will contribute scale to tubing and pipes when heated.

PRESENT YIELDS AND RECOMMENDATIONS FOR FUTURE SUPPLIES

Pumpage of ground water at Los Alamos in 1967 was 1.3 billion gallons. Two wells on the Pajarito Plateau produced 37 percent of this total (table 1); the heavy pumpage appeared to cause little or no change in water levels in the wells.

Information obtained from the drilling of the three deep wells on the Pajarito Plateau shows that the upper 1,000 feet of the Tesuque Formation is composed of coarse volcanic debris and arkosic sand. These coarse sediments yield larger amounts of water to wells than do the fine sediments that predominate in the formation farther to the east along the Rio Grande.

The Puye Formation attains greatest thickness in a north-trending depositional basin beneath the central part of the plateau (fig. 2). Partial saturation of the permeable conglomerate in the central part of the plateau contributes to the higher yields of the wells.

The main aquifer is at a depth of about 1,200 feet along the western edge of the plateau, and the depth

TABLE 2.—*Aquifer characteristics of selected wells in the Los Alamos area*

Supply well or test well [1]	Date drilled	Depth (feet) [2]	Depth to water (feet)	Pumping rate (gpm)	Specific capacity (gpm per ft of drawdown)	Aquifer [3]	Coefficient of transmissibility (gpd per sq ft)
L–1B	1960	1,750	40	560	5	QTst	17,000
L–5	1948	1,750	170	485	4	do	
G–1	1950	2,000	265	450	5	do	12,000
G–5	1951	1,840	445	555	7	do	12,000
P–1	1964	2,500	740	640	15	QTsp, QTst	55,000
P–2	1965	2,300	835	1,425	26	do	40,000
P–3	1966	2,550	740	1,400	38	do	343,000
T–1	1949	815	750	6	.5	QTsp	7,700
T–2	1950	1,205	1,166	2	.6	QTt	1,000
T–3	1960	1,821	1,173	88	6	QTsp, QTt, QTst	11,000
T–4	1960	1,065	968	16	2	QTsp	2,400
T–5	1949	2,000	970±5			QTsp, QTt	

[1] G, supply well in Guaje Canyon; L, supply well in Los Alamos Canyon; P, supply well on Pajarito Plateau; T, test well.
[2] Completed depth of well.
[3] QTsp, Puye Formation; QTst, Tesuque Formation; QTt, Tschicoma Formation.

T 3.—*Chemical analyses of water from selected wells in Los Alamos Canyon, Guaje Canyon, and Pajarito Mesa well fields*

[Analyses by Group H-7 of the Los Alamos Scientific Laboratory]

Supply well [1]	Date Collected	Temperature (°F)	Chemical constituents (parts per million)												Specific conductivity (micromhos at 25°C)
			Silica [2] (SiO_2)	Calcium (Ca)	Magnesium (Mg)	Sodium (Na)	Carbonate ($CaCO_3$)	Bicarbonate (HCO_3)	Chloride (Cl)	Fluoride (F)	Nitrate (NO_3)	Total dissolved solids	Total hardness (as $CaCO_3$)	pH	
-1B	5-28-68	87	37	8	1	195	0	262	17	2	0.2	409	24	8.1	600
-5	6-18-68	78	36	10	0	105	0	134	0	.9	.2	191	26	8.3	232
-1	5-28-68	80	84	12	.5	38	0	74	3	.4	.3	199	32	8.0	152
-5	5-25-68	78	60	18	3	23	0	74	3	.4	.4	163	56	7.8	158
-1	6-18-68	83	82	28	5	36	0	122	5	.3	.1	246	90	7.9	248
-2	6-18-68	73	81	13	2	21	0	58	0	.3	.3	176	40	7.6	114
-3	6-18-68	81	74	26	8	33	0	122	7	.3	.1	259	98	7.8	260

[1] G, supply well in Guaje Canyon; L, supply well in Los Alamos Canyon; P, supply well on Pajarito Plateau.
[2] Silica analyses are from samples collected in May 1967. Later samples have not been analyzed for silica.

decreases eastward with the gentle slope of the land surface to a depth of about 600 feet along the eastern edge (fig. 2). The water in the aquifer moves eastward toward the Rio Grande, which is the principal area for ground-water discharge (Cushman, 1965, p. D33).

Locations of future wells should be chosen carefully so as to avoid the relatively impermeable rocks of the Tschicoma Formation and the thick sections of basaltic rocks of Chino Mesa. These rocks are hard and are difficult to drill. Holes drilled in basalt are likely to be cr d because, in drilling, the bit may be deflected by ints or cavities. If rotary methods are used, it ma difficult to maintain fluid circulation in the hole at places where open joints occur. Additional wells capable of yielding from 1,000 to 1,500 gpm of water could be located at various sites near the center of the Pajarito Plateau.

REFERENCES

Cushman, R. L., 1965, An evaluation of aquifer and well characteristics of municipal well fields in Los Alamos and Guaje Canyons, near Los Alamos, New Mexico: U.S. Geol. Survey Water-Supply Paper 1809-D, 50 p.

Griggs, R. L., 1964, Geology and ground-water resources of the Los Alamos area, New Mexico: U.S. Geol. Survey Water-Supply Paper 1753, 107 p.

Kelley, V. C., 1952, Tectonics of the Rio Grande depression of central New Mexico, *in* New Mexico Geol. Soc. Guidebook, 3d Field Conf., The Rio Grande country: p. 93-105.

U.S. Public Health Service, 1962, Public Health Service drinking water standards, revised 1962: Public Health Service pub. 956, 61 p.

LA-7379-MS
Informal Report

UC-70
Issued: June 1978

Movement of Fluids and Plutonium from Shafts at Los Alamos, New Mexico

William D. Purtymun
Raymond Garde
Richard Peters

University of California

LOS ALAMOS SCIENTIFIC LABORATORY
Post Office Box 1663 Los Alamos, New Mexico 87545

An Affirmative Action/Equal Opportunity Employer

This report was prepared as an account of work sponsored by the United States Government. Neither the United States nor the United States Department of Energy, nor any of their employees, nor any of their contractors, subcontractors, or their employees, makes any warranty, express or implied, or assumes any legal liability or responsibility for the accuracy, completeness, or usefulness of any information, apparatus, product, or process disclosed, or represents that its use would not infringe privately owned rights.

UNITED STATES
DEPARTMENT OF ENERGY
CONTRACT W-7405-ENG. 36

MOVEMENT OF FLUIDS AND PLUTONIUM FROM SHAFTS AT LOS ALAMOS, NEW MEXICO

by

William D. Purtymun, Raymond Garde, and Richard Peters

ABSTRACT

The movement of fluids and plutonium from wastes disposed in shafts drilled into rhyolite tuff were studied under normal and test conditions. During normal operations of a waste treatment plant at the Los Alamos Scientific Laboratory (LASL), a $Fe(OH)_3$ (ferric hydroxide) sludge is mixed with cement to form a paste and disposed into the shafts. Under these conditions there was no indication of movement of fluids into the tuff; however, there was some movement of paste into open joints that intersected the shaft. As a special test, some $Fe(OH)_3$ sludge without cement was put into an experimental shaft. In this case, fluids moved a few meters from the shaft. The fluids carried trace amounts of plutonium from the shaft, but an inventory indicated more than 99% remained adsorbed or attached to the sludge in the shaft.

I. INTRODUCTION

Industrial waste from the LASL Plutonium Processing Facility is treated at a plant to remove plutonium and other radioactive contaminants.[1] The wastes are treated by chemical flocculation, sedimentation, and filtering processes, which produce an effluent that is released to the environment and a contaminated $Fe(OH)_3$ sludge that is mixed with a cement paste (waste-cement paste). The waste-cement paste is pumped into shafts at a controlled burial ground adjacent to the treatment plant.[2] These shafts are generally 2.4 m in diameter and range from 4.6 to 19.8 m deep.

The burial ground is located on the Pajarito Plateau, which was formed by a series of ashflows and ashfalls of rhyolite tuff.[3] At the site, the tuff is about 240 m thick and is underlain by a fanglomerate composed of cobbles and boulders in a matrix of sand and gravels. The main aquifer of the Los Alamos area lies at a depth of 350 m within the fanglomerate and there are no known perched aquifers above it.[4]

This study was conducted in two parts: (1) to determine the movement of fluids (water containing treated chemicals) and radioactive contaminants from a shaft filled with waste-cement paste under normal operating conditions, and (2) to determine the movement of fluids and plutonium under test conditions from $Fe(OH)_3$ sludge released into a smaller (60-cm-diam) shaft without the addition of cement. The second part of the study was experimental as sludge is not normally released or disposed of in this manner at LASL.

II. MOVEMENT OF FLUIDS AND RADIONUCLIDES FROM A WASTE CEMENT PASTE FILLED SHAFT

Test holes (TH) 10 cm in diameter and 29.6 cm deep were drilled at the shaft area in early 1968, prior to the development of the disposal field, to establish the geology and hydrology of the tuff. The shafts are located in the 18-m-wide berm between seepage ponds, which were used for effluent disposal in the late 1940s and early 1950s. Normally, the fluid

content of the tuff in undisturbed areas ranged from 4 to 6% by volume.[5,6] However, because of infiltration of effluents from the ponds, the fluid content of the tuff in cuttings from the test holes, drilled prior to the development of shafts, ranged from 7 to 12% by volume.

A shaft, located about 60 cm north from TH-7, was drilled to a depth of 17.7 m and filled with contaminated cement paste and capped by April 1969. The cement-paste volume released into the shaft was 85 m^3, of which about 28 m^3 was fluids. Test hole TH-7A, located about 60 cm from the eastern edge of the shaft, was completed after the shaft was filled. Cuttings from both test holes were analyzed for fluid content and gross-alpha and -beta activity.

The fluid content of cuttings from the test holes ranged from 8 to 14% by volume in the upper 3 m, reflecting the infiltration of fluids from precipitation. Prior to use of the disposal shafts, the fluid content of the tuff at TH-7, from a depth of 3 to 29.6 m, ranged from 7 to 10% by volume. After the shaft was filled, the fluid content of the tuff at TH-7A, from a depth of 3 to 24 m, ranged from 4 to 8% by volume, showing a decrease in the fluid content of 3 to 6% (Fig. 1). Below a depth of 24 m there was no significant change in fluid content of the tuff. The decrease in the fluid content of the tuff adjacent to and below the bottom of the shaft is apparently caused by the hydration of the cement. During the hydration process of the waste-cement paste, fluid was extracted from the tuff.

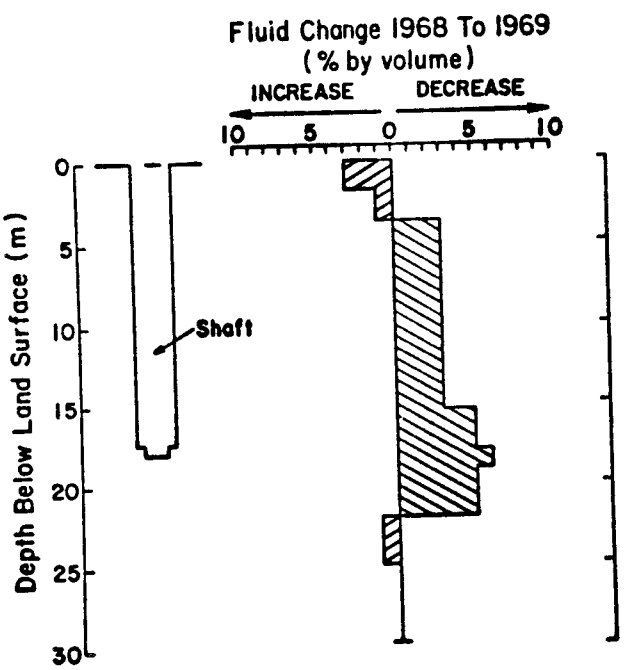

Fig. 1.
Change in fluid content of tuff adjacent to shaft prior to and after shaft was filled with cement paste.

The gross-alpha activity of cuttings from TH-7 ranged from 2 to 5 pCi/g, reflecting naturally occurring radioactive isotopes. There was no significant change in the activity in cuttings from TH-7A, which was drilled after the shaft was filled with contaminated cement paste.

Gross-beta activity ranged from <1 to 3 pCi/g in cuttings from TH-7 (1968). Activity in cuttings from hole TH-7A (1969) indicated only one significant change; the sample from the interval 23.5 to 25.0 m contained gross-beta activity of 40 pCi/g. The activity was lower, by a factor of 10 or more, above and below that depth interval. This is attributed to the test hole intersecting an open joint connected to the shaft, which was filled with the cement paste from an adjoining shaft. Such cement-paste filled joints have been observed when other shafts have been drilled adjacent to shafts that were previously filled and capped.

III. MIGRATION OF FLUIDS AND PLUTONIUM FROM SLUDGE

A small volume, 2.9 × 10^3 ℓ, of $Fe(OH)_3$ sludge was used to study the movement of fluids and plutonium in the tuff. This study is also applicable in evaluating the containment of similar sludge (dewatered to 35% solids) that is packaged in 208-ℓ drums and stored or buried in disposal pits dug into the tuff.

A 60-cm-diam, 6.1-m-deep shaft was used for this study. Four test holes (X series), 12.2 m deep, were drilled adjacent to the shaft (Fig. 2). The fluid content and plutonium concentrations from the cuttings were determined as baseline data. The test holes were later used to monitor the movement of fluids for this study. The subsurface fluid measurements were made by neutron logging equipment prior to and after each disposal event. About nine months after the study began, three test holes (C-series) were cored to a depth of about 11 m to recover cores for analyses to evaluate the movement of plutonium from the sludge.

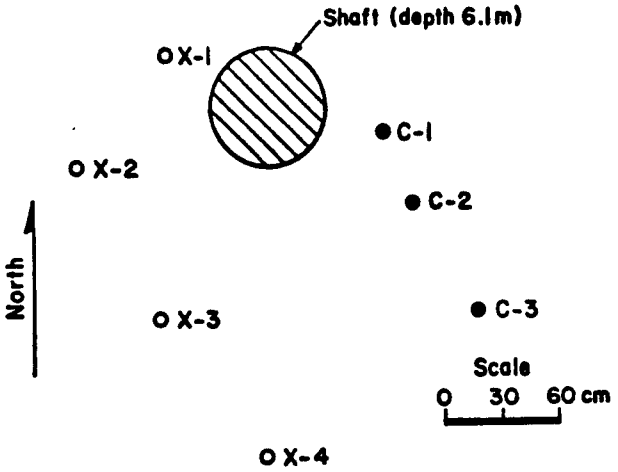

Fig. 2.
Plan view of shaft and test holes, X-series for monitoring fluid contents of tuff and C-series cored for plutonium data.

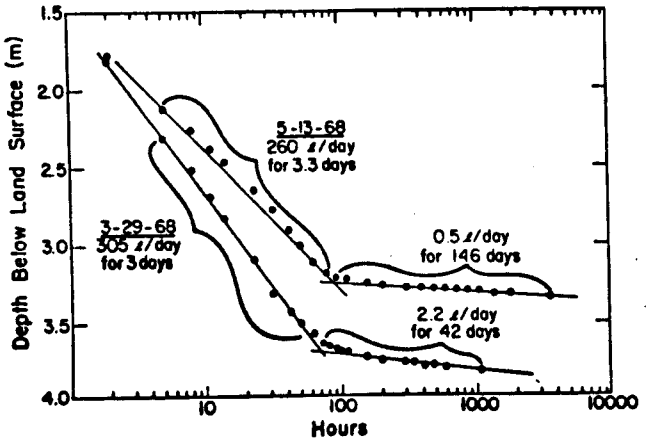

Fig. 3.
Fluid level declines in shaft receiving sludge on March 29 and May 13.

A. Movement of Fluids

About 1.5 × 10³ ℓ of sludge, with a fluid content of 82%, were pumped into the shaft on March 29, 1968. The rate of sludge-level decline, measured with a continuous water-stage recorder, was about 305 ℓ/day for the first three days and about 2.2 ℓ/day for the remaining 42 days (Fig. 3). Twenty-eight days after the study began, the fluids had moved outward from the shaft 1 m and downward about 2 m (Fig. 4). The maximum fluid content of the tuff, about 30 cm from the shaft, increased to about 12% by volume from a pretest measurement of 4 to 6% by volume.

An additional 1.4 × 10³ ℓ of sludge, with a fluid content of about 83%, were pumped into the shaft on May 13, 1968. The rate of sludge level decline was about 260 ℓ/day for 3.3 days, then sharply decreased to 0.5 ℓ/day for the remaining 146 days the recorder was in operation (Fig. 3). Seven days following the second release of sludge into the shaft, the fluids had moved outward from the shaft 1.5 m, while the downward movement remained at about 2 m. The fluid content of the tuff 30 cm from the shaft increased from about 12 to 16% by volume.

Fine particles in the sludge in the first release filled pore space in the tuff in the walls and the bottom of the shaft (Fig. 4). As a result, the fluid loss rate was slower during the second release and the accumulation of sludge at the bottom of the shaft caused the fluids to move horizontally from the shaft.

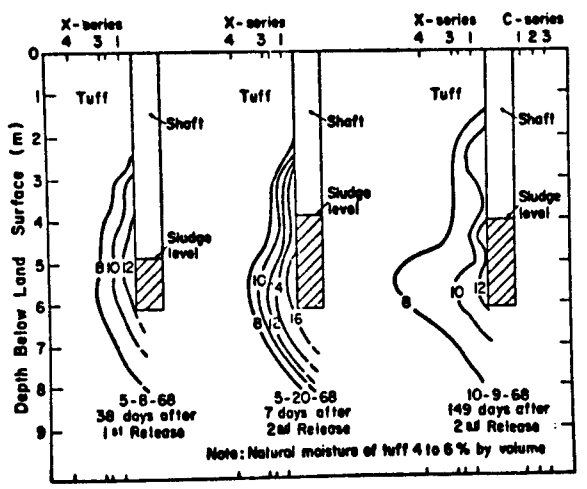

Fig. 4.
Cross section of shaft area showing isofluid contents (per cent by volume) in tuff.

About 150 days after the second release of sludge, the fluids had moved horizontally into the tuff more than 3 m. The vertical movement remained at about 2 m. The fluid content of the tuff about 30 cm from the shaft decreased from 16 to 12% by volume as the fluids were distributed to a greater distance from the shaft.

The porosity of the ashflow tuff ranges from 35 to 45% by volume, with fluid contents of less than 16%. Thus the tuff is not saturated and movement of fluid is under unsaturated conditions. Abrahams described the energy relationship of fluid to tuff

with an average porosity of 40% by volume.[7] The movement of fluids in the capillary size pores can be explained by one or more of the processes noted in Table I. The fluid content of the tuff near the shaft was 12% by volume after the initial release and increased to about 16% after the second release. The main movement processes in this fluid content range are capillarity and gravity. When the fluid content decreased below 10%, the major movement processes were diffusion and capillarity. The lack of vertical movement of fluids and the fluid content of the tuff during the initial period of the test indicated the major process of movement was by capillarity aided somewhat by gravity. During the later periods, the moisture content adjacent to the shaft decreased and the movement was mainly by diffusion and capillarity (Fig. 4).

The total volume of fluids in the tuff within the 8% contour on October 9, 1968, was estimated at 3.1 $\times 10^3$ ℓ, of which 1.6 $\times 10^3$ ℓ were fluids in the tuff prior to the study and 1.5 $\times 10^3$ ℓ were fluids that had moved into the tuff from the sludge (Fig. 3). The two releases of sludge contained about 2.9 $\times 10^3$ ℓ of fluids; thus the inventory accounts for about 60% of the fluids released. The remaining 40% of the fluids are retained in the shaft with the sludge or may have moved in the lower moisture range beyond the 8% contour. The major mechanism for transporting plutonium from the sludge was the fluid movement into the tuff.

B. Movement of Plutonium

Predisposal concentrations of ^{238}Pu and ^{239}Pu in the tuff were <0.02 pCi/g (analytical limits of detection) as determined from cuttings from the four X-series test holes (Fig. 2). The plutonium concentration in the 2.9 $\times 10^3$ ℓ of sludge pumped into the shaft was about 45 $\times 10^3$ pCi/ℓ, or about 1.3 $\times 10^{-4}$ Ci. About 90% of the plutonium was ^{239}Pu.

Cores analyzed from the C-series test holes, taken about seven months after the second release of sludge into the shaft, showed ^{238}Pu was detectable only in hole C-1, 30 cm from the shaft, at a depth of 4.6 to 5.5 m. The ^{239}Pu was detectable out to about 60 cm from the shaft at a depth of 5 to 5.5 m (Table II). The core from 1.8 to 2.1 m of hole C-1 contained 0.17 pCi/g of ^{239}Pu. However, this does not indicate differential movement between the ^{238}Pu and ^{239}Pu. The ^{239}Pu was detectable at greater distances from the shaft because of the larger amount of that isotope in the sludge.

The plutonium concentrations decreased outward from the shaft, following the same general pattern as the movement of fluids. The total plutonium (^{238}Pu and ^{239}Pu) in hole C-1 ranged from 0.33 to 1.52 pCi/g in the interval 4 to 5.5 m, where the fluid content of the tuff reached a maximum of 16% by volume on May 20, seven days after the second release (Fig. 5). The interval 4 to 5.5 m is opposite the sludge remaining in the shaft, which also may have contributed fine particles with attached plutonium that moved out with the fluids.

Measurable amounts of plutonium were found in about 1.3 m^3 of tuff adjacent to the shaft. The inventory in the tuff was estimated using two volumes (density of the tuff 1.47 g/cm^3) and two concentrations. The inner volume had an average concentration of 1.1 pCi/g and a mass of 9.8 $\times 10^5$ g (0.67 m^3), and the outer volume a concentration of 0.26 pCi/g and a mass of 9.3 $\times 10^5$ g (0.63 m^3). The amount of plutonium in the tuff was estimated at 1.1 $\times 10^{-6}$ Ci. Compared to the 1.3 $\times 10^{-4}$ Ci of plutonium contained in the $Fe(OH)_3$ sludge disposed in the shaft, the inventory indicates less than 1% of the plutonium moved from the shaft into the tuff.

The plutonium and sludge were probably retained by the tuff in part by the filtering of fine particles in the fluids by capillary size pores and in part by adsorption (ion exchange) in the tuff.

TABLE I

MOVEMENT PROCESSES AT VARIOUS FLUID CONTENTS IN TUFF

Movement Process	Fluid Content (% volume)	Tension (bars)
No apparent movements	<5	---
Diffusion & capillarity	5 ≃ 10	15.2
Capillarity & gravity	10 ≃ 22	0.34
Drainage by gravity	22 ≃ 39	---

IV. SUMMARY

The major transport mechanism for radionuclide migration from a sludge released into shafts in the tuff is by movement with fluids associated with the

TABLE II

PLUTONIUM ANALYSES FROM C-SERIES TEST HOLE NOVEMBER 1968

		Picocuries per Gram					
		^{238}Pu			^{239}Pu		
From	To	C-1	C-2	C-3	C-1	C-2	C-3
1.8	2.1	<0.02	<0.02	---	0.17	<0.02	---
2.7	3.0	0.04	0.02	---	<0.02	<0.02	---
3.4	3.7	0.06	---	<0.02	0.02	---	<0.02
4.0	4.3	0.05	<0.02	---	0.28	<0.02	---
4.6	4.9	0.15	<0.02	<0.02	0.86	<0.02	<0.02
5.2	5.5	0.12	<0.02	<0.02	1.4	0.06	<0.02
5.8	6.1	<0.02	<0.02	<0.02	0.06	<0.02	<0.02
6.4	6.7	<0.02	<0.02	<0.02	0.03	<0.02	<0.02
7.3	7.6	<0.02	<0.02	<0.02	<0.02	<0.02	<0.02
8.8	9.1	<0.02	<0.02	---	<0.02	<0.02	---
10.7	11.0	<0.02	---	---	<0.02	---	---

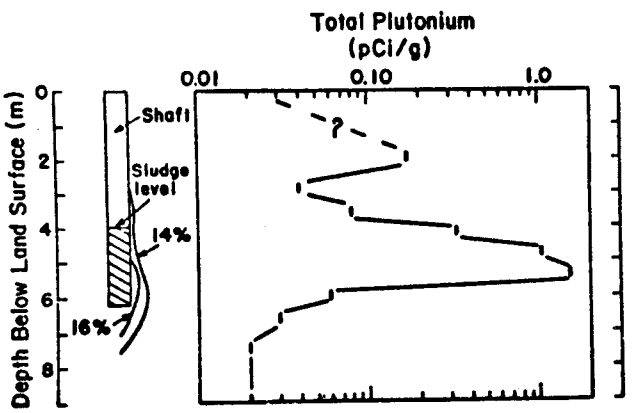

Fig. 5.
Cross section of shaft area showing maximum fluid content of tuff and sludge level in shaft in relation to total plutonium in cores from hole C-1.

wastes. Test holes drilled adjacent to a cement-paste filled shaft indicate no loss of fluids into the tuff from the hydration of the cement-paste mixture. Thus, movement or transport of contaminants is very unlikely because of the lack of fluids. Open joints in the tuff intersecting the shaft will allow early movement of the contaminated cement paste; however, upon hydration of the cement in the joint, this movement ceases.

The $Fe(OH)_3$ sludge released into a shaft during the study contained fluids that moved into the adjacent tuff, carrying some plutonium into the tuff with it. Trace amounts of ^{239}Pu were found about 60 cm from the shaft; however, the inventory indicates that 99% of the plutonium was retained in the sludge remaining in the shaft. Plutonium that moved with fluids in the tuff was probably retained by the filtering properties and adsorption (ion exchange) in the tuff.

REFERENCES

1. C. W. Christenson and L. A. Emelity, "Chemical Treatment and Cement Fixation of Radioactive Wastes," Jour. of Water Pollution Cont. Fed., Washington, D.C. (July 1970).

2. L. A. Emelity and C. W. Christenson, "Operational Practices in Treatment of Low- and Intermediate-Level Radioactive Wastes: Argonne and Los Alamos Laboratories, United States of America," in *Practices in the Treatment of Low- and Intermediate-Level Radioactive Wastes, International Atomic Energy Agency*, Vienna, Austria (1966).

3. R. L. Griggs, "Geology and Ground-Water Resources of the Los Alamos Area, New Mexico," U.S. Geol. Survey Water-Supply Paper 1753 (1964).

4. W. D. Purtymun and S. Johansen, "General Geohydrology of the Pajarito Plateau," New Mexico Geol. Soc. Guidebook, 25th Field Conf., Ghost Ranch, Central-Northern New Mexico (1974).

5. J. H. Abrahams, J. E. Weir, and W. D. Purtymun, "Distribution of Moisture in Soil and Near-Surface Tuff on the Pajarito Plateau, Los Alamos County, New Mexico," U.S. Geol. Survey Prof. Paper 424-D (1961).

6. W. D. Purtymun, "Underground Movement of Tritium from Solid-Waste Storage Shafts," Los Alamos Scientific Laboratory report LA-5286-MS (1973).

7. J. H. Abrahams, "Physical Properties and Movement of Water in the Bandelier Tuff, Los Alamos and Santa Fe Counties, New Mexico," U.S. Geol. Survey Admin. Rept., Albuquerque, New Mexico (1963).

Printed in the United States of America. Available from
National Technical Information Service
U.S. Department of Commerce
5285 Port Royal Road
Springfield, VA 22161

Microfiche $ 3.00

001-025	4.00	126-150	7.25	251-275	10.75	376-400	13.00	501-525	15.25
026-050	4.50	151-175	8.00	276-300	11.00	401-425	13.25	526-550	15.50
051-075	5.25	176-200	9.00	301-325	11.75	426-450	14.00	551-575	16.25
076-100	6.00	201-225	9.25	326-350	12.00	451-475	14.50	576-600	16.50
101-125	6.50	226-250	9.50	351-375	12.50	476-500	15.00	601-up	--1

1. Add $2.50 for each additional 100-page increment from 601 pages up.

New Mexico Geol. Soc. Guidebook, 25th Field Conf., Ghost Ranch (Central-Northern N.M.), 1974

GENERAL GEOHYDROLOGY OF THE PAJARITO PLATEAU

by

WILLIAM D. PURTYMUN and STEVEN JOHANSEN
Environmental Studies Group
University of California
Los Alamos Scientific Laboratory
Los Alamos, New Mexico

INTRODUCTION

The Pajarito Plateau, twenty miles northwest of Santa Fe in north-central New Mexico, forms an apron of volcanic and sedimentary rocks around the eastern flanks of the Jemez Mountains (Fig. 1). The plateau slopes gently eastward from the mountains toward the Rio Grande where it terminates in steep slopes and cliffs formed by down cutting of the river. It is dissected into a number of narrow mesas by south-eastward trending intermittent streams.

The main aquifer lies at depth of 600 to 1200 ft beneath the surface of the plateau in rocks of the Santa Fe Group. This is the only aquifer in the area capable of municipal and industrial water supply.

GEOLOGY

The plateau is formed by rocks of the Santa Fe Group of middle(?) Miocene to Pleistocene(?) age, and volcanic rocks of Pliocene and Pleistocene age (Griggs, 1964). The Santa Fe Group comprises the Tesuque and the Puye Formations and the basaltic rocks of Chino Mesa. These formations crop out along the eastern margin of the Pajarito Plateau.

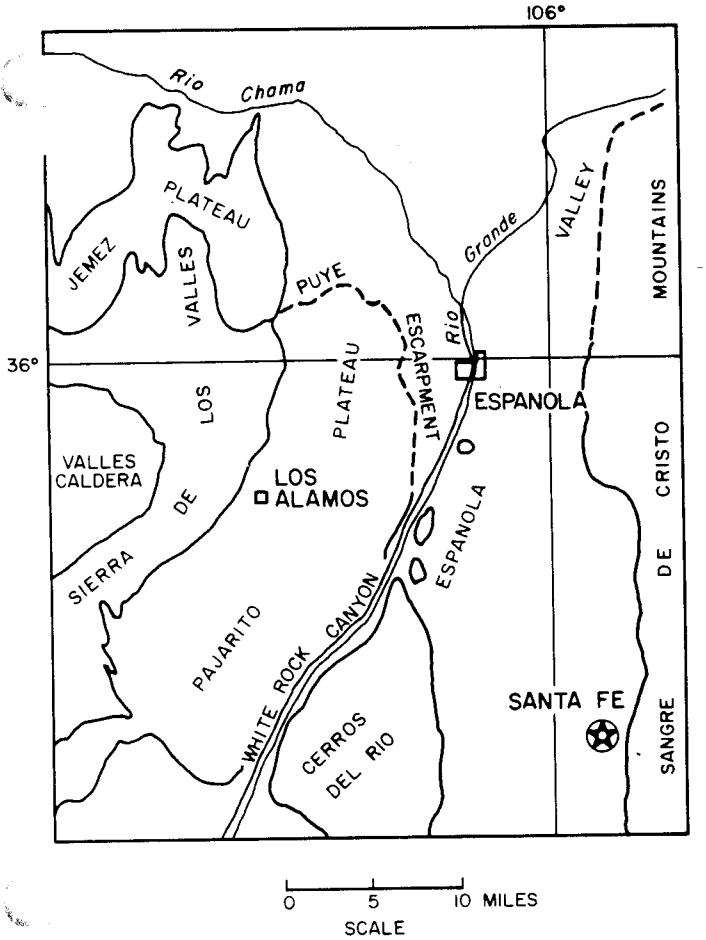

Figure 1. Geographic features in the vicinity of the Pajarito Plateau.

The Tesuque Formation consists of friable to moderately well cemented light-pinkish-gray to light-brown siltstone and sandstone that contains lenses of conglomerate and clay. Some basalt flows are interbedded in the unit. The sedimentary rocks were derived from two sources. The lower part of the formation consists principally of fine arkosic quartz sand derived from source areas east of the Rio Grande. The upper part consists of very coarse arkosic quartz sand, latitic gravels, and volcanic detritus, derived from sources both east and west of the Rio Grande (Griggs, 1964).

The Puye Formation is a poorly consolidated conglomerate channel-fill deposit overlain by a fanglomerate composed of volcanic debris. The channel-fill deposits are gray and consist of fragments of quartzite, schist, gneiss, and granite, ranging in size from sand to boulder. The fanglomerate is generally gray and consists of pebbles and cobbles of rhyolite, latite, quartz-latite, and pumice, in a matrix of silt and sand. Sorting is poor, but lenses of fairly well sorted pumiceous siltstone and water-laid pumice are present within the fanglomerate. The rocks were derived from flows associated with the volcanic rocks of the Jemez Mountains.

Basaltic rocks of Chino Mesa consist of basalt and basalt breccia that overlie the Puye Formation along the Rio Grande and interfinger with the conglomerate to the west beneath the Pajarito Plateau (Fig. 2). The basalt, which thickens southward along the river and thins westward, originated from volcanic vents near Chino Mesa (Fig. 1).

Major volcanic units in the area are the Tschicoma Formation of Pliocene age and the Bandelier Tuff of Pleistocene age.

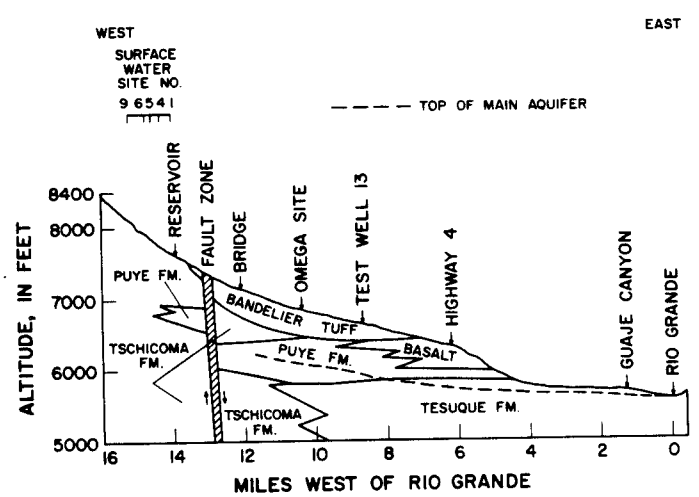

Figure 2. East-west geologic section through the Pajarito Plateau.

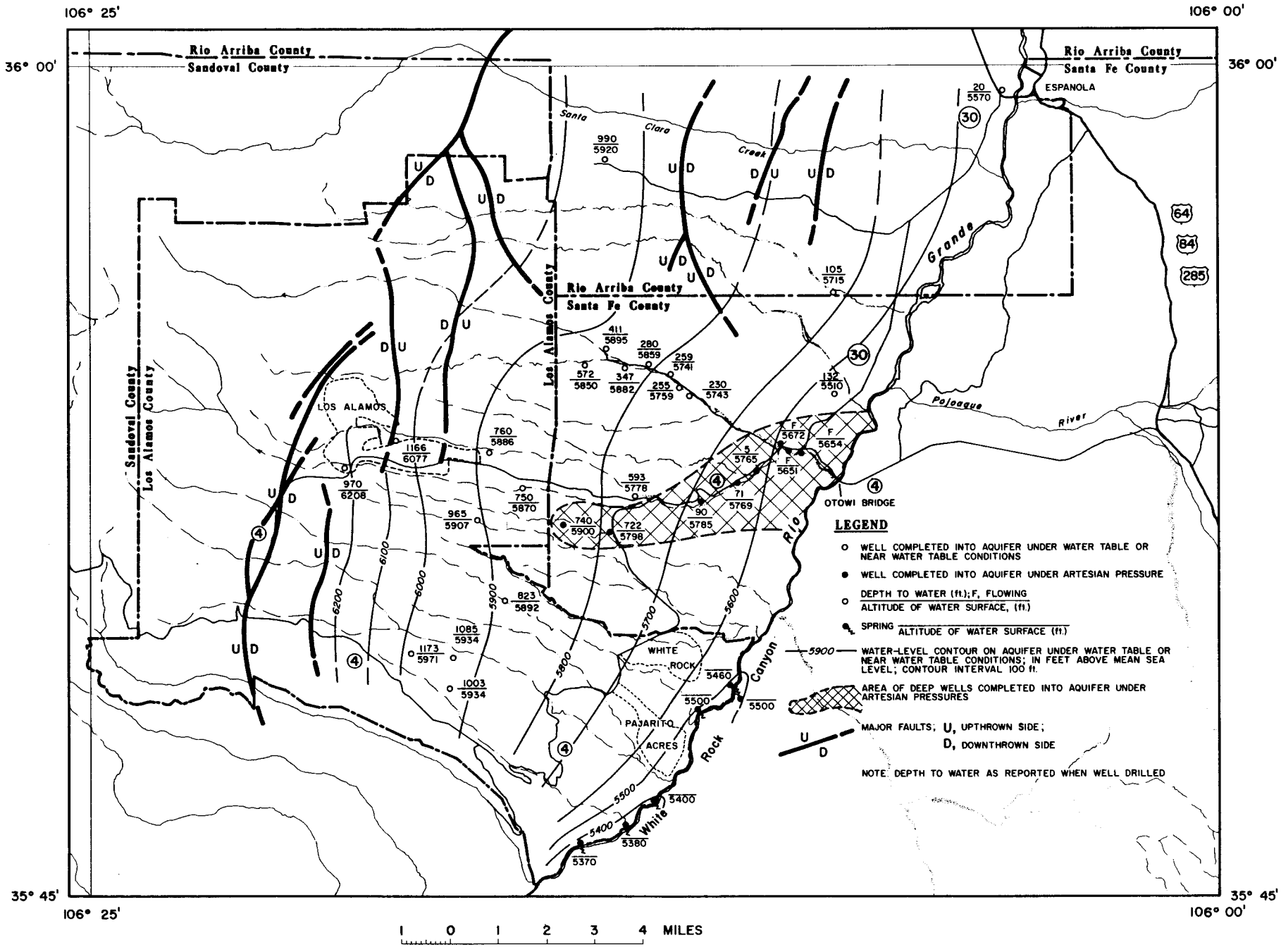

Figure 3. Generalized urs on top of main aquifer.

The Tschicoma Formation forms the mountains of the Sierra de los Valles, and is present in the subsurface beneath the tern edge of the plateau (Fig. 2). It was extruded through overlies the Tesuque Formation. The Tschicoma volcanics composed of latite, quartz-latite flows, and pyroclastic rocks. The Tschicoma Formation is overlain by the Bandelier Tuff along the flanks of the mountains. The Bandelier Tuff, a series of ash flows and ash falls of rhyolitic tuff, caps the Pajarito Plateau and unconformably overlies the Puye Formation and basaltic rocks of Chino Mesa in the central and eastern parts of the plateau.

The Tschicoma Formation, the Bandelier Tuff and basaltic rocks of Chino Mesa contain only small amounts of water which are perched above the main aquifer. The main aquifer is in the lower part of the Puye Formation and Tesuque Formation in the western and central part of the plateau and within the Tesuque Formation along the eastern edge of the plateau.

HYDROLOGY

The upper surface of the main aquifer rises westward from the Rio Grande through the Tesuque into the lower part of the Puye Formation beneath the central and western parts of the plateau (Fig. 2). The water in the aquifer moves from the major recharge area in the Valles Caldera eastward toward the Rio Grande where a part is discharged into the river through seeps and springs (Fig. 3).

The major recharge area for the aquifer is the intermountain basins formed by the Valles Caldera. The upper parts of the sediments in the basins are lacustrine deposits of clay, sand, gravels (Conover and others, 1963), which are underlain volcanic debris resulting from the collapse of the caldera. ments and volcanics in the basin are highly permeable and are saturated. The basin fill material recharges the main aquifer in sediments of the Tesuque Formation.

Minor amounts of recharge may occur in the deep canyons containing perennial streams on the flanks of the mountains. The intermittent streams in canyons which are cut into the plateau add little if any recharge to the main aquifer.

Gradient on the surface of the aquifer averages about 60 feet per mile beneath the plateau in the Puye Formation with the depth to water decreasing along with the gentle slope of the surface of the plateau from about 1200 feet to the west to about 600 feet to the east. The gradient of the aquifer steepens to about 100 feet per mile along the eastern edge of the plateau as the water in the aquifer moves into the less permeable sediments of the Tesuque Formation. The aquifer is under water table conditions in the western margin of the plateau and is artesian along the eastern edge and along the Rio Grande (Fig. 3).

The Rio Grande is the principal area for ground water discharge from the main aquifer. A gain in stream flow of the river as it passes through White Rock Canyon was first described by Spiegel and Baldwin (1963). Cushman (1965) estimated that the 11.5 mile reach of the canyon below Otowi Bridge receives a discharge from the main aquifer of 4300 to 5500 acre-feet annually.

The first water-supply wells for Los Alamos municipal and industrial supply were developed along the eastern edge of Pajarito Plateau in 1947. These wells are completed in the main aquifer and consist of six wells in the Los Alamos Canyon field and seven wells in the Guaje Canyon field. Well depth ranges from 870 to 2000 feet (Purtymun and Herceg, 1972).

Aquifer tests of wells located in the eastern well field, which penetrate about 1600 feet of the fine grained sediments of the Tesuque Formation, indicate an average coefficient of transmissibility of 20,000 g/d/ft of the aquifer (Cushman, 1965). These wells yield an average of 500 gpm with a specific capacity of 8 gpm/ft of drawdown.

The partial saturation of the coarse volcanic debris of the Puye Formation and coarse volcanic debris and arkosic sands of the Tesuque Formation has also led to the development of high yield wells for municipal and industrial supply in the central part of the Pajarito Plateau (Purtymun and Cooper, 1969). Three wells in the Pajarito field were developed from 1965 through 1968. These wells range in depth from 2300 to 2550 feet. The three wells have produced more than 40 percent of the 4700 acre-feet of water used at Los Alamos since 1968.

Aquifer tests of wells on the plateau indicate a coefficient of transmissibility range from 40,000 to 320,000 g/d/ft of the aquifer which includes an average of 250 feet of Puye Formation and 1550 feet of the Tesuque Formation. High yield wells in this area average 1000 gpm with a specific capacity of about 35 gpm/ft of drawdown.

The chemical quality of water may vary within the well fields due to local conditions within the aquifer. In general the quality of water is good; total dissolved solids range from about 200 mg/1 to less than 500 mg/1. Silica concentrations range from 35 to 80 mg/1 while total hardness (as $CaCO_3$) ranges from 25 to 100 mg/1.

REFERENCES

Conover, C. S., C. V. Theis, and R. L. Grieggs, 1963, Geology and hydrology of the Valle Grande and Valle Toledo, Sandoval County, New Mexico: U.S. Geol. Survey Water-Supply Paper 1619-Y.

Cushman, R. L., 1965, An Evaluation of aquifer and well characteristics of municipal well fields in Los Alamos and Guaje Canyons, near Los Alamos, New Mexico: U.S. Geol. Survey Water-Supply Paper 1809-D.

Griggs, R. L., 1964, Geology and ground-water resources of the Los Alamos Area, New Mexico: U.S. Geol. Survey Water-Supply Paper 1753.

Purtymun, W. D., and J. B. Cooper, 1969, Development of ground-water supplies on the Pajarito Plateau, Los Alamos County, New Mexico: U.S. Geol. Survey Prof. Paper 650-B.

Purtymun, W. D., and J. E. Herceg, 1972, Summary of Los Alamos municipal well-field characteristics, 1947-1971: Los Alamos Scientific Laboratory report LA-5040-MS.

Spiegel, Zane, and Brewster Baldwin, 1963, Geology and water resources of the Santa Fe Area, New Mexico: U.S. Geol. Survey Water-Supply Paper 1525.

UNITED STATES
DEPARTMENT OF THE INTERIOR
GEOLOGICAL SURVEY
Albuquerque, New Mexico

Distribution of moisture and radioactivity in the soil and tuff at the contaminated waste pit near Technical Area 21, Los Alamos, New Mexico

By

William D. Purtymun and William R. Kennedy[1/]

Prepared in cooperation with the U S. Atomic Energy Commission and the Los Alamos Scientific Laboratory, Los Alamos, New Mexico

November 1966

[1/] Group Leader H-6, Los Alamos Scientific Laboratory

Contents

	Page
Abstract	7
Introduction	8
Description of soil and tuff	38
Distribution of moisture in soil and tuff	40
Distribution of radioactivity in soil and tuff	42
Conclusions	45
References	46

Illustrations

Page

Figure 1.--Map of the Los Alamos area showing location of contaminated waste pit---------- 9

2.--Map of contamination waste pit near Technical Area 21 (DP-West) showing locations of test holes---------- 10

3.--Log and moisture content of soil and tuff in test hole DPS-1---------- 12

4.--Log and moisture content of soil and tuff in test hole DPS-2---------- 13

5.--Log and moisture content of soil and tuff in test hole DPS-3---------- 14

6.--Log and moisture content of soil and tuff in test hole DPS-4---------- 15

7.--Log and moisture content of soil and tuff in test hole DPS-5---------- 16

8.--Log and moisture content of soil and tuff in test hole DPS-6---------- 17

9.--Log and moisture content of soil and tuff in test hole DPS-7---------- 18

10.--Log and moisture content of soil and tuff in test hole DPS-8---------- 19

11.--Log and moisture content of soil and tuff in test hole DPS-9---------- 20

12.--Log and moisture content of soil and tuff in test hole DPS-10---------- 21

Illustrations - Concluded

Page

Figure 13.--Log and moisture content of soil and tuff in test hole DPS-11 ---------- 22

14.--Log and moisture content of soil and tuff in test hole DPS-12 ---------- 23

15.--Log and moisture content of soil and tuff in test hole DPS-13 ---------- 24

Tables

Page

Table 1.--Radiochemical analyses of soil and tuff from test hole DPS-1 ---------- 25

2.--Radiochemical analyses of soil and tuff from test hole DPS-2 ---------- 26

3.--Radiochemical analyses of soil and tuff from test hole DPS-3 ---------- 27

4.--Radiochemical analyses of soil and tuff from test hole DPS-4 ---------- 28

5.--Radiochemical analyses of soil and tuff from test hole DPS-5 ---------- 29

6.--Radiochemical analyses of soil and tuff from test hole DPS-6 ---------- 30

7.--Radiochemical analyses of soil and tuff from test hole DPS-7 ---------- 31

8.--Radiochemical analyses of soil and tuff from test hole DPS-8 ---------- 32

9.--Radiochemical analyses of soil and tuff from test hole DPS-9 ---------- 33

10.--Radiochemical analyses of soil and tuff from test hole DPS-10 ---------- 34

11.--Radiochemical analyses of soil and tuff from test hole DPS-11 ---------- 35

12.--Radiochemical analyses of soil and tuff from test hole DPS-12 ---------- 36

Tables - Concluded

Page

Table 13.--Radiochemical analyses of soil and tuff from test hole DPS-13---------- 37

14.--The range of gross alpha and gross beta radioactivities of soil and tuff---------- 43

Distribution of moisture and radioactivity
in the soil and tuff at the contaminated
waste pit near Technical Area 21,
Los Alamos, New Mexico

By

William D. Purtymun and William R. Kennedy[1/]

Abstract

The contaminated waste pit near Technical Area 21 was investigated to determine if waterborne radioactive contaminants had migrated from the pit into the adjacent soil and tuff. Thirteen test holes, ranging in depth from 25 to 50 feet, were drilled through the soil into the underlying tuff in the vicinity of the waste pit. No holes were drilled through the base of the pit as only the surface of the pit and adjacent land is considered for commercial use. The distribution of moisture in the soil and tuff penetrated by the test holes was determined by a neutron-scattering moisture probe. Samples of drill cuttings of the soil and tuff were analyzed for gross alpha and gross beta-gamma radioactivities, and plutonium and uranium.

The moisture content of the tuff adjacent to the test holes indicated that the tuff was not saturated. Radiochemical analyses of soil and tuff indicated no radioactive contamination.

[1/] Group Leader H-6, Los Alamos Scientific Laboratory

Introduction

The laboratories and test areas of the Los Alamos Scientific Laboratory are on the Pajarito Plateau in north-central New Mexico. The Pajarito Plateau, formed by a series of ashflow and ashfall tuff, is dissected into a number of finger-like mesas that slope eastward from the Sierra de los Valles toward the Rio Grande (fig. 1). Solid wastes, impregnated with or containing radioactive contamination, and sludges and some liquids that contain radioactive particles are buried in pits dug into the surface of these mesas.

One of the oldest contaminated waste pits is located near Technical Area 21 (DP-West). Between 1945 and 1947 the pit was filled with wastes containing mostly alpha radioactive contaminants.

The area of the waste pit is about 250,000 square feet; the original depth was about 20 feet. The present surface of the filled-in pit area is irregular. Drainage is to the south and grasses and oak shrubs grow in the fill material. Around the pit the surface of the mesa slopes gently to the south towards a small canyon which has nearly vertical walls (fig. 2). This canyon is confluent with Los Alamos Canyon a short distance downgradient from the disposal pit. At the confluence the floor of Los Alamos Canyon is about 400 feet below the surface of the mesa.

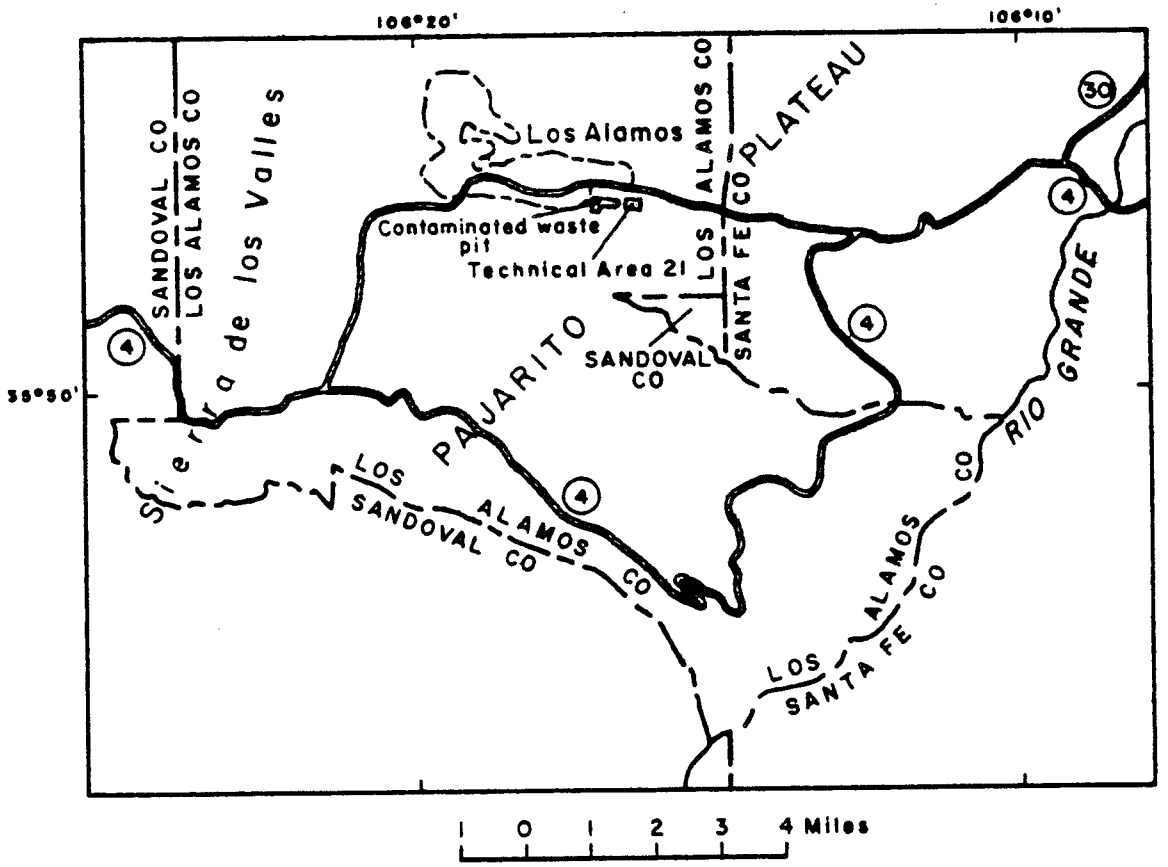

Figure 1.--Map of the Los Alamos area showing location of contaminated waste pit.

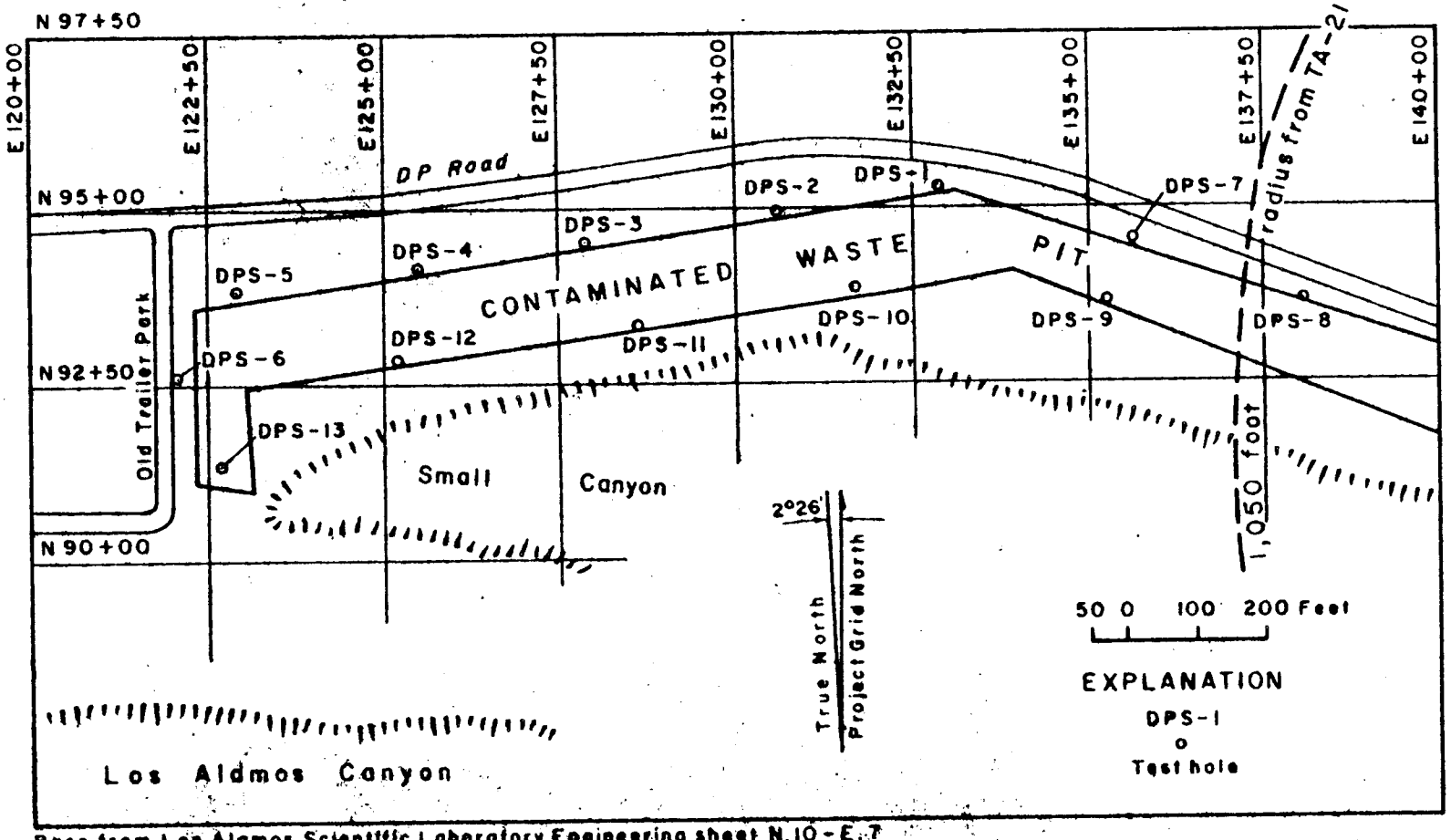

Base from Los Alamos Scientific Laboratory Engineering sheet N.10-E.7

Figure 2.--Map of contamination waste pit near Technical Area 21 (DP-West) showing locations of test holes.

Expansion of laboratory facilities and increased growth of the community of Los Alamos has caused a re-evaluation of present land use to determine if the land is being utilized in the best possible way. It was proposed by the Los Alamos Scientific Laboratory and the U.S. Atomic Energy Commission that a part of the filled-in contaminated waste pit, outside the radius of 1,050 feet from TA-21 (an area approved for commercial property), be leveled, filled where necessary, and sealed with asphalt, and used for a storage area for trailers and boats. Also, the land adjacent to the pit could be utilized for commercial use.

A joint study, requested by the Engineering Division, LASL, and the Construction and Maintenance Branch, AEC, was made by Group H-6 of the Los Alamos Scientific Laboratory and the Water Resources Division of the U.S. Geological Survey to determine if seepage of water from precipitation had caused migration of radioactive contaminants from the pit into the adjacent soil and tuff. The study was confined to an area slightly within and considerably beyond a radius of 1,050 feet from Technical Area 21 (fig. 2)--an area approved for commercial property.

Thirteen test holes ranging in depth from 25 to 50 feet were drilled in the vicinity of the outer edges of the waste pit (fig. 2). The log and moisture content of the soil and tuff penetrated by the test holes are shown in figures 3 through 15. Samples of soil and tuff were collected during drilling of the holes and were analyzed by Group H-6 for radioactive contamination. The results of these analyses are shown on tables 1 through 13.

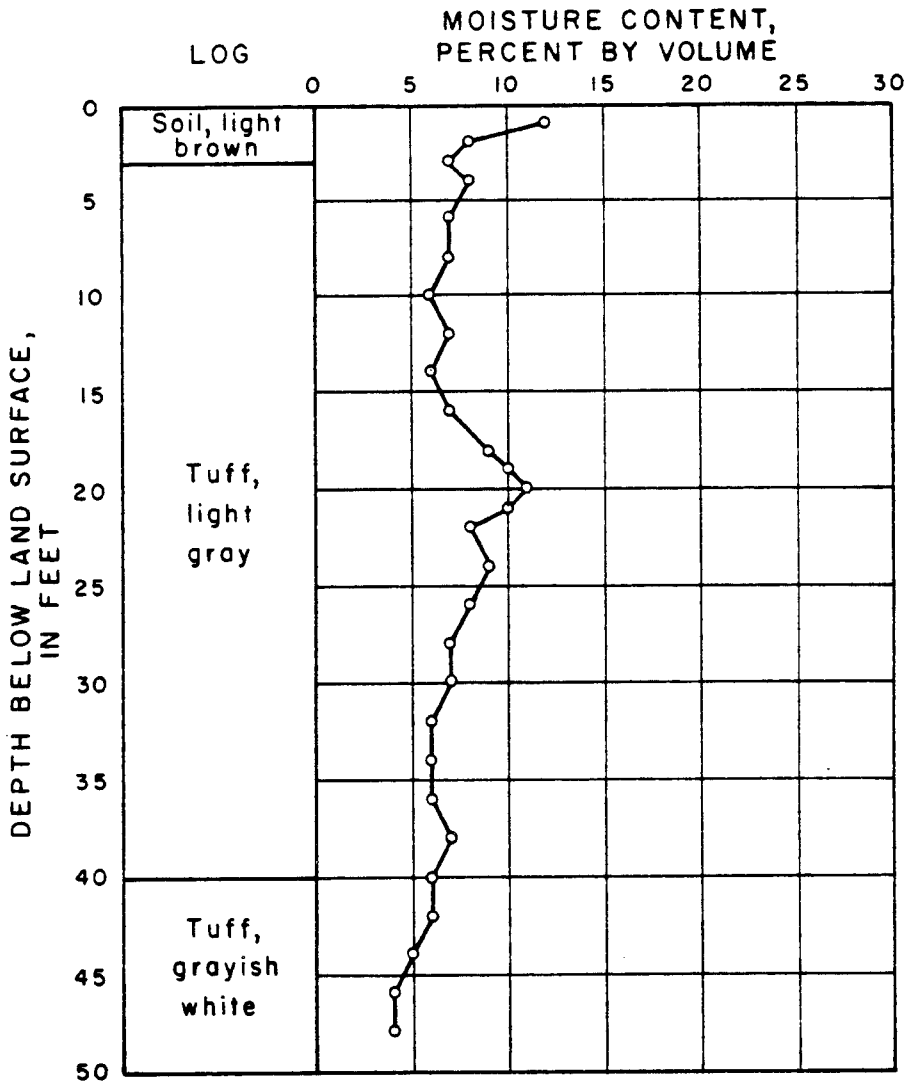

Location: Project grid, N95 + 13, E132 + 97
Date drilled: 2-7-66
Altitude: 7,190 feet above mean sea level
Depth: 50 feet
Diameter: 4-inches

Figure 3.--Log and moisture content of soil and tuff in test hole DPS-1

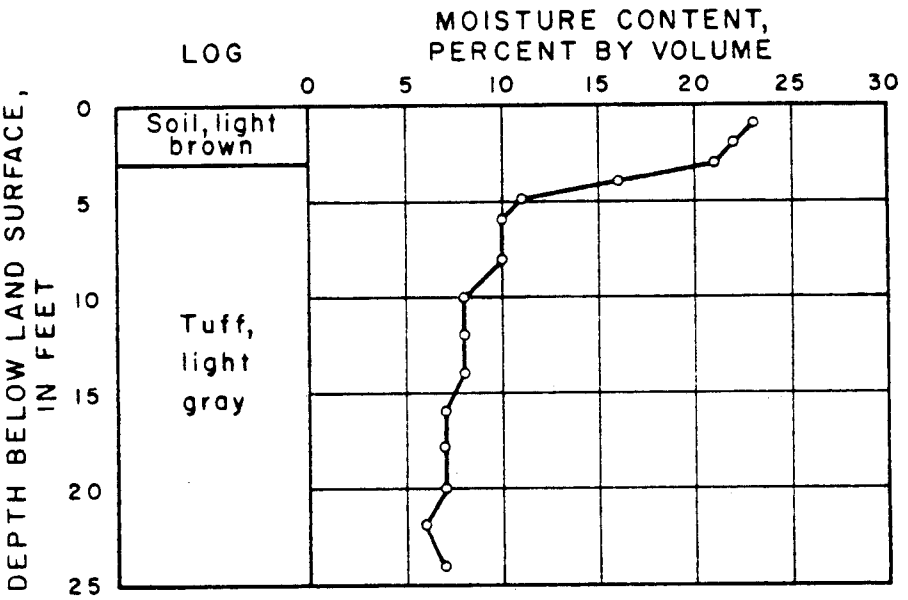

Location: Project grid, N94 + 78, E130 + 56
Date drilled: 2-7-66
Altitude: 7,191 feet above mean sea level
Depth: 25 feet
Diameter: 4-inches

Figure 4.--Log and moisture content of soil and tuff in test hole DPS-2

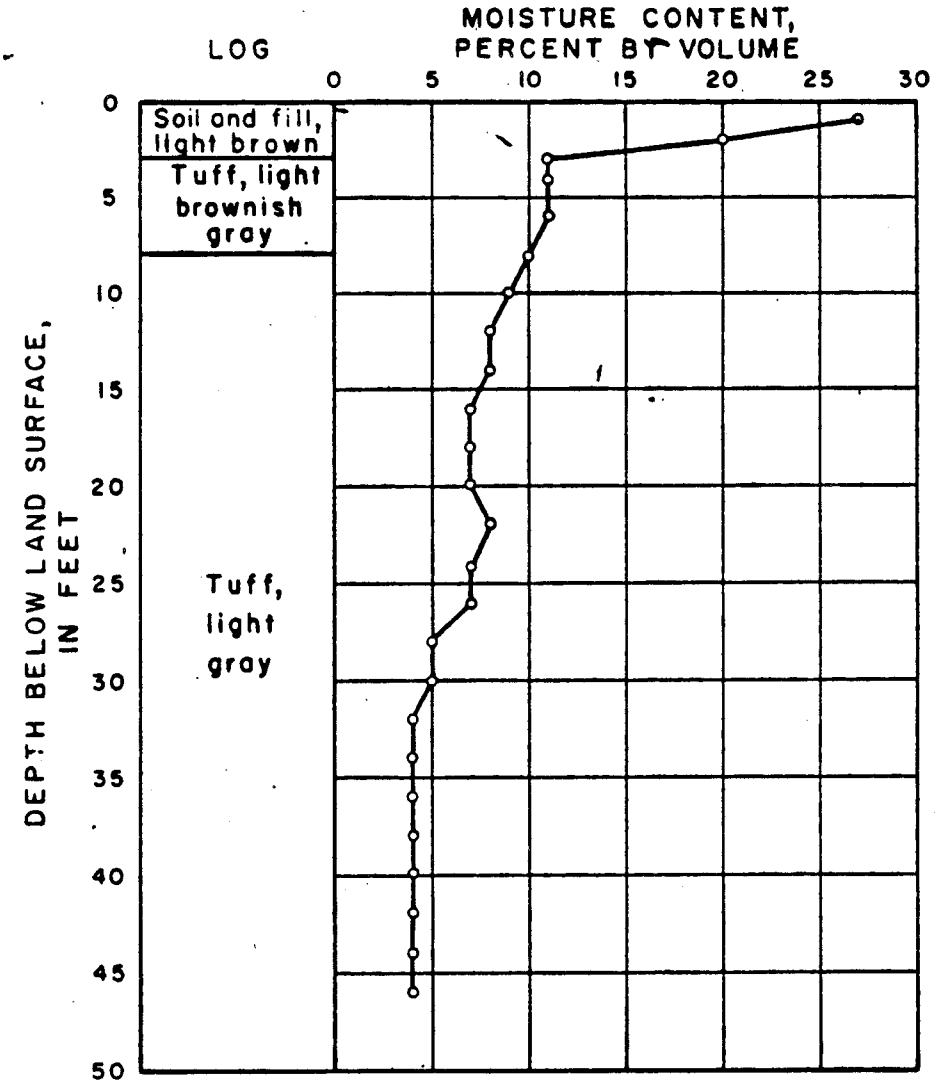

Location: Project grid, N94 + 43, E127 + 87
Date drilled: 2-7-66
Altitude: 7,194 feet above mean sea level
Depth: 50 feet
Diameter: 4-inches

Figure 5.--Log and moisture content of soil and tuff in test hole DPS-3

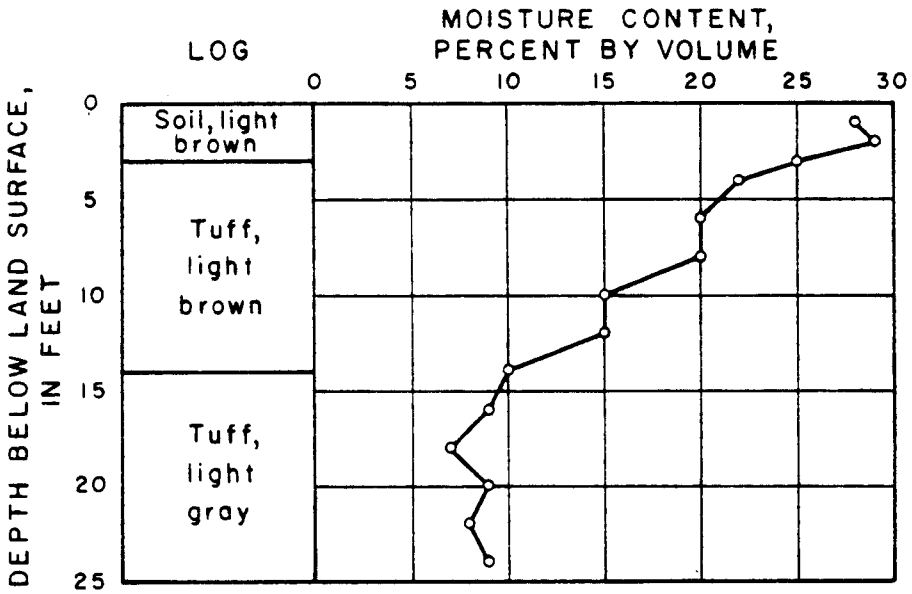

Location: Project grid, N94 + 16, E125 + 89
Date drilled: 2-7-66
Altitude: 7,202 feet above mean sea level
Depth: 25 feet
Diameter: 4-inches

Figure 6.--Log and moisture content of soil and tuff in test hole DPS-4

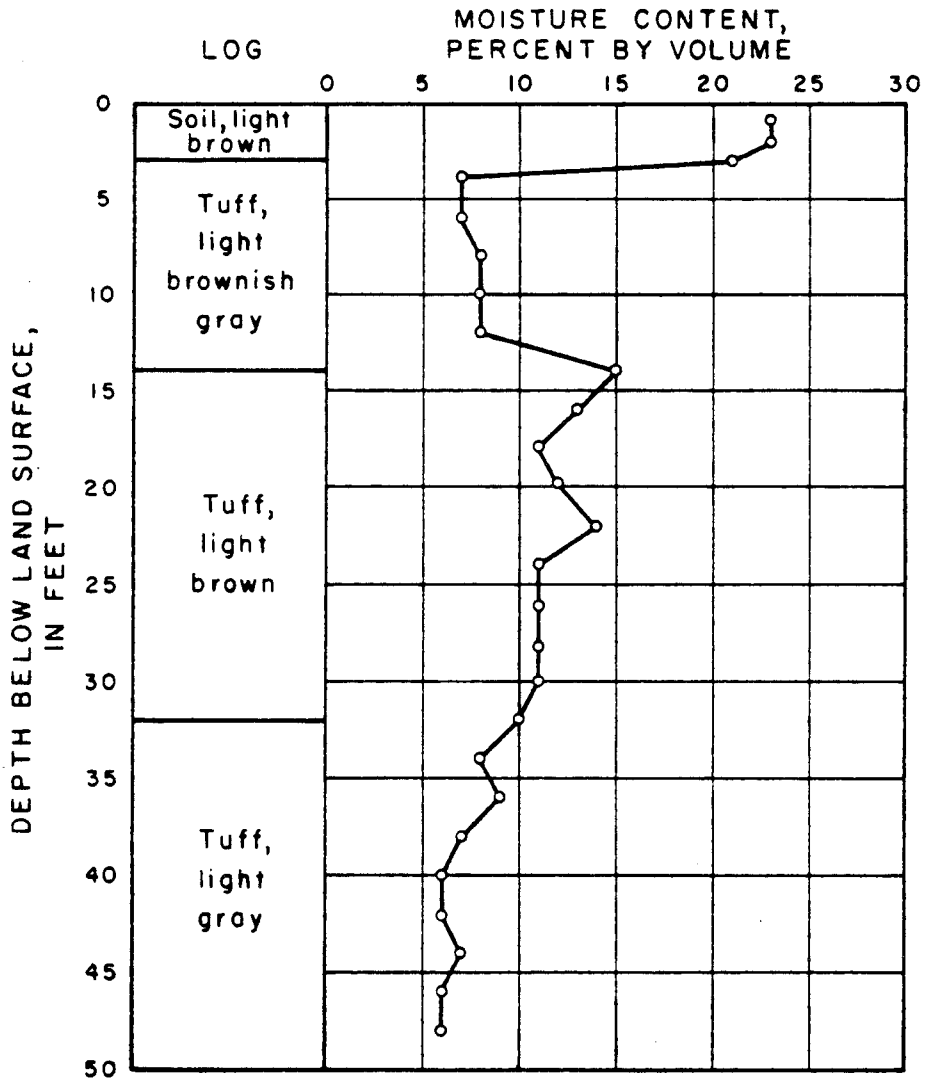

Location: Project grid, N93 + 80; E122 + 85
Date drilled: 2-7-66
Altitude: 7,214 feet above mean sea level
Depth: 50 feet
Diameter: 4-inches

Figure 7.--Log and moisture content of soil and tuff in test hole DPS-5

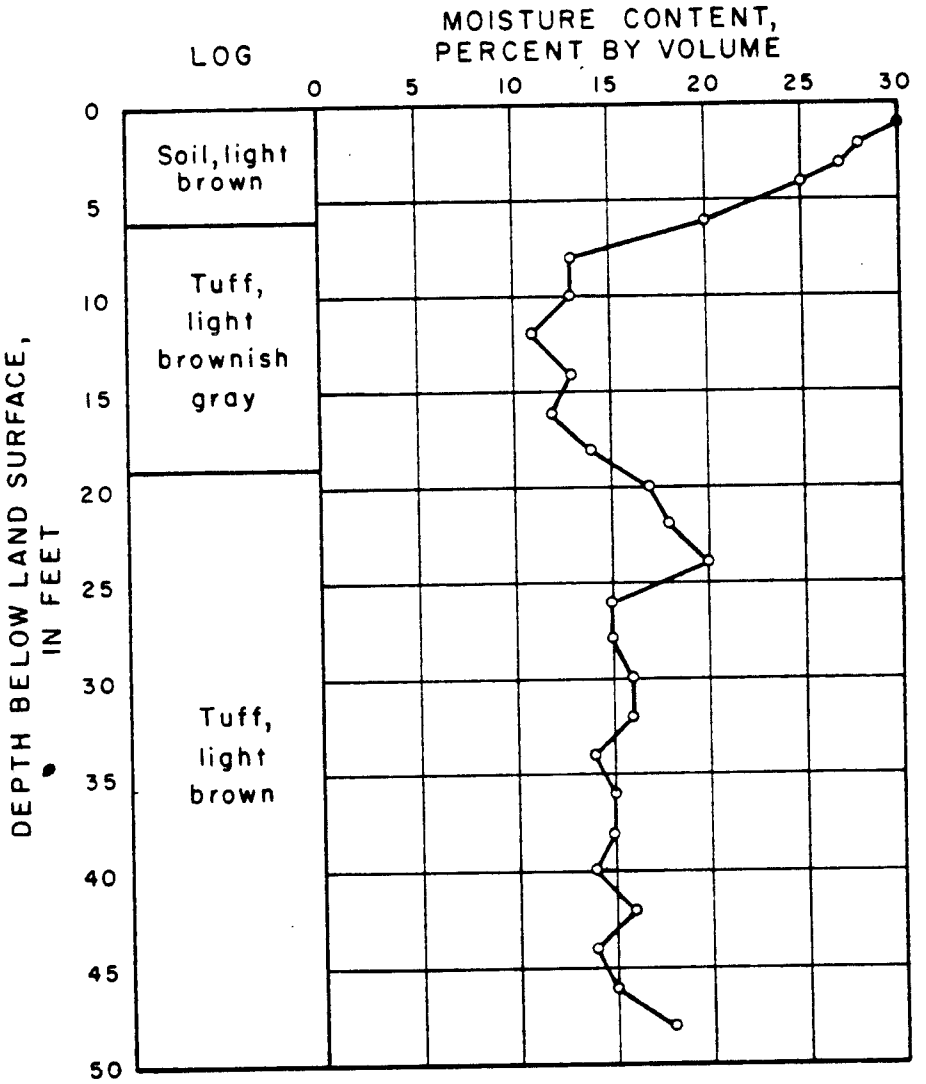

Location: Project grid, N92 + 58, E122 + 10
Date drilled: 2-8-66
Altitude: 7,216 feet above mean sea level
Depth: 50 feet
Diameter: 4-inches

Figure 8.--Log and moisture content of soil and tuff in test hole DPS-6

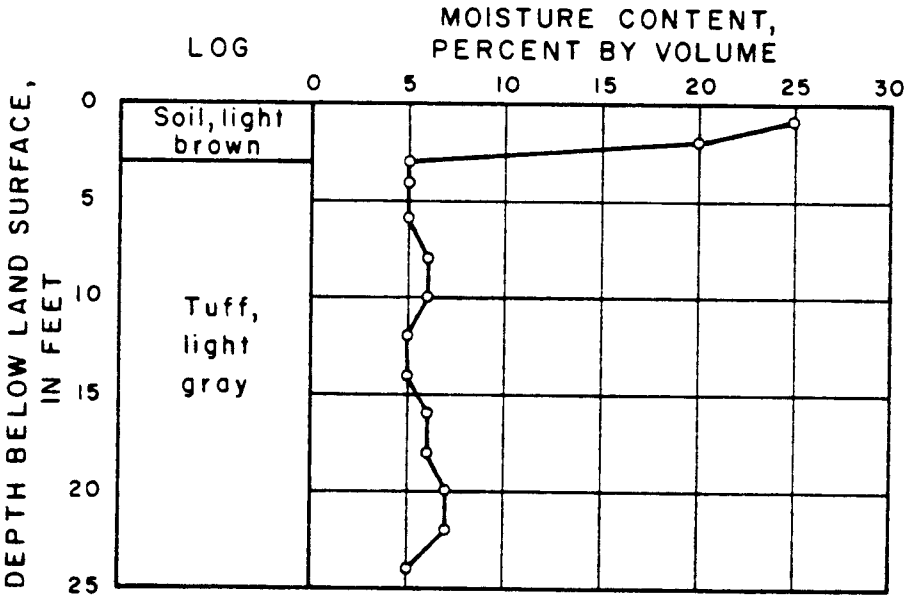

Location: Project grid, N94 + 41, E135 + 69
Date drilled: 2-8-66
Altitude: 7,185 feet above mean sea level
Depth: 25 feet
Diameter: 4-inches

Figure 9.--Log and moisture content of soil and tuff in test hole DPS-7

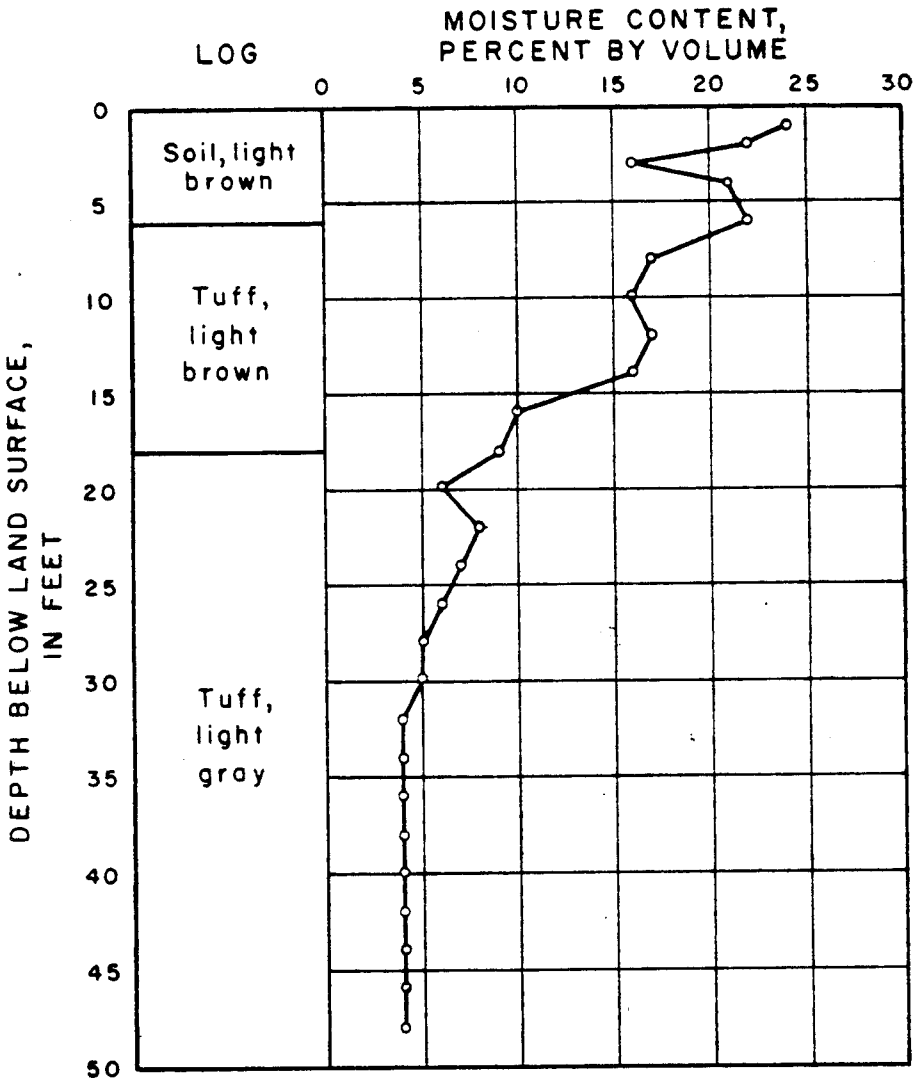

Location: Project grid, N93 + 66, E138 + 06
Date drilled: 2-8-66
Altitude: 7,181 feet above mean sea level
Depth: 50 feet
Diameter: 4-inches

Figure 10--Log and moisture content of soil and tuff in test hole DPS-8

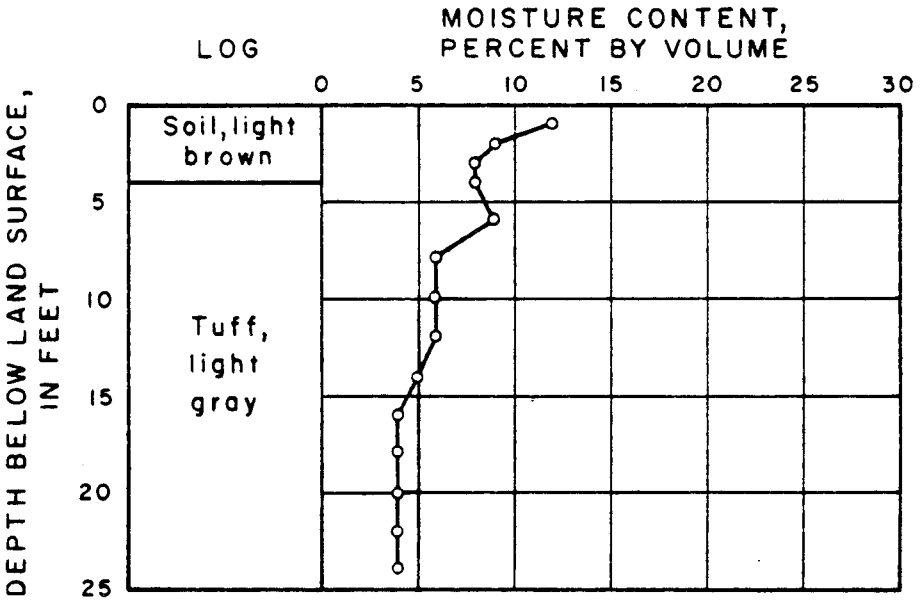

Location: Project grid, N93 + 57, E135 + 19
Date drilled: 2-9-66
Altitude: 7,180 feet above mean sea level
Depth: 25 feet
Diameter: 4-inches

Figure 11.--Log and moisture content of soil and tuff in test hole DPS-9

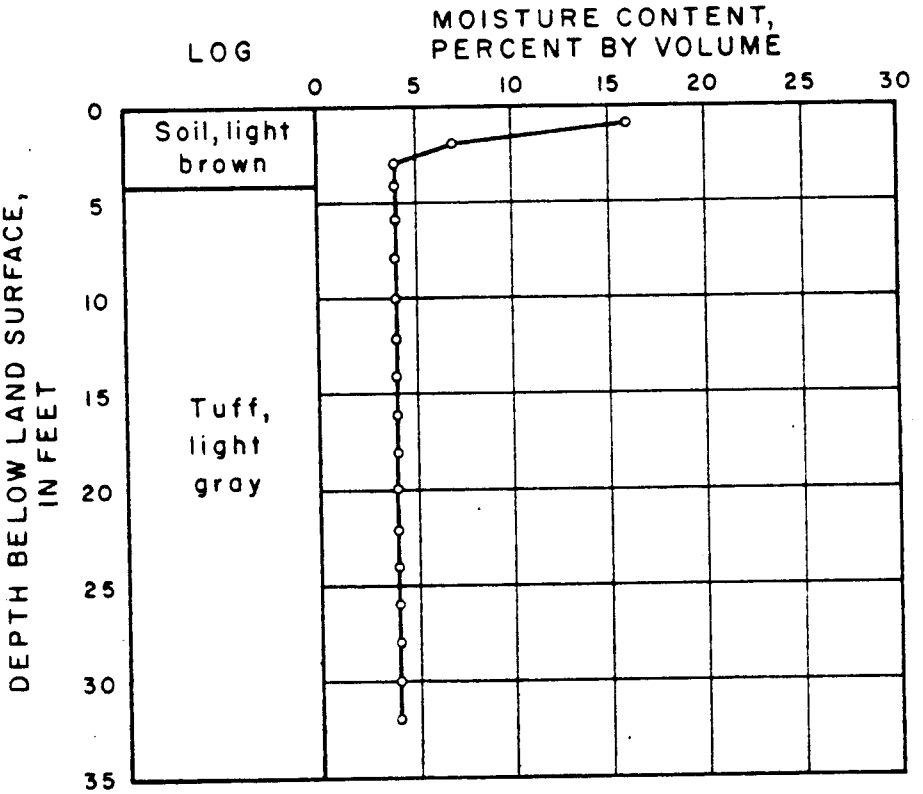

Location: Project grid, N93 + 66, E131 + 55
Date drilled: 2-9-66
Altitude: 7,182 feet above mean sea level
Depth: 35 feet
Diameter: 4-inches

Figure 12.--Log and moisture content of soil and tuff in test hole DPS-10

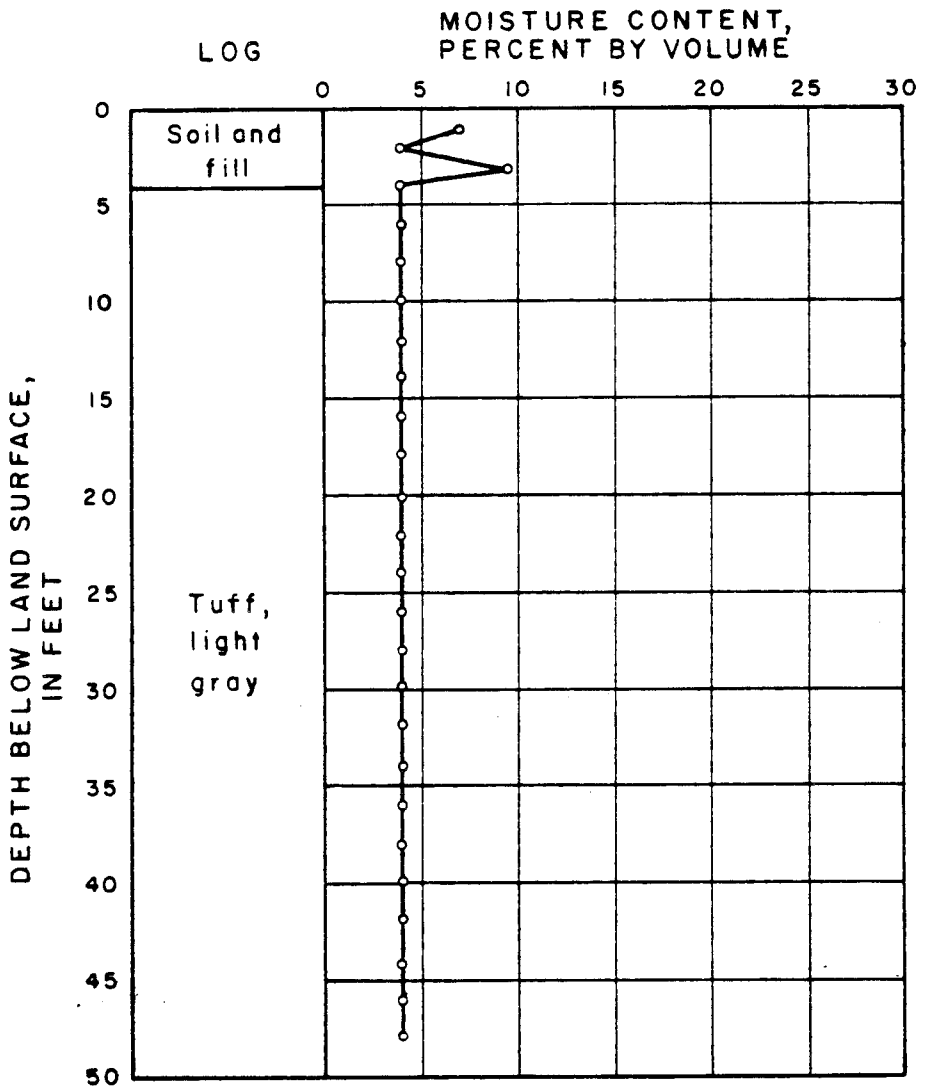

Location: Project grid, N93 + 21, E128 + 51
Date drilled: 2-9-66
Altitude: 7,192 feet above mean sea level
Depth: 50 feet
Diameter: 4-inches

Figure 13.--Log and moisture content of soil and tuff in test hole DPS-11

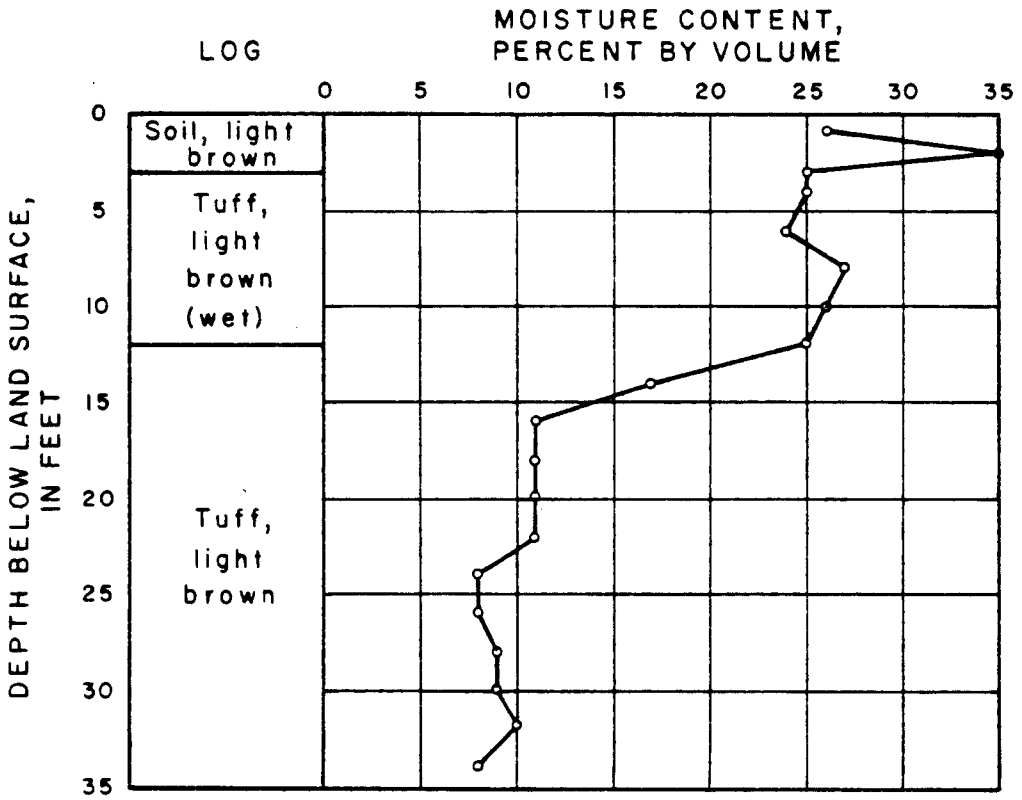

Location: Project grid, N92 + 79, E125 + 21
Date drilled: 2-9-66
Altitude: 7,192 feet above mean sea level
Depth: 36 feet
Diameter: 4-inches

Figure 14.--Log and moisture content of soil and tuff in test hole DPS-12

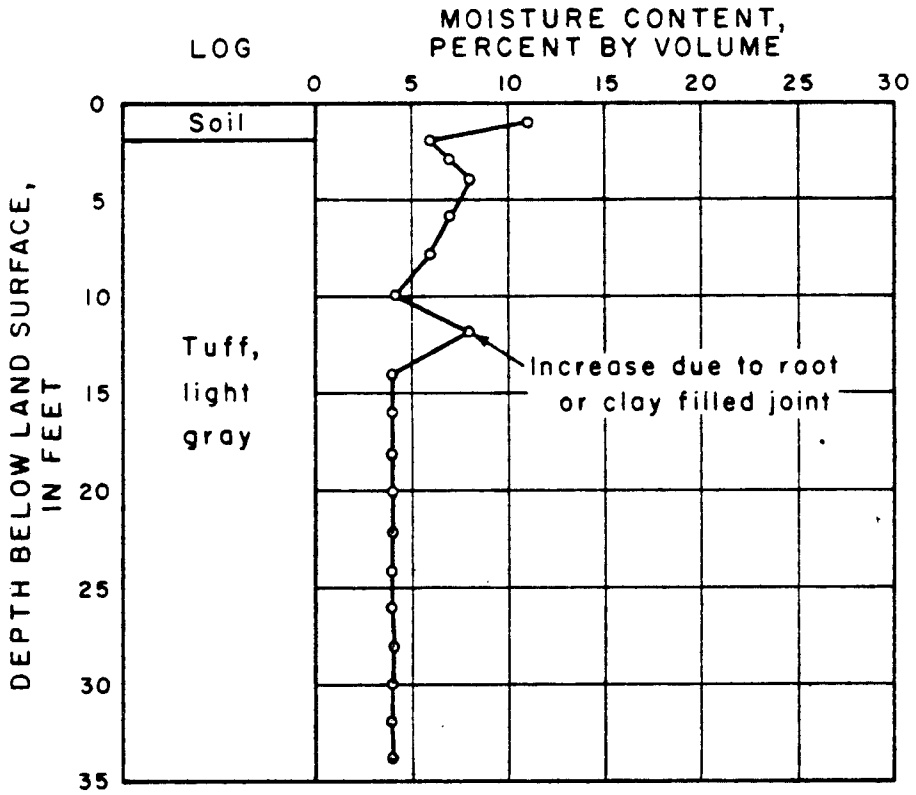

Location: Project grid, N91 + 39, E122 + 72
Date drilled: 2-9-66
Altitude: 7,210 feet above mean sea level
Depth: 35 feet
Diameter: 4-inches

Figure 15.--Log and moisture content of soil and tuff in test hole DPS-13

Table 1.--Radiochemical analyses of soil and tuff from test hole DPS-1.

Depth (feet)	Material	Gross alpha (d/m/g)[1/]	Gross beta-gamma (d/m/g)[1/]	Plutonium (d/m/g)[1/]	Uranium (μg/g)[2/]
0- 1	Soil	0.4	3.1	<0.4	<0.5
1- 2	Soil	.5	3.0	< .4	< .5
2- 3	Soil	.7	3.6	< .4	< .5
3- 5	Tuff	.3	2.4	< .4	< .5
5-10	Tuff	.3	6.0	< .4	< .5
10-15	Tuff	.6	2.7	< .4	< .5
15-20	Tuff	.7	3.6	< .4	< .5
20-25	Tuff	.4	2.2	< .4	< .5
25-30	Tuff	.3	1.0	< .4	< .5
30-35	Tuff	.2	1.2	< .4	< .5
35-40	Tuff	.3	.6	< .4	< .5
40-45	Tuff	.4	1.2	< .4	< .5
45-50	Tuff	.4	.0	< .4	< .5

1/ Disintegrations per minute per gram.

2/ Micrograms per gram.

Table 2.--Radiochemical analyses of soil and tuff from test hole DPS-2.

Depth (feet)	Material	Gross alpha (d/m/g)[1/]	Gross beta-gamma (d/m/g)[1/]	Plutonium (d/m/g)[1/]	Uranium (μg/g)[2/]
0- 1	Soil	0.9	9.1	<0.4	<0.5
1- 2	Soil	.5	2.8	< .4	< .5
2- 3	Soil	.8	.6	< .4	< .5
3- 5	Tuff	.6	.3	< .4	< .5
5-10	Tuff	.3	1.8	< .4	< .5
10-15	Tuff	.6	2.5	< .4	< .5
15-20	Tuff	.6	3.3	< .4	< .5
20-25	Tuff	.5	2.1	< .4	< .5

[1/] Disintegrations per minute per gram.

[2/] Micrograms per gram.

Table 3.--Radiochemical analyses of soil and tuff from test hole DPS-3.

Depth (feet)	Material	Gross alpha (d/m/g)[1/]	Gross beta-gamma (d/m/g)[1/]	Plutonium (d/m/g)[1/]	Uranium (μg/g)[2/]
0- 1	Soil	1.2	12.6	<0.4	<0.5
1- 2	Soil	.3	4.3	< .4	< .5
2- 3	Soil	.1	1.6	< .4	< .5
3- 5	Tuff	.1	1.5	< .4	< .5
5-10	Tuff	.6	1.3	< .4	< .5
10-15	Tuff	.3	.0	< .4	< .5
15-20	Tuff	.1	.0	< .4	< .5
20-25	Tuff	.1	.1	< .4	< .5
25-30	Tuff	.1	.1	< .4	< .5
30-35	Tuff	.5	1.6	< .4	< .5
35-40	Tuff	.4	.7	< .4	< .5
40-45	Tuff	.0	.1	< .4	< .5
45-50	Tuff	.1	.7	< .4	< .5

1/ Disintegrations per minute per gram.

2/ Micrograms per gram.

Table 4.--Radiochemical analyses of soil and tuff from test hole DPS-4.

Depth (feet)	Material	Gross alpha (d/m/g)[1/]	Gross beta-gamma (d/m/g)[1/]	Plutonium (d/m/g)[1/]	Uranium (μg/g)[2/]
0- 1	Soil	0.3	4.3	<0.4	<0.5
1- 2	Soil	1.1	4.9	< .4	< .5
2- 3	Soil	.0	.0	< .4	< .5
3- 5	Tuff	.2	.0	< .4	< .5
5-10	Tuff	.3	1.9	< .4	< .5
10-15	Tuff	.1	1.3	< .4	< .5
15-20	Tuff	.5	.6	< .4	< .5
20-25	Tuff	.9	4.6	< .4	< .5

[1/] Disintegrations per minute per gram.

[2/] Micrograms per gram.

Table 5.--Radiochemical analyses of soil and tuff from test hole DPS-5.

Depth (feet)	Material	Gross alpha (d/m/g)[1/]	Gross beta-gamma (d/m/g)[1/]	Plutonium (d/m/g)[1/]	Uranium (μg/g)[2/]
0- 1	Soil	0.5	4.5	<0.4	<0.5
1- 2	Soil	.9	4.8	< .4	< .5
2- 3	Soil	.3	2.7	< .4	< .5
3- 5	Tuff	.1	3.4	< .4	< .5
5-10	Tuff	.1	1.5	< .4	< .5
10-15	Tuff	.4	3.6	< .4	< .5
15-20	Tuff	.3	1.3	< .4	< .5
20-25	Tuff	.3	1.6	< .4	< .5
25-30	Tuff	1.0	7.6	< .4	< .5
30-35	Tuff	.5	3.1	< .4	< .5
35-40	Tuff	.2	.9	< .4	< .5
40-45	Tuff	.2	2.5	< .4	< .5
45-50	Tuff	.3	4.0	< .4	< .5

1/ Disintegrations per minute per gram.

2/ Micrograms per gram.

Table 6.--Radiochemical analyses of soil and tuff from test hole DPS-6.

Depth (feet)	Material	Gross alpha (d/m/g)[1/]	Gross beta-gamma (d/m/g)[1/]	Plutonium (d/m/g)[1/]	Uranium (μg/g)[2/]
0- 2	Soil	0.8	6.1	<0.4	<0.5
2- 5	Soil	.7	4.6	< .4	< .5
5-10	Soil and tuff	.8	4.0	< .4	< .5
10-15	Tuff	.6	3.3	< .4	< .5
15-20	Tuff	.8	5.2	< .4	< .5
20-25	Tuff	1.2	5.7	< .4	< .5
25-30	Tuff	.3	3.4	< .4	< .5
30-35	Tuff	.5	2.7	< .4	< .5
35-40	Tuff	.3	3.6	< .4	< .5
40-45	Tuff	.2	2.8	< .4	< .5
45-50	Tuff	.2	3.9	< .4	< .5

1/ Disintegrations per minute per gram.

2/ Micrograms per gram.

Table 7.--Radiochemical analyses of soil and tuff from test hole DPS-7.

Depth (feet)	Material	Gross alpha (d/m/g)[1/]	Gross beta-gamma (d/m/g)[1/]	Plutonium (d/m/g)[1/]	Uranium (μg/g)[2/]
0- 2	Soil	1.2	[illegible]	<0.4	<0.5
2- 5	Soil and tuff	.6	3.9	< .4	< .5
5-10	Tuff	.2	1.3	< .4	< .5
10-15	Tuff	.3	1.5	< .4	< .5
15-20	Tuff	.5	2.4	< .4	< .5
20-25	Tuff	.4	2.7	< .4	< .5

1/ Disintegrations per minute per gram.

2/ Micrograms per gram.

Table 8.--Radiochemical analyses of soil and tuff from test hole DPS-8.

Depth (feet)	Material	Gross alpha (d/m/g)1/	Gross beta-gamma (d/m/g)1/	Plutonium (d/m/g)1/	Uranium (µg/g)2/
0- 2	Soil	0.6	3.5	<0.4	<0.5
2- 5	Soil	.5	4.9	< .4	< .5
5-10	Soil and Tuff	.4	5.8	< .4	< .5
10-15	Tuff	.3	3.6	< .4	< .5
15-20	Tuff	.4	2.2	< .4	< .5
20-25	Tuff	.4	1.3	< .4	< .5
25-30	Tuff	.1	1.0	< .4	< .5
30-35	Tuff	.6	3.4	< .4	< .5
35-40	Tuff	.2	4.9	< .4	< .5
40-45	Tuff	.4	4.6	< .4	< .5
45-50	Tuff	.4	3.0	< .4	< .5

1/ Disintegrations per minute per gram.

2/ Micrograms per gram.

Table 9.--Radiochemical analyses of soil and tuff from test hole DPS-9.

Depth (feet)	Material	Gross alpha (d/m/g)[1/]	Gross beta-gamma (d/m/g)[1/]	Plutonium (d/m/g)[1/]	Uranium (μg/g)[2/]
0- 2	Soil	0.7	2.4	<0.4	<0.5
2- 5	Soil and Tuff	.5	2.1	< .4	< .5
5-10	Tuff	.4	3.7	< .4	< .5
10-15	Tuff	.5	1.8	< .4	< .5
15-20	Tuff	.5	3.7	< .4	< .5
20-25	Tuff	.3	1.0	< .4	< .5

1/ Disintegrations per minute per gram.

2/ Micrograms per gram.

Table 10.--Radiochemical analyses of soil and tuff from test hole DPS-10

Depth (feet)	Material	Gross alpha (d/m/g)[1/]	Gross beta-gamma (d/m/g)[1/]	Plutonium (d/m/g)[1/]	Uranium (μg/g)[2/]
0- 2	Soil	0.4	3.1	<0.4	<0.5
2- 5	Soil and Tuff	.3	3.0	< .4	< .5
5-10	Tuff	.8	2.5	< .4	< .5
10-15	Tuff	.6	2.7	< .4	< .5
15-20	Tuff	.6	4.3	< .4	< .5
20-25	Tuff	.5	2.7	< .4	< .5
25-30	Tuff	.2	2.1	< .4	< .5
30-35	Tuff	1.0	.7	< .4	< .5

1/ Disintegrations per minute per gram.

2/ Micrograms per gram.

Table 11.--Radiochemical analyses of soil and tuff from test hole DPS-11

Depth (feet)	Material	Gross alpha (d/m/g) 1/	Gross beta-gamma (d/m/g) 1/	Plutonium (d/m/g) 1/	Uranium (µg/g) 2/
0- 2	Soil	0.3	2.1	<0.4	<0.5
2- 5	Soil and Tuff	.6	4.0	< .4	< .5
5-10	Tuff	.4	1.3	< .4	< .5
10-15	Tuff	.5	1.9	< .4	< .5
15-20	Tuff	.5	2.8	< .4	< .5
20-25	Tuff	.5	1.2	< .4	< .5
25-30	Tuff	.7	3.0	< .4	< .5
30-35	Tuff	-	-	-	-
35-40	Tuff	.6	1.9	< .4	< .5
40-45	Tuff	.9	2.7	< .4	< .5
45-50	Tuff	.5	1.8	< .4	< .5

1/ Disintegrations per minute per gram.

2/ Micrograms per gram.

Table 12.--Radiochemical analyses of soil and tuff from test hole DPS-12

Depth (feet)	Material	Gross alpha (d/m/g)[1/]	Gross beta-gamma (d/m/g)[1/]	Plutonium (d/m/g)[1/]	Uranium (μg/g)[2/]
0- 2	Soil	0.8	1.2	<0.4	<0.5
2- 5	Soil and Tuff	.4	1.6	< .4	< .5
5-10	Tuff	.4	.4	< .4	< .5
10-15	Tuff	.3	1.0	< .4	< .5
15-20	Tuff	.4	.0	< .4	< .5
20-25	Tuff	.5	3.0	< .4	< .5
25-30	Tuff	.8	.9	< .4	< .5
30-35	Tuff	.4	.6	< .4	< .5

1/ Disintegrations per minute per gram.

2/ Micrograms per gram.

Table 13.--Radiochemical analyses of soil and tuff from test hole DPS-13

Depth (feet)	Material	Gross alpha (d/m/g)[1/]	Gross beta-gamma (d/m/g)[1/]	Plutonium (d/m/g)[1/]	Uranium (μg/g)[2/]
0- 2	Soil	1.0	4.3	<0.4	<0.5
2- 5	Tuff	.7	.0	< .4	< .5
5-10	Tuff	.4	2.1	< .4	< .5
10-15	Tuff	.7	2.8	< .4	< .5
15-20	Tuff	.6	.0	< .4	< .5
20-25	Tuff	.8	.9	< .4	< .5
25-30	Tuff	.9	1.9	< .4	< .5
30-35	Tuff	.4	.4	< .4	< .5

1/ Disintegrations per minute per gram.

2/ Micrograms per gram.

Description of soil and tuff

The light-brown clay soil cover of the mesa is derived from the weathering of the underlying tuff. The granules and sand-size particles of the soil consist mainly of quartz and sanidine crystals and fragments, and a few fragments of latite or rhyolite. The clay minerals making up most of the silt and clay fractions are montmorillonite and illite (Staritsky, 1949). The soil is generally thickest along the axis of the mesa and thinnest toward the edges of the canyon where the tuff is exposed. Near the pit the soil thickness ranges from 2 to 6 feet.

The rhyolite tuff underlying the soil is the Tshirege Member of the Bandelier Tuff of Pleistocene age (Griggs, 1964). The deepest test holes (depth 50 feet) penetrated only the uppermost ashflow.

The light brownish-gray and/the light-brown tuff (both partly weathered) are composed of quartz and sanidine crystals and/crystal fragments in a light brownish-gray or light-brown ash matrix that is in the process of breaking down into clay by weathering. A few rock fragments of latite or rhyolite are present. Pumice fragments are weathered to light-brown or light brownish-orange clays. The light-gray and/the grayish white tuff (both unweathered) consist of quartz and sanidine crystals and crystal fragments and a few rock fragments of pumice and latite or rhyolite in a gray ash matrix. The gray ash matrix contains pores that are capillary in size.

Numerous joints slightly open to closed, occur in most of the ashflow tuffs. The majority of the joints are near vertical although a few are nearly horizontal. Joints terminating in the soil zone are filled with brown clay.

Water moving through the soil zone to the tuff moves more readily into the tuff than into the clay filled joints as the tuff is more permeable than the clay. If water should move into an open joint, the extreme dryness of the tuff and capillary pores cause the water to be rapidly absorbed into the tuff that forms the joint face. Joints impede the movement of water because the water in the tuff is held in tension within the small pore spaces and the joints form breaks in the capillary pores through which movement occurs.

The total thickness of the Bandelier Tuff underlying the mesa at the disposal pit exceeds 800 feet. The tuff is in the zone of aeration; the zone of saturation is at a depth of about 1,200 feet below the surface of the mesa.

The fill material, covering the solid wastes in the pit, is composed of a mixture of soil and tuff. The tuff is being altered by weathering to silt and clay. The thickness of the fill material above the wastes is unknown.

Distribution of moisture in soil and tuff

Annual precipitation on the Pajarito Plateau is about 18 inches. Although water not removed by surface drainage infiltrates into the soil, the downward movement of water is impeded by the dense transition zone between the soil and tuff. Little if any water from precipitation moves into the underlying tuff, except in areas where the natural soil cover has been disturbed (Abrahams and others, 1961). Thus in the waste-pit area it is possible that moisture may have moved downward through the fill, thence downward and laterally into the tuff due to capillary action. Movement of water through the tuff is slow.

The moisture content in the soil and tuff adjacent to the walls of the test holes drilled around the waste pit was determined with a neutron-scattering moisture probe and with a portable electronic scaler The scaler readings were converted to moisture content (percent by volume) from a calibration chart. The holes were sealed after logging to avoid changing the conditions. The logging interval was 1 foot in the soil zone and 2 feet in the tuff. The moisture content of the soil and tuff, from normal infiltration of precipitation, decreases with depth. Significant increases of moisture content with depth in the tuff probably indicate lateral movement.

In the soil zone the moisture content ranged from less than 4 percent by volume (DPS-10, fig. 12 and DPS-13, fig. 15) near the contact of the soil and tuff to 35 percent (DPS-12, fig. 14) above the contact. The moisture content of the light brownish-gray and light-brown tuff (weathered) ranged from 8 percent to 27 percent by volume (DPS-12, fig. 14). The moisture content of the light-gray tuff was generally less than 10 percent in test holes pentrating this unit.

The distribution of moisture in the soil and tuff in eight of the test holes indicates moisture content generally decreases with depth. The moisture content of the soil and tuff in five test holes decreased from land surface to depths between 12 and 24 feet [test holes DPS-1 (fig. 3), DPS-4 (fig. 6), DPS-5 (fig. 7), DPS-6 (fig. 8), and DPS-7 (fig. 9)] then increases slightly. The moisture increase at these depths ranges from 2 percent by volume (DPS-7) to 7 percent (DPS-5 and DPS-6). The moisture content of the tuff is in the low moisture range, less than 20 percent by volume. The effective porosity of the tuff (void space available to transmit water) is estimated from laboratory determination of similar tuff to range between 35 to 40 percent by volume, thus moisture is being moved by capillary action, and the tuff is not saturated.

Distribution of radioactivity in soil and tuff

One hundred twenty-three samples of soil and tuff were collected from the thirteen test holes and analyzed for radioactive contamination (tables 1 through 13) to determine if water had moved contaminants into the adjacent soil and tuff. Six samples of soil and tuff were collected from an area known to be free of contamination (except by fallout) and were analyzed to establish the natural radiation of the soil and tuff.

The interval sampled varied from hole to hole for the first five feet, depending on the thickness of the soil zone; however, each hole was sampled in the tuff at five-foot intervals to total depth. The samples (soil and tuff) were analyzed for gross alpha and gross beta radioactivity and specific analyses for plutonium and uranium.

The radioactivities measured on the soil and tuff samples from the test holes varied in gross alpha radioactivity from 0.0 d/m/g (disintegrations per minute per gram) to 1.[illegible] d/m/g and in gross beta radioactivity from 0.0 d/m/g to 12.6 d/m/g. The analyses of the samples collected near the waste pit indicate that they contain no more radioactivity than those collected from an area far removed from the area of waste disposal (table 14). In general, all the surface samples (soil) analyzed had a slightly higher gross beta radioactivity than those samples taken at depth. This is probably due to radionuclide absorption of fall-out material.

Table 14.--The range of gross alpha and gross beta radioactivities of soil and tuff.

Material	Samples from test holes near the radioactive waste in the pit		Samples from test holes in an area where there is no radioactive waste contamination	
	Gross alpha[1/]	Gross beta[1/]	Gross alpha[1/]	Gross beta[1/]
	Range	Range	Range	Range
Soil	0.0 to 1.2	0.0 to 12.6	1.2 to 1.4	4 to 12.0
Tuff	0.0 to 1.2	0.0 to 7.6	.4 to 1.6	4.5 to 10.8

[1/] Distintegrations per minute per gram.

The specific analyses of the samples of soil and tuff, for plutonium and uranium, showed no indication of contamination from the wastes in the pit. Plutonium was less than 0.4 d/m/g and uranium was less than 0.5 μg/g (micrograms per gram). Analyses of soil and tuff from an area free from contamination contained less than 0.4 d/m/g of plutonium and less than 0.5 μg/g of uranium.

Conclusions

The moisture content of the tuff adjacent to the test holes and the pit was low, generally less than 10 percent by volume, thus the tuff is not saturated. Radiochemical analyses of the soil and tuff from the test holes showed no indication of radioactive contamination. The amount of water moving into the waste materials is not sufficient to cause migration of radioactive contaminates, or else the volume of and rate of movement has not been great enough to move the contaminates laterally into the tuff. No information is available on the radioactivity beneath the pit.

References

Abrahams, John H., Jr., Weir, James E , Jr., and Purtymun, William D., 1961, Distribution of moisture in soil and near-surface tuff on the Pajarito Plateau, Los Alamos County, New Mexico: U.S. Geol. Survey Prof. Paper 424-D, Art. 339, p. 142-145.

Griggs, R. L., 1964, Geology and ground-water resources of the Los Alamos area, New Mexico: U.S. Geol. Survey Water-Supply Paper 1753, 106 p., 1 pl., 20 figs.

Staritzky, Eugene, 1949, Report on the petrographic examination of local soil: Los Alamos Scientific Laboratory, LA-741, p. 12.

Written: November 1970

Distributed: May 1971

LA-4660
UC-41, HEALTH AND SAFETY
TID-4500

LOS ALAMOS SCIENTIFIC LABORATORY
of the
University of California
LOS ALAMOS • NEW MEXICO

Geology and Hydrology of Mesita del Buey

by

Report written by:

William D. Purtymun
William R. Kennedy

Work done by:

William D. Purtymun
Pablo O. Romero
Jack W. Aeby

CONTENTS

ABSTRACT..... 1

INTRODUCTION..... 1

GEOLOGY..... 2

Stratigraphy..... 2

Santa Fe Group..... 2

Bandelier Tuff..... 2

Guaje Member..... 3

Otowi Member..... 3

Tshirege Member..... 3

Unit 1..... 3

Unit 2..... 3

Soil and Alluvium..... 6

Geologic Structure..... 7

Joint Systems..... 7

HYDROLOGY..... 8

Soil and Tuff Moisture..... 8

Surface Water..... 9

Stream-Connected Aquifers..... 9

Main Aquifer..... 9

EROSION RATES OF TUFF..... 9

WASTE DISPOSAL AREAS..... 10

Area G..... 10

Area H..... 10

Area J..... 10

Area L..... 10

WASTE DISPOSAL AND THE GEOHYDROLOGIC ENVIRONMENT... 10

REFERENCES..... 11

APPENDIX A: Guidelines for Construction of Pits on Mesita del Buey..... 12

GEOLOGY AND HYDROLOGY OF MESITA DEL BUEY

by

William D. Purtymun and William R. Kennedy

ABSTRACT

Mesita del Buey is used for the disposal of wastes contaminated by radionuclides, of toxic or explosive chemicals, and of classified materials. These are buried in pits or shafts dug into the mesa surface. The mesa, covered by a clay-like soil, is underlain by a series of ashfalls of rhyolite tuffs from 240 to 590 ft thick. The tuffs are above the main aquifer of the Los Alamos area which lies at a depth of about 1,000 ft. Stream flow in adjacent canyons is intermittent. Water in the alluvium of the stream-connected aquifer in the canyon south of the mesa is recharged by storm runoff. The hydrologic characteristics and conditions of the soil, tuff, and seal material used to cover the wastes indicate no recharge to the stream-connected aquifer or main aquifer through the soil, buried wastes, or tuff at Mesita del Buey.

INTRODUCTION

Mesita del Buey is part of the Pajarito Plateau about 4 miles southeast of the community of Los Alamos, New Mexico (Fig. 1). The mesa, designated Technical Area 54, is used for the disposal of wastes contaminated by radionuclides, of toxic or explosive chemicals, and of classified materials. These are buried in pits or shafts dug into the mesa surface. Disposal operations on the mesa began in 1956.

The geology and hydrology of Mesita del Buey were studied. The mesa, covered by a clay-like soil, is underlain by a series of ashflows and ashfalls of rhyolite tuff. The ashflow units underlying the mesa top were mapped. Logs of a supply well and test holes in Pajarito Canyon, south of the mesa, were used to correlate the subsurface geology. Joint systems in the upper ashflows in the disposal areas were analyzed. Hydrologic data on soil and tuff moisture, surface water, stream-connected aquifers, and the main aquifer were collected. The erosion rates of the tuff were estimated. The study was to determine the geohydrologic pattern in relation to the disposal operations.

Mesita del Buey is a narrow southeast-trending mesa about 2 miles long and a quarter of a mile wide (Fig. 2). The mesa surface slopes gently from an altitude of about 6,900 ft near its western margin to about 6,600 ft near its eastern end. It is bounded on the north by an unnamed canyon and Canada del Buey, and on the south by Pajarito Canyon. The canyons have cut 50 to 100 ft below the surface of the mesa. The edges of the mesa are vertical or near-vertical cliffs, with steep slopes at their bases. The ashflows on the north-facing slopes at the foot of the mesa are covered with detrital alluvium, whereas those on the south-facing slopes are exposed.

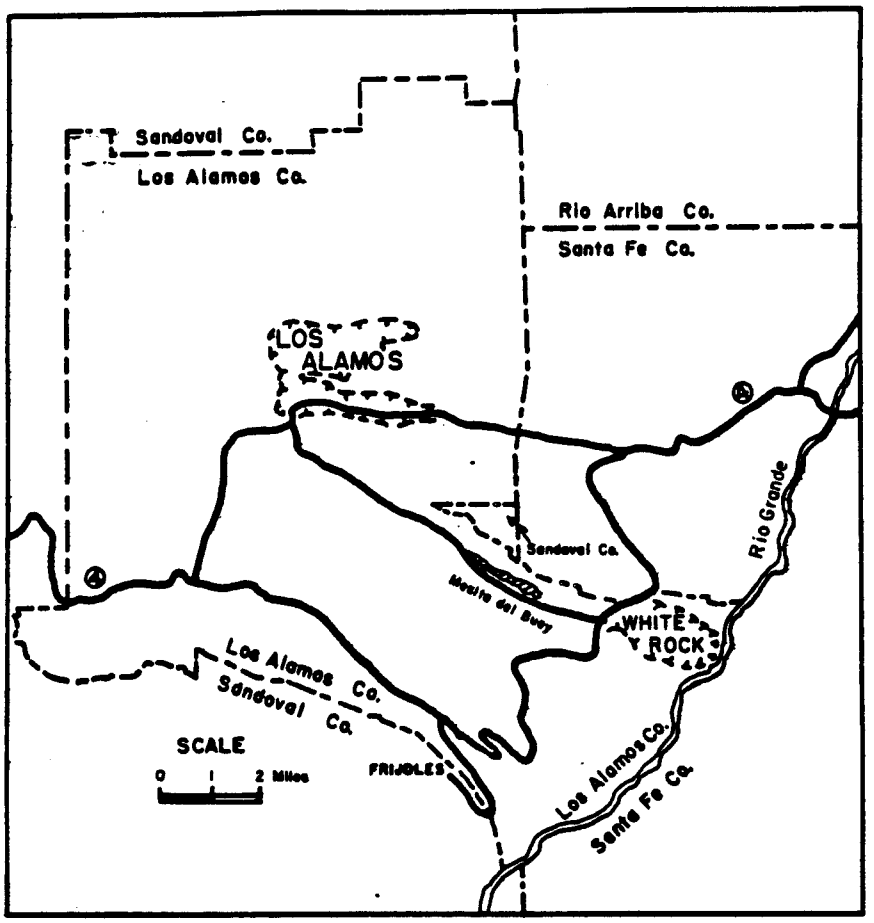

Fig. 1. Location of Mesita del Buey.

GEOLOGY

The Pajarito Plateau forms a topographic high area along the western part of the Rio Grande depression in north central New Mexico. Mesita del Buey is a part of the Pajarito Plateau. The plateau is formed by a series of Pleistocene ashfalls and ashflows of Bandelier Tuff.[1] In the subsurface are the sediments and volcanic rocks of the Santa Fe Group of Middle Miocene to Pleistocene age. The formations in the Santa Fe Group, from oldest to youngest, are the Tesuque and Puye with interbedded Chino Mesa basalt (Griggs'"basaltic rocks of Chino Mesa").

STRATIGRAPHY

Santa Fe Group. Santa Fe Group formations are not exposed at Mesita del Buey, but were penetrated by supply well PM-2 in Pajarito Canyon near the western part of the mesa. The Tesuque Formation consists of silty sandstones, sandstones with lenses of clay, and pebbly conglomerate. The well penetrated about 1,200 ft of this formation. The Puye Formation overlies the Tesuque. The lower 70 ft of the Puye is poorly consolidated channel-fill deposit; the upper 640 ft is volcanic debris. The Chino Mesa Formation is composed of basalt flow rocks and interbedded sediments. It overlies the main body of the Puye Formation, and only a thin section of the Puye overlies the basalts (Fig. 3). Supply well PM-2 penetrated about 270 ft of the Chino Mesa basalt.

Bandelier Tuff. The ashflows and ashfalls of the Bandelier Tuff overlie the Chino Mesa basalt (Fig. 3). The Bandelier has been divided into three members. In

ascending order, they are the Guaje, Otowi, and Tshirege Members.

Guaje Member. The Guaje Member is an ashfall pumice with a thin layer of water-laid pumiceous tuff that rests on the Puye Formation and the Chino Mesa basalt. The Guaje consists of gray lump-pumice fragments as large as 2 in. in diameter. Glass shards and crystals of quartz and sanidine are present in the cellular structure. The upper 2 to 3 ft is reworked pumice and tuff. The Guaje does not outcrop at Mesita del Buey, but below the surface it varies from about 30 to about 10 ft thick from west to east in Pajarito Canyon.

Otowi Member. The Otowi Member is a light gray, nonwelded, pumiceous, rhyolitic tuff. It contains quartz crystals, glass shards minor amounts of mafic minerals, and varying amounts of rock fragments of rhyolite, latite, and pumice in a fine-grained ash. The Otowi is mostly ashflows, but contains several beds of reworked tuff and pumice at the top. It does not outcrop at Mesita del Buey but is found subsurface (Fig. 3).

Tshirege Member. The Tshirege Member is a series of ashflows of rhyolite tuff which have been classified according to degrees of welding, i.e., nonwelded, moderately welded, and welded tuffs.[2] The nonwelded tuff has high porosity, only light cohesion of glassy fragments, and crumbly fracture. The moderately welded tuff has less porosity, moderate cohesion, slight deformation of glassy fragments, and a somewhat brittle fracture. The welded tuff has low porosity, good cohesion, a high degree of deformation by flattening of glassy fragments, and a brittle fracture. Most of the pores are capillary in size. The following shows porosity range in each classification.

	Range (Vol %)
Nonwelded tuff	40 to 60
Moderately welded tuff	30 to 55
Welded tuff	15 to 40

The Tshirege Member has been divided into three units, determined by Baltz et al.[3] where it outcrops in Mortandad Canyon. The Tshirege at Mesita del Buey was mapped using these units. At Mesita del Buey, as at Mortandad Canyon, Unit 1 has been subdivided into units 1a and 1b, and Unit 2 into 2a and 2b (Fig. 2). At Mesita del Buey, Unit 3, a nonwelded to moderately welded pumiceous tuff, is absent.

Unit 1. The lower unit of the Tshirege Member consists of two layers, similar in lithology but different in color and welding. The lower layer is designated Unit 1a and the upper, Unit 1b.

Unit 1a is a light orange to light brown, pumiceous tuff breccia. It contains numerous pumice lumps as much as 6 in. long, with small quartz crystals and rock fragments of latite and rhyolite. The tuff ranges from nonwelded to moderately welded and weathers to a steep slope. In places, a vertical wall with a talus slope at the base has formed. Unit 1a overlies the reworked sediments at the top of the Otowi Member. The upper part of the unit is exposed in Canada del Buey along the eastern edge of the mesa (Fig. 2). In the subsurface at the western part of the mesa, Unit 1a is about 30 ft thick, thinning to less than 10 ft to the east.

Unit 1b is a grayish brown tuff containing larger quartz crystals but fewer and smaller rock fragments of pumice, latite, and rhyolite. The unit is moderately welded and weathers to a vertical wall or steep talus slope. It is separated from the underlying Unit 1a by a notch, caused by weathering in a vertical wall, or is recognized as a talus slope lying on the bench formed at the top of Unit 1a. Unit 1b outcrops in lower Canada del Buey east of the mesa. Its thickness averages about 25 ft.

Unit 2. Unit 2 forms the walls and surface of Mesita del Buey. It consists of several ashflows, divided into lower

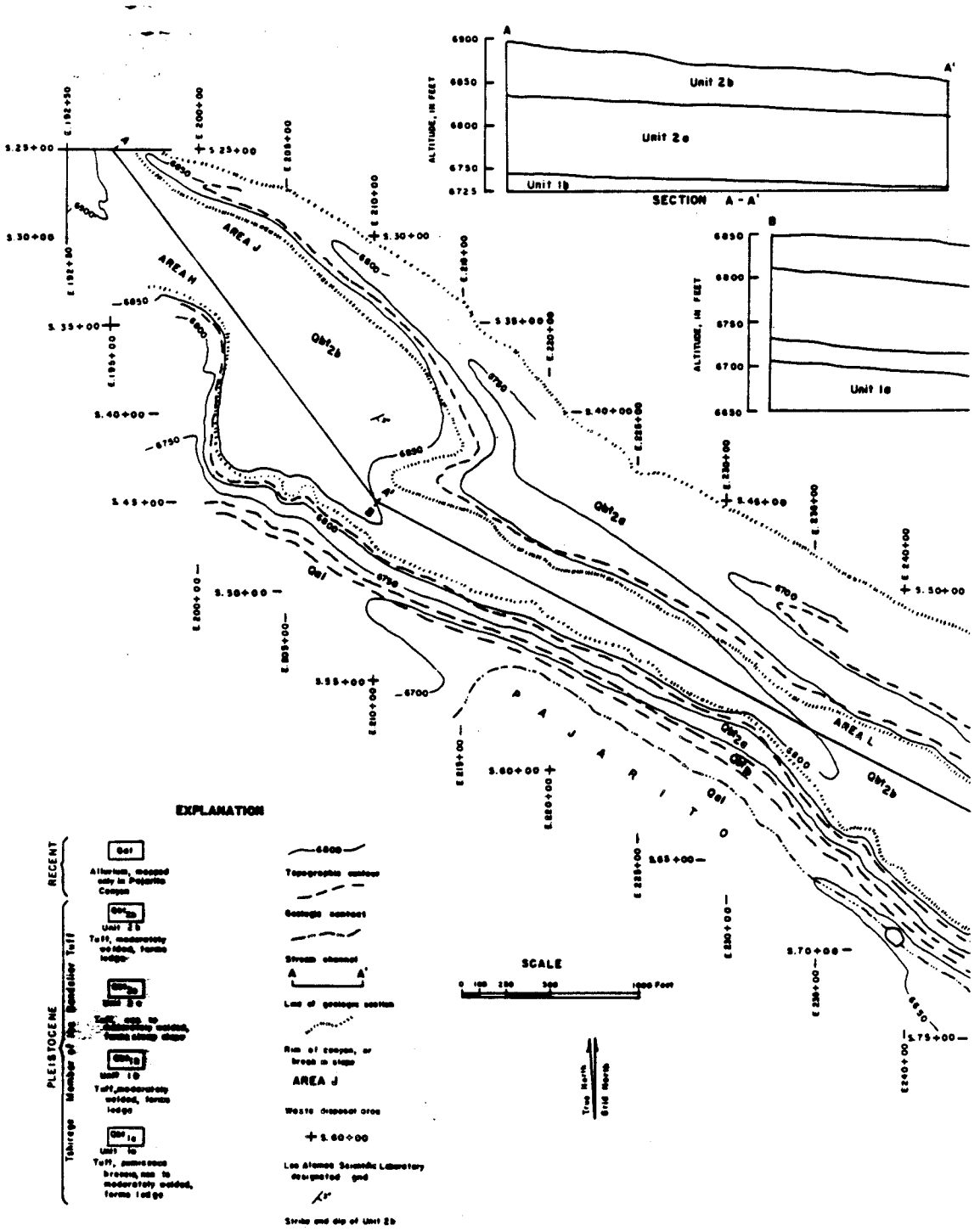

Fig. 2. Geologic map and sections of Mesita del Buey.

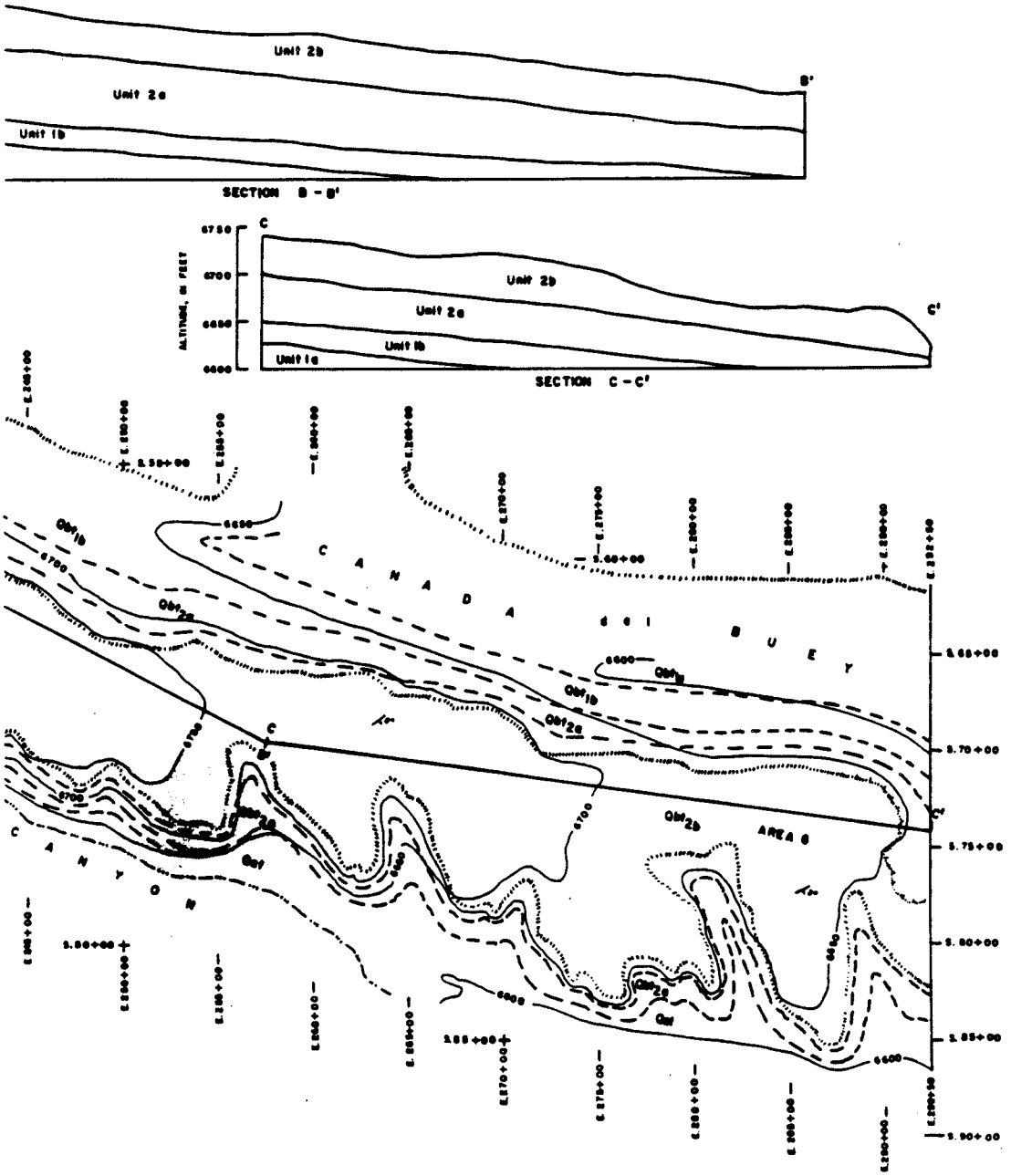
Unit 2b
Unit 2a
Unit 1b
B'
SECTION B - B'
C
ALTITUDE, in FEET
6750
6700
6650
6600
Unit 2b
Unit 2a
Unit 1b
Unit 1a
C'
SECTION C - C'
C A N A D A d e l B U E Y
C A N Y O N
AREA 6
Qbf1b
Qbf2a
Qbf2b
Qaf
6700
6650
6600
C
C'
E.292+00
S.65+00
S.70+00
S.75+00
S.80+00
S.85+00
S.90+00

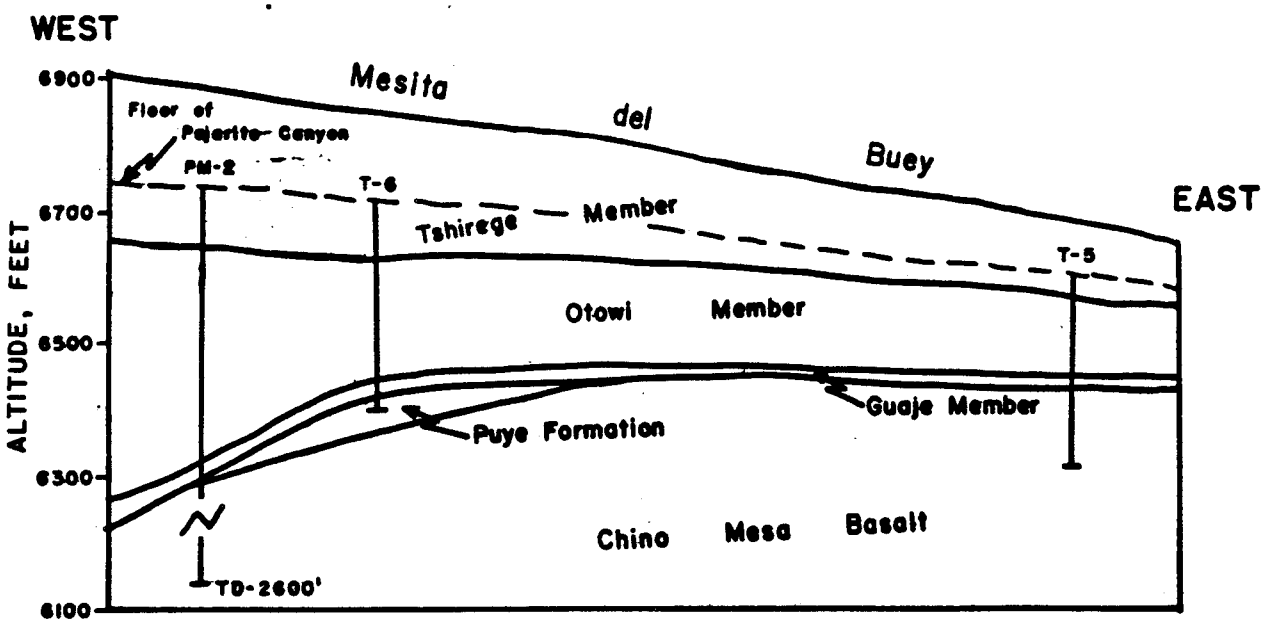

Fig. 3. Geologic cross section (East-West) showing relationship of the Chino Mesa basalt to the Bandelier Tuff.

Unit 2a and upper Unit 2b.

Unit 2a is a light-gray pumiceous tuff that contains rock fragments of pumice, latite, and rhyolite, with some quartz crystals in a light-gray ash. The pumice fragments are devitrified and dark brown. The rock fragments in the lower part of the unit may be as long as 3 in., but they decrease in size toward the top of the unit. The western part of the unit is a moderately welded tuff that forms a vertical wall along the canyons. Eastward, the welding decreases to a nonwelded unit where it forms a talus slope. There are two ashflows or ashfalls in Unit 2a. The upper part of the unit near the western margin of the mapped area (Fig. 2) is moderately welded tuff that becomes nonwelded as one progresses eastward. The nonwelded portion is apparently an ashfall containing numerous pumice fragments and some reworked tuff. Unit 1b is somewhat transitional into Unit 2a, and the contact is recognized by a gradual change in color and by a lithologic change. Unit 2a varies from about 85 ft thick on the west to about 30 ft thick to the east. Most of the thinning occurs in the upper ashfall.

Unit 2b is a light gray to brown, weathered rhyolite tuff with some pebble-size rock fragments of pumice, latite, and rhyolite and numerous crystals and crystal fragments of quartz and sanidine. It is a moderately welded to welded tuff that forms the upper walls and surface of the mesa. It forms ledges, benches, and vertical walls around the edge of the mesa. Unit 2b is separated from the underlying Unit 2a by an erosional contact, marked by a thin layer of silt, sand, and pumice. Unit 2b is composed of at least two ashflows that cooled as a single unit. The contact between these two flows is not evident where they outcrop, but in pits dug at Area "G" (Fig. 2) it is recognized by increased size and number of pumice fragments with an occasional deposit of reworked tuff and pumice. Unit 2b is about 60 ft thick.

Soil and Alluvium. The soil cover is 3 to 4 ft thick along the axis of the Mesa and thins toward the canyon rims where the tuff

is exposed. The light, brown, clay-like soil is derived from weathering of the tuff. The primary soil constituents are quartz and feldspar with the clay minerals montmorillonite and illite.[4]

The alluvium overlying weathered tuff in the stream channels north of the mesa is probably no more than 3 to 4 ft thick. It consists of sand-size quartz and sanidine crystals and crystal fragments, and pebble- to cobble-size fragments of latite, rhyolite, and pumice derived from weathering and erosion of the tuff.

The alluvium in Pajarito Canyon, south of the mesa, is 20 to 30 ft thick. About 1/2 mile southeast of Area "G" the canyon has cut to base level on the basalt, and the alluvium fans out on top of the basalt. The canyon heads on the flanks of the mountains and contains pebbles, cobbles, and boulders of latite and rhyolite, the volcanic flow rocks that form the mountains. The sand-grain-size material is derived in part from weathered tuff. Gravels from pits in this canyon have been used for road construction and concrete mix.

GEOLOGIC STRUCTURE

The Rio Grande depression near Los Alamos is 25 to 30 miles wide. Mesita del Buey lies within the depression. The estimated thickness of volcanic rocks and sediments overlying the basement complex of Precambrian crystalline rocks is about 12,000 ft.[8]

The upper ashflows at Mesita del Buey dip 2 to 3 degrees to the southeast. The ashflows of the Bandelier Tuff thin eastward because these younger rocks lie on top of the older basalt (Fig. 3). The basalts originated from volcanic centers to the east, and flow was north and west into the area, forming a topographic high before the tuff was laid down.

Joint Systems. The ashflows of the Bandelier tuff are broken into a number of blocks by joints, formed by shrinkage (tension) as the ashflow cooled. The near-vertical attitude of most of these joints and the curved form of some, are indicative of formation by cooling. The joints are more numerous in welded than in nonwelded tuffs because the welded tuffs were laid down at higher temperatures.

The joints are classified as master and minor joints. Master joints are numerous and long, and may pass through one or more ashflows. A single unit may contain several ashflows emplaced at different times, but the joint pattern of the older layer may tend to govern formation of joints in the younger layer as it cools. Also, two or more ashflows may be laid down in rapid succession and cool as a single unit with joints forming in the flows at the same time.

The master joints are vertical or nearly vertical and generally dip 70 degrees from the horizontal. The vertical trend may be straight or slightly curved. The dip is deflected slightly when the joint enters a unit with different density or degree of welding.

Minor joints dip at angles less than 70 degrees. They are more numerous near the tops of ashflows and do not persist as they intersect the master joints.

A joint traced vertically through an ashflow may be closed in places and open in others. Locally the opening may be as much as 2 in. wide, but most openings are less than 1/4 in. wide. Joints terminating in the base of the soil zone or in exposed tuff on the mesa surface are filled with light-brown clay which may extend 3 to 4 ft below the surface. Below the brown clay, the joint openings are filled, or the joint faces are plated, with a light-gray clay. The light-gray clay is derived from weathering of the tuff and from minerals leached from the tuff by water and precipitated along joint openings before development of the near-surface brown clay that seals the joint at the surface.

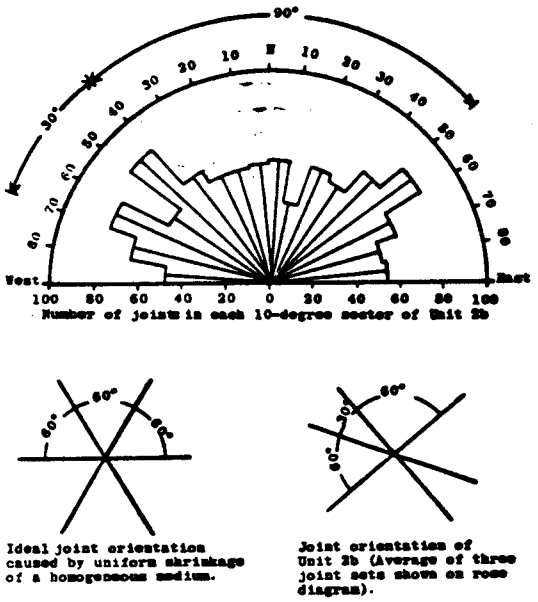

Fig. 4. Orientation of joints in Unit 2b.

The master joints are tension joints formed by the contraction of the tuff as it cooled. In a cooling homogeneous molten liquid, rupture occurs as three vertical fractures intersecting at angles of 120 degrees and radiating out from numerous centers.[6] If the centers are evenly distributed, the fractures bound vertical hexagonal columns. A rose diagram illustrating the orientation of joints formed from a homogeneous molten liquid would show three joint sets (a number of joints with the same characteristic pattern) intersecting at angles of 60 degrees (Fig. 4).

The heterogeneous characteristics of the tuff did not allow joint sets to form vertical hexagonal columns. A rose diagram prepared using the orientation of 1,078 master joints (492 in Area G (Fig. 2), 296 in Area L, and 290 in Areas J and H) showed the average of the three joint sets intersecting at angles of 30 and 90 degrees (Fig. 4). The three joint sets, N30°W to N50°W, N60°W to N80°W, and N40°E to N60°E, comprise 40% of the joints measured for the study.

The blocks formed by the joints range from a few square feet to as much as 500 ft^2 at the surface. In the walls of the pits there is about one master joint for every 7 ft of horizontal wall.

HYDROLOGY

The annual precipitation on the Pajarito Plateau is about 18 in. Most occurs in July and August as thunder showers. Some precipitation infiltrates the soil and tuff on the mesa, and the rest flows off into the canyons. Part of the surface flow in the canyons recharges stream-connected aquifers in the stream channel alluvium, and the rest is lost to evapotranspiration. Surface water drainage is eastward toward the Rio Grande. Water in the main aquifer lies at a depth of about 1,050 ft along the western margin of Mesita del Buey and at 850 ft at the eastern margin. Water in the aquifer moves eastward toward the Rio Grande.

SOIL AND TUFF MOISTURE

Part of the precipitation that falls on the Mesa surface infiltrates the soil and tuff. Where the soil cover has not been disturbed, little if any water from precipitation infiltrates the underlying tuff.[7]

Where the soil cover has been disturbed, as in the disposal areas, the moisture content of the tuff indicates that precipitation may have infiltrated to a depth of 10 ft. The moisture ranges from 2 to 8% by weight, decreasing with depth. Below 10 ft, the moisture content ranges from 0.5 to 2% by weight, showing that the moisture is redistributed by diffusion.

Tests of infiltration of precipitation in the tuff used to cover the waste in pits showed that moisture from a single storm may reach a depth of 6 ft, but in the weeks after the storm it is returned to the atmosphere by evaporation.

Open joints in the ashflow may allow precipitation to move into the tuff. The joints are now filled to a depth of 3 to

4 ft with clay that acts as a seal and prevents precipitation from infiltrating the tuff.

SURFACE WATER

Stream flow in the canyons north of Mesita del Buey is intermittent flow from storm runoff. These canyons head on the Pajarito Plateau and have a small drainage area. Stream channels in the canyons are narrow with few if any cut banks, indicating small and infrequent runoff.

Pajarito Canyon, south of the mesa, heads on the flanks of the mountains to the west and has a large drainage area. The intermittent flow in the canyon is from spring snowmelt and summer thunder showers. Gravel pits in the canyon usually contain ponded water. Some intermittent return flow occurs about 1 mile southwest of the mesa, where the alluvium laps on to a basalt flow.

STREAM-CONNECTED AQUIFERS

The alluvium in the canyons north of Mesita del Buey is thin and contains no perennial water owing to the small amount of runoff.

The intermittent stream in Pajarito Canyon, however, recharges a perennial body of water in the stream-connected aquifer in the alluvium. As is typical of stream-connected aquifers, the water table is highest during the spring from snowmelt and in late summer from showers. In the fall and early summer the water table declines. Gravel pits in the canyon have been dug into the top of the stream-connected aquifers.

MAIN AQUIFER

The top of the main aquifer (capable of municipal and industrial water supply) lies at a depth of about 1,200 ft along the flanks of the mountains to the west and slopes gently eastward toward the Rio Grande. The aquifer is recharged by precipitation on the mountains and in deep canyons cut into the western part of the Plateau.[8] The water moves eastward toward the Rio Grande where part is discharged into the river through seeps and springs. The rate of water movement computed from aquifer tests of supply wells is estimated to be 1 ft/day.[9] From Mesita del Buey to the Rio Grande is about 4 1/2 miles, so we estimate that any water will take over 60 years to move from beneath the mesa to the river.

EROSION RATES OF TUFF

Vital to the containment of wastes buried at Mesita del Buey is the rate at which the tuff encompassing the wastes erodes. Some of the wastes contain radionuclides with a very long half-life.

There is no practical method to determine the erosion rate of the tuff during the short time that the mesa has been used for waste disposal. Erosion rates can be approximated by relating the age of the tuff to its past erosion. Erosion rates based on these assumptions are conservative because the tuff probably eroded faster initially than at present. The area is more stable since the stream channels in Canada del Buey and Pajarito Canyon have cut to a temporary base level on the resistant basalt.

Radiometric dating indicates that the tuff was emplaced about 1.1 million years ago.[5] The thickness of Unit 3 tuff eroded from the surface of the mesa at Area G is estimated to be about 80 ft on the basis of geologic sections on the plateau where this unit is preserved. Its erosion rate for the past 1.1 million years is about 7.2×10^{-5} ft/year. Vertical downcutting in the canyons has been estimated at 1.9×10^{-4} ft/year in Canada del Buey and 1.6×10^{-4} ft/year in Pajarito Canyon. Wilden and Criley[5] estimated the vertical downcutting in major canyons to be 5 to 8×10^{-4} ft/year. At Area G, horizontal erosion at the top of the mesa is estimated to be about 4.5×10^{-4} ft/year.

Wastes are buried in the natural confines of the tuff to a level 2 ft below the mesa surface and then covered and mounded over with 6 to 8 ft of tuff. Considering the vertical erosion of 2 ft of tuff on the mesa top at a rate of 7.2×10^{-5} ft/year,

it would take 27,000 years for the mesa top to erode to the top of the wastes.

The edges of the pits are 50 ft or more from the edge of the mesa. Considering the horizontal erosion of 60 ft of tuff at a rate of 4.5×10^{-4} ft/year it would take more than 110,000 years for the tuff to erode far enough to expose the wastes in the pits.

WASTE DISPOSAL AREAS

There are four areas on Mesita del Buey used for disposal of wastes contaminated by radionuclides, of toxic or explosive chemicals, and of classified materials. The disposal areas are pits and shafts located according to guidelines set up by the U. S. Geological Survey, the U. S. Atomic Energy Commission, and the Health and Engineering Divisions of the Los Alamos Scientific Laboratory (Appendix A).

Access to the disposal areas is from Pajarito Road. The mesa is fenced from canyon to canyon at its western margin.

AREA G

Area G has been designated for the disposal of solid wastes and packaged sludges that contain radioactive nuclides. The solid wastes range from rubber gloves and glasswear to parts of buildings or trucks that cannot be cleaned.[16] The wastes are buried in pits or shafts dug into the mesa surface.

The pits are 100 ft wide, 600 ft long, and 30 to 35 ft deep. There is a ramp at each end of the long dimension to facilitate entering the pit with trucks to dispose of the wastes. The wastes are buried in 6- to 8- ft-deep layers, and each layer is covered with 1 to 2 ft of tuff. The pits are filled to 2 to 4 ft below the land surface and then covered with 6 to 8 ft of tuff, slightly mounded for surface-water drainage.

There are a number of shafts for disposal of organic material, oil, or solid wastes. The shafts are 2 to 6 ft in diameter and up to 64 ft deep. Special shafts for certain types of wastes have been prepared by lining them with concrete or by coating their walls with asphalt. The entire area surrounding the pits and shafts is fenced and locked.

The pits and most of the shafts extend into Unit 2b, and the deeper (64 ft) shafts extend through Unit 2b into the top of Unit 2a of the Tshirege Member of the Bandelier Tuff.

AREA H

Area H has been designated for the disposal of classified materials. The materials are placed in 6-ft-diam shafts about 60 ft deep. The area is fenced and locked. The shaft currently in use has a locked cover. Filled shafts are capped with 5 to 6 ft of concrete. The shafts extend through Unit 2b into the top of Unit 2a.

AREA J

Area J is used for the disposal of wastes from areas where explosive chemicals are processed. It consists of pits 50 ft wide, 250 ft long, and about 15 ft deep. There are ramps at the ends of the long dimension of the pits. The area is fenced but not locked. The pits extend into Unit 2b.

AREA L

Area L is used for the disposal of chemicals or possibly toxic materials in pits or shafts. The pit is 12 ft wide, 200 ft long, and about 12 ft deep with ramps on the long dimension. Shafts are 6 ft in diameter and about 60 ft deep. The area is fenced and locked. The pit extends into Unit 2b, and the shafts extend through Unit 2b into the top of Unit 2a.

WASTE DISPOSAL AND THE GEOHYDROLOGIC ENVIRONMENT

Total containment of contaminants is of paramount importance in the disposal of wastes at Mesita del Buey. Initial containment is accomplished with the burial of wastes in pits or shafts. After burial, the major means of transport of contaminants to the environment would be in the hydrologic cycle.

Transport of contamination by surface runoff on the mesa seems unlikely because the wastes are buried.

Little if any water from precipitation or surface runoff infiltrates through the seal material overlying wastes in filled pits. There is not enough water to leach the contaminants from the wastes and move them into the tuff. The bottoms of the pits are underlain by about 590 ft of tuff along the western part of the mesa and about 240 ft of tuff along the eastern edge. The hydrologic characteristics and conditions of the soil, seal material, and tuff indicate no recharge to the stream-connected aquifers or main aquifer through the surface soil, buried wastes, or underlying tuff at Mesita del Buey.

The natural moisture content of the unsaturated tuff is in the range in which moisture is redistributed by diffusion. Contaminants may be transported by diffusion if gases or volatile fluids are placed in shafts or pits. Diffusion may take place through the tuff where there are large amounts of pore space, through open joints, or along contacts between ashflows.

Vertical and horizontal erosion rates of the tuff surrounding the waste in pits or shafts indicate that under present climatic conditions the estimated life of the pits will be about 27,000 years. Routine maintenance to control erosion of the seal material will extend this life.

REFERENCES

1. R. L. Griggs, "Geology and Ground Water Resources of the Los Alamos Area, New Mexico," U. S. Geological Survey Water Supply Paper 1753, 1964.

2. W. D. Purtymun and F. C. Koopman, "Physical Characteristics of the Tshirege Member of the Bandelier Tuff with Reference to Use as Building and Ornamental Stone," U. S. Geological Survey open-file report, 1965.

3. E. H. Baltz, J. H. Abrahams, Jr., and W. D. Purtymun, "Preliminary Report on the Geology and Hydrology of Mortandad Canyon near Los Alamos, N. M., with Reference to Disposal of Liquid Low-Level Radioactive Wastes," U. S. Geological Survey open-file report, 1963.

4. Eugene Staritzky, "Report on the Petrographic Examination of Local Soils," Los Alamos Scientific Laboratory report LA-741 Series A (1949).

5. R. Wilden and E. E. Criley, "Geology of Los Alamos," in "Geologic Studies and Material Properties Investigations of Mesita de Los Alamos," Los Alamos Scientific Laboratory report LA-3728 (1968).

6. M. P. Billings, Structural Geology, Prentice-Hall, Inc., New York, 1942.

7. J. H. Abrahams, Jr., J. E. Weir, Jr., and W. D. Purtymun, "Distribution of Moisture in Soil and Near-Surface Tuff on the Pajarito Plateau, Los Alamos County, New Mexico," in short papers in geologic and hydrologic sciences. Articles 293-435, U. S. Geological Survey Prof. Paper 424-D, 1961.

8. R. L. Cushman, "An Evaluation of the Aquifer and Well Characteristics of the Municipal Well Fields in Los Alamos and Guaje Canyons near Los Alamos, N. M.," U. S. Geological Survey Water Supply Paper 1809-D, 1965.

9. C. W. Theis and C. S. Conover, "Pumping Test in the Los Alamos Canyon Well Field near Los Alamos, N. M.," U. S. Geological Survey Water Supply Paper 1619-I, 1962

10. J. W. Enders, "Solid Radioactive Waste Disposal at the Los Alamos Scientific Laboratory," in "Disposal of Radioactive Wastes into the Ground," International Atomic Energy Agency, Austria, 1967.

APPENDIX A

GUIDELINES FOR CONSTRUCTION OF PITS ON MESITA DEL BUEY*

These guidelines were formed during a meeting held at Los Alamos on June 23, 1965, with the following people in attendance: Salvatore Russo, Eng-3; Ben Williams, Eng-3; Dean Meyer, H-1; William Kennedy, H-6; C. W. Christenson, H-7; of the Los Alamos Scientific Laboratory; and Dr. C. V. Theis, F. C. Koopman, and William D. Purtymun of the U. S. Geological Survey.

Construction

Pits should be a minimum of 50 ft from the canyon rim.

Pits should be no deeper than adjacent canyon floors.

The long dimensions of pits should be parallel (as near as possible) to surface topographic contours.

Large open joints should be filled with seal material (tuff removed from pit during construction).

Drainage around open pits should be such that runoff from precipitation on the mesa does not enter the pit while it is being filled.

Size and shape of pit are not important.

Pit bottoms need not be level.

Burial of wastes

Burial of wastes in layers (layer of waste covered by layer of tuff) should be continued.

Wastes should be buried in the confines of the natural tuff. (If the soil zone is exceptionally thick, this unusual condition would indicate instability in that immediate area.) The wastes should be buried below the soil zone within the tuff.

Surface seal of pits

Pits can be filled with wastes to within 2 ft of the land surface.

Seal material (tuff) overlying the wastes should be 6 to 8 ft thick.

The surface of the seal material over the pit should be slightly rounded.

Adequate drainage should be provided to remove runoff from precipitation on the mesa.

Drainage ways should be located so that they do not cross the surface of a sealed pit.

Planting of native vegetation on the surface of sealed pits should be considered.

---

* From letter to S. E. Russo, LASL Group ENG-3, from F. C. Koopman, U. S. Geological Survey, June 30, 1965.

Copy I

UNITED STATES
DEPARTMENT OF THE INTERIOR
GEOLOGICAL SURVEY
Albuquerque, New Mexico

Physical characteristics of the Tshirege Member of the Bandelier Tuff with reference to use as a building and ornamental stone

By

W. D. Purtyman and F. C. Koopman

Report prepared for the Community Action Program, Santa Clara Indian Pueblo in cooperation with the U.S. Atomic Energy Commission and the University of California, Los Alamos Scientific Laboratory

September 1965

Contents

	Page
Introduction	4
Availability and accessibility	6
Physical characteristics of the Tshirege Member of the Bandelier Tuff	9
Welding	10
Density	12
Bearing capacities	13
Thermal conductivity	15
Chemical composition	16
Mineral composition	17
Pumice, rhyolite, and latite rock inclusions	18
Weathering and erosion characteristics	19
Color	20
Natural moisture content	21
Thickness	22
Joints	23
Conclusions	24
References	25

Illustrations

	Reference page
Figure 1.--Map showing topographic features in the region of the Santa Clara Indian Reservation and their relation to the Bandelier Tuff (shaded) of the Jemez Mountains ----------	6
2.--Diagrammatic cross section showing the relation of geologic formations in the area south of the Santa Clara Indian Reservation -----	6

Physical characteristics of the Tshirege Member of the Bandelier Tuff with reference to use as a building and ornamental stone

By

W. D. Purtymun and F. C. Koopman

Introduction

The suitability of the Tshirege Member of the Bandelier Tuff for insulation, ornament, building stone, and other uses is dependent on its availability, accessibility and physical properties. At the request of Mr. Paul Tafoya, Governor of Santa Clara Indian Pueblo and Mr. W. Williams, Advisor of the Community Action Program at Santa Clara, New Mexico, the information available as to its geographical and geological accessibility and its physical properties are presented in this report. The information will be useful in the Community Action Program for developing and enlarging the Puye Cliff Dwelling area as a tourist facility. It may also suggest other uses for the stone to anyone who may be interested.

The information contained in this report was abstracted from reports in the files of the U.S. Geological Survey, prepared for and in cooperation with the U.S. Atomic Energy Commission and the University of California's, Los Alamos Scientific Laboratory at Los Alamos, New Mexico. The reports that contain the information on the physical properties of the tuff were prepared from data collected during investigations related to the disposal of solid waste materials, industrial effluents, and studies pertaining to the development of ground-water supply at Los Alamos.

The fact that some of the tuff is suitable for building purposes was recognized by the historical cliff dwellers, and in modern times by the builders of the first houses at Los Alamos. It was found to have good insulating properties and good strength as well as beauty. It was used to construct four fireplaces at the Los Alamos Lodge. Among the newer buildings constructed of tuff are: the fire tower, those buildings of the Los Alamos Building and Loan Company, and the Gate Restaurant. Also, many stone fences, retaining walls, drainage ditches, and protective slope covers are constructed of tuff at Los Alamos. A few homes and fireplaces in Albuquerque are constructed of tuff.

Availability and accessibility

The tuff is available in large quantities and also reasonably accessible because of its favorable geographic location and geologic occurrence. It is the cap rock of a large plateau lying between the volcanic center, Sierra de los Valles, on the west and the Rio Grande on the east in North-central New Mexico (fig. 1). This tuff has

Figure 1 (caption on next page) belongs near here.

been sculptured by erosion into a picturesque arrangement of canyons, mesas, and cliffs roughly parallel to each other and all extending outward and downslope toward the river, away from the volcanic center to the west. This slope feature with all of its canyons and mesas is called the Pajarito Plateau (Hewitt, 1953). It was originally a nearly-smooth sloping surface formed as the result of the accumulation of hot volcanic ash material ejected from the volcanic center to the west (Valles Caldera).

Rocks exposed on or near the Pajarito Pleateau are the Tesuque Formation, Puye Conglomerate, the Tschicoma Formation, and the Bandelier Tuff. A generalized east-west geologic section showing their relationship in an area south of Santa Clara Indian Reservation is shown on figure 2. A detailed description of these formations can

Figure 2 (caption on next page) belongs near here.

be found in Griggs (1964) and Spiegel and Baldwin (1963).

Figure 1.--Map showing topographic features in the region of the Santa Clara Indian Reservation and their relation to the Bandelier Tuff (shaded) of the Jemez Mountains.

2.--Diagrammatic cross section showing the relation of geologic formations in the area south of the Santa Clara Indian Reservation.

The Bandelier Tuff was formed from a series of ash falls and ash flowes ejected from the volcanic center to the west. It is of rhyolitic composition and consists of three members that form a part of the Pajarito Plateau. From oldest to youngest, the members are the Guaje, Otowi, and Tshirege.

The Guaje Member consists of light-gray ash-fall pumice and water-laid pumiceous tuff. The base of the unit contains gray lumps of pumice as much as 2 inches in length. The average thickness of the Guaje ranges from 20 to 35 feet. Pumice from the Guaje Member is mined for use in concrete aggregate.

The Otowi Member consists of a light-gray, nonwelded, friable, pumiceous, rhyolite tuff that weathers to a gentle slope. Its thickness varies and may be as much as 400 feet beneath the central part of the plateau. The nonwelded friable unit would not be suitable as a building stone.

The Tshirege Member overlies the Otowi Member and it forms the cap rock of the finger-like mesas of the Pajarito Plateau. It was formed of a series of ash flows nonwelded into a series of rhyolite tuff. Because of its physical properties, described in the following section, some layers of the tuff are well suited to use as building and ornamental stone. A detailed description of the Tshirege Member is given in the following section.

The Tshirege Member is well exposed along the canyon walls and is also readily accessible under a thin mantle of surface soil on the mesa tops.

Physical characteristics of the Tshirege Member of the Bandelier Tuff

The tuffs of the Tshirege Member were formed by a series of ash flows and ash falls which are described as nonwelded, moderately welded, and welded tuff. The nonwelded, moderately welded, and welded tuff grade one into the other both vertically and horizontally.

Welding

The welding process of an ash-flow tuff begins after emplacement. The major factors affecting welding are heat at the time of emplacement, amount of volatiles in the mass, rate of cooling, and thickness of the ash flow. The degree of welding ranges from incipient stages marked by the sticking together or cohesion of glassy fragments to complete welding marked by the cohesion of the surfaces of glassy fragments accompanied by their deformation and elimination of pore space (Smith, 1960).

Zonal variation of welding occurs vertically within individual flows or within a series of flows that have cooled as a single unit. Single ash flows that have cooled as a unit may show a greater degree of welding near the center than near the upper and lower contacts. A series of ash flows that have been emplaced in rapid succession may cool as a single unit with the greatest degree of welding near the center.

Variation of welding occurs horizontally within individual flows with greater degree welding near the mountains (the source area). The degree of welding becomes less eastward across the plateau.

The tuffs in the Los Alamos area are classified according to the degree of welding--i.e., nonwelded, moderately welded, and welded tuffs. Welding results in increased cohesion and deformation of the glassy fragments in the tuff. Nonwelded tuff has high porosity, only slight cohesion of the glassy fragments, and crumbly fracture; moderately welded tuff has lesser porosity, moderate cohesion, slight deformation of the glassy fragments, and a somewhat brittle fracture; and welded tuff has lower porosity, good cohesion, a high degree of deformation by flattening of glassy fragments, and a brittle fracture.

The degree of welding influences most of the physical characteristics of the individual ash-flow tuff units.

The following shows a large range in porosity in each of the variations of tuff indicating that welding is only one of several factors determining porosity.

	Range in porosity (percent by volume)
Nonwelded tuff	40 to 60
Moderately welded tuff	30 to 55
Welded tuff	15 to 40

Density

The bulk density of nonwelded tuff is lower than in welded tuff. This is due to the compaction of the matrix (glass shards and ash) and closer arrangement of the quartz and sanidine, crystals, and rock fragments in the process of welding of a welded tuff. The specific gravity of the tuff matrix averages about 2.55. The range in bulk density of nonwelded to welded tuff depends on the porosity (i.e., the larger a porosity the smaller the buld density).

The following table shows a comparison of the bulk densities of the tuff (nonwelded to welded) with other building stone.

Building stone	Range in bulk density (lbs. in cu. ft.)
Nonwelded tuff	64- 95
Moderately welded tuff	72-115
Welded tuff	95-135
Brick[1/]	87-137
Granite[1/]	165-172
Marble[1/]	160-177
Sandstone[1/]	134-147
Concrete[1/]	170-190

1/ Handbook of Physics and Chemistry, 1958.

Bearing capacities

The bearing capacities of a tuff are dependent upon the density of tuff (i.e., the greater bearing capacities occur with the tuff of greater density). The density of the tuff is related to welding (i.e., density of the tuff increases from nonwelded tuff to welded tuff).

Data are available on the bearing capacities of the moderately welded tuff. The following table shows the relationship of density change to the resistance to crushing of a moderately welded tuff in the area of investigation.

Bulk density (lbs. per cu. ft.)	Resistance to crushing (lbs. per sq. ft.)
108	48,800
109	73,000
111	79,200
112 (probably with pumice inclusion)	69,200
113	99,200
114	115,600

Pumice fragment inclusion in a small sample of the tuff would decrease the bearing capacity as failure would most likely occur within the pumice fragment.

The following table is a comparison of the bearing capacities of a moderately welded tuff (density 108 and 114 lbs. per cu. ft.) and miscellaneous building stone. The bearing capacity is computed as 1/5 of rupture strength of the material.

Building stone	Bearing capacity (lbs. per sq. ft.)
Moderately welded tuff (108 lbs. per cu. ft.)	9,700
Moderately welded tuff (114 lbs. per cu. ft.)	23,000
Concrete 1/	23,000
Sandstone 1/	69,000
Brick 1/	86,000
Marble 1/	219,000
Granite 1/	279,000

1/ Handbook of Chemistry and Physics, 1958.

The moderately welded tuff is a good structural building stone as its bearing capacity is roughly comparable to concrete with a density or weight of about half that of concrete.

Thermal conductivity

The thermal conductivity of the tuff is related to porosity, thus, the thermal conductivity of a nonwelded tuff would be less than a welded tuff as more pore space is available for insulation.

The only data available on the thermal conductivity was made of a moderately welded tuff in one area investigated. The following table is a companion of the thermal properties of the tuff and miscellaneous building stone. A decrease in thermal conductivity increases the insulating value.

Building stone or material	Range of thermal conductivity (B.T.U. per hr. per sq. ft. and temp. gradient of 1°F per in. thickness)
Rock wool 1/	0.26- 0.29
Moderately welded tuff	.31- .38
Brick 1/	3 - 6
Concrete (set) 1/	6 - 9
Sandstone 1/	8 -16
Marble 1/	14 -20
Granite 1/	13 -28

1/ Handbook of Chemistry and Physics, 1958.

The moderately welded tuff is a better insulation than other building materials. A building constructed of a moderately welded tuff may not need additional insulation.

Chemical composition

The chemical composition of a rock may affect its usefulness in a concrete aggregate and for other purposes. The following table shows a representative analyses of the tuff.

Chemical constituents	Range in percent
Silica (SiO_2)	72.0 -78.2
Alumina (Al_2O_3)	11.2 -13.8
Ferric oxide (Fe_2O_3)	1.1 - 2.1
Ferrous oxide (FeO)	.21- .75
Magnesium oxide (MgO)	.02- .33
Calcium oxide (CaO)	.26- 1.17
Sodium oxide (Na_2O)	3.5 - 4.5
Potassium oxide (K_2O)	4.2 - 4.7
Water (H_2O)	.15- 2.8
Titanium oxide (TiO_2)	.10- .32
Phosphorous oxide (P_2O_5)	.10- .07
Manganese oxide (MnO)	.00- .98
Carbon dioxide (CO_2)	< .05

Mineral composition

The tuff is rhyolitic in composition and contains small rock fragments of rhyolite, latite and devitrified pumice and crystals and crystal fragments of sanidine, and quartz, in a matrix of glass shards and welded ash. Dark minerals are scarce although traces of crystal fragments of biotite, hornblende, and pyroxene have been observed (Griggs, 1964).

Seven samples of a moderately welded tuff were analyzed petrographically by C. S. Ross (written communication, July 7, 1960). Ross recalculated the proportions of phenocrysts in terms of proportion by weight. The results of all seven were similar, one of which is presented here:

Pore space	about 30 percent by volume
Phenocrysts	about 20 percent by weight
Sanidine	12 percent by weight
Quartz	6 percent by weight
Magnetite	1± percent by weight
Pyroxene	0.5± percent by weight

The ground mass is typical devitrified welded tuff. The devitrification products are very fine-grained, but show typical cristobalite-feldspar structure. Cavities contain radial groups of feldspar and tridymite. The rocks contain a few areas of altered andesite, and some brown birefracting clay like material (probably montmorillonite).

Pumice, rhyolite, and latite rock inclusions

Rock inclusions of pumice, rhyolite, and latite are found in the tuff. The frequency of occurrence of the rock fragments differs in individual ash flows and at different locations within the same ash flow.

The pumice fragments may be as much as two inches in length and one inch in diameter. The pumice is soft and friable and should cause no problem in cutting the tuff. The rhyolite and latite fragments are dark gray, hard, and may be as much as two or three inches across. These large rock fragments may cause some difficulty in cutting the tuff so that care should be taken in selecting tuff units that are void of these larger rock fragments.

Weathering and erosion characteristics

The surface of exposed tuff (nonwelded to welded) becomes "case hardened" as it is exposed to the weather. In this process, due to the porosity of the tuff, moisture is absorbed and some minerals are dissolved. The minerals are returned to the surface by evaporation as the tuff dries out where they are precipitated to form a rind. This rind forms a protective surface which resists the wearing away of the surface by wind and water. However, exposed pumice fragments weather out rapidly to enhance the beauty of the stone.

Lichens grow on tuff where moisture accumulates for brief periods. Lichens covered tuff has been used as ornamental stone for the construction of fences and walls of houses in Albuquerque, New Mexico.

The weathering characteristics of the tuff do not affect its use as a building stone; but on the contrary, it enhances the beauty of the stone.

Color

The color of the tuff ranges from very light gray to medium dark gray. Some units range from pinkish gray to light pink. Large fragments of pumice that appear much darker than the matrix in some units enhance the color of the tuff. Moderately welded units are generally lighter in color than the welded units. The coloring is inherent in the tuff and probably the result of minor changes in the chemical constituents and heat of emplacement. Weathering of the tuff changes the color very slightly.

Natural moisture content

The natural moisture content of the tuff forming the mesas between the eastward-trending canyons is generally less than five percent by volume. The low moisture content of the tuff is caused by the protective cap of clayey soil derived by weathering of the tuff near the surface. The soil is thickest near the axis of the mesas and thins toward the edges where the tuff is exposed. Precipitation that is not removed by surface drainage on the mesa tops infiltrates into the soil; however, the downward movement of this water is impeded or stopped by a dense transition zone between the soil and tuff and the water is returned to the atmosphere by evapotranspiration (Abrahams, Weir, and Purtymun, 1961).

The low natural moisture content of the tuff decreases the weight of the cut stone for handling and transportation, and should aid in quarrying and cutting.

Thickness

The Tshirege Member, consisting of a series of ash-flow tuffs ranging from nonwelded to welded, is about 800 feet thick along the western edge of the Pajarito Plateau. The Tshirege thins eastward to less than 50 feet. Some of the uppermost ash flows are beveled off by erosion eastward across the plateau. Outliers of tuff overlie the Puye Conglomerate along Puye Escarpment. Most all ash flows thin eastward from the source area (Sierra de los Valles).

Nonwelded ash flows in the lower part of the Tshirege Member may be as much as 200 feet thick near the center of the plateau. Individual moderately welded and welded ash flows in the upper part of the Tshirege Member range from 20 to 120 feet thick. The thickness of these moderately welded and welded tuff units permits a large source of quarry stone.

Joints

Joints are prominent in the tuff. They divide the rocks into many irregular blocks, many of which are prismatic or columnar. The joint density in a specific area will differ with different degrees of welding. The number of joints decreases with a decrease degree of welding (fewer joints are found in nonwelded tuff than in welded tuff). The numerically predominant joints are near vertical and are persistent in length and pass through several groups of tuff units. These joints tend to curve slightly. The joint face is relatively smooth and will add rustic beauty as use as a building stone. The presence of the joints should cause no difficulty in cutting the tuff, but aid in quarrying blocks of tuff.

Conclusions

Although no studies of Tshirege Member of the Bandelier Tuff were made to determine its suitability as a foundation rock, structural building stone, ornamental stone, or as an insulating material, the information obtained in earlier studies as to its availability, accessibility, and physical properties indicates that it is well suited to those and other uses. Furthermore, it has already been used for those and other purposes, and it promises to be a valuable resource to the Santa Clara Pueblo Indians and to other citizens of New Mexico.

References

Abrahams, J. H., Jr., Weir, J. E., Jr., and Purtymun, W. D., 1961, Distribution of moisture in soil and near-surface tuff on the Pajarito Plateau, Los Alamos County, New Mexico: in short papers in geologic and hydrologic sciences, Articles 293-435, U.S. Geol. Survey Prof. Paper 424-D, art. 339, p. 142-145.

Griggs, R. L., 1964, Geology and ground-water resources of the Los Alamos area, New Mexico: U.S. Geol. Survey Water-Supply Paper 1753, 104 p., 1 pl., 20 figs., 4 tbls.

Hewitt, E. L., 1953, The Pajarito Plateau and its ancient people: Albuquerque, Univ. of New Mexico Press, 174 p.

Hodgman, Charles D., Editor, 1958, Handbook of Chemistry and Physics: Cleveland, Chemical Rubber Publishing Co., 3,456 p.

Kelley, V. C., 1948, Los Alamos Project, Pumice Investigation: Final Report No. 2, Field Survey to Los Alamos Scientific Laboratory, 16 p., 1 fig.

Smith, R. L., 1960, Zones and zonal variations in welded ash flows: U.S. Geol. Survey Prof. Paper 354-F, 10 p., 2 pls.

Spiegel, Zane, and Baldwin, Brewster, 1963, Geology and water resources of the Santa Fe area, New Mexico: U.S. Geol. Survey Water-Supply Paper 1525, 258 p., 7 pls., 56 figs., 21 tbls.

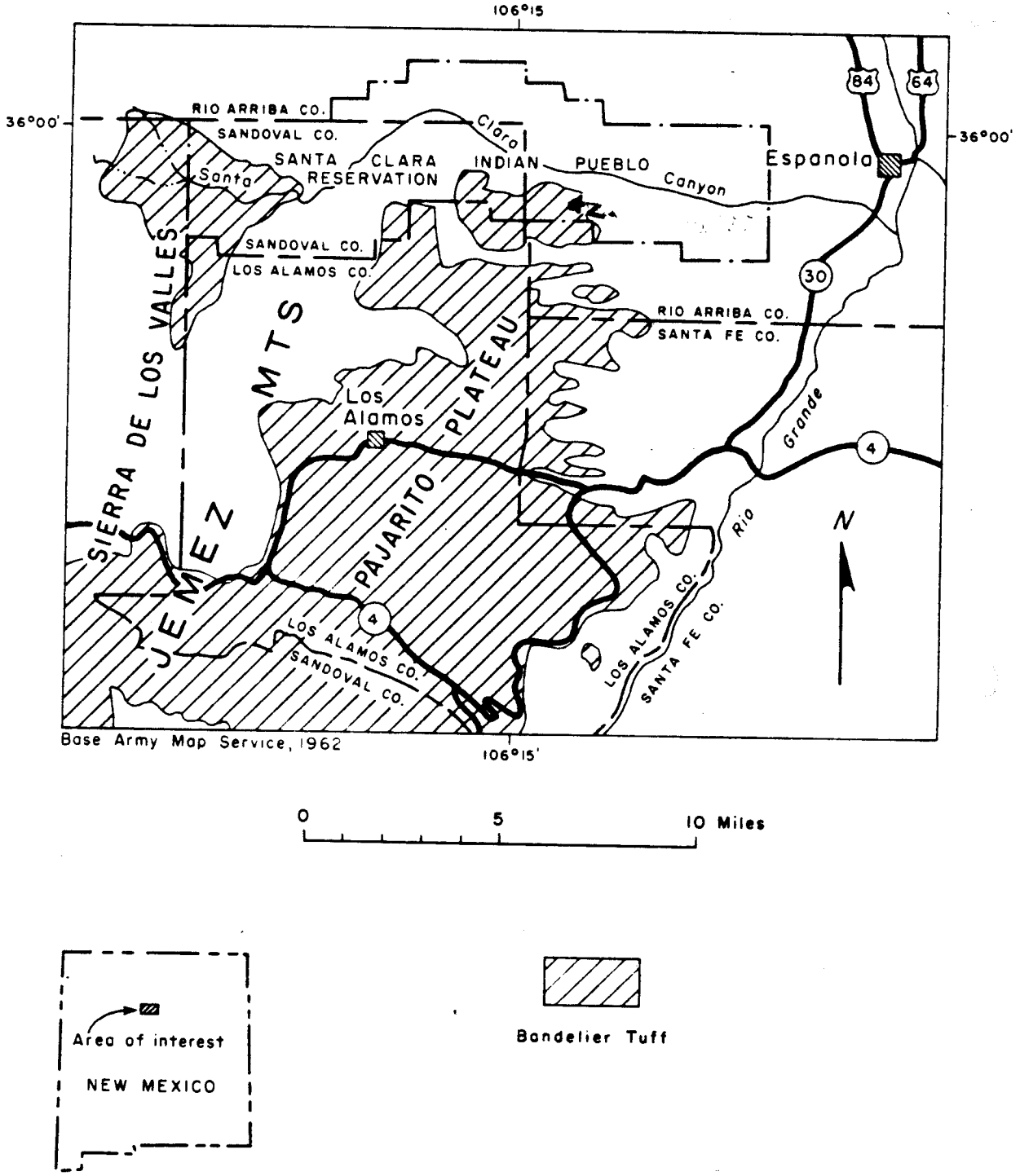

Figure 1.--Map showing topographic features in the region of the Santa Clara Indian Reservation and their relation to the Bandelier Tuff (shaded) of the Jemez Mountains.

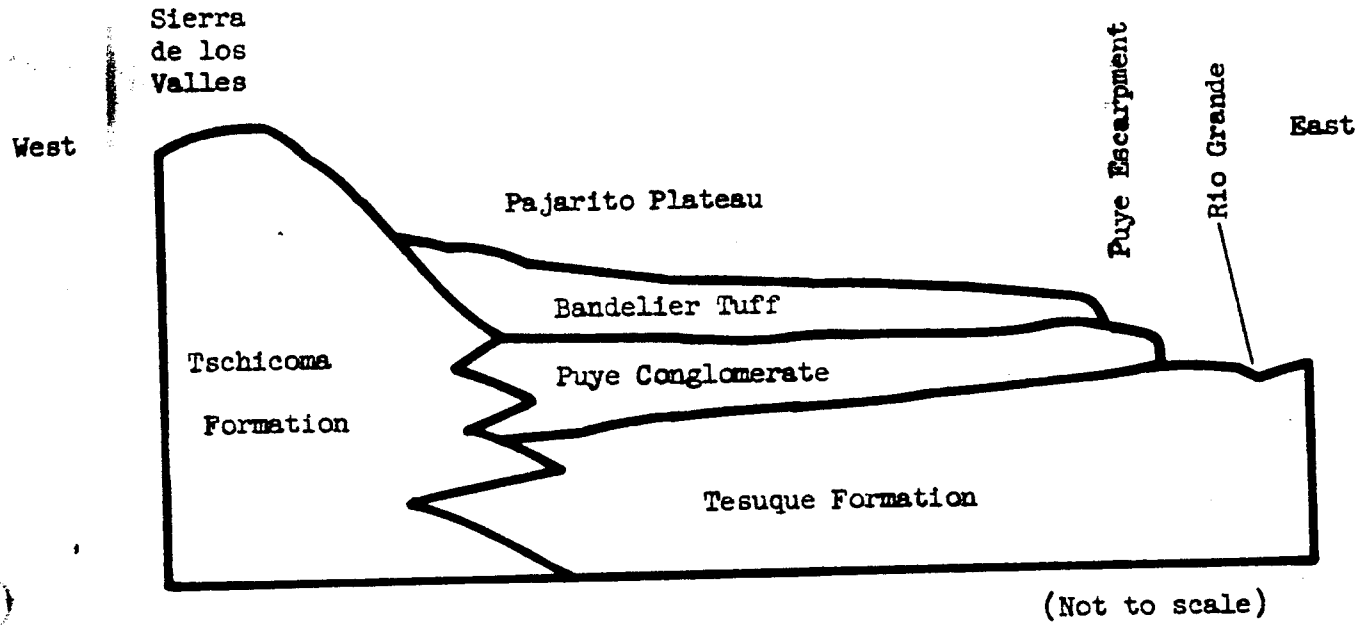

Figure 2.-- Diagrammatic cross section showing the relation of geologic formations in the area south of the Santa Clara Indian Reservation

LA-5725-MS
Informal Report

UC-11
Reporting Date: August 1974
Issued: October 1974

Air Volume and Energy Transfer Through Test Holes and Atmospheric Pressure Effects on the Main Aquifer

by

W. D. Purtymun
F. C. Koopman*
S. Barr
W. E. Clements

*Permanent address: U.S. Geological Survey, Albuquerque, NM 87106.

los alamos
scientific laboratory
of the University of California
LOS ALAMOS, NEW MEXICO 87544

UNITED STATES
ATOMIC ENERGY COMMISSION
CONTRACT W-7405-ENG. 36

AIR VOLUME AND ENERGY TRANSFER THROUGH TEST HOLES AND ATMOSPHERIC PRESSURE EFFECTS ON THE MAIN AQUIFER

by

W. D. Purtymun, F. C. Koopman, S. Barr, and W. E. Clements

ABSTRACT

Air volumes and energy transfer through test holes completed in the Bandelier Tuff and/or Puye Formation were monitored for 95 h at test hole DT-10 and for 34 h at test holes DT-10 and Alpha. Air transfer caused by atmospheric pressure changes at DT-10 during the 95-h study consisted of four cycles of four intake periods and four exhaust periods. The total volume of air taken into the reservoir was 2910 m^3 while 1425 m^3 of air were released from the reservoir. The largest volume of air transferred was 2400 m^3 during an intake period of 40 h with an atmospheric pressure change of 0.46 cmHg. The average energy in the air transferred during the intake period was 14.4 x 10^3 g-cal/m^3 while the average energy in the air of the exhaust period was 19.3 x 10^3 g-cal/m^3.

The 24-h study at test holes DT-10 and Alpha was made near the end of an exhaust period. About 1160 m^3 of air were released from the reservoir rocks at DT-10 with about 10 500 m^3 of air released from Alpha. A constriction in the casing to accommodate instrumentation reduced the volume of air transferred from DT-10. Energy in air transferred from DT-10 was 19.3 x 10^3 g-cal/m^3 and 12.3 x 10^3g-cal/m^3 from Alpha.

Atmospheric pressure changes cause water-level fluctuations in test holes penetrating the main aquifer. The changes in water-levels, atmospheric pressure and rates of air transferred during the 95-h study were correlatable. The barometric efficiency of the aquifer during the four cycles ranged from 51 to 88 percent. Larger barometric efficiencies resulted with smaller volumes of air transferred and smaller pressure changes.

I. INTRODUCTION

Test holes in the Bandelier Tuff and Puye Formation (a conglomerate) in north-central New Mexico transfer air to and from the tuff and conglomerate in response to changes in atmospheric pressure. The air enters the tuff and conglomerate through test holes during atmospheric highs and is released during atmospheric lows. This phenomenon has been recognized throughout the world and is especially prominent where wells or test holes penetrate unsaturated sections of rocks of volcanic origin. Though the phenomenon is well known, little effort has been made to determine volumes, rates, and pressures at which the air transfer takes place. A study was made to determine some of the parameters related to air exchange under normal atmospheric pressures.

A theoretical model was prepared to examine the air transfer in the reservoir rock in response to pressure changes of the test holes at land surface. The preliminary model is attached as Appendix A. An analytical model describing gas flow through a porous soil or rock in response to variation of atmospheric pressure is presented as Appendix B.

The study is of academic interest and covers only a short time interval. It may be kept in mind that some practical use of the phenomenon could be developed. One possible use would be energy extraction from reservoir rocks that have above-normal geothermal gradients by taking advantage of atmospheric pressure changes.

Changes in atmospheric pressure produce water-level fluctuations in wells or test holes penetrating confined aquifers. An assessment of pressure change on the water levels in a test hole was made in conjunction with the air transfer study.

The study was made in test holes on the Pajarito Plateau which lies between the Sierra de Los Valles and the Rio Grande in north-central New Mexico. The plateau is formed by the Bandelier Tuff, a series of ashflows and ashfalls of rhyolite tuff.[1] The tuff underlying this plateau is about 320 m thick along the flanks of the mountains and thins to less than 80 m along the Rio Grande. The porosity of the tuff ranges from about 15 percent in the welded units to as much as 60 percent in the nonwelded units.[2] The pores are mainly capillary in size. Open joints in the tuff also add to the porosity.

Atmospheric pressure changes resulting in slight air pressure change in the tuff to depths of 35 m have been detected.[3] The exchange of air through bore holes at a depth less than 35 m has been detected, indicating that a differential pressure does exist between the atmosphere and the upper 35 m of tuff. The soil cover on the mesa and case hardening of the tuff exposed on the edges of the mesa and canyon walls apparently form a partial barrier to transfer of air in and out of the tuff resulting from atmospheric pressure changes.

Underlying the tuff is the Puye Formation that is a conglomerate made up of silts, clays, gravels, and boulders. The upper part of the conglomerate and overlying tuff are in the zone of aeration. The main aquifer in the area of study lies at a depth of about 330 m and occurs in the lower part of the conglomerate. The water in the aquifer responds to atmospheric pressure changes in test holes in the area.

A. Test Holes Used in the Study

The studies were made at two test holes south of Los Alamos on the Pajarito Plateau. Test hole DT-10 is completed through the Bandelier Tuff and into the Puye Formation. Test hole Alpha is completed into the Bandelier Tuff. The tuff and upper part of the conglomerate are in the zone of aeration.

Test hole DT-10 is 433 m deep; the water level in the hole is 332 m below the land surface. The bore hole, 40.6 cm in diameter, contains casing 30.5 cm in diameter that is reduced in diameter to 10.2 cm at land surface to accommodate instrumentation. The casing is 433 m in length, with slots cut into the lower 105 m. About 4 m of the slotted casing extend above the water table. About 88 m^2 of conglomerate and 334 m^2 of tuff in the bore wall of the hole are exposed to the atmosphere between the casing and the bore wall. The reduction of the casing to accommodate the instrumentation and slots in the lower part of the casing restrict the air volume transfer.

Test hole Alpha is located about 1000 m west of DT-10. Alpha is completed within tuff in the zone of aeration at a depth of 58 m. It contains casing 61 cm in diameter that extends to a depth of 3 m, thus about 106 m^2 of tuff in the bore walls of the hole are exposed to the atmosphere. Instruments were placed in the casing at a

depth of about 3 m, thus the air volume transfer was not restricted.

B. Instrumentation

The parameters measured during the investigation were bore-hole air velocity, temperature, humidity, and atmospheric pressure. Air velocities were measured by a thermopile air-flow sensing sonde and recorder which were modified to use battery power. A second unit, similarly modified, consisted of a dual-thermistor air flow sensing sonde and recorder. Thermographs were used to measure temperature and humidity. Temperatures recorded by the thermographs were cross-checked by a thermistor-type temperature sonde and recorder. Instruments were calibrated and checked in the field by use of sling psychrometers, anemometers, and thermometers. Microbarograph records were cross-checked with the LASL Weather Section.

II. AIR VOLUME TRANSFER

The four parameters (air velocity, humidity, temperature, and atmospheric pressure) were recorded for 95 h from October 10 through 14, 1964, on test hole DT-10 and for 24 h on November 14, 1964, on test holes DT-10 and Alpha. The air transfer into and from the reservoir caused by changes in atmospheric pressure is described in cycles. The cycles consist of an exhaust period (air transfer from the reservoir to the atmosphere) and an intake period (air transfer from the atmosphere to the reservoir).

A. Test Hole DT-10

Four cycles of air transfer from test hole DT-10 occurred from 0500 on October 10 to 0400 on October 14. The four intake periods ranged from 4 to 40 h in length for a total of 57 h. The volume of air taken into the reservoir ranged from 40 m^3 to 2440 m^3 (Table I). Total volume of air taken into the reservoir during the four intake periods was 2910 m^3.

The four exhaust periods ranged from 2 to 18 h for a total of 38 h. The volume of air released from the reservoir to the atmosphere ranged from 5 m^3 to 540 m^3. Total volume of air released from the reservoir was 1425 m^3. During the 95 h the net increase of air to the reservoir was 1485 m^3.

The largest volume of air transferred during the 95 h was during the 40 h intake period from 1900 on October 11 to 1100 on October 13. During this period 2440 m^3 of air were taken into the reservoir rock. The atmospheric pressure was at 58.22 cmHg when the period began and at 58.63 when it ended. The atmospheric pressure increased during the initial part of the period then varied during the remainder of the 40 h (Fig. 1).

TABLE I

AIR VOLUME TRANSFERRED THROUGH TEST HOLE DT-10 DURING FOUR CYCLES

	Intake Period		Exhaust Period	
Cycle No.	Interval (h)	Volume (m^3)	Interval (h)	Volume (m^3)
1	7	310	18	540
2	4	40	9	540
3	40	2440	9	340
4	6	120	2	5

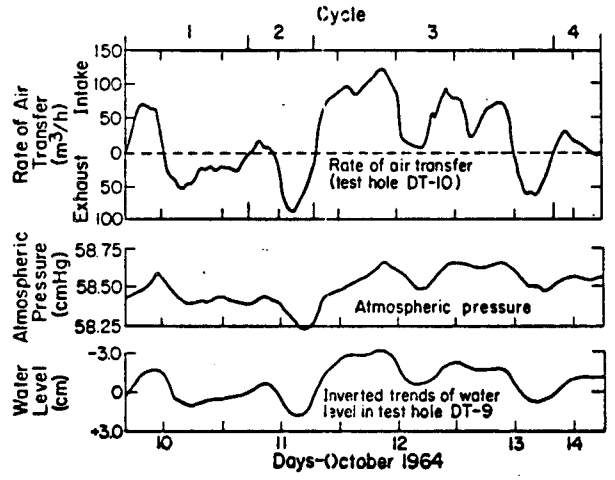

Fig. 1. Rate of air transfer in test hole DT-10; atmospheric pressure; and water level trends in test hole DT-9, October 10 through 14, 1964.

TABLE II

MAXIMUM ATMOSPHERIC PRESSURE CHANGE DURING FOUR CYCLES

Cycle No.	cmHg Intake[1]	cmHg Exhaust[2]
1	0.15	0.20
2	0.05	0.20
3	0.46	0.18
4	0.10	0.02

[1]Pressure Increase
[2]Pressure Decrease

The maximum atmospheric pressure change (0.46 cmHg) occurred during the first 15 h of the 40 h period (Table II). At this time the air-transfer rate was 114 m^3/h. The rate of air transferred increased with increasing atmospheric pressure from 2000 on October 11 to 0900 on October 12; however, for a short time (0200 to 0400 on October 12) the air-transfer rate decreased slightly while the atmospheric pressure was steadily increasing (Fig. 1).

The rate of air transfer for each of the four cycles varied from a few m^3/h to the maximum of 114 m^3/h. A general increase in atmospheric pressure during a period will result in an increased rate of air transfer. The larger volumes of air are transferred when maximum atmospheric pressure changes take place, resulting in periods of longer duration.

The transition pressure at which the periods change is dependent on the duration, volume of air transferred, and amount of atmospheric pressure change during the previous period. The transition pressure is generally greater at the beginning of the intake period than at the beginning of the exhaust period (Table III). The air pressure increases in the reservoir rock during the intake period and decreases during the exhaust period.

TABLE III

TRANSITIONAL PRESSURES OF INTAKE AND EXHAUST PERIODS AT TEST HOLE DT-10

	Intake Period			Exhaust Period		
Cycle No.	Start	End	Pressure Increase	Start	End	Pressure Decrease
1	58.34	58.44	+.10	58.44	58.32	0.12
2	58.32	58.32	.00	58.32	58.22	0.10
3	58.22	58.63	+.41	58.63	58.42	0.21
4	58.42	58.44	+.02	58.44	58.44	0.00

Periods of short duration in which small volumes of air were transferred occurred with only small atmospheric pressure changes. This resulted in a period change at or near the same transitional pressure at which the period began. (Table I and III, Cycle 2 intake period and Cycle 4 exhaust period).

B. Test Holes, DT-10 and Alpha

The volume and rate of air transferred by test holes DT-10 and Alpha were measured during an exhaust period of 24 h on November 14, 1964. Although the air transfer was in an exhaust period, the atmospheric pressure increased about 0.15 cmHg during the 24 h. The increased pressure indicated that the period was approaching the transitional pressure. About 10 500 m^3 were released from the reservoir rock through Alpha whereas 1160 m^3 were released through DT-10. The average rate of air transfer for the 24-h period was 438 m^3/h and 48 m^3/h from Alpha and DT-10, respectively. The volume of air and the rate at which the air was transferred from Alpha was about 9 times greater than that of DT-10, although the area of reservoir rock exposed in DT-10 was several times greater. It is concluded that the constriction of the casing at the land surface to 10 cm diameter in DT-10 impeded air transfer and also that vapor from the aquifer may have decreased the air permeability of the reservoir rock. In test hole Alpha measurements were made at a depth of 3 m, inside the open surface casing, thus, no physical restrictions were present that would impede the transfer of air.

III. ENERGY TRANSFER

The hourly gain or loss of energy caused by air transfer through test holes was computed for the 95 h at DT-10 and during the 24-h exhaust period at DT-10 and Alpha. The energy was computed from the measured parameters of temperature, moisture content, and volume of air transferred by use of psychrometric charts and tables at an atmosphere of 58.42 cmHg.[4] The tables are based on energy of dry air at -18°C (0°F) that has been made equal to 2520 g-cal (10 BTU). At -18°C the energy in dry air at a pressure of 58.42 cmHg is 5.8×10^3 g-cal/m^3.

The temperature of the reservoir rocks measured in test holes ranged from 11°C at 30 m to about 19°C at 340 m within the main aquifer. The temperature gradient is about 27°C per km within the normal range of 25°C to 35°C per km.[5]

The air temperature for the 95 h of the study at DT-10 in October ranged from a minimum of 4°C to 18°C. The average temperature of the air measured during the four intake periods was 13°C while the average moisture content was 4 g/m^3. The estimated energy in each cubic meter of air was 14.4×10^3 g-cal (Table IV). The amount of energy taken into the reservoir was about 41.9×10^6 g-cal.

The average temperature of air transferred during the exhaust period was 16°C with an average moisture content of 9 g/m^3. The estimated energy in each cubic meter of air was 19.3×10^3 g-cal. The amount of energy transferred from the reservoir to the atmosphere was 27.5×10^6 g-cal.

The heat of the reservoir rocks and of the aquifer warmed the air taken into the reservoir during the intake periods. The warmer air coupled with the increased moisture content (water vapor from the aquifer) resulted in an increase of about 5 g-cal/m^3 in the exhaust periods. The volume of air in the exhaust periods was about half of the volume of air in the intake periods, thus a net gain of about 14.4×10^6 g-cal was added to the reservoir during the 95-h study.

The air temperatures during the 24-h study on November 14 ranged from 1°C to 8°C. The average temperature during the exhaust cycle at Alpha was 7°C with a moisture content of 2 g/m^3 (Table V). The energy in a cubic meter of air was 12.3×10^3 g-cal. The total volume of air transferred

TABLE IV

ENERGY TRANSFERRED THROUGH TEST HOLE DT-10

DURING FOUR CYCLES

Period	Intake	Exhaust
Time Interval (h)	57	38
Volume of Air (m^3)	2,910	1,425
Average Temperature (°C)	13	16
Average Moisture Content (g/m^3)	4	9
Energy per Cubic Meter (g-cal)	14.4×10^3	19.3×10^3
Total Energy Transferred (g-cal)	41.9×10^6	27.5×10^6

from the reservoir was 10 500 m^3 which contained about 129.2×10^6 g-cal of energy.

The average temperature during exhaust period at DT-10 was 16°C during the same 24 h. The moisture content was 11 g/m^3 containing about 19.3×10^3 g-cal/m^3. The volume of air transferred to the atmosphere was 1 160 m^3 which contained about 22.4×10^6 g-cal of energy.

The energy per unit-volume was considerably less in the air that was transferred from Alpha than that from DT-10 due to the water vapor and higher temperature of the air released through DT-10. However, the amount of energy released from the reservoir through Alpha was about 6 times greater than that released through DT-10 due to the greater volume of air transferred through Alpha (Table V).

The larger volume of air transferred through Alpha in previous cycles results in cooling of the reservoir rocks with advancing Fall weather. The amount of energy in the air from Alpha during the exhaust period in November was less than that of the intake periods in October at DT-10 due to the cooling of the reservoir rocks during the previous cycles.

IV. ATMOSPHERIC PRESSURE EFFECTS ON MAIN AQUIFER

Test hole DT-9 is located about 950 m south of DT-10. The 500-m hole is completed into the same aquifer as DT-10. The aquifer is very sensitive to atmospheric pressure changes, earth shocks, and probable

TABLE V

ENERGY TRANSFERRED THROUGH TEST HOLES DT-10 AND

ALPHA DURING A 24-HOUR EXHAUST PERIOD

Test Hole	DT-10	Alpha
Volume of Air (m^2)	1,160	10,500
Average Temperature (°C)	16	7
Average Moisture Content (g/m^3)	11	2
Energy per cubic meter	19.3×10^3	12.3×10^3
Total Energy Transferred (g-cal)	22.4×10^6	129.2×10^6

earth tide effects. These effects (water-level fluctuation) are monitored by a semi-continuous water-stage recorder at DT-9.

The possible earth tide effects are recorded by minor water-level fluctuations in which the gravitational pull of the moon elongates and compresses the aquifer. These effects, estimated from the records by eliminating atmospheric effects range from 0.3 to 0.9 cm of water-level fluctuation.

Water-level fluctuations are also recorded from earth shocks. In general these must be the result of strong earth motion. Records of the Alaskan earthquake of 1964 caused a water-level fluctuation of more than 30 cm. Smaller fluctuations have occurred, generally less than 3 cm, which are attributed to major quakes in Mexico or Central America. These fluctuations are caused by expansion and compaction of the aquifer by surface waves of the earthquake.

Changes in atmospheric pressure cause water-level fluctuations. During a storm of December 1967 a fluctuation of over 18 cm was recorded. Minor changes in atmospheric pressure also cause water-level fluctuations. Water levels were plotted for the 95-h period along with atmospheric pressure and rates of air transfer at DT-10 (Fig. 1). Since the relationship is reversed the water levels on the figure are inverted for comparison. Increase in atmospheric pressure causes water-level decline while a decrease in pressure causes a water-level rise. The changes in water levels, atmospheric pressure and rates of air transfer are correlatable.

The barometric efficiency of the aquifer can be expressed in terms of a column of water. The ratio of water-level changes to pressure change expresses the barometric efficiency of the aquifer (Table VI). The barometric efficiency ranged from 51 to 88 percent for the four cycles. The smaller pressure changes with smaller volumes of air transferred resulted in the greater barometric efficiency.

The aquifer penetrated by DT-9 is not homogeneous but is made up of three different rock types (conglomerate, volcanic flow rock, and sandstone) with three different coefficients of transmissibility and probably three different head (water) pressures in each unit. The variation in barometric efficiency is the result of the different pressures within each unit.

V. CONCLUSIONS

The larger volume of air transfer occurs when atmospheric pressure change is at a maximum which results in air transfer periods of a long duration. The transitional pressure at which periods change is dependent on the amount of pressure change, duration of the period and volume of air transferred during the previous period. The transitional pressure at which periods change increases during the intake period and decreases during the exhaust period.

TABLE VI

BAROMETRIC EFFICIENCY

Cycle No.	Max Atmospheric (cmHg)	Max Atmospheric Pressure (cmH_2O)	Max Water-level Fluctuation (cmH_2O)	Barometric Efficiency (%)
1	.35	4.8	3.0	63
2	.25	3.4	2.6	76
3	.63	8.6	4.4	51
4	.12	1.6	1.4	88

The variation in barometric efficiency of the aquifer is the result of variation in head pressure in the different rock units of the aquifer. The larger barometric efficiency occurs with smaller atmospheric pressure change and a decrease in efficiency with increased pressure change.

REFERENCES

1. R. L. Griggs, "Geology and Ground Water Resources of the Los Alamos Area, New Mexico," U.S. Geological Survey Water Supply Paper 1753 (1964).

2. W. D. Purtymun and R. C. Koopman, "Physical Characteristics of the Tshirege Member of the Bandelier Tuff With Reference to Use as Building Ornamental Stone," U.S. Geological Survey Open File Report (1965).

3. J. L. Kunkler, "Measurements of Atmospheric Pressure and Subsurface-Gas Pressures in the Unsaturated Zone of the Bandelier Tuff, Los Alamos, New Mexico," U.S. Geological Survey Prof. Paper 650-D (1969).

4. W. Goodman, "Air Conditioning Analyses with Psychrometric Charts and Tables," McMillan Co., New York (1943).

5. D. E. White, "Characteristics of Geothermal Energy Resources" in Geothermal Energy, Ed. by Kinger and Otte, Stanford University Press (1973).

APPENDIX A

PRELIMINARY THEORETICAL EXAMINATION OF AIR VOLUME TRANSFER THROUGH TEST HOLES

Elementary theoretical considerations were made to gain insight into the phenomenon behind the observations of air transfer through test holes. The basic problem appears to be one of response of flow in the test hole - reservoir rock system to pressure changes at the mouth of the hole. The governing equations for flow in the hole and in the porous reservoir can be specified. An immediate consequence of the system structure is that the limiting flow is flow within the porous rock, hence this aspect is the focus of the analysis.

The steady flow through a porous medium (reservoir rock) is described by Darcy's law for fluid of constant density

$$\frac{\mu}{k}\vec{u} = -\nabla(p + \rho\Omega), \qquad (1)$$

where μ is the fluid viscosity $(ML^{-1}T^{-1})$, k the permeability (L^2), p is pressure (FL^{-2}), ρ is density (ML^{-3}), u is velocity (LT^{-1}), and Ω is an arbitrary potential with units of (T^{-2}). Ω is generally used to account for gravity in the seepage of water through soils.

A simple derivation of (1) from the fundamental equations for fluid flow will guide us in the extension to some nonsteady aspects of the flow. Writing the fundamental momentum-conservation equations

$$\frac{\partial}{\partial t}\vec{u} + \vec{u}\cdot\nabla\vec{u} = -\frac{1}{\rho}\nabla p - \nabla\Omega + \vec{F}. \qquad (2)$$

If the time dependence and inertial terms are neglected in (2) and if the friction term F is made proportional to the velocity through $-\frac{\mu}{\rho}\vec{u} = \vec{F}$ the results Eq. (1). Note that this is fundamentally different from the Stokes hypothesis for more pure fluid systems which puts the frictional

stress proportional to the rate of strain or velocity gradient. The present analysis retains the time dependence but neglects inertial effects. The analysis is made for air flow rather than liquid, therefore the role of gravity is reduced and Eq. (2) can be simplified to

$$\frac{\partial \vec{u}}{\partial t} + \frac{\mu}{\rho k}\vec{u} = -\frac{1}{\rho}\nabla p \cdot \qquad (3)$$

The assumption of constant density simplifies the mass continuity equation to

$$\nabla \cdot \vec{u} = 0. \qquad (4)$$

The calculation of the divergence of either Eq. (1) or (3), neglecting gravity, and use of Eq. (4), results in a soluble equation for the pressure field from which the velocity can be calculated using Eq. (1) or (3),

$$\nabla^2 p = 0 . \qquad (5)$$

Equation (5) forms a basis of a series of simple models described below, each with its interpretive value.

<u>(a) Two-dimensional, radially symmetric steady-state flow in a plane parallel to ground level (Fig. A-1)</u>. In this coordinate system, Eq. (5) becomes

$$\frac{d^2p}{dr^2} + \frac{1}{r}\frac{dp}{dr} = 0, \qquad (6)$$

where r is the radial distance from the center of the hole. Equation (6) can be solved by the substitution, $r = e^s$ or $s = \ln r$. Introducing the boundary conditions at the wall of the test hole, r_0, $p = 0$ and $u = u_0$, the solution is

$$p(r) = +\frac{\mu}{k} u_0 r_0 (\ln \frac{r_0}{r})$$

$$u(r) = u_0 \frac{r_0}{r} . \qquad (7)$$

Positive u, u_0 is directed from the wall radially outward. The selection of $p = 0$ as a boundary condition is arbitrary and $p = 0$ is not an absolute value but a departure from some equilibrium value. The gradient of p, and not p itself, is important.

Notice from Eq. (7) that the velocity drops off as the inverse of the distance from the wall. Hence u drops to 10% of u_0 at 10 r_0. Choice of 0.1 u_0 as a cutoff for effects of the bore hole with $r_0 = 0.2$ m suggests that the flow involves a volume with a radius of 2 m.

<u>(b) Two-dimensional time dependent symmetric flow in a plane parallel to the ground level</u>. Equation (3) yields the same pressure field as treated in (a). Introducing a periodic condition on pressure at the wall and p = const. at $r - Nr_0$ gives a pressure field,

$$p = \frac{\sin \nu t}{\ln N} \ln \frac{Nr_0}{r}, \qquad (8)$$

where ν is the frequency of the impressed boundary condition; α is its amplitude.

The periodic solution of Eq. (3) with the pressure field given by Eq. (8) is of the form

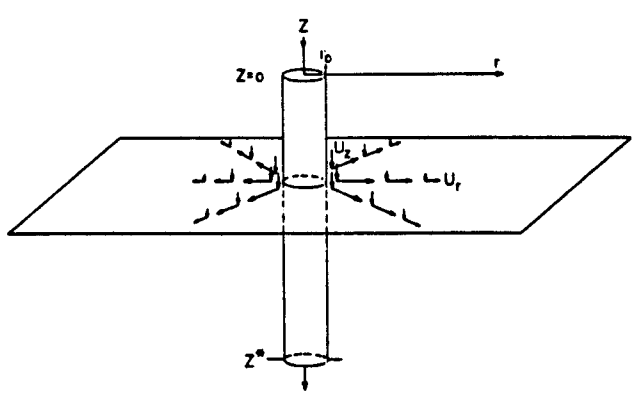

Fig. A-1. Schematic diagram of three-dimensional air transfer.

$$u(r,t) = \left(\frac{\alpha}{r \ln N}\right) \left(\frac{1}{k^2 \upsilon^2 + \mu^2}\right) [k\mu \sin \upsilon k^2 \cos \upsilon t] \tag{9}$$

Equation (9) shows that the velocity lags the external pressure by an amount

$$\tan^{-1} \left(- \frac{\mu}{\upsilon k}\right) - \frac{\pi}{2} . \tag{10}$$

This supports qualitatively the results depicted in Fig. 1 where the velocity maxima appear to be 1-3 h behind the pressure extremes.

(c) Three-dimensional, axisymmetric steady-state flow. The three-dimensional analog to section (a) is a readily tractable problem and it can provide some insight into the limitations of the assumptions in (a). The starting point is again Eq. (5), which in circular cylindrical coordinates is

$$\frac{\partial^2 p}{\partial r^2} + \frac{1}{r} \frac{\partial p}{\partial r} + \frac{\partial^2 p}{\partial z^2} = 0 . \tag{11}$$

The coordinate z is oriented along the axis of the bore hole. Equation (11) can be solved by the technique of separation of variables, setting $p(r,z) = R(r)\xi(z)$. This yields a pair of ordinary differential equations for R and ξ. The equation for R,

$$r^2 R'' - m^2 r^2 R = 0 , \tag{12}$$

has a solution

$$R(r) = a_1 K_0 (mr) + a_2 I_0 (mr) . \tag{13}$$

K_0 and I_0 are modified Bessel functions of the second and first kind respectively and are tabulated in many references (e.g. Abramowitz and Stegun (Ref. 1). The boundary condition of finite p at large r makes $a_2 = 0$.

The equation for ξ gives some conditions on the parameter, $m\xi$.

$$\xi'' = -m^2 \xi \tag{14}$$

has solutions of the form

$$\xi = b_1 e^{imz} + b_2 e^{-imz} . \tag{15}$$

Choosing the real solutions,

$$\xi = b_3 \cos mz + b_4 \sin mz . \tag{16}$$

If z is chosen to be zero at ground level and increases downward, the boundary conditions can be specified as $\xi = 0$ at $z = 0$, $p(r_0\ z) = \beta z$. The linear pressure gradient in the shaft is a reasonable hypothesis to account for flow into ($\beta < 0$) or out of ($\beta > 0$) the hole, although any specified pressure function would work as well. The first boundary condition makes $b_3 = 0$. All wavelengths, m, contribute to ξ according to a weighting function (Fourier coefficient) determined by the second boundary condition on ξ.

$$\xi = b_4 \int_0^\infty \sin mz\ S(m) dm . \tag{17}$$

S(m) is determined using the properties of the Fourier transform

$$S(m) = \int_0^z \frac{\beta z}{b_4} \sin mz\ dz$$

$$S(m) = \frac{\beta}{b_4} \left[\frac{1}{m^2} \sin mz^* - \frac{z^*}{m} \cos mz^*\right]. \tag{18}$$

In (18), z* is the bottom of the test hole. S(m) is, as shown in Fig. A-2, heavily weighted toward low wavenumbers, $m \to 0$. The transform pair, (17) and (18) determine the form of $\xi(z) = \beta z$ everywhere; the form of S(m) which also affects R(r) (i.e., Eq. (13) is the most valuable result of the present treatment). Putting together the solution for p:

$$p(r,z) = \int_0^\infty p_m(r,z,m) S(m) dm$$

$$= \int_0^\infty S(m) \frac{K_0(mr)}{K_0(mr_0)} az, dm, \tag{19}$$

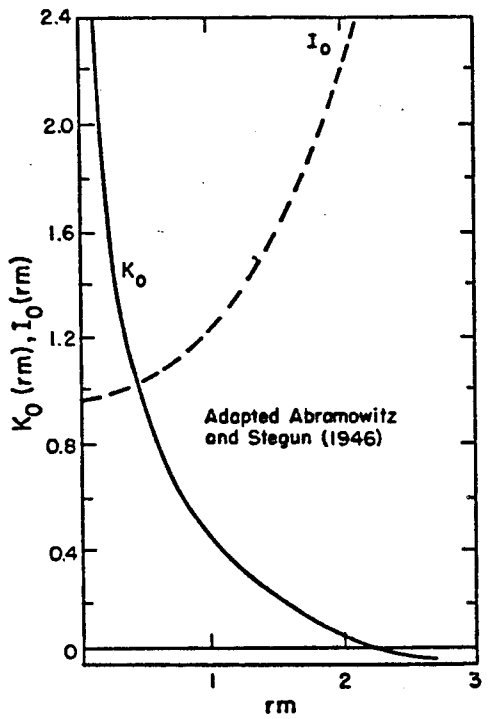

Fig. A-2. Plot of the modified Zeroth order Bessel functions of the first kind (I_o) and second kind (K_o).

where S(m) is given by (18). Equation (19) can be evaluated numerically using tabulated functions and the velocity can be similarly evaluated from

$$u_r = \frac{k}{\mu} \int_0^\infty mS(m) \frac{K_1(mr)}{K_0(mr_0)} dm$$

$$u_z = -\frac{k\beta}{\mu} \int_0^\infty S(m) \frac{K_0(mr)}{K_0(mr)} dm ,$$

which is just an application of (1). Rather than go into detailed evaluations, it is appropriate here to examine the results qualitatively. First the vertical component is constant at all heights for a given r but drops off according to $K_0(mr)$ for larger r. $K_0(mr)$ behaves like $[-\ell n(mr)]$ for small mr hence the three-dimensional flow exhibits properties very similar to the two-dimensional case in (a). The present case has some appealing aspects such as finite pressure for large r, and shows the nature of the streamlines in the reservoir rock; but the basic ideas of disturbed volume and time lag behavior are not likely to be much different.

The extension of case (c) to a time-dependent problem is conceptually straightforward and would be a reasonable extension to the present analysis. Some of the assumptions in this treatment in which second-order corrections could be made are:

(1) constant density

(2) neglect of gravity effects (related to (1)). However, these are likely to contribute only small adjustments to the results described above. Modeling experiments with pressure described as different functions of time and depth in the shaft would also be interesting additions.

REFERENCE

1. M. Abramowitz and I.A. Stegun, 1964, Handbook of Mathematical Functions, National Bureau of Standards, U.S. Govt. Printing Office, Washington, D.C. 1046 pp.

APPENDIX B

GAS FLOW IN A HOMOGENEOUS ISOTHERMAL POROUS SOIL OR ROCK DUE TO VARIATION OF ATMOSPHERIC PRESSURE

Atmospheric pressure variations induce pressure gradients in the soil and rocks of the earth's surface which result in a flow of the interstitial gas. An analytical model describing this flow can be developed from Darcy's law and the principle of conservation of mass.

Consider a homogeneous isothermal porous medium having a porosity ε (ratio of void to bulk volume) and permeability k $[L^2]$. The dynamic viscosity of the interstitial gas will be denoted by η $[M\ L^{-1}T^{-1}]$. We assume that the movement of the interstitial gas is governed by the local pressure gradient through Darcy's law.

$$\vec{v} = -\frac{k}{\eta}\ \vec{\nabla}P\ , \tag{1}$$

where P is the pressure $[M\ L^{-1}S^{-2}]$ and v is the volume flow rate per unit <u>geometric</u> area perpendicular to the direction of the flow. It should be noted that v has units of velocity $[L\ T^{-1}]$. Darcy's law is valid for Reynolds numbers less than 5. Reynolds numbers several orders of magnitude less than this are expected for atmospheric pressure-induced flow in soil or rock and, hence, the use of Darcy's law is justified here.

If we now look at a small volume τ of the porous medium and consider conservation of mass for the interstitial gas, then it is required that

$$\frac{\partial}{\partial t}\int \rho\varepsilon d\tau = -\oint (\rho\vec{v})\cdot d\vec{s}. \tag{2}$$

where ρ is the density $[M\ L^{-3}]$ and $d\vec{s}$ is the outward directed normal unit area vector to τ . Making use of the divergence theorem, equating integrands in the result, and eliminating $\vec{v}$ by the use of Darcy's law gives

$$\frac{\partial\rho}{\partial t} = \frac{k}{\varepsilon\eta}\ \vec{\nabla}\cdot(\rho\vec{\nabla}P). \tag{3}$$

The isothermal condition requires that P/ρ = constant; therefore, Eq. (3) can be written as

$$\frac{\partial P}{\partial t} = \frac{k}{\varepsilon\eta}\ \vec{\nabla}\cdot\ (P\vec{\nabla}P)\ . \tag{4}$$

We now make use of the fact that atmospheric pressure variations p are small compared to the mean pressure P_o and write

$$P = P_o + p\ . \tag{5}$$

Substituting Eq. (5) into Eq. (4) and linearizing the result gives

$$\frac{\partial p}{\partial t} = \frac{kP_o}{\varepsilon\eta}\nabla^2 p\ , \tag{6}$$

which can be written as

$$\nabla^2 p = \alpha^2\ \frac{\partial p}{\partial t}\ , \tag{7}$$

where

$$\alpha^2 = \frac{\varepsilon\eta}{kP_o}\ . \tag{8}$$

It should be noted that (7) is simply a diffusion equation for the pressure perturbation with the diffusion coefficient being α^{-2}. We will now discuss the solution of Eq. (7) for some particular cases.

CASE I: Transient Solution for a General Time-Dependent Pressure Perturbation at the Surface of an Infinitely Deep Plane Medium.

For local atmospheric pressure perturbations at the earth's surface the earth may be considered flat and of infinite extent and depth. In this case the problem can be considered one-dimensional. We will choose the z-axis perpendicular to the earth's surface with the positive direction upward. The boundary conditions are

$$p(0,t) = p^*(t) \tag{9}$$

$$p(-\infty, t) = \text{finite value}, \tag{10}$$

where $p^*(t)$ is the atmospheric pressure perturbation at the surface. For transient solutions the initial condition will be chosen as

$$p(z,0) = 0, \tag{11}$$

which requires no perturbation at $t = 0$ and, hence, no gas flow initially.

Under these conditions the transient solution for a general time-dependent perturbation at the surface can be found by use of Laplace transforms and is

$$p = -\frac{1}{2}\alpha z\pi^{-\frac{1}{2}}\int_0^t p^*(t-\lambda)\lambda^{-3/2} \exp(-\tfrac{1}{4}\alpha^2 z^2\lambda^{-1})d\lambda. \tag{12}$$

CASE II: Linear Pressure Perturbation at the Surface of Case I.

As an example of the use of the general solution (12) in Case I we now consider a linear pressure perturbation of the form

$$p = a\,t, \tag{13}$$

where a is a constant. Atmospheric pressure variation associated with the passage of a frontal system can to a first approximation be represented by this type of ramp function.

Substituting Eq. (13) in Eq. (12) and carrying out the indicated integration yields

$$p = (at + \tfrac{1}{2}a\alpha^2 z^2)\operatorname{erfc}(-\tfrac{1}{2}\alpha z t^{-\frac{1}{2}}) + a\alpha z(t/\pi)^{\frac{1}{2}}\exp(-\tfrac{1}{4}\alpha^2 z^2 t^{-1}) \tag{14}$$

where erfc denotes the complementary error function defined by

$$\operatorname{erfc}(x) = 1 - \operatorname{erf}(x) = 2\pi^{-\frac{1}{2}}\int_x^\infty \exp(-u^2)du. \tag{15}$$

The resulting velocity field is found by applying Darcy's law to Eq. (14). This gives

$$v = -2a\alpha(k/\eta)(t/\pi)^{\frac{1}{2}}[\tfrac{1}{2}\alpha z t^{-\frac{1}{2}}\pi^{\frac{1}{2}}\operatorname{erfc}(-\tfrac{1}{2}\alpha z t^{-\frac{1}{2}}) + \exp(-\tfrac{1}{4}\alpha^2 z^2 t^{-1})]. \tag{16}$$

At the surface ($z = 0$) Eq. (15) reduces to

$$v(z=0) = -2a\alpha(k/\eta)(t/\pi)^{\frac{1}{2}} = -2a[\varepsilon k/(\eta P_o\pi)]^{\frac{1}{2}}\, t^{\frac{1}{2}}. \tag{17}$$

Hence, in this case the volume flux from the surface will vary as $t^{\frac{1}{2}}$ as long as the linear pressure ramp continues.

CASE III: Established Sinusoidal Pressure Variation at the Surface.

Diurnal pressure variations have an oscillating nature. If we assume a pressure perturbation at the surface of the form

$$p^*(t) = \phi \sin(\omega t), \tag{18}$$

and if we only consider times such that the initial condition is unimportant, then the solution to Eq. (7) for the boundary conditions of Eq. (18) and Eq. (10) is

$$p = \phi \exp(\beta z)\sin(\omega t + \beta z) \tag{19}$$

where

$$\beta = (\omega/2)^{\frac{1}{2}}\alpha . \tag{20}$$

The corresponding velocity field is again found from Darcy's law and is

$$v = \frac{k}{\eta}\beta\ \phi\exp(\beta z)\ \left\{\sin(\omega t + \beta z) + \cos(\omega t + \beta z)\right\}. \tag{21}$$

At the surface (z = 0) Eq. (22) becomes

$$v(z = 0) = \phi\ [\varepsilon k\omega/(\ \eta P_o)]\sin(\omega t + \pi/4). \tag{22}$$

It should be noted that the velocity is 45° out of phase with the assumed surface pressure perturbation.

For average soils we can choose $\varepsilon = 0.5$, $k = 10^{-8}\text{cm}^2$, and $\eta = 1.8 \times 10^{-4}$ g $\text{cm}^{-1}\text{s}^{-1}$. A reasonable estimate of ϕ/P_o is 0.01 and we can let the period of oscillation be 24 hours. These values yield an amplitude of the surface velocity (flow rate per unit area) to be $4 \times 10^{-4}\text{cm s}^{-1}$.

LA-8635-MS

UC-11
Issued: December 1980

Geohydrology of White Rock Canyon of the Rio Grande from Otowi to Frijoles Canyon

W. D. Purtymun
R. J. Peters
J. W. Owens

GEOHYDROLOGY OF WHITE ROCK CANYON OF THE RIO GRANDE FROM OTOWI TO FRIJOLES CANYON

by

W. D. Purtymun, R. J. Peters, and J. W. Owens

ABSTRACT

Twenty-seven springs discharge from the Totavi Lentil and Tesuque Formation in White Rock Canyon. Water generally acquires its chemical characteristics from rock units that comprise the spring aquifer. Twenty-two of the springs are separated into three groups of similar aquifer-related chemical quality. The five remaining springs make up a fourth group with a chemical quality that differs due to localized conditions in the aquifer. Localized conditions may be related to recharge or discharge in or near basalt intrusion or through faults. Streams from Pajarito, Ancho, and Frijoles Canyons discharge into the Rio Grande in White Rock Canyon. The base flow in the streams is from springs. Sanitary effluent in Mortandad Canyon from the treatment plant at White Rock also reaches the Rio Grande.

I. INTRODUCTION

The Los Alamos Scientific Laboratory (LASL) and the communities of Los Alamos and White Rock are located on the Pajarito Plateau west of the Rio Grande. The eastern edge of the plateau terminates along White Rock Canyon. This canyon is formed by downcutting of the Rio Grande (Fig. 1). The elevation of the Rio Grande is about 1680 m at Otowi decreasing to 1620 m at the confluence of Frijoles Canyon, about 18 km to the south. The western rim of the canyon is formed by the Pajarito Plateau, which rises as much as 340 m above the river. The eastern rim of the canyon is formed by the uplands of La Mesita and Cerros del Rio that rise above the river 200 m to 380 m, respectively.

The Pajarito Plateau, west of the Rio Grande, is drained by Los Alamos, Sandia, Mortandad, Pajarito, Water, Ancho, Chaquihui, and Frijoles Canyons. The area east of the river is drained by Cañada Ancha and several smaller, unnamed canyons. With two exceptions, the canyons drop precipitiously into White Rock Canyon. The channels in Los Alamos Canyon and Cañada Ancha slope steeply to the river (Fig. 2).

Sanitary effluent from the treatment plant at White Rock forms a perennial flow in lower Mortandad Canyon that discharges into the Rio Grande. Base flow in streams in Pajarito and Ancho Canyons is from spring discharge from the Totavi Lentil. The springs provide perennial flow to the Rio Grande. The flow in lower Frijoles Canyon is intermittent, with discharge reaching the river when evapotranspiration rates are low. Some water is discharged directly into the river from alluvial fans at the mouth of Los Alamos and Frijoles Canyons.

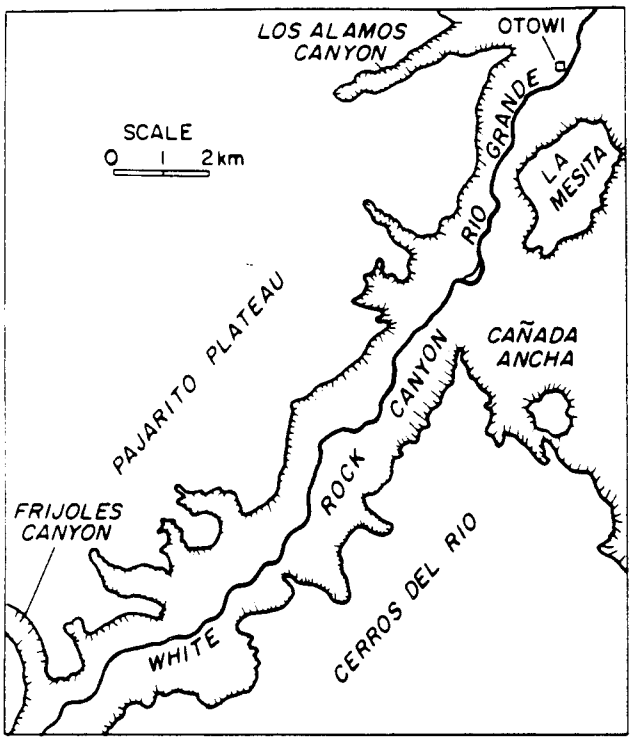

Fig. 1.
Topographic features adjacent to White Rock Canyon.

Twenty-seven springs and seeps are located in White Rock Canyon from Otowi to Frijoles Canyon. Of these, seven are located on the east side of the Rio Grande. These springs discharge ground water from the upper surface of the main aquifer of the Los Alamos area (west of White Rock Canyon), which rises westward from the river through the Tesuque Formation.[1,2] To the east the aquifer remains within the Tesuque Formation. East of the river, basalts intruded in and through the Tesuque Formation (at La Mesita and Cerros del Rio) form a partial barrier to ground water movement toward the river.[3]

In 1964, a study was made of the geohydrology of the White Rock Canyon.[4] The chemical quality of 21 springs and 3 streams was described. These springs and stations on the streams are used as a part of the present water quality monitoring system. The springs and streams are sampled on an average of every two years for chemical and radiochemical analyses. The purpose of this paper is to update the 1964 report. This will provide a better basis for interpreting of water quality data for the annual report issued by LASL, "Environmental Surveillance at Los Alamos."[5-7]

II. GEOLOGY

White Rock Canyon is located near the center of the Española Basin, which contains sediments and interbedded basalts.[8] The canyon was formed by the downcutting of the Rio Grande through the basaltic rocks of Chino Mesa. The basaltic rocks form the rim and upper parts of the canyon walls (Figs. 3, 3A, 3B, 3C). The Puye Formation underlies the basalts and is exposed in the canyon above the siltstones, sandstones, and interbedded basalts of the Tesuque Formation. The latter forms the lower part of the canyon walls and floor.

The Tesuque Formation and the Totavi Lentil (lower member of the Puye Formation) are described in detail as these units contain springs and seep areas. The description of the units is drawn largely from Griggs and are described from oldest to youngest.[9]

The Tesuque Formation is a sequence of light-colored sediments laid down as coalescing alluvial fan and flood plain deposits in the Rio Grande depression. It is composed of moderately well-cemented beds of fine to coarse grained arkosic siltstone and sandstone and some conglomerate and clay lenses. The Tesuque Formation also contains some volcanic debris and interbedded basalts. North of the confluence of Water Canyon and the Rio Grande the sediments are mostly fine-grained. They are shown in Figs. 3A-3C as TS(FG). South of the confluence of Water Canyon and the river, the outcrops of the Tesuque Formation contain interbedded basalt flows. The sediments above and below the basalts contain volcanic debris that is much coarser than the sandstone that is found in the Tesuque Formation to the north. These basalts and coarser sandstones are shown in Fig. 3C as TS(CG). The coarser sandstones and interbedded basalts are younger than the main body of the Tesuque Formation that is present from Otowi to Water Canyon.

The Puye Formation consists of two members. The lower member is a channel fill deposit named the Totavi Lentil. The upper member, the fanglomerate member, is composed of volcanic debris.

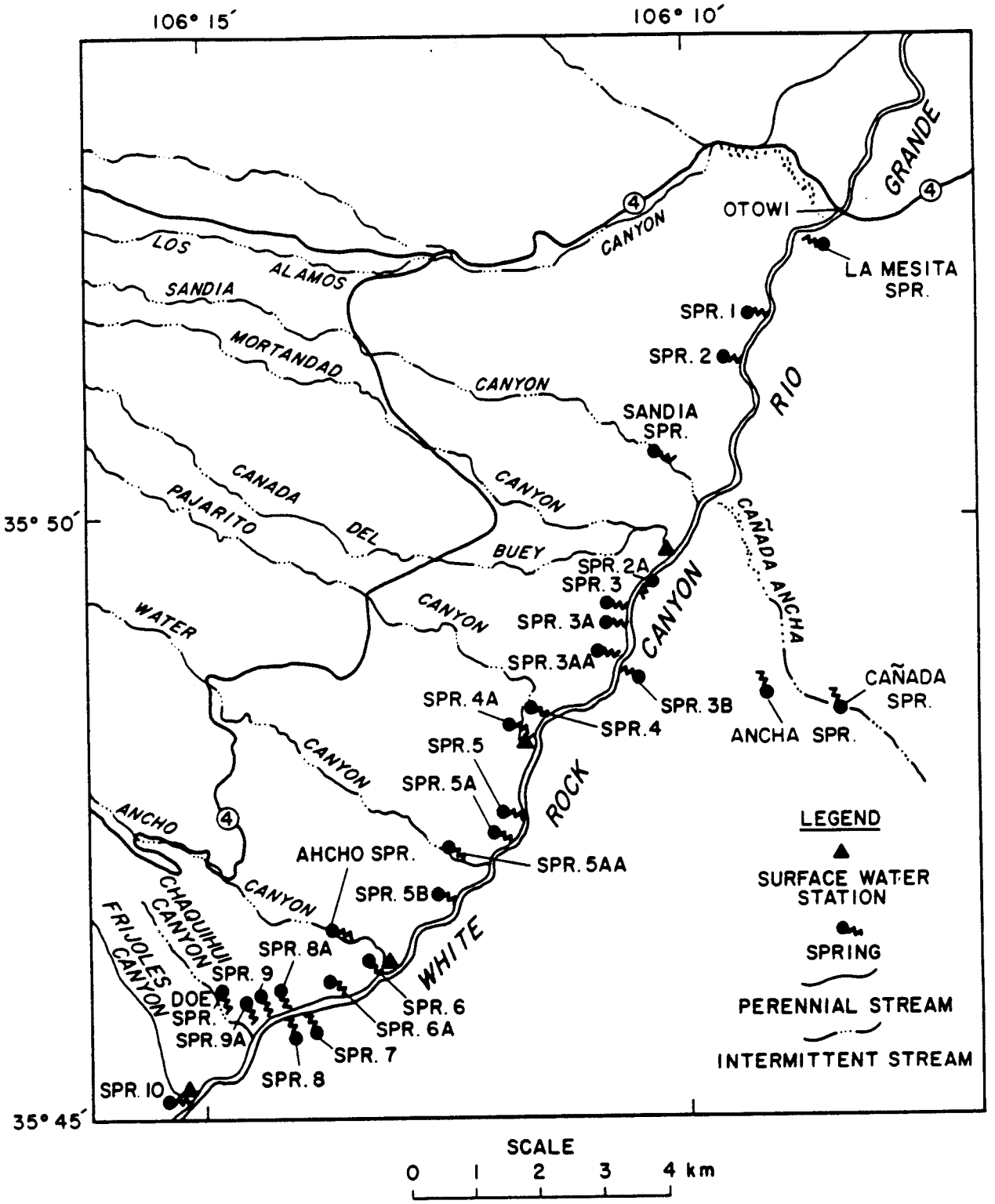

Fig. 2.
Generalized location of springs in White Rock Canyon.

The Totavi Lentil overlies the Tesuque Formation along the Rio Grande to a point below Ancho Canyon. Here it wedges out between the underlying Tesuque Formation and the overlying basaltic rocks of Chino Mesa (Fig. 3C). The Lentil consists mainly of subrounded to well-rounded quartzite and quartz pebbles and boulders. Sorting is generally poor, but well-sorted lenses of silt and sand are present. The thickness ranges from a few meters to about 15 m. The Totavi Lentil is shown in Figs. 3A-3C as QTp(TL).

The fanglomerate member of the Puye Formation is a gray fanglomerate composed of rhyolite, latite, quartz latite, some basalt, and water laid pumice in a matrix of silt and sand. The fanglomerate overlies the Totavi Lentil south of Los Alamos Canyon and wedges out between the lentil and basaltic rocks of Chino Mesa about 3 km south of Otowi. The fanglomerate does not outcrop along the eastern edge of White Rock Canyon. The fanglomerate member is shown as QTp in Fig. 3A. No springs or seeps issue from the fanglomerate member.

The basaltic rocks of Chino Mesa consist of numerous reddish-brown to black basalt flows. These are vesicular to dense and include interflow zones of clay, silt, and basalt fragments. The basalts rest on the Tesuque Formation south of Ancho Canyon and on the Totavi Lentil and fanglomerate member north of Ancho Canyon. Along Los Alamos Canyon, younger basalt flows overlie the fanglomerate member. Basalt intrusion through the Tesuque Formation forms numerous plugs in La Mesita and Cerros del Rio. The basaltic rocks of Chino Mesa are shown in Figs. 3A-3C as QTb. The basaltic rocks of Chino Mesa contain no springs or seeps.

Recent alluvium along the Rio Grande consists of silt to boulder-size debris of a variety of materials. Near Otowi the alluvium may be as much as 8 m thick; southward it forms a thin sheet overlying the Tesuque Formation. At the mouth of Los Alamos, Sandia, Mortandad, Pajarito, Ancho, and Frijoles Canyons large alluvial fans are deposited, causing the water to flow against the east canyon wall. The alluvium along the Rio Grande is not shown on Figs. 3A-3C as it was not of consequence to this study.

III. HYDROLOGY

Water from springs generally acquires its chemical characteristics by solution of minerals in the rock units that compose the aquifer. Based on similar water quality and aquifer characteristics, the springs have been separated into four groups: Group I—springs that discharge from the Totavi Lentil; Group II—springs that discharge from the Tesuque Formation coarse-grained sediments; Group III—springs that discharge from Tesuque Formation fine-grained sediments, and Group IV—springs that discharge near intrusion basalts or faults having a slightly different chemical characteristic because of localized conditions of the aquifer. These Group IV springs discharge from the fine-grained Tesuque Formation along the east side of the canyon. They are in the area of numerous basalt flows and intrusions that form La Mesita and Cerros del Rio.

High flow in the Rio Grande has covered some of the springs at times when samples were collected, so that in some years these data are missing. A near complete set of data was collected in 1978. These chemical data are considered to be representative of the quality of water from the individual springs. The missing data were filled in from the most recent years.

The chemical analyses were performed to determine the types of water and if chemical quality changes takes place with time. No samples were collected and analyzed for bacteria.

In comparing data from individual springs and streams over the years, some slight variation in chemical quality is evident. The chemical variations are small and are due to seasonal influences such as changes in air temperature and the effects of evapotranspiration on spring discharge. The variations in water quality are within the range normally expected and are not considered significant.

Radiochemical analyses of spring and stream water are performed along with chemical analyses. Radiochemical analyses are for gross alpha, gross beta, ^{137}Cs, ^{238}Pu, ^{239}Pu, ^{3}H, and total U. The concentrations of ^{137}Cs, ^{238}Pu, ^{239}Pu, and ^{3}H have been below limits of detection in samples collected since 1967. During 1978 the limits of detection for ^{137}Cs was <120 pCi/ℓ; ^{238}Pu, and ^{239}Pu were <0.02 pCi/ℓ;

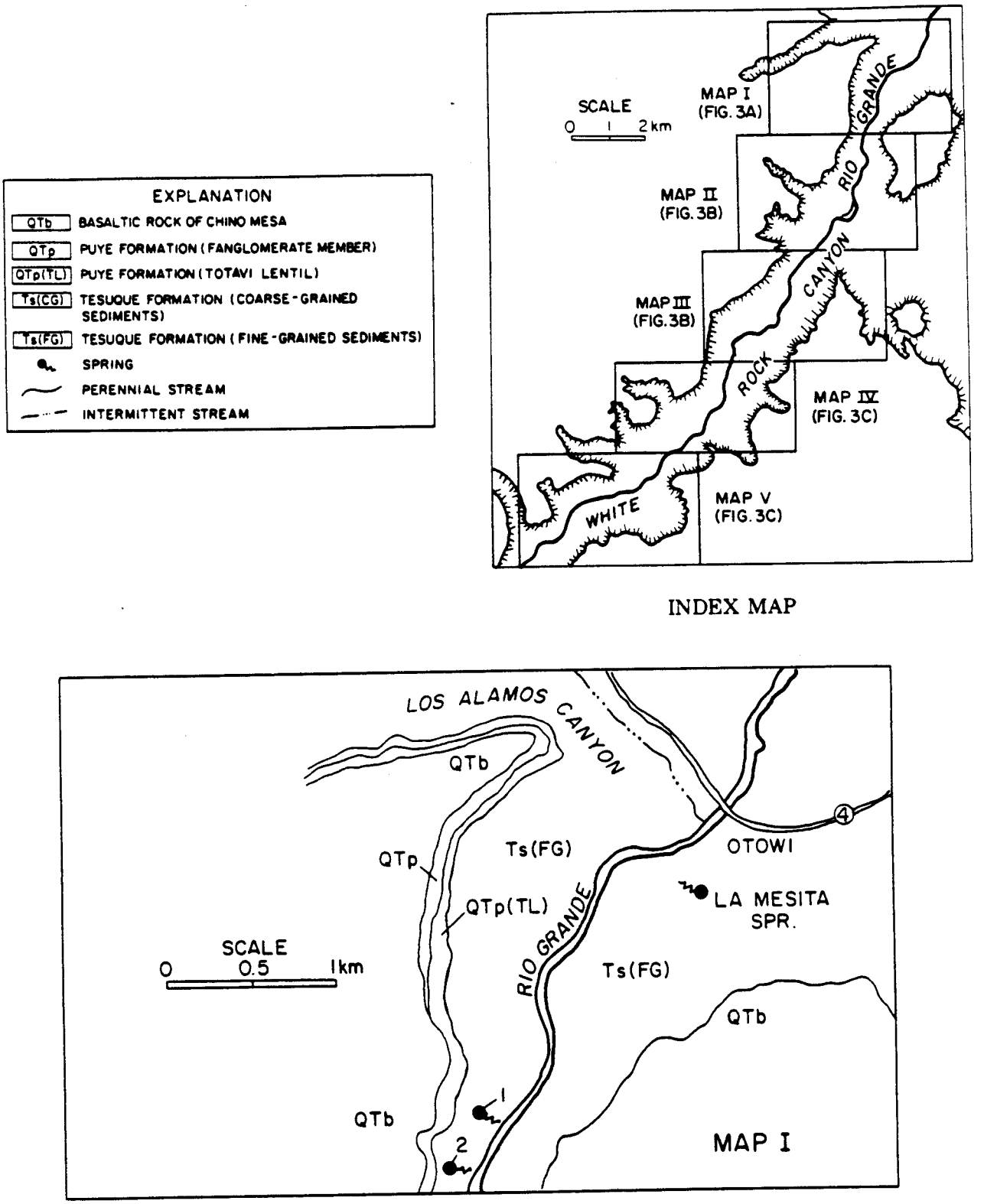

A. Map I.

Fig. 3.
Geologic map of White Rock Canyon.

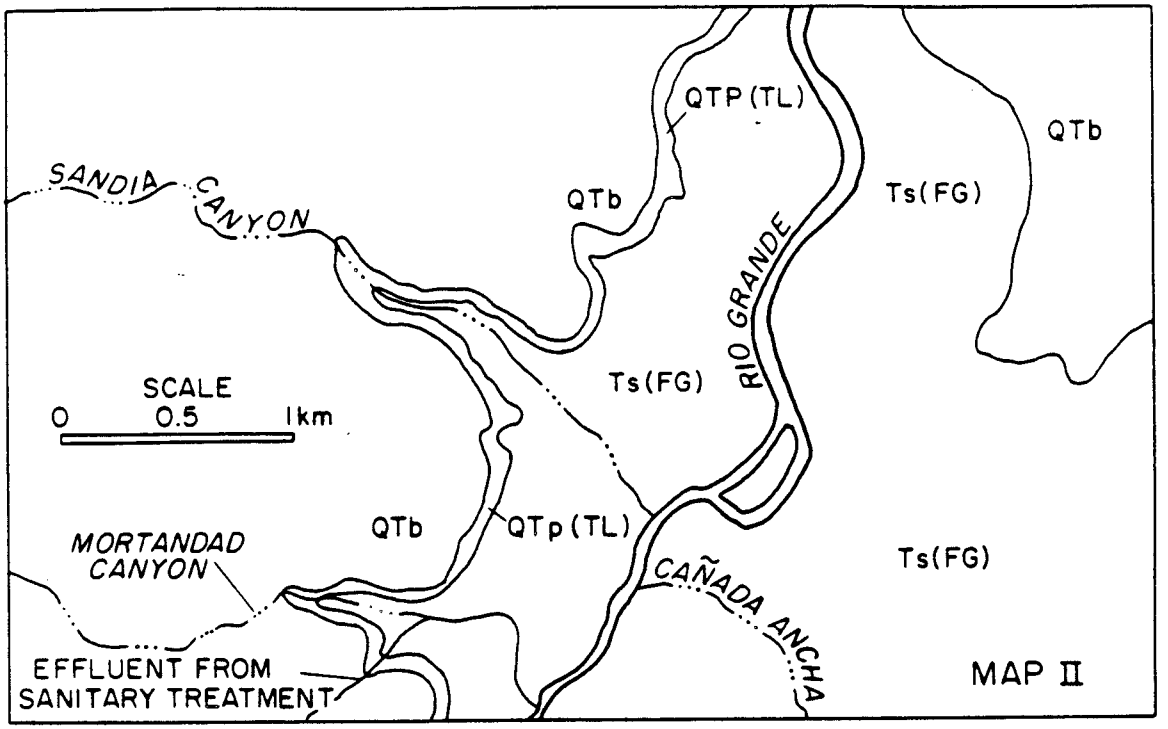

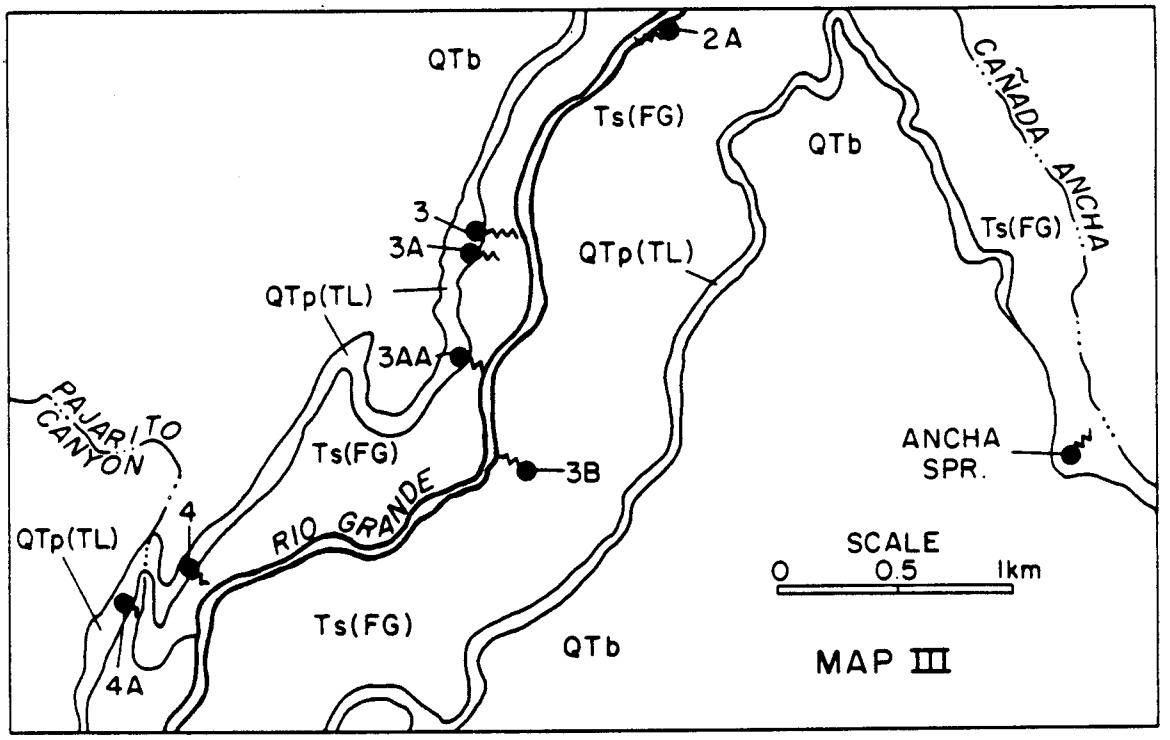

B. Maps II and III.

Fig. 3 (Cont).

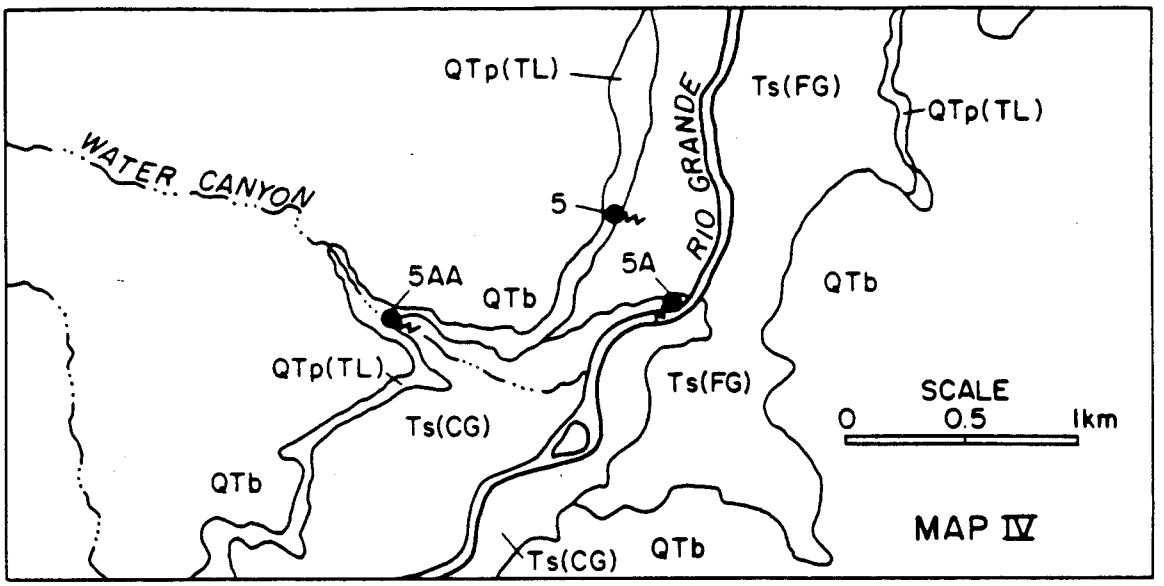

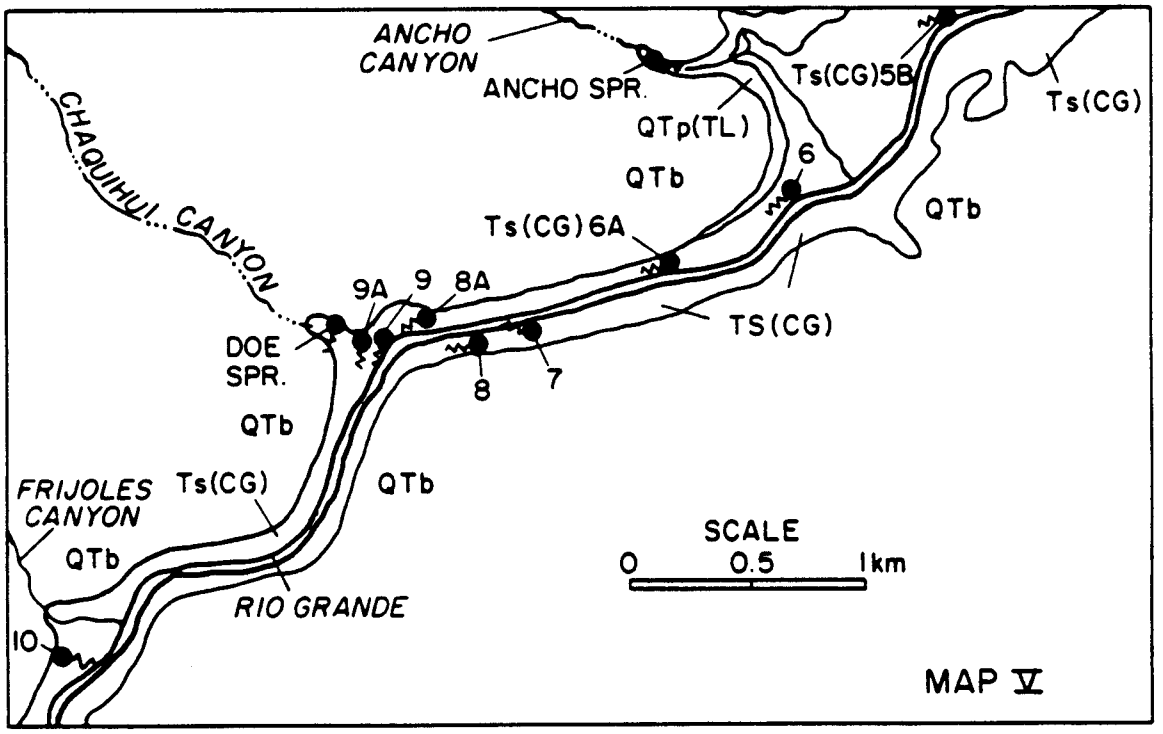

C. Maps IV and V.

Fig. 3 (Cont).

and ^3H was <1500 pCi/ℓ.[8] Thus, only the gross alpha, gross beta, and total U in water from the springs and streams are discussed. This radioactivity is natural, taken in the solution by the ground water moving through the aquifers.

A. Springs

The Group I springs (Totavi Lentil) are all on the west side of the river. They range in elevation from 1737 m in Sandia Canyon to the north to 1683 m near Pajarito Canyon and then increase in elevation to the south to 1737 m near Ancho Canyon where the Totavi Lentil wedges out between the coarse-grained Tesuque Formation and basaltic rocks of Chino Mesa (Figs. 3A-3C). Springs in this group form the base flow in Pajarito and Ancho Canyon (Table I). Discharge from all but two of the springs reaches the Rio Grande. The discharge in Sandia Canyon (Sandia Spring) and Water Canyon (Spring 5AA) is depleted by infiltration into the alluvium and evapotranspiration before reaching the river.

Discharge from the Group I springs is a calcium and bicarbonate water (Fig. 4). The average sulfate and chloride concentrations are about 4 mg/ℓ. Total dissolved solids (TDS) range from 112 to 210 mg/ℓ, with an average concentration of 163 mg/ℓ (Table II).

The Group II springs (Tesuque Formation, coarse-grained sediments) are located on both sides of White Rock Canyon. Six of the springs (Springs 5A, 5B, 6, 6A, 7 and 8) are located at the edge of the channel (Fig. 2). These springs discharge about 30 ℓ/s directly into the river. Springs in or near Chaquehui Canyon (Springs 8A, 9, 9A, and Doe) are located 40 to 60 m above the river. They provide water for large areas of vegetation. All discharge from Doe and Spring 9A is lost to infiltration or evaporation before reaching the river. Spring 10 discharges <0.1 ℓ/s from the edge of the alluvial fan at the mouth of Frijoles Canyon.

The discharge from the Group II springs is a sodium and bicarbonate water. The average sulfate and chloride concentrations are about 3 mg/ℓ. The TDS range from 154 to 262 mg/ℓ, with an average concentration of 183 mg/ℓ.

The Group III springs (Tesuque Formation, fine-grained sediments) are located on the west wall of the canyon below Otowi (Fig. 3A). The springs form large seep areas that are covered with vegetation. There is no discharge to the river because of the large losses to evapotranspiration.

Discharge from the Group III springs is also a sodium and bicarbonate water. Chemical concentrations in general are higher than in the Group I and Group II springs. Sulfate concentrations are about 10 mg/ℓ while chlorides are low at 3 mg/ℓ. The TDS ranges from 194 to 236 mg/ℓ, with an average of 215 mg/ℓ.

There are five springs in Group IV, La Mesita, Ancha, 2A, 3B, and Cañada (Fig. 2, Table II); these springs are located on the east side of the river. These springs discharge from the fine-grained Tesuque Formation where there are numerous basalt flows and plugs as well as faults.

La Mesita Spring is a seep area in and adjacent to a small channel that drains the steep western side of La Mesita (Fig. 1). La Mesita is formed by a series of intruded basalts. The seeps are in a part of the fine-grained Tesuque Formation. At the source are the remains of a gallery set into the bank above the channel. The water from the gallery was probably used by the now abandoned Denver and Rio Grande Railroad. La Mesita spring is about 20 m above the Rio Grande (Fig. 2). The spring discharges into the channel. The channel below the springs contains heavy growth of shrubs and trees, and only when evapotranspiration rates are low does water from the spring reach the Rio Grande. The discharge from La Mesita Spring is a sodium and bicarbonate water. Sulfate is about 12 mg/ℓ, chloride 6 mg/ℓ, and TDS about 286 mg/ℓ.

Ancha Spring is located about 2.6 km east of the Rio Grande in a small canyon cut into the Cerros del Rio (Fig. 2). The small canyon is a tributary to Cañada Ancha. Water from the spring issues from near the contact of the basalt with underlying volcanic sediments. Water from the spring does not reach Cañada Ancha. Discharge from the spring is a calcium and sulfate water. Sulfates are 212 mg/ℓ, chloride 5 mg/ℓ, and TDS 508 mg/ℓ, about twice the TDS concentrations found in other springs in White Rock Canyon.

Spring 2A is located on the east side of the river at about river level. The spring appears to discharge from fine-grained sediments of the Tesuque Formation; however, the chemical characteristics differ

TABLE I

RECORDS OF SPRINGS IN WHITE ROCK CANYON

	Elevation (m)	Topographic Situation	Temp (°C)	Discharge at Rio Grande (ℓ/s)	Remarks
Group I (Totavi Lentil)					
Sandia Spring	1737	Seep area in and adjacent to channel	22	0	Sandia Canyon
Spring 3	1695	Gravel terrace above river	22	1	
Spring 3A	1695	Gravel terrace above river	22	3	
Spring 3AA	1688	Gravel terrace above river	19	<1	
Spring 4	1683	Gravel slope above river	19	5.1	
Spring 4A	1683	Grravel terrace above channel	21	37	Pajarito Canyon
Spring 5	1698	Gravel on steep slope above river	21	0.6	
Spring 5AA	1756	Seep in channel forms pools	18	0	Water Canyon
Ancho Spring	1737	Gravels underlying basalt in channel	22	4.3	Ancho Canyon
Group II (Tesuque Fm. Coarse Grained)					
Spring 5A	1645	Fractures in basalt at edge of river	21	1.7	
Spring 5B	1646	Steep slope at edge of river	16	0.6	
Spring 6	1640	Fractures in basalt at edge of river	23	3.6	
Spring 6A	1638	Fractures in basalt at river level	22	9.5	
Spring 7	1637	Slope at edge of river	21	11	
Spring 8	1637	Slope at edge of river	22	4.4	
Spring 8A	1682	Seep in channel on canyon wall	22	1.6	
Spring 9	1679	Large seep area above river	20	0.5	
Spring 9A	1684	Seep area on canyon wall	19	0	Chaquihui Canyon
Doe Spring	1707	Seep area in channel and canyon wall	21	0	Chaquihui Canyon
Spring 10	1634	Edge of alluvial fan above river	19	<1	Frijoles Canyon
Group III (Tesuque Fm. Fine Grained)					
Spring 1	1711	Seep area on slope above river	18	0	
Spring 2	1707	Seep area on slope above river	17	0	
Group IV (Tesuque Fm. Fine Grained Near Basalt Intrusion or Faults)					
La Mesita Spring	1700	Seep area in and above channel	17	<1	Remains of gallery above channel
Ancha Spring	1760	Seep area in channel, volcanic sediments	21	0	
Spring 2A	1675	Gravel along edge of river	22	<1	
Spring 3B	1676	Terrace on slope above river	20	2	
Cañada Spring	1682	Seep area in Cañada Ancha	19	0	

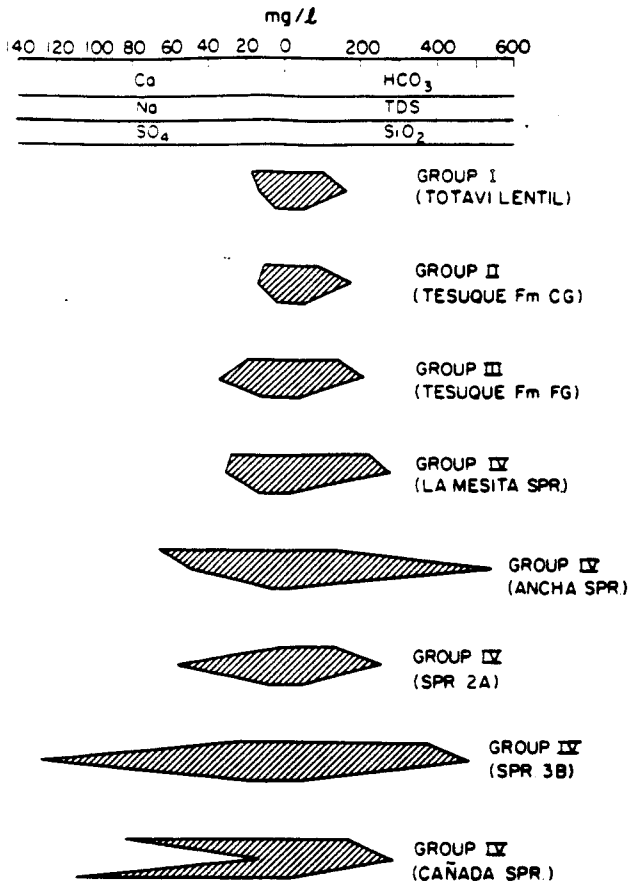

Fig. 4.
Graphic comparison of chemical characteristics of water from springs.

from other springs in the canyon. The discharge to the river is estimated at less than 0.1 ℓ/s. The discharge from spring 2A is a sodium and bicarbonate water. The sulfates are about 7 mg/ℓ, chlorides 2 mg/ℓ, and TDS 270 mg/ℓ.

Spring 3B is located east and about 30 m above the Rio Grande. The main discharge is from the top of a low mound on a moderate slope. The mound is composed of a blue clay containing gravels of rounded quartz and quartzite. The surface of the area is covered with black vescular basalt and red scoria. Numerous seeps supporting a thick cover of salt grass occur in the area. About 2 ℓ/s of discharge from the spring and seeps reach the river. Discharge from spring 3B is also a sodium and bicarbonate water. Sulfates are 16 mg/ℓ, chlorides 4 mg/ℓ, and TDS are elevated at 500 mg/ℓ.

Cañada Spring is located east of the Rio Grande in the channel of Cañada Ancha. It is a seep area in fine-grained sediments of the Tesuque Formation adjacent to a basalt plug. The discharge from the spring is a calcium and bicarbonate water. Sulfates are 106 mg/ℓ, chlorides 3 mg/ℓ, and TDS 298 mg/ℓ (Table II).

Gross alpha, gross beta and total U in water from the springs and streams are due to natural radioactivity taken into solution from the aquifer (Table III). Concentrations of gross alpha and gross beta were similar in Group I, II, and III springs. The concentration of total U in Groups I and II was slightly higher than Group III springs.

Gross alpha, gross beta, and total U were generally higher in Group IV springs (La Mesita, Ancha, 2A, 3B, and Cañada) than in water from Groups I, II, or III. Gross alpha, gross beta, and total U concentration in water from Spring 3B has been consistently higher than water from any of the other springs in the canyon. The radioactivity is natural occurring, leached from the rock units of the aquifer. Water from the Group IV springs is also highly mineralized.

The chemical quality of water from the four groups of springs is quite good. The maximum concentrations of SO_4, Cℓ, F, NO_3, and TDS are well below drinking water standards (Table IV). The concentrations of gross alpha, and total U in water from the Groups I, II, and III springs were below drinking water standards.[10] Measurements of gross alpha in water from the Group IV springs (La Mesita, Ancha, 2A, and 3B) range from 5.5 to 13 pCi/ℓ or above the standard of 5 pCi/ℓ. This may be due to presence of ^{226}Ra. Additional analyses are necessary to validate the water for domestic use. Total U in the Group IV is well below drinking water standards.[11]

B. Streams

Streams from Mortandad, Pajarito, Ancho, and Frijoles Canyons enter the Rio Grande between Otowi and Frijoles Canyons. Base flow in Mortandad is sanitary effluent from the treatment plant at White Rock. Base flow in Pajarito and Ancho Canyons is from springs discharging from the Totavi Lentil near the Rio Grande. Base flow in Frijoles Canyon is from a series of headwater springs located about 13 km west of the Rio Grande on the flanks of

TABLE II

WATER QUALITY OF SPRINGS AND STREAM IN WHITE ROCK CANYON

	mg/ℓ													μmho	pCi/ℓ		μg/ℓ
	SiO_2	Ca	Mg	Na	CO_3	HCO_3	SO_4	Cl	F	NO_3	PO_4	TDS	Total Hard	Specific (Cond.)	Gross Alpha	Gross Beta	Total U
Springs																	
Group I (Tetavi Lentil)																	
Sandia Spring	44	35	2.8	17	0	171	3	4	0.8	<2	<2	210	105	290	<0.5	4.2	0.8
Spring 3	58	15	1.3	14	0	83	4	3	0.4	2	<2	170	49	190	0.5	4.5	0.5
Spring 3A	48	15	1.4	14	0	98	4	2	0.4	2	<2	164	54	170	2.6	2.5	0.9
Spring 3AA[a]	36	20	<0.3	15	0	102	4	3	0.4	<2	<2	142	44	240	2.0	4.8	1.9
Spring 4	50	16	4.0	13	0	98	9	6	0.2	<2	<2	152	75	210	2.1	3.7	0.8
Spring 4A	62	14	4.3	12	0	105	5	5	0.5	<2	<2	180	77	200	1.7	1.1	0.7
Spring 5	62	14	4.6	12	0	105	5	4	0.4	<2	<2	112	72	210	0.7	1.7	0.1
Spring 5AA	52	16	4.0	12	0	105	3	4	0.5	<2	<2	188	83	210	2.4	5.4	0.1
Ancho Spring	70	8	2.5	10	0	73	2	2	0.3	<2	<2	146	57	130	<0.5	2.9	<0.1
Group II (Tesuque Fm. Coarse Grained)																	
Spring 5A	54	16	2.5	19	0	102	7	4	0.4	<2	<2	200	68	220	0.5	3.6	1.3
Spring 5B[b]	---	18	3.0	12	0	80	---	5	0.2	<2	---	262	58	190	<0.5	3.4	0.4
Spring 6	33	8	3.1	10	0	85	2	2	0.3	<2	<2	160	58	140	<0.5	2.3	0.6
Spring 6A	35	7	2.2	10	0	63	2	2	0.2	<2	<2	154	41	120	<0.5	2.5	<0.1
Spring 7	35	8	2.3	13	0	73	3	2	0.2	<2	<2	162	50	150	1.5	3.4	0.2
Spring 8	68	13	3.8	22	0	122	7	3	0.3	<2	<2	250	80	220	2.1	3.5	1.8
Spring 8A	72	6	1.7	11	0	66	2	2	0.3	<2	<2	160	35	120	<0.5	2.0	<0.1
Spring 9	70	8	2.5	11	0	173	2	2	0.4	<2	<2	170	60	130	<0.5	2.2	<0.1
Spring 9A	70	7	2.2	11	0	75	2	2	0.5	<2	<2	180	45	130	1.7	0.2	0.4
Doe Spring	66	8	2.5	11	0	73	2	2	0.5	<2	<2	158	42	140	<0.5	3.6	<0.1
Spring 10	62	8	2.5	11	0	78	2	2	0.5	<2	<2	160	70	140	0.7	1.3	<0.1
Group III (Tesuque Fm. Fine Grained)																	
Spring 1	32	24	1.9	32	0	170	13	3	0.7	<2	<2	194	77	290	1.0	3.9	2.3
Spring 2	30	13	0.5	47	0	117	6	3	1.0	<2	<2	236	50	280	0.9	1.8	2.2
Group IV (Tesuque Fm. Fine Grained Near Basalt Intrusions or Faults)																	
La Mesita Spring	19	27	0.6	29	0	222	12	6	0.3	8	<2	286	70	270	6.3	7.0	14
Ancha Spring[c]	16	66	23	49	0	144	212	5	0.3	12	<2	508	214	470	8	11	14
Spring 2A[b]	42	3	0.1	56	0	142	7	2	0.4	2	<2	270	20	280	5.5	4.5	8.0
Spring 3B	44	21	1.8	126	0	398	16	4	0.3	8	<2	500	61	620	13	11	20
Cañada Spring[c]	28	81	4.6	10	0	176	106	3	0.3	32	<2	298	178	350	3.2	5.1	3.7
Streams																	
Mortandad	88	16	7.6	75	5	132	37	29	0.9	60	40	552	95	600	<0.5	18	0.5
Pajarito	64	15	4.3	13	0	93	6	5	0.5	<2	<2	186	84	200	2.5	4.3	0.4
Ancho	68	9	2.8	10	0	102	2	2	0.4	<2	<2	160	50	140	<0.5	2.2	<0.1
Frijoles[d]	---	32	4.0	13	0	121	---	2	<0.1	2	---	246	102	260	1.7	3.0	0.9
Frijoles[e]	52	12	3.2	10	0	71	4	3	0.3	<2	<2	138	32	100	<0.5	3.4	<0.4

[a]November 1979.
[b]September 1977.
[c]May 1980.
[d]July 1977 after June 1977 wildfire.

TABLE III

GROSS ALPHA, GROSS BETA, AND TOTAL URANIUM IN WATER FROM SPRINGS
(Analyses in pCi/ℓ except as noted)

	Min	Max	$\bar{x}$	s
			Gross Alpha	
Group I	<0.5	2.4	1.4	0.9
Group II	<0.5	2.1	0.9	0.6
Group III	0.9	1.0	1.0	0.1
Group IV				
La Mesita	---	6.3	---	---
Ancha	---	8.0	---	---
Spring 2A	---	5.5	---	---
Spring 3B	---	13.0	---	---
Cañada	---	3.2	---	---
			Gross Beta	
Group I	1.1	5.4	3.4	1.5
Group II	0.2	3.6	2.6	1.1
Group III	1.8	3.9	2.8	1.5
Group IV				
La Mesita	---	7.0	---	---
Ancha	---	11.0	---	---
Spring 2A	---	4.5	---	---
Spring 3B	---	11.0	---	---
Cañada	---	5.1	---	---
			Total U*	
Group I	<0.01	1.9	0.6	0.6
Group II	<0.1	1.3	0.5	0.6
Group III	2.2	2.3	2.2	0.1
Group IV				
La Mesita	---	14.0	---	---
Ancha	---	14.0	---	---
Spring 2A	---	8.0	---	---
Spring 3B	---	20.0	---	---
Cañada	---	3.7	---	---

*μg/ℓ.

the mountains. A comparison of the chemical characteristics of the four streams is shown in Fig. 5 and detailed analyses are presented in Table II. Stream samples are collected above the confluence with the Rio Grande.

The chemical quality of water in Mortandad Canyon is typical of treated sanitary effluent. Sodium is 75 mg/ℓ, sulfate 37 mg/ℓ, chlorides 29 mg/ℓ, nitrates 60 mg/ℓ, and TDS at 552 mg/ℓ (Table II). Most chemical constituents are higher than found in natural waters of the region.

Base flow in Pajarito Canyon is principally a calcium and bicarbonate-type water similar to that discharging from springs in the Totavi Lentil (Table II). Sulfates are about 6 mg/ℓ, chlorides about 5 mg/ℓ, and TDS about 186 mg/ℓ. The base flow in Ancho Canyon is a sodium and bicarbonate water. Though the main base flow is from springs in the Totavi Lentil, water from the coarse-grained sediments of the Tesuque Formation is added to the flow. Consequently, the flow increases downgradient in the canyon. Sulfates and chlorides are about 2 mg/ℓ and TDS 160 mg/ℓ (Table II).

A wildfire in June 1977 burned about 26 km^2 of the drainage area in upper Frijoles Canyon. Investigation of the chemical quality of the stream at Bandelier National Monument Headquarters (about 4 km from the river) indicates slight post-fire increases in calcium, bicarbonate, chloride, fluoride, and TDS in the base flow when compared to data collected from 1957 through March 1977.[12] Analyses of the water from Frijoles stream at the Rio Grande in July 1977 indicated slightly higher concentrations of calcuim, bicarbonate, and TDS when compared to analyses of water collected in November 1979 (Table II). Principal ions in 1979 were calcium and bicarbonate with sulfate concentrations of 4 mg/ℓ, chlorides 3 mg/ℓ, and TDS 138 mg/ℓ (Table II). With continued flushing of the burn area by storm runoff and recovery of the vegetative cover, the quality of water in the stream will return to normal within 3 to 5 yr.

Gross alpha, gross beta, and total U concentrations are normal in water from the stream near the Rio Grande, with the exception of gross beta (18 pCi/ℓ) from Mortandad Canyon (Table V). Treated sanitary effluents almost always contain higher gross beta activity than natural waters due to higher concentrations of potassium.[7]

The chemical quality of water from the streams is generally quite good. The concentrations of SO_4, Cℓ, F, NO_3, and TDS meet the drinking water standards with the exception of NO_3 in sanitary effluents in Mortandad Canyon. The NO_3 of the effluents is about 20 mg/ℓ greater than permitted for domestic use (Table IV). The gross alpha and total U are below standards or criteria.[10]

The release of sanitary effluent in Mortandad Canyon has little or no effect on the chemical quality of water in the Rio Grande because of the dilution factor. The discharge of effluent at the Rio Grande is <0.03 m^3/s compared to the mean discharge of the Rio Grande of about 30 m^3/s.[13]

TABLE IV

COMPARISON OF MAXIMUM CONCENTRATIONS OF SELECT CHEMICAL AND RADIONUCLIDE CONCENTRATIONS WITH DRINKING WATER STANDARDS

	mg/ℓ					Gross	Total
	SO_4	Cℓ	F	NO_3	TDS	Alpha[b]	U[c]
Standards[a]	600	250	1.6	45	1000	5	1800
Springs							
Group I	9	6	0.8	2	210	2.6	1.9
Group II	7	5	0.5	<2	262	2.1	1.3
Group III	13	3	1.0	<2	236	1.0	2.3
Group IV	212	6	0.4	32	508	13	20
Streams							
Natural[d]	6	5	0.5	2	246	2.5	0.9
Effluent[e]	37	29	0.9	60	552	<0.5	0.5

[a]USEPA National Interim Primary Drinking Water Standards and NMEID Water Supply Regulations.[10,11]
[b]pCi/ℓ.
[c]μg/ℓ.
[d]Pajarito, Ancho, and Frijoles stream.
[e]Mortandad stream, sanitary effluent.

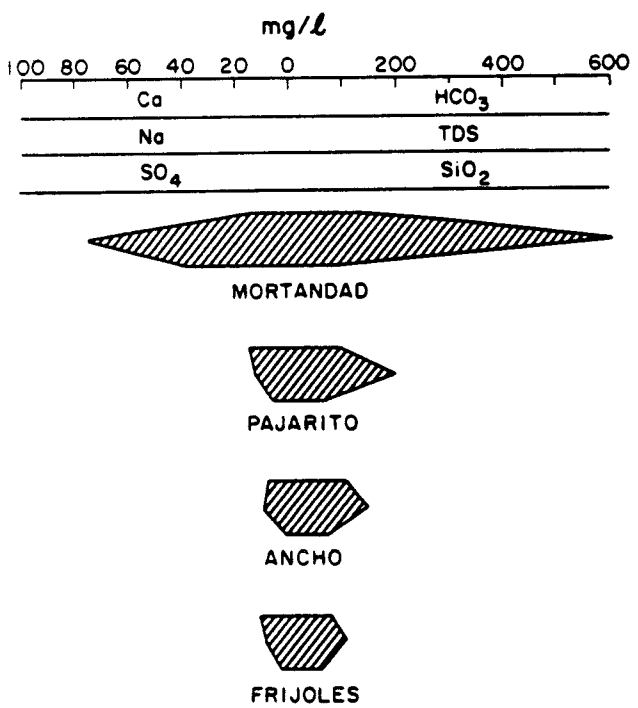

Fig. 5.
Graphic comparison of chemical characteristics of water from streams.

TABLE V

GROSS ALPHA, GROSS BETA, AND TOTAL U IN WATER FROM STREAMS

(Analyses in pCi/ℓ except as noted)

Stream	Gross Alpha	Gross Beta	Total U[a]
Mortandad	<0.5	18	0.5
Pajarito	2.5	4.3	0.4
Ancho	<0.5	2.2	<0.1
Frijoles	<0.5	3.4	<0.4

[a]μg/ℓ.

IV. SUMMARY AND CONCLUSIONS

Twenty-seven springs are located in the reach of White Rock Canyon from Otowi to the confluence of Frijoles Canyon. Chemical quality of water from the

springs is separated into four groups. Three groups have similar aquifer related chemical quality. Group I springs discharge a calcium and bicarbonate type water from the Totavi Lentil. Group II springs discharge a sodium and bicarbonate type water from coarse-grained sediments of the Tesuque Formation. Group III springs discharge a sodium and bicarbonate water from fine-grained sediments of the Tesuque Formation. Water from Group III springs contains slightly higher chemical concentrations than the water from Group II springs. Group IV consists of five springs, La Mesita, Ancha, 2A, 3B, and Cañada, each having slightly different chemical characteristics because of localized conditions of the aquifer. In general, chemical constituents in water from the Group IV springs are higher than those found in Groups I, II, and III springs.

Chemical quality of water from individual springs has varied slightly in samples collected from 1964 through 1979. The variations are normal due to seasonal variations and are not considered significant.

Four streams enter the Rio Grande in White Rock Canyon from Otowi to the confluence of Frijoles Canyon. The quality of water in Mortandad Canyon reflects the quality of treated sanitary effluent released from the plant at White Rock. The effluent has little or no effect on the quality of water in the Rio Grande because of the dilution factor. The quality of water in Pajarito Canyon reflects the base flow from Group I springs in the Totavi Lentil. The quality of water in Ancho Canyon reflects mainly the base flow from Group I springs in the Totavi Lentil, which is modified slightly by some discharge from the coarse-grained sediments of the Tesuque Formation before the stream reaches the Rio Grande. Base flow in Frijoles Canyon is from springs about 13 km west of the Rio Grande. The wildfire in June 1977 in the drainage area of Frijoles Canyon had only slight effect on the quality of water at the river.

The chemical quality of water from the springs and streams is good. The concentrations of SO_4, $C\ell$, F, NO_3, and TDS are below drinking water standards with the exception of NO_3 in sanitary effluents found in Mortandad Canyon. It should be noted that no bacteria samples were collected and analyzed. Thus, the chemical quality may be good, but the water from the springs and streams may not be potable due to bacteria.

REFERENCES

1. W. D. Purtymun and S. Johansen, "General Geohydrology of the Pajarito Plateau," N. M. Geol. Society Guidebook, 25th Field Conf., Ghost Ranch, Central Northern New Mexico (1974).

2. R. L. Boston, "General Geology and Hydrology of North-Central Santa Fe County, New Mexico," New Mexico State Engineer open-file report (1968).

3. Z. Spiegel and B. Baldwin, "Geology and Water Resources of the Santa Fe Area, New Mexico," U.S. Geol. Survey Water-Supply Paper 1525 (1963).

4. W. D. Purtymun, "Geology and Hydrology of White Rock Canyon from Otowi to the Confluence of Frijoles Canyon, Los Alamos and Santa Fe Counties, New Mexico," U.S. Geol. Survey open-file report (1966).

5. Environmental Surveillance Group H-8, "Environmental Surveillance at Los Alamos During 1977," Los Alamos Scientific Laboratory report LA-7283-MS (1978).

6. Environmental Surveillance Group H-8, "Environmental Surveillance at Los Alamos During 1978," Los Alamos Scientific Laboratory report LA-7800-ENV (1979).

7. Environmental Surveillance Group H-8, "Environmental Surveillance at Los Alamos During 1979," Los Alamos Scientific Laboratory report LA-8200-ENV (1980).

8. V. C. Kelley, "Tectonics of the Rio Grande Depression of Central New Mexico," N. M. Geol. Society Guidebook, 3rd Field Conference, Rio Grande County (1952).

9. R. L. Griggs, "Geology and Water Resources of the Los Alamos Area, New Mexico," U.S. Geol. Survey Water-Supply Paper 1753 (1964).

10. U.S. Environmental Protection Agency, "National Interim Primary Drinking Water Regulations," (EPA-570/9-76-003), EPA, Office of Water Supply (1976).

11. New Mexico Environmental Improvement Department, "Water Supply Regulations," New Mexico Environmental Improvement Department, Santa Fe, New Mexico (1977).

12. W. D. Purtymun and H. Adams, "Geohydrology of Bandelier National Monument, New Mexico," Los Alamos Scientific Laboratory report LA-8461-MS (1980).

13. U. S. Geological Survey, "Water Resources Data for New Mexico for Water Year 1978," U.S. Geol. Survey Water-Data Report NM-78-1 (1979).

Page Range	Domestic Price	NTIS* Price Code	Page Range	Domestic Price	NTIS* Price Code	Page Range	Domestic Price	NTIS* Price Code	Page Range	Domestic Price	NTIS* Price Code
001-025	$ 5.00	A02	151-175	$11.00	A08	301-325	$17.00	A14	451-475	$23.00	A20
026-050	6.00	A03	176-200	12.00	A09	326-350	18.00	A15	476-500	24.00	A21
051-075	7.00	A04	201-225	13.00	A10	351-375	19.00	A16	501-525	25.00	A22
076-100	8.00	A05	226-250	14.00	A11	376-400	20.00	A17	526-550	26.00	A23
101-125	9.00	A06	251-275	15.00	A12	401-425	21.00	A18	551-575	27.00	A24
126-150	10.00	A07	276-300	16.00	A13	426-450	22.00	A19	576-600	28.00	A25
									601-up	†	A99

†Add $1.00 for each additional 25-page increment or portion thereof from 601 pages up.

LA-8422-MS

Informal Report

Radiochemical Analyses of Samples from Beneath a Solid Radioactive Waste Disposal Pit at Los Alamos, New Mexico

University of California

LOS ALAMOS SCIENTIFIC LABORATORY
Post Office Box 1663 Los Alamos, New Mexico 87545

An Affirmative Action/Equal Opportunity Employer

This report was not edited by the Technical Information staff.

This work was supported by the US Department of Energy, Division of Waste Management, Low Level Waste Programs.

This report was prepared as an account of work sponsored by the United States Government. Neither the United States nor the United States Department of Energy, nor any of their employees, makes any warranty, express or implied, or assumes any legal liability or responsibility for the accuracy, completeness, or usefulness of any information, apparatus, product, or process disclosed, or represents that its use would not infringe privately owned rights. Reference herein to any specific commercial product, process, or service by trade name, mark, manufacturer, or otherwise, does not necessarily constitute or imply its endorsement, recommendation, or favoring by the United States Government or any agency thereof. The views and opinions of authors expressed herein do not necessarily state or reflect those of the United States Government or any agency thereof.

UNITED STATES
DEPARTMENT OF ENERGY
CONTRACT W-7405-ENG. 36

LA-8422-MS
Informal Report
UC-70
Issued: June 1980

Radiochemical Analyses of Samples from Beneath a Solid Radioactive Waste Disposal Pit at Los Alamos, New Mexico

W. D. Purtymun
M. A. Rogers
M. L. Wheeler

RADIOCHEMICAL ANALYSES OF SAMPLES FROM BENEATH A SOLID RADIOACTIVE WASTE DISPOSAL PIT AT LOS ALAMOS, NEW MEXICO

by

W. D. Purtymun, M. A. Rogers, M. L. Wheeler*

ABSTRACT

Solid radioactive wastes are disposed of by burial in pits excavated in rhyolite tuff at the Los Alamos Scientific Laboratory (LASL). Contaminants in the waste include fission products, uranium, and transuranic elements. In 1976, horizontal core holes were drilled beneath a waste disposal pit that was used from 1963 to 1966. Samples of the core were analyzed for gross alpha, gross beta, total uranium, ^{90}Sr, ^{137}Cs, ^{238}Pu, ^{239,240}Pu, and ^{241}Am. The measured gross alpha, gross beta, and uranium concentrations were above minimum detection limits; concentrations of the remaining radionuclides, all of which are man-made isotopes, were below the minimum detection limits. Statistical comparisons were made of the gross alpha, gross beta, and uranium data to identify any significant variations from natural concentrations in the tuff. The comparisons demonstrated that none of the radioactivity detected in the samples can be attributed to migration from the disposal pit.

I. INTRODUCTION

Shallow land burial has been used for disposal of solid radioactive wastes at LASL since the early 1940s. Previous studies have shown that there is little potential for migration of radionuclides from the wastes because of the geologic and hydrologic characteristics of the disposal sites.[1,2,3] The purpose of this investigation was to determine whether any radionuclides have migrated downward from a waste pit used in the early 1960s. Horizontal core holes were drilled beneath the pit from a nearby canyon wall, and samples of the core were analyzed for radioactive constituents known to be present in the pit. The results of these analyses were then compared with expected background values from non-contaminated areas.

II. THE STUDY SITE

A. Description and Location

The LASL technical areas (TA) are located on the Pajarito Plateau, a topographic high along the western side of the Rio Grande Valley in northern New Mexico. The Plateau slopes gently eastward from the base of the Sierra de los Valles to the cliffs overlooking the Rio Grande (Fig. 1). Southeast trending streams have dissected the Plateau into

---

*Authors listed in alphabetical order.

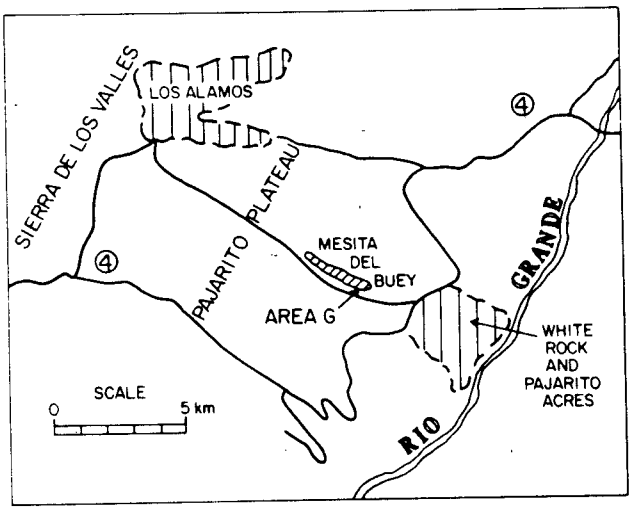

Fig. 1.
Physiographic features of the Los Alamos area showing location of Mesita del Buey.

narrow finger-like mesas. The majority of LASL's facilities, including waste disposal sites, are located on the tops of these mesas.

In 1956, Area G, TA-54, was designated for the disposal of solid radioactive waste (Fig. 1). The wastes range from rubber gloves and glassware to parts of obsolete buildings and equipment that cannot be decontaminated. They are buried in pits ranging in size from 9 to 30 m wide, 45 to 180 m long, and 4 to 10 m deep. The waste is placed in layers 1 to 2 m deep, and each layer is covered with approximately 0.5 m of crushed tuff. The pits are filled to within 1 m of the land surface, and covered with 1.5 to 2 m of crushed tuff. This final cover is slightly mounded above the original grade to encourage surface runoff. Some wastes are placed in vertical shafts, which range from 0.6 to 1.8 m in diameter, and up to 20 m deep.[4]

Solid waste Pit 3 at Area G was selected as the study location. It is typical of disposal pits at LASL (size and types of waste) and the surrounding terrain provided ready access to a drilling location. Further, there are no disposal shafts adjacent to Pit 3; possible lateral migration from wastes below the bottom of the pit is not a concern.

Pit 3, excavated in 1963, is 30 m wide, 160 m long, and about 8 m deep.[4] Waste was placed in the pit in seven layers, which were separated by crushed or broken tuff. A final cover of 3 m of crushed tuff was placed over the waste. Waste disposal records indicate the quantities and location of waste in the pit. The inventory of radionuclides in the pit shows that the amount of ^{3}H, ^{90}Sr, mixed activation and fission products is uncertain. A partial inventory shows 64 curies of $^{239,240}Pu$ and 58 curies of ^{241}Am when the pit was covered.[4] The total amounts probably do not exceed these figures by a factor of 2. The records also show about 10 curies of uranium, primarily ^{235}U and ^{238}U. The pit was filled and the final cover completed in 1966.

B. Geology

The surface and underlying rocks of the Pajarito Plateau are ash flows and ash falls of rhyolite tuff from the Jemez volcanic complex.[5] The tuff is underlain by partially lithified sediments, basalt, and other volcanic rocks. The study location, in Area G, is near the eastern end of one of the mesas (Mesita del Buey) forming the Plateau. This mesa trends southeast, and is about 3.2 km long by 0.4 km wide. The surface slopes from an elevation of about 2100 m near the western end to about 2010 m at its eastern end at Area G. It is bounded on the north and south by canyons cut 15 to 30 m below the mesa surface, and several small side drainages serate the edge of the mesa.

The sides of the mesa are vertical or near-vertical cliffs, with steep slopes at their base. The ash-flow tuffs on the north-facing slopes of the canyon walls are generally covered with talus, while those on the south-facing slopes are exposed. The surface of the mesa has a thin soil zone, up to a meter thick along the axis of the mesa and thinning toward the canyon rim where the tuff is exposed.

The Tshirege Member of the Bandelier Tuff forms the upper surface and underlies the mesa at Area G.[5,6,7] It is a rhyolite tuff composed of a basal ash fall, followed by a series of ash flows. The Tshirege has been divided into several units, with the lower four present at Mesita del Buey (Fig. 2).[8] These units are typically nonwelded to moderately welded, and composed of quartz and sanidine crystals and crystal fragments, with some rock fragments of latite, rhyolite, and pumice in an ash matrix. The units are distinguished from each other by the degree of welding, color, and the size and relative

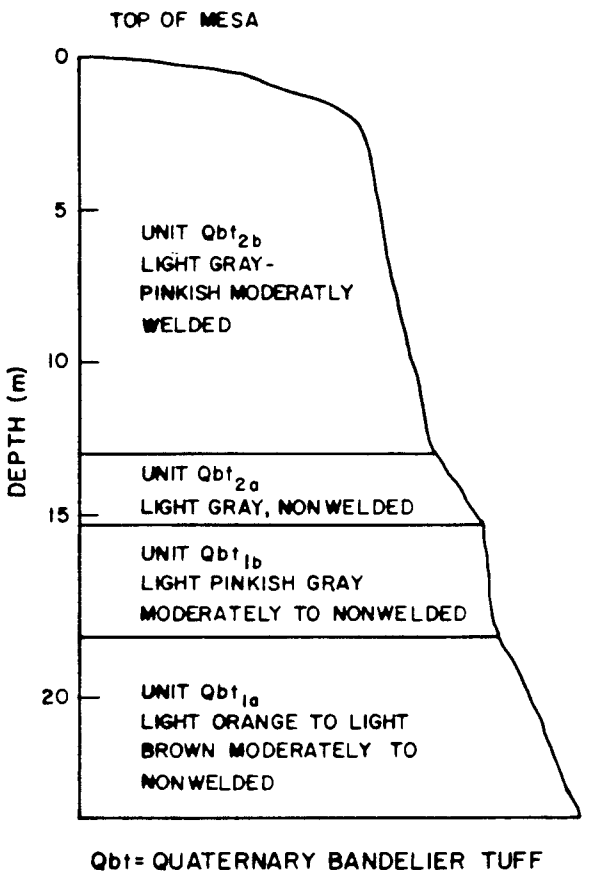

Fig. 2.
Geologic column showing stratigraphic units present at Mesita del Buey.

proportions of the crystal, rock and pumice fragments. The Bandelier Tuff contains numerous vertical or near vertical joints. These joints may be open or closed, or may have a filling of clay or caliche. Most of the joints do not cross into formations underlying the Bandelier Tuff.

C. Climatology

The climate of the Pajarito Plateau is semiarid; annual precipitation ranges from 35 to 50 cm and potential evaporation is on the order of 150 cm. Summer rainfall accounts for about 70% of the annual precipitation. The mean annual temperature is 9°C with extremes of 35°C in the summer and −25°C in the winter.

D. Hydrology

The undisturbed soils have significant accumulations of clay at the soil-tuff contact.[9] This clay is relatively impermeable, and retards the downward movement of infiltrated precipitation. As a result, the underlying tuff is quite dry, with moisture contents usually ranging from 2 to 5% by volume below a few meters.

The hydrologic characteristics of the undisturbed tuff vary with the degree of induration. The tuff has a saturated hydraulic conductivity on the order of 10^{-3} cm/min, and the conductivity decreases rapidly with decreasing water content.[10] At a water content of 5% by volume, the hydraulic conductivity of the tuff is less than 10^{-8} cm/min,[10] and water movement is primarily in the vapor phase through the bulk tuff or open joints.

The hydrologic characteristics of disturbed crushed tuff, used as a final cover over the waste trenches, are comparable to those of undisturbed tuff.[10] The hydraulic conductivity is somewhat higher because of greater effective porosity. Measurement of moisture distributions in the crushed tuff overlying buried waste show that the highest moisture contents (15-20% by volume) occur at depths of less than 3 m, with a continual decrease in moisture content below that depth. The high values are associated with spring snowmelt or summer thunderstorm activity, and within a few weeks the infiltrated water is returned to the atmosphere by evaporation or transpiration.[7]

There is no known perched water at Area G between the surface of the mesa and the main aquifer of the Los Alamos area. The main aquifer (capable of municipal and industrial water supply) lies at a depth of 250 m below the surface of the mesa. The movement of water in the aquifer is from the recharge area, an intermontane basin west of Los Alamos, to the Rio Grande where a part of the water is discharged to the river through seeps and springs.[11]

Stream flow in the canyon north and south of Area G is intermittent and occurs only during periods of heavy precipitation or spring snowmelt. The intermittent stream in the canyon to the south recharges a small body of water in the alluvium. The alluvium in the canyon north of Area G does not contain any perched water because of the relatively small amount of surface runoff in that drainage.

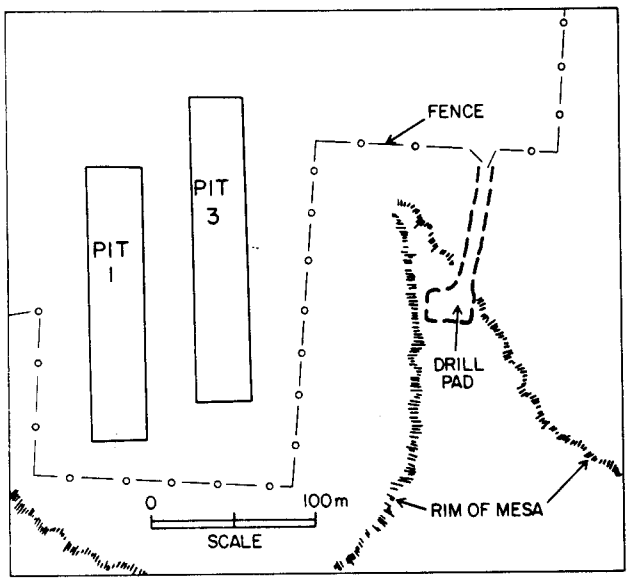

Fig. 3.
Southeastern part of Area G, showing location of waste pits and drill pad.

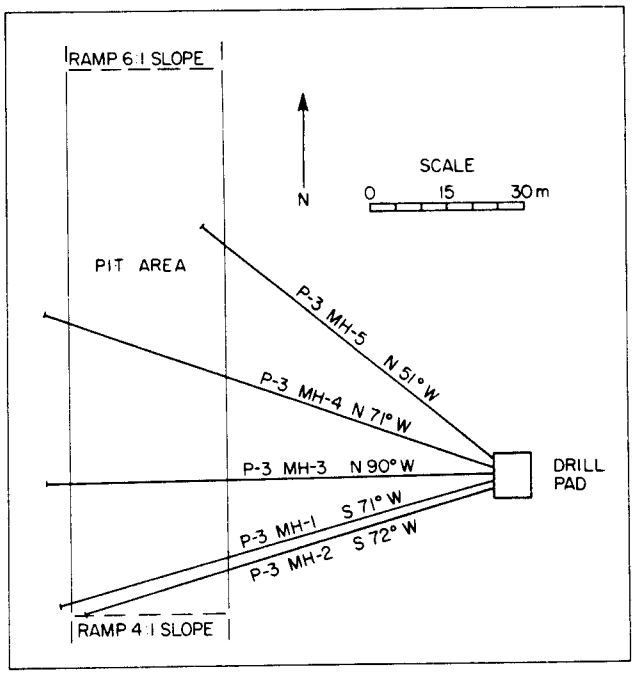

Fig. 4.
Orientation of core holes beneath Waste Pit 3, Area G.

III. METHODS OF STUDY

A. Sample Collection

For this study it was necessary to collect samples of the tuff from beneath Pit 3 for radiochemical analyses. Horizontal drilling to collect the samples was selected for two reasons.

1. Vertical holes would penetrate the wastes and possibly lead to cross-contamination of the samples.
2. Previous attempts at vertical coring in the tuff led to poor sample recovery.

A drill pad was constructed in a small canyon east of the pit (Fig. 3). Five horizontal holes (Fig. 4) were cored under the pit using air as a cuttings carrier to avoid contamination of the core by drilling mud or water. During drilling operations the air and cuttings from the holes were discharged into a closed tank partly filled with water. The water retained most of the cuttings. The air from the tank was exhausted through high-velocity filters to retain any remaining dust that might otherwise have been transmitted to the atmosphere. Water and cuttings from the tank were monitored for radioactive contamination, as was the ambient air in the area. No contamination was detected in the water, cuttings, or air.

The completion data on each core hole were published in a summary report by Reynolds Electrical and Engineering Company,[12] while the geologic desciption of cores from the holes was presented in a LASL publication.[13]

The starting elevation of each hole was below the bottom of the pit, and the holes were oriented at initial angles slightly above the horizontal. As coring of a given hole progressed, the angle decreased because of gravitational rotation of the coring assembly and drill stem. (The coring angle and compass orientation were determined periodically with down-hole survey instruments.) At some distance from the drilling face, the hole angle passed through the horizontal, and assumed a negative angle, plunging gently downward beneath the pit (Figs. 5 through 9). Thus, the core holes were not at a constant depth beneath the pit. Cores recovered for analyses ranged in depth from 0.0 to 3.4 m at the near (eastern) edge of the pit, to 3.1 to 7.2 m at the far (western) edge of the pit (Table I).

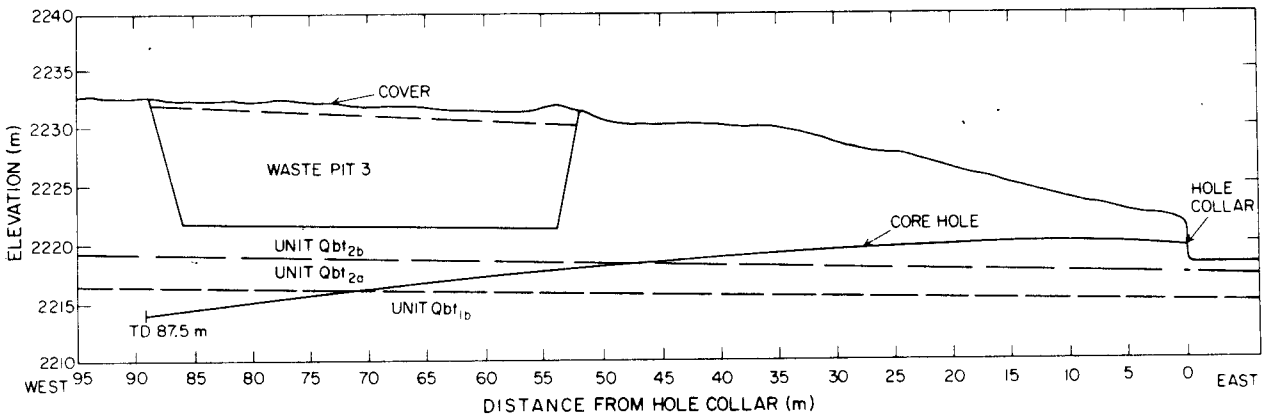

Fig. 5.
Cross section of the mesa showing the geologic units, pit 3, and the trace of core hole MH-1.

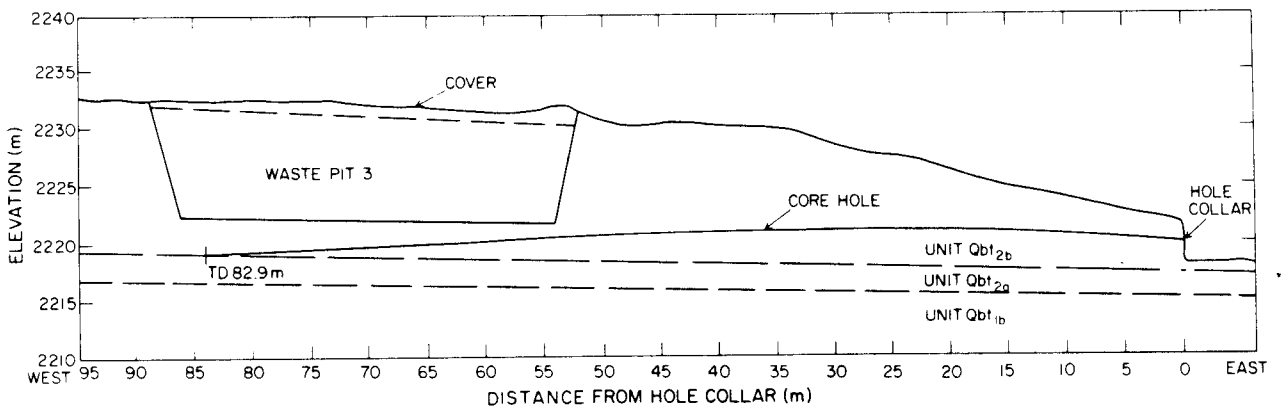

Fig. 6.
Cross section of the mesa showing geologic units, pit 3, and the trace of core hole MH-2.

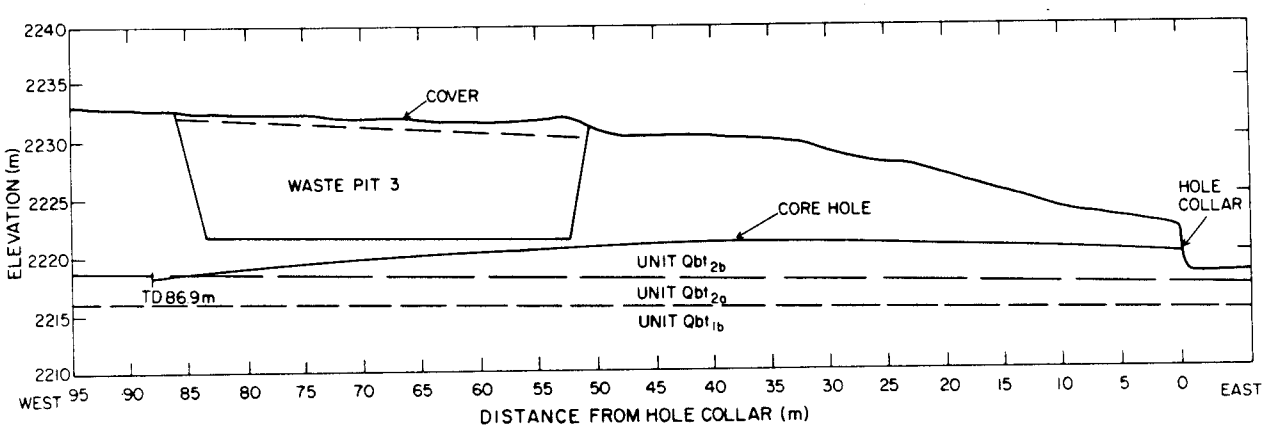

Fig. 7.
Cross section of the mesa showing the geologic units, pit 3, and the trace of core hole MH-3.

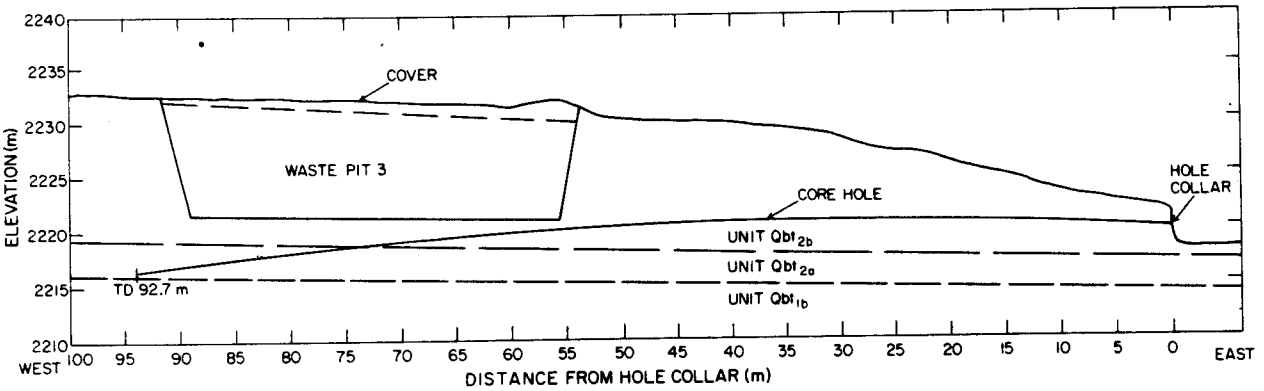

Fig. 8.
Cross section of the mesa showing geologic units, pit 3, and the trace of core hole MH-4.

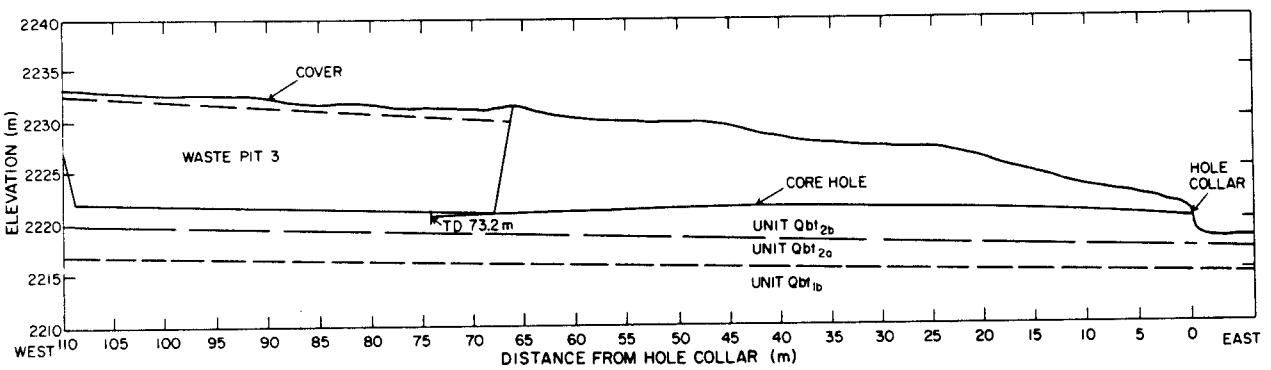

Fig. 9.
Cross section of the mesa showing geologic units, pit 3, and the trace of core hole MH-5.

Three of the stratigraphic units of the Bandelier Tuff were penetrated by the core holes. All holes were initiated in Unit 2b. Core holes MH-2 and MH-5 were completed in Unit 2b, holes MH-3 and MH-4 were completed in the upper part of Unit 2a, and hole MH-1 was completed in Unit 1b. The recovery for a given core run varied from 37 to 100%.[13] As the core was logged, samples were collected at intervals of about every 1.5 m from the collar to within 5.5 m of the pit, and at intervals of about every 0.3 m from that point to the end of the hole.[13]

B. Radiochemical Analyses

The core samples were analyzed for gross alpha, gross beta, ^{90}Sr, ^{238}Pu, ^{239,240}Pu, ^{241}Am, ^{137}Cs and total uranium. The following is a brief description of analytical methods. Detailed methods of analyses are presented in LA-7263-MS.[8]

The tuff cores were dried, ground, and sieved through No. 12 (~1.7 mm) screens. Separate aliquots of the prepared tuff were taken for each analysis. Tuff for gross alpha and gross beta analyses was leached with hot acid and the leachate evaporated onto a stainless steel planchet before counting in a thin window, dual gas proportional counter. Analytical results for gross alpha are reported with respect to ^{239}Pu as a standard, and for gross beta with respect to ^{90}Sr-^{90}Y as a standard. Aliquots of tuff for ^{238}Pu and ^{239,240}Pu analyses were spiked with ^{242}Pu to determine recovery percentages, while for ^{241}Am the aliquots were spiked with ^{243}Am. The Pu and Am were isolated by ion exchange, electroplated on a stainless steel disk, and counted on an alpha spectrometer. Aliquots of tuff for ^{137}Cs

TABLE I

HOLE LENGTH AND DEPTH BELOW PIT AT NEAR AND FAR EDGE

	Core Holes				
	MH-1	MH-2	MH-3	MH-4	MH-5
Total distance cored (m)	87.5	82.9	86.9	92.7	73.2
Hole length at near edge of pit (m)	53.2	53.6	51.8	54.9	67.1
Hole length at far edge of pit (m)	84.6	82.9[a]	82.3	87.8	73.2[b]
Depth beneath pit at near edge (m)	3.4	1.2	0.6	0.8	0.0
Depth beneath pit at far edge (m)	7.2	3.1	3.1	4.4	0.3

[a]Completed beneath pit.
[b]Completed in fill within pit.

analyses were counted directly with a Ge(Li) detector, coupled with a multichannel analyzer. Tuff for ^{90}Sr analyses was dissolved with acid. The sample was extracted with HDEHP to remove the ^{90}Y daughter and any interfering radionuclides. Stable Y was added as a chemical carrier. After allowing the ^{90}Y to re-equilibrate with the ^{90}Sr, the sample was re-extracted, the Y purified, and the sample counted on a gas proportional counter. Aliquots of tuff for total uranium analyses were irradiated by epithermal neutrons in a nuclear reactor and then counted with a Ge(Li) gamma ray spectrometer.

The minimum detection limits (MDL) for gross alpha and gross beta activity are 0.8 and 0.03 pCi/g, respectively. The MDL for ^{137}Cs is 0.5 pCi/g; for ^{238}Pu, $^{239,240}Pu$ and ^{241}Am, 0.005 pCi/g; for ^{90}Sr, 1.0 pCi/g; and for total uranium, 0.4 μg/g.

IV. RESULTS AND DISCUSSION

A. Strategy

The Bandelier Tuff contains naturally-occurring radionuclides, which emit alpha and/or beta radiation, including uranium. The presence of gross alpha, gross beta or uranium concentrations above expected background values would indicate possible migration of radionuclides from the waste pit to the underlying tuff. Further, elevated values in samples from beneath the pit compared with those from beside the pit, would be an additional indication of migration from the pit. Detection of the artificially produced radionuclides, ^{90}Sr, ^{137}Cs, ^{238}Pu, $^{239,240}Pu$, and ^{241}Am, would indicate migration from either the waste in the pit, or from surface deposition of fallout from atmospheric tests.

TABLE II

NATURAL AND FALLOUT CONCENTRATIONS OF RADIOACTIVITY AND RADIONUCLIDES IN REGIONAL SOILS AND SEDIMENTS

(Concentrations in pCi/g except as noted)

	Min	Max	$\bar{x}$
Gross Alpha	0.1	18	4
Gross Beta	0.2	13	5.2
^{137}Cs	<0.01	1.06	0.32
^{238}Pu	<0.001	0.010	<0.001
^{239}Pu	<0.001	0.045	0.008
^{90}Sr	<0.01	10	0.25
Total U[a]	<0.1	5.1	1.8

[a]μg/g.

Concentrations of man-made radionuclides occurring in surface soils and sediments have been determined for the period 1974-1978 in the area surrounding LASL, and are presented in Table II.[8] The natural uranium content of the tuff varies from unit to unit.[14] Concentrations measured in samples from outcrops are summarized in Table III. The data in Tables II and III are included for comparison with the analytical results for samples collected adjacent to and under the pit.

B. Analytical Results

The analytical results for samples from the core holes are summarized in Tables IV through VIII. Shown in the tables are the minimum, maximum, mean ($\bar{x}$), and twice the standard deviation (2S) for the number of analyses made in each core hole. The MDL for each analysis is shown in the respective table. The ± value following the minimum and maximum values is the analtyical errors (1S) associated with that particular analysis. In order to conclude, at the 95% confidence level, that a particular radionuclide is present in a sample, the reported value minus twice the analytical error must exceed the stated MDL. If the reported value minus twice the analytical error is less than MDL, it can only be

TABLE III

URANIUM CONCENTRATIONS IN OUTCROP SAMPLES OF BANDELIER TUFF

(concentration, μg/g)

Unit	Min	Max	$\bar{x}$
2b	3.9	6.3	5.0
2a	4.9	8.2	7.1
1b	7.2	8.2	7.8

concluded, at the 95% confidence level, that the radionuclide was not detected in the sample at concentrations above the MDL.

Each set of analyses is grouped according to the core holes from which the samples were collected. The analyses are further divided into those samples adjacent to the pit, and those samples underlying the pit. Data that might reflect naturally-occurring radioactivity (gross alpha, gross beta and uranium) were further subdivided into those samples from Unit 2b, Unit 2a, and Unit 1b. Unit 1b was encountered only in core hole MH-1 (Fig. 5).

A total of 354 samples were analyzed for gross alpha and gross beta (Tables IV and V). Of these, 191 samples were from under the pit, and 165 samples were from the area adjacent to the pit. All measured concentrations were above the minimum detection limits.

A total of 107 samples from the five core holes were analyzed for total uranium (Table VI). These included all samples showing alpha activity substantially above the mean value. Fifty-eight of the samples were from the area adjacent to the pit, while the remaining 49 samples were from under the pit. All measured concentrations were above the minimum detection limits.

A total of 43 analyses were made for ^{137}Cs from samples from the five holes. Of these, 11 were from the area adjacent to the pit, and 32 were from under the pit (Table VII). The ^{137}Cs concentrations were at or below the MDL of 0.50 pCi/g.

Forty-four samples from the five core holes were analyzed for ^{238}Pu and $^{239,240}Pu$ (Table VII). Of the 44 samples, 11 were from the area adjacent to the pit

TABLE IV

GROSS ALPHA ACTIVITY IN SAMPLES FROM CORE HOLES ADJACENT TO AND UNDER PIT 3
(concentrations in pCi/g)

	No. of Analyses	Min	Max	$\bar{x}$	2σ
Adjacent to Pit					
Unit 2b					
MH-1	22	2.0 ± 1.0	5.6 ± 2.4	3.5	2.0
MH-2	27	1.9 ± 1.0	5.7 ± 2.4	3.0	1.8
MH-3	18	1.9 ± 1.0	5.1 ± 2.2	2.7	2.0
MH-4	21	2.0 ± 1.0	3.9 ± 1.6	2.8	1.0
MH-5	65	1.6 ± 1.0	4.7 ± 2.0	2.9	1.2
Unit 2a					
MH-1	12	2.9 ± 1.4	8.7 ± 3.6	4.0	3.2
Under Pit					
Unit 2b					
MH-2	51	2.6 ± 1.2	6.4 ± 2.8	4.3	2.0
MH-3	52	2.1 ± 1.1	6.1 ± 2.6	3.8	1.8
MH-4	37	2.6 ± 1.2	8.3 ± 3.4	3.6	2.0
MH-5	5	2.6 ± 1.2	3.3 ± 1.6	3.0	0.6
Unit 2a					
MH-1	14	3.2 ± 1.4	5.5 ± 2.4	4.3	1.2
MH-4	18	2.6 ± 1.2	5.6 ± 2.4	3.8	2.0
Unit 1b					
MH-1	12	7.3 ± 3.0	13.0 ± 6.0	9.7	4.4

Note: MDL gross alpha 0.8 pCi/g, referenced to ^{239}Pu as standard.

and 33 were from the area under the pits. All analyses were below the MDL of 0.005 pCi/g.

Forth-three samples from the five core holes were analyzed for ^{241}Am (Table VIII). Of the 43 samples, 13 were from the area adjacent to the pit and 30 were from the area under the pit. The analyses were below the MDL of 0.005 pCi/g.

Forty-three samples from the five core holes were analyzed for ^{90}Sr (Table VIII). Of the 43 samples, 11 were from the area adjacent to the pit and 32 were from under the pit. All the analyses were below the MDL of 1.0 pCi/g.

C. Discussion

Gross alpha, gross beta, and uranium concentrations in the samples were all above the minimum detection limits. For each type of analysis, a composite of the sample analyses from all holes penetrating a particular unit under the pit was compared statistically with a composite of analyses for samples in the same unit in the area adjacent to the pit. Further, the analyses were grouped according to geologic unit and compared with each other. All comparisons were made at a 95% confidence level.

The comparison of results showed no significant differences in gross alpha, gross beta, or uranium concentrations in samples from under the pit compared with those away from the pit for Units 2a and 2b. Unit 1b was not encountered in the area away from the pit because of its stratigraphic position. The comparisons did show differences in gross alpha, gross beta, and uranium concentrations between units; results for 2a and 2b were similar,

TABLE V

GROSS BETA ACTIVITY IN SAMPLES FROM CORE HOLES ADJACENT TO AND UNDER PIT 3
(concentrations in pCi/g)

	No. of Analyses	Min	Max	$\bar{x}$	2σ
Adjacent to Pit					
Unit 2b					
MH-1	22	1.6 ± 0.6	6.1 ± 1.4	3.5	2.2
MH-2	27	0.8 ± 0.6	3.5 ± 1.0	2.0	1.4
MH-3	18	1.1 ± 0.4	5.2 ± 1.2	2.2	1.3
MH-4	21	1.1 ± 0.6	3.8 ± 1.0	1.9	1.6
MH-5	65	0.7 ± 0.6	3.7 ± 1.0	1.8	1.2
Unit 2a					
MH-1	12	2.4 ± 0.8	6.2 ± 1.4	3.8	2.4
Under Pit					
Unit 2b					
MH-2	51	−0.5 ± 0.4	5.0 ± 1.2	2.8	1.8
MH-3	52	1.3 ± 0.6	6.3 ± 1.4	2.8	2.0
MH-4	37	1.4 ± 0.6	5.1 ± 1.2	2.4	1.8
MH-5	5	1.7 ± 0.8	3.0 ± 0.8	2.2	1.0
Unit 2a					
MH-1	14	1.7 ± 0.8	4.3 ± 1.0	2.8	1.6
MH-4	18	1.1 ± 0.6	4.5 ± 1.2	2.3	1.8
Unit 1b					
MH-1	12	4.2 ± 1.2	6.5 ± 1.4	5.4	2.2

Note: MDL gross beta 0.03 pCi/g, referenced to ^{90}Sr as standard.

but concentrations in Unit 1b were significantly higher for all three types of analysis.

The analyses for man-made radionuclides indicate that such radionuclides are not present in the samples at concentrations above detection limits. The differences in gross alpha and gross beta concentrations between Unit 1b and Unit 2a or 2b are substantially greater than the magnitude of the minimum detection limits. Thus, man-made radionuclides known to be in the pit cannot be responsible for these differences.

The differences in measured uranium concentrations between the various units are of the same magnitude as the measured differences in gross alpha concentrations. Thus, the elevated concentration or uranium (an alpha emitter) in Unit 1b is considered to be the primary source of the higher gross alpha values for the unit. Other naturally-occurring alpha emitters, such as those belonging to the thorium decay series, are known to be present in the tuff,[15] and are also likely contributors to the elevated alpha values. Concentrations of uranium in outcrop samples (Table III) are similar to those in samples from beneath and beside the pit in the respective units.

The pattern of elevated gross beta concentrations was similar to that for gross alpha and uranium, and could not be accounted for by measured concentrations of man-made beta emitters. However, tritium (^{3}H), a naturally-occurring beta emitter, is also a

TABLE VI

TOTAL URANIUM IN SAMPLES FROM CORE HOLES ADJACENT TO AND UNDER PIT 3
(concentrations in $\mu g/g$)

	No. of Analyses	Min	Max	x	2σ
Adjacent to Pit					
Unit 2b					
MH-1	9	4.4 ± 1.0	5.0 ± 1.0	4.7	0.4
MH-2	11	4.5 ± 1.0	5.0 ± 1.0	4.7	0.3
MH-3	10	4.8 ± 1.0	5.2 ± 1.0	4.9	0.3
MH-4	10	4.3 ± 1.0	4.8 ± 1.0	4.6	0.4
MH-5	16	4.5 ± 1.0	6.2 ± 1.2	4.9	0.8
Unit 2a					
MH-1	2	4.7 ± 1.0	5.0 ± 1.0	4.8	0.4
Under Pit					
Unit 2b					
MH-2	9	4.1 ± 0.8	5.4 ± 1.0	4.8	0.9
MH-3	9	4.5 ± 1.0	5.3 ± 1.0	4.7	0.5
MH-4	4	4.7 ± 1.0	5.5 ± 1.0	5.0	0.7
MH-5	2	5.0 ± 1.0	5.9 ± 1.2	5.4	1.3
Unit 2a					
MH-1	7	4.9 ± 1.0	5.3 ± 1.0	5.1	0.1
MH-3	1	---	5.1 ± 1.0	5.1	1.0
MH-4	7	4.5 ± 1.0	5.3 ± 1.0	5.0	0.5
Unit 1b					
MH-1	10	6.7 ± 1.4	8.6 ± 1.8	7.4	1.2

Note: Total uranium MDL, 0.4 mg/g.

known contaminant in the waste pit, primarily as tritiated water (HTO). The possible migration of tritium was not investigated in this study because the cores were obtained by drilling with air. Tritiated water vapor in the air would thus be mixed with any tritiated water in the core, rendering useless any data on tritium content of the samples.

The movement of tritium (as tritiated water vapor) from disposal pits and shafts has been documented.[16,17] The tritiated water is incorporated in the natural flow of moisture in the tuff. This migration appears to be due primarily to the movement of water vapor through the open joints and fractures of the tuff. The movement through the bulk of the tuff is restricted, but is greater in zones of higher effective porosity.

It is thus feasible that tritium, while not specifically analyzed for, contributed to the elevated gross beta concentrations observed in Unit 1b. Only qualitative interpretations of possible tritium concentrations are possible; the technique used for gross beta determination is very imprecise for measurement of tritium concentrations. However, several observations argue against the possibility that the observed gross beta variations resulted from tritium in the samples. The concentration of potassium (and the associated ^{40}K, a natural beta emitter) vary by a factor of two among units.[15] It was previously noted that concentrations of uranium and thorium (and their associated decay chains) vary between Units 1b and 2a or 2b. Both decay chains contain numerous beta emitters, which would contribute to

TABLE VII

CESIUM AND PLUTONIUM IN SAMPLES FROM CORE HOLES ADJACENT TO AND UNDER PIT 3
(concentrations in pCi/g)

	No. of Analyses	Min	Max	$\bar{x}$	2σ
^{137}Cs					
Adjacent to Pit					
MH-1	2	−0.10 ± 0.40	0.20 ± 0.60	0.05	0.42
MH-2	2	−0.10 ± 0.80	0.00 ± 0.40	−0.05	0.14
MH-3	2	0.03 ± 0.20	0.30 ± 0.80	0.11	0.32
MH-4	2	0.00 ± 0.16	0.06 ± 0.16	0.03	0.08
MH-5	2	−0.03 ± 0.06	0.04 ± 0.04	0.01	0.10
Under Pit					
MH-1	11	−0.06 ± 0.36	0.50 ± 1.20	0.09	0.36
MH-2	7	−0.15 ± 0.60	0.20 ± 0.80	0.03	0.26
MH-3	6	−0.03 ± 0.12	0.30 ± 0.40	0.08	0.24
MH-4	6	−0.05 ± 0.40	0.04 ± 0.40	0.01	0.08
MH-5	2	−0.17 ± 0.40	−0.07 ± 0.12	−0.12	0.14
^{238}Pu					
Adjacent to Pit					
MH-1	3	−0.003 ± 0.006	0.001 ± 0.008	−0.003	0.004
MH-2	2	−0.002 ± 0.002	0.000 ± 0.002	−0.001	0.002
MH-3	2	−0.001 ± 0.001	0.000 ± 0.002	−0.000	0.000
MH-4	2	−0.001 ± 0.001	0.001 ± 0.002	−0.000	0.002
MH-5	2	0.001 ± 0.002	0.001 ± 0.010	0.001	0.000
Under Pit					
MH-1	13	−0.003 ± 0.003	0.001 ± 0.002	0.000	0.002
MH-2	6	−0.001 ± 0.002	0.001 ± 0.008	0.002	0.008
MH-3	5	−0.001 ± 0.001	0.000 ± 0.002	0.000	0.000
MH-4	6	−0.002 ± 0.002	0.000 ± 0.002	−0.001	0.002
MH-5	2	−0.001 ± 0.002	0.000 ± 0.004	0.000	0.002
^{239}Pu					
Adjacent to Pit					
MH-1	3	−0.004 ± 0.006	−0.001 ± 0.002	−0.002	0.004
MH-2	2	0.000 ± 0.002	0.001 ± 0.002	0.001	0.000
MH-3	2	−0.001 ± 0.001	0.000 ± 0.002	0.000	0.002
MH-4	2	−0.001 ± 0.001	0.000 ± 0.002	0.000	0.002
MH-5	2	−0.002 ± 0.001	−0.001 ± 0.006	−0.001	0.002
Under Pit					
MH-1	13	−0.001 ± 0.003	0.003 ± 0.003	0.000	0.002
MH-2	6	−0.002 ± 0.003	0.002 ± 0.010	0.000	0.002
MH-3	6	−0.001 ± 0.002	0.003 ± 0.004	0.000	0.004
MH-4	6	−0.002 ± 0.002	0.001 ± 0.002	0.000	0.002
MH-5	2	−0.001 ± 0.003	−0.003 ± 0.006	−0.002	0.002

Note: MDL for ^{137}Cs, 0.50 pCi/g; ^{238}Pu, ^{239}Pu, 0.005 pCi/g.

TABLE VIII

AMERICIUM AND STRONTIUM IN SAMPLES FROM CORE HOLES ADJACENT TO AND UNDER PIT 3
(concentrations in pCi/g)

	No. of Analyses	Min	Max	$\bar{x}$	2σ
^{241}Am					
Adjacent to Pit					
MH-1	3	0.000 ± 0.002	0.001 ± 0.002	0.000	0.002
MH-2	3	0.000 ± 0.002	0.001 ± 0.002	0.000	0.002
MH-3	3	0.001 ± 0.002	0.002 ± 0.006	0.001	0.002
MH-4	2	0.000 ± 0.002	0.003 ± 0.002	0.001	0.002
MH-5	2	0.000 ± 0.002	0.000 ± 0.002	0.000	0.002
Under Pit					
MH-1	12	0.000 ± 0.002	0.004 ± 0.004	0.000	0.002
MH-2	5	0.000 ± 0.002	0.001 ± 0.004	0.001	0.002
MH-3	5	0.000 ± 0.002	0.003 ± 0.006	0.001	0.002
MH-4	6	−0.002 ± 0.006	0.002 ± 0.002	0.000	0.002
MH-5	2	0.000 ± 0.002	0.000 ± 0.002	0.000	0.000
^{90}Sr					
Adjacent to Pit					
MH-1	2	0.40 ± 0.20	0.50 ± 0.20	0.45	0.14
MH-2	2	0.00 ± 0.40	0.20 ± 0.20	0.10	0.28
MH-3	3	0.10 ± 0.20	0.80 ± 1.80	0.43	0.70
MH-4	2	0.00 ± 0.08	0.10 ± 0.20	0.05	0.14
MH-5	2	0.10 ± 0.20	0.10 ± 0.20	0.10	0.00
Under Pit					
MH-1	12	0.02 ± 0.20	0.40 ± 0.20	0.24	0.44
MH-2	7	0.05 ± 0.20	0.20 ± 0.20	0.15	0.32
MH-3	6	−0.03 ± 0.40	0.40 ± 0.20	0.14	0.36
MH-4	5	0.00 ± 0.20	0.10 ± 0.20	0.06	0.10
MH-5	2	−0.10 ± 0.20	0.20 ± 0.20	0.05	0.42

Note: MDL for ^{241}Am 0.005 pCi/g; ^{90}Sr, 1.0 pCi/g.

the observed differences. Finally, the elevated gross beta concentrations were observed in the lowest unit penetrated (1b), with lower concentrations in the overlying Units 2a and 2b. If tritium in the waste pit were the source of the elevated gross beta concentrations, the concentrations would be higher immediately adjacent to the bottom of the pit. For these reasons, the possible presence of tritium in the samples is not considered to be the source of the observed differences in gross beta concentrations among stratigraphic units. Rather, these variations are attributed to natural beta emitters in the tuff.

V. SUMMARY AND CONCLUSIONS

A. Summary

Solid radioactive wastes from LASL are disposed of by burial in pits excavated in rhyolite tuff at LASL disposal sites. The semiarid climate, coupled with relatively low permeabilities of soil and underlying tuff, restricts the downward movement of water within waste materials. This study was performed in an attempt to detect the migration of radionuclides in waste to the tuff immediately underlying a waste pit.

Waste Pit 3, used from 1963 to 1966 was selected as the study location. Disposal records identified the presence of ^{3}H, ^{90}Sr, mixed activation and fission products, $^{239,240}Pu$, ^{241}Am, and uranium as contaminants in the waste.

The tuff at the study location has been divided into several stratigraphic units, distinguishable from each other by chemical and physical properties. The natural concentrations of uranium, as well as other natural radionuclides, vary from unit to unit.

In 1976, horizontal core holes were drilled in a fan-shaped array beneath the disposal pit from a drill pad in an adjacent drainage. The depth of the core holes beneath the bottom of the pit varied from nearly zero to more than seven meters. Samples of tuff adjacent to and beneath the pit were analyzed for radionuclides known to be present in the pit, as well as for gross alpha and gross beta radiation. The analytical results from samples beneath the pit were compared statistically with those from samples from beside the pit. The analytical results were also grouped according to stratigraphic units, and comparisons were made between units and with outcrop data for the respective units.

B. Conclusions

The man-made radionuclides known to be present in the pit, ^{90}Sr, ^{137}Cs, ^{238}Pu, $^{239,240}Pu$, and ^{241}Am, were not present in the samples at concentrations above the minimum detection limits.

Gross alpha and gross beta radiation, as well as uranium, was detected in the samples. However, the tuff contains naturally-occurring radionuclides, including uranium. There are no statistically significant differences in the concentrations of gross alpha, gross beta, or uranium in samples from under the pit compared with those adjacent to the pit within respective stratigraphic units.

Uranium concentrations varied between stratigraphic units, but the mean values from the cores were statistically indistinguishable from concentrations measured in outcrops. Similar variability in gross alpha concentrations between units is attributed to the observed variability in uranium, as well as to other naturally-occurring radionuclides.

Gross beta variations were also observed between stratigraphic units. Tritium, a known contaminant in the waste pit and a weak beta emitter, was not analyzed for because of potential cross-contamination with atmospheric tritium. However, the pattern of beta variations (increasing downward from the pit) provides a strong argument that tritium from the pit is not the source of the observed variability. Rather, the variations are attributed to other naturally-occurring radionuclides.

Thirteen years elapsed between the initial use of the disposal pit and this investigation. The state of the waste containers in the pit is uncertain, but many were undoubtedly ruptured at the time of disposal through compaction by heavy earthmoving equipment. Further, much of the waste, including some contaminated soil, was not in containers. Thus most of the radionuclides in the pit can be assumed to be available for dissolution by moving soil moisture. The actual rates of such dissolution are not known.

The expected water flow velocities in the solid and crushed tuff, on the order of fractions of a cm/year, suggest that no migrating solutions would be detectable at depths of more than a few centimeters beneath the pit. That expectation is not contradicted by this study, in that no radionuclides were detected in the samples whose presence can be attributed to migration from the pit.

VI. ACKNOWLEDGMENTS

This study would have been impossible without the assistance of Ken Larkin and the drilling personnel from Reynolds Electrical and Engineering Company. All analytical work was performed or directed by the Environmental Studies Group H-8, at LASL.

Their help is greatly appreciated. The statistical analyses were done by Willy Abeele, in the Environmental Science Group LS-6, at LASL. Without these analyses, the data collected by the study would have been very difficult to interpret. Finally, the authors are indebted to Ed Essington, also in LS-6, for his diligent and critical review of our initial draft.

REFERENCES

1. J. H. Abrahams, "Physical Properties and Movement of Water in the Bandelier Tuff, Los Alamos and Santa Fe Counties, New Mexico," U.S. Geol. Survey open-file report (1963).

2. J. H. Abrahams, J. E. Weir, and W. D. Purtymun, "Distribution of Moisture in Soil and Near-Surface Tuff on the Pajarito Plateau, Los Alamos County, New Mexico," U.S. Geol. Survey Prof. Paper 424 D (1961).

3. W. D. Purtymun and W. R. Kennedy, "Distribution of Moisture and Radioactivity in the Soil and Tuff at the Contaminated Waste Pit Near Technical Area 21, Los Alamos, New Mexico," U.S. Geol. Survey open-file report (1966).

4. M. A. Rogers, "History and Environmental Setting of LASL Near-Surface Land Disposal Facilities for Radioactive Wastes (Areas A, B, C, D, E, F, G, and T)," Los Alamos Scientific Laboratory report LA-6848-MS, Vols. 1 and 2 (1977).

5. R. L. Griggs, "Geology and Ground Water Resources of the Los Alamos Area, New Mexico," U.S. Geol. Survey Water-Supply Paper 1753 (1964).

6. W. D. Purtymun, "Geology and Hydrology of Area G, Mesita del Buey, Los Alamos County, New Mexico," U.S. Geol. Survey open-file report (1966).

7. W. D. Purtymun and W. R. Kennedy, "Geology and Hydrology of Mesita del Buey," Los Alamos Scientific Laboratory report LA-4660 (1971).

8. "Environmental Surveillance at Los Alamos During 1977," Los Alamos Scientific Laboratory report LA-7263-MS (1978).

9. J. W. Nyhan, L. W. Hocker, T. E. Calhoun, and D. L. Young, "Soil Survey of Los Alamos County," Los Alamos Scientific Laboratory report LA-6779-MS (1978).

10. M. L. Wheeler, W. J. Smith, A. F. Gallegos, "A Preliminary Evaluation of the Potential for Plutonium Release from Burial Grounds at Los Alamos Scientific Laboratory," Los Alamos Scientific Laboratory report LA-6694-MS (1977).

11. R. L. Cushman, "An Evaluation of Aquifer and Well Characteristics of Municipal Well Fields in Los Alamos and Guaje Canyons, Near Los Alamos, New Mexico," U.S. Geol. Survey Water-Supply Paper 1809-D (1965).

12. Reynolds Electric and Engineering Co., "Horizontal Monitoring Holes, Los Alamos, New Mexico, Completion Report," Contract E(26-1) 40 ERDA, October 1976.

13. W. D. Purtymun, M. L. Wheeler, and M. A. Rogers, "Geologic Description of Cores from Holes P-3 MH-1 through P-3 MH-5, Area G, Technical Area 54," Los Alamos Scientific Laboratory report LA-7308-MS (1978).

14. M. A. Rogers and B. W. Burton, "Trace Element Study of the Bandelier Tuff (Pleistocene), Pajarito Plateau, Los Alamos and Santa Fe Counties, North Central New Mexico," (in preparation).

15. B. W. Crowe, G. L. Linn, G. Heiken, M. L. Bevier, "Stratigraphy of the Bandelier Tuff in the Pajarito Plateau," Los Alamos Scientific Laboratory report LA-7225-MS (1978).

16. W. D. Purtymun, "Underground Movement of Tritium from Solid-Waste Storage Shafts," Los Alamos Scientific Laboratory report LA-5286-MS (1973).

17. M. L. Wheeler and J. L. Warren, "Tritium Containment after Burial of Contaminated Solid Wastes," Proceedings 23rd Conf. on Remote Systems Technology, San Francisco, California (1975).

LA-11135-MS

UC-70
Issued: November 1987

Environmental Status of Technical Area 49, Los Alamos, New Mexico

William D. Purtymun
Alan K. Stoker

Los Alamos
Los Alamos National Laboratory
Los Alamos, New Mexico 87545

ENVIRONMENTAL STATUS OF TECHNICAL AREA 49, LOS ALAMOS, NEW MEXICO

by

William D. Purtymun
Alan K. Stoker

ABSTRACT

In 1960 and 1961 a series of experiments involving high explosives and radioactive materials were conducted at Los Alamos, New Mexico, primarily to understand certain safety aspects of operational nuclear weapons. The experiments were conducted underground in large diameter holes as deep as 120 ft. The experiments were conducted in an area that was extensively studied in advance by the U. S. Geological Survey. The location was selected because it had geologic and hydrologic characteristics that assured complete containment of the experiments and precluded any possible contamination of groundwater. Important features verified by the USGS included the absence of any recharge and about 1200 feet of dry rock above the groundwater aquifer.

Residual materials dispersed by detonation of the high explosives remain at the bottom of the experimental holes. The materials of significance from an environmental standpoint include about 40 kg of plutonium, 93 kg of enriched uranium, at least 82 kg of depleted uranium, 13 kg of beryllium, and an undetermined amount of lead. The area is presently identified as a radioactive and hazardous material disposal area for purposes of compliance with Department of Energy and Environmental Protection Agency requirements.

Environmental monitoring has been carried out regularly since the time of the experiments. Results of measurements confirm that there has been no contamination of groundwater. Minor surface soil contamination dating from the time of the experimental operations has been detected in small surface drainages near the experimental area. None of the surface contamination has been measurable at Laboratory boundaries or points of public access on a state highway. Additional environmental studies will be conducted in the future under auspices of Department of Energy programs designed to assure appropriate management of buried transuranic waste and full compliance with requirements of the Comprehensive Environmental Response, Compensation, and Liability Act.

I. HISTORY AND BACKGROUND

A. Hydronuclear Experiments

Hydronuclear experiments were conducted underground at the Los Alamos Scientific Laboratory (LASL; the word "Scientific" was included in the name until 1980 when it was changed to "National"), Los Alamos, New Mexico, in 1960 - 1961. The experiments were conducted at Technical Area 49 (TA-49), located on Frijoles Mesa in the southwest corner of the Laboratory (Fig. 1). The experiments, conducted at the direction of President Eisenhower, were primarily to answer fundamental questions regarding certain safety aspects of four weapon systems that became operational in 1958. These experiments involved a combination of conventional (chemical) high explosives, usually in a nuclear weapon configuration, and fissile material whose quantity was reduced far below the amount required for a nuclear explosion. Between January 1960 and August 1961, a total of 35 hydronuclear experiments and 9 related calibration, equation-of-state, and criticality experiments, all involving some fissile material, were conducted (Thorn 1987). Other experiments involving high explosives and possibly some small amounts of radioactive tracers, but no fissile materials, were conducted starting in October 1959 and extending through the same period. The aerial photograph on the cover of this report shows TA-49 in late 1959.

B. Operations

The experiments involving fissile materials were conducted in 3- or 6-ft-diameter experimental holes at depths of 31 to 108 ft. Some of the other experiments were conducted in holes as deep as 120 ft. Several such experimental holes were augered and prepared for use in sequence. The experimental configuration was emplaced at the bottom of the hole, which was then stemmed (backfilled) with sand to contain the physical force of the high-explosive detonation. As the experiment was detonated, measurements and samples were taken through access tubes or pipes. After completion of measurements and sample collection, the experimental holes were backfilled with additional sand and sealed with concrete. Results of analyses were used to modify the next configuration in the series. The first series of nine hydronuclear experiments was conducted between January 12 and February 11, 1960 (Thorn 1987).

C. Materials Left in Place

All presently known remaining contamination at TA-49 is described in the next three sections.

1. Experimental Areas. Most materials were left in the experimental holes in which the experiments were conducted. The principal materials of interest from an environmental standpoint include plutonium, uranium, beryllium, and lead. A total of about 40.1 kg of plutonium, 93 kg of enriched uranium, at least 82 kg of depleted uranium, and 13 kg of beryllium were utilized. (No estimate of the amount of lead left from the experiments is presently available but will be determined from detailed review of engineering drawings during followup studies described later in Section IV of this report.) A small amount of fission products (less than 1 millicurie) would also be present.

Physical properties of the tuff and sand readily absorbed the energy of explosions and confined most of the materials within a maximum distance of 10 to 20 ft from the location of the experimental configuration. This confinement is indicated because in only one case was contamination from an

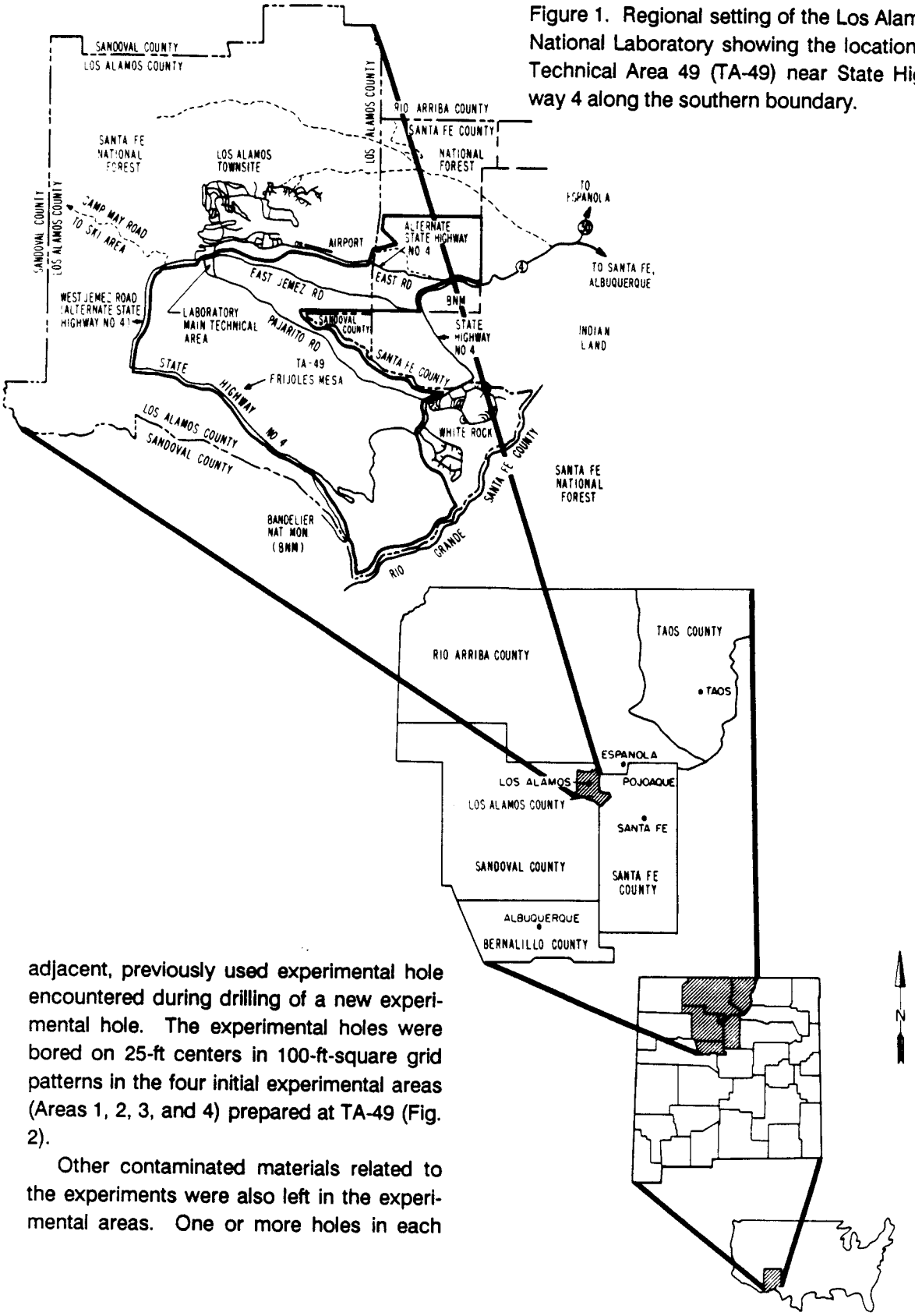

Figure 1. Regional setting of the Los Alamos National Laboratory showing the location of Technical Area 49 (TA-49) near State Highway 4 along the southern boundary.

adjacent, previously used experimental hole encountered during drilling of a new experimental hole. The experimental holes were bored on 25-ft centers in 100-ft-square grid patterns in the four initial experimental areas (Areas 1, 2, 3, and 4) prepared at TA-49 (Fig. 2).

Other contaminated materials related to the experiments were also left in the experimental areas. One or more holes in each

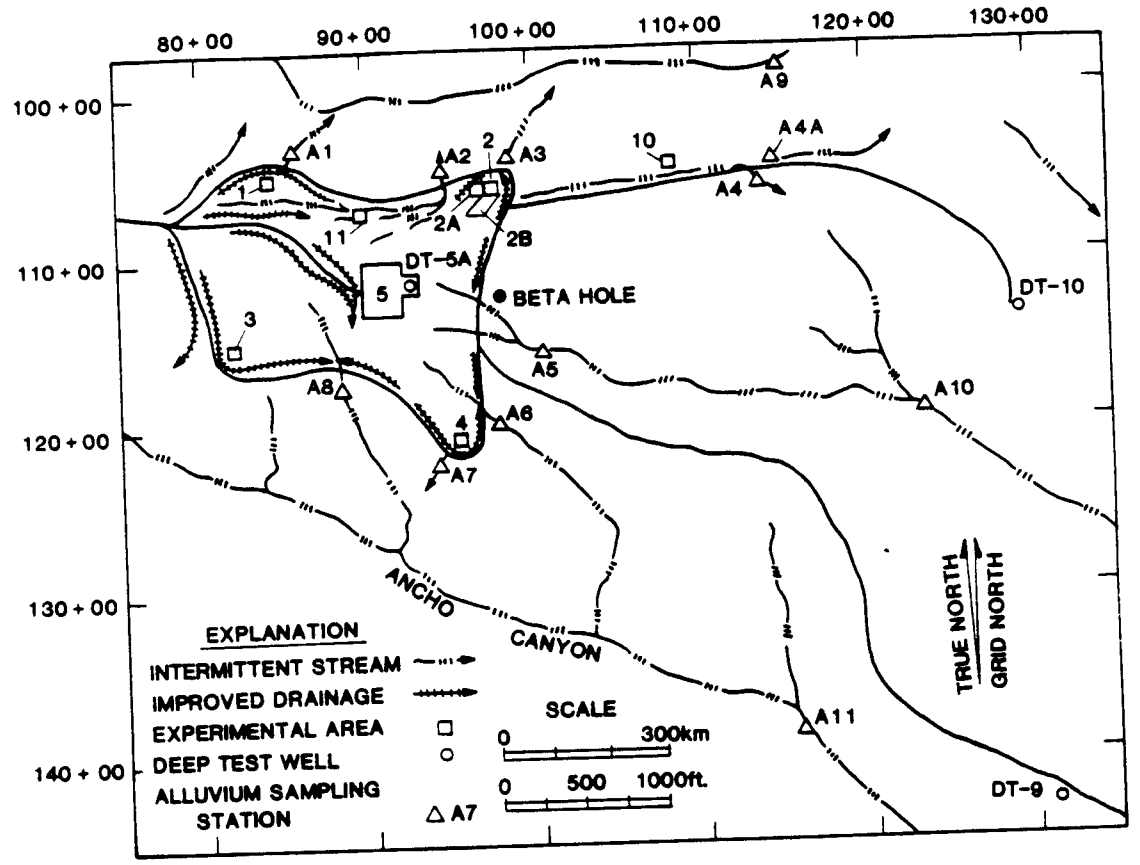

Figure 2. Map of TA-49 showing experimental areas, core holes, deep test wells, and sediment sampling locations.

experimental area were used to permit expansion of gases passing through the sample collection devices and probably contain some particulate contamination. Some of the holes were used to dispose of pipes and other equipment contaminated during the experiments. Steel boxes buried adjacent to the experimental holes were used to contain sample collection equipment and often became contaminated. These were filled with concrete and left in place.

2. Surface Contamination. Some plutonium contamination was measured at the surface in experimental Area 2 in December 1960 and was traced to cuttings from experimental hole 2-M drilled during October and November. Plutonium had apparently been dispersed through fractures in the tuff by detonation of an experiment in an adjacent experimental hole. All surface soil contamination measurable by standard procedures and instruments of the time was collected and placed back in experimental hole 2-M. The experimental hole was then filled with clean sand and capped with concrete. The entire surface of Area 2 was covered with 6 ft of compacted aggregate in January 1961 and sealed with a 4- to 6-in.-thick asphalt pad in September 1961. The asphalt pad can be seen in the upper right portion of the aerial photograph in Fig. 3, which was taken in

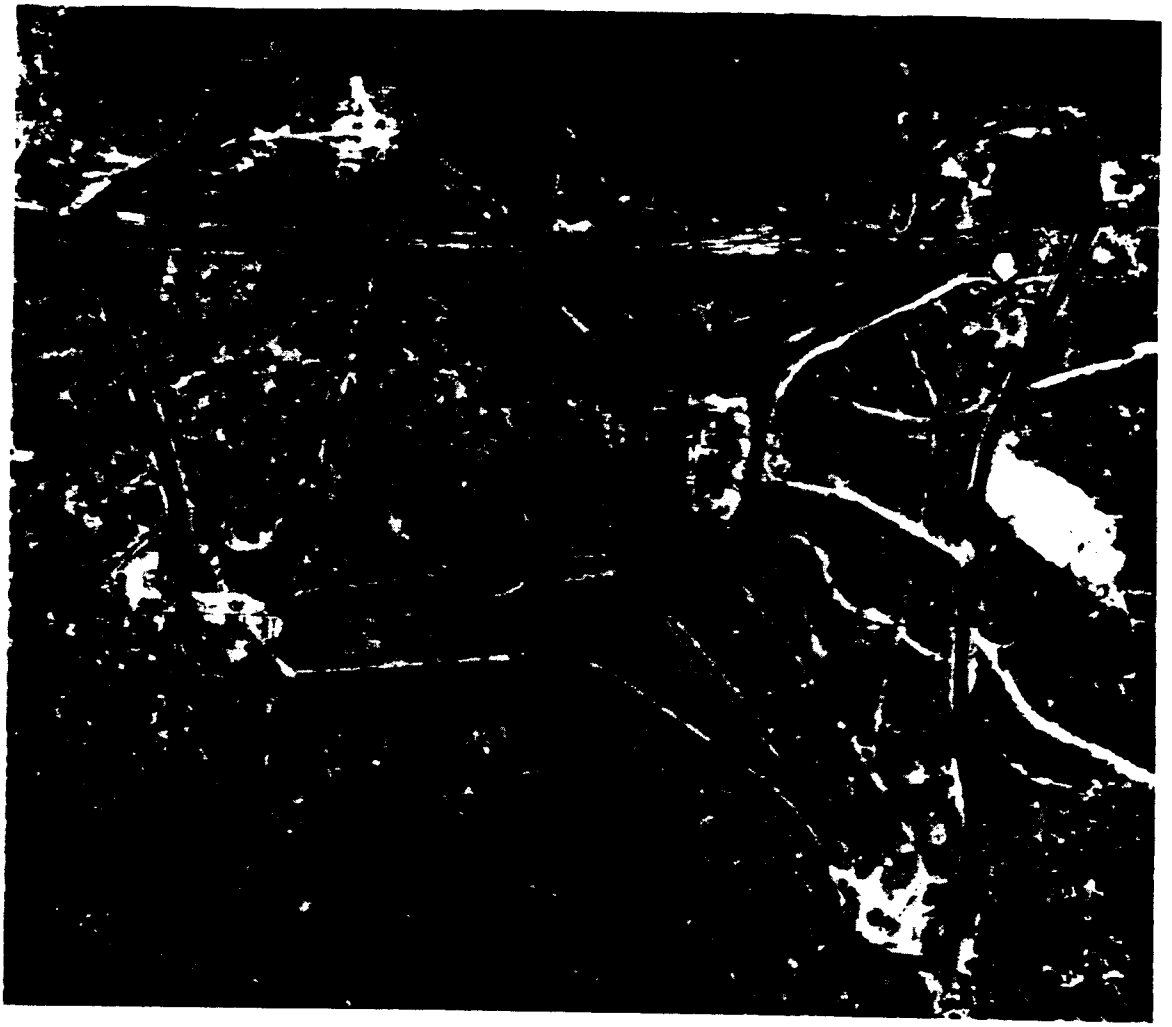

Figure 3. Aerial photograph of TA-49 from 1965. Note asphalt pad covering experimental area 2 in upper right.

1965. This inadvertent contamination incident left some remaining trace amounts of plutonium on the surface in the vicinity of TA-49. After closure of the original 100-ft-square experimental Area 2, additional experimental holes were constructed to the west (Area 2A) and south (Area 2B) as indicated in Fig. 2.

3. Contaminated Structures. Structures located in Area 11 (Fig. 2) of TA-49 were used for radiochemistry. They were decontaminated, demolished, and removed in September of 1971. Close inspection of the aerial photograph in Fig. 4, which was taken in 1974, shows the absence of the structures in Area 11. Contaminated materials were packaged and transported to the Laboratory's radioactive waste disposal facility at TA-54. Uncontaminated materials and debris were buried in a landfill about 1/2 mile northwest of the TA-49 experimental area. A contaminated subsurface drain field that served the radiochemistry facility was left in

Figure 4. Aerial photograph of TA-49 (1974). Note absence of structures in experimental area 11 in top center when compared was photograph in Figure 3 (1965).

place and represents a source of near-surface contamination remaining in the TA-49 vicinity.

II. SITE SELECTION AND EVALUATION

A. Reconnaissance Survey

The Water Resources Division of the U.S. Geological Survey (USGS), in cooperation with the U.S. Atomic Energy Commission (AEC) and LASL, in 1947 began a series of geologic studies and hydrologic investigations related to developing a water supply for Los Alamos and disposing of low-level radioactive liquid effluents. Because of this expertise, in January 1959, AEC and LASL requested the USGS make a preliminary study to locate a site for the hydronuclear experiments. The site was to be within the Laboratory at a distance from the Los Alamos townsite, have a flat area large enough to accommodate the experimental facilities, be able to contain the experiments,

and have geologic and hydrologic characteristics that would retain any residuals or contaminated materials from the experiments and preclude contamination of the water supply.

The study identified Frijoles Mesa as a favorable site. The mesa was relatively flat and large enough to accommodate the experimental facilities. The area was believed to have about 1200 ft of unsaturated tuff and sediments above the main aquifer. The mesa was not considered to be a source of recharge to the underlying aquifer. The mesa was selected as the site pending development of additional data related to the geology and hydrology. A detailed study was initiated by USGS in September 1959 at AEC's request.

B. Detailed Hydrogeologic Investigation

The USGS performed a detailed geologic and hydrologic investigation of Frijoles Mesa (TA-49). The field work began October 1959 and the most intensive part was finished by mid-May 1960.

The fundamental conclusion of the study was that "Recharge to the ground water from Frijoles Mesa is very small or nonexistent; thus no contaminants in solution are likely to be carried to the ground water beneath TA-49" (Wier 1962).

The hydrogeologic investigation of the mesa was focused on assuring containment of residual materials that would be left in the experimental holes. Three deep test wells ranging from 1409 to 1821 ft were drilled into the main aquifer of the Los Alamos area to determine thickness of the tuff and volcanic sediments and hydrologic characteristics of the aquifer. Deep test well DT-5A is located near the center of the four experimental areas (Fig. 2). Wells DT-9 and DT-10 are located down the groundwater gradient to the east. In addition, four core holes ranging in depth from 300 to 500 ft deep were drilled in the centers of the four experimental areas to detail the geology and hydrologic characteristics of the tuff beneath the areas. These holes were cased and left in place for future monitoring. Surface geology of the area was mapped and correlated with subsurface geology determined from logs of the test wells and core holes.

Soil moisture studies were made in 23 moisture access holes ranging from 10 to 49 ft deep, which were drilled on the mesa surface. Soil thickness was measured and mapped. The holes were logged with a neutron probe to determine moisture content of the soil and tuff near the mesa surface.

Data on soil and tuff characteristics were examined and mapped for a number of the 6-ft holes drilled for the experiments. Data were also collected from two holes, one drilled 692 ft into the tuff and the other drilled 968 ft deep through the tuff and into the top of the volcanic sediments. These two holes were later abandoned. Two 2-ft-diameter holes were drilled to a depth of about 189 ft, one on the mesa surface and the other in the adjacent canyon to the north. Both were completed in the tuff. None of the holes contained any perched water. Samples of tuff were collected for analyses of hydrologic properties (Wier 1962).

The geologic studies documented that the Bandelier Tuff is about 930 ft thick in the vicinity of TA-49 (Fig. 5). It is composed of three members (Griggs 1964). The upper member, the Tshirege Member, is about 640 ft thick composed of 6 units of nonwelded to welded ashflow tuffs (welded tuff exhibits higher density and cohesion) and a waterlaid sand between two ashflows (Fig. 6). The middle member, the Otowi Member, is composed of two nonwelded ashflows or ashfalls that are about 200 ft thick. The lower member, the Guaje Member, is an ashfall of pumice with a thickness of 90 ft. The volcanics and volcanic sediments, the Puye

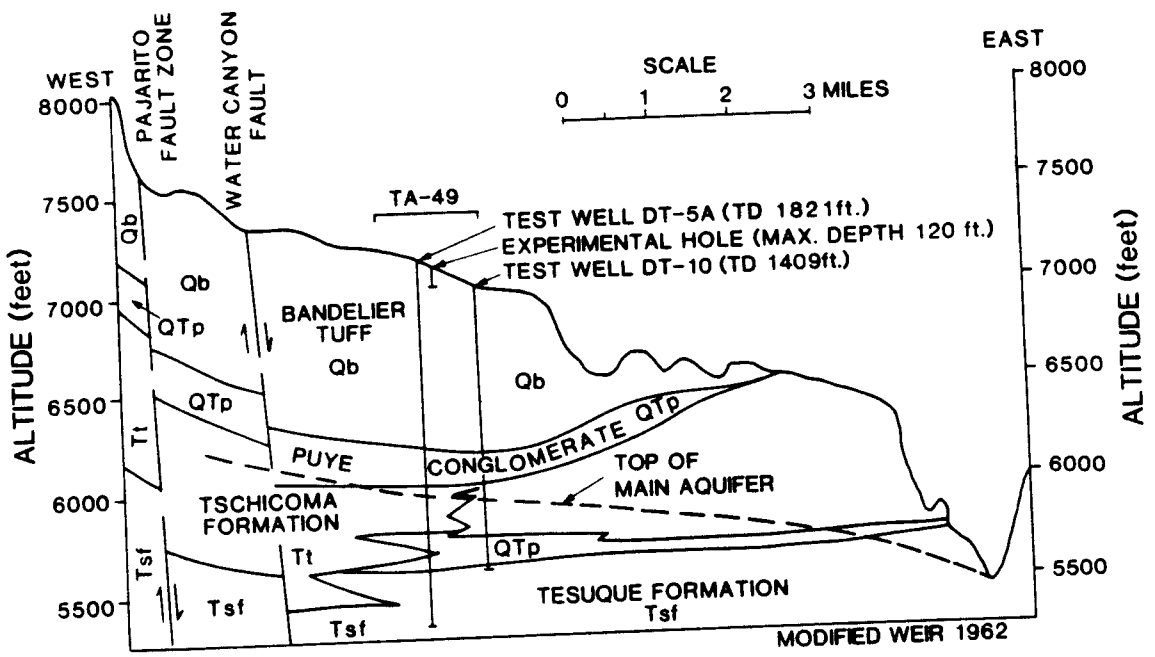

Figure 5. Geologic cross section through TA-49 from the Pajarito fault zone to the Rio Grande.

Conglomerate and the Tschicoma Formation, underlying the tuff are about 600-ft thick. They are in turn underlain by siltstones and sandstones of the Tesuque Formation, which exceeds a thickness of 2300 ft in the area (Fig. 5).

The three deep test wells indicated that the top of the main aquifer was at a depth of about 1170 ft near the center of the four experimental areas. The test wells and other holes drilled in the area indicated no perched water in the tuff or volcanics above the main aquifer in spite of the presence of potential perching beds. This absence of perched water indicates that no recharge to the main aquifer occurs through the plateau in the vicinity of TA-49.

The direction of groundwater movement in the deep aquifer is to the east-southeast toward the Rio Grande where a part of the water is discharged into the river through seeps and springs (Fig. 7). The rate of movement of the water determined from aquifer tests was estimated to be about 400 ft/yr for the upper 400 ft of the aquifer (Wier 1962). The aquifer tests indicated the average specific capacity of 15 gpm/ft of drawdown, an average field coefficient of permeability of 83 gpd/ft^2, and a transmissivity of 36,000 gpd/ft (Wier 1962).

As an additional benefit, these extensive hydrologic study data were utilized to develop an improved water supply for Los Alamos. The data resulted in siting and drilling high-yield (greater than 1000 gpm) water supply wells for the Laboratory and for the community on the Pajarito Plateau, 2 to 4 miles northeast of TA-49 (Purtymun 1969). In 1986 these wells accounted for 56 percent of the total water production for Los Alamos.

Hydrologic characteristics of the main aquifer on the Pajarito Plateau and at Frijoles Mesa were re-evaluated in 1984 using data from 5 water supply wells and 10 test holes. The rate of movement of water in the upper 490 ft of the aquifer was calculated to be

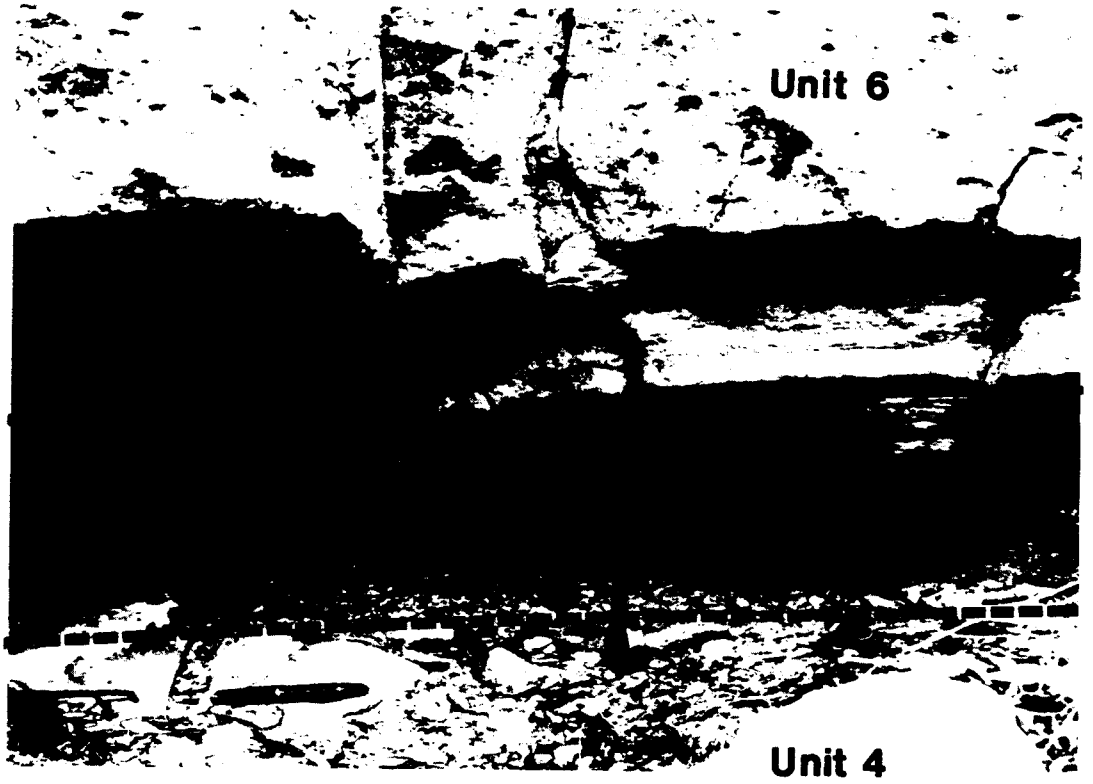

Figure 6. Ashflow units 4 and 6, and sand unit 5 of the Tshirege Member of the Bandelier Tuff at TA-49. Upper photograph shows outcrop one quarter mile northwest of Well DT-9; lower photograph shows units as penetrated by an Experimental Hole in TA-49 at about 60-foot depth.

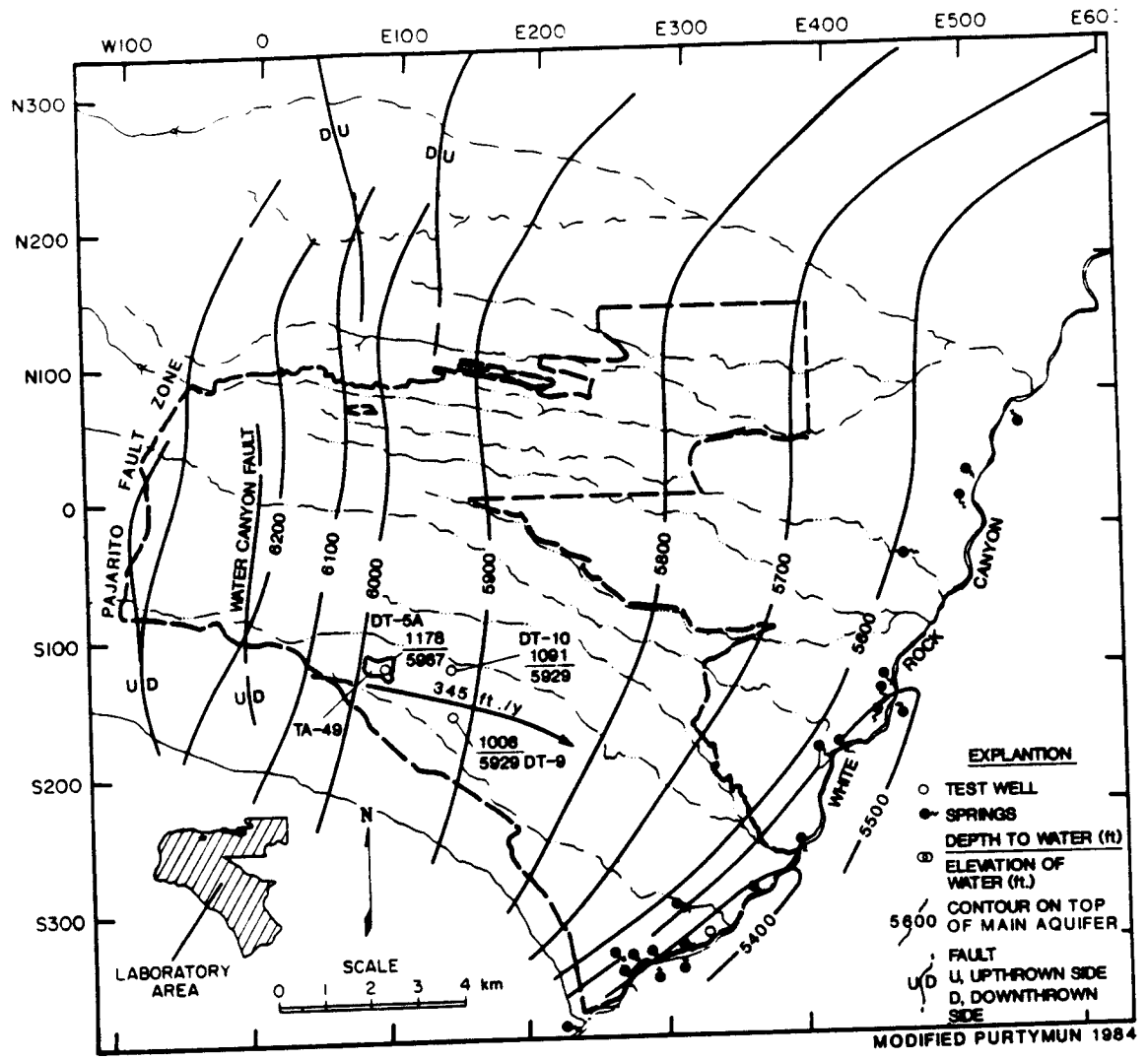

Figure 7. Map showing generalized contours on top of main aquifer and annual rate of movement of groundwater in the vicinity of TA-49.

about 345 ft/yr, which is similar to the rate calculated in 1960. The water is a sodium-bicarbonate type with total dissolved solids ranging from 124 to 142 mg/L.

A water-level recorder was operated from 1960 to 1968 and from 1970 to 1982 on well DT-9. The record indicated that the main aquifer is very sensitive to atmospheric pressure changes, earth shocks (earthquakes), and probable earth tide effects (Purtymun 1984). The water-level trends over a 22-year period indicate a general water-level decline from about 1003 to 1006 ft below the surface. The decline indicates deficient recharge, with only one period (1971) of recharge exceeding the normal discharge of the aquifer through springs in White Rock Canyon. The major recharge area for the aquifer is the intermountain basin formed by the Valles Caldera beyond the Sierra de los Valles, about 10 miles west of Frijoles Mesa (Purtymun 1984).

Laboratory analyses of the tuff from the core holes indicated very complex hydrologic properties. These properties depend strongly on the degree of welding of the tuff,

which ranges from nonwelded to welded. The porosity of the tuff at Frijoles Mesa ranged from 19 to 54 percent by volume, specific retention ranged from 11 to 27 percent, and specific yield from about 1 to 43 percent. The laboratory permeability ranged from less than 0.05 to 22 gpd/ft^2. The permeability of the tuff is related to the degree of welding of the tuff because porosity is governed by pore size and interconnection of pores. Lower permeabilities occur in welded tuffs and the larger permeabilities occur in the nonwelded tuffs. The striking characteristic of the tuff is its low moisture content. The tuff contains no free water; natural moisture content ranges from less than 4 to about 8 percent by volume.

Tuff has the capacity to retain plutonium, thereby limiting its movement, even if water were present, by the chemical process of ion exchange. Ion exchange capacity of the tuff was measured by both the USGS and LASL. The USGS results indicated a range of 0.5 to about 4 meq/100 g. LASL results indicated a range of about 0.7 to 2.8 meq/100 g. Calculations based on an ion exchange capacity of 1 meq/100 g indicated 100 g of tuff could retain 60 mg of plutonium. Laboratory experiments confirmed retention of at least 1 mg/100 g and suggested higher capacity but were terminated at that level.

Soil cover on the mesa surface is composed of layers starting with a weathered zone of tuff and clay, then a pumice, and finally an upper clayey soil zone. Measurements made with neutron moisture gaging equipment in the spring, summer, and fall of 1960 indicated little if any movement of precipitation into the tuff underlying the soil cover (Abrahams 1961). Annual evapotranspiration is greater than annual precipitation. Natural moisture content of the tuff ranges from less than 4 to about 8 percent by volume, indicating that movement of water could occur only in the vapor phase by diffusion. There is insufficient moisture available to move contaminants from the experimental holes toward the main aquifer. Data collected from Frijoles Mesa during drilling of experimental holes, test wells, surface and subsurface mapping, moisture monitoring of soil and tuff, as well as laboratory analyses of tuff, indicate the soil cover "...forms an almost perfect seal over the mesa surface and the near-surface joints" (Wier 1962). The mesa is not a recharge area for the main aquifer (Abrahams 1961 and Cushman 1965).

III. ENVIRONMENTAL SURVEILLANCE SINCE 1961

A. U. S. Geological Survey Surveillance (1961-1970)

From the time of the initial hydrogeologic study until about 1970, a joint cooperative effort between the USGS and LASL continued to perform periodic monitoring of the conditions in the vicinity of TA-49. This included measuring water levels and sampling the water in the main aquifer by the three deep test wells in 1963, 1967, 1969, and 1970. No changes in concentrations of naturally present radionuclides occurred and no plutonium was observed.

Water from the main aquifer discharges from Ancho Springs and other springs in White Rock Canyon about 4 miles east of TA-49 (Fig. 7). Water samples collected from Ancho Springs in 1961, 1962, 1963, 1965, and 1969 contained only background radioactivity showing no effect of the experiments at TA-49. Sediment samples taken in 1965 from Water Canyon and Ancho Canyon drainages adjacent to TA-49 and several other stations downgradient toward the Rio Grande showed no indication of plutonium contamination.

B. Los Alamos Surveillance (1971-1986)

Environmental surveillance of the entire Laboratory environs has been conducted by the Laboratory's Environmental Surveillance Group and reported annually since 1971 in a series of publicly available reports. Some of the data pertinent to TA-49 have been documented in these annual reports. Specifically, analyses of the main aquifer water samples from the deep test wells and springs have been reported regularly. Results for surface water and sediment samples at the Laboratory boundaries have been reported. Airborne radioactivity at a station near TA-49 has been reported. No data have shown any indication of contamination of the main aquifer or any offsite transport of plutonium contamination from TA-49 by surface water or airborne transport. The supplementary onsite monitoring and special studies in the immediate vicinity of TA-49 have been documented in a series of periodic internal memorandum reports.

C. Surface Conditions

Many radionuclides have an affinity for fine clay and silt particles in soil or sediments. These fine clay and silt particles with attached radionuclides are subject to transport with storm runoff. Sediment sampling stations were established downgradient from TA-49 in Water Canyon (the drainage area includes the north side of experimental Areas 1 and 2; Fig. 2) at State Road 4 (SR-4), and at the Rio Grande (Fig. 8). Other stations are located in Ancho Canyon (the drainage area includes the east and south portions of experimental Areas 3 and 4) at SR-4 and at the Rio Grande. There have been no data from measurements of radionuclides in samples from these stations that can be attributed to the hydronuclear experiments at TA-49. Data from these stations have been reported in the annual environmental surveillance report under sections on Perimeter and Onsite Sediment Stations (Environmental Surveillance Group 1986, 1987).

Eleven sediment stations were established in the immediate vicinity of TA-49 during 1975 in natural drainages from the four experimental areas (Areas 1, 2, 3, and 4; Fig. 2) and in three canyons downgradient from the experimental areas. A twelfth sediment station was added in 1981 as the drainage in the area was modified (Fig. 2). Sediments are typically collected in late fall after spring and summer runoff. The data collected annually indicate that only three onsite stations exhibit plutonium in excess of worldwide fallout. These stations are downgradient from and drain Area 11, the former site of the chemistry building (removed 1971), and the area adjacent to Area 2 where some surface plutonium contamination occurred during the experiments conducted in 1960.

Station A3 (Fig. 2) has shown the highest concentrations. The plutonium-239 concentrations for 12 analyses between 1975 and 1986 have ranged from 0.01 to 17 pCi/g with a mean of 3.5 pCi/g and standard deviation of 5.2 pCi/g. The plutonium-239 concentration in the 1986 sample was 10.7 pCi/g. Results over the past 12 years at the stations have shown no particular trend.

Background or fallout concentrations of plutonium on sediments in northern New Mexico are about 0.01 pCi/g (Environmental Surveillance Group 1986). The Environmental Protection Agency proposed screening level, to assure meeting proposed dose limits to the public for exposure to transuranic contamination over a large area, is about 15 pCi/g (USEPA 1977). Plutonium attached to sediments transported by storm runoff into Water or Ancho canyons is dispersed over a large area resulting in concentrations indistinguishable from background.

Beryllium analyses were first made in 1985. Surface runoff samples in 1985 from Water Canyon at SR-4 had levels less than detection limits for both water (50 mg/L) and

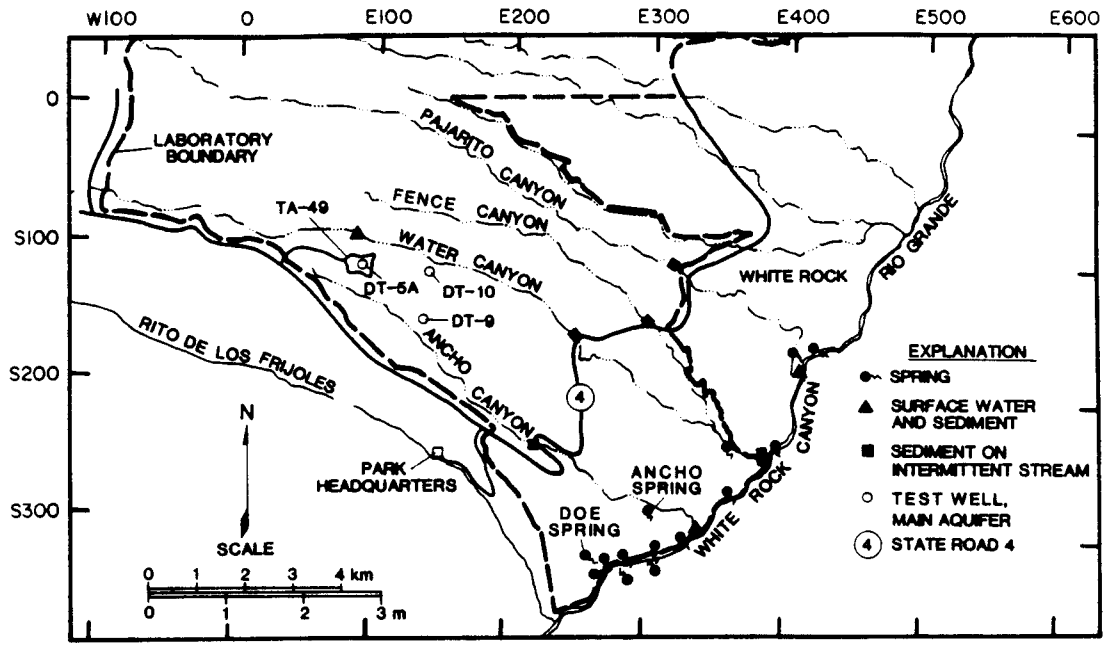

Figure 8. Sediment sampling stations in Water and Ancho Canyons, deep test wells at TA-49, and springs in White Rock Canyon.

suspended sediments (10 mg/L) (Environmental Surveillance Group 1986). Measurements of sediment samples from both Water and Ancho Canyons at SR-4 in 1986 also showed beryllium concentrations to be less than the limit of detection (Environmental Surveillance Group 1987).

The supplementary monitoring and special studies at TA-49 have been documented in a series of periodic internal memorandum reports.

D. Surveillance of the Main Aquifer

The three deep test wells described earlier were drilled from the surface of Frijoles Mesa into the main aquifer of the Los Alamos Area (Fig. 2). These test wells and the springs along White Rock Canyon of the Rio Grande are sampled to monitor water quality in the main aquifer. Pumps were temporarily installed in the test wells to perform aquifer tests in 1960. Water samples were collected at that time to establish background water quality. The pumps were removed upon completion of the tests. After 1960, water samples were bailed from the wells until permanent pumps were installed to facilitate and permit more frequent sampling. A pump was installed in well DT-5A in 1970 and one was installed in well DT-10 in 1978. Test well DT-9 is scheduled to receive a pump in 1987.

There has been no significant change in the chemical or radiochemical water quality parameters measured since the first samples were collected from the wells in 1960. All measurements are consistent with expectations for natural variation. Neither has there been any significant change in measurements of the water from the springs since the first samples were collected in 1964. The water samples from the wells and springs show no effects of the hydronuclear experiments at TA-49. These data have been

reported in the annual environmental surveillance report under sections on Onsite Monitoring and White Rock Canyon (Environmental Surveillance Group 1986, 1987).

E. Maintenance and Special Studies

In March 1975 the asphalt pad over experimental hole 2-M in Area 2 was found collapsed leaving an opening in the asphalt and underlying clay and gravel about 8 ft long, 6 ft wide, and 3 ft deep. In September 1976, the opening was filled with a rock and clay mixture, compacted, sealed with asphalt, and the entire asphalt pad above Area 2 was repaved.

Before being repaired, the opening in the pad apparently allowed water to move into experimental hole 2-M and through the fractures into the adjacent core hole 2 (USGS CH-2). The 500-ft-deep, 4-1/2-in.-diameter core hole had been drilled with mud in 1959 and was cased to the bottom with 2-in.-diameter galvanized pipe including a 20-ft slotted section at the bottom. About 50 ft of water was observed in the bottom of the hole in February and December of 1975. Unfiltered samples of water bailed in October 1977 and August 1978 contained 1.7 to 3.1 pCi/L of plutonium-239. In April and May 1979 and April through June 1980 the amount of water standing in the core hole was measured several times to be about 150 ft. The water, about 24 gal., was removed from the cased hole by bailing in June 1980. Three filtered samples of the bailed water contained a maximum plutonium-239 concentration of 5.5 pCi/L and the suspended sediment contained a maximum of 0.7 pCi/g. (These concentrations are small compared with guidance issued by the Department of Energy [DOE] for controlled areas of 100,000 pCi/L [US Department of Energy 1981]). This indicated water had moved plutonium from the experimental hole into the core hole. After the core hole was bailed dry, it did not yield any additional water. It has remained dry through April 1986, the time of the last inspection.

Concern related to the presence of water in the core hole resulted in initiating a special hydrologic investigation in the spring of 1980 to locate the source of the water, determine whether it resulted from infiltration through the broken asphalt above experimental hole 2-M, or whether water was moving into the tuff beneath the experimental area on a larger scale. This investigation focused on the upper 50 to 78 ft of the tuff at Area 2 and the sand unit that separates the two ash flows of moderately welded tuff units (Fig. 6). The sand unit is located at depths ranging from 70 to 80 ft and is up to 2 ft in thickness. The widespread sand unit is quite permeable and could transmit water to the core hole if sufficient water was available.

For the first part of the investigation, five 4-in.-diameter holes were augered to a depth of 123 ft, about 50 to 60 ft away from the edges of Areas 2, 2A, and 2B, to determine if the sand unit could be conducting water into the three experimental areas. These holes penetrated an upper moderately welded ashflow unit, the sand unit, and the underlying moderately welded unit. Cuttings from the holes were monitored for plutonium and the moisture contents were determined. The holes were also logged with the moisture neutron equipment. The sand and tuff penetrated by the auger holes contained no plutonium. The moisture of the cuttings and tuff determined in the laboratory and by the neutron logging indicated normal moisture concentrations ranging from less than 4 to 8 percent by volume. The data collected from the holes indicated that there was no recharge moving into the tuff beneath the three experimental areas nor was there any movement through the areas.

The second part of the investigation addressed six experimental holes that remained

unused in Areas 2A and 2B when the experiments of 1959-61 ended. Because of concern for safety, these experimental holes had been filled with sand in 1963. Thus there was a possibility that these sand-filled experimental holes were pathways for water from precipitation or run-off to enter core hole 2 in Area 2. Moisture access tubes were installed in the sand of three of these experimental holes and penetrated into the underlying tuff where possible. Moisture contents of the sand and tuff were determined with neutron moisture logging equipment. The moisture content of the sand in the unused experimental holes showed unsaturated conditions and therefore could not contribute to the presence of water in the core hole.

The conclusion from both parts of the special investigation was that the water in the core hole came through the depression formed by the collapse of asphalt above experimental hole 2-M. Apparently the water that was present was confined to the immediate vicinity of the core hole because of the seal formed by the mud used during the drilling. However, to limit any future possibility of infiltration, the integrity of the unused experimental holes in Areas 2A and 2B was improved by removing the upper 2 to 3 ft of sand and capping them with concrete in August 1981.

The La Mesa Fire in June 1977 burned across Frijoles Mesa and TA-49. The asphalt pad on Area 2 was not damaged. Some remaining buildings, structures, and cable ways from the 1959-61 experimental era and subsequent unrelated activities at TA-49 were damaged or destroyed. In 1984 special funding permitted cleanup of surface debris at TA-49. Debris was removed to a landfill pit at the western end of the mesa and covered with crushed tuff. Additional fill (clay and gravel) was placed over Areas 1 and 4. Cracks in the asphalt pad of Area 2 were sealed. Surface drainage of the area was improved.

IV. APPLICABLE ENVIRONMENTAL REGULATIONS AND DOE REQUIREMENTS

Federal regulations promulgated pursuant to the Resource Conservation and Recovery Act (RCRA) and the Comprehensive Environmental Response, Compensation, and Liability Act (CERCLA) impose requirements for some actions in relation to TA-49. A number of DOE Orders also require certain environmental monitoring, waste management, and evaluation studies. The following sections describe recent and planned future actions and programs responsive to the various requirements.

A. Designation as Hazardous Waste Site Under RCRA (Section 3016)

In accord with requirements of RCRA and DOE Order 5480.2, Hazardous and Radioactive Mixed Waste Management, the Laboratory identified TA-49 to DOE as a hazardous waste site for reporting to EPA in January 1986 as part of the biannual Federal Facility Hazardous Waste Activities Inventory. The four experimental areas have been collectively designated as Material Disposal Area AB. The information on Material Disposal Area AB reported to the EPA is presented in Appendix A. This information will be used by the EPA to maintain the required lists of Federal Hazardous Waste Activities. As new information is developed by the planned studies described in the subsequent sections, it will be incorporated in the biannual updates required by Section 3016 of RCRA.

B. Required Future Action Under CERCLA

In accord with the requirements of CERCLA and DOE Order 5480.14 CERCLA Program, TA-49 is being studied under the DOE

Albuquerque Operations Office Comprehensive Environmental Assessment and Response Program (CEARP). As part of the Phase 1 CEARP evaluation, TA-49 was evaluated for potential migration of contaminants by the EPA Hazard Ranking System (HRS) for chemical contaminants and the DOE's modification (mHRS) of that system for evaluation of radioactive contaminants. The overall migration mode scores were derived to be 6.7 based on the beryllium and 5.3 based on the plutonium. The HRS/mHRS scoring forms are reproduced as Appendix B. These scores reflect relatively low potentials for migration of contaminants. Facilities evaluated by the EPA must have scores of 28.5 or higher to be considered for inclusion on the National Priorities List. The site will receive additional field study under Phase 2 of CEARP. This will lead to an evaluation of risk that will form the basis for a decision on what, if any, remedial measures should be recommended for TA-49. The information provided to EPA as required by RCRA for the Federal Hazardous Waste Activities Inventory probably will be placed on the Federal Facility Docket required by the Superfund Amendments and Reauthorization Act of 1986 (SARA).

C. Routine Environmental Monitoring

The routine monitoring of groundwater in the main aquifer, surface water run-off, and sediments as described earlier in Section III.B of this report will be continued as part of the annual environmental surveillance program carried out by the Environmental Surveillance Group. These results will continue to be reported in the annual environmental surveillance reports (Environmental Surveillance Group 1986, 1987b). This monitoring satisfies the requirements of DOE Orders 5480.1, Environmental Protection, Safety, and Health Protection Programs, and 5484.1, Environmental Protection, Safety, and Health Protection Information Reporting Requirements. Supplementary onsite monitoring results will be included in periodic reports prepared for the Interim Waste Management Program or CEARP as appropriate.

D. DOE Radioactive Waste Area Monitoring

The Laboratory's Health, Safety, and Environment (HSE) Division conducts a continuing environmental surveillance program sponsored by the Interim Waste Management Program of DOE's Office of Defense Waste and Transportation Management. This program provides supplementary monitoring for the radioactive waste disposal areas within the Laboratory boundaries meeting the requirements of DOE Order 5480.2, Radioactive Waste Management (Environmental Science Group 1987). This cooperative effort among the Environmental Science, Environmental Surveillance, and Health and Environmental Chemistry Groups has an established program schedule whereby each designated waste area receives an intensive characterization at 5-year intervals and routine monitoring during other years. Designated Waste Disposal Area AB at TA-49 will be included in this program starting in 1987.

E. CEARP Remedial Investigation

Preliminary, summary information on TA-49 will be included in the CEARP Phase 1, Installation Assessment, document for Los Alamos, which is expected to be released in 1987. A detailed plan for field investigation of TA-49 will be prepared during 1987 under the auspices of the CEARP. This will result in a CEARP Phase 2, Confirmation, Site-Specific Monitoring Plan (US Department of Energy 1986). The Site-Specific Monitoring Plan will

include detailed evaluation of all known existing data. This evaluation will be the basis for developing a detailed sampling plan that will meet all the guidelines required by DOE under its applicable programs (including the Defense Buried TRU Waste program described in the following section) and those required by EPA for a Remedial Investigation under CERCLA. The Site-Specific Sampling Plan will be made available to the EPA and appropriate New Mexico agencies for information and review.

F. DOE Defense Buried TRU Waste Evaluation

Under the Defense Buried Transuranic (TRU) Waste Management Program, wastes resulting from defense programs with concentrations of transuranic elements greater than 100 nCi/g receive special attention. A significant portion of the contaminated sand and tuff at the bottoms of the experimental holes is presumed to have concentrations of plutonium exceeding this criterion. A crude estimate of the maximum volume of material meeting or exceeding the TRU criterion can be calculated by assuming the plutonium is distributed uniformly through an approximately 100 m^3 spherical volume (diameter between 5 and 6 m) at the bottom of each of 44 experimental holes for a total volume of about 4400 m^3. The approximately 2890 curies (total alpha activity in 40.1 kg of weapons grade plutonium assuming 0.072 Ci/g) would be distributed at an average level of 0.65 Ci/m^3 throughout the 4400 m^3. Using an average density of about 1.5 g/cm^3 for tuff, leads to a concentration estimate of about 430 nCi/g.

A similar crude estimate of the total volume of contaminated material that might have to be removed to get all the TRU waste can also be made. Assuming uniform distribution of the plutonium throughout rectangular solids having the same area as the experimental hole grid patterns and a thickness of 5 m results in an estimated volume of about 36,000 m^3. This volume would have an average concentration of about 50 nCi/g.

The Los Alamos National Laboratory (LANL) is presently preparing a Site Long-Range Plan (SLRP) for buried TRU waste. This plan will be part of a nationwide DOE program to provide a description of the approach, resources, and schedules to ensure uniform, coordinated CERCLA response at all DOE buried TRU waste sites. At LANL this will be accomplished largely by addressing all buried TRU waste sites in coordination with the CEARP, described in the previous section. TA-49 is on the list of designated buried TRU waste disposal areas at Los Alamos. It will be evaluated along with the other buried TRU waste disposal areas at Los Alamos for risk and possible remedial action from a consistent basis.

REFERENCES

J. H. Abrahams, J. E. Wier, and W. D. Purtymun, "Distribution of Moisture in Soil and Near-Surface Tuff On The Pajarito Plateau, Los Alamos County, New Mexico," US Geological Survey Professional Paper 424-D (1961).

R. L. Cushman, "An Evaluation of Aquifer and Well Characteristics of Municipal Well Fields in Los Alamos and Guaje Canyons Near Los Alamos, New Mexico," US Geological Survey Water-Supply Paper 1809-D (1965).

Environmental Science Group, Environmental Surveillance Group, and Health and Environmental Chemistry Group, "Environmental Surveillance of Low-Level Radioactive Waste Management Areas at Los Alamos During 1985," Los Alamos National Laboratory document LA-UR-87-139 (February 1987).

Environmental Surveillance Group, "Environmental Surveillance at Los Alamos During 1985," Los Alamos National Laboratory report LA-10721-ENV (April 1986).

Environmental Surveillance Group, "Environmental Surveillance at Los Alamos During 1986," Los Alamos National Laboratory report LA-10992-ENV (April 1987).

R. L. Griggs, "Geology and Ground-Water Resources of the Los Alamos Area, New Mexico," US Geological Survey Water-Supply Paper 1753 (1964).

W. D. Purtymun and J. B. Cooper, "Development of Ground Water Supplies on the Pajarito Plateau, Los Alamos County, New Mexico," US Geological Survey Professional Paper 650-B (1969), p. B149-B153.

W. D. Purtymun, F. C. Koopman, S. Barr, and W. E. Clements, "Air Volume and Energy Transfer Through Test Holes and Atmospheric Pressure Effects on the Main Aquifer," Los Alamos Scientific Laboratory report LA-5725-MS (1974).

W. D. Purtymun, "Hydrologic Characteristics of the Main Aquifer in the Los Alamos Area: Development of Ground Water Supplies," Los Alamos National Laboratory report LA-9957-MS (January 1984).

R. N. Thorn and D. R. Westervelt, "Hydronuclear Experiments," Los Alamos National Laboratory report LA-10902-MS (February 1987).

US Department of Energy Order 5484.1A, Chapter XI, "Requirements for Radiation Protection" (April 1981).

US Department of Energy, "Comprehensive Environmental Assessment and Response Program Phase 2: Generic Monitoring Plan" (Draft), Albuquerque Operations Office, U.S. DOE, Albuquerque, New Mexico.

US Environmental Protection Agency, "Proposed Guidance on Dose Limits for Persons Exposed to Transuranium Elements in the General Environment," U.S. Environmental Protection Agency, Office of Radiation Programs, Criteria and Standards Division, Report EPA 540/4-77-106, Washington D.C., 1977.

J. E. Wier and W. D. Purtymun, "Geology and Hydrology of Technical Area 49, Frijoles Mesa, Los Alamos County, New Mexico," US Geological Survey Open-File Report (1962).

APPENDIX A
INVENTORY OF FEDERAL AGENCY HAZARDOUS WASTE ACTIVITIES

A. RESPONSIBLE FEDERAL AGENCY: U.S. Department of Energy
1000 Independence Avenue SW
Washington, DC 20585

1. Responsible Field Organization: DOE - Los Alamos Area Office

2. Address: Los Alamos, N.M. 87545
(Street, City, State, Zip)

3. DOE Site Contact: Harold E. Valencia

4. Phone Number: (505) 667-5105 (Commercial) 843-5105 (FTS)

B. INSTALLATION/SITE LOCATION

1. Installation name: Los Alamos National Lab (LANL)

2. Federal Facility ID Number (GSA No.): NM0890010515

3. Address: P.O. Box 1663, Los Alamos, N.M. 87545
(Street, City, County, State, Zip Code)

4. Number of sites on this installation: 20

5. Site name and/or site number: Material Disposal Area AB

6. Address: Same as B.3. above
(Street, City, County) (State, Zip Code)

7. Coordinates: 35°49' 051" 106°14' 015"
(For a rural site with no street address)

C. HAZARDOUS WASTE MANAGEMENT STATUS

1.		O	C	Date closed
Storage:	Containers	| |	| |	
	Tanks	| |	| |	
	Surface impoundments	| |	| |	
	Waste Piles	| |	| |	

Installation LANL

Site Area AB

		O	C	
Treatment:	Tanks	| |	| |	
	Surface impoundments	| |	| |	
	Incinerators	| |	| |	
	Other (describe)	| |	| |	
Disposal:	Landfill	| |	|X|	Prior to 1980
	Land Treatment	| |	| |	
	Surface impoundment	| |	| |	
	Underground Injection Wells	| |	| |	
	Waste Piles	| |	| |	

O = Operating C = Closed

If the above space is not sufficient, or if the site has one or more operating or closed units in any technique, provide the necessary information in an attachment labelled Attachment C and enter "Attachment C" in the space provided for each technique.

2. Is Attachment C included with the inventory? Yes | | No | |

3. Indicate if any of the following forms were submitted for this site and, if so, the date of the original submittal:

	Yes	No	Date Submitted
RCRA S3010 Notification	| |	|X|	
RCRA Part A	| |	|X|	
RCRA Part B	| |	|X|	
RCRA Closure Plan	| |	|X|	

Installation LANL

Site Area AB

RCRA S3019 Exposure Assessment | | |X| _____

CERCLA S103 Notification | | |X| _____

4. If a RCRA Part B was submitted, what is its current status?

Permit Issued | | Permit Denied | | No Final Action | |

5. If a closure plan was submitted, what is its current status?

Closure Approved | | Closure Denied | | No Final Action | |

6. If the closure plan was approved, has closure been certified?

Yes | | No | |

7. If the site is no longer used for hazardous waste management, what other activities are currently carried on at the site? (e.g., pasture, building site, park): _____

_____

8. Is this a RCRA site, a CERCLA site, or both?

RCRA | | CERCLA |X| Both | |

D. WASTE TYPE

1.

	Waste Code	Estimated Amt. Handled FY85 (Amt/unit of measure)	Unit(s) Involved (Form Attachment C)		Waste Code	Estimated Amt. Handled FY85 (Amt/unit of measure)	Unit(s) Involved (Form Attachment C)
1				6			
2				7			
3				8			
4				9			
5				10			

Installation LANL

Site Area AB

Submit, as Attachment D, the following information: summarize the results of all waste analyses in tabular form, including the presence and approximate concentration ranges of measured hazardous constituents. See the guidance to this form for additional instructions.

If the above additional waste analysis information was submitted previously in a form indicated in C-3, indicate the kind of submittal, the date of the submittal and the location of this information in that submittal. Label this information "Attachment D." If any previously submitted information must be updated, update that information in Attachment D.

2. Is Attachment D included with the inventory? Yes |X| No | |

E. ENVIRONMENTAL CONTAMINATION

1. Has this site had releases to the environment? Yes | | No |X|

2. If yes, indicate in which media the release(s) occurred:

Air | | Surface Water | | Groundwater | | Subsurface Gas | |

3. If yes, when did the release(s) occur: _____

4. If yes, type and concentration of wastes or waste constituents involved in the release(s): _____

_____

5. If yes, give the extent of the release(s) in terms of the lateral extent of release, environmental impact of the release, and any other information necessary for EPA to assess the extent of the release: _____

_____

If the above space is not sufficient to answer each question, submit the necessary information in an attachment labeled Attachment E. If the information was submitted previously in a form indicated in C-3, indicate in Attachment E the kind of submittal, the date of the submittal and the location of the information in that submittal. If the previously submitted information needs to be updated, update that information in Attachment E.

6. Is Attachment E included with the inventory? Yes | | No |X|

Installation LANL

Site Area AB

F. ENVIRONMENTAL MONITORING DATA

1. Does this site have environmental monitoring data?

Yes |X| No | |

2. What statistical and analytical methods were used to analyze the data? Monitoring is for materials not regulated under RCRA.

3. How was the data obtained (e.g., grab sample, etc.)?

Groundwater (bailing); surface and drilled samples.

4. When was it obtained: 1960 - present

5. If the site is a land disposal site and it does not have environmental monitoring data, why not?

If the above space is not sufficient to answer each question, submit the necessary information in an attachment labelled Attachment F. If the information was submitted previously in a form indicated in C-3, indicate in Attachment F the kind of submittal, the date of the submittal and the location of the information in that submittal. If the previously submitted information needs to be updated, update that information in Attachment F.

6. Is Attachment F included with the inventory? Yes | | No | |

G. RESPONSE ACTIONS

1. Have response actions been undertaken for this site?

Yes | | No | |

2. Have response actions been studied for this site?

Yes | | No | |

3. Are these actions part of a CERCLA effort? Yes | | No | |

4. What kind of actions are already underway:

Study | | PA/SI | | RIFS | | Remedial Investigation | |

Remedial Action | | Removal | |

Installation LANL

Site Area AB

If the above space is not sufficient to answer each question, submit the necessary information in an attachment labelled Attachment G. If the information was submitted previously in a form indicated in C-3, indicate in Attachment G the kind of submittal, the date of the submittal, and the location of the information in that submittal. If the previously submitted information needs to be updated, update that information in Attachment G.

5. Is Attachment G included with the inventory? Yes | | No |X|

H. FOR DISPOSAL SITES ONLY

1. Describe the hydrogeology of the site: The main aquifer is 1200 ft below the site with an eastward flow of an average flow rate of 0.3 m/day.

2. Indicate the location of withdrawal wells and surface water within one mile of the site: There is intermittent streamflow in Water Canyon located about 2000 ft north of the site.

If the above space is not sufficient to answer each question, submit the necessary information in an attachment labelled Attachment H. If the information was submitted previously in a form indicated in C-3, indicate in Attachment H the kind of submittal, the date of the submittal, and the location of the information in that submittal.

If the previously submitted information needs to be updated, update that information in Attachment H.

3. Is Attachment H included with the inventory? Yes | | No |X|

ATTACHMENT D

Installation: LANL Site:

Area AB

EPA Hazardous Waste Number Code (from 40 CFR 261.21-.33)	Type of Analyses Used to Identify This Waste (Example: Analysis of waste stream directly, analysis of landfill leachate or other environmental monitoring result, analysis of surface impoundment contents, etc.)	Principal Constituents	Minimum Concentration (mg/l)	Maximum Concentration (mg/l)
P015	Analysis of material at disposal time.	Beryllium		

APPENDIX B

HAZARD RANKING SYSTEM/MODIFIED HAZARD RANKING SYSTEM (HRS/mHRS)

HRS/mHRS SUMMARY COVER SHEET

SITE NAME: Area AB, TA-49 LOTUS FILE NAME:

(AFTER KEYING IN SITE NAME, PRESS "ALT" & "A" KEYS SIMULTANEOUSLY)

FIELD OFFICE: Los Alamos Area Office. U.S. Department of Energy

EPA REGION: Region VI-Dallas

PERSON(S) IN CHARGE OF SITE: Harold Valencia, Area Manager
U.S. Department of Energy

NAME OF REVIEWER: J. Lynn Scholl DATE: February 17, 1987

GENERAL DESCRIPTION OF THE FACILITY:

(For example: landfill, surface impoundment, pile, container; types of hazardous substances; location of the facility; contamination route of major concern; types of information needed for rating; agency action, etc.)

The main concern at this area is beryllium, lead, high explosives, and radioactive material in shafts.

SCORES:	CHEMICAL	RADIOACTIVE	MAXIMUM
Sm =	6.67	5.26	6.67
Sgw =	11.53	9.11	11.53
Ssw =	0.00	0.00	0.00
Sa =	0.00	0.00	0.00
Sfe =	0.00	0.00	0.00
Sdc =	0.00	0.00	0.00

GROUND WATER ROUTE WORKSHEET Site: Area AB, TA-49

RATING FACTOR	VALUE / RANGE	SEL VAL	MULTI-PLIER	SCORE	MAX. SCORE	REF. SEC.	REFERENCES FOR EACH ASSIGNED SCORE
1. OBSERVED RELEASE	0 / 45	0	1	0	45	3.1	No observed release.
If Observed Release is Given a Score of 45, Proceed to Line 4							
If Observed Release is Given a Score of 0, Proceed to Line 2							
2. ROUTE CHARACTERISTICS						3.2	
A. Depth to Aquifer of Concern	0 1 2 3	0	2	0	6		Depth to top of aquifer approx. 1200 ft (LA-9957-MS, fig. 4; ENG-R 5277/6)
B. Net Precipitation	0 1 2 3	0	1	0	3		20 in. total annual precip.; 46 in. total evap.
C. Permeability of the Unsaturated Zone	0 1 2 3	2	1	2	3		(40 CFR 300, App.A, figs. 4, 5) Measurements range from 2E-5 to 5E-4 (LA-8962-MS, p.21)
D. Physical State	0 1 2 3	2	1	2	3		Powder.
TOTAL ROUTE CHARACTERISTICS SCORE				4	15		
3. CONTAINMENT	0 1 2 3	3	1	3	3	3.3	No liners.
4. WASTE CHARACTERISTICS						3.4	
Chemical							
A. Toxicity/Persistence	0 3 6 9 12 15 18	18	1	18	18		Beryllium, lead, high explosives.
B. Hazardous Waste Quantity	0 1 2 3 4 5 6 7 8	1	1	1	8		Quantity assumed to be less than forty drums.
Radioactive							
A. Maximum Observed	0 1 3 7 11 15 21 26	0	1	0	26		
B. Maximum Potential	0 1 3 7 11 15 21 26	15	1	15	26		Plutonium, uranium, americium.
TOTAL WASTE CHARACTERISTICS SCORE							
CHEMICAL				19	26		
RADIOACTIVE				15	26		
5. TARGETS						3.5	
A. Ground Water Use	0 1 2 3	3	3	9	9		
B. Distance to Nearest Well/Population Served	0 4 6 8 10 12 16 18 20 24 30 32 35 40	20	1	20	40		Distance to nearest supply well less than three miles. Population served greater than 10000. (LA-9957-MS, figs. 5, 10; LA-10721-ENV, p.13; ENG-R 92)
TOTAL TARGETS SCORE				29	49		

6. CALCULATION

If Line 1 is 45, Multiply 1 x 4 x 5

If Line 1 is 0, Multiply 2 x 3 x 4 x 5

CHEMICAL	6612	57330
RADIOACTIVE	5220	57330

7. NORMALIZATION

Divide Line 6 by 57330 and Multiply by 100

CHEMICAL Sgw =	11.53	100.00
RADIOACTIVE Sgw =	9.11	100.00
MAXIMUM Sgw =	11.53	100.00

NOTE: NE means Not Evaluated.

SURFACE WATER ROUTE WORKSHEET Site: Area AB, TA-49

RATING FACTOR	VALUE RANGE	SEL VAL	MULTI-PLIER	SCORE	MAX. SCORE	REF. SEC.	REFERENCES FOR EACH ASSIGNED SCORE
1. OBSERVED RELEASE	0 45	45	1	45	45	4.1	Observed release. (WDP 1983)
If Observed Release is Given a Value of 45, Proceed to Line 4							
If Observed Release is Given a Value of 0, Proceed to Line 2							
2. ROUTE CHARACTERISTICS						4.2	
A. Facility Slope and Intervening Terrain	0 1 2 3	NE	1	NE	3		
B. 1-yr. 24-hr. Rainfall	0 1 2 3	NE	1	NE	3		
C. Distance to Nearest Surface Water	0 1 2 3	NE	2	ERR	6		
D. Physical State	0 1 2 3	NE	1	NE	3		
TOTAL ROUTE CHARACTERISTICS SCORE				ERR	15		
3. CONTAINMENT	0 1 2 3	NE	1	NE	3	4.3	
4. WASTE CHARACTERISTICS						4.4	
Chemical							
A. Toxicity/Persistence	0 3 6 9 12 15 18	18	1	18	18		Beryllium, lead, high explosives.
B. Hazardous Waste Quantity	0 1 2 3 4 5 6 7 8	1	1	1	8		Assume quantity less than forty drums.
Radioactive							
A. Maximum Observed	0 1 3 7 11 15 21 26	0	1	0	26		
B. Maximum Potential	0 1 3 7 11 15 21 26	3	1	3	26		Plutonium, uranium, americium.
TOTAL WASTE CHARACTERISTICS SCORE							
CHEMICAL				19	26		
RADIOACTIVE				3	26		
5. TARGETS						4.5	
A. Surface Water Use	0 1 2 3	0	3	0	9		No surface water use within three miles.
B. Distance to Sensitive Environment	0 1 2 3	0	2	0	6		No sensitive environments within one mile.
C. Population Served/ Distance to Water Intake Downstream	0 4 6 8 10 12 16 18 20 24 30 32 35 40	0	1	0	40		No surface water intake within three miles.
TOTAL TARGETS SCORE				0	55		
6. CALCULATION							
If Line 1 is 45, Multiply 1 x 4 x 5					64350		
If Line 1 is 0, Multiply 2 x 3 x 4 x 5							
CHEMICAL				0			
RADIOACTIVE				0			
7. NORMALIZATION							
Divide Line 6 by 64350 and Multiply by 100							
CHEMICAL Ssw =				0.00	100.00		NOTE: NE means Not Evaluated.
RADIOACTIVE Ssw =				0.00	100.00		
MAXIMUM Ssw =				0.00	100.00		

AIR ROUTE WORK SHEET Site: Area AB, TA-49

RATING FACTOR	VALUE / RANGE	SEL VAL	MULTI-PLIER	SCORE	MAX. SCORE	REF. SEC.	REFERENCES FOR EACH ASSIGNED SCORE
1. OBSERVED RELEASE	0 45	0	1	0	45	5.1	No observed release.
Date and Location:							
Sampling Protocol:							
If Line 1 is 0, the Sa = 0. Enter on Line 5							
If Line 1 is 45, Then Proceed to Line 2.							
2. WASTE CHARACTERISTICS						5.2	
Chemical							
A. Reactivity and Incompatibility	0 1 2 3	0	1	0	3		
B. Toxicity	0 1 2 3	0	3	0	9		
C. Hazardous Waste Quantity	0 1 2 3 4 5 6 7 8	0	1	0	8		
Radioactive	0 2 5 8 12 16 20	0	1	0	20		
TOTAL WASTE CHARACTERISTICS SCORE							
CHEMICAL				0	20		
RADIOACTIVE				0	20		
3. TARGETS							
A. Population Within 4-Mile Radius	0 9 12 15 18 21 24 27 30	0	1	0	30		
B. Distance to Sensitive Environment	0 1 2 3	0	2	0	6		
C. Land Use	0 1 2 3	0	1	0	3		
TOTAL TARGETS SCORE				0	39		
4. CALCULATION							
Multiply 1 x 2 x 3							
CHEMICAL				0	35100		
RADIOACTIVE				0	35100		
5. NORMALIZATION							
Divide Line 4 by 35100 and Multiply by 100							
CHEMICAL Sa =				0.00	100.00		NOTE: NE means Not Evaluated.
RADIOACTIVE Sa =				0.00	100.00		
MAXIMUM Sa =				0.00	100.00		

SUMMARY CALCULATION OF TOTAL MIGRATION SCORE

		CHEMICAL	RADIOACTIVE	
Ground Water Route	(Sgw)	11.53	9.11	
Surface Water Route	(Ssw)	0.00	0.00	
Air Route	(Sa)	0.00	0.00	
Sum of Squares		133.02	82.90	
Square Root of Sum		11.53	9.11	
TOTAL MIGRATION SCORE	(Sm)	6.67	5.26	Square Root of Sum Divided by 1.73

DIRECT CONTACT WORKSHEET Site: Area AB, TA-49

RATING FACTOR	VALUE / RANGE		SEL VAL	MULTI-PLIER	SCORE	MAX. SCORE	REF. SEC.	REFERENCES FOR EACH ASSIGNED SCORE
1. OBSERVED INCIDENT	0	45	0	1	0	45	8.1	
If Observed Incident is Given a Score of 45, Proceed to Line 4								
If Observed Incident is Given a Score of 0, Proceed to Line 2								
2. ACCESSIBILITY	0 1 2 3		0	1	0	3	8.2	
3. CONTAINMENT	0	15	0	1	0	15	8.3	
4. WASTE CHARACTERISTICS								
Chemical Toxicity	0 1 2 3		0	5	0	15	8.4	
Radioactive	0 1 2 4 6 9 12 15		0	1	0	15		
5. TARGETS								
A. Population Within a 1-Mile Radius	0 1 2 3 4 5		0	4	0	20	8.5	
B. Distance to a Critical Habitat	0 1 2 3		0	4	0	12		
TOTAL TARGETS SCORE					0	32		

6. CALCULATION

If Line 1 is 45, Multiply 1 x 4 x 5

If Line 1 is 0, Multiply 2 x 3 x 4 x 5

CHEMICAL	0	21600
RADIOACTIVE	0	21600

7. NORMALIZATION

Divide Line 6 by 21600 and Multiply by 100

CHEMICAL Sdc =	0.00	100.00
RADIOACTIVE Sdc =	0.00	100.00
MAXIMUM Sdc =	0.00	100.00

NOTE: NE means Not Evaluated.

FIRE AND EXPLOSION WORKSHEET Site: Area AB, TA-49

RATING FACTOR	VALUE RANGE	SEL VAL	MULTI-PLIER	SCORE	MAX. SCORE	REF. SEC.	REFERENCES FOR EACH ASSIGNED SCORE
1. OBSERVED RELEASE	1 3	0	1	0	3	7.1	
2. WASTE CHARACTERISTICS						7.2	
A. Direct Evidence	0 3	0	1	0	3		
B. Ignitability	0 1 2 3	0	1	0	3		
C. Reactivity	0 1 2 3	0	1	0	3		
D. Incompatibility	0 1 2 3	0	1	0	3		
E. Waste Quantity							
Chemical	0 1 2 3 4 5 6 7 8	0	1	0	8		
Radioactive	0 1 2 3 5 6 8	0	1	0	8		
TOTAL WASTE CHARACTERISTICS SCORE							
CHEMICAL				0	20		
RADIOACTIVE				0	20		
3. TARGETS						7.3	
A. Distance to Nearest Population	0 1 2 3 4 5	0	1	0	5		
B. Distance to Nearest Building	0 1 2 3	0	1	0	3		
C. Distance to Sensitive Environment	0 1 2 3	0	1	0	3		
D. Land Use	0 1 2 3	0	1	0	3		
E. Population Within 2-Mile Radius	0 1 2 3 4 5	0	1	0	5		
F. Buildings Within 2-Mile Radius	0 1 2 3 4 5	0	1	0	5		
TOTAL TARGETS SCORE				0	24		

4. CALCULATION

Multiply 1 x 2 x 3

CHEMICAL	0	1440
RADIOACTIVE	0	1440

5. NORMALIZATION

Divide Line 4 by 1440 and Multiply by 100

CHEMICAL Sfe =	0.00	100.00
RADIOACTIVE Sfe =	0.00	100.00
MAXIMUM Sfe =	0.00	100.00

NOTE: NE means Not Evaluated.

LA-11332-MS

UC-11
Issued: August 1988

Water Supply at Los Alamos: Current Status of Wells and Future Water Supply

W. D. Purtymun
A. K. Stoker

Los Alamos National Laboratory
Los Alamos, New Mexico 87545

WATER SUPPLY AT LOS ALAMOS: CURRENT STATUS OF WELLS AND FUTURE WATER SUPPLY

by

W. D. Purtymun and A. K. Stoker

ABSTRACT

The municipal and industrial use of groundwater at the Los Alamos National Laboratory and Los Alamos County was about 1.5 billion gallons during 1986. From a total of 19 wells that range in age from 5 to 41 years, the water was pumped from 3 well fields. The life expectancy of a well in the area ranges from 30 to 50 years, dependent on the well construction and rate of corrosion of the casing and screen. Twelve of the wells are more than 30-years old and, of these, four cannot be used for production, three because of well damage (LA-1, LA-4, and G-3) and one (LA-6) because the quality of water is not suitable for use. Eight (LA-2, LA-3, LA-5, G-1, G-2, G-4, G-5, and G-6) of the twelve oldest wells are likely to be unsuitable for use in the next 10 years because of well deterioration and failure. The remaining 7 wells include 2 (LA-1B, G-1A) that are likely to fail in the next 20 years. Five of the younger wells in the Pajarito well field are in good condition and should serve for another two or three decades.

The program of maintenance and rehabilitation of pumps and wells has extended production capabilities for short periods of time. Pumps may be effectively repaired or replaced; however, rehabilitation of the well is only a short-term correction to increase the yield before it starts to decline again. The two main factors that prevent successful well rehabilitation are: (1) chemicals precipitated in the gravel pack and screen restrict or reduce the entrance of water to the well, which reduces the yield of the well, and (2) the screen and casing become corroded to a point of losing structural strength and subsequent failure allows the gravel pack and formation sand to enter the well. Both factors are due to long-term use and result in extensive damage to the pump and reduce the depth of the well, which in turn causes the yield to decline. Once such well damage occurs, rehabilitation is unlikely to be successful and the ultimate result is loss of the well. Two wells (LA-4 and G-3) were lost in 1987 because of such damage.

It is essential to implement a program to replace wells that have failed or will fail in the next 10 years to ensure a continued and reliable water supply. Any change in operation of the Laboratory or county that will require additional water adds to the urgency to develop a system of new wells. Rehabilitation of the older wells will not ensure a continued or reliable supply, or meet additional demands for water. This report presents the history of the wells and well fields, briefly describes the geology and hydrology of the area, includes a section on production and production capacity, and outlines development of additional water supply.

I. INTRODUCTION

A. Background

The Los Alamos National Laboratory and the communities of Los Alamos and White Rock are supplied by water pumped from deep wells in three well fields located in Los Alamos Canyon, Guaje Canyon, and on the Pajarito Plateau. These wells produce water from the main aquifer of the Los Alamos area that lies at depths varying from several hundred to more than a thousand feet below the mesa tops. The main aquifer is the only aquifer in the area that is capable of municipal and industrial water supply.

Water moves eastward through the aquifer from the major recharge area in the Valle Caldera, several miles west of Los Alamos, toward the Rio Grande, where a part is discharged into the river through seeps and springs. The upper surface of the main aquifer slopes gently downward through the lower part of the Puye Conglomerate beneath the central and western parts of the plateau and then through the Tesuque Formation down to the Rio Grande at the eastern margin of the plateau. The main aquifer is under water table conditions beneath the western and central part of the Pajarito Plateau; along the eastern margin and near the Rio Grande it is under artesian conditions.

This groundwater resource was developed as a result of the decision to make Los Alamos a permanent research facility after World War II. Water supply through the World War II period had been from surface water sources. During the winter of 1945-1946 surface water supply failed and for several weeks water had to be hauled from the Rio Grande. The U. S. Geological Survey began investigations in 1946 to develop a reliable water supply.

Studies were first made in the Valle Caldera, Valle Grande, and Valle Toledo, west of Los Alamos. The plan was to develop wells and transmission lines over the mountains to Los Alamos. The completion of test holes and aquifer tests indicated a potential water resource; however, the surface water and groundwater in the area were connected and pumping of the wells reduced stream flow. Fully appropriated surface water rights in the drainage area precluded use of the resource for water supply.

At the same time, additional studies were conducted north of Otowi along the Rio Grande and in the lower part of Los Alamos Canyon. These studies indicated that a water supply could be developed in lower Los Alamos Canyon.

The original six wells in the Los Alamos field were drilled and completed from 1946-1948. An additional well was completed in 1960. Water from the Los Alamos field is lifted vertically about 1,800 ft through four booster stations into storage to serve both Laboratory and community areas.

Water usage at the Laboratory and the community during the late 1940s continued to increase, and to meet this increased need, five wells were completed in 1950 and 1951 to form the Guaje Canyon field. Two wells were added to the field to replace declining yield of older wells in 1954 and 1965. Water from the Guaje field is lifted vertically about 1,500 ft through four booster stations into storage, mainly serving the northernmost community areas.

The Pajarito field consisting of five wells was developed from 1965-1982 to supply increased demand for water and to supplement the declining production from the wells in the Los Alamos and Guaje well fields. There are three booster stations that can lift water to White Rock or the Laboratory and the townsite area.

A small amount of the original surface water sources are still used for water supply. In 1986 this amounted to about 4% of the total production or about 28×10^6 gal.

The wells in the three well fields range in age from 5 to 41 years. Declining production from deteriorating wells in the Los Alamos and Guaje fields in the past few years has become significant. Recent attempts to rehabilitate older wells to restore production have failed and focus concern on the need for a comprehensive plan to ensure a reliable water supply for the long term. The purpose of this report is to review and evaluate the condition of the wells and well fields as to their reliability to meet future water demands. A rationale for constructing new wells is based on these conclusions and understanding of the geohydrology of the area.

B. Geology and Hydrology

The geology and hydrology of the wells and well fields have been presented in detail in

another report (Purtymun 1984a). A summary of the major geologic and hydrologic features is included through a series of figures appearing in that report. These figures will provide information for discussions of the wells and well fields in this report and can be referenced as a basis for understanding the geohydrology. Fundamental geologic and hydrologic data were compiled from observations and measurements from supply wells, stock wells, and test holes completed in the main aquifer or springs that discharge from the main aquifer (Fig. 1). The geologic data were used to prepare a diagrammatic section of geologic units (Fig. 2) and a geologic section showing the stratigraphy and structure from the Sierra de los Valles across the Pajarito Plateau to the Rio Grande (Fig. 3). The section shows the top of the main aquifer and its relation to the geologic units. The depth to water in the main aquifer was used to determine and map the surface of the main aquifer essential to defining the hydrologic gradient of the groundwater (Fig. 4). Interpretations of aquifer tests performed in the supply wells and test holes provided the basis for

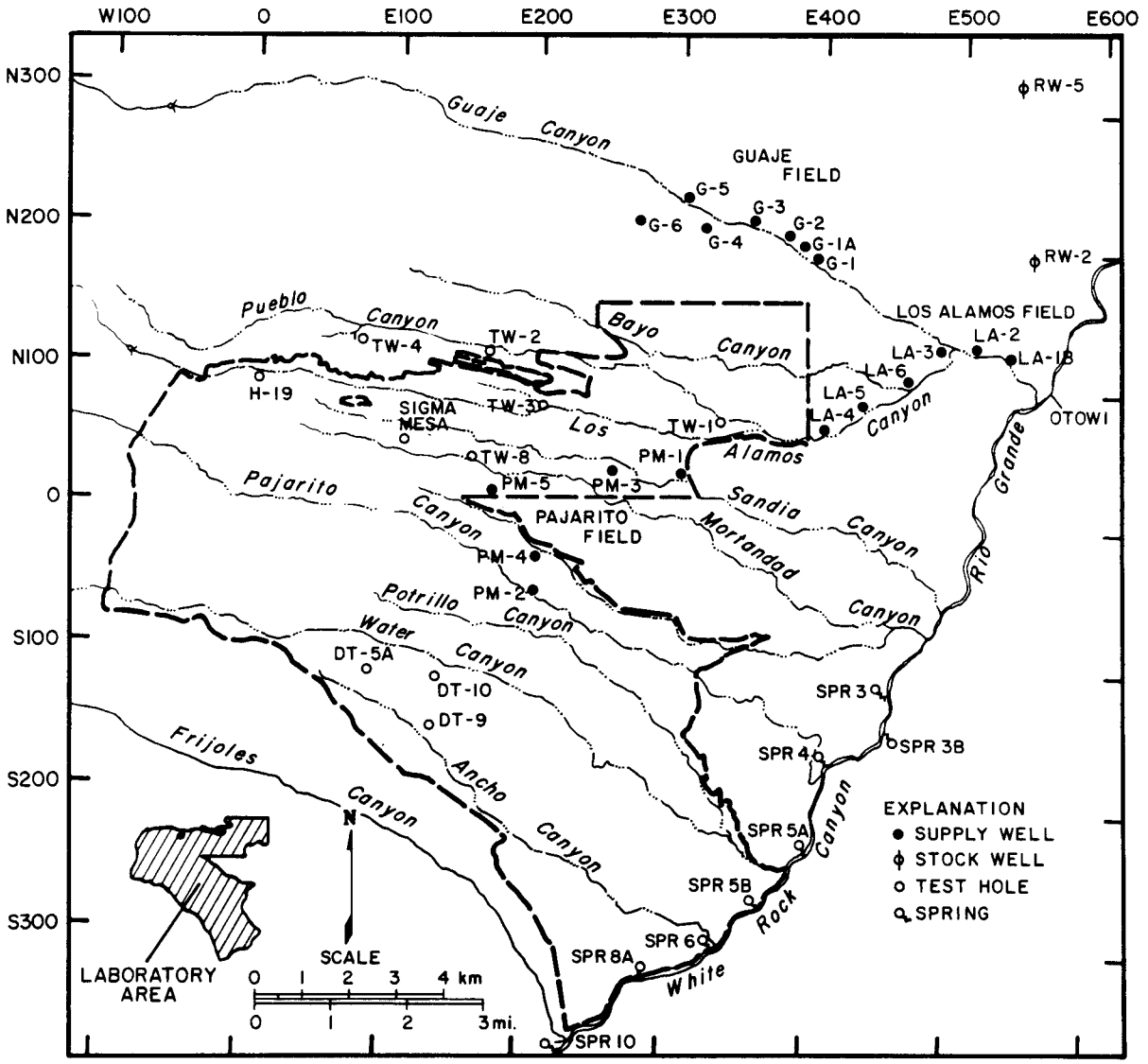

Figure 1. Location of supply, test, and stock wells completed or spring discharging from the main aquifer.

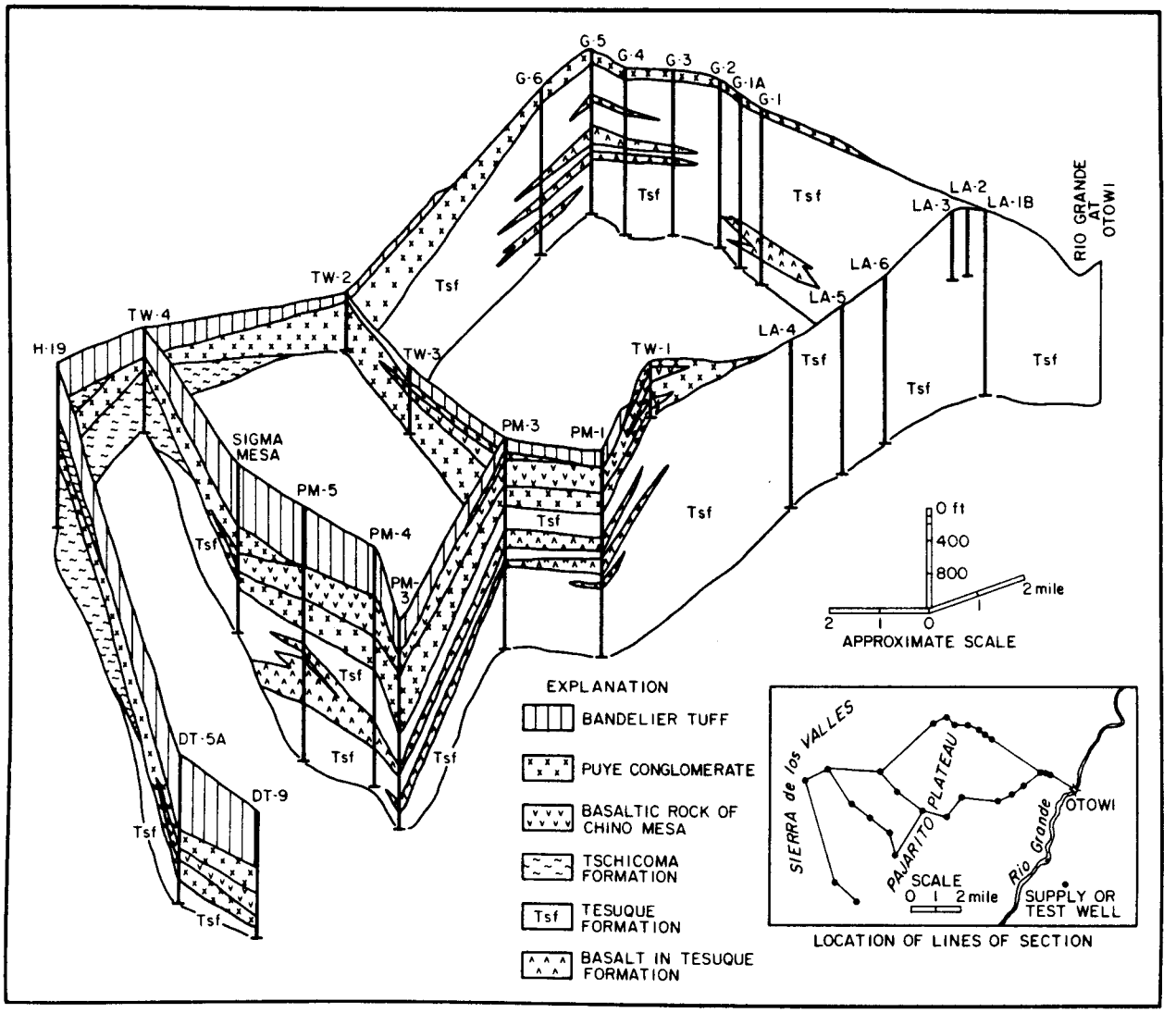

Figure 2. Diagrammatic section of geologic units in the Los Alamos area.

defining the hydrologic characteristics of the main aquifer (Fig. 5). The movement of water in the aquifer was inferred by combining the gradient and the hydrologic characteristics of the aquifer. Movement is basically perpendicular to the water surface contours, generally to the east and southeast toward the Rio Grande with estimated rates of flow in the aquifer ranging from about 20 to about 350 ft/yr (Fig. 6). Periodic water level data were used to determine trends of water level declines in wells or test holes completed in the main aquifer (Fig. 7). Water-level declines related to production are used for comparison of production per ft of water-level decline in the Los Alamos and Guaje fields and wells PM-1, PM-2, and PM-3 of the Pajarito field (Fig. 8). The basic chemical quality and graphic depiction of principal chemical quality parameters determined by analysis of samples from supply wells, test holes, stock wells, and springs shows basic similarity throughout the main aquifer (Figs. 9 and 10).

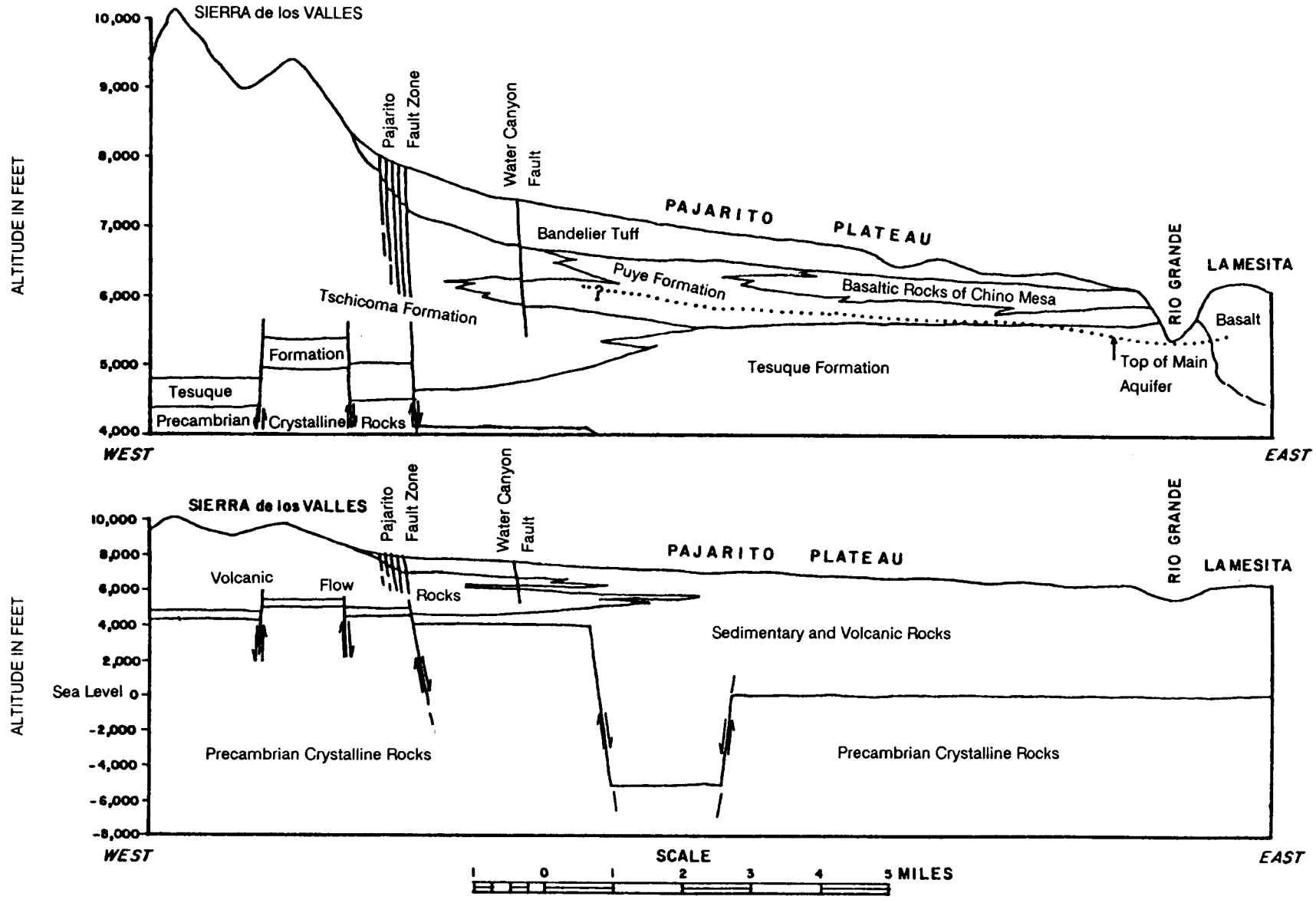

Figure 3. Geologic section showing stratigraphy and structure from the Sierra de los Valles, across the Pajarito Plateau to the Rio Grande.

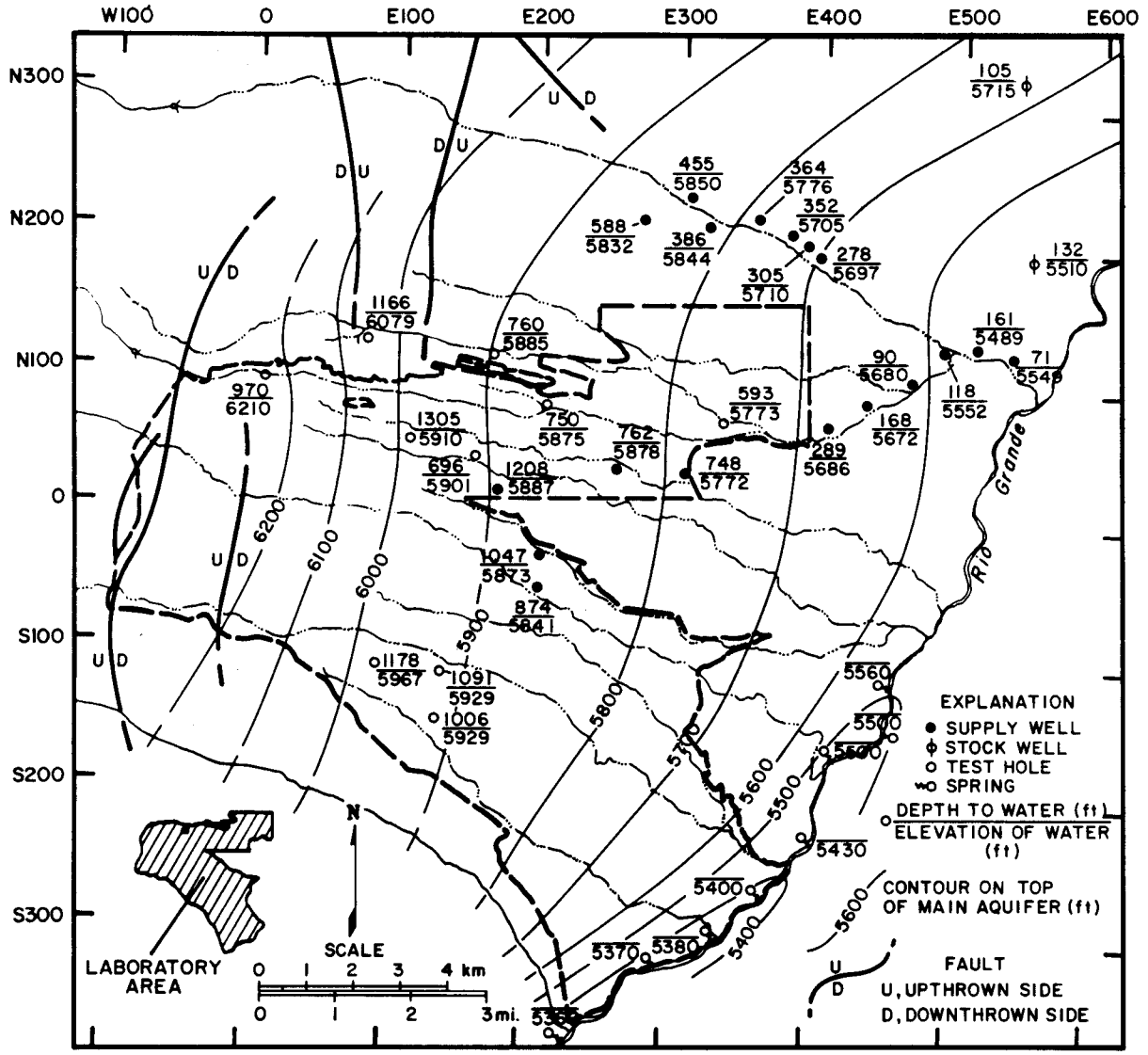

Figure 4. Generalized contours on the surface of the main aquifer.

C. Data Sources

The data presented in this report have been collected from a number of published and unpublished reports, unpublished notebooks, and operating records. Reports include the "Summary of Los Alamos Municipal Well Field Characteristics, 1947-1971" (Purtymun 1972) and the series of annual water supply reports covering the years 1972-1987 (Purtymun 1972a-1987). Other reports included Theis (1962), Cushman (1965, 1975), Purtymun (1977), and Purtymun (1984a). Well-field development and well locations were described in two reports from the U.S. Geological Survey (Purtymun 1965, 1969). A description of early developments of the Los Alamos and Guaje well fields is found in Griggs (1964) and Black (1951). Some data were taken from planning reports (Herkenhoff 1974; Keiser 1984). Measuring points of the various wells and well conditions were taken from an unpublished notebook from the U. S. Geological Survey. Notes and data collected during well rehabilitation or testing of the wells were reviewed. Notes and video tapes taken

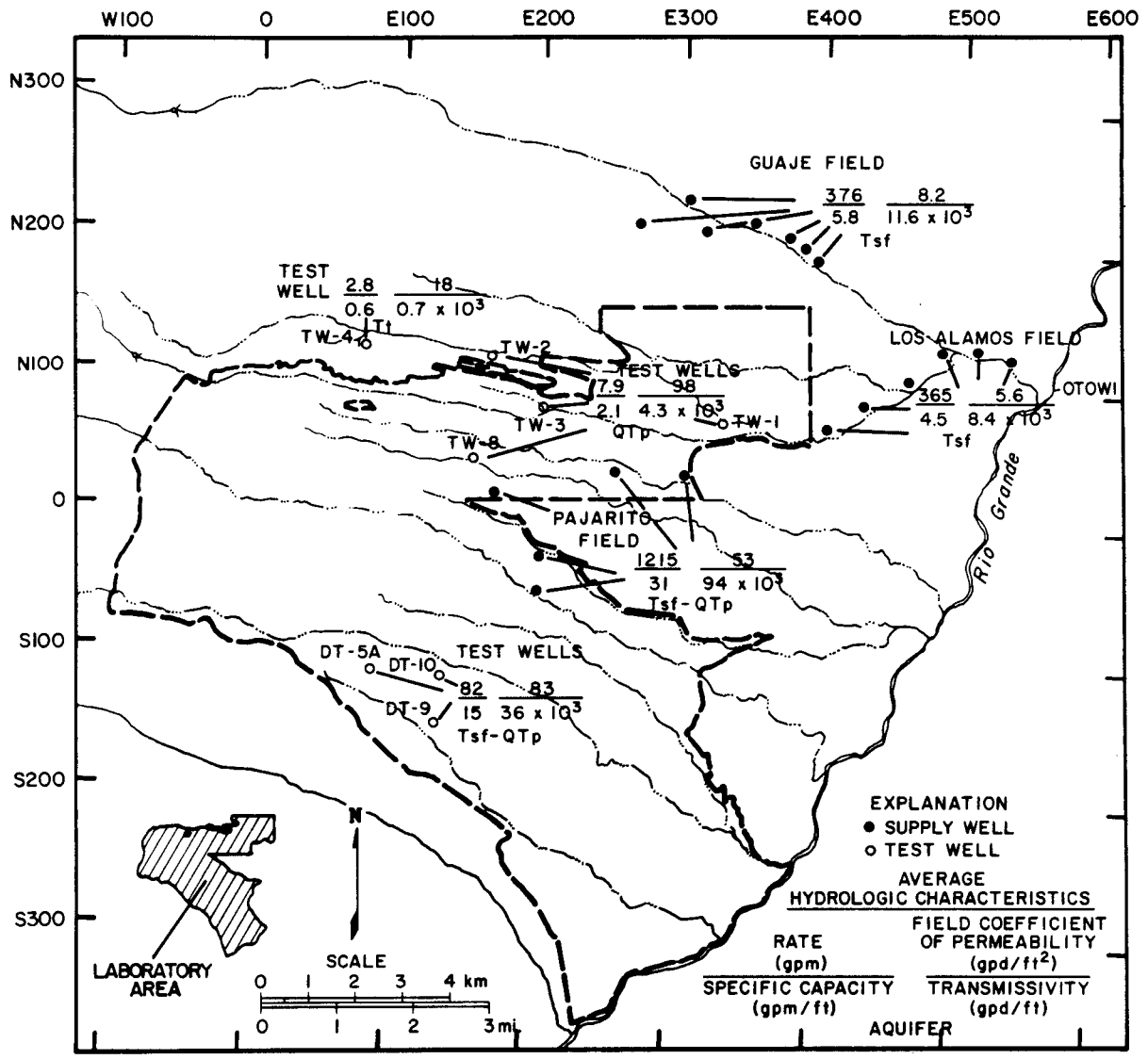

Figure 5. Hydrologic characteristics of the main aquifer.

while video logs were run in a number of wells provided details on well conditions. Some well data, mainly the depth setting of pumps, came from unpublished records of the Pan Am Utility Division.

II. WELL CONSTRUCTION AND REHABILITATION

Some of the important and unique characteristics of particular wells or groups of wells are directly dependent on the original techniques used for their construction. Much of the present understanding of well deterioration comes from observations related to well rehabilitation efforts over the years. This section provides summary descriptions of well construction techniques and rehabilitation as background to understanding subsequent discussions of individual well histories.

A. Well Construction

Three basic methods of well construction have been employed for the water production

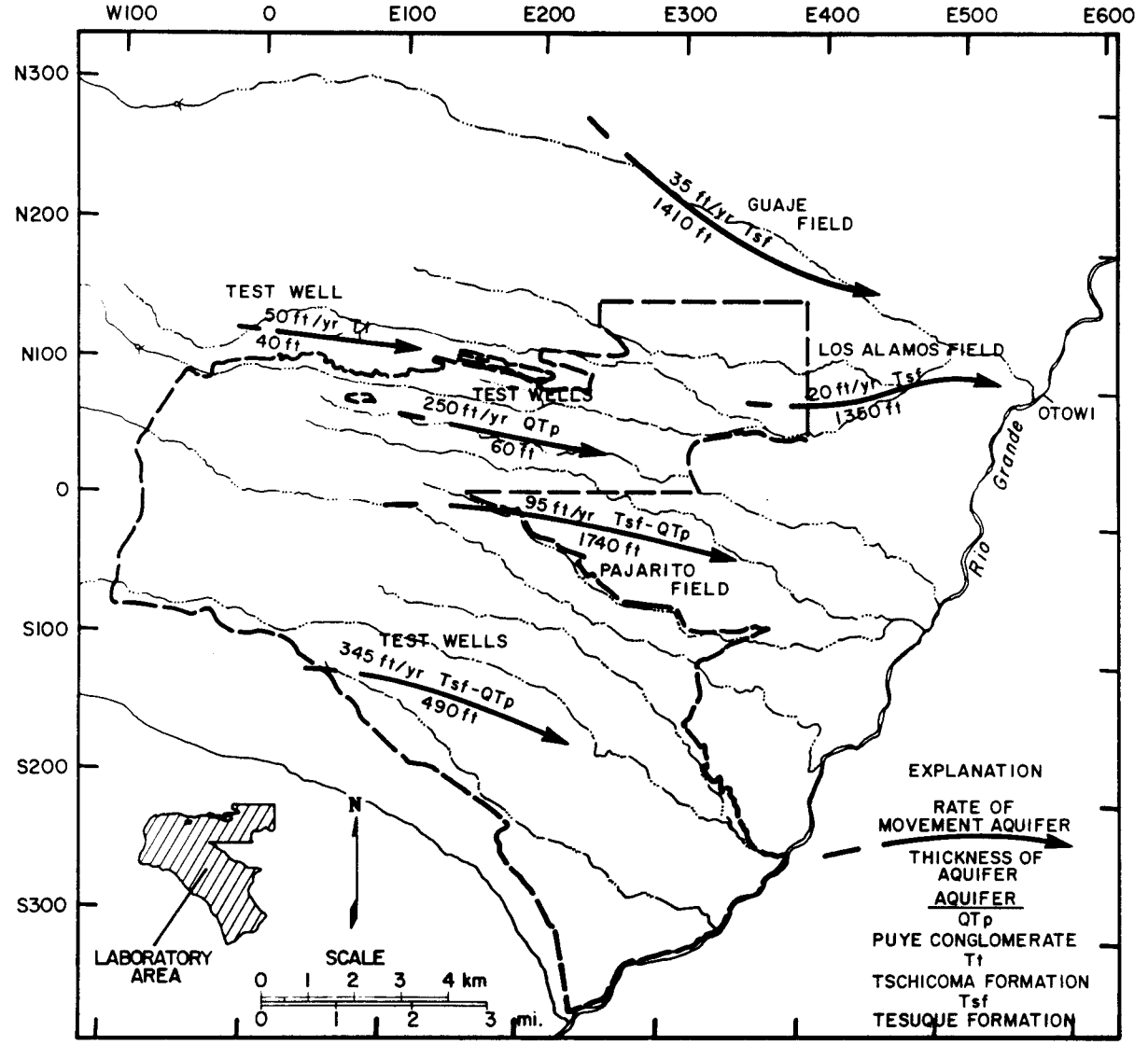

Figure 6. Rate of movement of water in the main aquifer.

wells. They generally correspond to specific time periods and reflect some evolution of understanding of the most effective methods for the local geohydrologic conditions.

Basic data on the construction of individual wells are presented in Table 1. This includes the year of completion, the total drilled depth of the pilot hole, the depth to which casing was installed, and the total length of screen or perforated casing installed. Additional information includes the most recent measurement of the depth to which sand has filled the well and the length of screen or perforations that remain uncovered. Additional detailed data on the individual well casing and screen parameters are summarized in Table 2.

Wells LA-1, -2, and -3 were constructed by drilling 16- or 19-in.-diameter holes. Geophysical logs were used to determine the depths of the most permeable zones of the aquifer. Sections of 12-in.-diameter screen were set opposite the permeable zones alternating with 10-in. slotted casing between the screen sections. The wells were gravel packed.

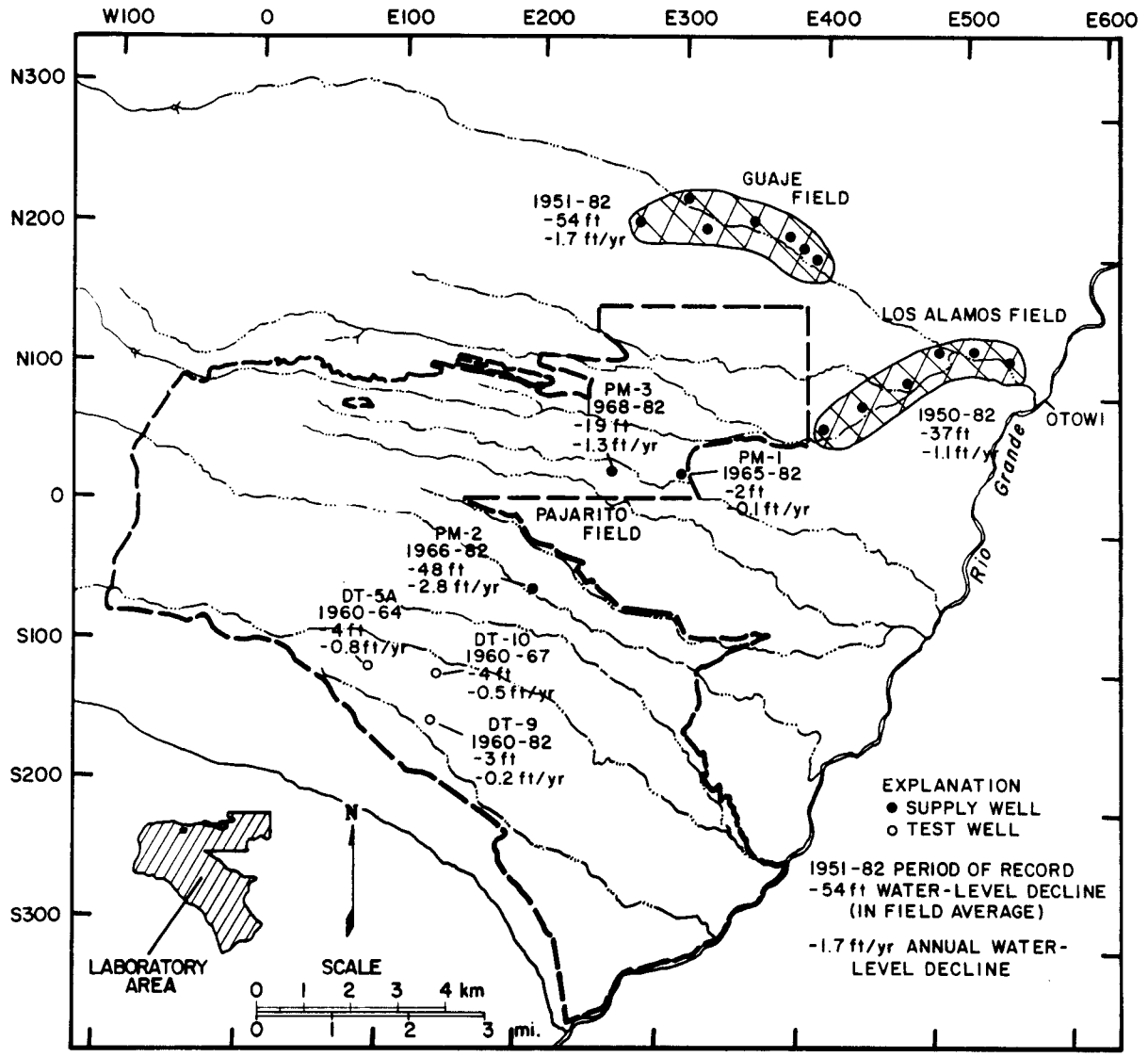

Figure 7. Water-level declines in well fields, supply, and test wells.

Wells LA-4, -5, and -6 in the Los Alamos field and wells G-1, -2, -3, -4, and -5 were started with a 20-in.-diameter surface casing (blank casing used to shut out shallow water) set and cemented in a 22-in.-diameter hole to a depth sufficient to seal out surface and near surface groundwater. Then an 11-1/2-in.-diameter pilot hole was drilled to the total depth of the well. It was reamed to 19-in.-diameter to the total depth of the pilot hole or a depth including the most permeable section of the aquifer. Selected depths opposite the most permeable zones in the aquifer were determined from geophysical logs. The intervals including these zones were underreamed to 27-in.-diameter and well screen sections placed opposite those zones. Blank casing is in the intervening zones. The wells were packed by pumping gravel through a drop line between the annulus of the hole and the casing or screen. This resulted in different thicknesses of the gravel pack in the well and is now believed to be poor design in well construction. The gravel pack will not settle and clean up during development because the gravel pack will separate in the sections of blank casing

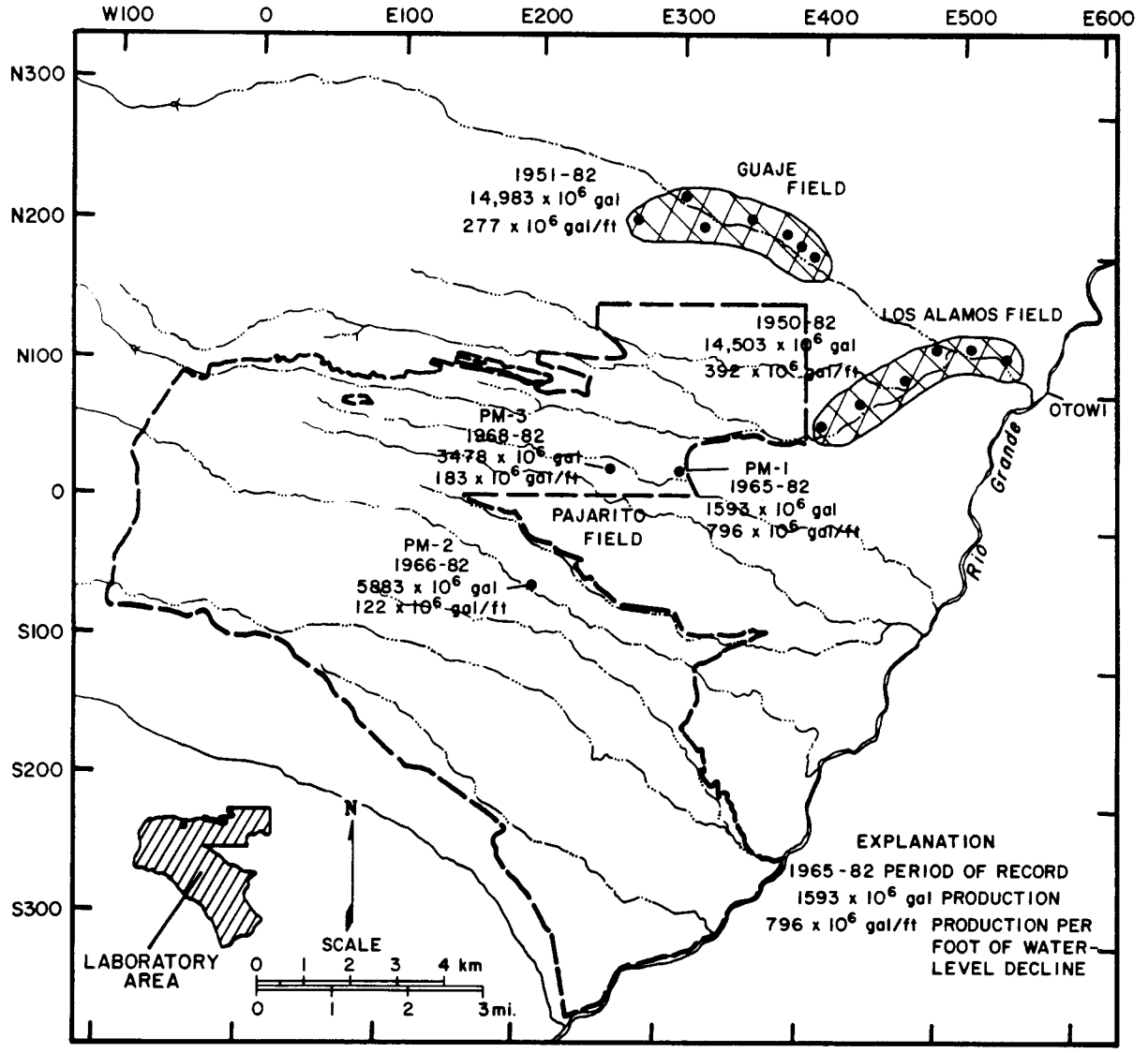

Figure 8. Water-level declines related to production from well fields and supply wells.

between sections of screen. Video logs of wells where several louvers were missing show that no gravel pack remains between the screen and hole wall. There was no apparent movement of gravel from the upper part of the well pack in the surface casing.

Well LA-1B was constructed in essentially the same fashion with two exceptions: the entire depth to be cased was reamed to 27-in.-diameter, and perforated casing was used instead of well screen.

The casing in these Los Alamos and Guaje wells is reduced from 12-in.- to 10-in.-diameter at depths well below the pump intake setting (Table 2). The 12-in.-diameter casing is necessary to allow setting of the line shaft turbine pump. Experience has shown that the intake to the pump should be set in blank casing. If the pump intake is set in the screen, the backwash from the pump, when it is shut off, will cause cavitation in the gravel pack, resulting in gravel pack separation in the screen opposite the pump intake. Formation

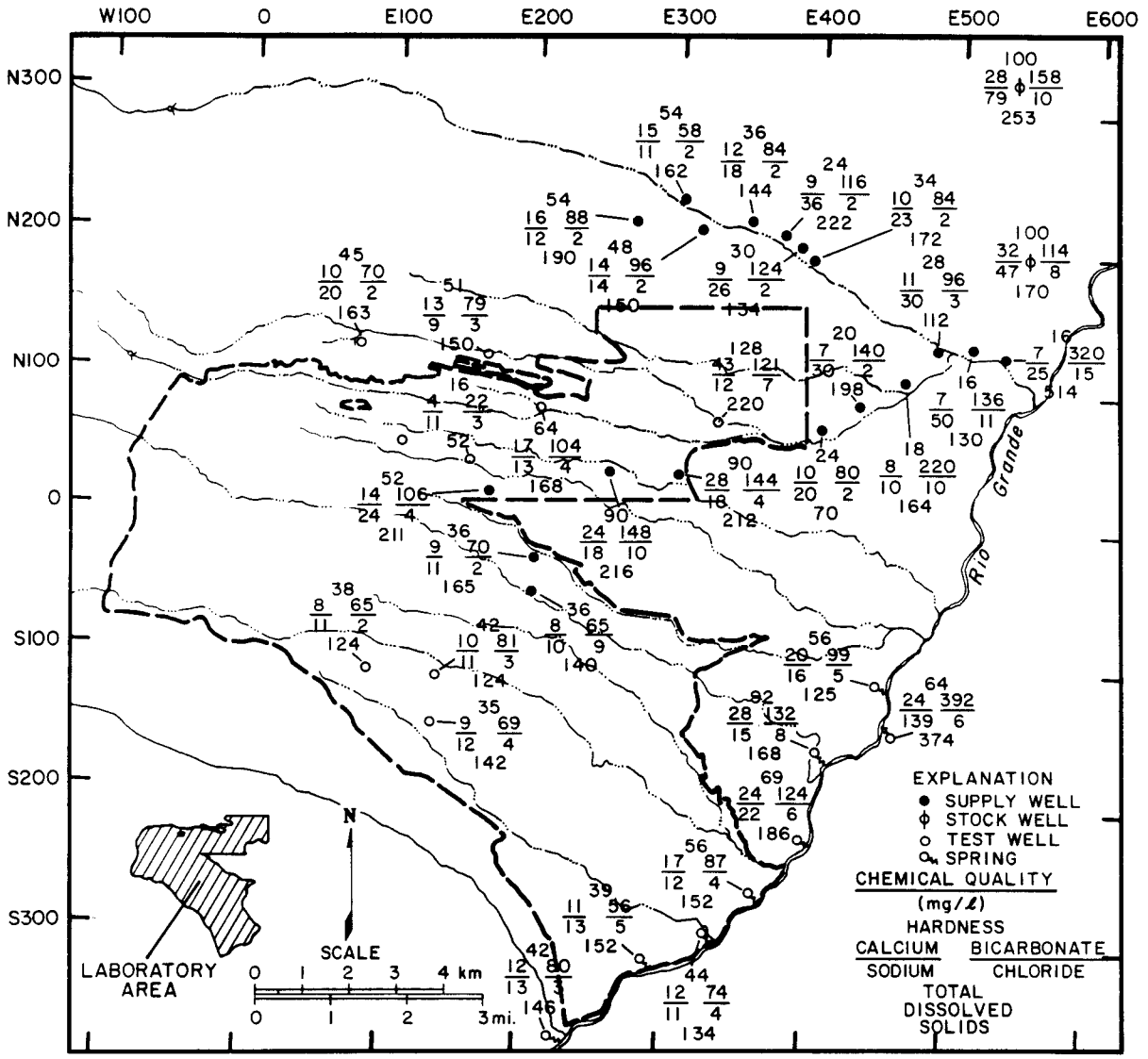

Figure 9. Chemical quality of water from springs, supply, test, and stock wells.

sand and gravel from the gravel pack will enter the well when the pump is restarted.

Well G-6 and all the wells in the Pajarito field were constructed by starting with a large diameter surface string cemented to keep out surface water. Then a 9-1/2-in.- or 11-1/2-in.-diameter pilot hole was drilled to total depth. Geophysical logs indicating permeable sections of the aquifer were used to determine completion depth of the well. The well was then reamed uniformly to completion depth to a diameter of 27-in. or 29-in. The well was cased with blank pipe to a depth of about 100 ft below the estimated pump setting. Continuous well screen was set extending to the bottom of the well. The casing and screen are uniform diameter for the entire depth, depending on the well, 12-, 14-, or 16-in.-diameter from top to bottom. The uniform thickness of gravel pack and the continuous screen in the lower part of the hole allowed better development of the wells and allows the gravel pack to move readily to fill voids. Separation of the gravel pack is less likely with this type of construction.

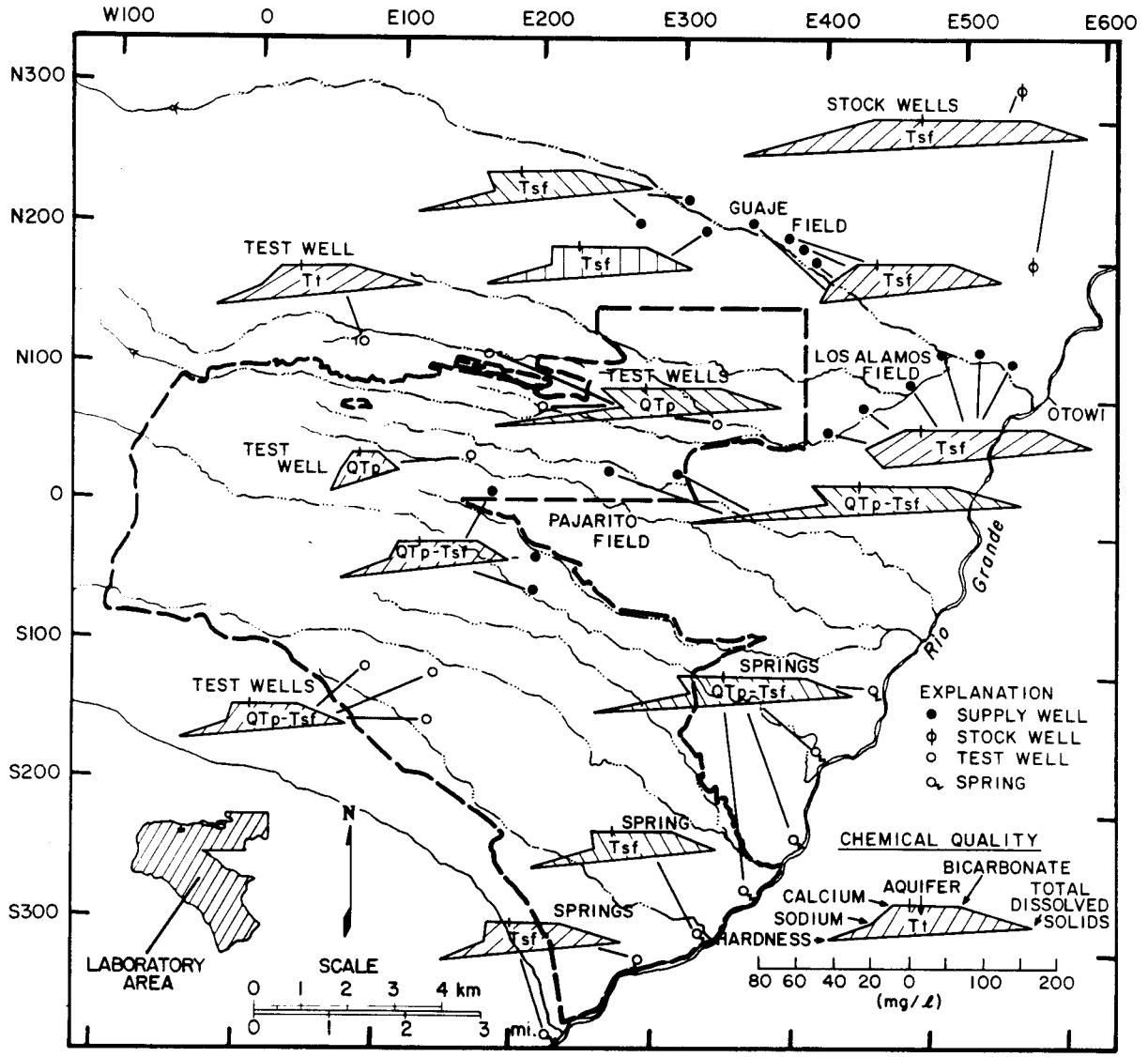

Figure 10. Graphic comparison of chemical constituents in water from springs, supply, test, and stock wells.

Well G-6 and all the wells in the Pajarito field are constructed with a 5 ft length of blank casing welded to the bottom of the screen. The end of the pipe is welded closed with a steel plate. At least 30 ft of sediments and scale should be left in the well to prevent the sand pump or bailer from damaging or separating the casing by bumping the steel plate.

B. Well Deterioration and Rehabilitation

Well yields decline over a period of time for various reasons. Chemical precipitation, especially calcium carbonate, in the gravel pack and screen tend to restrict the entrance of water into the well. The calcium carbonate formation in the

Table 1. Well Construction

		Completion Year	Depth of Pilot Hole (ft)	Cased Depth (ft)	Length of Screen or Perforation (ft)	Depth Open (ft)	Length of Screen or Perforation Open (ft)	Percentage of Screen or Perforation Open (%)
Los Alamos Field								
Well	LA-1	1946	1001	870	805	598 (60)	538 (60)	67
	LA-1B	1960	2256	1750	591	1655 (83)	576 (83)	97
	LA-2	1946	882	870	760	878 (62)	568 (63)	75
	LA-3	1947	910	870	760	816 (83)	701 (83)	92
	LA-4	1948	2019	1964	400	1907 (88)	378 (87)	95
	LA-5	1948	2024	1750	400	1954 (62)	400 (62)	100
	LA-6	1948	2030	1710	400	1200 (76)	210 (76)	53
Guaje Field								
Well	G-1	1950	2002	2000	490	1750 (62)	420 (62)	86
	G-1A	1954	2071	1519	563	1500 (73)	553 (73)	98
	G-2	1951	2006	1970	425	1707 (81)	385 (81)	91
	G-3	1951	1997	1792	400	1238 (88)	280 (87)	70
	G-4	1951	2002	1930	360	1172 (81)	180 (81)	50
	G-5	1951	1997	1840	400	703 (86)	100 (86)	25
	G-6	1964	2005	1530	825	1480 (79)	790 (79)	96
Pajarito Field								
Well	PM-1	1965	2501	2499	1549	2479 (73)	1534 (73)	99
	PM-2	1965	2600	2300	1291	2280 (87)	1276 (87)	99
	PM-3	1966	2552	2552	1591	2552 (66)	1591 (66)	100
	PM-4	1981	2920	2875	1594	2875 (81)	1594 (81)	100
	PM-5	1982	3120	3093	1632	3093 (82)	1532 (82)	100

Note: Numbers in parentheses indicate year of measurement.

Table 2. Well Casing and Screen

		Casing and Screen Diameter	Depth to Pump Intake Setting (ft)	Depth to Top of Upper Screen (ft)	Depth to Bottom of Lowest Screen (ft)	Location of Pump Intake Setting
Los Alamos Field						
Well	LA-1	12-in. to 465, alternate 10" and 12" to 870	--	60	865	--
	LA-1B	12-in. to 650 ft; 10-in. to 1750 ft	360	326	1694	Blank
	LA-2	12-in. to 495, alternate 10" and 12" to 870	380	105	865	Screen
	LA-3	12-in. to 445, alternate 10" and 12" to 870	340	105	865	Screen
	LA-4	12-in. to 754 ft; 10-in. to 1965 ft	460	754	1964	Blank
	LA-5	12-in. to 580 ft; 10-in. to 1750 ft	500	440	1746	Blank
	LA-6	12-in. to 600 ft; 10-in to 1790 ft	300	420	1778	Blank
Guaje Field						
Well	G-1	12-in. to 490 ft; 10-in. to 2000 ft	465	490	1980	Blank
	G-1A	12-in. to 663 ft; 10-in. to 1519 ft	496	563	1513	Screen
	G-2	12-in. to 600 ft; 10-in. to 1970 ft	500	425	1960	Blank
	G-3	12-in. to 695 ft; 10-in. to 1792 ft	500	400	1785	Blank
	G-4	12-in. to 720 ft; 10-in. to 1930 ft	610	360	1925	Blank
	G-5	12-in. to 739 ft; 10-in. to 1840 ft	600	400	1830	Blank
	G-6	12-in. to 1530 ft	710	825	1525	Blank
Pajarito Field						
Well	PM-1	12-in. to 2499 ft	900	945	2494	Blank
	PM-2	14-in. to 2300 ft	950	1004	2295	Blank
	PM-3	14-in. to 2552 ft	830	956	2547	Blank
	PM-4	16-in. to 2875 ft	1150	1260	2854	Blank
	PM-5	16-in. to 3093 ft	1384	1440	3072	Blank

Note: Screen or perforated sections in wells in Los Alamos and Guaje fields (except G-6) are located at select depth intervals opposite permeable section of the aquifer; wells in the Pajarito field and well G-6 contain screen through the aquifer.

gravel pack and screen is probably enhanced because of the pressure drop as the water enters the well. Sand moving into and lingering in the gravel pack also restricts the movement of water into the well. In some wells sand is carried through the gravel pack into the pump. This tends to wear the pump out. Other sand pulled through the gravel pack falls to the bottom of the well covering screens that reduce the amount of water entering the well. Some restoration of yield in older wells can be accomplished by rehabilitation.

Three methods of well rehabilitation have been used at Los Alamos to try to improve the yield of the older wells. These methods are: (1) brushing and swabbing the casing and screen to remove scale and to rework the gravel pack, (2) using a sand pump to remove scale and sand covering screen at the bottom of the well, and (3) an underwater explosive detonation technique in screened sections to remove scale and work the gravel pack, combined with sand pump removal of scale and sand, from the bottom of the well.

The working of the well with a brush and using the brush as a swab to create pressure differences to pull sand through the gravel pack in a screen section has been used on most of the wells. The brush dislodges chemical precipitate scale that has accumulated on the interior of the well screen and casing. This type of rehabilitation is followed by use of a sand pump to remove the sand and scale from the bottom of the well. In some cases a sand pump alone may be used to produce some swabbing effect and remove accumulations from the well. In general these simple rehabilitation measures increase the yield from the well for a short time and then the yield again declines. However, these methods can also cause additional deterioration of performance by physically damaging the well screens, especially in older wells. Older wells are more susceptible to damage because of corrosion weakening the screens. The use of a heavy wire brush in one of the older wells (LA-4) apparently damaged the screen, breaking out louvers in the screen, so that the sand entrance into the well could not be controlled.

A proprietary technique employing small explosive charges detonated in screened sections to break loose and remove scale and work or loosen up the gravel pack was employed in 1987 in one of the older wells (G-3, completed in 1951). The overall effect on the well was adverse as a number of louvers were broken from the screen by the detonations. Additional louvers were broken by subsequent use of a sand pump to remove sand and scale from the bottom of the well. The broken screen permits significant amounts of formation sand and gravel pack to enter the well, restricting yield and precluding further use in the water supply system.

However, this experience provided some of the most revealing information on the possible condition of many of the oldest wells in the Guaje and Los Alamos well fields. A small bucket was suspended below each section of explosive charges. The bucket caught some of the louvers broken from the screen as well as the scale, sand, and some of the gravel pack from the screen. The condition of the louvers indicated that the sections were almost completely rusted through, showing little or no competent metal remaining. The louvers were essentially cemented in place only by the chemical precipitates. The louvers were encrusted and cemented with the gravel, also indicating that the gravel pack itself is probably partially cemented by the formation of calcium carbonate in the gravel pack. Because of the extensive metal corrosion, use of acid to remove calcium carbonate deposits will probably result in complete failure of the screen and casing. The casing and screen in the older wells have been so weakened by rusting and corrosion that severe well damage is likely to result from any further attempts at rehabilitation.

Damaged screen and casing can sometimes be repaired by running a liner through the damaged section. This was done on well G-4 in 1976. The liner was set below the reduction of the casing from 12-in. to 10-in. As the well continued to produce sand with the pumpage, the liner lost its effectiveness within a short time.

Rehabilitation efforts of these older wells are only a short-term correction of well problems. The yields can be increased for only short periods of time before the yields continue their declines. The weakening of the well screens by corrosion and rust precludes any further rehabilitation in most of the wells in the Los Alamos and Guaje fields. Deterioration of casing and screen that allows sand to enter the well results in excessive wear on the pump, thus shortening the life of the pump.

III. HISTORIES OF THE WELL FIELDS

A. General Production and Performance Data

The total use of water for the Laboratory and the community increased by 230 x 10^6 gal. in 1976. Water use in 1977 declined to about 1500 x 10^6 gal. and has varied since 1977 from about 1450 x 10^6 gal. in 1979 to 1625 x 10^6 gal. in 1985 (Fig. 11). The decline in 1977 was attributed largely to a rate increase for water used in the community. A trend line projection of future water demands was made in 1985 based on water use data from 1977 through 1985. The projection suggested an annual increase of about 17 x 10^6 gal. The 1986 production fell below the projected production by about 105 x 10^6 gal. (Fig. 1) (Purtymun 1987).

The cumulative contribution to water production for each well through 1986 and cumulative totals for each well field are presented in Table 3. The annual production from each well field is charted in Fig. 12. Since the mid-1960s, production from the Los Alamos and Guaje fields has generally declined, while production from the Pajarito field has increased. Production from the Los Alamos field has decreased most rapidly in the last several years because of well deterioration and because it has the largest energy cost.

Changes in performance characteristics of individual wells give an indication of well condition and the degree of deterioration that has occurred with time. Data on pumping rates and specific capacities were presented for each well at the time it was completed and in 1986 (Table 4). The pumping rate is influenced by several factors including the proportion of the well screen that is open, the well's specific capacity, the aquifer drawdown, and the need to throttle the well because of snagging. The pumping rate, in turn, strongly influences the cost of producing water from a given well. The specific capacity is often an important indicator of well deterioration. It is an indicator of the pressure difference needed to move water from the aquifer into the well and is influenced by the amount of chemical precipitation and cementation in the gravel pack and the well screen.

The condition of the aquifer in the vicinity of each well is indicated by the change in non-pumping water levels presented in Table 5. These values indicate the ability of the aquifer to recover from pumpage and suggest the amount of water that has been "mined" from the vicinity of each well.

Particularly significant data will be highlighted in subsequent discussions of individual well histories.

B. History of the Los Alamos Well Field

The Los Alamos field is the oldest well field consisting of seven wells (Fig. 1). In 1986, the field produced 179 x 10^6 gal. or about 12% of

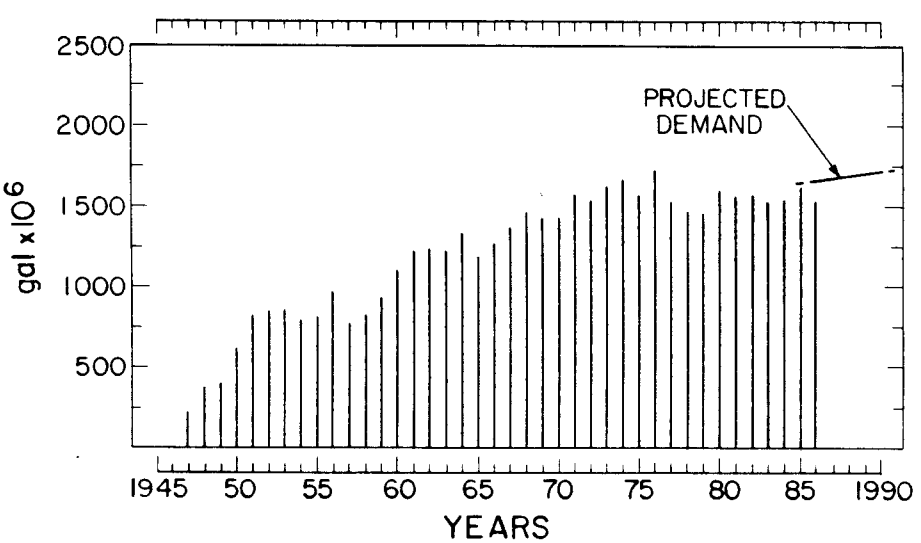

Figure 11. Water production 1947 to 1986 and projected demand 1986 to 1990 (Purtymun 1987).

Table 3. Production 1947-1986 and 1986

		1947-1986		1986	
		Pumpage x 10^6 gal	Percent of Total	Pumpage x 10^6 gal	Percent of Total
Los Alamos Field					
Well	LA-1	154	<1	0	0
	LA-1B	2,196	5	55	4
	LA-2	1,484	3	24	2
	LA-3	1,745	4	27	2
	LA-4	3,777	8	39	3
	LA-5	3,290	7	34	2
	LA-6	2,884	6	0	0
	Total	15,530	33	179	13
Guaje Field					
Well	G-1	2,630	6	30	2
	G-1A	3,380	7	130	9
	G-2	2,770	6	109	7
	G-3	2,183	5	27	2
	G-4	1,350	3	34	2
	G-5	3,082	6	52	4
	G-6	1,300	3	77	5
	Total	16,695	36	459	31
Pajarito Field					
Well	PM-1	1,941	4	74	5
	PM-2	6,330	14	84	6
	PM-3	4,429	10	246	16
	PM-4	1,539	3	307	20
	PM-5	149	<1	147	9
	Total	14,388	31	858	56
	Grand Total	46,613	100	1,496	100

the total well field production of 1,496 x 10^6 gal. (Table 3). The pumpage from the field from 1947 through 1986 has been 15,530 x 10^6 gal. At this writing, November 1987, production is from only three of the wells. Well LA-1 was abandoned in 1956 due to sand problem. Wells LA-4 and -5 are down for repairs. Damage to the screens of LA-4 may prevent the well from ever being put back on the line. Well LA-5 should be restored to production after the pump is repaired. Well LA-6 was taken out of active production in 1976 as the water from the well could no longer meet drinking water standards for arsenic content.

1. Well LA-1. Well LA-1 was used from 1947-1952 and again in 1955 and 1956, with a production of 154 x 10^6 gal. The well, completed in 1946, had large amounts of sand produced with the pumpage. The sand wore the pump out and reduced the pumping rate by covering the screen at the bottom of the well. Rehabilitation of the well has included reworking the gravel pack by

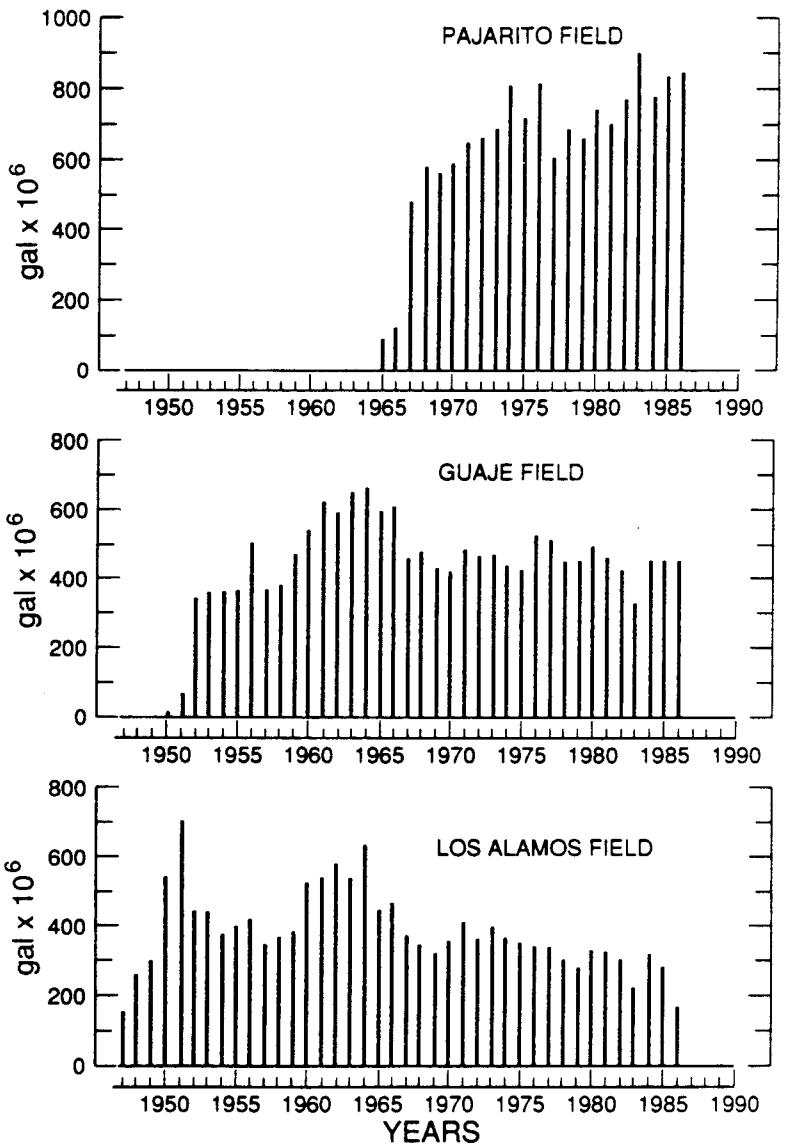

Figure 12. Annual production from Pajarito, Guaje, and Los Alamos fields.

swabbing the well and a reported treatment of acid to dissolve the scale. The acid not only removed the scale, but probably enlarged the screen openings and broke down the formation, which increased the sand content with the pumpage. The pump was pulled from the well in the late 1950s. It was open to 598 ft with only 67% of the 805 ft of screen open. Since that time, the well has been used only as an observation well to monitor the water level changes in the upper part of the aquifer in the lower part of the Los Alamos field. The water level fluctuations in the well reflect the pumpage from LA-1B. The condition of the well precludes its use for part of the water supply.

2. Well LA-1B. Well LA-1B, drilled to replace LA-1, is located about 150 ft northeast of LA-1. The pumpage from the well from 1960-1986 has been 2,196 x 10^6 gal. When the well

Table 4. Comparison of Pumping Rate and Specific Capacity

		Pumping Rate (gpm)			Specific Capacity (gpm/ft drawdown)		
		Completion	Current	Change (±)	Completion	Current	Change (±)
Los Alamos Field							
Well	LA-1	260 (47)	--	--	--	--	--
	LA-1B	558 (61)	573 (86)	+15	5.6 (61)	4.8 (86)	-0.8
	LA-2	423 (50)	312 (86)	-111	1.9 (50)	1.8 (86)	-0.1
	LA-3	345 (50)	338 (86)	-7	2.6 (50)	2.0 (86)	-0.6
	LA-4	631 (50)	552 (86)	-79	8.4 (50)	5.9 (86)	-2.5
	LA-5	535 (50)	419 (86)	-116	4.4 (50)	2.9 (86)	-1.5
	LA-6	623 (50)	--	--	11.8 (50)	--	--
Guaje Field							
Well	G-1	538 (50)	249 (86)	-289	5.0 (50)	1.5 (86)	-3.5
	G-1A	577 (55)	468 (86)	-109	11.3 (55)	11.4 (86)	+0.1
	G-2	550 (52)	382 (86)	-168	11.5 (52)	14.7 (86)	+3.2
	G-3	458 (52)	196 (86)	-262	9.5 (52)	1.9 (86)	-7.6
	G-4	395 (52)	211 (86)	-184	3.9 (52)	1.2 (86)	-2.7
	G-5	477 (52)	394 (86)	-83	8.2 (52)	9.6 (86)	+1.4
	G-6	392 (64)	293 (86)	-99	5.0 (64)	3.8 (86)	-1.2
Pajarito Field							
Well	PM-1	600 (65)	578 (86)	-22	15.0 (65)	26.3 (86)	+11.3
	PM-2	1425 (66)	1359 (86)	-66	22.6 (66)	21.2 (86)	-1.4
	PM-3	1342 (68)	1397 (86)	+55	47.9 (68)	58.2 (86)	+10.3
	PM-4	1460 (82)	1305 (86)	-155	35.6 (82)	37.3 (86)	+1.7
	PM-5	--	1199 (86)	--	--	--	--

Note: Numbers in parentheses are year of measurement.

Table 5. Comparison of Nonpumping Water Levels

		(ft)		
		Completion	Current	Change (± ft)
Los Alamos Field				
Well	LA-1	F (46)	34 (86)	-34
	LA-1B	+34 (60)	25 (86)	-59
	LA-2	F (46)	74 (86)	-74
	LA-3	F (47)	88 (86)	-88
	LA-4	189 (48)	284 (86)	-95
	LA-5	71 (48)	168 (86)	-97
	LA-6	2 (48)	92 (85)	-90
Guaje Field				
Well	G-1	192 (51)	279 (86)	-87
	G-1A	265 (55)	310 (86)	-45
	G-2	279 (52)	369 (86)	-90
	G-3	310 (52)	375 (86)	-65
	G-4	357 (52)	396 (86)	-39
	G-5	417 (52)	453 (86)	-36
	G-6	576 (64)	576 (86)	0
Pajarito Field				
Well	PM-1	746 (65)	748 (86)	-2
	PM-2	826 (66)	851 (86)	-25
	PM-3	743 (68)	763 (86)	-20
	PM-4	1050 (82)	1084 (86)	-34
	PM-5	--	--	--

Note: Numbers in parentheses are year of measurement; F indicates flowing well while +34 indicates flowing well (water level above land surface).

was completed, it was artesian with a head of about 34 ft. Pumpage has reduced the artesian pressure and the nonpumping water level had declined to 25 ft below land surface in 1986 or a total decline of about 59 ft (Table 5). The well was logged with the downhole video camera in 1983. At that time the well was open to a depth of 1,655 ft with 576 ft or 97% of the 591 ft of perforation open. The lower 95 ft of the well was filled with sand that had moved through the gravel pack and perforations into the well. The well pumping at 573 gallons per minute (gpm) has about 119 ft of drawdown and there is little, if any, sand produced with the pumpage. The video tape of the hole revealed a slight bend in the casing at a depth of 385 to 405 ft as indicated by the roll of the camera. The casing reduces in size from 12-in. to 10-in. at a depth of 650 ft (Table 2). As the well is cased with wrought iron pipe, no attempt should be made to bail or remove sand from the bottom of the well. Overall, the well is considered to be in fair condition and is likely to be usable for as much as 20 years more.

3. **Well LA-2.** The pumpage from well LA-2 from 1947-1986 was 1,484 x 10^6 gal. The well when completed was artesian. The nonpumping water level declined from flowing in 1946 to a depth of 76 ft below land surface. The pump was last removed from the well in 1962 and 1963. The well had accumulated little or no sand during the

one year of pumping. It appears that the well makes very little sand; however, the pumping rate must be held around 300 gpm with limited pumping time, 12 hours or less, or the pumping level will decline to the level of the pump intake. The well is considered to be in only fair condition and is likely to be usable for no more than another 10 years.

4. Well LA-3. The pumpage from well LA-3 from 1947-1986 was 1,745 x 10^6 gal. The pumping rate and the specific capacity have not changed significantly. The well was artesian when completed with nonpumping water level declining to about 88 ft below land surface in 1986. The pump was removed from the well in 1983. At that time, the well was open to a depth of about 816 ft; about 92% of the 760 ft of perforations was open. The scale was removed from the casing and perforations with a wire brush. The well produces sand with the pumpage at high discharge rates. The pumping rate should be maintained around 300 gpm, which will result in a drawdown of less than 150 ft. A drawdown greater than 150 ft will result in water and sand cascading into the well, which will cause excess wear on the pump and will decrease the well efficiency by sand accumulating and covering up the perforations. The well is considered to be in fair condition and is likely to be usable for no more than another 10 years.

5. Well LA-4. The pumpage from well LA-4 from 1948-1986 was 3,777 x 10^6 gal. The pumping rate decrease, the specific capacity decline from 8.6 to 5.9 gpm/ft of drawdown, and the 95 ft nonpumping water level decline indicate some deterioration of the well. The line shaft turbine pump failed in early 1987 and was pulled and replaced with a submersible. The hole was logged with the downhole video camera in July 1987 and was found open to 1,921 ft. A heavy wire brush was used to clean scale off the casing and screen. The scale and formation sand were removed to a depth of 1,942 ft in late July. The new pump was run in the hole, but testing indicated that the pumpage contained large amounts of sand. The well was shut down and several tests were run at discharge rates ranging from 351 to 525 gpm. The tests ranging from 2 to 4.5 hours indicated little or no sand in the pumpage. The well was put back on the line at about 525 gpm; however, after several hours of pumping, a large amount of sand occurred in the discharge. To prevent damage to the new pump and the pumps in the booster station the well was again taken off the line. The future action to be taken with the well has not been decided. Before removal of the pump early in 1987, the pumpage from the well contained little or no sand at a high pumping rate. The video log of the well in April 1987, before rehabilitation, indicated no damage to the casing or screen. The presence of large amounts of sand occurring periodically in the pumpage indicates that the casing, screen, or the reduction between the 12-in. and 10-in. was ruptured during the rehabilitation of the well.

The pump was pulled from the well in January 1988. Two video logs were run of the well. The log of February 3, 1988, was to the total depth of the well at 1 907 ft. The second log was run March 1, 1988, to a depth of about 780 ft. The logs indicated that the casing has separated at a depth of about 750 ft where the casing reduces from 12-in. to 10-in. diameter. It may be possible to repair the separation if the condition of the casing has not deteriorated because of corrosion and can stand the pressure of swedge inserted between the 12-in. and 10-in. diameter.

During 38 hours of pumping, including testing, during August 1987, about 35 ft of sediment had accumulated in the well. The depth of the well was reduced from 1942 ft to 1907 ft. The accumulation of sand in the well over a short period of pumping indicates the serious nature of the separation.

6. Well LA-5. The pumpage from well LA-5 from 1948-1986 was 3,290 x 10^6 gal. The well was sounded in 1962 (the last time the pump was removed from the well) at a depth of 1,954 ft. It was apparent that the pilot hole below the bottom of the casing was open for more than 200 ft. The pumping rate declined from 535 gpm in 1950 to 419 gpm in 1986 and the specific capacity decline from 4.4 to 2.9 gpm/ft of drawdown showed deterioration in the efficiency of the well. The nonpumping level declined about 97 ft from 1950 to 1986. The well produces little or no sand with the pumpage. The well is equipped with a line-shaft turbine pump, but needs a larger line-shaft to keep the pump in adjustment. In the summer of 1987, the line shaft separated. The well

is currently down for repairs. The well is considered to be in fair condition and is likely to be usable for no more than another 10 years.

7. **Well LA-6.** The production from well LA-6 was 2,884 x 10^6 gal. from 1948-1976. The well was taken off line in 1976 because of excessive arsenic in the water. The concentration of arsenic in the water had increased over time so that it could no longer be diluted with pumpage from other wells in the field to meet Federal Drinking Water Standards. During 1976, sand was used to pack off sections of the well from the bottom up to test various zones in an attempt to determine the source of the high arsenic concentrations (Purtymun 1977a). During this work, the tail pipe of a pump was lost in the sand at a depth of about 1,200 ft and, subsequently, a "fishing tool" and cable was lost at that depth trying to remove the tail pipe. The well had 400 ft of perforations or screen of which 210 ft or 53% of the perforations are above the tail pipe and fishing tool. Before these problems occurred, the well had been a good producer. The pumping rate declined only modestly and the specific capacity actually increased. With the effective depth of the well reduced to 1,200 ft, the well could sustain a pumping rate of about 580 gpm with a drawdown of about 60 ft. The well flowed water under artesian pressure at one time during construction. At the present time the well is not used in the system, nor are there any future plans to use the well because of the water quality.

C. History of the Guaje Well Field

The Guaje field consists of seven wells (Fig. 1). Wells G-1, -2, -3, -4, and -5 were completed in 1950-1951. Well G-1A was added in 1954 and G-6 was added in 1964 to offset the declining production of the other wells in the field. The production from the field during 1950-1986 was 16,695 x 10^6 gal. In 1986 the field produced 460 x 10^6 gal. or about 31% of the total well field production of 1,496 x 10^6 gal.

1. **Well G-1.** The pumpage from well G-1 was 2,630 x 10^6 gal. from 1950-1986. The well was last sounded in 1962 and was open to a depth of 1,750 ft with 576 ft or 86% of the screen open. No rehabilitation was undertaken at that time. The considerable decline in both pumping rate and specific capacity indicates significant deterioration of the well. The deterioration is probably a combination of scale forming on the screen, deterioration of the gravel pack, and sand covering the screen openings in the bottom of the well. The nonpumping water level declined from 192 ft in 1951 to 279 ft in 1986 or about 87 ft (Table 5). The well is considered to be in fair condition, but because of limited yield is likely to be usable for no more than 10 years.

2. **Well G-1A.** Well G-1A was drilled in 1954 to supplement the declining production of the five original wells in the well field. The well produced 3,380 x 10^6 gal. from 1954-1986 or about 20% of the total field production (Table 3). The pump was removed in 1973 and sediments were cleaned out of the well to a depth of 1,500 ft. The sediment left in the well covered only 10 ft of the 563 ft of screen in the well. The pumping rate has declined only modestly and the specific capacity has remained about constant. Overall, the well is considered to be in fair condition and is likely to be usable for as much as 20 years more.

3. **Well G-2.** The production from well G-2 was 2,770 x 10^6 gal. or about 17% of the total pumpage from 1950-1986. The pump was removed in 1981 for the first time since it was installed in 1950. During rehabilitation, the scale was removed from the casing and screen using a wire brush. The sand in the well was removed to a depth of 1,707 ft. A section of 1/2-in.-airline in the well prevented the removal of sand to the total depth of the well. Of the 425 ft of screen in the well, 385 ft or 91% of the screen was open. A video log was made of the well, which contained some interesting views of the screen and aquifer. The bore hole log showed water cascading through screened sections at depths of 285 to 295 ft, 300 to 310 ft, and 320 to 330 ft. The water level on December 18, 1981, was at 355 ft and on January 11, 1982, was at 333 ft. The water level in G2 fluctuates due to pumping of well G-1A about 1250 ft to the southwest. The pumping rate has declined from 550 gpm in 1952 to 382 gpm in 1986. The specific capacities appear to have increased from 11.7 gpm/ft of drawdown in 1952 to 14.7 gpm/ft of drawdown in 1986. The apparent increase is due to heavy pumpage of the well that does not allow the nonpumping level to make a

complete recovery and does not accurately measure well efficiency. The nonpumping water level has declined from 279 ft in 1953 to 382 ft in 1986. Overall, the well is considered to be in fair condition but because of declining yield is likely to be usable for no more than about 10 years.

4. Well G-3. The pumpage from well G-3 was 2,183 x 10^6 gal. from 1952-1986. Several attempts have been made to rehabilitate the well since 1975 to increase the yield. The rehabilitation efforts have failed to increase the yield. The pumping rate has declined from 458 gpm in 1950 and 196 gpm in 1986. The specific capacity of the well declined from 9.5 gpm/ft of drawdown in 1950 to 1.9 gpm/ft of drawdown in 1986 indicating significant well deterioration. During well rehabilitation in the winter of 1975-1976, the depth sounded was 1,558 ft. After the scale was removed from the casing and screen, the well was swabbed to try to work the gravel pack free of possible formation of calcium carbonate. The well was cleaned out to a depth of 1,601 ft before the pump was replaced in the well.

The pump was again removed from the well in January 1984, and the well was found to be filled with sediments to a depth of 1,304 ft. After rehabilitation, the sand and scale were removed from the well to a depth of 1,631 ft. The pumping rate and specific capacity declined rapidly from 1984-1986. The pump was removed from the well in June 1987. The well was logged to a depth of 1,492 ft. A proprietary explosive technique was tried to develop and rehabilitate the well. Small explosive charges were set off in 22 sections of screen to a depth of 1,492 ft. The well was examined with the downhole camera. The explosive shock waves had dislodged louvers leaving holes in the screen at 527, 757, 893, 957, and 1117, and in the section from 1,220 to 1,230 ft. Scale, formation sand, and gravel pack had entered and filled the hole to a depth of 1,431 ft. The well was developed by running a bailer up and down the hole to remove the remaining scale from the casing and screen as well as to move and open the gravel pack. At the end of 6 hours of development the hole was filled to a depth of 1,384 ft. After several days of additional development using a sand pump as a swab, the depth was at 1,238 ft. At that time only 280 ft of the 400 ft, or 70%, of screen in the well remained open. The sand and gravel pack were entering the hole faster than it could be removed. Further development and bailing of sand and gravel pack were terminated and the pump was replaced for further testing to assess the results of the explosive type of rehabilitation and development. Initial testing at a low discharge rate, 200 gpm, indicated that the well was making a large amount of sand. Additional testing is planned for late winter or early spring 1988. Depending on the amount of damage to the well screen, it may be that the well will no longer be usable.

5. Well G-4. Pumpage from well G-4 was 1,350 x 10^6 gal. from 1952-1986. The pump was removed from the well in 1981. The depth was at 1,172 ft. No rehabilitation was attempted. Only 100 ft or 25% of the 400 ft of screen in the well was open. Significant declines in both the pumping rate and the specific capacity of the well indicate serious deterioration (Table 4). The nonpumping water level declined from 357 ft in 1952 to 396 ft in 1986. The distance between G-4 and G-5 is about 2,500 ft; however, the pumping of one well affects the water levels in the other.

The well was badly damaged during construction. After completion in 1952, low yield from the well indicated well damage. The pump was pulled and a caliper log run of the well indicated that it was open to a depth of 1,381 ft. The caliper indicated no detectable breaks or holes in the screen or casing above 1,381 ft. An obstruction in the well prevented any removal of sediments below 1,381 ft. The pump was pulled from the well in February 1974, and the well was only open to a depth of 750 ft indicating that 1,215 ft of sediment had collected in the bottom of the well. Sediments were cleaned out to a depth of 1,185 ft when a sand pump was lost in the well. A video log of the hole was run to a depth of 1,167 ft and showed a few louvers out of the screen at a depth of about 765 ft. The sand pump was recovered and the well was cleaned out to a depth of 1,756 ft. A number of louvers, scrap iron, rags, and gloves were recovered at about 1,380 ft, the depth of the obstruction noted in 1952. A second run with the video log was made to a depth of 1,492 ft (limit of the equipment) that showed well screen damage from 1,270 to 1,290 ft, 1,312 to 1,332 ft, and 1,383 to 1,393 ft. It was quite evident that during construction and emplacement of the

gravel pack, the drop lines with external couplings feeding the gravel into the annulus between the casing and the hole wall tore the louvers from the screen. A slotted liner was run into the well to compensate for the damaged section. The liner, "belled-out" at the top, was 7-1/2 in. o.d. and was about 536 ft long. The bottom of the liner was set at 1,750 ft with the "belled-out" end set in the blank casing of the well at a depth of 1,214 ft. The yield of the well initially increased from about 280 gpm to around 400 gpm. At the higher yield, the well produced sand with the pumpage. The pump was pulled in 1981. Sand containing some gravel pack had accumulated to a depth of 1,150 ft. The well was cleaned out to a depth of 1,172 ft and the pump was replaced in the well. The pump failed and was pulled for repairs in 1985. The depth of the well was about 1,123 ft. No rehabilitation was attempted. The well is considered to be in poor condition and is unlikely to be usable for more than 10 years.

6. Well G-5. The pumpage from well G-5 was 3,082 x 10^6 gal. or 18% of total field production from 1952-1986 (Table 3). No major changes have occurred in the pumping rate, specific capacity, or nonpumping water level. The line shaft turbine originally installed in the well was replaced with a submersible in 1958. At that time the well was open to a depth of 673 ft. In 1975 the pump was removed for repairs and the sediments were removed to a depth of 912 ft. No attempt was made to remove sediments from the well below 912 ft because of significant well screen damage between 700 and 912 ft. The well bore filled with sand and gravel faster than it could be bailed from the hole. There were two badly damaged sections of screen at 710 to 714 ft and 738 to 740 ft. Large cobbles, 4 to 6-in. in diameter could be seen outside the casing with no gravel pack remaining in back of the damaged screen. The pump has been removed several times since 1975; however, due to the damage to the casing below 700 ft, no rehabilitation of the well has been undertaken other than removing scale for the screen and casing above the reduction in the casing at 700 ft. Sediments and sand had accumulated in the well to a depth of about 700 ft when the wells was measured again in 1979.

The damage to the casing probably occurred when the well was constructed or when the test pump was dropped into the well during testing in 1950. The pump was fished out of the well. Although only 100 of the 400 ft of screen in the well are above the 700 ft depth, the well has been and has continued to be one of the best and most reliable wells in the field (18% of total production from the field). However, because of its age and the damaged screen, the well is considered to be in poor condition and it is unlikely that it will be usable for more than 10 years.

7. Well G-6. Well G-6 was added to the well field in 1964 to replace the declining production from the other wells in the field. Since 1964, the production through 1986 was 1,300 x 10^6 gal. The pump was removed in April 1979 for repairs and the sand was removed from the well to a depth of 1,510 ft. In December of 1979, the pump was again removed for adjustment and the hole was open only to 1,480 ft. The pumping rate and the specific capacity have declined significantly. These changes and the amount of sand production indicates that considerable well deterioration has occurred in the past few years. At startup the pumpage contains excessive amounts of sand and gravel pack. The discharge is pumped to waste for the first few minutes to keep part of the sand and gravel pack out of the distribution system. The continued deterioration of the well, as shown by production characteristics, indicates that it should be replaced within 10 years.

D. History of the Pajarito Well Field

The Pajarito field consists of five wells (Fig. 1). The field was developed from 1965-1982. The field was developed to meet a small increasing demand for water and to supplement the declining production from the Los Alamos and Guaje fields. The production from the field from 1965-1986 was 14,388 x 10^6 gal. or 31% of all production (Table 3). Four of the wells in this field are considered high yield wells (pumping rates in excess of 1,000 gpm).

1. Well PM-1. The pumpage from well PM-1 was 1,941 x 10^6 gal. from 1965-1986. The pump was pulled in 1973 and was open to a depth of 2,479 ft. Only about 1% of the 1,549 ft of screen was covered with sediments. There was no rehabilitation of the well. The pump was repaired

and replaced in the well. The pumping rate has declined slightly and the specific capacity has increased from about 15 gpm/ft of drawdown in 1965 to 26.3 gpm/ft of drawdown in 1986. The increased specific capacity results from further developing the well by setting the gravel pack, as well as cleaning the gravel pack and aquifer of residual drilling muds. The further development of the well is also evident from the insignificant 2 ft change of the nonpumping water level (Table 5). The well produces sand in the pumpage at the start. A sand separator is used to remove sand from water as there is usage before the first storage tank, which separates the sand from the water. The well is considered to be in good condition and is likely to be usable for 20 to 30 years.

2. Well PM-2. The pumpage from well PM-2 was 6,330 x 10^6 gal. from 1966-1986. The pump was pulled for rehabilitation in 1987. The well was open to a depth of 2,283 ft. The blank casing and screen were worked over using a bailer or sand pump. This removed the outer scale from the casing and screen and reworked the gravel pack. The pumping rate, specific capacity, and nonpumping water level have only declined slightly. The well is a high-yield well and had a pumping rate of over 1,350 gpm in the fall of 1987. The well has produced more water than any other well in the three well fields. The well is considered to be in good condition and is likely to be usable for 20 to 30 years.

3. Well PM-3. Pumpage from well PM-3 was 4,429 x 10^6 gal. from 1966-1986. The pumping rate and the specific capacity have increased slightly since completion. The nonpumping water level has declined only 20 ft. The well has the lowest amount of drawdown and largest specific capacity of any well in the three well fields. Well PM-3 is a high-yield well with the production second highest of any well in the three fields. The pump, a line shaft turbine, has not been removed from the well since it was installed in 1966. The well is considered to be in good condition and is likely to be usable for 20 to 30 years.

4. Well PM-4. Well PM-4 is a relatively new well that was added to the field in 1982. The well produced 1,539 x 10^6 gal. from 1982-1986. The well is equipped with a line shaft turbine driven by a natural gas engine. A slight change in engine performance readily affects the pumping rate. The pumping rate declined from about 1,460 gpm in 1982 to about 1,305 gpm in 1986. This decline may have been caused by engine performance. This decline in gpm does not reflect well deterioration as the specific capacity increased slightly from 35.6 gpm/ft of drawdown to 37.3 gpm/ft of drawdown in 1986. The nonpumping water level declined from 1,050 ft to 1,084 ft during the same period. The well is considered to be in good condition and is likely to be usable for 30 years.

5. Well PM-5. Well PM-5 was the last well added to the system. The well was completed in 1982 and placed on line in 1985. The production from the well from 1985-1986 was 149 x 10^6 gal. The pumping rate is about 1,200 gpm. Due to the presence of drilling mud in the access line for the transducer, no water levels have been recorded since the well was tested. At that time the water level was about 1,210 ft below the surface of the mesa. The well is considered to be in good condition and is likely to be usable for 30 years.

IV. WELL FIELD PRODUCTION CAPACITIES

Well field and transmission system capacities limit the ability to meet peak demand requirements. Peak demand typically occurs during the summer months when temperatures and landscape irrigation requirements are highest. Current maximum production capabilities are only slightly greater than the historic maximum peak demand period. Maximum well field yields are given as the total of all wells in a field pumping at their rated current yields. Firm yield is taken to be the maximum yield reduced by the yield of the largest producing well in that field. Maximum yield and firm yield are over a 24-hour period. For the Los Alamos and Guaje lines, maximum transmission system capacities are determined by assuming all pumps in the booster stations are functioning. Firm transmission system capacity is the maximum reduced by the rated capacity of the largest pump. The Pajarito field can supply water to different parts of the distribution system, and transmission system capacity cannot be readily defined.

The maximum yield from the Los Alamos field in 1986 was 1,610 gpm or 2.32 million gallons per day (mgd), whereas the firm yield was 1,040 gpm or 1.50 mgd (Table 6). The booster capacity to transfer water through the four pumping stations into storage in the Laboratory and townsite has a maximum capacity of 3,000 gpm or 4.32 mgd, and a firm capacity of 2,000 gpm or 2.88 mgd (Table 6). The maximum and firm yield from the well field is much less than the maximum and firm capacity of the booster stations. The maximum yield from the Los Alamos well field could be nearly doubled to use maximum booster capacity. The increase cannot be accomplished by the rehabilitation of the present wells; it could be realized by the addition of new wells constructed with the latest methods.

The maximum yield for the Guaje field in 1986 was 2,000 gpm or 2.88 mgd, whereas the firm yield was 1,530 gpm or 2.20 mgd (Table 7). The four booster stations that transfer water from the field to the Laboratory and townsite have a maximum capacity of 3,000 gpm or 4.32 mgd, and a firm capacity of 2,000 gpm or 2.88 mgd (Table 7). The maximum yield from the well field could be increased by about 50% to make full use of the maximum booster capacity. This cannot be accomplished by well rehabilitation because of the current conditions of the wells, but it must be accomplished by addition of new wells to the field.

The maximum yield for the Pajarito field in 1986 was 5,845 gpm or 8.42 mgd, whereas the firm yield is 4,445 gpm or 6.40 mgd (Table 8). Wells PM-1 and -3 pump water to the community of White Rock or into storage that serves White Rock and Pajarito Acres. If necessary, water from storage can also be pumped into the next series of boosters, which will distribute the water to storage in the townsite area and the Laboratory. Wells PM-2, -4, and -5 pump to booster station 2, which backflows water for distribution in White Rock and Pajarito Acres or can pump it to Pajarito Booster 3 and then into storage for the Laboratory or townsite.

Table 6. Los Alamos Field

	Summary Well Capacity			
	Maximum Yield (1986)		Firm Yield (1986)	
Well	gpm	mgd	gpm	mgd
LA-1[a]	0	0	0	0
LA-1B	570	0.82	--	--
LA-2	300	0.43	300	0.43
LA-3	340	0.49	340	0.49
LA-4[b]	0	0	0	0
LA-5[c]	400	0.58	400	0.58
LA-6[d]	0	0	0	0
Total	1610	2.32	1040	1.50

[a]Well abandoned.
[b]Well damage; probably will never be placed back on line.
[c]Well down for repairs (November 1987).
[d]Standby - chemical problem.

Summary Booster Capacity

Maximum Booster Capacity - 3000 gpm: 4.32 gpd
Firm Booster Capacity - 2000 gpm: 2.88 gpd

Table 7. Guaje Field

	Summary Well Capacity			
	Maximum Yield (1986)		Firm Yield (1986)	
Well	gpm	mgd	gpm	mgd
G-1	250	0.36	250	0.36
G-1A	470	0.68	--	--
G-2	380	0.55	380	0.55
G-3[a]	0	0	0	0
G-4	210	0.30	210	0.30
G-5	395	0.57	395	0.57
G-6	295	0.42	295	0.42
Total	2000	2.88	1530	2.20

[a]Well damaged; probably never will be placed back on line.

Summary Booster Capacity

Maximum Booster Capacity - 3000 gpm: 4.32 gpd
Firm Booster Capacity - 2000 gpm: 2.88 gpd

Table 8. Pajarito Field

	Summary Well Capacity			
	Maximum Yield (1986)		Firm Yield (1986)	
Well	gpm	mgd	gpm	mgd
PM-1	580	0.83	580	0.83
PM-2	1360	1.96	1360	1.96
PM-3	1400	2.02	--	--
PM-4	1305	1.88	1305	1.88
PM-5	1200	1.73	1200	1.73
Total	5845	8.42	4445	6.40

Table 9. Peak Demand Periods - 1976
(June 11 - July 12)

No. of Days	32
Total Production	299×10^6 gal.
Average Daily Production	9.3×10^6 gal.

No. of Days Exceeding (gal.)	Days
10×10^6	14
9×10^6	9
8×10^6	4
7×10^6	3
$<7 \times 10^6$	2

Maximum and Firm Yield - 1986

Field	Maximum ($\times 10^6$ gpd)	Firm ($\times 10^6$ gpd)
Los Alamos	2.32	1.50
Guaje	2.88	2.20
Pajarito	8.42	6.40
	13.62	10.10

V. PEAK DEMAND

The historical maximum peak demand period occurred during the summer of 1976. The peak demand period was 32 days, from June 11 through July 12. During that time, 299×10^6 gal. was pumped or an average of 9.3×10^6 gpd. Fourteen days exceeded 10×10^6 gpd (Table 9).

The daily maximum yield from the three well fields in 1986 was 13.62×10^6 gal. and the firm yield was 10.1×10^6 gal. Thus, the system could probably meet a peak demand period similar to the one that occurred in 1976 if all major producing wells in the three fields are operating. However, the maximum and firm yields from the three fields can be expected to continue to decline as the older wells deteriorate. At present, six wells (LA-1, 2, -3, -4, -5, and -6) in the Los Alamos field and six wells in the Guaje field (G-1, -2, -3, -4, -5, and -6) will have to be replaced in the next 10 years to meet present and future demands.

VI. PUMPING SCHEDULE

The cost of operating various wells and well fields differ based on power consumption, which, in part, is based on yield and location. A detailed pumping schedule has been designed to minimize the cost of well field operations (Foreman 1985). The schedule does not consider the present well characteristics or conditions (1987). In general, when a well pumping rate falls below 300 gpm, it is excessively expensive to operate. The schedule is an idealized guideline; it can be modified as needed to accommodate the actual demand and to account for equipment down for maintenance or repair.

The schedule for operation of the wells (in hours/month) is detailed in Table 10. Pumping times for each well are based on expense of operation modified by considerations of controlling water quantity.

Table 10. Monthly Pumping Schedule (in hours) for Individual Wells[a]

Los Alamos Field

Wells LA-1B, -2, -3, -4, and -5 are to be pumped 18 hours monthly

Guaje Field	G-1	G-1A	G-2	G-3	G-4	G-5	G-6
January	36	350	350	200	200	350	350
February	36	300	300	100	100	300	160
March	36	300	300	100	100	300	160
April	36	400	400	200	200	400	355
May	36	400	400	200	200	400	355
June	36	400	400	200	200	400	355
July	36	400	400	200	200	400	355
August	36	400	400	200	200	400	355
September	36	400	400	200	200	400	355
October	36	300	400	200	200	400	355
November	36	300	400	200	200	400	355
December	36	300	300	100	100	400	160

Pajarito Field	PM-1	PM-2	PM-3	PM-4	PM-5
January	50	180	300	240	100
February	50	180	300	170	100
March	50	180	300	170	100
April	50	300	300	240	100
May	300	350	550	500	450
June	300	350	550	500	450
July	250	320	500	500	450
August	150	280	480	500	450
September	100	220	480	300	450
October	50	180	225	210	100
November	50	180	300	210	100
December	50	180	300	170	100

[a]Summary reference (Foreman 1985); at present time (1987) wells LA-4 and G-3 are not in use due to well damage.

The Los Alamos field is the most expensive to operate. Wells in this field need to be pumped a minimum of about 4 hours a week to prevent bacterial growth. They are pumped more than four hours a week just to meet actual demand or maintain fresh water in the lines.

The Guaje field is more cost effective to operate. Well G-1 is the most expensive well in the field and needs to be run 8 hours per week to prevent bacterial growth in the well and lines. All other wells in the Guaje field are generally not pumped more than the number of hours shown in Table 10 for each month. If circumstances require that some wells are used more than the ideal amount, then use in future months should be reduced so that the total number of pumping hours over the year is not exceeded.

The Pajarito field includes the highest yielding wells. Wells PM-1 and -3 are used mainly to serve White Rock and Pajarito Acres, with water being pumped to Pajarito Booster 2 only when absolutely necessary. The schedule indicates that most of the water used in White Rock and Pajarito Acres is pumped from PM-3 as it is less expensive to operate than PM-1. Water from wells PM-2, -4 and -5 is generally not directed to the White Rock tank unless that is the only way to meet actual demand in White Rock and Pajarito Acres. Wells PM-2 and PM-4 are located close to each other and excessive pumping in one well may affect the water level in the other well. Thus, the recommended total pumpage from the two wells is not normally exceeded.

VII. DEVELOPMENT OF ADDITIONAL WATER SUPPLY

Replacement of wells in the Los Alamos and Guaje fields and additions to the Pajarito field will be necessary to meet the current demand as well as the projected future demand. The status of all the existing wells is summarized in Table 11. The deterioration of the wells in the two older well fields will gradually reduce the yield until current demand cannot be met. As discussed in the section on well field histories, it is likely that at least six wells in the Los Alamos field and six wells in the Guaje field will have to be replaced in the next 10 years (Table 11).

The large number of wells in the Los Alamos vicinity and the long production histories provide a solid basis for recommendations for location and development of new and replacement wells. The recommendations in this report are elaborations of basic concepts presented in a previous report, "Hydrologic Characteristics of the Main Aquifer in the Los Alamos Area: Development of Ground Water Supplies" (Purtymun 1984a). That report contains sections describing drilling conditions, geologic and geophysical logs, and well construction techniques applicable in the Los Alamos area that should aid in the construction of new or replacement wells.

A. Geologic and Hydrologic Consideration

The main aquifer extends from the Rio Grande westward beneath the Pajarito Plateau and rises stratigraphically through the Tesuque Formation into the lower part of the Puye Conglomerate. The Puye Conglomerate is an important part of the main aquifer. The coarse volcanic debris within the conglomerate yields water readily to wells and, in part, allows the development of high-yield, low-drawdown wells in the area. The conglomerate attains its greatest thickness in a north-south trending basin beneath the central part of the plateau as shown in Fig. 13. The Tesuque Formation beneath the plateau is saturated and is the main source of water supply. The sediments of the Tesuque Formation become coarser westward from the Rio Grande; the upper beds become younger with the westward dip. This coarse sediment aids in the development of high-yield wells in the same general area.

The locations of future wells in this area must be chosen carefully because wells placed too far west will encounter hard volcanic rocks of the Tschicoma Formation, which do not yield water readily. A well that is completed in or near the outcrop of Tschicoma would not yield an appreciable amount of water because the rocks are relatively impermeable and they form a barrier to the east and southeast movement of groundwater in the main aquifer. Wells placed too far to the east encounter thick basalts, which constitute difficult drilling and may not yield water readily. The siltstones and fine-grained sandstones of the Tesuque Formation do not yield water as well as the coarser sediments found further to the west.

Proposed locations and staging for new and replacement wells in each of the three fields are discussed in the next three sections.

Table 11. Well Characteristics

Field and Well	Age	Yield (gpm)	Yield[a]	Well Condition[b]	Maximum Remaining Life	Remarks
Los Alamos Field						
LA-1	41	0	None	Poor	0	
LA-1B	27	573	Adequate	Fair	20	
LA-2	41	312	Adequate	Fair	10	
LA-3	40	338	Adequate	Fair	10	
LA-4	39	0	None	Poor	0	
LA-5	39	419	Adequate	Fair	10	Pump failure (1987)
LA-6	37	0	None	Poor	0	Arsenic above MPC[c]
Guaje Field						
G-1	37	249	Marginal	Fair	10	
G-1A	33	468	Adequate	Fair	20	
G-2	36	382	Adequate	Fair	10	
G-3	36	0	None	Poor	0	
G-4	36	211	Marginal	Poor	10	
G-5	36	394	Adequate	Poor	10	
G-6	23	293	Marginal	Poor	10	
Pajarito Field						
PM-1	22	578	Adequate	Good	20	
PM-2	22	1359	High	Good	30	
PM-3	21	1397	High	Good	30	
PM-4	6	1305	High	Good	40	Gas power
PM-5	5	1199	High	Good	40	

[a]Yield: Marginal - <300 gpm, expensive to operate; Adequate - 300-1000 gpm; and High - 1000+ gpm.

[b]Well Condition: Poor - damage to casing and screen; Fair - well deterioration due to corrosion and sanding; and Good - little, if any, well deterioration. Wells equipped with electric motors except PM-4.

[c]Maximum permissible concentrations for drinking water standards.

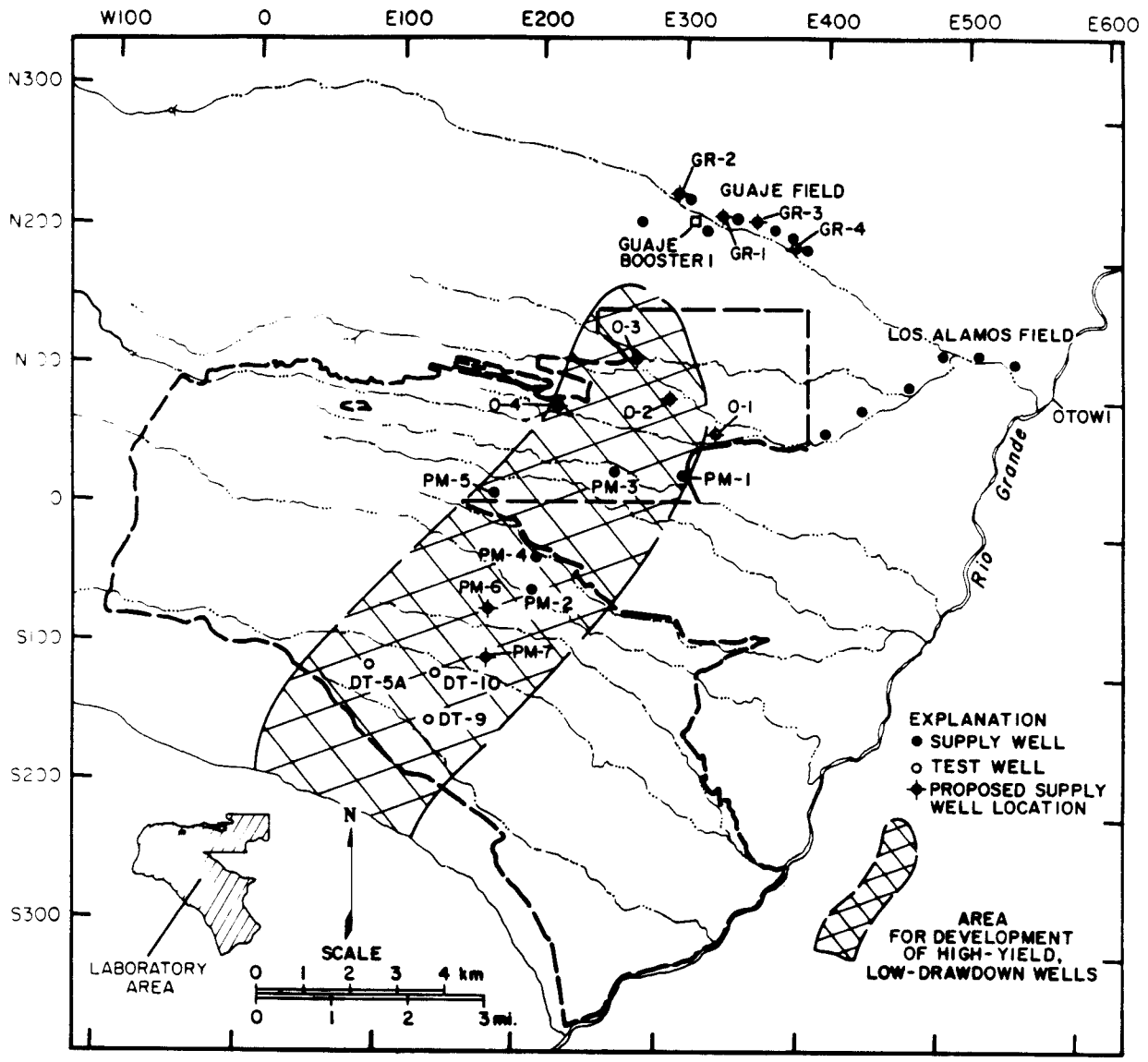

Figure 13. Proposed location for supply wells and areas for development of high-yield, low-drawdown wells.

B. Los Alamos Field

Within the next 10 years most, if not all, of the wells in the Los Alamos field will have to be replaced or relocated. The Los Alamos field is located east of Los Alamos in Santa Fe County on the San Ildefonso Pueblo Grant. The aquifer in this area is composed of siltstones and fine grained sandstones of the Tesuque Formation. Only low- to moderate-yield wells (300 to 500 gpm) can be located in this area. There has been some problem with the water quality; well LA-6 has been placed on standby because of arsenic concentrations in excess of standards for municipal use.

Location and development of additional wells for the Los Alamos field should be west of the present well field (Fig. 14). This is in an area where high yield and low drawdown (1,000 gpm with less than 100 ft drawdown) can be developed. The proposed location is on land controlled by the Department of Energy (Otowi Section). In this

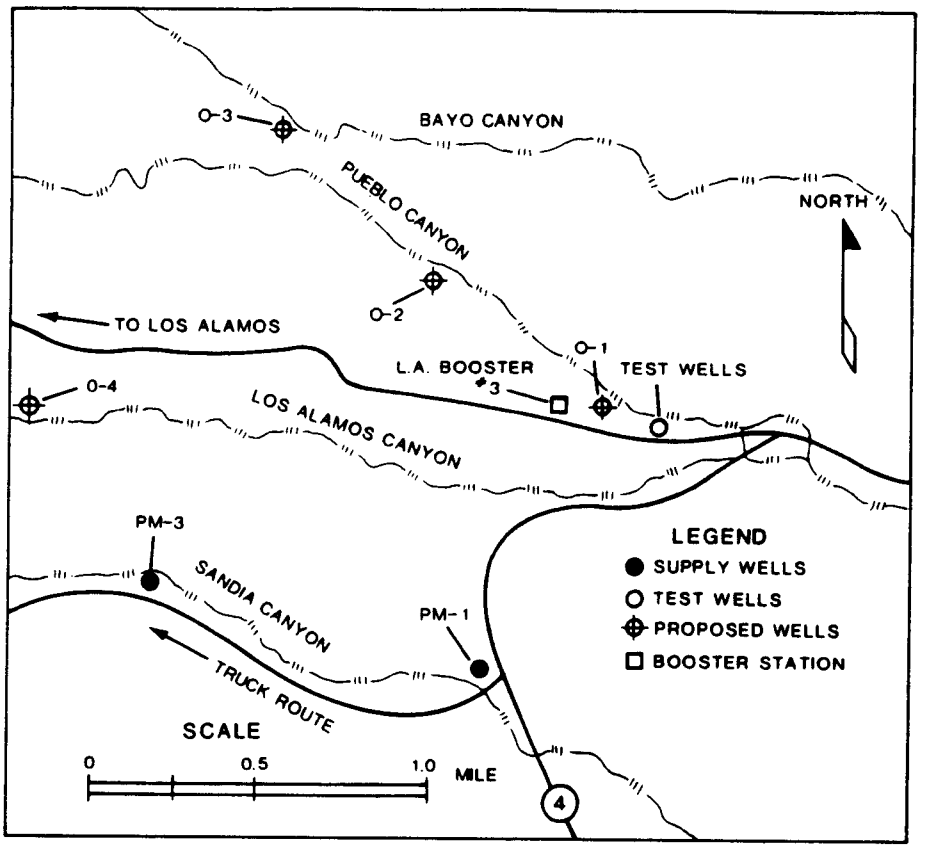

Figure 14. Proposed location for supply wells in the Otowi section.

area, the lower part of the Puye Formation is saturated and coarser sediments in the upper part of the Tesuque Formation are within the main aquifer (Table 12). Three wells could be developed in this area of lower Pueblo and adjacent to Los Alamos Canyon with adequate spacing so that cones of depression caused by pumping of the wells will not overlap. The wells should be drilled in sequence as shown (Otowi-1, -2, and -3 in Fig. 12) at about 3500 ft spacing. The well field could take advantage of the existing booster stations and water line from the Los Alamos field. Combined production rates from the three wells are expected to be at least 3,000 gpm, which will match the capacity of the booster stations. The quality of water from the wells is expected to be similar to that of well PM-1.

An alternate location for a well (Otowi-4) near the Otowi section would be in Los Alamos Canyon below TA-53 (Mason facility). The anticipated geologic log of the well is shown in Table 13. The chemical quality of water in the aquifer would be similar to the other wells in the Otowi section. The well could be used to supply TA-53 to the south or pumped into the Los Alamos line to the north at Booster No. 4 (Figs. 13 and 14).

C. Guaje Field

Within the next 10 years, six of the wells in the Guaje field should be replaced (Table 11). The five wells (G-1 through G-5) located in Guaje Canyon did not meet their full potential for yield and production due to well damage and poor construction. It is now known that screens in wells G-4 and G-5 were damaged during construction. The method of well construction in all five wells (underreaming opposite permeable sections of the aquifer and setting screen opposite the underreamed section) did not develop the wells to their full potential yield. Setting blank casing below the pump intake and screen to the bottom of future

Table 12. Anticipated Geologic Log of a Supply Well in Lower Pueblo Canyon

Elevation: 6400 to 6600 ft above sea level
Depth of Pilot Hole: 2500 ft
Hydrologic Data:
Depth to Water: 600 to 750 ft
Yield: Estimated 1000 gpm
Drawdown: Estimated 100 ft or less
Aquifer: Puye Conglomerate and Tesuque Formation

Stratigraphic Unit	Thickness (ft)	Depth (ft)
Alluvium		
Gravels and boulders	20	20
Puye Conglomerate		
Conglomerate	60	80
Basaltic Rocks of Chino Mesa		
Basalts and interflow breccia, may contain perched water, at a depth of 210 to 260 ft	205	285
Puye Conglomerate		
Conglomerate	165	450
Basaltic Rocks of Chino Mesa		
Basalts and interflow breccias	100	550
Puye Conglomerate		
Conglomerate	250	800
Tesuque Formation		
Siltstone, sandstone, and conglomerate with occasional basalt flow in upper 1200 ft of formation	1700	2500

well would allow better well development with higher resulting yields. The hydrologic characteristic of the aquifer indicates that wells with a moderate yield and low drawdown (500 to 1,000 gpm with about 100 ft of drawdown) can be developed within the present well field (Table 14).

Four wells could be developed that would replace the yield of the six wells (G-1 through G-6). The replacement wells should be spaced in a manner to cause minimum interference between the wells as they are pumped. The additional wells should not be located northwest or west of the existing wells because of the outcrop of Tschicoma in the area. The land is east of well G-1 within the San Ildefonso Pueblo Grant so the replacement well should be between G-1 and east of the Tschicoma outcrop near G-6.

The location of the wells should allow maximum spacing between the wells (Fig. 15). Construction should be done in a specific sequence with the hydrologic data collected during construction and testing evaluated to confirm the proposed location of the next well. The proposed sequence of construction would be Guaje replacement well 1 (GR-1) located about halfway between wells G-3 and G-4; a Guaje replacement

Table 13. Anticipated Geologic Log of O-4 (Otowi-4) in Los Alamos Canyon Below TA-33

Elevation: 6625 ft above sea level
Depth of Pilot Hole: 2800 ft
Hydrologic Data:
Depth to Water: 750 ft
Yield: Estimated 800-1500 gpm
Drawdown: Estimated 100 ft or less
Aquifer: Lower Puye Conglomerate and Tesuque Formation

Stratigraphic Unit	Thickness (ft)	Depth (ft)
Alluvium	20	20
Bandelier Tuff		
Ashflows and pumice	160	180
Puye Conglomerate		
Conglomerate	100	280
Basaltic Rocks of Chino Mesa		
Basalts and interflow breccia	80	360
Puye Conglomerate		
Conglomerate	500	860
Tesuque Formation		
Siltstone, sandstone, and conglomerate with possible basalt flows	1940	3800

well 2 (GR-2) located 150 ft from well G-5; Guaje replacement well 3 (GR-3) located midway between G-2 and G-3, and Guaje replacement well 4 (GR-4) located near well G-1. The existing wells with yields at or about 300 gpm should be left on the line as the replacement wells are drilled. The chemical quality of the replacement wells will be similar to the existing wells.

D. Pajarito Field

The Pajarito field is composed of five wells; four are developed as high yield wells (Table 11). The age and present condition of the wells suggest that there is no need for replacement in the next 20 years. New wells may be needed if additional water production is required to supplement the production from the three fields.

The Pajarito field north and west of PM-2, -4, or -5 cannot be expanded and still remain in the area where high-yield wells can be developed. Also, space is unavailable in Sandia Canyon for additional wells if space is maintained between wells to reduce interference or overlapping drawdown.

The suggested location for additional wells in the Pajarito field is southwest of well PM-2 (Fig. 13). The locations are chosen for maximum spacing between wells to minimize the interference between wells when they are pumping and to align the wells perpendicular to the movement of groundwater in the main aquifer.

One well, Pajarito 6 (PM-6), could be located about 3500 ft southwest of PM-2 at an elevation of about 6850 ft. This well is recommended if the proposed M-Division central

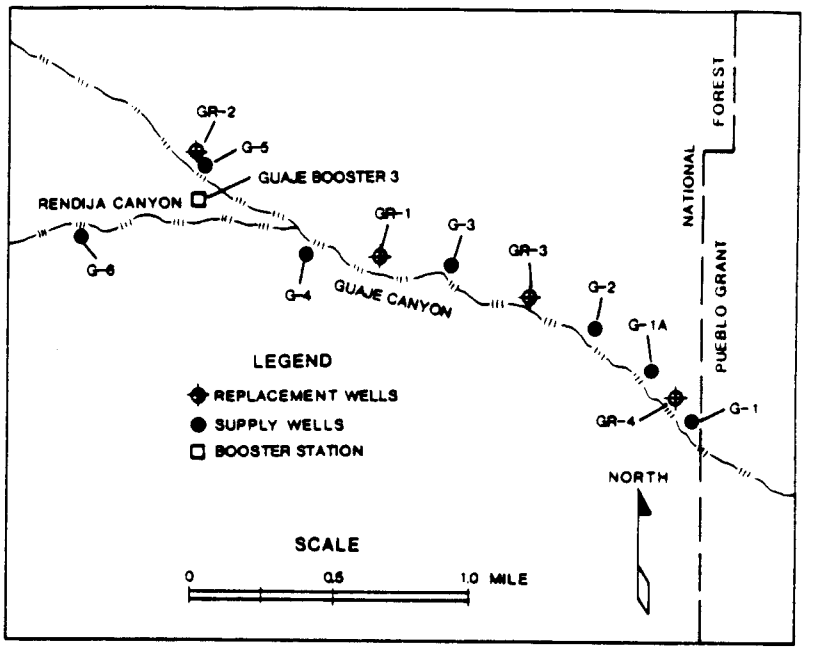

Figure 15. Proposed location for replacement wells in Guaje field.

Table 14. Anticipated Geologic Log of a Supply Well Near Well G-4 in Guaje Canyon

Elevation: 6230 ft above sea level
Depth of Pilot Hole: 2000 ft
Hydrologic Data:
Depth to Water: 400 ft
Yield: Estimated 500 gpm
Drawdown: Estimated 100 ft or less
Aquifer: Tesuque Formation

Stratigraphic Unit	Thickness (ft)	Depth (ft)
Alluvium		
Gravels and boulders	15	15
Puye Conglomerate		
Conglomerate	105	120
Tesuque Formation		
Siltstone and sandstone	380	500
Basalt and interflow breccia	30	530
Siltstone and sandstone	330	860
Basalt and interflow breccia	75	935
Siltstone and sandstone	30	965
Basalt and interflow breccia	20	980
Siltstone and sandstone	130	1110
Basalt and interflow breccia	40	1150
Siltstone and sandstone	850	2000

Table 15. Anticipated Geologic Log of Supply Wells on the Pajarito Plateau South of Well PM-2

Elevation: 6850 ft above sea level
Depth of Pilot Hole: 2850 ft
Hydrologic Data:
Depth to Water: 950 ft
Yield: Estimated 1000 gpm
Drawdown: Estimated 100 ft or less
Aquifer: Puye Conglomerate and Tesuque Formation

Stratigraphic Unit	Thickness (ft)	Depth (ft)
Bandelier Tuff		
Ashflow tuff and pumice	650	650
Basaltic rocks of Chino Mesa		
Basalt and interflow breccia	350	1000
Puye Conglomerate		
Conglomerate	650	1650
Tesuque Formation		
Sandstone and conglomerate	400	2050
Basalt and interflow breccia	50	2100
Sandstone and siltstone	200	2300
Basalt and interflow breccia	100	2400
Siltstone and sandstone	450	2850

complex is developed; this would provide a water source for the complex and preclude pumping the water to the reservoir string and feeding it back down to R-Site. A second well, Pajarito 7 (PM-7), may be located about 7000 ft southwest of PM-2 at an elevation of about 6800 ft (Fig. 11). High-yield wells can be developed at these locations (Table 14). The water quality should be similar to that of PM-2.

REFERENCES

Black 1951: Black and Veatch, Consulting Engineers, "Report on Water Supply, Los Alamos Project, Los Alamos, New Mexico," Kansas City, MO, Admin. Rept. to United States Atomic Energy Commission (1951).

Cushman 1965: R. L. Cushman, "An Evaluation of Aquifer and Well Characteristics of Municipal Well Fields in Los Alamos and Guaje Canyons Near Los Alamos, New Mexico," U.S. Geol. Survey Water-Supply Paper 1809-D (1965).

Cushman 1975: R. L. Cushman and W. D. Purtymun, "An Evaluation of Yield and Water Relations," Los Alamos Scientific Laboratory report LA-6086-MS (1975).

Foreman 1985: Gordon Foreman, "Instructions for Pumping Schedule," Los Alamos Informal Memorandum to PAA UWGW Well Operation (1985).

Griggs 1964: R. L. Griggs, "Geology and Ground-Water Resources of the Los Alamos Area, New Mexico," U.S. Geol. Survey Water-Supply Paper 1753 (1964).

Herkenhoff 1974: Gorden Herkenhoff and Associates, Engineers and Planners, "Comprehensive Plan for Water System Improvement, Los Alamos, New Mexico," Contract at (29-1) 2201, Albuquerque, NM (1974).

Keiser 1985: Raymond Keiser, Consulting Engineers, "Long Range Utilities Plan," ENG-11, Los Alamos, New Mexico (1985).

Purtymun 1965: W. D. Purtymun and J. B. Cooper, "Locations for Five Water-Supply Wells at Los Alamos, New Mexico," U.S. Geol. Survey Open-File report (1965).

Purtymun 1969: W. D. Purtymun and J. B. Cooper, "Development of Ground-Water Supplies on the Pajarito Plateau, Los Alamos County, New Mexico," U.S. Geol. Survey Prof. Paper 650-B (1969).

Purtymun 1972: W. D. Purtymun and J. E. Herceg, Compilers, "Summary of Los Alamos Municipal Well-Field Characteristics, 1947-1971," Los Alamos Scientific Laboratory report LA-5040-MS (1972).

Purtymun 1972a: W. D. Purtymun and J. E. Herceg, "Water Supply at Los Alamos During 1971," Los Alamos Scientific Laboratory report LA-5039-MS (1972).

Purtymun 1973: W. D. Purtymun and J. E. Herceg, "Water Supply at Los Alamos During 1972," Los Alamos Scientific Laboratory report LA-5296-MS (1973).

Purtymun 1974: W. D. Purtymun and J. E. Herceg, "Water Supply at Los Alamos During 1973," Los Alamos Scientific Laboratory report LA-5636-MS (1974).

Purtymun 1975: W. D. Purtymun, "Water Supply at Los Alamos During 1974," Los Alamos Scientific Laboratory report LA-5998-MS (1975).

Purtymun 1976: W. D. Purtymun, "Water Supply at Los Alamos During 1975," Los Alamos Scientific Laboratory report LA-6461-PR (1976).

Purtymun 1977: W. D. Purtymun, "Water Supply at Los Alamos During 1976," Los Alamos Scientific Laboratory report LA-6814-PR (1977).

Purtymun 1977a: W. D. Purtymun, "Hydrologic Characteristics of the Los Alamos Well Field with Reference to the Occurrence of Arsenic in Well LA-6," Los Alamos Scientific Laboratory report LA-7012-MS (1977).

Purtymun 1978: W. D. Purtymun, "Water Supply at Los Alamos During 1977," Los Alamos Scientific Laboratory report LA-7436-MS (1978).

Purtymun 1979: W. D. Purtymun, "Water Supply at Los Alamos During 1978," Los Alamos Scientific Laboratory report LA-8074-PR (1979).

Purtymun 1980: W. D. Purtymun, "Water Supply at Los Alamos During 1979," Los Alamos Scientific Laboratory report LA-8504-PR (1980).

Purtymun 1981: W. D. Purtymun and Max Maes, "Water Supply at Los Alamos During 1980," Los Alamos National Laboratory report LA-8977-PR (1981).

Purtymun 1983: W. D. Purtymun, N. M. Becker, and Max Maes, "Water Supply at Los Alamos During 1981," Los Alamos National Laboratory report LA-9734-PR (1983).

Purtymun 1984: W. D. Purtymun, N. M. Becker, and Max Maes, "Water Supply at Los Alamos During 1982," Los Alamos National Laboratory report LA-9896-PR (1984).

Purtymun 1984a: W. D. Purtymun, "Hydrologic Characteristics of the Main Aquifer in the Los Alamos Area: Development of Ground Water Supplies," Los Alamos National Laboratory report LA-9957-MS (1984).

Purtymun 1985: W. D. Purtymun, N. M. Becker, and Max Maes, "Water Supply at Los Alamos During 1983," Los Alamos National Laboratory report LA-10327-PR (1985).

Purtymun 1986: W. D. Purtymun, N. M. Becker, and M. N. Maes, "Water Supply at Los Alamos During 1984," Los Alamos National Laboratory report LA-10584-PR (1986).

Purtymun 1986a: W. D. Purtymun, N. M. Becker, and M. N. Maes, "Water Supply at Los Alamos During 1985," Los Alamos National report LA-10835-PR (1986).

Purtymun 1987: W. D. Purtymun, A. K. Stoker, and M. N. Maes, "Water Supply at Los Alamos During 1986," Los Alamos National Laboratory report LA-11046-PR (1987).

Theis 1962: C. V. Theis and C. S. Conover, "Pumping Test in the Los Alamos Canyon Well Field near Los Alamos, New Mexico," U.S. Geol. Survey Water-Supply Paper 1619-I 1962).

LA-11478-PR
Progress Report

UC-000
Issued: January 1989

Water Supply at Los Alamos During 1987

W. D. Purtymun
A. K. Stoker
M. N. Maes

Los Alamos
Los Alamos National Laboratory
Los Alamos, New Mexico 87545

WATER SUPPLY AT LOS ALAMOS DURING 1987

by

W. D. Purtymun, A. K. Stoker, and M. N. Maes

ABSTRACT

Municipal and industrial water supply during 1987 was 1594×10^6 gal. from wells in three fields and 34×10^6 gal. from the spring gallery in Water Canyon. About 2.8×10^6 gal. of nonpotable water from the Guaje Reservoir and 3.2×10^6 gal. from the Los Alamos Reservoir were used for irrigation; thus, the total water usage in 1987 was about 1634×10^6 gal. Water supply was satisfactory in that the production met demand and water quality in the distribution system was in compliance with state and federal regulations. However, in 1987 two wells were lost because of deterioration of the casing and screen. In spite of rehabilitation attempts to maintain the yield, production from the older wells continued to decline. A comprehensive evaluation of the wells and well fields made in late 1987 concluded that replacement wells and new wells were needed soon to ensure a reliable water supply for the Laboratory and the county of Los Alamos.

I. INTRODUCTION

This report summarizes production and aquifer conditions for water wells in the Los Alamos, Guaje, and Pajarito well fields (Fig. 1). The wells supply most of the water used for municipal and industrial purposes in Los Alamos County and the Los Alamos National Laboratory. The spring gallery in Water Canyon supplies the rest of the water to the system. A summary of data on the surface water from Guaje and Los Alamos Reservoirs that is used for irrigation is included in this report. The chemical quality of water from wells, the gallery (spring), and the distribution system is also discussed.

This report is a joint effort between the Laboratory Environmental Surveillance Group (HSE-8) and the Utilities Department of Pan American World Services (Pan Am). The purpose of this report is to ensure a continuing historical record and to provide guidance for management of water resources in its long-range planning for the water-supply system. We have issued 1 summary report for the period 1947–1971 and 16 annual reports that contain the results of our studies of these water supplies.[1–17] An additional report summarized the hydrology of the main aquifer with reference to future development of ground water supplies.[18] In late 1987 a report

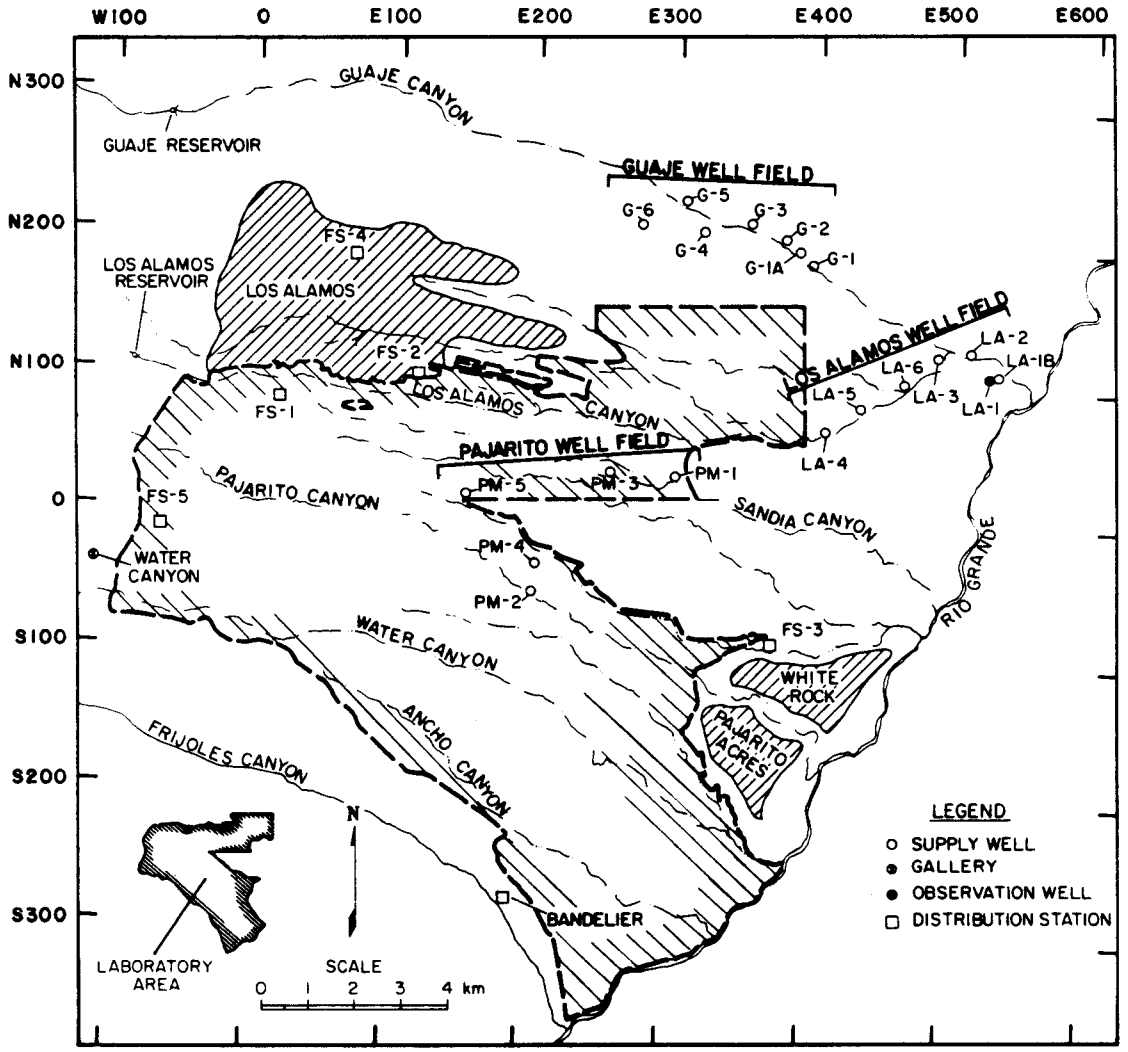

Fig. 1. Location of reservoirs, well fields, water-supply wells, and gallery water supply.

was prepared examining the current status of wells and the future water supply.[19] A part of the abstract of that report is included here to provide a complete historical record.

Pan Am, which is the support contractor to the Laboratory and the Department of Energy (DOE) at Los Alamos, maintains and operates the water-supply system. Water from the system is sold to the county for the communities of Los Alamos and White Rock.

After the water is pumped from the wells into distribution lines, it is lifted by booster pumps into reservoirs for storage. Water from the gallery flows by gravity through a microfilter and chlorination station and then is pumped into one of the system reservoirs for distribution. The entire water supply is disinfected before distribution to Los Alamos, White Rock, and Laboratory areas (Fig. 1).

Pan Am maintains a record of the hours of operation for each well along with records of daily and monthly water production. The monthly averages of water levels from nonpumping and

pumping wells are computed from air-line pressure or transducer data recorded continuously at each well. These data are used in calculating pumping rates, drawdown (the difference between water levels from nonpumping and pumping wells), and other well-field statistics that are included in this report. The Appendix contains annual pumping and production information for each water-supply well and gallery for the period of record.

Water for the Laboratory and for the Los Alamos and White Rock communities is supplied from 17 deep wells in 3 well fields and from 1 gallery. The well fields are located on the Pajarito Plateau and in the Los Alamos and Guaje Canyons east of the plateau (Fig.1). The wells are completed in the main aquifer, the only aquifer capable of municipal and industrial water supply in the area. The depth to water ranges from 25 to 30 ft (semiartesian) in the well field in lower Los Alamos Canyon to about 760 ft along the eastern edge of the Pajarito Plateau, and increases to about 1200 ft near the center of the plateau at Well PM-5. Water in the aquifer moves from the recharge area in the Valles Caldera eastward beneath the plateau to the Rio Grande, where a part is discharged into the river through seepage and springs.[18] The gallery, which is located west of the Laboratory on the flanks of the Sierra de los Valles, discharges water from a small aquifer perched in the volcanic rocks.

Water from the two reservoirs is used for irrigation of lawns during the summer. The reservoirs are in canyons on the flanks of the mountains. Los Alamos Reservoir is located west, and Guaje Reservoir, northwest, of Los Alamos. The source of water in the reservoirs is from springs, snowmelt, and summer run-off.

II. WELL-FIELD CHARACTERISTICS

Production from the three well fields increased 97×10^6 gal., from 1497×10^6 gal. in 1986 to 1594×10^6 gal. in 1987 (Table I). The months of heaviest production in 1987 were June, July, and August. The production during these months was 582×10^6 gal., an increase from 503×10^6 gal. for a similar period of heavy production in 1986. The months of lightest production were January, February, and March, with a production of 285×10^6 gal., an increase from 262×10^6 gal. for a similar period in 1986.

The difference in demand between periods of heavy and light production (summer and winter) is mainly because of water usage for lawn irrigation. The water levels in the wells respond accordingly, with the highest water levels observed during months of least production and the lowest water levels during months of greatest production.

The production and use of water at the Laboratory and the community increased from about 230×10^6 gal. in 1947 to 1700×10^6 gal. in 1976. However, water usage in 1977 declined to about 1500×10^6 gal. and has varied since then from about 1450×10^6 gal. in 1979 to about 1628×10^6 gal. in 1987 (Fig. 2). The decline in 1977 and the lower demand since then have been attributed largely to a rate increase for water used in the community and to water-saving measures in the community and the Laboratory. Much of the landscaping in the community has been changed from lawns and shrubs, which require watering, to southwestern landscaping (native plants and gravels), which requires little if any water other than normal rainfall.

A projection of future water demand was made in 1985 based on production data from 1977 through 1985. This projection indicated an annual increase of about 17×10^6 gal., or about 1%

Table I

Production from Wells and Gallery 1947–1987
(in Millions of Gallons)

Year	Los Alamos Field	Guaje Field	Pajarito Field	Water Canyon Gallery	Production Total
1947	147	0	0	84	231
1948	264	0	0	97	361
1949	302	0	0	92	394
1950	547	3	0	54	604
1951	702	68	0	39	809
1952	448	350	0	48	846
1953	444	372	0	39	855
1954	380	374	0	40	794
1955	407	375	0	33	815
1956	437	506	0	23	966
1957	350	378	0	40	768
1958	372	395	0	60	827
1959	391	478	0	54	923
1960	530	533	0	48	1 111
1961	546	624	0	54	1 224
1962	577	597	0	67	1 241
1963	539	654	0	51	1 244
1964	627	665	0	45	1 337
1965	447	571	99	72	1 189
1966	450	613	127	82	1 272
1967	373	464	481	56	1 374
1968	345	474	584	65	1 468
1969	331	435	569	80	1 415
1970	360	423	595	65	1 443
1971	412	484	657	37	1 590
1972	380	467	662	40	1 549
1973	406	475	685	49	1 615
1974	369	453	802	35	1 659
1975	356	431	749	42	1 578
1976	343	531	817	41	1 732
1977	345	515	614	57	1 531
1978	302	444	690	45	1 481
1979	289	456	662	44	1 451
1980	339	485	743	32	1 599
1981	336	469	701	45	1 551
1982	317	422	773	46	1 558
1983	221	338	904	38	1 501
1984	326	460	780	34	1 600
1985	290	456	841	37	1 624
1986	179	460	858	28	1 525
1987	217	485	892	34	1 628
	15 743	17 183	15 285	2 072	50 283

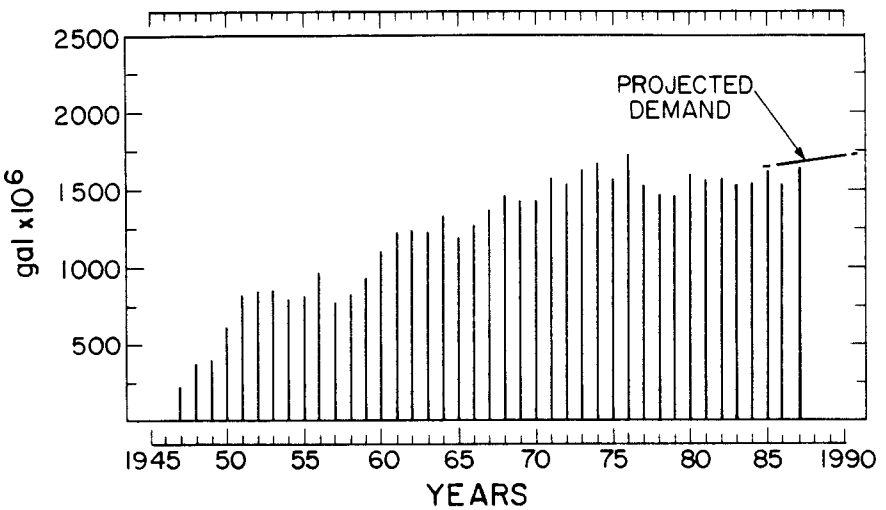

Fig. 2. Water production and usage from 1947 to 1986, and projected demand from 1986 to 1990.

per year. The actual increase has been about 0.6% per year, with production this year falling about 75×10^6 gal. below the projected amount (Fig. 2).

The peak demand period for 1987 was a 16-day period, July 2–17, when production was 134×10^6 gal., or about 8.4×10^6 gal./day (Table II). The demand for water during this period was up 43×10^6 gal. from the peak demand period of 14 days in 1986.

Table II

Peak Demand Periods 1982–1987

	Demand Period					
	June 23–July 11 1982	June 30–July 11 1983	June 8–June 18 1984	June 29–July 16 1985	July 28–August 10 1986	July 2–July 17 1987
No. of days	19	12	11	18	14	16
Total production (gal.)	145×10^6	91×10^6	81×10^6	138×10^6	91×10^6	134×10^6
Average daily production (gal.)	8.1×10^6	7.6×10^6	7.4×10^6	7.7×10^6	6.5×10^6	8.4×10^6
No. of days exceeding						
10×10^6 gal.	—	—	—	—	—	—
9×10^6 gal.	1	—	—	3	—	4
8×10^6 gal.	9	6	2	4	2	7
7×10^6 gal.	9	2	6	9	2	4
$<7 \times 10^6$ gal.	0	4	3	2	10	1

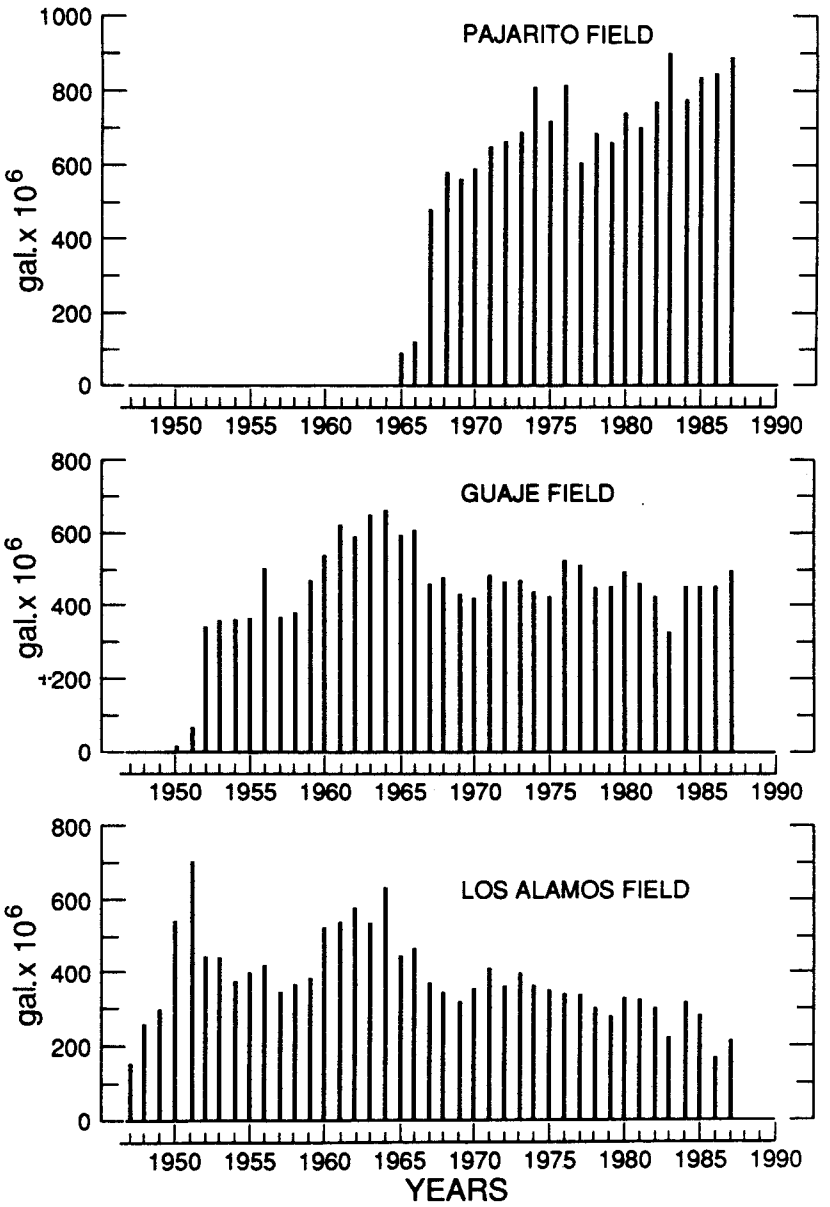

Fig. 3. Comparison of annual production from three well fields.

The cumulative production total since 1947 from the three well fields and gallery is $50\,283 \times 10^6$ gal. (Table I), with $15\,743 \times 10^6$ gal. (31%) from the Los Alamos field, $17\,183 \times 10^6$ gal. (34%) from the Guaje field, $15\,285 \times 10^6$ gal. (31%) from the Pajarito field, and 2072×10^6 gal. (4%) from the gallery in Water Canyon.

Although cumulative well-field productions are nearly equal, they do not reflect current proportionate contributions because production generally declines with the age of the well field. The wells in the Los Alamos field were constructed in the period 1947 through 1960, with production peaking in 1951 and declining since that time (Fig. 3); wells in Guaje field were constructed in

Table III

Production Characteristics for 1986 and 1987

	Production					
	Amount (10^6 gal.)		Well Field (%)		Total Production (%)	
	1986	1987	1986	1987	1986	1987
Los Alamos Field						
Well LA-1	—	—	—	—	—	—
Well LA-1B	54.9	97.3	31	45	4	6
Well LA-2	24.1	39.6	13	18	2	2
Well LA-3	26.9	50.9	15	23	2	3
Well LA-4	38.8	1.6	22	<1	2	<1
Well LA-5	34.6	27.9	19	13	2	2
Well LA-6	—	—	—	—	—	—
Subtotal	179.3	217.3	100	99	12	13
Guaje Field						
Well G-1	30.3	29.2	7	6	2	2
Well G-1A	130.4	122.5	28	25	9	7
Well G-2	109.3	109.7	24	23	7	7
Well G-3	26.7	<0.1	6	<1	2	<1
Well G-4	33.9	25.1	7	5	2	2
Well G-5	52.4	116.7	11	24	3	7
Well G-6	76.7	81.4	17	17	5	5
Subtotal	459.7	484.6	100	100	30	30
Pajarito Field						
Well PM-1	73.9	102.4	9	12	5	6
Well PM-2	84.4	28.3	10	3	6	2
Well PM-3	244.8	250.2	28	28	16	16
Well PM-4	307.4	392.2	36	44	20	24
Well PM-5	147.3	118.6	17	13	9	7
Subtotal	857.8	891.7	100	100	56	55
Water Canyon (Gallery)	28.2	34.2	100	100	2	2
Total	1525.0	1627.8	—	—	100	100

the period 1950 through 1964, with production peaking in 1964 and declining since then. Wells in the Pajarito field were constructed in the period 1966 through 1982, with peak production occurring in 1983.

The present yields generally reflect the age of the wells in the three fields. In 1987 about 55% of total production came from the Pajarito field, 30% from the Guaje field, 13% from the Los Alamos field, and 2% from the Water Canyon gallery (Table III).

A. Los Alamos Well Field

The Los Alamos well field includes six supply wells and one observation well. Three wells (LA-1, -2, and -3) were completed in 1947 to depths of about 870 ft. Because Well LA-1 produced excessive sand with the water, which rapidly wore out the pumps, it was replaced by Well LA-1B in 1960. During the period from 1948 to 1950, Wells LA-4, -5, and -6 were completed, to depths of about 2000 ft. Well LA-1B was completed at a depth of 1750 ft.

The 1987 production came from four of these wells (LA-1B, -2, -3, and -5). The pump in Well LA-4 failed in 1986 and was removed in 1987. Rehabilitation of the well caused separation of the casing, which permitted excessive sand to enter the well. Repair of the separation is doubtful because of the age of the well and weakness of the casing. Well LA-6 was placed on standby in 1977 because the water contained an excess of natural arsenic.[20]

Production from the Los Alamos well field increased about 38×10^6 gal., from 179×10^6 gal. in 1986 to 217×10^6 gal. in 1987 (Table III). The well field contributed about 13% of the total 1987 production, a slight increase over the 12% contribution in 1986.

The average pumping rates in 1987 ranged from 252 to 589 gallons per minute (gpm) (Table IV). The combined pumping rate of the field declined from 2194 gpm in 1986 to 1559 gpm in 1987, partly because of the loss of Well LA-4. There was little or no change in the specific capacities of the wells in use in 1987 when compared with the capacities of those same wells in 1986.

The water levels in the individual wells fluctuated with the amount of production. For example, water levels for 1987 showed a decline due to increased production from the three wells in the lower part of the field (Wells LA-1B, -2, and -3) when compared to water levels and production reported from those wells in 1986. The water level in Well LA-4 rose after that well was out of service for a year. The reduced production from Well LA-5 because it was down for several months as a result of pump failure caused little or no change in the water level (Fig. 4 and Table V). The decline of the average water level in the Los Alamos field from 1986 to 1987 was about 24 ft.

B. Guaje Well Field

The Guaje well field includes seven wells ranging in depth from 1500 to 2000 ft. Wells G-1, -2, -3, -4, and -5 were completed in 1950, Well G-1A was completed and placed in service in 1954, and Well G-6 was placed in service in 1964.

The 1987 production came from six of these wells. Rehabilitation of Well G-3 damaged a number of screens, causing the well to pump a large amount of sand. It is unlikely that this well will be placed back in service.

Production from the Guaje field increased about 25×10^6 gal., from 460×10^6 gal. in 1986 to 485×10^6 gal. in 1987. The well field contributed about 30% of the total production in 1987, the same as in 1986 (Table III).

The average pumping rate of the six wells ranged from 208 to 457 gpm (Table IV). The loss of Well G-3 in 1987 and the continued deterioration of the other six wells because of age resulted in a decline of the combined pumping rate of 244 gpm, from 2193 gpm in 1986 to 1949 gpm in

Table IV

Average Pumping Rate and Specific Capacity, 1986 and 1987

	Average Pumping Rate (gpm)		Average Specific Capacity (gpm/ft of drawdown)	
	1986	1987	1986	1987
Los Alamos Field				
Well LA-1	—	—	—	—
Well LA-1B	573	589	4.8	4.9
Well LA-2	312	252	1.8	1.3
Well LA-3	338	313	2.0	1.8
Well LA-4	552	0	—	—
Well LA-5	419	405	2.9	2.8
Subtotal	2194	1559	2.9	2.7
Guaje Field				
Well G-1	249	235	1.5	1.4
Well G-1A	468	457	11.4	10.9
Well G-2	382	404	14.7	12.2
Well G-3	196	0	—	—
Well G-4	211	208	1.2	1.2
Well G-5	394	379	9.6	9.0
Well G-6	293	266	3.8	3.5
Subtotal	2193	1949	7.0	6.4
Pajarito Field				
Well PM-1	578	586	26.3	27.9
Well PM-2	1359	1340	21.2	23.9
Well PM-3	1397	1397	58.2	55.9
Well PM-4	1305	1289	37.3	35.8
Well PM-5	1199	1220	—	—
Subtotal	5838	5832	35.8	35.9
Water Canyon (Gallery)	54	65	—	—
Total	10 279	9405	—	—

1987. The specific capacities of the individual wells declined slightly, with an overall decline of <1 gpm/ft of drawdown.

The water levels in nonpumping wells in the lower part of Guaje field (Wells G-1, -1A, and -2) remained about the same or rose slightly. The increased production from the upper part of the field (Wells G-4, -5, and -6) caused a slight decline in water level (Fig. 5 and Table V). The overall decline in the well field was about 7 ft.

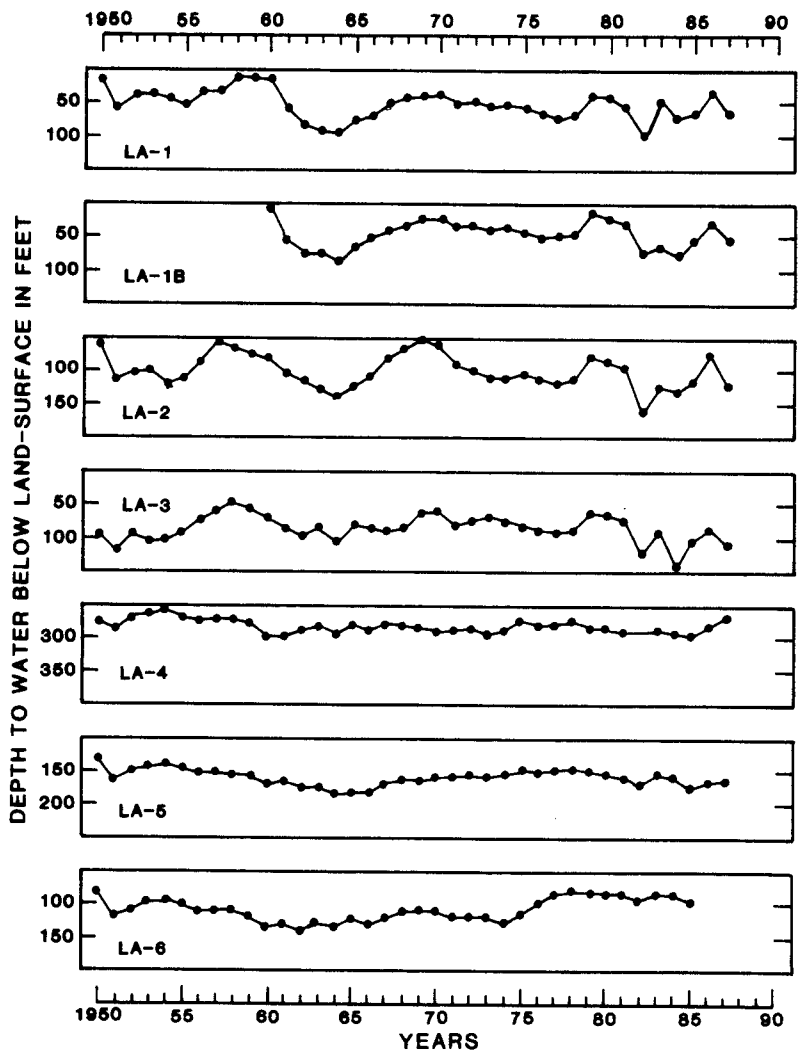

Fig. 4. Nonpumping water levels in the Los Alamos well field.

C. Pajarito Well Field

The Pajarito well field includes five wells. The wells were completed over a 17-year period, from 1965 through 1982, and range in depth from 2300 to 3100 ft. Because they are located on the Pajarito Plateau, the depths to water range from about 750 ft at Well PM-1 to more than 1200 ft at Well PM-5.

The production from the Pajarito well field in 1987 was about 892×10^6 gal., an increase of 34×10^6 gal. more than the 858×10^6 gal. produced by this field in 1986 (Table III). The field contributed about 55% of the total 1987 production, slightly less than the 56% contribution in 1986. The production from Well PM-4 represented 44% of the total Pajarito field production and 24% of the total water produced at Los Alamos in 1987.

The average pumping rates of the Pajarito wells ranged from 586 to 1397 gpm. Four of the wells (PM-2, -3, -4, and -5) had high yields, with pumping rates over 1000 gpm (Table IV). The

Table V

Average Water Levels for Nonpumping and Pumping Wells and Average Drawdown, 1986 and 1987

	Average Water Levels					
	Nonpumping (ft)		Pumping (ft)		Drawdown (ft)	
	1986	1987	1986	1987	1986	1987
Los Alamos Field						
Well LA-1	34	7	—	—	—	—
Well LA-1B	25	60	144	187	119	121
Well LA-2	74	129	252	319	178	190
Well LA-3	88	118	255	289	167	171
Well LA-4	284	269	377	357	93	88
Well LA-5	168	167	310	314	142	147
Well LA-6	—	—	—	—	—	—
Average per field	112	136				
Guaje Field						
Well G-1	279	280	450	451	171	171
Well G-1A	310	320	351	362	41	42
Well G-2	369	366	395	399	26	33
Well G-3	—	—	—	—	—	—
Well G-4	396	398	574	573	178	175
Well G-5	453	462	494	504	41	42
Well G-6	576	595	654	671	78	76
Average per field	397	404				
Pajarito Field						
Well PM-1	748	752	770	773	22	21
Well PM-2	851	851	915	907	64	56
Well PM-3	763	763	787	788	24	25
Well PM-4	1084	1081	1119	1117	35	36
Well PM-5	—	—	—	—	—	—
Average per field	862	862				

pumping rate from the individual wells varied slightly from 1986 to 1987; however, the combined rate in 1987 (5832 gpm) was nearly unchanged from the 1986 combined rate (5838 gpm).

The specific capacities of the wells in 1987 ranged from 23.9 to 55.9 gpm/ft of drawdown. There was no significant change in the specific capacities between 1986 and 1987 (Table IV).

The water levels in these wells fluctuated very little in response to the amount of water pumped from the individual wells. There was no change in the average nonpumping levels between 1986 and 1987 (Table V and Fig. 6).

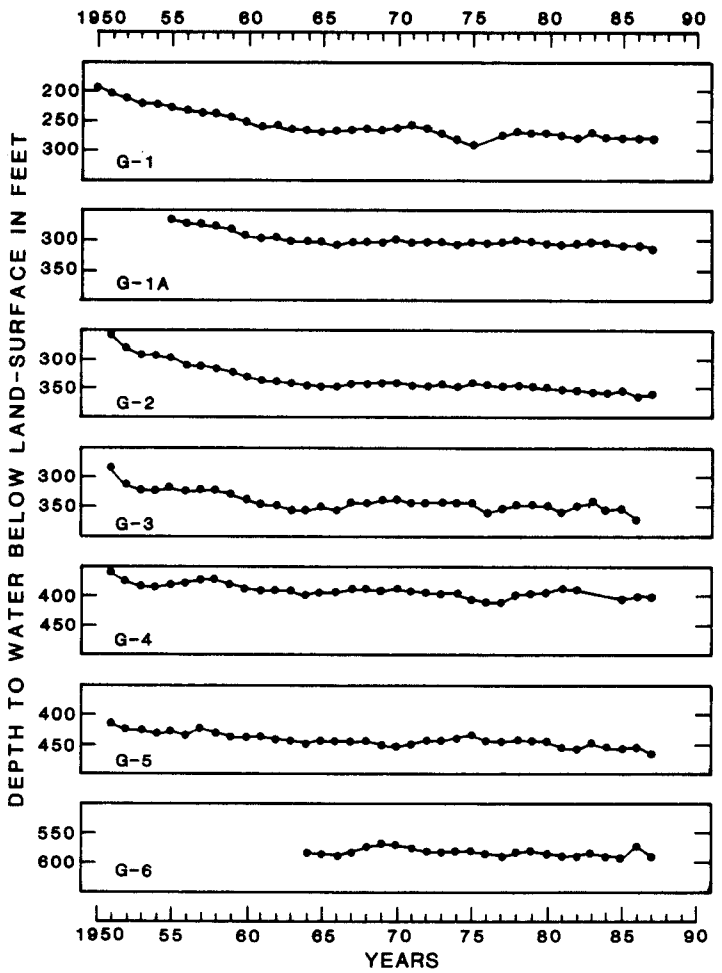

Fig. 5. Nonpumping water levels in the Guaje well field.

D. Pump Failures and Repairs

The line-shaft turbine pump in Well LA-4 failed in late August 1986 and was removed in early 1987 to be replaced with a submersible pump. The well was logged with a down-hole video camera in July 1987, which showed it was open to a depth of 1921 ft. After the well was logged, a heavy wire brush was used to clean the scale off the casing and screen. The scale and formation sand pulled into the well during the cleaning operation were removed to a depth of 1942 ft before the submersible pump was set in the well. The pump failed because of electrical problems. It was pulled, repaired, and returned to the well, but when the well was placed on line production contained a large amount of sand. Test runs at several pumping rates (tested over a 38-h period) could not reduce the sand to acceptable levels where the pump, system lines and tanks, and booster pumps would not sustain damage. The pump was removed a second time in January 1988 and the well was again logged with the video camera. The heavy wire brush had apparently caused the casing to separate at the point where the size of the casing was reduced from 12 to 10 in. in diameter, at a depth of about 754 ft. It is probable that the well cannot be repaired and will be lost as a producing well in the Los Alamos field.

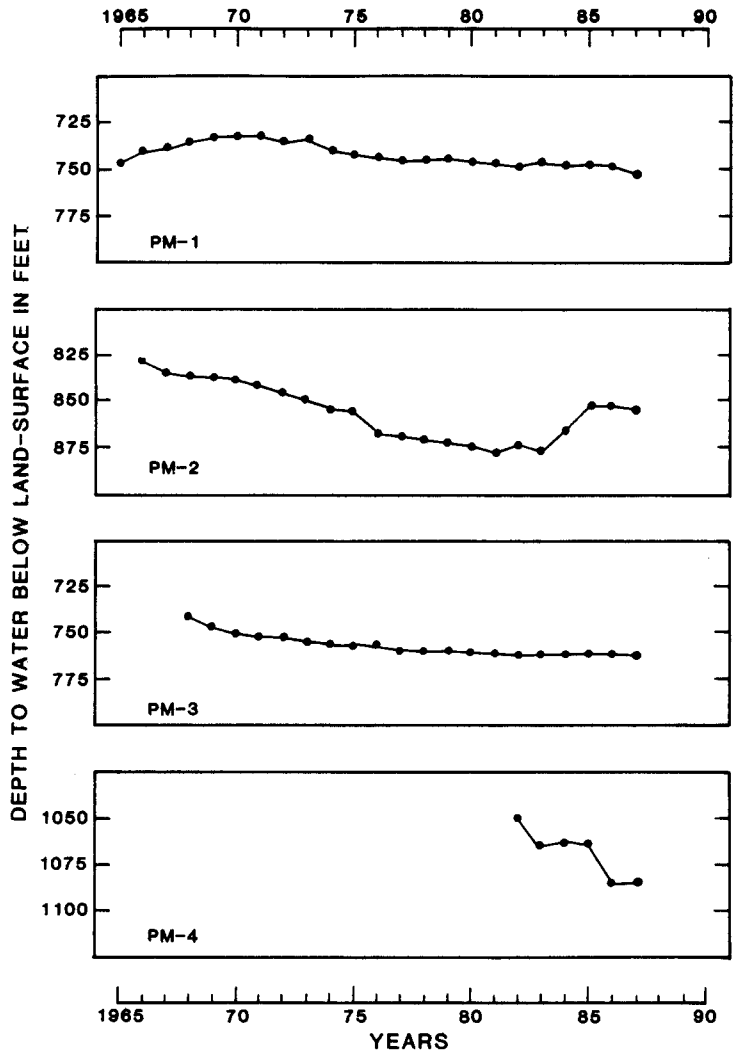

Fig. 6. Nonpumping water levels in the Pajarito well field (no water-level data for Well PM-5).

The line shaft in Well LA-5 separated in July 1987, causing the well to be down from August 1987 through January 1988. The pump motor and part of the line shaft were pulled and repaired, and the difficult job of adjusting the line shaft is in progress. The well should be back on line before the heavy demand period that usually begins in late May.

The pumping rate of Well G-3 declined to about 150 gpm by July 1986 and the well was placed on standby. The specific capacity of the well had declined steadily since 1979, indicating well deterioration. The pump was pulled in June 1987 and the well was logged to a depth of 1492 ft. Well rehabilitation was attempted using an explosive technique. Shock waves were produced by the explosives to break up scale and any chemical precipitates in the screens and gravel pack that limited water flow into the well. The well screen sections were weakened from corrosion as a result of age and the explosives broke out a number of louvers from the screen sections,

allowing formation sand and gravel pack to enter the well. The present condition of the well is such that it will probably never be returned to service.

The pump in Well PM-2 was pulled for rehabilitation and repair in March 1987. A video log of the well determined the depth to be 2283 ft. A sand pump and bailer were used to remove the scale from the casing and screen and to loosen the gravel pack. The well was placed back in service in September 1987.

E. Current Status of Wells and Future Water Supply

In the fall of 1987 a comprehensive study was made of the water-supply system to determine the current status of the wells and to evaluate the future water supply for Los Alamos.[19] A brief summary of the resulting report is presented here.

The three well fields include 19 supply wells ranging in age from 5 to 41 years. The life expectancy of a well in the area ranges from 30 to 50 years.

Twelve of the wells are more than 30 years old and, of these, four cannot be used for production, three because of well damage (LA-1 and -4 and G-3) and one (LA-6) because the water is not suitable for use. The other eight (LA-2, -3, and -5 and G-1, -2, -4, -5, and -6) are likely to become unsuitable for use in the next 10 years because of well deterioration and screen failure.

The newer seven wells include two (LA-1B and G-1A) that are likely to fail in the next 20 years. The five wells in the Pajarito well field are in good condition and should serve for another 20 to 30 years.

The program of maintenance and rehabilitation of pumps and wells has extended production capabilities for short periods of times. Pumps may be effectively repaired or replaced, but rehabilitation of wells is only a short-term correction that will restore some of the yield before the yield continues to decline.

The report concludes that it is essential to implement a program to replace wells that have failed, or will fail in the next 10 years, to ensure a continued and reliable water supply.

III. WATER CANYON GALLERY

The spring gallery in Water Canyon is dug back about 30 ft into the Bandelier tuff. The gallery or tunnel is framed with timbers and sheet metal to keep the wall and ceiling from collapsing. The floor of the gallery is constructed to form a basin. About 1 mile of water line connects the gallery to the microfilter station, located near S-Site along the southwestern edge of the Laboratory. The water flows through the microfilter station, then is chlorinated, and is pumped into a tank for storage and distribution.

The water occurs in the fractures of a welded tuff, which is underlain by a nonwelded tuff (tuff with few fractures that prevents water from moving downward), creating a perched aquifer. Recharge to the perched aquifer is rapid. In the spring when snowmelt occurs, the discharge from the gallery increases and causes increased suspended sediment. When the sediment concentration in the water reaches the limits allowed for a municipal water supply, a turbidity-monitoring device switches the flow to a waste to keep the sediments out of the distribution system.

The gallery is a valuable source of water supply. During 1987 about 2% of the total municipal and industrial water supply was obtained from the gallery (Table III). The production from the gallery increased about 6×10^6 gal., from 28×10^6 gal. in 1986 to 34×10^6 gal. in 1987. Since 1947 the total production from the gallery has been 2072×10^6 gal. (Table I).

IV. GUAJE AND LOS ALAMOS RESERVOIRS

Water from Guaje and Los Alamos reservoirs was used for the municipal and industrial water supply at Los Alamos during the early days of the Manhattan Project. Use of the water from the reservoirs for the municipal supply was discontinued about 1959 because of intermittent periods of turbidity caused by storm run-off and because of difficulties in maintaining bacteriological levels below the limits allowed for a municipal water supply.

Both of the reservoirs and adjacent areas are now open for recreational use. The water from the reservoirs is available for irrigation of lawns and shrubs in the community and Laboratory. Parts of the line are above ground and are subject to freezing; thus water use from the reservoirs is limited to the period from late spring to early fall.

Guaje Reservoir in upper Guaje Canyon has a capacity of 0.25×10^6 gal. and a drainage area of 5.6 sq miles. The reservoir is for diversion rather than storage, as perennial flow is maintained by springs in the canyon above the reservoir. Water flows by gravity through 6.8 miles of distribution line for irrigation of lawns and shrubs at Los Alamos Middle School and Guaje Pines Cemetery. The line from the reservoir is not a part of, nor is it connected to, the distribution system for the municipal water supply.

The annual production from Guaje Reservoir when it was used for the municipal water supply from 1947 through 1958 ranged from an estimated 24×10^6 to 213×10^6 gal. (Table VI). There is no record of the amount of water used for irrigation from 1959 through 1971, but since 1972 the amount of water used for irrigation has ranged from 2.4×10^6 to 9.7×10^6 gal. The amount used in 1987 was 2.8×10^6 gal., up from the 2.4×10^6 gal. used in 1986.

Los Alamos Reservoir in upper Los Alamos Canyon has a capacity of 13.4×10^6 gal. and a drainage area of 6.4 sq miles. The reservoir is used for storage and recreation. The water flows by gravity through about 2.6 miles of distribution lines for irrigation of lawns and shrubs at the Laboratory's Health Research Building, the Los Alamos High School, and Mesa School. The line from the reservoir is not a part of, nor is it connected to, the distribution system for the municipal water supply.

The annual production from Los Alamos Reservoir when it was used for the municipal water supply from 1947 through 1958 ranged from 4.8×10^6 to 54.8×10^6 gal. (Table VI). There is no record of water usage from the reservoir from 1959 through 1978, but since 1978 the amount of water used for irrigation has ranged from 0.9×10^6 to 3.2×10^6 gal. The amount of water from the reservoir used for irrigation in 1987 was 3.2×10^6 gal., up from the 1.5×10^6 gal. used in 1986.

V. QUALITY OF WATER

The quality of water is monitored to determine whether water from the wells, gallery, and the distribution system meets federal requirements (standards) for a municipal water supply. Water

Table VI

Production from Guaje and Los Alamos Reservoirs for 1947–1958 and 1972–1987

Year	Guaje Reservoir[a] (10^6 gal.)	Los Alamos Reservoir (10^6 gal.)
Municipal Water-Supply Production		
1947	87.8	21.7
1948	119.8	21.9
1949	116.1	14.7
1950	79.9	20.6
1951	41	10.5
1952	131	33.6
1953	58	14.8
1954	66	16.9
1955	71	18.1
1956	24	4.8
1957	213	54.8
1958	193	49.4
Irrigation Production		
1972	5.8	—
1973	9.7	—
1974	4.9	—
1975	5.3	—
1976	4.4	—
1977	4.1	—
1978	2.8	—
1979	3.7	1.3
1980	4.7	2.3
1981	2.7	2.1
1982	3.4	2.8
1983	3.4	1.4
1984	3.0	1.3
1985	2.8	0.9
1986	2.4	1.5
1987	2.8	3.2

[a]Production from Guaje Reservoir for 1951–1958 is estimated.

samples are collected and analyzed from the wells and gallery and from six stations in the distribution system (five at fire stations and one at Bandelier National Monument).

Primary drinking water standards are related directly to safety of the drinking water supply.[21] Table VII shows the standards and maximum concentrations observed in samples from the wells and distribution system. Federal primary standards for fluoride have been raised to 4 mg/L

(Ref. 21), and proposed New Mexico regulations when they go into effect will be raised to that level.[22]

Table VII

Comparison of Standards for Drinking Water with Maximum Concentrations of Chemicals and Radiochemicals in Water Supply

	Standards	Maximum Concentrations of Chemicals and Radiochemicals in Water: Supply Wells and Gallery	Maximum Concentrations of Chemicals and Radiochemicals in Water: Distribution System
Primary Standards[a] (mg/L)			
Ag	0.05	<0.001	<0.001
As	0.05	0.044	0.017
Ba	1.0	0.084	0.107
Cd	0.01	<0.0005	<0.0005
Cr	0.05	0.022	0.011
F	4.0	3.2	1.0
Hg	0.002	0.0003	<0.0002
NO_3(N)	10	<1	<1
Pb	0.05	0.092	0.031
Se	0.01	<0.002	<0.002
Secondary Standards[b] (mg/L)			
Cl	250	17	45
Cu	1.0	0.266	0.024
F	2.0	3.2	1.0
Fe	0.3	0.095	0.110
Mn	0.05	<0.009	<0.001
SO_4	250	39	10
Zn	5.0	0.250	0.096
Total dissolved solids	500	430	276
pH (no units)	6.5–8.5	8.6	8.4
Radiochemical Standards[a] (10^{-9} μCi/mL)			
^{137}Cs	200	42	71
^{238}Pu	15	0.011	0.012
$^{239,240}Pu$	15	–0.044	0.037
Gross alpha	15	–5.0	2.4
Gross beta	—	3.2	42
Total uranium[c] (μg/L)	1800	6.0	2.0
^{3}H (10^{-6} μCi/mL)	20	0.3	2.1

[a]Reference 21.
[b]Reference 23.
[c]Reference 24.

The maximum concentrations of all chemicals were below the standards except for one analysis for lead reported in water from Well PM-5. After this finding three additional samples from Well PM-5 were collected and analyzed for lead. The concentrations in the three samples were below the limits of detection of 0.001 mg/L. Samples from the well taken in previous years showed that the lead concentrations in those samples were at the limits of detection. The report of the sample with 0.092 mg/L of lead is probably the result of contamination of the sample when it was collected and does not reflect the quality of water from the well.

Secondary drinking water standards, which are related more to the quality of water as determined by public acceptance of the municipal water supply, are intended as guidelines.[23] The quality of water from the wells and gallery was within the secondary drinking water standards. Water in the distribution system met all standards, primary and secondary.

Water from the wells, gallery, and distribution system was in compliance with the radiochemical standards[21] (Table VII).

Radiochemical and chemical analyses of water from Well LA-6 were not included in Table VII; detailed results were reported in the annual environmental surveillance report[25] for 1987. Well LA-6 was placed on standby in 1977 because it contained natural arsenic that exceeded drinking water standards. The well remains on standby. The arsenic concentrations found in this well in 1987 were 0.147 mg/L, compared with the standard of 0.05 mg/L.

Individual primary, secondary, radiochemical, and miscellaneous chemical analyses for each well, gallery, and station in the distribution system are presented in "Environmental Surveillance at Los Alamos During 1987."[25] In summary, water in the distribution system is in compliance with federal and state primary, secondary, and radiochemical standards.

VI. SUMMARY

Operations of wells and well fields in 1987 were satisfactory. Though production during the year increased, the system was able to handle the increase even during the peak demand period. Trends showing water levels in the wells were as expected considering the current amount of production. The loss of two wells during the year did not overload the system. However, the loss of the two wells and the declining yield from the older wells indicate the need to add new wells to the system to handle future demand and to allow for any increase in demand for water at the Laboratory and the community. Future operations of the wells and water-supply system should be continued as in past years. Continued collection of hydrologic data from the wells and well fields is necessary to evaluate present and future wells and well-field operations.

ACKNOWLEDGMENTS

Statistics on well production were collected by personnel from Pan Am and were compiled for this report by the Environmental Surveillance Group (HSE-8).

REFERENCES

1. W. D. Purtymun and J. E. Herceg, Compilers, "Summary of Los Alamos Municipal Well-Field Characteristics, 1947–1971," Los Alamos Scientific Laboratory report LA-5040-MS (1972).

2. W. D. Purtymun and J. E. Herceg, "Water Supply at Los Alamos During 1971," Los Alamos Scientific Laboratory report LA-5039-MS (1972).

3. W. D. Purtymun and J. E. Herceg, "Water Supply at Los Alamos During 1972," Los Alamos Scientific Laboratory report LA-5296-MS (1973).

4. W. D. Purtymun and J. E. Herceg, "Water Supply at Los Alamos During 1973," Los Alamos Scientific Laboratory report LA-5636-MS (1974).

5. W. D. Purtymun, "Water Supply at Los Alamos During 1974," Los Alamos Scientific Laboratory report LA-5998-MS (1975).

6. W. D. Purtymun, "Water Supply at Los Alamos During 1975," Los Alamos Scientific Laboratory report LA-6461-PR (1976).

7. W. D. Purtymun, "Water Supply at Los Alamos During 1976," Los Alamos Scientific Laboratory report LA-6814-PR (1977).

8. W. D. Purtymun, "Water Supply at Los Alamos During 1977," Los Alamos Scientific Laboratory report LA-7436-MS (1978).

9. W. D. Purtymun, "Water Supply at Los Alamos During 1978," Los Alamos Scientific Laboratory report LA-8074-PR (1979).

10. W. D. Purtymun, "Water Supply at Los Alamos During 1979," Los Alamos Scientific Laboratory report LA-8504-PR (1980).

11. W. D. Purtymun and Max Maes, "Water Supply at Los Alamos During 1980," Los Alamos National Laboratory report LA-8977-PR (1981).

12. W. D. Purtymun, N. M. Becker, and Max Maes, "Water Supply at Los Alamos During 1981," Los Alamos National Laboratory report LA-9734-PR (1983).

13. W. D. Purtymun, N. M. Becker, and Max Maes, "Water Supply at Los Alamos During 1982," Los Alamos National Laboratory report LA-9896-PR (1984).

14. W. D. Purtymun, N. M. Becker, and Max Maes, "Water Supply at Los Alamos During 1983," Los Alamos National Laboratory report LA-10327-PR (1985).

15. W. D. Purtymun, N. M. Becker, and Max Maes, "Water Supply at Los Alamos During 1984," Los Alamos National Laboratory report LA-10584-PR (1986).

16. W. D. Purtymun, N. M. Becker, and Max Maes, "Water Supply at Los Alamos During 1985," Los Alamos National Laboratory report LA-10835-PR (1986).

17. W. D. Purtymun, A. K. Stoker, and M. N. Maes, "Water Supply at Los Alamos During 1986," Los Alamos National Laboratory report LA-11046-PR (1987).

18. W. D. Purtymun, "Hydrologic Characteristics of the Main Aquifer in the Los Alamos Area: Development of Ground Water Supplies," Los Alamos National Laboratory report LA-9957-MS (1984).

19. W. D. Purtymun and A. K. Stoker, "Water Supply at Los Alamos: Current Status of Wells and Future Water Supply," Los Alamos National Laboratory report LA-11332-MS (1988).

20. W. D. Purtymun, "Hydrologic Characteristics of the Los Alamos Well Field with Reference to the Occurrence of Arsenic in Well LA-6," Los Alamos Scientific Laboratory report LA-7012-MS (1977).

21. "National Interim Primary Drinking Water Regulations," U.S. Environmental Protection Agency report EPA-570/9-003 (U.S. Government Printing Office, Washington, DC, 1976).

22. "Preliminary Draft of Regulations Governing Water Supplies," New Mexico Environmental Improvement Division, New Mexico Health and Environment Department, Santa Fe, New Mexico (December 1987).

23. "National Secondary Drinking Water Regulations," U.S. Environmental Protection Agency, *Federal Register* **44**(140) (July 19, 1979).

24. International Commission on Radiological Protection, "Recommendations of the International Commission on Radiological Protection," adopted January 17, 1977, *Annals at the ICRP* No. 3 (1977).

25. Environmental Surveillance Group (HSE-8), "Environmental Surveillance at Los Alamos During 1987," Los Alamos National Laboratory report LA-11306-ENV (May 1988).

Appendix

Annual Statistics on Aquifer Characteristics

Well LA-1

Year	Pump Time (h)	Production (10^6 gal.)	Pump Rate (gpm)	Water Level (Nonpumping) (ft)
1947	3468	54.0	259.5	—
1948	2988	34.7	193.6	—
1949	1361	26.7	327.0	—
1950	563	10.5	310.8	19.0
1951	1215	14.6	200.3	59.0
1952	286	3.4	198.1	40.0
1953	0	0.0	0.0	36.0
1954	0	0.0	0.0	44.0
1955	690	9.7	234.3	51.0
1956	39	0.0	0.0	33.0
1957	0	0.0	0.0	33.0
1958	0	0.0	0.0	10.0
1959	0	0.0	0.0	13.0
1960	0	0.0	0.0	13.0
1961	0	0.0	0.0	59.0
1962	0	0.0	0.0	84.0
1963	0	0.0	0.0	90.0
1964	0	0.0	0.0	95.0
1965	0	0.0	0.0	76.0
1966	0	0.0	0.0	70.0
1967	0	0.0	0.0	52.0
1968	0	0.0	0.0	42.0
1969	0	0.0	0.0	38.0
1970	0	0.0	0.0	37.0
1971	0	0.0	0.0	51.0
1972	0	0.0	0.0	49.0
1973	0	0.0	0.0	55.0
1974	0	0.0	0.0	53.0
1975	0	0.0	0.0	58.0
1976	0	0.0	0.0	69.0
1977	0	0.0	0.0	74.0
1978	0	0.0	0.0	68.0
1979	0	0.0	0.0	38.0
1980	0	0.0	0.0	40.0
1981	0	0.0	0.0	51.0
1982	0	0.0	0.0	98.0
1983	0	0.0	0.0	46.0
1984	0	0.0	0.0	71.0
1985	0	0.0	0.0	63.0
1986	0	0.0	0.0	34.0
1987	0	0.0	0.0	70.0

Appendix (cont)

Well LA-1B

Year	Pump Time (h)	Production (10^6 gal.)	Pump Rate (gpm)	Water Level Nonpumping (ft)	Water Level Pumping (ft)	Drawdown (ft)	Specific Capacity (gpm/ft)
1960	415	36.3	1457.8	7.0	111.0	104.0	14.0
1961	3727	124.7	557.6	54.0	154.0	100.0	5.6
1962	3936	129.1	546.7	72.0	169.0	97.0	5.6
1963	3649	117.4	536.2	74.0	170.0	96.0	5.6
1964	4174	130.3	520.3	81.0	183.0	102.0	5.1
1965	3007	97.9	542.6	63.0	170.0	107.0	5.1
1966	2589	83.9	540.1	50.0	169.0	119.0	4.5
1967	2519	84.9	561.7	39.0	153.0	114.0	4.9
1968	2183	74.0	565.0	32.0	147.0	115.0	4.9
1969	2244	75.7	562.2	22.0	142.0	120.0	4.7
1970	2369	79.7	560.7	22.0	143.0	121.0	4.6
1971	2633	89.1	564.0	31.0	162.0	131.0	4.3
1972	2215	75.3	566.6	31.0	163.0	132.0	4.3
1973	2628	87.2	553.0	37.0	170.0	133.0	4.2
1974	2282	73.9	539.7	35.0	161.0	126.0	4.3
1975	2308	74.4	537.3	42.0	168.0	126.0	4.3
1976	2521	79.6	526.2	50.0	176.0	126.0	4.2
1977	2782	84.2	504.4	47.0	167.0	120.0	4.2
1978	2306	75.6	546.3	42.0	162.0	120.0	4.6
1979	1354	45.9	564.6	13.0	134.0	121.0	4.7
1980	1955	62.9	536.3	21.0	146.0	125.0	4.3
1981	2299	73.9	537.7	26.0	144.0	118.0	4.5
1982	3707	108.1	486.0	71.0	180.0	109.0	4.5
1983	407	12.1	495.0	61.0	160.0	99.0	5.0
1984	2673	96.9	604.0	75.0	201.0	126.0	4.8
1985	1919	68.5	595.0	55.0	179.0	124.0	4.8
1986	1598	54.9	573.0	25.0	144.0	119.0	4.8
1987	2753	97.3	589.0	66.0	187.0	121.0	4.9

Appendix (cont)

Well LA-2

Year	Pump Time (h)	Production (10^6 gal.)	Pump Rate (gpm)	Water Level Nonpumping (ft)	Water Level Pumping (ft)	Drawdown (ft)	Specific Capacity (gpm/ft)
1947	963	27.6	477.7	—	—	—	—
1948	3659	59.3	270.1	—	—	—	—
1949	1654	41.8	421.2	—	—	—	—
1950	614	15.6	423.5	59.0	285.0	226.0	1.9
1951	2415	57.7	398.2	111.0	305.0	194.0	2.1
1952	1980	46.3	389.7	101.0	300.0	199.0	2.0
1953	2201	47.2	357.4	100.0	301.0	201.0	1.8
1954	2601	56.8	364.0	116.0	—	—	—
1955	2223	49.4	370.4	110.0	—	—	—
1956	1805	44.2	408.1	84.0	—	—	—
1957	1066	29.6	462.8	53.0	277.0	224.0	2.1
1958	1166	31.1	444.5	60.0	270.0	210.0	2.1
1959	1599	40.7	424.2	71.0	303.0	232.0	1.8
1960	2169	51.6	396.5	76.0	305.0	229.0	1.7
1961	2149	44.4	344.3	101.0	313.0	212.0	1.6
1962	1823	35.7	326.4	111.0	314.0	203.0	1.6
1963	1999	40.7	339.3	127.0	332.0	205.0	1.7
1964	1924	34.2	296.3	137.0	347.0	210.0	1.4
1965	1911	39.8	347.1	121.0	330.0	209.0	1.7
1966	1070	21.4	333.3	108.0	340.0	232.0	1.4
1967	238	4.9	343.1	78.0	304.0	226.0	1.5
1968	502	11.3	375.2	64.0	305.0	241.0	1.6
1969	155	3.8	408.6	50.0	297.0	247.0	1.7
1970	341	7.2	351.9	59.0	310.0	251.0	1.4
1971	1787	31.8	296.6	88.0	318.0	230.0	1.3
1972	2189	39.3	299.2	96.0	322.0	226.0	1.3
1973	2625	46.7	296.5	106.0	334.0	228.0	1.3
1974	2033	36.8	301.7	109.0	325.0	216.0	1.4
1975	2310	40.2	290.0	103.0	320.0	217.0	1.3
1976	2488	39.9	267.3	113.0	322.0	209.0	1.3
1977	2775	42.5	255.3	118.0	314.0	196.0	1.3
1978	2299	39.5	286.4	112.0	338.0	226.0	1.3
1979	1353	26.2	323.0	75.0	316.0	241.0	1.3
1980	1960	33.8	287.4	84.0	318.0	234.0	1.2
1981	1991	34.4	300.0	94.0	336.0	242.0	1.2
1982	3174	51.2	269.0	161.0	348.0	187.0	1.4
1983	2752	54.5	330.0	121.0	321.0	200.0	1.6
1984	2753	53.7	325.0	130.0	323.0	193.0	1.7
1985	2027	37.1	305.0	112.0	291.0	179.0	1.7
1986	1289	24.1	312.0	74.0	252.0	178.0	1.8
1987	2619	39.6	252.0	129.0	319.0	190.0	1.3

Appendix (cont)

Well LA-3

Year	Pump Time (h)	Production (10^6 gal.)	Pump Rate (gpm)	Water Level Nonpumping (ft)	Water Level Pumping (ft)	Drawdown (ft)	Specific Capacity (gpm/ft)
1947	1476	64.9	732.8	—	—	—	—
1948	3647	82.5	377.0	—	—	—	—
1949	1505	41.7	461.8	—	—	—	—
1950	2793	57.8	344.9	97.0	231.0	134.0	2.6
1951	3554	66.9	313.7	116.0	233.0	117.0	2.7
1952	2514	58.6	388.5	94.0	218.0	124.0	3.1
1953	3104	69.7	374.2	103.0	229.0	126.0	3.0
1954	2595	57.3	368.0	101.0	225.0	124.0	3.0
1955	2195	48.7	369.8	91.0	226.0	135.0	2.7
1956	1849	42.1	379.5	74.0	222.0	148.0	2.6
1957	1080	26.1	402.8	56.0	219.0	163.0	2.5
1958	1612	33.6	347.4	49.0	225.0	176.0	2.0
1959	1821	35.0	320.3	54.0	231.0	177.0	1.8
1960	2174	38.4	294.4	68.0	230.0	162.0	1.8
1961	1939	34.7	298.3	85.0	189.0	104.0	2.9
1962	2361	45.4	320.5	93.0	192.0	99.0	3.2
1963	2128	42.5	332.9	81.0	197.0	116.0	2.9
1964	2574	50.4	326.3	104.0	217.0	113.0	2.9
1965	1961	43.3	368.9	79.0	220.0	141.0	2.6
1966	2236	46.1	343.6	81.0	219.0	138.0	2.5
1967	2274	47.4	347.4	86.0	218.0	132.0	2.6
1968	2127	42.7	334.6	82.0	251.0	169.0	2.0
1969	2072	40.1	322.6	58.0	246.0	188.0	1.7
1970	2303	44.0	318.4	55.0	241.0	186.0	1.7
1971	2556	45.4	296.0	77.0	250.0	173.0	1.7
1972	2205	39.7	300.1	73.0	251.0	178.0	1.7
1973	977	20.3	346.3	65.0	248.0	183.0	1.9
1974	2291	43.5	316.5	73.0	244.0	171.0	1.9
1975	2306	43.3	313.0	80.0	253.0	173.0	1.8
1976	2474	42.3	285.0	88.0	260.0	172.0	1.7
1977	2779	47.3	283.7	89.0	248.0	159.0	1.8
1978	2308	42.4	306.4	87.0	250.0	163.0	1.9
1979	1343	28.1	348.1	58.0	243.0	185.0	1.9
1980	1952	35.1	299.9	61.0	237.0	176.0	1.7
1981	2297	41.5	301.1	70.0	240.0	170.0	1.8
1982	3691	54.9	247.0	118.0	246.0	128.0	1.9
1983	949	14.7	258.0	89.0	203.0	129.0	2.0
1984	838	16.6	329.0	142.0	301.0	159.0	2.0
1985	2078	41.9	336.0	104.0	280.0	176.0	1.9
1986	1328	26.9	338.0	88.0	255.0	167.0	2.0
1987	2710	50.9	313.0	118.0	289.0	171.0	1.8

Appendix (cont)

Well LA-4

Year	Pump Time (h)	Production (10^6 gal.)	Pump Rate (gpm)	Water Level Nonpumping (ft)	Water Level Pumping (ft)	Drawdown (ft)	Specific Capacity (gpm/ft)
1948	1570	42.7	453.3	—	—	—	—
1949	940	37.5	664.9	—	—	—	—
1950	4350	164.9	631.8	278.0	353.0	75.0	8.4
1951	4909	173.6	589.4	285.0	357.0	72.0	8.2
1952	3429	119.6	581.3	267.0	339.0	72.0	8.1
1953	3034	109.1	599.3	264.0	335.0	71.0	8.4
1954	2133	78.2	611.0	255.0	329.0	74.0	8.3
1955	2647	94.5	595.0	268.0	341.0	73.0	8.2
1956	3402	120.0	588.9	273.0	346.0	73.0	8.1
1957	2844	105.4	617.7	270.0	345.0	75.0	8.2
1958	2973	110.3	618.3	270.0	342.0	72.0	8.6
1959	3084	113.5	613.4	275.0	346.0	71.0	8.6
1960	4084	145.6	594.2	296.0	365.0	69.0	8.6
1961	3687	129.7	586.3	296.0	365.0	69.0	8.5
1962	3688	129.3	584.3	286.0	359.0	73.0	8.0
1963	3718	130.5	585.0	280.0	351.0	71.0	8.2
1964	4500	155.0	574.1	291.0	361.0	70.0	8.2
1965	3110	111.4	597.0	279.0	349.0	70.0	8.5
1966	3279	115.6	587.6	285.0	356.0	71.0	8.3
1967	2127	77.1	604.1	278.0	350.0	72.0	8.4
1968	2276	81.7	598.3	280.0	351.0	71.0	8.4
1969	1694	61.8	608.0	282.0	358.0	76.0	8.0
1970	2333	83.5	596.5	286.0	363.0	77.0	7.7
1971	2519	89.0	588.9	287.0	373.0	86.0	6.8
1972	2322	82.6	592.9	282.0	367.0	85.0	7.0
1973	2616	92.4	588.7	294.0	377.0	83.0	7.1
1974	2306	82.2	594.1	286.0	367.0	81.0	7.3
1975	2319	82.3	591.5	272.0	355.0	83.0	7.1
1976	2802	98.2	584.1	277.0	373.0	96.0	6.1
1977	2741	96.4	586.2	278.0	374.0	96.0	6.1
1978	2248	80.1	594.2	271.0	368.0	97.0	6.1
1979	2964	104.6	587.9	280.0	376.0	96.0	6.1
1980	3322	115.3	578.5	284.0	385.0	101.0	5.7
1981	2573	89.4	579.1	289.0	393.0	104.0	5.6
1982	0	0	0	—	—	—	—
1983	1840	61.5	577.0	287.0	392.0	105.0	5.3
1984	2695	87.1	539.0	290.0	383.0	93.0	5.8
1985	2667	86.4	540.0	292.0	378.0	86.0	6.3
1986	1172	38.8	552.0	284.0	377.0	93.0	5.9
1987	38	1.6	—	269.0	357.0	88.0	—

Appendix (cont)

Well LA-5

Year	Pump Time (h)	Production (10^6 gal.)	Pump Rate (gpm)	Water Level Nonpumping (ft)	Water Level Pumping (ft)	Drawdown (ft)	Specific Capacity (gpm/ft)
1948	1171	40.4	575.0	—	—	—	—
1949	1763	58.5	553.0	—	—	—	—
1950	4052	130.1	535.1	131.0	254.0	123.0	4.4
1951	6004	187.4	520.2	162.0	272.0	110.0	4.7
1952	3425	109.6	533.3	147.0	259.0	112.0	4.8
1953	3278	103.9	528.3	141.0	257.0	116.0	4.6
1954	2546	80.1	524.4	137.0	259.0	122.0	4.3
1955	3158	97.3	513.5	145.0	267.0	122.0	4.2
1956	3476	104.5	501.1	150.0	276.0	126.0	4.0
1957	2868	86.0	499.8	150.0	277.0	127.0	3.9
1958	3009	89.9	498.0	151.0	277.0	126.0	4.0
1959	3088	93.5	504.6	155.0	280.0	125.0	4.0
1960	4088	119.1	485.6	168.0	288.0	120.0	4.0
1961	3534	100.3	473.0	165.0	288.0	123.0	3.8
1962	3735	107.7	480.6	172.0	—	—	—
1963	3726	105.0	469.7	171.0	—	—	—
1964	4236	118.8	467.4	184.0	—	—	—
1965	1740	50.5	483.7	180.0	—	—	—
1966	2817	79.3	469.2	180.0	—	—	—
1967	2533	73.7	484.9	168.0	—	—	—
1968	2233	63.3	472.5	161.0	300.0	139.0	3.4
1969	2402	68.5	475.3	161.0	298.0	137.0	3.5
1970	2353	66.1	468.2	157.0	300.0	143.0	3.3
1971	2659	74.4	466.3	155.0	302.0	147.0	3.2
1972	2301	64.4	466.5	153.0	304.0	151.0	3.1
1973	2476	68.3	459.7	156.0	308.0	152.0	3.0
1974	1903	52.5	459.8	154.0	306.0	152.0	3.0
1975	2318	63.9	459.4	149.0	309.0	160.0	2.9
1976	2799	77.6	462.1	150.0	310.0	160.0	2.9
1977	2665	74.8	467.8	147.0	303.0	156.0	3.0
1978	2274	64.9	475.8	145.0	299.0	154.0	3.1
1979	2964	84.0	472.4	149.0	301.0	152.0	3.1
1980	3316	92.2	463.6	153.0	300.0	147.0	3.2
1981	3523	96.5	456.5	158.0	304.0	146.0	3.1
1982	3654	102.3	467.0	168.0	299.0	136.0	3.4
1983	2842	78.1	458.0	154.0	295.0	141.0	3.2
1984	2889	72.1	416.0	156.0	281.0	125.0	3.1
1985	2153	55.8	432.0	174.0	308.0	134.0	3.2
1986	1376	34.6	419.0	168.0	310.0	142.0	2.9
1987	1148	27.9	405.0	167.0	314.0	147.0	2.8

Appendix A (cont)

Well LA-6

Year	Pump Time (h)	Production (10^6 gal.)	Pump Rate (gpm)	Water Level Nonpumping (ft)	Water Level Pumping (ft)	Drawdown (ft)	Specific Capacity (gpm/ft)
1948	116	4.9	704.0	—	—	—	—
1949	2451	95.8	651.4	—	—	—	—
1950	4490	167.9	623.2	83.0	136.0	53.0	11.8
1951	5882	201.6	571.2	115.0	160.0	45.0	12.7
1952	3168	110.3	580.3	108.0	151.0	43.0	13.5
1953	3177	113.8	597.0	95.0	139.0	44.0	13.6
1954	2894	107.1	616.8	92.0	135.0	43.0	14.3
1955	2911	108.0	618.3	97.0	140.0	43.0	14.4
1956	3438	125.8	609.9	106.0	149.0	43.0	14.2
1957	2833	102.4	602.4	107.0	152.0	45.0	13.4
1958	2957	106.9	602.5	108.0	131.0	43.0	14.0
1959	3096	108.3	583.0	115.0	158.0	43.0	13.6
1960	4084	138.6	565.6	130.0	172.0	42.0	13.5
1961	3284	112.5	571.0	129.0	171.0	42.0	13.6
1962	3886	129.4	555.0	135.0	175.0	40.0	13.9
1963	2953	102.9	580.8	125.0	171.0	46.0	12.6
1964	4244	138.3	543.1	132.0	172.0	40.0	13.6
1965	3145	103.8	550.1	120.0	160.0	40.0	13.8
1966	3173	104.0	546.3	129.0	169.0	40.0	13.7
1967	2511	85.4	566.8	118.0	158.0	40.0	14.2
1968	2111	71.6	565.3	109.0	150.0	41.0	13.8
1969	2402	81.6	566.2	109.0	151.0	42.0	13.5
1970	2337	79.1	564.1	106.0	149.0	43.0	13.1
1971	2472	82.5	556.2	119.0	160.0	41.0	13.6
1972	2317	79.2	569.7	117.0	155.0	38.0	15.0
1973	2638	90.6	572.4	118.4	155.0	37.0	15.5
1974	2337	79.8	569.1	120.0	156.0	36.0	15.8
1975	1571	51.9	550.6	113.0	151.0	38.0	14.5
1976	175	5.1	485.7	96.0	—	—	—
1977	—	—	—	82.0	—	—	—
1978	33	1.1	572.7	77.0	142.0	65.0	8.8
1979	6	0.2	555.6	80.0	146.0	66.0	8.4
1980	4	0.1	520.8	82.0	142.0	60.0	8.7
1981	2.3	0.08	579.8	84.0	141.0	57.0	10.2
1982	—	—	—	90.0	—	—	—
1983	—	—	—	81.0	—	—	—
1984	—	—	—	83.0	—	—	—
1985	—	—	—	92.0	—	—	—
1986	—	—	—	—	—	—	—
1987	—	<0.1	—	—	—	—	—

Appendix (cont)

Well G-1

Year	Pump Time (h)	Production (10^6 gal.)	Pump Rate (gpm)	Water Level Nonpumping (ft)	Water Level Pumping (ft)	Drawdown (ft)	Specific Capacity (gpm/ft)
1950	0	2.8	0.0	195.0	—	—	—
1951	1168	37.7	538.0	202.0	309.0	107.0	5.0
1952	2476	75.5	508.2	213.0	295.0	82.0	6.2
1953	3275	97.3	495.2	221.0	292.0	71.0	7.0
1954	2616	77.8	495.7	221.0	290.0	69.0	7.2
1955	2406	70.5	448.4	226.0	295.0	69.0	7.1
1956	2958	83.2	468.8	235.0	303.0	68.0	6.9
1957	2098	55.9	444.1	236.0	307.0	71.0	6.3
1958	2460	68.1	461.4	238.0	308.0	70.0	6.6
1959	2952	82.4	465.2	245.0	314.0	69.0	6.7
1960	3564	96.0	448.9	254.0	325.0	71.0	6.3
1961	4236	112.4	442.2	260.0	333.0	73.0	6.1
1962	3431	93.6	454.7	258.0	342.0	84.0	5.4
1963	4519	114.9	423.8	265.0	348.0	83.0	5.1
1964	4374	113.8	433.6	269.0	352.0	83.0	5.2
1965	3530	90.7	428.2	268.0	352.0	84.0	5.1
1966	4074	102.6	419.7	269.0	363.0	94.0	4.5
1967	2615	69.9	445.5	266.0	362.0	96.0	4.6
1968	2996	78.9	438.9	264.0	366.0	102.0	4.3
1969	2657	68.3	428.4	266.0	376.0	110.0	3.9
1970	2712	64.7	397.6	264.0	377.0	113.0	3.5
1971	2908	67.9	389.2	258.0	378.0	120.0	3.2
1972	2865	66.1	384.5	264.0	389.0	125.0	3.1
1973	2997	67.5	375.4	271.0	403.0	132.0	2.8
1974	2767	62.3	375.3	283.0	412.0	129.0	2.9
1975	2467	55.7	376.3	293.0	411.0	118.0	3.2
1976	2962	65.1	366.3	—	—	—	—
1977	2734	57.9	353.0	275.0	426.0	151.0	2.3
1978	2656	56.0	351.4	270.0	419.0	149.0	2.4
1979	2998	61.7	342.9	271.0	422.0	151.0	2.3
1980	3459	68.3	329.0	273.0	428.0	155.0	2.1
1981	4427	81.6	307.2	275.0	444.0	169.0	1.8
1982	3678	69.0	313.0	278.0	443.0	165.0	1.9
1983	2871	52.2	303.0	272.0	443.0	171.0	1.8
1984	3804	62.8	275.0	276.0	448.0	172.0	1.5
1985	3004	48.3	268.0	278.0	450.0	172.0	1.6
1986	2027	30.3	249.0	279.0	450.0	171.0	1.5
1987	2070	29.2	235.0	280.0	451.0	171.0	1.4

Appendix (cont)

Well G-1A

Year	Pump Time (h)	Production (10^6 gal.)	Pump Rate (gpm)	Water Level Nonpumping (ft)	Water Level Pumping (ft)	Drawdown (ft)	Specific Capacity (gpm/ft)
1954	108	4.6	709.0	—	—	—	—
1955	1531	53.0	577.0	265.0	316.0	51.0	11.3
1956	3130	107.7	573.5	273.0	323.0	50.0	11.5
1957	2470	87.0	587.0	274.0	327.0	53.0	11.1
1958	2670	92.5	577.4	279.0	331.0	52.0	11.1
1959	2965	102.7	577.3	284.0	333.0	49.0	11.8
1960	3641	122.8	562.1	291.0	342.0	51.0	11.0
1961	4297	147.3	571.3	298.0	350.0	52.0	11.0
1962	3972	136.1	571.1	295.0	344.0	49.0	11.7
1963	4525	149.7	551.4	301.0	350.0	49.0	11.3
1964	3852	129.3	559.4	302.0	353.0	51.0	11.0
1965	3505	116.5	554.0	302.0	353.0	51.0	10.9
1966	3964	133.4	560.9	306.0	355.0	49.0	11.4
1967	2720	91.3	559.4	302.0	351.0	49.0	11.4
1968	3089	103.2	556.8	302.0	352.0	50.0	11.1
1969	2695	90.7	560.9	303.0	356.0	53.0	10.6
1970	2772	92.5	556.2	300.0	357.0	57.0	9.8
1971	3313	111.8	562.4	303.0	361.0	58.0	9.7
1972	2879	94.0	544.2	302.0	361.0	59.0	9.2
1973	2760	87.9	530.8	302.0	362.0	60.0	8.8
1974	2974	92.7	519.5	307.0	355.0	48.0	10.8
1975	2740	85.3	518.9	304.0	351.0	47.0	11.0
1976	2983	91.6	511.8	302.0	350.0	48.0	10.7
1977	2942	88.7	502.5	302.0	350.0	48.0	10.5
1978	2631	77.9	493.5	300.0	345.0	45.0	11.0
1979	2974	88.0	493.9	301.0	345.0	44.0	11.0
1980	3480	103.2	494.4	305.0	345.0	40.0	12.4
1981	4212	131.2	519.1	307.0	347.0	40.0	13.0
1982	3618	109.7	505.0	305.0	347.0	42.0	12.0
1983	2901	86.7	498.0	301.0	336.0	35.0	14.2
1984	3789	113.9	501.0	302.0	345.0	43.0	11.7
1985	4430	128.4	483.0	306.0	348.0	42.0	11.5
1986	4644	130.4	468.0	310.0	351.0	41.0	11.4
1987	4468	122.5	457.0	320.0	362.0	42.0	10.9

Appendix (cont)

Well G-2

Year	Pump Time (h)	Production (10^6 gal.)	Pump Rate (gpm)	Water Level Nonpumping (ft)	Water Level Pumping (ft)	Drawdown (ft)	Specific Capacity (gpm/ft)
1951	123	3.9	528.5	259.0	—	—	—
1952	2372	78.3	550.2	279.0	327.0	48.0	11.5
1953	3254	105.6	540.9	290.0	334.0	44.0	12.3
1954	2682	86.3	536.3	291.0	335.0	44.0	12.2
1955	2487	78.8	528.1	299.0	345.0	46.0	11.5
1956	3109	95.8	513.6	310.0	357.0	47.0	10.9
1957	2458	76.1	516.0	311.0	360.0	49.0	10.5
1958	2707	80.1	493.2	315.0	361.0	46.0	10.7
1959	2938	84.6	479.9	320.0	363.0	43.0	11.2
1960	3535	96.6	455.4	328.0	370.0	42.0	10.8
1961	3982	105.3	440.7	336.0	375.0	39.0	11.3
1962	4076	99.8	408.1	338.0	374.0	36.0	11.3
1963	4563	105.7	386.1	344.0	379.0	35.0	11.0
1964	4541	105.3	386.5	346.0	380.0	34.0	11.4
1965	3535	82.6	389.4	346.0	381.0	35.0	11.1
1966	3994	94.7	395.2	349.0	383.0	34.0	11.6
1967	2743	67.6	410.7	344.0	379.0	35.0	11.7
1968	2732	66.5	405.7	344.0	379.0	35.0	11.6
1969	2679	68.6	426.8	344.0	381.0	37.0	11.5
1970	2431	62.8	430.5	343.0	381.0	38.0	11.3
1971	3420	87.4	425.9	345.0	384.0	39.0	10.9
1972	2887	73.4	423.7	348.0	388.0	40.0	10.6
1973	2816	72.4	428.5	344.0	385.0	41.0	10.5
1974	3056	82.0	447.2	347.0	390.0	43.0	10.4
1975	2724	74.5	455.8	341.0	384.0	43.0	10.6
1976	2990	81.1	452.1	344.0	388.0	44.0	10.3
1977	2981	80.4	449.5	346.0	388.0	42.0	10.7
1978	2562	71.6	451.9	345.0	386.0	41.0	11.0
1979	2975	80.0	448.0	347.0	388.0	41.0	11.0
1980	3478	92.4	443.0	350.0	389.0	39.0	11.4
1981	1432	38.3	445.8	352.0	390.0	38.0	11.7
1982	2833	25.7	476.0	352.0	399.0	47.0	10.1
1983	624	16.5	441.0	356.0	399.0	43.0	10.3
1984	2018	43.7	361.0	358.0	385.0	27.0	13.4
1985	4339	96.6	371.0	352.0	381.0	29.0	12.8
1986	4769	109.3	382.0	369.0	395.0	26.0	14.7
1987	4526	109.7	404.0	366.0	399.0	33.0	12.2

Appendix (cont)

Well G-3

Year	Pump Time (h)	Production (10^6 gal.)	Pump Rate (gpm)	Water Level Nonpumping (ft)	Water Level Pumping (ft)	Drawdown (ft)	Specific Capacity (gpm/ft)
1951	192	7.3	633.7	281.0	—	—	—
1952	2379	65.4	458.2	310.0	358.0	48.0	9.5
1953	3192	76.4	398.9	322.0	360.0	38.0	10.5
1954	2675	66.1	411.8	322.0	370.0	48.0	8.6
1955	2369	69.4	488.3	316.0	368.0	52.0	9.4
1956	3149	87.9	465.2	324.0	380.0	56.0	8.3
1957	2517	70.2	464.8	324.0	385.0	61.0	7.6
1958	2562	69.5	452.1	323.0	386.0	63.0	7.2
1959	2931	74.6	424.2	326.0	395.0	69.0	6.1
1960	3591	82.5	382.9	335.0	407.0	72.0	5.3
1961	3612	79.9	368.7	343.0	414.0	71.0	5.2
1962	4057	83.7	343.9	348.0	418.0	70.0	4.9
1963	4555	86.7	317.2	352.0	422.0	70.0	4.5
1964	4487	78.6	292.0	355.0	424.0	69.0	4.2
1965	3498	65.6	312.6	350.0	419.0	69.0	4.5
1966	3991	73.7	307.8	353.0	420.0	67.0	4.6
1967	2752	52.9	320.4	344.0	418.0	74.0	4.3
1968	3086	56.5	305.1	341.0	418.0	77.0	4.0
1969	2672	50.8	316.9	338.0	417.0	79.0	4.0
1970	2736	55.4	337.5	336.0	419.0	83.0	4.1
1971	3337	64.2	320.6	342.0	423.0	81.0	4.0
1972	2838	50.9	298.9	341.0	421.0	80.0	3.7
1973	2843	47.3	277.3	341.0	418.0	77.0	3.6
1974	3006	49.3	273.3	342.0	424.0	82.0	3.3
1975	2632	43.1	272.9	341.0	428.0	87.0	3.1
1976	2971	82.6	463.4	359.0	447.0	88.0	5.3
1977	2961	78.9	444.1	353.0	448.0	95.0	4.7
1978	2590	66.4	427.5	345.0	443.0	98.0	4.4
1979	3014	69.0	381.0	345.0	450.0	105.0	3.6
1980	3448	61.8	298.6	348.0	453.0	105.0	2.8
1981	4315	66.6	257.2	357.0	467.0	110.0	2.3
1982	3550	51.0	239.0	349.0	459.0	110.0	2.2
1983	2183	31.3	239.0	340.0	463.0	123.0	1.9
1984	1211	19.0	267.0	355.0	475.0	120.0	2.2
1985	1587	22.1	232.0	351.0	470.0	119.0	2.0
1986	2266	26.7	196.0	375.0	492.0	117.0	1.7
1987	—	<0.1	—	—	—	—	—

Appendix (cont)

Well G-4

Year	Pump Time (h)	Production (10^6 gal.)	Pump Rate (gpm)	Water Level Nonpumping (ft)	Water Level Pumping (ft)	Drawdown (ft)	Specific Capacity (gpm/ft)
1951	—	12.5	—	357.0	477.0	120.0	—
1952	2401	56.9	395.0	374.0	474.0	100.0	3.9
1953	2677	55.2	343.7	380.0	472.0	92.0	3.7
1954	2256	58.8	434.4	383.0	526.0	143.0	3.0
1955	1172	22.7	322.8	378.0	481.0	103.0	3.1
1956	1800	33.9	313.9	377.0	491.0	114.0	2.8
1957	1324	24.2	304.6	373.0	498.0	125.0	2.4
1958	1970	35.9	303.7	370.0	490.0	120.0	2.5
1959	1819	31.6	289.5	378.0	494.0	116.0	2.5
1960	2457	37.0	251.0	385.0	509.0	124.0	2.0
1961	2787	45.0	269.1	389.0	512.0	123.0	2.2
1962	2738	41.7	253.8	386.0	505.0	119.0	2.1
1963	3519	46.4	219.8	388.0	504.0	116.0	1.9
1964	3561	42.9	200.8	396.0	499.0	103.0	1.9
1965	2100	23.8	188.9	394.0	492.0	98.0	1.9
1966	2219	33.6	252.4	391.0	498.0	107.0	2.4
1967	2690	44.8	277.6	388.0	509.0	121.0	2.3
1968	2083	31.4	251.2	386.0	509.0	123.0	2.0
1969	1309	17.4	221.5	387.0	505.0	118.0	1.9
1970	606	7.7	211.8	384.0	504.0	120.0	1.8
1971	1640	21.0	213.4	389.0	503.0	114.0	1.9
1972	2840	33.3	195.4	391.0	507.0	116.0	1.7
1973	3006	37.2	206.3	392.0	521.0	129.0	1.6
1974	2672	34.3	213.9	392.0	519.0	127.0	1.7
1975	1977	41.0	345.6	403.0	559.0	156.0	2.2
1976	2859	57.8	336.9	406.0	571.0	165.0	2.0
1977	2954	62.4	352.1	406.0	589.0	183.0	1.9
1978	2607	49.5	316.5	398.0	589.0	191.0	1.7
1979	2974	52.9	296.4	395.0	586.0	191.0	1.6
1980	2235	35.6	265.7	394.0	580.0	186.0	1.4
1981	432	8.2	316.4	385.0	573.0	188.0	1.7
1982	3657	65.2	297.0	386.0	578.0	192.0	1.5
1983	2604	42.2	270.0	—	—	—	—
1984	3766	49.7	220.0	—	—	—	—
1985	1747	21.7	207.0	402.0	572.0	170.0	1.2
1986	2678	33.9	211.0	396.0	574.0	178.0	1.2
1987	2011	25.1	208.0	398.0	573.0	175.0	1.2

Appendix (cont)

Well G-5

Year	Pump Time (h)	Production (10^6 gal.)	Pump Rate (gpm)	Water Level Nonpumping (ft)	Water Level Pumping (ft)	Drawdown (ft)	Specific Capacity (gpm/ft)
1951	—	6.7	—	414.0	—	—	—
1952	2579	73.8	476.9	422.0	480.0	58.0	8.2
1953	1433	37.8	439.6	425.0	467.0	42.0	10.5
1954	2617	80.9	515.2	429.0	473.0	44.0	11.7
1955	2529	80.4	529.9	427.0	472.0	45.0	11.8
1956	3052	97.0	529.7	431.0	478.0	47.0	11.3
1957	2385	64.1	447.9	424.0	466.0	42.0	10.7
1958	1523	49.1	537.3	428.0	477.0	49.0	11.0
1959	2917	101.7	581.1	435.0	495.0	60.0	9.7
1960	2828	98.0	577.6	437.0	501.0	64.0	9.0
1961	3908	134.0	571.5	438.0	507.0	69.0	8.3
1962	4186	142.0	565.4	440.0	511.0	71.0	8.0
1963	4528	151.0	555.8	441.0	513.0	72.0	7.7
1964	4532	150.4	553.1	446.0	516.0	70.0	7.9
1965	3520	117.1	554.5	443.0	516.0	73.0	7.6
1966	2555	83.2	542.7	445.0	520.0	75.0	7.2
1967	2405	80.0	554.4	444.0	519.0	75.0	7.4
1968	2513	81.2	538.5	443.0	517.0	74.0	7.3
1969	2649	83.3	524.1	450.0	520.0	70.0	7.5
1970	2771	88.9	534.7	453.0	521.0	68.0	7.9
1971	2657	88.3	553.9	450.0	521.0	71.0	7.8
1972	2902	92.4	530.7	441.0	514.0	73.0	7.3
1973	3003	97.5	541.1	444.0	515.0	71.0	7.6
1974	2054	69.0	559.9	440.0	513.0	73.0	7.7
1975	2266	74.7	549.4	433.0	500.0	67.0	8.2
1976	2955	95.0	535.8	442.0	504.0	62.0	8.6
1977	2836	92.1	541.3	444.0	504.0	60.0	9.0
1978	2608	84.2	538.4	442.0	502.0	60.0	9.0
1979	2766	86.5	521.5	442.0	502.0	60.0	8.7
1980	2896	89.0	512.4	442.0	502.0	60.0	8.5
1981	2124	66.7	523.4	451.0	528.0	77.0	6.8
1982	1219	38.2	522.0	455.0	510.0	55.0	9.5
1983	2904	73.2	420.0	445.0	492.0	47.0	8.9
1984	3838	115.4	501.0	452.0	507.0	55.0	9.4
1985	2193	67.9	516.0	453.0	509.0	56.0	9.2
1986	2219	52.5	394.0	453.0	494.0	41.0	9.6
1987	5732	116.7	379.0	462.0	504.0	42.0	9.0

Appendix (cont)

Well G-6

Year	Pump Time (h)	Production (10^6 gal.)	Pump Rate (gpm)	Water Level Nonpumping (ft)	Water Level Pumping (ft)	Drawdown (ft)	Specific Capacity (gpm/ft)
1964	1912	45.0	392.3	581.0	659.0	78.0	5.0
1965	3200	74.9	390.1	582.0	660.0	78.0	5.0
1966	3931	92.2	390.9	585.0	658.0	73.0	5.4
1967	2454	57.8	392.6	580.0	653.0	73.0	5.4
1968	2597	56.2	360.7	574.0	647.0	73.0	4.9
1969	2698	55.6	343.5	568.0	636.0	68.0	5.1
1970	2765	51.0	307.4	569.0	634.0	65.0	4.7
1971	2932	42.8	243.3	573.0	629.0	56.0	4.3
1972	2516	57.0	377.6	578.0	670.0	92.0	4.1
1973	2991	65.3	363.9	579.0	667.0	88.0	4.1
1974	2950	63.8	360.5	579.0	665.0	86.0	4.2
1975	2717	56.7	347.8	577.0	659.0	82.0	4.2
1976	2966	57.8	324.8	584.0	662.0	78.0	4.2
1977	2954	54.4	306.9	586.0	659.0	73.0	4.2
1978	2218	38.4	288.9	581.0	645.0	64.0	4.5
1979	1030	18.2	295.1	579.0	645.0	66.0	4.8
1980	1789	34.5	321.5	583.0	670.0	87.0	3.7
1981	4302	76.5	296.4	586.0	673.0	87.0	3.4
1982	3763	63.6	281.0	588.0	669.0	81.0	3.5
1983	1960	35.4	301.0	582.0	668.0	86.0	3.5
1984	3010	55.3	306.0	589.0	666.0	77.0	3.9
1985	3980	71.4	299.0	586.0	664.0	78.0	3.8
1986	4420	76.7	293.0	576.0	654.0	78.0	3.8
1987	5100	81.4	266.0	595.0	671.0	76.0	3.5

Appendix (cont)

Well PM-1

Year	Pump Time (h)	Production (10^6 gal.)	Pump Rate (gpm)	Water Level Nonpumping (ft)	Water Level Pumping (ft)	Drawdown (ft)	Specific Capacity (gpm/ft)
1965	2754	99.2	600.3	746.0	786.0	40.0	15.0
1966	3086	108.0	583.3	740.0	779.0	39.0	15.0
1967	2870	111.0	644.6	737.0	781.0	44.0	14.6
1968	1846	68.1	614.8	735.0	769.0	34.0	18.1
1969	951	34.4	602.9	733.0	766.0	33.0	18.3
1970	1781	66.2	619.5	733.0	769.0	36.0	17.2
1971	2728	101.0	617.1	733.0	766.0	33.0	18.7
1972	2415	84.9	585.9	735.0	762.0	27.0	21.7
1973	1688	46.5	459.1	736.0	755.0	19.0	24.2
1974	2649	96.3	605.9	740.0	768.0	28.0	21.6
1975	2567	94.8	615.5	741.0	766.0	25.0	24.6
1976	2933	106.8	606.9	744.0	767.0	23.0	26.4
1977	2969	105.4	591.7	745.0	767.0	22.0	26.9
1978	2544	90.6	593.3	745.0	767.0	22.0	27.0
1979	2350	83.4	591.5	744.0	766.0	22.0	26.9
1980	2786	98.5	588.6	746.0	769.0	23.0	25.7
1981	2789	98.5	588.6	747.0	769.0	22.0	26.8
1982	2820	99.6	589.0	748.0	770.0	22.0	26.8
1983	2464	86.5	585.0	747.0	769.0	22.0	26.6
1984	2667	92.8	580.0	749.0	772.0	23.0	25.6
1985	2760	95.4	576.0	749.0	770.0	21.0	27.4
1986	2130	73.9	578.0	748.0	770.0	22.0	26.3
1987	2912	102.4	586.0	752.0	773.0	21.0	27.9

Appendix (cont)

Well PM-2

Year	Pump Time (h)	Production (10^6 gal.)	Pump Rate (gpm)	Water Level Nonpumping (ft)	Water Level Pumping (ft)	Drawdown (ft)	Specific Capacity (gpm/ft)
1966	221	18.9	1425.3	826.0	889.0	63.0	22.6
1967	4336	370.0	1422.2	834.0	888.0	54.0	26.3
1968	3865	328.2	1415.3	838.0	889.0	51.0	27.8
1969	3304	279.9	1411.9	838.0	890.0	52.0	27.2
1970	3529	300.6	1419.7	839.0	893.0	54.0	26.3
1971	4035	339.5	1402.3	841.0	898.0	57.0	24.6
1972	4611	385.3	1392.7	845.0	902.0	57.0	24.4
1973	4571	380.6	1387.7	849.0	907.0	58.0	23.9
1974	5443	450.9	1380.7	853.0	912.0	59.0	23.4
1975	4644	385.3	1382.8	854.0	913.0	59.0	23.4
1976	5382	442.0	1368.8	866.0	924.0	58.0	23.6
1977	3306	272.8	1375.3	868.0	924.0	56.0	24.6
1978	4743	388.4	1364.9	871.0	928.0	57.0	23.9
1979	4671	381.8	1262.2	872.0	924.0	52.0	26.2
1980	5023	409.6	1359.2	873.0	931.0	58.0	23.4
1981	4551	370.1	1355.4	876.0	934.0	58.0	23.4
1982	4319	359.3	1386.0	874.0	934.0	60.0	23.1
1983	1922	157.9	1369.0	876.0	935.0	59.0	23.2
1984	996	81.6	1365.0	866.0	930.0	64.0	21.7
1985	1749	143.3	1365.0	851.0	916.0	65.0	21.0
1986	1036	84.4	1359.0	851.0	915.0	64.0	21.2
1987	351	28.3	1340.0	851.0	907.0	56.0	23.9

Appendix (cont)

Well PM-3

Year	Pump Time (h)	Production (10^6 gal.)	Pump Rate (gpm)	Water Level Nonpumping (ft)	Water Level Pumping (ft)	Drawdown (ft)	Specific Capacity (gpm/ft)
1968	2327	187.4	1342.2	743.0	771.0	28.0	47.9
1969	3241	254.7	1309.8	746.0	772.0	26.0	50.4
1970	2905	227.8	1306.9	750.0	774.0	24.0	54.5
1971	2774	216.3	1299.6	751.0	774.0	23.0	56.5
1972	2445	192.1	1309.5	752.0	775.0	23.0	56.9
1973	3256	257.8	1319.6	755.0	778.0	23.0	57.4
1974	3241	255.3	1312.9	756.0	779.0	23.0	57.1
1975	3421	269.3	1312.0	757.0	780.0	23.0	57.0
1976	3171	268.3	1410.2	758.0	784.0	26.0	54.2
1977	2792	235.5	1405.8	758.0	784.0	26.0	54.1
1978	2516	211.0	1397.6	759.0	784.0	25.0	55.9
1979	2359	197.2	1393.0	760.0	784.0	24.0	58.0
1980	2796	234.4	1397.2	760.0	785.0	25.0	55.9
1981	2784	232.4	1391.3	761.0	786.0	25.0	55.6
1982	2831	238.1	1402.0	762.0	785.0	23.0	60.9
1983	2496	207.6	1386.0	762.0	785.0	23.0	60.3
1984	3317	275.6	1385.0	762.0	787.0	25.0	55.4
1985	2643	221.2	1395.0	762.0	784.0	22.0	63.4
1986	2920	244.8	1397.0	763.0	787.0	24.0	58.2
1987	2984	250.2	1397.0	763.0	788.0	25.0	55.9

Appendix (cont)

Well PM-4

Year	Pump Time (h)	Production (10^6 gal.)	Pump Rate (gpm)	Water Level Nonpumping (ft)	Water Level Pumping (ft)	Drawdown (ft)	Specific Capacity (gpm/ft)
1982	869	76.2	1460	1050	1091	41	35.6
1983	5267	452.5	1432	1066	1101	35	40.9
1984	4059	325.8	1338	1065	1104	39	34.3
1985	4759	379.2	1328	1066	1101	35	37.9
1986	3925	307.4	1305	1084	1119	35	37.3
1987	5071	392.2	1289	1081	1117	36	35.8

Appendix (cont)

Well PM-5

Year	Pump Time (h)	Production (10^6 gal.)	Pump Rate (gpm)	Water Level Nonpumping (ft)	Water Level Pumping (ft)	Drawdown (ft)	Specific Capacity (gpm/ft)
1985	—	2.0	—	—	—	—	—
1986	2047	147.3	1199	—	—	—	—
1987	1620	118.6	1220	—	—	—	—

Appendix (cont)

Water Canyon Gallery

Year	Time (h)	Production (10^6 gal.)	Discharge Rate (gpm)
1947	8760	84.0	159.8
1948	8784	97.0	184.0
1949	8760	92.0	175.0
1950	8760	54.0	102.7
1951	8760	39.0	74.2
1952	8784	48.0	91.1
1953	8760	39.0	74.2
1954	8760	40.0	76.1
1955	8760	33.0	62.8
1956	8784	23.0	43.6
1957	8760	40.0	76.1
1958	8760	60.0	114.2
1959	8760	54.0	102.7
1960	8784	48.0	91.1
1961	8760	54.0	102.7
1962	8760	67.0	127.5
1963	8760	51.0	97.0
1964	8784	45.0	85.4
1965	8760	72.0	137.0
1966	8760	82.0	156.0
1967	8760	56.0	106.5
1968	8784	65.0	123.3
1969	8760	80.0	152.2
1970	8760	65.0	123.7
1971	8760	37.0	70.4
1972	8784	40.0	75.9
1973	8760	49.0	93.2
1974	8760	35.0	66.6
1975	8760	42.0	79.9
1976	8784	41.0	77.8
1977	8760	57.0	108.4
1978	8760	45.0	86.2
1979	8760	44.0	83.7
1980	8784	32.0	60.7
1981	8760	45.5	86.6
1982	8760	45.9	94.9
1983	8760	38.2	72.7
1984	8784	34.0	65.4
1985	8760	36.6	69.6
1986	8760	28.2	53.6
1987	8760	34.2	65.1

LA-7308-MS
Informal Report

UC-70
Issued: May 1978

Geologic Description of Cores from Holes P-3 MH-1 Through P-3 MH-5, Area G, Technical Area 54

William D. Purtymun
Merlin L. Wheeler
Margaret Anne Rogers

los alamos
scientific laboratory
of the University of California
LOS ALAMOS, NEW MEXICO 87545

An Affirmative Action/Equal Opportunity Employer

UNITED STATES
DEPARTMENT OF ENERGY
CONTRACT W-7405-ENG. 36

GEOLOGIC DESCRIPTION OF CORES FROM HOLES P-3 MH-1 THROUGH P-3 MH-5, AREA G, TECHNICAL AREA 54

by

William D. Purtymun
Merlin L. Wheeler
Margaret Anne Rogers

ABSTRACT

Five horizontal holes were cored beneath Pit 3 near the southeast edge of Mesita del Buey at Area G. The pit, filled and covered by 1966, contains solid radioactive wastes. The holes were cored to obtain samples of the tuff underlying the pit to determine if there has been any migration of radionuclides by infiltration of water in the past 10 yr. The five holes were collared in Unit 2b of the Tshirege Member of the Bandelier Tuff; three of the holes plunged downward into Unit 2a. This report describes the rock units penetrated by core holes and the joint characteristics observed. The locations of core samples selected for analyses are related to the floor of the pit.

I. INTRODUCTION

Mesita del Buey is a narrow, southeast-trending mesa near the eastern margin of the Pajarito Plateau (Fig. 1). The mesa slopes gently from an elevation of about 2100 m near its western edge to about 2000 m at its eastern edge. It is covered with a thin clay soil, underlain by a series of ashflows of rhyolite tuff.[1] Southeast-trending canyons to the north and south of the mesa have cut 15 to 40 m below the mesa surface.

Area G, Technical Area 54 (TA-54), has been designated by the Los Alamos Scientific Laboratory (LASL) for the disposal and storage of solid radioactive wastes. These wastes are placed in shafts or pits dug into the surface of the mesa. Studies made by the U. S. Geological Survey in 1973-74 emphasized the need to determine if any contamination from these wastes had moved into the underlying tuff.[2]

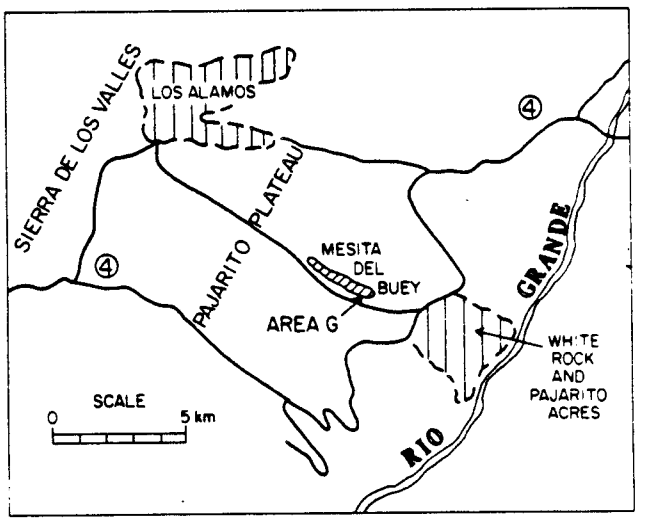

Fig. 1.
Location of Mesita del Buey on the Pajarito Plateau.

Pit 3, one of the older pits in Area G, was excavated in 1963 and covered by 1966. It is located in the southeastern part of the area (Fig. 2). Since Pit 3 waste was buried over 10 yr ago, this area is one of the better sites at LASL for studying the possible migration of radionuclides. Five horizontal holes were cored under Pit 3 using air as a cuttings carrier to avoid contamination of the core by water (Fig. 3). A vertical hole was also cored through the tuff and into the top of the underlying basalt, to obtain geologic information. The coring was done during the period from April 6 through May 23, 1976, by Reynolds Electrical and Engineering Company (REECo) of Las Vegas, Nevada. Construction and completion data for each core hole were published in a summary report prepared by REECo.[3]

The holes were oriented to pass about 1 m beneath the pit. The elevation of the floor of the pit ranged from 2021.3 to 2021.6 m above sea level. The core holes were collared at elevations ranging from 2019.6 to 2019.9 m and were oriented at angles of 00°57' to 4°00' above a horizontal plane (Table I). As coring of a given hole progressed, the vertical angle decreased due to gravitational forces and rotation of the coring assembly and drill stem. At some distance from the collar, the hole returned to horizontal and assumed a negative angle plunging gently downward beneath the pit.

During drilling operations, the air and cuttings from the hole were collected through air lines and discharged into a closed tank partially filled with water. The water retained most of the cuttings. The air from the tank was exhausted through high-velocity filters to retain any remaining dust that might otherwise have been transmitted into the atmosphere. Water and cuttings from the tank were monitored for radioactive contamination, as was ambient air in the area. No contamination was detected in the water, cuttings, or air.

The cores were about 4.8 cm in diameter. Each was packaged in plastic wrap and boxed according to hole and distance from hole collar. Later, in the laboratory, the cores were described, and sections of core were removed for radiochemical analyses.

Core runs varied in length from 1.5 to 6.1 m. In most runs, the first part of the core was lost due to abrasion in the core barrel and erosion of the core by the cuttings carrier (air). Thus all cores were described from the end of a run. A core was sampled about every 1.5 m to within a distance of 5.5 m of the pit. From that point onward the core was sampled about every 0.3 m. Where possible, every other sample included joints or fractures within the core. Core

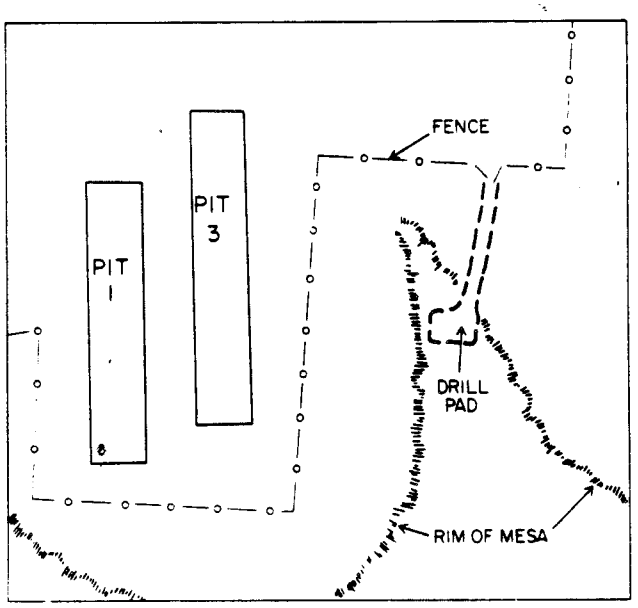

Fig. 2.
Southeastern part of Area G showing location of waste pits and drill pad.

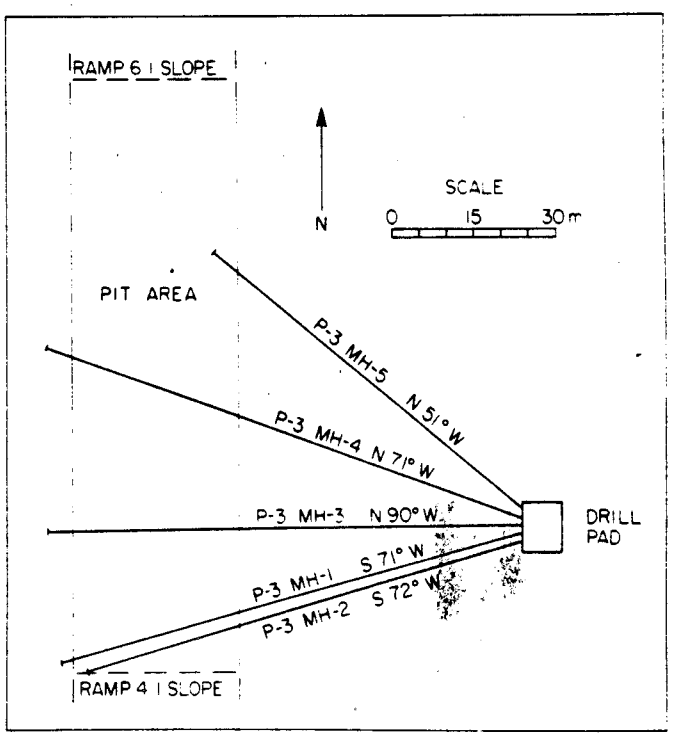

Fig. 3.
Orientation of core holes beneath Pit 3, Area G.

TABLE I

SUMMARY OF CORE HOLE DATA

	Core Holes				
	P-3 MH-1	P-3 MH-2	P-3 MH-3	P-3 MH-4	P-3 MH-5
Hole collar elevation (m)	2019.6	2019.8	2019.7	2019.8	2019.9
Initial angle above horizontal	00°57'	03.°00'	03°15'	03°00'	04°00'
Hole orientation	S73°W	S72°W	N90°W	N70°W	N51°W
Distance to horizontal (m)	12	34	38	28	42
Total distance cored (m)	87.5	82.9	86.9	92.7	73.2
Total core recovered (%)	56	74	59	51	75
Unit 2b cored (m)	45.1	82.9	85.4	69.5	73.2
Unit 2b core recovered (%)	75	74	58	52	75
Unit 2a cored (m)	42.5	---	1.5	23.2	---
Unit 2a core recovered (%)	37	---	100	49	---
Hole length at near edge of pit (m)	53.2	53.6	51.8	54.9	67.1
Hole length at far edge of pit (m)	84.6	82.9[a]	82.3	87.8	73.2[b]
Depth beneath pit at near edge (m)	3.4	1.2	0.6	0.8	0.0
Depth beneath pit at far edge (m)	7.2	3.1	3.1	4.4	0.3

[a]Completed beneath pit.
[b]Completed in fill within the pit.

sections, 5 to 6 cm in length, were stored in glass jars pending radiochemical analyses.

A radiochemical analyses sheet and core log were prepared. The sample number, depth, and designation of sample type were noted. BLK designated core with no joints or fractures; JO, core with open joint, light weathering on the joint surface; JFB; core with joint filled or plated with brown clay; and JFC, core with joint filled or plated with caliche and minor amounts of brown clay. Laboratory numbers ranged from MAR-77.00751 to MAR-77.01104,* for a total of 354 samples selected from the 5 core holes.

*Laboratory numbers, Analytical Chemistry Data Base, Group H-8, LASL.

II. GEOLOGY

Mesita del Buey is underlain by the Tshirege Member of the Bandelier Tuff. The geology and hydrology have been described in previous reports.[4,5] The units of the Tshirege Member important to this study were Unit 2b (Qbt_{2b}) and the underlying Unit 2a (Qbt_{2a}).

Unit 2b is a light gray to light pinkish-brown, moderately welded tuff that contains quartz and sanidine crystals and crystal fragments in an ash matrix. The unit contains some fragments of latite.

rhyolite, and pumice, which vary in size from less than 1 cm to over 5 cm in length. The pumice fragments, light to dark gray, are devitrified and increase in size and frequency near the contact with Unit 2a. Unit 2b color changes from a light pinkish-brown at the hole collars to light gray above the contact with the underlying unit. It is a moderately welded tuff at the hole collars grading into a nonwelded tuff at the contact.

The contact zone between Units 2b and 2a is a medium sand composed of quartz, sanidine, and reworked tuff in a matrix of ash. It is slightly more cohesive than the lower part of Unit 2b and the underlying Unit 2a.

The cored upper part of Unit 2a is a light gray, nonwelded tuff composed of quartz and sanidine crystals and crystal fragments with some rock fragments of latite, rhyolite, and pumice in an ash matrix. The pumice fragments are light gray to dark brown and decrease in size downward from the contact.

The two units at Area G dip gently to the southeast. Unit 2b, forming the upper surface and edge of the mesa, thins to the southeast as the result of deposition and erosion. Unit 2a also thins to the southeast; however, this is the result of deposition of the flow over a topographic high on older basalts.[5]

The thickness of Unit 2b in the southeast part of Area G (Pit 3) is about 11 m and is composed of a single ash flow. At the contact with Unit 2a the sand ranges from less than 2 cm to as much as 8 cm thick, dipping gently to the southeast. In this area, Unit 2a is about 10 m thick and is composed of two ashflows. Only the upper flow was penetrated by the core holes.

After completion of core hole P-3 MH-5, the last horizontal hole under Pit 3, a vertical hole was drilled to the Bandelier Tuff-basalt contact. The hole penetrated about 48.7 m of the Bandelier Tuff before entering the basalt. No cores or cuttings of the tuff were recovered, so correlation of the various units or members of the Bandelier Tuff was not possible. The hole was completed in the basalt at a depth of 50 m.

III. HORIZONTAL CORE HOLES

The horizontal core holes were cored from a drill pad located in a small canyon east of Pit 3 and were oriented to penetrate different areas beneath the pit (Figs. 2 and 3). Pit 3 is 30.5 m wide, 200 m long, and about 9 m deep. It was laid out with a north-south orientation and had ramps with slopes of 6:1 at one end and 4:1 at the other end of the long dimension to allow trucks to enter and discharge wastes. The wastes within the pit were buried in 1.5- to 2-m layers, and covered with 0.2 to 0.6 m of tuff that was excavated when the pit was dug. The pit was filled to 0.5 to 1 m below the surface of the mesa and then covered with 1.5 to 3 m of tuff, slightly mounded to encourage surface runoff. The pit was completed in the lower ashflow of Unit 2b. The contact between Unit 2b and Unit 2a lies at a depth of 3 to 3.5 m below the floor of the pit.

Core hole P-3 MH-1, cored to a distance of 87.5 m, assumed the horizontal at about 12 m then plunged gently downward through Unit 2b into Unit 2a (Fig. 4). The hole entered the area beneath the southern part of the pit at a distance of 53.2 m from the hole collar and a depth of 3.4 m below the pit floor and exited at a distance of 84.6 m and a depth of 7.2 m below the pit floor (Table I). Sample numbers in this interval were MAR-77.00784 through MAR-77.00805 (see Appendix A).

Core hole P-3 MH-2, cored to a distance of 82.9 m, assumed the horizontal at about 34 m and then plunged downward in Unit 2b (Fig. 5). The hole entered the area beneath the pit at a distance of 53.6 m from the hole collar and a depth of 1.2 m below the pit floor. The end of the hole was 3.1 m below the pit floor (Table I). Sample numbers in this interval were MAR-77.00838 to MAR-77.00888 (see Appendix B).

Core hole P-3 MH-3, cored to a distance of 86.9 m, assumed the horizontal at about 38 m and then plunged downward through Unit 2b into the upper part of Unit 2a (Fig. 6). The hole entered the area beneath the central part of the pit at a distance of 51.8 m and a depth of 0.6 m from the hole collar and a depth of 0.6 m below the pit floor and exited at a distance of 82.3 m and a depth of 3.1 m below the pit floor. The entire hole was within Unit 2b (Table I). The sample numbers in this interval were MAR-77.00907 through MAR-77.00945 (see Appendix C).

Core hole P-3 MH-4, cored to a distance of 92.7 m, assumed the horizontal at about 28 m and then plunged downward through Unit 2b into Unit 2a (Fig. 7). The hole entered the area beneath the northern two-thirds of the pit. The point of entry beneath the pit was 54.9 m from the hole collar and

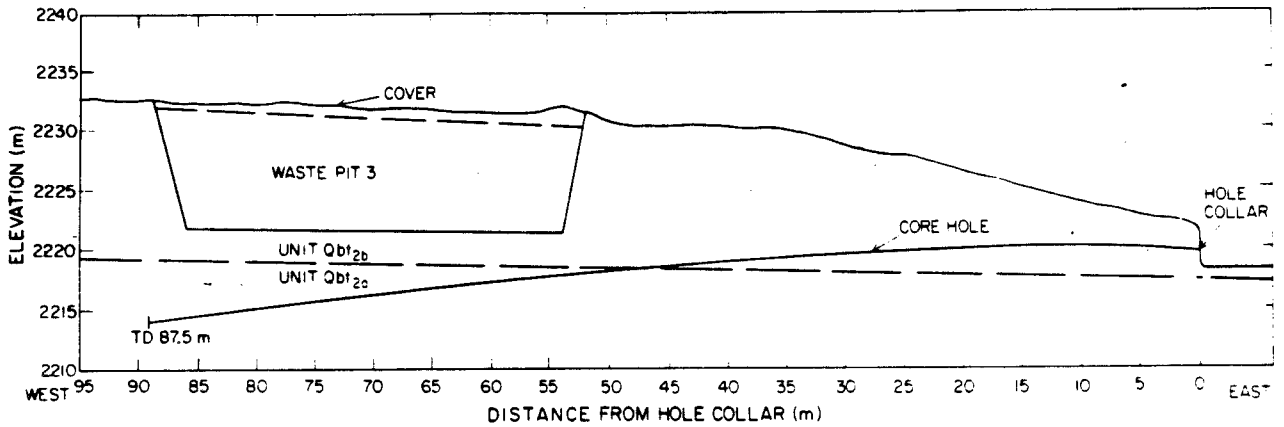

Fig. 4.

Cross section of the mesa showing the geologic units, Waste Pit 3, and the trace of core hole P-3 MH-1.

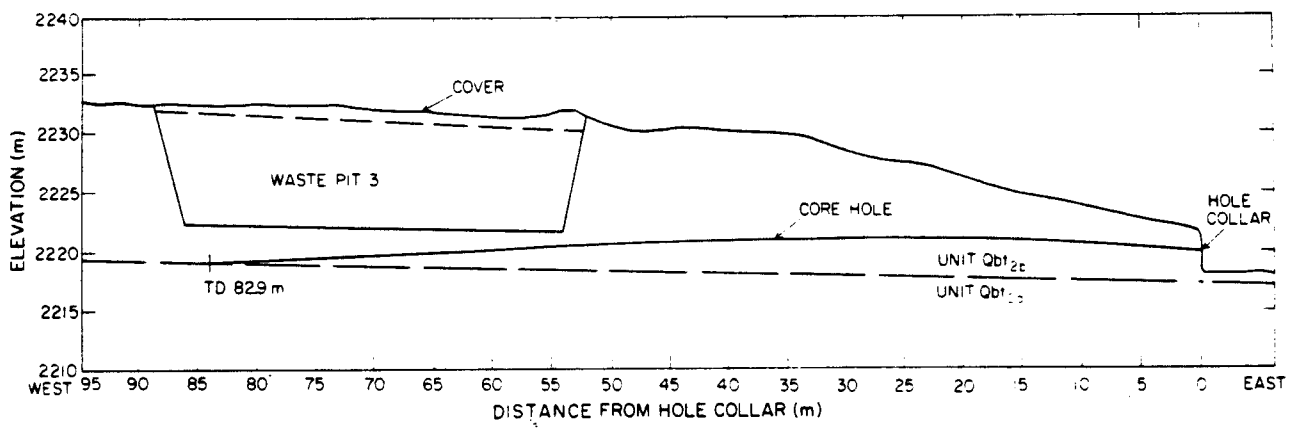

Fig. 5.

Cross section of the mesa showing the geologic units, Waste Pit 3, and the trace of core hole P-3 MH-2.

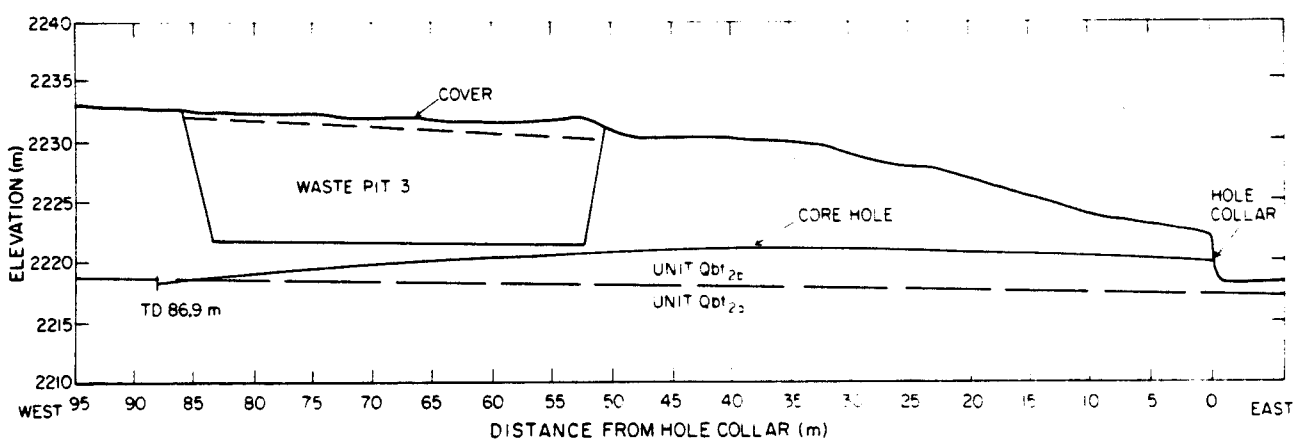

Fig. 6.

Cross section of the mesa showing geologic units, Waste Pit 3, and the trace of core hole P-3 MH-3.

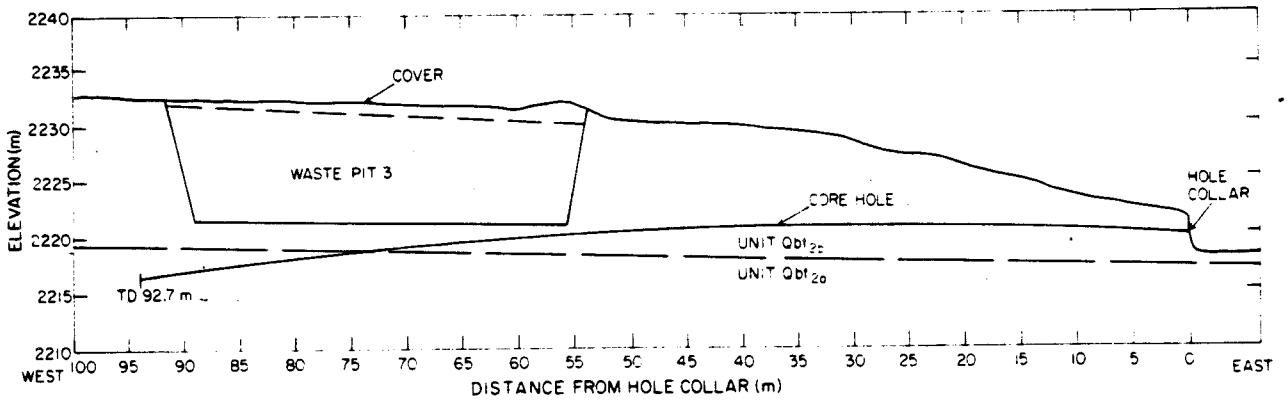

Fig. 7.
Cross section of the mesa showing geologic units, Waste Pit 3, and the trace of core hole P-3 MH-4.

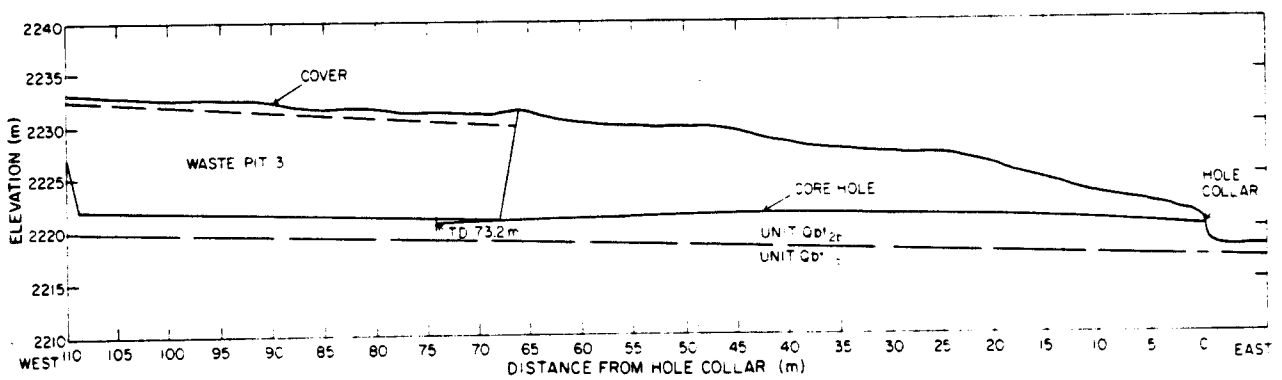

Fig. 8.
Cross section of the mesa showing geologic units, Waste Pit 3, and the trace of core hole P-3 MH-5.

0.8 m below the pit floor and the point of exit was at 87.8 m from the hole collar and 4.4 m below the pit floor. The sample numbers in this interval were MAR-77.00980 through MAR-77.01032 (see Appendix D).

Core Hole P-3 MH-5, cored to a distance of 73.2 m, assumed the horizontal at 42 m and then plunged gently downward in Unit 2b (Fig. 8). The hole entered the area beneath the northern half of the pit at a distance of 67.1 m and terminated beneath the pit at a distance of 73.2 m (Table I). The hole appeared to have penetrated the crushed-tuff backfill in the pit. The hole terminated at a depth of 0.3 m below the pit floor. Only 0.6 m of tuff was recovered in the 6.1-m length of hole cored beneath the pit. The sample numbers beneath the pit were MAR-77.01100 through MAY-77.01104 (see Appendix E).

IV. JOINT CHARACTERISTICS AND CORE RECOVERY

The orientation of joints and fractures in the north-south walls of Pit 3 was determined after the pit was dug, prior to the disposal of wastes. The major joints were vertical or near vertical with dips greater than 70°. The joints were filled or plated with brown clay or caliche. A few were open with only light weathering of the joint face. Joints open at depth within the pit were totally filled with clay beneath the thin soil zone.

There were 199 joints logged in cores from Unit 2b (Table II). Joints filled or plated with brown clay made up 72% of the joints, joints that were open with slightly weathered surfaces made up 19%, while joints filled or plated with caliche and minor amounts of brown clay made up the remaining 9%.

TABLE II

JOINT CHARACTERISTICS OF CORE

	No. of Joints	%
Unit 2b		
Joints open, slight weathering on joint face	38	19
Joints filled or plated with brown clay	144	72
Joints filled or plated with caliche	17	9
Unit 2a		
Joints open, slight weathering	3	18
Joints filled or plated with brown clay	14	82

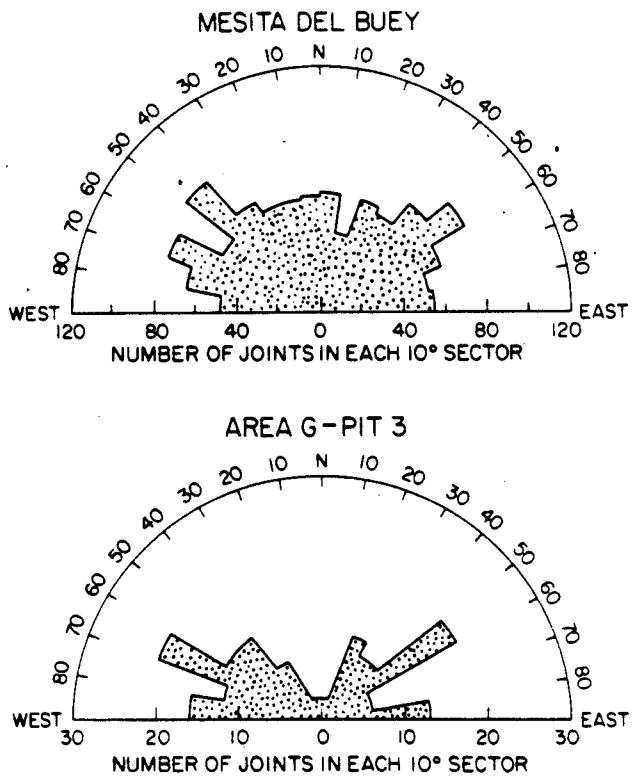

Fig. 9.
Joint orientation in Unit 2b on Mesita del Buey and in the walls of Pit 3, Area G.

There were 17 joints logged in Unit 2a, of which 82% were filled or plated with brown clay and the remaining 18% were open with a slightly weathered surface. Joints filled or plated with caliche did not occur in this unit.

The joint orientation for 166 joints in Unit 2b of Pit 3 indicated two major sets, N40°W to N70°W and N20°E to N60°E (Fig. 9). The number of joints in these two sets comprised 57% of the joints measured. A rose diagram of 1078 joints in Unit 2b at Mesita del Buey indicated three major joint sets: N30°W to N50°W, N60°W to N80°W, and N40°E to N60°E (Fig. 9). These three joint sets constitute 40% of the 1078 joints measured.[5] The orientation of the major joint sets at Pit 3 and on Mesita del Buey were comparable. These are tension joints, which formed as the ash flow cooled.

The joint frequency in Pit 3 averaged one joint for every 2.2 m along the pit wall. This frequency compares favorably with the joint frequency found in other pits in the area, which ranged from one joint for every 1.8 to 2.1 m of pit wall.

The joint frequency in Unit 2b for holes P-3 MH-1, P-3 MH-2, and P-3 MH-5 was one joint per 0.9 to 1.0 m of core recovered, or one joint per 1.2 to 1.4 m of holes cored (Table III). This joint frequency is higher than that observed in Pit 3, which was one joint per 2.2 m. The joint frequency in holes P-3 MH-3 and P-3 MH-4 was one joint per 1.6 to 1.7 m of core recovered, or one joint per 2.8 to 3.3 m of holes cored (Table III). This frequency brackets the observed frequency in Pit 3. The joint frequency in Unit 2a was one joint per 0.8 m (P-3 MH-3), 1.2 m (P-3 MH-4), and 2.6 m (P-3 MH-1) of core recovered. Minor joints were probably not completely mapped on the wall of the pit, because of difficulties in identifying them. However, these minor joints were prominent in the cores, which tended to break along joint faces. Thus, as seen in holes P-3 MH-1, P-3 MH-2, and P-3 MH-5, joint frequency was higher in the cores than in the pit walls.

An evaluation was made to determine if variations in joint frequency or core recovery were related to the orientation and intersection of the core holes with the major joint sets. No relationship was established.

TABLE III

CORE RECOVERY AND JOINT FREQUENCY

	P3 MH-1	P3 MH-2	P-3 MH-3	P-3 MH-4	P-3 MH-5
Core recovered (%)	75	74	58	52	75
Joint frequency (per m)[a]	0.9	1.0	1.6	1.7	1.0
Joint frequency (per m)[b]	1.2	1.4	2.8	3.3	1.4

[a]Per meter of core recovered.
[b]Per meter of hole cored.

Variations in the tuff such as degree of welding, size of pumice and other rock fragments, and orientation of joints intersecting the core will affect the amount of core recovered. Other factors such as the type of coring assembly, the drilling pressure, the rotation speed, length of the core run, and the volume and velocity of the cuttings carrier also affect core recovery. Core recovery in Unit 2b for holes P-3 MH-1, P-3 MH-2, and P-3 MH-5 ranged from 74 to 75%, while in holes P-3 MH-3 and P-3 MH-4 recovery was lower, at 52 and 58% (Table I). Core recovery in Unit 2a was 37 % for hole P-3 MH-1, 100% for hole P-3 MH-3, and 49% for hole P-3 MH-4. This unit is very friable. In hole P-3 MH-3 the core barrel was pushed into Unit 2a with little or no rotation or circulation of air to remove cuttings: thus recovery was 100%.

The majority of joints logged in the cores intersected the core at angles of 30° to 90°. Intersection of the core at angles of less than 30° caused some of the core to break up in the barrel because of drill stem and outer coring assembly rotation. As a result, these sections of core were eroded and dispersed by the the cuttings carrier (air).

V. CONCLUSIONS

Cores were obtained at depths ranging from 0 to 7.2 m beneath the pit, from two units of a rhyolite tuff. The core holes were oriented to enter different locations beneath the pit. The sections of the core from beneath the pit were sampled at intervals of 0.3 m for radiochemical analyses. When possible, every other sampled section included a joint or fracture. Sufficient samples were obtained from the five core holes to aid in evaluating possible migration of radionuclides from solid wastes in the pit into the underlying tuff.

Core recovery from the five holes ranged from 52% to 75%, with joint frequencies ranging from 0.9 to 1.7 m of core recovered. The largest percentage of the joints were filled or plated with brown clay. The remainder were open with joint faces slightly weathered or plated with caliche. Joint orientations on the mesa and in the pit indicate that the joints formed as the ashflows cooled.

REFERENCES

1. R. L. Griggs, "Geology and Ground Water Resources of the Los Alamos Area, New Mexico," U.S. Geol. Survey Water-Supply Paper 1753 (1964).

2. T. E. Kelly, "Evaluation of Monitoring of Radioactive Solid Waste Burial Sites at Los Alamos, New Mexico," U. S. Geol. Survey open-file report (1975).

3. Reynolds Electric and Engineering Co., "Horizontal Monitoring Holes, Los Alamos, New Mexico, Completion Report," Contract E (26-1)-410 ERDA, October 1976.

4. W. D. Purtymun, "Geology and Hydrology of Area G, Mesita del Buey, Los Alamos County, New Mexico," U. S. Geol. Survey Admin. report (1966).

5. W. D. Purtymun and W. R. Kennedy, "Geology and Hydrology of Mesita del Buey," Los Alamos Scientific Laboratory report LA-4660 (1971).

APPENDIX A

CORE LOG P3-MH-1
(HORIZONTAL DISTANCE IN METERS)

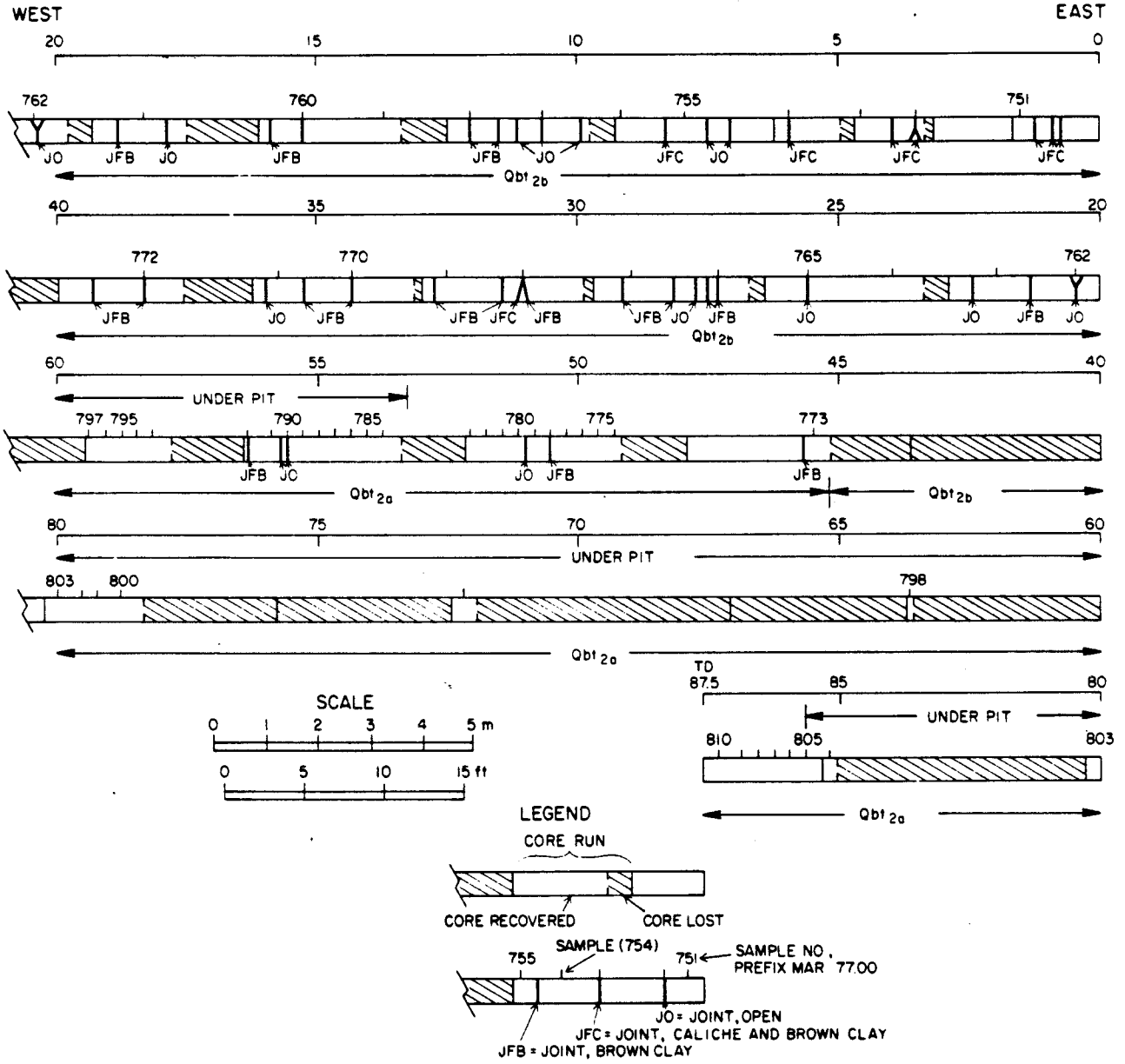

APPENDIX B

CORE LOG P3-MH-2
(HORIZONTAL DISTANCE IN METERS)

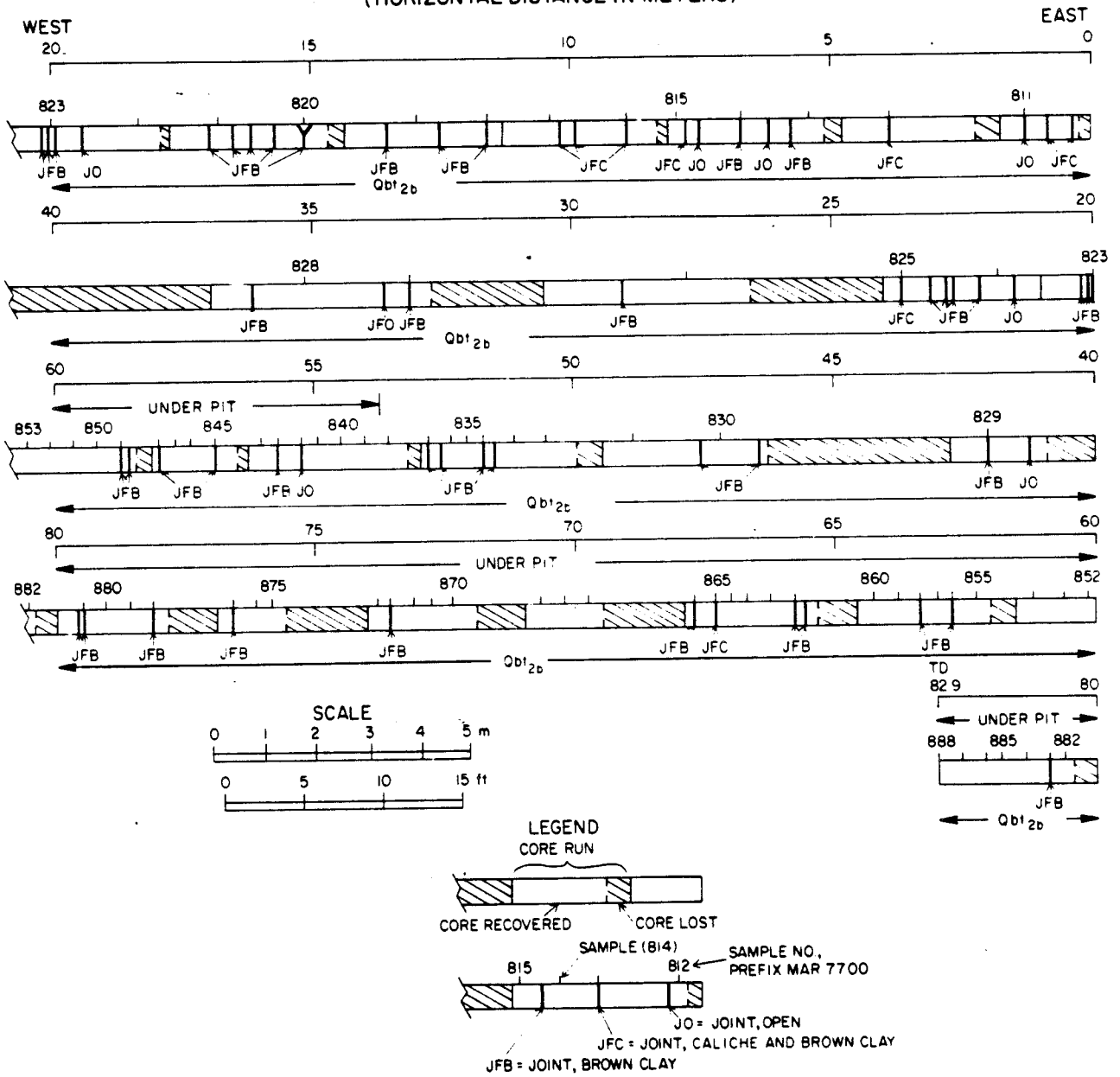

APPENDIX C

CORE LOG P3-MH-3
(HORIZONTAL DISTANCE IN METERS)

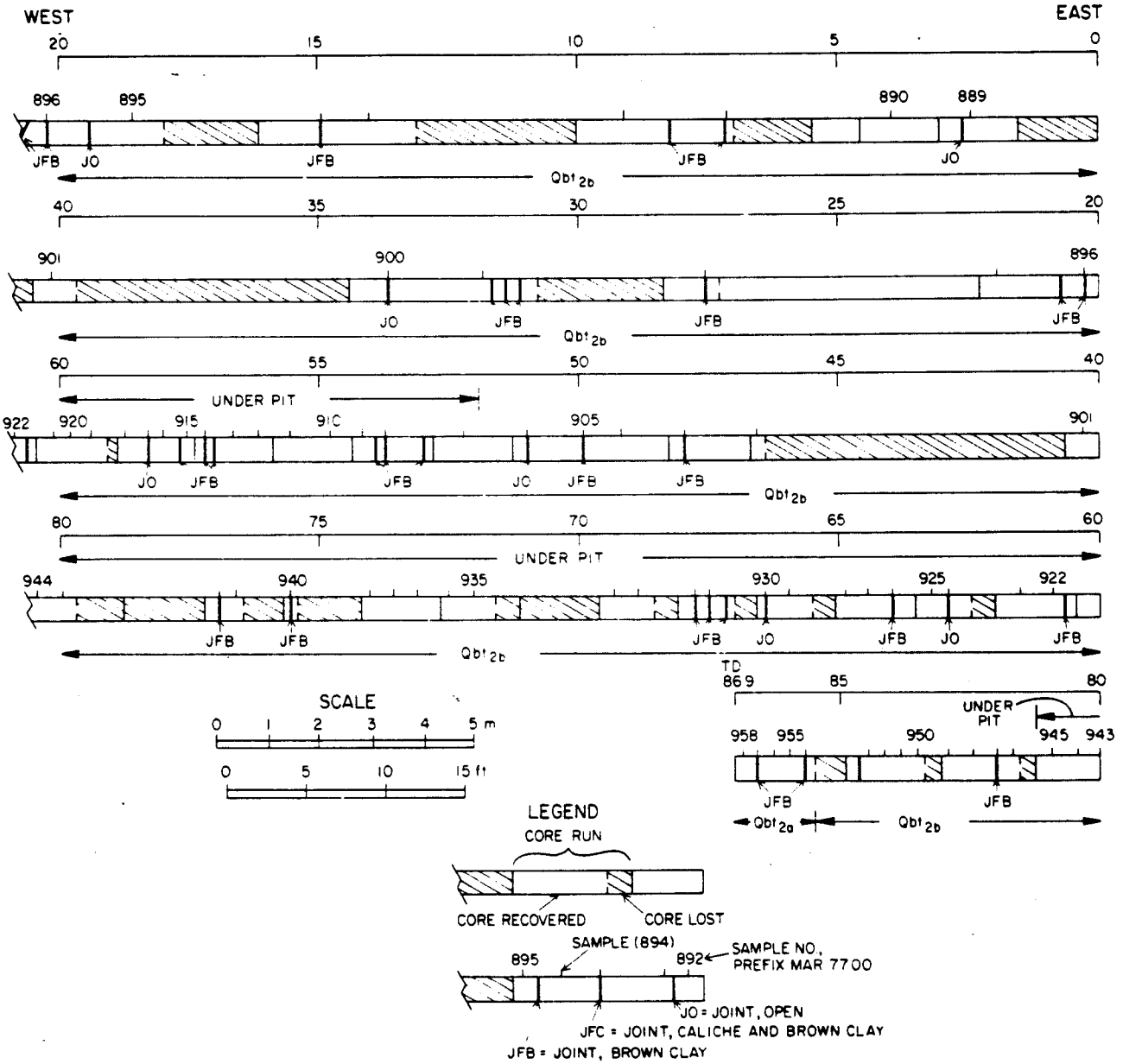

APPENDIX D

CORE LOG P3-MH-4
(HORIZONTAL DISTANCE IN METERS)

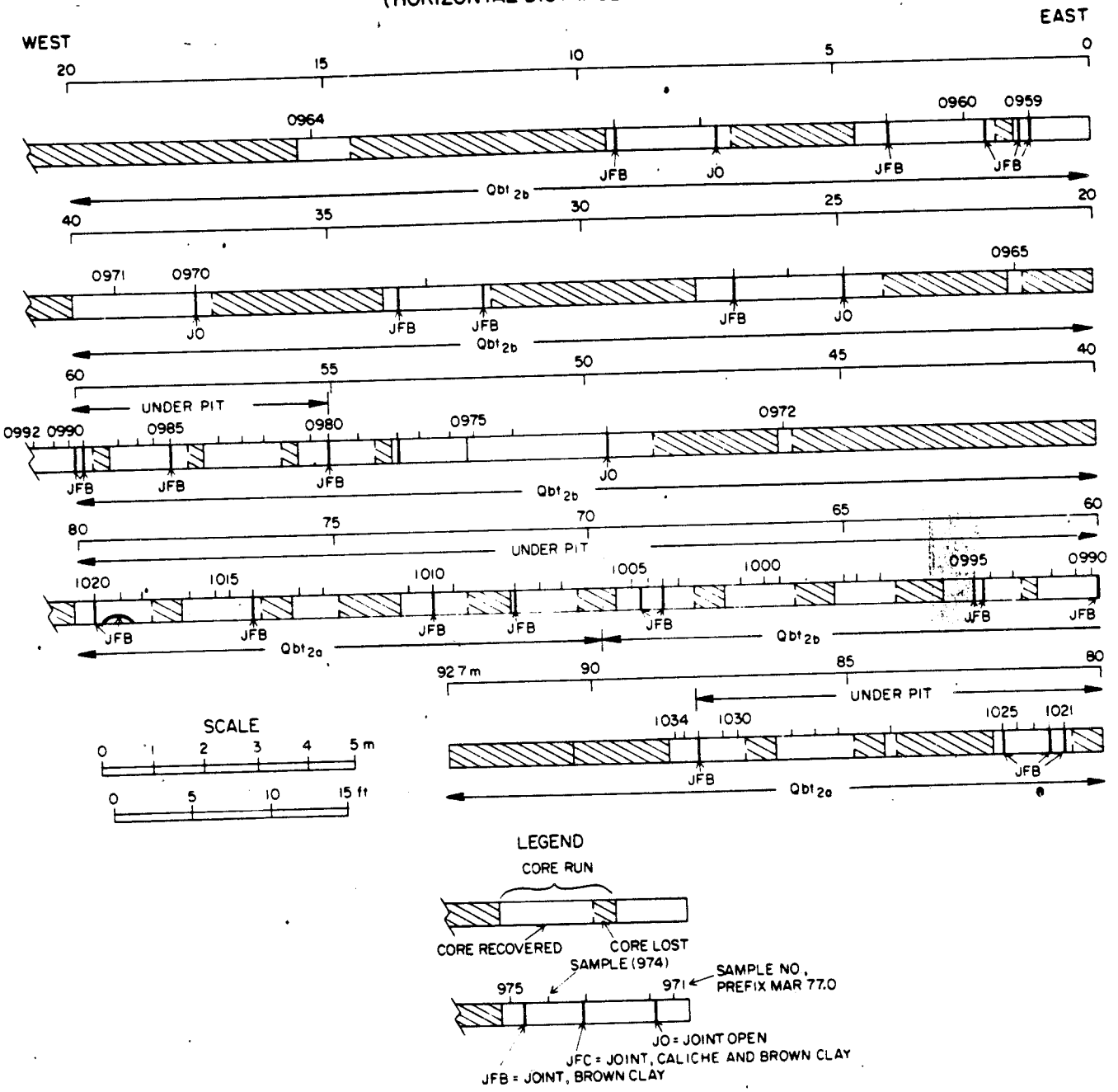

APPENDIX E

CORE LOG P3-MH-5
(HORIZONTAL DISTANCE IN METERS)

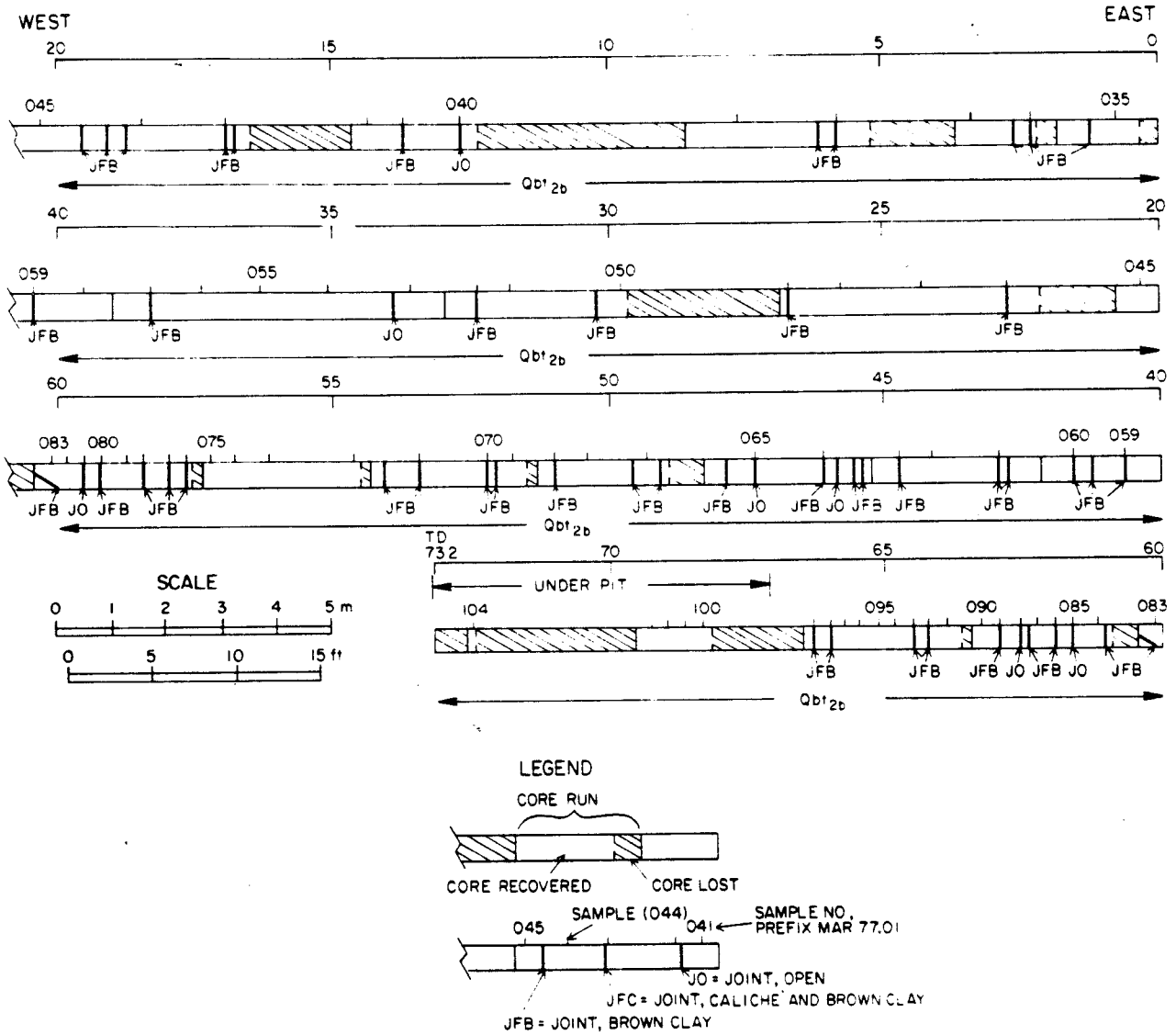

☆ U S GOVERNMENT PRINTING OFFICE 1978—777-089 92

PUK CA-SA-01

UNITED STATES
DEPARTMENT OF THE INTERIOR
GEOLOGICAL SURVEY
Albuquerque, New Mexico

The distribution of moisture in the soil and underlying tuff at Technical Area 49, Frijoles Mesa, Los Alamos County, New Mexico

By

William D. Purtymun

Prepared in cooperation with and for administrative release only to the Atomic Energy Commission and University of California, Los Alamos Scientific Laboratory, Los Alamos, New Mexico

Not reviewed for conformance to Geological Survey nomenclature or editorial standards

June 1962

Contents

	Page
Abstract	1
Introduction	3
Description of the soil and underlying tuff	6
Rhyolite tuff	7
Water-laid pumice	9
Transition zone and clayey soil	10
Moisture distribution in the soil and underlying tuff	12
Conclusions	14

Illustrations

(All illustrations in pocket)

	Reference Page
Figure 1. Index map of part of Los Alamos and adjacent counties, New Mexico, showing the location of Technical Area 49 (TA-49) and Frijoles Mesa ---	3
2. Location of test areas and moisture-measurement test holes in TA-49, Los Alamos County, N. Mex. ----------	3

Tables

Page

Table 1. Moisture content and lithologic log of test hole 1M-1, Technical Area 49 ---------- 15

2. Moisture content and lithologic log of test hole 1M-2, Technical Area 49 ---------- 16

3. Moisture content and lithologic log of test hole 1M-3, Technical Area 49 ---------- 17

4. Moisture content and lithologic log of test hole 1M-3A, Technical Area 49 ---------- 18

5. Moisture content and lithologic log of test hole 2M-1, Technical Area 49 ---------- 19

6. Moisture content and lithologic log of test hole 2M-2, Technical Area 49 ---------- 20

7. Moisture content and lithologic log of test hole 2M-3, Technical Area 49 ---------- 21

8. Moisture content and lithologic log of test hole 3M-1, Technical Area 49 ---------- 22

9. Moisture content and lithologic log of test hole 3M-2, Technical Area 49 ---------- 23

10. Moisture content and lithologic log of test hole 3M-3, Technical Area 49 ---------- 24

11. Moisture content and lithologic log of test hole 4M-1, Technical Area 49 ---------- 25

12. Moisture content and lithologic log of test hole 4M-2, Technical Area 49 ---------- 26

Tables - Continued

Page

Table 13. Moisture content and lithologic log of test hole 4M-3, Technical Area 49 ---------- 27

14. Moisture content and lithologic log of test hole 4M-4, Technical Area 49 ---------- 28

15. Moisture content and lithologic log of test hole 5M-1, Technical Area 49 ---------- 29

16. Moisture content and lithologic log of test hole 5M-2, Technical Area 49 ---------- 30

17. Moisture content and lithologic log of test hole 6M-1, Technical Area 49 ---------- 31

18. Moisture content and lithologic log of test hole 9M-1, Technical Area 49 ---------- 32

19. Moisture content and lithologic log of test hole 9M-2, Technical Area 49 ---------- 33

20. Moisture content and lithologic log of test hole 9M-3, Technical Area 49 ---------- 34

21. Moisture content and lithologic log of test hole 9M-4, Technical Area 49 ---------- 35

22. Moisture content and lithologic log of test hole 10M-1, Technical Area 49 ---------- 36

23. Moisture content and lithologic log of test hole 10M-2, Technical Area 49 ---------- 37

PUB-LAB-001

The distribution of moisture in the soil and underlying tuff at Technical Area 49, Frijoles Mesa, Los Alamos County, New Mexico

By

William D. Purtymun

Abstract

Twenty-three moisture test holes were constructed in February and March 1960 to study the moisture distribution in the soil and underlying tuff at Technical Area 49, on the northern segment of Frijoles Mesa, in north-central New Mexico. Radioactive contaminants are buried within the tuff in this area, and sufficient infiltration of water from precipitation could cause them to move into nearby surface and ground-water supplies.

Moisture measurements, tabulated in this report, indicate that only small and insignificant amounts of water infiltrate the soil and underlying tuff in Technical Area 49, except at sites where construction work has disturbed the natural soil cover or changed the pattern of surface drainage.

The periodic moisture measurements, made by a neutron-scattering moisture probe for a 2-year period, indicated the moisture content of the soil and transition zone varied due to weather conditions. The moisture content of the tuff remained the same, varied due to weather conditions, or increased slightly in the upper few feet of tuff in 21 of the test holes. The moisture content in the tuff, up to a depth of 16 feet, in two test holes increased from 13½ to 28 percent by volume, indicating some infiltration of water.

Introduction

Technical Area 49 (TA-49) is ~~located~~ on the northern segment of Frijoles Mesa in Los Alamos County, about 5 miles south of the city of Los Alamos, in north-central New Mexico (fig. 1). The mesa is

Figure 1.--Index map of part of Los Alamos and adjacent counties, New Mexico, showing the location of Technical Area 49 (TA-49) and Frijoles Mesa.

underlain by a series of ash falls and flows of rhyolite tuff more than 900 feet thick. The surface of the mesa slopes gently eastward about 150 feet per mile and contains shallow arroyos which drain into deep-cut eastward-trending canyons that bound the mesa on the north and south.

TA-49 is used as a test area by the Los Alamos Scientific Laboratory. Within TA-49 are smaller test areas known as Areas 1, 2, 3, 4, 5, 6, and 10 (fig. 2). All other locations within TA-49

Figure 2.--Location of test areas and moisture-measurement test holes in TA-49, Los Alamos County, N. Mex.

are known as Area 9.

Clayey soil caps most of the mesa and overlies a transition zone between the soil and the underlying welded rhyolite tuff, (except in Areas 2 and 10 where a layer of water-laid pumice occurs between the transition zone and the clayey-soil cover).

Radioactive contaminants are buried in the tuff in Areas 1, 2, 3, 4, and 10 at depths up to 100 feet below the surface of the mesa. Sufficient infiltration of water from precipitation could remove these contaminants from the tuff and move them outward into the deep canyons that bound the mesa, or perhaps even move them downward to the main ground-water body which lies 1,000 to 1,200 feet below the surface of the mesa.

This study was made in cooperation with the Los Alamos Scientific Laboratory to determine the moisture distribution in the soil cover and underlying tuff at TA-49. Twenty-three test holes were drilled in February and March 1960 to study the thickness of the soil and the changes in moisture content in the soil and underlying tuff.

The test holes range in depth from 9 to 50 feet and are ~~located~~ ~~are and~~ in or near test areas, roadside drainage ditches, and arroyos. The holes were drilled with a wagon drill which used air to remove the cuttings. All holes except those in Area 3 were drilled to diameters slightly greater than 2 inches, and plastic tubing was forced into the holes by the hydraulic lift of the wagon drill so as to insure a tight fit between the walls of the holes and the tubing. Three test holes in Area 3 were drilled 2.5 inches in diameter, and the annular space between the hole wall and tubing was packed with ground tuff.

Moisture content of the soil cover and tuff was measured at various depths in the plastic-lined holes with a neutron-scattering moisture probe which had previously been calibrated for use in plastic tubing. The moisture-content measurements made in these holes are believed to be within 1 percent of the natural moisture content of the soil or tuff.

The test holes are designated by Area number, "M" for moisture test, and the number of the hole within the Area. Test hole 2M-3 is in Area 2, is a moisture-test hole, and is the third hole drilled in that Area. In Area 1 a subscript "A" was added to an offset hole drilled near test hole 1M-3. The locations of the test holes are based on the Los Alamos grid system, which is a rectangular system of squares numbered in feet south and east of established base lines (fig. 2).

The report "Geology and hydrology of Technical Area 49, Frijoles Mesa, Los Alamos County, New Mexico," by James E. Weir, Jr. and William D. Purtymun, on file with the Atomic Energy Commission at Los Alamos, contains basic data obtained during the first six months of the study. This report as a continued study summarizes moisture-content measurements made in the 23 test holes in the TA-49 area during the period March-April 1960 to March-April 1962. Included, also, are lithologic logs of the test holes and other data pertinent to the continuation, by the Los Alamos Scientific Laboratory, of moisture measurements in these test holes.

Description of the soil and underlying tuff

During the drilling of the test holes, the air-returned cuttings were observed, and a visual lithologic log was made (tables 1-23). The transition zone could not be distinguished, in the sample cuttings, from the overlying clayey-soil zone. Therefore, the clayey soil and the transition zone were logged as a single unit.

Rhyolite tuff

The moisture test holes are bottomed in a single ash flow composed of welded rhyolite tuff, which is as much as 60 feet thick near the center of the mesa. The air-returned cuttings of tuff that were logged during drilling of the test holes varied in color from light brownish-red, light tan, light pink, and very light gray to white. Unweathered tuff is very light gray to white. The darker colors probably represent different degrees of weathering that occurred prior to development of the soil cover or weathering that is occurring at present because of variations of moisture content in the tuff.

The tuff contains phenocrysts of quartz and sanidine ranging in size from medium to coarse sand, gray devitrified pumice fragments up to three-quarters of an inch, and gray to light-brown rhyolite and latite fragments. Some of the quartz crystals are clear and have well developed crystal faces; others are dipyramidal in crystal form and contain white globular inclusions. Mineralogic analysis indicates the tuff also contains a small percentage of magnetite and pyroxene and some clay, which is probably montmorillonite.

Natural moisture content in the tuff of cores taken from a depth of 20 to 70 feet ranges from 0.8 to 8.7 percent by volume. Porosity ranges from 38 to 54 percent by volume and specific retention from 16 to 27 percent by volume. The higher porosities occur near the surface. Vertical permeability ranges from 0.1 to 6 gpd (gallons per day) per square foot. The horizontal permeability ranges from 0.2 to 5 gpd per square foot.

Percolation of water could occur through open joints where the soil mantle has been stripped off, leaving the tuff exposed. Movement of water through the unjointed tuff would be slow, as indicated by the range of permeabilities of 0.1 to 6 gpd per square foot.

Water-laid pumice

A layer of fairly well sorted, water-worn pumice fragments was found in test holes in Areas 2 and 10. The layer is 2 to 4 feet thick and overlies the transition zone and is overlain by clayey soil. The pumice is brownish-gray to brown, with cellular structure of frothy glass containing phenocrysts of quartz and sanidine. A few layers of clay and some intermixed brown clay were found in the pumice layer along with roots.

The layer of pumice probably is highly permeable, because it is loosely consolidated and the fragments are well sorted and well rounded. The clay layers probably impede downward movement of water.

Transition zone and clayey soil

The transition zone is composed of partly weathered, but angular, tuff fragments in a matrix of brown clay which contains a few roots. Thickness ranges from a few inches to 4 feet. The zone grades upward into clayey soil except where it is overlain by pumice. The base of the transition zone grades into and is irregularly disconformable with the top of the underlying tuff. Joints and cracks in the upper part of the tuff are clay filled.

The brown clayey soil which occurs on most of the mesa contains percentages of particle sizes estimated as follows: 20 percent sand, 30 percent silt, and ~~59~~ 50 percent clay. Sand-size particles are crystals and fragments of quartz.

The soil thickness appears to depend upon the amount of water available for weathering the underlying tuff. The thickest soil zones are found along shallow slow-draining ditches, arroyo channels, and relatively flat areas where water collects and stands (fig. 2). Soil and transition zone thickness, combined, range from 1 to 9 feet in the test holes.

The clay in the transition zone is nearly impervious and virtually eliminates percolation through this zone. The weathered angular tuff fragments usually are isolated in the clay matrix and contribute little to the bulk permeability of the zone.

Percolation of water through the clayey soil is small where the soil is relatively undisturbed. Any movement of water through the soil would be very slow and would occur only during exceptionally long wet periods, which are rare in the region.

The road metal used in some of the test and parking areas consist of crushed tuff, sometimes mixed with soil. A fill of crushed tuff alone would transmit water rapidly, but an admixture of soil impedes infiltration of water.

Moisture distribution in the soil and underlying tuff

Moisture measurements reported in tables 1 through 23 cover a 2-year period. Three to four series of measurements were made in 1960, two in 1961, and one in 1962. The tables of individual test holes show depths below HI (height of instrument which is at the top of the shield of the neutron probe), depths below land surface, material in which the moisture measurement was made, and moisture content in percent by volume at various dates and depths. The log of the test hole appears beneath the moisture measurements and remarks concerning changes in moisture content below the logs.

The moisture measurements in the fill and soil cover, which includes the transition zone, varied due to prevailing weather conditions. The moisture content in the test holes was highest in March and April as the result of late winter snow and generally was lowest in the months August through October due to the high evapotranspiration rate during the summer and early fall. The moisture content also varied with prevailing weather conditions in the fill and pumice of test hole 2M-2 and in the pumice of test holes 2M-1 and 10M-1. No significant change in moisture content occurred in the pumice of test holes ~~2M-1 and~~ 10M-2.

The moisture content of the tuff in test holes 2M-3, 3M-1, 3M-2, 4M-1, 4M-2, 4M-4, 5M-1, 5M-2, 9M-1, and 9M-2 varied or increased slightly due to prevailing weather conditions or because of new drainage constructed near the holes. The increases in moisture content were slight and, in most instances, were confined to the upper few feet of the tuff.

Test holes 1M-3 and 1M-3A showed an increase in moisture content in the tuff ~~up~~ to a depth of 16 feet. The moisture content increased from 14½ percent to 28 percent by volume in the 2-year period, which indicates some infiltration of water. This condition was caused by ponding of water in a nearby arroyo due to construction work (fig. 2).

Conclusions

The moisture measurements made during the 2-year period of observation indicate that water, from precipitation, rarely infiltrates the undisturbed soil cover into the underlying tuff. The increase or variation in moisture content in the tuff, which was observed in test holes 1M-3 and 1M-3A, is caused primarily by changes in the natural conditions that existed prior to construction in the area. Drainage in the arroyo south of test holes 1M-3 and 1M-3A, where water is presently impounded, should be improved, or water may move into the radioactive materials buried in Area 1 within the next few years.

Table 1.--Moisture content and lithologic log of test hole 1M-1, Technical Area 49

Location: 104 + 40S
85 + 48E

Depth below HI (feet)	Depth below land surface (feet)	Material	Moisture content (percent by volume) Mar. 28, 1960	May 3, 1960	June 29, 1960	Oct. 5, 1960	Mar. 28, 1961	Sept. 5, 1961	Mar. 8, 1962
3	1	Soil	37.5	35	30	17.5	36.5	29	38
4	2	do.	23.5	25	24.5	14	31	15	30
5	3	do.	6.5	6.5	6.5	5.5	5.5	5.5	6
6	4	do.	9	10	9.5	7	6.5	7.5	8
8	6	Tuff	9.5	9.5	9.5	7.5	7	7.5	8
10	8	do.	6	6	5.5	5.5	5.5	5.5	6
12	10	do.	3.5	3.5	3.5	3.5	3.5	3.5	4
14	12	do.	3.5	3.5	3.5	3.5	3	3	3.5
16	14	do.	3	3	3.5	3	3	3	3.5
18	16	do.	3.5		3.5	3	3	3	3
23	21	do.	4			3.5	3.5	3.5	4
28	26	do.	3.5			3	3	3	3.5
33	31	do.	3.5			4	4	4.5	4.5
38	36	do.				12	12	9.5	7.5
43	41	do.	4			4	3.5	4	4
48	46	do.	4			4	4	4	4

Lithologic log

Description of material	Thickness (feet)	Depth (feet)
Soil, brown, clayey	4.6	4.6
Tuff, light brownish red	7.4	12
Tuff, white to very light gray	3	15
Tuff, light pink	34	49

Remarks

No significant change in moisture content in the tuff except at 36 feet below land surface, which probably is a clay-filled crack that is drying out since penetration by the test hole.

Table 2.--Moisture content and lithologic log of test hole 1M-2, Technical Area 49

Location: 104 + 63S
83 + 39E

Depth below HI (feet)	Depth below land surface (feet)	Material	Moisture content (percent by volume)							
			Mar. 15, 1960	Mar. 31, 1960	May 3, 1960	June 29, 1960	Oct. 7, 1960	Mar. 28, 1961	Aug. 29, 1961	Mar. 8, 1962
3	1.5	Tuff	37	38	39.5	39	37.5	40	38	23
4	2.5	do.	8.5	7.5	9	11	10.5	16.5	12.5	7
5	3.5	do.	4.5	4.5	4.5	5	4.5	4.5	7.5	6
6	4.5	do.	4.5	4.5	4.5	4.5	4.5	4.5	6	5
8	6.5	do.	4	3.5	4	4.5	4.5	4	4.5	4
10	8.5	do.	4	3.5	3	3	3	<3	<3	<3
12	10.5	do.	3	3.5	3	3	3.5	<3	<3	<3
14	12.5	do.	3	3	3	3	3	<3	<3	<3
16	14.5	do.	3		3	3	3	<3	<3	<3
18	16.5	do.	3	3		4	3	<3	<3	<3

Lithologic log

Description of material	Thickness (feet)	Depth (feet)
Fill, broken tuff	0.5	0.5
Soil, brown	0.5	1
Tuff, white to very light gray	18	19

Remarks

No significant change in moisture content of the tuff below 2.5 feet below land surface.

Table 3.--Moisture content and lithologic log of test hole 1M-3, Technical Area 49

Location: 105 + 92S
84 + 95E.

Depth below HI (feet)	Depth below land surface (feet)	Material	Moisture content (percent by volume)							
			Mar. 16, 1960	Mar. 30, 1960	Apr. 21, 1960	June 29, 1960	Oct. 5, 1960	Mar. 28, 1961	Aug. 29, 1961	Mar. 8, 1962
3	1	Soil	37	32		27				
4	2	do.	45	41.5	39.5	36	33.5	36.5	31.5	31.5
5	3	do.	27	23	27	26	10.5	19	15.5	34.5
6	4	do.	21	18	18.5	21	21	25	21	16.5
7	5	Tuff	18	16	20.5		21.5	26	23	21.5
8	6	do.	24.5	24.5	26.5	25.5	25	28	25.5	23.5
9	7	do.	27	27	27		26	27	26	27
10	8	do.	28	27.5	27.5	26.5	26	27.5	26.5	29
12	10	do.	30	30	30	28.5	27.5	28.5	29	33
13	11	do.	32	33				32		30
14	12	do.	29.5	29	29	29.5	28	28.5	29	31
16	14	do.	34	30.5	29.5	27.5	27.5	27	27.5	29.5
18	16	do.	39	35.5	35.5	32.5	30	31	30	28
20	18	do.	40	36.5	34		26.5	26	24.5	29.5

Lithologic log

Description of material	Thickness (feet)	Depth (feet)
Soil, brown, clayey	4	4
Tuff, light brownish red	15	19

Remarks

Moisture content varies in soil zone and tuff. Ponded water nearby may be infiltrating the tuff.

Table 4.--Moisture content and lithologic log of test hole 1M-3A, Technical Area 49

Location: 105 + 92S
85 + 02E

Depth below HI (feet)	Depth below land surface (feet)	Material	Moisture content (percent by volume)							
			Apr. 21, 1960	May 3, 1960	June 30, 1960	Oct. 5, 1960	Mar. 28, 1961	July 13, 1961	Aug. 29, 1961	Mar. 8, 1962
4	1	Soil		40.5	35.5	25	38.5	34.5	36.5	39
5	2	do.	37.5	38.5	30	33.5	42	31.5	29.5	40.5
6	3	do.	31.5	31	31	25.5	39.5	26	32	34.5
7	4	Tuff	33	30	31.5	27.5	38	27.5	30	31.5
8	5	do.	32	31.5	33	28.5	39	29.5	30	31
9	6	do.	30.5	31.5	32	29	39.5	30.5	31.5	31.5
10	7	do.	27	28	28	28.5	34.5	30.5	29.5	27.5
11	8	do.	24.5	23	25.5	27	31	29.5	29	26.5
12	9	do.		18.5	23	26	29.5	30	28.5	26.5
13	10	do.	21.5				30	31.5	31	28
14	11	do.		19.5	24	27.5	31	31		
15	12	do.	13				28	30	29	27.5
16	13	do.		13	16	9	23.5	24		23
17	14	do.	8.5				15	18	19	19.5
18	15	do.		7.5	8		11	14		17
19	16	do.	7					11.5	13.5	15.5
21	18	do.						7	9.5	12
23	20	do.	5			5.5	6	6	6.5	8
25	22	do.						4.5		
28	25	do.	5			4	4.5		4	4.5
33	30	do.	4.5			4	4		4	4.5
38	35	do.	4			4	4		4	4.5
43	40	do.	4			4	4		4	4.5
47	44	do.	4.5			4	4		4	4.5

Lithologic log

Description of material	Thickness (feet)	Depth (feet)
Soil, brown	3.2	3.2
Tuff, light gray	45.8	49

Remarks

Moisture contents in soil varied due to prevailing weather conditions. Moisture content in tuff increased from 7 to 20 feet below land surface due to infiltration of water from nearby pond in arroyo.

Table 5.--Moisture content and lithologic log of test hole 2M-1, Technical Area 49

Location: 104 + 73S
99 + 28E

Depth below HI (feet)	Depth below land surface (feet)	Material	Moisture content (percent by volume)						
			Mar. 28, 1960	May 3, 1960	June 29, 1960	Oct. 5, 1960	Apr. 3, 1961	Aug. 31, 1961	Mar. 8, 1962
3	1	Pumice	24	23	20.5	20.5	15	5	7.5
4	2	do.	25	24.5	24	28.5	20	17	16
5	3	do.	27.5	28	27.5	27	28	27	26.5
6	4	do.	22	23.5	23.5	24	26	24.5	24.5
7	5	do.	23.5	24.5	25	10.5	23.5	25	25
8	6	do.	5.5	5.5	5.5	<3	11	8.5	10
10	8	Tuff	2.5	2.5	2.5	<3	<3	<3	3
12	10	do.	2.5	2.5	2.5	<3	<3	<3	<3
14	12	do.	2.5	2.5	2.5	<3	<3	<3	<3
16	14	do.	2.5	2.5	2.5	<3	<3	<3	<3
18	16	do.				<3	<3	<3	<3
23	21	do.				<3	<3	<3	<3
28	26	do.	4			3.5	<3.5	3.5	4
33	31	do.				<3	3.5	3.5	<3
38	36	do.				<3	<3	<3	<3
43	41	do.	3.5			<3	<3	<3	<3
48	46	do.	3			<3	<3		

Lithologic log

Description of material	Thickness (feet)	Depth (feet)
Soil, brown, clayey	0.5	0.5
Pumice, tan	6.5	7
Tuff, white	3	10
Tuff, light gray	39	49

Remarks

No significant change in moisture content in the tuff.

Table 6.--Moisture content and lithologic log of test hole 2M-2, Technical Area 49

Location: 107 + 12S
100 + 05E

Depth below HI (feet)	Depth below land surface (feet)	Material	Moisture content (percent by volume)					
			Mar. 28, 1960	May 3, 1960	Oct. 7, 1960	Apr. 3, 1961	Aug. 31, 1961	Mar. 8, 1962
2	1	Fill	37	32.5	23	41	36	36
3	2	do.	34	33.5	26.5	32.5	28.5	30
4	3	do.	32.5	32.5	29.5	38	33	32.5
5	4	do.	23	23.5	18	33.5	31	29
6	5	do.	20.5	19	15	24	26.5	22.5
7	6	Pumice	12.5	11.5	8.5	10	9.5	11
8	7	do.	7	6.5	6.5	5	5.5	5.5
9	8	do.		29.5	30.5	25.5	29.5	28.5
10	9	do.	6	6	5.5	7.5	5.5	6

Lithologic log

Description of material	Thickness (feet)	Depth (feet)
Fill, crushed tuff and soil	5.5	5.5
Pumice, tan	4.5	10

Remarks

Moisture contents of fill and pumice varied due to prevailing weather conditions. High moisture content at 8 feet is probably a clay layer in the pumice.

Table 7.--Moisture content and lithologic log of test hole 2M-3, Technical Area 49

Location: 106 + 66S
96 + 01E

Depth below HI (feet)	Depth below land surface (feet)	Material	Moisture content (percent by volume)							
			Mar. 13, 1960	Apr. 1, 1960	May 3, 1960	June 29, 1960	Oct. 7, 1960	Apr. 3, 1961	Sept. 5, 1961	Mar. 8, 1962
3	1	Soil	33.5	33	30.5	24	14	33.5	22	22.5
4	2	do.	35	35.5	33.5	31	16.5	25	14.5	16.5
5	3	do.	40	40	37.5	35	17	19	15.5	29
6	4	do.	37.5	33.5	30	31.5	21.5	32	24	11.5
7	5	do.	22	21	20	19.5	15	13.5	10	12.5
8	6	Tuff	17.5	18	17.5	17	13.5	13	11.5	11.5
9	7	do.	12	14.5						
10	8	do.	11.5	12.5	13.5	13.5	11.5	12	11	8.5
12	10	do.	5.5	6	6.5	7.5	8.5	8.5	8	7
14	12	do.	4.5	5	5	5	6	7	6	6.5
16	14	do.	5	5	5	5	5.5	5.5	5.5	6.5
18	16	do.	5	5	5	4.5	5	4.5	5	4.5
20	18	do.	4.5	4.5					4.5	4.5

Lithologic log

Description of material	Thickness (feet)	Depth (feet)
Soil, brown, clayey	5	5
Tuff, light gray	11	16
Tuff, light pink	3	19

Remarks

No significant change in moisture content in the tuff below 10 feet below land surface.

Table 8.--Moisture content and lithologic log of test hole 3M-1, Technical Area 49

Location: 115 + 97S
82 + 03E

Depth below HI (feet)	Depth below land surface (feet)	Material	Moisture content (percent by volume)							
			Mar. 17, 1960	Apr. 5, 1960	May 4, 1960	June 30, 1960	Oct. 7, 1960	Mar. 28, 1961	Aug. 29, 1961	Mar. 20, 1962
2	1	Tuff	35.5	35.5	33.5	33.5	30	40	38.5	36.5
3	2	do.	16	15.5	16.5	18.5	18	33	34.5	14.5
4	3	do.	6	6	7	8	7.5	12	13.5	9
5	4	do.	4.5	4.5	4.5	5	5.5	6	8.5	7
6	5	do.	4	3.5	3.5	4	4	4.5	6	6.5
8	7	do.	3.5	3.5	3.5	3.5	3.5	3.5	4	5
10	9	do.	4	4	4	4	3.5	3.5	3.5	4
12	11	do.	3.5	3.5	4	4	3.5	4	3.5	3.5
14	13	do.	3.5		3.5	3.5	<3.5	3.5	3.5	3.5
16	15	do.	4	3.5	3.5	3.5	<3.5	3.5	3.5	3.5
18	17	do.			3.5	4	3.5	3.5	3.5	3.5
20	19	do.	3.5	4					3.5	<3.5
23	22	do.					<3.5	<3.5	<3.5	<3.5
28	27	do.					<3.5	<3.5	<3.5	<3.5
33	32	do.					<3.5	<3.5	<3.5	<3.5
38	37	do.					<3.5	<3.5	<3.5	<3.5
43	42	do.					<3.5	<3.5	<3.5	<3.5
48	47	do.					<3.5	<3.5	<3.5	<3.5

Lithologic log

Description of material	Thickness (feet)	Depth (feet)
Soil, brown, clayey	0.9	0.9
Tuff, light gray	49.1	50

Remarks

Moisture content increased in the tuff to a depth of 5 feet below land surface due to change in drainage during the fall of 1960.

Table 9.--Moisture content and lithologic log of test hole 3M-2, Technical Area 49

Location: 114 + 82S
82 + 67E

Depth below HI (feet)	Depth below land surface (feet)	Material	Moisture content (percent by volume)							
			Mar. 17, 1960	Apr. 7, 1960	May 4, 1960	June 29, 1960	Oct. 7, 1960	Mar. 28, 1961	Aug. 29, 1961	Mar. 20, 1962
3	1.5	Soil	39	38	38	38	36.5	40.5	39.5	44
4	2.5	do.	30	31.5	33.5	33	33.5	39	41	30
5	3.5	Tuff	17	17	15.5	17	17	17	29	17
6	4.5	do.			10	10	11	14	15	12.5
8	6.5	do.			5.5	5.5	5.5	6	6	4.5
10	8.5	do.			5.5	5.5	6	4.5	5	4
12	10.5	do.			3.5	3.5	3.5	3.5	3.5	<3.5
14	12.5	do.			4	3.5	3.5	<3.5	3.5	4
16	14.5	do.			4.5	4.5	4.5	4	4	3.5
18	16.5	do.			3.5	3.5	3.5	3.5	3.5	3.5

Lithologic log

Description of material	Thickness (feet)	Depth (feet)
Soil, brown, clayey	2.6	2.6
Tuff, light gray	16.4	19

Remarks

No significant change in moisture content occurred in the tuff below 4.5 feet below land surface.

Table 10.--Moisture content and lithologic log of test hole 3M-3, Technical Area 49

Location: 114 + 56S
79 + 96E

Depth below HI (feet)	Depth below land surface (feet)	Material	Moisture content (percent by volume)							
			Mar. 17, 1960	Apr. 1, 1960	May 4, 1960	June 29, 1960	Oct. 7, 1960	Mar. 28, 1961	Aug. 29, 1961	Mar. 20, 1962
2	1	Fill	25.5	30.5	27	25	23	36.5	33	30.5
3	2	do.	38	42	38.5	38.5	37.5	41.5	39	40
4	3	do.	11.5	10.5	8.5	8.5	7.5	11.5	10.5	10
5	4	do.	6.5	6.5	6.5	7	7.5	6	8	7.5
6	5	Soil	7		7	8	8	7	8	8
8	7	do.			5.5	5.5	6	6	6	7
10	9	Tuff			4.5	4.5	4.5	4	4.5	4.5
12	11	do.			4.5	4.5	4.5	4	4.5	4.5
14	13	do.			3.5	4	4	3.5	3.5	3.5
16	15	do.			4	4	4	3.5	3.5	3.5
18	17	do.			3.5	3.5	3.5	<3.5	<3.5	<3.5

Lithologic log

Description of material	Thickness (feet)	Depth (feet)
Fill, crushed tuff	4	4
Soil, brown	3	7
Tuff, light gray	13	20

Remarks

No significant moisture changes occurred in the tuff.

Table 11.--Moisture content and lithologic log of test hole 4M-1, Technical Area 49

Location: 121 + 29S
96 + 44E

Depth below HI (feet)	Depth below land surface (feet)	Material	Moisture content (percent by volume) Mar. 17, 1960	Apr. 7, 1960	May 2, 1960	Oct. 7, 1960	Mar. 29, 1961	Mar. 20, 1962
2	1	Soil	32.5	31.5	25	20	31.5	32
3	2	Tuff	18.5	18.5	21.5	25	32.5	37
4	3	do.	10.5	10	13.5	15	21.5	24.5
5	4	do.	6	6				12.5
6	5	do.	6.5			5.5	6	12.5
8	7	do.			4	4	4.5	6.5
10	9	do.			3.5	<3.5	<3.5	5
12	11	do.			<3.5	<3.5	<3.5	4.5
14	13	do.			<3.5	<3.5	<3.5	4
16	15	do.			<3.5	<3.5	<3.5	4
18	17	do.				<3.5	<3.5	5
23	22	do.				<3.5	<3.5	3.5
28	27	do.				<3.5	<3.5	3.5
33	32	do.	4.5	4		4	4	4
38	37	do.				<3.5	<3.5	<3.5
43	42	do.	3.5	3.5		3.5	3.5	3.5
48	47	do.				3.5	3.5	4

Lithologic log

Description of material	Thickness (feet)	Depth (feet)
Soil, brown	1.9	1.9
Tuff, light gray	13.1	15
Tuff, light brown	2	17
Tuff, light gray	32	49

Remarks

September 19, 1961.--Casing broke off at ground level and hole filled with water. March 20, 1962.--Reading high. No significant change in moisture content of the tuff occurred 4 feet below land surface prior to September 1961.

Table 12.--Moisture content and lithologic log of test hole 4M-2, Technical Area 49

Location: 120 + 57S
94 + 70E

Depth below HI (feet)	Depth below land surface (feet)	Material	Moisture content (percent by volume)						
			Mar. 23, 1960	May 3, 1960	June 29, 1960	Oct. 5, 1960	Mar. 29, 1961	Sept. 8, 1961	Mar. 20, 1962
2	0.5	Soil		10	8	11	31		
3	1.5	Tuff	30.5	28	26.5	26	38	31.5	25
4	2.5	do.	11.5				29.5	25	34
5	3.5	do.		15.5	17	16		8.5	18
6	4.5	do.	6.5	5	5.5	6	5.5	7	7
8	6.5	do.		7	8	8	6.5	5	7
10	8.5	do.		4.5	4.5	4.5	4.5	4	4
12	10.5	do.		5	5.5	5.5	5	5	4.5
14	12.5	do.		5.5	5.5	6	5	4	4
16	14.5	do.		<3.5	<3.5	<3.5	<3.5	<3.5	5
18	16.5	do.			<3.5	<3.5	<3.5	<3.5	<3.5

Lithologic log

Description of material	Thickness (feet)	Depth (feet)
Soil, brown	1.2	1.2
Tuff, light gray	6.8	8
Tuff, light brown	1	9
Tuff, light gray	11	20

Remarks

No significant change in moisture content occurred below 3.5 feet below land surface in the tuff.

Table 13.--Moisture content and lithologic log of test hole 4M-3, Technical Area 49

Location: 122 + 76S
96 + 94E

Depth below HI (feet)	Depth below land surface (feet)	Material	Moisture content (percent by volume) Mar. 17, 1960	May 3, 1960	June 29, 1960	Oct. 7, 1960	Mar. 20, 1962
3	1	Fill	39	32	25	21.5	32.5
4	2	do.	39.5	38.5	37	37	41.5
5	3	do.	28.5	25	24	26	37.5
6	4	Tuff	10.5	9	9.5	9.5	22.5
7	5	do.	5.5	5	5.5	6.5	19.5
9	7	do.		5	5	5.5	18.5
11	9	do.		3.5	4	4	8
13	11	do.		3.5	3.5	3.5	4
15	13	do.		3.5	3.5	3.5	4
17	15	do.		4.5	4.5	4.5	4.5
19	17	do.			3.5	4	4

Lithologic log

Description of material	Thicknes (feet)	Depth (feet)
Fill, crushed tuff	3	3
Tuff, light gray	16	19

Remarks

March 29, 1961.--Casing broke off at ground level and hole filled with water.
March 20, 1962.--Moisture reading high.
No significant change in moisture content in the tuff prior to March 1961.

Table 14.--Moisture content and lithologic log of test hole 4M-4, Technical Area 49

Location: 118 + 72S
94 + 94E

Depth below HI (feet)	Depth below land surface (feet)	Material	Moisture content (percent by volume)							
			Mar. 18, 1960	Apr. 7, 1960	May 3, 1960	June 29, 1960	Oct. 7, 1960	Mar. 27, 1961	Sept. 8, 1961	Mar. 20, 1962
3	1	Soil	35	35.5	32.5	31	21	33.5	23.5	33
4	2	do.	39.5	40	38.5	39	34	36.5	34	34.5
5	3	Tuff	21	21	20	21	20.5	19.5	26	23
6	4	do.	10	8.5	7	7.5	8.5	6.5	8	8.5
8	6	do.			6	6	6.5	5.5	6.5	7
10	8	do.			4.5	5	5	4.5	4.5	5
12	10	do.			4	4	4	3.5	3.5	4
14	12	do.			4	3.5	3.5	<3.5	<3.5	<3.5
16	14	do.			<3.5	<3.5	<3.5	<3.5	<3.5	<3.5
18	16	do.				<3.5	<3.5	<3.5		<3.5

Lithologic log

Description of material	Thickness (feet)	Depth (feet)
Soil, brown	2.9	2.9
Tuff, light gray	9.1	12
Tuff, light brown	3	15
Tuff, light gray	4	19

Remarks

No significant changes in moisture content occurred in the tuff below 6 feet below land surface.

Table 15.--Moisture content and lithologic log of test hole 5M-1, Technical Area 49

Location: 111 + 32S
94 + 36E

Depth below HI (feet)	Depth below land surface (feet)	Material	Moisture content (percent by volume)							
			Mar. 14, 1960	Apr. 7, 1960	Apr. 30, 1960	May 6, 1960	Oct. 5, 1960	Apr. 6, 1961	Aug. 28, 1961	Mar. 20, 1962
3	0.5	Soil	11.5	30	34.5	14.5	<3.5	37.5	6.5	28
4	1.5	do.	11.5	30	34.5	33	12	36	17	34
5	2.5	Tuff	10	11	11.5	10.5	6	7	5.5	6
6	3.5	do.	7.5	7	8	7.5	6	6.5	5.5	6.5
8	5.5	do.		8	9.5	8.5	8	7.5	7	7.5
10	7.5	do.	8		9	8	7.5	7.5	7	8
12	9.5	do.				6.5	6.5	6	5.5	6
14	11.5	do.	4.5		4.5	4.5	4.5	4.5	4.5	4.5
16	13.5	do.	4.5		5.5	5	4.5	4.5	4.5	5.5
18	15.5	do.	4.5		4.5	4.5	4	4	4	4.5
20	17.5	do.				4.5	4	4	4	4.5
25	22.5	do.				4	4	4	4	4
30	27.5	do.				4.5	4	4	4	4.5
35	32.5	do.				4.5	4	4	4.5	4.5
40	37.5	do.				4.5	4	4	4	4.5

Lithologic log

Description of material	Thickness (feet)	Depth (feet)
Soil, brown	2.2	2.2
Tuff, light gray	36.8	39

Remarks

No significant changes in moisture content occurred in the tuff below 5.5 feet below land surface.

Table 16.--Moisture content and lithologic log of test hole 5M-2, Technical Area 49

Location: 111 + 05S
92 + 38E

Depth below HI (feet)	Depth below land surface (feet)	Material	Moisture content (percent by volume) Apr. 1, 1960	May 2, 1960	Oct. 7, 1960	Apr. 3, 1961	Aug. 31, 1961	Mar. 9, 1962
3	1	Soil	37	33	25.5	37	36.5	36.5
4	2	do.	40.5	37.5	35	40.5	37.5	44
5	3	do.	28	27	22.5	38.5	24.5	38.5
6	4	Tuff	25.5	26.5	25	26	23.5	24.5
7	5	do.	22	20	22	20.5	21	28
8	6	do.	11.5	10	11.5	14.5	14	14
10	8	do.	7	7	7.5	9	10	12
12	10	do.	<3.5	<3.5	<3.5	3.5	3.5	4.5
14	12	do.	<3.5	<3.5	<3.5	<3.5	3.5	3.5
16	14	do.	<3.5	<3.5	<3.5	<3.5	<3.5	<3.5
18	16	do	<3.5		<3.5	<3.5	<3.5	3.5

Lithologic log

Description of material	Thickness (feet)	Depth (feet)
Soil, brown	3.3	3.3
Tuff, white to light gray	15.7	19

Remarks

No significant changes in moisture content occurred in the tuff below 6 feet below land surface.

Table 17.--Moisture content and lithologic log of test hole 6M-1, Technical Area 49

Location: 102 + 15S
68 + 83E

Depth below HI (feet)	Depth below land surface (feet)	Material	Moisture content (percent by volume)							
			Mar. 14, 1960	Apr. 5, 1960	May 3, 1960	June 30, 1960	Oct. 7, 1960	Mar. 28, 1961	Aug. 29, 1961	Mar. 20, 1962
3	1	Soil	48	37	28	23	16	32.5	31.5	29
4	2	do.	42.5	44	41.5	37.5	28	42.5	42	39.5
5	3	do.	45	45.5	45	44.5	43	46.5	44.5	44.5
6	4	do.		44	44.5	43.5	43.5	45	42.5	42
7	5	do.		38.5	39	39	38	41	39	38.5
8	6	do.		34.5	37	36	34.5	36	36.5	35
9	7	do.		20.5	23.5	23	22	22	30	24.5
10	8	do.		15.5	19.5	19	19.5	19	21	21
12	10	Tuff	10	10	8	8.5	9	7	8	9
14	12	do.	6	6	6	6	6.5	5.5	5.5	6.5
16	14	do.	6.5	7	8	8	8.5	7	8	9
18	16	do.	4.5	4.5	4.5	4.5	4.5	4	4.5	4.5

Lithologic log

Description of material	Thickness (feet)	Depth (feet)
Soil, dark brown, moist	9	9
Tuff, light yellowish brown	1	10
Tuff, light gray	9	19

Remarks

No significant change in moisture content occurred in the tuff.

Table 18.--Moisture content and lithologic log of test hole 9M-1, Technical Area 49

Location: 116 + 67S
88 + 44E

Depth below HI (feet)	Depth below land surface (feet)	Material	Moisture content (percent by volume) Mar. 16, 1960	Mar. 30, 1960	May 3, 1960	Oct. 7, 1960	May 6, 1961	Aug. 29, 1961	Mar. 20, 1962
3	1	Soil	43	40.5	30.5	8	29	13.5	36
4	2	do.	44	42.5	33.5	12.5	38.5	35.5	28.5
5	3	do.	40.5	40	37.5	14	41.5	19.5	33.5
6	4	do.	32	31.5	28	19.5	27.5	20	27
7	5	do.	24.5	24.5	22.5	16.5	20	16.5	20.5
8	6	do.	20	20.5	19	14	18	15	15.5
10	8	Tuff	18.5	20	20	18	18.5	18	15
12	10	do.	13.5	11.5	13	12	12	12.5	15.5
14	12	do.	10.5	13.5	10	14.5	15	15.5	12.5
16	14	do.	10	8.5	8	7.5	6.5	7.5	9.5
18	16	do.	14	7.5			6	6.5	

Lithologic log

Description of material	Thickness (feet)	Depth (feet)
Soil, brown	6.9	6.9
Tuff, light tan	12.1	19

Remarks

Moisture content in the tuff varied to a depth of 16 feet. This is probably due to a new channel cut near the moisture hole.

Table 19.--Moisture content and lithologic log of test hole 9M-2, Technical Area 49

Location: 113 + 40S
98 + 15E

Depth below HI (feet)	Depth below land surface (feet)	Material	Moisture content (percent by volume)							
			Mar. 14, 1960	Apr. 7, 1960	Apr. 30, 1960	May 6, 1960	Oct. 7, 1960	Apr. 6, 1961	Sept. 14, 1961	Mar. 8, 1962
3	1	Soil	36.5	31	30	32	24.5	29	28	29
4	2	so.	37.5	42	41	43	38	41	38.5	40
5	3	do.	38	45	45	45	45.5	45.5	43.5	44.5
6	4	do.	45	46.5	45	46	44.5	47	45	46.5
7	5	do.	41.5	44	42	43	42	46	45	45.5
8	6	do.	23.5	26.5	24.5	26.5	26.5	31.5	29.5	30
10	8	Tuff	11.5	12.5	10.5	14.5	14.5	17	17	17.5
12	10	do.	4.5	4.5	4.5	6.5	5.5	5.5	6.5	6.5
14	12	do.	4.5	4.5	4.5	5	4.5	4.5	4.5	4.5
16	14	do.	7	9		8	6.5	6	6.5	5
18	16	do.	11.5	8.5		7	6.5	6	7	6

Lithologic log

Description of material	Thickness (feet)	Depth (feet)
Soil, brown	6.9	6.9
Tuff, light gray	12.1	19

Remarks

No significant changes in moisture content occurred in the tuff below 10 feet below land surface.

Table 20.--Moisture content and lithologic log of test hole 9M-3, Technical Area 49

Location: 117 + 02S
104 + 57E

Depth below HI (feet)	Depth below land surface (feet)	Material	Moisture content (percent by volume)						
			Mar. 14, 1960	Apr. 30, 1960	May 6, 1960	Oct. 7, 1960	Apr. 6, 1961	Sept. 19, 1961	Mar. 20, 1962
3	1	Soil	43.5	34	38.5	11	39.5	30	35.5
4	2	do.	42	34	39.5	13	41	26	33
5	3	do.	43.5	41.5	42.5	36.5	46	40	41.5
6	4	do.	8	6.5	7.5	7	11	7.5	7
7	5	Tuff	6		6	6.5	6.5	7.5	7
8	6	do.	5.5	5.5	6	6.5	5.5	6.5	6.5
10	8	do.	5.5		5.5	6	5	6	6
12	10	do.	5		5	5	4.5	5.5	5.5
14	12	do.	4.5		4.5	4.5	4.5	4.5	4.5
16	14	do.	4.5		4.5	4.5	4	4.5	4.5
18	16	do.	4.5		4.5	4.5	4	4.5	4.5

Lithologic log

Description of material	Thickness (feet)	Depth (feet)
Soil, brown	4.2	4.2
Tuff, light reddish brown	13.8	18
Tuff, light brown	1	19

Remarks

No significant changes in moisture content occurred in the tuff.

Table 21.--Moisture content and lithologic log of test hole 9M-4, Technical Area 49

Location: 113 + 93S
100 + 40E

Depth below HI (feet)	Depth below land surface (feet)	Material	Moisture content (percent by volume)					
			Mar. 25, 1960	May 3, 1960	Oct. 7, 1960	Apr. 6, 1961	Sept. 8, 1961	Mar. 8, 1962
3	1	Fill	19	27	20	27	5.5	21.5
4	2	do.	26.5	25.5	28.5	31	4.5	5.5
5	3	do.	21.5	39	32	38	6	7
6	4	do.	39.5	28	30	32	6.5	6.5
8	6	do.		22	25	25	21	20.5
10	8	do.		21.5	22.5	20	22	20.5
12	10	do.		5.5	5.5	5.5	5.5	5
14	12	do.		4	4	3.5	4	4
16	14	Tuff		<3.5	<3.5	3.5	3.5	<3.5
18	16	do.		<3.5	<3.5	<3.5	<3.5	<3.5

Lithologic log

Description of material	Thickness (feet)	Depth (feet)
Fill, soil and crushed tuff	12.4	12.4
Tuff, light gray	6.6	19

Remarks

No significant changes in moisture content occurred in the tuff.

Table 22.--Moisture content and lithologic log of test hole 10M-1, Technical Area 49

Location: 104 + 96S
110 + 31E

Depth below HI (feet)	Depth below land surface (feet)	Material	Moisture content (percent by volume) May 4, 1960	Oct. 5, 1960	Mar. 29, 1961	Sept. 5, 1961	Mar. 9, 1962
2	0.5	Soil	8	<3.5	26.5	6	17
3	1.5	do.	22	5.5	27.5	10	18
4	2.5	Pumice	23.5	8	14.5	31.5	16.5
5	3.5	do.	4.5	5.5	7	23	13.5
6	4.5	do.	5	4	4.5	19.5	15.5
8	6.5	Tuff	<3.5	<3.5	<3.5	<3.5	3
10	8.5	do.	<3.5	<3.5	<3.5	<3.5	<3.5
12	10.5	do.	<3.5	<3.5	<3.5	<3.5	<3.5
14	12.5	do.	<3.5	<3.5	<3.5	<3.5	<3.5
16	14.5	do.	<3.5	<3.5	<3.5	<3.5	<3.5
18	16.5	do.	<3.5	<3.5	3.5	3.5	3.5
20	18.5	do.		3.5	3.5	3.5	3.5
24	22.5	do.		3.5	3.5	3.5	3.5
26	26.5	do.		4	4	4	4

Lithologic log

Description of material	Thickness (feet)	Depth (feet)
Soil, brown	2.4	2.4
Pumice, light gray	2.1	4.5
Tuff, light gray	24.5	29

Remarks

No significant changes in moisture content occurred in the tuff.

Table 23.--Moisture content and lithologic log of test hole 10M-2, Technical Area 49

Location: 104 + 54S
108 + 69E

Depth below HI (feet)	Depth below land surface (feet)	Material	Moisture content (percent by volume)					
			Mar. 28, 1960	May 4, 1960	Oct. 5, 1960	Mar. 29, 1961	Sept. 5, 1961	Mar. 9, 1962
2	1	Fill	37	33	14	36	24.5	33
3	2	do.	39	36.5	15	35	11	22
4	3	do.	32	33	12	14	5.5	7
5	4	do.	19	22	15	11	6.5	10
6	5	Pumice	27	28.5	32.5	31	28.5	28.5
8	7	do.	6.5	6	6.5	6.5	6.5	6
10	9	do.	5	4.5	4.5	4.5	5	4.5
12	11	do.	3.5	3.5	3.5	3.5	<3.5	3.5
14	13	Tuff	<3.5	<3.5	<3.5	<3.5	<3.5	<3.5
16	15	do.	<3.5	<3.5	<3.5	<3.5	<3.5	<3.5
18	17	do.	<3.5	<3.5	<3.5	<3.5	<3.5	<3.5
20	19	do.	<3.5		<3.5	<3.5	<3.5	

Lithologic log

Description of material	Thickness (feet)	Depth (feet)
Fill, soil and crushed tuff, mixed	4	4
Pumice, light gray	8	12
Tuff, light gray	8	20

Remarks

No significant changes in moisture content occurred in the pumice or tuff.

UNITED STATES
DEPARTMENT OF THE INTERIOR
GEOLOGICAL SURVEY
Albuquerque, New Mexico

Geology of the microseismograph station at S-Site, Los Alamos County, New Mexico

By

William D. Purtymun

Administrative report

Prepared for and in cooperation with the U.S. Atomic Energy Commission and the University of California, Los Alamos Scientific Laborarory.

October 1968

Contents

	Page
Abstract	4
Introduction	5
Geology	6
Santa Fe Group	8
Volcanic rocks of the Jemez Mountains	9
Structure	10
S-Site	12
Summary	15
References cited	16

Illustrations

Page

Figure 1.--Physiographic map of the Los Alamos area and generalized geologic sections ---------- 7

2.--Geology in the vicinity of S-Site, Los Alamos County, New Mexico ---------- 13

Geology of the microseismograph station at S-Site,

Los Alamos County, New Mexico

By

William D. Purtymun

Abstract

The Bandelier Tuff crops out at the surface of the Pajarito Plateau at S-Site. Underlying the tuff are rocks of the Puye, Tschicoma, and Tesuque Formations. Beneath the Tesuque Formation, and above the Precambrian basement complex which is at a depth of about 4,300 feet, the rocks probably consist of sandstone, conglomerate, shale, and limestone.

S-Site is on the western edge of a buried depositional basin in the Tesuque Formation beneath the central part of the Pajarito Plateau. This basin is filled with volcanic debris of the Puye Formation. A deep sediment-filled trough, caused by down-faulting of the Precambrian rocks underlies the depositional basin.

The western edge of S-Site is bounded by the Pajarito fault zone, a series of normal faults downthrown to the east. East of the site a minor fault cuts rhyolitic rocks of the Bandelier Tuff.

Introduction

The University of California, Los Alamos Scientific Laboratory, has established a three-component microseismograph station on the western edge of the Pajarito Plateau in Los Alamos County, north-central New Mexico. The station is located in Building TA-16-80 in Technical Area 16 (TA-16) known as S-Site. At the request of Mr. C. W. Trask and Mr. Dean Keller, Engineer I, Los Alamos Scientific Laboratory, through Mr. Harry Standring, U.S. Atomic Energy Commission, and Mr. William Kennedy, Group H-6, Los Alamos Scientific Laboratory, an investigation was made to determine the geology and geologic structure of the area. The investigation is a part of the continuing geologic and hydrologic site studies which are a part of Contract AT (29-1) 1739 modification 8 between the U.S. Geological Survey, the U.S. Atomic Energy Commission, and Los Alamos Scientific Laboratory.

Much of the information for the investigation was abstracted from previous reports of the U.S. Geological Survey prepared for and in cooperation with the U.S. Atomic Energy Commission and Los Alamos Scientific Laboratory at Los Alamos, New Mexico. These reports contain data on the geology and structure of the area which were collected during investigations for the disposal of liquid and solid radioactive wastes and for studies of ground-water development at Los Alamos. Data also were abstracted from other geologic reports of the area. This report presents a general description of the geology and structure of the Pajarito Plateau with particular reference to S-Site.

Geology

The Pajarito Plateau forms an apron around the east flank of the Sierra de los Valles, slopes gently eastward, and terminates along the Puye Escarpment and White Rock Canyon (fig. 1). The plateau is structurally a part of the Rio Grande depression--a complex series of en echelon faulted troughs or basins that extend from southern Colorado southward along the Rio Grande valley to Mexico (Kelly, 1952, p. 93).

In the Rio Grande depression, Precambrian basement rocks--granite, gneiss, schist, and quartzite--have been faulted downward to great depths (fig. 1). A sequence of rocks believed to consist of sandstone, conglomerate, shale, and limestone of Paleozoic and Mesozoic age overlie the Precambrian rocks. The upper part of the depression contains rocks to Tertiary and Quaternary age that are "basin fill" sediments and volcanics.

In the Pajarito Plateau area rock units exposed, or buried in the near subsurface, are, in ascending stratigraphic order, the Tesuque Formation of Pliocene age, the Puye Formation of Pliocene age, the basaltic rocks of Chino Mesa of Tertiary age (Santa Fe Group), the Tschicoma Formation of Pliocene age, and the Bandelier Tuff or Pleistocene age (volcanic rocks of the Jemez Mountains). The stratigraphic relation of these rocks on the Pajarito Plateau is shown on figure 1. Section A-A' (fig. 1) is a generalized illustration of the near-surface geology and structure in the Los Alamos area. A detailed description is given by Griggs (1964, p. 16-74).

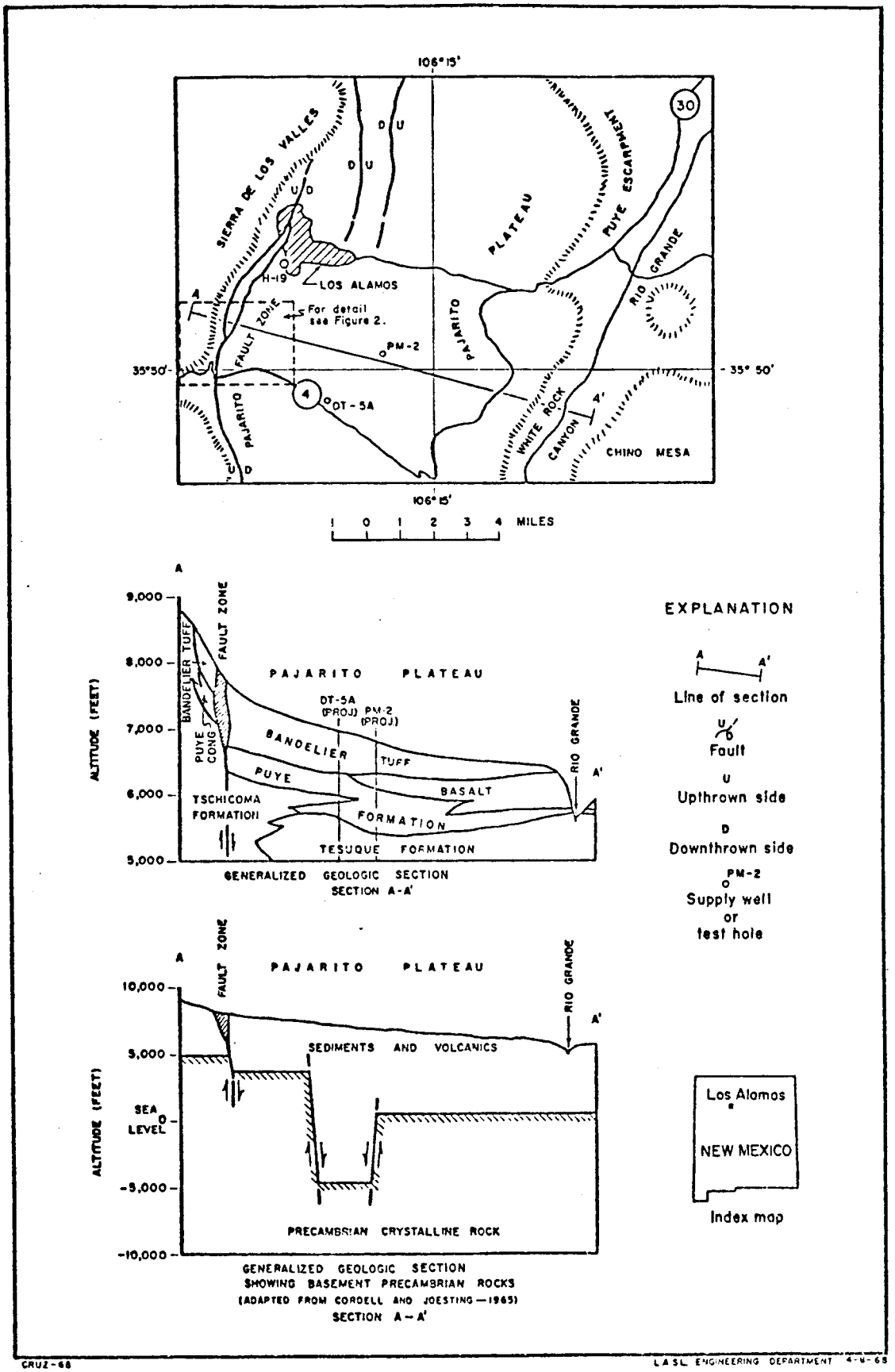

Figure 1.--Physiographic map of the Los Alamos area and generalized geologic sections.

Santa Fe Group

The Tesuque Formation of the Santa Fe Group consists of siltstones, sandstones, clay lenses, and conglomerate, and some interbedded basalt. The formation crops out in the bottom of the canyon walls along the Rio Grande; it is in the subsurface beneath the Pajarito Plateau. Near the Rio Grande the thickness of the formation exceeds 2,600 feet.

The Puye Formation of the Santa Fe Group overlies the Tesuque Formation. It forms the Puye Escarpment and crops out along White Rock Canyon. The Puye is composed of two members. The lower member, the Totavi Lentil, is a thin, poorly consolidated conglomerate; the upper unnamed fanglomerate member is a poorly to well consolidated fan deposit of volcanic detritus derived from the Tschicoma Formation. Near the Rio Grande the Puye is only 60 to 80 feet thick. The formation thickens northward and westward on the Pajarito Plateau (Griggs, 1964, p. 29).

The basaltic rocks of Chino Mesa originated from vents near Chino Mesa (fig. 1). They consist of a series of flows and interflow breccias that are as much as 500 feet thick along the Rio Grande. The basalts thin westward beneath the Pajarito Plateau where they are interbedded with the fanglomerate member of the Puye Formation.

Volcanic rocks of Jemez Mountains

The volcanic rocks of the Jemez Mountains in the report area include the Tschicoma Formation and the Bandelier Tuff. The Tschicoma Formation forms the core of and crops out on the flanks of the Sierra de los Valles and is in the subsurface along the western edge of the plateau. It is composed of latite, quartz latite, and rhyolitic flow rocks (Ross and others, 1961, p. 139). Along the western edge of the plateau some of the younger flows intertongue with the Puye Formation.

The Bandelier Tuff forms the upper surface of the Pajarito Plateau. The Guaje Pumice Bed, an ash-fall pumice, is the lower part of the Otowi Member. The Otowi Member is generally a nonwelded ashflow of rhyolite tuff. The upper Tshirege Member is a series of nonwelded to welded ashflows of rhyolite tuff (Purtymun and Koopman, 1965, p. 11). The tuff is as much as 1,000 feet thick along the western edge of the plateau near Los Alamos. It thins eastward to less than 50 feet along White Rock Canyon. The upper ashflows of the Bandelier Tuff dip gently eastward toward the river at 1 to 2 degrees.

Structure

The most prominent structural feature of the Pajarito Plateau is the Pajarito fault zone which trends northward along the western edge of the plateau. It is a part of the complex fault system that formed the Rio Grande depression. The fault zone consists of normal faults that are downthrown to the east and displace rocks of the Bandelier Tuff, Puye Formation, and Tschicoma Formation (fig 1). The displacement, estimated from the fault scarp west of S-Site, is from 400 to 500 feet. The amount of displacement decreases northward where, at a point north of Los Alamos, all visible traces of the fault disappear (fig. 1). The movement along the fault zone has been in small increments which began prior to the deposition of the Bandelier Tuff and continued into post-Bandelier time (Willden and Criley, 1966, p. 6). The displacement of the older rocks is greater than the displacement of the younger rocks. The major fault in this zone extends into and displaces the Precambrian rocks.

North of Los Alamos and east of the Pajarito fault zone, two normal faults (fig. 1) cut the Bandelier Tuff, the Puye Formation, and the Tschicoma Formation. These faults, downthrown to the west, form a graben between them and the Pajarito fault zone. They are a part of the fault system which formed the Rio Grande depression.

Beneath the central part of the Pajarito Plateau a north-trending depositional basin is formed in the Tesuque Formation (fig. 1). The basin is filled with volcanic debris of the Puye Formation, overlain by the Bandelier Tuff. The eastern edge of the basin is formed by thick flows of basalt from Chino Mesa, 2 to 4 miles west of the Rio Grande (John and others, 1967, p. 28).

A gravity survey indicated that the deepest part of the Rio Grande depression (top of the Precambrian rocks) is in a north-trending trough near the center of the plateau, (Cordell and Joesting, 1965). The bottom of this sediment-filled trough lies about 5,000 feet below sea level (fig. 1).

S-Site

S-Site (TA-16) in which the microseismograph station is located, is on the Pajarito Plateau at the western edge of the Rio Grande depression (fig. 2).

Knowledge of the subsurface geology in this area is poor, due to the lack of nearby test holes; however, an estimate of the geologic units present and their thickness was made from geologic logs of test holes DT-5A, PM-2, and H-19 (fig. 1) and a gravity survey. The thickness and average depth below land surface to the tops of the units are listed below:

Geologic unit	Thickness (feet)	Average depth below land surface to top of unit (feet)
Bandelier Tuff	800	0
Puye Formation	500	800
Tschicoma Formation	1,000	1,300
Tesuque Formation and earlier sediments	2,000	2,300
Precambrian rocks	-	4,300

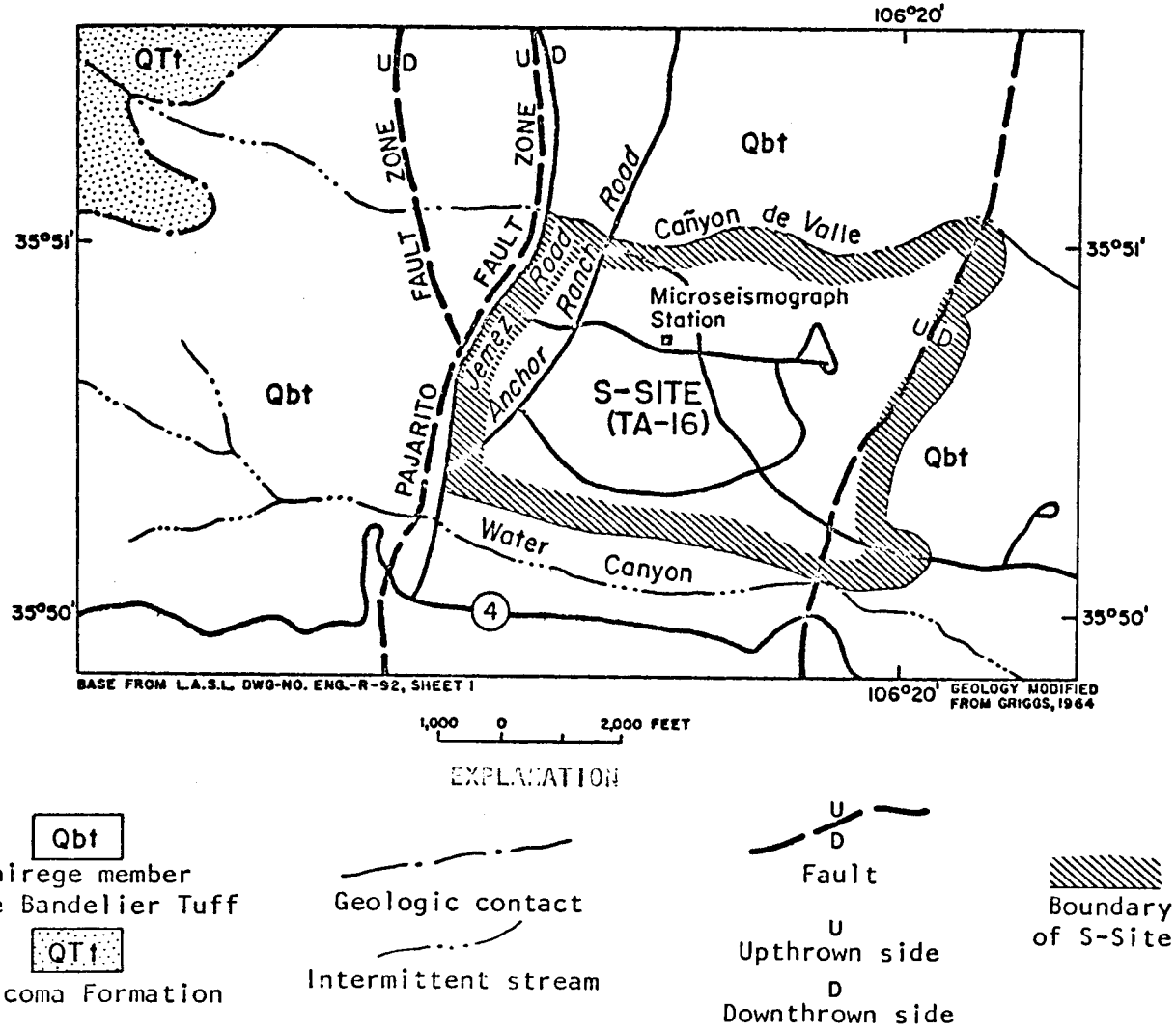

Figure 2.--Geology in the vicinity of S-Site, Los Alamos County, New Mexico.

The rock cropping out at the S-Site area is the moderately welded to welded unit of the Tshirege Member of the Bandelier Tuff. The unit is about 60 feet thick and it is separated from an underlying moderately welded unit by sheet-wash sand and gravel that marks an erosional unconformity. The sand and gravel bed is exposed in a north-trending fault scarp about 4,200 feet east of the station and along the walls of Cañyon de Valle and Water Canyon. The scarp results from a minor normal fault downthrown to the east, in the Bandelier Tuff (fig. 2). The measured displacement at the fault is 88 feet on the north wall of Cañyon de Valle.

The northward-trending Pajarito fault zone branches into two major faults about 3,000 feet west of the microseismograph station (fig. 2). Movement along both the Pajarito fault zone and the minor normal fault, east of the station, has probably been in small increments that began prior to the deposition of the tuff and continued into post-Bandelier time.

Summary

S-Site is on the western edge of the Rio Grande depression, a major structural feature formed by a complex fault system that extends northward through New Mexico. The microseismograph station at S-Site is on the west edge of a buried depositional basin that is filled with volcanic debris of the Puye Formation and younger rocks. The basin trends northward near the center of the plateau and overlies a deeper sediment-filled trough formed by downfaulting of the Precambrian basement rocks.

The surface of S-Site is capped by moderately welded to welded tuff of the Tshirege Member of the Bandelier Tuff. Nonwelded to welded units of the tuff are estimated to be about 800 feet thick at the site and to be underlain by about 3,500 feet of volcanic debris, volcanic flow rocks and sediments. The Precambrian basement complex is estimated to be at a depth of about 4,300 feet. On the west, the site is bounded by the north-trending Pajarito fault zone, which is the major surface structural feature in the area. The fault zone forms the boundary between the western edge of the plateau and the flanks of the mountains. The major faults in the zone, downthrown to the east, break the rocks of the Bandelier Tuff, Puye, and Tschicoma Formations, and extends into the Precambrian crystalline rocks. The site is bounded on the east by a minor fault which has cut the rhyolitic rocks of the Bandelier Tuff.

References cited

Cordell, Lindreth, and Joesting, H. R., 1965, Geophysical investigations in the Rio Grande graben and Valles Caldera: U.S. Geol. Survey manuscript rept. in files of Crustal Studies Branch.

Griggs, R. L., 1964, Geology and ground-water resources of the Los Alamos area, New Mexico: U.S. Geol. Survey Water-Supply Paper 1753, 106 p. 20 figs.

John, E. C., Enyart, E., Purtymun, W. D., 1967, Records of wells, test holes, springs, and surface-water stations in the Los Alamos area; U.S. Geol. Survey open-file rept., 129 p., 10 figs.

Kelly, V. C., 1952, Tectonics of the Rio Grande depression of central New Mexico, in The Rio Grande Country, 1952: New Mexico Geol. Soc. Guidebook, 3rd Field Conf., p. 93-105.

Purtymun, W. D., and Koopman, F. C., 1965, Physical characteristics of the Tshirege Member of the Bandelier Tuff with reference to use as a building and ornamental stone: U.S. Geol. Survey open-file rept., 25 p., 2 figs.

Ross, C. S., Smith, R. L., and Bailey, R. A., 1961, Outline of the geology of the Jemez Mountains, New Mexico, in The Albuquerque Country, 1961: New Mexico Geol. Soc. Guidebook, 12th Field Conf., p. 129-143.

Willden, Ronald, and Criley, E. E., 1966, Study of possibilities of seismic hazards in the vicinity of Los Alamos, New Mexico: U.S. Geol. Survey manuscript rept. in files of Crustal Studies Branch.

los alamos
scientific laboratory
of the University of California
LOS ALAMOS, NEW MEXICO 87544

LA-5286-MS
Informal Report
UC-41
ISSUED: May 1973

Underground Movement of Tritium from Solid-Waste Storage Shafts

by

William D. Purtymun

UNDERGROUND MOVEMENT OF TRITIUM
FROM SOLID-WASTE STORAGE SHAFTS

by

William D. Purtymun

ABSTRACT

Tritium from contaminated wastes placed in storage shafts has been transported by moisture into the adjacent tuff. A study made to determine the extent and geologic factors governing this movement indicates that 100 pCi/ml levels have moved westward a distance of 105 ft in 4 yr. Major movement has been along the contact between the two ashflows penetrated by the shafts, with secondary transport through open joints and through the tuff matrix. Evaporation from surface soil and tuff and transpiration from plants has been a contributing factor in the release of tritium to the atmosphere.

INTRODUCTION

Shafts in Area G, Technical Area 54 on the Mesita del Buey, are used for the storage of solid wastes (Fig. 1). The surface soil in this area is underlain by a series of ashflows of rhyolite tuff,[1] into which the shafts are completed.

Shafts 1 through 14 were drilled with a bucket auger in the spring of 1966, and are 2 and 3 ft in diameter and 20 ft deep. Wastes, packaged in plastic bags or metal containers, were placed in these unlined (except shaft 14) shafts, which were capped with concrete when filled. Storage records indicate that the shafts were filled and capped prior to 1970 and that all except shaft 14 received some waste contaminated with tritium.

Shafts 39 through 48 were drilled, also with a bucket auger, in June 1970. They are 2 ft in diameter and 25 ft deep. Samples of tuff were collected as the shafts were being drilled to determine

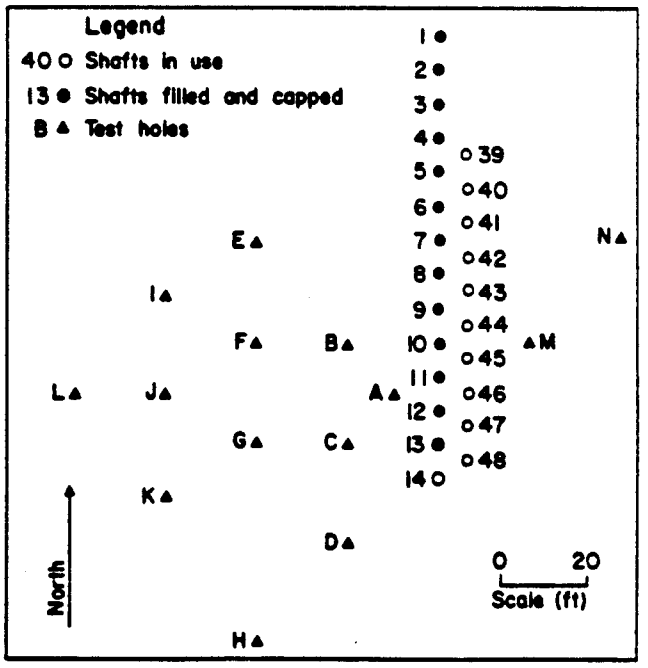

Fig. 1. Planview of shafts and test holes in Area G, TA-54.

the levels of tritium in moisture in the tuff. The moisture content of the tuff was determined and tritium analyses were made on water distilled from the tuff samples (Table I).

The water distilled from the tuff contained above-background concentrations of tritium, indicating leakage of tritium from the wastes in the nearby shafts 1 through 13. The largest concentrations of tritium were in moisture from samples collected in shafts 47 and 48. These two shafts are adjacent to shafts 12 and 13 (Fig. 1), which received an unknown amount of tritium associated with a classified shipment of wastes in July 1966 and September 1966.

A study was made in August 1970 to determine the extent of the movement of tritium with moisture into the tuff and to delineate some of the geologic factors related to this movement. Fourteen test holes were laid out and drilled, 12 to the west of the burial shafts and 2 to the east. This concentration of observation points to the west was chosen because shafts 39 through 48 (to the east), which were open at the time, permitted air exchange from the tuff to the atmosphere and could have affected natural migration of tritiated moisture through the tuff.

TABLE I

TRITIUM ANALYSES OF MOISTURE FROM DRILL CUTTINGS SHAFTS 39 THROUGH 49

Shaft No.	Depth (ft)	Moisture Content (% by wt)	Tritium (pCi/ml)
39	25	1.2	52,800
40	15	2.0	7,400
40	25	1.0	15,100
41	15	1.1	116,000
41	25	1.4	6,800
42	15	1.4	70,700
42	25	0.9	10,600
43	15	1.2	3,100
43	25	0.2	23,000
44	15	1.6	4,640
44	25	0.6	1.780
45	15	1.0	211,000
45	25	0.8	178,000
46	15	0.9	30,800
46	25	0.5	6,810
47	15	0.9	221,000
47	25	0.7	1,180,000
48	15	2.3	171,000
48	25	0.8	325,000

The test holes, 6 in. in diameter and 50 ft deep, were drilled with a power auger. Tuff samples representing 5-ft intervals were collected from the auger cuttings. The holes were thoroughly cleaned before each 5-ft sample run, and the results of the tritium analyses indicated that there was little, if any, cross-contamination between samples from successive 5-ft intervals.

The samples of tuff cuttings were collected in plastic bags and returned to the laboratory for analysis. Each sample was placed in a 600-ml beaker, filling it to about 3 cm from the top. A 50-ml beaker was nestled in the top of the cuttings, and a large watch glass filled with ice was placed on the top of the 600-ml beaker. The beaker and tuff were heated to drive out the water vapor which condensed on the bottom side of the watch glass. The condensate dripped into the 50-ml beaker and was retained for further analysis. Preparation of surface soil and tuff samples were made in this same manner.

Water from vegetation in the area was analyzed to determine if the vegetation contained tritiated moisture or was transpiring it to the atmosphere. To establish tritium content, a sample of vegetation was collected, cut into small pieces, and subjected to the same distillation process as the soil and tuff samples. Transpired moisture was collected as a condensate in a plastic bag tied over a plant or a portion of the plant for 24 h.

A 0.5-ml aliquot of the water obtained from the soil, tuff, or vegetation was mixed with 15 ml of a dioxane-base liquid scintillation cocktail and counted in a liquid scintillation counter for 100 minutes. Instrument background was determined by assaying a similarly prepared sample containing

only blank reagents. The detection limit for the above method was about 5 pCi/ml of water.

PHYSICAL CHARACTERISTICS OF THE TUFF

The test holes and the burial shafts penetrated two ashflows. The upper flow is about 17 ft thick at the shafts, thinning slightly to the west due to erosion of its upper surface, and dipping somewhat to the southeast. The shafts were completed into the top of the lower ashflow which is about 40 ft thick.

The ashflows are similar in composition. Both are moderately welded light gray tuff composed of quartz and sanidine crystals and crystal fragments, with rhyolite, latite, and pumice rock fragments in a matrix of gray ash. Laboratory determinations indicate that porosity of the tuff ranges from 36 to 44% by volume. The contact between the upper and lower flows is characterized by a zone of reworked tuff fragments and by an increase in the size and number of the pumice fragments in the base of the upper ashflow. Within Area G, the zone of reworked tuff may be very thin or nonexistent, or as much as 3 ft thick.

During cooling, the ashflows were broken into a number of large blocks by vertical or near vertical joints. Since both flows cooled as a single unit, the joints extend through both. Joint openings may range to as much as 1/2 in., with those terminating at the surface of the mesa being filled with a light brown clay to a depth of 3 to 4 ft. The joint frequency is about 1 per 7 ft of lateral distance as observed in the walls of 11 storage pits at TA-54.

Measurements of moisture content of the samples indicated that precipitation had infiltrated into the tuff to a depth of over 10 ft. The moisture content in this 10-ft interval ranged from 3 to 8% by weight, decreasing with depth. From a depth of 10 ft to 50 ft the moisture content ranged from 0.4 to about 3% by weight. This low value lies in the regime where moisture transport is primarily by diffusion in the vapor phase. The movement of the tritium is by exchange with natural airborne moisture in the tuff.

UNDERGROUND MOVEMENT OF TRITIUM

Tritium concentrations were determined for water distilled from 140 samples of tuff collected from the 14 test holes (Table II). In general the tritium concentrations increased to a maximum between depths of 10 and 30 ft and then decreased with depth.

Isotritium contours were constructed at depths of 10 to 15 ft, 20 to 25 ft, 30 to 35 ft, and 40 to 45 ft (Figs. 2 and 3). Test holes and burial shafts were used for control points on Fig. 2 while only the test holes were used on Fig. 3. The irregularities in the isotritium contours just east of the shafts are due to the movement of the tritium through open joints which provide a much more rapid means of migration than movement through the tuff matrix. The effect of these joints is apparent only near the shafts due to the close spacing of control points used in construction of the contours. West of the shafts where control points (test holes) are located on 20 ft centers the effect of the joints on movement of the tritium is not apparent. The contours are elongated to the west of the shafts showing the principal movement of the tritium.

Isotritium contours were also constructed for a vertical plane extending east and west through shaft 13 (Fig. 4). The contours show that the major movement of tritium took place along the contact between the two ashflows. The abundance of pumice fragments in the lower part of the upper ashflow and the presence of the reworked tuff between the two flows causes a greater porosity and permeability in the contact region as compared to the matrix or joints in the overlying or underlying tuff. The tritiated moisture migrating along the contact serves as a source for movement into the upper and lower ashflows.

A comparison of the isotritium contours in planview (Figs. 2 and 3) just above and below the contact shows that migration of the tritium was not uniform along the contact but greater in a westerly direction. This is due to a thickening of the layer

TABLE II

TRITIUM ANALYSES OF MOISTURE FROM DRILL CUTTINGS
TEST HOLES A THROUGH N (pCi/ml)

Depth (ft)	A	B	C	D	E	F	G
0- 5	68,000	5,370	7,510	383	294	531	729
5-10	94,700	11,800	22,300	6,310	1,100	538	1,610
10-15	196,000	8,270	55,500	13,800	439	632	4,190
15-20	159,000	12,900	44,800	14,300	1,010	1,860	7,060
20-25	471,000	13,200	39,700	18,800	744	2,620	9,310
25-30	275,000	9,850	32,800	19,900	611	3,750	9,370
30-35	140,000	6,390	22,900	15,000	516	3,190	7,490
35-40	211,000	4,470	13,900	9,200	742	2,160	6,550
40-45	116,000	4,590	4,790	4,380	918	1,405	3,680
45-50	79,000	4,170	4,950	1,470	816	1,107	3,650

Depth (ft)	H	I	J	K	L	M	N
0- 5	42	41	77	42	37	4,830	250
5-10	30	144	267	154	157	6,680	2,410
10-15	131	182	3,720	405	249	6,920	6,140
15-20	197	320	5,490	876	205	7,480	8,790
20-25	445	195	7,210	912	145	5,780	9,400
25-30	430	207	6,340	1,060	127	4,100	9,820
30-35	512	196	969	1,060	122	3,690	9,290
35-40	330	140	1,230	728	87	2,780	7,760
40-45	278	144	966	801	57	3,020	6,250
45-50	235	136	844	569	44	2,550	4,710

of reworked tuff lying along the contact which increases the rate of movement in that direction.

The tuff in the ashflows is not homogenous. It is broken by joints, and porosity varies within the tuff matrix. The contact between the two ashflows adds to the inhomogeneity. Thus the extent of the migration can only be approximated. About 4 yr after the wastes were stored in shafts 12 and 13, a 100 pCi/ml contour has moved to a distance of about 105 ft west of the shafts along the contact between the two ashflows (Fig. 4), and the 100 pCi/ml contour extrapolated beneath the shafts is at a depth of about 97 ft below the surface of the mesa. There is a second contact beneath the lower ashflow (Fig. 4), however, and this contact would slow the vertical migration of tritiated water vapors through the tuff by allowing them to move laterally along the more permeable contact. In general, the volume of tuff containing the tritiated moisture has assumed the shape of an irregular lens, shortened to the east and elongated to the west (Fig. 4).

Little water from precipitation infiltrates through the soil into the underlying tuff.[1] There is not enough water to leach the tritium from the wastes and move it through the 240 ft of dry tuff and 610 ft of dry volcanic rocks and sediments to the main aquifer that lies at a depth of about 850 ft at Area G.

RELEASE OF TRITIUM TO THE ATMOSPHERE

Intake of air during periods of high atmospheric pressure and exhaust of air during periods of low pressure have been noted for burial shafts and test holes in the tuff in Area G. The soil and weathered surface tuff forms a partial barrier against the exchange of air between the underlying

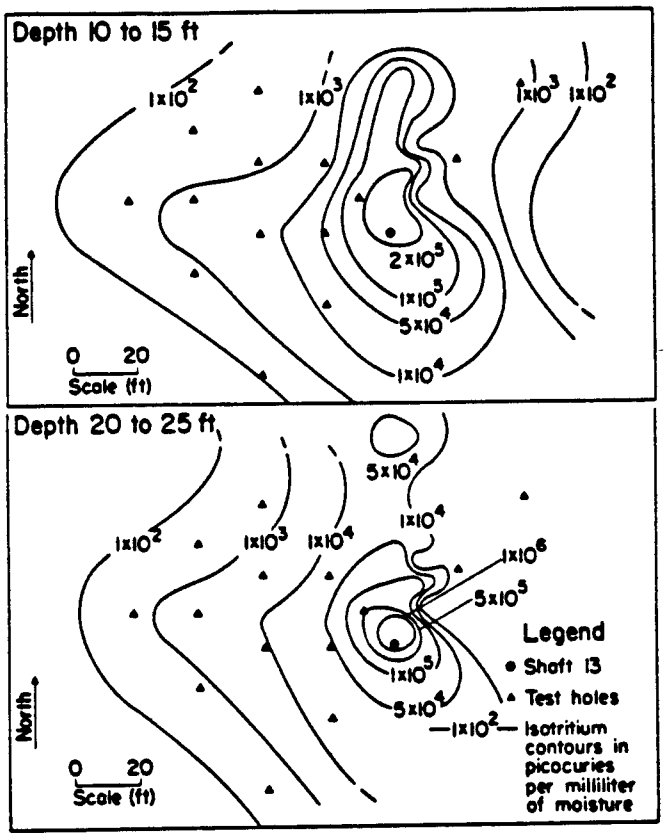

Fig. 2. Isotritium concentrations in picocuries per milliliter of moisture in planview at depths of 10 to 15 ft and 20 to 25 ft.

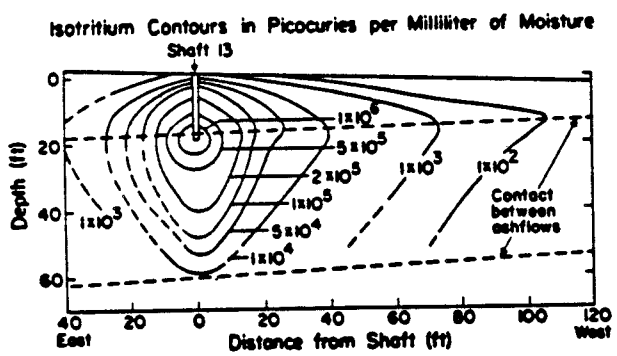

Fig. 4. Isotritium concentrations in picocuries per milliliter of moisture in section east and west of shaft 13.

tuff and the atmosphere.[2] Air was pumped from shaft 47 to determine if measurable amounts of tritium could be released to the atmosphere during an atmospheric low.

The air in the shafts is nearly saturated with water vapor. The measured relative humidity

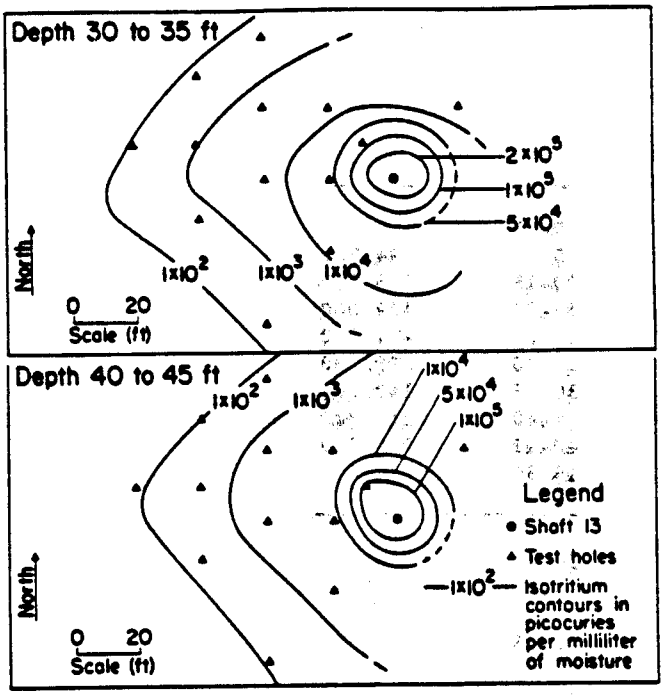

Fig. 3. Isotritium concentrations in picocuries per milliliter of moisture in planview at depths of 30 to 35 ft and 40 to 45 ft.

varied from 94 to 98% at a temperature of about 70°F. Prior to receiving wastes, shaft 47 was sealed at the surface and air pumped out of the unlined shaft at a rate of about 2.5 cfm for 24 h. Moisture was collected in a condenser at the pump and analyzed for tritium. The tritium concentration was 577,000 pCi/ml of water, about half the concentration found in moisture from a sample of tuff collected from a depth of 25 ft (Table I).

A number of samples of surface soil were collected west of shaft 13 out to a distance of 120 ft (Table III). Tritiated moisture concentrations generally decreased with distance from shafts 12 and 13. The sample collected at 80 ft consisted of tuff since there was no soil cover at that point. We therefore conclude that tritium is being released to the atmosphere as a result of evaporation of soil moisture near the shafts.

In an effort to determine whether or not vegetation has any influence on the transfer of tritiated moisture from the disposal shafts to the atmosphere, five samples of vegetation and moisture

TABLE III

MOISTURE CONTENT AND TRITIUM ANALYSES OF MOISTURE FROM SOIL AND TUFF WEST OF SHAFT 13, AUGUST 5, 1970

Distance (ft)	Moisture Content (% by wt)	Tritium (pCi/ml)
5	8.8	1,100
10	17.3	327
20	10.2	131
40	7.0	40
60	6.4	68
80	2.7	122
100	7.1	30
120	8.2	21

transpired from vegetation were collected in the immediate vicinity of the disposal shafts (Table IV). These analyses indicate that there is an uptake of tritium by plants from the soil and tuff and that tritiated moisture is being transpired to the atmosphere. Measurements from two samples collected about 0.5 miles west of the shafts are included for comparison. No attempt was made to determine the amount of tritiated moisture being released to the atmosphere due to transpiration from plants and evaporation from surface soil adjacent to the shafts.

STORAGE OF TRITIUM-CONTAMINATED WASTES

Containment is the goal of every waste storage operation. To attain this goal, new packaging techniques for tritium-contaminated wastes were initiated. Small items are placed in 55 gal drums, which are then filled with asphalt, sealed, and lowered into the shafts. Large objects present a more complex problem. The walls and bottom of the receiving shaft are coated with asphalt, and the waste is emplaced in the shaft and encased in asphalt.

Additional measures would provide even better containment performance for these disposal shafts. Location and depth should be chosen to preclude the penetration of two ashflows. This may not always be possible due to the location of the disposal site. Furthermore, the frequency of joints and fractures in the ashflow tuffs makes it difficult to locate shafts where open joints and fractures do not intersect the walls. Therefore, the walls of all shafts should be coated by spraying with asphalt to help retain the tritium by sealing any contact between ashflows as well as any open joints or fractures, and by decreasing the porosity of the tuff matrix.

SUMMARY

The transport of tritium is by exchange with the natural water in the tuff and subsequent movement of this moisture in the vapor phase. Primary movement from the shafts was along the contact between two ashflows, and secondary movement was through open joints and through the tuff matrix.

TABLE IV

TRITIUM ANALYSES OF MOISTURE FROM PLANTS

Location	Type of Plant	Type of Sample	Tritium (pCi/ml)
40 ft South of Shaft 13	Ragweed	DIS	392
40 ft South of Shaft 13	Tumble Weed	DIS	398
At Shaft 13	Unknown	SWT	101,000
85 ft North of Shaft 13	Chamisa	SWT	17,700
At Shaft 14	Unknown	DIS	7,970
0.5 Mile West of Area G	Chamisa	SWT	<5
0.5 Mile West of Area G	Unknown	SWT	<5

DIS - Analyses made of moisture distilled from plant by heating.
SWT - Analyses made of moisture transpired from plant.

This migration has caused 100 pCi/ml concentrations of tritiated moisture to be displaced about 105 ft west of the shafts in 4 yr. Since the tuff is not homogenous, the tritium-contaminated volume has formed the shape of an irregular lens truncated to the east of the shaft and elongated to the west.

Tritiated moisture has migrated to the surface of the mesa where evaporation from the soil and exposed tuff and transpiration from plants is releasing it to the atmosphere. This effect is most noticeable in an area adjacent to the shafts and decreases with distance outward.

New storage techniques include encasing tritium-contaminated wastes in asphalt to prevent migration from the shafts. Additional precautions could be taken by spraying the walls of all shafts with asphalt in order to seal contacts between ash-flows and open joints and fractures and to reduce the porosity of the tuff matrix.

REFERENCES

1. W. D. Purtymun, "Geology and Hydrology of Mesita del Buey," Los Alamos Scientific Laboratory report LA-4660 (1971).
2. J. L. Kunkler, "Measurement of Atmospheric Pressure and Subsurface Gas Pressure in the Unsaturated Zone of the Bandelier Tuff, Los Alamos, New Mexico," U.S. Geol. Survey Prof. Paper 650-D (1969).

☆ U. S. GOVERNMENT PRINTING OFFICE: 1973 — 784-278/23

CM:449(160)

Informal Report

Geohydrology of the Pajarito Plateau with Reference to Quality of Water, 1949-1972

PRELIMINARY REPORT
SUBJECT TO REVISION

by

William D. Purtymun

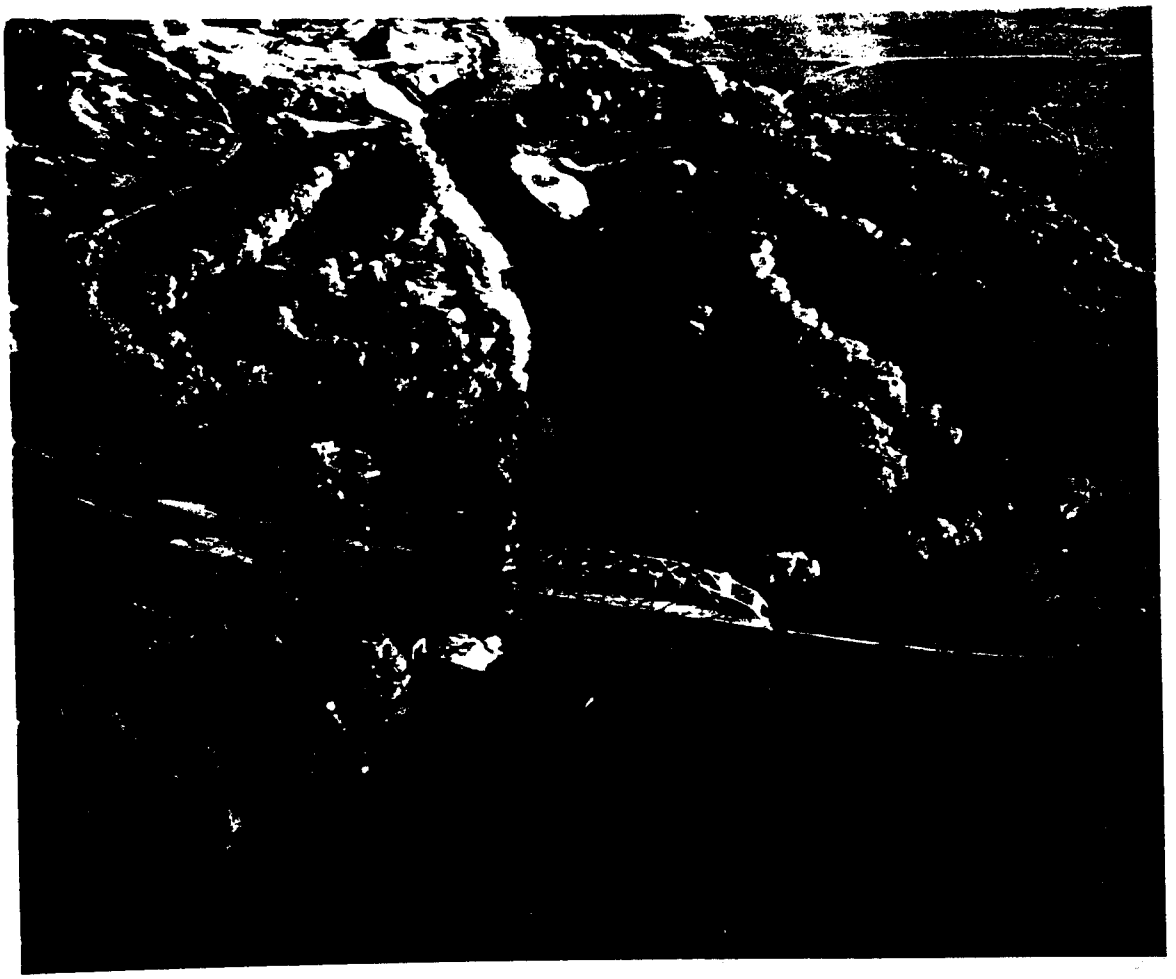

December 1975

GEOHYDROLOGY OF PAJARITO PLATEAU

WITH REFERENCES TO QUALITY OF WATER, 1949-1972

By

William D. Purtymun

CONTENTS

ABSTRACT 1
I. INTRODUCTION 1
A. Geography 1
B. Geology 4
1. Santa Fe Group 5
2. Volcanic Rock of the Jemez Mountains 8
3. Alluvium and Soil 9
4. Structure 9
C. Hydrology 12
1. Surface Water 12
2. Water in the Alluvium 14
3. Perched Aquifers in the Puye Formation and Basaltic Rocks of Chino Mesa 14
4. Main Aquifer of the Los Alamos Area 14
D. Methods of Study 16
1. Chemical Analyses of Water 16
2. Radiochemical Analyses of Water 18
3. Radiochemical Analyses of Sediments 19
4. Particle Size Distribution of Sediments 19
5. Inventory of Plutonium in Sediments in Drainage Areas 4, 5, and 7 20
6. Flood-frequency and Maximum Discharge 22
II. DRAINAGE AREA 1 (BARRANCA CANYON) 23
A. Radiochemical Analyses of Sediments 24
B. Flood-frequency and Maximum Discharge 26
III. DRAINAGE AREA 2 (BAYO CANYON) 26
A. Chemical Analyses of Storm Runoff 27
B. Radiochemical Analyses of Sediments 27
C. Flood-frequency and Maximum Discharge 29
IV. DRAINAGE AREA 3 30
V. DRAINAGE AREA 4 (ACID-PUEBLO CANYON) 30
A. Sewage and Industrial Treatment Plants 32
1. Chemical Quality of Sewage and Industrial Effluents 34
2. Radiochemical Quality of Sewage and Industrial Effluents 37

B. Surface Water 39
1. Chemical Quality of Surface Water 41
2. Radiochemical Quality of Surface Water 46
C. Water in Alluvium 49
1. Chemical Quality of Water in Alluvium 50
2. Radiochemical Quality of Water in Alluvium 54
D. Radiochemical Analyses of Sediments 56
E. Inventory of Plutonium in Channel Sediments 61
F. Flood-frequency and Maximum Discharge 63
VI. DRAINAGE AREA 5 (LOS ALAMOS AND DP CANYONS) 63
A. Industrial Waste Treatment Plants 66
1. Sewage Treatment Plant 66
2. Seepage Pits for Industrial Effluents 66
a. Retention of Plutonium in the Tuff 69
b. Movement of Plutonium in the Tuff 71
c. Observation January 1967 73
3. Industrial Treatment Plant Building 35 74
4. Industrial Plant Building 257 75
a. Radiochemical Analyses of Tuff ..... from Test Holes and Shafts 77
5. Chemical Quality of Sewage and Industrial Effluents 78
6. Radiochemical Quality of Sewage and Industrial Effluents 79
B. Surface Water, DP Canyon 83
1. Chemical Quality of Surface Water 83
2. Radiochemical Quality of Surface Water 86
C. Surface Water, Los Alamos Canyon 88
1. Chemical Quality of Surface Water 88
2. Radiochemical Analyses of Surface Water 90
D. Water in Alluvium, Los Alamos Canyon 90
1. Chemical Quality of Water in Alluvium 90
2. Radiochemical Quality of Water in Alluvium 93
E. Storm Runoff DP-Los Alamos Canyon 95
1. Transport of Radionuclides 97

F. Radiochemical Analyses of Sediments.....103
G. Inventory of Plutonium in Channel Sediments.....107
H. Flood-frequency and Maximum Discharge.....111
VII. DRAINAGE AREA 6 (SANDIA CANYON).....113
A. Industrial Waste Treatment Plants.....113
B. Surface Water.....113
1. Chemical Quality of Surface Water.....113
2. Radiochemical Quality of Surface Water.....116
C. Water in Alluvium.....117
1. Chemical Quality of Water in Alluvium.....117
2. Radiochemical Analyses of Water in Alluvium.....117
D. Radiochemical Analyses of Sediments.....118
E. Flood-frequency and Maximum Discharge.....119
VIII. DRAINAGE AREA 7 (MORTANDAD CANYON).....119
A. Geologic and Hydrologic Investigations.....121
1. Preliminary Report of the Geology and Hydrology.....121
2. Distribution of Radioactivity in Alluvium.....123
3. Disposal of Industrial Effluent in Mortandad Canyon.....124
4. Occurrence of Tritium in the Shallow Alluvial Aquifer, 1966-1969.....125
5. Despersion and Movement of Tritium in the Shallow Aquifer..125
B. Industrial Waste Treatment.....126
1. Chemical Quality of Effluent.....127
2. Radiochemical Quality of Effluent.....131
C. Surface Water.....135
1. Chemical Quality of Surface Water.....136
2. Radiochemical Quality of Surface Water.....141
D. Water in Alluvium.....142
1. Chemical Quality of Water in Alluvium.....144
2. Inventory of Chemicals Released and in Storage.....153
3. Radiochemical Quality of Water in Alluvium.....154
E. Inventory of Plutonium in Solution in Storage.....159
F. Storm Runoff and Transport of Radionuclides.....160
G. Radiochemical Analyses of Cuttings from Test Hole.....161

H. Radiochemical Analyses of Sediments.....162
1. Sediment Analyses Mortandad Canyon.....163
2. Sediment Analyses 10-Site Canyon.....166
I. Inventory of Plutonium in Channel Sediments.....168
J. Flood-frequency and Maximum Discharge.....170
IX. DRAINAGE AREA 8.....171
X. DRAINAGE AREA 9 (CAÑADA DEL BUEY).....171
A. Surface Water.....173
1. Chemical Quality of Surface Water.....173
2. Radiochemical Quality of Surface Water.....174
B. Radiochemical Analyses of Sediments.....174
C. Flood-frequency and Maximum Discharge.....175
XI. DRAINAGE AREA 10 (PAJARITO CANYON).....175
A. Surface Water.....177
1. Chemical Quality of Surface Water.....177
2. Radiochemical Quality of Surface Water.....178
B. Radiochemical Analyses of Sediments.....179
C. Flood-frequency and Maximum Discharge.....180
XII. DRAINAGE AREA 11 (WATER CANYON).....181
A. Surface Water.....181
1. Chemical Quality of Surface Water.....183
2. Radiochemical Quality of Surface Water.....184
B. Radiochemical Analyses of Sediments.....185
C. Flood-frequency and Maximum Discharge.....187
XIII. DRAINAGE AREA 12.....188
XIV. DRAINAGE AREA 13 (ANCHO CANYON).....188
A. Surface Water.....188
1. Chemical Quality of Surfaee Water.....188
2. Radiochemical Quality of Surface Water.....191
B. Radiochemical Analyses of Sediments.....192
C. Flood-frequency and Maximum Discharge.....193
XV. DRAINAGE AREA 14.....194
XVI. DRAINAGE AREA 15 (CHAQUEHUI CANYON).....194
A. Surface Water.....194
1. Chemical Quality of Surface Water.....194
2. Radiochemical Quality of Surface Water.....197

B. Radiochemical Analyses of Sediment.....198
C. Flood-frequency and Maximum Discharge.....198
XVII DRAINAGE AREA 16.....198
XVIII PERCHED WATER IN PUYE FORMATION.....199
A. Chemical Quality of Water.....201
B. Radiochemical Quality of Water.....202
XIX. PERCHED WATER IN BASALTIC ROCKS OF CHINO MESA.....202
A. Chemical Quality of Water.....204
B. Radiochemical Quality of Water.....207
XX. MAIN AQUIFER OF THE LOS ALAMOS AREA.....210
A. Test Well 1.....210
1. Geologic and Hydrologic Characteristics.....210
2. Chemical Quality of Water.....212
3. Radiochemical Quality of Water.....213
B. Test Well 2.....214
1. Geologic and Hydrologic Characteristics.....214
2. Chemical Quality of Water.....215
3. Radiochemical Quality of Water.....216
C. Test Well 3.....217
1. Geologic and Hydrologic Characteristics.....217
2. Chemical Quality of Water.....218
3. Radiochemical Quality of Water.....220
D. Test Well 4.....221
1. Geologic and Hydrologic Characteristics.....221
2. Chemical Quality of Water.....222
3. Radiochemical Quality of Water.....223
E. Test Hole 5.....223
1. Geologic Characteristics.....224
F. Test Hole T-6.....224
1. Geologic Characteristics.....224
G. Test Hole T-7.....225
1. Geologic Characteristics.....225
H. Test Well 8.....225
1. Geologic and Hydrologic Characteristics.....225
2. Chemical Quality of Water.....226

3. Radiochemical Quality of Water.....227
I. Test Well DT-5A.....228
1. Geologic and Hydrologic Characteristics.....228
2. Chemical Quality of Water.....229
3. Radiochemical Quality of Water.....230
J. Test Well DT-9.....231
1. Geologic and Hydrologic Characteristics.....231
2. Chemical Quality of Water.....232
3. Radiochemical Quality of Water.....233
K. Test Well DT-10.....234
1. Geologic and Hydrologic Characteristics.....234
2. Chemical Quality of Water.....235
3. Radiochemical Quality of Water.....235
L. Test Hole H-19.....237
1. Geologic and Hydrologic Characteristics.....237
M. San Ildefonso Stock Wells.....237
1. Chemical Quality of Water.....238
2. Radiochemical Quality of Water.....238
N. Buckman Well.....239
1. Chemical Quality of Water.....239
XXI. SUMMARY.....240
XXII. SELECTED REFERENCES.....249
XXIII. APPENDICES.....254

Illustrations

Figure 1. Physiographic features in North-Central New Mexico 3

Figure 2. Geologic map and sections showing stratigraphic units and basement Precambrian Rocks beneath the Pajarito Plateau 6

Figure 3. Major faults and contours on the top of the main aquifer of the Los Alamos area 11

Figure 4. Drainage areas and points of intermittent stream discharge 17

Figure 5. Drainage Area 1 (Barranca Canyon) showing location of sediment sampling station 25

Figure 6. Drainage Area 2 (Bayo Canyon) and Drainage area 3 showing locations of sampling stations 28

Figure 7. Drainage Area 4 (Pueblo Canyon) 31

Figure 8. Sampling stations, Geologic Map, and Cross-Section of Drainage Area 4 (Pueblo Canyon) 33

Figure 9. Drainage Area 5 (DP-Los Alamos Canyons) showing geology and sampling stations 64

Figure 10. Seepage Pits for Industrial Effluents 67

Figure 11. Shaft disposal area for sludges fixed in sludges 76

Figure 12. Channel bed sediment sampling stations in DP-Los Alamos Canyons 100

Figure 13. Drainage Area 6 (Sandia Canyon) showing sampling stations 112

Figure 14. Drainage Area 7 (Mortandad Canyon) showing geology and sampling stations 120

Figure 15. Drainage Area 8 and Drainage Area 9 (Cañada del Buey) showing location of sampling stations 172

Figure 16. Drainage Area 10 (Pajarito Canyon) showing location of sampling stations 176

Figure 17. Drainage Area 11 (Water Canyon) showing locations of sampling stations 187

Figure 18. Drainage Area 12 and Drainage Area 13 (Ancho Canyon) showing locations of sampling stations.....189
Figure 19. Drainage Area 14, Drainage Area 15 (Chaquehui Canyon) showing location of sampling stations and Drainage Area 16.....195
Figure 20. Cross-section and map showing perched water in the Puye Formation and Basaltic Rock of Chino Mesa.....200
Figure 21. Location of Test Wells and Test Holes.....211

ABSTRACT

The facilities of Los Alamos Scientific Laboratory are located on the Pajarito Plateau in North-Central New Mexico. The plateau is formed by ashfall and ashflow units of the Bandelier Tuff. The tuff is underlain by volcanic debris of the Puye Formation which in places interfingers with the Basaltic Rocks of Chino Mesa. The Puye Formation is underlain by sediments of the Tesuque Formation.

Southeastward intermittent streams that drain into the Rio Grande have cut deep canyons into the Bandelier Tuff. The intermittent runoff in the canyons occur from storm runoff and the release of treated sewage or industrial effluents. The effluents do not reach the Rio Grande as surface flow.

There are two major ground water systems in the canyons. A near surface ground water system occurs in the larger canyon in the alluvium which is underlain by the tuff. This system is recharged by the intermittent storm runoff or release of effluents. A deep ground water system, the main aquifer, occurs in the lower part of the volcanic debris and sediments of Puye and Tesuque Formation.

The movement of water from the recharge area in the Valles Caldera and canyons cut into the flanks of the mountains and western part of the plateau eastward toward the Rio Grande, where a part is discharged into the river.

There are sixteen drainage areas on the plateau that encompass the Laboratory Reservation. Hydrogeologic data have been collected in twelve of these areas. The remaining four areas are small with no well defined drainage, thus, have not warranted study.

Treated sewage effluents are released into Drainage Area 4 (Acid-Pueblo Canyon), 5 (DP-Los Alamos Canyon), 6 (Sandia Canyon), 10 (Pajarito Canyon) and 11 (Water Canyon). Pueblo Canyon receives the largest volume of effluents from the two community sewage treatment plants. The volume released into the remaining drainage areas are small. The chemical quality of the sewage effluents released into the canyons have dominated the chemical quality of the water in the stream and shallow ground water aquifer in the alluvium of the canyons.

Two drainage areas, 5 (Los Alamos Canyon) and 7 (Mortandad Canyon) are currently receiving effluents from treatment plants that operate to reduce radionuclide concentrations. Drainage Area 6 (Sandia Canyon) receives some effluents as the result of blow-down from the power plant at TA-3. Drainage Area 11 (Water Canyon) receives some water from industrial process at nearby technical areas. These canyons also receive sewage effluent as previously mentioned.

The chemical quality of water in the streams or shallow aquifers in the alluvium of these canyons reflect the chemical quality of the type of effluent released, such as sewage or industrial effluents. The base flow in these canyons are from the release of effluents. In general, the chemical quality of the water improves downgradient from the effluent outfall as the chemical ions in the effluent adjust to the environment.

Drainage Area 4 (Acid-Pueblo Canyon) received industrial effluents containing radionuclides until 1964. Drainage Area 5 (DP-Los Alamos Canyons) received this type of effluents from 1952 to present, and Drainage Area 7 (Mortandad Canyon) also received this type of effluents from 1963 to present.

Residual radionuclides remain in the Acid Pueblo Canyon drainage although the release of effluents ceased in 1964. The radionuclide concentration decreased downgradient in the canyon from the old effluent outfall. The radioactive materials are attached to the alluvial materials in the stream channel. They, in part, are resuspended in water in the stream.

Radionuclides in solution in the stream and shallow aquifer in alluvium and attached to alluvial material are found in DP-Los Alamos Canyon. The concentrations generally decrease down stream from the outfall in DP Canyon and below the junction of DP with Los Alamos Canyon. The radionuclides have an affinity for the alluvial material in the channels of both canyons. There is no high build up of radionuclide near the effluent outfalls. Storm runoff during the summer, transports and disperses the alluvial material and attached radionuclides down the canyon to the Rio Grande.

Radionuclides in solution in the stream and shallow aquifer in the alluvial material are found in Mortandad Canyon. The concentrations also

decrease downgradient from the effluent outfall. Although the radionuclides are dispersed by storm runoff down the canyon, there has been no transport off the Laboratory Reservation. This is due to the small drainage area that results in low volumes of storm runoff and thick sections of unsaturated alluvium that has been able to adsorp all runoff since hydrologic observations began in 1960.

The chemical quality of water from perched aquifers in the Puye Formation and Basaltic Rocks of Chino Mesa in Pueblo Canyon indicate recharge from the stream in Pueblo Canyon. There is no indication of contamination of these perched aquifers by radionuclides released from the treatment plant at TA-45 from 1943 to 1964.

The chemical quality of water from eight test wells completed into the main aquifer have shown no change during the period of study. The quality of water reflects no contamination by sewage or industrial effluents. Radionuclides occuring in the waters are natural and do not indicate any contamination from the release of industrial effluents on the plateau.

I. INTRODUCTION

The Community of Los Alamos and the Laboratories of the Los Alamos Scientific Laboratory are located on the Pajarito Plateau in north-central New Mexico. The community and the Laboratory have grown from a few hundred people in 1943 to over 16,000 with about 4,000 employed in the Laboratory.

Geologic and hydrologic studies began in 1947 to evaluate the water resources of the area and to study the problems associated with the treatment and release of industrial and sewage effluents into canyon disposal areas. The purpose of this report is to evaluate the impact of the Laboratory on the surface and shallow ground water aquifers in the alluvium in canyon drainage areas and to provide compilation of basic data for future reference. The study covers drainage areas that form discharge points from ERDA-LASL controlled property.

The study includes geologic and hydrologic conditions in the drainage areas including channel geology, occurrence and movement of surface and ground water, chemical and radiochemical quality of water, radiochemical analyses of sediments, transport of sediments in storm runoff (in canyons where data is available), particle-size distribution of sediments, and flood-frequency and maximum discharge in the drainage area. The study also includes basic data collected in the surveillance monitoring program, 1949-1972, special studies, and in part develops new data necessary for completion of the study.

A. Geography

The Pajarito Plateau forms an apron 8 to 16 km wide and 32 to 40 km long around the eastern flanks of the Sierra de los Valles

(Fig. 1). The surface of the plateau slopes gently eastward from an altitude of about 2290 m along the flanks of the mountains to about 1430 m along the eastern edge where it terminates along the Puye Escarpment and White Rock Canyon. The plateau is drained by southeast and eastward trending streams that have cut deep canyons into the surface of the plateau.

The Rio Grande lies to the east of the plateau. It drops from an altitude of about 1680 m at Otowi (mouth of Los Alamos Canyon) to about 1630 m at the junction with Frijoles Canyon. North of Otowi the Rio Grande lies in a broad valley, while to the south it is confined in a deep narrow canyon (White Rock Canyon).

The mountain peaks of the Sierra de Los Valles rise to an altitude of about 3,525 m near the head of Santa Clara Canyon and to an altitude of 3110 m near the head of Frijoles Canyon. The crest of the north-south trending range of peaks and ridges forms a surface water divide. Streams originating on the eastern slopes and Pajarito Plateau flow directly into the Rio Grande. Streams on the western sloped follow a more circuitous course and enter the Rio Grande 48 km to the south.

The climate and vegetation change westward from the Rio Grande to the crest of the Sierra de Los Valles along with the change in altitude. The average precipitation increases from about 23 cm along the Rio Grande to as much as 76 cm along the crest of the mountains. The average precipitation on the plateau is about 46 cm. About 70 percent of this amount occurs in July and August during summer thunder showers.

The average July temperatures at the lower altitude is about 23° C and on the plateau is about 19° C while average January

shown on Fig. 2.

A detailed discussion of the geology of the area is presented by Griggs[1] and Bailey et al.[2]

1. Santa Fe Group

The Santa Fe Group in ascending order, consists of the Tesuque Formation, the Puye Formation, and basaltic rocks of Chino Mesa.

The Tesuque Formation is a sequence of light-colored sediments laid down as coalescing alluvial-fan and flood-plain deposits in the Rio Grande depression. These sedimentary rocks were derived from highlands to the north, and possibly in part from the Sangre de Cristo Mountains to the east. The separate beds are composed of friable to moderately well-cemented, light-pink-grey to light-brown siltstone and sandstone that contain lenses of conglomerate and clay. Bedding generally is poorly developed except locally in fine-grained material.

The Puye Formation consists of two members. The lower member is a poorly consolidated, channel-fill deposit. A fanglomerate overlies the lower member and is composed of volcanic debris.

The lower member of the Puye Formation overlies the Tesuque Formation along the Rio Grande and in Los Alamos and Guaje Canyons. It is grey, poorly consolidated conglomerate consisting of fragments of quartzite, schist, gneiss, and granite ranging in size from sand to boulders; well-sorted lenses of silt and sand are present sporadically. The materials making up the conglomerate were derived principally from igneous and metamorphic rocks to the north and northeast. They were deposited on a broad flood plain and in channels of the ancestral Rio Grande. A zone near

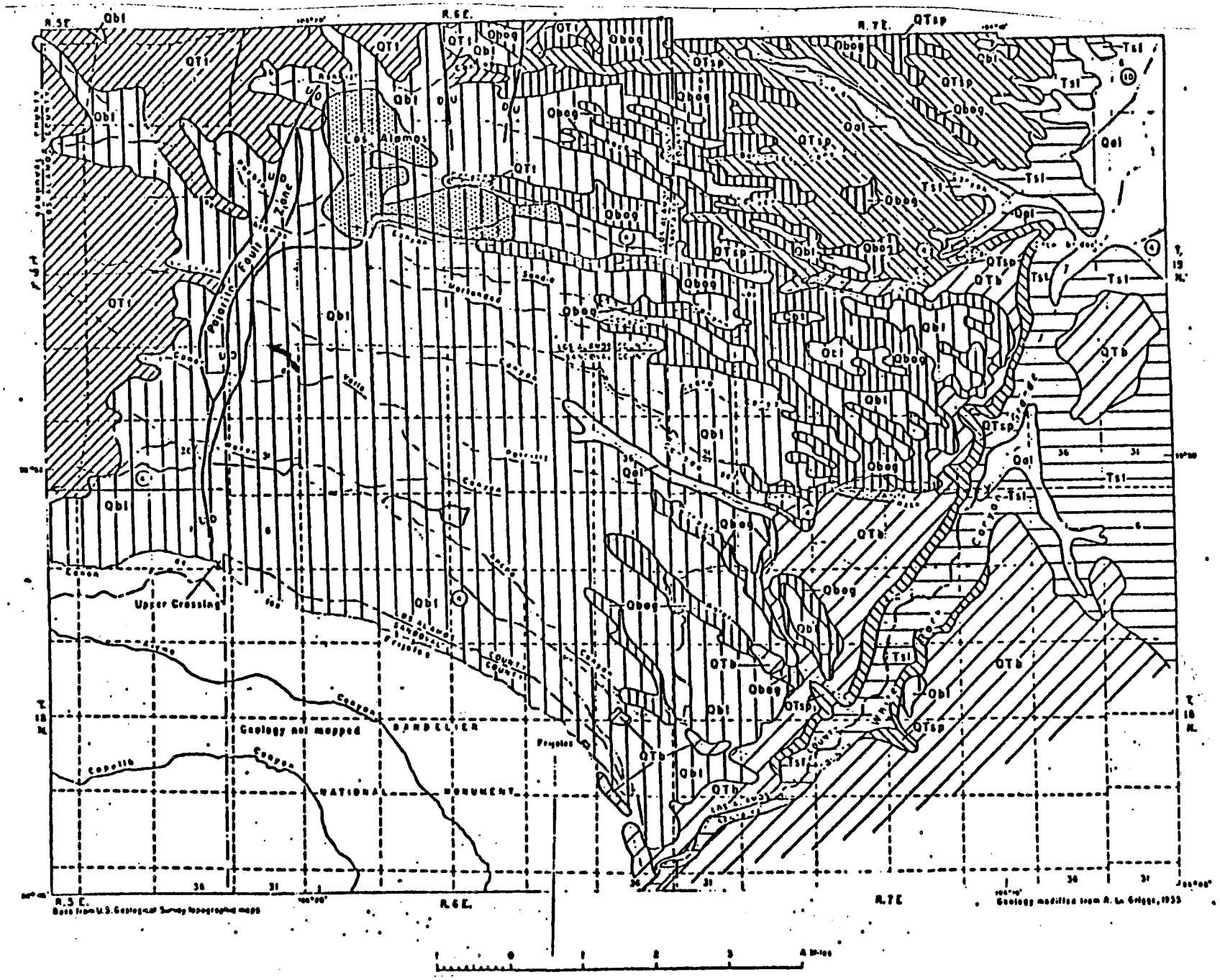

Fig. 2. Geologic map of the [illegible]rito Plateau

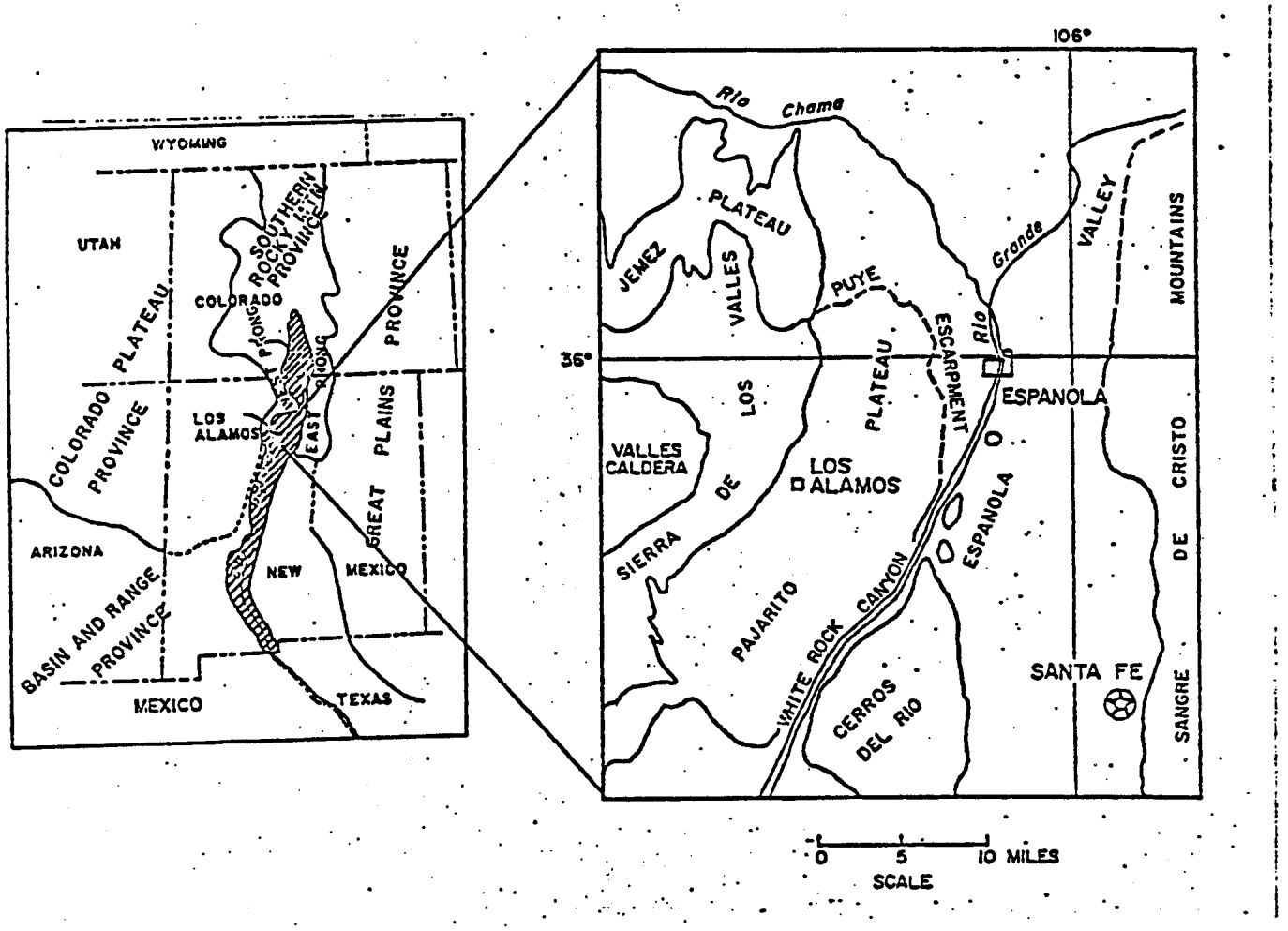

Fig. 1. Physiographic features in North-Central New Mexico.

temperature at the valley is -6° C and on the plateau -7° C. At higher altitudes on the mountain crests, temperatures are lower so that snow on the peaks lasts until late May or early June.

Cottonwoods, willows, and box elders are found along the Rio Grande and in the lower part of the canyons cut into the plateau. The eastern two-thirds of the plateau is covered with piñon and cedar while the western third and lower flanks of the mountains are covered with pine. Spruce, fir, and aspen intermingle with the pine on the upper slopes of the mountains. Alpine meadows are found on some of the south facing slopes of the higher peaks.

The upper surface of the plateau is sparsely covered with gamma grass while a variety of grasses occur in the canyon floors. The banks of the perennial streams are stabilized with this growth of grass.

B. Geology

Drainage areas or streams that head on the flanks of the mountains are cut into the rocks of the Tschicoma Formation. Canyons on the Pajarito Plateau are cut into and are underlain by the Bandelier Tuff. Along the eastern edge of the pleateau, the channel is cut through the Puye Formation into the Tesuque which floors the valley north of Otowi and forms the lower canyon walls along the Rio Grande in White Rock Canyon. The basaltic rocks of Chino Mesa are in places interbedded in the sediments of the Puye Formation.

The rock units described, from oldest to youngest, are the Tesuque Formation, Puye Formation and basaltic rock of Chino Mesa of the Santa Fe Group; the Tschicoma Formation and Bandelier Tuff of the volcanic rocks of the Jemez Mountains, and alluvium and soil of recent age. The generalized stratigraphic relations are

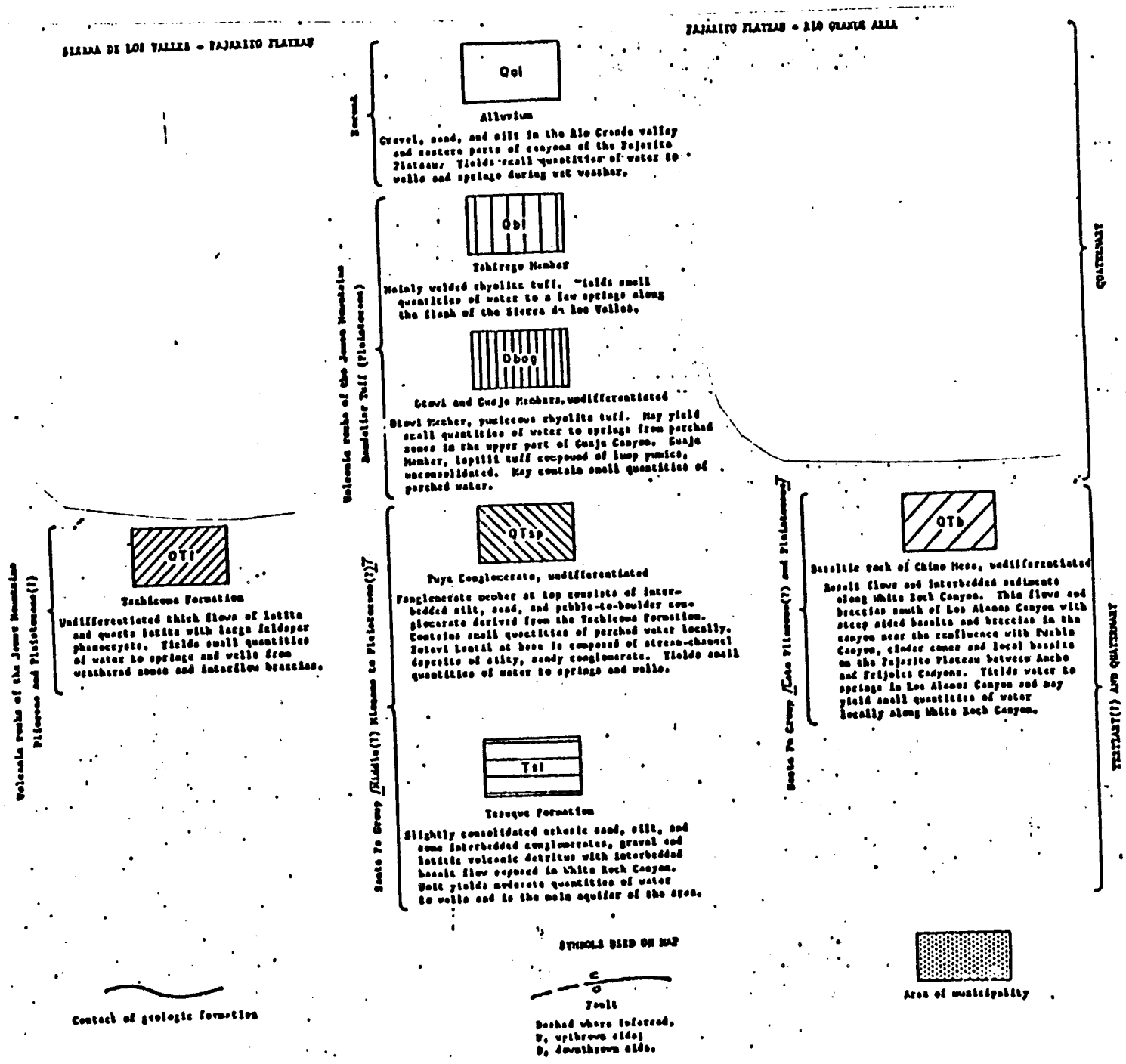

Fig 2A. Geologic and Hydrologic description of rock units.

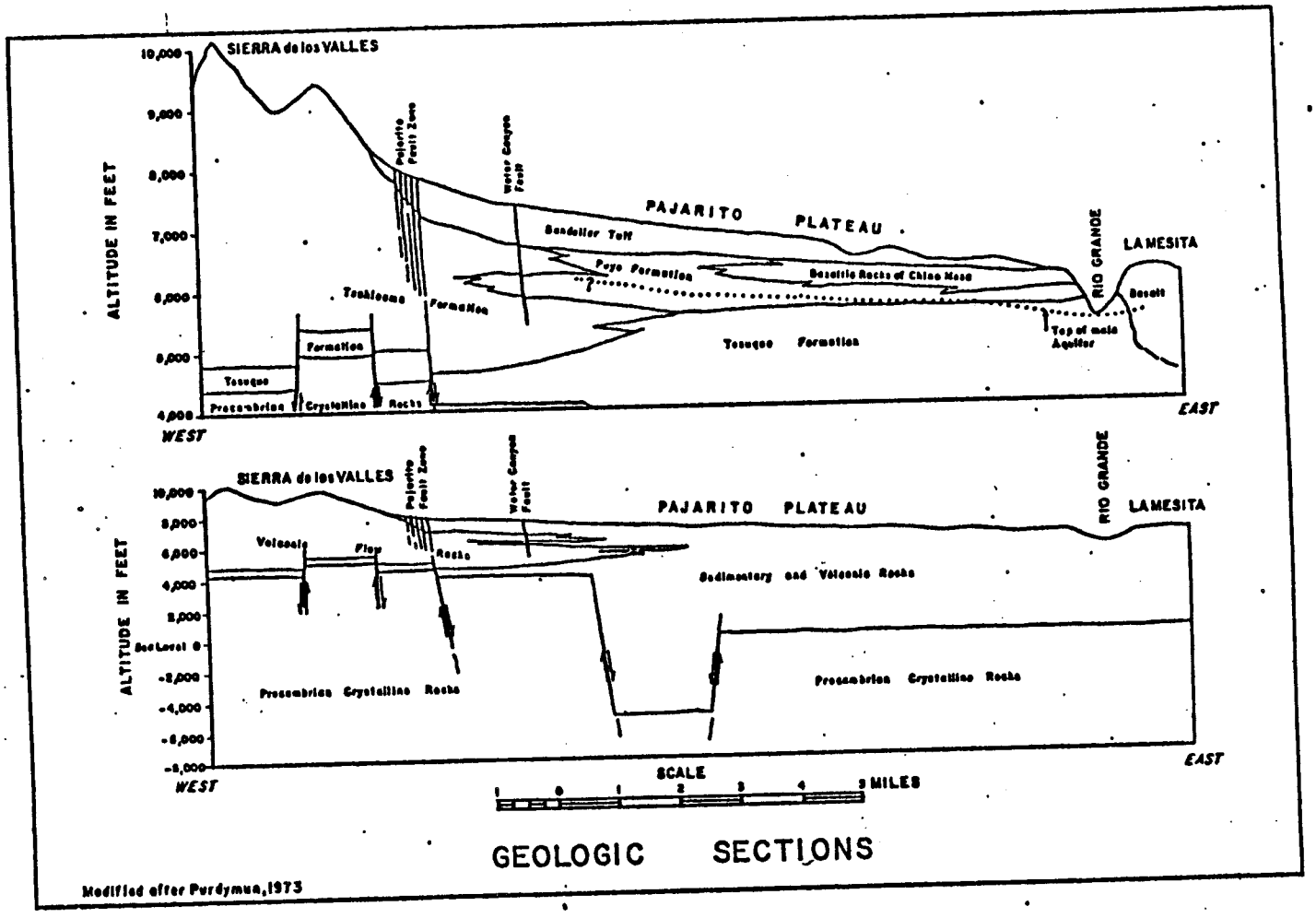

Fig. 2B Geologic sections showing stratigraphic units and basement Precambrian rocks beneath the Pajarito Plateau.

the top is composed of a mixture of pegmatitic rocks and volcanic debris. This mixed zone represents a change in source of sediments from igneous and metamorphic terrane to the north to the igneous and volcanic terrane to the west.

The upper member of the Puye Formation is a fanglomerate composed of pebbles, cobbles, and boulders of rhyolite, latite, quartz latite, and pumice in a grey matrix of silt and sand. These rocks were derived from flows associated with the volcanic rocks of the Jemez Mountains. Sorting is poor, but tongues and lenses of fairly well-sorted pumiceous siltstone and water-lain pumice are present within the fanglomerate. The degree of cementation varies from friable to well-cemented. In upper Guaje and Los Alamos Canyons, the fanglomerate member consists of angular boulders; eastward it grades to silt, sand, gravels, and rounded boulders.

The basaltic rocks of Chino Mesa originated from volcanic vents on the Cerros del Rio to the southeast of the Los Alamos area. The basalts cap the mesas of Cerros del Rio and form the steep walls of White Rock Canyon. The basalts flowed north and northwest into the Los Alamos area interfingering with the Puye Formation.

The basalts consist of five units which range in color from grey to black. They contain varying amounts of olivine, pyroxene, and plagioclase feldspar and range from fine-grained to glassy. Individual flows vary in thickness from a few feet to over 50 feet. Sediments may be found between the individual flows.

The basalts outcrop in the lower parts of the major canyons that drain the Pajarito Plateau from Otowi to Frijoles Canyon in

White Rock Canyon.

2. Volcanic rocks of the Jemez Mountains

Volcanic rocks of the Jemez Mountains along the eastern flanks of the Sierra de los Valles and on the Pajarito Plateau consist of the Tschicoma Formation and the younger Bandelier Tuff.

The Tschicoma Formation is composed of undifferentiated latite and quartz latite flows and pyroclastic rocks that are highly fractured and jointed; some intervals contain weathered zones and interflow breccia. These rocks form the core and flanks of the Sierra de los Valles.

The Bandelier Tuff is composed chiefly of ashfall and ashflow tuff and some thin, water-lain sediments. The formation has been divided into three members: Guaje, Otowi, and Tshirege, from the oldest to the youngest. The Bandelier Tuff forms the upper part of the Pajarito Plateau. Physical characteristics of the tuff are presented as Appendix A.

The Guaje Member of the Bandelier Tuff is an ashfall pumice and water-laid pumiceous tuff that rests unconformably on older rocks. The base of the unit contains grey lump-pumice fragments as much as 2 inches in length. Glass shards and crystals of quartz and sanidine are present in the cellular structure of partly devitrified pumice. Rounded pebble-size fragments of light-red rhyolite are present near the top.

The Otowi Member of the Bandelier Tuff is a light-grey, non-welded, pumiceous rhyolite tuff that weathers to a gently slope; it is conformable with the underlying Guaje. Quartz crystals, glass shards, minor amounts of mafic minerals, and varying amounts of rhyolite, latite, and pumice fragments included in a fine-grained

ash compose the tuff. Most of the rock fragments are rounded. The Otowi consists of ashflows primarily but it contains several beds of silt and water-laid pumice near the top.

The Tshirege Member of the Bandelier Tuff, is composed of a series of ashflows of rhyolite tuff that contains at least one thin, water-laid bed near the top. The Tshirege unconformably overlies the Otowi and forms the caprock of the fingerlike mesas of the Pajarito Plateau. The rhyolite tuffs range from nonwelded to welded. The thin, water-laid bed is composed of material derived from the underlying tuff.

3. Alluvium and soil

Alluvium from the Sierra de los Valles and the Pajarito Plateau has been deposited in the canyons of the plateau. Near the heads of the canyons bedrock commonly is exposed in the lower parts; but further down the canyons alluvium may be several hundred feet wide and as much as 80 feet thick.

Alluvial deposits in the canyons heading on the flanks of the Sierra de los Valles contain cobbles and boulders with accompanying clay, silt, sand, and gravel derived from the Tschicoma Formation and Bandelier Tuff. Deposits in the canyons heading on the Pajarito Plateau contain clay, silt, sand, and gravel derived from the Bandelier Tuff.

Clayey soil derived from weathering of the Bandelier Tuff covers most of the fingerlike mesas of the Pajarito Plateau.

4. Structure

The Rio Grande depression is a structurally low area that constitutes the valley through which the Rio Grande flows.[3] The Pajarito Plateau is part of the depression although it forms a

topographic high area along the western margin of the valley.

The most prominent structural features of the Pajarito Plateau is the Pajarito fault zone which trends northward along the western edge of the plateau. It is a part of the complex fault system that formed the Rio Grande depression. The fault zone consists of normal faults that are downthrown to the east and displace rocks of the Bandelier Tuff, Puye Formation, and Tschicoma Formation (Fig. 2). The displacement, estimated from the fault scarp west of S-Site, is from 120 to 150 m. The amount of displacement decreases northward where, at a point north of Los Alamos, all visible traces of the fault disappear (Fig. 3). The movement along the fault zone has been in small increments which began prior to the deposition of the Bandelier Tuff and continued into post-Bandelier time. The displacement of the older rocks is greater than the displacement of the younger rocks. The major fault in this zone extends into and displaces the Precambrian rocks.

North of Los Alamos and east of the Pajarito fault zone, two normal faults (Fig. 3) cut the Bandelier Tuff, the Puye Formation, and the Tschicoma Formation. These faults, downthrown to the west, form a graben between them and the Pajarito fault zone. They are a part of the fault system which formed the Rio Grande depression.

Beneath the central part of the Pajarito Plateau a north-trending depositional basin is formed in the Tesuque Formation. The basin is filled with volcanic debris of the Puye Formation, overlain by the Bandelier Tuff. The eastern edge of the basin is formed by thick flows of basalt from Chino Mesa, 3 to 6 km west of the Rio Grande.

A gravity survey indicated that the deepest part of the

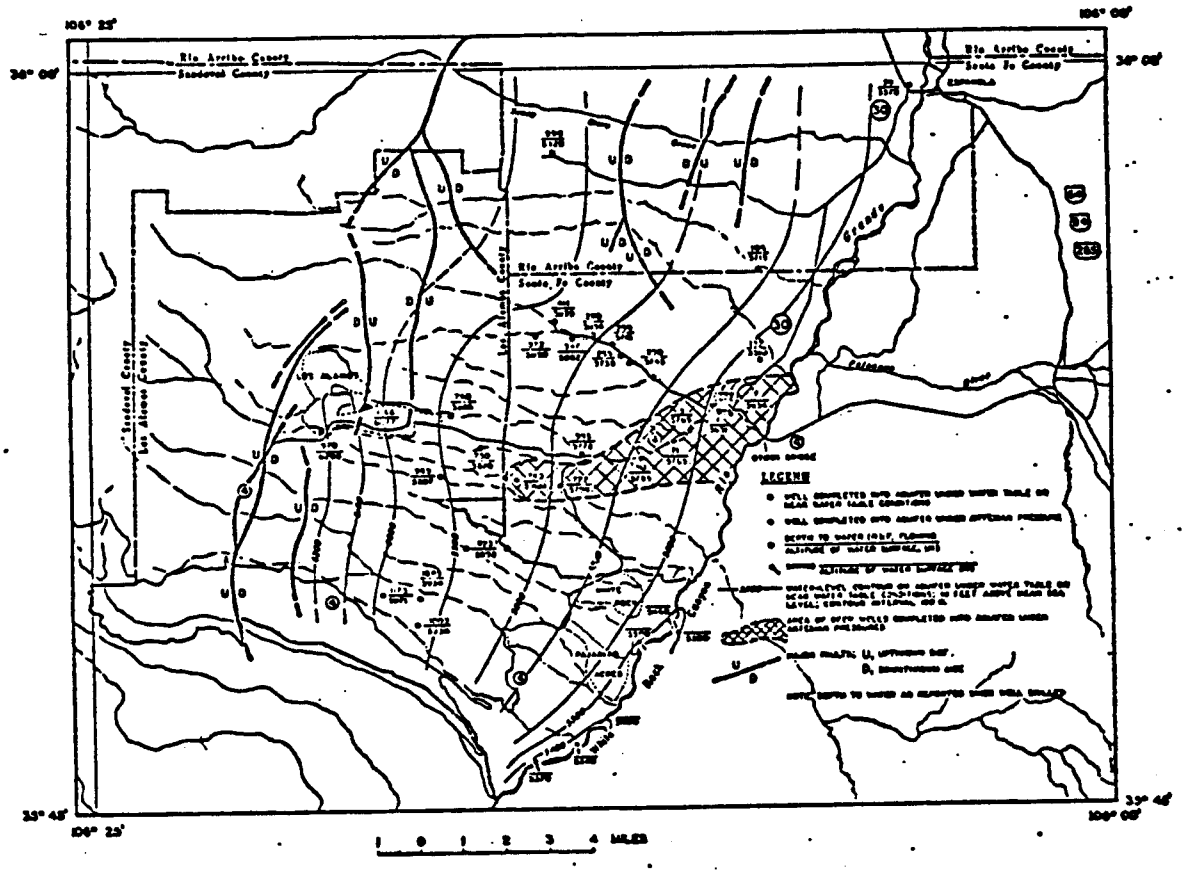

Fig. 3. Major faults and contours on the top of the main aquifer of the Los Alamos area.

Rio Grande depression (top of the Precambrian rocks) is in a north-trending trough near the center of the plateau. The bottom of this sediment-filled trough lies about 1,500 m below sea level (Fig. 2).

C. Hydrology

The master stream of north-central New Mexico, the Rio Grande flows southeastward along the eastern edge of the Pajarito Plateau and ultimately receives all runoff from the eastern flanks of the Sierra de los Valles and Pajarito Plateau. Rito de los Frijoles and Santa Clara Creek to the south and north of the drainage areas studied are the only perennial streams that discharge into the Rio Grande. Intermittent streams that cross the plateau flow into the Rio Grande only during periods of excess precipitation.

Surface flow in the intermittent streams is from either effluents released from industrial waste treatment plants and sewage treatment plants of from precipitation recharge of small aquifers in the alluvium along the canyon bottom.

A perched water body occurs in the Puye Formation and basaltic rocks of Chino Mesa in lower Pueblo, Los Alamos, and Sandia Canyon. The main aquifer (aquifer capable of water supply) lies at a depth of about 370 m along the western edge of the plateau and at a depth of about 180 m along the eastern edge.

The Bandelier Tuff is above the main zone of saturation and does not contain any known bodies of perched water in the Los Alamos area. Hydrologic characteristics of the tuff are presented in Appendix B.

1. Surface Water

Records from the gauging station at Otowi on the Rio Grande

indicate that for 71 years of record the average discharge is about 43 m^3/sec. The drainage area above Otowi is about 14,300 sq. miles in southern Colorado and northern New Mexico. The maximum discharge of 691 m^3/sec occurred on May 2, 1920 and is the greatest since at least 1884 and probably since 1741. The minimum discharge of 1.7 m^3/sec occurred in July of 1902.[4] Total sediment load passing the gauging station at Otowi during 1969 was 1.6 x 10^6 t. Some extremes listed for chemical quality and sediment loads for the period 1946 through 1969 are listed below.[5]

Dissolved solids: Maximum, 1,030 mg/l Aug. 5, 1963; minimum, 135 mg/l May 1-31, 1969. Hardness: Maximum, 702 mg/l Aug. 5, 1963; minimum, 83 mg/l May 22-26, 1960, June 22-28, 1968. Specific conductance: Maximum daily, 1,310 micromhos Aug. 5, 1963; minimum daily, 165 micromhos June 13, 1952. Water temperatures (1948-69): Maximum 31° C Aug. 4, 5, 1954; minimum, freezing point on many days during winter months. Sediment concentrations (1947-69): Maximum daily, 43,500 mg/l Aug. 21, 1955; maximum daily, 11 mg/l July 27, 1963. Sediment loads (1947-69): Maximum daily, 3.3 x 10^5 t Aug. 23, 1961; minimum daily, 2.7 t July 27, 1963.

Perennial flow occurs in the upper reaches of Los Alamos, Pajarito, Canon de Valle and Water Canyon. The flow is from perched water zones in the Tschicoma Formation and Bandelier Tuff. Perennial flow in sections of Pueblo, Los Alamos, Sandia, and Mortandad are from the release of effluents from industrial waste treatment plants, sewage plants, and blow down water from cooling process. These effluents do not leave the boundaries of

the ERDA property as surface flow but infiltrate to recharge small bodies of water in the alluvium of the canyon bottoms. Only during periods of excessive precipitation, snowmelt, or heavy summer showers, does runoff from most of the stream reach the Rio Grande. Occurrence of surface water is treated in each major drainage area investigated in this report. Hydrology of Santa Clara, Guaje Los Alamos, and Frijoles Canyon as related to low-flow investigations are presented in Appendix C.

2. Water in the alluvium

Water in the alluvium is recharged from surface flow from either effluents, cooling water, or storm runoff. Water in the alluvium occurs in Pueblo, Los Alamos, Mortandad, and Pajarito Canyon and probably is perched seasonally in the upper reach and perennially in the lower parts of other canyons that receive effluents or runoff from the Pajarito Plateau and Sierra de los Valles. The occurrence of water in the alluvium is treated in each of the major drainage areas investigated in this report.

3. Perched Water in the Puye Formation and basaltic rocks of Chino Mesa

Perched water recharged from water in the alluvium occurs in lower Pueblo, Los Alamos and Sandia Canyons. A part of this perched water discharges from springs in Los Alamos and Sandia Canyons. The movement and quality of water in the perched aquifer are treated as a part of this report.

4. Main aquifer of the Los Alamos area

The main aquifer in the Los Alamos area is in the Santa Fe Group. The potentiometric surface (Fig. 3) rises from the Rio Grande westward through the Tesuque Formation into the lower

part of the Puye Conglomerate which interfingers with Tschicoma Formation (Fig. 2). The position of the potentiometric surface in the Tschicoma Formation is not known beneath the western edge of the plateau. Brecciated zones within the Tschicoma Formation may contain water but where encountered in wells such zones have not yielded more than 0.3 to 0.6 l/sec.

The gradient of the potentiometric surface beneath the Pajarito Plateau averages about 370 m along the western edge of the plateau to about 180 m at the confluence of Pueblo and Los Alamos Canyons. Water in the aquifer moves eastward toward the Rio Grande where some water is discharged through springs in the channel and along the banks (Fig. 3). Recharge to the main aquifer occurs on the flanks of the mountain or from the Valles Caldera to the west of Los Alamos.[6] The movement of water in the supply wells in lower Los Alamos Canyon is estimated to be about 110 m/yr.[7] Aquifer tests in the main aquifer south of Los Alamos also indicates slow movement of water in the range 55 m/yr to 220 m/yr. The transit time from recharge of the aquifer to discharge along the Rio Grande is unknown; however, tritium age dating of water from supply wells in Los Alamos, Guaje, and the Pajarito well field indicate that the water has been in transit from the recharge area for periods much greater than 50 years. Tritium analyses (electolysis enrichment method) were below limits of detection (0.5 tritium units).

The main aquifer is separated from water in the alluvium in canyon bottoms and from the perched aquifers in lower Pueblo. Los Alamos, and Sandia Canyons by from 200 to over 300 m of

of unsaturated volcanics and sediments. Geologic and hydrologic data collected during testing and monitoring of test holes penetrating the main aquifer are considered in a latter part of the report.

D. Method of Investigation

The study areas include all drainage areas on ERDA controlled property. The drainage areas were outlined on the basis of point of discharge at ERDA-LASL boundary (Fig. 4). All data that was available concerning the geohydrology of surface water, shallow ground water in the alluvium, and transport of sediments was used. List of published and unpublished reports that were used are found in Appendix D.

1. Chemical analyses of water

The chemical quality of surface and ground water in the alluvium was determined by methods as outlined in "Standard methods for examination of water and waste water"[8] and "Methods for the Collection and analyses of water samples."

The average concentration of sodium (Na), Chloride (CL), fluoride (F), nitrate (NO_3), total dissolved solids (TDS), specific conductance, and pH of a number of analyses for a sampling station is used in the tables in the text of this report to show trends in concentration in the disposal area, and over a period of time at a single station. These specific ions and chemical characteristics were used as they will readily reflect quality of water change that may occur. Complete chemical analyses from each station for the period 1967-1972 is presented in Appendix E for the drainage areas.

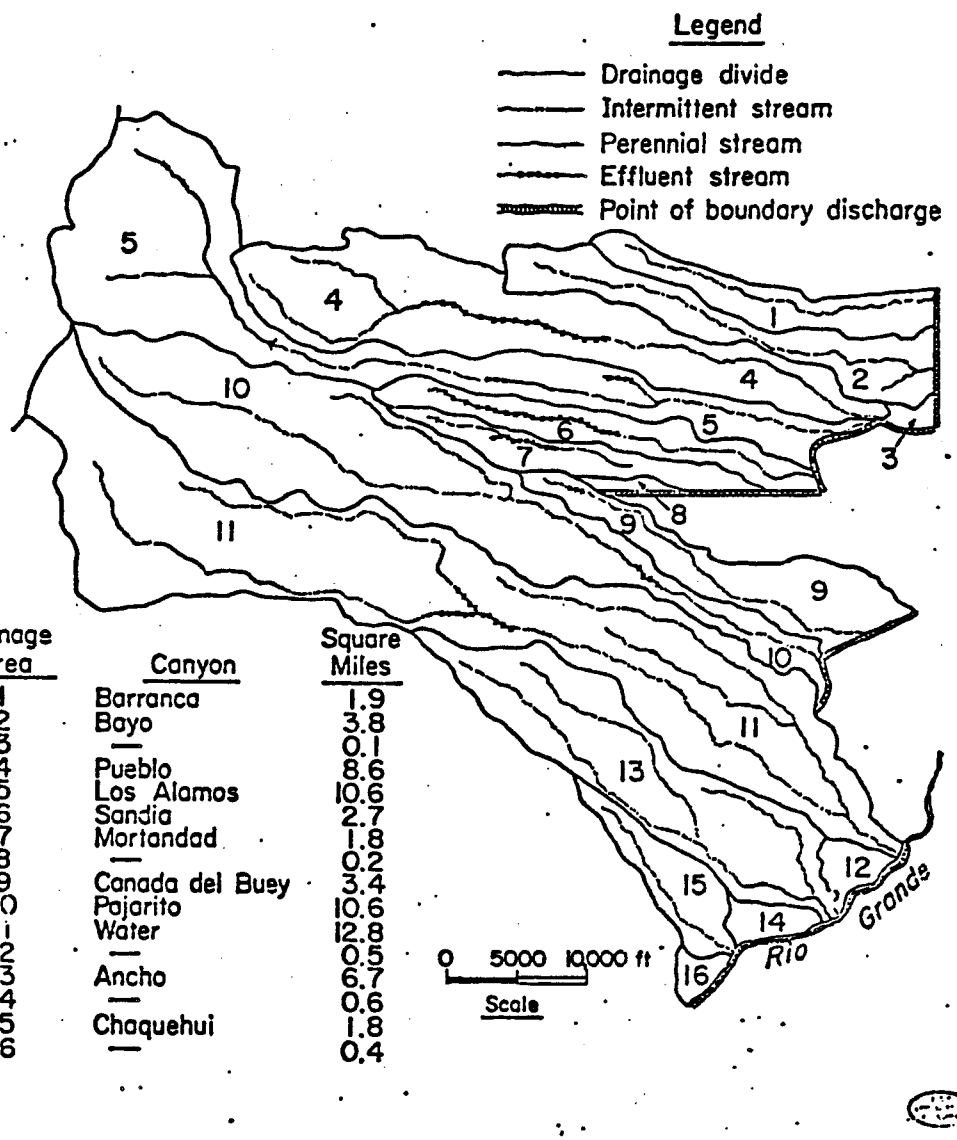

Drainage Area	Canyon	Square Miles
1	Barranca	1.9
2	Bayo	3.8
3	—	0.1
4	Pueblo	8.6
5	Los Alamos	10.6
6	Sandia	2.7
7	Mortandad	1.8
8	—	0.2
9	Canada del Buey	3.4
10	Pajarito	10.6
11	Water	12.8
12	—	0.5
13	Ancho	6.7
14	—	0.6
15	Chaquehui	1.8
16	—	0.4

Fig. 4. Drainage areas and points of intermittent stream discharge.

2. Radiochemical analyses of water

The radiochemcial data is presented in two parts for each hydrologic regime, surface water, water in alluvium, perched aquifers and main aquifer, covering the periods 1958 through 1967 and 1968 through 1972. During the period 1958 through 1967 analyses were made for gross beta and plutonium. The procedures for analyses for plutonium used Bismuth Phosphate Coprecipitation Method. This method had a limits of detection of 0.5 pCi/l (picocuries per liter). The limits of detection for gross beta activity during this same period was 14 pCi/l and total uranium 0.5 μg/l.

During the period 1967 through 1972, analyses were made for gross alpha and beta, ^{238}Pu, ^{239}Pu, ^{3}H, and total uranium. Procedures used for sample preparation and gross alpha, beta, and gamma screening are outlined in Radioassay Procedures for Environmental Samples.[10] The determination of specific alpha emitters was performed using an alpha spectrometer and internal tracers for recovery corrections. Purification and concentrations were done by ion exchange and electrodeposition or by coprecipitation. Uranium was determined fluorometrically unless specific uranium isotopes were required. The methods used in the period 1967 through 1972 were better in that the limits of detection were lower. Limits of detections for gross alpha and beta activity were 1 pCi/l, plutonium 0.05 pCi/l and total uranium 0.4 μg/l.

The average concentration of a number of analyses for a sampling station is used in the tables in the text of this report to show general trends in concentrations in the disposal area.

Many of the individual analyses are below the limits of detection. The limits of detection rather than zero has been used to compute the average. Complete radiochemical analyses from each station for the period 1967-1972 is presented in Appendix C for the drainage areas.

3. Radiochemical analyses of sediments

Stream channel bed material is referred to as sediments. These sediments were collected with 7.6 cm scoop across the main channel to a depth of about 3 cm. Suspended sediments are classed as having a mean diameter less than 6 mm and are those sediments that remain in suspension in water for a period of time without contact with the bottom. The suspended sediments were collected with a single-stage sampler, cumulative sampler, or a DH-48 sampler during flood or storm runoff.

The procedures used for radiochemical analyses of channel bed sediments and suspended sediments are outlined in "Standard Analytical Procedures for Soil."[11] Plutonium was analyzed by using an alpha spectrometer after concentration and purification by ion-exchange chemistry with internal tracers added for recovery corrections.

4. Particle-size Distribution of Sediments

The particle-size distribution was made by mechanical shaker (Ro-Tap) through a series of different size mesh screens. The size distribution was made of the sediments having a particle size diameter of less than 3.96 millimeters, according to the Wentworth Grade Scale. The particle-size distribution

Grade	Size Range (Millimeters)
Granules	2.36 - 3.96
Sand	
Very Coarse	1.17 - 2.36
Coarse	.589 - 1.17
Medium	.295 - .589
Fine	.147 - .295
Very Fine	.074 - .147
Silt and Clay	Less than .074

is expressed as percent by weight of the channel bed sediments.

The sediments are derived from chemical and mechanical weathering of the acid volcanic rocks (Tschicoma and Puye Formations and Bandelier Tuff). The granules are composed principally of tuff, pumice, latite, and rhyolite rock fragments with minor amounts of quartz and sanidine crystals. The fractions of fine to coarse sand consist mainly of quartz and sanidine crystals and crystal fragments with minor amounts of rock fragments. The silt and clay fraction are composed mainly of clay minerals montmorillonite and illite.

5. Inventory of Plutonium in Sediments of Drainage Area 4, 5, and 7

Drainage Area 4 (Acid-Pueblo Canyon), Drainage Area 5 (Los Alamos -DP Canyon) and Drainage Area 7 (Mortandad Canyon) have received treated liquid effluents that have contained some plutonium. An inventory was made to determine the amount of plutonium released into the canyon in preceeding years.

Plutonium in the waste when released is adsorbed or retained with the finer material in the channel alluvium. The concentrations of plutonium tend to build up at the point of effluent discharge in the channel during the fall through the spring. This large concentration is reduced by transport during storm runoff, especially the heavy summer showers.

The fine particle in the alluvium in the channel have the greater affinity for the plutonium; however, most of the plutonium is in the coarser alluvium as it is more abundant. The finer sediments in the alluvium are carried out of the canyons (Acid-Pueblo and DP-Los Alamos) as suspended sediments with the storm runoff, while the larger materials are being transported as bed material. The bed material lags behind, moving short distances with each succeeding runoff event.

Storm runoff reaches the Rio Grande from Acid-Pueblo and DP-Los Alamos Canyons. There has been no runoff in the drainage area of Mortandad Canyon to the Laboratory boundary (Santa Fe-Los Alamos County Line) since hydrologic investigation began in the canyon in 1960. This is due to the small drainage area and the thickness of unsaturated alluvium in the canyon.

The inventory is based on (1) mass of sediments in a section of the channel, and (2) the average concentration of plutonium in sediments in that section.

The annual amounts of plutonium released from the Treatment Plants into the canyon were compiled from records furnished by H-7. The estimate from the TA-45 Plant 1943-1950 was taken from LA-5282-MS. The mass of sediments is compiled from channel width,

length of section, a thickness of 0.15 m, and a specific gravity of 1.57. The mass of the sediments and concentration of plutonium were used to compute the amount of plutonium in the section. The inventory in the canyon was made from data collected in 1968, 1970, and 1972 and is presented in the Drainage Areas 4, 5, and 7 sections of the report.

6. Flood-Frequency and Maximum Discharge

The sixteen drainage areas considered in the study contain only intermittent streams at the ERDA Boundary, with the exception of Drainage Area 13 (Ancho Canyon). The lower reach of Ancho contains a perennial stream fed by springs from the main aquifer in the lower part of the Puye Formation and upper part of the Tesuque Formation.

There are three gauging stations on the plateau; mouth of DP Canyon, mid-reach of Los Alamos Canyon and upper Mortandad Canyon. There are no gauging stations on the channels of the sixteen drainage areas, thus, theoretical flood-frequency and maximum discharge were compiled from a method devised by Scott.[12] The methods used, consist of defining the relationship between existing flood data and the physical and climatic characteristics of the gauged sites or drainage basin. The data was extrapolated by use of regression analyses using this relationship and basin characteristics to determine flood frequency and maximum discharge.

The peak discharges of 2, 5, 10, 25, and 50 year recurrence intervals were determined for each of the drainage areas containing a well defined channel from nomographs presented by Scott for Region 1 which includes the Rio Grande water shed in north central New Mexico.

The climatic data used with the nomographs as determined at Los Alamos was a mean minimum January temperature of 8° F and a maximum 24 hour 2 year rainfall of 4.3 cm.. The area of each drainage area, in square in km^2 above the ERDA-LASL Boundary was determined by use of a planimeter. The main channel slope, was compiled from elevations taken from topographic maps. Using points at 10 and 85 percent of the distance from discharge point at the boundary and drainage divide. The difference in altitude between those two points divided by the distance between the points was used to compute the main channel slope for drainage areas. The channel slopes are present as dimensionless ratios of average vertical distance change (negative to horizontal distance traversed).

The flood frequency or "recurrence interval" is the average interval of time between floods of a given magnitude. A flood with a recurrence interval of 50 years is the annual flood that is equaled or exceeded once in 50 years, with long term average. The concept implies no regularity in the time of recurrence of a given magnitude flood. It is possible for two or more 50 year floods to occur within a short period of time, or many more than 50 years may elapse before the occurrence of one 50 year flood.

Frequencies may be expressed in terms of probabilities, i.e. the probability of the occurrence of a 10 year flood in any given year is 1 in 10 or 0.1; the probability of a 50 year flood in any given year is 1 in 50, or 0.02.

II. DRAINAGE AREA 1 (BARRANCA CANYON)

Barrance Canyon contains an intermittent stream. Runoff occurs during heavy summer thunder showers and possibly some snow

melt in the upper reaches of the canyon. There is no effluent discharge into the canyon from either sewage or industrial waste treatment plants. No data is available on chemical or radiochemical quality of the storm runoff.

A. Radiochemical analyses of sediments

Samples of sediments from the stream channel were collected in Barranca Canyon above the junction with Guaje Canyon, about 0.5 miles east of the boundary (Fig. 5).

Particle size distribution of sediments in the stream channel was made of the sample collected in 1965. The sediments were derived from the Bandelier Tuff and Puye Formation.

Particle-size Distribution of Sediments

Grade	Distribution (percent by weight)
Granules	10
Sand	
Very Coarse	17.5
Coarse	27.0
Medium	21.0
Fine	11.5
Very Fine	5.5
Silt and Clay	7.5

Radiochemical analyses were made of sediments collected November 24, 1965 and February 5, 1970. No activity found in the sediments were in the range as would be expected from world wide fallout.

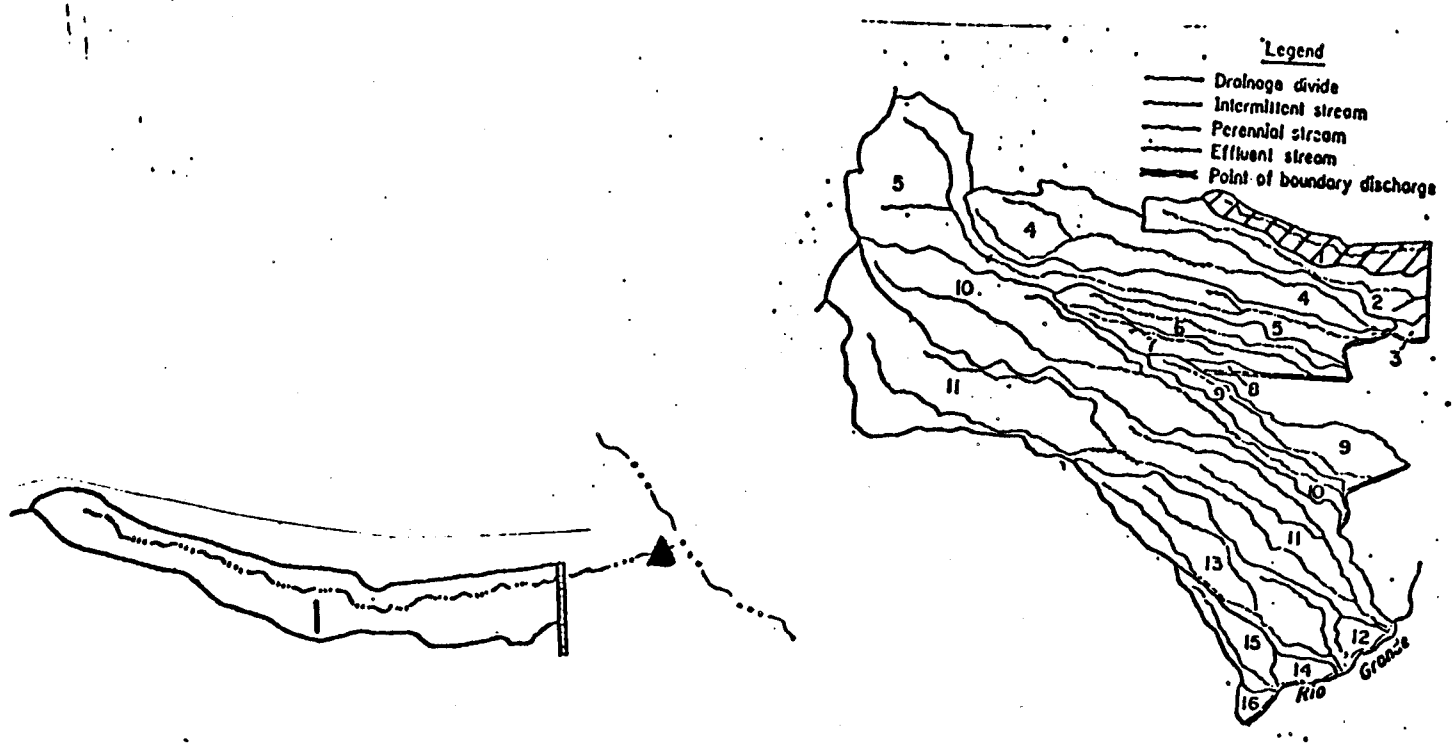

Fig. 5. Drainage Area 1 (Barranca Canyon) showing location of sediment sampling station.

11-5-65	
Gross alpha	3 c/m/g
Gross beta	1 c/m/g
Gross Gamma	28 c/m/g
2-5-70	
Gross alpha	2 pCi/g
Gross beta	3 pCi/g
Gross gamma	1 pCi/g
Plutonium-238	0.005 pCi/g
Plutonium-239	.007 pCi/g

B. Flood-frequency and Maximum Discharge

Barranca Canyon heads on the Pajarito Plateau at an altitude of about 2, 195 m. The flood frequency and maximum discharge are based on the following data:

Drainage Area - 4.9 km^2

Main Channel Slope - 0.039

Frequency	Maximum Discharge (m^3/sec)
2-year	1.5
5-year	4.1
10-year	6.7
25-year	12
50-year	14

III. DRAINAGE AREA 2 (BAYO CANYON)

Bayo Canyon contains only an intermittent stream. Runoff occurs during heavy summer thunder showers with some possible snow melt in the upper reaches of the canyon. There is no effluent discharge into the canyon; however, prior to 1965, a technical area used for testing, was located in the canyon. The site was abandoned and the area was cleaned up in 1965.

A. Chemical analyses of storm runoff

Chemical analyses was made of storm runoff that occurred at Station 1 in August 22, 1957 (Fig. 6).

Determination	Concentrations
Chemical (mg/l)	
Sodium	4.8 mg/l
Carbonate	0 mg/l
Bicarbonate	117 mg/l
Chloride	8.0 mg/l
Fluoride	1.0 mg/l
Nitrate	2.0 mg/l
Specific Conductance (μmhos)	227
pH	7.2

No radiochemical analyses were performed on the sample.

B. Radiochemical analyses of sediments

Two sediment sampling stations were established in the canyon. They are located near the middle of the canyon (Station 1) and the other about Bayo Canyon above the junction with Los Alamos Canyon about 2.4 km east of the boundary (Station 2).

Particle size distribution of the sediments at the two stations are shown below. The sediments are derived from the Bandelier Tuff and Puye Formation:

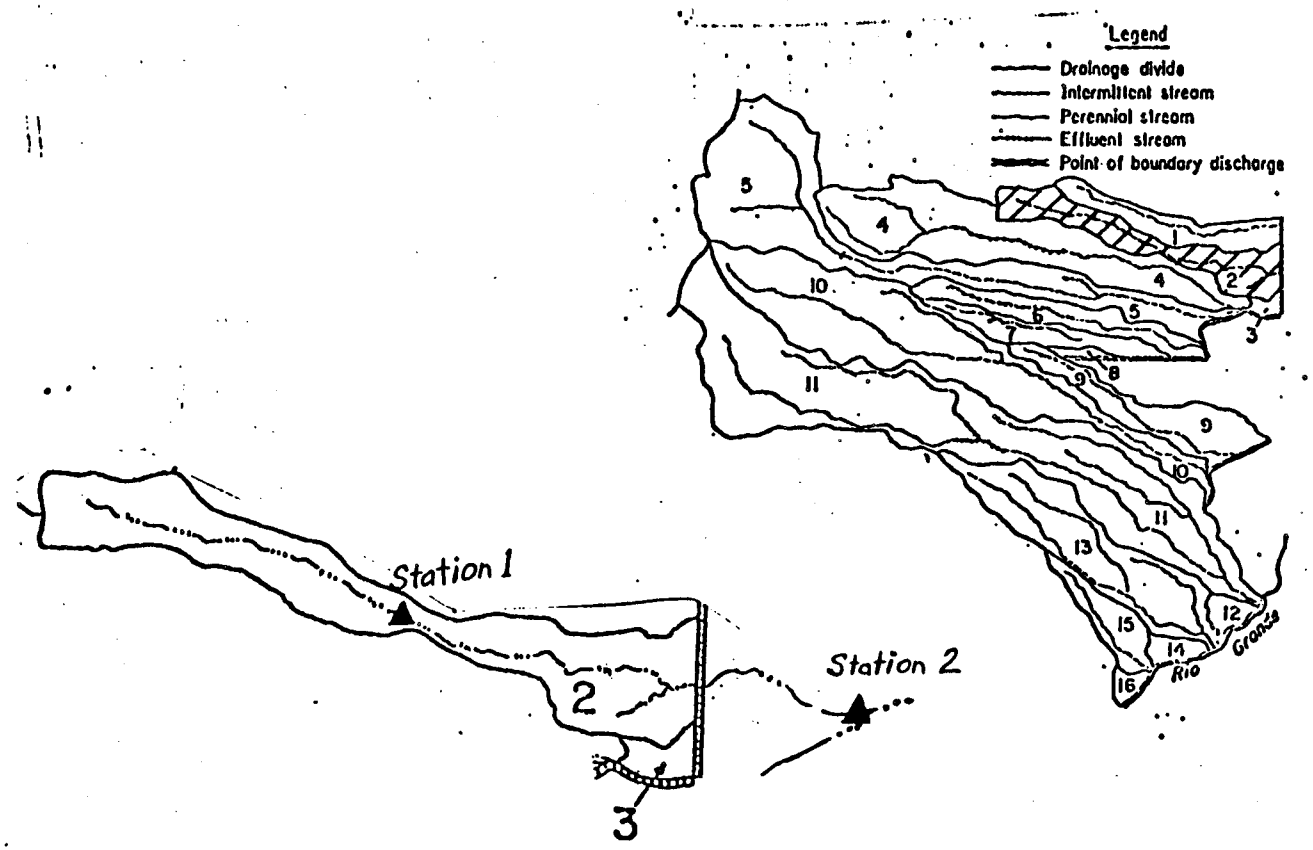

Fig. 6. Drainage Area 2 (Bayo Canyon) and Drainage Area 3 showing locations of sampling stations.

Particle-size Distribution of Sediments

Grade	Distribution (percent by weight) Station 1	Station 2
Granules	2.0	2.0
Sand		
Very Coarse	40.5	24.5
Coarse	40.5	46.5
Medium	10.5	16.0
Fine	3.5	6.5
Very Fine	1.5	1.5
Silt and Clay	2.0	2.5

Radiochemical analyses were made of sediments from the two stations collected November 24, 1965 and February 5, 1970. The activity is in the range that would be expected from world wide fallout.

Determination	Station 1 11-24-65	Station 1 2-5-70
Gross alpha	1 cm/g	<1 pCi/g
Gross beta	<1 cm/g	<1 pCi/g
Gross gamma	<1 cm/g	<1 pCi/g
Plutonium-238	--	<0.001 pCi/g
Plutonium-239	--	.004 pCi/g

Determination	Station 2 11-24-65	Station 2 2-5-70
Gross alpha	3 cm/g	<1 pCi/g
Gross beta	21 cm/g	<1 pCi/g
Gross gamma	<1 cm/g	<1 pCi/g
Plutonium-238	--	< .001 pCi/g
Plutonium-239	--	.004 pCi/g

C. Flood-frequency and Maximum Discharge

Bayo Canyon heads on the Pajarito Plateau at an altitude of

about 2,036 m. The flood-frequency and maximum discharge at the boundary is based on the following data:

Drainage Area - 9.8 km^2

Main channel slope - 0.028

Frequency Frequency	Maximum Discharge (m^3/sec)
2-year	2.4
5-year	6.1
10-year	8.5
25-year	17
50-year	19

IV. DRAINAGE AREA 3

Drainage Area 3 is on the south facing wall of Los Alamos Canyon. No major drainage channel developed in the 0.25 km^2 drainage area. No data are available on chemical or radioachemical quality of storm runoff.

V DRAINAGE AREA 4 (ACID-PUEBLO CANYON)

Stream flow is perennial in the upper and lower reaches of Pueblo Canyon from the release of treated sewage effluent from the Pueblo and Bayo Plants (Fig. 7). Storm runoff adds to the volume of flow either from winter snow melt or summer thunderstroms. During the period 1951 through 1963, industrial effluents from TA-45 were released into Acid Canyon, a small tributary to Pueblo Canyon. The Central Sewage Treatment Plant released effluents into the middle reach of the canyon from 1947 through 1966.

The stream flow in Pueblo Canyon recharges a shallow body of ground water in the alluvium. As the water in the alluvium moves downgradient, water is lost to evapotranspiration while some moves into two shallow perched water bodies in the Puye Formation and

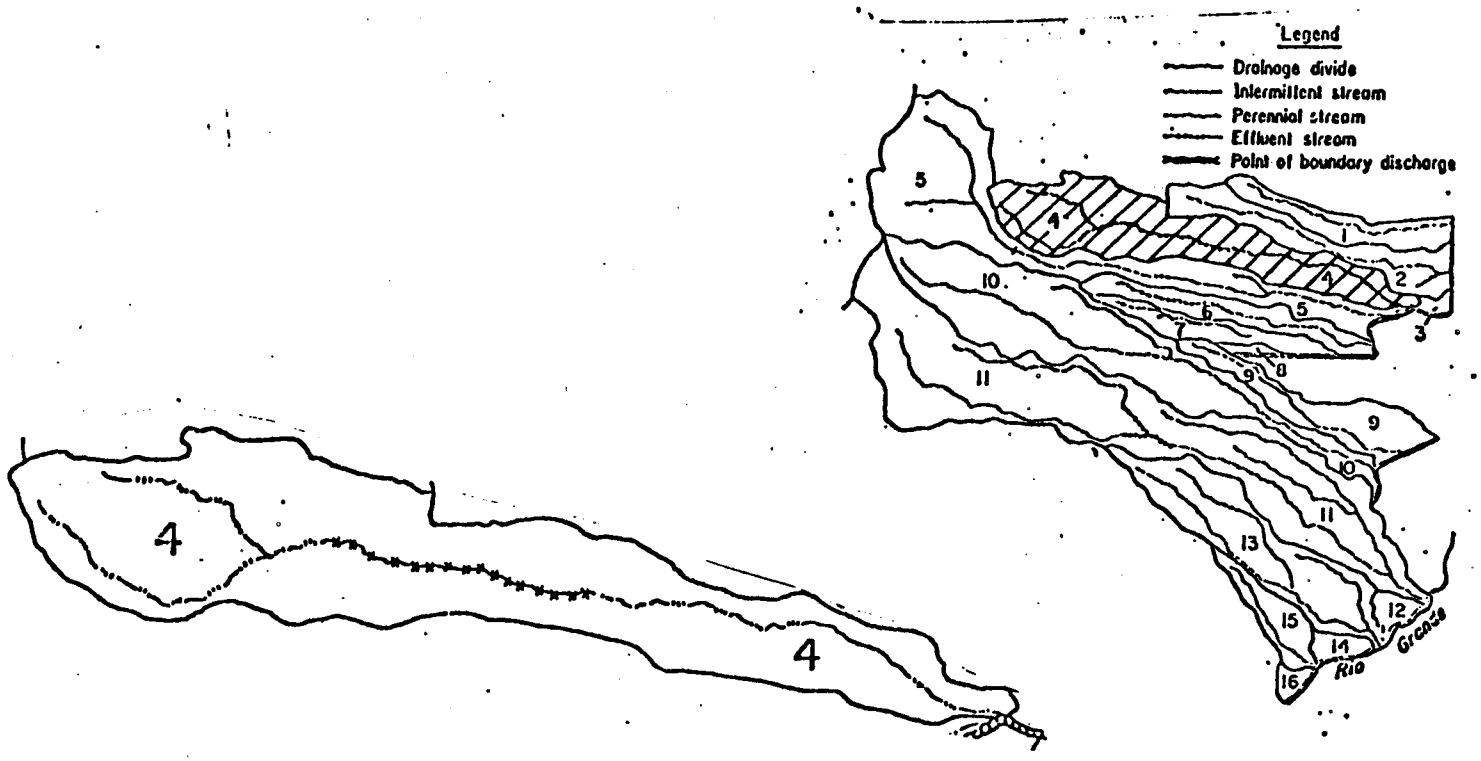

Fig. 7. Drainage Area 4 (Pueblo Canyon).

Basaltic Rocks of Chino Mesa (Fig. 8)

A. Sewage and Industrial Treatment Plants

Sewage has been treated and released at three plants in Pueblo Canyon during the interval between 1951 and 1971. The oldest plant in operation is the Pueblo Plant which began operations in the mid 1940's and is still in operation. The yearly volume of sewage effluent released increased from 375 x 10^3 m^3 in 1956 to 875 x 10^3 m^3 in 1961.

The release in 1970 was about 780 x 10^3 m^3. From April through September, about 90 percent of the effluent is pumped to the golf course for irrigation.

The central treatment plant operated from the late 1940's to about 1966 when the effluent was then treated at the Bayo Plant. The earlier release from the plant ranged from 570 x 10^3 m^3 to 760 x 10^3 m^3 annually; however, after 1954, when a part of the effluents were pumped to the power plant for use, the releases into Pueblo Canyon dropped, ranging from 75 x 10^3 m^3 to 150 x 10^3 m^3 per year to 1966 when all the effluents were then treated at Bayo Plant.

The Bayo Plant became operational in 1963 with the effluent released into Pueblo Canyon. The plant was enlarged and in 1966 began treating sewage previously processed at the central treatment plant. The release in 1972 was about 900 x 10^3 m^3.

The industrial waste treatment plant at TA-45 was in operation from January 1951 through June 1963. Several small batches of waste were treated until June 1964 prior to complete abandonment of the plant. Plutonium, the major waste contaminate, was removed

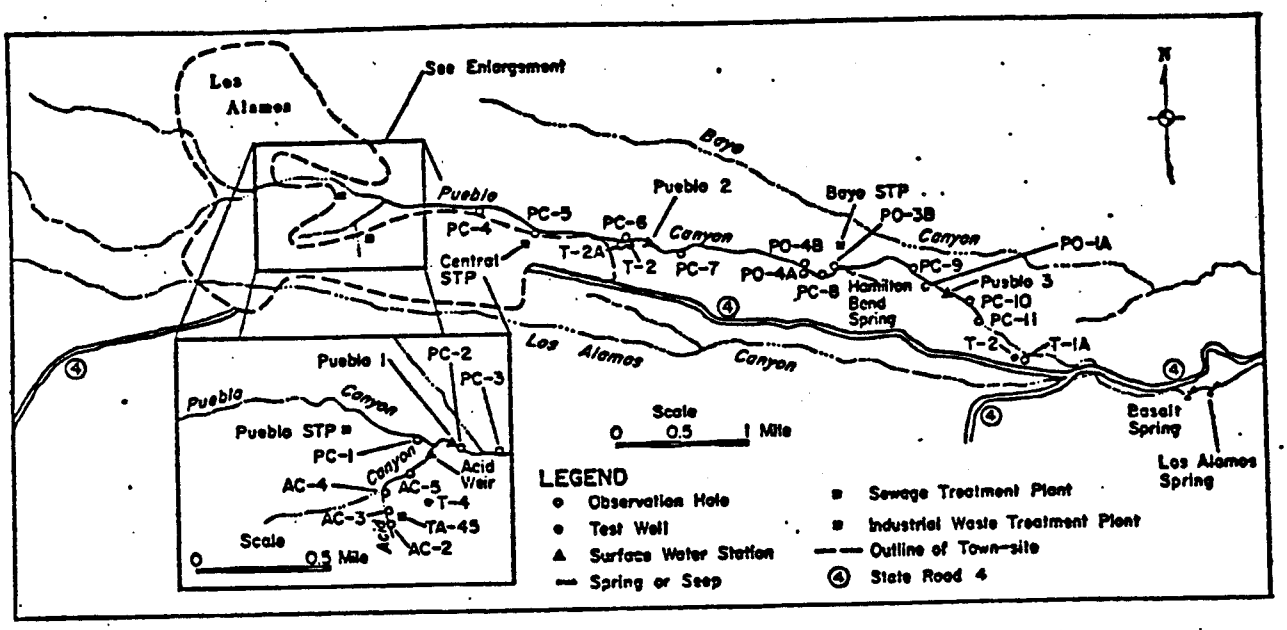

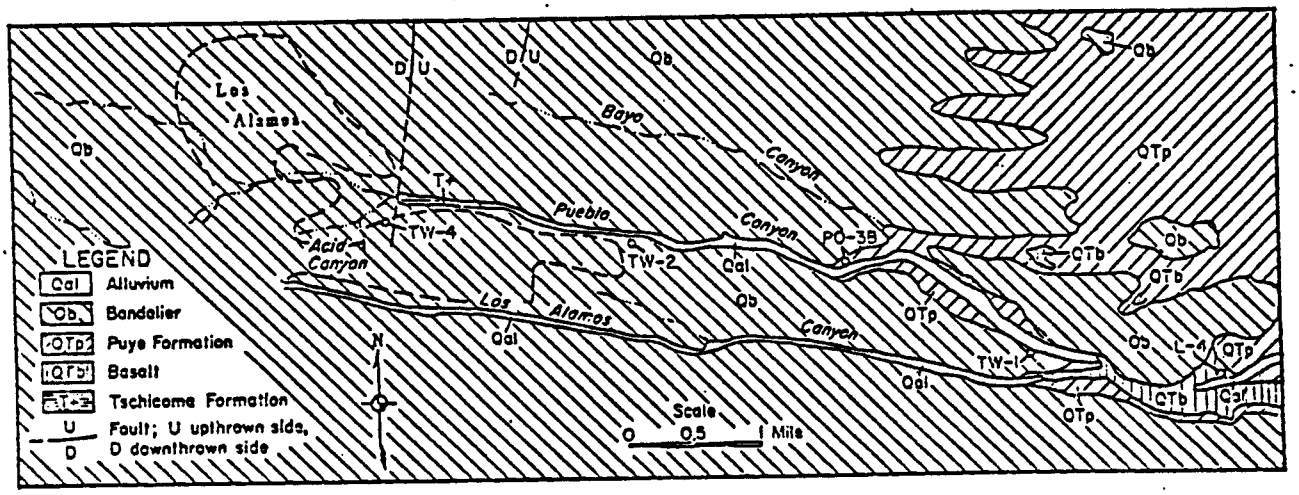

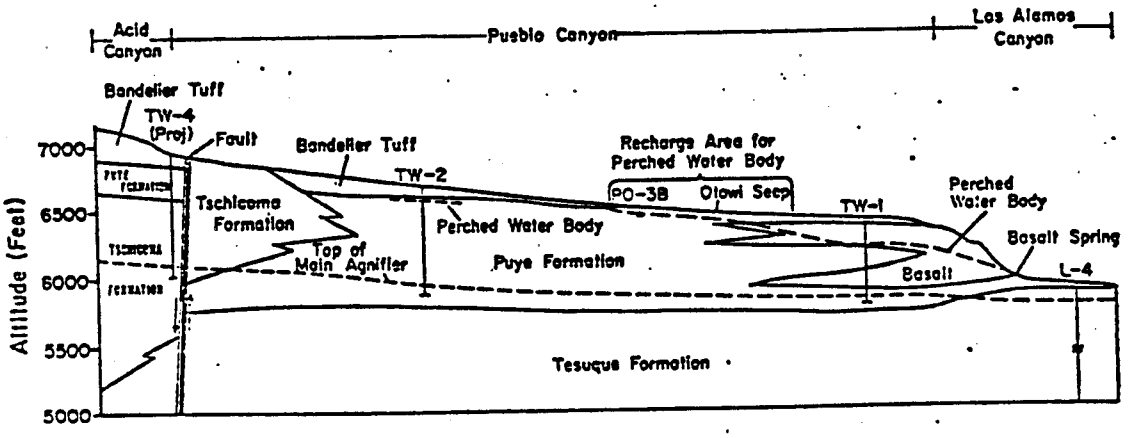

Fig. 8. Sampling stations, geologic map, and cross-section of Drainage Area 4 (Pueblo Canyon).

from liquid wastes by chemical treatment with ferric sulfate and lime, which forms a flocculent that precipitates to the bottom of settling tanks. The precipitate (ferric hydroxide) carries nearly all of the plutonium with it. The sludge is removed from the bottom of the tank, packaged, and buried in pits.

An average of 9×10^3 of waste were released into Acid Canyon between 1946 and 1951. The volume of waste released increased from 15×10^3 m^3 in 1951 to a maximum of about 65×10^3 m^3 in 1962, then decreased to about 0.7×10^3 m^3 in 1964 as the new plant at TA-50 became operational. The wastes were released from the treatment plant in batches of 55 m^3 to 75 m^3 rather than by continuous flow. The effluents were released into Acid Canyon. The effluents made up the bulk of the flow in the canyon except some occasional runoff from storms.

1. Chemical quality of sewage and industrial effluents

The chemical quality of effluents from the Pueblo, Central (now abandoned), and the Pueblo Sewage treatment plants have remained about the same over the years.

Chemical Quality of Sewage Effluent

(Average of a number of samples, analyses in mg/l except as noted).

Plant	Pueblo				Central		Bayo	
Year	1952	1961	1971	1972	1952	1961	1971	1972
Number of Samples	1	1	2	4	1		2	4
Calcium	--	--	26	14	--		13	14
Magnesium	--	--	3	6	--		2	5
Sodium	--	94	88	76	--	114	89	78
Carbonates	--	0	0	0	--	0	0	0
Bicarbonates	176	121	120	140	210	158	160	118
Phosphate	--	35	--	--	--	22	--	--
Chloride	32	34	36	31	30	46	30	55
Fluoride	1.6	1.6	.8	.7	1.6	2.6	1.5	1.2
Nitrate	40	30	66	26	35	43	31	57
Dissolved Solids	350 [a]	400 [a]	420	403	370 [a]	400 [a]	374	408
Hardness	--	49	74	66	--	37	41	55
Conductance[b]	540	620	500	475	570	620	500	450
pH[c]	--	7.0	72	7.2	--	7.1	7.2	7.3

[a] Estimated, Ref. 12 p 270

[b] Micromhos at 25° C

[c] No units

The chemical ions and physical characteristics are greater than found in natural occurring water. Metal ion analyses of effluent from the Pueblo and Bayo Plants were made in 1971 and 1972. The results indicated some trace amounts of metal ions in the effluents.

The chemical ions and physical characteristics are greater than found in natural occurring water. Metal ion analyses of effluent from the Pueblo and Bayo Plants were made in 1971 and 1972. The results indicated some trace amounts of metal ions in the effluents.

Metal Ion Analyses
(Average of three analyses in parts per billion)

	Pueblo	Bayo
In Solution		
Cadmium	1.3	.91
Beryllium	.29	1.4
Lead	<1.0	3.8
Mercury	0.5	< .02
Particulates		
Cadmium	.48	.30
Beryllium	< .25	< .25
Lead	6.5	4.7
Mercury	.34	.05

The chemical quality of the effluents released into the canyon reflects the quality of influents to the plant and chemicals used to neutralize undesirable constituents and remove radionuclides. The effluents are highly mineralized when compared to naturally occurring waters. The high pH is the result of treatment of the effluents with lime as part of the process to remove radionuclides. In general, the chemical ion concentrations vary with the ever changing quality of the influents.

Chemical Analyses of Industrial Effluents[a]
(Analyses in mg/l, except as noted)

Year	1952	1953	1954	1955	1956	1957	1958	1959	1960	1961	1962	1963	1964
Calcium	14	74	116	96	55	15	10	80	82	28	76	27	4
Magnesium	3	49	60	--	0	38	16	5	5	1	2	1	1
Sodium	46	162	35	87	105	57	680	78	118	87	102	99	69
Carbonates	38	3	68	289	--	138	336	162	467	100	154	82	60
Bicarbonates	132	46	140	314	284	280	599	193	530	140	201	151	130
Chloride	54	290	57	18	9	9	229	1	83	48	61	24	10
Fluoride	5	2	10	4	4	14	80	3	10	7	2	2	2
Nitrate (N)[b]	24	130	178	10	24	2	200	12	3	7	4	1	1
Hardness	46	390	537	240	88	195	90	219	225	70	200	68	10
Conductance[c]	--	--	--	--	1200	1380	600	630	795	650	1110	640	450
pH	--	--	9.1	11.5	11.4	11.2	11.0	11.8	11.6	11.0	10.9	10.8	10.5

[a] Weekly composite sample (one analysis from each years record)
[b] N x 4.4 = NO_3
[c] Micromhos at 25° C

2. Radiochemical Quality of Sewage and Industrial Effluents

Radiochemical analyses of sewage effluent from the Pueblo and Bayo Plants have been made on samples collected in 1971 and 1972. The results show only traces of radionuclides which are background.

Radiochemical Analyses of Sewage Effluents
(Average 7 samples collected in 1971 and 1972
in pCi/l except as noted)

Determination	Pueblo	Bayo
Gross alpha	1	2
Gross beta	9	30
Plutonium-238	0.05	0.05
Plutonium-239	0.05	0.05
Cesium-137	350	350
Tritium	1,000	1,000
Total Uranium[a]	1.6	1.8

[a] µg/l

The volume of effluent and concentrations of gross alpha, gross beta, total plutonium and tritium released as effluent after treatment at the plant for the period 1951 through 1964 were compiled from plant records by Group H-7 (H7-LAE-434).

Average Annual Radiochemical Quality of Effluents released from TA-45 (1951-1964)

		Picocuries per liter			
Year	Amount (M^3)	Gross alpha	Gross beta	Total Pu	^3H [a] ($x\ 10^3$)
1951	22080	111	--	59.3	140
1952	28540	144	--	38.5	110
1953	27610	139	--	41.7	110
1954	38910	112	--	56.2	77
1955	39910	102	--	54.8	75
1956	39720	150	--	26.4	76
1957	43310	200	--	20.7	69
1958	40580	94.6	--	22.4	74
1959	46110	38	--	26.5	65
1960	40870	86.5	31000	64.1	73
1961	52850	176	9600	100	57
1962	64110	115	19000	61	47
1963	30880	232	26000	97.4	97
1964	891	94	150	45	1300

[a] Estimated

Major treatment during operation of the plant was to reduce the amount of plutonium received in the liquid waste. During the period 1943 through 1964, about 170 millicuries of plutonium were released into the canyon.

Annual Amount of Radionuclides Released
with Effluents from TA-45

Year	Millicuries			
	Gross alpha	Gross beta	Total Pu	^{3}H[a]
1943-50[a]	--	--	143[b]	--
1951	2.4	--	1.3	3090
1952	4.1	--	1.1	3140
1953	3.8	--	1.2	3040
1954	4.4	--	2.2	2990
1955	4.1	--	2.2	2990
1956	6.0	--	1.0	3020
1957	8.7	--	.9	2990
1958	3.8	--	.9	3000
1959	1.8	--	1.2	2990
1960	3.5	1270	2.6	2980
1961	9.3	507	5.2	3010
1962	7.4	1220	3.9	3010
1963	3.0	803	3.0	3000
1964	.04	.1	.04	1160
Total (1943-1964)	--	--	170.	--

[a] Estimated
[b] LA-5282-MS[13]

B. Surface Water

Stream flow in Pueblo during the period 1951 through 1964 consisted of effluents from the two sewage treatment plants (Pueblo and Central) and from the industrial waste treatment plant (TA-45) near Acid Canyon, a tributary canyon to Pueblo. Precipitation and snowmelt occasionally added to the volume of flow.

The average discharge from 1957 to 1964 in Pueblo Canyon, just

below the junction with Acid Canyon, was about 56 l/sec, from September through April and about 14 l/sec from May through August. Near test Well 2 (added flow from the central plant) the average discharge was about 45 l/sec from September through April and 14 l/sec from May through August (Fig. 8). The decrease in stream flow May through August reflected decreased release from the sewage-treatment plants because most of the effluent was used for irrigation and cooling water at the power plant. Stream flow during summer usually ended near observation well PO-4A but during the summer extended to near Pueblo 3 or beyond (Fig. 8).

The same characteristics of discharge occurred in upper Pueblo Canyon from the sewage treatment plant during the period 1964 through 1971; however, stream flow generally ended near or east of test Well 2 during the summer and extended to near Hamilton Bend Springs in the winter. The new sewage-treatment plant at Bayo began operations in 1964 and by 1966 the the Central treatment plant was closed. This caused a shift in release of effluent in the lower part of the canyon.

The stream flow decreased down the canyon as water moved into the alluvium. The alluvium is thin in the upper reaches of the canyon and thinkens to about 18 m to the east. Slight or little losses of surface water were noted where the alluvium overlies the Tschicoma Formation (Fig. 8). The alluvium in the stream channel overlying the Tschicoma Formation is thin. The rocks of the formation are quite hard and resist down cutting of the stream channel. To the east where the channel is underlain by the Bandelier Tuff, the alluvium thickens as the tuff erodes and weathers quite easy. As the alluvium thickens in this section of the stream, storage

capacities of the alluvium increase which is accompanied by an increased loss of surface flow as it infiltrates into the alluvium. Surface water losses also occur to evaporation and transpiration by plants and trees.

The surface water loss in the canyon is estimated at about 5 l/sec per km when discharge at the confluence of Acid and Pueblo Canyons is about 60 l/sec. As discharge increases, these losses increase due to water taken into bank storage which is later partly released as the discharge declines. Loss from bank storage occurs from evapotranspiration and some water is held as soil moisture.

Surface water stations for monitoring the chemical and radiochemical quality of the surface water were established at Acid Weir, Pueblo 1, Pueblo 2, and Pueblo 3 in 1954.

1. Chemical quality of surface water

The chemical quality of water from Acid Weir from 1954 to 1964 reflect the chemical quality of the effluent released from the treatment plant.

Chemical Quality of Surface Water at Acid Weir
(Average of a number of analyses)

Chemical Constituents	Period 1953-1964	Period 1965-1972
Chemical (mg/l)		
Chloride	33	77
Fluoride	3.9	1.4
Nitrate	83	4.4
Total Dissolved solids	735	320
Conductance (μmhos)	670	240
pH	8.4	7.5

The water was basic and fluoride and nitrate concentrations were high as were total dissolved solids. The high chlorides in the period 1965-1972 are probably from leaching from salt-sand mixtures stored at the head of the canyon by the county. Runoff in Acid Canyon during the period 1964-1972 consisted mainly of storm runoff, release of water from the pool at the High School, and runoff from lawn watering in the residential area. The yearly average shows general decline in concentrations of fluoride and nitrate and in total dissolved solids, conductance, and pH. The chloride concentrations have increased 1970 through 1972.

Chemical Quality of Surface Water from Acid Weir
(Average yearly analyses in mg/l except as noted)

Year	No. of samples	Na	Cl	F	NO_3	TDS	Conductance[a]	pH[b]
1953	9	--	29	4.1	157	435[c]	670	--
1954	10	--	37	5.2	242	545[c]	840	--
1955	6	--	36	5.2	304	640[c]	980	--
1956	10	--	32	5.7	50	583	---	8.6
1957	3	72	23	3.8	36	345[c]	530	7.9
1958	6	66	25	5.1	23	350[c]	540	8.1
1959	3	87	45	4.0	26	400[c]	610	8.3
1960	1	85	44	3.9	16	335[c]	515	8.6
1961	1	78	29	2.0	29	420	480	8.5
1962	2	94	39	2.2	26	400	380	9.4
1963	2	72	24	2.0	13	356	400	8.3
1965	1	38	14	1.7	4	246	240	7.6
1970	2	98	165	1.7	4	437	520	7.7
1971	1	41	52	.9	4	276	220	7.1
1972	2	86	73	1.9	4	305	395	7.4

[a] Micromhos at 25° C

[b] No units

[c] Estimated

Surface water stations were established at Pueblo 1, Pueblo 2, and Pueblo 3 in Pueblo Canyon (Fig. 8). The chemical quality of the water at the three stations reflect the chemical quality of the sewage effluent from the Pueblo, Central (abandoned) and Bayo Plants.

Chemical Quality of Surface Water at Pueblo 1, 2, and 3
(Average of a number of analyses) 1953 through 1972

Chemical (mg/l)	Pueblo 1	Pueblo 2	Pueblo 3
Chemical (mg/l)			
Chloride	30	30	28
Fluoride	2.0	1.6	1.7
Nitrate	52	34	13
Total Dissolved Solids	365	342	409
Conductance (μmhos)	450	410	400
pH	7.3	7.5	7.4

The chemical quality of water at Pueblo 1 shows little or no effect of the release of effluent from the industrial waste treatment plant at TA-45 which ceased operations in 1964.

Quality of Surface Water at Pueblo 1
(Average of Yearly Analyses in mg/l except as noted)

Year	No. of samples	Na	Cl	F	NO_3	TDS	Conductance [a]	pH [b]
1953	9	--	31	2.2	61	350 [c]	535	--
1954	11	--	30	2.4	77	350 [c]	541	--
1955	6	--	32	3.3	153	470 [c]	725	--
1956	8	--	35	2.5	14	445	--	8.0
1957	6	65	24	2.3	38	275 [c]	426	7.5
1958	12	56	24	1.6	30	280 [c]	435	7.5
1959	5	62	26	1.4	35	320 [c]	496	7.4
1961	1	45	16	1.0	22	340	360	7.7
1962	2	70	28	1.6	53	403	480	6.9
1963	2	60	33	2.0	35	348	360	7.2
1970	2	81	40	1.4	44	374	400	7.0
1971	1	82	28	1.0	57	376	400	7.0
1972	2	75	41	3.3	53	416	430	7.1

[a] Micromhos at 25° C

[b] No units

[c] Estimated

The chemical quality of water at Pueblo 1 reflects the chemical quality of the effluent from the Pueblo Sewage Treatment Plant.

The chemical quality of water at Pueblo 2 reflects the combined release of sewage effluent from 1953 to 1964 from the Pueblo and Central Plant, and after 1964 only the release from the Pueblo Plant.

Quality of Surface Water at Pueblo 2
(Average Yearly Analyses in mg/l except as noted)

Year	No. of samples	Na	Cl	F	NO_3	TDS	Conductance[a]	pH[b]
1953	8	--	32	1.2	42	305[c]	470	--
1954	9	--	32	1.2	60	310[c]	475	--
1955	2	--	34	2.5	64	360[c]	557	--
1956	9	--	34	2.4	26	444	--	8.2
1957	4	63	27	2.3	25	280[c]	437	7.6
1958	12	64	27	1.7	24	265[c]	409	7.8
1959	5	72	31	1.5	35	325[c]	497	7.3
1961	1	38	12	1.0	13	294	285	7.8
1962	1	61	25	1.2	30	325	320	7.2
1963	3	71	30	1.5	40	398	302	7.5
1964	2	84	31	2.0	40	390	420	7.5
1970	2	81	44	1.3	22	402	410	7.5
1971	1	72	28	.6	26	330	360	7.3
1972	2	73	39	3.3	31	363	395	7.7

[a] Micromhos at 25° C
[b] No Units
[c] Estimated

The quality of water at Pueblo 3 from 1957 through 1964 reflects return flow from Hamilton Bend Springs and flow through the alluvium. The quality of water at Pueblo 3 in 1970 through 1972 reflects mainly the quality of sewage effluent released from the Bayo Plant.

Quality of Surface Water at Pueblo 3
(Average Yearly Analyses in mg/l except as noted)

Year	No. of samples	Na	Cl	F	NO_3	TDS	Conductance[a]	pH[b]
1957	1	48	18	2.0	20	210	320	7.9
1958	7	51	22	1.4	22	215	331	7.6
1959	5	71	32	1.6	20	310	478	7.4
1961	2	59	17	.7	18	465	440	7.7
1963	1	65	28	2.0	9	362	420	7.5
1964	2	115	47	2.0	22	455	435	7.8
1970	2	84	22	1.0	61	376	344	7.0
1971	1	74	26	1.2	66	416	380	6.9
1972	2	76	39	3.3	44	385	450	7.3

[a] Micromhos at 25° C

[b] No Units

[c] Estimated

Metal ion analyses were made of surface water from Acid Weir, Pueblo 1, Pueblo 2, and Pueblo 3 in 1971 and 1972. The analyses show some traces of metal ions.

Metal Ion Analyses
(Average of two analyses in μg/l)

Metal Ion	Acid Weir	Pueblo 1	Pueblo 2	Pueblo 3
In Solution				
Cadmium	3.3	3.7	3.9	3.2
Beryllium	.25	.25	.25	.25
Lead	3.0	2.0	3.0	5.2
Mercury	0.02	.05	.02	.14
Particulate				
Cadmium	.35	7.0	.25	.75
Beryllium	.25	.25	.25	.25
Lead	.16	7.1	2.8	11.1
Mercury	.11	.34	.06	.14

2. Radiochemical Quality of Surface Water

The treated effluents were released directly into Acid Canyon, thus the direct release of effluents into the canyon and lack of

dilution of radioactivity in the surface flow in Acid Canyon was greater than in Pueblo Canyon. The plutonium and gross beta activity generally decreased downgradient from Acid Weir in Acid Canyon to Pueblo 3 in Pueblo Canyon. Due to the "slug" type of release, the radiochemical quality varied according to the time the sample was collected.

The highest concentration of plutonium reported in Acid Canyon was 17.1 pCi/l at Acid Weir in May 1959, with Pueblo 1, 2 and 3 having plutonium concentrations of less than the limits of detection (<0.5 pCi/l). Another high period of plutonium occurred in surface water during April 1963 when the plutonium was 13.6 pCi/l at Acid Weir, <0.5 pCi/l at Pueblo 1 and <0.5 pCi/l at Pueblo 2.

Plutonium in Surface Water
(Average of a number of analyses in pCi/l)

Year	Acid Weir	Pueblo 1	Pueblo 2	Pueblo 3
1958	4.2	0.6	<.5	.7
1959	4.5	<.5	<.5	<.5
1960	0.6	--	--	<.5
1961	1.3	<.5	<.5	<.5
1962	2.0	<.5	2.7	--
1963	7.6	<.5	1.0	<.5
1964	--	--	<.5	<.5
1965	<.5	--	--	--

The highest concentrations of gross beta activity occurred in July 1959. The activity decreased from 586 pCi/l at Acid Weir to 2,610 pCi/l at Pueblo 1. The samples were collected during the decline of a release of industrial effluents.

Gross Beta in Surface Water
(Average of a number of analyses, pCi/l)

Year	Acid Weir	Pueblo 1	Pueblo 2	Pueblo 3
1958	694	75	55	326
1959	285	447	<14	<14
1960	245	--	--	27
1961	225	<14	<14	52
1962	110	<14	18	--
1963	78	<14	22	17
1964	--	--	20	22
1965	<14	--	--	--

The above concentrations of plutonium and gross beta activity reflect the changing conditions in the canyon while the industrial effluents were being released.

The radiochemical results of surface water analyses in 1970 through 1972 show the condition in the canyon when the source of the plutonium and other radionuclides in the water is due to resuspension from those nuclides previously adsorped or exchanged with ions of the alluvial materials in the channel sediments. Plutonium and gross beta activity are higher in Acid Canyon (Acid Weir) than in Pueblo Canyon. In general, the concentrations decrease downgradient in the canyon. The residual of industrial effluents is still within the Acid-Pueblo Canyon system.

Radiochemical Analyses of Surface Water 1970 through 1972
(Average of 5 analyses in pCi/l, except where noted)

	Acid Weir	Pueblo 1	Pueblo 2	Pueblo 3
Gross alpha	<3	<1	<1	<1
Gross beta	153	36	15	14
Plutonium-238	.08	.08	.05	.05
Plutonium-239	1.87	.07	.27	.06
Cesium-137	<350	<350	<350	<350
Tritium	1970	<1000	<1000	<1000
Natural Uranium[a]	1.3	1.0	1.0	1.0

[a] Micrograms per liter

C. Water in Alluvium

Stream flow infiltrates into the alluvium to maintain small bodies of water perched on the underlying tuff and Puye Formation. The water in the alluvium moves downgradient and water is lost into the tuff and fanglomerate.

The laboratory analyses indicate that the coefficient of permeability of the tuff ranges from 3×10^{-5} m/day for a welded tuff to 9×10^{-1} m/day for a nonwelded tuff. Water moving through the tuff does not completely saturate the matrix because of noncommunicating pore space which are mostly of capillary size. Infiltration of water into the tuff is considered small due to the hydrologic characteristics of the tuff. Also infiltration of water into the Tschicoma Formation is considered small due to the characteristics of the rocks (generally seen in outcrops and dense with no open fractures) and that there is very little surface water loss in the reach of the channel underlain by the Tschicoma.

The stream channel is cut down to the tuff-fanglomerate contact between observation Well PO-4A and Hamilton Bend Spring (Fig. 8). The top of the Puye Formation in this area is characterized by a water laid lens of tuffaceous sediment.

As the alluvium thins due to the resistance to erosion of the sediment, water in the alluvium is returned to the surface in the seep area at Hamilton Bend Spring. A similar resistant layer of sediments occurs at Otowi Seep.

The sediment lenses are thin and underlain by fanglomerate debris which is quite permeable. The area underlain by the Puye Formation is the major recharge area for the perched aquifer that discharges in part in Los Alamos Canyon at Basalt and Los Alamos

Springs (Fig. 6).

A series of shallow observation holes were constructed in Acid and Pueblo Canyons (Fig. 5). Drive points and corrugated metal pipe were driven or dug 4 to 6 feet into the alluvium to obtain samples of water moving through the alluvium. The observation holes in Acid Canyon were designated "AC" (AC-3, AC-4, AC-5) while the observation holes in Pueblo Canyon were designated as "PC" (PC-1, PC-2, PC-3, PC-4, PC-5, PC-6, PC-7, PC-8, PC-9, PC-10, PC-11). Collection of water samples (pumped) from these holes was dependent on stream flow for recharge, therefore at times when the stream was not flowing, the hole would be dry. Storm runoff occasionally destroyed a hole so that by 1964, most of this sampling network was gone.

In 1957, sixteen test holes were drilled up to depths of 23 m in the area of Hamilton Bend Springs for additional geologic and hydrologic information. Three were incorporated into the monitoring net PO-1A (destroyed 1967), PO-4A and PO-4B. PO-1A, PO-4A, and PO-4B were completed into the alluvium. A fourth test hole in this series, PO-3B, was completed at a depth of about 17 m in the Puye Formation, and is also used as a part of the monitoring net. Recharge is from water in the alluvium. Water in the alluvium is also discharged at Hamilton Bend Springs and Otowi Seep which are a part of the monitoring net.

1. Chemical Quality of Water in the Alluvium

Chemical quality of water in the alluvium in Acid Canyon (AC-series holes) in the period 1954 through 1964 reflects chemical quality of industrial effluents while water in the alluvium in Pueblo Canyon (PC and PO series holes) reflect the quality of

sewage effluents predominating. Surface water in the canyon recharges water in the alluvium.

The chemical quality of water in the alluvium in Acid Canyon varied markedly between sampling periods, but the water was highly mineralized. In Pueblo Canyon the chemical quality of water in the alluvium was somewhat better, having a lower fluoride ion and nitrate concentration and a slight decrease in mineral concentration as shown by a decrease in conductance.

The trends or significant changes in the chemical quality of water as it moves downgradient through the alluvium in Acid and Pueblo Canyons is partly obscured by the dilution effect of snowmelt and storm runoff, changes in volume of effluent released from the sewage treatment plants, slug-type release of water from the industrial waste treatment plant, and changing of effluents released from both sewage and industrial plants. The chemical quality of water in Acid Canyon was unstable due to the high pH. In Pueblo Canyon the pH of the water in the alluvium decreased abruptly to an average pH of 7.5 or less. A general trend, however, during the period of operation of the industrial plant indicates that the chemical quality of water generally improves downgradient in the canyon. The quality of water was best during the winter and early spring when stream flow is at a maximum due to increased release of sewage effluents and snowmelt, and poorest during the late spring and early summer when sewage effluent release and storm runoff is at a minimum.

Chemical Quality of Water in Alluvium in Acid and Pueblo Canyons 1954 through 1965
(Average of a number of analyses in mg/l except as noted)

Observation Hole	No of analyses	CL	F	NO_3	TDS	Conductance[a]	pH[b]
AC-3	25	30	3.4	38	481	590	10.4
4	29	38	4.4	35	765	665	10.0
5	8	26	3.0	65	553	610	9.6
PC-1	24	27	1.8	22	300[c]	460	7.5
2	31	28	2.2	28	542	505	7.4
3	29	27	2.3	33	430	495	7.5
4	23	30	1.9	40	432	485	7.3
5	9	32	1.8	42	315[c]	485	7.3
6	37	25	1.3	12	373	380	7.4
7	21	30	1.6	28	338	470	7.4
8	16	29	1.1	36	275[c]	425	7.4
9	25	29	1.2	6	430	370	7.4
10	30	27	1.4	19	379	350	7.3
11	13	29	1.5	28	361	390	7.2
PO-1A	9	27	1.2	7	327	380	7.4
PO-4A	15	25	1.7	23	318	400	7.1
PO-4B	10	28	.9	10	330	370	7.2
Hamilton Bend Springs	31	30	.8	18	336	405	7.5
Otowi Seep	4	33	1.6	2	275[c]	422	7.5
PO-3B[d]	7	13	0.4	6	190	200	7.2

[a] Micromhos at 25° C

[b] No Units

[c] Estimated

[d] Completed in Puye Formation

Monitoring of water in the alluvium during the period 1970 through 1972 was performed at Observation Holes PO-4A and PO-4B and at Hamilton Bend Springs. The chemical quality of the surface water in the canyon which recharges the water in the alluvium.

Quality of Water in the Alluvium 1970 through 1972
(Average of several analyses)

Station	PO-4A	PO-4B	Hamilton Bend Spr.	PO-3B[a]
No. of Samples	3	1	4	5
Chemical (mg/l)				
Calcium	21	12	17	27
Magnesium	5	10	7	10
Sodium	63	66	72	28
Carbonate	0	0	0	0
Bicarbonate	85	116	118	76
Chloride	35	30	38	32
Fluoride	2.5	1.0	2.5	4.0
Nitrate	34	6	16	2.1
Dissolved Solids	344	299	423	281
Total Hardness	73	70	68	107
Conductance[b]	347	360	367	270
pH[c]	7.2	7.0	7.6	7.0

[a] Completed in Puye Formation

[b] Micromhos at 25° C

[c] No Units

Metal ion analyses were made of water from PO-4A and Hamilton Bend Springs. Traces of metal ions in the water are a bit lower than found in surface water in the canyon.

Metal Ion Analyses
(Average of a number of analyses in μg/l)

	PO-4A	Hamilton Bend Spr.	PO-3B
No of Analyses	1	1	2
In Solution			
Cadmium	1.1	.18	15
Beryllium	<.25	<.25	< .25
Lead	3.5	4.5	3.0
Mercury	.13	<.02	.25
Particulate			
Cadmium	.68	.72	5.8
Beryllium	<.25	<.25	<.25
Lead	4.5	4.8	18
Mercury	.27	<.02	.8

2. Radiochemical Quality of Water in the Alluvium

Water in the alluvium is recharged directly from stream flow; thus as with the surface water, concentrations of plutonium and gross beta activity were highest in Acid Canyon due to the direct release of effluents and lack of dilution by sewage effluents which occurs in Pueblo Canyon. In general, as with the surface water, the concentrations of radionuclides decrease downgradient in the canyons.

Plutonium in Water in the Alluvium, 1958 through 1964
(Average of a number of analyses in pCi/l)

Years	1958	1959	1960	1961	1962	1963	1964	1965
Station								
AC-3	5.3	2.9	<.5	--	14.6	18.2	--	--
AC-4	1.9	41.9	4.0	1.3	--	--	--	--
AC-5	4.9	--	<.5	--	--	--	--	--
PC-1	<.5	<.5	--	--	--	--	--	--
PC-2	<.5	10.9	--	--	--	--	--	--
PC-3	1.3	<.5	<.5	<.5	--	--	--	--
PC-4	.5	<.5	--	--	<.5	<.5	--	--
PC-5	.5	.5	--	--	--	--	--	--
PC-6	1.8	<.5	<.5	<.5	<.5	.9	.8	
PC-7	<.5	<.5	--	--	--	--	--	--
PC-8	<.5	<.5	--	--	--	--	--	--
PC-9	.7	<.5	--	--	<.5	<.5	<.5	--
PC-10	<.5	<.5	<.5	<.5	<.5	<.5	<.5	<.5
PC-11	--	<.5	<.5	2.7	<.5	<.5	.9	<.5
PO-1A	1.9	<.5	<.5	--	--	--	<.5	--
PO-4A	<.5	<.5	<.5	--	--	--	<.5	<.5
PO-4B	<.5	<.5	<.5	--	--	--	--	<.5
Hamilton Bend Springs	<.5	<.5	<.5	<.5	<.5	1.0	.9	--
Otowi Seep	<.5	<.5	<.5	--	3.8	<.5	.8	<.5
PO-3B	<.5	<.5	<.5	—	<.5	<.5	<.5	—

Gross Beta in Water in the Alluvium 1958 through 1965
(Average of a number of analyses, analyses in picocuries per liter)

Year	1958	1959	1960	1961	1962	1963	1964	1965
Station								
AC-3	788	347	1260	---	108	260	---	---
AC-4	810	621	165	198	---	---	---	---
AC-5	1080	---	---	---	---	---	---	---
PC-1	< 14	< 14	< 14	---	---	---	---	---
PC-2	26	< 14	---	---	---	---	---	---
PC-3	28	22	15	135	---	---	---	---
PC-4	337	< 14	---	---	900	22	---	---
PC-5	< 14	< 14	---	---	---	---	---	---
PC-6	32	< 14	16	90	< 14	31	< 14	---
PC-7	260	< 14	---	---	---	---	---	---
PC-8	98	< 14	---	---	---	---	---	---
PC-9	53	< 14	---	---	< 14	48	< 14	---
PC-10	< 14	< 14	< 14	48	17	31	< 14	< 14
PC-11	---	144	< 14	< 14	< 14	16	57	< 14
PO-1A	268	< 14	< 14	---	---	---	18	
PO-4A	69	< 14	< 14	---	---	---	< 14	< 14
PO-4B	27	< 14	< 14	---	---	---	---	< 14
Hamilton Bend Springs	< 14	< 14	< 14	< 14	< 14	< 14	< 14	< 14
Otowi Seep	38	< 14	< 14	---	< 14	87	< 14	---
PO-3B		< 14	< 14	< 14	---	< 14	< 14	---

[a] Six analyses, Gross beta reported 3/58, 1270 pCi/l; 5/58, 189 pCi/l, 6/58 14 pCi/l.

The maximum concentration of plutonium in water in the alluvium was 180 pCi/l from hole AC-4 in May of 1959. Gross beta

Radiochemical Analyses of Water in the Alluvium
1970 through 1972
(Average of a number of analyses in pCi/l)

Station	PO-4A	PO-4B	Hamilton Bend spr.	PO-3B
No. of Analyses	3	1	4	5
Gross alpha	1	4	2	1
Gross beta	6	10	6	6
Plutonium 238	.05	.05	.05	.08
Plutonium-239	.06	.05	.06	.06
Cesium-137	350	350	350	350
Tritium	1,100	1,100	1,200	15,000
Total Uranium[a]	1.2	0.5	1.1	0.7

[a] Micrograms per liter.

Effluent from the Bayo Plant covered the return flow from Otowi Seep. Radiochemical analyses from the three stations were background with the exception of trace amounts of plutonium-239 and tritium reported in one sample from PO-4A and Hamilton Bend Spring.

D. Radiochemical analyses of Sediments

Samples of sediments have been collected in Acid and Pueblo Canyons from 1954 to the present to determine the amount of adsorption of radionuclides with the sediment materials.

Particle size distribution of the sediments at stations are shown on the following table.

Particle Size Distribution of Sediments

Grade	Distribution (Percent by weight)						
Granules	AC-4	Acid Weir	PC-1	PC-5	PC-7	PC-9	Rd. 4
Sand	4.5	6.5	3.0	10.5	5.0	2.0	1.0
Very Coarse	47.0	42.5	36.5	34.5	28.0	10.0	17.0
Coarse	44.0	39.5	50.5	37.0	31.0	40.0	50.5
Medium	2.0	6.0	7.0	11.0	19.0	21.0	19.0
Fine	1.0	1.5	1.0	3.0	11.5	9.5	7.0
Very Fine	1.0	1.0	.5	1.5	2.5	6.5	2.0
Silt and Clay	.5	3.0	1.5	3.0	3.0	11.0	3.5

Sediments from the channel at AC-4 and Acid Weir were derived from the Bandelier Tuff. In Acid Canyon sediments from PC-1, PC-5, PC-7, PC-9 and at State Road 4 were derived from the Tschicoma Formation and Bandelier Tuff. Sediments from PC-9 and at State Road 4 may contain some reworked material from the Puye Formation.

Samples of sediments collected from the stream channel in the period 1954 through 1961 when the industrial plant was in operation were analyzed for gross alpha and gross beta activity. The gross alpha and gross beta activity increased in October 1958 due to a release of untreated effluents. The gross alpha and beta activity was considerably lower in Pueblo Canyon than in Acid Canyon. In general the activity decreased with increased distance from the effluent outfall above AC-3. There is no apparent build up of radionuclides in the sediments in Acid Canyon due to the sediment transport by storm runoff which moves the radionuclide attached to the sediments downstream dispersing them over a larger area.

Gross Alpha Activity of Sediments from Acid and Pueblo Canyon
1954 through 1961 (Analyses in picocuries per dry gram)

Location	1954	1955	1956	1957	1958	1959	1960	1961
AC-3	1600	2600	34	390	2900	360	120	130
AC-4	320	500	140	170	1600	220	67	40
AC-5	190	---	120	64	52	100	57	37
Acid Weir	---	---	---	---	34	50	48	220
Pueblo 1	35	---	2	---	11	5	3	57
PC-2	16	---	3	---	6	9	3	20
PC-4	52	---	---	---	3	---	41	10
PC-5	9	---	---	---	----	4	11	11
PC-6	4	---	---	---	---	4	9	10
PC-7	54	---	---	---	---	2	5	120
PO-4A	---	---	---	---	---	4	2	33

Gross Beta Activity of Sediments from Acid and Pueblo Canyon
1954 through 1961
(Analyses in counts per minute per dry gram)

Location	1956	1957	1958	1959	1960	1961
AC-3	360	370	11,320	990	1500	70
AC-4	142	70	10,440	290	730	60
AC-5	11	90	440	155	480	120
Acid Weir	---	---	830	107	340	3650
Pueblo 1	< 1	---	120	50	< 1	120
PC-2	17	---	120	7	40	20
PC-4	---	---	370	---	90	< 1
PC-5	---	---	---	---	< 1	< 1
PC-6	---	---	----	60	20	10
PC-7	---	---	---	10	40	190
PO-4A	---	---	---	20	70	< 1

The radionuclides adsorbed on the sediments are also dispersed throughout the canyons by the intermittent release of industrial effluents and sewage effluents released into the canyon.

On November 24 and 25, 1965 a series of sediment samples from Acid and Pueblo Canyons were analyzed for gross alpha, beta, and gamma activity.

Radiochemical Analyses of Sediments, November 1965
(Analyses in counts per minute per dry gram)

Location	Gross Alpha	Gross Beta	Gross Gamma
AC-3	27	5	<1
Acid Weir	22	20	6
PC-1	1	19	16
PC-5	1	6	<1
PC-7	3	<1	30
PC-9	3	32	6
Road 4	4	9	14

The gross alpha activity decreases downgradient while there appears to be no pattern for the distribution of gross beta and gamma activity.

On April 16, 1970 another set of samples were collected of sediment in Acid and Pueblo canyons. Analyses indicated residual gross alpha, beta, and plutonium-239 in Acid Canyon. In general concentrations decreased downgradient from the effluent discharge points.

Radiochemical Analyses of Sediments, April 1970
(Analyses in picocuries per dry gram)

Location	Gross Alpha	Gross Beta	Gross Gamma	Pu238	Pu 239
AC-4	41	11	7	0.19	29.0
Acid Weir	36	14	7	.21	25.0
PC-1	2	2	<1	<.001	.04
PC-2	8	2	2	.08	4.9
PC-5	8	12	<1	.011	4.6
PC-7	4	2	<1	<.001	1.2
PC-9	1	<1	<1	<.001	.40
Road 4	3	4	<1	.006	1.1

Additional samples were collected and analyzed from two stations in 1971 and 1972. One of the stations is in the middle reach of the canyon (PC-6), and the other is at the above boundary discharge point at State Road 4. All theree analyses at the two stations show residual gross alpha, beta, and plutonium-239 which was released into the canyon from the treatment plant prior to 1965. The plutonium is bound to sediments in the stream channel and is subject to transport as suspended or bed load material during periods of storm runoff.

Radiochemical Analyses of Sediments 1971 and 1972
(Analyses in picocuries per dry gram, except as noted)

	PC-6			State Road 4		
	5-7-71	10-14-71	10-11-72	5-7-71	10-14-71	10-11-72
Gross Alpha	7	10	< 1	2	4	< 1
Gross Beta	2	2	4	2	2	4
Plutonium-238	.016	.007	.012	.006	.001	< .002
Plutonium-239	2.93	2.20	2.55	.761	.391	.370
Cesium-137	--	< 1.5	3.4	--	<1.5	3.9
Natural Uranium[a]	0.19	.22	.42	.12	.10	.32

[a] micrograms per gram

E. Inventory of Plutonium in Channel Sediments

The four sections of the channel in the canyon considered in the inventory are the section in Acid Canyon from the old outfall at TA-45 to the confluence with Pueblo Canyon, (0-480 m) and three sections in Pueblo Canyon from that point to the confluence with Los Alamos Canyon (480 to 10,280 m) as shown on Fig. 8. The physical characteristics of the four sections of channel are shown as follows:

Physical Characteristics of Channel
Acid-Pueblo Canyon

1. 0 to 480 m (Acid Canyon)
   Width 1.5 m Depth 0.15 m
   Sp. g. 1.57 Weight 170 x 10^6 g

2. 480 m to 2,600 m
   Width 2.5 m Depth 0.15 m
   Sp. g. 1.57 Weight 1,790 x 10^6 g

3. 2,600 m to 6,800 m
   Width 2.5 m Depth 0.15 m
   Sp. g. 1.57 Weight 2,967 x 10^6 g

4. 6,800 m to 10,280 m (Confluence)
   Width 4 m Depth 0.15 m
   Sp. g. 1.57 Weight 3,278 x 10^6 g

The computation showed the concentrations and amounts of plutonium at each section of the canyon for February 1970 and October 1972, and are presented in the following table.

A. Acid-Pueblo Canyon (February, 1970)

Section	Station	Concentration µCi/g	Concentration Ave	Total Pu mCi	% of Total Pu
0- 480	AC4	29.1			
	Acid Weir	24.8	27.0	4.6	25
480- 2,600	PC-2	4.98			
	PC-5	4.71	4.84	8.7	48
2,600- 6,800	PC-7	1.15			
	PC-9	.398	.775	2.3	13
6,800-10,280	PC-9	.398			
	SR-4	1.14	.770	2.5	14
Total		--	--	18.1	100

B. Acid-Pueblo Canyon (October, 1972)

Section	Station	Concentration µCi/g	Concentration Ave	Total Pu mCi	% of Total Pu
0- 480	AP-1	2.5			
	AP-2	2.3			
	AP-3	6.9			
	AP-4	50			
	AP-5	13			
	AP-6	12			
	AP-7	11	14.0	2.4	21
480- 2,600	AP-8	2.1			
	PC-5	2.6	2.4	4.3	37
2,600- 6,800	AP-9	.36			
	AP-10	1.2	.78	2.3	20
6,800-10,280	AP-10	1.2			
	SR-4	.37	.78	2.6	22
Total		--	--	11.6	100

The recap of the plutonium inventories in the canyon is presented as follows, for comparison.

Section (m)	Total Plutonium (mCi) Feb. 1970	Total Plutonium (mCi) Oct. 1972
0- 480	4.6	2.4
480- 2,600	8.7	4.3
2,600- 6,800	2.3	2.3
6,000-10,280	2.5	2.6
Total	18.1	11.6

The inventory in Acid-Pueblo Canyon indicates that form the outfall to the confluence with Los Alamos Canyon, in February, 1970 only 18.1 or 11% of the 170 mCi of plutonium released into the canyon remains in the sediments. In October, 1972, only 11.6 mCi or 7% remained of the 170 mCi. The largest changes occur in the upper sections of the canyon (0-2600 m) which contain the greatest amounts of plutonium. The amounts in the lower section (2600 to 10,280 m) appear to be somewhat in equilibrium, with the input transport equal to output. for the two years of data the transport is about 3.25 mCi per year.

F. Flood Frequency and Maximum Discharge

Acid Canyon heads on the Pajarito Plateau at an altitude of about 2,220 m and has a drainage area of about 0.8 km^2. It is tributary to Pueblo Canyon on the western part of the Pajarito Plateau. Pueblo Canyon heads on the flanks of the Sierra de los Valles at an altitude of about 2,7400 m and has cut a deep canyon into the Pajarito Plateau.

The flood-frequency and maximum discharge at the boundary are based on the following data:

Drainage Area	22.3 km^2
Main Channel Slope	-0.33

Frequency	Maximum-Discharge (m^3/sec)
2-year	3.1
5-year	7.1
10-year	10
25-year	17
50-year	21

VI DRAINAGE AREA V (LOS ALAMOS-DP CANYONS)

Los Alamos Canyon drainage area extends to the drainage divide on the flanks of the Sierra de los Valles and enters the Rio Grande to the east near Otowi (Fig. 9). Major tributaries are Pueblo Canyon just east of the AEC boundary and DP Canyon near the center of the plateau. DP Canyon is of prime importance, as an industrial treatment plant releases low level radioactive effluents into the canyon. The alluvium in the canyon is thin in the upper reaches and thickens eastward to about 20 feet near the eastern edge of the plateau. The alluvium is underlain by tuff in the western and central part of the canyon and conglomerate and basalt in the eastern part.

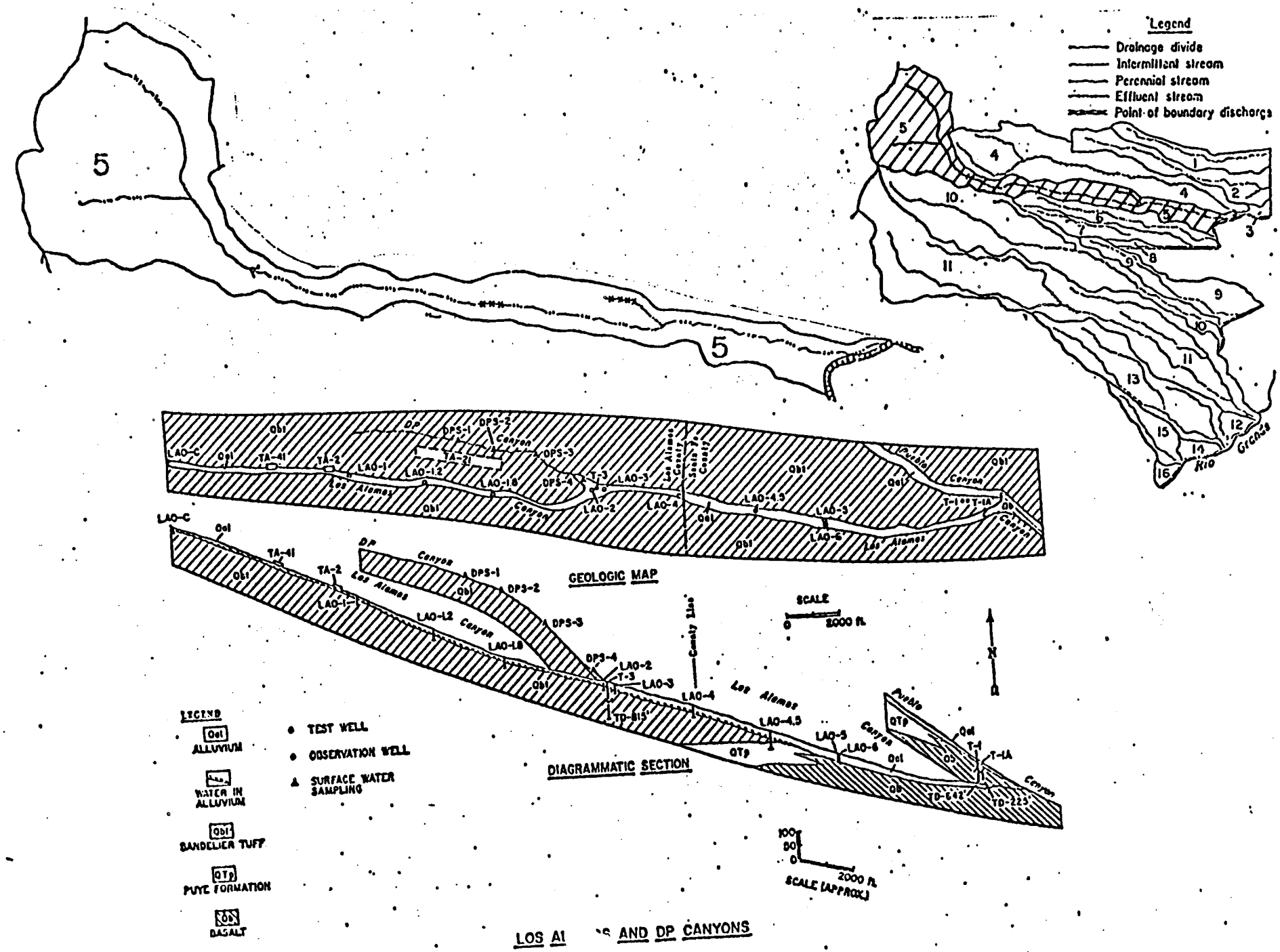

LOS AL[illegible]S AND DP CANYONS

Fig. 9. Drainage Area 5 (DP-Los Alamos Canyons) showing geology and

In the upper reach on the flanks of the mountains, perennial surface flow occurs. A part is impounded at Los Alamos Reservoir and is used for lawn irrigation at parts of the Laboratory in a system that is independent of the municipal water supply.

Surface flow in the canyon across the plateau is intermittent. There is some release of water from the TA-41 cooling tower and sewage effluent from TA-2 and TA-41. Storm runoff in the canyon during the summer may reach the Rio Grande. The sewage effluent, water from the cooling tower, and storm runoff maintain, along with inflow of water in the alluvium from DP Canyon, recharge the water in the alluvium that is perched on the tuff (Fig. 9). As the water in the alluvium moves downgradient some is lost to evapotranspiration while the rest moves into the underlying tuff, conglomerate, and basalt. The major area of loss of water in the alluvium occurs in the lower reach of the canyon on the plateau where the alluvium is underlain by conglomerate and basalt. Infiltration of water from the alluvium into the conglomerate and basalt replenishes the body perched in the basalt in Pueblo Canyon. The water from the perched zone discharges from the base of the basalts (Basalt Spring) in Los Alamos Canyon to the east (Fig. 9).

DP Canyon heads on the plateau and has a small drainage area. The canyon is tributary to Los Alamos Canyon near the center of the plateau. The alluvium in the upper reach of the canyon is thin or non-existent; however, in the lower reach of the canyon the alluvium thickens rapidly to about 6 m at the junction with

Los Alamos Canyon. The canyon is cut into and underlain by tuff.

Initial disposal of liquid waste at TA-21 was into seepage pits dug into the tuff near the head of the canyon. In 1952, a treatment plant was constructed and put into operation. The plant processed 7.5 x 10^3 m^3 of liquid waste are released into DP Canyon along with the sewage effluent.

Treated sewage effluent is released into the canyon from the plant at the eastern edge of TA-21. The stream flow in the canyon is intermittent. Intermittent flow consists of industrial and sewage effluents and storm runoff. The industrial and sewage effluent maintains an intermittent stream which infiltrates into the alluvium in the lower reach of the canyon. Only during storm runoff in the canyon does surface flow reach Los Alamos Canyon.

A. Sewage and Industrial Treatment Plants

Sewage from Technical Area 21 is treated prior to release into DP Canyon at a plant near the eastern edge of the area. The oldest waste treatment or retention facilities for industrial effluents have been located at TA-21. Wastes have been handled by three different methods in the period 1943 through 1972.

1. Sewage Treatment Plant

The sewage treatment plant treats and releases about 30 x 10^3 m^3 of effluent per year. The plant services the facilities at TA-21 and enters the canyon between sampling stations DPS-3 and DPS-4 (Fig. 9).

2. Seepage Pits for Industrial Effluent

The seepage pits near Building 35 are the oldest used for the disposal of liquid wastes at Los Alamos. Wastes from the processing

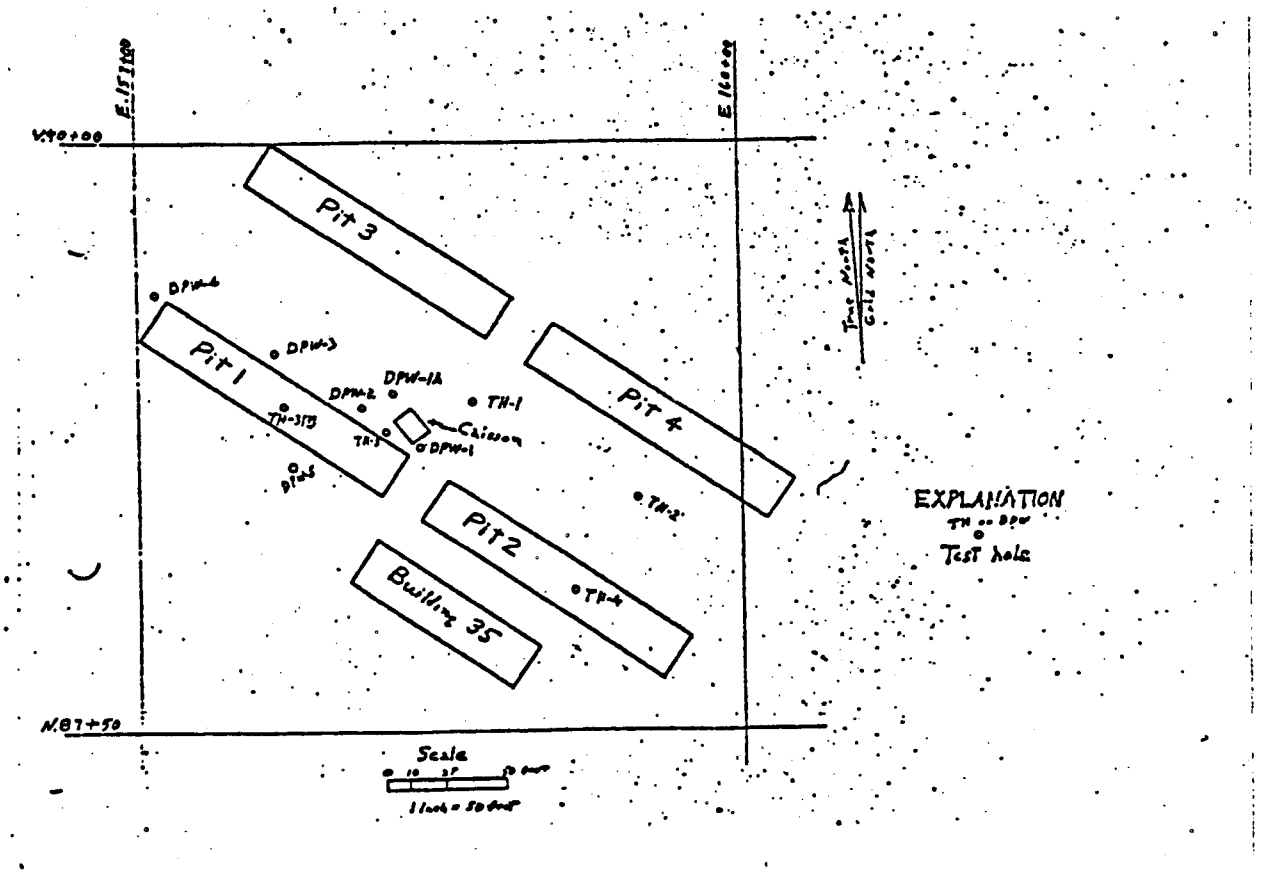

Fig. 10. Seepage pits for industrial effluents.

of plutonium at TA-21 were released into pits during the period 1943 to 1952. The use of the pits was discontinued in 1952 when a treatment plant (Building 35) was installed to remove plutonium and other radionuclides. The effluents from the plant are released into DP Canyon, a southeast trending canyon north of the pit area.

The disposal area consists of 4 pits that are about 365 m long, 60 m wide and about 2 m deep (Fig. 10). The pits are filled with about 1.2 m of sand, gravel and boulders with berms extended around the individual pits. Effluents were released through a distribution system into pits 1 and 2 and through overflow pipes into pits 3 and 4 respectively. In January 1967 the outline of the gravel portion of the pits was obscured by the growth of grasses and weeds and erosion of the berms. A new road has covered part of Pit 1 and construction has destroyed some of the berm around Pit 3.

The pits are probably excavated into Unit 3 of the Tshirege Member of the Bandelier Tuff. The lower part of this unit is nonwelded tuff grading up into a moderately welded tuff which underlies the pits. Joints are more numerous in the upper part of the unit due to the denser welding. Most of the joints are oriented vertical or near vertical. The total thickness of the unit is about 34 m. It is underlain by a moderately to densely welded tuff.

The total thickness of the Bandelier Tuff underlying the mesa at Building 35 exceeds 240 m. The tuff is in the zone of areation; the top of the main zone of saturation is about 350 m below the surface of the mesa.

The amount of effluents released into the pits during the period 1943 to 1952 has been estimated to range from 7.5×10^3 to 11×10^3 m^3 a year. The concentration of plutonium in the effluents during this period has been estimated at 60 c/m/ml (counts per minute per milliliter) with an average fluoride concentration (associated with the wastes) of 160 ppm (parts per million). In addition, 39.5 m^3 of effluent highly concentrated with ammonium citrate was released into the pits from June 1951 to July 1952. The plutonium concentration of this waste averaged about 7,000 c/m/ml and the fluoride concentrations were about 200 ppm.

The pits were not used from 1952 to January 1965. Since January 1965, pits 1 and 2 have received an average of 280 m^3 gallons a month or a total of 6.8×10^3 m^3 of low level radioactive effluent from DP-East.

A study was made in 1953 to determine the retention characteristics of the tuff with regard to plutonium while another study was made in 1961 to determine the movement of plutonium in the tuff.[14] The results of these studies are summarized in the following sections.

a. Retention of Plutonium in the Tuff

Five test holes were drilled in and around the pits in 1953. Material from the test holes was analyzed to determine the relative amounts of plutonium and the ion exchange capacities of tuff adjacent to and underlying the pits. Location of test holes are shown in Fig. 10. The exact location of the TH-3 in pit 1 is unknown. Plutonium and ion exchange capacities of the tuff are shown in the following tables:

Plutonium in Tuff from Test Holes, 1953

TH-1 Depth (m)	TH-1 Plutonium (d/m/g)[a]	TH-2 Depth (m)	TH-2 Plutonium (d/m/g)[a]	TH-3 Depth (m)	TH-3 Plutonium (d/m/g)[a]
Surface	70	Surface	9	Surface	8
0.6	4	0.6	3	0.3	400
1.2	4	1.2	2	0.6	36,100
1.8	4	1.8	2	0.9	45,600
1.8 to 3.0	2	2.4	1	3.6	1,400
3.0 to 4.3	2	3.0	4	4.6	5,000
4.6	4	3.6	3	4.9	5,100
		4.3	3	5.2	720
		4.9	4	5.5	24
		5.5	2	5.8	12
		6.1	3	6.1	12

TH-1 Depth (m)	TH-1 Plutonium (d/m/g)[a]	TH-5 Depth (m)	TH-5 Plutonium (d/m/g)[a]
Surface	410	Surface	32
0.3	600	0.6	9
0.6	10	1.2	8
0.9	80	1.8	4
1.2	3,400	2.4	3
1.5	530	3.0	2
1.8	80	3.3	2
2.1	1,800	3.6	450
2.4	40	3.8	1,510
2.7	380	4.0	1,330
3.0	2,400		

[a] Disintegrations per minute per gram.

[b] Angle hole, point of intersection with pit.

Note: TH-1 and TH-2 are vertical holes in earth filled berm.
TH-3 and TH-4 are vertical holes in pits.
TH-5 is angle hole of 45 degrees extending under pit.

Ion Exchange Capacity

TH-3 at 5.5 m 0.7 milliequivalent per 100 grams
TH-4 at 1.5 m 3.2 milliequivalent per 100 grams
TH-5 at 3.7 m 1.7 milliequivalent per grams

It was concluded from the study that plutonium is readily retained by the various earth media (clay, sand, and gravel) and that

the retention is greater in the finer materials.[13] The horizontal migration of plutonium is very small within 6.1 m of the surface, (TH-1 and TH-2). Other observations were that the ion exchange capacity of the tuff is inadequate to account for the retention of plutonium. THe retention of plutonium in the tuff is mostly due to absorption, and the effect of ion exchange is of secondary importance.

b. Movement of plutonium in the tuff

The study in 1961 was to determine the movement of plutonium and effluent in the tuff. A shaft (caisson) 9.1 m deep, 1.8 m wide, and 3.6 m long was dug near pit 1 (Fig. 10). Horizontal holes were cored into the wall of the shaft at 0.6 m depth intervals so as to terminate beneath pit 1. A vacuum cup system was placed in the horizontal holes to obtain samples of the effluent moving through the tuff for chemical and radiochemical analyses. Six additional vertical or near vertical holes were drilled to a depth of about 30.4 m around pit 1. The vertical holes and some of the horizontal holes in the shaft were used to determine the moisture content of the tuff by use of a neutron moisture-scattering probe. About 798 m^3 of tap water was released into pit 1 in July 1961. A month later, 653 m^3 of effluent containing plutonium was added. It was concluded from the study that plutonium had penetrated to a depth of at least 8.5 m in the tuff beneath the pits and that this penetration at depth takes place mainly along joints. Clay formed in joints and in devitrified fragments by weathering will sorb plutonium and result in localized areas of high plutonium concentrations. The low concentrations of aluminum and silica in the effluent in all samples indicated the absence of colloidal

clays that might provide a means of transporting plutononium through the tuff. The chemical quality of the effluent through the tuff indicated an inverse relationship between the gross alpha (plutonium) and pH of the effluent (high pH, low concentrations of gross alpha; low pH, high concentrations of gross alpha). Hardness and total dissolved solids increased at depth, suggesting the dissolution of materials from the tuff. The movement of effluents through the tuff is predominantly downward beneath the pits aided by open joints.

The amount of plutonium that was reported from cores and rock samples taken during construction of the experimental facility for the study in 1961 are presented in the following table:

Gross Alpha in Cuttings from Test Holes

Horizontal holes in caisson

Depth (m)	No. Cores	Average Gross alpha a/	Gross alpha a (Max.)	All Cores (Mis.)
1.8	10	3,003	6,613	4
2.4	7	1,306	2,850	11
3.0	8	1,143	1,872	12
3.7	6	821	1,729	414
4.3	9	749	2,094	1
4.9	9	732	1,305	8
5.5	4	517	923	141
6.1	7	183	506	45
6.7	4	15	20	11
7.3	8	402	1,038	175
7.8	10	13	88	2
8.5	6	28	156	2

Vertical or near vertical holes around pit

Hole No.	No. of Samples	Depth (m)	Gross alpha[a] (Avg.)	(Max.)	(Min.)
1	10	23	2	3	1
1-A	10	25	24	24	9
2	11	28	698	3,722	142
3	11	30	3	7	2
4	13	30	1.5	2	1
5	7	28	3	6	1

a/ Counts per minute per gram.

Note: Hole DPW-1A angled at 11 1/2 degrees toward pit 1
Hole DPW-2 angled at 19 degrees toward pit 1.

C. Observations January 1967

Effluents from DP-East have at times partially filled the shaft near Pit 1, thus creating a more localized point for infiltration of liquids (Fig. 10). Test holes DPW-1A and DPW-3 contained some effluent at the time of observation. It is supposed that the water in DPW-3 moved down the outside of the casing from water ponded in the pit. Radiochemical analyses of water from these holes contained only background amounts of gross alpha and gross beta gamma radioactivity and no plutonium or uranium. Results of analyses of water for tritium shown below are approximations and are subject to revision.

DPW-1A - 462 dpm
DPW-3
Effluent running into shaft - 2,000 dpm

A sample of weathered tuff collected beneath the gravel fill of pit 1 near the shaft contained 978 c/m/g (counts per minute per gram) of gross alpha radioactivity.

The January 1967 measurements of hole DPW-1 show the effect of the 1.9 million gallons of effluent from DP-East in which the maximum concentrations of water have moved from a depth of 3.7 m (40 percent, August 1961) to 12 m (41 percent, January 1967). The hole is next to the shaft. The moisture measurements in DPW-2 and DPW-5 show a general decrease in the moisture content of the tuff from August 1961 to January 1967. The indication is that most of the effluents released into pit 1 have moved down in the area of the shaft, a focal point for collection and infiltration of effluents into the tuff.

The studies have shown that the movement of the effluents in the tuff underlying the seepage pits is mostly downward beneath the pits. The plutonium moves with the effluents and the data indicate that most of the plutonium is retained by absorption in the upper 6.1 m of the tuff. Some, however, may move to greater depths through open joints.

The construction of a solid waste disposal pit in the area may necessitate the drilling of several holes to determine the amount of contamination present as well as the structure and lithology of the underlying rock. The number and depth of the holes would depend on the size, depth and location of the proposed pit.

3. Industrial Treatment Plant Bldg. 35.

The industrial waste treatment plant at Bldg. 35 operated from 1952 to late 1967. The treatment plant was similar to that operated at TA-45. The treatment was virtually the same, with plutonium and americium the major contaminates. Many wastes from this area contained high concentrations of inert salts that would

interfere with the usual treatment of plutonium and americium wastes. These wastes were treated separately. Chemical wastes, such as hydrofluoric acid used in processing plutonium, were neutralized and discharged with other effluents from the plant into DP Canyon.

The sludge at Bldg. 35 was also packaged and buried in the solid disposal pits on the mesa. The plant has a somewhat smaller capacity than that at TA-45 with an annual discharge into DP Canyon of 7.5×10^3 m^3 to 15×10^3 m^3. After 1967, operations were transferred to a new plant at Building 257.

4. Industrial Treatment Plant Bldg. 257

The new plant at Bldg. 257 began operation in late 1967 and had a slightly greater capacity for treatment of effluents that the old plant at Bldg. 35. The treatment of the liquid wastes was essentially the same with some modification of newer equipment such as pressure type filters rather than gravity flow and some changes in filter media.

A new process introduced at the plant was the treatment and disposal of sludges resulting from chemical and physical treatment.

The sludge from the plant is fed through a pug mill that mixes the sludge with cement with the resulting slurry pumped into shafts adjacent to the plant. Other wastes containing high concentrations of chemicals or radionuclides may be processed along with the sludges for disposal. The cement sets up, fixing the contaminants in the cement.

The shafts 2.4 m in diameter range in depth from 5.5 to 19.5 m. They are located in berm areas adjacent to old seepage pits (Fig. 11). The shafts are completed into the ashflow units

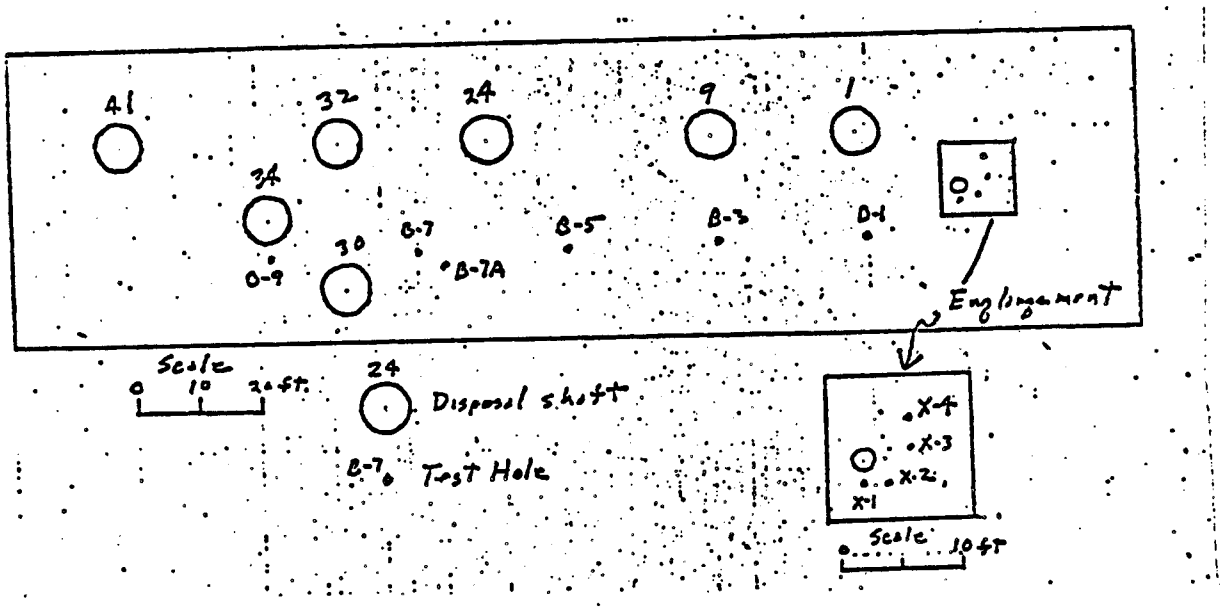

Fig. 11. Shaft disposal area for sludges fixed in cement.

of the Tshirege Member of the Bandelier Tuff.

a. Radiochemical Analyses of Tuff from Test Holes and Shafts

Samples of tuff were collected from the wall of shafts as they were being dug and analyses were made of moisture for tritium.

Tritium Analyses of Moisture from Samples of Tuff from Test Holes and Shafts

Source	Number of Samples	Average of a number of analyses Picocuries per milliliter Tritium
Test Hole B-1	11	88
Test Hole B-3	11	317
Test Hole B-5	11	183
Test Hole B-7	11	4336
Test Hole B-9	10	501
Shaft 1	10	5420
Shaft 9	6	1480
Shaft 24	4	4887
Shaft 30	3	5397
Shaft 32	2	1306
Shaft 34	8	2192
Shaft 41	7	495

The tritium has moved with the moisture from the old seepage pits into the tuff. The tuff is not saturated. There is no free water, as the tuff has a larger porosity made up mostly of capillary size pores. Where there is a moisture gradient, the moisture will tend to move to the lower moisture concentration by diffusion and capillary action.

5. Chemical Quality of Sewage and Industrial Effluents

- Samples of effluent from the sewage treatment plant were collected immediately below the effluent outfall for chemical analyses. The individual analyses varied slightly but were in the same general range in the few analyses shown. The effluents contained chemical concentrations as one would expect from sewage treatment plants. The effluents are similar to the Pueblo and Bayo Plants.

Chemical Analyses of Sewage Effluent

(Analyses in mg/l except where noted)

Determinations	12-5-67	5-5-69	8-5-69
Calcium	20	16	16
Magnesium	12	4	7
Sodium	160	230	175
Carbonate	0	0	0
Bicarbonate	280	394	190
Chloride	35	50	35
Fluoride	3	2	4
Nitrate	.9	1.3	13
Dissolved Solids	383	458	442
Total Hardness	100	55	70
Specific Conductance[a]	580	800	520
pH[b]	7.5	7.4	8.2

[a] Microhms

[b] No units

The chemical quality of effluent released from the industrial plant varied due to the changing quality of water received. In general, the effluents released into the canyon were highly

mineralized as compared to natural occurring water in the area. The table shows one weekly composite collected during the first week of July for each year, 1960 through 1972.

Chemical Quality of Industrial Effluents[a]

(Analyses in mg/l except where noted)

	1960	1961	1962	1963	1964	1965	1966	1967	1968	1969	1970	1971	197
Calcium	4	1	2	4	4	44	64	56	22	8	26	8	1
Magnesium	2	1	<1	1	1	1	2	10	<1	<1	29	2	
Sodium	532	485	423	272	413	195	270	690	280	340	270	490	68
Carbonate	314	560	428	118	690	315	1740	130	37	300	300	260	11
Bicarbonate	478	626	558	296	920	430	2036	210	212	505	420	910	79
Chloride	370	405	234	290	665	45	178	598	72	40	113	55	9
Fluoride	60	140	20	30	140	0.9	15	15	11	44	7	20	1
Nitrate (N)[b]	67	25	5	10	26	13	104	23	45	34	11	48	19
Total Hardness	16	7	6	12	15	115	170	180	54	20	185	30	6
Conductance[c]	1600	4000	1860	2000	5600	1880	4400	3200	900	2140	2260	2240	270
pH[d]	11.3	11.8	11.4	10.9	12.1	11.7	12.0	11.4	9.8	11.5	11.5	10.3	8.

[a] Weekly Composite 1st week of July of year noted

[b] Micromhos

[c] No Units

[d] n x 4.4 = NO_3

6. Radiochemical Quality of Sewage and Industrial Effluent

Radiochemical analyses was made of effluent from the sewage treatment plant. The samples were collected below the effluent outfall. Traces of americium were found in the samples collected on 8-5-69 and 7-16-70. The presence of trace amounts of americium and plutonium may be due to some contamination getting into the sewage collection system from laboratories at TA-21 processing or working with these isotopes.

Radiochemical Analyses of Sewage Effluent

(Analyses in picocuries per liter)

Determination	12-5-69	5-5-69	8-5-69	2-16-70
Gross Alpha	3	3	< 2	3
Gross Beta	14	20	13	14
Plutonium 238	<.05	<.05	<.05	.16
Plutonium 239	<.05	<.05	<.05	.14
Americium 241	--	--	.07	.08
Radium 226	<.15	--	--	
Tritium	<50,000	<50,000	<50,000	8,000

The volume of effluent from the waste treatment plant at TA-21 has ranged from 6228 to 16,220 m^3 annually. The major waste treated contained plutonium and americium with some mixed fission products.

Average Annual Concentrations Gross Alpha, Gross Beta, and Total Plutonium in Effluents Released

Year	Volume (m^3)	Picocuries per liter Gross Alpha	Gross Beta	Total Pu
1952	16220	--	--	20
1953	14400	76	--	76
1954	11520	88	--	88
1955	9436	120	--	100
1956	11690	68	--	65
1957	16170	66	--	64
1958	9987	58	--	56
1959	9138	107	--	92
1960	8408	227	--	206
1961	9251	626	--	582
1962	11660	309	--	251
1963	12150	2800	--	174
1964	6228	26	--	181
1965	9594	140	--	103
1966	10920	93	--	81
1967	7832	290	--	290

Average Annual Concentrations Gross Alpha, Gross Beta, and Total Plutonium in Effluents Released (Continued)

Year	Volume (m^3)	Picocuries per liter Gross Alpha	Gross Beta	Total Pu
1967[a]	3509	--	--	22
1968	11360	450	2700	140
1969	13290	220	4700	120
1970	10850	--	4700	140
1971	9839	--	3100	72
1972	8780	--	1800	148

[a]1952-1967 Bldg. 35
1967-1972 Bldg. 257

The average annual concentrations of gross alpha of the effluents released ranged from 26 to 626 pCi/l during the period of record. For four years of record (1968-1972), the gross beta activity ranged from 18 to 4700 pCi/l while total plutonium for 21 years of record ranged from 20 to 583 pCi/l.

Average annual concentrations of tritium, cesium-137, strontium-89, and 90 of effluents released from the waste treatment plants were available for select years.

Average Annual Concentrations of
Tritium, Cesium-137, and Strontium 89, and 90

Year	Picocuries per liter			
	Tritium	Cs 137	Sr 89	Sr 90
1952	120,000	--	--	--
1953	140,000	--	--	--
1954	170,000	--	--	--
1955	210,000	--	--	--
1956	170,000	--	--	--
1957	120,000	--	--	--
1958	200,000	--	--	--
1959	220,000	--	--	--
1960	240,000	--	--	--
1961	220,000	--	--	--
1962	170,000	--	--	--
1963	160,000	--	--	--
1964	320,000	--	--	--
1965	210,000	--	--	--
1966	180,000	--	--	--
1967	260,000	--	--	--
1968	--	1,100	--	--
1969	--	--	--	--
1970	--	--	160	240
1971	--	--	43	61
1972	420,000	--	74	120

The annual amounts of gross alpha and plutonium were computed from average annual concentrations and volumes of effluents.

Annual Amounts of Radionuclides Released with
Effluents DP-West (DP-35 and 257)

Year	Millicuries		
	Gross Alpha	Gross Beta	Total Pu
1952	--	--	.3
1953	1.1	--	1.1
1954	1.0	--	1.0
1955	1.1	--	.9
1956	.8	--	.8
1957	1.1	--	1.0
1958	.6	--	.6
1959	1.0	--	.8
1960	1.9	--	1.7
1961	5.8	--	5.4
1962	3.6	--	2.9
1963	34	--	2.2
1964	.2	--	1.1
1965	1.3	--	1.0

Annual Amounts of Radionuclides Released with Effluents DP-West (DP-35 and 257) (Continued)

Year	Millicuries Gross Alpha	Gross Beta	Total Pu
1966	1.0	--	.9
1967	2.3	--	2.4
1968	5.1	31	1.6
1969	2.9	65	1.6
1970	--	51	1.5
1971	--	30	.7
1972	--	16	1.3
Total	--	--	30.8

B. Surface Water, DP Canyon

Stream flow in DP Canyon is intermittent and is from the release of sewage and industrial effluents. The effluents do maintain some perennial flow in various sections of the canyon, however, all effluents move into the alluvium in the lower reach of the canyon. The effluents, except for periods of extreme precipitation, do not reach Los Alamos Canyon as surface flow, but move into the canyon as groundwater in the alluvium.

There are four surface water stations in the canyon (Fig. 9). Due to the thin alluvium in the upper and middle reach of the canyon, and the limited access in the lower canyon, there are no observation holes in the alluvium. A surface water gauging station was established at the mouth of DP-Canyon as a part of a study to determine transport of radionuclides in storm runoff.

1. Chemical Quality of Surface Water

The chemical quality of the surface water in the canyon reflects the quality of industrial and sewage effluents released from the treatment plants. In general, the quality of water improves as it moves down gradient in the canyon. The following

table presents the average chemical quality for each station by years. There has been a general improvement in the quality of effluents released into the canyon as seen by a general decline of chemical constituents in surface water at DPS-1. The quality of the water improves down gradient in the canyon from DPS-1 to DPS-4. A general summary is shown below, while the following table summarizes annual concentrations.

Chemical Quality of Surface Water
(average of a number of analyses in mg/l
except as noted, 1967 through 1972)

Station	DPS-1	DPS-2	DPS-3	DPS-4[a/]
No of Analyses	19	8	7	26
Sodium	357	225	277	140
Chloride	161	74	85	79
Fluoride	10.9	10.1	12.1	7.4
Nitrate	134	66	92	62
Total Dissolved Solids	1175	708	657	695
Conductance[b/]	1560	860	1040	740
pH[c]	9.5	9.1	9.1	7.9

a/ Analyses 1962 through 1972

b/ Micromhos

c/ No Units

Quality of Surface Water at DPS-1, DPS-2, DPS-3, and DPS-4

(Average of a number of analyses in mg/l)

Source	Year	No. of Analyses	Na	Cl	F	NO_3	TDS	Conductance [a]	pH [b]
DPS-1	1967	2	630	410	9.5	104	1740	2440	9.7
DPS-1	1968	3	670	215	23	381	1950	2730	10.1
DPS-1	1969	2	375	92	32	53	1100	1700	10.7
DPS-1	1970	5	241	140	6.0	118	878	1080	9.6
DPS-1	1971	4	233	76	4.7	62	893	1110	9.3
DPS-1	1972	3	206	137	2.5	88	932	1130	7.9
DPS-2	1967	1	290	75	8.0	140	669	900	8.5
DPS-2	1968	2	250	65	9.4	101	746	980	9.4
DPS-2	1969	2	282	103	12.0	26	716	920	9.8
DPS-2	1970	2	188	85	13.0	48	714	920	9.1
DPS-2	1971	1	68	15	3.7	35	642	330	8.2
DPS-3	1967	1	310	85	10	28	799	960	8.8
DPS-3	1968	2	325	88	16	150	676	1220	9.1
DPS-3	1969	2	293	75	12	31	409	930	9.0
DPS-3	1970	2	200	93	10	84	814	1000	9.3
DPS-4	1962	2	143	134	15	40	771	745	7.4
DPS-4	1963	2	132	113	13	41	742	740	7.5
DPS-4	1964	3	109	106	5.6	57	734	983	7.8
DPS-4	1965	2	110	109	15	40	656	910	7.8
DPS-4	1967	2	253	103	7.7	145	757	990	7.9
DPS-4	1968	2	200	85	6.2	370	607	850	8.1
DPS-4	1969	2	198	60	5.0	35	390	660	8.0
DPS-4	1970	4	103	45	11	18	464	550	8.5
DPS-4	1971	4	113	47	5.0	36	531	530	7.8
DPS-4	1972	3	214	58	4.1	30	493	600	8.0

a/ Micromhos

/ No Units

Select trace metal ion analyses were made of water from two stations, DPS-1 and DPS-4 in 1971 and 1972. They indicate some trace metals in the surface water.

Metal Ion Analyses

(range and average of 5 analyses in μg/l)

Station	DPS-1 Min	DPS-1 Max	DPS-1 Av	DPS-4 Min	DPS-4 Max	DPS-4 Av
In solution						
Cadmium	0.8	13.2	6.9	0.4	7.2	3.6
Beryllium	<0.25	0.48	0.30	< .25	--	< .25
Lead	<1.0	5.0	1.8	<1.0	5.0	1.8
Mercury	<0.02	0.22	0.09	< .02	—	< .02
Particulates						
Cadmium	< .25	.89	0.43	< .25	.50	30
Beryllium	< .25	—	<.25	< .25	—	< .25
Lead	<1.0	5.2	2.8	<1.0	4.3	1.8
Mercury	<0.02	0.11	0.04	< .02	—	< .02

2. Radiochemical Quality of Surface Water

Radiochemical analyses of surface water from 1961 through 1965 indicated some Gross beta and plutonium in at DPS-4 from the treatment plant at Building 35. Analyses from 1967 through 1972 show a general decrease in the concentration of radionuclides down gradient in the canyon.

Gross Beta and Plutonium in Surface Water at DPS-4
(average of a number of analyses in picocuries per liter, 1961-1965)

Year	No. of Analyses	Gross Beta	Plutonium
1961	2	91	<0.5
1962	3	139	<0.5
1963	2	197	0.7
1964	3	71	0.9
1965	3	50	0.7

DP CANYON

SURFACE FLOW SAMPLING SITES

RADIOCHEMICAL QUALITY OF WATER

SOURCE	YEAR	MAX. # SAMPLES	GROSS ALPHA	GROSS BETA	^{238}Pu	^{239}Pu	^{241}Am	^{226}Ra	^{234}U	^{137}Cs	^{90}Sr	^{3}H	^{238}U
DPS-1	1967	1	63	51700	3.87	76.10	1.29	-.15	32.10	34000	28600	542000	.021
DPS-1	1968	3	34	14307	4.25	28.82	4.52	.17	56.30	13400	11360	2002	.021
DPS-1	1969	3	14	2060	5.55	9.10	3.58	.24	32.63	3490	800	430	.021
DPS-1	1970	5	7	1202	.81	2.20	1.19	-.15	12.33	692	568	402	.021
DPS-1	1971	4	22	1392	1.16	2.07	.60	-.15	12.31	1203	716	356	.738
DPS-1	1972	3	13	2469	.32	5.68	.33	-.00	-.00	-355	-	396100	7.100
DPS-2	1967	1	4	6690	.38	2.70	.63	-.15	4.40	2740	5810	660	.021
DPS-2	1968	2	7	4695	.30	2.10	.82	-.15	11.70	3165	2620	413	.021
DPS-2	1969	2	22	1055	2.29	3.64	1.70	-.15	57.30	2260	350	670	.021
DPS-2	1970	2	8	990	1.14	1.33	.58	-.15	26.45	450	534	381	.021
DPS-2	1971	1	5	640	5.64	.72	.25	-.00	2.11	523	376	195	.021
DPS-2	1972	-	-	-	-.00	-.00	-.00	-.00	-.00	-	-	-	-.000
DPS-3	1967	1	5	290	.21	.77	-.05	-.15	9.30	310	2260	927	.021
DPS-3	1968	2	6	1525	.43	2.63	1.42	.18	16.20	1445	3180	549	.021
DPS-3	1969	2	19	940	3.05	4.23	1.00	-.15	54.10	530	500	140	.021
DPS-3	1970	2	24	945	1.40	1.09	.62	-.15	88.60	395	453	459	.021
DPS-3	1971	-	-	-	-.00	-.00	-.00	-.00	-.00	-	-	-	-.000
DPS-3	1972	-	-	-	-.00	-.00	-.00	-.00	-.00	-	-	-	-.000
DPS-4	1967	1	-2	1800	.13	.14	-.05	.35	2.05	-240	632	410000	-.000
DPS-4	1968	2	6	625	.09	.08	.08	.17	3.35	-240	435	476000	-.000
DPS-4	1969	4	2	418	.44	.52	.35	-.15	2.71	-243	380	346250	-.000
DPS-4	1970	4	1	457	.13	.21	.20	-.00	1.53	-234	233	162250	-.000
DPS-4	1971	4	3	370	.11	.13	.08	-.00	1.72	-306	315	103250	.600
DPS-4	1972	3	2	609	.11	.27	.25	-.00	-.00	-354	-	172500	3.300
DPS-E	1967	1	3	14	-.05	-.05	-.00	-.15	-.00	-	-	-50000	-.000
DPS-E	1968	-	-	-	-.00	-.00	-.00	-.00	-.00	-	-	-	-.000
DPS-E	1969	2	2	17	-.05	-.05	.07	-.00	-.00	-	-	-50000	-.000
DPS-E	1970	1	3	14	.16	.14	.08	-.00	-.00	-	-	8000	-.000
DPS-E	1971	-	-	-	-.00	-.00	-.00	-.00	-.00	-	-	-	-.000
DPS-E	1972	-	-	-	-.00	-.00	-.00	-.00	-.00	-	-	-	-.000

C. Surface Water, Los Alamos Canyon

Los Alamos Canyon heads on the flanks of the mountains and has a small perennial stream and a spring that feeds into the reservoir. Surface flow below the reservoir is intermittent due to overflow from the reservoir and storm runoff. Small amounts of waste water are released from TA-2 and some treated sewage effluent from a treatment plant near TA-41. Due to only intermittent flow below the reservoir, samples are collected when flow occurs in this reach of the canyon.

1. Chemical Quality of Surface Water

Water samples have been collected and analyzed from above and at the reservoir. The following table presents results of some of the earlier analyses.

Quality of Surface Water at and above

Los Alamos Reservoir

	Milligrams per liter				µmhos	
Date	Sodium	Chloride	Fluoride	Nitrate	Conductance	pH
6/7/61 1/	3	1.0	0.1	.2	65	7.4
6/12/58 2/	3	1.2	.4	.3	80	7.1
10/1/52 3/	3	5	2.0	<.1	—	8.0

1/ 1.1 Mile above Reservoir

2/ 0.2 Mile above Reservoir

3/ Reservoir

Later analyses from 1967 through 1972 are shown below.

Quality of Water in Los Alamos Reservoir

(Analyses 1967-1972 in mg/l except as noted)

Date	Sodium	Chloride	Fluoride	Nitrate	Dissolved Solids	Conductance [a]	pH [b]
12/67	8	3	.2	.4	80	120	7.3
4/69	6	2	<.1	.4	85	110	7.3
5/71	7	<1	<.1	.4	110	140	7.1
5/72	7	2	<.1	.4	98	140	7.0

[a] Micromhos at 25° C

[b] No units

The stream flow in the canyon below the reservoir is intermittent. The following table lists miscellaneous analyses taken in this reach of canyon.

Intermittent Stream Flow
(Analyses in mg/l except as noted)

Date	Sodium	Chloride	Fluoride	Nitrate	Dissolved Solids	Conductance [a]	pH [b]
5/67 1/	38	28	<.1	.9	180	210	7.5
8/69 1/	79	26	.5	2.2	250	280	7.7
12/67 1/	70	35	.3	13	260	290	7.6
8/57 3/	12	4	1.2	2.3	—	240	7.6
4/58 4/	9	5	.6	2.2	—	130	7.5
6/58 4/	19	11	.4	5.2	—	210	7.7

1/ Near obs. Well LAO-1

2/ Near Obs. Well LAO-4.5

3/ Flood Flow at Highway 4

4/ Snow melt at Highway 4

[a] Micromhos at 25° C

[b] No Units

2. Radiochemical Analyses of Surface Water

Radiochemical analyses of surface water from sources other than storm runoff are shown on the following table. The analyses only reflect background radioactivity except the tritium concentration at LAO-4.5. The surface flow at LAO-4.5 is return flow from the alluvium and the tritium is from the effluents in DP-Canyon.

Radiochemical Analyses of Surface Water in Los Alamos Canyon

(Average of a number of analyses in picocuries per liter except as noted)

Source	No of Analyses	Date	Gross Alpha	Gross Beta	^{238}Pu	^{239}Pu	^{3}H	Total Uranium 1/
Reservoir	1	1971	2	2	<.05	<.05	—	<.4
At LAO-1	3	1969	<1	17	<.05	<.06	$<1x10^3$	.7
At LAO-1.8	1	1964	<1	4	<.05	<.05	—	1.5
At LAO-4.5	1	1967	<1	18	<.05	<.05	$160x10^3$	1.1

1/ μg/l

D. Water in Alluvium, Los Alamos Canyon

The alluvium in the canyon ranges from about 6 ft thick at LAO-C to about 20 ft at LAO-5. The alluvial aquifer is recharged from the release of sewage effluent from TA-41, cooling water, and intermittent storm runoff. Recharge also moves into the aquifer from the alluvium at the mouth of DP Canyon. There are 9 shallow observation wells in the Canyon (Fig).

1. Chemical Quality of Water in Alluvium

The chemical quality of water from wells in the alluvium from test holes LAO-C, LAO-1, and LAO-1.8 show concentrations of chemical constituents above what would be expected in natural water. These concentrations are due to runoff from storm drains and probably outfalls from Technical Areas, HRL, TA-41, and TA-2.

Quality of Water in Alluvium

(Average of a number of analyses in mg/l except as noted)

Source	No. of Analyses	Sodium	Chloride	Fluoride	Nitrate	Dissolved Solids	Conductance[a]	pH
LAO-C	7	39	47	0.5	2.6	223	265	7.5
LAO-1	22	80	38	0.8	4.4	356	415	7.4
LAO-1.8	2	47	30	< .1	.4	203	245	7.4
LAO-2	18	96	49	7.1	17	461	535	7.6
LAO-3	20	126	52	6.6	18	370	515	7.6
LAO-4	10	68	38	1.4	9.2	280	340	7.4
LAO-4.5	14	47	30	0.3	1.7	261	270	7.3
LAO-5	6	36	36	0.4	1.3	215	240	7.3
LAO-6	2	50	30	0.3	.4	211	270	7.4

[a] µmhos

The following table presents an annual recap of certain chemical constituents from 1967 through 1972 for each test hole. In general there were slight chemical changes at each station during the years 1967 through 1972. The quality of the water at LAO-2 reflects the inflow from DP-Canyon which receives industrial effluents. The quality of the water improves down gradient in the canyon from LAO-2 to LAO-6.

Quality of Water in Alluvium

(Average of a number of analyses)

			Milligrams per Liter					µmhos	
Source	Year	No. of Analyses	Sodium	Chloride	Fluoride	Nitrate	Dissolved Solids	Conductance	pH
LAO-C	1970	1	28	21	1.0	4.4	166	160	7.5
LAO-C	1971	2	37	46	.2	.4	249	190	7.5
LAO-C	1972	4	53	74	.4	2.4	253	345	7.5
LAO-1	1967	2	132	32	.6	2.1	406	505	7.2
LAO-1	1968	3	82	33	1.7	1.8	246	335	7.4
LAO-1	1969	2	83	47	.3	1.8	295	370	7.3
LAO-1	1970	4	54	26	.9	3.5	434	335	7.8
LAO-1	1971	4	74	27	.6	6.6	414	470	7.3
LAO-1	1972	4	75	50	.7	5.7	397	475	7.4
LAO-1.8	1969	2	47	30	< .1	.4	203	245	7.4
LAO-2	1967	1	180	73	7.0	7.5	594	760	7.3
LAO-2	1968	3	94	39	8.1	9.6	334	440	7.6
LAO-2	1969	2	37	37	5.0	7.9	369	410	7.6
LAO-2	1970	3	96	44	6.3	20	479	510	7.
LAO-2	1971	2	91	33	5.6	18	431	490	7.5
LAO-2	1972	3	97	55	4.4	24	472	573	7.5
LAO-3	1967	2	139	57	7.5	25	451	550	7.4
LAO-3	1968	2	84	30	8.5	4.4	362	405	7.6
LAO-3	1969	2	115	54	5.0	15	394	500	7.6
LAO-3	1970	4	85	43	7.0	13	445	490	7.7
LAO-3	1971	3	82	40	5.2	17	439	500	7.4
LAO-3	1972	4	109	69	4.9	27	484	615	7.5
LAO-4	1967	2	100	36	.6	7.0	294	360	7.3
LAO-4	1968	3	66	31	1.5	1.8	285	315	7.5
LAO-4	1969	2	65	35	2.3	.9	217	280	7.5
LAO-4	1970	1	57	40	2.0	18	284	370	7.1
LAO-4.5	1969	2	58	32	< .1	.9	277	270	7.6
LAO-4.5	1970	5	38	32	.5	1.3	265	275	7.2
LAO-4.5	1971	3	36	30	< .1	3.9	280	255	7.3
LAO-4.5	1972	4	55	27	.4	.9	222	270	7
LAO-5	1967	1	42	28	.4	2.6	208	240	7.2

Source	Year	No. of Analyses	Sodium	Chloride	Fluoride	Nitrate	Dissolved Solids	Conductance	pH
LAO-5	1968	2	17	25	.8	.4	224	250	7.2
LAO-5	1969	2	52	33	< .1	.9	210	240	7.4
LAO-6	1968	1	49	26	.5	< .4	227	295	7.4
LAO-6	1969	1	51	33	.1	.4	195	250	7.3

Water from 5 observation wells were analyzed for metal ions in 1971 and 1972. The average is presented in the following table. In general, the metal ion concentration increases below the confluence with DP Canyon due to the recharge consisting partly of effluents from the Industrial Treatment Plant at TA-21.

Metal Ion Analyses of Water in Alluvium

(Average of a number of analyses in μg/l)

Source	LAO-C	LAO-1	LAO-2	LAO-3	LAO-4.5
No of Analyses	4	5	4	5	4
In Solution					
Cadmium	2.1	4.5	3.7	2.6	2.8
Beryllium	< .25	< .25	< .25	.27	< .25
Lead	4.8	1.3	4.8	1.9	<1.0
Mercury	< .02	.07	< .02	.38	< .02
Particulate					
Cadmium	2.1	.65	1.35	1.30	.55
Beryllium	1.7	< .25	.78	.77	.42
Lead	22.6	10.7	10.2	12.3	13.2
Mercury	.11	.07	.5	.04	< .02

2. Radiochemical Analyses of Water in Alluvium

The earlier analyses , 1966 and 1968, are shown on the following table. Traces of radionuclides were reported in the canyon.

Radiochemical Analyses of Water in Alluvium 1966-1967

(Average of a number of analyses)

Source	Year	No. of Analyses	Picocuries per liter		µg/l
			Gross Beta	Plutonium	Total Uranium
LAO-1	1966	3	17	<.5	< .5
LAO-1	1967	1	113	<.5	< .5
LAO-2	1966	2	32	.6	< .5
LAO-3	1966	3	32	<.5	2.6
LAO-4	1966	2	<14	<.5	< .5
LAO-4	1967	1	15	<.5	< .5
LAO-5	1966	1	<14	<.5	< .5

The recap of radiochemical analyses from 1967 through 1972 are presented on the following table. The increase in radionuclides is noted at LAO-2 where the industrial effluents from DP Canyon recharge the water in the alluvium. As in DP Canyon, the concentration of radionuclides decrease downgradient due to ion exchange and adsorption with alluvial materials and dilution with water moving through the alluvium.

LOS ALAMOS CANYON

ALLUVIAL AQUIFER OBSERVATION WELLS

RADIOCHEMICAL QUALITY OF WATER

SOURCE	YEAR	MAX. # SAMPLES	GROSS ALPHA	GROSS BETA	^{238}Pu	^{239}Pu	^{241}Am	^{226}Ra	^{234}U	^{137}Cs	^{90}Sr	^{3}H	^{238}U
LAO-C	1970	1	-1	4	-.05	-.05	-.00	-.00	-.00	-	-	-1000	1.200
LAO-C	1971	2	-1	3	-.05	-.05	-.00	-.00	-.00	-345	-	-1000	-.400
LAO-C	1972	4	-1	5	.06	.07	.13	-.00	-.00	-353	-	-1225	1.100
LAO-1	1967	1	-1	50	-.05	-.05	-.00	.19	-.00	-	-	-	1.300
LAO-1	1968	3	3	37	-.05	.08	-.05	.16	.32	-240	-	-	-.000
LAO-1	1969	3	-1	36	-.05	.06	-.00	-.00	-.00	-	-	-	.800
LAO-1	1970	4	-1	76	.05	-.00	-.00	-.00	-.00	-	-	-	.500
LAO-1	1971	4	1	94	.05	.27	-.00	-.00	-.00	-345	-	20750	.800
LAO-1	1972	4	1	127	.17	.18	-.05	-.00	-.00	-354	-	19575	.700
LAO-1.2	1969	2	1	5	-.05	-.05	-.00	-.00	-.00	-	-	-	.600
LAO-1.2	1970	1	-1	3	-.05	-.05	-.00	-.00	-.00	-	-	-	-.400
LAO-1.8	1969	2	1	5	-.05	-.05	-.00	-.00	-.00	-	-	-	1.000
LAO-2	1967	1	-1	91	-.05	-.05	-.00	.30	-.00	-	-	-	2.000
LAO-2	1968	3	3	59	-.05	.06	-.05	-.15	-.00	-250	-	-	1.600
LAO-2	1969	2	1	77	.10	.60	-.00	-.00	-.00	-	-	-	1.600
LAO-2	1970	3	-1	80	-.05	.14	-.00	-.00	-.00	-250	-	-	.600
LAO-2	1971	2	1	101	.15	.33	-.00	-.00	-.00	-340	-	52000	.900
LAO-2	1972	3	2	188	.09	.19	.12	-.00	-.00	-354	-	153300	2.700
LAO-3	1967	1	-1	45	-.05	.05	-.00	.19	-.00	-	-	214000	4.900
LAO-3	1968	3	2	61	.07	.08	-.05	.24	-.00	-240	-	125667	.800
LAO-3	1969	2	2	49	-.05	.06	-.00	-.00	-.00	-	-	350000	1.400
LAO-3	1970	4	2	56	-.05	.08	-.00	-.00	-.00	-230	-	73000	.930
LAO-3	1971	3	3	95	.07	.08	-.00	-.00	-.00	333	-	37667	1.200
LAO-3	1972	4	3	92	.10	.15	-.05	-.00	-.00	-355	-	186850	3.000
LAO-4	1967	1	-1	9	-.05	.06	-.00	-.00	-.00	-	-	222000	.800
LAO-4	1968	3	5	16	.05	.05	-.05	-.15	-.00	-240	-	61000	1.200
LAO-4	1969	2	-1	9	-.05	-.05	-.00	-.00	-.00	-	-	55500	.400
LAO-4	1970	1	-1	10	-.05	-.05	-.00	-.00	-.00	-	-	66000	-.400
LAO-4.5	1969	3	-1	5	-.05	-.05	-.00	-.00	-.00	-	-	43000	.700
LAO-4.5	1970	5	1	26	.06	.07	-.00	-.00	-.00	-	-	77750	.400
LAO-4.5	1971	3	1	5	.07	.08	-.00	-.00	-.00	-	-	24000	.700
LAO-4.5	1972	4	2	10	.09	.06	.05	-.00	-.00	-353	-	28175	1.300
LAO-5	1967	1	-1	4	-.05	-.05	-.00	-.00	-.00	-	-	126000	-.400
LAO-5	1968	2	1	8	-.05	.09	-.05	-.15	-.00	-240	-	70000	1.200
LAO-5	1969	2	-1	5	-.05	-.05	-.00	-.00	-.00	-	-	55500	.800
LAO-6	1968	1	2	18	.17	.25	-.00	-.15	-.00	-240	-	75000	.400
LAO-6	1969	1	-1	7	-.05	-.05	-.00	-.00	-.00	-240	-	51000	-.400

E. Storm Runoff DP - Los Alamos Canyon

A gaging station was constructed at the mouth of DP Canyon in the Spring of 1967. A second gaging station was established on Los Alamos Canyon above the junction with DP Canyon in the Spring of 1968. The following table presents a recap of flow events from 1970 through 1972 at each station.

Storm Runoff at DP-Canyon Gaging Station

Year	Month	No. of Events	Total Discharge m^3
1970	April	7 1/	5300
	May	1	615
	June	5	2220
	July	5	3945
	Aug	9	11590
	Sept	4	2465
1971	April	1	125
	July	9	22200
	Aug	3	11590
	Sept	4	6660
	Oct	4	10230
	Dec	1	6040
1972	July	3	740
	Aug	4	1480
	Sept	4	46000
	Oct	2	50500

1/ Snowmelt (7 day)

Storm Runoff at Los Alamos Gaging Station

Year	Month	No. of Events	Total Discharge m^3
1970	April	17 a/	44000
	June	3	2465
	July	4	6290
	Aug	9	51800
	Sept	8	9600
1971	July	5	13600
	Aug	1	615
	Oct	2	1970
1972	Sept	4	37000

a/ 17 days of snowmelt runoff

2. Transport of radionuclides in storm runoff

A study to determine transport of radionuclides in storm runoff was made at DPS-4 at the mouth of DP Canyon (Fig. 9).

Storm Runoff and Transport of Radionuclides in DP Canyon, Los Alamos County, New Mexico.[15]

ABSTRACT

Effluents from the waste treatment plant at Los Alamos Scientific Laboratory's Technical Area 21 are released into DP Canyon. The radionuclides remaining in the effluents are bound to stream-channel sediments which are later carried out of the canyon by storm runoff.

A study was made to determine the runoff volume, the suspended-sediment load, and the amount of radio-activity carried out of DP Canyon by storm runoff. During the summer of 1967, precipitation resulted in 23 runoff events that carried ≈88 000 kg of suspended sediments out of the canyon in ≈36 800 m^3 of water. Less than 74 μCi of gross alpha emitter and ≈40 100 μCi of gross beta were carried out of the canyon in solution. The suspended sediments carried out ≈70 μCi of gross alpha emitters and ≈11 300 μCi of gross beta emitters. About 31 000 μCi of ^{90}Sr left the canyon in solution, as did traces of ^{238}Pu, ^{239}Pu, and ^{241}Am.

Cumulative samplers to collect samples of storm runoff (water and suspended sediments) were installed in the wall of the gauging station at DPS-4 in 1967. Samples were collected of the runoff events during the summer of 1967 and 1968. The chemical quality of the water is shown on the following table.

Chemical Quality of Storm Runoff
(Average of a number of analyses, 1967 and 1968)

Year	No. of Analyses	Na	Cl	F	NO_3	TDS	Conductance	pH
1967	14	103	47	4.5	13	354	490	8.6
1968	10	125	38	4.1	6	343	550	11.6

Radiochemical analyses of surface runoff for the similar period are presented on the following table. The analyses indicate that some radionuclides are

being transported out of the canyon.

DP CANYON

SURFACE FLOW SAMPLING SITES

RADIOCHEMICAL QUALITY OF WATER

(FLOOD FLOW CONDITIONS)

SOURCE	YEAR	MAX. # SAMPLES	GROSS ALPHA	GROSS BETA	^{238}Pu	^{239}Pu	^{241}Am	^{226}Ra	^{234}U	^{137}Cs	^{90}Sr	^{3}H	^{238}U
DPS-4	1967	10	-2	1089	.16	.19	.27	-.15	1.09	-240	831	-	-.000
DPS-4	1968	15	4	770	.35	1.11	.91	-.15	3.44	328	444	-	-.000

Trace concentrations of radionuclides were detected in solution of the runoff at DPS-4, thus indicating the transport of radioactivity out of the effluent release area.

In 1968, cumulative samplers were installed in the stream channel in Los Alamos Canyon, one above the junction with DP Canyon and three below the junction. The runoff was collected from four events; however, plugging of the intake on some of the samplers during an event caused loss of sample for that station. The samples were collected to see if a measurable amount of radioactivity carried out of DP Canyon diluted with runoff in Los Alamos Canyon could be detected.

The average of a number of water samples from cumulative samplers at the four stations in Los Alamos are shown on the following table for the year 1968. The locations are shown on Fig. 12.

		Average of a number analyses - (picocuries per liter)			
Source	Number of Analyses	Gross Alpha	Gross Beta	^{238}Pu	^{239}Pu
LAS-1	4	<2	12	.08	.10
LAS-2	1	<2	220	<.05	.19
LAS-3	4	<2	288	<.05	.12
LAS-4	1	<2	830	.12	.17

Suspended sediments from the runoff were also analyzed and are shown on the following table for the year 1968.

Source	Number of Samples	Average of a number of analyses Picocuries per dry gram	
		Gross Alpha	Gross Beta
LAS-1	4	5	5
LAS-2	1	6	52
LAS-3	4	9	38
LAS-4	1	13	92

The results indicate that measurable amounts of radionuclides are found in solution and in the suspended sediments in Los Alamos Canyon, having been carried out of DP Canyon.

A series of samples were collected of storm runoff with a DH-48 sediment sampler at the gauging station in Los Alamos and DP Canyon in the summer of 1968. The samples were collected at intervals through an event. The discharge and sediment concentrations were determined. The fluids were separated from the suspended sediments and were analysed for gross alpha and gross beta activity. The investigation was made to determine if sediment and radioactivity changed with time through a runoff event. The following tables recaps the data.

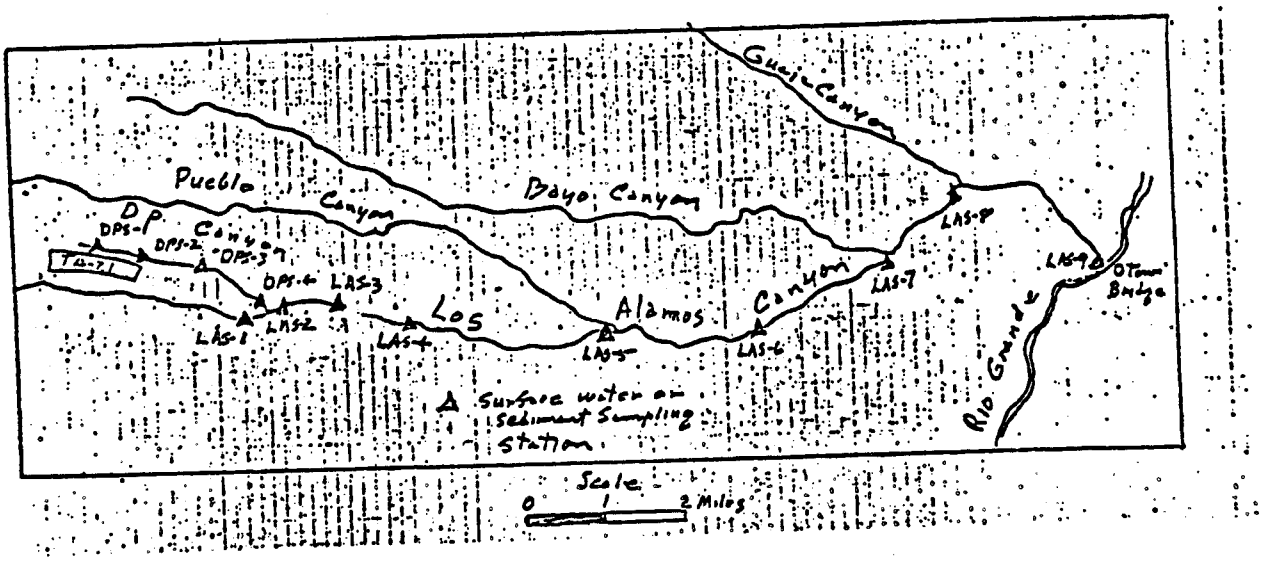

Fig. 12. Channel bed sediment sampling stations in DP-Los Alamos Canyons.

DP Canyon, July 30, 1968

Hour	Discharge (l/sec)	Suspended Sediment Concentration (mg/l)	In Solution (pCi/l) Gross Alpha	In Solution (pCi/l) Gross Beta	Suspended Sediment (pCi/g) Gross Alpha	Suspended Sediment (pCi/g) Gross Beta
14:50	1540	19,500	<1	1800	39	1120
15:00	1540	11,200	<1	1700	43	1050
15:30	1410	20,400	<1	1080	17	520
16:15	525	9,920	3	1360	15	670
17:00	270	4,010	0	1150	48	1170
18:20	165	1,340	14	1190	47	1680

A second set of samples were collected on July 31, 1968. Discharge, sediment concentrations and gross alpha and gross beta activity were determined from the sample in solution and in the suspended sediment. The results are presented as follows:

DP Canyon, July 31, 1968

Hour	Discharge (l/sec)	Suspended Sediment Concentration (mg/l)	In Solution (pCi/l) Gross Alpha	In Solution (pCi/l) Gross Beta	Suspended Sediment (pCi/g) Gross Alpha	Suspended Sediment (pCi/g) Gross Beta
13:50	56	1,080	<1	920	64	890
14:20	1730	43,000	<1	1080	9	260
14:30	1640	26,000	<1	820	14	300
14:45	2040	13,000	<1	770	10	350
14:50	1700	11,000	<1	860	52	390
15:00	1410	37,000	<1	1180	6	210
15:05	1260	37,000	3	1190	9	210
15:10	1220	48,000	8	1190	6	180
15:20	1190	27,000	<1	1090	7	220
15:30	1020	56,000	14	1220	4	140
15:40	570	4,900	8	1000	21	650

DP Canyon, July 31, 1968
(Continued)

Hour	Discharge (l/sec)	Suspended Sediments Concentration (mg/l)	In Solution (pCi/l) Gross Alpha	In Solution (pCi/l) Gross Beta	Suspended Sediments (pCi/g) Gross Alpha	Suspended Sediments (pCi/g) Gross Beta
15:50	480	4800	6	1100	79	610
16:00	490	4400	8	1070	16	650
16:10	480	4600	19	1120	20	520
16:20	440	2500	41	1060	15	790

A series of samples were collected from DP Canyon and Los Alamos Canyon above the confluence with DP for comparison on August 6, 1968.

DP and Los Alamos Canyon, August 6, 1968

Hour	Discharge (l/sec)	Suspended Sediments Concentration (mg/l)	In Solution (pCi/l) Gross Alpha	In Solution (pCi/l) Gross Beta	Suspended Sediments (pCi/g) Gross Alpha	Suspended Sediments (pCi/g) Gross Beta
DP Canyon						
15:35	690	24,000	19	1180	3	227
15:55	525	18,000	<1	920	3	191
16:15	450	7,700	3	710	4	300
16:30	305	5,900	11	800	93	324
16:45	240	5,400	3	740	2	280
17:00	210	2,800	8	730	4	420
17:15	160	1,700	3	760	10	580
17:30	135	1,800	14	840	2	590
17:45	120	1,000	3	832	<1	620
Los Alamos Canyon						
15:40	2040	20,000	6	16	6	6
16:10	1560	10,000	<1	14	8	6
16:25	1130	9,400	<1	11	4	6
16:45	880	6,800	<1	18	2	4
16:55	760	5,800	<1	18	3	6
17:15	680	4,200	11	17	5	7
17:40	590	4,800	<1	<1	<1	<1

Only trace concentrations of gross alpha activity were found in solution in the runoff in both DP and Los Alamos Canyons. Gross beta activity in solution and gross alpha and gross beta activity indicate transport of radionuclides out

of DP Canyon which receives industrial effluent. A comparison of the activity in the runoff of DP Canyon and Los Alamos Canyon indicates magnitude of measureable concentrations being transported. In general, the sediment concentrations decrease with discharge. In DP Canyon, the activity concentrations vary throughout the event.

F. Radiochemical Analyses of Sediments

Channel sediments in DP Canyon are derived from weathering of the Bandelier Tuff. Sediments in Los Alamos Canyon are derived from weathering of the Bandelier Tuff and Tschicoma Formation.

Particle-size distribution of channel sediments at stations are shown on the following table.

Particle-Size Distribution

(Percent by Weight)

Source	DPS-1	DPS-4	LAO-C	LAO-1	LAO-3
Granules	8.0	4.0	16.5	< 0.5	0.5
Sand					
Very Coarse	48.5	42.5	38.0	23.0	13.0
Coarse	29.0	36.0	32.0	53.0	40.0
Medium	8.0	10.5	10.5	18.5	23.5
Fine	3.0	4.5	2.0	4.0	11.0
Very Fine	1.5	1.0	.5	.5	4.5
Silt and Clay	2.0	1.5	.5	.5	7.5

Channel sediments were collected in DP Canyon in 1967 and 1968 for radiochemical analyses.

Source	Number of Samples	Average of a number of analyses Picocuries per dry gram. Gross alpha	Gross beta	^{238}Pu	^{239}Pu
DPS-1	2	16	536	.62	7.68
DPS-2	1	3	140	.12	1.32
DPS-3	1	2	122	.12	.79
DPS-4	3	3	29	.07	.65

The concentration of radioactivity and radionuclides in the channel sediments is greater near the effluent outfall from the treatment plant at TA-21 in DP Canyon with the concentrations decreasing downgradient in DP Canyon and Los Alamos Canyon to the Rio Grande. The radionuclides in the effluent are being adsorbed or exchanged with clay minerals in the channel sediments. Storm runoff is moving the sediments downgradient in the canyon dispersing them over a larger area. It appears that there is a build-up in the sediments near the effluent outfall during the fall, winter, and spring when storm runoff is at a minimum. Heavy thunder showers during the summer transport the sediments downgradient in the canyon so that a large build up of radionuclides at the outfall does not occur.

Channel sediments were collected from DP and Los Alamos Canyon in November, 1965 and analyzed for gross alpha, beta, and gamma activity. The results are shown in the following table.

Radiochemical Analyses of Sediments, November 1965

(Analyses in Counts per Minute per Dry Gram)

Location	Gross Alpha	Gross Beta	Gross Gamma
DPS-1	6	566	130
DPS-4	3	25	8
LAO-C	2	7	30
LAO-1	2	8	2
LAO-3	2	4	12
Rd-4	1	<1	< 1

A similar set of samples were collected and analyzed for gross alpha, gross beta, and plutonium in the spring of 1970. The results are shown on the following table.

Radiochemical Analyses of Sediments, February and March, 1970

(Analyses in picocuries per dry gram)

Location	Gross Alpha	Gross Beta	^{238}Pu	^{239}Pu
DPS-1	28	391	15.8	2.69
DPS-4	5	92	.219	1.40
LAO-C	2	1	< .001	< .001
LAO-1	1	4	.026	.101
LAO-3	2	9	.09	.189
LAO-4	2	12	.011	.153
LAO-6	2	9	.032	.364
Rd-4	2	8	.003	.845

Samples of sediments from the stream channel were collected in February 1970, from Los Alamos Canyon, one above the junction with DP Canyon and the rest downgradient to the Rio Grande (Fig. 12). The averages of the samples of the channel sediments are shown on the following table.

		Average of a number of samples Picocuries per dry gram			
Source	Number of Samples	Gross alpha	Gross beta	^{238}Pu	^{239}Pu
LAS-1	3	3	45	.07 1/	.87 1/
LAS-2	2	4	16	.08 1/	2.39 1/
LAS-3	4	3	61	.08 2/	.50 2/
LAS-4	3	12	124	.04 1/	.45 1/
LAS-5	3	2	16	.05	.16
LAS-6	2	2	9	.02	.56
LAS-7	2	1	11	.03	.16
LAS-8	2	2	6	.02	12

1/ Average 2 analyses

2/ Average 3 analyses

Samples were analyzed from two stations at LAO-3 and State Road 4 in 1971 and 1972.

Radiochemical Analyses of Sediments 1971 and 1972

(Analyses in picocuries per dry gram except as noted)

	LAO-3			Rd. 4		
	5/7/71	10/14/71	10/10/72	5/7/71	10/14/71	10/10/72
Gross Alpha	3	18	<1	2	<1	<1
Gross Beta	1	73	2	4	<1	6
^{238}Pu	.007	2.45	.037	.007	.003	.004
^{239}Pu	.961	1.36	.370	.112	.054	.004
^{137}Cs	—	103	7.3	—	3.4	4.6
Total Uranium	0.81	.16	.40	.09	.02	.33

The results of the analyses of channel sediments indicate that storm runoff is transporting radionuclides out of DP Canyon and into Los Alamos Canyon and probably measurable amounts to the Rio Grande.

G. Inventory of Plutonium in Channel Sediments

The inventory of plutonium was made of channel sediment of DP and Los Alamos Canyon to the Rio Grande. The physical characteristics of the channel used in computing the inventory for July 1968, August 1968, February 1970, and October 1972, are shown below.

Physical Characteristics of Channel

DP-Los Alamos Canyon

1. 0 to 1 800 m (DP Canyon)
   Width 1.5 m Depth 0.15 m
   Sp. g. 1.57 Weight 459 x 10^6 g

2. 1 800 m to 6 600 m (Los Alamos Canyon)
   Width 2.5 m Depth 0.15 m
   Sp. g. 1.57 Weight 2 832 x 10^6 g

Confluence Pueblo-Los Alamos to Rio Grande

1. Confluence to 4 800 m
   Width 3 m Depth 0.15 m
   Sp. g. 1.57 Weight 3 408 x 10^6 g

Physical Characteristics of Channel
(Continued)

Confluence Pueblo-Los Alamos to Rio Grande

2. 4 800 m to 7 2 00 m (Rio Grande)
Width 4 m Depth 0.15 m
Sp. g. 1.57 Weight 2 261 x 10^6 g

The concentrations of plutonium at each station, average at each station, and total amount at each section are presented in the following table.

Concentrations and Total Plutonium in Sections of Channel

DP-Los Alamos Canyon (May, 1968)

Section	Station	Concentration µCi/g	Concentration Ave.	Total mCi	% of Total Pu
0-1 800	DPS-1	16.20			
	DPS-4	.84	8.5	3.9	78
1 800-6 600	LAS-3	.65			
	LAS-5	.15	.40	1.1	22
TOTAL		—	—	5.0	100

Los Alamos Canyon (July, 1968)

1 800-6 600	LAS-2	4.39			
	LAS-3	.72			
	LAS-4	.68			
	LAS-5	.22	1.5	0.4	—
TOTAL		—	—	0.4	

DP-Los Alamos Canyon (August, 1968)

0-1 800	DPS-1	0.41			
	DPS-2	1.44			
	DPS-3	.91			
	DPS-4	.88	0.91	.4	27
1 800-6 600	LAS-2	.60			
	LAS-3	.37			
	LAS-4	.30			
	LAS-5	.23	.38	1.1	73
TOTAL		—	—	1.5	100

Concentrations and Total Plutonium in Sections of Channel
(Continued)

DP-Los Alamos Canyon (February, 1970)

Section	Station	Concentration µCi/g	Concentration Ave.	Total Pu mCi	% of Total Pu
0-1 800	DPS-1	18.4			
	DPS-4	1.62	10.1	4.6	81
1 800-6 600	LAS-2	.198			
	LAS-3	.156			
	LAS-4	.396			
	LAS-5	.848	0.4	1.1	19
TOTAL		--	--	5.7	100

DP-Los Alamos Canyon (October, 1972)[1]

0-1 800	DP-5	0.76			
	DP-6	19			
	DP-7	.93	6.9	3.2	86
1 800-6 600	DP-9	.20			
	DP-10	.30			
	SR-4	.01	.17	.5	14
TOTAL		--	--	3.7	100

1/ DP Series Ecology Section

Los Alamos Canyon [Confluence LA-Pueblo to Rio Grande] (May, 1968)

Confluence-4 800	LAS-6	.62			
	LAS-8	.34	.48	1.6	62
4 800-7 200	LAS-8	.34			
	LAS-9	.24	.29	1.0	38
TOTAL		--	--	2.6	100

Los Alamos Canyon [Confluence LA-Pueblo to Rio Grande], (August, 1968)

Confluence-4 800	LAS-6	.53			
	LAS-8	.02	.28	1.0	100
4 800-7 200	LAS-8	.02			
	LAS-9	<.01	.01	<.02	--
TOTAL		--	--	1.0	100

Los Alamos Canyon [Confluence LA-Pueblo to Rio Grande] (February, 1970)

Confluence-4 800	LAS-6	.860			
	LAS-7	.338	.60	2.0	65
4 800-7 200	LAS-8	.591			
	LAS-9	.364	.48	1.1	35
TOTAL		--	--	3.1	100

The inventories are considered in DP Canyon (0-1800 m) and Los Alamos Canyon (1800 to 6600) to the confluence with Pueblo Canyon, Recap is as follows:

	Total Plutonium (mCi)				
Section (m)	May 1968	July 1968	Aug. 1968	Feb. 1970	Oct. 1972
0-1 800	3.9	—	.4	4.6	3.2
1 800-6 600	1.1	0.4	1.1	1.1	.5
TOTAL	5.0	—	1.5	5.7	3.7

The inventory in DP-Los Alamos Canyon for 1968 reflects the transport by storm runoff. The May concentrations decrease through August as the material containing plutonium moves out into Los Alamos Canyon with summer runoff. The channel in this reach (0-1 800) has a very thin alluvium cover and a steep gradient. Runoff is above normal due to the developed area. In the lower reach (May, 1968, February, 1970 and October, 1972), the transport appears to have equalized, with input equal to output.

The inventory in the canyon in May, 1968, indicates that from the outfall to the confluence with Pueblo only 5.0 mCi or 21% of the 24.1 mCi (1952-1967) released remains in the Canyon. In August, only 1.5 mCi or 6% of the 24.1 mCi remained. Transport out of this reach of the canyon by storm runoff for the year was about 3.5 mCi. In February, 1970, about 5.7 mCi or 21% of the 27.3 mCi (1952-1969) of plutonium remained in this reach. The October 1972 sampling indicated about 3.7 mCi or 8% of 30.8 mCi (1952-1972) remained in the canyon.

The inventories are considered in Los Alamos Canyon from the junction of Pueblo Canyon to the Rio Grande (0-7 200 m). The recap of the total amount of plutonium in the two sections in this reach of channel are as follows:

Los Alamos Canyon from Junction with Pueblo to Rio Grande

Section (m)	Total Plutonium (mCi) May 1968	Aug. 1968	Feb. 1970
0-4 800	1.6	1.0	2.0
4 800-7 200	1.0	<.02	1.1
TOTAL	2.6	≈1.0	3.1

The inventory in Los Alamos Canyon from the confluence of Pueblo to the Rio Grande in May 1968, was 2.6 mCi which decreased to ≈1.0 in August with the transport of plutonium with summer runoff.

The inventory of February 1970, combining both DP-Los Alamos (5.7 mCi) and Acid-Pueblo (18.1 mCi) and below the confluence (3.1 mCi), indicates a total of 26.9 mCi of plutonium in the three separate reaches ≈14% of the amounts released into DP-Los Alamos (27.3 mCi, 1952-1969) and Acid-Pueblo (170 mCi, 1943-1964). If one considers the inventory in each of the three segments of the three canyons or combinations of segments and assumes all plutonium is tied up in the sediments, the loss of plutonium or transport to the Rio Grande is about 80 to 90% of all plutonium released from the treatment plants.

H. Flood Frequency and Maximum Discharge

Los Alamos Canyon heads on the flanks of the Sierra de los Valles at an altitude of about 3170 m. The flood frequency and maximum discharges at boundary are based on the following data.

Drainage Area - 27.5 km^2

Main Channel Slope - 0.040

Frequency Frequency	Maximum Discharge (m^3/sec)
2-year	3.0
5-year	6.8
10-year	11
25-year	16
50-year	20

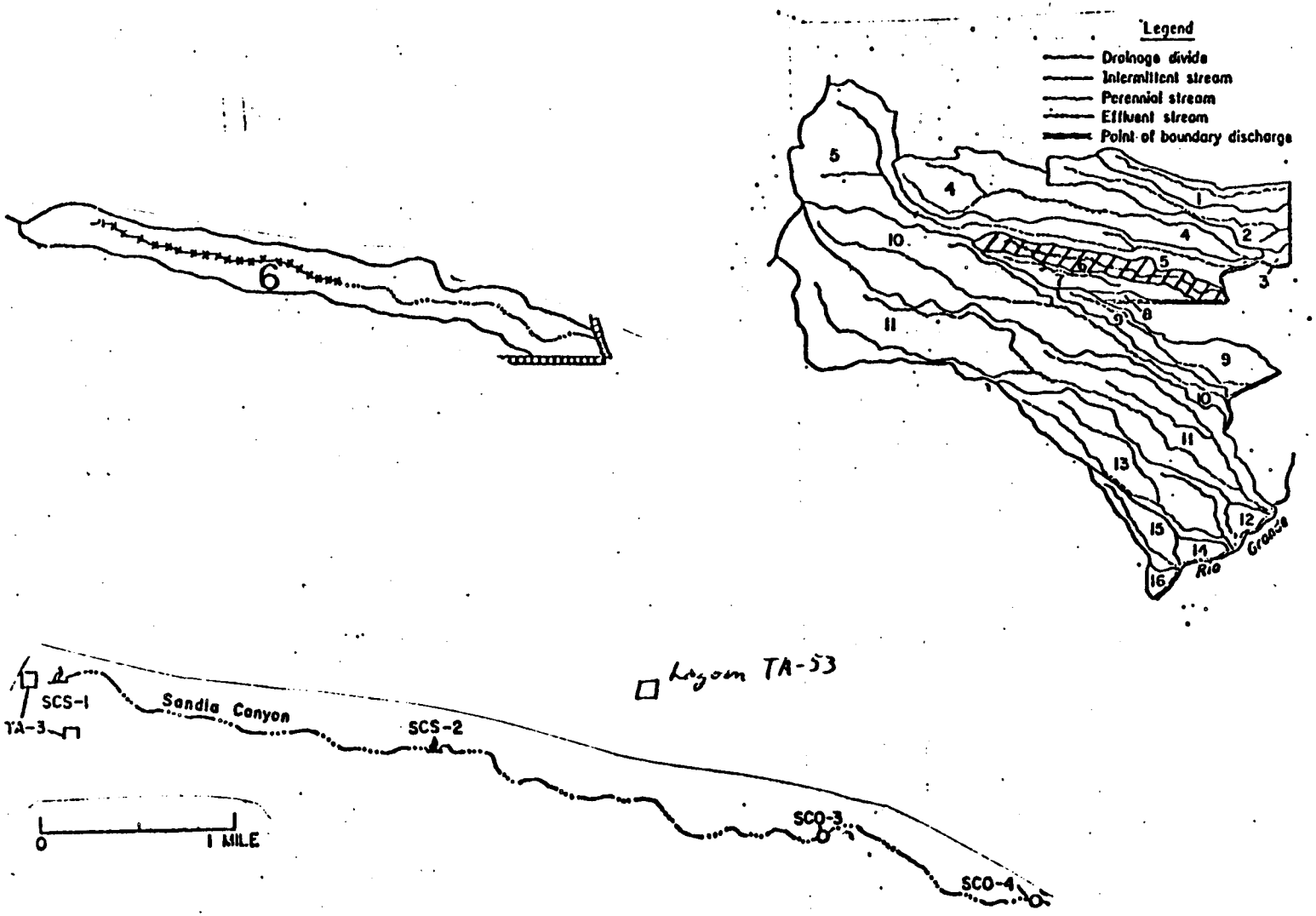

Fig. 13. Drainage Area 6 (Sandia Canyon) showing sampling stations.

VII. DRAINAGE AREA 6 (SANDIA CANYON)

Sandia Canyon heads on the Pajarito Plateau and is tributary to the Rio Grande. The alluvium in the upper reach of the canyon is thin in the western part of the plateau, but thickens to about 12 m at State Road 4. The alluvium is underlain by the Bandelier Tuff.

The stream in the upper reach of the canyon is perennial from the release of effluents from the sewage treatment plant and power plant at TA-3 (Fig. 13). The flow extends eastward to near the center of the plateau where all flow is lost to evapotranspiration or infiltration into the underlying tuff. Only during heavy thundershowers during the summer does the intermittent storm runoff extend in the canyon across the plateau to the Rio Grande.

A. Industrial Waste Treatment Plants

The sewage treatment plant serves the office-type complex of laboratories and shops that are centrally located in the TA-3 area. About 75 percent of the effluent is cycled into the power plant for cooling purposes. The combined release of effluents from the sewage treatment and power plant is about 2.3×10^5 m^3 of effluent per year into Sandia Canyon. Sewage lagoons at TA-53 are located on the mesa between Sandia and Los Alamos Canyons. Overflow from the lagoons does not reach the channel in either of the canyons.

B. Surface Water

Effluents from the treatment plants and surface water are sampled at two stations, SCS-1 and SCS-2 (Fig. 13).

1. Chemical Quality of Surface Water

The chemical quality of water at SCS-1 below the outfall from both treatment plants reflects the quality of effluent released into the canyon. As shown on the following table, the quality of the water improves downgradient in the stream.

Chemical Quality of Surface Water, 1969-1972
(Average of a number of analyses in mg/l except as noted)

Station	SCS-1	SCS-2
No. of Analyses	12	12
Sodium	200	150
Chloride	282	66
Fluoride	27.5	3.6
Nitrate	18	17
Total Dissolved Solids	1260	730
Conductance a/	1515	730
pH b	6.4	7.1

a/ Micromhos
b/ No Units

The following table presents averages of analyses by years of the two stations.

Chemical Quality of Surface Water
(Average of a number of analyses in mg/l except as noted)

Source	Year	No. of Analyses	Na	Cl	F	NO_3	TDS	Conductance a/	pH b/
SCS-1	1969	1	375	45	55	<.4	1738	1120	7.7
SCS-1	1970	3	104	55	.3	28	826	690	6.9
SCS-1	1971	4	206	49	2.1	22	1565	3465	5.6
SCS-1	1972	4	117	48	52	22	913	785	5.5
SCS-2	1969	1	190	50	6.0	12	680	720	7.9
SCS-2	1970	3	153	75	1.7	25	850	840	7.3
SCS-2	1971	4	153	75	2.5	22	795	850	7.6
SCS-2	1972	4	107	64	4.2	4.2	591	510	5.6

a/ Micromhos at 25° C
b/ No Units

The chemical treatment of water for use at the power plant resulted in release of hexavalent chromate. The use of chromate in treatment of water for cooling at the power plant was discontinued in April 1972. The concentrations varied downgradient in the channel, showing no apparent trends.

Hexavalent Chromate in Surface Water

(Average of a number of analyses in mg/l)

Station	Year	No of Analyses	Hexavalent Chromate
SCS-1	1969	1	0.07
SCS-1	1970	4	8.5
SCS-1	1971	2	11.2
SCS-1	1972	4	.18
SCS-2	1969	1	2.4
SCS-2	1970	4	5.4
SCS-2	1971	2	7.3
SCS-2	1972	4	1.3

Select trace metal ion analyses were made of water from the two stations. The following table shows some metal ions in the surface water that are probably the result of treatment of the water used in the cooling process at the Power Plant.

METAL ION ANALYSES

(Range and average of a number of analyses in µg/l)

Station	SCS-1[a] Min	SCS-1[a] Max	SCS-1[a] Av	SCS-2[b] Min	SCS-2[b] Max	SCS-2[b] Av
In Solution						
Cadmium	<0.25	18.8	8.6	0.4	6.8	3.2
Beryllium	<0.25	—	<0.25	<0.25	0.28	0.27
Lead	<1.0	25.0	7.5	<1.0	2.5	1.5
Mercury	< .02	—	<	<0.02	—	<0.02
Particulates						
Cadmium	<0.25	2.8	1.4	<0.25	0.56	0.36
Beryllium	<0.25	—	<0.25	<0.25	—	<0.25
Lead	<1.0	11.9	8.1	<1.0	1.8	1.2
Mercury	<0.02	0.32	0.15	<0.02	0.43	0.18

a/ Four analyses

b/ Three analyses

2. Radiochemical Quality of Surface Water

The radiochemical analyses of surface water from stations SCS-1 and SCS-2 showed only traces of radionuclides which may have been released with sewage influent from laboratories in the TA-3 complex. The following table presents an annual average of radionuclides for the years 1969 through 1972.

SANDIA CANYON

(Average of a number of analyses in pCi/l except as noted)

SURFACE FLOW SAMPLING SITES

RADIOCHEMICAL QUALITY OF WATER

SOURCE	YEAR	MAX. # SAMPLES	GROSS ALPHA	GROSS BETA	^{238}Pu	^{239}Pu	^{241}Am	^{226}Ra	^{234}U	^{137}Cs	^{90}Sr	^{3}H	23
SCS-1	1969	1	-1	8	-.05	-.05	-.00	-.00	-.00	-	-	8700	3.1
SCS-1	1970	5	-1	14	.06	.05	-.00	-.00	-.00	-	-	32600	-.4
SCS-1	1971	4	1	16	.07	.07	-.00	-.00	-.00	-230	-	4675	2.1
SCS-1	1972	4	1	17	.11	.06	-.00	-.00	-.00	-150	-	3350	1.2
SCS-2	1969	1	-1	11	-.05	-.05	-.00	-.00	-.00	-	-	710[illegible]	-.4
SCS-2	1970	5	-1	11	-.05	-.05	-.00	-.00	-.00	-	-	170	-.4
SCS-2	1971	4	-1	11	-.05	-.05	-.00	-.00	-.00	-240	-	7[illegible]	-.4
SCS-2	1972	4	1	16	.08	.06	.07	-.00	-.00	753	-	4[illegible]	1.2

a/ Analyses in µg/l

C. Water in Alluvium

Two observation holes were drilled into the alluvium (SCO-3 and SCO-4) in the middle and lower reach of the canyon. They did not encounter any water. After storm runoff in the canyon in early September, 1969 water did infiltrate into the alluvium near hole SCO-4 and a sample was collected and analyzed.

1. Chemical Quality of Water in Alluvium

The chemical quality of the water in the alluvium recharged from storm runoff showed some effects from the effluent released from the power plant with the presence of chromate.

Analyses of Water in Alluvium at SCO-4

(Sept. 1969, mg/l except as noted)

Sodium	Chloride	Fluoride	Chromate	Nitrate	Dissolved Solids	Conductance [a]
80	15	<0.1	0.18	1.3	320	350

[a] micromhos

2. Radiochemical Quality of Water in Alluvium

The radiochemical analyses indicated only background amounts of radionuclides.

Radiochemical Analyses of Water in Alluvium at SCO-4

(Sept. 1969, in pCi/l except as noted)

Gross Alpha	Gross Beta	^{238}Pu	^{239}Pu	^{3}H	Total Uranium [a]
<1	2	<0.05	<0.05	$<4 \times 10^{3}$	0.4

[a] Micrograms per liter

D. Radiochemical Analyses of Sediments

Sediments from the stream channel have been collected for particle size distribution analysis. The particle size distribution of sediments at stations are shown on the following table.

Grade	Stations (Distribution by weight) Near SCS-2	Near SCO-4	State Road 4
Granules	20.5	9.0	6.0
Sand			
Very Coarse	23.0	22.5	12.0
Coarse	35.0	43.5	44.0
Medium	15.0	14.0	19.0
Fine	4.5	6.5	11.0
Very Fine	1.0	2.5	4.0
Silt and Clay	1.0	2.0	4.0

Sediments from the stream channel near SCS-2, SCO-3 and at State Road 4 were collected for analyses in 1965 and 1970. The results of the analyses indicate only background amounts of radionuclides.

Radiochemical Analyses of Sediments

(Analyses in pCi/g except as noted)

Source (Near)	Year	Gross Alpha	Gross Beta	^{238}Pu	^{239}Pu
Power Plant	1970	1	2	<0.001	0.004
SCS-2 [a]	1965	1	2	—	—
SCS-2	1970	2	1	<0.001	<0.001
SCS-3 [a]	1965	1	17	—	—
SCS-3	1970	1	< 1	<0.001	<0.001
State Rd 4 [a]	1965	2	<1	—	—
State Rd 4	1970	2	2	<0.001	0.003

[a] Counts per minute per dry gram

E. Flood Frequency and Maximum Discharge

Sandia Canyon heads on the Pajarito Plateau at an altitude of about 2290 m and is tributary to the Rio Grande. The flood-frequency and maximum discharge at the boundary are based on the following data:

Drainage Area 7.0 km^2

Main Channel slope 0.028

Frequency	Maximum Discharge (cubic ft per second)
2-year	2.0
5-year	5.4
10-year	8.5
25-year	16
50-year	18

VIII. Drainage Area 7 (Mortandad Canyon

Mortandad Canyon heads on the Pajarito Plateau and is tributary to the Rio Grande (Fig. 14). The main industrial treatment plant at TA-50 releases effluent into the canyon. The plant began treating liquid waste in 1963. The plant releases 54 x 10^3 m^3 of effluent annually into the canyon. An additional 26 x 10^3 to 125 x 10^3 m^3 of waste water from TA-48, New Sigma and storm runoff enter the canyon annually. The stream in the upper reach of the canyon is perennial from the release of industrial effluents and cooling water. Storm runoff adds to the volume of flow; however, since 1960, when hydrologic observations began, all storm runoff as well as effluent has infiltrated into the alluvium west of the discharge boundary due to the small drainage area and large volume of unsaturated alluvium. The alluvium in the canyon thickens from less than 1 m

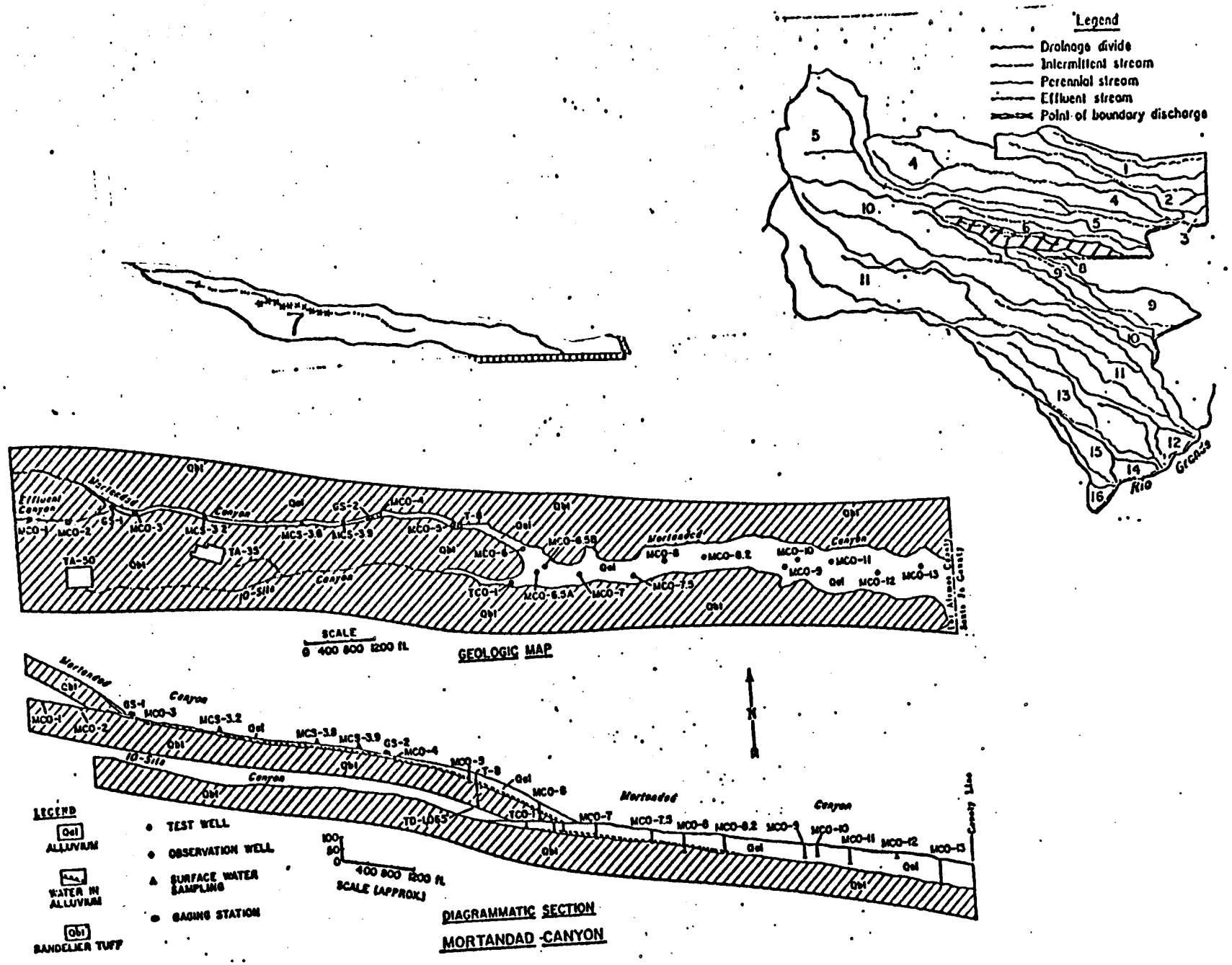

Fig. 14. Drainage Area 7 (Mortandad Canyon) showing geology and sampling stations.

in the upper reaches to more than 40 m at the boundary.

The perennial flow from the effluents and intermittent storm runoff recharges a small body of water in the alluvium that is perched on the underlying tuff. As the water in the alluvium moves eastward, steady losses to evapotranspiration with minor losses into the tuff occur so that the water in the alluvium is of limited extent and does not extend to the surface water discharge boundary at the Santa Fe-Los Alamos County line.

B. Geologic and Hydrologic Investigations

Prior to release of effluents into Mortandad Canyon, studies were made to determine the geologic and hydrologic characteristics of the canyon in regard to the disposal of low-level radioactive liquid wastes. A series of additional studies have been made in the canyon as it receives the bulk of the effluent from the treatment wastes generated by the laboratory. An abstract of the results from these reports is presented in the following section.

1. Preliminary Report of the Geology and Hydrology[16]

The preliminary report (1963) summarizes the studies October 1960 through June 1961

ABSTRACT

The U.S. Geological Survey, in cooperation with the U.S. Atomic Energy Commission and the Los Alamos Scientific Laboratory, selected the upper part of Mortandad Canyon near Los Alamos, New Mexico as a site for disposal of treated, liquid, low-level radioactive waste. This report summarizes the part of a study of the geology and hydrology that was done from October 1960 through June 1961. Additional work is being continued.

Mortandad Canyon is a narrow, east-southeast-trending canyon about 9-1/2 miles long that heads on the central part of the Pajarito Plateau at an altitude of about 7,340 feet. The canyon is tributary to the Rio Grande. The drainage area of the part of Mortandad Canyon that was investigated is about 2 square miles, and the total drainage area is about 4.9 square miles.

The Pajarito Plateau is capped by the Bandelier Tuff of Pleistocene age. Mortandad Canyon is cut in the Bandelier, and alluvium covers the floor of the canyon to depths ranging from less than 1 foot to as much as 100 feet. The Bandelier is underlain by silt, sand, conglomerate, and interbedded basalt of the Santa Fe Group of Miocene, Pliocene, and Pleistocene age. Some ground water is perched in the alluvium in the canyon; however, the top of the main aquifer is in the Santa Fe Group at a depth of about 990 feet below the canyon floor.

Joints in the Bandelier Tuff probably were caused by shrinkage of the tuff during cooling. The joints range from hairline cracks to fissures several inches wide. Water can infiltrate along the open joints where the Bandelier is at the surface; however, soil, alluvial fill, and autochthonous clay inhibit infiltration on the tops of mesas, and probably in the alluvium-floored canyons, also.

Thirty-three test holes, each less than 100 feet deep, were drilled in 10 lines across Mortandad Canyon from the western margin of the study area to just west of the Los Alamos-Santa Fe county line. Ten of the holes were cased for observation wells to measure water levels and collect water samples from the alluvium. Twenty-three of the holes were cased to seal out water and were used as access tubes to accomodate a neutron-neutron probe for determining the moisture content of the alluvium and tuff.

The source of recharge for the perched ground-water body in the alluvium in Mortandad Canyon is the precipitation in the drainage area of the canyon. During the winter of 1960-61, a snowpack 1-2 feet thick accumulated in the narrow shaded upper part of the canyon. The alluvium beneath the snowpack received some recharge because of diurnal melting during the winter. In March 1961 the snow-melt water saturated most of the thin alluvium in the upper part of the canyon, and a surface stream began to flow. The maximum flow of the surface stream was about 250 gpm (gallons per minute). Water from the stream infiltrated into the alluvium at the front of the surface stream and in the reach upstream from the front. A ground-water mound was formed beneath the channel by water infiltrating from the stream. The front of the surface stream and the front of the ground-water mound advanced eastward to about the middle of the area studied. From this point eastward, the alluvium is thick enough to absorb and transmit the amount of flow in 1961. Late in April the front of the surface stream retreated, and by the first of May the surface flow stopped. During and after this period the ground-water mound decayed, and ground-water levels dropped in the upper part of the canyon as water drained into the channel and downgradient through the alluvium.

The amount of recharge was small in the wide lower part of the canyon during the period of study. The rise in ground-water levels and the increase in moisture content of the alluvium in the lower part of the canyon indicate that water moved downgradient by underflow through the alluvium from the recharge area in the upper part of the canyon. Moisture measurements indicate that only a little water moved into the underlying Bandelier Tuff from the saturated alluvium in the part of the canyon studied.

A deep test well was drilled in Mortandad Canyon near the middle of the area studied. The top of the main aquifer in the well was between the depths of 985 and 990 feet below the bottom of the canyon. The water rose almost 30 feet in the well, indicating that confining beds exist in the lower part of the Puye Conglomerate. The piezometric surface of the main aquifer slopes eastward,

indicating that the main aquifer is recharged mainly west of the Pajarito Plateau, and that it discharges the water near the Rio Grande. Samples of water from the main aquifer and the alluvium had no radioactivity above that of a standard sample of water.

The infiltration and movement of waste liquid will follow the same general pattern as that of the perched ground water in the alluvium. The liquid will infiltrate in the upper and middle reaches of the part of the canyon studied and move eastward through the alluvium. The data indicate that the alluvium in the lower reach will absorb and transmit the predicted discharge of 500,000 gallons of waste per week. Little of the liquid will move downward into the Bandelier Tuff in the area studied, and probably none will reach the main aquifer in the Santa Fe Group. The movement of ground-water in the part of the canyon east of the Los Alamos-Santa Fe County line was not determined.

The clay in the alluvium probably will remove most of the radioactive waste material by sorption and base exchange. This might eventually build up relatively high concentrations of radioactive material which would move slowly downgradient through the alluvium. Further work will be necessary, before and after waste is discharged from the plant, to obtain quantitative hydrologic data and to determine the movements of the water in the alluvium below the area studied.

A progress report was issued in 1964 covering the period 1961 to June 1963. Data included are surface water records, quality of water prior to the release of effluents as well as radiochemical analyses of sediments from the stream channel and observation holes.[17]

2. Distribution of Radioactivity in Alluvium[18]

A short paper was prepared in 1966 which describes radioactivity in the alluvium of Mortandad Canyon.

ABSTRACT

Fine particles in alluvial material in a disposal area for liquid radioactive wastes at Los Alamos have greater affinity for radionuclides than coarse particles; however, most of the radioactivity is in the coarse material, which is more abundant. The radioactivity in the alluvium is dispersed by waste water and storm runoff and decreases with distance from the point of effluent outfall. Most of the radionuclides are retained in the upper 3 feet of the deposits, resulting in very little change in the quality of the ground water perched in the alluvium.

3. Disposal of Industrial Effluents in Mortandad Canyon[19]

A report was submitted in 1967 describing a study to determine the movement of effluents in Mortandad Canyon and evaluate the possibility of contamination of surface and ground water outside the canyon disposal area.

ABSTRACT

Mortandad Canyon is cut into the Bandelier Tuff, which forms the Pajarito Plateau. The drainage area above and within the disposal area is small. The alluvium is thin in the upper canyon but thickens eastward into the middle and lower canyon.

The canyon has no natural perennial streamflow. Surface water entering the disposal area is storm runoff, waste water from cooling process at New Sigma and TA-48, and industrial effluents from the waste treatment plant at TA-50. The storm runoff, waste water and effluents infiltrate into the alluvium to recharge a body of water perched in the alluvium overlying the tuff. As the water moves through the alluvium some is lost to evapotranspiration while the remainder infiltrates into the tuff.

An inventory of surface water and water in the alluvium from July 1963 to June 1965 indicated that a greater amount of water was lost into the tuff in the upper canyon than in the middle and lower canyon of the disposal area becuase the alluvium overlying the tuff in the upper canyon is more permeable (silty sand) than the alluvium overlying the tuff in the middle and lower canyon (sandy silt). The movement of water in the tuff is downward beneath the disposal area into the unsaturated volcanic rocks and sediments of the Puye Conglomerate.

The upper part of the main aquifer in the Los Alamos area is in the Puye Conglomerate, about 1,000 feet beneath the canyon floor. The water in the main aquifer is moving at about 70 feet per year toward the Rio Grande. The Rio Grande, about 6 miles east of the disposal area, is the natural discharge for the main aquifer.

The chemical and radiochemical quality of water in the alluvium improves downgradient in the disposal area due to dilution of the effluent by storm runoff and waste water, and by adsorption of certain ions and radionuclides by clay minerals. Water in the main aquifer showed no sign of chemical or radiochemical contamination.

The geology and hydrology of Mortandad Canyon is ideal for the disposal of low-level radioactive effluents. The small drainage area and the volume of alluvium (to absorb the storm runoff) reduces chances for storms to flush contaminates to the Rio Grande. Chemical and radiochemical contamination is confined to the disposal area. The disposal area has an environment that reduces the contamination in the effluents, and the slow movement of water in the main aquifer beneath the disposal area would allow ion-exchange and half life decay of any radionuclides

that should reach the aquifer, so that no contamination would remain in the water when it reached its natural discharge area.

4. Occurance of Tritium in the Shallow Alluvial Aquifer, 1966-1969 [20]

The occurance and dispersion of tritium in water in the alluvium was described in a section of a 1973 report.

ABSTRACT

Tritium was detected in the stream-connected aquifer in the alluvium of the canyon. Concentrations were greater in the lower part of the canyon. The tritium was probably residual from liquid waste released in early operations of the treatment plant at TA-50 (1963 through 1966) or from TA-35 in the late 1950's or early 1960's.

It was estimated in February 1967 that storage of water in the alluvium in the lower canyon was about 19.0 million liters. The average tritium concentration (MCO-6, MCO-7, MCO-7.5, and MCO-8) for February was 490 pCi/ml; thus, it was estimated that the water in storage contained about 9.3 Ci of tritium. In May 1969 the storage was estimated at 14.4 million liters with an average tritium concentration of 80 pCi/ml or about 1.2 Ci of tritium in the total water in storage.

The tritium concentrations decrease with time due to the dilution of the water with the inflow of waste effluents and storm runoff into the alluvium and tritium losses to evapotranspiration.

5. Dispersion and Movement of Tritium in the Shallow Aquifer [21]

A report in 1974 describes the movement and dispersion of tritium in ground water in the alluvium.

ABSTRACT

Twenty (20) Ci of tritium discharged into Mortandad Canyon in November 1969 were used to determine the dispersion and movement of the tritium in a shallow aquifer in the alluvium. It took 388 days for the peak concentration to move 3,027 m from the effluent outfall to the eastern end of the aquifer. The concentration decreased from 77,700 pCi/ml to 310 pCi/ml in that distance. Ground water in transit storage contained about 0.9 Ci of tritium prior to the release of the 20 Ci. About 3.9 Ci of tritium remained in transit storage at the end of 1970. The remaining 17.0 Ci were lost with evapotranspiration, infiltration with ground water into the underlying tuff, or suspended with soil moisture above the aquifer.

The rate of movement of water in the alluvium and field coefficient of permeability were described for the three sections of the canyon using tritium and chloride ion as tracers.

Canyon Location	Type of Unit	Velocity of Tracers (m/day)	Coefficient of Permeability (m/da
Upper	Coarse Sand	18	141
Middle	Silty-Sand-Clay	5	50
Lower	Silty-Sand-Clay	2	7.6

B. Industrial Waste Treatment

Liquid wastes, products of research by the Los Alamos Scientific Laboratory, are treated at the waste treatment plant at TA-50. The liquid wastes contain a varying amount of chemical and radiochemical constituents. However, the treatment of the influents to reduce harmful contamination is about the same regardless of the chemical and radiochemical quality of the liquid wastes. The chemical composition of the influent is changed by the addition of certain chemicals during treatment.

The chemicals are added at several stages during treatment. Sodium hydroxide is added to the liquid wastes as it arrives at the plant to neutralize the acid and to raise the pH. Ferric sulfate and calcium hydroxide are added as the influent enters flocculator clarifiers; this precipitates out the radioactivity that was carried in suspension or was otherwise insoluble. The precipitate is collected as a sludge in settling basins, dried, mixed with vermiculite, placed in barrels, and buried in disposal pits on the plateau. Flocculation removes most of the plutonium and fission products. If, however, the liquid waste still contains excessive radioactivity it is acidized with nitric acid and passed through ion exchange columns where artificial resins remove most of the remaining radionuclides, generally strontium 90, cesium 137, and other fission products. The waste is again treated with sodium hydroxide to raise the pH to about 11 before transfer to holding tanks prior to disposal.

Concentrations of sodium, calcium, carbonate, bicarbonate, nitrate, and chlorides, as well as total dissolved solids, are higher than found in native waters. If the wastes are acidized for the ion-exchange columns, high nitrate and conductivity are characteristic of the effluent.

Careful control is maintained throughout the entire treatment operation by frequent collection and analysis of the influent at the different stages of treatment. The resulting effluent is discharged into the disposal area when the radioactivity is less than 10 percent of the MPC (maximum permissible concentration) as recommended by the International Committee on Radiation Protection.

1. Chemical Quality of Effluent

The liquid wastes vary in chemical and radiochemical constituents when they arrive at the plant; however, the resulting effluents reflect the chemical treatment of a weekly composite, as shown on the following table.

Chemical Quality of Effluents [a]

(Analyses in mg/l except where noted)

	1963	1964	1965	1966	1967	1968	1969	1970	1971	1972
Calcium	40	37	20	56	129	167	25	32	48	12
Magnesium	3	< 1	4	< 1	< 1	< 1	1	5	2	2
Sodium	96	280	205	135	100	135	2250	500	740	215
Carbonate	139	280	290	130	230	340	2350	158	120	20
Bicarbonate	199	370	415	160	320	448	2610	282	720	290
Chloride	10	37	25	19	10	24	52	35	140	10

Chemical Quality of Effluents[a]
(Analyses in mg/l except where noted)
(Continued)

	1963	1964	1965	1966	1967	1968	1969	1970	1971	1972
Fluoride	2	2	3	1	3	2.6	.2	.9	3.2	< .1
Nitrate (n)[b]	3	29	6.0	7	7.9	6.0	74	223	280	52.8
Cyanide	< 1	< 1	< 1	< 1	< 1	< 1	< 1	< 1	< 1	< 1
Total Dissolved Solids							4258	2132	2118	768
Conductance[c]	760	1980	1760	1280	1380	2090	4500	2400	2520	1140
pH[b]	11.3	11.6	11.5	11.5	11.4	11.7	12.1	10.9	9.7	8.9

a/ Weekly Composite, 1st week of July, filter Sample; if ion-exchange column used, nitrate and calcium higher.

b/ N x 4.4 = NO_3

c/ Micromhos

d/ No Units

The average annual chemical quality of the effluents is presented in the following table.

The Average Annual Chemical Quality of Industrial Effluent from TA-50.

Effluent TA-50	Chemical Constituents											
	Milligrams per liter											
Year	Calcium (Ca)	Magnesium (Mg)	Sodium (Na)	Carbonate (CO_3)	Bicarbonate (HCO_3)	Chloride (Cl)	Fluoride (F)	Nitrate (NO_3)	Dissolved solids	Total hardness	Specific conductance (μmhos at 25°C)	pH
1963[a]	52	1.4	188	302	376	28	1.7	63	830	135	1730	11.6
1964	36	0.9	219	280	386	41	2.5	97	960	94	1950	11.6
1965	40	0.8	196	278	367	30	2.2	131	860	109	2070	10.9
1966	52	3.2	151	213	292	17	1.4	50	660	145	1280	11.4
1967	110	3.1	120	226	306	21	2.3	55	570	289	1520	11.2
1968	100	2.7	153	265	353	28	3.2	63	618	259	1630	11.2
1969	91	2.3	286	300	428	34	2.7	131	940	235	1990	11.2
1970	56	4.8	406	354	472	38	2.1	551	1500	155	2340	11.2
1971	42	3.9	433	218	641	169	2.7	372	1590	120	2450	9.2
1972	30	3.6	571	91	506	108	1.2	766	1670	91	2570	8.8

A measure of the effect of the effluents on plant growth is the sodium-adsorption ratio (SAR) and conductance. The SAR approximates the base exchange of sodium in the effluent and is a measure of the alkali hazard that could occur and in turn would effect plant growth in the canyon. It is expressed in equivalents per million as:

$$SAR = \sqrt{\frac{Na}{\frac{Ca + Wg}{z}}}$$

The sodium (alkali) hazard is based on SAR of 0 - 10, low, 11 - 18, medium, 19 - 26, high; and above 26 very high.

The salinity hazard is based on the conductance or mineral concentration in solution of the effluent that is available for precipitation into the soil that in turn can effect plant growth. The classification is based on 100 to 250 µmhos, low; 250 to 750 µhmos, medium; 750 to 2250 µmhos, high; and above 2250 µmhos very high. The following table shows the sodium (alkali) and salinity hazard of the effluent based on average annual concentration.

	Effluent - TA-50			
Year	SAR	Sodium (Alkali) Hazard	Conductance (µmhos/cm)	Salinity Hazard
1962	--	--	--	--
1963	7.0	Low	1730	High
1964	6.9	Low	1950	High
1965	8.4	Low	2070	High
1966	5.5	Low	1280	High
1967	3.1	Low	1520	High
1968	4.1	Low	1630	High
1969	8.1	Low	1990	High
1970	14	Medium	2340	very high
1971	17	Medium	2450	very high
1972	26	High	2570	very high

Waste water is discharged into the disposal area from New Sigma and TA-48 from cooling processes in the laboratories. The water is originally from the municipal supply from Los Alamos. No chemicals are added; however, the chemical quality may have been changed slightly by use, due to evaporation losses as shown on the following table:

Chemical Quality of Waste Water TA-48 and New Sigma

(Analyses in mg/l except as noted)

Source	Year	Sodium	Chloride	Fluoride	Nitrate	Dissolved Solids	Conductance a/	pH
TA-48	1962	36	6	0.8	1.3	192	218	7.7
TA-48	1965	44	2	0.8	.4	210	240	8.0
New Sigma	1962	34	4	1.6	1.8	162	180	8.3
New Sigma	1965	32	2	0.4	2.2	599	640	7.8

a/ Micromhos

B. Radiochemical Quality of Effluent

After treatment and release, the effluents contain some radionuclides. The following table presents the average annual concentrations in the effluent.

Average Annual Radiochemical Quality of Effluents, TA-50

Year	Amount (M^3)	pCi/l Gross Alpha	Gross Beta	Total Pu	^{89}Sr	^{90}Sr
1963	27390	194	12700	58.4	5430	1450
1964	51400	70	52000	37.7	1200	1700
1965	49000	109	16600	71.2	860	1260
1966	52810	70	7500	31.0	460	670
1967	59680	128	6300	70.7	890	220
1968	60290	86	5400	43.0	540	130
1969	54480	24	6600	120	1000	240
1970	53180	160	11000	94	250	370
1971	45680	230	24000	150	270	690
1972	57080	240	6700	148 a/	62	[illegible]

a/ ^{238}Pu 130; ^{239}Pu 18

The annual and total amount of radionuclides released in effluents from TA-50 is presented in the following table.

Annual Amount of Radionuclides Released with Effluents, TA-50

Year	mCi Gross Alpha	Gross Beta	Total Pu	^{89}Sr	^{90}Sr
1963	5.3	348	1.6	148.7	39.7
1964	3.6	2670	1.9	64.9	87.4
1965	5.3	813	3.5	42.1	61.7
1966	3.7	396	1.6	24.3	35.4
1967	7.6	376	4.2	53.1	13.1
1968	5.2	326	2.6	32.6	7.8
1969	1.3	360	6.5	54.5	13.1
1970	8.5	585	5.0	13.3	19.7
1971	10.5	1096	6.8	12.3	31.5
1972	13.7	382	8.4 a/	3.5	5.5
	64.7	7352	42.1	449.3	314.9

a/ ^{238}Pu, 7.4; ^{239}Pu, 1.0.

In addition to the effluents released from the treatment plant at TA-50, a smaller plant was operated at TA-35 from 1956 through 1963. The effluents were released into 10-Site Canyon. The volume of effluent was not sufficient to move as surface flow into Mortandad Canyon. Storm runoff entered Mortandad Canyon between MCO-6 and MCO-7. The effluents contained mainly strontium and cesium. The annual average concentrations of radionuclides are shown on the following table.

Average Annual Radiochemical Quality of Effluents, TA-35

		pCi/l		
Year	Amount (M^3)	Gross Beta	^{89}Sr	^{90}Sr
1956	682.5	—	1 370 000	241 000
1957	1630	1 430 000	130 000	22 600
1958	1391	119 000	73 000	7 700
1959	667.5	6 600 000[a/]	38 900	5 990
1960	1248	76 000	27 200	4 800
1961	1541	64 000[a/]	5 840	650
1962	1241	82 000[a/]	7 410	820
1963	399.5	310 000	250[a/]	250[a/]

a/ Estimated

The annual and total amounts of ^{89}Sr and ^{90}Sr released from TA-35 into 10-Site Canyon are presented in the following table.

Annual Amounts of ^{89}Sr and ^{90}Sr Released with Effluents, TA-35

Year	mCi	
	^{89}Sr	^{90}Sr
1956	935	164
1957	212	36.8
1958	101	10.7
1959	25.9	4.0
1960	33.9	5.9
1961	9.0	1.0
1962	8.9	.9
1963	0.1	0.1 a/
TOTAL	1 325.8	223.4

a/ Estimated

C. Surface Water

Surface water entering the canyon consists of effluent from TA-50, storm runoff and waste water. The effluent from TA-50 for the period 1964 (first full year of discharge) to 1972 has ranged from 46 x 10^3 to 60 x 10^3 m^3 or an annual average of about 54 x 10^3 m^3. Waste water from TA-48 has ranged from 1.6 x 10^3 to 2.0 x 10^3 m^3 annually. Six (6) release of waste water from New Sigma have occurred ranging from 2 to 6 weeks in time. The releases were 1962 (18 x 10^3 m^3), 1963 (37 x 10^3 m^3), 1964 (19 x 10^3 m^3), 1965 (18 x 10^3 m^3), and 1969 (48 x 10^3 m^3). The average annual runoff and waste water entering the canyon from 1962 through 1972 has ranged from 26 x 10^3 to 125 x 10^3 m^3 or an annual average of about 63 x 10^3 m^3. Thus, over a period of time the dilution of effluent to runoff and waste water has been about one to one. The volume of water entering the canyon is measured at Gauging Station 1 (Fig. 14). The following table shows annual volume of effluent, storm runoff, and waste water passing through Gauging Station 1.

Volume of Effluent Storm Runoff and Waste Water at Gauging Station 1

	Effluent TA-50 (x 10^3 m^3)	Storm-runoff and Waste Water (x 10^3 m^3)	Total (x 10^3 m^3)
1961	--	--	--
1962	--	70	70
1963	27[a]	125	152
1964	51	59	110
1965	49	75	124
1966	53	35	88
1967	60	79	139
1968	60	52	112
1969	54	93	147
1970	53	50	103
1971	46	29	75
1972	57	26	83

[a] Operations July-December

A second gauging station GS-2 was operated about 1370 m downgradient from GS-1 from March 1962 through December 1965. The annual surface water loss between the two stations ranged from 51 x 10^3 m^3 to 115 x 10^3 m^3. The loss was to evapotranspiration and infiltration into the alluvium and underlying tuff. Water infiltrating into the alluvium recharges the water in the alluvium that is preched on the underlying tuff. The water in the alluvium moved downgradient into the lower section of the canyon east of GS-1. During the period of record, about 74% of the surface water passing through GS-1 was lost before reaching GS-2. The following table presents the annual records of surface water passing by Gauging Stations 1 and 2 and losses between the two stations.

Surface Discharge at Gauging Stations 1 and 2 and Loss between Stations 1962-1964 (In Cubic Meters)

Year	Gauging Station 1	Gauging Station 2	Surface Water loss between Stations
1962[a]	70	19	51
1963	152	37	115
1964	110	28	82

a/ March through December

Surface water sampling stations are at GS-1, MCS-3.8, MCS-3.9, and GS-2. The surface flow at stations MCS-3.8 and MCS-3.9 is return flow from the alluvium. The increased gradient in the channel causes thinning of the alluvium causing water in the alluvium moving downgradient to flow on the surface for 30 to 60 m.

1. Chemical Quality of Surface Water

The chemical quality of the surface flow after June 1963 reflects the release of treated industrial effluents from TA-50. The following table presents average chemical quality of surface water at the four stations from 1962 through 1972.

Chemical Quality of Surface Water, 1962-1972
(Average of a number of analyses in mg/l except as noted)

Station	GS-1	MCS-3.8	MCS-3.9	GS-2[a]
No. of Analyses	37	16	19	3
Sodium	183	134	148	122
Chloride	15	20	31	14
Fluoride	1.2	2.0	1.3	1.3
Nitrate	24	33	11	29
Total Dissolved Solids	494	555	636	443
Conductance[b]	570	600	720	500
pH[c]	9.6	8.4	8.3	—

a Samples collected during release of effluents from New Sigma.

b Micromhos

c No Units

The return flow at MCS-3.8 and 3.9 indicates dissolution of chemical ions in the alluvium as seen by the increase in total dissolved solids concentration. Analyses of water at GS-2 were taken during the release of waste water from New Sigma Bldg. The following table presents average annual quality of water at GS-1 from 1962 to 1972.

Quality of Surface Water at Gauging Station 1
(Average of a number of analyses in mg/l except as noted)

Year	No. of Analyses	Na	Cl	F	NO_3	TDS	Conductance[a]	pH[b]
1962	2	40	6	0.8	1.3	212	240	7.6
1963	2	70	10	1.2	1.3	324	440	8.7
1964	6	146	19	1.3	63	566	670	9.8
1965	5	245	16	1.4	36	921	1150	10.2
1966	3	109	20	1.8	35	412	500	10.4
1967	2	86	5	1.2	1.3	255	415	10.2
1968	2	56	13	0.8	.9	194	260	9.4
1969	1	22	5	<.1	2.2	244	220	9.0
1970	6	881	16	1.7	40	1309	1190	11.1
1971	4	139	38	1.9	36	517	620	11.0
1972	4	221	15	1.0	44	479	520	7.7

[a] Microhmos
[b] No Units

The chemical quality varies due to the change in quality of the effluent from TA-50. The nitrate concentrations have increased in the latter part of the period due to a greater use of the ion-exchange columns which use nitric acid as part of the treatment process.

The following table presents the average annual chemical quality of water at MCS-3.8 for the years 1963 through 1971.

Quality of Surface Water at MCS-3.8
(Average of a number of analyses in mg/l except as noted)

Year	No. of Analyses	Na	Cl	F	NO_3	TDS	Conductance[a]	pH[b]
1963	2	78	7	0.8	4.8	328	405	8.6
1964	5	186	36	4.6	119	742	440	8.0
1965	4	128	11	1.8	19	583	520	8.4
1966	2	100	35	1.5	15	385	540	9.5
1967	1	149	24	1.4	16	346	460	8.0
1968	1	115	5	1.0	9.7	318	440	8.2
1971	1	185	30	3.0	490	1186	1400	8.3

[a] Microhmos at 25° C

[b] No Units

The next table presents the quality of water at MCS-3.9 for the years 1963 through 1972.

Quality of Surface Water at MCS-3.9
(Average of a number of analyses in mg/l except as noted)

Year	No. of Analyses	Na	Cl	F	NO_3	TDS	Conductance[a]	pH[b]
1963	1	43	6	.4	<.4	221	290	7.7
1964	3	152	29	.9	114	748	920	8.0
1965	2	114	12	1.6	37	552	600	9.6
1966	2	102	32	1.5	15	437	500	8.6
1967	2	132	20	1.2	15	356	400	7.9
1968	1	110	15	2.2	11	260	370	8.3
1970	1	260	20	1.0	246	662	820	8.5
1971	3	280	104	1.5	303	1390	1300	8.2
1972	4	139	39	1.5	299	1098	1235	7.8

[a] Micromhos at 25° C

[b] No Units

Analyses from Stations MCS-3.8 and MCS-3.9 are of return flow from the alluvium, in which the nitrate increase in the latter part of the period, is quite prominent. Total dissolved solids also shows a large increase in concentration.

The following table shows analyses of water at Gauging Station GS-2 which is mainly waste water from New Sigma Bldg.

Quality of Surface Water at Gauging Station 2
(Average of a number of analyses in mg/l except as noted)

Year	No. of Analyses	Na	Cl	F	NO_3	TDS	Conductance[a]	pH[b]
1962	1	48	6	.8	.2	232	250	7.7
1964	2	151	17	1.8	10.0	544	600	9.5
1965	1	167	20	1.3	10.0	552	640	10.2

[a] Micromhos at 25° C
[b] No Units

Selected metal ions were analyzed from samples of water collected at Gauging Station 1 in 1971 and 1972 and from MCS-3.9 in 1971.

Metal Ion Analysis
(Average of a number of analyses in μg/l)

Source	Gauging Station 1	MCS-3.9
No. of Analyses	3	2
In Solution		
Cadmium	2.6	5.4
Beryllium	.26	<.25
Lead	<1.0	9.2
Mercury	.26	<.02
Particulates		
Cadmium	0.30	0.38
Beryllium	<.25	<.25
Lead	1.2	<1.0
Mercury	.41	< .02

2. Radiochemical Quality of Surface Water

The surface water in Mortandad Canyon at GS-1 and GS-2, prior to the release of effluents from TA-50, contained less than 0.5 pCi/l of plutonium and gross beta was near or below 14 pCi/l. The following table presents radiochemical quality of water from 1962 through 1965.

Radiochemical Quality 1967-1965

Station	Year	No. of Analyses	pCi/l Gross Beta	pCi/l Total Pu	µg/l Total Uranium
GS-1	1964	6	570	6.0	1.1
GS-1	1965	5	1200	2.5	.8
MCS-3.8	1963	2	18	<.5	.7
MCS-3.8	1964	5	180	4.5	<.5
MCS-3.8	1965	4	140	1.2	.8
MCS-3.9	1963	1	<14	<.5	<.5
MCS-3.9	1964	3	100	2.9	<.5
MCS-3.9	1965	2	80	<.5	<.5
GS-2	1962	1	<14	<.5	<.5
GS-2	1964	2	490	2.7	.8
GS-2	1965	4	140	1.2	<.5

There was no analyses of surface water in 1966. The following table presents the radiochemical quality of water from 1967 through 1972.

MORTANDAD CANYON

SURFACE FLOW SAMPLING SITES

RADIOCHEMICAL QUALITY OF WATER

SOURCE	YEAR	MAX. # SAMPLES	GROSS ALPHA	GROSS BETA	^{238}Pu	^{239}Pu	^{241}Am	^{226}Ra	^{234}U	^{137}Cs	^{90}Sr	^{3}H	^{238}U
GS-1	1967	1	-1	343	-.05	-.05	-.00	.38	.40	-240	-	-50	.021
GS-1	1968	2	-1	292	.46	.42	-.05	-.15	.88	255	-	-50	.271
GS-1	1969	2	10	1174	6.46	6.64	-.00	-.15	1.18	3020	169	241	.621
GS-1	1970	8	19	3338	19.80	5.60	3.06	-.15	2.01	6336	385	87	.021
GS-1	1971	5	31	1604	25.35	5.06	4.51	-.15	4.16	3556	233	31	.021
GS-1	1972	4	12	520	8.68	.97	.77	-.00	-.00	718	-	23475	3.250
MCS-3.9	1967	1	-1	97	-.05	-.05	-.00	-.15	-.00	-	-	82	.821
MCS-3.9	1968	2	1	193	.12	.22	-.05	-.15	-.00	-240	-	-	3.121
MCS-3.9	1969	1	-1	142	.22	.17	-.00	-.00	-.00	-	-	6	1.221
MCS-3.9	1970	2	2	309	.35	.28	-.00	-.00	-.00	-	87	391	1.472
MCS-3.9	1971	4	10	817	3.14	.34	-.00	-.15	-.00	323	167	45	5.571
MCS-3.9	1972	4	12	523	5.97	.90	.86	-.00	-.00	-350	-	46933	8.430
GS-2	1971	1	95	312	1.05	5.00	3.02	-.15	2.03	390	89	28	.021

In general the surface water near the effluent outfall contains the largest concentrations of radioactivity which decrease with increase distance from the outfall.

D. Water in Alluvium

Water in the alluvium is recharged from industrial effluents, storm run-off and waste water. As the water in the alluvium moves downgradient in the canyon, loss to evapotranspiration and into the underlying tuff is of limited extent.

The volume of water in the alluvium was calculated from the known volume of saturation in the alluvium as determined by test drilling, and subsequent water level in test holes as the volume of water fluctuates, dependent on amount of recharge. The following table presents the volume of water in storage in the aquifer as of December 31 for the years 1961 through 1972 and the annual volume of surface and ground water loss in the canyon. The calculations are based on volume of inflow at Gauging Station 1 for the year and changes in storage.

Storage in Aquifer and Surface and Ground Water Loss

Year	Storage in aquifer[a] ($x\ 10^3\ m^3$)	Annual surface and ground water loss in canyon ($x\ 10^3\ m^3$)
1961	20	--
1962	20	70
1963	22	150
1964	24	108
1965	25	123
1966	20	93
1967	30	129
1968	24	118
1969	25	146
1970	20	108
1971	29	66
1972	23	89

[a] Storage as of December 31

Storage in the aquifer has ranged from 20 x 10^3 m^3 to 30 x 10^3 m^3 from the years 1961 through 1972. The volume of loss has ranged from 70 x 10^3 m^3 to 146 x 10^3 m^3. The volume of water in storage has remained fairly constant for the period of record. The loss from storage has been essentially equal to the volume of surface water inflow for the year, thus, the aquifer has remained of limited extent, within the project boundaries.

The canyon has been subdivided into three sections to facilitate computation of storage. This division is sometimes used to compute the mass of radionuclides or chemicals in storage. The following table presents the volume of water in storage in the alluvium in the three sections of the canyon from 1961 through 1972 as of December 31.

Volume in Storage in Three Sections of Aquifer, 1961-1972

	Volume in x 10^3 m^3 [a]			
Year	Upper	Middle	Lower	Total
1961	3.2	3.3	13.3	19.8
1962	2.4	5.7	11.8	19.9
1963	2.1	3.5	16.5	22.1
1964	5.9	4.7	13.2	23.8
1965	3.9	6.3	14.9	25.1
1966	2.8	3.1	14.2	20.1
1967	6.7	5.1	18.3	30.1
1968	5.2	4.7	14.3	24.2
1969	2.9	5.6	16.6	25.1
1970	2.5	2.9	14.4	19.8
1971	4.8	7.1	16.9	28.8
1972	4.4	5.0	13.5	22.9

[a] As of December 31

Water samples were collected from ten (10) observation holes (Fig. 10). The depth to water ranges from about 1.2 m at Observation Hole MCO-3 to 24 m at Observation Hole MCO-8. The water levels will vary dependent on the volume of water entering the canyon as surface flow.

1. Chemical Quality of Water in Alluvium

Samples were collected and analyzed prior to the release of effluents from TA-50 to provide a base line of the chemical quality changes that would occur in water in the alluvium.

The following table presents a summary of the chemical quality of water prior to the release of effluents from TA-50.

Chemical Quality of Water in Alluvium, 1961-1962

(average of a number of analyses in mg/l except as noted)

Obs. Hole	No. of Analyses	Na	Cl	F	NO_3	TDS	Conductance[a]	pH[b]
MCO-1	1	95	10	1.0	0.5	175[c]	270	7.1
MCO-2	1	115	12	1.0	1.5	188[c]	290	7.0
MCO-3	3	52	7	0.7	0.9	398	420	7.1
MCO-4	3	48	7	0.7	0.8	370	440	7.2
MCO-5	3	28	7	0.7	0.8	203	270	6.7
MCO-6	3	16	8	0.7	1.1	325	350	6.6
MCO-7	3	15	7	0.7	1.1	283	240	6.7
MCO-7.5	2	18	8	0.4	1.4	230[c]	350	6.8
MCO-8	3	16	7	0.7	0.9	175	230	6.8

[a] Micromhos at 25° C

[b] No Units

[c] Estimated

Observation Holes MCO-1 and MCO-2 were drilled in or near the stream channel to depths of less than 2 m. The chemical quality is essentially the same as the stream or cooling water discharged from TA-48. No samples were collected after 1962.

Observation Hole MCO-3 is located 122 m west of the effluent outfall. The hole was drilled to a depth of 3.6 m. The depth to water is about 1 m. The average chemical quality of water from 1961 through 1972 is presented on the following table.

Chemical Quality of Water, MCO-3
(average of a number of analyses in mg/l except as noted)

Year	No. of Analyses	Na	Cl	F	NO_3	TDS	Conductance[a]	pH[b]
1961	1	59	8	1.0	0.9	250[c]	380	7.0
1962	2	48	7	0.4	0.8	398	460	7.2
1963	9	109	15	0.9	45	458	540	7.6
1964	10	165	28	2.2	73	673	740	8.1
1965	5	100	13	1.6	22	428	460	8.6
1966	3	89	16	1.2	13	359	400	8.6
1967	2	100	14	1.2	8.8	253	290	8.5
1968	2	84	12	1.4	5.3	229	310	9.0
1969	2	237	5	3.0	7.0	567	660	8.8
1970	4	210	20	1.0	761	738	790	8.6
1971	4	256	69	2.6	260	964	1215	9.1
1972	4	234	28	1.6	285	977	1075	8.2

[a] Micromhos at 25° C
[b] No Units
[c] Estimated

Observation Hole MCO-4 is located 1460 m east of the effluent outfall. The hole was drilled to a depth of 5.8 m. The water level is about 3.7 m. The average chemical quality of water from 1961 through 1972 is presented on the following table.

Chemical Quality of Water, MCO-4
(average of a number of analyses in mg/l except as noted)

Year	No. of Analyses	Na	Cl	F	NO_3	TDS	Conductance[a]	pH[b]
1961	1	52	8	1.0	1.0	210[c]	320	6.8
1962	2	44	6	0.4	0.5	371	440	7.2
1963	9	72	11	0.5	37	387	415	7.4
1964	10	140	26	0.7	96	605	750	7.6
1965	5	144	15	1.2	57	455	640	7.9
1966	3	113	26	0.9	26	433	500	7.9
1967	2	140	22	1.6	18	341	435	7.6
1968	2	128	10	1.6	8.8	296	395	8.0
1969	2	118	10	<0.1	22	293	390	8.2
1970	5	158	18	0.7	202	624	740	7.8
1971	4	262	77	1.0	392	1108	1300	7.6
1972	4	262	42	1.4	299	1018	1175	7.6

[a] Micromhos at 25° C

[b] No Units

[c] Estimated

Observation Hole MCO-5 is located 1841 m east of the effluent outfall. The hole was drilled to a depth of about 11.5 m. The water level is about 6.4 m. The average chemical quality of water from 1961 through 1962 is presented on the following table.

Chemical Quality of Water, MCO-5
(average of a number of analyses in mg/l except as noted)

Year	No. of Analyses	Na	Cl	F	NO_3	TDS	Conductance[a]	pH[b]
1961	1	29	6	1.0	1.0	186	220	6.5
1962	2	28	8	0.4	0.6	220	320	6.9
1963	8	36	7	0.4	3.5	222	241	7.1
1964	10	102	22	0.4	89	494	601	7.4
1965	5	101	13	0.3	44	396	496	7.6
1966	4	133	27	0.2	40	411	608	7.7
1967	1	164	13	1.0	0.8	315	350	7.5
1968	2	128	15	0.4	8.8	307	360	7.5
1969	2	118	12	<0.1	28	281	375	8.3
1970	1	131	10	<0.1	20	546	660	7.5
1971	4	209	46	0.4	367	926	1100	7.3
1972	4	199	57	0.5	216	808	955	7.5

[a] Microhmos at 25° C
[b] No Units

Observation Hole MCO-6 is located 2234 m east of the effluent outfall. The hole was drilled to a depth of 21.6 m. The water level is about 11 m. The average chemical quality of water from 1961 through 1972 is presented on the following table.

Chemical Quality of Water, MCO-6

(average of a number of analyses in mg/l except as noted)

Year	No. of analyses	Na	Cl	F	NO_3	TDS	Conductance[a]	pH[b]
1961	1	15	7	1.0	1.4	140[c]	210	6.5
1962	1	28	9	0.4	0.8	325	350	6.7
1963	9	36	7	0.4	6.2	218	240	7.1
1964	10	96	21	0.4	95	475	590	7.5
1965	5	104	12	0.4	43	412	470	7.5
1966	3	112	30	0.2	31	462	480	7.7
1967	2	183	14	0.4	16	404	460	7.6
1968	2	120	10	0.9	9.7	312	335	8.1
1969	2	121	10	<0.1	24	312	370	8.2
1970	5	102	18	0.7	114	483	550	7.4
1971	4	226	45	0.8	409	1000	1195	7.5
1972	4	231	73	0.8	246	920	1100	7.6

[a] Microhmos at 25° C

[b] No Units

[c] Estimated

Observation Hole MCO-7 is located 2554 m east of the effluent outfall. The hole was drilled to a depth of 20.7 m. The water level is about 12.2 m. The average chemical quality of water from 1961 through 1972 is presented on the following table.

Chemical Quality of Water, MCO-7

(average of a number of analyses in mg/l except as noted)

Year	No. of Analyses	Na	Cl	F	NO_3	TDS	Conductance[a]	pH[b]
1961	1	14	7	1.0	1.4	237	220	6.6
1962	2	16	7	0.4	0.7	330	260	6.8
1963	6	23	6	0.4	3.1	222	245	7.1
1964	10	32	12	0.4	33	235	288	7.3
1965	5	48	8	0.4	22	258	310	7.3
1966	3	71	25	0.1	28	309	452	7.5
1967	2	140	18	0.2	15	362	435	7.5
1968	2	112	15	0.2	6.6	314	360	7.6
1969	2	122	15	<0.1	15	360	375	8.2
1970	3	90	13	0.2	35	357	407	7.4
1971	4	166	28	0.6	374	872	995	7.2
1972	4	170	74	0.3	217	785	925	7.5

[a] Microhmos at 25° C

[b] No Units

Observation Hole MCO-7.5 is located 2844 m east of the effluent outfall. The hole was drilled to a depth of 18.3 m. The water level is about 13.7 m. The average chemical quality of water from 1962 through 1972 is presented on the following table.

Chemical Quality of Water, MCO-7.5

(average of a number of analyses in mg/l except as noted)

Year	No. of Analyses	Na	Cl	F	NO_3	TDS	Conductance [a]	pH [b]
1962	2	18	8	0.4	1.4	905	350	6.8
1963	5	17	6	0.4	2.2	237	336	7.2
1964	10	23	12	0.4	39	370	349	7.3
1965	5	50	13	0.5	60	340	408	7.1
1966	3	69	28	<0.1	35	391	460	7.4
1967	2	145	20	<0.1	26	426	465	7.6
1968	2	123	10	0.4	3.5	322	390	7.6
1969	2	110	8	<0.1	7.9	454	395	8.0
1970	2	86	8	0.1	35	303	400	7.4
1971	3	190	24	0.5	378	889	973	7.1
1972	4	166	77	0.2	216	792	930	7.4

[a] Microhmos at 25° C

[b] No Units

Observation Hole MCO-8 is located 3027 m east of the effluent outfall. The hole was drilled to a depth of 25.3 m. The water level is about 21.3 m. The average chemical quality of water from 1962 through 1972 is presented on the following table.

Chemical Quality of Water, MCO-8

(average of a number of analyses in mg/l except as noted)

Year	No. of Analyses	Na	Cl	F	NO_3	TDS	Conductance[a]	pH[b]
1961	1	23	6	1.0	1.2	200	240	6.7
1962	2	9	8	0.4	0.6	151	225	6.9
1963	4	13	5	0.5	3.3	292	172	7.1
1964	10	14	8	0.4	21	203	239	7.4
1965	5	30	10	0.6	51	274	324	7.4
1966	3	38	18	0.1	31	328	363	7.3
1967	2	86	16	0.6	26	327	465	7.4
1968	2	69	22	0.3	18	311	370	7.4
1969	2	84	25	<0.1	8.8	404	365	8.0
1970	4	50	11	0.3	18	310	345	7.6
1971[c]	—	—	—	—	—	—	—	—
1972	3	107	57	0.3	216	718	820	7.4

[a] Micromhos at 25° C

[b] No

[c] 1971 observation Hole dry

The release of effluents into the canyon from TA-50 has significantly changed the chemical quality of water in the alluvium. The following table shows the increase of certain chemical and physical constituents. There was no change in fluoride. Total dissolved solids increase about three fold. The major change is seen by the release of a predominately alkaline effluent with a high concentration of sodium. This has resulted in a change from a slightly acid water to a basic water in the alluvium.

Chemical Quality of Water 1962 and 1972

(average of analyses from seven observation holes)

	1962	1972
Sodium (mg/l)	28	196
Chloride (mg/l)	0.8	242
Fluoride (mg/l)	0.7	0.7
Nitrate (mg/l)	1.0	55
Total Dissolved Solids (mg/l)	292	860
Conductance (μmhos)	330	1000
pH	6.8	7.6

Select metal ions were analyzed in water from observation holes in 1971 and 1972. Traces of the few constituents found are slightly higher than what would be expected in natural waters.

Metal Ion Analyses, 1971-1972

(average of a number of analyses in μg/l)

Source	MCO-3	MCO-4	MCO-5	MCO-6	MCO-7	MCO-7.5
No. of Analyses	4	2	3	3	4	3
In Solution						
Cadmium	5.0	5.2	4.8	3.2	6.9	0.33
Beryllium	<0.25	0.26	0.35	0.40	<0.25	<0.25
Lead	26	16	9.3	1.7	2.9	1.7
Mercury	0.05	<0.02	<0.02	<0.02	<0.02	<0.02
Particulates						
Cadmium	0.86	0.69	1.4	2.2	0.53	3.2
Beryllium	0.35	0.46	0.73	1.7	0.53	2.6
Lead	22	27	26	32	37	57
Mercury	0.12	0.10	0.08	0.11	0.10	0.19

2. Inventory of Chemical Released and in Storage

An inventory of chemicals released into the canyon was estimated using the annual average concentration and volume of effluent for the period July 1963 through December 1972. The inventory of chemicals in solution in the aquifer was made prior to release of effluents and in December 1972 by using the average annual concentrations from seven (7) Observation Holes and the volume of water in storage. The following table presents mass of chemical released with effluent, the mass in storage prior to release of effluents and the mass in storage after 10 years of effluent release.

Inventory of Chemicals in Effluents Released and in Storage in the Aquifer

	kg x 10^3		
	Effluents	In Storage	
Chemical	1963-1972	1962	1972
Calcium	32	0.2	0.9
Magnesium	1.4	.08	.3
Sodium	143	.6	4.9
Carbonate	126	0	0
Bicarbonate (as $CaCO_3$)	210	1.8	5.1
Chloride	26	.1	1.2
Fluoride	1.1	.01	.01
Nitrate	120	.06	5.7
Total Dissolved Solids	519	6.4	20.9
TOTAL	989.5	9.2	39.0

The inventory of chemicals released into the canyon are estimated at 989 x 10^3 kg. This increased the mass from 9.2 x 10^3 kg in 1962 (pre-release) to 39.0 x 10^3 kg in 1972 (after 10 years of release). The amount of chemicals unaccounted for in the inventory were taken up by plants, base exchange with alluvial material in the stream channel or carried into the underlying tuff by infiltrating water.

The sodium (alkali) and salinity hazard of water in storage in the aquifer was compiled from annual average concentration of sodium, calcium, and magnesium (SAR) and conductance.

Sodium and Salinity Hazard
in Storage in the Aquifer

Year	SAR	Sodium (Alkali Hazard)	Conductance (μmhos/cm)	Salinity Hazard
1962	2.1	low	360	medium
1963	3.2	low	360	medium
1964	1.1	low	510	medium
1965	5.5	low	440	medium
1966	5.4	low	470	medium
1967	7.2	low	400	medium
1968	5.9	low	360	medium
1969	6.7	low	410	medium
1970	5.9	low	560	medium
1971	7.9	low	1160	high
1972	9.6	low	1000	high

3. Radiochemical Quality of Water in Alluvium

Samples were collected and analyzed prior to release of effluents from TA-50 to provide a base line of the radiochemical changes that would occur in water in the alluvium.

The following table presents a summary of the radiochemical quality of water prior to the release of effluents from TA-50.

Radiochemical Quality of Water in Alluvium

(average of a number of analyses, 1961-1962)

Obs. Hole	No. of Analyses	pCi/l		µg/l
		Gross Beta	Total Pu	Total Uranium
MCO-1	3	<14	<0.5	<0.5
MCO-2	3	<14	<0.5	<0.5
MCO-3	5	<14	<0.5	<0.5
MCO-4	5	<14	<0.5	<0.5
MCO-5	5	<14	<0.5	<0.5
MCO-6	5	<14	<0.5	<0.5
MCO-7	5	<14	1.8	<0.5
MCO-7.5	1	<14	3.1	<0.5
MCO-8	5	<14	<0.5	<0.5

The following table presents radiochemical data 1963 through 1965 after effluents were released into the canyon.

Radiochemical Quality 1963-1965

(average of a number of analyses)

Obs. Hole	Year	No. of Analyses	pCi/l Gross Beta	pCi/l Total Pu	µg/l Total Uranium
MCO-3	1963	2	14	6.5	<0.5
MCO-3	1964	10	247	3.2	<0.5
MCO-3	1965	5	131	1.7	3.8
MCO-4	1963	4	54	1.8	<0.5
MCO-4	1964	10	136	4.1	<0.5
MCO-4	1965	5	130	1.6	<0.5
MCO-5	1963	1	23	<0.5	<0.5
MCO-5	1964	10	105	2.2	<0.5
MCO-5	1965	5	34	1.4	<0.5
MCO-6	1963	3	26	<0.5	1.5
MCO-6	1964	10	64	2.0	<0.5
MCO-6	1965	5	32	2.0	<0.5
MCO-7	1963	3	<14	<0.5	<0.5
MCO-7	1964	10	38	<0.5	0.6
MCO-7	1965	5	15	<0.5	<0.5
MCO-7.5	1963	2	<14	<0.5	<0.5
MCO-7.5	1964	9	30	0.5	0.5
MCO-7.5	1965	6	17	<0.5	<0.5
MCO-8	1963	3	<14	<0.5	<0.5
MCO-8	1964	10	16	0.7	1.5
MCO-8	1965	6	<14	<0.5	<0.5

The concentrations of plutonium were greater near the effluent discharge area and decreased downgradient in the canyon. Only trace concentrations of plutonium were noted at observation hole MCO-7 by 1965. Gross beta emitter in the water showed the same general pattern as the plutonium decreasing in concentration downgradient in the canyon. The gross beta activity may have extended to hole MCO-7.5. Total uranium showed no apparent increase or trend in the canyon.

There were no radiochemical analyses of water in the alluvium in 1966. The following table presents a recap of radiochemical analyses from 1967 through 1972.

MORTAR DAD CANYON

ALLUVIAL AQUIFER OBSERVATION WELLS

RADIOCHEMICAL QUALITY OF WATER

SOURCE	YEAR	MAX. # SAMPLES	GROSS ALPHA	GROSS BETA	^{238}Pu	^{239}Pu	^{241}Am	^{226}Ra	^{234}U	^{137}Cs	^{90}Sr	^{3}H	^{238}U
MCO-3	1967	1	-1	116	-.05	.14	-.00	-.15	-.00	-	-	-	1.300
MCO-3	1968	2	1	166	.27	.22	-.05	-.15	2.77	-240	-	-	.700
MCO-3	1969	1	7	93	.27	.35	-.00	-.00	-.00	-	-	-	.90[illegible]
MCO-3	1970	5	6	505	1.03	.47	.20	-.15	-.00	345	92	-	1.90[illegible]
MCO-3	1971	4	21	1471	14.31	1.60	-.00	-.15	-.00	2090	314	40500	9.00[illegible]
MCO-3	1972	4	11	612	3.94	.35	.50	-.00	-.00	382	-	47100	7.58[illegible]
MCO-4	1967	1	-1	83	-.05	.06	-.00	-.15	-.00	-	-	-	-.40
MCO-4	1968	2	1	83	.13	.43	-.05	-.15	1.48	-240	-	-	1.20
MCO-4	1969	3	3	129	.14	.12	-.00	-.00	-.00	-	-	-	1.70
MCO-4	1970	6	3	141	.11	.08	-.00	-.15	-.00	-230	-	-	1.5
MCO-4	1971	4	3	418	.23	.07	-.00	-.00	-.00	-277	179	49250	3.7
MCO-4	1972	4	9	343	.93	.16	.10	-.00	-.00	-350	-	64475	6.0
MCO-5	1967	1	2	9	-.05	-.05	-.00	-.15	-.00	-	-	-	[illegible]
MCO-5	1968	2	1	45	.11	.63	3.81	-.15	-.00	-240	-	-	.7
MCO-5	1969	2	-1	29	.05	.09	-.00	-.00	-.00	-	-	-	[illegible]
MCO-5	1970	2	4	25	.06	-.05	-.00	-.00	-.00	-	-	-	1.
MCO-5	1971	4	1	186	.09	-.05	-.00	-.00	-.00	-263	175	64000	2.
MCO-5	1972	4	3	112	.14	.07	.19	-.00	-.00	-350	-	78250	
MCO-6	1967	1	2	7	-.05	.09	-.00	-.00	-.00	-	-	-	4.
MCO-6	1968	2	6	27	.07	.79	-.05	.36	-.00	-240	-	-	1.
MCO-6	1969	2	4	18	-.05	.06	-.00	-.15	-.00	-	-	-	[illegible]
MCO-6	1970	6	4	31	-.05	-.05	-.00	-.15	-.00	-230	-	-	.9
MCO-6	1971	4	2	168	.05	-.05	-.00	-.00	-.00	-240	-	51500	.7
MCO-6	1972	4	2	132	.08	-.05	.22	-.00	-.00	-350	-	59500	3.5
MCO-7	1967	1	2	2	-.05	.05	-.00	-.00	-.00	-	-	-	1.5
MCO-7	1968	2	1	10	-.05	.11	-.05	-.15	-.00	-240	-	-	.8
MCO-7	1969	2	5	9	-.05	.05	-.00	.19	-.00	-	-	-	.7
MCO-7	1970	4	2	17	-.05	.06	-.00	-.00	-.00	-230	-	-	-.4
MCO-7	1971	4	-1	105	.09	-.05	-.00	-.00	-.00	-265	-	84000	.7
MCO-7	1972	4	2	73	.12	.06	.08	-.00	-.00	-350	-	68875	1.8
MCO-7.5	1967	1	3	11	-.05	.06	-.00	-.15	-.00	-	-	-	3.6
MCO-7.5	1968	2	2	9	.11	.32	.10	.56	-.00	-240	-	-	.8
MCO-7.5	1969	2	1	39	.10	.15	-.00	-.00	-.00	-	-	-	.8
MCO-7.5	1970	3	7	32	.32	.37	-.00	-.00	-.00	-240	-	-	-.4
MCO-7.5	1971	3	1	68	.12	-.05	-.00	-.00	-.00	-277	-	122000	.7
MCO-7.5	1972	4	1	70	.08	.12	1.08	-.00	-.00	-350	-	49525	1.80
MCO-8	1967	1	-1	10	-.05	-.05	-.00	-.15	-.00	-	-	-	-.40
MCO-8	1968	2	-1	8	.05	.11	-.05	-.00	-.00	-240	-	-	1.70
MCO-8	1969	2	1	22	-.05	-.05	-.00	-.00	-.00	-	-	-	.90
MCO-8	1970	4	-1	10	.06	-.05	-.00	-.00	-.00	-230	-	-	.80
MCO-8	1971	-	-	-	-.00	-.00	-.00	-.00	-.00	-	-	-	-.00
MCO-8	1972	3	1	46	.10	.52	.31	-.00	-.00	-350	-	129733	.90

During 1972, gross alpha activity decreased from 11 pCi/l to less than 1 pCi/l downgradient in the aquifer. Gross beta decreased from 612 to 46 pCi/l. The concentration of plutonium was greater for ^{238}Pu than ^{239}Pu as shown on the preceeding table. The influent to the plant was carrying more ^{238}Pu than ^{239}Pu for treatment. The ^{238}Pu decreased from 3.94 to 0.10 pCi/l downgradient in the canyon. The ^{239}Pu varied from <0.5 to 0.52 pCi/l showing no particular trend. The ^{241}Am in the aquifer also varied in the canyon showing no particular trend. Tritium increased from 47 x 10^3 to 129 x 10^3 pCi/l downgradient in the canyon. The increase was due to the release of 20 curies of tritium with effluent in 1969 and shows residual from movement downgradient.

E. Inventory of Plutonium in Solution in Storage

An inventory was made of the total plutonium in solution in the aquifer by using the average concentration in three sections of the aquifer and volume of water in storage as of December 1972. The following table shows data used in estimating inventory.

Inventory of Plutonium In Solution

Section	Obs Hole	Total Pu (pCi/l)	Av. Pu (pCi/l)	Volume in Aquifer x 10^3 m^3	Total Pu µCi
Upper	MCO-3	4.29	--		
	MCO-4	1.09	2.69	4.4	11.8
Middle	MCO-4	1.09	--		
	MCO-5	.21	--		
	MCO-6	.13	0.72	5.0	3.6
Lower	MCO-6	.13	--		
	MCO-7	.18	--		
	MCO-8	.6	0.28	13.6	3.8
TOTAL	—	--	--	--	19.2

The total amount of plutonium in solution in the aquifer as of December 1972, was estimated to be 19.2 µCi. The amount of plutonium released with the effluent from 1963 through 1972 was 21.9 mCi (21.9 x 10^3 µCi). Thus, only a small fraction (0.08%) of plutonium released was present in solution in the

F. Storm Runoff and Transport of Radionuclides

Three stations were established and equipped with cumulative samplers at GS-1, GS-2, and midway between GS-1 and GS-2. The stations were equipped with 5 samplers each. The water from the samplers was combined for radiochemical analyses for flow events on July 11, 1967 and September 14, 1967.

The average of the radiochemical analyses for storm runoff event July 11, 1967, are shown on the following table. Total volume of runoff was about 560 m^3 through the GS-1 gauging station.

Runoff event July 11, 1967 m pCi/l

	Source		
	Upper	Middle	Lower
Gross alpha	2	2	<1
Gross beta	94	163	205
^{238}Pu	.13	.17	.12
^{239}Pu	.13	.56	.37
^{234}U	.25	.69	1.13
^{226}Ra	<.15	<.15	<.15
^{137}Cs	<240	<240	<240

The radiochemical analyses of storm runoff that occurred on September 14, 1967 are shown on the following table. The voluem of storm runoff was about 1.1×10^3 m^3 through the GS-1 gauging station.

Storm runoff September 14, 1972
(analyses in pCi/l except as noted)

	Upper	Middle	Lower
Gross alpha	2	1	3
Gross beta	35	123	80
^{238}Pu	.18	.32	.18
^{239}Pu	.22	.09	.67
^{226}Ra	<.15	<.15	<.15
^{137}Cs	<240	<240	<240
Total Uranium	<.4	.5	16.9

Sediments from the upper station were analyzed for gross alpha and gross beta for the runoff event that occurred on July 11, 1967. The analyses were made of the five samples collected at 0.0 m, 0.3 m, 0.6 m, 0.9 m, 1.2 m above the stream channel to determine the distribution of radionuclides at various heights within a flow event.

The anlayses indicate that the concentrations of radioactivity decrease with increasing height above the channel. The sediment concentrations also decrease with increasing height above the channel, the heavier and larger sediments being transported as channel bed sediments. The larger and heavier suspended sediments decrease with the increased height above the channel with lighter and finer suspended sediments near the top of the flow.

Sediments analyzed; runoff event 9/11/67

Height above stream channel (m)	Picocuries per dry gram	
	Gross alpha	Gross beta
0.0	171	234
0.3	175	297
0.6	44	68
0.9	15	72
1.2	14	28

In general the finer sediments (clay and silts) contain the greater amount of radionuclides; however, the transport of the finer material is greater over a period of flow along the base of the channel due to a greater concentration of a mixture of sediment sizes and duration of flow (tail-off of runoff decreases with time).

G. Radiochemical Analyses of Cuttings from Test Holes

Twenty-seven (27) test holes were drilled in seven lines across the canyon

in the fall of 1960. The test holes are located above the stream channel. Samples were collected and analyzed of the upper 0.6 m of the hole for gross alpha and beta emitters. Locations are the same as observation holes. The following table presents average activity for a number of holes drilled in the line.

Radiochemical Analyses of Cuttings
(average of a number of analyses in counts per minute per dry gram)

Location	No. of Holes	Gross alpha		Gross beta	
		0.3m	0.6m	0.3m	0.6m
Line 1	3	1.3	3.0	1.4	13
Line 2	2	1.6	5.2	1.8	<.5
Line 3	2	1.3	< .5	1.0	<.5
Line 4	3	1.0	2.7	1.4	<.5
Line 5	4	1.3	2.4	1.2	1.0
Line 6	6	0.8	2.3	1.0	1.8
Line 8	7	1.4	20	1.8	22

The analyses show background in most of the cuttings. The gross beta activity at Line 1 may be in part from TA-46. Line 8 shows excessive amounts of gross beta activity that may be in part from effluents released from Ten-Site. There were also some liquid effluents released from Ten-site into Ten-Site Canyon which is confluent to Mortandad upgradient from Line 8 and below Line 6.

H. Radiochemical Analyses of Sediments

Channel sediments in Mortandad and tributary canyons are derived from weathering of the Bandelier Tuff. Particle-size distribution of channel sediments at stations are shown on the following table.

Particle-Size Distribution

(Percent by Weight)

Source	Near New Sigma	GS-1	MCS-3.8	MCO-5	Near TSC-1	MCO-12
Granules	4.5	15.0	18.0	11.0	1.5	5.5
Sand						
Very Coarse	16.0	32.0	26.0	20.5	35.0	22.5
Coarse	52.5	28.5	42.5	41.0	41.0	42.5
Medium	21.5	13.0	9.5	17.5	11.5	16.5
Fine	5.0	6.0	1.5	6.5	4.5	5.5
Very Fine	.3	2.0	0.5	1.0	2.0	1.5
Silt and Clay	.2	3.5	1.0	2.5	3.0	6.0

The very fine sand and silt and clay size fractions make up less than percent by weight of the channel sediments. These sediments have the greatest capacity for adsorption and ion-exchange of radionuclides in the liquid effluents.

1. Sediment Analyses Mortandad Canyon

Radiochemical analyses of alluvium from the stream channel were made prior to the release of effluents from TA-50. The results are presented in the following table. The samples were collected at the surface of the channel and at depths of 0.3, 0.6 and 0.9 m below the channel.

Radiochemical Analyses of Sediments, May, 1963

(Counts per minute per day gram)

Type of activity	Depth below land surface (m)	Sampling Stations						
		Gaging Station No. 1	MCO-3	MCS-3.8	MCO-4	MCO-5	MCO-6	MCO-7
Gross alpha	Surface	1	<1	2	1	2	2	1
	0.3	1	1	2	1	< 1	1	< 1
	0.6	3	1	2	<1	2	2	1
	0.9	2	-	2	1	1	3	3
Gross beta	Surface	159	2	2	27	10	36	28
	0.3	22	13	32	2	< 1	<1	<1
	0.6	11	< 1	< 1	4	<1	9	< 1
	0.9	3	-	< 1	31	15	8	21

Another set of surface sediments were collected in November, 1965 and analyzed for gross alpha, beta, and gamma activity. The results are shown on the following table.

Radiochemical Analyses of Sediments
November, 1965

(Analyses in Counts per Minute per Dry Gram)

Location	Gross Alpha	Gross Beta	Gross Gamma
Near New Sigma	1	23	32
GS-1	5	189	74
MCS-3.8	3	60	4
MCO-5	24	36	72
MCO-12	1	< 1	< 1

A similar set of samples were collected and analyzed for gross alpha, gross beta, and plutonium in the spring of 1970. The results are shown on the following table.

Radiochemical Analyses of Sediments
February and March, 1970

(Analyses in picocuries per dry Gram)

Location	Gross Alpha	Gross Beta	^{238}Pu	^{239}Pu
Near New Sigma	2	2	<.002	<0.002
GS-1	76	350	42	46
MCS-3.8	8	36	1.33	2.44
MCO-5	6	30	.697	2.14
MCO-7	3	6	.188	.209
MCO-12	3	5	.003	.016

Additional samples were collected in 1971 and 1972 at MCO-5.

Radiochemical Analyses of Sediments at
MCO-5, 1971 and 1972

(Analyses in picocuries per dry gram)

	5-14-71	10-14-71	10-10-72
Gross Alpha	6	4	2
Gross Beta	31	20	24
^{238}Pu	1.61	.044	1.98
^{239}Pu	1.11	.384	.78
^{137}Cs	-	130	63
Total Uranium	.07	.19	.67

The results of the 1965 and 1970 analyses indicate no sediment transport out of the disposed area or off the AEC controlled property.

2. Sediment Analyses Ten-Site Canyon

Samples of sediments in Ten-Site Canyon were collected and analyzed for radionuclides due to the release of effluents from TA-35. The earliest analyses were made in 1956. The following table show results of analyses of surface sediments from 1956 through 1961.

The high activity in the Canyon is due to strontium. The major isotope of strontium released into the canyon is ^{89}Sr as shown by inventory of radionuclides treated at the site and released with liquid effluents.

Radiochemical Analyses of Sediments
1956-1961

	Distance from outfall in meters				
	At Outfall	60	400	670	930
Gross Beta 1/					
1956	824,000	885,000	29,600	2,000	1,200
1957	23,480	3,270	2,510	750	20
1958	87,420	1,910	2,440	130	-
1959	2,801	237	294	33	< 1
1960	830	370	1,470	260	< 1
1961	2,130	590	1,530	1,440	850
Strontium 2/					
1956	320,000	210,000	56,000	42,000	2,000
1957	3,800	1,400	87	350	14
1958	2,500	750	1,400	69	10
1959	61	39	110	34	-
1960	130	76	89	76	-
1961	30	22	20	20	-

1/ Counts per minute per dry gram
2/ Picocuries per dry gram

Results of analyses of samples collected in 1965 are shown on the following table.

Radiochemical Analyses, November 1965
(Analyses in counts per minute per dry gram)

Location	Gross Alpha	Gross Beta	Gross Gamma
At Outfall	4	10	16
Near TSCO-1	1	10	< 1

The results of analyses of samples collected in 1970 are presented on the following table.

Radiochemical Analyses, February 1970
(Analyses in picocuries per dry gram)

Location	Gross Alpha	Gross Beta	^{238}Pu	^{239}Pu
At Outfall	3	7	0.063	0.113
Near TSCO-1	2	4	0.044	0.369

I Inventory of Plutonium in Channel Sediments

There has been no transport of sediments out of the disposal area to the disposal area to the boundary since hydrologic observations in the canyon began.[21] The area of the canyon considered for the inventory was determined by the results of analyses that indicated above ground concentration of plutonium in the channel.

The physical characteristics of the channel used in the inventory are presented below.

Physical Characteristics of Channel

1. 0 to 1 460 m
   Width 1 m Depth 0.15 m
   Sp. g. 1.57 Weight 344 x 10^6 g

2. 1 460 m to 3 040 m
   Width 2 m Depth 0.15 m
   Sp. g. 1.57 Weight 744 x 10^6 g

The inventories were estimated using the following concentrations for February 1970 and October 1972.

Concentrations and Total Plutonium
in Sections of Channel

February, 1970

Section	Station	Concentration µCi/g	Ave.	Total Pu mCi	% of Total Pu
0-1 460	GS-1	87.9			
	MCS-3.8	3.8	45.8	15.8	93
1 460-3 040	MCO-5	2.8			
	MCO-7	.40	1.6	1.2	7
TOTAL		--	--	17.0	100

October, 1972

Section	Station	Concentration µCi/g	Ave.	Total Pu mCi	% of Total Pu
0-1 460	M-1	223			
	M-2	117			
	M-3	91			
	M-4	48			
	M-5	124			
	M-6	24			
	M-7	21			
	M-8	9.1	82	28.2	85
1 460-3 040	MCO-5	2.8			
	M-9	11	6.9	5.1	15
TOTAL		--	--	33.3	100

The recap for 1970 and 1972 is presented below.

Mortandad Canyon

Section	Total Plutonium (mCi) Feb. 1970	Oct. 1972
0-1 460	15.8	28.2
1 460-3 040	1.5	5.1
TOTAL	17.0	33.3

The inventory in Mortandad Canyon for February 1970 shows about 17.0 mCi of Pu in the reach from 0 to 3 040 m. The total release from 1963 through 1969 was 21.9 mCi. The remaining 4.9 mCi has been carried past MCO-8 by storm runoff, but not to MCO-12 where the sediments contained only background amounts of Pu. The inventory in October, 1972 shows about 33.3 mCi of Pu in the reach from 0-3 040 m. The release during the period 1964 to 1972 was 42.1 mCi. The remaining 8.8 mCi were carried east of MCO-8 by storm runoff but not to MCO-12 (Fig. 14).

J. Flood Frequency and Maximum Discharge

There has been no runoff out of the canyon disposal area to the AEC boundary since hydrologic observation began in 1960. The canyon heads on tha Pajarito Plateau and has a small drainage area. Total drainage area west of the county line is about 4.7 km^2 with 1.2 km^2 above GS-1, and an additional 2.1 km^2 from GS-1 to Obs. Hole MCO-8. Observations indicate that most, if not all, surface runoff into the canyon occurs in the 3.3 km^2 west of Obs. Hole MCO-8. The canyons contributing runoff are Mortandad, Effluent and Ten-Site canyon. East of MCO-8, the remaining 1.4 km^2 are relatively flat with no major or minor canyons entering from adjacent mesas.

The stream channel east of MCO-6 braids out on the canyon floor as the canyon begins to widen and alluvium thickens. The small drainage area with thick sections of unsaturated alluvium allows rapid infiltration of storm runoff to date.

As the channel is not well defined in the lower section of the canyon, the method for flood-frequency and maximum discharge analyses as described by Scott is not applicable. However, as the channel is well defined west of MCO-6, the flood-frequency and maximum discharge was computed at GS-1. The drainage area is 1.2 km^2 with a mean channel slope of 0.029.

Flood-Frequency and Maximum Discharge
at Gaging Station 1

Frequency	Max. Discharge m^3/sec.
2-year	1.1
5-year	3.4
10-year	5.4
25-year	12
50-year	14

The maximum discharge during the period 1962 through 1972 was estimated to be about 2.3 in which 11 x 10^3 m^3 of water passed through the gaging station. This occurred on July 31, 1968 and caused flooding in the canyon which ended between MCO-10 and MCO-12. The runoff did not reach the AEC boundary. The events predicted by use of Scott's method for the 12 years of record appear high.

The increased construction in the area (TA-35, TA-55) will increase the storm runoff into the canyon. At a maximum discharge of 2.8 to 3.4 m^2/sec at GS-1, the flood flow will probably reach the boundary and move on to Indian land.

IX. DRAINAGE AREA 8

Drainage area 8 is a small mesa top and slope which contain no defined drainage (Fig. 15). No data has been collected in the area which is about 0.5 km^2.

X. DRAINAGE AREA 9 (Cañada del Buey)

Cañada del Buey heads on the Pajarito Plateau. It has cut a canyon in the Bandelier Tuff which is quite narrow and deep just north of TA-46. The stream flow in the canyon is intermittent. One small stretch near TA-46 contains some surface flow from waste water released from the operations of a cooling tower (Fig. 15). The alluvium in the canyon is quite thin and contains little or no known perched water in tha alluvium.

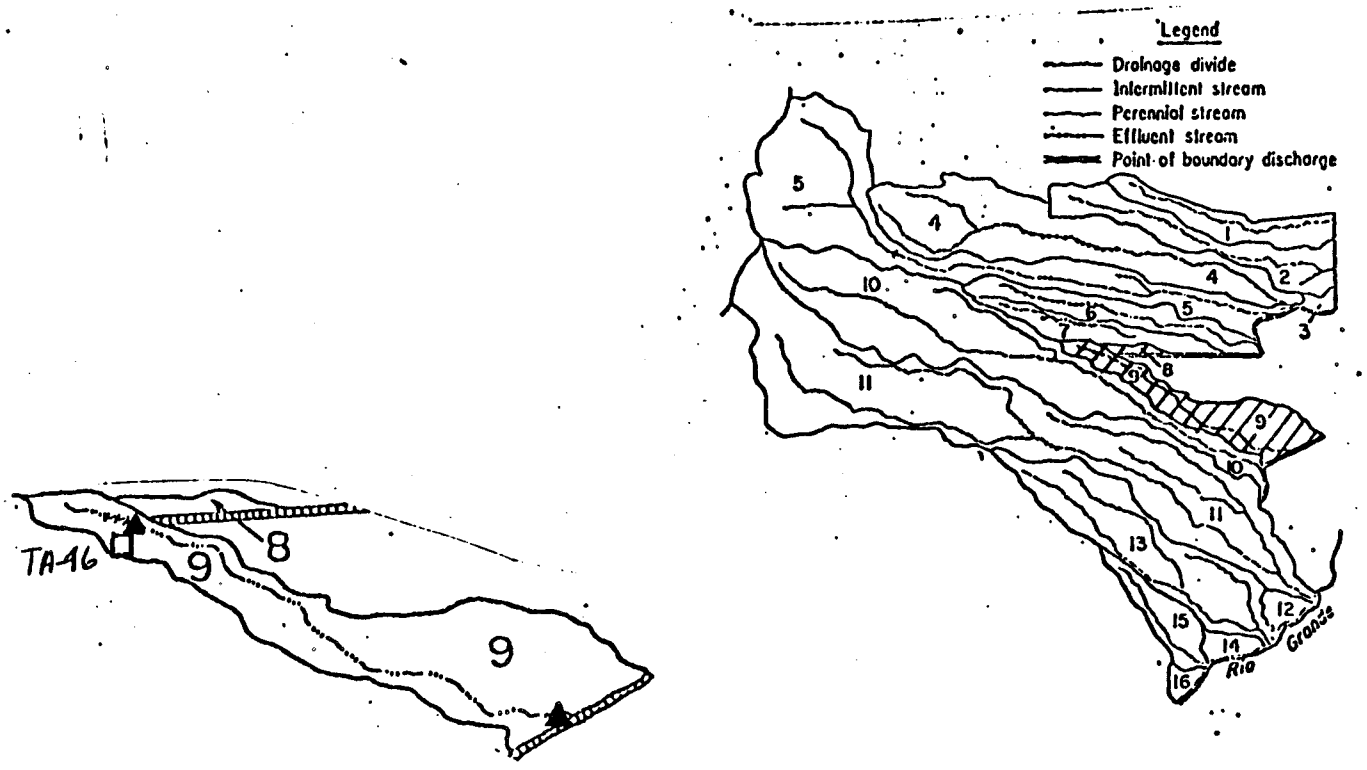

Fig. 15. Drainage Area 8 and Drainage Area 9 (Canada del Buey) showing location of sampling stations.

A. Surface Water

Intermittent flow in the canyon is from storm runoff, though a small reach of the canyon contain perennial flow from waste water released on the south wall of the canyon from TA-46. It is this waste water that is sampled for chemical and radiochemical constituents.

1. Chemical Quality of Surface Water

The chemical quality of the water in the canyon reflects the release of waste water from TA-46. The following table presents the quality of water in the canyon from 1967 through 1972.

Chemical Quality of Surface Water in Canada del Buey
Near TA-46, in mg/l except as noted

Year	No. of Analyses	Na	Cl	F	NO_3	TDS	Conductance[a]	pH[b]
1967	1	41	5	2.6	9.7	183	170	8.0
1971	1	24	5	0.8	17	184	180	7.3
1972	1	17	6	1.0	4.4	162	140	7.3

[a] Microhmos at 25° C
[b] No Units

Select trace metal ion analyses were made of the water in 1971 and 1972 at the same station.

Metal Ion Analyses
µg/l

	1971	1972
In Solution		
Cadmium	0.92	0.25
Beryllium	<0.25	<0.25
Lead	<1.0	5.5
Mercury	<0.02	<0.02
Particulates		
Cadmium	0.49	<0.25
Beryllium	<0.25	<0.25
Lead	2.9	<1.0
Mercury	<0.02	--

The chemical quality of the water is good. The concentration dissolved is low, in the range of water in the municipal water supply.

2. Radiochemical Quality of Surface Water

Radiochemical quality of surface water in Cañada del Buey below TA-46 is shown below for the year 1970 through 1971.

Radiochemical Quality of Surface Water in Cañada del Buey Near TA-48

pCi/l except as noted

	1970	1971	1972
Gross Alpha	1	2	<1
Gross Beta	5	3	2
^{238}Pu	< 0.05	< 0.05	0.20
^{239}Pu	< 0.05	< 0.05	<0.05
^{137}Cs	-	-	<350
Tritium	-	-	1,100
Total Uranium a/	0.4	0.4	1.8

a/ µg/l

B. Radiochemical Analyses of Sediments

Channel sediments in Cañada del Buey are derived from the Bandelier Tuff. The particle size distribution was made of sediments in the canyon at the AEC Boundary on State Road 4.

	Particle-Size Distribution (Percent by Weight)
Granules	2.0
Sand	
Very Coarse	31.5
Coarse	40.0
Medium	13.5
Fine	7.0
Very Fine	3.0
Silt and Clay	2.0

Radiochemical analyses at the same station for the year 1965 and 1970 are shown below.

Radiochemical Quality of Sediments in Cañada del Buey at State Road 4

	1965 1/	1970 2/
Gross Alpha	2	1
Gross Beta	<1	1
Gross Gamma	14	-
^{238}Pu	-	<0.002
^{239}Pu	-	0.009

1/ Counts per minute per dry gram

2/ Picocuries per dry gram

C. Flood - Frequency and Maximum Discharge

Cañada del Buey heads on the Pajarito Plateau at an altitude of 2 210 ft. The flood-frequency and maximum discharge are based on the following data:

Drainage Areas 3.4 sq mi Main Channel Slope 110 ft/mi

Frequency	Maximum Discharge (Cfs)
2 Year	2.6
5 Year	6.2
10 Year	9.4
25 Year	19
50 Year	21

XI. DRAINAGE AREA 10 (Pajarito Canyon)

Pajarito Canyon heads on the flanks of the Sierra de los Valles and thus drains a large area (Fig. 16). The stream channel is cut into the Bandelier Tuff across the Pajarito Plateau. The alluvium is thin in the upper reaches of the canyon and thickens eastward. Stream flow in the canyon is intermittent from storm runoff and snowmelt. The intermittent flow recharges water which moves downgradient in the alluvium overlying the tuff. Water in the alluvium is seasonal and dependent on intermittent flow for recharge.

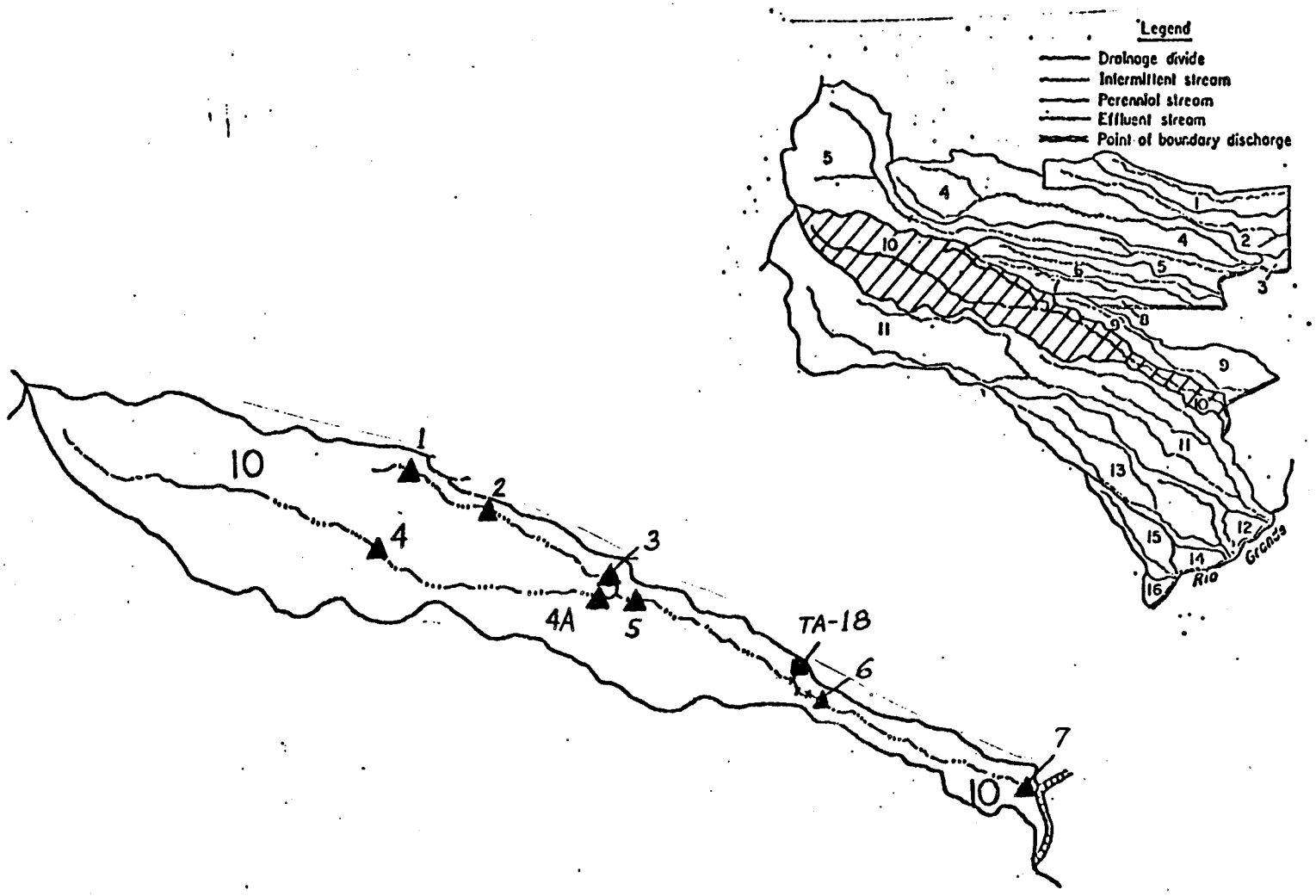

Fig. 16. Drainage Area 10 (Pajarito Canyon) showing location of sampling stations.

A. Surface Water

There is only minor release of water or treated sewage effluent into the canyon, mainly from TA-18. There is one surface water sampling station in the canyon below TA-18. The canyon bottom in this area has been excavated for gravel or base coarse. There are no observation holes in the canyon.

1. Chemical Quality of Surface Water

Water samples for chemical analyses are collected from one of the gravel pits below TA-18. The following table presents the quality of water from near TA-18.

Chemical Quality of Water in Pajarito Canyon Near TA-18
in mg/l except as noted

Year	No. of analyses	Na	Cl	F	NO_3	TDS	Conductance[a]	pH[b]
1962	1	46	11	0.4	0.9	204	210	7.0
1967	2	36	11	1.5	0.9	186	210	7.9
1971	1	24	5	0.8	1.8	184	180	7.3
1972	1	17	6	1.0	0.4	162	140	7.3

a Micromhos at 25° C

b No Units

Select trace metal ion analyses were made of water in 1971 and 1972 at the same station

Metal Ion Analyses
(In parts per Billion)

	1971	1972
In Solution		
Cadmium	1.6	0.38
Beryllium	<0.25	<0.25
Lead	<1.0	4.5
Mercury	<0.02	<0.02
Particulates		
Cadmium	0.64	<0.25
Beryllium	<0.25	<0.25
Lead	5.8	<1.0
Mercury	<0.02	-

The chemical quality of the water is good as shown by low total dissolved solids.

2. Radiochemical Quality of Surface Water

The radiochemical quality of water from the gravel pit near TA-18 for 1962 and 1967 is presented on the following table.

Radiochemical Quality of Surface Water 1962 and 1967
(Picocuries per liter, except as noted)

	1962	1967
No. of Analyses	1	2
Gross Beta	<14	< 1.4
Total Plutonium	< 0.4	< 0.4
Total Uranium [a]	< 0.5	< 0.5

[a] μg/l

B. Radiochemical Analyses of Sediments

Main stems of Pajarito Canyon west of TA-18 consist of two canyons, Pajarito and Two-Mile Canyons, which head on the flanks of the mountains. The sediments in the canyon are derived from weathering of the Tschicoma Formation and Bandelier Tuff.

Particle size distribution from stations in the drainage area are shown on the following table while locations are shown on Figure .

Particle-Size Distribution
(Percent by Weight)

Stations	1	2	3	4	5	6	7
Granules	8.5	3.0	17.5	8.0	20.5	2.5	14.5
Sand							
Very Coarse	22.5	24.0	36.0	22.0	44.0	15.0	34.0
Coarse	41.0	46.0	34.0	31.5	26.0	52.0	33.5
Medium	17.5	19.5	8.0	22.0	6.0	26.0	8.0
Fine	5.5	5.0	2.0	11.5	2.0	3.0	2.0
Very Fine	2.0	1.0	0.5	3.5	1.0	0.5	2.0
Silt and Clay	3.0	1.5	1.5	1.5	0.5	0.5	5.0

The following table presents the radiochemical analyses of sediments collected in 1965.

Sediment Analyses, 1965
(Counts per minute per dry gram)

Station	Gross Alpha	Gross Beta	Gross Gamma
1	1	<1	20
2	1	<1	8
3	1	<1	8
4	1	<1	18
5	2	8	4
6	3	<1	48
7	3	<1	<1

A second set of samples were collected in 1970 from similar stations. The results are shown on the following table.

Sediment Analyses, 1970
(pCi/g)

Station	Gross Alpha	Gross Beta	^{238}Pu	^{239}Pu
1	1	<1	.018	.003
2	2	1	.019	<.002
3	1	<1	.016	.038
4	2	<1	<.002	.004
4A	2	2	<.002	.003
5	2	2	<.002	.009
6	<1	<1	<.002	<.002
7	2	2	<.002	.008

Four (4) samples were collected from station 7 (Pajarito Canyon at State Road 4) in 1971 and 1972. The analyses are shown on the following table.

Sediment Analyses 1971 & 1972
(pCi/g except as noted)

	5-7-71	10-14-71	4-5-72	10-10-72
Gross Alpha	2	5	-	2
Gross Beta	4	18	-	12
^{238}Pu	0.002	0.001	-	0.003
^{239}Pu	0.002	0.002	-	0.026
^{137}Cs	-	4.1	1.9	9.1
Total Uranium	0.07	0.05	0.18	0.58

The radiochemical analyses of sediments in the drainage area are low, in the range of worldwide fallout.

C. Flood-Frequency and Maximum Discharge

Pajarito Canyon heads on the flanks of the mountains at an altitude of 3 170 m. The flood-frequency and maximum discharge are based on the following data.

Drainage Area 27.4 km^2; Main Channel Slope -0.039.

Frequency	Maximum Discharge (m^3/sec)
2-year	3.0
5-year	7.1
10-year	10
25-year	16
50-year	20

XII. DRAINAGE AREA II (WATER CANYON)

Water Canyon heads on the flanks of the mountains where it has cut canyons into the Tschicoma Formation and Bandelier Tuff. Across the plateau the canyons are cut into the Bandelier Tuff while along the eastern edge where the canyon joins the Rio Grande the canyon is cut into basalts of Chino Mesa and underlying Tesuque Formation. The alluvium is thin in canyons on the flanks of the mountains where the channel gradient is steep, and the alluvium thickens across the plateau. Near State Road 4 gravels have been removed for use as base coarse.

A. Surface Water

A perennial stream occurs in Upper Valles Canyon which is tributary to Water Canyon near the center of the plateau. Several springs discharge from perched layers in the tuff in Upper Water Canyon (Fig. 17). One of the larger Springs (Water Canyon-S-Site Supply) furnishes a part of the water supply for the S-Site area. Waste water from several areas in S-Site is released into Valles Canyon and Water Canyon. This water moves into the alluvium a short distance downgradient from the junction of these two canyons. The stream flow in the remainder of Water Canyon is intermittent and results from storm runoff and snow melt. There are no observation holes in the alluvium that have been used as a part of the monitoring net.

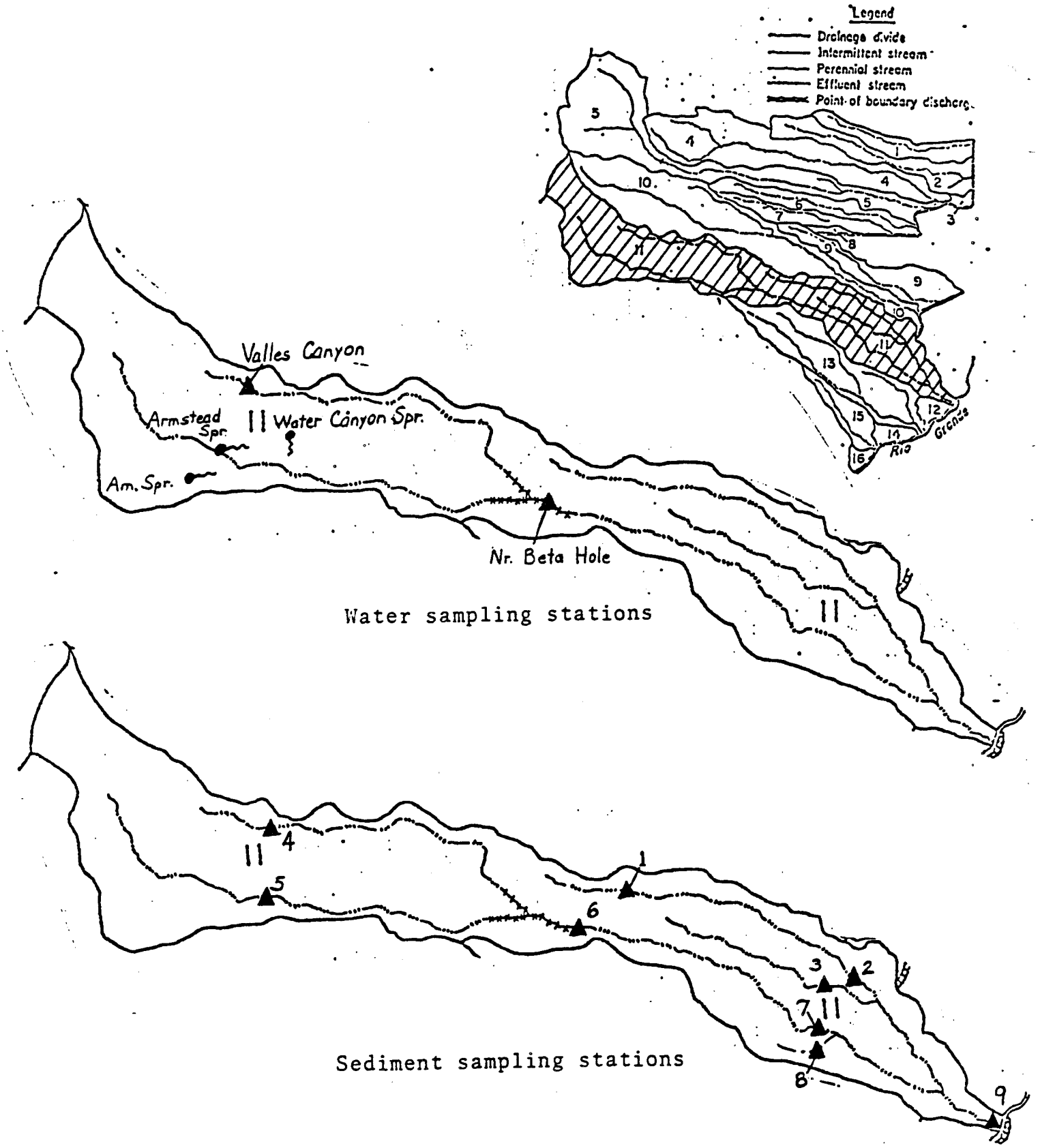

Fig. 17. Drainage Area 11 (Water Canyon) showing locations of sampli stations.

1. Chemical Quality of Surface Water

Springs that discharge from perched zones in the Bandelier Tuff on the flanks of the mountains are American Springs, Armstead Spring, and Water Canyon (S-Site Water Supply). Other sources of surface water is waste water near Beta Hole. Beta Hole is drilled through a thin section of alluvium near the north side of the canyon and completed 187 ft into the tuff, and is dry. The following table presents the chemical quality of water.

Chemical Quality of Surface Water
(mg/l except as noted)

Sources	Year	No. of Analyses	Na	Cl	F	NO3	TDS	Conductance[a]	pH[b]
Am. Spr.	1952	1	5	2	0.4	0.7	80[c]	120	7.1
Am. Spr.	1967	1	8	3	<.4	.4	112	100	7.4
Am. Spr.	1969	1	10	3	<.4	.2	147	105	7.4
Am. Spr.	1970	1	4	1	<.4	.1	80[c]	120	7.2
Armstead Spr.	1958	1	6	2	.4	.5	70[c]	105	7.4
Armstead Spr.	1961	1	4	1	.2	.2	65[c]	100	6.9
Armstead Spr.	1969	1	5	2	<.4	.2	123	130	7.3
Valle Canyon	1961	1	3	<1	<.4	<.1	-	70	6.9
Water Canyon	1952	1	2	5	1.0	<.1	-	-	-
Water Canyon	1967	1	8	5	<.4	.2	37	70	7.9
Water Canyon	1969	1	9	<1	<.4	.1	112	140	7.5
Water Canyon	1970	1	4	<1	<.4	1.7	86	120	6.9
Water Canyon	1971	1	6	2	.9	.3	98	140	7.2
Water Canyon	1972	3	7	1	.9	.2	83	120	7.8
Near Beta Hole	1970	1	19	8	3.9	.2	255	280	7.8
Near Beta Hole	1971	1	25	5	.9	.2	160	150	7.3
Near Beta Hole	1972	1	27	14	.4	.1	162	190	7.0

[a] Micromhos at 25° C

[b] No Units

[c] Estimated

Select trace metal ion analyses have been made of water from Water Canyon (S-Site Supply) and at the station near Beta Hole.

Metal Ion Analyses

(In μg/l)

	Water Canyon		Near Beta Hole	
In Solution	1971	1972	1971	1972
Cadmium	0.40	<0.25	1.5	<0.25
Beryllium	<0.25	<0.25	<0.25	<0.25
Lead	1.3	<1.0	2.0	5.5
Mercury	<0.02	<0.02	<0.02	<0.02
Particulates				
Cadmium	<0.25	<0.25	0.44	<0.25
Beryllium	<0.25	<0.25	<0.25	<0.25
Lead	2.2	<1.0	2.2	<1.0
Mercury	<0.02	<0.02	<0.02	<0.13

The total dissolved solids concentration of surface water in the canyon is low, showing only minor deterioration of water used in processes at S-Site.

2. Radiochemical Quality of Surface Water

Radiochemical analyses of surface water were made of samples collected from American Springs, Water Canyon (S-Site Supply), Valle Canyon, and near Beta Hole. The results are shown on the following table.

Radiochemical Analyses
(pCi/l except as noted)

Source	Year	No. of Analyses	Gross Alpha	Gross Beta	^{238}Pu	^{239}Pu	Total Uranium[a/]
American Spr.	1967	1	2	7	<0.05	<0.05	0.4
American Spr.	1969	1	<1	3	<0.05	<0.05	0.5
American Spr.	1970	1	<1	10	<0.05	<0.05	0.4
Water Canyon	1967	1	2	6	<0.05	<0.05	1.3
Water Canyon	1969	1	4	6	<0.05	<0.05	2.5
Water Canyon	1970	1	2	5	<0.05	<0.05	0.4
Water Canyon	1971	1	<1	< 1	<0.05	<0.05	<0.4
Water Canyon	1972	3	<1	7	<0.05	<0.05	0.2
Valle Canyon	1967	1	<1	6	<0.05	<0.05	<0.4
Valle Canyon	1969	1	<1	2	<0.05	<0.05	0.6
Near Beta Hole	1970	1	1	2	<0.05	<0.05	2.1
Near Beta Hole	1971	1	2	2	<0.05	<0.05	0.7
Near Beta Hole	1972	1	<1	3	<0.05	<0.05	1.3

[a] μg/l

The analyses show only background amounts of radionuclides except for the one 1972 analysis from near Beta Hole where traces of plutonium 238 were reported in the water.

B. Radiochemical Analyses of Sediments

A number of canyons are tributary to Water Canyon. Sediment samples for particle-size distribution and radiochemical analyses were collected from channels in the tributary canyons as well as in Water Canyon.

Particle-size distribution from stations in the drainage area are shown on the following table while locations are shown on Fig. 17.

Particle-Size Distribution
(Percent by Weight)

Stations	1	2	3	4	5	6	7	8	9
Granules	7.0	3.0	3.5	40.0	25.0	3.0	2.5	11.0	3.0
Sand									
Very Coarse	51.5	35.5	50.5	27.0	34.5	30.5	28.0	32.5	27.0
Coarse	34.0	41.5	41.0	18.0	28.5	44.5	56.5	36.0	48.0
Medium	4.0	11.5	3.5	5.0	7.0	14.0	15.0	11.0	15.0
Fine	1.0	4.5	0.5	3.5	2.0	5.5	4.0	4.5	4.5
Very Fine	0.5	1.5	0.5	3.0	0.5	2.0	1.5	3.5	1.0
Silt and Clay	0.5	1.5	0.5	2.5	1.5	1.0	2.5	2.0	1.0

The following table presents radiochemical analyses of sediments collected in the drainage area in 1965.

Sediment Analyses, 1965
(Counts per minute per dry gram)

Station	Gross Alpha	Gross Beta	Gross Gamma
1	5	1	46
2	2	<1	34
3	1	2	24
4	2	<1	28
5	<1	8	36
6	<1	<1	2
7	1	18	4
8	2	<1	12
9	1	11	12

In 1970 a series of samples were collected at the same stations and analyzed for gross alpha and beta activity as well as plutonium.

Sediment Analyses, 1970
(Picocuries per dry gram)

Station	Gross Alpha	Gross Beta	^{238}Pu	^{239}Pu
1	3	4	<0.002	0.006
2	1	2	<0.002	<0.002
3	3	3	<0.002	0.004
4	2	4	<0.002	0.011
5	4	4	<0.002	0.022
6	1	1	<0.002	0.050
7	2	2	<0.002	0.003
8	2	2	<0.002	<0.002
9	<1	<1	0.010	<0.002

Additional channel samples were collected at Station 1, near Beta Hole and Station 7 in 1971 and 1972.

Sediment Analyses, 1971 and 1972
(Picocuries per dry gram)

Station	Date	Gross Alpha	Gross Beta	^{238}Pu	^{239}Pu	^{137}Cs	Total Uranium
1	10-71	11	8	0.005	0.007	<1.5	2.8
1	11-72	1	7	0.008	0.004	4.6	5.2
Near Beta Hole	5-71	1	1	0.004	0.001	-	-
Near Beta Hole	10-71	<1	4	<0.003	0.004	4.5	0.44
7	5-71	1	<1	<0.001	<0.001	-	-
7	10-71	5	4	<0.001	0.001	<1.5	0.15
7	10-72	3	14	<0.003	<0.003	4.8	0.09

The results of the radiochemical analyses of sediments indicate only background amounts of radionuclides except the total Uranium in samples from Station 1 which is in Potrillo Canyon. The uranium is probably due to tests or experiments that are or were done in the area.

C. Flood-Frequency and Maximum Discharge

Water Canyon heads on the flanks of the mountains at an altitude of 3 170 m. Some perennial flow occurs in the main stem of Valles and Water Canyons on the flanks of the mountains. The remainder of the channel carries only intermittent storm runoff. The flood-frequency and maximum discharge is based on the following data:

Drainage Area 33.2 km^2

Main Channel Slope-0.050

Frequency	Maximum Discharge m^2/sec
2-Year	2.8
5-Year	6.8
10-Year	9.6
25-Year	14
50-Year	18

XIII. DRAINAGE AREA 12

Drainage area 12 is a steep canyon wall on the west side of the Rio Grande and contains no well defined drainage (Fig. 18). The area is about 1.3 km^2. No data has been collected in the area.

XIV. DRAINAGE AREA 13 (ANCHO CANYON)

Ancho Canyon heads on the middle of the Pajarito Plateau. The canyon is cut into the Bandelier Tuff on the plateau, and through the basaltic rocks of Chino Mesa and Tesuque Formation at the eastern edge as the channel drops into the Rio Grande.

A. Surface Water

Stream flow in the channel on the plateau is intermittent. In the lower reaches of the canyon is a perennial stream fed by springs in the Totavi Lentil (Fig. 18). The stream reaches the Rio Grande. There are no known releases of effluent from Technical Areas within the drainage area. There is probably some small volumes of water perched in the alluvium seasonally.

1. Chemical Quality of Surface Water

Spring and surface water stations are located in the lower reach of the canyon. Ancho Spring discharges from the Totavi Lentil which is overlain by basalt. The underlying Tesuque Formation also adds to the volume of flow. The chemical analyses from these two stations are shown on the following table.

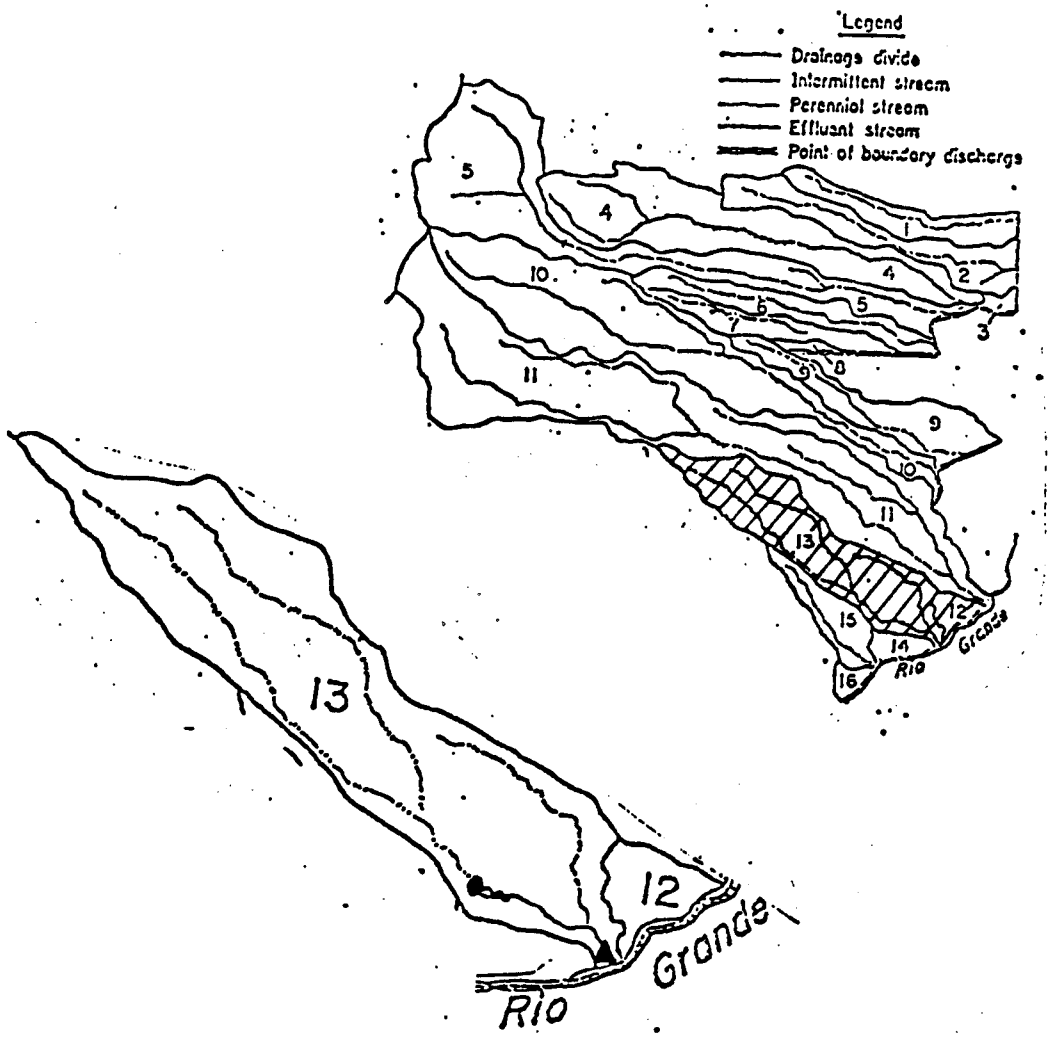

Water sampling stations

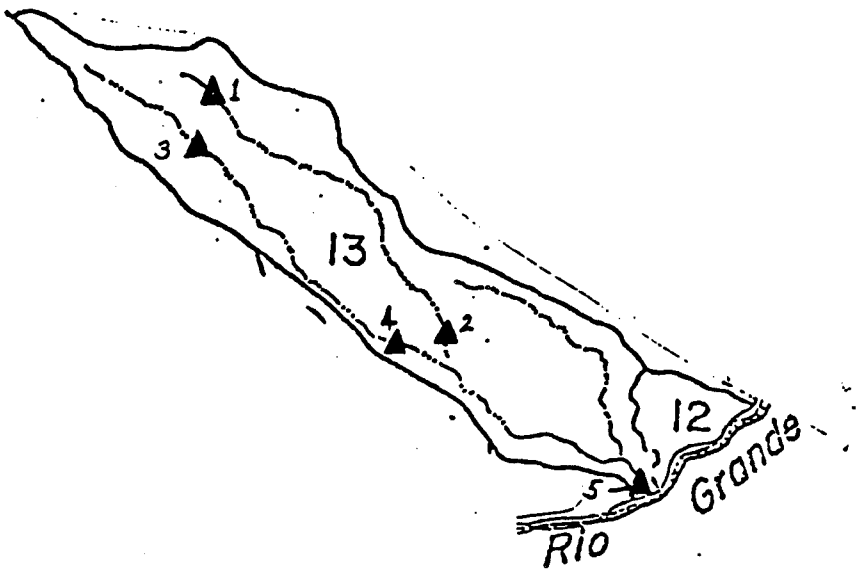

Sediment sampling stations

Fig. 18. Drainage Area 12 and Drainage Area 13 (Ancho Canyon) showing locations of sampling stations.

Chemical Quality of Surface Water
(Average of a number of analyses in mg/l except as noted)

Source	Year	No. of Analyses	Na	Cl	F	NO_3	TDS	Conductance[a]	pH[b]
Ancho Spr.	1952	2	7	6	1.6	.2	146	-	7.7
Ancho Spr.	1953	4	8	4	.3	.5	168	-	7.8
Ancho Spr.	1954	2	9	2	.4	.6	115	-	7.5
Ancho Spr.	1955	1	9	2	.4	.2	673	-	7.2
Ancho Spr.	1956	3	12	3	.4	.5	148	-	7.9
Ancho Spr.	1957	1	12	3	.5	.4	148	-	7.9
Ancho Spr.	1959	2	10	2	.4	.4	90[c]	140	7.7
Ancho Spr.	1960	1	10	3	.4	.5	85[c]	130	7.8
Ancho Spr.	1961	1	10	3	.4	.9	85[c]	130	7.8
Ancho Spr.	1962	1	8	3	.4	2.2	183	165	7.6
Ancho Spr.	1963	1	13	3	.4	3.6	124	140	7.6
Ancho Spr.	1965	1	7	3	.5	2.2	124	140	7.7
Ancho Spr.	1969	1	19	3	.1	.4	206	260	8.5
Ancho Spr.	1971	1	12	2	.1	.9	162	200	7.9
Near Rio Grande	1963	1	15	5	.8	.4	204	240	8.1
Near Rio Grande	1964	1	11	4	.4	.4	271	240	8.8
Near Rio Grande	1967	1	17	1	.8	.4	203	260	7.6
Near Rio Grande	1969	1	21	2	.5	.4	156	270	8.4
Near Rio Grande	1971	1	12	2	.1	.4	158	140	8.6

[a]Micromhos at 25° C
[b]No Units
[c]Estimated

Select trace metal ions analyses were made from Ancho Spring and the stream near the Rio Grande in 1971.

Metal Ion Analyses
(In μg/l)

	Ancho Spring	Stream Near Rio Grande
In Solution		
Cadmium	1.7	1.5
Beryllium	< .25	< .25
Lead	<1.0	<1.0
Mercury	< .02	< .02
Particulates		
Cadmium	< .25	.25
Beryllium	< .25	< .25
Lead	<1.0	2.6
Mercury	< .02	< .02

The chemical quality of water from the spring is low in total dissolved solids and shows no effect of Laboratory operations.

2. Radiochemical Quality of Surface Water

Radiochemical analyses of surface water were made of samples collected from Ancho Spring and from the stream near the Rio Grande. The results of samples from 1960 through 1967 are shown on the following table.

Radiochemical Analyses, 1960-1967
(pCi/l except as noted)

Source	Year	Gross Beta	Total Plutonium	Total Uranium a/
Ancho Spr.	1960	<14	<0.4	<0.5
Ancho Spr.	1961	<14	< .4	< .5
Ancho Spr.	1962	<14	< .4	.5
Ancho Spr.	1963	<14	< .4	3.1
Ancho Spr.	1965	<14	< .4	< .5
Nr. Rio Grande	1963	27	< .4	< .5
Nr. Rio Grande	1964	6	< .4	< .5
Nr. Rio Grande	1967	4	< .4	< .5

a/ μg/l

Radiochemical analyses from the two stations from 1969 and 1971 are shown on the following table.

Radiochemical Analyses, 1969-1971
(Picocuries per liter, except as noted)

Source	Year	Gross Alpha	Gross Beta	238 Pu	239 Pu	Total Uranium
Ancho Spr.	1969	<1	1	<0.05	<0.05	0.4
Ancho Spr.	1971	<1	<1	<0.05	<0.05	<0.4
Nr. Rio Grande	1969	<1	2	<0.05	<0.05	0.7
Nr. Rio Grande	1971	<1	1	<0.05	<0.05	<0.4

The analyses show only background concentrations of radionuclides.

B. Radiochemical Analyses Sediments

The sediments in the canyon at stations 1, 2, 3, and 4 are derived from weathering of the Bandelier Tuff while those at Station 5 are a combination of weathering of the Bandelier Tuff, basaltic rocks of Chino Mesa, Puye Formation, and Tesuque Formation. Particle-size distribution from stations in the drainage are shown on the following table.

Particle-Size Distribution
(Percent by Weight)

Station	1	2	3	4	5
Granules	3.0	1.0	10.5	8.5	5.5
Sand					
Very Coarse	48.5	21.0	53.5	26.0	43.0
Coarse	35.0	44.5	29.5	27.5	41.5
Medium	9.0	16.5	4.0	13.5	6.5
Fine	3.0	8.5	2.0	10.0	1.5
Very Fine	1.0	4.5	1.0	4.5	1.0
Silt and Clay	0.5	3.0	1.0	5.0	1.0

The following table presents radiochemical analyses of sediments collected in the drainage area in 1965. Locations are shown on Fig. 18.

Sediment Analyses, 1965
(Counts per minute per day gram)

Station	Gross Alpha	Gross Beta	Gross Gamma
1	2	<1	12
2	2	14	46
3	1	<1	26
4	1	15	14
5	1	1	8

Similar stations were sampled and analysed in 1970. The results are shown on the following table.

Sediment Analyses, 1970
pCi per dry gram

Station	Gross Alpha	Gross Beta	^{238}Pu	^{239}Pu
1	2	<1	<0.002	<0.002
2	2	2	<0.002	<0.002
3	<1	1	<0.002	0.006
4	1	<1	<0.002	<0.002
5	1	1	0.010	0.007

The results of the analyses indicate that radiochemical concentrations in the sediment in the drainage area are background.

C. Flood-Frequency and Maximum Discharge

Ancho Canyon heads on the Pajarito Plateau at an altitude of 2 220 m. Stream flow in the canyon is intermittent except in the lower reach. In the lower reach to the Rio Grande, the stream flow is perennial at less than 0.2 m^2/sec. Flood-frequency and maximum discharge is based on the following data:

Drainage Area 17.4 km^2
Main Channel Slope-0.045

Frequency	Maximum Discharge (m^2/sec)
2-Year	2.3
5-Year	5.4
10-Year	8.2
25-Year	14
50-Year	17

XV DRAINAGE AREA 14

Drainage area 14 is a steep wall on the west side of the Rio Grande and contains no well defined drainage (Fig. 19). The area is about 1.6 km^2. No data has been collected in this drainage.

XVI. DRAINAGE AREA 15 (CHAQUEHUI CANYON)

Chaquehui Canyon heads on the eastern part of the Pajarito Plateau. The canyon is cut into the Bandelier Tuff and through the basaltic rocks of Chino Mesa and Tesuque Formation as the Channel drops steeply to the Rio Grande. There are no observation holes in the canyon though there is water perched locally in the alluvium.

A. Surface Water

Stream flow in the channel is intermittent. Near the eastern reaches of the canyon water from springs and seeps in the Tesuque Formation maintains a small stream and several large pools which infiltrate into the alluvium prior to reaching the Rio Grande (Fig. 19). There are no release of effluents into the drainage area.

1. Chemical Quality of Surface Water

A sampling station has been established from one of the pool areas below the spring discharge from the sandstones and silt-

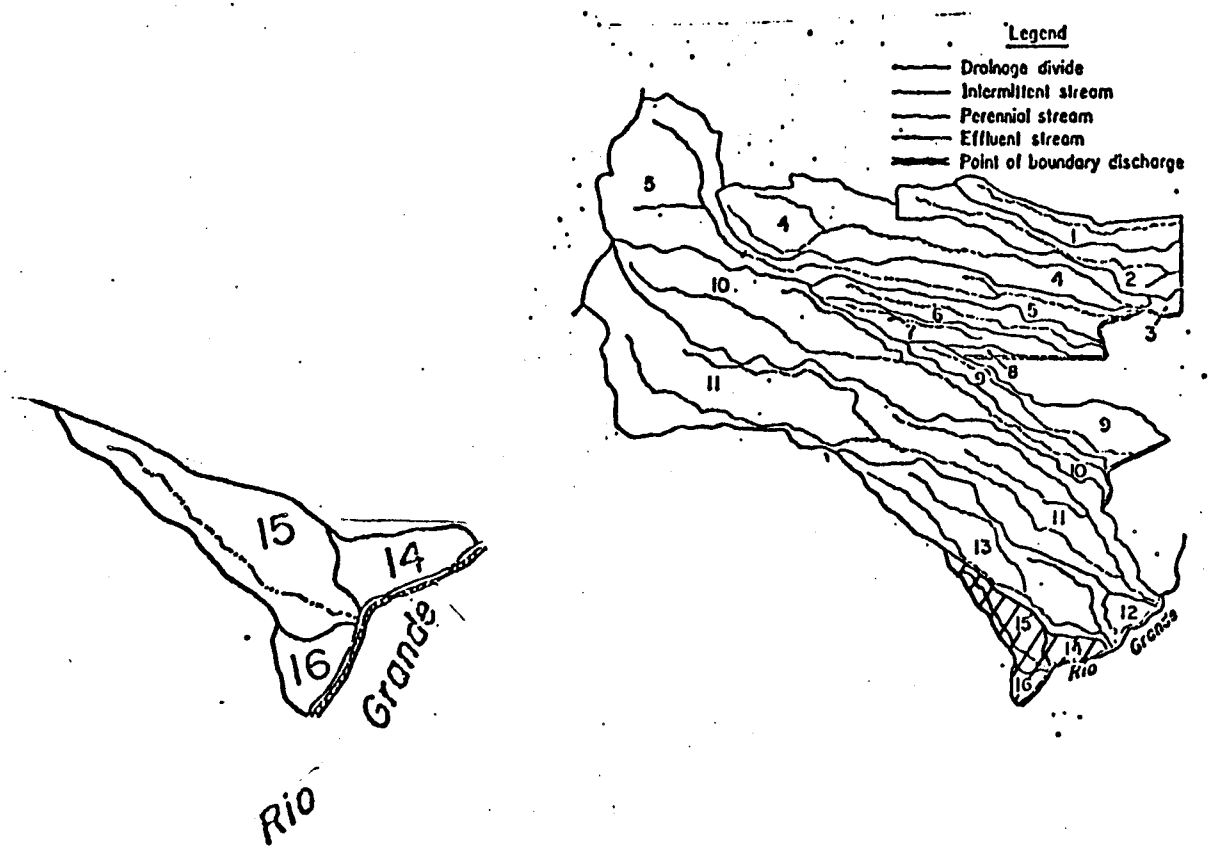

Fig. 19. Drainage Area 14, Drainage Area 15 (Chaquehui Canyon), and Drainage Area 16.

stones of the Tesuque Formation. The following table recaps the chemical analyses from this station which is called Doe Spring.

Chemical Quality of Water from Doe Spring
(In mg/l except as noted)

Year	Analyses	Na	Cl	F	NO_3	TDS	Conductance[a]	pH[b]
1956	1	15	2	0.3	2.6	180	240[c]	7.6
1957	1	11	2	.6	2.6	170[c]	260	7.8
1959	1	11	2	.4	1.3	160[c]	250	7.7
1960	1	12	2	.5	.4	170[c]	260	7.3
1961	1	11	1	.5	.4	165[c]	240	7.7
1962	1	9	2	.4	.9	186	220	7.5
1963	1	10	2	.4	.4	129	140	7.5
1965	1	13	5	.2	.4	218	240	7.8
1967	1	23	1	.3	.9	304	320	7.9
1969	1	22	3	.2	<.4	153	180	8.4
1971	1	21	4	.3	.9	219	260	8.0

a Micromhos at 25° C

b No Units

c Estimated

Trace metal ion analyses were made from Doe Spring in 1971.

Metal Ion Analyses
(In μg/l)

In Solution	Doe Spring
Cadmium	1.9
Beryllium	<0.25
Lead	<1.0
Mercury	<0.02
Particulates	
Cadmium	<0.25
Beryllium	<0.25
Lead	<1.0
Mercury	<0.25

The chemical quality of water from the spring is low. The increase in total dissolved solids in 1965 and 1967 may show the effect of residual from storm runoff in the pool.

2. Radiochemical Quality of Surface Water

The recap of radiochemical analyses from 1957 through 1967 are presented as follows:

Radiochemical Analyses of Water
from Doe Spring, 1957-1967
(pCi/l except as noted)

Year	Gross Beta	Total plutonium	Total Uranium[a]
1959	<14	<.4	<.5
1960	<14	<.4	<.5
1962	<14	<.4	<.5
1963	<14	<.4	1.2
1965	<14	<.4	<.5
1967	26	<.4	.5

[a] μg/l

The recap of radiochemical analyses 1969 and 1971.

Radiochemical Quality of Water from Doe Spring
1969-1971
(pCi/l, except as noted)

	1969	1971
Gross Alpha	<1	<1
Gross Beta	1	3
^{238}Pu	<0.05	<0.05
^{239}Pu	<0.05	<0.05
Total Uranium[a]	0.4	0.6

[a] μg/l

The analyses show no radionuclide above limits of detection except uranium which is natural occurring in the discharge from the spring aquifer.

B. Radiochemical Analyses of Sediments

There were no particle-size distribution made of sediments in the canyon. One set of sediment analyses were analyzed from the mouth of the canyon in September 1969.

Radiochemical Analyses of Sediments
(pCi per dry gram)

Gross Alpha	2
Gross Beta	3
^{238}Pu	0.003
^{239}Pu	0.003

The levels of radioactivity are background or in the case of plutonium are no greater than world-wide fallout from atmospheric testing.

C. Flood Frequency and Maximum Discharge

Chaquehui Canyon heads on the Pajarito Plateau at an altitude of m Stream flow is intermittent except for a short reach near the eastern reach (Fig. 19). The flood-frequency and miximum discharge is based on the following data:

Drainage Area 4.7 km^2
Main Channel Slope-0.078

Frequency	Maximum Discharge (m^2/sec)
2-year	1.1
5-year	3.0
10-year	4.5
25-year	8
50-year	10

XVII DRAINAGE AREA 16

Drainage Area 16 is a steep wall on the west side of the Rio Grande and contains no well defined drainage (Fig. 19). The area is about 1.0 km^2.

No data has been collected in this drainage.

XVIII PERCHED WATER IN THE PUYE FORMATION

The only known body of water perch in the Puye Formation above the main aquifer occurs in the mid-reach of Drainage Area 4 (Pueblo Canyon). Other areas of perched water in the Puye may occur, but the limited number of deep test holes (seven test holes 300 m) did not encounter water perched in the Puye (Fig. 20).

Test well 2 A was drilled in 1947 to a depth of 40.5 m. The well has been equipped with a pump. The hole penetrated alluvium, Bandelier Tuff, and was completed in the fanglomerate. The fanglomerate is a slightly cemented unit of sand, gravels, and boulders with silt and clay lenses. The following table presents the geologic log.

Geologic Log of TW-2A
(Altitude of Land Surface 2026 m)

Unit	Thickness (m)	Depth (m)
Alluvium	3.4	3.4
Bandelier Tuff		
Otowi Member	6.4	9.8
Guaje Member	9.8	19.6
Puye Formation (fanglomerate)	21.3	40.9

The following table presents some of the hydrologic characteristics as were determined by an aquifer test.

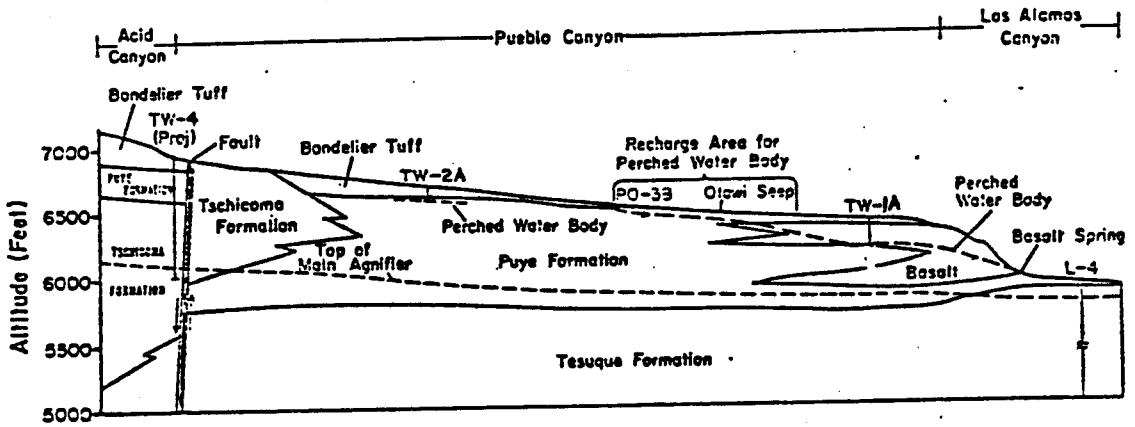

Cross-Section showing perched water in Puye Formation and Basaltic Rocks of Chino Mesa.

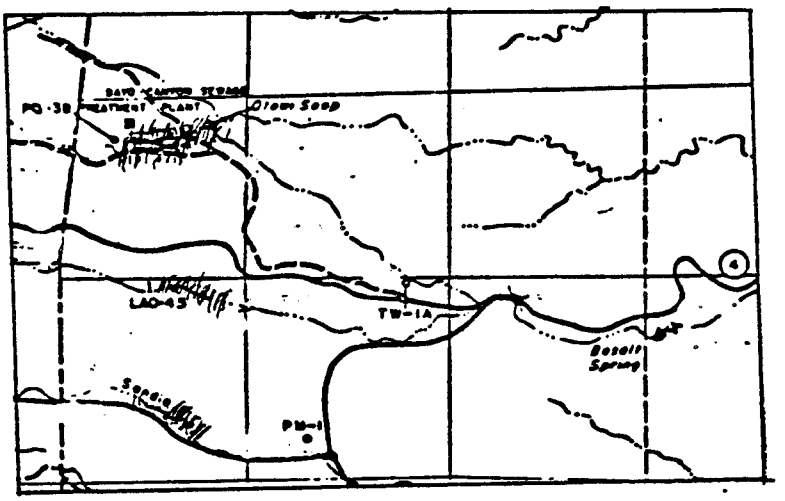

Recharge Area

Location of Recharge Area to perched aquifer at TW-1A, PM-1 and Basalt Spring.

Figure 20. Cross-section and map showing perched water in the Puye Formation and Basaltic Rocks of Chino Mesa.

Aquifer Test TW-2A (1952)

Thickness of Aquifer (m)	1.5
Duration of Test (hrs)	4.5
Pumping rate (l/sec)	0.018
Water level prior to Test (m)	35.4
Total Drawdown (m)	3.1
Specific Capacity [(l/sec)/(m)]	
First 4 hr	0.062
Entire Test	0.062
Transmissivity (m^2/day)	0.62
Hydrologic Conductivity (m/day)	0.41

The aquifer is of limited areal extent. The changes in water levels over a period of time indicate that the aquifer is hydraulically connected to the stream flow in Pueblo Canyon. The water level response to recharge to the aquifer is estimated at 4 to 6 months at Test Well 2A.

A. Chemical Quality of Water

Water samples have been collected from the test hole from 1951 through 1965. The following table presents a summary of the chemical quality to 1965.

Chemical Quality of Water TW-2A
(Average of a number of analyses in mg/l)

Year	No. of Analyses	Na	Cl	F	NO_3	TDS
1951	1	-	2	0.4	2	109
1952	2	-	2	.2	2	115
1953	8	-	3	.4	.2	116
1956	8	12	7	.5	2	144
1957	2	11	8	.4	.4	130[a]
1958	4	8	27	.6	4	140[a]
1959	7	11	16	.5	4	130[a]
1960	6	14	15	.4	31	170[a]
1961	4	16	16	.7	7.9	179
1962	3	15	14	.5	14	164
1963	3	20	16	.6	19	188
1964	3	16	16	.5	24	148
1965	2	18	10	.9	15	172

[a] Estimated

The quality of water has change over the period of year probably reflecting the quality of water in the stream. The most noticeable increase has been in chlorides, nitrates and total dissolved solids.

B. Radiochemical Quality of Water

A summary of the radiochemical analyses from 1958 through 1965 are presented in the following table.

Radiochemical Quality of Water, TW-2A
(Average of a number of Analyses in pCi/l except as noted)

Year	No. of Analyses	Gross Beta	Total Plutonium	Total Uranium
1958	2	14	0.5	0.5
1959	10	14	0.5	0.5
1960	10	14	0.5	0.5
1961	2	14	0.5	0.5
1962	4	14	0.5	0.5
1963	3	14	0.5	0.5
1964	3	14	0.5	0.5
1965	2	14	0.5	0.5

[a] mg/l

The results of the analyses show that the concentrations of radioactivity were below limits of detection.

XIX PERCHED WATER IN BASALTIC ROCKS

Perched water was encountered in the basaltic rocks of Chino Mesa penetrated by Test Well 1A in the lower part of Pueblo Canyon (Fig. 20). The pilot hole for Supply Well PM-1 at Sandia Canyon also penetrated the same body of water in the basalts at a depth of 136 to 141 m. The section of perched water was cased and grouted with cement slury out of the supply well. The geologic log of a section of PM-1 is as follows.

Partial Geologic Log of PM-1
(Altitude of Land Surface 1987 m)

Unit	Thickness (m)	Depth[a] (m)
Bandelier Tuff		
Otowi Member	36.6	36.6
Guaje Member	13.7	50.3
Basaltic Rocks of Chino Mesa	104.2	154.5
Puye Formation (silt and clay)	13.1	167.6

[a] Total depth of Well 762.3 m

Test Well 1 A was drilled in 1949 to a depth of 68.6 m. The test hole penetrated the Puye Formation and Basaltic rocks of Chino Mesa as shown on the geologic log.

Geologic Log of TW-1A
(Altitude of Land Surface 1942 m)

Unit	Thickness (m)	Depth (m)
Puye Formation (fanglomerate)	15.2	15.2
Basaltic Rocks of Chino Mesa	35.1	50.3
Puye Formation (fanglomerate)	3.4	53.7
Basaltic Rocks of Chino Mesa	14.9	68.6

The well is equipped with a pump. The following table summarizes the hydrologic characteristics of the aquifer that occurs in an interflow breccia, the contact between two basalt flows. The water in the aquifer is under artesian head.

Aquifer Test TW-1A (1952)

Thickness of aquifer (m)	0.9
Duration of Test (hrs)	1128
Pumping Rate (l/sec)	0.21
Water Level Prior to Test (m)	55.7
Total Drawdown (m)	1.4
Specific Capacity [(l/sec)(m)]	
(First 4 hrs)	2.1
(Entire Test)	0.16
Transmissivity (m^2/day)	103
Hydrologic Conductivity (m/day)	114

No aquifer tests were made at Supply Well PM-1; however a bailing test indicated a yield of about 3×10^{-1} l/sec with a drawdown of 2 m.

Recharge to the aquifer occurs in Pueblo Canyon in the area from Observation Hole PO-3B to Otowi Seep and in Los Alamos Canyon in the vicinity of Observation Hole LAO-4.5 (Fig. 20). The surface flow in the recharge reach of Pueblo Canyon is mainly effluent from the Bayo Sewage Treatment Plant while storm runoff in Los Alamos Canyon contributes most of the recharge. The movement of water is eastward where a part is discharged from the basaltic rocks at Basalt Spring. The discharge of the spring varies according to the volume of recharge entering the aquifer. The discharge ranges from 0.9 to 2.1 l/sec during the year. Based on water-level response to stream flow it was estimated that the recharge from near Observation Hole PO-3B to Otowi Seep takes one to two months to reach Test Well 1A with another 2 to 3 months to reach Basalt Spring.

A. Chemical Quality of Water

Water samples for analyses were collected from 1951 through 1971 from test 1A. The following table presents an annual summary.

Chemical Quality of Water TW-1A
(Average of a number of analyses in mg/1)

Year	No. of Analyses	Na	Cl	F	NO_3	TDS
1951	4	46	24	0.6	27	298
1952	3	34	19	.5	23	243
1953	9	26	12	.5	14	216
1954	5	-	15	.8	26	465
1955	6	-	10	1.1	27	311
1956	5	-	13	.6	18	279
1957	2	-	31	.6	14	230[a]
1958	10	25	26	.5	12	195[a]
1959	8	15	54	.5	-	165[a]
1960	6	36	23	.6	19	230[a]
1961	4	40	25	.6	24	319
1962	3	53	26	.7	31	340
1963	1	60	27	1.2	62	388
1964	4	53	30	1.2	35	313
1968	2	85	33	2.1	18	318
1969	1	77	27	1.8	13	339
1971	2	60	37	2.1	31	318

[a] Estimated

A summary of the average chemical quality of water from Basalt Spring is shown on the following table.

Chemical Quality of Water, Basalt Spring
(Average of a number of analyses in mg/l)

Year	No. of Analyses	Na	Cl	F	NO_3	TDS
1951	1	-	16	0.5	8	220
1952	4	-	15	.4	13	215
1953	3	-	16	.4	10	198
1954	3	-	16	.4	15	195[a]
1955	2	-	16	.5	12	198[a]
1956	18	17	17	.6	18	212
1957	3	16	13	.5	14	191[a]
1958	6	13	13	.6	11	169[a]
1959	5	14	15	.4	10	190[a]
1960	2	15	13	.5	8	175[a]
1961	1	14	14	.5	8	174[a]
1962	2	20	17	.8	13	256
1963	2	24	20	1.2	13	198
1964	1	20	20	.8	13	229
1965	2	10	14	.8	13	197
1967	1	25	15	.3	13	150
1968	1	24	14	.6	13	168
1969	2	24	14	.3	9	207
1971	2	15	11	.6	13	220
1972	2	19	14	.4	10	197

[a] Estimated

The chemical quality of water from Test Well 1A is quite similar to that in the stream at Pueblo 3. The concentrations of the chemical have generally increased with time.

The quality of water from Basalt Spring is quite similar though the concentrations are lower. This is probably due to changes that occur during transit in the aquifer that reduces the concentrations in the aquifer material.

The following table presents results of metal ion analyses for TW-1 and Basalt Springs.

Metal Ion Analyses
(Average of a number of Analyses in μg/l)

Year	TW-1A 1971	Basalt Springs 1971	Basalt Springs 1972
No. of Analyses	2	2	2
In Solution			
Cadmium	4.3	2.8	0.65
Beryllium	.31	<0.25	<0.25
Lead	1.6	<1.0	<1.0
Mercury	<0.02	<0.02	<0.02
Particulates			
Cadmium	8.8	0.33	<0.25
Beryllium	.48	<0.25	<0.25
Lead	470	0.65	2.2
Mercury	0.07	<0.02	0.04

The 470 μg/l of lead in particulates from TW-1A is probably from pump column or lead packer connecting screen to casing at the bottom of the well.

B. Radiochemical Quality of Water

One sample of water was collected from a depth of ≈140 m in the inflow breccias at Supply Well PM-1 for total plutonium and tritium analyses. Plutonium was below limits of detection of <0.5 pCi/l as was the tritium $<50 \times 10^3$ pCi/l.

The following table presents an annual summary of the radiochemical analyses of water from Test Well 1A from 1958 through 1964.

Radiochemical Quality of Water, TW-1A
(Average of a number of analyses in pCi/l except as noted)

Year	No. of Analyses	Gross Beta	Total Plutonium	Total Uranium[a]
1958	3	<14	<0.5	<0.5
1959	8	<14	<0.5	<0.5
1960	8	<14	<0.5	<0.5
1961	2	<14	<0.5	<0.5
1962	4	<14	<0.5	<0.5
1963	1	<14	<0.5	<0.5
1964	4	<14	<0.5	<0.5

[a] µg/l

The analyses results were below limits of detection. A summary of the analyses made in 1968, 1969, and 1971 are shown below:

Radiochemical Quality of Water, TW-1A
(Average of a number of analyses in pCi/l, except as noted)

Year	1968	1969	1971
No. of Analyses	2	1	2
Gross Alpha	1	2	1
Gross Beta	12	7	- [a]
^{238}Pu	<0.05	<0.05	<0.05
^{239}Pu	<0.05	<0.05	<0.05
Total Uranium[b]	1.1	1.3	0.4

[a] Sample 6-1, 189 pCi/l; 9-1, 7 pCi/l. Sample 6-1 is probably analytical error or cross contamination of sample.

[b] µg/l

An annual summary of the radiochemical analyses of water from Basalt Spring from 1957 through 1965 is shown on the following table.

Radiochemical Quality of Water, Basalt Springs
(Average of a number of analyses in pCi/l, except as noted)

Year	No. of Analyses	Gross Beta	Total Plutonium	Total Uranium[a]
1957	1	<14	<0.5	<0.5
1958	4	<14	<0.5	<0.5
1959	5	<14	<0.5	<0.5
1960	4	<14	<0.5	<0.5
1961	2	<14	<0.5	<0.5
1962	2	<14	<0.5	1.0
1963	2	<14	<0.5	1.5
1964	1	<14	<0.5	2.0
1965	2	<14	<0.5	0.6

[a] μg/l

The annual summary of radiochemical analyses from 1967 through 1972 are shown on the following table.

Radiochemical Quality of Water, Basalt Springs
(Average of an number of analyses in pCi/l except as noted)

Year	1967	1968	1969	1970	1971	1972
No. of Analyses	1	1	2	1	2	2
Gross Alpha	1	1	<1	<1	1	<1
Gross Beta	4	4	4	5	2	4
^{238}Pu	<0.05	<0.05	<0.05	<0.05	<0.05	<0.05
^{239}Pu	<0.05	<0.05	<0.05	<0.05	<0.05	<0.05
Total Uranium[a]	1.2	1.0	1.6	0.4	1.6	3.0

[a] μg/l

The radiochemical analyses show natural or less than detectable amounts of radionuclides. The total uranium is natural occurring. The variation in concentration probably has to do with seasonal change in discharge from the spring and time of year samples are collected.

XX MAIN AQUIFER OF THE LOS ALAMOS AREA

Eleven (11) test holes have been drilled on the plateau to determine the thickness of the geologic units and water-bearing formations (Fig. 21). Seven (7) of the test holes have been completed as wells and are used in part for monitoring the chemical and radiochemical quality of water in the main aquifer. The geologic logs and hydrologic characteristics of the units penetrated by the test holes are presented. A summary of the chemical and radiochemical quality of water in the main aquifer is included in the following sections. Complete chemical and radiochemical quality of water data or of the last samples analyzed are found in Appendix G and H respectively.

A. Test Well 1

Test Well 1 was completed in 1950. It was the one of a series of test holes drilled in the period 1949 to 1950 to determine geologic and hydrologic characteristics of the main aquifer.[23] The test hole is located in lower Pueblo Canyon (Fig. 21).

1. Geologic and Hydrologic Characteristics

The test hole penetrated the Puye Formation and Basaltic Rocks of Chino Mesa as shown by the log.

Geologic Los of TW-1
(Altitude at Land Surface 1942 m)

Unit	Thickness (m)	Depth (m)
Puye Formation (fanglomerate)	15.2	15.2
Basaltic Rocks of Chino Mesa	35.0	50.2
Puye Formation (fanglomerate)	3.4	53.6
Basaltic Rocks of Chino Mesa	24.1	77.7
Puye Formation (fanglomerate)	47.2	124.9
Basaltic Rocks of Chino Mesa	30.5	155.4
Puye Formation (fanglomerate)	29.0	184.4
Puye Formation (conglomerate)	11.3	195.7

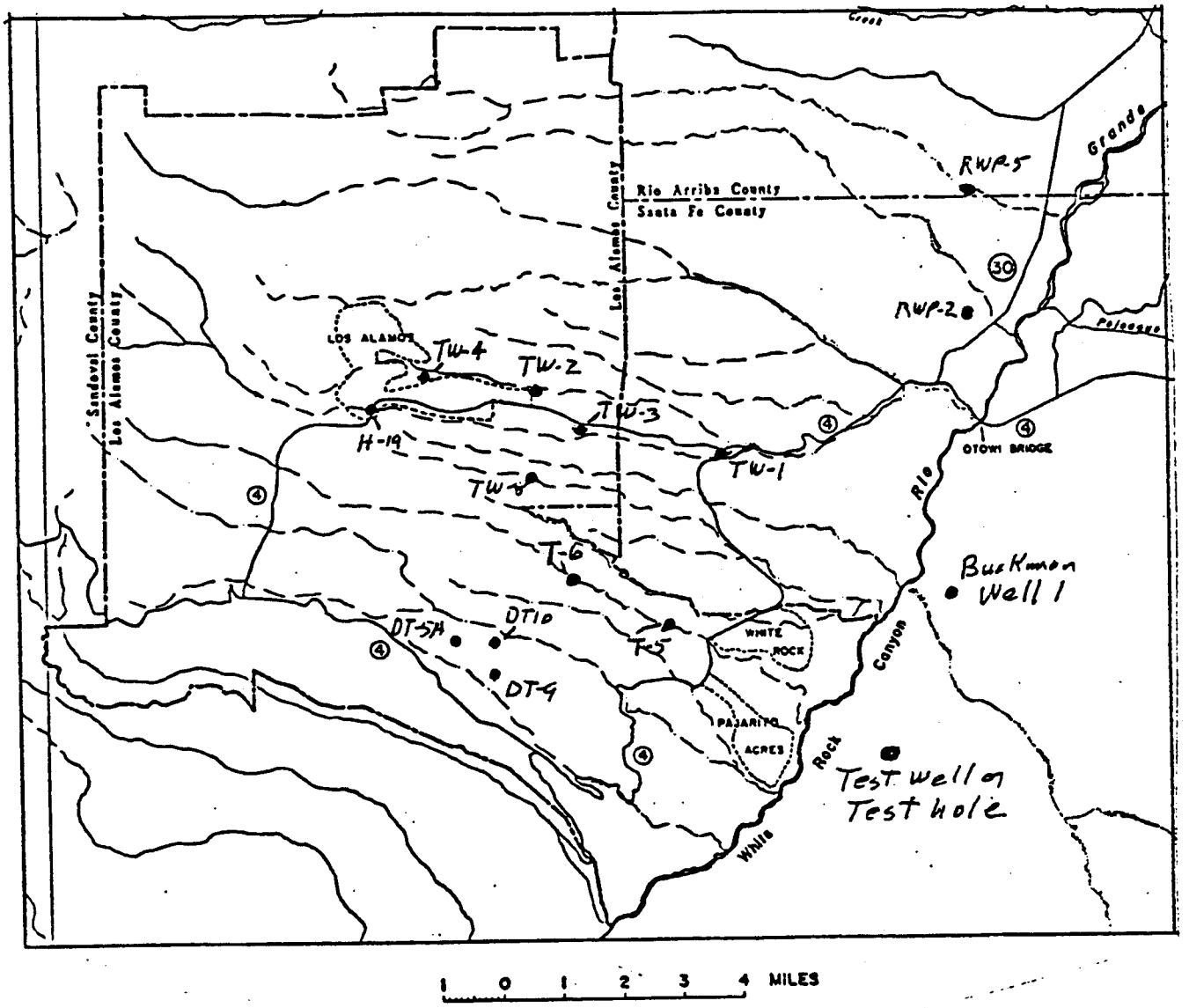

Figure 21. Location of test wells and test holes

The well was equipped with a pump until 1960. The following table summarizes the hydrologic characteristics of the aquifer that occurs in a conglomerate of sand, gravels, and boulders of the Puye Formation.

Aquifer Test TW-1 (1952)

Thickness of Aquifer (m)	5.8
Duration of test (hrs)	246
Pumping Rate (l/sec)	0.15
Water level prior to test (m)	180.4
Total Drawdown (m)	11.8
Specific Capacity [(l/sec)/(m)]	
(First 4 hrs)	0.1
(Entire test)	0.01
Transmissivity (m^2/day)	2.5
Hydrologic Conductivity (m/day)	0.45

2. Chemical Quality of Water

Chemical analyses of water form TW-1 were made from 1952 through 1970 as shown on the following table.

Chemical Quality of Water TW-1
(Average of a number of analyses in mg/l)

Year	No. of Analyses	Na	Cl	F	NO_3	TDS
1952	18	16	8	1.3	1.8	161
1953	10	18	5	1.1	2.2	161
1954	2	--	10	1.3	2.5	147
1955	1	--	10	1.1	3.4	194
1956	8	20	5	1.4	3.5	191
1957	10	20	5	1.1	3.1	131
1958	6	17	5	1.0	7.4	120[a]
1959	2	18	4	1.1	6.9	120[a]
1960	3	18	5	1.0	6.8	120[a]
1961	5	17	4	1.3	4.3	149
1962	1	19	4	1.2	10.4	178
1963	1	34	6	0.8	0.4	186
1965	1	17	8	0.7	0.8	149
1967	1	21	14	0.7	0.4	173
1969	1	33	8	0.1	0.4	188
1970	1	11	8	0.5	0.4	161

[a] Estimated

The samples prior to 1961 were pumped while after that date, samples were collected with a sampling bailer. There has been no significant change in the chemical quality of water from 1952 through 1970.

3. Radiochemical Quality of Water

The following table presents the radiochemical quality of water from 1958 through 1964.

Radiochemical Quality of Water TW-1
(Average of a number of analyses in pCi/l except as noted)

Year	No. of Analyses	Gross Beta	Total Plutonium	Total Uranium[a]
1958	2	<14	<0.5	0.5
1959	3	<14	<0.5	--
1960	6	<14	<0.5	--
1961	2	<14	<0.5	<0.5
1962	2	<14	<0.5	1.5
1963	1	<14	<0.5	0.7
1965	1	<14	<0.5	<0.5
1967	1	<14	<0.5	<0.5

[a] μg/l

A similar table presents data collected in 1969 and 1970.

Radiochemical Quality of Water TW-1
(Analyses in pCi/l except as noted)

	1969	1970
Gross Alpha	1	<1
Gross Beta	4	5
^{238}Pu	<0.05	<0.05
^{239}Pu	<0.05	<0.05
Total Uranium[a]	<0.4	<0.4

[a] μg/l

Analyses indicate natural or less than detectable amounts of radionuclides.

B. Test Well 2

Test Well 2 was completed in 1949. It was also one of the series of test holes drilled in the period of 1949 through 1950.[23] The test hole is located in the mid reach of Pueblo Canyon (Fig. 21).

1. Geologic and Hydrologic Characteristics

The test hole penetrated the alluvium, Bandelier Tuff, and was completed in the lower part of the Puye Formation as shown by the log.

Geologic Log of TW-2
(Altitude of Land Surface 2026 m)

Units	Thickness (m)	Depth (m)
Alluvium	3.4	3.4
Bandelier Tuff		
Otowi Member	6.1	9.5
Guaje Member	9.7	19.2
Puye Formation (fanglomerate)	194.1	213.3
Puye Formation (conglomerate)	27.1	240.4

The well is equipped with a pump. The following table summarizes the hydrologic characteristics of the aquifer that occurs in a conglomerate of sand, gravels, and boulders in the Puye Formation.

Aquifer Test TW-2 (1952)

Thickness of Aquifer (m)	7.3
Duration of Test (hrs)	760
Pumping Rate (l/sec)	0.42
Water Level prior to Test (m)	231.8
Total Drawdown (m)	2.3
Specific Capacity [(l/sec)/(m)]	
(First 4 hrs)	0.23
(Entire Test)	0.21
Transmissivity (m^2/day)	87
Hydrologic Conductivity (m/day)	12

2. Chemical Quality of Water

Chemical analyses of water from TW-2 were made from 1951 through 1972 as shown on the following table.

Chemical Quality of Water TW-2
(Average of a number of analyses in mg/l)

Year	No. of Analyses	Na	Cl	F	NO_3	TDS
1951	10	8	6	0.5	0.5	159
1952	14	8	5	0.7	0.4	158
1953	3	9	4	0.5	0.3	146
1954	1	-	4	0.8	0.5	172
1955	1	-	3	0.4	3.0	164
1958	1	9	7	0.4	0.1	-
1960	3	10	3	0.4	0.3	102[a]
1961	4	10	2	0.7	0.5	158
1962	4	11	3	0.9	1.9	152
1963	3	10	2	0.4	1.7	119
1964	3	9	3	0.5	1.3	130
1968	1	19	4	1.0	1.2	95[a]
1969	1	17	3	0.1	<0.4	90
1970	1	11	5	0.5	1.6	98
1971	1	10	5	0.8	<0.4	86
1972	1	10	6	0.5	0.4	78

[a] Estimated

In general, the chemical quality of the water has changed slightly with a decrease in total dissolved solids. Other ions have remained about the same concentration.

Metal ion analyses are presented in the following table.

Metal Ion Analyses
(Analyses in g/l)

In Solution	6-1-71
Cadmium	1.1
Beryllium	<0.25
Lead	11
Mercury	<0.02
Particulates	
Cadmium	2.1
Beryllium	<0.25
Lead	43
Mercury	<0.02

The concentration of lead in the particulates is probably due to pump column or lead packer connecting screen to casing.

3. Radiochemical Quality of Water

The following table presents the radiochemical quality water from 1958 through 1964.

Radiochemical Quality of Water TW-2
(Average of a number of analyses in pCi/l except as noted)

Year	No. of Analyses	Gross Beta	Total Plutonium	Total Uranium[a]
1958	1	<14	<0.5	<0.5
1959	1	<14	<0.5	<0.5
1960	7	<14	<0.5	-
1961	8	<14	<0.5	--
1962	3	<14	<0.5	1.5
1963	3	<14	<0.5	0.8
1964	3	<14	<0.5	<0.5

The following table presents data collected from 1968 through 1972.

Radiochemical Quality of Water TW-2
(Analyses in pCi/l except as noted)

	1968	1969	1970[a]	1971	1972
Gross Alpha	<1	1	<1	2	<1
Gross Beta	2	1	1	2	<1
^{238}Pu	<0.05	<0.05	<0.05	<0.05	<0.05
^{239}Pu	<0.05	<0.05	<0.05	<0.05	<0.05
Total Uranium[b]	1.1	0.4	0.7	0.4	<0.4

[a] Average of 2 analyses
[b] μg/l

Radioactivity is background or below limits of detection.

C. Test Well 3

Test Well 3 was completed in 1949. It was one of the series of test holes drilled during the period 1949-1950.[23] The test hole is located in the mid-reach of Los Alamos Canyon (Fig. 21).

1. Geologic and Hydrologic Characteristics

The test hole penetrated the Bandelier Tuff, and was completed in the lower part of the Puye Formation as shown by log.

Geologic Log of TW-3
(Altitude of Land Surface 2019 m)

Units	Thickness (m)	Depth (m)
Bandelier Tuff		
Otowi Member	42.7	42.7
Guaje Member	10.7	53.4
Puye Formation (fanglomerate)	27.7	81.1
Basaltic Rocks of Chino Mesa	21.9	103.0
Puye Formation (fanglomerate)	126.5	229.5
Puye Formation (conglomerate)	18.9	248.4

The well is equipped with a pump. The following table summarizes the hydrologic characteristics of the aquifer that occurs in a conglomerate of sand, gravels, and boulders of the Puye Formation.

Aquifer Test TW-3 (1952)

Thickness of Aquifer (m)	7.6
Duration of Test (hrs)	720
Pumping Rate (l/sec)	0.42
Water Level prior to Test (m)	228.9
Total Drawdown (m)	4.6
Specific Capacity [(l/sec)/(m)]	
(First 4 hrs)	0.10
(Entire Test)	0.10
Transmissivity (m^2/day)	97
Hydrologic Conductivity (m/day)	13

2. Chemical Quality of Water

Chemical analyses of water from TW-3 were made from 1951 through 1972 as shown on the following table.

Chemical Quality of Water TW-3
(Average of a number of analyses in mg/l)

Year	Analyses	Na	Cl	F	NO_3	TDS
1951	7	25	4	0.5	1.1	186
1952	4	17	6	0.6	1.8	194
1953	3	11	4	0.7	0.5	195
1954	3	--	5	0.3	0.6	185
1956	7	16	6	0.5	1.6	200
1957	5	14	4	0.4	0.8	205
1958	1	13	7	0.4	1.1	200
1959	4	13	5	0.5	0.7	140[a]
1960	3	14	5	0.4	0.7	145[a]
1961	3	16	5	0.6	0.4	176
1962	3	14	5	0.6	2.6	199
1963	1	17	5	0.4	2.4	200
1964	2	13	5	0.4	0.7	199
1965	2	11	5	0.7	1.3	156
1967	3	24	10	0.4	1.3	160
1968	1	24	4	0.4	1.2	201
1969	1	22	5	<0.1	0.4	124
1970	1	15	5	<0.1	3.1	180
1971	1	15	5	0.6	0.4	106
1972	1	19	6	0.5	<0.4	94

[a] Estimated

Chemical concentrations varied slightly over the years but showed no significant changes in concentrations. Total dissolved solids decreased in concentrations during the past few years.

Metal Ion Analyses
(Analyses in μg/l)

	6-3-71
In Solution	
Cadmium	2.8
Beryllium	<0.25
Lead	3.5
Mercury	<0.02
Particulates	
Cadmium	5.6
Beryllium	<0.25
Lead	8.2
Mercury	<0.02

3. Radiochemical Quality of Water

The following table presents the radiochemical quality of water from 1958 through 1965.

Radiochemical Quality of Water TW-3
(Average of a number of analyses in pCi/l except as noted)

Year	No. of Analyses	Gross Beta	Total Plutonium	Total Uranium
1958	2	<14	<0.5	--
1959	8	<14	<0.5	--
1960	10	<14	<0.5	--
1961	8	<14	<0.5	--
1962	4	<14	<0.5	1.1
1963	1	<14	<0.5	5.0
1964	2	<14	<0.5	<0.5
1965	2	<14	<0.5	<0.5

The following table presents data collected from 1967 through 1972.

Radiochemical Quality of Water TW-3
(Average of a number of analyses in pCi/l except as noted)

	1967	1968	1969	1970	1971	1972
No. of Analyses	2	1	2	2	1	1
Gross Alpha	<1	<1	<1	3	2	<1
Bross Beta	5	3	2	3	4	2
^{238}Pu	<0.05	<0.05	<0.05	<0.05	<0.05	<0.05
^{239}Pu	<0.05	<0.05	<0.05	<0.05	<0.05	<0.05
Total Uranium[a]	1.3	2.4	0.4	0.7	0.4	<0.4

[a] μg/l

There were no significant concentrations of radionuclides as indicated by the analyses.

D. Test Well 4

Test Well 4 was completed in 1950. It was one of a series of test holes drilled in the period 1949-1950.[23] The test hole is located on the western part of the plateau near the old Waste Treatment Plant (TA-45) at the head of Acid Canyon (Fig. 21).

1. Geologic and Hydrologic Characteristics

The test hole penetrated the Bandelier Tuff, Puye Formation and is completed into the Tschicoma Formation as shown by the log.

Geologic Log of TW-4
(Altitude of Land Surface m)

Units	Thickness (m)	Depth (m)
Bandelier Tuff		
Tshirege Member	85.3	85.3
Otowi Member	26.8	112.1
Guaje Member	8.2	120.3
Puye Formation (fanglomerate)	73.2	193.5
Tschicoma Formation	173.7	367.2

The well has been equipped with a pump. It was removed in 1973. The following table summarizes the hydrologic characteristics of the aquifer that occurs in a brecciated zone in the volcanic flow rocks of latite of the Tschicoma Formation.

Aquifer Test TW-4 (1952)

Thickness of Aquifer (m)	6.4
Duration of Test (hrs)	720
Pumping Rate (l/sec)	0.18
Water Level prior to Test (m)	255.6
Total Drawdown (m)	1.5
Specific Capacity [(l/sec)/(m)]	
(First 4 hrs)	0.24
(Entire Test)	0.12
Transmissivity (m^2/day)	9.3
Hydrologic Conductivity (m/day)	1.5

2. Chemical Quality of Water

The pump on TW-4 was installed in 1952. It was out of service from 1954 through 1960. It failed again in 1966 and was removed from the well in 1973. Chemical analyses of water from the well were made during the period when the pump was in service as shown on the following table.

Chemical Quality of Water TW-4
(Average of a number of analyses in mg/l)

Year	No. of Analyses	Na	Cl	F	NO_3	TDS
1952	8	8	5	0.2	0.3	101
1953	1	5	2	0.1	0.3	180
1961	1	11	5	0.3	0.4	95[a]
1962	2	10	3	0.6	3.9	191
1963	4	12	3	0.5	1.4	172
1964	4	9	2	0.4	4.4	141
1965	3	15	3	0.6	1.3	129

[a] Estimated

Chemical concentrations and total dissolved solids varied in concentrations but indicated no significant changes occurred from 1952 to 1965.

3. Radiochemical Quality of Water

The following table presents the radiochemical quality of water from TW-4 from 1961 through 1965. No analyses have been made since the pump failed in 1965.

Radiochemical Quality of Water TW-4
(Average of a number of analsyes in pCi/l except as noted)

Year	No. of Analyses	Gross Beta	Total Plutonium	Total Uranium[a]
1961	1	<14	<0.5	<0.5
1962	2	<14	<0.5	<0.5
1963	4	<14	<0.5	0.5
1964	4	< 14	<0.5	1.8
1965	3	<14	<0.5	0.9

No significant concentrations of activity were detected.

E. Test Hole T-5

Test Hole T-5 was completed in 1950. It was one of the series of test holes drilled in the period 1949-1950.[23] The test hole is located in the

Lower reach of Pajarito Canyon near State Road 4 (Fig. 21).

1. Geologic Characteristics

The test hole penetrated the alluvium and Bandelier Tuff and was completed into the Basaltic Rocks of Chino Mesa as shown by the log.

Geologic Log of TH-5
(Altitude of Land Surface 2009 m)

Units	Thickness (m)	Depth (m)
Alluvium	7.0	7.0
Bandelier Tuff		
Tshirege Member	5.2	12.2
Otowi Member	36.6	48.8
Guaje Member	3.4	52.2
Basaltic Rocks of Chino Mesa	28.0	80.2

The test hole did not encounter any water bearing zone beneath the alluvium. Water in the alluvium was cased from the hole.

F. Test Hole T-6

Test hole T-6 was completed in 1950. It was part of the series of test holes drilled in the period 1949-1950.[23] The test hole is located in mid reach of Pajarito Canyon (Fig. 21) and State Road 4 (Fig. 21).

1. Geologic Characteristics

The test hole penetrated the alluvium, Bandelier Tuff, and is completed in the Puye Formation as shown by the log.

Geologic Log of T-6
(Altitude of Land Surface 2042 m)

Units	Thickness (m)	Depth (m)
Alluvium	7.6	7.6
Bandelier Tuff		
Tshirege Member	18.3	25.9
Otowi Member	54.9	80.8
Guaje Member	6.1	86.9
Puye Formation (fanglomerate)	4.6	91.5

The test hole did not encounter any water in the geologic units penetrated beneath the alluvium.

G. Test Hole T-7

Test hole T-7 was completed in 1950. It was also part of a drilling program of 1949-1950.[23] The test hole is located in the midreach of Ancho Canyon (Fig. 21).

1. Geologic Characteristics

The test hole penetrated alluvium, Bandelier Tuff, and were completed in the Basaltic Rocks of Chino Mesa as shown by the log.

Geologic Log of T-7
(Altitude of Land Surface 1897 m)

Units	Thickness (m)	Depth (m)
Alluvium	3.0	3.0
Bandelier Tuff		
Otowi Member	10.7	13.7
Basaltic Rock of Chino Mesa	3.0	16.7

The lower Guaje Member of the Bandelier Tuff was not penetrated at the test hole. The unit was eroded off or never deposited prior to the deposition of the Otowi Member.

The test hole did not encounter any water in any of the units penetrated.

H. Test Well 8

Test well 8 was completed in 1960. The test hole was drilled to delineate the geologic and hydrologic characteristics of units underlying Mortandad Canyon (Fig. 21). The test hole was completed prior to use of the canyon as a area to receive treated industrial effluents.[16,24]

1. Geologic and Hydrologic Characteristics

The test hole penetrated alluvium, Bandelier Tuff, Puye Formation, Basaltic Rocks of Chino Mesa and is completed in the Puye Formation as shown by the log.

Geologic Log of TW-8
(Altitude of Land Surface 2095 m)

Units	Thickness (m)	Depth (m)
Alluvium	12.0	12.0
Bandelier Tuff		
Tshirege Member	6.1	18.1
Otowi Member	117.3	135.4
Guaje Member	13.7	149.1
Puye Formation (fanglomerate)	27.4	176.5
Basaltic Rocks of Chino Mesa	44.2	220.7
Puye Formation (fanglomerate)	103.6	324.3

The well was not equipped with a pump until January of 1973. The following data summarizes the hydrologic characteristics of the aquifer that occurs in a fanglomerate of sand, gravels, and boulders of the Puye Formation.

Aquifer Test TW-8 (1960)

Thickness of Aquifer (m)	24.4
Duration of Test (hrs)	2.0
Bailing Rate (l/sec)	1.0
Water Level prior to Test (m)	293.4
Total Drawdown (m)	0.10[a]
Specific Capacity [(l/sec)/(m)]	
Estimated	2[b]
Transmissivity (m^2/day)	30
Hydrologic Conductivity (m/day)	1.2

[a]Residual drawdown 5 min after bailing ended
[b]Estimated

2. Chemical Quality of Water

There was no pump on TW-8 during the period of the report. Samples were collected with a sampling bailer. The following table presents the chemical quality of water.

Chemical Quality of Water TW-8
(Analyses in mg/l)

Year	Na	Cl	F	NO_3	TDS
1960	12	2	0.7	3.0	216
1961	15	2	0.4	2.0	463
1963[a]	15	2	0.4	2.2	187
1965	10	3	0.2	0.9	113
1967	13	1	0.1	0.4	141
1969	23	3	0.1	1.8	148

[a] Average of 2 analyses

The concentrations have varied slightly; however, as samples are bailed from the well, the indication is that there has been no significant change in the quality during the period.

3. Radiochemical Quality of Water

The following table presents the radiochemical quality of water from 1960 through 1965.

Radiochemical Quality of Water TW-8
(Analyses in pCi/l except as noted)

Year	Gross Beta	Total Plutonium	Total Uranium[a]
1960	<14	<0.5	<2.5
1961	<14	<0.5	<2.5
1963[b]	<14	<0.5	<0.5
1965	<14	<0.5	<0.5

[a] μg/l
[b] Average of 2 analyses

The following table presents data collected at different dates during 1969.

Radiochemical Quality of Water TW-8
(Analyses in pCi/l except as noted)

	1-10-69	1-14-69	2-14-69	11-6-69
Gross Alpha	<1	2	<1	<1
Gross Beta	2	3	1	3
^{238}Pu	<0.05	<0.05	<0.05	<0.05
^{239}Pu	<0.05	<0.05	<0.05	<0.05
Total Uranium[a]	0.5	0.4	0.4	0.4

[a] μg/l

No significant concentration of radionuclides were detected.

I Test Well DT-5A

Test well DT-5A was completed in 1960. It was drilled as a series of 3 deep test holes (DT-9, DT-10) to determine the geologic and hydrologic characteristics of the rock units underlying a small test area.[24,25] The test hole is located on the Pajarito Plateau south of Water Canyon (Fig. 21).

1. Geologic and Hydrologic Characteristics

The test hole penetrated rocks of the Bandelier Tuff, Puye, Tschicoma, and Tesuque Formations as shown by the log.

Geologic Log of DT-5A
(Altitude of Land Surface 2177 m)

Units	Thickness (m)	Depth (m)
Bandelier Tuff		
Tshirege Member	195.4	195.4
Otowi Member	60.4	255.8
Guaje Member	27.7	283.5
Puye Formation (fanglomerate)	72.2	355.7
Tschicoma Formation	38.4	394.1
Puye Formation (fanglomerate)	42.1	436.2
Tschicoma	7.9	444.1
Puye Formation (fanglomerate)	5.5	449.6
Puye Formation (conglomerate)	15.8	465.4
Tesuque Formation	89.6	555.0

The well was equipped with a pump for the aquifer test. It was later removed. The following data summarizes the hydrologic characteristics of the aquifer which occurs in the Puye Formation (fanglomerate and conglomerate), Tschicoma and Tesuque Formations.

Aquifer Test DT-5A (1960)

Thickness of Aquifer (m)	106.7[a]
Duration of Test (hrs)	25
Pumping Rate (l/sec)	5.1
Water Level prior to Test (m)	357.5
Total Drawdown (m)	4.3
Specific Capacity [(l/sec)/(m)] (Entire Test)	1.2
Transmissivity (m^2/day)	136
Hydrologic Conductivity (m/day)	1.2

[a] Saturated section that should yield water readily to the well.

2. Chemical Quality of Water

Except for the sample collected in 1960 which was pumped, the remainder of the samples were collected with a smapling bailer. The following table presents the chemical quality of water.

Chemical Quality of Water DT-5A
(Analyses in mg/l)

Year	Na	Cl	F	NO_3	TDS
1960	14	1	0.2	2.0	147
1963	13	1	0.4	0.9	185
1967	14	4	0.4	<0.4	126
1969	19	3	<0.1	<0.4	120
1970	11	5	0.4	0.4	101

There has been no significant change in the quality of water during the period 1960 through 1970.

3. Radiochemical Quality of Water

The following table presents radiochemical quality of water as determined upon completion of the well in 1960.

Radiochemical Quality of Water DT-5A[a]
(Analyses in pCi/l except as noted)

	5-1-60
Alpha Activity	<1.3
Beta Activity	7.3
Radium (Ra)	<0.1
Total Uranium[b]	0.9

[a] Analyses U. S. Geol. Survey
[b] μg/l

The data collected in 1960, 1963, and 1967 is presented as follows:

Radiochemical Quality of Water DT-5A
(Analyses in pCi/l except as noted)

Year	Gross Beta	Total Plutonium	Total Uranium[a]
1960	<14	<0.5	1.0
1963	<14	<0.5	<0.5
1967[b]	<14	<0.5	<0.5
1967[c]	<14	<0.5	<0.5

[a] μg/l
[b] Zone Sample 390 m
[c] Zone Sample 527 m

Data for samples collected in 1969 and 1970 are shown as follows:

Radiochemical Quality of Water DT-5A
(Analyses in pCi/l except as noted)

	2-24-69	4-24-70
Gross Alpha	<1	3
Gross Beta	3	2
^{238}Pu	<0.05	<0.05
^{239}Pu	<0.05	<0.05
Total Uranium[a]	0.4	0.4

[a] μg/l

Analyses detected no significant concentrations of radionuclides.

J. Test Well DT-9

Test well DT-9 was completed in 1960. The well drilled for geologic and hydrologic data as previously mentioned. It is located on the plateau south of Water Canyon (Fig. 21).

1. Geologic and Hydrologic Characteristics

The test well penetrated rock units of the Bandelier Tuff, Puye, Tschicoma and Tesuque Formations as shown by the log.

Geologic Log of DT-9
(Altitude of Land Surface m)

Units	Thickness (m)	Depth (m)
Bandelier Tuff		
Tshirege Member	206.0	206.0
Otowi Member	38.4	244.4
Guaje Member	14.6	259.0
Puye Formation (fanglomerate)	22.6	281.6
Tschicoma Formation	72.5	354.1
Puye Formation (fanglomerate)	47.8	401.9
Puye Formation (conglomerate)	11.6	413.5
Tesuque Formation	43.9	457.4

The well was equipped with a pump for the aquifer test. After the test, the pump was removed. The well has been equipped with a semi-continuous water stage recorder to determine the regional trends of water-level change of the

main aquifer. The well is located in a remote area away from the influence of pumpage for water supply. The regional decline from 1960 through 1968 has been about 0.61 m or 7.6 cm per year. The recorder has shown that the aquifer is very sensitive to atmospheric pressure changes, earth shocks, and probable earth tide effects.[26] The following data recaps the hydrologic characteristics of the aquifer which occurs in the Puye Formation (fanglomerate and conglomerate) Tschicoma and Tesuque Formation.

Aquifer Test DT-9 (1960)

Thickness of Aquifer (m)	91.4[a]
Duration of Test (hrs)	24
Pumping Rate (l/sec)	5.6
Water Level prior to Test (m)	305.7
Total Drawdown (m)	1.2
Specific Capacity [(l/sec)/(m)] (Entire Test)	4.6
Transmissivity (m^2/day)	760
Hydrologic Conductivity (m/day)	8.2

[a] Saturated section that should yield water readily to the well.

2. Chemical Quality of Water

Except for the sample collected in 1960 which was pumped, the remainder of the samples were collected with a sampling bailer. The following table presents the chemical quality of water.

Chemical Quality of Water
(Analyses in mg/l)

Year	Na	Cl	F	NO_3	TDS
1960	12	2	0.3	<0.4	136
1969	19	3	<0.1	1.3	160
1970	10	5	<0.1	<0.4	120
1971	14	4	<0.1	0.9	160

There was no significant change in quality of water during the period 1960 through 1971.

3. Radiochemical Quality of Water

The following table presents radiochemical data as determined upon completion of the well in 1960.

Radiochemical Quality of Water DT-9[a]
(Analyses in pCi/l except as noted)

	5-7-60
Alpha Activity	1.4
Beta Activity	3.6
Radium (Ra)	<0.1
Total Uranium[b]	0.8

[a] Analyses U. S. Geol. Survey
[b] μg/l

Samples were collected during the aquifer test at intervals of 4, 12, 16, and 24 hrs after pumping began. Gross Beta was <14 pCi/l; total Plutonium was <0.5 pCi/l and total uranium was <0.5 μg/l in the four samples analyzed.

The following table presents analyses collected in 1969 and 1970.

Radiochemical Quality of Water DT-9
(Analyses in pCi/1 except as noted)

	2-20-69	4-28-70
Gross Alpha	<1	<1
Gross Beta	1	2
^{238}Pu	<0.05	<0.05
^{239}Pu	<0.05	<0.05
Total Uranium[a]	0.8	0.9

[a] μg/1

No significant concentrations of radionuclides were detected in the analyses.

K. Test Well DT-10

Test well DT-10 was completed in 1960 as a part of the three wells located south of Water Canyon, to determine geologic and hydrologic conditions underlying the plateau (Fig. 21).

1. Geologic and Hydrologic Conditions

The test hole penetrated rock units of the Bandelier Tuff, Basaltic Rocks of Chino Mesa, Tschicoma, and Puye Formations as shown by the log.

Geologic Log of DT-10
(Altitude of Land Surface 2139 m)

Units	Thickness (m)	Depth (m)
Bandelier Tuff		
Tschirege Member	204.8	204.8
Otowi Member	47.8	252.6
Guaje Member	10.7	263.3
Puye Formation (fanglomerate)	32.9	296.2
Tschicoma Formation	12.2	308.4
Basaltic Rocks of Chino Mesa	82.0	390.4
Puye Formation (fanglomerate)	22.9	413.3
Puye Formation (Conglomerate)	14.0	427.3
Tesuque Formation	2.1	429.4

The well was equipped for test purposes only. The following test purposes only. The following data recaps the hydrologic characteristics of the aquifer

that occurs in the Puye (fanglomerate and conglomerate) and Tschicoma Formations. The well only penetrated a thin section of the Tesuque Formation (2 m).

Aquifer Test DT-10 (1961)

Thickness of Aquifer (m)	60.9[a]
Duration of Test (hrs)	16
Pumping Rate (l/sec)	4.9
Water Level prior to Test (m)	330.7
Total Drawdown (m)	1.5
Specific Capacity [(l/sec)/(m)]	
Entire Test	3.3
Transmissivity (m^2/day)	447
Hydrologic Conductivity (m/day)	7.4

[a] Saturated section that should yield water readily to the well.

2. Chemical Quality of Water

Samples were collected from the well with a sampling bailer. The following table presents the chemical quality of water.

Chemical Quality of Water DT-10
(Analyses in mg/l)

Year	Na	Cl	F	NO_3	TDS
1960	11	3	0.2	1.0	138
1963	14	3	0.4	0.9	185
1967	12	6	0.1	<0.4	141
1969	19	3	<0.1	0.9	155
1970	10	3	0.4	<0.4	118

There was no significant change in the quality of water during the period 1960 through 1970.

3. Radiochemical Quality of Water

The following table presents radiochemical data as determined upon

completion of the well in 1960.

Radiochemical Quality of Water DT-10[a]
(Analyses in pCi/l except as noted)

	5-5-60
Alpha Activity	<0.8
Beta Activity	8.7
Radium (Ra)	<0.1
Total Uranium[b]	1.0

[a] Analyses U. S. Geol. Survey
[b] μg/l

The following data was collected in 1960 and 1963.

Radiochemical Quality of Water DT-10
(Analyses in pCi/l except as noted)

Date	Gross Beta	Total Plutonium	Total Uranium[a]
5-5-60	<14	<0.5	<1.0
9-20-60[b]	<14	<0.5	<4.0
11-13-63	<14	<0.5	0.7
2-15-67	<14	<0.5	<0.5

[a] μg/l
[b] 4 samples collected during aquifer test.

The following data was collected in 1969 and 1970.

Radiochemical Quality of Water DT-10
(Analyses in pCi/l except as noted)

	2-24-69	4-30-70
Gross Alpha	<1	<1
Gross Beta	1	2
^{238}Pu	<0.05	<0.05
^{239}Pu	<0.05	<0.05
Total Uranium[a]	1.2	0.4

[a] μg/l

There were no significant concentrations of radioactivity detected in the aquifer at Well DT-10 during the period 1960 through 1970.

L. Test Hole H-19

Test hole H-19 was completed in 1949. It was drilled for geologic and hydrologic information related to the development of possible water supply.[1] The test hole is located in upper Los Alamos Canyon (Fig. 21).

1. Geologic and Hydrologic Characteristics

The test hole penetrated rock units of alluvium, Bandelier Tuff, Puye and Tschicoma Formation as shown by the log.

Geologic Log of H-19
(Altitude of Land Surface 2188 m)

Units	Thickness (m)	Depth (m)
Alluvium	8.2	8.2
Bandelier Tuff		
Tshirege Member	52.7	60.9
Otowi Member	65.5	126.4
Guaje Member	17.4	143.8
Tschicoma Formation	105.8	249.6
Puye Formation (fanglomerate)	119.2	368.8
Tschicoma Formation	82.3	451.1
Puye Formation (conglomerate)	3.0	454.1
Tschicoma Formation	155.4	609.5

The test hole encountered a large thickness of relatively impermeable latites and rhyolites of the Tschicoma Formation which decreased the hydrologic Conductivity of the main aquifer. The yield would not be sufficient for completion as a supply well. The top of the main aquifer is about 295 m in the test hole. No records exist of aquifer tests. The hole was abandoned and casing pulled in 1949.

M. San Ildefonso Stock Wells

Two stock wells located to the northeast of the Los Alamos area were sampled to obtain background data on the chemical and radiochemical quality

of water in the main aquifer. The wells are located in the flat area east of the Puye Escarpment (Fig. 21).

Well RWP-2 is at an altitude of 1680 m. The well is completed into the Tesuque Formation and has a reported water level of 40.0 m. Well RWP-5 is at an altitude of 1742 m and is also completed into the Tesuque Formation. The water-level is reported at a depth of 32.0 m. Both wells are equipped with windmills.

1. Chemical Quality of Water

The following table summarizes the chemical quality of water in 1967.

Chemical Quality of Water, RWP-2, RWP-5
(Analyses in mg/l)

	RWP-2	RWP-5
Na	47	79
Cl	8	10
F	0.1	0.2
NO_3	0.9	3.1
TDS	170	253

Chemical quality indicates low to moderate TDS which is characteristic of water in the Tesuque Formation.

2. Radiochemical Quality of Water

The following table summarizes the radiochemical Quality in 1967.

Radiochemical Quality, RWP-2, RWP-5
(Analyses in pCi/l except as noted)

	RWP-2	RWP-5
Gross Alpha	4	2
Gross Beta	10	14
^{238}Pu	<0.05	<0.05
^{239}Pu	<0.05	<0.05
Total Uranium[a]	1.8	2.3

[a] μg/l

There is no significant concentrations of radionuclides as seen by the analyses.

N. Buckman Well

This is an abandoned well that was used for water to service the railroad that ran from Alamosa, Colorado to Santa Fe. The railroad was abandoned in 1940. The well is located across the Rio Grande from Los Alamos (Fig. 21).

The well is completed in the main aquifer which is the Tesuque Formation. The total depth is unknown, but when sounded in 1964, it was only open to 13.1 m. The well was flowing about 0.3 l/sec on August 25, 1964.

1. Chemical and Radiochemical Quality of Water

The following tables summarize the quality of water from the well.

Chemical Quality
(Analyses in mg/l)

	8-25-64
Na	48
Cl	4
F	0.4
NO_3	5.3
TDS	247

Radiochemical Quality
(Analyses in pCi/l except as noted)

	8-25-64
Gross Beta	<14
Total Plutonium	< 0.5
Total Uranium[a]	2.0

[a] μg/l

There were no significant concentrations of ions or radionuclides in the water when compared with other waters of the main aquifer.

XXI SUMMARY

The surface water and ground water in the alluvium are separated from water in the main aquifer by several hundred meters of unsaturated volcanic tuff and sediments. The surface water recharges the shallow aquifers in the alluvium in the canyon drainage areas. As the stream flow is intermittent and mainly dependent on the release of effluents from sewage and industrial treatment plants, the quality of water in the stream and the shallow aquifer is dominated by the quality of the effluents released after treatment. The water in the stream and in the alluvium is not a source of municipal, industrial, or agriculture use. There is no surface flow of effluents beyond the Laboratory boundaries. The following section summarizes the conditions in the drainage areas.

Drainage Area 1 (Barranca Canyon)

The drainage area of about 4.9 km^2 receives no effluent discharges. The canyon contains only intermittent storm runoff. No water samples have been collected and analyzed. Radiochemical analyses of sediments show only background concentrations of radionuclides.

Drainage Area 2 (Bayo Canyon)

The drainage area of about 9.8 km^2 receives no effluent discharges. The canyon was used as a test area until 1964. It contains only intermittent storm runoff. Chemical concentrations of storm runoff taken while the area was in operation are normal. Radiochemical analyses of sediments show no indication of contamination from the operations of the test area.

Drainage Area 3

The drainage area of 0.3 km^2 contains no well defined channel nor receives any effluent discharge.

Drainage Area 4 (Acid-Pueblo Canyon)

The drainage area of 22.3 km^2 receives effluent from two community sewage treatment plants and did receive industrial effluents containing radionuclides from 1943 through 1964. The release of sewage effluents maintain a base flow in a part of the canyon and recharges the water in the alluvium, a small body of perched water in the Puye Formation in the mid-reach of the canyon, and a second body of perched water in the Basaltic Rocks of Chino Mesa in the lower part of the canyon. The chemical quality of water in the stream, aquifers in alluvium, perched water in the volcanic sediments, and basalts is dominated by the quality of sewage effluents released. The intermittent release of industrial effluents during the period of operation of the treatment plant elevated for short periods of time the chemical concentrations of the sewage effluents in the canyon.

The industrial effluents contained some mixed fission products, but the major concern is the amount of plutonium released. In general, these concentrations decreased downgradient in the canyon from the effluent outfall both in solution and in sediments of the channel. This is due mainly to the uptake of the radionuclide by sediments in the stream channel. The concentrations are normally higher near the outfall decreasing downgradient in the channel. The accumulation of radionuclide and sediments are flushed and dispersed down the canyon by storm runoff.

The maximum reported concentration of plutonium in solution during the period 1958 through 1972 was 18.2 pCi/l that occurred in 1963 in the shallow water in the alluvium. About 8 pCi/l occurred in 1971 in surface flow at Acid Weir. This later analyses indicate resuspension of the plutonium into solution from the sediments or underlying tuff bedrock. The concentration guides for uncontroled areas for plutonium in solution is 5×10^3 pCi/l.

Thus, the highest concentraion reported in the canyon is below recommended levels for uncontrolled areas.

The total amount of plutonium released in the canyon during the period 1943 to 1964 was estimated at 170 mCi. The major amounts remaining in the canyon are believed to be adsorped by or attached to the channel sediment. An inventory made in 1972 indicated that the sediments only contain about 12 mCi. The remaining 168 mCi have been flushed by storm runoff into Los Alamos Canyon.

Drainage Area 5 (DP-Los Alamos Canyon)

The drainage area of 27.5 km^2 receives effluent from two sewage treatment plants (one near TA-21 and the other near TA-41) and an industrial waste treatment plant that processes radioactive influents. The volume of the sewage and industrial effluents released into DP and Los Alamos Canyon are low. They rapidly infiltrate into the alluvium. The stream flow in Los Alamos Canyon is impounded by a dam on the flanks of the mountain to the west of the plateau. Stream flow is intermittent in the canyons of the plateau. The major volumes of stream flow occur during the summer from heavy showers; however, a heavy snow pack can produce runoff for one to two months during the late spring.

The chemical quality of water in the short reaches of base flow below the plants is reflected in the similar quality of water in the alluvium. This is quite evident as the industrial and sewage effluent from DP Canyon move into the mid-reach of Los Alamos Canyon. As in Pueblo Canyon, the chemical quality of the water improves downgradient in the canyon.

Plutonium is the major radionuclide in the industrial effluents. The highest concentration of plutonium in solution was about 77 pCi/l reported in 1967. In 1972, the highest concentration was about 6 pCi/l. These concentrations decrease downgradient in the canyon. The concentration of plutonium

recommended for uncontrolled areas is 5×10^3 pCi/l thus, the highest concentration reported is below this level.

The total amount of plutonium released in the canyon during the period 1952 to 1972 was about 30.8 mCi. An inventory in 1972 indicated an estimated 3.7 mCi remained in the canyon to the junction of Pueblo Canyon. The remainder 27.1 mCi was flushed during storm runoff events into the lower reach of Los Alamos Canyon and to the Rio Grande.

Drainage Area 6 (Sandia Canyon)

The drainage area of 7.0 km^2 receives sewage effluent and blow-down of process water from the TA-3 power plant. The stream in the upper reach of the canyon is perennial with the release of the effluents. The chemical quality of the water in the stream and alluvium reflects the quality of effluent released. No radionuclides are released into the canyon. Sediments analyses indicate only background concentration of radioactivity.

Drainage Area 7 (Mortandad Canyon)

The drainage area of 4.7 km^2 receives cooling or waste water from TA-48 and industrial effluent from the waste treatment plant at TA-50. The stream below the effluent outfall is perennial for in short reach due to the release of effluents. The chemical quality of water in the stream and alluvium reflects the quality of the effluents released from the treatment plant. The average annual total dissolved solids in the stream range from about 320 to 1300 mg/l while that in the alluvium ranged from 360 to 1130 mg/l. In general the chemical quality improved downgradient in the canyon. The water is the poorest quality in any of the drainage areas; however, it is not used for any type of supply nor does the water move past the Laboratory boundary as surface flow or through the aquifer in the alluvium. The volume of surface water and effluent recharge to the aquifer in the alluvium is only sufficient to maintain the aquifer of limited extent within the upper reach

of the canyon.

Radionuclides released with the effluent are bound to sediments in the stream channel. The sediments are subject to transport by storm runoff; however, since hydrologic observations began in 1960, storm runoff has not reached the Laboratory boundary. In general, the concentration of radioactivity in solution and sediments decrease downgradient in the canyon.

Plutonium is a major radionuclide released with the effluents. The highest concentration reported in solution has been about 30 pCi which is below recommended levels for uncontrolled areas.

About 42.1 mCi of plutonium, 449 mCi of strontium 89, and 315 mCi of strontium 90 have been released into the canyon from the plant at TA-50. An additional 1,326 mCi of strontium 89 and 223 mCi of strontium 90 were released from 10-Site into a small tributary canyon to Mortandad. There has been little or no transport of these radionuclides into Mortandad. All radionuclide released have remained in the canyon as volume of storm runoff has been to small to allow transport to the Laboratory boundary.

Drainage Area 8

The drainage area of 0.5 km^2 contains no well defined channel nor receives any effluent discharge.

Drainage Area 9

The drainage area of 8.8 km^2 receives only a small volume of effluents from a cooling process.

The chemical quality of the water in a small reach of the stream is good and contains only natural concentrations of radionuclides. The analyses of channel sediments also show no indication of contamination by radionuclide from Laboratory operations.

Drainage Area 10 (Pajarito Canyon)

The drainage area of 27.5 km^2 receives a small volume of sewage effluent. As the canyon has a large drainage area on the flanks of the mountain intermittent snow melt and summer thundy showers provide enough runoff to recharge a small body of water in the alluvium.

The chemical quality of water in the stream is not objectional (low TDS) nor does it contain concentrations of radionuclides that indicate contamination.

Drainage Area 11 (Water Canyon)

The drainage area of 33.3 km^2 receives small volumes of sewage and industrial process water. The volume is sufficient to maintain a small reach of perennial flow in the mid reach of the canyon. The chemical quality of the surface flow is not objectionable (low TDS) nor does it contain concentrations of radionuclides that indicate contamination. Sediment analyses show only background concentrations of radionuclides except in one canyon that is trubutary canyon from the north that contains above background concentration of total uranium. This is due to testing adjacent mesas and transport into the canyon by runoff.

Drainage Area 12

The drainage area of 1.3 km^2 contains no well defined channel nor receives any effluent discharge.

Drainage Area 13 (Ancho Canyon)

The drainage area of 17.4 km^2 contains a perennial stream in its lower reach to the Rio Grande. The canyon receives no effluent releases. The chemical and radiochemical quality of the water are normal. Sediment analyses show only natural or background concentrations of radionuclides.

Drainage Area 14

The drainage area of 1.6 km^2 contains no well defined channel nor

receives any effluent discharge.

Drainage Area 15 (Choquehui Canyon)

The drainage area of 4.7 km^2 contain a small spring bed reach of perennial flow above the Rio Grande. The canyon receives no effluent releases. Chemical and radiochemical analyses of water are normal showing no indication of Laboratory operations. Sediment analyses show only natural or background concentrations of radionuclides.

Drainage Area 16

The drainage area 1.0 of km^2 contains no well defined channel nor does it receive any effluent discharge.

The chemical quality of the surface and ground water in the alluvial aquifer pore no environmental or health problems as the result of past Laboratory activities. The water are contained with in the Laboratory areas. The chemical quality in some canyon may be poor; however, the quality generally improves as it moves downgradient.. The water is not a source of municipal, industrial, or agricultural useage.

The areas of present release of radioactive industrial effluents is controlled. The largest concentrations of plutonium found in solution are below recommended limits for uncontrolled areas. The bulk of radionuclides is attached or absorbed in alluvial materially in the channels below the plaint outfall. Estimated inventories of plutonium in Acid-Pueblo and DP-Los Alamos Canyons indicate that about 195 mCi have been transported past the Laboratory boundries by storm runoff into Lower Los Alamos Canyon and to the Rio Grande in the past 30 years. Trace of plutonium above the limits of detection ($\approx$ 0.05 pCi/g) can be found in sediments of lower Los Alamos Canyon.

Sediment volumes in the Rio Grande at Otowi Bridge have ranged from 0.6×10^6 to 6.8×10^6 t with an average of about 2.2×10^6 t for the 24 year period from 1948 through 1971. Considering the mixing of 195 mCi of plutonium with the average annual sediment load for a single year the average plutonium concentration in sediment of the river would be 9×10^{-5} pCi/g. Using an average annual release of 6.5 mCi of plutonium (195 mCi/30 years) with the average annual sediment load the sediment concentration in the river would be about 2.7×10^{-5} pCi/g. Thus it appears due to the dispersion of the radionuclide the effect that can be measured of transport of radionuclides in the Rio Grande would be slight.

Four test wells completed into the main aquifer in canyon receiving radioactive industrial effluent exhibit no change in chemical quality nor any trace of radionuclides that can be attributed to the release of the effluents. The chemical and radiochemical quality of water from the remainder of the test wells completed into the main aquifer also show no effect of the Laboratorys or Community release of industrial or sewage effluents.

The industrial and sewage effluents infiltrate into the alluvium of the Canyon to recharge bodies of water perched on the tuff. As the water move downgradient some is lost to evapotranspiration and the remainder move into the underlying tuff. The movement of water in the tuff is downward and the rates of movement vary due to the different hydrologic characteristics of the tuff. The volcanic debris of the Paye Formation and Basaltic Rocks of Chino Mesa contain lenses of silt and clay that would tend to perch and distribute over a large area any water moving downward to the main aquifer. In general several hundred meters of unsaturated tuff, volcanics debris and basalts separate the water in the alluvium and main aquifer.

The movement of water in the main aquifer is at about 110 m/yr. toward the natural discharge area of the Rio Grande. It would take over 100 years

based on this rate of movement for the water in the main aquifer to reach the river from the central part of the plateau. Thus if any contaminates, chemical or radiochemical, should reach the aquifer the transit time from point of contamination to discharge area would allow chemical and ion or base exchange reactions to take place so no contamination would remain in the water at the natural discharge area.

XXII Selected References

1. R. L. Griggs, "Geology and Ground-Water Resources of the Los Alamos Area, New Mexico," U.S. Geol. Survey Water-Supply Paper 1753 (1964).

2. R. A. Bailey, R. S. Smith, and C. S. Ross, "Stratigraphic Nomenclature of the Volcanic Rocks in the Jemez Mountains, New Mexico," U. S. Geol. Survey Bull. 1274-P (1969).

3. V. C. Kelley, "The Rio Grande Depression from Taos to Santa Fe," New Mex. Geol. Soc. Seventh Field Conf., Southeastern Sangre de Cristo Mountains, New Mexico (1956).

4. U. S. Geol. Survey, "Water Resources Data for New Mexico, Pt. 1 Surface Water Records," Albuquerque, New Mexico (1970).

5. U. S. Geol. Survey, "Water Resources Data for New Mexico, Pt. 2 Water Quality Records," Albuquerque, New Mexico (1969).

6. R. L. Cushman, "An Evaluation of Aquifer and Well Characteristics of Municipal Well Field in Los Alamos and Guaje Canyons near Los Alamos, New Mexico," U. S. Geol. Survey Water-Supply Paper 1809-D (1965).

7. C. V. Theis and C. S. Canover, "Pumping Tests in the Los Alamos Canyon Well Field near Los Alamos, New Mexico," U. S. Geol. Survey Water-Supply Paper 1619-I (1962).

8. American Public Health Assoc. Inc., "Standard Methods for the Examination of Water and Wastewater," 1790 Broadway, NY, New York 10019, Vol. 12 (1965).

9. J. D. Hem, "Study and Intrepretation of the Chemical Characteristics of Natural Water," U. S. Geol. Survey Water-Supply Paper 1473 (1959).

10. P. E. Trujillo Jr., "Analytical Proceedures," In Environmental Monitoring in the Vicinity of the Los Alamos Scientific Laboratory, Jan. through June 1971, Los Alamos Scientific Laboratory Dept. LA-4871-MS (1972).

11. P. E. Trujillo Jr. "Standard Analytical Procedures for Soil" Manuscript Group H-6, Los Alamos Scientific Laboratory (1970).

12. F. H. Rainwater and L. L. Thatcher, "Methods for Collection and Analyses of Water Samples," U. S. Geol. Survey Water-Supply Paper 1454 (1960).

13. T. E. Hakonson, J. W. Nyhan, L. J. Johnson, and K. V. Bostick, "Ecological Investigations of Radioactive Materials in Waste Discharge Areas at Los Alamos for the Period July 1, 1972 through March 31, 1973," Los Alamos Scientific Laboratory Dept. LA-5282-MS (1972).

14. C. W. Christenson and R. G. Thomas, "Movement of Plutonium through Los Alamos Tuff," in Second Ground Disposal of Radioactive Waste Conf., U. S. Dept. of Commerce TID-7628 (1962).

15. William D. Purtymun, "Storm Runoff and Transport of Radionuclides in DP Canyon, Los Alamos County, New Mexico," Los Alamos Scientific Laboratory Dept. LA-5744 (1974).

16. E. H. Baltz, J. H. Abrahams, and W. D. Purtymun, "Preliminary Report of the Geology and Hydrology of Mortandad Canyon near Los Alamos, N. Mex., with reference to disposal of Liquid Low Level Radioactive Wastes," U. S. Geol. Survey Open-file Rept. (1963).

17. W. D. Purtymun, "Progress Report on the Hydrology of Mortandad Canyon Disposal System for Treated Low-level Radioactive Wastes, July 1961 to June 1963," U. S. Geol. Survey Admin. Rept. (1964).

18. W. D. Purtymun, G. L. Johnson, and E. C. John, "Distribution of Radioactivity in Alluvium of a Disposal Area at Los Alamos, New Mexico," U. S. Geol. Survey Prof. Paper 550-D (1966).

19. W. D. Purtymun, "The Disposal of Low-level Radioactive Effluents in Mortandad Canyon, Los Alamos County, New Mexico," U. S. Geol. Survey Admin. Rept. (1968).

20. W. D. Purtymun, "Regional Survey of Tritium in Surface and Ground Water in the Los Alamos Area, New Mexico, August 1966 through May 1969," Los Alamos Scientific Laboratory Rept. LA-5234-MS (1973).

21. W. D. Purtymun, "Despersion and Movement of Tritium in a Shallow Aquifer in Mortandad Canyon at the Los Alamos Scientific Laboratory," Los Alamos Scientific Laboratory Rept. LA-5716-MS (1974).

22. U. S. Dept. of Agriculture, "Diagnore and Improvement of Saline and Alkali Soils," U. S. Dept. of Agriculture Handbook 60 (1954).

23. Black and Veatch Consulting Engineers, "Ground-Water Observation Wells," Los Alamos, New Mexico," Admin. Rept. prepared for U. S. A.E.C. (1950).

24. E. E. John, E. Euyart, and W. D. Purtymun, "Records of Wells, Test Holes, Springs and Surface Water Stations in the Los Alamos Area, New Mexico," U. S. Geol. Survey Open-file Rept. (1967).

25. J. E. Weir and W. D. Purtymun, "Geology and Hydrology of Technical Area 49, Frijoles Mesa, Los Alamos County, New Mexico," U. S. Geol. Survey Admin. Rept. (1962).

26. W. D. Purtymun, F. C. Koopman, S. Barr and W. E. Clements, "Air Volume and Energy Transfer Through Test Holes and Atmospheric Pressure Effects on the Main Aquifer," Los Alamos Scientific Laboratory Rept. LA-5725-MS (1974).

XXII. Appendices

Contents

		Page
A.	Physical Characteristics of the Bandelier Tuff	255
B.	Hydrologic Characteristics of the Bandelier Tuff	263
C.	Low Flow Investigations in Santa Clara, Guaje, Los Alamos and Frijoles Canyons.	273
D.	Geologic, Hydrologic, and Waste Disposal Reports	292
E.	Chemical Analyses of Surface and near Surface Ground Water in the Drainage Areas, 1967 through 1972	296
F.	Radiochemical Analyses of Surface and near Surface Ground Water in the Drainage Areas 1967 through 1972	317
G.	Chemical Analyses of Water from the Main Aquifer	341
H.	Radiochemical Analyses of Water from the Main Aquifer	343

Appendix A

Physical Characteristics of the Bandelier Tuff

The Bandelier Tuff is formed by a series of ash flows and ash falls which are described as nonwelded, moderately welded, and welded tuff. The nonwelded, moderately welded, and welded tuff grade one into the other both vertically and horizontally.

The upper Tshirege Member, is about 250 m thick along the western edge of the Pajarito Plateau and thins eastward to less than 15 m. Individual moderately welded and welded ash flows in the upper part of the Tshirege Member range from 6 to 40 m thick. Some of the uppermost ash flows are beveled off by erosion eastward across the plateau. Outliers of tuff overlie the Puye formation along Puye Escarpment. Most all ash flows thin eastward from the source area (Sierra de los Valles). Nonwelded ash flows of the Otowi Member may be as much as 90 m thick near the center of the plateau.[1/]

I. Welding

The welding process of an ash flow tuff begins after emplacement. The major factors affecting welding are heated at the time of emplacement, amount of volatiles in the mass, rate of cooling, and thickness of the ash flow.[2/] The degree of welding ranges from incipient stages marked by the sticking together or cohesion of glassy fragments to complete welding marked by the cohesion of the surfaces of glassy fragments accompanied by their deformation and elimination of pore space.

Zonal variation of welding occurs vertically within individual flows or within a series of flows that have cooled as a single unit.[3] Single ash flows that have cooled as a unit may show a greater degree of welding near the center than near the upper and lower contacts. A series of ash flows that have been emplaced in rapid succession may cool as a single unit with

the greatest degree of welding near the center.

Variation of welding occurs horizontally within individual flows with greater degree welding near the mountains (the source area). The degree of welding becomes less eastward across the plateau.

The tuffs in the Los Alamos area are classified according to the degree of welding--i. e., nonwelded, moderately welded, and welded tuffs. Welding results in increased cohesion and deformation of the glassy fragments in the tuff. Nonwelded tuff has high porosity, only slight cohesion of the glassy fragments, and crumbly fracture; moderately welded tuff has lesser porosity, moderate cohesion, slight deformation of the glassy fragments, and a somewhat brittle fracture; and welded tuff has lower porosity, good cohesion, a high degree of deformation by flattening of glassy fragments, and a brittle fracture.[4]

The degree of welding influences most of the physical characteristics of the individual ash-flow tuff units.

The following shows a large range in porosity in each of the variations of tuff indicating that welding is only one of several factors determining porosity.

	Range in porosity (percent by volume)
Nonwelded tuff	40 to 60
Moderately welded tuff	30 to 55
Welded tuff	15 to 40

The surface of ex-osed tuff (nonwelded to welded) becomes "case hardened" as it is exposed to the weather. In this process, due to the porosity of the tuff, moisture is absorbed and some minerals are dissolved. The minerals are returned to the surface by evaporation as the tuff dries out where they are precipitated to form a rind. This rind forms a protective surface which resist the wearing away of the surface by wind and water. However, exposed

pumice fragments weather out rapidly leaving small covities in tuff surface.

II. Density

The density of nonwelded tuff is lower than in welded tuff. This is due to the compaction of the matrix (glass shards and ash) and closer arrangement of the quartz and samidine, crystals, and rock fragments in the process of welding of a welded tuff. The specific gravity of the tuff matrix averages about 2.55. The range in bulk density of nonwelded to welded tuff depends on the porosity (i. e., the larger a porosity the smaller the density).

The following table shows a comparison of the densities of pumice and the tuff (nonwelded to welded) with other rock types.

Rock Type	Range in density (gm/cm^3)
pumice (nonwelded)	< 1.0
Nonwelded tuff	1.02-1.52
Moderately welded tuff	1.15-1.84
Welded tuff	1.52-2.16
Granite	2.64-2.76
Marble	2.60-2.84
Sandstone	2.14-2.36
Basalt	2.4 -3.1

III. Bearing capacities

The bearing capacities of a tuff are dependent upon the density of tuff (i. e., the greater bearing capacities occur with the tuff of greater density). The density of the tuff is related to welding (i. e., density of the tuff increases from nonwelded tuff to welded tuff).

Data are available on the bearing capacities of the moderately welded tuff. The following table shows the relationship of density change to the resistance to crushing of a moderately welded tuff.

Density (gm/cm^3)	Resistance to crushing (kg/m^2)
1.73	2.4×10^5
1.74	3.7×10^5
1.77	3.9×10^5
1.79 (probably with pumice inclusion)	3.4×10^5
1.81	4.8×10^5
1.83	5.6×10^5

Rock inclusions of pumice, rhyolite, and latite are found in the tuff. The frequency of occurrence of the rock fragments differs in individual ash flows and at different locations within the same ash flow.

The pumice fragments may be as much as 5 cm in length and 2 cm in diameter. The pumice is soft and friable. Pumice fragment inclusion in a small sample of the tuff would decrease the bearing capacity as failure would most likely occur within the pumice fragment. The rhyolite and latite fragments are dark gray, hard, and may be as much as two or three inches across. These large rock fragments would add strength to the matrix of tuff.

The following table is a comparison of the bearing capacities of a moderately welded tuff (density 1.73 and ~ 1.82 g/cm^3) and miscellaneous rock type. The bearing capacity is computed as 1/5 of rupture strength of the material.

Rock Type	Bearing capacity (kg/m^2)
Moderately welded tuff (1.73 g/cm^3)	4.7×10^4
Moderately welded tuff (1.82 g/cm^3)	1.1×10^5
Sandstone	3.4×10^5
Limestone	8.4×10^5
Marble	1.1×10^6
Granite	1.4×10^6

IV. Thermal Conductivity

The thermal conductivity of the tuff is related to porosity, thus, the

thermal conductivity of a nonwelded tuff would be less than a welded tuff as more pore space is available for insulation.

The only data available on the thermal conductivity was made of a moderately welded tuff in one area investigated. The following table is a companion of the thermal properties of the tuff and miscellaneous rock types. A decrease in thermal conductivity increases the insulating value.

Rock Type	Range of thermal conductivity $\left(\frac{\text{cal, gm-cm}}{\text{hr x cm}^2 \text{ x } ^\circ\text{C}}\right)$
Moderately welded tuff	0.38-0.47
Limestone	4.9 -11
Sandstone	9.9 -20
Marble	17-25
Granite	16-35

V. Mineral composition

The tuff is rhyolitic in composition and contains small rock fragments of rhyolite, latite and devitrified pumice and crystals and crystal fragments of sanidine, and quartz, in a matrix of glass shards and welded ash. Dark minerals are scarce although traces of crystal fragments of biotite, hornblende, and pyroxene have been observed.[2]

Seven samples of a moderately welded tuff were analyzed petrographically by C. S. Ross (written communication, July 7, 1960). Ross recalculated the proportions of phenocrysts in terms of proportion by weight. The results of all seven were similar, one of which is presented here:

Pore space	about 30 percent by volume
Phenocrysts	about 20 percent by weight
Sanidine	12 percent by weight
Quartz	6 percent by weight
Magnetite	1 percent by weight
Pyroxene	0.5 ± percent by weight

The ground mass is typical devitrified welded tuff. The devitrification

products are very fine grained, but show typical cristobalite feldspar structure. Cavities contain radial groups of feldspar and tridymite. The rocks contain a few areas of altered andesite, and some brown firefracting clay like material (probably montmorillonite).

VI. Chemical composition

The color of the tuff ranges from very light gray to medium dark gray. Some units range from pinkish gray to light pink. Large fragments of pumice that appear much darker than the matrix in some units enhance the color of the tuff. Moderately welded units are generally lighter in color than the welded units. The coloring is inherent in the tuff and probably the result of minor changes in the chemical constituents and heat of emplacement.

In general the tuff is composed namely of silica and alumina. The range in chemical constituents is shown on the following table.

Chemical constituents	Range (in percent)
Silica (SIO_2)	72.0-78.2
Alumina (Al_2O_3)	11.2-13.8
Ferric oxide (Fe_2O_3)	1.1-2.1
Ferrous oxide (FeO)	.21-.75
Magnesium oxide (MgO)	.02-.33
Calcium oxide (CaO)	.26-1.17
Sodium oxide (Na_2O)	3.5-4.5
Potassium oxide (K_2O)	4.2-4.7
Water (H_2O)	.15-2.8
Titanium oxide (TiO_2)	.10- .32
Phosphorous oxide (P_2O_5)	.10- .07
Manganese oxide (MnO)	.00- .98
Carbon dioxide (CO_2)	<.05

VII. Joints

Joints and joint systems are prominent in the Tshirege Member. The joints divide the rocks into multitudinous polygonal blocks, many of which are prismatic or columnar.

The joints can be classified into two groups, master joints and minor joints. The term "master joint" signifies those joints that are numerically predominant, are most persistent in length, and pass through several groups of beds.[5]

The master joints can be traced vertically across two or more units of the Tshirege Member. They are vertical or near vertical, dipping more than 80°. The overall vertical trends of the individual master joints are relatively straight; however, they curve slightly through individual units and upon entering a unit of different degree of welding, may be deflected slightly.

The minor joints dip at angles from about 40° to 80° and in most instances, intersect the master joints. These joints are not as persistent as master joints.

Master joint systems in Mortandad Canyon display orientation differences of about 60°.[6] Joint systems mapped at Mesita del Buey also indicate orientation differences of 60°.[7] The angular differences between these joint systems suggest that these sets are conjugate tension joints caused by shrinkage during cooling of the rocks.

REFERENCES

1. R. L. Griggs, "Geology and Ground Water Resources of the Los Alamos Area, New Mexico," U. S. Geol. Survey Water-Supply Paper 1753, (1964).
2. C. S. Ross and R. L. Smith, "Ash-Flow Tuffs: Their Origin and Geologic Relations and Identification," U. S. Geol. Survey Prof. Paper 366 (1961).
3. R. L. Smith, "Zones and Zonal Variation in Welded Ash Flows", U. S. Geol. Survey Prof. Paper 354-F, (1960).
4. W. D. Purtymun and F. C. Koopman, "Physical characteristics of the Tshirage Member of the Bandelier Tuff with Reference to Use as Building and Ornamental Stone," U. S. Geol. Survey Open-File Rept. (1965).
5. V. C. Kelley and N. M. Clinton, "Fracture Systems and Tectonic Elements of the Colorado Plateau," Univ. N. Mex. Pub. in Geol. No. 6 (1960).
6. E. H. Baltz, J. H. Abrahams, and W. D. Purtymun, "Preliminary Report on the Geology and Hydrology of Mortandad Canyon near Los Alamos, New Mexico," U. S. Geol. Survey Open-File Rept. (1963).
7. W. D. Purtymun, "Geology and Hydrology of Mesita del Buey," Los Alamos Scientific Laboratory Rept. LA-4660 (1971).

Appendix B

Hydrologic Characteristics of the Bandelier Tuff

The natural moisture content of the tuff forming the mesas between the eastward-trending canyons is generally less than five percent by volume. Thus, movement of moisture is under unsaturated conditions. The low moisture content of the tuff is caused by the protective cap of clay soil derived by weathering of the tuff near the surface. The hydrologic characteristics of the tuff depend largely upon the degree of welding of the individual ash flows.

I. Hydrologic Effects of Soil

The surfaces of the finger-like mesas which form the Pajarito Plateau are covered by a clayey soil derived by weathering of the underlying tuff of the Tshirege Member. The soil is thickest near the axes of the mesas and thins toward the edges where the tuff is exposed. Thick sections of soil have also developed along slow draining arroyos cut into the surfaces of mesas and in relatively flat areas where water collects and stands. The greatest known thickness of woil is at Frijoles Mesa where 2.7 m was logged in a shallow test hole located in a relatively flat area.

Petrographic examination of the soil derived from the Tshirege Member was made by Staritzky of the Los Alamos Scientific Laboratory.[1] He found that the size distribution of the "sand" fraction (greater than 50 microns in diameter) varied between 15 and 38 percent, the "silt" fraction (2 to 50 microns in diameter) varied between 58 and 73 percent, and the "clay fraction" (less than 2 microns in diameter) varied between 4 and 12 percent. Mineralogically, the principal constituents of the soil were quartz and feldspar, and the most important secondary constituents are the clay minerals, montmorillonite and illite. Monmorillonite is known to have the highest base-exchange capacity

(85 to 100 millequivalents per 100 grams) and illite the next highest (25 to 30 millequivalents per 100 grams) among the clay minerals.

A study of the natural distribution of moisture in soil and in near surface tuff was made at Frijoles Mesa during a 2-year period. The moisture content in the soil cover, including the transition zone from the soil to weathered tuff, varied according to prevailing weather conditions. The moisture content was highest in March and April as the result of late winter snows and thawing and was generally lowest in the months of August through October owing to high evapotranspiration rates. Water from precipitation rarely infiltrated through the undisturbed soil cover into the underlying tuff and only in an extremely low moisture range (less than 5 percent moisture by volume) within the upper 1 m of the tuff.[2]

The upper two units of moderately welded tuff (thickness about 36.5 m) at Frijoles Mesa blow air through open joints in response to a declining atmospheric pressure therefore, the soil cover, which prevents most of the precipitation from infiltrating into the underlying tuff, also impedes the exchange air from the atmosphere to the tuff.[3]

II. Hydrologic Characteristics of Nonwelded, Moderately Welded and Welded Tuff

The hydrologic characteristics of tuff related to porosity, specific yield, specific retention, pore size distribution and hydrologic conductivity were determined of in six units of the Tshirege member at Frijoles Mesa. These hydrologic characteristics were determined in the laboratory under saturated conditions. As saturated conditions rarely occur in the tuff, these parameters maybe of only general interest.

The porosity of the tuff at Frijoles Mesa ranged from 19 to 54 percent by volume; the lowest porosities are in the welded tuffs. Specific yield and specific retention decrease with a decrease in porosity. Specific yield is

greater than specific retention in a nonwelded tuff (high porosity); however, as the porosity decreases the difference become smaller and low porosity specific retention in a welded tuff may be greater than specific yield.

The relationship of porosity to pore size depends on the degree of welding, thickness of the flow, and position in the flow. The larger pore sizes and greater porosities are near the top of the flow and decrease vertically through the flow. This is due to the larger pores formed by escaping gases near the top and compaction and baking of the middle and lower portion of the flow as it cools.

The hydrologic conductivity is indirectly related to porosity depending upon pore size and the degree of interconnection of the pores. The permeability of the tuff matrix decreases with depth for the same reasons that the porosity decreases.

Hydrologic characteristics of the Tshirege Member of the Bandelier Tuff, as determined in the laboratory are shown in the following table.

Hydrologic characteristics of
of the Tshirege Member
at Frijoles Mesa

Hydrologic Characteristics						
Unit	Depth below surface of mesa (m)	Degree of welding	Porosity (percent)	Specific yield (percent)	Specific retention (percent)	Range of Hydrologic Conductivity (m/day)
6	0-19.5	Moderate	38-54	18-34	16-27	0.004-0.25
5	19.5-20.1	None (sand)	-	-	-	1.4 -2.4
4	20.1-41.1	Moderate	33-54	11-43	12-22	0.012-0.53
3	41.1-53.3	Nonwelded	48	34	14	0.9
2	53.3-83.5	Welded	19-37	.6-26	11-21	.08-2 0.003-0.08
1B	83.5-152.7	Nonwelded	-	-	-	50-2.1

III. Movement of Water

The Tshirege Member is dry beneath the surfaces of the finger like mesas. The moisture content of the tuff generally is less than 5 percent by volume, even though the specific retention ranges from 11 to 27 percent. Beneath the canyons, which contain perennial or intermittent streams, the moisture content of the tuff may be as much as 60 percent by volume; however, the water movement through the tuff is as unsaturated flow. Test holes drilled through alluvium and into the tuff in Water and Mortandad Canyons penetrated thick sections (up to 55 m) of wet tuff (up to 60 percent moisture by volume); however, no free water moved into the test holes.

Holes through which instruments can be used to measure moisture content of the bore wall were holes constructed in the tuff beneath the stream channel in upper Mortandad Canyon and these holes contained no free water, although the welded tuff beneath the stream contained as much as 25 percent moisture by volume. Specially constructed moisture access holes in the tuff underlying water perched in the alluvium in lower Mortandad Canyon had moisture contents of the tuff as much as 45 percent by volume but the rock yielded no free water. The welded and nonwelded tuff in the canyon are transmitting water downward into the tuff by unsaturated flow.

The water in the tuff moves an unsaturated flow. The majority of the pores are of capillary size. The energy relationship with moisture content of a moderately welded tuff was determined by Abrahams[4] (Fig. 1). The saturated moisture content of the tuff was about 41 percent by volume. When moisture contents are below 4 percent there is no movement of water; from 4 to 8 percent moisture is redistributed by diffusion; from 8 to 23 percent distribution is by gravity and capillarity and above 23 percent the movement is by drainage from gravity.

A study of the movement of water through the tuff was made at Mesita del

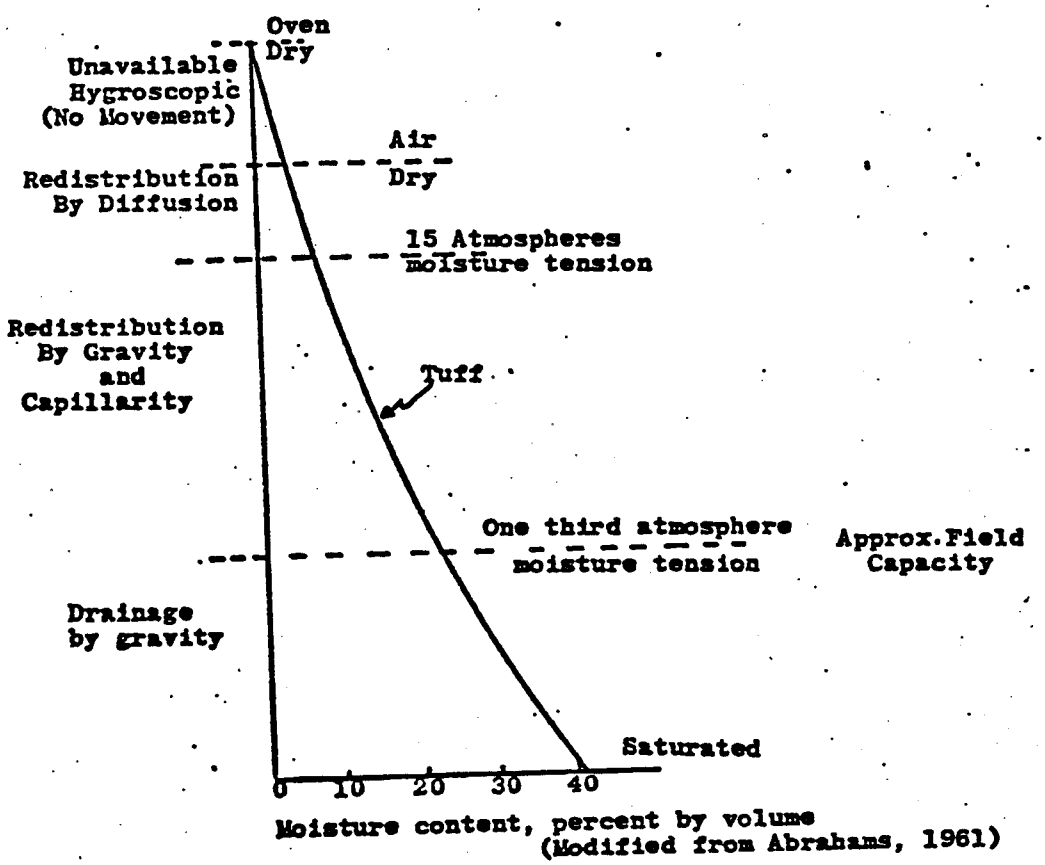

Figure 1. Energy relationships with moisture content of tuff.

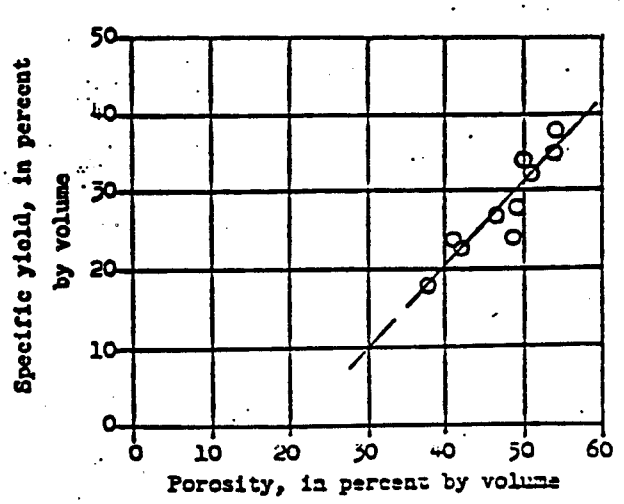

Figure 2. Relationship of specific yield to porosity of the tuff.

Buey. The movement of water from an infiltration pit was monitored by a series of moisture access tubes set in the tuff and a neutron-scattering moisture prob and scaler. The average infiltration rate from a m^3 pit under a constant head of 23 cm of water averaged about 0.34 m/day for a period of about 160 days. The wetted front moving into the tuff was sharpest during the first part of the test. After about 2 months of infiltration moisture had moved downward more than 4.5 m moisture content ranged as follows: 35 percent by volume at 0.6 m below the pit, 30 percent at 0.9 m, 25 percent at 4 m, and 20 percent at 4.6 m.

IV. Hydrologic effects of welding

The uppermost ash flow at Frijoles Mesa exhibits zonal variations of welding in a single cooling unit by vertical changes in porosity. The moderately welded flow is about 24 m thick near the center of the mesa. The greatest porosities are in the upper and basal parts of the flow. Lesser porosities (zone of denser welding) are in the lower one third of the flow, and the pore size decreases with increased depth. The following table presents the hydrologic characteristics at different intervals in a single ash flow tuff.

Hydrologic characteristics of an ash-flow tuff at Frijoles Mesa

Height above base of flow (m)	Porosity (percent)	Specific yield (percent)	Specific retention (percent)	Hydrologic Conductivity (m/day)		Pore size distribution (percent of porosity)	
				vertical	horizontal	> .01 mm	< .01 mm
17.9	54	35	19	10.082	-	-	-
47 14.3	50	34	16	0.12	0.12	39	61
47 14.3	54	38	16	0.25	0.21	26	74
12.2	51	34	17	0.16	0.16	20	80
	49	28	21	0.041	-		
6.7	41	24	17	0.004	0.082	20	80
6.1	47	27	20	0.082	0.082	15	85

Hydrologic characteristics of an ash-flow tuff at Frijoles Mesa (cont'd)

Height above base of flow (m)	Porosity (percent)	Specific yield (percent)	Specific retention (percent)	Hydrologic Conductivity (m/day)		Pore size distribution (percent of porosity)	
				vertical	horizontal	>.01 mm	<.01 mm
5.8	42	23	19	0.041	0.033		
3.6	38	18	20	0.037	0.041		
1. 0.3	51	33	18	0.041	-	17	83
1. 0.3	49	24	25	0.037	0.082	20	80

A decrease in porosity in an ash-flow tuff results in a decrease in specific retention increases proportionately (Fig. 2). The hydrologic conductivity is related to pore size and pore-size distribution rather than porosity. The permeability of the tuff matrix decreases at increased depth with a general decrease in the percentage of pore sizes greater than 0.1 mm.

Variations in vertical and horizontal permeability in the lower one third of the flow may be due to movement and compaction of the ash flow as it cooled. Movement of flow as it cools could result in elongation of the pores in a horizontal plant, and the greatest permeability probably is in this direction. Three of the five horizontal hydrologic conductivities in the lower one third of the flow are greater than the vertical conductivities, however, the conductivity measurements were taken in random directions and no attempt was made at orientation to the probable direction of movement of the flow.

V. Hydrologic effects of joints and contacts

Joints and the fractures in the tuff are capable of transmitting fluid and may offset the relative inability for the adjacent rock to transmit fluid. The interconnection of the joint system is an important aspect of the

hydrologic regime.

Joints in moderately welded to welded tuff of the Tshirege Member range from closed to open. Locally the amount of opening is as much a 5 cm, however, the majority of joints are open less than 1 cm. All joints terminating at the base of the soil zone, which covers the surfaces of the mesas, are filled with a light-brown clay. The depth of clay filling varies from 0.9 to 1.2 m below the soil zone at Mesita del Buey and Frijoles Mesa. The joint openings are plated with clay to depths of 21 m at Frijoles Mesa. Some of the joints are filled or plated with a light-gray clay. The light-gray clay is derived from weathering of the tuff and is composed of minerals leached from the tuff by water. This clay was precipitated along the joint openings prior to the development of the soil zone. The joints are interconnected and master joints transect one or more flows. Joints are more numerous and open in ash flows of moderately welded to welded tuffs than in nonwelded tuff.

Joints that are interconnected in the moderately welded and welded units of tuff could provide paths for rapid movement, water was introduced directly into these open joints. Water would be dispersed through joint systems.

Joints in the moderately welded to welded tuffs will transmit water depending upon the amount of opening and the degree of interconnection between different joint systems. More than 15,000 m^3 of drilling fluid was lost while drilling 300 m of Bandelier Tuff at Frijoles Mesa. Most of the loss was in the upper 150 m in the Tshirege Member which here consist of moderately welded to welded tuff in which open joints are numerous. During grouting of a casing in a large diameter hole at Frijoles Mesa (a 76 cm dia., 15.2 m depth casing filled with water to prevent collapse) the bottom seal in the casing ruptured, and the water from within the casing drained into the formation within 3 hours. The number and orientation of joints in the hole were determined before the casing was installed. A joint near the bottom was open 1 to 3 cm for about

1.2 m. The 6.9 m^3 of water moved into the joint and downward into the joint systems of the underlying flow. Abbreviation of another large-diameter hole 15.2 deep and located 7.6 m to the north failed to disclose and trace of the water.

The experiment at Mesita del Buey indicated that water from the infiltration pit moved downward through a moderately welded tuff into a pumice zone which is more porous and permeable. Movement in the pumiceous zone was lateral. Infiltration into a moderately welded tuff underlying the pumice zone was from near the center of the saturated area in the pumiceous lense. The moisture content of the top moderately welded tuff was much lower than the underlying pumiceous zone, which indicates that specific retention of the pumice zone is greater.

Vertical infiltration through the Tshirege Member would be affected by zonal variations of welding as well as by horizontal contacts between flows.

Vertical changes in hydrologic conductivity caused by contacts between flows tend to perch infiltrating water. In the stream channel in Mortandad Canyon, water is returned to the surface from underflow in the alluvium and in a moderately welded tuff at the contact with a nonwelded tuff.

Industrial wastes discharged into surface water in Acid Canyon move into the joints and tuff of the Tshirege Member, are perched on the top of the Otowi Member, and then move laterally along the contact into a seep area at the junction of Acid and Pueblo Canyons.

Results of an infiltration experiment in the soil near TA-50 indicated that precipitation that is not removed by surface drainage infiltrates into the soil on the mesas of the Pajarito Plateau; however, the downward movement of this water is impeded or stopped by the dense transition zone between the soil and tuff and the water is returned to the atmosphere by evapotranspiration.[2]

REFERENCES

1. Eugene Staritzky, "Report on the Petrographic Eramination of Local Soil," Los Alamos Scientific Laboratory Dept. LA-741 (1949).
2. J. H. Abrahams, J. E. Weir, and W. D. Purtymun, "Distribution of Moisture in Soil and Near Surface Tuff on the Pajarito Plateau, Los Alamos County, New Mexico, "U. S. Geol. Survey Prof. Paper 424-D (1961).
3. W. D. Purtymun and Others, "Air Volume and Energy Transfer Through Test Holes and Atmospheric Effect on the Main Aquifer," Los Alamos Scientific Laboratory Rept. LA-5725-MS (1974).
4. J. H. Abrahams, "Physical Properties of and Movement of water in the Bandelier Tuff," U. S. Geol. Survey Open-File Dept. (1963).

Appendix C

Low Flow Investigations in Santa Clara, Guaje, Los Alamos, and Frijoles Canyons

Surface water drainage accross the Pajarito Plateau is eastward from the Sierra de los Valles to the Rio Grande, the master stream in north-central New Mexico (Fig. 1). The eastward trending intermittent and perennial streams have cut deep canyon into the plateau. Two of the major canyons, Santa Clara and Frijoles, contain surface water which during a part of the year discharge into the Rio Grande, Guaje and Los Alamos Canyon contain perennial streams in their upper reaches. Only during periods of excessive precipitation (heavy snow melt or summer thunder showers) cause surface water in these two canyons to reach the Rio Grande.

The geology and hydrology of the area have been discussed in previous sections of this report. The low flow investigations were made in 1958, 1959, and 1960.[1,2] While the State Engineer summarizes stream flow at the gaging station in Santa Clara Canyon for the years 1937 through 1941 and 1950.[3] The U. S. Geological Survey summarizes the stream flow at gaging stations in Frijoles Canyon for the years 1960 through 1967.[4] The present study utalizes data from these investigations and reports. Low flow data has been supplemented by additional measurements in Santa Clara and Guaje Canyons and by the collection of water samples for chemical and radiochemical analyses.

Geologic sections were prepared along the stream channels of Santa Clara, Guaje, Los Alamos, and Frijoles Canyons using existing geologic maps modified by field investigations. Subsurface correlations were interpreted from outcrops and logs of near-by wells or test holes. The low-flow stations are shown on cross-section and results of measurements on tables of respective sections in the text.

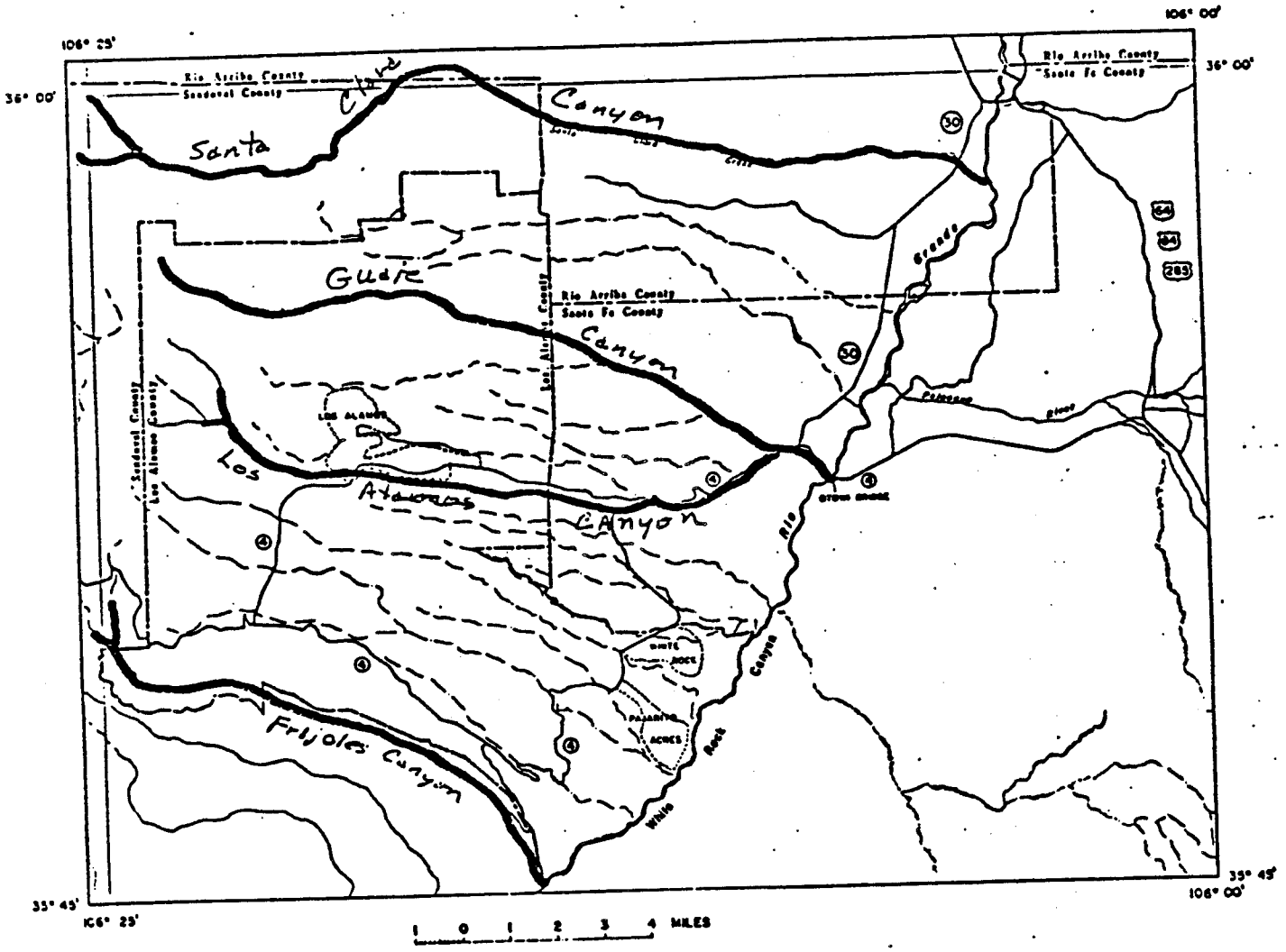

Figure 1. Map of Los Alamos Area showing location of low-flow investigations in Santa Clara, Guaje, Los Alamos, and Frijoles Canyons.

The purpose of the low flow studies was to relate geology and geologic structure to loss or gain in stream flow in evaluating recharge or discharge to stream connected aquifers (aquifers in the alluvium) or the main aquifer.

Low-flow measurements were made with a pygmy current meter except as noted. The report is presented in English units to correspond with initial studies. The conversion factors to metric are presented if conversion is desired

Conversion of English to Metric Units

Multiply	By	To Obtain
Inches (in)	2.54	Centimeters (cm)
Feet (ft)	0.3048	Meters (m)
Miles (mi)	1.609	Kilometers (km)
Square miles (sq. mi)	2.59	Square Kilometers (km^3)
Cubic feet/sec (cfs)	28.32	Liters/sec (l/sec)
Acre-feet (Ac. ft)	1233	Cubic Meters (m^3)

I. SANTA CLARA CANYON

The effective drainage area (area in which base flow increases, generally in mountain front underlain by the Tschicoma Formation) of Santa Clara Canyon is about 27 sq. mi. The canyon contains the largest stream flow of the three canyons. The stream is fed by precipitation percolating through the coalluvium overlying the Tschicoma Formation on the Canyon walls and emerging in the stream channel as surface flow. The flow starts about 1.2 mi west of the initial point at an altitude of about 9,200 ft (Fig. 2). The largest flow increase, in reach investigated, is between stations 3 and 8 and generally continues to increase to station 26 (Table 1). In this reach of the canyon the gradient of the stream channel is about 230 ft/mi and is underlain by the Tschicoma Formation. East of station 26 there is a steady decline in flow as the gradient of the channel decrease to an average of about 115 ft/mi where the

Puye and Tesuque Formations underlie the stream. It is evident that the alluvium begins to thicken east of station 26 thus a part of the flow is lost into the stream connected aquifer in the alluvium and underlying Puye while the rest is lost to evapotranspiration.

Two small recreational reservoirs (3 and 4) were built in the canyon by Santa Clara Pueblo above station 26 prior to the 1958 through 1960 seepage investigations (Figure 3). Two additional reservoirs were built between stations 3, 8, and 11 prior to seepage run made in June 1967. There was no apparent loss of water from the reservoirs into the underlying formations as indicated by the 1967 measurements. Water below station 34 is diverted from the stream for irrigation during a part of the year. A shallow well near station 31 (48 ft deep in alluvium) is used to fill stock tanks on the plateau south of the canyon.

A gaging station was operated by the U. S. Geological Survey near station 34 for the water year (October through September) 1937, 1938, 1939, 1940 and 1951 (New Mexico State Engineer, 1959 p. 229). The annual runoff (volume of water to cover entire watershed) ranged from 1.3 to 3 inches (Table 2).

II. GUAJE CANYON

Guaje Canyon has an effective drainage area of about 6 sq mi above the reservoir. Base flow in the canyon is maintained by two springs which discharge at an altitude of about 8,850 ft (between stations 4 and 6 above reservoir) from a zone at the base of the Bandelier Tuff.[5] A small amount of flow is added to the stream from coalluvium on the canyon walls above the reservoir (Fig. 3). Surface water losses occur eastward from the reservoir (Table 3). The amount of flow is sufficient (with no diversion from the reservoir) to extend near mile 6 before being depleted to evapotranspiration and infiltration into the underlying alluvium and formations. The gradient of the stream channel underlain by the Tschicoma Formation is about 300 to 500 ft/mi decreasing to

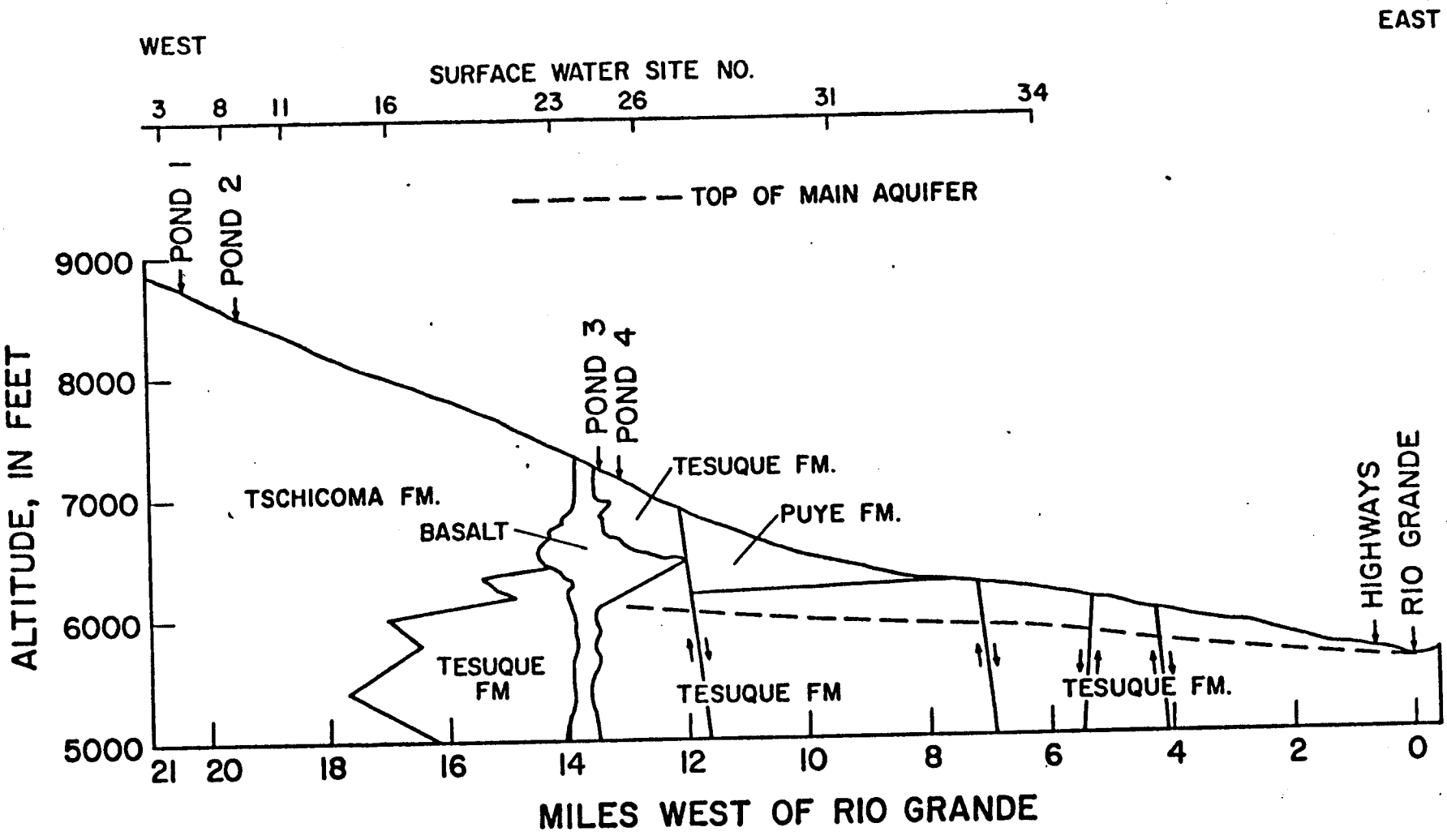

Figure 2. Geologic section of Santa Clara Canyon showing location of low flow measurements.

Table 1. Santa Clara Canyon Low Flow Measurements
(cubic feet per second)

	1958	1959				1960		1967
	Oct. 14-15	Apr. 14	June 2	Aug 31	Oct 12-14	May 16-17	June 20-22	June 30
3	2.0	2.2	2.7	2.6	2.2	5.4	1.9	--
8	4.0	4.0	4.9	4.1	3.4	7.1	2.0	3.6
11	4.0	4.1	5.2	4.8	3.8	8.6	2.8	3.5
16	4.6	5.4	4.9	5.6	4.5	8.6	2.8	3.4
23	4.5	5.4	5.2	6.1	4.3	7.9	3.7	3.4
26	3.9	6.0	5.3	4.9	4.2	8.8	4.3	3.2
31	5.5	5.0	4.6	5.3	3.4	8.3	3.6	2.7
34	3.1	3.6	3.9	4.3	3.2	7.4	2.1	--

Table 2. ~~Annual Runoff at Gaging Station in~~
Santa Clara Canyon

WATER YEAR	ANNUAL RUNOFF	
	(Acre-feet)	(Inches)
1937	3,368	1.8
1938	3,039	1.7
1939	2,630	1.4
1940	2,825	1.5
1941	5,602	3.0
1950	2,460	1.3

- Drainage area 34.5 sq. mi.

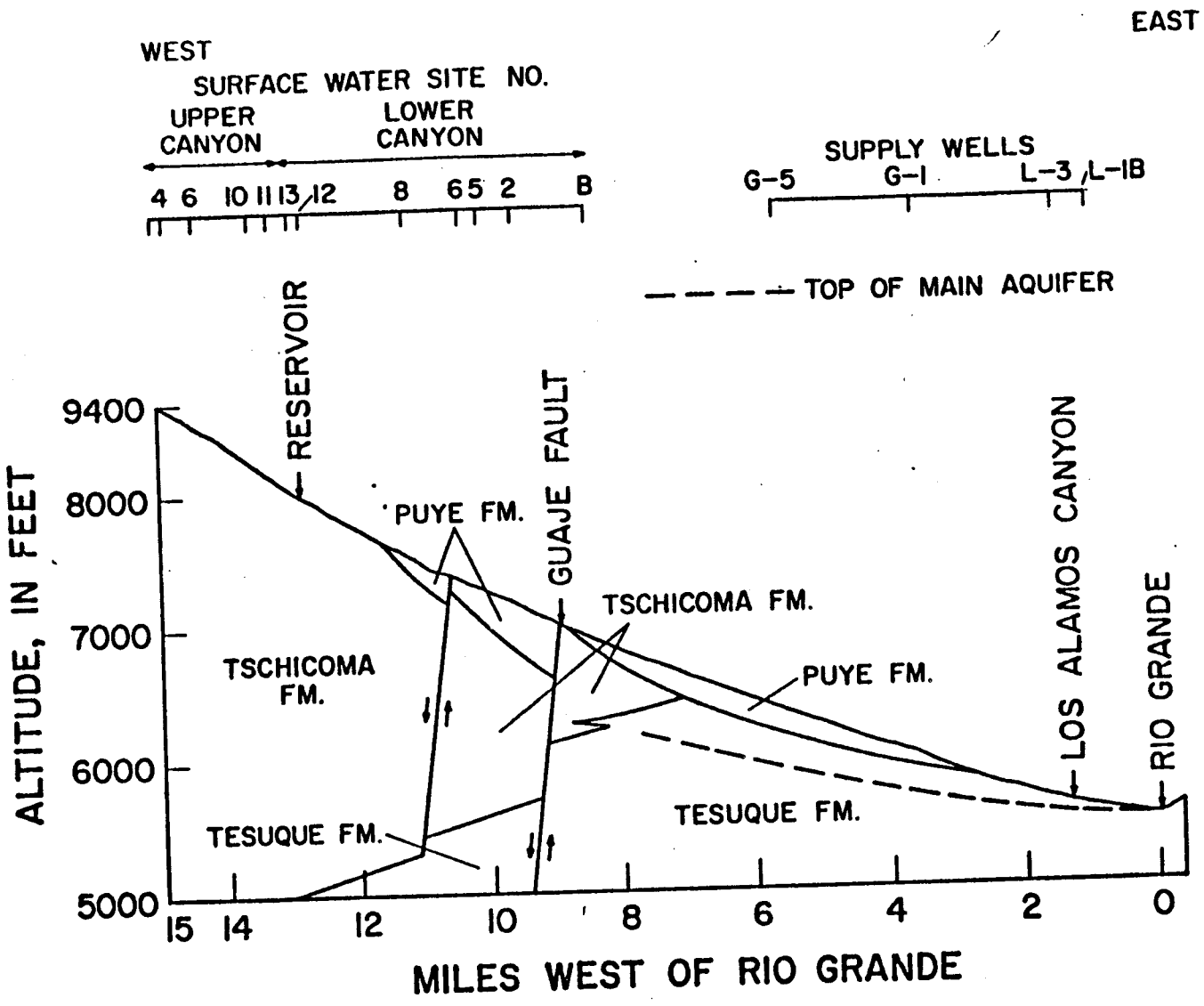

Figure 3. Geologic section of Guaje Canyon showing location of low flow measurements.

Table 3. Guaje Canyon Low Flow Measurements
(cubic feet per second)

	1958	1959				1960		1967	
Site No.	Oct 17	Apr 15	June 3	Sept 1&4	Oct 12-14	May 16-17	June 20-22	May 3a/	June 9a/
4	0.2	0.2	0.3	0.5	0.2	0.4	0.3		
6	0.4	0.4	0.4	1.0	0.4	1.0	0.5		
10	0.4	0.4	0.5	2.0	0.4	1.1	0.5		
11	0.5	0.5	0.5	2.0	0.4	1.0	0.6		
13	0.4	0.6	0.4	2.7	0.5	1.5	0.5	0.34	0.31
Dam b/									
12	0.3	0.7	0		0	0.9	0	0.36	0.34
8	0.3	0.8	0.04		0.01	0.8	0.04	0.29	0.26
6	0.2	0.5	0.02		0	1.0	0.05	0.24	0.21
5	0.03	0.3	0		0	1.0	0	0.17	0.15
2	0.05	0.4	0.04		0.08	1.2	0.1	0.21	0.18
B	0	—	0		0	0.9	0	0	0

a/ Measurements with par~~tial~~shall flume

b/ Water diverted to Los Alamos on all runs except Apr. 15, 1959

about 210 ft/mi where the channel underlain by the Puye to 100 ft/mi where underlain by the Tesuque Formation. The alluvium is thin overlying the Tschicoma and thickens eastward accross the plateau.

North-south trending faults form two small structural basins accross the canyon between mile 3 and 6 (Fig. 3). The channels in these basins are underlain by as much as 20 ft of alluvium and an unknown thickness of volcanic debris of the Puye Formation and are in the area of surface water loss by evapotranspiration and infiltration into the underlying rocks. Return flow occurs in small amounts along the trace of the eastern most fault. This flow rapidly infiltrates into alluvium east of the fault. A test hole drilled near Station 2 in the structural basin encountered about 17 ft of alluvium and was completed at a depth of about 103 ft in the Puye. Both the alluvium below the stream channel and underlying conglomerate appeared to be saturated. The return flow at the fault trace indicates a impermeable boundary formed by the Tschicoma Formation to the eastward movement of water in the alluvium and upper part of the Puye.

A structural feature influencing the movement of water in the main aquifer is the two structural basins formed by faulting in Guaje Canyon. The surface of the main aquifer rises north-westward in the Guaje well field east of the structural basins; however, a change in direction of movement of water indicated by the contours to the south of the structural basins shows that the impermeable rocks of the Tschicoma Formation form a boundary to the eastward movement of water in the main aquifer (Fig. 3, main test of report). Surface water infiltrating into the volcanic debris of the structural basins would move north-south around the Tschicoma Formation. There appears to be a saturated thickness of volcanic debris (about 100 ft) where surface water loss to the alluvium and underlying rock may be a part of direct recharge to the main aquifer.

Guaje Reservoir is contained by a small concrete dam about 25 ft along and 11 ft high with a storage capacity of about 250,000 gal. It is located in a narrow part of the canyon at an altitude of about 8,020 ft. Water can be diverted from the reservoir through a pipe line up to the plateau to Los Alamos. The water was used as a part of the water supply unit 1959. Since that time it has been used periodically for irrigation during the summer. Discharge measurements of the stream above and below the dam (when no water was being diverted) indicated no loss from the reservoir by infiltration into the underlying rocks.

III. LOS ALAMOS CANYON

Los Alamos Canyon has effective drainage area of about 6 sq mi above the reservoir. Base flow in the canyon is maintained by a spring between stations 6 and 9 at an altitude of about 8,000 ft from fractured zone in the Tschicoma Formation (Fig. 4). Base flow above the reservoir is small; however, with snowmelt runoff the excess flow which tops the reservoir will extend across the plateau to near state highway 4 (Table 4). The gradient of the channel underlain by the Tschicoma Formation is about 310 ft/mi on the flanks of the mountains while across the plateau where the channel is underlain by the Bandelier tuff the gradient decreases to about 160 ft/mi (Fig. 5). The channel crosses the Pajarito Fault Zone near Mile 2. Near Mile 7.8 there is some return flow as the alluvium thins where it is underlain basalt interbedded with the Puye Formation. The basalts form a series of falls in the channel between mile 9.5 and 10.5 (Fig. 4). Near mile 10.5 there is a spring in the basalt that discharges about 25 gpm into the stream channel; the flow only moves about one quarter of a mile downstream before infiltrating into the underlying alluvium.

Eight shallow observation wells are drilled through the alluvium into the tuff or basalt between Miles 5 and 9. The stream flow which during the spring tops the reservoir and during heavy summer thunder showing maintain some water

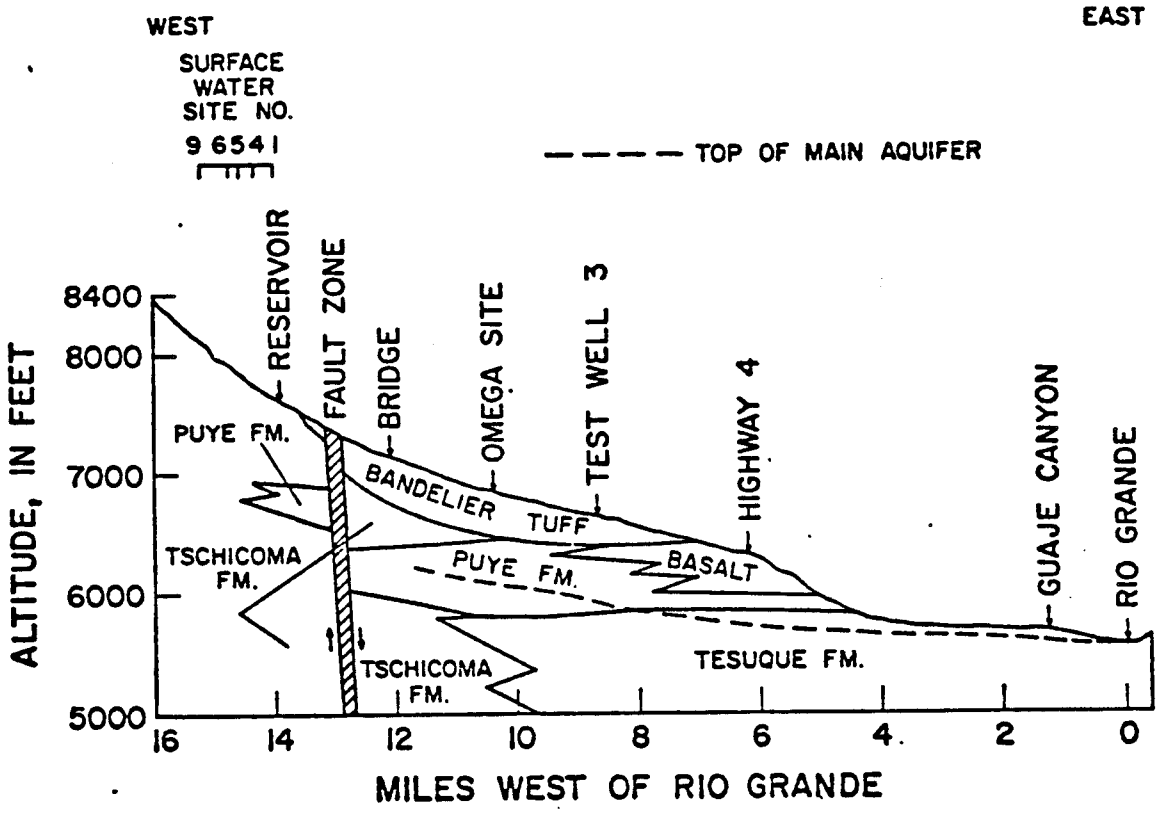

Figure 4. Geologic section of Los Alamos Canyon showing location of low flow measurements.

Table 4. Los Alamos Canyon Low Flow Measurements (cubic feet per second)

	1958		1959		1961
Site No.	May 23	Oct. 30	Apr. 15	May 15	Apr. 27
9	—	0.0	0.0	0.0	—
6	—	0.4	0.3	0.4	—
4	—	0.1	0.4	0.4	—
2	—	0.1	0.4	0.4	—
1	—	0.1	0.5	0.5	—
Dam					
1	—	—	—	—	3.2 a/
2	—	—	—	—	3.2
3	9.0 a/	—	—	—	2.9
4	—	—	—	—	3.1
5	6.3	—	—	—	1.2
6	5.5	—	—	—	0.3

a/ Runoff over dam.

in the alluvium of this stream connected aquifer. The amount of water in the aquifer is seasonal dependent in stream flow. As the water in the alluvium some is lost to evapotranspiration while the rest moves into the tuff and basalt. Stream flow lost into the basalt is the source of recharge for water discharge from the spring near mile 10.5. There is no apparent perched water between the stream connected aquifer in the alluvium and basalt and the main aquifer based on data from a test hole near mile 6.5 which penetrates about 60 ft into the top of the main aquifer.

Los Alamos Reservoir is contained by an earth filled dam that has a storage capacity of about 13 million gal. Water is diverted through a pipe line to Los Alamos. The water was used as a part of the water supply until 1959.

IV. FRIJOLES CANYON

Frijoles Canyon has an effective drainage area of about 9 sq mi on the flanks of the mountains west of the Pajarito Fault Zone (Fig. 5). The canyon differs, however, as it is cut into the Bandelier Tuff on the flanks of the mountains. The slope of the channel west of the fault zone is about 380 ft/mi while to the west it decreases to about 150 ft/mi on the western two thirds of the plateau where the channel is underlain by tuff. In the eastern third the slope of the channel increase to about 390 ft/mi where it is underlain by basalt interbedded with the Puye Formation. The basalt forms two falls which have retarded the down cutting of the canyon to the west.

The base flow in the canyon is maintained by springs emerging from densely welded tuff from an altitude of about 8,430 ft in both the north and west fork of the canyon. The flow increases eastward from seepage from the coalluvium on the canyon walls (Table 5). The increase is to the fault zone, which may be attributed to water moving down along the brecciated zone from higher elevations or to thinning of the tuff and alluvium near the fault. The surface water losses across the plateau appear to be mainly from evapotranspiration.

The alluvium in the canyon appears to be thin as there is no increase in flow between stations 26 and 30 where channel is cut on basalt and conglomerate. The tuff underlying the channel west of the fault zone and western part of the plateau is probably small as the permeability of the tuff is low.

A gaging station was operated near the Pajarito fault zone during water years 1960, 1961, and 1962 (Table 6). The station was moved during the latter part of 1962 to near station 22 in the lower reach of the canyon. Records were obtained for the water year 1964 through 1969. The annaul runoff for the upper gaging station ranged from 2.5 to 2.8 in and from 0.6 to 1.3 in at the lower station for the years of record.

V. CHEMICAL AND RADIOCHEMICAL QUALITY OF WATER

Water samples were collected during the low-flow investigations 1958 and 1960. They were analyzed for bicarbonate, sodium, and chloride ions as well as conductance to determine if changes in quality of the surface flow could be correlated with increase gain or loss of flow in the stream.[6,7] The results of these analyses indicated no particular trends to increased gain or loss with flow as gain or loss were small. The results did show a general increase in these ions and specific conductance down gradient in the stream as ions were adsorbed by the water from the channel material.

Chemical and radiochemical analyses of surface water from the stream in the four canyons are shown on Table 7. The low concentration of ions and total dissolved solids are as one would expect of high mountain streams. The quality of water from a stream connected aquifer in the alluvium in Guaje Canyon is quite simialr to the quality of surface water in the canyon.

The radiochemical quality of the water shows only traces of natural occuring activity. Results of analyses ^{238}Pu and ^{239}Pu in the four smaples were below limits of detection of 0.05 pCi/l.

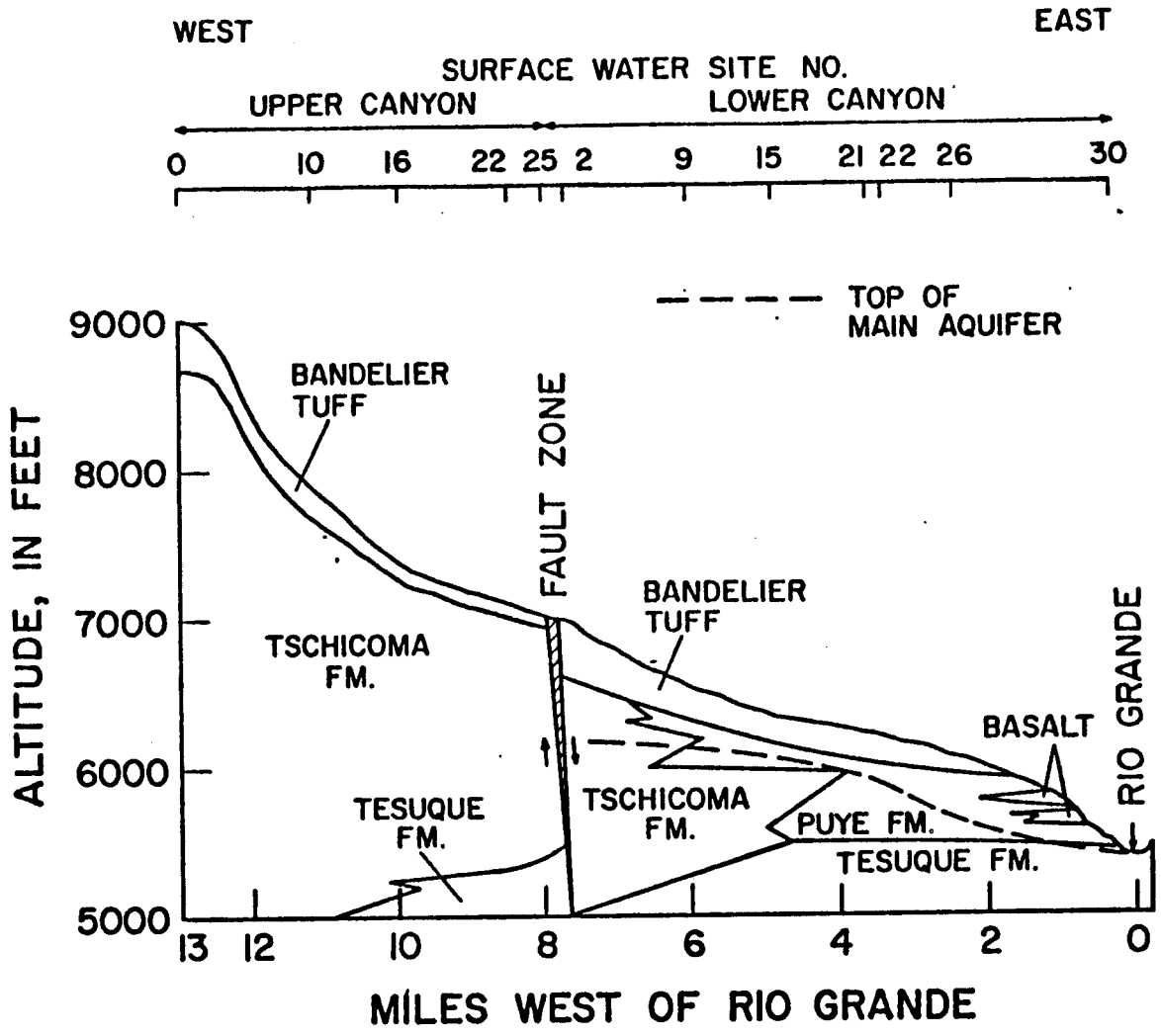

Figure 5. Geologic section of Frijoles Canyon showing location of low flow measurements.

Table 5. Frijoles Canyon Low Flow Measurements (cubic feet per second)

	1958	1959					1960	
Site No.	Oct. 20	Apr. 16	Apr. 29	June 2 & 3	Sept. 2 & 3	Oct. 12 -14	May 16-17	June 20-22
10	--	--	0.9	0.5	0.3	0.1	0.9	0.5
16	--	--	1.4	0.9	0.6	0.6	1.4	0.9
25	--	--	2.1	1.5	1.2	1.2	1.6	1.2
2	1.9	2.7	--	1.6	--	1.4	2.1	1.2
9	1.2	2.6	--	1.5	1.2	1.0	1.5	0.8
15	1.5	2.4	--	1.1	1.2	1.1	--	0.9
21	1.2	2.2	--	1.3	1.2	1.0	1.7	1.0
22	1.3	2.6	--	1.1	1.1	1.0	1.5	0.8
26	1.2	1.6	--	1.1	1.2	0.8	1.4	0.8
30	--	--	--	--	0.7	0.5	1.2	0.3

Table 6. Annual Runoff at Gaging Station in Frijoles Canyon

Water Year	Annual Runoff	
	Acre Feet	Inches
1960	1,332	2.8
1961	1,180	2.5
1962	1,240	2.6
1963	--	
1964	580	0.6
1965	830	0.8
1966	735	0.8
1967	673	0.7
1968	1260	1.3
1969	1040	1.1

Gaging station moved in 1963; drainage area 1960 - 1962, 8.9 sq. mi.; 1964 - 1969, 17.5 sq. mi.

Table 7. Chemical and Radiochemical Quality of surface and ground water in alluvium.

	Santa Clara Station 16	Guaje Station 13	Los Alamos Station 1	Frijoles Station 25	Guaje Canyon near Station 2 (Alluvium)
Date Collected	4-25-69	4-24-69	4-23-69	5-13-69	4-15-70
Chemical (Milligrams per liter)					
Calcium	6	6	6	6	12
Magnesium	.5	3.0	2.0	3.0	5
Sodium	10	9	6	13	7
Carbonate	0	0	0	0	0
Bicarbonate	22	38	26	34	36
Chloride	1	1	2	1	0
Fluoride	0.0	0.0	0.0	0.2	0.4
Nitrate	0.1	0.1	0.1	0.1	0.2
Dissolved Solids	82	120	86	111	111
Total Hardness as C_aCO_3	16	26	21	28	50
Conductance in Micromhos at 25°C	54	75	56	80	80
pH	7.3	7.8	7.3	7.4	7.7
Radiochemical					
Gross Alpha 1/	0.00±0.76	0.00±0.58	0.35±0.89	0.00±0.87	0.0±1.2
Gross Beta 1/	3.1 ±1.9	2.4 ±1.2	2.2 ±1.3	3.9 ±1.3	2.4±1.3
Uranium (Natural) 2/	0.2 ± 0.4	0.5 ±0.4	0.6 ±0.4	0.8 ±0.4	0.0±0.4

1/ Picocuries per liter
2/ Micrograms per liter

VI. SUMMARY

Precipitation on the slopes of the mountains is the source of surface flow found in canyons cut into the Pajarito Plateau. The major loss of stream flow on the plateau is due to evapotranspiration; however, eastward across the plateau surface flow recharges stream connected aquifers in the alluvium. The amount of water in the alluvium is seasonal dependent on stream flow. As the water in the alluvium moves downgradient some infiltrates into the underlying rocks and some is lost to evapotranspiration. An aquifer perched in basalts in Los Alamos Canyon is recharged in part from water in the alluvium.

The main aquifer and stream connected aquifers are separated by a thickness of unsaturated rocks. The slope on the surface of the main aquifer indicates recharge area is on the flanks of the mountains, brecciated zone along major faults that along the western edge of the plateau, and deep canyons cut into the flanks of the mountains and western part of the plateau. The structural basin in Guaje Canyon may be a part of the recharge area to the main aquifer.

Appendix D

Geologic, Hydrologic and Waste

Disposal Reports

(Selected Report no listed in References)

Geologic and Hydrologic Reports

1. V. C. Kelley, "Tectonus of the Rio Grande Depression of Central New Mexico," New Mex. Geol. Soc. Third Field Conf., Rio Grande Country (1952).
2. C. S. Ross, R. L. Smith, R. A. Bailey, "Outline of the Geology of the Jemez Mountains, New Mexico," New Mexico Geol. Soc. Twelth Field Conf., Albuquerque Country (1961).
3. J. H. Abrahams, E. H. Baltz, and W. D. Purtymun, "Movement of Perched Ground Water in Alluvium near Los Alamos, New Mexico," U. S. Geol. Survey Prof. Paper 450-B (1962).
4. Fane Spiegel and Brewster Baldwin, "Geology and Water Resources of the Santa Fe Area, New Mexico," U. S. Geol. Survey Water-Supply Paper (1963).
5. W. D. Purtymun, "Geology and Hydrology of White Rock Canyon from Otowi to the Confluence of Frijoles Canyon, Los Alamos and Santa Fe Countries, New Mexico," U. S. Geol. Survey Admin. Rept (1966).
6. W. D. Purtymun, "Geology of the Microseismograph Station at S-Site, Los Alamos County, New Mexico," U. S. Geol. Survey Admin. Rept. (1968).
7. M. Dean Keller, Comiler, "Geologic Studies and Material Properties Investigations of Mesita de Los Alamos," Los Alamos Scientific Laboratory Rept. LA-3728 (1968).
8. W. D. Purtymun and J. B. Cooper, "Development of Ground-Water Supplies on the Pajarito Plateau, Los Alamos County, New Mexico," U. S. Geol. Survey Prof. Paper 650-B (1969).

REFERENCES

1. U. S. Geological Survey, "Surface Water Supply of the United States, Part 8, 1959, Western Gulf of Mexico Basins," U. S. Geol. Survey Water-Supply Paper 1632 (1962).
2. U. S. Geological Survey, "Surface Water Supply of the United States, Part 8, 1960, Western Gulf of Mexico Basins, U. S. Geological Survey Water-Supply Paper 1712 (1963).
3. New Mexico State Engineer, "Hydrologic Summary, New Mexico Stream Flow and Reservoir Contents 1888-1954," New Mexico State Engineer Tech. Rept. 7.
4. U. S. Geological Survey, "Water Resources Data for New Mexico, Part 1, 1960 through 1969," Albuquerque, New Mexico (1960-1969).
5. H. T. Stearns, "Ground-Water Supplies for Los Alamos," Consulting Engineer Rept to USAEC (1948).
6. U. S. Geological Survey, "Quality of Surface Water of the United States, Part 7 and 8, 1959, Lower Mississippi River Basin and Western Gulf of Mexico Basins," U. S. Geol. Water-Supply Paper 1744 (1961).
7. U. S. Geol. Survey, "Quality of Surface Water of the United States, Parts 7 and 8, 1960, Lower Mississippi River Basin and Western Gulf of Mexico Basins," U. S. Geol. Survey Water-Supply Paper 1814 (1962).

9. Dames and Moore, Consulting Engineers, "Report of Geologic, Foundation, Hydrologic, and Seismic Investigations for the Plutonium Processing Facility at the Los Alamos Scientific Laboratory," Engineering Rept. to AEC and LASL (1972).

10. W. D. Purtymun and Steven Johansen, "General Geohydrology of the Pajarito Plateau," New Mexico Geol. Soc. Twenty-Fifth Field Conf., Ghost Ranch Central - Northern, New Mexico (1974).

Waste Disposal

1. C. W. Christenson, "Radioactive Waste Disposal Practice at Los Alamos," First Session on Ind. Radioactive Waste Disposal, Hearings, before Spec. Sub. Comm. on Radiation, V. 1, Eighty-sixth Cong., U. S. Gov't. Printing Office (1959).

2. L. A. Emelity, C. W. Christenson, and W. H. Kline, "Operational Practice in Treatment of Low - and Intermediate - Level Radioactive Wastes," International Atomic Agency, Vienna, Austria (1966).

3. J. P. Hutchinson and C. W. Christenson, "Treatment of Radioactive Wastes by Chemical Precipitation and Ion-Exchange at Los Alamos, New Mexico, U. S. Gov't. Printing Office, TID-11048 (1960).

4. L. A. Emelity, R. Garde, and C. W. Christenson, "Waste Management in a Small, Widely Dispersed Mountain Community," Los Alamos Scientific Laboratory Rept. LA-DC-13156 (1971).

5. J. H. Abrahams, "Geologic and Hydrologic Environment of Radioactive Waste-Disposal Sites at Los Alamos, New Mexico," U. S. Geol. Survey Admin. Rept. (1963).

6. J. E. Weir and others, "The Hydrology and Chemical and Radiochemical Quality of Surface and Ground Water at Los Alamos, New Mexico, 1949-1955," U. S. Geol. Survey Admin. Rept. (1963).

7. J. H. Abrahams, "Hydrology and the Chemical and Radiochemical Quality of Surface and Ground Water at Los Alamos, New Mexico, January 1956 through June 1957," U. S. Geol. Survey Admin. Rept. (1966).

8. J. H. Abrahams and W. D. Purtymun, "The Hydrology and the Chemical and Radiochemical Quality of Surface and Ground Water at Los Alamos, New Mexico, July 1957 through June 1961," U. S. Geol. Survey Admin. Rept. (1966).

9. W. D. Purtymun, J. H. Abrahams, and J. R. Arrett, "Hydrology of Waste Disposal Systems at Los Alamos, New Mexico, 1949 through 1961," U. S. Geol. Survey Unpub. Rept.

10. W. D. Purtymun, "The Chemical and Radiochemical Quality of Surface and Ground Water at Los Alamos, New Mexico, July 1961 through June 1962," U. S. Geol. Survey Admin. Rept. (1966).

11. W. D. Purtymun, "The Chemical and Radiochemical Quality of Surface and Ground Water at Los Alamos, New Mexico, July 1962 through June 1963," U. S. Geol. Survey Admin. Rept. (1966).

12. W. D. Purtymun, "The Chemical and Radiochemical Quality of Surface and Ground Water at Los Alamos, New Mexico, July 1963 through June 1974," U. S. Geol. Survey Admin Rept. (1966).

13. W. D. Purtymun and E. A. Enyart, "The Chemical and Radiochemical Quality of Surface and Ground Water at Los Alamos, New Mexico, July 1964 through June 1965," U. S. Geol. Survey Admin. Rept. (1966).

14. W. D. Purtymun and J. L. Kumkler, "The Chemical and Radiochemical Quality of Surface and Ground Water at Los Alamos, New Mexico, July 1965 through June 1966," U. S. Geol. Survey Admin. Rept. (1967).

15. W. D. Purtymun and J. L. kumkler, "The Chemical and Radiochemical Quality of Surface and Ground Water at Los Alamos, New Mexico, July 1966 through June 1967," U. S. Geol. Survey Admin. Rept. (1969).

16. W. R. Kennedy, "Los Alamos Environmental Monitoring Program," Los Alamos Scientific Laboratory Rept. LA-3639-MS (1970).

17. W. R. Kennedy, W. D. Purtymun, and H. F. Schults, "Los Alamos Environmental Monitoring Program, July through December 1970," Los Alamos Scientific Laboratory Rept. LA-4672-MS (1971).

18. J. E. Herceg, Compiler, "Environmental Monitoring in the Vicinity of the Los Alamos Scientific Laboratory, January through June 1971," Los Alamos Scientific Laboratory Rept. LA-4871-MS (1972).

19. J. E. Herceg, Compiler, "Environmental Monitoring in the Vicinity of the Los Alamos Scientific Laboratory, July through December 1971," Los Alamos Scientific Laboratory Rept. LA-4970 (1972).

20. J. E. Herceg, Compiler, "Environmental Monitoring in the Vicinity of the Los Alamos Scientific Laboratory, Calendar Year 1972," Los Alamos Scientific Rept. LA-5184 (1973).

21. W. D. Purtymun, "Plutonium in Stream Channel Alluvium in the Los Alamos Area, New Mexico," Los Alamos Scientific Laboratory Rept. LA-4561 (1971).

22. Unpublished Data, "Chemical and Radiochemical Quality of Surface and Ground Water from 1952 through 1957" Compiled data by source, in File Group H-8, Los Alamos Scientific Laboratory.

23. Unpublished Data, "Radiochemical Analyses, Results for Water Samples," Series of Memos from 1958 through 1970 (Some Memos Missing), in Files Group H-8, Los Alamos Scientific Laboratory.

24. Unpublished Data, "Chemical Quality of Surface and Ground Water," U. S. Geol. Survey, Analyses Cards for Individual Sources, in Files Group H-8 Los Alamos Scientific Laboratory.

Chemical Analyses of Surface and Near Surface Ground Water in the Drainage Areas 1967 through 1972

Source DRAINAGE AREA 4 (ACID-PUEBLO CANYON)	Date of Collection	Chemical Constituents, Milligrams per liter: Calcium (Ca)	Magnesium (Mg)	Sodium (Na)	Carbonate (CO_3)	Bicarbonate (HCO_3)	Chloride (Cl)	Fluoride (F)	Nitrate (NO_3)	Dissolved solids	Total hardness	Specific conductance (micromhos at 25°C)	pH
Acid Weir	4-17-70	56	14	147	0	60	310	.4	1.3	629	200	280	7.8
"	11-17-70	23	0	50	0	125	20	3	1.3	244	58	248	7.6
"	10-14-71	16	2	41	0	104	52	.9	5.3	272	48	216	7.1
"	4-5-72	29	6	72	0	88	114	1.11	4.8	370	96	480	7.4
"	10-11-72	19	4	100	0	160	32	.7	5.3	240	64	310	7.4
Pueblo 1	4-16-70	20	5	78	0	16	40	3.8	52.8	340	70	400	7.0
"	11-19-70	19	5	84	0	74	39	5.	39.6	407	70	400	7.0
"	10-14-71	16	7	82	0	96	28	6.0	56.8	476	68	400	7.0
"	4-5-72	14	9	75	0	68	48	5.94	51.3	446	72	440	7.1
"	10-11-72	16	2	75	0	96	34	.7	54.6	386	48	420	7.1
Pueblo 2	4-16-70	16	7	78	0	64	50	3.6	37.4	319	70	420	7.9
"	11-19-70	15	6	84	0	94	37	5	83.6	486	63	400	7.2
"	10-15-71	14	5	72	0	96	28	4.6	24.6	330	56	300	7.3
"	4-5-72	18	6	75	0	92	44	5.43	42.9	378	68	420	7.8
"	10-11-72	14	4	71	0	108	34	.7	26.8	346	52	370	7.6
Pueblo 3	4-16-70	20	5	83	0	80	20	4	57.2	376	70	288	6.8
"	11-19-70	18	7	84	0	120	23	5	70.4	377	75	400	7.1
"	10-14-71	13	7	74	0	96	26	4.8	65.6	416	60	350	6.9
"	4-5-72	16	4	75	0	96	34	5.57	41.1	392	56	420	7.3
"	10-11-72	18	3	78	0	156	44	1.1	44.9	378	56	480	7.3
Hom. Bend Sprs.	4-17-70	16	10	78	0	132	30	2.6	4.4	612	80	340	7.8
"	11-19-70	17	4	70	0	100	43	4	22.0	341	57	370	7.2
"	4-5-72	16	7	67	0	120	38	2.59	18.1	370	68	380	7.7
"	10-11-72	19	5	71	0	120	42	.8	19.4	370	68	380	7.6

APPENDIX E

(Continued)

Source DRAINAGE AREA 4 (ACID-PUEBLO CANYON)	Date of Collection	Chemical Constituents: Milligrams per liter: Calcium (Ca)	Magnesium (Mg)	Sodium (Na)	Carbonate (CO_3)	Bicarbonate (HCO_3)	Chloride (Cl)	Fluoride (F)	Nitrate (NO_3)	Dissolved solids	Total hardness	Specific conductance (micromhos at 25°C)	pH
Acid Weir	4-17-70	56	14	147	0	60	310	.4	1.3	629	200	280	7.8
"	11-17-70	23	0	50	0	125	20	3	1.3	244	58	248	7.6
"	10-14-71	16	2	41	0	104	52	.9	5.3	273	48	216	7.1
"	4-5-72	29	6	72	0	88	114	1.11	11.8	370	96	480	7.4
"	10-11-72	19	4	100	0	160	32	.7	5.3	240	64	310	7.4
Pueblo 1	4-16-70	20	5	78	0	16	40	3.8	52.8	340	70	400	7.0
"	11-19-70	19	5	84	0	74	39	5.	39.6	407	70	400	7.0
"	10-14-71	16	7	82	0	96	28	6.0	56.8	476	68	400	7.0
"	4-5-72	14	9	75	0	68	48	5.94	51.3	446	72	440	7.1
"	10-11-72	16	2	75	0	96	34	.7	54.6	386	48	420	7.1
Pueblo 2	4-16-70	16	7	78	0	64	50	3.6	37.4	319	70	420	7.9
"	11-19-70	15	6	84	0	94	37	5	83.6	486	63	400	7.2
"	10-15-71	14	5	72	0	96	28	4.6	24.6	330	56	360	7.3
"	4-5-72	18	6	75	0	92	44	5.43	42.9	378	68	420	7.8
"	10-11-72	14	4	71	0	108	34	.7	26.8	346	52	370	7.6
Pueblo 3	4-16-70	20	5	83	0	80	20	4	57.2	376	70	288	6.8
"	11-19-70	18	7	84	0	120	23	5	70.4	377	75	400	7.1
"	10-14-71	13	7	74	0	96	26	4.8	65.6	416	60	380	6.9
"	4-5-72	16	4	75	0	96	34	5.57	41.1	392	56	420	7.3
"	10-11-72	18	3	78	0	156	44	1.1	44.9	378	56	480	7.3
Hom. Bend Sprs.	4-17-70	16	10	78	0	132	30	2.6	4.4	612	80	340	7.8
"	11-19-70	17	4	70	0	100	43	4	22.0	341	57	370	7.2
"	4-5-72	16	7	67	0	120	38	2.59	18.1	370	68	380	7.7
"	10-11-72	19	5	71	0	120	42	.8	19.4	370	68	380	7.6

Source	Date of Collection	Chemical Constituents, Milligrams per liter: Calcium (Ca)	Magnesium (Mg)	Sodium (Na)	Carbonate (CO_3)	Bicarbonate (HCO_3)	Chloride (Cl)	Fluoride (F)	Nitrate (NO_3)	Dissolved solids	Total hardness	Specific conductance (micromhos at 25°C)	pH
DRAINAGE AREA 4 (ACID-PUEBLO CANYON)													
Acid Weir	4-17-70	56	14	147	0	60	310	.4	1.3	629	200	280	7.8
"	11-17-70	23	0	50	0	125	20	3	1.3	244	58	248	7.6
"	10-14-71	16	2	41	0	104	52	.9	5.3	273	48	216	7.1
"	4-5-72	29	6	72	0	88	114	1.11	11.8	370	96	480	7.4
"	10-11-72	19	4	100	0	160	32	.7	5.3	240	64	310	7.4
Pueblo 1	4-16-70	20	5	78	0	16	40	3.8	52.8	340	70	400	7.0
"	11-19-70	19	5	84	0	74	39	5.	39.6	407	70	400	7.0
"	10-14-71	16	7	82	0	96	28	6.0	56.8	476	68	400	7.0
"	4-5-72	14	9	75	0	68	48	5.94	51.3	446	72	440	7.1
"	10-11-72	16	2	75	0	96	34	.7	54.6	386	48	420	7.1
Pueblo 2	4-16-70	16	7	78	0	64	50	3.6	37.4	319	70	420	7.9
"	11-19-70	15	6	84	0	94	37	5	83.6	486	63	400	7.2
"	10-15-71	14	5	72	0	96	28	4.6	24.6	330	56	340	7.3
"	4-5-72	18	6	75	0	92	44	5.43	42.9	378	68	420	7.8
"	10-11-72	14	4	71	0	108	34	.7	26.8	346	52	370	7.6
Pueblo 3	4-16-70	20	5	83	0	80	20	4	57.2	376	70	288	6.8
"	11-19-70	18	7	84	0	120	23	5	70.4	377	75	400	7.1
"	10-14-71	13	7	74	0	96	26	4.8	65.6	416	60	350	6.9
"	4-5-72	16	4	75	0	96	34	5.57	41.1	392	56	420	7.3
"	10-11-72	18	3	78	0	156	44	1.1	44.9	378	56	480	7.3
Ham. Bend Sprs.	4-17-70	16	10	78	0	132	30	2.6	4.4	612	80	340	7.8
"	11-19-70	17	4	70	0	100	43	4	22.0	341	57	370	7.2
"	4-5-72	16	7	67	0	120	38	2.59	18.1	370	68	380	7.7
"	10-11-72	19	5	71	0	120	42	.8	19.4	370	68	380	7.6

Source	Date of Collection	Chemical Constituents: Milligrams per liter: Calcium (Ca)	Magnesium (Mg)	Sodium (Na)	Carbonate (CO_3)	Bicarbonate (HCO_3)	Chloride (Cl)	Fluoride (F)	Nitrate (NO_3)	Dissolved solids	Total hardness	Specific conductance (micromhos at 25°C)	pH
PO-3B	4-17-70	24	14	29	0	84	30	4.0	1.8	274	120	280	7.0
"	11-19-70	28	7	34	0	86	32	8.8	30.8	341	100	260	7.1
"	10-14-71	21	8	28	0	40	34	4.0	15.0	258	84	240	6.7
"	4-5-72	30	8	26	0	72	32	1.3	13.3	288	108	284	7.3
"	10-11-72	32	11	23	0	100	30	2.2	.4	242	124	270	7.1
PO-4A	4-16-70	20	10	68	0	76	25	3	44	339	90	320	6.9
"	4-5-72	30	1	62	0	84	45	3.6	33.2	368	80	400	7.3
"	10-11-72	13	4	38	0	96	32	.8	23.8	324	48	320	7.3
PO-4B	4-17-70	12	10	66	0	116	30	1.0	5.7	299	70	360	7.0
Test Well TW-1A	5-1-68	32	7	90	0	134	37	1.3	13.2	288	110	420	7.7
"	6-10-68	22	12	91	0	114	29	3.0	17.6	347	104	500	7.4
"	2-25-69	20	11	77	0	132	27	2.6	15	339	94	340	7.3
"	6-1-71	27	7	42	0	80	45	1.8	12.3	262	96	380	7.2
"	9-1-71	29	9	75	0	124	30	2.5	57.2	374	108	420	7.4
Basalt Spring	12-6-67	36	14	25	0	86	15	0.3	13.2	150	210	225	7.4
"	5-1-68	32	10	24	0	86	14	.6	11.4	168	120	260	8.1
"	5-12-69	27	7	24	0	72	13	.3	8.8	212	98	240	8.7
"	8-11-69	27	9	24	0	84	14	.3	10.6	202	106	245	7.9
"	5-7-71	30	11	15	0	92	10	.3	12.3	214	120	240	7.5
"	8-31-71	27	13	15	0	88	12	.9	11.4	225	120	230	7.5
"	2-17-72	30	9	21	0	84	14	.2	12.2	238	112	220	7.9
"	7-31-72	30	10	17	0	88	14	.7	9.7	156	116	240	7.7

(Continued)

Source DRAINAGE AREA 5 (DP CANYON)	Date of Collection	Chemical Constituents: Milligrams per liter: Calcium (Ca)	Magnesium (Mg)	Sodium (Na)	Carbonate (CO_3)	Bicarbonate (HCO_3)	Chloride (Cl)	Fluoride (F)	Nitrate (NO_3)	Dissolved solids	Total hardness	Specific conductance (micromhos at 25°C)	pH
DPS-1	12-5-67	12	10	400	40	240	190	4	136.4	859	70	1080	10.0
"	4-30-68	20	17	900	500	900	225	12.6	981.2	3,130	120	4400	11.2
"	6-19-68	20	10	680	200	670	265	18	26.4	1698	90	2380	10.2
"	10-4-68	14	9	430	12	260	155	37	13.64	1024	38	1400	8.9
"	5-5-69	16	2	500	190	610	150	22	30.8	1264	50	1640	10.0
"	8-5-69	28	0	250	260	310	35	42	70.4	932	70	1760	11.1
"	6-24-70	8	2	250	90	340	165	10	35.2	982	30	1240	10.1
"	8-14-70	14	5	270	60	310	110	5	123.2	808	55	1200	9.4
"	9-24-70	14	2	140	50	230	65	3	8.8	442	45	620	9.4
"	11-17-70	20	1	295	45	220	220	6	255.2	1194	55	1200	9.8
"	12-1-70	24	2	250	20	220	140	6	176.0	964	70	1140	9.3
"	2-10-71	22	5	300	240	392	125	9.3	123.2	1222	76	1520	11.2
"	5-7-71	19	5	275	68	528	90	2.0	61.6	1098	68	1320	8.9
"	8-16-71	6	3	190	72	356	52	4.2	1.8	648	28	840	9.4
"	11-4-71	24	5	167	0	296	38	3.4	62.9	606	80	760	7.7
"	2-17-72	38	6	240	0	464	178	3.5	137.3	1287	120	1450	7.8
"	7-31-72	42	6	144	0	300	66	2.5	65.6	682	128	840	7.9
"	11-2-72	48	11	235	0	312	166	1.6	66.0	832	164	1100	7.9
DPS-2	12-5-67	16	12	290	0	240	75	8	140.8	669	90	900	8.5
"	4-30-68	20	5	250	38	258	80	8.8	158.4	778	70	1060	9.3
"	6-19-68	20	12	250	0	290	50	10	44.0	714	100	900	9.4
"	5-5-69	16	2	370	100	470	95	13	39.6	976	50	1220	9.6
"	8-5-69	16	10	195	70	220	110	11	13.2	456	80	620	9.9
"	2-16-70	28	10	145	20	350	60	17	48.4	700	110	840	9.0

APPENDIX E

(Continued)

Source	Date of Collection	Chemical Constituents, Milligrams per liter: Calcium (Ca)	Magnesium (Mg)	Sodium (Na)	Carbonate (CO_3)	Bicarbonate (HCO_3)	Chloride (Cl)	Fluoride (F)	Nitrate (NO_3)	Dissolved solids	Total hardness	Specific conductance (micromhos at 25°C)	pH
DPS-2	8-14-70	22	2	230	50	320	110	9	484	728	65	1000	9.1
"	1-20-71	30	4	68	0	128	15	3.7	35.2	642	92	330	8.2
DPS-3	12-5-67	16	7	310	0	300	85	10	127.6	799	70	960	8.8
"	4-30-68	24	0	290	40	292	95	13.5	198.0	890	60	1260	9.3
"	6-19-68	40	22	360	0	360	80	17	46.8	462	190	1180	8.4
"	5-5-69	16	5	420	100	490	105	18	57.2	514	60	1300	9.6
"	8-5-69	12	10	165	0	220	45	6	4.4	304	70	560	8.4
"	2-16-70	24	12	150	50	350	65	12	96.8	860	110	1000	7.3
"	8-14-70	18	1	250	50	310	120	8	66.0	768	50	1000	9.3
DPS-4	12-5-67	36	10	210	0	240	85	8	74.8	575	130	780	8.3
"	4-29-68	32	10	210	0	218	115	8.5	70.4	658	120	980	8.1
"	9-30-68	25	8	190	0	250	55	3.8	457.6	556	94	720	8.1
"	5-5-69	24	2	230	0	270	80	1	48.4	276	70	760	8.2
"	8-4-69	20	10	165	0	250	40	8	22.0	504	90	560	7.9
"	2-16-70	28	12	94	20	200	40	5	30.8	482	120	520	9.0
"	6-24-70	20	2	103	0	230	45	8	17.6	482	60	540	8.2
"	8-14-70	24	2	109	20	260	40	7	8.8	446	70	600	8.9
"	11-17-70	23	7	105	0	225	55	4	13.2	444	85	540	7.8
"	2-12-71	22	11	115	0	200	45	5.9	39.6	612	100	600	7.5
"	5-7-71	24	4	120	0	220	70	5.6	44.0	536	76	800	8.2
"	8-16-71	27	4	123	0	256	40	4.8	22.4	540	84	680	8.1
"	11-4-71	19	2	94	0	188	30	3.7	21.1	434	56	480	7.4
"	2-16-72	27	2	143	0	188	88	4.2	49.3	564	76	680	7.8
"	7-31-72	21	6	128	0	240	46	4.7	19.4	486	76	600	8.4

APPENDIX E

(Continued)

Source	Date of Collection	Chemical Constituents, Milligrams per liter: Calcium (Ca)	Magnesium (Mg)	Sodium (Na)	Carbonate (CO_3)	Bicarbonate (HCO_3)	Chloride (Cl)	Fluoride (F)	Nitrate (NO_3)	Dissolved solids	Total hardness	Specific conductance (micromhos at 25°C)	pH
DPS-4	11-2-72	21	5	100	0	212	40	34	22.0	428	72	520	7.8
DPE-STP	12-5-67	20	12	160	0	280	33	3	0.9	383	100	580	7.5
"	5-5-69	16	4	230	0	344	50	2	1.3	458	55	800	7.4
"	8-5-69	16	7	175	0	190	35	4	13.2	442	70	570	8.2

Source DRAINAGE AREA 5 (LOS ALAMOS CANYON	Date of Collection	Chemical Constituents Milligrams per liter: Calcium (Ca)	Magnesium (Mg)	Sodium (Na)	Carbonate (CO_3)	Bicarbonate (HCO_3)	Chloride (Cl)	Fluoride (F)	Nitrate (NO_3)	Dissolved solids	Total hardness	Specific conductance (micromhos at 25°C)	pH
L.A. Reservoir	12-7-67	20	0	8	0	44	3	.2	3.5	79	50	66	7.3
"	4-23-69	6	2	6	0	26	2	.0	.4	86	21	56	7.3
"	5-7-71	10	9	7	0	44	0	0	.4	110	60	70	7.1
"	5-5-72	8	6	7	0	44	2	0	.4	98	44	78	7.0
S.W. at LAO-1	5-5-67	14	2	38	0	60	28	0	.9	179	43	208	7.5
"	8-11-69	16	4	79	0	96	26	.5	2.2	251	58	280	7.7
S.W. at LAO-4.5	12-5-67	28	10	70	0	114	35	.3	13.2	260	110	292	7.6
LAO-C	11-25-70	16	7	25	0	72	21	1	4.4	166	68	160	7.5
"	8-16-71	22	6	37	0	84	45	.1	.4	246	80	300	7.7
"	11-5-71	24	10	40	0	60	46	.2	.9	252	100	280	7.3
"	2-17-72	27	7	60	0	64	92	.03	.9	272	96	350	7.6
"	5-5-72	18	7	37	0	68	56	0	.4	186	72	300	7.1
"	7-31-72	19	5	50	0	100	42	.5	.4	226	68	284	7.4
"	11-2-72	30	10	64	0	84	106	.3	.9	328	116	440	7.2
LAO-1	12-5-67	28	12	125	0	94	35	.7	8.8	357	120	400	7.1
"	4-29-68	24	5	112	0	84	60	.8	3.9	220	80	440	7.4
"	6-19-68	14	0	70	0	78	14	3.0	1.3	258	36	268	7.7
"	10-4-68	14	3	65	0	110	24	1.5	.9	261	48	300	7.2
"	5-5-69	22	5	79	0	70	64	.1	1.8	309	74	400	7.3
"	8-5-69	18	5	86	0	80	29	.5	2.2	281	64	340	7.3
"	2-16-70	28	12	52	0	100	30	0	5.1	344	120	330	5.1
"	6-24-70	16	5	42	0	76	33	.7	.9	255	60	280	7.5
"	8-13-70	24	7	69	0	100	25	.8	2.6	358	90	400	7.8
"	11-17-70	20	12	52	0	86	14	2	4.4	774	100	320	7.6

Source	Date of Collection	Chemical Constituents, Milligrams per liter: Calcium (Ca)	Magnesium (Mg)	Sodium (Na)	Carbonate (CO_3)	Bicarbonate (HCO_3)	Chloride (Cl)	Fluoride (F)	Nitrate (NO_3)	Dissolved solids	Total hardness	Specific conductance (micromhos at 25°C)	pH
LAO-1	2-12-71	35	12	64	0	92	25	1.4	7.9	404	138	410	7.3
"	5-7-71	35	11	70	0	92	25	.4	7.0	418	132	500	7.0
"	8-16-71	29	7	80	0	108	33	.3	6.6	430	100	500	7.4
"	11-5-71	24	9	82	0	108	22	.3	6.2	404	96	470	7.5
"	2-17-72	21	8	54	0	84	60	.4	6.1	356	84	420	7.5
"	5-5-72	21	7	68	0	80	70	.9	3.1	338	80	460	7.1
"	7-31-72	35	11	92	0	112	36	.3	7.9	498	132	560	7.6
"	11-2-72	24	8	86	0	124	34	1.0	5.3	394	92	460	7.2
LAO-1.2	5-5-69	17	4	66	0	72	42	0	.9	260	60	300	7.5
"	8-5-69	17	5	74	0	78	35	0	.4	239	64	300	7.4
"	8-13-70	16	6	53	0	90	30	0	2.2	234	65	300	7.1
LAO-1.8	5-5-69	18	4	42	0	58	33	0	.4	182	62	240	7.5
"	8-5-69	19	5	51	0	76	27	0	.4	223	70	252	7.4
LAO-2	12-5-67	24	12	180	0	204	73	7	74.8	594	110	760	7.3
"	4-29-68	12	5	127	0	100	45	14.7	7.0	366	50	430	7.8
"	6-19-68	16	2	41	0	68	25	7	.4	208	48	284	7.5
"	9-30-68	28	5	115	0	210	47	2.4	22	428	90	600	7.5
"	5-5-69	4	1	74	0	86	34	6.0	2.2	267	28	320	7.7
"	8-4-69	20	5	140	0	220	39	4.0	13.2	472	72	500	7.6
"	2-16-70	28	10	100	2	210	45	4	39.6	512	110	540	8.6
"	5-11-70	16	7	81	0	186	45	8	13.2	458	70	450	7.5
"	8-13-70	18	4	109	0	240	40	7	9.8	468	60	540	7.1
"	8-16-71	21	3	102	0	216	39	5.6	19.8	472	64	580	7.6
"	11-14-71	13	5	80	0	156	26	5.6	16.7	390	52	400	7.1

Source	Date of Collection	Chemical Constituents: Milligrams per liter: Calcium (Ca)	Magnesium (Mg)	Sodium (Na)	Carbonate (CO_3)	Bicarbonate (HCO_3)	Chloride (Cl)	Fluoride (F)	Nitrate (NO_3)	Dissolved solids	Total hardness	Specific conductance (micromhos at 25°C)	pH
LAO-1	2-12-71	35	12	64	0	92	25	1.4	7.9	404	138	410	7.3
"	5-7-71	35	11	70	0	92	25	.4	7.0	418	132	500	7.0
"	8-16-71	29	7	80	0	108	33	.3	6.6	430	100	500	7.4
"	11-5-71	24	9	82	0	108	22	.3	6.2	404	96	470	7.5
"	2-17-72	21	8	54	0	84	60	.4	6.1	356	84	420	7.5
"	5-5-72	21	7	68	0	80	70	.9	3.1	338	80	460	7.1
"	7-31-72	35	11	92	0	112	36	.3	7.9	498	132	560	7.6
"	11-2-72	24	8	86	0	124	34	1.0	5.3	394	92	460	7.2
LAO-1.2	5-5-69	17	4	66	0	72	42	0	.9	260	60	300	7.5
"	8-5-69	17	5	74	0	78	35	0	.4	239	64	300	7.4
"	8-13-70	16	6	53	0	90	30	0	2.2	234	65	300	7.1
LAO-1.8	5-5-69	18	4	42	0	58	33	0	.4	182	62	240	7.5
"	8-5-69	19	5	51	0	76	27	0	.4	223	70	252	7.4
LAO-2	12-5-67	24	12	180	0	204	73	7	74.8	594	110	760	7.3
"	4-29-68	12	5	127	0	100	45	14.7	7.0	366	50	430	7.8
"	6-19-68	16	2	41	0	68	25	7	.4	208	48	284	7.5
"	9-30-68	28	5	115	0	210	47	2.4	22	428	90	600	7.5
"	5-5-69	4	1	74	0	86	34	6.0	2.2	267	28	320	7.7
"	8-4-69	20	5	140	0	220	39	4.0	13.2	472	72	500	7.6
"	2-16-70	28	10	100	2	210	45	4	39.6	512	110	540	8.6
"	5-11-70	16	7	81	0	186	48	8	13.2	458	70	450	7.5
"	8-13-70	18	4	109	0	240	40	7	8.8	468	60	540	7.1
"	8-16-71	21	3	102	0	216	39	5.6	19.8	472	64	580	7.6
"	11-14-71	13	5	80	0	156	26	5.6	16.7	390	52	400	7.1

APPENDIX E

(Continued)

Source	Date of Collection	Chemical Constituents, Milligrams per liter: Calcium (Ca)	Magnesium (Mg)	Sodium (Na)	Carbonate (CO_3)	Bicarbonate (HCO_3)	Chloride (Cl)	Fluoride (F)	Nitrate (NO_3)	Dissolved solids	Total hardness	Specific conductance (micromhos at 25°C)	pH
LAO-2	2-17-72	26	4	87	0	180	82	3.9	41.8	520	80	640	7.6
"	7-31-72	19	7	111	0	232	48	4.7	21.6	486	76	600	7.6
"	11-2-72	16	5	92	0	200	36	4.6	15.4	412	60	480	7.4
LAO-3	12-5-67	40	7	152	0	190	53	8	26.0	474	130	540	7.2
"	4-29-67	24	10	127	0	136	60	7	22.4	422	100	560	7.7
"	6-20-68	17	3	82	0	102	30	10	4.0	335	56	380	7.6
"	9-30-68	18	2	85	0	150	30	7	4.4	398	54	430	7.7
"	5-5-69	26	4	127	0	160	70	5	22.0	430	84	580	7.8
"	8-4-69	17	4	102	0	150	37	5	8.8	357	60	420	7.5
"	2-16-70	28	17	80	10	190	35	5	22.0	468	140	460	7.7
"	6-24-70	16	7	81	0	186	48	8	13.2	458	70	520	7.6
"	8-13-70	16	6	100	0	210	35	7	8.8	414	65	540	7.2
"	11-17-70	16	6	79	0	170	52	8	8.8	440	65	430	7.3
"	5-7-71	21	7	86	0	168	50	5.5	22.0	430	80	520	7.3
"	8-16-71	21	4	82	0	180	41	4.7	15.4	427	68	520	7.7
"	11-4-71	19	5	77	0	180	30	5.6	14.1	432	68	460	7.2
"	2-16-72	24	6	114	0	152	78	4.7	28.8	482	84	580	7.6
"	5-5-72	26	9	97	0	196	82	4.1	28.2	508	100	700	7.2
"	7-31-72	26	7	130	0	126	76	4.8	39.2	510	92	680	7.7
"	11-2-72	18	6	92	0	204	38	5.8	13.2	434	68	500	7.4
LAO-4	12-5-67	36	10	117	0	150	45	.4	8.8	338	130	380	7.3
"	4-29-68	20	12	66	0	74	40	1.3	4.4	220	100	300	7.5
"	6-20-68	19	3	66	0	104	27	3	.9	366	60	300	7.5
"	10-4-68	18	6	67	0	130	27	.4	<.1	270	70	340	7.6

Source	Date of Collection	Chemical Constituents, Milligrams per liter: Calcium (Ca)	Magnesium (Mg)	Sodium (Na)	Carbonate (CO_3)	Bicarbonate (HCO_3)	Chloride (Cl)	Fluoride (F)	Nitrate (NO_3)	Dissolved solids	Total hardness	Specific conductance (micromhos at 25°C)	pH
LAO-4	5-5-69	14	4	60	0	66	37	.6	.9	196	52	264	7.6
"	8-4-69	18	6	70	0	104	32	4.0	.4	238	70	300	7.4
"	8-13-70	22	7	57	0	180	40	2	1.8	284	85	370	7.1
LAO-4.5	5-5-69	16	0	57	0	78	32	0	.9	214	40	260	7.5
"	8-4-69	19	7	59	0	96	31	0	.4	339	76	280	7.3
"	2-16-70	24	10	39	0	100	30	0	1.8	208	100	240	8.2
"	5-11-70	20	7	33	0	88	25	.6	.9	279	80	260	7.6
"	6-24-70	20	7	30	0	80	28	.6	1.3	232	80	260	7.6
"	8-13-70	22	8	46	0	120	40	.2	1.8	242	90	320	7.0
"	11-17-70	24	6	43	0	272	38	1	1.3	362	85	284	8.4
"	2-12-71	22	9	37	0	88	40	.4	4.4	309	94	264	7.2
"	8-16-71	19	6	37	0	88	30	.1	3.1	236	72	270	7.7
"	11-4-71	14	10	35	0	88	20	.1	4.8	296	76	230	7.1
"	2-16-72	32	5	100	0	120	30	.2	.7	262	108	300	7.7
"	5-5-72	18	7	37	0	88	30	.2	.4	204	72	272	7.3
"	7-31-72	14	9	41	0	108	20	.5	.9	180	72	232	7.7
"	11-2-72	19	9	42	0	112	26	.8	.9	244	84	270	7.3
LAO-5	12-5-67	28	10	42	0	62	28	.4	2.6	209	110	240	7.2
"	6-20-68	18	5	45	0	64	24	.8	.4	212	64	240	7.2
"	10-4-68	16	5	44	0	90	26	.8	<.1	235	60	256	7.3
"	5-5-69	14	9	48	0	56	31	0	1.3	185	72	224	7.3
"	8-4-69	17	7	56	0	74	35	0	.4	220	70	260	7.4
LAO-6	10-4-68	18	5	49	0	200	26	.5	<.1	227	64	296	7.4
"	5-5-69	18	5	51	0	66	33	.1	.4	195	64	248	7.3

Source	Date of Collection	Chemical Constituents, Milligrams per liter: Calcium (Ca)	Magnesium (Mg)	Sodium (Na)	Carbonate (CO_3)	Bicarbonate (HCO_3)	Chloride (Cl)	Fluoride (F)	Nitrate (NO_3)	Dissolved solids	Total hardness	Specific conductance (micromhos at 25°C)	pH
DRAINAGE AREA 6 (SANDIA CANYON)													
SCS-1	9-5-69	0	0	375	0	340	45	55	<.1	1738	0	1120	7.7
"	1-13-70	40	10	70	0	176	50	1.4	30.8	612	160	560	6.3
"	6-29-70	36	17	77	0	32	55	3	26.4	837	160	600	7.4
"	9-24-70	40	11	164	0	70	60	3	26.4	1028	145	900	7.2
"	3-8-71	38	14	78	0	32	55	2.6	21.1	700	152	660	6.7
"	6-1-71	30	12	90	0	60	40	1.6	22.0	732	124	640	7.0
"	9-14-71	58	34	575	--	--	45	2.6	26.4	4130	284	7000	2.1
"	12-6-71	30	15	81	0	36	54	1.4	17.6	696	136	560	6.7
"	3-3-72	54	15	170	0	144	66	1.8	4.4	754	196	840	7.5
"	6-9-72	4	8	156	0	148	34	179	18.0	1782	43	1300	—
"	8-31-72	32	14	97	0	140	64	19	29.5	760	136	620	7.3
"	11-6-72	22	11	42	0	88	28	9.7	35.2	354	100	380	7.1
SCS-2	9-5-69	40	12	140	0	100	50	6	11.9	690	150	720	7.9
"	1-12-70	40	14	185	0	80	95	1.3	26.4	1016	160	1000	7.1
"	9-24-70	36	7	109	0	100	50	2	17.6	610	120	640	7.6
"	12-21-70	59	15	166	0	80	80	1.9	30.8	930	208	850	7.1
"	3-15-71	38	16	144	0	80	75	3.2	24.2	802	160	840	7.1
"	6-1-71	37	11	173	0	72	65	2.1	17.6	856	138	1060	8.2
"	9-14-71	35	14	115	0	100	50	2.9	13.6	686	144	660	7.8
"	12-6-71	35	11	160	0	84	108	1.6	30.8	834	132	840	7.1
"	3-3-72	27	12	143	0	64	50	1.8	13.5	674	116	700	7.2
"	6-9-72	26	8	94	0	104	72	3.8	4.8	598	96	600	—
"	8-31-72	26	6	85	0	136	44	2.6	3.1	456	88	500	7.8
"	11-6-72	35	11	104	0	136	90	8.8	13.2	606	132	240	7.2
SCO-4	9-5-69	32	7	80	0	140	15	0	1.3	320	60	350	—

APPENDIX E

(Continued)

Source	Date of Collection	Chemical Constituents, Milligrams per liter: Calcium (Ca)	Magnesium (Mg)	Sodium (Na)	Carbonate (CO_3)	Bicarbonate (HCO_3)	Chloride (Cl)	Fluoride (F)	Nitrate (NO_3)	Dissolved solids	Total hardness	Specific conductance (micromhos at 25°C)	pH
DRAINAGE AREA 7 (MORTANDAD CANYON)													
GS-1	12-6-67	44	0	127	132	170	5	2.0	8.8	291	110	600	11.2
"	4-30-68	32	2	50	6	102	10	.9	1.8	142	90	240	9.2
"	10-7-68	36	0	61	38	116	15	.7	.4	245	90	288	9.6
"	9-5-69	24	7	43	0	120	5	.0	2.2	244	90	220	9.0
"	6-22-70	44	5	185	44	148	13	1.4	382.8	876	130	860	9.4
"	7-21-70	6	1	430	180	270	21	.9	822.8	1735	20	2000	10.6
"	9-24-70	8	1	147	160	290	10	2	13.2	478	25	700	10.9
"	11-17-70	7	2	385	135	290	22	2	501.6	1358	25	1460	10.9
"	12-1-70	34	2	385	0	130	20	3	545.6	1558	93	1600	8.3
"	12-21-70	21	1	111	0	128	10	1.1	162.8	518	56	500	7.6
"	2-12-71	54	3	84	0	96	15	1.9	79.2	523	148	470	8.0
"	6-2-71	70	2	170	12	376	35	3.5	22.0	716	186	960	8.1
"	9-13-71	54	8	130	0	236	49	2.5	24.2	546	168	680	7.7
"	12-6-71	30	7	59	0	148	36	1.6	1.8	300	104	380	7.6
"	3-3-72	13	5	240	0	312	28	1.3	95.0	706	52	840	7.6
"	6-9-72	21	7	94	0	180	10	1.6	7.9	462	80	520	7.7
"	8-31-72	19	3	116	0	224	10	1.5	70.4	522	60	540	8.0
"	11-6-72	14	4	35	0	104	10	1.0	8.8	224	52	200	7.3
MCS-3.9	12-6-67	20	7	113	0	110	15	1.0	13.2	-	80	310	8.0
"	4-30-68	20	7	110	0	130	15	2.2	11.4	260	80	370	8.3
"	9-23-70	30	4	260	0	210	20	1.0	246	662	90	820	8.5
"	3-8-71	42	5	290	36	164	30	1.5	602.8	1308	124	1500	9.1
"	9-13-71	40	6	315	0	328	151	1.9	225.3	1134	124	1360	8.1

APPENDIX E

(Continued)

Source	Date of Collection	Chemical Constituents, Milligrams per liter: Calcium (Ca)	Magnesium (Mg)	Sodium (Na)	Carbonate (CO_3)	Bicarbonate (HCO_3)	Chloride (Cl)	Fluoride (F)	Nitrate (NO_3)	Dissolved solids	Total hardness	Specific conductance (micromhos at 25°C)	pH
MCS- 3.9	12-6-71	35	7	235	0	260	132	1.1	79.2	828	116	1040	7.5
"	3-3-72	30	9	285	0	248	54	1.5	248.6	902	112	1080	7.8
"	6-9-72	21	9	200	32	304	48	1.1	435.6	1278	88	1520	7.8
"	8-31-72	34	6	315	0	464	28	1.5	277.2	1242	108	1340	8.2
"	11-6-72	26	3	240	0	356	26	2.0	233.2	970	76	1000	7.7
MCO-3	12-6-67	20	5	74	8	92	8	1.0	8.8	255	70	232	8.7
"	4-30-68	20	7	78	6	100	10	1.7	7.0	206	80	278	9.2
"	10-7-68	18	4	91	10	86	15	1.2	3.1	252	60	340	8.9
"	6-2-69	64	7	320	20	80	5	6	31	820	190	1000	9.1
"	9-5-69	18	6	154	0	160	5	0	10.6	314	70	320	8.5
"	1-12-70	20	7	78	0	100	15	1.1	17.6	320	60	400	8.3
"	6-22-70	28	7	180	52	166	15	1.4	294.8	805	100	860	9.2
"	9-24-70	16	2	260	30	210	25	1.0	171.6	612	50	700	9.3
"	12-21-70	35	2	320	0	168	25	1.3	576.4	1214	96	1200	7.5
"	3-25-71	21	4	340	160	248	20	1.5	629.2	1392	68	1640	10.5
"	6-3-71	24	1	250	36	300	20	5.2	237.6	890	64	1200	9.4
"	9-13-71	30	5	230	16	308	122	2.4	123.2	908	96	1140	8.8
"	12-6-71	30	5	205	0	236	114	1.4	405	666	96	880	7.7
"	3-10-72	18	5	170	12	184	26	2.2	134.6	652	64	600	8.5
"	6-9-72	50	7	310	0	324	38	1.2	426.8	1256	152	1500	7.9
"	8-31-72	51	6	285	0	340	28	1.1	422.4	1270	152	1400	8.0
"	11-2-72	22	5	173	0	296	20	1.7	162.8	730	76	800	8.3

Source	Date of Collection	Chemical Constituents: Milligrams per liter: Calcium (Ca)	Magnesium (Mg)	Sodium (Na)	Carbonate (CO_3)	Bicarbonate (HCO_3)	Chloride (Cl)	Fluoride (F)	Nitrate (NO_3)	Dissolved solids	Total hardness	Specific conductance (micromhos at 25°C)	pH
MCO-4	12-6-67	24	7	101	0	108	18	2	13.2	274	90	310	7.5
"	4-30-68	16	12	127	0	220	15	2.1	12.8	284	90	380	7.9
"	10-7-68	14	3	130	0	158	5	1.1	8.8	308	48	410	8.0
"	6-2-69	24	10	120	0	120	5	0	26.4	260	100	430	8.1
"	9-8-69	20	2	115	0	150	5	0	20.7	326	60	350	8.4
"	1-12-70	40	2	97	0	140	15	.8	35.2	406	110	540	7.8
"	5-14-70	28	7	84	0	130	18	.8	61.6	414	100	480	8.0
"	6-23-70	28	10	100	0	146	18	1.0	123.2	502	110	600	7.6
"	9-23-70	40	8	270	0	210	20	0	334.4	750	135	960	7.9
"	12-21-70	48	14	240	0	184	23	1.1	462.0	1050	176	1100	7.5
"	3-8-71	53	14	330	0	160	25	1.0	668.3	1330	188	1500	7.6
"	6-3-71	40	3	240	0	184	30	1.6	492.8	1110	114	1300	7.6
"	9-13-71	40	10	230	0	276	1	1.0	299.2	1106	140	1300	7.7
"	12-6-71	43	7	250	0	252	144	.6	110.0	838	136	1100	7.5
"	3-3-72	34	7	261	0	232	58	1.2	229.7	872	112	1020	7.6
"	6-9-72	37	12	250	0	280	46	1.3	338.8	1044	140	1300	7.5
"	8-31-72	40	6	245	0	340	34	1.7	334.4	1102	124	1260	7.7
"	11-6-72	30	8	290	0	388	32	1.5	286.0	1052	108	1120	7.7
MCO-5	12-6-67	12	7	164	0	162	13	1.0	.9	315	60	350	7.5
"	4-30-68	12	5	140	0	156	20	.5	8.8	300	50	390	7.5
"	10-7-68	7	1.4	115	0	122	10	.2	11.0	314	24	330	7.5
"	6-2-69	12	4	124	0	100	20	0	27.3	252	45	400	8.1
"	9-8-69	12	7	112	0	140	5	0	29.5	310	60	350	8.5

APPENDIX E

(Continued)

Source	Date of Collection	Chemical Constituents, Milligrams per liter: Calcium (Ca)	Magnesium (Mg)	Sodium (Na)	Carbonate (CO_3)	Bicarbonate (HCO_3)	Chloride (Cl)	Fluoride (F)	Nitrate (NO_3)	Dissolved solids	Total hardness	Specific conductance (micromhos at 25°C)	pH
MCO-5	9-23-70	32	10	131	0	150	10	0	198.0	546	120	660	7.5
"	3-8-71	58	20	250	0	152	25	.4	541.2	1116	228	1260	7.2
"	6-3-71	56	14	190	0	144	20	.2	506.0	1104	196	1320	7.2
"	9-13-71	37	13	185	0	160	50	.6	290.4	822	144	1000	7.5
"	12-6-71	30	8	210	0	172	88	.2	132.0	664	108	820	7.4
"	3-3-72	30	9	200	0	180	86	.1	128.5	634	112	820	7.6
"	6-9-72	34	10	144	0	185	58	.3	162.8	774	124	940	7.3
"	8-31-72	42	14	275	0	264	48	.8	286.0	986	160	1160	7.6
"	11-6-72	30	12	177	0	236	36	.8	277.2	836	124	880	7.4
MCO-6	12-6-67	16	5	141	0	154	3	.5	8.8	334	60	310	7.5
"	4-30-68	12	10	140	0	140	15	1.6	10.1	344	70	380	8.3
"	10-7-68	6	1	99	0	106	5	.2	9.7	281	22	290	7.9
"	6-2-69	12	1	137	0	90	15	0	26.4	296	35	400	7.8
"	9-8-69	24	7	105	0	140	5	0	22.0	328	90	340	8.5
"	1-12-70	20	10	80	0	150	15	.3	26.4	346	80	380	7.8
"	5-14-70	22	7	79	0	122	18	.8	39.6	399	85	460	7.5
"	6-23-70	20	7	77	0	120	15	.8	48.4	388	80	460	7.5
"	9-23-70	28	10	120	0	140	20	.9	171.6	524	110	660	7.1
"	12-22-70	48	10	152	0	156	20	.6	286.0	756	160	800	7.2
"	3-8-71	58	17	210	0	160	25	.6	475.2	1010	212	1180	8.0
"	6-3-71	54	14	230	0	124	25	2.0	576.4	1206	194	1500	7.1
"	9-13-71	37	14	205	0	168	35	.6	365.2	936	148	1080	7.4
"	12-6-71	40	11	260	0	192	96	0	220.0	848	144	1020	7.4

A N A E

(Continued)

Source	Date of Collection	Chemical Constituents, Milligrams per liter: Calcium (Ca)	Magnesium (Mg)	Sodium (Na)	Carbonate (CO_3)	Bicarbonate (HCO_3)	Chloride (Cl)	Fluoride (F)	Nitrate (NO_3)	Dissolved solids	Total hardness	Specific conductance (micromhos at 25°C)	pH
MCO-6	3-3-72	32	12	261	8	236	126	.7	134.6	814	128	1060	7.9
"	6-9-72	32	10	174	0	220	72	.5	215.6	886	120	1100	7.3
"	8-31-72	35	13	245	0	256	54	4.0	294.8	986	140	1160	7.6
"	11-6-72	37	12	240	0	276	40	4.0	334.4	996	140	1080	7.5
MCO-7	12-6-67	28	5	121	0	144	18	.3	8.8	323	90	320	7.4
"	4-30-68	20	10	132	0	144	20	.1	7.0	338	90	400	7.8
"	10-7-68	11	2	93	0	130	10	.2	6.2	289	34	320	7.4
"	6-24-69	20	2	128	0	130	20	0	13.2	380	60	400	7.9
"	9-8-69	16	5	115	0	140	10	0	17.6	340	60	350	8.5
"	1-12-70	20	7	67	0	150	10	0	17.6	304	80	320	7.5
"	6-23-70	20	8	103	0	126	15	.3	30.8	412	85	440	7.4
"	9-24-70	14	4	100	0	130	15	.2	57.2	354	60	460	7.3
"	3-8-71	40	15	144	0	132	20	.1	277.2	662	160	780	7.3
"	6-3-71	58	12	155	0	124	25	.6	466.4	950	194	1160	7.0
"	9-13-71	62	19	175	0	120	25	.03	431.2	1036	236	1100	7.2
"	12-6-71	46	16	190	0	136	42	0	325.6	870	186	940	7.2
"	3-3-72	40	11	200	0	172	86	.11	191.8	714	144	900	7.7
"	6-9-72	40	12	136	0	188	90	<.1	158.4	738	148	900	—
"	8-31-72	40	15	178	0	196	66	.5	281.6	883	160	960	7.5
"	11-6-72	42	10	165	0	212	54	.4	237.6	828	144	940	7.3
MCO-7.5	12-6-67	24	12	148	0	150	23	0	17.6	440	110	460	7.4
"	4-30-68	20	12	140	0	162	15	.8	6.6	342	100	420	8.1
"	10-7-68	18	0	106	0	150	5	0	.9	303	46	360	7.2

APPENDIX E

(Continued)

Source	Date of Collection	Chemical Constituents, Milligrams per liter: Calcium (Ca)	Magnesium (Mg)	Sodium (Na)	Carbonate (CO_3)	Bicarbonate (HCO_3)	Chloride (Cl)	Fluoride (F)	Nitrate (NO_3)	Dissolved solids	Total hardness	Specific conductance (micromhos at 25°C)	pH
MCO-7.5	6-4-69	16	5	120	0	130	10	0	8.8	576	60	390	7.8
"	9-8-69	28	7	100	0	180	5	0	6.6	332	100	400	8.3
"	1-12-70	16	10	72	0	150	10	.2	17.6	234	80	340	7.4
"	9-23-70	18	5	100	0	140	5	0	48.4	372	65	460	7.3
"	6-3-71	40	11	140	0	140	20	1.3	299.2	834	146	920	7.2
"	9-13-71	56	17	160	0	124	25	.2	404.8	916	208	1000	7.0
"	12-6-71	59	14	200	0	120	28	0	435.6	916	204	1000	7.0
"	3-3-72	48	13	210	0	140	58	.2	315.9	846	172	980	7.6
"	6-9-72	45	9	136	0	172	94	<.1	176.0	742	148	920	—
"	8-31-72	42	14	170	0	184	84	.3	140.8	782	160	960	7.4
"	11-6-72	48	10	150	0	196	70	.3	237.6	800	160	900	7.3
MCO-8	12-6-67	40	12	93	0	134	18	1.0	22.0	339	150	360	7.3
"	4-30-68	32	14	78	0	130	20	.6	176	308	140	400	7.3
"	10-7-68	28	8	60	0	130	5	0	19.8	314	105	340	7.2
"	6-4-69	28	5	83	0	110	20	0	7.5	302	90	360	7.7
"	9-8-69	28	10	85	0	140	10	0	9.7	506	110	370	8.4
"	1-12-70	38	6	47	0	120	10	0	13.2	278	120	320	7.7
"	6-23-70	24	7	50	0	140	10	0	17.6	313	90	340	7.6
"	9-23-70	24	6	50	0	140	10	0	22.0	322	85	360	7.3
"	12-22-70	27	11	55	0	120	13	.5	26.4	328	112	360	7.7
"	6-9-72	61	16	94	0	128	46	<.1	250.8	770	216	820	—
"	8-31-72	54	18	116	0	144	60	.3	184.8	678	212	860	7.4
"	11-6-72	54	17	110	0	144	64	.4	215.6	706	204	780	7.4

APPENDIX E

(Continued)

Source	Date of Collection	Chemical Constituents: Milligrams per liter										Specific conductance (micromhos at 25°C)	pH
		Calcium (Ca)	Magnesium (Mg)	Sodium (Na)	Carbonate (CO_3)	Bicarbonate (HCO_3)	Chloride (Cl)	Fluoride (F)	Nitrate (NO_3)	Dissolved solids	Total hardness		
DRAINAGE AREA 9 (CAÑADA DEL BUEY)													
TA-46	5-18-67	10	4	41	0	80	5	2.6	.9	183	42	164	8.0
"	5-7-71	16	8	24	0	80	5	.8	1.8	184	72	176	7.3
"	5-3-72	11	4	17	0	60	6	1.0	.4	162	44	136	7.3
DRAINAGE AREA 10 (PAJARITO CANYON)													
TA-18	5-9-67	19	5	44	0	120	10	.3	.4	214	70	232	7.4
"	5-7-71	26	10	16	0	76	20	0	.4	184	104	200	7.0
"	5-3-72	30	9	15	0	68	30	0	17.6	192	112	260	7.1
DRAINAGE AREA 11 (WATER CANYON)													
Amer. Spr.	12-7-67	16	10	8	0	60	3	0	1.8	112	80	100	7.4
"	4-23-69	10	4	10	0	54	3	0	.9	147	39	104	7.4
"	7-30-70	11	5	4	0	56	1	0	.4	—	48	120	7.2
Water Cany.	12-7-67	12	7	8	0	46	5	.1	.9	37	60	70	7.9
"	7-17-68	6	6	9	0	40	0	0	.4	112	40	72	7.5
"	7-30-70	8	2	4	0	42	0	0	7.5	86	30	86	6.9
"	7-29-71	8	6	6	0	76	2	.2	1.3	98	44	64	7.2
"	2-14-72	10	7	6	0	44	2	0	1.3	80	52	74	7.6
"	7-21-72	10	7	8	0	52	<1	.3	.9	38	52	80	7.9
"	12-21-72	8	8	7	0	52	<1	.2	.4	132	52	72	8.0
Near Beta Hole	4-15-70	12	5	19	0	100	8	.9	.9	255	50	280	7.8
"	5-10-71	11	8	25	0	84	5	.2	.9	160	60	150	7.3
"	5-3-72	11	8	27	0	80	14	.1	.4	162	60	192	7.0

Source	Date of Collection	Chemical Constituents Milligrams per liter: Calcium (Ca)	Magnesium (Mg)	Sodium (Na)	Carbonate (CO_3)	Bicarbonate (HCO_3)	Chloride (Cl)	Fluoride (F)	Nitrate (NO_3)	Dissolved solids	Total hardness	Specific conductance (micromhos at 25°C)	pH
DRAINAGE AREA 13 (ANCHO CANYON)													
Ancho at RG	9-17-67	14	4	21	0	68	2	0.5	.4	156	50	272	8.4
11	8-25-71	16	5	12	8	76	2	<.1	.4	158	60	140	8.6
DRAINAGE AREA 15 (CHAQUEHUI CANYON)													
Doe Spring	9-17-69	12	4	22	0	64	3	0.2	<.1	153	46	180	8.4
	8-12-71	16	5	21	0	84	4	0.3	0.9	219	60	260	7.9

Radiochemical Analyses of Surface and Near Surface Ground Water in Drainage Areas, 1967 through 1972

Source	Date Collected	Gross Alpha	Gross Beta	^{238}Pu	^{239}Pu	^{241}Am	^{226}Ra	^{234}U	^{137}Cs	^{90}Sr	^{3}H	^{233}U
		PICOCURIES PER LITER										µg/l
Drainage Area 4 (Acid-Pueblo Canyon)												
Acid Weir	4-16-70	<1	346	<0.05	0.07	—	—	—	—	—	3×10^3	<0.4
"	11-19-70	3	105	<.05	.48	—	—	—	—	—	3×10^3	.7
"	10-4-71	6	52	.18	7.98	—	—	—	<300	—	1.6×10^3	2.1
"	4-5-72	1	146	<.05	.11	—	—	—	<350	—	1.5×10^3	2.6
"	10-11-72	3	118	<.05	.72	—	—	—	<350	—	$<1 \times 10^3$	.8
Pueblo 1	4-16-70	<1	17	<.05	<.05	—	—	—	—	—	$<1 \times 10^3$	.5
"	11-19-70	<1	25	<.05	<.05	—	—	—	—	—	$<1 \times 10^3$	1.1
"	10-14-71	<1	7	.07	.08	—	—	—	<300	—	$<1 \times 10^3$	<.4
"	4-5-72	1	8	.16	.13	—	—	—	<350	—	$<1 \times 10^3$	2.6
"	10-11-72	<1	11	.05	<.05	—	—	—	<350	—	$<1 \times 10^3$	.2
Pueblo 2	4-16-70	<1	21	<.05	<.05	—	—	—	—	—	$<1 \times 10^3$	1.3
"	11-19-70	<1	19	<.05	.08	—	—	—	—	—	$<1 \times 10^3$	<.4
"	10-15-71	<1	9	.07	1.02	—	—	—	<300	—	$<1 \times 10^3$	.4
"	4-5-72	1	13	<.05	.09	—	—	—	<350	—	$<1 \times 10^3$	2.6
"	10-11-72	<1	14	<.05	.13	—	—	—	<350	—	$<1 \times 10^3$	<.2
Pueblo 3	4-16-70	<1	10	<.05	<.05	—	—	—	—	—	$<1 \times 10^3$	<.4
"	11-19-70	<1	12	<.05	<.05	—	—	—	—	—	$<1 \times 10^3$	1.0
"	10-14-71	<1	6	.06	<.05	—	—	—	<350	—	$<1 \times 10^3$	<.4
"	4-5-72	2	18	<.05	.11	—	—	—	<350	—	$<1 \times 10^3$	2.6
"	10-11-72	<1	23	.06	<.05	—	—	—	<350	—	$<1 \times 10^3$	.6

APPENDIX F

(Continued)

Page 2 of 24

Source	Date Collected	Gross Alpha	Gross Beta	^{238}Pu	^{239}Pu	^{241}Am	^{226}Ra	^{234}U	^{137}Cs	^{90}Sr	^{3}H	^{238}U
		PICOCURIES PER LITER										µg/l
H.B. Spr	4-17-70	<1	4	<0.05	<0.05	—	—	—	—	—	<1 X10³	<0.4
"	11-19-70	2	8	<.05	<.05	—	—	—	—	—	<1 X10³	.5
"	4-5-72	3	7	<.05	.09	—	—	—	<350	—	<1 X10³	3.3
"	10-11-72	<1	6	<.05	<.05	—	—	—	<350	—	1.8 X10³	.2
PO-3B	4-16-70	<1	7	<.05	<.05	—	—	—	—	—	15 X10³	<.4
"	11-19-70	<1	8	<.05	<.05	—	—	—	—	—	13 X10³	<.4
"	10-14-71	<1	6	.05	<.05	—	—	—	<300	—	1.4 X10³	<.4
"	4-5-72	2	6	<.05	.08	—	—	—	<350	—	14 X10³	2.0
"	10-11-72	<1	5	.22	.06	—	—	—	<350	—	22 X10³	<.2
PO-4A	4-16-70	<1	5	<.05	<.05	—	—	—	—	—	<1 X10³	1.5
"	4-5-72	2	7	<.05	.08	—	—	—	<350	—	<1 X10³	2.0
"	10-11-72	<1	7	<.05	.05	—	—	—	<350	—	1.3 X10³	<.2
PO-4B	4-16-70	4	10	<.05	<.05	—	—	—	—	—	<1 X10³	.5
Test Well TW-1A	5-1-68	1	10	<0.05	<.05	—	—	—	—	—	<1 X10³	1.7
"	6-10-68	1	14	<.05	<.05	—	—	—	—	—	<1 X10³	.4
"	2-25-69	2	7	<.05	<.05	—	—	—	—	—	<1 X10³	1.3
"	6-1-71	2	189	<.05	<.05	—	—	—	—	—	<1 X10³	.4
"	9-1-71	<1	<1	<.05	<.05	—	—	—	<350	—	<1 X10³	<.4
Basalt Spr	12-16-67	1	4	<.05		—	—	—	—	—	—	.4
"	5-1-68	1	4	<.05		—	—	—	—	—	—	.4

Page 3 of 24

Source	Date Collected	Gross Alpha	Gross Beta	^{238}Pu	^{239}Pu	^{241}Am	^{226}Ra	^{234}U	^{137}Cs	^{90}Sr	^{3}H	^{238}U
		PICOCURIES PER LITER										µg/l
Basalt Spr	5-12-68	<1	4	<0.05	<0.05	—	—	—	—	—	—	1.0
"	8-11-69	<1	3	<.05	<.05	—	—	—	—	—	—	2.3
"	10-20-70	<1	5	<.05	<.05	—	—	—	—	—	—	0.4
"	5-7-71	2	2	<.05	<.05	—	—	—	—	—	—	1.4
"	8-31-71	<1	<1	<.05	<.05	—	—	—	—	—	$<1\times10^3$	1.8
"	2-17-72	<1	3	<.05	<.05	—	—	—	<360	—	$<1\times10^3$	3.4
"	7-31-72	<1	4	<.05	<.05	—	—	—	<350	—	$<1\times10^3$	2.6

LASL-ERDA-OFFICIAL

APPENDIX F

(Continued)

Source	Date Collected	Gross Alpha	Gross Beta	^{238}Pu	^{239}Pu	^{241}Am	^{226}Ra	^{234}U	^{137}Cs	^{90}Sr	^{3}H	^{238}U
		PICOCURIES PER LITER										µg/l
Drainage Area 5 (DP Canyon)												
DPS-1	12-5-67	63	51,700	3.87	76.1	1.29	<0.15	32.1	34,000	28,600	542×10^3	–
"	4-30-68	7	32,000	1.53	6.57	1.97	<.15	10.1	33,000	23,000	$1,980 \times 10^3$	–
"	4-18-68	79	9,200	9.37	76.6	8.46	.21	104	5,200	11,200	287×10^3	–
"	10-4-68	16	1,720	1.85	3.3	3.13	<.15	54.8	2,000	880	3796×10^3	–
"	5-5-69	23	2,170	8.71	13.1	4.68	<.15	70.3	3,500	1,110	630×10^3	–
"	8-5-69	14	2,850	4.76	11.1	4.20	.32	18.6	5,700	860	500×10^3	–
"	11-4-69	4	1,160	3.25	3.1	1.85	–	9.0	1,270	430	160×10^3	–
"	6-24-70	5	1,240	1.19	2.88	1.18	–	9.2	900	580	490×10^3	–
"	8-14-70	7	740	.72	1.68	.92	–	13.5	660	410	110×10^3	–
"	9-24-70	12	510	.72	2.31	1.37	<.15	15.1	250	210	62×10^3	–
"	11-17-70	2	1,110	.54	1.53	.85	–	10.1	350	610	750×10^3	–
"	12-1-70	11	2,410	.87	2.62	1.63	<.15	13.7	1,300	1,200	600×10^3	–
"	2-12-71	<1	980	.46	.65	.24	–	.92	1,600	310	190×10^3	–
"	5-7-71	62	2,875	1.45	3.79	1.22	–	–	1,700	–	123×10^3	–
"	8-16-71	16	615	2.75	3.47	.72	<.15	25.6	1,050	837	655×10^3	–
"	11-4-71	9	1,100	.05	.38	.21	<.15	10.4	460	1,002	454×10^3	2.3
"	2-17-72	2	843	<.05	.53	–	–	–	<370	–	$1,120 \times 10^3$	10.1
"	7-31-72	17	3,960	.29	16.2	.55	–	–	<350	–	57×10^3	6.7
"	11-2-72	19	2,604	.63	.31	.11	–	–	<350	–	11.5×10^3	4.4
DPS-2	12-5-67	4	6,690	.38	2.70	.63	<.15	4.40	2,740	5810	660×10^3	–

APPEN

(Continued)

Source	Date Collected	PICOCURIES PER LITER Gross Alpha	Gross Beta	^{238}Pu	^{239}Pu	^{241}Am	^{226}Ra	^{234}U	^{137}Cs	^{90}Sr	^{3}H	μg/l ^{238}U
DPS-2	4-30-68	5	6,090	0.36	1.39	0.44	<0.15	9.70	4,220	3,350	536 x10^3	—
"	6-18-68	8	3,300	.24	2.80	1.20	<.15	13.7	2,116	1,860	287 x10^3	—
"	5-5-69	20	1,360	3.68	4.97	2.19	<.15	33.1	2,260	350	798 x10^3	—
"	8-5-69	44	750	.89	2.31	1.21	<.15	81.5	—	—	542 x10^3	—
"	2-16-70	12	1,390	2.04	2.33	.97	<.15	42.0	740	620	511 x10^3	—
"	8-14-70	4	590	.23	.33	.19	—	10.9	<220	447	250 x10^3	—
"	1-20-71	5	640	5.64	.72	.25	—	2.11	523	376	195 x10^3	—
DPS-3	12-5-67	5	2,920	.21	.77	<.05	<.15	9.30	310	2,260	927 x10^3	—
"	4-30-68	6	130	.24	1.77	1.65	.21	13.9	1,560	3,470	686 x10^3	—
"	6-18-68	6	2,920	.61	3.48	1.19	<.15	18.5	1,330	3,890	412 x 10^3	—
"	5-5-69	10	840	5.31	5.99	2.81	.19	34.4	1,120	530	876 x 10^3	—
"	8-5-69	27	1,040	.79	2.46	1.00	<.15	54.1	530	506	146 x10^3	—
"	2-16-70	45	1,140	2.60	1.94	1.08	<.15	167	330	530	732 x10^3	—
"	8-14-70	3	750	.20	.24	.16	—	10.2	460	376	185 x10^3	—
DPS-4	12-5-67	<2	1800	.13	.14	<.05	.35	2.05	<240	632	410 x10^3	—
"	4-30-68	<2	730	.07	.05	<.05	<.15	3.56	<240	517	679 x10^3	—
"	9-31-68	9	520	.11	.11	.11	.19	3.13	<240	352	273 x10^3	—
"	2-5-69	<1	520	<.05	.08	.14	<.15	2.46	<240	271	258 x10^3	—
"	5-5-69	3	430	.11	.16	.16	—	4.25	<240	589	702 x10^3	—
"	8-5-69	2	510	.19	.83	.37	—	2.12	<240	—	372 x10^3	—

APPENDIX F

(Continued)

		PICOCURIES PER LITER										µg/l
Source	Date Collected	Gross Alpha	Gross Beta	^{238}Pu	^{239}Pu	^{241}Am	^{226}Ra	^{234}U	^{137}Cs	^{90}Sr	^{3}H	^{238}U
DPS-4	10-22-69	3	210	1.41	0.99	0.72	–	2.05	<240	–	53X10³	–
	2-16-70	<1	480	<.05	.14	.19	–	2.41	–	–	318X10³	–
	6-24-70	<2	420	.10	.54	.37	–	1.23	<250	–	117X10³	–
	8-14-70	<1	440	.14	.09	.12	–	1.30	<220	200	99X10³	–
	11-17-70	<1	480	.24	.05	.10	–	1.16	<230	270	115X10³	–
	2-12-71	<1	480	.07	<.05	<.05	–	2.80	<230	–	101X10³	–
	5-12-71	9	700	.09	<.05	.10	–	–	–	–	108X10³	–
	8-16-71	<1	4	.13	.16	.07	–	1.15	<340	360	78X10³	–
	11-4-71	3	300	.15	.28	.08	–	1.20	<340	269	126X10³	0.6
	2-16-72	<1	482	<.05	.07	–	–	–	<360	–	308X10³	4.6
	7-31-72	2	598	.08	.46	.26	–	–	<360	–	136X10³	3.6
	11-2-72	5	798	.09	.27	<.05	–	–	<350	–	73.5X10³	1.8
DPE-STP	12-5-67	3	14	<.05	<.05	–	–	–	–	–	<50X10³	.9
	5-5-69	3	20	<.05	<.05	–	–	–	–	–	<50X10³	.9
	8-5-69	<2	13	<.05	<.05	.07	–	–	–	–	<50X10³	1.3
	2-16-70	3	14	.16	.14	.08	–	–	–	–	8X10³	.6

APPENDI
(Continued)

Source	Date Collected	Gross Alpha	Gross Beta	^{238}Pu	^{239}Pu	^{241}Am	^{226}Ra	^{234}U	^{137}Cs	^{90}Sr	^{3}H	^{238}U
		PICOCURIES PER LITER										µg/l
Drainage Area 5 (Los Alamos Canyon)												
Reservoir	12-7-67	<1	6	<0.05	<0.05	—	<0.15	—	—	—	<50X10³	0.8
"	4-23-69	<1	2	<.05	<.05	—	—	—	—	—	<50X10³	.6
"	5-7-71	2	2	<.05	<.05	—	—	—	—	—	<50X10³	.4
"	5-3-72	<1	<1	<.05	<.05	—	—	—	—	—	<1X10³	1.5
SW. of LAO-1	2-5-69	<1	20	<.05	<.05	—	—	—	—	—	—	<.4
"	5-5-69	<1	17	<.05	<.05	—	—	—	—	—	<1X10³	<.4
"	8-11-69	<1	13	<.05	.06	—	—	—	—	—	—	1.5
SW at LAO-1.5	4-11-69	<1	4	<.05	.05	—	—	—	—	—	<50X10³	1.5
SW. of LAO-1.5	12-5-67	<1	18	<.05	<.05	—	<.15	—	—	—	160X10³	1.1
LAO-C	11-25-70	<1	4	<.05	<.05	—	—	—	<340	—	<1X10³	1.2
"	8-16-71	<1	<1	<.05	<.05	—	—	—	<350	—	<1X10³	<.4
"	11-5-71	<1	<1	<.05	<.05	—	—	—	—	—	<1X10³	<.4
"	2-17-72	<1	6	<.05	.14	—	—	—	<360	—	<1X10³	2.3
"	5-5-72	<1	2	.09	<.05	—	—	—	<350	—	<1X10³	<.4
"	7-31-72	<1	4	<.05	<.05	0.06	—	—	<350	—	<1X10³	1.8
"	11-2-72	<1	9	<.05	<.05	.19	—	—	<350	—	1.9X10³	<.4
LAO-1	12-5-67	<1	50	<.05	<.05	—	.19	—	—	—	<50X10³	1.3
"	4-29-68	3	52	<.05	<.05	—	.19	—	—	—	<50X10³	<.4
"	6-19-68	<1	20	<.05	<.05	—	<.15	—	—	—	<50X10³	<.4
"	10-4-68	4	40	<.05	.13	<.05	<.15	.32	<240	—	<50X10³	—

APPENDIX F

(Continued)

		PICOCURIES PER LITER										µg/l
Source	Date Collected	Gross Alpha	Gross Beta	^{238}Pu	^{239}Pu	^{241}Am	^{226}Ra	^{234}U	^{137}Cs	^{90}Sr	^{3}H	^{238}U
LAO-1	5-5-69	<1	26	<0.05	<0.05	–	–	–	–	–	<50x10³	<0.4
"	8-5-69	<1	40	<.05	<.05	–	–	–	–	–	<50x10³	<.4
"	11-4-69	<1	42	<.05	.07	–	–	–	–	–	<50x10³	1.5
"	2-16-70	<1	88	<.05	.05	–	–	–	–	–	4x10³	<.4
"	2-24-70	<1	36	<.05	.05	–	–	–	–	–	6x10³	.9
"	8-13-70	<1	71	<.05	<.05	–	–	–	–	–	11x10³	<.4
"	11-17-70	<1	107	.09	.06	–	–	–	–	–	41x10³	<.4
"	2-12-71	<1	148	<.05	<.05	–	–	–	–	–	24x10³	.8
"	5-7-71	<2	78	.06	.09	–	–	–	–	–	76x10³	1.6
"	8-16-71	<1	93	.05	<.05	–	–	–	<340	–	33x10³	<.4
"	11-4-71	<1	55	.05	.90	–	–	–	<350	–	8.5x10³	<.4
"	2-17-72	<1	76	<.05	.07	–	–	–	<360	–	26x10³	1.3
"	5-5-72	<1	53	.46	<.05	–	–	–	<350	–	11.7x10³	<.2
"	7-13-72	2	222	<.05	.06	<0.05	–	–	<350	–	14.9x10³	1.0
"	11-2-72	2	157	.10	.55	<0.05	–	–	<350	–	25.7x10³	<.2
LAO-1.2	5-5-69	<1	4	<.05	<.05	–	–	–	–	–	<50x10³	.7
"	8-5-69	2	6	<.05	<.05	–	–	–	–	–	19x10³	<.4
"	8-13-70	<1	3	<.05	<.05	–	–	–	–	–	6x10³	<.4
LAO-1.8	5-5-69	<1	4	<.05	<.05	–	–	–	–	–	<50x10³	.9
	8-5-69	2	5	<.05	.05	–	–	–	–	–	<50x10³	1.1

APPENDIX F

(Continued)

Source	Date Collected	PICOCURIES PER LITER Gross Alpha	Gross Beta	^{238}Pu	^{239}Pu	^{241}Am	^{226}Ra	^{234}U	^{137}Cs	^{90}Sr	^{3}H	µg/l ^{238}U
LAO-2	12-5-67	<1	91	<0.05	0.05	–	0.30	–	–	–	390×10^3	2.6
"	4-29-68	3	57	<.05	<.05	–	<.15	–	–	–	115×10^3	2.0
"	6-19-68	<1	44	<.05	.06	–	<.15	–	–	–	27×10^3	<.4
"	9-31-68	4	77	<.05	.08	<0.05	<.15	–	<250	–	180×10^3	2.4
"	8-4-69	2	86	<.05	.43	–	–	–	–	–	210×10^3	2.2
"	11-5-69	<1	68	.15	.78	–	–	–	–	–	–	1.0
"	2-16-70	<1	80	<.05	.10	–	–	–	–	–	280×10^3	.6
"	5-11-70	<1	73	<.05	.20	–	–	–	<250	–	–	<.4
"	8-13-70	<1	87	<.05	.14	–	–	–	–	–	86×10^3	.7
"	8-16-71	<1	106	<.05	.16	–	–	–	<340	–	59×10^3	1.0
"	11-4-71	2	95	.25	.51	–	–	–	<340	–	45×10^3	.8
"	2-16-72	<1	162	<.05	<.05	–	–	–	<360	–	245×10^3	3.6
"	7-31-72	2	239	.12	.05	.12	–	–	<350	–	145×10^3	4.2
"	11-2-72	3	163	.11	.46	.12	–	–	<350	–	71×10^3	<.2
LAO-3	12-5-67	<1	45	<.05	.05	–	.19	–	–	–	215×10^3	4.9
"	4-29-68	2	103	<.05	<.05	–	.28	2.00	<240	–	220×10^3	–
"	6-20-68	<1	34	<.05	<.05	–	<.15	–	–	–	70×10^3	.7
"	9-30-68	3	45	.11	.15	<.05	.30	–	<240	–	35×10^3	.9
"	5-5-69	2	45	<.05	<.05	–	–	–	–	–	505×10^3	1.7
"	8-4-69	2	53	<.05	.08	–	–	–	–	–	192×10^3	1.0

APPENDIX F

(Continued)

Source	Date Collected	PICOCURIES PER LITER Gross Alpha	Gross Beta	^{238}Pu	^{239}Pu	^{241}Am	^{226}Ra	^{234}U	^{137}Cs	^{90}Sr	^{3}H	µg/l ^{238}U
LAO-3	2-16-70	3	9	<0.05	<0.05	–	–	–	–	–	46 X 10³	<0.4
"	6-24-70	<1	65	<.05	.07	–	–	–	–	–	97 X 10³	1.6
"	8-13-70	3	75	<.05	.07	–	–	–	–	–	90 X 10³	1.3
"	11-17-70	<1	74	<.05	.12	–	–	–	<230	–	59 X 10³	<.4
"	5-7-71	<1	190	.10	<.05	–	–	–	<350	–	21 X 10³	.4
"	8-16-71	<1	49	.05	.12	–	–	–	<370	–	58 X 10³	1.8
"	11-4-71	4	45	<.05	.08	–	–	–	410	–	34 X 10³	1.4
"	2-16-72	<1	62	<.05	.05	–	–	–	<370	–	191 X 10³	3.6
"	5-5-72	2	69	<.05	<.05	–	–	–	<350	–	226 X 10³	2.8
"	7-31-72	4	109	.25	.41	<0.05	–	–	<350	–	259 X 10³	5.5
"	11-2-72	5	127	<.05	.10	<0.05	–	–	<350	–	71 X 10³	.2
LAO-4	12-5-67	<1	9	<.05	.06	–	–	–	–	–	222 X 10³	.8
"	4-29-68	3	17	<.05	<.05	–	<0.15	–	–	–	71 X 10³	.4
"	6-20-68	<1	10	<.05	.05	–	<.15	–	–	–	59 X 10³	.4
"	10-4-68	11	20	.06	<.05	<.05	<.15	–	<240	–	53 X 10³	1.8
"	5-5-69	<1	9	<.05	<.05	–	–	–	–	–	55 X 10³	<.4
"	8-4-69	<1	10	<.05	<.05	–	–	–	–	–	56 X 10³	.4
"	8-13-70	<1	10	<.05	<.05	–	–	–	–	–	66 X 10³	<.4
LAO-4.5	5-5-69	<1	3	<.05	<.05	–	–	–	–	–	56 X 10³	.9
"	8-4-69	<1	8	<.05	<.05	–	–	–	–	–	41 X 10³	.8

APPEN X

(Continued)

		PICOCURIES PER LITER										µg/l
Source	Date Collected	Gross Alpha	Gross Beta	^{238}Pu	^{239}Pu	^{241}Am	^{226}Ra	^{234}U	^{137}Cs	^{90}Sr	^{3}H	^{238}U
LAO-4.5	11-4-69	1	4	<0.05	<0.05	—	—	—	—	—	32 X10³	<0.1
"	2-16-70	2	71	<.05	.19	—	—	—	—	—	173 X10³	.4
"	5-11-70	<1	8	<.05	<.05	—	—	—	—	—	—	<.4
"	6-24-70	<1	6	.11	<.05	—	—	—	—	—	44 X10³	<.4
"	8-13-70	<1	4	<.05	<.05	—	—	—	—	—	54 X10³	<.4
"	11-17-70	2	42	<.05	<.05	—	—	—	—	—	40 X10³	<.4
"	2-12-71	<1	7	<.05	<.05	—	—	—	—	—	34 X10³	1.2
"	8-16-71	<1	1	.09	.11	—	—	—	<340	—	26 X10³	<.4
"	11-4-71	2	6	.06	.18	—	—	—	<350	—	12 X10³	<.4
"	2-16-72	<1	6	<.05	<.05	—	—	—	<360	—	34 X10³	2.6
"	5-5-72	<1	3	.20	.06	—	—	—	<350	—	28 X10³	<.2
"	7-31-72	<1	8	<.05	.08	0.06	—	—	<350	—	18.2 X10³	2.1
"	11-2-72	3	12	<.05	<.05	<.05	—	—	<350	—	32.5 X10³	<.2
LAO-5	12-5-67	<1	4	<.05	<.05	—	—	—	—	—	126 X10³	<.1
"	6-20-68	<1	10	<.05	<.05	—	—	—	—	—	70 X10³	1.8
"	10-4-68	<1	7	<.05	<.05	<.05	<0.15	—	<240	—	76 X10³	.16
"	5-5-69	<1	3	<.05	<.05	—	—	—	—	—	61 X10³	.9
"	8-4-69	<1	7	<.05	<.05	—	—	—	—	—	50 X10³	.16
LAO-6	10-4-68	2	18	.17	.25	—	<.15	—	<240	—	75 X10³	.4
"	5-5-69	<1	7	<.05	<.05	—	—	—	<240	—	51 X10³	<.4

APPENDIX F

(Continued)

		PICOCURIES PER LITER										µg/l
Source	Date Collected	Gross Alpha	Gross Beta	^{238}Pu	^{239}Pu	^{241}Am	^{226}Ra	^{234}U	^{137}Cs	^{90}Sr	^{3}H	^{238}U
LAS-1	7-31-68	1	21	0.05	<0.05	–	–	1.11	<240	–	–	–
"	8-5-68	<1	12	.06	.05	–	–	2.06	<240	–	–	–
"	8-18-68	<1	8	.17	.27	–	–	.74	<240	–	–	–
"	9-22-68	<1	7	<.05	.05	–	–	.94	<240	–	–	–
"	7-23-71	<1	9	<.05	<.05	–	–	–	<300	–	<1X10³	<0.4
"	7-29-71	<1	3	.12	<.05	–	–	–	<300	–	<1X10³	.5
"	8-29-71	<1	6	.06	.05	–	–	–	<310	–	<1X10³	<0.4
LAS-2	8-18-68	<1	220	<.05	.19	–	–	–	<240	–	–	.5
"	7-29-71	<1	131	<.05	<.05	–	–	–	<300	–	4.5X10³	<.4
"	8-29-71	<1	111	<.05	.07	–	–	–	<300	–	6.8X10³	.4
LAS-3	7-31-68	2	470	<.05	<.05	–	–	–	<240	–	–	.7
"	8-5-68	<1	320	<.05	.09	–	–	–	<240	–	–	1.1
"	8-18-68	<1	220	<.05	.17	–	–	–	<240	–	–	.7
"	9-22-68	<1	140	<.05	.08	–	–	–	<240	–	–	.09
"	7-23-71	<1	236	<.05	<.05	–	–	–	<300	58.5	11X10³	<.4
"	7-29-71	<1	116	.07	.09	–	–	–	<308	–	3.2X10³	<.4
"	8-29-71	<1	224	.08	<.05	–	–	–	<310	<6.0	17.5X10³	<.4
LAS-4	7-31-68	1	830	.12	.17	–	–	–	<240	–	–	.8

APPENI

(Continued)

Source	Date Collected	Gross Alpha	Gross Beta	^{238}Pu	^{239}Pu	^{241}Am	^{226}Ra	^{234}U	^{137}Cs	^{90}Sr	^{3}H	^{238}U
		PICOCURIES PER LITER										µg/l
Drainage Area 6 (Sandia Canyon)												
SCS-1	2-6-69	2	14	<0.05	<0.05	—	—	—	—	—	—	<0.4
"	9-5-69	<1	8	<.05	<.05	—	—	—	—	—	8.7×10^3	3.1
"	1-13-70	<1	12	<.05	.05	—	—	—	—	—	17×10^3	<.4
"	3-19-70	<1	16	<.05	<.05	—	—	—	—	—	127×10^3	<.4
"	6-29-70	<1	17	<.05	<.05	—	—	—	—	—	10×10^3	<.4
"	9-24-70	<1	13	<.05	<.05	—	—	—	—	—	8×10^3	<.4
"	12-22-70	<1	11	<.05	.05	—	—	—	—	—	$<1 \times 10^3$	<.4
"	3-8-71	<1	15	<.05	<.05	—	—	—	—	—	5×10^3	<.4
"	6-1-71	<1	22	<.12	.12	—	—	—	—	—	7×10^3	<.4
"	9-14-71	<1	14	.10	.08	—	—	—	<330	—	2.7×10^3	2.9
"	12-6-71	3	12	<.05	<.05	—	—	—	<140	—	4×10^3	<.4
"	3-3-72	<1	9	<.05	.06	—	—	—	280	—	3×10^3	<.2
"	6-9-72	<1	19	.16	<.05	—	—	—	<160	—	1×10^3	.5
"	8-31-72	<1	22	.13	.09	—	—	—	<105	—	3.9×10^3	3.8
"	11-6-72	3	19	.09	<.05	—	—	—	<50	—	5.5×10^3	<.2
SCS-2	2-6-69	<1	11	<.05	<.05	—	—	—	—	—	—	<.4
"	9-5-69	<1	10	<.05	<.05	—	—	—	—	—	7.1×10^3	.4
"	1-12-70	<1	12	<.05	<.05	—	—	—	—	—	22×10^3	<.4
"	3-19-70	<1	12	<.05	<.05	—	—	—	—	—	26×10^3	<.4
"	9-24-70	<1	8	<.05	<.05	—	—	—	—	—	7×10^3	<.4

APPENDIX F
(Continued)

		PICOCURIES PER LITER										µg/l
Source	Date Collected	Gross Alpha	Gross Beta	^{238}Pu	^{239}Pu	^{241}Am	^{226}Ra	^{234}U	^{137}Cs	^{90}Sr	^{3}H	^{238}U
SCS-2	12-21-70	<1	12	<0.05	<0.05	—	—	—	—	—	23×10^3	<0.4
"	3-15-71	<1	21	<.05	<.05	—	—	—	—	—	10×10^3	<.4
"	6-1-71	<1	17	<.05	<.05	—	—	—	—	—	10×10^3	<.4
"	9-14-71	<1	6	<.05	<.05	—	—	—	<340	—	5.8×10^3	<.4
"	12-6-71	<1	10	<.05	<.05	—	—	—	<140	—	6×10^3	<.4
"	3-3-72	<1	11	<.05	.08	—	—	—	1,960	—	4×10^3	<.2
"	6-9-72	<1	14	.09	.05	—	—	—	<356	—	34×10^3	1.8
"	8-31-72	<1	15	.14	.06	.08	—	—	<356	—	4.7×10^3	2.0
"	11-6-72	3	22	<.05	<.05	.05	—	—	<356	—	5.1×10^3	1.1
SCO-4	9-5-69	<1	2	<.05	<.05	—	—	—	—	—	$<4 \times 10^3$	.4

Source	Date Collected	Gross Alpha	Gross Beta	^{238}Pu	^{239}Pu	^{241}Am	^{223}Ra	^{234}U	^{137}Cs	^{90}Sr	^{3}H	^{238}U
		PICOCURIES PER LITER										µg/l
Drainage Area 7 (Mortandad Canyon)												
GS-1	12-6-67	<1	343	<0.05	<0.05	—	0.38	0.40	<240	—	<50x10³	—
"	4-30-68	<1	364	.32	.41	—	<.15	.88	<240	—	<50x10³	—
"	10-7-68	<1	219	.59	.42	<0.05	<.15	—	270	—	<50x10³	0.5
"	6-2-69	12	2,206	12.5	13.2	—	<.15	1.18	5,808	169	53x10³	—
"	9-5-69	7	148	.42	.08	—	<.15	—	<240	—	428x10³	.7
"	1-12-70	2	1,560	1.50	.13	.27	—	.95	690	326	304x10³	—
"	3-17-70	14	1,280	7.14	3.63	17.6	<.15	.86	7,740	794	65x10³	—
"	6-22-70	2	1,520	.34	.19	.09	—	5.17	2,780	375	35x10³	—
"	7-21-70	29	904	28.0	18.5	.89	<.15	.58	2,030	32	24x10³	—
"	9-24-70	5	924	3.92	1.78	.38	—	.23	1,420	91	44x10³	—
"	11-17-70	11	1,240	14.6	5.44	2.56	.15	.73	2,380	67	41x10³	—
"	12-1-70	74	19,300	50.7	11.1	2.64	.15	4.56	32,300	1,260	171x10³	—
"	12-21-70	12	811	12.8	3.99	.08	.15	2.96	1,350	134	10x10³	—
"	2-12-71	12	2,340	14.7	2.20	.19	.15	1.80	4,320	489	54x10³	—
"	3-15-71	27	879	32.5	4.21	1.78	.15	3.72	1,670	116	8x10³	—
"	6-3-71	363	2,120	266.0	16.9	188	.15	—	8,120	—	17x10³	—
"	9-13-71	15	2,246	11.5	1.77	1.24	.15	9.20	3,410	126	20x10³	—
"	12-6-71	4	434	2.03	.23	.55	—	2.01	260	201	55x10³	—
"	3-3-72	3	714	5.6	.54	—	—	—	—	—	14x10³	3.3
"	6-9-72	18	562	13.3	1.18	—	—	—	1,330	—	45.6x10³	4.4

APPENDIX F

(Continued)

		PICOCURIES PER LITER										µg/l
Source	Date Collected	Gross Alpha	Gross Beta	^{238}Pu	^{239}Pu	^{241}Am	^{226}Ra	^{234}U	^{137}Cs	^{90}Sr	^{3}H	^{238}U
GS-1	8-31-72	12	6.12	12.2	1.73	0.99	—	—	475	—	29.4x10³	5.1
"	11-6-72	15	192	3.6	.43	—	—	—	350	—	4.9x10³	<.2
MCS-3.9	12-6-67	<1	97	<.05	<.05	—	<0.15	—			82x10³	.8
"	4-30-68	<1	230	.18	.29	—	<.15	2.95	<240		<50x10³	—
"	10-7-68	2	156	.05	.15	<.05	<.15	—	<240		—	3.1
"	9-8-69	<1	142	.22	.17	—	—	—	—		6x10³	1.2
"	3-17-70	3	265	.31	.27	—	—	—	—	72	718x10³	1.2
"	9-23-70	<1	353	.39	.29	—	—	—	—	101	63x10³	1.7
"	3-8-71	3	483	1.76	.23	—	—	—	280	—	49x10³	7.5
"	6-3-71	22	1,770	6.64	.59	—	—	—	490	—	31x10³	10.1
"	9-13-71	9	659	2.17	.43	—	<.15	—	380	1	45x10³	5.5
"	12-6-71	7	354	2.05	.09	—	—	—	<140	154	55x10³	9.1
"	3-3-72	2	279	.95	.24	—	—	—	—	—	—	8.3
"	6-9-72	.8	550	1.14	.07	—	—	—	<350	—	6.9x10³	8.2
"	8-31-72	15	610	16.0	2.67	1.53	—	—	<350	—	95.6x10³	10.8
"	8-6-72	24	651	5.8	.61	.19	—	—	<350	—	44.3x10³	6.4
GS-2	1-18-71	95	312	1.05	5.00	3.02	<0.15	2.03	390	89	28x10³	—
MCO-3	12-6-67	<1	116	<.05	.14	—	<.15	—	<240	—	<50x10³	1.3
"	4-30-68	2	214	.13	.13	—	<.15	2.77	<240	—	<50x10³	—
"	10-7-68	<1	117	.41	.31	<.05	<.15	—	—	—	<50x10³	.7

APPENI

(Continued)

		PICOCURIES PER LITER										µg/l
Source	Date Collected	Gross Alpha	Gross Beta	^{238}Pu	^{239}Pu	^{241}Am	^{226}Ra	^{234}U	^{137}Cs	^{90}Sr	^{3}H	^{238}U
MCO-3	9-8-69	7	9.3	0.27	0.35	—	—	—	—	—	17×10^3	0.9
"	1-12-70	13	150	1.76	.42	—	<0.15	—	<240	—	2910×10^3	1.2
"	3-17-70	2	294	.79	.60	—	—	—	—	32	272×10^3	<.4
"	6-22-70	5	975	.97	.51	—	—	—	—	191	64×10^3	2.3
"	9-24-70	6	345	1.29	.68	0.20	—	—	—	54	46×10^3	2.1
"	12-21-70	3	760	.33	.13	—	—	—	450	—	49×10^3	3.5
"	3-15-71	23	2,170	29.0	3.88	—	<0.15	—	7,010	—	25×10^3	—
"	6-3-71	37	2,630	21.9	1.65	—	—	—	750	—	20×10^3	13.7
"	9-13-71	14	616	5.04	.64	—	<0.15	—	440	412	46×10^3	8.4
"	12-6-71	8	466	1.31	.24	—	—	—	160	215	41×10^3	4.9
"	3-10-72	3	213	6.93	.48	—	—	—	—	—	49×10^3	5.2
"	6-9-72	8	729	1.94	.20	—	—	—	445	—	35.6×10^3	12.4
"	8-31-72	8	875	2.28	.34	.27	—	—	<356	—	54.1×10^3	9.1
"	11-6-72	26	629	4.6	.37	.72	—	—	<350	—	49.7×10^3	3.6
MCO-4	12-6-67	<1	83	<.05	.06	—	<.15	—	—	—	69×10^3	<.4
"	4-30-68	2	137	.21	.56	—	<.15	1.48	<240	—	$<50 \times 10^3$	—
"	10-7-68	<1	28	<.05	.30	<.05	<.15		<240	—	$<50 \times 10^3$	1.2
"	6-2-69	2	122	<.05	<.05	—	—	—	—	—	18×10^3	1.1
"	9-8-69	<1	77	<.05	.17	—	—	—	—	—	18×10^3	<.4
"	11-6-69	7	188	.33	.14	—	—	—	—	—	17×10^3	3.6

APPENDIX F

(Continued)

		PICOCURIES PER LITER										µg/l
Source	Date Collected	Gross Alpha	Gross Beta	^{238}Pu	^{239}Pu	^{241}Am	^{226}Ra	^{234}U	^{137}Cs	^{90}Sr	^{3}H	^{238}U
MCO-4	1-12-70	10	76	0.34	0.12	–	<0.15	–	<230	–	2180X10³	1.0
"	3-17-70	4	109	<.05	.10	–	–	–	<230	–	1060X10³	.4
"	5-14-70	<1	114	<.05	.08	–	–	–	–	–	522X10³	1.3
"	6-23-70	<1	125	<.05	<.05	–	–	–	–	–	242X10³	.9
"	9-23-70	2	174	<.05	<.05	–	–	–	–	–	102X10³	1.8
"	12-21-70	<1	248	.12	<.05	–	–	–	<230	–	58X10³	3.5
"	3-8-71	<1	422	.12	.05	–	–	–	<230	–	60X10³	3.7
"	6-3-71	3	512	.15	.05	–	–	–	<350	–	41X10³	3.8
"	9-13-71	2	437	.35	.16	–	–	–	<340	211	41X10³	3.1
"	12-6-71	5	306	.29	.07	–	–	–	<140	147	58X10³	4.0
"	3-3-72	2	219	.89	.26	–		–	–	–	96X10³	12.0
"	6-9-72	9	313	.53	.07	–	–	–	<350	–	45X10³	6.9
"	8-31-72	5	331	.93	.15	<0.05	–	–	<350	–	53X10³	3.1
"	11-6-72	20	509	1.38	.17	.15	–	–	<350	–	63X10³	2.0
MCO-5	12-6-67	2	9	<.05	<.05	–	<.15	–	–	–	222X10³	<.4
"	4-30-68	1	68	.12	.05	–	<.15	–	–	–	83X10³	.6
"	10-7-68	<1	21	.09	1.20	3.81	<.15	–	<240	–	57X10³	<.4
"	6-2-69	<1	29	<.05	.07	–	–	–	–	–	17X10³	.6
"	9-8-69	<1	28	.06	.10	–	–	–	–	–	27X10³	.7
"	3-17-70	7	19	.05	<.05	–	–	–	–	–	141X10³	.4

APPENDIX

(Continued)

Source	Date Collected	PICOCURIES PER LITER Gross Alpha	Gross Beta	^{238}Pu	^{239}Pu	^{241}Am	^{226}Ra	^{234}U	^{137}Cs	^{90}Sr	^{3}H	µg/l ^{238}U
MCO-5	9-23-76	<1	36	0.06	<0.05	–	–	–	–	–	303 X 10³	0.6
"	3-8-71	<1	216	<.05	<.05	–	–	–	<220	–	82 X 10³	1.5
"	6-3-71	<1	178	.20	<.05	–	–	–	<356	–	86 X 10³	1.4
"	9-13-71	2	278	<.05	<.05	–	–	–	<346	175	69 X 10³	1.3
"	12-6-71	<1	71	.07	<.05	–	–	–	<146	–	59 X 10³	1.3
"	3-3-72	<1	63	<.05	.08	–	–	–	–	–	79 X 10³	2.1
"	6-9-72	1	52	.24	<.05	–	–	–	<350	–	64 X 10³	3.6
"	8-31-72	2	127	<.05	.08	.08	–	–	<350	–	109 X 10³	3.1
"	11-6-72	6	204	.20	.08	.30	–	–	<350	–	61 X 10³	2.0
MCO-6	12-6-67	2	7	<.05	.09	–	–	–	–	–	144 X 10³	4.6
"	4-30-68	10	31	<.05	.32	–	.54	–	–	–	77 X 10³	1.9
"	10-7-68	1	22	.10	1.26	<.05	.19	–	<240	–	61 X 10³	<.4
"	6-2-69	<1	10	<.05	.05	–	–	–	–	–	18 X 10³	<.4
"	9-8-69	7	26	<.05	.07	–	<.15	–	–	–	17 X 10³	.6
"	1-12-70	11	20	<.05	.05	–	<.15	–	<230	–	27 X 10³	<.4
"	3-17-70	10	21	<.05	<.05	–	<.15	–	–	–	1320 X 10³	<.4
"	5-14-70	<1	27	<.05	<.05	–	–	–	–	–	1120 X 10³	2.0
"	6-23-70	<1	40	<.05	<.05	–	–	–	–	–	642 X 10³	1.3
"	9-23-70	1	32	<.05	<.05	–	–	–	–	–	343 X 10³	<.4
"	12-22-70	<1	45	<.05	<.05	–	–	–	–	–	148 X 10³	.7

APPENDIX F

(Continued)

		PICOCURIES PER LITER										µg/l
Source	Date Collected	Gross Alpha	Gross Beta	^{238}Pu	^{239}Pu	^{241}Am	^{226}Ra	^{234}U	^{137}Cs	^{90}Sr	^{3}H	^{238}U
MCO-6	3-8-71	<1	224	<0.05	<0.05	–	–	–	–	–	79 X10³	1.3
"	6-3-71	<1	172	.06	<.05	–	–	–	–	–	61 X10³	.9
"	9-13-71	<1	152	<.05	<.05	–	–	–	<340	–	56 X10³	1.3
"	12-6-71	3	125	<.05	<.05	–	–	–	<140	–	47 X10³	2.4
"	3-3-72	<1	93	<.05	<.05	–	–	–	–	–	51 X10³	3.9
"	6-9-72	1	53	.14	<.05	–	–	–	<300	–	65 X10³	3.1
"	8-31-72	1	160	.06	<.05	0.19	–	–	<350	–	62 X10³	3.9
"	11-6-72	6	222	.09	<.05	.25	–	–	<350	–	61 X10³	3.1
MCO-7	12-6-67	2	2	<.05	.05	–	–	–	–	–	143 X10³	1.5
"	4-30-68	2	8	<.05	.95	–	<0.15	–	–	–	154 X10³	1.2
"	10-7-68	<1	12	<.05	.16	<.05	<.15	–	<240	–	67 X10³	<.4
"	6-24-69	1	11	<.05	.06	–	–	–	–	–	29 X10³	.9
"	9-8-69	8	6	<.05	<.05	–	.19	–	–	–	27 X10³	.4
"	1-12-70	3	20	<.05	<.05	–	–	–	<230	–	22 X10³	.4
"	3-17-70	3	10	<.05	.07	–	–	–	–	–	45 X10³	<.4
"	6-23-70	<1	14	<.05	<.05	–	–	–	–	–	899 X10³	<.4
"	9-23-70	2	23	<.05	<.05	–	–	–	–	–	639 X10³	<.4
"	3-8-71	<1	44	<.05	<.05	–	–	–	<230	–	212 X10³	.8
"	6-3-71	<1	168	<.05	<.05	–	–	–	<350	–	126 X10³	1.2
"	9-13-71	<1	134	.19	<.05	–	–	–	<340	–	89 X10³	<.4

APPENDIX

(Continued)

		PICOCURIES PER LITER										µg/l
Source	Date Collected	Gross Alpha	Gross Beta	^{238}Pu	^{239}Pu	^{241}Am	^{226}Ra	^{234}U	^{137}Cs	^{90}Sr	^{3}H	^{238}U
MCO-7	12-6-71	<1	72	<0.05	<0.05	—	—	—	<140	—	79 X10³	<0.4
"	3-3-72	<1	70	<.05	.07	—	—	—	—	—	66 X10³	1.3
"	6-9-72	<1	45	.19	<.05	—	—	—	<350	—	56 X10³	3.1
"	8-31-72	<1	57	.07	<.05	0.11	—	—	<350	—	51 X10³	2.0
"	11-6-72	3	119	.17	<.05	<.05	—	—	<350	—	72 X10³	.8
MCO-7.5	12-6-67	3	11	<.05	.06	—	<.15	—	—	—	230 X10³	3.6
	4-30-68	4	13	.12	<.05	—	.56	—	—	—	196 X10³	1.2
	10-7-68	<1	5	.09	.59	.10	—	—	<240	—	118 X10³	<.4
	6-4-69	2	9	<.05	<.05	—	—	—	—	—	48 X10³	1.1
	9-8-69	<1	69	.15	.24	—	—	—	—	—	33 X10³	.4
	1-12-70	7	35	.25	.27	—	—	—	<240	—	24 X10³	.4
	3-17-70	8	36	.49	.70	—	—	—	—	—	40 X10³	<.4
	9-23-70	6	26	.22	.14	—	—	—	—	—	177 X10³	<.4
	6-3-71	2	95	.26	<.05	—	—	—	<350	—	183 X10³	1.1
	9-13-71	<1	56	.05	<.05	—	—	—	<340	—	146 X10³	<.4
	12-6-71	<1	54	<.05	<.05	—	—	—	<140	—	104 X10³	.6
	3-3-72	<1	74	<.05	.30	—	—	—	—	—	183 X10³	1.5
	6-9-72	1	52	.08	.06	—	—	—	<350	—	58 X10³	2.9
	8-31-72	<1	56	.09	.05	.37	—	—	<350	—	77 X10³	1.8
	11-6-72	2	99	.08	<.05	1.78	—	—	<350	—	88 X10³	1.1

APPENDIX F

(Continued)

		PICOCURIES PER LITER										µg/l
Source	Date Collected	Gross Alpha	Gross Beta	^{238}Pu	^{239}Pu	^{241}Am	^{226}Ra	^{234}U	^{137}Cs	^{90}Sr	^{3}H	^{238}U
MCO-8	12-6-67	<1	10	<0.05	<0.05	–	<0.15	–	–	–	510 X10³	<0.1
	4-30-68	1	11	.05	<.05	–	<.15	–	–	–	360 X10³	2.7
	10-7-68	<1	8	.05	.16	<0.05	–	–	<240	–	238 X10³	.6
	6-4-69	<1	8	<.05	<.05	–	–	–	–	–	136 X10³	1.3
	9-8-69	2	36	<.05	<.05	–	–	–	–	–	134 X10³	<.4
	1-12-70	<1	6	<.05	<.05	–	–	–	<230	–	78 X10³	.4
	3-17-70	<1	15	<.05	<.05	–	–	–	–	–	84 X10³	<.4
	6-23-70	<1	8	<.05	<.05	–	–	–	–	–	49 X10³	1.3
	9-23-70	1	9	.07	<.05	–	–	–	–	–	208 X10³	.4
	12-22-70	<1	8	.06	<.05	–	–	–	<230	–	348 X10³	.4
	6-9-72	1	32	.19	<.05	–	–	–	<350	–	122 X10³	1.5
	8-31-72	<1	48	.06	1.46	0.32	–	–	<350	–	126 X10³	1.1
	11-6-72	1	58	<.05	<.05	.30	–	–	<350	–	141 X10³	<.2

APPENDI.

(Continued)

Source	Date Collected	Gross Alpha	Gross Beta	^{238}Pu	^{239}Pu	^{241}Am	^{226}Ra	^{234}U	^{137}Cs	^{90}Sr	^{3}H	^{238}U
		PICOCURIES PER LITER										µg/l
Drainage Area 9 (Canada del Buey)												
Nr. TA-46	3-19-70	1	5	<0.05	<0.05	—	—	—	—	—	11 X10³	0.4
"	5-7-71	2	3	<.05	<.05	—	—	—	—	—	20 X10³	.4
"	5-3-72	<1	2	.20	<.05	—	—	—	<350	—	1 X10³	1.8
Drainage Area 10 (Pajarito Canyon)												
Nr. TA-18	5-7-71	2	2	<0.05	<0.05	—	—	—	—	—	11 X10³	0.4
	5-2-71	<1	3	.10	.06	—	—	—	<350	—	3 X10³	3.1
Drainage Area 11 (Water Canyon)												
Am. Spr.	12-7-67	2	7	<0.05	<0.05	—	—	—	—	—	1.7 X10³	0.4
"	4-23-69	<1	3	<.05	<.05	—	—	—	—	—	1.5 X10³	.5
"	7-30-70	<1	10	<.05	<.05	—	—	—	—	—	<1 X10³	.4
Water Canyon	12-7-67	2	6	<.05	<.05	—	—	—	—	—	<1 X10³	1.3
"	7-17-69	4	6	<.05	<.05	—	—	—	—	—	<1 X10³	2.5
"	7-30-70	2	5	<.05	<.05	—	—	—	—	—	<1 X10³	.4
"	7-29-71	<1	<1	<.05	<.05	—	—	—	—	—	<1 X10³	<.4
"	2-14-72	<1	3	<.05	<.05	—	—	—	<290	—	<1 X10³	.2
"	7-8-72	<1	11	<.05	<.05	—	—	—	<350	—	<1 X10³	2.9
"	12-20-72	—	—	<.05	<.05	—	—	—	<350	—	<1 X10³	—

APPENDIX F

(Continued)

Source	Date Collected	Gross Alpha	Gross Beta	^{238}Pu	^{239}Pu	^{241}Am	^{226}Ra	^{234}U	^{137}Cs	^{90}Sr	^{3}H	^{238}U (µg/l)
		PICOCURIES PER LITER										
Drainage Area 11 (Cont.) (Water Canyon)												
Valle Canyon	12-7-67	<1	6	<0.05	<0.05	–	–	–	–	–	–	<0.4
"	4-23-69	<1	2	<.05	<.05	–	–	–	–	–	–	.6
Nr. Beta Hole	4-15-70	1	2	<.05	<.05	–	–	–	–	–	<1X10³	2.1
"	5-10-71	2	2	<.05	<.05	–	–	–	–	–	<1X10³	.7
"	5-2-72	<1	3	.11	.06	–	–	–	<350	–	<1X10³	1.3
Drainage Area 13 (Ancho Canyon)												
Ancho at RG	9-17-69	<1	2	<0.05	<0.05	–	–	–	–	–	<1X10³	0.7
"	8-25-71	<1	<1	<.05	<.05	–	–	–	<350	–	<1X10³	<.4
Drainage Area 15 (Chaquehui Canyon)												
Doe Spr	9-17-69	<1	1	<0.05	<0.05	–	–	–	–	–	–	0.4
	8-25-71	<1	<1	<0.05	<0.05	–	–	–	–	–	<1X10³	0.6

APPENDIX

Chemical Analyses of Water from the Main Aquifer

1 of 2 Pages

Source	Date of Collection	Chemical Constituents, Milligrams per liter: Calcium (Ca)	Magnesium (Mg)	Sodium (Na)	Carbonate (CO_3)	Bicarbonate (HCO_3)	Chloride (Cl)	Fluoride (F)	Nitrate (NO_3)	Dissolved solids	Total hardness	Specific conductance (micromhos at 25°C)	pH
TW-1	2-25-69	30	2	33	0	114	8	<0.1	0.4	188	94	205	7.5
"	5-1-70	32	7	11	0	118	8	.5	<.4	161	110	240	7.5
TW-2	6-10-68	14	3	19	0	62	4	1.0	1.3	—	50	130	7.9
"	2-25-69	8	3	17	0	49	3	<.1	<.4	90	32	160	8.3
"	9-24-70	14	5	11	0	70	5	.5	1.7	198	55	240	7.8
"	6-1-71	13	3	10	0	52	5	.8	<.4	86	44	140	8.3
"	10-11-72	10	2	10	0	40	6	.5	.4	46	32	140	8.5
TW-3	11-13-67	29	31	24	0	82	10	0.8	<0.4	171	200	175	7.5
"	11-17-67	28	10	25	0	100	5	0.4	2.6	191	110	170	7.5
"	6-10-69	19	6	24	0	86	4	0.4	1.3	201	72	180	8.0
"	2-25-69	17	5	22	0	88	5	<.1	.4	124	64	145	8.0
"	9-23-70	20	5	15	0	100	5	<.1	1.7	180	73	160	7.6
"	6-3-71	18	5	15	0	84	5	.6	.4	106	64	160	7.8
"	10-12-72	19	5	19	0	92	6	.5	<.4	94	68	140	7.6
TW-4	10-19-64	10	6	13	0	71	<1	0.4	0.9	163	99	160	8.0
"	6-8-65	10	5	20	0	70	2	<.1	.4	163	45	150	7.9
DT-54	2-15-67	9	3	13	0	58	4	0.9	<0.4	121	36	180	
"	2-15-67	8	3	14	0	60	4	.1	<.4	130	34	180	
"	2-24-69	8	2	19	0	52	3	<.1	.4	120	28	180	
"	9-24-70	12	5	16	0	54	5	.4	.4	101	50	150	

APPENDIX G

(Continued)

2 of 2 Pages

Source	Date of Collection	Chemical Constituents: Milligrams per liter: Calcium (Ca)	Magnesium (Mg)	Sodium (Na)	Carbonate (CO_3)	Bicarbonate (HCO_3)	Chloride (Cl)	Fluoride (F)	Nitrate (NO_3)	Dissolved solids	Total hardness	Specific conductance (micromhos at 25°C)	pH
TW-8	2-14-67	10	4	13	0	64	<1	<0.1	<0.4	141	44	220	7.7
"	1-19-69	11	3	23	0	66	3	<.1	1.7	146	40	220	7.8
DT-9	2-20-69	10	4	19	0	56	3	<0.1	1.3	160	40	180	7.3
"	4-28-70	12	5	10	0	53	5	<.1	<.4	170	50	150	7.8
"	11-5-71	11	5	14	0	72	4	<.1	.9	160	48	200	7.2
DT-10	2-24-69	10	5	19	0	60	3	<.1	0.9	155	44	200	7.7
"	4-30-70	20	7	10	0	62	3	.4	<.4	118	60	150	7.9
RWP-2	12-7-67	32	5	47	0	114	8	0.1	0.9	170	100	200	8.1
RWP-5	12-7-67	28	7	79	0	158	10	0.2	3.1	253	100	270	7.6
Cuckman W-1	8-25-64	4	<1	48	14	113	4	0.4	5.3	247	12	240	8.9

APPENDIX II

(Continued)

2 of 2 pages

Source	Date Collected	Gross Alpha	Gross Beta	^{238}Pu	^{239}Pu	^{241}Am	^{226}Ra	^{234}U	^{137}Cs	^{90}Sr	^{3}H	^{238}U
		PICOCURIES PER LITER										µg/l
DT-5A	2-24-69	<1	3	<0.05	<0.05	–	–	–	–	–	–	0.4
"	4-24-70	3	2	<.05	<.05	–	–	–	–	–	$<1\times10^{-3}$	0.4
TW-8	1-10-69	<1	2	<0.05	<0.05	–	–	–	–	–	–	0.5
"	1-14-69	2	3	<.05	<.05	–	–	–	–	–	–	.4
"	2-14-69	<1	1	<.05	<.05	–	–	–	–	–	–	.4
"	11-6-69	<1	3	<.05	<.05	–	–	–	–	–	–	.4
DT-9	2-20-69	<1	1	<0.05	<0.05	–	–	–	–	–	–	0.8
"	4-28-70	<1	2	<.05	<.05	–	–	–	–	–	$<1\times10^{3}$	.9
DT-10	2-24-69	<1	1	<0.05	<0.05	–	–	–	–	–	–	1.2
"	4-30-70	<1	2	<.05	<.05	–	–	–	–	–	$<1\times10^{3}$	.4
RWP-2	12-7-67	4	10	<0.05	<0.05	–	–	–	–	–	–	1.8
RWP-5	12-7-67	2	14	<0.05	<0.05	–	–	–	–	–	–	2.3

APPENDIX H

Radiochemical Analyses of Water from the Main Aquifer

1 of 2 Pages

Source	Date Collected	Gross Alpha	Gross Beta	^{238}Pu	^{239}Pu	^{241}Am	^{226}Ra	^{234}U	^{137}Cs	^{90}Sr	^{3}H	^{238}U
		PICOCURIES PER LITER										µg/l
TW-1	2-29-69	1	<0.05	<0.05	<0.05	–	–	–	–	–	<1X10³	<0.4
"	5-1-70	<1	<.05	<.05	<0.05	–	–	–	–	–	<1X10³	<0.4
TW-2	6-10-68	<1	2	<0.05	<0.05	–	–	–	–	–	–	1.1
"	2-25-69	1	1	<.05	<.05	–	–	–	–	–	–	.4
"	4-7-70	<1	1	<.05	<.05	–	–	–	–	–	<1X10³	.4
"	9-24-70	<1	1	<.05	<.05	–	–	–	–	–	<1X10³	1.0
"	6-1-71	2	2	<.05	<.05	–	–	–	–	–	<1X10³	.4
"	10-12-72	<1	<1	<.05	<.05	–	–	–	<350	–	<1X10³	<.2
TW-3	11-13-67	<1	8	<0.05	<0.05	–	–	–	–	–	–	0.5
"	11-17-67	<1	3	<.05	<.05	–	–	–	–	–	–	2.2
"	6-10-68	<1	3	<.05	<.05	–	–	–	–	–	–	2.4
"	2-25-69	<1	2	<.05	<.05	–	–	–	–	–	–	1.0
"	11-5-69	<1	2	<.05	<.05	–	–	–	–	–	–	.4
"	4-7-70	4	4	<.05	<.05	–	–	–	–	–	<1X10³	.4
"	9-23-70	<1	1	<.05	<.05	–	–	–	–	–	<1X10³	2.0
"	6-3-71	2	4	<.05	<.05	–	–	–	–	–	<1X10³	.4
"	10-12-71	<1	2	<.05	<.05	–	–	–	<350	–	<1X10³	<.4
"												

LA-9957-MS

Hydrologic Characteristics of the Main Aquifer in the Los Alamos Area:

Development of Ground Water Supplies

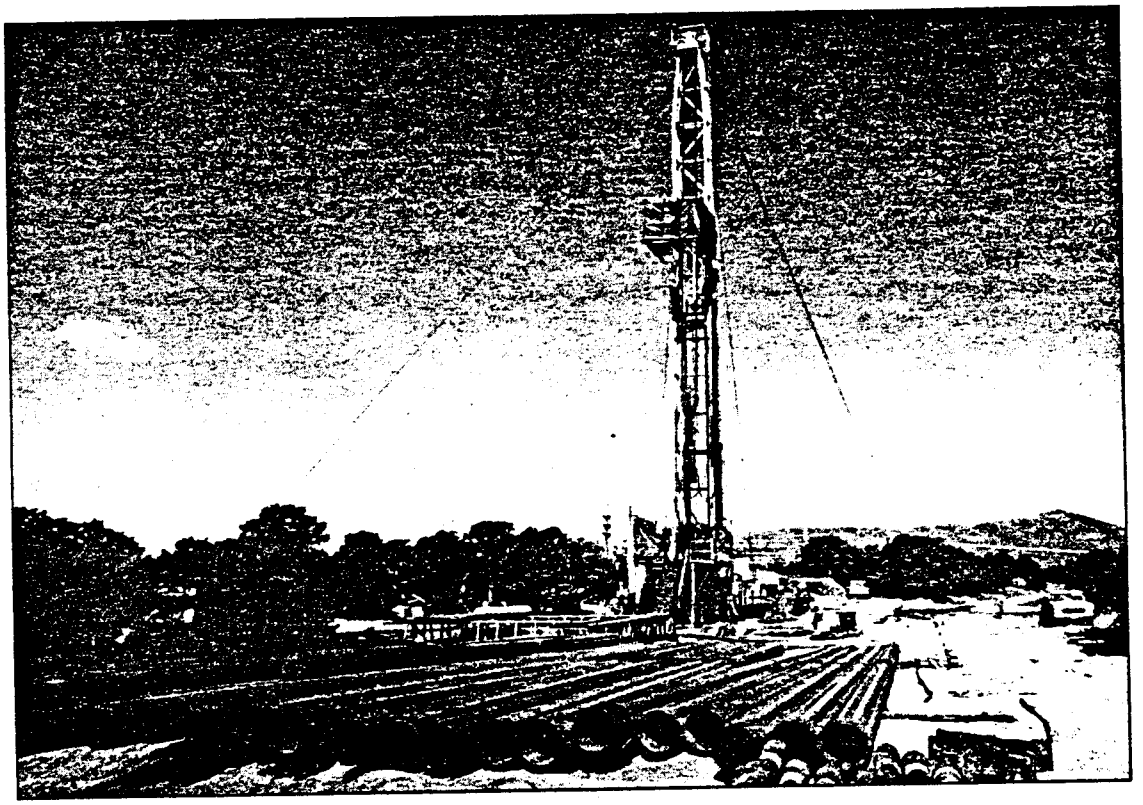

Los Alamos
Los Alamos National Laboratory
Los Alamos, New Mexico 87545

An Affirmative Action/Equal Opportunity Employer

Edited by Sharon Crane
Prepared by Kathy Derouin, Group HSE-8
Cover design by Gloria Sharp

DISCLAIMER

This report was prepared as an account of work sponsored by an agency of the United States Government. Neither the United States Government nor any agency thereof, nor any of their employees, makes any warranty, express or implied, or assumes any legal liability or responsibility for the accuracy, completeness, or usefulness of any information, apparatus, product, or process disclosed, or represents that its use would not infringe privately owned rights. Reference herein to any specific commercial product, process, or service by trade name, trademark, manufacturer, or otherwise, does not necessarily constitute or imply its endorsement, recommendation, or favoring by the United States Government or any agency thereof. The views and opinions of authors expressed herein do not necessarily state or reflect those of the United States Government or any agency thereof.

LA-9957-MS

UC-11
Issued: January 1984

Hydrologic Characteristics of the Main Aquifer in the Los Alamos Area: Development of Ground Water Supplies

W. D. Purtymun

Los Alamos National Laboratory
Los Alamos, New Mexico 87545

Los Alamos National Laboratory is operated by the University of California for the United States Department of Energy under contract W-7405-ENG-36.

HYDROLOGIC CHARACTERISTICS OF THE MAIN AQUIFER IN THE LOS ALAMOS AREA: DEVELOPMENT OF GROUND WATER SUPPLIES

by

W. D. Purtymun

ABSTRACT

Deep wells completed into the main aquifer have furnished 40.5×10^9 gal. of water for the Los Alamos National Laboratory and for the communities of Los Alamos and White Rock from 1947 through 1982. The main aquifer is within the siltstones and sandstones of the Tesuque Formation along the Rio Grande, and it rises westward into the lower part of the Puye Conglomerate beneath the central and western part of the Pajarito Plateau. The Laboratory and communities of Los Alamos and White Rock are located on the Pajarito Plateau.

Supply, test, and stock wells have been used to collect hydrologic data from the aquifer beneath the Pajarito Plateau and to the east along the Rio Grande. Hydrologic characteristics of springs along the Rio Grande, which are in the discharge area from the main aquifer, are included to supplement the data from the wells. Hydrologic characteristics of the aquifer determined from tests and observations are the saturated thickness, pumping or production rates of the wells, drawdown, specific capacity, field coefficient of permeability, transmissivity, rate of water movement in the aquifer, production from wells and fields, water-level trends of the aquifer, rates of water-level decline, and production per foot of water-level decline.

Chemical quality of water in the aquifer varies according to the formations yielding water to the wells. Based on hydrologic characteristics of existing wells, suggested locations for four additional wells were made in areas to develop high-yield low-drawdown (1000-gpm/100-ft) supply wells. These locations are recommended in long-range planning for future water supply as the demand for water increases at the Laboratory and in the communities. A well to replace well G-4 in the Guaje Field is recommended to offset declining production in the field.

I. INTRODUCTION

The Los Alamos National Laboratory and the communities of Los Alamos and White Rock are supplied by water pumped from deep wells in three well fields located in Los Alamos Canyon, in Guaje Canyon, and on the Pajarito Plateau. Production from these wells is from the main aquifer of the Los Alamos area. The main aquifer is the only aquifer that is capable of municipal and industrial supply. In addition to the 18 supply wells that penetrate into the main aquifer, 10 test wells and 2 stock wells in the Los Alamos area are completed into the main aquifer.

A. Purpose and Scope

Hydrologic data have been collected from 1947 through 1982 from supply and test wells. The data have been collected and published to ensure a continuing historical record to provide guidance for water management resources and long-range planning for the water supply sytem.[1-14] The purpose of this report is to evaluate this hydrologic data and to describe the hydrology of the main aquifer to provide support for long-range planning of locations for additional wells.

B. Geography

The facilities of the Los Alamos National Laboratory and the communities of Los Alamos and White Rock are located on the Pajarito Plateau. The Pajarito Plateau forms an apron 8 to 16 miles wide and 30 to 40 miles long around the eastern flanks of the Sierra de los Valles (Fig. 1). The surface of the plateau slopes gently eastward from an altitude of about 7800 ft along the flanks of the mountains to about 6200 ft along the eastern edge, where it terminates along the Puye Escarpment and White Rock Canyon. The plateau is drained by southeast- and eastward-trending streams that have cut deep canyons into the surface of the plateau.

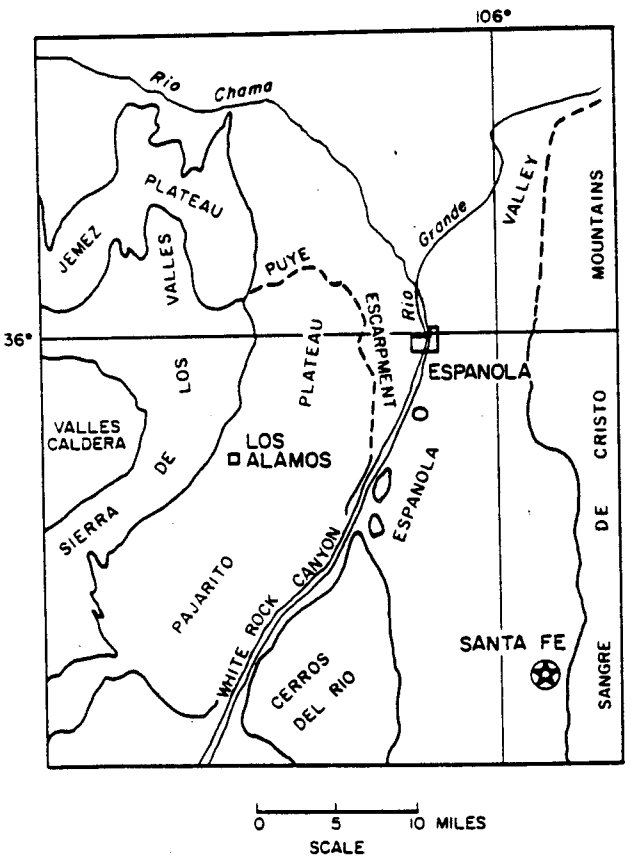

Fig. 1. Topographic features in the Los Alamos area.

The Rio Grande lies to the east of the plateau. It drops from an altitude of about 5500 ft at Otowi (mouth of Los Alamos Canyon) to about 5360 ft at the junction with Frijoles Canyon. North of Otowi the Rio Grande lies in a broad valley, whereas to the south it is confined in a deep narrow canyon (White Rock Canyon).

The mountain peaks of the Sierra de Los Valles rise to an altitude of about 11 500 ft near the head of Santa Clara Canyon and to an altitude of 10 200 ft near the head of Frijoles Canyon. The crest of the north/south-trending range of peaks and ridges forms a surface water divide. Streams originating on the eastern slopes and Pajarito Plateau flow directly into the Rio Grande. Streams on the western slopes follow a more circuitous course and enter the Rio Grande 75 miles to the south.

The climate and vegetation change westward from the Rio Grande to the crest of the Sierra de Los Valles, along with the change in altitude. The average precipitation increases from about 10 in. along the Rio Grande to as much as 30 in. along the crest of the mountains. The average annual precipitation on the plateau is about 18 in. About 70% of the precipitation occurs in July and August during summer thundershowers.

C. Definitions of Terms

A few of the hydrologic terms are defined for the convenience of the reader.

- Aquifer. A body of rocks or formations that contains sufficient permeable material to conduct ground water and to yield economically significant quantities of water to wells or springs.
- Saturated Thickness. The zone of complete saturation, which includes permeable and relatively impermeable rock units.
- Pumping or Production Rate. Reported in gallons per minute (gpm).
- Drawdown. The distance the water level in a well is lowered by pumping (ft).
- Specific Capacity. The rate of discharge of a water well per unit of drawdown (gpm/ft).
- Transmissivity. The rate at which water in an aquifer is transmitted through a unit width of the aquifer under unit hydraulic gradient (gpd/ft).

- Field Coefficient of Permeability. The rate of flow of water in gallons per day through 1 sq ft under a hydraulic gradient of 100% at prevailing temperature in the aquifer (gpd/ft^2).
- Rate of Movement in the Aquifer. Derived from the equation $V = PI/p$, where P = field coefficient of permeability in gpd/ft^2 (converted to ft^3), I = hydraulic gradient, and p = per cent porosity of saturated thickness ranging from 15% for fine sediments to 20% for sandstones and conglomerates.
- Production. Reported in gallons (gal.).

II. GEOLOGY

Drainage areas or streams that head on the flanks of the mountains are cut into the rocks of the Tschicoma Formation. Canyons on the Pajarito Plateau are cut into and are underlain by the Bandelier Tuff. Along the eastern edge of the plateau, the channel is cut through the Puye Conglomerate into the Tesuque Formation, which floors the valley north of Otowi on the Rio Grande and forms the lower canyon walls along the Rio Grande in White Rock Canyon (Fig. 1). The basaltic rocks of Chino Mesa are in places interbedded in the sediments of the Puye Conglomerate.

The rock units described, from oldest to youngest, are the Tesuque Formation, Puye Conglomerate, and basaltic rock of Chino Mesa of the Santa Fe Group; the Tschicoma Formation and Bandelier Tuff of the volcanic rocks of the Jemez Mountains; and alluvium and soil of recent age. The generalized geology, stratigraphy, and structure are presented as a basis for understanding hydrology of the main aquifer. Detailed geology can be found in Refs. 15-19. The geologic nomenclature used in this report is from Griggs.[17]

The generalized stratigraphic relations are shown on the geologic cross-section through the Pajarito Plateau, Fig. 2. A diagrammatic section correlation of rock units between supply and test wells is shown in Fig. 3.

A. Santa Fe Group

The Santa Fe Group, in ascending order, consists of the Tesuque Formation, Puye Conglomerate, and basaltic rocks of Chino Mesa (Fig. 2).

The Tesuque Formation is the oldest geologic formation to be considered in this report. It consists of a poorly to moderately cemented light-pink siltstone, silty sandstone, and a few lenses of pebbly conglomerate and clay. The sand-sized particles are dominantly quartz and feldspar; minor amounts of biotite, muscovite, and magnetite are also present. Rock fragments are rhyolite, gneiss, schist, limestone, and quartzite. Basalt flows are interbedded with the sediments of the Tesuque Formation. They generally are about 50 ft thick and contain interflow breccias of sediments.

The Tesuque Formation crops out along the Rio Grande and in lower Los Alamos and Guaje Canyons and underlies the Pajarito Plateau (Fig. 2).

Many individual beds in this formation are permeable and, where saturated, will yield water to a well. Some of the beds are relatively impermeable, and they restrict vertical and lateral movement of water within the formation. Beneath the Pajarito Plateau, coarse volcanic rock fragments of latite, basalt, rhyolite, tuff, and pumice predominate in the upper 1000 ft of the Tesuque Formation. These coarse sediments yield larger amounts of water to wells than do the finer sediments that predominate in the formation farther to the east along the Rio Grande.

The interbedded basalt flows in the Tesuque Formation may be fairly dense; when thin, they may be highly jointed and yield large amounts of water. Sediments of the interflow breccias between basalt flows are coarse and should yield water readily.

The Puye Conglomerate overlies the Tesuque Formation and consists of poorly to well-cemented detritus, which ranges in size from clay to large boulders (Fig. 2). The rocks that compose the conglomerate are latite, quartz latite, dacite, rhyolite, basalt, and pumice. Lenses and tongues of silt, clay, or pumice are common. The basal bed of the conglomerate is a slightly consolidated channel-fill deposit distinctive in composition, consisting of pegmatite gravel and boulders of quartzite, granite, gneiss, schist, and fragments of basalt and limestone.

The Puye Conglomerate crops out along the Rio Grande and thickens westward beneath the Pajarito Plateau. Along the western edge of the plateau, it interfingers in the subsurface with flow rocks of the Tschicoma Formation (Fig. 2). The Puye Conglomerate is highly permeable and, when saturated, it yields large amounts of water to wells.

The basaltic rocks of Chino Mesa consist of a series of basalt flows and interflow breccias. Individual flows generally are less than 50 ft thick; however, a series of flows may form a single thick-basalt unit. Interflow breccias of broken fragments of basalt and sediments may occur between individual flows.

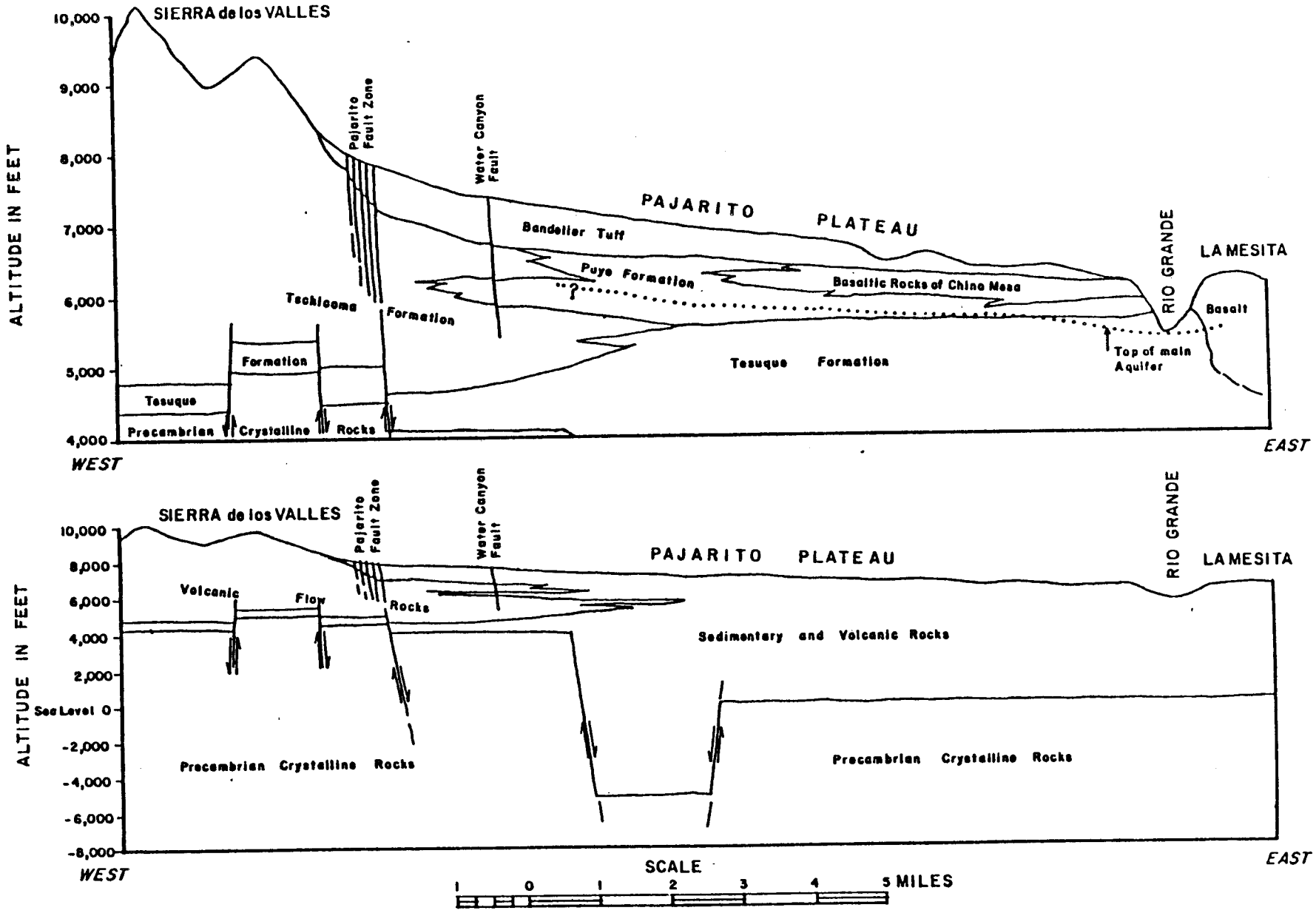

Fig. 2. Geologic section showing stratigraphy and structure from the Sierra de los Valles across the Pajarito Plateau to the Rio Grande.

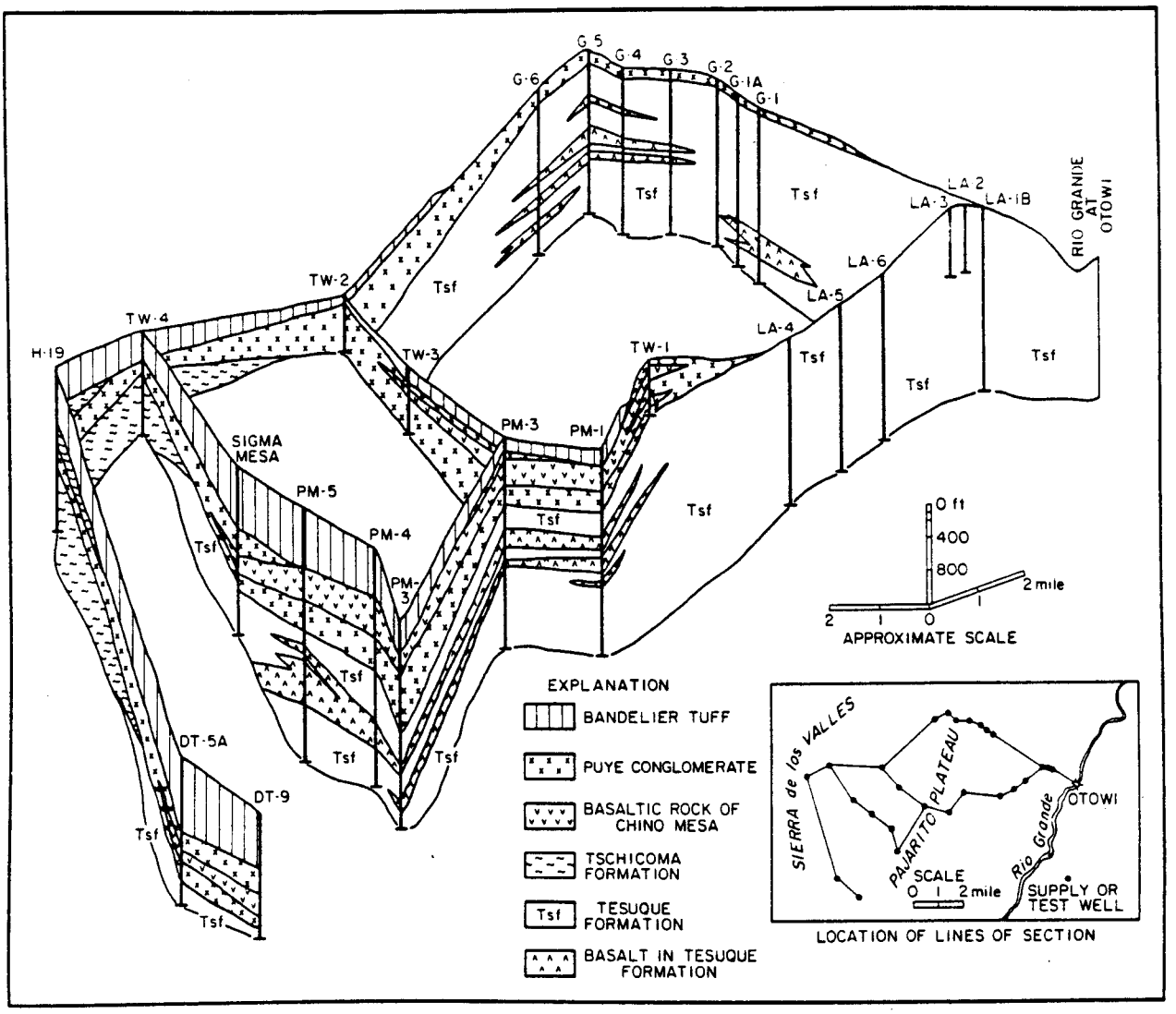

Fig. 3. Diagrammatic section of geologic units in the Los Alamos area.

A thick section of these rocks crops out along the Rio Grande in White Rock Canyon south of Los Alamos Canyon. The rocks thin westward beneath the Pajarito Plateau, where they interfinger in the subsurface with sediments of the Puye Conglomerate.

The basalt flows were extruded from centers east of the Rio Grande, and they flowed north, northwest, and west across the present course of the river. They form the eastern edge of a north/south-trending basin beneath the central part of the Pajarito Plateau (Fig. 3). The basin is filled with conglomerate that interfingers with the basalt; deposition of the conglomerate and emplacement of the basalts were contemporaneous. Thick sections of basalt into the subsurface and along the eastern margin of the Pajarito Plateau occur where the flows filled topographic lows in the Puye Conglomerate.

Thin basalt flows, separated by interflow breccias beneath the central part of the Pajarito Plateau, are permeable and when saturated, will yield water readily. Open joints and cavities in thick-basalt flows also yield water; however, along the Rio Grande (White Rock Canyon), steepening of the contours on the surface of the main aquifer indicates that thick-basalt flows form a barrier to movement of ground water (Fig. 4).

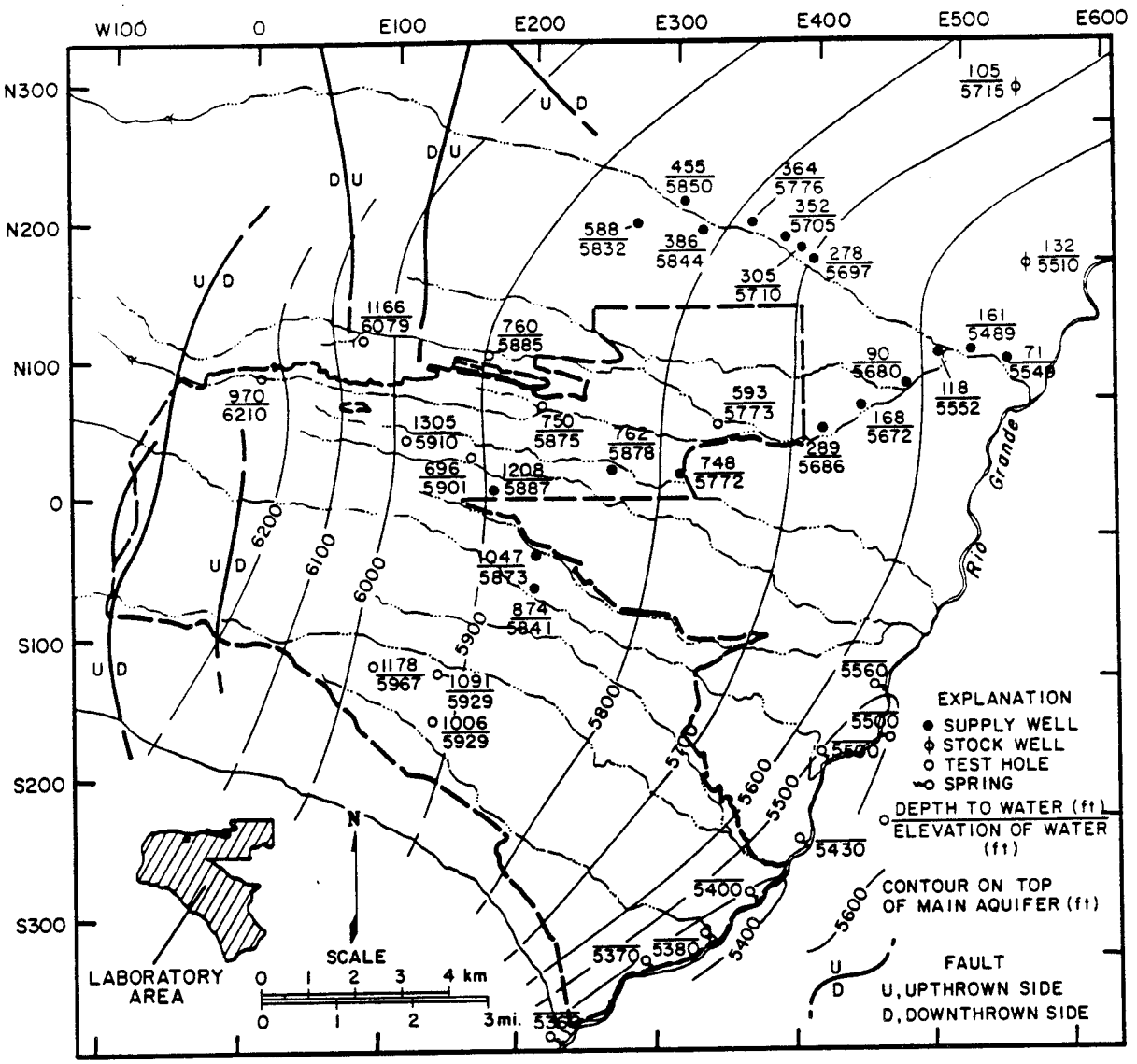

Fig. 4. Generalized contours on the surface of the main aquifer.

B. Volcanic Rocks of the Jemez Mountains

Volcanic rocks of the Jemez Mountains, along the eastern flanks of the Sierra de los Valles and on the Pajarito Plateau, consist of the Tschicoma Formation and the younger Bandelier Tuff (Fig. 2).

The Tschicoma Formation consists of flow and pyroclastic rocks composed of latite, quartz latite, dacite, and andesite. Interflow breccias of broken fragments of flow rocks and sediments occur between flows.

The Tschicoma Formation forms the Sierra de los Valles west of the Pajarito Plateau and is present in the subsurface beneath the western part of the plateau, where it interfingers with the Puye Conglomerate (Figs. 2 and 3).

The Tschicoma Formation has low permeability and thus retards and restricts the movement of ground water. Open joints and interflow breccias within the formation, which could yield appreciable amounts of water, are limited.

The Bandelier Tuff consists of a series of ash fall and ash flow tuff that is light grained and rhyolitic. The tuff contains quartz and sanidine crystals, pumice, and small fragments of other igneous rock in a matrix of fine ash shards.

The tuff overlies the older rocks and forms the surface of the Pajarito Plateau. The thickness ranges from about 1000 ft along the western margin of the plateau, where it laps onto the Tschicoma Formation, to less than 50 ft along the Rio Grande, where it overlies the Puye Conglomerate or the basaltic rocks of Chino Mesa (Fig. 2).

The tuff is above the main ground-water body and only in areas on the flanks of the Sierra de los Valles does it contain small amounts of perched water, which discharges from springs.

C. Alluvium and Soil

Alluvium from the Sierra de los Valles and the Pajarito Plateau has been deposited in the canyons of the plateau. Near the heads of the canyons, bedrock commonly is exposed in the lower parts, but farther down the canyons, alluvium may be several hundred feet wide and as much as 80 ft thick.

Alluvial deposits in the canyons heading on the flanks of the Sierra de los Valles contain cobbles and boulders with accompanying clay, silt, sand, and gravel derived from the Tschicoma Formation and Bandelier Tuff. Deposits in the canyons heading on the Pajarito Plateau contain clay, silt, sand, and gravel derived from the Bandelier Tuff. The alluvium contains some water in the larger canyons; however, the amount is insufficient for water supply.

Clayey soil derived from weathering of the Bandelier Tuff covers most of the fingerlike mesas of the Pajarito Plateau.

D. Structure

The Rio Grande depression is a structurally low area that constitutes the valley through which the Rio Grande flows.[20] The Pajarito Plateau is part of the depression, although it forms a topographic high area along the western margin of the valley.

The most prominent structural features of the Pajarito Plateau is the Pajarito fault zone, which trends northward along the western edge of the plateau. It is a part of the complex fault system that formed the Rio Grande depression. The fault zone consists of normal faults that are downthrown to the east and that displace rocks of the Bandelier Tuff, Puye Conglomerate, and Tschicoma Formation (Fig. 2). The displacement, estimated from the fault scarp, is from 400 to 500 ft. The amount of displacement decreases northward where, at a point north of Los Alamos, all visible traces of the fault disappear. The movement along the fault zone has been in small increments, which began before the deposition of the Bandelier Tuff and continued into post-Bandelier time. The displacement of the older rocks is greater than the displacement of the younger rocks. The major fault in this zone extends into and displaces the Precambrian rocks.

North of Los Alamos and east of the Pajarito fault zone, two normal faults cut the Bandelier Tuff, the Puye Formation, and the Tschicoma Formation. These faults, downthrown to the west, form a graben between them and the Pajarito fault zone. They are a part of the fault system that formed the Rio Grande depression.

Beneath the central part of the Pajarito Plateau, a north-trending depositional basin is formed in the Tesuque Formation. The basin is filled with volcanic debris of the Puye Conglomerate, overlain by the Bandelier Tuff. The eastern edge of the basin is formed by thick flows of basalt from Chino Mesa, 5 to 10 miles west of the Rio Grande (Fig. 2).

A gravity survey indicated that the deepest part of the Rio Grande depression (top of the Precambrian rocks) is in a north-trending trough near the center of the plateau. The bottom of this sediment-filled trough lies about 5000 ft below sea level (Fig. 2).[21]

III. MAIN AQUIFER OF THE LOS ALAMOS AREA

The main aquifer of the Los Alamos area is the only aquifer capable of municipal and industrial water supply. The upper surface of the main aquifer rises westward from the Rio Grande through the Tesuque Formation into the lower part of the Puye Conglomerate, beneath the central and western parts of the plateau (Fig. 2).[22] The water in the aquifer moves from the major recharge area in the Valles Caldera eastward toward the Rio Grande, where a part is discharged into the river through seeps and springs (Fig. 4).

The major recharge area for the aquifer is the intermountain basin formed by the Valles Caldera. The upper parts of the sediments in the basin are lacustrine deposits of clay, sand, and gravels, which are underlain by volcanic debris resulting from collapse of the caldera.[23] The sediments and volcanics in the basin are highly permeable and are saturated. The saturated "basin fill" recharges the main aquifer in sediments of the

Tesuque Formation. Minor amounts of recharge may occur in the deep canyons containing perennial streams on the flanks of the mountains. The intermittent streams in the canyon, which are cut into the plateau, add little, if any, recharge to the main aquifer.

Radiometric methods to date the age of the water in the main aquifer (time in transit from recharge to discharge) have been made using tritium and carbon-14. Tritium concentrations in water from wells from the Los Alamos and Guaje well fields have been less than 0.5 tritium units. Based on a natural occurrence of eight tritium units in precipitation (before hydrogen bomb tests), the age of the water in the aquifer in the two well fields is greater than 50 yr. Carbon-14 analyses of water from a well in the Pajarito Field at the eastern edge of the well have indicated that the age of water in the main aquifer is about 1400 yr. The radiometric age of water in the main aquifer indicates a slow rate of movement from the recharge area in the Valles Caldera.

The gradient on the surface aquifer, beneath the Sierra de los Valles and the western part of the Pajarito Plateau in the Los Alamos area, is about 120 ft per mile in the Tschicoma Formation interbedded with the Puye Conglomerate. As water in the aquifer moves into the more permeable sediments of the Puye Conglomerate in the central part of the plateau, the gradient increases to 60 to 80 ft per mile. The gradient decreases to 80 to 100 ft per mile along the eastern edge of the plateau as the water in the aquifer moves into the less permeable sediments of the Tesuque Formation (Fig. 4). The depth to the aquifer ranges from about 1200 ft along the western edge of the plateau, decreasing to about 600 ft along the eastern edge.

The Rio Grande is the principal area for ground water discharges from the main aquifer. A gain in streamflow in the Rio Grande in a 26-mile reach from the gaging stations at Otowi to Cochiti was computed at about 25 cfs.[24] Further investigation indicated that the river gained flow from Otowi to the mouth of the Frijoles Canyon, a distance of about 11.5 miles. Below Frijoles Canyon the Rio Grande is a losing stream.[25] Water from the river is lost to underlying sediments. It is estimated that the 11.5-mile reach of the canyon below Otowi receives a discharge from the main aquifer of 4300 to 5500 acre-feet annually.[26]

The main aquifer extends to the south into Bandelier National Monument. The movement of water in the Monument trends more to the south than east, as in the Los Alamos area. The depth to water along the western edge of the Pajarito Plateau in the Monument ranges from 1000 to about 1200 ft, with a gradient of 60 to 80 ft per mile. The Rio Grande above the mouth of Frijoles Canyon is a gaining stream, whereas below Frijoles Canyon the Rio Grande is a losing stream. Thus, the surface of the aquifer north of Frijoles Canyon is slightly above the river level, but the surface of the aquifer to the south is at an elevation below the river level.[25]

The main aquifer extends to the north of Los Alamos beneath the Pajarito Plateau around the northwestern flanks of the Sierra de los Valles. Water movement is to the east and northeast in the Puye Conglomerate and the Tesuque Formation beneath the Pajarito Plateau and within the Tesuque Formation in the Española Valley.

The thickness of the main aquifer is unknown; however, the Rio Grande depression contains over 15 000 ft of volcanic rocks and sediments that overlie the Precambrian crystalline rocks.[21] These volcanic rocks and sediments are potential aquifer.

The volcanic rocks and sediments that fill the depression are apparently saturated. Water quality will deteriorate at increased depth. Most of the wells in the depression yield fresh [less than 1000 mg/ℓ total dissolved solids (TDS)] to slightly saline water (1000 to 3000 mg/ℓ TDS).[27] The deepest well in the Los Alamos area penetrated about 2250 ft of sediments in the depression. The TDS concentrations from this well are about 500 mg/ℓ. It is estimated that the water in the depression will be fresh to a depth of 6000 to 7000 ft before the TDS will exceed 1000 mg/ℓ. Thus, the main aquifer in the area has a saturated thickness of at least 6000 ft before chemical quality may restrict the use of the aquifer for municipal and industrial supply.

A. Supply, Test, and Stock Wells

The Los Alamos Field is composed of five producing wells (LA-1B, 2, 3, 4, and 5). One well (LA-6) is on standby to be used only in case of an emergency because the water contains excessive amounts of arsenic. The field was constructed in 1946 and 1948. One well (LA-1B) was added to the field in 1960 (Fig. 5).

The Guaje Field is composed of seven wells. The field was constructed in 1950 and 1951. Well G-1A was added to the field in 1954 and well G-6 was added in 1964.

The Pajarito Field is composed of wells PM-1, 2, and 3, which were constructed in 1965 and 1966; well PM-4, added to the system in 1982; and well PM-5, completed in 1982 but not added to the system until late 1983.

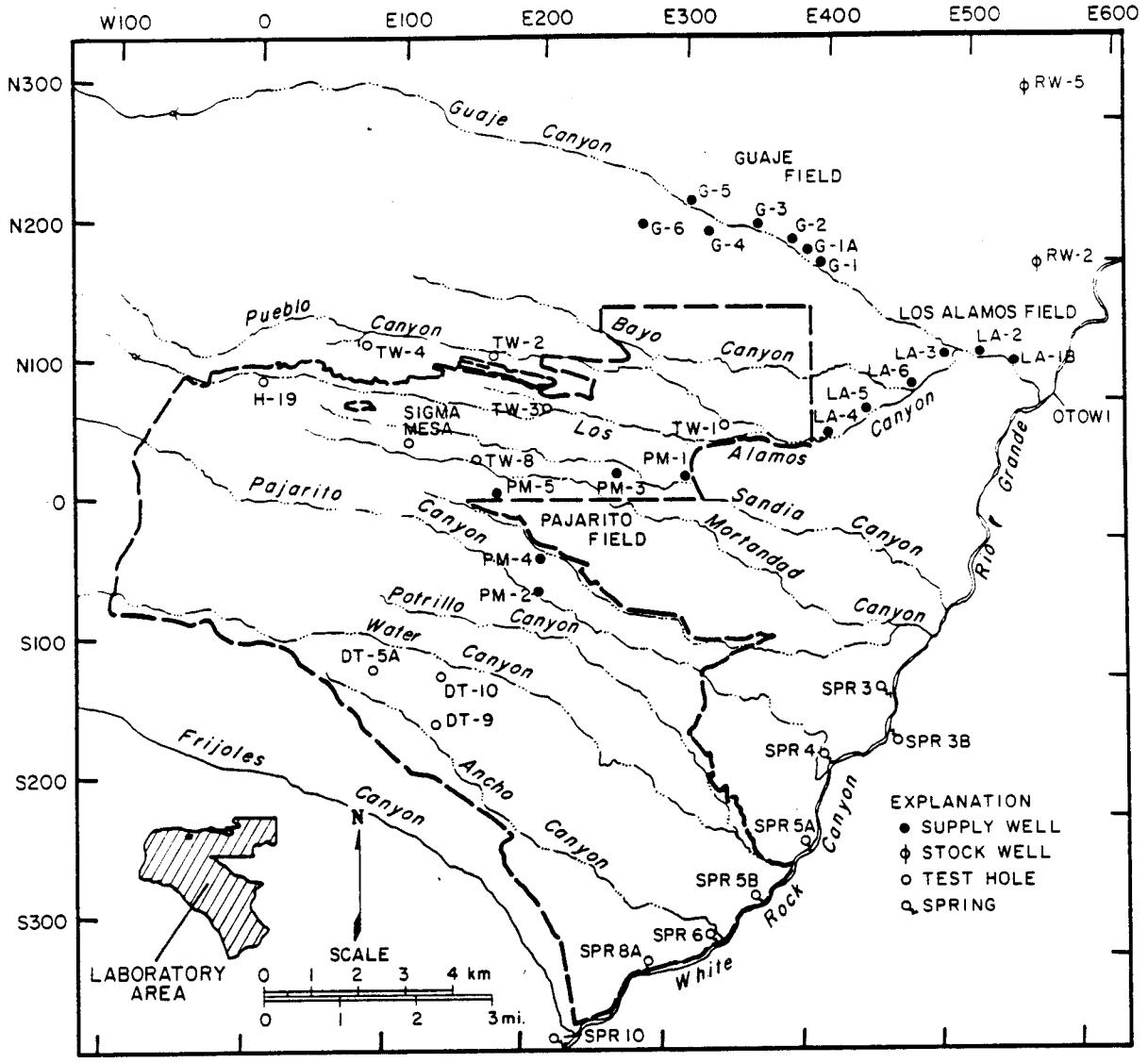

Fig. 5. Location of supply, test, and stock wells and springs in the Los Alamos area.

Construction and hydrologic data for the individual supply wells are presented in Appendix A.

Test wells TW-1, 2, 3, 4, and H-19 were drilled in 1949 through 1950 to determine the geologic and hydrologic characteristics of formations underlying the Pajarito Plateau. Test wells TW-1, 2, 3, and 4 are cased and are used as part of a well net that monitors the main aquifer.[28] Test well H-19 was abandoned uncased.

Test wells DT-5A, DT-9, and DT-10 were drilled in 1960 to evaluate the geologic and hydrologic conditions of a test site.[29] Test well TW-8 was drilled in 1960 to determine the geologic and hydrologic condition beneath a canyon disposal area for treated liquid low-level radioactive effluents.[30] Sigma Mesa was a test hole drilled in 1979 to determine geologic and hydrologic conditions related to possible development of geothermal energy for use at the Laboratory. The hole was scheduled for a depth of 10 000 to 12 000 ft; however, construction problems (lost circulation) terminated the hole at a depth of 2292 ft.

Two stock wells, equipped with windmills located on San Ildefonso Pueblo, were drilled in 1954 and 1955.

Nothing is known about hydrologic characteristics of the main aquifer, except for original water levels and chemical quality.

Construction and hydrologic data for the individual test and stock wells are presented in Appendix B.

Eight springs in White Rock Canyon were used in construction of the contours on the surface of the main aquifer and aid in interpretation of chemical quality of water in the main aquifer.[25] Hydrologic data for the springs are presented in Appendix C.

B. Production and Water-Level Fluctuations

Water from the wells in the Los Alamos Field is lifted vertically about 1800 ft through four booster stations into storage in the Laboratory and community areas. The water from the Guaje Field is lifted vertically about 1500 ft through four booster stations into storage. In the Pajarito Field, wells PM-1 and PM-3 supply the community of White Rock. The water is produced from the wells to storage. Wells PM-2, 4, and 5 can be used to supply White Rock, or their output can be lifted about 800 ft vertically into the Laboratory or community area through two booster stations.

The total production from well in the three wells fields from 1947 through 1982 has been 40 496 × 10^6 gal. (Table I). Production from three test wells in the southern area of the Laboratory (DT-5A, DT-9, and DT-10) was measured during testing after completion in 1960.

The main aquifer beneath the western and central part of the Pajarito is under water table conditions, whereas along the eastern margin and Rio Grande it is under artesian conditions.[26] In 1946 a number of test holes were drilled along the Rio Grande, north of Otowi and in the lower part of Los Alamos Canyon, to determine if a water supply could be developed in this area.[31] Three test holes along the Rio Grande drilled to a depth of 475 to 495 ft were artesian, as were the four test holes ranging in depth from 375 to 475 ft in lower Los Alamos Canyon.[31]

Supply wells LA-1 (abandoned and replaced by LA-1B), LA-2, and LA-3, which were completed in late 1946 and 1947 and cased to a depth of 870 ft, also were artesian and flowed when completed.[32] Pumpage soon reduced the artesian pressure, and water levels were below the well head. Other wells in Los Alamos Field (LA-4, -5, and -6) probably encountered semiartesian conditions, as did some of the wells in Guaje Canyon (G-1, G-1A, and G-2) and in the Pajarito Field (PM-1 and -3).

The hydrostatic pressures increased with depth. In 1960 the water levels in the lower part of the Los Alamos Field (LA-1, -2, and -3) ranged from 13 to 76 ft below the well head. Well LA-1B, 150 ft northeast of abandoned well LA-1, was drilled to a depth of 2256 ft and was cased and gravel packed to 1750 ft. The well began flowing during development. The well flow increased to about 100 gpm. The well was shut in and pressures measured over a 30-day period. Shut-in pressure was 13 psi, which is equal to a head of water 34 ft above the land surface.[26] Pumpage in the first month reduced the artesian pressure so that the water levels were below land surface. If the well is not pumped for several months, the water level rises in the well; several times in the last 20 yr, the well flowed for short periods of time before artesian pressures were reduced by pumpage.

Months of heavy production generally occur in June, July, and August and months of light production are in December, January, and February. The differences in demand for periods of heavy-to-light production (summer to winter) are mainly due to the use of water for lawn and yard irrigation. As a result, the water levels in the wells fluctuate with production. The highest water level occurs during the winter and lowest water level occurs during the summer.

1. Los Alamos Field. The wells in the Los Alamos Field produced 14 503 × 10^6 gal. of water from 1947 through 1982. This pumpage was 36% of the total pumpage from the three well fields (Table I).

Water levels in the individual wells have generally declined in response to the pumpage. The water-level declines from 1950 through 1982 in wells LA-2, -3, -4, -5, and -6 have ranged from 7 ft in LA-6 to 72 ft in LA-2. The water-level decline in well LA-1B from 1960 through 1982 has been 64 ft. In general, the largest amount of water-level decline has occurred in the lower part of the field (LA-1B, -2, and -3) and the least amount of decline in the upper part of the field (LA-4, -5, and -6). The average decline in the lower part of the field has been 52 ft from 1950 through 1982, whereas the lower field has produced 35% of the water from the field. The average water-level decline in the upper part of the field has been 21 ft from 1950 through 1982, whereas the upper field has produced 65% of the water from the field (Table I).

TABLE I

PRODUCTION FROM THE LOS ALAMOS, GUAJE, AND PAJARITO WELL FIELDS
1947-82

	Pumpage (10^6 gal.)	Percentage of Field	Percentage of Total
Los Alamos Field			
Well LA-1[a]	154	1	<1
Well LA-1B	1964	14	5
Well LA-2	1305	9	3
Well LA-3	1644	11	4
Well LA-4	3503	24	9
Well LA-5	3049	21	8
Well LA-6[b]	2884	20	7
Total	14 503	100	~36
Guaje Field			
Well G-1	2402	16	6
Well G-1A	2937	20	7
Well G-2	2520	17	6
Well G-3	2040	13	5
Well G-4	1217	8	3
Well G-5	2790	19	7
Well G-6	1077	7	3
Total	14 983	100	37
Pajarito Field			
Well PM-1	1593	14	4
Well PM-2	5863	53	14
Well PM-3	3478	32	9
Well PM-4	76	1	<1
Well PM-5	---	---	---
Total	11 010	100	~27
Total	40 496	---	~100

[a]Production 1946 to 1952 and 1955 to 1956 (well abandoned).
[b]Production from 1948 to 1976, well on standby production, pumped to wastes 1977 to 1982.

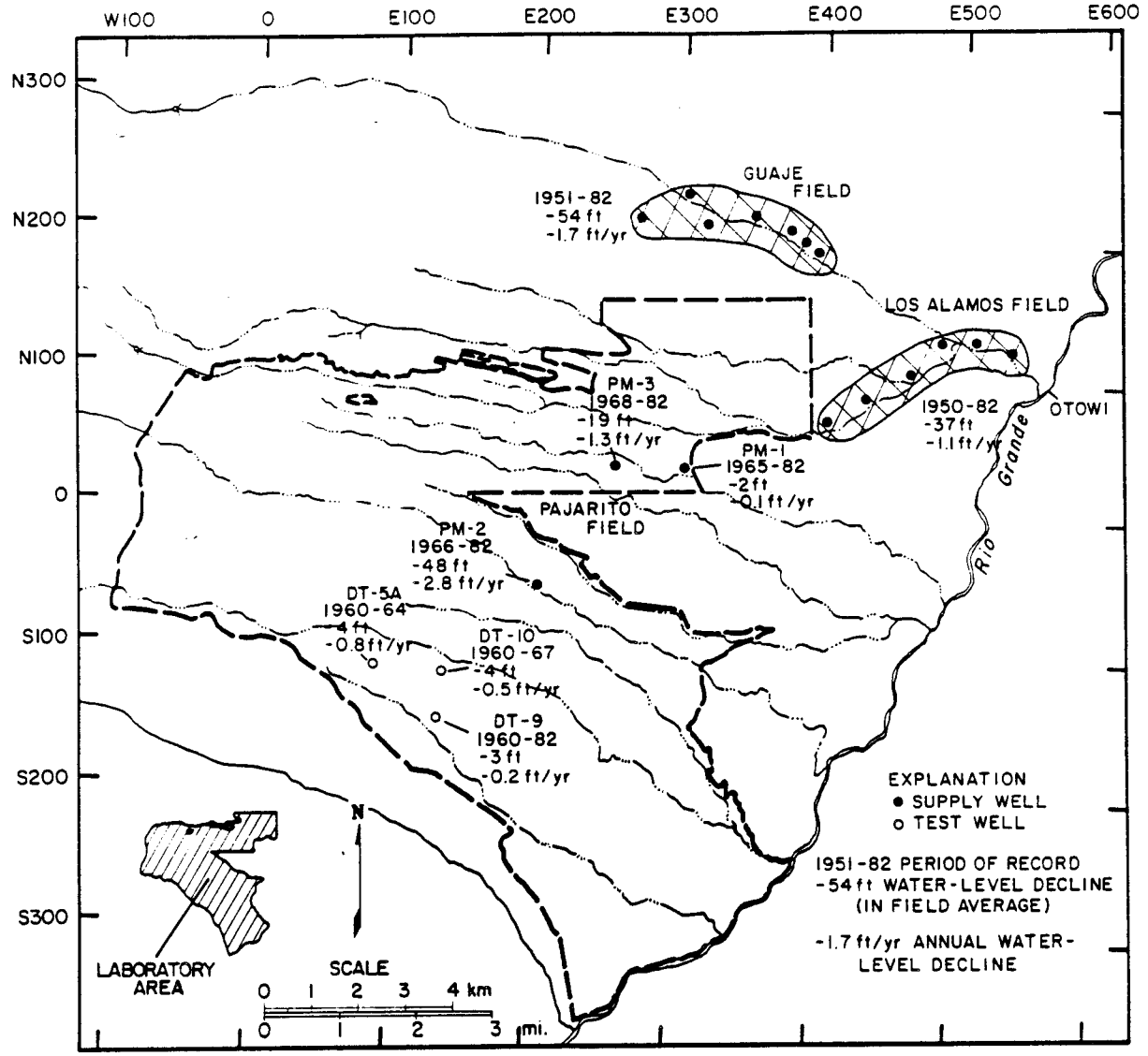

Fig. 6. Water-level declines in well fields and supply and test wells.

The average water-level decline in the Los Alamos Field from 1950 through 1982 has been 37 ft, with an average annual rate of decline of 1.1 ft/yr (Fig. 6). Production of 14 503 × 10^6 gal. and a water-level decline of 37 ft equal the production of 392 × 10^6 gal. of water per foot of water-level decline in the field (Fig. 7).

2. Guaje Field. The wells in the Guaje Field produced 14 983 × 10^6 gal. of water from 1951 through 1982. This pumpage was 37% of the total pumpage from the three well fields (Table I).

Water levels in the individual wells have responded to the amount of pumpage resulting in a general decline. Water-level declines from 1951 through 1982 in wells G-1, -1A, -2, -3, -4, and -5 have ranged from 29 to 93 ft. The water level in well G-6 from 1964 through 1982 has been 7 ft. The largest decline has been in the lower part of the field (G-1, -1A, -2, and -3), where production has been the greatest. The average decline has been about 75 ft, whereas about 66% of the total production from the field has been from these wells. The average decline in the upper field (G-4, -5, and -6) has been about 26 ft.

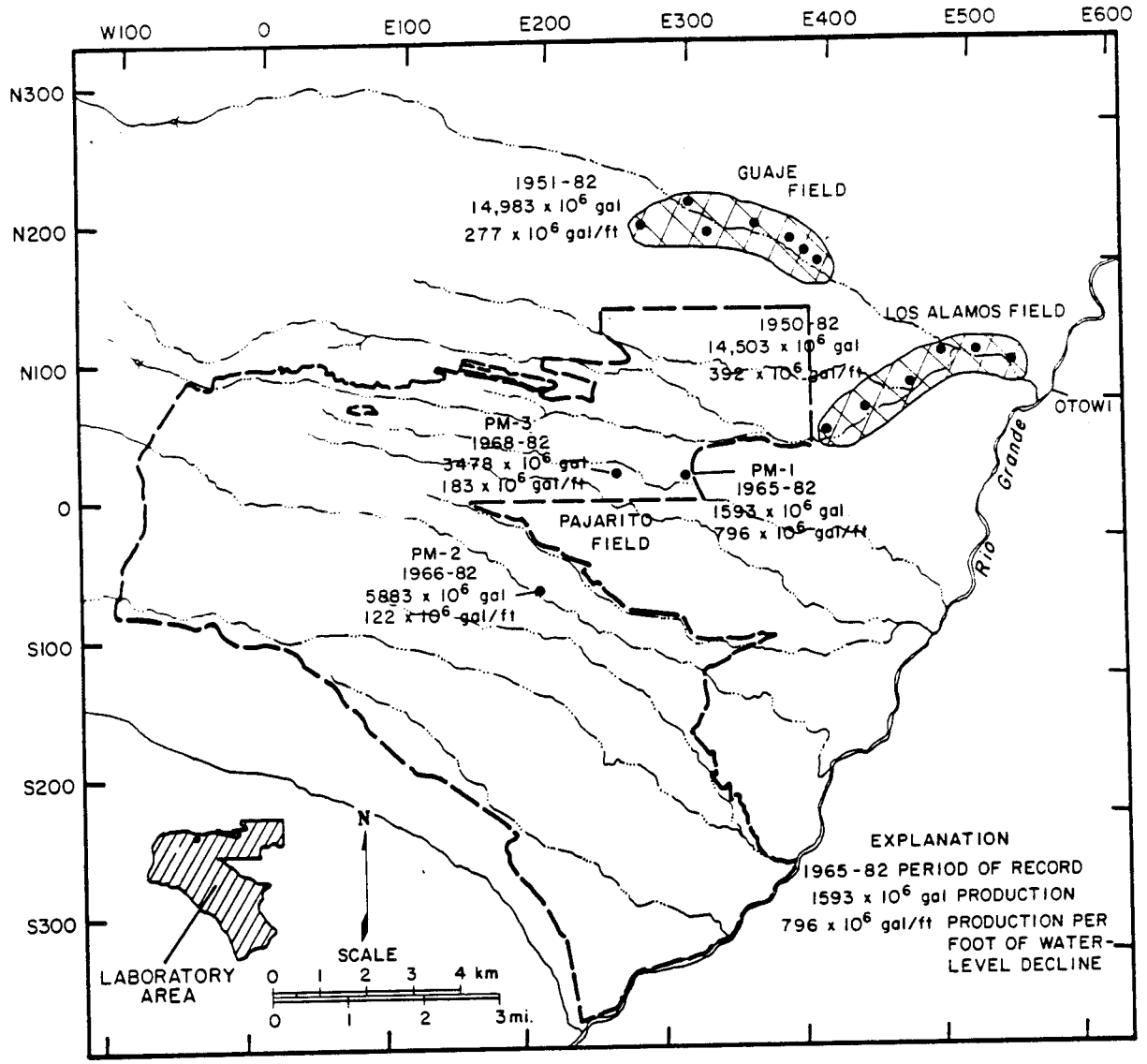

Fig. 7. Water-level declines related to production from well fields and supply wells.

while 34% of the total production has been from these wells.

The larger amount of production from the lower field is based on greater pumping rates. The declines are as anticipated for amount of pumpage and are not considered significant.

The average water-level decline in the Guaje Field for the period 1951 through 1982 has been 54 ft with an average annual rate of decline of 1.7 ft/yr (Fig. 6). The production of 14 983 × 10^6 gal. and a water-level decline of 54 ft equal the production of 277 × 10^6 gal. of water per foot of water-level decline in the field (Fig. 7).

3. Pajarito Field. The well in the Pajarito Field produced 11 010 × 10^6 gal. for the period 1965 through 1982. The pumpage was mainly from PM-1, -2, and -3, because production from PM-4 began in July 1982 and construction of the transmission system of PM-5 has not yet been completed. The pumpage from the field was 27% of the total pumpage from the three well fields (Table I). The water levels in the individual wells respond to the amount of pumpage, resulting in a general water-level decline.

The water level in well PM-1 declined 2 ft from 1965 through 1982 or at a rate of about 0.1 ft/yr (Fig. 6). The

pumpage during this period was about 1593×10^6 gal. or 14% of the field total (Fig. 6 and Table I). The water level declined during production of 796×10^6 gal./ft for the period 1965 through 1982. As the well PM-1 was pumped, the well continued to develop while allowing new water-bearing beds to contribute to the pumpage from the well. This is evident in the specific capacity, which increased each year from 15 gpm/ft in 1965 to 27 gpm/ft in 1982. This has resulted in the highest ratio in these wells of production to total water-level decline (Fig. 7).

The water level in well PM-2 declined 48 ft from 1966 through 1982, at a rate of 2.8 ft/yr (Fig. 6). The pumpage during this period was 5863×10^6 gal., or about 53% of the field total. This is a high-yield well with a pumping rate of about 1400 gpm.

In the 18 years that well PM-2 was in operation, it produced 14% of the total production from all three well fields (Table I). The production during the period 1966 through 1982 was 5863×10^6 gal. with a water-level decline of 42 ft. This equals the production of 122×10^6 gal./ft of water-level decline (Fig. 7). Specific capacities varied slightly at about 23 gpm/ft but showed no significant trends for the period 1966 through 1982. There was little indication from the specific capacity that there was any further development of the well after it was placed in service.

The water level in well PM-3 declined 19 ft from 1968 through 1982, at a rate of 1.3 ft/yr (Fig. 6). The pumpage during this period was 3478×10^6 gal. or about 32% of the field total (Table I).

PM-3 is a high-yield well with a pumping rate of 1400 gpm. In 15 yr of service, it has produced 9% of the total water produced at Los Alamos from 1947 through 1982 (Table I). The specific capacity of the well has increased from 48 gpm/ft in 1968 to about 61 gpm/ft in 1982. Based on specific capacity and production rates, this is the best well in the system. The water level has declined during production of 183×10^6 gal./ft during the period 1968 through 1982 (Fig. 7).

Well PM-4 was completed in 1982 and was placed in production in July. The well produced 76×10^6 gal. for the remaining 6 months of 1982. Water level, nonpumping and pumping, rose slightly as the well developed while it was pumped. The pumping cleaned out the drilling mud and fine silts, clays, and sands that were left in the gravel pack and water-bearing formations when the well was drilled. The specific capacity increased from 30.0 gpm/ft to 36.8 gpm/ft from July to December. It is also a high-yield well with a pumping rate of 1470 gpm and a high specific capacity. Based on production rates and specific capacity, this is the second best well in the system.

Well PM-5 was completed in 1982 and has not been equipped or connected to the system. Tests of the well indicate that the pump will be rated at about 1225 gpm, which will result in a drawdown of about 144 ft, with a specific capacity of about 8.5 gpm/ft of drawdown. The well will probably develop with pumpage when put into production, resulting in a smaller drawdown and a greater specific capacity.

4. Test Wells. Test well DT-5A was pumped for a 24-h period for testing early in 1960. The amount of water produced was about 0.1×10^6 gal. The water level recovered after the test and showed no effect of the pumpage. During the period 1960 through 1964 after the test, the well was not equipped with a pump. During this period the water level declined about 4 ft or at a rate of 0.8 ft/yr (Fig. 6). The decline is under normal conditions (lack of recharge), not as the result of pumpage.

The test well DT-5A was equipped with a pump in 1970. Since that time, the well has produced about 0.3×10^6 gal. for collection of samples for chemical and radiochemical analyses. The well is pumped twice a year at about 5 gpm for about 2 days before sampling. The amount of water removed from the aquifer is small, and if any decline occurred from pumpage, it would be insignificant and immeasurable from one pumping period to the next (6 months later).

Test well DT-9 was pumped for a 24-h period early in 1960. The amount of water produced was about 0.1×10^6 gal. The water levels recovered after that and showed no effect of the pumpage. During the period 1960 to 1982 after the test, the well was not equipped with a pump. Water was bailed out for sample collection. No more than 500 gal. have been removed from the well since 1960. The small amount of water removed from the well would not result in significant water-level changes in the aquifer.

The well DT-9 is 0.75 mile south of well DT-10 and 1.25 miles southeast of well DT-5A, so that the small amount of water pumped from these wells will not affect the water level of well DT-9 (Fig. 2). Well DT-9 was equipped with a water stage recorder from 1960 to 1968 and 1970 to 1982. A continuous water-level record was obtained from the recorder. Water-level data were compiled into average annual measurements to illustrate

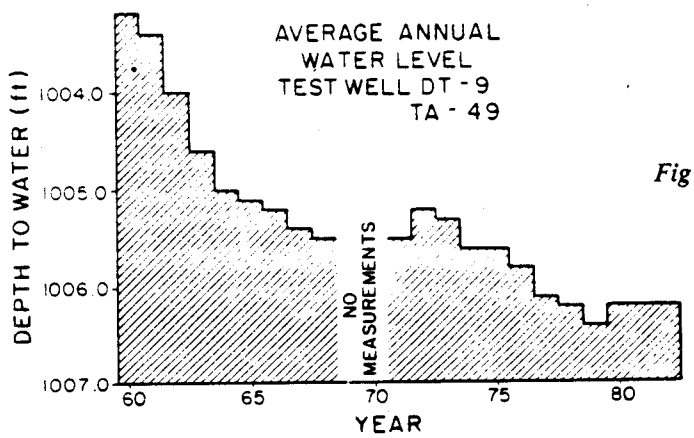

Fig 8. Average annual water levels in Test Well DT-9, 1960 to 1968 and 1971 to 1982.

water-level trends over a period of 22 yr. This reflects normal water-level fluctuations and trends for the region. The water level in the well declined from 1003 ft to 1006 ft from 1960 through 1982 (or at an average rate of about 0.1 ft/yr) (Fig. 8). The most rapid decline occurred from 1960 to 1968,when the decline was 2.3 ft or about 0.3 ft/yr (Fig. 8). The annual average water level rose 0.3 ft from 1971 to 1972, then declined 1.2 ft to 1979. Since 1979 the water level has remained about the same. The fluctuation of water levels reflects normal regional water-level trends. The decline in water levels shows deficient recharge, with only one period (1971) of recharge exceeding the normal discharge of the aquifer in White Rock Canyon.

The well and records from the water stage recorder were used in a special study, "Air Volume and Energy Transfer Through Test Holes and Atmospheric Pressure Effects on the Main Aquifer."[33] The main aquifer is very sensitive to atmospheric pressure changes, earth shocks, and probable earth tide effects. These effects (water-level fluctuation) were monitored by a continuous water stage record on well DT-9.

The possible earth tide effects are recorded by minor water-level fluctuations in which the gravitational pull of the moon elongates and compresses the aquifer. These effects, estimated from records by eliminating atmospheric effects, range from 0.01 to 0.03 ft of water-level fluctuation.

Water-level fluctuations are also recorded from earth shocks. In general, these are the result of strong earth motion. Records of the Alaskan earthquake of 1964 caused a water-level fluctuation of more than 1 ft in well DT-9. Small fluctuations have occurred, generally less than 0.10 ft, which are attributed to major earthquakes in Mexico or Central America. These water-level fluctuations are caused by expansion and compaction of the aquifer by surface waves of the earthquake.[33]

Test holes or wells in the Bandelier Tuff and Puye Conglomerate transfer air to and from the tuff and conglomerate in response to changes in atmospheric pressure. Test holes tend to "blow air" during barometric lows and to "suck air" during barometric highs. The air is transferred to and from the unsaturated zone above the main aquifer. The changes in atmospheric pressure also cause water-level fluctuations. During a storm in December 1967, a fluctuation of over 0.6 ft was recorded. Minor changes in atmospheric pressure also cause water-level fluctuations.

During a special study, October 10 through 14, 1964, four cycles of pressure changes were correlated with four cycles of water-level fluctuations. Increased atmospheric pressure caused water-level declines, and a decrease in pressure caused the water level to rise. The changes in water level, atmospheric pressure, and rates of air transfer from the test holes were correlated.[33]

The barometric efficiency of the aquifer can be expressed in terms of a column of water. The ratio of water-level changes to pressure changes expresses the barometric efficiency of the aquifer. During the four cycles of water-level and atmospheric pressure changes, the barometric efficiency of the aquifer ranged from 51 to 88%. The smaller pressure changes with smaller volumes of air transferred resulted in greater barometric efficiency.

The aquifer penetrated by DT-9 is not homogeneous but is made up of three different formations (conglomerate, basalts, and sandstones) with three different transmissibilities and probably three different pressure

heads (water pressures in each unit). The variations in barometric efficiency are the result of the combined different pressures within each formation.[33]

Test well DT-10 was equipped with a pump for a 24-h period for testing in early 1960. The amount of water produced was about 0.1×10^6 gal. The water level recovered after the test and showed no measurable effect of the pumping. During the period 1960 to 1967, the water level declined about 4 ft or at an annual rate of 0.5 ft/yr. The well was not equipped with a pump during this period. Water-level decline was normal, not from pumpage, but because of lack of recharge to the aquifer.

It was not until 1979 that well DT-10 was equipped with a pump. The well is pumped twice a year at a rate of about 6 gpm for a period of 4 h. The amount of water produced during the past 4 yr is small (0.02×10^6 gal.). Any resulting water decline caused by pumpage would be too small to measure from one pumping period to the next pumping period.

Test well TW-8 was bailed for testing in December 1960. The amount of water removed during the test was about 2.0×10^3 gal. Recovery to the original water level was completed 8 min after the bailing ended.[33] The water-level decline from 1960 to 1965 was about 1 ft or about 0.2 ft/yr. This is a normal water-level decline.

In 1972 a pump was installed on TW-8. The well is pumped at about 6 gpm for a 2-h period twice a year. Thus, since 1972 about 0.03×10^6 gal. of water have been pumped from the well for collection of samples.

C. Hydrologic Characteristics

Hydrologic characteristics, pumping rates, specific capacities, transmissivities, and field coefficients of permeability were determined during aquifer tests or during periods of production from the wells or test holes (Fig. 9). The rock type or formation that forms the aquifer determines the hydrologic characteristics of the particular well or test hole (Table II). Wells in the Los Alamos and Guaje Fields are complete in the Tesuque Formations. Basalt flow occurs in the Tesuque Formation within the Guaje Field but is absent in the Los Alamos Field. Test well TW-4 is complete in the Tschicoma Formation. Supply wells in the Pajarito Field and test wells DT-5A, DT-9, and DT-10 are complete in the Puye Conglomerate and Tesuque Formation. Test wells TW-1, -2, -3, and -8 are complete in the Puye Conglomerate. Various thicknesses of saturation and different amounts of fines, such as silts, clays, and very fine sands in the various rock types. result in different hydrologic characteristics.

1. Tesuque Formation. The wells in the Los Alamos Field are completed in the fine sediments of the Tesuque Formation. The sediments contain no interbedded basalts (Fig. 3). The saturated thicknesses penetrated by the wells range from 709 to 1700 ft with an average of 1350 ft. At an average pumping rate of 365 gpm, the average specific capacity is 4.5 gpm/ft of drawdown, an average drawdown of 91 ft. Based on production characteristics of the well field, a drawdown of >125 ft results in excessive sand produced with water, which shortens the life of the pumps.

The field coefficient of permeability ranges from 3.0 to 9.3 gpd/ft^2 with an average of 5.6 gpd/ft^2. Transmissivity of the aquifer ranges from 2.5×10^3 to 15.7×10^3 gpd/ft with an average 8.4×10^3 gpd/ft (Fig. 9). The rate of movement of water in the aquifer, based on hydrologic characteristics and gradient on the top of the main aquifer in the Los Alamos Field, is estimated at 20 ft/yr within the upper 1350 ft of the aquifer (Fig. 10).

2. Tesuque Formation with Interbedded Basalts. All wells in the Guaje Well Field penetrated the sediments with interbedded basalts, except one well, G-2 (Fig. 3). The saturated thickness of the aquifer ranged from 942 to 1722 ft with an average of 1410 ft. At an average pumping rate of 376 gpm, the average specific capacity was 5.8 gpm/ft of drawdown or an average drawdown of 65 ft.

The field coefficient of permeability ranged from 5.3 to 11.3 gpd/ft^2 with an average of 8.2 gpd/ft^2. The average transmissivity of the aquifer in the Guaje Field is 11.6×10^3 gpd/ft.

The rate of movement of water in the upper 1410 ft of the aquifer of sediments and basalts in the Guaje Field is estimated at 35 ft/yr (Fig. 10).

3. Tschicoma Formation. Test well TW-4 was completed into a brecciated zone within the Tschicoma Formation. The saturated thickness was about 40 ft, and the specific capacity was low at 0.6 gpm/ft during a pumping rate of 2.8 gpm. The transmissivity low was at 0.75×10^3 gpd/ft and the field coefficient of permeability averaged 19 gpd/ft^2. The rate of movement of water in the 40 ft of the aquifer in the brecciated zone is estimated at 50 ft/yr (Fig. 10).

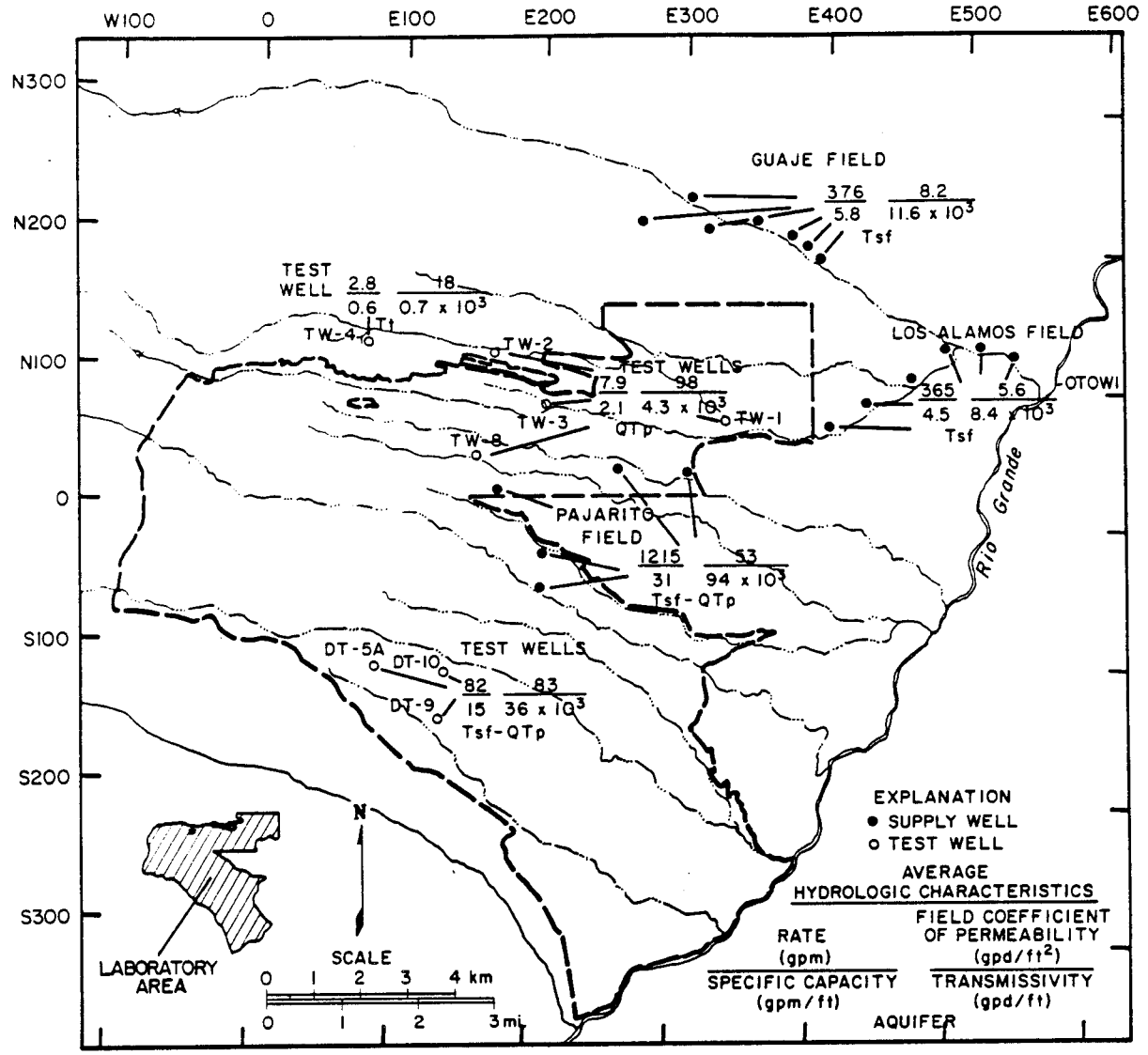

Fig. 9. Hydrologic characteristics of the main aquifer.

Test well H-19 encountered water in the lower part of the Puye Conglomerate underlain by a massive flow of Tschicoma Formation would yield very little water to the well. Tests indicated that the saturated section of the Tschicoma Formation (joints and brecciated zone between the flows) was relatively impermeable and was not a source of water supply.[17]

4. Tesuque Formation and Puye Conglomerate. The well in the Pajarito Field and test wells DT-5A, DT-9, and DT-10 penetrated the main aquifer in the lower part of the Puye Conglomerate and the Tesuque Formation. The Pajarito Field and test wells are located on the Pajarito Plateau. Beneath the plateau, the Tesuque Formation contains interbedded basalt flows.

The saturated thickness of the Puye Conglomerate in the Pajarito Field ranged from 50 to 535 ft with an average thickness of 270 ft, although the saturated thickness of the underlying Tesuque Formation ranged from 890 to 1700 ft with an average thickness of 1470 ft. At an average pumping rate of 1215 gpm, the average specific capacity is 31 gpm/ft of drawdown or an average drawdown of 40 ft (Fig. 9).

The field coefficient of permeability of the combined Puye Conglomerate and Tesuque Formation is 53 gpd/ft^2 with an average transmissivity of 94 × 10^3 gpd/ft.

TABLE II

AVERAGE HYDROLOGIC CHARACTERISTICS OF THE MAIN AQUIFER IN THE LOS ALAMOS AREA

	Saturated Thickness (ft)	Rate (gpm)	Specific Capacity (gpm/ft)	Field Coefficient of Permeability (gpd/ft^2)	Transmissivity (10^3 gpd/ft)
Los Alamos Field (Tesuque Formation)	1350	365	4.5	5.6	8.4
Guaje Field (Tesuque Formation and interbedded basalt)	1410	376	5.8	8.2	11.6
Pajarito Field (Tesuque Formation and Puye Conglomerate)	1740	1215	31	53	94
Test Hole TW-4 (Tschicoma Formation)	40	2.8	0.6	18	0.7
Test Holes DT-5A, -9, and -10 (Tesuque Formation and Puye Conglomerate)	490	82	15	83	36
Test Holes TW-1, -2, -3, and 8 (Puye Conglomerate)	60	7.9	2.1	98	4.3

Rate of movement of water in the combined thickness of 1740 ft of Puye Conglomerate and Tesuque Formation is 95 ft/yr (Fig. 10).

The saturated thickness of the Puye Conglomerate in the three test wells (DT-5A, -9, and -10) ranged from 310 to 355 ft with an average of 340 ft. The saturated underlying Tesuque Formation ranged from 15 to 290 ft with an average of 150 ft. At a pumping rate of 82 gpm, the average specific capacity was 15 gpm/ft of drawdown or about 5.5 ft of drawdown (Fig. 9).

The average field coefficient of permeability of the Puye Conglomerate and Tesuque Formation penetrated by the test holes was 83 gpd/ft^2, where the average transmissivity was 36 × 10^3 gpd/ft. The rate of movement of water in the 490 ft of aquifer penetrated by the test hole was 345 ft/yr (Fig. 10).

5. Puye Conglomerate. Test wells on the plateau that are complete within the main aquifer in the Puye Conglomerate are TW-1, -2, -3, and -8 (Fig. 3). The saturated thickness of the conglomerate ranges from 29 to 97 ft with an average of 60 ft. At an average pumping rate of 7.9 gpm, the specific capacity is 2.0 gpm/ft of drawdown or an average drawdown of 17 ft. The average field coefficient of permeability is about 98 gpd/ft^2 with an average transmissivity of 4.3 × 10^3 gpd/ft (Fig. 9). The rate of movement of water in the Puye Conglomerate with an average thickness of 60 ft is about 250 ft/yr (Fig. 10).

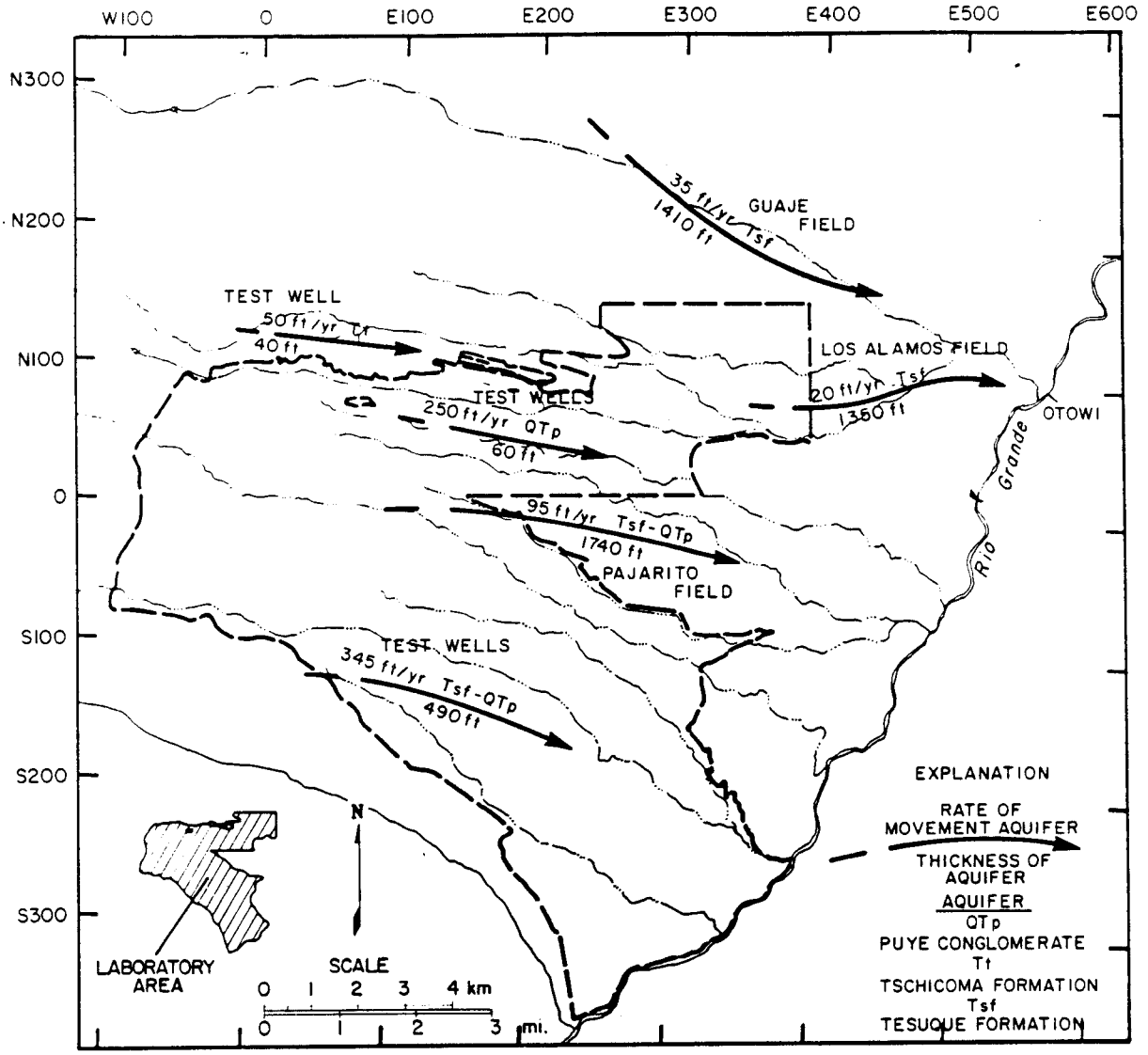

Fig. 10. Rate of movement of water in the main aquifer.

D. Quality of Water

The quality of water is monitored from the supply well to determine if the water meets the Federal primary, secondary, and radiochemical standards for municipal supplies.[34,35] The water is collected at the well heads after a period of pumping so that the water sampled represents what is in the aquifer adjacent to the well. Quality of water from a well depends on the depth of well, the lithology of the aquifer, and yields from individual beds within the aquifer. The quality of water from the individual wells varies because of local aquifer conditions within the same aquifer.

Primary drinking water standards relate directly to the safety of drinking water supplies.[34] Ten primary standards are compared with maximum concentrations from the wells (Table III), whereas detailed analyses from individual wells are presented in Appendix D (Table III). The maximum concentrations from wells are within the standards with the exception of fluoride of 2.6 mg/ℓ

TABLE III

CHEMICAL AND RADIOCHEMICAL QUALITY OF WATER FROM SUPPLY WELLS

Chemical	Units	Maximum Concentration Supply Well	Standards
Chemical Standards[a]			
Primary			
Ag	mg/ℓ	<0.0005	0.05
As	mg/ℓ	0.048	0.05
Ba	mg/ℓ	0.09	1.0
Cd	mg/ℓ	<0.001	0.01
Cr	mg/ℓ	0.022	0.05
F	mg/ℓ	2.6	2.0
Hg	mg/ℓ	<0.0002	0.002
NO_3	mg/ℓ	7.6	45
Pb	mg/ℓ	0.005	0.05
Se	mg/ℓ	<0.003	0.01
Chemical Standards[b]			
Secondary			
Cl	mg/ℓ	16	250
Cu	mg/ℓ	0.013	1.0
Fe	mg/ℓ	0.325	0.3
Mn	mg/ℓ	0.008	0.05
SO_4	mg/ℓ	27	250
Zn	mg/ℓ	0.12	5.0
TDS	mg/ℓ	408	500
pH	---	8.1	6.5 - 8.5
Radiochemical Standards[a]			
^{137}Cs	10^{-9} μCi/mℓ	40 ± 60	200
^{238}Pu	10^{-9} μCi/mℓ	0.018 ± 0.024	7.5
^{239}Pu	10^{-9} μCi/mℓ	0.010 ± 0.010	7.5
Gross Alpha	10^{-9} μCi/mℓ	11 ± 6.0	15
^{3}H	10^{-6} μCi/mℓ	4.2 ± 0.6	20
Total U	10^{-9} μg/ℓ	7.0 ± 1.4	1800

[a]Reference 34.
[b]Reference 35.

from well LA-1B in the Los Alamos Field. Mixing water with that from other wells in the field reduces the fluoride concentrations to acceptable limits within the distribution system.

Secondary standards are not related to the safety of drinking water but, instead, refer to the aesthetic quality.[35] Listed are eight constituents from the wells that are below the secondary standards (Table III). Secondary constituents from individual wells are listed in Appendix E.

Radiochemical standards relate to the safety of drinking water.[34] Radioactivity in the water from the wells occurs naturally in the aquifer. Gross alpha activity from the water from well PM-4 ($20 \pm 8.0 \times 10^{-9}$ μCi/mℓ) is above the standard (15×10^{-9} μCi/mℓ). Further analyses indicated gross alpha was $0.0 \pm 0.8 \times 10^{-9}$ μCi/mℓ. Analyses were performed for ^{226}Ra. It was 0.03×10^{-9} μCi/mℓ, much less than the 5×10^{-9} μCi/mℓ drinking water standard. The high gross alpha reported initially probably reflects contamination of the sample after collection. All other radioactive concentrations were below the standards (Table III). Radiochemical analyses from individual wells are listed in Appendix F.

Water from well LA-6, Los Alamos Field, is not used for municipal supply because the arsenic concentration in the water exceeds the primary standards. The water cannot be mixed with other water from the well field to reduce the arsenic concentrations in the distribution system to a level below the standards.[36]

Routine analyses determine whether water quality deteriorates with continued production. Some of these analyses, along with some of the primary and secondary constituents, are used to discuss the quality of water from the well fields, supply wells, and test wells (Fig. 11).

1. Los Alamos Field. Predominate chemical constituents in water from the Los Alamos Field are sodium-bicarbonate (Fig. 12). The water from the well field is very soft with total hardness ranging from 16 to 28 mg/ℓ. (Hardness classification: soft, 1 to 60 mg/ℓ; moderately hard, 61 to 120 mg/ℓ; hard, 121 to 180 mg/ℓ; and very hard, >180 mg/ℓ.)[37]

The TDS range from 70 to 514 mg/ℓ. The high 514 mg/ℓ occurs in water from well LA-1B. The maximum concentration of chloride is about 15 mg/ℓ, but fluorides range from 0.4 to 2.5 mg/ℓ. Dilution in the distribution system reduces the fluoride from well LA-1B (2.5 mg/ℓ) to levels below the standards for municipal use.

The arsenic-bearing water at well LA-6 is from a deep source and is circulated upward through a permeable fault zone that crosses or lies adjacent to the well. The high arsenic concentration in water from the well (range 0.141 to 0.203 mg/ℓ) precludes using this water for the municipal supply. It was calculated that the arsenic level from the well would have to be at a concentration of 0.100 mg/ℓ or less, at a pumping rate of 300 gpm, in order to dilute it enough by pumpage from the other wells in the field to lower it to an acceptable level in the distribution system.[36]

2. Guaje Field. Water from wells in the upper part of the Guaje Field (G-5 and -6) is a calcium bicarbonate type changing downgradient to a calcium sodium bicarbonate type at well G-4 to a sodium bicarbonate water in the lower part of the well field (G-1, -1A, -2, and -3). The transition from one type of water to another in the field is probably because the basalts in the upper part of the field yield more water than those in the lower field (Fig. 12). The water from the field is soft, with hardness ranging from 24 to 54 mg/ℓ. The hardness of the water decreases from the upper part of the field into the lower part of the field. The TDS range from 134 to 220 mg/ℓ. The chloride concentrations in water from the wells are about 2 mg/ℓ, but fluoride concentrations are 0.8 mg/ℓ or less.

3. Pajarito Field. Water from wells PM-1 and -3 contains calcium bicarbonate. As a result, the water is hard, with a hardness of about 90 mg/ℓ. The well penetrated a thickness of saturated basalt in the sediments of the Tesuque Formation, which may have caused the high concentration of calcium and magnesium resulting in the hard water. The general chemical quality of the water from the two wells is similar, with TDS of 212 and 216 mg/ℓ in PM-1 and -3, respectively. Chlorides are 4 and 10 mg/ℓ and fluorides are about 0.4 mg/ℓ in water from each well.

The water from wells PM-2, -4, and -5 is similar in quality, being a sodium bicarbonate water (Fig. 12). The water is soft, ranging from 36 to 52 mg/ℓ, but the TDS range from 140 to 211 mg/ℓ. Chlorides are low at 9 mg/ℓ or less; fluorides are 0.3 mg/ℓ.

4. Test Wells. Water from TW-1, -2, and -3 is a calcium bicarbonate water. The water quality is not exactly the same at each of the wells. Water from TW-1

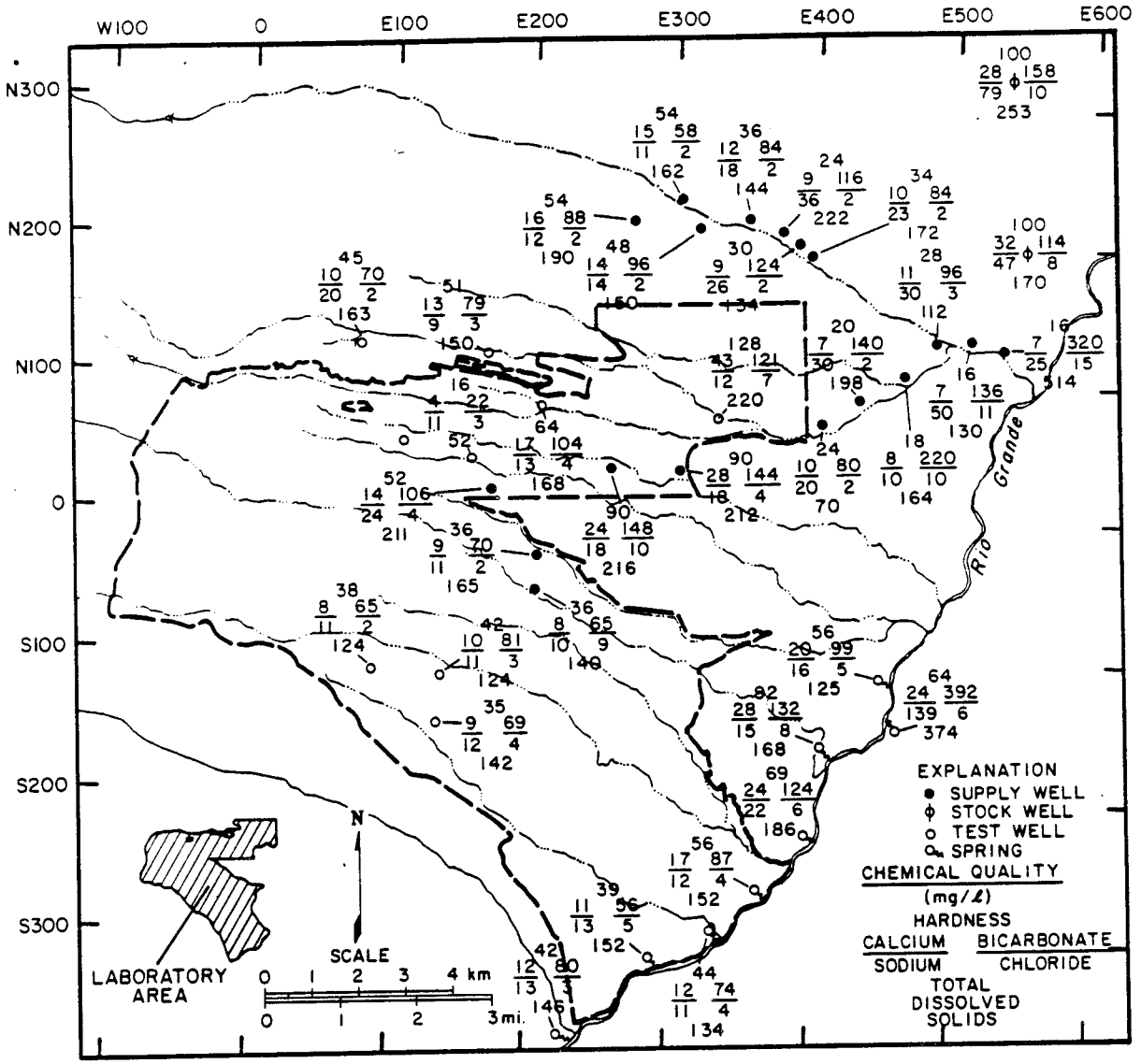

Fig. 11. Chemical quality of water from supply, test, and stock wells.

is hard at 128 mg/ℓ, and TDS are 220 mg/ℓ, where chloride is 7 mg/ℓ and fluoride is 0.4 mg/ℓ. Water from TW-2 is soft at 51 mg/ℓ, and TDS are 150 mg/ℓ, where chloride is 3 mg/ℓ and fluoride is 0.5 mg/ℓ. Water from TW-3 is moderately hard at 64 mg/ℓ, and TDS are 168 mg/ℓ, where chloride is 4 mg/ℓ and fluoride is 0.4 mg/ℓ.

Water from TW-4 and -8 is a sodium bicarbonate water, which is different in chemical quality (Fig. 12). Water from TW-4 is soft at 45 mg/ℓ with TDS of 163 mg/ℓ. The chlorides are about 2 mg/ℓ, where fluorides are <0.4 mg/ℓ. Water from TW-8 is soft at 16 mg/ℓ with TDS of 52 mg/ℓ. Chlorides are about 3 mg/ℓ, where fluorides are 0.2 mg/ℓ.

Water from DT-5A, -9, and -10 is of a sodium bicarbonate type. The quality of water is quite similar from all three test wells. The water is soft, ranging from 35 to 42 mg/ℓ. The concentrations of TDS range from 124 to 142 mg/ℓ with chloride concentrations of 4 mg/ℓ or less and fluoride of 0.3 mg/ℓ or less.

5. Stock Wells. Water from the stock wells RW-2 and -5 is similar in chemical quality and is a sodium

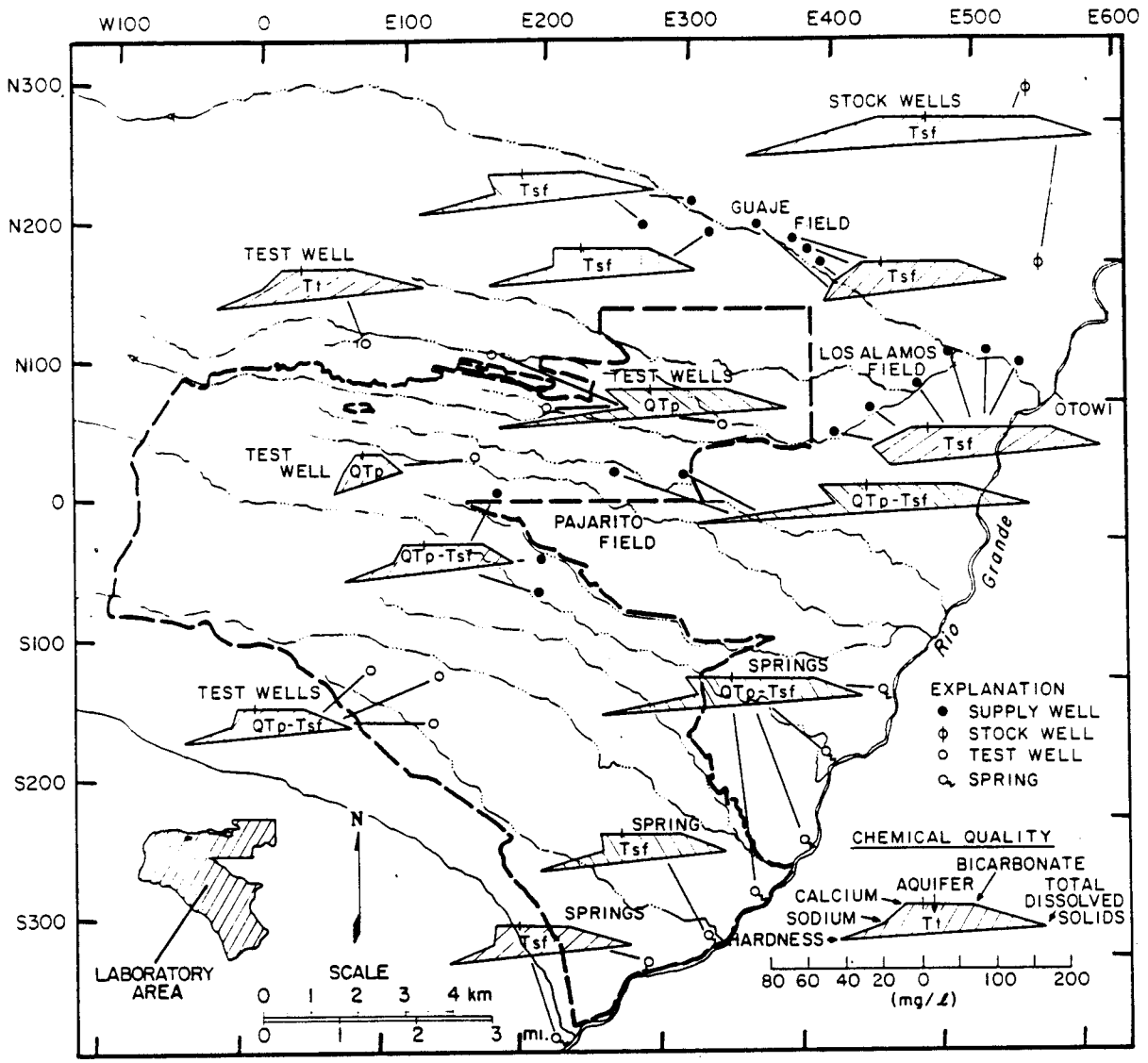

Fig. 12. Graphic comparison of chemical constituents in water from supply, test, and stock wells.

bicarbonate type water (Fig. 12). There is a large amount of calcium and magnesium in the water, which results in a moderately hard water with a hardness of 100 mg/ℓ. The TDS are 170 and 253 mg/ℓ, where chlorides are 10 mg/ℓ or less. The fluoride concentrations are 0.2 mg/ℓ or less.

6. Springs. The quality of water from the springs varies; however, it is combined in four groups for the purpose of this report. The springs discharge from the main aquifer.

The water from Spring 3B is a sodium bicarbonate type with TDS of about 610 mg/ℓ. The water is moderately hard at 64 mg/ℓ, where chlorides are 6 mg/ℓ and fluorides are 0.6 mg/ℓ. The spring discharges from basalts in the Tesuque Formation along a fault or dike. The quality of water is different from that of any other spring in this area of White Rock Canyon.

The quality of water from the spring changes from a calcium bicarbonate to a sodium bicarbonate water south between Spring 5A to Spring 8A in White Rock

Canyon (Fig. 12). The spring discharge is from the main aquifer.

Water from Springs 3, -4, -5A, and -5B is of the calcium bicarbonate type, and water quality varies. Water from Spring 3 is soft with a hardness of 56 mg/ℓ; the TDS are 125 mg/ℓ, where chlorides are 5 mg/ℓ and fluorides are 0.4 mg/ℓ. Water from Spring 4 is moderately hard at 92 mg/ℓ; the TDS are 168 mg/ℓ, where chlorides are 8 mg/ℓ and fluorides are 0.5 mg/ℓ. Water from Spring 5A is moderately hard at 69 mg/ℓ; the TDS are 186 mg/ℓ, where chlorides are 6 mg/ℓ and fluorides are 0.3 mg/ℓ. Water from Spring 5B is soft at 56 mg/ℓ; the TDS are 152 mg/ℓ, where chlorides are 4 mg/ℓ and fluorides are 0.5 mg/ℓ.

The water from Spring 6 is transitional from a calcium bicarbonate water to a sodium bicarbonate water (Fig. 12). The concentrations of calcium and sodium are almost equal at 12 mg/ℓ and 11 mg/ℓ, respectively. The water is soft at 44 mg/ℓ, where the TDS are 134 mg/ℓ. The chlorides are low at 4 mg/ℓ, as are the fluorides at 0.3 mg/ℓ.

Water from Springs 8A and 10 is a sodium bicarbonate water. The water chemical quality from these springs is similar. The water is soft with hardnesses of 39 and 42 mg/ℓ, respectively. The TDS of water from Spring 8A are 152 mg/ℓ and those from Spring 10 are 146 mg/ℓ. The chloride concentrations are 5 mg/ℓ or less, and fluoride concentrations are 0.4 mg/ℓ.

IV. DEVELOPMENT OF ADDITIONAL WATER SUPPLY

The main aquifer extends from the Rio Grande westward beneath the Pajarito Plateau and rises stratigraphically through the Tesuque Formation into the lower part of the Puye Conglomerate. The Puye Conglomerate becomes an important part of the main aquifer. The conglomerate attains its greatest thickness in the north/south-trending basin beneath the central part of the plateau. The coarse volcanic debris within the conglomerate yields water readily to wells and, in part, allows the development of high-yield, low-drawdown wells in this area. The Tesuque Formation beneath the Pajarito Plateau is saturated and is the main source of water supply for municipal and industrial use. The sediments of the Tesuque Formation become coarser westward from the Rio Grande; the upper bed becomes younger with the westward dip. This coarse sediment aids in the development of high-yield wells in this area.[38]

The locations of future wells in this area must be chosen carefully, because wells placed too far west will encounter flow rock of the Tschicoma Formation, which does not yield water readily. Wells placed too far to the east encounter vast thicknesses of basalt, which will not only constitute difficult drilling but may also not yield water readily (Fig. 2).[39]

A. Los Alamos Field

The Los Alamos Field is composed of five producing wells in lower Los Alamos Canyon (Fig. 5). The well and two booster stations and transmission lines are on San Ildefonso Pueblo land. The combined production rate from the field in 1982 was about 2050 gpm,[13] and the booster stations are equipped to handle 2300 gpm. Thus, to reach full capacity of the system an additional 250 gpm could be developed.

The Los Alamos Field was developed in 1946 through 1948, but one well (LA-1B) was added in 1960. Of the six original wells in the field, only four (LA-2, -3, -4, and -5) are still in use. Well LA-1 was abandoned when its yield declined, owing to partial filling of the well with fine sand and sediments. Well LA-6 is on standby for emergency use only because arsenic concentrations in the water are above standards for municipal use. Of the four original wells (1946-1948) in service, the combined pumping rate has declined from 1935 gpm in 1950 to 1562 gpm in 1982. The specific capacity has also declined from 4.3 gpm/ft to 2.5 gpm/ft indicating that over the past 30 yr, some wells have deteriorated. Screen openings are corroded and gravel pack material is filled with fine sand, silts, or clay. To ensure continued production from the field, future plans should include additional wells to offset production decline in the older wells.

The present location of the field is on Pueblo land in an area where only low- to moderate-yield wells (300 to 500 gpm) can be developed. The present spacing between wells in the Los Alamos field restricts any future well locations in that field, because any closer spacing would result in interference between wells, thus causing rapid water-level decline in this section of the field.

Location and development of additional wells for the Los Alamos Field should be west of the present field in lower Pueblo Canyon (Fig. 13). This is in an area where high yield and low drawdown (1000 gpm with less than 100 ft of drawdown) can be developed. In this area, the lower part of the Puye Conglomerate is saturated and the

coarser sediments in the upper part of the Tesuque Formation are within the main aquifer. Two wells could be developed in this area that could use the existing Los Alamos Field transmission and booster system (Fig. 13). Combined production rates from the two wells should be at least 2000 gpm or about the output of the five presently producing wells in the field.

The anticipated geologic section of wells drilled in the lower Pueblo Canyon area is presented in Table IV. The pilot hole should be at least 2500 ft deep. This would allow about 1800 ft of saturated thickness for development of the well.

The water quality should be similar to that of supply well PM-1. The water will probably have a hardness of about 90 mg/ℓ, a TDS concentration of 212 mg/ℓ, and chloride and fluoride concentrations of 4 mg/ℓ and 0.3 mg/ℓ, respectively.

TABLE IV

ANTICIPATED GEOLOGIC LOG OF A SUPPLY WELL IN LOWER PUEBLO CANYON

Elevation: 6400 to 6600 ft above sea-level datum
Depth of Pilot Hole: 2500 ft
Hydrologic Data:
Depth to water: 600 to 750 ft
Yield: Estimated 1000 gpm
Drawdown: Estimated 100 ft or less
Aquifer: Puye Conglomerate and Tesuque Formation

Stratigraphic Unit	Thickness (ft)	Depth (ft)
Alluvium		
Gravel and boulders	20	20
Puye Conglomerate		
Conglomerate	60	80
Basaltic rocks of Chino Mesa		
Basalts and interflow breccia, may contain perched water, at a depth of 210 to 260 ft	205	285
Puye Conglomerate		
Conglomerate	165	450
Basaltic rocks of Chino Mesa		
Basalts and interflow breccias	100	550
Puye Conglomerate		
Conglomerate	250	800
Tesuque Formation		
Siltstone, sandstone, and conglomerate with occasional basalt flow in upper 1200 ft of formation	1700	2500

B. Guaje Field

The Guaje Field is composed of seven producing wells. The combined production of the field in 1982 was 2630 gpm. The booster stations and transmission lines can handle 2700 gpm; thus, to reach full capacity, an additional 70 gpm could be developed in the field.

The Guaje Field was developed in 1950 through 1951, with one well (G-1A) added in 1954 and another well (G-6) added in 1964. The five wells in the field in 1950 through 1951 had a combined production rate of 2387 gpm in 1952 and an average specific capacity of 7.9 gpm/ft. The pumping rate had declined to 1847 gpm, and the average specific capacity declined to 5.0 gpm/ft in 1982. The wells deteriorated because of age, corrosion of the screen openings, the well filling with sediments, gravel pack filled with fine sediments, and mainly, the damage to screen sections of the wells, especially wells G-4 and G-5.[6] The yield from the wells will continue to decline with time because of deterioration of the casing, screen, and gravel pack. To ensure continued production from the field and maximum use of existing booster and distribution systems, one replacement well should be considered and other wells should be rehabilitated.[11]

A replacement well should be considered, because at present, the spacing of existing wells in the Guaje Field is adequate with minor interference occurring when the wells are pumped. An additional well in the field would cause excessive drawdown because of the proximity of other wells. An additional well in the field should not be located northwest or west of the existing wells because of the outcrop of Tschicoma Formation in these areas. A well that is finished in or near the outcrop of Tschicoma would not yield an appreciable amount of water because the rocks are relatively impermeable and they form a barrier to east and southeast movement of ground water in the main aquifer. Land ownership will not permit locating a well southeast of well G-1 in Guaje Canyon (Fig. 5).

A replacement well should be considered for well G-4. Maximum yield from the well was 434 gpm with a specific capacity of 3.0 gpm/ft of drawdown in 1954. In 1982 the yield had declined to 297 gpm with a specific capacity of 1.5 gpm/ft of drawdown. At times, the well produces a lot of sand with the pumpage.

Well G-4 was completed at a depth of 1930 ft in 1951. In November 1953 the well was filled with sediments to about 1129 ft. Attempts to remove the sediments from the well were abandoned at a depth of 1486 ft because the bailer would stick and gravel pack was being bailed from the well. The presence of gravel pack indicated that the casing was ruptured. In October 1954 the well was opened to 1386 ft. About 110 ft of the 360 ft of screen buried below the 1380-ft level reduced the yield of the well because sediment continued to accumulate. In 1968 the well had filled with sediments to a depth of 765 ft. When sediments were being removed from the well, a large amount of gravel pack was present, so it was cleaned only to a depth of 798 ft. The well was filled with sediments to a depth of 750 ft in 1975. At this time, the sediments were cleaned out to a depth of 1750 ft. A video log of the hole was made with a television camera, which indicated minor breaks in the screen above the depth of 1230 ft with major breaks in sections of the screen below a depth of 1230 ft. A slotted liner was set from 1214 to 1750 ft; however, after the well was back in operation, pumpage sometimes contained a large amount of sand. In 1981 the hole was opened only to a depth of 1150 ft. Only 22 ft of sediments were cleaned out of the well because the bailer tended to stick in the well. Well G-4 should be replaced because of the damaged screen. The well will continue to deteriorate with sand accumulation until the yield will be insufficient to continue economical operation. It can be replaced with a well that should produce at least 500 gpm with less than 100 ft of drawdown.

The replacement well should be located at least 150 ft south of well G-4; however, a distance of 300 to 500 ft would be preferable because drilling would be less likely to affect the cavities caused by pumpage of sand from G-4. The pilot hole should be at least 2000 ft deep. This would allow a saturated section of about 1600 ft to develop the well. The stratigraphic section penetrated by the replacement well should be similar to those penetrated by well G-4 (Table V). The water quality should also be similar to that of well G-4. The TDS should be about 150 mg/ℓ, with soft water at 48 mg/ℓ. Chloride should be less than 5 mg/ℓ and fluorides should be about 0.2 mg/ℓ.

TABLE V

ANTICIPATED GEOLOGIC LOG OF A SUPPLY WELL NEAR WELL G-4 IN GUAJE CANYON

Elevation: 6230 ft above sea-level datum
Depth of Pilot Hole: 2000 ft
Hydrologic Data:
Depth To Water: 400 ft
Yield: Estimated 500 gpm
Drawdown: Estimated 100 ft or less
Aquifer: Tesuque Formation

Stratigraphic Unit	Thickness (ft)	Depth (ft)
Alluvium		
Gravels and boulders	15	15
Puye Conglomerate		
Conglomerate	105	120
Tesuque Formation		
Siltstone and sandstone	380	500
Basalt and interflow breccia	30	530
Siltstone and sandstone	330	860
Basalt and interflow breccia	75	935
Siltstone and sandstone	30	965
Basalt and interflow breccia	20	980
Siltstone and sandstone	130	1110
Basalt and interflow breccia	40	1150
Siltstone and sandstone	850	2000

Well G-3 had a pumping rate of 410 gpm and a specific capacity of 8.6 gpm/ft of drawdown in 1954. The pumping rate has declined to 240 gpm, with a specific capacity of 2.1 gpm/ft of drawdown in 1982. Television logs of the well indicate that the casing and screens are in good condition. The well should be rehabilitated by some method (acid, shock, jetting screens with high pressure, or swabbing) to try to increase the yield of the well.

Well G-5 is missing large sections of the screen below a depth of 700 ft. As the well continues to be a good producer with little drawdown (520 gpm with specific capacity of 9.5 gpm/ft), no attempt should be made to repair or rehabilitate the well. A replacement well should

be considered in the future for this well if yield and specific capacity decline.

C. Pajarito Field

The Pajarito Field is composed of four producing wells. One well that was just completed should be added to the system in late 1983. The four wells can produce about 4800 gpm and when the fifth well is added to the system, the production should be about 6000 gpm. These wells are high-yield wells in an area capable of developing wells with pumping rates >1000 gpm. The development of additional wells in the field is not imminent; however, if additional wells are to be developed, locations should be in areas where high yield and low drawdown can be expected.

The Pajarito Field north and west of PM-2, -4, or -5 cannot be expanded and still remain in the area where high-yield wells can be developed. Also, space is unavailable in Sandia Canyon for additional wells, if space is maintained between wells to reduce interference or overlapping of drawdown. Adding wells in lower Pueblo Canyon has already been discussed.

The suggested location for additional wells in the Pajarito Field is to the southwest of well PM-2 (Fig. 13). The locations are chosen for maximum spacing between wells to minimize the interference between wells when they are pumping and to align the wells at right angles to the movement of ground water in the main aquifer, which is west to east.

One additional well could be located about 3500 ft southwest of PM-2 at an elevation of about 6850 ft, with a second well located about 7000 ft southwest of PM-2 at an elevation of about 6800 ft. The quality of water at these locations should be similar to that of PM-2. The TDS should be about 140 mg/ℓ with a chloride value of 9 mg/ℓ and fluoride value of 0.3 mg/ℓ. The water is soft with hardness of 36 mg/ℓ.

The pilot hole at these locations should be at least 2800 ft, which would result in a saturated section of about 1800 ft to develop a high-yield well. The anticipated geologic section at the two locations is shown in Table VI.

D. Drilling Conditions

Cable tool and rotary methods of drilling have been used to construct water supply wells in the Los Alamos area. The cable tool and rotary method has been used to drill the upper section of unsaturated material (alluvium, Bandelier Tuff, Puye Conglomerate, and Basaltic Rocks of Chino Mesa) above the main aquifer. Rotary drilling has been used to complete the well in the saturated sediments and volcanic rocks within the main aquifer, the lower part of the Puye Conglomerate, and the Tesuque Formation.

The alluvium or soil at most sites is thin. The alluvium (Guaje or Pueblo Canyons) may cover large, very hard boulders of latite, rhyolite, or quartz latite.

The Bandelier Tuff is a soft, friable, porous, and permeable rock. The drilling should progress easily. A thick section of tuff may cause major circulation problems if it is drilled with the rotary using drilling mud as a cutting carrier. Drilling by cable tool should cause no lost circulation problems; using air foam as a cutting carrier with the rotary should reduce the lost circulation problem and should allow the upper section of the hole to be cased above the main aquifer. The wall of the borehole in the Bandelier Tuff holds up well when it is drilled by either cable tool or rotary.

The Puye Conglomerate contains numerous latite, rhyolite, and quartz latite boulders that are quite hard. The formation is slightly consolidated to consolidated. Drilling will be slow, and in some cases, circulation of drilling fluid when using the rotary method may be difficult.

The basaltic rocks of Chino Mesa are hard and contain joints and small cavities. Drilling these rocks will be slow and difficult, and if rotary methods are used, circulation may be difficult to maintain. Using air foam as a cutting carrier through the basalts reduces the circulation problem. For completion of the well, it will probably be necessary to set a surface string of casing through these basalts. The pilot hole in basalts is likely to become crooked because when the hard rocks are drilled, the bits are deflected by joints and interflow breccias between flows of different hardnesses.

The Tesuque Formation of siltstones and sandstones is drilled easily by rotary methods using mud as a cuttings carrier. The interbedded basalts in the sediments are hard to drill and will, in most cases, cause problems in maintaining the circulation using a mud rotary. The formation is completely saturated at most of the locations (Guaje Canyon is the exception). If sufficient penetration of the aquifer is made and a high head of water can be maintained in the drill hole, reverse circulation using air down a drop line in the drill stem has been successful in maintaining circulation at depth in

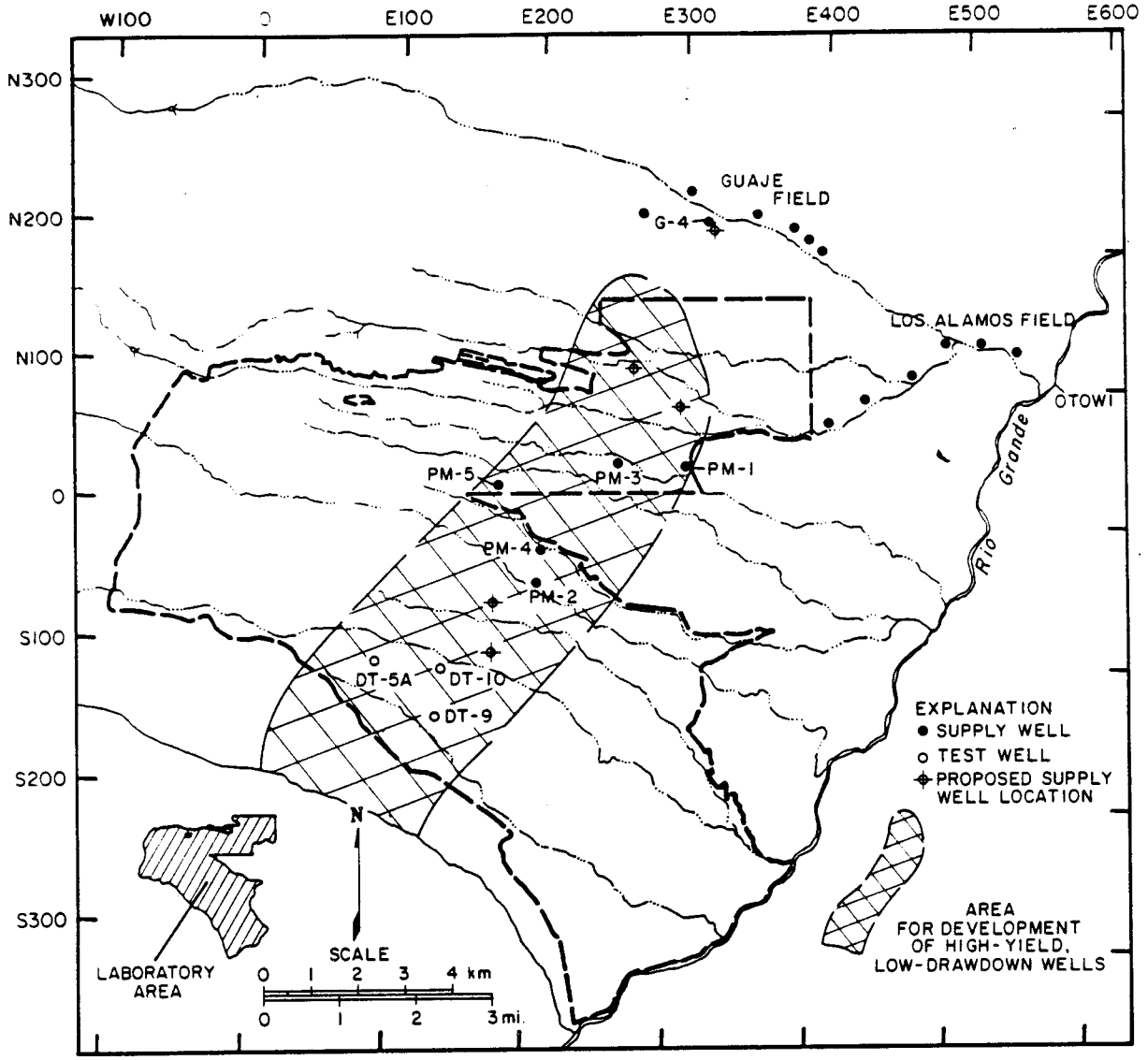

Fig. 13. Proposed locations for additional supply wells and area for development of high-yield, low-drawdown wells.

the Tesuque Formation when the sediments contain interbedded basalts.

E. Geology and Geophysical Logs

The depth at which a supply well will be completed is determined from geologic and geophysical logs. During drilling of the pilot hole, cuttings should be caught at 5-ft-depth intervals when using a cable tool or at 10-ft-depth intervals when using a rotary. Cuttings are then described by a geologist and a geologic log is prepared. The geologic log is used to correlate and compare rock units with hydrologic characteristics of geophysical logs.

Geophysical logs to be run in the pilot hole are (1) Compensated Neutron-Formation Density, (2) Dual Induction—SFL with Linear Correlation Log, (3) Microlog, and (4) Temperature Log. These logs, along with the geologic log, will aid in determining the water-bearing

TABLE VI

ANTICIPATED GEOLOGIC LOG OF SUPPLY WELLS ON THE PAJARITO PLATEAU SOUTH OF WELL PM-2

Elevation: ~6850 ft
Depth of Pilot Hole: 2850 ft
Hydrologic Data:
Depth to Water: 950 ft
Yield: Estimated 1000 gpm
Drawdown: Estimated 100 ft or less
Aquifer: Puye Conglomerate and Tesuque Formation

Stratigraphic Unit	Thickness (ft)	Depth (ft)
Bandelier Tuff		
Ashflow tuff and pumice	650	650
Basaltic rocks of Chino Mesa		
Basalt and interflow breccia	350	1000
Puye Conglomerate		
Conglomerate	650	1650
Tesuque Formation		
Sandstone and conglomerate	400	2050
Basalt and interflow breccia	50	2100
Sandstone and siltstone	200	2300
Basalt and interflow breccia	100	2400
Siltstone and sandstone	450	2850

characteristics of the Puye Conglomerate and Tesuque Formation within the main aquifer.

F. Well Construction

Well construction should provide for a surface string of blank casing, adequately cemented, to seal out water encountered in the alluvium (Pueblo and Guaje Canyon). It will also be necessary to seal out, with casing, any water encountered above the main aquifer. Samples of water encountered above the main aquifer should be obtained for chemical and radiochemical analyses, where possible, if drilling with cable tool or air rotary.

Most of the water-bearing beds of the Tesuque Formation contain fine sediments so poorly consolidated that a gravel pack around the casing and screen section of the well will be required to reduce the entry of fine material into the well. Perforated pipe or screen should be placed through the entire saturated section of the well except in the upper 200 to 250 ft of the saturated section. The pump intake is usually set 200 to 250 ft below the top of the aquifer. Blank pipe should be set through this section to prevent "cavitation" of the pump bowls in order to obtain the maximum efficiency of the pump.

Two gage lines (2-in. i.d.) attached outside the casing should extend from the surface and enter the casing at 200 to 250 ft below the top of the main aquifer or near the top of the screen section. One gage line houses the air line and continuously monitors the water levels; the second gage line is used for the water-level measurement equipment or well-surveying instruments.

V. SUMMARY AND CONCLUSIONS

The main aquifer of the Los Alamos area is the only aquifer capable of municipal and industrial water supply. The main aquifer extends from the Rio Grande westward beneath the Pajarito Plateau and rises westward stratigraphically through the Tesuque Formation into the lower part of the Puye Conglomerate. The water in the aquifer moves eastward toward the Rio Grande, where it discharges through a series of springs and seeps. The depth of the main aquifer varies from about 1200 ft along the western margin of the plateau to about 600 ft at the confluence of Pueblo and Los Alamos Canyons. At the Rio Grande, some wells encountered water in the aquifer under artesian pressures. The main aquifer extends north and south of the Los Alamos area and is estimated to be over 6000 ft thick.

The Puye Conglomerate is highly permeable and, where it is saturated beneath the Pajarito Plateau, will yield large amounts of water to wells. The Tesuque Formation is composed of siltstones, sandstones, and some conglomerate. Many of the individual beds in the Tesuque Formation are highly permeable and, where saturated, will yield water to a well. Beneath the Pajarito Plateau, coarse volcanic rock fragments are in the upper 1000 ft of the Tesuque Formation, and they yield more water to wells than do the finer sediments, which predominate in the formation farther to the east along the Rio Grande.

In the Los Alamos area, 18 supply wells, 10 test wells, and 2 stock wells are supplied by the main aquifer. Hydrologic characteristics of the main aquifer were determined from some of these wells. The hydrologic characteristics reflect the permeability and thickness of the formations.

The Los Alamos Field is completed in siltstones and sandstones of the Tesuque Formation. With a saturated thickness of about 1350 ft, the average specific capacity is about 4.5 gpm/ft of drawdown at a pumping rate of 365 gpm. The average transmissivity is 8.4×10^3 gpd/ft with a field coefficient of permeability of 5.6 gpd/ft^2. The average rate of movement in the upper 1350 ft of aquifer in the Los Alamos Field is about 20 ft/yr. The production from the field in 1947 to 1982 has been 14.5×10^9 gal. or about 36% of the total water pumped for use at Los Alamos. This has resulted in an average water-level decline in the field of 37 ft or about 1.1 ft/yr. The average production per foot of water-level decline has been 392×10^6 gal./ft.

The Guaje Field is completed in siltstones and sandstones with some interbedded basalt flows and breccias of the Tesuque Formation. The average saturated thickness of 1410 ft has an average specific capacity of 5.8 gpm/ft of drawdown at a pumping rate of 376 gpm. The average transmissivity is 11.6×10^3 gpd/ft with a field coefficient of permeability of 8.2 gpd/ft^2. The average rate of movement is about 35 ft/yr. The production in 1951 through 1982 from the field has been 14.9×10^9 gal. or about 37% of total water pumped for use at Los Alamos. This has resulted in an average water-level decline in the field of 54 ft or about 1.7 ft/yr. The average production per foot of water-level decline has been 277×10^6 gal./ft.

The Pajarito Field is completed in siltstones, sandstones, and conglomerates that are interbedded with basalt and basalt breccias of the Puye Conglomerate and Tesuque Formation. The lower part of the Puye Conglomerate is also saturated within the field. The average saturated thickness of 1740 ft has an average specific capacity of 31 gpm/ft of drawdown at a pumping rate of 1215 gpm. The average transmissivity is 94×10^3 gpd/ft with an average field coefficient of permeability of 53 gpd/ft^2. The average rate of movement in the 1740 ft of Puye Conglomerate and Tesuque Formation is 95 ft/yr. Production from the field from 1965 to 1982 has been 11.0×10^9 gal. or about 27% of the total water pumped at Los Alamos.

There are five wells in the field, but most of the production has been from three wells: PM-1, -2, and -3. Well PM-4 was placed in service in July 1982, and well PM-5 was completed but had not been connected to the transmission line by the end of 1982. The production from well PM-1 has been about 1.6×10^9 gal. from 1965 to 1982 resulting in a water-level decline of 2 ft. The average production per foot of water-level decline has been 796×10^6 gal./ft. The production from well PM-2 has been 5.9×10^9 gal. from 1966 to 1982. This well has produced the most water of the individual wells (14% of the total water pumped at Los Alamos in 1950 through 1982). The water level declined 48 ft from 1966 to 1982 or about 2.8 ft/yr. The average production per foot of water-level decline has been 122×10^9 gal./ft. The production of well PM-3 has been 3.5×10^9 gal. from 1968 to 1982. This has resulted in a water-level decline of 19 ft with an average production of 183×10^6 gal./ft of drawdown.

Test well TW-4 is completed into a brecciated zone in the Tschicoma Formation. At a pumping rate of 2.8 gpm, the specific capacity is 0.6 gpm/ft of drawdown. The 40-ft zone of saturation has a transmissivity of 0.7×10^3 gpd/ft and a field coefficient of permeability of 18 gpd/ft^2. The rate of movement in the brecciated zone is about 50 ft/yr.

Test wells DT-5A, -9, and -10 penetrated a saturated thickness of 345 ft at the Tesuque Formation and lower part of the Puye Conglomerate. The test well had an average specific capacity of 15 gpm/ft of drawdown at a pumping rate of 82 gpm. The average transmissivity is 36×10^3 gpd/ft with an average field coefficient of permeability of 83 gpd/ft^2. The amount of pumpage from these test wells is low, thereby causing no significant change in water levels; however, water-level decline in well DT-5A from 1960 to 1964 was 4 ft and in well DT-10 it was 4 ft from 1960 to 1967. At well DT-9, the average annual water levels were recorded from 1960 to 1968 and 1970 to 1982. The most rapid decline occurred from 1960 to 1968, about 2.3 ft. The water level rose about 0.3 ft from 1971 to 1972, then declined about 1.2 ft to 1979. Since 1979 the water level has remained about the same. The water-level declines reflect decreases in recharge resulting in natural water-level declines.

Test Wells TW-1, -2, -3, and -8 penetrated a 60-ft saturated section in the lower part of the Puye Conglomerate. At a pumping rate of 8 gpm, the average specific capacity is 2.1 gpm/ft of drawdown. The average

transmissivity is 4.3×10^3 gpd/ft with an average field coefficient of permeability of 98 gpd/ft^2. The average rate of water movement in the 60-ft saturated section of the aquifer is about 250 ft/yr.

Based on hydrologic characteristics of the wells, high-yield and low-drawdown (1000 gpm/100 ft) wells can be developed near the center of the Pajarito Plateau in a northeast-trending zone. Two high-yield and low-drawdown wells can be developed in lower Pueblo Canyon as replacement wells or wells to supplement production from the Los Alamos Field. Two high-yield and low-drawdown wells can be located on the Pajarito Plateau southwest of well PM-2 to supplement the production from the Pajarito Field to meet future increased demand.

A replacement well for well G-4 in the Guaje Field should be considered to offset decline in production in the field as well efficiency declines in the field. The well could be constructed to produce 500 gpm with less than 100 ft of drawdown.

REFERENCES

1. W. D. Purtymun and J. E. Herceg, "Summary of Los Alamos Municipal Well-Field Characteristics, 1947-1971," Los Alamos Scientific Laboratory report LA-5040-MS (1972).

2. W. D. Purtymun and J. E. Herceg, "Water Supply at Los Alamos During 1971," Los Alamos Scientific Laboratory report LA-5039-MS (1972).

3. W. D. Purtymun and J. E. Herceg, "Water Supply at Los Alamos During 1972," Los Alamos Scientific Laboratory report LA-5296-MS (1973).

4. W. D. Purtymun and J. E. Herceg, "Water Supply at Los Alamos During 1973," Los Alamos Scientific Laboratory report LA-5636-MS (1974).

5. W. D. Purtymun, "Water Supply at Los Alamos During 1974," Los Alamos Scientific Laboratory report LA-5998-MS (1975).

6. W. D. Purtymun, "Water Supply at Los Alamos During 1975," Los Alamos Scientific Laboratory report LA-6461-MS (1976).

7. W. D. Purtymun, "Water Supply at Los Alamos During 1976," Los Alamos Scientific Laboratory report LA-6814-PR (1977).

8. W. D. Purtymun, "Water Supply at Los Alamos During 1977," Los Alamos Scientific Laboratory report LA-7436-MS (1978).

9. W. D. Purtymun, "Water Supply at Los Alamos During 1978," Los Alamos Scientific Laboratory report LA-8074-PR (1979).

10. W. D. Purtymun, "Water Supply at Los Alamos During 1979," Los Alamos Scientific Laboratory report LA-8504-PR (1980).

11. W. D. Purtymun and Max Maes, "Water Supply at Los Alamos During 1980," Los Alamos National Laboratory report LA-8977-MS (1981).

12. W. D. Purtymun, N. M. Becker, and M. Maes, "Water Supply at Los Alamos During 1981," Los Alamos National Laboratory report LA-9737-PR (1983).

13. W. D. Purtymun, N. M. Becker, and M. Maes, "Water Supply at Los Alamos During 1982," Los Alamos National Laboratory report LA-9896-PR.

14. R. L. Cushman and W. D. Purtymun, "An Evaluation of the Yield and Water-Level Relationships," Los Alamos Scientific Laboratory report LA-6086-MS (1975).

15. C. S. Ross, R. L. Smith, and R. A. Bailey, "Outline of Geology of the Jemez Mountains, New Mexico," New Mexico Geological Society Guidebook of the Albuquerque Country, 12th Field Conf. (1961).

16. R. L. Smith, R. A. Bailey, and C. S. Ross, "Structural Evolution of the Valles Caldera, New Mexico and Its Bearing on Emplacement of Ring Dikes," US Geol. Surv. Prof. Pap. 424-D (1961).

17. R. L. Griggs, "Geology and Ground-Water Resources of the Los Alamos Area, New Mexico," US Geol. Surv. Water-Supply Pap. 1753 (1964).

18. R. A. Bailey, R. L. Smith, and C. S. Ross, "Stratigraphic Nomenclature of the Volcanic Rock of the Jemez Mountains, New Mexico," US Geol. Surv. Bull. 1274-P (1969).

19. R. L. Smith, R. A. Bailey, and C. S. Ross, "Geologic Map of the Jemez Mountains, New Mexico," US Geol. Surv. Misc. Geol. Inv. Map I-571 (1970).

20. V. C. Kelley, "The Rio Grande Depression from Taos to Santa Fe," New Mexico Geological Society Guidebook of the Southeastern Sangre de Cristo Mountains, New Mexico, 7th Field Conf. (1956).

21. A. J. Budding, "Gravity Survey of the Pajarito Plateau, Los Alamos and Santa Fe Counties, New Mexico," Los Alamos Scientific Laboratory report LA-7419-MS (1978).

22. W. D. Purtymun and S. Johansen, "General Geohydrology of the Pajarito Plateau," New Mexico Geol. Society Guidebook, Ghost Ranch (Central-Northern, New Mexico), 25th Field Conf. (1974).

23. C. S. Conover, C. V. Theis, and R. L. Griggs, "Geology and Hydrology of the Valle Grande and Valle Toledo, Sandoval County, New Mexico," US Geol. Surv. Water-Supply Pap. 1619-Y (1963).

24. Z. E. Spiegel, "Geology and Water Resources of the Santa Fe Area, New Mexico," US Geol. Surv. Water-Supply Pap. 1525 (1963).

25. W. D. Purtymun, R. J. Peters, and J. W. Owens, "Geohydrology of White Rock Canyon of the Rio Grande from Otowi to Frijoles Canyon," Los Alamos Scientific Laboratory report LA-8635-MS (1980).

26. R. L. Cushman, "An Evaluation of Aquifer and Well Characteristics of Municipal Well Fields in Los Alamos and Guaje Canyons Near Los Alamos, New Mexico," US Geol. Surv. Water-Supply Pap. 1809-D (1965).

27. T. E. Kelly, "Reconnaissance Investigation of Ground Water in the Rio Grande Drainage Basin—With Special Emphasis on Saline Ground-Water Resources," US Geol. Surv. Hydrol. Atlas HA-510 (1974).

28. J. E. Weir, J. H. Abrahams, J. R. Waldron, and W. D. Purtymun, "The Hydrology and the Chemical and Radiochemical Quality of Surface and Ground Water at Los Alamos, New Mexico, 1945-55," US Geol. Surv. Open-File report (1962).

29. J. E. Weir and W. D. Purtymun, "Geology and Hydrology of Technical Area 49, Frijoles Mesa, Los Alamos County, New Mexico," US Geol. Surv. Open-File report (1962).

30. E. H. Baltz, J. H. Abrahams, and W. D. Purtymun, "Preliminary Report on the Geology and Hydrology of Mortandad Canyon near Los Alamos, New Mexico—With Special Reference to Disposal of Liquid Low-Level Radioactive Wastes," US Geol. Surv. Open-File report (1963).

31. Black and Veatch, Consulting Engineers, "Report on Water Supply, Los Alamos Project, Los Alamos, New Mexico," Kansas City, Mo., Admin. report prepared for US Atomic Energy Commission (1946).

32. C. V. Theis and C. S. Conover, "Pumping Test in the Los Alamos Canyon Well Field near Los Alamos, New Mexico," US Geol. Surv. Water-Supply Pap. 1619-I (1962).

33. W. D. Purtymun, F. C. Koopman, S. Barr, and W. E. Clements, "Air Volume and Energy Transfer Through Test Holes and Atmospheric Pressure Effects on the Main Aquifer," Los Alamos Scientific Laboratory report LA-5725-MS (1974).

34. US Environmental Protection Agency, "National Interim Primary Drinking Water Regulations," Office of Water Supply report EPA-570/9-76-003 (1976).

35. US Environmental Protection Agency, "National Secondary Drinking Water Regulations," Federal Register, Vol. 44, No. 140 (July 19, 1979).

36. W. D. Purtymun, "Hydrologic Characteristics of the Los Alamos Well Field with Reference to the Occurrence of Arsenic in Well LA-6," Los Alamos Scientific Laboratory report LA-7012-MS (1977).

37. American Society for Testing Materials, "Manual on Water," ASTM Special Tech. Pub. No. 422, 3rd ed. (ASTM, Philadelphia, 1969).

38. W. D. Purtymun and J. B. Cooper, "Development of Ground-Water Supplies on the Pajarito Plateau, Los Alamos County, New Mexico," US Geol. Surv. Prof. Pap. 650-B (1969), B149-B153.

39. W. D. Purtymun and J. B. Cooper, "Locations for Five Water-Supply Wells at Los Alamos, New Mexico," US Geol. Surv. Open-File report (1965).

APPENDIX A

CONSTRUCTION AND HYDROLOGIC DATA FOR WELLS IN LOS ALAMOS, GUAJE, AND PAJARITO FIELDS

	Los Alamos Field						
	LA-1[a]	LA-1B	LA-2	LA-3	LA-4	LA-5	LA-6
Date of Completion (yr)	1946	1960	1946	1947	1948	1948	1948
Elevation of LSD (ft)	5625	5620	5650	5670	5975	5840	5770
Construction							
Depth drilled (ft)	1001	2256	882	910	2019	2084	7030
Depth completed (ft)	870	1750	870	870	1965	1750	1790
Diameter (in.) [b]	10	12 (650 ft) 10	10	10	12 (754 ft) 10	12 (630 ft) 10	12 (597 ft) 10
Water Levels							
Date	1982	1982	1982	1982	1981	1982	1982
Depth below LSD (ft)	40	71	161	118	289	168	90
Elevation (ft)	5585	5549	5489	5552	5686	5672	5680
Water-Level Fluctuations							
Period	1950-1982	1960-1982	1950-1982	1950-1982	1950-1981	1950-1982	1950-1982
Change (ft)	-79	-64	-72	-21	-11	-45	-7
Annual rate (ft/yr)	-2.4	-2.8	-2.2	-0.6	-0.3	-1.4	-0.2
Aquifer							
Formation	Tsf	Tsf	Tsf	Tsf	Tsf	Tsf	Tsf
Saturated thickness (ft)	830	1679	709	752	1676	1582	1700
Yield							
Date	1950	1982	1982	1982	1981	1982	1981
Rate (gpm)	366	486	269	247	579	467	580
Drawdown (ft)	293	109	187	128	104	136	57
Specific capacity (gpm/ft)	0.8	4.5	1.4	1.9	5.6	3.4	10.2
Transmissivity (gpd/ft)	--	15 700	2500	2500	9600	4800	15 500
Field coefficient of permeability (gpd/ft^2)	---	9.3	3.5	3.3	5.7	3.0	9.1
Production							
Period (yr)	1947-1956	1960-1982	1947-1982	1948-1982	1948-1982	1948-1982	1948-1975
Pumpage (10^6 gal.)	353	1964	1305	1644	3503	3049	2884

APPENDIX A (cont)

	Los Alamos Field						
	LA-1[a]	LA-1B	LA-2	LA 3	LA-4	LA-5	LA-6
Quality of Water							
Date	1952	2-28-80	2-28-80	2-28-0	2-28-80	2-28-80	2-28-80
Chemical (mg/ℓ)							
SiO_2	29	40	26	24	30	36	26
Ca	7	7	7	1	10	7	8
Mg	1	0.4	0.2	0.2	0.2	0.2	0.2
Na	80	25	50	30	20	30	10
CO_3	0	0	0	0	0	0	0
HCO_3	177	320	136	96	80	140	220
SO_4	20	37	13	7	3	5	22
Cl	18	15	11	3	2	2	10
F	1.3	2.5	1.2	0.5	0.4	0.9	1.6
NO_3	1.8	2.3	2.5	2.4	2.0	2.3	2.3
TDS	---	514	130	112	70	198	364
Hardness	22	16	16	28	24	20	18
Specific conductance (μmho)	385	330	270	550	200	200	300
pH	---	8.4	8.5	8.4	8.5	8.7	8.7
Radiochemical							
Total uranium (μg/ℓ)	---	5.7 ± 1.2	4.5 ± 1.0	3.5 ± 0.8	0.9 ± 0.8	4.8 ± 0.8	3.1 ± 0.8
Temperature (°F)	63	83	75	67	83	77	84

APPENDIX A (cont)

	Guaje Field						
	G-1	G-1A	G-2	G 3	G-4	G-5	G-6
Date of Completion (yr)	1950	1954	1951	1951	1951	1951	1964
Elevation of LSD (ft)	5975	6015	6055	6140	6230	6305	6420
Construction							
Depth drilled (ft)	2100	2071	2006	1996	2002	1997	2005
Depth completed (ft)	2000	1519	1996	1792	1930	1840	1530
Diameter (in.)[b]	10 (490 ft) 10	12 (8663 ft) 10	12 (8600 ft) 10	12 (8695 ft) 10	12 (8720 ft) 10	12 (8739 ft) 10	12
Water Levels							
Depth below LSD (ft)	278	305	352	364	386	455	588
Elevation (ft)	5697	5710	5703	5776	5844	5850	5832
Water-Level Fluctuations							
Period (yr)	1951-1982	1955-1982	1951-1982	1951-1982	1951-1982	1951-1982	1964-1982
Change (ft)	-83	-40	-93	-83	-29	-41	-7
Annual rate (ft/yr)	-2.6	-1.4	-2.9	-2.6	-0.9	-1.3	-0.4
Aquifer							
Formation	Tsf	Tsf	Tsf	Tsf	Tsf	Tsf	Tsf
Saturated thickness (ft)	1722	1214	1644	1428	1544	1385	942
Yield							
Date	1982	1982	1982	1982	1982	1982	1982
Rate (gpm)	313	505	476	239	297	522	281
Drawdown (ft)	165	42	47	112	192	55	81
Specific capacity (gpm/ft)	1.9	12.0	10.1	2.1	1.5	9.5	3.5
Transmissivity (gpd/ft)	12 000	11 000	15 000	7500	17 500	12 000	6300
Coefficient of permeability (gpd/ft^2)	7.0	9.1	9.1	5.3	11.3	8.7	6.7
Production							
Period (yr)	1950-1982	1954-1982	1951-1982	1951-1982	1951-1982	1951-1982	1952-1982
Pumpage (10^6 gal.)	2386	2921	2504	2084	1202	2774	1062

APPENDIX A (cont)

	Guaje Field						
	G-1	G-1A	G-2	G 3	G-4	G-5	G-6
Quality of water							
Date	2-28-80	2-28-80	2-28-80	2-28-80	2-28-80	2-28-80	2 24-80
Chemical (mg/ℓ)							
SiO_2	86	78	78	54	52	64	70
Ca	10	9	9	12	14	15	16
Mg	0.5	0.5	0.6	1.5	2.5	3.7	3.6
Na	23	26	36	18	14	11	12
CO_3	0	0	0	0	0	0	0
HCO_3	84	124	116	84	96	88	88
SO_4	4	4	4	4	3	4	3
Cl	2	2	2	2	2	2	2
F	0.5	0.5	0.8	0.3	0.2	0.2	0.2
NO_3	2.1	2.1	1.9	2.5	2.7	2.9	1.8
TDS	172	134	222	144	150	162	190
Hardness	34	30	24	36	48	54	54
Specific conductance (μmho)	130	200	200	300	160	130	200
pH	8.3	8.4	8.5	8.3	8.2	8.2	7.9
Radiochemical							
Total uranium (μg/ℓ)	1.0 + 0.8	0.7 + 0.8	0.9 + 0.8	0.8 + 0.8	1.0 + 0.8	0.8 + 0.8	2.4 + 0.8
Temperature (°F)	78	84	85	82	79	78	83

APPENDIX A (cont)

	Pajarito Field				
	PM-1	PM-2	PM-3	PM-4	PM-5
Date of Completion	1965	1965	1966	1981	1982
Elevation of LSD (ft)	6520	6715	6640	6920	7095
Construction					
Depth drilled (ft)	2501	2600	2552	2920	3120
Depth completed (ft)	2499	2300	2552	2875	3093
Diameter (in.)[b]	12	14	14	16	16
Water Levels					
Date	1982	1982	1982	1982	1982
Depth below LSD (ft)	748	874	762	1047	1208
Elevation (ft)	5772	5841	5878	5873	5887
Water-Level Fluctuations					
Period (yr)	1965-1982	1966-1982	1968-1982	1981-1982	---
Change (ft)	-2	-48	-19	<5	---
Annual rate (ft/yr)	-0.1	-2.8	-1.3	---	---
Aquifer					
Formation	QTp-Tsf	QTp-Tsf	QTp-Tsf	QTp-Tsf	QTp-Tsf
Saturated thickness (ft)	1751	1426	1790	1828	1885
Yield					
Date	1982	1982	1982	1982	1982
Rate (gpm)	589	1386	1402	1473	1225
Drawdown (ft)	22	60	23	40	144
Specific capacity (gpm/ft)	26.8	23.1	60.9	36.8	8.5
Transmissivity (gpd/ft)	55 000	40 000	320 000	44 000	10 000
Field coefficient of permeability (gpd/ft^2)	31	28	179	24	5.3
Production					
Period (yr)	1965-1982	1966-1982	1968-1982	1982	---
Pumpage (10^6 gal.)	1593	5863	3478	76	---
Quality of Water					
Date	3-18-81	3-18-81	3-18-81	8-3-81	8-4-81
Chemical (mg/ℓ)					
SiO_2	77	81	88	87	86
Ca	28	8	24	9	14
Mg	6.9	3.1	8.4	3	4
Na	18	10	18	11	24
CO_3	0	0	0	0	0
HCO_3	144	65	148	70	106
SO_4	5	3	7	4	10
Cl	4	9	10	2	4
F	0.3	0.3	0.4	0.3	0.3
NO_3	2.0	<0.1	1.8	2	8
TDS	212	140	216	165	211
Hard	90	36	90	36	52
Specific conductance (μmho)	260	130	250	120	190
pH	8.0	7.8	8.3	8.2	8.2
Radiochemical					
Total uranium (μg/ℓ)	2.4 ± 0.8	0.0 ± 0.8	1.0 ± 0.8	0.8 ± 0.8	2.2 ± 0.4
Temperature (°F)	71	69	71	69	73

[a]Well was abandoned in 1956; data were not used in the average hydrologic characteristics. It is located 150 ft SW of well LA-1B.

[b]Wells have two different diameter sizes of casing; i.e., 12 (650 ft) 10 reads: 12-in. diameter to 650 ft, then 10-in. diameter to completed depth of well.

Note: QTp = Puye Conglomerate; Tsf = Tesuque Formation.

APPENDIX B

CONSTRUCTION AND HYDROLOGIC DATA FOR TEST AND STOCK WELLS

	Test Wells				
	TW-1	TW-2	TW-3	TW-4	TW-5A
Date of Completion	1950	1949	1949	1950	1960
Elevation of LSD (ft)	6370	6645	6625	7245	7145
Construction					
Depth drilled (ft)	642	789	815	1205	1821
Depth completed (ft)	642	789	815	1205	1821
Diameter (in.)	8	8	10	6	8
Water levels					
Date	1951	1951	1951	1951	1964
Depth below LSD (ft)	593	760	750	1166	1178
Elevation (ft)	5773	5885	5875	6079	5967
Water-Level Fluctuations					
Period	---	---	---	---	1960-1964
Changes (ft)	---	---	---	---	–4
Annual rate (ft/yr)	---	---	---	---	–0.8
Aquifer					
Formations	QTp	QTp	QTp	Tt	QTp-Tsf
Saturated thickness (ft)	49	29	65	39	643
Yield					
Date	1951	1951	1951	1951	1960
Rate (gpm)	2.4	6.7	6.6	2.8	81
Drawdown (ft)	38.9	7.5	15.0	4.8	14.2
Specific capacity (gpm/ft)	<0.1	1.0	0.5	0.6	5.7
Transmissivity (gpd/ft)	200	7000	7800	750	11 000
Field coefficient of permeability (gpd/ft^2)	4	241	120	19	17
Quality of Water					
Date	2-28-81	9-17-81	3-31-81	6-8-65	9-16-81
Chemical (mg/ℓ)					
SiO_2	49	79	84	---	72
Ca	43	13	17	10	8
Mg	7.7	3.8	6.0	5	2.5
Na	12	9	13	20	11
CO_3	0	0	0	0	0
HCO_3	121	79	104	70	65
SO_4	3	3	3	---	1
Cl	7	3	4	2	2
F	0.4	0.5	0.4	<0.4	0.2
NO_3	2.4	6.2	4.1	0.4	3.9
TDS	220	150	168	163	124
Hardness	128	51	64	45	38
Specific conductance (μmho)	320	150	190	150	120
pH	8.0	8.0	7.9	7.9	7.9
Radiochemical					
Total uranium (μg/ℓ)	6.1 ± 1.2	0.1 ± 0.8	0.7 ± 0.8	0.5 ± 0.5	0.0 ± 0.8
Temperature (°F)	70	71	74	70	70

APPENDIX B (cont)

	Test Wells					Stock Wells	
	TW-8	DT-9	DT-10	Sigma Mesa	H-19	RW-2	RW-5
Date of Completion	1960	1960	1960	1979	1949	1954	1955
Elevation of LSD (ft)	6870	6935	7020	7215	7180	5642	5820
Construction							
Depth drilled (ft)	1065	1501	1409	2292	2000	161	132
Depth completed (ft)	1065	1501	1408	---	2000 a	161	132
Diameter (in.)	8	12	12	---	---	---	---
Water Levels							
Date	1965	1982	1967	1979	1949	1954	1955
Depth below LSD (ft)	969	1006	1091	1305.b	970	132	105
Elevation (ft)	5901	5929	5929	5910	6210	5510	5715
Water-Level Fluctuations							
Period	1960-1965	1960-1982	1960-1967	---	---	---	---
Change (ft)	-1	-3	-4	---	---	---	---
Annual rate (ft/yr)	-0.2	-0.2	-0.5	---	---	---	---
Aquifer							
Formations	QTp	QTp-Tsf	QTp-Tsf	QTp-Tsf	Tt-QTp	Tsf	Tsf
Saturated thickness (ft)	97	498	324	987	1030	---	---
Yield							
Date	1960	1960	1960	---	---	---	---
Rate (gpm)	16	88	78	---	---	---	---
Drawdown (ft)	8.0	4.0	4.9	---	---	---	---
Specific capacity (gpm/ft)	2	22	16	---	---	---	---
Transmissivity (gpd/ft)	2400	61 000	36 100	---	---	---	---
Field coefficient of permeability (gpd/ft^2)	25	122	111	---	---	---	---
Quality of Water							
Date	4-6-81	4-10-81	4-2-81	---	---	12-7-67	12-7-67
Chemical (mg/ℓ)							
SiO_2	50	72	58	---	---	---	---
Ca	4	9	10	---	---	32	28
Mg	0.9	3.1	3.5	---	---	5	7
Na	11	12	11	---	---	47	79
CO_3	7	0	0	---	---	0	0
HCO_3	22	69	81	---	---	114	158
SO_4	<1	2	1	---	---	---	---
Cl	3	4	3	---	---	8	10
F	2	<0.2	0.3	---	---	0.1	0.2
NO_3	4.4	4.3	<0.4	---	---	0.9	3.1
TDS	52	142	124	---	---	170	253
Hardness	16	35	42	---	---	100	100
Specific conductance (μmho)	90	150	130	---	---	200	270
pH	9.8	8.0	8.3	---	---	8.1	7.6
Radiochemical							
Total uranium (μg/ℓ)	0.0 ± 0.8	0.8 ± 0.8	0.8 ± 0.8	---	---	1.8 ± 0.4	2.3 ± 0.8
Temperature (°F)	67	70	67	---	---	67	66

[a]Hole abandoned.

[b]Water level interpreted from geophysical logs.

Note: Tsf = Tesuque Formation; QTp = Puye Conglomerate; and Tt = Tschicoma Formation.

APPENDIX C

HYDROLOGIC DATA FOR SPRINGS IN WHITE ROCK CANYON

	Spring 3	Spring 3B	Spring 4	Spring 5A	Spring 5B	Spring 6	Spring 8A	Spring 10
Elevation of LSD (ft)	5560	5500	5500	5430	5400	5380	5370	5360
Aquifer	QTp	Tsf	QTp	Tsf	Tsf	Tsf	Tsf	Tsf
Discharge at Rio Grande (gpm)	20	30	80	30	10	60	30	20
Quality of Water								
Date	10-13-81	10-13-81	10-13-81	10-13-81	10-14-81	10-14-81	10-14-81	10-15-81
Chemical (mg/ℓ)								
SiO_2	52	46	60	60	64	74	75	69
Ca	20	24	28	24	17	12	11	12
Mg	1.6	2.0	5.7	2.7	4.4	3.6	2.8	3.2
Na	16	139	15	22	12	11	13	13
CO_3	0	0	0	0	0	0	0	0
HCO_3	99	392	132	124	87	74	56	80
SO_4	4	4	6	7	2	2	3	3
Cl	5	6	8	6	4	4	5	4
F	0.4	0.6	0.5	0.3	0.5	0.3	0.4	0.4
NO_3	2.6	8.4	<0.4	1.7	2.0	<0.4	<0.4	1.7
TDS	125	374	168	186	152	134	152	146
Hardness	56	64	92	69	56	44	39	42
Specific conductance (μmho)	210	610	220	240	150	140	130	120
pH	8.1	7.5	7.0	7.4	7.4	7.0	9.0	7.8
Radiochemical								
Total uranium (μg/ℓ)	2.3 ± 0.8	19 ± 4.0	1.5 ± 0.8	2.2 ± 0.8	1.9 ± 0.8	1.0 ± 0.8	1.7 ± 0.8	1.7 ± 0.8
Temperature (°F)	72	68	66	70	61	73	72	66

Note: Tsf = Tesuque Formation and QTp = Puye Conglomerate.

APPENDIX D

CHEMICAL QUALITY OF WATER FROM MUNICIPAL SUPPLY AND DISTRIBUTION

Primary Chemical Quality Required for Municipal Use
(Concentrations in mg/ℓ)

	Ag	As	Ba	Cd	Cr	F	Hg	NO_3	Pb	Se
Los Alamos Field										
Well LA-1B	<0.0005	0.039	0.06	<0.001	0.022	2.6	<0.0002	1.2	<0.003	<0.003
Well LA-2	<0.0005	0.013	0.09	<0.001	0.020	1.9	<0.0002	1.8	<0.003	<0.003
Well LA-3	<0.0005	0.009	0.06	<0.001	0.010	0.7	<0.0002	1.7	<0.003	<0.003
Well LA-5	<0.0005	0.032	0.07	<0.001	0.010	1.0	<0.0002	1.4	<0.003	<0.003
Guaje Field										
Well G-1	<0.0005	<0.005	0.06	<0.001	0.008	0.4	<0.0002	1.2	<0.003	<0.003
Well G-1A	<0.0005	0.009	0.04	<0.001	0.006	0.5	<0.0002	1.2	<0.003	<0.003
Well G-2	<0.0005	0.048	0.03	<0.001	0.011	1.0	<0.0002	0.9	<0.003	<0.003
Well G-3	<0.0005	0.018	0.02	<0.001	0.005	0.4	<0.0002	1.0	0.004	<0.003
Well G-4	<0.0005	<0.005	0.02	<0.001	0.004	0.3	<0.0002	1.5	<0.003	<0.003
Well G-5	<0.0005	<0.005	0.02	<0.001	0.002	0.3	<0.0002	3.0	<0.003	<0.003
Well G-6	<0.0005	<0.005	0.02	<0.001	0.005	0.3	<0.0002	0.6	<0.003	<0.003
Pajarito Field										
Well PM-1	<0.0005	<0.005	0.09	<0.001	0.010	0.3	<0.0002	1.1	<0.003	<0.003
Well PM-2	<0.0005	<0.005	0.02	<0.001	0.004	0.2	<0.0002	0.4	<0.003	<0.003
Well PM-3	<0.0005	<0.005	0.05	<0.001	0.003	0.3	<0.0002	0.7	0.005	<0.003
Well PM-4	<0.0005	<0.005	0.04	<0.001	0.006	0.3	<0.0002	7.6	<0.003	<0.003
Well PM-5	<0.0005	<0.005	0.04	<0.001	0.002	0.4	<0.0002	3.0	<0.003	<0.003
Los Alamos Well LA-6	<0.0005	0.185		<0.001	0.014	2.3	<0.0002	0.4	0.006	<0.003
USEPA Maximum Contaminant Level	0.05	0.05	1.0	0.01	0.05	2.0	0.002	45	0.05	0.01

APPENDIX E

SECONDARY CHEMICAL QUALITY FOR MUNICIPAL USE
(concentrations in mg/ℓ)

	Cl	Cu	Fe	Mn	SO_4	Zn	TDS	pH
Los Alamos Field								
Well LA-1B	16	0.003	0.028	<0.002	27	<0.01	408	7.9
Well LA-2	16	0.006	0.100	0.008	12	<0.01	204	8.5
Well LA-3	4	<0.002	0.007	<0.002	5	<0.01	162	8.3
Well LA-5	2	<0.002	<0.005	<0.002	3	<0.01	170	8.6
Guaje Field								
Well G-1	3	0.003	0.007	0.010	<2	0.02	162	7.9
Well G-1A	3	0.013	0.006	<0.002	<2	0.02	152	8.3
Well G-2	3	<0.002	0.010	<0.002	2	<0.01	168	8.3
Well G-3	3	0.010	0.018	<0.002	<2	0.12	120	8.3
Well G-4	3	0.012	0.062	0.002	3	0.09	126	8.2
Well G-5	3	<0.002	0.012	0.002	4	<0.01	160	8.3
Well G-6	3	<0.002	<0.005	<0.002	2	<0.01	134	7.6
Pajarito Field								
Well PM-1	6	<0.002	<0.005	<0.002	2	<0.01	188	7.6
Well PM-2	2	0.003	<0.005	<0.002	2	0.04	134	8.0
Well PM-3	8	0.001	<0.005	<0.002	3	0.01	203	8.0
Well PM-4	2	<0.002	0.020	0.003	4	<0.01	169	8.2
Well PM-5	3	<0.002	0.050	0.005	10	<0.01	211	8.2
Water Canyon								
Gallery	<1	<0.002	0.325	<0.002	2	0.02	114	7.5
Los Alamos Well LA-6	4	0.011	0.908	<0.002	2	0.07	222	8.6
Secondary Standards	250	1.0	0.3	0.05	250	5.0	500	6.5 - 8.5

APPENDIX F

RADIOCHEMICAL QUALITY OF WATER FROM MUNICIPAL SUPPLY AND DISTRIBUTION

Station	1982 Date	Radiochemical						
		^{137}Cs (10^{-9} μCi/mℓ)	^{238}Pu (10^{-9} μCi/mℓ)	^{239}Pu (10^{-9} μCi/mℓ)	Gross Alpha (10^{-} μCi/mℓ)	Gross Beta (10^{-9} μCi/mℓ)	^{3}H (10^{-6} μCi/mℓ)	Total U (μg/ℓ)
Los Alamos Field								
Well LA-1B	3-30	−50 ± 80	−0.004 ± 0.014	−0.004 ± 0.012	11 ± 6.0	6.4 ± 2.4	---	5.0 ± 1.0
Well LA-2	3-30	19 ± 40	0.009 ± 0.020	−0.019 ± 0.000	9.0 ± 4.0	4.1 ± 1.8	0.3 ± 0.6	3.9 ± 0.8
Well LA-3	3-30	−80 ± 40	0.004 ± 0.012	−0.012 ± 0.008	1.5 ± 1.4	6.5 ± 2.0	1.2 ± 0.6	4.6 ± 1.0
Well LA-5	3-30	−10 ± 34	−0.005 ± 0.010	−0.010 ± 0.010	3.3 ± 2.0	3.8 ± 1.8	0.9 ± 0.6	7.0 ± 1.4
Guaje Field								
Well G-1	3-30	40 ± 60	−0.006 ± 0.012	−0.012 ± 0.012	0.1 ± 1.2	2.4 ± 1.6	3.4 ± 0.6	0.9 ± 0.8
Well G-1A	3-30	−2 ± 80	0.007 ± 0.030	−0.007 ± 0.020	0.3 ± 1.0	28 ± 6.0	1.8 ± 0.6	1.0 ± 0.8
Well G-2	3-30	−7 ± 38	0.005 ± 0.016	−0.014 ± 0.012	0.8 ± 1.2	0.8 ± 1.4	0.3 ± 0.6	0.9 ± 0.8
Well G-3	3-30	−40 ± 40	0.004 ± 0.014	−0.013 ± 0.000	1.0 ± 1.2	2.1 ± 1.6	4.1 ± 0.6	1.6 ± 0.8
Well G-4	3-30	40 ± 60	0.014 ± 0.038	0.010 ± 0.600	1.1 ± 1.2	1.2 ± 1.4	0.2 ± 0.6	1.0 ± 0.8
Well G-5	3-30	−40 ± 80	−0.005 ± 0.000	−0.016 ± 0.010	1.0 ± 1.0	3.8 ± 1.6	0.7 ± 0.6	1.3 ± 0.4
Well G-6	3-30	19 ± 40	0.009 ± 0.026	−0.009 ± 0.038	5.9 ± 2.4	7.7 ± 2.2	0.8 ± 0.6	1.7 ± 0.8
Pajarito Field								
Well PM-1	3-30	−50 ± 40	−0.010 ± 0.020	−0.050 ± 0.100	0.7 ± 1.4	8.1 ± 2.4	0.5 ± 0.6	1.8 ± 0.8
Well PM-2	3-30	20 ± 40	0.010 ± 0.040	−0.020 ± 0.040	1.1 ± 1.2	1.9 ± 1.6	0.3 ± 0.6	0.0 ± 0.8
Well PM-3	3-30	30 ± 20	−0.014 ± 0.014	−0.005 ± 0.014	1.0 ± 1.4	13 ± 3.2	4.2 ± 0.6	1.6 ± 0.8
Well PM-4	8-3	10 ± 48	0.012 ± 0.020	−0.012 ± 0.034	0.0 ± 0.8	18 ± 4.0	0.5 ± 0.6	0.8 ± 0.8
Well PM-5	8-4	36 ± 34	0.018 ± 0.024	0.004 ± 0.024	3.9 ± 2.2	3.2 ± 1.6	0.4 ± 0.6	2.2 ± 0.4
Los Alamos Field								
Well LA-6	3-30	−30 ± 40	−0.005 ± 0.000	−0.015 ± 0.030	2.9 ± 2.2	4.0 ± 1.8	0.5 ± 0.6	3.8 ± 0.8

☆ U.S. GOVERNMENT PRINTING OFFICE: 1984-0-776-026/4003

Los Alamos

Los Alamos National Laboratory
Los Alamos, New Mexico 87545

memorandum

TO: Anthony F. Drypolcher,
HSE-8 Associate Group Leader, MS E518

DATE: November 12, 1985

FROM: William D. Purtymun, HSE-8

MAIL STOP/TELEPHONE: K490/7-0810

SYMBOL: HSE8-85-1388

SUBJECT: REPORT "GEOLOGY AND HYDROLOGY OF AREA P NEAR S-SITE"

The subject report was prepared as you requested and is attached. Could you please see that Stan gets a copy?

WDP:brm

Attachment: a/s

Cy: T. Buhl, HSE-8, MS K490

GEOLOGY AND HYDROLOGY OF AREA P NEAR S-SITE

by

William D. Purtymun

I. INTRODUCTION

Area P (Landfill) is located on the western margin of the Pajarito Plateau within the boundaries of Los Alamos National Laboratory. The Pajarito Plateau, formed by a series of ashflows and ashfall tuffs, forms an apron around the east flank of the Sierra de los Valles (Fig. 1). The surface of the plateau slopes gently eastward and terminates along the Puye Escarpment and White Rock Canyon above the Rio Grande. The surface of the mesa has been dissected into a number of narrow mesas by southeast trending streams.

This report was requested by the Regulatory Compliance Section of the Environmental Surveillance Group (HSE-8). It was prepared from published reports and reconnaissance of the area.

II. GENERAL GEOLOGY

The Pajarito Plateau is structurally a part of the Rio Grande depression--a complex series of faulted troughs or basins that extend from southern Colorado along the Rio Grande to northern Mexico (Kelley 1952). The basement rock has been down faulted in the depression to as much as 10,000 to 15,000 feet below sea level (Fig. 2). The depression is filled with sediment and volcanic rocks.

The rocks that outcrop along the edges of and form the surface of the Pajarito Plateau are from oldest to youngest:

the Tesuque Formation, Puye Conglomerate, Basaltic Rocks of Chino Mesa, Tschicoma Formation, and Bandelier Tuff (Fig. 2). For a detailed description of these rock units, see Griggs (1964). The most important rock unit at Area P is the Bandelier Tuff.

The Bandelier Tuff forms the upper surface of the Pajarito Plateau. It is composed of a series of ashfalls and ashflows of rhyolite tuff. The three members of the Bandelier Tuff in ascending order are Guaje member, a lump pumice; the Otowi Member, a massive nonwelded ashflow; and the Tshirege Member, a series of moderately welded to welded ashflows (Purtymun and Koopman 1965). The Tshirege Member forms the surface of the mesa at Area P.

The most prominent structural feature of the Pajarito Plateau is the Pajarito Fault Zone, which tends northward along the western edge of the plateau (Fig. 3). The fault is downthrown to the east and displaces rocks of the Bandelier Tuff, Puye Conglomerate and Tschicoma Formation (Fig. 2). The displacement is estimated at about 400 ft (Budding 1976). Two smaller faults occur north and east of the Fault Zone (Fig. 3). They are the Los Alamos Fault (displacement 20 ft) and the Guaje Mountain Fault (displacement 10 to 50 ft). The Water Canyon Fault is the most important fault in this study as it occurs near Area P (see section III).

III. LOCAL GEOLOGY

Area P (Landfill) lies near the western margin of the Pajarito Plateau in a saddle of a short eastern trending narrow mesa. A scarp due to the Water Canyon fault lies to the west of the landfill. To the north, the Canon de Valle has cut through the scarp and drains an area to the west on

the flanks of the Sierra de los Valles. A small canyon has cut into the edge of the scarp to the south of the saddle. This south edge of the saddle slopes gently to the south. The explosive burning facility occupies the saddle and gently sloping part of the saddle to the south.

Area P (Landfill) occupies the northern part of the saddle that slopes gently to the north for about 400 feet and then becomes very steep as Canon de Valle has cut a deep canyon into the Bandelier Tuff. To the east of Area P the saddle rises gently to the top of the narrow mesa that terminates about a mile to the east as Canon de Valle turns abruptly to the south (Fig. 4).

The Bandelier Tuff (Tshirege Member) forms the saddle and underlies the Explosive Burning Facility and part of the landfill. About 50 feet of tuff in the saddle appear to be a moderately welded tuff, while about 80 feet of welded tuff is exposed beneath the moderately welded tuff in the south wall of Canon de Valle (Fig. 5).

The following geologic section is estimated from logs of Test Hole DT-5A and PM-2 and log of supply Well PM-2 (Purtymun 1968):

Geologic Unit	Thickness (ft)	Average Depth Below Land Surface to Top of Unit (ft)
Bandelier Tuff	800	0
Puye Conglomerate	500	800
Tschicoma Formation	~~1000~~	1300
Tesuque Formation and Earlier Volcanics and Sediments	2000	2300
Precambrian Rocks	--	4300

The Water Canyon fault lies about 2 miles east of the Pajarito Fault Zone (Fig. 3). It is a normal fault with a displacement of about 30 ft as measured between marker beds in the Bandelier tuff. The fault is downthrown to the east and is abut 2.5 to 3 miles long (Budding 1976).

The scarp formed west of Area P appears to be an erosional scarp. The Water Canyon fault lies east (Fig. 4). The outcrop of the upper units of the Bandelier Tuff on the north wall of Canon de Valle shows no breaks (bed dip to the west) northwest, north, and northeast of Area P. Several hundred yards east of Area P these beds are broken by the Water Canyon fault. The fault zones of broken tuff weather rapidly with the formation of silt and clay. These zones tend to restrict the movement of water rather than promote the movement. East of fault the beds dip gently to the east.

The elevation of the saddle is about 7460 ft above sea level. The main aquifer (aquifer capable of municipal and industrial supply) lies at an elevation of about 6230 feet above sea level, or 1230 feet below the saddle in the Puye Conglomerate.

IV. LOCAL HYDROLOGY

Surface runoff from Area P is into Canon de Valle. Canon de Valle heads on the flanks of the Sierra de los Valles to the west and is tributary to a major intermittent stream in Water Canyon about 2 miles to the southeast. Water Canyon is tributary to the Rio Grande about 6 miles to the east in White Rock Canyon.

The stream in Canon de Valle below Area P is probably intermittent due to small drainage areas on the flanks of the mountain. It contains some water used in cooling machining processes from facilities to the west. This water forms base flow of the stream.

Canon de Valle is over 100 feet deep at the saddle near Area P. The canyon in this area of the plateau contains only a thin section of alluvium (probably less than 10 feet thick), which could contain water from the stream perched on the underlying tuff. This is a common occurrence with water in major stream channels that cross the plateau. In Water Canyon, about 2.5 miles to the southeast, water in a shallow observation well fluctuates with the amount of runoff in the intermittent stream. It is dry most of the time. In this area, a 200-foot deep/2-foot diameter well cased through the alluvium to shut out the water is completed in the tuff. This well has contained no water for the past 25 years.

Based on other test holes and supply wells on the plateau (Frijoles Mesa, Supply Wells PM-2, 3, 4, and 5), there is no known perched water beneath the alluvium in the stream channel and the top of the main aquifer.

The top of the main aquifer lies at a depth of about 1230 feet below the surface in rocks of the Puye Conglomerate at Area P. The main aquifer is recharged from precipitation in the mountains to the west, deep canyons cut into the mountains, and from ground water in the Valles Caldera west of the Sierra de los Valles. The movement of water is from the recharge area eastward toward the Rio Grande where part of the water is discharged into the river through seeps and springs. The movement of water in the upper 500-feet of

aquifer at Frijoles Mesa to the southwest has been calculated at about 345 feet per year, while to the east the movement in the upper 1740 feet of supply well is much less at 95 feet per year (Purtymun 1984). The movement of the water in the main aquifer is probably near an average of the two rates at about 200 feet per year in the upper 1000 ft of the aquifer. A thick section of Tschicoma Formation lying within the main aquifer has a low permeability and tends to restrict the movement of water.

V. AREA P

The landfill at Area P is located on the south wall of Canon de Valles. The elevation is about 7400 ft. The south wall of the canyon contains a thick growth of live oak, pine, and wild rose.

The Bandelier Tuff that forms the Pajarito Plateau consists of a series of ashflow and ash falls that are described as nonwelded, moderately welded, and welded. The tuff at the landfill overlies a welded tuff and laps on to a moderately welded tuff (Fig. 5). The hydrologic characteristics of the tuff depend on degree of welding; the denser the welding, the lower porosity and hydraulic conductivity. The porosity of a moderately welded tuff will range from 30 to 55 percent by volume, while that of a welded tuff will range from 15 to 40% by volume. The saturated hydraulic conductivity for a moderately welded tuff ranges from 0.1 to 1.7 ft/day, while the welded tuff ranges from 0.009 to 0.26 ft/day. The tuff at Area P is not saturated.

The tuff is dry with natural moisture contents ranging from one to six percent by volume. Soil development on the tuff and north facing slopes has restricted most, if not

all, infiltration from precipitation into the underlying tuff.

The landfill is an on-sloping bench of moderately welded tuff underlain by a welded tuff (Fig. 5). The landfill was built from west to east. To the west the surface of the landfill has been capped with soil and tuff. There is no indication of water or leachate leaving the toe of the older part of the landfill.

To the west, on the recently used part of the landfill, there is a considerable erosion, subsidence and evidence of water entering the landfill. At the toe of the landfill in this area the water appears (at time of precipitation, not continuous flow) as surface flow on the top of the welded tuff.

The toe of the dump in the older part extends over the welded tuff, to the canyon bottom; however, the main part of the landfill is well above flood stage of Canon de Valle. There are some cans and other debris scattered below the main toe of the dump.

The landfill may not be located in the best possible area; however, there are some positive geologic and hydrologic conditions at the present location.

(1) The landfill is underlain by a welded tuff, which has a low porosity and a low hydraulic conductivity.

(2) The landfill is above the maximum flood level of Canon de Valle with exception of minor amounts of material that is scattered below the main toe of the landfill.

(3) It is in an area where all runoff water can be diverted from the landfill.

(4) About 1200 ft of unsaturated volcanics and sediments lie between the landfill and main aquifer of the Los Alamos Area.

(5) The Water Canyon Fault zone lies about 400 ft east of the landfill.

The depth to the top of the main aquifer, combined with the underlying relatively impermeable welded tuff, indicates that the present location of the landfill could be ideal with stabilization and runon and runoff control.

REFERENCES

Budding, A. J. and Purtymun, W. D., "Seismicity of the Los Alamos Area Based on Geologic Data," Los Alamos Scientific Laboratory report LA-6278-MS (1976).

Griggs, R. L., "Geology and Ground-Water Resources of the Los Alamos Area, New Mexico," U.S. Geol. Survey Water Supply Paper 1753 (1964).

Kelley, V. C., "Tectonics of the Rio Grande Depression of Central New Mexico," in The Rio Grande Country, NM Geol. Soc Guidebook, 3rd Field Conference (1952).

Purtymun, W. D. and Koopman, F. C., "Physical Characteristics of the Tshirege member of the Bandelier Tuff with Reference to Use as a Building and Ornamental Stone," U.s. Geol. Survey Open-File report (1965).

Purtymun, W. D., "Geology of the Microseismograph Station at S-Site, Los Alamos County, New Mexico," U.S. Geol. Survey Admin report (1968).

Purtymun, W. D., "Hydrologic Characteristics of the Main Aquifer in the Los Alamos Area: Development of Water Supplies," Los Alamos National Laboratory report LA-9957-MS (1984).

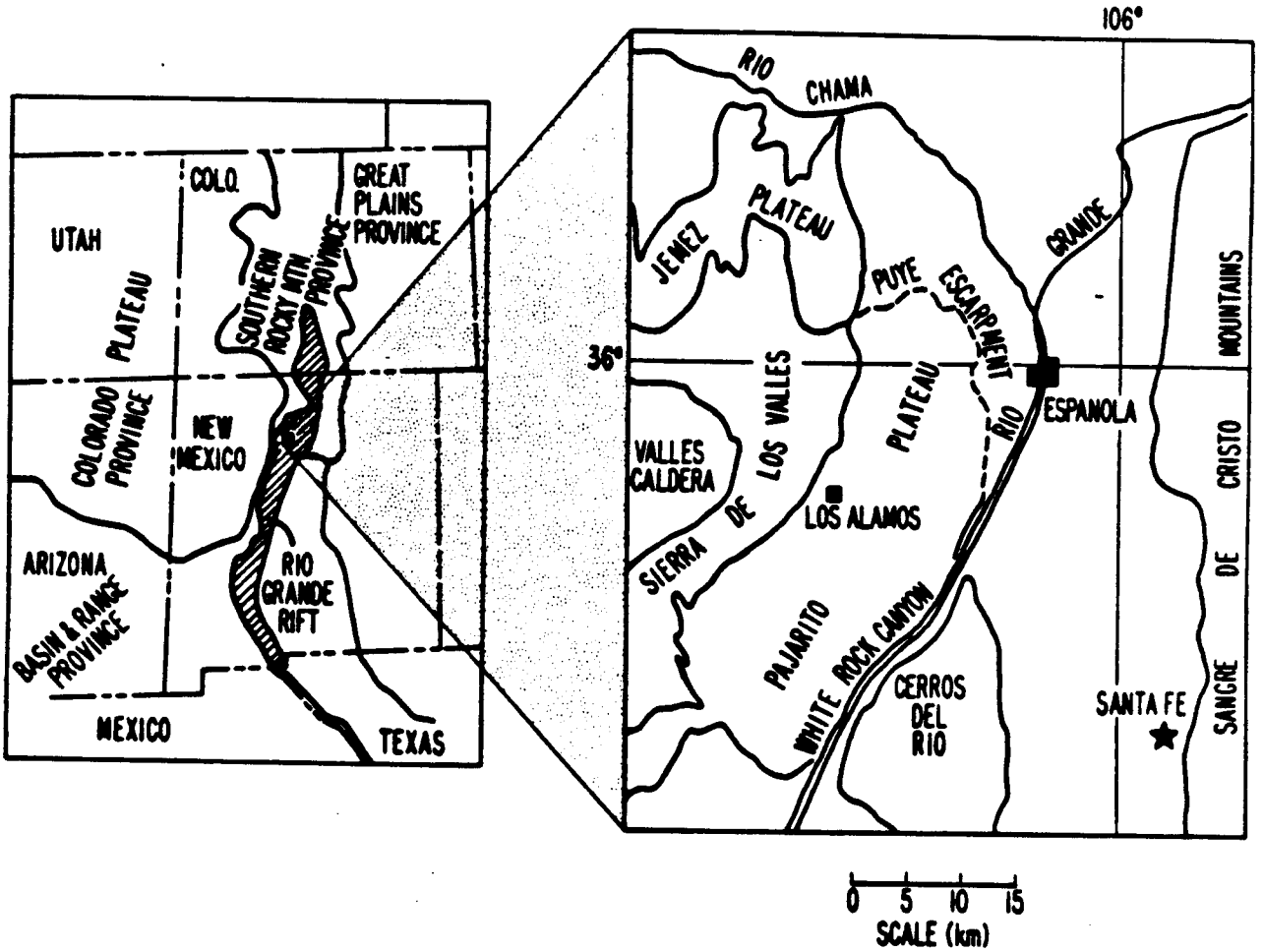

Fig. 1. Physiographic features of the Los Alamos Area.

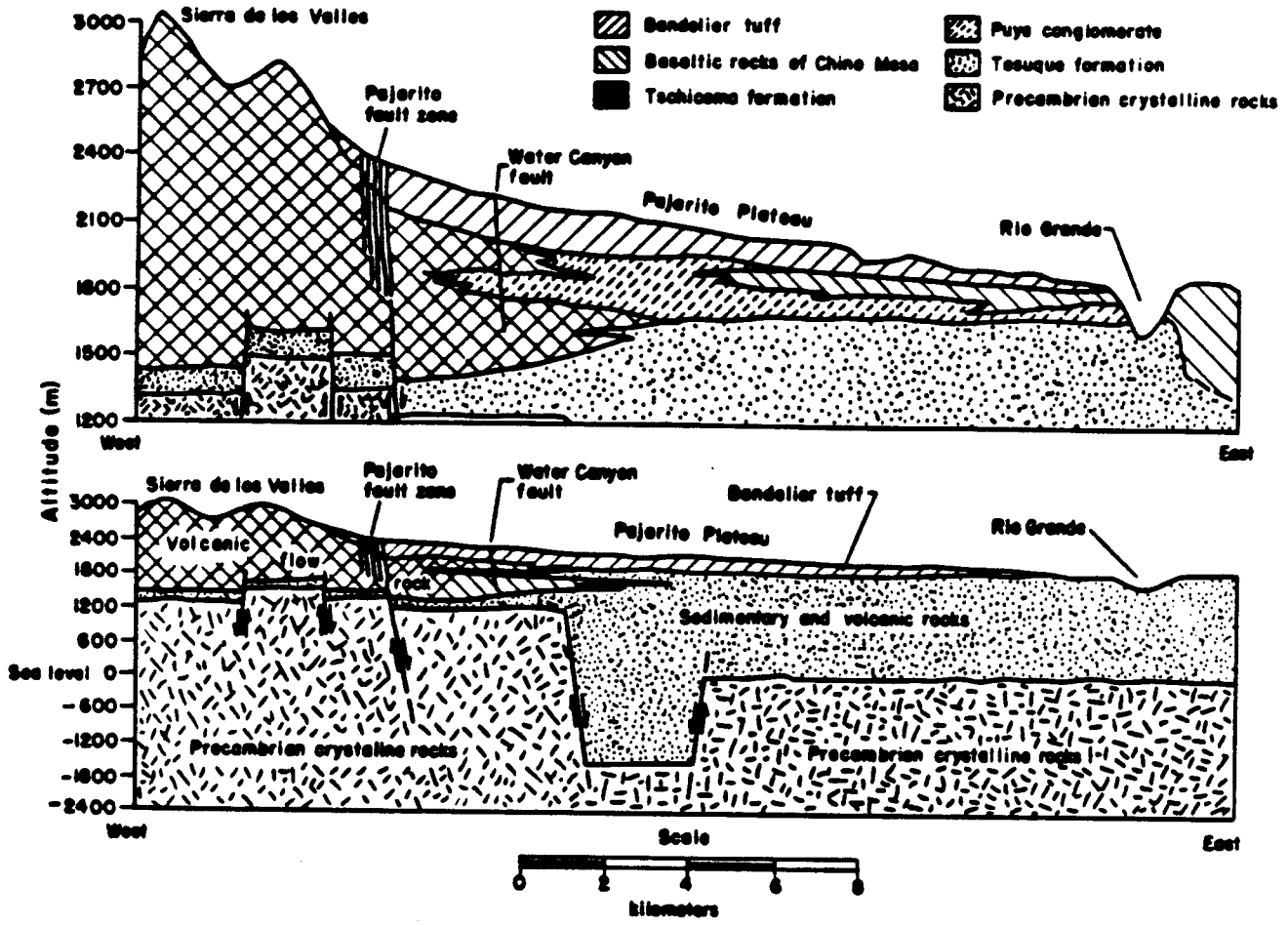

Fig. 2. Geologic section showing stratigraphic relationship of geologic unit.

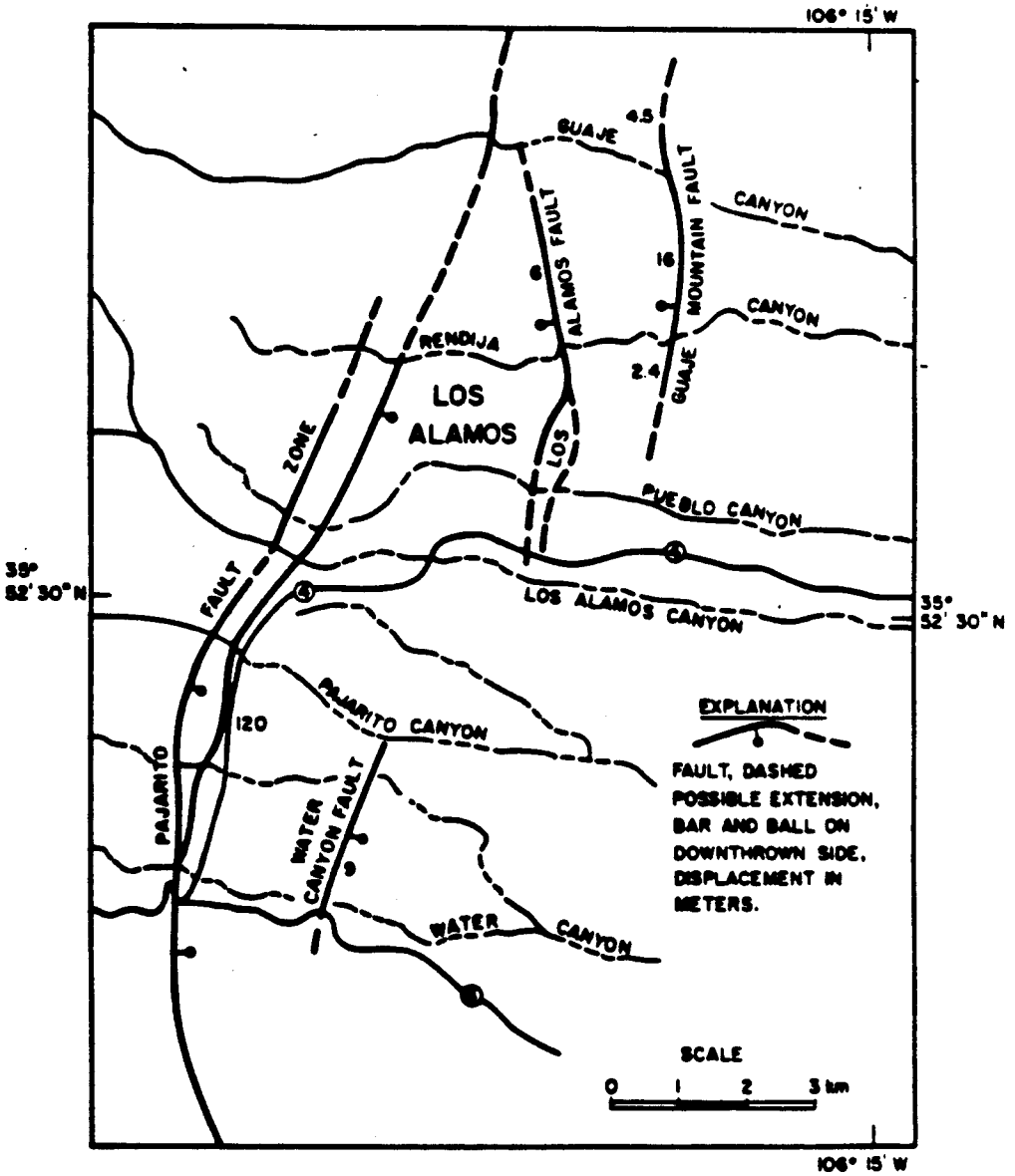

Fig. 3. Map showing faults in the Los Alamos Area.

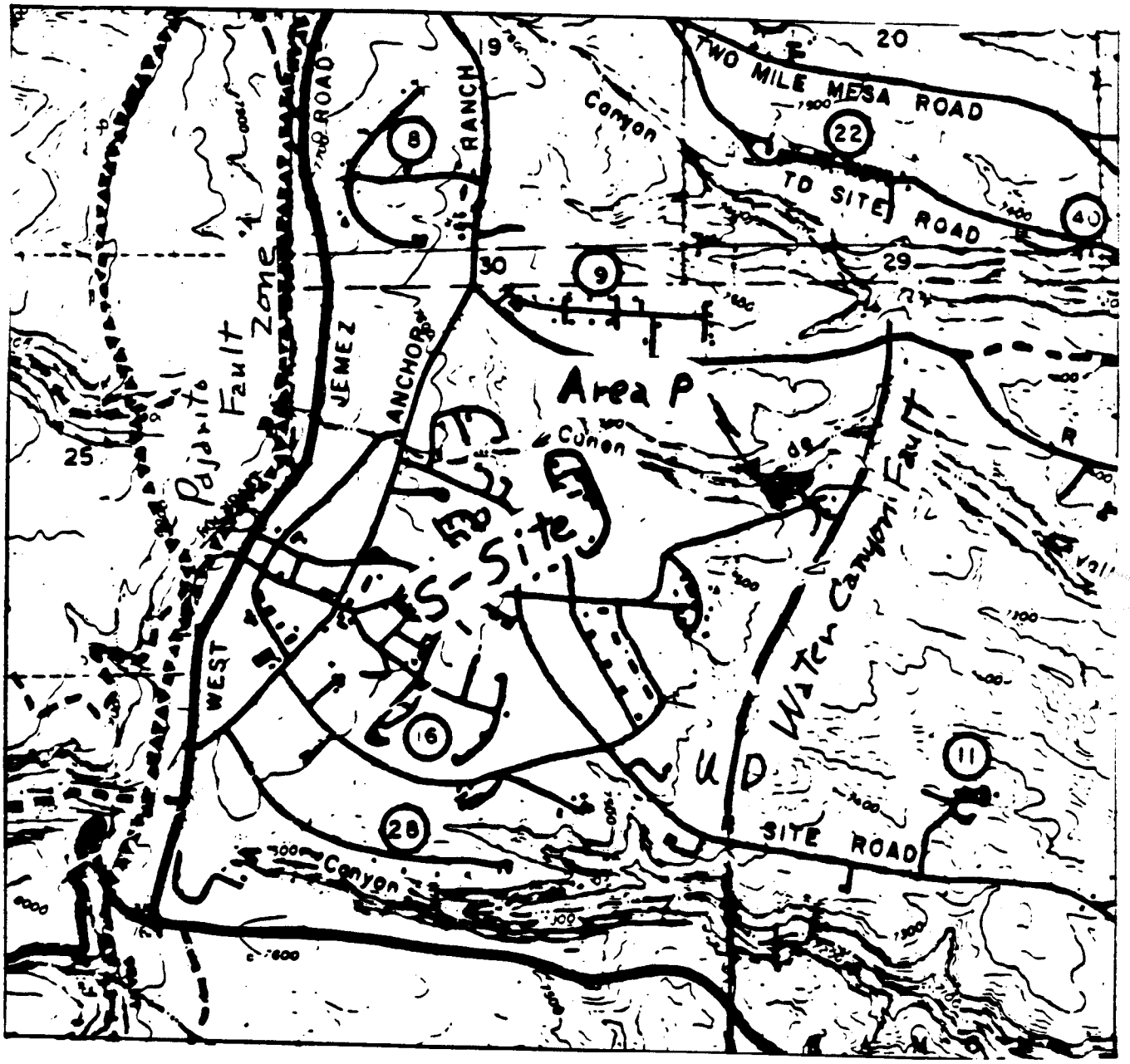

Fig. 4. Map showing S-Site, Area P and nearby faults.

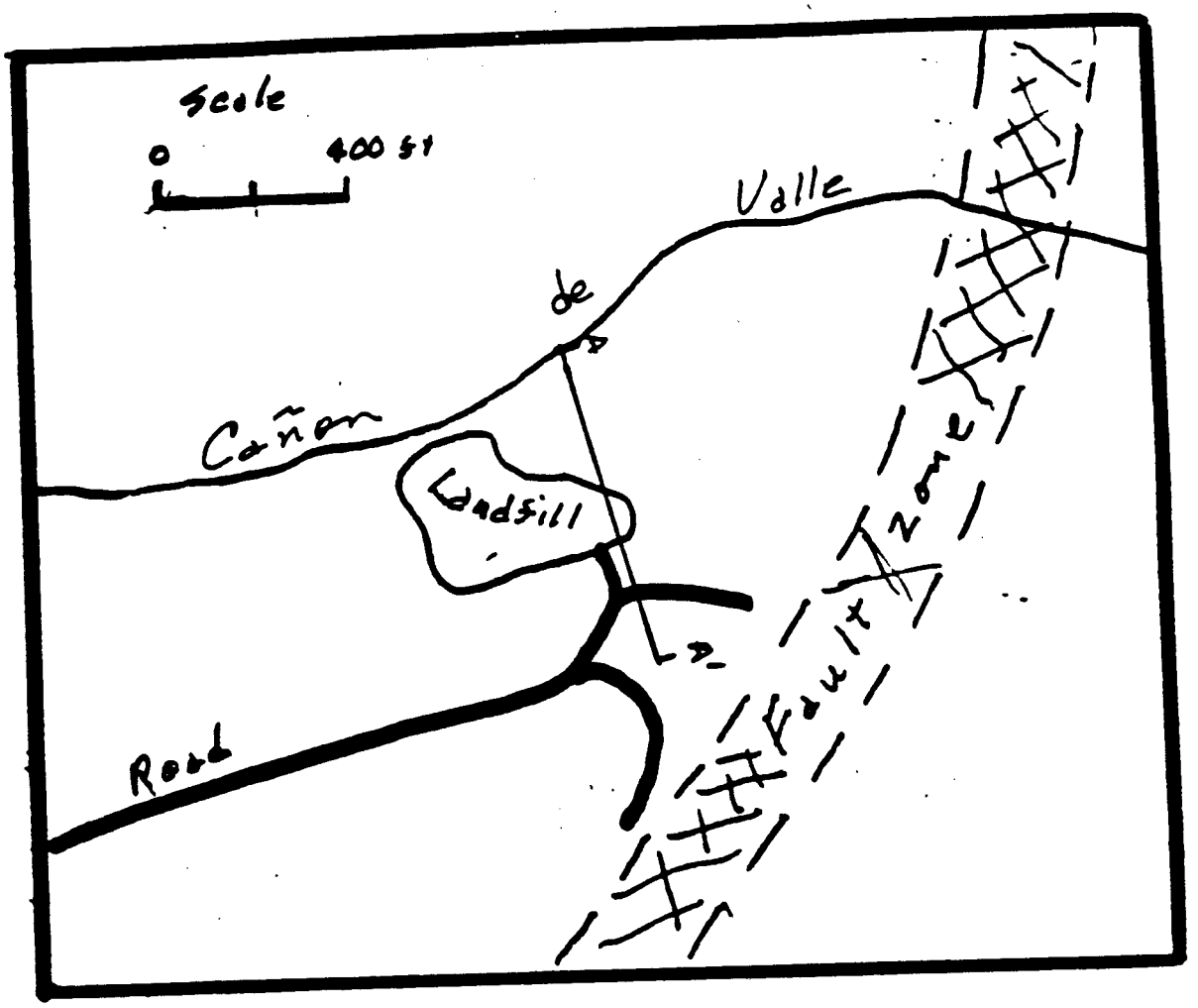

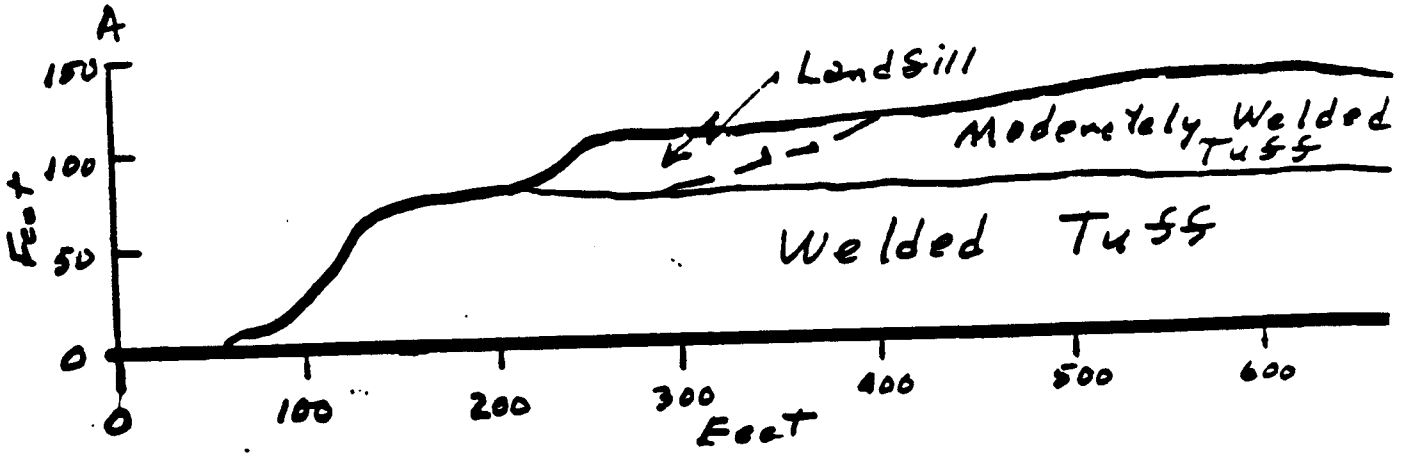

Fig. 5. Map showing landfill at Area P and generalized geologic section.

DANIEL B. STEPHENS & ASSOCIATES, INC.

CONSULTANTS IN GROUND-WATER HYDROLOGY SOCORRO, NEW MEXICO

FINAL DATA REPORT ON LABORATORY ANALYSES OF SOIL HYDRAULIC PROPERTIES OF WELDED TUFFS AT LOS ALAMOS NATIONAL LABORATORY

PREPARED FOR

LOS ALAMOS NATIONAL LABORATORY

JANUARY, 1988

DANIEL B. STEPHENS & ASSOCIATES, INC.
CONSULTANTS IN GROUND-WATER HYDROLOGY

• GROUND-WATER CONTAMINATION • UNSATURATED ZONE INVESTIGATIONS • WATER SUPPLY DEVELOPMENT •

January 5, 1988

Mr. Fred Brown
Hydrogeologist
Los Alamos National Laboratory
Group HSE-8
Los Alamos, NM 87545

Subject: Results of Testing for Hydraulic Properties of Welded Tuff

Dear Mr. Brown:

Please find enclosed the final data report on laboratory analyses for hydraulic properties of 10 cores of welded tuff. This report constitutes completion of the analyses requested.

We are continuing our own in-house research on unsaturated hydraulic conductivity using the additional cores that you provided us. I will report to you the results of the investigation when they have been completed.

We would like to point out that the porosity values we have reported are those computed from degree of saturation to water, and therefore represent the effective porosity to that fluid.

Daniel B. Stephens & Associates, Inc. cannot verify that samples are representative of the formation from which they were collected, and we do not assume any responsibility for interpretations or analyses based on this data.

We are very grateful to provide this service to Los Alamos National Laboratory. Please do not hesitate to call us if you have any questions.

Sincerely yours,

Daniel B. Stephens & Associates, Inc.

Warren B. Cox
Laboratory Manager

WBC:bdf
Enclosure

P.O. BOX 740 SOCORRO, NEW MEXICO 87801 (505) 835-3162

Final Data Report on Laboratory Analyses

Of

Soil Hydraulic Properties

Of

Welded Tuffs

At

Los Alamos National Laboratory

Prepared For

Los Alamos National Laboratory

January, 1988

DANIEL B. STEPHENS & ASSOCIATES, INC.

LIST OF TABLES

1. Summary of Tests Performed

2. Unit Conventions

3. Summary of Sample Characteristics

4. Summary of Saturated Hydraulic Conductivity Tests

5. Summary of Moisture Retention Characteristics

6. Summary of Initial Moisture Content, Dry Bulk Density and Porosity

7. Summary of Unsaturated Hydraulic Parameters

SCOPE OF WORK

Scope of Work

Daniel B. Stephens & Associates, Inc. (DBS) was requested by Los Alamos National Laboratory of Los Alamos, New Mexico, to perform laboratory analyses for properties of soil, as outlined in written communication of September 9, 1987. The scope of work included the following laboratory tests on 10 cores:

1. Sample Preparation
2. Saturated Hydraulic Conductivity
3. Moisture Retention (main drainage curve), Hanging Column Method, 2 points
4. Moisture Retention (main drainage curve), Pressure Plate Method, 4 points
5. Initial Moisture Content, Bulk Density and Porosity
6. Unsaturated Hydraulic Conductivity

In execution of the foregoing request, DBS has performed the work as summarized below and in Table 1.

The cores of welded tuff were cut by hand to fit soil retaining rings in which all tests were performed. Descriptions of the sample characteristics are presented in Table 3. Laboratory analyses to determine the hydraulic properties of the ten samples are summarized in Tables 4-7. The sample reference numbers were taken as those marked on the outside of each individual sample bag.

Included in this data report are summary tables, graphs where presentation in this form was required, and raw laboratory data. The Principles and Methods section describes the basic principles of the analyses and methods of calculation. All calculation results are expressed in metric units according to Table 2.

Table 1. Summary of Tests Performed

Sample Number	Hydraulic Conductivity		Moisture Retention		Initial Moisture Content	Porosity	Dry Bulk Density
	Saturated	Unsaturated	Hanging Column	Pressure Plate			
7-8	X	X	X	X	X	X	X
11-12	X	X	X	X	X	X	X
16-17	X	X	X	X	X	X	X
21-22	X	X	X	X	X	X	X
25-26	X	X	X	X	X	X	X
35-36	X	X	X	X	X	X	X
42-43	X	X	X	X	X	X	X
61-62	X	X	X	X	X	X	X
75-76	X	X	X	X	X	X	X
80-81	X	X	X	X	X	X	X

Table 2. Unit Conventions

Hydraulic Conductivity: cm/sec

Moisture Content: % volume

Bulk Density: g/cc

Porosity: dimensionless (cm^3/cm^3)

Note: Unless otherwise stated, lengths are in units of centimeters, and masses are in units of grams.

SAMPLE CHARACTERISTICS

Table 3. Summary of Sample Characteristics

Sample No.	Depth (ft)	Color	Texture	Comments
7-8	Unknown	Reddish Brown	Volcanic Ash	Contained Olivine Crystals
11-12	Unknown	Reddish Brown	Volcanic Ash	Contained Olivine Crystals
16-17	Unknown	Reddish Brown	Volcanic Ash	Contained Olivine Crystals
21-22	Unknown	Reddish Brown	Volcanic Ash	Contained Olivine Crystals
25-26	Unknown	Reddish Brown	Volcanic Ash	Contained Olivine Crystals
35-36	Unknown	Reddish Brown	Volcanic Ash	Contained Olivine Crystals
42-43	Unknown	Reddish Brown	Volcanic Ash	Contained Olivine Crystals
61-62	Unknown	Reddish Brown	Volcanic Ash	Contained Olivine Crystals
75-76	Unknown	Reddish Brown	Volcanic Ash	Contained Olivine Crystals and a small area of clay at one end
80-81	Unknown	Reddish Brown	Volcanic Ash	Contained Olivine Crystals

SATURATED HYDRAULIC CONDUCTIVITY

Table 4. Summary of Saturated Hydraulic Conductivity Tests

Sample No.	K_s (cm/sec)
7-8	1.58E-04
11-12	2.84E-04
16-17	2.78E-04
21-22	2.00E-04
25-26	9.18E-05
35-36	2.25E-05
42-43	8.57E-05
61-62	5.15E-04
75-76	2.28E-04
80-81	4.41E-05

FALLING HEAD TEST DATA

JOB NAME: Los Alamos
JOB NUMBER: 87-L-070
SAMPLE NUMBER: 7-8
RING NUMBER: 14
DEPTH: unknown
TYPE OF WATER USED: 0.01N CaCl2 SOLUTION
SAMPLE X-SECTION AREA: 22.060 (sq. cm)
STANDPIPE X-SECTION AREA: 0.785 (sq. cm)
SAMPLE LENGTH: 3.0 (cm)

DATE (1987)	TIME (DAY)	DEL T (SEC)	TEMP (C)	RESERVOIR HEAD(CM)	SAMPLE HEAD(CM)	K SAT (CM/SEC)	K SAT @ 20 C (CM/SEC)
TEST # 1:							
11/5	0.00		19.0	0.0	70.5		
11/5	0.00	705	19.0	0.0	24.8	1.58E-04	1.61E-04
TEST # 2:							
11/5	0.00		19.0	0.0	70.5		
11/5	0.00	590	19.0	0.0	30.4	1.52E-04	1.55E-04

AVERAGE K SAT: 1.58E-04 (CM/SEC)

COMMENTS:

LABORATORY ANALYSIS BY: S. Stoller
CALCULATIONS MADE BY: S. Stoller
CHECKED BY: W. Cox

FALLING HEAD TEST DATA

JOB NAME: Los Alamos
JOB NUMBER: 87-L-070
SAMPLE NUMBER: 11-12
RING NUMBER: 22
DEPTH: unknown
TYPE OF WATER USED: 0.01N CaCl2 SOLUTION
SAMPLE X-SECTION AREA: 22.060 (sq. cm)
STANDPIPE X-SECTION AREA: 0.785 (sq. cm)
SAMPLE LENGTH: 3.0 (cm)

DATE (1987)	TIME (DAY)	DEL T (SEC)	TEMP (C)	RESERVOIR HEAD(CM)	SAMPLE HEAD(CM)	K SAT (CM/SEC)	K SAT @ 20 C (CM/SEC)
TEST # 1:							
11/10	839:33		15.0	0.0	74.6		
11/10	845:39	423	15.0	0.0	29.4	2.35E-04	2.59E-04
TEST # 2:							
11/10	854:11		15.0	0.0	74.6		
11/10	900:20	369	15.0	0.0	28.3	2.80E-04	3.09E-04

AVERAGE K SAT: 2.84E-04 (CM/SEC)

COMMENTS:

LABORATORY ANALYSIS BY: S. Stoller
CALCULATIONS MADE BY: S. Stoller
CHECKED BY: W. Cox

FALLING HEAD TEST DATA

JOB NAME: Los Alamos
JOB NUMBER: 87-L-070
SAMPLE NUMBER: 16-17
RING NUMBER: 2
DEPTH: unknown
TYPE OF WATER USED: 0.01N CaCl2 SOLUTION
SAMPLE X-SECTION AREA: 22.060 (sq. cm)
STANDPIPE X-SECTION AREA: 0.785 (sq. cm)
SAMPLE LENGTH: 3.0 (cm)

DATE (1987)	TIME (DAY)	DEL T (SEC)	TEMP (C)	RESERVOIR HEAD(CM)	SAMPLE HEAD(CM)	K SAT (CM/SEC)	K SAT @ 20 C (CM/SEC)
TEST # 1:							
11/5	0.00		19.0	0.0	69.8		
11/5	0.00	302	19.0	0.0	32.7	2.68E-04	2.73E-04
TEST # 2:							
11/5	0.00		19.0	0.0	69.8		
11/5	0.00	276	19.0	0.0	34.0	2.78E-04	2.83E-04

AVERAGE K SAT: 2.78E-04 (CM/SEC)

COMMENTS:

LABORATORY ANALYSIS BY: S. Stoller
CALCULATIONS MADE BY: S. Stoller
CHECKED BY: W. Cox

FALLING HEAD TEST DATA

JOB NAME: Los Alamos
JOB NUMBER: 87-L-070
SAMPLE NUMBER: 21-22
RING NUMBER: F
DEPTH: unknown
TYPE OF WATER USED: 0.01N CaCl2 SOLUTION
SAMPLE X-SECTION AREA: 22.060 (sq. cm)
STANDPIPE X-SECTION AREA: 0.785 (sq. cm)
SAMPLE LENGTH: 3.0 (cm)

DATE (1987)	TIME (DAY)	DEL T (SEC)	TEMP (C)	RESERVOIR HEAD(CM)	SAMPLE HEAD(CM)	K SAT (CM/SEC)	K SAT @ 20 C (CM/SEC)
TEST # 1:							
11/5	0.00		19.0	0.0	76.1		
11/5	0.00	364	19.0	0.0	38.7	1.98E-04	2.02E-04
TEST # 2:							
11/5	0.00		19.0	0.0	76.1		
11/5	0.00	497	19.0	0.0	30.7	1.95E-04	1.99E-04

AVERAGE K SAT: 2.00E-04 (CM/SEC)

COMMENTS:

LABORATORY ANALYSIS BY: S. Stoller
CALCULATIONS MADE BY: S. Stoller
CHECKED BY: W. Cox

FALLING HEAD TEST DATA

JOB NAME: Los Alamos
JOB NUMBER: 87-L-070
SAMPLE NUMBER: 25-26
RING NUMBER: C
DEPTH: unknown
TYPE OF WATER USED: 0.01N CaCl2 SOLUTION
SAMPLE X-SECTION AREA: 22.060 (sq. cm)
STANDPIPE X-SECTION AREA: 0.785 (sq. cm)
SAMPLE LENGTH: 3.0 (cm)

DATE (1987)	TIME (DAY)	DEL T (SEC)	TEMP (C)	RESERVOIR HEAD(CM)	SAMPLE HEAD(CM)	K SAT (CM/SEC)	K SAT @ 20 C (CM/SEC)
TEST # 1:							
11/5	0.00		19.0	0.0	76.5		
11/5	0.00	1116	19.0	0.0	29.6	9.08E-05	9.25E-05
TEST # 2:							
11/5	0.00		19.0	0.0	76.5		
11/5	0.00	736	19.0	0.0	41.3	8.94E-05	9.11E-05

AVERAGE K SAT: 9.18E-05 (CM/SEC)

COMMENTS:

LABORATORY ANALYSIS BY: S. Stoller
CALCULATIONS MADE BY: S. Stoller
CHECKED BY: W. Cox

FALLING HEAD TEST DATA

JOB NAME: Los Alamos
JOB NUMBER: 87-L-070
SAMPLE NUMBER: 35-36
RING NUMBER: G
DEPTH: unknown
TYPE OF WATER USED: 0.01N CaCl2 SOLUTION
SAMPLE X-SECTION AREA: 22.060 (sq. cm)
STANDPIPE X-SECTION AREA: 0.785 (sq. cm)
SAMPLE LENGTH: 3.0 (cm)

DATE (1987)	TIME (DAY)	DEL T (SEC)	TEMP (C)	RESERVOIR HEAD(CM)	SAMPLE HEAD(CM)	K SAT (CM/SEC)	K SAT @ 20 C (CM/SEC)
TEST # 1:							
11/10	845:16		15.0	0.0	70.7		
11/10	941:03	3347	15.0	0.0	36.9	2.07E-05	2.29E-05
TEST # 2:							
11/10	942:22		15.0	0.0	70.7		
11/10	1110:48	5306	15.0	0.0	26.1	2.00E-05	2.21E-05

AVERAGE K SAT: 2.25E-05 (CM/SEC)

COMMENTS:

LABORATORY ANALYSIS BY: S. Stoller
CALCULATIONS MADE BY: S. Stoller
CHECKED BY: W. Cox

FALLING HEAD TEST DATA

JOB NAME: Los Alamos
JOB NUMBER: 87-L-070
SAMPLE NUMBER: 42-43
RING NUMBER: 4
DEPTH: unknown
TYPE OF WATER USED: 0.01N CaCl2 SOLUTION
SAMPLE X-SECTION AREA: 22.060 (sq. cm)
STANDPIPE X-SECTION AREA: 0.785 (sq. cm)
SAMPLE LENGTH: 3.0 (cm)

DATE (1987)	TIME (DAY)	DEL T (SEC)	TEMP (C)	RESERVOIR HEAD(CM)	SAMPLE HEAD(CM)	K SAT (CM/SEC)	K SAT @ 20 C (CM/SEC)
TEST # 1:							
11/10	841:17		15.0	0.0	76.5		
11/10	904:42	1405	15.0	0.0	29.6	7.21E-05	7.96E-05
TEST # 2:							
11/10	905:46		15.0	0.0	76.5		
11/10	923:33	1067	15.0	0.0	33.3	8.32E-05	9.18E-05

AVERAGE K SAT: 8.57E-05 (CM/SEC)

COMMENTS:

LABORATORY ANALYSIS BY: S. Stoller
CALCULATIONS MADE BY: S. Stoller
CHECKED BY: W. Cox

FALLING HEAD TEST DATA

JOB NAME: Los Alamos
JOB NUMBER: 87-L-070
SAMPLE NUMBER: 61-62
RING NUMBER: A4
DEPTH: unknown
TYPE OF WATER USED: 0.01N CaCl2 SOLUTION
SAMPLE X-SECTION AREA: 22.060 (sq. cm)
STANDPIPE X-SECTION AREA: 0.785 (sq. cm)
SAMPLE LENGTH: 3.0 (cm)

DATE (1987)	TIME (DAY)	DEL T (SEC)	TEMP (C)	RESERVOIR HEAD(CM)	SAMPLE HEAD(CM)	K SAT (CM/SEC)	K SAT @ 20 C (CM/SEC)
TEST # 1:							
11/10	840:53		15.0	0.0	79.8		
11/10	844:18	265	15.0	0.0	28.8	4.11E-04	4.53E-04
TEST # 2:							
11/10	855:36		15.0	0.0	79.8		
11/10	859:14	218	15.0	0.0	27.4	5.23E-04	5.78E-04

AVERAGE K SAT: 5.15E-04 (CM/SEC)

COMMENTS:

LABORATORY ANALYSIS BY: S. Stoller
CALCULATIONS MADE BY: S. Stoller
CHECKED BY: W. Cox

FALLING HEAD TEST DATA

JOB NAME: Los Alamos
JOB NUMBER: 87-L-070
SAMPLE NUMBER: 75-76
RING NUMBER: 19
DEPTH: unknown
TYPE OF WATER USED: 0.01N CaCl2 SOLUTION
SAMPLE X-SECTION AREA: 22.060 (sq. cm)
STANDPIPE X-SECTION AREA: 0.785 (sq. cm)
SAMPLE LENGTH: 3.0 (cm)

DATE (1987)	TIME (DAY)	DEL T (SEC)	TEMP (C)	RESERVOIR HEAD(CM)	SAMPLE HEAD(CM)	K SAT (CM/SEC)	K SAT @ 20 C (CM/SEC)
TEST # 1:							
11/10	840:27		15.0	0.0	76.1		
11/10	849:03	576	15.0	0.0	26.8	1.93E-04	2.13E-04
TEST # 2:							
11/10	855:03		15.0	0.0	76.1		
11/10	903:29	506	15.0	0.0	26.8	2.20E-04	2.43E-04

AVERAGE K SAT: 2.28E-04 (CM/SEC)

COMMENTS:

LABORATORY ANALYSIS BY: S. Stoller
CALCULATIONS MADE BY: S. Stoller
CHECKED BY: W. Cox

FALLING HEAD TEST DATA

JOB NAME: Los Alamos
JOB NUMBER: 87-L-070
SAMPLE NUMBER: 80-81
RING NUMBER: 18
DEPTH: unknown
TYPE OF WATER USED: 0.01N CaCl2 SOLUTION
SAMPLE X-SECTION AREA: 22.060 (sq. cm)
STANDPIPE X-SECTION AREA: 0.785 (sq. cm)
SAMPLE LENGTH: 3.0 (cm)

DATE (1987)	TIME (DAY)	DEL T (SEC)	TEMP (C)	RESERVOIR HEAD(CM)	SAMPLE HEAD(CM)	K SAT (CM/SEC)	K SAT @ 20 C (CM/SEC)
TEST # 1:							
11/10	840:02		15.0	0.0	74.9		
11/10	921:11	2469	15.0	0.0	27.4	4.35E-05	4.80E-05
TEST # 2:							
11/10	923:49		15.0	0.0	74.0		
11/10	1015:03	3074	15.0	0.0	25.9	3.65E-05	4.02E-05

AVERAGE K SAT: 4.41E-05 (CM/SEC)

COMMENTS:

LABORATORY ANALYSIS BY: S. Stoller
CALCULATIONS MADE BY: S. Stoller
CHECKED BY: W. Cox

MOISTURE RETENTION

Table 5. Summary of Moisture Retention Characteristics

Sample No.	Pressure Head (cm of water)	Moisture Content (cm^3/cm^3)
7-8	-0.0	51.8
	-100.0	49.4
	-195.0	49.0
	-1019.8	15.0
	-3059.4	13.9
	-5099.0	12.5
	-15297.0	8.3
11-12	-0.0	56.1
	-98.0	53.3
	-198.0	52.7
	-1019.8	37.6
	-3059.4	29.3
	-5099.0	26.1
	-15297.0	19.9
16-17	-0.0	54.9
	-101.0	53.6
	-199.0	52.9
	-1019.8	42.2
	-3059.4	29.2
	-5099.0	26.0
	-15297.0	20.4
21-22	-0.0	56.2
	-97.0	56.1
	-1019.8	28.1
	-3059.4	22.8
	-5099.0	19.5
	-15297.0	12.4
25-26	-0.0	52.0
	-98.5	51.4
	-1019.8	23.3
	-3059.4	21.3
	-5099.0	16.6
	-15297.0	10.0

Table 5. Summary of Moisture Retention Characteristics (continued)

Sample No.	Pressure Head (cm of water)	Moisture Content (% vol)
35-36	-0.0	42.8
	-205.0	41.4
	-1019.8	30.2
	-3059.4	14.2
	-5099.0	13.4
	-15297.0	9.4
42-43	-0.0	42.3
	-100.5	42.3
	-209.0	42.2
	-1019.8	33.5
	-3059.4	30.5
	-5099.0	28.9
	-15297.0	22.8
61-62	-0.0	36.4
	-95.5	34.8
	-202.0	32.6
	-1019.8	19.3
	-3059.4	11.2
	-5099.0	10.4
	-15297.0	7.9
75-76	-0.0	41.6
	-95.0	37.9
	-199.0	33.1
	-1019.8	24.0
	-3059.4	12.5
	-5099.0	11.6
	-15297.0	8.3
80-81	-0.0	34.6
	-1019.8	27.5
	-3059.4	18.3
	-5099.0	17.1
	-15297.0	10.7

MOISTURE RETENTION DATA - HANGING COLUMN
(PORE SIZE DISTRIBUTION)

JOB NAME: LOS ALAMOS
JOB NUMBER: 87-L-070
SAMPLE NUMBER: 7-8
RING NUMBER: 14
DEPTH: unknown
SAMPLE VOLUME: 66.18 (cc)
SATURATED WEIGHT AT 0 CM TENSION
(WITH CAP AND RING): 189.1 (g)
TARE RING: 72.1 (g)
TARE CAP: 0.0 (g)
DRY WEIGHT OF SAMPLE: 82.7 (g)
SATURATED MOISTURE CONTENT: 51.8 (% vol)
INITIAL VOLUME OF WATER IN SAMPLE: 34.3 (cc)

DATE (1987)	TIME	SUCTION (CM)	BURET VOL (CC)	CHANGE VOL (CC)	CHANGES VOL (CC)	MOISTURE CONTENT(% VOL) DRYING	WETTING
11/23	1025	0.0	37.1	--	--	51.8	0.0
11/25	800	100.0	35.5	1.6	1.6	49.4	0.0
11/30	810	195.0	35.2	0.3	1.9	49.0	0.0

COMMENTS:

LABORATORY ANALYSIS PERFORMED BY: S. Stoller
CALCULATION MADE BY: S. Stoller
CHECKED BY: W. Cox

MOISTURE RETENTION DATA - 15 BAR PRESSURE PLATE
(PORE SIZE DISTRIBUTION)

JOB NAME: LOS ALAMOS
JOB NUMBER: 87-L-070
SAMPLE NUMBER: 7-8
RING NUMBER: 14
DEPTH: unknown
SAMPLE VOLUME: 66.18 (cc)
SATURATED WEIGHT AT 0 CM TENSION
(WITH CAP AND RING): 189.1 (g)
TARE RING: 72.1 (g)
TARE CAP: 0.0 (g)
DRY WEIGHT OF SAMPLE: 82.7 (g)
SATURATED MOISTURE CONTENT: 51.8 (% vol)
INITIAL VOLUME OF WATER IN SAMPLE: 30.1 (cc)
WEIGHT FROM HANGING COLUMN, W/O CAP: 184.9 (g)
FINAL TENSION ON HANGING COLUMN: 195.0 (cm)

DATE (1987)	TIME	PRESSURE (BAR)	WEIGHT W/RING(G)	CHANGE WT (G)	CHANGES WT (G)	MOISTURE CONTENT (% VOL)
11/30	845	0.0	184.9	--	--	--
12/2	735	1.0	164.7	20.2	20.2	15.0
12/6	830	3.0	164.0	0.7	20.9	13.9
12/8	840	5.0	163.1	0.9	21.8	12.5
12/13	1655	15.0	160.3	2.8	24.6	8.3

COMMENTS:

LABORATORY ANALYSIS PERFORMED BY: S. Stoller
CALCULATION MADE BY: S. Stoller
CHECKED BY: W. Cox

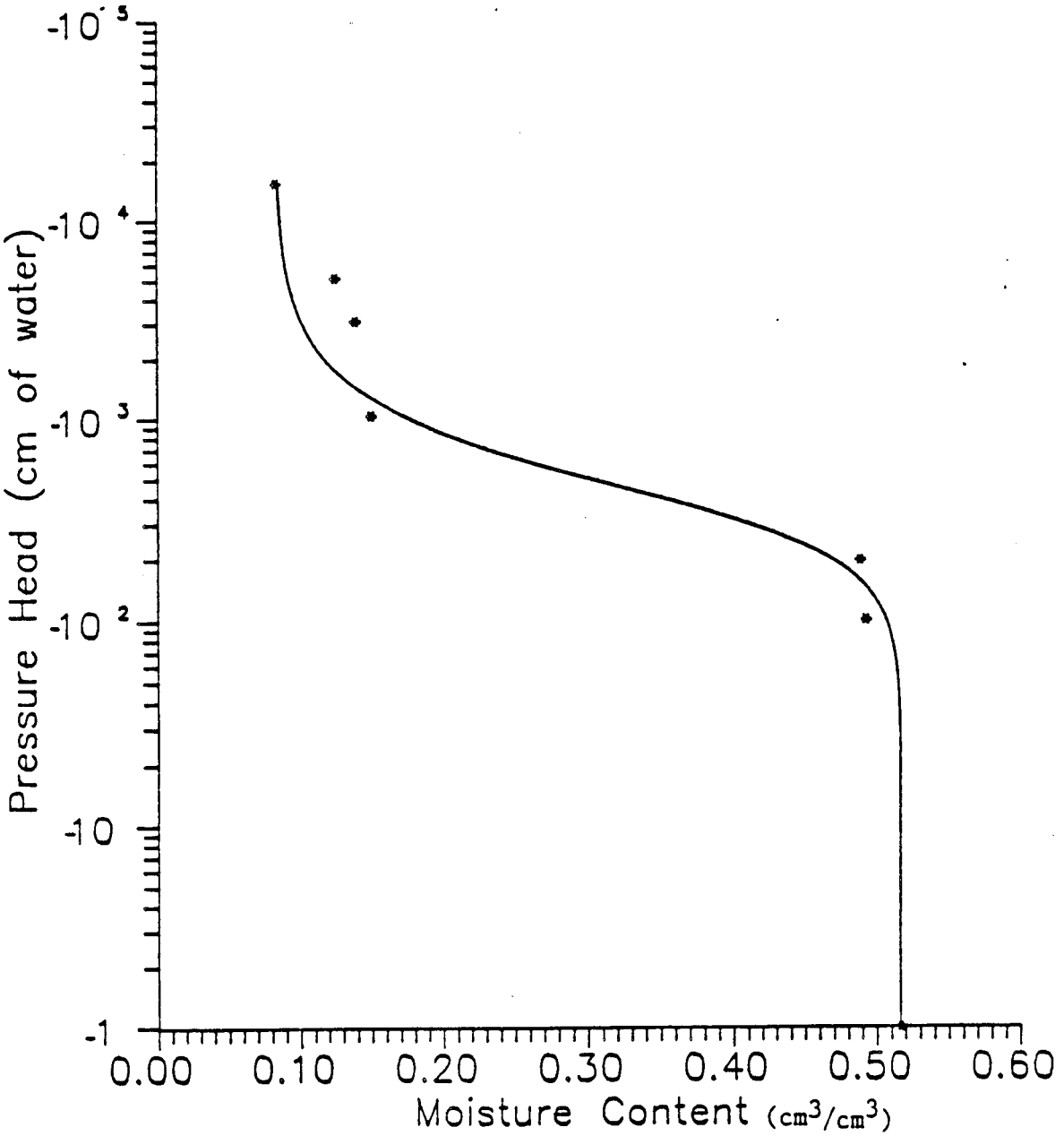

FIGURE NUMBER:	Pressure Head (cm of water) vs. Moisture Content (cm^3/cm^3), Sample No. 7-8.				DANIEL B. STEPHENS & ASSOCIATES, INC.
FOR:	PROJECT NO:	DATE:	PLOTTED BY:	CHECKED BY:	
Los Alamos	87-L-070	1/4/88	SLS	WBC	

MOISTURE RETENTION DATA - HANGING COLUMN
(PORE SIZE DISTRIBUTION)

JOB NAME: LOS ALAMOS
JOB NUMBER: 87-L-070
SAMPLE NUMBER: 11-12
RING NUMBER: 22
DEPTH: unknown
SAMPLE VOLUME: 66.18 (cc)
SATURATED WEIGHT AT 0 CM TENSION
(WITH CAP AND RING): 193.6 (g)
TARE RING: 73.3 (g)
TARE CAP: 0.0 (g)
DRY WEIGHT OF SAMPLE: 83.2 (g)
SATURATED MOISTURE CONTENT: 56.1 (% vol)
INITIAL VOLUME OF WATER IN SAMPLE: 37.1 (cc)

DATE (1987)	TIME	SUCTION (CM)	BURET VOL (CC)	CHANGE VOL (CC)	CHANGES VOL (CC)	MOISTURE CONTENT(% VOL) DRYING	WETTING
11/23	1025	0.0	36.4	--	--	56.1	0.0
11/25	800	98.0	34.6	1.8	1.8	53.3	0.0
11/30	810	198.0	34.2	0.4	2.2	52.7	0.0

COMMENTS:

LABORATORY ANALYSIS PERFORMED BY: S. Stoller
CALCULATION MADE BY: S. Stoller
CHECKED BY: W. Cox

MOISTURE RETENTION DATA - 15 BAR PRESSURE PLATE
(PORE SIZE DISTRIBUTION)

JOB NAME:	LOS ALAMOS
JOB NUMBER:	87-L-070
SAMPLE NUMBER:	11-12
RING NUMBER:	22
DEPTH:	unknown
SAMPLE VOLUME:	66.18 (cc)
SATURATED WEIGHT AT 0 CM TENSION (WITH CAP AND RING):	193.6 (g)
TARE RING:	73.3 (g)
TARE CAP:	0.0 (g)
DRY WEIGHT OF SAMPLE:	83.2 (g)
SATURATED MOISTURE CONTENT:	56.1 (% vol)
INITIAL VOLUME OF WATER IN SAMPLE:	32.6 (cc)
WEIGHT FROM HANGING COLUMN, W/O CAP:	189.1 (g)
FINAL TENSION ON HANGING COLUMN:	198.0 (cm)

DATE (1987)	TIME	PRESSURE (BAR)	WEIGHT W/RING(G)	CHANGE WT (G)	CHANGES WT (G)	MOISTURE CONTENT (% VOL)
11/30	845	0.0	189.1	--	--	--
12/2	740	1.0	181.4	7.7	7.7	37.6
12/6	830	3.0	175.9	5.5	13.2	29.3
12/8	840	5.0	173.8	2.1	15.3	26.1
12/13	1700	15.0	169.7	4.1	19.4	19.9

COMMENTS:

LABORATORY ANALYSIS PERFORMED BY: S. Stoller
CALCULATION MADE BY: S. Stoller
CHECKED BY: W. Cox

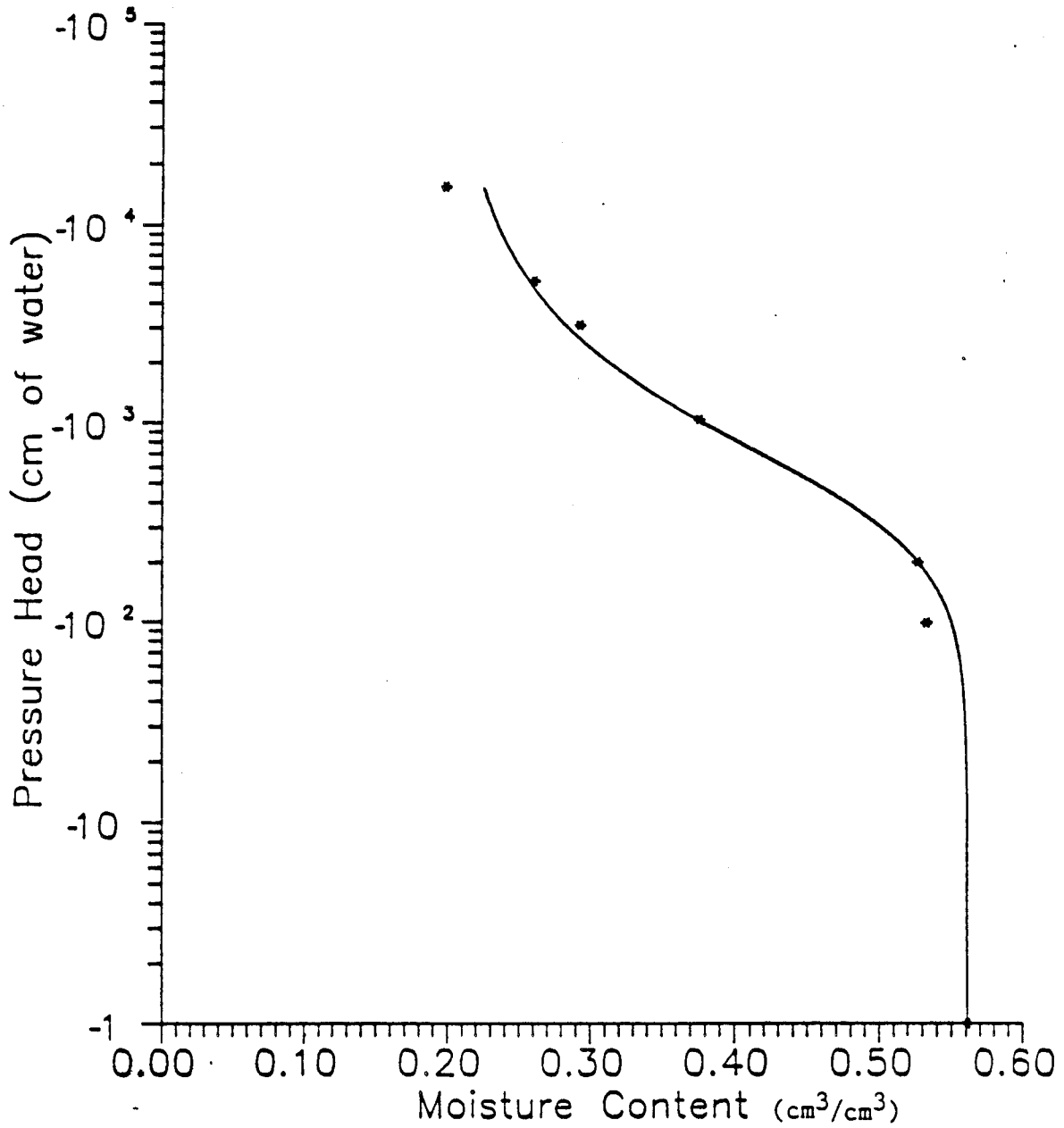

FIGURE NUMBER:	Pressure Head (cm of water) vs. Moisture Content (cm^3/cm^3), Sample No. 11-12				DANIEL B. STEPHENS & ASSOCIATES, INC.
FOR: Los Alamos	PROJECT NO: 87-L-070	DATE: 1/4/88	PLOTTED BY: SLS	CHECKED BY: WBC	

MOISTURE RETENTION DATA - HANGING COLUMN
(PORE SIZE DISTRIBUTION)

JOB NAME: LOS ALAMOS
JOB NUMBER: 87-L-070
SAMPLE NUMBER: 16-17
RING NUMBER: 2
DEPTH: unknown
SAMPLE VOLUME: 66.18 (cc)
SATURATED WEIGHT AT 0 CM TENSION
(WITH CAP AND RING): 193.6 (g)
TARE RING: 73.1 (g)
TARE CAP: 0.0 (g)
DRY WEIGHT OF SAMPLE: 84.2 (g)
SATURATED MOISTURE CONTENT: 54.9 (% vol)
INITIAL VOLUME OF WATER IN SAMPLE: 36.3 (cc)

DATE (1987)	TIME	SUCTION (CM)	BURET VOL (CC)	CHANGE VOL (CC)	CHANGES VOL (CC)	MOISTURE CONTENT(% VOL) DRYING	WETTING
11/23	1025	0.0	33.7	--	--	54.9	0.0
11/25	800	101.0	32.9	0.8	0.8	53.6	0.0
11/30	810	199.0	32.4	0.5	1.3	52.9	0.0

COMMENTS:

LABORATORY ANALYSIS PERFORMED BY: S. Stoller
CALCULATION MADE BY: S. Stoller
CHECKED BY: W. Cox

MOISTURE RETENTION DATA - 15 BAR PRESSURE PLATE
(PORE SIZE DISTRIBUTION)

JOB NAME: LOS ALAMOS
JOB NUMBER: 87-L-070
SAMPLE NUMBER: 16-17
RING NUMBER: 2
DEPTH: unknown
SAMPLE VOLUME: 66.18 (cc)
SATURATED WEIGHT AT 0 CM TENSION
(WITH CAP AND RING): 193.6 (g)
TARE RING: 73.1 (g)
TARE CAP: 0.0 (g)
DRY WEIGHT OF SAMPLE: 84.2 (g)
SATURATED MOISTURE CONTENT: 54.9 (% vol)
INITIAL VOLUME OF WATER IN SAMPLE: 33.4 (cc)
WEIGHT FROM HANGING COLUMN, W/O CAP: 190.7 (g)
FINAL TENSION ON HANGING COLUMN: 199.0 (cm)

DATE (1987)	TIME	PRESSURE (BAR)	WEIGHT W/RING(G)	CHANGE WT (G)	CHANGES WT (G)	MOISTURE CONTENT (% VOL)
11/30	845	0.0	190.7	--	--	--
12/2	740	1.0	185.2	5.5	5.5	42.2
12/6	830	3.0	176.6	8.6	14.1	29.2
12/8	840	5.0	174.5	2.1	16.2	26.0
12/13	1700	15.0	170.8	3.7	19.9	20.4

COMMENTS:

LABORATORY ANALYSIS PERFORMED BY: S. Stoller
CALCULATION MADE BY: S. Stoller
CHECKED BY: W. Cox

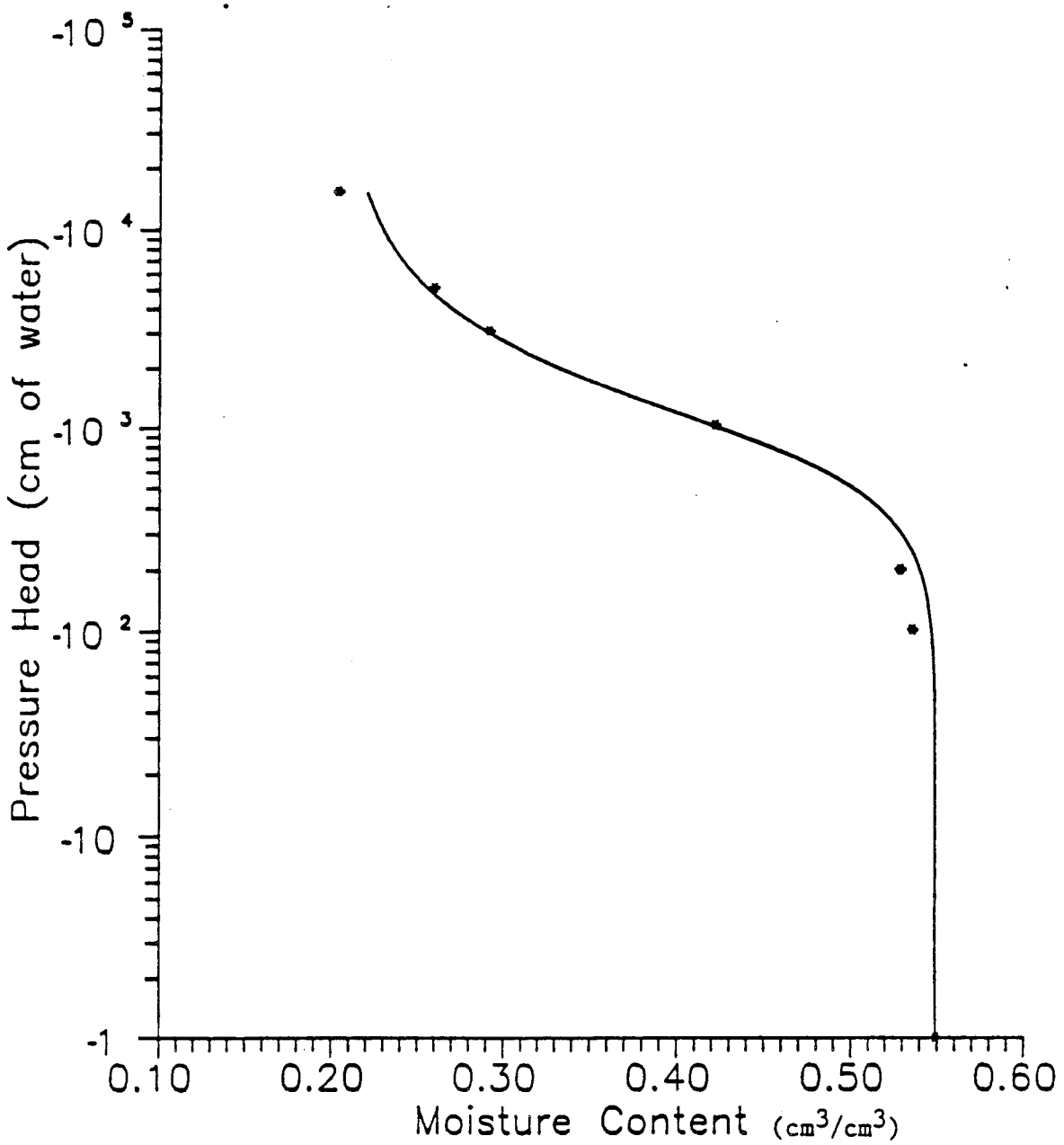

FIGURE NUMBER:	Pressure Head (cm of water) vs. Moisture Content (cm^3/cm^3), Sample No. 16-17				DANIEL B. STEPHENS & ASSOCIATES, INC.
FOR: Los Alamos	PROJECT NO: 87-L-070	DATE: 1/4/88	PLOTTED BY: SLS	CHECKED BY: WBC	

MOISTURE RETENTION DATA - HANGING COLUMN
(PORE SIZE DISTRIBUTION)

JOB NAME: LOS ALAMOS
JOB NUMBER: 87-L-070
SAMPLE NUMBER: 21-22
RING NUMBER: F
DEPTH: unknown
SAMPLE VOLUME: 66.18 (cc)
SATURATED WEIGHT AT 0 CM TENSION
(WITH CAP AND RING): 194.0 (g)
TARE RING: 73.8 (g)
TARE CAP: 0.0 (g)
DRY WEIGHT OF SAMPLE: 83.0 (g)
SATURATED MOISTURE CONTENT: 56.2 (% vol)
INITIAL VOLUME OF WATER IN SAMPLE: 37.2 (cc)

DATE (1987)	TIME	SUCTION (CM)	BURET VOL (CC)	CHANGE VOL (CC)	CHANGES VOL (CC)	MOISTURE CONTENT(% VOL) DRYING	WETTING
11/23	1025	0.0	34.5	--	--	56.2	0.0
11/25	800	97.0	34.4	0.1	0.1	56.1	0.0
11/30	810	198.0	37.6	-3.2	-3.1	60.9	0.0

COMMENTS:

LABORATORY ANALYSIS PERFORMED BY: S. Stoller
CALCULATION MADE BY: S. Stoller
CHECKED BY: W. Cox

MOISTURE RETENTION DATA - 15 BAR PRESSURE PLATE
(PORE SIZE DISTRIBUTION)

JOB NAME: LOS ALAMOS
JOB NUMBER: 87-L-070
SAMPLE NUMBER: 21-22
RING NUMBER: F
DEPTH: unknown
SAMPLE VOLUME: 66.18 (cc)
SATURATED WEIGHT AT 0 CM TENSION
(WITH CAP AND RING): 194.0 (g)
TARE RING: 73.8 (g)
TARE CAP: 0.0 (g)
DRY WEIGHT OF SAMPLE: 83.0 (g)
SATURATED MOISTURE CONTENT: 56.2 (% vol)
INITIAL VOLUME OF WATER IN SAMPLE: 32.7 (cc)
WEIGHT FROM HANGING COLUMN, W/O CAP: 189.5 (g)
FINAL TENSION ON HANGING COLUMN: 198.0 (cm)

DATE (1987)	TIME	PRESSURE (BAR)	WEIGHT W/RING(G)	CHANGE WT (G)	CHANGES WT (G)	MOISTURE CONTENT (% VOL)
11/30	845	0.0	189.5	--	--	--
12/2	740	1.0	175.4	14.1	14.1	28.1
12/6	830	3.0	171.9	3.5	17.6	22.8
12/8	840	5.0	169.7	2.2	19.8	19.5
12/13	1710	15.0	165.0	4.7	24.5	12.4

COMMENTS:

LABORATORY ANALYSIS PERFORMED BY: S. Stoller
CALCULATION MADE BY: S. Stoller
CHECKED BY: W. Cox

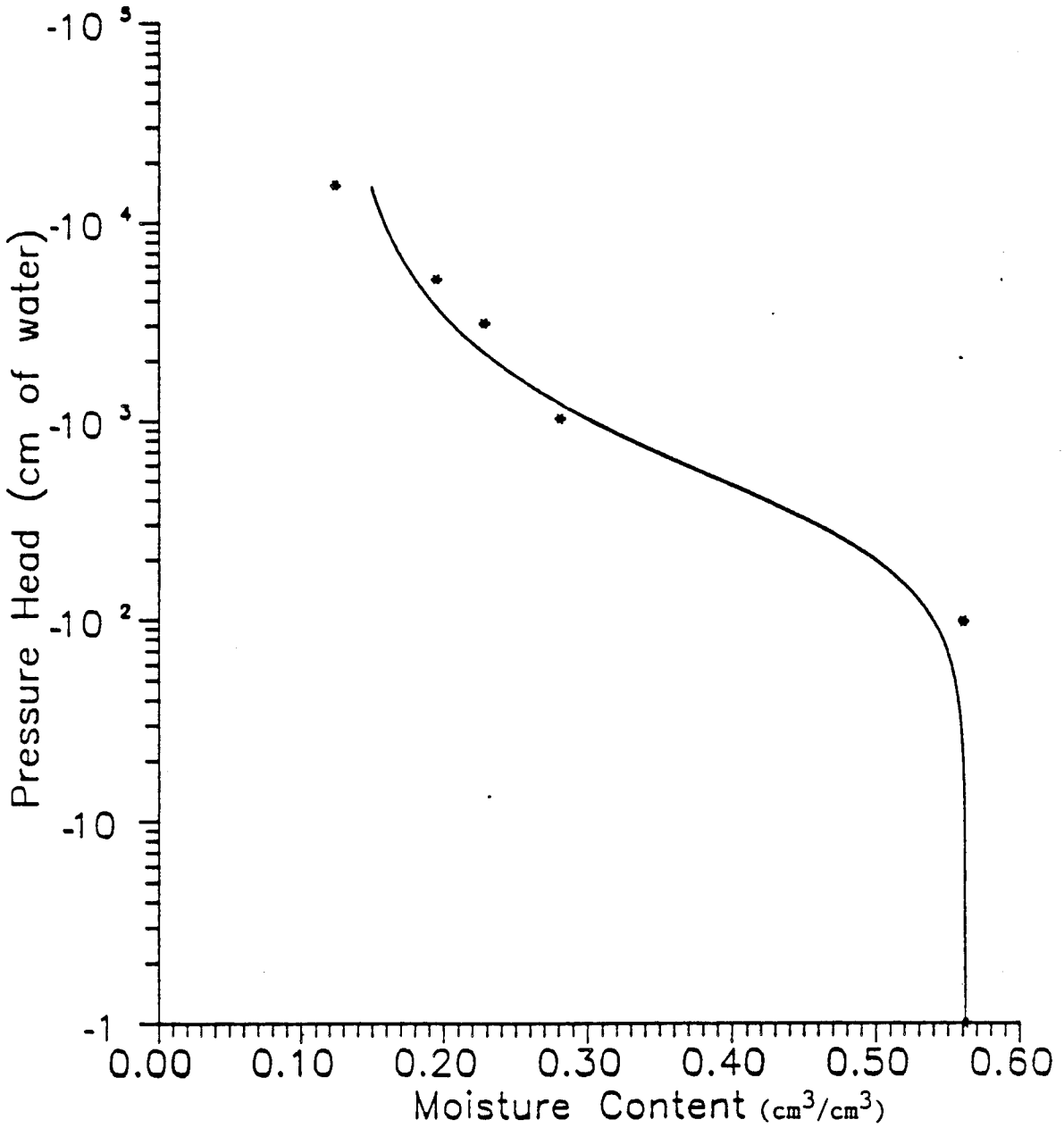

FIGURE NUMBER:	Pressure Head (cm of water) vs. Moisture Content (cm^3/cm^3), Sample No. 21-22				DANIEL B. STEPHENS & ASSOCIATES, INC.
FOR: Los Alamos	PROJECT NO: 87-L-070	DATE: 1/4/88	PLOTTED BY: SLS	CHECKED BY: WBC	

MOISTURE RETENTION DATA - HANGING COLUMN
(PORE SIZE DISTRIBUTION)

JOB NAME: LOS ALAMOS
JOB NUMBER: 87-L-070
SAMPLE NUMBER: 25-26
RING NUMBER: C
DEPTH: unknown
SAMPLE VOLUME: 66.18 (cc)
SATURATED WEIGHT AT 0 CM TENSION
(WITH CAP AND RING): 198.3 (g)
TARE RING: 72.8 (g)
TARE CAP: 0.0 (g)
DRY WEIGHT OF SAMPLE: 91.1 (g)
SATURATED MOISTURE CONTENT: 52.0 (% vol)
INITIAL VOLUME OF WATER IN SAMPLE: 34.4 (cc)

DATE (1987)	TIME	SUCTION (CM)	BURET VOL (CC)	CHANGE VOL (CC)	CHANGES VOL (CC)	MOISTURE CONTENT(% VOL) DRYING	WETTING
11/23	1025	0.0	35.6	--	--	52.0	0.0
11/25	800	98.5	35.2	0.4	0.4	51.4	0.0
11/30	810	203.0	36.5	-1.3	-0.9	53.3	0.0

COMMENTS:

LABORATORY ANALYSIS PERFORMED BY: S. Stoller
CALCULATION MADE BY: S. Stoller
CHECKED BY: W. Cox

MOISTURE RETENTION DATA - 15 BAR PRESSURE PLATE
(PORE SIZE DISTRIBUTION)

JOB NAME: LOS ALAMOS
JOB NUMBER: 87-L-070
SAMPLE NUMBER: 25-26
RING NUMBER: C
DEPTH: unknown
SAMPLE VOLUME: 66.18 (cc)
SATURATED WEIGHT AT 0 CM TENSION
(WITH CAP AND RING): 198.3 (g)
TARE RING: 72.8 (g)
TARE CAP: 0.0 (g)
DRY WEIGHT OF SAMPLE: 91.1 (g)
SATURATED MOISTURE CONTENT: 52.0 (% vol)
INITIAL VOLUME OF WATER IN SAMPLE: 30.9 (cc)
WEIGHT FROM HANGING COLUMN, W/O CAP: 194.8 (g)
FINAL TENSION ON HANGING COLUMN: 203.0 (cm)

DATE (1987)	TIME	PRESSURE (BAR)	WEIGHT W/RING(G)	CHANGE WT (G)	CHANGES WT (G)	MOISTURE CONTENT (% VOL)
11/30	845	0.0	194.8	--	--	--
12/2	740	1.0	179.3	15.5	15.5	23.3
12/6	830	3.0	178.0	1.3	16.8	21.3
12/8	840	5.0	174.9	3.1	19.9	16.6
12/13	1710	15.0	170.5	4.4	24.3	10.0

COMMENTS:

LABORATORY ANALYSIS PERFORMED BY: S. Stoller
CALCULATION MADE BY: S. Stoller
CHECKED BY: W. Cox

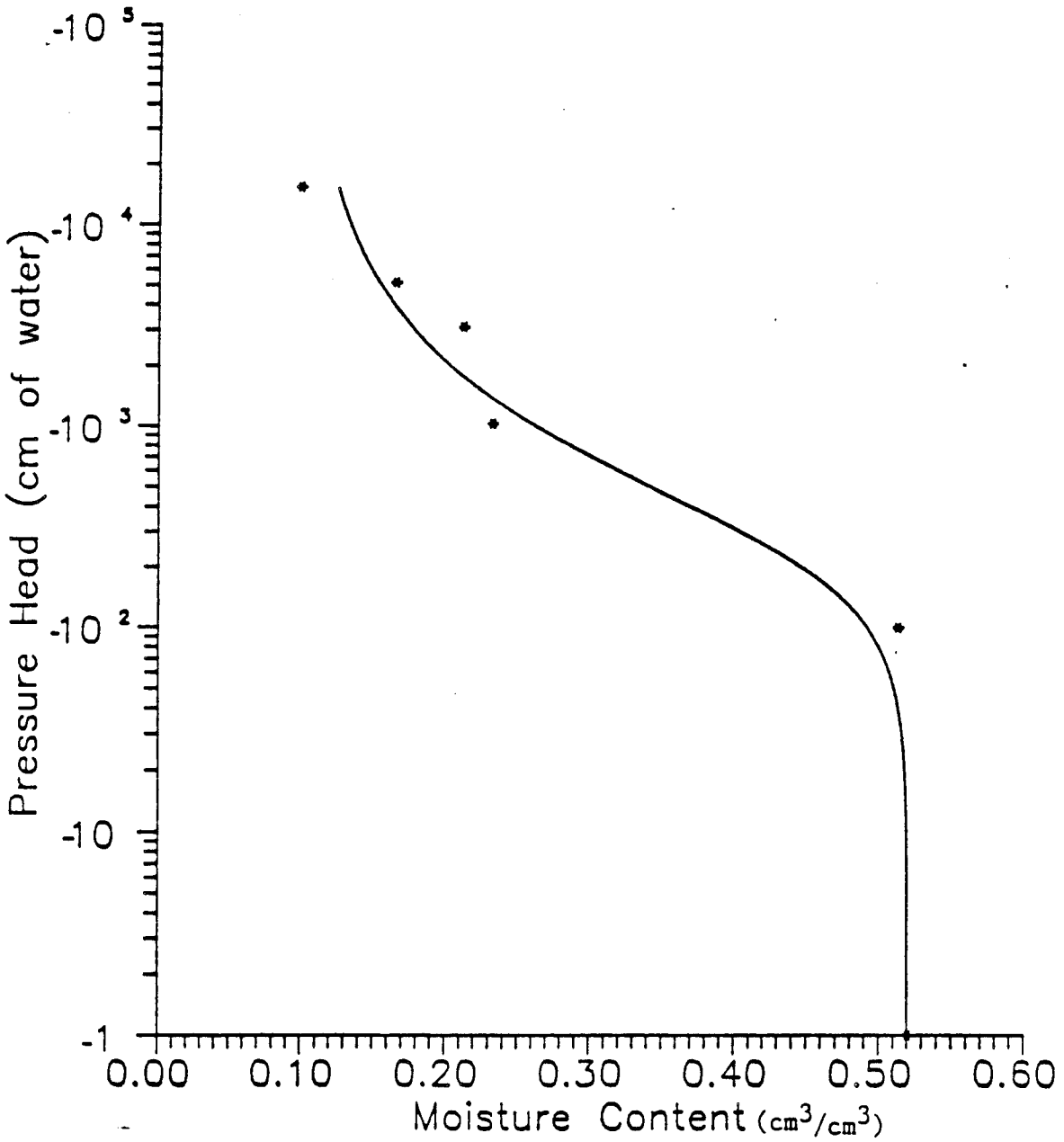

FIGURE NUMBER:	Pressure Head (cm of water) vs. Moisture Content (cm^3/cm^3), Sample No. 25-26				DANIEL B. STEPHENS & ASSOCIATES, INC.
FOR: Los Alamos	PROJECT NO: 87-L-070	DATE: 1/4/88	PLOTTED BY: SLS	CHECKED BY: WBC	

MOISTURE RETENTION DATA - HANGING COLUMN
(PORE SIZE DISTRIBUTION)

JOB NAME: LOS ALAMOS
JOB NUMBER: 87-L-070
SAMPLE NUMBER: 35-36
RING NUMBER: G
DEPTH: unknown
SAMPLE VOLUME: 66.18 (cc)
SATURATED WEIGHT AT 0 CM TENSION
(WITH CAP AND RING): 208.4 (g)
TARE RING: 73.3 (g)
TARE CAP: 0.0 (g)
DRY WEIGHT OF SAMPLE: 106.8 (g)
SATURATED MOISTURE CONTENT: 42.8 (% vol)
INITIAL VOLUME OF WATER IN SAMPLE: 28.3 (cc)

DATE (1987)	TIME	SUCTION (CM)	BURET VOL (CC)	CHANGE VOL (CC)	CHANGES VOL (CC)	MOISTURE CONTENT(% VOL) DRYING	WETTING
11/24	1120	0.0	33.0	--	--	42.8	0.0
11/28	1125	96.0	32.1	0.9	0.9	41.4	0.0
11/30	810	205.0	32.1	0.0	0.9	41.4	0.0

COMMENTS:

LABORATORY ANALYSIS PERFORMED BY: S. Stoller
CALCULATION MADE BY: S. Stoller
CHECKED BY: W. Cox

MOISTURE RETENTION DATA - 15 BAR PRESSURE PLATE
(PORE SIZE DISTRIBUTION)

JOB NAME: LOS ALAMOS
JOB NUMBER: 87-L-070
SAMPLE NUMBER: 35-36
RING NUMBER: G
DEPTH: unknown
SAMPLE VOLUME: 66.18 (cc)
SATURATED WEIGHT AT 0 CM TENSION
(WITH CAP AND RING): 208.4 (g)
TARE RING: 73.3 (g)
TARE CAP: 0.0 (g)
DRY WEIGHT OF SAMPLE: 106.8 (g)
SATURATED MOISTURE CONTENT: 42.8 (% vol)
INITIAL VOLUME OF WATER IN SAMPLE: 27.0 (cc)
WEIGHT FROM HANGING COLUMN, W/O CAP: 207.1 (g)
FINAL TENSION ON HANGING COLUMN: 205.0 (cm)

DATE (1987)	TIME	PRESSURE (BAR)	WEIGHT W/RING(G)	CHANGE WT (G)	CHANGES WT (G)	MOISTURE CONTENT (% VOL)
11/30	845	0.0	207.1	--	--	--
12/2	740	1.0	200.1	7.0	7.0	30.2
12/6	830	3.0	189.5	10.6	17.6	14.2
12/8	840	5.0	189.0	0.5	18.1	13.4
12/13	1715	15.0	186.3	2.7	20.8	9.4

COMMENTS:

LABORATORY ANALYSIS PERFORMED BY: S. Stoller
CALCULATION MADE BY: S. Stoller
CHECKED BY: W. Cox

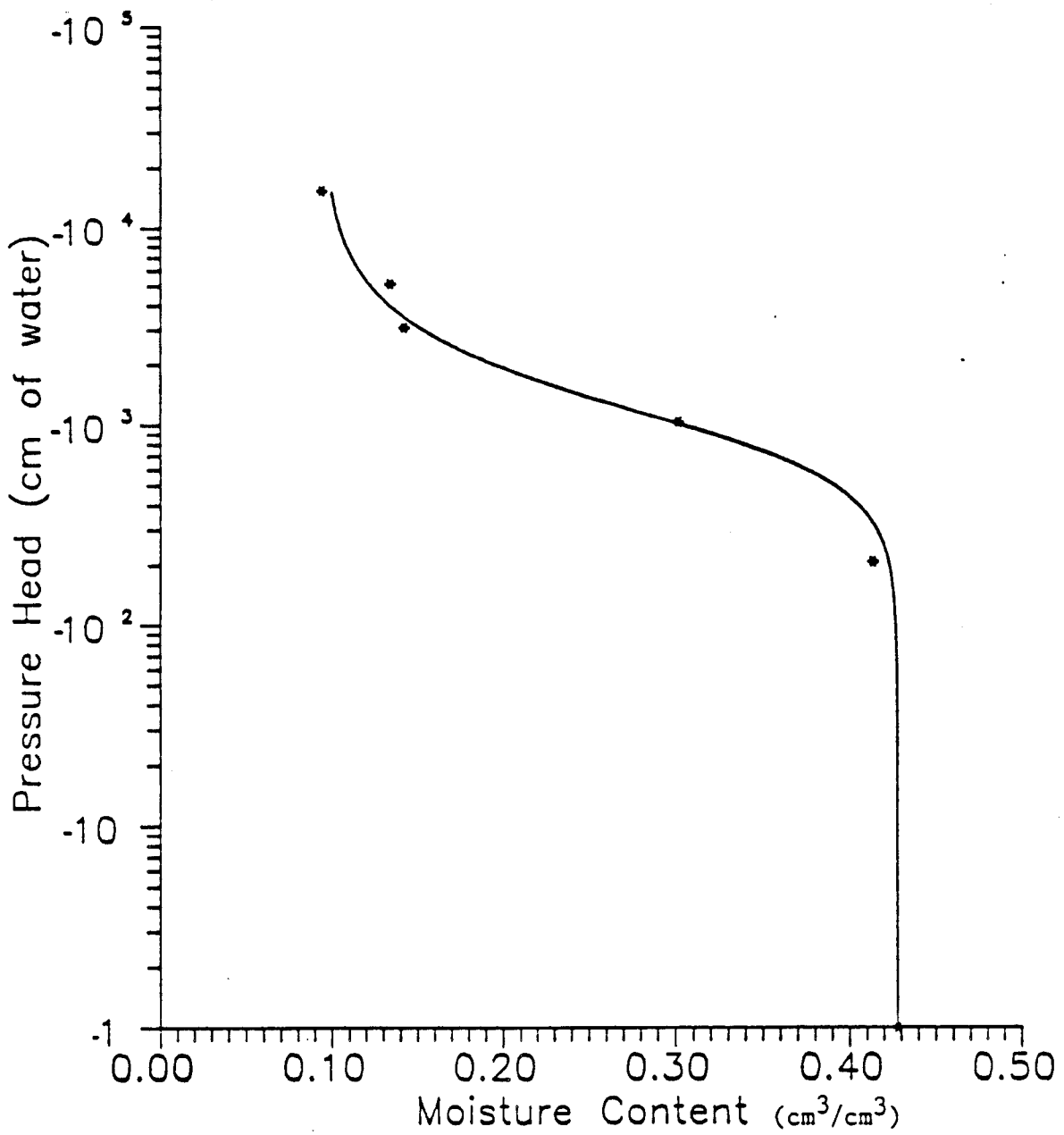

FIGURE NUMBER:	Pressure Head (cm of water) vs. Moisture Content (cm^3/cm^3), Sample No. 35-36				DANIEL B. STEPHENS & ASSOCIATES, INC.
FOR: Los Alamos	PROJECT NO 87-L-070	DATE: 1/4/88	PLOTTED BY: SLS	CHECKED BY: WBC	

MOISTURE RETENTION DATA - HANGING COLUMN
(PORE SIZE DISTRIBUTION)

JOB NAME: LOS ALAMOS
JOB NUMBER: 87-L-070
SAMPLE NUMBER: 42-43
RING NUMBER: 4
DEPTH: unknown
SAMPLE VOLUME: 66.18 (cc)
SATURATED WEIGHT AT 0 CM TENSION
(WITH CAP AND RING): 208.0 (g)
TARE RING: 72.6 (g)
TARE CAP: 0.0 (g)
DRY WEIGHT OF SAMPLE: 107.4 (g)
SATURATED MOISTURE CONTENT: 42.3 (% vol)
INITIAL VOLUME OF WATER IN SAMPLE: 28.0 (cc)

DATE (1987)	TIME	SUCTION (CM)	BURET VOL (CC)	CHANGE VOL (CC)	CHANGES VOL (CC)	MOISTURE CONTENT(% VOL) DRYING	WETTING
11/24	1120	0.0	32.7	--	--	42.3	0.0
11/28	1125	100.5	32.7	0.0	0.0	42.3	0.0
11/30	810	209.0	32.6	0.1	0.1	42.2	0.0

COMMENTS:

LABORATORY ANALYSIS PERFORMED BY: S. Stoller
CALCULATION MADE BY: S. Stoller
CHECKED BY: W. Cox

MOISTURE RETENTION DATA - 15 BAR PRESSURE PLATE
(PORE SIZE DISTRIBUTION)

JOB NAME: LOS ALAMOS
JOB NUMBER: 87-L-070
SAMPLE NUMBER: 42-43
RING NUMBER: 4
DEPTH: unknown
SAMPLE VOLUME: 66.18 (cc)
SATURATED WEIGHT AT 0 CM TENSION
(WITH CAP AND RING): 208.0 (g)
TARE RING: 72.6 (g)
TARE CAP: 0.0 (g)
DRY WEIGHT OF SAMPLE: 107.4 (g)
SATURATED MOISTURE CONTENT: 42.3 (% vol)
INITIAL VOLUME OF WATER IN SAMPLE: 26.4 (cc)
WEIGHT FROM HANGING COLUMN, W/O CAP: 206.4 (g)
FINAL TENSION ON HANGING COLUMN: 209.0 (cm)

DATE (1987)	TIME	PRESSURE (BAR)	WEIGHT W/RING(G)	CHANGE WT (G)	CHANGES WT (G)	MOISTURE CONTENT (% VOL)
11/30	845	0.0	206.4	--	--	--
12/2	740	1.0	202.2	4.2	4.2	33.5
12/6	830	3.0	200.2	2.0	6.2	30.5
12/8	840	5.0	199.1	1.1	7.3	28.9
12/13	1720	15.0	195.1	4.0	11.3	22.8

COMMENTS:

LABORATORY ANALYSIS PERFORMED BY: S. Stoller
CALCULATION MADE BY: S. Stoller
CHECKED BY: W. Cox

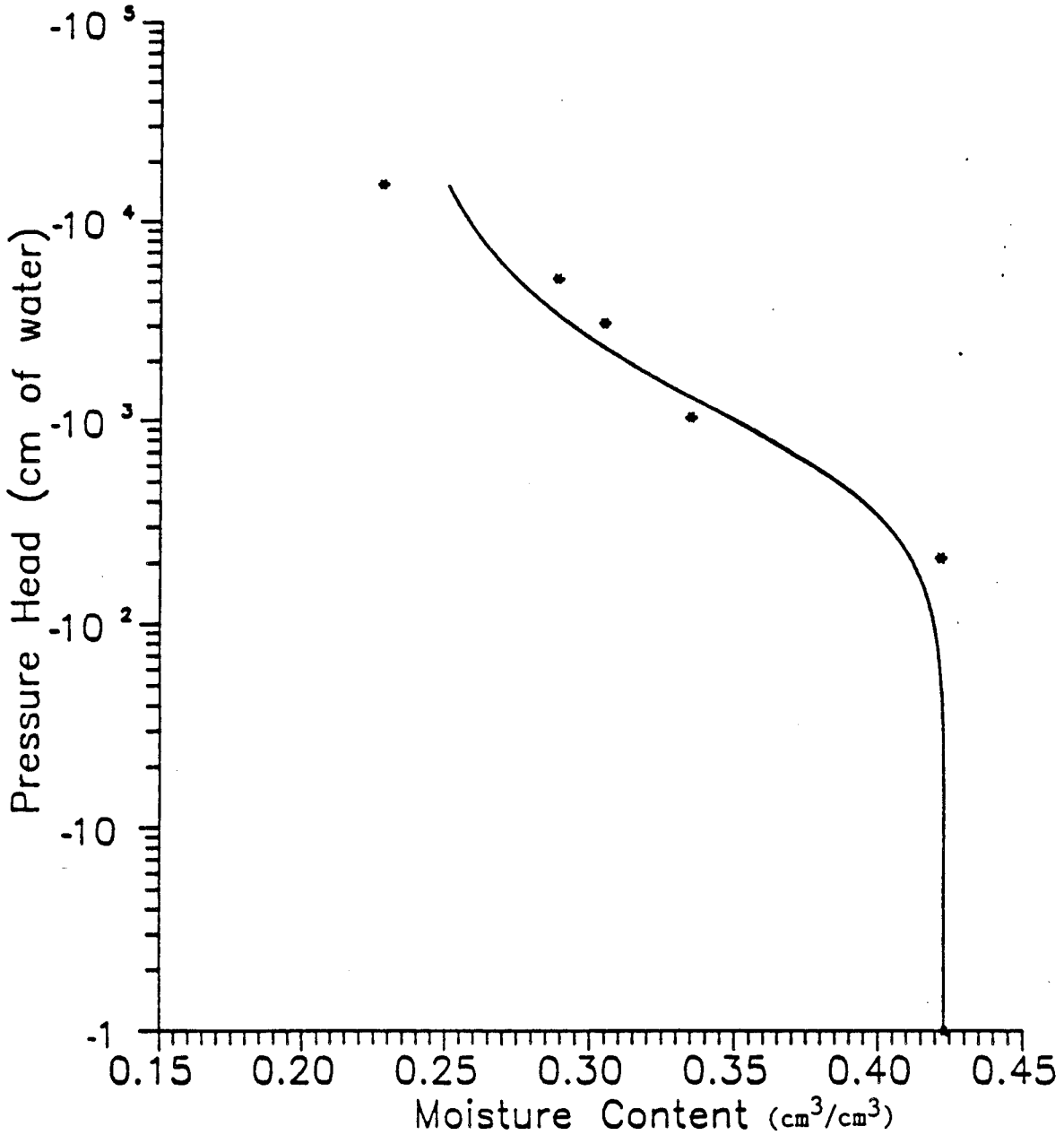

FIGURE NUMBER:	Pressure Head (cm of water) vs. Moisture Content (cm^3/cm^3), Sample No. 42-43				DANIEL B. STEPHENS & ASSOCIATES, INC.
FOR: Los Alamos	PROJECT NO: 87-L-070	DATE: 1/4/88	PLOTTED BY: SLS	CHECKED BY: WBC	

MOISTURE RETENTION DATA - HANGING COLUMN
(PORE SIZE DISTRIBUTION)

JOB NAME: LOS ALAMOS
JOB NUMBER: 87-L-070
SAMPLE NUMBER: 61-62
RING NUMBER: A4
DEPTH: unknown
SAMPLE VOLUME: 66.18 (cc)
SATURATED WEIGHT AT 0 CM TENSION
(WITH CAP AND RING): 210.1 (g)
TARE RING: 73.4 (g)
TARE CAP: 0.0 (g)
DRY WEIGHT OF SAMPLE: 112.6 (g)
SATURATED MOISTURE CONTENT: 36.4 (% vol)
INITIAL VOLUME OF WATER IN SAMPLE: 24.1 (cc)

DATE (1987)	TIME	SUCTION (CM)	BURET VOL (CC)	CHANGE VOL (CC)	CHANGES VOL (CC)	MOISTURE CONTENT(% VOL) DRYING	WETTING
11/24	1120	0.0	36.1	--	--	36.4	0.0
11/28	1125	95.5	35.0	1.1	1.1	34.8	0.0
11/30	810	202.0	33.6	1.4	2.5	32.6	0.0

COMMENTS:

LABORATORY ANALYSIS PERFORMED BY: S. Stoller
CALCULATION MADE BY: S. Stoller
CHECKED BY: W. Cox

MOISTURE RETENTION DATA - 15 BAR PRESSURE PLATE
(PORE SIZE DISTRIBUTION)

JOB NAME: LOS ALAMOS
JOB NUMBER: 87-L-070
SAMPLE NUMBER: 61-62
RING NUMBER: A4
DEPTH: unknown
SAMPLE VOLUME: 66.18 (cc)
SATURATED WEIGHT AT 0 CM TENSION
(WITH CAP AND RING): 210.1 (g)
TARE RING: 73.4 (g)
TARE CAP: 0.0 (g)
DRY WEIGHT OF SAMPLE: 112.6 (g)
SATURATED MOISTURE CONTENT: 36.4 (% vol)
INITIAL VOLUME OF WATER IN SAMPLE: 20.8 (cc)
WEIGHT FROM HANGING COLUMN, W/O CAP: 206.8 (g)
FINAL TENSION ON HANGING COLUMN: 202.0 (cm)

DATE (1987)	TIME	PRESSURE (BAR)	WEIGHT W/RING(G)	CHANGE WT (G)	CHANGES WT (G)	MOISTURE CONTENT (% VOL)
11/30	845	0.0	206.8	--	--	--
12/2	740	1.0	198.8	8.0	8.0	19.3
12/6	830	3.0	193.4	5.4	13.4	11.2
12/8	840	5.0	192.9	0.5	13.9	10.4
12/13	1720	15.0	191.2	1.7	15.6	7.9

COMMENTS:

LABORATORY ANALYSIS PERFORMED BY: S. Stoller
CALCULATION MADE BY: S. Stoller
CHECKED BY: W. Cox

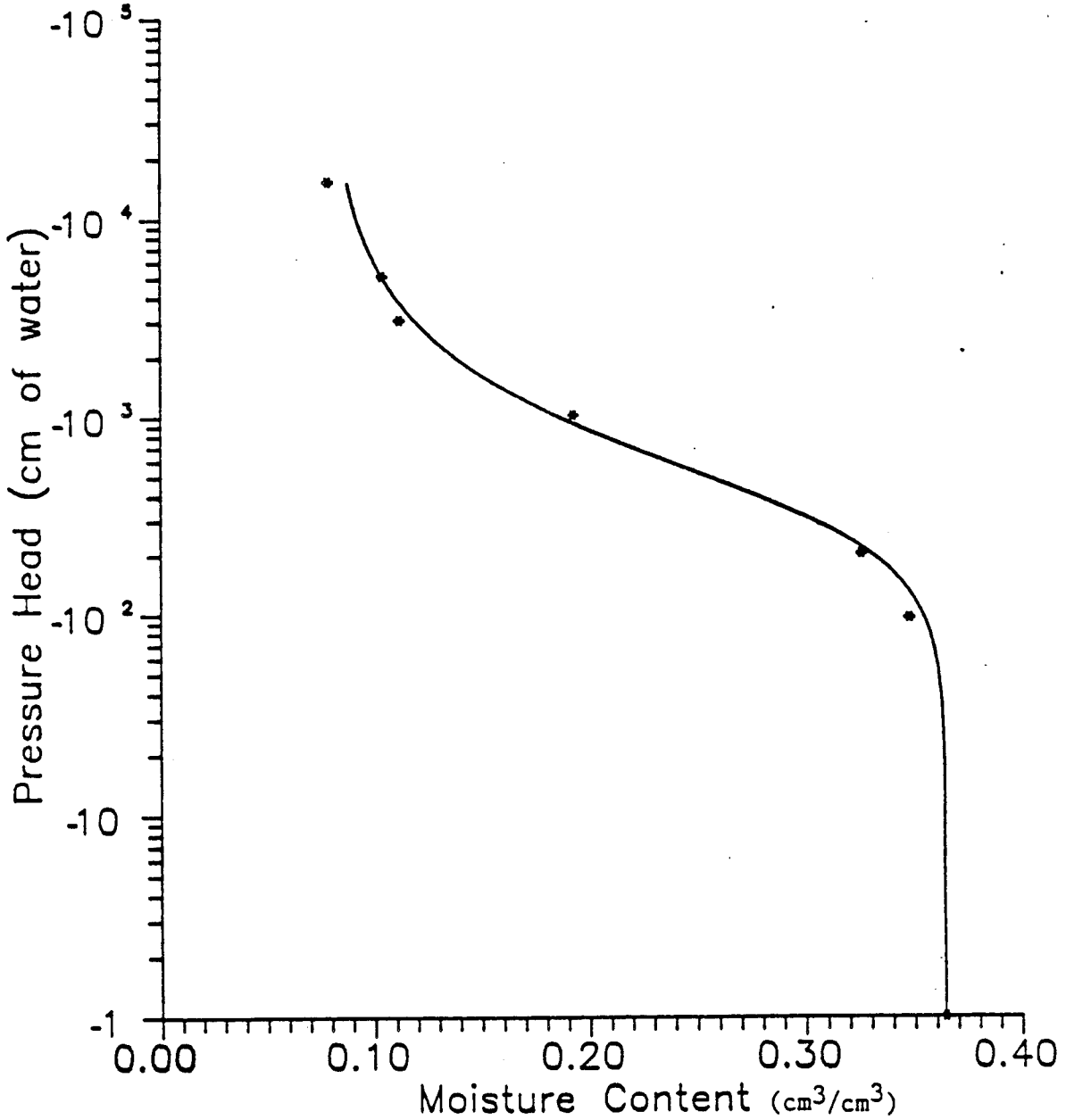

FIGURE NUMBER:	Pressure Head (cm of water) vs. Moisture Content (cm^3/cm^3), Sample No. 61-62				DANIEL B. STEPHENS & ASSOCIATES, INC.
FOR: Los Alamos	PROJECT NO: 87-L-070	DATE: 1/4/88	PLOTTED BY: SLS	CHECKED BY: WBC	

MOISTURE RETENTION DATA - HANGING COLUMN
(PORE SIZE DISTRIBUTION)

JOB NAME: LOS ALAMOS
JOB NUMBER: 87-L-070
SAMPLE NUMBER: 75-76
RING NUMBER: 19
DEPTH: unknown
SAMPLE VOLUME: 66.18 (cc)
SATURATED WEIGHT AT 0 CM TENSION
(WITH CAP AND RING): 204.5 (g)
TARE RING: 73.4 (g)
TARE CAP: 0.0 (g)
DRY WEIGHT OF SAMPLE: 103.6 (g)
SATURATED MOISTURE CONTENT: 41.6 (% vol)
INITIAL VOLUME OF WATER IN SAMPLE: 27.5 (cc)

DATE (1987)	TIME	SUCTION (CM)	BURET VOL (CC)	CHANGE VOL (CC)	CHANGES VOL (CC)	MOISTURE CONTENT(% VOL) DRYING	WETTING
11/24	1120	0.0	34.4	--	--	41.6	0.0
11/28	1125	95.0	32.0	2.4	2.4	37.9	0.0
11/30	810	199.0	28.8	3.2	5.6	33.1	0.0

COMMENTS:

LABORATORY ANALYSIS PERFORMED BY: S. Stoller
CALCULATION MADE BY: S. Stoller
CHECKED BY: W. Cox

MOISTURE RETENTION DATA - 15 BAR PRESSURE PLATE
(PORE SIZE DISTRIBUTION)

JOB NAME: LOS ALAMOS
JOB NUMBER: 87-L-070
SAMPLE NUMBER: 75-76
RING NUMBER: 19
DEPTH: unknown
SAMPLE VOLUME: 66.18 (cc)
SATURATED WEIGHT AT 0 CM TENSION
(WITH CAP AND RING): 204.5 (g)
TARE RING: 73.4 (g)
TARE CAP: 0.0 (g)
DRY WEIGHT OF SAMPLE: 103.6 (g)
SATURATED MOISTURE CONTENT: 41.6 (% vol)
INITIAL VOLUME OF WATER IN SAMPLE: 21.9 (cc)
WEIGHT FROM HANGING COLUMN, W/O CAP: 198.9 (g)
FINAL TENSION ON HANGING COLUMN: 199.0 (cm)

DATE (1987)	TIME	PRESSURE (BAR)	WEIGHT W/RING(G)	CHANGE WT (G)	CHANGES WT (G)	MOISTURE CONTENT (% VOL)
11/30	845	0.0	198.9	--	--	--
12/2	740	1.0	192.9	6.0	6.0	24.0
12/6	830	3.0	185.3	7.6	13.6	12.5
12/8	840	5.0	184.7	0.6	14.2	11.6
12/13	1725	15.0	182.5	2.2	16.4	8.3

COMMENTS:

LABORATORY ANALYSIS PERFORMED BY: S. Stoller
CALCULATION MADE BY: S. Stoller
CHECKED BY: W. Cox

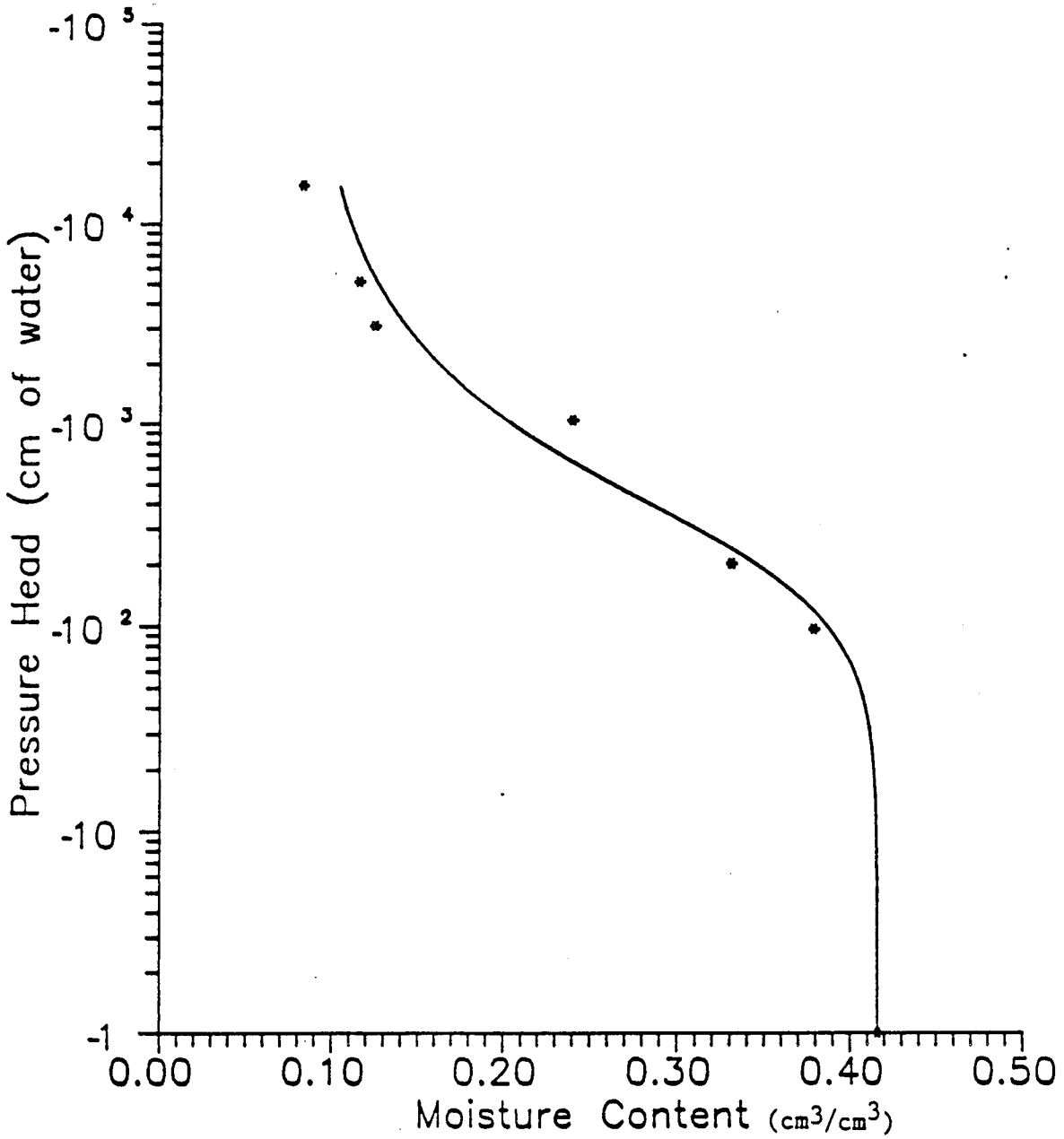

FIGURE NUMBER:	Pressure Head (cm of water) vs. Moisture Content (cm^3/cm^3), Sample No. 75-76				DANIEL B. STEPHENS & ASSOCIATES, INC.
FOR: Los Alamos	PROJECT NO: 87-L-070	DATE: 1/4/88	PLOTTED BY: SLS	CHECKED BY: WBC	

MOISTURE RETENTION DATA - HANGING COLUMN
(PORE SIZE DISTRIBUTION)

JOB NAME: LOS ALAMOS
JOB NUMBER: 87-L-070
SAMPLE NUMBER: 80-81
RING NUMBER: 18
DEPTH: unknown
SAMPLE VOLUME: 66.18 (cc)
SATURATED WEIGHT AT 0 CM TENSION
(WITH CAP AND RING): 215.1 (g)
TARE RING: 73.1 (g)
TARE CAP: 0.0 (g)
DRY WEIGHT OF SAMPLE: 119.1 (g)
SATURATED MOISTURE CONTENT: 34.6 (% vol)
INITIAL VOLUME OF WATER IN SAMPLE: 22.9 (cc)

DATE (1987)	TIME	SUCTION (CM)	BURET VOL (CC)	CHANGE VOL (CC)	CHANGES VOL (CC)	MOISTURE CONTENT(% VOL) DRYING	WETTING
11/24	1120	0.0	34.0	--	--	34.6	0.0
11/28	1125	98.5	34.1	-0.1	-0.1	34.8	0.0
11/30	810	205.0	38.1	-4.0	-4.1	40.8	0.0

COMMENTS:

LABORATORY ANALYSIS PERFORMED BY: S. Stoller
CALCULATION MADE BY: S. Stoller
CHECKED BY: W. Cox

MOISTURE RETENTION DATA - 15 BAR PRESSURE PLATE
(PORE SIZE DISTRIBUTION)

JOB NAME: LOS ALAMOS
JOB NUMBER: 87-L-070
SAMPLE NUMBER: 80-81
RING NUMBER: 18
DEPTH: unknown
SAMPLE VOLUME: 66.18 (cc)
SATURATED WEIGHT AT 0 CM TENSION
(WITH CAP AND RING): 215.1 (g)
TARE RING: 73.1 (g)
TARE CAP: 0.0 (g)
DRY WEIGHT OF SAMPLE: 119.1 (g)
SATURATED MOISTURE CONTENT: 34.6 (% vol)
INITIAL VOLUME OF WATER IN SAMPLE: 21.4 (cc)
WEIGHT FROM HANGING COLUMN, W/O CAP: 213.6 (g)
FINAL TENSION ON HANGING COLUMN: 205.0 (cm)

DATE (1987)	TIME	PRESSURE (BAR)	WEIGHT W/RING(G)	CHANGE WT (G)	CHANGES WT (G)	MOISTURE CONTENT (% VOL)
11/30	845	0.0	213.6	--	--	--
12/2	740	1.0	210.4	3.2	3.2	27.5
12/6	830	3.0	204.3	6.1	9.3	18.3
12/8	840	5.0	203.5	0.8	10.1	17.1
12/13	1725	15.0	199.3	4.2	14.3	10.7

COMMENTS:

LABORATORY ANALYSIS PERFORMED BY: S. Stoller
CALCULATION MADE BY: S. Stoller
CHECKED BY: W. Cox

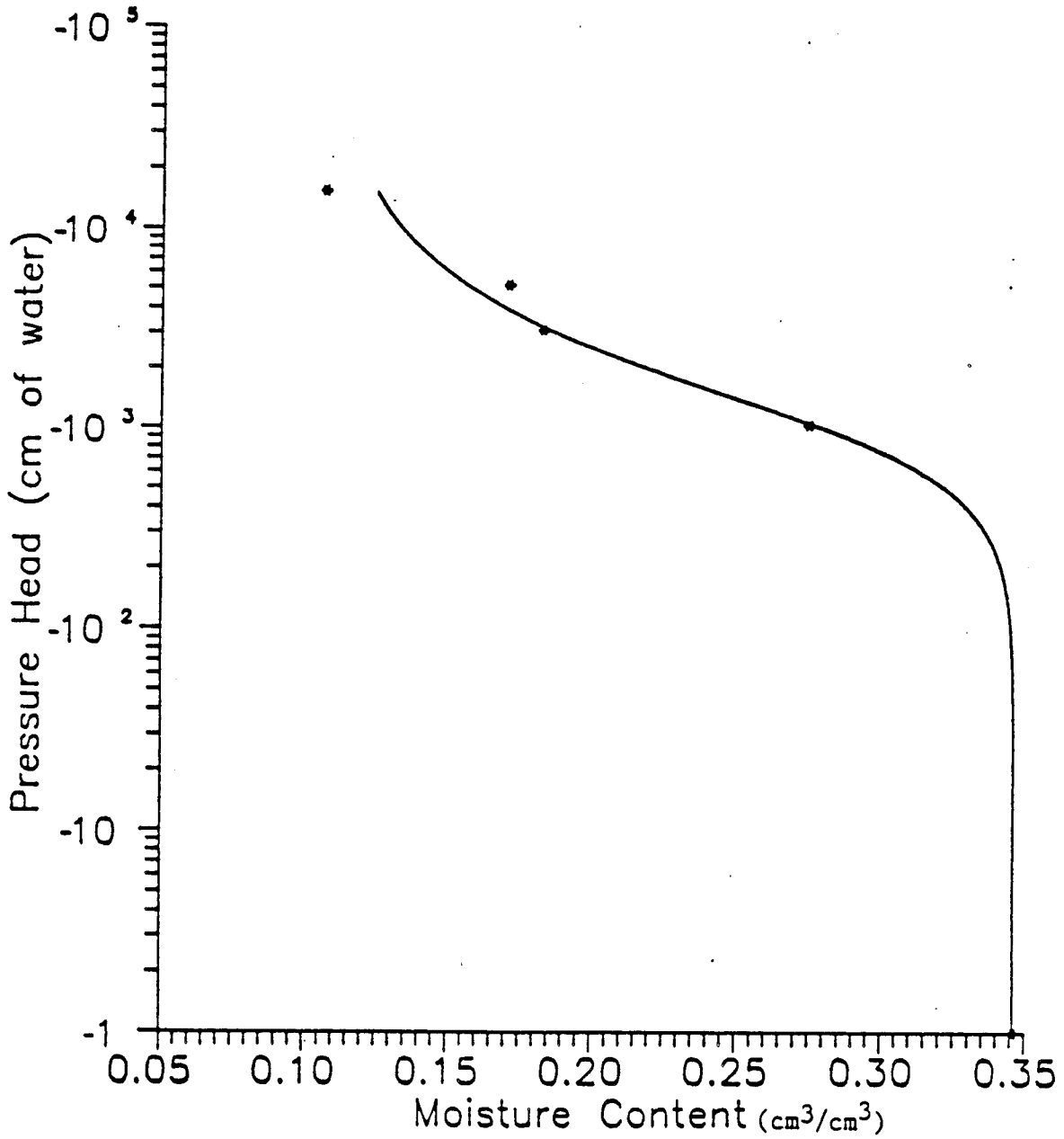

FIGURE NUMBER:	Pressure Head (cm of water) vs. Moisture Content (cm^3/cm^3), Sample No. 80-81				DANIEL B. STEPHENS & ASSOCIATES, INC.
FOR: Los Alamos	PROJECT NO: 87-L-070	DATE: 1/4/88	PLOTTED BY: SLS	CHECKED BY: WBC	

INITIAL MOISTURE CONTENT, DRY BULK DENSITY AND POROSITY

Table 6. Summary of Initial Moisture Content, Dry Bulk Density and Porosity

Sample No.	Initial Moisture Content Gravimetric (g/g)	Initial Moisture Content Volumetric (cm^3/cm^3)	Dry Bulk Density (g/cc)	Porosity* (% vol)
7-8	28.30	35.36	1.25	51.8
11-12	14.90	18.74	1.26	56.1
16-17	17.46	22.21	1.27	54.9
21-22	15.90	19.95	1.25	56.2
25-26	13.94	19.19	1.38	52.0
35-36	14.51	23.42	1.61	42.8
42-43	22.53	36.57	1.62	42.3
61-62	11.55	19.64	1.70	36.4
75-76	14.77	23.12	1.57	41.6
80-81	11.17	20.10	1.80	34.6

*Taken as saturated moisture content

DATA FOR INITIAL MOISTURE CONTENT,
BULK DENSITY, AND POROSITY

JOB NAME: LOS ALAMOS
JOB NUMBER: 87-L-070
SAMPLE NUMBER: 11-12
RING NUMBER: 22
DEPTH: unknown

FIELD WIEGHT OF SAMPLE (W/CAP AND RING): 168.9 (g)
TARE WEIGHT, RING: 73.3 (g)
TARE WEIGHT, PAN: 0.0 (g)
SAMPLE VOLUME: 66.18 (cc)
DATE AND TIME INTO OVEN: 12/13/87 1700
DATE AND TIME OUT OF OVEN: 12/17/87 940

DRY WEIGHT OF SAMPLE: 83.2 (g)
DRY BULK DENSITY: 1.26 (g/cc)
PARTICLE DENSITY: 2.65 (g/cc)
(METHOD: ASSUME MEAN PARTICLE DENSITY = 2.65 g/cc)

CALCULATED POROSITY: 52.56 (% vol)

INITIAL MOISTURE CONTENT (VOLUMETRIC): 18.74 (% vol)

INITIAL MOISTURE CONTENT (GRAVIMETRIC): 14.90 (%)

COMMENTS:

LABORATORY ANALYSIS PERFORMED BY: S. Stoller
CALCULATIONS MADE BY: S. Stoller
CHECKED BY: W. Cox

DATA FOR INITIAL MOISTURE CONTENT,
BULK DENSITY, AND POROSITY

JOB NAME:	LOS ALAMOS
JOB NUMBER:	87-L-070
SAMPLE NUMBER:	16-17
RING NUMBER:	2
DEPTH:	unknown

FIELD WIEGHT OF SAMPLE (W/CAP AND RING):	172.0 (g)
TARE WEIGHT, RING:	73.1 (g)
TARE WEIGHT, PAN:	0.0 (g)
SAMPLE VOLUME:	66.18 (cc)
DATE AND TIME INTO OVEN:	12/13/87 1700
DATE AND TIME OUT OF OVEN:	12/17/87 940
DRY WEIGHT OF SAMPLE:	84.2 (g)
DRY BULK DENSITY:	1.27 (g/cc)
PARTICLE DENSITY:	2.65 (g/cc)
(METHOD: ASSUME MEAN PARTICLE DENSITY = 2.65 g/cc)	
CALCULATED POROSITY:	51.99 (% vol)
INITIAL MOISTURE CONTENT (VOLUMETRIC):	22.21 (% vol)
INITIAL MOISTURE CONTENT (GRAVIMETRIC):	17.46 (%)

COMMENTS:

LABORATORY ANALYSIS PERFORMED BY:	S. Stoller
CALCULATIONS MADE BY:	S. Stoller
CHECKED BY:	W. Cox

DATA FOR INITIAL MOISTURE CONTENT,
BULK DENSITY, AND POROSITY

JOB NAME: LOS ALAMOS
JOB NUMBER: 87-L-070
SAMPLE NUMBER: 21-22
RING NUMBER: F
DEPTH: unknown

FIELD WIEGHT OF SAMPLE (W/CAP AND RING): 170.0 (g)
TARE WEIGHT, RING: 73.8 (g)
TARE WEIGHT, PAN: 0.0 (g)
SAMPLE VOLUME: 66.18 (cc)
DATE AND TIME INTO OVEN: 12/13/87 1700
DATE AND TIME OUT OF OVEN: 12/17/87 940

DRY WEIGHT OF SAMPLE: 83.0 (g)
DRY BULK DENSITY: 1.25 (g/cc)
PARTICLE DENSITY: 2.65 (g/cc)
(METHOD: ASSUME MEAN PARTICLE DENSITY = 2.65 g/cc)

CALCULATED POROSITY: 52.67 (% vol)

INITIAL MOISTURE CONTENT (VOLUMETRIC): 19.95 (% vol)

INITIAL MOISTURE CONTENT (GRAVIMETRIC): 15.90 (%)

COMMENTS:

LABORATORY ANALYSIS PERFORMED BY: S. Stoller
CALCULATIONS MADE BY: S. Stoller
CHECKED BY: W. Cox

DATA FOR INITIAL MOISTURE CONTENT,
BULK DENSITY, AND POROSITY

JOB NAME: LOS ALAMOS
JOB NUMBER: 87-L-070
SAMPLE NUMBER: 25-26
RING NUMBER: C
DEPTH: unknown

FIELD WIEGHT OF SAMPLE (W/CAP AND RING): 176.6 (g)
TARE WEIGHT, RING: 72.8 (g)
TARE WEIGHT, PAN: 0.0 (g)
SAMPLE VOLUME: 66.18 (cc)
DATE AND TIME INTO OVEN: 12/13/87 1700
DATE AND TIME OUT OF OVEN: 12/17/87 940

DRY WEIGHT OF SAMPLE: 91.1 (g)
DRY BULK DENSITY: 1.38 (g/cc)
PARTICLE DENSITY: 2.65 (g/cc)
(METHOD: ASSUME MEAN PARTICLE DENSITY = 2.65 g/cc)

CALCULATED POROSITY: 48.05 (% vol)

INITIAL MOISTURE CONTENT (VOLUMETRIC): 19.19 (% vol)

INITIAL MOISTURE CONTENT (GRAVIMETRIC): 13.94 (%)

COMMENTS:

LABORATORY ANALYSIS PERFORMED BY: S. Stoller
CALCULATIONS MADE BY: S. Stoller
CHECKED BY: W. Cox

DATA FOR INITIAL MOISTURE CONTENT,
BULK DENSITY, AND POROSITY

JOB NAME:	LOS ALAMOS
JOB NUMBER:	87-L-070
SAMPLE NUMBER:	35-36
RING NUMBER:	G
DEPTH:	unknown

FIELD WIEGHT OF SAMPLE (W/CAP AND RING):	195.6 (g)
TARE WEIGHT, RING:	73.3 (g)
TARE WEIGHT, PAN:	0.0 (g)
SAMPLE VOLUME:	66.18 (cc)
DATE AND TIME INTO OVEN:	12/13/87 1700
DATE AND TIME OUT OF OVEN:	12/17/87 940
DRY WEIGHT OF SAMPLE:	106.8 (g)
DRY BULK DENSITY:	1.61 (g/cc)
PARTICLE DENSITY:	2.65 (g/cc)
(METHOD: ASSUME MEAN PARTICLE DENSITY = 2.65 g/cc)	
CALCULATED POROSITY:	39.10 (% vol)
INITIAL MOISTURE CONTENT (VOLUMETRIC):	23.42 (% vol)
INITIAL MOISTURE CONTENT (GRAVIMETRIC):	14.51 (%)

COMMENTS:

LABORATORY ANALYSIS PERFORMED BY:	S. Stoller
CALCULATIONS MADE BY:	S. Stoller
CHECKED BY:	W. Cox

DATA FOR INITIAL MOISTURE CONTENT,
BULK DENSITY, AND POROSITY

JOB NAME: LOS ALAMOS
JOB NUMBER: 87-L-070
SAMPLE NUMBER: 42-43
RING NUMBER: 4
DEPTH: unknown

FIELD WIEGHT OF SAMPLE (W/CAP AND RING): 204.2 (g)
TARE WEIGHT, RING: 72.6 (g)
TARE WEIGHT, PAN: 0.0 (g)
SAMPLE VOLUME: 66.18 (cc)
DATE AND TIME INTO OVEN: 12/13/87 1700
DATE AND TIME OUT OF OVEN: 12/17/87 940

DRY WEIGHT OF SAMPLE: 107.4 (g)
DRY BULK DENSITY: 1.62 (g/cc)
PARTICLE DENSITY: 2.65 (g/cc)
(METHOD: ASSUME MEAN PARTICLE DENSITY = 2.65 g/cc)

CALCULATED POROSITY: 38.76 (% vol)

INITIAL MOISTURE CONTENT (VOLUMETRIC): 36.57 (% vol)

INITIAL MOISTURE CONTENT (GRAVIMETRIC): 22.53 (%)

COMMENTS:

LABORATORY ANALYSIS PERFORMED BY: S. Staller
CALCULATIONS MADE BY: S. Staller
CHECKED BY: W. Cox

DATA FOR INITIAL MOISTURE CONTENT,
BULK DENSITY, AND POROSITY

JOB NAME: LOS ALAMOS
JOB NUMBER: 87-L-070
SAMPLE NUMBER: 61-62
RING NUMBER: A4
DEPTH: unknown

FIELD WIEGHT OF SAMPLE (W/CAP AND RING): 199.0 (g)
TARE WEIGHT, RING: 73.4 (g)
TARE WEIGHT, PAN: 0.0 (g)
SAMPLE VOLUME: 66.18 (cc)
DATE AND TIME INTO OVEN: 12/13/87 1700
DATE AND TIME OUT OF OVEN: 12/17/87 940

DRY WEIGHT OF SAMPLE: 112.6 (g)
DRY BULK DENSITY: 1.70 (g/cc)
PARTICLE DENSITY: 2.65 (g/cc)
(METHOD: ASSUME MEAN PARTICLE DENSITY = 2.65 g/cc)

CALCULATED POROSITY: 35.80 (% vol)

INITIAL MOISTURE CONTENT (VOLUMETRIC): 19.64 (% vol)

INITIAL MOISTURE CONTENT (GRAVIMETRIC): 11.55 (%)

COMMENTS:

LABORATORY ANALYSIS PERFORMED BY: S. Stoller
CALCULATIONS MADE BY: S. Stoller
CHECKED BY: W. Cox

DATA FOR INITIAL MOISTURE CONTENT,
BULK DENSITY, AND POROSITY

JOB NAME: LOS ALAMOS
JOB NUMBER: 87-L-070
SAMPLE NUMBER: 75-76
RING NUMBER: 19
DEPTH: unknown

FIELD WIEGHT OF SAMPLE (W/CAP AND RING): 192.3 (g)
TARE WEIGHT, RING: 73.4 (g)
TARE WEIGHT, PAN: 0.0 (g)
SAMPLE VOLUME: 66.18 (cc)
DATE AND TIME INTO OVEN: 12/13/87 1700
DATE AND TIME OUT OF OVEN: 12/17/87 940

DRY WEIGHT OF SAMPLE: 103.6 (g)
DRY BULK DENSITY: 1.57 (g/cc)
PARTICLE DENSITY: 2.65 (g/cc)
(METHOD: ASSUME MEAN PARTICLE DENSITY = 2.65 g/cc)

CALCULATED POROSITY: 40.93 (% vol)

INITIAL MOISTURE CONTENT (VOLUMETRIC): 23.12 (% vol)

INITIAL MOISTURE CONTENT (GRAVIMETRIC): 14.77 (%)

COMMENTS:

LABORATORY ANALYSIS PERFORMED BY: S. Stoller
CALCULATIONS MADE BY: S. Stoller
CHECKED BY: W. Cox

DATA FOR INITIAL MOISTURE CONTENT,
BULK DENSITY, AND POROSITY

JOB NAME:	LOS ALAMOS
JOB NUMBER:	87-L-070
SAMPLE NUMBER:	80-81
RING NUMBER:	18
DEPTH:	unknown

FIELD WIEGHT OF SAMPLE (W/CAP AND RING):	205.5 (g)
TARE WEIGHT, RING:	73.1 (g)
TARE WEIGHT, PAN:	0.0 (g)
SAMPLE VOLUME:	66.18 (cc)
DATE AND TIME INTO OVEN:	12/13/87 1700
DATE AND TIME OUT OF OVEN:	12/17/87 940
DRY WEIGHT OF SAMPLE:	119.1 (g)
DRY BULK DENSITY:	1.80 (g/cc)
PARTICLE DENSITY:	2.65 (g/cc)
(METHOD: ASSUME MEAN PARTICLE DENSITY = 2.65 g/cc)	
CALCULATED POROSITY:	32.09 (% vol)
INITIAL MOISTURE CONTENT (VOLUMETRIC):	20.10 (% vol)
INITIAL MOISTURE CONTENT (GRAVIMETRIC):	11.17 (%)

COMMENTS:

LABORATORY ANALYSIS PERFORMED BY:	S. Stoller
CALCULATIONS MADE BY:	S. Stoller
CHECKED BY:	W. Cox

UNSATURATED HYDRAULIC PROPERTIES

Table 7. Summary of Parameters for Calculating Unsaturated Hydraulic Conductivity

Sample No.	α (cm^{-1})	N (dimension-less)	θ_r (cm^3/cm^3)	θ_s (cm^3/cm^3)	K_s (cm/sec)
7-8	0.00272	2.49734	0.083	0.518	1.58E-04
11-12	0.00231	1.73884	0.199	0.561	2.84E-04
16-17	0.00119	2.04731	0.204	0.549	2.78E-04
21-22	0.00313	1.73941	0.124	0.562	2.00E-04
25-26	0.00371	1.69308	0.100	0.520	9.18E-05
35-36	0.00108	2.44961	0.094	0.428	2.25E-05
42-43	0.00164	1.66466	0.228	0.423	8.57E-05
61-62	0.00263	1.93720	0.079	0.364	5.15E-04
75-76	0.00452	1.65070	0.083	0.416	2.28E-04
80-81	0.00098	1.96205	0.107	0.346	4.41E-05

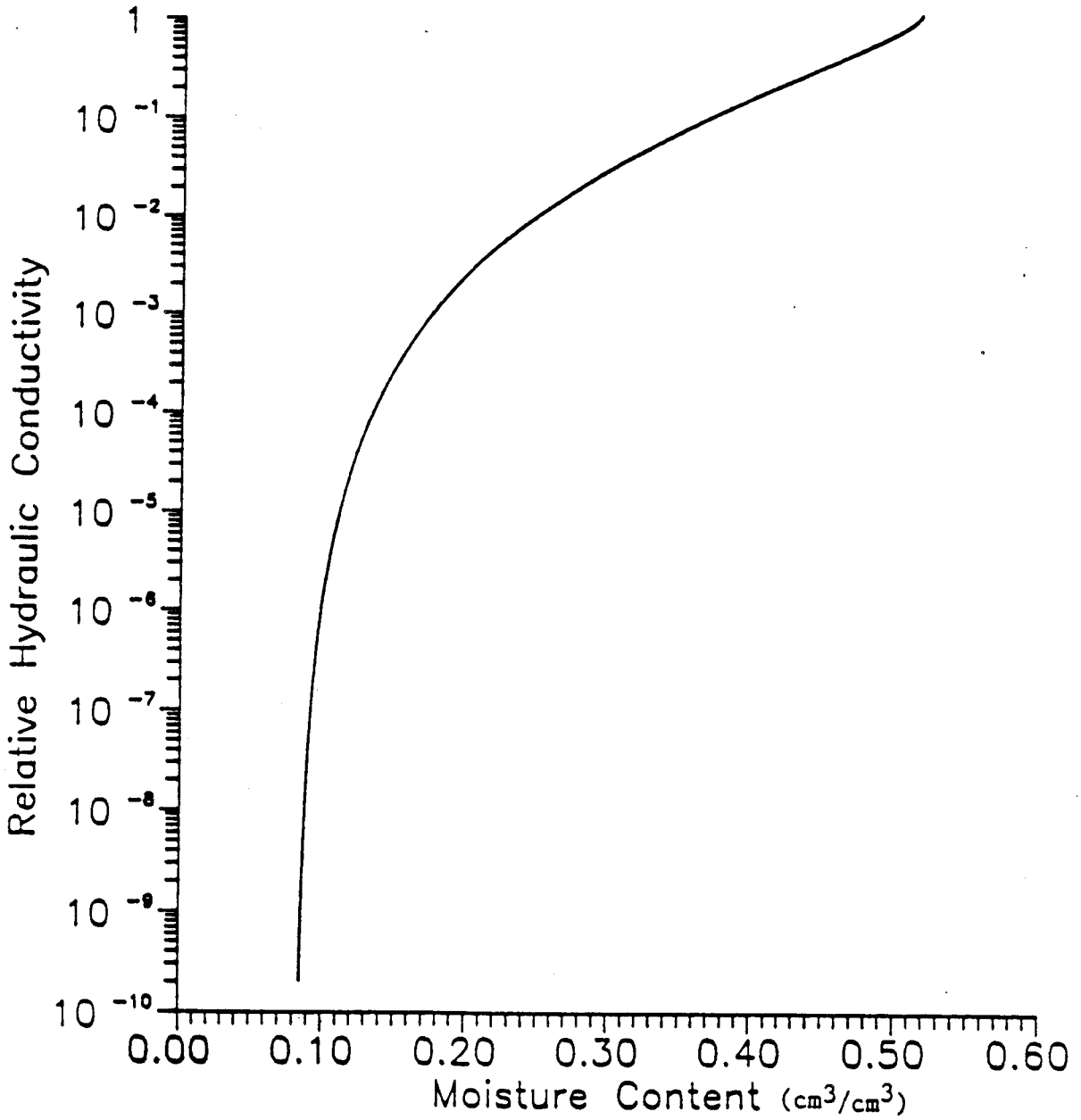

FIGURE NUMBER:	Relative Hydraulic Conductivity vs. Moisture Content (cm^3/cm^3), Sample No. 7-8				DANIEL B. STEPHENS & ASSOCIATES, INC.
FOR: Los Alamos	PROJECT NO: 87-L-070	DATE: 1/4/88	PLOTTED BY: SLS	CHECKED BY: WBC	

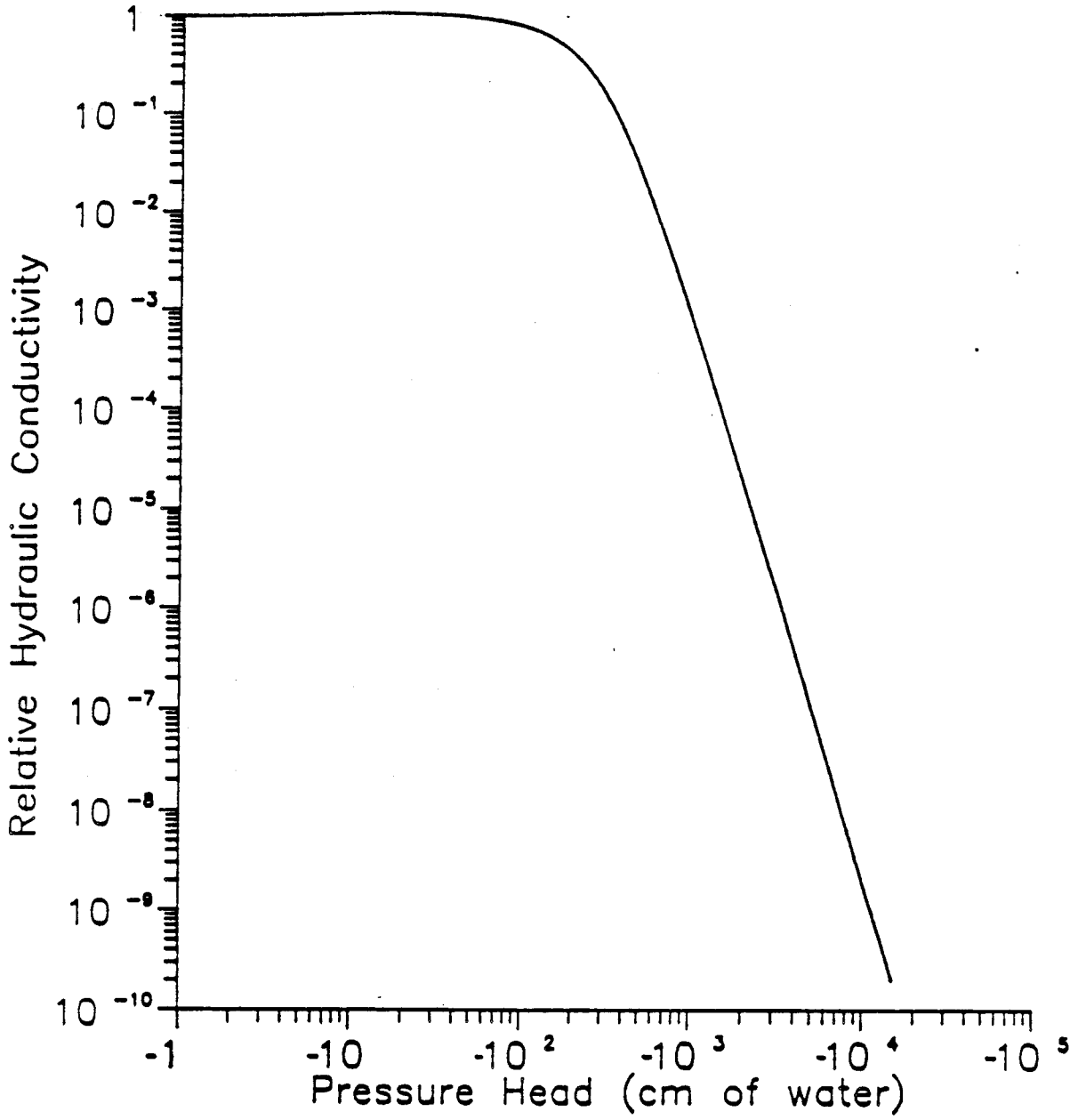

FIGURE NUMBER:	Relative Hydraulic Conductivity vs. Pressure Head (cm of water), Sample No.7-8				DANIEL B. STEPHENS & ASSOCIATES, INC.
FOR: Los Alamos	PROJECT NO: 87-L-070	DATE: 1/4/88	PLOTTED BY: SLS	CHECKED BY: WBC	

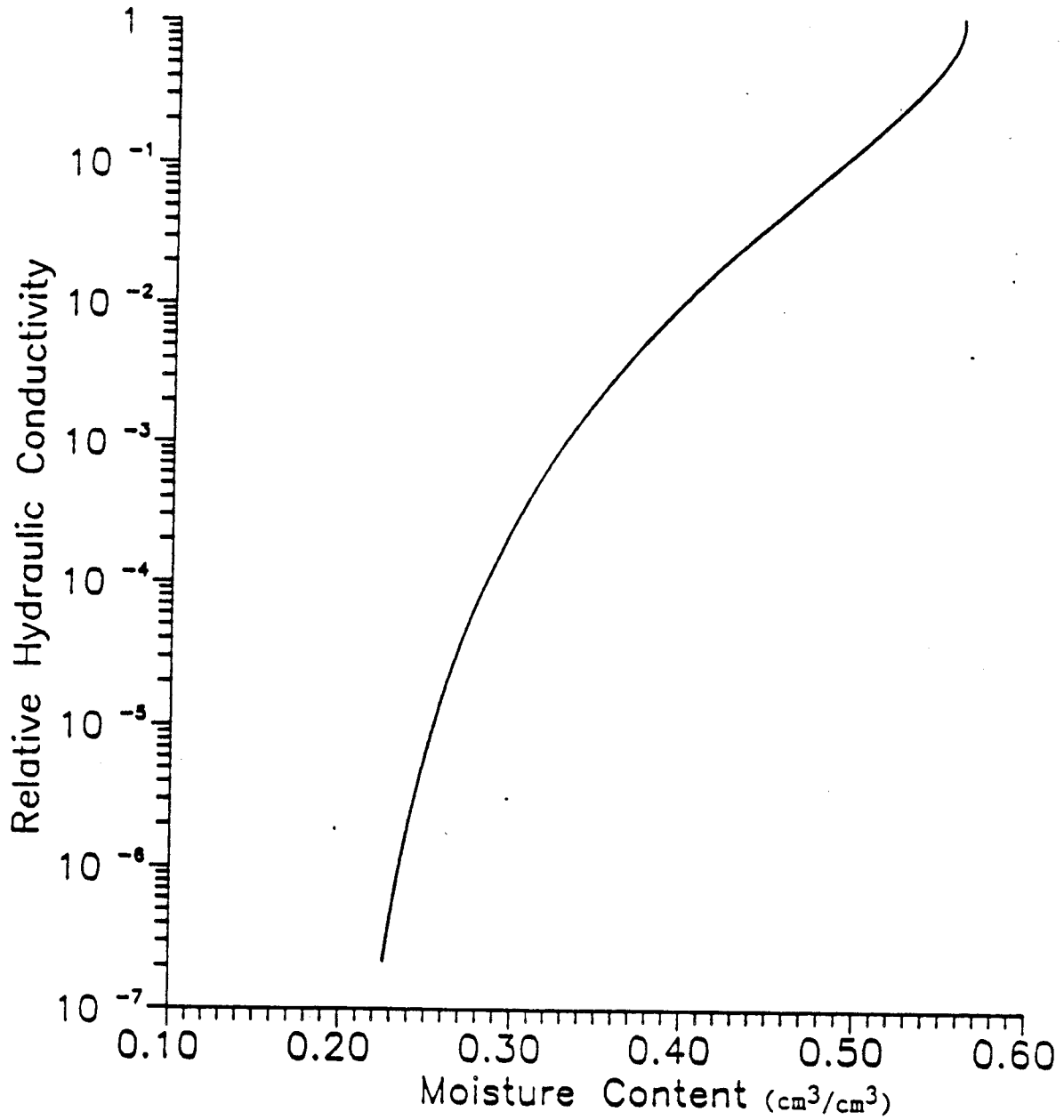

FIGURE NUMBER:	Relative Hydraulic Conductivity vs. Moisture Content (cm^3/cm^3), Sample No. 11-12				DANIEL B. STEPHENS & ASSOCIATES, INC.
FOR: Los Alamos	PROJECT NO: 87-L-070	DATE: 1/4/88	PLOTTED BY: SLS	CHECKED BY: WBC	

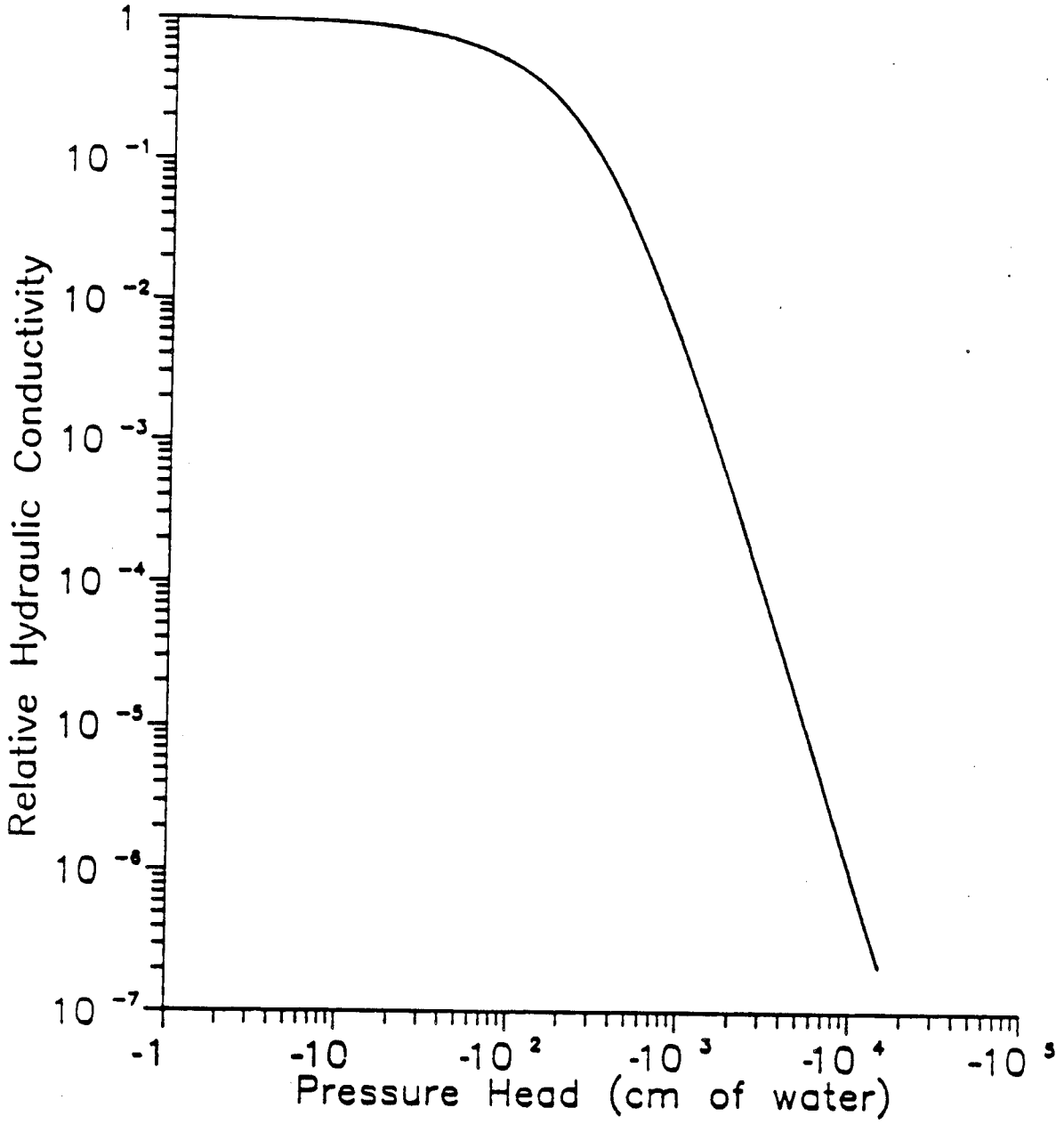

FIGURE NUMBER:	Relative Hydraulic Conductivity vs. Pressure Head (cm of water), Sample No. 11-12				DANIEL B. STEPHENS & ASSOCIATES, INC.
FOR: Los Alamos	PROJECT NO: 87-L-070	DATE: 1/4/88	PLOTTED BY: SLS	CHECKED BY: WBC	

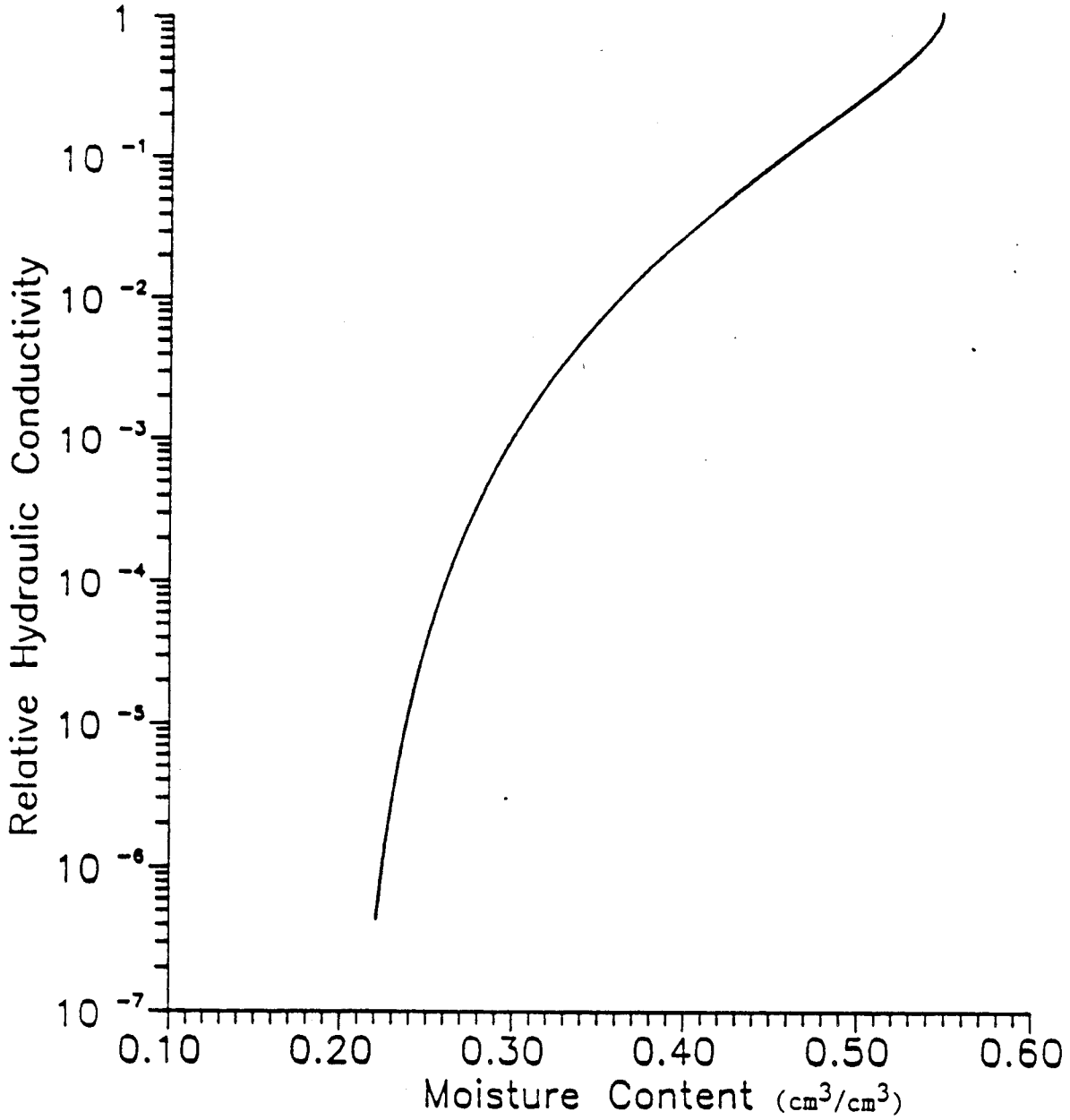

FIGURE NUMBER:	Relative Hydraulic Conductivity vs. Moisture Content (cm^3/cm^3), Sample No. 16-17				DANIEL B. STEPHENS & ASSOCIATES, INC.
FOR: Los Alamos	PROJECT NO: 87-L-070	DATE: 1/4/88	PLOTTED BY: SLS	CHECKED BY: WBC	

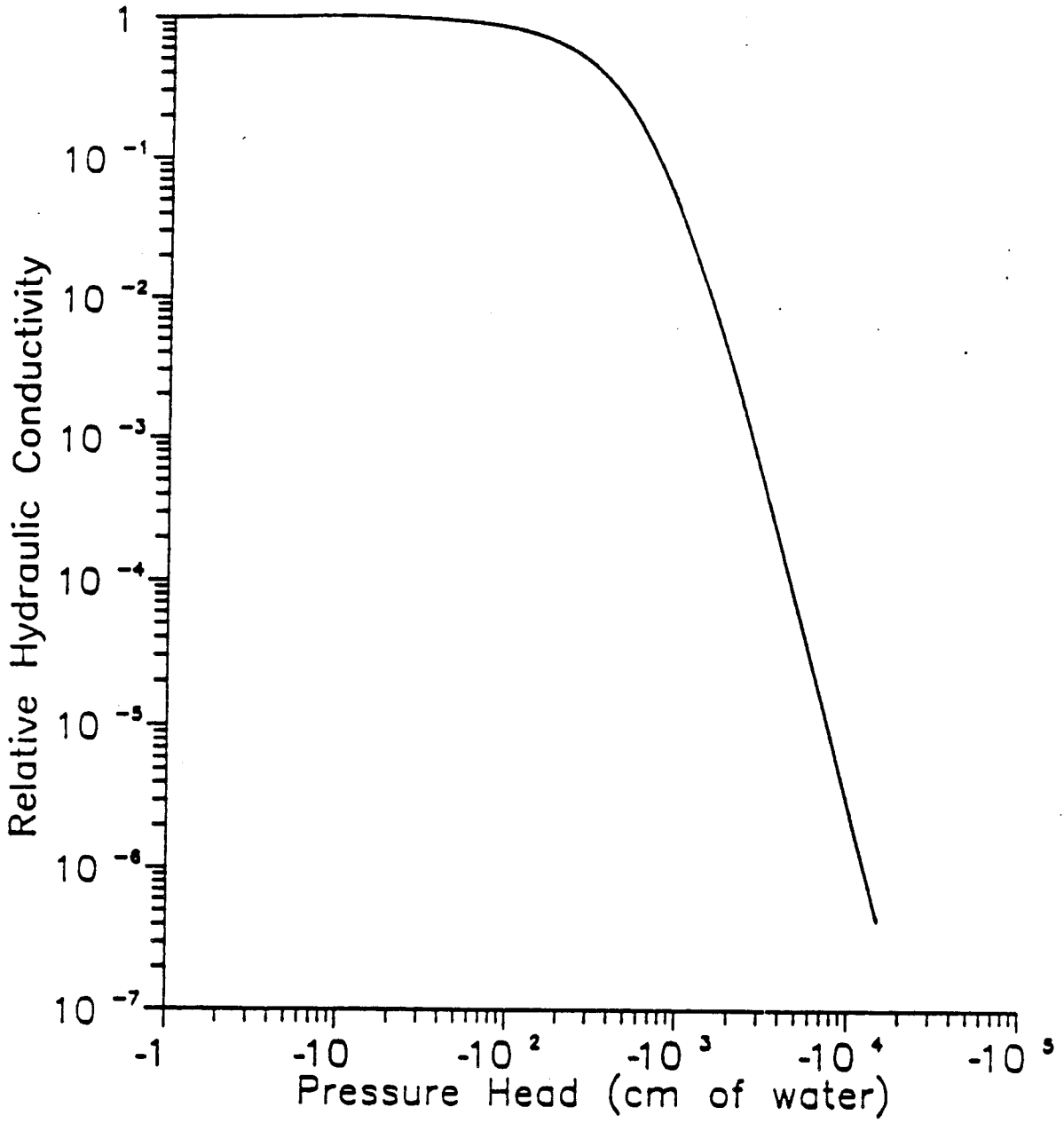

FIGURE NUMBER:	Relative Hydraulic Conductivity vs. Pressure Head (cm of water), Sample No. 16-17				DANIEL B. STEPHENS & ASSOCIATES, INC.
FOR: Los Alamos	PROJECT NO: 87-L-070	DATE: 1/4/88	PLOTTED BY: SLS	CHECKED BY: WBC	

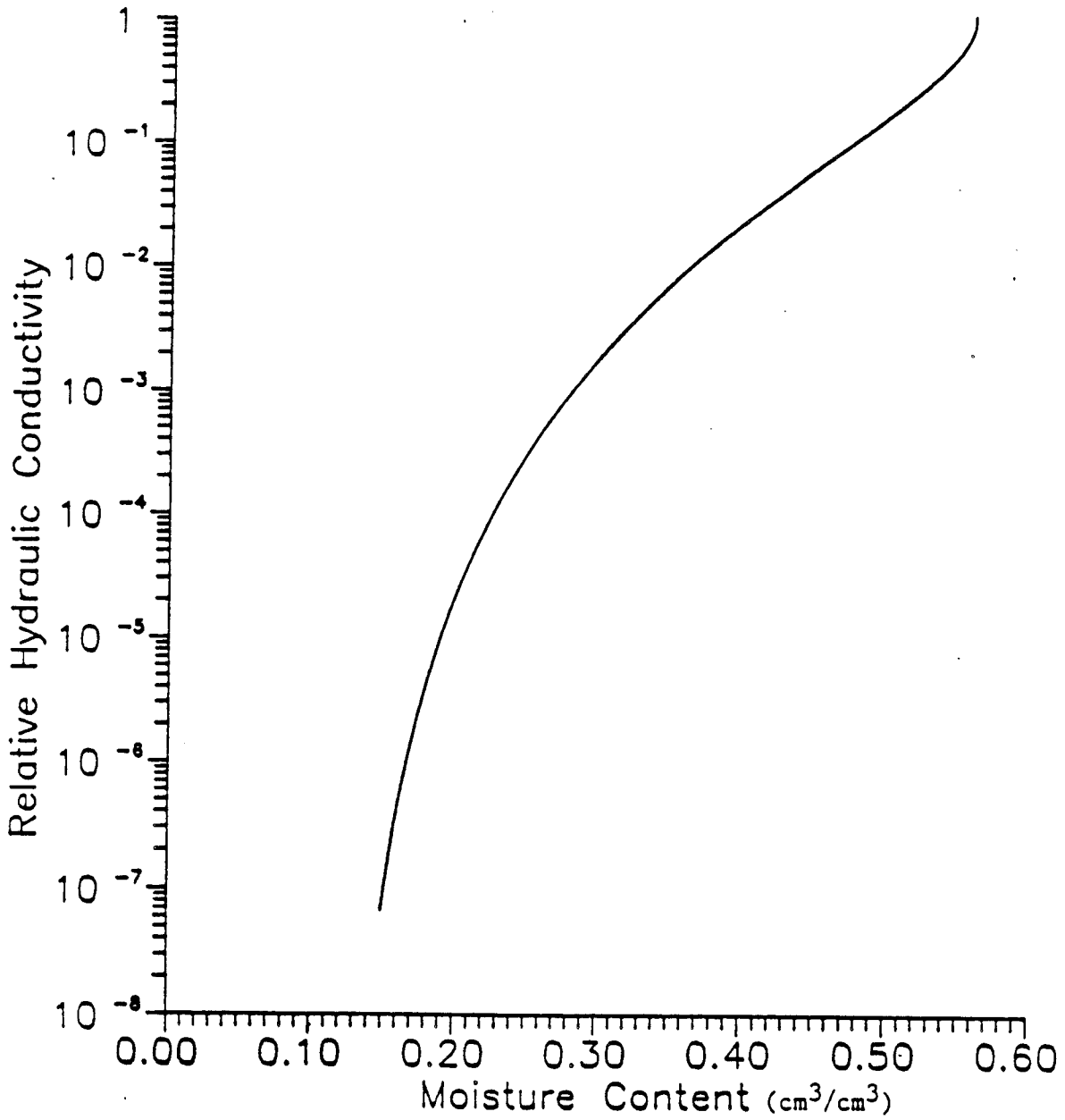

FIGURE NUMBER:	Relative Hydraulic Conductivity vs. Moisture Content (cm^3/cm^3), Sample No. 21-22				DANIEL B. STEPHENS & ASSOCIATES, INC.
FOR: Los Alamos	PROJECT NO: 87-L-070	DATE: 1/4/88	PLOTTED BY: SLS	CHECKED BY: WBC	

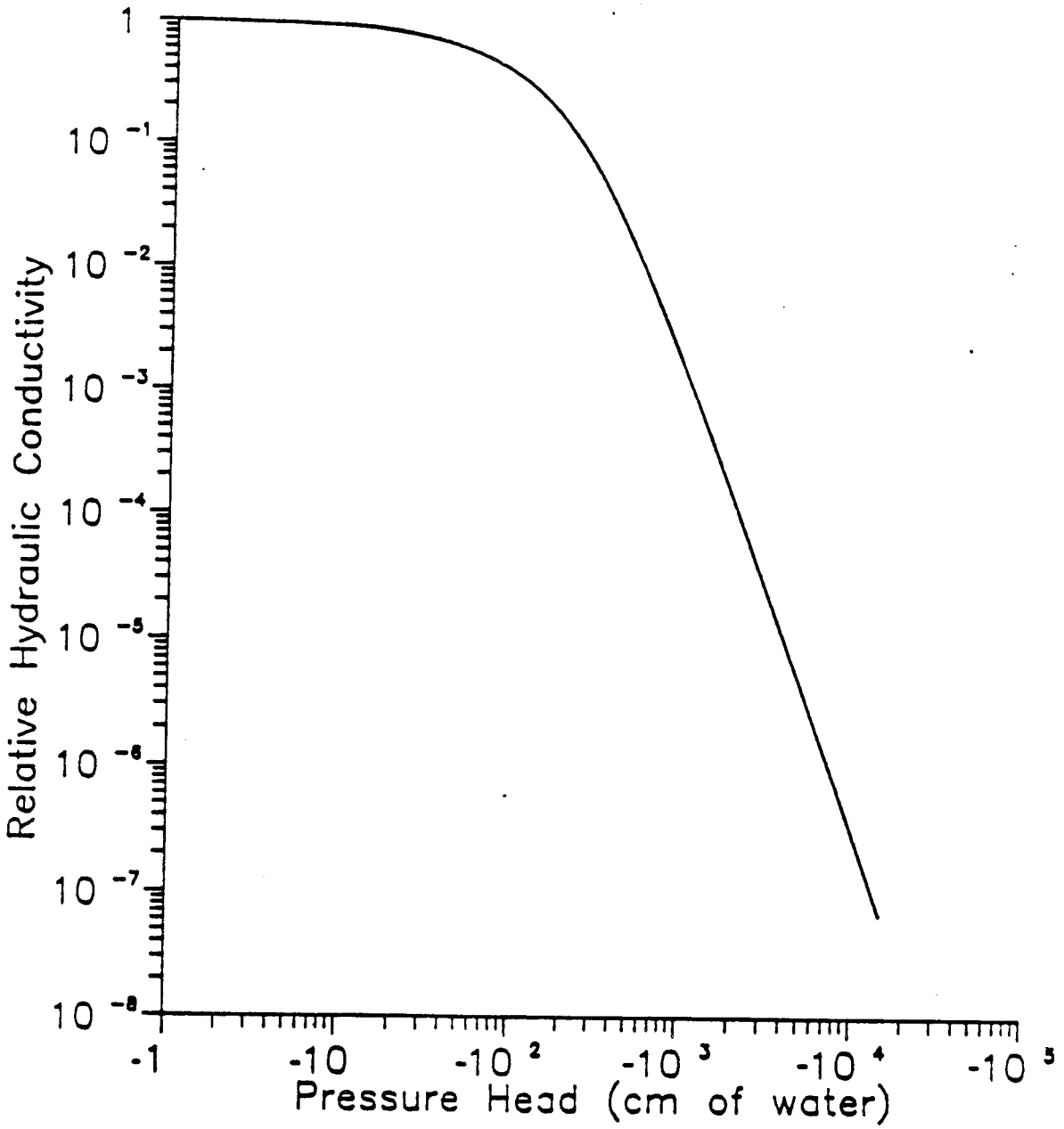

FIGURE NUMBER:	Relative Hydraulic Conductivity vs. Pressure Head (cm of water), Sample No. 21-22				DANIEL B. STEPHENS & ASSOCIATES, INC.
FOR: Los Alamos	PROJECT NO: 87-L-070	DATE: 1/4/88	PLOTTED BY: SLS	CHECKED BY: WBC	

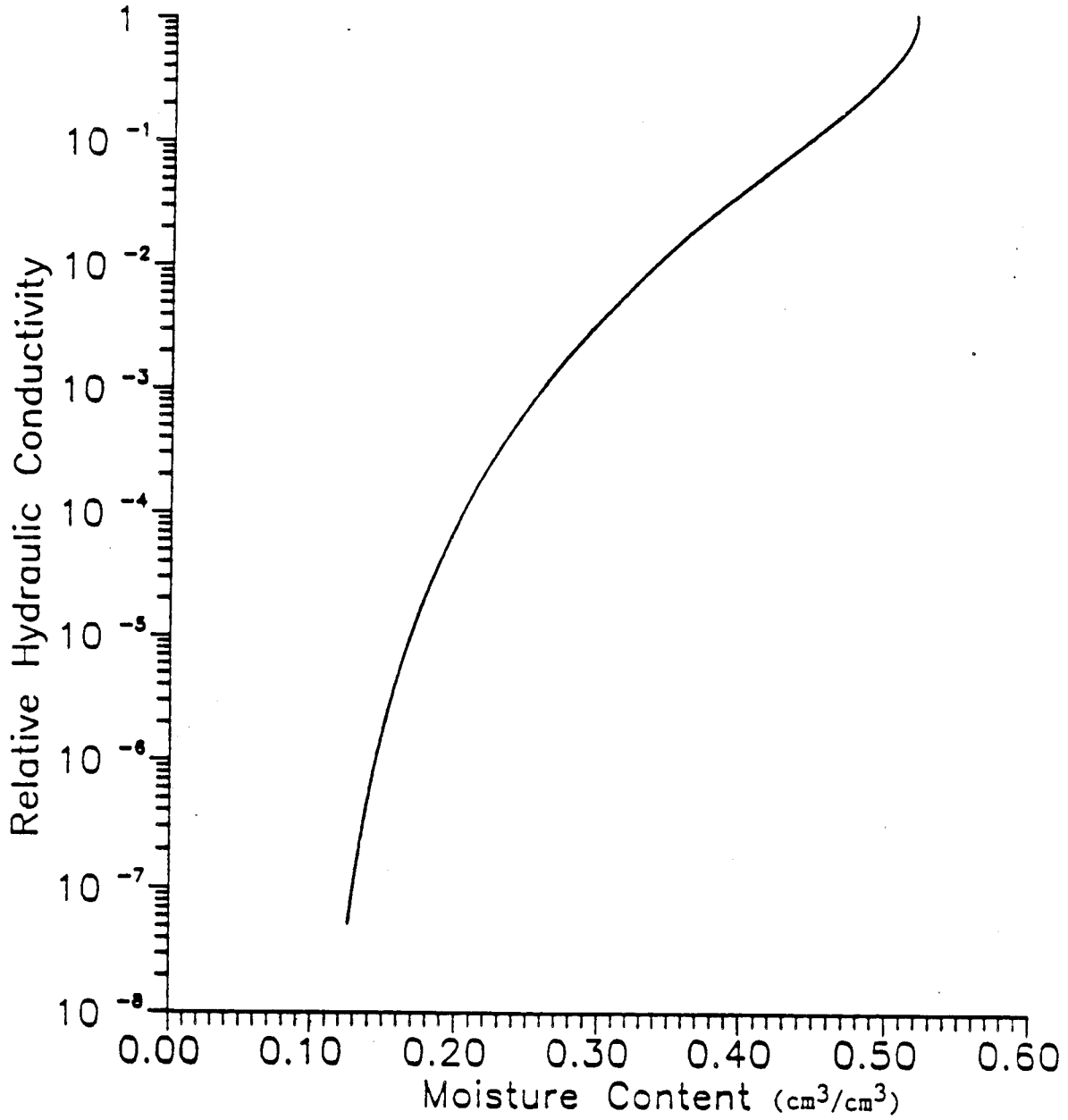

FIGURE NUMBER:	Relative Hydraulic Conductivity vs. Moisture Content (cm^3/cm^3), Sample No. 25-26				DANIEL B. STEPHENS & ASSOCIATES, INC.
FOR: Los Alamos	PROJECT NO: 87-L-070	DATE: 1/4/88	PLOTTED BY: SLS	CHECKED BY: WBC	

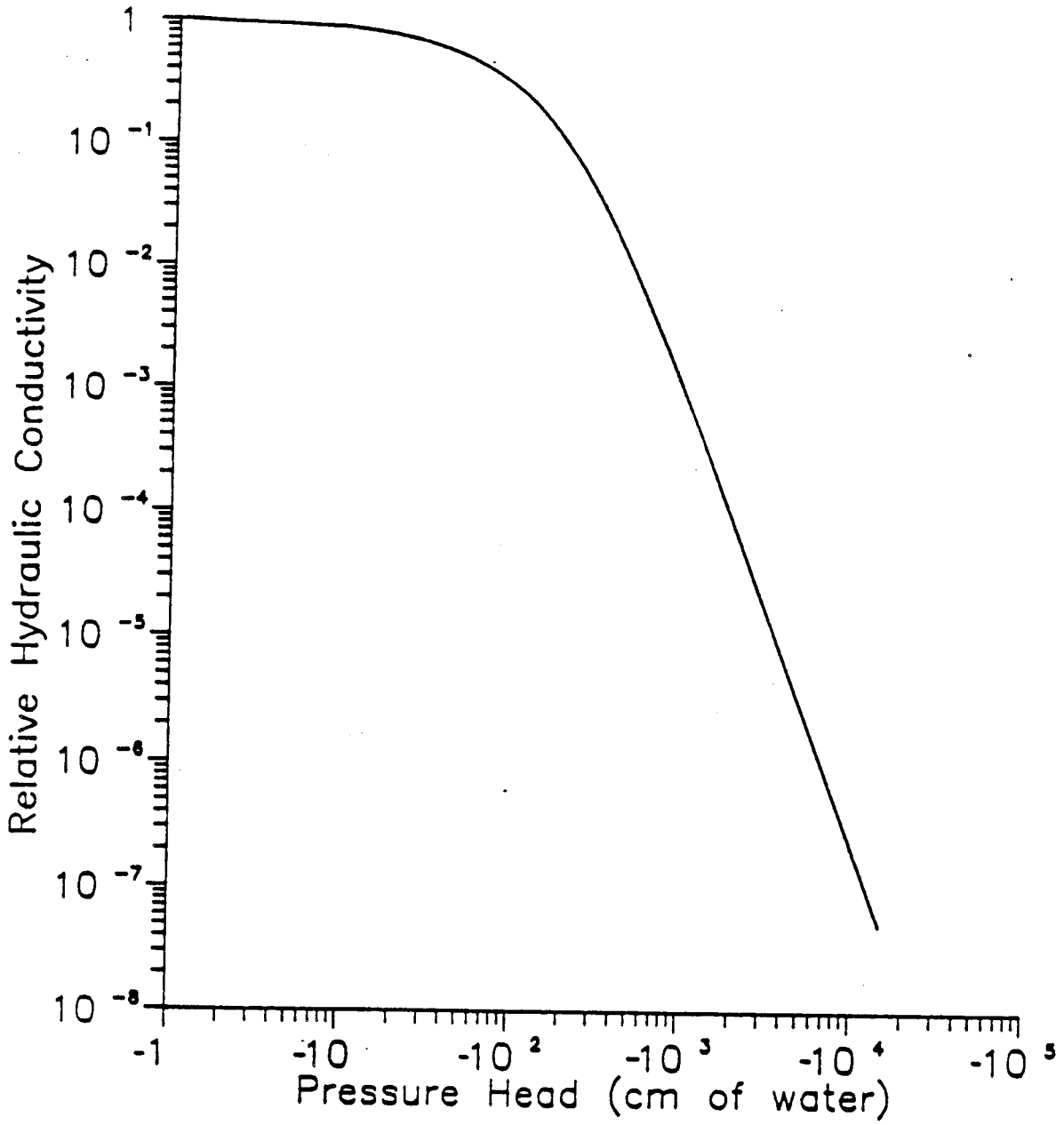

FIGURE NUMBER	Relative Hydraulic Conductivity vs. Pressure Head (cm of water), Sample No. 25-26				DANIEL B. STEPHENS & ASSOCIATES, INC.
FOR: Los Alamos	PROJECT NO: 87-L-070	DATE: 1/4/88	PLOTTED BY: SLS	CHECKED BY: WBC	

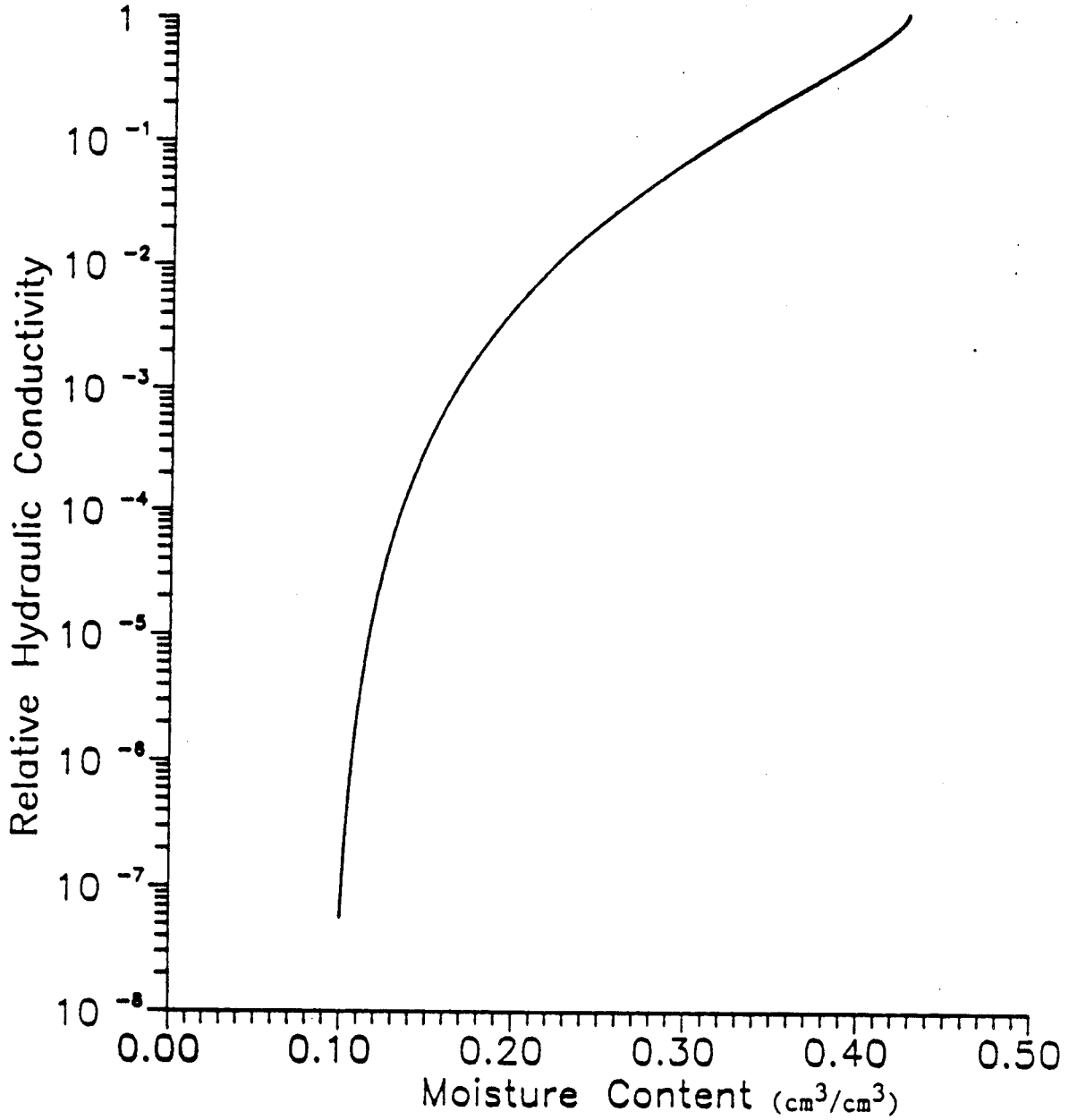

FIGURE NUMBER:	Relative Hydraulic Conductivity vs. Moisture Content (cm^3/cm^3), Sample No. 35-36				DANIEL B. STEPHENS & ASSOCIATES, INC.
FOR: Los Alamos	PROJECT NO: 87-L-070	DATE: 1/4/88	PLOTTED BY: SLS	CHECKED BY: WBC	

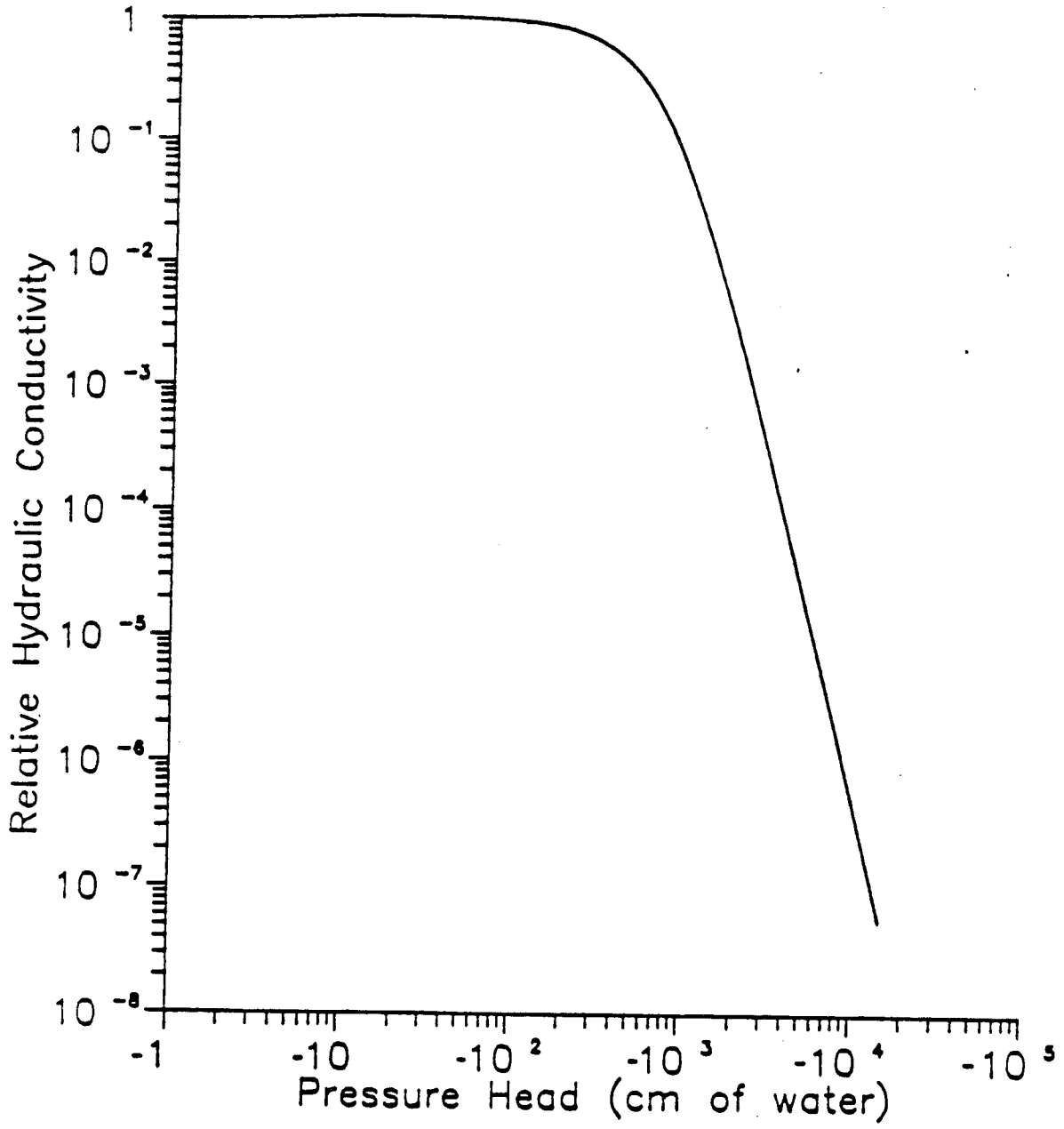

FIGURE NUMBER	Relative Hydraulic Conductivity vs. Pressure Head (cm of water), Sample No. 35-36				DANIEL B. STEPHENS & ASSOCIATES, INC.
FOR: Los Alamos	PROJECT NO: 87-L-070	DATE: 1/4/88	PLOTTED BY: SLS	CHECKED BY: WBC	

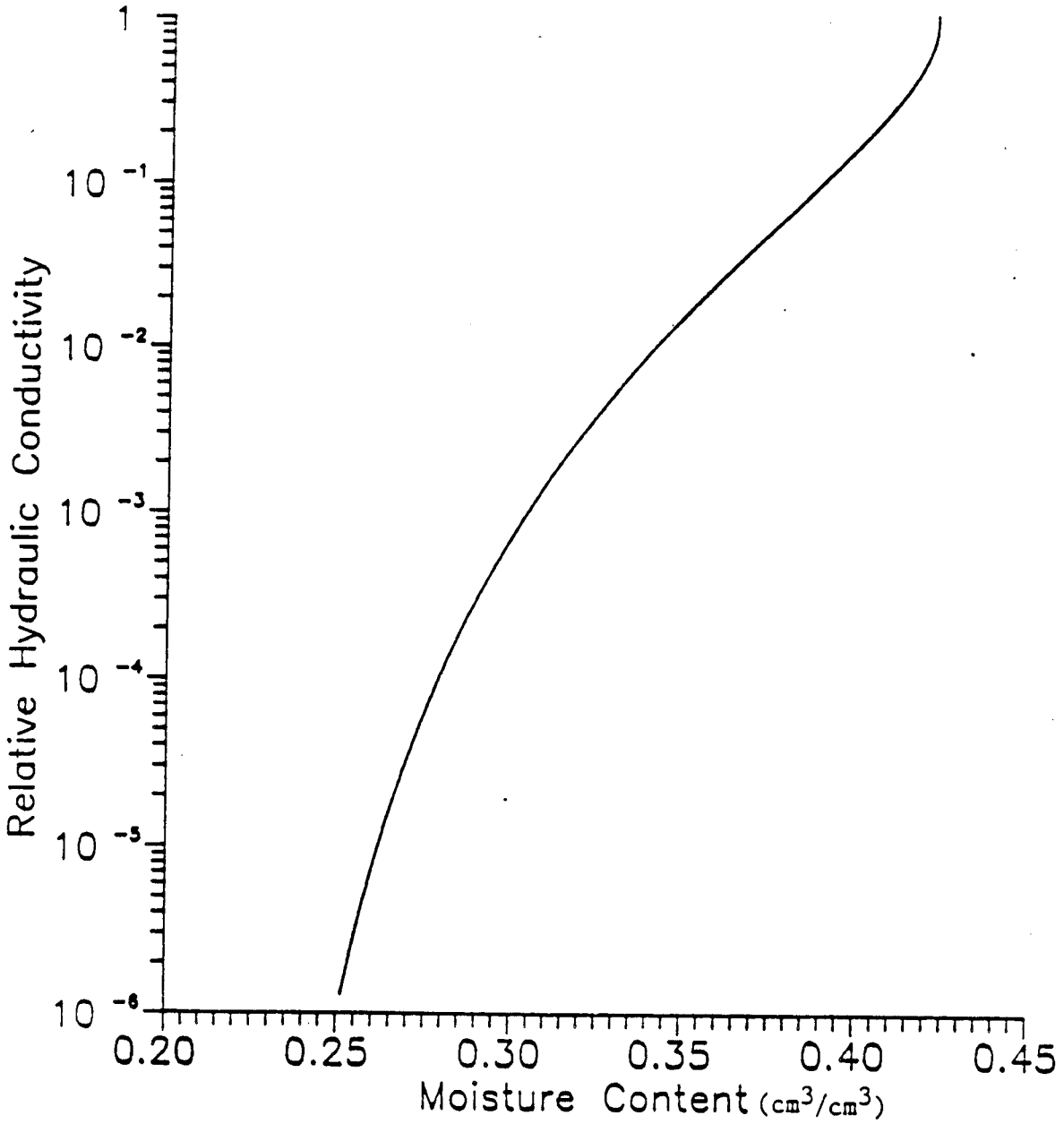

FIGURE NUMBER:	Relative Hydraulic Conductivity vs. Moisture Content (cm^3/cm^3), Sample No. 42-43				DANIEL B. STEPHENS & ASSOCIATES, INC.
FOR: Los Alamos	PROJECT NO: 87-L-070	DATE: 1/4/88	PLOTTED BY: SLS	CHECKED BY: WBC	

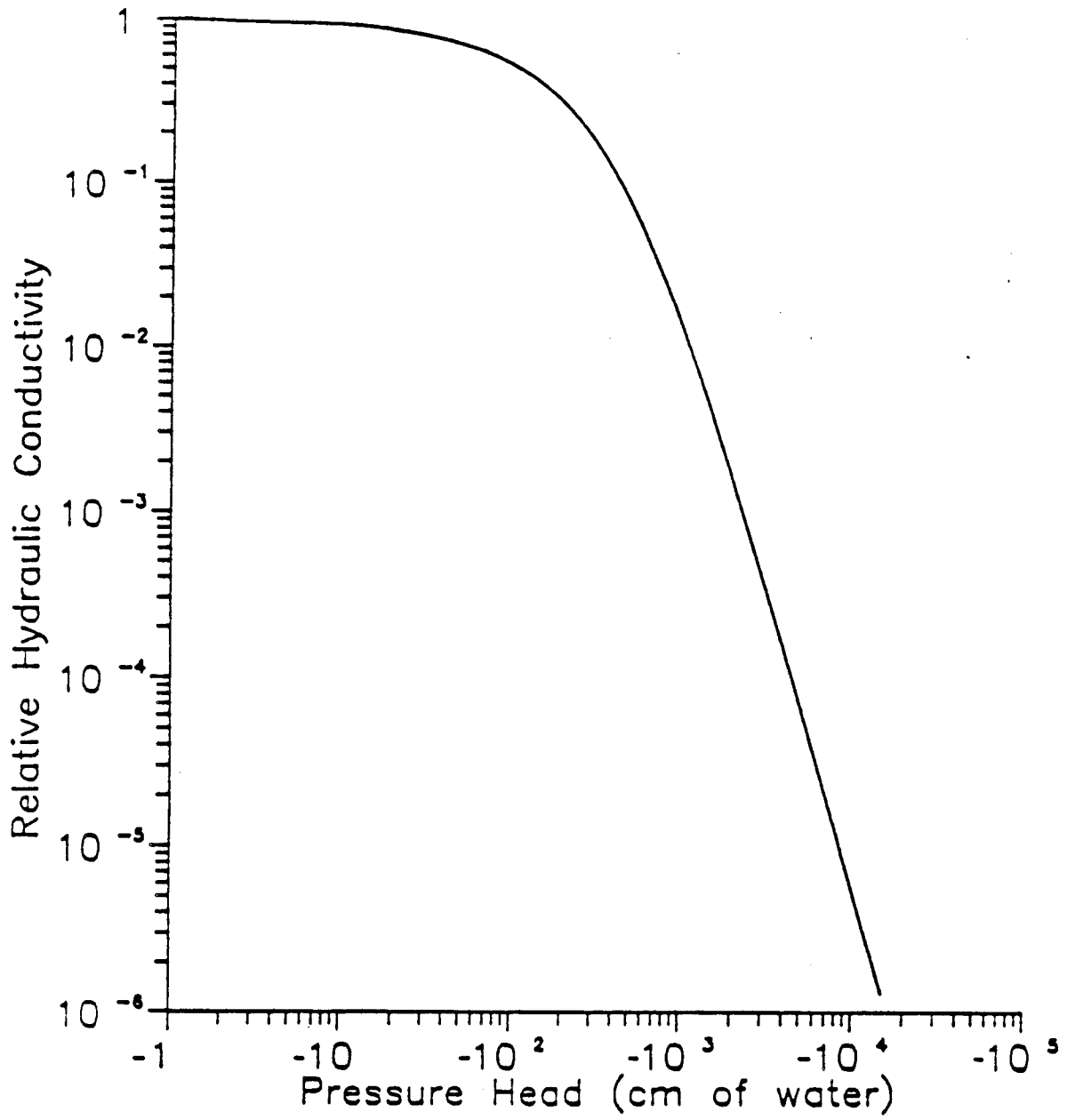

FIGURE NUMBER	Relative Hydraulic Conductivity vs. Pressure Head (cm of water), Sample No. 42-43				DANIEL B. STEPHENS & ASSOCIATES, INC.
FOR: Los Alamos	PROJECT NO: 87-L-070	DATE: 1/4/88	PLOTTED BY: SLS	CHECKED BY: WBC	

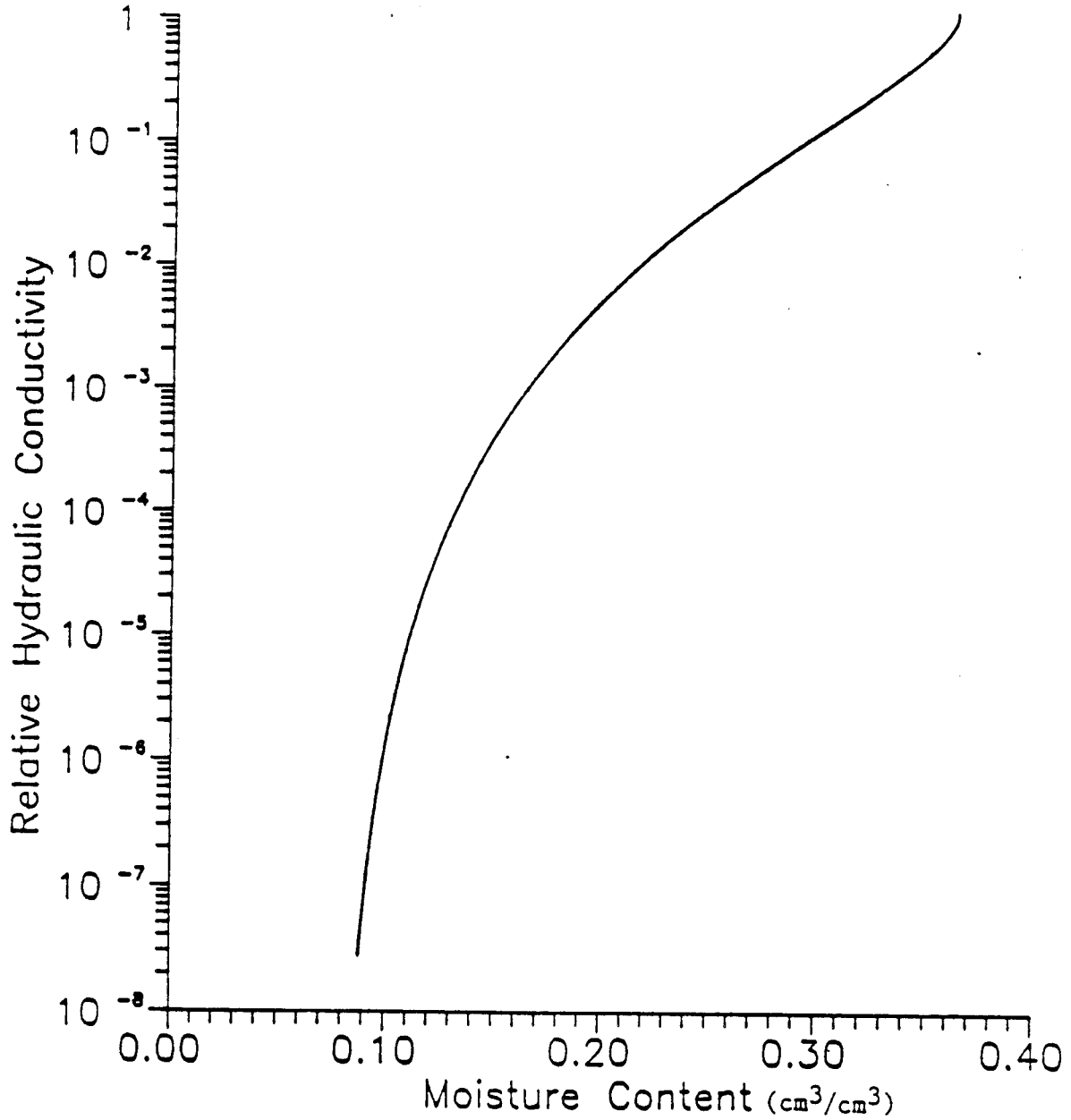

FIGURE NUMBER	Relative Hydraulic Conductivity vs. Moisture Content (cm^3/cm^3), Sample No. 61-62				DANIEL B. STEPHENS & ASSOCIATES, INC.
FOR: Los Alamos	PROJECT NO: 87-L-070	DATE: 1/4/88	PLOTTED BY: SLS	CHECKED BY: WBC	

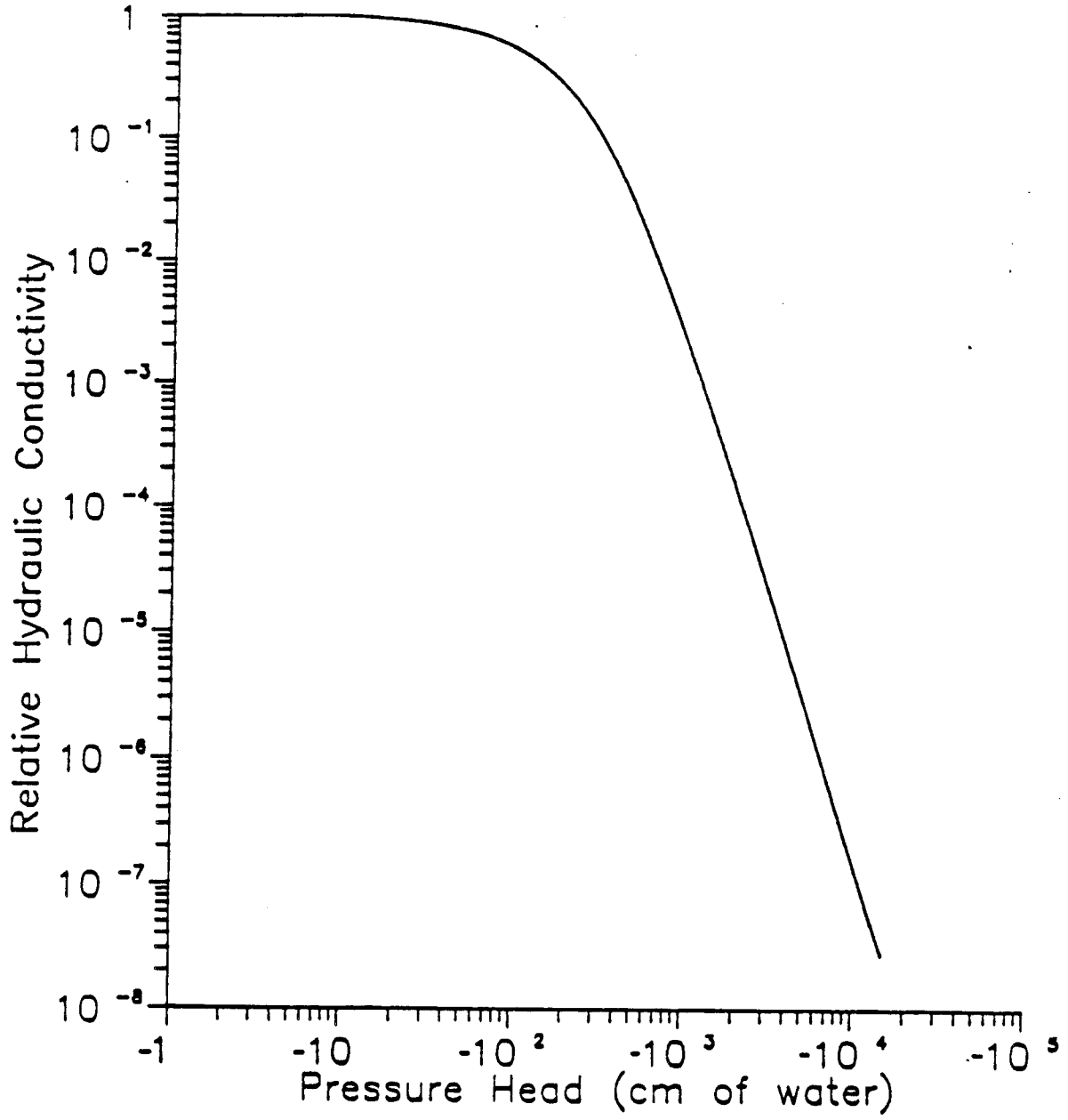

FIGURE NUMBER	Relative Hydraulic Conductivity vs. Pressure Head (cm of water), Sample No. 61-62				DANIEL B. STEPHENS & ASSOCIATES, INC.
FOR: Los Alamos	PROJECT NO: 87-L-070	DATE: 1/4/88	PLOTTED BY: SLS	CHECKED BY: WBC	

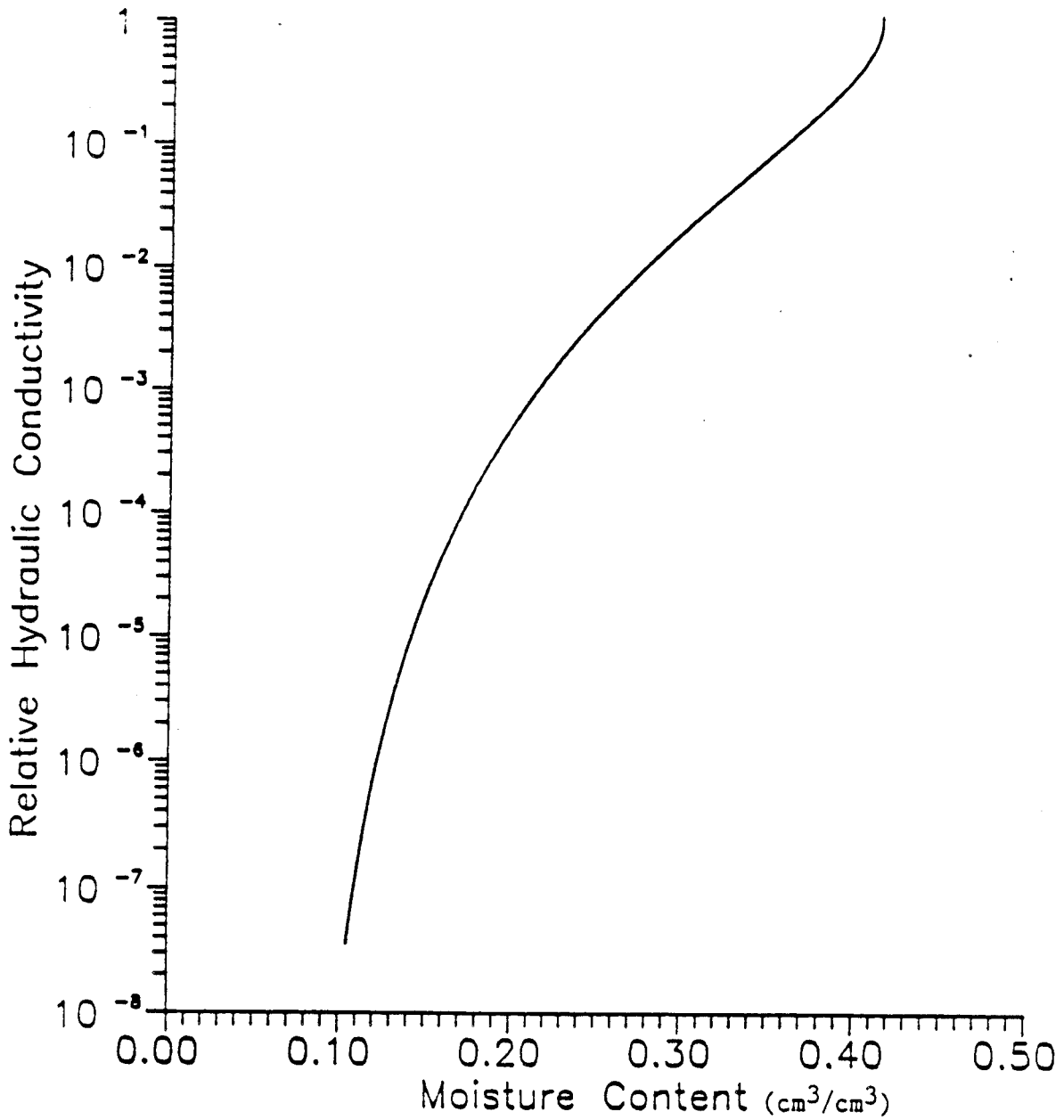

FIGURE NUMBER	Relative Hydraulic Conductivity vs. Moisture Content (cm^3/cm^3), Sample No. 61-62				DANIEL B. STEPHENS & ASSOCIATES, INC.
FOR: Los Alamos	PROJECT NO: 87-L-070	DATE: 1/4/88	PLOTTED BY: SLS	CHECKED BY: WBC	

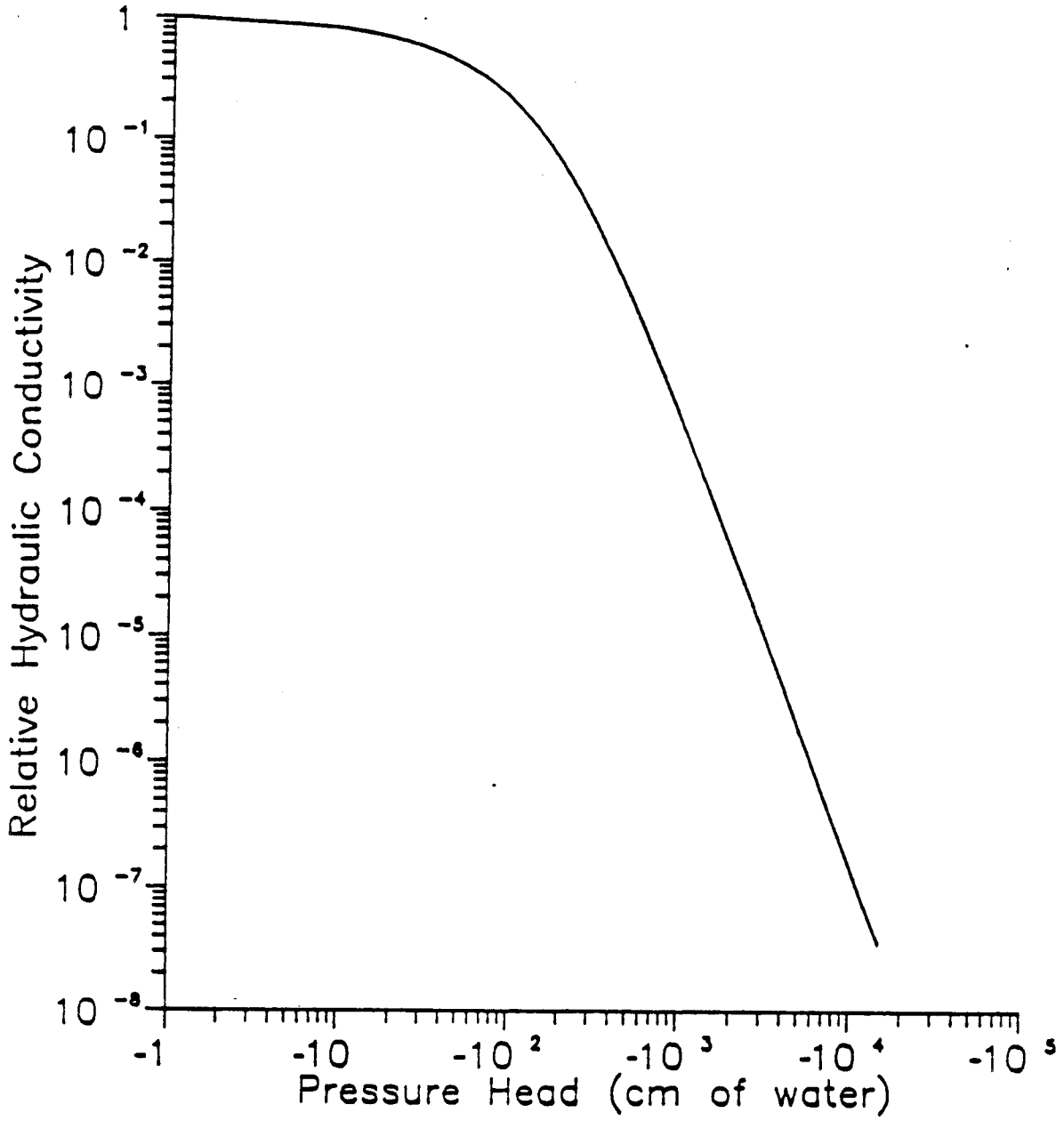

FIGURE NUMBER	Relative Hydraulic Conductivity vs. Pressure Head (cm of water), Sample No. 75-76				DANIEL B. STEPHENS & ASSOCIATES, INC.
FOR: Los Alamos	PROJECT NO: 87-L-070	DATE: 1/4/88	PLOTTED BY: SLS	CHECKED BY: WBC	

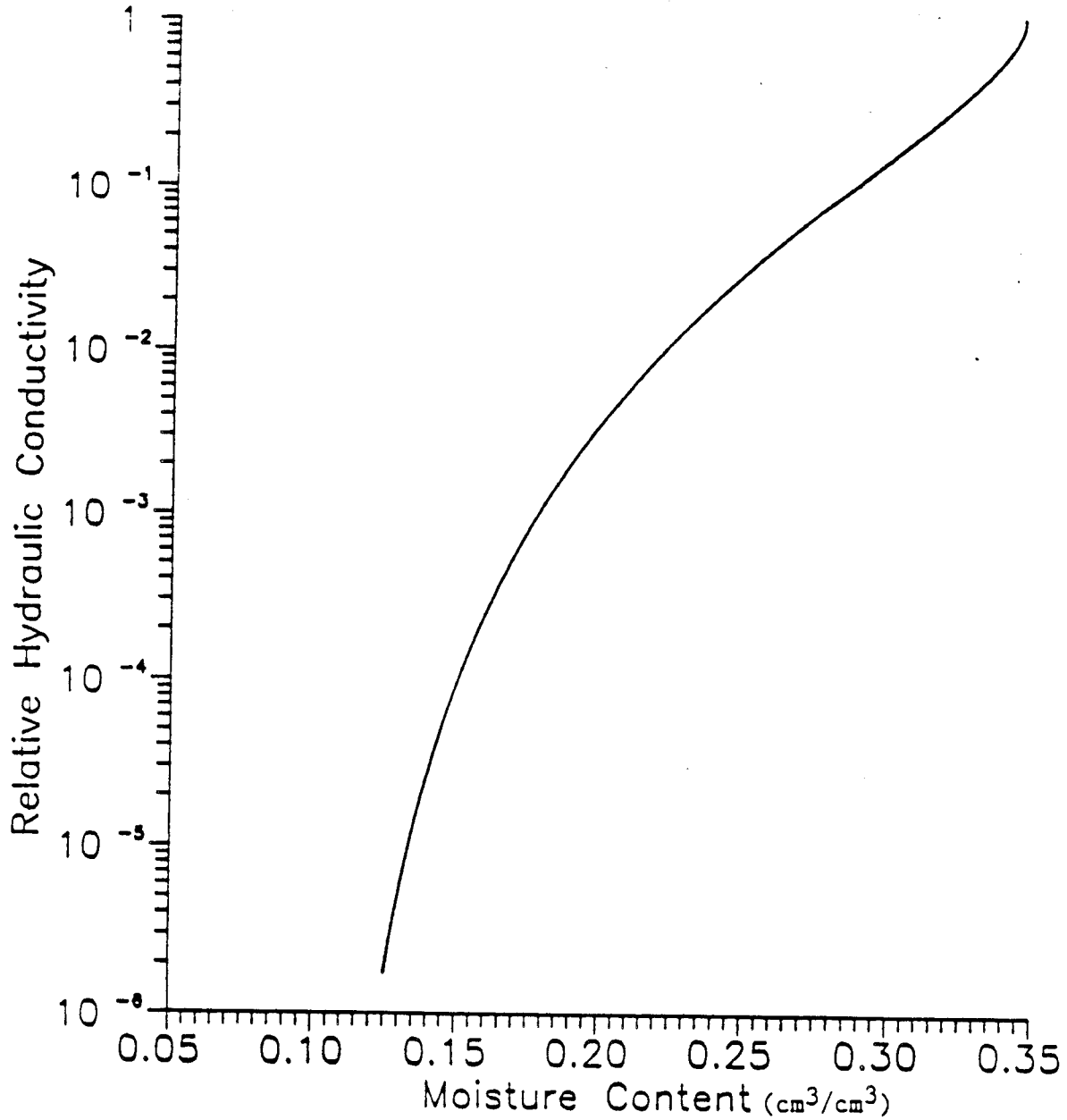

FIGURE NUMBER	Relative Hydraulic Conductivity vs. Moisture Content (cm^3/cm^3), Sample NO. 80-81				DANIEL B. STEPHENS & ASSOCIATES, INC.
FOR: Los Alamos	PROJECT NO: 87-L-070	DATE: 1/4/88	PLOTTED BY: SLS	CHECKED BY: WBC	

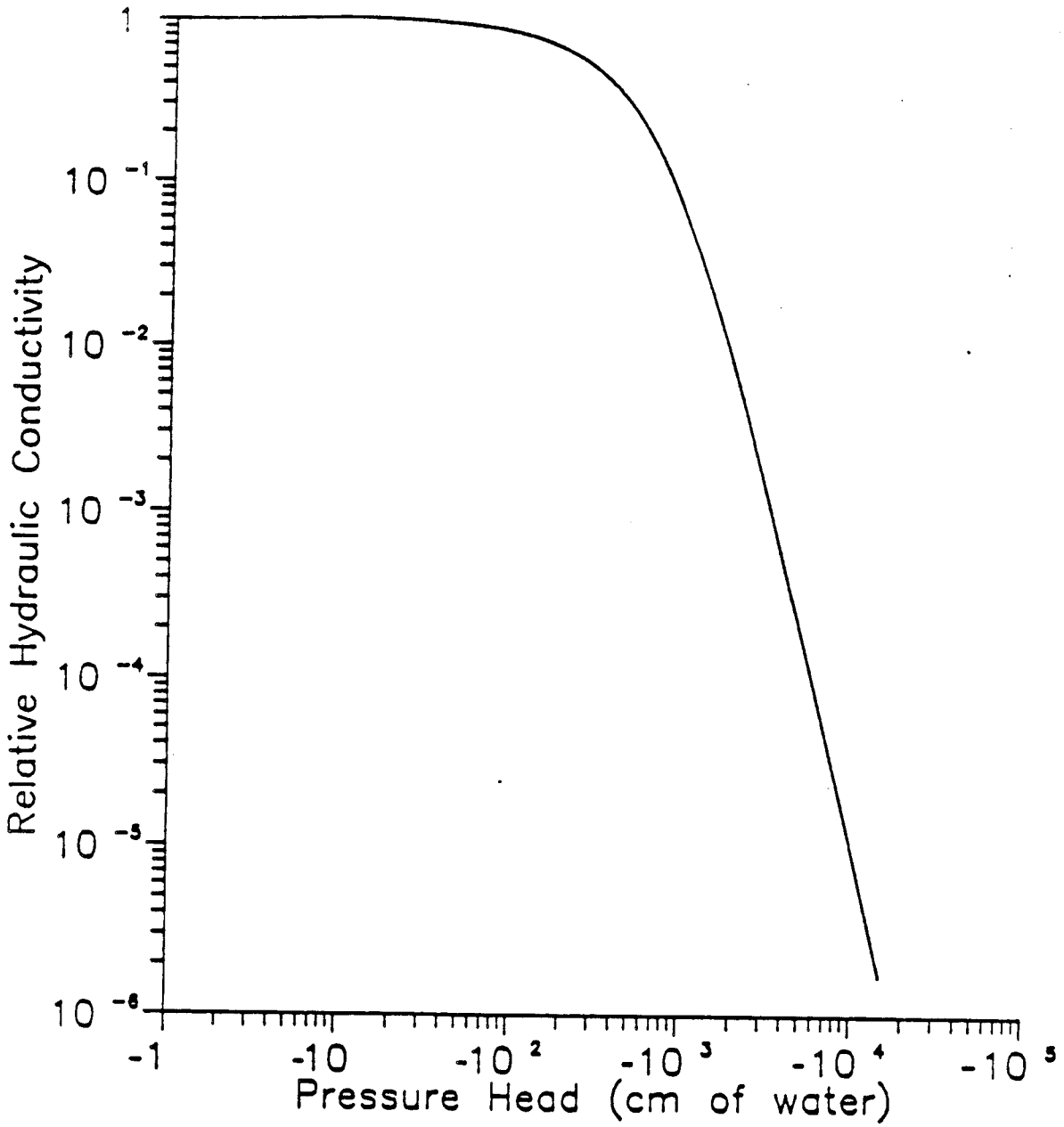

FIGURE NUMBER	Relative Hydraulic Conductivity vs. Pressure Head (cm of water), Sample No. 80-81				DANIEL B. STEPHENS & ASSOCIATES, INC.
FOR: Los Alamos	PROJECT NO: 87-L-070	DATE: 1/4/88	PLOTTED BY: SLS	CHECKED BY: WBC	

PRINCIPLES AND METHODS

SATURATED HYDRAULIC CONDUCTIVITY

Method

The saturated hydraulic conductivity of a soil sample can be measured in two types of laboratory apparatus: a constant head permeameter or a falling head permeameter.

Constant head. The hydraulic conductivity K is defined here as the ratio of q, the volume flux of water passing through a unit cross sectional area of soil per unit time, and ($\Delta h/L$) or gradient of hydraulic head in the direction of flow, corrected to 20°C:

$$K = (q/[\Delta h/L])(V_T/V_{20}) \qquad (1)$$

where $V_{20,T}$ is the kinematic viscosity at 20°C and observed temperature, T.

A soil sample of length, L, and cross-sectional area, A, is placed in a sample holder which prevents any loss of soil or change in volume and establishes laminar unidirectional flow through the sample. A constant head differential, Δh, is then set up across the sample and maintained. Periodic readings of volumetric outflow are taken until stable values for conductivity, K are obtained. Temperature of the fluid is measured with a thermometer. Figure B-1 is a diagram of the apparatus used. A constant head system is best suited to samples with conductivities greater than 10^{-4} cm/sec.

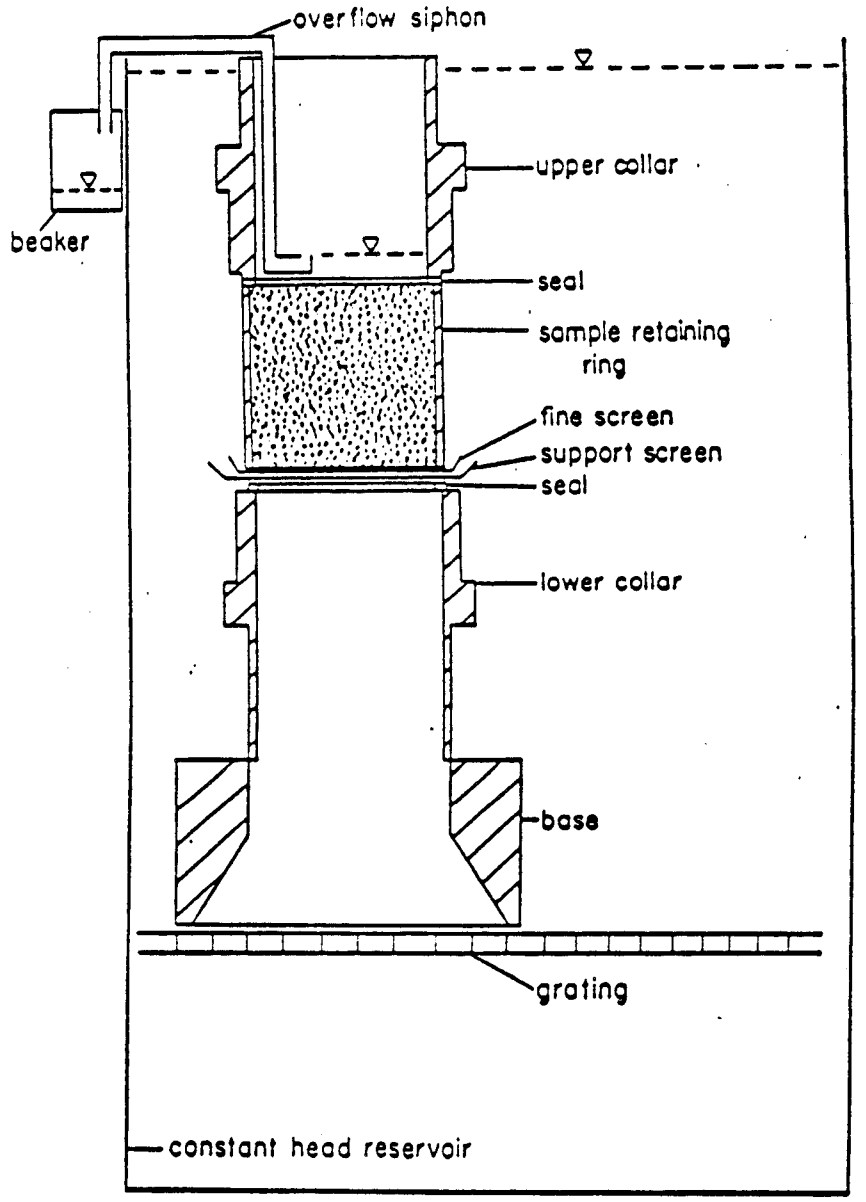

Figure B-1. Constant Head Permeameter

Falling head. A soil sample of length L and cross sectional area, A, is placed in a sample holder which has a standpipe with cross-sectional area, a. A head of H_1, is established in the standpipe above the sample, then the water level is allowed to fall to H_2 in time t. Figure B-2 is a diagram of the apparatus used. A falling head system is best suited to samples with conductivities less than 10^{-4} cm/sec. The hydraulic conductivity, is then defined as:

$$K = (a \times L/A \times t) \ \ell n \ (H_1/H_2)(V_T/V_{20}) \qquad (2)$$

Procedures:

Constant head. Cylinders containing the soil sample are covered on both ends with loose fitting caps and placed in a shallow pan containing de-aired water. The samples are allowed to wet slowly from below for 24 hours. The samples are removed from the pan, and two screens are placed over one end; a very stiff one of coarse mesh for support and a fine one of either 80 to 100 mesh to prevent any sample from being washed out. The cylinder, with screens attached, is then clamped into the sample retainer and placed in the permeameter. The level of the water in the permeameter reservoir is then slowly raised over a period of hours. When the level in the reservoir reaches to within a few centimeters above the top of the sample, a siphon is placed in the sample retainer assembly to remove water from above

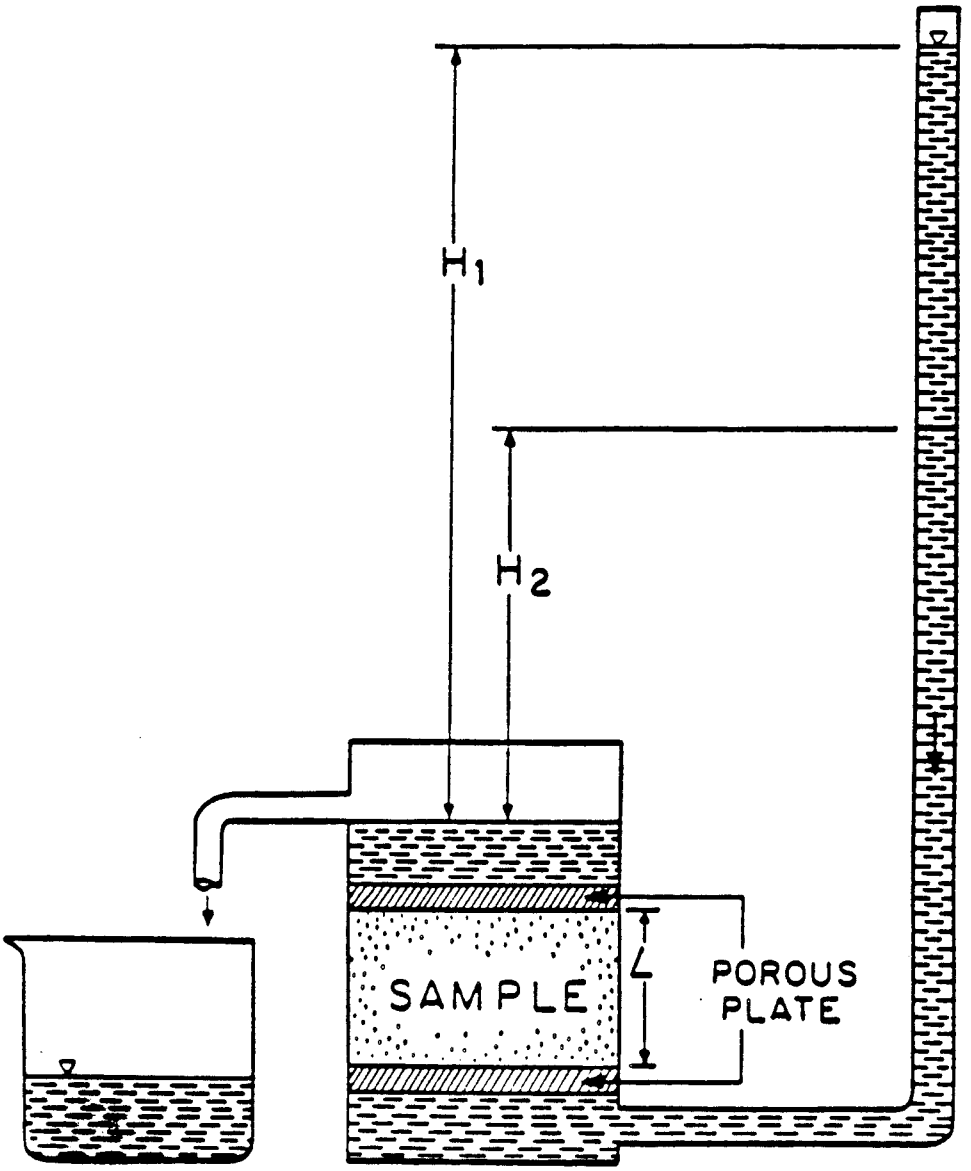

Figure B-2. Falling Head Permeameter

the sample. Water flows upward through the sample due to the hydraulic head difference across the sample. Periodic measurements of discharge and the head difference across the sample are made, and the hydraulic conductivity is calculated. A correction to 20 C is then applied for differences in kinematic viscosity. Measurement continues until the calculated hydraulic conductivity value stabilizes.

Falling head. Saturation of the sample is obtained by the same procedures described under constant head test. Screens are also attached as outlined under constant head test. The ring with screens is then placed in the falling head sample retainer and set in a constant head reservoir. Water is added to the standpipe and the difference between the water level in the standpipe and that in the constant head reservoir are recorded over time. The water level in the standpipe is allowed to fall, while the fluid level in the lower level is constant. After a period of time the difference in water levels between that in the standpipe and that in the constant head reservoir are measured and the elapsed time noted. Correction is applied for kinematic viscosity.

Calculations:

Experimental values are substituted into the appropriate equation as outlined under methods.

MOISTURE RETENTION - HANGING COLUMN
(PORE SIZE DISTRIBUTION)

Principle

Use of pore size distribution as a soil characteristic is based upon acceptance of the capillary model. This model is described by:

$$h' = 2 \cos \gamma / \rho g r \qquad (3)$$

where h' is the height to which a liquid will rise in a clean capillary tube of radius r, γ is the surface tension of the liquid, ρ is its density, and g is acceleration due to gravity. If water is extracted from an initially saturated sample of soil by a tension equal to h', the volume of water extracted is equal to the volume of pores having an effective radius greater than the radius, r. As the tension applied to the sample increases, additional water drains from progressively smaller pores.

Method

The key component of the apparatus for measuring the retention of moisture at different pressure heads or pore size distribution is a fritted glass porous plate that conducts water, but when wet the plate is impermeable to air. The fritted glass

plates have an air-entry pressure of about 300 to 400 cm of water. These plates are affixed in a glass funnel which is connected to a buret with stopcock by means of flexible tubing. A diagram of the apparatus is shown in Figure 3. A soil sample is placed on the plate and tension, h' is applied to the sample by positioning the fluid level in the buret at different levels below the center of the sample. Water flows out of the sample into the buret until equilibrium is achieved. The tension is again increased or decreased to obtain another state of equilibrium between moisture held by capillary forces in the sample and the applied tension.

Laboratory Procedure

Air is first removed from the porous plate by allowing de-aired water to pass continuously through it for 24 hours. The funnel with porous plate and the buret are supported on vertical rods by means of clamps. A saturated sample within its sample ring is then placed on the porous plate, making certain that good hydraulic contact is established between the soil particles and the plate. With the stopcock of the buret closed, the initial level of the water in the buret is recorded.

The buret is then lowered a small increment to about 10 to 15 cm below the center of the soil sample. When the stopcock is opened, the soil may begin to desaturate, and the drainage will flow into the buret. When drainage has ceased, the stopcock is

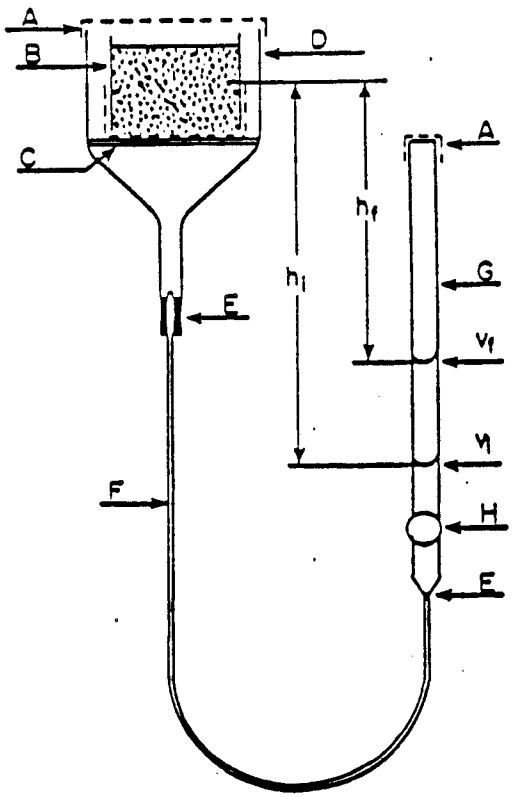

A Aluminum foil covers
B Sample in cylinder
C Fritted glass porous plate (part of D)
D Büchner funnel with porous plate
E Joints must be secure
F Flexible tubing
G Burette, least division not more than 0.1% sample volume
H Stopcock of burette
h_i cm of water suction, initial
h_f cm of water suction, final
v_i Burette reading, initial
v_f Burette reading, final

Figure B-3. Hanging Column Apparatus

closed and we record the water level in the buret and the vertical distance from the bottom of the meniscus of the water in the buret to the middle of the soil sample. The procedure is repeated in a stepwise manner until the maximum tension desired is reached. A reversal of the process is used to gather data on the wetting behavior of the sample.

Calculation

Saturated moisture content , θ_{sat} , (volume percent) is determined as follows:

$$\theta \text{ sat} = [\text{M sat} - \text{M dry}]/[V_T \times \rho_w] \times 100 \quad (\% \text{ vol}) \quad (4)$$

where M sat = mass of sample saturated, M dry = mass of sample, oven dried to a constant weight, V_T = volume of the sample, ρ_w = density of the water at temp when saturated mass was determined. The quantity $[\text{M sat} - \text{M dry}]/\rho_w$ is the volume, in cubic centimeters, of water initially contained in the sample volume. The drainage is subtracted from the initial volume of water and then divided by the sample volume to arrive at the moisture content in percent volume at the given value of tension.

$$[V_i - V_D]/V_T \times 100 = \theta_{h'} \quad (\% \text{ vol}) \quad (5)$$

where V = volume of water initial, V_D = cumulative volume drained from sample, V_T = volume of sample, $\theta_{h'}$ = moisture content at the tension value h'. This gives then a paired set of values of tension, or pressure head, versus volumetric moisture content.

MOISTURE RETENTION - PRESSURE PLATE

Principle

The operation of the pressure plate moisture extractor requires maintaining a pressure difference between the liquid phase of the water in the soil and water on the opposite side of a porous plate which supports the soil sample. The sample and porous plate are sealed in a rigid container so that positive gas pressure applied above the plate causes flow to occur across the plate (Figure B-4). The porous ceramic plate is supported by a fine mesh screen which also provides a passage way for the extracted solution. The water beneath the plate is open to the atmosphere through the outflow tube. The illustration in Figure B-5 shows a magnified view of soil particles in contact with the plate inside the pressure plate extractor during an extraction run.

As soon as air pressure inside the chamber is raised above atmospheric pressure, the higher pressure inside the chamber forces excess water through the microscopic pores in the plate. Air, however, will not flow through the pores of the plate, because the plate remains saturated due to its high air-entry pressure. When the pressure in the chamber increases, water leaves the sample until the tension of the water

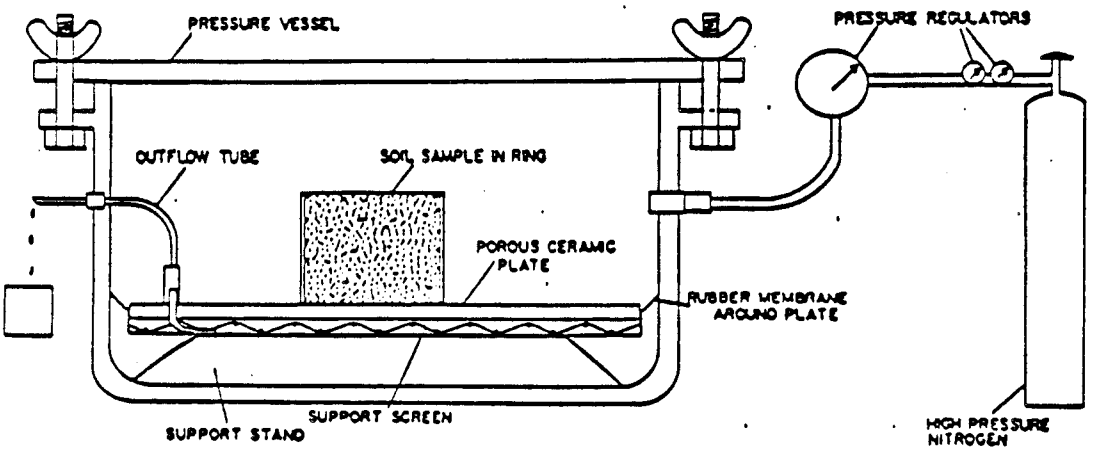

Figure B-4. Pressure Plate Extractor

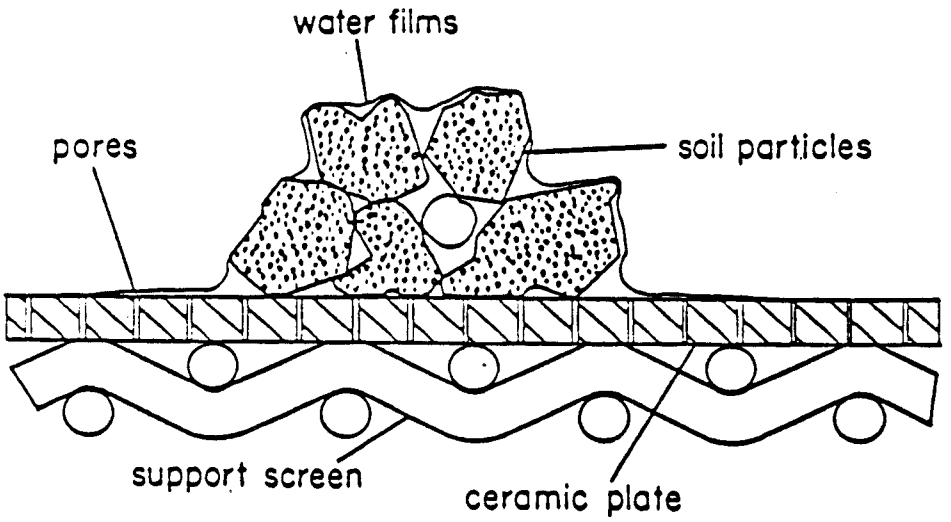

Figure B-5. Magnified View of Soil Particles

due to capillary and adsorptive forces is in equilibrium with the applied pressure.

Method

Moisture retention is obtained using a pressure plate extractor (Soil Moisture Inc., Santa Barbara, CA, Model 1500), with 1, 3 and 15 bar ceramic plates. Pressure is provided by high pressure nitrogen from cylinders.

Laboratory Procedure

The porous ceramic plate is placed is a shallow pan with deaired distilled water and allowed to stand overnight. The plate is then removed from the pan and placed in the extractor. De-aired distilled water is poured over the plate to the limit allowed by the rubber skirt, which generally just submerges the plate. The pressure plate is sealed and pressure brought to 50% of the plates maximum rated pressure. This pressure is maintained until outflow ceases. The extractor is opened and any excess water around the plate is removed.

The soil samples in their sample rings are then placed on the plate, making certain good hydraulic contact is established. The extractor is then sealed and the pressure brought to the level desired. The pressure is maintained until outflow ceases. The extractor is then opened and the samples weighed quickly on an electronic top-loading balance. Subsequently, the samples are

returned to the extractor, and the pressure is increased to the next increment.

Calculations

The decrease in mass of water in the sample during a period of applied pressure is converted to an equivalent decrease in volume of water according to:

$$V_w = \Delta m/\rho_T \qquad \text{(cc)} \qquad (6)$$

where Δm = change in mass of soil sample (g), ρ_T = density of water at temperature of experiment (g/cc), V_w = equivalent volume of water (cc).

Volumes of water calculated from equation 6 are then used to determine the moisture content at that pressure:

$$\theta_p = (V_i - \Sigma\Delta V_w)/V_T \times 100 \qquad \text{(\% vol)} \qquad (7)$$

where θ_p = moisture content at pressure p(% vol), V_i = initial volume of water in sample (cc), $\Sigma\Delta V_w$ = cumulative water volume change (cc), V_T = total volume of the sample (cc).

INITIAL MOISTURE CONTENT

Method

Core method, with oven drying.

Laboratory Procedure

The field weight of the soil sample is determined as soon as possible after the sample is removed from the packing container. The tare of the ring which holds the sample, as well as the mass of the caps for the ends of the ring, are determined. The volume of soil in the sample ring is also calculated. After all specified analyses have been performed on the sample, the sample is removed from its ring and spread in an aluminum pan. When necessary, soil aggregates are broken up by motar and pestal. Care is taken not to change the natural particle size distribution. The sample is placed in a convection oven at 110° C for at least 24 hours until dried to a constant weight.

Calculations

The initial moisture content is determined on a percent volume basis according to:

$$\theta_i = [M_i - M_f]/[V_T \times \rho] \times 100 \quad (\%vol) \qquad (8)$$

where θ_i = initial moisture content (% vol), M_i = initial mass of soil only (g), M_f = final mass of soil only (g), V_T = total

volume of sample (cc), ρ = density of pore fluid in the soil when initial mass was determined (g/cc). The density of the pore fluid initially present in the sample is assumed to be 1.0 g/cc.

BULK DENSITY

Method

Core method, with oven drying.

Laboratory Procedure

The volume of the soil sample is determined from sample geometry measurements, and the sample is dried in the oven at 110 C until no additional mass loss occurs.

Calculations

$$\rho_b = M_D/V_T \qquad (g/cc) \qquad (9)$$

where ρ_b = dry bulk density (g/cc), M_D = mass of oven dried soil sample (g), V_T = total volume of soil sample (cc).

POROSITY

Method

Calculated from bulk density and measured or assumed values of particle density.

Laboratory Procedure

Bulk density, ρ_b, is determined by oven drying, as described in the section outlining the bulk density determination. For this series of analyses particle density, ρ_s, is assumed to be 2.65 g/cc.

Calculation

$$n = [1 - (\rho_b/\rho_s)] \times 100 \qquad \text{(percent)} \qquad (10)$$

UNSATURATED HYDRAULIC CONDUCTIVITY

Method

Mualem (1976) described the theoretical basis for a procedure used to estimate unsaturated hydraulic conductivity from the soil-water release curve according to the following equations;

$$K_r = S_e^{\frac{1}{2}}\left[\int_0^{S_e} 1/h(x)dx / \int_0^1 1/h(x)\ dx\right]^2 \qquad (11)$$

where K_r = relative hydraulic conductivity, $h = h(S_e)$ is the negative pressure head, given here as a function of dimensionless moisture content:

$$S_e = \theta - \theta_r / \theta_s - \theta_r \qquad (12)$$

where subscripts s and r indicate saturated and residual values of the soil moisture (θ). The expression relating dimensionless moisture content to the pressure head, and thus the soil moisture release curve is given by:

$$S_e = [\ 1/1+(\alpha h)^n]^m \qquad m = 1 - 1/n \qquad (13)$$

where α, and n are obtained by a non-linear least squares numerical procedure applied to measured moisture retention data using the technique developed by Van Genuchten (1978).

Laboratory procedure

The data input to the computer model of Van Genuchten (1978)

consists of the saturated moisture content, residual moisture content and values of observed pressure head versus moisture content. The residual moisture content is taken to be the moisture content at -15 bars. The paired values of observed pressure head and moisture content are obtained as described under the procedures for determining moisture retention by the hanging column and pressure plate methods. Saturated moisture content is determined through gravimetric measurements and sample geometry.

References

Mualem, Y., 1976, A New Model for Predicating the Hydraulic Conductivity of Unsaturated Porous Media, Water Resources Research, vol. 12, no. 3, p. 513-522.

Van Genuchten, R., 1978, Calculating the Unsaturated Hydraulic Conductivity With a New Closed-Form Analytical Model, Research Report No. 78-WR-08, Princeton University, Department of Civil Engineering, September 1978, 65pp.

Pumping Tests in the Los Alamos Canyon Well Field Near Los Alamos, New Mexico

By C. V. THEIS *and* C. S. CONOVER

CONTRIBUTIONS TO THE HYDROLOGY OF THE UNITED STATES

GEOLOGICAL SURVEY WATER-SUPPLY PAPER 1619-I

Prepared in cooperation with the U.S. Atomic Energy Commission

UNITED STATES GOVERNMENT PRINTING OFFICE, WASHINGTON : 1962

UNITED STATES
DEPARTMENT OF THE INTERIOR
GEOLOGICAL SURVEY
Albuquerque, New Mexico

Geology and hydrology of Technical Area 49, Frijoles Mesa, Los Alamos County, New Mexico

by

James E. Weir, Jr., and William D. Purtymun

A study of the possible contamination of ground water by radioactive wastes

Prepared in cooperation with the Atomic Energy Commission

1962

For administrative release only to the Atomic Energy Commission

Not reviewed for conformance to
Geological Survey nomenclature or editorial standards

Contents

	Page
Abstract	1
Introduction	6
Location and setting	7
Previous work	9
Personnel and acknowledgments	10
Purpose and scope of report	11
Techniques used and data collected	14
Surface mapping	15
Test drilling	17
Deep wells	18
Exploratory large-diameter auger holes	27
Core holes	29
Shallow holes for moisture measurements	30
Geophysical logs	31
Down-hole mapping	34
Laboratory investigations	37
Tests and analyses of rock samples	38
Spencer J. Buchanan and Associates	38
Health Division - Group H-7	38
Geological Survey	39
Geology and hydrology	43
Santa Fe Group (middle(?) Miocene To Pleistocene(?))	46
Undifferentiated unit	49
Physical characteristics	49
Water-bearing characteristics	69

Contents - Continued

Page

Geology and hydrology - Continued

Santa Fe Group - Continued

Puye Conglomerate (upper Pliocene(?)) ---------- 70

Totavi Lentil ---------- 70

Physical characteristics ---------- 70

Water-bearing characteristics ---------- 71

Fanglomerate member ---------- 73

Physical characteristics ---------- 73

Water-bearing characteristics ---------- 75

Basaltic rocks of Chino Mesa ---------- 76

Physical characteristics ---------- 76

Water-bearing characteristics ---------- 77

Volcanic rocks of the Jemez Mountains ---------- 78

Tschicoma Formation (Pliocene and Pleistocene(?)) ---------- 80

Physical characteristics ---------- 80

Water-bearing characteristics ---------- 82

Bandelier Tuff (Pleistocene) ---------- 83

Guaje Member ---------- 84

Otowi Member ---------- 85

Tshirege Member ---------- 89

Alluvium ---------- 90

Geology and water-bearing properties of the Tshirege Member of the Bandelier Tuff ---------- 91

Unit 1A ---------- 114

Contents - Continued

Page

Geology and water-bearing properties of the Tshirege Member of the Bandelier Tuff - Continued

Unit 1A - Continued

Physical characteristics ---------- 114

Water-bearing characteristics ---------- 115

Unit 1B ---------- 116

Physical characteristics ---------- 116

Water-bearing characteristics ---------- 120

Unit 2 ---------- 121

Physical characteristics ---------- 121

Water-bearing characteristics ---------- 122

Unit 3 ---------- 124

Physical characteristics ---------- 124

Water-bearing characteristics ---------- 127

Unit 4 ---------- 128

Physical characteristics ---------- 128

Water-bearing characteristics ---------- 129+130

Unit 5 ---------- 132

Physical characteristics ---------- 132

Water-bearing characteristics ---------- 136

Unit 6 ---------- 137

Physical characteristics ---------- 137

Water-bearing characteristics ---------- 148

Soil cover and related material ---------- 149

Contents - Continued

Page

Geology and water-bearing properties of the Tshirege Member of the Bandelier Tuff - Continued

Soil cover and related material - Continued

Weathered tuff ---------- 150

Water-laid pumice ---------- 151

Soil cover ---------- 152

Moisture distribution in the upland soil and underlying tuff -- 154

Test holes in well drained areas ---------- 156

Test holes in areas receiving runoff from well drained areas ---------- 158

Infiltration from stream flow ---------- 161

Recharge of the main aquifer ---------- 164

Water-level changes ---------- 168

Pumping tests ---------- 170

Tests at well DT-5A ---------- 171

Tests at well DT-9 ---------- 172

Tests at well DT-10 ---------- 173

Velocity of ground-water movement ---------- 175

Quantity of water moving through the aquifer ---------- 176

Quality of water ---------- 177

Age of ground water in principal aquifer ---------- 181

Conclusions ---------- 185

Suggested continuing study ---------- 188

Selected references ---------- 190

Appendix ---------- 192

Tables

		Page
Table 1.	Casing schedule for well DT-5A	21
2.	Casing schedule for well DT-9	23
3.	Casing schedule for well DT-10	25
4.	Rock samples for petrographic, chemical, spectographic, and X-ray analysis by the Geological Survey	40
5.	Sample log of well DT-5A	51
6.	Sample log of well DT-9	57
7.	Sample log of well DT-10	63
8.	Sample log of well DT-5P	86
9.	Type section of units in Tshirege Member of the Bandelier Tuff	92
10.	Log of core hole 1	96
11.	Log of core hole 2	98
12.	Log of core hole 3	101
13.	Log of core hole 4	104
14.	Mineral constituents of the Tshirege Member of the Bandelier Tuff at TA-49, Los Alamos County, N. Mex.	107
15.	Chemical analyses of the Tshirege Member, Bandelier Tuff at TA-49, Los Alamos County, N. Mex.	109 ~~Pocket~~
16.	Results of semiquantitative spectrographic analyses of the Tshirege Member of the Bandelier Tuff at TA-49, Los Alamos County, N. Mex.	110 ~~Pocket~~

Tables - Continued

		Page
Table 17.	Results of hydrologic laboratory analyses of the Tshirege Member of the Bandelier Tuff at TA-49, Los Alamos County, N. Mex.	112 ~~Pocket~~
18.	Sample log of Beta hole	117
19.	Sample log of Alpha hole	125
20.	Summary of results of moisture measurements in test holes located in well drained areas	157
21.	Summary of results of moisture measurements in test holes in areas that receive runoff from well drained areas	159
22.	Partial chemical analyses of water samples from deep wells at TA-49, Los Alamos County, N. Mex.	179
23.	Radiochemical and chemical analyses of water from deep test wells at TA-49, Los Alamos County, N. Mex.	180A ~~Pocket~~
24.	Particle-size distribution in percent by weight for samples from TA-49, Los Alamos County, N. Mex.	193
25.	Pore-size distribution and soil-tension samples from TA-49, Los Alamos County, N. Mex.	194
26.	Reconnaissance notes for large-diameter holes in Areas 1, 2, 3, 4, and 10, TA-49, Los Alamos County, N. Mex.	195

Illustrations--short list

		Page
Figure 1.	Index map of part of Los Alamos and adjacent counties, New Mexico	7
2.	Layout of large-diameter holes in Areas 1, 2, 3, 4, and 10	34 A
3.	Deleted.	
4.	Geologic map of the Los Alamos area ---Pocket	44
5.	Geologic cross section through Frijoles Mesa	44 A
6.	Geologic map and cross section of TA-49 --Pocket	91
7.	Structure contours on unit Qbt_2 ---------Pocket	121
8.	Deleted. Sand Unit 5 in Shaft Area 11	132 A
9.	Deleted. Sand Unit 5 in Shaft Area 11	132 B
10.	Deleted. Outcrop of Unit 5	132 C
11.	Water-laid sand of unit Qbt_5	132 D
12.	Deleted. Sand Unit 5 in Shaft Area 11	132 E
13.	Structure contours on the top of unit Qbt_5 Pocket	(135)
14.	Outcrop of curved joint face in unit Qbt_6	137 A
15.	Maps of walls of selected large-diameter holes in Area 1 ---Pocket	(138)
16.	Maps of walls of selected large-diameter holes in Area 2 ---Pocket	(138)
17.	Maps of walls of selected large-diameter holes in Area 3 ---Pocket	(138)

Illustrations--short list - Continued

Page

Figure 18. Maps of walls of selected large-diameter holes in Area 4 ---------- Pocket (138)

19. Isopach map of unit Qbt_6 ---------- Pocket (147)

20. Thickness of soil in TA-49 ---------- Pocket (152)

21. Graph of moisture content and lithology in test hole 1M-2 ---------- 154 A

22. Graph of moisture content and lithology in test hole 2M-1 ---------- 154 B

23. Graph of moisture content and lithology in test hole 2M-2 ---------- 154 C

24. Graph of moisture content and lithology in test hole 3M-1 ---------- 154 D

25. Graph of moisture content and lithology in test hole 3M2 ---------- 154 E

26. Graph of moisture content and lithology in test hole 3M-3 ---------- 154 F

27. Graph of moisture content and lithology in test hole 4M-1 ---------- 154 G

28. Graph of moisture content and lithology in test hole 4M-2 ---------- 154 H

29. Graph of moisture content and lithology in test hole 4M-3 ---------- 154 I

Illustrations--short list - Continued

		Page
Figure 30.	Graph of moisture content and lithology in test hole 4M-4	154 J
31.	Graph of moisture content and lithology in test hole 5M-2	154 K
32.	Graph of moisture content and lithology in test hole 9M-4	154 L
33.	Graph of moisture content and lithology in test hole 10M-1	154 M
34.	Graph of moisture content and lithology in test hole 10M-2	154 N
35.	Graph of moisture content and lithology in test hole 1M-1	154 O
36.	Graph of moisture content and lithology in test hole 1M-3	154 P
37.	Graph of moisture content and lithology in test hole 1M-3A	154 Q
38.	Graph of moisture content and lithology in test hole 2M-3	154 R
39.	Graph of moisture content and lithology in test hole 5M-1	154 S
40.	Graph of moisture content and lithology in test hole 6M-1	154 T

Illustrations--short list - Continued

		Page
Figure 41.	Graph of moisture content and lithology in test hole 9M-1	154 U
42.	Graph of moisture content and lithology in test hole 9M-2	154 V
43.	Graph of moisture content and lithology in test hole 9M-3	154 W
44.	Graph of measurements of flow downstream from well DT-5A	161 A
45.	Generalized contours on the piezometric surface of the main aquifer	166 A
46.	Hydrograph of water levels measured and from recorder charts at well DT-5A	168 A
47.	Hydrograph of water levels measured and from recorder charts at well DT-9	168 B
48.	Hydrograph of water levels measured and from recorder charts at well DT-10	169 A
49.	Deleted. Work Over Rig on DT-9 During Aquifer tests	170A
50.	Deleted. Discharge from Well DT-9 during Aquifer test	170B
51.	Semilogarithmic graph of recovery of water level in well DT-5A	171 A

Illustrations--short list - Continued

		Page
Figure 52.	Semilogarithmic graph of recovery of water level in well DT-9	172 A
53.	Semilogarithmic graph of recovery of water level in well DT-10	174 A

Appendix

Figure 54A.	Gamma ray-neutron logs of well DT-5	Pocket (2)
54B.	Induction log of well DT-5	Pocket (3)
54C.	Temperature log of well DT-5	Pocket (4)
55A.	Gamma ray-neutron logs of well DT-5A	Pocket (5)
55B.	Induction-electrical and spontaneous-potential logs of well DT-5A	Pocket (6)
55C.	Microlog and microcaliper logs of well DT-5A	Pocket (7)
55D.	Laterolog of well DT-5A, TA-49	Pocket (8)
55E.	Temperature log of well DT-5A	Pocket (9)
55F.	Sonic log of well DT-5A	Pocket (10)
56A.	Gamma ray-neutron logs of the upper 1,301 feet of well DT-9	Pocket (11)
56B.	Gamma-ray log from depth of 1,094 to 1,501 feet of well DT-9	Pocket (12)
56C.	Induction-electrical and spontaneous-potential logs of well DT-9	Pocket (13)
56D.	Laterolog of well DT-9	Pocket (14)

Illustrations--short list - Continued

		Page
Figure 56E.	Temperature log of well DT-9 ----------	Pocket (15)
56F.	Sonic log of well DT-9 --- ----------	Pocket (16)
57A.	Gamma ray-neutron log of well DT-10 ----------	Pocket (17)
57B.	Induction-electrical and spontaneous-potential logs of well DT-10 ----------	Pocket (18)
57C.	Temperature log of well DT-10 ----------	Pocket (19)
57D.	Sonic log of well DT-10 ----------	Pocket (20)
58.	Gamma-ray log of core hole 1 ----------	Pocket (24)
59A.	Gamma-ray log of core hole 2 ----------	Pocket (27)
59B.	Gamma ray-neutron log of upper 201 feet of core hole 2 ----------	Pocket (23)
59C.	Electrical log of the upper 368 feet of core hole 2 ----------	Pocket (24)
59D.	Temperature log of the upper 200 feet of core hole 2 ----------	Pocket (25)
60.	Gamma-ray log of core hole 3 in Area 3 ----------	Pocket (26)
61.	Gamma-ray log of core hole 4 in Area 4 ----------	Pocket (27)
62A.	Gamma ray-neutron logs of Alpha hole ----------	Pocket (28)
62B.	Induction log of Alpha hole, TA-49 ----------	Pocket (29)

Illustrations--long list

		Reference page
Figure 1.	Index map of part of Los Alamos and adjacent counties, New Mexico, showing the location of Technical Area 49 (TA-49) ----------	7
2.	Layout of large-diameter holes in Areas 1, 2, 3, 4, and 10 showing holes mapped and described. (Areas shown on figure 6.) ----------	34 A
3.	Deleted.	
4.	Geologic map of the Los Alamos area, New Mexico Pocket	44
5.	Geologic cross section through Frijoles Mesa from the Pajarito fault to the Rio Grande. Location is shown on figure 4. Description of units is shown on figures 4 and 6 ----------	44 A
6.	Geologic map and cross section showing location of exploratory drill holes, TA-49, Los Alamos County, N. Mex. ---------- Pocket	91
7.	Structure contours on unit Qbt_2 of the Tshirege Member of the Bandelier Tuff, TA-49, Los Alamos County, N. Mex. ---------- Pocket	121
8.	~~Deleted.~~ Sandunits 5, in Shaft Area 11	132A
9.	Deleted. " " " " "	132B
10.	Deleted " " " " "	132C

Illustrations--long list - Continued

Reference page

Figure 11. Water-laid sand of unit Qbt_5 of the Tshirege Member of the Bandelier Tuff underlain and overlain by weathered iron-stained ~~unit Qbt~~ and flows $_4$, southeast wall of west hole in Area 10, TA-49, Los Alamos County, N. Mex. ---------- ~~Pocket~~ ---- (132 B

12. Deleted. Sand Unit in Shaft Area 11 132E

13. Structure contours on the top of unit Qbt_5 of the Tshirege Member of the Bandelier Tuff, TA-49, Los Alamos County, N. Mex. ---------- Pocket (135)

14. Outcrop of curved joint face in unit Qbt_6 of the Tshirege Member of the Bandelier Tuff. North side of New Mexico Highway 4, about 1.5 miles west of entrance to TA-49, Los Alamos County, N. Mex. ---------- 137 4

15. Maps of walls of selected large-diameter holes in Area 1, TA-49, Los Alamos County, N. Mex Pocket (138)

16. Maps of walls of selected large-diameter holes in Area 2, TA-49, Los Alamos County, N. Mex. Pocket (138)

17. Maps of walls of selected large-diameter holes in Area 3, TA-49, Los Alamos County, N. Mex. --Pocket (138)

18. Maps of walls of selected large-diameter holes in Area 4, TA-49, Los Alamos County, N. Mex. Pocket (138)

19. Isopach map of unit Qbt_6 of the Tshirege Member of the Bandelier Tuff, TA-49, Los Alamos County, N. Mex. ---------- Pocket ------- (147)

Illustrations--long list - Continued

Reference page

Figure 20. Thickness of soil and location of moisture-measurement test holes in TA-49, Los Alamos County, N. Mex. ---------- Pocket ---------- (152)

21. Graph of moisture content and lithology in test hole 1M-2, TA-49, Los Alamos County, N. Mex. ---- 154 A

22. Graph of moisture content and lithology in test hole 2M-1, TA-49, Los Alamos County, N. Mex. ---- 154 B

23. Graph of moisture content and lithology in test hole 2M-2, TA-49, Los Alamos County, N. Mex. ---- 154 C

24. Graph of moisture content and lithology in test hole 3M-1, TA-49, Los Alamos County, N. Mex. ---- 154 D

25. Graph of moisture content and lithology in test hole 3M-2, TA-49, Los Alamos County, N. Mex. ---- 154 E

26. Graph of moisture content and lithology in test hole 3M-3, TA-49, Los Alamos County, N. Mex. ---- 154 F

27. Graph of moisture content and lithology in test hole 4M-1, TA-49, Los Alamos County, N. Mex. ---- 154 G

28. Graph of moisture content and lithology in test hole 4M-2, TA-49, Los Alamos County, N. Mex. ---- 154 H

29. Graph of moisture content and lithology in test hole 4M-3, TA-49, Los Alamos County, N. Mex. ---- 154 I

30. Graph of moisture content and lithology in test hole 4M-4, TA-49, Los Alamos County, N. Mex. ---- 154 J

Illustrations--long list - Continued

		Reference page	
Figure 31.	Graph of moisture content and lithology in test hole 5M-2, TA-49, Los Alamos County, N. Mex. -----	154	K
32.	Graph of moisture content and lithology in test hole 9M-4, TA-49, Los Alamos County, N. Mex. -----	154	L
33.	Graph of moisture content and lithology in test hole 10M-1, TA-49, Los Alamos County, N. Mex. ----	154	M
34.	Graph of moisture content and lithology in test hole 10M-2, TA-49, Los Alamos County, N. Mex. ----	154	N
35.	Graph of moisture content and lithology in test hole 1M-1, TA-49, Los Alamos County, N. Mex. -----	154	O
36.	Graph of moisture content and lithology in test hole 1M-3, TA-49, Los Alamos County, N. Mex. -----	154	P
37.	Graph of moisture content and lithology in test hole 1M-3A, TA-49, Los Alamos County, N. Mex. ----	154	Q
38.	Graph of moisture content and lithology in test hole 2M-3, TA-49, Los Alamos County, N. Mex. -----	154	R
39.	Graph of moisture content and lithology in test hole 5M-1, TA-49, Los Alamos County, N. Mex. -----	154	S
40.	Graph of moisture content and lithology in test hole 6M-1, TA-49, Los Alamos County, N. Mex. -----	154	T
41.	Graph of moisture content and lithology in test hole 9M-1, TA-49, Los Alamos County, N. Mex. -----	154	U

Illustrations--long list - Continued

		Reference page
Figure 42.	Graph of moisture content and lithology in test hole 9M-2, TA-49, Los Alamos County, N. Mex. -----	154 V
43.	Graph of moisture content and lithology in test hole 9M-3, TA-49, Los Alamos County, N. Mex. -----	154 W
44.	Graph of measurements of flow downstream from well DT-5A as compared to discharge at well during pumping test April 30-May 1, 1960, at TA-49 ----------	161 A
45.	Generalized contours on the piezometric surface of the main aquifer, Los Alamos area, N. Mex. ----	166 A
46.	Hydrograph of water levels measured and from recorder charts at well DT-5A, TA-49, Los Alamos County, N. Mex. ----------	168 A
47.	Hydrograph of water levels measured and from recorder charts at well DT-9, TA-49, Los Alamos County, N. Mex. ----------	168 B
48.	Hydrograph of water levels measured and from recorder charts at well DT-10, TA-49, Los Alamos County, N. Mex. ----------	169 A
49.	Deleted. Workover Rig DT-9	170 A
50.	Deleted. Discharge DT-9 during aquifer test	170 B
51.	Semilogarithmic graph of recovery of water level in well DT-5A May 1 and 2, 1960, after pumping 25 hours at an average rate of 81 gpm ----------	171 A

Illustrations--long list - Continued

		Reference page
Figure 52.	Semilogarithmic graph of recovery of water level in well DT-9 May 7 and 8, 1960, after pumping 24 hours at an average rate of 88 gpm ----------	172 A
53.	Semilogarithmic graph of recovery of water level in well DT-10, September 22 and 23, 1960, after 16 hours of pumping at an average rate of 78 gpm ----	174 A

Appendix

Figure 54A.	Gamma ray-neutron logs of well DT-5, TA-49, Los Alamos County, N. Mex. ----------	Pocket (2)
54B.	Induction log of well DT-5, TA-49, Los Alamos County, N. Mex. ----------	Pocket (3)
54C.	Temperature log of well DT-5, TA-49, Los Alamos County, N. Mex. ----------	Pocket (4)
55A.	Gamma ray-neutron logs of well DT-5A, TA-49, Los Alamos County, N. Mex. ----------	Pocket (5)
55B.	Induction-electrical and spontaneous-potential logs of well DT-5A, TA-49, Los Alamos County, N. Mex. -	Pocket (6)
55C.	Microlog and microcaliper logs of well DT-5A, TA-49, Los Alamos County, N. Mex. ----------	Pocket (7)
55D.	Laterolog of well DT-5A, TA-49, Los Alamos County, N. Mex. ----------	Pocket (8)
55E.	Temperature log of well DT-5A, TA-49, Los Alamos County, N. Mex. ----------	Pocket (9)
55F.	Sonic log of well DT-5A, TA-49, Los Alamos County, N. Mex. ----------	Pocket (10)

Illustrations--long list - Continued

Page

Figure 56A. Gamma ray-neutron logs of the upper 1,301 feet of well DT-9, TA-49, Los Alamos County, N. Mex. -- Pocket (11)

56B. Gamma-ray log from depth of 1,094 to 1,501 feet of well DT-9, TA-49, Los Alamos County, N. Mex. ---------- Pocket (12)

56C. Induction-electrical and spontaneous-potential logs of well DT-9, TA-49, Los Alamos County, N. Mex. ---------- Pocket (13)

56D. Lateralog of well DT-9, TA-49, Los Alamos County, N. Mex. ---------- Pocket (14)

56E. Temperature log of well DT-9, TA-49, Los Alamos County, N. Mex. ---------- Pocket (15)

56F. Sonic log of well DT-9, TA-49, Los Alamos County, N. Mex. ---------- Pocket (16)

57A. Gamma ray-neutron log of well DT-10, TA-49, Los Alamos County, N. Mex. ---------- Pocket (17)

57B. Induction-electrical and spontaneous-potential logs of well DT-10, TA-49, Los Alamos County, N. Mex. ---------- Pocket (18)

57C. Temperature log of well DT-10, TA-49, Los Alamos County, N. Mex. ---------- Pocket (19)

57D. Sonic log of well DT-10, TA-49, Los Alamos County, N. Mex. ---------- Pocket 20

Illustrations--long list - Continued

		Page
Figure 58.	Gamma-ray log of core hole 1 in Area 1, TA-49, Los Alamos County, N. Mex.	Pocket (21)
59A.	Gamma-ray log of core hole 2 in Area 2, TA-49, Los Alamos County, N. Mex.	Pocket (22)
59B.	Gamma ray-neutron log of upper 201 feet of core hole 2 in Area 2, TA-49, Los Alamos County, N. Mex.	Pocket (23)
59C.	Electrical log of the upper 368 feet of core hole 2 in Area 2, TA-49, Los Alamos County, N. Mex.	Pocket (24)
59D.	Temperature log of the upper 200 feet of core hole 2 in Area 2, TA-49, Los Alamos County, N. Mex.	Pocket (25)
60.	Gamma-ray log of core hole 3 in Area 3, TA-49, Los Alamos County, N. Mex.	Pocket (26)
61.	Gamma-ray log of core hole 4 in Area 4, TA-49, Los Alamos County, N. Mex.	Pocket (27)
62A.	Gamma ray-neutron logs of Alpha hole, TA-49, Los Alamos County, N. Mex.	Pocket (28)
62B.	Induction log of Alpha hole, TA-49, Los Alamos County, N. Mex.	Pocket (29)

Geology and hydrology of Technical Area 49

Frijoles Mesa, Los Alamos County, New Mexico

By

James E. Weir, Jr. and William D. Purtymun

Abstract

Frijoles Mesa is a part of the Pajarito Plateau, a dissected ash-flow field that laps onto the Sierra de los Valles to the west and terminates in cliffs along White Rock Canyon to the east. Technical Area 49 (TA-49) occupies about 2 square miles on the northern segment of Frijoles Mesa near the center of the plateau, about 5 miles south of Los Alamos.

The rocks exposed at the surface at TA-49 are of the Bandelier Tuff of Pleistocene age. Subsurface rocks of the Santa Fe Group of Middle(?) Miocene to Pleistocene(?) age and the Tschicoma Formation of Pliocene and Pleistocene(?) age were penetrated by three deep test holes. The rocks of the Santa Fe Group, in ascending order, are: the undifferentiated unit, the Puye Conglomerate, and the basaltic rocks of Chino Mesa. Interbedded with the rocks of the Santa Fe Group are rocks of the Tschicoma Formation.

The undifferentiated unit consists of sediments laid down as alluvial-fan and flood-plain deposits. Above the undifferentiated unit is the Puye Conglomerate, which consists of two members. The lower member is a poorly consolidated channel-fill deposit called the Totavi Lentil. Overlying the Totavi Lentil is the fanglomerate member that is made up of volcanic debris. Interbedded with the fanglomerate member are the basaltic rocks of Chino Mesa and latite and quartz-latite ~~flow rocks~~ tuff of the Tschicoma Formation.

The Bandelier Tuff overlies the fanglomerate member. It consists of ash-fall and ash-flow rocks that are draped over the older rocks, filling the lows and smoothing out the topography of the older rocks. The Bandelier Tuff consists of three members. In ascending order they are: the Guaje Member, an ash-fall pumice and water-laid pumiceous tuff; the Otowi Member, a friable ash-flow tuff; and the uppermost Tshirege Member, a series of ash-flow tuffs with one thin water-laid bed near the top.

The Tshirege Member forms the finger-like mesa at TA-49. It is the most important geologic unit because test operations will place contaminants in these rocks ABOUT ~~within~~ 100 feet BELOW ~~of~~ the mesa surface. There these contaminants could be removed by water and carried into the zone of saturation.

The X-ray and chemical analyses of the tuff from the Tshirege Member indicate that they are rhyolitic in composition. Hydrologic analysis of the tuff indicated the following ranges: porosity, 19.3 to 54.7 percent; specific retention, 11.3 to 27.3 percent; specific yield, 0.6 to 42.6; permeability, 0.04 to 22 gpd (gallons per day) per square foot for consolidated samples, and 34 to 59 gpd per square foot for unconsolidated samples. Moisture content ranged from 0.2 to 8.7 percent by volume beneath the mesa, but moisture contents of tuff from a test hole in Water Canyon north of the mesa ranged from 13.3 to 36.3 percent by volume, which indicates some infiltration of water.

The soil cover on the mesa surface is characterized by a weathered zone, a water-laid pumice zone, and a soil zone. The top few feet of the Tshirege Member is composed of partly weathered tuff fragments in a matrix of clay. The weathered zone grades up into a brown clayey soil except along the northern edge of the mesa, where a layer of water-laid pumice occurs between the weathered zone and the soil zone.

Periodic moisture readings of the soil and underlying tuff, made by a neutron-scattering moisture probe, indicate little or no infiltration of water from precipitation through the soil zone. Other data collected during drilling, mapping, and hydrologic analysis of rocks of the Guaje, Otowi, and Tshirege Members of the Bandelier Tuff indicate that the soil forms a nearly perfect seal on the mesa surface and that the Bandelier Tuff has a large bulk permeability. Where the soil cover has been removed or disturbed, water in sufficient quantities would move almost vertically through the Bandelier Tuff into the Puye Conglomerate and eventually into the zone of saturation.

Stream flow in A NATURAL STREAM CHANNEL ON ~~an arroyo on~~ the surface of the mesa was measured at two moisture test holes about 700 feet apart. There was very little loss of flow between the two test holes after the channel and bank material had become saturated. No change in moisture content in the channel material or underlying tuff was detected below a depth of 3.5 feet in either of the test holes. The moisture content increased 16 percent by volume in the upper 3.5 feet while the stream was flowing. Six days after the flow ended, capillary return to the surface and evaporation had decreased this moisture content by as much as 13 percent.

The zone of saturation, or main aquifer, lies 1,000 to 1,200 feet below the mesa surface at TA-49 in rocks of the Santa Fe Group and Tschicoma Formation. No perched water was found above the zone of saturation. The gradient on the piezometric surface of the main aquifer is east-southeastward toward the Rio Grande about ~~60~~ 50 feet per mile. Data indicated that the recharge area to the main aquifer is west of TA-49 on the slopes of the Sierra de los Valles and the western part of the Pajarito Plateau. The specific capacity of three wells finished in the main aquifer range from 5.7 to 22 gpm (gallons per minute) per foot of drawdown. Pumping tests indicate an average coefficient of permeability of 180 gpd per foot per foot. The velocity of water in the main aquifer is approximately 400 feet per year. The quantity of water passing through the upper 650 feet of the aquifer beneath the test areas at TA-49 is approximately 370 acre-feet per year.

Tritium analyses indicate that the water in the main aquifer ranges in age from 13 to 20 years. The cause of differences in age could be that the water deeper in the aquifer moves more slowly and is actually older, or that some young water is being added to the aquifer by local recharge from canyon sources such as Water Canyon to the north or Frijoles Canyon to the south.

Introduction

The Los Alamos Area Office, U.S. Atomic Energy Commission, requested support from the Geological Survey for a project at Technical Area 49 (TA-49) informally in conference September 29, 1959. The request was confirmed by a copy of a letter (JO-462) from Mr. William Ogle of the Los Alamos Scientific Laboratory to Mr. Paul Wilson, Manager of the Los Alamos Area Office.

The work of the Geological Survey was aimed at 1) providing geological information to the AEC about the rocks that underlie the area, and 2) defining the direction and rate of movement of water in the zone of aeration and the movement of ground water in the zone of saturation beneath the project area eastward to the Rio Grande.

Fieldwork began in late October 1959 and was completed in September 1960, although the most intensive part of the fieldwork was finished by May 10, 1960.

Location and setting

Much of Los Alamos County south of the city of Los Alamos is used for test operations by the Los Alamos Scientific Laboratory. Various installations and areas in the upland surface and the canyon bottoms are designated "technical areas."

Technical Area 49 occupies about 2 square miles on the northern segment of Frijoles Mesa, 5 miles (about 10 road miles) south of Los Alamos (fig. 1). Frijoles Mesa is a part of the Pajarito

Figure 1.--Index map of part of Los Alamos and adjacent counties, New Mexico, showing the location of Technical Area 49 (TA-49).

Plateau, which is a dissected ash-flow field that laps onto the Sierra de los Valles (fig. 4) to the west and terminates in cliffs along White Rock Canyon to the east. The area is in the former Roman Vigil Grant, which is not sectionized, but projections of land divisions into the Grant area indicate that TA-49 is mainly in secs. 3 and 4, T. 18 N., R. 6 E., with minor parts of the area in secs. 33 and 34, T. 19 N., R. 6 E. and sec. 2, T. 18 N., R. 6 E.

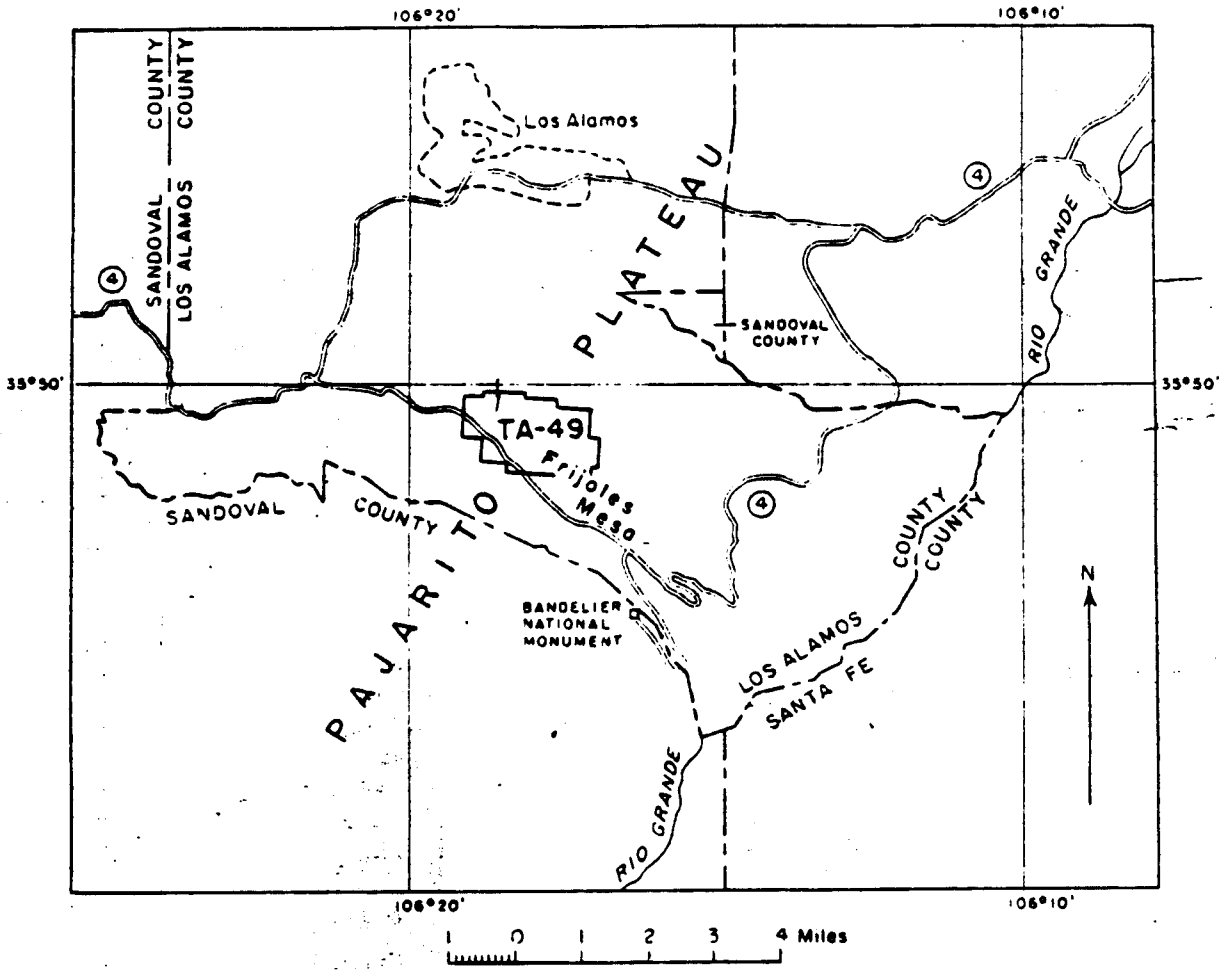

Figure 1.--Index map of part of Los Alamos and adjacent counties, New Mexico, showing the location of Technical Area 49 (TA-49).

LASL AEC OFFICIAL

The northern segment of Frijoles Mesa slopes gently eastward from an altitude of about 7,200 feet near the western edge of TA-49 to an altitude of about 7,000 feet at its dissected eastern end. It is bounded on the north by Water Canyon, which has been cut 300 to 400 feet below the plateau surface, and on the south by Ancho Canyon, whose floor is 100 to 200 feet below the relatively flat upland.

Frijoles Mesa and the adjacent canyons support moderate to dense vegetative growth. Pinon pine and juniper are the predominant trees, and there is a sparse growth of ponderosa pine, mainly in the canyons. Grama grass predominates as surface cover, and a few scrub oak, mostly shinnery oak, grow in isolated patches.

Water and Ancho Canyons drain eastward and are almost parallel. They empty into the Rio Grande in White Rock Canyon. Water Canyon heads on the slopes of the Sierra de los Valles. In the reach of Water Canyon, north of TA-49, a small intermittent flow of unknown origin occurs. Ancho Canyon heads near the entrance to TA-49 (fig. 6) and does not contain a perennial stream in its upper reach.

Drainage channels on the mesa trend generally east-southeastward with the gradient of the mesa surface, and many minor channels braid out on top of the mesa in flatter areas. Short tributary canyons drain into the two major canyons north and south of TA-49. The eastern part of TA-49 is drained by a rather well-developed dendritic system of channels and canyons. Most minor drainageways empty runoff into Ancho Canyon to the south.

Previous work

Geology and ground-water conditions in the Los Alamos area have been studied by the Geological Survey and the Atomic Energy Commission under a cooperative program since 1949. An administrative report to the AEC by Griggs (1955) describes the general aspects of the geology of Los Alamos County. Surface geology on figure 4 is taken mainly from Griggs' geologic map, and stratigraphic nomenclature proposed by Griggs is used in this report.

The geology and ground-water conditions in Los Alamos County are described in a classified report by Baltz and others (1959), which appraised several areas as to the feasibility of the experimental work. The investigations in TA-49 are a result of this report.

Personnel and acknowledgements

Work was done under the supervision of W. E. Hale, District Engineer, Ground Water Branch, U.S. Geological Survey, in Albuquerque.

The writers extend thanks to the personnel of the Los Alamos Scientific Laboratory, especially Mr. Robert W. Newman, Group Leader, J-6 Group, for close cooperation in facilitating the fieldwork. Appreciation also is expressed to the Zia Company, especially Messrs. W. C. Francis and W. P. Junge, for direct operational aid in almost all phases of the fieldwork. ~~Three to four~~ employees of the Zia Company were made available to collect cutting samples and to log drilling time. The cooperation of Buchanan and Associates in the core-drilling phase of operations is acknowledged. Support and cooperation of all people associated with work at TA-49 was in every way complete and gratifying.

Purpose and scope of report

The study at TA-49 was made to determine whether ground water, either perched or in the zone of saturation, might be contaminated by radioactive materials that would be buried 30 to 120 feet below the surface of the mesa. This report describes the geology and hydrology ~~of the mesa~~ at TA-49, with emphasis on the rocks within about 100 feet of the surface, particularly their hydrologic properties.

The investigations having to do with the possibility that contaminants might be leached from the rock in which they were emplaced consisted of geologic mapping, subsurface geologic studies, observing and advising on drilling operations, interpreting geophysical logs of holes, conducting pumping tests, and making water-level measurements in wells. Rock samples were collected and sent to Geological Survey laboratories for petrographic description, chemical and X-ray analysis, and measurement of physical properties. Rock sampling was very intensive as an insurance against the possibility of missing information that could not be obtained later. The samples have been catalogued and are stored in the Geological Survey office at Los Alamos and are available to interested parties for future study.

The tuff exposed in TA-49 had previously been mapped as a single unit; however, it was necessary, for the purpose of this study, to subdivide the rock into seven informal stratigraphic units. Six of these units are exposed in Water Canyon and are recognizable in the subsurface beneath Frijoles Mesa on the basis of cores, drill cuttings, or geophysical logs. The seventh unit is known only in the subsurface.

Information on the main aquifer of the Los Alamos area, which is 1,000 to 1,200 feet below the mesa surface, was obtained from three deep test wells. (The main aquifer in the Los Alamos area is the zone of saturation in the undifferentiated unit of the Santa Fe Group. The top of the zone of saturation in the main aquifer seems to rise westward into the upper units of the Santa Fe Group and the Tschicoma Formation. However, the water in the upper part of the Santa Fe Group and the Tschicoma Formation may be perched. The water in the main aquifer is under artesian pressure.) Hydrologic characteristics of the aquifer were estimated from drill cuttings, geophysical logs, and a pumping test on each of the three deep wells. The data obtained from these deep wells provide the basis for estimates of the average rate and direction of ground-water movement in the principal aquifer.

The results of laboratory investigations of physical and chemical characteristics of the rocks and chemical analyses of ground-water samples are tabulated in order to make them readily available for future study, but a detailed interpretation of these data is beyond the scope of this report.

Techniques used and data collected

Most phases of the project were carried on simultaneously. Cores were described at the drilling sites. Drill cuttings were examined with a binocular microscope during periods when other operations were not pressing. Pumping tests were run on wells DT-5A, DT-9, and DT-10 to determine well performance and aquifer characteristics.

The locations of wells, large-diameter holes, and test holes used in this report are listed in the following table.

TA-49 Area. Los Alamos grid locations, of test holes.

(See figs. 6 and 20.)

Deep wells		
DT-5P	111 + 32 south	94 + 36 east
DT-5	110 + 99	93 + 03
DT-5A	111 + 47	93 + 03
DT-9	142 + 81	131 + 27
DT-10	113 + 27	129 + 94
Exploratory large-diameter holes		
Alpha	111 + 16 south	97 + 54 east
Beta	83 + 63	91 + 89
Gamma and Gamma "A"	133 + 20	104 + 00
Core holes		
CH-1	104 + 98 south	84 + 37 east
CH-2	105 + 70	97 + 85
CH-3	114 + 94	82 + 06
CH-4	120 + 33	95 + 68
Shallow holes for moisture measurements		
1M-1, 2, 3, and 3A	105 + 00 south	84 + 00 east
2M-1, 2, and 3	106 + 00	98 + 00
3M-1, 2, and 3	115 + 00	82 + 00
4M-1, 2, 3, and 4	120 + 00	96 + 00
5M-1	111 + 32	94 + 36
5M-2	111 + 05	92 + 38
6M-1	102 + 15	68 + 83
9M-1	116 + 67	88 + 44

Los Alamos grid locations - Continued

Shallow holes for moisture measurements - Continued

9M-2	113 + 40	98 + 15
9M-3	117 + 02	104 + 57
9M-4	113 + 93	100 + 40
10M-1	104 + 96	110 + 31
10M-2	104 + 54	108 + 69

Large-diameter holes used for experimental purposes by the Los Alamos Scientific Laboratory. Layout of holes in areas shown on figure 2.

Area 1	105 + 00 south	84 + 00 east
Area 2	106 + 00	98 + 00
Area 3	115 + 00	82 + 00
Area 4	120 + 00	96 + 00
Area 10	105 + 00	109 + 00
WCM-1	111 + 20	92 + 20
WCM-2	145 + 00	102 + 20

Location of well in
The Los Alamos area, by section, township, range

(See fig. 4.)

T-1, 1A	sec. 20, T. 19 N., R. 7 E.
T-2, 2A	sec. 14, T. 19 N., R. 6 E.
T-3	sec. 13, T. 19 N., R. 6 E.
T-4	sec. 16, T. 19 N., R. 6 E.
H-19	sec. 17, T. 19 N., R. 6 E.
L-3	sec. 14, T. 19 N., R. 7 E.

Surface mapping

Geologic mapping on aerial photographs was begun early in December 1959. Stratigraphic relations were established in the area of maximum exposures on the south wall of Water Canyon.

The exposures were examined about every 400 to 500 yards to make certain of adequate control. Contacts were referred to the many vertical control points established in the field by Laboratory personnel engaged in mapping TA-49 topographically. Control points were located on the aerial photographs,and geologic contacts were drawn on the photographs (scale 1:7,000) in the field by stereoscopic methods.

The unit contacts on the photographs did not completely agree with the topographic contours. Therefore, the geologic contacts were adjusted to agree with the topographic base map. The geologic map is sufficiently accurate for all purposes anticipated. Segments of many contacts were drawn through areas where rock exposures are poor, and in these areas the contact alinement may not be exact. The areas of best exposure are along the road leading from the mesa just east of Area 10 into Water Canyon, the northern walls of canyons, and a few places in the bottoms of arroyo channels.

Test drilling

Thirty-seven exploratory holes were drilled ranging in depth from 7 to 1,821 feet and in diameter from 2 inches to 2 feet. The five deep test wells are designated by "DT" and the number of a nearby area. These test wells include the pilot hole, DT-5P, and the wells DT-5, DT-5A, DT-9, and DT-10. Three holes, arbitrarily called Alpha, Beta, and Gamma, were drilled with a bucket auger on top of the mesa, in Water Canyon and in Ancho Canyon. A core hole was drilled in Areas 1 through 4 (fig. 2). These holes are designated by "CH" and an area number. Twenty-five shallow test holes were drilled with a wagon drill. These are designated by the number of the nearby area, a "M" for "moisture" to indicate the purpose of the holes, and the number of the hole in the area.

Deep wells

Five wells were drilled to obtain hydrologic and geologic information about the main aquifer. The wells were located to give the widest distribution of subsurface geologic control and the best hydrologic control (fig. 6). Consideration was given to choosing the best sites for monitoring ground water for possible contamination.

Well DT-5P, just east of Area 5, was an air rotary hole drilled to determine the presence or absence of perched water (saturated zones above and separated from the main aquifer). It was completed at a depth of 692 feet as a dry hole.

Well DT-5, about 50 feet west of DT-5P, was unsuccessful. It was drilled with air rotary equipment. The air return was mostly lost into cracks and crevices in the tuff, and the hole was abandoned at a depth of 927 feet. Few samples of drill cuttings were obtained, and these were not described because samples from nearby well DT-5P had already been described. Three side-wall samples were taken from depths of 390, 490, and 500 feet to obtain undisturbed samples from that interval to supplement unsuccessful vertical coring in Areas 1 and 2.

Well DT-5A, 50 feet south of well DT-5, was drilled with rotary equipment, using mud as a drilling fluid. Circulation was very poor in the upper 520 feet of the hole. Twelve-inch casing was installed and cemented at this depth (TABLE 1). Below 520 feet, circulation was maintained and cuttings samples were obtained to the total depth of 1,821 feet.

Well DT-9 (fig. 6) was begun as a 20-inch hole using cable-tool equipment. The hole was reduced to 16 inches at a depth of 395 feet, and drilled at that diameter to a depth of 1,300 feet, at which point it was logged geophysically and then cased with 12-inch pipe. An 11-inch hole was drilled from 1,300 to 1,501 feet and an 8-inch liner was installed (table 2).

Well DT-10 (fig. 6) was drilled with cable-tool equipment 16 inches in diameter to a depth of 1,125 feet below the land surface, at which point 12-inch casing was installed. An 11-inch hole was drilled from 1,125 feet to 1,408 feet, and an 8-inch liner was installed (table 3).

Table 1.--Casing schedule for well DT-5A

Altitude of land surface 7,143.32 feet

Description	Depth below land surface (feet)		Length (feet)		Altitude of top of section (feet)
	Top	Bottom	Slotted	Blank	
		12-inch I. C. casing			
Blank	+0.3	519.7		520	7,143.62
		8-inch I. D. casing			
Blank	+.5	1,171.5		1,172	7,143.82
Slotted	1,171.5	1,191.5	20		5,971.82
Blank	1,191.5	1,279.5		88	5,951.82
Slotted	1,279.5	1,289.5	10		5,863.82
Blank	1,289.5	1,335.5		46	5,853.82
Slotted	1,335.5	1,381.5	46		5,807.82
Blank	1,381.5	1,415.5		34	5,761.82
Slotted	1,415.5	1,445.5	30		5,727.82
Blank	1,445.5	1,535.5		90	5,697.82
Slotted	1,535.5	1,555.5	20		5,607.82
Blank	1,555.5	1,591.5		36	5,587.82
Slotted	1,591.5	1,615.5	24		5,551.82
Blank	1,615.5	1,635.5		20	5,527.82
Slotted	1,635.5	1,655.5	20		5,507.82
Blank	1,655.5	1,708.5		53	5,487.82
Slotted	1,708.5	1,728.5	20		5,434.82

See footnote at end of table

Table I.—Casing schedule for well DT-5A - Continued

Description	Depth below land surface (feet)		Length (feet)		Altitude of top of section (feet)
	Top	Bottom	Slotted	Blank	
		8-inch I. D. casing - Continued			
Blank	1,728.5	1,740.5		12	5,414.82
Slotted	1,740.5	1,750.5	10		5,402.82
Blank	1,750.5	1,768.5		18	5,392.82
Slotted	1,768.5	1,788.5	20		5,374.82
Blank	1,788.5	1,819.5		31	5,354.82
Bottom of hole					5,323.82
Total 8-inch I. D. casing			220	1,600	

1/ Extension of casing above land surface.

Table 2.--Casing schedule for well DT-9

Altitude of land surface 6,937.32

Description	Depth below land surface (feet) Top	Bottom	Length (feet) Slotted	Blank	Altitude of top of section (feet)
		12-inch I. D. casing			
Blank	+2.0 1/	819.0		821.0	6,939.32
Slotted	819.0	878.8	59.8		6,118.32
Blank	878.9	903.2		24.4	6,058.52
Slotted	903.2	934.5	31.3		6,034.12
Blank	934.5	958.5		24.0	6,002.82
Slotted	958.5	982.6	24.1		5,978.82
Blank	982.6	1,002.4		19.8	5,954.72
Slotted	1,002.4	1,036.4	34.0		5,934.92
Blank	1,036.4	1,057.4		21.0	5,900.92
Slotted	1,057.4	1,093.4	36.0		5,879.92
Blank	1,093.4	1,142.0		48.6	5,843.92
Slotted	1,142.0	1,208.4	66.4		5,795.32
Blank	1,208.4	1,266.2		57.8	5,728.92
Slotted	1,266.2	1,310.5	44.3		5,671.12
Blank	1,310.5	1,333.0		22.5	5,626.82
Bottom of 12-inch I. D. casing					5,604.32
Total 12-inch I. D. casing			295.9	1,039.1	

1/ See footnote at end of table

Table 2.--Casing schedule for well DT-9 - Continued

Description	Depth below land surface (feet)		Length (feet)		Altitude of top of section (feet)
	Top	Bottom	Slotted	Blank	
		8-inch I. D. casing			
Swage	1,313.1	1,317.2		4.1	5,624.22
Slotted	1,317.2	1,500.0	182.8		5,620.12
Bottom of 8-inch I. D. casing					5,437.32
Total 8-inch I. D. casing			182.8	4.1	

Top of 8-inch casing swage to 11 inches O. D. and run as liner to total depth of 1,500 feet, which telescopes 19.9 feet into the 12-inch casing.

1/ Extension of casing above land surface.

Table 3.--Casing schedule for well DT-10

Altitude of land surface 7,019.41

Description	Depth below land surface (feet) Top	Bottom	Length (feet) Slotted	Blank	Altitude of top of section (feet)
		12-inch I. D. casing			
Blank	+1.9 1/	1,078.4		1,080.3	7,021.31
Slotted	1,078.4	1,128.0	49.6		5,941.01
Bottom of 12-inch I. D. casing					5,891.41
Total 12-inch I. D. casing			49.6	1,080.3	
		8-inch I. D. casing			
Swage	1,096	1,097		1	5,923.41
Slotted	1,097	1,118	21		5,922.41
Blank	1,118	1,196		78	5,901.41
Slotted	1,196	1,206	10		5,823.41
Blank	1,206	1,228		22	5,813.41
Slotted	1,228	1,258	30		5,791.41
Blank	1,258	1,268		10	5,761.41
Slotted	1,268	1,278	10		5,751.41
Blank	1,278	1,302		24	5,741.41
Slotted	1,302	1,322	20		5,717.41
Blank	1,322	1,332		10	5,697.41
Slotted	1,332	1,342	10		5,687.41
Blank	1,342	1,368		26	5,677.41
Slotted	1,368	1,408	40		5,671.41
Bottom of hole					5,631.41
Total 8-inch I. D. casing			141	171	

1/ See footnote at end of table

Table 3.--Casing schedule for DT-10 - Continued

Top of 8-inch casing swaged out to 11 inches O. D. and run as liner to a total depth of 1,408 feet, which extends the 8-inch casing 32 feet into the 12-inch casing.

1/ Projecting above land surface.

Exploratory large-diameter auger holes

The large-diameter holes Beta, in Water Canyon, and Gamma, in Ancho Canyon (fig. 6), were drilled with a bucket auger, mainly to determine whether perched water was present beneath the canyon bottoms. The large-diameter hole Alpha was drilled on the mesa surface primarily for geologic information.

Beta hole was drilled 2 feet in diameter to a depth of 180 feet. The hole was dry. Gamma hole was drilled 2 feet in diameter but was abandoned at a depth of 7 feet because of the hardness of the tuff, and a nearby 4-inch hole called Gamma A was drilled to a depth of 54 feet with the wagon drill. The hole was dry. Alpha hole was drilled 2 feet in diameter to a depth of 189 feet to obtain geologic information. The hole was dry.

Core holes

Four core holes were drilled, one in each of Areas 1 through 4 in TA-49, mainly to obtain 2-inch diameter core samples for geologic study. Air was used as a cuttings carrier in order to obtain cores free of drilling mud and to detect zones of perched water.

The parts of the cores not used in the tests are stored in the Geological Survey office at Los Alamos. The core holes were cased with 2-inch pipe slotted in the lower 20 feet. Logs of the cores are in tables 10 through 13.

Shallow holes for moisture measurements

Twenty-three holes were drilled on the mesa surface in TA-49 (fig. 20) and two in Water Canyon (fig. 6) for the purpose of measuring moisture content and the changes in moisture content with time and depth. Areas 1 through 4 and Area 10 were of special interest because potential ground-water contaminants would be left in the ground as a result of the experimental work in these areas. These holes were drilled with a wagon drill and are 2.5 inches in diameter. They were cased with 2-inch plastic pipe.

A rough visual log was made at the time the holes were drilled by observing color changes of the air-returned cuttings and the general drilling conditions. These logs are plotted beside the graphs of moisture content. (See figs. 21-43.)

Holes WCM-1 and WCM-2, in Water Canyon, were drilled with a wagon drill using air as a cuttings carrier. These borings penetrated water in the thin alluvium at the level of water in the nearby stream, and air drilling could not be continued. The holes were drilled about 2.5 inches in diameter and cased with 2-inch plastic pipe; WCM-1 was cased to a depth of 9.9 feet with perforations the entire length; WCM-2 was cased to 9.4 feet with perforations in its lower 6 feet.

Geophysical logs

Electrical, radioactivity, temperature, and sonic logs were run in wells DT-5, DT-5A, DT-9, DT-10, Alpha hole, and in core holes in Areas 1 through 4. (See figs. 54A-62B.)

Most of the logs were run by Schlumberger Well Surveying Corporation. Gamma-ray logs in the completed core holes were run with equipment of the Geological Survey because of the small hole diameter. The Survey also gamma-ray logged the lower 307 feet of well DT-9.

The electrical logs were used primarily to select principal water-bearing zones ~~of greatest permeability~~ for setting perforated casing. To a lesser extent these logs were used to select stratigraphic contacts.

Induction logs and laterologs were run on wells DT-5A and DT-9. Induction logs were run on well DT-10 and Alpha hole. The induction logs were not useable because of the very high resistivity of the rocks penetrated and the large diameter of the bore holes (especially Alpha hole).

Laterologs were run in wells DT-5A and DT-9 because of their better definition of units in rocks of high resistivity. The laterolog strikingly indicated the position of volcanic flows interbedded in the Santa Fe Group (figs. 55D and 56D); however, in the Bandelier Tuff at well DT-5A, the laterolog apparently did not define lithologic boundaries that were indicated on the other geophysical logs. A microlog and caliper log were run on well DT-5A.

The radioactivity logs, mainly gamma-ray, were the most useful of the logs for picking geologic contacts. The gamma-ray log yielded useable results in holes that contained no liquid or were only partly filled and holes with casing installed. The only geophysical log of the lower 307 feet of DT-9 was the gamma-ray log run with Geological Survey equipment. A study of this log showed changes in gamma radiation sufficiently well to aid in accurately choosing contacts between stratigraphic units penetrated by the well.

Temperature logs were run on wells DT-5A, DT-9, and DT-10 to obtain the general geothermal gradient and temperature of water.

Sonic logs were run only in holes or parts of holes containing liquid; consequently, these logs were run in only DT-5A, DT-9, and DT-10. The sonic logs were used to a limited extent in corroborating the upper and lower boundaries of hard layers of volcanic rocks in the aquifer. The sonic log for DT-5A also was used to estimate values of porosity.

Data on the interval between 300 and 500 feet below the mesa surface was almost entirely determined from the geophysical logs. The logs were also used to make more precise determinations of stratigraphic contacts.

Down-hole mapping

A large number of holes in Areas 1 through 4 and in Area 10 were dug with a bucket auger as part of the experiments conducted by the Los Alamos Scientific Laboratory at TA-49. These holes were 3 to 6 feet in diameter and 49 to 108 feet in depth. Thirty-nine of the holes were inspected in the course of this investigation and detailed geologic maps were made in 19 of the 39. This provided an opportunity to examine the structure and lithology of freshly exposed tuff and provided information on the post-depositional history of the tuff as well as a basis for interpretations of water movement.

Figures 15-18 contain the geologic maps of the holes, and table 26 includes reconnaissance notes on the holes that were inspected but not mapped. The system of designating the holes and the location of the ones that were inspected are shown on figure 2. These holes are numbered according to area and are

Figure 2.--Layout of large-diameter holes in Areas 1, 2, 3, 4, and 10 showing holes mapped and described. (Areas are shown on figure 6.)

alphabetized within each area (except Area 10). Hole 1-A was mapped early in the study as a 3-foot diameter hole and later was examined in reconnaissance as a 6-foot diameter hole.

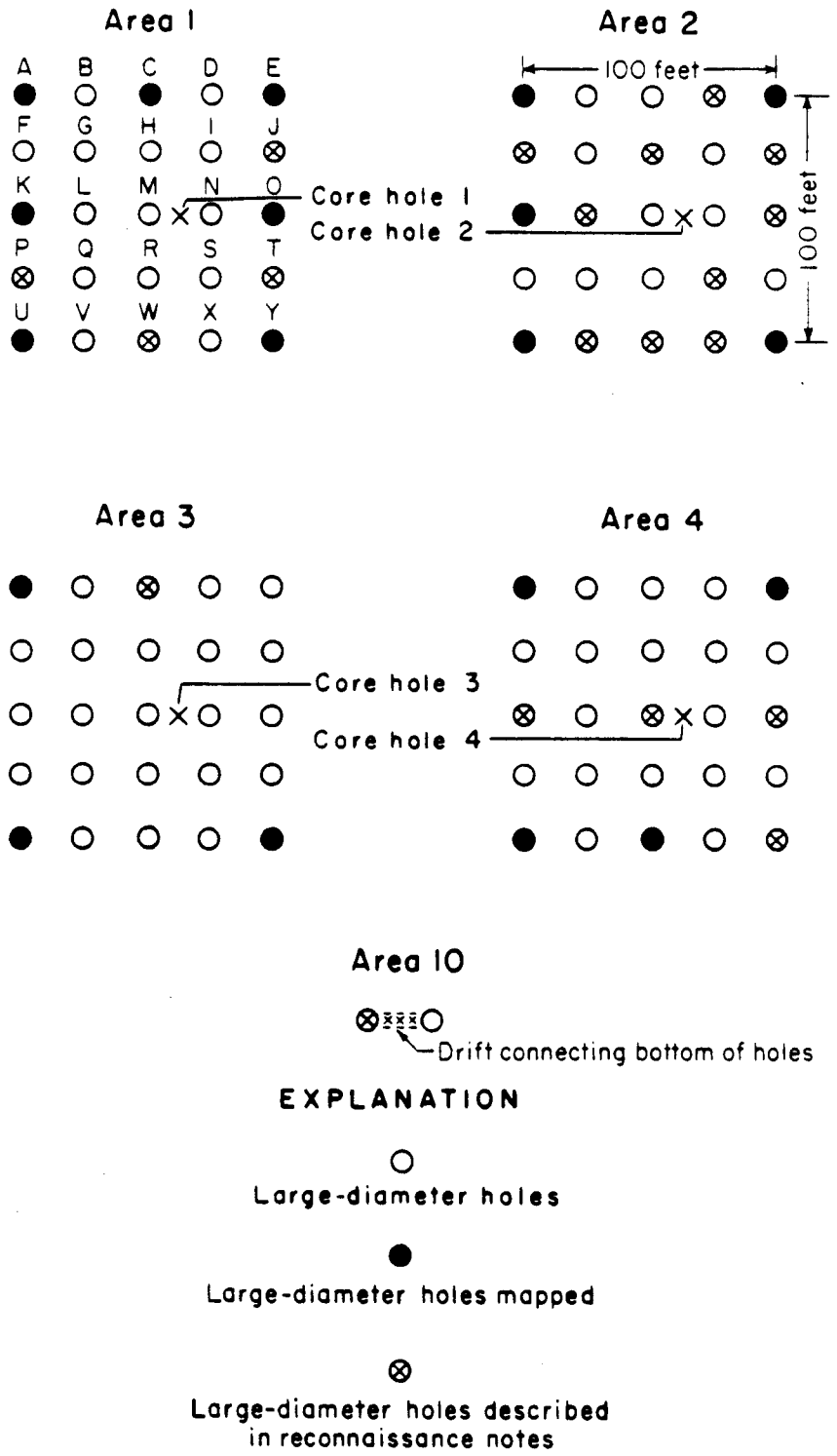

Figure 2.--Layout of large-diameter holes in Areas 1, 2, 3, 4, and 10 showing holes mapped and described. (Areas shown on figure 6.)

The down-hole maps were plotted in the field on tubes covered with ruled cross-section paper at a scale of 1 inch equals 2 feet. The maps were reduced to 1 inch equals 6 feet for inclusion in this report.

Samples were collected at 5-foot intervals in the holes that were mapped for possible future study. The samples were hand-specimen size and were collected at random from the hole walls. Cuttings samples of each 5-foot interval also were obtained from these holes.

Laboratory investigations

Numerous analyses were run on the samples that were collected at TA-49 to obtain data on the physical characteristics of the tuff and soil. Sampling was most intensive in the interval between 30 and 120 feet beneath the surface of the mesa. Physical-properties tests and mineralogic and chemical analyses of rocks were made by Buchanan and Associates laboratories. Samples of rock were analyzed mineralogically and chemically by laboratories of the Geological Survey (tables 14, 15, and 16).

Hydrologic analyses were run by the Geological Survey on 36 rock samples to aid in evaluating water movement in the zone of aeration (table 17).

Tests and analyses of rock samples

Spencer J. Buchanan and Associates

About 150 samples of rock from TA-49 were tested under the direction of Buchanan and Associates, consulting engineers, Bryan, Tex. Tests performed included strength tests, thermal conductivity, specific heat, particle-size distribution, density, specific gravity, moisture content, porosity, and permeability. Moisture content was determined for about 70 samples and porosity for about 30 samples, mostly 5-inch cores from the walls of the large-diameter holes. Permeability to air was determined for 10 samples of core from the 4 core holes, and particle-size distribution was determined on 9 crushed specimens of the 10 samples analyzed for permeability.

Chemical (spectrographic) and mineralogical analyses were run on 9 of the core samples for which permeability was determined. Also, maximum stress, moisture content, density, and specific gravity determinations were made on these samples. The results of the tests and analyses were transmitted to the University of California Laboratory at Los Alamos.

Health Division - Group H-7

About 12 samples, including cores from the core holes, 5-inch diameter side-wall cores and unconsolidated samples from the large-diameter holes, and air cuttings from the core holes were analyzed by Group H-7 for ion-exchange capacity.

Geological Survey

~~Suites of~~ drill-cuttings samples from hole DT-5P, wells DT-5A, DT-9, and DT-10 were studied with a binocular microscope and described. The air cuttings from hole DT-5P were washed and described wet. Rotary mud-returned cuttings from well DT-5A and cable-tool cuttings from wells DT-9 and -10 had been washed when they were collected, and descriptions were made of the damp samples without further processing.

Bucket-auger samples from Alpha and Beta holes were examined with the binocular microscope and described. The bit-ground cuttings and chunk samples, if available, were examined. Some friable intervals in these holes did not yield chunk samples.

Mineralogic and chemical analyses were run on 16 samples by the Geochemistry and Petrology Branch. Two of the 16 samples analyzed chemically by the rapid-rock method (Shapiro and Brannock, 1956) also were analyzed by the classical method (Hillebrand, 1900) as a check on the relative accuracy of the rapid-rock analyses. Table 4 lists the samples and types of analyses made of each.

Table 4.--Rock samples for petrographic, chemical, spectographic, and x-ray analysis by the Geological Survey.

Laboratory Serial No.	Hole No.	Depth	Washington, D.C. Mineralogic	Washington, D.C. Chemical Rapid rock	Washington, D.C. Chemical classical	Denver, Colorado Chemical (spectrographic)	Denver, Colorado Mineralogic (diffractometer)
155572 (282123 1/)	2-U	52	X	X		X	X
573 (124 1/)	4-A	85	X	X		X	X
574 (125 1/)	2-Y	78	X	X		X	X
929	CH-1	45.5	X				
930	2-H	30	X	X		X	X
931	CH-2	65	X				
932	CH-2	130-132	X	X		X	X
933	CH-3	54	X				
934	CH-3	100	X				
935	4-Y	78	X	X		X	X
936	CH-3	46.5		X			
937	CH-4	83		X			
156056	CH-1	38-40		X	X	X	X
057	3-Y	105		X	X	X	X
058	3-C	58	X	X		X	X
059	2-H	58	X	X		X	X

Determinations of permeability, porosity, specific yield, specific retention, and moisture content were made on most of the 36 samples analyzed by the Hydrologic Laboratory of the Ground Water Branch, Denver, Colo. Specific gravity and dry unit weight were determined for most of these samples. Mechanical analyses were run on 7 samples.

Approximate pH was determined on 9 samples. Moisture tension was determined on 10 samples and pore-size distribution was determined for 5 of those samples.

Permeability determinations were made on consolidated tuff and some of the unconsolidated samples. Unconsolidated samples were packed into ~~the~~ a permeameter cylinder.

A water sample from each deep test well was analyzed to obtain radio-chemical and chemical background concentrations in ground water. Samples from DT-5A, DT-9, and DT-10 were collected near the end of pumping tests. A bailed sample was collected from DT-10.

Water samples were collected during drilling and development from wells DT-5A, DT-9, and DT-10 to determine whether there might be chemical differences in water from different depth intervals in the aquifer.

Tritium concentration was determined in two samples from well DT-9 and one sample from well DT-5A. One sample from DT-9 was collected from the bailer when the well was 1,325 feet deep and the other sample was collected after the well was completed and near the end of the pumping test. The sample from well DT-5A was collected near the end of the pumping test.

Geology and hydrology

A detailed study of the geology of Los Alamos County was not made during the course of this investigation. The reader is referred to a report on this area by Griggs (1955).

A detailed study of the geology and hydrology of TA-49 was made. The most important deposits in respect to the occurrence of ground water are volcanic and sedimentary rocks of Tertiary and Quaternary age. In TA-49, only rocks of Quaternary age are exposed at the surface; however, three deep test wells have been completed in rocks of Tertiary age that are exposed elsewhere in the Los Alamos area. In TA-49, rocks of Quaternary age are not less than 1,000 feet thick and probably are not more than about 1,300 feet thick. The thickness of the rocks of Tertiary age is unknown. The distribution of rocks in the Los Alamos area is shown in figure 4. The general sequence

Figure 4.--Geologic map of Los Alamos area, New Mexico.

of rock units and the general structural relations of the rocks of hydrologic importance are shown on a geologic cross section (figure 5)

Figure 5.--Geologic cross section through Frijoles Mesa from the Pajarito fault to the Rio Grande. Location is shown on figure 4. Descriptions of units are shown on figures 4 and 6.

based on test drilling and geologic mapping in TA-49 and on the geologic map.

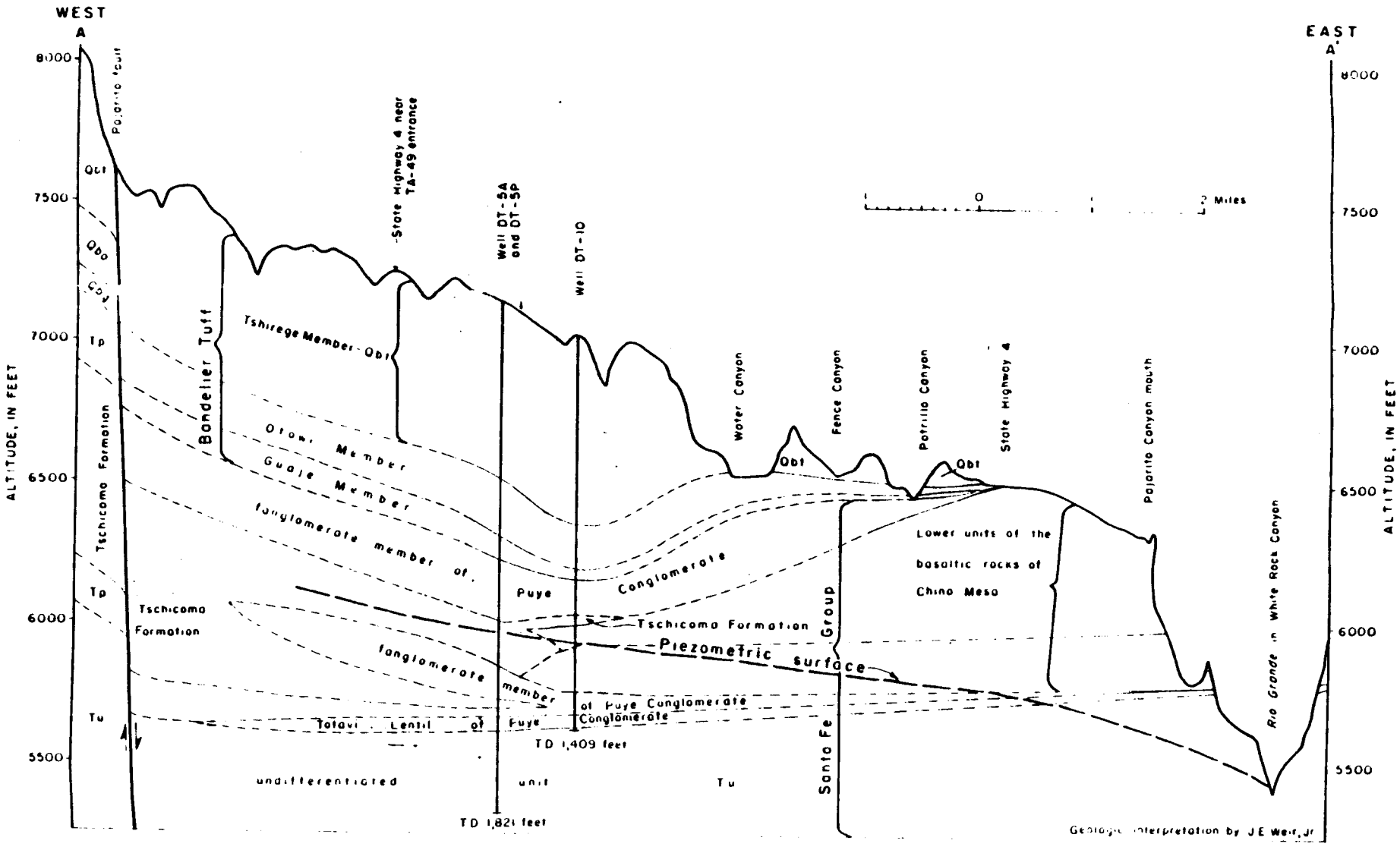

Figure 5 -- Geologic cross section through Frijoles Mesa from the Pajarito fault to the Rio Grande Location is shown on fig 4. Description of units is shown on figs 4 and 6

444

The rock units described in this report are (ascending): the Santa Fe Group of Middle(?) Miocene to Pleistocene(?) age, the volcanic rocks of the Jemez Mountains of Pliocene and Pleistocene age, and the alluvium of Pleistocene and Recent age.

Santa Fe Group

At TA-49, the Santa Fe Group of Middle(?) Miocene to Pleistocene(?) age is composed of: an undifferentiated unit; the Puye Conglomerate, which consists of the Totavi Lentil and the fanglomerate member; and the lower two units of the basaltic rocks of Chino Mesa.

The undifferentiated unit is a sequence of light-colored sediments laid down as coalescing alluvial-fan and flood-plain deposits in the Rio Grande depression. These sedimentary rocks seem to have been derived from the highlands to the north but may have been derived, in part, from the Sangre de Cristo Mountains to the east. The undifferentiated unit crops out along the Rio Grande and in Los Alamos and Guaje Canyons. It is present in the subsurface under most of the Pajarito Plateau.

The Puye Conglomerate consists of a thin basal river gravel overlaid by fan deposits of interlayered boulders, gravel, silt, and sand. The basal unit, called the Totavi Lentil, is arkosic and quartzitic debris, from sand to boulder size, derived principally from igneous and metamorphic rocks to the north and northeast. These gravels were deposited on the broad flood plain and channels of a large river, and they wedge out eastward and westward at the limits of the old riverbeds. The fan deposits that lap onto the Totavi Lentil are called the fanglomerate member and are composed of debris derived from volcanic rocks, mainly latite, quartz latite, and andesite, which crop out on the Sierra de los Valles to the west.

The Totavi Lentil of the Puye Conglomerate disconformably overlies the undifferentiated unit along the Rio Grande and also conformably overlies it in Los Alamos and Guaje Canyons. In the Los Alamos area, the Totavi Lentil crops out in Guaje and Los Alamos Canyons and southward along the Rio Grande to a point below the mouth of Ancho Canyon, where it wedges out between the underlying undifferentiated unit and the overlying basaltic rocks of Chino Mesa. It is found in the subsurface under most of the Pajarito Plateau.

The fanglomerate member of the Puye Conglomerate conformably overlies the Totavi Lentil. A zone near the top of the Totavi Lentil is composed of a mixture of pegmatitic rocks and volcanic debris. This mixed zone represents a change in source of the sediments from igneous and metamorphic terrane to volcanic terrane. The fanglomerate member interfingers with the easternmost flows of the Tschicoma Formation beneath the Pajarito Plateau and with the lower units of the basaltic rocks of Chino Mesa. The sediments of the upper part of the fanglomerate member were derived from the Tschicoma Formation, which formed the high mountain mass of the Sierra de los Valles to the west prior to the ash falls and flows of the Bandelier Tuff. The fanglomerate member consists mainly of latite, quartz latite, and andesite. In upper Guaje and Los Alamos Canyons, the fanglomerate member consists of angular boulders and grades to silt, sand, gravel, and rounded boulders eastward. The fanglomerate member is exposed in the Los Alamos area in Guaje, Rendija, Pueblo, and Los Alamos Canyons and is found in the subsurface under most of the Pajarito Plateau. It forms gray cliffs on the west side of the Rio Grande north of its junction with Los Alamos Canyon.

The basaltic rock of Chino Mesa consists of five mappable units, which originated from volcanic vents near Chino Mesa to the southeast of the Los Alamos area.[a]

The lower two units of the basaltic rock of Chino Mesa crop out along the Rio Grande south of Otowi Bridge. Unit 1 rests unconformably on the undifferentiated unit south of Ancho Canyon and to the north interfingers with the Totavi Lentil along the Rio Grande, with the upper flow of the unit conformable to the Totavi. To the west beneath the Pajarito Plateau the unit 1 interfingers with the fanglomerate member and the Tschicoma Formation.

Unit 2 of the basaltic rocks of Chino Mesa conformably overlies unit 1 and interfingers with the fanglomerate member and Tschicoma Formation west of the Rio Grande. East of the Rio Grande unit 2 interfingers with the upper unit of the undifferentiated unit and wedges out beneath flows of unit 4.

Unit 3 of the basaltic rock of Chino Mesa crops out in lower Los Alamos, Sandia, and Mortandad Canyons west of the Rio Grande and on Chino Mesa east of the river. It consists of basalt flows on a dissected surface. Unit 3 rests disconformably on unit 2 and unconformably on the Puye Conglomerate. It is equivalent in part to the old alluvium.

---

a/ In Griggs' original manuscript report (1955) the basalt units were numbered 1-5 from youngest to oldest. In this report the units are numbered from oldest to youngest, in conformance with accepted stratigraphic practice.

Unit 4 of the basaltic rock of Chino Mesa consists of basalt flows capping the mesas south of Los Alamos Canyon west of the Rio Grande and on the eastern side of the Rio Grande south of Otowi Bridge. Unit 4 rests unconformably on the Puye Conglomerate and the undifferentiated unit and butts against unit 3 in lower Los Alamos Canyon.

Unit 5 of the basaltic rock of Chino Mesa consists of cinder cones and local basalt flows. It overlies with unconformity all older rock in which it is in contact. Where the Bandelier Tuff overlies the basaltic rock of Chino Mesa the contact is an unconformity.

Only the two lower units, 1 and 2, of the basaltic rock of Chino Mesa have been penetrated at TA-49. These were found in well DT-10. Basaltic rocks of Chino Mesa were not present in other wells that penetrated the same stratigraphic sequence.

The old alluvium consists of clays and gravels and is present on the mesa northeast of Guaje Canyon, west of Totavi in Los Alamos Canyon, lower Mortandad Canyon, and at the north end of Chino Mesa. It was deposited unconformably upon the Puye Conglomerate. The old alluvium is overlaid unconformably by the Bandelier Tuff. A flow, unit 3 of the basaltic rock of Chino Mesa, tongues out into the old alluvium west of Totavi. At the north end of Chino Mesa it is overlaid unconformably by the flows of unit 4. As the old alluvium is not present at TA-49, it is not discussed further.

Undifferentiated unit

Physical characteristics

The undifferentiated unit of the Santa Fe Group is composed of friable to moderately well-cemented beds of light-pinkish-gray to light-brown siltstones and sandstones with some conglomerate and clay lenses. Bedding is generally poorly developed except for horizontal bedding found locally in the fine-grained material. The sand-size detritus is made up dominantly of quartz and feldspar and minor amounts of chalcedony, biotite, muscovite, and magnetite. Rock fragments consist of rhyolite, latite, gneiss, schist, limestone, and quartzite. The fragments of quartz, feldspar, gneiss, schist, quartzite, and limestone were derived from the east side of the Rio Grande valley and areas to the north. The fragments of volcanic origin, consisting of latite, rhyolite, tuff, and pumice, were derived from the west and occur mainly in the upper part of the unit.

Cuttings from the undifferentiated unit recovered in wells DT-5A, DT-9, and DT-10 (tables 5, 6, and 7) are a mixture of easterly and westerly derived sediments containing quartz, feldspar, quartzite, latite, rhyolite, and pumice.

At TA-49 three wells, DT-5A, DT-9, and DT-10, are bottomed in the unit. Well DT-5A penetrated 294 feet, DT-9 penetrated 144 feet, and DT-10 penetrated 7 feet. In well DT-10 the lower 7 feet of the boring was assigned to the unit by interpretation of electrical and gamma-ray-neutron logs. The total thickness of the unit in the region exceeds 2,400 feet, based on well information and exposures in lower Los Alamos Canyon (fig. 4).

The undifferentiated unit probably thins to the east and west toward the margins of Rio Grande trough in the region. The west boundary of the trough is not well known but may pass through the approximate longitude of Valle Grande. The upper surface of the undifferentiated unit ~~apparently~~ slopes about 1 degree southward in the TA-49 area.

Table 5.--Sample log of well DT-5A

Drilled by rotary with mud for carrier

Total depth 1,821 feet

Completed pilot hole January 25, 1960

Altitude of land surface 7,143.78 feet

	Thickness (feet)	Depth (feet)
Bandelier Tuff		
Tshirege Member:		
Sidewall cores from hole DT-5:		
Unit 1B		
Tuff, ~~light-gray to~~ light-pinkish-gray, highly friable; greenish glass shards; rhyolite rock fragments ----------		370
Unit 1A		
Tuff, light gray to light tan, pumiceous ----------		490
Tuff, light gray to pinkish gray, pumiceous, apparently friable --		500

Table 5.--Log of well DT-5A - Continued

	Thickness (feet)	Depth (feet)
No samples recovered due to lack of circulation ---	520	520
Unit 1A		
Tuff, light-gray to light-pinkish-gray; quartz and sanidine crystals and fragments; mafic minerals in fine-grained ash matrix; light-yellowish-gray pumice with cellular structure; light-red rhyolite rock fragments occur from 560 to 641 feet; light-gray rhyolite rock fragments occur from 580 to 641 feet; fragments of light-gray siltstone occur from 610 to 615 feet ----------	121±	641

Table 5.--Log of well DT-5A #-Continued

	Thickness (feet)	Depth (feet)
Bandelier Tuff - Continued		
Otowi Member:		
Tuff, light-gray, pumiceous; quartz and sanidine crystals and fragments with minor amounts of mafic minerals in a fine-grained ash matrix. Light- or dark-gray and light-red rhyolite; light-red and gray latite; white to light-gray pumice fragments throughout member ----------	198	839
Guaje Member:		
Pumice, light-gray, contains some rhyolite and latite rock fragments ----------	91	930
Santa Fe Group		
Puye Conglomerate		
Fanglomerate member:		
Conglomerate composed of rhyolite, latites, andesite(?), and light-colored igneous debris. Other rock fragments include light-red sandstone, pumice, and light-tan clays. Some gravels appear well rounded --------	237	1,167

Table 5.--Log of well DR-5A - Continued

	Thickness (feet)	Depth (feet)
Tschicoma Formation		
Undifferentiated latite and quartz latite:		
Latite flow rock, light-gray to dark-gray; interflows of greenish-gray siltstone, rhyolite, and tuff fragments and clays occur from 1,221 to 1,225 feet and from 1,259 to 1,264 feet -----	126	1,293
Santa Fe Group		
Puye Conglomerate		
Panglomerate member:		
Conglomerate composed of rhyolite, latites, andesites(?) and light-colored igneous debris. Other rock fragments include light-gray and white siltstone; light-gray and greenish-gray sandstone. Some fragments appear well rounded. Light-gray ash containing some of the above rock fragments occurs from 1,415 to 1,431 feet ---------	138	1,431

Table 5.--Log of well DF-5A - Continued

	Thickness (feet)	Depth (feet)
Tschicoma Formation		
Undifferentiated latite and quartz latite:		
Latite flow rock, dark-gray, some of appears glassy ----------	26	1,457
Santa Fe Group		
Puye Conglomerate		
Fanglomerate member:		
Conglomerate consisting of rhyolite, latite, and other igneous debris; light-gray sandstone and brown clay ----------	18	1,475
Totavi Lentil:		
Conglomerate composed of bull quartz, quartzite, and much granitic debris. Also abundant volcanic rock debris; gray and brown sandstone fragments -------	52	1,527

Table 5.--Log of well DT-5A - Continued

	Thickness (feet)	Depth (feet)
Undifferentiated unit:		
Siltstone and sandstone, light-pinkish-gray, yellow and brown with lenses of conglomerate; arkosic is some zones but containing much volcanic debris. Light-gray and brown siltstones occur from 1,555 to 1,580 feet; pumiceous zones from 1,585 to 1,595 feet and 1,760 to 1,780 feet. Cuttings are finer from 1,775 to 1,820 feet ----------	294	1,821

Table 6.--Sample log of well DT-9

Drilled by cable tool

Total depth 1,501 feet

Completed February 19, 1960

Altitude of land surface 6,937.3 feet

	Thickness (feet)	Depth (feet)
Bandelier Tuff		
Tshirege Member		
Unit 4:		
Tuff, light-brownish-tan, welded; composed of quartz and sanidine crystals and fragments; light-gray glassy and gray rhyolite in an ash matrix; dark-green mafic minerals; light-yellowish-gray pumice fragments with dark mafic minerals parallel to the cellular structure of the pumice; minor amounts of clay weathered from pumice fragments occur from 48 to 58 feet ----------	58	58

Table 6.--Log of well DT-9 - Continued

	Thickness (feet)	Depth (feet)
Bandelier Tuff - Continued		
Tshirege Member - Continued		
Unit 3:		
Tuff, light gray, containing quartz and sanidine crystals and fragments; fragments of light-tan and white pumice and dark-gray rhyolite in an ash matrix. Sanidine crystals increase in quantity from 74 to 116 feet ----------	58	116
Unit 2:		
Tuff, light-purplish-gray, welded, dense; composed of sanidine crystals and fragments up to granule size; a few quartz crystals and fragments; light-gray to gray rhyolite fragments; matrix is gray glassy ash; green mafic minerals coated with an iron stain ----------	98	214

Table 6.--Log of well DT-9 - Continued

	Thickness (feet)	Depth (feet)
Bandelier Tuff - Continued		
Tshirege Member - Continued		
Unit 1B:		
Tuff, light-gray to reddish-orange, pumiceous, containing some rhyolite rock fragments. Light-gray tuff from 280 to 308 feet contains sanidine; iron-stained quartz crystals and fragments; gray glassy rhyolite fragments; light-gray pumice fragments. Light reddish-orange tuff occurs from 308 to 390 feet and is composed of sanidine and quartz crystals, with some dark-colored inclusions in the quartz crystals; light-gray and light-orange pumice with streaks of dark-gray glass along the cell structure; and a few fragments of dark-gray rhyolite. Light-gray pumice fragments occur from 390 to 462 feet ----------	248	462

Table 6.--Log of well DT-9 - Continued

	Thickness (feet)	Depth (feet)
Bandelier Tuff - Continued		
Tshirege Member - Continued		
Unit 1A:		
Tuff, gray, friable, pumiceous; sanidine and quartz crystals in equal amounts; light-gray and gray glassy rhyolite fragments; some yellowish-orange pumice fragments included. Large light-gray pumice fragments occur from 609 to 618 feet ----------	214	676
Otowi Member:		
Tuff, light-gray, friable; containing light-gray and light-pink pumice fragments; quartz and sanidine crystals and fragments in a glassy ash matrix; light-red, gray, and glassy gray rhyolite; green mafic minerals. Light-red volcanic rock fragments with black and gray glassy bands occur from 756 to 766 feet ----------	126	802

Table 6.--Log of well DT-9 - Continued

	Thickness (feet)	Depth (feet)
Bandelier Tuff - Continued		
Guaje Member:		
Pumice, light-gray ----------	48	850
Santa Fe Group		
Puye Conglomerate		
Fanglomerate member:		
Conglomerate, gray; composed of rhyolite, latite, and light-colored igneous debris; some particles are fine to very coarse and appear to be subrounded. Brown clay up to 60 percent occurs from 918 to 924 feet ----------	74	924
Tschicoma Formation		
Undifferentiated latite and quartz latite:		
Latite and quartz latite ~~flow rocks~~, dark-gray. Inter-flow zones from 1,058 to 1,078 feet and from 1,114 to 1,143 feet contain latite and quartz-latite rock fragments; brown clay; yellow and milky quartz fragments. Water encountered at approximately 1,005 feet ----------	238	1,162

Table 6.--Log of well DT-9 - Continued

	Thickness (feet)	Depth (feet)
Santa Fe group:		
Puye conglomerate:		
Fanglomerate member:		
Conglomerate, gray; composed of rhyolite latite, and quartz-latite fragments with some of the fine to coarse fragments shwoing well-rounded grains. Also fragments of light-gray siltstone and light-yellowish-brown clay ----------	157	1,319
Totavi lentil:		
Conglomerate, gray; rhyolite, latite, and quartzite rock fragments; minerals noted were quartz, white orthoclase, pink microcline, biotite, magnetite, tourmaline, and chalcedony; sand-size particles appear subrounded to well rounded ----------	38	1,357
Undifferentiated unit:		
Siltstone, silty sandstone, and sandstone with occasional conglomerate; light-brown; composed of rhyolite, latite, quartzite, and some pumice.----------	144	1,501

Table 7.--Sample log of well DT-10

Drilled by cable tool

Total depth, 1,409 feet

Completed March 13, 1960

Altitude of land surface 7,019.4 feet

	Thickness (feet)	Depth (feet)
Bandelier Tuff		
Tshirege Member		
Unit 6:		
Tuff, light-gray; medium to very coarse; prominent sanidine phenocrysts with larger phenocrysts containing white globular inclusions; black mafic minerals; large assortment of volcanic rock fragments ----------	29	29
Unit 5:		
Not noted in samples.		
Unit 4:		
Tuff, light-gray to light-red, welded; composed of sanidine, quartz, and mafic minerals with some rock fragments of white and gray glassy rhyolite and brown latite ----------	52	81

Table 7.--Log of well DT-10 - Continued

	Thickness (feet)	Depth (feet)
Bandelier Tuff - Continued		
Tshirege Member - Continued		
Unit 3:		
Tuff, light-reddish-brown; containing sanidine, quartz, and black and green mafic minerals with some rock fragments of gray glassy and reddish rhyolite and latite. Light-yellow devitrified pumice occurs from 128 to 138 feet ----------	57	138
Unit 2:		
Tuff, reddish-brown to light-gray; contains sanidine, quartz, pink orthoclase, and a few fragments of chalcedony and sand-size rock fragments of gray glassy rhyolite and latite ----------	90	228

Table 7.--Log of well DT-1C - Continued

	Thickness (feet)	Depth (feet)
Bandelier Tuff - Continued		
Tshirege Member - Continued		
Unit 1B:		
Tuff, light-gray to very light-orange; pumiceous, contains sanidine, quartz, dark mafic minerals, and feldspar with prominent alteration rings; rock fragments of rhyolite and latite. Large pumice fragments occur from 348 to 370 feet. White to light-gray pumice with reddish-orange rhyolite occur from 408 to 476 feet -	248	476
Unit 1A:		
Tuff, white to light-gray, pumiceous; brown stains on sanidine fragments; orange pumice fragments with streaks of dark-brown glass along cellular structure; dark-green mafic minerals; an abundance of latite and rhyolite rock fragments ----------	196	672

829 feet
259
78

Table 7.--Log of well DT-10 - Continued

	Thickness (feet)	Depth (feet)
Bandelier tuff - Continued		
Otowi member:		
Tuff, light-reddish-tan; white, very light-gray, and bright-orange pumice fragments; dark-green mafic minerals; latite, and light-gray rhyolite ~~rock~~ fragments. Various volcanic rocks with layered structure occur from 754 to 765 feet -----	157	829
Guaje member:		
Pumice, light-gray ----------	35	864
Santa Fe group:		
Puye conglomerate:		
Fanglomerate member:		
Conglomerate; samples from 864 to 972 feet contain medium-gray, gray, and brown latite and rhyolite fragments and pebbles; subangular to subrounded; large vesicular fragments of black basalt. Sand-size fraction contains sanidine and white pumice fragments -	108	972

Table 7.--Log of well DT-10 - Continued

	Thickness (feet)	Depth (feet)
Tschicoma Formation		
Undifferentiated latite and quartz latite:		
Latite flow, ~~rock~~, dark-gray, vesicular, very fine crystalline; mafic minerals appear to be altered; unweathered basalt fragments are included in latite ----------	40	1,012
Santa Fe Group		
Basaltic rocks of Chino Mesa		
Unit 2:		
Basalt, ~~Tsb~~ $_2$, dark-red, vesicular ----	96	1,108
Unit 1:		
Basalt, reddish-brown to black, dense, containing olivine, and drusy green minerals on some basalt fragments --	173	1,281
Puye Conglomerate		
Fanglomerate member:		
Conglomerate, consisting of dark-gray latite, red glassy rhyolite; and brown clays and silts ----------	75	1,356

Table 7.--Log of well DT-10 - Continued

	Thickness (feet)	Depth (feet)
Santa Fe group - Continued		
Puye conglomerate - Continued		
Totavi lentil:		
Conglomerate, consisting of feldspathic quartzsite, gray and brown latite, and red and light-gray rhyolite ------	46	1,402
Undifferentiated unit:		
Siltstone, sandstone and occasional conglomerate; no samples recovered, interpretation from gamma log ---------	7	1,409

Water-bearing characteristics

At TA-49 the undifferentiated unit is saturated, but inasmuch as it is overlain by much more permeable saturated rocks, little could be learned about the water-bearing characteristics of the undifferentiated unit from the pumping tests on wells DT-5A, DT-9, and DT-10. Several inferences can be made, however, about its water-bearing properties on the basis of its lithologic characteristics, and by extrapolation of conditions in the Los Alamos Canyon well field. Pumping tests on city supply well L3 indicated a transmissibility of about 2,500 gpd (gallons per day) per foot for approximately the upper 1,000 feet for the unit (Theis and Conover, 19~~50~~61). Therefore, a moderate to low permeability for the undifferentiated unit is indicated. Variations in lithologic character both laterally and vertically in the undifferentiated unit probably result in differences in permeability and differences in velocity within the aquifer. Movement through beds having relatively higher permeability would be more rapid than through less permeable beds.

Puye Conglomerate

Totavi Lentil

Physical characteristics

The Totavi Lentil is a gray, poorly consolidated conglomerate made up of fragments of quartzite, schist~~s~~, gneiss, and granite. It consists mainly of subrounded to well-rounded quartzite and quartz. Sorting generally is poor but well-sorted lenses of silt and sand are present sporadically. At TA-49 samples from DT-5A, DT-9, and DT-10 indicate that the Totavi Lentil consists of massive quartz, quartzite, and granitic debris. Sand-size particles consist of quartz, white feldspar, pink microcline, biotite, magnetite, tourmaline, and chalcedony, partly subrounded to well rounded.

At TA-49 the thickness of the lentil in wells DT-5A, DT-9, and DT-10 are 52, 38, and 46 feet respectively, indicating a southeastward thinning. Regionally the thickness of the unit ranges from 0 to 89 feet. It wedges out eastward in the vicinity of Canada Ancha and also wedges out in the subsurface westward ~~(fig. 5)~~. It is thickest (89 feet) at well T-2 in upper Pueblo Canyon and thinnest (10 feet) at hole H-19. At wells T-1 and T-3 there is 37 and 62 feet, respectively, of Totavi. Well T-4 was too shallow to penetrate the unit. The part of the lentil beneath TA-49 dips southward about 1 degree, a dip that possibly is typical of the slope of the wide channel in which the unit was deposited.

Water-bearing characteristics

The Totavi Lentil is saturated at TA-49. It has a moderately high porosity and permeability, and readily transmits water. A pumping test of well DT-10 indicates a relatively high transmissibility for the Totavi and THE overlying conglomerate member and included basalt. The basalt probably has a disproportionate effect on the transmissibility of the composite section of rocks. Transmissibilities for the Totavi Lentil alone were obtained elsewhere in the Los Alamos area from wells T-1, T-2, and T-3. (See fig. 4.) Pumping tests of these wells indicate coefficients of transmissibility as follows:

Wells	Transmissibility (gpd per foot)
T-1	160
T-2	7,000
T-3	7,800

The differences may be due, in part, to a smaller thickness of the unit at T-1, but they also reflect differences in lithologic character. It is inferred that velocity of water movement in the Totavi is greater than in the undifferentiated unit--an inferrence that is corroborated by interpretation of tritium analyses discussed in a later section of this report.

The heterogeneity, cross-bedding, and interlayering of silt and sand with conglomerate should result in a highly dispersive flow pattern in the Totavi.

Fanglomerate member

Physical characteristics

The Fanglomerate member is a gray conglomerate, composed of pebbles, cobbles, and boulders of rhyolite, latite, quartz latite, and pumice in a matrix of silt and sand. These rocks ~~are~~ WERE derived from flows associated with the volcanic rocks of the Jemez Mountains. Sorting is poor but there are tongues and lenses of fairly well-sorted pumiceous siltstone and water-laid pumice in the fanglomerate. The degree of cementation varies from friable to well cemented. The Fanglomerate member contains large angular boulders in upper Guaje and Pueblo Canyons grading into finer and rounded material to the east.

In the western half of the Pajarito Plateau, the flows ~~rocks~~ of the Tschicoma Formation are interbedded with the Fanglomerate member by replacement and in the eastern half of the plateau some of the basaltic rocks of Chino Mesa are interbedded with the Fanglomerate member. The Fanglomerate member does not crop out at TA-49. It is interbedded with the Tschicoma Formation in the subsurface. At well DT-10 it is interbedded also with units 1 and 2 of the basaltic rocks of Chino Mesa. The Puye, Tschicoma, and the basaltic rocks apparently ~~were deposited in~~ FORMED a shallow trough trending southward beneath the western side of Pajarito Plateau (fig. 5).

At TA-49 well DT-5A penetrated 393 feet of the Fanglomerate member. Wells DT-9 and DT-10 penetrated 231 feet and 183 feet of the member, respectively. Known thickness ranges from 209 feet exposed in lower Guaje Canyon to 637 feet penetrated in well T-2 in Pueblo Canyon.

Water-bearing characteristics

At TA-49 the lower beds of the Fanglomerate member are saturated where they are interbedded with the Tschicoma Formation and basaltic rocks of Chino Mesa. Elsewhere in the Los Alamos area, wells T-1A and T-2A in Pueblo Canyon penetrated perched water in zones of relatively low permeability in the Fanglomerate member. At TA-49 the unit probably has a moderate to low permeability; however, some beds may have high permeabilities and may readily transmit water. In general, permeability and transmissibility in the Fanglomerate member are less than in the underlying Totavi Lentil.

Basaltic rocks of Chino Mesa

Physical characteristics

Units 1 and 2 of the basaltic rocks of Chino Mesa were found at TA-49 in well DT-10. Unit 1 consists mainly of a reddish-brown to black, dense basalt containing olivine. In well DT-10 it is 173 feet thick and overlies the lower layer of the Fanglomerate member of the Puye Conglomerate. Unit 2 is mostly a dark-red vesicular basalt. At well DT-10 it overlies unit 1 and is 96 feet thick. It is overlaid by a latite flow of the Tschicoma Formation.

On the basis of the sonic log (fig. 57D), several intervals in the basalt units penetrated by well DT-10 are moderately to strongly jointed. These intervals are: about 1,125 to 1,130 feet, which may be an interflow zone; 1,175 to 1,210 feet; and 1,254 to 1,284 feet, which may be the most strongly jointed but may be partly a brecciated interval at the base of unit 1. These zones drilled somewhat faster than other intervals in the basalt. A 22-foot interflow or brecciated zone at the base of unit 2 is shown by the gamma-ray log also.

Water-bearing characteristics

At TA-49 unit 1 and the lower 22 feet of unit 2 of basaltic rock of the Chino Mesa penetrated by well DT-10 are in the zone of saturation and seemingly transmit considerable quantities of water through joints and interflow zones. About 3 miles downgradient these basalts are above the zone of saturation and the water they transmit passes into the underlying units of the Santa Fe group. The upper parts of units 1 and 2 of the basaltic rocks of Chino Mesa [redacted] are vesicular and thus may have a high porosity but largely a low interstitial permeability. Cracks and joints formed as a result of shrinkage commonly transmit water very readily. The movement of water through a labyrinth of interconnected joints would be almost as free and unimpeded as flow through small channels. Dispersion might be limited locally within the basaltic rocks by dense relatively impervious parts of the basalt flows. Thus contaminants entering a strongly jointed zone might tend to stay in this zone for some distance downgradient. Elsewhere in the Los Alamos area, the basalt units appear to be above the main zone of saturation and contain perched water locally, as along White Rock Canyon where several small springs and seeps occur that apparently issue from partly saturated interflow zones.

Volcanic rocks of the Jemez Mountains

Volcanic rocks of the Jemez Mountains along the eastern flanks of the Sierra de los Valles and on the Pajarito Plateau are composed of the Tschicoma Formation of Pliocene and Pleistocene(?) age and the younger Bandelier Tuff of Pleistocene age. The Tschicoma Formation consists of undifferentiated latite and quartz latite that are flow ~~rocks~~ and pyroclastic rocks associated with the volcanic rocks of the Jemez Mountains. They are highly fractured and jointed and some intervals contain weathered zones and interflow breccias. The latite and quartz latite rocks are widely exposed on the Sierra de los Valles (fig. 4) and are present in the subsurface beneath the Pajarito Plateau (fig. 5). These rocks were penetrated by wells DT-5A, DT-9, and DT-10 at TA-49 (figs. 5 and 6) and by test well T-4 in the city of Los Alamos and hole H-19 in upper Los Alamos Canyon. The lower part of this ~~series~~ sequence is interbedded with the fanglomerate member of the Puye Conglomerate and also with the basaltic rocks of Chino Mesa.

The Bandelier Tuff forms the Pajarito Plateau. The Bandelier Tuff laps on to the undifferentiated latite and quartz latite along the western edge of the plateau and terminates to the east in cliffs, steep slopes, and as filling in buried canyons cut in basalt along the Rio Grande. The tuff is composed of ash-fall pumice, ash flows, and water-laid volcanic ash and pumice.

Table 8.--Sample log of well DT-5P

Drilled by rotary with air for carrier

Total depth 692 feet

Completed November 21, 1959

Altitude of land surface 7,144 feet

	Thickness (feet)	Depth (feet)
Bandelier Tuff:		
Tshirege Member:		
Unit 6:		
Tuff, light-gray, pumiceous; contains dipyramidal quartz crystals, some of which are clear with white inclusions; sanidine crystals and fragments; white and yellow pumice fragments; latite and quartz latite rock fragments ----------	73	73
Unit 5:		
Not recognized in cuttings ----------	2	75
Unit 4:		
Tuff, light-purplish-gray; consists mainly of quartz and sanidine crystals and fragments; light-red rhyolite fragments --	44	119
Unit 3:		
Tuff, light-purplish-gray, pumiceous; includes latite and rhyolite rock fragments; quartz is very coarse sand size, clear, dipyramidal crystals; sanidine fragments are pitted. Samples decrease from 50 to 90 percent then [illegible] ----------	63	182

Tschicoma Formation

Physical characteristics

The undifferentiated latite and quartz latite of the Tschicoma Formation contains large phenocrysts of plagioclase and smaller phenocrysts of quartz, biotite, hornblende, and augite in a fine-grained matrix of plagioclase, orthoclase, augite, magnetite, and varying amounts of glass. Interflow zones contain greenish-gray siltstone, clay, and rock fragments of tuff, rhyolite, and latite.

At TA-49 well DT-5A penetrated two layers of latite and quartz latite of the Tschicoma Formation. The upper layer is 126 feet thick and contains two interflow zones 4 and 5 feet thick ~~(table 5)~~ composed of clay, latite, tuff, and rhyolitic fragments. The lower layer is 26 feet thick. Well DT-9 penetrated 238 feet of undifferentiated latite and quartz latite interbedded with the Fanglomerate member.

Well DT-10 penetrated 40 feet of the undifferentiated latite and quartz latite unit of the Tschicoma Formation. Several interflow zones composed of dark-red silt and clay were penetrated. At well DT-10 the undifferentiated latite and quartz latite of the Tschicoma Formation lie on unit 2 of the basaltic rocks of Chino Mesa and are overlain by the upper part of the Fanglomerate member of the Puye Conglomerate.

The latite and quartz latite rocks were emplaced as viscous lava flows, and generally are highly jointed and fractured owing to shrinkage and flow deformation. Normally, these rocks have two or more joint or fracture systems that intersect.

Water-bearing characteristics

At TA-49 the uppermost part of the Tschicoma Formation is in the zone of saturation in the vicinity of wells DT-5A and DT-9. The joints and fractures in these rocks provide space for water storage and avenues of great permeability and the interflow zones commonly contain some breccia that is permeable.

Elsewhere in the Los Alamos area water was found in the Tschicoma in well T-4 and hole H-19 (fig. 4). Several springs issue from interflow and contact zones between layers in the undifferentiated latite and quartz latite unit. Some of these springs are located in Guaje, Los Alamos, Pajarito, and Water Canyons, and Canon de Valle.

Bandelier Tuff

The Bandelier Tuff consists chiefly of ash-fall and ash-flow tuff. Some thin water-laid sediments are included in the Bandelier. The unit is divided into three members: Guaje, Otowi, and Tshirege, from oldest to youngest. The Guaje Member rests unconformably on older rocks and consists of pyroclastic debris, partly water-laid. It is draped over the older topography. The Otowi Member is conformable to the underlying Guaje Member and consists of pumiceous tuff of ash-flow origin and locally near the top contains a few generally thin layers of water-laid sediments. The Tshirege Member unconformably overlies the Otowi and forms the cap of the Pajarito Plateau. In this report it is subdivided into seven units, composed mainly of ash-flow tuff at least one of which is water-laid. The units of the Tshirege are numbered 1A, 1B, and 2 through 6 from bottom to top.

Guaje member

The Guaje member consists of ash-fall pumice and water-laid pumiceous tuff. Near the base gray lump-pumice fragments ~~up to~~ as much as 2 inches in length occur. Fragments of glass shards, and quartz and sanidine crystals are found in a cellular structure of the partly devitrified pumice. Some rounded, pebble-size fragments of light-red rhyolite are found near the top of the unit.

At TA-49 the Guaje member is ~~found~~ present in the subsurface in all three deep test wells. It is 48 feet thick in DT-9, 35 feet thick in DT-10 and 91 feet thick in DT-5A.

At TA-49 the Guaje member is above the main zone of saturation and the unit contains no perched water. Elsewhere in the Los Alamos area the Guaje contains perched water locally, as at hole H-19 in upper Los Alamos Canyon. The interstices and intercellular spaces in the pumice are small. The porosity of the Guaje averages about 40 percent but permeability generally is low. Fractures and joints are not pronounced in the Guaje member, and barely perceptible joints apparently are closed or filled by alteration material.

Otowi Member

The Otowi Member consists of a light-gray pumiceous rhyolite tuff that is friable and weathers to a gentle slope and odd teepee-LIKE shapes. Quartz crystals, glass shards, and minor amounts of mafic minerals and varing amounts of rhyolite, latite, and pumice fragments are included in a fine-grained ash. The rock fragments are rounded. The Otowi is an ash flow and contains several water-laid beds of ash and pumice near the top. Where the unit is exposed, some of the joints are hair-line cracks that are filled with brown clay containing roots, and some curvilinear joints are open and enlarged by weathering.

At TA-49 the Otowi is present only in the subsurface but it crops out in Water and Ancho Canyons about 0.5 mile east of TA-49. The CONTACT BETWEEN THE Otowi and overlying Tshirege Member is erosional.

At TA-49 the top of the Otowi is from 641 to 676 feet below the surface in the deep test wells. The unit is 157 feet thick in DT-10, 126 feet in DT-9, and 198 feet in DT-5A. Well DT-5P penetrated 51 feet of the Otowi Member (table 8).

The Otowi Member may yield water to springs in upper Guaje Canyon but it does not contain perched water at TA-49. Porosity of the Otowi Member ranges from 45 to 50 percent. Interstices in the Otowi are small and permeability probably is low.

Table 8.--Log of DT-5P - Continued

	Thickness (feet)	Depth (feet)
Bandelier Tuff - Continued		
Tshirege Member - Continued		
Unit 2:		
Tuff, light-pinkish-gray; groundmass is very fine sand to silt-size ash with abundant sanidine phenocrysts and some quartz ----------	100	202
Unit 1B:		
Tuff, light-tan, pumiceous; quartz and sanidine crystals and fragments; light-tan pumice fragments; gray and light-red rhyolite and gray latite rock fragments; pumice fragments have dark-gray streaks along cellular structure from 379 to 412 feet; light-tan pumice; very fine-size quartz and sanidine crystals and fragments; 95 percent of sample was lost when washed from 448 to 485 ----------	203	485
Unit 1A:		
Tuff, light-pinkish-gray, pumiceous; light-gray and yellowish-orange pumice fragments; quartz and sanidine fragments and crystals; gray latite, light-red and gray rhyolite rock fragments; rock fragments increase from 556 to 641 feet ----------	156	641

Table 8.--Log of DT-5P - Continued

	Thickness (feet)	Depth (feet)
Bandelier Tuff - Continued		
Otowi Member:		
Pumice, light-tan, some welded tuff fragments; light-gray and light-reddish rhyolite: 80 to 98 percent of samples lost when washed ---	51	692

Note: Hole was drilled with a 4½-inch rock bit using air to cool the bit and clean the hole. Perched water was not present. Color determination was made from dry samples. Samples were washed and described while wet. Correlations are based on drill cuttings from hole 5P and on gamma-ray log of hole DT-5 which is about 50 feet to the northeast of 5P.

Tshirege Member

The Tshirege Member forms the finger-like mesas of the Pajarito Plateau. It is composed of a series of ash flows of rhyolite tuff and contains at least one thin water-laid bed near the top. The rhyolite tuff is composed of quartz and sanidine crystals and fragments, some mafic minerals, and zenoliths of gray rhyolite and latite in a fine ash matrix. The tuff varies from friable to welded. The thin water-laid bed is composed of material derived from the underlying ash flow.

The Tshirege Member is entirely above the main zone of saturation at TA-49, and it contains no perched water. Adjacent to and beneath the canyons it probably contains perched water.

The Tshirege Member is the most important geologic unit in Area 49 insofar as test operations are concerned and this unit is treated in detail in a special section following the discussion of the alluvium.

Alluvium

Alluvium in Water Canyon ~~on~~ AT the northern edge of TA-49 consists of material derived from the Tschicoma Formation that forms the Sierra de los Valles and from the Bandelier Tuff of Frijoles Mesa into which Water Canyon is cut.

The alluvium is a poorly sorted mixture of silt, clay derived from weathered tuff, and ~~larger~~ SAND particles derived from the latites and quartz latites ~~rocks~~ of the Tschicoma Formation. The sand~~-size~~ particles consist of quartz, sanidine, dark minerals, and fragments of tuff, pumice, latite, quartz latite, and rhyolite.

The alluvium in Water Canyon ranges in thickness from 6 to about 14 feet. Test holes ~~WMB-1~~ WCM-1 and 2 penetrated about 14 feet of clay, silt, and minor amounts of gravel overlying 2 to 4 feet of gravel at the base of the alluvium. At Beta hole the alluvium consists of 8 feet of silt and gravel. The stream channel in many places is cut 6 to 10 feet into the alluvium.

Clays and silts are almost impermeable when saturated but gravels or gravels with minor amounts of clay and silts will readily transmit water. In test holes WCM-1 and 2 water was (temporarily) perched in the alluvium on top of the lowest exposed unit of the Tshirege Member of the Bandelier Tuff indicating the permeability of the alluvium is greater than that of the underlying tuff.

Ancho Canyon, on the southern edge of TA-49, heads in Frijoles Mesa which is underlain by the Bandelier Tuff. Alluvium is very thin or absent in Ancho Canyon. For this reason it was not mapped on figure 6.

Geology and water-bearing properties of the Tshirege Member of the Bandelier Tuff

The Tshirege Member ranges in thickness from about 1,000 feet in upper Frijoles Canyon to less than 100 feet along the Rio Grande.

At TA-49 the Tshirege Member has been divided into seven units (fig. 6). Unit 1A is the oldest and known only in the subsurface.

Figure 6.--Geologic map and cross section showing location of exploratory drill holes, TA-49, Los Alamos County, N. Mex.

~~Description of subsurface units are shown on figure 4.~~

The other six units, units 1B, and 2 through 6, crop out in Water Canyon and are described in a measured section (table 9).

Correlation of the units in the subsurface were made by gamma-ray-neutron and lithologic logs of the four core holes (tables 10-13) and wells DT-5P, DT-5, DT-5A, DT-9, and DT-10.

Table 9.--Type section of units in the Tshirege Member of the Bandelier Tuff

South wall of Water Canyon - NW¼NE¼ sec. 3 (projected) T. 18 N., R. 6 E.

Measured by E. H. Baltz and W. D. Purtymun

	Thickness (feet)
Bandelier Tuff:	
Tshirege Member:	
Unit 6:	
Tuff, light-grayish-pink, weathers brownish-pink, rhyolitic, moderately welded; fine-grained ash matrix; small pumice fragments; scattered quartz and sanidine crystals; approximate horizontal sheeting that may be bedding; conchoidal joints; forms cliffs, caps mesa. Lower contact is irregular ------	56+
Unit 5:	
Sand, light-gray with intermixed limonitic stains, water-laid; mostly medium-grained but contains fragments up to pebble size; composed of reworked tuff containing stream-worn quartz and sanidine crystals and tuff fragments; foreset and topset bedding is well developed; forms notch near top of mesa; lower contact is irregular. Joints of underlying unit 4 are filled with sand ------	3.8

Table 9.--Type section of units in the Tshirege Member - Continued

	Thickness (feet)
Bandelier Tuff - Continued	
Tshirege Member - Continued	
Unit 4:	
Tuff, light-pinkish-gray; fine-grained; 10 percent quartz crystals; small light-pink to dark-gray rhyolite fragments; small pumice fragments up to ½ inch in length; no bedding present but lenses of disk-shaped pumice up to 6 inches in length and 2 inches thick in dense pinkish-gray matrix; weathering grades up into sand of units; forms cliff; lower contact is gradational ----------	41
Unit 3:	
Tuff, light-gray, very pumiceous, friable; 20 to 30 percent granule size quartz and sanidine crystals; pumice fragments up to 1 inch in length; this description applies to lower 3 feet. Remainder of unit, except for upper 2 feet, is covered and forms slope. Small valley cut into this unit. Lower contact is covered ----------	40

Table 9.--Typical section of units in the Tshirege Member - Continued

	Thickness (feet)
Bandelier Tuff - Continued	
Tshirege Member - Continued	
Unit 2:	
Tuff, light-pinkish-gray, weathering light-brownish-gray; dense, welded; 20 to 30 percent coarse-grained quartz and feldspar crystals and fragments; 10 percent pebble-size pumice fragments; gray rhyolite rock fragments; matrix crystals of fine-grained glassy material; forms cliffs consisting of two beds separated by a slight notch; lower contact with unit 1B is concealed but on north wall of canyon is irregular ---------	100

Table 9.--Type section of units in the Tshirege Member - Continued

	Thickness (feet)
Bandelier Tuff - Continued	
Tshirege Member - Continued	
Unit 1B:	
Tuff, gray to pinkish-gray, weathers pink to light-orange; cobble-size gray rhyolite; quartz and feldspar crystals and fragments; pumice fragments in ash matrix; weathering around quartz crystal and fragments are yellow stained; pumice weathers to brown clay; internal stratification lacking but rock fragments and pumice are in lenses; maybe two or more ash falls with irregular contacts; weathers to steep slope pitted by weathering out of pumice fragments in places. Probably is an explosive breccia ----------	134+

Table 10.--Log of core hole 1

Cored by rotary with air for carrier

Total depth 501 feet

Completed December 6, 1959

Altitude of land surface 7,170

	Thickness (feet)	Depth (feet)
Bandelier Tuff		
Tshirege Member		
Unit 6:		
Tuff, light-gray to purplish-gray pumiceous; zenoliths of gray, red and dark-gray rock fragments; medium-size quartz and sanidine crystals and fragments; dark-gray devitrified pumice up to ½ inch in length; sand-size brownish-yellow mafic minerals. Tuff is dense from 58 to 71 feet; 42.0 feet of core recovered ---------	71	71
Unit 5:		
No recovery, interpretation from gamma-ray log ----------	2	73
Unit 4:		
Tuff, light-gray to light-tan; medium- to granule-size quartz and sanidine crystals and fragments; devitrified pumice up to 1 inch in length; grayish-blue latite rock fragments; 5.4 feet of core recovered -	41	114

Table 10.--Log of core hole 1 - Continued

	Thickness (feet)	Depth (feet)
Bandelier Tuff - Continued		
Tshirege Member - Continued		
Unit 3:		
Tuff, light-red, arkosic; abundant sanidine and quartz phenocrysts; some zenolithic material of latite(?) up to pebble size recovered in the interval from 184 to 186 feet; 0.0 foot of core recovered ----------	76	190
Unit 2:		
Tuff, purplish-gray, welded, dense; zenoliths of medium-gray latite; coarse-size quartz and sanidine crystals and fragments. Near vertical fracture brown clay plated 261 to 262 feet; 48.7 feet of core recovered ----------	94	284
Unit 1B:		
Tuff, light-pinkish-gray; zenoliths of medium-gray latite(?); vertical fracture brown clay plated about 315 feet; 8.6 feet of core recovered ----------	217	501

Correlations based on recovered core and gamma-ray logs.

Table 11.--Log of core hole 2

Cored by rotary with air for carrier

Total depth of hole 501 feet

Completed November 30, 1959

Altitude of land surface 7,137

	Thickness (feet)	Depth (feet)
Bandelier Tuff		
Tshirege Member		
Unit 6:		
Tuff, very light-gray to light-pinkish-gray, pumiceous; very fine-grained ashy matrix; quartz crystals are clear with well developed faces and range from very fine-grained to large-granule size; xenoliths of light-red dense igneous rock; pumice fragments up to 3/4 inch in length; limonite stains on fractures; 47.8 feet of core recovered ----------	78	78
Unit 5:		
No recovery, interpretation from gamma-ray log ----------	2	80

Table 11.--Log of core hole 2 - Continued

	Thickness (feet)	Depth (feet)
Bandelier Tuff - Continued		
Tshirege Member - Continued		
Unit 4:		
Tuff, light-gray with slight lavender cast; very coarse to granule quartz and feldspar crystal fragments; devitrified pumice fragments up to 1 inch in length; zenoliths of light grayish-green dense rock; 40 feet of core recovered ----------	56	136
Unit 3:		
No recovery ----------	55	191
Unit 2:		
Tuff, light-purplish-gray, dense, welded; quartz and sanidine crystals up to granule size; devitrified pumices up to ½ inch in length; zenoliths of dark-gray rock fragments up to ½ inch in length; 67.9 feet of core recovered ----------	101	292

Table 11.--Log of core hole 2 - Continued

	Thickness (feet)	Depth (feet)
Bandelier Tuff - Continued		
Tshirege Member - Continued		
Unit 1B:		
Tuff, light-pinkish-gray, pumiceous; quartz and sanidine crystals up to granule size; devitrified pumice 3/4 inch in length and 3/8 inch wide; 3.8 feet of core recovered ---------	195	487
Unit 1A:		
No recovery ----------	14	501

Correlation based on recovered core and gamma-ray logs.

Table 12.--Log of core hole 3

Cored by rotary with air for carrier

Total depth 300 feet

Completed February 3, 1960

Altitude of land surface 7,170

	Thickness (feet)	Depth (feet)
Bandelier Tuff		
Tshirege Member		
Unit 6:		
Tuff, light-gray to light-pinkish-gray; fine-grained groundmass with medium- to very coarse-grained quartz and sanidine crystals and fragments; granule-size purplish-brown devitrified pumice; granule to pebble-size medium-brown latite; strongly jointed zone from 23 to 28 feet and 34 to 37 feet; 44.3 feet of core recovered ----------	75	75
Unit 5:		
No recovery, interpretation from gamma-ray log ----------	2	77

Table 12.--Log of core hole 3 - Continued

	Thickness (feet)	Depth (feet)
Bandelier Tuff - Continued		
Tshirege Member - Continued		
Unit 4:		
Tuff, light-purplish-pink; fine-grained groundmass with 50 percent sanidine and abundant very coarse-grained medium-gray rock fragments; elongated devitrified pumice fragments up to 1 inch in length; decrease in rock fragments and pumice from 105 to 111 feet; 15.5 feet of core recovered ----	44	121
Unit 3:		
Tuff, purplish-pink to gray, very pumiceous; no core recovery; sample taken with basket ----------	72	193
Unit 2:		
Tuff, light-gray to purplish-gray, welded, dense; quartz and sanidine crystals and fragments up to granule size; light-gray phenocrysts of rhyolite rock fragments; devitrified pumice fragments up to ½ inch in length and mafic mineral stains occur from 194 to 200 feet; 77.5 feet of core recovered ----	82	275

Table 12.--Log of core hole 3 - Continued

	Thickness (feet)	Depth (feet)
Bandelier Tuff - Continued		
Tshirege Member - Continued		
Unit 1B		
Tuff, light-purplish-pink to gray, dense, welded; granule-size quarts and sanidine crystals and fragments; purplish-pink devitrified pumice fragments; gray rhyolite rock fragments; gray rhyolite fragments increase from 295 to 300 feet; 23.2 feet of core recovered ----------	25	300

Note: Correlation based on recovered core and gamma-ray logs.

Table 13.--Log of core hole 4

Cored by rotary with air for carrier

Total depth 303 feet

Completed February 5, 1960

Altitude of land surface 7,116 feet

	Thickness (feet)	Depth (feet)
Bandelier Tuff		
Tshirege Member		
Unit 6:		
Tuff, light-gray to light-pinkish-gray; very fine-grained groundmass with very coarse-grained phenocrysts of quartz and sanidine; light-purplish-gray devitrified pumice up to 3/4 inch in length; granule-size medium-gray latite rock fragments; 44.1 feet of core recovered ----------	62	62
Unit 5:		
No recovery, interpretation from gamma-ray log ----------	2	64

Table 13.--Log of core hole 4 - Continued

	Thickness (feet)	Depth (feet)
Bandelier Tuff - Continued		
Tshirege Member - Continued		
Unit 4:		
Tuff, light-purplish-gray; very fine-grained groundmass with about 50 percent quartz and sanidine phenocrysts; some purplish-brown devitrified pumice; medium-gray latite and quartz latite rock fragments; tuff appears dense and size of rock fragments increase from 104 to 109 feet; 28.6 feet of core recovered ----------	61	125
Unit 3:		
No recovery ----------	52	177
Unit 2:		
Tuff, light-purplish-gray, dense, welded; quartz and sanidine crystals and fragments up to granule size; medium-gray to dark-gray rhyolite rock fragments; a few light-gray devitrified pumice fragments as much as ¼ inch in length; 79.0 feet of core recovered --	111	288

Table 13.--Log of core hole 4 - Continued

	Thickness (feet)	Depth (feet)
Bandelier Tuff - Continued		
Tshirege Member - Continued		
Unit 1B:		
Tuff, light-purplish-pink to light-purplish-gray; granule size quartz and sanidine size quartz and sanidine crystals and fragments; light-gray rhyolite rock fragments; some mafic staining; pebble-size devitrified pumice fragments; 4.7 feet of core recovered ----------	15	303

Note: Correlation based on recovered core and gamma-ray logs.

Table 14.--Mineral constituents of the Tshirege member of the Bandelier tuff at TA-49, Los Alamos County, N. Mex.[1]

Results are coded according to the following system: 1 = 75-100 percent, 2 = 50-75 percent, 3 = 25-50 percent, 4 = 10-25 percent, 5 = 0-10 percent, 2-3 = 35-65 percent, 4-5 = 5-15 percent.

Sample location		Stratigraphic	Mineral constituents[2]					Remarks
Hole	Depth (feet)	Unit	Feldspar	Quartz	Tridymite	Cristobalite	Clay	
CH-1	38-40	Qbt_6	2	5	4	4	-	
2-H	30	Qbt_6	2-3	5	4	4	-	
2-H	58	Qbt_6	2	4	5	4	5	
2-U	52	Qbt_6	3	5	5	3	5	Feldspar (sanidine?). Clay (montmorillonitic).
2-Y	78	Qbt_5	3	4-5	5	3	5	Feldspar (sanidine?).
CH-2	130-132	Qbt_4	2	4	5	4	5	
3-C	58	Qbt_6	2	5	4	4	-	
3-Y	105	Qbt_4	2	5	4	4	5	
4-A	85	Qbt_4	3	5	5	2	5	Feldspar (sanidine?). Clay (montmorillonitic).
4-Y	78	Qbt_4	2	4	5	4	5	

1/ Analyst: Theodore Botinelly of the Geochemistry and Petrology Branch of the U.S. Geological Survey

2/ Quantities are estimated on the basis of peak heights of diffractometer patterns. A precise identification of the clays was not made; on the basis of bulk patterns and patterns of oriented samples the clays probably are montmorillonite. The feldspars probably are sanidine based on some minor shifts of peak positions in the sa

The X-ray analyses of samples from units 4, 5, and 6 of the Tshirege Member indicate~~s~~ that these rocks are 25 to ~~50~~ 75 percent feldspar that is largely sanidine, 0 to 25 percent quartz, 0 to 25 percent tridymite, and 10 to 75 percent cristobalite. Some of the samples contain as much as 10 percent clay, probably montmorillonite (table 14). Chemical analyses of samples from these units show the following ranges in percentage of constituents analyzed: silica (SiO_2) 72.0-78.2, alumina (Al_2O_3) 11.2-13.8, ferric oxide (Fe_2O_3) 1.1-2.1, ferrous oxide (FeO) 0.21-0.75, magnesium oxide (MgO) 0.02-0.33, calcium oxide (CaO) 0.26-1.17, sodium oxide (Na_2O) 3.5-4.5, potassium oxide (K_2O) 4.2-4.7, water (H_2O) ~~0.28~~ 0.15-2.8, titanium oxide (TiO_2) 0.10-0.32, phosphorus oxide (P_2O_5) 0.01-0.07, manganese oxide (MnO) 0.00-0.08, and carbon dioxide (CO_2) less than 0.05 (table 15). Spectrographic analyses (table ~~16~~ 16) of samples from these units showed rather uniform content of major and minor elemental constituents analyzed.

Table 15.--Chemical analyses of the Tshirege member, Bandelier tuff at TA-49, Los Alamos County, N. Mex.

Hole designation	Depth (feet)	Stratigraphic unit	Constituents (Percent) SiO_2	Al_2O_3	Fe_2O_3	FeO	MgO	CaO	Na_2O	K_2O	H_2O	TiO_2	P_2O_5	MnO	CO_2	Sum
CH-1	38-40	Qbt_6	72.7	13.5	2.0	0.50	0.33	1.0	4.5	4.5	0.55	0.32	0.07	0.08	<0.05	100
CH-1[1/]	38-40	Qbt_6	73.71	13.53	1.77	.75	.16	1.17	4.50[2/]	4.49[2/]	.11[3/] .18	.14	.01	.01	-	100.52
2-H	30	Qbt_6	72.0	13.5	2.1	.24	.28	.67	3.7	4.3	2.8	.26	.06	.06	< .05	100
2-H	58	Qbt_6	73.6	13.1	1.9	.25	.32	.51	3.9	4.6	1.3	.26	.06	.06	< .05	100
2-U	52	Qbt_6	75.6	12.7	1.2	.34	.12	.59	4.0	4.6	.46	.18	.05	.04	< .05	100
2-Y	78	Qbt_5	78.2	11.2	1.4	.35	.12	.30	3.5	4.2	.32	.17	.03	.04	< .05	100
CH-2	130-132	Qbt_4	77.2	12.0	1.1	.28	.04	.41	4.1	4.4	.28	.14	.02	.06	< .05	100
3-C	58	Qbt_6	74.6	12.8	1.7	.21	.12	.53	4.2	4.7	.75	.22	.05	.06	< .05	100
3-Y	105	Qbt_4	74.8	12.7	1.5	.28	.16	.66	4.1	4.7	.51	.22	.04	.06	< .05	100
3-Y[1/]	105	Qbt_4	74.78	12.51	1.50	.38	.04	.87	4.12[2/]	4.70[2/]	.41[3/] .15	.21	-	.00	-	99.67
CH-3	46.5	Qbt_6	72.6	13.8	1.9	.18	.20	.61	4.3	4.5	1.2	.27	.06	.07	< .05	99.99
4-A	85	Qbt_4	77.0	12.1	1.2	.23	.02	.26	4.0	4.6	.44	.10	.02	.04	< .05	100
4-Y	78	Qbt_4	76.5	12.4	1.2	.25	.05	.26	4.2	4.6	.29	.14	.02	.06	< .05	100
CH-4	83	Qbt_4	76.6	12.4	1.2	.29	.09	.29	4.2	4.5	.42	.13	.02	.08	< .05	100.22

Except as otherwise noted, samples were analyzed by rapid methods similar to those described in USGS Bulletin 1036-C.

Analysts: Paul L. D. Elmore, Samuel D. Botts, Ivan H. Barlow, and Gillison Chloe.

1/ Rock analysis done by classical or conventional methods as described by Hillebrand (1900). Analyst: M. K. Carron.

2/ Determined by flame photometer by W. W. Brannock.

3/ Upper figure for H_2O^+, lower figure for H_2O^-. The H_2O^+ quantity for sample from hole 3-Y at 105 feet determined from loss on ignition minus H_2O^-.

109 ~~117~~

H.

Table 16.--Results of semiquantitative spectrographic analyses of the Tshirege member of the Bandelier tuff at TA-49, Los Alamos County, N. Mex.

Hole designation	Stratigraphic unit in Tshirege member	Depth (feet)	Constituents (Percent)																												
			Si	Al	Fe	Mg	Ca	Na	K	Ti	Mn	Ba	Be	Ce	Co	Cr	Cu	Ga	La	Mo	Nb	Nd	Ni	Pb	Sc	Sn	Sr	V	Y	Yb	Zr
CH-1	Qbt_6	38-40	M	M	1.5	0.3	0.7	3	3	0.15	0.07	0.07	0.00015	0.015	0.0003	0.0007	0.0007	0.003	0.007	d	0.003	0.007	0.0003	0.003	0.0007	0	0.015	0.0015	0.003	0.0003	0.03
2-H	Qbt_6	30	M	M	1.5	.3	.7	3	3	.15	.03	.03	.0003	.015	.0003	.0015	.0007	.003	.007	d	.003	.007	.0007	.003	.0007	d	.007	.0015	.003	.0003	.03
2-H	Qbt_6	58	M	M	1.5	.15	.3	3	3	.15	.03	.03	.0003	.015	0	.0007	.0003	.003	.007	d	.003	.007	.0003	.003	.0007	d	.007	.0015	.003	.0003	.03
2-U	Qbt_6	52	M	M	1.5	.07	.3	3	3	.15	.03	.03	.00015	.015	0	.0007	.0003	.003	.007	d	.003	.007	0	.003	0	0	.007	.0007	.003	.0003	.03
2-Y	Qbt_5	78	M	7	1.5	.07	.15	3	3	.07	.03	.015	.0003	.015	0	.00015	.0003	.0015	.015	d	.007	.007	0	.003	0	0	.003	.0007	.007	.0007	.03
CH-2	Qbt_4	130-132	M	M	.7	.07	.3	3	3	.07	.07	.015	.0003	d	0	.00015	.00015	.003	.003	0	.003	0	0	.0015	0	0	.003	0	.003	.0003	.015
3-C	Qbt_6	58	M	M	1.5	.15	.3	3	3	.15	.03	.03	.0003	.03	0	.0007	.0003	.0015	.015	d	.003	.015	.0003	.003	.0007	d	.007	.0007	.007	.0007	.03
3-Y	Qbt_4	105	M	M	1.5	.15	.3	3	3	.15	.03	.03	.0003	.015	0	.0003	.0003	.003	.007	d	.003	.007	.0003	.007	d	d	.007	.0007	.003	.0003	.03
4-A	Qbt_4	85	M	7	.7	.03	.15	3	3	.07	.03	.015	.0003	.015	0	d	.00015	.003	.007	d	.003	d	0	.003	0	0	.003	0	.003	.0003	.03
4-Y	Qbt_4	78	M	M	.7	.07	.3	3	3	.07	.03	.015	.0003	.015	0	d	.0003	.003	.007	0	.003	.007	0	.0015	0	d	.003	0	.003	.0003	.03

Analyst: R. G. Havens

Symbols used: M - Major constituent; i.e. greater than 10 percent.

0 - Constituent analyzed but not found.

d - Constituent barely detectible, concentration uncertain.

Note: The following constituents were analyzed but not found: P, Ag, As, Au, B, Bi, Cd, Dy, Er, Eu, Gd, Ge, Hf, Hg, Ho, In, Ir, Li, Lu, Os, Pd, Pr, Pt, Re, Rh, Ru, Sb, Sm, Ta, Tb, Te, Th, Tl, Tm, U, W, Zn.

Approximate visual detection limits (Revised August 1956) for the elements determined by the semiquantitative spectrographic methods

Element	Percent	Element	Percent	Element	Percent	Element	Percent	Element	Percent	Element	Percent	Element	Percent	Element
Si	0.002	Al	0.001	Fe	0.0008	Mg	0.0005	Ca	0.005	Na 1/	0.05 (0.0005)	K 1/	0.7 (0.002)	Ti
P	.2	Mn	.0002	Ag	.0001	As 1/	.1 (.01)	Au	.002	B	.002	Ba	.0002	Be
Bi	.001	Cd	.005	Ce	.02	Co	.0005	Cr	.0001	Cs 1/	2 (0.02)	Cu	.0001	Dy
Er	.005	Eu	.05	Ga	.0002	Gd	.005	Ge	.001	Hf	.01	Hg 1/	1 (0.002)	Ho
In	.001	Ir	.01	La	.002	Li 1/	.02 (0.00006)	Lu	.01	Mo	.0005	Nb	.001	Nd
Ni	.0003	Os	.01	Pb	.001	Pd	.0003	Pr	.05	Pt	.003	Rb 1/	10. (0.006)	Re
Rh	.005	Ru	.01	Sb	.01	Sc	.0005	Sm	.001	Sr	.0002	Sn	.01	Ta
Tb	.1	Te 1/	.1 (.01)	Th	.02	Tl	.01	Tm	.01	U	.05	V	.001	W
Y	.001	Yb	.0005	Zn	.02	Zr	.001							

1/ A different exposure is required for the detectabilities shown in parentheses.

Note: Some combinations of elements affect the detectabilities. Approximate values are given. In unusually favorable materials, concentrations somewhat lower than the values given may be detected. In unfavorable materials the given detectabil

The following ranges in permeability were obtained by analysis of samples (table 17) from units 1B, 2, 3, 4, 5, and 6 of the Tshirege Member: 0.04-22 gpd per square foot for consolidated samples, 34-59 gpd per square foot for unconsolidated samples that were repacked in permeameter cylinders; specific yield 0.6-42.6 percent; porosity 19.3-54.7 percent; specific retention 11.3-27.3 percent; dry unit weight 1.17-2.05 grams per cubic centimeter; specific gravity (grain density) 2.32-2.58 grams per cubic centimeter; moisture content 0.2-36.3 percent by volume, 0.1-43.2 percent of dry weight; and approximate pH 7.5-7.9. Mechanical analyses made on seven unconsolidated samples from units 1B, 3, and 5 (table 24) indicated rather large ranges in particle sizes from clay through medium gravel. Samples from units 1B and 3 probably have little value as these are mostly bit-cut samples. Samples from unit 5 are unconsolidated samples obtained while mapping large-diameter holes. Pore-size distribution of 10 samples from units 4, 5, and 6 are shown on table 25.

The porosity and permeability of the Tshirege Member depends upon the degree of welding and amount of weathering of individual ash flows. Joints and fractures are numerous, especially in the welded units. The joints and fractures that are open probably would transmit water rapidly.

Table 17.--Results of hydrologic laboratory analyses of the Tshirege member of the Bandelier tuff at TA-49, Los Alamos County, N. Mex.

Laboratory sample No.	Field No.	Stratigraphic unit	Depth (feet)	Approximate pH	Moisture content: dry weight (percent)	Moisture content: volume (percent)	Specific gravity	Dry unit weight (g per cc)	Specific retention (percent)	Porosity (percent)	Specific yield (percent)	Coefficient of permeability (gpd per square foot)
60-HM 11[c]	CH-1	Qbt_6	15	7.5			2.57	1.19	19.2	53.7	34.5	2
15[c]	CH-3	Qbt_6	20		1.5	1.9	2.58	1.24	27.3	51.9	24.6	.1
59-HM 197	2-W	Qbt_6	30		.6	.8	2.57	1.28	16.3	50.2	33.9	3
197[h]	2-W	Qbt_6	30		-	-	-	-	-	-	-	[a]3
60-HM 6	2-O	Qbt_6	30		1.0	1.1	2.58	1.17	16.2	54.7	38.5	6
6[h]	2-O	Qbt_6	30		-	-	-	-	-	-	-	[a]5
7	1-A	Qbt_6	30		.6	.8	2.58	1.26	17.7	51.2	33.5	4
7[h]	1-A	Qbt_6	30		-	-	-	-	-	-	-	[a]4
21	3-A	Qbt_6	30	7.8	5.9	4.7	2.58	1.21	23.0	53.1	30.1	.9
21[h]	3-A	Qbt_6	30									[a].2
18[c]	CH-4	Qbt_6	33	7.8			2.57	1.31	20.5	49.0	28.5	1
1	4-U	Qbt_6	40				2.53	1.33	20.0	46.6	26.6	2
1[h]	4-U	Qbt_6	40									[a]2
59-HM 196	2-D	Qbt_6	55		2.0	3.0	2.56	1.50	16.8	41.4	24.6	.1
196[h]	2-D	Qbt_6	55									[a]2
60-HM 9	2-F	Qbt_6	56		1.9	2.6	2.57	1.38	15.4	46.3	30.9	4
9[h]	2-F	Qbt_6	56									[a]3
8	1-A	Qbt_6	58		3.0	4.7	2.55	1.58	19.8	38.0	18.2	.9
8[h]	1-A	Qbt_6	58									[a]1
22	3-A	Qbt_6	58		.8	1.2	2.57	1.48	19.5	42.4	22.9	1
22[h]	3-A	Qbt_6	58									[a].8
2	4-U	Qbt_6	60				2.58	1.26	17.9	51.2	33.3	1
59-HM 198	4-A	Qbt_6	64		6.6	8.7	2.57	1.32	24.6	48.6	24.0	.9
198[h]	4-A	Qbt_6	64									[a]2
60-HM 10	4-U	Qbt_5	61				2.55	1.57				[b]59
59-HM 199	4-A	Qbt_5	66				2.58	1.47				[b]34
60-HM 3	4-U	Qbt_4	67		.3	.4	2.56	1.17	11.7	54.3	42.6	13
3[h]	4-U	Qbt_4	67									[a]13
5	4-U	Qbt_4	82		.3	.4	2.57	1.33	14.7	48.2	33.5	4
5[h]	4-U	Qbt_4	82									[a]4
23	3-A	Qbt_4	88	7.7	.5	.7	2.57	1.33	11.6	48.2	36.6	5
23[h]	3-A	Qbt_4	88									[a]8
4	4-U	Qbt_4	104		1.3	2.2	2.54	1.71	21.8	32.7	10.9	.3
4[h]	4-U	Qbt_4	104									[a].4
29	Alpha	Qbt_3	135	7.9	2.2	2.9	2.56	1.32	14.2	48.4	34.2	22
28	Alpha	Qbt_3	175		.2	.3						
16[c]	CH-3	Qbt_2	195		.1	.2	2.54	1.59	11.3	37.4	26.1	2
13[c]	CH-2	Qbt_2	197				2.55	1.83	12.3	28.2	15.9	.2
19[c]	CH-4	Qbt_2	202		.1	.2	2.54	2.05	17.3	19.3	2.0	.04
17[c]	CH-3	Qbt_2	205		.1	.2	2.55	2.02	20.2	20.8	.6	.08
31[c]	CH-2	Qbt_2	255		.1	.2	2.57	1.84	20.8	28.4	7.6	.2
12[c]	CH-1	Qbt_2	265	7.7			2.56	1.85	14.4			.2
14[c]	CH-2	Qbt_2	270				2.55	1.84	13.9	27.8	13.9	.3
20[c]	CH-4	Qbt_2	274	7.7	.1	.2	2.56	1.81	17.2	29.3	12.1	.2
32[c]	CH-2	Qbt_{1B}	295	7.9	.1	.2	2.56	1.81	17.3	29.3	12.0	.2
24	Beta	Qbt_{1B}	10		22.9	27.0						
25	Beta	Qbt_{1B}	65		14.1	13.3						
30	Beta	Qbt_{1B}	105		17.8		2.32					
26	Beta	Qbt_{1B}	135	7.7	43.2	36.3						[b]50
27	Beta	Qbt_{1B}	180		16.3	17.3						

a Horizontal permeability parallel to axes of 6-inch sidewall cores.

b Repacked samples

c Vertical cores

h Horizontal cores cut from larger samples

Unit 1A

Physical characteristics

Unit 1A consists of light-gray to light-pinkish-gray, pumiceous, friable rhyolite tuff that contains quartz and sanidine crystals and fragments, and rhyolite and latite fragments, and minor amounts of dark-green mafic minerals. Some of the sanidine fragments are stained dark-brown.

Unit 1A overlies the Otowi Member and does not crop out at TA-49. Unit 1A is 214 feet thick in well DT-9, 196 feet thick in DT-10, and 156 feet thick in DT-5P. It is an ash flow, the eastern end of which is deposited in a depression in older rocks beneath TA-49. It thickens southeastward from TA-49 then thins eastward and wedges out between unit 1B of the Tshirege Member and Otowi Member of the Bandelier Tuff (fig. 5).

Water-bearing characteristics

Unit 1A is dry at TA-49. Little is known of its potential water-bearing properties; however, mud circulation was maintained through this unit in well DT-5A, and its fracture permeability must be relatively low.

Joints and fractures are probably present in unit 1A, but because it is a friable unit they probably are closed or only slightly open. Water percolating through open joints and fractures in the unit probably would cause the alteration of the tuff to clay and would eventually seal them.

Unit 1B

Physical characteristics

Unit 1B is a light-gray to very light-orange rhyolite tuff that contains quartz and feldspar crystals and fragments, large to small pumice fragments, and gray subrounded rhyolite and latite ~~rock-~~ fragments as much as cobble size. Unit 1B is an explosion breccia. Cuttings, samples, and outcrops show yellow weathering stains around quartz crystals and fragments. The pumice weathers to a brown clay. Stratification is lacking, but rock fragments and pumice commonly occur in lenses. The contact with the overlying unit 2 is irregular.

Beta hole, in Water Canyon, penetrated 172 feet of unit 1B (table 18). Drill cuttings from the bottom 75 feet of the boring contain nodules of brown clay as much as 6 inches long, which probably are the weathered product of large pumice fragments. The clay nodules are platy and fibrous near the center and grade to highly altered cellular pumice at the edges.

Table 18.--Sample log of Beta hole

Drilled by rotary bucket

Total depth 180 feet

Completed February 25, 1960

Altitude of land surface 6,801 feet

	Thickness (feet)	Depth (feet)
Recent alluvium ----------	8	8
Bandelier Tuff		
Tshirege Member		
Unit 1B:		
Tuff, light-pinkish-tan to light-gray, pumiceous, friable; quartz and sanidine fragments and crystals up to granule size; mafic mineral stains and some mafic minerals; devitrified pumice fragments up to ½ inch in length; light-yellowish pumice; gray glassy pumice; dark-gray pumice fragments; some rhyolite ~~rock~~ fragments; samples from 61 to 81 feet are light red. Samples from 105 to 180 feet contain brown nodules of clay up to 6 inches in length; these appear to be large pumice fragments that altered to clay; the clay appears platy in places and near edge grades into highly altered cellular pumice; some gray rhyolite and light-red latite ~~rock~~ fragments are found in this interval ----------	~~172~~	~~180~~

Table 18.--Sample log of Beta hole - Continued

	Thickness (feet)	Depth (feet)
Bandelier Tuff - Continued		
Tshirege Member - Continued		
Drilling stopped at 180 feet in a rhyolite and latite tuff breccia, edges of fragments subrounded; ground mass a light-brownish-tan, pumiceous, friable tuff ---------	172	180

Unit 1B weathers to a light pink or orange and is pitted by the weathering out of large pumice fragments. On the north wall of Water Canyon unit 1B is characterized by a steep slope that is broken by a bench about 20 feet below the contact with unit 2. This bench extends from TA-49 eastward to Highway 4.

At TA-49 unit 1B ranges in thickness from 195 feet in core hole 2 to 248 feet in wells DT-9 and DT-10. Core holes 1, 3, and 4 are bottomed in the unit and penetrated 217 feet, 25 feet, and 15 feet, respectively. Wells DT-5, DT-5P, and DT-5A penetrated 203 feet of unit 1B.

Water-bearing characteristics

Free water was not found in unit 1B at TA-49, but cuttings from unit 1B from Beta hole contained considerably more moisture than samples from lithologically similar units higher in the section.

Interstices in the matrix of unit 1B probably are small and its permeability is low, although locally the porosity may be relatively high. Clay nodules in cuttings from Beta hole in Water Canyon contained 45 to 60 percent moisture by volume, but other samples, composed mostly of ash, contained 13 to 36 percent moisture (table 17). Moisture content of a core from unit 1B, core hole 2, is less than 1 percent.

The section of unit 1B penetrated by the Beta hole is weathered and highly altered due to water infiltrating from the canyon floor.

Unit 2

Physical characteristics

Unit 2 is a light-pinkish-gray to purplish-gray rhyolite tuff. It is hard, welded, and contains coarse sand- to granule-size phenocrysts of quartz and sanidine crystals and fragments, light-gray to gray rhyolite and latite rock fragments, and gray pumice fragments up to ½-inch long in a fine-grained, glassy ash. The outcrop of unit 2 stands as cliffs, which weather to a light brownish gray, and consists of two beds of about equal thickness separated by a slight notch. Unit 2 exhibits columnar jointing in the form of hexagonal pinnacles standing 10 to 20 feet in height and from 5 to 8 feet in diameter, west of Beta hole in Water Canyon.

Unit 2 ranges in thickness from 82 feet in core hole 3 to 111 feet in core hole 4 at TA-49. Thicknesses of unit 2 penetrated in other core holes and wells are as follows: core hole 1, 94 feet; core hole 2, 101 feet; well DT-5, 100 feet; well DT-9, 98 feet; and well DT-10, 90 feet. In the measured section in Water Canyon unit 2 is 100 feet thick. Structure contours on the top of unit 2 indicate a gentle 1- to 2-degree dip southeasterly with an undulating surface (fig. 7).

Figure 7.--Structure contours on unit $_4bt_2$ Tshirege Member of the Bandelier Tuff, TA-49, Los Alamos County, N. Mex.

Water-bearing characteristics

Unit 2 is dry at TA-49. The natural moisture content of the rock in unit 2 is about 0.2 percent by volume, based on five samples from core holes 2, 3, and 4. The porosity of the five samples from unit 2 that were tested range from 19 to 37 percent by volume and specific retention ranged from 11 to 21 percent by volume (table 17). Permeability was 0.04 to 2 gpd per square foot.

The fill used in building the leveled area where Gamma and Gamma "A" holes are located is composed of broken tuff and soil. Gamma hole penetrated about 6 feet of fill, and Gamma "A" hole penetrated about 10 feet of fill overlying unit 2. Spring snowmelt percolated into the fill, and perched above welded tuff of unit 2. This perched water ran into Gamma and Gamma "A" holes. Gamma hole is 2 feet in diameter and 7.15 feet deep. It was dry when drilled on February 26, 1960, but on May 2, 1960 the water level was 5.85 feet. Gamma "A" hole is 4 inches in diameter and 54 feet deep. It was dry when drilled on February 26, 1960, and on March 30 the water level was 43.6 feet. The hole was dry on May 2, 1960. Gamma "A" hole is cased with 10 feet of 4-inch steel casing which extends 1.90 feet above land surface. The water gained entry into the well through 1.90 feet of uncased fill above unit 2.

Although the permeability of unit 2 is low, the open joints and fractures in it would transmit water rapidly. Columnar jointing is present locally in the outcrop. A core taken at 261 feet in core hole 1 contained a nearly vertical joint plated with clay which indicates that water had percolated through joints and fractures in the rocks to fairly great depth. Weathering of the tuff adjacent to the joint probably occurred during the deposition of unit 5, which is a fluvial sand. The low moisture content indicates that water presently is not moving through unit 2.

Unit 3

Physical characteristics

Unit 3 is a friable and pumiceous light-gray rhyolite tuff that contains medium to very coarse sand-size phenocrysts of sanidine and quartz crystals and fragments, gray and white devitrified pumice fragments up to ½-inch in length, an abundance of light-gray pumice, and gray rhyolite and latite rock fragments in a fine-grained glassy ash matrix. Some quartz fragments are coated with a yellow weathering stain and others are clear. Sanidine fragments appear to be pitted. Surface exposures of unit 3 are very poor. The unit weathers to a slope on which soil has developed. The best description of unit 3 is based on cuttings from Alpha hole (table 19). Core recovery from the unit was poor.

At TA-49 the thickness of unit 3 ranges from 40 feet at the measured section in Water Canyon to 76 feet in core hole 1. Thicknesses of the unit penetrated in other borings are as follows: DT-9, 58 feet; and DT-10, 57 feet.

Table 19.--Sample log of Alpha hole

Drilled by rotary bucket

Total depth 189 feet; diameter 2 feet

Completed February 6, 1960

Altitude of land surface 7,125 feet

	Thickness (feet)	Depth (feet)
Bandelier Tuff		
Tshirege Member		
Unit 6:		
Tuff, light-gray, moderately welded; contains fine- to medium-size quartz and sanidine crystals and fragments; yellowish-tan to gray pumice and gray devitrified pumice fragments; light-red latite and gray rhyolite rock fragments in a fine-grained light-gray ash matrix. Hard layer was encountered at 54 feet	76	76
Unit 5:		
Sand, light-gray, friable; fine- to coarse-size quartz and sanidine fragments subrounded; quartz has coating of yellow weathering stain; fragments of tuff and pumice	2	78

Table 19.--Sample log of Alpha hole - Continued

	Thickness (feet)	Depth (feet)
Bandelier Tuff - Continued		
Tshirege Member - Continued		
Unit 4:		
Tuff, light-gray; medium to coarse quartz and sanidine crystals and fragments; gray devitrified pumice; light-gray rhyolite rock fragments, subrounded; friable zone 78 to 85 feet; moderately welded 85 to 128 feet ----------	50	128
Unit 3:		
Tuff, light-gray, friable; medium-size quartz and sanidine crystals and fragments; gray and white devitrified pumice fragments up to ½ inch in length; gray rhyolite rock fragments, pebble size; coating of yellow weathering stain around quartz fragments; large amount of very light-gray pumice; samples from 166 to 189 are pinkish-gray and moderately welded ----------	61	189

Water-bearing characteristics

Unit 3 is dry at TA-49. Natural moisture content ranged from 0.2 to 2.9 percent by volume (table 17). One chunk sample had a porosity of 48 percent by volume and a permeability of 22 gpd per square foot.

The few joints that can be seen on the outcrop are filled with brown clay, produced by weathering of the tuff. Joints at depth presumably are open because drilling fluid was lost in this unit. The maintenance of circulation of either air or mud during drilling was difficult. Only a small amount of cuttings was recovered from unit 3; the rest were probably carried into open joints.

Unit 4

Physical characteristics

Unit 4 is a light-gray to light-pinkish-gray rhyolite tuff that contains phenocrysts and fragments of medium sand- to granule-size quartz and sanidine crystals in a moderately welded ash matrix. Also present are fragments of pink to light-gray rhyolite and dark-gray pumice. Some of the pumice fragments are devitrified. Unit 4 is not bedded at the measured section in Water Canyon; however, lenses of disk-shaped dark-gray pumice fragments as much as 6 inches long and 2 inches thick are present in a dense pinkish-gray tuff.

In the outcrop the moderately welded tuff contains clay filled joints and fractures. In the large-diameter holes, joints are open as much as ½ to 2 inches. Air blowing from open joints in response to declining barometric pressure indicates that the joints are interconnected in hole 4-U. Parts of this unit form cliffs in the canyon walls.

Four samples from unit 4 of the Tshirege Member of the Bandelier Tuff were analyzed petrographically by C. S. Ross of the Geological Survey (written communication, July 7, 1960). Ross recalculated the proportions of phenocrysts to represent proportion by weight. The following are results of these analyses.

Sample from Hole 4-Y, depth 78 feet

Pore space about 30 percent

Phenocrysts about 27 percent by weight

Sanidine 15 percent

Quartz 10 percent

Magnetite 1± percent

Pyroxene 0.5± percent

Groundmass is typical devitrified, welded tuff showing usual submicroscopic intergrowth of cristobalite and feldspar. Gas-phase reaction resulted in additions to sanidine phenocrysts, and tridymite and feldspar in cavities. Dark porous areas up to 15mm in diameter represent pumice fragments. A few small areas of andesitic rock are present.

Sample from Hole 4-A, depth 85 feet

Pore space about 30 percent

Phenocrysts about 32 percent by weight

Sanidine 22 percent

Quartz 11 percent

Pyroxene 0.7 percent (ortha, dominant; clino, present)

Magnetite 1.0 percent

Groundmass is devitrified shards containing unusual feldspar-cristobalite aggregates. Vesicular cavities contain gas-phase tridymite and feldspar. The sanidine phenocrysts contain secondary addition of feldspar (gas-phase) material. The sample contains an unusually large proportion of pumice grains.

Sample from ~~of~~ Core hole 3, depth 100 feet

Pore space about 30 percent

Phenocrysts about 38 percent by weight

Sanidine 24 percent

Quartz 12 percent

Pyroxene (largely clino) 1 percent

Magnetite 1 percent

No zircon observed

Groundmass contains abundant tridymite and gas-phase, secondary growth on sanidine. Devitrification products are unusually coarse grained. Sample contains inclusions of andesite.

Sample from Core hole 2, depth 130 to 132 feet

Pore space about 30 percent

Phenocrysts about 34 percent by weight

Sanidine 30 percent

Quartz 12 percent

Magnetite 1± percent

Pyroxene 0.5 percent

The groundmass is a typical devitrified welded tuff, the devitrification product being cristobalite and feldspar. Gas-phase reaction has resulted in secondary growths on the sanidine and development of tridymite and feldspar in vesicules. Plate-like crystals of tridymite are unusually large as are the gas-phase and devitrification minerals.

~~132~~ 128 D

Water-bearing characteristics

Unit 4 was dry at TA-49. Natural moisture content was very low, ranging from 0.4 to 2.2 percent by volume. The porosity of four samples of unit 4 ranged from 32.7 to 54.3 percent by volume, and specific retention ranged 11.6 to 21.8 percent by volume. The porosity decreased with depth due to the denser welding within the flow. The specific retention increased with a decrease in porosity due to a decrease in pore size which would tend to hold water under tension. Vertical permeabilities ranged from 13 gpd per square foot for the more porous tuff to 0.3 gpd per square foot for the less porous tuff found lower in the section. Horizontal permeabilities ranged from 0.4 to 13 gpd per square foot and decreased with depth. The horizontal permeability in one sample from hole 3-A was 8, and vertical permeability was 5 gpd per square foot (table 17). This difference of permeability may be related to possible near horizontal orientation of interstices in the ash-flow rock.

Joints in outcrops of unit 4 contain weathered brownish clay. Joints in the unit in large diameter holes varied from closed to open. In the upper part of the unit, joints are filled with sand from unit 5, indicating that these joints and fractures were open during the deposition of unit 5. In some of the large-diameter holes (figs. 15, 17, and 18) the tuff of unit 4 is friable and weathered below the contact with unit 5.

If water were transmitted by percolation to unit 5, it would further percolate downward through the permeable sand-filled joints to the open joints.

Unit 5

Physical characteristics

Unit 5 is friable water-laid medium to coarse sand composed of worn quartz and sanidine crystals and fragments of reworked tuff as large as boulder size.

Topset and foreset bedding is well developed. Some limonite stains and a few stringers of brown clay are oriented with the cross-bedding in the unit (fig. 11). Unit 5 weathers to form a

Figure ~~11~~ 12.--Water-laid sand of unit Qbt_5 of the Tshirege Member of the Bandelier Tuff underlain by weathered iron-stained unit Qbt_4, southeast wall of west hole in Area 10, TA-49, Los Alamos County, N. Mex.

notch on cliffs between the underlying and overlying units.

Figure 8.- Sand Unit 5 in Shaft at Area 11

Figure 9.- Stand Unit 5 in Shoshone Area 11

Photograph by Roy Stone
Los Alamos Scientific Laboratory

Figure 10.--Outcrop of unit Qbt_5 of the Tshirege Member of the Bandelier Tuff at head of a small canyon 0.4 mile northwest of well DT-9, TA-49, Los Alamos County, N. Mex.

ST 1326

Photograph by Roy Stone
Los Alamos Scientific Laboratory

Figure 11.--Water-laid sand of unit Qbt_5 of the Tshirege Member of the Bandelier Tuff underlain and overlain by weathered iron-stained ash flows. Southeast wall of west hole in area 10, TA-49, Los Alamos County, N. Mex.

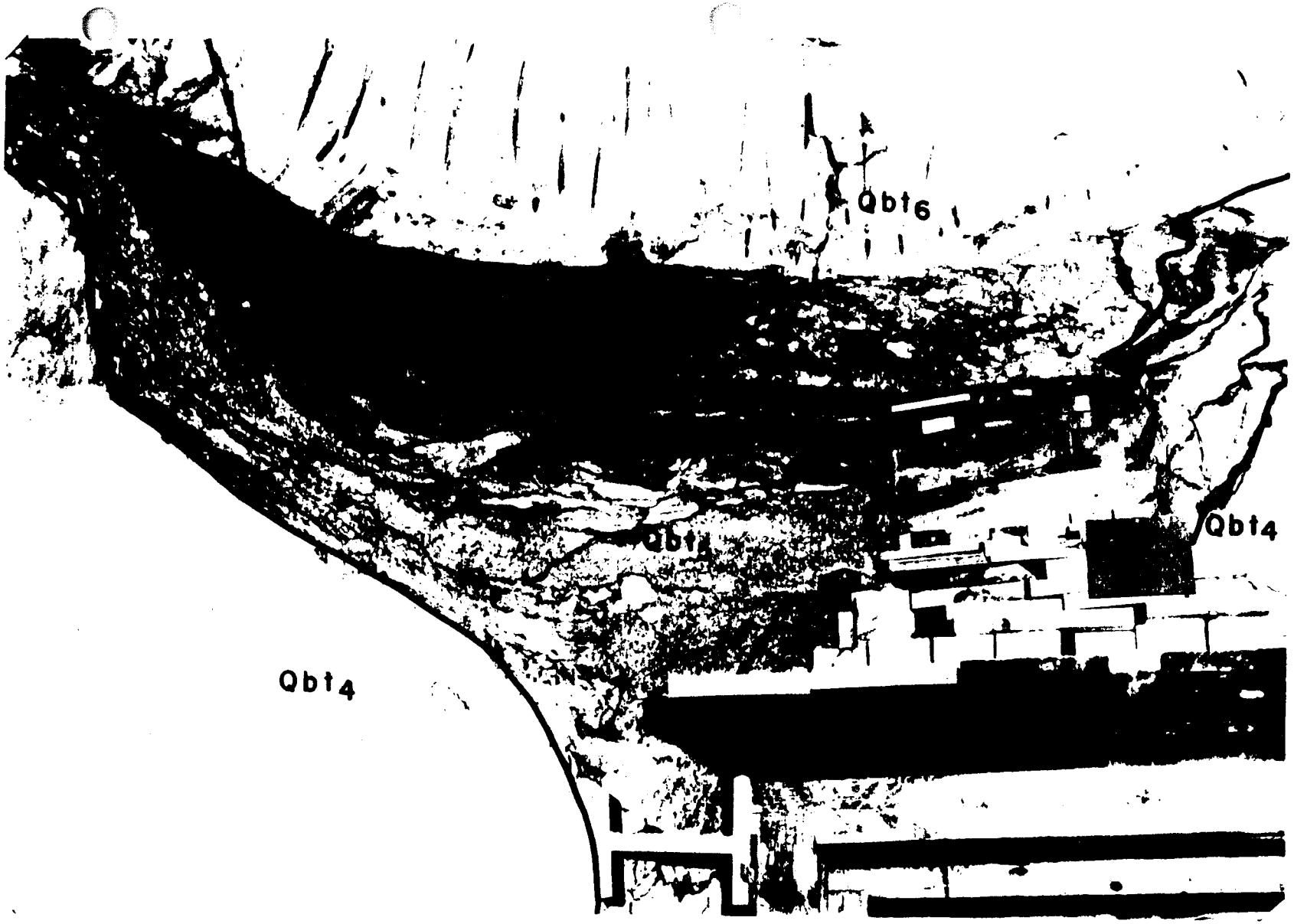

Photograph by Roy Stone
Los Alamos Scientific Laboratory

Figure 12.--Stream channel in unit Qbt_4 of the Tshirege Member of the Bandelier Tuff filled with sand of unit Qbt_5. East wall of west hole in area 10, TA-49, Los Alamos, N. Mex.

A sample from unit 5 of the Tshirege Member of the Bandelier Tuff was analyzed petrographically by C. S. Ross of the Geological Survey (written communication, July 7, 1960). Ross recalculated the proportions of phenocrysts to represent proportion by weight. The following is the result of the analysis.

Hole 2-Y, depth 78 feet

Sample is about one-third phenocrysts

Sanidine 22 percent

Quartz 11 percent

Magnetite 1± percent

Pyroxene 0.5± percent

THE fine fraction is devitrified glass composed dominantly of sub-microscopic intergrowths of cristobalite and feldspar.

There are irregular zones around sanidine phenocrysts which may represent an addition of material by gas-phase reaction. In pore spaces, tridymite, sanidine, and slender needles of hornblende have been formed.

At TA-49 the thickness of unit 5 ranges from 0 in large-diameter hole 4-Y (fig. 18) to about 4 feet in a channel intercepted by large-diameter holes in Area 10. Structure contours on top of unit 5 indicate a dip of about 1 degree to the southeast (fig. 13).

Figure 13.--Structure contours on the top of unit bt_5 of the Tshirege Member of the Bandelier Tuff, TA-49, Los Alamos County, N. Mex.

Water-bearing characteristics

Unit 5 was dry at TA-49, and there is little evidence to indicate that the unit has transmitted water in recent times.

Unit 5 is a permeable sand composed mainly of well-sorted quartz and sanidine crystals and crystal fragments. Joints and fractures in the overlying unit 6 are closed and terminate at or near the contact. Only a few fractures transect the sand and continue into unit 4 where most of them are sand filled (fig. 18).

Tuff adjacent to joints and fractures below the sand-filled zone is weathered as much as $\frac{1}{4}$ to 1 inch on each side. Water that caused these weathered joint and fracture surfaces probably moved through the joints and fractures during the deposition of unit 5.

Unit 5 has a permeability of 34 to 59 gpd per square foot (table 17) and should transmit water readily. The abundance of sand-filled and open fractures in the upper part of unit 4 would tend to transmit the water downward rapidly.

Unit 6

Physical characteristics

Unit 6 is a light-gray to pinkish-gray rhyolite tuff. It is a moderately welded ash-flow tuff containing phenocrysts of quartz and sanidine that range in size from medium to coarse sand, gray devitrified pumice fragments as much as 3/4-inch in diameter; and gray to light-brown rhyolite and latite rock fragments. Some of the quartz crystals are clear and have well developed crystal faces and some are dipyramidal in crystal form and contain white globular inclusions. Mineralogic analyses indicate a small percent of magnetite and pyroxene and some clay which is probably montmorillonite (table 14). The sand-size mafic minerals are brownish yellow as the result of weathering. Some horizontal sheeting occurs at the outcrops. Curvilinear joints were present in the large-diameter holes and in the outcrops (fig. 14). The

Figure 14.--Outcrop of curved joint face in unit bt_6 of the Tshirege Member of the Bandelier Tuff. North side of New Mexico Highway 4, about 1.5 miles west of the entrance to TA-49, Los Alamos County, N. Mex.

unit unconformably overlies unit 5 and forms cliffs. It caps the mesa at TA-49.

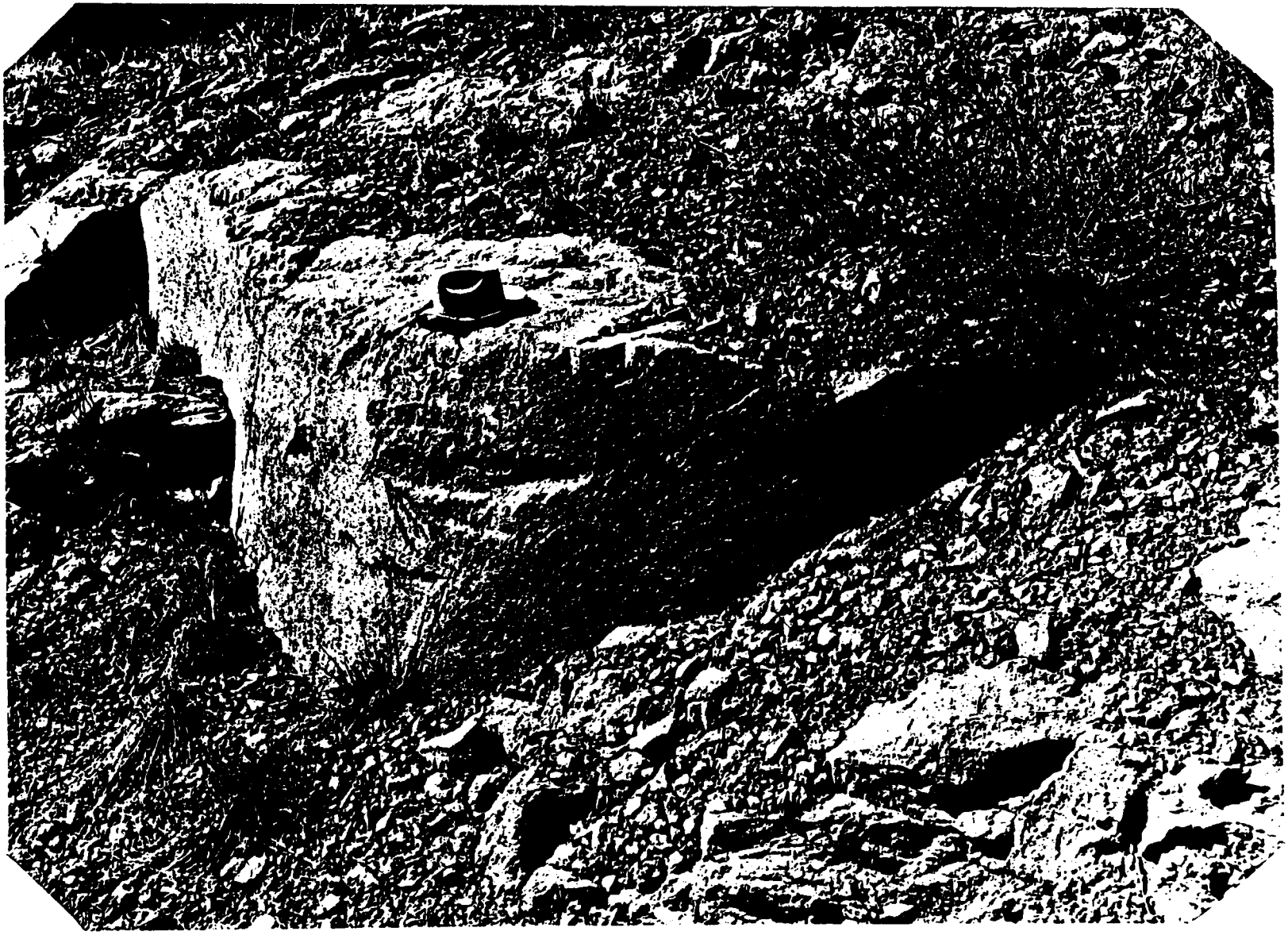

Photograph by Roy Stone, Los Alamos Scientific Laboratory

Figure 14.--Outcrop of curved joint face in unit Qbt_6 of the Tshirege Member of the Bandelier Tuff. North side of New Mexico Highway 4, about 1.5 miles west of entrance to TA-49, Los Alamos County, N. Mex.

The joints in unit 6 generally are of two types: master joints, THAT having northerly trends and nearly vertical attitudes, and minor joints (figs. 15, 16, 17, and 18) THAT having varying trends and dips

Figure 15.--Maps of walls of selected large-diameter holes in Area 1, TA-49, Los Alamos County, N. Mex.

16.--Maps of walls of selected large-diameter holes in Area 2, TA-49, Los Alamos County, N. Mex.

17.--Maps of walls of selected large-diameter holes in Area 3, TA-49, Los Alamos County, N. Mex.

18.--Maps of walls of selected large-diameter holes in Area 4, TA-49, Los Alamos County, N. Mex.

varying from nearly vertical to horizontal.

The master joints are tectonic in origin, and probably are related to major faults of the region, such as the Pajarito fault west of TA-49. Almost every large-diameter hole intersected at least one master joint that is continuous through unit 6, and some that cut through unit 5 into unit 4. Many minor joints terminate at the master joints. Near the surface the master joints are filled with clay, most of which was formed in place by weathering of the tuff, but some of the clay may have washed in from the soil zone above. At depth these joints commonly are open and many have a thin clay plate on both faces of the open joint. Most of these clay plates are altered tuff adjacent to joint faces, caused by water that formerly percolated through the open joints.

The minor joints probably were caused mainly by cooling of the volcanic ash flow, although some of them probably are related to faulting and gentle folding. A nearly horizontal brecciated zone is present in unit 6 about 15 to 20 feet below the surface. The rocks in this zone are broken by numerous irregular minor joints, most of which are open.

Joints could not be projected from a hole to another 25 feet away because of the change in strike and dip and numerous intersections of one joint with others. In some cases it was impossible to match joints on opposite walls of a hole due to the change in strike and intersections. However, interconnection of joints between holes was evident during various experiments in the area conducted by the University of California.

Seven samples from unit 6 of the Tshirege Member of the Bandelier Tuff were analyzed petrographically by C. S. Ross (written communication, July 7, 1960). Ross recalculated the proportions of phenocrysts to represent proportions by weight. The following is a discussion of each of these analyses.

Sample from core hole 1, depth 45.5 feet

Pore space about 30 percent

Phenocrysts about 20 percent by weight

Sanidine 12 percent

Quartz 6 percent

Magnetite 1± percent

Pyroxene 0.5± percent

Groundmass is typical devitrified welded tuff. The devitrification products are very fine grained, but show the typical cristobalite-feldspar structure. Cavities contain radial groups of feldspar and tridymite. The rock contains a few areas of altered andesite.

Sample from core hole 2, depth 65 feet

Typical welded tuff differing from others in no essential way.

Phenocrysts about 24 percent by weight

Sanidine 14 percent

Quartz 7 percent

Pyroxene (clino and ortho) 1 percent

Magnetite 1 percent

Pink, well-rounded zircon

Feldspar and tridymite in cavities

Sample from hole 2-U, depth 52 feet

Pore space about 30 percent

Phenocrysts about 27 percent by weight

Sanidine 20 percent

Quartz 5 percent

Magnetite 1 percent

Pyroxene (clino, dominant; ortho, present)

The groundmass is made up of shards which have been partly devitrified. There is some indication of gas-phase mineralization. Minute minerals, probably tridymite and feldspar, have developed in cavities and feldspar has been deposited on ~~ruins~~ RIMS of sanidine grains. The rock contains very small amounts of altered andesite grains.

Sample from hole 2-H, depth 30 feet

Pore space about 35 percent

Phenocrysts about 20 percent by weight

Sanidine 12 percent

Quartz 4 percent

Magnetite 1 percent

Pyroxene 0.5± percent

Groundmass is in part devitrified shards (feldspar and cristobalite). Brown birefracting clay-like material is probably montmorillonite, 15± percent of the groundmass. This is the only sample in the group which shows any alteration. All other changes are deuteric ones comprising devitrification and gas-phase reaction.

Sample from Hole 2-H, depth 58 feet

Pore space about 30 percent

Phenocrysts about 13 percent by weight

Sanidine 8 percent

Quartz 3 percent

Magnetite 1± percent

Pyroxene 0.5± percent (ortho, sparse; clino, dominant)

Trace of zircon

Much of the magnetite is intergrown with pyroxene. Some altered inclusions of an older andesitic rock are present. Groundmass is devitrified glass shards. Feldspar and tridymite occur in vesicular pore space. A little clay material has developed.

Sample from core hole 3, depth 54 feet

Similar to Area 2 core hole at a depth of 65 feet.

Sample from Hole 3-C, depth 58 feet

Pore space about 30 percent

Phenocrysts about 23 percent by weight

Sanidine 15 percent

Quartz 8 percent

A little secondary growth (gas phase) on the feldspar, but other gas-phase materials are too fine grained to be conspicuous. Groundmass material is devitrified glass. The devitrification products are cristobalite and feldspar. Tridymite and feldspar have developed as gas-phase products in cavities. The groundmass is in part made up of pumice fragments up to 10 mm in diameter which occur as darker colored porous areas.

The thickness of unit 6 at TA-49 ranged from zero near well DT-9, where it has been stripped away by erosion, to 80 feet near core hole 2. An isopach map (fig. 19) indicates that unit 6 is

Figure 19.--Isopach map of unit $\mathfrak{u}bt_6$ of the Tshirege Member of the Bandelier Tuff, TA-49, Los Alamos County, N. Mex.

thickest along the crest of the mesa at TA-49 where it has been eroded the least.

The base of the unit dips about 1 degree in a general southeasterly direction. The eroded upper surface of the unit along the crown of Frijoles Mesa slopes generally eastward at about 150 feet per mile.

Water-bearing characteristics

Unit 6 was dry at TA-49. Natural moisture content of samples ranged from 0.8 to 8.7 percent by volume (table 17), and porosity ranged from 38 to 54 percent by volume and specific retention from 15 to 27 percent by volume. The higher porosities were found in samples taken near the surface. Vertical permeability of samples ranged from 0.1 to 6 gpd per square foot. The horizontal permeability ranged from 0.2 to 5 gpd per square foot.

Joints in unit 6 near the surface are filled with clay. At depth many of these joints are open. The open joint face may appear unweathered as if jointing has just taken place, or the open joint face may contain a thin layer of clay, which is the product of weathering of the tuff. Tuff adjacent to these clay-plated joint faces are weathered to a light brown in zones from ½ to 5 inches wide parallel to the joint. The weathered zones also occur above horizontal and low angle joints indicating that water moved from the open joint into the tuff by capillarity. (See map of hole 2A, fig. 16.) Water probably percolated through these joints prior to and during the development of the soil.

Percolation of water could occur through open joints where the soil mantle has been stripped off leaving the tuff exposed. Movement would be rapid in the large interconnected joints filling the smaller joints where it would be absorbed by the tuff. Large joints that transect the unit would carry water rapidly into the underlying unit. Movement of water through the unjointed tuff would be slow as indicated by the range of permeabilities of 0.1 to 6 gpd per square foot.

Soil cover and related material

The mantle rock at TA-49 is characterized by a weathered zone, a water-laid pumice, and a soil zone. The top few feet of unit 6 is composed of broken, partly weathered tuff fragments in a matrix of clay. The weathered tuff grades upward into a clayey soil, except in Areas 2 and 10, where a layer of water-laid pumice occurs between the weathered zone and soil zone.

The weathered zone and soil zone are composed of materials weathered in place from the underlying tuff. The soil zone may contain some material that was washed into the area. The water-laid pumice was washed in during the early stages of development of the soil, and the overlying soil developed from it. The pumice layer occurs only locally and was deposited in a low area on Frijoles Mesa. The brown clay found throughout the soil mantle and associated materials probably is largely montmorillonite (table 14).

Weathered tuff

The weathered tuff is composed of angular tuff fragments that are slightly weathered in a matrix of brown clay, which contains a few roots. Thickness ranges from a few inches to 4 feet. The base of the weathered zone grades into and is irregularly disconformable with the top of the welded tuff of unit 6. Joints and cracks in the upper part of unit 6 are clay filled. Some clay filling is found in joints as deep as 65 feet below the land surface and some roots occur as deep as 40 feet (figs. 15, 16, 17, and 18).

The nearly impervious clay of the weathered zone virtually eliminates percolation through the zone. Weathered angular tuff fragments usually are isolated in the clay matrix of the zone and contribute little to bulk permeability of the zone.

Where roots in the zone are decayed, some water might move through the weathered zone via openings left by the roots. However, these openings should tend to close as water is introduced owing to the swelling properties of the clay.

Water-laid pumice

A layer of fairly well sorted, water-worn pumice fragments occurs in Areas 2 and 10 at TA-49. The layer is 2 to 4 feet thick and overlies the weathered tuff zone. The pumice is brownish gray to brown, has a cellular structure of frothy glass, and contains phenocrysts of quartz and sanidine. A few layers of clay, some intermixed brown clay, and roots are present in the pumice layer.

The layer of pumice probably is highly permeable because it is loosely consolidated and the fragments are well sorted and well rounded.

Where the pumice layer has been exposed by construction, as in the ditch adjacent to the road north of Area 2, water could infiltrate rapidly during wet weather. Probably this water would be perched temporarily on the underlying weathered zone. The pumice could also transmit some water laterally along the top of the weathered zone. A very small amount of water may percolate through the weathered zone into the tuff of unit 6; however, most of the water infiltrating the pumice layer probably is returned to the atmosphere by transpiration and evaporation.

Soil cover

A brown clay soil caps most of the mesa at TA-49. Percentages of various particle sizes in the soil are estimated as follows: 20 percent sand, 30 percent silt, and 50 percent clay. Sand-size particles are crystals and fragments of quartz.

The soil thickness seems to depend on the amount of water available for weathering the underlying tuff. The thickest soil zones are found along shallow, slow-draining ditches, streambeds, and relatively flat areas where water collects and stands. Soil thickness ranges from 0.5 to 9 feet in the shallow test holes drilled for soil-moisture studies. The greatest known thickness of soil (9 feet) at TA-49 occurs on a relatively flat area north of Area 6 (fig. 20).

Figure 20.--Thickness of soil and location of moisture-measurement test holes in TA-49, Los Alamos County, N. Mex.

The weathered zone could not be distinguished from the soil in logging the cuttings during drilling so the soil and weathered zone are logged as a single unit (figs. 21-43). The pumice layer is shown in test holes where it was penetrated in Areas 2 and 10. The thickness of soil is closely related to topographic slope; the soil thins rapidly away from the crown of the mesa, as indicated by the contours on figure 20.

Tubes formed by the decay of roots may transmit water through the soil zone. However, these openings would tend to close as they were wetted because of the swelling properties of the clay.

Percolation of water through the soil zone is small where the soil is relatively undisturbed and would take place only during exceptionally long wet periods, which are rare in the region.

Moisture distribution in the upland soil and underlying tuff

Twenty-three test holes were drilled for use in studying the soil thickness and distribution of moisture in the soil and underlying tuff of unit 6 of the Tshirege member of the Bandelier tuff. The test holes were located around test areas, roadside drainage ditches, and stream channels (fig. 20). Measurements were made of the moisture content of the soil and tuff at various depths by a neutron-scattering moisture probe. Moisture content determined by the probe ~~appear to be~~ are 1 to 2 percent higher than those made in the laboratory.

Measurements were made at least twice during the period from March to June 1960 and are depicted on graphs of moisture content and lithologic logs (figs. 21 ~~through~~ - 43).

Figures 21-43.--Graphs of moisture content and lithology in test holes, TA-49, Los Alamos County, N. Mex.

Figure 21.--Graph of moisture content and lithology in test hole 1M-2, TA-49, Los Alamos County, N. Mex.

Location.- 104 + 63.11 S 83 + 39.13 E
Depth.- 19 ft
Drilled.- 2/24/60
Altitude.- 7,170 ft

Explanation of log

- Backfill, tuff
- Soil, brown, clayey
- Tuff, brown
- Tuff, tan
- Tuff, gray or white
- Pumice

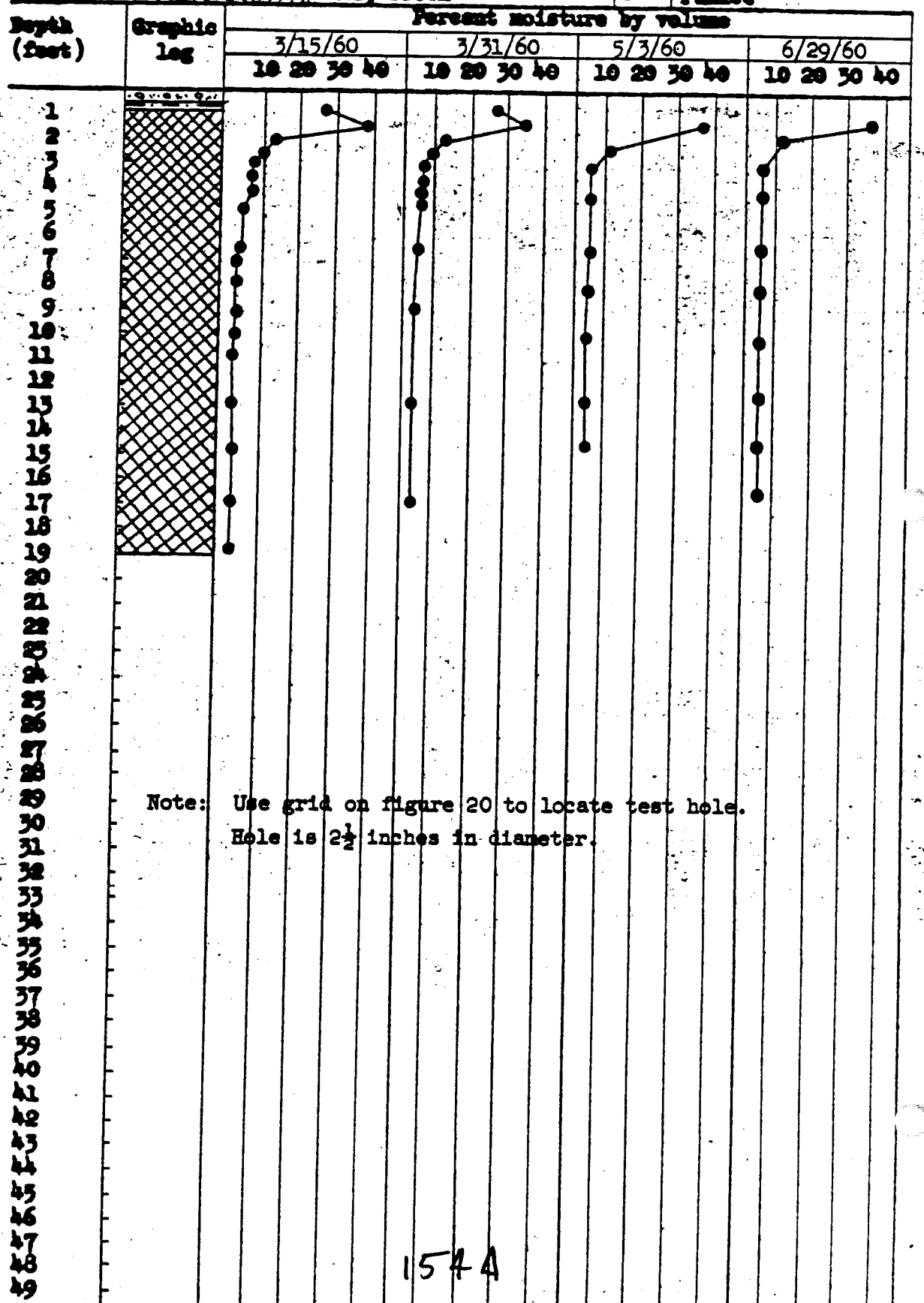

Note: Use grid on figure 20 to locate test hole.
Hole is $2\frac{1}{2}$ inches in diameter.

154A

Figure 22.--Graph of moisture content and lithology in test hole 2M-1, TA-49, Los Alamos County, N. Mex.

Location.- 104 + 72.67 S 99 + 28.26 E
Depth.- 49 ft
Drilled.- 2/17/60
Altitude.- 7,129 ft

Explanation of log

- Backfill, tuff
- Soil, brown, clayey
- Tuff, brown
- Tuff, tan
- Tuff, gray or white
- Pumice

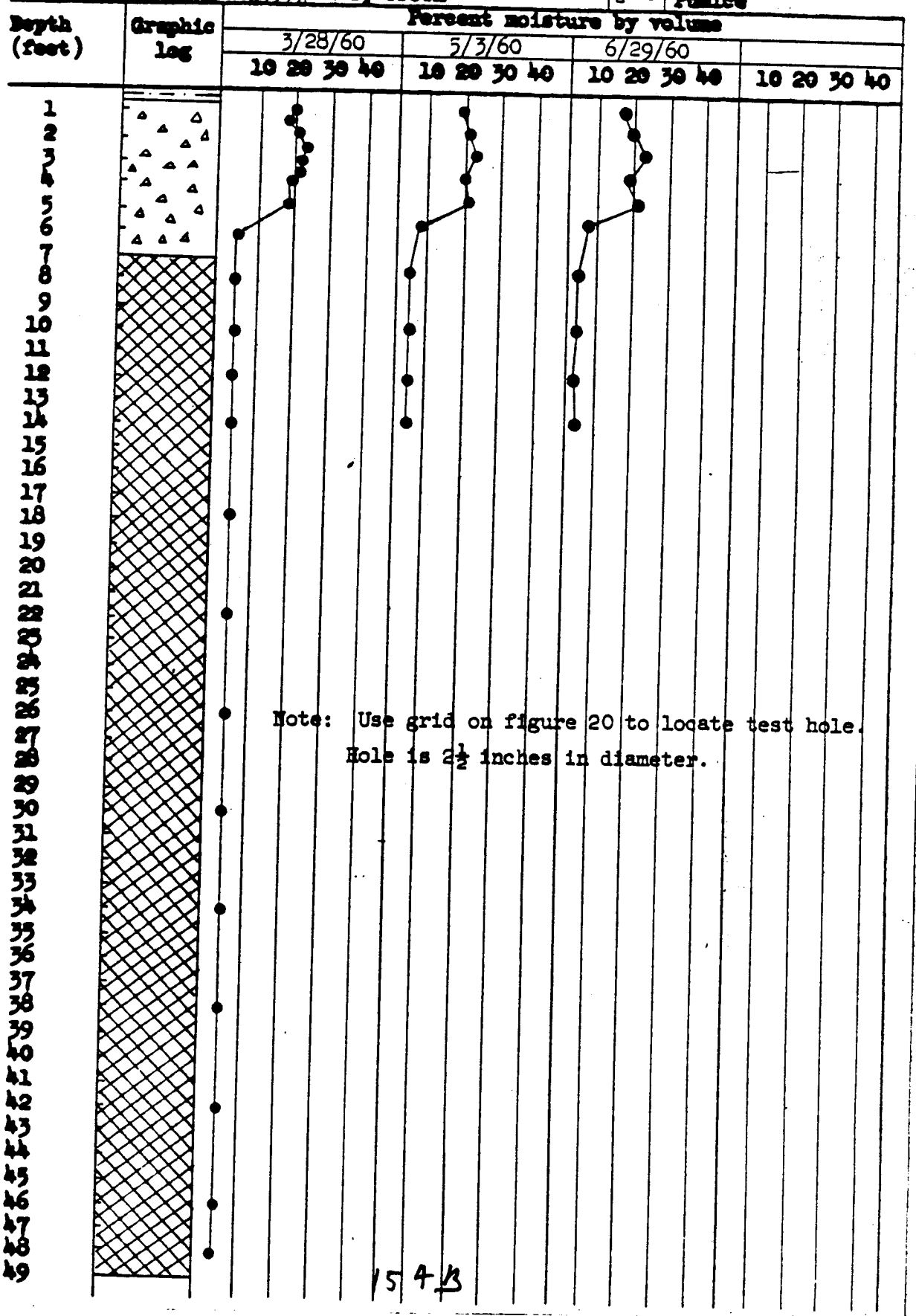

Note: Use grid on figure 20 to locate test hole. Hole is 2½ inches in diameter.

Figure 23.--Graph of moisture content and lithology in test hole 2M-2, TA-49, Los Alamos County, N. Mex.

Location.- 107 + 11.61 S 100 + 04.79 E
Depth.- 10 ft
Drilled.- 2/17/60
Altitude.- 7,131 ft

Explanation of log

- Backfill, tuff
- Soil, brown, clayey
- Tuff, brown
- Tuff, tan
- Tuff, gray or white
- Pumice

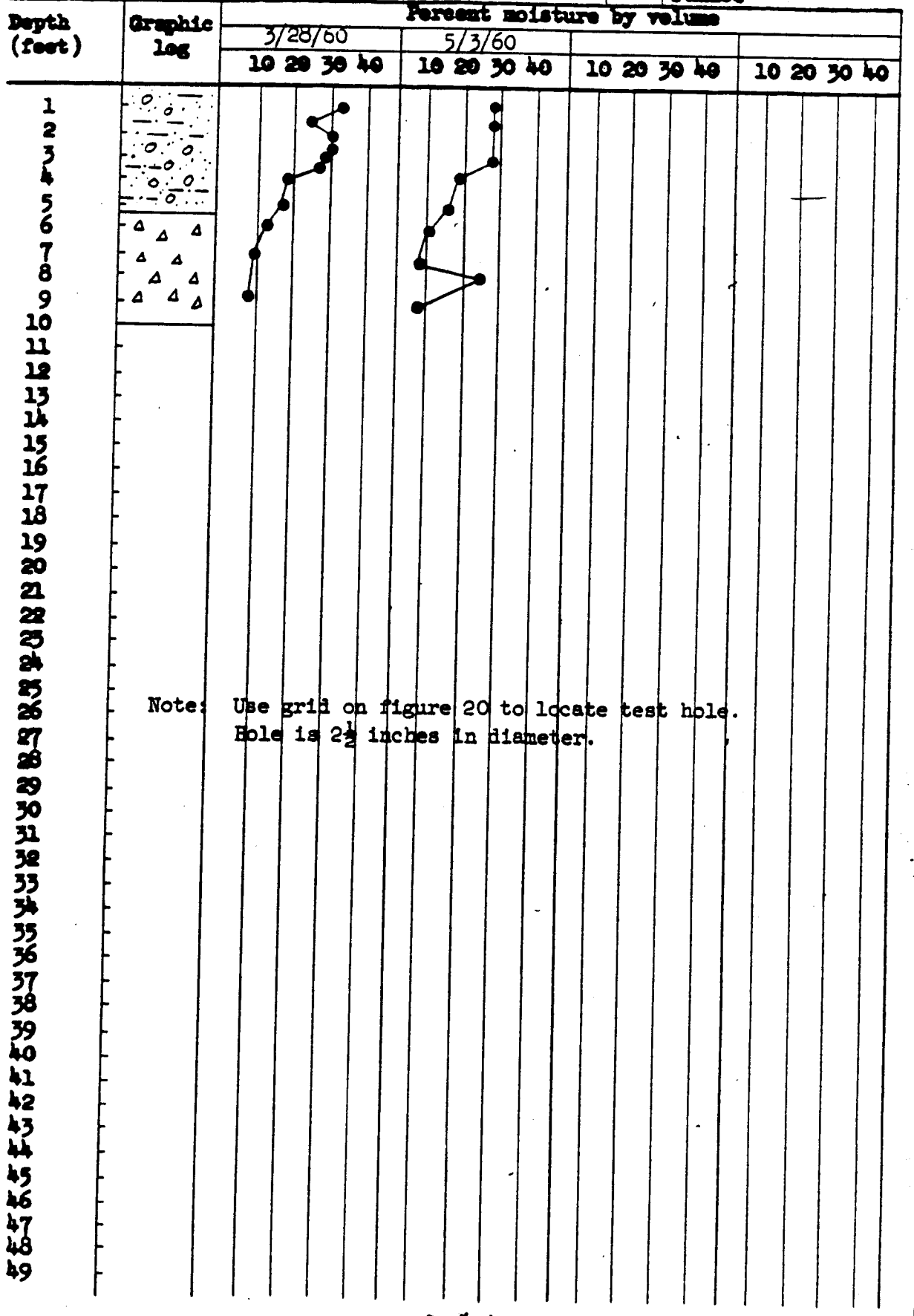

Note: Use grid on figure 20 to locate test hole.
Hole is 2½ inches in diameter.

Figure 24.--Graph of moisture content and lithology in test hole 3M-1, TA-49, Los Alamos County, N. Mex.

Location.- 115 + 97.11 S 82 + 03.29 E
Depth.- 50 ft
Drilled.- 2/15/60
Altitude.- 7,163 ft

Explanation of log

- Backfill, tuff
- Soil, brown, clayey
- Tuff, brown
- Tuff, tan
- Tuff, gray or white
- Pumice

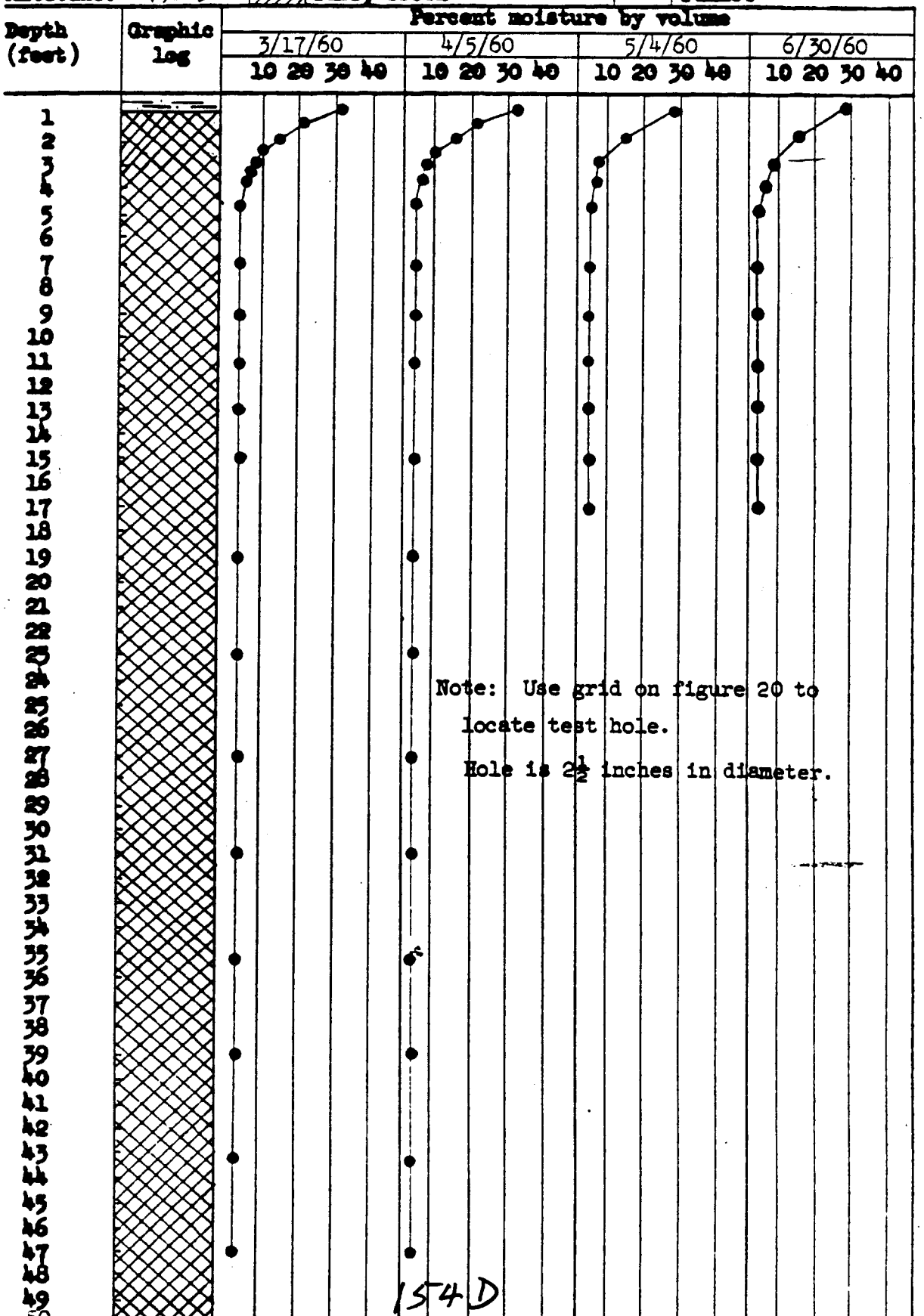

154D

Figure 25.--Graph of moisture content and lithology in test hole 3M-2, TA-49, Los Alamos County, N. Mex.

Location.- 114 + 81.53 S 82 + 67.46 E
Depth.- 19 ft
Drilled.- 2/15/60
Altitude.- 7,169 ft

Explanation of log

- Backfill, tuff
- Soil, brown, clayey
- Tuff, brown
- Tuff, tan
- Tuff, gray or white
- Pumice

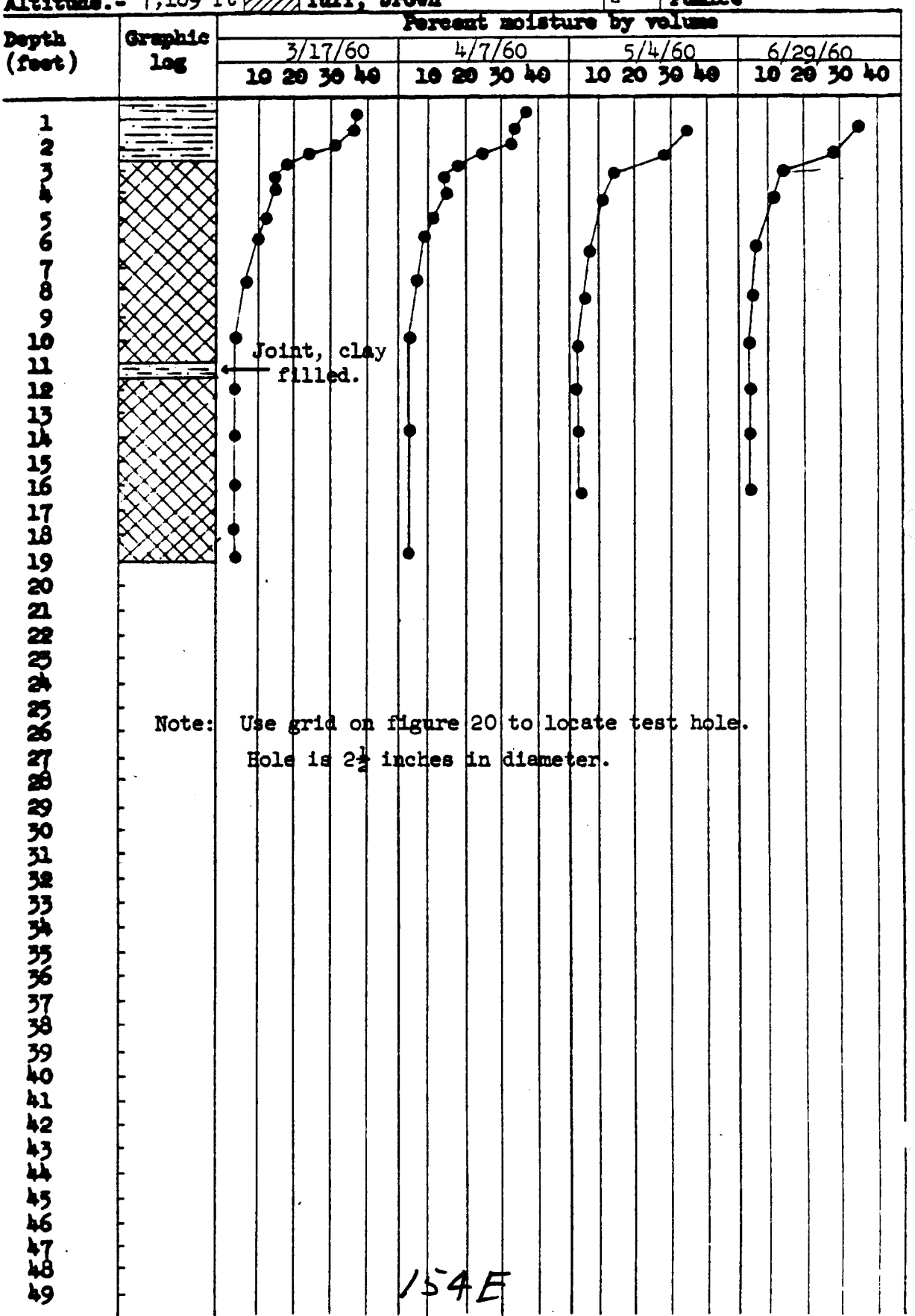

Figure 26.--Graph of moisture content and lithology in test hole 3M-3, TA-49, Los Alamos County, N. Mex.

Location.- 114 + 56.29 S 79 + 95.70 E
Depth.- 20 ft
Drilled.- 2/15/60
Altitude.- 7,174 ft

Explanation of log

- Backfill, tuff
- Soil, brown, clayey
- Tuff, brown
- Tuff, tan
- Tuff, gray or white
- Pumice

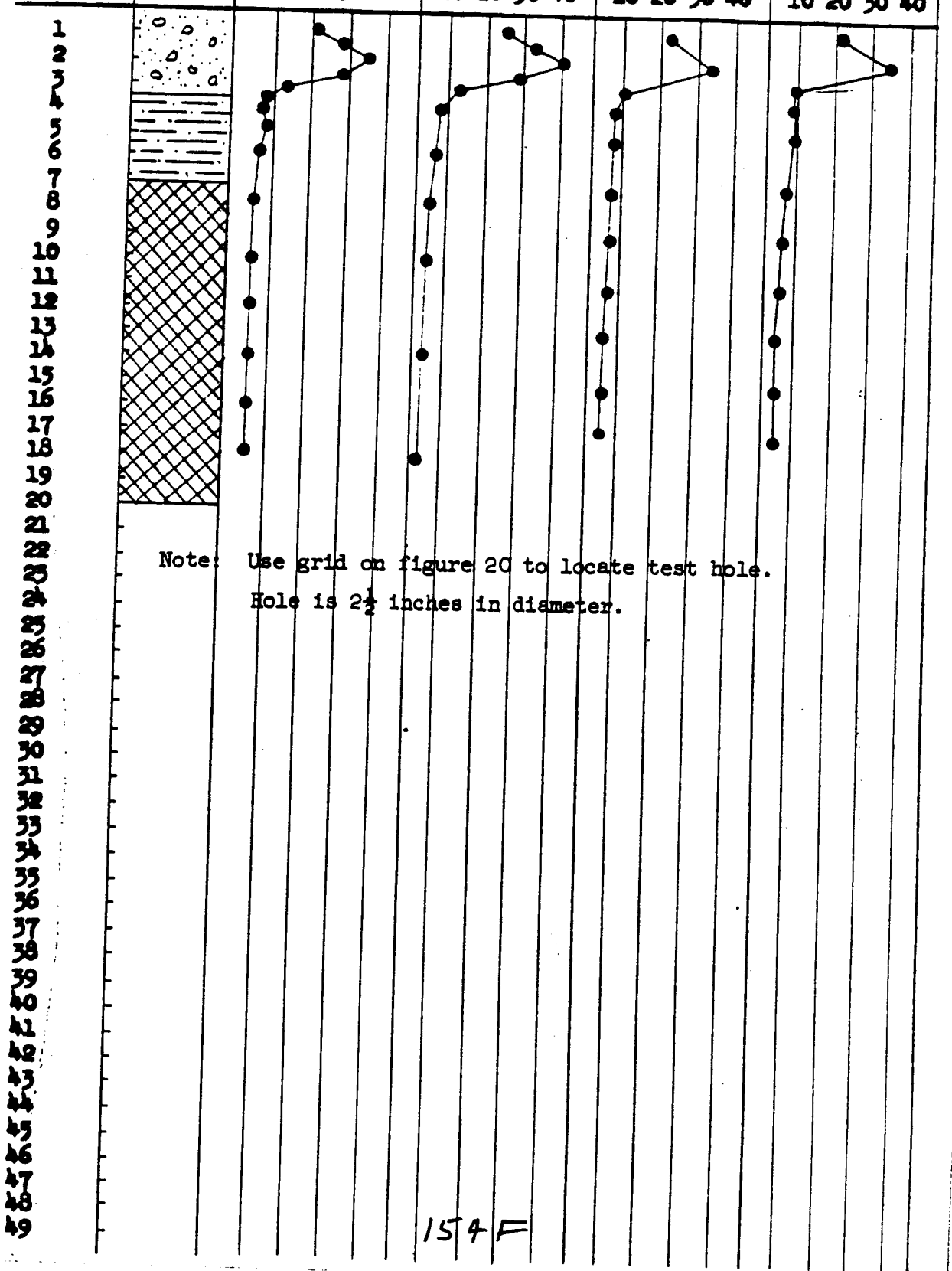

Note: Use grid on figure 20 to locate test hole.
Hole is 2½ inches in diameter.

154F

Figure 27.--Graph of moisture content and lithology in test hole 4M-1, TA-49, Los Alamos County, N. Mex.

Location.- 121 + 29.23 S 96 + 43.59 E
Depth.- 49 ft
Drilled.- 2/16/60
Altitude.- 7,112 ft

Explanation of log

- Backfill, tuff
- Soil, brown, clayey
- Tuff, brown
- Tuff, tan
- Tuff, gray or white
- Pumice

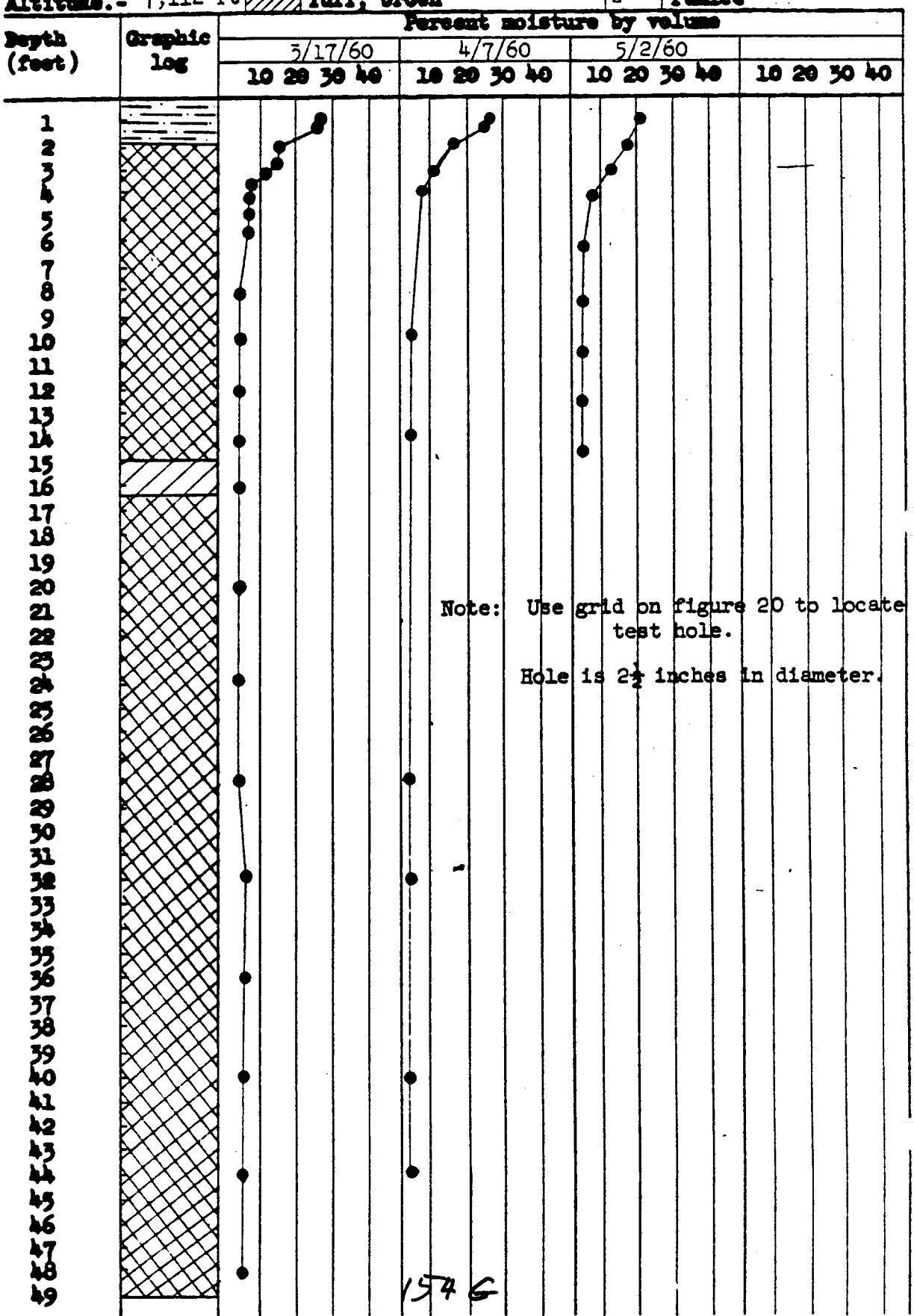

LASL-AEC-OFFICIAL

Figure 28.--Graph of moisture content and lithology in test hole 4M-2, TA-49, Los Alamos County, N. Mex.

Location.- 120 + 56.96 S 94 + 70.47 E
Depth.- 20 ft
Drilled.- 2/15/60
Altitude.- 7,116 ft

Explanation of log

- Backfill, tuff
- Soil, brown, clayey
- Tuff, brown
- Tuff, tan
- Tuff, gray or white
- Pumice

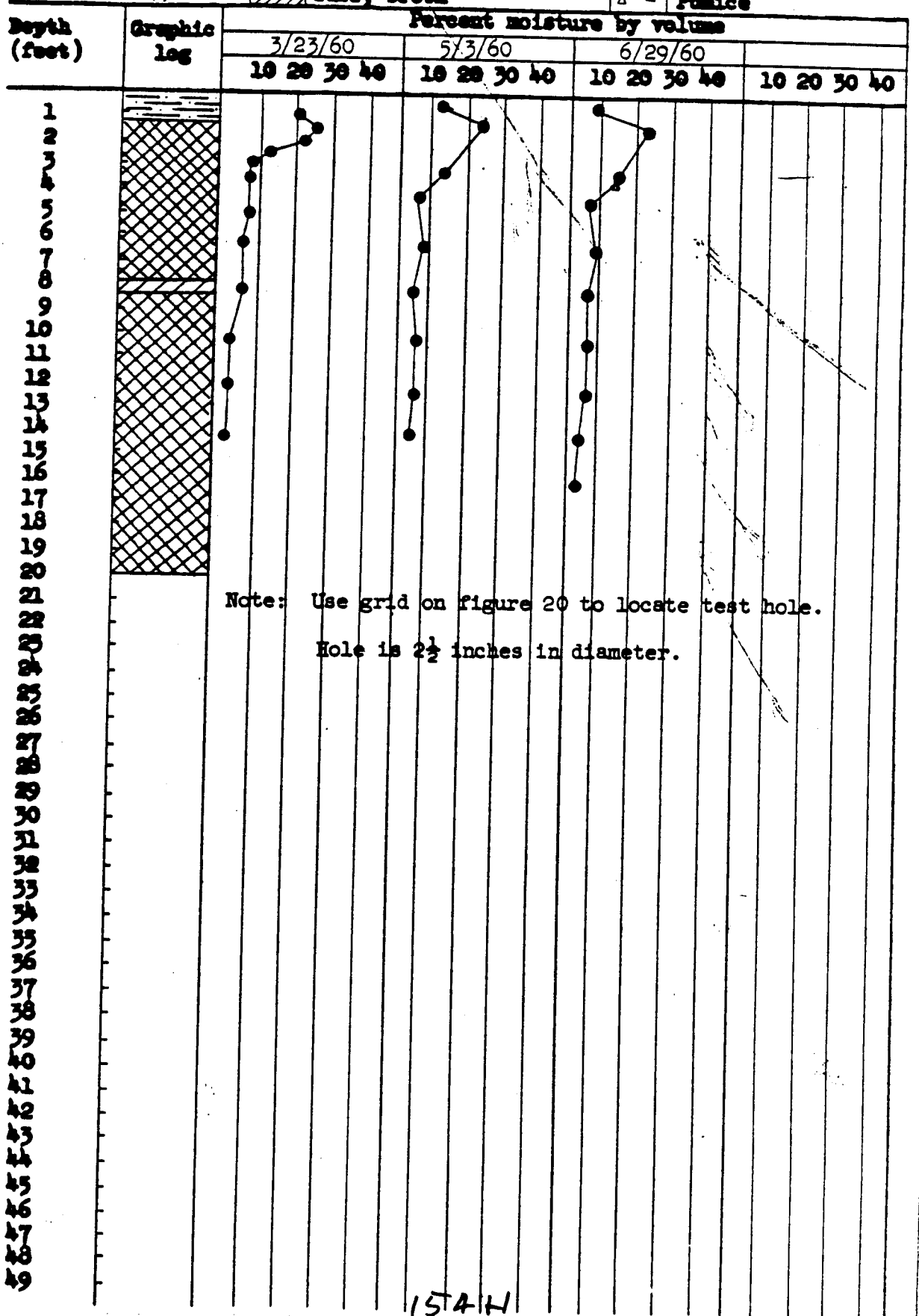

154H

Figure 29.--Graph of moisture content and lithology in test hole 4M-3, TA-49, Los Alamos County, N. Mex.

Location.- 122 + 76.04 S 96 + 93.84 E
Depth.- 19 ft
Drilled.- 2/15/60
Altitude.- 7,107 ft

Explanation of log
- Backfill, tuff
- Soil, brown, clayey
- Tuff, brown
- Tuff, tan
- Tuff, gray or white
- Pumice

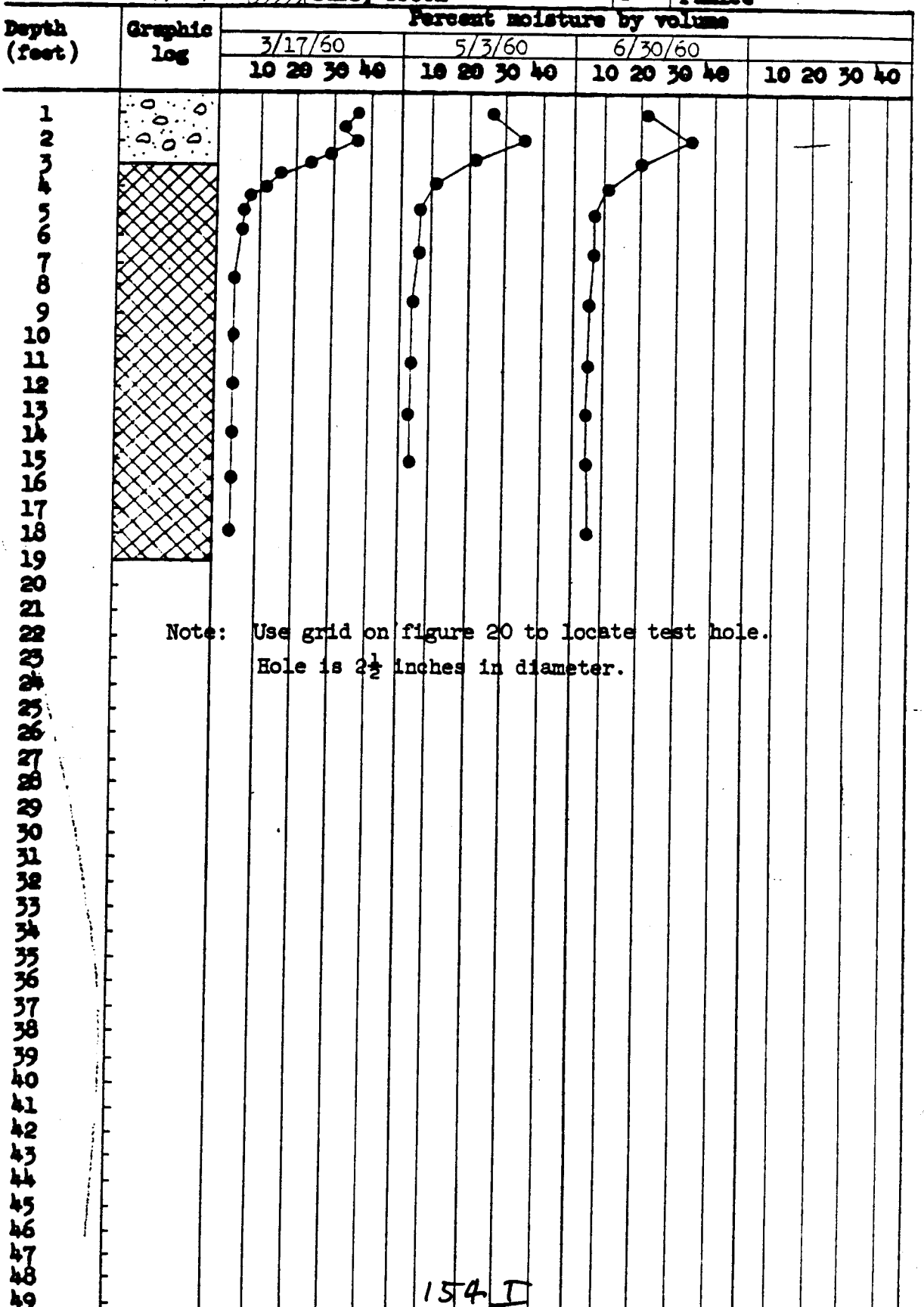

Note: Use grid on figure 20 to locate test hole.
Hole is 2½ inches in diameter.

Figure 30.--Graph of moisture content and lithology in test hole 4M-4, TA-49, Los Alamos County, N. Mex.

Location.- 118 + 71.52 S 94 + 93.95 E
Depth.- 19 ft
Drilled.- 2/16/60
Altitude.- 7,122 ft

Explanation of log

- Backfill, tuff
- Soil, brown, clayey
- Tuff, brown
- Tuff, tan
- Tuff, gray or white
- Pumice

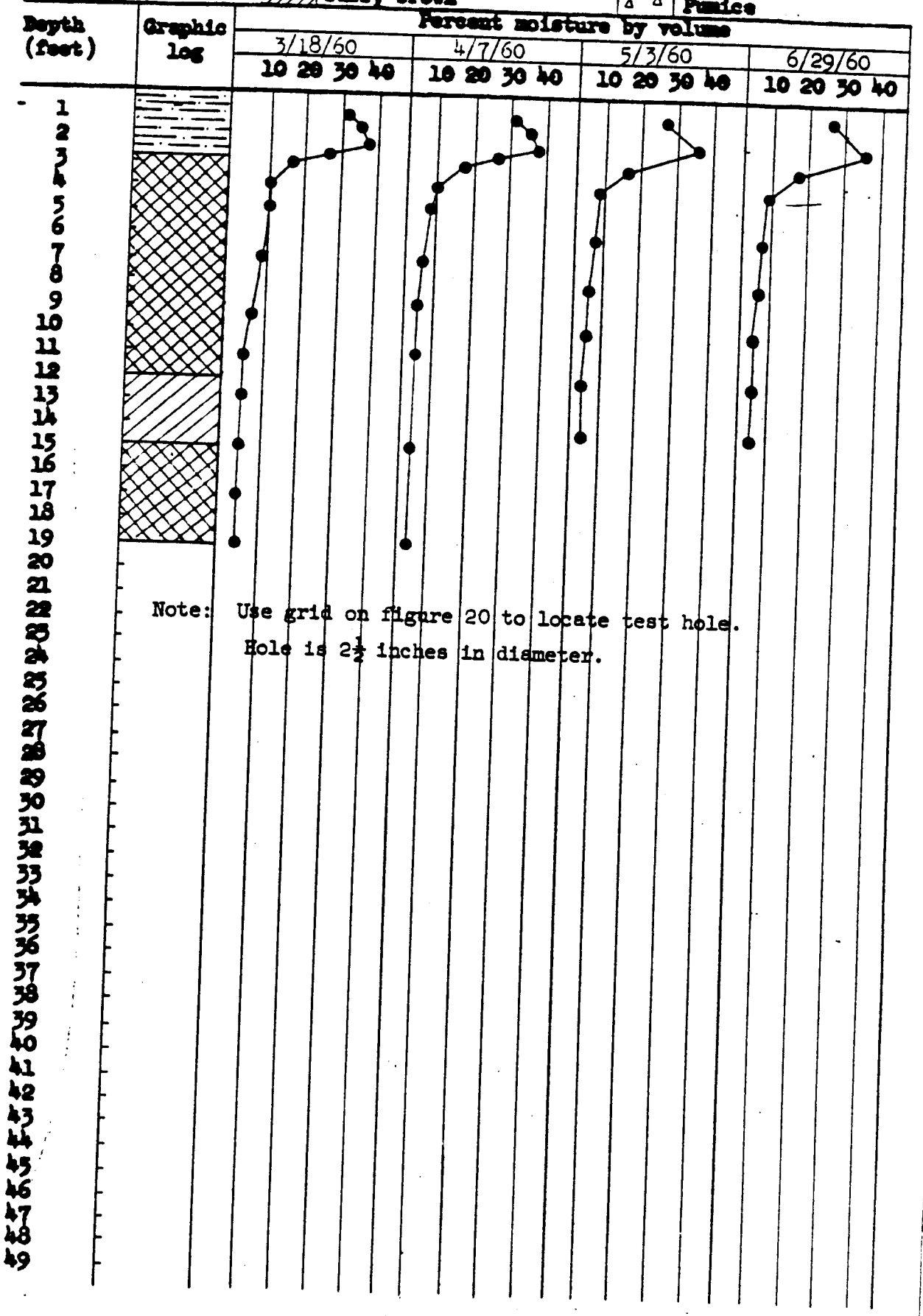

Figure 51.--Graph of moisture content and lithology in test hole 5M-2, TA-49, Los Alamos County, N. Mex.

Location.- 111 + 04.87 S 92 + 37.59 E
Depth.- 19 ft
Drilled.- 2/16/60
Altitude.- 7,146 ft

Explanation of log

- Backfill, tuff
- Soil, brown, clayey
- Tuff, brown
- Tuff, tan
- Tuff, gray or white
- Pumice

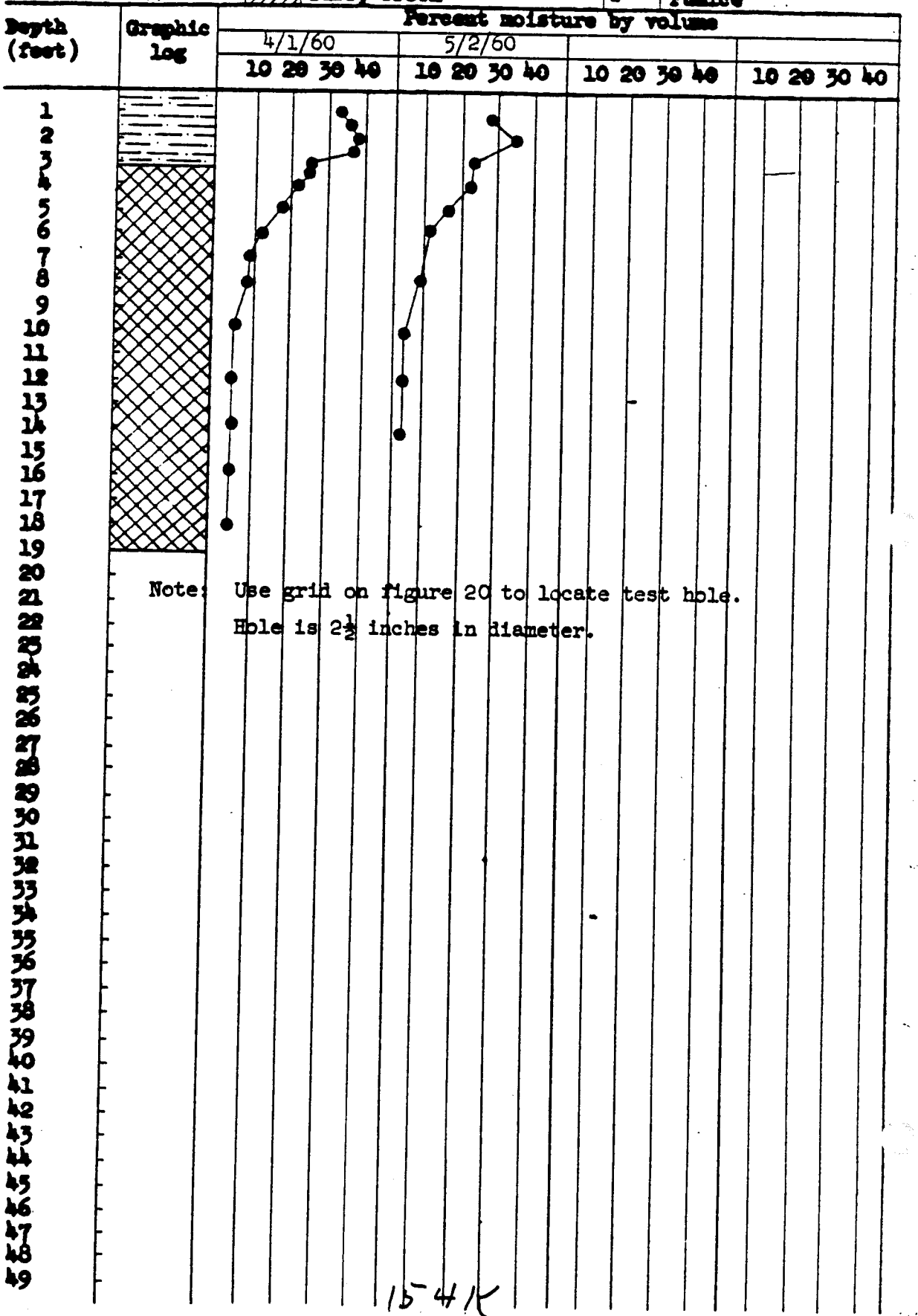

Note: Use grid on figure 20 to locate test hole.
Hole is 2½ inches in diameter.

LASL-AEC-OFFICIAL

15-41K

Figure 32.--Graph of moisture content and lithology in test hole 9M-4, TA-49, Los Alamos County, N. Mex.

Location.- 113 + 93.43 S 100 + 40.05 E
Depth.- 19 ft
Drilled.- 2/16/60
Altitude.- 7,097 ft

Explanation of log

- Backfill, tuff
- Soil, brown, clayey
- Tuff, brown
- Tuff, tan
- Tuff, gray or white
- Pumice

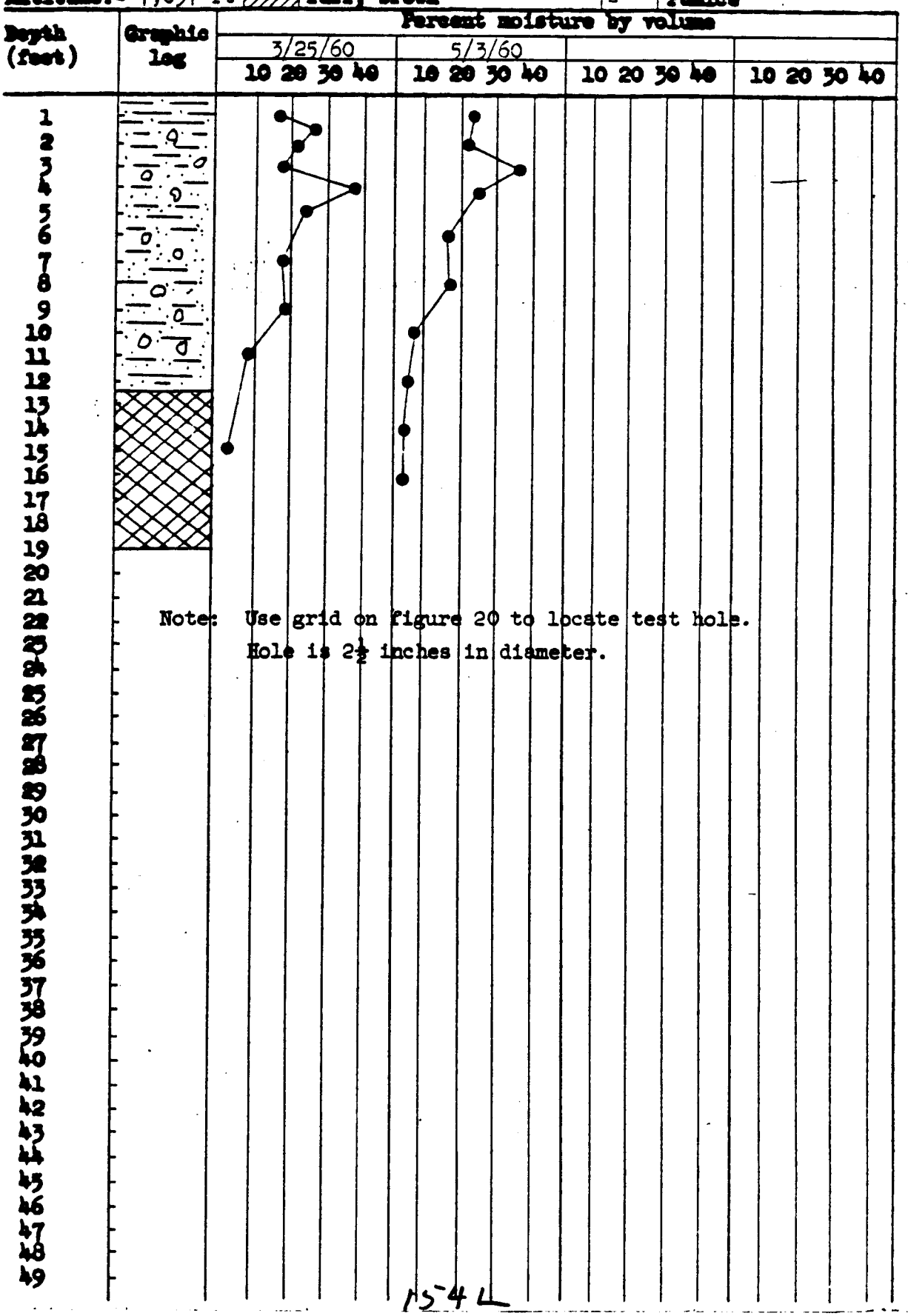

Note: Use grid on figure 20 to locate test hole.
Hole is 2½ inches in diameter.

LAST ALL OFFICIAL

Figure 33.--Graph of moisture content and lithology in test hole 10M-1, TA-49, Los Alamos County, N. Mex.

Location.- 104 + 95.62 S 110 + 30.66 E
Depth.- 29 ft
Drilled.- 2/23/60
Altitude.- 7,090 ft

Explanation of log

- Backfill, tuff
- Soil, brown, clayey
- Tuff, brown
- Tuff, tan
- Tuff, gray or white
- Pumice

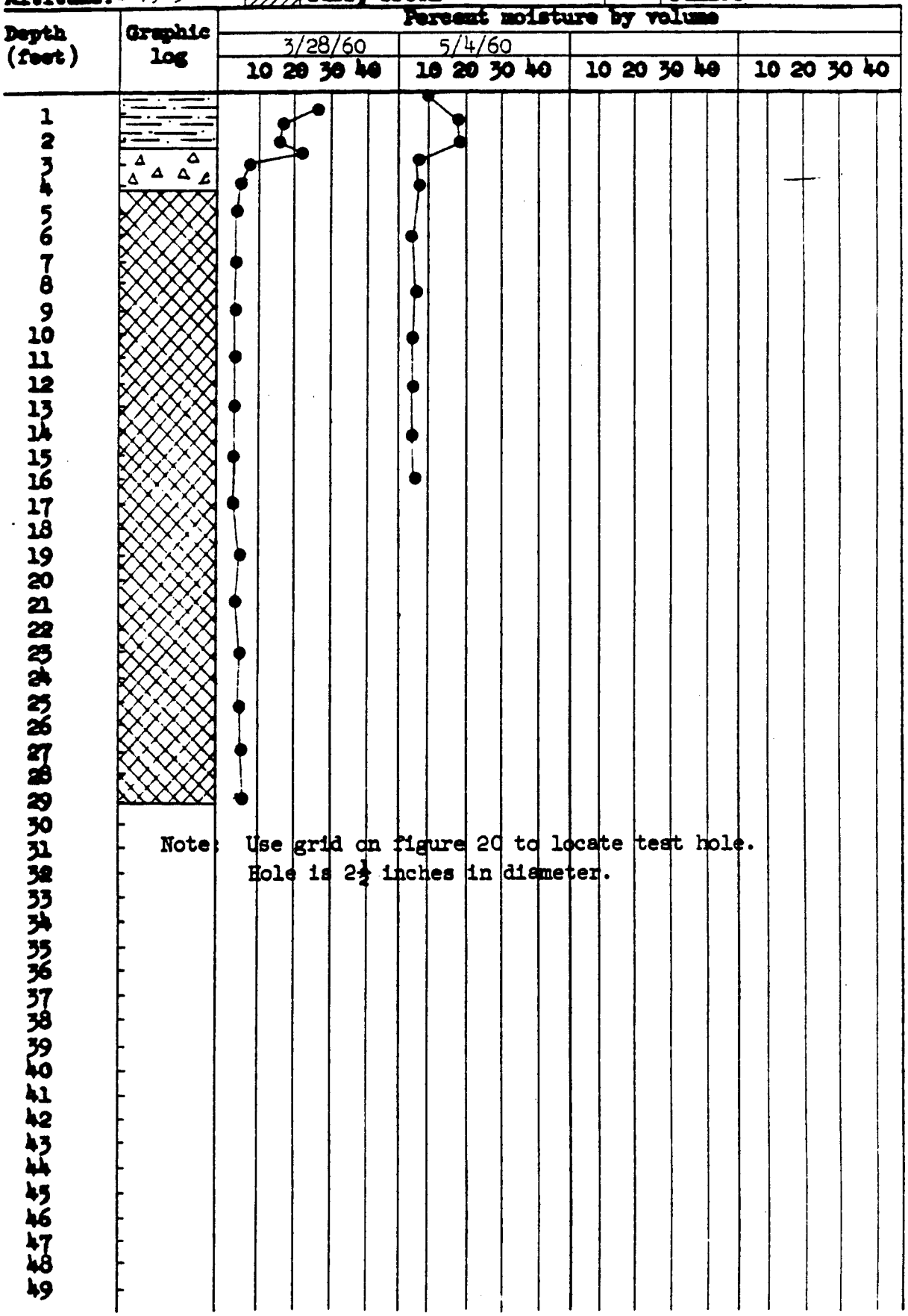

Note: Use grid on figure 20 to locate test hole.
Hole is 2½ inches in diameter.

Figure 34.--Graph of moisture content and lithology in test hole 10M-2, TA-49, Los Alamos County, N. Mex.

Location.- 104 + 53.61 S 108 + 68.66 E
Depth.- 20 ft
Drilled.- 2/23/60
Altitude.- 7,093 ft

Explanation of log

- Backfill, tuff
- Soil, brown, clayey
- Tuff, brown
- Tuff, tan
- Tuff, gray or white
- Pumice

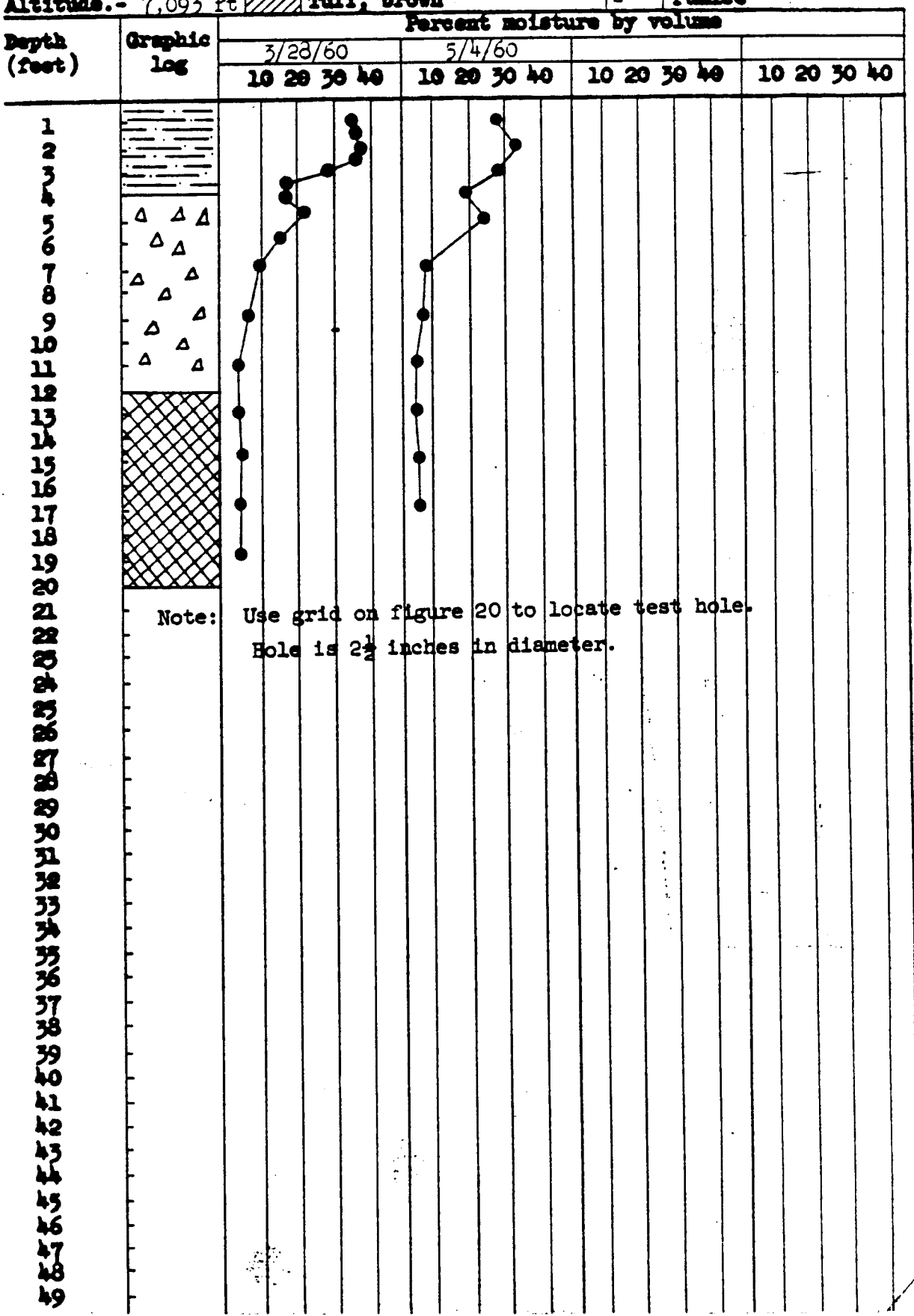

Figure 35.--Graph of moisture content and lithology in test hole 1M-1, TA-49, Los Alamos County, N. Mex.

Location.- 104 + 40.33 S 85 + 48.24 E
Depth.- 49 feet
Drilled.- 2/27/60
Altitude.- 7,162 ft

Explanation of log

- Backfill, tuff
- Soil, brown, clayey
- Tuff, brown
- Tuff, tan
- Tuff, gray or white
- Pumice

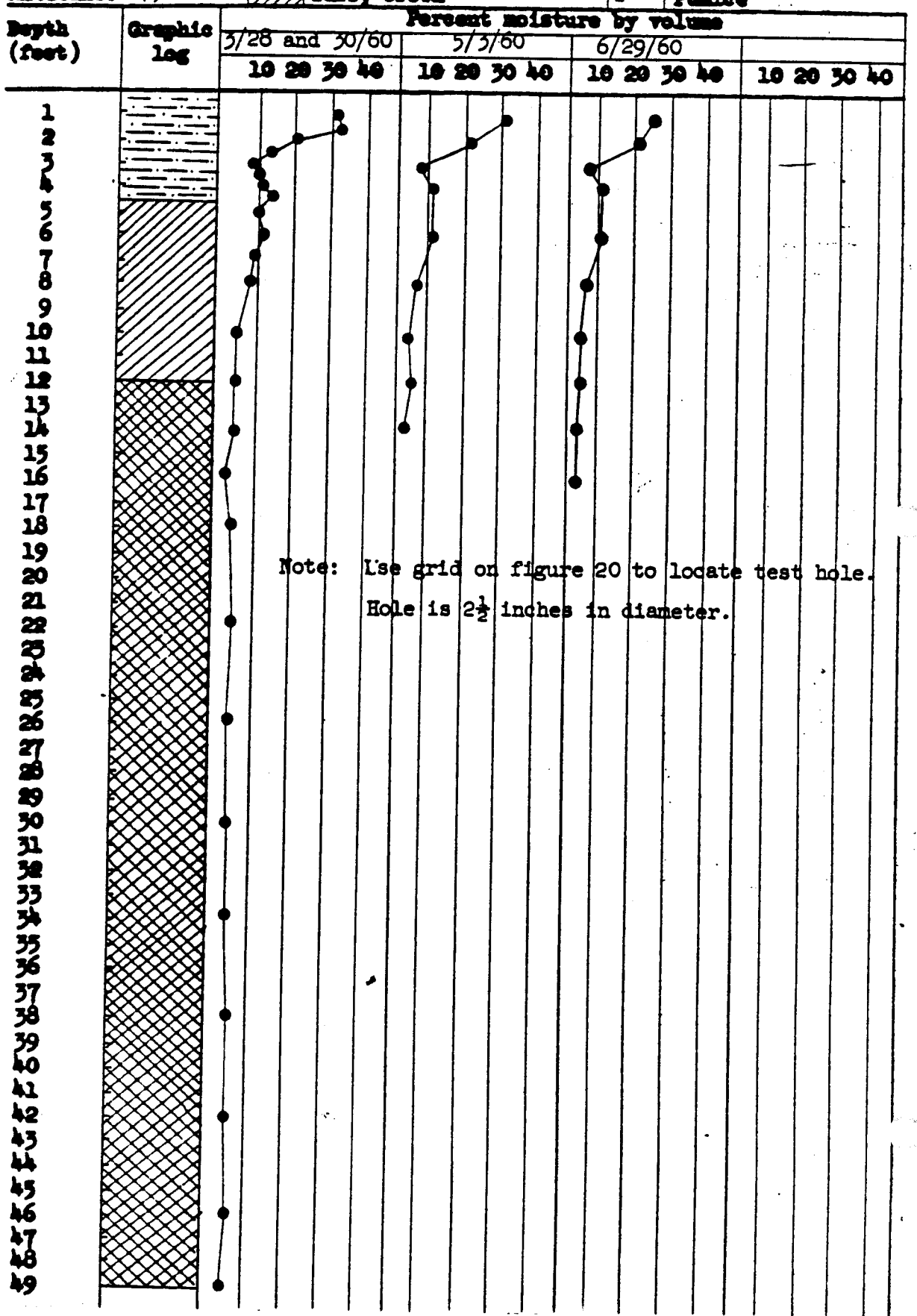

Note: Use grid on figure 20 to locate test hole. Hole is $2\frac{1}{2}$ inches in diameter.

Figure 36.--Graph of moisture content and lithology in test hole 1M-3, TA-49, Los Alamos County, N. Mex.

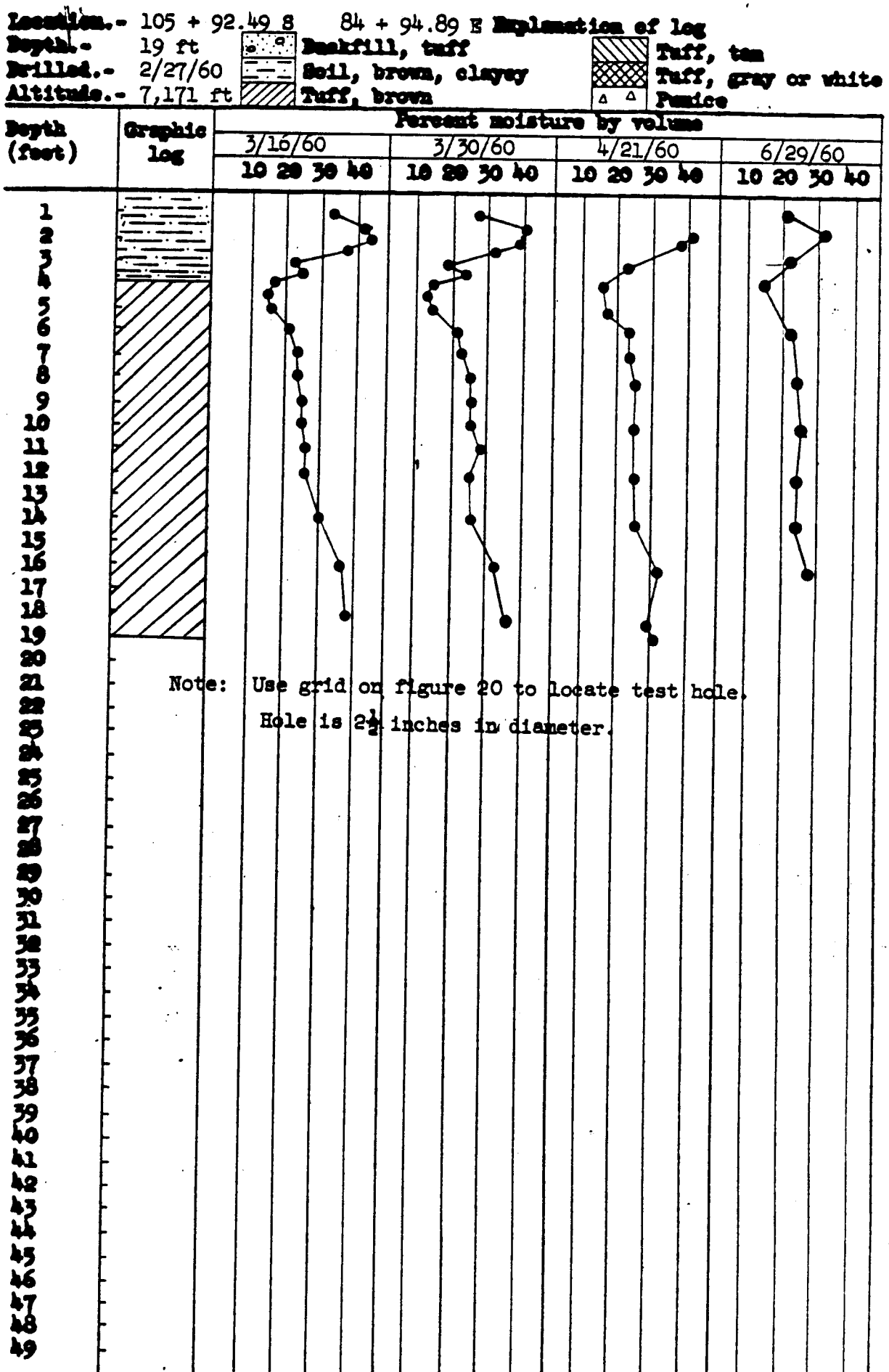

Figure 37.--Graph of moisture content and lithology in test hole 1M-5A, TA-49, Los Alamos County, N. Mex.

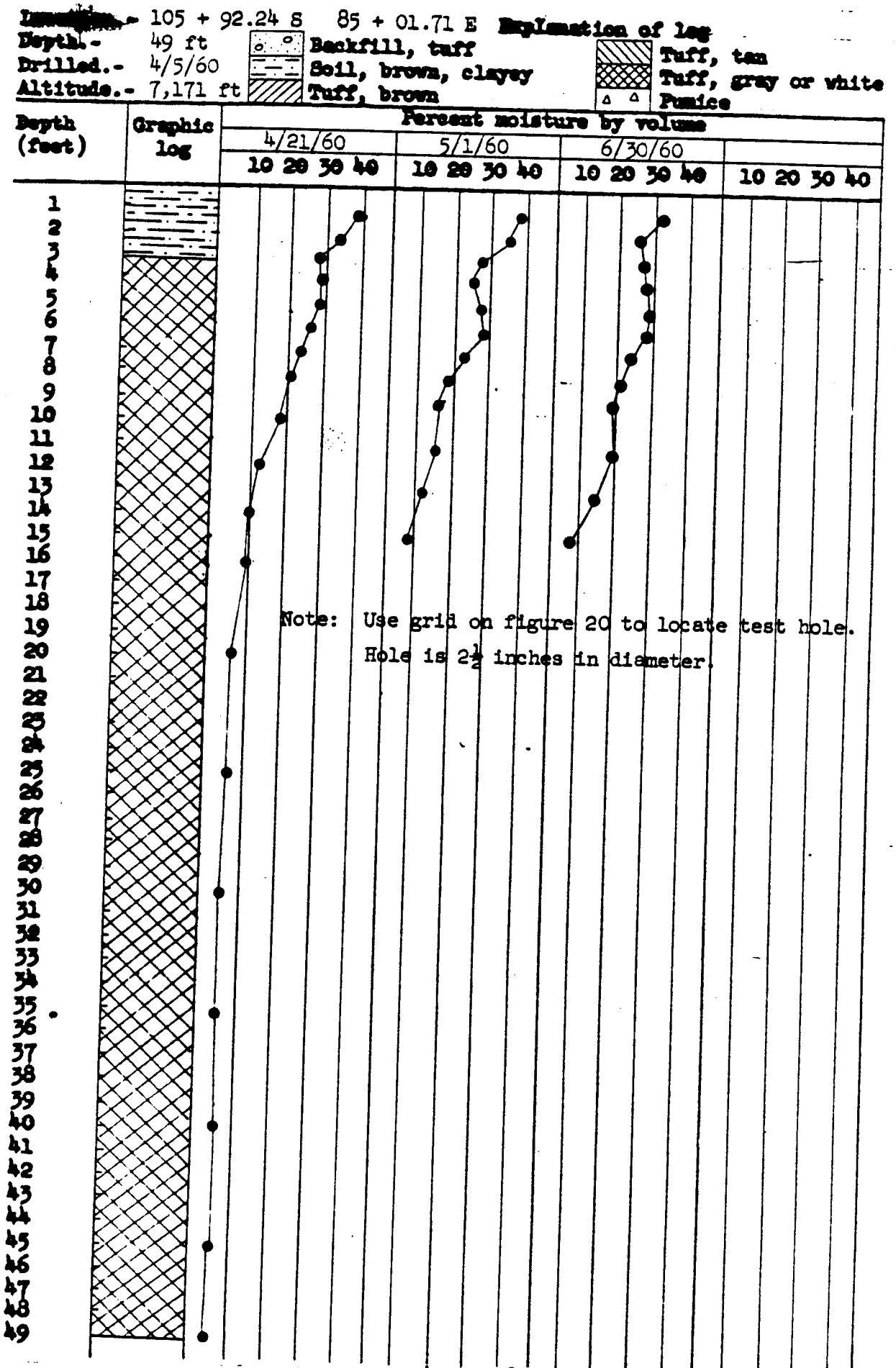

Figure 38.--Graph of moisture content and lithology in test hole 2M-3, TA-49, Los Alamos County, N. Mex.

Location.- 106 + 66.28 S 96 + 00.67 E
Depth.- 19 ft
Drilled.- 2/17/60
Altitude.- 7,141 ft

Explanation of log

- Backfill, tuff
- Soil, brown, clayey
- Tuff, brown
- Tuff, tan
- Tuff, gray or white
- Pumice

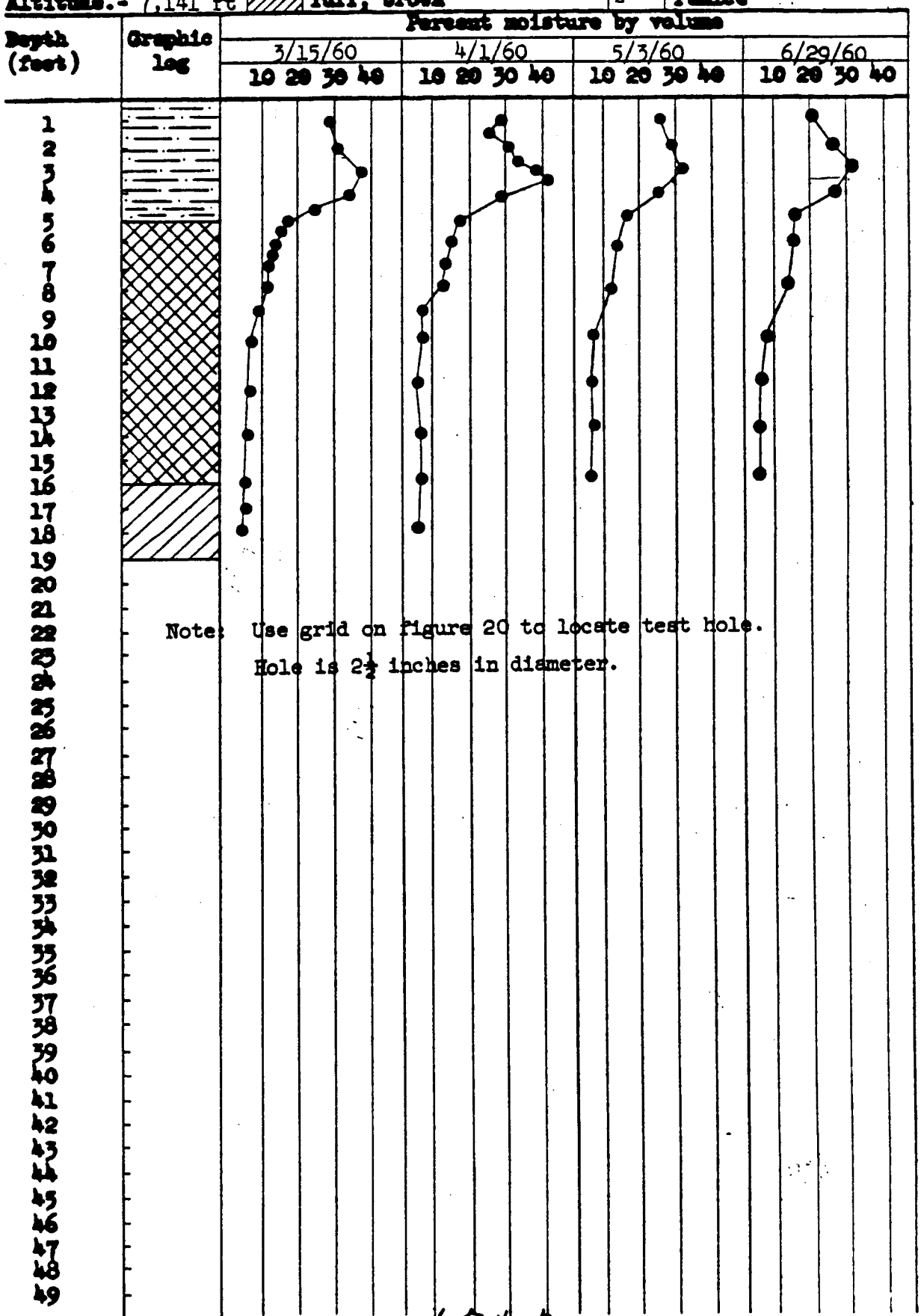

LASL-AEC-OFFICIAL

Figure 39.--Graph of moisture content and lithology in test hole DM-1, TA-49, Los Alamos County, N. Mex.

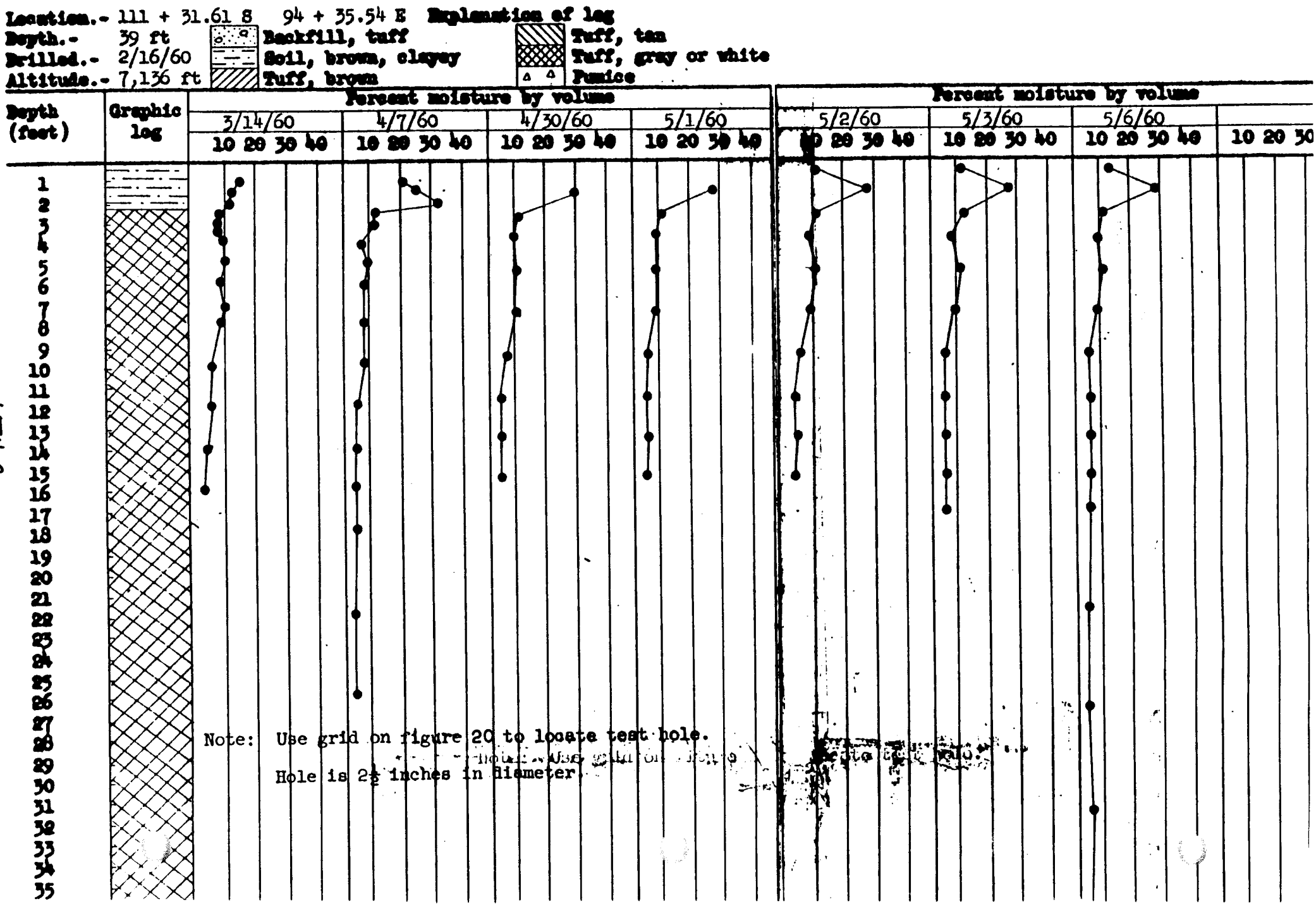

Figure 40.--Graph of moisture content and lithology in test hole 6M-1, TA-49, Los Alamos County, N. Mex.

Location.- 102 + 14.74 S 68 + 83.02 E
Depth.- 19 ft
Drilled.- 2/24/60
Altitude.- 7,210 ft

Explanation of log

- Backfill, tuff
- Soil, brown, clayey
- Tuff, brown
- Tuff, tan
- Tuff, gray or white
- Pumice

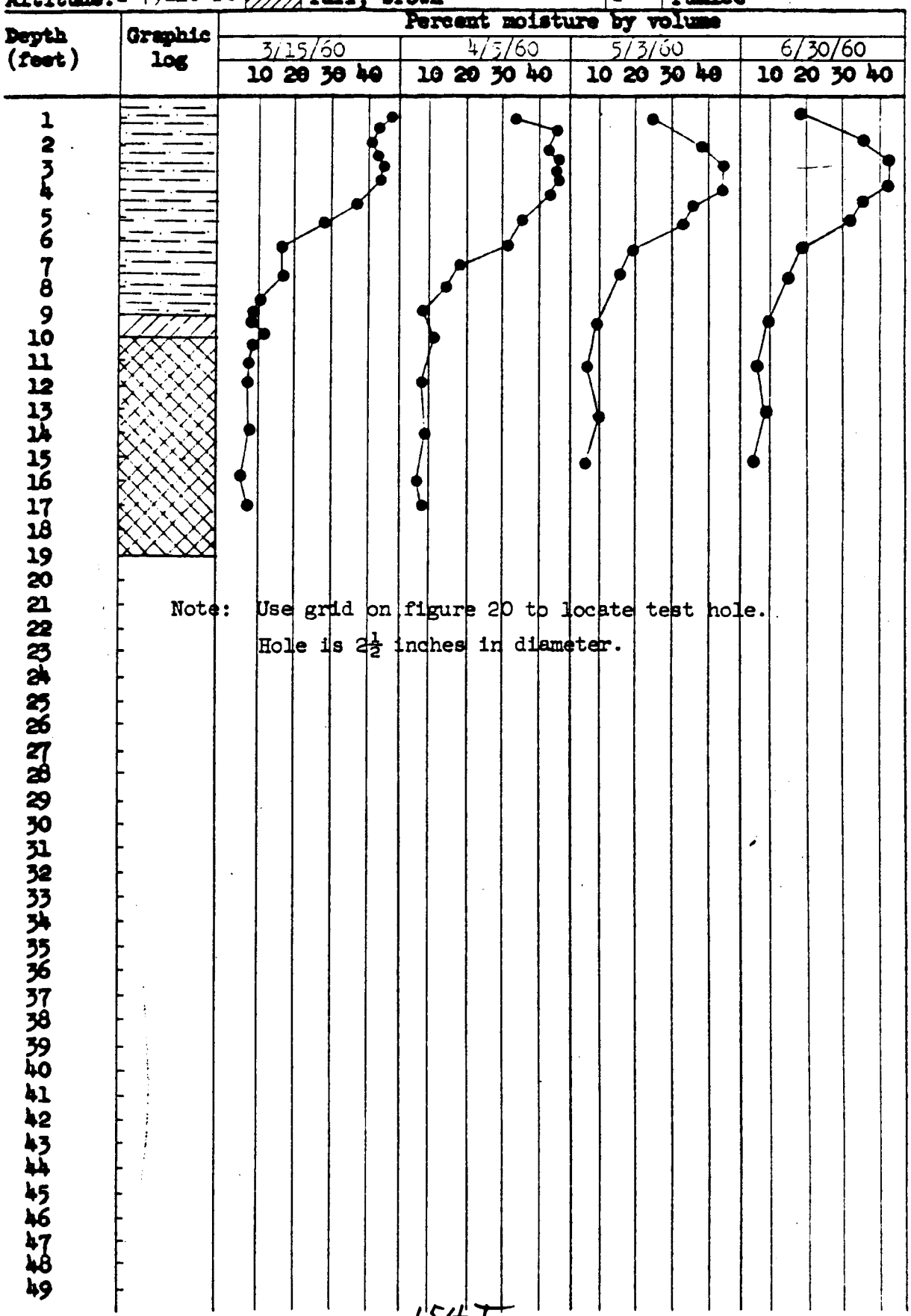

Note: Use grid on figure 20 to locate test hole.
Hole is $2\frac{1}{2}$ inches in diameter.

LASL ARC OFFICIAL

Figure 41.--Graph of moisture content and lithology in test hole 9M-1, TA-49, Los Alamos County, N. Mex.

Location.- 116 + 67.49 S 88 + 43.84 E
Depth.- 19 ft
Drilled.- 2/24/60
Altitude.- 7,115 ft

Explanation of log

- Backfill, tuff
- Soil, brown, clayey
- Tuff, brown
- Tuff, tan
- Tuff, gray or white
- Pumice

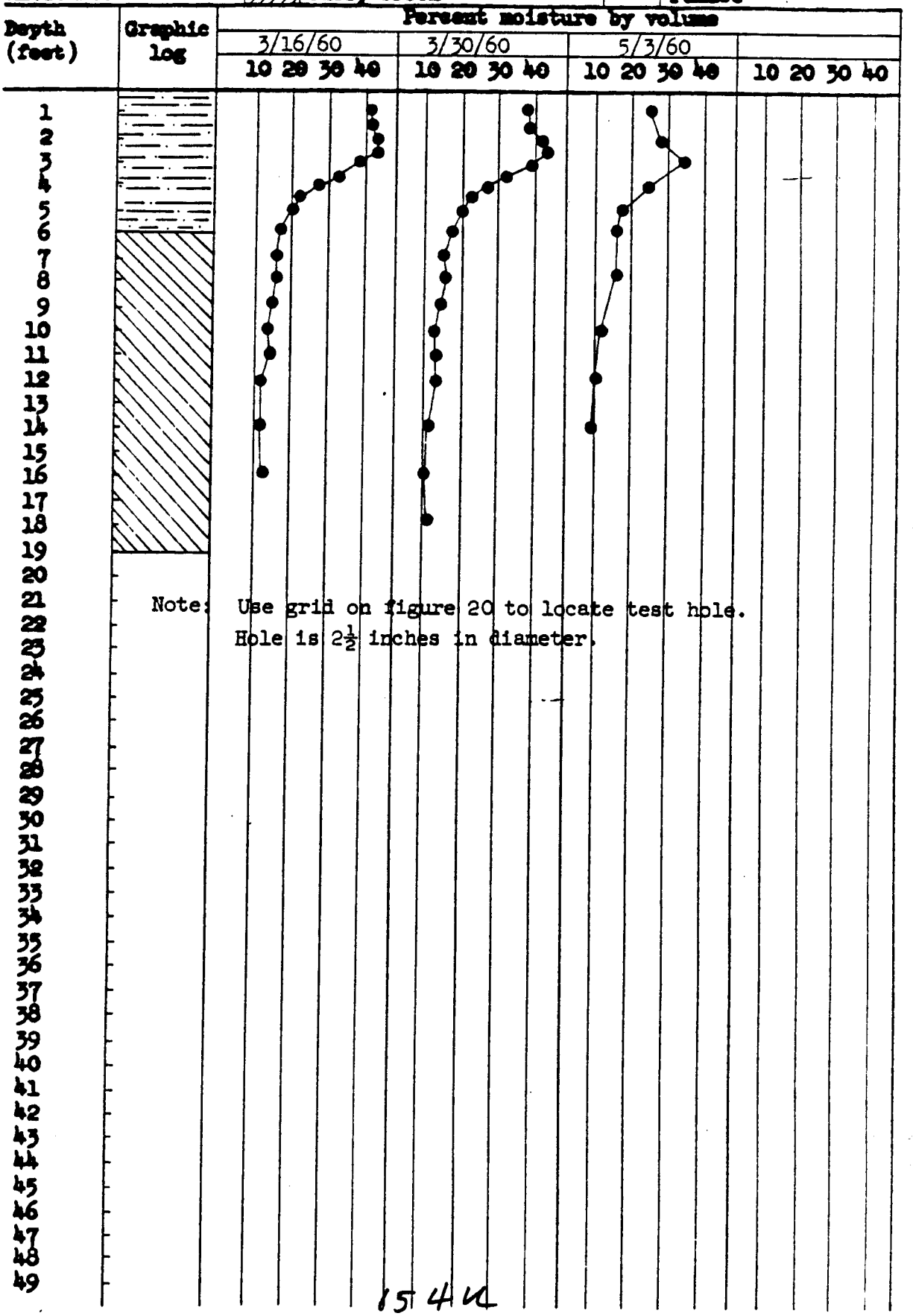

1544

Figure 42.--Graph of moisture content and lithology in test hole 9M-2, TA-49, Los Alamos County, N. Mex.

Location.- 113 + 40.39 S 98 + 14.81 E
Depth.- 19 ft
Drilled.- 3/4/60
Altitude.- 7,104 ft

Explanation of log

- Backfill, tuff
- Soil, brown, clayey
- Tuff, brown
- Tuff, tan
- Tuff, gray or white
- Pumice

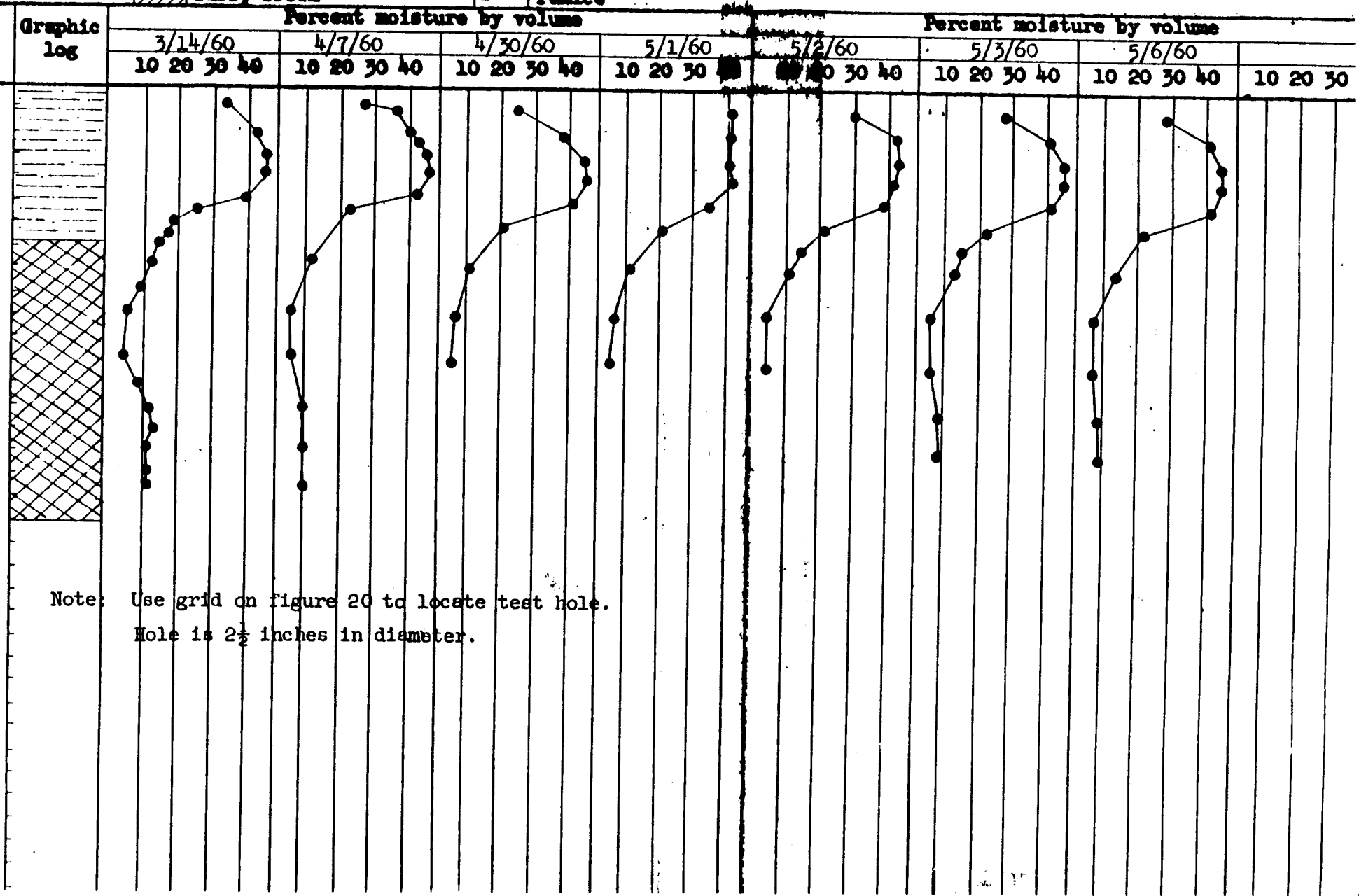

Note: Use grid on figure 20 to locate test hole.
Hole is 2½ inches in diameter.

Figure 43.--Graph of moisture content and lithology in test hole 9M-3, TA-49, Los Alamos County, N. Mex.

Location.- 117 + 01.88 S 104 + 56.98 E
Depth.- 19 ft
Drilled.- 2/17/60
Altitude.- 7,049 ft

Explanation of log
Backfill, tuff
Soil, brown, clayey
Tuff, brown
Tuff, tan
Tuff, gray or white
Pumice

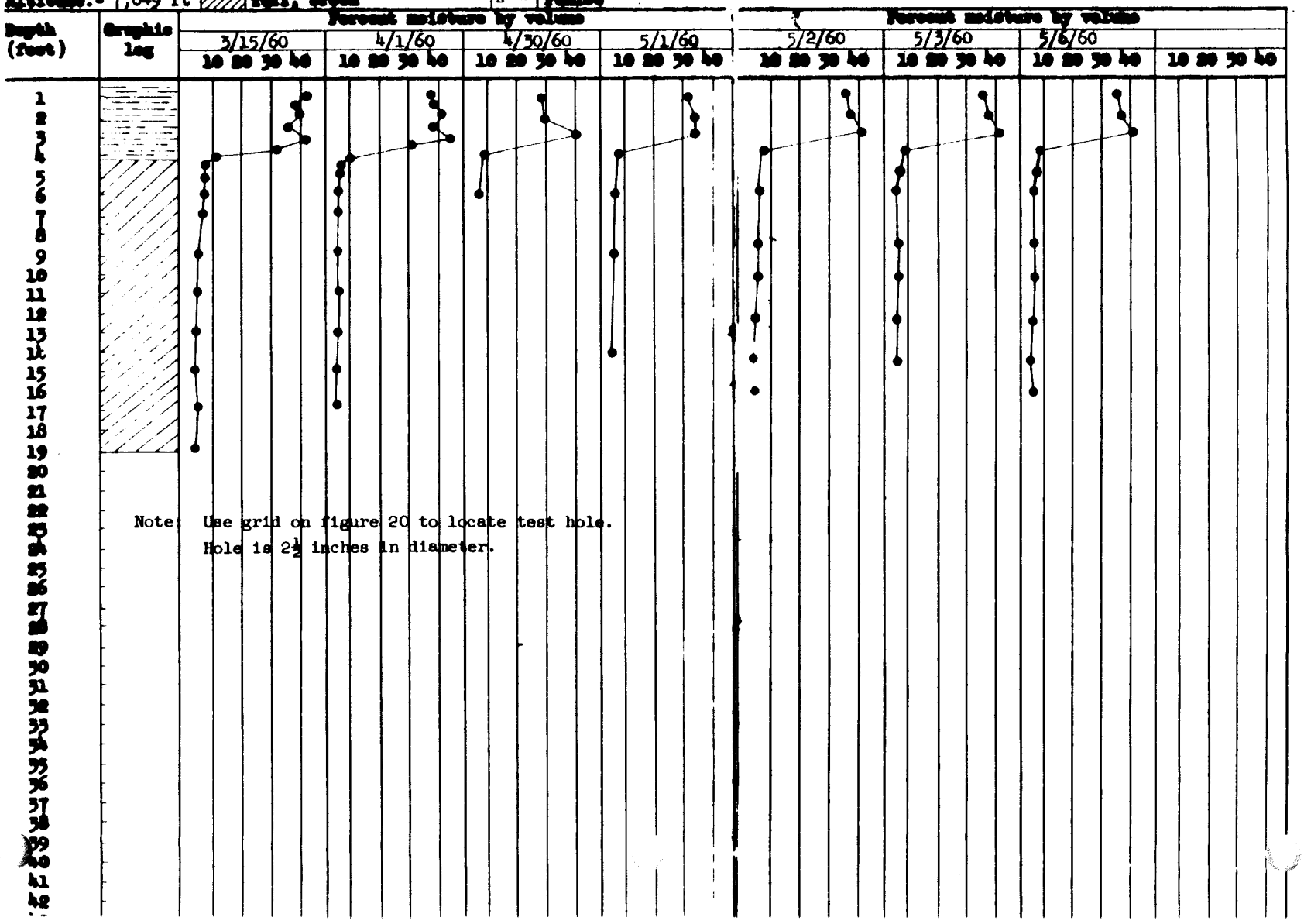

Note: Use grid on figure 20 to locate test hole.
Hole is 2½ inches in diameter.

154 W

Moisture content of the soil ranged from 48 percent by volume near the surface in March to 8 percent at depth. The moisture content of the near-surface tuff, WHERE IT WAS covered by a thin soil, ranged from 37 percent by volume to less than 4 percent at depth in test holes in well-drained areas. Moisture content was highest in the upper few feet of soil and tuff in March and April as a result of the late winter snow; it decreased in June due to the higher evapotranspiration rates of early summer. Moisture content of the tuff at depth remained constant in the period March to June except in test hole 1M-3A where an increase of 1 to 3.5 percent by volume was noted between 4 and 13 feet.

Test holes in well-drained areas

Holes 1M-2; 2M-1 and -2; 3M-1, -2, and -3; 4M-1, -2, -3, and -4; 5M-2; 9M-4; and 10M-1 and -2 are located in well-drained areas and penetrated an average soil or soil and backfill thickness of 3.5 feet (table 20). At the average depth of 4.7 feet in these holes, moisture content decreased from about 30 percent to 10 percent by volume. At the average depth of 8.8 feet, the moisture content decreased further to 5 percent.

The clay soil had retained most of the moisture that fell as snow or rain and the moisture content in the upper part of this soil varied due to evaporation, transpiration, and prevailing weather conditions prior to and during moisture readings. Near the base of the soil zone, no apparent change in moist re content was noted during the period of March to June (figs. 21-34).

The tuff just below the soil zone contained as much as 37 percent moisture by volume. Moisture content in the tuff of unit 6 decreased to less than 10 percent a few feet below the soil. No significant changes in moisture content were noted in the tuff during the period March to June.

The moisture content did not change in the pumice layer during the period March to June. Measurements made in test hole 2M-2 (fig. 23) indicated a moisture content of 25 percent in the pumice layer at 8 feet on May 3, 1960. This anomalously high reading probably is in a thin clay layer in the pumice zone.

Table 20.--Summary of results of moisture measurements in test holes located in well-drained areas

Test hole	Soil thickness (feet)	Depth at which moisture decreases to 10% by volume (feet)	Depth at which moisture decreases to 5% by volume (feet)
1M-2	1.0 1/	2.5	7.0
2M-1	.5 2/	5.5	7.0
2M-2	5.5 1,2/	6.5	9+
3M-1	.9	2.5	4.5
3M-2	2.6	6.0	9.0
3M-3	7.0 1/	3.0	14.0
4M-1	1.9	3.0	7.0
4M-2	1.2	4.0	13.0
4M-3	3.0 1/	4.0	7.0
4M-4	2.9	4.0	10.0
5M-2	3.3	6.5	9.0
9M-4	12.4 1/	9.0	12.0
10M-1	2.4 2/	3.0	5.0
10M-2	4.0 2/	6.5	10.0
Average	3.5	4.7	8.8

1/ Backfill composed of soil and tuff.

2/ Soil overlies pumice.

Test holes in areas THAT receiv~~ing~~e runoff

from well-drained areas

Test holes 1M-1 and -3A; 2M-3; 5M-1; 6M-1; and 9M-1, -2, and -3 are located on or near arroyos, drainage ditches, and flat areas THAT DRAIN SLOWLY. ~~of slow drainage.~~ Graphs of moisture readings in these holes are shown on figures 35 ~~through~~ 43.

The average soil thickness of this group of test holes is 5.3 feet (table 21). At an average depth of 9.5 feet, the moisture content decreased to 10 percent by volume, but the moisture content was above 5 percent to depths of more than 19 feet in all but one of the holes. In test hole 1M-1 (fig. 35) the moisture content decreased to 5 percent by volume at 10 feet.

Moisture content determined in the soil penetrated by these test holes varied with evaporation, transpiration, and prevailing weather conditions. No significant change in moisture content of the soil was noted during the period of March to June.

Table 21.--Summary of results of moisture measurements in test holes in areas that receive runoff from well-drained areas

Test hole	Soil thickness (feet)	Depth at which moisture decreases to 10% by volume (feet)	Depth at which moisture decreases to 5% by volume (feet)
1M-1	4.6	6.5	10
1M-3A	3.2	14.0	49+
2M-3	5.0	8.5	19+
5M-1	2.2	6.5	39+
6M-1	9.0	9.0	19+
9M-1	6.9	19+	-
9M-2	6.9	8.5	19+
9M-3	4.2	4.0	19+
Average	5.3	9.5	-

No significant change in moisture content in the tuff was noted, except in hole 1M-3A (fig. 20), where THE moisture content increased 1 to 3.5 percent by volume between 4 and 13 feet in the tuff from May 3 to June 30, 1960. Test hole 1M-3A is located on the bank of an arroyo, and the bank is about 5 feet above the bottom of the channel. Construction near test hole 1M-3A caused water to pond 2 to 4 inches deep in the arroyo during wet periods. The thin soil and sand in the channel of the arroyo may have allowed the ponded water to infiltrate downward and laterally into the tuff as shown by the increase of moisture from 1 percent to 3.5 percent at a depth of 4 to 13 feet. Between 13 and 20 feet a small increase in moisture content is suggested, but between 20 and 49 feet the moisture content remained about 6 to 8 percent.

The specific retention of samples of unit 6 ranges from ~~19~~ 15 to 27 percent by volume (table 17). On June 30, 1960, in test hole 1M-3A the moisture content of the tuff ranged from 27.5 percent at 4 feet to 29 percent at 5 feet, suggesting that there may have been some free water in that interval. The increase of 1 to 3.5 percent in moisture content at various depths during the period from May to June may indicate a slow downward movement of moisture in the vicinity of test hole 1M-3A. This indicated movement of moisture into the tuff is brought about by the ponding of water in an area where it was formerly allowed to drain.

Infiltration from stream flow

Water discharged from well DT-5A during the pumping test was measured frequently in the natural stream channel near test holes 9M-2 and 9M-3 (fig. 20). The results of these measurements and measurements of discharge from the well are shown graphically on figure 44.

Figure 44.--Graph of measurements of flow downstream from well DT-5A as compared to discharge at well during pumping test April 30-May 1, 1960 at TA-49.

Moisture content of soil and rock penetrated in three test holes adjacent to the stream channel was measured on April 30, May 1, 2, 3, and 6, 1960 thus monitoring infiltration from the stream during and after the pumping test. Results of moisture measurements in these three holes, 5M-1, 9M-2, and 9M-3, are shown in figures 39, 42, and 43. From the discharge pipe at the well to near test hole 5M-1 the water flowed in a natural channel partially filled and dammed by drill cuttings from well DT-5A (fig. 20). Downstream from the partial dam to test hole 9M-3 the natural channel is cut into the soil. The bottom of the channel consists mostly of silt, sand, and gravel, but some tuff is exposed.

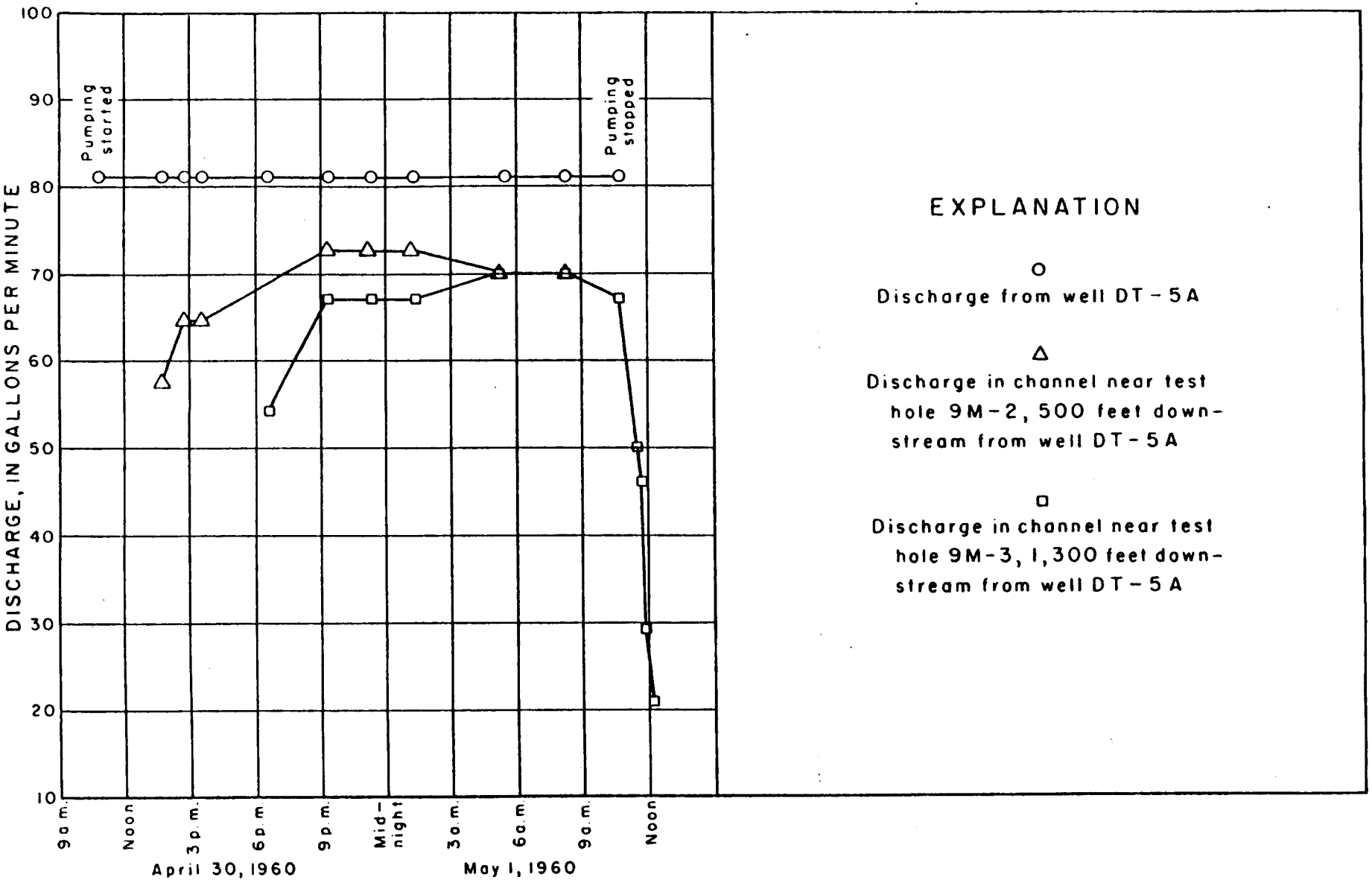

Figure 44.--Graph of measurements of flow downstream from well DT-5A as compared to discharge at well during pumping test April 30-May 1, 1960 at TA-49.

30.

Pumping started at 10:45 a.m. on April ~~1~~. From 10:45 a.m. to 9:15 p.m. flow measurements in the channel at test holes 9M-2 and 9M-3 showed varying flow losses owing to infiltration of water into the drill cuttings, ponding of water near test hole 5M-1, evaporation, and infiltration of water into the tuff and silty clay adjacent to and beneath the stream channel. Flow losses during this first period of the test became progressively less with continued saturation of more of the drill cuttings, stream-bed and stream-bank materials. Flow measurements at test holes 9M-2 and 9M-3 during the period from 9:15 p.m. April 30 to 1:10 a.m. on May 1, 1960, indicated that the flow and losses were at equilibrium. During this time flow loss between well DT-5A and test hole 9M-2 was 1.5 gpm per 100 feet of channel. The flow loss was 0.7 gpm per 100 feet of channel between test holes 9M-2 and 9M-3. The stream banks between test holes 9M-2 and 9M-3 were saturated sometime between about 2 a.m. and 7 a.m. on May 1, 1960, when flow in the channel measured at the test holes became about equal. Flow loss from the well DT-5A to test hole 9M-2 increased to 1.9 gpm per 100 feet of channel from 5:45 a.m. to 8:10 a.m. May 1, 1960.

The greater flow loss in the upper reach of the channel, both during the period of equilibrium and the period of no apparent loss in the lower reach, probably can be attributed to continued but slightly changing percolation into the drill cuttings. Additional vertical infiltration from the pond at the head of the channel may have occurred during this period as air bubbles rose to the surface of the pond at different times during and after the pumping test.

The moisture content measured in test hole 5M-1 did not change during the test. This indicates no lateral movement of water from the pond 22 feet from the test hole (fig. 39) although vertical infiltration from the pond probably occurred.

In test hole 9M-2 at a depth of 1.5 feet in the soil, the moisture content increased 16 percent from April 30 to May 1 (fig. 42). From May 1 to May 6, 1960, capillary return to the surface and evaporation decreased this moisture content by 13 percent. At a depth of 2.5 feet the moisture content increased 3 percent from April 30 to May 2, 1960. Below 2.5 feet there was no significant change in moisture content of the tuff.

In test hole 9M-3 the moisture content increased 6 percent at 1.5 feet from April 30 to May 3, 1960 (fig. 43). At a depth of 2.5 feet the moisture content increased 8 percent during the same period. At a depth of 3.5 feet and below there was no significant change in moisture content.

In the lower reach of the channel it is apparent that there was very little loss of flow after the channel and bank material was saturated. No change in moisture content was detected below 3.5 feet in depth in either of test holes 9M-2 or 9M-3. Any lateral filtration of water from the pond near test hole 5M-1 was not detected indicating that any infiltration would have been downward probably along vertical and near vertical joints into the underlying tuff.

Recharge to the main aquifer

Data obtained during the investigation indicate that Frijoles Mesa is not part of the ground-water recharge area in the region. Perched water was not found beneath TA-49.

The soil cover on the mesa at TA-49 prevents most of the precipitation from infiltrating into the underlying rocks. The clay-like soil forms an almost perfect seal over the mesa surface and the near-surface joints. This is evidenced by open joints in units 4 and 6 which blow air (figs. 15, 17, and 18) in response to declining barometric pressure. A very low moisture content (table 17) was found in the upper 300 feet of the Tshirege Member. The moisture-meter surveys indicate little or no increase in moisture content below the undisturbed soil zone. Where the soil cover has been disturbed, removed, or water allowed to pond, infiltration into the underlying tuff takes place slowly (fig. 37).

Decreasing flow downstream in perennial streams in Water Canyon to the north and Frijoles Canyon to the south indicates that some recharge may occur beneath the deeper canyons of the Pajarito Plateau. Available data do not show how much of the decrease in flow in the canyons is caused by evapotranspiration and how much is recharge to the bedrock.

The general shape and slope of the piezometric surface (fig. 45)

Figure 45.--Generalized contours on the piezometric surface of the main aquifer, Los Alamos area, New Mexico.

---

indicate the main source of recharge to the aquifer is west of Frijoles Mesa. The Pajarito fault zone and the slopes of the mountains, which receive relatively high precipitation, probably are part of the main source of recharge.

Some recharge from Frijoles Canyon can be inferred because of the configuration of the contours on the piezometric surface (fig. 45) in that area.

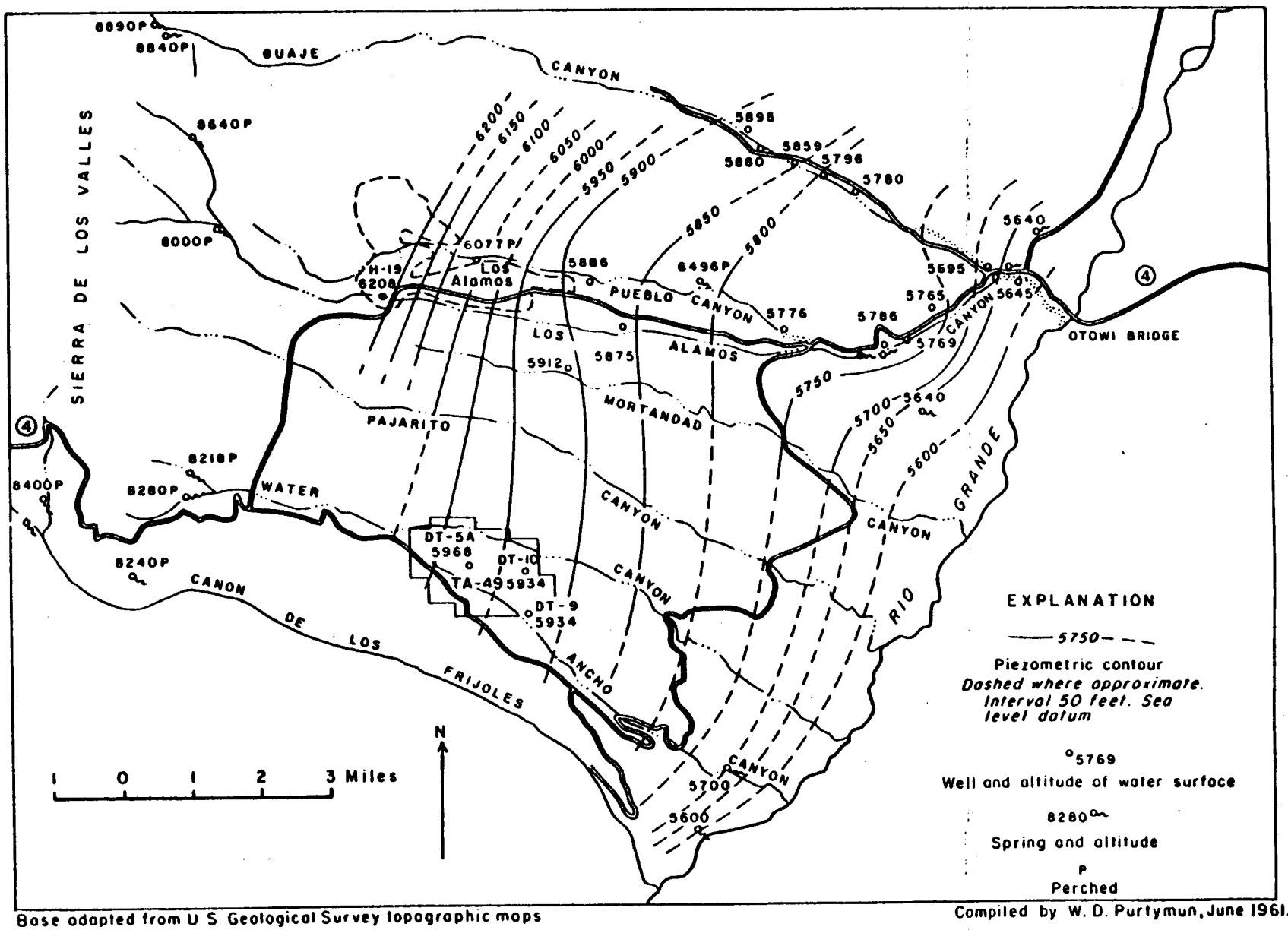

Base adapted from U S Geological Survey topographic maps

Compiled by W. D. Purtymun, June 1961.

Figure 45.--Generalized contours on the piezometric surface of the main aquifer, Los Alamc rea, N. Mex.

LASL AEC OFFICIAL

LASL AEC OFFICIAL

Depth to the piezometric surface of the main aquifer beneath TA-49 ranged from about 1,004 feet below the land surface at DT-9 to 1,172 feet at DT-5A. Much of the difference in water levels in different wells is due to topographic position; however, the altitude of the piezometric surface of the water is almost 40 feet higher in well DT-5A than in wells DT-9 and DT-10, which are respectively 0.8 mile southeast and 0.7 mile east of DT-5A.

The gradient on the piezometric surface is east-southeastward toward the Rio Grande at about 50 feet per mile (fig. 45).

Water-level changes

Water-level measurements in well DT-5A (fig. 46) indicate that

Figure 46.--Hydrograph of water levels measured and from recorder charts at well DT-5A, TA-49, Los Alamos County, N. Mex.

the water level was near 1,173 feet below the land surface after the well was developed. One level measured April 30, 1960, is anomalously low owing to residual drawdown after the aquifer test run on the well.

The water level in well DT-9 (fig. 47) declined about 3 feet

Figure 47.--Hydrograph of water levels measured and from recorder charts at well DT-9, TA-49, Los Alamos County, N. Mex.

during the period of drilling of the well. This decline probably represents difference of head in successively deeper water-bearing strata. The water level in 1960 was about 1,003 feet below land surface.

During April a recorder was operated at DT-9 and a microbarograph was operated at TA-49. Changes in water level in the well correlate qualitatively with changes in barometric pressure, but the amplitude of the water-level fluctuations indicates an additional effect that probably is caused by something other than barometric pressure.

LASL-AEC-OFFICIAL

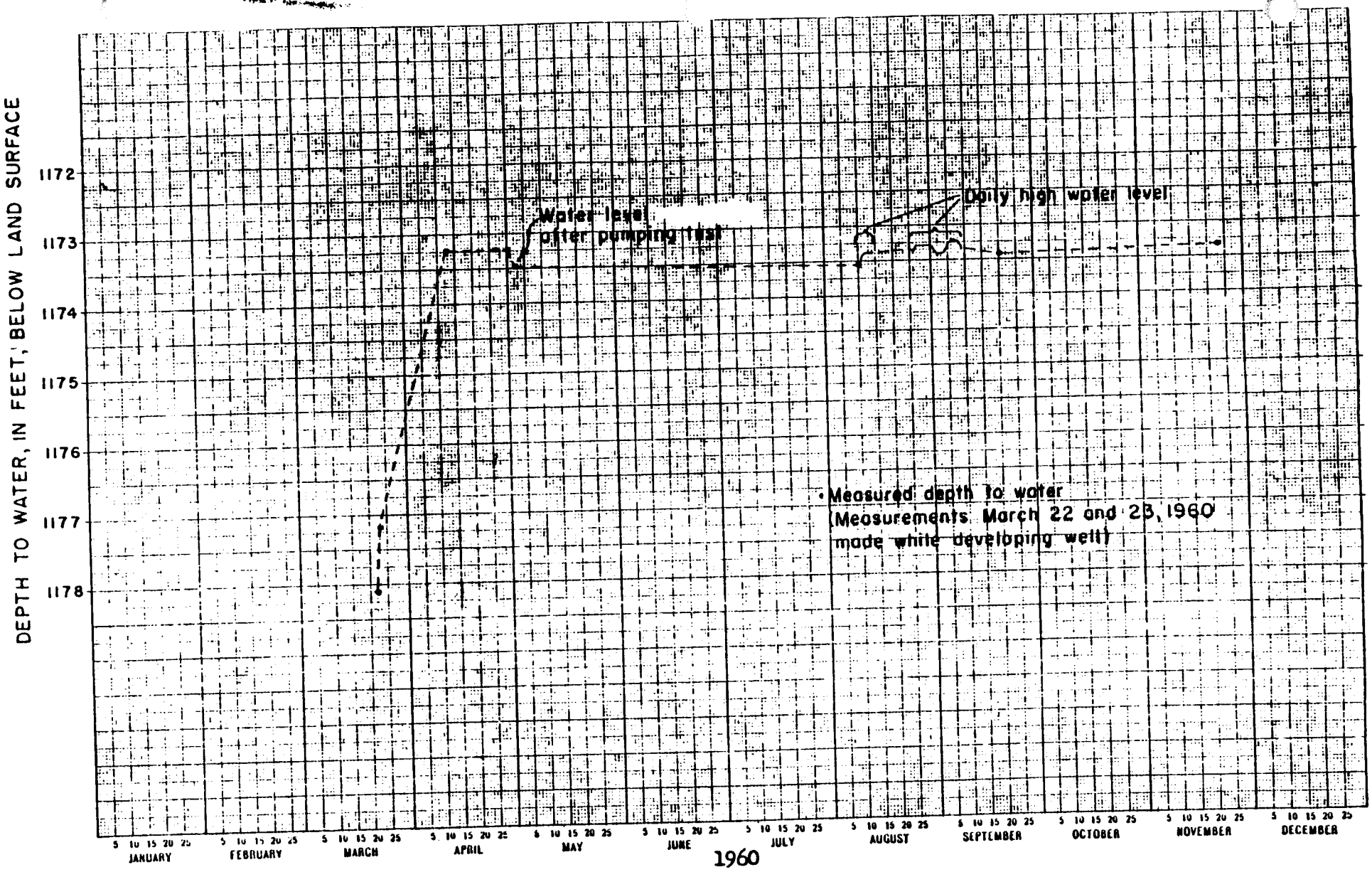

Figure 46.--Hydrograph of water levels measured and from recorder charts at well DT-5A, TA-49, Los Alamos County, N. Mex.

TA 49 168 A

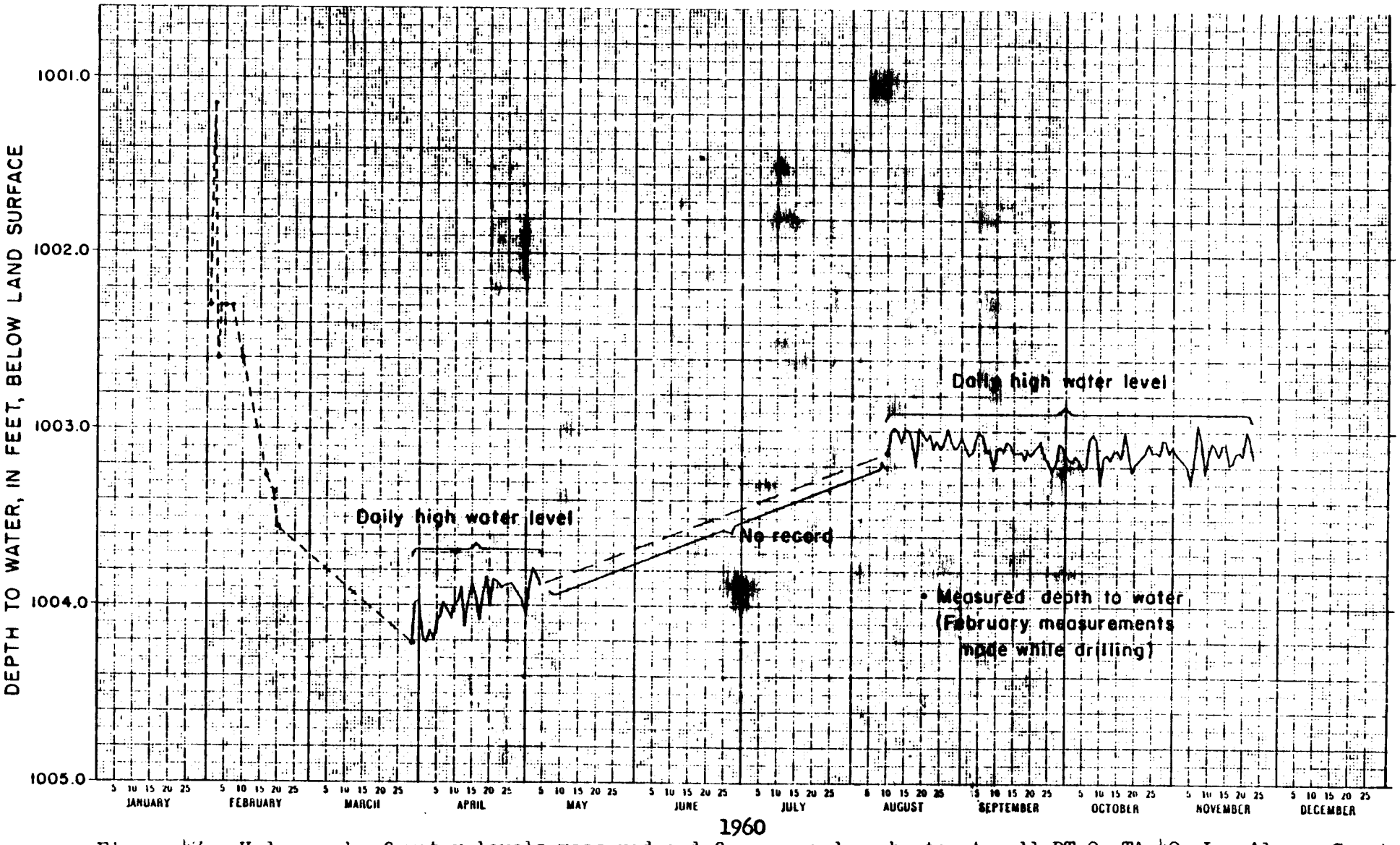

Figure 47.--Hydrograph of water levels measured and from recorder charts at well DT-9, TA-49, Los Alamos County, N. Mex.

Measurements of water level at well DT-10 (fig. 48) show a decline

Figure 48.--Hydrograph of water levels measured and from recorder charts at well DT-10, TA-49, Los Alamos County, N. Mex.

of slightly more than 1 foot during drilling. The change apparently represents a slightly lower head in the lower beds of the Puye conglomerate aquifer. A recorder was operated for 1 week on well DT-10, and daily fluctuations, though barely perceptible, correlate with barometric pressure changes. The water level in this well was about 1,085 feet below land surface during 1960.

LASL-AEC-OFFICIAL

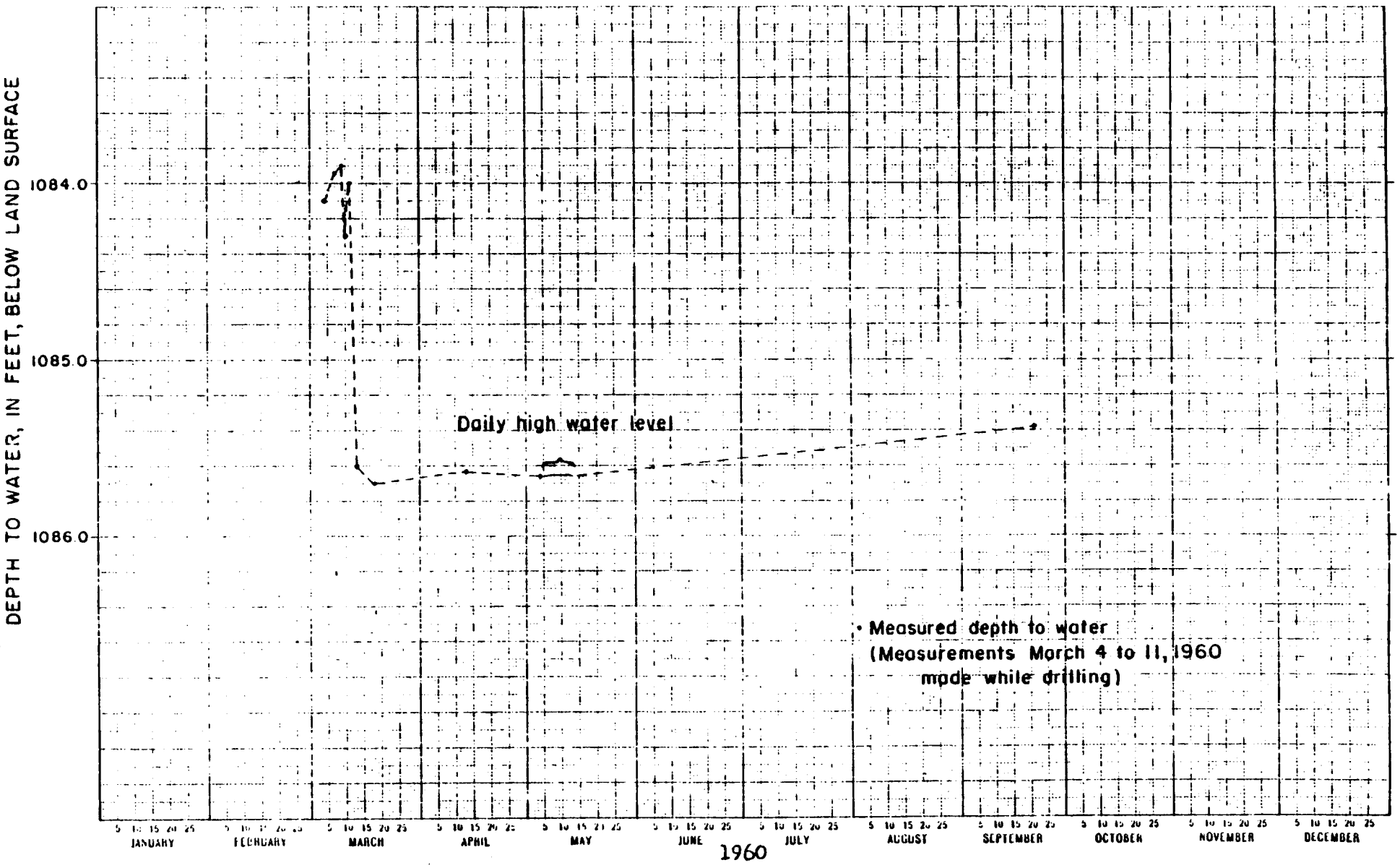

Figure 48.--Hydrograph of water levels measured and from recorder charts at well DT-10, TA-49, Los Alamos County, N. Mex.

Pumping tests

Pumping tests approximately 16 to 24 hours in length were run on wells DT-5A, DT-9, and DT-10 (Figures 49, 50). The pump used for the tests was a 40-horsepower submersible turbine. Discharge was measured by means of parshall flumes set near the well. Measurements of water levels were made with an electrical water-level indicator inside a 1-inch plastic tube banded to the pump. Drawdown and recovery were read directly on a steel tape fastened to the electrical lead for the probe. Recovery of water level after pumping in both wells was analyzed by the method devised by Theis (1935) and later described by Wenzel (1942).

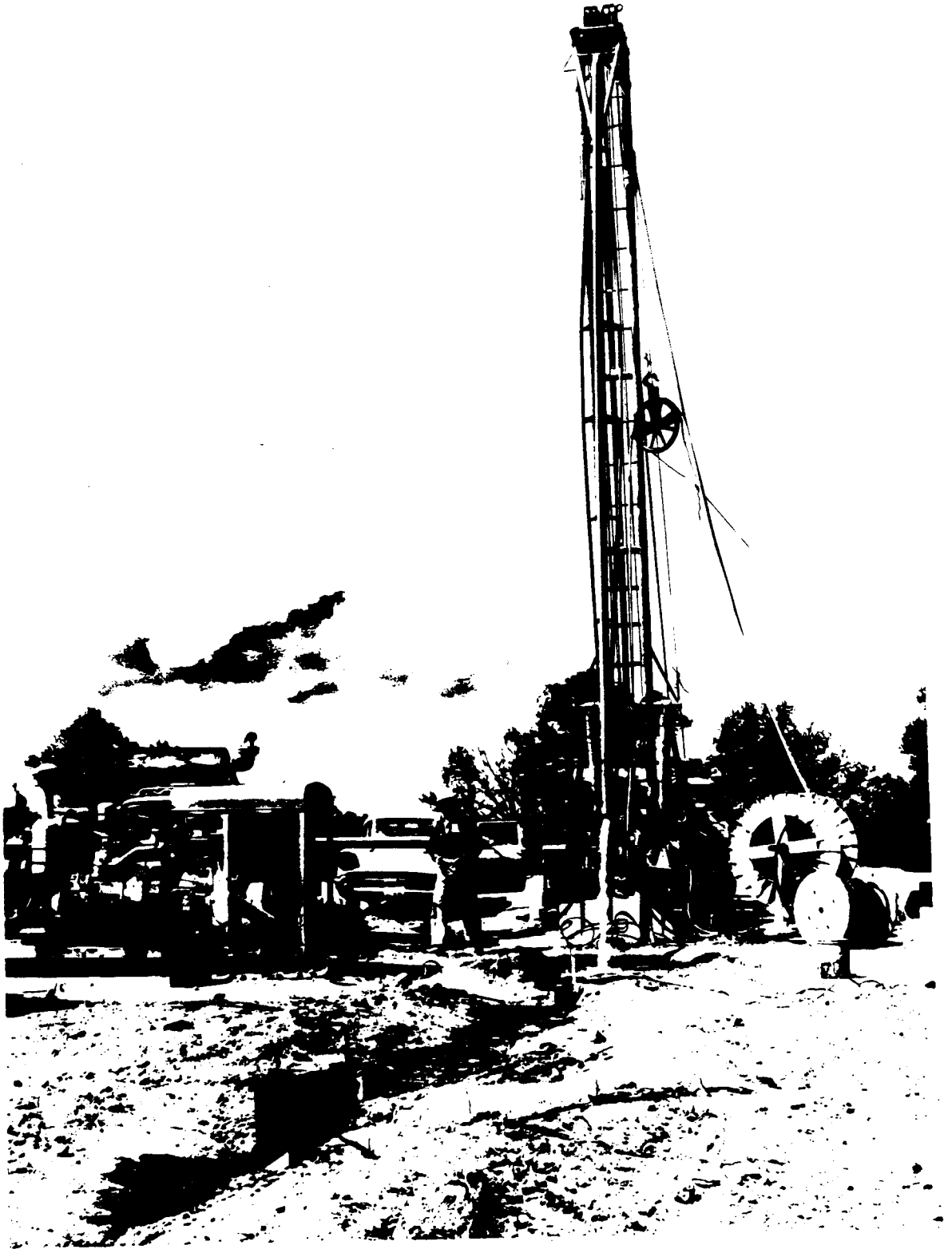

Figure 49.– Work over Rig on Well DT-9 during aquifer test

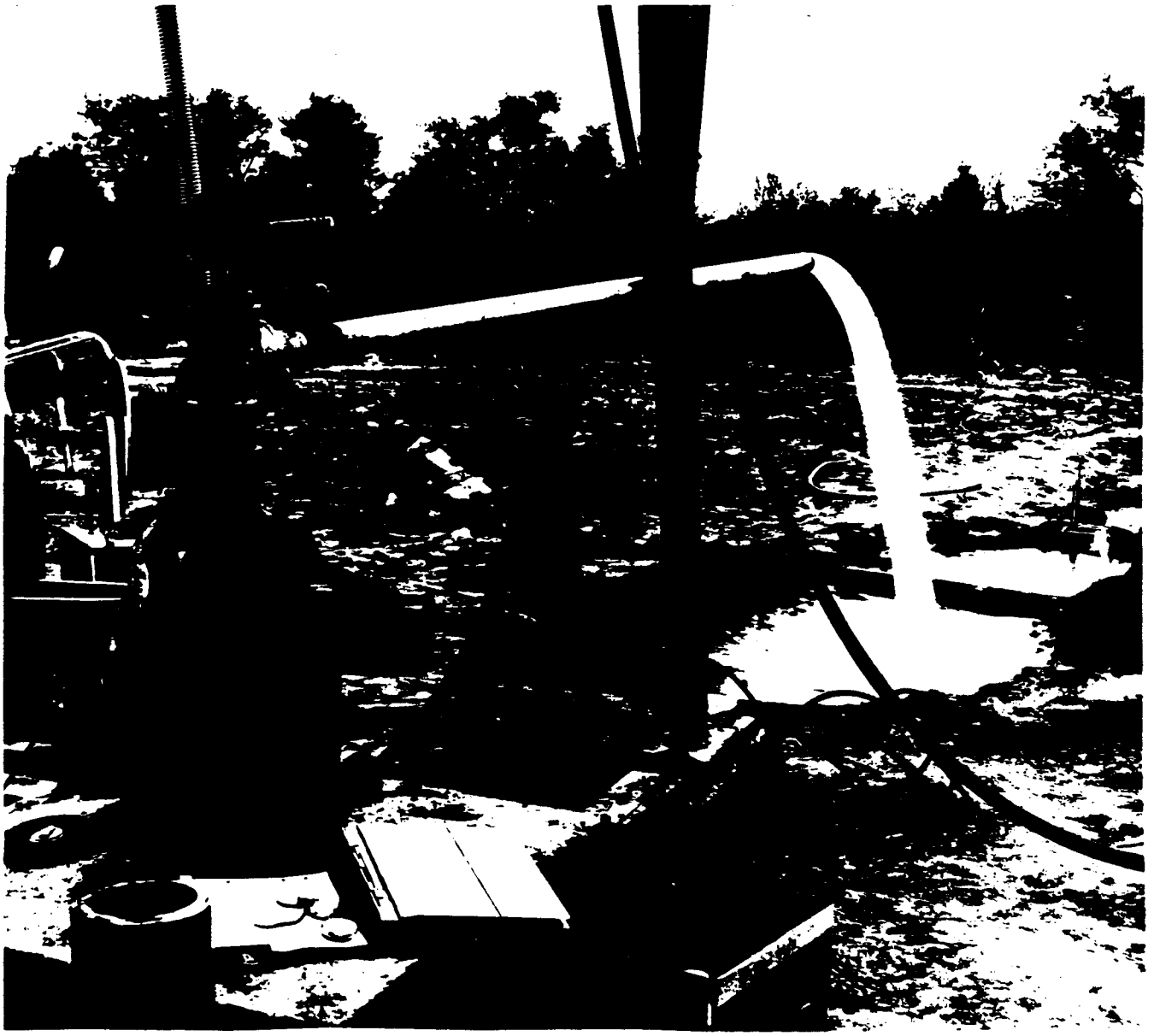

Figure - 50 Discharge from Well DT-4 during aquifer test

Tests at well DT-5A

Well DT-5A was pumped at a rate of 81 gpm for slightly more than 25 hours April 30 and May 1, 1960. The pump intake was set at 1,287 feet below the land surface for the test. Maximum drawdown during pumping was 14.1 feet indicating a specific capacity for the well of 5.7 gpm per foot of drawdown. Discharged water had a small amount of sand in it during the first 10 minutes of pumping, after which it cleared and remained clear. Temperature of the water pumped was 70°F.

Analysis of water-level recovery after pumping (fig. 51) indicates

Figure 51.--Semilogarithmic graph of recovery of water level in well DT-5A May 1 and 2, 1960, after pumping 25 hours at an average rate of 81 gpm.

a transmissibility, T, of 11,000 gpd per foot for the aquifer here. Approximately 350 feet of the saturated beds penetrated should readily yield water to the well, as indicated by the electrical log. Thus field permeability should be $\frac{11,000}{350}$ or 30 gpd per foot per foot. A comparison of this field permeability with that of well DT-9 suggests that only 20 percent of the potential water-bearing beds is yielding water. As the well was drilled by the rotary method it is inferred that about 80 percent of the saturated interval is plugged with drilling mud. If the well is to be used for water supply the specific capacity probably could be improved further by surging and by use of mud-cutting chemicals.

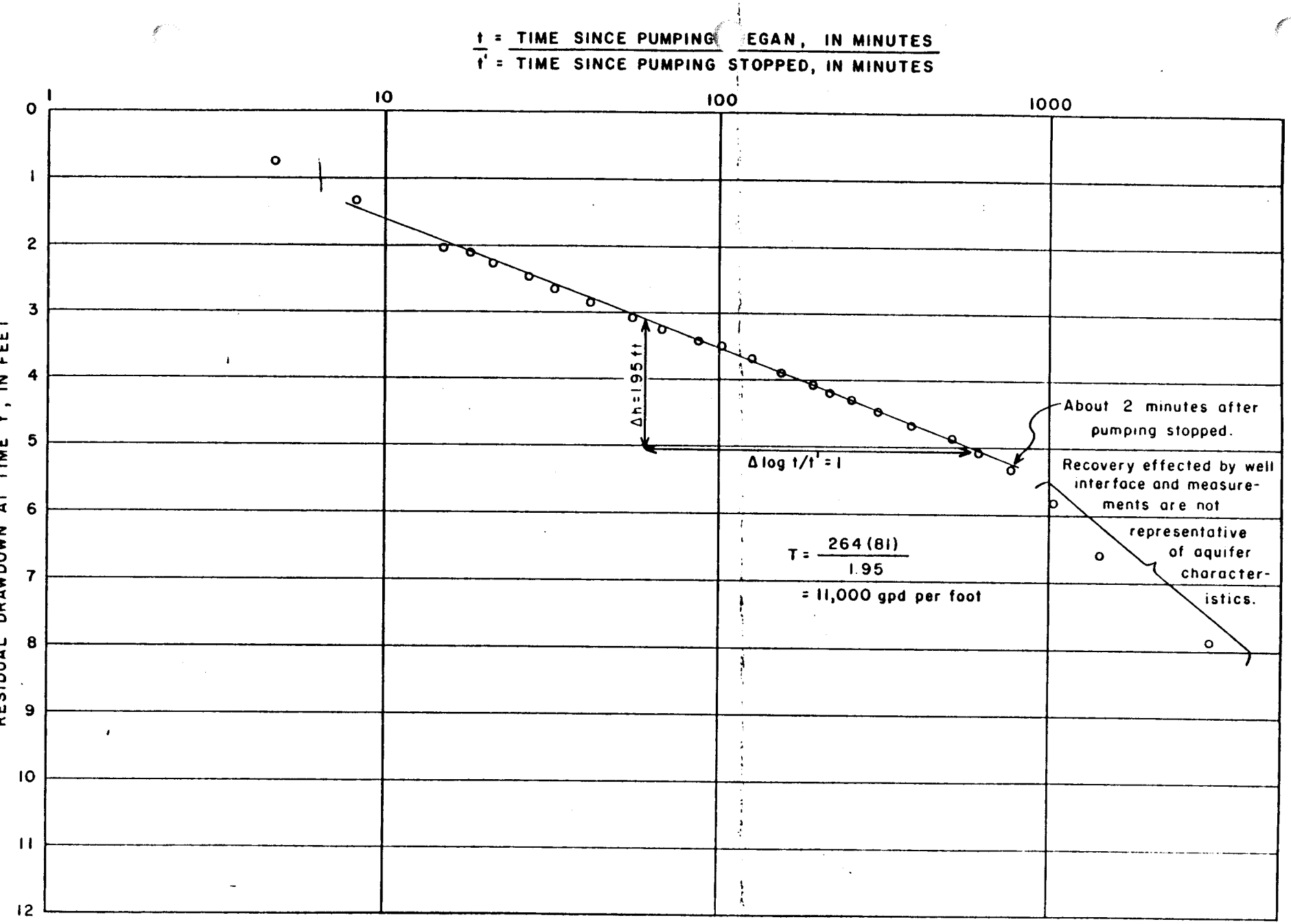

Figure 51.--Semilogarithmic graph of recovery of water level in well DT-5A May 1 and 2, 1960, after pumping 25 hours at an average rate of 81 gpm.

Tests at well DT-9

A pumping test was run on well DT-9 May 6 and 7, 1960. The pump was set at 1,117 feet below the land surface, and the well was pumped at 88 gpm--maximum discharge for the pump--for 24 hours.

Maximum drawdown during pumping was 3.95 feet, giving a specific capacity for the well of 22 gpm per foot of drawdown. The discharge was free of sand and sediment throughout the pumping test, and the water temperature was 70° F.

Recovery of water level was analyzed to determine transmissibility of the aquifer in the vicinity of the well (fig. 52). As determined,

Figure 52.--Semilogarithmic graph of recovery of water level in well DT-9 May 7 and 8, 1960, after pumping 24 hours at an average rate of 88 gpm.

the transmissibility, T, is 61,000 gpd per foot. ~~From~~ DATA geophysical logs and examination of drill cuttings, ~~it is estimated~~ INDICATE that about 300 feet of a total of 500 feet of saturated aquifer penetrated will readily yield water. Thus, field permeability should be $\frac{61,000}{300}$, or approximately 200 gpd per foot per foot.

The coefficient of permeability as determined at well DT-9 is more representative of the aquifer in the Santa Fe Group than the transmissibility determined at well DT-5A.

LASL AEC OFFICIAL

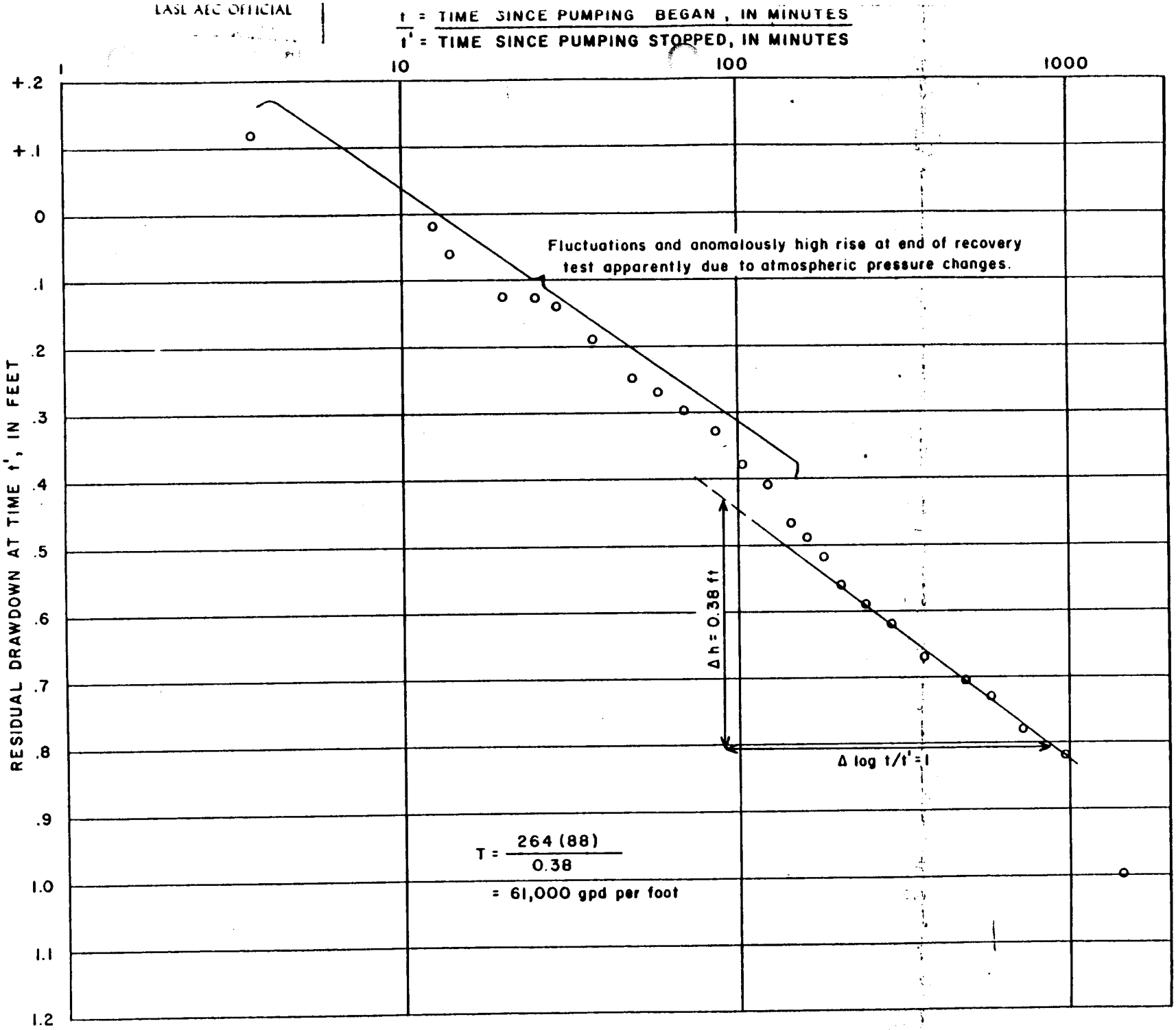

Figure 52.--Semilogarithmic graph of recovery of water level in well DT-9 May 7 and 8, 1960, after pumping 24 hours at an average rate of 88 gpm.

Tests at well DT-10

An attempt was made (May 1960) to install a pump in well DT-10. An obstruction was found in the well at 1,100 feet, where the casing is reduced with a liner from 12 to 8 inches in diameter. (See table 16.) The obstruction was later swaged out and the pump installed in September 1960.

A 16-hour pumping test was made on well DT-10 September 21 and 22, 1960. The pump was set at 1,185 feet below the land surface, and the average rate of pumping during the test was 78 gpm with a drawdown of 4.8 feet. The specific capacity of the well is 16 gpm per foot of drawdown. The discharge was free of sediment and clear in appearance except during the first minute of pumping, when a foamy, detergent-like substance came out with the water. Some rusty pipe scale was included in the water during the first few minutes of pumping, but this cleared up in a very short time. The temperature of the water during pumping was 67°F, which was 3 degrees cooler than water from the wells DT-5A and DT-9. Well DT-10 is finished in the upper part of the main aquifer, and the lower temperature of water from DT-10 tends to corroborate the stratigraphic analysis that indicates there may be a hydraulic separation between the Puye Conglomerate and the underlying undifferentiated unit of the Santa Fe Group. The cooler water suggests that there may be recharge into the aquifer nearby, possibly along Water Canyon.

Transmissibility of the Puye Conglomerate, as determined from analysis of water-level recovery (fig. 53), is 36,100 gpd per foot.

Figure 53.--Semilograthmic graph of recovery of water level in well DT-10, September 22 and 23, 1960, after 16 hours of pumping at an average rate of 78 gpm.

~~It is estimated~~ DATA from geophysical logs and examination of the drill cuttings INDICATE that about 200 feet of the saturated section penetrated by DT-10 readily yields water to the well. Therefore, field permeability is about 180 gpd per foot per foot, a figure that compares favorably with the field permeability of 200 determined at well DT-9.

LASL-AEC-OFFICIAL

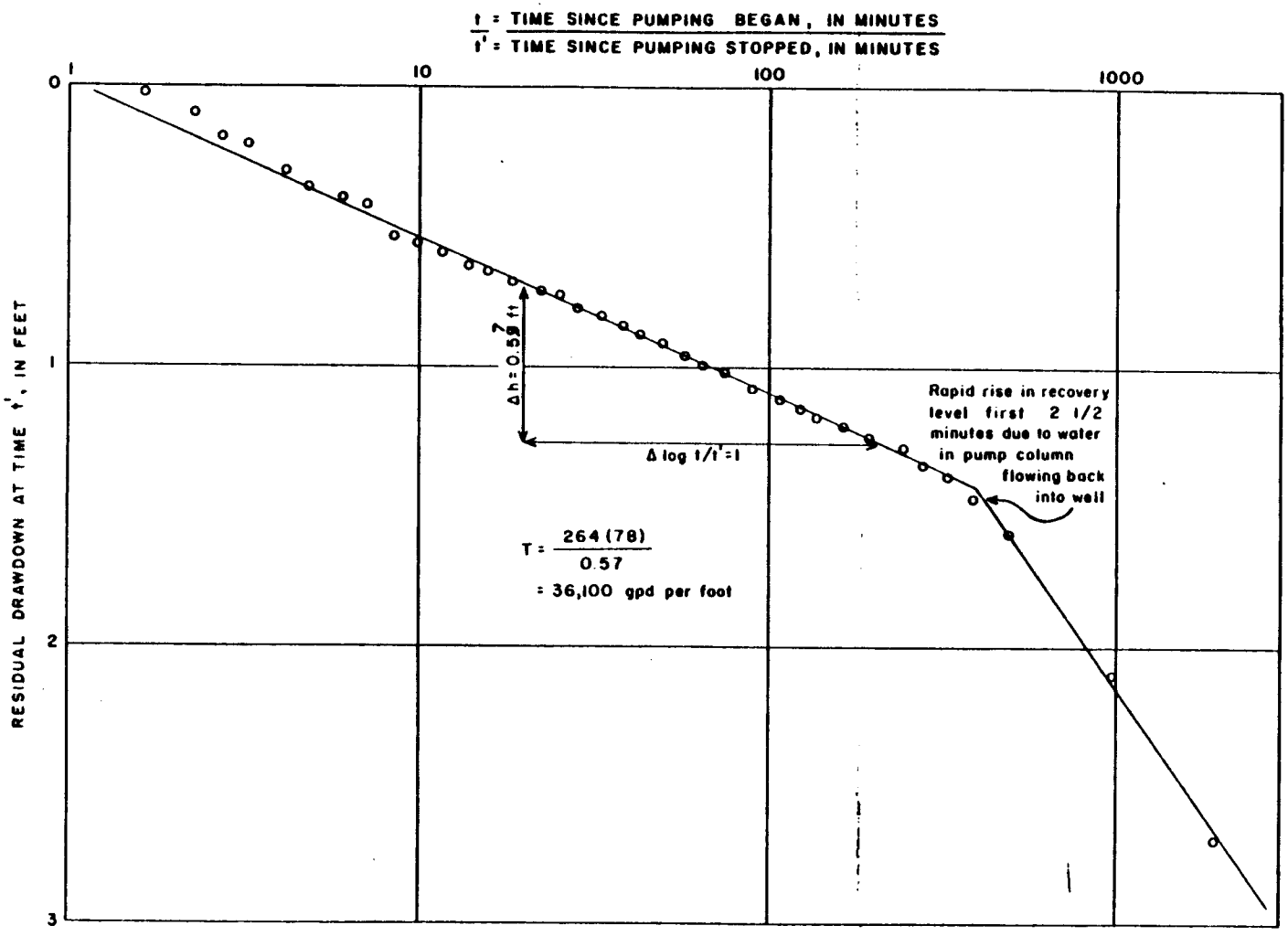

Figure 53.--Semilogarithmic graph of recovery of water level in well DT-10, September 22 and 23, 1960, after 16 hours of pumping at an average rate of 78 gpm.

174A

Velocity of ground-water movement

Velocity of flow in an aquifer can be computed by the following equation:

$$V \text{ (in feet per day)} = \frac{PI}{p}$$

wherein:

P = field permeability, gpd per foot per foot (gallons converted to cubic feet)

I = gradient, feet per foot

p = porosity of the aquifer, percent

The average permeability of the aquifer, as determined by pumping tests at wells DT-9 and DT-10, is approximately ~~190~~ 180 gpd per square foot, which is more representative of the aquifer than the value obtained at DT-5A. The gradient on the piezometric surface between wells DT-5A and DT-10 is about 60 feet per mile. Porosity is estimated to be 25 percent, an average value based on porosity determinations for many materials of the same character as those common in the Santa Fe Group. If these values are substituted in the above equation, the velocity is $\frac{180}{(7.48)\ 0.25} \cdot \frac{60}{(5{,}280)} = 1.098$ feet per day, or roughly 400 feet per year.

V =

Quantity of water moving through the aquifer

The quantity of ground water passing through a given cross-sectional area of the aquifer can be estimated from the equation

$$Q \text{ in gpd} = PIAp$$

where A is the cross-sectional area of the aquifer. The average estimated thicknesses of beds readily yielding water to the deeper wells DT-5A and DT-9 are 350 and 300 feet, respectively, or, averaged together, 325 feet. The width of the affected area beneath TA-49 at right angles to the east-southeast direction of movement of the ground water is about 2,000 feet. Then:

$$Q = (180) \cdot \frac{60}{5{,}280} \cdot (325)\,(2{,}000)\,0.25$$

$$= 331{,}440 \text{ gpd}$$

or approximately 370 acre-feet per year passing through the cross-section of the aquifer beneath the test areas at TA-49.

Quality of water

Water samples were collected while wells DT-9 and -10 were being drilled to determine whether there was a change in chemical constituents at depth (table 22). A single field conductance was made on a sample from well DT-5A at the end of the development period.

Analysis of water from various depths in wells DT-9 and -10 indicates a decrease in specific conductance in both wells and a decrease in carbonate concentration with depth in well DT-10. The pH of water in both wells also decreases with depth. This may indicate contamination by drilling mud of the water sampled. The analyses, though possibly contaminated, indicate that there is a small difference between chemical composition of the water within the Tschicoma Formation and members of the Santa Fe Group.

Water samples were collected at the end of the pumping tests on wells DT-5A, -9, and -10, and a single bailer sample was collected from well DT-10 upon completion. Water from the three wells is soft and is low in dissolved solids (table 23). The specific conductance is low, and the pH is near 7. Calcium, magnesium, and sodium are the principal cations, while more than 90 percent of the anions are bicarbonate. The silica content is high. The high silica concentrations are typical of water that is recharged or moves through extrusive felsic rocks, such as those which occur in the Los Alamos area.

The water from wells DT-5A, 9, and 10 is similar to water found in the test and supply wells in the area. The water is of good quality for domestic and most industrial use, but the silica scale produced when the water is heated may be objectionable for certain industrial uses.

Radiochemical analyses from wells DT-5A, 9, and 10 are shown on table ~~28~~ 23. The analyses indicate that the concentration of radionuclides is well below the tolerance limits and the data are included for future background study.

Table ~~21~~ 22.--~~Partial~~ chemical analyses of water ~~samples~~ from deep wells at TA-49, Los Alamos County, ~~New Mexico~~

(Analyses by U.S. Geological Survey, Quality of Water Branch, Albuquerque, N. Mex.

(Constituents in parts per million except as otherwise indicated in column head.)

Well No.	Depth of well (feet)	Date of collection	Stratigraphic unit	Temperature (°F)	Silica (SiO_2)	Bicarbonate (HCO_3)	Carbonate (CO_3)	Hardness as ($CaCO_3$) Calcium and magnesium	Specific conductance (micromhos at 25° C)	Specific conductance, ~~measured in~~ field (micromhos at 25° C)	pH
DT-5A	1,821	3-25-60	Santa Fe Group							420	
DT-10	1,120	3- 8-60	Puye conglomerate	65	54	202	15	103	617	520	8.9
	1,221	3- 8-60		66	41	157	3	56	506		8.4
	1,248	3- 8-60		67	43	154	9	77	488	400	8.7
	1,256	3- 9-60		68	37	160	5	67	529	370	8.4
	1,338	3-11-60		67						290	
	1,424	3-11-60		66						290	
	1,430	3-13-60		65						115	
	1,430	3-13-60		65						180	
DT-9	1,048	2- 2-60	Santa Fe Group	68	68	98	0	32	260		8.2
	1,060	2- 3-60			72	76	0	28	157		8.0

Table 21.--Partial chemical analyses of water samples from deep wells - Continued

Well No.	Depth of well (feet)	Date of collection	Stratigraphic unit	Temperature (°F)	Silica (SiO_2)	Bicarbonate (HCO_3)	Carbonate (CO_3)	Hardness as ($CaCO_3$) Calcium and magnesium	Specific conductance (micromhos at 25° C)	Specific conductance, measured in field (micromhos at 25° C)	pH
DT-9	1,220	2- 6-60	Santa Fe Group		64	110	0	38	299		8.2
	1,286	2- 9-60	Continued	49	65	112	1	41	326		8.3
	1,327	2-16-60		68	56	88	0	28	191		7.7
	1,501	2-20-60		68	60	78	0	33	155	185	7.5
	1,501	5- 7-60		71						145	

Table 22.--Radiochemical and chemical analyses of water from deep test wells at TA-4[illegible], Los Alamos County, N. Mex.

(Results in parts per million and equivalents per million except as otherwise noted.)

	Well DT-5A		Well DT-9		Well DT-10			
Analysis No.	3681		3688		3684[a]		4[illegible]74	
Date of collection:	5-1-60		5-7-60		5-5-60		5-22-60	
Chemical components								
	ppm	epm	ppm	epm	ppm	epm	ppm	epm
SiO_2	76	-	6[illegible]	-	65	-	65	-
Al	.2	-	.2	-	.1	-	-	-
Fe	.21	-	.4	-	.00	-	.01	-
Mn	.00	-	.00	-	.00	-	-	-
Ca	8.8	0.43[illegible]	12	0.599	12	0.5[illegible]	12	0.60
Mg	2.[illegible]	.238	1.2	.099	2.[illegible]	.238	2.9	.24
Na	14	.609	12	.522	11	.478	12	.52
K	1.8	.046	1.2	.031	1.2	.031	-	-
Cations (epm)	-	1.332	-	1.2[illegible]1	-	1.346	-	-
HCO_3	68	1.115	68	1.115	80	1.311	78	1.28
CO_3	0	.000	0	.000	0	.000	0	.00
SO_4	8.7	.181	3.7	.077	3.7	.077	-	-
Cl	.5	.014	2.0	.056	2.2	.062	-	-
F	.2	.011	.3	.016	.2	.011	.2	.01
NO_3	2.0	.032	.0	.000	1.[illegible]	.016	-	-
PO_4	.00	-	.28	-	.21	-	-	-
Anions (epm)	-	1.3[illegible]3	-	1.264	-	1.477	-	-
Difference:								
Cations - anions (epm)	-	-.021	-	-.013	-	-0.31	-	-
Physical characteristics and computed values								
Dissolved solids (ppm)								
Res. on evap. at 180°C	147		136		138		-	
Calculated	148		134		138		-	
Suspended solids (ppm)								
Hardness as $CaCO_3$ (ppm)	34		35		42		42	
Non-carbonate	0		0		0		0	
Specific conductance (micromhos at 2[illegible]°C)	132		125		135		131	
pH	7.6		7.[illegible]		7.3		7.7	
Color	0		0		0		-	
Radiochemical data								
Alpha activity (μμc/l)	< 1.3		1.4 ± 0.7		< 0.8			
as of	6-28-60		6-30-60		6-2[illegible]-60			
Beta activity (μμc/l)	7.3 ± 1.1		3.6 ± 0.5		8.7 ± 1.3			
as of	6-20-60		6-21-60		6-21-60			
Radium (Ra) (μμc/l)	< 0.1		0.1 ± 0.1		0.1 ± 0.1			
Uranium (U) (μg/l)	0.[illegible] ± 0.1		0.8 ± 0.1		1.[illegible] ± [illegible]			

Age of ground water in the principal aquifer

Tritium content in ground water sometimes can be used to determine the age of the water (von Buttlar and Libby, 1955, and von Buttlar and Wendt, 1958) and, with sufficient sampling, sometimes can be used as a tracer to obtain direction and rate of movement of ground water. The rate of movement of ground water may be determined by referring anomalously high tritium concentrations in ground water to recharge occurring soon after the hydrogen-bomb experiments. At the time of the explosion, large quantities of tritium were released into the atmosphere and returned to the earth's surface in precipitation. The first hydrogen-bomb experiment, in November 1952, released some tritium to the atmosphere, but the first experiment to release large quantities was in March 1954. Several series of tests were made between March 1954 and October 1958 (Telegadas, 1959).

Samples of rainfall at Los Alamos taken in June 1954, after the second hydrogen-bomb explosion, had 1,160 to 1,550 T.U. A tritium unit (T.U.) is defined as one atom of tritium in 10^{18} atoms of hydrogen. A sample collected Feb. 7, 1954, from Rito de los Frijoles, a stream that drains an area typical of recharge area to the north, at Bandelier National Monument, had 27.2 ±0.4 T.U. (von Buttlar and Libby, 1955) and is thought to be representative of rain and snow that fell on the recharge area between hydrogen-bomb explosions 1 and 2, in November 1952 and March 1954, respectively. Water from this era of recharge may appear in wells in TA-49 in about 1975 as water having an approximate tritium concentration of about 7 T.U. Average pre-bomb tritium content in precipitation is thought to have been about 8 T.U., based on analyses of Chicago precipitation by Kaufman and Libby (1954) and von Buttlar and Libby (1955). The only pre-hydrogen-bomb tritium analyses available are those made at Chicago. Assuming that water in the aquifer at TA-49 has not been enriched with tritium by local recharge, the age of water in the aquifer can be determined from samples collected from deep test wells, provided the samples contain detectable quantities of tritium.

Three samples of water from two of the deep test wells contained detectable quantities of tritium. As the half life of tritium is 12.26 years, the ages of samples could be computed. The following table includes the results of tritium analyses and computed ages of samples:

Well No.	Date collected	Date analyzed	Depth of well when collected	Tritium units (T.U.)	Computed ages of samples (years)
DT-5A	5- 1-60	11--60	1,821	2.6	19.9 or 20
DT-9	2-16-60	11--60	1,325	3.8	13.1 or 13
DT-9	5- 7-60	11-60	1,501	3.5	14.6 or 15

The significance of apparent differences in age cannot be fully assessed; however, it seems reasonable that water deeper in the aquifer moves more slowly and is actually older. Probably both samples that indicate relatively younger water are mixtures of water near the top of the zone of saturation with deeper water. More hydrologic data would be needed to determine which zones contribute most of the water in order to evaluate differing concentrations with depth in the aquifer.

Moreover, some young water may be added to the aquifer by local recharge from canyon sources such as Water Canyon. Thus, samples may be mixtures of a very small amount of local recharge water with older water coming from major areas of recharge on the mountain slopes to the west.

The Pajarito fault zone presumably is the most likely principal recharge area, as recharge should readily percolate downward here through fractured rock. The fault zone is about 3.7 miles, or 20,000 feet, up the ground-water gradient from TA-49. Assuming that the fault zone and vicinity are the main area of recharge and that the three samples analyzed are undiluted and unenriched water from the recharge area, then

$$\frac{\text{20,000 feet (distance to recharge area)}}{\text{15.9 years (average age of samples analyzed)}} = \text{1,260 feet per year,}$$

or about 1,300 feet per year is the approximate velocity of ground-water movement. This computed velocity is considerably greater than the velocity (400 feet per year) computed from pumping-test data and gradient of the piezometric surface. This line of reasoning does not allow any appreciable period of time for the movement of water from the surface in the recharge area down to the aquifer, which probably is a valid concept if open fractures are the route of downward movement.

The approximate location of the recharge area can be determined by using these age-of-water data in another way:

$$\text{400 feet per year} \times \text{15.9 years} = \text{6,300 feet}$$

Thus, a part of the area of recharge may be nearer to TA-49 than the Pajarito fault zone, probably along Water Canyon and other nearby canyons east of the Pajarito fault zone. Relegating any appreciable time to vertical movement in the zone of aeration would have the effect of making the recharge area closer to the point of sampling or increasing velocity of movement in the zone of saturation.

Conclusions and suggestions

Data obtained from the large-diameter holes indicates that little, if any, recharge to the ground water presently occurs at Frijoles Mesa. Clayey soil and clay filling the near-surface parts of joints are a barrier to infiltration of water into joints. The effectiveness of this impervious seal is indicated by blowing of air from open joints at depth in response to declining barometric pressure. At some time in the past, joints in the Bandelier Tuff have carried percolating water, as indicated by alteration of joint faces in the rock. This percolation presumably occurred before the soil mantle was developed.

The moisture readings in the test holes indicate that water rarely infiltrates the mesa surface to depths greater than the thickness of the soil and that a soil cover as much as 2 feet thick seemingly prevents natural infiltration to the underlying bedrock. Locally, where the soil cover is thin or absent and in some places on the mesa that receive runoff from well-drained areas, some small amount of infiltration into the tuff does occur.

Moisture determinations made in test holes adjacent to a natural channel that carried water discharged from well DT-5A during a pumping test indicate that infiltration took place laterally into the soil and related weathered materials. Moisture measurements in the holes made after flow stopped in the channel indicate that water that had moved laterally from the stream was returned to the surface by capillarity and evaporated. Some water was lost continually from a disturbed part of the channel in the upper reach throughout the period of flow. A part of this loss could have gone downward into the tuff.

The large loss of drilling mud and water into the 930 feet of Bandelier Tuff penetrated by wells DT-5 and DT-5A probably was into open joints. Data are not available to determine whether the water lost in drilling the two wells moved downward through the Bandelier Tuff and into the Puye Conglomerate. It is likely that this liquid is entrapped in the labyrinth of interconnected joints and is slowly being absorbed by the tuff adjacent to the joints.

No perched water was observed in the interval between the mesa surface at TA-49 and the main zone of saturation at a depth of somewhat more than 1,000 feet. The absence of perched water and the large bulk permeability of the Bandelier Tuff indicate that it would transmit water rapidly. Water that has access to the tuff and joint systems, if in sufficient quantities, will move with ease almost vertically downward into the Puye Conglomerate and eventually into the zone of saturation.

Soil materials for sealing abandoned test areas are available on the mesa. Soil for sealing purposes should be obtained in places as far away from testing areas as possible because wherever natural soil is scalped, chances are increased for infiltration of water into the tuff. Adequate drainage on the mesa should be maintained to prevent infiltration from ponded water.

Recharge to the ground water from Frijoles Mesa is very small or nonexistent; thus, no contaminants in solution are likely to be carried to the ground water beneath TA-49. However, if contaminants should reach the main ground-water body, several conditions, mainly hydrologic, exist that tend to decrease hazards resulting from such contamination:

1. Presently no ground water is used downgradient in the Los Alamos area from TA-49. The Rio Grande, into which the ground water is naturally discharged, is the nearest point of hazardous contamination of water supplies.

2. Some dilution of the contaminated water would occur in the aquifer and further dilution would occur in the Rio Grande as the contaminants were slowly discharged into it.

3. At the slow migration rate of ground water in the Los Alamos area, it would take about 80 years for contaminants to move from a point in the aquifer beneath TA-49 to the Rio Grande.

4. Ion exchange or adsorption of dissolved contaminants onto materials through which the contaminated water passes will reduce the concentration of radioactive contaminants. This was investigated by the Health Division of the Los Alamos Scientific Laboratory for the upper part of the Bandelier Tuff at TA-49. The aquifer materials also presumably will absorb some of the contaminants.

Suggested continuing study

Water samples for radiometric analysis should be collected annually from wells DT-5A, 9, and 10 to determine whether contamination is taking place. If well DT-5A could be pumped steadily and the water used at TA-49, it would be advantageous to monitoring because a slightly greater part of the aquifer could be sampled in this way. Samples from the other wells could be obtained with a bailer. The well that is pumped should be provided with an air line to record its water level and a measuring tube (about 1 inch in diameter) should be provided also so that air-line recordings can be checked periodically by direct measurement. A continuous water-level recorder should be installed in the well DT-9. The wells that are not used for water supply should be pumped once every 5 to 10 years for a period of 1 to 3 months and sampled for radiochemical analyses.

Moisture readings should be made in the test holes four times each year to determine whether there is infiltration of water. The frequency of moisture readings can be decreased in some of the holes when data indicate that the results are not significant.

Compacted soil should be used to seal the abandoned test areas, and the casings of the core holes in these areas should be extended through the soil cover. The core holes could then be used for measuring the moisture content of the compacted soil cover and underlying tuff and for gamma-ray logging.

It would be informative to sink an angular drift to a point a few feet beneath a large-diameter hole and inject water into the large-diameter hole to sample the water filtering into the angular drift by means of porous cups or drip-catching jugs. Injection water could be spiked with a radioactive tracer. Radiometric analyses of water samples should indicate whether contaminants will pass through tuff or joints in the tuff.

SELECTED REFERENCES
~~LITERATURE CITED~~

Griggs, R. L., 1955, Geology and ground-water resources of the Los Alamos area, N. Mex.: Administrative report released to AEC, 230 p., 17 pls., 17 figs., 5 tables. (Being revised for publication as a U.S. Geol~~ogical~~ Survey Water-Supply Paper.)

Hillebrand, W. F., 1900, Some principles and methods of rock analysis: U.S. Geol. Survey Bull. 980, 71 p., 1 pl., 10 figs.

Kaufman, Sheldon, and Libby, W. F., 1954, The natural distribution of tritium: Phys. Rev., v. 93, no. 6, p. 1337-1344.

Shapiro, Leonard, and Brannock, W. W., 1956, Rapid analysis of silicate rocks--a contribution to geochemistry: U.S. Geol. Survey Bull. 1036-C, p. 19-56, figs. 4-12.

Telegadas, Kosta, 1959, Announced nuclear detonations, United States, United Kingdom, Union of Soviet Socialist Republics, in Fallout from nuclear weapons tests, Hearings before the Special Subcommittee on Radiation of the Joint Committee on Atomic Energy, Eighty-sixth Congress: Washington, U.S. Govt. Printing Office, v. 3, p. 2517-2533.

Theis, C. V., 1935, The relation between the lowering of the piezometric surface and the rate and duration of discharge of a well using ground-water storage: Am. Geophys. Union Trans., pt. 2, p. 519-524, [August].

Theis, C. V., and Conover, C. S., 1961, Pumping test on wells at Los Alamos, New Mexico: U.S. Geol. Survey open-file report, 42 p.

von Buttlar, Haro, and Libby, W. F., 1955, Natural distribution of cosmic-ray produced tritium, II: Jour. Inorg. and Nuclear Chemistry, v. 1, p. 75-91.

von Buttlar, Haro, and Wendt, Immo, 1958, Ground-water studies in New Mexico using tritium as a tracer: Amer. Geophys. Union, v. 39, no. 4, p. 660-668.

Wenzel, L. K., 1942, Methods for determining permeability of water-bearing materials with special reference to discharging-well methods: U.S. Geol. Survey Water-Supply Paper 887, 192 p., 6 pls., 17 figs.

Appendix

Data contained herein was collected during the course of investigation of TA-49, Los Alamos County, N. Mex. It is not specifically considered in this report and is appended for possible use by future investigators.

Table 29.--Particle-size distribution in percent by weight for samples from TA-49, Los Alamos County, N. Mex.

Lab. No.	Source of sample	Depth (feet)	Stratigraphic unit in Tshirege Mbr.	Diameter of particles in millimeters									
						Sand					Gravel		
				<0.004 clay	0.004-0.0625 silt	0.0625-0.125 v. fine	0.125-0.25 fine	.25-.5 medium	.5-1 coarse	1-2 v. coarse	2-4 v. fine	4-8 fine	8-16 medium
60NM10	4-U	61	5	2.7	10.2	7.0	20.9	27.0	25.2	6.4	0.5	0.1	-
59NM199	4-A	66	5	3.9	11.0	7.3	9.6	17.9	24.3	20.1	4.9	.8	0.2
60NM24	Beta	10	1B	30.0	11.4	3.2	6.8	24.2	14.6	9.8	-	-	-
60NM25	Beta	65	1B	8.0	35.0	11.9	14.3	12.5	14.6	2.8	.7	.2	-
60NM26	Beta	135	1B	42.7	20.2	9.7	13.1	6.3	4.4	.6	.4	1.3	1.3
60NM27	Beta	180	1B	13.0	28.8	8.7	10.4	12.5	16.9	6.0	3.1	.6	-
60NM28	Alpha	175	3	3.9	24.3	10.4	11.4	14.6	16.4	19.0	-	-	-

225/193

Table 25.--Pore-size distribution and soil-moisture tension of samples from TA-49, Los Alamos County, N. Mex.

Lab. sample No.	Source of sample	Depth (feet)	Stratigraphic unit	Pore-size distribution (cm of water)					Moisture content at 1/3 atmosphere tension (percent)
				1	15	30	60	150	
60NM6	2-0	30	Qbt_6			-			40.05
60NM7	1-A	30	Qbt_6			-			40.86
60NM1	4-U	40	Qbt_6	45.80	43.81	41.54	41.88	40.46	38.74
60NM9	2-F	56	Qbt_6			-			29.60
60NM8	1-A	58	Qbt_6			-			40.55
60NM2	4-U	60	Qbt_6	48.45	46.18	44.06	44.72	43.41	42.62
60NM10	4-U	61	Qbt_5			-			4.49
60NM3	4-U	67	Qbt_4	39.51	38.22	40.09	35.18	22.30	20.68
60NM5	4-U	82	Qbt_4	36.95	34.76	33.11	33.17	29.96	24.54
60NM4	4-U	104	Qbt_4	33.57	32.23	30.38	30.96	31.22	29.14

Table ~~25~~ 26.--Reconnaissance notes for large-diameter holes in areas 1, 2, 3, 4, and 10, TA-49, Los Alamos County, N. Mex.

Area 1

Hole 1-A Diameter - 6 feet

Depth (feet)	
0-2	Soil
2-15	Vertical joint in west wall is 2 inches clay filled. In southwest wall vertical joint is ½ inch clay filled. Northeast wall has vertical joint 1/8 inch clay filled. South wall has vertical joint ¼ inch clay filled. North wall has two joints that are ¼ inch clay filled.
15	Northeast wall has horizontal joint open ¼ inch.
35	Vertical joints are open ¼ to ½ inch. Large fracture zone on northeast wall has joint openings ¼ to 1 inch.
50	Fracture zone on east wall contains joint openings ¼ to ½ inch.
55	Joints on north and west walls join at apex and are open ¼ inch.

Table ~~25~~ 26.--Reconnaissance notes for large-diameter holes - Continued

Area 1 - Continued

Hole 1-J

Depth (feet)	
0-3	Soil
3	Near vertical joint on southeast and southwest walls meet in apex down hole at 28 feet.
5	Horizontal joint is open 1/8 inch.
15	Low dipping joint system around hole has openings up to $\frac{1}{2}$ inch.
35	Apex of near vertical joint on northeast wall. Joint is open 1/8 inch.
52	Flat-lying joints are open 1/8 to $\frac{1}{4}$ inch.

Table 26.--Reconnaissance notes for large-diameter holes - Continued

Area 1 - Continued

Hole 1-P

Depth (feet)	
0-2	Soil, 2 feet thick on north wall, thins to 6 inches on the south wall.
2	Two vertical joints on north wall are 1 foot apart and contain $\frac{1}{4}$ inch of clay filling. East wall shows vertical joint which is 1 inch clay filled. Vertical joint on south wall is 1/16 inch clay filled. Vertical joint on west wall is complement of joint on north wall.
4	On northeast wall apex of joint dips steeply to the southeast.
16	Fracture zone.
25	Apex with limbs upward of two joints which are open 1/8 inch in places on the north and west walls. Well-developed, flat-lying joint is open 1/8 to $\frac{1}{4}$ inch.
30-35	Flat-lying joints which are open 1/8 to $\frac{1}{4}$ inch.
40	Vertical joints on north and northeast walls split and die out.
50	Well-developed joint system on north wall is open $\frac{1}{4}$ to $\frac{1}{2}$ inch.

Table 26.--Reconnaissance notes for large-diameter holes - Continued

Area 1 - Continued

Hole 1-T

Depth (feet)	
0-3	Soil, flat-lying joints under soil zone are clay filled.
3	Vertical joint on northwest wall is $\frac{1}{4}$ inch clay filled. Northeast wall shows a vertical joint which is 1 inch clay filled with white altered tuff $\frac{1}{4}$ inch on each joint face. Vertical joint on south wall is 1 inch clay filled.
17	Joint system exposed on east wall contains joints that are open 1/8 to $\frac{1}{4}$ inch.
21	Flat-lying joints extending around hole are open $\frac{1}{4}$ inch locally.
30	Vertical joint on south wall is open $\frac{1}{4}$ inch.
40	Apex of joint on northeast wall dips steeply to southeast and is open $\frac{1}{4}$ inch.
58	North-northeast wall contains joint which is open 1 inch. Trace of joint across hole on west wall is open $\frac{1}{2}$ to 1 inch. This is the same joint that has an apex at 40 feet.

Table 26.--Reconnaissance notes for large-diameter holes - Continued

Area 1 - Continued

Hole 1-W

Depth (feet)	
0-3	Soil
3	Northwest wall has vertical joint $\frac{1}{4}$ inch clay filled. Vertical joint on northeast wall is $\frac{1}{4}$ inch clay filled. Vertical joint on east wall is $\frac{1}{4}$ inch clay filled. Southwest wall has vertical joint 1/8 inch clay and root filled.
10	Southeast wall shows vertical joint with 1 to 3 inches of white alteration material in joint. Joint continued down hole to a depth of 25 feet.
15	Intersection of curved joint on west wall and joint on northwest wall. Intersection of joint is open $\frac{1}{4}$ to $\frac{1}{2}$ inch. Joint continues down hole on northwest wall. Flat-lying joint is open 1/8 inch.
25-40	Joint on southeast wall is open 1/8 inch passing through as intensely fractured zone. Joint on east wall is open 1/8 inch passing through intensely fractured zone.

Note: Below 40 feet most joints are open slightly.

Table 26.--Reconnaissance notes for large-diameter holes - Continued

Area 2

Hole 2-D Diameter - 6 feet; depth - 57 feet

Depth (feet)	
0-1	Soil
1-5	Pumice, water-laid.
5-6	Weathered zone, tuff fragments in matrix of brown clay.
15	Joints on northeast and west wall are clay filled 1 to $1\frac{1}{2}$ inches.
20	Horizontal joints around hole are clay filled $\frac{1}{4}$ to $\frac{1}{2}$ inch.
23	Joints mentioned at 15 feet come to apex on southwest wall, strike southeast and dip steeply southwest, and are 1 inch alteration filled.
27	Joint on north side of hole is open and clay filled locally up to $\frac{1}{4}$ inch.
32	Joint on south wall terminates against a joint system which dips to the northwest at about 30 feet.
42-43	Apex of joints mentioned at 27 and 32 feet strike east and dip steeply southward. Hole is strongly jointed. Northeast and southeast walls have large plucked zones. Joints on northeast wall are flat to steeply dipping northward and are open 1/8 to $\frac{1}{4}$ inch with some alteration lining.
43-57	Northern half of hole has many joints striking northwest and dipping steeply to the northeast.

Table ~~25~~ 26.--Reconnaissance notes for large-diameter holes - Continued

Area 2 - Continued

Hole 2-F Diameter - 6 feet; depth - 58 feet

Depth (feet)	
0-1.4	Soil, containing roots.
1.4-5	Pumice, water-laid, some clay, roots up to 3/4 inch thick. Bottom of pumice zone dips slightly to the north.
5-7	Weathered zone, tuff fragments in matrix of brown clay.
16	Northeast wall has several joints that are vertical, strike north, and are clay filled $\frac{1}{4}$ inch.
16-18	Numerous flat-lying joints are clay filled up to 1/8 inch.
20	Northeast wall has north-northeast striking joints that dip steeply to the northeast and are clay filled 1/8 to $\frac{1}{4}$ inch. Large medium gray devitrified pumice fragments up to 3 inches in length are found to a depth of 22 feet.
23	Irregular joints strike east-west and dip about 45° to the north. These joints circle the hole and are open locally up to $\frac{1}{4}$ inch.
25	Joints on southeast wall are clay filled. West wall contains irregular joints that are open 1/8 to 3/8 inch.
28	Hole diameter now 6.4 feet.
29	Flat-lying joints are open 1/8 to $\frac{1}{4}$ inch.
34	Irregular joints on north wall are open 1/8 to $\frac{1}{4}$ inch.

Table ~~25~~ 26.--Reconnaissance notes for large-diameter holes - Continued

Area 2 - Continued

Hole 2-F - Continued

Depth (feet)	
35-38	System of low angle joints around the hole. Joints strike east-west and are open locally up to 1/8 inch.
40-58	On the north side of hole is system of joints striking northwest, dipping steeply east that are open $\frac{1}{4}$ to $\frac{1}{2}$ inch. There is a large plucked zone on the north side of the hole from 49 to 58 feet. Hole is belled to 7 feet in diameter from 52 to 58 feet.

Table 26.--Reconnaissance notes for large-diameter holes - Continued

Area 2 - Continued

Hole 2-H Diameter - 6 feet; depth - 58 feet

Depth (feet)	
0-1	Fill, broken tuff.
1-2	Soil, clayey, brown.
2-5	Pumice, water-laid, about 3 feet thick on north and west wall, thins to 1 foot on southeast wall.
5-7	Weathered zone, tuff fragments in a brown clay matrix.
7	North-northeast striking joint dips to the west 80° to 85° and is clay filled 1 inch.
13	West-northwest striking joints on northwest side of hole dip with a slight angle and are clay filled.
18-22	East-west striking joints are clay and root filled up to $\frac{1}{4}$ inch. Apex on north side of hole.
22-26	East-west striking joints dip to the northwest at 15° to 30° and are open 1/8 to $\frac{1}{2}$ inch, clay lined.
30-34	Several west-northwest striking joints dip 45° to the north and are clay filled 1/8 inch.
35-42	Intersecting near flat-lying joint systems circle the hole. Above the joints tuff is light pinkish brown and is evidently altered by water. Below the joints the tuff is light gray.

Table 26.--Reconnaissance notes for large-diameter holes - Continued

Area 2 - Continued

Hole 2-H - Continued

Depth (feet)	
48	East-west striking joint dips 80° to 85° north and is open 1/8 to $\frac{1}{4}$ inch.
50-58	Northwest striking joint is tangent to hole on northeast wall causing bad pluck from 50 to 58 feet.

Table ~~25~~ 26.--Reconnaissance notes for large-diameter holes - Continued

Area 2 - Continued

Hole 2-J Diameter - 6 feet; depth - 58 feet

Depth (feet)	
0-2	Fill, broken tuff with about 6 inches of brown clayey soil near bottom.
2-5	Pumice, water-laid.
5	Northwest striking joint on west wall of hole caused pluck out.
11	Broken zone on south wall of hole.
11-19	Light gray tuff contains dark gray devitrified pumice fragments up to 1½ inches in length.
22-29	Northwest striking joint on west wall of hole is clay and root filled.
33-36	East-west striking joint dips north at 20° to 30° and is open up to ¼ inch. Northwest striking joint now striking north and drifts to center of hole at bottom, dipping about 80° east. Light pink alteration in joints that are open locally.
41	Northwest striking joint system dips 15° to 30° north and is open up to 1/8 inch.
45-58	Small pluck out on north wall between 45 and 58 feet. Bottom of hole is in relatively unjointed rock.

Table ~~25~~ 26.--Reconnaissance notes for large-diameter holes - Continued

Area 2 - Continued

Hole 2-L Diameter - 6 feet; depth - 58 feet

Depth (feet)	
0-2	Soil
2-10	On north wall a northeast striking vertical joint is clay filled ½ inch to a depth of 10 feet. Below 10 feet this joint is open. North-northwest wall shows vertical joint that is ¼ inch clay filled. Southwest wall shows vertical joint striking northeast that is 2 inches, clay filled. At 10 feet there is a system of flat-lying joints.
20	System of flat-lying joints are open locally up to 1/16 inch.
34	On north wall a joint is open ¼ inch with pink weathered tuff on each side forming clay lining of joint surface. Triangular pluck hole on south wall.
36	Triangle-shaped pluck hole on east wall.
44	Joints are clay and root filled.
54	Most joints are closed. Some are open locally up to 1/16 inch.

Table 26.--Reconnaissance notes for large-diameter holes - Continued

Area 2 - Continued

Hole 2-0 Diameter - 6 feet; depth - >8 feet

Depth (feet)	
0-1	Soil, brownish, clayey.
1-5	Pumice, water-laid, pieces up to 1 inch in length, subrounded with some clay interlayered. Base of pumice dips slightly to the northeast.
5-7	Weathered zone composed of large, angular pieces of tuff in a matrix of brown clay.
7-15	Master joint on northeast and south walls striking north-northeast, dipping steeply, is clay filled $\frac{1}{2}$ inch with a few roots. Joint on northwest wall strikes north-northwest and is 1 inch clay filled but is open locally. Joint on west-southwest wall strikes north and is $\frac{1}{4}$ inch clay filled. On south wall is a system of vertical joints striking east-west.
15-21	A flat-lying joint dips at a low angle to the north-northwest and is open up to 1/8 inch. Several minor joints terminate against this flat-lying joint. At 17 feet tuff appears more dense than above.
23-26	Badly broken zone dipping slightly north-northeast.

Table ~~25~~ 26.--Reconnaissance notes for large-diameter holes - Continued

Area 2 - Continued

Hole 2-0 - Continued

Depth (feet)	
31	Master joint on northeast wall is clay filled and locally open ½ inch. On west wall a system of vertical joints originates in a broken zone at 26 feet. Joints in system strike north-northeast and are clay filled and open locally up to ¼ inch.
37	Pluck out of master joint on northeast wall where joint is open 3/4 inch; opening extends 1.5 feet into the face of the hole. Tuff contains devitrified pumice fragments up to 1 inch across.
40	Joint on northeast wall, dipping moderately to the north, and connecting joint on west wall with master joint.
41-50	Large triangular pluck from intersecting joints on southwest wall. Master joint on northeast wall is now hair line. West-northwest striking joint, complement of plucked out joint at 40 to 41 feet. This joint has roots and brown clay at 45 feet.
54	Apex of north-northwest striking joint on west wall. Rock has considerable amounts of granule to pebble-size devitrified pumice fragments.
55	Joint on northwest wall dips moderately to southeast. Apex is at 55 feet.

Table 26.--Reconnaissance notes for large-diameter holes - Continued

Area 2 - Continued

Hole 2-S Diameter - 6 feet; Depth - 58 feet

Depth (feet)	
0-3	Soil, clayey, brown.
3-5	Pumice, water-laid.
5	Vertical joint north-northeast wall clay filled 1/32 inch. Vertical joint on southwest wall is ½ inch clay filled. Vertical joint on west wall is 1 inch clay and root filled.
17	Joint system, clay filled triangular pluck 8 inches across.
22	East wall shows joint striking northeast.
24	Vertical joint on west wall becomes irregular with various branches that are clay filled.
32-35	Vertical joint on west wall splits and dies out at 35 feet. Joints are clay and root filled 1/8 inch. Horizontal joints at 35 feet are open up to ¼ inch.
40	Joint system about 1 foot east of north line is open ¼ inch. Small irregular closed fractures are found at various places around hole.
49-57	Joints and pluck on east wall. Southwest wall has vertical joint. Joint trending east dips 45° west. Joints are clay filled and open locally up to 1 inch.

Table 26.--Reconnaissance notes for large-diameter holes - Continued

Area 2 - Continued

Hole 2-V Diameter - 6 feet; depth - 58 feet

Depth (feet)	
0-4	Soil, brown with pumice pockets on southwest wall.
4-5	Weathered zone, tuff fragments in a matrix of brown clay.
10	Master joint on northeast wall strikes south-southwest and is 1 inch clay filled.
9-15	Vertical joint tangent to north-northeast wall strikes east-southeast and intersects master joint. Joint on southwest wall strikes northwest and causes pluck at 15 feet, where joint is tangent to hole.
18	Flat-lying brecciated zone around hole. Devitrified pumice fragments in tuff are as much as 1 inch in length. Joint on southwest wall strikes northeast and is open ½ inch.
28	Southwest striking joint intersects tangential joint on northeast wall. Southwest wall has badly broken zone from 18 to 28 feet. Joints in this zone are open. Joint originating in broken zone at 26 feet strikes northeast and apparently is the same as the joint that intersects tangent joint on northwest wall at this depth.

Table ~~25~~ 26.--Reconnaissance notes for large-diameter holes - Continued

Area 2 - Continued

Hole 2-V - Continued

Depth (feet)	
38	Tangential joint now single trace near north wall striking southeast. Joint that originates in broken zone at 26 feet dips steeply southeast, and trace on wall of hole is drifting eastward.
50	Roots in joints on west wall.
57	Northeast striking joint has roots at 57 feet. Bottom of hole strongly jointed. Hole belled to 6 feet 8 inches from 50 to 58 feet.

General note: Hole is in moderately jointed rock. Tuff penetrated is fairly dense and not strongly jointed except 50 to 58 feet.

Table 25.--Reconnaissance notes for large-diameter holes - Continued

Area 2 - Continued

Hole 2-W Diameter - 6 feet; depth - 58 feet

Depth (feet)	
0-3.6	Soil, brown.
4	Master Joint on west side of hole is 1 inch clay filled.
12	Master joint dips to north and is clay and root filled up to 1 inch. Tuff is light gray and dense. Small joints are clay filled.
19	Master joint is 2.9 feet west of north and is clay filled 1/8 inch. Two joints dip 45° north at 18 feet. Joint on southwest wall, 2.5 feet from master joint, is clay filled $\frac{1}{4}$ inch.
26	Northeast striking joint is tangent to hole on south wall. It causes pluck out from 26 feet to bottom.
30	Two joints dip 45° into master joint 2.7 feet west of north.
37	Roots in plucked zone in south edge of hole.
44	Master joint 2.2 feet west of north is open locally up to $\frac{1}{4}$ inch.
51-58	Roots in pluck zone on south wall. Joints appear to strike northeast.

Table ~~25~~ 26.--Reconnaissance notes for large-diameter holes - Continued

Area 2 - Continued

Hole 2-X Diameter - 6 feet; depth - 56 feet

Depth (feet)	
0-2.5	Soil zone, brown clay, slightly pumiceous with large roots throughout. Soil thickens slightly on west wall and grades into pumice zone on east wall.
2.5-4	Pumice with brown clay and roots.
4-5.5	Weathered zone with tuff and some pumice in a matrix of brown clay. One system of vertical joints occurs below the weathered zone on the northeast wall. A few flat-lying joints found on southwest wall are about 1/8 inch clay filled.
10	Major vertical joint strikes north-northeast and is 1/8 inch clay filled. One joint dips steeply east.
20	Major joint on northeast wall dips to the northwest at a low angle. A few irregular minor joints, which dip to the east and south, are found on the north wall. Irregular minor joints found on the south wall are flat-lying.
30-41	Hole is badly broken between major joints on west wall, southward around hole to major joint on northeast wall.

Table ~~25~~ 26.--Reconnaissance notes for large-diameter holes - Continued

Area 2 - Continued

Hole 2-X - Continued

Depth (feet)	
45	Major joints on north-northeast and southwest walls strike southwest and apparently are same system. Intersection on southwest wall open up to 3/4 inch locally, but intersections on northeast wall are open 1/8 inch. South and east walls ~~is~~ are badly broken between these major joints. Vertical joints are found on the north wall from 42 feet to the bottom of hole.

Table 26.--Reconnaissance notes for large-diameter holes - Continued

Area 3

Hole 3-C Diameter - 6 feet; depth - 87 feet

Depth (feet)	
0-3	Soil and fill.
3	Joint striking south-southwest dips north and is $\frac{1}{4}$ inch clay filled.
7	System of flat-lying joints.
15	System of joints striking north-northeast dip about 20° west. Joint mentioned at 3 feet now vertical and open 1/16 inch.
21	Joint mentioned at 3 feet now dipping about 80° south.
28-30	Brecciated zone, system of joints striking east-northeast dipping from 10° to 20° north.
33	Joint mentioned at 3 feet now vertical, strike to north at 28 feet. South wall shows joint that strikes northeast. Pluck along joint which is open up to $\frac{1}{2}$ inch.
33-45	Joint in southeast wall that is clay filled $\frac{1}{2}$ inch. At 45 feet joint mentioned at 3 feet is here closed.
53	Southeast wall is badly broken. Northwest wall contains vertical joint striking west-northwest and is 1/8 inch clay filled.
58	Joint mentioned at 53 feet terminates against apex of northeast striking joint which is tangent to hole on northwest wall. Clay filling up to $\frac{1}{4}$ inch thick. Several plucks along each fracture.

Table ~~25~~ 26.--Reconnaissance notes for large-diameter holes - Continued

Area 3 - Continued

Hole 3-C - Continued

Depth (feet)	
63	Southwest limb of joint that showed apex at 58 feet is here a hair line. Northeast joint plucked out, has clay filling. Joint on southeast wall strikes east, dips 85° south, and is open ½ inch. West wall contains north striking vertical joint that is clay lined and is open 1/8 inch. North wall contains vertical, north striking joint.
72	Joint on southeast wall terminates.
78	Water-laid sand on north wall is 2.5 feet thick. Two joints below sand are 2 and 6 inches wide and extend to bottom of hole at 87 feet. Sand is 0.85 feet thick on west wall, 0.5 feet thick on east wall, and 0.4 feet thick on south wall.
78-87	Joints beneath sand strike northeast and are closed. Joints on north wall are filled with sand and range from 2 inches to over 1 foot wide. Some pieces of tuff are found in the sand filling. Tunnel drift to the north is about 2 feet in diameter. It intersects two northeast-striking, sand-filled joints about 2 inches wide, 2 feet apart, approximately 8 feet from the wall of the large-diameter hole.

Table 25.--Reconnaissance notes for large-diameter holes - Continued

Area 3 - Continued

Hole 3-C - Continued

Note: Hole 3-C was re-examined after shot in hole 3-A. As the working caisson was set, only the bottom 8 feet of hole was re-examined. The sand-filled joints on the north wall were open as much as 1 foot from the hole face where the sand was shaken out by the concussion of the shot. Partial collapse of the 24-inch drift occurred about 8 feet from the hole between the two northeast-striking joints. The drift was partly filled with rubble at this point.

Table 26.--Reconnaissance notes for large-diameter holes - Continued

Area 4

Hole 4-K Diameter - 6 feet; Depth - 58 feet

Depth (feet)	
	Soil and weathered zone are covered with casing.
8	Southwest wall shows apex of joint, which is clay and root filled up to 1 inch, and strikes west-northwest, dips 70° northeast. East wall has joint which strikes north-northeast with apex upward at 10 feet. Joint is 2 inches clay filled. Northwest wall shows vertical joint striking northwest, clay filled up to 6 inches near top and 2 inches at 9 feet.
15	Joint on southwest wall is clay and root filled. Joint on northwest wall is here clay and root filled about 1 inch. Tuff has devitrified pumice fragments up to 1 inch in length.
18	Pluck out at joint on southwest wall. Joint on northwest wall splits. Northernmost joint strikes northwest, is clay filled ½ inch, and terminates at 40 feet. Westernmost joint dies out at 22 feet.
26	Dip of the joint on southwest wall at 8 feet is now 80°, northeast several marked plucks from this joint, which is clay and root filled 1 inch.
33	Joint described at 26 feet is here trending vertical reverses in dip farther down. It is now striking west-northwest and dipping 80° south-southeast.

Table 26.--Reconnaissance notes for large-diameter holes - Continued

Area 4 - Continued

Hole 4-K - Continued

37	Tuff is less strongly jointed below this depth.
42	On the northeast wall is a system of vertical north-northwest striking joints that are clay filled.
58	Joint mentioned on southwest wall at 8, 26, and 33 feet is now vertical and strikes northeast.

Table 26.--Reconnaissance notes for large-diameter holes - Continued

Area 4 - Continued

Hole 4-M Diameter - 6 feet

Depth (feet)	
0-5	Soil entirely stripped off. East wall shows large vertical joint that strikes northwest and is 1 inch clay filled. North wall has 3/4-inch clay-filled joint that strikes northwest. Southwest wall has 2 vertical joints that are one foot apart and are 1 inch clay filled. South wall has vertical fracture striking north which is 1½ inch clay filled.
10	Brecciated zone on northeast wall.
15	Joint system on north-northeast wall contains joints that are open up to ½ inch.
20	Flat-lying joints all around hole. Joint on north wall now ¼ inch clay filled.
25	Vertical joints mentioned from 0 to 5 feet still persist. Flat-lying joints at 24 and 28 feet.
30	Joint on south wall is now open ¼ inch.
35	Pluck out along joints, on southwest wall.
40	Joint splits at 33 feet on south wall, dips eastward at 45°, and both branches are open up to 1/16 inch.
50	Vertical joints still persist and are ½ to 1 inch clay filled.

Table ~~25~~ 26.--Reconnaissance notes for large-diameter holes - Continued

Area 4 - Continued

Hole 4-O Diameter - 7 feet; Depth - 58 feet

Depth (feet)	
0-2	Soil and weathered zone.
2-26	Northwest and southeast wall of hole has vertical joints that are 1 inch clay filled and strike northwest. On southeast wall a joint strikes north, is near vertical, and contains clay filling up to 3 inches. Hole walls appear to be tight except for the above-mentioned joints.
26-32	Northeast wall of hole contains apex of joint. West limb dips at 45° to 30 feet and intersects vertical northwest striking joint on northwest wall. East limb of joint is vertical and 1 to 3 inches clay filled.
32	Northeast wall is brecciated.
35	Hole reduced in diameter about 4 to 6 inches.
41	Northwest striking joint is 1 to 3 inches clay filled and contains a few roots.
48	Southwest wall has northwest striking joint that shows apex with limbs downward. Limbs are clay filled up to 1 inch. Joints noted at 41 feet here are dipping (45° or less) and are clay filled. On southeast wall joint strikes northwest, persists to bottom of hole, and is 1 inch clay filled.

Table 26.--Reconnaissance notes for large-diameter holes - Continued

Area 4 - Continued

Hole 4-Y Diameter - 6 feet; Depth - 69 feet

Depth (feet)	
0-2	Soil zone is thin on weathered tuff zone.
7	Southeast wall has joint that is clay filled and strikes northwest, dips 80° northeast.
22	South wall has north-northwest striking joint which dips west at 85°.
28	Pluck out from above joint, which appears to be ¼ inch clay filled. Joint mentioned at 7 feet is here open 1/16 inch.
29	Northwest wall shows apex upward of joint. This joint strikes east-northeast and dips 80° to the northwest. Also on the northwest wall is a vertical joint that strikes south-southeast.
32-45	Southeast wall of hole is badly broken along upward apex at joint.
46	Hole badly broken on southwest wall. Master joint is vertical and strikes east-southeast. It is open ½ inch.
51	Very few joints except master joint mentioned at 46 feet.
57	Southeast wall contains a system of high angle joints.
62	Water-laid sand, 1½ feet thick on north wall and very thin or stripped away on the other walls of the hole.

Table 25.--Reconnaissance notes for large-diameter holes - Continued

Area 4 - Continued

Hole 4-Y - Continued

Depth (feet)	
62-69	Wall of hole contains very friable tuff below sand. West wall contains joint striking north-northeast, dipping 85° north. West wall has joint which is vertical and strikes north-northeast. These two joints apparently are not the same.

Table 26.--Reconnaissance notes for large-diameter holes - Continued

Area 10

Area 10 contains two 6-foot diameter holes 25 feet apart and drilled to a depth of about 60 feet. The two holes are connected at the bottom by a horizontal drift. Only the westernmost hole and the drift were examined.

West hole

Diameter - 6 feet
(except for bottom 12 feet, which is 13 feet)

Depth (feet)	
0-1	Back-fill, broken tuff. Most of soil is stripped off.
1-3.5	Pumice, layered, light gray with brownish clay lenses included.
3.5-5	Weathered zone containing partially weathered tuff fragments in a matrix of brown clay.
5	Joint on south wall is ¼ inch clay filled and strikes north-northeast. Tuff has pebble-size, purplish devitrified pumice fragments.
10	Broken zone.
17	Joint mentioned at 5 feet persists through broken zone, but is only 1/8 inch clay filled. Joint on east-northeast wall originates in broken zone, strikes northeast, and is ¼ inch clay filled.
18-23	Badly broken zone. Joints are irregular; roots noted in north striking joint on northeast wall.

Table 25.--Reconnaissance notes for large-diameter holes - Continued

Area 10 - Continued

West hole - Continued

Depth (feet)	
33	Joints strike northwest and north and are open 1/8 to 1½ inches.
48	Top of 13-foot diameter hole. Joint striking south-southwest. Joints on north-northeast wall are ¼ inch clay filled.
50	Top of weathered zone in tuff above sand dips to the northeast.
54	Top of sand dips to the northwest at a low angle. Sand is stripped away on southwest wall and thickens to about 2 feet on east wall near drift. Joints found about 2 feet below sand are sand filled and open from ¼ to 2 inches. Tuff below sand is weathered, highly pumiceous, and friable. Joint in bottom of west hole is open several feet below bottom of hole.

Area 10

The drift extends east-west between the two large diameter vertical holes. On entering the drift from the east hole, weathered pumiceous tuff extends upward on the north wall and then cuts across the top of the drift to the south wall a few feet east of the portal to west hole. The tuff is about 9 feet thick on the north side of the drift and contains an abundance of quartz and irregular brownish iron-stained streaks.

Appendix

Figures 54A
Through 62B
consists of
geophysical logs
of Core Holes, Test Wells,
and Obs Holes
were not reproduced
for This Report -
One Set Available
in Original Report

Figure 54A.--Gamma ray-neutron logs of well DT-5, TA-49

Los Alamos County, N. Mex.

Figure 54B--Induction log of well DT-5, TA-49

Los Alamos County, N. Mex.

(3)

LOS ALAMOS SCIENTIFIC LABORATORY

Figure 54C.--Temperature log of well DT-5, TA-49,

Los Alamos County, N. Mex.

(4)

Figure 55A.--Gamma ray-neutron logs of well DT-5A, TA-49, Los Alamos County, N. Mex.

Figure 55B.--Induction-electrical and spontaneous-potential logs of well DT-5A, TA-49

Los Alamos County, N. Mex.

(4)

Figure 55C.--Microlog and microcaliper log of well DT-5A, TA-49, Los Alamos County, N. Mex.

Figure 55D.--Laterolog of well DT-5A, TA-49

Los Alamos County, N. Mex.

Figure 55E.--Temperature log of well DT-5A, TA-49

Los Alamos County, N. Mex.

Figure 55F.--Sonic log of well DT-5A, TA-49

Los Alamos County, N. Mex.

COUNTY LOS ALAMOS, NEW MEXICO
FIELD or LOCATION UNDESIGNATED
WELL DEEP HOLE #1

Log Depth
RUN No.
Date
First Reading
Last Reading
Feet Measur
Csg. Schlum
Csg. Driller
Depth Reach
Bottom Drill
Mud Nat.
Dens. Vi
Mud Resist.
" Res. BH
" pH
" Wtr. Lo
" Rmf
Bit Size
Span:
3'
Opr. Rig Tim
Truck No.
Recorded By
Witness

(10)

Figure 56A.--Gamma ray-neutron logs of the upper 1,301 feet of well DT-9, TA-49, Los Alamos County, N. Mex.

Figure 56B.--Gamma-ray log from depth of 1,094 to 1,501 feet of well DT-9, TA-49, Los Alamos County, N. Mex.

Figure 56C.--Induction-electrical and spontaneous-potential logs of well DT-9, TA-49

Los Alamos County, N. Mex.

COUNTY LOS ALAMOS, NEW MEXICO
FIELD or
LOCATION UNDESIGNATED

RUN
Date
First R
Last R
Feet M
Csg. S
Csg. D
Depth
Bottom
Depth
Mud M
Dens.
Mud R
" R
R
R
" F
" S
Bit Si
Spcg
Opr.
Truck
Record
Witne

(13)

Figure 56D.--Lateralog of well DT-9, TA-49

Los Alamos County, N. Mex.

Figure 56E.--Temperature log of well DT-9, TA-49

Los Alamos County, N. Mex.

COUNTY LOS ALAMOS, NEW MEX.
FIELD or LOCATION UNDESIGNATED

Date
First Rec
Last Rea
Footage
Max. De
Bottom
Hole Siz
Casing S
Depth D
Mud Da
Fluid Lev
Max. Ter
Cementa
Circulatic
A-Cem
1)
2)
3)
4)
B-Loca
1)
2)
Truck No
Recorded
Witnesse

Figure 56F.--Sonic log of well DT-9, TA-49

Los Alamos County, N. Mex.

COUNTY LOS ALAMOS, NEW MEXICO
Lo
R
Date
First
Last
Feet
Csg.
Csg.
Dept
Botto
Mud
Dens
Mud
"
"
"
"
Bit Si
Span
Opr.
Truck
Recor
Witn

Figure 57A.--Gamma ray-neutron log of

well DT-10, TA-49

Los Alamos County, N. Mex.

SCHLUMB

COUNTY LOS ALAMOS, NEW MEX.
FIELD or LOCATION UNDESIGNATED
WELL T.A. 49
COMPANY THE ZIA COMPANY

Log Depths Measur

RUN NO.
Date
First Reading
Last Reading
Footage Measured
Max. Depth Reach
Bottom Driller
Maximum Temp. °
Fluid Nature
Fluid Level
Casing Size
Casing Weight
Casing Size
Casing Weight
Bit Size
Bit Size
No. Counters Used
Type Equipment
Type Panel
Opr. Rig Time
Truck No.
Observer
Witness

(17)

Figure 57B.--Induction-electrical and spontaneous-potential logs of well DT-10, TA-49

Los Alamos County, N. Mex.

Figure 57C.--Temperature log of well DT-10, TA-49.

Los Alamos County, N. Mex.

SCHI

COUNTY LOS ALAMOS, NEW MEXICO
FIELD or
LOCATION UNDESIGNATED
WELL D.T. 10

Date 3-
First Readin
Last Readin
Footage Me
Max. Depth
Bottom Drill
Hole Size
Casing Size
Depth Datur
Mud Data
Fluid Level
Max. Temp.
Cementatior
Circulation
A-Cemen
1) Dat
2) Am
3) Cal
4) Dep
B-Locatior
1) Cas
2) Dat
Truck No.
Recorded By
Witnessed B

Figure 57D.--Sonic log of well DT-10, TA-49

Los Alamos County, N. Mex.

Figure 58.--Gamma ray log of core hole 1 in Area 1, TA-49, Los Alamos County, N. Mex.

Figure 59A.--Gamma log of core hole 2 in Area 2, TA-49,

Los Alamos County, N. Mex.

Figure 59B.--Gamma ray-neutron log of upper 210 feet of core hole 2 in Area 2, TA-49, Los Alamos County, N. Mex.

SCHLUM

COUNTY
FIELD or LOCATION
WELL
COMPANY

Log Depth Mec

RUN NO

Date
First Reading
Last Reading
Footage Measu
Max. Depth Rec
Bottom Driller
Maximum Temp
Fluid Nature
Fluid Level
Casing Size
Casing Weight
Casing Size
Casing Weight
Bit Size
Bit Size
No. Counters U
Type Equipment
Type Panel
Opr. Rig Time
Truck No.
Observer
Witness

Figure 59C.--Electrical log of the upper 368 feet of core hole 2 in Area 2, TA-49, Los Alamos County, N. Mex.

Figure 59D.--Temperature log of the upper 200 feet of core hole 2 in Area 2, TA-49 Los Alamos County, N. Mex.

Figure 60.--Gamma-ray log of core hole 3 in Area 3, TA-49, Los Alamos County, N. Mex.

Figure 61.--Gamma-ray log of core hole 4 in Area 4, TA-49, Los Alamos County, N. Mex.

Property of Field Mus. U. S. Atomic Energy Commission

Figure 62A.--Gamma ray-neutron logs of Alpha hole, TA-49

Los Alamos County, N. Mex.

Figure [illegible]--Induction log of Alpha hole, TA-[illegible]

Los Alamos County, N. Mex.

Fig. 62B
Induction log of
Alpha Hole, TA-49